7041 (32)

NASA

Earth Resources
A Continuing
Bibliography
with Indexes

NASA SP-7041(32)
January 1982

NEWARK PUBLIC LIBRARY

JUN 8 1982

U. S. GOVT. PUBS.
DEPOSITORY 376

National Aeronautics and
Space Administration

es Earth Resourc
s Earth Resources
arth Resources E
th Resources Ear
Resources Earth
esources Earth R
sources Earth Re

NAS 1.21:

ACCESSION NUMBER RANGES

Accession numbers cited in this Supplement fall within the following ranges:

IAA (A-10000 Series)	A81-40833 – A81-49982
STAR (N-10000 Series)	N81-28047 – N81-34139

This bibliography was prepared by the NASA Scientific and Technical Information Facility operated for the National Aeronautics and Space Administration by PRC Government Information Systems.

NASA SP-7041 (32)

EARTH RESOURCES

A Continuing Bibliography
With Indexes
Issue 32

A selection of annotated references to unclassified reports and journal articles that were introduced into the NASA scientific and technical information system and announced between October 1 and December 31, 1981 in

- *Scientific and Technical Aerospace Reports (STAR)*
- *International Aerospace Abstracts (IAA).*

Scientific and Technical Information Branch 1982
National Aeronautics and Space Administration
Washington, DC

READEX FICHE best copy available

This supplement is available as NTISUB/038/093 from the National Technical Information Service (NTIS), Springfield, Virginia 22161 at the price of $10.50 domestic; $21.50 foreign for standing orders. Please note: Standing orders are subscriptions which do not terminate at the end of a year, as do regular subscriptions, but continue indefinitely unless specifically terminated by the subscriber.

INTRODUCTION

The technical literature described in this continuing bibliography may be helpful to researchers in numerous disciplines such as agriculture and forestry, geography and cartography, geology and mining, oceanography and fishing, environmental control, and many others. Until recently it was impossible for anyone to examine more than a minute fraction of the earth's surface continuously. Now vast areas can be observed synoptically, and changes noted in both the earth's lands and waters, by sensing instrumention on orbiting spacecraft or on aircraft.

This literature survey lists 580 reports, articles, and other documents announced between October 1 and December 31, 1981 in *Scientific and Technical Aerospace Reports (STAR)*, and *International Aerospace Abstracts (IAA)*.

The coverage includes documents related to the identification and evaluation by means of sensors in spacecraft and aircraft of vegetation, minerals, and other natural resources, and the techniques and potentialities of surveying and keeping up-to-date inventories of such riches. It encompasses studies of such natural phenomena as earthquakes, volcanoes, ocean currents, and magnetic fields; and such cultural phenomena as cities, transportation networks, and irrigation systems. Descriptions of the components and use of remote sensing and geophysical instrumentation, their subsystems, observational procedures, signature and analyses and interpretive techniques for gathering data are also included. All reports generated under NASA's Earth Resources Survey Program for the time period covered in this bibliography will also be included. The bibliography does not contain citations to documents dealing mainly with satellites or satellite equipment used in navigation or communication systems, nor with instrumentation not used aboard aerospace vehicles.

The selected items are grouped in nine categories. These are listed in the Table of Contents with notes regarding the scope of each category. These categories were especially chosen for this publication, and differ from those found in *STAR* and *IAA*.

Each entry consists of a standard bibliographic citation accompanied by an abstract. The citations and abstracts are reproduced exactly as they appeared originally in *STAR*, or *IAA*, including the original accession numbers from the respective announcement journals. This procedure, which saves time and money, accounts for the variation in citation appearance.

Under each of the nine categories, the entries are presented in one of two groups that appear in the following order:

IAA entries identified by accession number series A81-10,000 in ascending accession number order;

STAR entries identified by accession number series N81-10,000 in ascending accession number order.

After the abstract section, there are five indexes:

subject, personal author, corporate source, contract number and report/accession number.

AVAILABILITY OF CITED PUBLICATIONS

IAA ENTRIES (A81-10000 Series)

All publications abstracted in this Section are available from the Technical Information Service, American Institute of Aeronautics and Astronautics, Inc. (AIAA), as follows: Paper copies of accessions are available at $7.00 per document up to a maximum of 40 pages. The charge for each additional page is $0.25. Microfiche[1] of documents announced in *IAA* are available at the rate of $3.00 per microfiche on demand, and at the rate of $1.25 per microfiche for standing orders for all *IAA* microfiche. The price for the *IAA* microfiche by category is available at the rate of $1.50 per microfiche plus a $1.00 service charge per category per issue. Microfiche of all the current AIAA Meeting Papers are available on a standing order basis at the rate of $1.50 per microfiche.

Minimum air-mail postage to foreign countries is $1.00 and all foreign orders are shipped on payment of pro-forma invoices.

All inquiries and requests should be addressed to AIAA Technical Information Service. Please refer to the accession number when requesting publications.

STAR ENTRIES (N81-10000 Series)

One or more sources from which a document announced in *STAR* is available to the public is ordinarily given on the last line of the citation. The most commonly indicated sources and their acronyms or abbreviations are listed below. If the publication is available from a source other than those listed, the publisher and his address will be displayed on the availability line or in combination with the corporate source line.

Avail: NTIS. Sold by the National Technical Information Service. Prices for hard copy (HC) and microfiche (MF) are indicated by a price code followed by the letters HC or MF in the *STAR* citation. Current values for the price codes are given in the tables on page vii.

Documents on microfiche are designated by a pound sign (#) following the accession number. The pound sign is used without regard to the source or quality of the microfiche.

Initially distributed microfiche under the NTIS SRIM (Selected Research in Microfiche) is available at greatly reduced unit prices. For this service and for information concerning subscription to NASA printed reports, consult the NTIS Subscription Section, Springfield, Va. 22161.

NOTE ON ORDERING DOCUMENTS: When ordering NASA publications (those followed by the * symbol), use the N accession number. NASA patent applications (only the specifications are offered) should be ordered by the US-Patent-Appl-SN number. Non-NASA publications (no asterisk) should be ordered by the AD, PB, or other *report* number shown on the last line of the citation, not by the N accession number. It is also advisable to cite the title and other bibliographic identification.

Avail: SOD (or GPO). Sold by the Superintendent of Documents, U.S. Government Printing Office, in hard copy. The current price and order number are given following the availability line. (NTIS will fill microfiche requests, at the standard $4.00 price, for those documents identified by a # symbol.)

---

(1) A microfiche is a transparent sheet of film, 105 by 148 mm in size, containing as many as 60 to 98 pages of information reduced to micro images (not to exceed 26:1 reduction).

Avail: NASA Public Document Rooms. Documents so indicated may be examined at or purchased from the National Aeronautics and Space Administration, Public Documents Room (Room 126), 600 Independence Ave., S.W., Washington, D.C. 20546, or public document rooms located at each of the NASA research centers, the NASA Space Technology Laboratories, and the NASA Pasadena Office at the Jet Propulsion Laboratory.

Avail: DOE Depository Libraries. Organizations in U.S. cities and abroad that maintain collections of Department of Energy reports, usually in microfiche form, are listed in *Energy Research Abstracts*. Services available from the DOE and its depositories are described in a booklet, *DOE Technical Information Center - Its Functions and Services* (TID-4660), which may be obtained without charge from the DOE Technical Information Center.

Avail: Univ. Microfilms. Documents so indicated are dissertations selected from *Dissertation Abstracts* and are sold by University Microfilms as xerographic copy (HC) and microfilm. All requests should cite the author and the Order Number as they appear in the citation.

Avail: USGS. Originals of many reports from the U.S. Geological Survey, which may contain color illustrations, or otherwise may not have the quality of illustrations preserved in the microfiche or facsimile reproduction, may be examined by the public at the libraries of the USGS field offices whose addresses are listed in this introduction. The libraries may be queried concerning the availability of specific documents and the possible utilization of local copying services, such as color reproduction.

Avail: HMSO. Publications of Her Majesty's Stationery Office are sold in the U.S. by Pendragon House, Inc. (PHI), Redwood City, California. The U.S. price (including a service and mailing charge) is given, or a conversion table may be obtained from PHI.

Avail:- BLL (formerly NLL): British Library Lending Division, Boston Spa, Wetherby, Yorkshire, England. Photocopies available from this organization at the price shown. (If none is given, inquiry should be addressed to the BLL.)

Avail: Fachinformationszentrum, Karlsruhe. Sold by the Fachinformationszentrum Energie, Physik, Mathematik GMBH, Eggenstein Leopoldshafen, Federal Republic of Germany, at the price shown in deutschmarks (DM).

Avail: Issuing Activity, or Corporate Author, or no indication of availability. Inquiries as to the availability of these documents should be addressed to the organization shown in the citation as the corporate author of the document.

Avail: U.S. Patent and Trademark Office. Sold by Commissioner of Patents and Trademarks, U.S. Patent and Trademark Office, at the standard price of 50 cents each, postage free.

Other availabilities: If the publication is available from a source other than the above, the publisher and his address will be displayed entirely on the availability line or in combination with the corporate author line.

ADDRESSES OF ORGANIZATIONS

American Institute of Aeronautics
and Astronautics
Technical Information Service
555 West 57th Street, 12th Floor
New York, New York 10019

British Library Lending Division,
Boston Spa, Wetherby, Yorkshire,
England

Commissioner of Patents and
Trademarks
U.S. Patent and Trademark Office
Washington, D.C. 20231

Department of Energy
Technical Information Center
P.O. Box 62
Oak Ridge, Tennessee 37830

ESA-Information Retrieval Service
ESRIN
Via Galileo Galilei
00044 Frascati (Rome) Italy

Fachinformationszentrum Energie, Physik,
Mathematik GMBH
7514 Eggenstein Leopoldshafen
Federal Republic of Germany

Her Majesty's Stationery Office
P.O. Box 569, S.E. 1
London, England

NASA Scientific and Technical Information
Facility
P.O. Box 8757
B. W. I. Airport, Maryland 21240

National Aeronautics and Space
Administration
Scientific and Technical Information
Branch (NST-41)
Washington, D.C. 20546

National Technical Information Service
5285 Port Royal Road
Springfield, Virginia 22161

Pendragon House, Inc.
899 Broadway Avenue
Redwood City, California 94063

Superintendent of Documents
U.S. Government Printing Office
Washington, D.C. 20402

University Microfilms
A Xerox Company
300 North Zeeb Road
Ann Arbor, Michigan 48106

University Microfilms, Ltd.
Tylers Green
London, England

U.S. Geological Survey
1033 General Services Administration
Building
Washington, D.C. 20242

U.S. Geological Survey
601 E. Cedar Avenue
Flagstaff, Arizona 86002

U.S. Geological Survey
345 Middlefield Road
Menlo Park, California 94025

U.S. Geological Survey
Bldg. 25, Denver Federal Center
Denver, Colorado 80225

NTIS PRICE SCHEDULES

Schedule A

STANDARD PAPER COPY PRICE SCHEDULE

(Effective January 1, 1982)

Price Code	Page Range	North American Price	Foreign Price
A01	Microfiche	$ 4.00	$ 8.00
A02	001-025	6.00	12.00
A03	026-050	7.50	15.00
A04	051-075	9.00	18.00
A05	076-100	10.50	21.00
A06	101-125	12.00	24.00
A07	126-150	13.50	27.00
A08	151-175	15.00	30.00
A09	176-200	16.50	33.00
A10	201-225	18.00	36.00
A11	226-250	19.50	39.00
A12	251-275	21.00	42.00
A13	276-300	22.50	45.00
A14	301-325	24.00	48.00
A15	326-350	25.50	51.00
A16	351-375	27.00	54.00
A17	376-400	28.50	57.00
A18	401-425	30.00	60.00
A19	426-450	31.50	63.00
A20	451-475	33.00	66.00
A21	476-500	34.50	69.00
A22	501-525	36.00	72.00
A23	526-550	37.50	75.00
A24	551-575	39.00	78.00
A25	576-600	40.50	81.00
	601-up	-- 1/	-- 2/

A99 - Write for quote

1/ Add $1.50 for each additional 25 page increment or portion thereof for 601 pages up

2/ Add $3.00 for each additional 25 page increment or portion thereof for 601 pages and more

Schedule E

EXCEPTION PRICE SCHEDULE

Paper Copy & Microfiche

Price Code	North American Price	Foreign Price
E01	$ 6.50	$ 13.50
E02	7.50	15.50
E03	9.50	19.50
E04	11.50	23.50
E05	13.50	27.50
E06	15.50	31.50
E07	17.50	35.50
E08	19.50	39.50
E09	21.50	43.50
E10	23.50	47.50
E11	25.50	51.50
E12	28.50	57.50
E13	31.50	63.50
E14	34.50	69.50
E15	37.50	75.50
E16	40.50	81.50
E17	43.50	88.50
E18	46.50	93.50
E19	51.50	102.50
E20	61.50	123.50

E99 - Write for quote

N01	30.00	45.00

TABLE OF CONTENTS

Subject Categories

Abstracts in this Bibliography are grouped under the following categories: *page:*

01 AGRICULTURE AND FORESTRY 197
Includes crop forecasts, crop signature analysis, soil identification, disease detection, harvest estimates, range resources, timber inventory, forest fire detection, and wildlife migration patterns.

02 ENVIRONMENTAL CHANGES AND CULTURAL RESOURCES 213
Includes land use analysis, urban and metropolitan studies, environmental impact, air and water pollution, geographic information systems, and geographic analysis.

03 GEODESY AND CARTOGRAPHY 221
Includes mapping and topography.

04 GEOLOGY AND MINERAL RESOURCES 225
Includes mineral deposits, petroleum deposits, spectral properties of rocks, geological exploration, and lithology.

05 OCEANOGRAPHY AND MARINE RESOURCES 231
Includes sea-surface temperature, ocean bottom surveying imagery, drift rates, sea ice and icebergs, sea state, fish location.

06 HYDROLOGY AND WATER MANAGEMENT 243
Includes snow cover and water runoff in rivers and glaciers, saline intrusion, drainage analysis, geomorphology of river basins, land uses, and estuarine studies.

07 DATA PROCESSING AND DISTRIBUTION SYSTEMS 257
Includes film processing, computer technology, satellite and aircraft hardware, and imagery.

08 INSTRUMENTATION AND SENSORS 269
Includes data acquisition and camera systems and remote sensors.

09 GENERAL 277
Includes economic analysis.

SUBJECT INDEX **A-1**
PERSONAL AUTHOR INDEX **B-1**
CORPORATE SOURCE INDEX **C-1**
CONTRACT NUMBER INDEX **D-1**
REPORT/ACCESSION NUMBER INDEX **E-1**

TYPICAL CITATION AND ABSTRACT FROM *STAR*

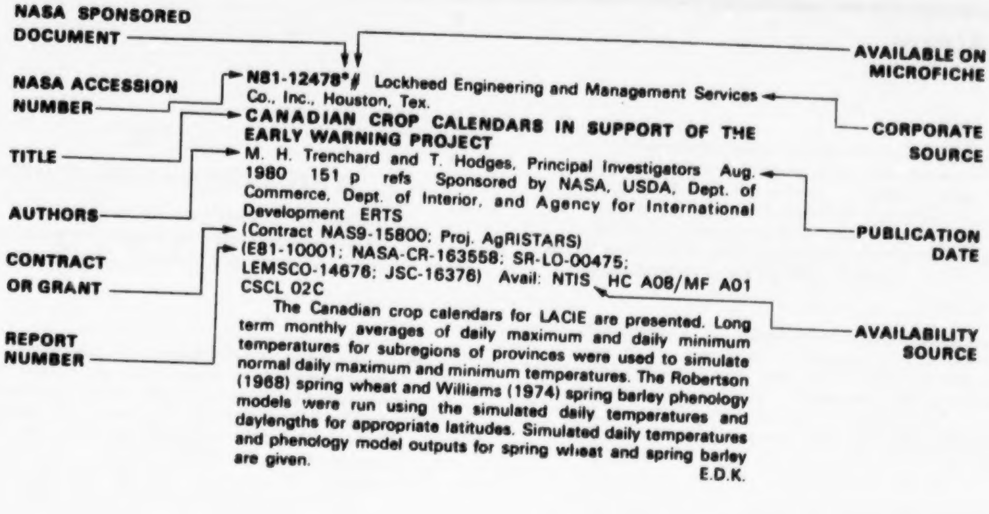
NASA SPONSORED DOCUMENT
AVAILABLE ON MICROFICHE
NASA ACCESSION NUMBER
CORPORATE SOURCE
TITLE
AUTHORS
PUBLICATION DATE
CONTRACT OR GRANT
REPORT NUMBER
AVAILABILITY SOURCE

N81-12478*# Lockheed Engineering and Management Services Co., Inc., Houston, Tex.

CANADIAN CROP CALENDARS IN SUPPORT OF THE EARLY WARNING PROJECT

M. H. Trenchard and T. Hodges, Principal Investigators Aug. 1980 151 p refs Sponsored by NASA, USDA, Dept. of Commerce, Dept. of Interior, and Agency for International Development ERTS

(Contract NAS9-15800; Proj. AgRISTARS)

(E81-10001; NASA-CR-163558; SR-LO-00475; LEMSCO-14676; JSC-16376) Avail: NTIS HC A08/MF A01 CSCL 02C

The Canadian crop calendars for LACIE are presented. Long term monthly averages of daily maximum and daily minimum temperatures for subregions of provinces were used to simulate normal daily maximum and minimum temperatures. The Robertson (1968) spring wheat and Williams (1974) spring barley phenology models were run using the simulated daily temperatures and daylengths for appropriate latitudes. Simulated daily temperatures and phenology model outputs for spring wheat and spring barley are given.

E.D.K.

TYPICAL CITATION AND ABSTRACT FROM *IAA*

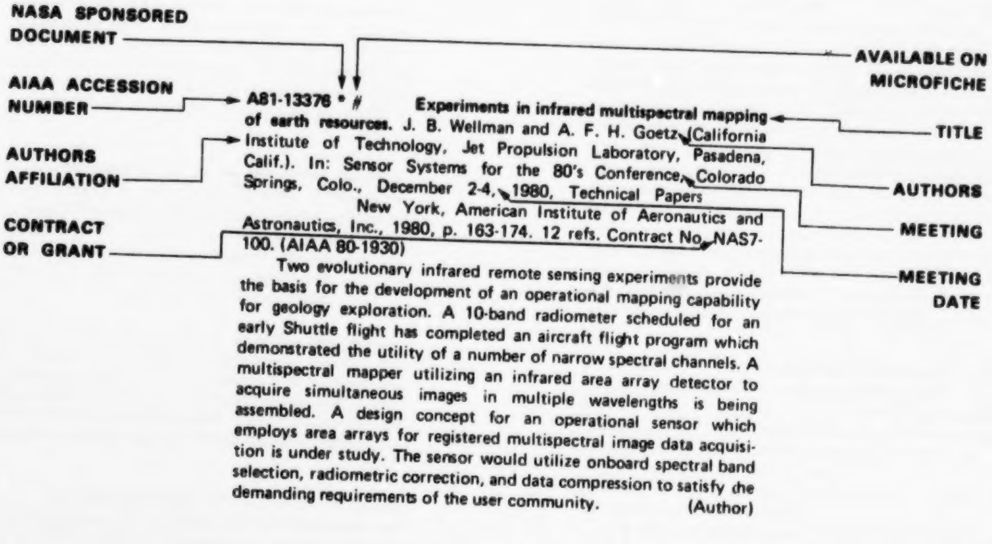
NASA SPONSORED DOCUMENT
AVAILABLE ON MICROFICHE
AIAA ACCESSION NUMBER
TITLE
AUTHORS AFFILIATION
AUTHORS
MEETING
CONTRACT OR GRANT
MEETING DATE

A81-13376 * # **Experiments in infrared multispectral mapping of earth resources.** J. B. Wellman and A. F. H. Goetz (California Institute of Technology, Jet Propulsion Laboratory, Pasadena, Calif.). In: Sensor Systems for the 80's Conference, Colorado Springs, Colo., December 2-4, 1980, Technical Papers New York, American Institute of Aeronautics and Astronautics, Inc., 1980, p. 163-174. 12 refs. Contract No. NAS7-100. (AIAA 80-1930)

Two evolutionary infrared remote sensing experiments provide the basis for the development of an operational mapping capability for geology exploration. A 10-band radiometer scheduled for an early Shuttle flight has completed an aircraft flight program which demonstrated the utility of a number of narrow spectral channels. A multispectral mapper utilizing an infrared area array detector to acquire simultaneous images in multiple wavelengths is being assembled. A design concept for an operational sensor which employs area arrays for registered multispectral image data acquisition is under study. The sensor would utilize onboard spectral band selection, radiometric correction, and data compression to satisfy the demanding requirements of the user community. (Author)

TABLE OF CONTENTS

EARTH RESOURCES

A Continuing Bibliography (Issue 32)

JANUARY 1982

01

AGRICULTURE AND FORESTRY

Include crop forecasts, crop signature analysis, soil identification, disease detection, harvest estimates, range resources, timber inventory, forest fire detection, and wildlife migration patterns.

A81-41485 # **Results of ground surveys, carried out in conjunction with satellite and aerial studies, of the state of winter wheat on the Kursk test polygon (Rezul'taty nazemnykh podsputnikovykh i podsamoletnykh issledovanii sostoianiia ozimoi pshenitsy na testovom uchastke Kurskogo poligona).** N. V. Beliaeva and T. M. Vasiukhina. In: Some results on the investigation of earth resources by aerial and polygon methods. Leningrad, Gidrometeoizdat, 1980, p. 51-63. 12 refs. In Russian.

A81-41486 # **Determination of the types and state of crops from multispectral aerial photographs (Opredelenie vidov i sostoianiia sel'skokhoziaistvennykh kul'tur po materialam mnogozonal'noi aerofotos'emki).** T. M. Vasiukhina and N. K. Vinnichenko. In: Some results on the investigation of earth resources by aerial and polygon methods. Leningrad, Gidrometeoizdat, 1980, p. 64-72. 5 refs. In Russian.

A81-41487 # **Evaluation of the possibility of using spectral-band and multispectral aerial photographs for the large-scale survey of natural pastures (Otsenka vozmozhnosti ispol'zovaniia spektrozonal'nykh i mnogozonal'nykh aerofotosnimkov dlia krupnomasshtabnogo obsledovaniia prirodnykh kormovykh ugodii).** N. V. Beliaeva, V. B. Golub, and E. V. Tsvetaeva. In: Some results on the investigation of earth resources by aerial and polygon methods. Leningrad, Gidrometeoizdat, 1980, p. 73-79. 7 refs. In Russian.

A81-41488 # **The possibilities of the automated classification of agricultural objects on the basis of their multispectral aerial-spaceborne images (Vozmozhnosti avtomatizirovannoi klassifikatsii sel'skokhoziaistvennykh ob'ektov po ikh mnogozonal'nym aerokosmicheskim izobrazheniiam).** G. G. Andreev. In: Some results on the investigation of earth resources by aerial and polygon methods. Leningrad, Gidrometeoizdat, 1980, p. 80-85. 5 refs. In Russian.

The paper examines software aspects of the automated processing of aerial and spaceborne images of agricultural regions; the purpose of the processing is to classify agricultural objects on the basis of their photometric features and to identify these objects with crops. Particular attention is given to a method that involves the use of a chain of recognition algorithms. Applications of this method are considered. B.J.

A81-41489 # **Practical application of the method of empty blocks for the computerized determination of the boundaries of agricultural objects (Prakticheskoe primenenie metoda pustykh blokov dlia vydeleniia granits sel'skokhoziaistvennykh ob'ektov s pomoshch'iu EVM).** G. G. Andreev and L. N. Choban. In: Some results on the investigation of earth resources by aerial and polygon methods. Leningrad, Gidrometeoizdat, 1980, p. 86-92. In Russian.

An important problem in the machine analysis of multispectral images of agricultural objects is the determination of the boundaries of these objects. The criterion of empty blocks (a method for verifying nonparametric statistical hypotheses) is proposed as a method for determining these boundaries. Algorithms of the main program and the learning program are presented along with examples of computation on the EC-1022 computer. B.J.

A81-43181 **Agricultures's needs related to satellite hydrology.** E. T. Engman (U.S. Department of Agriculture, Hydrology Laboratory, Beltsville, MD). In: Satellite hydrology; Proceedings of the Fifth Annual William T. Pecora Memorial Symposium on Remote Sensing, Sioux Falls, SD, June 10-15, 1979. Minneapolis, MN, American Water Resources Association, 1981, p. 19-25. 10 refs.

A81-43221 * **Survey of in-situ and remote sensing methods for soil moisture determination.** T. J. Schmugge (NASA, Goddard Space Flight Center, Laboratory for Atmospheric Sciences, Greenbelt, MD), T. J. Jackson (U.S. Department of Agriculture, Hydrology Laboratory, Beltsville, MD), and H. L. McKim (U.S. Army, Cold Regions Research Engineering Laboratory, Hanover, NH). In: Satellite hydrology; Proceedings of the Fifth Annual William T. Pecora Memorial Symposium on Remote Sensing, Sioux Falls, SD, June 10-15, 1979. Minneapolis, MN, American Water Resources Association, 1981, p. 333-352. 152 refs.

General methods for determining the moisture content in the surface layers of the soil based on in situ or point measurements, soil water models and remote sensing observations are surveyed. In situ methods described include gravimetric techniques, nuclear techniques based on neutron scattering or gamma-ray attenuation, electromagnetic techniques, tensiometric techniques and hygrometric techniques. Soil water models based on column mass balance treat soil moisture contents as a result of meteorological inputs (precipitation, runoff, subsurface flow) and demands (evaporation, transpiration, percolation). The remote sensing approaches are based on measurements of the diurnal range of surface temperature and the crop canopy temperature in the thermal infrared, measurements of the radar backscattering coefficient in the microwave region, and measurements of microwave emission or brightness temperature. Advantages and disadvantages of the various methods are pointed out, and it is concluded that a successful monitoring system must incorporate all of the approaches considered. A.L.W.

A81-43224 * **Soil moisture applications of the heat capacity mapping mission.** J. L. Heilman (Texas A&M University, College Station, TX) and D. G. Moore (South Dakota State University, Brookings, SD). In: Satellite hydrology; Proceedings of the Fifth Annual William T. Pecora Memorial Symposium on Remote Sensing, Sioux Falls, SD, June 10-15, 1979. Minneapolis, MN, American Water Resources Association, 1981, p. 371-376. 5 refs. Contract No. NAS5-2406.

Results are presented of ground, aircraft and satellite investigations conducted to evaluate the potential of the Heat Capacity Mapping Mission (HCMM) to monitor soil moisture and the depth of shallow ground water. The investigations were carried out over eastern South Dakota to evaluate the relation between directly measured soil temperatures and water content at various stages of canopy development, aircraft thermal scanner measurements of apparent canopy temperature and the reliability of actual HCMM data. The results demonstrate the possibility of evaluating soil moisture on the basis of HCMM apparent canopy temperature and day-night soil temperature difference measurements. Limitations on the use of thermal data posed by environmental factors which influence energy balance interactions, including phase transformations, wind patterns, topographic variations and atmospheric constituents are pointed out. A.L.W.

A81-43262 **A multistage mapping approach for an irrigated croplands inventory.** L. Tinney, J. Holloway, J. Baggett, and J. Estes (California, University, Santa Barbara, CA). In: Satellite hydrology; Proceedings of the Fifth Annual William T. Pecora Memorial Symposium on Remote Sensing, Sioux Falls, SD, June 10-15, 1979. Minneapolis, MN, American Water Resources Association, 1981, p. 694-696.

A81-43264 **Selected irrigation acreage estimates in northern Florida from Landsat data.** K. B. Webster, R. J. Musgrove (Suwannee River Water Management District, White Springs, FL), J. R. Lucas (Technicolor Graphic Services, Inc.; U.S. Geological Survey, EROS Data Center, Sioux Falls, SD), and A. L. Higer (U.S. Geological Survey, Miami, FL). In: Satellite hydrology; Proceedings of the Fifth Annual William T. Pecora Memorial Symposium on Remote Sensing, Sioux Falls, SD, June 10-15, 1979. Minneapolis, MN, American Water Resources Association, 1981, p. 701-705. Research supported by the U.S. Geological Survey.

A81-43265 * **Mapping irrigated lands in Western Kansas from Landsat.** T. H. L. Williams and J. Poracsky (Kansas, University, Lawrence, KS). In: Satellite hydrology; Proceedings of the Fifth Annual William T. Pecora Memorial Symposium on Remote Sensing, Sioux Falls, SD, June 10-15, 1979. Minneapolis, MN, American Water Resources Association, 1981, p. 707-714. 19 refs. Grant No. NGL-17-004-024.

A description is presented of a multidate visual interpretation technique for identifying and mapping irrigated lands in Western Kansas based on gray tone interpretation of Landsat imagery. The technique provides detailed maps of irrigated lands that can be updated yearly (from 1972 onwards) and used as the basis for calculations of water use and its temporal trends. A review of remote sensing work on irrigated lands indicates that three different types of study have evolved, involving various combinations of desired final data and the means of arriving at it. Attention is given to crop characteristics, the development of an interpretation technique, the interpretation procedure, the computer assisted output, and aspects of verification and accuracy. It is pointed out that the considered technique is likely to be applicable to similar situations of a semi-arid area dominated by a small number of crops. G.R.

A81-43266 **Mapping irrigated cropland on the High Plains using Landsat.** G. P. Thelin, T. L. Johnson, and R. A. Johnson (U.S. Geological Survey, Reston, VA). In: Satellite hydrology; Proceedings of the Fifth Annual William T. Pecora Memorial Symposium on Remote Sensing, Sioux Falls, SD, June 10-15, 1979. Minneapolis, MN, American Water Resources Association, 1981, p. 715-721.

A program has been recently undertaken to determine water use in the High Plains. The High Plains aquifer, the focus of the study, covers approximately 450,000 square kilometers. The study, called the High Plains Regional Aquifer-System Analysis is developing a computer model designed to simulate the ground water system throughout the High Plains aquifer. Three difference methods for mapping irrigated cropland were evaluated. The first method employed visual interpretation of classified source materials. The second method employs interpretation of Landsat multispectral images, and the third the digital analysis of Landsat data. It was found that digital analysis of Landsat multispectral data provides an efficient method of mapping irrigated cropland. After evaluating the three different methods for mapping the areal extent of irrigated cropland, plans are being made to complete the task of mapping for the entire extent of the High Plains Regional aquifer. G.R.

A81-43536 **Rainforest species on large-scale color photos.** B. J. Myers and M. L. Benson (Commonwealth Scientific and Industrial Research Organization, Div. of Forest Research, Canberra, Australia). *Photogrammetric Engineering and Remote Sensing*, vol. 47, Apr. 1981, p. 505-513. 16 refs.

The extreme variability and complexity of tropical rainforests preclude any detailed floristic classification from conventional small-scale black-and-white aerial photographs. This paper describes a study conducted in north Queensland of the use of large-scale color, color infrared, and black-and-white aerial photographs for the identification of tree species as a basis for rainforest classification. Normal color transparency film at 1:2000 scale was the best combination of film and scale for species identification. Six forest areas studied by five interpreters had a total of 111 different dominant and codominant species. In the test stands, 55 different rainforest species were correctly identified at least once. Twenty-four species were identified with more than 75 percent accuracy and 11 of these were correctly identified in every case examined by the five interpreters. Directions for future research are suggested. (Author)

A81-43537 **Extravisual damage detection - Defining the standard normal tree.** P. A. Murtha and J. A. McLean (British Columbia, University, Vancouver, Canada). *Photogrammetric Engineering and Remote Sensing*, vol. 47, Apr. 1981, p. 515-522. 9 refs. Research supported by the Natural Sciences and Engineering Research Council of Canada.

Large-scale color-infrared aerial photographs of an interior British Columbia Douglas-fir stand are examined by optical visual analysis techniques for evidence of tree damage. Red-, green-, and blue-filter optical densitometric measurements were taken from developed film dye-layers, and the red:green-, red:blue-, and green:blue-filter density ratios were calculated. Damages were classified according to type, and the trees were field-checked for accuracy of species designation, height, age, and other pathological conditions. Results of a diameter increment analysis indicated that diameter increments were related to damage classification, with damage type III Ob having a reduced radial increment of less than 0.05. Damage types III Oa and III Ob had darker or lighter magenta hues than neighboring normal trees, although they could not be separated visually by crown characteristics. Selective logging makes desirable the removal of slow growing trees, and this technique makes possible the thinning of damage type III Ob and III Ob/II E trees for selective logging programs. D.L.G.

A81-43540 * **Vegetable crop management with remote sensing.** C. H. Blazquez (NASA, Kennedy Space Center, Cocoa Beach, FL), R. A. Elliott (Systems Control, Inc. /VT/, Champlain Technology Industries, West Palm Beach, FL), and G. J. Edwards (Florida, University, Lake Alfred, FL). *Photogrammetric Engineering and Remote Sensing*, vol. 47, Apr. 1981, p. 543-547. 12 refs.

Repetitive aerial photography with color infrared (ACIR) and black-and-white infrared (B and WIR) films was taken of potato and tomato fields in southwest Florida during the spring season of 1975. Color differences observed in the photographs revealed different levels of soil moisture in the fields, improper ditch arrangements, poor stands of plants, and areas where late blight (Phytophthora infestans) (Mont.)d.By and early blight (Alternaria solani) (Ell. and Mart.) Jones and Grout. were defoliating potato plants. Photographs of fields before planting also indicated areas where excessive rock formations existed which would make field preparation costly. Preplanting photographs also pinpointed areas with different water table levels. (Author)

A81-43727 **Rainbow 80; Fall Technical Meeting, Niagara Falls, NY, October 7-10, 1980, ASP Technical Papers.** Meeting sponsored by the American Society of Photogrammetry and American Congress on Surveying and Mapping. Falls Church VA, American Society of Photogrammetry, 1981. 358 p.

Topics discussed include new uses of photogrammetric techniques, current digital processing for interfacing cartography, and photogrammetry and land remote sensing and data acquisition. Particular consideration is given to remote sensing plant science applications, such as the use of remote sensing data in predicting vegetative variables, detecting crop stress, and interpreting landscape patterns. Imaging radar used in geology, hydrospherics, and environmental impact assessment are also discussed. J.F.

A81-43732 **Mountain pine beetle damage surveys with high-altitude panoramic photography.** B. B. Eav, R. D. Dillman, J. C. Prill, and R. E. Hinkle (Lockheed Engineering and Management Services Co., Inc., Houston, TX). In: Rainbow 80; Fall Technical Meeting, Niagara Falls, NY, October 7-10, 1980, ASP Technical Papers. Falls Church, VA, American Society of Photogrammetry, 1981, p. DA-1-D-1 to DA-1-D-14. 10 refs. U.S. Department of Agriculture Contract No. 53-3187-8-25.

An investigation of the potential of high altitude panoramic photography obtained with Itek KA-80A optical bar camera, compared with conventional surveys, for improving the efficiency of statewide mountain pine beetle (Dendroctonus ponderosa Hopkins) damage assessment involved the development of an appropriate survey design. The survey design initially developed for a small scale test using data from the Black Hills National Forest in South Dakota was a two-stage sampling with probability proportional to size in each stage. This design was refined and modified to include a third stage for application on a large scale in the Colorado Front Range comprising 5.5 million acres. Results indicate that optical bar surveys are a realistic alternative to conventional survey techniques and potentially more cost effective. (Author)

A81-43737 **The effect of sensor bandpass and spectral response in crop stress detection.** M. J. Duggin (New York, State University, Syracuse, NY) and P. N. Slater (Arizona, University, Tucson, AZ). In: Rainbow 80; Fall Technical Meeting, Niagara Falls, NY, October 7-10, 1980, ASP Technical Papers. Falls Church, VA, American Society of Photogrammetry, 1981, p. RS-2-C-1 to RS-2-C-12. 8 refs. Research supported by the U.S. Department of Agriculture and New York State Department of Environmental Conservation.

In order to map and to quantify vegetative disease using remote sensing it is necessary to be able to analyze the data to discern contrasts between healthy and diseased vegetative canopies, or between canopies affected by disease to different levels of severity. In order to perform such quantitative analysis, it is necessary to consider the interaction between the spectral reflectance of the target and the spectral response of the remote sensing device. While such interaction will be small for spectrally flat targets (e.g. white sand), they have been found to be larger for vegetation. Calculations are made to compare the contrasts obtained by using the outputs of each channel within each band of the Landsat multispectral scanners (MSS's) when looking at identical pairs of vegetative targets. Similar calculations are performed for Kodak color-infrared film (EK 2448) and for Kodak black-and-white infrared film (EK 2424). (Author)

A81-43738 * **Waveband evaluation of proposed thematic mapper in forest cover classification.** R. S. Latty and R. M. Hoffer (Purdue University, West Lafayette, IN). In: Rainbow 80; Fall Technical Meeting, Niagara Falls, NY, October 7-10, 1980, ASP Technical Papers. Falls Church, VA, American Society of Photogrammetry, 1981, p. RS-2-D-1 to RS-2-D-12. 31 refs. Contract No. NAS9-15889.

This study involved the evaluation of the characteristics of multispectral scanner data relative to forest cover type mapping, using NASA's NS-001 multispectral scanner to simulate the proposed Thematic Mapper (TM). The objectives were to determine: (1) the optimum number of wavebands to utilize in computer classifications of TM data; (2) which channel combinations provide the highest expected classification accuracy; and (3) the relative merit of each channel in the context of the cover classes examined. Transformed divergence was used as a measure of statistical distance between spectral class densities associated with each of twelve cover classes. The maximum overall mean pair-wise transformed divergence was used as the basis for evaluating all possible waveband combinations available for use in computer-assisted forest cover classifications. (Author)

A81-43740 * **Remote sensing aided procedure for conifer growth modeling in the northeastern Sierra Nevada.** H. G. Smith and S. Khorram (California, University, Berkeley, CA). In: Rainbow 80; Fall Technical Meeting, Niagara Falls, NY, October 7-10, 1980, ASP Technical Papers. Falls Church, VA, American Society of Photogrammetry, 1981, p. RS-2-F-1 to RS-2-F-13. 10 refs. Grant No. NGL-05-003-404.

The objective of this study was to use remotely-sensed data with ground-acquired data for preparing inputs to a mathematical model for generation of a potential conifer growth map of a wildland area. The study area, jointly selected by the resource managers of the U.S. Forest Service at the Plumas National Forest and researchers, covers approximately 500 sq km in the northeastern scrapment of Sierra Nevada. The approach involved a computerized databank based on both remotely-sensed and ground-acquired data. The remotely-sensed data included Landsat Multispectral Scanner (MSS) data, NOAA-5 Very High Resolution Radiometer (VHRR) data and U-2 Color infrared photography. The ground data included U.S. Geological Survey (USGS) topographic maps, Defense Mapping Agency (DMA)/USGS digital terrain data, soil maps, and vegetation data. The results included a series of maps for the final product as well as the intermediate products. The intermediate products were potential evapotranspiration, aspect, and soil plant available water. (Author)

A81-43741 * **Look direction dependence of radar backscattering cross section for agricultural fields.** W. P. Waite, H. C. MacDonald, J. S. Demarcke, and B. H. Corbell (Arkansas, University, Fayetteville, AR). In: Rainbow 80; Fall Technical Meeting, Niagara Falls, NY, October 7-10, 1980, ASP Technical Papers. Falls Church, VA, American Society of Photogrammetry, 1981, p. RS-2-G-1 to RS-2-G-14. 9 refs. Contracts No. NAS9-14251; No. JPL-954940.

Analysis of multifrequency-multipolarization scatterometer data acquired by NASA Johnson Space Center during the 1978 Colby Agricultural Soil Moisture Experiment provides evidence that the effects of row orientation remain quite severe for relatively bare fields over a wide range of radar frequencies. In addition, Seasat satellite radar imagery from areas in Louisiana shows dominant row orientation effects even beneath substantial amounts of vegetation cover. The multiparameter nature of the Colby data set, and the continuous angular change in field patterns observed in the Louisiana test area provide much finer definition of microwave sensitivity to row orientation than has been possible in the past. (Author)

A81-43743 * **Use of Seasat satellite radar imagery for the detection of standing water beneath forest vegetation.** H. C. MacDonald, W. P. Waite, and J. S. Demarcke (Arkansas, University, Fayetteville, AR). In: Rainbow 80; Fall Technical Meeting, Niagara Falls, NY, October 7-10, 1980, ASP Technical Papers. Falls Church, VA, American Society of Photogrammetry, 1981, p. RS-3-B-1 to RS-3-B-13. 13 refs. Contract No. JPL-954940.

The Seasat synthetic aperture radar, operating at a 23-cm, L-band wavelength, detected anomalous tonal patterns in areas having relatively uniform vegetable canopy. These anomalously high radar returns were shown to be related more to the underlying terrain (areas of standing water) than to the vegetation canopy. These results show that L-band radars, imaging forested terrain in a Seasat configuration, are sensitive to gross changes in vegetation, and may even penetrate the vegetation canopy, providing an unmistakable radar signature. Properly designed space imaging radar shuttle experiments, using multiple frequency and polarization radars of various depression angles, may provide documentation for a flood-monitoring capability. Height, configuration, and density of the biomass in conjunction with frequency and incidence angle of the imaging system are shown to be important factors in formulating a backscatter model, but the relative significance of each is yet to be determined. J.F.

A81-43744 * **Active microwave measurements for estimating soil moisture in Oklahoma.** T. J. Jackson (U.S. Department of Agriculture, Hydrology Laboratory, Beltsville, MD), A. Chang, and T. J. Schmugge (NASA, Goddard Space Flight Center, Greenbelt, MD). In: Rainbow 80; Fall Technical Meeting, Niagara Falls, NY, October 7-10, 1980, ASP Technical Papers. Falls Church, VA, American Society of Photogrammetry, 1981, p. RS-3-C-1 to RS-3-C-10. 8 refs.

Previous research has shown that active and passive microwave sensors can be used to estimate near surface soil moisture. An advantage of the active systems is that they have the capability of high spatial resolution from satellite platforms. Most of the previous research has been conducted on agricultural fields. This study examined the use of active microwave data for estimating the average surface soil moisture for several watersheds located near Chicasha, Oklahoma. Data were collected using P, L, and C band scatterometers, mounted on the National Aeronautics and Space Administration C130B aircraft flying at an altitude of 300 m. Soil moisture data were collected in conjunction with three flights during May 1978. Our results indicated that relationships between the scatterometer data and soil moisture do exist and agree with the results obtained at the University of Kansas. (Author)

A81-44637 **Crop reporting from space - Problems, promises, potential.** D. Paarlberg. In: Commercial operations in space - 1980-2000; Proceedings of the Eighteenth Goddard Memorial Symposium, Washington, DC, March 27, 28, 1980. San Diego, CA, American Astronautical Society; Univelt, Inc., 1981, p. 111-115. (AAS 80-062)

Crop reporting from space is in a transitional stage, gradually becoming operational. Research, experimentation and development continue. A three-year experimental program marginally met its target for accuracy with regard to wheat production in the USSR, 90 percent accurate 90 percent of the time. Remote sensing is being used by the Department of Agriculture to improve the accuracy of its crop reports in the United States. It has not been possible to estimate costs and benefits with acceptable accuracy. The best method of releasing remote-sensed crop report data seems to be wide simultaneous distribution to the general public, free of direct cost. (Author)

A81-45428 **A photo interpretation approach to forest regrowth monitoring using side-looking airborne radar - Grant County, Oregon.** N. E. Hardy (Toronto, University, Mississauga, Ontario, Canada). *International Journal of Remote Sensing*, vol. 2, Apr.-June 1981, p. 135-144. 11 refs.

A preliminary project was devised to study the forest monitoring potential of side-looking airborne radar. A group of ten photo interpreters was assembled to evaluate the forest regrowth content of a radar image. A series of 20 cutting locations was selected from U.S. Forest Service data. Categories and category associations were tabulated from each participant's results. Some success was achieved in distinguishing between five major forest categories. Little success was achieved in attempting to subdivide the image content into highly specific categories. It was concluded that the radar has the potential to segregate categories, but interpreters must possess as much radar interpretation expertise as forestry expertise. (Author)

A81-45432 * **Infrared-temperature variability in a large agricultural field.** J. P. Millard (NASA, Ames Research Center, Moffett Field, CA), R. C. Goettelman (EAL Corp., Richmond, CA), and M. J. LeRoy (DCA Corp., Palo Alto, CA). *International Journal of Remote Sensing*, vol. 2, July-Sept. 1981, p. 201-211.

Dunnigan Agro-Meteorological Experiment airborne thermal scanner images of a large varying-terrain barley field are acquired and analyzed. Temperature variability that may occur within instantaneous fields of view (IFOV) is defined (coefficient of variation: standard deviation/mean temperature in degrees C), and the percentage of the area within various IFOV's within + or - 1, 2, 3, and 5 degrees of the mean is determined. With the exception of very rugged terrain, over 80% of the area within 4, 16, 65 and 258 ha cells was at temperatures within + or - 3 C of the mean cell temperature. Remote measurements of field temperature appeared to be slightly influenced by pixel size in the range 4 ha to 259 ha, and the area percentage within any pixel which contributes within + or - 1, 2, 3, and 5 degrees C of the mean, is nominally the same. In conclusion, no great advantage is found in utilizing a small IFOV instead of a large one for remote sensing of crop temperature. D.L.G.

A81-46026 **Machine processing of remotely sensed data and soil information systems and remote sensing and soil survey; Proceedings of the Sixth Annual Symposium, Purdue University, West Lafayette, IN, June 3-6, 1980.** Symposium sponsored by the International Society of Soil Science, American Society of Agronomy, IEEE, et al. Edited by P. G. Burroff and D. B. Morrison. New York, Institute of Electrical and Electronics Engineers, Inc., 1980. 397 p. Members, $22.50; nonmembers, $30.

Papers included in this volume cover the general areas of data processing and analysis, data processing systems, crop inventory, forestry, land use, soil survey, and soil information. The following topics are discussed: the current and future need for land resource information, future earth resource data acquisition systems, current soil information systems, remote sensing and soil survey, and the future requirements of resource data storage, retrieval, analysis, and utilization. Plans for the U.S. operational land satellite program, soil information needs, nonfederal information requirements, and research priorities for the 1980's are outlined. V.L.

A81-46031 **Application of multispectral reflectance studies of soils - Pre-Landsat.** S. J. Kristof, M. F. Baumgardner, R. A. Weismiller, and S. Davis (Purdue University, West Lafayette, IN). In: Machine processing of remotely sensed data and soil information systems and remote sensing and soil survey; Proceedings of the Sixth Annual Symposium, West Lafayette, IN, June 3-6, 1980. New York, Institute of Electrical and Electronics Engineers, Inc., 1980, p. 52-62. 12 refs.

Results of preliminary studies on the reflectance properties of soils as related to their other physical and chemical properties are presented. Laboratory studies of the spectral properties of 250 soil samples representing 22 soil series, ten textures, and four drainage profiles were carried out to determine the visible and infrared spectral bands most suitable for observing soil variations. The application of the digital analysis of multispectral data to soil mapping was then studied on the basis of double-beam spectrophotometer and airborne multispectral scanner data taken of ten areas characterized by vegetation, bare soil and water features. Analysis of the field data confirmed the relationships found between soil reflectance and color, organic matter content, moisture content and texture, and indicated the usefulness of multispectral mapping in soil surveys. A.L.W.

A81-46032 * **An assessment of Landsat data acquisition history on identification and area estimation of corn and soybeans.** M. M. Hixson, M. E. Bauer (Purdue University, West Lafayette, IN), and D. K. Scholz (U.S. Geological Survey, EROS Data Center, Sioux Falls, SD). In: Machine processing of remotely sensed data and soil information systems and remote sensing and soil survey; Proceedings of the Sixth Annual Symposium, West Lafayette, IN, June 3-6, 1980. New York, Institute of Electrical and Electronics Engineers, Inc., 1980, p. 72-77. 9 refs. Contract No. NAS9-15466.

During the past decade, numerous studies have demonstrated the potential of satellite remote sensing for providing accurate and timely crop area information. This study assessed the impact of Landsat data acquisition history on classification and area estimation accuracy of corn and soybeans. Multitemporally registered Landsat MSS data from four acquisitions during the 1978 growing season were used in classification of eight sample segments in the U.S. Corn Belt. The results illustrate the importance of selecting Landsat acquisitions based on spectral differences in crops at certain growth stages. (Author)

A81-46033 * **Crop classification with a Landsat/radar sensor combination.** R. Y. Li, F. T. Ulaby (University of Kansas Center for Research, Inc., Lawrence, KS), and J. R. Eyton (South Carolina, University, Columbia, SC). In: Machine processing of remotely sensed data and soil information systems and remote sensing and soil survey; Proceedings of the Sixth Annual Symposium, West Lafayette, IN, June 3-6, 1980. New York, Institute of Electrical and Electronics Engineers, Inc., 1980, p. 78-87. 9 refs. Contract No. NAS9-15421.

A combined Landsat/radar approach to classification of remotely sensed data, with emphasis on crops, was undertaken. Radar data were obtained by microwave radar spectrometers over fields near Eudora, Kansas and Landsat image data were obtained for the same test site. After Landsat digital images were registered and test-cells extracted, a comparable set of radar image pixels were simulated to match the Landsat pixels. The combined data set is then used for classification, and the results are examined with the best combination of sensor variables identified. Finally, the usefulness of radar in a simulated cloud-cover situation is demonstrated. The major conclusion derived from this study is that the combination of radar/optical sensors is superior to either one alone. (Author)

A81-46034 # **Comparison of Landsat-2 and field spectrometer reflectance signatures of south Texas rangeland plant communities.** A. J. Richardson, D. E. Escobar, H. W. Gausman, and J. H. Everitt (U.S. Science and Education Administration, Weslaco, TX). In: Machine processing of remotely sensed data and soil information systems and remote sensing and soil survey; Proceedings of the Sixth Annual Symposium, West Lafayette, IN, June 3-6, 1980. New York, Institute of Electrical and Electronics Engineers, Inc., 1980, p. 88-97. 27 refs.

A81-46035 * **A model of plant canopy polarization response.** V. C. Vanderbilt (Purdue University, West Lafayette, IN). In: Machine processing of remotely sensed data and soil information systems and remote sensing and soil survey; Proceedings of the Sixth Annual Symposium, West Lafayette, IN, June 3-6, 1980. New York, Institute of Electrical and Electronics Engineers, Inc., 1980, p. 98-108. 30 refs. Contract No. NAS9-15466.

Sensors to remotely measure the linear polarization of ground scenes have been proposed for the Multispectral Resource Sampler (MRS), a satellite sensor system proposed to complement the Thematic Mapper. At present justification for a sensor on MRS to measure scene polarization is limited. This paper discusses a model for the amount of linearly polarized light reflected by the shiny leaves of such crops as wheat, corn, and sorghum. The theory demonstrates that, potentially, measurements of the linearly polarized light from a crop canopy may be used as an additional feature to discriminate between crops. Examination of the model suggests that, potentially, satellite polarization measurements may be used to monitor crop development stage, leaf water content, leaf area index, hail damage, and certain plant diseases. The model adds to the understanding of the potential information content of scene polarization measurements acquired by future satellite sensor systems such as MRS. (Author)

A81-46036 * **Procedure M - A framework for stratified area estimation.** R. J. Kauth, R. C. Cicone, and W. A. Malila (Michigan, Environmental Research Institute, Ann Arbor, MI). In: Machine processing of remotely sensed data and soil information systems and remote sensing and soil survey; Proceedings of the Sixth Annual Symposium, West Lafayette, IN, June 3-6, 1980. New York, Institute of Electrical and Electronics Engineers, Inc., 1980, p. 109-119. 20 refs. Contract No. NAS9-15476.

This paper describes Procedure M, a systematic approach to processing multispectral scanner data for classification and acreage estimation. A general discussion of the rationale and development of the procedure is given in the context of large-area agricultural applications. Specific examples are given in the form of test results on acreage estimation of spring small grains. (Author)

A81-46047 **Use of Landsat digital data to assist in mapping soils on Arizona rangelands.** E. H. Horvath, D. F. Post (Arizona, University, Tucson, AZ), W. M. Lucas (Santa Fe National Forest, Santa Fe, NM), and R. A. Weismiller (Purdue University, West Lafayette, IN). In: Machine processing of remotely sensed data and soil information systems and remote sensing and soil survey; Proceedings of the Sixth Annual Symposium, West Lafayette, IN, June 3-6, 1980. New York, Institute of Electrical and Electronics Engineers, Inc., 1980, p. 235-240. 17 refs. Research supported by the U.S. Bureau of Land Management and Coronado National Forest.

The outline and results of more than three years of field and laboratory studies are presented. Spectral maps generated from Landsat satellite data were used to aid in soil and vegetation surveys of five sites in southeastern Arizona. The sites are rangeland with varied physiography and relief, but generally sparse vegetation. It was found that spectral maps show a very positive correlation with grey tones or color patterns on photographs, and can be an excellent auxiliary tool for locating boundaries of mapping units. They can also aid in the location of representative sites for pedon descriptions, and could be used as an aid to quality control and map correlation studies in the field. The type and/or color of the geologic parent material was the dominant factor affecting the response recorded by the satellite. (Author)

A81-46050 **A case study of soil erosion detection by digital analysis of the remotely sensed multispectral Landsat scanner data of a semi-arid land in southern India.** V. Guruswamy, S. J. Kristof, and M. Baumgardner (Purdue University, West Lafayette, IN). In: Machine processing of remotely sensed data and soil information systems and remote sensing and soil survey; Proceedings of the Sixth Annual Symposium, West Lafayette, IN, June 3-6, 1980. New York, Institute of Electrical and Electronics Engineers, Inc., 1980, p. 266-272. 9 refs.

A81-46051 * **Development of a digital data base for reflectance-related soil information.** E. R. Stoner (NASA, Earth Resources Laboratory, Bay St. Louis, MS) and L. L. Biehl (Purdue University, West Lafayette, IN). In: Machine processing of remotely sensed data and soil information systems and remote sensing and soil survey; Proceedings of the Sixth Annual Symposium, West Lafayette, IN, June 3-6, 1980. New York, Institute of Electrical and Electronics Engineers, Inc., 1980, p. 273-279. 5 refs. Contract No. NAS9-15466.

A digital soils data base established for inclusion of soil reflectance data, physical, chemical, and engineering measurements, and site information is discussed. Initial data are taken from 500 soil samples covering the spectral range of 0.5 to 2.3 microns. Information obtained from each observation includes spectral data, and identification records with the soil and spectral observation parameters. The LARSPEC software system is available to retrieve and manipulate information, and scattergrams of identification and spectral data allow the initiation of statistical analyses of soil data. In addition, soil characteristics, graphical displays of reflectance spectra, and identification information examples are given. D.L.G.

A81-46054 * # **Bulk processing techniques for very large areas - Landsat classification of California.** W. Newland (Technicolor Graphic Services, Inc., Moffett Field, CA), D. Peterson, and S. Norman (NASA, Ames Research Center, Moffett Field, CA). In: Machine processing of remotely sensed data and soil information systems and remote sensing and soil survey; Proceedings of the Sixth Annual Symposium, West Lafayette IN, June 3-6, 1980. New York, Institute of Electrical and Electronics Engineers, Inc., 1980, p. 306-318. 6 refs.

In 1977, California Law AB452 was passed to provide a mandate for the California Department of Forestry (CDF) to design and implement an information system to assess the forest land base for multiple uses and values. In connection with this mandate, a land-cover map of the entire state, emphasizing forest types, was produced. In producing this map, the latest techniques in digital image mosaicking were combined with the highspeed processing capability available on the ILLIAC IV parallel processor and other computer systems at the Ames Research Center (ARC). An operational and very responsive analysis method was developed at ARC that permitted on-time response to weekly workshops conducted with CDF field personnel to identify all 1,200 spectral classes and to produce final products. Over 100,000,000 acres were classified in the period between December 1, 1978, and April 15, 1979. All analyses were conducted using existing software. G.R.

A81-46055 * # **Procedure 1 and forestland classification using Landsat data.** R. F. Nelson (NASA, Goddard Space Flight Center, Greenbelt, MD) and R. M. Hoffer (Purdue University, West Lafayette, IN). In: Machine processing of remotely sensed data and soil information systems and remote sensing and soil survey; Proceedings of the Sixth Annual Symposium, West Lafayette, IN, June 3-6, 1980. New York, Institute of Electrical and Electronics Engineers, Inc., 1980, p. 319-325. 10 refs.

Procedure 1 (P-1) was developed for the Large Area Crop Inventory Experiment (LACIE) and has been used extensively to develop land-use classification of agricultural areas. The P-1 approach requires that pixels (also called dots) of known identity must be located in the study scene. The entire area is clustered and the spectral classes formed are identified using the dots. The analyst need only locate and identify the dots. The rest of the work is done by the computer. The objective of the reported study was to evaluate the effectiveness of P-1's automated approach in a complex forest-land situation. The study site was located in the eastern half of the San

Juan National Forest in southwestern Colorado. The study showed that P-1 performed as well as the Multicluster Blocks approach on the rugged study area.
G.R.

A81-46056 **Change vector analysis - An approach for detecting forest changes with Landsat.** W. A. Malila (Michigan, Environmental Research Institute, Ann Arbor, MI). In: Machine processing of remotely sensed data and soil information systems and remote sensing and soil survey; Proceedings of the Sixth Annual Symposium, West Lafayette, IN, June 3-6, 1980. New York, Institute of Electrical and Electronics Engineers, Inc., 1980, p. 326-336. 9 refs. U.S. Department of Agriculture Contract No. 53-3197-8-19.

Periodic multiresource surveys and effective management of forest resources would be facilitated by capabilities for accurate detection of disturbances and other changes in land cover. Current techniques are not as effective and efficient as desired. This paper describes a recently developed digital method for change detection using multidate Landsat data. The method employs calculation of spectral change vectors from two different dates, prompting its name - Change Vector Analysis. The concept and a stratification procedure are described and their features are compared to other approaches. An implementation was tested that utilizes a linear transformation of Landsat data channels and spatial-spectral clustering of multidate data for the definition of spectrally homogeneous stand-like 'blobs'. Maps of two types of change, harvesting and regrowth, were produced and analyzed for a test site in Northern Idaho. (Author)

A81-46404 * **Sampling Landsat classifications for crop area estimation.** M. M. Hixson, B. J. Davis, and M. E. Bauer (Purdue University, West Lafayette, IN). *Photogrammetric Engineering and Remote Sensing,* vol. 47, Sept. 1981, p. 1343-1348. 8 refs. Contract No. NAS9-14970.

An investigation was conducted to evaluate the effect of several sampling alternatives on the accuracy of crop area estimates made from classification of Landsat Multispectral Scanner (MSS) data. The specific objective was to assess the precision and the bias associated with alternative sampling schemes involving different numbers of several sampling unit sizes. The estimates achieved using the 5 by 6 nm segments were found to have the least precision of any sampling scheme tested. The estimates become more precise as the segment size decreases and more segments are taken. The precision of the 5 by 6 nm segments was significantly less than that of the pixel samples. None of the sampling schemes was significantly biased on the average, and none of the average estimates differed significantly from the population parameter. The maximum absolute deviation, however, was directly related to sampling unit size and should be considered in selection of a sampling unit.
G.R.

A81-46406 * **Microdensitometry to identify saline rangelands on 70-mm color-infrared aerial film.** J. H. Everitt, A. H. Gerbermann, and M. A. Alaniz (U.S. Department of Agriculture, Weslaco, TX). *Photogrammetric Engineering and Remote Sensing,* vol. 47, Sept. 1981, p. 1357-1362. 15 refs. NASA Order S-58376-G.

Many of the world's rangelands are affected by salinity. The detection of these areas is important to range and resource managers who are concerned with productivity, condition, and animal carrying capacity. The reported study was conducted along a north-to-south flight line 24 km long and 1.6 wide in Starr County, TX. Everitt et al. (1977) described seven different native range sites (four nonsaline and three saline) along this flight line. The study showed that photointerpretation by microdensitometry could be used to identify saline range sites quantitatively on CIR (0.50 to 0.90 micrometers) aerial film (scales 1:19,000, 1:42,000, and 1:80,000) exposed in May 1976, June 1976, and June 1979. Microdensitometer readings made on CIR film using white or blue light generally gave the best separation between saline and nonsaline range sites. The differences in microdensitometry readings among saline and nonsaline range sites were caused by less plant cover on the saline sites.
G.R.

A81-46895 * **Remote sensing of thermal radiation from an aircraft - An analysis and evaluation of crop-freeze protection methods.** R. A. Sutherland, H. E. Hannah, A. F. Cook, and J. D. Martsolf (Florida, University, Gainesville, FL). *Journal of Applied Meteorology,* vol. 20, July 1981, p. 813-820. 17 refs. Research supported by the University of Florida; Contract No. NAS10-8920.

Thermal images from an aircraft-mounted scanner are used to evaluate the effectiveness of crop-freeze protection devices. Data from flights made while using fuel oil heaters, a wind machine and an undercanopy irrigation system are compared. Results show that the overall protection provided by irrigation (at approximately 2 C) is comparable to the less energy-efficient heater-wind machine combination. Protection provided by the wind machine alone (at approximately 1 C) was found to decrease linearly with distance from the machine by approximately 1 C/100 m. The flights were made over a 1.5 hectare citrus grove at an altitude of 450 m with an 8-14 micron detector. General meteorological conditions during the experiments, conducted during the nighttime, were cold (at approximately -6 C) and calm with clear skies. (Author)

A81-47354 **The space engineering use efficiency for forest study.** P. I. Moroz and V. S. Kudriavtsev (Vsesoiuznoe Ob'edinenie Lesproekt, Moscow, USSR). *International Astronautical Federation, International Astronautical Congress, 32nd, Rome, Italy, Sept. 6-12, 1981, Paper 81-108.* 7 p.

The principal factors determining the economic effect of space information use are given. They include an increase in labor productivity, a cut in expenditure and a shortening of periods of work by traditional means of replacement, an improvement in the nature-protective functions of forests, and a release of funds and their use in other industrial spheres. The use of space information for forestry purposes is seen as giving a considerable economic effect and as making it possible to solve tasks on a new qualitative level. The formula used in computing the economic effect is given.
C.R.

A81-49344 **Assessing winter wheat dry matter production via spectral reflectance measurements.** J. K. Aase and F. H. Siddoway (U.S. Department of Agriculture, Northern Plains Soil and Water Research Center, Sidney, MT). *Remote Sensing of Environment,* vol. 11, Sept. 1981, p. 267-277. 27 refs.

A field experiment was located on a Williams loam soil, 11 km northwest of Sydney, MT. 'Roughrider', a winterhardy hard red winter wheat (Triticum aestivum L.) cultivar, was seeded to seven strands of from 0 to 100% (100% = 1,570,000 plants per hectare). On clear mornings, a hand-held radiometer was used to measure reflectances, corresponding to the Landsat multispectral scanner bands. Relationships between the normalized difference vegetation index as determined from late tillering until the beginning of flowering growth stages, and end-of-season straw and total dry matter clearly established the potential of remote sensing for predicting straw and total dry-matter yield. The prediction of dry-matter production is useful in providing an estimate of residue production for erosion control and as a potential source for feed and energy.
B.J.

A81-49347 **Thermal vegetation canopy model studies.** J. A. Smith, K. J. Ranson, D. Nguyen, L. Balick (Colorado State University, Fort Collins, CO), L. E. Link (U.S. Army, Environmental Laboratory, Vicksburg, MS), L. Fritschen (Washington, University, Seattle, WA), and B. Hutchison (NOAA, Atmospheric Turbulence and Diffusion Laboratory, Oak Ridge, TN). *Remote Sensing of Environment,* vol. 11, Sept. 1981, p. 311-326. 29 refs. Grants No. DACW39-77-C-0073; No. DAAG29-79-C-0199.

An iterative-type thermal model applicable to forest canopies was tested with data from two diverse forest types. The model framework consists of a system of steady-state energy budget equations describing the interactions of short- and long-wave radiation within three horizontally infinite canopy layers. A state-space formulation of the energy dynamics within the canopy is used which permits a factorization of canopy geometrical parameters from canopy optical and thermal coefficients as well as environmental driving variables. Two sets of data characterizing a coniferous (Douglas-fir) and deciduous (oak-hickory) canopy were collected to evaluate the thermal model. The results show that the model approximates measured mean canopy temperatures to within 2 C for relatively clear weather conditions and deviates by a maximum of 3 C for very hazy or foggy conditions.
(Author)

A81-49755 # **Forestry priorities and their implications for the Canadian Remote Sensing Program.** L. Sayn-Wittgenstein (DENDRON Resource Surveys, Ltd., Ottawa, Canada). In: Canadian

Symposium on Remote Sensing, 6th, Halifax, Canada, May 21-23, 1980, Proceedings. (A81-49751 24-43) Ottawa, Canadian Aeronautics and Space Institute, 1981, p. 33-35.

A81-49756 # **Operational applications for analysis of agricultural crops and cultural practices.** A. R. Mack (Department of Agriculture, Research Branch, Ottawa, Canada). In: Canadian Symposium on Remote Sensing, 6th, Halifax, Canada, May 21-23, 1980, Proceedings. Ottawa, Canadian Aeronautics and Space Institute, 1981, p. 37-42. 20 refs.

The evaluation of crop growth and field crop acreage from aerial imagery was begun by Agriculture Canada in the mid 1960's. By 1970, the studies were enlarged to include spectral data on crops and soils using a wide range of photographic and electronic measuring systems carried over the fields by both aircraft and satellites. During the last 15 years, these studies have repeatedly shown that certain groups of crops, types of crop losses, and crop growing conditions could be readily determined and their areal distribution in a crop district, region, or province accurately measured (e.g., corn, oil seeds, cereal crops, and fallowland). Growing conditions have been evaluated in recent years from Landsat imagery in dryland cereal growing areas for spring wheat and winter wheat.

B.J.

A81-49760 # **Application of temporal Landsat forest digital data for updating the Yukon RRAMS data base using Aries.** Y. J. Lee (Pacific Forest Research Centre, Victoria, British Columbia, Canada). In: Canadian Symposium on Remote Sensing, 6th, Halifax, Canada, May 21-23, 1980, Proceedings. Ottawa, Canadian Aeronautics and Space Institute, 1981, p. 73-80. 9 refs.

The paper examines the effectiveness of temporal Landsat forest digital data as input to update the Yukon information retrieval system for renewable resources and management statistics (Yukon RRAMS). The temporal Landsat MSS data for a portion of the Lake Laberge Ecoregion were enhanced to emphasize softwood and hardwood stands. These enhanced images were used to locate training areas for supervised maximum likelihood classification. The results of the supervised classification were geometrically corrected and referenced to UTM grid cells. A summary of percentage occupancy in each 1/4-UTM grid cell by forest land classes was available for direct input to update the Yukon RRAMS data base.

B.J.

A81-49764 * # **Technical aspects of forest inventory demonstrations using Landsat data - Projects in the Pacific Northwest States.** D. L. Peterson, G. Gnauk (NASA, Ames Research Center, Moffett Field, CA), and D. Noren (ESL, Inc., Sunnyvale, CA). In: Canadian Symposium on Remote Sensing, 6th, Halifax, Canada, May 21-23, 1980, Proceedings. Ottawa, Canadian Aeronautics and Space Institute, 1981, p. 105, 106.

A81-49766 # **Integration and comparison of SAR and MSS data for potato crop area estimation.** D. G. Goodenough, P. M. Teillet, and B. Guindon (Canada Centre for Remote Sensing, Ottawa, Canada). In: Canadian Symposium on Remote Sensing, 6th, Halifax, Canada, May 21-23, 1980, Proceedings. Ottawa, Canadian Aeronautics and Space Institute, 1981, p. 127-142. 9 refs. Research supported by the Department of Agriculture of Canada and New Brunswick Department of Agriculture and Rural Development.

Airborne SAR and Landsat MSS imagery was obtained in the summer of 1978 for an agricultural site located near Grand Falls, New Brunswick. In order to compare the performances of these two sensors, it was necessary to overlay the imagery on a common map (UTM) grid. Landsat imagery was corrected on the DICS system at CCRS. For the high-resolution airborne SAR data, a new rectification procedure was developed which models the aircraft flight parameters and uses terrain information in the form of a digital terrain model to remove image distortions introduced by topographic relief. In addition, using a feature selection technique, it was determined which combination of MSS and radar channels provided the greatest separability among the major target types in the Grand Falls area (i.e., potatoes, grains, pasture, fallow, and forest). B.J.

A81-49770 # **SAR image response over a conifer regeneration site.** E. Wedler, S. Pala, and A. Jano (Ministry of Natural Resources, Ontario Centre for Remote Sensing, Toronto, Canada). In: Canadian Symposium on Remote Sensing, 6th, Halifax, Canada, May 21-23, 1980, Proceedings. Ottawa, Canadian Aeronautics and Space Institute, 1981, p. 179-186. 5 refs.

A81-49782 # **Principal components enhancements versus classifications of Landsat images for forestry applications (Les accentuations numériques d'images Landsat contre les classifications automatisees pour la cartographie vegetale).** J. Beaubien (Ministère de l'Environnement, Centre de Recherches Forestières des Laurentides, Sainte-Foy, Quebec, Canada). In: Canadian Symposium on Remote Sensing, 6th, Halifax, Canada, May 21-23, 1980, Proceedings. Ottawa, Canadian Aeronautics and Space Institute, 1981, p. 301-305. In French.

Studies on the potential of Landsat data applied to forest vegetation inventory are becoming numerous; most are based on automated classifications, mainly supervised classification. As a result of two projects in Quebec, on the Laurentian Plateau and on the North Shore, the usefulness of two algorithms, i.e., classifications and principal component digital enhancements, is compared and discussed. Good color enhancement seems to give more information on forest vegetation cover than automated classifications. Color enhancement can be used in the field and interpreted as a color aerial photograph. The interpreter's knowledge and experience in forestry are used to produce a vegetation map based on field sampling. Classifications offer the advantages of automatically producing a map and of rapidly yielding the area occupied by each class; but depending on the complexity of the forest territory concerned and on the training sets, precision of results can be variable, especially when dealing with many classes.

(Author)

A81-49784 # **Rapeseed - Guidelines for operational monitoring.** R. J. Brown, F. J. Ahern, R. A. Ryerson, K. P. B. Thomson, D. G. Goodenough, J. A. McCormick, and P. M. Teillet (Canada Centre for Remote Sensing, Ottawa, Canada). In: Canadian Symposium on Remote Sensing, 6th, Halifax, Canada, May 21-23, 1980, Proceedings. Ottawa, Canadian Aeronautics and Space Institute. 1981, p. 321-330. 8 refs.

Ground spectral measurements, airborne multispectral scanner (MSS) and Landsat MSS data were used to determine the phenological window during which rapeseed can be separated from its confusion crops on Landsat imagery. Ground spectroscopy measurements were used to predict the probability of correct classification of rapeseed and the results were confirmed using Landsat imagery acquired on three dates throughout the growing season. It was found that there are two phenological windows during which rapeseed can be reliably distinguished. One window corresponds to the period when the rapeseed is in bloom and the other when peas and the small grains are ripening.

(Author)

A81-49785 # **Research on assessment of the recreational value of forests using Landsat digital data.** H. Amano. In: Canadian Symposium on Remote Sensing, 6th, Halifax, Canada, May 21-23, 1980, Proceedings. Ottawa, Canadian Aeronautics and Space Institute, 1981, p. 331-337. 6 refs.

The process of assessing the recreational values of forests and benefits thereof to the urban society by utilizing Landsat and complementary Japanese National Statistics is described. The study area selected (about 800,000 ha) was the Northern Kanto districts of Japan, located within 100 km north of Tokyo. Landsat data tapes were used to produce a digital map which consisted of seven land use classes. From this digital map, the forest distribution pattern and the degree of separability between forested and urban areas were expressed as Morisita's and Gini's index, respectively. The results show that the Landsat digital map is valuable for the estimation of quantitative recreation values of forest in relation to the urban area. In addition, Landsat data are in digital form, so that such maps can easily be processed.

(Author)

A81-49786 # **Colour - The critical photointerpretation element in the identification of rangeland plant communities on colour and colour-infrared aerial photography.** E. K. Watson and A. L. van Ryswyk. In: Canadian Symposium on Remote Sensing, 6th, Halifax, Canada, May 21-23, 1980, Proceedings. Ottawa, Canadian Aeronautics and Space Institute, 1981, p. 339-349. 11 refs. Research supported by the Department of the Agriculture of Canada.

Although a review of the literature shows that color-infrared is preferred over ordinary color film for range vegetation identification, the identification of variably colored grasses, forbs and shrubs becomes difficult due to the following properties of color-infrared film: (1) blue and green plants appear as similar magenta hues; (2) senescent yellow and white grasses both appear white; (3) purples, reds and red-browns appear as hues of yellow; and (4) the interaction of non-green flowers or stems with the color of the plant to yield a color shift. The elements of photointerpretation for the identification of some dominant range plant species are presented, with emphasis on the interactions of plant colors with multidate-multiscale color and color-infrared photography. Among the elements of photointerpretation treated are growth form distribution, habitat, pattern and texture. O.C.

A81-49787 # **Photointerpretation of fire damage to trees in a ponderosa pine/bunchgrass community.** P. A. Murtha, A. H. Johnson, and R. M. Strang (British Columbia, University, Vancouver, Canada). In: Canadian Symposium on Remote Sensing, 6th, Halifax, Canada, May 21-23, 1980, Proceedings. Ottawa, Canadian Aeronautics and Space Institute 1981, p. 351-359. 16 refs. Research supported by the Natural Sciences and Engineering Research Council, British Columbia Ministry of Agriculture, and Environment Canada.

This paper reports on the application of a new technique for photointerpretation of fire damage to trees in a ponderosa pine/bunchgrass community in British Columbia, reviews pertinent details of a 1978 fire-ecology study, and discusses aspects of photointerpretation of vegetation damage. Photointerpreted damage classes and optical densitometry to determine spectral-ratio deviations are suggested for photointerpretation of fire-related tree damage. The approach was tested on large-scale color-infrared aerial photographs of the fire-ecology plots. The results indicate that a combination of visual photointerpretation and calculated spectral ratio deviations provide a reliable photointerpretation technique for determination of fire impact on trees in the rangeland plant community. The remote sensing results are supported by independently-derived ground-based fire data. (Author)

A81-49789 # **The application of thermography for locating potential frost pockets in forest cutovers.** G. R. Lawrence (Ministry of Natural Resources, Ontario Centre for Remote Sensing, Toronto, Canada) and A. Banner (Intertech Remote Sensing, Ltd., Ottawa, Canada). In: Canadian Symposium on Remote Sensing, 6th, Halifax, Canada, May 21-23, 1980, Proceedings. Ottawa, Canadian Aeronautics and Space Institute, 1981, p. 369-376. 14 refs.

Cutover areas in three study sites were imaged in May with the aid of an airborne thermal scanner. Profiles of ground temperature, air temperature at 10 cm, and radiant temperature using a PRT-10 were prepared on two nights in November under similar weather conditions at a selected ground truth site. The data were compared with air temperature measurements done at the time of the overflight. The effects of nocturnal air drainage and pooling are successfully shown by the imagery. The study suggests that thermography holds promise for delineating relative frost hazards across forest cutovers. C.R.

A81-49791 # **The application of remote sensing techniques for an ecological land survey of the snow goose colony at Cape Henrietta Maria, Hudson Bay.** G. H. Wickware, D. W. Cowell (Environment Canada, Lands Directorate, Burlington, Ontario, Canada), R. A. Sims (Environment Canada, Canadian Forestry Service, Sault Ste. Marie, Ontario, Canada), and R. K. Ross (Canadian Wildlife Service, Ottawa, Canada). In: Canadian Symposium on Remote Sensing, 6th, Halifax, Canada, May 21-23, 1980, Proceedings. Ottawa, Canadian Aeronautics and Space Institute, 1981, p. 387-395. 10 refs.

A large expanding snow goose colony in the Cape Henrietta Maria area of Hudson Bay was studied with the aid of a multilevel remote sensing program. Training sites for each habitat were selected using 1:2000 scale 70 mm color and color infrared photography, while land systems were delineated using 1:60,000 scale black and white photography. Population estimates were made by means of a modified technique employed by Kerbes (1975), and a stratified random sample of all negatives within the colony's boundaries was selected to give overall areal coverage of 10%. Results of nesting density counts show a large increase in breeding pairs with only a small increase in the areal extent of the colony itself, and highest nest concentrations occur in the thicket meadow marsh and the graminoid brackish meadow marsh which are nearest to fluvially dominated areas and areas with a high density of brackish coastal lakes and ponds. D.L.G.

A81-49794 # **The discrimination of cereal crops and legumes using reflectance data in the Landsat bandpasses.** M. J. Duggin (New York, State University, Syracuse, NY) and G. C. Cooney (McQuarie University, Sydney, Australia). In: Canadian Symposium on Remote Sensing, 6th, Halifax, Canada, May 21-23, 1980, Proceedings. Ottawa, Canadian Aeronautics and Space Institute, 1981, p. 421-426. 5 refs. Research supported by the U.S. Department of Agriculture.

An example of the type of feasibility study which could usefully precede remote sensing surveys of, for example, different crop types or forest stands consisting of different tree types, is examined. The ground-level reflectance properties of several cereal crops and legumes are measured radiometrically for the Landsat satellite multispectral scanner (MSS) bandpasses on two occasions during the growth season. Multivariate analysis of the variance of the reflectance factor variables for the scanner bandpasses MSS 4 (500-600 nm), MSS 5 (600-700 nm), MSS 6 (700-800 nm), MSS 7 (800-1100 nm) and for log (base 10) MSS 7/5 shows that on each date the nine plant types are separable on the basis of reflectance properties. C.R.

A81-49799 # **Thermal inertia mapping of some areas of Quebec based on aerial and HCMM satellite data (Cartographie de l'inertie thermique de certains secteurs du Québec à partir de données aériennes et du satellite H.C.M.M.).** M. Bernier, R. Brochu, and F. Bonn (Sherbrooke, Université, Sherbrooke, Quebec, Canada). In: Canadian Symposium on Remote Sensing, 6th, Halifax, Canada, May 21-23, 1980, Proceedings. Ottawa, Canadian Aeronautics and Space Institute, 1981, p. 473-482. 17 refs. In French.

An example of the application of aerial and HCMM data to the construction of thermal inertia maps indicating soil moisture contents in regions of eastern Canada is presented. The aerial data was obtained in two flights at 1800 m over agricultural lands in the vicinity of Sherbrooke by means of thermography during day and night flights and multispectral photography during the day flight; preliminary treatment involved the division of the 5 x 1.25 km area into 400 pixels 125 m on a side and the acquisition of soil type, soil drainage, soil utilization and slope data for each pixel. Soil temperatures estimated from the thermographic data and albedos computed from an average of the reflectivities in the yellow-green, red and infrared spectral bands are used to derive the thermal inertia of each pixel. Examination of the thermal inertia distribution in comparison with soil drainage data indicates that the values of thermal inertia may be used to determine soil moisture in agricultural areas only if the complex relation between soil and vegetation temperature has been determined. In the case of HCMM data, obtained in the wavelength bands 0.5-1.1 and 10.5-12.0 microns with a pixel size of 481.5 m covering the entire southeast of Quebec, it is found that the resolution is too low to allow the use of the concept of thermal inertia in differentiating between regions of differing soil water content. A.L.W.

A81-49810 # **A simulation of Thematic Mapper performance in an agricultural application.** F. J. Ahern, R. J. Brown, D. G. Goodenough, and K. P.-B. Thomson (Canada Centre for Remote Sensing, Ottawa, Canada). In: Canadian Symposium on Remote Sensing, 6th, Halifax, Canada, May 21-23, 1980, Proceedings. Ottawa, Canadian Aeronautics and Space Institute, 1981, p. 585-596. 13 refs.

The Thematic Mapper (TM) to be flown on Landsat-D is expected to furnish significantly improved agricultural classification over the present Landsat multispectral scanner (MSS) because of its improved spectral bands and greater spatial, spectral, and radiometric resolution. It is noted that the expected performance of the TM in an agricultural application has been simulated from airborne MSS data as part of a CCRS project entitled The Saskatchewan Rangeland/Rapeseed Study. The performance of the TM is compared with the simulated and actual performance of the present Landsat multispectral scanner. It is pointed out that the TM bands can be combined in a number of familiar and unfamiliar color composites. Some of these are created and displayed to demonstrate their value for agricultural applications. Using restricted versions of the simulated TM data set, the improvements in spectral classification with varying band combinations and varying radiometric and spatial resolution are determined. C.R.

A81-49615 # **Evaluation of Thematic Mapper bands - A first step in feature selection.** K. Staenz, F. J. Ahern, and R. J. Brown (Canada Centre for Remote Sensing, Ottawa, Canada). In: Canadian Symposium on Remote Sensing, 6th, Halifax, Canada, May 21-23, 1980, Proceedings. Ottawa, Canadian Aeronautics and Space Institute, 1981, p. 625-634. 16 refs.

It is pointed out that the Thematic Mapper (TM) on Landsat-D will produce more than 10 times the data than the present Landsat Multispectral Scanner (MSS) because of its increased dimensionality (7 bands) and improved ground resolution (30 m). However, the impact upon image analysis can be reduced by analyzing a subset of the data and thus reducing the dimensionality. A study is made to identify these possible subsets. The correlation between the reflectance factors of nine common crop types and one soil type in the first six TM spectral bands is determined. In similar fashion, the correlations between the Landsat MSS bands are calculated as a test of the available data set and procedure. C.R.

N81-28120# Joint Publications Research Service, Arlington, Va.
USE OF SATELLITE PICTURES FOR AGRICULTURE
D. Gergishvili *In its* USSR Rept.: Space, No. 9 (JPRS-77388) 2 Mar. 1981 p 26-27 refs Transl. into ENGLISH from Komunisti (USSR), 24 Jul. 1980 p 4

Avail: NTIS HC A03/MF A01

The functions of the hydrometeorological station in Telavi, Soviet Georgia, are described. Agroclimatic conditions affecting the grape crop are monitored to provide protection against natural hazards. Weather forecasts are produced, aerological, agrometeorological, hydrological, and meteorological data are collected, and environmental pollution monitored. The use of weather satellite data has improved their forecasting ability by 3.2 percent, and the accuracy of hail forecasting by 3.7 percent. J.D.H.

N81-29487*# Department of Agriculture, Houston, Tex.
LARGE AREA APPLICATION OF A CORN HAZARD MODEL
Pat Ashburn and T. W. Taylor, Principal Investigators Mar. 1981 15 p refs Sponsored by NASA, USDA, Dept. of Commerce, Dept. of the Interior, and Agency for International Development ERTS
(Proj. AgRISTARS)
(E81-10164; NASA-CR-160985; EW-UL-04074; JSC-17130) Avail: NTIS HC A02/MF A01 CSCL 02C

An application test of the crop calendar portion of a corn (maize) stress indicator model developed by the early warning, crop condition assessment component of AgRISTARS was performed over the corn for grain producing regions of the U.S.S.R. during the 1980 crop year using real data. Performance of the crop calendar submodel was favorable; efficiency gains in meteorological data analysis time were on a magnitude of 85 to 90 percent. Author

N81-29488*# Lockheed Engineering and Management Services Co., Inc., Houston, Tex.
A TEMPORAL/SPECTRAL ANALYSIS OF SMALL GRAIN CROPS AND CONFUSION CROPS
W. R. Johnson, Principal Investigators Mar. 1981 76 p refs Sponsored by NASA, USDA, Dept. of Commerce, Dept. of the Interior, and Agency for International Development ERTS
(Contract NAS9-15800; Proj. AgRISTARS)
(E81-10167; NASA-CR-160983; SR-L1-04054;
LEMSCO-15676; JSC-17128) Avail: NTIS HC A05/MF A01 CSCL 02C

Spectral data from the LANDSAT-2 satellite were used to study the growth cycles of fields of wheat, barley, alfalfa, corn, sunflowers, soybeans, rye, flax, oats, millet, grass, and hay. Signatures of pastures, trees, and idle fallow were also studied. The growth cycles were portrayed in the form of temporal plots of the greeness-brightness transformation vector applied to average channel pixel values within the fields, all of which were in three counties in North Dakota. The plots of each crop reveal characteristics which can be used in crop classification procedures. A.R.H.

N81-29489*# National Aeronautics and Space Administration. Goddard Space Flight Center, Greenbelt, Md.
EFFECT OF FOREST CANOPY CLOSURE ON INCOMING SOLAR RADIANCE
C. Lisette Dottavio, Principal Investigator Apr. 1981 29 p refs Sponsored by NASA, USDA, Dept. of Commerce, Dept. of the Interior, and Agency for International Development ERTS (Proj. AgRISTARS)
(E81-10170; NASA-TM-82113; RR-G1-04065) Avail: NTIS HC A03/MF A01 CSCL 02F

In order to better understand the physical processes involved in defoliation assessment from remotely sensed data, a field study was designed to investigate the effect of forest canopy closure and other environmental variables on incoming solar radiation. Diffuse radiation measurements were recorded in red, infrared, and middle infrared wavelengths using the Mark 2 three band field radiometer. Results to date indicate that the percent canopy closure is the single most important variable affecting incoming solar radiation. In the visible and near infrared regions, interaction between time of day and date (defined later as solar zenith angle) also affect radiometric response. Aspect has only limited influence on radiance response. These same variables do not influence middle infrared response, however. Uniformity of the forest canopy appears to be more important. These results are compared to LANDSAT MSS classification results of gypsy moth defoliation. A.R.H.

N81-29494*# Lockheed Engineering and Management Services Co., Inc., Houston, Tex.
EVALUATION OF GRAVIMETRIC GROUND TRUTH SOIL MOISTURE DATA COLLECTED FOR THE AGRICULTURAL SOIL MOISTURE EXPERIMENT, 1978 COLBY, KANSAS, AIRCRAFT MISSION
L. M. Arya and D. E. Phinney, Principal Investigators Oct. 1980 307 p Sponsored by NASA, USDA, Dept. of Commerce, Dept. of the Interior, and Agency for International Development ERTS
(Contract NAS9-15800; Proj. AgRISTARS)
(E81-10114; NASA-CR-160966; SM-LO-00441;
LEMSCO-14600; JSC-16357) Avail: NTIS HC A14/MF A01 CSCL 08M

Soil moisture data acquired to support the development of algorithms for estimating surface soil moisture from remotely sensed backscattering of microwaves from ground surfaces are presented. Aspects of field uniformity and variability of gravimetric soil moisture measurements are discussed. Moisture distribution patterns are illustrated by frequency distributions and contour plots. Standard deviations and coefficients of variation relative to degree of wetness and agronomic features of the fields are examined. Influence of sampling depth on observed moisture content an variability are indicated. For the various sets of measurements, soil moisture values that appear as outliers are flagged. The distribution and legal descriptions of the test fields are included along with examinations of soil types, agronomic features, and sampling plan. Bulk density data for experimental fields are appended, should analyses involving volumetric moisture content be of interest to the users of data in this report. A.R.H.

N81-29495*# Texas A&M Univ., College Station. Dept. of Mathematics.
DEVELOPMENT OF ADVANCED ACREAGE ESTIMATION METHODS Final Report, 1 Nov. 1979 - 31 Oct. 1980
L. F. Guseman, Jr., Principal Investigator Dec. 1980 133 p refs Sponsored by NASA, USDA, Dept. of Commerce, Dept. of the Interior, and Agency for International Development ERTS
(Contract NAS9-14689; Proj. AgRISTARS)
(E81-10160; NASA-CR-161004; SR-TI-04112) Avail: NTIS HC A07/MF A01 CSCL 08B

The use of the AMOEBA clustering/classification algorithm was investigated as a basis for both a color display generation technique and maximum likelihood proportion estimation procedure. An approach to analyzing large data reduction systems was formulated and an exploratory empirical study of spatial correlation in LANDSAT data was also carried out. Topics addressed include: (1) development of multiimage color images; (2) spectral spatial classification algorithm development; (3) spatial correlation studies; and (4) evaluation of data systems. A.R.H.

N81-29499*# Virginia Polytechnic Inst. and State Univ., Blacksburg.

NATIONWIDE FORESTRY APPLICATIONS PROGRAM. ANALYSIS OF FOREST CLASSIFICATION ACCURACY

Russell G. Congalton, Roy A. Mead, Richard G. Oderwald, and Joel Heinen, Principal Investigators 20 Jan. 1981 93 p refs Sponsored by NASA, USDA, Dept. of Commerce, Dept. of Interior, and Agency for International Development ERTS
(Proj. AgRISTARS)
(E81-10183; NASA-CR-160949; RR-U1-04066; JSC-17123) Avail: NTIS HC A05/MF A01 CSCL 02F

The development of LANDSAT classification accuracy assessment techniques, and of a computerized system for assessing wildlife habitat from land cover maps are considered. A literature review on accuracy assessment techniques and an explanation for the techniques development under both projects are included along with listings of the computer programs. The presentations and discussions at the National Working Conference on LANDSAT Classification Accuracy are summarized. Two symposium papers which were published on the results of this project are appended. A.R.H.

N81-29500*# Science and Education Administration, Phoenix, Ariz. Water Conservation Lab.

SOIL MOISTURE INFERENCES FROM THERMAL INFRARED MEASUREMENTS OF VEGETATION TEMPERATURES

R. D. Jackson, Principal Investigator Mar. 1981 14 p refs Sponsored by NASA, USDA, Dept. of Commerce, Dept. of Interior, and Agency for International Development ERTS
(Proj. AgRISTARS)
(E81-10184; NASA-CR-160954; EW-U1-04068; JSC-17125) Avail: NTIS HC A02/MF A01 CSCL 08M

Thermal infrared measurements of wheat (Triticum durum) canopy temperatures were used in a crop water stress index to infer root zone soil moisture. Results indicated that one time plant temperature measurement cannot produce precise estimates of root zone soil moisture due to complicating plant factors. Plant temperature measurements do yield useful qualitative information concerning soil moisture and plant condition. Author

N81-29504*# Environmental Research Inst. of Michigan, Ann Arbor.

USERS MANUAL FOR THE US BASELINE CORN AND SOYBEAN SEGMENT CLASSIFICATION PROCEDURE Procedures Report, 15 Nov. 1979 - 14 Mar. 1981

Robert Horvath, Robert Colwell, Principal Investigators, C. Hay, M. Metzler, O. Mykolenko, J. Odenweller, and D. Rice Mar. 1981 274 p Sponsored by NASA, USDA, Dept. of Commerce, Dept. of the Interior, and Agency for International Development Prepared in cooperation with California Univ., Berkeley ERTS
(Contracts NAS9-15476; NAS9-14565; Proj. AgRISTARS)
(E81-10190; NASA-CR-160975; FC-E1-00712;
ERIM-152400-1-X) Avail: NTIS HC A12/MF A01 CSCL 02C

A user's manual for the classification component of the FY-81 U.S. Corn and Soybean Pilot Experiment in the Foreign Commodity Production Forecasting Project of AgRISTARS is presented. This experiment is one of several major experiments in AgRISTARS designed to measure and advance the remote sensing technologies for cropland inventory. The classification procedure discussed is designed to produce segment proportion estimates for corn and soybeans in the U.S. Corn Belt (Iowa, Indiana, and Illinois) using LANDSAT data. The estimates are produced by an integrated Analyst/Machine procedure. The Analyst selects acquisitions, participates in stratification, and assigns crop labels to selected samples. In concert with the Analyst, the machine digitally preprocesses LANDSAT data to remove external effects, stratifies the data into field like units and into spectrally similar groups, statistically samples the data for Analyst labeling, and combines the labeled samples into a final estimate. J.M.S.

N81-29505*# National Oceanic and Atmospheric Administration, Houston, Tex. National Earth Satellite Service.

THE ENVIRONMENTAL VEGETATION INDEX: A TOOL POTENTIALLY USEFUL FOR ARID LAND MANAGEMENT

T. I. Gray, Jr. and D. G. McCrary, Principal Investigators Mar. 1981 6 p refs Repr. from Vol. of Extended Abstr.: 15th Conf. on Agr. and Forest Meteorol. and 5th Conf. on Biometeorol., 1981 p 205-207 Presented at the 15th Conf. on Agr. and Forest Meteorol. and 5th Conf. on Biometeorol., Anaheim, Calif., 1-3 Apr. 1981 Sponsored by NASA, USDA, Dept. of Commerce, Dept. of the Interior, and Agency for International Development ERTS
(Proj. AgRISTARS)
(E81-10191; NASA-CR-160978; EW-NI-04076; JSC-17132) Avail: NTIS HC A02/MF A01 CSCL 02C

The NOAA-6 AVHRR data sets acquired over South Texas and Mexico during the spring of 1980 and after Hurricane Allen passed inland are analyzed. These data were processed to produce the Gray-McCrary Index (GMI's) for each pixel location over the selected area, which area contained rangeland and cropland, both irrigated and nonirrigated. The variations in the GMI's appear to reflect well the availability of water for vegetation. The GMI area maps are shown to delineate and to aid in defining the duration of drought; suggesting the possibility that time changes over a selected area could be useful for irrigation management. Author

N81-29507*# Lockheed Engineering and Management Services Co., Inc., Houston, Tex.

DESCRIPTIVE AND SENSITIVITY ANALYSES OF WATBALI: A DYNAMIC SOIL WATER MODEL

W. W. Hildreth, Principal Investigator Mar. 1981 87 p refs Sponsored by NASA, USDA, Dept. of Commerce, Dept. of the Interior, and Agency for International Development ERTS
(Contract NAS9-15800; Proj. AgRISTARS)
(E81-10193; NASA-CR-160980; SM-LO-04021;
LEMSCO-16572; JSC-16846) Avail: NTIS HC A05/MF A01 CSCL 08M

A soil water computer model that uses the IBM Continuous System Modeling Program III to solve the dynamic equations representing the soil, plant, and atmospheric physical or physiological processes considered is presented and discussed. Using values describing the soil-plant-atmosphere characteristics, the model predicts evaporation, transpiration, drainage, and soil water profile changes from an initial soil water profile and daily meteorological data. The model characteristics and simulations that were performed to determine the nature of the response to controlled variations in the input are described the results of the simulations are included and a change that makes the response of the model more closely represent the observed characteristics of evapotranspiration and profile changes for dry soil conditions is examined. A.R.H.

N81-29508*# Lockheed Engineering and Management Services Co., Inc., Houston, Tex.

EVALUATION OF SPRING WHEAT AND BARLEY CROP CALENDER MODELS FOR THE 1979 CROP YEAR

C. V. Nazare and J. G. Carnes, Principal Investigators Feb. 1981 35 p refs Sponsored by NASA, USDA, Dept. of Commerce, Dept. of the Interior, and Agency for International Development ERTS
(Contract NAS9-15800; Proj. AgRISTARS)
(E81-10197; NASA-CR-160977; FC-L1-04030;
LEMSCO-15936; JSC-16850) Avail: NTIS HC A03/MF A01 CSCL 02C

During the Large Area Crop Inventory Experiment, spring wheat planting date and crop development stage estimates based on historical normals were improved by the use of the Feyerherm planting date and Robertson spring wheat crop calendar models. The Supporting Research Crop Calendar Project element modified the Robertson model to reduce bias at cardinal growth stages within the growing season. These models were tested in 1980 along with a state-of-the-art barley model (Williams) against a ground-truth data set from 49 calendar year 1979 segments in the U.S. Great Plains spring wheat and barley region. Author

N81-29511*# Lockheed Engineering and Management Services Co., Inc., Houston, Tex.

EVALUATION OF LARGE AREA CROP ESTIMATION TECHNIQUES USING LANDSAT AND GROUND-DERIVED DATA

M. L. Amis, R. K. Lennington, M. V. Martin, W. G. McGuire, and S. S. Shen, Principal Investigators Mar. 1981 136 p refs Sponsored by NASA, USDA, Dept. of Commerce, Dept. of the Interior, and Agency for International Development
(Proj. AgRISTARS)
(E81-10200; NASA-CR-160998; DC-LI-04051;
LEMSCO-15763; JSC-17116) Avail: NTIS HC A06/MF A01 CSCL 02C

The results of the Domestic Crops and Land Cover Classification and Clustering study on large area crop estimation using LANDSAT and ground truth data are reported. The current crop area estimation approach of the Economics and Statistics Service of the U.S. Department of Agriculture was evaluated in terms of the factors that are likely to influence the bias and variance of the estimator. Also, alternative procedures involving replacements for the clustering algorithm, the classifier, or the regression model used in the original U.S. Department of Agriculture procedures were investigated. J.M.S.

N81-30507# Department of Agriculture, Washington, D.C. Statistical Research Div.
CROP AREA ESTIMATION USING GROUND-GATHERED AND SAMPLED LANDSAT DATA
James Weldon Mergerson May 1981 23 p refs
(PB81-192783; AGESS-810408) Avail: NTIS HC A02/MF A01 CSCL 02C

A comparative study in which a procedure using ground gathered data and classified LANDSAT data for estimating crop area were compared to procedures using ground gathered data and sampled LANDSAT data is described. Data from parts of Iowa and Missouri were used. Unitemporal data were used in Iowa and multitemporal data were used in Missouri. Results indicate that some sampling schemes can be used without any significant difference in the crop area estimates, but with a large reduction in cost for corn, soybeans, and winter wheat. GRA

N81-30508# Georgia Inst. of Tech., Atlanta. Applied Sciences Lab.
AGRICULTURAL WATER DEMAND PREDICTION USING REMOTE SENSING TECHNOLOGY FOR GEORGIA RESOURCE MANAGEMENT
John R. Jensen and Donald L. Chery Dec. 1980 57 p refs Sponsored by Dept. of Interior Prepared in cooperation with Georgia Univ., Athens
(PB81-184137; W81-02428; ERC-07-80; OWRT-A-083-GA(1)) Avail: NTIS HC A04/MF A01 CSCL 02C

A method to assess the amount of water pumped from aquifers or the effect of intensive agriculture on watershed water balance (WWB) is discussed. Certain measurements are needed to model WWB. The major flow components are (1) rainfall input, and (2) out flows of evapotranspiration (ET) and surface and subsurface discharge. ET is determined by careful selection and analysis of LANDSAT digital data to determine an agriculture region's land cover; ET was used in a hydrologic water balance model. Digital image processing of LANDSAT-3 data discriminated major field crops and forests in Tift County, Georgia, for a water use assessment. GRA

N81-30511# Department of Agriculture, Washington, D.C. Statistical Reseach Div.
AGRISTARS (AGRICULTURE AND RESOURCES INVENTORY SURVEYS THROUGH AEROSPACE REMOTE SENSING) DC/LC (DOMESTIC CROPS AND LAND ROVER) PROJECT SUMMARY CROP AREA ESTIMATES FOR KANSAS AND IOWA, 1980
David D. Kleweno and Charles E. Miller Mar. 1981 20 p refs
(PB81-196909; AGESS-810414) Avail: NTIS HC A02/MF A01 CSCL 02B

The major crop area estimation element of the 1980 AgRISTARS DC/LC project as implemented by the Economics and Statistics Service is described. Data from NASA Earth resources monitoring satellites, LANDSAT II and III, were used in conjunction with conventionally gathered ground data to provide 1980 crop area estimates of harvested winter wheat in Kansas and planted soybeans and corn in Iowa. GRA

N81-31595 Arizona Univ., Tucson.
SPECTRAL PROPERTIES OF ARIZONA SOILS AND RANGELANDS AND THEIR RELATIONSHIP TO LANDSAT DIGITAL DATA Ph.D. Thesis
Emilio Hubert Horvath 1981 196 p
Avail: Univ. Microfilms Order No. 8116702

The relationships between the spectral properties of Arizona soils and rangelands and their characteristics were studied. The per cent reflectance of soils was determined using a multispectral hand-held radiometer, and the spectral response of Arizona rangeland sites was measured by scanners aboard on orbiting satellite. These spectral properties were related, by means of stepwise multiple regressions, to various soil and site characteristics. It was shown that for central and southern Arizona rangelands, it is possible to define specific relationships between site characteristics and satellite measured spectral response. Less than ten site characteristics and their interactions explain considerable portions of the variability between mapping units for a given survey. These relationships are unique for specific locations, but they could easily be developed for a survey area and effectively used in the mapping process. Dissert. Abstr.

N81-31596*# National Oceanic and Atmospheric Administration, Houston, Tex.
METEOROLOGICAL SATELLITE DATA: A TOOL TO DESCRIBE THE HEALTH OF THE WORLD'S AGRICULTURE
T. I. Gray, Jr., D. G. McCrary, Principal Investigators, and L. Scott Feb. 1981 12 p refs Sponsored by NASA, USDA, Dept. of Commerce, Dept. of the Interior, and Agency for International Development Prepared in cooperation with Lockheed Engineering and Management Services Co., Inc., Houston, Tex. ERTS
(Contract NAS9-15800; Proj. AgRISTARS)
(E81-10204; NASA-CR-160953; EW-NI-04042;
LEMSCO-15978; JSC-17112) Avail: NTIS HC A02/MF A01 CSCL 02C

Local area coverage data acquired aboard the TIROS-N satellite family by the advanced very high resolution radiometer systems was examined to determine the agricultural information current. Albedo differences between channel 2 and channel 1 of the advanced very high resolution radiometer LAC (called EVI) are shown to be closely correlated to the Ashburn vegetative index produced from LANDSAT multispectral scanner data which have been shown to vary in response to 'greenness', soil moisture, and crop production. The statistical correlation between the EVI and the Ashburn Vegetative Index (+ or - 1 deg) is 0.86. Author

N81-31597*# Lockheed Engineering and Management Services Co., Inc., Houston, Tex.
A DESCRIPTION OF THE REFORMATTED SPRING SMALL GRAINS LABELING PROCEDURE USED IN TEST 2, PART 2 OF THE US/CANADA WHEAT AND BARLEY EXPLORATORY EXPERIMENT
W. F. Palmer and E. R. Magness, Principal Investigator Feb. 1981 42 p refs Sponsored by NASA, USDA, Dept of Commerce, Dept. of the Interior and Agency for International Development ERTS
(Contract NAS9-15800; Proj. AgRISTARS)
(E81-10206; NASA-CR-160969; FC-LO-04000;
LEMSCO-15404; JSC-16827) Avail: NTIS HC A03/MF A01 CSCL 02C

The reformatted spring small grains labeling procedure is designed to be used for assigning crop identification labels to a predetermined and selected number of dots. The development and description of this procedure is presented. Author

N81-31598*# Lockheed Engineering and Management Services Co., Inc., Houston, Tex.
CLASSIFICATION OF WHEAT: BADHWAR PROFILE SIMILARITY TECHNIQUE
Wills W. Austin Oct. 1980 32 p refs Sponsored by NASA, USDA, Dept. of Commerce, Dept. of the Interior, and Agency for International Development ERTS
(Contract NAS9-15800; Proj. AgRISTARS)
(E81-10207; NASA-CR-160970; SR-LO-00499;
LEMSCO-15305; JSC-16826) Avail: NTIS HC A03/MF A01 CSCL 02C

The Badwar profile similarity classification technique used successfully for classification of corn was applied to spring wheat classifications. The software programs and the procedures used to generate full-scene classifications are presented, and numerical results of the acreage estimations are given. J.M.S.

N81-31599*# Lockheed Engineering and Management Services Co., Inc., Houston, Tex.
WEATHER ANALYSIS AND INTERPRETATION PROCEDURES DEVELOPED FOR THE US/CANADA WHEAT AND BARLEY EXPLORATORY EXPERIMENT
M. H. Trenchard, Principal Investigator Nov. 1980 49 p refs Sponsored by NASA, USDA, Dept. of Commerce, Dept. of the

Interior, and Agency for International Development ERTS
(Contract NAS9-15800; Proj. AGRISTARS)
(E81-10208; NASA-CR-160971; FC-LO-04014;
LEMSCO-15612; JSC-16840) Avail: NTIS HC A03/MF A01
CSCL 02C

Procedures and techniques for providing analyses of meteorological conditions at segments during the growing season were developed for the U.S./Canada Wheat and Barley Exploratory Experiment. The main product and analysis tool is the segment-level climagraph which depicts temporally meteorological variables for the current year compared with climatological normals. The variable values for the segment are estimates derived through objective analysis of values obtained at first-order station in the region. The procedures and products documented represent a baseline for future Foreign Commodity Production Forecasting experiments. Author

N81-31614# Department of Agriculture, Washington, D.C. Economics and Statistics Service.
CROP AREA ESTIMATES USING GROUND-GATHERED AND LANDSAT DATA. A MULTITEMPORAL APPROACH: MISSOURI, 1979
James Weldon Mergerson Feb. 1981 30 p refs
(PB81-186751; AGESS-810223) Avail: NTIS
HC A03/MF A01 CSCL 02D

Four channel data were used for the unitemporal approach. Eight channel data consisting of four channels from each of two dates were used for the multitemporal approach. The multitemporal data set and the two corresponding unitemporal data sets were analyzed using various procedures. Results indicated that the use of multitemporal data can significantly improve the precision of crop area estimates for corn, soybeans, and winter wheat, obtained using the unitemporal approach. GRA

N81-32576*# Lockheed Engineering and Management Services Co., Inc., Houston, Tex.
ANALYSIS OF US SPRING WHEAT AND SPRING BARLEY PERIODIC GROUND TRUTH Interim Report
T. Hodges, Principal Investigator Jan. 1981 51 p refs Sponsored by NASA, USDA,, Dept. of Commerce, Dept. of the Interior and Agency for International Development ERTS
(Contract NAS9-15800; Proj. AgRISTARS)
(E81-10203; NASA-CR-161005; SR-L0-04012;
LEMSCO-15698; JSC-16837) Avail: NTIS HC A04/MF A01
CSCL 02C

An attempt to document the size and geographic distribution of phenological differences between spring wheat and spring barley in the U.S. Great Plains is described. Severe inconsistencies found in the two sets of data taken at 51 segments in Montana, North Dakota, and South Dakota are discussed. A.R.H.

N81-32577*# Department of Agriculture, Houston, Tex.
YIELD MODEL DEVELOPMENT (YMD) IMPLEMENTATION PLAN FOR FISCAL YEARS 1981 AND 1982
Russell A. Ambroziak, Principal Investigator Mar. 1981 136 p Sponsored by NASA, USDA, Dept. of Commerce, Dept. of the Interior and Agency for International Development ERTS
(Proj. AgRISTARS)
(E81-10211; NASA-CR-160951; YM-J1-C0618; JSC-16857)
Avail: NTIS HC A07/MF A01 CSCL 02C

A plan is described for supporting USDA crop production forecasting and estimation by (1) testing, evaluating, and selecting crop yield models for application testing; (2) identifying areas of feasible research for improvement of models; and (3) conducting research to modify existing models and to develop new crop yield assessment methods. Tasks to be performed for each of these efforts are described as well as for project management and support. The responsibilities of USDA, USDC, USDI, and NASA are delineated as well as problem areas to be addressed. A.R.H.

N81-32578*# Lockheed Engineering and Management Services Co., Inc., Houston, Tex. Remote Sensing Technology Implementation Project.
PHOTOGRAPHIC TECHNOLOGY DEVELOPMENT PROJECT: TIMBER TYPING IN THE TAHOE BASIN USING HIGH ALTITUDE PANORAMIC PHOTOGRAPHY Final Report
J. F. Ward Jun. 1981 42 p refs Sponsored in part by Dept. of Agriculture Original Contains Color Illustrations
(Grant NGR-53-3182-0-29)
(NASA-CR-161082; LEMSCO-15691) Avail: NTIS
HC A03/MF A01 CSCL 14E

Procedures were developed and tested for using KA-80A optical bar camera panoramic photography for timber typing forest land and classifying nonforest land. The study area was the south half of the Lake Tahoe Basin Management Unit. Final products from this study include four timber type map overlays on 1:24,000 orthophoto maps. The following conclusions can be drawn from this study: (1) established conventional timber typing procedures can be used on panoramic photography if the necessary equipment is available, (2) The classification and consistency results warrant further study in using panoramic photography for timber typing; and (3) timber type mapping can be done as fast or faster with panoramic photography than with resource photography while maintaining comparable accuracy. A.R.H.

N81-32588# Army Engineer Topographic Labs., Fort Belvoir, Va
LANDFORM-VEGETATION RELATIONSHIPS IN THE NORTHERN CHIHUAHUAN DESERT
Melvin B. Satterwhite and Judy Ehlen 29 Mar. 1981 21 p refs
(AD-A102896; ETL-R020) Avail: NTIS HC A02/MF A01 CSCL 08/6

The description and monitoring of environmental resources in arid regions can be a formidable undertaking requiring substantial resources. These efforts can be expedited by using remote sensing techniques. There remains, however, a need for correlating features that are readily extracted from the imagery with anticipated soil and vegetation conditions on the ground. Landform features provide a basis for the assessment of soil and vegetation conditions and these features can be readily identified from aerial photography and, to a certain extent, from LANDSAT imagery. The purpose of this study was to evaluate landform features as a basis for the assessment of soil and vegetation conditions. The study was conducted on 650,000 hectares in the northern Chihuahuan Desert (south-central New Mexico and western Texas). Landform conditions and plant communities were identified from an analysis of stereo panchromatic aerial photography, and were evaluated in detail by intensive field investigations. Soil conditions of the various landforms identified from the imagery were established by the laboratory analysis of field samples. The distribution of the plant communities was closely correlated to landform conditions and the edaphic factors affecting plant-available soil-water, soil texture, soil depth, infiltration, and slope. GRA

N81-33339# European Space Agency, Paris (France).
COHERENT AND INCOHERENT RADAR SCATTERING FROM ROUGH SURFACES AND VEGETATED AREAS
T. D. Guyenne, comp. and G. Levy, comp. May 1981 166 p refs Proceedings of ESA-EARSeL Workshop, Alpbach, Austria, 16-20 Mar. 1981 Sponsored in cooperation with Austrian Solar and Space Agency and DFVLR
(ESA-SP-166; ISSN-0379-6566) Avail: NTIS
HC A08/MF A01

The comparison of scatterometer results and radar images with respect to the physical information content is presented. Scatterometer systems, imaging radar systems, synthetic aperture radar (SAR), volume and surface scatter theories and their applications are studied. Scatterometer measurements on crop and soil surfaces, scatterometer calibration, and optimal polarization concept in radar imaging are discussed.

N81-33349# Centre National de la Recherche Scientifique, Toulouse (France). Centre d'Etude Spatiale des Rayonnements.
SCATTEROMETER MEASUREMENTS ON CROP AND SOIL SURFACES
Thuy LeToan *In* ESA Coherent and Incoherent Radar Scattering from Rough Surfaces and Vegetated Areas May 1981 p 99-110 refs
Avail: NTIS HC A08/MF A01

Scatterometer experiments on soil moisture detection and crop monitoring are summarized. Radar backscatter is found to be correlated to and sensitive to the soil moisture of the upper layer 0 to 5 cm at frequencies of 4 to 5 GHz and at an angle of incidence of 0 to 20 deg. The influence of soil texture on dielectric properties of moist soils led to defining a moisture parameter that accounts for this dependence. Research on crop identification and monitoring pointed out the large fluctuations of backscattering coefficient with time during the growing season, thus the need of multidate data for crop identification potentialities of radar for crop parameter detection and growth stage determination. Author (ESA)

N81-33542*# Texas A&M Univ., College Station. Remote Sensing Center.
DRYLAND PASTURE AND CROP CONDITIONS AS SEEN BY HCMM Progress Report, Jan. - Apr. 1980
J. C. Harlan, Principal Investigator, W. D. Rosenthal, and Bruce J. Blanchard Apr. 1980 19 p Original contains imagery. Original imagery may be purchased from NASA Goddard Space Flight Center, (code 601), Greenbelt, Md. 20771. Domestic users send orders to 'Attn: National Space Science Data Center'; non-domestic users send orders to 'Attn: World Data Center A for Rockets and Satellites'. HCMM
(Contract NAS5-24383)
(E81-10080; NASA-CR-164749; PR-3712-9) Avail: NTIS HC A02/MF A01 CSCL 02C

Daily antecedant precipitation indexes (API) values were calculated from precipitation amounts at each rain gage on the Washita River watershed; daytime thermal IR data from the watershed on July 24 was compared to July 13 daytime IR data covering the same area. Surface moisture conditions on the 13th were drier. A good relationship is apparent between thermal temperature difference around each rain gage site and the corresponding API value on July 24, 1978. Thirty-six hour day/night registered IR data at each rain gage on October 16/17 was compared to the corresponding daily API. Thermal patterns associated with an October 8 storm were still detectable but not as strongly as day/day differences between July 24 and 13. Analysis began on the IR data from the 10 HCMM CCT's tapes, received as well as on GOES visible and IR data for July 21 and 28, 1978. The spatial and thermal resolution in the latter were too gross to detect minor soil moisture differences which were detectable during the same period on HCMM thermal data. A.R.H.

N81-33543*# Dartmouth Coll., Hanover, N.H.
AN INVESTIGATION OF VEGETATION AND OTHER EARTH RESOURCE/FEATURE PARAMETERS USING LANDSAT AND OTHER REMOTE SENSING DATA. 1: LANDSAT. 2: REMOTE SENSING OF VOLCANIC EMISSIONS Semiannual Status Report, 1 Feb. - 31 Jul. 1981
Richard W. Birnie and Richard E. Stoiber, Principal Investigators 31 Jul. 1981 44 p refs Original contains imagery. Original photography may be purchased from the EROS Data Center, Sioux Falls, S.D. 57198. ERTS
(Contract NCC5-22)
(E81-10081; NASA-CR-164750; SASR-3) Avail: NTIS HC A03/MF A01 CSCL 08F

The application of a classification algorithm for mixture landscapes to LANDSAT data in order to inventory one-half million acres of forest land in northern Maine is reported as well as efforts to develop a user-oriented mapping system for forestry applications. Ash samples and ash leachates from volcanoes around the world were cataloged and analyzed. An instrument developed for remotely sensing HCl gas is being calibrated and evaluated. A real-time computer line for the COSPEC is under investigation in order to facilitate analysis of SO2 emission at a more detailed level than possible before. Evidence of increased magmatic gas component from Mt. St. Helens is documented and volcanic activity in Nicaragua is summarized. A.R.H.

N81-33545*# Texas A&M Univ., College Station. Remote Sensing Center.
MEASUREMENT OF SOIL MOISTURE TRENDS WITH AIRBORNE SCATTEROMETERS Progress Report, 1 Jan. 1980 - Jan. 1981
M. J. McFarland, Cheryl Jones, Sidney W. Theis, and Wesley D. Rosenthal, Principal Investigators 1 Jan. 1981 49 p ERTS
(Grant NsG-5134)
(E81-10078; NASA-CR-164752; RSC-3458-5) Avail: NTIS HC A03/MF A01 CSCL 08M

Soil moisture data collected in conjunction with aircraft data approximately 4 miles northwest of Dalhart, Texas are summarized. Ground data were collected in 22 fields extending along two parallel 11-mile lines running east-west. The sample fields included corn, pasture, millet and fallow fields selected for their suitability for analysis with aircraft data. A NASA C130 flew every other day along the two flight lines. Two passes were flown on each line with various sensors operating on each pass. The sensor included a PRT-5, NS001 thematic mapper, MMS, L and C band passive microwave radiometers and 13.3, 4.75, 1.6 and .4 GHz scatterometers. In addition, low and medium altitude color infrared photography and special calibration data were gathered. The ground work, the fields, procedures in the field and lab, and the final data sets are described. A.R.H.

N81-33546*# Lockheed Engineering and Management Services Co., Inc., Houston, Tex.
INTERIM CATALOG GROUND DATA SUMMARY, DATA ACQUISITION YEAR 1978
V. L. Cook and H. M. Doyle, Principal Investigators Mar. 1981 37 p Sponsored by NASA, USDA, Dept. of Commerce, Dept. of the Interior, and Agency for International Development ERTS
(Contract NAS9-15800; Proj. AgRISTARS)
(E81-10132; NASA-CR-161035; MU-L1-04056; LEMSCO-16325; JSC-17120) Avail: NTIS HC A03/MF A01 CSCL 02C

Those sample segment number for which aircraft data were acquired and/or field inventory data were produced in 1978 are listed by states. Detail specifications, background information, description of the format, sources of information, and an explanation of procedures for the catalog are included. A.R.H.

N81-33549*# National Aeronautics and Space Administration. Lyndon B. Johnson Space Center, Houston, Tex.
A COMPARATIVE STUDY OF THE THEMATIC MAPPER AND LANDSAT SPECTRAL BANDS FROM FIELD MEASUREMENT DATA
G. D. Badhwar and K. E. Henderson, Principal Investigators Mar. 1981 21 p refs Sponsored by NASA, USDA, Dept. of Commerce, Dept. of the Interior, and Agency for International Development ERTS
(Proj. AgRISTARS)
(E81-10165; NASA-TM-84032; SR-J0-04029; JSC-16849) Avail: NTIS HC A02/MF A01 CSCL 02C

Principal component and factor analysis techniques were applied to the spectral data collected over 27 field plots of various crops under varying agronomic conditions. The spectral data was integrated over the proposed thematic mapper bands and LANDSAT MSS spectral bands. The results were examined to compare the discrimination power of the thematic mapper. Author

N81-33554*# Minnesota Univ., St. Paul. Dept. of Soil Science.
A PROJECT TO EVALUATE MOISTURE STRESS AND PHENOLOGICAL FACTORS IN CORN AND SOYBEAN AREAS OF SOUTHWESTERN AND SOUTH-CENTRAL MINNESOTA
R. H. Rust and Pierre Robert, Principal Investigators *In its* A Study of Minn. Land and Water Resources Using Remote Sensing, Vol. 14 1 Jan. 1981 18 p refs Original contains color imagery. Original photography may be purchased from the EROS Data Center, Souix Falls, S.D. 57198. ERTS

Avail: NTIS HC A05/MF A01 CSCL 02C

The capability of aerial color infrared photography for identifying and locating soilscapes most susceptible to drought development or those having different soil drainages was evaluated. Although west central and southwestern Minnesota had a significant precipitation deficit during the 1980 crop season, indications of plant stress were not observed either from ground observation or through interpretation of imagery at the selected sampling sites. Well-drained soil was more depleted during the 'maximium green peak' period than the poorly drained soil. The recharge was more evident on the poorly drained site in the fall. Measurements of leaf water potential and leaf temperature for corn and soybean leaves were made by multispectral band scanner and recorded for analysis. A.R.H.

N81-33555*# National Aeronautics and Space Administration. Lyndon B. Johnson Space Center, Houston, Tex.
AgRISTARS: FOREIGN COMMODITY PRODUCTION

FORECASTING. PROGRAM REVIEW PRESENTATION TO LEVEL 1, INTERAGENCY COORDINATION COMMITTEE
Semiannual Project Management Report

Roy Eason, Principal Investigator 6 Nov. 1980 123 p Sponsored by NASA, USDA, Dept. of Commerce, Dept. of the Interior, and Agency for International Development Original contains imagery. Original photography may be purchased from the EROS Data Center, Sioux Falls, S.D. 57198. ERTS
(Proj. AgRISTARS)
(E81-10168; NASA-TM-84030; FC-J0-04010; JSC-16835)
Avail: NTIS HC A06/MF A01 CSCL 02C

Accomplishments made since March 1980 in developing and testing procedures to provide more objective and reliable crop production forecasts several times during the growing season as well as improved preharvest estimates for a range of countries and crops are summarized. Results of classification procedures verification and simulated aggregation tests are included as well as evaluations of crop stage model performance. The status of wheat/barley and corn/soybean experiments is examined and the extension of the methods used in the experiments to multicrop sampling and aggregation is considered. The foreign similarity region approach, objectives and scopes for FY-81, and major changes in the FY81/82 plan are examined. A.R.H.

N81-33558*# Kansas Univ., Lawrence. Space Technology Center.

CROP PHENOLOGY AND LANDSAT-BASED IRRIGATED LANDS INVENTORY IN THE HIGH PLAINS: APPENDICES
Final Report

[1981] 201 p refs ERTS
(Grant NAG2-57)
(E81-10172; NASA-CR-164565) Avail: NTIS
HC A10/MF A01 CSCL 02C

Data collected in an effort to produce a master crop calendar in map and tabular format for the High Plains Aquifer are presented. Contents include: a key to the counties in the High Plains Aquifer; USDA Economics and Statistic Service data for 1979; Agricultural Stabilization and Conservation Service data for 1979 and 1980; Cooperative Extension Service data for 1979 and 1980; recording methods from questionnaire; scatterplots portraying ASCS, Extension and ESS data; crop irrigation maps; and weekly summary based optimal LANDSAT dates. A bibliography is included. A.R.H.

N81-33559*# Kansas Univ., Lawrence. Space Technology Center.

CROP PHENOLOGY AND LANDSAT-BASED IRRIGATED LANDS INVENTORY IN THE HIGH PLAINS **Final Report**

E. A. Martinko, Principal Investigator, J. Poracsky, E. R. Kipp, H. Krieger, and K. Gunn [1981] 139 p ERTS
(Grant NAG2-57)
(E81-10173; NASA-CR-164566) Avail: NTIS
HC A07/MF A01 CSCL 02C

The need to determine the volume of ground water being pumped from the High Plains region aquifer (HPRA) for irrigation can be met using a LANDSAT based remote sensing system. Crop calendar differences in such a large area (most of Nebraska, half of Kansas, the Texas and Oklahoma Panhandle areas, a portion of South Dakota, and the eastern parts of Wyoming, Colorado, and New Mexico) can introduce local influences on the interpretation of the algorithms employed. A method is described for determining the optimal dates for inventorying various crops grown on these irrigated lands in support of an effort to identify irrigated and develop a computer model for predicting aquifer response to changes in ground water development. A crop calendar for the crops grown in the HPRA is presented. A.R.H.

N81-33561*# Purdue Univ., Lafayette, Ind. Lab. for Applications of Remote Sensing.

EVALUATION OF LANDSAT DATA ANALYSIS FOR FOREST SURVEY **Final Report**

R. P. Mroczynski, R. M. Hoffer, and R. F. Nelson, Principal Investigators 1980 47 p refs Sponsored by NASA and US Forest Service Original contains imagery. Original photography may be purchased from the EROS Data Center, Sioux Falls, S.D. 57198. ERTS
(E81-10175; NASA-CR-164754 LARS-TR-101880) Avail: NTIS HC A03/MF A01 CSCL 02F

LANDSAT classification results are compared to current survey statistics for forest/non-forest classes in the northeastern aspen-birch survey unit in Minnesota. The results help to provide: the first step in a land change monitoring system; estimates of cost of local and regional land use statistics obtained from LANDSAT; and information regarding the degree of information that can be extracted from LANDSAT. The possibility of detecting disturbance on survey plots was determined. This possible application of forest survey ground plots as training material for computer-aided LANDSAT classification is discussed. T.M.

N81-33564*# Tulsa Univ., Okla. Div. of Mathematical Sciences.

MAXIMUM LIKELIHOOD ESTIMATION FOR MIXTURE MODELS

R. A. Redner, Principal Investigator Oct. 1980 51 p refs Sponsored by NAsA, USDA, Dept. of Commerce, Dept. of the Interior and Agency for International Development Prepared in cooperation with Lockhead Engineering and Management Services Co., Inc., Houston, Tex. ERTS
(Contract NAS9-15800; Proj. AgRISTARS)
(E81-10178; NASA-CR-160967; SR-J0-04007;
LEMSCO-14880; JSC-16832) Avail: NTIS HC A04/MF A01
CSCL 12A

The maximum likelihood estimation of parameters in mixture model is discussed, the use of ancillary information in the maximum likelihood process is shown, and the strong consistency of the maximum likelihood estimator is proven. A study of these three areas leads to a threshold maximum estimator which estimates the number of classes in a mixture model. This estimator, along with the iteration procedure by which it is calculated, is described. Local and global results for the procedure are given. A.R.H.

N81-33565*# Lockheed Engineering and Management Services Co., Inc., Houston, Tex.

AUSTRALIAN TRANSITION YEAR SPECIAL STUDIES

R. W. Payne and T. E. Armstrong, Principal Investigators Jan. 1981 110 p Sponsored by NASA, USDA, Dept. of Commerce, Dept. of the Interior and Agency for International Development Original contains color imagery. Original photography may be purchased from the EROS Data Center, Sioux Falls, S.D. 57198. ERTS
(Contract NAS9-15800; Proj. AgRISTARS)
(E81-10179; NASA-CR-160968; FC-L0-00464;
LEMSCO-14808; JSC-16368) Avail: NTIS HC A06/MF A01
CSCL 02C

The processing of Australian data during LACIE transition year resulted in identification of the major issues in classification, sampling/aggregation, yield, and production. Classification issues which were identified and/or partially resolved are those concerned with early-season and late-season wheat varieties, abandonment, confusion crops, and ancillary data problems, especially crop calendar problems. Labeling accuracy results and ground-truth data from a New South Wales sample segment are included with results, conclusions, and recommendations for crop labeling and labeling-related issues. A.R.H.

N81-33573*# National Aeronautics and Space Administration. Lyndon B. Johnson Space Center, Houston, Tex.

A CROP MOISTURE STRESS INDEX FOR LARGE AREAS AND ITS APPLICATION IN THE PREDICTION OF SPRING WHEAT PHENOLOGY

P. C. Doraiswamy and D. R. Thompson, Principal Investigtors Mar. 1981 28 p refs Sponsored by NASA, USDA, Dept. of Commerce, Dept. of the Interior and Agency for International Development Prepared in cooperation with Lockheed Engineering and Management Services Co., Inc., Houston, Tex. ERTS
(Contract NAS9-15800; Proj. AgRISTARS)
(E81-10202; NASA-TM-84035; SR-L1-04064; JSC-17121;
LEMSCO-16216) Avail: NTIS HC A03/MF A01 CSCL 02C

An agrometeorological crop phenology model for spring wheat is presented which incorporates the photothermal concept suggested by the Robertson crop calendar model for spring grains. This model differs from the Robertson model in that it incorporates a crop moisture stress index as a model parameter. The data used to assess the effects of moisture stress on phenological development were derived from the literature. In certain parts of the model, it is suggested that remotely sensed spectral data may be used as inputs. The model is applicable to large area forecasting and incorporates the influence of soil moisture deficit on phenological development. Model outputs representing a moisture-stressed condition and an adequate moisture condition are discussed for growth observations in North Dakota and Montana. A.R.H.

N81-33575*# National Aeronautics and Space Administration. Lyndon B. Johnson Space Center, Houston, Tex.

EXPERIMENT PLAN: ROW AND ROUGHNESS EFFECTS ON DEPENDENCE OF ACTIVE MICROWAVE MEASUREMENTS OF SOIL MOISTURE

J. F. Paris and L. M. Arya, Principal Investigators Oct. 1980 38 p refs Sponsored by NASA, USDA, Dept. of Commerce, Dept. of the Interior, and Agency for International Development Prepared in cooperation with Lockheed Engineering and Management Services Co., Inc., Houston, Tex. ERTS
(Proj. AgRISTARS)
(E81-10209; NASA-TM-84048; SM-J0-00613; JSC-16822; LEMSCO-15181) Avail: NTIS HC A03/MF A01 CSCL 08M

To increase understanding of the effects of agricultural tillage practices and aspect angle on the interpretation of active microwave data over bare agricultural fields, an experiment is planned for determining the effects of different combinations of row spacings and heights at L-band, C-band, and Ku-band for viewing angles of 10 deg, 20 deg, 30 deg, 40 deg, and 50 deg and for HH polarization. The objectives give scope, approach, test site description, and data requirements for the experiment. The data is to be gathered at the Prairie View A&M University, Texas test site and at Jornada, New Mexico. A data analysis plan is proposed including error analysis for estimating the modulation function. A.R.H.

N81-33588# Battelle Inst., Frankfurt am Main (West Germany). Abt. Laser und Optik.

EXPERIMENTAL INVESTIGATION OF THE PHYSICAL FUNDAMENTALS FOR REMOTE SENSING OF SOIL AND VEGETATION MOISTURE BY ACTIVE INFRARED REFLECTANCE SPECTROSCOPY USING CO2 LASER TECHNIQUE
Final Report

Joerg Boscher and Frank Lehman (Zentralstelle fuer Geo-Photogrammetrie und Fernerkundung) Bonn Bundesministerium fuer Forschung und Technologie Dec. 1980 39 p refs In GERMAN; ENGLISH summary Sponsored by Bundesministerium fuer Forschung und Technologie
(BMFT-FB-W-80-037; BF-R-64-028-01; ISSN-0170-1339) Avail: NTIS HC A03/MF A01; Fachinformationszentrum, Karlsruhe, West Germany DM 8.20

The application of active infrared spectroscopy to remote sensing of soil moisture was examined. The reflectance of water and dry and moist soil samples, including selected minerals and natural soils, was measured with the emission lines of the CO2 laser. The reflectance spectra of the samples change in a characteristic way with increasing moisture. Spectral differences of the dry materials are reduced with increasing water content, enabling the use of the ratio of the reflected intensities of two CO2 laser lines to determine the moisture content of surfaces. The airborne remote sensing system (DIALEX) developed for differential absorption spectroscopy of gases can be employed for two channel reflectance spectroscopy. Applications of this moisture sensing method in the fields of mineral deposits prospecting, agriculture and forestry are discussed. Author (ESA)

N81-33598# Technicolor Graphic Services, Inc., Sioux Falls, S. Dak.

A SELECTED BIBLIOGRAPHY: REMOTE SENSING APPLICATIONS IN WILDLIFE MANAGEMENT

David M. Carneggie, Donald O. Ohlen, and Lawrence R. Pettinger 23 Feb. 1981 24 p
(Contract DI-14-08-0001-16439)
(PB81-215881) Avail: NTIS HC A02/MF A01 CSCL 13B

This bibliography cites 165 selected technical reports, journal articles, and other publications on remote sensing applications for wildlife management. Developments in the use of remotely sensed data for wildlife habitat mapping, habitat inventory, habitat evaluation, and wildlife census are covered. The works cited were published between 1947 and 1979. GRA

02

ENVIRONMENTAL CHANGES AND CULTURAL RESOURCES

Includes land use analysis, urban and metropolitan studies, environmental impact, air and water pollution, geographic information systems, and geographic analysis.

A81-41061 # **Hurricane 'Flossie' /September 1978/ observed in the north Atlantic, by the Meteosat satellite (L'uragano 'Flossie' /Settembre 1978/ visto dal Meteosat sul nord Atlantico).** S. Zanni (Centro Nazionale di Meteorologia e Climatologia Aeronautica, Rome, Italy). *Rivista di Meteorologia Aeronautica*, vol. 41, Jan.-Mar. 1981, p. 33-42. 14 refs. In Italian.

The behavior of hurricane Flossie (September 1978) in the north Atlantic in terms of the monthly mean September circulation is interpreted. Some brief remarks and meteosynoptic suggestions regarding Flossie's genesis and development are presented, also in analogy with other similar hurricanes in this segment of the Atlantic ocean mainly in fall, season of highest tropical storm activity. Finally some interpretations of two Meteosat infra-red and water vapour images which show the maximum stage of Flossie moving sharply northward to the Atlantic extra-tropical latitudes are presented. (Author)

A81-41404 **Stratospheric sulfate from the Gareloi eruption, 1980 - Contribution to the 'ambient' aerosol by a poorly documented volcanic eruption.** W. A. Sedlacek, E. J. Mroz, and G. Heiken (California, University, Los Alamos, NM). *Geophysical Research Letters*, vol. 8, July 1981, p. 761-764. 5 refs.

While sampling stratospheric aerosols during July-August 1980 a plume of 'fresh' volcanic debris was observed in the Northern Hemisphere. The origin of this material seems to be a poorly documented explosive eruption of Gareloi volcano in the Aleutian Islands. The debris was sampled at an altitude of 19.2 km - almost twice the height of observed eruption clouds. Such remote, unobserved or poorly documented eruptions may be a source that helps maintain the 'ambient' stratospheric aerosol background. (Author)

A81-42281 # **Remote sensing and mapping of pastures (Distantsionnaia indikatsiia i kartirovanie pastbishch).** B. V. Vinogradov. *Issledovanie Zemli iz Kosmosa*, May-June 1981, p. 35-45. 24 refs. In Russian.

Aerial and space surveys were used to study the composition, structure, phenology, and dynamics of pastures. The topography method of pastural survey is discussed at several levels, ranging from the detailed (population) and elementary (biogenetic) to the local and regional. The most up-to-date method involves the determination of pastural changes caused by overgrazing. This is done by comparing repeated aerial and space photographs of the same territory and recording the pastural modifications of land use by means of overgrazing and desertification indicators during a single flight. J.F.

A81-43261 * **Application of remote sensing for California irrigated lands assessment.** L. Tinney, J. Estes (California, University, Santa Barbara, CA), S. Wall, and R. Colwell (California, University, Berkeley, CA). In: Satellite hydrology; Proceedings of the Fifth Annual William T. Pecora Memorial Symposium on Remote Sensing, Sioux Falls, SD, June 10-15, 1979. Minneapolis, MN, American Water Resources Association, 1981, p. 689-693. Grant No. NsG-2208.

Recognizing the need for land use data as an input to State water planning, the California Department of Water Resources (DWR) and its predecessor agencies have conducted land use surveys since the late 1940's. In 1957 the California Water Plan was established. A statewide assessment is compiled every four to five years to review overall water resource conditions. Satellite remote sensing imagery, such as available from Landsat, has been recognized by DWR as a potential source of land use data. Analysis of Landsat imagery in connection with 'calibrating' data from low altitude photography and/or field checks can provide an economical means for providing a large scale, single year base inventory of general land use. The purpose of the Applications Pilot Test is to develop and document the use of Landsat for such an inventory. Towards the overall goal of developing an operational methodology that DWR could cost effectively implement four tasks have been specified. G.R.

A81-43263 **Remote sensing of bank erosion along the Missouri River, South Dakota.** P. H. Rahn (South Dakota School of Mines and Technology, Rapid City, SD). In: Satellite hydrology; Proceedings of the Fifth Annual William T. Pecora Memorial Symposium on Remote Sensing, Sioux Falls, SD, June 10-15, 1979. Minneapolis, MN, American Water Resources Association, 1981, p. 697-700.

In South Dakota, rapid erosion and deposition occurs below the main stem dams on the Missouri River. A description is presented of the use of Landsat imagery to quantify the amount of erosion in a reach below Gavins Point Dam. Landsat imagery of the entire reach below Gavins Point Dam was obtained and compared and images were chosen based on available cloud-free days, for the days of May 30, 1973 and February 23, 1976. It is pointed out that satellite imagery adds a new dimension to fluvial studies by allowing for repetitive (temporal) coverage of a stream reach. The considered study shows that it is possible to periodically assess areas of erosion and deposition for the Missouri River. G.R.

A81-43523 # **Remote methods and desert conservation (Distantsionnye metody i okhrana prirody pustyn').** N. G. Kharin. Moscow, Izdatel'stvo Nauka, 1980. 104 p. 124 refs. In Russian.

The application of remote sensing methods in the study of desert resources for the prevention of destructive processes and the planning of desert reclamation are examined. Problems in the monitoring of natural resources to which remote methods may successfully be applied are considered, including the study of vegetation damage, land use, soil erosion and salinization, water resources and pollution and natural disasters, and space-borne, aerial and ground-based methods used in resource monitoring are presented. The application of multispectral aerospace photography for the thematic mapping of desert areas is then examined, with attention given to the determination of optimum spectral regions, the characteristics of the photographs obtained, map correction, and the feasibility of using the maps in the planning of conservation measures. Attention is also given to the application of remote methods in the mapping of conservation zones in desert regions and the study of natural preserves in arid regions. A.L.W.

A81-43533 **Comparison of sampling procedures and data analysis for a land-use and land-cover map.** K. Fitzpatrick-Lins (U.S. Geological Survey, Reston, VA). *Photogrammetric Engineering and Remote Sensing*, vol. 47, Mar. 1981, p. 343-351. 9 refs.

The accuracy of the Tampa, Florida Land-Use and Land-Cover Map produced by the U.S. Geological Survey at a scale of 1:250,000 was estimated by the use of two separate sample selections, a manual sample selection, and a computer automated sample selection. A comparison of these two methods favors the second. The manual sample selection used a stratified systematic unaligned sampling technique. The computer-based automated sample selection first used a stratified systematic unaligned sampling technique followed by a random selection stratified by category to assure that all categories were adequately sampled. With the manual sample selection only six of the 26 categories were adequately represented, and nine were not represented at all. Using the computer-based sample selection, all 26 categories were represented. B.J.

A81-43534 **Spatial correlation effects upon accuracy of supervised classification of land cover.** J. B. Campbell (Virginia Polytechnic Institute and State University, Blacksburg, VA). *Photogrammetric Engineering and Remote Sensing*, vol. 47, Mar. 1981, p. 355-363. 19 refs.

The Landsat 1 multispectral scanner imaged south central Virginia at six dates during the 1974 growing season. The examination of selected parcels of forest reveals the presence of positive continuity between MSS values at adjacent pixels, the degree of continuity varies from date to date, and according to MSS bands at a

given date. In at least some cases, it can be shown that estimates of category variances based on values at contiguous pixels yield low values relative to those based on random samples of the same area. These biased estimates can lead to overestimation of contrast between categories and to errors in supervised classification. Erroneously classified pixels may tend to cluster, thus increasing the opportunity for misinterpretation of errors as genuine land-cover parcels.
B.J.

A81-43733 * **Urban area update procedures using Landsat data.** D. L. Toll (NASA, Goddard Space Flight Center, Greenbelt, MD), J. A. Royal (General Electric Co., Space Systems Div., Beltsville, MD), and J. B. Davis (U.S. Bureau of Census, Geography Div., Washington, DC). In: Rainbow 80; Fall Technical Meeting, Niagara Falls, NY, October 7-10, 1980, ASP Technical Papers. Falls Church, VA, American Society of Photogrammetry, 1981, p. RS-1-E-1 to RS-1-E-17. 18 refs.

Landsat digital enhancements and classification maps are shown to be useful for updating the urban expansion of standard metropolitan statistical areas on a macro scale. Automated procedures for detecting nonurban to urban land coverage change using multitemporal Landsat data are investigated for five metropolitan areas, showing an overall delineation similar to that obtained from large scale aerial photography. The evaluated change detection procedures include image differencing, principal component transformation prior to differencing, and post classification comparison. Results show that image differencing techniques in MSS band 5 provide the most accurate land cover change detections.
J.F.

A81-43739 **From landforms to avian habitat - A look at topology.** J. E. Skaley (Cornell University, Ithaca, NY). In: Rainbow 80; Fall Technical Meeting, Niagara Falls, NY, October 7-10, 1980, ASP Technical Papers. Falls Church, VA, American Society of Photogrammetry, 1981, p. RS-2-E-1 to RS-2-E-8. 8 refs.

A landscape approach, in which basic topological relationships among shapes and patterns in the terrain are identified, has been used to predict local climate and potential songbird habitat. Geometric models and topological relationships among basic patterns are shown to provide a focus for quantifying and understanding relationships between terrain features. Three case studies are presented, exemplifying nature's tendency to repeat basic shapes and patterns which can be used to predict landscape properties. Illustrations are provided, showing topological shapes related to landform features, forest canopy characteristics, air flow patterns, and heating and cooling patterns. Associations between avian groups and different topological features and canopy structures are given. It is suggested that these relationships be examined in greater detail as a way of quantifying the interpretation process and improving landscape analysis.
J.F.

A81-43748 **Use of remote sensing in landscape stratification for environmental impact assessment.** J. A. Stanturf (Cornell University, Ithaca, NY) and D. G. Heimbuch (Heimbuch-Stanturf, Inc., Ithaca, NY). In: Rainbow 80; Fall Technical Meeting, Niagara Falls, NY, October 7-10, 1980, ASP Technical Papers. Falls Church, VA, American Society of Photogrammetry, 1981, p. PS-2-A-1 to PS-2-A-11. 22 refs.

Landscape units, used in environmental impact assessment, are delineated by integrating remotely sensed data and available single-factor data. A remote sensing approach to landscape stratification is described, and shown to be superior to other approach that require single-factor maps under certain conditions. Flow charts show the steps necessary for developing classification criteria, delineating units and a map legend, and using the landscape units in impact assessment. The approach is then applied to assess impacts of a transmission line to illustrate the method.
J.F.

A81-43749 * **Texture measurements from Seasat - SAR images for urban land use interpretation.** F. Fasler (California Institute of Technology, Jet Propulsion Laboratory, Pasadena, CA). In: Rainbow 80, Fall Technical Meeting, Niagara Falls, NY, October 7-10, 1980, ASP Technical Papers. Falls Church, VA, American Society of Photogrammetry, 1981, p. PS-2-B-1 to PS-2-B-10. 9 refs. Contract No. NAS7-100.

Different grey tones in Seasat Synthetic Aperture Radar (SAR) images for the same type of urban land cover considerably impair the possibilities of establishing automatic classification procedures for these types of data. Since the orientation of the main features like street patterns and buildings with respect to the azimuth angle of the radar antenna is the crucial factor for the observed differences in grey tone, prior information on these elements and special processing of the data would be required to eliminate this effect. Another approach suggested in this paper is to make use of the textural information in the image rather than of its grey tone. For different study sites within the Los Angeles urbanized area texture measures could be derived which result in characteristic values for specific types of land cover and are largely independent of the azimuth angle effect. At the same time the results for the study area indicate an improvement of the overall separability for the different land cover types included in the analysis.
(Author)

A81-44515 * # **Measurements of CF2Cl2, CFCl3, and N2O in the lower stratosphere between 2 deg S and 73 deg N latitude.** J. F. Vedder, E. C. Y. Inn, B. J. Tyson, C. A. Boitnott (NASA, Ames Research Center, Atmospheric Experiments Branch, Moffett Field, CA), and D. O'Hara (EAL Corp., Richmond, CA). *Journal of Geophysical Research*, vol. 86, Aug. 20, 1981, p. 7363-7368. 20 refs.

Mixing ratios are presented for CF2Cl2, CFCl3, and N2O in the lower stratosphere. They are derived from measurements made on samples collected by a high-altitude aircraft during a survey in the northern hemisphere in the summer of 1977. The vertical distributions of the mixing ratios of these species show a decrease with increasing altitude and a marked decrease at a given altitude with increasing latitude from 2 deg S to 73 deg N latitude. These results agree with measurements at similar latitudes in the fall of 1976 and with results of other experiments. The experimental apparatus and procedures are described in greater detail than in previous papers.
(Author)

A81-44526 # **Aerosol formation, transformation, and effects in Denver's emissions plume.** C. C. Van Valin, R. F. Pueschel, and D. L. Wellman (NOAA, Environmental Research Laboratories, Boulder, CO). *(International Association of Meteorology and Atmospheric Physics, International Conference on Budget and Cycles of Trace Gases and Aerosols, 4th, Boulder, CO, Aug. 12-18, 1979.) Journal of Geophysical Research*, vol. 86, Aug. 20, 1981, p. 7463-7470. 22 refs.

During November and December 1978, a field study was conducted with the primary objective to identify the factors and substances that cause the reduction of visibility and the gray-brown color of the polluted air mass, the 'brown cloud', during winter pollution episodes. Gases and aerosols over the Denver metropolitan area and at varying distances downwind were measured with a research aircraft. Near the principal emissions source area, the particle number distribution was found to be dominated by nucleus mode aerosols, the O3 concentration was much lower than background, and the NO concentration was greater than that of NO2. After a few hours reaction during sunlight, the O3 concentrations were greater than background, most of the NO had been converted to NO2, and the accumulation mode particles were comparatively more numerous than in the young pollution cloud. A mechanism has been identified for the removal of NO2 from the atmosphere during periods of high relative humidity.
G.R.

A81-44684 **Texture analysis and urban land use classification.** C. A. Harlow, R. W. Conners, M. M. Trivedi, D. A. DiRosa, and R. E. Vasquez-Espinosa (Louisiana State University, Baton Rouge, LA). In: SOUTHEASTCON '81; Proceedings of the Region 3 Conference and Exhibit, Huntsville, AL, April 5-8, 1981. Piscataway, NJ, Institute of Electrical and Electronics Engineers, Inc., 1981, p. 115-119. 10 refs.

Image processing techniques have been applied to the analysis of urban scenes. Many characteristics of land use patterns are given by the spatial variations of the gray shades in the image. Texture analysis is an image processing technique developed to analyze spatial variations in gray shades. A texture analysis technique based upon the Spatial Gray Level Dependence Method (SGLDM) has been developed. This method utilizes statistical and structural analysis and is therefore called a statistical and structural texture analysis procedure (SSA). The SSA texture analysis procedure has been applied to the analysis and classification of a digitized photograph of a complex urban scene. (Author)

A81-44701 **A comparison of automatic classification algorithms for land use map by remotely sensed data.** S. Fujimura and H. Toyota (Tokyo, University, Tokyo, Japan). In: SOUTHEASTCON '81; Proceedings of the Region 3 Conference and Exhibit, Huntsville, AL, April 5-8, 1981. Piscataway, NJ, Institute of Electrical and Electronics Engineers, Inc., 1981, p. 299-303.

The results of various supervised classification algorithms for the preparation of land use maps based on remotely sensed multispectral data are compared in order to illustrate some of the problems in the selection of the most suitable algorithm. Multispectral data obtained in the Fukuyama district of Japan was classified by the maximum likelihood method, the linear discriminant function method, the minimum Euclidean distance method and the correlation method with and without normalization of the mean, and the correct classification rates of the various methods were analyzed. The relative accuracies of the methods are found not to be in the order predicted under the assumption of a normal data distribution. Further analysis reveals this to be due to the lack of generality of the training data. It is thus recommended that when the statistical properties of the training data vary greatly from one category to another, the minimum Euclidean distance method or the linear discriminant function method be used rather than the more common maximum likelihood method. A.L.W.

A81-44862 **ISS-b experimental results on global distributions of ionospheric parameters and thunderstorm activity.** N. Matuura (Ministry of Posts and Telecommunications, Radio Research Laboratories, Nakaminato, Ibaraki, Japan), M. Kotaki, S. Miyazaki, E. Sagawa, and I. Iwamoto (Ministry of Posts and Telecommunications, Radio Research Laboratories, Koganei, Tokyo, Japan). *(International Astronautical Federation, International Astronautical Congress, 31st, Tokyo, Japan, Sept. 22-27, 1980.) Acta Astronautica,* vol. 8, May-June 1981, p. 527-548. 19 refs.

Experimental results from the Ionosphere Sounding Satellite-b (ISS-b) are presented, with emphasis on the global distribution of such ionospheric parameters as (1) critical frequency (foF2); (2) the probability of occurrence of spread echoes; (3) nighttime electron temperature and ionic constituents of the ambient plasma; and (4) thunderstorms detected by means of radio technique. Detailed maps are presented for all four missions of the satellite, for a period lasting from August 1978 to June 1979. O.C.

A81-45406 # **Investigation of the efficiency of the optical sounding of aerosol by the use of spectral photometers (Issledovanie effektivnosti opticheskogo zondirovaniia aerozolia s ispol'zovaniem spektral'nykh fotometrov).** B. S. Kostin. In: Investigation of atmospheric aerosol by means of laser sounding.
Novosibirsk, Izdatel'stvo Nauka, 1980, p. 70-83. 12 refs. In Russian.

A method is developed for the analysis of the efficiency of the optical sounding of atmospheric aerosol by spectral photometers; the method is based on the comparison of results obtained from the inversion of optical measurements with data from direct measurements of the microstructure of atmospheric aerosol. This approach makes it possible to compare the absolute values of particle concentrations. It is shown that, within the limits of measurement error, the inversion results agree well with direct-measurement data. F.G.M.

A81-45434 **Land use mapping of Hong Kong from Landsat images - An evaluation.** C. P. Lo (University of Hong Kong, Hong Kong). *International Journal of Remote Sensing,* vol. 2, July-Sept. 1981, p. 231-252. 15 refs.

Landsat 70 mm film images are evaluated for planimetric accuracy and the accuracy of land use interpretation for the production of land use maps of Hong Kong. Maps are produced for a 1061 sq km area at a scale of 1:250,000 using a Fairey additive viewer, and at a scale of 1:88,500 using manual interpretation, demonstrating that information can be improved with further enlargement of the Landsat segment despite resolution limitations. An urban land use map at a scale of 1:25,000 is also generated with a computer assisted method of Landsat data analysis, demonstrating lower accuracy due to the intensity of urban land use. Although the maps do not reach the accuracy of aerial photography, they are of an acceptable planimetric and semantic accuracy, and are relatively cheap while allowing frequent revisions. D.L.G.

A81-45437 **Procedures for change detection using Landsat digital data.** P. J. Howarth (McMaster University, Hamilton, Ontario, Canada) and G. M. Wickware (Environment Canada, Canada Centre for Inland Waters, Burlington, Ontario, Canada). *International Journal of Remote Sensing,* vol. 2, July-Sept. 1981, p. 277-291. 17 refs. Research supported by the Natural Sciences and Engineering Research Council of Canada, Prairie Regional Office of Parks.

Procedures in applying complementary methods of band ratioing and post-classification change detection to monitor a large remote area are presented. Work by Wickware and Howarth (1980) demonstrating the use of band ratioing and post-classification detection is also presented, including methods for detecting, displaying and measuring environment change. Band ratioing, classification, change matrices, binary theme prints and conflict character assignment maps are found to provide a practical sequence for analyzing hydrologic and vegetation changes. In addition, the amount of information required is found to depend on the complexity of the problem and the level and type of resource management decision to be made. D.L.G.

A81-45862 **A differential inversion method for high resolution atmospheric remote sensing.** M. M. Abbas (Drexel University, Philadelphia, PA). In: Remote sensing of atmospheres and oceans; Proceedings of the Interactive Workshop on Interpretation of Remotely Sensed Data, Williamsburg, VA, May 23-25, 1979. New York, Academic Press, Inc., 1980, p. 1-14; Discussion, p. 15-18. 7 refs.

The spectral lines of atmospheric gases may be fully resolved with high resolution observations by techniques, such as infrared heterodyne spectrometers. An inversion method suitable for such observations is discussed and is found to have several advantages over conventional methods. The method is based on matching the derivatives of the observed radiances or transmittances with the calculated values for the modeled atmosphere. The proposed method provides a significant narrowing of the weighting functions and improvement in the overall accuracy of the retrieved profiles. The method is applied to inversion of ozone absorption lines in the earth's atmosphere and the results are compared with those obtained with a conventional method. (Author)

A81-45870 * **Role of multiple scattering in ozone profile retrieval from satellite measurements in the ultraviolet.** S. L. Taylor, P. K. Bhartia, V. G. Kaveeshwar, K. F. Klenk (Systems and Applied Sciences Corp., Riverdale, MD), A. J. Fleig (NASA, Goddard Space Flight Center, Greenbelt, MD), and C. L. Mateer (Department of the Environment, Atmospheric Environment Service, Downsview, Ontario, Canada). In: Remote sensing of atmospheres and oceans; Proceedings of the Interactive Workshop on Interpretation of Remotely Sensed Data, Williamsburg, VA, May 23-25, 1979. New York, Academic Press, Inc., 1980, p. 219-229; Discussion, p. 230, 231. 6 refs.

The retrieval of the ozone profile from satellite ultraviolet measurements can be extended to greater depths when multiple scattering is taken into account. The sensitivity of the multiple-scattered wavelength radiances to geophysical variables are discussed and results of profile inversions of Nimbus 4 backscatter ultraviolet data for coincident ground-truth measurements with and without multiple scattering are presented. (Author)

A81-46044 **The use of CIR and airborne multispectral scanner techniques for wetland soils mapping of highway corridors.** A. E. Redfield (Dames and Moore, Washington, DC) and K. S. Thom (General Electric Co., Space Div., Lanham, MD). In: Machine processing of remotely sensed data and soil information systems and remote sensing and soil survey; Proceedings of the Sixth Annual Symposium, West Lafayette, IN, June 3-6, 1980.
New York, Institute of Electrical and Electronics Engineers, Inc., 1980, p. 205-213. 9 refs. Research sponsored by the U.S. Department of Transportation.

This paper summarizes the results of an investigation aimed at evaluating the potential advantages of state-of-the-art airborne remote sensing for highway siting and planning tasks, specifically in wetland areas. The basic objectives of the study were to develop methodologies using remotely sensed data for mapping wetlands soils and drainage, to evaluate the relative merits and usefulness of the various methods developed, to generate a selection of output products from the remote sensor data for display to highway planners and photointerpreters, and to provide recommendations for implementation of remote sensing techniques in the highway planning and siting process. To accomplish these objectives, remote sensor and ground truth data were acquired for selected test sites in Florida, Michigan, and Minnesota. One of several test sites in Michigan has been selected as representative of the study objectives and methodology. (Author)

A81-46046 **The methodology of CIAT's land resource study of tropical America.** T. T. Cochrane (International Centre for Tropical Agriculture, Cali, Columbia). In: Machine processing of remotely sensed data and soil information systems and remote sensing and soil survey; Proceedings of the Sixth Annual Symposium, West Lafayette, IN, June 3-6, 1980. New York, Institute of Electrical and Electronics Engineers, Inc., 1980, p. 227-234. 23 refs.

A description is given of an agricultural land resource evaluation program aimed at the effective development and transfer of germplasma-oriented technology to Central and South America. The study reduces land information to a common base in terms of land systems that are defined as repetitive patterns of climate, soils and landscape, delineated directly onto satellite and side-looking radar imagery. The system facilitates the analysis of the land resource data with other information, including economic parameters, and is playing an increasingly important role as a dynamic land resource data bank for the region's crop, pasture and agro-forestry production. O.C.

A81-46407 * **Analysis of landfills with historic airphotos.** T. L. Erb, W. R. Philipson, W. L. Teng, and T. Liang (Cornell University, Ithaca, NY). *Photogrammetric Engineering and Remote Sensing*, vol. 47, Sept. 1981, p. 1363-1369. Research supported by the New York State Dept. of Health; Grant No. NGL-33-010-071.

An investigation is conducted regarding the value of existing aerial photographs for waste management, including landfill monitoring. The value of historic aerial photographs for documenting landfill boundaries is shown in a graph in which the expansion of an active landfill is traced over a 40-year period. Historic aerial photographs can also be analyzed to obtain general or detailed land-use and land-cover information. In addition, the photographs provide information regarding other elements of the physical environment, including geology, soils, and surface and subsurface drainage. The value of historic photos is discussed, taking into account applications for inventory, assessing contamination/health hazards, planning corrective measures, planning waste collection and facilities, developing inactive landfills, and research concerning improved land-filling operations. G.R.

A81-47001 **Radiation studies in the atmosphere (Radiatsionnye issledovaniia v atmosfere).** Edited by K. Ia. Kondrat'ev and N. E. Ter-Markariants. Leningrad, Gidrometeoizdat (Glavnaia Geofizicheskaia Observatoriia, Trudy, No. 434), 1980. 151 p. In Russian.

Attention is given to such topics as the basic problems of the physics and chemistry of contemporary changes of climate, the Global Aerosol-Radiation Experiment (GAREX) of 1977, determination of effective values of the refractive index of atmospheric aerosol, algorithms for the effective evaluation of atmospheric transparence from lidar sounding, and angular anisotropy of reflection from snow cover and desert. Also considered are a method for the aerial measurement of integral fluxes of long-wave and short-wave radiation, statistical characteristics of the albedo of the earth-atmosphere system over the Atlantic, the effect of diffraction on the accuracy of absolute measurements of direct solar radiation, and an evaluation of the presence of aerosol in the atmosphere over the tropical Atlantic from measurements of direct solar radiation. F.G.M.

A81-47002 # **Basic problems of the physics and chemistry of contemporary changes of climate (Osnovnye problemy fiziki i khimii sovremennykh izmenenii klimata).** K. Ia. Kondrat'ev. In: Radiation studies in the atmosphere. Leningrad, Gidrometeoizdat, 1980, p. 3-14. 26 refs. In Russian.

The paper reviews various problems of the physics and chemistry of contemporary changes of global climate, associated with the influence of changes of atmospheric composition on radiation conditions and climate. Particular attention is given to the analysis of anthropogenic changes in the greenhouse effect. The possibilities of investigating climate parameters and the factors determining climate by means of space observations are briefly examined. F.G.M.

A81-47359 **An atmospheric study by 'Spectrum-15' onboard of the Salyut-6 orbital station.** D. Mishev (B'lgarska Akademiia na Naukite, Tsentralna Laboratoriia po Kosmicheski Izsledvaniia, Sofia, Bulgaria). *International Astronautical Federation, International Astronautical Congress, 32nd, Rome Italy, Sept. 6-12, 1981, Paper 81-120.* 10 p. 8 refs.

The multichannel spectrometer system, Spectrum-15, on board the Salyut-6 orbital station, is used to investigate the air pollution over large cities and industrial centers. The Spectrum-15 instrument has 15 channels, each bandwidth of which is not greater than 20 nm. It uses an objective width focus distance of 300 mm, a relative aperture of 1:4, and an angle-of-sight of 8 deg. The instrument is used in several study programs to define atmospheric transparency, determine aerosol indices of atmospheric scatter, and study the dependence of frequency on the atmospheric transfer function. The preliminary data processing of results from these investigations are presented in graphic form and interpreted. A list of the various program investigations carried out thus far is given, along with their corresponding dates and orbits as well as the cosmonaut who performed the study. J.F.

A81-47430 **Potential for detection of natural disasters via Meteosat.** A. Robson, J. Morgan (ESA, European Space Operations Centre, Darmstadt, West Germany), R. W. Herschy (Department of Transport/Department of the Environment, Water Data Unit, Reading, England), and J. Zschau (Kiel, Neue Universität, Kiel, West Germany). *International Astronautical Federation, International Astronautical Congress, 32nd, Rome, Italy, Sept. 6-12, 1981, Paper 81-262.* 19 p. 11 refs.

The use of Meteosat satellite capabilities in the detection of natural disasters is discussed. The satellites, which are positioned in geosynchronous orbit above the prime meridian, carry on imaging radiometer with coverage of a 65 deg great circle arc about the subsatellite point in one visible and two infrared channels every half hour. Disasters which may be observed by the radiometer system include hurricanes, extratropical depressions, drought situations and flooding; the resulting ground-processed images may then be distributed by the satellite to over 200 digital and analog receiving stations to be used in ameliorating the effects of the disasters. The Meteosat satellites are also part of a data collection system in which environmental sensors known as data collection platforms transmit data to the satellite on one of 66 reporting channels in the 402 MHz band and the satellite retransmits the data to the ground following conversion to the 1675 MHz band. The data collection platforms can be used to gather data in real time for purposes of water management and for applications in earth motion studies such as storm surge prediction and earthquake prediction. A.L.W.

A81-47433 **Analysis of the November 23, 1980 earthquake as a design basis for satellite emergency communication.** G. Berretta (ESA, Paris, France), P. Daly, H. Fromm, D. Tits (ESA, European Space Research and Technology Centre, Noordwijk, Netherlands), and S. Rossignoli (Fabbrica Italiana Apparecchiature Radioelettriche, Milan, Italy). *International Astronautical Federation, International Astronautical Congress, 32nd, Rome, Italy, Sept. 6-12, 1981, Paper 81-269.* 23 p. 12 refs.

The earthquake that occurred in Italy in November 1980 is discussed in order to show how satellites can be used for communication during emergencies. Five functions are identified where human intervention could reduce the consequences of earthquakes; these are predicting the occurrence of the earthquake, locating the earthquake focus, evaluating the damage and identifying life lines, localizing the survivors in need, and providing communications. Satellites are shown to be applicable in all these functions. It is proposed that a

Direct Television Broadcasting satellite be used for emergency communication. The features offered by this satellite are listed, among them the fact that the communications link to the area of the disaster is immediately available and that no installation with specialized personnel is required. It is also noted that the TV receiving antenna that would be used for emergency communication is already pointed toward the satellite. C.R.

A81-48682 # **Dynamic ecosystem of the Aral Basin studied from satellite imagery (Dinamika ekosistem basseina Arala po materialam kosmofotos'emok).** A. V. Sadov (Vsesoiuznyi Nauchno-Issledovatel'skii Institut Gidrogeologii i Inzhenernoi Geologii, Moscow, USSR). *Issledovanie Zemli iz Kosmosa,* July-Aug. 1981, p. 18-26. 12 refs. In Russian.

The possibilities and methods of studying changes in the environment of the Aral Basin and adjacent territories based on an analysis of satellite imagery are presented. The analysis is carried out by means of ecological interpretations, including the identification of the spatial boundaries of the ecosystem, an estimation of their stability to technogenetic effects, and the determination of their resulting changes. Satellite imagery is shown to be valuable for the construction of prognosis maps: an economic assessment of the territories involved is made and the probable lines of development of the anthropogenic process are plotted; this is used to construct prognosis maps of the evolution of the territory. J.F.

A81-49174 **Satellite observations of England and northwestern Europe.** J. L. Foster, J. P. Ormsby, and R. J. Gurney. *Weather,* vol. 36, Sept. 1981, p. 252-259. 8 refs.

The Heat Capacity Mapping Mission (HCMM) satellite, launched in April 1978 into a sun-synchronous orbit at an altitude of 620 km, acquired high-quality thermal infrared data suitable for studying the thermal properties of the terrestrial surface. HCMM data taken over England, Wales, and northwestern Europe on May 30, 1978 illustrate the effect of large urban areas on the weather and climate of the area. The urban heat island effect is evident, the larger cities being 10 K hotter than surrounding areas in the early afternoon. Many of the urban areas appear as dark areas of lower albedo, and well defined heat islands show as white blotches due to the higher surface temperature. The heat islands are much more distinct on the daytime thermal infrared images than on the nighttime images. Areas having a low building density and little or no industry are also detected on HCMM daytime thermal infrared imagery, since even a single block of buildings can start the process of heat island formation (Landsberg, 1970). Central business areas of London and the West Midlands are about 8 K warmer than their surrounding rural areas, but there is some systematic variation within each urban area, corresponding to local land use. J.F.

A81-49346 **Determination of beach sand parameters using remotely sensed aircraft reflectance data.** R. A. Shuchman (Michigan, Environmental Research Institute, Ann Arbor, MI) and D. K. Rea (Michigan, University, Ann Arbor, MI). *Remote Sensing of Environment,* vol. 11, Sept. 1981, p. 295-310. 16 refs. Research supported by the University of Michigan; Contracts No. N0014-74-C-0273; No. N0014-78-C-0458.

A81-49407 # **The distribution of the trace gases H2O, NO2, and HNO3 in the middle atmosphere on the basis of LIMS measurements (Über die Verteilung der Spurengase H2O, NO2 und HNO3 in der mittleren Atmosphäre aus LIMS-Messungen).** H. Fischer, C. Lüdecke (München, Universität, Munich, West Germany), and J. C. Gille (National Center for Atmospheric Research, Boulder, CO). *(Deutsche Meteorologen-Tagung und Internationales Alfred-Wegener-Symposium, Berlin, West Germany, Feb. 25-29, 1980.) Annalen der Meteorologie,* no. 15, 1980, p. 29-32. 7 refs. In German.

The trace gases H2O, NO2, and HNO3 are important factors in the photochemical reactions of the stratosphere. The Limb Infrared Monitor of the Stratosphere (LIMS) experiment was started to obtain global data for a detailed study of the chemistry-radiation-dynamics system of the atmosphere, taking into account the atmospheric region extending from the upper troposphere to the lower mesosphere. The LIMS instrument was placed on board of the polar Satellite Nimbus 7. A horizon-scanning procedure is employed in the studies. The current status of data evaluation is considered, giving attention to comparisons with ground truth data and the computer program for the evaluation of the satellite data. The obtained profiles for H2O, HNO3, and NO2 are shown. G.R.

A81-49431 # **Aerosol sounding by means of aircraft-borne optical radar (Aerosolsondierung mittels Flugzeuglidar).** P. Mörl, M. E. Reinhardt, and W. Renger (Deutsche Forschungs- und Versuchsanstalt für Luft- und Raumfahrt, Institut für Physik der Atmosphäre, Oberpfaffenhofen, West Germany). *(Deutsche Meteorologen-Tagung und Internationales Alfred-Wegener-Symposium, Berlin, West Germany, Feb. 25-29, 1980.) Annalen der Meteorologie,* no. 15, 1980, p. 167, 168. 5 refs. In German.

Optical radar measurements conducted with the aid of aircraft provide the possibility to perform rapid surveys on a regional scale regarding the existence and location of atmospheric haze. Typical applications are related to the study of smog layers, and the survey of solid-particle pollutant emission in the case of great industrial complexes. Studies conducted by the German Meteorological Service make use of a Nd-YAG laser which provides 20-ns pulses at 1.064 and 0.532 micrometers. Operational data concerning the optical radar system are discussed, taking into account the backscattering profile produced by the laser pulse. Attention is also given to the auxiliary equipment, and aspects of data processing and evaluation. First results related to pilot missions are briefly considered. G.R.

A81-49433 # **Comparative measurements of stratospheric CH4 and CO concentrations with spectrograph and correlation radiometers (Vergleichende Messungen stratosphärischer CH4- und CO-Konzentrationen mit Spektrograph und Korrelationsradiometern).** D. Rabus and F. Fergg (München, Universität, Munich, West Germany). *(Deutsche Meteorologen-Tagung und Internationales Alfred-Wegener-Symposium, Berlin, West Germany, Feb. 25-29, 1980.) Annalen der Meteorologie,* no. 15, 1980, p. 171, 172. 5 refs. In German.

A81-49752 # **The integration of remote sensing in environmental decision making for the Maritimes.** A. C. Hamilton (New Brunswick, University, Fredericton, Canada). In: Canadian Symposium on Remote Sensing, 6th, Halifax, Canada, May 21-23, 1980, Proceedings. Ottawa, Canadian Aeronautics and Space Institute, 1981, p. 1-7.

An examination of the integration of remote sensing in decision-making for the Maritime environment shows that for basic land and ocean information the requirement is for sensors such as SAR that will reveal properties that hitherto were elusive or undetectable. For operational monitoring, the main requirement in addition to what is now routinely available is for dependable, frequent, weather-independent imagery. For management and policy decision-making there is an institutional requirement and a technical requirement. The institutional requirement is for better facilities to convert data to information and for decision-makers to learn the use of information interactively. The technical requirement is for finer and more dependable spectral resolution particularly for forestry, agriculture, and land classification. B.J.

A81-49759 # **Multistage remote sensing in exploratory ecodistrict land classification.** E. B. Wiken, T. W. Pierce, and G. R. Ironside (Environment Canada, Lands Directorate, Ottawa, Canada). In: Canadian Symposium on Remote Sensing, 6th, Halifax, Canada, May 21-23, 1980, Proceedings. Ottawa, Canadian Aeronautics and Space Institute, 1981, p. 63-71. 5 refs.

The Northern Land Use Information Series attempts to provide broad and consistent coverage of land resources in the Northwest Territories at a scale of 1:250,000. The map series includes an ecological overview of terrestrial ecosystems, the focus being the mapping and description of ecodistricts. The combined use of Landsat, aerial photographs, and 35 mm color slides has proved to be effective in the prefield, field, and postfield activities of the ecological land classification. The benefits have included improved map boundary definition and ecodistrict descriptions; reduced time, material, and manpower inputs; and improved field reconnaissance work through better direction to the various ecodistricts as well as to representative locales within each district. B.J.

A81-49773 # **Interpreter evaluations of airborne radar imagery for ecological and land/use cover classification in southern Manitoba.** C. D. A. Rubec (Environment Canada, Lands Directorate, Ottawa, Canada) and J. Cihlar (Canada Centre for Remote Sensing, Ottawa, Canada). In: Canadian Symposium on Remote Sensing, 6th, Halifax, Canada, May 21-23, 1980, Proceedings.
Ottawa, Canadian Aeronautics and Space Institute, 1981, p. 203-215. 6 refs.

Synthetic aperture radar images flown over two test areas in southwestern Manitoba were used successfully for classification and mapping of land cover, land use and general vegetation types. The criteria affecting interpretation success are similar to those commonly used with aerial photography. Radar images have specific patterns, shapes and associations that can be related to ground features. However, radar image tone and texture can present problems to interpreters. Experience with other types of images, and personal knowledge of the study area, all increase interpreter success with radar images. Summer X band, HH polarized images are the optimal source of synthetic aperture radar data for ecological and land use mapping applications in prairie regions of Canada. (Author)

A81-49781 # **Applications of remote sensing to construction impact assessment at the Roberts Bank Port, British Columbia.** G. F. Tomlins and K. P. B. Thomson (Canada Centre for Remote Sensing, Ottawa, Canada). In: Canadian Symposium on Remote Sensing, 6th, Halifax, Canada, May 21-23, 1980, Proceedings.
Ottawa, Canadian Aeronautics and Space Institute, 1981, p. 289-299. 18 refs.

A81-49783 # **Land use/cover mapping for Halifax County - Remote sensing alternatives.** N. A. Prout (Intera Environmental Consultants, Ltd., Ottawa, Canada). In: Canadian Symposium on Remote Sensing, 6th, Halifax, Canada, May 21-23, 1980, Proceedings. Ottawa, Canadian Aeronautics and Space Institute, 1981, p. 307-320. 12 refs.

A81-49788 # **Interpretation techniques applied to mixed terrains (Techniques d'interprétation appliquées aux terrains mixtes).** E. J. Langham (Environment Canada, National Hydrology Research Institute, Hull, Quebec, Canada), Y. Heymann (Société Française des Etudes et de La Recherche Economique et Statistique, France), and A. I. Rivard. In: Canadian Symposium on Remote Sensing, 6th, Halifax, Canada, May 21-23, 1980, Proceedings.
Ottawa, Canadian Aeronautics and Space Institute, 1981, p. 361-367. In French.

Results of the application of the supervised classification technique in conjunction with image color enhancement to land-use classification based on Landsat data obtained over a region previously studied by aerial photography and ground observations are presented. Data was obtained of the French department of Lot, a region composed of woods, pasture land, agricultural fields and vineyards. Due to the smallness of the fields and the mixture of vine and ground spectral signatures in a single area, it was found that nonsupervised classification of false-color images was unable to provide more than a general classification of land use. When principle component color enhancement is used together with the supervised classifier, it was possible not only to identify calcareous underbrush and other types of wooded terrains, but to distinguish vineyards from other crops. A.L.W.

A81-49790 # **Spectral measurement of rangeland.** K. P. B. Thomson, F. J. Ahern, R. J. Brown, K. Staenz (Canada Centre for Remote Sensing, Ottawa, Canada), D. H. McCartney, and J. Waddington (Department of Agriculture, Melfort, Saskatchewan, Canada). In: Canadian Symposium on Remote Sensing, 6th, Halifax, Canada, May 21-23, 1980, Proceedings. Ottawa, Canadian Aeronautics and Space Institute, 1981, p. 377-386. 6 refs.

A project carried out by the Canada Centre for Remote Sensing during the summer of 1979 at the Experimental Rangeland Site near Pathlow, Saskatchewan in which the biomass/spectral reflectance relationship was addressed is discussed. It is noted that this site is representative of the rangeland under current use in Saskatchewan. The remote sensing data comprised Landsat MSS data (July 27 and September 19) and airborne multispectral scanner data (July 27 and September 14). Analysis of the data was found to show good correlations between Landsat MSS parameters and green biomass in the July period but not in September. Similar results were obtained for the Thematic Mapper Bands, which were simulated from the airborne MSS data. C.R.

A81-49792 # **Remote sensing and land use planning.** P. S. T. Lee (U.S. Department of Agriculture, Remote Sensing Branch, Washington, DC). In: Canadian Symposium on Remote Sensing, 6th, Halifax, Canada, May 21-23, 1980, Proceedings.
Ottawa, Canadian Aeronautics and Space Institute, 1981, p. 397-403. 8 refs.

Changes in land use were measured in Central Arizona using sensing techniques, and a framework was developed to provide timely information on land use planning purposes. A land use classification system is presented, which defines major land use categories as agricultural land; urban or build-up land; range, forest and barren land; and water. Landsat data are registered and digitized to estimate acreages of changes for various land use classes. Total acreages or urban land have increased from 136 thousand acres in 1972, to 304 thousand acres in 1979, representing a 122% increase; 65% of which comes from range and other land, and 35% of which comes from formerly agricultural land. About 55,000 acres of rangeland have been converted to farmland due to more water irrigation; however, this does not offset the loss of agricultural land to urban expansion, and a net loss of 15,000 acres of farmland and 186,000 acres of rangeland is found in Maricopa county. D.L.G.

A81-49798 # **Landsat data as a basis for regional environmental assessment within the Columbia Plateau.** L. S. Leonhart (Rockwell International Corp., Richland, WA) and J. G. Stephan (Battelle Pacific Northwest Laboratories, Richland, WA). In: Canadian Symposium on Remote Sensing, 6th, Halifax, Canada, May 21-23, 1980, Proceedings. Ottawa, Canadian Aeronautics and Space Institute, 1981, p. 459-471.

It is pointed out that initial assessments of the area involved classification of four contiguous Landsat scenes recorded during the summer of 1975 and about 300 1978 high-altitude (U-2) photographs. The mosaic thus obtained was segregated into ten land-cover classes. The classified land-cover data were machine-integrated with digital irrigation well-location data obtained from the U.S. Geological Survey's Ground-Water Site Inventory. The resulting ground-water multisource data product was required by hydrologists in order to segregate potential artificial recharge areas from artificial groundwater discharge areas. It is noted that related studies have employed Landsat data and aerial imagery to identify linear structures and other geologic features which may have a significant bearing on the tectonic and/or hydrologic setting to the Columbia Plateau. C.R.

A81-49803 # **Resource inventory and terrain analysis in north western Manitoba from integrated remote sensing data.** V. H. Singhroy (J. D. Mollard and Associates, Ltd., Regine, Saskatchewan, Canada) and R. Dixon (Manitoba Remote Sensing Centre, Winnipeg, Canada). In: Canadian Symposium on Remote Sensing, 6th, Halifax, Canada, May 21-23, 1980, Proceedings. Ottawa, Canadian Aeronautics and Space Institute, 1981, p. 513-523. 10 refs.

It is noted that continued growth in northern Manitoba communities demands the acquisition and compilation of data pertaining to the regional resource potential of large areas. In the majority of cases, planners, resource managers, and environmental consultants are faced with the problem of limited and scattered data which inhibit comprehensive regional planning. A simple integrated approach and techniques involved in using multistage remote sensing data in the production of a regional resource base map are demonstrated. Enhanced Landsat data, black and white, color infrared and thermal infrared photographs are used to generate regional vegetation and terrain geology maps prior to field investigation. Field sampling verifies the accuracy of the units identified and produces a valuable data base for detailed analysis and planning. C.R.

A81-49806 # **Current resource mapping and environmental monitoring applications using Landsat MSS data in Scotland.** G. C. Stove (MacAuley Institute for Soil Research, Aberdeen, Scotland) and K. E. Bagot (Royal Aircraft Establishment, Farnborough, Hants., England). In: Canadian Symposium on Remote Sensing, 6th, Halifax, Canada, May 21-23, 1980, Proceedings. Ottawa, Canadian Aeronautics and Space Institute, 1981, p. 551-557.

Photogrammetric digital mapping facilities and the advanced, IDP3000 image analyzer are used to enhance and measure a variety of peatland and land cover types, leading to the compilation of a 1:100,000-scale Peat Resource and Land Cover Map of the Isle of Lewis. Further development of multispectral classification techniques based on stretched band ratios for selective terrain features has resulted in the compilation of a land use/land cover map of the Buchan area of northeast Scotland. In addition, optimizing the stretched band intensity differences by means of principal components analysis has made it possible to distinguish between phytoplankton blooms, coastal sediment re-circulation patterns and submerged coastal and river-mouth bars. A similar enhancement technique outlines mountain snow cover and distinguishes between cloud and snow. O.C.

N81-29496*# National Aeronautics and Space Administration. Earth Resources Labs., Bay St. Louis, Miss.
EVALUATION OF MULTIBAND, MULTITEMPORAL, AND TRANSFORMED LANDSAT MSS DATA FOR LAND COVER AREA ESTIMATION
E. R. Stoner, G. A. May (Dept. of Agriculture, Houston, Tex.), and M. T. Kalcic, Principal Investigators Apr. 1981 25 p refs
Sponsored by NASA, USDA, Dept. of Commerce, Dept. of the Interior, and Agency for International Development ERTS
(Proj. AgRISTARS)
(E81-10161; NASA-TM-82289; DC-Y1-04089; NSTL/ERL-196) Avail: NTIS HC A02/MF A01 CSCL 02C

Sample segments of ground-verified land cover data collected in conjunction with the USDA/ESS June Enumerative Survey were merged with LANDSAT data and served as a focus for unsupervised spectral class development and accuracy assessment. Multitemporal data sets were created from single-date LANDSAT MSS acquisitions from a nominal scene covering an eleven-county area in north central Missouri. Classification accuracies for the four land cover types predominant in the test site showed significant improvement in going from unitemporal to multitemporal data sets. Transformed LANDSAT data sets did not significantly improve classification accuracies. Regression estimators yielded mixed results for different land covers. Misregistration of two LANDSAT data sets by as much and one half pixels did not significantly alter overall classification accuracies. Existing algorithms for scene-to scene overlay proved adequate for multitemporal data analysis as long as statistical class development and accuracy assessment were restricted to field interior pixels. A.R.H.

N81-29517# California Univ., Livermore. Lawrence Livermore Lab. Environmental Sciences Div.
REMOTE SENSING OF SOIL RADIONUCLIDE FLUXES IN A TROPICAL ECOSYSTEM
B. Clegg, J. Koranda, W. Robinson, and G. Holladay 6 Nov. 1980 7 p refs Submitted for publication
(Contract W-7405-eng-48)
(UCRL-84501) Avail: NTIS HC A02/MF A01

A transponding geostationary satellite is being used to collect surface environmental data to describe the fate of soil-borne radionuclides. The remote, former atomic testing grounds at the Eniwetok and Bikini Atolls present a difficult environment in which to collect continuous field data. Land-based, solar-powered microprocessor and environmental data systems remotely acquire measurements of net and total solar radiation, rain, humidity, temperature, and soil-water potentials. For the past year, the water flux model predicts wet season plant transpiration rates nearly equal to the 6 to 7 mm/d evaporation pan rate, which decreases to 2 to 3 mm/d for the dry season. Radioisotopic analysis confirms the microclimate-estimated 1:3 to 1:20 soil to plant dry matter concentration ratio. This ratio exacerbates the dose to man from intake of food plants. Nephelometer measurements of airborne particulates presently indicate a minimum respiratory radiological dose. DOE

N81-30656 Institut d'Aeronomie Spatiale de Belgique, Brussels.
ATMOSPHERIC NITRIC ACID AND CHLOROFLUOROMETHANE 11 FROM INTERFEROMETRIC SPECTRA OBTAINED AT THE OBSERVATOIRE DU PIC DU MIDI
C. Lippens and C. Muller 1980 31 p refs Submitted for publication
(Aeronomica-Acta-A-227-1980) Avail: Issuing Activity

A modified interferometer was used to obtain absorption spectra and emission spectra (reduced from the difference between the reference spectrum and transformed emission data). The data obtained lead to a value of 12 billion mol/cu cm nitric acid at an altitude of 22km; chlorofluoromethane 11 is found in the troposphere at 148 + or - 12ppt. No evidence of peroxy nitric acid, nitrous acid or ammonia was observed. The difficulties in observing hydrogen peroxide and obtaining accurate values for ozone and chlorofluoromethane 12 are discussed. The integrated peroxynitric acid column is found to be smaller than 10 to the 15th power mol/sq cm. Author (ESA)

N81-30695# Pennsylvania State Univ., University Park. Dept. of Meteorology.
ENVIRONMENTAL MEASUREMENTS OF POWER PLANT COOLING TOWER AND STACK PLUMES Final Report
D. W. Thomson, ed., R. G. dePena, ed., and J. A. Pena, ed. 1981 180 p refs
(Contracts DE-AS02-76EV-02463; AT(11-1)-2463; E(11-1)-2463)
(DOE/EV-02463/6) Avail: NTIS HC A09/MF A01

The focus of this program was to establish the reality and magnitude of any environmental changes caused by the plumes from large evaporative cooling towers through a comprehensive set of measurements taken from a research aircraft. Results are divided into three sections: structure and dynamics of cooling tower plumes; chemical transformation of SO2 to sulfates in coal-fired power plant plumes; and drift deposition studies. DOE

N81-31680*# Science Applications, Inc., La Jolla, Calif.
SATELLITE MEASUREMENTS OF TROPOSPHERIC AEROSOLS Final Report
M. Griggs Aug. 1981 64 p refs
(NASA-CR-3459; SAI-131-80-578-LJ) Avail: NTIS HC A04/MF A01 CSCL 13B

This investigation uses LANDSAT 2 radiance data and ground-truth measurements of the aerosol optical thickness, obtained previously from five inland sites, to study the usefulness and limitations of the near infrared radiance over inland bodies of water. The linear relationship between LANDSAT 2 MSS7 and aerosol content found in this study can be used to estimate the aerosol content with a standard deviation of 0.42N. Analysis of the data for MSS6 and MSS7 suggest that the larger uncertainty is mostly due to water turbidity, with little contribution from the adjacency effect. The relationship found is best applied to determine an average aerosol content over a period of time at a given target, or an area average at a given time over several targets close together. Author

N81-32581*# Aerospace Corp., El Segundo, Calif. Electronics Research Lab.
MILLIMETER-WAVE SENSING OF THE ENVIRONMENT: A BIBLIOGRAPHIC SURVEY
E. Schneider and E. E. Epstein 29 May 1981 308 p
(Contract NAS6-2960)
(NASA-CR-156879; ATR-81-(7805-1)) Avail: NTIS HC A14/MF A01 CSCL 13B

This literature survey was conducted to examine the field of millimeter wave remote sensing of the environment and collect all relevant observations made in the atmospheric windows near 90, 140, and 230 GHz of ocean, terrain, man-made features, and the atmosphere. Over 170 articles and reports were examined; bibliographic references are provided for all and abstracts are quoted when available. Selected highlights were extracted from the pertinent articles. T.M.

N81-32586# Army Engineer Topographic Labs., Fort Belvoir, Va.
REMOTE SENSING FOR ENGINEERING SITE SELECTION
Jack N. Rinker and Robert E. Frost 13 May 1981 15 p refs
(AD-A102810; ETL-R018) Avail: NTIS HC A02/MF A01 CSCL 14/5

For any significant construction, e.g., airstrip, bridge, dam, powerplant, industrial park, canal, etc., there is the first phase of site selection and evaluation. One goal of this phase is to obtain information about surficial materials (granular, cohesive, permeable, nonuniform, etc.), thickness of the soil mantle, nature of the bedrock, drainage, presence of unstable materials and conditions, presence of subsurface solution cavities, fractures, joints, faults, etc. Remote sensing techniques in the form of manual analysis of photo index sheets and LANDSAT for regional information, and of stereo aerial photography for local details.

provides an economical and rapid means of obtaining this first assessment. An experienced team can quickly produce surficial geology/soils maps, drainage maps, land use/land cover maps, etc., highlight potential problem areas, select preferred sites and alternates, and indicate probable impacts on the environment of any given action. This image-derived information sets the basis for establishing a logical ground sampling program, and provides the framework for correlating a large variety of information. As yet, it is not possible to provide very much of this needed terrain information by digital, or automatic, image analysis procedures.
Author (GRA)

N81-32708*# National Aeronautics and Space Administration. Langley Research Center, Hampton, Va.
NASA PARTICIPATION IN THE 1980 PERSISTENT ELEVATED POLLUTION EPISODE/NORTHEAST REGIONAL OXIDANT STUDY (PEPE/NROS) PROJECT: OPERATIONAL ASPECTS
G. L. Maddrea, Jr. and R. J. Bendura Sep. 1981 136 p refs
(NASA-TM-83170; L-14584) Avail: NTIS HC A07/MF A01
CSCL 13B

A field experiment designed to further understand the formation and transport of visibility reducing aerosols and to characterize regional scale air masses and urban plumes is described. Measurements were made primarily in the Ohio River Valley region. The NASA participation included obtaining measurements for the determination of mixing layer height and ozone profiles by using airborne remote sensor systems such as the ultraviolet differential absorption lidar, the high spectral resolution lidar, and the laser absorption spectrometer. Other NASA systems included the microwave atmospheric remote sensor, tethered balloons, an in situ measurements aircraft, and several photometer/transmissiometer systems. T.M.

N81-33720# Science Applications, Inc., La Jolla, Calif. Electronics Vision and Systems Div.
SATELLITE MEASUREMENTS OF ATMOSPHERIC AEROSOLS Annual Report, 15 Nov. 1980 - 26 Aug. 1981
M. Griggs 26 Aug. 1981 21 p refs
(Contract N00014-77-C-0489)
(AD-A103493; SAI-131-81-275-LJ) Avail: NTIS
HC A02/MF A01 CSCL 04/1

Analysis of NOAA-6 AVHRR data and ground-truth measurements at two locations has found a radiance-aerosol content relationship which agrees very well with that previously determined for LANDSAT 2 Data. A new technique was developed to use AVHRR Channels 1 and 2 radiances to infer aerosol size distribution information, in addition to the optical thickness. The technique was successfully tested with a small data set obtained in a ground-truth experiment on the USNS Hayes. Author (GRA)

03

GEODESY AND CARTOGRAPHY

Includes mapping and topography.

A81-42554 # Analysis of the geometry of a frame photograph (K analizu geometrii kadrovogo fotosnimka). V. G. Tarakanov (Leningradskoe Vysshee Voenno-Topograficheskoe Komandnoe Uchilishche, Leningrad, USSR). *Geodeziia i Aerofotos'emka,* vol. 1, 1981, p. 82-86. In Russian.

A principle of surface mapping is developed for describing the basic geometric relationships of frame photographs. In particular, the principle can be used to obtain relationships between the coordinate points of a region and image coordinate points on aerial photographs in addition to scale formulas for aerial photographs. The proposed mapping principle (and methods for the description of single photos and stereopairs that derive from this principle) is characterized by relative simplicity, universality, and efficiency. B.J.

A81-42556 # The use of spaceborne photography for topographic mapping (Ispol'zovanie kosmicheskikh snimkov pri topograficheskom kartografirovanii). T. V. Vereshchaka (Moskovskii Institut Inzhenerov Geodezii, Aerofotos'emki i Kartografii, Moscow, USSR). *Geodeziia i Aerofotos'emka,* vol. 1, 1981, p. 95-102. In Russian.

Various aspects of the application of spaceborne photography to topographic mapping are considered. Spaceborne photography is found to be useful in such tasks as the systematic analysis of terrain changes, the interpretation of aerial photographs for the compilation and modification of topographic maps, and the editing of topographic maps. Spaceborne photography is also considered in relation to the formation of systems of conditional markings, and the geographic principles underlying combinations of conditional markings. B.J.

A81-42846 # Measurement of lengths, angles, and areas on the earth's spheroid (Izmerenie dlin, uglov i ploshchadei na zemnom sferoide). V. I. Khizhnichenko. *Geodeziia i Kartografiia,* May 1981, p. 6-8. In Russian.

In order to evaluate geometrical distortions of images obtained by satellite television systems, it is necessary to know the lengths, areas, and angles of triangles specified by three points on the surfaces of the spheroidal earth. This paper presents approximate formulas for calculating the lengths, angles, and areas of spheroidal triangles, whose vertices are specified by geographic coordinates. The analysis is carried out relative to auxiliary angular coordinates on a single sphere; the resulting formulas are obtained with allowance for the ellipsoidality of the spheroid. This method was successfully used to evaluate geometrical distortions of images of the earth's surface obtained by the Meteor-Priroda space system. B.J.

A81-42847 # Topographic and cartographic applications of photogrammetry (O topograficheskom i kartograficheskom primenenii fotogrammetrii). N. V. Sukhot'ko. *Geodeziia i Kartografiia,* May 1981, p. 52-55. In Russian.

Papers concerning the topographic and cartographic applications of photogrammetry presented at the 16th congress of the International Photogrammetry Society (July 1980) are briefly reviewed. Particular consideration is given to the compilation of detailed digital maps and the cartographic processing of digital data; the improvement and refinement of topographic maps; general large-scale mapping with the aim of urban and rural planning; mapping using satellite remote sensing systems; orthophototransformation and photomapping; pollution mapping; and the general mapping of earth resources. Basic directions in the development of photogrammetry are described. P.T.H.

A81-43524 # Gravimetric studies of the earth's crust in the oceans (Gravimetricheskie issledovaniia zemnoi kory okeanov). A. G. Gainanov. Moscow, Izdatel'stvo Moskovskogo Universiteta, 1980. 240 p. 271 refs. In Russian.

Methods of marine gravimetry are described, and maps of the gravity anomalies in the Pacific, Atlantic, and Indian Oceans are presented and described. Gravimetric and seismic data were used to construct density models of the oceanic crust, as well as of the lithosphere of mid-oceanic ridges, trenches, and continental margins. In addition, the use of gravimetry to survey for petroleum resources in the ocean is considered. B.J.

A81-45427 * An examination of spectral band ratioing to reduce the topographic effect on remotely sensed data. B. Holben and C. Justice (NASA, Goddard Space Flight Center, Earth Resources Branch, Greenbelt, MD). *International Journal of Remote Sensing,* vol. 2, Apr.-June 1981, p. 115-133. 33 refs.

Spectral-band ratioing of radiance data is examined as a means of reducing the topographic effect in multispectral data. A ground-based nadir-pointing two-channel radiometer filtered for the red and photographic IR portions of the spectrum was used to measure the topographic effect associated with a uniform surface inclined from horizontal to 60 deg at 16 compass points and for several solar elevations. It is found that ratioing reduced the topographic effect in the field-measured radiance data by an average of 83%, that the remaining topographic effect could be further reduced by subtracting the scattered-light component of the global irradiance before ratioing, and that ratioing was not effective in reducing the topographic effect on shaded surfaces illuminated solely by scattered light. It is concluded that additional variations in ratios can be expected for Landsat data owing to sensor calibration and quantization. F.G.M.

A81-45828 * # Orbit determination requirements for TOPEX. B. D. Tapley, B. E. Schutz, J. Ries, G. Rosborough (Texas, University, Austin, TX), and G. H. Born (California Institute of Technology, Jet Propulsion Laboratory, Pasadena, CA). *American Astronautical Society and American Institute of Aeronautics and Astronautics, Astrodynamics Specialist Conference, Lake Tahoe, NV, Aug. 3-5, 1981, AAS Paper 81-158.* 30 p. 15 refs.

The error sensitivity of orbit calculations in support of the NASA Ocean Surface Topography Mapping Experiment (TOPEX), which require an accuracy on the order of 5 cm, is investigated. The contributions of errors in the gravitational, atmospheric drag and solar radiation pressure models to the computed orbit are analyzed for the cases of an ideal data distribution and realistic laser ranging data coverage. It is found that the major contributor to radial orbital error is the error in the geopotential model, accounting for orbital errors of 30 to 70 cm, with the effects of solar radiation pressure, drag modeling, tracking station coordinate errors making lesser contributions. It is concluded that TOPEX accuracy goals cannot be met using ground-based laser ranging data without improving the geopotential model. A.L.W.

A81-46678 Stereoorthophotos as aids in the mapping of high mountain regions (Stereoorthophotos als Hilfsmittel der Hochgebirgskartierung). R. Finsterwalder (München, Technische Universität, Munich, West Germany). *Bildmessung und Luftbildwesen,* vol. 49, Sept. 1, 1981, p. 161-164. 7 refs. In German.

The appropriate representation of the characteristics of high mountain regions is very difficult. Contour lines, for instance, cannot adequately show sharp edges and discontinuities present in mountainous terrain. The difficulties can be reduced by making use of orthophotos. Finsterwalder (1972) and Pillewizer (1976) have conducted studies in this direction, taking into account orthophotos which could not be viewed stereoscopically. However, the third dimension is in mountainous areas especially important for the interpretation of aerial photographs. The use of a second orthophoto makes it now possible to view orthophotos also stereoscopically, and to obtain, thereby, additional information for the map-plotting procedure. Attention is given to the production of stereoorthophotos, the study of the two orthophotos and the contour line image in the stereoscope, and the drawing procedure. The implementation of the considered method is illustrated with the aid of three examples involving stereo models. G.R.

A81-47938 # Differential Doppler experiment /DIDEX/ for geodetic applications. J. Kazmierski (Instytut Lotnictwa, Warsaw, Poland), J. Latka, and J. B. Zielinski (Polska Akademia Nauk, Centrum Badan Kosmicznych, Warsaw, Poland). In: Scientific and engineering uses of satellite radio beacons; Proceedings of the

Symposium, Warsaw, Poland, May 19-23, 1980. (A81-47901 23-46) Warsaw, Panstwowe Wydawnictwo Naukowe, 1981, p. 443-448.

The proposed DIDEX (Differential Doppler Experiment) of the Intercosmos program uses a mother spacecraft and two subsatellites to measure the Doppler shift of a two-way microwave radio signal. The space vehicles have an altitude of about 300 km and an orbital plane inclination of 85 deg. The two-way Doppler shift is measured by transmitting a known signal to the two subsatellites from the mother spacecraft and coherently transponding the observed signal back to the reference system. The reference oscillator generates a 10 MHz signal stable to one part in 10 to the 11th over a 1-100 sec interval. The receivers are of the phase-locked type; the phase-locked loops have 5 Hz noise bandwidths which are broadened to 50 Hz during signal acquisition. An accuracy of 0.05 mm/sec for velocity measurements is required, and a signal frequency of 3-5 GHz is used. The influence of the ionosphere on measurement accuracy is considered when (1) the mother spacecraft moves in a homogeneous ionosphere with a velocity difference between the two subsatellites and (2) the mother satellite moves in an ionosphere with a horizontal gradient electron concentration. The DIDEX procedure is shown to correct measurement errors, taking into account only the first term containing the influence of the ionosphere. J.F.

A81-48678 # **Optimization of Doppler measurements in the satellite network of Eastern Europe (Optimizatsiia Dopplerovskikh izmerenii v kosmicheskoi seti Vostochnoi Evropy).** Ts. Gergov and N. Georgiev (B'lgarska Akademiia na Naukite, Tsentralna Laboratoriia po Vissha Geodeziia, Sofia, Bulgaria). *Vissha Geodeziia,* no. 7, 1981, p. 13-19. 5 refs. In Russian.

Photographic observations and optimal Doppler observations from the Intercosmos program were used in a modeling study to determine the feasibility of constructing a three-dimensional geodetic network. Optimal Doppler measurements were assessed in an effort to obtain the highest accuracy in the determination of station coordinates. It is found that a three-dimensional network of satisfactory geodetic accuracy cannot be established on the basis of only Doppler measurements of earth chord length. Network accuracy is increased by the inclusion of the orienting elements Lambda and Phi of the earth chords, defined by available photographic observations in conjunction with Doppler measurements. B.J.

A81-48679 # **A 'meteorological' method for calculating vertical refraction (O 'meteorologicheskom' metode ucheta vertikal'noi refraktsii).** O. A. Mozzhukhin (Gor'kovskii Inzhenerno-Stroitel'nyi Institut, Gorki, USSR). *Vissha Geodeziia,* no. 7, 1981, p. 57-63. 8 refs. In Russian.

Attention is given to the so-called meteorological method for assessing the influence of refraction in geodetic leveling. The theoretical background and experimental verification of the method are discussed along with its limits of application. Empirical ratios of systematic and random errors due to refraction are obtained for geodetic measurements as a function of distances to the observation points. B.J.

A81-48696 # **Lineaments - Problems and directions of studies by means of aerial and space tools and methods (Lineamenty - Problemy i napravleniia issledovanii s pomoshch'iu aerokosmicheskikh sredstv i metodov).** V. I. Makarov. *Issledovanie Zemli iz Kosmosa,* July-Aug. 1981, p. 109-115. 35 refs. In Russian.

Divergences of opinion existing among investigators of lineaments are examined. Problems involving the definition, origin, age, classification, and depth of lineaments, and their relationship to planetary fracture systems are examined. Emphasis is placed on the use of remote sensing methods to study lineaments. B.J.

A81-49811 # **Generation and use of digital elevation data for large areas.** P. J. Letts (DIPIX Systems, Ltd., Ottawa, Canada) and G. Rochon (Université Laval, Quebec, Canada). In: Canadian Symposium on Remote Sensing, 6th, Halifax, Canada, May 21-23, 1980, Proceedings. Ottawa, Canadian Aeronautics and Space Institute, 1981, p. 597-602.

It is noted that while the integration of topographical data in the analysis of remotely sensed images has several advantages, technical difficulties often make this operation impracticable. On the basis of contours digitized from standard cartographic maps, a new approach to the generation of a digital terrain model is presented, along with the use of these data in the transformations of satellite-measured radiances. It is thus possible to modify the radiances either as a function of the ground solar illumination or of the look angles of the satellite, or even of the reflection characteristics of the observed surfaces. C.R.

N81-30496*# Phoenix Corp., McLean, Va.
SPACE BASED TOPOGRAPHIC MAPPING EXPERIMENT USING SEASAT SYNTHETIC APERTURE RADAR AND LANDSAT 3 RETURN BEAM VIDICON IMAGERY Final Report
Gerald L. Mader 20 Jul. 1981 35 p refs Prepared for JPL
(Contract JPL-955998)
(NASA-CR-164675; JPL-9950582) Avail: NTIS HC A03/MF A01 CSCL 08B

A technique for producing topographic information is described which is based on same side/same time viewing using a dissimilar combination of radar imagery and photographic images. Common geographic areas viewed from similar space reference locations produce scene elevation displacements in opposite direction and proper use of this characteristic can yield the perspective information necessary for determination of base to height ratios. These base to height ratios can in turn be used to produce a topographic map. A test area covering the Harrisburg, Pennsylvania region was observed by synthetic aperture radar on the Seasat satellite and by return beam vidicon on by the LANDSAT - 3 satellite. The techniques developed for the scaling re-orientation and common registration of the two images are presented along with the topographic determination data. Topographic determination based exclusively on the images content is compared to the map information which is used as a performance calibration base. A.R.H.

N81-30505# Los Alamos Scientific Lab., N. Mex.
SEASAT SATELLITE INVESTIGATION OF THE STRUCTURE OF WESTERN NEBRASKA AND ITS APPLICATION TO THE EVALUATION OF GEOTHERMAL RESOURCES
J. Stix 1981 20 p refs Presented at the Intern. Symp. of Remote Sensing of Environ., Ann Arbor, Mich., 11-15 May 1981
(Contract W-7405-eng-36)
(LA-UR-81-1454; CONF-810557-1) Avail: NTIS HC A02/MF A01

Seasat synthetic aperture radar (SAR) satellite imagery was used to interpret the structural framework and the geothermal potential of an area in western Nebraska. Lineaments were mapped from the imagery and then compared to known structure. It was found that Seasat does record surface manifestations of subtle basement structures, particularly faulting. Four areas with geothermal potential were delineated using Seasat and other data. It is concluded that Seasat imagery is a useful reconnaissance exploration tool in the interpretation of regional structure within areas of little topographic relief. DOE

N81-31601*# Smithsonian Astrophysical Observatory, Cambridge, Mass.
SATELLITE TO SATELLITE DOPPLER TRACKING (SSDT) FOR MAPPING OF THE EARTH'S GRAVITY FIELD Final Report, 1 Apr. 1980 - 31 Mar. 1981
G. Colombo, E. M. Gaposchkin, and M. Grossi Sep. 1981 107 p refs
(Grant NAG5-36)
(NASA-CR-164722) Avail: NTIS HF A06/MF A01 CSCL 08G

Two SSDT schemes were evaluated: a standard, low-low, SSDT configuration, which both satellites are in basically the same low altitude nearly circular orbit and the pair is characterized by small angular separation; and a more general configuration in which the two satellites are in arbitrary orbits, so that different configurations can be comparatively analyed. The standard low-low SSDT configuration is capable of recovering 1 deg X 1 deg surface anomalies with a strength as low as 1 milligal, located on the projected satellite path, when observing from a height as large as 300 km. The Colombo scheme provides an important complement of SSDT observations, inasmuch as it is sensitive to radial velocity components, while keeping at the same performance level both measuring sensitivity and measurement resolution. T.M.

N81-31604*# GeoScience Research Corp., Salisbury, Md.
TERRAIN PROFILING FROM SEASAT ALTIMETRY
R. L. Brooks Mar. 1981 59 p refs Sponsored by NASA, National Geodetic Survey and USGS
(NASA-CR-156878) Avail: NTIS HC A03/MF A01 CSCL 08B

To determine their applicability for terrain profiling, Seasat altimeter measurements were analyzed for the following geographic areas: (1) Andean salars of southern Bolivia; (2) Alaska; (3) south-central Arizona; (4) imperial Valley of California; (5) Yuma Valley of Arizona; and (6) Great Salt Lake Desert. Analysis of the data over all of these geographic areas shows that the satellite altimeter servo did not respond quickly enough to changing terrainn features. However, it is demonstrated that retracking of the archived surface return waveforms yields surface elevations over smooth terrain accurate to + or - 1 m when correlated with large scale maps. The retracking algorithm used and its verification over the salars of southern Bolivia are described. Results are presented for each of the six geographic areas. A.R.H.

N81-32574*# Wisconsin Univ., Madison.
INVESTIGATION OF ANTARCTIC CRUST AND UPPER MANTLE USING MAGSAT AND OTHER GEOPHYSICAL DATA Quarterly Status Technical Progress Report
C. R. Bentley, Principal investigator 4 Mar. 1981 1 p ERTS
(Contract NAS5-25977)
(E81-10113; NASA-CR-164107; QSTPR-4) Avail: NTIS HC A02/MF A01 CSCL 09B

The compatibility of Univac-formatted tapes with the in-house computer was investigated and a decision was made to switch to IBM-formatted tapes. A NASA software package was adapted for use with data when they become available. Auxiliary geophysical and geological data and literature continue to be compiled and studied so that when data tapes arrive, real analysis may begin. A.R.H.

N81-33522# Institut fuer Angewandte Geodaesie, Frankfurt am Main (West Germany).
POSITION MEASUREMENTS IN COLOMBIA BY MEANS OF SATELLITE OBSERVATIONS [POSITIONSBESTIMMUNGEN IN KOLUMBIEN MITTELS SATELLITENBEOBACHTUNGEN]
Walter Etling *In its* Rept. on Cartography and Geodesy, Ser. 1: Original Rept., No. 80 1980 p 5-11 In GERMAN; ENGLISH summary
Avail: NTIS HC A05/MF A01

A number of positions on the Earth were determined by means of Doppler measurements using the Navy navigation satellite system in support of a seismic measurement compaign conducted in Colombia. The transformation of the initial geocentric system to the required terrestrial coordinate systems is discussed. It is shown that the positions of the points to be measured can be determined with an accuracy sufficient for cartographic purposes using only a restricted number of satellite passages. Experimentation under conditions pertaining to Colombia is also commented on. Author (ESA)

N81-33525# Institut fuer Angewandte Geodaesie, Frankfurt am Main (West Germany).
OVSUP: A PROGRAM FOR COMPUTER-AIDED DISENTANGLEMENT OF OVERLAPPING ZONES [OVSUP: EIN PROGRAMM ZUR EDV-GESTUETZTEN ENTFLECHTUNG DER UEBERLAPPUNGSSTELLAN VERBREITER LINIENHAFTER KARTENELSENENTE]
Roland Schittenhelm *In its* Rept. on Cartography and Geodesy, Ser. 1: Original Rept., No. 80 1980 p 75-82 refs In GERMAN; ENGLISH summary

Avail: NTIS HC A05/MF A01

A computer program (OVSUP) was developed to disentangle overlapping zones of broadened cartographic line elements by computing the amount of displacement of single points. OVSUP is run in combination with a subroutine OVPREC which finds the beginning and the end of such overlapping zones automatically. A survey is made of the program structure, the functioning of its subroutines, and the conditions for application. The computer output is in the form of a vector containing the coordinates of the displaced points. A practical application illustrates the procedure. Author (ESA)

N81-33526# Institut fuer Angewandte Geodaesie, Frankfurt am Main (West Germany).
PHOTOGRAMMETRY IN CHINA
Zhi-zhou Wang (Wuhan Coll. of Geodesy, Photogrammetry and Cartography, China) *In its* Rept. on Cartography and Geodesy, Ser. 1: Original Rept., No. 80 1980 p 83-89 In GERMAN; ENGLISH summary

Avail: NTIS HC A05/MF A01

Past and present developments in China in the field of photogrammetry and survey are summarized. The production of topographic maps at scales 1 : 100,000 and 1 : 50,000 produced by topogrammetic techniques is discussed. Base map production at scale 1 : 10,000 using aerial imagery, analytical block adjustment, computer bundle adjustment, and preliminary orthophoto production is described. Photogrammetric research on digital correlation of stereophotography on production and application of digital terrain models, and on geometrical remote sensing data processing are treated. Author (ESA)

N81-33527# Institut fuer Angewandte Geodaesie, Frankfurt am Main (West Germany).
REPORTS ON CARTOGRAPHY AND GEODESY, SERIES 1: ORIGINAL REPORTS, NUMBER 81 [NACHRICHTEN AUS DEM KARTEN- UND VERMESSUNGSWESEN, REIHE 1: ORIGINALBEITRAERE]
1980 134 p refs In GERMAN; ENGLISH summary Original contains color illustrations
(ISSN-0469-4236) Avail: NTIS HC A07/MF A01

The application of automatic data processing to cartography is discussed. Software development, with contributions to object extraction, network synthesis, graphical kernel systems, and height model construction is considered. Configuration descriptions of global cartographic data base systems and applications in the fields of geological surveys, electrical supply grids, and marine navigation are presented.

N81-33578# Air Force Inst. of Tech., Wright-Patterson AFB, Ohio. School of Engineering.
AN EVALUATION OF DETAIL IN DYNAMIC VISUAL DISPLAYS M.S. Thesis
Mary A. Smart 1 Dec. 1980 111 p refs
(AD-A103378; AFIT/GCS/EE/80-14) Avail: NTIS HC A06/MF A01 CSCL 09/2

This report has its basis in the Airborne Electronic Terrain Mapping System (AETMS), an aircraft mapping system based on an idea proposed by L.A. Tamburino and developed by the Air Force Avionics Laboratory. A constantly changing background provides the basis for an interesting investigation on the hypothesis that a dynamic background will distract the operator's attention away from important details on the display. The software developed provides an overlay of symbols onto the terrain map generated by the AETMS and is contained in this report. A symbol and color set is suggested for the AETMS. An experiment to determine a master symbol and color set is suggested. The experiment suggests using both simple vector symbols and Fourier transformed symbols to help define the master set. Author (GRA)

N81-33581# Analytic Sciences Corp., Reading, Mass.
MILITARY GEODESY AND GEOSPACE SCIENCE, UNIT ONE
Warren G. Heller and A. Richard LeSchack Feb. 1981 191 p refs
(Contract F19628-77-C-0152; AF Proj. 3204)
(AD-A104038; SCIENTIFIC-5; AFGL-TR-81-0028) Avail: NTIS HC A09/MF A01 CSCL 08/5

Unit One introduces the student to Mapping, Charting, and Geodesy. Basic concepts and principles are presented that will be applied during the remainder of the course. The subjects to be covered include: Earth modeling; Coordinate systems; and Techniques of mapping, charting, and geodesy. All of these areas are part of the science of geodesy, which is defined by the three principal subjects with which it is concerned: The size and shape of the earth; The relative location of points on or near the surface of the earth; and The earth's gravity field. The first two areas are referred to as geometric geodesy; the third is physical geodesy. The geometric and physical (or gravitational) aspects of geodesy are closely related to one another, since the physical surface of the earth does not deviate greatly from an equipotential surface of the gravity field. The material of Unit One is organized into three chapters, each examining geodesy from a different point of view: Geometric geodesy (Chapter Two) -- including material on relevant aspects of cartography and surveying; Physical geodesy (Chapter Three); and Satellite geodesy (Chapter Four) -- emphasizing the unique contributions to geodesy resulting from the use of Earth satellites. GRA

N81-33589# Geological Survey, Denver, Colo. Federal Center.

TOPOGRAPHIC SLOPE CORRECTION FOR ANALYSIS OF THERMAL INFRARED IMAGES Interim Report

Kenneth Watson Mar. 1981 14 p refs
(Contract NASA Order-S-40256-B)
(PB81-211781; USGS-GD-81-002) Avail: NTIS HC A02/MF A01 CSCL 08B

A simple topographic slope correction was developed using a linearized thermal model and assuming slopes less than about twenty degrees. The correction can be used to analyze individual thermal images or composite products such as temperature difference or thermal inertia. Simple curves are provided for latitudes of 30 and 50 degrees. The form is easily adapted for analysis of HCMM images using the Defense Mapping Agency digital terrain data. GRA

N81-33760*# National Aeronautics and Space Administration. Wallops Flight Center, Wallops Island, Va.

GULF OF MEXICO SATELLITE RADAR ALTIMETRY Final Report

C. G. Parra, R. G. Forsythe, and C. L. Parsons Aug. 1981 231 p refs
(NASA-TM-73295) Avail: NTIS HC A11/MF A01 CSCL 08C

The dynamic topography of the sea surface was measured. The radar altimeter measurements yield average ocean topographic data which are mapped. Seasonal deviations from a 3 year mean topography are presented. The altimeters are also instrumented with sample and hold gates which provide information about the shape and amplitude of the return waveform. Parameters including ocean surface wind speed and the significant wave height are determined. One hundred eighty six wind speed and significant wave height histograms are presented. E.A.K.

04

GEOLOGY AND MINERAL RESOURCES

Includes mineral deposits, petroleum deposits, spectral properties of rocks, geological exploration, and lithology.

A81-41908 **Tiwi geothermal project - The Philippines.** R. Aquino (De La Salle University, Manila, Philippines), S. Aquino (Philippine National Oil Co., Manila, Philippines), and A. Alcaraz. In: Geothermal energy projects: Planning and management. New York and Oxford, Pergamon Press, 1980, p. 168-205. 5 refs.

An account is given of the Philippines' Tiwi geothermal field development and related research projects. Among the topics covered are: (1) preliminary research studies throughout the Philippine archipelago, considering such potential sites as direct volcanic exhalations, shallow volcanic sources, deep-seated plutonic sources, and deep faulting in regions of high geothermal gradient; (2) fault systems detected by aerial photographic surveys, such as the plug-dome fault systems, radial fault systems, and arcuate fault systems; (3) performance figures on test drill holes at six different locations; (4) mechanical details of the Tiwi steam-gathering system; (5) the National Power Corporation's organization of responsibilities; and (6) detailed comparisons of energy demand, sources and their costs in the Philippines as seen by the Ten-Year Energy Program for the period 1979-88. O.C.

A81-42276 # **The use of imagery of the earth to study the structure of degassing zones within oil and gas basins (Ispol'zovanie kosmicheskikh snimkov zemli pri izuchenii stroeniia zon degazatsii neftegazonosnykh basseinov).** G. I. Amurskii and M. S. Bondureva (Vsesoiuznyi Nauchno-Issledovatel'skii Institut Prirodnykh Gazov, Moscow, USSR). *Issledovanie Zemli iz Kosmosa,* May-June 1981, p. 5-10. 6 refs. In Russian.

Space imagery is used to identify and trace the local faults and fracture zones of several anticlinal structures in Central Asia. These zones, favorable to the vertical migration of stratified fluids, exhibit an increased permeability, and are therefore subject to degassing and the accumulation of gaseous sulfur. J.F.

A81-42277 # **Concerning the hydrogeological significance of faults on platform regions, as revealed by space imagery (O gidrogeologicheskoi roli razryvnykh narushenii platformennykh oblastei, vyiavliaemykh na kosmicheskikh snimkakh).** M. I. Burleshin and A. V. Sadov (Vsesoiuznyi Nauchno-Issledovatel'skii Institut Gidrogeologii i Inzhenernoi Geologii, Moscow, USSR). *Issledovanie Zemli iz Kosmosa,* May-June 1981, p. 11-17. 9 refs. In Russian.

The characteristics of faults revealed by space imagery are compared with those observed by traditional methods. A hydrogeological interpretation of several faults in the Turanian plate is given, along with the fundamental methods of this interpretation. It is concluded that space imagery may be used to recognize developing faults which would influence the thickness, composition, and plicated structure of the platform rock. Space imagery may also reveal areas of extended rock overlap, influencing rock permeability, and may thus be used to find underground mineral water. Finally, space imagery is important for the accurate definition of hydrogeological region boundaries and the development and revision of hydrogeological maps. J.F.

A81-42278 # **Ring structures of Precambrian shields, based on the interpretation of space imagery (Kol'tsevye struktury Dokembriiskikh shchitov po dannym deshifrirovaniia kosmicheskikh snimkov).** V. M. Moralev (Akademiia Nauk SSSR, Institut Litosfery, Moscow, USSR) and M. Z. Glukhovskii (Proizvodstvennoe Geologicheskoe Ob'edinenie Aerologiia, Moscow, USSR). *Issledovanie Zemli iz Kosmosa,* May-June 1981, p. 18-22. 5 refs. In Russian.

Space imagery interpretations were used to identify two types of ring structures found in Precambrian shields. Large ring structures, reaching a diameter of 900-1200 km, are considered relicts of ancient sedimentary-volcanic basins, corresponding to structures of primary lithospheric cleavage. The second type of ring structures, having a 50-400 km diameter, mainly represent granite-gneiss domes and magmatic diapirs, surrounded by zones of ultrabasite-basic granulite. J.F.

A81-42279 # **Fitoexomorphogenic analysis of geological environment changes in the South Aral Sea, based on aerial and space imagery (Fitoekzomorfogennyi analiz izmenenii geologicheskoi sredy Iuzhnogo Priaral'ia po aero- i kosmicheskim snimkam).** A. L. Revzon (Vsesoiuznyi Nauchno-Issledovatel'skii Institut Gidrogeologii i Inzhenernoi Geologii, Moscow, USSR). *Issledovanie Zemli iz Kosmosa,* May-June 1981, p. 23-27. 6 refs. In Russian.

A81-42280 # **Space research on seismic regions (Kosmicheskie issledovaniia v seismoaktivnykh regionakh).** B. N. Khovanskii (Gosudarstvennyi Nauchno-Issledovatel'skii i Proizvodstvennyi Tsentr Priroda, USSR). *Issledovanie Zemli iz Kosmosa,* May-June 1981, p. 28-34. 10 refs. In Russian.

Space images have been used to identify fracture zones of high seismic and tectonic activity, where a relatively high percentage of seismic dislocations and earthquake epicenters are located. The combination of space imagery interpretation with the analysis of foreshock data, obtained by geodetic and geophysical methods, is shown to provide an accurate means of long range prediction of earthquake time, location, and intensity. J.F.

A81-42289 # **Geological interpretation in an interactive mode in automated systems of digital image processing (Geologicheskoe deshifrirovanie v dialogovom rezhime v avtomatizirovannykh sistemakh tsifrovoi obrabotki izobrazhenii).** T. P. Belikova, V. E. Gendler, and L. P. Iaroslavskii (Akademiia Nauk SSSR, Institut Problem Peredachi Informatsii; Proizvodstvennoe Geologicheskoe Ob'edinenie Aerologiia, Moscow, USSR). *Issledovanie Zemli iz Kosmosa,* May-June 1981, p. 102-112. 6 refs. In Russian.

The geological interpretation of aerial and space images in automated systems is discussed. Examples are presented using the method of adaptive amplitude transformation for image preparation in interactive mode processing. Brightness characteristics of geological objects and the peculiarities of their interpretation during space photography are discussed. Regions of plicated land masses, formed by Ordovician deposition, are shown at several levels, using the adaptive mode quantization method, and corresponding geological maps are presented with explanations of their symbols. The method of contrast-degree intensification is discussed, whereby the original phototone values are transformed on the basis of a distribution curve of tonal image points. Interactive processing of aerial and space images is shown to dramatically increase the number of objects distinguished, as well as to improve the reliability of the interpretation. J.F.

A81-43215 **Optical and digital analyses of Landsat data depicting hydrogeological features of the Daryacheh-Ye-Namak area, Iran.** M. S. Akhavi (Nova Scotia Land Survey Institute, Lawrencetown, Canada). In: Satellite hydrology; Proceedings of the Fifth Annual William T. Pecora Memorial Symposium on Remote Sensing, Sioux Falls, SD, June 10-15, 1979. Minneapolis, MN, American Water Resources Association, 1981, p. 278-283. 13 refs.

Optical and digital processing techniques were used to detect and map hydrogeological and water resources features at the Daryacheh-Ye-Namak (salt lake) area, north-central Iran. Analyses of optically and digitally enhanced Landsat images, aided by field information, made it possible to depict the changing areal extent and depth of a shallow salt lake occurring in the western section of this internal lacustrine basin. Also, salt surfaces having possible economic value were classified and other pertinent hydrogeologic observations were made using enhanced Landsat data. (Author)

A81-43227 **Correlation of geologic structure inferred from computer enhanced Landsat imagery with underground water supplies in Arizona.** R. Schowengerdt, C. E. Glass (Arizona, University, Tucson, AZ), L. Ethridge (Phillips Petroleum Co., Bartlesville, OK), and E. M. Babcock. In: Satellite hydrology; Proceedings of the Fifth

Annual William T. Pecora Memorial Symposium on Remote Sensing, Sioux Falls, SD, June 10-15, 1979. Minneapolis, MN, American Water Resources Association, 1981, p. 387-397. 12 refs. U.S. Department of the Interior Grant No. B-066-ARIZ.

Photolineaments of the entire northeast quadrant of Arizona were mapped from standard EROS Data Center false color Landsat composites. Photolineaments were also mapped using computer-enhanced Landsat imagery of two intensive study sites. A third source of geological-structure data was existing large-scale lineament maps derived from aerial photography of the study sites. A spatially distributed parameter obtained from these maps, lineament density, was mathematically correlated with water well survey data (specific capacity, specific conductance, transmissivity, and water temperature) to establish the most useful combination of data for extension of lineament signatures through the entire northeast quadrant. Results from this initial study indicate that Landsat imagery may be used to survey large areas for lineaments, and to cue the hydrogeologist to promising regions, which can then be mapped at aerial photography scales. B.J.

A81-43228 **Landsat data for locating shallow glacial aquifers in eastern South Dakota.** P. H. Rahn (South Dakota School of Mines and Technology, Rapid City, SD) and D. G. Moore (South Dakota State University, Brookings, SD). In: Satellite hydrology; Proceedings of the Fifth Annual William T. Pecora Memorial Symposium on Remote Sensing, Sioux Falls, SD, June 10-15, 1979. Minneapolis, MN, American Water Resources Association, 1981, p. 398-406. 11 refs. U.S. Geological Survey Contract No. 14-08-0001-13576.

A81-43230 **Ground water exploration programs in Africa.** L. Zall and O. Russell (Earth Satellite Corp., Washington, DC). In: Satellite hydrology; Proceedings of the Fifth Annual William T. Pecora Memorial Symposium on Remote Sensing, Sioux Fall, SD, June 10-15, 1979. Minneapolis, MN, American Water Resources Association, 1981, p. 416-425. 12 refs.

As part of regional ground water exploration programs in Tanzania, Upper Volta, Benin, and Ghana, ground water exploration guide maps were prepared using digitally processed and photographically enlarged Landsat imagery. Digital processing of Landsat data permits the enhancement of spectral gray levels or subtle tonal variations, such as those caused by lithologic changes, geological structure, or the variation of soil moisture. Such imagery also emphasizes linear features, fractures, or faults that can be missing or difficult to interpret from unprocessed imagery. These guide maps substantially increased the efficiency of operation and decreased the time and expense necessary to complete these programs. B.J.

A81-43232 **Applications of aerospace data for detection of submarine springs in Jamaica.** F. A. Kohout (U.S. Geological Survey, Woods Hole, MA), D. R. Wiesnet (NOAA, National Earth Satellite Service, Washington, DC), M. Deutsch, J. A. Shanton (U.S. Geological Survey, Reston, VA), and M. C. Kolipinski (U.S. National Park Service, San Francisco, CA). In: Satellite hydrology; Proceedings of the Fifth Annual William T. Pecora Memorial Symposium on Remote Sensing, Sioux Falls, SD, June 10-15, 1979.

Minneapolis, MN, American Water Resources Association, 1981, p. 437-445. 8 refs. Research sponsored by the United Nations.

A project carried out in Jamaica in 1971 by the United Nations Development Programme, the Jamaica Geological Survey, and NASA is discussed. The findings of the underwater SCUBA investigations are correlated with anomalies shown in the aircraft data and with Apollo IX spacecraft photography and TIROS-N satellite imagery. Remote sensing of submarine springs is seen as having the potential of performing at least two useful functions: (1) the discovery of submarine discharge may help to identify geologic or geomorphic structures on the mainland where there would be high probability of drilling successful wells, and (2) periodic observation of the thermal or turbidity anomalies associated with a submarine spring can serve as an outpost system for monitoring hydrologic changes brought about by future expolitation of the aquifer. C.R.

A81-43730 * **Use of imaging radar for geology and archeology.** M. Daily (California Institute of Technology, Jet Propulsion Laboratory, Pasadena, CA). In: Rainbow 80; Fall Technical Meeting, Niagara Falls, NY, October 7-10, 1980, ASP Technical Papers. Falls Church, VA, American Society of Photogrammetry, 1981, p. DA-1-B-1 to DA-1-B-13.

Imaging radar is shown to be a useful sensor for geological analysis as a standal one sensor in clouded regions or as a complementary data source with visible NIR systems. Radar image tone is a function of the radar system parameters (imaging geometry, frequency, polarization) and a function of the target (local slope, electrical properties, and surface roughness). Substantial topographic texture enhancement can be achieved for large scale features by using specular returns associated with steep-incidence radars or shadows associated with grazing-incidence systems. Texture enhancement also allows radar to image lineaments and archeological features, such as canals and causeways. Future multispectral radars may achieve better discrimination of subresolution structures. Seasat radar images of several geographic locations are provided. J.F.

A81-44061 # **The possibility of using an aerial thermal survey for studying the structure of the salt bed in the Gulf of Kara-Bogaz-Gol (O vozmozhnosti primeneniia teplovoi aeros'emki dlia izucheniia stroeniia solianogo plasta Zaliva Kara-Bogaz-Gol).** V. I. Gornyi (Vsesoiuznoe Aerogeologicheskoe Nauchno-Proizvodstvennoe Ob'edinenie Aerogeologiia, Leningrad, USSR). *Akademiia Nauk SSSR, Doklady,* vol. 259, no. 2, 1981, p. 321-323. 5 refs. In Russian.

A81-45430 * **A radar image time series.** F. Leberl, H. Fuchs (Graz, Technische Universität, Graz, Austria), and J. P. Ford (California Institute of Technology, Jet Propulsion Laboratory, Pasadena, CA). *International Journal of Remote Sensing,* vol. 2, Apr.-June 1981, p. 155-183. 13 refs. Contract No. NAS7-100.

A set of ten side-looking radar images of a mining area in Arizona that were aquired over a period of 14 yr are studied to demonstrate the photogrammetric differential-rectification technique applied to radar images and to examine changes that occurred in the area over time. Five of the images are rectified by using ground control points and a digital height model taken from a map. Residual coordinate errors in ground control are reduced from several hundred meters in all cases to + or - 19 to 70 m. The contents of the radar images are compared with a Landsat image and with aerial photographs. Effects of radar system parameters on radar images are briefly reviewed. F.G.M.

A81-46039 **Lineament mapping in northern Sweden from Landsat images using orthogonal image transforms.** L. C. Andersson and H. Hauska (Lulea, Hogskola, Lulea, Sweden). In: Machine processing of remotely sensed data and soil information systems and remote sensing and soil survey; Proceedings of the Sixth Annual Symposium, West Lafayette, IN, June 3-6, 1980.
New York, Institute of Electrical and Electronics Engineers, Inc., 1980, p. 147-157. Styrelsen for Teknisk Utveckling Contracts No. 76-6669; No. 77-6345.

A81-46194 **Geomorphic mapping from Landsat-3 Return Beam Vidicon /RBV/ imagery.** G. R. Cochrane and G. H. Browne (Auckland, University, Auckland, New Zealand). *Photogrammetric Engineering and Remote Sensing,* vol. 47, Aug. 1981, p. 1205-1213. 17 refs.

Landsat-3 Return Beam Vidicon (RBV) imagery of eastern North Island of New Zealand is useful for regional geomorphic mapping. Three broad tectono-physiographic regions - Western Taupo volcanic plateau zone, Central blockfaulted Mesozoic greywacke zone, and Eastern Inland Hawke Bay zone of dissected Tertiary hill country - are recognized and their features discussed. Some previously unmapped lineaments are noted. Ten geomorphic categories - coastal dunes, raised marine terraces, alluvial terraces, volcanic cones, dip slopes, large landslides, undissected plateau, dissected plateau, undulating hill country, and steep hill country - have been successfully mapped from the RBV data. The principal advantages of RBV images for geomorphic mapping are their improved geometric accuracy and their relatively high spatial resolution (40 m). Limitations in differentiating land-water interfaces are present. Landsat RBV imagery can be used to supplement future studies in the earth sciences, especially in remote or poorly mapped areas. (Author)

A81-47353 **Ore-controlling space geological objects and their assessment techniques applied to mineral prediction.** A. L. Stavtsev (Ministerstvo Geologii SSSR, Ob'edinenie Aerogelogiia, Moscow, USSR). *International Astronautical Federation, International Astronautical Congress, 32nd, Rome, Italy, Sept. 6-12, 1981, Paper 81-107.* 4 p.

The importance of rupture dislocations is assessed, and it is noted that faults and fault zones are commonly well exhibited on space images. The combined analysis of fault identification charts and maps of the distribution of known mineral deposits makes it possible to assess the role of rupture dislocations in the spatial distribution of minerals and to delineate, through analogy, promising areas for mineral extraction. Attention is also given to the analysis of the ore-controlling importance of ring structures and to the combined application of identified space images and geological and geophysical data to a computerized mineral prediction. It is concluded that the application of space images to mineral exploration provides geologists with ample opportunity for studying the spatial distribution of metallic and nonmetallic ores and predicting their potential occurrences. C.R.

A81-48683 # **The informational estimation of the effectiveness of using satellite imagery in hydrogeological research (Opyt informatsionnoi otsenki effektivnosti primeneniia kosmicheskikh snimkov v gidrogeologicheskikh issledovaniiakh).** M. I. Burleshin and V. N. Koloskova (Vsesoiuznyi Nauchno-Issledovatel'skii Institut Gidrogeologii i Inzhenernoi Geologii, Moscow, USSR). *Issledovanie Zemli iz Kosmosa,* July-Aug. 1981, p. 27-31. 6 refs. In Russian.

An informational approach is used to estimate the effectiveness of using satellite imagery in the hydrogeological mapping of the Ustiurt Plateau. Satellite imagery and intermediate and final schemes of the hydrogeological interpretation are represented as data channels. Based on information theory, a quantitative estimation and a comparison of the contents of hydrogeological maps, compiled by terrestrial mapping and space imagery interpretation, are made. J.F.

A81-48684 # **The use of satellite imagery for studying the structural features of the Caspian oil and gas region (Primenenie kosmicheskikh materialov dlia izucheniia strukturnykh osobennostei pri-Kaspiiskoi neftegazonosnoi provintsii).** L. F. Volchegurskii and V. G. Pronin (Vsesoiuznoe Aerogeologicheskoe Nauchno-Proizvodstvennoe Ob'edinenie Aerogeologiia, Moscow, USSR). *Issledovanie Zemli iz Kosmosa,* July-Aug. 1981, p. 32-38. 8 refs. In Russian.

Based on a study of satellite imagery, the boundaries of the Caspian oil and gas region are defined, and the linear structures, interpreted as faults or zones of faults, are distinguished. Ring structures, corresponding to the structures of the different horizons of the sedimentary cover and bedplate, are discussed. Based on the data obtained by satellite imagery, a detailed scheme of the oil and gas geological regionalization is presented. Such a study is then used to define the individual oil and gas zones within the range of the Caspian region, to trace the extended faults which play a significant role in forming these oil and gas zones, to select regions of seismic research, and to reinterpret the structural maps. J.F.

A81-48685 # **The interrelation of linear and isometric objects on satellite imagery and the oil and gas structures of the Buzuluk Basin (O vzaimosviazi lineinykh i izometrichnykh ob'ektov na kosmicheskikh snimkakh i neftegazonosnykh struktur Buzulukskoi vpadiny).** D. M. Trofimov and B. I. Dmitrieva (Moskovskii Gosudarstvennyi Universitet, Moscow, USSR). *Issledovanie Zemli iz Kosmosa,* July-Aug. 1981, p. 39-44. 5 refs. In Russian.

A81-48690 # **Complex processing of satellite images and the geological interpretation (Kompleksnaia obrabotka kosmicheskikh snimkov i geologicheskaia interpretatsiia).** V. S. Iudin (Akademiia Nauk SSSR, Institut Geologii i Geofiziki, Novosibirsk, USSR). *Issledovanie Zemli iz Kosmosa,* July-Aug. 1981, p. 70-75. 20 refs. In Russian.

A correlation between the appearance of natural formations in geological and geophysical measurements and their representation on satellite images is established, based on the data of standard survey regions. The contents of the images, subjected to computer processing, can provide much information on geological processes. A comprehensive analysis using the indicated correlated dependences is used to produce a preliminary classification of tectonic structures and can reveal several phenomena of deep-seated processes in the regions. The obtained results may be used to find valuable mineral deposits. J.F.

A81-48691 # **Interactive system for the regional prognosis of raw mineral resources, based on ground-based and satellite imagery data (Dialogovaia sistema regional'nogo prognozirovaniia mineral'no-syr'evykh resursov po dannym nazemnykh i kosmicheskikh s'emok).** B. A. Chumachenko, V. V. Marchenko, E. P. Vlasov, E. A. Nemirovskii, and V. A. Iakovlev (Mezhdunarodnyi Nauchno-Issledovatel'skii Institut Problem Upravleniia, Moscow, USSR). *Issledovanie Zemli iz Kosmosa,* July-Aug. 1981, p. 76-82. 5 refs. In Russian.

The interactive system 'Region' is used for forecasting potential areas of raw mineral resources from ground and space survey data. Mathematical models which forecast and estimate the prospective ore content and heuristic models concerning the regularity of ore location are stored in one data bank. Data of aerospace, ground-based, geological, geophysical, and geochemical images as well as their descriptions are kept in a second regional bank. Data from both banks are processed by a logical-statistical program. An algorithm for distinguishing images with standard patterns is performed, and a program for the classification of nonstandard patterns is carried out, based on a taxonomy method. Algorithmic programs of simulated modeling are then performed, producing a variety of prognosis solutions. J.F.

A81-49767 # **Experimental use of real time SAR imagery in support of oil exploration in the Beaufort Sea.** J. B. Mercer (Dome Petroleum, Ltd., Calgary, Alberta, Canada), R. T. Lowry, and S. K. Leving (Intera Environmental Consultants, Ltd., Ottawa, Canada). In: Canadian Symposium on Remote Sensing, 6th, Halifax, Canada, May 21-23, 1980, Proceedings. Ottawa, Canadian Aeronautics and Space Institute, 1981, p. 143-152. 8 refs. Research supported by Dome Petroleum, Ltd.

SAR imagery, generated in real-time, has been used for the first time to support an Arctic marine operation. During the latter portion of Dome Petroleum's late season drilling program (November 1979) in the Beaufort Sea, the SAR-580 flew daily missions to provide near real-time 'snap shots' of the ice conditions in the vicinity of the operations. The aim of the program was to assist both the icebreaker support of the drillship and the subsequent navigation back to harbor. To provide the context for this SAR application, a review of Beaufort Sea ice conditions is presented along with a brief discussion of the problems and techniques of the interpretation of the SAR imagery. The downlink and operational performance of the SAR are described along with an outline of an improved system. B.J.

A81-49769 # **Applicability of airborne SAR data to geological mapping.** S. Pala, R. Mussakonski, and E. Wedler (Ministry of Natural Resources, Ontario Center for Remote Sensing, Toronto, Canada). In: Canadian Symposium on Remote Sensing, 6th, Halifax, Canada, May 21-23, 1980, Proceedings. Ottawa, Canadian Aeronautics and Space Institute, 1981, p. 169-177.

Airborne SAR data, obtained over the Canadian Shield in the vicinity of Sudbury and Haliburton, is analyzed to establish its usefulness and its limitations as a geological mapping tool. Various inherent geological features in volcanic, igneous and metamorphic rock groups are examined on the radar imagery in an effort to determine what can and cannot be detected. An attempt has been made to recognize all the known geological features on the SAR imagery. The characteristics of radar data from X and L bands, both parallel and cross-polarized, were individually studied for the purpose of identifying the usefulness of each band. Successful use of SAR imagery as a geological mapping tool will depend upon the attributes and limitations of the data to distinguish those surface elements necessary for mapping. The techniques used and the results obtained are described. The radar and terrain characteristics which were useful, or which created limitations, are examined and discussed.
B.J.

A81-49802 # **Geological and terrain analysis of the Annapolis County region of Nova Scotia - An application of digital Landsat, radar and colour infrared data.** V. H. Singhroy (J. D. Mollard and Associates, Ltd., Regina, Saskatchewan, Canada), W. D. Bruce (Canada Centre for Remote Sensing, Ottawa, Canada), and G. R.

Stevens (Acadia University, Wolfville, Nova Scotia, Canada). In: Canadian Symposium on Remote Sensing, 6th, Halifax, Canada, May 21-23, 1980, Proceedings. Ottawa, Canadian Aeronautics and Space Institute, 1981, p. 501-511. 15 refs.

It is pointed out that in areas where detailed geological information is lacking and rock outcrops are covered by thick glacial drift, a comprehensive exploration program must involve both field geologists and remote sensing scientists. The contribution of remotely sensed data to the understanding of the structural and glacial geology of the Annapolis County region where exploration programs are active is assessed. Optical and digital processing of Landsat data, together with visual interpretation of radar and color imagery, are found to be valuable in delineating significant geological features. It is noted that multidate digital Landsat data have contributed to the delineation of glacial lineaments, major faults, and 'convectional cells'. Also discussed is the contribution of color infrared data in the verification of digital Landsat themes. C.R.

A81-49809 # **Detection of changes in a coal surface mining area by ratioing multidate Landsat digital data.** D. O. Ohlen (Technicolor Graphic Services, Inc., Sioux Falls, SD). In: Canadian Symposium on Remote Sensing, 6th, Halifax, Canada, May 21-23, 1980, Proceedings. Ottawa, Canadian Aeronautics and Space Institute, 1981, p. 581, 582.

Two procedures are compared for determining change in a coal surface mining area in southern Montana using ratioed multidate Landsat data. Subscenes of Landsat band 5 multispectral scanner data acquired in July 1976 and June 1977 are selected. Each subscene is geometrically corrected to a U.S. Geological Survey 7.5 minute topographic map based and resampled using a 100-meter square pixel. The first procedure used in determining the ranges of ratioed data associated with land cover change involves a comparison of a line printer output of pixel values of the ratioed data with the actual changes that occurred in land cover. The second procedure involves interactive manipulation of the minimum and maximum brightness values in a histogram of the ratioed data to determine which pixels become brighter or darker during the test period. Although the two procedures produce similar results, neither procedure gives results adequate for identifying changes produced by surface mining. C.R.

N81-29143* National Aeronautics and Space Administration, Washington, D. C.
NASA SELECTS SCIENTIFIC INVESTIGATIONS FOR EARTH DYNAMICS STUDIES
21 Aug. 1981 9 p
(NASA-News-Release-81-129; P81-10131) Avail: NASA Scientific and Technical Information Facility, P.O. Box 8757, B.W.I. Airport, Md. 21240 CSCL 22A

Forty two domestic investigators affiliated with U.S. universities, governmental agencies, or private concerns and 14 investigators from France, West Germany, the Netherlands, Switzerland, Spain, Sweden, Australia, New Zealand, Venezuela, and Canada were selected to use precise geodetic data obtained by laser ranging and very long base interferometry in a study of the Earth's tectonic plate movement, crustal deformation, and rotational dynamics. The studies to be made and the principal investigators for each are listed. A.R.H.

N81-30502# Rice Univ., Houston, Tex. Dept. of Geology.
METHODS DEVELOPMENT AND APPLICATIONS EVALUATIONS OF NURE AERIAL RECONNAISSANCE SURVEY DATA FOR URANIUM RESOURCE EVALUATION: BEEVILLE/BAY CITY AND CRYSTAL CITY QUADRANGLES, TEXAS Final Report
John A. S. Adams, Sam F. Harrill, and J. E. Oddo Apr. 1981 115 p refs Prepared for Bendix Field Engineering Corp., Grand Junction, Colo.
(Contracts DE-AC08-76NV-01183; DE-AC13-76GJ-01664) (GJBX-69(81)) Avail: NTIS HC A06/MF A01

The NURE open-file reports on the aerial gamma spectrometric, hydrologic, and stream-sediment surveys of some 50,000 square kilometers of land area in south Texas were studied in regard to their utility in identifying regions of high or higher favorability for uranium deposits. Substantial agreement was found between the NURE aerial data and the ground and helicopter data as regards the general radioelement distributions in the stratigraphic units studied. The vehicle-mounted gamma-ray spectrometer used systematically gave some 30 percent higher thorium concentration estimates when compared with those from the NURE aerial data. The NURE aerial data are adequate in number to characterize the major stratigraphic units, but they may not be quantitative enough for detailed comparisons from one quadrangle to another, and the optimum sampling area for each formation is not known. DOE

N81-31594 Stanford Univ., Calif.
ATMOSPHERIC CORRECTION TO LANDSAT DATA FOR LIMONITE DISCRIMINATION Ph.D. Thesis
William Stephen Kowalik 1981 400 p
Avail: Univ. Microfilms Order No. 8115805

A simple equation describing the radiance measured by the LANDSAT satellites over Lambertian surfaces was used to model the effects of the additive path-radiance and skylight irradiance terms when band ratios are used. The model results show that if the path-radiance and skylight are not corrected, than ratio values (longer wavelength in numerator) increase significantly when proceeding from poorly-illuminated to well-illuminated topographic slopes of the same surface material. After a modeled pathradiance correction, this tendency is reduced, for example, in the 5/4 ratio by a factor of 4X across moderately steep topography. LANDSAT data for 183 test sites (pixel size) in the Yerington District, Nevada were studied from each of 6 images to test the conclusions from the modeling in a mineral exploration framework. The 183 test sites represent three major rock types: (1) limonitically-altered Jurassic quartz monzonite: (2) nonlimonitically altered Jurassic granodiorite rocks; and (3) Teritary volcanic rocks. Field and lab work on each site have characterized the rock type, intensity of iron oxide mineral development, surface topographic orientation, percentage vegetation cover, and vegetation species present. Dissert. Abstr.

N81-32576*# Instituto de Pesquisas Espaciais, Sao Jose dos Campos (Brazil).
VISUAL ENHANCEMENT OF IMAGES OF NATURAL RESOURCES: APPLICATIONS IN GEOLOGY [REALCE VISUAL DE IMAGENS DE RECURSOS NATURAIS: APLICACOES EM GEOLOGIA]
Nelson deJesusParada, Principal Investigator, Gilberto Neto, Evandro O. Araujo, Nelson D. A. Mascarenhas, and Ricardo C. M. deSouza Dec. 1980 55 p refs In PORTUGUESE; ENGLISH summary Presented at the 32nd Reuniao Anual da SBPC, Rio de Janeiro, 6-12 Jul. 1980 Sponsored by NASA ERTS
(E81-10181; NASA-CR-164693; INPE-1952-RPE/267) Avail: NTIS HC A04/MF A01 CSCL 08G

The principal components technique for use in multispectral scanner LANDSAT data processing results in optimum dimensionality reduction. A powerful tool for MSS IMAGE enhancement, the method provides a maximum impression of terrain ruggedness; this fact makes the technique well suited for geological analysis. A.R.H.

N81-32587# Army Engineer Topographic Labs., Fort Belvoir, Va.
IDENTIFYING IGNEOUS ROCKS IN AN ARID ENVIRONMENT ON AERIAL PHOTOGRAPHY BY PHOTO TONE AND PHOTO TEXTURE
Judy Ehlen 15 May 1981 26 p refs
(AD-A102809; ETL-R019) Avail: NTIS HC A03/MF A01 CSCL 14/5

Work concerning identifying igneous rock types on aerial photography began in the late 1940's and early 1950's (Belcher, and others, 1951; Frost, and others, 1953). Even now, the only igneous rocks thought by many to be identifiable on aerial photography are granite, basalt, and some pyroclastic rocks (Military Geology, 1956; von Bandat, 1962; Way, 1973; and Lillesand and Kiefer, 1979). Recent work has shown, however, that other specific igneous lithologies, such as andesite and monzonite, can be identified successfully by air photo analysis (Ehlen, 1981). The purpose of this study was to determine how, and to what level of classification, igneous rocks can be identified by air photo interpretation procedures. Thus, the specific objectives were: (1) to further evaluate established igneous rock identification criteria for arid and semiarid environments, (2) to discover new photo pattern indicators for igneous rocks in these climates, and (3) to develop a classification for igneous rocks based on their photo patterns, similar to a petrologic classification. GRA

N81-32592# High Life Helicopters, Inc., Puyallup, Wash.
AIRBORNE GAMMA-RAY SPECTROMETER AND MAGNETOMETER SURVEY
1980 78 p
(Contract DE-AC13-79GJ-01692)
(DE81-027157; GJBX-211(81)) Avail: NTIS
HC A05/MF $11.00

An airborne combined radiometric and magnetic survey was performed over the area covered by the Toronto, Buffalo, Kingston, Rochester, and Elmira, 1:250,000 National Topographic Map Series (NTMS), quadrangle maps. The survey was part of DOE's National Uranium Resource Evaluation (NURE) program. Data were collected by a helicopter equipped with a gamma-ray spectrometer with a large crystal volume, and with a high sensitivity proton precession magnetometer. The radiometric system was calibrated at the Walker Field Calibration pads and the Lake Mead Dynamic Test Range. Data quality was ensured during the survey by daily test flights and equipment checks. Radiometric data were corrected for live time, aircraft and equipment background, cosmic background, atmospheric radon, Compton scatter, and altitude dependence. The corrected data were statistically evaluated, plotted, and contoured to produce anomaly maps based on the radiometric response of individual geological units. The anomalies were interpreted and an interpretation map produced. DOE

N81-33548*# College of William and Mary, Williamsburg, Va. Dept. of Geology.
MINERALOGICAL, OPTICAL, AND GEOCHEMICAL PROPERTIES OF JOHN H. KERR RESERVOIR SEDIMENT SAMPLES FOR AgRISTARS POLLUTION RESEARCH
Karen L. Bice and Stephen C. Clement, Principal Investigators
Aug. 1981 18 p refs Sponsored by NASA, USDA, Dept. of Commerce, Dept. of Interior, and Agency for International Development ERTS
(Contract NAS1-16042; Proj. AgRISTARS)
(E81-10155; NASA-CR-165762) Avail: NTIS
HC A02/MF A01 CSCL 08F

X-ray diffraction and spectroscopy were used to investigate and compare the mineralogical and chemical properties of two Kerr Reservoirs sediment samples. The index of refractions of the kaolinite present in each sample was determined also. The sediments are composed primarily of illite, kaolinite, quartz, and minor amounts of chlorite. The most abundant elements in the sediment samples are silicon, aluminum, and iron. The kaolinite of sample K-10-80 has a higher index of refraction than that of sample K-3-81. Author

N81-33584# High Life Helicopters, Inc., Puyallup, Wash.
AIRBORNE GAMMA-RAY SPECTROMETER AND MAGNETOMETER SURVEY. CANYON CITY QUADRANGLE (OREGON), VOLUME 2 Final Report
1981 212 p refs Prepared jointly with QEB, Inc.
(Contract DE-AC13-79GJ-01692)
(DE81-028682; GJBX-240-81-V2-(Canyon-City)) Avail: NTIS
HC A10/MF A01

Fourteen uranium anomalies are listed and are shown on the uranium anomaly interpretation map. Potassium (%K), equivalent uranium (ppM eU), equivalent thorium (eT), eU/eT, eU/K, eT/K, and magnetic pseudo contour maps are presented. Stacked profiles showing geologic strip maps along each flight-line, together with sensor data, and ancillary data are included. Geologic unit designations are given for each of the 14 uranium anomalies. All maps and profiles were prepared on a scale of 1:250,000, but have been reduced to 1:500,000 for presentation. DOE

N81-33585# High Life Helicopters, Inc., Puyallup, Wash.
AIRBORNE GAMMA-RAY SPECTROMETER AND MAGNETOMETER SURVEY, SALEM QUADRANGLE (OREGON), VOLUME 2 Final Report
1981 126 p refs Prepared in cooperation with QEB, Inc., Lakewood, Colo.
(Contract DE-AC13-79GJ-01692)
(DE81-028681; GJBX-240-81-Vol-2-(Salem)) Avail: NTIS
HC A07/MF A01

Five uranium anomalies which meet the minimum statistical requirements are tabulated and are shown on the uranium anomaly interpretation map. Potassium (%K), equivalent uranium (ppM eU), equivalent thorium (eT), eU/eT, eU/K, eT/K, and magnetic pseudo-contour maps are presented. Stacked profiles showing geologic strip maps along each flight-line, together with sensor data, and ancillary data are included. All maps and profiles were prepared on a scale of 1:250,000, but were reduced to 1:500,000 for presentation. Each of the anomalies occurs over the Eocene Tyee and Burpee formation (Teme), a rhythmically banded, feldspathic and micaceous, massive bedded sandstone, and siltstone. Anomalies 1, 2, 3, and 4 are in the northwest corner of the map. Anomalies 2 and 3 are near faults, so may be due to radon leaking from the faults. Anomaly No. 5 is in the southwest corner of the map. DOE

05

OCEANOGRAPHY AND MARINE RESOURCES

Includes sea-surface temperature, ocean bottom surveying imagery, drift rates, sea ice and icebergs, sea state, fish location.

A81-41350 **Method for estimation of ocean current velocity from satellite images.** E. Mollo-Christensen (MIT, Cambridge, MA), P. Cornillon, and A. D. S. Mascarenhas, Jr. *Science,* vol. 212, May 8, 1981, p. 661, 662. 6 refs. Contracts No. N00014-79-C-0413; No. N00014-75-C-0291.

Barotropic instability waves on a shear interface propagate at the average speed of the water on the two sides. Assuming the instability to be excited by tidal oscillations, the phase speed is the wavelength divided by the tidal period. If the water is at rest on one side of the shear layer the current speed on the other side can be calculated. This method, applied to the Gulf Stream beyond Cape Hatteras as seen in satellite images, gives estimates of current speed in general agreement with in situ observations. (Author)

A81-41490 # **Evaluation of the effect of sea-ice roughness on the microwave emission of the ice (Otsenka vliianiia sherokhovatosti morskogo l'da na ego radioteplovoe izluchenie).** P. A. Nikitin. In: Some results on the investigation of earth resources by aerial and polygon methods. Leningrad, Gidrometeoizdat, 1980, p. 93-97. In Russian.

Formulas of geometric optics are used to calculate the effect of the surface roughness of sea ice on its microwave emission. The ice was modeled as a homogeneous isothermal medium with a normal distribution of elementary-area inclinations. Available data on Arctic sea ice were used as input parameters. It is found that, in the case of horizontal polarization, emissivity increments due to roughness can exceed by 30% the amplitudes of possible variations of the microwave emissivity of Arctic water surfaces. B.J.

A81-41755 **Satellite aided coastal zone monitoring and vessel traffic system.** J. L. Baker (Baker Development Corp., Sherwood Forest, MD). *(Institute of Navigation, Annual Meeting, 36th, U.S. Naval Postgraduate School, Monterey, CA, June 23-26, 1980.) Navigation,* vol. 27, Winter 1980-1981, p. 290-304.

A technique used to continuously monitor the location of cooperating vessels within the 200-nautical-mile U.S. coastal zone is discussed. Using the ATS-3 satellite, the LORAN-C navigational system is based on the 'roll call' technique, and is similar to shore-based ship traffic advisory systems using radar. A description and demonstration of the operational system are given, including the onboard, satellite, communications, display, and control systems. Capabilities of the system include search and rescue, coastal zone management, avoidance of collisions and grounding, ships entering territorial waters, military, and research and exploration. In conclusion, the system is shown to be operational in any weather, relatively inexpensive, able to communicate with all commercial or government satellites, andd possessing unlimited range. D.L.G.

A81-41974 * **Seasat data applications by commercial users.** D. R. Montgomery (California Institute of Technology, Jet Propulsion Laboratory, Pasadena, CA). *Marine Geodesy,* vol. 4, no. 4, 1980, p. 387-416. 9 refs. Contract No. NAS7-100.

The Seasat Program was initiated as a proof-of-concept mission to evaluate the effectiveness of a study of remotely sensed oceanographic phenomena from a satellite platform. From its inception the Seasat Program has been user-oriented. The user comprised three major segments of the ocean community, including academic users, users within various government agencies, and commercial users. Commercial users represent a broad spectrum of commercial marine industries. The commercial users proposed to NASA to carry out a pilot demonstration to assess the utility of Seasat data in the private sector. The commercial users' program is considered along with case studies that utilize Seasat data, and aspects of real-time system operation. Attention is given to the potential value of an employment of synthetic aperture radar, the altimeter, the scatterometer, and the scanning multichannel microwave radiometer. G.R.

A81-41996 * **Oceanic Satellite Data Distribution System.** D. R. Montgomery (NASA, Washington, DC). *Marine Technology Society Journal,* vol. 14, no. 6, 1980, p. 28-30.

The Satellite Data Distribution System (SDDS) serves to process satellite-derived ocean observations, generate ocean analysis and forecast products, and distribute the products to a limited set of commercial users. The SDDS functions in series with the U.S. Navy Fleet Numerical Oceanography Center (FNOC) to provide products on a near-real-time basis to commercial marine industries. Conventional meteorological and oceanographic observations provided to FNOC serve as the input set to the numerical analysis and forecast models. Large main-frame computers are used to analyze and forecast products on a routine, operational basis (at 6-hour and 12-hour synoptic times). The products, reformatted to meet commercial users needs, are transferred to a NASA-owned computer for storage and distribution. Access to the information is possible either by a commercial dial-up packet-switching network or by a direct computer-computer connection. J.F.

A81-41997 * **Future plans for NASA's Oceanic Processes Program.** W. S. Wilson (NASA, Office of Space and Terrestrial Applications, Oceanic Processes Branch, Washington, DC). *Marine Technology Society Journal,* vol. 14, no. 6, 1981, p. 26, 27.

NASA's Oceanic Processes Program has the objectives to develop a scientific basis for viewing the oceans from space and to demonstrate the utility of such an undertaking. There are currently four flight projects concerning the oceanic area. These projects are related to the National Oceanic Satellite System (NOSS), the Dynamic Ocean Topography Experiment (TOPEX), the Gravity Satellite (GRAVSAT), and a Synthetic Aperture Radar (SAR) mission. NOSS is being planned as a limited operational demonstration of viewing the oceans from space. It is to provide a capability to observe surface winds, waves, temperature, color, ice cover, and currents. It is scheduled for launch in 1986. TOPEX and GRAVSAT are being planned as research missions and are both scheduled for launch about 1986. The SAR mission is being planned to provide a spaceborne capability to observe the surface of the land and the oceans. G.R.

A81-42026 **Imaging ocean waves by synthetic aperture radars with long integration times.** C. L. Rufenach (NOAA, Wave Propagation Laboratory, Boulder, CO) and W. R. Alpers (Hamburg, Universität; Max-Planck-Institut für Meteorologie, Hamburg, West Germany). *IEEE Transactions on Antennas and Propagation,* vol. AP-29, May 1981, p. 422-428. 25 refs. NOAA-supported research; Grant No. NATO-SRG-10.

The effect of long integration time on synthetic aperture radar imagery of moving ocean waves is examined in view of the fact that Seasat images have resulted in a coherent integration time of 2.5 s (one-look processing) when processed to the full resolution of 6.25 m. First, the orbital motion on image formation is investigated, with results based on a Bessel series expansion of the phase term. Image patterns are evaluated numerically for a monochromatic wave traveling in the azimuthal direction. Then, the effect of the coherence time of the ocean wave field on the azimuthal resolution is examined. It is concluded that the scene coherence time for ocean wave imagery is usually several seconds, and therefore, for most radars and sea states, it is not the limiting factor in the imaging process; the orbital acceleration associated with long waves is usually more important for the degradation in the azimuthal resolution. K.S.

A81-42066 # **A comparison of Seasat 1 altimeter measurements of wave height with measurements made by a pitch-roll buoy.** D. J. Webb (Institute of Oceanographic Sciences, Wormley, Surrey, England). *Journal of Geophysical Research,* vol. 86, July 20, 1981, p. 6394-6398. 13 refs.

Measurements of significant wave-height, made by pitch-roll buoy on eight occasions taken during the Joint Air-Sea Interaction Experiment, were compared with the Seasat 1 radar altimeter measurements. Wave heights were estimated from the leading edge of the smoothed pulse, and the significant wave height was found to be between 0.8 and 2.3 m. The mean value for the ratio of the radar altimeter measurements to the buoy measurements was 0.96 + or - 0.04, and the standard deviation of each value was 0.10. The variance was found to be consistent with the spatial variations in the wave field and other known sources of error, on six occasions, whereas, on two occasions, the variance was found to be larger, thus indicating that some other factor may be involved. K.S.

A81-42067 * # **Microwave radiometer measurement of tidally induced salinity changes off the Georgia coast.** B. M. Kendall (NASA, Langley Research Center, Hampton, VA), and J. O. Blanton (Skidaway Institute of Oceanography, Savannah, GA). *Journal of Geophysical Research*, vol. 86, July 20, 1981, p. 6435-6441. 7 refs. NASA-supported research; Contract No. DE-AS09-80EV-1033.

A quasi-synoptic survey of tidally induced salinity changes off the Georgia coast was performed by using a L band microwave radiomater onboard a NASA aircraft. Salinity maps were obtained for ebb and flood conditions in order to define the salinity distributions near rivers and sounds and major changes that occur from ebb flow to flood flow. The Savannah River plume dominated the salinity regime and extended out from the Savannah River mouth about 12 km during ebb tidal conditions. The plume merged into a band of low salinity water extending along the Georgia-South Carolina coast which was produced by the many river sources of freshwater entering the coastal waters. The changes in salinity observed offshore of the river plume area were consistent with estimates of the changes that would occur over a typical tidal excursion perpendicular to the observed gradient. (Author)

A81-42102 # **Satellite scatterometer.** A. Kühnle. *Dornier-Post* (English Edition), no. 2, 1981, p. 9, 10.

Research in the use of microwave instruments to measure ocean wind-vector fields and wave spectra is briefly discussed. The principle of determining wind vectors is examined, and a mathematical model of radar backscattering by capillary waves on the ocean surface is described. The existence of a satellite scatterometer developed in Western Europe is noted. F.G.M.

A81-42131 **Sea ice detection using enhanced infrared satellite data.** G. L. Hufford (NOAA, Satellite Field Services Station, Anchorage, AK). *Mariners Weather Log*, vol. 25, Jan.-Feb. 1981, p. 1-6.

A81-42215 * **Remote sensing of oceanic phytoplankton - Present capabilities and future goals.** W. E. Esaias (NASA, Langley Research Center, Hampton, VA). In: Primary productivity in the sea. New York, Plenum Publishing Corp., 1980, p. 321-337. 29 refs.

A description is given of current work in the development of sensors, and their integration into increasingly powerful systems, for oceanic phytoplankton abundance estimation. Among the problems relevant to such work are phytoplankton ecology, the spatial and temporal domains, available sensor platforms, and sensor combinations. Among the platforms considered are satellites, aircraft, tethered balloons, helicopters, ships, and the Space Shuttle. Sensors discussed include microwave radiometers, laser fluorosensors, microwave scatterometers, multispectral scanners, Coastal Ocean Dynamics Radar (CODAR), and linear array detectors. Consideration is also given to the prospects for such future sensor systems as the National Oceanic Satellite System (NOSS) and the Airborne Integrated Mapping System (AIMS). O.C.

A81-42228 **Application of remote sensing to monitoring and studying dispersion in ocean dumping.** R. W. Johnson and C. W. Ohlhorst (NASA, Langley Research Center, Hampton, VA). In: Ocean dumping of industrial wastes. New York, Plenum Publishing Corp., 1981, p. 175-191. 19 refs.

Remotely sensed wide area synoptic data provides information on ocean dumping that is not readily available by other means. A qualitative approach has been used to map features, such as river plumes. Results of quantitative analyses have been used to develop maps showing quantitative distributions of one or more water quality parameters, such as suspended solids or chlorophyll a. Joint NASA/NOAA experiments have been conducted at designated dump areas in the U.S. coastal zones to determine the applicability of aircraft remote sensing systems to map plumes resulting from ocean dumping of sewage sludge and industrial wastes. A second objective is related to the evaluation of previously developed quantitative analysis techniques for studying dispersion of materials in these plumes. It was found that plumes resulting from dumping of four waste materials have distinctive spectral characteristics. The development of a technology for use in a routine monitoring system, based on remote sensing techniques, is discussed. G.R.

A81-42553 # **Investigation of illumination in the image plane of the receiving optical system for the aerial or spaceborne photography of the world ocean (Issledovanie osveshchennosti v ploskosti izobrazheniia priemnoi opticheskoi sistemy pri aerokosmicheskoi s'emke akvatorii mirovogo okeana).** V. V. Polovinko (Moskovskii Institut Inzhenerov Geodezii, Aerofotos'emki i Kartografii, Moscow, USSR). *Geodeziia i Aerofotos'emka*, vol. 1, 1981, p. 73-82. 10 refs. In Russian.

The illumination in the image plane of the receiving optical system for the aerial or spaceborne photography of the ocean is studied as a function of the optical properties of the cloudless atmosphere, the ocean, and the receiving system. Equations are obtained for the brightness of ocean areas whose emission is detected by the receiving system in the visible and IR ranges. Equations describing the aerial and spaceborne photography are presented. B.J.

A81-42622 * **Wave direction measured by four different systems.** M. G. Mattie (U.S. Army, Coastal Engineering Research Center, Ft. Belvoir, VA), S. V. Hsiao (California Institute of Technology, Jet Propulsion Laboratory, Pasadena, CA), and D. D. Evans (Hughes Aircraft Co., Radar Systems Group, El Segundo, CA). *IEEE Journal of Oceanic Engineering*, vol. OE-6, July 1981, p. 87-93. 13 refs. Contract No. NAS7-100.

A March 1977 wave direction measurement experiment is reported in which four systems were used to provide offshore wave-direction information: (1) synthetic aperture radar (SAR), (2) a coastal imaging radar, (3) an offshore pressure-gage array, and (4) aerial photography. From the coastal radar images and aerial photographs, the direction and length of the principal wavetrains were measured by a manual analysis. The SAR images were processed using fast Fourier transform to give two-dimensional wave spectra. Scatter diagrams are presented which intercompare the measurements of all four systems, and show good agreement among all imaging systems. It is concluded that aerial photography and SAR will prove more useful when wave measurements are needed over a large area or when there are rapidly changing wave characteristics. O.C.

A81-43206 **Iceberg detectability problems using SAR and SLAR systems.** M. E. Kirby and R. T. Lowry (Intera Environmental Consultants, Ltd., Ottawa, Canada). In: Satellite hydrology; Proceedings of the Fifth Annual William T. Pecora Memorial Symposium on Remote Sensing, Sioux Falls, SD, June 10-15, 1979.

Minneapolis, MN, American Water Resources Association, 1981, p. 200-212. 10 refs. Research supported by the Intertech Remote Sensing, Ltd.

The application of synthetic aperture radar (SAR) and real aperture side-looking airborne radar (SLAR) systems for the identification of icebergs involves an understanding of the complicated interactions between the radar beams and the multi-faceted bergs. This paper summarizes the major problems that have been encountered in iceberg census research from selected portions of SLAR and SAR airborne experiments that were recently conducted. Since little radar iceberg data have been gathered from space satellites, the airborne systems offer attractive simulation possibilities. These systems have been used here to address such topics as iceberg detectability in relation to resolution, depression angle, sea clutter, and iceberg size and type. (Author)

A81-43244 **Multispectral kelp resource surveys.** J. R. Jensen (Georgia, University, Athens, GA), J. E. Estes (California, University, Santa Barbara, CA), and M. Mel (Geoscientific and Consulting, Playa Del Rey, CA). In: Satellite hydrology; Proceedings of the Fifth Annual William T. Pecora Memorial Symposium on Remote Sensing, Sioux Falls, SD, June 10-15, 1979.

Minneapolis, MN, American Water Resources Association, 1981, p. 533-542. 23 refs.

A multispectral approach to monitoring kelp resources is reported. Four dates of high-altitude color-infrared aerial photography (1:125,000), four dates of Landsat digital imagery, and two dates of X-band radar imagery were analyzed yielding kelp acreage estimates for beds along the Southern California Bight. These estimates were compared with statistics compiled by a private photogrammetric engineering firm responsible for monitoring Southern California beds. The practicality of monitoring kelp using these remote sensing systems is discussed. (Author)

A81-43245 **Remote sensing of coastal pollutants using multispectral data.** W. Philpot and V. Klemas (Delaware, University, Newark, DE). In: Satellite hydrology; Proceedings of the Fifth Annual William T. Pecora Memorial Symposium on Remote Sensing, Sioux Falls, SD, June 10-15, 1979. Minneapolis, MN, American Water Resources Association, 1981, p. 543-549. 6 refs.

In this paper we describe an attempt to use Landsat multispectral imagery for detection and classification of pollutants in coastal waters. The analysis technique applied to the Landsat data is the eigenvector (principal components) analysis. This proved to be a fairly useful method for detecting iron acid waste off the coast of Delaware and in the New York Bight, and may prove a useful technique for inland waters as well. A qualitative relationship between the apparent water color and the concentration and depth of a pollutant is described. (Author)

A81-43246 * **Aerospace remote sensing of the coastal zone for water quality and biotic productivity applications.** E. B. Pritchard and R. C. Harriss (NASA, Langley Research Center, Marine and Applications Technology Div., Hampton, VA). In: Satellite hydrology; Proceedings of the Fifth Annual William T. Pecora Memorial Symposium on Remote Sensing, Sioux Falls, SD, June 10-15, 1979. Minneapolis, MN, American Water Resources Association, 1981, p. 550-562. 25 refs.

Remote sensing can provide the wide area synoptic coverage of surface waters which is required for studies of such phenomena as river plume mixing, phytoplankton dynamics, and pollutant transport and fate, but which is not obtainable by conventional oceanographic techniques. The application of several remote sensors (aircraftborne and spacecraftborne multispectral scanners, passive microwave radiometers, and active laser systems) to coastal zone research is discussed. Current measurement capabilities (particulates, chlorophyll a, temperature, salinity, ocean dumped materials, other pollutants, and surface winds and roughness) are defined and the results of recent remote sensing experiments conducted in the North Atlantic coastal zone are presented. The future development of remote sensing must rely on an integrated laboratory research program in optical physics. Recent results indicate the potential for separation of particulates into subsets by remote sensors. (Author)

A81-43247 **Digital analysis of Landsat MSS data and application for coastal marine environment.** H. Ochiai (Toba Merchant Marine College, Toba, Japan) and Y. Suzuki (Facom Information Processing Co., Tokyo, Japan). In: Satellite hydrology; Proceedings of the Fifth Annual William T. Pecora Memorial Symposium on Remote Sensing, Sioux Falls, SD, June 10-15, 1979. Minneapolis, MN, American Water Resources Association, 1981, p. 563-569.

This paper presents the techniques of image analysis of remote sensing data obtained by Landsat in the study of marine environment applications in the coastal area of Japan. In the analysis of remote sensing data for a specific object, thematic analysis with feature extraction and classification techniques for pattern recognition has become more popular. In the digital analysis, spectral characteristics of the data can be expressed quantitatively. Many flexible techniques can also be incorporated to find out the most effective method of analysis of remote sensing and field application. In an analysis of the marine environment, the classification per area is more effective than the classification per pixel. For relatively simple methods with a wide variety of application, methods have been developed in which imagery is classified and analyzed concerning the similarity of spectral data. (Author)

A81-43248 **Satellite observations of a geothermal submarine spring off Florida west coast.** F. A. Kohout (U.S. Geological Survey, Woods Hole, MA), R. C. Munson (NOAA, Norfolk, VA), R. M. Turner (U.S. Geological Survey, Reston, VA), and W. R. Royal. In: Satellite hydrology; Proceedings of the Fifth Annual William T. Pecora Memorial Symposium on Remote Sensing, Sioux Falls, SD, June 10-15, 1979. Minneapolis, MN, American Water Resources Association, 1981, p. 570-578. 20 refs.

A81-43250 **Combined satellite imagery for study of coastal circulation, Onslow Bay, North Carolina.** C. W. Welby and L. J. Pietrafesa (North Carolina State University, Raleigh, NC). In: Satellite hydrology; Proceedings of the Fifth Annual William T. Pecora Memorial Symposium on Remote Sensing, Sioux Falls, SD, June 10-15, 1979. Minneapolis, MN, American Water Resources Association, 1981, p. 585-592. 18 refs. Research supported by the North Carolina State University; U.S. Bureau of Land Management Contract No. 025-08; Contract No. EY-71-5-09-0902.

A photo-optical technique using satellite imagery has been devised to study surface and near surface circulation patterns in the shallow shelf waters of Raleigh and Onslow bays, North Carolina. The NOAA-5 VHRR thermal imagery was matched photographically to the scale of the Landsat 70 mm transparencies, and the transparencies were superimposed in a color additive viewer, taking advantage of the scaling and rotational capabilities of the viewer. Various combinations of filters together with positive and negative transparencies were used to enhance the imagery for interpretation. Through photographic enlargement and the projection capabilities of the viewer, imagery has been studied at scales between approximately 1:850,000 and 1:250,000. Combination of the imagery types enables the interpreter to differentiate between cold and warm water masses, to interpret circulation patterns at the instant of imaging, and to identify the patterns of suspended matter distribution and dispersion in the shallow bays. With this information the interpreter can improve his understanding of the relative effects of varying forces on water mass movement. (Author)

A81-43251 * **Satellite detection of oil on the marine surface.** M. J. Wilson, P. E. O'Neill (NASA, Washington, DC), and J. E. Estes (California, University, Santa Barbara, CA). In: Satellite hydrology; Proceedings of the Fifth Annual William T. Pecora Memorial Symposium on Remote Sensing, Sioux Falls, SD, June 10-15, 1979. Minneapolis, MN, American Water Resources Association, 1981, p. 593-602. 14 refs.

The ability of two widely dissimilar spaceborne imaging sensors to detect surface oil accumulations in the marine environment has been evaluated using broadly different techniques. Digital Landsat multispectral scanner (MSS) data consisting of two visible and two near infrared channels has been processed to enhance contrast between areas of known oil coverage and background clean surface water. These enhanced images have then been compared to surface verification data gathered by aerial reconnaissance during the October 15, 1975, Landsat overpass. A similar evaluation of oil slick imaging potential has been made for digitally enhanced Seasat-A synthetic aperture radar (SAR) data from July 18, 1979. Due to the premature failure of this satellite, however, no concurrent surface verification data were collected. As a substitute, oil slick configuration information has been generated for the comparison using meteorological and oceanographic data. The test site utilized in both studies was the extensive area of natural seepage located off Coal Oil Point, adjacent to the University of California, Santa Barbara. (Author)

A81-43539 * **Drift and dispersion studies of ocean-dumped waste using Landsat imagery and current drogues.** V. Klemas and W. D. Philpot (Delaware, University, Newark, DE). *Photogrammetric Engineering and Remote Sensing,* vol. 47, Apr. 1981, p. 533-542. 27 refs. Research supported by Du Pont de Nemours and Co.; Contract No. NAS5-20983.

The drift and dispersion of industrial acid wastes dumped 64 km off the Delaware coast were investigated using 16 Landsat images. Waste plume drift velocities and spread rates were obtained, and principal component analysis was performed to discriminate the acid waste from other pollutants. Waste plumes averaged drifting rates from 0.59 km/hr to 3.39 km/hr into the southwest quadrant, and remained above the thermocline, which formed at depths ranging from 13 m to 24 m. Rapid waste movement toward shore occurred primarily during storms, although plumes were rapidly dispersed and diluted at spread rates in excess of 4 cm/sec. Landsat data analysis also indicates plume width increase of about 1.5 cm/sec during calm sea conditions, which is also in agreement with Falk's (1974) estimates of plume dilution. D.L.G.

A81-43967 # **Features of the radar detection of sea surface nonuniformities (Osobennosti obnaruzheniia neodnorodnostei morskoi poverkhnosti radiolokatsionnym metodom).** A. I. Kalmykov and A. P. Pichugin (Akademiia Nauk Ukrainskoi SSR, Institut Radiofiziki i Elektroniki, Kharkov, Ukrainian SSR). *Akademiia Nauk SSSR, Izvestiia, Fizika Atmosfery i Okeana,* vol. 17, July 1981, p. 754-761. 9 refs. In Russian.

Amplitude (mean and fluctuation) and spectral characteristics of radar scattering by both a uniform sea surface and nonuniformities in the form of slicks are presented. It is shown that scattering from slicks within a broad range of incidence angles can be described in the framework of a selective scattering model (the two-scale model). Using typical examples of obtained results, the possibilities of processing radar signals are discussed, with the aim of detecting slicks and determining their main parameters. J.F.

A81-44861 **Satellite determination of the mesoscale variability of the sea surface temperature.** P. Y. Deschamps, R. Frouin (Lille I, Université, Villeneuve-d'Ascq, Nord, France) and L. Wald (Paris, Ecole Nationale Supérieur des Mines, Valbonne, Alpes-Maritimes, France). *Journal of Physical Oceanography,* vol. 11, June 1981, p. 864-870. 21 refs. Research supported by the Centre National de la Recherche Scientifique, Centre National d'Etudes Spatiales, and Centre National pour l'Exploitation des Océans.

Satellite infrared data have been used to investigate the mesoscale variability of the SST (sea surface temperature) field. A statistical analysis of the SST field has been performed by means of the structure function. Results give the equivalent power-law exponent n of the spatial variance density spectrum. The exponent n was found to vary from 1.5 to 2.3 with a mean value of 1.8 in the range of scales 3-100 km which is in agreement with previous one-dimensional analysis from shipborne and airborne measurements. These observed values of n are discussed and compared with the values predicted by turbulence theories. A.L.W.

A81-45436 **Particular features of the ocean glitter pattern observed from a sun-synchronous orbit.** J. C. Kosik (Centre National d'Etudes Spatiales, Toulouse, France) and G. Paci (ESA, Earth Observation Programme Office, Toulouse, France). *International Journal of Remote Sensing,* vol. 2, July-Sept. 1981, p. 265-275. 6 refs.

An analysis method is developed to locate the point of maximum sea surface glitter for a scanner on a sun-synchronous orbit. A simulation of the ocean glitter effect is conducted, and sun glint avoidance methods are discussed. Results show the spread of the glitter pattern over a large area around the point of specular reflection. Patterns suggest symmetry features which may be used to develop a simplified analysis of the glitter problem. Possible benefits of the simplified computation method include the extension to any type of scanning system, and plotting the latitude and scanning angle of specular reflection for descending and ascending daylight passes respectively. The method is also applied to two specific problems, and the solutions are discussed. D.L.G.

A81-45861 **Remote sensing of atmospheres and oceans; Proceedings of the Interactive Workshop on Interpretation of Remotely Sensed Data, Williamsburg, VA, May 23-25, 1979.** Workshop sponsored by the U.S. Navy and Institute for Atmospheric Optics and Remote Sensing; Contract No. N00014-79-G-0039. Edited by A. Deepak (Institute for Atmospheric Optics and Remote Sensing, Hampton, VA). New York, Academic Press, Inc., 1980. 655 p. $45.

The workshop focused on the current state of knowledge as well as on the results of the latest investigations in the fields of remote sensing of oceanographic, terrestrial, and atmospheric quantities. Topics discussed include: recent advances in inversion methods, atmospheric temperature sounding, interpretation of aerosol sounding, and gaseous constituent retrievals. Other topics are: remote sounding by microwaves, sounding of sea surface temperature, ocean color, and winds, and interpretation of recent results from space.

V.L.

A81-45881 **Application of the truncated normal distribution technique to the derivation of sea surface temperatures.** H. E. Fleming (NOAA, National Environmental Satellite Service, Washington, DC). In: Remote sensing of atmospheres and oceans; Proceedings of the Interactive Workshop on Interpretation of Remotely Sensed Data, Williamsburg, VA, May 23-25, 1979.

New York, Academic Press, Inc., 1980, p. 503-544; Discussion, p. 545. Navy-supported research.

The truncated normal distribution technique is applied to the derivation of sea surface temperatures from high-resolution satellite measurements in the 11-micron window region. The purpose of this technique is to remove cloud contamination from the measurements. This procedure produces sea surface temperature maps on a mesoscale level so that a reasonably small-scaled temperature structure, such as that found in the Gulf Stream, can be determined. Because not all the cloud contamination is removed by the truncated normal distribution technique, the resulting temperature fields are modified by an error detection and correction technique. Results from both simulated and real data are presented. No attempt has been made to account for atmospheric attenuation by water vapor; therefore, the results are accurate in only a relative sense. (Author)

A81-46104 **Spaceborne synthetic aperture radar for oceanography.** Edited by R. C. Beal (Johns Hopkins University, Laurel, MD), P. S. DeLeonibus (NOAA, Washington, DC), and I. Katz (Johns Hopkins University, Laurel, MD). Baltimore, MD, Johns Hopkins University Press (Johns Hopkins Oceanographic Studies, No. 7), 1981. 215 p. $19.50.

Topics discussed include the structure of short gravity waves on the ocean surface, the statistical characteristics of wind generated short gravity waves, and SAR ocean imaging mechanisms. Papers are presented on the variability of winds over the ocean, the problems in ocean wave hindcasting, and surface signs of internal ocean dynamics. C.R.

A81-46105 * **The structure of short gravity waves on the ocean surface.** O. M. Phillips (Johns Hopkins University, Baltimore, MD). In: Spaceborne synthetic aperture radar for oceanography. Baltimore, MD, Johns Hopkins University Press, 1981, p. 24-31. 14 refs. NASA-supported research.

A brief review is given of the salient properties of short gravity waves and the way in which their structure is modified by longer waves or swell, by variable currents, and by internal waves. It is noted that an underlying swell produces a mottled pattern in synthetic aperture radar (SAR) imagery, and an expression is derived giving the fractional modulation in backscattering cross section of the ocean surface in terms of the slope of an underlying swell, the wind direction, and the direction of swell propagation relative to the angle of observation. The expression provides the possibility in appropriate circumstances of estimating the swell slope by remote sensing, in addition to the wavelength and direction of propagation, which can be measured directly from the imagery. An account is also given of the refraction of waves in variable currents and internal waves. C.R.

A81-46107 **SAR ocean imaging mechanisms.** R. O. Harger (Maryland, University, College Park, MD). In: Spaceborne synthetic aperture radar for oceanography. Baltimore, MD, Johns Hopkins University Press, 1981, p. 41-52. 14 refs.

It is noted that in applying synthetic aperture radar (SAR) to oceanography the basic SAR theory must be extended to account for scattering from a time-varying surface that satisfies nonlinear hydrodynamic restraints. A model that assumes a two-scale ocean surface is discussed. Nonlinear electromagnetic and hydrodynamic interactions produce a complex image dependence on the two scales. A spectral expansion of the image is given, and the contributions from the nonlinear interactions and scattering mechanism are identified. Under certain conditions, the image is a linear, space-variant transformation, decomposable into three more easily understood transformations, of an effective reflectivity density at a reference time. C.R.

A81-46109 # **The wind speed dependency of ocean microwave backscatter.** D. B. Ross (NOAA, Sea-Air Interaction Laboratory, Miami, FL). In: Spaceborne synthetic aperture radar for oceanography. Baltimore, MD, Johns Hopkins University Press, 1981, p. 75-86. 21 refs.

Seasat SAR imagery of the ocean is analyzed in terms of the forcing atmosphere and the forcing ocean. In comparison with other types of measurements of surface wind speed, rainfall, wave roughness conditions, and air-sea temperature differences, it is found that the short ocean waves responsible for the radar backscatter are strongly coupled to the local wind and are modulated by rainfall rate and air-sea temperature differences, especially when the sign of the difference is changing rapidly. C.R.

A81-46110 * # **The study of mesoscale ocean winds.** W. L. Jones, E. M. Bracalente (NASA, Langley Research Center, Hampton, VA), and V. E. Delnore (Kentron International, Inc., Hampton, VA). In: Spaceborne synthetic aperture radar for oceanography. Baltimore, MD, Johns Hopkins University Press, 1981, p. 87-94. 11 refs.

SAR data gathered over the U.S. East Coast are used to infer near-surface wind speed, using a simplified model to relate the strength of the 30 to 40 cm SAR backscatter to surface wind speed. It is found that the SAR backscatter is nearly isotropic with a wind speed exponent of 0.4. Using this exponent, the model is tested against an independent data set. Subsequent agreement between wind speeds simultaneously determined by SAR and the Seasat-A Satellite Scatterometer (SASS) is within 0.7 m/s rms. A one-dimensional Fourier transform of the SAR-derived wind field shows an increasing energy content in rough agreement with the Van der Hoven spectrum. C.R.

A81-46112 * **Spatial evolution of ocean wave spectra.** R. C. Beal (Johns Hopkins University, Applied Physics Laboratory, Laurel, MD). In: Spaceborne synthetic aperture radar for oceanography. Baltimore, MD, Johns Hopkins University Press, 1981, p. 110-127. 24 refs. NASA-Navy-supported research; Contract No. NOAA-MO-A01-78-00-4330.

The spatially evolving deep water synthetic aperture radar (SAR) directional spectra of a mixed ocean wave system are compared with a comprehensive set of surface and aircraft measurements. The evolution of the SAR spectra, at least for ocean wavelengths greater than 80 m, is seen as generally consistent with the auxiliary data set in both time and space. From the spatial evolution of the angular component of the spectra, it is possible to project back to an apparent remote storm source that is also consistent with the storm location via GOES satellite imagery. The data provide compelling evidence that the spatial evolution of SAR ocean wave spectra can be a useful tool in global ocean wave monitoring and forecasting. C.R.

A81-46113 * **Refraction of coastal ocean waves.** R. A. Shuchman and E. S. Kasischke (Michigan, Environmental Research Institute, Ann Arbor, MI). In: Spaceborne synthetic aperture radar for oceanography. Baltimore, MD, Johns Hopkins University Press, 1981, p. 128-135. 16 refs. NASA-supported research; Contract No. NOAA-MO-A01-78-00-4339.

Refraction of gravity waves in the coastal area off Cape Hatteras, NC as documented by synthetic aperture radar (SAR) imagery from Seasat orbit 974 (collected on September 3, 1978) is discussed. An analysis of optical Fourier transforms (OFTs) from more than 70 geographical positions yields estimates of wavelength and wave direction for each position. In addition, independent estimates of the same two quantities are calculated using two simple theoretical wave-refraction models. The OFT results are then compared with the theoretical results. A statistical analysis shows a significant degree of linear correlation between the data sets. This is considered to indicate that the Seasat SAR produces imagery whose clarity is sufficient to show the refraction of gravity waves in shallow water. C.R.

A81-46115 # **Detection of the Gulf Stream.** R. M. Hayes (U.S. Coast Guard, Washington, DC). In: Spaceborne synthetic aperture radar for oceanography. Baltimore, MD, Johns Hopkins University Press, 1981, p. 146-160. 44 refs.

Aircraft and satellite thermal infrared and visual indicators are used to locate Gulf Stream boundaries, which are compared with those apparent in Seasat synthetic aperture (SAR) imagery. Emphasis in the analysis is on orbits 400 and 931, which capture the semipermanent Gulf Stream meander that develops when the current passes over the Charleston Rise. Results demonstrate that identifiable linear features in the SAR imagery are correlated with the current velocity shear zone. Gulf Stream detection is seen as related to modulation of the small gravity wave field at the boundary of the swift current yielding long, distinct, linear features in the radar imagery. It is noted that tonal and/or textural contrast of the water within and outside the Gulf Stream arising from a sea surface temperature-induced difference in the effect of wind stress on surface roughness may also contribute to Gulf Stream detection. Backscatter measurements made along transects across the Gulf Stream are given in order to characterize the signature of a SAR-to-scene transfer function that reveals the nature of the Gulf Stream radar cross section at the boundaries. C.R.

A81-46116 * # **A search for cold water rings.** R. E. Cheney (NASA, Goddard Space Flight Center, Greenbelt, MD). In: Spaceborne synthetic aperture radar for oceanography. Baltimore, MD, Johns Hopkins University Press, 1981, p. 161-170. 23 refs.

SAR imagery obtained by Seasat in the Sargasso Sea during 1978 is examined for cold ring signatures. One orbit on August 26 is thought to have imaged the edge of a cold ring, although the ring's position was not well known at the time. During another orbit on September 23, drifting buoy and expendable bathythermography data furnished conclusive evidence that the ring was centered directly in the SAR swath. Although some suggestive patterns are visible in the images, it is not clear that cold rings can be identified by SAR, even though dynamically similar features, such as the Gulf Stream and warm rings, can be accurately detected. The suggestion is made that cold rings may be imaged inadequately because of their lack of surface temperature gradient. C.R.

A81-46117 # **Tracking of a warm water ring.** D. E. Lichy, M. G. Mattie, and L. J. Mancini (U.S. Army, Coastal Engineering Research Center, Fort Belvoir, VA). In: Spaceborne synthetic aperture radar for oceanography. Baltimore, MD, Johns Hopkins University Press, 1981, p. 171-182. 7 refs.

The imaging of a warm water ring off the East Coast of the U.S. by the Seasat synthetic aperture radar (SAR) on descending orbit six times during September and October of 1978 is discussed. The location and microwave response of SAR imagery for the rings are compared with NOAA-5 thermal infrared imagery and frontal analysis maps from the U.S. Naval Oceanographic Office. Centers of the rings are found to coincide within about 10 km. The diameters of the warm water rings delineated on the SAR imagery turn out to be smaller than on NOAA-5 imagery. The distinguishing features of the warm water ring area on the SAR imagery are concentric curvilinear features less than 1 km wide and as long as 150 km. The ability of the SAR to track warm water rings and the type of microwave return are discussed. C.R.

A81-46919 # **Nimbus-7 Coastal-Zone Colour Scanner data processing for Earthnet - Experience to date.** L. Fusco (ESA, Earthnet Programme Office, Frascati, Italy). *ESA Bulletin,* no. 27, Aug. 1981, p. 36-42.

A status report is given for the Earthnet program office's acquisition, preprocessing, archiving and distribution to users of Coastal Zone Color Scanner (CZCS) data from the Nimbus-7 satellite. These data are being used to demonstrate the usefulness of satellite coastal waters monitoring in such major issues as: (1) the optimum qualification and quantification of suspended materials and (2) definition of the requirements for future ocean monitoring equipment. In addition to detailed tabulations of Nimbus-7 and CZCS performance parameters, a list is given of the individual research objectives of the European countries participating in the data sharing program and examples are given of raw data products, system-corrected products, geophysical data products, and the Nimbus-7 CZCS data catalogue. O.C.

A81-47004 # **Correlation between integral and spectral albedos of clouds over water surfaces (Sootnoshenie integral'nogo i spektral'nogo al'bedo oblakov nad vodnoi poverkhnost'iu).** V. I. Binenko. In: Radiation studies in the atmosphere. Leningrad, Gidrometeoizdat, 1980, p. 29-32. 5 refs. In Russian.

An analysis is presented of airborne measurements conducted during 1971-1972 in the framework of the KENEX cloud program;

cumulus cloud cover over the Black Sea, the Sea of Azov, the Karskii Sea, and Ladozhskii Lake was investigated. The results were used to determine correlations between integral (0.3-3.0 microns) and spectral (0.6-0.92, 0.76, 0.69-0.74, 0.4-0.65, 0.676, 0.457, 0.391, and 0.369 micron) cloud albedos over water surfaces. F.G.M.

A81-47021 # **Application of GOES visible-infrared data to quantifying mesoscale ocean surface temperatures.** G. A. Maul (NOAA, Atlantic Oceanographic and Meteorological Laboratories, Miami, FL). *Journal of Geophysical Research,* vol. 86, Sept. 20, 1981, p. 8007-8021. 29 refs. Research supported by the U.S. Department of Energy.

The investigation is concerned with the possibility to use data from the Geostationary Operational Environmental Satellite (GOES) for the solution of sea surface temperature problems, taking into account the Gulf of Mexico as the test area because it is ringed with upper air stations from which atmospheric corrections can be calculated. A theoretical error analysis, with which to explain the + or - 1 to + or - 4 K errors being reported, is conducted. On the basis of the error analysis, an objective procedure is developed to quantify the satellite-derived temperatures from GOES at an acceptable level of accuracy. The procedure is applied to the Gulf of Mexico for October 1977. In the considered case, data from two research ships are available to serve as surface verification information. The described procedure, which is labor intensive, is not considered as an alternative to the GOSSTCOMP. The goal is rather to determine with it the temperature patterns well enough so that they may be used to study the physics of certain dynamical oceanographic processes. G.R.

A81-47022 **Satellite-tracked drift buoy observations of the near-surface flow in the eastern mid-latitude North Pacific.** G. J. McNally (California, University, La Jolla, CA). *Journal of Geophysical Research,* vol. 86, Sept. 20, 1981, p. 8022-8030. 20 refs. Contract No. N00014-75-C-0152.

The considered observations show that the large-scale coherent flow is essentially always along the isobars of sea level pressure, 20 - 30 deg to the right of the surface winds, at approximately 1.5% of the wind speed during the periods of strong persistent atmospheric forcing normally observed in the fall, winter, and spring seasons. Mesoscale energetics with time and length scales of 30 days and 100 km are clearly seen in near surface flow in the summer months. The large-scale, coherent flow observed during the fall through spring seasons is essentially unaltered over the upper 30 m of the mixed layer. Vertical shear in the large-scale flow is clearly observed when the drifters are drogued to depths of 100 m or more. This suggests that the droguing technique used is effective and therefore the lack of difference in the current observations of undrogued drifters and those drogued at 30 m is due to a lack of vertical shear in the horizontal currents over the upper 30 m during periods of strong persistent atmospheric forcing. G.R.

A81-47099 **Remote sounding of atmosphere and ocean for climate research /Appleton Lecture/.** J. T. Houghton (Science Research Council, Rutherford and Appleton Laboratories, Chilton, Oxon, England). *IEE Proceedings, Part A - Physical Science, Measurement and Instrumentation, Management and Education, Reviews,* vol. 128, pt. A, no. 6, Sept. 1981, p. 442-448. 23 refs.

A description is presented of different types of satellite-borne remote sounding techniques of importance for the World Climate Research Program (WCRP). The WCRP is concerned with the attainment of a better understanding of climate and climatic change, particularly on time scales in the range from weeks to decades. The Global Atmospheric Research Program culminated in 1979 in the Global Weather Experiment, during which the atmosphere was observed as completely as possible for the period of a year. The purpose of the Global Weather Experiment was to investigate to what extent the atmosphere's large-scale circulation can be modelled and predicted by large numerical models. A particularly important remote sounding measurement from satellites is that of the temperature structure of the atmosphere below the satellite. In the case of remote temperature sounding, it is necessary to improve operational algorithms and procedures which make more complete use of the data. Improved sampling is needed for radiation-budget measurements. G.R.

A81-47344 **The first ESA remote sensing satellite /ERS/ - The programme and the system.** D. Lennertz and C. Honvault (ESA, Earth Observation Programme Dept., Toulouse, France). *International Astronautical Federation, International Astronautical Congress, 32nd, Rome, Italy, Sept. 6-12, 1981, Paper 81-90.* 14 p.

The European Space Agency is currently developing the first ESA Remote Sensing Satellite (ERS) system which will, as its first mission, monitor the ice and ocean regions. The objectives of the mission are both to increase scientific understanding of coastal zones and ocean processes and to develop economic applications related to a better knowledge of ocean parameters and sea state conditions. The payload of ERS-1 includes: (1) active microwave instrumentation, combining the functions of a synthetic aperture radar, a wave scatterometer, and a wind scatterometer, in order to measure wind fields and wind spectra; (2) a radar altimeter, for measuring significant wave heights; and (3) an ocean color monitor for measuring sea surface temperature and ocean color. The ERS-1 payload will be launched by ARIANE-2 in 1987 on a sun-synchronous orbit at 675 km. It will provide worldwide coverage, compatible with the duty cycles of its payload instruments and ensure real time acquisition through its own station network. The resulting data products will be listed by level, ranging from raw data to quick-look data to preprocessed products. Various ground segments associated with the satellite are presented. J.F.

A81-47348 **Radar altimeter for ocean remote sensing.** S. Pardini, R. Ronconi, R. Somma (Selenia S.p.A., Rome, Italy), and G. Picardi (Roma, Università, Rome, Italy). *International Astronautical Federation, International Astronautical Congress, 32nd, Rome, Italy, Sept. 6-12, 1981, Paper 81-94.* 10 p. European Space Agency Contract No. 4428/80.

Ocean radar altimetry is based on the electromagnetic backscattering of the ocean surface in response to a narrow pulse waveform under near normal incidence. The altimeter described is used to determine the satellite altitude over the sea surface, the significant wave height, and wind speeds. The instrument requires accuracy, implying high precision in radar measurements of the pertinent return echo parameters. Problem areas such as pull-in phase initialization and tracking phase are discussed and the adopted solution includes using two separated loops. The RF/IF unit and the signal processor are also discussed. A radar altimeter functional block diagram is given, as are error signals of range and slope discriminators and the deterministic simulation of loops operation. Finally the main parameters include a peak power of 400 W, a frequency of 13.5 GHz and an antenna gain of 40 dB. J.F.

A81-48548 * **The National Oceanic Satellite System.** W. J. Hussey (NOAA, National Earth Satellite Service, Suitland, MD). In: EASCON '80; Electronics and Aerospace Systems Conference, Arlington, VA, September 29-October 1, 1980, Conference Record. New York, Institute of Electrical and Electronics Engineers, 1980, p. 295-305.

It is noted that satellites equipped with microwave sensors will make possible the collection of oceanic data on a global basis under all weather conditions. The National Oceanic Satellite System (NOSS), which will provide a five-year operational demonstration of satellite sensing of oceanic phenomena, is described. The system will measure parameters characterizing the wind, sea surface temperature, waves, ice, water mass definition, and horizontal surface currents. The benefits expected from NOSS are listed. They include improvements in sea ice boundary analyses, which will assist fishing operations near the ice edge, and improvements in the ability to forecast severe storms. Each of NOSS's primary sensors - the Scatterometer, Altimeter, Coastal Zone Color Scanner, and Large Antenna Multichannel Microwave Radiometer - is described, and a table giving sensor characteristics is included. C.R.

A81-48681 # **Infrared imagery for studying the Kara-Bogaz-Gol Bay (Teplovaia s'emka pri izuchenii zaliva Kara-Bogaz-Gol).** V. I. Gornyi (Vsesoiuznoe Aerogeologicheskoe Nauchno-Proizvodstvennoe Ob'edinenie Aerogeologiia, Leningrad, USSR). *Issledovanie Zemli iz Kosmosa,* July-Aug. 1981, p. 11-17. 8 refs. In Russian.

Results of theoretical and experimental studies of the thermal field of the surface of the salt stratum of the Kara-Bogaz-Gol Bay and several dry salt lakes of West Turkmenia are presented. The dependence of diurnal fluctuations of the surface temperature of the moist salt stratum on the air humidity is shown. To substantiate the possibility of using infrared satellite imagery for studying the salt stratum of the Bay, aerial infrared images of the salt cover are presented, illustrating the good imaging properties of the surface's thermal field relative to the composition, structure, and moisture of the salt. It is concluded that infrared satellite imagery can be used to study the hydrological and hydrochemical conditions of the Bay. J.F.

A81-48687 # **An analysis of the data of synchronous measurements from the Meteor satellite and ships at the eastern coast of the Caspian Sea (Analiz dannykh sinkhronnykh izmerenii s ISZ 'Meteor' i sudov u Vostochnogo poberezh'ia Kaspiiskogo Moria).** G. P. Vaniushin, V. N. Diadiunov, and S. M. Sazhin (Vsesoiuznyi Nauchno-Issledovatel'skii Institut Morskogo Rybnogo Khoziaistva i Okeanografii; Gosudarstvennyi Nauchno-Issledovatel'skii Tsentr Izucheniia Prirodnykh Resursov, Moscow, USSR). *Issledovanie Zemli iz Kosmosa,* July-Aug. 1981, p. 54-60. 16 refs. In Russian.

Data were obtained from synchronous measurements by the Meteor satellite and ships at the eastern coast of the Caspian Sea on Sept. 22, 1978. Results of the investigation, which involved 26 hydrological stations, were used to show the relationship between the brightness of the water medium, the concentration of chlorophyll, the suspension of inorganic matter, and the values of relative transparency. J.F.

A81-49126 **Satellites for oceanography - The promises and the realities.** R. Goody (Harvard University, Cambridge, MA). *Oceanus,* vol. 24, Fall 1981, p. 3-5.

The problems encountered in assimilating satellite data into oceanographic research are discussed. The possibilities offered by satellites are illustrated by describing the Coastal Zone Color Scanner, the infrared sounder, the active radar scatterometer, and the synthetic aperture radar. It is stressed that remote sensing techniques from satellites are here to stay, and the oceanographic community is urged to embrace them. It is pointed out that if oceanographic science is to profit to a maximum, planning must start for combinations of measurements from satellites, aircraft, buoys, ships, and islands. C.R.

A81-49127 * **Oceanography from satellites.** W. S. Wilson (NASA, Oceanic Processes Branch, Washington, DC). *Oceanus,* vol. 24, Fall 1981, p. 9-16. 14 refs.

It is pointed out that oceanographers have benefited from the space program mainly through the increased efficiency it has brought to ship operations. For example, the Transit navigation system has enabled oceanographers to compile detailed maps of sea-floor properties and to more accurately locate moored subsurface instrumentation. General descriptions are given of instruments used in satellite observations (altimeter, color scanner, infrared radiometer, microwave radiometer, scatterometer, synthetic aperture radar). It is pointed out that because of the large volume of data that satellite instruments generate, the development of algorithms for converting the data into a form expressed in geophysical units has become especially important. C.R.

A81-49128 **The promise of satellite altimetry.** C. Wunsch (MIT, Cambridge, MA). *Oceanus,* vol. 24, Fall 1981, p. 17-26. 5 refs.

The contributions that an altimetric satellite could make to oceanography are discussed. It is noted that such a satellite would provide a global view of the surface elevation of the ocean every few days. Since the surface elevation can be related to the velocity at depth fairly easily, a new altimetric mission could give a fast, quantitative measure of the state of the ocean. But its real value is that by combining altimetric measurements with the equations of motion, the altimeter could be used to provide accurate data for numerical models of the global circulation, both to analyze the state of the sea and, potentially, to forecast it. A description is given of the Ocean Topography Experiment (Topex). C.R.

A81-49129 **The future for satellite-derived surface winds.** J. J. O'Brien (Florida State University, Tallahassee, FL). *Oceanus,* vol. 24, Fall 1981, p. 27-31.

It is noted that cautious agreement exists that the scatterometer is capable of measuring wind speed in many weather situations to within 2 meters per second (approximately 5 miles per hour). It is also able to measure wind direction. If the orbit of a satellite carrying a scatterometer were adjusted to altitudes of about 2,400 km, the satellite could cover the entire globe in a few days. For the first time, it would be possible to have a global distribution of wind estimates every week or so. What is more, with a satellite wind-observing system, the Ekman drift current could be calculated on a regular basis. These estimates could be used for search and rescue operations, as well as for pollution transport problems. C.R.

A81-49130 * # **Remote sensing in biological oceanography.** W. E. Esaias (NASA, Langley Research Center, Hampton, VA). *Oceanus,* vol. 24, Fall 1981, p. 32-38.

The main attribute of remote sensing is seen as its ability to measure distributions over large areas on a synoptic basis and to repeat this coverage at required time periods. The way in which the Coastal Zone Color Scanner, by showing the distribution of chlorophyll a, can locate areas productive in both phytoplankton and fishes is described. Lidar techniques are discussed, and it is pointed out that lidar will increase the depth range for observations. C.R.

A81-49132 **Climate, the oceans, and remote sensing.** F. P. Bretherton (National Center for Atmospheric Research, Boulder, CO). *Oceanus,* vol. 24, Fall 1981, p. 49-55.

It is noted that an understanding of the workings of the climate system and an ability to predict year-to-year variations and long-term changes resulting from man's activities will require extensive observations of the ocean. The surface temperature and flux of heat through the surface are identified as key variables for the atmospheric circulation. The wind stress on the surface and the net of evaporation less rainfall are also seen as important factors in oceanic circulation. The long-term redistribution of heat by the ocean currents and year-to-year fluctuations in heat storage are identified as central climatic variables. It is thought that satellite observations, because of their global perspective, may play a key role in many of these areas. C.R.

A81-49133 * **Commercial applications of satellite oceanography.** D. R. Montgomery (California Institute of Technology, Jet Propulsion Laboratory, Pasadena, CA). *Oceanus,* vol. 24, Fall 1981, p. 56-65. 11 refs. Contract No. NAS7-100.

It is shown that in the next decade the oceans' commercial users will require an operational oceanographic satellite system or systems capable of maximizing real-time coverage over all ocean areas. Seasat studies suggest that three spacecraft are required to achieve this. Here, the sensor suite would measure surface winds, wave heights (and spectral energy distribution), ice characteristics, sea-surface temperature, ocean colorimetry, height of the geoid, salinity, and subsurface thermal structure. The importance of oceanographic data being distributed to commercial users within two hours of observation time is stressed. Also emphasized is the importance of creating a responsive oceanographic satellite data archive. An estimate of the potential dollar benefits of such an operational oceanographic satellite system is given. C.R.

A81-49378 **Compact and highly sensitive fluorescence lidar for oceanographic measurements.** U. Gehlhaar, K. P. Gunther, and J. Luther (Oldenburg, Universität, Oldenburg, West Germany). *Applied Optics,* vol. 20, Oct. 1, 1981, p. 3318-3320. 12 refs. Research supported by the Deutsche Forschungsgemeinschaft.

A compact and highly sensitive helicopter-borne fluorescence lidar is described. The single channel system is based on a high power, tunable laser. From an altitude of 70 m, selective detection of the tracer dye rhodamine B of less than 10 to the -10th g/cu cm in natural waters is achieved. (Author)

A81-49426 # **Theoretical investigations concerning the measurement of the plankton concentration with the aid of satellites (Theoretische Untersuchungen zur Messung der Plaktonkonzentration mit Hilfe von Satelliten).** G. Metzig (Köln, Universitat, Cologne, West Germany) and M. Kerschgens (Bonn, Universitat, Bonn, West Germany). *(Deutsche Meteorologen-Tagung und Internationales Alfred-Wegener-Symposium, Berlin, West Germany, Feb. 25-29, 1980.) Annalen der Meteorologie,* no. 15, 1980, p. 154, 155. 5 refs. In German.

A description is presented of a theoretical model which provides information regarding the possibilities to determine plankton concentrations in the ocean by remote sensing. The model makes use of the theory of radiation transport. Radiative flux in the ocean and radiation densities in the atmosphere are computed for fifteen spectral intervals in the range from 0.3 to 0.76 micrometers. The mathematical procedure consists of a combination of an iterative solution scheme and a modified two-stream method. The preliminary objective of the considered study is related to a calculation of the change in the surface albedo of the sea by plankton, and the possibilities which exist for measuring this change with an instrument located at the upper boundary of the atmosphere. G.R.

A81-49649 # **Atlantic hurricane season of 1980.** M. B. Lawrence and J. M. Pelissier (NOAA, National Hurricane Center, Miami, FL). *Monthly Weather Review,* vol. 109, July 1981, p. 1567-1582.

A summary of the 1980 hurricane season is presented. Eleven named tropical cyclones were tracked, of which nine reached hurricane force. Allen, an intense storm, affected a number of Caribbean countries before making landfall on the Texas coast. (Author)

A81-49656 # **The occurrence of vertical tilt in tropical cyclones.** J. E. Huntley and J. W. Diercks (U.S. Navy, Naval Oceanography Command Center - Joint Typhoon Warning Center, GU). *Monthly Weather Review,* vol. 109, Aug. 1981, p. 1689-1700. 8 refs.

Satellite imagery and aircraft reconnaissance data are presented to show that the tropical cyclones of the western North Pacific often possess significant horizontal displacements between their surface and 700 mb circulation centers during the development stage. Because of the frequency of aircraft reconnaissance during their existence and the range of peak intensities recorded, Super Typhoon Tip, Typhoon Abby and Tropical Depression 01 were selected to illustrate this phenomenon. This observational evidence raises questions as to whether: (1) the displacement between surface and upper level centers are related to the fields of convergence which are necessary to organize and intensify a tropical cyclone, or merely a reaction to upper level shearing flow; and (2) a numerical model initialized with a weak, sloping vortex would spin up to typhoon strength. O.C.

A81-49657 # **Eastern North Pacific tropical cyclones of 1980.** E. B. Gunther (NOAA, Eastern Pacific Hurricane Center, Redwood City, CA). *Monthly Weather Review,* vol. 109, Aug. 1981, p. 1701-1712.

A81-49754 # **Operational use of satellite imagery in the Canadian ice program.** T. F. Mullane (Ice Forecasting Central, Ottawa, Canada). In: Canadian Symposium on Remote Sensing, 6th, Halifax, Canada, May 21-23, 1980, Proceedings.
Ottawa, Canadian Aeronautics and Space Institute, 1981, p. 17-32. 7 refs.

The need to provide timely and accurate ice information in support of marine transportation and offshore exploration has increased steadily in recent years. The near real-time reception of NOAA and Landsat imagery provides comprehensive and detailed information on ice conditions. This paper reviews the development and operational use of satellite imagery at Ice Forecasting Central. Imagery acquisition, enhancement, and analysis are considered. The capabilities and limitations of the imagery for the definition of ice features are examined, and developments in automated interpretation processes are presented. B.J.

A81-49758 # **The use of satellite imagery as an aid to the Canadian Coast Guard ice operations.** B. Dawe (Remotec Applications, Inc., St. John's, Newfoundland, Canada), A. Collins (Canada Centre for Remote Sensing, Ottawa, Canada), L. Humphries, and G. Warren (Canadian Coast Guard, St. John's, Newfoundland, Canada). In: Canadian Symposium on Remote Sensing, 6th, Halifax, Canada, May 21-23, 1980, Proceedings. Ottawa, Canadian Aeronautics and Space Institute, 1981, p. 53-61. 5 refs.

A81-49771 # **Airborne impulse radar sounding of sea ice.** J. R. Rossiter, K. A. Butt, J. B. Gamberg, and T. F. Ridings (Newfoundland, Memorial University, St. John's, Canada). In: Canadian Symposium on Remote Sensing, 6th, Halifax, Canada, May 21-23, 1980, Proceedings. Ottawa, Canadian Aeronautics and Space Institute, 1981, p. 187-194. 14 refs. Research supported by the Canadian Marine Drilling, Ltd., Esso Resources Canada, Ltd., and National Research Council of Canada; Department of Supply and Services Contract No. 1SU-78-00347.

Airborne impulse radar, operated from a helicopter and a Twin-Otter, was used in March-April 1979 to estimate the physical properties of sea ice in the Beaufort Sea and Lake Melville, Labrador. Concurrent measurements included: thickness, salinity, temperature, crystal fabric, electrical properties of the ice, simultaneous aerial photography, and synthetic aperture radar imagery. Impulse radar center-frequencies of 80, 100, and 200 MHz appear to give the best trade-off of penetration vs resolution and antenna size. Data collected below 30 m elevation have reduced side-scatter from the ice surface. Speeds below 50 m/s are required with the current hardware to achieve coherence from scan-to-scan. Thickness estimates are excellent for fresh and brackish ice, and are good for underformed first-year sea ice about 1-2 m thick. Areas of fresh water melt pools that have only experienced surface refreezing show thickness profiles that warrant further examination. Bottom returns from multilayer ice are sporadic, although floes up to 14 m have been sounded. Ridges are not usually penetrated, but can be easily detected. (Author)

A81-49772 # **The Lake Melville/Labrador offshore synthetic aperture radar study - Winter 1979.** R. D. Worsfold, S. K. Parashar, and D. C. Strong (Remotec Applications, Inc., St. John's, Newfoundland, Canada). In: Canadian Symposium on Remote Sensing, 6th, Halifax, Canada, May 21-23, 1980, Proceedings.
Ottawa, Canadian Aeronautics and Space Institute, 1981, p. 195-202. 11 refs. Research supported by the Newfoundland Department of Regional and Economic Expansion.

A81-49774 # **Single and multiple parameter microwave signatures of sea ice.** R. E. Hawkins, C. E. Livingstone, A. L. Gray (Canada Centre for Remote Sensing, Ottawa, Canada), K. Okamoto (Ministry of Posts and Telecommunications, Radio Research Laboratories, Tokyo, Japan), L. D. Arsenault (Cold Regions Remote Sensing, Stittsville, Ontario, Canada), D. Pearson (Intera Environmental Consultants, Ltd., Ottawa, Canada), and T. L. Wilkinson (Waterloo, University, Waterloo, Ontario, Canada). In: Canadian Symposium on Remote Sensing, 6th, Halifax, Canada, May 21-23, 1980, Proceedings. Ottawa, Canadian Aeronautics and Space Institute, 1981, p. 217-229. 19 refs.

Simultaneous 13.3 GHz dual-polarized fanbeam scatterometer data, 19.35 GHz horizontally polarized profiling radiometer data and nadir-looking aerial photography with corresponding X- and L-band SAR (Synthetic Aperture Radar) imagery were collected with the CCRS Convair-580 in March 1979 in the Beaufort Sea and in the eastern Arctic in April 1979. This data set was analyzed to compile statistics on 11 WMO (World Meteorological Organization) classes of sea ice, ranging from calm open water to multiyear ice and ice island. (Author)

A81-49775 # **Radar detection of sea-ice ridges and icebergs in frozen oceans at incidence angles from 0 deg to 90 deg.** D. Pearson (Intera Environmental Consultants, Ltd., Ottawa, Canada), C. E. Livingstone, R. K. Hawkins, A. L. Gray (Canada Centre for Remote Sensing, Ottawa, Canada), L. D. Arsenault (Cold Regions for Remote Sensing, Stittsville, Ontario, Canada), T. L. Wilkinson (Waterloo, University, Waterloo, Ontario, Canada), and K. Okamoto (Ministry of Posts and Telecommunications, Radio Research Laboratories, Tokyo, Japan). In: Canadian Symposium on Remote Sensing, 6th, Halifax, Canada, May 21-23, 1980, Proceedings.
Ottawa, Canadian Aeronautics and Space Institute, 1981, p. 231-241. 5 refs.

Dual-polarized 13.3 GHz scatterometer data and X-band SAR data, collected in the Beaufort Sea and in the eastern Arctic, during the SURSAT sea-ice experiment deployments in March 1979 and April 1979 respectively, have been analyzed to determine the radar contrasts (signal to sea-ice clutter) between sea-ice ridges and the surrounding sea ice in the Beaufort Sea and between icebergs and the surrounding sea ice in the eastern Arctic. The effects of radar resolution cell size on ridge detectability were examined using aerial photography to estimate ridge dimensions. Over the incidence angle range observed, the contrast between ridges and the surrounding sea-ice is nearly independent of incidence angle for all ice types. Cross-polarized radars produce larger ridge contrasts than like-polarized radars, with the largest contrasts and greatest polarization dependence being observed for rough first-year ridges in smooth first-year ice and the smallest contrasts and least polarization dependence being observed for multiyear ridges in multiyear ice. The contrast between icebergs and the first-year ice background is nearly independent of incidence angle over the observed range. Cross-polarized radars enhance iceberg detectability but synthetic aperture radars operated at satellite incidence angles are found to be unsuitable for iceberg detection. (Author)

A81-49776 # **SAR processing of partially coherent and sinusoidally dynamic ocean waves.** R. K. Raney (Canada Centre for Remote Sensing, Ottawa, Canada). In: Canadian Symposium on Remote Sensing, 6th, Halifax, Canada, May 21-23, 1980, Proceedings. Ottawa, Canadian Aeronautics and Space Institute, 1981, p. 243-247. 6 refs.

The surface of the ocean as observed by a Synthetic Aperture Radar (SAR) evidences both random and deterministic dynamics that have a major impact on the resulting image. This paper explores selected image properties when both effects are present. It is shown that the average response of the SAR is not sensitive to misfocus, whether caused by processor maladjustment or scene dynamics. On the other hand, impulse response and frequency response are critically affected by focus, with a sensitivity that is proportional to the space-bandwidth product of the SAR. Thus, accelerations in a wave scene cannot give rise to wave-like contrasts already present. Orbital motions of surface reflecting wavelets may cause a Doppler shifted image position to occur, which will lead to wave-like contrasts in the image if focus and coherence are maintained. This paper points out that the shift is constant with range for azimuthal waves. In contrast, range dependence occurs in most azimuthal SAR wave imagery. These facts suggest that orbitally derived Doppler shift cannot be the dominant imaging mechanism for oceanic waves. (Author)

A81-49777 # **Digital image analysis of SAR imagery for the detection of icebergs.** W. E. Kirby (Intera Environmental Consultants, Ltd., Ottawa, Canada). In: Canadian Symposium on Remote Sensing, 6th, Halifax, Canada, May 21-23, 1980, Proceedings. Ottawa, Canadian Aeronautics and Space Institute, 1981, p. 249-262. 7 refs.

In the spring of 1979, four-channel SAR data sets over iceberg-infested waters were obtained as part of the Sursat program. Portions of this imagery were digitized and analyzed to evaluate the utility of present image processing methods in isolating icebergs and for incorporation into future iceberg prediction models. It is found that: (1) level slicing of the raw data was not suitable for isolating icebergs from the background pack ice, especially in the XHH band; (2) median filtering significantly reduced radar speckle and improved the identification of the icebergs; (3) supervised classification methods resulted in significant data gaps, and were found to be time-consuming; (4) the two-dimensional parallelepiped plots are valuable in assessing the results of the classification procedures; and (5) none of the techniques used could isolate the icebergs from the background pack ice, since the methods function in feature space where the distributions of the spectral intensities determine the classifications. O.C.

A81-49779 # **Optimizing imaging radar parameters for ice reconnaissance.** R. T. Lowry (Intera Environmental Consultants, Ltd., Ottawa, Canada) and H. G. Hengeveld (Department of the Environment, Atmospheric Environment Service, Downsview, Ontario, Canada). In: Canadian Symposium on Remote Sensing, 6th, Halifax, Canada, May 21-23, 1980, Proceedings. Ottawa, Canadian Aeronautics and Space Institute, 1981, p. 273-283. 6 refs.

A81-49805 # **Airborne remote sensing of sea surface chlorophyll and temperature along the outer British Columbia coast.** G. A. Borstad, R. M. Brown (Search Oceanography, Ltd., Sidney, British Columbia, Canada), and J. F. R. Gower (Institute of Ocean Sciences, Sidney, British Columbia, Canada). In: Canadian Symposium on Remote Sensing, 6th, Halifax, Canada, May 21-23, 1980, Proceedings. Ottawa, Canadian Aeronautics and Space Institute, 1981, p. 541-549. 12 refs. Department of Supply and Services Contract No. 1SB-79-00097.

A81-49807 # **Meteosat experience in assisting commercial fishing (Météosat et l'experience d'aide à la pêche).** J.-C. Favard (Centre National d'Etudes Spatiales, Toulouse, France), J.-M. Stretta, and J. Citeaux (Office de la Recherche Scientifique et Technique d'Outre-Mer, Bondy, Seine-Saint-Denis, France). In: Canadian Symposium on Remote Sensing, 6th, Halifax, Canada, May 21-23, 1980, Proceedings. Ottawa, Canadian Aeronautics and Space Institute, 1981, p. 561-565. 5 refs. In French.

A81-49967 * **Regression techniques for oceanographic parameter retrieval using space-borne microwave radiometry.** R. Hofer (Ciba-Geigy AG, Basel, Switzerland) and E. G. Njoku (California Institute of Technology, Jet Propulsion Laboratory, Pasadena, CA). *IEEE Transactions on Geoscience and Remote Sensing,* vol. GE-19, Oct. 1981, p. 178-189. 18 refs. Research supported by the U.S. National Academy of Sciences; Contract No. NAS7-100.

Variations of conventional multiple regression techniques are applied to the problem of remote sensing of oceanographic parameters from space. The techniques are specifically adapted to the scanning multichannel microwave radiometer (SMRR) launched on the Seasat and Nimbus 7 satellites to determine ocean surface temperature, wind speed, and atmospheric water content. The retrievals are studied primarily from a theoretical viewpoint, to illustrate the retrieval error structure, the relative importances of different radiometer channels, and the tradeoffs between spatial resolution and retrieval accuracy. Comparisons between regressions using simulated and actual SMMR data are discussed; they show similar behavior. (Author)

N81-28668# World Meteorological Organization, Geneva (Switzerland). Commission for Marine Meteorology.
REPORTS ON MARINE SCIENCE AFFAIRS. REPORT 14: SATELLITE DATA REQUIREMENTS FOR MARINE METEOROLOGICAL SERVICES
G. D. Hamilton 1980 53 p refs
(WMO-548; ISBN-92-63-10548-0; Rept-14) Avail: NTIS MF A01; print copy available from WMO, Geneva

The applications of satellite data in marine meteorology are reviewed, and the specific requirements for quantitative data gathered by satellite are discussed. The analysis of satellite derived parameters includes surface winds, sea and swell, surface visibility, ice accretion, precipitation, cloud cover, air temperature, humidity, sea surface temperature, surface currents, atmospheric pressure, surf and breakers, storm surge, and sea ice. The availability and access to satellite data for the various marine user groups is examined. A tabular summary of satellites of utility to marine meteorology, their sensors, and observable parameters is provided. Author (ESA)

N81-30168# British Aerospace Dynamics Group, Bristol (England). Space and Communications Div.
COASTAL OCEANS MONITORING SATELLITE SYSTEM (COMSS) SYSTEM EVALUATION STUDY Final Report
Paris ESA Jan. 1981 131 p refs
(Contract ESA-3632/78/F-CG(SC))
(ESS/SS-1035; ESA-CR(P)-1433) Avail: NTIS HC A07/MF A01

The individual sensors, launcher (Ariane) and platform are defined. Payloads A and B are described with emphasis on an ocean color monitor, imaging microwave radiometer, synthetic aperture radar and supporting units. Orbits and coverage, configuration options, power and mission profile and data handling are detailed. Satisfaction of payload power remains the most severe problem (for the power subsystem parameters considered) for payload A unless the operating duty cycles are restricted which can be accommodated within the ARIANE shroud. Sufficient mass margin (over 100 kg) exists to allow the inclusion of additional small instruments. These have to operate infrequently or at very low average power to avoid further aggravating the power problem. Wideband type tape recorders (around 5-10 GB

capacity) should be carried to provide reasonable orbit cover. For Payload B, the provisional scatterometer parameters (notably power and data) appear to be very demanding. Consequently, the duty cycles of operation of other instruments have to be severely restricted if the scatterometer operates frequently.
Author (ESA)

N81-30498# Instituto de Pesquisas Espaciais, Sao Jose dos Campos (Brazil).
FOLLOWING OCEANOGRAPHIC PHENOMENA ON THE SOUTH COAST OF BRAZIL WITH REMOTE SENSING FROM ORBITAL DISTANCE [ACOMPANHAMENTO DE FENOMENOS OCEANOGRAFICOS DA COSTA SUL DO BRASIL POR SENSORIAMENTO REMOTO A DISTANCIA ORBITAL]
Emmanuel Gama deAlemida and Keiko Tanaka Jan. 1981 35 p refs In PORTUGUESE; ENGLISH summary
(INPE-1975-RPE/280) Copyright. Avail: NTIS HC A03/MF A01

Data obtained by the very high resolution radiometer (VHRR) on the NOAA-5 satellite show thermal contrast due to cold upwelled water which occurs along the coast of Rio de Janeiro State. Coastal station data, VHRR data, and a mathematical model based on Ekman's theory suggest a possible interpretation of mesoscale oceanic phenomena. It is concluded that: (1) when surface winds are from 22.5 deg (true), the thermal VHRR imagery indicates a cool surface plume that extends south of Cabo Frio; (2) when the wind direction increases to 67.5 deg (true) the cool plume changes to a SW direction; and (3) when the wind direction becomes than 135 deg (true), there is no cool water present near the coast.
A.R.H.

N81-30765# National Oceanic and Atmospheric Administration, Rockville, Md.
NOAA CLIMATE PROGRAM PLAN
Jan. 1981 57 p refs
(PB81-193815; NOAA-81022305) Avail: NTIS HC A04/MF A01 CSCL 04B

The overall goal of the NOAA Climate Program is to develop and deliver improved climate data, information, and prediction services and to expand understanding of climate processes through focused physical, dynamic, and statistical climate research. Particular emphasis will be directed to studies of the impacts of natural climate variability on commercially important marine fisheries.
GRA

N81-30780# National Oceanic and Atmospheric Administration, Rockville, Md. Office of Marine Pollution Assessment.
ENVIRONMENTAL ASSESSMENT OF THE ALASKAN CONTINENTAL SHELF: REPORTS OF PRINCIPAL INVESTIGATORS. VOLUME 1: REACTORS - BIRDS, PLANKTON, LITTORAL, BENTHOS Annual Reports
1980 815 p refs Sponsored in part by Bureau of Land Management 3 Vol.
(PB81-196263) Avail: NTIS HC A99/MF A01 CSCL 08A

Simulation modeling of marine bird population energetics, food consumption, and sensitivity to perturbation was performed. Shorebird dependence on Arctic littoral habitats was studied as well as the distribution, abundance, and feeding ecology of birds associated with pack ice. A study of the population numbers and productivity of colonial seabirds is included. Plankton studies in the Bering Sea and an environmental assessment of selected habitats in the Arctic littoral system are also included. The distribution, abundance, community structure, and trophic relationships of the benthos of the Northeastern Gulf of Alaskan from Yakutat Bay to Cross Sound and the distribution, abundance, diversity, and productivity of the Western Sea benthos were studied.
E.D.K.

N81-31605*# GeoScience Research Corp., Salisbury, Md.
ICE SHEET ALTIMETRY Final Report
R. L. Brooks Mar. 1981 32 p refs
(Contract NAS6-3117)
(NASA-CR-156877) Avail: NTIS HC A04/MF A01 CSCL 14B

Generalized surface slopes were computed for the Antarctic and Greenland ice sheets by differencing plotted contour levels and dividing them by the distance between the contours. It was observed that more than 90% of the ice sheets have surface slopes less than 1%. Seasat test mode-1 Seasat altimeter measurements over Greenland were analyzed by comparisons with collinear and intersecting normal mode Seasat altimeter passes. Over the ice sheet, the computed surface elevations from test mode-1 measurements were consistently lower by about 45 m and the AGC levels were down by approximately 6 dB. No test mode-1 data were acquired over Antarctica. It is concluded that analysis of the existing altimeter data base over the two ice sheets is crucial in designing a future improved altimeter tracking capability. It is recommended that additional waveform retracking be performed to characterize ice sheet topography as a function of geographic area and elevation.
A.R.H.

N81-31803# Defense Mapping Agency Hydrographic and Topographic Center, Washington, D.C.
INTERPRETATION OF HYDROGRAPHIC FEATURES SEEN IN THE WATERS OFF CAPE COD Final Report, M.S. Thesis
Charles Leonard Reed May 1981 193 p refs
(AD-A102343) Avail: NTIS HC A09/MF A01 CSCL 08/10

A study was conducted to determine the origin of features appearing in a LANDSAT image (1724-14472; 17 July 1974) of the waters off Cape Cod by multitemporal and multispectral analysis techniques. Acquisition of ancillary data supplemented imagery from five different sensors, including visible, near infrared, and microwave, representing fifteen discrete times over a five-year period. Digital data for the LANDSAT image was evaluated multispectrally. Various water reflectance models were applied to the digital data to determine whether features related to reflected light from the ocean bottom, turbidity, or surface reflectance. Parameters were estimated from historical data. Results of model calculations were compared with the observed radiances at several locations in the scene. Multitemporal analysis affirmed that the following detailed information can be determined from space imagery: Rapid rates of coastal change, possible uncharted shoals, and theorized surface manifestations of internal waves. In all cases multisensor imagery increased the reliability of the derived information. Multispectral analysis provided additional evidence for attributing variations of reflectance in deep ocean to the effects of surface reflection and also appears to be the primary cause of reflectivity of patterns over the shoal areas around Nantucket Island.
Author (GRA)

N81-31807# National Oceanic and Atmospheric Administration, Miami, Fla. Atlantic Oceanographic and Meteorological Labs.
DRIFTING BUOY DATA FROM THE TROPICAL PACIFIC OCEAN DURING NORPAX EQUATORIAL TEST SHUTTLE EXPERIMENT
Donald V. Hansen, Carol C. Duckett, William Patzert, Gerald McNalley, and Edmund Kerut Sep. 1980 79 p
(Grant NSF OCE-16827)
(PB81-198939; NOAA-TM-ERL-AOML-45; NOAA-81031705) Avail: NTIS HC A05/MF A01 CSCL 08C

The core project of the Test Shuttle experiment was serial CTD and XBT sampling between 20 degrees N and 17 degrees S along 150 degrees W at approximately monthly intervals and weekly AXBT sampling on 150 degrees W and 158 degrees W. These observations were collected between Hawaii and Tahiti, spanning the North Equatorial Current (NEC), the North Equatorial Counter Current (NECC) and the South Equatorial Current (SEC).
GRA

N81-31808# National Advisory Committee on Oceans and Atmosphere, Washington, D.C. Task Group on Services to Ocean Operations.
OCEAN SERVICES FOR THE NATION. NATIONAL OCEAN GOALS AND OBJECTIVES FOR THE 1980'S
Victoria J. Jones, ed. Jan. 1981 82 p
(PB81-200602; NACOA-18) Avail: NTIS HC A05/MF A01 CSCL 08J

The goals include: ocean observation and prediction; navigation and positioning, mapping and charting, ocean data and information dissemination; monitoring the ocean; and a new ocean measurement capability. These goals are to provide improved Arctic and Antarctic Ocean information.
GRA

N81-33342# Deutsche Forschungs- und Versuchsanstalt fuer Luft- und Raumfahrt, Oberpfaffenhofen (West Germany).
IMAGING RADAR SYSTEMS
F. Schlude *In* ESA Coherent and Incoherent Radar Scattering from Rough Surfaces and Vegetated Areas May 1981 p 29-39 refs

Avail NTIS HC A08/MF A01

Imaging systems are classified and described. A description of design procedure and problems is provided. Factors affecting image quality of thin point target distributions are analyzed and limitations of this model are pointed out. The imaging of quasi-continuous point distributions and its application to ocean surface imaging are considered. A comparison is made of systems combining imaging and Fourier transformation used in oceanographic research. The technical data of various systems is summarized.
Author (ESA)

N81-33344# Kansas Univ Center for Research, Inc., Lawrence Remote Sensing Lab

SEA SURFACE SCATTERING

Richard K. Moore *In* ESA Coherent and Incoherent Radar Scattering from Rough Surfaces and Vegetated Areas May 1981 p 53-61 refs

Avail NTIS HC A08/MF A01

Basic mechanisms of sea-surface scattering are described for a two-scale model. The basic concept of Bragg resonance is illustrated with a sinusoidal component of the ocean spectrum. Factors affecting the overall spectrum of ocean waves are listed. Sketches show the geometry associated with using a scatterometer to calculate windspeed in measurements of radar backscatter from the wind driven sea. The model described is quasi-empirical based upon theoretical calculations and measurements with both spacecraft and aircraft. Problems in accurate determination of model parameters are discussed for aircraft and spacecraft. Details are given of research on capillary wave distribution, the satellite altimeter and other non-imaging techniques for determining wave spectra are set out. Unknown quantities including surface expression of bottom topography are mentioned. Author (ESA)

N81-33539*# Environmental Research and Technology, Inc., Concord, Mass

COMPARATIVE ANALYSIS OF SEA ICE FEATURES USING SIDE-LOOKING AIRBORNE RADAR (SLAR) AND LANDSAT IMAGERY Final Report

James C. Barnes and Clinton J. Bowley, Principal Investigators Cleveland NASA. Lewis Research Center Mar. 1981 71 p refs Original contains imagery Original photography may be purchased from the EROS Data Center, Sioux Falls, S.D. 57198 ERTS

(Contract NAS3-21924)

(E81-10044, NASA-CR-165335, P-3970-F) Avail NTIS HC A04/MF A01 CSCL 08L

A comparative analysis of sea ice features was carried out using X-Band, real aperture side-looking airborne radar (SLAR) and LANDSAT imagery. The SLAR data were collected by the NASA/LeRC C-131 aircraft on flights over the Mackenzie Delta and Prudhoe-Barrow areas of the southern Beaufort Sea and the Norton Sound area of the eastern Bering Sea. The LANDSAT data were for dates as near as possible to the dates of the SLAR missions. The analysis of the data sample available for the investigation indicates the SLAR imagery has distinct advantages over LANDSAT for identifying certain features and ice types. It is further indicated that the capability for SLAR observe ice through clouds is essential for an operational ice information system.
R.C.T.

N81-33763# Defense Mapping Agency Hydrographic and Topographic Center, Washington, D.C. Hydrographic/Topographic Center

DERIVATION OF SHALLOW OCEAN BOTTOM REFLECTANCE VALUES FROM COLOR AERIAL PHOTOGRAPHY

Donald J. Gerson, Lynn K. Fehrenbach, Kenneth R. Piech, and David W. Gaucher Jun. 1981 22 p refs

(AD-A101105) Avail NTIS HC A02/MF A01 CSCL 08/10

An alternative to the field survey method of acquiring hydrographic data is described. The technique involves the use of digitized color aerial photography in the derivation of the percentage of reflectance of shallow ocean bottom materials. These spectral reflectance values can then be used in an algorithm for calculating water depths. The reflectances that were derived in this study show a close relative comparison to ground truth information. After a discussion of the causes of discrepancies between derived and actual reflectance values, it is concluded that this method of data acquisition merits further investigation due to its high geometric fidelity, its simplicity, and its cost and time saving benefits.
Author (GRA)

06

HYDROLOGY AND WATER MANAGEMENT

Includes snow cover and water runoff in rivers and glaciers, saline intrusion, drainage analysis, geomorphology of river basins, land uses, and estuarine studies.

A81-41158 # **Determination of moisture from NOAA polar orbiting satellite sounding radiances.** C. M. Hayden, W. L. Smith, and H. M. Woolf (NOAA, National Earth Satellite Service, Madison, WI). *Journal of Applied Meteorology*, vol. 20, Apr. 1981, p. 450-466. 11 refs.

A method is analyzed by which lower troposphere moisture fields can be deduced from radiances measured by satellite. A retrieval technique is described, and the method is evaluated statistically using both synthesized radiances and actual satellite measurements. The TIROS operational vertical sounder (TOVS) measurements made in the 6.7 micron water vapor absorption band are investigated. Three major changes to current operational methods are reported: (1) the surface contribution to the outgoing radiance is subtracted before making temperature and moisture retrievals, allowing a better definition of low-level moisture gradients. (2) The temperature/moisture solution is subjected to a one channel iteration to ensure that the radiative transfer equation is satisfied for low-level moisture, which is beneficial in cases of extreme dryness. (3) In areas of extensive cloud cover, a cloud moisture model is introduced to allow a definition of the atmospheric moisture below the cloud. It was found that the moisture in the surface -700 mb and 850-500 mb layers and particularly the horizontal gradient pattern can be well defined.
E.B.

A81-41723 # **The use of satellite data in predicting spring flow in the basins of the upper Ob' and upper Enisei (Opyt primeneniia kosmicheskoi informatsii dlia tselei prognoza vesennego stoka v basseinakh rek verkhnei Obi i verkhnego Eniseia).** N. V. Vostriakova. In: Problems of the utilization and protection of the natural resources of Siberia (Problemy ispol'zovaniia i okhrany prirodnykh resursov Sibiri). Novosibirsk, Izdatel'stvo Nauka, 1980, p. 26-30. 7 refs. In Russian.

A81-42095 **Insights into errors of SMS-inferred GATE convective rainfall.** J. A. Augustine, C. G. Griffith, W. L. Woodley (NOAA, Office of Weather Research and Modification, Boulder, CO), and J. G. Meitin (Cooperative Institute for Research in Environmental Sciences, Boulder, CO). *Journal of Applied Meteorology*, vol. 20, May 1981, p. 509-520. 7 refs. NOAA-supported research.

It is noted that, in the mean, the Griffith/Woodley rain estimation technique underestimated the radar-measured rain of each of the three phases of GATE, to varying degrees, and that the satellite-derived rain at the isohyets were generally too extensive relative to radar-measured patterns. Three possible error sources are investigated. They are: (1) the method of apportionment of satellite-derived rain at the surface; (2) resolution degradation of the digital satellite imagery; and (3) anomalous behavior of convective clouds in the tropical Atlantic relative to those of the Florida derivation data set. To correct the satellite-derived rain patterns, a new method of apportionment is tested by recomputing the GATE satellite rain estimates. The relative error caused by resolution degradation is quantified by comparing rain estimates produced from full resolution imagery to estimates derived from degraded imagery for an 8 deg latitude by 12 deg longitude area in the eastern tropical Pacific ocean over a 54 h period. The remaining differences between the GATE satellite and radar estimates are considered to be attributable to different conditions prevailing in Florida and in GATE.
C.R.

A81-42126 **Satellite detection of seiches in Great Salt Lake, Utah.** M. Matson and C. P. Berg (NOAA, National Earth Satellite Service, Washington, DC). *Water Resources Bulletin*, vol. 17, Feb. 1981, p. 122-128. 21 refs.

On June 15, 1977, an unusual brightness anomaly was detected in the north arm of Great Salt Lake, Utah, on NOAA-5 Very High Resolution Radiometer (VHRR) visible band imagery and on Landsat-2 multispectral visual band imagery. Retrospective inspection of NOAA-3, 4, and 5 satellite imagery from 1974-77 revealed 12 previous cases of the anomaly, whereas post monitoring documented nine other cases through May 1978. Comparison of lake levels in the north arm with meteorological parameters leads to the conclusion that the anomalous brightness is associated with wind induced seiches in the north arm. Apparently the wind induces a lower water depth, turbulence, and mixing throughout the water column in the western third of the north arm, thus increasing the brightness of the surface waters chiefly from sediment resuspension.
(Author)

A81-42229 * **Simulation modeling of estuarine ecosystems.** R. W. Johnson (NASA, Langley Research Center, Hampton, VA). In: Estuarine and wetland processes. New York, Plenum Publishing Corp., 1980, p. 541-559. 18 refs.

A simulation model has been developed of Galveston Bay, Texas ecosystem. Secondary productivity measured by harvestable species (such as shrimp and fish) is evaluated in terms of man-related and controllable factors, such as quantity and quality of inlet fresh-water and pollutants. This simulation model used information from an existing physical parameters model as well as pertinent biological measurements obtained by conventional sampling techniques. Predicted results from the model compared favorably with those from comparable investigations. In addition, this paper will discuss remotely sensed and conventional measurements in the framework of prospective models that may be used to study estuarine processes and ecosystem productivity.
(Author)

A81-43176 **Satellite hydrology; Proceedings of the Fifth Annual William T. Pecora Memorial Symposium on Remote Sensing, Sioux Falls, SD, June 10-15, 1979.** Symposium sponsored by the American Water Resources Association. Edited by M. Deutsch (U.S. Geological Survey, Reston, VA), D. R. Wiesnet (NOAA, Washington, DC), and A. Rango (NASA, Goddard Space Flight Center, Greenbelt, MD). Minneapolis, MN, American Water Resources Association, 1981. 743 p. $85.

Philosophical and technical backgrounds for the application of remote sensing by earth scientists are presented. Interests and activities of participating agencies of the United States and Canadian governments, universities, and the private sector in implementing satellite technology in a diverse array of water-related programs are described. Consideration is then given to applications of satellite data to the various aspects of the hydrologic cycle and man's impact on it: meteorology, snow and ice, surface water, soil moisture, ground water, wetlands, coastal zone, water quality and environment, and water use and management.
B.J.

A81-43177 **Remote sensing in hydrology - A challenge to scientists.** J. S. Cragwall, Jr. (U.S. Geological Survey, Reston, VA). In: Satellite hydrology; Proceedings of the Fifth Annual William T. Pecora Memorial Symposium on Remote Sensing, Sioux Falls, SD, June 10-15, 1979. Minneapolis, MN, American Water Resources Association, 1981, p. 3-5.

Hydrologic applications of remote sensing by satellites are briefly reviewed. Specific applications discussed include: shallow ground water exploration, inventorying of surface waters, estimation of water withdrawal and consumption, assessment of sea and polar ice conditions, and the relay of hydrologic data to collecting points by satellites. Some of the problems yet to be solved are: better resolution in the thermal infrared and microwave parts of the spectrum, a quick-look capability that can be used for planning purposes, and an improved ability to incorporate land surface features into hydrologic models, which means solving the associated problems of large-scale data storage and processing.
V.L.

A81-43178 **Satellite applications in river and flood forecasting.** R. A. Clark (NOAA, National Weather Service, Silver Spring, MD). In: Satellite hydrology; Proceedings of the Fifth Annual William T. Pecora Memorial Symposium on Remote Sensing, Sioux Falls, SD, June 10-15, 1979. Minneapolis, MN, American Water Resources Association, 1981, p. 6-8.

Several applications of satellites to river and flood forecasting are described. Areas in which satellites offer a great potential for improved forecasts include areal estimates of snow cover, data relay, improved rainfall estimates in data sparse regions, and better definition of areal variation of soil moisture. (Author)

A81-43179 * **NASA water resources/hydrology remote sensing program in the 1980's.** M. A. Calabrese and P. G. Thome (NASA, Washington, DC). In: Satellite hydrology; Proceedings of the Fifth Annual William T. Pecora Memorial Symposium on Remote Sensing, Sioux Falls, SD, June 10-15, 1979. Minneapolis, MN, American Water Resources Association, 1981, p. 9-15. 19 refs.

A81-43180 **Corps of Engineers utilization of satellites for hydrologic purposes.** V. K. Hagen (U.S. Army, Corps of Engineers, Washington, DC). In: Satellite hydrology; Proceedings of the Fifth Annual William T. Pecora Memorial Symposium on Remote Sensing, Sioux Falls, SD, June 10-15, 1979. Minneapolis, MN, American Water Resources Association, 1981, p. 16-18.

Activities of the U.S. Army Corps of Engineers in the application of satellites to hydrologic studies are reviewed starting with its initial experiment in 1972. Specific applications discussed include: water control management, runoff estimation, land use, monitoring changes, flooded area identification, and location of important features such as dams and lakes. Most of the current research relates to improved sensors or advanced applications of satellite imagery. V.L.

A81-43182 **A review of Canada's present and future remote sensing activities relating to hydrology.** E. J. Langham (National Hydrology Research Institute, Ottawa, Canada). In: Satellite hydrology; Proceedings of the Fifth Annual William T. Pecora Memorial Symposium on Remote Sensing, Sioux Falls, SD, June 10-15, 1979. Minneapolis, MN, American Water Resources Association, 1981, p. 26-32. 12 refs.

The presentation reviews the technical resources in Canada for acquisition and processing remotely sensed data with particular attention to airborne and satellite borne instrumentation, satellite data reception, and data analysis systems used by various agencies. It then goes on to give examples of applications of these data from various subdisciplines of hydrology. (Author)

A81-43183 **Satellite versus conventional methods in hydrology.** D. G. Anderson (U.S. Geological Survey, Reston, VA). In: Satellite hydrology; Proceedings of the Fifth Annual William T. Pecora Memorial Symposium on Remote Sensing, Sioux Falls, SD, June 10-15, 1979. Minneapolis, MN, American Water Resources Association, 1981, p. 33-36. 21 refs.

Remote sensing applications research efforts are discussed under three broad categories: (1) replace conventional methods with satellite based approaches; (2) combine conventional and satellite data; and (3) emphasize problems unique to solution by the use of satellite data. It is pointed out that most applications of satellite data in each of the three categories require a combination of field observations and related experience for reasonable analysis. Satellite and conventional data tend to be complementary and techniques using both types of data should be considered in hydrologic studies. V.L.

A81-43184 **An introduction to satellite hydrology.** G. K. Moore (U.S. Geological Survey, EROS Data Center, Sioux Falls, SD). In: Satellite hydrology; Proceedings of the Fifth Annual William T. Pecora Memorial Symposium on Remote Sensing, Sioux Falls, SD, June 10-15, 1979. Minneapolis, MN, American Water Resources Association, 1981, p. 37-41. 5 refs.

A81-43186 **Adapting GOES DCS for use by Corps of Engineers.** T. D. Buckelew (U.S. Army, Corps of Engineers, Waltham, MA). In: Satellite hydrology; Proceedings of the Fifth Annual William T. Pecora Memorial Symposium on Remote Sensing, Sioux Falls, SD, June 10-15, 1979. Minneapolis, MN, American Water Resources Association, 1981, p. 48-50.

New England Division, Corps of Engineers, working with private industry, has demonstrated a random reporting capability for collecting data using a standard 1500 Hz channel on NOAA's Geostationary Environmental Operational Satellite (GOES). In the random reporting system, hundreds of data collection platforms (DCP's) transmit on a single channel at proper time intervals to ensure an acceptable probability of reception. Several techniques have been incorporated to improve reception probabilities, the main ones being a short message (less than 3 seconds) and an adaptive algorithm programmed into each platform. This algorithm assures sufficient transmission during critical times, yet relieves the system of superfluous messages during normal periods when no new or important information has been generated. The demonstration has confirmed that, even without the adaptive feature, at least 200 platforms will report successfully (with 90 percent probability) within an hour. (Author)

A81-43187 **Satellite telemetry of hydrologic data in California.** C. A. McCullough (California, Dept. of Water Resources, Div. of Flood Management, Sacramento, CA). In: Satellite hydrology; Proceedings of the Fifth Annual William T. Pecora Memorial Symposium on Remote Sensing, Sioux Falls, SD, June 10-15, 1979. Minneapolis, MN, American Water Resources Association, 1981, p. 51-53.

Telemetry of hydrologic data in California is beginning to use a satellite as part of the communication path. At present a snow water content sensor and ten precipitation gages report through a satellite. In addition, fire weather data passes through the satellite to aid in suppression of forest and range fires. Large amounts of real-time data are essential to water management and include stream flow, precipitation, wind, snow water content, temperature water quality, and reservoir stage. The present system collects data from about 180 locations, part of which are tied into a computer. Eventually it will process all the data. The emphasis is on real-time data for flood forecasting, water supply forecasting, and water operations. Use of satellites eliminates radio rath problems in mountain terrain and decreases use of mountaintop repeaters that are subject to climatic problems. Changes in the satellite facilities available to us are needed to achieve real-time data acquisition capability. (Author)

A81-43188 **Monitoring Canada's water resources in remote regions by satellite telemetry.** I. A. Reid (Environment Canada, Environmental Management Service, Ottawa, Canada), C. Pesant (Quebec, Ministère des Richesses Naturelles, Direction Générale des Eaux, Quebec, Canada), and B. E. Goodison (Environment Canada, Atmospheric Environment Service, Downsview, Ontario, Canada). In: Satellite hydrology; Proceedings of the Fifth Annual William T. Pecora Memorial Symposium on Remote Sensing, Sioux Falls, SD, June 10-15, 1979. Minneapolis, MN, American Water Resources Association, 1981, p. 54-59. 17 refs.

Since 1894 much activity has taken place with respect to monitoring, cataloguing, and managing Canada's inland waters. In 1979, the formal active network of the Water Survey of Canada consists of 2749 stations across Canada. Agencies at both the federal and provincial levels and some publicly owned companies are endeavoring to employ the advantages of telemetry by satellites. The Atmospheric Environment Service (AES) of Environment Canada is becoming actively involved in satellite telemetry to provide better service to the Canadian public. Currently, some 300 meterological and climatological stations provide real-time weather observations during all or part of the day utilizing human resources. Satellite telemetry would provide a less expensive yet reliable means of getting the necessary observations from remote areas. Environmental Management Service (EMS), also part of Environment Canada, joined NASA in an experiment to retransmit hydrometric data by satellite with the launch of Landsat in 1972. At present EMS has 40 Data Collection Platforms deployed across Canada. G.R.

A81-43191 **A satellite derived technique for estimating rainfall from thunderstorms and hurricanes.** R. A. Scofield and V. J. Oliver (NOAA, National Environmental Satellite Service, Washington, DC). In: Satellite hydrology; Proceedings of the Fifth Annual William T. Pecora Memorial Symposium on Remote Sensing, Sioux Falls, SD, June 10-15, 1979. Minneapolis, MN, American Water Resources Association, 1981, p. 70-76. 7 refs.

The purpose of this paper is threefold: (1) to summarize the Scofield/Oliver technique for making rainfall estimates from convective systems, (2) to present the results using the technique in real time on major flash flood producing thunderstorms in Mississippi (April 1979) and on Hurricane Anita (September 1977) as the storm advanced into northeastern Mexico, and (3) to discuss some possible reasons why the technique often underestimates the copious rainfall associated with the slow moving remnants of tropical storms. The flash flood producing thunderstorms occurred in Mississippi on April 11-13, 1979. Results showed that the 48-hour estimated heavy rainfall pattern was quite similar to the observed. As Hurricane Anita approached the coastal area, the San Antonio Weather Service Forecast Office (WSFO) was concerned with potential flooding in the Rio Grande basin and in Brownsville, Texas. During the critical time period from September 1-2, 1977, rainfall estimates were provided to the San Antonio WSFO. The results indicated that the rainfall estimates from Hurricane Anita were quite comparable with the ground truth rain gauge measurements. (Author)

A81-43192 **Utilizing GOES imagery to determine convective storm characteristics in data deficient regions.** J. P. Jolly (J. P. Jolly and Associates, Ottawa, Canada). In: Satellite hydrology; Proceedings of the Fifth Annual William T. Pecora Memorial Symposium on Remote Sensing, Sioux Falls, SD, June 10-15, 1979. Minneapolis, MN, American Water Resources Association, 1981, p. 77-83.

In many developing countries there is a scarcity of continuous recording precipitation gauges. This hinders or prevents hydrologic analyses for small or medium-sized basins. Using GOES-obtained enhanced infrared imagery and a recently developed technique, which related heights and expansion/contraction characteristics of cumulonimbus clouds to one-half hour rainfall amounts, convective storms were analyzed. The relations between cloud brightness levels on enhanced infrared imageries and one-half hour rainfall amounts were verified using regional recorded daily rainfall totals from which particular storm rainfall characteristics were estimated. (Author)

A81-43193 **Rain estimation over several areas of the globe using satellite imagery.** W. L. Woodley, C. G. Griffith (NOAA, National Hurricane and Experimental Meteorology Laboratory, Coral Gables, FL), and J. A. Augustine (NOAA, Weather Modification Program Office, Boulder, CO). In: Satellite hydrology; Proceedings of the Fifth Annual William T. Pecora Memorial Symposium on Remote Sensing, Sioux Falls, SD, June 10-15, 1979.

Minneapolis, MN, American Water Resources Association, 1981, p. 84-91. 7 refs. NOAA-supported research; U.S. Bureau of Reclamation Contract No. 8-07-83-V0016.

A computer-automated technique to estimate rainfall using digital, infrared geosynchronous satellite imagery has been developed and tested. The method requires time histories of convective entities at discrete temperature thresholds and a set of empirical relationships. Development of tracking software and access to a large computer now permit rain estimates for large (10-million sq km) areas down to individual clouds. Rain estimates for several areas of the globe (Florida, the tropical Atlantic Ocean and western Africa, the eastern tropical Pacific Ocean and tropical South America, two flash flood situations, and the U.S. High Plains) are presented. The satellite-inferred rainfalls are compared to ground truth when available. (Author)

A81-43197 * **Modeling the terrestrial hydrology for the global atmosphere - The future role of satellite data.** J. D. Lin, P. Bock, and J. J. Alfano (Connecticut, University, Storrs, CT). In: Satellite hydrology; Proceedings of the Fifth Annual William T. Pecora Memorial Symposium on Remote Sensing, Sioux Falls, SD, June 10-15, 1979. Minneapolis, MN, American Water Resources Association, 1981, p. 124-138. 14 refs. Grant No. NsG-5075.

A global terrestrial hydrology model has been developed for the transport and storage of moisture and heat in the ground surface layer where the hydrological parameters react to diurnal and seasonal changes in the atmosphere. The spatial and temporal variability of land surface features is considered in the model by means of large scale parameterizations. The model can be either forced by the atmosphere using conventional meteorological data or coupled to an atmospheric general circulation model (GCM) for interactive studies. The global surface is divided into 4 deg longitude by 5 deg latitude cells while the ground is represented by a thin surface layer, a bulk layer (the root zone), and a deep layer (the ground water zone). Results are presented from a seven-day global experiment which was conducted utilizing the GLAS GCM (NASA Goddard Laboratory for Atmospheric Sciences). The model has demonstrated its capability to predict, over a large region, the overall soil moisture storage and major flux exchanges with the atmosphere above and the ground water below. (Author)

A81-43198 **A statistical approach to rainfall estimation using satellite data.** L. F. Whitney, Jr. and L. D. Herman (NOAA, National Environmental Satellite Service, Washington, DC). In: Satellite hydrology; Proceedings of the Fifth Annual William T. Pecora Memorial Symposium on Remote Sensing, Sioux Falls, SD, June 10-15, 1979. Minneapolis, MN, American Water Resources Association, 1981, p. 139-143. 6 refs.

A statistical approach is used in an attempt to estimate convective rainfall using satellite data. The objective is to furnish rainfall estimates in a form suitable as input to hydrologic models which forecast river flow. These models require area-averaged rainfall over periods of 6 hours in watersheds covering 500 or more square miles. It is noted that from among the variables used, a screening regression method selected those which best explain area-averaged rainfall. In both cases studied, the selected variables correlate with rainfall at above 0.8. However, since meteorological conditions in each case were very different, neither regression equation was a good estimator of the rainfall in the other case. Some of the most important variables selected are IR-temperature gradients along the tropospheric shear, ratio of IR-temperature to IR-temperature gradient along the low-level wind, low-level dewpoint, low-level dewpoint gradient along the high-level wind, and low-level dewpoint advection. It is noted that although these preliminary results are encouraging, many more cases must be included and any positive results checked against independent data. C.R.

A81-43199 **Roles of satellites in hydrology.** D. G. Anderson (U.S. Geological Survey, Reston, VA). In: Satellite hydrology; Proceedings of the Fifth Annual William T. Pecora Memorial Symposium on Remote Sensing, Sioux Falls, SD, June 10-15, 1979. Minneapolis, MN, American Water Resources Association, 1981, p. 144-155. 26 refs.

The usefulness of satellite data in hydrologic applications is demonstrated by examples involving three areas (Arctic region; Ouachita River, Arkansas/Louisiana; and Albemarle-Pamlico Sounds, North Carolina). The data used included data from four satellite systems (Apollo, Landsat, Nimbus, and Heat Capacity Mapping Mission), covering the visible, thermal, and infrared bands and ranging in resolution from 30 m to 50 km. It is shown that data from satellites, if analyzed at the initial stage of a hydrologic study, can provide valuable conceptual information on the hydrologic systems involved. V.L.

A81-43200 **Satellite snow mapping techniques with emphasis on the use of Landsat.** C. J. Bowley and J. C. Barnes (Environmental Research and Technology, Inc., Concord, MA). In: Satellite hydrology; Proceedings of the Fifth Annual William T. Pecora Memorial Symposium on Remote Sensing, Sioux Falls, SD, June 10-15, 1979. Minneapolis, MN, American Water Resources Association, 1981, p. 158-164. 18 refs.

The types of satellite data that have been used to map snow cover and the interpretative techniques that have evolved are reviewed with emphasis on the application of snow covered areas from Landsat to runoff prediction. It is pointed out that the experience of the data interpreter is highly valuable in estimating snow covered area during partial cloud cover conditions, and when interpreting snow cover in areas of heavy forest cover, mountain shadows, and bare rock terrain. The application of remote sensing in portions of the spectrum other than the visible is also discussed. V.L.

A81-43201 **Application of snow covered area to runoff forecasting, in the Sierra Nevada, California.** J. F. Hamnaford and A. J. Brown (California, Dept. of Water Resources, Snow Surveys Branch, Sacramento, CA). In: Satellite hydrology; Proceedings of the Fifth Annual William T. Pecora Memorial Symposium on Remote Sensing, Sioux Falls, SD, June 10-15, 1979.
Minneapolis, MN, American Water Resources Association, 1981, p. 165-172.

Results of a four-year project to explore the application of snow covered area (SCA) obtained from satellite imagery to hydrologic forecasting are summarized. Data describing SCA are found to have greatest hydrologic application during the period of snow melt in the spring and early summer rather than during the period of snow pack accumulation. SCA provides the source of near real-time data from within the watershed during a period when snow pack conditions are changing rapidly and snow melt runoff rates are high. SCA data may be most useful for detection and monitoring of conditions within the basin that depart from natural or experienced conditions. V.L.

A81-43202 **Satellite Image Atlas of the earth's glaciers.** R. S. Williams, Jr. and J. G. Ferrigno (U.S. Geological Survey, Reston, VA). In: Satellite hydrology; Proceedings of the Fifth Annual William T. Pecora Memorial Symposium on Remote Sensing, Sioux Falls, SD, June 10-15, 1979. Minneapolis, MN, American Water Resources Association, 1981, p. 173-182. 24 refs.

In June 1977, a project was initiated to prepare a 'Satellite Image Atlas of Glaciers'. It is pointed out that there exist sufficient Landsat, NOAA, and other satellite data in various archives for this project. The preparation of such an atlas is considered a timely effort because of the wide variety of impending and ongoing U.S. and international climatological studies. The primary objective of the atlas is to provide a pictorial inventory either in the form of a Landsat or other satellite image, or as a tabular listing of the best available Landsat or other satellite images of extant glaciers. Such an atlas should provide a means of obtaining a better estimate of the total area of the planet covered by glaciers. Attention is given to image selection, the contents of the atlas, the Antarctic ice sheet, Iceland, and Svalbard.

G.R.

A81-43203 **The satellite record of the winter of 1978-79 in North America.** D. R. Wiesnet and C. P. Berg (NOAA, National Environmental Satellite Service, Washington, DC). In: Satellite hydrology; Proceedings of the Fifth Annual William T. Pecora Memorial Symposium on Remote Sensing, Sioux Falls, SD, June 10-15, 1979. Minneapolis, MN, American Water Resources Association, 1981, p. 183-187. 9 refs.

The satellite record of the winter 1978-79 is reviewed to demonstrate the utility of NOAA/NESS (National Oceanic and Atmospheric Administration/National Environment Satellite Service) satellite data to record snow cover on a continental basis, which is a good measure of winter's severity. Results examined in the light of a 13-year record show a clear trend toward increased winter snow cover. It is also shown that the severity of the 1978-79 North American winter, as measured by satellite-determined snow cover, was a regional rather than a hemispheric or global phenomenon.

V.L.

A81-43204 **Potentials of mapping buried glacier ice with Landsat thermal imagery.** R. Lougeay (New York, State University, Geneseo, NY). In: Satellite hydrology; Proceedings of the Fifth Annual William T. Pecora Memorial Symposium on Remote Sensing, Sioux Falls, SD, June 10-15, 1979. Minneapolis, MN, American Water Resources Association, 1981, p. 189-192. 5 refs. Research supported by the State University of New York Research Foundation.

Field observations and the analysis of Landsat imagery of the Wrangell Mountains of Alaska provide information on the nature and extent of buried glacier ice. Spectral bands 5, 7, and false color composite imagery from existing Landsat multispectral data proved most useful for mapping glacial margins and large masses of active but buried glacier ice. Signal contrasts between bare detritus and vegetation cover were most strongly pronounced on band 5, while band 7 displayed stronger contrasts between the microtopographic texture of the moraine covered ice masses and adjacent etrital surfaces of talus or outwash. When the mantle of morainic detritus is thinner than the diurnal thermal damping depths, strong signal contrasts between ice cored moraines and dry glacial drift deposits are present.

B.J.

A81-43205 **Prediction of water yield using satellite imagery and a snowmelt simulation model.** W. O. Rasmussen and P. F. Ffolliott (Arizona, University, Tucson, AZ). In: Satellite hydrology; Proceedings of the Fifth Annual William T. Pecora Memorial Symposium on Remote Sensing, Sioux Falls, SD, June 10-15, 1979. Minneapolis, MN, American Water Resources Association, 1981, p. 193-196. 14 refs.

A computer simulation model has been developed for estimating the impacts of alternate land management activities on winter water yield in snow covered areas. The model uses satellite imagery to delineate the areal extent of the snow covered area near peak snow-pack accumulation. A degree-day snowmelt technique is used to predict daily melt, with daily stream flow being computed from recession analysis. The model has been structured in an interactive format to facilitate operation by users at remote locations using readily available data sets.

(Author)

A81-43207 * **Passive microwave sensing of snow characteristics over land.** A. T. C. Chang, D. K. Hall, J. L. Foster, A. Rango, and J. C. Shiue (NASA, Goddard Space Flight Center, Application Directorate, Greenbelt, MD). In: Satellite hydrology; Proceedings of the Fifth Annual William T. Pecora Memorial Symposium on Remote Sensing, Sioux Falls, SD, June 10-15, 1979. Minneapolis, MN, American Water Resources Association, 1981, p. 213-217. 11 refs.

Truck-mounted, airborne, and spaceborne systems with various radiometers ranging in wavelength from 0.8 to 21 cm were used to measure the brightness temperatures of snow-covered areas at test sites near Steamboat Springs and Walden, Colorado. The brightness temperature at a short wavelength (0.8 cm) was found to decrease more rapidly with increasing snow depth than the brightness temperature at a longer wavelength (6 cm). More scattering of the shorter-wavelength radiation by the snow crystals results in a lower brightness temperature. The longer-wavelength (6 cm) radiation penetrates through meters of dry snowpack and is useful for the assessment of the underlying ground conditions. B.J.

A81-43208 **Landsat derived snow cover as an input variable for snow melt runoff forecasting in South Central Colorado.** B. A. Shafer (Soil Conservation Service, Denver, CO), J. K. Marron (Soil Conservation Service, Arvada, CO), and C. F. Leaf. In: Satellite hydrology; Proceedings of the Fifth Annual William T. Pecora Memorial Symposium on Remote Sensing, Sioux Falls, SD, June 10-15, 1979. Minneapolis, MN, American Water Resources Association, 1981, p. 218-224. 5 refs.

Landsat imagery for the period 1973-78 was used to calculate snow covered area on six drainages in South Central Colorado. Snow covered area was used as a predictor variable to forecast both short-term and seasonal snow melt runoff volumes. The Leaf-Brink Subalpine Water Balance simulation model was adapted to use snow covered area as an input parameter to predict residual volume runoff. Areal snow cover was also used in a statistical model to forecast runoff and is compared to current water equivalent index methods of forecasting. Results indicate that Landsat derived snow cover is highly correlated with seasonal stream flow volumes. Snow cover extent is an important variable for forecast purposes once the main snow melt season begins but is of limited value before that time.

(Author)

A81-43209 * **Monitoring snow with microwaves.** W. H. Stiles and F. T. Ulaby (University of Kansas Center for Research, Inc., Lawrence, KS). In: Satellite hydrology; Proceedings of the Fifth Annual William T. Pecora Memorial Symposium on Remote Sensing, Sioux Falls, SD, June 10-15, 1979. Minneapolis, MN, American Water Resources Association, 1981, p. 225-229. Contract No. NAS5-23777.

Results of an experimental study concerned with the active and passive microwave response to snow pack are discussed. Comprehensive ground truth measurements and preliminary investigations indicate that the primary factors affecting the microwave response are snow water equivalent and snow wetness. The most important conclusion of the study is that the scattering and emission behavior of snow varies drastically as a function of frequency between 1 GHz and 37 GHz, which suggests that the multifrequency operation has the potential to provide estimates on several snow parameters, primarily wetness profile and water equivalent, simultaneously. V.L.

A81-43210 **Operational use of satellite data for snow inventory and runoff forecast.** G. Ostrem, T. Andersen (Norges Vassdrags- og Elektrisitetsvesen, Oslo, Norway), and H. Odegaard (IBM Norway, Oslo, Norway). In: Satellite hydrology; Proceedings of the Fifth Annual William T. Pecora Memorial Symposium on Remote Sensing, Sioux Falls, SD, June 10-15, 1979. Minneapolis, MN, American Water Resources Association, 1981, p. 230-234. 8 refs. Research supported by the Norges Vassdrags- og

Elektrisitetsvesen and Norges Teknisk-Naturvitenskapelige Forskningsrad.

A method has been developed whereby NOAA and TIROS data are used to evaluate remaining snow in mountain watersheds and to predict the corresponding melt water volume. The method can only be used in vegetation free or almost vegetation free high mountain basins and only during the snow melt period after some 20% of the landscape has become snow free. The relation between the remaining snow cover (as expressed in per cent or in square km) and the subsequent melt water inflow is determined empirically. The method has been used for monitoring water reservoirs in southern Norway but can be also used in other areas. V.L.

A81-43211 * **The use of radar imagery for surface water investigations.** M. L. Bryan (California Institute of Technology, Jet Propulsion Laboratory, Pasadena, CA). In: Satellite hydrology; Proceedings of the Fifth Annual William T. Pecora Memorial Symposium on Remote Sensing, Sioux Falls, SD, June 10-15, 1979. Minneapolis, MN, American Water Resources Association, 1981, p. 238-251. 28 refs. Contract No. NAS7-100.

The paper is concerned with the interpretation of hydrologic features using L-band (HH) imagery collected by aircraft and Seasat systems. Areas of research needed to more precisely define the accuracy and repeatability of measurements related to the conditions of surfaces and boundaries of fresh water bodies are identified. These include: the definition of shoreline, the nature of variations in surface roughness across a water body and along streams and lake shores, and the separation of ambiguous conditions which appear similar to lakes. V.L.

A81-43212 **An examination of fluvial morphological characteristics of western Amazon streams from Apollo-Soyuz photographs.** R. K. Holz and V. R. Baker (Texas, University, Austin, TX). In: Satellite hydrology; Proceedings of the Fifth Annual William T. Pecora Memorial Symposium on Remote Sensing, Sioux Falls, SD, June 10-15, 1979. Minneapolis, MN, American Water Resources Association, 1981, p. 252-259. 9 refs.

Empirical formulas are tested in estimating the hydrologic properties of certain South American rivers. The study reveals the lack of precise understanding of regime behavior in tropical streams and the difficulty of transferring the results of research on humid midlatitude and semiarid midlatitude streams to those of the humid tropical areas. The results show that the low sinuosity Amazon Basin streams transport much finer sediment than do streams of equivalent sinuosity previously described for semiarid regions. Many of the fluvial complexities of the western Amazon Basin are seen as resulting from the relative abilities of different rivers to rework coarse, relict alluvium that was deposited during the relatively arid full-glacial phases of the Pleistocene. C.R.

A81-43213 **Hydrologic land use classification using Landsat.** R. J. Cermak, A. Feldman, and R. P. Webb (U.S. Army, Hydrologic Engineering Center, Davis, CA). In: Satellite hydrology; Proceedings of the Fifth Annual William T. Pecora Memorial Symposium on Remote Sensing, Sioux Falls, SD, June 10-15, 1979. Minneapolis, MN, American Water Resources Association, 1981, p. 262-269. 8 refs.

Experience with land use classification from Landsat multispectral imagery is described. Land use is required for the estimation of hydrologic model parameters. The land use classification procedure used is an unsupervised, noninteractive approach requiring no special image processing equipment. Watershed land use was determined from Landsat digital data, entered into a geographic data bank, and compared with a conventional land use classification. Hydrologic simulation model parameters were estimated from land use and other basin characteristics. The generated discharge frequency curves, corresponding to the alternative land use classifications, permitted the hydrologic significance of accuracy in land use identification to be assessed. (Author)

A81-43214 **Landsat data for regulatory permit monitoring.** A. N. Williamson (U.S. Army, Engineer Waterways Experiment Station, Vicksburg, MS). In: Satellite hydrology; Proceedings of the Fifth Annual William T. Pecora Memorial Symposium on Remote Sensing, Sioux Falls, SD, June 10-15, 1979. Minneapolis, MN, American Water Resources Association, 1981, p. 270-277.

The U.S. Army Corps of Engineers Regulatory Permit Program for activities in navigable inland or ocean waters was revised in July 1975. The major impact of the revisions is the requirement for a Department of the Army permit for the water disposal of dredged or fill material in virtually every water body in the U.S. The immensity of these requirements dictated that methods must be found that would provide a cost-effective way to detect and periodically monitor activities requiring permits. One candidate for this application was the Landsat satellite. The multispectral scanner (MSS) on board the satellite could provide relatively inexpensive and repetitive coverage of large areas of terrain on a regular basis. However, there were some questions regarding the ability of the MSS to resolve small terrain features, the applicability of currently available automatic data processing techniques and the cost of using Landsat MSS data for monitoring activities. An investigation of the various factors is discussed. Given an understanding of certain limitations concerning the acquired data, an interpreter can extract from a Landsat-derived image information that is valuable from the standpoint of the Regulatory Permit Program. G.R.

A81-43216 **Improving stream flow estimates through the use of Landsat.** G. J. Allord (U.S. Geological Survey, Water Resources Div., Madison, WI) and F. L. Scarpace (Wisconsin, University, Madison, WI). In: Satellite hydrology; Proceedings of the Fifth Annual William T. Pecora Memorial Symposium on Remote Sensing, Sioux Falls, SD, June 10-15, 1979. Minneapolis, MN, American Water Resources Association, 1981, p. 284-291. 7 refs.

Using new estimates of land cover in multiple regression techniques, the standard error of estimate (SE) for the least annual 7-day low flow for 2- and 10-year recurrence intervals of ungaged sites are lowered by 9 percent each. The SE of flood frequency in the 'Driftless Area' of Wisconsin for 10-, 50-, and 100-year recurrence intervals are lowered by 14 percent. Four of nine basin characteristics determined from satellite imagery are significant variables in the multiple regression techniques, whereas only 1 of the 12 characteristics determined from topographic maps is significant. The percentages of land cover categories in each basin are determined by merging basin boundaries, digitized from quadrangles, with a classified Landsat scene. Both the basin boundary X-Y polygon coordinates and the satellite coordinates are converted to latitude-longitude for merging compatibility. C.R.

A81-43217 **Flood applications of satellite imagery.** J. Kruus, H. L. Ferguson (Environment Canada, Atmospheric Environment Service, Ottawa, Canada), M. Deutsch (U.S. Geological Survey, Reston, VA), and P. L. Hansen (New Brunswick, Dept. of the Environment, Fredericton, Canada). In: Satellite hydrology; Proceedings of the Fifth Annual William T. Pecora Memorial Symposium on Remote Sensing, Sioux Falls, SD, June 10-15, 1979. Minneapolis, MN, American Water Resources Association, 1981, p. 292-301. 7 refs.

Various techniques that can be used to derive information relevant to floods from satellite imagery are illustrated. Multistage sampling makes use of Landsat images and aerial photography at various scales to outline flood damage from a regional scale to single fields. It is noted that multispectral composites may be made to enhance such features as standing water or floodplain indicators for measurement of photointerpretation. Temporal composites are useful in comparing flood levels on various dates or, if one of the images shows the normal stage, in measuring flooded area. It is noted that digital mapping methods may also be used in detecting, mapping, and measuring the area covered by water at various stages for derivation of a stage storage curve. C.R.

A81-43218 **A note on indirect detection of seiches in Great Salt Lake, Utah, by NOAA and Landsat satellite imagery.** M. Matson, C. P. Berg, and D. R. Wiesnet (NOAA, National Earth Satellite Service, Washington, DC). In: Satellite hydrology; Proceedings of the Fifth Annual William T. Pecora Memorial Symposium on Remote Sensing, Sioux Falls, SD, June 10-15, 1979. Minneapolis, MN, American Water Resources Association, 1981, p. 303-307. 5 refs.

On June 15, 1977, an unusual reflectance anomaly was detected in the north arm of Great Salt Lake, Utah, on NOAA-5 Very High Resolution Radiometer (VHRR) visible band imagery, and later on

Landsat-2 multispectral visual band imagery. Comparison of north arm lake levels with meteorological parameters leads to the conclusion that the anomalous reflectance is associated with wind induced seiches in the north arm. Apparently, the wind induces anomalous current patterns and higher than usual current speeds and waves in the western part of the north arm; these currents and waves then entrain the fine grained sediments of the shallow lake bottom, thus increasing the turbidity and hence the reflectance of surface waters. (Author)

A81-43219 Assessing the Red River of the North 1978 flooding from NOAA satellite data. C. P. Berg, D. R. Wiesnet, and M. Matson (NOAA, National Earth Satellite Service, Washington, DC). In: Satellite hydrology; Proceedings of the Fifth Annual William T. Pecora Memorial Symposium on Remote Sensing, Sioux Falls, SD, June 10-15, 1979. Minneapolis, MN, American Water Resources Association, 1981, p. 309-315. 5 refs.

Thermal infrared (IR) Very High Resolution Radiometer (VHRR) data from the polar-orbiting NOAA-5 satellite are used to map the spring 1978 flooding on the Red River of the North. The twice-daily VHRR-IR coverage provides good flood extent mapping capability for small rivers having broad flood plains such as the Red River of the North (basin area 101,519 square kilometers). Flood extent is delineated using computer-enhanced, enlarged thermal IR images mapped onto 1:1,000,000 base maps and compared to ground-based hydrologic data. The resulting maps show the flood-inundated areas and the changes that occur as the flood proceeds downstream. (Author)

A81-43220 A preliminary analysis of SAR mapping of the Manitoba flood, May 1979. R. T. Lowry (Intera Environmental Consultants, Ltd., Ottawa, Canada), N. Mudry (Manitoba, Dept. of Mines, Natural Resources and Environment, Winnipeg, Canada), and E. J. Langham. In: Satellite hydrology; Proceedings of the Fifth Annual William T. Pecora Memorial Symposium on Remote Sensing, Sioux Falls, SD, June 10-15, 1979. Minneapolis, MN, American Water Resources Association, 1981, p. 316-323.

A preliminary evaluation is presented of SAR imagery obtained of the flooding of the Red River in Manitoba in May, 1979 as part of the Sursat Program to determine Canadian needs for a surveillance satellite and the appropriate sensors to be used to meet those needs. The area of the flooding was mapped with an airborne synthetic aperture radar based on the ERIM four-channel SAR which consists of two dual polarized radars operating in the L and X bands, which was operated in the steep mode to simulate satellite observations. The imagery was processed to obtain maps of 1:250,000 and 1:500,000 scale which can be used to establish the actual extent of the flooding. The X-band is found to provide a better image, in part due to its higher resolution and shorter wavelength. Results demonstrate that an airborne SAR can provide all-weather flood area delineation, although satellite-borne radar, with steep depression angles, lower resolution and lower frequency, may not be able to delineate floods without special image processing. A.L.W.

A81-43226 Ground water and satellites - An overview/introduction. W. A. Pettyjohn (Oklahoma State University, Stillwater, OK). In: Satellite hydrology; Proceedings of the Fifth Annual William T. Pecora Memorial Symposium on Remote Sensing, Sioux Falls, SD, June 10-15, 1979. Minneapolis, MN, American Water Resources Association, 1981, p. 385, 386.

Remote sensing reports have improved dramatically in the past few years because of highly sophisticated automatic data processing. Unfortunately, much of the information is of limited practical value to local, state, or federal agencies, as well as other potential users. Satellite data, in several disciplines, has been less than satisfactory, not because it isn't suited to a specific application, but rather because so few use it. This is the result of poor communication, which can be overcome, in part, by publishing our findings more widely and by producing applications oriented, readable reports. (Author)

A81-43229 Hydrogeologic interpretations of Landsat imagery in arid zones of South and West Africa. W. Kruck (Bundesanstalt für Geowissenschaften und Rohstoffe, Hanover, West Germany). In: Satellite hydrology; Proceedings of the Fifth Annual William T. Pecora Memorial Symposium on Remote Sensing, Sioux Falls, SD, June 10-15, 1979. Minneapolis, MN, American Water Resources Association, 1981, p. 408-415. 8 refs.

A81-43231 Observations on Lake Ontario basin hydrogeology from optical enhancements of Landsat imagery. A. Falconer, L. Myers (Library of Parliament, Ottawa, Canada), and M. Deutsch (U.S. Geological Survey, Reston, VA). In: Satellite hydrology; Proceedings of the Fifth Annual William T. Pecora Memorial Symposium on Remote Sensing, Sioux Falls, SD, June 10-15, 1979. Minneapolis, MN, American Water Resources Association, 1981, p. 427-436. 8 refs. U.S. Geological Survey Contracts No. 14-08-0001-13169; No. 14-08-0001-3185.

Before the close of the International Hydrological Decade (IHD), the launch of Landsat 1 in 1972 made possible the collection and analysis of satellite images showing the entire Lake Ontario drainage basin. An assessment was made of Landsat imagery and prelaunch aircraft analog data to determine their usefulness in assisting IHD investigators to define the regional hydrological characteristics of the basin. By using a composite of July data from MSS bands 4, 5, and 7, reprocessing of standard EDC products leads to the production of a low-cost detailed synoptic view of vegetation distribution and land use in the Lake Ontario basin. A temporal series of two scene Landsat mosaics of the western Lake Ontario region provide an information base for interpreting hydrological conditions from snow distribution, ice melting patterns, and vegetation anomalies indicative of ground water discharge or the presence of shallow aquifers. B.J.

A81-43233 * Ground water applications of the heat capacity mapping mission. J. L. Heilman (Texas A & M University, College Station, TX) and D. G. Moore (South Dakota State University, Brookings, SD). In: Satellite hydrology; Proceedings of the Fifth Annual William T. Pecora Memorial Symposium on Remote Sensing, Sioux Falls, SD, June 10-15, 1979. Minneapolis, MN, American Water Resources Association, 1981, p. 446-449. U.S. Geological Survey Contract No. 14-08-0001-12510; Contract No. NAS5-24206.

The paper discusses the ground water portion of a hydrologic investigation of eastern South Dakota using data from the Heat Capacity Mapping Mission (HCMM) satellite. The satellite carries a two-channel radiometer (0.5-1.1 and 10.5-12.5 microns) in a sun synchronous orbit and collects data at approximately 0230 and 1330 local standard time with repeat coverage of 5 to 16 days depending on latitude. It is shown that HCMM data acquired at appropriate periods of the diurnal and annual temperature cycle can provide useful information on shallow ground water. V.L.

A81-43234 * Landsat classification of coastal wetlands in Texas. R. J. Finley (Texas, University, Austin, TX), S. McCulloch (Texas Natural Resources Information System, Austin, TX), and P. Harwood (National Governor's Association, Council of State Planning Agencies, Washington, DC). In: Satellite hydrology; Proceedings of the Fifth Annual William T. Pecora Memorial Symposium on Remote Sensing, Sioux Falls, SD, June 10-15, 1979. Minneapolis, MN, American Water Resources Association, 1981, p. 453-462. 15 refs. Contract No. NAS5-20986.

Through a multiagency study of Landsat imagery applications, an analysis of Texas coastal wetlands shows that five Level III categories of wetlands can be delineated using image interpretation: topographically low marshes, topographically high marshes, tidal flats, sea grass and algal flats, and vegetated dredged material. Image interpretation involves optical enlargement of 1:1,000,000 scale, Landsat transparencies to a scale of 1:125,000 and mapping on a stable film base. Digital classification procedures, resulting in 1:24,000 scale line printer maps as output, require several iterations to display welands effectively. Accuracies of 65% were achieved for all wetland categories combined. B.J.

A81-43235 Accuracy evaluation of Landsat digital classification of vegetation in the Great Dismal Swamp. P. T. Gammon (U.S. Geological Survey, Suffolk, VA), W. G. Rohde (U.S. Geological Survey, EROS Data Center, Sioux Falls, SD), and V. Carter (U.S. Geological Survey, Reston, VA). In: Satellite hydrology; Proceedings of the Fifth Annual William T. Pecora Memorial Symposium on Remote Sensing, Sioux Falls, SD, June 10-15, 1979.

Minneapolis, MN, American Water Resources Association, 1981, p. 463-473. 9 refs.

A81-43236 * **Using Landsat MSS data with soils information to identify wetland habitats.** C. L. Ernst and R. M. Hoffer (Purdue University, Lafayette, IN). In: Satellite hydrology; Proceedings of the Fifth Annual William T. Pecora Memorial Symposium on Remote Sensing, Sioux Falls, SD, June 10-15, 1979.
Minneapolis, MN, American Water Resources Association, 1981, p. 474-478. 6 refs. Grant No. NGL-15-005-186.

A previous study showed that certain fresh water wetland vegetation types can be spectrally separated when a maximum likelihood classification procedure is applied to Landsat spectral data. However, wetland and upland types which have similar vegetative life forms (e.g., upland hardwoods and hardwood swamps) are often confused because of spectral similarity. Therefore, the current investigation attempts to differentiate similar wetland and upland types by combining Landsat multispectral scanner (MSS) data with soils information. The Pigeon River area in northern Indiana used in the earlier study was also employed in this investigation. A layered classification algorithm which combined soils and spectral data was used to generate a wetland classification. The results of the spectral/soils wetland classification are compared to the previous classification that had been based on spectral data alone. The results indicate wetland habitat mapping can be improved by combining soils and other ancillary data with Landsat spectral data. (Author)

A81-43237 * **Improvements in lake volume predictions using Landsat data.** J. C. Gervin (NASA, Goddard Space Flight Center, Greenbelt, MD) and S. F. Shih (Florida, University, Belle Glade, FL) In: Satellite hydrology; Proceedings of the Fifth Annual William T. Pecora Memorial Symposium on Remote Sensing, Sioux Falls, SD, June 10-15, 1979. Minneapolis, MN, American Water Resources Association, 1981, p. 479-484. NASA-supported research.

A cumulative error in the water balance budget for Lake Okeechobee produces a one million acre-foot discrepancy in the predicted water volume over a 4-year period. The major source of error appears to be complex shoreline marshes that comprise 20 percent of the lake surface. The water balance budget model presently treats these marshes as open water. Using Landsat data, the vegetation in the lake's littoral zone was classified multispectrally to provide a data base for determining water budget information. First, the acreage of a given plant species in the littoral zone was obtained with satellite data. Second, the surface area occupied by plants (which therefore could not be considered open water) was used to adjust the vegetation acreage giving an effective water surface. Based on this information, more detailed representations of evapotranspiration and total water surface (and hence total lake volume) could be provided to the water balance budget computation. (Author)

A81-43238 * **Landsat hydrobiological classification for an inland fresh water marsh within Everglades National Park.** P. W. Rose and P. C. Rosendahl (U.S. National Park Service, South Florida Research Center, Homestead, FL). In: Satellite hydrology; Proceedings of the Fifth Annual William T. Pecora Memorial Symposium on Remote Sensing, Sioux Falls, SD, June 10-15, 1979.
Minneapolis, MN, American Water Resources Association, 1981, p. 485-491. NASA-supported research.

The considered investigation is concerned with the application of Landsat Multispectral Scanner (MSS) data to the classification of vegetative communities and the establishment of flow vectors for the Shark River Slough in Everglades National Park, Florida. A systematic array of 'ground truth' was established utilizing comprehensive hydrologic field data and conventional high altitude infrared aerial photography. A control network was defined that represented all hydrobiological zones (those wetland vegetative communities that directly influence the rate of overland sheet flow) in the Shark River Slough. These data were then directly applied to the Landsat imagery utilizing an interactive multispectral processor which generated hydrographic maps of the slough and defined the surface radiance characteristics of each hydrobiological system. It was found that the application of Landsat imagery for hydrologic applications in a wetlands area, such as the Shark River Slough in Everglades National Park, is definitely a viable tool for resource management. G.R.

A81-43239 * **A comparison of remote sensing techniques for Minnesota wetlands classification.** L. F. Werth (Lockheed Electronics Co., Inc., Houston, TX) and M. P. Meyer (Minnesota, University, St. Paul, MN). In: Satellite hydrology; Proceedings of the Fifth Annual William T. Pecora Memorial Symposium on Remote Sensing, Sioux Falls, SD, June 10-15, 1979.
Minneapolis, MN, American Water Resources Association, 1981, p. 492-498. 8 refs. Research supported by the University of Minnesota and NASA.

A wetland classification study in a typically complex 650 sq km test site in east central Minnesota compared the time, cost and accuracy of manually interpreted 1:24,000 scale color infrared aerial photographs with digital analysis of Landsat data. The comparison was between the same general wetland and non-wetland classes; accuracy of both systems was evaluated with intensive ground verification. For the same general classes, the overall mapping accuracy was 96 percent for the aerial photo interpretation and 71 percent for Landsat double-date classification. Results with maximum likelihood and SECHO classifiers were the same, 71 percent while mapping accuracy with a layered classifier was only 66 percent. Compared to a general geometric correction and a single-date data set, geographic position and classification accuracy improved when a precision geometric correction and a double-date data set were used. Landsat digital analysis was faster, 24 vs. 90 days, but photointerpretation was more economical at $0.15/hectare (including all costs of procurement, processing and analysis), compared with Landsat costs of $0.35/hectare (not including costs of data procurement, processing prior to delivery to user and related overhead). (Author)

A81-43240 **Landsat interpretation of prairie lakes and wetlands of eastern South Dakota.** R. G. Best and D. G. Moore (South Dakota State University, Brookings, SD). In: Satellite hydrology; Proceedings of the Fifth Annual William T. Pecora Memorial Symposium on Remote Sensing, Sioux Falls, SD, June 10-15, 1979. Minneapolis, MN, American Water Resources Association, 1981, p. 499-506. 15 refs. U.S. Geological Survey Contract No. 14-08-0001-13576.

Spectral and morphometric properties of prairie lakes and wetlands can be interpreted on Landsat MSS imagery. Multispectral interpretations for developing water quality sampling strategies are discussed and illustrated. Photographic enhancement techniques including contrast enhancement to depict qualitative turbidity differences, thematic extraction of open water bodies, and temporal compositing for determining the occurrence and distribution of emergent vegetation are presented and illustrated. The statistical accuracy of morphometric measurements, including area length, breadth, mean breadth, and shoreline development index were calculated. Models for estimating average depth and volume were developed and evaluated. (Author)

A81-43241 * **A technique for improved assessment of flow resistance characteristics of natural wetlands using Landsat data.** J. C. Gervin (NASA, Goddard Space Flight Center, Greenbelt, MD) and S. F. Snih (Florida, University, Bell Glade, FL). In: Satellite hydrology; Proceedings of the Fifth Annual William T. Pecora Memorial Symposium on Remote Sensing, Sioux Falls, SD, June 10-15, 1979.
Minneapolis, MN, American Water Resources Association, 1981, p. 507-511. NASA-supported research.

In the past, one value of the roughness coefficient has frequently been used to represent the flow resistance characteristics of the entire natural wetland throughout the year. To improve the simulation of water flow through these natural vegetation communities, Landsat imagery and in situ flow measurements could be combined to produce a more detailed representation of flow resistance. The vegetation in a typical marshland drainage basin in south Florida was classified into five major categories using Landsat data. Flow measurements were then performed at characteristic sites in the basin. The measurements were taken at various depths during months of significant flow to examine the effect of seasonal growth. This information can be compared with the areal extent of the vegetation measured by satellite to more accurately simulate resistance to water flow in natural marshland drainage basins. (Author)

A81-43242 **Using Landsat imagery to study the Okavango Swamp, Botswana.** S. M. Hutton and T. Dincer. In: Satellite hydrology; Proceedings of the Fifth Annual William T. Pecora

Memorial Symposium on Remote Sensing, Sioux Falls, SD, June 10-15, 1979. Minneapolis, MN, American Water Resources Association, 1981, p. 512-519. 20 refs.

A81-43243 * **Computer-implemented remote sensing techniques for measuring coastal productivity and nutrient transport systems.** M. K. Butera (NASA, Earth Resources Laboratory, Bay St. Louis, MS). In: Satellite hydrology; Proceedings of the Fifth Annual William T. Pecora Memorial Symposium on Remote Sensing, Sioux Falls, SD, June 10-15, 1979. Minneapolis, MN, American Water Resources Association, 1981, p. 522-532. 21 refs.

An automatic technique has been developed to measure marsh plant production by inference from a species classification derived from Landsat MSS data. A separate computer technique has been developed to calculate the transport path length of detritus and nutrients from their point of origin in the marsh to the shoreline from Landsat data. A nutrient availability indicator, the ratio of production to transport path length, was derived for each marsh-identified Landsat cell. The use of a data base compatible with the Landsat format facilitated data handling and computations. (Author)

A81-43249 * **Applications of Landsat imagery to a coastal inlet stability study.** Y.-H. Wang (Texas A & M University, Galveston, TX). In: Satellite hydrology; Proceedings of the Fifth Annual William T. Pecora Memorial Symposium on Remote Sensing, Sioux Falls, SD, June 10-15, 1979. Minneapolis, MN, American Water Resources Association, 1981, p. 579-584. 6 refs. NASA-sponsored research.

Polcyn and Lyzenga (1975) and Middleton and Barber (1976) have demonstrated that it is possible to correlate the radiance values of a multispectral imagery, such as Landsat imagery, with the depth related information. The present study is one more example of such an effort. Two sets of Landsat magnetic tape were obtained and displayed on the screen of an Image-100 computer. Spectral analysis was performed to produce various signatures, their extent, and location. Subsequent ground truth observations and measurements were gathered by means of hydrographic surveys and low altitude aerial photographs for interpretation and calibration of the Landsat data. Finally, a coastal engineering assessment based on the Landsat data was made. Recommendations regarding the navigational canal alignment and dredging practice are presented in the light of inlet stability. (Author)

A81-43252 **Using enhanced Landsat images for calibrating real time estuarine water quality models.** J. M. Hill (Louisiana State University, Baton Rouge, LA) and D. S. Graham (Tudor Engineering Co., San Francisco, CA). In: Satellite hydrology; Proceedings of the Fifth Annual William T. Pecora Memorial Symposium on Remote Sensing, Sioux Falls, SD, June 10-15, 1979.
Minneapolis, MN, American Water Resources Association, 1981, p. 603-614. 20 refs. Research supported by the U.S. Environmental Protection Agency; Grant No. NOAA-04-158-44046.

A study of the effects of silvicultural activities and associated channelization upon the quality of the receiving waters of Apalachicola Bay in north Florida is utilizing Landsat images and data to verify real time estuarine water quality models. Management of estuarine water resources requires that accurate mathematical paradigms of circulation and quality be made in order to evaluate the effects of different alternative scenarios. For such paradigms to be predictive in estuaries, it has been demonstrated that they must be in so called 'real time' in which the timestep is much shorter than the tidal period. Verification of such models requires good synoptic data. These are usually impossible to acquire as the time required to traverse the estuary by boats results in measurements being taken over most of the tidal cycle, while continuous observations taken at fixed points provide inadequate spatial resolution at practical staffing levels. Circulation patterns in several specially enhanced Landsat images show good comparison to output of finite element two-dimensional (2-D) vertically averaged models of Apalachicola Bay, hence, information can be applied to both calibrate and verify estuarine water quality models. (Author)

A81-43253 * **An application of Landsat and computer technology to potential water pollution from soil erosion.** W. J. Campbell (NASA, Goddard Space Flight Center, Greenbelt, MD). In: Satellite hydrology; Proceedings of the Fifth Annual William T. Pecora Memorial Symposium on Remote Sensing, Sioux Falls, SD, June 10-15, 1979. Minneapolis, MN, American Water Resources Association, 1981, p. 616-621. 5 refs.

Agricultural activity has been recognized as the primary source of nonpoint source water pollution. Water quality planners have needed information that is timely, accurate, easily reproducible, and relatively inexpensive to utilize to implement 'Best Management Practices' for water quality. In this paper, a case study shows how the combination of satellite data, which can give accurate land-cover/land-use information, and a computerized geographic information system, can assess nonpoint pollution at a regional scale and be cost effective. (Author)

A81-43254 * **Bay of Fundy verification of a system for multidate Landsat measurement of suspended sediment.** J. C. Munday, Jr. (Virginia Institute of Marine Science; College of William and Mary, Gloucester Point, VA), T. T. Afoldi (Canada Centre for Remote Sensing, Ottawa, Canada), and C. L. Amos (Geologic Survey of Canada, Bedford Institute of Oceanography, Dartmouth, Nova Scotia, Canada). In: Satellite hydrology; Proceedings of the Fifth Annual William T. Pecora Memorial Symposium on Remote Sensing, Sioux Falls, SD, June 10-15, 1979. Minneapolis, MN, American Water Resources Association, 1981, p. 622-640. 39 refs. Grant No. NGL-47-022-005.

A system for automated multidate Landsat CCT MSS measurement of suspended sediment concentration (S) has been implemented and verified on nine sets (108 points) of data from the Bay of Fundy, Canada. The system employs 'chromaticity analysis' to provide automatic pixel-by-pixel adjustment of atmospheric variations, permitting reference calibration data from one or several dates to be spatially and temporally extrapolated to other regions and to other dates. For verification, each data set was used in turn as test data against the remainder as a calibration set: the average absolute error was 44 percent of S over the range 1-1000 mg/l. The system can be used to measure chlorophyll (in the absence of atmospheric variations), Secchi disk depth, and turbidity. (Author)

A81-43255 **Assessment and classifications of selected Illinois lakes through the application of space technology.** D. J. Schaeffer, R. P. Clarke, D. F. Sefton (Illinois Environmental Protection Agency, Springfield, IL), and D. H. P. Boland (USAF, Wright-Patterson AFB, OH). In: Satellite hydrology; Proceedings of the Fifth Annual William T. Pecora Memorial Symposium on Remote Sensing, Sioux Falls, SD, June 10-15, 1979.
Minneapolis, MN, American Water Resources Association, 1981, p. 641-648. 8 refs.

Selected Illinois lakes were assessed and classified by: (1) applying a complete linkage clustering algorithm to Landsat MSS data and interpreting the clusters by comparing the spectral composition and uniqueness of each with water quality data, field evaluations, lake morphology, and watershed characteristics; and (2) using Landsat spectral ranks as independent variables and contact-sensed data as dependent variables for the development of multiple regression models to obtain estimates of trophic indicator parameters and multivariate trophic indices and, subsequently, lake trophic state rankings and groupings. Cluster analysis of the raw spectral data established distinctive lake groups, each comprised of water bodies having similar optical and physical properties. The spectral properties of each lake provided an integrated characterization of water quality and related use impairment problems. The trophic parameter estimates, as well as lake clusters and rankings derived from them, were in general agreement with contact-sensed data and with the raw spectral data. (Author)

A81-43256 **Thermal patterns of Lake Michigan and Lake Superior from satellite remote sensors and its uses.** H. W. Hoffman (NOAA, National Weather Service, Rosemont, IL). In: Satellite hydrology; Proceedings of the Fifth Annual William T. Pecora Memorial Symposium on Remote Sensing, Sioux Falls, SD, June 10-15, 1979. Minneapolis, MN, American Water Resources Association, 1981, p. 650-653.

Average surface water temperature maps have been drawn for Lake Michigan and Lake Superior in order to understand short- and long-range thermal patterns. The data used were generated over a two-year period from the Very High Resolution Radiometer on NOAA-4 and -5 satellites. Results indicate that the waters of Lake Michigan and Lake Superior as observed from satellite imagery act in similar manner as any other large and deep body of water in that fluctuations in water temperature occur very gradually, except for upwelling effects near the shore. The high specific heat of these water bodies has a profound effect on climatic conditions of adjacent air and land masses. V.L.

A81-43257 **Lake Ontario dynamics and water quality observations using thematically enhanced Landsat data.** A. Falconer (Spectral Data Corp., Regional Remote Sensing Facility, Nairobi, Kenya), M. Deutsch (U.S. Geological Survey, Reston, VA), and L. Myers (Library of Parliament, Ottawa, Canada). In: Satellite hydrology; Proceedings of the Fifth Annual William T. Pecora Memorial Symposium on Remote Sensing, Sioux Falls, SD, June 10-15, 1979. Minneapolis, MN, American Water Resources Association, 1981, p. 655-661. 15 refs. U.S. Geological Survey Contracts No. 14-08-0001-13169; No. 14-08-0001-13185.

The considered study is concerned with the use of satellite data for the identification of phenomena observed in western Lake Ontario. Ships and aircraft have been generally employed for gathering knowledge about the Great Lakes. It is pointed out that space technology has the potential to greatly increase the efficiency and effectiveness of lake monitoring programs. Satellites such as Landsat can obtain synoptic and repetitive views useful for guiding ships and aircraft to areas where more detailed studies are needed. An investigation is conducted of the techniques for photo-optical reprocessing of Landsat images and computer processing of digital Landsat data to enhance water quality information and to determine the appropriate use of each method. It is found that Landsat is an excellent source of synoptic data indicative of the dynamics of Lake Ontario and its water quality conditions. Landsat data needs to be specially processed (thematically enhanced) to depict anomalies indicative of water quality of dynamics. G.R.

A81-43258 * **Application of digital image processing techniques and information systems to water quality monitoring of Lake Tahoe.** A. Y. Smith and R. J. Blackwell (California Institute of Technology, Jet Propulsion Laboratory, Pasadena, CA). In: Satellite hydrology; Proceedings of the Fifth Annual William T. Pecora Memorial Symposium on Remote Sensing Sioux Falls, SD, June 10-15, 1979. Minneapolis, MN, American Water Resources Association, 1981, p. 662-672. 8 refs.

The Tahoe basin occupies over 500 square miles of territory located in a graben straddling the boundary between California and Nevada. Lake Tahoe contains 126 million acre-feet of water. Since the 1950's the basin has experienced an ever increasing demand for land development at the expense of the natural watershed. Discharge of sediment to the lake has greatly increased owing to accelerated human interference, and alterations to the natural drainage patterns are evident in some areas. In connection with an investigation of the utility of a comprehensive system that takes into account the causes as well as the effects of lake eutrophication, it has been attempted to construct an integrated and workable data base, comprised of currently available data sources for the Lake Tahoe region. Attention is given to the image based information system (IBIS), the construction of the Lake Tahoe basin data base, and the application of the IBIS concept to the Lake Tahoe basin. G.R.

A81-43259 * **Trophic state determination for shallow coastal lakes from Landsat imagery.** C. W. Welby, A. M. Witherspoon (North Carolina State University, Raleigh, NC), and R. E. Holman, III (North Carolina Div. of Environmental Management, Edenton, NC). In: Satellite hydrology; Proceedings of the Fifth Annual William T. Pecora Memorial Symposium on Remote Sensing, Sioux Falls, SD, June 10-15, 1979. Minneapolis, MN, American Water Resources Association, 1981, p. 674-680. 20 refs. Contract No. NAS8-31984.

A study has been carried out to develop a photo-optical technique by which Landsat imagery can be used to monitor trophic states of lakes. The proposed technique uses a single number to characterize the trophic state, and a feature within the satellite scene is used as an internal standard for comparison of the lakes in time. By use of the technique it is possible to assess in retrospect the trophic state of each individual lake. V.L.

A81-43356 # **Annual and interannual variations in outgoing longwave radiation over the tropics.** T. R. Heddinghaus and A. F. Krueger (NOAA, Climate Analysis Center, Washington, DC). *Monthly Weather Review,* vol. 109, June 1981, p. 1208-1218. 25 refs. NOAA-supported research.

Four years of satellite observations of the outgoing longwave radiation have been used to study the distribution of cloudiness and rainfall over the tropics. Annual and interannual variations are described, partially with the help of an eigenvector analysis. Interannual variations in the outgoing longwave radiation are particularly interesting since they tend to follow the Southern Oscillation. Consequently, it can be used to monitor changes in the large-scale circulation over the tropics. (Author)

A81-43538 **Remote sensing of dinoflagellate blooms in a turbid estuary.** J. C. Munday, Jr. and P. L. Zubkoff (Virginia Institute of Marine Science, Gloucester Point, VA). *Photogrammetric Engineering and Remote Sensing,* vol. 47, Apr. 1981, p. 523-531. 36 refs.

Dinoflagellate blooms in sediment-laden waters of the York River, Virginia consistently produced reflectance decreases in visible bands, but produced equivocal changes in the photographic infrared. The equivocal infrared changes are due to simultaneous variations in chlorophyll and inorganic suspended sediment concentrations, as interpreted with a reflectance model. Equations are developed to show what conditions of changing chlorophyll and sediment can produce invariant reflectance. Color photography of dinoflagellate blooms in turbid estuaries portrays chlorophyll distributions with limited accuracy. The complexity of the spatial distributions necessitates remote sensing for synoptic mapping. (Author)

A81-43543 **Mapping wetlands using orthophotoquads and 35-mm aerial photographs.** R. A. Mead (Virginia Polytechnic Institute and State University, Blacksburg, VA) and P. T. Gammon (U.S. Geological Survey, Suffolk, VA). *Photogrammetric Engineering and Remote Sensing,* vol. 47, May 1981, p. 649-652. 11 refs.

A U.S. Geological Survey 7.5-minute orthophotoquad is used in combination with 35-mm color-infrared aerial transparencies to inventory and map North Carolina wetland areas of interest to regional or local land managers. Orthophotoquads are rectified black-and-white aerial photographs produced in the 7.5-minute, 1:24,000 scale standard map series. These orthophotoquads provide a mapping base of uniform scale upon which many vegetation and land-use boundaries may be delineated. The 35-mm aerial photographs, flown at a larger scale, for example, 1:6,000, along selected transects within the orthophotoquad afford identification of different wetland types. The vegetation types identified on the 35-mm infrared photographs thus assist the interpreter in identifying the desired wetland types on the total wetland area within the quad. In areas where orthophotoquads are available, this method permits resource managers to map wetlands without the need for expensive large format photography. (Author)

A81-43544 * **Multisensor analysis of hydrologic features with emphasis on the Seasat SAR.** J. L. Foster and D. K. Hall (NASA, Goddard Space Flight Center, Greenbelt, MD). *Photogrammetric Engineering and Remote Sensing,* vol. 47, May 1981, p. 655-664. 13 refs.

Synthetic aperture radar (SAR) imagery of the Wind River Range area in Wyoming is compared with visible and near-infrared imagery of the same area. Data from the Seasat L-Band SAR and an aircraft X-Band SAR are compared with Landsat Return Beam Vidicon (RBV) visible data and near-infrared aerial photography and topographic maps of the same area. It is noted that visible and near-infrared data provide more information than the SAR data when conditions are the most favorable. The SAR penetrates clouds and snow, however, and data can be acquired day or night. Drainage density detail is good on SAR imagery because individual streams show up well owing to riparian vegetation; this causes higher radar reflections which result from the 'rough' surface which vegetation creates. In the winter image, the X-Band radar data show high returns because of cracks on the lake ice surfaces. High returns can also be seen in the L-Band SAR imagery of the lakes due to ripples on the surface induced by wind. It is concluded that the use of multispectral data would optimize analysis of hydrologic features. C.R.

A81-43545 * **Use of ocean color scanner data in water quality mapping.** S. Khorram (California, University, Berkeley, CA). *Photogrammetric Engineering and Remote Sensing,* vol. 47, May

1981, p. 667-676. 53 refs. Research supported by the University of California; Grant No. NsG-5256.

Remotely sensed data, in combination with in situ data, are used in assessing water quality parameters within the San Francisco Bay-Delta. The parameters include suspended solids, chlorophyll, and turbidity. Regression models are developed between each of the water quality parameter measurements and the Ocean Color Scanner (OCS) data. The models are then extended to the entire study area for mapping water quality parameters. The results include a series of color-coded maps, each pertaining to one of the water quality parameters, and the statistical analysis of the OCS data and regression models. It is found that concurrently collected OCS data and surface truth measurements are highly useful in mapping the selected water quality parameters and locating areas having relatively high biological activity. In addition, it is found to be virtually impossible, at least within this test site, to locate such areas on U-2 color and color-infrared photography. C.R.

A81-43548 **Hydrogeology of glacial deposits from aerial photographs.** E. K. Sauer (Saskatchewan, University, Saskatoon, Canada). *Photogrammetric Engineering and Remote Sensing*, vol. 47, June 1981, p. 811-822. 28 refs.

It is pointed out that aerial photographs present a unique vertical perspective of certain landscape features which exist as expressions of the hydrogeology of an area. Geological processes interpreted from aerial photographs define ground-water systems and boundary conditions in glaciated terrain. The ground-water flow system within this framework is indicated on black-and-white photographs by springs, tone patterns, vegetation indicators, salinity of surface soils, slope instability, and apparent anomalies in streams and floodplains. Direct and indirect evidence of recharge and storage is often evident because of the landscape features. Discharge phenomena tend to be the most apparent, however. G.R.

A81-43549 **Wetland mapping from digitized aerial photography.** F. L. Scarpace, B. K. Quirk, R. W. Kiefer, and S. L. Wynn (Wisconsin, University, Madison, WI). *Photogrammetric Engineering and Remote Sensing*, vol. 47, June 1981, p. 829-838. 32 refs.

Computer classification of digitized aerial imagery for wetland mapping was investigated. A comparison was made between digital and manual interpretation of a high altitude color infrared photograph. The resulting computer classification was approximately 90 percent accurate. Digital analysis of aerial imagery provides high resolution information and could provide an operational method for monitoring and mapping wetlands. (Author)

A81-43742 * **Mapping the Great Salt Lake shoreline and associated waterfowl habitat from Landsat data.** J. Boissonnault (Utah, University, Salt Lake City, UT) and R. G. Witt (NASA, Goddard Space Flight Center, Greenbelt, MD). In: Rainbow 80; Fall Technical Meeting, Niagara Falls, NY, October 7-10, 1980, ASP Technical Papers. Falls Church, VA, American Society of Photogrammetry, 1981, p. RS-3-A-1 to RS-3-A-7.

A81-43745 * **Manual versus digital Landsat analysis for modeling river flooding.** W. R. Philipson and W. R. Hafker (Cornell University, Ithaca, NY). In: Rainbow 80; Fall Technical Meeting, Niagara Falls, NY, October 7-10, 1980, ASP Technical Papers. Falls Church, VA, American Society of Photogrammetry, 1981, p. RS-3-D-1 to RS-3-D-10. 8 refs. Grant No. NGL-33-010-171. DI Project A-089-NY.

The comparative value of manual versus digital image analysis for determining flood boundaries is being examined in a study of the use of Landsat data for modeling flooding of the Black River, in northern New York. The work is an extension of an earlier study in which Black River flooding was assessed through visually interpreted, multi-date Landsat band 7 images. Based on the results to date, it appears that neither color-additive viewing nor digital analysis of Landsat data provide improvement in accuracy over visual analysis of band 7 images, for delineating the boundaries of flood-affected areas. (Author)

A81-43746 **Preliminary survey of HCMM satellite thermal imagery as applied to hydrospherics.** D. R. Wiesnet, D. F. McGinnis, Jr., M. Matson, and J. A. Pritchard (NOAA, National Environmental Satellite Service, Washington, D.C.). In: Rainbow 80; Fall Technical Meeting, Niagara Falls, NY, October 7-10, 1980, ASP Technical Papers. Falls Church, VA, American Society of Photogrammetry, 1981, p. RS-3-E-1 to RS-3-E-12. 14 refs.

NASA's Heat Capacity Mapping Mission satellite, launched April 26, 1978 to an orbital altitude of 620 km, provides day/night thermal (10.5-12.5 micron) coverage on a regular basis. The satellite, having exceptional thermal and spatial resolution, has been used to study hydrospheric features. Estuarine tidal circulation monitoring is demonstrated in large systems; some degree of tidal circulation is inferred from thermal patterns even in small estuaries. Details of transient circulation features such as eddies are studied synoptically, and details of tidal currents are readily mapped. Attempts to estimate soil moisture from thermal patterns and/or thermal inertia measurements are complicated by canopy temperatures and geomorphology. Delineation and measurement of urban heat islands are shown to be useful for demographic studies and for determinining the effect of anthropogenic changes on mesoscale climates. J.F.

A81-43747 **Southern Chesapeake Bay circulation and suspended sediment transport analyzed using Landsat imagery.** J. C. Munday, Jr. and M. S. Fedosh (College of William and Mary, Gloucester Point, VA). In: Rainbow 80; Fall Technical Meeting, Niagara Falls, NY, October 7-10, 1980, ASP Technical Papers. Falls Church, VA, American Society of Photogrammetry, 1981, p. RS-3-F-1 to RS-3-F-5. 12 refs.

Fifty dates of Landsat images of the southern Chesapeake Bay are under study for circulation patterns and suspended sediment transport as a function of wind, tide, and fresh water inflow conditions. Methods of analysis include visual interpretation and color-coded density slicing of MSS 5 images coupled with color-additive viewing of MSS 4 to 7 images. At the Bay mouth, flood tide plumes are prominent on the north side, and ebb plumes carrying James River sediments on the south. A turbidity increase follows the progressive tidal wave of maximum current in its passage up the Bay. Plumes are oriented downwind. Winter and spring turbidities, in association with strong northerly winds, are higher than in summer. (Author)

A81-45429 * **Water quality mapping from Landsat digital data.** S. Khorram (California, University, Berkeley, CA; North Carolina State University, Raleigh, NC). *International Journal of Remote Sensing*, vol. 2, Apr.-June 1981, p. 145-153. 37 refs. Research supported by the University of California; Grant No. NsG-5256.

A81-46045 * **Mapping alpine soils using color positive and color infrared photographs.** S. Burns (Colorado, University, Boulder, CO). In: Machine processing of remotely sensed data and soil information systems and remote sensing and soil survey; Proceedings of the Sixth Annual Symposium, West Lafayette, IN, June 3-6, 1980. New York, Institute of Electrical and Electronics Engineers, Inc., 1980, p. 214-220. 11 refs. Grant No. NGL-06-003-200.

During a soil survey of the Indian Peaks area of the Colorado Front Range, it was found that large scale color positive photographs taken in the autumn were extremely useful for mapping alpine soils. Smaller scale color infrared photos were also helpful for delineation of mapping units. The soil mapping units were deduced on the basis of landforms and snow accumulation which is reflected in patterns of vegetational communities. (Author)

A81-46405 * **Manual versus digital Landsat analysis for delineating river flooding.** W. R. Philipson and W. R. Hafker (Cornell University, Ithaca, NY). *Photogrammetric Engineering and Remote Sensing*, vol. 47, Sept. 1981, p. 1351-1356. 8 refs. Grant No. NGL-33-010-171. DI Project A-089-NY.

It has been found that flood boundary information derived from Landsat images, acquired at different flood stages, could be used to develop an empirical model for estimating the extent of flooding on the basis of in situ measurements of river discharge. An investigation was undertaken to determine whether improved results might have been obtained through digital image analysis or by including other Landsat spectral bands. The study area encompasses a highly flood-prone reach of the Black River in Lewis County, NY. It was found that visual analysis of aerial photographs and a Landsat band 7 image gave similar results. Visual and digital analysis of Landsat band 7 data gave similar results, and digital analysis of Landsat band 7 data gave results which were at least as good as digital analysis of combinations of spectral bands. G.R.

A81-47356 **Monitoring of snow covered area using satellite data.** H. Ochiai (Toba Merchant Marine College, Toba, Mie, Japan) and K. Takeda (Science and Technology Agency, National Institute of Natural Resources, Tokyo, Japan). *International Astronautical Federation, International Astronautical Congress, 32nd, Rome, Italy, Sept. 6-12, 1981, Paper 81-114.* 12 p.

It is pointed out that the detection of snow regions in Japan by Landsat MSS and RBV is recognized as being more effective than the snow depth distribution maps compiled from data from snow survey stations. High-resolution data obtained by NOAA AVHRR is also considered suitable for monitoring snow covered areas. C.R.

A81-47647 * # **Airborne simultaneous spectroscopic detection of laser-induced water Raman backscatter and fluorescence from chlorophyll a and other naturally occurring pigments.** F. E. Hoge (NASA, Wallops Flight Center, Wallops Island, VA) and R. N. Swift (EG & G Washington Analytical Services Center, Inc., Pocomoke City, MD). *Applied Optics,* vol. 20, Sept. 15, 1981, p. 3197-3205. 22 refs.

The airborne laser-induced spectral emission bands obtained simultaneously from water Raman backscatter and the fluorescence of chlorophyll and other naturally occurring waterborne pigments are reported here for the first time. The importance of this type data lies not only in its single-shot multispectral character but also in the application of the Raman line for correction or calibration of the spatial variation of the laser penetration depth without the need for in situ water attenuation measurements. The entire laser-induced fluorescence and Raman scatter emissions resulting from each separate 532-nm 10-nsec laser pulse are collected and spectrally dispersed in a diffraction grating spectrometer having forty photomultiplier tube detectors. Results from field experiments conducted in the North Sea and the Chesapeake Bay/Potomac River are presented. Difficulties involving the multispectral resolution of the induced emissions are addressed, and feasible solutions are suggested together with new instrument configurations and future research directions. (Author)

A81-47676 # **Use of water Raman emission to correct airborne laser fluorosensor data for effects of water optical attenuation.** M. Bristow, D. Nielsen, D. Bundy, and R. Furtek (U.S. Environmental Protection Agency, Environmental Monitoring Systems Laboratory, Las Vegas, NV). *Applied Optics,* vol. 20, Sept. 1, 1981, p. 2889-2906. 42 refs.

It is shown that the interference from changes in optical attenuation experienced during airborne fluorosensor measurements of fluorophore concentrations in surface waters can be eliminated, by normalizing the fluorescence signal with the concurrent water Raman signal. In a remote, chlorophyll a concentration monitoring application of the principle in fresh waters, the Raman-corrected chlorophyll a fluorescence measurements were found to (1) be highly correlated with chlorophyll a ground truth data, and (2) have a water Raman signal reciprocal that varied directly as the beam attenuation coefficient. It is suggested that this latter relationship be exploited as a technique for remotely sensing changes in surface water optical attenuation. O.C.

A81-48554 * # **Airborne microwave radiometer remote sensing of lake ice.** C. T. Swift, R. F. Harrington, and H. F. Thornton (NASA, Langley Research Center, Hampton, VA). In: EASCON '80; Electronics and Aerospace Systems Conference, Arlington, VA, September 29-October 1, 1980, Conference Record.

New York, Institute of Electrical and Electronics Engineers, 1980, p. 369-373. 5 refs.

The NASA Langley C-Band Stepped Frequency Microwave Radiometer was used to conduct airborne remote sensing measurements of the Great Lakes ice cover during the winters of 1978 and 1979. In order to evaluate the use of microwave radiometry for remote sensing of fresh water ice, an initial experiment was conducted in February 1978. After the results were analyzed an algorithm was developed, and a more comprehensive mission was completed in March 1979, which related the thermal emission from lake ice to meaningful geophysical quantities. A clear discrimination of pressure ridges and rubble from base ice was observed, and evidence was found which showed gradual changes in the thickness of the base itself. Results indicate that passive microwave sensors can provide a measure of lake ice within uncertainties presented by the attenuation coefficient, and the changes in surface reflectivity imposed by surface roughness. D.L.G.

A81-48941 **Suburban soil loss and runoff simulation assisted by interpretation of large scale aerial photography.** J. R. Jensen (South Carolina, University, Columbia, SC) and Z. Berger (Exxon Product Research Co., Houston, TX). *Remote Sensing Quarterly,* vol. 3, Jan. 1981, p. 4-20. 27 refs.

A81-48942 * **Landsat observations of snowcover depletion and flooding in the Chesapeake Bay area during the winter of 1979.** J. Foster (NASA, Goddard Space Flight Center, Earth Survey Applications Div., Greenbelt, MD). *Remote Sensing Quarterly,* vol. 3, Jan. 1981, p. 21-28.

A81-48944 **A report on the use of remote sensing techniques for the supervision of New England coastal salt marshes.** D. E. Wallace (Nebraska, University, Omaha, NE). *Remote Sensing Quarterly,* vol. 3, Jan. 1981, p. 45-53. 9 refs.

A81-49757 * # **Landsat - What is operational in water resources.** E. M. Middleton (NASA, Goddard Space Flight Center, Greenbelt, MD) and J. C. Munday, Jr. (Virginia Institute of Marine Science, Gloucester Point, VA). In: Canadian Symposium on Remote Sensing, 6th, Halifax, Canada, May 21-23, 1980, Proceedings. Ottawa, Canadian Aeronautics and Space Institute, 1981, p. 43-52. 35 refs.

Applications of Landsat data in hydrology and water quality measurement were examined to determine which applications are operational. In hydrology, the principal applications have been surface water inventory, and land cover analysis for (1) runoff modeling and (2) abatement planning for non-point pollution and erosion. In water quality measurement, the principal applications have been: (1) trophic state assessment, and (2) measurement of turbidity and suspended sediment. The following applications were found to be operational: mapping of surface water, snow cover, and land cover (USGS Level 1) for watershed applications; measurement of turbidity, Secchi disk depth, suspended sediment concentration, and water depth. B.J.

A81-49761 # **Utilisation and benefits of SLAR in operational ice data acquisition.** H. G. Hengeveld (Department of the Environment, Atmospheric Environment Service, Downsview, Ontario, Canada). In: Canadian Symposium on Remote Sensing, 6th, Halifax, Canada, May 21-23, 1980, Proceedings.
Ottawa, Canadian Aeronautics and Space Institute, 1981, p. 81-88. 8 refs.

Since 1978, the SLAR system on the Atmospheric Environment Service ice reconnaissance aircraft has been used operationally to provide ice services during more than 3000 hours of reconnaissance flight time. The radar has been modified to include a dry silver processor/display, roll compensation, and sensitivity time control, and is employed together with visual observations and laser surface profiles for the in-flight generation of ice charts. Methods of direct relay of imagery to the user in conjunction with ice charts have been assessed. Primary benefits in the use of SLAR in ice reconnaissance are the large increase in data available to users, the ability to support users during storms, and the accumulation of high data range image records. Future developments will include the use of onboard CRT displays, the improvement of sensitivity time control circuits, and experiments involving improved radar design. B.J.

A81-49778 # **Application of synthetic aperture radar data to snow cover monitoring.** B. E. Goodison, S. E. Waterman (Department of the Environment, Atmospheric Environment Service, Downsview, Ontario, Canada), and E. J. Langham (Environment Canada, National Hydrology Research Institute, Ottawa, Canada). In: Canadian Symposium on Remote Sensing, 6th, Halifax, Canada, May 21-23, 1980, Proceedings. Ottawa, Canadian Aeronautics and Space Institute, 1981, p. 263-271. 10 refs.

As part of the Canadian Sursat (Surveillance Satellite) project, airborne X and L band synthetic aperture radar (SAR) data were obtained for a study site in the Ottawa area in November, 1978 and March, 1979, representing snow-free and snow-covered conditions, respectively. Coincident ground based measurements of snowpack properties, soil moisture, and meteorological parameters were collected. The SAR data were used in the form of 70 mm positive transparencies, which were analyzed with the aid of an image analyzer/density slicer. The SAR imagery of the snow-covered site showed a marked change in appearance particularly in the X-band data. In general, the non-forested areas of the study site exhibited a higher X-band radar return in the presence of the snow cover. Variations in the X-band return appear to be a complex function of snowpack properties, including depth, density, free water and water equivalent. In particular, areas of ice and dense snow were observed to produce relatively high radar returns. The L-band data showed little or no relationship between radar return and snowpack properties. The results suggest that SAR data could prove useful for detecting snow cover in non-forested areas. (Author)

A81-49796 # **Airborne estimation of water quality parameters in Lake Ontario.** H. H. Zwick (Canada Centre for Remote Sensing, Ottawa, Canada), S. C. Jain, S. A. Gluckstein (Moniteq, Ltd., Concord, Ontario, Canada), and T. A. Calwell (Genesys Group, Ltd., Ottawa, Canada). In: Canadian Symposium on Remote Sensing, 6th, Halifax, Canada, May 21-23, 1980, Proceedings. Ottawa, Canadian Aeronautics and Space Institute, 1981, p. 443-451. 24 refs.

A81-49797 # **Use of Landsat images in the monitoring and study of the LG 2 reservoir during the filling period (Les images Landsat dans la surveillance et l'étude du réservoir de LG 2 durant la période de remplissage).** P. Laframboise (Société de Développement de la Baie James, Montreal, Canada) and A. Bachand (Société d'Energie de la Baie James, Montreal, Canada). In: Canadian Symposium on Remote Sensing, 6th, Halifax, Canada, May 21-23, 1980, Proceedings. Ottawa, Canadian Aeronautics and Space Institute, 1981, p. 453-457. 5 refs. In French.

The extent of processes associated with the filling of the reservoir behind the LG 2 dam, a part of the La Grande Rivière hydroelectric system in northern Quebec, has been monitored by the use of Landsat 2 and 3 images. Images were acquired starting before the initiation of filling on November 27, 1978 through the end of the following year from the Landsat MSS and RBV instruments. The major stages of dam filling were studied by the visual analysis of the images, including the ecology and physiography of the site before filling, the elevation of vegetation by the rising ice cover, and the turbidity and location of partially flooded vegetation during the free-water period. The major factor limiting the surveillance of the reservoir has been the availability of suitable images, particularly during the summer months. A.L.W.

A81-49800 **The detection of groundwater discharges /springs/ using aerial thermography.** G. R. Lawrence, D. White (Ministry of Natural Resources, Ontario Centre for Remote Sensing, Toronto, Canada), and I. Deslauriers (Associated Realty Consultants, Goderich, Ontario, Canada). In: Canadian Symposium on Remote Sensing, 6th, Halifax, Canada, May 21-23, 1980, Proceedings. Ottawa, Canadian Aeronautics and Space Institute, 1981, p. 483-491.

A81-49968 * # **Freshwater ice thickness observations using passive microwave sensors.** D. K. Hall, J. L. Foster, A. T. C. Chang, and A. Rango (NASA, Goddard Space Flight Center, Hydrological Sciences Branch, Greenbelt, MD). *IEEE Transactions on Geoscience and Remote Sensing*, vol. GE-19, Oct. 1981, p. 189-193. 11 refs.

Walden Reservoir, a freshwater lake in north-central Colorado, was overflown six times by a NASA C-130 aircraft between January 1977 and April 1980. The aircraft was equipped with four microwave radiometers operating between 0.81 and 6.0 cm in wavelength (37.0 to 5.0 GHz). The 6.0-cm radiometer data showed a good relationship with ice thickness based on a sample of four ice thickness values. The 1.67- and 1.35-cm radiometer data showed weaker relationships with ice thickness. The 0.81-cm sensor data showed no positive relationship with ice thickness. None of the relationships was statistically significant because of the small sample size. The 6.0-cm sensor data in the nadir-viewing mode was found to have the most potential of all the wavelengths studied, for use in remotely determining ice thickness. The 6.0-cm radiometer probably sensed the entire thickness of the ice on the reservoir (ranging from 25.4 to 67.3 cm in thickness) and was apparently not significantly affected by the snow overlying the ice. The shorter wavelengths are scattered by the snow overlying the ice and are more suitable for snow studies than for ice thickness studies. (Author)

N81-29520# Environmental Research Inst. of Michigan, Ann Arbor. Infrared and Optics Lab.
A REMOTE SENSING TECHNIQUE TO MONITOR CLADOPHORA IN THE GREAT LAKES Final Report, 1975 - 1977
Fred J. Tanis Jul. 1980 38 p refs
(Grant EPA-R-803611)
(PB81-173841; EPA-600/3-80-075) Avail: NTIS HC A03/MF A01 CSCL 08H

The feasibility of using an airborne multispectral scanner to monitor shoreline algae problems is demonstrated. Multispectral data were collected at two sites on the U.S. Lake Ontario shoreline. Computer generated color maps were produced to show spatial distribution of Cladophora in the nearshore zone and to estimate standing crop. Spectral features of Cladophora were related to measured standng crop. GRA

N81-30509# Minnesota Univ., Minneapolis. Remote Sensing Lab.
SATELLITE MONITORING OF SNOW EXTENT AND CONDITION IN AGRICULTURAL, TRANSITIONAL, AND FORESTED LAND COVER AREAS Final Report
T. M. Lillesand, D. E. Meisner, A. L. Downs, and R. L. Deuell Dec. 1980 38 p refs
(Grant DOC/NA80AA-D-0019)
(PB81-188625; NOAA-81021104; RSL-RR-80-6) Avail: NTIS HC A03/MF A01 CSCL 08L

GOES and TIROS/NOAA-6 satellite data were evaluated visually and digitally to assess their potential for aiding the process of state wide snow extent mapping in Minnesota. This state contains a geographic continuum spanning from a large open agricultural area, through a partially forested transitional zone, to a heavily forested area. The ability to discriminate snow extent statewide was found to be influenced by the state of sensing and the cover types involved. GRA

N81-33550*# Minnesota Univ., Minneapolis. Space Science Center.
A STUDY OF MINNESOTA LAND AND WATER RESOURCES USING REMOTE SENSING, VOLUME 14 Progress Report, 31 Dec. 1980
1 Jan 1981 97 p refs Original contains color imagery. Original photography may be purchased from the EROS Data Center, Sioux Falls, S.D. 57198 ERTS
(Grant NGL-24-005-263)
(E81-10166; NASA-CR-164768) Avail: NTIS HC A05/MF A01 CSCL 05B

Techniques developed for processing and interpreting imagery and for correlating data obtained in the field as well as by aerial and satellite photography are described with particular emphasis on monitoring water quality in lakes, detecting ground water levels, and evaluating moisture stress to plants.

N81-33552*# Minnesota Univ., Duluth. Dept. of Physics.
LAKEWIDE MONITORING OF SUSPENDED SOLIDS USING SATELLITE DATA
Michael Sydor, Principal Investigator *In its* A Study of Minn. Land and Water Resources Using Remote Sensing, Vol. 14 1 Jan. 1981 29 p Original contains imagery. Original photography may be purchased from the EROS Data Center, Sioux Falls, S.D. 57198 ERTS

Avail: NTIS HC A05/MF A01 CSCL 08H

In anticipation of using LANDSAT and Nimbus 7 coastal zone color scanner data to observe the decrease in suspended solids in Lake Superior following cessation of the dumping of taconite tailings, a series of lakewide sampling cruises was conducted to make radiometric measurements at a lake level. A means for identifying particulates and measuring their concentration from LANDSAT data was developed. The initial distribution of chemical parameters in the extreme western arm of the lake, where the concentration gradients are high, is to be based on the LANDSAT data. Subsequent lakewide dispersal and distribu-

tion is to be based on the coastal zone color scanner data
A.R.H.

N81-33553*# Minnesota Univ., St. Paul. Geological Survey.
SYNERGISTIC RELATIONSHIPS AMONG REMOTE-SENSING AND GEOPHYSICAL MEDIA: GEOLOGICAL AND HYDROLOGICAL APPLICATIONS Final Report
David L. Southwick, Joseph E. Goebel, Matt Walton, Lawrence G. Batten, and James Heutmaker, Principal Investigators *In its* A Study of Minn. Land and Water Resources Using Remote Sensing, Vol. 14 1 Jan. 1981 29 p ref ERTS

Avail: NTIS HC A05/MF A01 CSCL 08G

Skylab photographs, side-looking radar imagery, published soil maps, topographic maps, conventional aerial photography as well as LANDSAT imagery under wet and dry changes for several years were analyzed over selected areas in Minnesota to test their usefulness in detecting near-surface ground water. Results show that optical density read from LANDSAT data is not a reliable discriminator of depth to shallow ground water when one band of one scene is used alone, and is little improved when several bands of several scenes are used synergistically. The method is enhanced if information from soil maps is included in the analysis, especially for discriminating boggy ground from better drained areas. It appears, however, that in areas where soil maps and good topographic maps already exist, the depth to ground water can be predicted from those media as well as (if not better than) it can be predicted from remote imagery. The LANDSAT method used demonstrated no capability for recognizing deeper categories of ground water.
A.R.H.

N81-33560*# Cornell Univ., Ithaca, N. Y. School of Civil and Environmental Engineering.
CORNELL UNIVERSITY REMOTE SENSING PROGRAM Semiannual Status Report, 1 Dec. 1980 - 31 May 1981
Warren R. Philipson, Principal Investigator, Ta Liang, and John A. Stanturf Jun. 1981 115 p refs ERTS
(Grant NGL-33-010-171)
(E81-10174; NASA-CR-164567; SASR-18) Avail: NTIS HC A06/MF A01 CSCL 05B

A preliminary methodology was developed for siting windmills and selecting test sites for locating anemometers in Erie, Niagra, and Orleans Counties, New York. Overlays were derived fom historic airphotos (1938-1968) of the Love Canal area in an effort to show changes and delineate drainage areas. Projects in progress include assessing scenic views in Hamilton County, New York; developing algorithms for predicting vineyard yield; and a study of the spectral effects of sulfur dioxide on bean yield. Spin-off research includes developing a remote sensing method for improving lake sampling strategies, using digital analysis of LANDSAT data to characterize acid lakes; and studying advanced technologies for environment management and monitoring.
A.R.H.

N81-33577*# National Aeronautics and Space Administration. Langley Research Center, Hampton, Va.
A COMPARISON OF OBSERVED AND ANALYTICALLY DERIVED REMOTE SENSING PENETRATION DEPTHS FOR TURBID WATER
W. Douglas Morris, J. W. Usry, William G. Witte, Charles H. Whitlock, and E. A. Guraus Sep. 1981 23 p refs
(NASA-TM-83176) Avail: NTIS HC A02/MF A01 CSCL 08H

The depth to which sunlight will penetrate in turbid waters was investigated. The tests were conducted in water with a single scattering albedo range, and over a range of solar elevation angles. Two different techniques were used to determine the depth of light penetration. It showed little change in the depth of sunlight penetration with changing solar elevation angle. A comparison of the penetration depths indicates that the best agreement between the two methods was achieved when the quasisingle scattering relationship was not corrected for solar angle. It is concluded that sunlight penetration is dependent on inherent water properties only.
E.A.K.

N81-33593# Hydrocomp, Inc., Mountain View, Calif.
EVALUATION OF REMOTE SENSING DATA FOR INPUT INTO HYDROLOGICAL SIMULATION PROGRAM-FORTRAN (HSPF) Final Report, Mar. 1979 - Jun. 1980
D. D. Franz and S. M. Lieu Jun. 1981 107 p refs
(Contract EPA-68-01-5801)
(PB81-209561; EPA-600/3-81-037) Avail: NTIS HC A06/MF A01 CSCL 08H

The feasibility of using a remotely sensed data base as input into the hydrologic simulation program-FORTRAN was evaluated (HSPF). Data from LANDSAT and conventionally obtained data were used to set up the input parameters of HSPF. Simulations were run to compare the two sets of data. The remotely sensed data performed as least as well as the conventional one when compared with observed data. in addition, it was estimated to offer savings of 30 to 50 percent in the cost of set up and operations.
GRA

N81-33599# Maine Univ., Orono. Land and Water Resources Center.
QUANTIFICATION OF NON-POINT SOURCE SEDIMENTATION THROUGH DENSITOMETRIC ANALYSIS OF COLOR INFRARED AERIAL PHOTOGRAPHY
Terrence J. Keating, Jerry D. Lowry, and Rachel S. Smith Apr. 1981 79 p refs Sponsored by Dept. of Interior
(PB81-209157; W81-03252; OWRT-A-049-ME(2)) Avail: NTIS HC A05/MF A01 CSCL 13B

A method for the detection, quantification, and location of nonpoint pollution sources upon the use of aerial color infrared photography was established. An airborne small format camera system was flown simultaneous to minimal selected ground sampling. This allowed measurement of ground levels of turbidity and suspended solids over relatively large watershed areas. Calibration of monitored rivers was used to assess firm response to given pollutant types; with quantification by densitometry. Suspended solids concentrations from firm density values are estimated.
GRA

07

DATA PROCESSING AND DISTRIBUTION SYSTEMS

Includes film processing, computer technology, satellite and aircraft hardware, and imagery.

A81-41055 **Multispectral texture analysis (Multispektrale Texturanalyse).** M. Dehn (Karlsruhe, Universität, Karlsruhe, West Germany). *Bildmessung und Luftbildwesen,* vol. 49, July 1, 1981, p. 101-110. 5 refs. In German. Research supported by the Deutsche Forschungsgemeinschaft.

The multispectral quality of texture analysis for the classification of land use grades is investigated. A test image, composed of various FMP scenes, is classified using image element features. Extracted texture parameters computed from several spectral bands were found to give better results than the information derived from only one spectral band and greatly reduced the number of incorrect classification allocations. The data to be classified required a detailed investigation in order to extract the parameters which would best describe the object classes. Calculation of the feature extraction parameters required from 60 to 90 minutes for 512 x 512 image elements.

J.F.

A81-41057 **A rectification technique for digital orthophoto production (Ein Entzerrungsverfahren zur Herstellung digitaler Orthophotos).** W. Göpfert (Institut für angewandte Geodäsie, Frankfurt am Main, West Germany). *Bildmessung und Luftbildwesen,* vol. 49, July 1, 1981, p. 117-125. 9 refs. In German.

Digital geometrical image processing is applied to a digital/analog converted aerial photograph to produce a digital orthophoto. A rubber stretch algorithm, specifically the multiquadratic interpolation approach, is used as a geometric processing method. DTM data, as well as photogrammetric model evaluation, are used as input data types. Corresponding gray value transfer characteristics are generated to radiometrically adjust the various photographs to be mosaicked. During the digital/analog conversion, optimal image contrasting and selective detail enhancement are obtained. As an example, a digital orthophoto of scale 1:25,000 is produced from 1:62,000 aerial photography using as input terrain profile data obtained through analytical photogrammetry.

J.F.

A81-41479 # **Accuracy of transmission of spectral contrasts in multispectral aerial photography, with application to problems of object recognition (O tochnosti peredachi spektral'nykh kontrastov pri mnogozonal'nom aerofotografirovanii primenitel'no k zadacham raspoznavaniia obe'ktov).** Iu. A. Dzhemard'ian, S. V. Komissarenko, and V. G. Skrotskii. In: Some results on the investigation of earth resources by aerial and polygon methods. Leningrad, Gidrometeoizdat, 1980, p. 20-24. In Russian.

An analysis is presented of systematic and random errors arising in the multispectral aerial photography of earth resources; the multispectral method under consideration involves photochemical processing and microphotometry of the multispectral negatives. The use of two recognition models for crop identification on the Kursk test polygon is examined.

B.J.

A81-41480 # **Experience with the determination of optical image distortions of landscape elements on IR aerial photographs (Opyt opredeleniia opticheskikh iskazhenii izobrazheniia elementov landshafta na IK aerosnimkakh).** V. A. Kharitonov and V. V. Gorbachev. In: Some results on the investigation of earth resources by aerial and polygon methods. Leningrad, Gidrometeoizdat, 1980, p. 25-33. 8 refs. In Russian.

The paper considers the use of photographic photometry to determine optical image distortions on infrared aerial photographs due to the nonuniformity of angular distribution of reflected radiation. An analysis of experimental aerial photography data confirms the effectiveness of this method. It is concluded that it is necessary to allow for the angular-distribution nonuniformity in the qualitative processing of aerial and spaceborne photographs. B.J.

A81-41481 # **Experience with image combination in multispectral aerial photography (Opyt sovmeshcheniia izobrazhenii mnogozonal'noi aeros'emki).** A. N. Belinskii and I. M. Bokshtein. In: Some results on the investigation of earth resources by aerial and polygon methods. Leningrad, Gidrometeoizdat, 1980, p. 34-37. In Russian.

An interactive method for the combination of images simultaneously obtained in different spectral regions is described. The image combination algorithm consists of four operations: elimination of the nonuniformity of illumination, adaptive quantization, determination of contours, and the correlation of reference sections and the final combination of images. The use of this technique in the automated classification of multispectral images is considered. B.J.

A81-41482 # **Machine method for the equalization of average phototone in an aerial photograph field (Mashinnyi metod vyravnivaniia srednego fototona po poliu aerofotoizobrazheniia).** G. G. Andreev and N. N. Koptseva. In: Some results on the investigation of earth resources by aerial and polygon methods. Leningrad, Gidrometeoizdat, 1980, p. 38-41. In Russian.

The paper examines aspects of the computer correction of the phototone of aerial photographs whose purpose is to eliminate distortions caused by the nonuniformity of the lens illumination distribution function. A block diagram for the correction program on the EC-1022 computer is presented. The method can be used at the first stage of the machine processing of aerial photographic images.

B.J.

A81-41484 # **The use of the spectral and physical-geographic characteristics of natural objects for the interpretation of multispectral satellite images (Ispol'zovanie spektral'nykh i fiziko-geograficheskikh kharakteristik prirodnykh obrazovanii pri deshifrirovanii mnogozonal'nykh sputnikovykh izobrazhenii).** N. K. Vinnichenko. In: Some results on the investigation of earth resources by aerial and polygon methods. Leningrad, Gidrometeoizdat, 1980, p. 45-50. In Russian.

Various aspects of the thematic interpretation of multispectral satellite images on the basis of the spectral and physical-geographic characteristics of natural objects on the earth's surface are considered. A block diagram describing the use of a priori information for the analysis of multispectral satellite images is presented. B.J.

A81-42555 # **Determination of the external-orientation elements of single photographs and stereopairs (Opredelenie elementov vneshnego orientirovaniia odinochnykh snimkov i stereopar).** I. T. Antipov (Nauchno-Issledovatel'skii Institut Prikladnoi Geodezii, USSR) and T. A. Bashkova. *Geodeziia i Aerofotos'emka,* vol. 1, 1981, p. 87-94. In Russian.

The paper formulates principles for the determination of the external-orientation elements (EOE) of single aerial photographs and stereopairs for their use in photogrammetry. A system of normal equations is developed for transformation to the inclined plane at all photograph points; the solution of these equations makes it possible to obtain quantities that characterize the position of the inclined plane. The EOEs of a photograph are determined from these quantities. A method is proposed for EOE determination in the processing of aerial photographs by analog steroephotogrammetry.

B.J.

A81-42631 **A measure of reliability for classification of earth satellite data.** M. Alvo and M. Goldberg (Ottawa, University, Ottawa, Canada). *IEEE Transactions on Systems, Man, and Cybernetics,* vol. SMC-11, Apr. 1981, p. 312-318. 13 refs.

A measure is presented which may be used to indicate reliability or confidence in the classification of individual Landsat imagery pixels; in turn permitting comparisons, on an individual pixel basis, of classifications obtained from successive images. The immediate neighborhood in spectral space of each vector value of the class is compared with that of the modal vector by means of a modified chi-square goodness-of-fit statistic. A normalization technique based on simultaneous interference, which requires only the specification of a significance level (the usual alpha in statistics) is described, and the satisfactory performance of the measures is demonstrated through both simulated data and Landsat imagery. O.C.

A81-43185 **The GOES data collection system.** M. L. Nelson (NOAA, National Environmental Satellite Service, Washington, DC). In: Satellite hydrology; Proceedings of the Fifth Annual William T. Pecora Memorial Symposium on Remote Sensing, Sioux Falls, SD, June 10-15, 1979. Minneapolis, MN, American Water Resources Association, 1981, p. 45-47.

A brief look at the Geostationary Operational Environmental Satellite (GOES) Data Collection System (DCS) is provided. The basic configuration of the system is identified by describing the major elements and their functions. The basic design criteria, together with system development has led to a truly operational program. The National Environmental Satellite Service (NESS) and many users have accumulated years of experience with this program so that it is now possible to identify the useful features. This background also has made it possible for NESS and the users to plan for additional capabilities. System improvements and how they benefit the users are explained. Finally, the growth of the system in terms of number of platforms and users are given. (Author)

A81-43189 **U.S. geological survey application of satellite telemetry for the support of hydrologic data collection.** W. G. Shope and R. W. Paulson (U.S. Geological Survey, Reston, VA). In: Satellite hydrology; Proceedings of the Fifth Annual William T. Pecora Memorial Symposium on Remote Sensing, Sioux Falls, SD, June 10-15, 1979. Minneapolis, MN, American Water Resources Association, 1981, p. 60-64.

The network of hydrologic stations operated by the Geological Survey's Water Resources Division is discussed. Attention is given to the idea of using a satellite data collection system in order to automate the link between the field site sensor and the computer networks. It is noted that this automation would not only save manpower but would also shorten the collection cycle from weeks or months to hours. The satellite system comprises a satellite in orbit, a network of small battery-operated radio transmitters (called Data Collection Platforms, or DCP's), and one or more earth receiving stations. It is noted that monitoring the networks through the use of real-time data provides the Geological Survey with a valuable operational tool that will result in better quality data and greater efficiencies in network management. C.R.

A81-43222 **Characteristics of microwave emission of significance to satellite remote sensing of soil water.** R. W. Newton (Texas A & M. University, College Station, TX). In: Satellite Hydrology; Proceedings of the Fifth Annual William T. Pecora Memorial Symposium on Remote Sensing, Sioux Falls, SD, June 10-15, 1979. Minneapolis, MN, American Water Resources Association, 1981, p. 353-362. 18 refs.

Newton (1977) developed a method of interpreting passive microwave emission measurements in terms of average soil moisture over a predicted soil depth. In order to test the approach for a relatively wide range of soil water and soil temperature profile shapes, an analytical model is used to predict the microwave emission at four frequencies of soil water and soil temperature profiles measured by Jackson (1973) over a soil moisture range from saturation through dry down as well as at both day and night periods. It was determined that the average soil water parameter developed by Newton and its associated depth could be estimated from microwave emission measurements within a minimum of ambiguity. It was also found that the depth associated with the average soil water parameter is only slightly dependent on the soil temperature profile, which indicates that an improvement in depth of penetration will probably not be obtained from night measurements. B.J.

A81-43531 **Correlation techniques and devices.** G. Konecny and D. Pape (Hannover, Universität, Hanover, West Germany). *(International Society for Photogrammetry, Congress, 14th, Hamburg, West Germany, July 13-25, 1980.) Photogrammetric Engineering and Remote Sensing,* vol. 47, Mar. 1981, p. 323-333. 69 refs.

Image correlation techniques are reviewed according to the photogrammetric and mathematical fundamentals as well as the techniques for video-conversion, correlation, and rectification of video signals. The historical development of automatic image correlation devices from the Hobrough Stereomat, via the Bunker Ramo UNAMACE to the Hobrough Gestalt System and the Bendix AS-11-BX is then traced. Reference is made to the Rastar Correlator under development at the University of Hannover, based on designs by Hobrough and completed by Pape. Finally, other experimental attempts at image correlation, such as (coherent) optical correlation and digital off-line correlation, are summarized. (Author)

A81-43532 **Automation in photogrammetry.** J. B. Case (U.S. Defense Mapping Agency, Washington, DC). *(International Society for Photogrammetry, Congress, 14th, Hamburg, West Germany, July 13-25, 1980.) Photogrammetric Engineering and Remote Sensing,* vol. 47, Mar. 1981, p. 335-341. 39 refs.

All functional aspects of photogrammetry, i.e., triangulation mensuration, elevation data extraction, planimetric data extraction, and rectification and orthorectification, are now being automated to some degree. Automation extends from computer control of comparators and analog stereo plotters, through the analytical stereoplotters, to orthophoto printers and fully automated correlation equipment. The drive towards automation has been triggered not only by the continuing necessity to reduce costs, but also by the need to generate new products (e.g., DTM, land use, etc.) and to utilize other than conventional mapping photography. These have led, in turn, to the necessity for data editing and data management systems. The trend in the future will be towards the ever-increasing use of digital image processing technology. Examples of several levels of automation in photogrammetry are described. (Author)

A81-43546 **A capture-recapture approach for estimation of detection probabilities in aerial surveys.** L. D. Maxim (Everest Consulting Associates, Princeton, NJ), L. Harrington (Mathtech, Inc., Arlington, VA), and M. Kennedy. *Photogrammetric Engineering and Remote Sensing,* vol. 47, June 1981, p. 779-788. 17 refs.

A simple approach for estimating detection probabilities from imagery when ground truth data are non-existent is presented. Based upon what are termed capture-recapture statistics, the method requires only an independent examination of the imagery by two or more observers. In its simplest form the approach requires the assumptions that detections are independent and that no false positives occur. When data from three or more observers are available, checks upon model assumptions can be performed and less restrictive models can be developed. The approach is illustrated with several numerical examples. (Author)

A81-43734 * **Training site statistics from Landsat and Seasat satellite imagery registered to a common map base.** J. Clark (California Institute of Technology, Jet Propulsion Laboratory, Pasadena, CA). In: Rainbow 80; Fall Technical Meeting, Niagara Falls, NY, October 7-10, 1980, ASP Technical Papers. Falls Church, VA, American Society of Photogrammetry, 1981, p. RS-1-F-1 to RS-1-F-9. 5 refs. Contract No. NAS7-100.

Landsat and Seasat satellite imagery and training site boundary coordinates were registered to a common Universal Transverse Mercator map base in the Newport Beach area of Orange County, California. The purpose was to establish a spatially-registered, multi-sensor data base which would test the use of Seasat synthetic aperture radar imagery to improve spectral separability of channels used for land use classification of an urban area. Digital image processing techniques originally developed for the digital mosaics of the California Desert and the State of Arizona were adapted to spatially register multispectral and radar data. Techniques included control point selection from imagery and USGS topographic quadrangle maps, control point cataloguing with the Image Based Information System, and spatial and spectral rectifications of the imagery. The radar imagery was pre-processed to reduce its tendency toward uniform data distributions, so that training site statistics for selected Landsat and pre-processed Seasat imagery indicated good spectral separation between channels. (Author)

A81-43736 **On the analysis of remote sensing data to predict selected vegetative variables.** R. K. Blystone and M. J. Duggin (New York, State University, Syracuse, NY). In: Rainbow 80; Fall Technical Meeting, Niagara Falls, NY, October 7-10, 1980, ASP Technical Papers. Falls Church, VA, American Society of Photogrammetry, 1981, p. RS-2-B-1 to RS-2-B-11. 17 refs. Research supported by the U.S. Department of Agriculture.

An empirical approach is used to predict biological variables from remote sensing data. The empirical use of an association as a predictor model when analyzing an image is shown to be dangerous, since there may be many possible associations of remote sensing data with various biological variables. Moreover, use of ratios of recorded radiance values do not always work for a given situation. Approaches for formulating a better empirical predictor model, which would be applicable to a single image or limited ground area at one point in time are outlined. A regression model is constructed in which remotely sensed radiance values are the independent variables and the vegetative property of interest is the dependent variable. The necessity of constructing an economical multiple linear regression (MLR) model is discussed, and the importance of using training data to develop the MLR and test data for determining the adequacy of its predictions is explained. J.F.

A81-45431 **A comparison between two photographic methods for the determination of relative bidirectional reflectance.** P. J. Curran, T. J. Munday, and E. J. Milton (Reading, University, Reading, Berks., England). *International Journal of Remote Sensing,* vol. 2, Apr.-June 1981, p. 185-188. 5 refs. Research supported by the Natural Environment Research Council and University of Reading.

Two simple photographic methods have recently been proposed for the measurement of relative bidirectional reflectance (Lillesand and Kiefer 1979, Curran 1980). These two methods were used to calculate the relative bidirectional reflectance of ten contrasting surfaces. The photographic relative bidirectional reflectance so recorded, was then compared with the radiometric bidirectional reflectance for each surface. Two conclusions were drawn: first, that relative bidirectional reflectance can be measured using these simple photographic techniques, and second, that there was no significant difference between the Lillesand and Kiefer and Curran methods for photographically deriving relative bidirectional reflectance. (Author)

A81-45433 * **Application of digital terrain data to quantify and reduce the topographic effect on Landsat data.** C. O. Justice, S. W. Wharton, and B. N. Holben (NASA, Goddard Space Flight Center, Earth Resources Branch, Greenbelt, MD). *International Journal of Remote Sensing,* vol. 2, July-Sept. 1981, p. 213-230. 29 refs.

Landsat multispectral scanner (MSS) data are integrated with 30 m US Geological Survey digital terrain data to quantify and reduce topographic effects on imagery of a forested mountain ridge in central Pennsylvania. Spectral band ratioing slightly decreased variation of Landsat data for 50% of the transects and could not eliminate direct-light topographic effects. A Lambertian model increased topographic effect, and a modified Lambertian model decreased variation produced by the original model, but gave higher variances than found in the raw Landsat data. A non-Lambertian model, however, decreased variation by 86%, reducing topographic effects. The study demonstrated that high quality digital terrain data can be used to develop and test improved radiative transfer models, and enhance the utility of MSS data. D.L.G.

A81-46040 * **Maximum likelihood estimation of label imperfection probabilities and its use in the identification of mislabeled patterns.** C. B. Chittineni (Lockheed Engineering and Management Services Co., Houston, TX). In: Machine processing of remotely sensed data and soil information systems and remote sensing and soil survey; Proceedings of the Sixth Annual Symposium, West Lafayette, IN, June 3-6, 1980. New York, Institute of Electrical and Electronics Engineers, Inc., 1980, p. 158-170. 18 refs. Contract No. NAS9-15800.

Estimating label imperfections and the use of estimations in the identification of mislabeled patterns are discussed. Expressions are presented for the asymptotic variances of the probability of correct classification and proportion, and for the maximum likelihood estimates of classification errors and a priori probabilities. Models are developed for imperfections in the labels and classification errors, and expressions are derived for the probability of imperfect label identification schemes resulting in wrong decisions. The expressions are used in computing thresholds and the techniques are given practical applications. The imperfect label identification scheme in the multiclass case is found to amount to establishing a region around each decision surface, and decisions of the label correction scheme are found in close agreement with the analyst-interpreter interpretations of the imagery films. As an example, the application of the maximum likelihood estimation to the processing of Landsat MSS data is discussed. D.L.G.

A81-46041 * **Context distribution estimation for contextual classification of multispectral image data.** J. C. Tilton, P. H. Swain, and S. B. Vardeman (Purdue University, West Lafayette, IN). In: Machine processing of remotely sensed data and soil information systems and remote sensing and soil survey; Proceedings of the Sixth Annual Symposium, West Lafayette, IN, June 3-6, 1980. New York, Institute of Electrical and Electronics Engineers, Inc., 1980. p. 171-180. NSF Grant No. MCS-78-04366; Contract No. NAS9-15466.

A classification algorithm incorporating contextual information in a general, statistical manner is presented. Methods are investigated for obtaining adequate estimates of the context distribution (a statistical characterization of context) upon which the classification algorithm depends. Finally, a method of estimating optimal algorithm parameters prior to performing preliminary classifications is explored. (Author)

A81-46042 **Stratification of Landsat data by uniformity productivity of soils.** J. Schubert, P. Chagarlamudi (Deloitte, Haskins and Sells Associates, Ottawa, Canada), J. A. Shields, and A. R. Mack (Agriculture Canada, Land Resource Research Institute, Ottawa, Canada). In: Machine processing of remotely sensed data and soil information systems and remote sensing and soil survey; Proceedings of the Sixth Annual Symposium, West Lafayette, IN, June 3-6, 1980. New York, Institute of Electrical and Electronics Engineers, Inc., 1980, p. 186-194. 11 refs.

The goal of this study was to develop and verify methods to use Landsat data for mapping and quantifying the productivity of soil areas on which the annual yields of spring wheat exposed to the same weather conditions are generally different. The study was done in two parts. First, a calibration study was done to determine which features visible on Landsat imagery were associated with different relative productivities. Then, in a two-part accuracy verification study, Uniform Productivity Area (UPA) boundaries were drawn on three map sheets (1:250,000 Canadian National Topographic System) and the relative productivity of each UPA within 25 townships in the Canadian Prairies were estimated. The boundaries were compared with known soil productivity area boundaries and the relative productivity ratings were compared with reported yields. (Author)

A81-46043 **Interactive processing of Landsat image for morphopedological studies.** D. Chaume and N. P. Thien (IBM France, S.A., Paris, France). In: Machine processing of remotely sensed data and soil information systems and remote sensing and soil survey; Proceedings of the Sixth Annual Symposium, West Lafayette, IN, June 3-6, 1980. New York, Institute of Electrical and Electronics Engineers, Inc., 1980, p. 195-204. 5 refs.

A study of the Gale area of the Mandingue plateau was studied by means of the ERMAN II earth resources management system and a novel, interactive image processing system. Training fields belonging to the different morphopedological units were determined from four photographs of the study area, and a model of transformation between corresponding coordinates on images and photographs was calculated from a set of landmarks. The coordinates of the subimages were obtained by applying the model of transformation to the coordinates on the photographs. Separate models of deformation were in addition calculated for smaller areas, corresponding to each aerial photograph. O.C.

A81-46052 * # **Inventory estimation on the massively parallel processor.** P. D. Argentiero, J. P. Strong, and D. W. Koch (NASA, Goddard Space Flight Center, Greenbelt, MD). In: Machine processing of remotely sensed data and soil information systems and remote sensing and soil survey; Proceedings of the Sixth Annual Symposium, West Lafayette, IN, June 3-6, 1980. New York, Institute of Electrical and Electronics Engineers, Inc., 1980, p. 286-293. 6 refs.

This paper describes algorithms for efficiently computing inventory estimates from satellite based images. The algorithms incorporate a one dimensional feature extraction which optimizes the pairwise sum of Fisher distances. Biases are eliminated with a premultiplication by the inverse of the analytically derived error matrix. The technique is demonstrated with a numerical example using statistics obtained from an actual Landsat scene. Attention was given to implementation of the Massively Parallel processor (MPP). A timing analysis demonstrates that the inventory estimation can be performed an order of magnitude faster on the MPP than on a conventional serial machine. (Author)

A81-46192 **Simulation of orbital image-sensor geometry.** R. B. Forrest. *Photogrammetric Engineering and Remote Sensing*, vol. 47, Aug. 1981, p. 1187-1193. 5 refs.

The essential dynamic aspects of orbital image-sensor geometry are modeled in a FORTRAN computer program presented and described in the paper. Parameters are listed for the Landsat MSS, and the program is sufficiently versatile that it can be modified to simulate other image-sensor geometries and formats. The program is organized to provide earth-surface coordinate outputs (latitude/longitude, local Cartesian) for any number of image coordinate inputs (pixel row/column numbers). Individual terrain heights may be specified for each image point of interest. (Author)

A81-46197 **Alternative 'scale up' estimators for aerial surveys where both detection and classification errors exist.** L. D. Maxim (Everest Consulting Associates, Princeton Junction, NJ), L. Harrington (Mathtech, Rosslyn, VA), and M. Kennedy. *Photogrammetric Engineering and Remote Sensing*, vol. 47, Aug. 1981, p. 1227-1239. 16 refs.

Four statistical estimators are proposed, characterized, and illustrated in order to scale up observed aerial survey counts of objects, for cases when both detection and classification errors are present. The context of the study is for an individual image or frame, and matrix methods are used for extensions to related aspects of the sampling theory. The model presented considers detection and classification as a two-stage process. Partial ground truth enables efficient estimators to be constructed or it can be used in place of either detection or identification probabilities. Of the four numerical examples presented, three make use of partial ground truth. Results may be used in agriculture and in the study of environmental pollutants. K.S.

A81-46378 * **Correlation function studies for snow and ice.** F. Vallese and J. A. Kong (MIT, Cambridge, MA). *Journal of Applied Physics*, vol. 52, Aug. 1981, p. 4921-4925. 13 refs. Research supported by the Charles Stark Draper Laboratory; Grant No. NAG5-141; Contract No. F19628-80-C-0052.

The random medium model is used to characterize snow and ice fields in the interpretation of active and passive microwave remote sensing data. A correlation function is used to describe the random permittivity fluctuations with the associated mean and variance and correlation lengths; and several samples are investigated to determine typical correlation functions for snow and ice. It is shown that correlation functions are extracted directly from appropriate ground truth data, and an exponential correlation function is observed for snow and ice with lengths corresponding to the actual size of ice particles or air bubbles. Thus, given that a medium has spatially stationary statistics and a small medium, the random medium model can interpret remote sensing data where theoretical parameters correspond to actual physical parameters of the terrain. D.L.G.

A81-46402 * **Radiometry with nighttime DMSP images in digital form.** T. A. Croft (SRI International, Menlo Park, CA). *Photogrammetric Engineering and Remote Sensing*, vol. 47, Sept. 1981, p. 1319-1325. 10 refs. NASA-supported research.

The USAF Defense Meteorological Satellite Program (DMSP) spacecraft sends images to earth in the form of numbers. It has been common practice to erase the only digital records, the magnetic tapes, for reuse, after films (resembling photographs) have been created from the numbers. While the DMSP images have been widely used, their application in research has been hindered by both the lack of digital data and the lack of an authoritative source of related technical information. The character of the digital form is considered. Each image is essentially a three-dimensional list (X,Y,Z) in which X and Y represent the position coordinates of a pixel and Z is its associated radiance. Only the value of Z is given and the X-Y position must be deduced from adjunct information. Each original scan composed of 1464 pixels represents an area on the earth's surface about 3 km wide and 3000 km long. Strengths and weaknesses of the system with respect to research applications are considered, and concepts for the design of a nocturnal imager are discussed. G.R.

A81-46917 # **Large-area histograms from Meteosat images.** K. O. Röska (ESA, European Space Operations Centre, Darmstadt, West Germany). *ESA Bulletin*, no. 27, Aug. 1981, p. 13-15.

The possibility of building multidimensional histograms from multichannel Meteosat images that improve feature identification and interpretation capabilities is demonstrated. Two-dimensional histograms of large and meteorologically uniform areas are given as examples, together with an automatic feature identification technique having modest computational requirements. The two histogram types produced by the method are infrared/visible and infrared/water vapor. O.C.

A81-47007 # **Angular anisotropy of reflection from various types of underlying surface. I - Snow cover. II - Desert (Uglovaia anizotropiia otrazheniia razlichnykh tipov podstilaiushchei poverkhnosti. I - Snezhnyi pokrov. II - Pustynia).** V. I. Korzov and K. Ia. Kondrat'ev. In: Radiation studies in the atmosphere.

Leningrad, Gidrometeoizdat, 1980, p. 43-63. 14 refs. In Russian.

Aerial measurements of the angular anisotropy of reflection of short-wave radiation from snow cover were performed with instruments aboard the IL-18 aircraft. Measurements of relative spectral brightness and spectral albedo are used to calculate coefficients of brightness, anisotropy of reflection, and asymmetry of reflection in the solar-vertical plane. These characteristics were used to analyze the angular anisotropy of reflection from snow cover as a function of solar height, flight altitude, angles of sight, and wavelength. Aerial measurements of the angular anisotropy of reflection from desert regions are also analyzed. Coefficients of brightness, anisotropy of reflection, and asymmetry in the solar-vertical plane are used to analyze the angular anisotropy of reflection from the desert as a function of wavelength, solar height, flight altitude, and angles of sight. F.G.M.

A81-47349 **Use of elevation models for landform analysis by Seasat-SAR imagery.** A. Apolloni (Calabira, Università, Cosenza, Italy), A. Carrara (CNR, IRPI, Cosenza, Italy), and P. Murino (Napoli, Università, Naples, Italy). *International Astronautical Federation, International Astronautical Congress, 32nd, Rome, Italy, Sept. 6-12, 1981, Paper 81-98*. 17 p. 35 refs.

Results are presented of a study of the feasibility of applying Seasat-SAR data to the identification and classification of slope instability phenomena. The study was carried out for the Buonamico Basin area of southern Calabria, a region characterized by rugged topography, strong relief, steep irregular slopes and a very dense stream network frequently subject to landslides and erosion. The imagery obtained was processed to remove radar speckle, then calibrated geometrically with reference to a digital terrain topographic map and calibrated radiometrically according to scattering area and direction. The resulting imagery is found to be strongly influenced by radar beam geometry, although the dominant landform features may be detected. On the basis of these results, it is recommended that (1) mountain zones be covered by at least two passes by an airborne or spaceborne system; (2) radiometric calibration be performed using properly smoothed digital terrain maps; and (3) radar data be compared with a large set of optically acquired and ground-based data. A.L.W.

A81-47351 **Application of delta modulation in on-board and ground video data processing systems for the purposes of remote sensing.** D. Mishev and P. Petrov (B'lgarska Akademiia na Naukite, Tsentralna Laboratoriia po Kosmicheski Izsledvaniia, Sofia, Bulgaria). *International Astronautical Federation, International Astronautical Congress, 32nd, Rome, Italy, Sept. 6-12, 1981, Paper 81-102*. 18 p. 8 refs.

The possibilities of delta modulation in the processing of multispectral video-data for remote sensing are discussed. It is noted that delta modulation allows the development of flexible digit systems for express analysis of a considerable amount of video data in a real time scale. Certain space-invariant operations and scale transformations are shown in data processing systems using delta modulation. The natural features of the method are analyzed for the case of differential and gradient operations over multispectral images. On the basis of this method, an efficient computational procedure of comparison with a reference pattern is developed. The possibilities of delta modulation in express video-processing ground systems are demonstrated by means of specialized devices operating in real time,

for example, the analyzer of multispectral homogeneities. An on-board system for data acquisition and data processing based on delta modulation is described.
C.R.

A81-47352 **Image quality for SPOT satellite - Specifications and budget.** G. Begni (Centre National d'Etudes Spatiales, Paris, France). *International Astronautical Federation, International Astronautical Congress, 32nd, Rome, Italy, Sept. 6-12, 1981, Paper 81-104*. 12 p.

The SPOT satellite, based on the CCD detector arrays, is to provide high resolution images of the earth surface in the visible and near-infrared domain as well as allow nadir viewing. The data products delivered by the ground image segment of the SPOT satellite program will be distributed over three levels in accordance with required accuracy. The products are rated on their radiometric and geometrical qualities: the radiometric image quality is the restitution accuracy of the measurement made by the satellite; its specifications lie in the accuracy of the signal to noise ratio, linearity, the relative accuracy between spectral bands, the relative multitemporal accuracy, the absolute accuracy, and the transfer function. Specifications of the geometrical image quality usually apply to vertical viewings and scenes with restricted altitude variations: localization accuracy, changes in lengths, anisomorphism, local coherence, multispectral superimposability, and relief restitution.
J.F.

A81-48473 **Image correlation algorithms.** B. Makarovic (International Institute for Aerial Survey and Earth Sciences, Enschede, Netherlands). *ITC Journal,* no. 1, 1981, p. 32-59. 25 refs.

Concepts and techniques for image correlation in photogrammetry are reviewed. The discussion includes the definition of image correlation systems, a classification of the various approaches, a brief description of the basic operations involved and their modifications, identification of the problem areas and possible solutions, and an estimate of the development trends. Image correlation is considered in the context of automatic generation of x-(or epipolar) parallaxes.
V.L.

A81-4[illegible]52 **Radar-optical-topographic transformations for scene content analysis.** C. A. McPherson, J. J. Hwang, and E. L. Hall (Tennessee, University, Knoxville, TN). In: EASCON '80; Electronics and Aerospace Systems Conference Arlington, VA, September 29-October 1, 1980, Conference Record. New York, Institute of Electrical and Electronics Engineers, 1980, p. 355-359. 6 refs. Contract No. F07401-78-C-0193.

A general method for transformations from one image to another is described and demonstrated for a typical radar-optical-topographic scene. The technique requires no visual correlation of pixels, although a knowledge of the position and orientation of the radar imaging system is needed. The theoretical concept of optical to radar transformation is explained through a mathematical model of the process, which derives a set of equations from six radar and three optical reference pixels. The technique is implemented by locating the position and orientation information of the chosen radar scene from previously generated data files, and selecting the region of the aerial photography that is assumed to contain the radar image. An error analysis is made, and the calculation error is reduced through software and visual inspection. Due to the ease of use and versatility of the technique, it requires less time than those methods which require a visual correlation of pixels within the two scenes, and is applicable to other types of scene matching.
D.L.G.

A81-48693 # **Selection of reference zones for the automatic coordinate control of space images (Vybor opornykh uchastkov dlia avtomaticheskoi koordinatnoi priviazki kosmicheskoi videoinformatsii).** G. A. Avanesov, V. A. Vavaev, and V. E. Verbin (Akademiia Nauk SSSR, Institut Kosmicheskikh Issledovanii, Moscow, USSR). *Issledovanie Zemli iz Kosmosa,* July-Aug. 1981, p. 91-95. 16 refs. In Russian.

Initial prerequisites and experimental data are presented, concerning an approach for selecting the reference zones for the automation of the coordinate control of images of the earth's surface, using data from space imagery systems. Based on the analysis of experimental results using actual images, a conclusion is made about the possible volume of an automatic catalog of standard reference zones. The main aspects of the method for selecting reference zones on the earth's surface include: (1) scanning and contouring on images of characteristic zones, satisfying geographical and physical requirements; (2) selecting the spectral range to describe the standard reference zones; (3) selecting the reference zones from contour zones on images, satisfying the maximum criterion for the parameter of nonuniformity; and (4) studying the temporal instability of the reference zones and determining the possible periods of dynamic correction of standards.
J.F.

A81-48694 # **Geometric correction of scanner images of the earth's surface (K voprosu o geometricheskoi korrektsii skanernykh snimkov zemnoi poverkhnosti).** V. I. Khizhnichenko. *Issledovanie Zemli iz Kosmosa,* July-Aug. 1981, p. 96-103. 7 refs. In Russian.

Space images of the earth, obtained from on-board TV scanning systems, are subject to geometric distortions, caused by a number of factors. The correction of these distortions is accomplished by computer, and the processing algorithms are developed for maximum speed to meet operational requirements. Expressions are obtained for recalculation of the coordinates of pixels, accomplished during the correction process, based on a mathematical model of scanner image acquisition. Examples of the processing of actual images of the earth's surface using the algorithms are presented.
J.F.

A81-48772 # **Derivation of formulas for the correlation of coordinate points of different-scale photographs and quasi-photographs (Vyvod formul sootnosheniia koordinat tochek raznomasshtabnykh fotosnimkov i kvazisnimkov).** M. V. Shul'min. *Geodeziia i Aerofotos'emka,* no. 3, 1981, p. 55-60. In Russian.

Formulas are derived that correlate the coordinate points of a place depicted on different-scale photographs obtained by aerial cameras with different focal distances and on processed photographs (so-called quasi-photographs). Electronic stereoscopic equipment has been developed for the image transformation of the different-scale photographs; this equipment makes it possible to transform photographic signals into electrical video signals on the basis of the mathematical relationships that have been derived. The application of this method of stereotopographic cartography is discussed. B.J.

A81-48773 # **The influence of the accuracy of determining the elements of the external orientation of a stereopair on the processing of aerial photographs on the basis of adjusting elements (Vliianie tochnosti opredeleniia elementov vneshnego orientirovaniia stereopary na protsess obrabotki aerosnimkov po ustanovochnym elementam).** T. A. Bashkova. *Geodeziia i Aerofotos'emka,* no. 3, 1981, p. 67-73. In Russian.

The paper investigates a method for determining the external-orientation elements of stereopairs by means of double photogrammetric resection. Attention is given to the influence of mean square errors in the external-orientation elements on the accuracy of computation of adjusting elements for scales of stereophotogrammetric devices and coordinate points.
B.J.

A81-48943 **A practical method for the verification of computer-processed Landsat data.** J. Hadley, Jr. (Northeast Ohio Four-County Regional Planning and Development Organization, Akron, OH) and T. L. Nash (Akron, University, Akron, OH). *Remote Sensing Quarterly,* vol. 3, Jan. 1981, p. 29-37. 9 refs. Research supported by the University of Akron.

A data verification technique is presented which can be adapted for use at most map scales and is relatively inexpensive, efficient, and requires a minimum of staff training. The technique is presented in the context of a study designed to test the reliability of processed LANDSAT cover data for Ohio for three distinct physiographic areas of the state. It is found to be adequate for generating the data's accuracy of statistics. It is noted that the methodology can be replicated for use with other polygon or grid cell geocoded information systems by altering, if necessary, the cell size used for pixel alignment.
C.R.

A81-49345 * **ICAP - An Interactive Cluster Analysis Procedure for analyzing remotely sensed data.** S. W. Wharton (NASA, Goddard Space Flight Center, Earth Resources Branch, Greenbelt, MD) and B. J. Turner (Pennsylvania State University, University Park, PA). *Remote Sensing of Environment,* vol. 11, Sept. 1981, p. 279-293. 30 refs.

An Interactive Cluster Analysis Procedure (ICAP) was developed to derive classifier training statistics from remotely sensed data. ICAP differs from conventional clustering algorithms by allowing the analyst to optimize the cluster configuration by inspection, rather than by manipulating process parameters. Control of the clustering process alternates between the algorithm, which creates new centroids and forms clusters, and the analyst, who can evaluate and elect to modify the cluster structure. Clusters can be deleted, or lumped together pairwise, or new centroids can be added. A summary of the cluster statistics can be requested to facilitate cluster manipulation. The principal advantage of this approach is that it allows prior information (when available) to be used directly in the analysis, since the analyst interacts with ICAP in a straightforward manner, using basic terms with which he is more likely to be familiar. Results from testing ICAP showed that an informed use of ICAP can improve classification, as compared to an existing cluster analysis procedure. (Author)

A81-49768 # **An investigation of the autocorrelation function of radar images.** L. Alexander (General Electric Co., Space Div., Philadelphia, PA) and H. Kritikos (Pennsylvania, University, Philadelphia, PA). In: Canadian Symposium on Remote Sensing, 6th, Halifax, Canada, May 21-23, 1980, Proceedings. Ottawa, Canadian Aeronautics and Space Institute, 1981, p. 153-160. 12 refs.

Three digital radar data sets are examined and their autocorrelation functions are computed. The autocorrelation functions are found to be substantially lower than those of visible images. The effects of resampling on imagery with this lower correlation coefficient are examined. The implication of these findings for information extraction from radar images is that spatial properties contribute a significant amount of information to classification success. The implication of the result for data compression suggests the improved performance of the Even Discrete Sine Transform for the compression of radar imagery. B.J.

A81-49780 # **Cartographic accuracy of synthetic aperture radar imagery.** E. E. Derenyi and J. L. Szabo (New Brunswick, University, Fredericton, Canada). In: Canadian Symposium on Remote Sensing, 6th, Halifax, Canada, May 21-23, 1980, Proceedings. Ottawa, Canadian Aeronautics and Space Institute, 1981, p. 287, 288. Research supported by the Department of Energy, Mines and Resources of Canada.

The cartographic accuracy of microwave imagery is investigated to ascertain geometric characteristics of imagery recorded by a synthetic aperture radar installed in the Convair-580 aircraft. Imagery is acquired in three passes, each line approximately 60 km long, with a sensor operating in a shallow angle mode at a depression angle of 24.4 deg to the center of the beam. Accuracy of the geographic position of points from SAR imagery is found to be a function of the density of control points and the length of the strip, and it is concluded that SAR-850 imagery has potential as a source of information for the revision of 1:50,000 scale maps when mathematical transformation and digital mapping techniques are employed. D.L.G.

A81-49793 # **Digital enhancements for vegetation mapping in a subarctic environment.** I. L. Johnston and P. J. Howarth (McMaster University, Hamilton, Ontario, Canada). In: Canadian Symposium on Remote Sensing, 6th, Halifax, Canada, May 21-23, 1980, Proceedings. Ottawa, Canadian Aeronautics and Space Institute, 1981, p. 405-412. 17 refs. Research supported by McMaster University; Natural Sciences and Engineering Research Council of Canada Grant No. A-5586.

Experiments have been undertaken to determine the most appropriate digital Landsat enhancements for mapping subarctic vegetation. Landsat data of the Hook Point area in northern Ontario recorded in June, July, and September were used in the study. Linear contrast stretch, band ratioing, video filtering and principal components enhancements were applied to the data. A visual assessment of the results was made to determine the capabilities of each enhancement to differentiate bog, fen and transitional vegetation cover. The effect of the enhancement algorithms on the digital values was also studied in small test areas. The different color renditions between a standard color composite and an atmospherically corrected composite demonstrate the effects of the solar and atmospheric corrections. The linear contrast stretch provided more vegetation information than the composites. However, band ratioing, video filtering and principal components enhancements did not provide satisfactory images of the vegetation. B.J.

A81-49795 # **Computer analysis of Tiros-N/NOAA-6 satellite data for operational snow cover mapping.** S. E. Waterman, W. D. Hogg, A. J. Hanssen, and V. L. Polavarapu (Department of the Environment, Atmospheric Environment Service, Downsview, Ontario, Canada). In: Canadian Symposium on Remote Sensing, 6th, Halifax, Canada, May 21-23, 1980, Proceedings.
Ottawa, Canadian Aeronautics and Space Institute, 1981, p. 435-442. 11 refs.

A81-49804 * # **Investigation of multispectral remote sensing of snow cover using a solar radiation model.** S. E. Waterman (Department of the Environment, Atmospheric Environment Service, Downsview, Ontario, Canada). In: Canadian Symposium on Remote Sensing, 6th, Halifax, Canada, May 21-23, 1980, Proceedings. Ottawa, Canadian Aeronautics and Space Institute, 1981, p. 525-540. 29 refs. Grant No. NGL-06-003-200.

A solar radiation model is described which is able to calculate, for given atmospheric and topographic input conditions, the spectral distributions of the direct and diffuse components of the total irradiance incident upon a target surface. The irradiance includes both upwelling radiation backscattered toward the earth's surface and radiation reflected toward the target from other terrain surfaces. Spectral reflectance data for two dissimilar snow types are fed into the model, along with a geometric description of the topography of the snow covered terrain. These data permit the calculation of the exitance of the target over the wavelength limits of a given sensor and, hence, the apparent contrast between the two snow types for the given input conditions. The results show that the contrast between the two snow types, all other factors being constant, is greatest in the near infrared wavelengths. C.R.

A81-49808 # **Role of aerial photographs in classification of Landsat data.** W. A. Miller, G. R. Johnson (Technicolor Graphic Services, Inc., Sioux Falls, SD), and W. G. Rhode. In: Canadian Symposium on Remote Sensing, 6th, Halifax, Canada, May 21-23, 1980, Proceedings. Ottawa, Canadian Aeronautics and Space Institute, 1981, p. 575, 576. 5 refs.

A81-49812 # **Histogram estimation for multiple-detector sensors.** W. M. Strome (Canada Centre for Remote Sensing, Ottawa, Canada). In: Canadian Symposium on Remote Sensing, 6th, Halifax, Canada, May 21-23, 1980, Proceedings. Ottawa, Canadian Aeronautics and Space Institute, 1981, p. 603-608.

It is shown that with relatively minor modification, peak and valley seeking clustering algorithms can be made more effective by adjusting the histograms of radiometrically corrected multidetector per channel data, such as those from the Landsat MSS as described. The slightly more complicated procedure produces a histogram which much more closely approximates the original intensity probability distribution function than that of either the raw or radiometrically corrected data. C.R.

A81-49813 # **Comparative experimental study on the use of original and compressed multispectral Landsat data of the Bayuda desert.** K. A. Ulbricht (Deutsche Forschungs- und Versuchsanstalt fur Luft- und Raumfahrt, Institut für Nachrichtentechnik, Oberpfaffenhofen, West Germany). In: Canadian Symposium on Remote Sensing, 6th, Halifax, Canada, May 21-23, 1980, Proceedings. Ottawa, Canadian Aeronautics and Space Institute, 1981, p. 609-616. 5 refs.

An excerpt from a multispectral Landsat scene, compressed by a ratio of 6.4/1, is investigated to determine the effect of the compression on the image contents. The study is based on several years of image processing activities on Landsat scenes of North African territories, in particular the Landsat image of February 5, 1973, of the Bayuda desert in the Sudan. This image was submitted to supervised maximum likelihood classification before and after compression of data as a function of the rejection class parameter sigma. Different approaches to the use of circular or rectangular training areas, before and after their compression, for classification on original and compressed scene, were used in investigating the influence of compression on image contents. With the aid of five training areas for classification, partitioning of classified image,

original as well as compressed, is given on a percentage basis as a function of sigma.
C.R.

A81-49814 # **Acquisition and preprocessing of images collected by future European Space Agency satellites.** J.-P. Antikidis (ESA, Earth Observation Programme Office, Toulouse, France). In: Canadian Symposium on Remote Sensing, 6th, Halifax, Canada, May 21-23, 1980, Proceedings. Ottawa, Canadian Aeronautics and Space Institute, 1981, p. 617-624.

Various efforts planned by the European Space Agency (ESA) for the development of systems in which instruments and processing are defined as a whole are discussed. Analysis of the different requirements has led the Agency to envisage specific payloads that would allow objectives to be attained in land applications, coastal ocean monitoring, and global ocean monitoring. It is noted that the ERS-1 system will have a satellite consisting of a multimission platform equipped with an 1800 W solar generator and a Fine Attitude Measurement System; the payload will comprise an Ocean Color Monitor, a multichannel Imaging Microwave Radiometer, and a Synthetic Aperture Radar.
C.R.

A81-49818 # **Geometric accuracy of Landsat images processed by NASDA.** Y. Yamamoto (National Space Development Agency of Japan, Tokyo, Japan). In: Canadian Symposium on Remote Sensing, 6th, Halifax, Canada, May 21-23, 1980, Proceedings. Ottawa, Canadian Aeronautics and Space Institute, 1981, p. 661-663.

N81-29497*# Lockheed Engineering and Management Services Co., Inc., Houston, Tex.
AN ANALYSIS OF HAZE EFFECTS ON LANDSAT MULTISPECTRAL SCANNER DATA
W. R. Johnson and M. L. Sestak, Principal Investigators Mar. 1981 40 p refs Sponsored by NASA, USDA, Dept of Commerce, Dept. of the Interior, and Agency for International Development ERTS
(Contract NAS9-15800; Proj. AgRISTARS)
(E81-10162; NASA-CR-160984; SR-L1-04071;
LEMSCO-15971; JSC-17127) Avail: NTIS HC A03/MF A01
CSCL 02C

Early season changes in optical depth change brightness, primarily along the soil line; and during crop development, changes in optical depth change both greenness and brightness. Thus, the existence of haze in the imagery could cause an unsuspecting analyst to interpret the spectral appearance as indicating an episodal event when, in fact, haze was present. The techniques for converting LANDSAT-3 data to simulate LANDSAT-2 data are in error. The yellowness and none such computations are affected primarily. Yellowness appears well correlated to optical depth. Experimental evidence with variable background and variable optical depth is needed, however. The variance of picture elements within a spring wheat field is related to its equivalent in optical depth changes caused by haze. This establishes the sensitivity of channel 1 (greenness) pixels to changes in haze levels. The between field picture element means and variances were determined for the spring wheat fields. This shows the variability of channel data on two specific dates, emphasizing that crop development can be influenced by many factors. The atmospheric correction program ATCOR reduces segment data from LANDSAT acquisitions to a common haze level and improves the results of analysis.
A.R.H.

N81-29498*# Lockheed Engineering and Management Services Co., Inc., Houston, Tex.
THE MULTICATEGORY CASE OF THE SEQUENTIAL BAYESIAN PIXEL SELECTION AND ESTIMATION PROCEDURE
M. D. Pore and T. B. Dennis, Principal Investigators Nov. 1980 22 p refs Sponsored by NASA, USDA, Dept. of Commerce, Dept. of Interior, and Agency for International Development ERTS
(Contract NAS9-15800; Proj. AgRISTARS)
(E81-10182; NASA-CR-160965; SR-LO-00478;
LEMSCO-14807; JSC-16378) Avail: NTIS HC A02/MF A01
CSCL 12A

A Bayesian technique for stratified proportion estimation and a sampling based on minimizing the mean squared error of this estimator were developed and tested on LANDSAT multispectral scanner data using the beta density function to model the prior distribution in the two-class case. An extention of this procedure to the k-class case is considered. A generalization of the beta function is shown to be a density function for the general case which allows the procedure to be extended.
Author

N81-29501*# Lockheed Engineering and Management Services Co., Inc., Houston, Tex.
CONVERSION OF SPU-UNIVERSAL DISK FILE TO JSC-UNIVERSAL TAPE STORAGE: CONVRT USER'S GUIDE
W. E. Ryland, Principal Investigator Sep. 1980 12 p Sponsored by NASA, USDA, Dept. of Commerce, Dept. of Interior, and Agency for International Development ERTS
(Contract NAS9-15800; Proj. AgRISTARS)
(E81-10185; NASA-CR-160938; EW-LO-00706;
LEMSCO-15608; JSC-16821) Avail: NTIS HC A02/MF A01
CSCL 09B

The CONVRT, program which runs on a DEC PDP 11/70 computer, reads data files on disk in the SPU-Universal format and reformats the data to JSC Universal and output on tape.
A.R.H.

N81-29502*# Lockheed Engineering and Management Services Co., Inc., Houston, Tex.
MAXIMUM LIKELIHOOD CLUSTERING WITH DEPENDENT FEATURE TREES
C. B. Chittineni, Principal Investigator Jan. 1981 54 p refs Sponsored by NASA, USDA, Dept. of Commerce, Dept. of the Interior, and Agency for International Development ERTS
(Contract NAS9-15683; Proj. AgRISTARS)
(E81-10186; NASA-CR-160939; SR-L1-04031;
LEMSCO-15683; JSC-16853) Avail: NTIS HC A04/MF A01
CSCL 12A

The decomposition of mixture density of the data into its normal component densities is considered. The densities are approximated with first order dependent feature trees using criteria of mutual information and distance measures. Expressions are presented for the criteria when the densities are Gaussian. By defining different types of nodes in a general dependent feature tree, maximum likelihood equations are developed for the estimation of parameters using fixed point iterations. The field structure of the data is also taken into account in developing maximum likelihood equations. Experimental results from the processing of remotely sensed multispectral scanner imagery data are included.
A.R.H.

N81-29503*# Elogic, Inc., Houston, Tex.
NEW OUTPUT IMPROVEMENTS FOR CLASSY
M. E. Rassbach, Principal Investigator Mar. 1981 37 p Sponsored by NASA, USDA, Dept. of Commerce, Dept. of the Interior, and Agency for International Development ERTS
(Contract NAS9-15981; Proj. AgRISTARS)
(E81-10189; NASA-CR-160974; SR-XI-04053; NAS-811)
Avail: NTIS HC A03/MF A01 CSCL 02C

Additional output data and formats for the CLASSY clustering algorithm were developed. Four such aids to the CLASSY user are described. These are: (1) statistical measures; (2) special map types; (3) formats for standard output; and (4) special cluster display method.
A.R.H.

N81-29506*# National Oceanic and Atmospheric Administration, Houston, Tex.
CHARACTERISTICS, OF TIROS, GOES, DMSP AND LANDSAT SYSTEMS
T. I. Gray, Jr., D. G. McCrary, and T. A. Armstrong, Principal Investigators (Lockheed Engineering and Management Services Co., Inc., Houston, Tex.) Mar. 1981 21 p Sponsored by NASA, USDA, Dept. of Commerce, Dept. of the Interior, and Agency for International Development
(Proj. AgRISTARS)
(E81-10192; NASA-CR-160979; EW-N1-04075; JSC-17131)
Avail: NTIS HC A02/MF A01 CSCL 02C

The characteristics of the TIROS, GOES, DMSP and LANDSAT systems of satellites are described. The data listed for each system are altitude of orbit, inclination/position, orbit type, orbits per day, expected operational lifetime and the sensor systems. The sensor systems are described as to wavelength of each channel, resolution, field of view and other pertinent information. Data information such as availability rate, collection method, primary use/application and how to obtain additional information is also given.
Author

N81-29509*# Lockheed Engineering and Management Services Co., Inc., Houston, Tex.
COMPUTER PROGRAM DOCUMENTATION USER INFORMATION FOR THE RSO-TAPE PRINT PROGRAM (RSO-PRNT)
P. M. Gibbs, Principal Investigator Nov. 1980 11 p ERTS
(Contract NAS9-15800)
(E81-10198; NASA-CR-161000; JSC-17015; LEMSCO-15903)
Avail: NTIS HC A02/MF A01 CSCL 09B

A user's guide for the RSOPRNT, a TRASYS Master Restart Output Tape (RSO) reader is presented. Background information and sample runstreams, as well as, references, input requirements and options, are included. J.M.S.

N81-29510*# Lockheed Engineering and Management Services Co., Inc., Houston, Tex.
ESTIMATION OF PROPORTIONS IN MIXED PIXELS THROUGH THEIR REGION CHARACTERIZATION
C. B. Chittineni, Principal Investigator Mar. 1981 38 p refs
Sponsored by NASA, USDA, Dept. of Commerce, Dept. of the Interior, and Agency for International Development ERTS
(Contract NAS9-15800; Proj. AgRISTARS)
(E81-10199; NASA-CR-161001; SR-L1-04067; LEMSCO-16021; JSC-17124) Avail: NTIS HC A03/MF A01 CSCL 12A

A region of mixed pixels can be characterized through the probability density function of proportions of classes in the pixels. Using information from the spectral vectors of a given set of pixels from the mixed pixel region, expressions are developed for obtaining the maximum likelihood estimates of the parameters of probability density functions of proportions. The proportions of classes in the mixed pixels can then be estimated. If the mixed pixels contain objects of two classes, the computation can be reduced by transforming the spectral vectors using a transformation matrix that simultaneously diagonalizes the covariance matrices of the two classes. If the proportions of the classes of a set of mixed pixels from the region are given, then expressions are developed for obtaining the estmates of the parameters of the probability density function of the proportions of mixed pixels. Development of these expressions is based on the criterion of the minimum sum of squares of errors. Experimental results from the processing of remotely sensed agricultural multispectral imagery data are presented. A.R.H.

N81-29522# Itek Corp., Lexington, Mass. Optical Systems Div.
CONCEPTUAL DESIGN OF AN AUTOMATED MAPPING SATELLITE SYSTEM (MAPSAT) Final Technical Report
26 Mar. 1981 303 p refs
(Contract DI-14-08-0001-18656)
(PB81-185555; ITEK-81-8449A-2; USGS/NMD-81-001) Avail: NTIS HC A14/MF A01 CSCL 08B

A concept for mapping and monitoring the Earth's surface from space involves obtaining elevation data from the use of the epipolar-plane condition in space. This greatly simplifies the mapping problem by permitting the automated processing of stereo data into digital elevation data. Multicolored image maps at 1:50,000 scale with 20-m contours are indicative of the products which are within the capability of the Mapsat system. Mapsat would provide continuity with respect to LANDSATS 1-3, including the same basic data transmission system. GRA

N81-30499# General Electric Co., Lanham, Md. Space Div.
INTERACTIVE DIGITAL IMAGE PROCESSING FOR TERRAIN DATA EXTRACTION Interim Report, 18 Sep. 1979 - 17 Sep. 1980
Howard L. Heydt, Thomas F. Wescott, and Christopher J. Peterson Nov. 1980 181 p refs
(Contract DAAK70-79-C-0153)
(AD-A101321; ETL-0241) Avail: NTIS HC A09/MF A01 CSCL 09/2

Man-machine interactive digital image processing techniques were applied to the extraction of terrain analysis data from aerial imagery were investigated. Emphasis is given to the extraction of vegetation data elements from digitized panchromatic photograhy, with a small amount of attention given to thermal infrared and side-looking radar imagery. Vegetation data elements listed in the USAETL Terrain Analysis Procedural Guide for Vegetation are addressed in varying degrees of depth. Interactive digital techniques are developed for vegetation/land cover boundary extraction, and for the extraction of several forest related data elements. The extraction techniques are developed using an interactive digital image analysis system-the General Elecric DIAL (Digital Image Analysis Laboratory). Results are compared in two cases to those achieved via existing manual analysis procedures. Author (GRA)

N81-30723# Environmental Research Inst. of Michigan, Ann Arbor. Radar and Optics Div.
FOURIER MODULUS IMAGE CONSTRUCTION Final Technical Report, 7 Sep. 1979 - 30 Sep. 1980
James E. Fienup May 1981 70 p refs
(Contract F30602-80-C-0002)
(AD-A101728; RADC-TR-81-63) Avail: NTIS HC A04/MF A01 CSCL 04/1

This report describes the investigation of a new method for recovering diffraction-limited images through the turbulent atmosphere. It consists of an iterative algorithm that constructs an image from Fourier modulus data which is measured by stellar speckle interferometry. Research results indicate that the method has the potential for providing diffraction-limited images of Earth-orbiting satellites. Image construction experiments were performed on Fourier modulus data computer-simulated to include the effects of atmospheric turbulence, diffraction, photon (Poisson statistics) noise, and a finite number of short-exposure images. The quality of the constructed images was found to degrade in a gradual and predictable manner as the signal-to-noise ratio decreases. The rms error of the constructed images was found to vary approximately as the square root of the rms error of the Fourier modulus data. Diffraction-limited images were constructed for levels of photon noise that would be expected for imaging satellites through a 1.6-meter telescope. Image construction experiments were performed on the Fourier modulus of a number of different objects of varying complexity. Interpretation of the results was complicated by a tendency of the algorithm to stagnate at local minimum having the appearance of a good quality image superimposed by a pattern of stripes. Nevertheless, results were suggestive that the solution is usually unique. GRA

N81-30852# L N K Corp., Inc., Silver Spring, Md.
KNOWLEDGE-BASED IMAGE ANALYSIS Progress Report, 1 Sep. 1978 - 1 Dec. 1980
George C. Stockman, Barbara A. Lambird, David Lavine, and Laveen N. Kanal Apr. 1981 243 p refs
(Contract DAAK70-77-C-0110)
(AD-A101319; ETL-0258) Avail: NTIS HC A11/MF A01 CSCL 09/2

The work reported was directed toward employing a priori knowledge in the automatic analysis of aerial imagery. Major objectives of the research were directed toward (1) map-guided registration; (2) verification of geographic data bases extracted from imagery; (3) enrichment of geographic data bases; and (4) automatic terrain feature extraction using multiple sources of knowledge and multi-level decision making. The key component in all of the work was the matching of existing iconic structure in a geographic data base (GDB) with detected image structure. By using iconic knowledge, the image interpretation paradigm becomes a three step process. First, some primitive features of the imagery must be recognized without any area-specific knowledge. Second, the imagery is aligned or registered with the knowledge base by drawing correspondences between the image features and their iconic analogues in the GDB. The matching is formalized by derivation of a transformation which maps points (x,y) of the image to points (u,v) in GDB coordinates. The final step of the process is the analysis of those parts of the image which were not successfully interpreted in steps 1 and 2. This implies a top-down search for image structures which correspond to features in the GDB. Section 2 of the report treats primitive extraction. The emphasis is currently on lineal, point, and region features only. A method for automatically inferring a rotation and translation transforming image to map is given in Section 3. Classification of registered regions is discussed in Section 4. Verification of lineal GDB features in gray-scale imagery is introduced in Section 5. Author (GRA)

N81-31600*# Elogic, Inc., Houston, Tex.
IMPROVED VERSION OF THE SPLIT ROUTINE FOR CLASSY
M. E. Rassbach, Principal Investigator Mar. 1981 16 p
Sponsored by NASA, USDA, Dept. of Commerce, Dept. of the Interior, and Agency for International Development ERTS
(Contract NAS9-15981; Proj. AGRISTARS)

(E81-10210; NASA-CR-160973; SR-IX-04046) Avail: NTIS HC A02/MF A01 CSCL 02C

The theoretical basis for a new version of the SPLIT routine for CLASSY is developed. (The SPLIT routine is used to guess the positions of the parts of a cluster which is not normally distributed.) The proposed routine would be a faster, more accurate replacement for the existing SPLIT routine, which was developed on an ad hoc basis.

J.M.S.

N81-31613# Royal Aircraft Establishment, Farnborough (England).

A TECHNIQUE FOR LINE EXTRACTION FROM LANDSAT MULTI-SPECTRAL SCANNER SATELLITE DATA WITH SOME APPLICATIONS OF THE TECHNIQUE

A. H. Benny Jan. 1981 42 p refs

(RAE-TR-81010; RAE-SPACE-592; BR78637) Avail: NTIS HC A03/MF A01

An automated technique is described for extracting lines from LANDSAT multispectral scanner images by means of density contour threading of the data. Lines are stored in the form of a series of X, Y coordinate pairs, sufficient coordinates being present to define each line with the required amount of detail. At a given contour level all possible lines are constructed which thread through the grid such that all locations to one side have a higher or similar value and all locations to the other side have a lower value. The image will in general yield several separate contour lines at any specified contour level. The method of searching for individual contour lines is based upon the observation that a line must run between any two adjacent pixels if one of them has a lower radiance value and the other a higher value than the selected level for the boundary line. If the selected level is the same as a pixel value, the line must run through that pixel, and to avoid missing this condition the test is altered to include the case in which one pixel has a lower value and the other a value greater than or equal to the selected level.

Author (ESA)

N81-31615# National Oceanic and Atmospheric Administration, Washington, D. C. National Earth Satellite Service.

SATELLITE IDENTIFICATION OF SURFACE RADIANT TEMPERATURE FIELDS OF SUBPIXEL RESOLUTION

Jeff Dozier Dec. 1980 17 p refs Sponsored in part by National Academy of Sciences - National Research Council

(PB81-184038; NOAA-TM-NESS-113; NOAA-81021710) Avail: NTIS HC A02/MF A01 CSCL 04B

A method is presented for identifying from NOAA TIROS-N series satellite data the magnitudes and subpixel areal coverages of two different surface radiant temperatures. The method utilizes the different response of the Planck function at different wavelengths.

GRA

N81-32602# National Oceanic and Atmospheric Administration, Boulder, Colo. Environmental Research Lab.

CATEGORIZATION OF NORTHERN GREEN BAY ICE COVER USING LANDSAT 1 DIGITAL DATA: A CASE STUDY

George A. Leshkevich Jan. 1981 25 p refs

(PB81-200438; NOAA-TM-ERL-GLERL-33; NOAA-81032301) Avail: NTIS HC A02/MF A01 CSCL 08I

Northern Green Bay ice cover on February 13, 1975, was analyzed using LANDSAT 1 digital data on the computer facilities at the Environmental Research Institute of Michigan. Training sets, consisting of selected areas in the LANDSAT scene that represent various ice types, were entered based upon the tone, texture, and location of the ice within the bay. The classification algorithm used in the analysis consisted of a modified maximum likelihood procedure using the multivariate Gaussian probability density function. It was found that seven ice types could be differentiated in the ice cover, that new (thin) ice could be distinguished from water, and that ice could be distinguished from relatively thin cloud cover.

GRA

N81-33345# Canada Centre for Remote Sensing, Ottawa (Ontario).

WAVE ORBITAL VELOCITY, FADE AND SAR RESPONSE TO AZIMUTH WAVES

R. K. Raney *In* ESA Coherent and Incoherent Radar Scattering from Rough Surfaces and Vegetated Areas May 1981 p 63-70 refs Submitted for publication

Avail: NTIS HC A08/MF A01

Orbital velocity bunching as an explanation of the response of SAR is proposed, and the restraint of the coherence time of the scattering centers is considered. Key results in random scene image theory as applied to the azimuth wave problem are summarized. Doppler shifts are shown to be a function of wave and sensor geometry. The first order consequence of orbital motion is shown to induce a redistributed scatterer density that may be considered independently from specific SAR performance parameters and the new density can be convolved with the SAR transfer function to derive the expected output image. Focus perturbation of azimuth wave imagery is observed to occur, but only for a specific subset of wave length and wave height circumstances. Scatterer fade is shown to be of central importance in the SAR transfer function.

Author (ESA)

N81-33347# Kansas Univ., Lawrence. Remote Sensing Lab.

A REVIEW OF VOLUME SCATTER THEORIES FOR MODELING APPLICATIONS

A. K. Fung *In* ESA Coherent and Incoherent Radar Scattering from Rough Surfaces and Vegetated Areas May 1981 p 83-92 refs

(Grants NSF ENG-79-09374; DAAG29-80-K-0018)
Avail: NTIS HC A08/MF A01

Volume scatter theories commonly applied to develop scatter models for vegetation, snow and sea ice are reviewed. These include the first-order theories based on the Born approximation and the renormalization method, and the multiple scatter theories based on the radiative transfer method and the matrix doubling method. The merits of these scattering theories are compared with those developed by Twersky and Rytov. Applications of the scatter models developed from a first-order theory and a multiple scatter theory are illustrated.

Author (ESA)

N81-33348# Marconi Co. Ltd., Chelmsford (England).

SCATTERING THEORY WITH APPLICATION TO SYNTHETIC APERTURE RADAR

S. Rotheram *In* ESA Coherent and Incoherent Radar Scattering from Rough Surfaces and Vegetated Areas May 1981 p 93-98 refs

Avail: NTIS HC A08/MF A01

A Green's function scattering theory is outlined analogous to the T-matrix scattering theory of quantum mechanics and using an integral equation of the Lippman Schwinger type. To apply the scattering theory to microwave imaging the Green's function representations are combined with a system model. A number of SAR imaging mechanisms are identified. These include complex Bragg waves, azimuthal tilting, a motion effect cut-off and a temporal resolution effect. An application to SAR 580 processing is indicated.

Author (ESA)

N81-33350# Illinois Univ. at Chicago Circle, Chicago. Communications Lab.

OPTIMAL POLARIZATION CONCEPT IN RADAR IMAGING

Wolfgang-M. Boerner *In* ESA Coherent and Incoherent Radar Scattering from Rough Surfaces and Vegetated Areas May 1981 p 129-142 refs Sponsored also by Humboldt Fellowship National Science and Engineering Research Council of Canada and NATO

(Contracts N00014-80-C-0708; N00014-80-C-0073; Grant DRXR-OPR-P-17227-EL)
Avail: NTIS HC A08/MF A01

Polarization as a factor of electromagnetic scattering is discussed. Due to the vector nature of electromagnetic waves, electromagnetic remote sensing and inverse scattering techniques, if applied rigorously, require incorporation of polarization information into their formulation. By applying this approach to existing and some novel theories, improvements in quality and fidelity of the reconstructed profiles and/or images can be obtained. The development of methods and theories of vector inverse scattering for the electromagnetic polarization-dependent case or in the more complicated seismic case of p and s-wave interaction in elastic media, as for example in Vertical Seismic Profiling, is advocated. Radar scattering matrices and radar measurables are described, as are polarization descriptors.

Author (ESA)

N81-33351# Kansas Univ. Center for Research, Inc., Lawrence. Remote Sensing Lab.

SCATTEROMETER CALIBRATION AND DATA CORRECTION

Richard K. Moore *In* ESA Coherent and Incoherent Radar Scattering from Rough Surfaces and Vegetated Areas May 1981 p 149-163
Avail: NTIS HC A08/MF A01

Calibration of radars used for scatterometer purposes and the calibrations necessary to recover the scattering coefficient from the data are discussed. If calibration permits repeatable measurements the system has good relative calibration. Absolute calibration is needed to compare measurements made by different systems or when design data for new systems is needed. Relative calibration may best be done by using a sample of the transmitted signal as a test signal to determine receiver response. Absolute calibration requires either separate calibrations of each part, which are then combined, or the return from a standard target may be used to calibrate the entire system. Surface and volume scatter calculations are illustrated for various situations. Author (ESA)

N81-33528# Institut fuer Angewandte Geodaesie, Frankfurt am Main (West Germany).
PARTIALLY AUTOMATED OBJECT EXTRACTION FROM AERIAL PHOTOGRAPHS AND LAND MAPS [TEILAUTOMATISCHE OBJELTEXTRAKTION AUS LUFTBILDERN UND LANDKARTEN]
U. Bausch, W. D. Groch, W. Kestner, and M. Sties *In its* Rept. on Cartography and Geodesy, Ser. 1 1980 p 7-22 refs In GERMAN; ENGLISH summary

Avail: NTIS HC A07/MF A01

Object controlled object extraction procedures are presented. Compared with systematic area covering methods such procedures are expected to use less computer time at lower error rates. The principles of methods for extracting linear, surface, and point features are explained, and their accuracy and quality are discussed. The local judgement of gray value profiles for the determination of object outlines is dealt with in detail. One dimensional operators are introduced assigning evaluation numbers to the image points of an image extract. The higher the number, the higher the probability is for a point to lie on a contour. In this way candidates for an object outline are filtered from the selected image range. The various methods were simulated on a computer and tested using different imagery material. Results are shown. Author (ESA)

N81-33541*# Washington Univ., Seattle. Dept. of Geological Sciences.
COMPARISON OF LABORATORY REFLECTANCE SPECTRA AND LANDSAT MULTISPECTRAL IMAGES OF HAWAIIAN LAVA FLOWS
Diane L. Evans, Tom G. Farr, and John B. Adams, Principal Investigators 1981 34 p refs Submitted for publication Sponsored by NASA Original contains imagery. Original photography may be purchased from the EROS Data Center, Sioux Falls, S.D. 57198 ERTS
(E81-10061; NASA-CR-164748) Avail: NTIS HC A03/MF A01 CSCL 08K

Laboratory reflectance spectra of samples with known compositions were compared to LANDSAT multispectral image of Hawaii. The technique used involves determining what the spectral response of a material of interest is at different wavelengths based on laboratory measurements, and searching a stack of spatially registered multispectral images for picture elements with the desired spectral signature. A relatively simple atmospheric correction was employed that combined the effects of gaseous absorption, Rayleigh, and anisotropic aerosol scattering. Laboratory spectal reflectance measurements of surface samples from Hawaii were found to allow mapping of a similar material over many square kilometers in the Hawaii LANDSAT frame, and that correspondence with the known geology and vegetation is excellent. The technique can be generalized to incorporate any bandpasses, and, therefore, has potential for identifying and mapping rock and vegetation types remotely. A.R.H.

N81-33544*# North Carolina State Univ., Raleigh. School of Engineering.
THE USE OF CHARGE TRANSFER DEVICES FOR LANDSAT PATTERN CLASSIFICATION Final Report
[1981] 23 p Sponsored by NASA Original contains imagery. Original photography may be purchased from the EROS Data Center, Sioux Falls, S.D. 57198 ERTS
(E81-10087; NASA-CR-164751) Avail: NTIS HC A02/MF A01 CSCL 05B

Several techniques were developed and tested for increasing the performance of analog or analog/binary systems which perform calculations of Gaussian pattern classification of multispectral data. All the techniques involve scaling of data parameters. The two major sources of inaccuracies in the system are random noise and unpredictable shifts in the zero point. Input scaling, covariance scaling, and x-u scaling are discussed. Application of the these techniques with the prototype system developed resulted in successful classification of land and water with zero errors. A.R.H.

N81-33547*# Vermont Univ., Burlington. School of Natural Resources.
THE DEVELOPMENT OF A REMOTE SENSING APPLICATIONS PROGRAM FOR VERMONT Annual Summary Report, 1 Jun. 1980 - 31 May 1981
Roy A. Whitmore, Jr., Principal Investigator 31 May 1981 59 p Original contains color imagery. Original photography may be purchased from the EROS Data Center, Sioux Falls, S.D. 57198 ERTS
(Grant NsG-7453)
(E81-10149; NASA-CR-164871) Avail: NTIS HC A04/MF A01 CSCL 08F

Ancillary hardware was obtained to expedite computer processing of remotely sensed data and demonstrations were held to acquaint general and technical interest groups with the facilities and service available. Systems were developed for handling and analyzing data. A Vermont land cover classification scheme and a remote sensing inventory and information system were devised. Specific applications discussed included (1) detecting forest insect defoliation; (2) Brighton land cover/land use mapping or planning; (3) Morristown farmland inventory and agricultural land study; (4) site analysis for a proposed wood-fired electric power plant; and (5) LANDSAT hands-on training course for State of New Hampshire personnel. The acquisition and testing of equipment for small-format aerial photography is also reported. A.R.H.

N81-33551*# Minnesota Univ., St. Paul. Remote Sensing Lab.
DEVELOPMENT OF ALTERNATIVE DATA ANALYSIS TECHNIQUES FOR IMPROVING THE ACCURACY AND SPECIFICITY OF NATURAL RESOURCE INVENTORIES MADE WITH REMOTE SENSING DATA
Thomas M. Lillesand, Principal Investigator *In its* A Study of Minn. Land and Water Resources Using Remote Sensing, Vol. 14 1 Jan. 1981 14 p ERTS

Avail: NTIS HC A05/MF A01 CSCL 05B

The applicability of digital LANDSAT data in updating the Minnesota Lake Land Management Information System and in assessing the trophic status of lakes was investigated. Data from various combinations of training, classification, and geometric correction techniques were compared to a photointerpreted reference data set consisting of ground-verified samples and six randomly selected photographs covering approximately one quarter of the study area. For a reconnaissance inventory, the training via polygons selected from aerial photographs with a canonical analysis minimum distance classifier is the most accurate and efficient analysis technique. The applications test project resulted in disappointing thematic classification results per se, but did contribute to the development of mechanisms for implementing a LANDSAT data processing capability in the State Planning Agency on a permanent basis. A.R.H.

N81-33556*# Science and Education Administration, Weslaco, Tex.
METHODS OF EDITING CLOUD AND ATMOSPHERIC LAYER AFFECTED PIXELS FROM SATELLITE DATA Quarterly Progress Report, 5 Dec. 1980 - 5 Jun. 1981
Paul R. Nixon, Craig L. Wiegand, Arthur J. Richardson, Michael P. Johnson, and Benjamin G. Goodier, Principal Investigators Jun. 1981 12 p ref ERTS
(NASA Order S-75406-B)
(E81-10169; NASA-CR-164769; QR-1; QR-2) Avail: NTIS HC A02/MF A01 CSCL 05B

Removal of such pixels prior to interpretation would avoid erroneous conclusions about Earth surface conditions such as extent and severity of, for example, droughts and freezes and their probable economic impact due to crop losses. The results of a cluster screening procedure applicable to daytime satellite coverage when reflective (VIS) and emissive (IR) band data are obtained were examined. For a 3 Jul 78 HCMM daytime scene, twenty-eight VIS digital values each accounted for over 1.0% of the pixels in the south Texas test area. The VIS digital value of 42, associated with land features, exceeded all others in frequency of occurrence, accounting for 5.6% of all pixels in the daytime scene. The most common IR digital count value was 80 which was common to both land and water. It accounted for 2.6% of the pixels. T.M.

N81-33557*# National Aeronautics and Space Administration. Earth Resources Labs., Bay St. Louis, Miss.

AN EVALUATION OF MSS P-FORMAT DATA REGISTRATION

Marcellus H. Graham and Raymond C. Luebbe, Principal Investigators Apr. 1981 57 p Sponsored by NASA, USDA, Dept. of Commerce, Dept. of the Interior, and Agency for International Development Prepared in cooperation with Dept. of Agriculture, Washington, D.C. ERTS
(Proj. AgRISTARS)
(E81-10171; NASA-TM-84033; DC-Y1-04069; NSTL/ERL-197) Avail: NTIS HC A04/MF A01 CSCL 02C

Twelve LANDSAT scenes of the P-format were analyzed for registration accuracy based on the hotline oblique mercator (HOM) tick marks contained in the annotation record. Independently chosen ground control points were used to evaluate each scene. The results indicate that 8 out of the 12 showed either good or fairly good registration and that the registration information provided with the MSS data can be used as a starting point from which to make a more precise registration. Author

N81-33562*# Lockheed Engineering and Management Services Co., Inc., Houston, Tex.

AS-BUILT DESIGN SPECIFICATION OF THE AUTOMATIC REGISTRATION SYSTEM FOR THE CARTOGRAPHIC TECHNOLOGY LABORATORY

N. Y. Chu and R. L. Nugent, Principal Investigators Dec. 1980 224 p ERTS
(Contract NAS9-15800)
(E81-10176; NASA-CR-160961; LEMSCO-15904; JSC-17017) Avail: NTIS HC A10/MF A01 CSCL 08B

The function of each processor comprising the automatic registration system is described. This document is intended to be used concurrently with the automatic registration system manual. The system is designed to be used on the PDP 11/45 computer. A.R.H.

N81-33563*# Elogic, Inc., Houston, Tex.

MAXIMUM LIKELIHOOD LABELING

M. E. Rassbach, Principal Investigator Feb. 1981 21 p Sponsored by NASA, USDA, Dept. of Commerce, Dept. of the Interior and Agency for International Development ERTS
(Contract NAS9-15981; Proj. AgRISTARS)
(E81-10177; NASA-CR-160948; SR-X1-04041; NAS-811) Avail: NTIS HC A02/MF A01 CSCL 12A

A method of identifying or labeling the cluster produced by any clustering algorithm has been designed and developed. This associates an externally defined label with each cluster, using a few prelabelled input points. Author

N81-33574*# Telespazio, S.p.A., Rome (Italy).

SOME METHODS OF MULTITEMPORAL ANALYSIS OF LANDSAT IMAGES RESULTING FROM A STUDY ON VENICE LAGOON

Angelo Zandonella, Principal Investigator 1980 5 p refs Presented at the Intern. Conf. on Image Anal. and Process., Pavia, Italy, Oct. 1980 Sponsored by NASA ERTS
(E81-10205; NASA-CR-164770) Avail: NTIS HC A02/MF A01 CSCL 08H

Two methods of analysis were developed. The first method concerns the multitemporal calibration of LANDSAT images. It consists of a projection, onto a common signals feature space, of images recorded in different time periods. The second method relates to multitemporal analysis of gravity center classes in the same feature space. The results obtained are discussed. T.M.

N81-33587# Dornier-Werke G.m.b.H., Friedrichshafen (West Germany).

POSSIBLE APPLICATIONS OF COMMUNICATION SATELLITES FOR RESEARCH TASKS IN POLAR REGIONS Final Report

Gerhard Bommas, Erhard Hanka, Jork Haussmann, Walther Klages, Paul Stuerzenhofaecker, and Joachim Thomas Bonn Bundesministerium fuer Forschung und Technologie Dec. 1980 245 p refs In GERMAN; ENGLISH summary Sponsored by Bundesministerium fuer Forschung und Technologie
(BMFT-FB-W-80-029; ISSN-0170-1339) Avail: NTIS HC A11/MF A01; Fachinformationszentrum, Karlsruhe, West Germany DM 41

The possibilities of using communication satellites to establish beyond-the-horizon communications within Antartica, and between Antartica and the Federal Republic of Germany is examined. Communication is shown to be possible using the following satellites: Marisat for the transmission of speech, telex and data, GOES for the transmission of meteorological data, and TIROS-N for the reception of cloud pictures. The coverage of geostationary satellites is limited to a latitude of approximately 80 deg. Links, south of 80 deg are to be established by means of HF. Line of sight communication up to 50 km is simply established with VHF equipment. Author (ESA)

08

INSTRUMENTATION AND SENSORS

Includes data acquisition and camera systems and remote sensors.

A81-41476 **Some results on the investigation of earth resources by aerial and polygon methods (Nekotorye rezul'taty issledovaniia prirodnykh resursov s pomoshch'iu samoletnykh i poligonnykh sredstv).** Edited by N. K. Vinnichenko and A. P. Tishchenko. Leningrad, Gidrometeoizdat (Nauchno-Issledovatel'skii Tsentr Izucheniia Prirodnykh Resursov, Trudy, No. 10), 1980. 119 p. In Russian.

Papers are presented on integrated aerial-satellite remote sensing systems, the resolution of TV scanning systems, the transfer of spectral contrasts in multispectral photography, and pseudocolor representation of multispectral aerial images. Consideration is also given to the use of spectral and physical-geographic characteristics of natural objects on the earth's surface for the interpretation of multispectral satellite photographs, the determination of the types and state of crops from multispectral aerial images, and the automated classification of agricultural objects from their multispectral aerial images.

B.J.

A81-41477 # **Aerial data acquisition systems using test-ground polygons (Aviatsionnye sredstva sbora informatsii na kontrol'no-izmeritel'nykh poligonakh).** N. K. Vinnichenko, A. D. Dobrozrakov, and V. P. Iakovlev. In: Some results on the investigation of earth resources by aerial and polygon methods. Leningrad, Gidrometeoizdat, 1980, p. 3-12. In Russian.

Consideration is given to a remote sensing system based on the integration of satellite-borne and airborne sensors. It is shown that, when integrated into a satellite remote sensing system, aerial data acquisition systems (i.e., aircraft and helicopter platforms) can perform the independent function of data acquisition on test-ground polygons, and can solve various auxiliary problems in the interests of promoting the operation of the satellite system.

B.J.

A81-41483 # **Pseudocolor representation of multispectral aerial images by means of a three-channel projector (Psevdotsvetnoe predstavlenie mnogozonal'nykh aeroizobrazhenii s pomoshch'iu trekhkanal'nogo proektora).** A. N. Belinskii. In: Some results on the investigation of earth resources by aerial and polygon methods. Leningrad, Gidrometeoizdat, 1980, p. 42-44. In Russian.

Attention is given to the use of a three-channel projector for the synthesis of color images of one region of the earth's surface obtained at three different wavelengths. Results on the visual interpretation of several pseudocolor images of agricultural lands are discussed.

B.J.

A81-41915 # **The effect of angular distribution models on the estimation of the earth's albedo.** H. Jacobowitz (NOAA, Earth Sciences Laboratory, Marlow Heights, MD). *American Meteorological Society and Canadian Meteorological Oceanographic Society, Conference on Atmospheric Radiation, Toronto, Canada, June 16-18, 1981, Paper.* 3 p.

The considered investigation is concerned with the differences between the models that have been utilized in processing the narrow-angle data and the consequent effects of the differences on the estimation of the earth's albedo. The processing of the Nimbus-7 Earth Radiation Budget (ERB) narrow-angle data into hemispheric albedoes first made use of angular distribution models which consisted of angular distributions for three surface types, including cloud-land, ocean, and for latitudes greater than 65 deg snow and ice. A comparison of the zonal profiles of albedo utilizing these models with that derived from the wide-angle sensors showed rather large differences. To assess the cause of these differences, Stowe et al. (1980) conducted a comparison between these models and a preliminary one derived from a composite 9 day set of ERB radiance data. Data for a comparison between wide and narrow channel estimates of zonal means of the earth's albedo are presented in a table.

G.R.

A81-41916 # **A new numerical treatment of the source function in the radiative transfer equation.** H. E. Fleming (NOAA, National Earth Satellite Service, Washington, DC). *American Meteorological Society and Canadian Meteorological Oceanographic Society, Conference on Atmospheric Radiation, Toronto, Canada, June 16-18, 1981, Paper.* 4 p.

A81-41919 * # **A radiometric model of an earth radiation budget radiometer optical system with diffuse-specular surfaces.** M. R. Luther (NASA, Langley Research Center, Hampton, VA). *American Meteorological Society and Canadian Meteorological Oceanographic Society, Conference on Atmospheric Radiation, Toronto, Canada, June 16-18, 1981, Paper.* 9 p. 11 refs.

The Earth Radiation Budget Experiment (ERBE) is to fly on NASA's Earth Radiation Budget Satellite (ERBS) and on NOAA F and NOAA G. Large spatial scale earth energy budget data will be derived primarily from measurements made by the ERBE nonscanning instrument (ERBE-NS). A description is given of a mathematical model capable of simulating the radiometric response of any of the ERBE-NS earth viewing channels. The model uses a Monte Carlo method to accurately account for directional distributions of emission and reflection from optical surfaces which are neither strictly diffuse nor strictly specular. The model computes radiation exchange factors among optical system components, and determines the distribution in the optical system of energy from an outside source. Attention is also given to an approach for implementing the model and results obtained from the implementation.

G.R.

A81-41920 * # **Performance evaluation of a spaceborne scatterometer.** W. L. Grantham, E. M. Bracalente, W. L. Jones, Jr., L. C. Schroeder (NASA, Langley Research Center, Hampton, VA), C. L. Britt, Jr. (Research Triangle Institute, Hampton, VA), and F. J. Wentz (Remote Sensing Systems, Sausalito, CA). *Institute of Electrical and Electronics Engineers, Oceans '81 Conference, Boston, MA, Sept. 16-18, 1981, Paper.* 7 p. 7 refs.

Study results are presented showing performance capability of a spaceborne scatterometer to operationally measure ocean surface wind speed and direction. In addition, a research mode is described which will allow development of improved radar signatures for ocean, sea ice, and land targets. The study results show that a scatterometer can meet the operational requirements of + or - 2 m/s wind speed accuracy (or + or - 10%, whichever is greater) and + or - 20 deg wind direction accuracy over most of the expected ocean surface conditions. The six beam scatterometer design evaluated is shown to be skillful (greater than 90% correct) in specifying the correct wind vector solution (with a 180 deg ambiguity) from the multiple solutions derived; further improvement must rely on meteorological and pattern recognition techniques now under study.

(Author)

A81-41995 **What has been learned from the scanning multi-channel microwave radiometers /SMMRs/.** J. Alishouse (NOAA, National Earth Satellite Service, Washington, DC). *Marine Technology Society Journal,* vol. 14, no. 6, 1980, p. 12, 13.

Two SMMRs have been flown, one on Seasat and the other on Nimbus-7. The two radiometers are essentially identical. Both have five frequencies, 6.63, 10.69, 18, 21, and 37 GHz and dual polarizations. Two algorithms have been used in the Seasat SMMR data processing to derive geophysical parameters. One is a nonlinear, least squares, iterative estimation technique, a type of Kalman filtering. The other is a regression technique with coefficients derived from simulation. The regression is essentially linear. Attention is given to sea surface temperature, sea surface wind speed, total precipitable water (water vapor), and corrections for the altimeter and the scatterometer.

G.R.

A81-42284 # **The signal-to-noise ratio of a space photographic system (Otnoshenie signal-shum kosmicheskoi fotograficheskoi sistemy).** L. M. Matiiasevich (Gosudarstvennyi Nauchno-Issledovatel'skii i Proizvodstvennyi Tsentr Priroda, USSR). *Issledovanie Zemli iz Kosmosa,* May-June 1981, p. 66-76. 11 refs. In Russian.

The concept of the signal-to-noise ratio is discussed in relation to a spaceborne photographic system used for the remote sensing of earth resources. The problems of a numerical determination of this value are considered, and it is shown that the signal is best characterized by three parameters: the density component (signal amplitude), the spatial dimension, and the frequency. A means for the practical application of this ratio is discussed. J.F.

A81-42285 # **Concerning the possibility of improving the spectroradiometric accuracy of remote sensing of the earth by means of multispectral band scanners (O vozmozhnom povyshenii spektroradiometricheskoi tochnosti pri distantsionnykh issledovaniiakh zemli s pomoshch'iu mnogozonal'nykh s'emochnykh sistem).** A. A. Bogdanov, V. N. Nalimov, A. G. Sychev, V. I. Tarnopol'skii, and G. N. Tolstykh (Akademiia Nauk SSSR, Institut Kosmicheskikh Issledovanii; Vsesoiuznyi Nauchno-Issledovatel'skii Institut Optiko-Fizicheskikh Izmerenii, Moscow, USSR). *Issledovanie Zemli iz Kosmosa,* May-June 1981, p. 77-84. 7 refs. In Russian.

Possibilities are discussed for decreasing the uncertainty of an object's emission spectrum by improving the accuracy of the calibration method and by applying a special processing method to the obtained data. It is shown that in measuring object brightness in several spectral bands, the true spectral dependence of brightness values can be determined by the method of successive approximation. The application of this technique to the remote sensing of the earth's surface by spaceborne multispectral band scanners is considered. J.F.

A81-42286 # **Concerning the reliability estimation of information obtained from several sources in earth survey tasks (Ob otsenke dostovernosti informatsii ot neskol'kikh istochnikov v zadache zemleobzora).** O. P. Nesterenko, Iu. A. Smol'ianinov, and S. D. Nadberezhnyi. *Issledovanie Zemli iz Kosmosa,* May-June 1981, p. 85-88. In Russian.

The problem of formulating a reliability estimation of information obtained simultaneously from satellite-borne remote sensing systems is presented. A complete a posteriori probability of the true message is averaged from several observed results and set as a function of a priori distribution. J.F.

A81-42671 * **Calibration validation for the GEOS 3 altimeter.** C. F. Martin (EG & G Washington Analytical Services Center, Inc., Riverdale, MD) and R. Kolenkiewicz (NASA, Goddard Space Flight Center, Greenbelt, MD). *Journal of Geophysical Research,* vol. 86, July 10, 1981, p. 6369-6381. 18 refs.

An absolute calibration of the altitude data is needed for some applications of the large quantity of altimeter data taken by the GEOS 3 intensive mode altimeter. The considered calibration technique is based on the use of a gravimetric geoid model and satellite passes which are nearly overhead at island laser tracking sites. Near overhead passes of GEOS 3 were achieved at Bermuda. Two of these passes were tracked by the Bermuda laser. The reported investigation has the objective to obtain a best estimate of the GEOS 3 altimeter calibration bias, using the two available passes and reconciling differences between them. Assuming that orbits with accurate altitudes over Bermuda are obtained, discrepancies between the two passes could be due to incorrect time tagging of the altimeter data. To assist in the resolution of the timing question, additional GEOS 3 passes through the calibration area were selected. On the basis of the obtained results, it is recommended to add 10.24 ms to GEOS 3 altimeter time tags before using the data. G.R.

A81-43071 * **Passive microwave techniques for geophysical sensing of the earth from satellites.** D. H. Staelin (MIT, Cambridge, MA). *IEEE Transactions on Antennas and Propagation,* vol. AP-29, July 1981, p. 683-687. 61 refs. Grant No. NAG5-10.

Passive microwave techniques for geophysical probing from aircraft and space have employed frequencies 1-300 GHz and have yielded information about atmospheric temperature and composition profiles and about surface parameters such as sea state, ice and snow type and extent, soil moisture, etc. The initially scientific program is now evolving into various operational spacecraft observatory systems; this mini-review summarizes recent accomplishments and future opportunities. (Author)

A81-43190 * **Advanced technology for satellite data collection systems.** C. E. Cote and J. E. Painter (NASA, Goddard Space Flight Center, Greenbelt, MD). In: Satellite hydrology; Proceedings of the Fifth Annual William T. Pecora Memorial Symposium on Remote Sensing, Sioux Falls, SD, June 10-15, 1979. Minneapolis, MN, American Water Resources Association, 1981, p. 65-67. 6 refs.

Technological developments in satellite data collection are aimed at relieving constraints of existing systems to permit expanded capability at lower costs in future operations. Constraints imposed by the limited electromagnetic spectrum available in the UHF band and the cost of user equipment are principal targets for improvement through technology. This paper describes ongoing developmental activities in system and component areas which will become available for the next generation of operations. (Author)

A81-43223 * **Potential application of satellite radar to monitor soil moisture.** F. T. Ulaby, G. A. Bradley, and M. C. Dobson (University of Kansas Center for Reserach, Inc., Lawrence, KS). In: Satellite hydrology; Proceedings of the Fifth Annual William T. Pecora Memorial Symposium on Remote Sensing, Sioux Falls, SD, June 10-15, 1979. Minneapolis, MN, American Water Resources Association, 1981, p. 363-370. 29 refs. Contract No. NAS9-14052.

The microwave backscattering characteristics of soils as a function of moisture content are reviewed as a basis for the evaluation of the applicability of satellite radar to soil moisture determinations. Results of experiments showing the dependence of the complex dielectric constant, power reflection coefficient and backscattering coefficient of soil on its volumetric moisture content are presented. Results of a research program using the truck-mounted University of Kansas microwave active spectrometer to determine if, by the proper choice of sensor frequency, polarization and incidence, the sensor dynamic range in response to moisture variations may be greater than its response to other variations are considered in detail, and the optimum conditions of frequency (between 4 and 5 GHz), angular incidence (between 7 and 20 deg from nadir) and polarization (HH) obtained are indicated. An empirical model for the backscattering coefficient as a function of gravimetric moisture content derived on the basis of the experimental data is presented, and it is noted that available airborne and spaceborne data confirm the results of the ground-based sensors. A.L.W.

A81-43225 * **Requirements of space-borne microwave radiometers for detecting soil moisture contents.** H.-H. K. Burke (Environmental Research and Technology, Inc., Concord, MA) and W. J. Burke (Boston College, Chestnut Hill, MA). In: Satellite hydrology; Proceedings of the Fifth Annual William T. Pecora Memorial Symposium on Remote Sensing, Sioux Falls, SD, June 10-15, 1979. Minneapolis, MN, American Water Resources Association, 1981, p. 377-383. 13 refs. Contracts No. NAS5-25529; No. NAS5-25527.

A multilayer radiative transfer model for predicting the relationship between soil moisture content and microwave emission is summarized. Attention is also given to the performance of various microwave sensors for soil moisture retrieval; here, the requirements of a satellite sensor system for monitoring large-scale soil moisture conditions are discussed. These requirements are presented in terms of (1) the wavelength, (2) atmospheric contamination, (3) polarization, (4) frequency of observation, and (5) spatial resolution. Each parameter is discussed in terms of microwave response. Previous aircraft data with extensive ground truth information are used to support the theories proposed. Trade-offs between the parameters and an optimum sensor system for space monitoring soil moisture information are discussed. C.R.

A81-43260 * **Land subsidence measured by satellite radar altimetry.** W. B. Krabill (NASA, Wallops Flight Center, Wallops Island, VA) and R. L. Brooks (GeoScience Research Corp., Salisbury, MD). In: Satellite hydrology; Proceedings of the Fifth Annual William T. Pecora Memorial Symposium on Remote Sensing, Sioux Falls, SD, June 10-15, 1979. Minneapolis, MN, American Water Resources Association, 1981, p. 683-688. Contract No. NAS6-2639.

Radar altimeter measurements from the GEOS-3 and SEASAT satellites are being evaluated to assess their potential contribution to terrain mapping. The primary evaluation area is the San Joaquin Valley of southern California; 40,000/sq km of the Valley have been mapped at a contour interval of 10 m from the satellite altimeter measurements. The accuracy of the altimeter derived terrain elevations is being assessed by comparison with 1:24,000 and digitized 1:250,000 maps and by intercomparisons at the crossover altimeter intersections. Comparisons of the altimeter derived elevations with historical maps archived at the U.S. Geological Survey confirms the USGS 1926-1972 subsidence contours for this area. Preliminary results from a similar analysis in the Houston-Galveston area of subsidence also demonstrates a capability of measuring land subsidence by satellite altimetry. (Author)

A81-43530 **Hardware aspects of digital mapping.** G. Petrie (Glasgow, University, Glasgow, Scotland). *(International Society for Photogrammetry, Congress, 14th, Hamburg, West Germany, July 13-25, 1980.) Photogrammetric Engineering and Remote Sensing,* vol. 47, Mar. 1981, p. 307-320. 28 refs.

The respective merits of digitizing photogrammetrically produced graphic plots and direct photogrammetric digitizing are described. The characteristics of various types of photogrammetric digitizing units are discussed, including representative examples of large multistation systems. Particular consideration is given to the trend toward the implementation of standard hardware interfaces and the incorporation of graphic displays into photogrammetric digitizing systems. A summary is then given of experiences with interactive graphic systems interfaced directly to stereoplotting machines reported by a number of North American mapping agencies. B.J.

A81-43547 * **Aircraft active microwave measurements for estimating soil moisture.** T. J. Jackson (U.S. Science and Education Administration, Hydrology Laboratory, Beltsville, MD), A. Chang, and T. J. Schmugge (NASA, Goddard Space Flight Center, Greenbelt, MD). *Photogrammetric Engineering and Remote Sensing,* vol. 47, June 1981, p. 801-805. 7 refs.

Both active and passive microwave sensors are sensitive to variations in near-surface soil moisture. The principal advantage of active microwave systems for soil moisture applications is that high spatial resolution can be retained even at satellite attitudes. The considered investigation is concerned with the use of active microwave scatterometers for estimating near-surface soil moisture. Microwave scatterometer data were obtained during a series of three aircraft flights over a group of Oklahoma research watersheds during May 1978. Data were obtained for the C, L, and P bands at angles of incidence between 5 and 50 degrees. The best results were obtained using C band data at incidence angles of 10 and 15 degrees and soil moisture depth of 0 to 15 cm. These results were in excellent agreement with the conclusions of the truck-mounted scatterometer measurement program reported by Ulaby et al. (1978, 1979). G.R.

A81-43735 **Relating ground level reflected radiance measurements in the Landsat MSS bandpasses to satellite altitudes.** M. J. Duggin (New York, State University, Syracuse, NY) and P. J. Ellis (Department of Scientific and Industrial Research, Physics and Engineering Laboratory, Lower Hutt, New Zealand). In: Rainbow 80; Fall Technical Meeting, Niagara Falls, NY, October 7-10, 1980, ASP Technical Papers. Falls Church, VA, American Society of Photogrammetry, 1981, p. RS-1-G-1 to RS-1-G-10. 16 refs. Research supported by the U.S. Department of Agriculture and New York State Department of Environmental Conservation.

Ground truth radiometers (GTRS) are used to test the feasibility of resource discrimination, mapping and quantification using Landsat digital multispectral scanner (MSS) data. The effect on differences of target spectral response for healthy and diseased vegetation is studied. The differences between recorded output from GTRS and the Landsat MSSs when viewing the same target under identical conditions are calculated. The average obtained for the mean normalized signal (NS) values in each bandpass of each MSS was used as a standard to which NS values calculated for the GTRs were compared. Although differences of up to 13% occurred in MSS 7, and two large differences (up to 20%) were found in MSS 5, general agreement (differences of 5% or less) was usual. This indicates that the GTRs, which are simple and inexpensive, can provide satisfactory ground reflectance data, which can be related accurately to Landsat data. J.F.

A81-45836 * # **Earth applications orbit analysis for a shuttle-mounted Multispectral Mapper.** J. M. Driver and C. C. H. Tang (California Institute of Technology, Jet Propulsion Laboratory, Mission Design Section, Pasadena, CA). *American Astronautical Society and American Institute of Aeronautics and Astronautics, Astrodynamics Specialist Conference, Lake Tahoe, NV, Aug. 3-5, 1981, AAS Paper 81-182.* 24 p. 8 refs. Contract No. NAS7-100.

The earth remote sensing problem of orbit design to acquire images with inherent geometric and geodetic accuracy is addressed. The basis for precise orbit modeling is discussed. Various orbit propagation tools are compared. Orbit characteristics for a nominal case at shuttle altitude are displayed. Modeling Parameter sensitivities are evaluated to determine limits on orbit propagation accuracy versus time. It is found that attainable propagation accuracies are sufficient for image quality assessment over the short term at the 15m pixel size desired for a Multispectral Mapper. (Author)

A81-45872 * **Progress in passive microwave remote sensing - Nonlinear retrieval techniques.** D. H. Staelin (MIT, Cambridge, MA). In: Remote sensing of atmospheres and oceans; Proceedings of the Interactive Workshop on Interpretation of Remotely Sensed Data, Williamsburg, VA, May 23-25, 1979. New York, Academic Press, Inc., 1980, p. 259-274; Discussion, p. 275, 276. 10 refs. Contract No. NAS5-22929.

A variety of nonlinear retrieval methods have been applied to passive microwave remote sensing problems. These problems can be characterized in part by the degree to which their underlying physics and statistics can be understood and characterized in a simple way. Four examples of varying complexity are considered here; the simplest problem requires only analytic expressions for retrievals, whereas the most complex problem has been handled only with pattern classification techniques. The four examples are: (1) Doppler measurements of winds at 70 to 100 km, (2) retrieval of atmospheric water vapor profiles using the opaque 183-GHz water vapor resonance, (3) retrieval of snow accumulation rate by means of combined theoretical and empirical procedures, and (4) classification of diverse polar terrain by means of pattern recognition techniques. (Author)

A81-45873 * **Inversion of multiwavelength radiometer measurements by three-dimensional filtering.** P. W. Rosenkranz and W. T. Baumann (MIT, Cambridge, MA). In: Remote sensing of atmospheres and oceans; Proceedings of the Interactive Workshop on Interpretation of Remotely Sensed Data, Williamsburg, VA, May 23-25, 1979. New York, Academic Press, Inc., 1980, p. 277-310; Discussion, p. 310, 311. 18 refs. Contract No. NAS5-22929.

Remote sensing data from satellites typically have three dimensions: scan position, spacecraft position, and wavelength. Inversion of the radiometric data to infer geophysical parameters is a filtering problem in which the dimension of wavelength (or channel number) is transformed into a dimension of geophysical parameters, and the most general solution is a three-dimensional filter. Linear filters have the advantages of computational speed and easily described transfer functions; but often the measurements are nonlinear functions of the parameters to be inferred. To the extent that the nonlinear inversion problem is overdetermined, it can be modeled by a critically determined linear problem. As an example, inversion of Scanning Multichannel Microwave Radiometer (SMMR) data by means of a three-dimensional Wiener Filter is described. Atmospheric water vapor content, rain liquid water content, surface wind speed and surface temperature are the parameters inferred from the measurements. Nonprecipitating liquid water and water vapor scale height are also modeled but not retrieved. The a priori statistics on which the filter is trained have the effect of governing the selection of a trade-off point of noise as a function of resolution (in all three retrieval dimensions). (Author)

A81-45879 * **Atmospheric correction of Nimbus-7 Coastal Zone Color Scanner imagery.** H. R. Gordon (Miami, University, Coral Gables, FL), J. L. Mueller (NASA, Goddard Space Flight Center, Laboratory for Atmospheric Sciences, Greenbelt, MD), and R. C. Wrigley (NASA, Ames Research Center, Moffett Field, CA). In: Remote sensing of atmospheres and oceans; Proceedings of the Interactive Workshop on Interpretation of Remotely Sensed Data, Williamsburg, VA, May 23-25, 1979. New York, Academic Press, Inc., 1980, p. 457-481; Discussion, p. 482, 483. 11 refs. Contract No. NAS5-22963.

The Coastal Zone Color Scanner (CZCS) on Nimbus-7 is a scanning radiometer designed to view the ocean in six spectral bands (centered at 443, 520, 550, 670, 750, and 11,500 nm) for the purpose of estimating sea surface chlorophyll and temperature distributions. In the visible bands, the atmosphere obscures the imagery to the extent that at 443 nm, at most, only 20 percent of the observed radiance originates from beneath the sea surface. Retrieving this subsurface radiance from the imagery is complicated by the highly variable nature of the aerosol's contribution. In this paper, an algorithm for the removal of these atmospheric effects from CZCS imagery is described, a preliminary application of the algorithm to an image with very strong horizontal variations in the aerosol optical thickness is presented, and retrieval of the spatial distribution of the aerosol optical thickness is discussed. (Author)

A81-46028 * **Parallel processing implementations of a contextual classifier for multispectral remote sensing data.** H. J. Siegel, P. H. Swain, and B. W. Smith (Purdue University, West Lafayette, IN). In: Machine processing of remotely sensed data and soil information systems and remote sensing and soil survey; Proceedings of the Sixth Annual Symposium, West Lafayette, IN, June 3-6, 1980. New York, Institute of Electrical and Electronics Engineers, Inc., 1980, p. 19-29. 19 refs. Contract No. NAS9-15466.

The applicability of parallel processing schemes to the implementation of a contextual classification algorithm which exploits the spatial and spectral context of a multispectral remote sensing pixel to achieve classification is examined. Two algorithms for classifying each multivariate pixel taking into account the probable classifications of neighboring pixels are presented which make use of a size three horizontally linear neighborhood, and the serial computational complexity of the more efficient algorithm is shown to grow in proportion to the number of pixels and the cube of the number of possible categories. The implementation of the more efficient algorithm on a CDC Flexible Processor system and on a multimicroprocessor system such as the proposed PASM is then discussed. It is noted that the use of N processors to perform the calculations N times faster than a single processor overcomes the principal disadvantage of contexual classifiers, i.e., their computational complexity.

A.L.W.

A81-46029 **Automatic processing of computer compatible tapes with data from multispectral scanners installed in Landsat satellites.** N. Scquizzato (Comisión Nacional de Investigaciones Espaciales, Buenos Aires, Argentina). In: Machine processing of remotely sensed data and soil information systems and remote sensing and soil survey; Proceedings of the Sixth Annual Symposium, West Lafayette, IN, June 3-6, 1980. New York, Institute of Electrical and Electronics Engineers, Inc., 1980, p. 30-39.

The design and operation of the STAI (Spanish acronym for ground data analysis system) for the digital processing of multispectral remote sensing data on computer compatible tapes are discussed. The interactive system consists of a central processing unit, main memory system, nine-track magnetic tape unit, magnetic tape controller, teletype, high-speed paper tape reader/punch, interface extension unit, sensor data input processor, black and white film recorder, tape playback unit, moving window display, color monitor, color film printing subsystem, operator panel, and tape operating system. Features to be added in the future include a table digitizer, color film digitizer and processor, and electrostatic printer plotter. Landsat CCTs can be displayed and processed using the moving window display as a first step in classification. Images are displayed at a vertical scale of 1:100,000 and horizontal scales of either 1:100,000 or 1:50,000.

A.L.W.

A81-46030 **The Lulea Image Processing System /LIPS/ - A versatile approach to earth resources data processing.** H. Hauska (Lulea, Hogskola, Lulea, Sweden). In: Machine processing of remotely sensed data and soil information systems and remote sensing and soil survey; Proceedings of the Sixth Annual Symposium, West Lafayette, IN, June 3-6, 1980. New York, Institute of Electrical and Electronics Engineers, Inc., 1980, p. 40-46. 14 refs. Styrelsen for Teknisk Utveckling Contracts No. 76-6669; No. 77-6345.

The minicomputer-based Lulea Image Processing System (LIPS), which was developed for earth resources data processing applications, is presented. The system was designed according to the available hardware (Nord 10/S CPU), and the criteria of ease of use, flexibility, portability, efficiency, ease of maintenance and batch capability. Image data files contain information on image identity and processing history as well as the image data itself quantized in grey scale values. The software is structured in two levels corresponding to a control program and processing level programs in the form of a pseudo-overlay. The modular processing modules include provisions for preprocessing, hard copy image output, orthogonal transformation, geometric correction, classification and the estimation of statistical parameters. Future improvements to the system include a color digital display system to provide true interactivity, and an image reading device.

A.L.W.

A81-46038 * **Radar image preprocessing.** V. S. Frost, J. A. Stiles, J. C. Holtzman (University of Kansas Research Center, Inc., Lawrence, KS), and D. N. Held (California Institute of Technology, Jet Propulsion Laboratory, Pasadena, CA). In: Machine processing of remotely sensed data and soil information systems and remote sensing and soil survey; Proceedings of the Sixth Annual Symposium, West Lafayette, IN, June 3-6, 1980. New York, Institute of Electrical and Electronics Engineers, Inc., 1980, p. 140-146. 14 refs. Research supported by the California Institute of Technology; Contract No. NAS7-100; Grant No. DAAG29-77-G-0075.

Standard image processing techniques are not applicable to radar images because of the coherent nature of the sensor. Therefore there is a need to develop preprocessing techniques for radar images which will then allow these standard methods to be applied. A random field model for radar image data is developed. This model describes the image data as the result of a multiplicative-convolved process. Standard techniques, those based on additive noise and homomorphic processing are not directly applicable to this class of sensor data. Therefore, a minimum mean square error (MMSE) filter was designed to treat this class of sensor data. The resulting filter was implemented in an adaptive format to account for changes in local statistics and edges. A radar image processing technique which provides the MMSE estimate inside homogeneous areas and tends to preserve edge structure was the result of this study. Digitally correlated Seasat-A synthetic aperture radar (SAR) imagery was used to test the technique.

(Author)

A81-46196 **Does the use of two radiometers correct for irradiance changes during measurements.** E. J. Milton (Durham, University, Durham, England). *Photogrammetric Engineering and Remote Sensing,* vol. 47, Aug. 1981, p. 1223-1225. 9 refs.

The method of inter-calibrating two field radiometers proposed by Duggin (1980) is critically assessed. It is claimed that by this method it is possible to correct for the effects of variations in total solar irradiation upon hemispherical directional reflectance during a series of measurements. However, this is questioned because in theory, the non-Lambertian nature of most natural surfaces prevents such a correction. Furthermore, it is shown that in practice, intra-canopy shadow effects are likely to confound the proposed method. Uniform irradiation conditions are seen as the only suitable environment for the field measurement of reflectance factors.

(Author)

A81-46241 * # **Magnetic space-based field measurements.** R. A. Langel (NASA, Goddard Space Flight Center, Geophysics Branch, Greenbelt, MD). *American Astronautical Society, Goddard Memorial Symposium on International Space Technical Applications, 19th, Arlington, VA, Mar. 26, 27, 1981, Paper 81-077.* 18 p. 18 refs.

Satellite measurements of the geomagnetic field began with the launch of Sputnik 3 in May 1958 and have continued sporadically in the intervening years. A list of spacecraft that have made significant contributions to an understanding of the near-earth geomagnetic field is presented. A new era in near-earth magnetic field measurements began with NASA's launch of Magsat in October 1979. Attention is given to geomagnetic field modeling, crustal magnetic anomaly studies, and investigations of the inner earth. It is concluded that satellite-based magnetic field measurements make global surveys practical for both field modeling and for the mapping of large-scale crustal anomalies. They are the only practical method of accurately modeling the global secular variation. Magsat is providing a significant contribution, both because of the timeliness of the survey and because its vector measurement capability represents an advance in the technology of such measurements.

G.R.

A81-46401 **Identification of subresolution high temperature sources using a thermal IR sensor.** M. Matson (NOAA, National Earth Satellite Service, Washington, DC) and J. Dozier (California, University, Santa Barbara, CA). *Photogrammetric Engineering and Remote Sensing,* vol. 47, Sept. 1981, p. 1311-1318. 14 refs.

Simultaneous use of the 3.8-micron and 11-micron thermal infrared channels on board the 3rd-generation NOAA-6 environmental satellite provides the capability to detect subresolution scale high-temperature sources, and to estimate both the temperature and size of such sources. Examples presented include gas flares from oil fields in the Middle East and steel mills in the midwestern United States. (Author)

A81-46461 **First Shuttle payload loading to begin.** C. Covault. *Aviation Week and Space Technology,* vol. 114, June 29, 1981, p. 54, 55, 57, 59.

The first Office of Space and Terrestrial Applications (OSTA 1) Space Shuttle payload, a multi-instrument array aimed at the development of oil and mineral exploration from space, will be carried into orbit by the second Columbia Orbiter mission. The Spacelab pallet mounting of the package incorporates: (1) the Shuttle imaging radar (SIR-A), which will study geological formations; (2) the Shuttle multispectral infrared radiometer; (3) a feature identification and location experiment; (4) an ocean color experiment; and (5) an air pollution measurement-from-satellite experiment. In one of the two OSTA 1 experiments to be conducted from the Shuttle cabin, photographic studies will be made of lightning propagation across thunderstorms. O.C.

A81-46679 **The European SAR-Project Convair 580 (Die Europäische SAR-Kampagne CV 580).** A. Sieber (Deutsche Forschungs- und Versuchsanstalt für Luft- und Raumfahrt, Institut für Hochfrequenztechnik, Oberpfaffenhofen, West Germany) and P. Hartl (Berlin, Technische Universität, Berlin, West Germany). *Bildmessung und Luftbildwesen,* vol. 49, Sept. 1, 1981, p. 165-170. In German.

The considered investigation is concerned with the possibilities and problems regarding an employment of Synthetic Aperture Radar (SAR) sensors in space missions with earth observation applications. The significance of the SAR Project for the European Microwave Remote Sensing program is discussed, taking into account the Microwave Remote Sensing Experiment, the establishment of national and international user organizations, and the support of research work related to radar systems. The organization of the entire project is considered along with the observational parameters for the SAR system. Test areas in Germany have been selected for a calibration of the SAR systems. Investigations related to snow and ice are to be conducted in Switzerland and Austria, while questions of glaciology and hydrology are to be studied in Greenland. G.R.

A81-46924 # **Radar methods for studying the earth (Radiolokatsionnye metody issledovaniia zemli).** Iu. A. Mel'nik, S. G. Zubkovich, V. D. Stepanenko, Iu. P. Sokolov, V. A. Gubin, V. E. Dulevich, S. V. Pereslegin, A. A. Veretiagin, V. M. Glushkov, and Iu. A. Iurkov. Moscow, Izdatel'stvo Sovetskoe Radio, 1980. 288 p. 118 refs. In Russian.

The principles of earth radar studies are presented. Models of reflection and characteristics of radar signals from land and water surfaces as well as atmospheric formations are discussed in detail. The methods for constructing and substantiating the parameters of active radar and radiometer systems used in observations of the earth's surface and meteorological objects from flight vehicles and satellites are presented. Methods for studying the active and passive radar methods used in cartography, geology, hydrology, oceanography, studies of vegetation cover, ice reconnaissance, and other geophysical fields are also discussed. J.F.

A81-47338 **Data collection and location by satellite - The Argos system.** J. L. Bessis (Centre Nationale d'Etudes Spatiales, Paris, France). *International Astronautical Federation, International Astronautical Congress, 32nd, Rome, Italy, Sept. 6-12, 1981, Paper 81-80.* 18 p. 11 refs.

A description is given of the data collection and platform location functions of the Argos system, carried onboard NOAA meteorological satellites, whose environmental concerns include meteorology, oceanography, offshore phenomena, hydrology, biology, vulcanology, and seismology. The system comprises such user platforms as buoys, balloons, fixed or offshore stations, animals, etc., on-board equipment, a data processing center, and a data distribution system for Argos users. It is shown that platform results are available within hours after their acquisition by satellite, and are readily accessible by means of telephone or telex network from anywhere in the world. Flowcharts are presented for the management responsibilities of the various managing agencies, the user platform, the on-board data collection system, the data processing center, and software. O.C.

A81-47342 **Passive microwave systems.** E. Schanda (Bern, Universität, Berne, Switzerland). *International Astronautical Federation, International Astronautical Congress, 32nd, Rome, Italy, Sept. 6-12, 1981, Paper 81-88.* 14 p. 20 refs.

Passive microwave sensors are presently applied on spaceborne platforms for investigations of large scale phenomena in geoscience and hydrology as well for the regular observation of meteorological features. Results of ground-based and airborne experiments over well-controlled test areas together with the present experience in synoptic earth observations from space can now be used for defining sensor systems for operational application in various fields of geoscience. Two examples are discussed: First the elements of a microwave payload for the global observation of the extent, the development and the hydrological state of the snow cover. Second, a payload for the measurement of the three-dimensional distribution of several minor constituents and of the temperature of the middle atmosphere by technique of limb sounding from Spacelab. (Author)

A81-47345 **Program and instrumentation of the satellite experiment Bulgaria-1300 II.** D. Mishev, K. Serafimov (B'lgarska Akademiia na Naukite, Tsentralna Laboratoriia po Kosmicheski Izsledvaniia, Sofia, Bulgaria), Iu. Trifonov, and I. Vetlov (Academy of Sciences, Intercosmos Council, Moscow, USSR). *International Astronautical Federation, International Astronautical Congress, 32nd Rome, Italy, Sept. 6-12, 1981, Paper 81-91.* 6 p.

The Bulgaria-1300 II complex will study the relationship between various natural formations with reflected and emitted electromagnetic radiation in the visual, near infrared, and VHF range of the spectrum. The studies, which will be spaceborne, airborne, and ground-based, will give descriptions of natural formations and their state based on objective physical characteristics. The Bulgaria-1300 II spacecraft, which will be launched in solar synchronous orbit, incorporates a four-channel scanner of low selective capability (MSU-M), a two-channel scanner of average selective capability (MSU-S), four VHF radiometers in the centimeter range, and a 32-channel spectrometer system in the visible and near-infrared range. The complex will operate in various modes, including direct data transmission, onboard data recording and sequential transmission to earth. Basic instrumental parameters of the spectrometer SMP-32 and the radiometers RM1 - RM4 are given, and the MSU-M and MSU-S scanners are discussed in greater detail. J.F.

A81-47360 **Meteorological applications of the ARGOS system.** J. L. Bessis (Centre National d'Etudes Spatiales, Paris, France). *International Astronautical Federation, International Astronautical Congress, 32nd, Rome, Italy, Sept. 6-12, 1981, Paper 81-121.* 15 p. 10 refs.

Attention is given to the way in which the ARGOS system can improve the meteorological network by using drifting buoys in connection with oceanographic data and balloons. Also discussed is the way in which moored meteorological buoys can be used to increase the forecasting period for weather analysis. C.R.

A81-47407 **New complex for ionosphere-magnetosphere study 'Intercosmos-Bulgaria-1300'.** K. Serafimov, I. Kutiev, S. Chapk'nov, M. Gogoshev, A. Bochev, Ts. Dachev, I. Ivanov (B'lgarska Akademiia na Naukite, Tsentralna Laboratoriia po Kosmicheski Izsledvaniia, Sofia, Bulgaria), V. Adasko, V. Balebanov, and A. Iosifian (Akademiia Nauk SSSR, Institut Kosmicheskikh Issledovanii, Moscow, USSR). *International Astronautical Federation, International Astronautical Congress, 32nd, Rome, Italy, Sept. 6-12, 1981, Paper 81-212.* 10 p.

The instrumentation for the Intercosmos-Bulgaria-1300 program to study ionospheric and magnetospheric interactions is described. Scientific objectives and observations such as regularities in the appearance of localized regions of electric fields and excitation

mechanisms on stable auroral red arcs are discussed, and a table of measurement parameters and the respective instruments is given. Accuracies of 0.1% for the electric field and 0.002% for the magnetic field are expected. Fundamental space physics problems are covered, and the selection process of the most effective parameters for the satellite and its orbit is presented. Finally, the scientific payload, based on plasma, high-energy, electromagnetic and optical equipment systems is analyzed, including the Foton-1, which scans the UV spectrum between 110-260 nm, providing information for aeronomic studies and the identification of high-energy impact ionization processes.
D.L.G.

A81-47409 **First results of the Intercosmos satellite IK-21.** K. Bischoff, E. Orlicek, K.-H. Schmelovsky, G. Zimmermann (Deutsche Akademie der Wissenschaften, Institut für Kosmosforschung, Berlin, East Germany), H.-J. Fischer (Gesellschaft für Weltraumforschung und Raumfahrt, East Germany), T. Hettenyi (Budapesti Muszaki Egyetem, Budapest, Hungary), G. Terekhin (Akademiia Nauk SSSR, Institut Kosmicheskikh Issledovanii, Moscow, USSR), and F. Wiegmann (Dresden, Technische Universität, Dresden, East Germany). *International Astronautical Federation, International Astronautical Congress, 32nd, Rome, Italy, Sept. 6-12, 1981, Paper 81-214.* 14 p.

First results of technical tests on the data collection system for Intercosmos-21 are presented, including results from multispectral measurements in the visual and NIR ranges. The general communication and electronics structures are given, and optical details of instruments are shown. Maximum power consumption during transmission is 14 W, with a mean power consumption of 1.5 W. The satellite consists of two channel receivers at 400 MHz, a transmitter at 460 MHz, two transmitters at 136 MHz, two magnetic recorders and control electronics. Depending on the geographical distribution of platforms, the number of suitable contacts and total contact time can be limited, and a time window is introduced to avoid erroneous transmissions during near horizontal passages. Results of the tests confirm calculations based on laboratory measurements, with a preliminary error rate of .0001, which agrees well with calculations based on measured receiver sensitivity 0.1 microvolts at 60 ohms.
D.L.G.

A81-48331 **A top-down approach to the use of simulation in computer system design.** I. C. Anderson (IBM Corp., Raleigh, NC), L. E. Deimel, Jr., R. J. Fornaro, and D. F. McAllister (North Carolina State University, Raleigh, NC). In: Summer Computer Simulation Conference, Seattle, WA, August 25-27, 1980, Proceedings. Arlington, VA, AFIPS Press, 1980, p. 89-93. 5 refs.

The process used in the design of the Edit Processor (EP) component of the Integrated Photogrammetric Instrument Network (IPIN) is described; IPIN is a network of instrumentation and minicomputers being assembled by the Defense Mapping Agency Aerospace Center to produce a data base of digitized terrain information from aerial stereophotographs. The top-down refinement of the EP simulation model proved to be an effective flexible tool to accompany the successive-refinement design process. The use of the multiple-server simplication for determining gross parameters of a system such as the EP is especially attractive and warrants further study to quantify the scope of its usefulness.
B.J.

A81-48553 * **Advanced synthetic aperture radar for remote sensing.** K. Krishen, T. K. Sampsel (NASA, Johnson Space Center, Experiment Systems Div., Houston, TX), and W. E. Brown, Jr. (California Institute of Technology, Jet Propulsion Laboratory, Pasadena, CA). In: EASCON '80; Electronics and Aerospace Systems Conference, Arlington, VA, September 29-October 1, 1980, Conference Record. New York, Institute of Electrical and Electronics Engineers, 1980, p. 362-368. 5 refs.

A program initiated by NASA was formed to address some key earth resources synthetic aperture radar (SAR) needs. Major steps in the SAR system development are summarized, and the objective of the advanced SAR (ASAR) program is defined. The program rationale and specific objectives are discussed, including system calibration, wide-band technique evaluation, a system resolution of 10 m or better at 45 deg, and an airborne system to cover four bands within 1 to 10 GHz. The ASAR conceptual system design, consisting of a modulator, transmitter, antenna, receiver, calibrator, and data system modules is also presented, and ASAR capability expansions are discussed. The program, scheduled for 1983, will provide a data source which is not available to applications investigations at this time, and will produce design approaches that are flexible and multimission to the maximum extent for application to a Shuttle or a freeflyer system.
D.L.G.

A81-48689 # **The characteristics of combining devices with different survey bands aboard a satellite (Osobennosti kompleksirovaniia na bortu ISZ priborov s razlichnymi polosami obzora).** A. A. Astashkin, V. K. Saul'skii, and G. R. Uspenskii. *Issledovanie Zemli iz Kosmosa,* July-Aug. 1981, p. 66-69. In Russian.

Several devices, having different resolutions and survey bands, are combined aboard satellites for the remote sensing of earth resources. A method is presented for calculating the satellite orbital parameters which will allow a complete coverage of the earth by each of the bands individually. Three devices are considered: a scanning television system with a survey band of 800 km and a resolution of 200 m, a multispectral system with a survey band of 200 km and a resolution of 50 m, and a television system with a survey band of 50-100 km and a resolution of 25 m. The requirements for the accurate maintenance of orbital height needed to accomplish a multi-band global survey are also determined.
J.F.

A81-48945 * **Early results from Magsat.** R. A. Langel (NASA, Goddard Space Flight Center, Geophysics Branch, Greenbelt, MD), R. H. Estes, and M. A. Mayhew (Business and Technological Systems, Inc., Seabrook, MD). *Nature,* vol. 293, Sept. 17, 1981, p. 190-192.

Papers presented at the May 27, 1981 meeting of the American Geophysical Union concerning early results from the Magsat satellite program, which was designed to study the near-earth magnetic fields originating in the core and lithosphere, are discussed. The satellite was launched on October 30, 1979 into a sun-synchronous (twilight) orbit, and re-entered the atmosphere on June 11, 1980. Instruments carried included a cesium vapor magnetometer to measure field magnitudes, a fluxgate magnetometer to measure field components and an optical system to measure fluxgate magnetometer orientation. Early results concerned spherical harmonic models, fields due to ionospheric and magnetospheric currents, the identification and interpretation of fields from lithospheric sources. The preliminary results confirm the possibility of separating the measured field into core, crustal and external components, and represent significant developments in analytical techniques in main-field modelling and the physics of the field sources.
A.L.W.

A81-49134 * **Satellite oceanography - The instruments.** R. H. Stewart (California Institute of Technology, Jet Propulsion Laboratory, Pasadena; California, University, Scripps Institution of Oceanography, La Jolla, CA). *Oceanus,* vol. 24, Fall 1981, p. 66-74. NASA-supported research.

It is pointed out that no instrument is sensitive to only one oceanographic variable; rather, each responds to a combination of atmospheric and oceanic phenomena. This complicates data interpretation and usually requires that a number of observations, each sensitive to somewhat different phenomena, be combined to provide unambiguous information. The distinction between active and passive instruments is described. A block diagram illustrating the steps necessary to convert data from satellite instruments into oceanographic information is included, as is a diagram illustrating the operation of a radio-frequency radiometer. Attention is also given to the satellites that carry the various oceanographic instruments. C.R.

A81-49753 # **The Surveillance Satellite Program and the future of microwave remote sensing.** A. L. Vankoughnett (National Research Council, Canada Centre for Space Science, Ottawa, Canada), R. K. Raney (Canada Centre for Remote Sensing, Ottawa, Canada), and E. J. Langham (Environment Canada, Inland Waters Directorate, Hull, Quebec, Canada). In: Canadian Symposium on Remote Sensing, 6th, Halifax, Canada, May 21-23, 1980, Proceedings. Ottawa, Canadian Aeronautics and Space Institute, 1981, p. 9-16. 8 refs.

The principal elements of the Canadian Surveillance Satellite (Sursat) program were participation in the NASA Seasat satellite experiment and a complementary research and development program. The Sursat program demonstrated the capabilities of spaceborne radiometers, scatterometers, and altimeters to monitor weath-

er and sea state parameters such as ocean surface temperature, ocean surface wind speed and direction, and ocean wave height. It also demonstrated the possibility of producing high-resolution images of the earth from space using Seasat SAR and the possibility that such images could provide information required by operational agencies for monitoring of ice coverage and drift. This paper describes the Sursat program and its conclusions and speculates about future microwave remote sensing activities in Canada.
B.J.

A81-49765 # **The airborne SAR project - Conclusions and applications.** D. R. Inkster, R. T. Lowry, N. A. Prout (Intera Environmental Consultants, Ltd., Ottawa, Canada), R. K. Raney, and K. P. B. Thomson (Canada Centre for Remote Sensing, Ottawa, Canada). In: Canadian Symposium on Remote Sensing, 6th, Halifax, Canada, May 21-23, 1980, Proceedings. Ottawa, Canadian Aeronautics and Space Institute, 1981, p. 119-126. 7 refs.

The extensive set of SAR imagery produced during the Airborne SAR Project (ASP) is examined along with some general research results. Maps of image areas are presented; data quality is examined; and the accessibility of the data to the public for future work is described. Results from the ice, oceans, lands, and human activities experiments are reviewed. Particular attention is given to ice surveillance research, including two recently completed industry-government pilot projects.
B.J.

A81-49801 # **Benefits of using airborne remote sensing for Thematic Mapping.** R. A. Ryerson (Canada Centre for Remote Sensing, Ottawa, Canada). In: Canadian Symposium on Remote Sensing, 6th, Halifax, Canada, May 21-23, 1980, Proceedings. Ottawa, Canadian Aeronautics and Space Institute, 1981, p. 493-500. 5 refs.

Preliminary results of the benefit-cost analysis now being done on the CCRS Airborne Remote Sensing Program are presented. Using material verified by users, the analysis demonstrates that Airborne Remote Sensing (ARS) is often a cost effective and accurate source of data. What is more, ARS provides a permanent record which can be consulted for additional interpretation long after imaging. A comparison is made between 1:10,000 panchromatic and 1:60,000 CIR with respect to user/industry supplied acquisition costs, interpretation costs, number of images, and total cost of mapping a hypothetical area using new and archived CIR and panchromatic film. In every case, the CIR was found to cost less. Significant specific benefits are illustrated using examples of imagery, dollar benefits of the use of remote sensing are calculated, and nonquantifiable results are described.
C.R.

N81-29408*# National Aeronautics and Space Administration Wallops Flight Center, Wallops Island, Va.
ALTIMETER RAIN DETECTION Final Report
E. J. Walsh Jul. 1981 19 p refs
(NASA-TM-73291) Avail: NTIS HC A02/MF A01 CSCL 14B

The implementation of a rain detection capability for the NOSS Radar altimeter design is proposed which would require only minor hardware modifications to the Seasat altimeter design is proposed. The expected level of performance is indicated.
A.R.H.

N81-29480*# California Univ. at Los Angeles. Inst. of Geophysics and Planetary Physics.
GEOMAGNETIC FIELD MAPPING FROM A SATELLITE: SPATIAL POWER SPECTRA OF THE GEOMAGNETIC FIELD AT VARIOUS SATELLITE ALTITUDES RELATIVE TO NATURAL NOISE SOURCES AND INSTRUMENT NOISE

M. G. McLeod and P. J. Coleman, Jr. *In* Alabama Univ. UAH/NASA Workshop on the Use of a Tethered Satellite System May 1976 5-32 refs

(Publ-1810) Avail: NTIS HC A11/MF A01 CSCL 08G

The spectra for the field are presented together with power spectra of the natural magnetospheric and ionospheric noise and a power spectrum of instrumental noise for a typical fluxgate magnetometer. The source of these data is described. The implications of these data relative to desirable instrument frequency resonse, stability and resolution specification as well as the implications relative to desirable spacecraft position and orientation accuracy specifications and desirable environmental (temperature, magnetic noise) specifications are discussed. Implications of these power spectra relative to choice of a suitable magnetometer and relative to desirable methods of data processing are considered. Finally, implications for desirable orbit and mission duration are discussed.
T.M.

N81-29482*# Phoenix Corp., McLean, Va.
REDUCTION AND ANALYSIS OF SATELLITE MAGNETOMETER DATA
Robert D. Regan *In* Alabama Univ. UAH/NASA Workshop on the Use of a Tethered Satellite System May 1978 p 59-91 refs Submitted for publication

Avail: NTIS HC A11/MF A01 CSCL 08N

The broad-scale magnetic anomalies that appear in regional complications of aeromagnetic data, and in regional and global maps are discussed. Satellite data can be of value in defining such anomalies and invaluable, especially when utilized with airborne data, in their interpretation. The reduction and interpretation of satellite magnetometer data differ significantly from the standard techniques that are routinely applied to conventional measurements. The reduction of the data is discussed and its morphology is detailed. Interpretational techniques that are applicable are presented.
T.M.

N81-29512# Defense Mapping Agency Aerospace Center, St. Louis, Mo. Dept. of Aerospace Cartography.
THE SENSOR IMAGE SIMULATOR Interim Report, Oct. 1979 - May 1981
Marshall B. Faintich, Paul C. Figura, and E. W. Quinn (Goodyear Aerospace Corp., Akron, Ohio) 22 Jun. 1981 21 p refs Proposed for presentation at the 3rd Iterservice/Ind. Training Equipment Conf., Orlando, Fla., 30 Nov. - 2 Dec. 1981
(AD-A101172) Avail: NTIS HC A02/MF A01 CSCL 09/2

The primary objective of the digital sensor simulation investigations being conducted at the Defense Mapping Agency (DMA) is to establish an editing and analysis capability for the digital culture and terrain data bases. For purposes of quality control and data base applicability investigations, DMA has developed the Sensor Image Simulator (SIS), a very high speed data base edit station and static scene simulator that allows for interactive query and manipulation of individual features in the data base displays and/or simulated sensor scenes to determine the corresponding data base elements responsible for the simulated features. The SIS was installed at DMA in 1981, and is designed to play a key role in determining the applicability of prototype data bases for use in advanced training simulators, as well as to ensure the quality of, and coherence between, the various digital data bases prior to new data insertion into the master cartographic data base files.
Author (GRA)

N81-30325*# National Aeronautics and Space Administration Wallops Flight Center, Wallops Island, Va.
RADAR ALTIMETER WAVEFORM MODELED PARAMETER RECOVERY
Aug. 1981 59 p refs
(NASA-TM-73294) Avail: NTIS HC A04/MF A01 CSCL 17I

Satellite-borne radar altimeters include waveform sampling gates providing point samples of the transmitted radar pulse after its scattering from the ocean's surface. Averages of the waveform sampler data can be fitted by varying parameters in a model mean return waveform. The theoretical waveform model used is described as well as a general iterative nonlinear least squares procedures used to obtain estimates of parameters characterizing the modeled waveform for SEASAT-1 data. The six waveform parameters recovered by the fitting procedure are: (1) amplitude; (2) time origin, or track point; (3) ocean surface rms roughness; (4) noise baseline; (5) ocean surface skewness; and (6) altitude or off-nadir angle. Additional practical processing considerations are addressed and FORTRAN source listing for subroutines used in the waveform fitting are included. While the description is for the Seasat-1 altimeter waveform data analysis, the work can easily be generalized and extended to other radar altimeter systems.
A.R.H.

N81-30342# Universite Catholique de Louvain (Belgium). Lab. de Telecommunications et d'Hyperfrequences.
STUDY OF THE INFLUENCE OF THE ATMOSPHERE ON THE PERFORMANCE OF AN IMAGING MICROWAVE RADIOMETER

A. Guissard Paris ESA Jul. 1980 248 p refs
(Contract ESTEC-4124/79/NL-DG(SC))
(ESA-CR(P)-1421) Avail: NTIS HC A11/MF A01

Errors induced by the intervening atmosphere on the determination of ground parameters from a set of radiometers operating in two polarization states and in the frequency range from 5 to 90 GHz were analyzed. The precision with which the atmospheric parameters themselves are measurable was studied. Methods for estimating parameters from measurements performed in a noisy environment are discussed. The radiative transfer problem through a scattering medium is reviewed and an approximate scalar form of the radiative equation proposed, valid under the assumption that the depolarizing effect can be neglected. A complete model for the atmosphere is discussed, and analytical expressions for the attenuations from atmospheric gases, clouds and rain are given for the frequency range of interest. Models for the radiative behavior of sea and sea ice are discussed. Finally the performance of the multichannel radiometer is analyzed for several typical situations. Author (ESA)

N81-32595# Zeiss (Carl), Oberkochen (West Germany). Abt fuer Geodaesie und Photogrammetrie.
APPLICATION OF NEW PRECISION MEASURING SYSTEMS FOR PHOTOGRAMMETRIC COMPARATORS Final Report
Reiner Schwebel Bonn Bundesministerium fuer Forschung und Technologie Dec. 1980 23 p refs In GERMAN; ENGLISH summary Sponsored by Bundesministerium fuer Forschung und Technologie
(BMFT-FB-T-80-134; ISSN-0340-7608) Avail: NTIS HC A02/MF A01

A technique for high precision two-dimensional coordinates measurements was developed and led to the construction of a high precision comparator. The system is based on Abbe's comparator principle makes use of a precision metrological x-y grid and linear pulse generators, and is free of mechanical driving error. The maximum error of scale, coordinate system and interpolation unit is below 0.5 microns and the temperature dependence attains at most 0.5 microns per degree C. A computer interface permits such online applications as controlled aerotriangulation or multiple photogrammetry in astronomy and industry. Author (ESA)

N81-33340# Deutsche Forschungs- und Versuchsanstalt fuer Luft- und Raumfahrt, Oberpfaffenhofen (West Germany). Inst fuer Hochfrequenztechnik.
INTRODUCTION TO THE WORKSHOP
A. Sieber *In* ESA Coherent and Incoherent Radar Scattering from Rough Surfaces and Vegetated Areas May 1981 p 13-17 refs
Avail: NTIS HC A08/MF A01

Research objectives in the use of scatterometers and imaging radar systems are discussed. System design for scatterometers and imaging radars, differences between scatterometers and imaging radars with respect to the measurement of scattered energy, and processing and evaluation of scatterometer data are included. Suggestions for work on theoretical models are given. These topics are related to data evaluation of synthetic aperture radar. Author (ESA)

N81-33540*# EG & G Washington Analytical Services Center, Inc., Riverdale, Md. Applied Systems Dept.
A STUDY OF THE EFFECTS OF THE ATMOSPHERE ON THEMATIC MAPPER OBSERVATIONS
William A. Pearce, Principal Investigator 1 Oct. 1977 139 p refs ERTS
(Contract NAS5-23639)
(E81-10056; NASA-CR-166660; EGG-004-77) Avail: NTIS HC A07/MF A01 CSCL 08B

The impact of Rayleigh and aerosol light scattering and the scattering of light by the ground both within and beyond the instantaneous field of view of the sensor are included in a Monte Carlo computer code used to simulate the transport of radiation from its source (the Sun) to satellite-borne receivers. The problem of signature contamination by atmospheric scattering is addressed. The specifications of the details of the computer code and of the model for the atmosphere-Earth-receiver system are described. Specifications of the thematic mapper scheduled to be launched on LANDSAT-D are summarized. Model observations of ground patterns and calibration effects are discussed. General formalism, spread and modulation transfer functions, and image enhancement are considered. The impact of the atmosphere on classification and classification errors is examined. Recommendations are included. A.R.H.

09

GENERAL

Includes economic analysis.

A81-42231 **Environmental satellites.** E. P. McClain (NOAA, National Earth Satellite Service, Washington, DC). In: McGraw Hill encyclopedia of environmental science. New York, McGraw Hill Book Co., Inc., 1980. 16 p. 13 refs.

The meteorological and oceanographic applications of the Geostationary Operational Environmental Satellite (GOES) and Improved TIROS Operational Satellite (ITOS) are discussed. Brief descriptions of the satellites, including the solar activity monitors and data collection systems are given. Meteorological applications involve disaster warning, frost forecasting, search and rescue, and snow cover information. Oceanographic applications both in operations and research, include sea surface temperatures to aid oil tankers along the eastern seaboard, upwelling processes, ocean current systems, and ice mapping. Other spacecraft for meteorological and environmental studies launched by NASA are the Landsat 3, designed for high resolution, Nimbus 7, equipped with imagers and sounders, and Seasat 1, used for observations of the oceans. D.L.G.

A81-42287 # **Efficiency criteria of space systems for studying the earth's natural resources (Kriterii effektivnosti kosmicheskikh kompleksov dlia izucheniia prirodnykh resursov zemli).** V. S. Avduevskii, A. A. Astashkin, V. K. Saul'skii, and G. R. Uspenskii. *Issledovanie Zemli iz Kosmosa,* May-June 1981, p. 89-95. 11 refs. In Russian.

Criteria for evaluating the efficiency of space systems, used to study the earth's natural resources, are discussed. The procedure is based on the determination of additional user income gained from the application of the space system: costs of design, development, and operation; and values characterizing the ability of the system to complete the user tasks. The approach is illustrated by values projected for Landsat-D. J.F.

A81-42288 # **Main tasks and methods of operational planning of experiments concerning the observations of the earth from space (Osnovnye zadachi i metody operativnogo planirovaniia eksperimentov po issledovaniiu zemli iz kosmosa).** M. Iu. Beliaev. *Issledovanie Zemli iz Kosmosa,* May-June 1981, p. 96-101. 5 refs. In Russian.

The effective operational planning of geophysical experiments, involving the use of manned spacecrafts for the remote sensing of earth resources, is discussed. Operational planning is considered as one of the tasks of the overall control of a complex space system and can be reduced to several individual tasks. The proposed solution of the problems is performed in an interactive mode, and an algorithm for the operational planning of geophysical experiments is presented. J.F.

A81-42513 **Large scale human benefits of space industrialization.** C. L. Gould (Rockwell International Corp., Pittsburgh, PA). In: Update on space. Volume 1. Granada Hills, CA, National Behavior Systems, 1981, p. 30-63.

Space industrialization is defined as a new technology in which the special environmental properties of outer space are used for the social and economic benefit of the people of the earth. A study conducted in connection with a NASA Contract on Space Industrialization is discussed. Part One of this study identified the potential goals for space industrialization and looked at ways to realize those goals. Part Two was concerned with the programs and problems of actually bringing about the goals. Space can be used to provide very large scale benefits either supported by the government in public services, supported by private industry or some combination thereof. World problems related to the population explosion are considered and attractive opportunities gained from space are discussed. These opportunities can be divided into four categories, related to services, products, energy, and human activities. G.R.

A81-43535 **Skylab in retrospect.** E. E. Derenyi (New Brunswick, University, Fredericton, Canada). *Photogrammetric Engineering and Remote Sensing,* vol. 47, Apr. 1981, p. 495-499. 7 refs.

Investigations conducted at the University of New Brunswick into the accuracy attainable for horizontal control extension using Skylab/EREP S-190A and S-190B imagery are reviewed. Single image and multiple image processing are discussed and it is shown that simple space resection procedures can give results compatible with more sophisticated aerial triangulation techniques. The RMSE values in X and Y coordinates ranged from 35 m to 75 m for S-190A photography and was on the order of 20 m photography for the S-190B imagery. The results obtained and the experience gained form a basis for predictions and recommendations pertinent to future space photography missions. In particular, the expected performance of the Large Format Camera, proposed for use in the Space Shuttle missions of the early 1980's, is discussed. (Author)

A81-43750 **Landsat technology transfer to the private and public sectors through community colleges and other locally available institutions.** R. H. Rogers, C. L. Wilson, R. H. Dye (Michigan, Environmental Research Institute, Ann Arbor, MI), and E. Jaworksi (Eastern Michigan University, Ypsilanti, MI). In: Rainbow 80; Fall Technical Meeting, Niagara Falls, NY, October 7-10, 1980, ASP Technical Papers. Falls Church, VA, American Society of Photogrammetry, 1981, p. PS-2-C-1 to PS-2-C-13. 5 refs.

NASA transferred Landsat technology to practicing professionals in the private sectors through community colleges and other locally available institutions. 'Hands on' interactive analysis training and demonstrations are offered through the use of color desk-top computer terminals communicating with a host computer by telephone lines. Features of the terminals and associated training materials are reviewed, including low cost, portability, interactive control, and special display features. Operational steps used to process Landsat data are enumerated. Plans for the of use of these features in training and demonstration projects are discussed. Results of the transfer project show that a gradual expansion of the user facility can be expected as confidence and available capital increase, and as the system shows potential for easily merging other sources of data into the Landsat analysis process. J.F.

A81-43981 # **Aerial thermal survey in the study of earth resources (Teplovaia aeros'emka pri izuchenii prirodnykh resursov).** B. V. Shilin. Leningrad, Gidrometeoizdat, 1980. 248 p. 119 refs. In Russian.

The principles of the thermal or infrared aerial surveying of earth resources are presented. Particular consideration is given to the operation of thermal sensors and to the selection of optimum survey conditions. Various applications of this technique are considered, including the study of anomalous temperature fields, geological mapping, the study of water bodies, the investigation of snow and ice cover, and hydrological and hydrogeological surveys. B.J.

A81-44635 **Commercial operations in space - 1980-2000; Proceedings of the Eighteenth Goddard Memorial Symposium, Washington, DC, March 27, 28, 1980.** Symposium sponsored by AAS, AIAA, AMA, et al. Edited by J. L. McLucas (Communications Satellite Corp., Washington, DC) and C. Sheffield (Earth Satellite Corp., Washington, DC). San Diego, CA, American Astronautical Society (Science and Technology Series. Volume 51); Univelt, Inc., 1981. 211 p. $30.

The need to revitalize American industry is considered along with questions of space industrialization, materials science and engineering in space, materials engineering in space, space power systems, earth resources, commercial launch operations, research opportunities, and international opportunities. Attention is given to the Space Shuttle power extension package, the orbital transfer of large space structures with nuclear electric rockets, a satellite power system overview of system studies and critical technology, electric orbit transfer vehicles, the mixed-mode principle and advanced chemical rocket engine concepts, crop reporting from space, the Space Industrialization Act and the government role in the commercialization of space, the airlines in the 80's and 90's, approaches to private sector involvement with government in technology development, innovation of space technology through joint endeavors between NASA and private industry, and the economic and political climate for exploitation of space riches. G.R.

A81-46234 # **European industrial space projects.** G. C. Bernardini (Italeco S.p.A., Rome, Italy). *American Astronautical Society, Goddard Memorial Symposium on International Space Technical Applications, 19th, Arlington, VA, Mar. 26, 27, 1981, Paper 81-053.* 8 p.

The efforts of an Italian civil engineering firm (ITALECO S.p.A.) to profitably use Landsat data are recounted. The data did not bring the commercial benefits hoped for, primarily because of the absence of repeatable and reliable rules for converting the esoteric art of Landsat interpretation into science and engineering practice. At present, the only role for Landsat, from a commercial viewpoint, is that of a source with which to supplement the information available from standard methods. C.R.

A81-46238 # **Development of Marine Observation Satellite-1.** K. Matsumoto (National Space Development Agency of Japan, Earth Observation Systems Dept., Tokyo, Japan). *American Astronautical Society, Goddard Memorial Symposium on International Space Technical Applications, 19th, Arlington, VA, Mar. 26, 27, 1981, Paper 81-060.* 9 p.

The program of MOS-1, the first Japanese earth observation satellite system to be developed for experimental purposes, is outlined. The mission objectives are to establish fundamental technologies common to both marine and land observation satellites, observe the sea surface and atmosphere using visible, infrared, and microwave radiometers, and verify the performance of these sensors. A table giving the characteristics of the MOS-1 sensors is included, and the data collection system transponder is described. Also included is a schematic diagram of the MOS-1 communication system. The various systems making up the ground segment are also described. C.R.

A81-47346 **SPOT status of development.** M. Courtois (Centre National d'Etudes Spatiales, Toulouse, France). *International Astronautical Federation, International Astronautical Congress, 32nd, Rome, Italy, Se, 6-12, 1981, Paper 81-92.* 11 p.

The System Probatoire d'Observation de la Terre (SPOT), a general purpose remote sensing satellite system, will be launched in May, 1984 within the French National Space Program. The SPOT mission objectives include the compilation of a worldwide data base for cartographic and earth resource exploration purposes, improvements in vegetative species discrimination, and the evaluation of photointerpretation methods and the linear array camera in space. The SPOT satellite consists of the SPOT 'bus', a standard multipurpose platform, and the payload; it will weigh 1750 kg at the start of the mission and operate in a circular sun-synchronous near-polar orbit at an altitude of 832 km. The HRV (high resolution visual) instrument is designed to operate in either a panchromatic mode (broad spectral band) with a ground sampling mesh of 10 m x 10 m or a multispectral mode (three narrower color bands) with a ground sampling mesh of 20 m x 20 m. This flexibility will enable the specific target scenes to be sampled more frequently as well as provide for stereo coverage of important areas. Linear arrays of CCD detectors will combine a high data rate (25 m bits/sec/data channel) with good radiometric resolution. Data from the satellite will be accessible through the central facility in France or through authorized X-band direct read-out stations. J.F.

A81-47350 **Physical and technical foundations for the development of subsatellite systems for the exploration of natural earth resources.** T. K. Ismailov (Akademiia Nauk Azerbaidzhanskoi SSR, Institut Kosmicheskikn Issledovanii Prirodnykh Resursov, Baku, Azerbaidzhan SSR). *International Astronautical Federation, International Astronautical Congress, 32nd, Rome, Italy, Sept. 6-12, 1981, Paper 81-101.* 10 p. 5 refs.

The importance of organizing a subsatellite environmental service is stressed. The principal objective of this service would be the prompt and regular collection, processing, and transmission of the results obtained from both contact and remote measurements of a large number of physicochemical, biometric, optical, and geometric characteristics of natural objects. The measurements would be taken at specified control points on the earth's surface using observation and measurement platforms (air, continental, and marine) either synchronously or quasi-synchronously with space facilities. C.R.

A81-47355 **Soviet remote sensing of the earth's resources and interpretation of space data with reference to the Caspian Sea, Siberia and the Arctic Ocean.** J. Popescu (British Broadcasting Corp., Monitoring Service, Reading, Berks., England). *International Astronautical Federation, International Astronautical Congress, 32nd, Rome, Italy, Sept. 6-12, 1981, Paper 81-112.* 8 p. 11 refs.

Soviet remote sensing of the earth's resources, including population, by unmanned and manned satellites is discussed. Multiscanning equipment is described, and it is noted that photographs and remote sensing data are used for making maps, prospecting, research, farming, civil engineering, weather forecasting, and protecting the environment. Attention is given to the increased importance of the data transmitted by crews on board the Salyut-6 space lab. C.R.

A81-47826 **What does space remote sensing provide (Qu'apporte la télédétection spatiale).** P. Gonfreville (Centre National d'Etudes Spatiales, Paris, France). *L'Aéronautique et l'Astronautique,* no. 89, 1981, p. 3-20. In French.

The capabilities and advantages of space remote sensing in the gathering of data for the management of natural resources and national development are discussed. The principles and operational characteristics of space remote sensing are considered with particular reference to the Landsat and SPOT systems. Attention is then given to specific applications of space remote sensing in the fields of cartography, including topographic and thematic mapping, agriculture, including national agricultural statistics, crop prediction and agricultural management, forests and natural vegetation, inland water resources, regional management for economic and social development, mineral and petroleum exploration, oceanography and other types of large inventories. A.L.W.

A81-47829 **Evaluation of the 1980 Cosmos program (Bilan du programme Cosmos 1980).** D. Laurent. *L'Aéronautique et l'Astronautique,* no. 89, 1981, p. 44-50. In French.

In the year 1980, the Soviet Union effected 89 rocket launches sending into orbit 110 satellites. The present paper examines the 88 of these satellites not launched as part of specific space programs but within the framework of the diversified Cosmos program. Of the 78 satellites launched for military applications, 30 were for purposes of photographic reconnaissance, 25 were for telecommunications, seven for navigation, five for electronic surveillance, five for early warning, three for ocean surveillance and three for interception. Six satellites for civilian applications were launched: four for purposes of earth resource detection and two Molniya satellites unable to be placed in their desired orbits. Four Cosmos satellites were sent up with scientific missions, including ocean observations, and geophysical experiments. As to general trends over the last five years, 1980 witnessed an increase in space activities compared to the previous year, continuing emphasis on the military sector and a preference for orbital inclinations of 72.9 and 82.3 deg. A.L.W.

A81-48527 **Requirements on the data/information system.** R. Bernstein (IBM Scientific Center, Palo Alto, CA). In: EASCON '80; Electronics and Aerospace Systems Conference, Arlington, VA, September 29-October 1, 1980, Conference Record.

New York, Institute of Electrical and Electronics Engineers, 1980, p. 20-26. 6 refs.

The paper examines current problems concerning the development and implementation of satellite systems of earth observation, and suggests some approaches and solutions for the future that involve software, system, and data standardization, and the development of a global digital data base. Advanced sensors produce digital data at rates of tens of millions of bits per second; communication systems exist that are capable of disseminating the data on a worldwide basis at millions of bits per second; and ground processing systems are currently operational that are preprocessing the sensor data and making them available to the user community. It is likely that future problems will involve managing the acquisition and distribution of these data, and providing the data to the users in a timely manner, in a suitable form, and at the lowest possible cost. B.J.

A81-48549 **The SPOT satellite mission, applications aspects and data products.** J.-P. Fouquet (Ambassade de France aux Etats Unis, Washington, DC). In: EASCON '80; Electronics and

Aerospace Systems Conference, Arlington, VA, September 29-October 1, 1980, Conference Record. New York, Institute of Electrical and Electronics Engineers, 1980, p. 306, 307.

A brief description of the SPOT satellite system is given. It is pointed out that the first mission's (1984) payload will comprise two identical optical instruments, which are described in detail, two onboard recorders, and an image telemetry system at 8 GHz (X-band). The SPOT system will be used mainly in cartography, geology, and agriculture. With regard to cartography, it is noted that the telescopes, because they can be pointed, will provide the cartographic user with a capability for quasi-vertical coverage and slant or stereo coverage. In geology, stereo data will be very useful in the reconnaissance exploration for the study of geomorphic features. In agriculture, the system's ground resolution will enable agricultural users to control small fields or to use SPOT data as samples for Landsat D data with which compatibility is studied. Tables giving the characteristics of the system's first payload and standard SPOT products are included. C.R.

A81-48936 **Remote sensing in development.** C. K. Paul (U.S. Agency for International Development, Washington, DC) and A. C. Mascarenhas (Dar es Salaam, University, Dar es Salaam, Tanzania). *Science*, vol. 214, Oct. 9, 1981, p. 139-145. 12 refs.

It is pointed out that in developing countries remote sensing is used to acquire statistics on crops and to locate petroleum and mineral deposits. To an ever greater extent, it is also being used for forest monitoring and subsurface water location. Among the problems related to Third World use of the technology are sensitivity about the dissemination of data with high spatial resolution, exploitation by multinational companies, absorptive capacity of countries for advanced technology, autonomy in acquiring resource information, and competing foreign policy interest of the industrialized world in the global search for raw materials. The attitude of Third World countries toward the use of remote sensing is seen as depending on the development model they adopt. C.R.

A81-49468 # **International monitoring from space /Problems of international law/ (Mezhdunarodnyi kontrol' s ispol'zovaniem kosmicheskikh sredstv /Mezhdunarodno-pravovye problemy/).** I. I. Kotliarov. Moscow, Izdatel'stvo Mezhdunarodnye Otnosheniia, 1981. 120 p. 232 refs. In Russian.

The work considers various aspects of monitoring and surveillance with regard to international laws and agreements on environment protection, disarmament, the use of space, etc. The use of spacecraft for purposes of such monitoring is discussed in detail. B.J.

A81-49751 **Canadian Symposium on Remote Sensing, 6th, Halifax, Canada, May 21-23, 1980, Proceedings.** Symposium sponsored by CASI, Canada Centre for Remote Sensing, Environment Canada, et al. Edited by T. T. Alfoldi (Canada Centre for Remote Sensing, Ottawa, Canada). Ottawa, Canadian Aeronautics and Space Institute, 1981. 715 p. In English and French.

Aspects of remote sensing technology and operational experience are reviewed, with reference to Canadian Programs. Particular attention is given to such applications as land use, forestry, agriculture, geology, hydrology, and pollution monitoring. A special section is devoted to radar (particularly SAR) applications and technology. B.J.

A81-49762 # **The remote sensing satellite program of the European Space Agency (Le programme de satellites de télédétection de L'Agence Spatiale Européenne).** D. Breton (ESA, Earth Observation Programme Office, Toulouse, France). In: Canadian Symposium on Remote Sensing, 6th, Halifax, Canada, May 21-23, 1980, Proceedings. Ottawa, Canadian Aeronautics and Space Institute, 1981, p. 89-96. In French.

The main directions of ESA activities in remote sensing are: the Earthnet program; remote sensing activities that will be implemented during the first Spacelab mission; and project definition, system studies of instruments, and technological activities relating to the ESA remote sensing satellite program. This paper examines the ESA remote sensing satellite program; attention is given to the objectives of the program, the Canadian Sursat requirements, the results of past studies, and ongoing or projected activities. B.J.

A81-49763 # **Present state of remote sensing development in Poland.** J. Konieczny and A. Linsenbarth (Instytut Geodezji i Kartografii, Warsaw, Poland). In: Canadian Symposium on Remote Sensing, 6th, Halifax, Canada, May 21-23, 1980, Proceedings. Ottawa, Canadian Aeronautics and Space Institute, 1981, p. 97-101.

A brief description is presented of the development of remote sensing in Poland as well as of the main aims and achievements of the Polish Center for Remote Sensing (OPOLIS). The instrumentation system of OPOLIS is reviewed, and various applications of remote sensing in Poland are examined, including land use mapping, agriculture, forest surveys, water pollution studies, air pollution studies, disaster surveying, and geological surveys. B.J.

N81-31030# Committee on Science and Technology (U S House).

NASA AUTHORIZATION, 1982, VOLUME 4

Washington GPO 1981 1248 p Hearings before the Subcomm on Space Sci and Appl of the Comm on Sci. and Technol., 97th Congr., 1st Sess., No 7, 28 Jan., 20, 23, 27 Feb., and 2, 4-5, 10-11 Mar. 1981

(GPO-79-432-Vol-4) Avail: Subcommittee on Space Science and Applications

Progress and accomplishments of the year are reviewed and requests for funding are examined in the areas of space sciences, shuttle related activities, space flight operations, a space applications, and aeronautics. The numerical aerodynamics simulation which will reduce the cost of aircraft design, chemical propulsion, large space structures, power systems, information systems, and the Venus Orbiting Imaging Radar spacecraft are discussed. Space processing, Spacelab payloads, and possible space shuttle configurations are also examined. A.R.H.

N81-32086*# Denver Research Inst., Colo. Program for Transfer Research and Impact Studies.

SPACE BENEFITS: THE SECONDARY APPLICATION OF AEROSPACE TECHNOLOGY IN OTHER SECTORS OF THE ECONOMY

[1981] 240 p refs

(Contract NASw-3113)

(NASA-CR-164733) Avail: NTIS HC A11/MF A01 CSCL 05A

Some 585 examples of the beneficial use of NASA aerospace technology by public and private organizations are described to demonstrate the effects of mission-oriented programs on technological progress in the United States. General observations regarding technology transfer activity are presented. Benefit cases are listed in 20 categories along with pertinent information such as communication link with NASA; the DRI transfer example file number, and individual case numbers associated with the technology and examples used; and the date of the latest contract with user organizations. Subject, organization, geographic, and field center indexes are included. A.R.H.

N81-32564*# National Aeronautics and Space Administration. Ames Research Center, Moffett Field, Calif.

FIELD STUDY FOR REMOTE SENSING: AN INSTRUCTOR'S MANUAL

William H. Wake, ed. (California State Coll., Bakersfield) and Garth A. Hull, ed. 1981 93 p refs Proceedings of the LANDSAT C Educator's/User's Workshop, Santa Maria, Calif., 2-4 Mar. 1978; sponsored by the National Council for Geographic Education and Univ. of Western Illinois, Macomb

(NASA-CP-2155; A-8336; LC-78-61696) Avail: NTIS HC A05/MF A01 CSCL 05I

The need for and value of field work (surface truthing) in the verification of image identification from high atitude infrared and multispectral space sensor images are discussed in this handbook which presents guidelines for developing instructional and research procedures in remote sensing of the environment.

N81-32565*# International Business Machines Corp., White Plains, N.Y. General Business Group.

AN INDUSTRIAL PERSPECTIVE OF THE LANDSAT OPPORTUNITY

Barbara F. Williams *In* NASA. Ames Research Center Field Study for Remote Sensing 1981 p 1-3

Avail: NTIS HC A05/MF A01 CSCL 05B

The feasibility of enhancing LANDSAT products to provide the greatest usability low cost data possible can be determined through government sponsorship and finance of one or more task forces composed of a critical number of experts in multiple disciplines from many industries and academia. The synergism of multiple minds addressing singular problems without the creation of permanent or perpetual structures must yield output in the form of implementable specifications, even if presented as alternatives. Changes are needed within the spacecraft in order to account for Sun angle changes. The use of pointing accuracy to make geometric corrections (and possible radiometric corrections, is needed more than onboard data reduction and information extraction, which assume a proper knowledge of application and reduce potential utilization. Multilinear arrays need to be investigated and methods for sensor calibration and for determining the effects of atmospheric inversion, as well as the best way to back out the modulation transfer function must be determined. A.R.H.

N81-32566*# California State Coll., Bakersfield. Dept. of Physics and Earth Sciences.

THE WORKSHOP

William H. Wake *In* NASA. Ames Research Center Field Study for Remote Sensing 1981 p 5-7

Avail: NTIS HC A05/MF A01 CSCL 05B

The plan is presented for a two day workshop held to provide educational and training experience in the reading, interpretation, and application of LANDSAT and correlated larger scale imagery, digital printout maps, and other collateral material for a large number of participants with widely diverse levels of expertise, backgrounds, and occupations in government, industry, and education. The need for using surface truth field studies with correlated aerial imagery in solving real world problems was demonstrated. A.R.H.

N81-32567*# California State Coll., Bakersfield. Dept. of Physics and Earth Science.

WHY SURFACE-TRUTH FIELD STUDY IS NEEDED IN REMOTE-SENSING INSTRUCTION

William H. Wake *In* NASA. Ames Research Center Field Study for Remote Sensing 1981 p 9-15 ref

Avail: NTIS HC A05/MF A01 CSCL 05I

Especially designed field studies are needed in remote sensing technology transfer courses regardless of the field work provided by the students'/trainees' major disciplines because the remote sensing discipline has unique emphases and needs. Modification of existng schedules to include field work provides the equivalent of extending the duration of the program with the added benefit of enhancing learning achievements per actual program day. The process of surface truth field instruction, levels of student capabilities and stages in the development of surface truth field studies are discussed. A.R.H.

N81-32571*# Sonoma State Univ., Calif. Dept. of Geography.

LANDSAT C WORKSHOP FIELD/LABORATORY EXERCISES

Joseph W. Frasca *In* NASA. Ames Research Center Field Study for Remote Sensing 1981 p 45-59 refs

Avail: NTIS HC A05/MF A01 CSCL 05I

Collection of ground information and supportive materials are absolutely necessary to verify and substantiate data extracted by the interpretation process regardless of sensor type and scale. Field observation and notes, the use of topographic and thematic maps, crop calendars, and climate records are just four examples of supportive materials which often are used in conjunction with remotely sensed materials. Illustration of this integrated multisensor approach is provided by four examples from the March, 1978 Santa Maria LANDSAT C Conference and Workshop. Four distinctive window sites were selected to demonstrate the usefulness of remotely sensed materials to solve geographic problems. A.R.H.

SUBJECT INDEX

Earth Resources/*A Continuing Bibliography (Issue 32)* JANUARY 1982

Typical Subject Index Listing

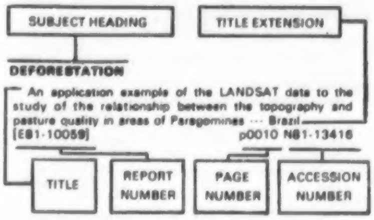
SUBJECT HEADING
TITLE EXTENSION
DEFORESTATION
An application example of the LANDSAT data to the study of the relationship between the topography and pasture quality in areas of Paragominas --- Brazil
[E81-10059] p0010 N81-13416
TITLE
REPORT NUMBER
PAGE NUMBER
ACCESSION NUMBER

The subject heading is a key to the subject content of the document. The title is used to provide a description of the subject matter. When the title is insufficiently descriptive of the document content, the title extension is added, separated from the title by three hyphens. The (NASA or AIAA) accession number and the page number are included in each entry to assist the user in locating the abstract in the abstract section (of this supplement). If applicable, a report number is also included as an aid in identifying the document. Under any one subject heading, the accession numbers are arranged in sequence with the AIAA accession numbers appearing first.

A

AERIAL PHOTOGRAPHY

Machine method for the equalization of average phototone in an aerial photograph field p0257 A81-41482

The possibilities of the automated classification of agricultural objects on the basis of their multispectral aerial-spaceborne images p0197 A81-41488

Remote sensing of bank erosion along the Missouri River, South Dakota p0213 A81-43263

A capture-recapture approach for estimation of detection probabilities in aerial surveys p0258 A81-43546

The possibility of using an aerial thermal survey for studying the structure of the salt bed in the Gulf of Kara-Bogaz-Gol p0226 A81-44061

AERIAL RECONNAISSANCE

Benefits of using airborne remote sensing for Thematic Mapping p0275 A81-49801

AERONAUTICAL ENGINEERING

NASA authorization, 1982, volume 4 [GPO-79-432-VOL-4] p0279 N81-31030

AEROSOLS

Stratospheric sulfate from the Gareloi eruption, 1980 - Contribution to the 'ambient' aerosol by a poorly documented volcanic eruption p0213 A81-41404

Aerosol formation, transformation, and effects in Denver's emissions plume p0214 A81-44526

Investigation of the efficiency of the optical sounding of aerosol by the use of spectral photometers p0215 A81-45406

Radiation studies in the atmosphere p0216 A81-47001

An atmospheric study by 'Spectrum-15' onboard of the Salyut-6 orbital station [IAF PAPER 81-120] p0216 A81-47359

Aerosol sounding by means of aircraft-borne optical radar p0217 A81-49431

Satellite measurements of tropospheric aerosols [NASA-CR-3459] p0219 N81-31680

NASA participation in the 1980 Persistent Elevated Pollution Episode/Northeast Regional Oxidant Study (PEPE/NROS) Project: Operational aspects [NASA-TM-83170] p0220 N81-32708

Satellite measurements of atmospheric aerosols [AD-A103493] p0220 N81-33720

AEROSPACE ENGINEERING

NASA authorization, 1982, volume 4 [GPO-79-432-VOL-4] p0279 N81-31030

AEROSPACE TECHNOLOGY TRANSFER

Landsat technology transfer to the private and public sectors through community colleges and other locally available institutions p0277 A81-43750

Space Benefits: The secondary application of aerospace technology in other sectors of the economy [NASA-CR-164733] p0279 N81-32086

AFRICA

Hydrogeologic interpretations of Landsat imagery in arid zones of South and West Africa p0248 A81-43229

Ground water exploration programs in Africa p0226 A81-43230

AGRICULTURE

Agricultures's needs related to satellite hydrology p0197 A81-43181

An application of Landsat and computer technology to potential water pollution from soil erosion p0250 A81-43253

Interpretation techniques applied to mixed terrains p0218 A81-49788

A simulation of Thematic Mapper performance in an agricultural application p0204 A81-49810

Use of satellite pictures for agriculture p0205 N81-28120

Agricultural water demand prediction using remote sensing technology for Georgia resource management [PB81-184137] p0207 N81-30508

AgRISTARS (Agriculture And Resources Inventory Surveys Through Aerospace Remote Sensing) DC/LC (Domestic Crops and Land Rover) project summary crop area estimates for Kansas and Iowa, 1980 [PB81-196909] p0207 N81-30511

Meteorological satellite data: A tool to describe the health of the world's agriculture [E81-10204] p0207 N81-31596

Crop area estimates using ground-gathered and LANDSAT data: A multitemporal approach: Missouri, 1979 [PB81-186751] p0208 N81-31614

AGRISTARS PROJECT

Users manual for the US baseline corn and soybean segment classification procedure [E81-10190] p0206 N81-29504

AgRISTARS (Agriculture And Resources Inventory Surveys Through Aerospace Remote Sensing) DC/LC (Domestic Crops and Land Rover) project summary crop area estimates for Kansas and Iowa, 1980 [PB81-196909] p0207 N81-30511

AgRISTARS: Foreign commodity production forecasting. Program review presentation to level 1, Interagency Coordination Committee [E81-10168] p0209 N81-33555

AGROCLIMATOLOGY

Weather analysis and interpretation procedures developed for the US/Canada wheat and barley exploratory experiment [E81-10208] p0207 N81-31599

AGROMETEOROLOGY

Use of satellite pictures for agriculture p0205 N81-28120

Yield Model Development (YMD) implementation plan for fiscal years 1981 and 1982 [E81-10211] p0208 N81-32577

AIR POLLUTION

Measurements of CF2Cl2, CFCl3, and N2O in the lower stratosphere between 2 deg S and 73 deg N latitude p0214 A81-44515

Aerosol formation, transformation, and effects in Denver's emissions plume p0214 A81-44526

An atmospheric study by 'Spectrum-15' onboard of the Salyut-6 orbital station [IAF PAPER 81-120] p0216 A81-47359

The distribution of the trace gases H2O, NO2, and HNO3 in the middle atmosphere on the basis of LIMS measurements --- Limb Infrared Monitor of Stratosphere p0217 A81-49407

Aerosol sounding by means of aircraft-borne optical radar p0217 A81-49431

Comparative measurements of stratospheric CH4 and CO concentrations with spectrograph and correlation radiometers p0217 A81-49433

Atmospheric nitric acid and chlorofluoromethane 11 from interferometric spectra obtained at the Observatoire du Pic du Midi [AERONOMICA-ACTA-A-227-1980] p0219 N81-30656

Environmental measurements of power plant cooling tower and stack plumes [DOE/EV-02463/6] p0219 N81-30695

NASA participation in the 1980 Persistent Elevated Pollution Episode/Northeast Regional Oxidant Study (PEPE/NROS) Project: Operational aspects [NASA-TM-83170] p0220 N81-32708

AIR WATER INTERACTIONS

A comparison of Seasat 1 altimeter measurements of wave height with measurements made by a pitch-roll buoy p0231 A81-42066

Satellite detection of seiches in Great Salt Lake, Utah p0243 A81-42126

A note on indirect detection of seiches in Great Salt Lake, Utah, by NOAA and Landsat satellite imagery p0247 A81-43218

The structure of short gravity waves on the ocean surface p0234 A81-46105

The wind speed dependency of ocean microwave backscatter p0234 A81-46109

The study of mesoscale ocean winds p0235 A81-46110

Spatial evolution of ocean wave spectra p0235 A81-46112

Satellite-tracked drift buoy observations of the near-surface flow in the eastern mid-latitude North Pacific p0236 A81-47022

The future for satellite-derived surface winds p0237 A81-49129

Climate, the oceans, and remote sensing p0237 A81-49132

Airborne estimation of water quality parameters in Lake Ontario p0254 A81-49796

Following oceanographic phenomena on the South Coast of Brazil with remote sensing from orbital distance [INPE-1975-RPE/280] p0240 N81-30498

Sea surface scattering p0241 N81-33344

AIRBORNE EQUIPMENT

Use of ocean color scanner data in water quality mapping p0251 A81-43545

Radar methods for studying the earth --- Russian book p0273 A81-46924

Aerosol sounding by means of aircraft-borne optical radar p0217 A81-49431

The airborne SAR project: Conclusions and applications p0275 A81-49765

AIRBORNE/SPACEBORNE COMPUTERS

An evaluation of detail in dynamic visual displays [AD-A103378] p0222 N81-33578

ALASKA

Sea ice detection using enhanced infrared satellite data p0232 A81-42131

Potentials of mapping buried glacier ice with Landsat thermal imagery p0246 A81-43204

Environmental assessment of the Alaskan continental shelf: Reports of principal investigators. Volume 1: Receptors - birds, plankton, littoral, benthos [PB81-196263] p0240 N81-30780

Terrain profiling from Seasat altimetry [NASA-CR-156878] p0222 N81-31604

ALBEDO

Correlation between integral and spectral albedos of clouds over water surfaces p0235 A81-47004

Theoretical investigations concerning the measurement of the plankton concentration with the aid of satellites p0237 A81-49426

ALGAE

A remote sensing technique to monitor Cladophora in the Great Lakes [PB81-173841] p0254 N81-29520

ALLUVIUM

An examination of fluvial morphological characteristics of western Amazon streams from Apollo-Soyuz photographs p0247 A81-43212

Applications of Landsat imagery to a coastal inlet stability study p0250 A81-43249

ALTIMETERS

Calibration validation for the GEOS 3 altimeter p0270 A81-42871

The promise of satellite altimetry --- for oceanography p0237 A81-49128

AMAZON REGION (SOUTH AMERICA)

An examination of fluvial morphological characteristics of western Amazon streams from Apollo-Soyuz photographs p0247 A81-43212

ANGULAR CORRELATION

Angular anisotropy of reflection from various types of underlying surface. I - Snow cover. II - Desert p0260 A81-47007

ANGULAR DISTRIBUTION

The effect of angular distribution models on the estimation of the earth's albedo p0269 A81-41915

ANNUAL VARIATIONS

Annual and interannual variations in outgoing longwave radiation over the tropics p0251 A81-43356

ANTARCTIC REGIONS

Satellite Image Atlas of the earth's glaciers p0246 A81-43202

Ice sheet altimetry
[NASA-CR-156877] p0240 N81-31605
Ocean services for the nation. National ocean goals and objectives for the 1980's
[PB81-200602] p0240 N81-31808
Investigation of Antarctic crust and upper mantle using Magsat and other geophysical data
[E81-10113] p0222 N81-32574
Possible applications of communication satellites for research tasks in polar regions
[BMFT-FB-W-80-029] p0267 N81-33587

ANTICLINES
The use of imagery of the earth to study the structure of degassing zones within oil and gas basins
p0225 A81-42276

APPROPRIATIONS
NASA authorization, 1982, volume 4
[GPO-79-432-VOL-4] p0279 N81-31030

AQUIFERS
Landsat data for locating shallow glacial aquifers in eastern South Dakota p0226 A81-43228
Applications of aerospace data for detection of submarine springs in Jamaica p0226 A81-43232
Mapping irrigated cropland on the High Plains using Landsat p0198 A81-43266

ARCHAEOLOGY
Use of imaging radar for geology and archeology
p0226 A81-43730

ARCTIC OCEAN
Soviet remote sensing of the earth's resources and interpretation of space data with reference to the Caspian Sea, Siberia and the Arctic Ocean
[IAF PAPER 81-112] p0278 A81-47355
Single and multiple parameter microwave signatures of sea ice p0238 A81-49774
Radar detection of sea-ice ridges and icebergs in frozen oceans at incidence angles from 0 deg to 90 deg
p0238 A81-49775
Environmental assessment of the Alaskan continental shelf: Reports of principal investigators. Volume 1: Reactors - birds, plankton, littoral, benthos
[PB81-196263] p0240 N81-30780
Ocean services for the nation. National ocean goals and objectives for the 1980's
[PB81-200602] p0240 N81-31808

ARCTIC REGIONS
Roles of satellites in hydrology p0245 A81-43199
The use of satellite imagery as an aid to the Canadian Coast Guard ice operations p0238 A81-49758

ARID LANDS
Hydrogeologic interpretations of Landsat imagery in arid zones of South and West Africa p0248 A81-43229
Remote methods and desert conservation --- Russian book p0213 A81-43523
A comparison between two photographic methods for the determination of relative bidirectional reflectance
p0259 A81-45431
A case study of soil erosion detection by digital analysis of the remotely sensed multispectral Landsat scanner data of a semi-arid land in southern India p0201 A81-46050
The environmental vegetation index: A tool potentially useful for arid land management --- Texas and Mexico, plant growth stress due to water deficits
[E81-10191] p0206 N81-29505
Identifying igneous rocks in an arid environment on aerial photography by photo tone and photo texture
[AD-A102809] p0228 N81-32587

ARIZONA
Prediction of water yield using satellite imagery and a snowmelt simulation model p0246 A81-43205
Correlation of geologic structure inferred from computer enhanced Landsat imagery with underground water supplies in Arizona p0225 A81-43227
A radar image time series p0226 A81-45430
Use of Landsat digital data to assist in mapping soils on Arizona rangelands p0201 A81-46047
Remote sensing and land use planning
p0218 A81-49792
Role of aerial photographs in classification of Landsat data p0262 A81-49808
Spectral properties of Arizona soils and rangelands and their relationship to LANDSAT digital data
p0207 N81-31595
Terrain profiling from Seasat altimetry
[NASA-CR-156878] p0222 N81-31604

ARRID LANDS
Landform-vegetation relationships in the northern Chihuahuan Desert
[AD-A102896] p0208 N81-32588

ASIA
The use of imagery of the earth to study the structure of degassing zones within oil and gas basins
p0225 A81-42276
Concerning the hydrogeological significance of faults on platform regions, as revealed by space imagery
p0225 A81-42277
Ring structures of Precambrian shields, based on the interpretation of space imagery p0225 A81-42278
Space research on seismic regions p0225 A81-42280

ATLANTIC OCEAN
Hurricane 'Flossie' /September 1978/ observed in the north Atlantic, by the Meteosat satellite
p0213 A81-41061
Microwave radiometer measurement of tidally induced salinity changes off the Georgia coast p0232 A81-42067
Remote sensing of coastal pollutants using multispectral data p0233 A81-43245
Aerospace remote sensing of the coastal zone for water quality and biotic productivity applications
p0233 A81-43246
Combined satellite imagery for study of coastal circulation, Onslow Bay, North Carolina
p0233 A81-43250
Satellite determination of the mesoscale variability of the sea surface temperature p0234 A81-44861
The study of mesoscale ocean winds
p0235 A81-46110
Tracking of a warm water ring p0235 A81-46117
Radiation studies in the atmosphere
p0216 A81-47001
Atlantic hurricane season of 1980 p0238 A81-49649
Meteosat experience in assisting commercial fishing
p0239 A81-49807
Following oceanographic phenomena on the South Coast of Brazil with remote sensing from orbital distance
[INPE-1975-RPE/280] p0240 N81-30498
Interpretation of hydrographic features seen in the waters off Cape Cod
[AD-A102343] p0240 N81-31803

ATMOSPHERIC ATTENUATION
Atmospheric correction of Nimbus-7 Coastal Zone Color Scanner imagery p0271 A81-45879
Study of the influence of the atmosphere on the performance of an imaging microwave radiometer
[ESA-CR(P)-1421] p0275 N81-30342

ATMOSPHERIC CHEMISTRY
Basic problems of the physics and chemistry of contemporary changes of climate p0216 A81-47002

ATMOSPHERIC COMPOSITION
Passive microwave techniques for geophysical sensing of the earth from satellites p0270 A81-43071
Measurements of CF2Cl2, CFCl3, and N2O in the lower stratosphere between 2 deg S and 73 deg N latitude
p0214 A81-44515
Aerosol formation, transformation, and effects in Denver's emissions plume p0214 A81-44526
A differential inversion method for high resolution atmospheric remote sensing p0215 A81-45862
The distribution of the trace gases H2O, NO2, and HNO3 in the middle atmosphere on the basis of LIMS measurements --- Limb Infrared Monitor of Stratosphere
p0217 A81-49407
Comparative measurements of stratospheric CH4 and CO concentrations with spectrograph and correlation radiometers p0217 A81-49433

ATMOSPHERIC MOISTURE
Determination of moisture from NOAA polar orbiting satellite sounding radiances p0243 A81-41158
Modeling the terrestrial hydrology for the global atmosphere - The future role of satellite data
p0245 A81-43197

ATMOSPHERIC OPTICS
Investigation of the efficiency of the optical sounding of aerosol by the use of spectral photometers
p0215 A81-45406
Radiation studies in the atmosphere
p0216 A81-47001
Correlation between integral and spectral albedos of clouds over water surfaces p0235 A81-47004
An atmospheric study by 'Spectrum-15' onboard of the Salyut-6 orbital station
[IAF PAPER 81-120] p0216 A81-47359
Methods of editing cloud and atmospheric layer affected pixels from satellite data --- in south Texas test area
[E81-10169] p0266 N81-33556

ATMOSPHERIC PHYSICS
Radiation studies in the atmosphere
p0216 A81-47001
Basic problems of the physics and chemistry of contemporary changes of climate p0216 A81-47002

ATMOSPHERIC RADIATION
A radiometric model of an earth radiation budget radiometer optical system with diffuse-specular surfaces
p0269 A81-41919
Radiation studies in the atmosphere
p0216 A81-47001

ATMOSPHERIC REFRACTION
A 'meteorological' method for calculating vertical refraction p0221 A81-48679

ATMOSPHERIC SCATTERING
Role of multiple scattering in ozone profile retrieval from satellite measurements in the ultraviolet
p0215 A81-45870
Fourier modulus image construction
[AD-A101728] p0264 N81-30723
A study of the effects of the atmosphere on thematic mapper observations
[E81-10056] p0276 N81-33540
Cornell University Remote Sensing Program
[E81-10174] p0255 N81-33560

ATMOSPHERIC SOUNDING
Determination of moisture from NOAA polar orbiting satellite sounding radiances p0243 A81-41158
A new numerical treatment of the source function in the radiative transfer equation --- for vertical atmospheric temperature and humidity profile retrieval from satellite radiance measurements p0269 A81-41916
Remote sensing of atmospheres and oceans; Proceedings of the Interactive Workshop on Interpretation of Remotely Sensed Data, Williamsburg, VA, May 23-25, 1979
p0234 A81-45861
A differential inversion method for high resolution atmospheric remote sensing p0215 A81-45862
Inversion of multiwavelength radiometer measurements by three-dimensional filtering p0271 A81-45873
Remote sounding of atmosphere and ocean for climate research /Appleton Lecture/ p0236 A81-47099
Passive microwave systems
[IAF PAPER 81-88] p0273 A81-47342
Aerosol sounding by means of aircraft-borne optical radar p0217 A81-49431

ATMOSPHERIC TEMPERATURE
Passive microwave techniques for geophysical sensing of the earth from satellites p0270 A81-43071
A 'meteorological' method for calculating vertical refraction p0221 A81-48679

AUSTRALIA
Rainforest species on large-scale color photos
p0198 A81-43536
Australian transition year special studies
[E81-10179] p0210 N81-33565

AUTOCORRELATION
An investigation of the autocorrelation function of radar images p0262 A81-49768

AZIMUTH
Wave orbital velocity, fade and SAR response to azimuth waves p0265 N81-33345

B

BACKSCATTERING
Look direction dependence of radar backscattering cross section for agricultural fields p0199 A81-43741
Role of multiple scattering in ozone profile retrieval from satellite measurements in the ultraviolet
p0215 A81-45870
The wind speed dependency of ocean microwave backscatter p0234 A81-46109
Radar altimeter for ocean remote sensing
[IAF PAPER 81-94] p0236 A81-47348
Altimeter rain detection
[NASA-TM-73291] p0275 N81-29408
A review of volume scatter theories for modeling applications p0265 N81-33347

BANDPASS FILTERS
The effect of sensor bandpass and spectral response in crop stress detection p0199 A81-43737

BARLEY
Infrared-temperature variability in a large agricultural field p0200 A81-45432
Evaluation of spring wheat and barley crop calender models for the 1979 crop year
[E81-10197] p0206 N81-29508
A description of the reformatted spring small grains labeling procedure used in test 2, part 2 of the US/Canada wheat and barley exploratory experiment
[E81-10206] p0207 N81-31597
Weather analysis and interpretation procedures developed for the US/Canada wheat and barley exploratory experiment
[E81-10208] p0207 N81-31599
Analysis of US spring wheat and spring barley periodic ground truth
[E81-10203] p0208 N81-32576

BAROTROPIC FLOW
Method for estimation of ocean current velocity from satellite images p0231 A81-41350

BARREN LAND
Remote sensing and land use planning
p0218 A81-49792

BAY ICE
Categorization of Northern Green Bay ice cover using LANDSAT 1 digital data: A case study
[PB81-200436] p0265 N81-32602

BAYES THEOREM
The multicategory case of the sequential Bayesian pixel selection and estimation procedure
[E81-10182] p0263 N81-29498

BAYS (TOPOGRAPHIC FEATURE)
Remote sensing of coastal pollutants using multispectral data p0233 A81-43245

BAYS (TOPOGRAPHIC FEATURES)
Combined satellite imagery for study of coastal circulation, Onslow Bay, North Carolina
p0233 A81-43250
Using enhanced Landsat images for calibrating real time estuarine water quality models p0250 A81-43252
Bay of Fundy verification of a system for multidate Landsat measurement of suspended sediment
p0250 A81-43254
Infrared imagery for studying the Kara-Bogaz-Gol Bay
p0236 A81-48681

BEACHES
Determination of beach sand parameters using remotely sensed aircraft reflectance data p0217 A81-49346

BEAUFORT SEA (NORTH AMERICA)
Operational use of satellite imagery in the Canadian ice program p0238 A81-49754
Experimental use of real time SAR imagery in support of oil exploration in the Beaufort Sea p0227 A81-49767

READEX FICHE best copy available

Airborne impulse radar sounding of sea ice p0238 A81-49771

Single and multiple parameter microwave signatures of sea ice p0238 A81-49774

Radar detection of sea-ice ridges and icebergs in frozen oceans at incidence angles from 0 deg to 90 deg p0238 A81-49775

Comparative analysis of sea ice features using Side-Looking Airborne Radar (SLAR) and LANDSAT imagery --- Beaufort Sea and Bering Sea [E81-10044] p0241 N81-33539

BEDROCK

Ring structures of Precambrian shields, based on the interpretation of space imagery p0225 A81-42278

Applicability of airborne SAR data to geological mapping p0227 A81-49769

BEETLES

Mountain pine beetle damage surveys with high-altitude panoramic photography p0199 A81-43732

BERING SEA

Comparative analysis of sea ice features using Side-Looking Airborne Radar (SLAR) and LANDSAT imagery --- Beaufort Sea and Bering Sea [E81-10044] p0241 N81-33539

BERMUDA

Calibration validation for the GEOS 3 altimeter p0270 A81-42671

BIBLIOGRAPHIES

Millimeter-wave sensing of the environment: A bibliographic survey [NASA-CR-156879] p0219 N81-32581

A selected bibliography: Remote sensing applications in wildlife management [PB81-215881] p0211 N81-33598

BIOMASS

Assessing winter wheat dry matter production via spectral reflectance measurements p0202 A81-49344

BIRDS

From landforms to avian habitat - A look at topology p0214 A81-43739

The application of remote sensing techniques for an ecological land survey of the snow goose colony at Cape Henrietta Maria, Hudson Bay p0204 A81-49791

Environmental assessment of the Alaskan continental shelf: Reports of principal investigators. Volume 1: Reactors - birds, plankton, littoral, benthos [PB81-196263] p0240 N81-30780

BLIGHT

Vegetable crop management with remote sensing p0198 A81-43540

The effect of sensor bandpass and spectral response in crop stress detection p0199 A81-43737

BOLIVIA

Utilizing GOES imagery to determine convective storm characteristics in data deficient regions p0245 A81-43192

Terrain profiling from Seasat altimetry [NASA-CR-156878] p0222 N81-31604

BOTSWANA

Using Landsat imagery to study the Okavango Swamp, Botswana p0249 A81-43242

BRAZIL

Following oceanographic phenomena on the South Coast of Brazil with remote sensing from orbital distance [INPE-1975-RPE/280] p0240 N81-30498

BRIGHTNESS

Investigation of illumination in the image plane of the receiving optical system for the aerial or spaceborne photography of the world ocean p0232 A81-42553

A temporal/spectral analysis of small grain crops and confusion crops --- North Dakota [E81-10167] p0205 N81-28498

BRIGHTNESS TEMPERATURE

Passive microwave sensing of snow characteristics over land p0246 A81-43207

Survey of in-situ and remote sensing methods for soil moisture determination p0197 A81-43221

Characteristics of microwave emission of significance to satellite remote sensing of soil water p0258 A81-43222

Inversion of multiwavelength radiometer measurements by three-dimensional filtering p0271 A81-45873

Radiometry with nighttime DMSP images in digital form --- satellite earth observations p0260 A81-46402

Airborne microwave radiometer remote sensing of lake ice p0253 A81-48554

Study of the influence of the atmosphere on the performance of an imaging microwave radiometer [ESA-CR(P)-1421] p0275 N81-30342

BUOYS

Drifting buoy data from the tropical Pacific Ocean during NORPAX equatorial test shuttle experiment [PB81-198939] p0240 N81-31807

C

CALIBRATING

Calibration validation for the GEOS 3 altimeter p0270 A81-42671

Does the use of two radiometers correct for irradiance changes during measurements p0272 A81-46196

Advanced synthetic aperture radar for remote sensing p0274 A81-48553

Scatterometer calibration and data correction p0265 N81-33351

CALIFORNIA

Satellite telemetry of hydrologic data in California p0244 A81-43187

Application of remote sensing for California irrigated lands assessment p0213 A81-43261

Texture measurements from Seasat - SAR images for urban land use interpretation p0214 A81-43749

Bulk processing techniques for very large areas - Landsat classification of California p0201 A81-46054

CAMERAS

Skylab in retrospect p0277 A81-43535

CANADA

A review of Canada's present and future remote sensing activities relating to hydrology p0244 A81-43182

Monitoring Canada's water resources in remote regions by satellite telemetry p0244 A81-43188

Bay of Fundy verification of a system for multidate Landsat measurement of suspended sediment p0250 A81-43254

Extravisual damage detection - Defining the standard normal tree p0198 A81-43537

Stratification of Landsat data by uniformity productivity of soils p0259 A81-46042

Canadian Symposium on Remote Sensing, 6th, Halifax, Canada, May 21-23, 1980, Proceedings p0279 A81-49751

The integration of remote sensing in environmental decision making for the Maritimes p0217 A81-49752

Forestry priorities and their implications for the Canadian Remote Sensing Program p0202 A81-49755

The use of satellite imagery as an aid to the Canadian Coast Guard ice operations p0238 A81-49758

Multistage remote sensing in exploratory ecodistrict land classification p0217 A81-49759

Application of temporal Landsat forest digital data for updating the Yukon RRAMS data base using Aries --- Renewable Resources And Management Statistics p0203 A81-49760

Integration and comparison of SAR and MSS data for potato crop area estimation p0203 A81-49766

Applications of remote sensing to construction impact assessment at the Roberts Bank Port, British Columbia p0218 A81-49781

Land use/cover mapping for Halifax County - Remote sensing alternatives p0218 A81-49783

Photointerpretation of fire damage to trees in a ponderosa pine/bunchgrass community p0204 A81-49787

The application of remote sensing techniques for an ecological land survey of the snow goose colony at Cape Henrietta Maria, Hudson Bay p0204 A81-49791

Thermal inertia mapping of some areas of Quebec based on aerial and HCMM satellite data p0204 A81-49799

Geological and terrain analysis of the Annapolis County region of Nova Scotia - An application of digital Landsat, radar and colour infrared data p0227 A81-49802

CANADIAN SPACE PROGRAMS

The Surveillance Satellite Program and the future of microwave remote sensing p0274 A81-49753

CANOPIES (VEGETATION)

Soil moisture applications of the heat capacity mapping mission p0197 A81-43224

On the analysis of remote sensing data to predict selected vegetative variables p0258 A81-43736

The effect of sensor bandpass and spectral response in crop stress detection p0199 A81-43737

A model of plant canopy polarization response p0201 A81-46035

Does the use of two radiometers correct for irradiance changes during measurements p0272 A81-46196

Remote sensing of thermal radiation from an aircraft - An analysis and evaluation of crop-freeze protection methods p0202 A81-46895

Thermal vegetation canopy model studies p0202 A81-49347

Effect of forest canopy closure on incoming solar radiance [E81-10170] p0205 N81-28499

Soil moisture inferences from thermal infrared measurements of vegetation temperatures [E81-10184] p0206 N81-29500

CAPE HATTERAS (NC)

Method for estimation of ocean current velocity from satellite images p0231 A81-41350

Refraction of coastal ocean waves p0235 A81-46113

CAPILLARY WAVES

Sea surface scattering p0241 N81-33344

CARBON DIOXIDE LASERS

Experimental investigation of the physical fundamentals for remote sensing of soil and vegetation moisture by active infrared reflectance spectroscopy using CO2 laser technique [BMFT-FB-W-80-037] p0211 N81-33588

CASPIAN SEA

Soviet remote sensing of the earth's resources and interpretation of space data with reference to the Caspian Sea, Siberia and the Arctic Ocean [IAF PAPER 81-112] p0278 A81-47355

The use of satellite imagery for studying the structural features of the Caspian oil and gas region p0227 A81-48684

An analysis of the data of synchronous measurements from the Meteor satellite and ships at the eastern coast of the Caspian Sea p0237 A81-48687

CATALOGS (PUBLICATIONS)

Interim catalog ground data summary, data acquisition year 1978 [E81-10132] p0209 N81-33546

CELESTIAL GEODESY

Measurement of lengths, angles, and areas on the earth's spheroid p0221 A81-42846

CENSUS

The application of remote sensing techniques for an ecological land survey of the snow goose colony at Cape Henrietta Maria, Hudson Bay p0204 A81-49791

CENTRAL AMERICA

The methodology of CIAT's land resource study of tropical America p0216 A81-46046

CHARGE TRANSFER DEVICES

The use of charge transfer devices for LANDSAT pattern classification [E81-10087] p0266 N81-33544

CHESAPEAKE BAY (US)

Southern Chesapeake Bay circulation and suspended sediment transport analyzed using Landsat imagery p0252 A81-43747

Landsat observations of snowcover depletion and flooding in the Chesapeake Bay area during the winter of 1979 p0253 A81-48942

Remote sensing in biological oceanography p0237 A81-49130

CHINA

Photogrammetry in China p0222 N81-33526

CHLOROPHYLLS

Atmospheric correction of Nimbus-7 Coastal Zone Color Scanner imagery p0271 A81-45879

Airborne simultaneous spectroscopic detection of laser-induced water Raman backscatter and fluorescence from chlorophyll a and other naturally occurring pigments p0253 A81-47647

Use of water Raman emission to correct airborne laser fluorosensor data for effects of water optical attenuation p0253 A81-47676

An analysis of the data of synchronous measurements from the Meteor satellite and ships at the eastern coast of the Caspian Sea p0237 A81-48687

Remote sensing in biological oceanography p0237 A81-49130

Airborne remote sensing of sea surface chlorophyll and temperature along the outer British Columbia coast p0239 A81-49805

CITIES

Urban area update procedures using Landsat data p0214 A81-43733

CITRUS TREES

Remote sensing of thermal radiation from an aircraft An analysis and evaluation of crop-freeze protection methods p0202 A81-46895

CLASSIFICATIONS

Hydrologic land use classification using Landsat p0247 A81-43213

Accuracy evaluation of Landsat digital classification of vegetation in the Great Dismal Swamp p0248 A81-43235

Using Landsat MSS data with soils information to identify wetland habitats p0249 A81-43236

Assessment and classifications of selected Illinois lakes through the application of space technology p0250 A81-43255

Spatial correlation effects upon accuracy of supervised classification of land cover p0213 A81-43534

A comparison of automatic classification algorithms for land use map by remotely sensed data p0215 A81-44701

Parallel processing implementations of a contextual classifier for multispectral remote sensing data p0272 A81-46028

Procedure M - A framework for stratified area estimation --- in multispectral scanner data processing p0201 A81-46036

Maximum likelihood estimation of label imperfection probabilities and its use in the identification of mislabeled patterns --- with application to Landsat MSS data processing p0259 A81-46040

Context distribution estimation for contextual classification of multispectral image data p0259 A81-46041

Stratification of Landsat data by uniformity productivity of soils p0259 A81-46042

Bulk processing techniques for very large areas - Landsat classification of California p0201 A81-46054

Sampling Landsat classifications for crop area estimation p0202 A81-46404

ICAP - An Interactive Cluster Analysis Procedure for analyzing remotely sensed data p0261 A81-49345

Principal components enhancements versus classifications of Landsat images for forestry applications p0203 A81-49782

Interpretation techniques applied to mixed terrains p0218 A81-49788

Role of aerial photographs in classification of Landsat data p0262 A81-49808

A temporal/spectral analysis of small grain crops and confusion crops --- North Dakota [E81-10167] p0205 N81-28498

Development of advanced acreage estimation methods [E81-10160] p0205 N81-29495

Evaluation of multiband, multitemporal, and transformed LANDSAT MSS data for land cover area estimation --- North Central Missouri
[E81-10161] p0219 N81-29486

Nationwide forestry applications program. Analysis of forest classification accuracy
[E81-10183] p0206 N81-29499

Maximum likelihood clustering with dependent feature trees
[E81-10186] p0263 N81-29502

New output improvements for CLASSY
[E81-10189] p0263 N81-29503

Users manual for the US baseline corn and soybean segment classification procedure
[E81-10190] p0206 N81-29504

Estimation of proportions in mixed pixels through their region characterization
[E81-10199] p0264 N81-29510

Evaluation of large area crop estimation techniques using LANDSAT and ground-derived data --- Missouri
[E81-10200] p0206 N81-29511

Classification of wheat: Badhwar profile similarity technique
[E81-10207] p0207 N81-31598

Improved version of the split routine for CLASSY
[E81-10210] p0264 N81-31600

Identifying igneous rocks in an arid environment on aerial photography by photo tone and photo texture
[AD-A102809] p0228 N81-32587

Categorization of Northern Green Bay ice cover using LANDSAT 1 digital data: A case study
[PB81-200438] p0265 N81-32602

A study of the effects of the atmosphere on thematic mapper observations
[E81-10056] p0276 N81-33540

The use of charge transfer devices for LANDSAT pattern classification
[E81-10087] p0266 N81-33544

AgRISTARS: Foreign commodity production forecasting. Program review presentation to level 1, Interagency Coordination Committee
[E81-10168] p0209 N81-33555

Maximum likelihood labeling
[E81-10177] p0267 N81-33563

Maximum likelihood estimation for mixture models
[E81-10178] p0210 N81-33564

CLIMATE

NOAA Climate Program plan
[PB81-193815] p0240 N81-30765

CLIMATOLOGY

The satellite record of the winter of 1978-79 in North America p0246 A81-43203

Basic problems of the physics and chemistry of contemporary changes of climate p0216 A81-47002

Remote sounding of atmosphere and ocean for climate research /Appleton Lecture/ p0236 A81-47099

Climate, the oceans, and remote sensing p0237 A81-49132

CLOUD COVER

Correlation between integral and spectral albedos of clouds over water surfaces p0235 A81-47004

Methods of editing cloud and atmospheric layer affected pixels from satellite data --- in south Texas test area
[E81-10169] p0266 N81-33556

CLOUD PHOTOGRAPHY

Possible applications of communication satellites for research tasks in polar regions
[BMFT-FB-W-80-029] p0267 N81-33587

CLUMPS

ICAP - An Interactive Cluster Analysis Procedure for analyzing remotely sensed data p0261 A81-49345

COAL

Detection of changes in a coal surface mining area by ratioing multidate Landsat digital data p0228 A81-49809

COASTAL ECOLOGY

Landsat classification of coastal wetlands in Texas p0248 A81-43234

Computer-implemented remote sensing techniques for measuring coastal productivity and nutrient transport systems p0250 A81-43243

A report on the use of remote sensing techniques for the supervision of New England coastal salt marshes p0253 A81-48944

Applications of remote sensing to construction impact assessment at the Roberts Bank Port, British Columbia p0218 A81-49781

The application of remote sensing techniques for an ecological land survey of the snow goose colony at Cape Henrietta Maria, Hudson Bay p0204 A81-49791

COASTAL WATER

Satellite aided coastal zone monitoring and vessel traffic system p0231 A81-41755

Microwave radiometer measurement of tidally induced salinity changes off the Georgia coast p0232 A81-42067

Application of remote sensing to monitoring and studying dispersion in ocean dumping p0232 A81-42228

Remote sensing of coastal pollutants using multispectral data p0233 A81-43245

Aerospace remote sensing of the coastal zone for water quality and biotic productivity applications p0233 A81-43246

Digital analysis of Landsat MSS data and application for coastal marine environment p0233 A81-43247

Satellite observations of a geothermal submarine spring off Florida west coast p0233 A81-43248

Applications of Landsat imagery to a coastal inlet stability study p0250 A81-43249

Combined satellite imagery for study of coastal circulation, Onslow Bay, North Carolina p0233 A81-43250

Drift and dispersion studies of ocean-dumped waste using Landsat imagery and current drogues p0233 A81-43539

Refraction of coastal ocean waves p0235 A81-46113

An analysis of the data of synchronous measurements from the Meteor satellite and ships at the eastern coast of the Caspian Sea p0237 A81-48687

Remote sensing in biological oceanography p0237 A81-49130

Airborne remote sensing of sea surface chlorophyll and temperature along the outer British Columbia coast p0239 A81-49805

Current resource mapping and environmental monitoring applications using Landsat MSS data in Scotland p0218 A81-49806

Coastal Oceans Monitoring Satellite System (COMSS) system evaluation study
[ESS/SS-1035] p0239 N81-30168

Following oceanographic phenomena on the South Coast of Brazil with remote sensing from orbital distance
[INPE-1975-RPE/280] p0240 N81-30498

COASTAL ZONE COLOR SCANNER

Atmospheric correction of Nimbus-7 Coastal Zone Color Scanner imagery p0271 A81-45879

Nimbus-7 Coastal-Zone Colour Scanner data processing for Earthnet Experience to date p0235 A81-46919

Remote sensing in biological oceanography p0237 A81-49130

COHERENT SCATTERING

Coherent and incoherent radar scattering from rough surfaces and vegetated areas --- conferences
[ESA-SP-166] p0208 N81-33339

Introduction to the workshop --- on coherent and incoherent radar scattering from rough surfaces and vegetated areas p0276 N81-33340

COLD WATER

A search for cold water rings p0235 A81-46116

COLOMBIA

Position measurements in Colombia by means of satellite observations p0222 N81-33522

COLOR

Colour - The critical photointerpretation element in the identification of rangeland plant communities on colour and colour-infrared aerial photography p0203 A81-49786

COLOR PHOTOGRAPHY

Some results on the investigation of earth resources by aerial and polygon methods --- Russian book p0269 A81-41476

Pseudocolor representation of multispectral aerial images by means of a three-channel projector p0269 A81-41483

Rainforest species on large-scale color photos p0198 A81-43536

The use of CIR and airborne multispectral scanner techniques for wetland soils mapping of highway corridors p0215 A81-46044

Mapping alpine soils using color positive and color infrared photographs p0252 A81-46045

Nimbus-7 Coastal-Zone Colour Scanner data processing for Earthnet Experience to date p0235 A81-46919

COLORADO

Passive microwave sensing of snow characteristics over land p0246 A81-43207

Landsat derived snow cover as an input variable for snow melt runoff forecasting in South Central Colorado p0246 A81-43208

Monitoring snow with microwaves p0246 A81-43209

Mapping irrigated cropland on the High Plains using Landsat p0198 A81-43266

Mountain pine beetle damage surveys with high-altitude panoramic photography p0199 A81-43732

Aerosol formation, transformation, and effects in Denver's emissions plume p0214 A81-44526

Mapping alpine soils using color positive and color infrared photographs p0252 A81-46045

Procedure 1 and forestland classification using Landsat data p0201 A81-46055

Freshwater ice thickness observations using passive microwave sensors p0254 A81-49968

COLUMBIA RIVER BASIN (ID-OR-WA)

Landsat data as a basis for regional environmental assessment within the Columbia Plateau p0218 A81-49798

COMMUNICATION NETWORKS

Data collection and location by satellite - The Argos system
[IAF PAPER 81-80] p0273 A81-47338

COMMUNICATION SATELLITES

Possible applications of communication satellites for research tasks in polar regions
[BMFT-FB-W-80-029] p0267 N81-33587

COMPARATORS

Application of new precision measuring systems for photogrammetric comparators
[BMFT-FB-T-80-134] p0276 N81-32595

COMPUTER COMPATIBLE TAPES

Automatic processing of computer compatible tapes with data from multispectral scanners installed in Landsat satellites p0272 A81-46029

COMPUTER GRAPHICS

Geological interpretation in an interactive mode in automated systems of digital image processing p0225 A81-42289

Hardware aspects of digital mapping p0271 A81-43530

Interactive processing of Landsat image for morphopedological studies p0259 A81-46043

Interactive system for the regional prognosis of raw mineral resources, based on ground-based and satellite imagery data p0227 A81-48691

The sensor image simulator
[AD-A101172] p0275 N81-29512

Interactive digital image processing for terrain data extraction
[AD-A101321] p0264 N81-30499

OVSUP: A program for computer-aided disentanglement of overlapping zones p0222 N81-33525

Photogrammetry in China p0222 N81-33526

Reports on cartography and geodesy, series 1: Original reports, Number 81
[ISSN-0469-4236] p0222 N81-33527

COMPUTER NETWORKS

A top-down approach to the use of simulation in computer system design --- of Edit Processor of Integrated Photogrammetric Instrument Network p0274 A81-48331

COMPUTER PROGRAMMING

OVSUP: A program for computer-aided disentanglement of overlapping zones p0222 N81-33525

COMPUTER PROGRAMS

Machine method for the equalization of average phototone in an aerial photograph field p0257 A81-41482

Nationwide forestry applications program. Analysis of forest classification accuracy
[E81-10183] p0206 N81-29499

Conversion of SPU-Universal disk file to JSC-Universal tape storage: CONVRT user's guide
[E81-10185] p0263 N81-29501

New output improvements for CLASSY
[E81-10189] p0263 N81-29503

Descriptive and sensitivity analyses of WATBALI: A dynamic soil water model
[E81-10193] p0206 N81-29507

Improved version of the split routine for CLASSY
[E81-10210] p0264 N81-31600

Visual enhancement of images of natural resources: Applications in geology
[E81-10181] p0228 N81-32575

COMPUTER SYSTEMS DESIGN

A top-down approach to the use of simulation in computer system design --- of Edit Processor of Integrated Photogrammetric Instrument Network p0274 A81-48331

COMPUTER SYSTEMS PROGRAMS

As-built design specification of the automatic registration system for the cartographic technology laboratory
[E81-10176] p0267 N81-33562

COMPUTER TECHNIQUES

Experience with image combination in multispectral aerial photography p0257 A81-41481

Practical application of the method of empty blocks for the computerized determination of the boundaries of agricultural objects p0197 A81-41489

Main tasks and methods of operational planning of experiments concerning the observations of the earth from space p0277 A81-42288

Rain estimation over several areas of the globe using satellite imagery p0246 A81-43193

Correlation of geologic structure inferred from computer enhanced Landsat imagery with underground water supplies in Arizona p0225 A81-43227

Computer-implemented remote sensing techniques for measuring coastal productivity and nutrient transport systems p0250 A81-43243

An application of Landsat and computer technology to potential water pollution from soil erosion p0250 A81-43253

Bay of Fundy verification of a system for multidate Landsat measurement of suspended sediment p0250 A81-43254

Automation in photogrammetry p0258 A81-43532

Waveband evaluation of proposed thematic mapper in forest cover classification p0199 A81-43738

Land use mapping of Hong Kong from Landsat images An evaluation p0215 A81-45434

Machine processing of remotely sensed data and soil information systems and remote sensing and soil survey; Proceedings of the Sixth Annual Symposium, Purdue University, West Lafayette, IN, June 3-6, 1980 p0200 A81-46026

Parallel processing implementations of a contextual classifier for multispectral remote sensing data p0272 A81-46028

A practical method for the verification of computer-processed Landsat data p0261 A81-48943

Computer analysis of Tiros-N/NOAA-6 satellite data for operational snow cover mapping p0262 A81-49795

The use of charge transfer devices for LANDSAT pattern classification
[E81-10087] p0266 N81-33544

COMPUTERIZED SIMULATION

Simulation of orbital image-sensor geometry p0260 A81-46192

A top-down approach to the use of simulation in computer system design --- of Edit Processor of Integrated Photogrammetric Instrument Network p0274 A81-48331

CONFERENCES

Satellite hydrology; Proceedings of the Fifth Annual William T. Pecora Memorial Symposium on Remote Sensing, Sioux Falls, SD, June 10-15, 1979 p0243 A81-43176

Rainbow 80; Fall Technical Meeting, Niagara Falls, NY, October 7-10, 1980, ASP Technical Papers p0198 A81-43727

Commercial operations in space - 1980-2000, Proceedings of the Eighteenth Goddard Memorial Symposium, Washington, DC, March 27, 28, 1980 p0277 A81-44635

Remote sensing of atmospheres and oceans; Proceedings of the Interactive Workshop on Interpretation of Remotely Senced Data, Williamsburg, VA, May 23-25, 1979 p0234 A81-45861

Machine processing of remotely sensed data and soil information systems and remote sensing and soil survey; Proceedings of the Sixth Annual Symposium, Purdue University, West Lafayette, IN, June 3-6, 1980 p0200 A81-46026

Canadian Symposium on Remote Sensing, 6th, Halifax, Canada, May 21-23, 1980, Proceedings p0279 A81-49751

Field Study for Remote Sensing: An instructor's manual [NASA-CP-2155] p0279 N81-32564

LANDSAT C workshop field/laboratory exercises p0280 N81-32571

Coherent and incoherent radar scattering from rough surfaces and vegetated areas --- conferences [ESA-SP-166] p0208 N81-33339

CONIFERS

Extravisual damage detection - Defining the standard normal tree p0198 A81-43537

Remote sensing aided procedure for conifer growth modeling in the northeastern Sierra Nevada p0199 A81-43740

Thermal vegetation canopy model studies p0202 A81-49347

SAR image response over a conifer regeneration site p0203 A81-49770

Photointerpretation of fire damage to trees in a ponderosa pine/bunchgrass community p0204 A81-49787

CONSTRUCTION

Remote sensing for engineering site selection [AD-A102810] p0219 N81-32586

CONTEXT

Parallel processing implementations of a contextual classifier for multispectral remote sensing data p0272 A81-46028

Context distribution estimation for contextual classification of multispectral image data p0259 A81-46041

CONTINENTAL SHELVES

Environmental assessment of the Alaskan continental shelf. Reports of principal investigators. Volume 1. Reactors - birds, plankton, littoral, benthos [PB81-196263] p0240 N81-30780

CONTOURS

A technique for line extraction from LANDSAT multi-spectral scanner satellite data with some applications of the technique [RAE-TR-81010] p0265 N81-31613

COORDINATE TRANSFORMATIONS

Derivation of formulas for the correlation of coordinate points of different-scale photographs and quasi-photographs p0261 A81-48772

Position measurements in Colombia by means of satellite observations p0222 N81-33522

COORDINATES

Selection of reference zones for the automatic coordinate control of space images p0261 A81-48693

CORN

An assessment of Landsat data acquisition history on identification and area estimation of corn and soybeans p0200 A81-46032

Large area application of a corn hazard model --- Soviet Union [E81-10164] p0205 N81-28497

Users manual for the US baseline corn and soybean segment classification procedure [E81-10190] p0206 N81-29504

AgRISTARS (Agriculture And Resources Inventory Surveys Through Aerospace Remote Sensing) DC/LC (Domestic Crops and Land Rover) project summary crop area estimates for Kansas and Iowa, 1980 [PB81-196900] p0207 N81-30511

Crop area estimates using ground-gathered and LANDSAT data. A multitemporal approach: Missouri, 1979 [PB81-186751] p0208 N81-31614

A project to evaluate moisture stress and phenological factors in corn and soybean areas of southwestern and south-central Minnesota p0209 N81-33554

COSMOS SATELLITES

Evaluation of the 1980 Cosmos program p0278 A81-47829

COST EFFECTIVENESS

Benefits of using airborne remote sensing for Thematic Mapping p0275 A81-49801

CROP CALENDARS

Selected irrigation acreage estimates in northern Florida from Landsat data p0198 A81-43264

Large area application of a corn hazard model --- Soviet Union [E81-10164] p0205 N81-28497

Evaluation of spring wheat and barley crop calender models for the 1979 crop year [E81-10197] p0206 N81-29508

Crop phenology and LANDSAT-based irrigated lands inventory in the high plains: Appendices [E81-10172] p0210 N81-33558

Crop phenology and LANDSAT-based irrigated lands inventory in the high plains [E81-10173] p0210 N81-33559

Australian transition year special studies [E81-10179] p0210 N81-33565

CROP GROWTH

The effect of sensor bandpass and spectral response in crop stress detection p0199 A81-43737

Infrared-temperature variability in a large agricultural field p0200 A81-45432

Stratification of Landsat data by uniformity productivity of soils p0259 A81-46042

Operational applications for analysis of agricultural crops and cultural practices p0203 A81-49756

A temporal/spectral analysis of small grain crops and confusion crops --- North Dakota [E81-10167] p0205 N81-28498

Weather analysis and interpretation procedures developed for the US/Canada wheat and barley exploratory experiment [E81-10208] p0207 N81-31599

Dryland pasture and crop conditions as seen by HCMM [E81-10080] p0209 N81-33542

A crop moisture stress index for large areas and its application in the prediction of spring wheat phenology [E81-10202] p0210 N81-33573

CROP IDENTIFICATION

Accuracy of transmission of spectral contrasts in multispectral aerial photography, with application to problems of object recognition p0257 A81-41479

Results of ground surveys, carried out in conjunction with satellite and aerial studies, of the state of winter wheat on the Kursk test polygon p0197 A81-41485

Determination of the types and state of crops from multispectral aerial photographs p0197 A81-41486

The possibilities of the automated classification of agricultural objects on the basis of their multispectral aerial-spaceborne images p0197 A81-41488

Selected irrigation acreage estimates in northern Florida from Landsat data p0198 A81-43264

An assessment of Landsat data acquisition history on identification and area estimation of corn and soybeans p0200 A81-46032

Crop classification with a Landsat/radar sensor combination p0200 A81-46033

Comparison of Landsat-2 and field spectrometer reflectance signatures of south Texas rangeland plant communities p0201 A81-46034

A model of plant canopy polarization response p0201 A81-46035

Procedure M - A framework for stratified area estimation --- in multispectral scanner data processing p0201 A81-46036

Operational applications for analysis of agricultural crops and cultural practices p0203 A81-49756

Rapeseed - Guidelines for operational monitoring p0203 A81-49784

The discrimination of cereal crops and legumes using reflectance data in the Landsat bandpasses p0204 A81-49794

A simulation of Thematic Mapper performance in an agricultural application p0204 A81-49810

Evaluation of Thematic Mapper bands - A first step in feature selection p0205 A81-49815

A description of the reformatted spring small grains labeling procedure used in test 2, part 2 of the US/Canada wheat and barley exploratory experiment [E81-10206] p0207 N81-31597

Classification of wheat: Badhwar profile similarity technique [E81-10207] p0207 N81-31598

Scatterometer measurements on crop and soil surfaces p0208 N81-33349

CROP INVENTORIES

Practical application of the method of empty blocks for the computerized determination of the boundaries of agricultural objects p0197 A81-41489

A multistage mapping approach for an irrigated croplands inventory p0198 A81-43262

Crop reporting from space - Problems, promises, potential [AAS 80-062] p0200 A81-44637

An assessment of Landsat data acquisition history on identification and area estimation of corn and soybeans p0200 A81-46032

Procedure M - A framework for stratified area estimation --- in multispectral scanner data processing p0201 A81-46036

Sampling Landsat classifications for crop area estimation p0202 A81-46404

Remote sensing in development --- for developing nations p0279 A81-48936

Integration and comparison of SAR and MSS data for potato crop area estimation p0203 A81-49766

Development of advanced acreage estimation methods [E81-10160] p0205 N81-29495

The multicategory case of the sequential Bayesian pixel selection and estimation procedure [E81-10182] p0263 N81-29498

Users manual for the US baseline corn and soybean segment classification procedure [E81-10190] p0206 N81-29504

Estimation of proportions in mixed pixels through their region characterization [E81-10199] p0264 N81-29510

Crop area estimation using ground-gathered and sampled LANDSAT data [PB81-192783] p0207 N81-30507

Atmospheric nitric acid and chlorofluoromethane 11 from interferometric spectra obtained at the Observatoire du Pic du Midi [AERONOMICA-ACTA-A-227-1980] p0219 N81-30656

Crop area estimates using ground-gathered and LANDSAT data. A multitemporal approach: Missouri, 1979 [PB81-186751] p0208 N81-31614

Analysis of US spring wheat and spring barley periodic ground truth [E81-10203] p0208 N81-32576

Yield Model Development (YMD) implementation plan for fiscal years 1981 and 1982 [E81-10211] p0208 N81-32577

AgRISTARS: Foreign commodity production forecasting. Program review presentation to level 1, Interagency Coordination Committee [E81-10168] p0209 N81-33555

Maximum likelihood estimation for mixture models [E81-10178] p0210 N81-33564

Australian transition year special studies [E81-10179] p0210 N81-33565

CROP VIGOR

Some results on the investigation of earth resources by aerial and polygon methods --- Russian book p0269 A81-41476

Results of ground surveys, carried out in conjunction with satellite and aerial studies, of the state of winter wheat on the Kursk test polygon p0197 A81-41485

Determination of the types and state of crops from multispectral aerial photographs p0197 A81-41486

Vegetable crop management with remote sensing p0198 A81-43540

Relating ground level reflected radiance measurements in the Landsat MSS bandpasses to satellite altitudes p0271 A81-43735

A model of plant canopy polarization response p0201 A81-46035

Meteorological satellite data: A tool to describe the health of the world's agriculture [E81-10204] p0207 N81-31596

Weather analysis and interpretation procedures developed for the US/Canada wheat and barley exploratory experiment [E81-10208] p0207 N81-31599

CYCLONES

The occurrence of vertical tilt in tropical cyclones p0238 A81-49656

Eastern North Pacific tropical cyclones of 1980 p0238 A81-49657

D

DAMAGE ASSESSMENT

Extravisual damage detection - Defining the standard normal tree p0198 A81-43537

Mountain pine beetle damage surveys with high-altitude panoramic photography p0199 A81-43732

Photointerpretation of fire damage to trees in a ponderosa pine/bunchgrass community p0204 A81-49787

DAMS

Remote sensing of bank erosion along the Missouri River, South Dakota p0213 A81-43263

Use of Landsat images in the monitoring and study of the LG 2 reservoir during the filling period p0254 A81-49797

DATA ACQUISITION

Aerial data acquisition systems using test-ground polygons p0269 A81-41477

The methodology of CIAT's land resource study of tropical America p0216 A81-46046

First results of the Intercosmos satellite IK-21 [IAF PAPER 81-214] p0274 A81-47409

Acquisition and preprocessing of images collected by future European Space Agency satellites p0263 A81-49814

Scatterometer calibration and data correction p0265 N81-33351

DATA BASES

Development of a digital data base for reflectance-related soil information p0201 A81-46051

Evaluation of remote sensing data for input into Hydrological Simulation Program-FORTRAN (HSPF) --- modeling the Occoquan watershed in Virginia using LANDSAT imagery for parameter estimation [PB81-209561] p0255 N81-33593

DATA COLLECTION PLATFORMS
Remote sensing of oceanic phytoplankton - Present capabilities and future goals p0232 A81-42215
The GOES data collection system p0257 A81-43185
Adapting GOES DCS for use by Corps of Engineers --- for flood control p0244 A81-43186
U.S. geological survey application of satellite telemetry for the support of hydrologic data collection p0258 A81-43189
Advanced technology for satellite data collection systems p0270 A81-43190
Data collection and location by satellite - The Argos system [IAF PAPER 81-80] p0273 A81-47338
Physical and technical foundations for the development of subsatellite systems for the exploration of natural earth resources [IAF PAPER 81-101] p0278 A81-47350
Meteorological applications of the ARGOS system [IAF PAPER 81-121] p0273 A81-47360
DATA COMPRESSION
Comparative experimental study on the use of original and compressed multispectral Landsat data of the Bayuda desert p0262 A81-49813
DATA CONVERSION ROUTINES
Conversion of SPU-Universal disk file to JSC-Universal tape storage: CONVRT user's guide [E81-10185] p0263 N81-29501
DATA CORRELATION
Correlation of geologic structure inferred from computer enhanced Landsat imagery with underground water supplies in Arizona p0225 A81-43227
Correlation techniques and devices --- for photogrammetry p0258 A81-43531
An investigation of the autocorrelation function of radar images p0262 A81-49768
As-built design specification of the automatic registration system for the cartographic technology laboratory [E81-10176] p0267 N81-33562
DATA MANAGEMENT
Interim catalog ground data summary. data acquisition year 1978 [E81-10132] p0209 N81-33546
DATA PROCESSING
A review of Canada's present and future remote sensing activities relating to hydrology p0244 A81-43182
Machine processing of remotely sensed data and soil information systems and remote sensing and soil survey. Proceedings of the Sixth Annual Symposium, Purdue University, West Lafayette, IN, June 3-6, 1980 p0200 A81-46026
Automatic processing of computer compatible tapes with data from multispectral scanners installed in Landsat satellites p0272 A81-46029
The Lulea Image Processing System /LIPS/ - A versatile approach to earth resources data processing p0272 A81-46030
A practical method for the verification of computer-processed Landsat data p0261 A81-48943
Evaluation of multiband, multitemporal, and transformed LANDSAT MSS data for land cover area estimation --- North Central Missouri [E81-10161] p0219 N81-29496
Maximum likelihood clustering with dependent feature trees [E81-10186] p0263 N81-29502
Computer program documentation user information for the RSO-tape print program (RSOPRNT) [E81-10198] p0264 N81-29509
Reports on cartography and geodesy. series 1: Original reports, Number 81 [ISSN-0469-4236] p0222 N81-33527
DATA PROCESSING EQUIPMENT
Hardware aspects of digital mapping p0271 A81-43530
DATA REDUCTION
Regression techniques for oceanographic parameter retrieval using space-borne microwave radiometry p0239 A81-49967
Reduction and analysis of satellite magnetometer data p0275 N81-29482
An analysis of haze effects on LANDSAT multispectral scanner data [E81-10162] p0263 N81-29497
Knowledge-based image analysis [AD-A101319] p0264 N81-30852
Methods of editing cloud and atmospheric layer affected pixels from satellite data --- in south Texas test area [E81-10169] p0266 N81-33556
DATA SAMPLING
Comparison of sampling procedures and data analysis for a land-use and land-cover map p0213 A81-43533
DATA SYSTEMS
Oceanic Satellite Data Distribution System p0231 A81-41996
The GOES data collection system p0257 A81-43185
Adapting GOES DCS for use by Corps of Engineers --- for flood control p0244 A81-43186
Requirements on the data/information system --- of satellite systems for earth resources observation p0278 A81-48527
DATA TRANSMISSION
Program and instrumentation of the satellite experiment Bulgaria-1300 II [IAF PAPER 81-91] p0273 A81-47345
DEFOLIATION
Effect of forest canopy closure on incoming solar radiance [E81-10170] p0205 N81-28499
An investigation of vegetation and other Earth resource/feature parameters using LANDSAT and other remote sensing data. 1: LANDSAT. 2: Remote sensing of volcanic emissions [E81-10081] p0208 N81-33543
DELTA MODULATION
Application of delta modulation in on-board and ground video data processing systems for the purposes of remote sensing [IAF PAPER 81-102] p0260 A81-47351
DEMOGRAPHY
The application of remote sensing techniques for an ecological land survey of the snow goose colony at Cape Henrietta Maria, Hudson Bay p0204 A81-49791
DESERTS
Remote methods and desert conservation --- Russian book p0213 A81-43523
Angular anisotropy of reflection from various types of underlying surface. I - Snow cover. II - Desert p0260 A81-47007
Comparative experimental study on the use of original and compressed multispectral Landsat data of the Bayuda desert p0262 A81-49813
Terrain profiling from Seasat altimetry [NASA-CR-156878] p0222 N81-31604
Landform-vegetation relationships in the northern Chihuahuan Desert [AD-A102896] p0208 N81-32588
DEVELOPING NATIONS
Hydrogeologic interpretations of Landsat imagery in arid zones of South and West Africa p0248 A81-43229
Using Landsat imagery to study the Okavango Swamp, Botswana p0249 A81-43242
Remote sensing in development --- for developing nations p0279 A81-48936
DICIDUOUS TREES
Thermal vegetation canopy model studies p0202 A81-49347
DIFFRACTION PATTERNS
Fourier modulus image construction [AD-A101728] p0264 N81-30723
DIFFUSE RADIATION
Effect of forest canopy closure on incoming solar radiance [E81-10170] p0205 N81-28499
DIGITAL DATA
Hardware aspects of digital mapping p0271 A81-43530
Water quality mapping from Landsat digital data p0252 A81-45429
Use of Landsat digital data to assist in mapping soils on Arizona rangelands p0201 A81-46047
Development of a digital data base for reflectance-related soil information p0201 A81-46051
Radiometry with nighttime DMSP images in digital form --- satellite earth observations p0260 A81-46402
Application of temporal Landsat forest digital data for updating the Yukon RRAMS data base using Aries --- Renewable Resources And Management Statistics p0203 A81-49760
An investigation of the autocorrelation function of radar images p0262 A81-49768
Research on assessment of the recreational value of forests using Landsat digital data p0203 A81-49785
Detection of changes in a coal surface mining area by ratioing multidate Landsat digital data p0228 A81-49809
Categorization of Northern Green Bay ice cover using LANDSAT 1 digital data: A case study [PB81-200436] p0265 N81-32602
Methods of editing cloud and atmospheric layer affected pixels from satellite data --- in south Texas test area [E81-10169] p0266 N81-33556
DIGITAL SIMULATION
The sensor image simulator [AD-A101172] p0275 N81-29512
DIGITAL TECHNIQUES
A rectification technique for digital orthophoto production p0257 A81-41057
Geological interpretation in an interactive mode in automated systems of digital image processing p0225 A81-42289
Flood applications of satellite imagery p0247 A81-43217
Ground water exploration programs in Africa p0226 A81-43230
Accuracy evaluation of Landsat digital classification of vegetation in the Great Dismal Swamp p0248 A81-43235
Digital analysis of Landsat MSS data and application for coastal marine environment p0233 A81-43247
Lake Ontario dynamics and water quality observations using thematically enhanced Landsat data p0251 A81-43257
Hardware aspects of digital mapping p0271 A81-43530
Automation in photogrammetry p0258 A81-43532
Wetland mapping from digitized aerial photography p0252 A81-43549
Rainbow 80: Fall Technical Meeting, Niagara Falls, NY, October 7-10, 1980, ASP Technical Papers p0198 A81-43727
Urban area update procedures using Landsat data p0214 A81-43733
Manual versus digital Landsat analysis for modeling river flooding p0252 A81-43745
Application of digital terrain data to quantify and reduce the topographic effect on Landsat data p0259 A81-45433
Land use mapping of Hong Kong from Landsat images An evaluation p0215 A81-45434
Procedures for change detection using Landsat digital data p0215 A81-45437
Automatic processing of computer compatible tapes with data from multispectral scanners installed in Landsat satellites p0272 A81-46029
The Lulea Image Processing System /LIPS/ - A versatile approach to earth resources data processing p0272 A81-46030
Radar image preprocessing --- of SEASAT-A SAR data p0272 A81-46038
Lineament mapping in northern Sweden from Landsat images using orthogonal image transforms p0226 A81-46039
Inventory estimation on the massively parallel processor --- from satellite based images p0259 A81-46052
Bulk processing techniques for very large areas - Landsat classification of California p0201 A81-46054
Change vector analysis - An approach for detecting forest changes with Landsat p0202 A81-46056
Manual versus digital Landsat analysis for delineating river flooding p0252 A81-46405
Applications of remote sensing to construction impact assessment at the Roberts Bank Port, British Columbia p0218 A81-49781
Digital enhancements for vegetation mapping in a subarctic environment p0262 A81-49793
Generation and use of digital elevation data for large areas p0221 A81-49811
Interactive digital image processing for terrain data extraction [AD-A101321] p0264 N81-30499
Development of alternative data analysis techniques for improving the accuracy and specificity of natural resource inventories made with remote sensing data p0266 N81-33551
DISASTERS
Potential for detection of natural disasters via Meteosat [IAF PAPER 81-263] p0216 A81-47430
Analysis of the November 23, 1980 earthquake as a design basis for satellite emergency communication [IAF PAPER 81-269] p0216 A81-47433
DISPLAY DEVICES
An evaluation of detail in dynamic visual displays [AD-A103378] p0222 N81-33578
DOPPLER EFFECT
Differential Doppler experiment /DIDEX/ for geodetic applications p0221 A81-47938
Optimization of Doppler measurements in the satellite network of Eastern Europe p0221 A81-48678
DOPPLER NAVIGATION
Position measurements in Colombia by means of satellite observations p0222 N81-33522
DOPPLER RADAR
Satellite To Satellite Doppler Tracking (SSDT) for mapping of the Earth's gravity field [NASA-CR-164722] p0223 N81-31601
DRAINAGE
A technique for improved assessment of flow resistance characteristics of natural wetlands using Landsat data p0249 A81-43241
Remote sensing for engineering site selection [AD-A102810] p0219 N81-32586
DRAINAGE PATTERNS
A technique for improved assessment of flow resistance characteristics of natural wetlands using Landsat data p0249 A81-43241
Cornell University Remote Sensing Program [E81-10174] p0255 N81-33560
DREDGED MATERIALS
Landsat data for regulatory permit monitoring p0247 A81-43214
DROUGHT
The environmental vegetation index: A tool potentially useful for arid land management --- Texas and Mexico, plant growth stress due to water deficits [E81-10191] p0206 N81-29506
DUMPING
Application of remote sensing to monitoring and studying dispersion in ocean dumping p0232 A81-42228
Drift and dispersion studies of ocean-dumped waste using Landsat imagery and current drogues p0233 A81-43539

E

EARTH ALBEDO
The effect of angular distribution models on the estimation of the earth's albedo p0269 A81-41915
EARTH CRUST
Gravimetric studies of the earth's crust in the oceans --- Russian book p0221 A81-43524
Magnetic space-based field measurements [AAS PAPER 81-077] p0272 A81-46241

NASA selects scientific investigations for Earth dynamics studies [NASA-NEWS-RELEASE-81-129] p0228 N81-29143

Satellite To Satellite Doppler Tracking (SSDT) for mapping of the Earth's gravity field [NASA-CR-164722] p0223 N81-31601

Investigation of Antarctic crust and upper mantle using Magsat and other geophysical data [E81-10113] p0222 N81-32574

EARTH HYDROSPHERE

Preliminary survey of HCMM satellite thermal imagery as applied to hydrospherics p0252 A81-43746

EARTH OBSERVATIONS (FROM SPACE)

Passive microwave techniques for geophysical sensing of the earth from satellites p0270 A81-43071

Radar methods for studying the earth --- Russian book p0273 A81-46924

EARTH ORBITS

Simulation of orbital image-sensor geometry p0260 A81-46192

EARTH RADIATION BUDGET EXPERIMENT

The effect of angular distribution models on the estimation of the earth's albedo p0269 A81-41915

A radiometric model of an earth radiation budget radiometer optical system with diffuse-specular surfaces p0269 A81-41919

EARTH RESOURCES

Large scale human benefits of space industrialization p0277 A81-42513

EARTH SURFACE

Concerning the possibility of improving the spectroradiometric accuracy of remote sensing of the earth by means of multispectral band scanners p0270 A81-42285

Angular anisotropy of reflection from various types of underlying surface I - Snow cover II - Desert p0260 A81-47007

Selection of reference zones for the automatic coordinate control of space images p0261 A81-48693

Geometric correction of scanner images of the earth's surface p0261 A81-48694

Experimental investigation of the physical fundamentals for remote sensing of soil and vegetation moisture by active infrared reflectance spectroscopy using CO2 laser technique [BMFT-FB-W-80-037] p0211 N81-33588

EARTHQUAKES

Space research on seismic regions p0225 A81-42280

Analysis of the November 23, 1980 earthquake as a design basis for satellite emergency communication [IAF PAPER 81-269] p0216 A81-47433

ECOLOGY

Remote sensing of oceanic phytoplankton - Present capabilities and future goals p0232 A81-42215

Remote methods and desert conservation --- Russian book p0213 A81-43523

Multistage remote sensing in exploratory ecodistrict land classification p0217 A81-49759

The application of remote sensing techniques for an ecological land survey of the snow goose colony at Cape Henrietta Maria, Hudson Bay p0204 A81-49791

ECONOMIC DEVELOPMENT

What does space remote sensing provide p0278 A81-47826

Space Benefits: The secondary application of aerospace technology in other sectors of the economy [NASA-CR-164733] p0279 N81-32086

ECONOMIC FACTORS

Efficiency criteria of space systems for studying the earth's natural resources p0277 A81-42287

Large scale human benefits of space industrialization p0277 A81-42513

ECOSYSTEMS

Simulation modeling of estuarine ecosystems p0243 A81-42229

Dynamic ecosystem of the Aral Basin studied from satellite imagery p0217 A81-48682

EDITING

A top-down approach to the use of simulation in computer system design --- of Edit Processor of Integrated Photogrammetric Instrument Network p0274 A81-48331

EDUCATION

Field Study for Remote Sensing: An instructor's manual [NASA-CP-2155] p0279 N81-32564

Why surface-truth field study is needed in remote-sensing instruction p0280 N81-32567

ELECTRIC POWER PLANTS

Environmental measurements of power plant cooling tower and stack plumes [DOE/EV-02463/6] p0219 N81-30695

ELECTROMAGNETIC NOISE

Geomagnetic field mapping from a satellite: Spatial power spectra of the geomagnetic field at various satellite altitudes relative to natural noise sources and instrument noise [PUBL-1810] p0275 N81-29480

ELEVATION

Use of elevation models for landform analysis by Seasat-SAR imagery [IAF PAPER 81-98] p0260 A81-47349

EMERGENCIES

Analysis of the November 23, 1980 earthquake as a design basis for satellite emergency communication [IAF PAPER 81-269] p0216 A81-47433

ENERGY BUDGETS

Thermal vegetation canopy model studies p0202 A81-49347

ENERGY SPECTRA

Spatial evolution of ocean wave spectra p0235 A81-46112

ENVIRONMENT EFFECTS

Basic problems of the physics and chemistry of contemporary changes of climate p0216 A81-47002

Applications of remote sensing to construction impact assessment at the Roberts Bank Port, British Columbia p0218 A81-49781

ENVIRONMENT MODELS

Simulation modeling of estuarine ecosystems p0243 A81-42229

ENVIRONMENT PROTECTION

Remote methods and desert conservation --- Russian book p0213 A81-43523

ENVIRONMENTAL MONITORING

Environmental satellites p0277 A81-42231

Satellite hydrology; Proceedings of the Fifth Annual William T. Pecora Memorial Symposium on Remote Sensing, Sioux Falls, SD, June 10-15, 1979 p0243 A81-43176

Corps of Engineers utilization of satellites for hydrologic purposes p0244 A81-43180

The GOES data collection system p0257 A81-43185

Monitoring Canada's water resources in remote regions by satellite telemetry p0244 A81-43188

Landsat data for regulatory permit monitoring p0247 A81-43214

Remote methods and desert conservation --- Russian book p0213 A81-43523

Use of remote sensing in landscape stratification for environmental impact assessment p0214 A81-43748

Commercial operations in space - 1980-2000; Proceedings of the Eighteenth Goddard Memorial Symposium, Washington, DC, March 27, 28, 1980 p0277 A81-44635

Procedures for change detection using Landsat digital data p0215 A81-45437

First Shuttle payload loading to begin p0273 A81-46461

Soviet remote sensing of the earth's resources and interpretation of space data with reference to the Caspian Sea, Siberia and the Arctic Ocean [IAF PAPER 81-112] p0278 A81-47355

Monitoring of snow covered area using satellite data [IAF PAPER 81-114] p0253 A81-47356

Potential for detection of natural disasters via Meteosat [IAF PAPER 81-263] p0216 A81-47430

Analysis of the November 23, 1980 earthquake as a design basis for satellite emergency communication [IAF PAPER 81-269] p0216 A81-47433

A report on the use of remote sensing techniques for the supervision of New England coastal salt marshes p0253 A81-48944

International monitoring from space /Problems of international law/ --- Russian book p0279 A81-49468

Canadian Symposium on Remote Sensing, 6th, Halifax, Canada, May 21-23, 1980, Proceedings p0279 A81-49751

The integration of remote sensing in environmental decision making for the Maritimes p0217 A81-49752

The Surveillance Satellite Program and the future of microwave remote sensing p0274 A81-49753

Present state of remote sensing development in Poland p0279 A81-49763

Current resource mapping and environmental monitoring applications using Landsat MSS data in Scotland p0218 A81-49806

Detection of changes in a coal surface mining area by ratioing multidate Landsat digital data p0228 A81-49809

Use of satellite pictures for agriculture p0205 N81-28120

A remote sensing technique to monitor Cladophora in the Great Lakes [PB81-173841] p0254 N81-29520

Conceptual design of an automated mapping satellite System (MAPSAT) [PB81-185555] p0264 N81-29522

Environmental measurements of power plant cooling tower and stack plumes [DOE/EV-02463/6] p0219 N81-30695

NOAA Climate Program plan [PB81-193815] p0240 N81-30765

Lakewide monitoring of suspended solids using satellite data --- Lake Superior water reclamation p0254 N81-33552

ENVIRONMENTAL SURVEYS

Use of remote sensing in landscape stratification for environmental impact assessment p0214 A81-43748

EQUATORIAL REGIONS

Drifting buoy data from the tropical Pacific Ocean during NORPAX equatorial test shuttle experiment [PB81-198939] p0240 N81-31807

ERROR ANALYSIS

Accuracy of transmission of spectral contrasts in multispectral aerial photography, with application to problems of object recognition p0257 A81-41479

Insights into errors of SMS-inferred GATE convective rainfall p0243 A81-42095

Spatial correlation effects upon accuracy of supervised classification of land cover p0213 A81-43534

Maximum likelihood estimation of label imperfection probabilities and its use in the identification of mislabeled patterns --- with application to Landsat MSS data processing p0259 A81-46040

ERS-1 (ESA SATELLITE)

The first ESA remote sensing satellite /ERS/ - The programme and the system [IAF PAPER 81-90] p0236 A81-47344

Acquisition and preprocessing of images collected by future European Space Agency satellites p0263 A81-49814

ESA SATELLITES

The remote sensing satellite program of the European Space Agency p0278 A81-49762

ESTUARIES

Simulation modeling of estuarine ecosystems p0243 A81-42229

Using enhanced Landsat images for calibrating real time estuarine water quality models p0250 A81-43252

Remote sensing of dinoflagellate blooms in a turbid estuary p0251 A81-43538

EUROPE

The European SAR-Project Convair 580 p0273 A81-46679

Satellite observations of England and north-western Europe p0217 A81-49174

EUTROPHICATION

Trophic state determination for shallow coastal lakes from Landsat imagery p0251 A81-43259

EVAPORATION

Descriptive and sensitivity analyses of WATBALI: A dynamic soil water model [E81-10193] p0206 N81-29507

EVAPOTRANSPIRATION

Modeling the terrestrial hydrology for the global atmosphere - The future role of satellite data p0245 A81-43197

Improvements in lake volume predictions using Landsat data p0248 A81-43237

Agricultural water demand prediction using remote sensing technology for Georgia resource management [PB81-184137] p0207 N81-30508

A crop moisture stress index for large areas and its application in the prediction of spring wheat phenology [E81-10202] p0210 N81-33573

EVERGALDES (FL)

Landsat hydrobiological classification for an inland fresh water marsh within Everglades National Park p0249 A81-43238

F

FADING

Wave orbital velocity, fade and SAR response to azimuth waves p0265 N81-33345

FARM CROPS

Spatial correlation effects upon accuracy of supervised classification of land cover p0213 A81-43534

Operational applications for analysis of agricultural crops and cultural practices p0203 A81-49756

Rapeseed - Guidelines for operational monitoring p0203 A81-49784

Evaluation of large area crop estimation techniques using LANDSAT and ground-derived data --- Missouri [E81-10200] p0206 N81-29511

Crop area estimation using ground-gathered and sampled LANDSAT data [PB81-192783] p0207 N81-30507

AgRISTARS: Foreign commodity production forecasting. Program review presentation to level 1, Interagency Coordination Committee [E81-10168] p0209 N81-33555

Crop phenology and LANDSAT-based irrigated lands inventory in the high plains: Appendices [E81-10172] p0210 N81-33558

Crop phenology and LANDSAT-based irrigated lands inventory in the high plains [E81-10173] p0210 N81-33559

FARMLANDS

Pseudocolor representation of multispectral aerial images by means of a three-channel projector p0269 A81-41483

A multistage mapping approach for an irrigated croplands inventory p0198 A81-43262

Remote sensing of bank erosion along the Missouri River, South Dakota p0213 A81-43263

Mapping irrigated lands in Western Kansas from Landsat p0198 A81-43265

Mapping irrigated cropland on the High Plains using Landsat p0198 A81-43266

Look direction dependence of radar backscattering cross section for agricultural fields p0199 A81-43741

Infrared-temperature variability in a large agricultural field p0200 A81-45432

Remote sensing and land use planning p0218 A81-49792

Evaluation of gravimetric ground truth soil moisture data collected for the agricultural soil moisture experiment, 1978 Colby, Kansas, aircraft mission [E81-10114] p0206 N81-29494

Satellite monitoring of snow extent and condition in agricultural, transitional, and forested land cover areas [PB81-188625] p0254 N81-30509

Dryland pasture and crop conditions as seen by HCMM
[E81-10080] p0209 N81-33542
Measurement of soil moisture trends with airborne scatterometers --- Texas
[E81-10088] p0209 N81-33545
A project to evaluate moisture stress and phenological factors in corn and soybean areas of southwestern and south-central Minnesota p0209 N81-33554
Crop phenology and LANDSAT-based irrigated lands inventory in the high plains: Appendices
[E81-10172] p0210 N81-33558
Crop phenology and LANDSAT-based irrigated lands inventory in the high plains
[E81-10173] p0210 N81-33559

FEDERAL BUDGETS
NASA authorization, 1982, volume 4
[GPO-79-432-VOL-4] p0279 N81-31030

FIELD OF VIEW
Infrared-temperature variability in a large agricultural field p0200 A81-45432
The characteristics of combining devices with different survey bands aboard a satellite p0274 A81-48689

FISHERIES
Remote sensing in biological oceanography p0237 A81-49130
Meteosat experience in assisting commercial fishing p0239 A81-49807

FISHES
NOAA Climate Program plan
[PB81-193815] p0240 N81-30765

FLAGELLATA
Remote sensing of dinoflagellate blooms in a turbid estuary p0251 A81-43538

FLATS (LANDFORMS)
Infrared imagery for studying the Kara-Bogaz-Gol Bay p0236 A81-48681

FLOOD CONTROL
Adapting GOES DCS for use by Corps of Engineers --- for flood control p0244 A81-43186

FLOOD PLAINS
Use of Landsat images in the monitoring and study of the LG 2 reservoir during the filling period p0254 A81-49797

FLOOD PREDICTIONS
The use of satellite data in predicting spring flow in the basins of the upper Ob' and upper Enisei p0243 A81-41723
Satellite applications in river and flood forecasting p0243 A81-43178
A satellite derived technique for estimating rainfall from thunderstorms and hurricanes p0244 A81-43191
A statistical approach to rainfall estimation using satellite data p0245 A81-43198
Improving stream flow estimates through the use of Landsat p0247 A81-43216
Manual versus digital Landsat analysis for modeling river flooding p0252 A81-43745

FLOODS
Flood applications of satellite imagery p0247 A81-43217
Assessing the Red River of the North 1978 flooding from NOAA satellite data p0248 A81-43219
A preliminary analysis of SAR mapping of the Manitoba flood, May 1979 p0248 A81-43220
Manual versus digital Landsat analysis for modeling river flooding p0252 A81-43745
Manual versus digital Landsat analysis for delineating river flooding p0252 A81-46405
Landsat observations of snowcover depletion and flooding in the Chesapeake Bay area during the winter of 1979 p0253 A81-48942

FLORIDA
Improvements in lake volume predictions using Landsat data p0249 A81-43237
A technique for improved assessment of flow resistance characteristics of natural wetlands using Landsat data p0249 A81-43241
Satellite observations of a geothermal submarine spring off Florida west coast p0233 A81-43248
Applications of Landsat imagery to a coastal inlet stability study p0250 A81-43249
Using enhanced Landsat images for calibrating real time estuarine water quality models p0250 A81-43252
Comparison of sampling procedures and data analysis for a land-use and land-cover map p0213 A81-43533
Vegetable crop management with remote sensing p0198 A81-43540
Remote sensing of thermal radiation from an aircraft - An analysis and evaluation of crop-freeze protection methods p0202 A81-46895

FLUORESCENCE
Airborne simultaneous spectroscopic detection of laser-induced water Raman backscatter and fluorescence from chlorophyll a and other naturally occurring pigments p0253 A81-47647
Use of water Raman emission to correct airborne laser fluorosensor data for effects of water optical attenuation p0253 A81-47676
Compact and highly sensitive fluorescence lidar for oceanographic measurements p0237 A81-49378

FLUOROHYDROCARBONS
Atmospheric nitric acid and chlorofluoromethane 11 from interferometric spectra obtained at the Observatoire du Pic du Midi
[AERONOMICA-ACTA-A-227-1980] p0219 N81-30656

FOREST FIRES
Photointerpretation of fire damage to trees in a ponderosa pine/bunchgrass community p0204 A81-49787

FOREST MANAGEMENT
Extravisual damage detection - Defining the standard normal tree p0198 A81-43537
Remote sensing aided procedure for conifer growth modeling in the northeastern Sierra Nevada p0199 A81-43740
Change vector analysis - An approach for detecting forest changes with Landsat p0202 A81-46056
The space engineering use efficiency for forest study
[IAF PAPER 81-108] p0202 A81-47354
Forestry priorities and their implications for the Canadian Remote Sensing Program p0202 A81-49755
The application of thermography for locating potential frost pockets in forest cutovers p0204 A81-49789

FORESTS
Spatial correlation effects upon accuracy of supervised classification of land cover p0213 A81-43534
Waveband evaluation of proposed thematic mapper in forest cover classification p0199 A81-43738
Use of Seasat satellite radar imagery for the detection of standing water beneath forest vegetation p0199 A81-43743
A photo interpretation approach to forest regrowth monitoring using side-looking airborne radar - Grant County, Oregon p0200 A81-45428
Bulk processing techniques for very large areas - Landsat classification of California p0201 A81-46054
Procedure 1 and forestland classification using Landsat data p0201 A81-46055
Thermal vegetation canopy model studies p0202 A81-49347
Application of temporal Landsat forest digital data for updating the Yukon RRAMS data base using Aries --- Renewable Resources And Management Statistics p0203 A81-49760
Present state of remote sensing development in Poland p0279 A81-49763
Technical aspects of forest inventory demonstrations using Landsat data - Projects in the Pacific Northwest States p0203 A81-49764
SAR image response over a conifer regeneration site p0203 A81-49770
Principal components enhancements versus classifications of Landsat images for forestry applications p0203 A81-49782
Research on assessment of the recreational value of forests using Landsat digital data p0203 A81-49785
Effect of forest canopy closure on incoming solar radiance
[E81-10170] p0205 N81-28499
Nationwide forestry applications program. Analysis of forest classification accuracy
[E81-10183] p0206 N81-29499
Interactive digital image processing for terrain data extraction
[AD-A101321] p0264 N81-30499
Agricultural water demand prediction using remote sensing technology for Georgia resource management
[PB81-184137] p0207 N81-30508
Satellite monitoring of snow extent and condition in agricultural, transitional, and forested land cover areas
[PB81-188625] p0254 N81-30509
An investigation of vegetation and other Earth resource/feature parameters using LANDSAT and other remote sensing data. 1: LANDSAT. 2: Remote sensing of volcanic emissions
[E81-10081] p0209 N81-33543
Evaluation of LANDSAT data analysis for forest survey --- northeastern aspen-birch survey unit in Minnesota - Carlton County
[E81-10175] p0210 N81-33561

FRAME PHOTOGRAPHY
Analysis of the geometry of a frame photograph p0221 A81-42554

FRANCE
Interpretation techniques applied to mixed terrains p0218 A81-49788

FRESH WATER
Landsat hydrobiological classification for an inland fresh water marsh within Everglades National Park p0249 A81-43238
Freshwater ice thickness observations using passive microwave sensors p0254 A81-49968

FROST
The application of thermography for locating potential frost pockets in forest cutovers p0204 A81-49789

FROST DAMAGE
The application of thermography for locating potential frost pockets in forest cutovers p0204 A81-49789

G

GAMMA RAY SPECTRA
Methods development and applications evaluations of NURE aerial reconnaissance survey data for uranium resource evaluation: Beeville/Bay City and Crystal City quadrangles, Texas
[GJBX-69(81)] p0228 N81-30502
Airborne gamma-ray spectrometer and magnetometer survey
[DE81-027157] p0229 N81-32592
Airborne gamma-ray spectrometer and magnetometer survey. Canyon City quadrangle (Oregon), volume 2
[DE81-028682] p0229 N81-33584
Airborne gamma-ray spectrometer and magnetometer survey, Salem quadrangle (Oregon), volume 2
[DE81-028681] p0229 N81-33585

GARP ATLANTIC TROPICAL EXPERIMENT
Insights into errors of SMS-inferred GATE convective rainfall p0243 A81-42095

GEOBOTANY
An investigation of vegetation and other Earth resource/feature parameters using LANDSAT and other remote sensing data. 1: LANDSAT. 2: Remote sensing of volcanic emissions
[E81-10081] p0209 N81-33543

GEOCHEMISTRY
Mineralogical, optical, and geochemical properties of John H. Kerr Reservoir sediment samples for AgRISTARS pollution research
[E81-10155] p0229 N81-33548

GEODESY
Differential Doppler experiment /DIDEX/ for geodetic applications p0221 A81-47938

GEODETIC SURVEYS
Measurement of lengths, angles, and areas on the earth's spheroid p0221 A81-42846
Optimization of Doppler measurements in the satellite network of Eastern Europe p0221 A81-48678
A 'meteorological' method for calculating vertical refraction p0221 A81-48679
Terrain profiling from Seasat altimetry
[NASA-CR-156878] p0222 N81-31604
Position measurements in Colombia by means of satellite observations p0222 N81-33522
Military geodesy and geospace science, unit one
[AD-A104038] p0222 N81-33581

GEODYNAMICS
NASA selects scientific investigations for Earth dynamics studies
[NASA-NEWS-RELEASE-81-129] p0228 N81-29143

GEOLOGICAL FAULTS
The use of imagery of the earth to study the structure of degassing zones within oil and gas basins p0225 A81-42276
Concerning the hydrogeological significance of faults on platform regions, as revealed by space imagery p0225 A81-42277
Ore-controlling space geological objects and their assessment techniques applied to mineral prediction
[IAF PAPER 81-107] p0227 A81-47353
The use of satellite imagery for studying the structural features of the Caspian oil and gas region p0227 A81-48684

GEOLOGICAL SURVEYS
Tiwi geothermal project - The Philippines p0225 A81-41908
An introduction to satellite hydrology p0244 A81-43184
U.S. geological survey application of satellite telemetry for the support of hydrologic data collection p0258 A81-43189
Landsat data for locating shallow glacial aquifers in eastern South Dakota p0226 A81-43228
Ground water exploration programs in Africa p0226 A81-43230
Aerial thermal survey in the study of earth resources --- Russian book p0277 A81-43981
Application of digital terrain data to quantify and reduce the topographic effect on Landsat data p0259 A81-45433
Lineament mapping in northern Sweden from Landsat images using orthogonal image transforms p0226 A81-46039
The informational estimation of the effectiveness of using satellite imagery in hydrogeological research p0227 A81-48683
Geological and terrain analysis of the Annapolis County region of Nova Scotia - An application of digital Landsat, radar and colour infrared data p0227 A81-49802
Conceptual design of an automated mapping satellite System (MAPSAT)
[PB81-185555] p0264 N81-29522
Methods development and applications evaluations of NURE aerial reconnaissance survey data for uranium resource evaluation: Beeville/Bay City and Crystal City quadrangles, Texas
[GJBX-69(81)] p0228 N81-30502
Atmospheric correction to LANDSAT data for limonite discrimination p0228 N81-31594
Remote sensing for engineering site selection
[AD-A102810] p0219 N81-32586

GEOMAGNETISM
Magnetic space-based field measurements
[AAS PAPER 81-077] p0272 A81-46241
Early results from Magsat --- studies of near-earth magnetic fields p0274 A81-48945
Geomagnetic field mapping from a satellite: Spatial power spectra of the geomagnetic field at various satellite altitudes relative to natural noise sources and instrument noise
[PUBL-1810] p0275 N81-29480
Reduction and analysis of satellite magnetometer data p0275 N81-29482

Investigation of Antarctic crust and upper mantle using Magsat and other geophysical data
[E81-10113] p0222 N81-32574

GEOMETRIC RECTIFICATION (IMAGERY)

A rectification technique for digital orthophoto production p0257 A81-41057

Correlation techniques and devices --- for photogrammetry p0258 A81-43531

Automation in photogrammetry p0258 A81-43532

A radar image time series p0228 A81-45430

Application of digital terrain data to quantify and reduce the topographic effect on Landsat data
p0259 A81-45433

Geometric correction of scanner images of the earth's surface p0261 A81-48694

Integration and comparison of SAR and MSS data for potato crop area estimation p0203 A81-49766

Geometric accuracy of Landsat images processed by NASDA p0263 A81-49818

Development of alternative data analysis techniques for improving the accuracy and specificity of natural resource inventories made with remote sensing data
p0266 N81-33551

An evaluation of MSS P-format data registration
[E81-10171] p0267 N81-33557

GEOMETRICAL OPTICS

Evaluation of the effect of sea-ice roughness on the microwave emission of the ice p0231 A81-41490

GEOMORPHOLOGY

An examination of fluvial morphological characteristics of western Amazon streams from Apollo-Soyuz photographs p0247 A81-43212

Landsat interpretation of prairie lakes and wetlands of eastern South Dakota p0249 A81-43240

Interactive processing of Landsat image for morphopedological studies p0259 A81-46043

Geomorphic mapping from Landsat-3 Return Beam Vidicon /RBV/ imagery p0228 A81-46194

GEOPHYSICS

Main tasks and methods of operational planning of experiments concerning the observations of the earth from space p0277 A81-42288

GEORGIA

Microwave radiometer measurement of tidally induced salinity changes off the Georgia coast p0232 A81-42067

Suburban soil loss and runoff simulation assisted by interpretation of large scale aerial photography
p0253 A81-48941

Agricultural water demand prediction using remote sensing technology for Georgia resource management
[PB81-184137] p0207 N81-30508

GEOS 3 SATELLITE

Calibration validation for the GEOS 3 altimeter
p0270 A81-42671

GEOTHERMAL RESOURCES

Tiwi geothermal project - The Philippines
p0225 A81-41908

Satellite observations of a geothermal submarine spring off Florida west coast p0233 A81-43248

Seasat satellite investigation of the structure of western Nebraska and its application to the evaluation of geothermal resources
[LA-UR-81-1454] p0223 N81-30505

GLACIAL DRIFT

Hydrogeology of glacial deposits from aerial photographs p0252 A81-43548

GLACIERS

Satellite Image Atlas of the earth's glaciers
p0246 A81-43202

Potentials of mapping buried glacier ice with Landsat thermal imagery p0246 A81-43204

Geological and terrain analysis of the Annapolis County region of Nova Scotia - An application of digital Landsat, radar and colour infrared data p0227 A81-49802

GLACIOLOGY

The European SAR-Project Convair 580
p0273 A81-46679

GLOBAL ATMOSPHERIC RESEARCH PROGRAM

Remote sounding of atmosphere and ocean for climate research /Appleton Lecture/ p0236 A81-47099

GOES SATELLITES

Characteristics, of TIROS, GOES, DMSP and LANDSAT systems
[E81-10192] p0263 N81-29506

GOVERNMENT/INDUSTRY RELATIONS

Space Benefits. The secondary application of aerospace technology in other sectors of the economy
[NASA-CR-164733] p0279 N81-32086

An industrial perspective of the LANDSAT opportunity
p0279 N81-32585

GRAINS (FOOD)

Procedure M - A framework for stratified area estimation --- in multispectral scanner data processing
p0201 A81-46036

The discrimination of cereal crops and legumes using reflectance data in the Landsat bandpasses
p0204 A81-49794

A temporal/spectral analysis of small grain crops and confusion crops --- North Dakota
[E81-10167] p0205 N81-28498

The multicategory case of the sequential Bayesian pixel selection and estimation procedure
[E81-10182] p0263 N81-29498

A description of the reformatted spring small grains labeling procedure used in test 2, part 2 of the US/Canada wheat and barley exploratory experiment
[E81-10206] p0207 N81-31597

Measurement of soil moisture trends with airborne scatterometers --- Texas
[E81-10088] p0209 N81-33545

AgRISTARS: Foreign commodity production forecasting. Program review presentation to level 1, Interagency Coordination Committee
[E81-10168] p0209 N81-33555

Australian transition year special studies
[E81-10179] p0210 N81-33565

GRASSLANDS

Evaluation of the possibility of using spectral-band and multispectral aerial photographs for the large-scale survey of natural pastures p0197 A81-41487

Remote sensing and mapping of pastures
p0213 A81-42281

GRAVIMETRY

Gravimetric studies of the earth's crust in the oceans --- Russian book p0221 A81-43524

Evaluation of gravimetric ground truth soil moisture data collected for the agricultural soil moisture experiment, 1978 Colby, Kansas, aircraft mission
[E81-10114] p0205 N81-29494

GRAVITATIONAL FIELDS

Satellite To Satellite Doppler Tracking (SSDT) for mapping of the Earth's gravity field
[NASA-CR-164722] p0223 N81-31601

GRAVITY ANOMALIES

Gravimetric studies of the earth's crust in the oceans --- Russian book p0221 A81-43524

Differential Doppler experiment /DIDEX/ for geodetic applications p0221 A81-47938

GRAVITY WAVES

The structure of short gravity waves on the ocean surface p0234 A81-46105

Refraction of coastal ocean waves p0235 A81-46113

GRAVSAT SATELLITE

Future plans for NASA's Oceanic Processes Program
p0231 A81-41997

GREAT BRITAIN

Satellite observations of England and north-western Europe p0217 A81-49174

GREAT LAKES (NORTH AMERICA)

Airborne microwave radiometer remote sensing of lake ice p0253 A81-48554

GREAT PLAINS CORRIDOR (NORTH AMERICA)

Determination of moisture from NOAA polar orbiting satellite sounding radiances p0243 A81-41158

Analysis of US spring wheat and spring barley periodic ground truth
[E81-10203] p0208 N81-32576

Crop phenology and LANDSAT-based irrigated lands inventory in the high plains: Appendices
[E81-10172] p0210 N81-33558

Crop phenology and LANDSAT-based irrigated lands inventory in the high plains
[E81-10173] p0210 N81-33559

GREAT SALT LAKE (UT)

Satellite detection of seiches in Great Salt Lake, Utah
p0243 A81-42126

A note on indirect detection of seiches in Great Salt Lake, Utah, by NOAA and Landsat satellite imagery
p0247 A81-43218

Mapping the Great Salt Lake shoreline and associated waterfowl habitat from Landsat data p0252 A81-43742

GREENHOUSE EFFECT

Basic problems of the physics and chemistry of contemporary changes of climate p0216 A81-47002

GREENLAND

Ice sheet altimetry
[NASA-CR-156877] p0240 N81-31605

GROUND TRUTH

Results of ground surveys, carried out in conjunction with satellite and aerial studies, of the state of winter wheat on the Kursk test polygon p0197 A81-41485

Relating ground level reflected radiance measurements in the Landsat MSS bandpasses to satellite altitudes
p0271 A81-43735

Alternative 'scale up' estimators for aerial surveys where both detection and classification errors exist
p0260 A81-46197

Evaluation of gravimetric ground truth soil moisture data collected for the agricultural soil moisture experiment, 1978 Colby, Kansas, aircraft mission
[E81-10114] p0205 N81-29494

Evaluation of large area crop estimation techniques using LANDSAT and ground-derived data --- Missouri
[E81-10200] p0206 N81-29511

Satellite measurements of tropospheric aerosols
[NASA-CR-3459] p0219 N81-31680

Field Study for Remote Sensing. An instructor's manual
[NASA-CP-2155] p0279 N81-32564

The workshop --- use and application of remotely sensed data p0280 N81-32566

Why surface-truth field study is needed in remote-sensing instruction p0280 N81-32567

LANDSAT C workshop field/laboratory exercises
p0280 N81-32571

Analysis of US spring wheat and spring barley periodic ground truth
[E81-10203] p0208 N81-32576

Interim catalog ground data summary, data acquisition year 1978
[E81-10132] p0209 N81-33546

A comparative study of the thematic mapper and LANDSAT spectral bands from field measurement data
[E81-10165] p0209 N81-33549

Lakewide monitoring of suspended solids using satellite data --- Lake Superior water reclamation
p0254 N81-33552

Evaluation of LANDSAT data analysis for forest survey --- northeastern aspen-birch survey unit in Minnesota - Carlton County
[E81-10175] p0210 N81-33561

As-built design specification of the automatic registration system for the cartographic technology laboratory
[E81-10176] p0267 N81-33562

Experiment plan: Row and roughness effects on dependence of active microwave measurements of soil moisture
[E81-10209] p0211 N81-33575

GROUND WATER

Survey of in-situ and remote sensing methods for soil moisture determination p0197 A81-43221

Soil moisture applications of the heat capacity mapping mission p0197 A81-43224

Ground water and satellites - An overview/introduction
p0248 A81-43226

Correlation of geologic structure inferred from computer enhanced Landsat imagery with underground water supplies in Arizona p0225 A81-43227

Ground water exploration programs in Africa
p0226 A81-43230

Ground water applications of the heat capacity mapping mission p0248 A81-43233

Satellite observations of a geothermal submarine spring off Florida west coast p0233 A81-43248

Hydrogeology of glacial deposits from aerial photographs p0252 A81-43548

Use of Seasat satellite radar imagery for the detection of standing water beneath forest vegetation
p0199 A81-43743

Landsat data as a basis for regional environmental assessment within the Columbia Plateau
p0218 A81-49798

The detection of groundwater discharges /springs/ using aerial thermography p0254 A81-49800

Synergistic relationships among remote-sensing and geophysical media: Geological and hydrological applications --- detecting near-surface ground water in Minnesota p0255 N81-33553

GULF OF MEXICO

Simulation modeling of estuarine ecosystems
p0243 A81-42229

Satellite observations of a geothermal submarine spring off Florida west coast p0233 A81-43248

Application of GOES visible-infrared data to quantifying mesoscale ocean surface temperatures
p0238 A81-47021

Gulf of Mexico satellite radar altimetry
[NASA-TM-73285] p0224 N81-33760

GULF STREAM

Method for estimation of ocean current velocity from satellite images p0231 A81-41350

Detection of the Gulf Stream p0235 A81-46115

A search for cold water rings p0235 A81-46116

Tracking of a warm water ring p0235 A81-46117

H

HABITATS

Using Landsat MSS data with soils information to identify wetland habitats p0249 A81-43236

From landforms to avian habitat - A look at topology
p0214 A81-43739

The application of remote sensing techniques for an ecological land survey of the snow goose colony at Cape Henrietta Maria, Hudson Bay p0204 A81-49791

Nationwide forestry applications program. Analysis of forest classification accuracy
[E81-10183] p0206 N81-29499

Environmental assessment of the Alaskan continental shelf: Reports of principal investigators. Volume 1: Reactors - birds, plankton, littoral, benthos
[PB81-196263] p0240 N81-30780

HAWAII

Comparison of laboratory reflectance spectra and LANDSAT multispectral images of Hawaiian lava flows
[E81-10061] p0266 N81-33541

HAZE

An analysis of haze effects on LANDSAT multispectral scanner data
[E81-10162] p0263 N81-29497

Some methods of multitemporal analysis of LANDSAT images resulting from a study on Venice Lagoon
[E81-10205] p0267 N81-33574

HEAT ISLANDS

Preliminary survey of HCMM satellite thermal imagery as applied to hydrospherics p0252 A81-43746

Satellite observations of England and north-western Europe p0217 A81-49174

HEAT SOURCES

Identification of subresolution high temperature sources using a thermal IR sensor p0273 A81-46401

HIGH RESOLUTION
A differential inversion method for high resolution atmospheric remote sensing p0215 A81-45862
HIGHWAYS
The use of CIR and airborne multispectral scanner techniques for wetland soils mapping of highway corridors p0215 A81-46044
HISTOGRAMS
Large-area histograms from Meteosat images p0260 A81-46917
Histogram estimation for multiple-detector sensors p0262 A81-49812
HONG KONG
Land use mapping of Hong Kong from Landsat images - An evaluation p0215 A81-45434
HURRICANES
Hurricane 'Flossie' /September 1978/ observed in the north Atlantic, by the Meteosat satellite p0213 A81-41061
A satellite derived technique for estimating rainfall from thunderstorms and hurricanes p0244 A81-43191
Atlantic hurricane season of 1980 p0238 A81-49649
HYDROELECTRICITY
Operational use of satellite data for snow inventory and runoff forecast p0246 A81-43210
HYDROGEOLOGY
Concerning the hydrogeological significance of faults on platform regions, as revealed by space imagery p0225 A81-42277
Fitoexomorphogenic analysis of geological environment changes in the South Aral Sea, based on aerial and space imagery p0225 A81-42279
Optical and digital analyses of Landsat data depicting hydrogeological features of the Daryacheh-Ye-Namak area, Iran p0225 A81-43215
Correlation of geologic structure inferred from computer enhanced Landsat imagery with underground water supplies in Arizona p0225 A81-43227
Landsat data for locating shallow glacial aquifers in eastern South Dakota p0226 A81-43228
Hydrogeologic interpretations of Landsat imagery in arid zones of South and West Africa p0248 A81-43229
Ground water exploration programs in Africa p0226 A81-43230
Observations on Lake Ontario basin hydrogeology from optical enhancements of Landsat imagery p0248 A81-43231
Satellite observations of a geothermal submarine spring off Florida west coast p0233 A81-43248
Hydrogeology of glacial deposits from aerial photographs p0252 A81-43548
Aerial thermal survey in the study of earth resources --- Russian book p0277 A81-43981
The informational estimation of the effectiveness of using satellite imagery in hydrogeological research p0227 A81-48683
A study of Minnesota land and water resources using remote sensing, Volume 14
[E81-10166] p0254 N81-33550
HYDROGRAPHY
The detection of groundwater discharges /springs/ using aerial thermography p0254 A81-49800
Interpretation of hydrographic features seen in the waters off Cape Cod
[AD-A102343] p0240 N81-31803
Derivation of shallow ocean bottom reflectance values from color aerial photography
[AD-A101105] p0241 N81-33763
HYDROLOGY
Environmental satellites p0277 A81-42231
Satellite hydrology. Proceedings of the Fifth Annual William T. Pecora Memorial Symposium on Remote Sensing, Sioux Falls, SD, June 10-15, 1979 p0243 A81-43176
Remote sensing in hydrology - A challenge to scientists p0243 A81-43177
NASA water resources/hydrology remote sensing program in the 1980's p0244 A81-43179
Corps of Engineers utilization of satellites for hydrologic purposes p0244 A81-43180
Agricultures's needs related to satellite hydrology p0197 A81-43181
A review of Canada's present and future remote sensing activities relating to hydrology p0244 A81-43182
Satellite versus conventional methods in hydrology p0244 A81-43183
An introduction to satellite hydrology p0244 A81-43184
Satellite telemetry of hydrologic data in California p0244 A81-43187
U.S. geological survey application of satellite telemetry for the support of hydrologic data collection p0258 A81-43189
Utilizing GOES imagery to determine convective storm characteristics in data deficient regions p0245 A81-43192
Modeling the terrestrial hydrology for the global atmosphere - The future role of satellite data p0245 A81-43197
A statistical approach to rainfall estimation using satellite data p0245 A81-43198
Roles of satellites in hydrology p0245 A81-43199
The use of radar imagery for surface water investigations p0247 A81-43211
An examination of fluvial morphological characteristics of western Amazon streams from Apollo-Soyuz photographs p0247 A81-43212
Hydrologic land use classification using Landsat p0247 A81-43213
Improving stream flow estimates through the use of Landsat p0247 A81-43216
A note on indirect detection of seiches in Great Salt Lake, Utah, by NOAA and Landsat satellite imagery p0247 A81-43218
Assessing the Red River of the North 1978 flooding from NOAA satellite data p0248 A81-43219
A preliminary analysis of SAR mapping of the Manitoba flood, May 1979 p0248 A81-43220
Survey of in-situ and remote sensing methods for soil moisture determination p0197 A81-43221
Characteristics of microwave emission of significance to satellite remote sensing of soil water p0258 A81-43222
Soil moisture applications of the heat capacity mapping mission p0197 A81-43224
Requirements of space-borne microwave radiometers for detecting soil moisture contents p0270 A81-43225
Ground water and satellites - An overview/introduction p0248 A81-43226
Applications of aerospace data for detection of submarine springs in Jamaica p0226 A81-43232
Landsat hydrobiological classification for an inland fresh water marsh within Everglades National Park p0249 A81-43238
A technique for improved assessment of flow resistance characteristics of natural wetlands using Landsat data p0249 A81-43241
Using Landsat imagery to study the Okavango Swamp, Botswana p0249 A81-43242
Assessment and classifications of selected Illinois lakes through the application of space technology p0250 A81-43255
A multistage mapping approach for an irrigated croplands inventory p0198 A81-43262
Remote sensing of bank erosion along the Missouri River, South Dakota p0213 A81-43263
Mapping irrigated lands in Western Kansas from Landsat p0198 A81-43265
Multisensor analysis of hydrologic features with emphasis on the Seasat SAR p0251 A81-43544
Use of Seasat satellite radar imagery for the detection of standing water beneath forest vegetation p0199 A81-43743
Aerial thermal survey in the study of earth resources --- Russian book p0277 A81-43981
The European SAR-Project Convair 580 p0273 A81-46679
Infrared imagery for studying the Kara-Bogaz-Gol Bay p0236 A81-48681
An analysis of the data of synchronous measurements from the Meteor satellite and ships at the eastern coast of the Caspian Sea p0237 A81-48687
Remote sensing in development --- for developing nations p0279 A81-48936
Landsat - What is operational in water resources p0253 A81-49757
Use of Landsat images in the monitoring and study of the LG 2 reservoir during the filling period p0254 A81-49797
Landsat data as a basis for regional environmental assessment within the Columbia Plateau p0218 A81-49798
Agricultural water demand prediction using remote sensing technology for Georgia resource management
[PB81-184137] p0207 N81-30508
HYDROLOGY MODELS
Modeling the terrestrial hydrology for the global atmosphere - The future role of satellite data p0245 A81-43197
A statistical approach to rainfall estimation using satellite data p0245 A81-43198
Application of snow covered area to runoff forecasting, in the Sierra Nevada, California p0245 A81-43201
Prediction of water yield using satellite imagery and a snowmelt simulation model p0246 A81-43205
Evaluation of remote sensing data for input into Hydrological Simulation Program-FORTRAN (HSPF) --- modeling the Occoquan watershed in Virginia using LANDSAT imagery for parameter estimation
[PB81-209561] p0255 N81-33593
HYDROMETEOROLOGY
The use of satellite data in predicting spring flow in the basins of the upper Ob' and upper Enisei p0243 A81-41723
Satellite applications in river and flood forecasting p0243 A81-43178
Monitoring Canada's water resources in remote regions by satellite telemetry p0244 A81-43188
Use of satellite pictures for agriculture p0205 N81-28120

I

ICE ENVIRONMENTS
Optimizing imaging radar parameters for ice reconnaissance p0239 A81-49779
ICE MAPPING
Sea ice detection using enhanced infrared satellite data p0232 A81-42131
Satellite Image Atlas of the earth's glaciers p0246 A81-43202
Correlation function studies for snow and ice p0260 A81-46378
The use of satellite imagery as an aid to the Canadian Coast Guard ice operations p0238 A81-49758
Airborne impulse radar sounding of sea ice p0238 A81-49771
The Lake Melville/Labrador offshore synthetic aperture radar study - Winter 1979 p0238 A81-49772
Single and multiple parameter microwave signatures of sea ice p0238 A81-49774
Radar detection of sea-ice ridges and icebergs in frozen oceans at incidence angles from 0 deg to 90 deg p0238 A81-49775
Digital image analysis of SAR imagery for the detection of icebergs p0239 A81-49777
Application of synthetic aperture radar data to snow cover monitoring p0253 A81-49778
Freshwater ice thickness observations using passive microwave sensors p0254 A81-49988
Ice sheet altimetry
[NASA-CR-156877] p0240 N81-31605
Categorization of Northern Green Bay ice cover using LANDSAT 1 digital data: A case study
[PB81-200438] p0265 N81-32602
Comparative analysis of sea ice features using Side-Looking Airborne Radar (SLAR) and LANDSAT imagery --- Beaufort Sea and Bering Sea
[E81-10044] p0241 N81-33539
ICE REPORTING
Remote sensing in hydrology - A challenge to scientists p0243 A81-43177
Iceberg detectability problems using SAR and SLAR systems p0232 A81-43206
The first ESA remote sensing satellite /ERS/ - The programme and the system
[IAF PAPER 81-90] p0236 A81-47344
Operational use of satellite imagery in the Canadian ice program p0238 A81-49754
Utilisation and benefits of SLAR in operational ice data acquisition p0253 A81-49761
The airborne SAR project - Conclusions and applications p0275 A81-49765
Experimental use of real time SAR imagery in support of oil exploration in the Beaufort Sea p0227 A81-49767
ICEBERGS
Iceberg detectability problems using SAR and SLAR systems p0232 A81-43206
Radar detection of sea-ice ridges and icebergs in frozen oceans at incidence angles from 0 deg to 90 deg p0238 A81-49775
Digital image analysis of SAR imagery for the detection of icebergs p0239 A81-49777
ICELAND
Satellite Image Atlas of the earth's glaciers p0246 A81-43202
IDAHO
Change vector analysis - An approach for detecting forest changes with Landsat p0202 A81-46056
IGNEOUS ROCKS
Identifying igneous rocks in an arid environment on aerial photography by photo tone and photo texture
[AD-A102809] p0228 N81-32587
ILLINOIS
Users manual for the US baseline corn and soybean segment classification procedure
[E81-10190] p0206 N81-29504
ILLUMINATING
Investigation of illumination in the image plane of the receiving optical system for the aerial or spaceborne photography of the world ocean p0232 A81-42553
IMAGE CONTRAST
Accuracy of transmission of spectral contrasts in multispectral aerial photography, with application to problems of object recognition p0257 A81-41479
IMAGE CORRELATORS
Correlation techniques and devices --- for photogrammetry p0258 A81-43531
Image correlation algorithms p0261 A81-48473
IMAGE ENHANCEMENT
Machine method for the equalization of average phototone in an aerial photograph field p0257 A81-41482
Sea ice detection using enhanced infrared satellite data p0232 A81-42131
Flood applications of satellite imagery p0247 A81-43217
Correlation of geologic structure inferred from computer enhanced Landsat imagery with underground water supplies in Arizona p0225 A81-43227
Observations on Lake Ontario basin hydrogeology from optical enhancements of Landsat imagery p0248 A81-43231
Satellite detection of oil on the marine surface p0233 A81-43251
Using enhanced Landsat images for calibrating real time estuarine water quality models p0250 A81-43252
Lake Ontario dynamics and water quality observations using thematically enhanced Landsat data p0251 A81-43257
Automation in photogrammetry p0258 A81-43532
Operational use of satellite imagery in the Canadian ice program p0238 A81-49754

Principal components enhancements versus classifications of Landsat images for forestry applications p0203 A81-49782

Interpretation techniques applied to mixed terrains p0218 A81-49788

Digital enhancements for vegetation mapping in a subarctic environment p0262 A81-49793

Current resource mapping and environmental monitoring applications using Landsat MSS data in Scotland p0218 A81-49806

Visual enhancement of images of natural resources: Applications in geology
[E81-10181] p0228 N81-32575

IMAGE PROCESSING

Multispectral texture analysis p0257 A81-41055

A rectification technique for digital orthophoto production p0257 A81-41057

Experience with image combination in multispectral aerial photography p0257 A81-41481

Machine method for the equalization of average phototone in an aerial photograph field p0257 A81-41482

Practical application of the method of empty blocks for the computerized determination of the boundaries of agricultural objects p0197 A81-41489

Geological interpretation in an interactive mode in automated systems of digital image processing p0225 A81-42289

Optical and digital analyses of Landsat data depicting hydrogeological features of the Daryacheh-Ye-Namak area, Iran p0225 A81-43215

Ground water exploration programs in Africa p0226 A81-43230

Digital analysis of Landsat MSS data and application for coastal marine environment p0233 A81-43247

Application of digital image processing techniques and information systems to water quality monitoring of Lake Tahoe p0251 A81-43258

Selected irrigation acreage estimates in northern Florida from Landsat data p0198 A81-43264

Skylab in retrospect p0277 A81-43535

A capture-recapture approach for estimation of detection probabilities in aerial surveys p0258 A81-43546

Rainbow 80; Fall Technical Meeting, Niagara Falls, NY, October 7-10, 1980, ASP Technical Papers p0198 A81-43727

Urban area update procedures using Landsat data p0214 A81-43733

Training site statistics from Landsat and Seasat satellite imagery registered to a common map base p0258 A81-43734

Manual versus digital Landsat analysis for modeling river flooding p0252 A81-43745

Southern Chesapeake Bay circulation and suspended sediment transport analyzed using Landsat imagery p0252 A81-43747

Texture analysis and urban land use classification p0214 A81-44684

A radar image time series p0226 A81-45430

Procedures for change detection using Landsat digital data p0215 A81-45437

Earth applications orbit analysis for a shuttle-mounted Multispectral Mapper
[AAS PAPER 81-182] p0271 A81-45836

Parallel processing implementations of a contextual classifier for multispectral remote sensing data p0272 A81-46028

The Lulea Image Processing System /LIPS/ - A versatile approach to earth resources data processing p0272 A81-46030

An assessment of Landsat data acquisition history on identification and area estimation of corn and soybeans p0200 A81-46032

Crop classification with a Landsat/radar sensor combination p0200 A81-46033

Comparison of Landsat-2 and field spectrometer reflectance signatures of south Texas rangeland plant communities p0201 A81-46034

Procedure M - A framework for stratified area estimation --- in multispectral scanner data processing p0201 A81-46036

Radar image preprocessing --- of SEASAT-A SAR data p0272 A81-46038

Lineament mapping in northern Sweden from Landsat images using orthogonal image transforms p0226 A81-46039

Maximum likelihood estimation of label imperfection probabilities and its use in the identification of mislabeled patterns --- with application to Landsat MSS data processing p0259 A81-46040

Context distribution estimation for contextual classification of multispectral image data p0259 A81-46041

Stratification of Landsat data by uniformity productivity of soils p0259 A81-46042

Interactive processing of Landsat image for morphopedological studies p0259 A81-46043

Inventory estimation on the massively parallel processor --- from satellite based images p0259 A81-46052

Bulk processing techniques for very large areas - Landsat classification of California p0201 A81-46054

Procedure 1 and forestland classification using Landsat data p0201 A81-46055

SAR ocean imaging mechanisms p0234 A81-46107

Application of delta modulation in on-board and ground video data processing systems for the purposes of remote sensing
[IAF PAPER 81-102] p0260 A81-47351

Image correlation algorithms p0261 A81-48473

Radar-optical-topographic transformations for scene content analysis p0261 A81-48552

Complex processing of satellite images and the geological interpretation p0227 A81-48690

Selection of reference zones for the automatic coordinate control of space images p0261 A81-48693

Geometric correction of scanner images of the earth's surface p0261 A81-48694

Derivation of formulas for the correlation of coordinate points of different-scale photographs and quasi-photographs p0261 A81-48772

The influence of the accuracy of determining the elements of the external orientation of a stereopair on the processing of aerial photographs on the basis of adjusting elements p0261 A81-48773

ICAP - An Interactive Cluster Analysis Procedure for analyzing remotely sensed data p0261 A81-49345

SAR processing of partially coherent and sinusoidally dynamic ocean waves p0239 A81-49776

Digital image analysis of SAR imagery for the detection of icebergs p0239 A81-49777

Landsat data as a basis for regional environmental assessment within the Columbia Plateau p0218 A81-49798

Generation and use of digital elevation data for large areas p0221 A81-49811

Histogram estimation for multiple-detector sensors p0262 A81-49812

Comparative experimental study on the use of original and compressed multispectral Landsat data of the Bayuda desert p0262 A81-49813

Acquisition and preprocessing of images collected by future European Space Agency satellites p0263 A81-49814

Evaluation of Thematic Mapper bands - A first step in feature selection p0205 A81-49815

Geometric accuracy of Landsat images processed by NASDA p0263 A81-49818

Estimation of proportions in mixed pixels through their region characterization
[E81-10199] p0264 N81-29510

Evaluation of large area crop estimation techniques using LANDSAT and ground-derived data --- Missouri
[E81-10200] p0206 N81-29511

The sensor image simulator
[AD-A101172] p0275 N81-29512

Interactive digital image processing for terrain data extraction
[AD-A101321] p0264 N81-30499

Knowledge-based image analysis
[AD-A101319] p0264 N81-30852

A technique for line extraction from LANDSAT multi-spectral scanner satellite data with some applications of the technique
[RAE-TR-81010] p0265 N81-31613

Visual enhancement of images of natural resources: Applications in geology
[E81-10181] p0228 N81-32575

Partially automated object extraction from aerial photographs and land maps p0266 N81-33528

The development of a remote sensing applications program for Vermont
[E81-10149] p0266 N81-33547

A study of Minnesota land and water resources using remote sensing, Volume 14
[E81-10166] p0254 N81-33550

Development of alternative data analysis techniques for improving the accuracy and specificity of natural resource inventories made with remote sensing data p0266 N81-33551

An evaluation of MSS P-format data registration
[E81-10171] p0267 N81-33557

Maximum likelihood labeling
[E81-10177] p0267 N81-33563

Some methods of multitemporal analysis of LANDSAT images resulting from a study on Venice Lagoon
[E81-10205] p0267 N81-33574

Topographic slope correction for analysis of thermal infrared images
[PB81-211781] p0224 N81-33589

IMAGE RECONSTRUCTION

Geometric accuracy of Landsat images processed by NASDA p0263 A81-49818

Fourier modulus image construction
[AD-A101728] p0264 N81-30723

IMAGE RESOLUTION

A measure of reliability for classification of earth satellite data p0257 A81-42631

Image quality for SPOT satellite - Specifications and budget
[IAF PAPER 81-104] p0261 A81-47352

An analysis of haze effects on LANDSAT multispectral scanner data
[E81-10162] p0263 N81-29487

A study of the effects of the atmosphere on thematic mapper observations
[E81-10066] p0276 N81-33540

IMAGING PROCESSING

Space based topographic mapping experiment using Seasat synthetic aperture radar and LANDSAT 3 return beam vidicon imagery
[NASA-CR-164875] p0223 N81-30498

IMAGING TECHNIQUES

A review of Canada's present and future remote sensing activities relating to hydrology p0244 A81-43182

Use of imaging radar for geology and archeology p0226 A81-43730

Simulation of orbital image-sensor geometry p0260 A81-46192

Radiometry with nighttime DMSP images in digital form --- satellite earth observations p0260 A81-46402

Manual versus digital Landsat analysis for delineating river flooding p0252 A81-46405

Applicability of airborne SAR data to geological mapping p0227 A81-49769

Airborne estimation of water quality parameters in Lake Ontario p0254 A81-49796

IMPERIAL VALLEY (CA)

Terrain profiling from Seasat altimetry
[NASA-CR-156878] p0222 N81-31604

IMPROVED TIROS OPERATIONAL SATELLITES

Characteristics, of TIROS, GOES, DMSP and LANDSAT systems
[E81-10192] p0263 N81-29506

INCOHERENT SCATTERING

Coherent and incoherent radar scattering from rough surfaces and vegetated areas --- conferences
[ESA-SP-166] p0208 N81-33339

Introduction to the workshop --- on coherent and incoherent radar scattering from rough surfaces and vegetated areas p0276 N81-33340

INDIA

A case study of soil erosion detection by digital analysis of the remotely sensed multispectral Landsat scanner data of a semi-arid land in southern India p0201 A81-46050

INDIANA

Using Landsat MSS data with soils information to identify wetland habitats p0249 A81-43236

Users manual for the US baseline corn and soybean segment classification procedure
[E81-10190] p0206 N81-29504

INDUSTRIAL PLANTS

Identification of subresolution high temperature sources using a thermal IR sensor p0273 A81-46401

INDUSTRIAL WASTES

Drift and dispersion studies of ocean-dumped waste using Landsat imagery and current drogues p0233 A81-43539

INFESTATION

Mountain pine beetle damage surveys with high-altitude panoramic photography p0199 A81-43732

The development of a remote sensing applications program for Vermont
[E81-10149] p0266 N81-33547

INFORMATION DISSEMINATION

Landsat technology transfer to the private and public sectors through community colleges and other locally available institutions p0277 A81-43750

INFORMATION RETRIEVAL

Computer program documentation user information for the RSO-tape print prugram (RSOPRNT)
[E81-10198] p0264 N81-29509

INFORMATION SYSTEMS

Application of digital image processing techniques and information systems to water quality monitoring of Lake Tahoe p0251 A81-43258

Physical and technical foundations for the development of subsatellite systems for the exploration of natural earth resources
[IAF PAPER 81-101] p0278 A81-47350

Requirements on the data/information system --- of satellite systems for earth resources observation p0278 A81-48527

Reports on cartography and geodesy, series 1: Original reports, Number 81
[ISSN-0469-4236] p0222 N81-33527

The development of a remote sensing applications program for Vermont
[E81-10149] p0266 N81-33547

Development of alternative data analysis techniques for improving the accuracy and specificity of natural resource inventories made with remote sensing data p0266 N81-33551

INFORMATION THEORY

Concerning the reliability estimation of information obtained from several sources in earth survey tasks p0270 A81-42286

INFRARED IMAGERY

Sea ice detection using enhanced infrared satellite data p0232 A81-42131

Utilizing GOES imagery to determine convective storm characteristics in data deficient regions p0245 A81-43192

Rain estimation over several areas of the globe using satellite imagery p0245 A81-43193

Infrared-temperature variability in a large agricultural field p0200 A81-45432

Identification of subresolution high temperature sources using a thermal IR sensor p0273 A81-46401

Microdensitometry to identify saline rangelands on 70-mm color-infrared aerial film p0202 A81-46406

The application of thermography for locating potential frost pockets in forest cutovers p0204 A81-49789

Soil moisture inferences from thermal infrared measurements of vegetation temperatures
[E81-10184] p0206 N81-29500
Topographic slope correction for analysis of thermal infrared images
[PB81-211781] p0224 N81-33589

INFRARED PHOTOGRAPHY
Experience with the determination of optical image distortions of landscape elements on IR aerial photographs p0257 A81-41430
Applications of aerospace data for detection of submarine springs in Jamaica p0226 A81-43232
Wetland mapping from digitized aerial photography p0252 A81-43549
The use of CIR and airborne multispectral scanner techniques for wetland soils mapping of highway corridors p0215 A81-46044
Mapping alpine soils using color positive and color infrared photographs p0252 A81-46045
Methods of editing cloud and atmospheric layer affected pixels from satellite data --- in south Texas test area
[E81-10169] p0266 N81-33556
Quantification of non-point source sedimentation through densitometric analysis of color infrared aerial photography
[PB81-209157] p0255 N81-33599

INFRARED RADIATION
Satellite identification of surface radiant temperature fields of subpixel resolution
[PB81-184038] p0265 N81-31615
Satellite measurements of atmospheric aerosols
[AD-A103493] p0220 N81-33720

INFRARED SPECTROMETERS
A differential inversion method for high resolution atmospheric remote sensing p0215 A81-45862
First results of the Intercosmos satellite IK-21
[IAF PAPER 81-214] p0274 A81-47409

INFRARED SPECTROSCOPY
Experimental investigation of the physical fundamentals for remote sensing of soil and vegetation moisture by active infrared reflectance spectroscopy using CO2 laser technique
[BMFT-FB-W-80-037] p0211 N81-33588

INLAND WATERS
Landsat data for regulatory permit monitoring p0247 A81-43214
Landsat hydrobiological classification for an inland fresh water marsh within Everglades National Park p0249 A81-43238

INLETS (TOPOGRAPHY)
Applications of Landsat imagery to a coastal inlet stability study p0250 A81-43249

INSTRUMENT PACKAGES
A radiometric model of an earth radiation budget radiometer optical system with diffuse-specular surfaces p0269 A81-41919

INTERCOSMOS SATELLITES
Program and instrumentation of the satellite experiment Bulgaria-1300 II
[IAF PAPER 81-91] p0273 A81-47345
New complex for ionosphere-magnetosphere study 'Intercosmos-Bulgaria-1300'
[IAF PAPER 81-212] p0273 A81-47407
First results of the Intercosmos satellite IK-21
[IAF PAPER 81-214] p0274 A81-47409

INTERFEROMETRY
Atmospheric nitric acid and chlorofluoromethane 11 from interferometric spectra obtained at the Observatoire du Pic du Midi
[AERONOMICA-ACTA-A-227-1980] p0219 N81-30656
Fourier modulus image construction
[AD-A101728] p0264 N81-30723

INTERNATIONAL LAW
International monitoring from space /Problems of international law/ --- Russian book p0279 A81-49468

IONOSPHERIC SOUNDING
ISS-b experimental results on global distributions of ionospheric parameters and thunderstorm activity p0215 A81-44862
New complex for ionosphere-magnetosphere study 'Intercosmos-Bulgaria-1300'
[IAF PAPER 81-212] p0273 A81-47407

IOWA
Users manual for the US baseline corn and soybean segment classification procedure
[E81-10190] p0206 N81-29504
Crop area estimation using ground-gathered and sampled LANDSAT data
[PB81-192783] p0207 N81-30507
Atmospheric nitric acid and chlorofluoromethane 11 from interferometric spectra obtained at the Observatoire du Pic du Midi
[AERONOMICA-ACTA-A-227-1980] p0219 N81-30656

IRAN
Optical and digital analyses of Landsat data depicting hydrogeological features of the Daryacheh-Ye-Namak area, Iran p0225 A81-43215

IRRADIANCE
Does the use of two radiometers correct for irradiance changes during measurements p0272 A81-46196
Investigation of multispectral remote sensing of snow cover using a solar radiation model p0262 A81-48804

IRRIGATION
Application of remote sensing for California irrigated lands assessment p0213 A81-43261
A multistage mapping approach for an irrigated croplands inventory p0198 A81-43262
Selected irrigation acreage estimates in northern Florida from Landsat data p0198 A81-43264
Mapping irrigated lands in Western Kansas from Landsat p0198 A81-43265
Mapping irrigated cropland on the High Plains using Landsat p0198 A81-43266
Remote sensing and land use planning p0218 A81-49792
Agricultural water demand prediction using remote sensing technology for Georgia resource management
[PB81-184137] p0207 N81-30508
Crop phenology and LANDSAT-based irrigated lands inventory in the high plains: Appendices
[E81-10172] p0210 N81-33558
Crop phenology and LANDSAT-based irrigated lands inventory in the high plains
[E81-10173] p0210 N81-33559

ITALY
European industrial space projects
[AAS PAPER 81-053] p0278 A81-46234
Use of elevation models for landform analysis by Seasat-SAR imagery
[IAF PAPER 81-98] p0260 A81-47349
Analysis of the November 23, 1980 earthquake as a design basis for satellite emergency communication
[IAF PAPER 81-269] p0216 A81-47433
Some methods of multitemporal analysis of LANDSAT images resulting from a study on Venice Lagoon
[E81-10205] p0267 N81-33574

J

JAMAICA
Applications of aerospace data for detection of submarine springs in Jamaica p0226 A81-43232

JAPAN
Digital analysis of Landsat MSS data and application for coastal marine environment p0233 A81-43247
A comparison of automatic classification algorithms for land use map by remotely sensed data p0215 A81-44701
Monitoring of snow covered area using satellite data
[IAF PAPER 81-114] p0253 A81-47356
Research on assessment of the recreational value of forests using Landsat digital data p0203 A81-49785

JAPANESE SPACE PROGRAM
Development of Marine Observation Satellite-1
[AAS PAPER 81-060] p0278 A81-46238

K

KANSAS
Mapping irrigated lands in Western Kansas from Landsat p0198 A81-43265
Look direction dependence of radar backscattering cross section for agricultural fields p0199 A81-43741
Crop classification with a Landsat/radar sensor combination p0200 A81-46033
Sampling Landsat classifications for crop area estimation p0202 A81-46404
Evaluation of gravimetric ground truth soil moisture data collected for the agricultural soil moisture experiment, 1978 Colby, Kansas, aircraft mission
[E81-10114] p0205 N81-29494
Atmospheric nitric acid and chlorofluoromethane 11 from interferometric spectra obtained at the Observatoire du Pic du Midi
[AERONOMICA-ACTA-A-227-1980] p0219 N81-30656

L

LABRADOR
Airborne impulse radar sounding of sea ice p0238 A81-49771
The Lake Melville/Labrador offshore synthetic aperture radar study - Winter 1979 p0238 A81-49772

LAGOONS
Some methods of multitemporal analysis of LANDSAT images resulting from a study on Venice Lagoon
[E81-10205] p0267 N81-33574

LAKE ICE
Airborne microwave radiometer remote sensing of lake ice p0253 A81-48554
Airborne impulse radar sounding of sea ice p0238 A81-49771
The Lake Melville/Labrador offshore synthetic aperture radar study - Winter 1979 p0238 A81-49772
Freshwater ice thickness observations using passive microwave sensors p0254 A81-49968

LAKE MICHIGAN
Thermal patterns of Lake Michigan and Lake Superior from satellite remote sensors and its uses p0250 A81-43256
Determination of beach sand parameters using remotely sensed aircraft reflectance data p0217 A81-49346

LAKE ONTARIO
Observations on Lake Ontario basin hydrogeology from optical enhancements of Landsat imagery p0248 A81-43231
Lake Ontario dynamics and water quality observations using thematically enhanced Landsat data p0251 A81-43257
Airborne estimation of water quality parameters in Lake Ontario p0254 A81-49796
A remote sensing technique to monitor Cladophora in the Great Lakes
[PB81-173841] p0254 N81-29520

LAKE SUPERIOR
Thermal patterns of Lake Michigan and Lake Superior from satellite remote sensors and its uses p0250 A81-43256
Lakewide monitoring of suspended solids using satellite data --- Lake Superior water reclamation p0254 N81-33552

LAKE TAHOE (CA-NV)
Application of digital image processing techniques and information systems to water quality monitoring of Lake Tahoe p0251 A81-43258
Photographic technology development project: Timber typing in the Tahoe Basin using high altitude panoramic photography
[NASA-CR-161082] p0208 N81-32578

LAKES
The use of radar imagery for surface water investigations p0247 A81-43211
Optical and digital analyses of Landsat data depicting hydrogeological features of the Daryacheh-Ye-Namak area, Iran p0225 A81-43215
Improvements in lake volume predictions using Landsat data p0248 A81-43237
Landsat interpretation of prairie lakes and wetlands of eastern South Dakota p0249 A81-43240
Assessment and classifications of selected Illinois lakes through the application of space technology p0250 A81-43255
Trophic state determination for shallow coastal lakes from Landsat imagery p0251 A81-43259

LAND ICE
Potentials of mapping buried glacier ice with Landsat thermal imagery p0246 A81-43204

LAND MANAGEMENT
European industrial space projects
[AAS PAPER 81-053] p0278 A81-46234
Development of alternative data analysis techniques for improving the accuracy and specificity of natural resource inventories made with remote sensing data p0266 N81-33551

LAND USE
Multispectral texture analysis p0257 A81-41055
Evaluation of the possibility of using spectral-band and multispectral aerial photographs for the large-scale survey of natural pastures p0197 A81-41487
Remote sensing and mapping of pastures p0213 A81-42281
Hydrologic land use classification using Landsat p0247 A81-43213
Improving stream flow estimates through the use of Landsat p0247 A81-43216
Application of remote sensing for California irrigated lands assessment p0213 A81-43261
Comparison of sampling procedures and data analysis for a land-use and land-cover map p0213 A81-43533
Mapping wetlands using orthophotoquads and 35-mm aerial photographs p0251 A81-43543
Urban area update procedures using Landsat data p0214 A81-43733
Training site statistics from Landsat and Seasat satellite imagery registered to a common map base p0258 A81-43734
Texture measurements from Seasat - SAR images for urban land use interpretation p0214 A81-43749
Texture analysis and urban land use classification p0214 A81-44684
A comparison of automatic classification algorithms for land use map by remotely sensed data p0215 A81-44701
Land use mapping of Hong Kong from Landsat images An evaluation p0215 A81-45434
The methodology of CIAT's land resource study of tropical America p0216 A81-46046
Bulk processing techniques for very large areas - Landsat classification of California p0201 A81-46054
Procedure 1 and forestland classification using Landsat data p0201 A81-46055
Change vector analysis - An approach for detecting forest changes with Landsat p0202 A81-46056
Analysis of landfills with historic airphotos p0216 A81-46407
A practical method for the verification of computer-processed Landsat data p0261 A81-48943
Satellite observations of England and north-western Europe p0217 A81-49174
Multistage remote sensing in exploratory ecodistrict land classification p0217 A81-49759
Present state of remote sensing development in Poland p0279 A81-49763
Interpreter evaluations of airborne radar imagery for ecological and land/use cover classification in southern Manitoba p0218 A81-49773
Land use/cover mapping for Halifax County - Remote sensing alternatives p0218 A81-49783
Interpretation techniques applied to mixed terrains p0218 A81-49788

Remote sensing and land use planning p0218 A81-49792
Landsat data as a basis for regional environmental assessment within the Columbia Plateau p0218 A81-49798
Thermal inertia mapping of some areas of Quebec based on aerial and HCMM satellite data p0204 A81-49799
Current resource mapping and environmental monitoring applications using Landsat MSS data in Scotland p0218 A81-49806
Evaluation of multiband, multitemporal, and transformed LANDSAT MSS data for land cover area estimation --- North Central Missouri
[E81-10161] p0219 N81-29496
Evaluation of large area crop estimation techniques using LANDSAT and ground-derived data --- Missouri
[E81-10200] p0206 N81-29511
Interactive digital image processing for terrain data extraction
[AD-A101321] p0264 N81-30499
Remote sensing for engineering site selection
[AD-A102810] p0219 N81-32586
The development of a remote sensing applications program for Vermont
[E81-10149] p0266 N81-33547
Evaluation of LANDSAT data analysis for forest survey --- northeastern aspen-birch survey unit in Minnesota - Carlton County
[E81-10175] p0210 N81-33561

LANDFILLS
Analysis of landfills with historic airphotos p0216 A81-46407

LANDSAT D
Efficiency criteria of space systems for studying the earth's natural resources p0277 A81-42287
A simulation of Thematic Mapper performance in an agricultural application p0204 A81-49810
Evaluation of Thematic Mapper bands - A first step in feature selection p0205 A81-49815

LANDSAT SATELLITES
Comparative experimental study on the use of original and compressed multispectral Landsat data of the Bayuda desert p0262 A81-49813
Characteristics, of TIROS, GOES, DMSP and LANDSAT systems
[E81-10192] p0263 N81-29506

LANDSAT 3
LANDSAT C workshop field/laboratory exercises p0280 N81-32571

LARGE AREA CROP INVENTORY EXPERIMENT
Evaluation of large area crop estimation techniques using LANDSAT and ground-derived data --- Missouri
[E81-10200] p0206 N81-29511
Australian transition year special studies
[E81-10179] p0210 N81-33565

LAVA
Comparison of laboratory reflectance spectra and LANDSAT multispectral images of Hawaiian lava flows
[E81-10061] p0266 N81-33541

LEAVES
A model of plant canopy polarization response p0201 A81-48035

LEGUMINOUS PLANTS
The discrimination of cereal crops and legumes using reflectance data in the Landsat bandpasses p0204 A81-49794

LIGHT SCATTERING
An examination of spectral band ratioing to reduce the topographic effect on remotely sensed data p0221 A81-45427
Airborne simultaneous spectroscopic detection of laser-induced water Raman backscatter and fluorescence from chlorophyll a and other naturally occurring pigments p0253 A81-47647
Use of water Raman emission to correct airborne laser fluorosensor data for effects of water optical attenuation p0253 A81-47676
A study of the effects of the atmosphere on thematic mapper observations
[E81-10056] p0276 N81-33540
A comparison of observed and analytically derived remote sensing penetration depths for turbid water
[NASA-TM-83176] p0255 N81-33577

LIGHT TRANSMISSION
Satellite measurements of atmospheric aerosols
[AD-A103493] p0220 N81-33720

LIMNOLOGY
A note on indirect detection of seiches in Great Salt Lake, Utah, by NOAA and Landsat satellite imagery p0247 A81-43218
Hydrogeologic interpretations of Landsat imagery in arid zones of South and West Africa p0248 A81-43229
Observations on Lake Ontario basin hydrogeology from optical enhancements of Landsat imagery p0248 A81-43231
Landsat interpretation of prairie lakes and wetlands of eastern South Dakota p0249 A81-43240
Assessment and classifications of selected Illinois lakes through the application of space technology p0250 A81-43255

LIMONITE
Atmospheric correction to LANDSAT data for limonite discrimination p0228 N81-31594

LINE SPECTRA
A differential inversion method for high resolution atmospheric remote sensing p0215 A81-45862
A technique for line extraction from LANDSAT multi-spectral scanner satellite data with some applications of the technique
[RAE-TR-81010] p0265 N81-31613

LINEAR FILTERS
Inversion of multiwavelength radiometer measurements by three-dimensional filtering p0271 A81-45873

LITHOSPHERE
Ring structures of Precambrian shields, based on the interpretation of space imagery p0225 A81-42278
Gravimetric studies of the earth's crust in the oceans --- Russian book p0221 A81-43524
Early results from Magsat --- studies of near-earth magnetic fields p0274 A81-48945

LONG WAVE RADIATION
Annual and interannual variations in outgoing longwave radiation over the tropics p0251 A81-43356

LOUISIANA
Landsat data for regulatory permit monitoring p0247 A81-43214
Look direction dependence of radar backscattering cross section for agricultural fields p0199 A81-43741

M

MAGNETIC SIGNATURES
Reduction and analysis of satellite magnetometer data p0275 N81-29482

MAGNETIC SURVEYS
Magnetic space-based field measurements
[AAS PAPER 81-077] p0272 A81-46241
Early results from Magsat --- studies of near-earth magnetic fields p0274 A81-48945
Geomagnetic field mapping from a satellite: Spatial power spectra of the geomagnetic field at various satellite altitudes relative to natural noise sources and instrument noise
[PUBL-1810] p0275 N81-29480
Investigation of Antarctic crust and upper mantle using Magsat and other geophysical data
[E81-10113] p0222 N81-32574
Airborne gamma-ray spectrometer and magnetometer survey
[DE81-027157] p0229 N81-32592
Airborne gamma-ray spectrometer and magnetometer survey. Canyon City quadrangle (Oregon), volume 2
[DE81-028682] p0229 N81-33584
Airborne gamma-ray spectrometer and magnetometer survey, Salem quadrangle (Oregon), volume 2
[DE81-028681] p0229 N81-33585

MAGNETIC TAPES
Conversion of SPU-Universal disk file to JSC-Universal tape storage: CONVRT user's guide
[E81-10185] p0263 N81-29501

MAGNETOSPHERE
New complex for ionosphere-magnetosphere study 'Intercosmos-Bulgaria-1300'
[IAF PAPER 81-212] p0273 A81-47407

MAINE
An investigation of vegetation and other Earth resource/feature parameters using LANDSAT and other remote sensing data. 1: LANDSAT. 2: Remote sensing of volcanic emissions
[E81-10061] p0209 N81-33543

MAN ENVIRONMENT INTERACTIONS
Simulation modeling of estuarine ecosystems p0243 A81-42229
Fitoexomorphogenic analysis of geological environment changes in the South Aral Sea, based on aerial and space imagery p0225 A81-42279
Application of digital image processing techniques and information systems to water quality monitoring of Lake Tahoe p0251 A81-43258
Dynamic ecosystem of the Aral Basin studied from satellite imagery p0217 A81-48682

MANITOBA
A preliminary analysis of SAR mapping of the Manitoba flood, May 1979 p0248 A81-43220
Interpreter evaluations of airborne radar imagery for ecological and land/use cover classification in southern Manitoba p0218 A81-49773
Resource inventory and terrain analysis in north western Manitoba from integrated remote sensing data p0218 A81-49803

MAPPING
Topographic and cartographic applications of photogrammetry p0221 A81-42847
A multistage mapping approach for an irrigated croplands inventory p0198 A81-43262
Mapping irrigated lands in Western Kansas from Landsat p0198 A81-43265
Mapping irrigated cropland on the High Plains using Landsat p0198 A81-43266
Remote sensing aided procedure for conifer growth modeling in the northeastern Sierra Nevada p0199 A81-43740
Land use mapping of Hong Kong from Landsat images - An evaluation p0215 A81-45434
Lineament mapping in northern Sweden from Landsat images using orthogonal image transforms p0226 A81-46039
Cartographic accuracy of synthetic aperture radar imagery p0262 A81-49780
Geomagnetic field mapping from a satellite: Spatial power spectra of the geomagnetic field at various satellite altitudes relative to natural noise sources and instrument noise
[PUBL-1810] p0275 N81-29480
The sensor image simulator
[AD-A101172] p0275 N81-29512
Conceptual design of an automated mapping satellite System (MAPSAT)
[PB81-185555] p0264 N81-29522
Space based topographic mapping experiment using Seasat synthetic aperture radar and LANDSAT 3 return beam vidicon imagery
[NASA-CR-164675] p0223 N81-30496
Ocean services for the nation. National ocean goals and objectives for the 1980's
[PB81-200602] p0240 N81-31808
Airborne gamma-ray spectrometer and magnetometer survey
[DE81-027157] p0229 N81-32592
OVSUP: A program for computer-aided disentanglement of overlapping zones p0222 N81-33525
Photogrammetry in China p0222 N81-33526
Reports on cartography and geodesy, series 1: Original reports, Number 81
[ISSN-0469-4236] p0222 N81-33527
Partially automated object extraction from aerial photographs and land maps p0266 N81-33528
As-built design specification of the automatic registration system for the cartographic technology laboratory
[E81-10176] p0267 N81-33562
An evaluation of detail in dynamic visual displays
[AD-A103378] p0222 N81-33578

MARINE BIOLOGY
Simulation modeling of estuarine ecosystems p0243 A81-42229
Landsat hydrobiological classification for an inland fresh water marsh within Everglades National Park p0249 A81-43238
Remote sensing in biological oceanography p0237 A81-49130

MARINE ENVIRONMENTS
Digital analysis of Landsat MSS data and application for coastal marine environment p0233 A81-43247
Satellites for oceanography - The promises and the realities p0237 A81-49126
Satellite oceanography - The instruments p0274 A81-49134
The Surveillance Satellite Program and the future of microwave remote sensing p0274 A81-49753
NOAA Climate Program plan
[PB81-193815] p0240 N81-30765

MARINE METEOROLOGY
Hurricane 'Flossie' /September 1978/ observed in the north Atlantic, by the Meteosat satellite p0213 A81-41061
Performance evaluation of a spaceborne scatterometer p0269 A81-41920
Rain estimation over several areas of the globe using satellite imagery p0245 A81-43193
The wind speed dependency of ocean microwave backscatter p0234 A81-46109
The study of mesoscale ocean winds p0235 A81-46110
Meteorological applications of the ARGOS system
[IAF PAPER 81-121] p0273 A81-47360
The National Oceanic Satellite System p0236 A81-48548
The future for satellite-derived surface winds p0237 A81-49129
Climate, the oceans, and remote sensing p0237 A81-49132
Atlantic hurricane season of 1980 p0238 A81-49649
The occurrence of vertical tilt in tropical cyclones p0238 A81-49656
Eastern North Pacific tropical cyclones of 1980 p0238 A81-49657
Meteosat experience in assisting commercial fishing p0239 A81-49907
Regression techniques for oceanographic parameter retrieval using space-borne microwave radiometry p0239 A81-49967
Reports on Marine Science Affairs. Report 14: Satellite data requirements for marine meteorological services
[WMO-548] p0239 N81-28668
Altimeter rain detection
[NASA-TM-73291] p0275 N81-29408

MARINE RESOURCES
Multispectral kelp resource surveys p0232 A81-43244

MARITIME SATELLITES
Satellite aided coastal zone monitoring and vessel traffic system p0231 A81-41755
Development of Marine Observation Satellite-1
[AAS PAPER 81-060] p0278 A81-46238
Satellites for oceanography - The promises and the realities p0237 A81-49126
Oceanography from satellites p0237 A81-49127
The promise of satellite altimetry --- for oceanography p0237 A81-49128
Commercial applications of satellite oceanography p0237 A81-49133
Satellite oceanography - The instruments p0274 A81-49134

MARKING

Maximum likelihood labeling
[E81-10177] p0267 N81-33563

MARSHLANDS

Accuracy evaluation of Landsat digital classification of vegetation in the Great Dismal Swamp
p0248 A81-43235

Landsat hydrobiological classification for an inland fresh water marsh within Everglades National Park
p0249 A81-43238

Using Landsat imagery to study the Okavango Swamp, Botswana p0249 A81-43242

Computer-implemented remote sensing techniques for measuring coastal productivity and nutrient transport systems p0250 A81-43243

A report on the use of remote sensing techniques for the supervision of New England coastal salt marshes
p0253 A81-48944

MATHEMATICAL MODELS

Remote sensing aided procedure for conifer growth modeling in the northeastern Sierra Nevada
p0199 A81-43740

Large area application of a corn hazard model --- Soviet Union
[E81-10164] p0205 N81-28497

Evaluation of spring wheat and barley crop calender models for the 1979 crop year
[E81-10197] p0206 N81-29508

Atmospheric correction to LANDSAT data for limonite discrimination p0228 N81-31594

Improved version of the split routine for CLASSY
[E81-10210] p0264 N81-31600

Yield Model Development (YMD) implementation plan for fiscal years 1981 and 1982
[E81-10211] p0208 N81-32577

A review of volume scatter theories for modeling applications p0265 N81-33347

Maximum likelihood estimation for mixture models
[E81-10178] p0210 N81-33564

A crop moisture stress index for large areas and its application in the prediction of spring wheat phenology
[E81-10202] p0210 N81-33573

Topographic slope correction for analysis of thermal infrared images
[PB81-211781] p0224 N81-33589

MATRICES (MATHEMATICS)

A review of volume scatter theories for modeling applications p0265 N81-33347

MAXIMUM LIKELIHOOD ESTIMATES

Maximum likelihood estimation of label imperfection probabilities and its use in the identification of mislabeled patterns --- with application to Landsat MSS data processing p0259 A81-46040

Context distribution estimation for contextual classification of multispectral image data
p0259 A81-46041

Maximum likelihood clustering with dependent feature trees
[E81-10186] p0263 N81-29502

Maximum likelihood labeling
[E81-10177] p0267 N81-33563

Maximum likelihood estimation for mixture models
[E81-10178] p0210 N81-33564

MEDITERRANEAN SEA

Satellite determination of the mesoscale variability of the sea surface temperature p0234 A81-44861

MERCATOR PROJECTION

An evaluation of MSS P-format data registration
[E81-10171] p0267 N81-33557

MESOSCALE PHENOMENA

Satellite determination of the mesoscale variability of the sea surface temperature p0234 A81-44861

The study of mesoscale ocean winds
p0235 A81-46110

Application of GOES visible-infrared data to quantifying mesoscale ocean surface temperatures
p0236 A81-47021

METEOROLOGICAL PARAMETERS

Progress in passive microwave remote sensing - Nonlinear retrieval techniques --- for meteorological parameters
p0271 A81-45872

METEOROLOGICAL RADAR

Performance evaluation of a spaceborne scatterometer
p0269 A81-41920

METEOROLOGICAL SATELLITES

Remote sounding of atmosphere and ocean for climate research /Appleton Lecture/ p0236 A81-47099

Reports on Marine Science Affairs. Report 14: Satellite data requirements for marine meteorological services
[WMO-548] p0239 N81-28668

Characteristics, of TIROS, GOES, DMSP and LANDSAT systems
[E81-10192] p0263 N81-29506

METEOROLOGICAL SERVICES

Rain estimation over several areas of the globe using satellite imagery p0245 A81-43193

METEOROLOGY

Environmental satellites p0277 A81-42231

Radiation studies in the atmosphere
p0216 A81-47001

Basic problems of the physics and chemistry of contemporary changes of climate p0216 A81-47002

METEOSAT SATELLITE

Large-area histograms from Meteosat images
p0260 A81-46917

Potential for detection of natural disasters via Meteosat
[IAF PAPER 81-263] p0216 A81-47430

MEXICO

The environmental vegetation index: A tool potentially useful for arid land management --- Texas and Mexico, plant growth stress due to water deficits
[E81-10191] p0206 N81-29505

MICHIGAN

Categorization of Northern Green Bay ice cover using LANDSAT 1 digital data: A case study
[PB81-200438] p0265 N81-32602

MICRODENSITOMETERS

Microdensitometry to identify saline rangelands on 70-mm color-infrared aerial film p0202 A81-48406

MICROWAVE ANTENNAS

Differential Doppler experiment /DIDEX/ for geodetic applications p0221 A81-47938

MICROWAVE EMISSION

Evaluation of the effect of sea-ice roughness on the microwave emission of the ice p0231 A81-41490

Microwave radiometer measurement of tidally induced salinity changes off the Georgia coast p0232 A81-42067

Monitoring snow with microwaves p0246 A81-43209

Characteristics of microwave emission of significance to satellite remote sensing of soil water p0258 A81-43222

Potential application of satellite radar to monitor soil moisture p0270 A81-43223

Requirements of space-borne microwave radiometers for detecting soil moisture contents p0270 A81-43225

MICROWAVE IMAGERY

Aircraft active microwave measurements for estimating soil moisture p0271 A81-43547

Correlation function studies for snow and ice
p0260 A81-46378

Airborne microwave radiometer remote sensing of lake ice p0253 A81-48554

The Surveillance Satellite Program and the future of microwave remote sensing p0274 A81-49753

Cartographic accuracy of synthetic aperture radar imagery p0262 A81-49780

Freshwater ice thickness observations using passive microwave sensors p0254 A81-49968

Scattering theory with application to synthetic aperture radar p0265 N81-33348

MICROWAVE RADIOMETERS

What has been learned from the scanning multi-channel microwave radiometers /SMMRs/ p0269 A81-41995

Study of the influence of the atmosphere on the performance of an imaging microwave radiometer
[ESA-CR(P)-1421] p0275 N81-30342

MICROWAVE SCATTERING

Satellite scatterometer p0232 A81-42102

Passive microwave sensing of snow characteristics over land p0246 A81-43207

Monitoring snow with microwaves p0246 A81-43209

Active microwave measurements for estimating soil moisture in Oklahoma p0199 A81-43744

The wind speed dependency of ocean microwave backscatter p0234 A81-46109

Single and multiple parameter microwave signatures of sea ice p0238 A81-49774

Evaluation of gravimetric ground truth soil moisture data collected for the agricultural soil moisture experiment, 1978 Colby, Kansas, aircraft mission
[E81-10114] p0205 N81-29494

Measurement of soil moisture trends with airborne scatterometers --- Texas
[E81-10088] p0209 N81-33545

Experiment plan: Row and roughness effects on dependence of active microwave measurements of soil moisture
[E81-10209] p0211 N81-33575

MICROWAVE SENSORS

Progress in passive microwave remote sensing - Nonlinear retrieval techniques --- for meteorological parameters
p0271 A81-45872

The European SAR-Project Convair 580
p0273 A81-46679

Passive microwave systems
[IAF PAPER 81-88] p0273 A81-47342

The National Oceanic Satellite System
p0236 A81-48548

MICROWAVE SPECTROMETERS

Passive microwave techniques for geophysical sensing of the earth from satellites p0270 A81-43071

MILLIMETER WAVES

Millimeter-wave sensing of the environment: A bibliographic survey
[NASA-CR-156879] p0219 N81-32581

MINERAL EXPLORATION

Ore-controlling space geological objects and their assessment techniques applied to mineral prediction
[IAF PAPER 81-107] p0227 A81-47353

Complex processing of satellite images and the geological interpretation p0227 A81-48690

Interactive system for the regional prognosis of raw mineral resources, based on ground-based and satellite imagery data p0227 A81-48691

Remote sensing in development --- for developing nations p0279 A81-48936

Methods development and applications evaluations of NURE aerial reconnaissance survey data for uranium resource evaluation: Beeville/Bay City and Crystal City quadrangles, Texas
[GJBX-69(81)] p0228 N81-30502

Atmospheric correction to LANDSAT data for limonite discrimination p0228 N81-31594

Airborne gamma-ray spectrometer and magnetometer survey
[DE81-027157] p0229 N81-32592

Airborne gamma-ray spectrometer and magnetometer survey. Canyon City quadrangle (Oregon), volume 2
[DE81-028682] p0229 N81-33584

Airborne gamma-ray spectrometer and magnetometer survey. Salem quadrangle (Oregon), volume 2
[DE81-028681] p0229 N81-33585

MINERALOGY

Mineralogical, optical, and geochemical properties of John H. Kerr Reservoir sediment samples for AgRISTARS pollution research
[E81-10155] p0229 N81-33548

MINES (EXCAVATIONS)

A radar image time series p0226 A81-45430

MINICOMPUTERS

A top-down approach to the use of simulation in computer system design --- of Edit Processor of Integrated Photogrammetric Instrument Network p0274 A81-48331

MINNESOTA

Assessing the Red River of the North 1978 flooding from NOAA satellite data p0248 A81-43219

A comparison of remote sensing techniques for Minnesota wetlands classification p0249 A81-43239

Satellite monitoring of snow extent and condition in agricultural, transitional, and forested land cover areas
[PB81-188625] p0254 N81-30509

A study of Minnesota land and water resources using remote sensing, Volume 14
[E81-10166] p0254 N81-33550

Synergistic relationships among remote-sensing and geophysical media: Geological and hydrological applications --- detecting near-surface ground water in Minnesota p0255 N81-33553

A project to evaluate moisture stress and phenological factors in corn and soybean areas of southwestern and south-central Minnesota p0209 N81-33554

Evaluation of LANDSAT data analysis for forest survey --- northeastern aspen-birch survey unit in Minnesota - Carlton County
[E81-10175] p0210 N81-33561

MISSISSIPPI

A satellite derived technique for estimating rainfall from thunderstorms and hurricanes p0244 A81-43191

MISSOURI

Evaluation of multiband, multitemporal, and transformed LANDSAT MSS data for land cover area estimation --- North Central Missouri
[E81-10161] p0219 N81-29496

Evaluation of large area crop estimation techniques using LANDSAT and ground-derived data --- Missouri
[E81-10200] p0206 N81-29511

Crop area estimation using ground-gathered and sampled LANDSAT data
[PB81-192783] p0207 N81-30507

Crop area estimates using ground-gathered and LANDSAT data. A multitemporal approach: Missouri, 1979
[PB81-186751] p0208 N81-31614

MISSOURI RIVER (US)

Remote sensing of bank erosion along the Missouri River, South Dakota p0213 A81-43263

MOISTURE CONTENT

Determination of moisture from NOAA polar orbiting satellite sounding radiances p0243 A81-41158

Monitoring snow with microwaves p0246 A81-43209

Aircraft active microwave measurements for estimating soil moisture p0271 A81-43547

Application of multispectral reflectance studies of soils - Pre-Landsat p0200 A81-46031

Assessing winter wheat dry matter production via spectral reflectance measurements p0202 A81-49344

MONTANA

Use of remote sensing in landscape stratification for environmental impact assessment p0214 A81-43748

Assessing winter wheat dry matter production via spectral reflectance measurements p0202 A81-49344

Detection of changes in a coal surface mining area by ratioing multidate Landsat digital data
p0228 A81-49809

A crop moisture stress index for large areas and its application in the prediction of spring wheat phenology
[E81-10202] p0210 N81-33573

MOTHS

Effect of forest canopy closure on incoming solar radiance
[E81-10170] p0205 N81-28499

MOUNTAINS

Mountain pine beetle damage surveys with high-altitude panoramic photography p0199 A81-43732

Application of digital terrain data to quantify and reduce the topographic effect on Landsat data
p0259 A81-45433

Mapping alpine soils using color positive and color infrared photographs p0252 A81-46045

Stereoorthophotos as aids in the mapping of high mountain regions p0221 A81-46678

MULTISPECTRAL BAND SCANNERS

Application of digital terrain data to quantify and reduce the topographic effect on Landsat data
p0259 A81-45433

Simulation of orbital image-sensor geometry p0260 A81-46192

Sampling Landsat classifications for crop area estimation p0202 A81-46404

MULTISPECTRAL PHOTOGRAPHY

Some results on the investigation of earth resources by aerial and polygon methods --- Russian book p0269 A81-41476

Aerial data acquisition systems using test-ground polygons p0269 A81-41477

Accuracy of transmission of spectral contrasts in multispectral aerial photography, with application to problems of object recognition p0257 A81-41479

Experience with image combination in multispectral aerial photography p0257 A81-41481

Pseudocolor representation of multispectral aerial images by means of a three-channel projector p0269 A81-41483

The use of the spectral and physical-geographic characteristics of natural objects for the interpretation of multispectral satellite images p0257 A81-41484

Determination of the types and state of crops from multispectral aerial photographs p0197 A81-41486

Evaluation of the possibility of using spectral-band and multispectral aerial photographs for the large-scale survey of natural pastures p0197 A81-41487

The possibilities of the automated classification of agricultural objects on the basis of their multispectral aerial-spaceborne images p0197 A81-41488

Practical application of the method of empty blocks for the computerized determination of the boundaries of agricultural objects p0197 A81-41489

Roles of satellites in hydrology p0245 A81-43199

Potentials of mapping buried glacier ice with Landsat thermal imagery p0246 A81-43204

Remote sensing of coastal pollutants using multispectral data p0233 A81-43245

Relating ground level reflected radiance measurements in the Landsat MSS bandpasses to satellite altitudes p0271 A81-43735

Earth applications orbit analysis for a shuttle-mounted Multispectral Mapper [AAS PAPER 81-182] p0271 A81-45836

Automatic processing of computer compatible tapes with data from multispectral scanners installed in Landsat satellites p0272 A81-46029

A technique for line extraction from LANDSAT multi-spectral scanner satellite data with some applications of the technique [RAE-TR-81010] p0265 N81-31613

Crop area estimates using ground-gathered and LANDSAT data. A multitemporal approach: Missouri, 1979 [PB81-186751] p0208 N81-31614

MULTIVARIATE STATISTICAL ANALYSIS

Maximum likelihood estimation for mixture models [E81-10178] p0210 N81-33564

N

NASA PROGRAMS

Future plans for NASA's Oceanic Processes Program p0231 A81-41997

NASA water resources/hydrology remote sensing program in the 1980's p0244 A81-43179

NASA authorization, 1982, volume 4 [GPO-79-432-VOL-4] p0279 N81-31030

NATIONAL OCEANIC SATELLITE SYSTEM

Future plans for NASA's Oceanic Processes Program p0231 A81-41997

The National Oceanic Satellite System p0236 A81-48548

NATURAL GAS EXPLORATION

The use of imagery of the earth to study the structure of degassing zones within oil and gas basins p0225 A81-42276

The use of satellite imagery for studying the structural features of the Caspian oil and gas region p0227 A81-48684

The interrelation of linear and isometric objects on satellite imagery and the oil and gas structures of the Buzuluk Basin p0227 A81-48685

NEBRASKA

Seasat satellite investigation of the structure of western Nebraska and its application to the evaluation of geothermal resources [LA-UR-81-1454] p0223 N81-30505

NEW ENGLAND (US)

A report on the use of remote sensing techniques for the supervision of New England coastal salt marshes p0253 A81-48944

NEW MEXICO

Landform-vegetation relationships in the northern Chihuahuan Desert [AD-A102896] p0208 N81-32588

NEW YORK

Manual versus digital Landsat analysis for modeling river flooding p0252 A81-43745

Manual versus digital Landsat analysis for delineating river flooding p0252 A81-46405

Cornell University Remote Sensing Program [E81-10174] p0255 N81-33560

NEW ZEALAND

Geomorphic mapping from Landsat-3 Return Beam Vidicon /RBV/ imagery p0226 A81-46194

NICARAGUA

An investigation of vegetation and other Earth resource/feature parameters using LANDSAT and other remote sensing data. 1: LANDSAT. 2: Remote sensing of volcanic emissions [E81-10081] p0209 N81-33543

NIGHT

Radiometry with nighttime DMSP images in digital form --- satellite earth observations p0260 A81-46402

NITRIC ACID

Atmospheric nitric acid and chlorofluoromethane 11 from interferometric spectra obtained at the Observatoire du Pic du Midi [AERONOMICA-ACTA-A-227-1980] p0219 N81-30656

NORTH AMERICA

A description of the reformatted spring small grains labeling procedure used in test 2, part 2 of the US/Canada wheat and barley exploratory experiment [E81-10206] p0207 N81-31597

Weather analysis and interpretation procedures developed for the US/Canada wheat and barley exploratory experiment [E81-10208] p0207 N81-31599

NORTH CAROLINA

Roles of satellites in hydrology p0245 A81-43199

Accuracy evaluation of Landsat digital classification of vegetation in the Great Dismal Swamp p0248 A81-43235

Combined satellite imagery for study of coastal circulation, Onslow Bay, North Carolina p0233 A81-43250

Trophic state determination for shallow coastal lakes from Landsat imagery p0251 A81-43259

Mapping wetlands using orthophotoquads and 35-mm aerial photographs p0251 A81-43543

NORTH DAKOTA

Assessing the Red River of the North 1978 flooding from NOAA satellite data p0248 A81-43219

A temporal/spectral analysis of small grain crops and confusion crops --- North Dakota [E81-10167] p0205 N81-28498

A crop moisture stress index for large areas and its application in the prediction of spring wheat phenology [E81-10202] p0210 N81-33573

NORTHERN HEMISPHERE

Measurements of CF2Cl2, CFCl3, and N2O in the lower stratosphere between 2 deg S and 73 deg N latitude p0214 A81-44515

Eastern North Pacific tropical cyclones of 1980 p0238 A81-49657

NORWAY

Satellite Image Atlas of the earth's glaciers p0246 A81-43202

Operational use of satellite data for snow inventory and runoff forecast p0246 A81-43210

NUTRIENTS

Computer-implemented remote sensing techniques for measuring coastal productivity and nutrient transport systems p0250 A81-43243

O

OCEAN BOTTOM

Applications of aerospace data for detection of submarine springs in Jamaica p0226 A81-43232

Gravimetric studies of the earth's crust in the oceans --- Russian book p0221 A81-43524

Interpretation of hydrographic features seen in the waters off Cape Cod [AD-A102343] p0240 N81-31803

Derivation of shallow ocean bottom reflectance values from color aerial photography [AD-A101105] p0241 N81-33763

OCEAN COLOR SCANNER

Use of ocean color scanner data in water quality mapping p0251 A81-43545

OCEAN CURRENTS

Method for estimation of ocean current velocity from satellite images p0231 A81-41350

Drift and dispersion studies of ocean-dumped waste using Landsat imagery and current drogues p0233 A81-43539

The structure of short gravity waves on the ocean surface p0234 A81-46105

Detection of the Gulf Stream p0235 A81-46115

Tracking of a warm water ring p0235 A81-46117

Satellite-tracked drift buoy observations of the near-surface flow in the eastern mid-latitude North Pacific p0236 A81-47022

Drifting buoy data from the tropical Pacific Ocean during NORPAX equatorial test shuttle experiment [PB81-198939] p0240 N81-31807

OCEAN DATA ACQUISITIONS SYSTEMS

Oceanic Satellite Data Distribution System p0231 A81-41996

Remote sensing of oceanic phytoplankton - Present capabilities and future goals p0232 A81-42215

Development of Marine Observation Satellite-1 [AAS PAPER 81-060] p0278 A81-46238

Nimbus-7 Coastal-Zone Colour Scanner data processing for Earthnet Experience to date p0235 A81-46919

Meteorological applications of the ARGOS system [IAF PAPER 81-121] p0273 A81-47360

The National Oceanic Satellite System p0236 A81-48548

Commercial applications of satellite oceanography p0237 A81-49133

Satellite oceanography - The instruments p0274 A81-49134

Coastal Oceans Monitoring Satellite System (COMSS) system evaluation study [ESS/SS-1035] p0239 N81-30168

Drifting buoy data from the tropical Pacific Ocean during NORPAX equatorial test shuttle experiment [PB81-198939] p0240 N81-31807

Ocean services for the nation. National ocean goals and objectives for the 1980's [PB81-200602] p0240 N81-31808

OCEAN DYNAMICS

Future plans for NASA's Oceanic Processes Program p0231 A81-41997

OCEAN SURFACE

What has been learned from the scanning multi-channel microwave radiometers /SMMRs/ p0269 A81-41995

Imaging ocean waves by synthetic aperture radars with long integration times p0231 A81-42026

A comparison of Seasat 1 altimeter measurements of wave height with measurements made by a pitch-roll buoy p0231 A81-42066

Satellite scatterometer p0232 A81-42102

Investigation of illumination in the image plane of the receiving optical system for the aerial or spaceborne photography of the world ocean p0232 A81-42553

Features of the radar detection of sea surface nonuniformities p0234 A81-43967

Particular features of the ocean glitter pattern observed from a sun-synchronous orbit p0234 A81-45436

Orbit determination requirements for TOPEX --- NASA ocean surface TOPography mapping EXperiment [AAS PAPER 81-158] p0221 A81-45828

Atmospheric correction of Nimbus-7 Coastal Zone Color Scanner imagery p0271 A81-45879

Application of the truncated normal distribution technique to the derivation of sea surface temperatures p0234 A81-45881

The structure of short gravity waves on the ocean surface p0234 A81-46105

SAR ocean imaging mechanisms p0234 A81-46107

The wind speed dependency of ocean microwave backscatter p0234 A81-46109

The study of mesoscale ocean winds p0235 A81-46110

Spatial evolution of ocean wave spectra p0235 A81-46112

Refraction of coastal ocean waves p0235 A81-46113

A search for cold water rings p0235 A81-46116

Correlation between integral and spectral albedos of clouds over water surfaces p0235 A81-47004

Application of GOES visible-infrared data to quantifying mesoscale ocean surface temperatures p0236 A81-47021

Satellite-tracked drift buoy observations of the near-surface flow in the eastern mid-latitude North Pacific p0236 A81-47022

Radar altimeter for ocean remote sensing [IAF PAPER 81-94] p0236 A81-47348

The future for satellite-derived surface winds p0237 A81-49129

SAR processing of partially coherent and sinusoidally dynamic ocean waves p0239 A81-49776

Airborne remote sensing of sea surface chlorophyll and temperature along the outer British Columbia coast p0239 A81-49805

Radar altimeter waveform modeled parameter recovery --- SEASAT-1 data [NASA-TM-73294] p0275 N81-30325

Interpretation of hydrographic features seen in the waters off Cape Cod [AD-A102343] p0240 N81-31803

Imaging radar systems --- ocean surface imaging p0240 N81-33342

Sea surface scattering p0241 N81-33344

Wave orbital velocity, fade and SAR response to azimuth waves p0265 N81-33345

Scattering theory with application to synthetic aperture radar p0265 N81-33348

Gulf of Mexico satellite radar altimetry [NASA-TM-73295] p0224 N81-33760

OCEAN TEMPERATURE

Satellite determination of the mesoscale variability of the sea surface temperature p0234 A81-44861

Atmospheric correction of Nimbus-7 Coastal Zone Color Scanner imagery p0271 A81-45879

Application of the truncated normal distribution technique to the derivation of sea surface temperatures p0234 A81-45881

Tracking of a warm water ring p0235 A81-46117

Application of GOES visible-infrared data to quantifying mesoscale ocean surface temperatures p0236 A81-47021

OCEANOGRAPHIC PARAMETERS

A comparison of Seasat 1 altimeter measurements of wave height with measurements made by a pitch-roll buoy p0231 A81-42066

Aerospace remote sensing of the coastal zone for water quality and biotic productivity applications p0233 A81-43246

Detection of the Gulf Stream p0235 A81-46115

The first ESA remote sensing satellite /ERS/ - The programme and the system [IAF PAPER 81-90] p0236 A81-47344

Regression techniques for oceanographic parameter retrieval using space-borne microwave radiometry p0239 A81-49967

OCEANOGRAPHY

Seasat data applications by commercial users p0231 A81-41974

Future plans for NASA's Oceanic Processes Program p0231 A81-41997

Remote sensing of oceanic phytoplankton - Present capabilities and future goals p0232 A81-42215

Application of remote sensing to monitoring and studying dispersion in ocean dumping p0232 A81-42228

Environmental satellites p0277 A81-42231

Use of ocean color scanner data in water quality mapping p0251 A81-43545

Remote sensing of atmospheres and oceans: Proceedings of the Interactive Workshop on Interpretation of Remotely Sensed Data, Williamsburg, VA, May 23-25, 1979 p0234 A81-45861

Spaceborne synthetic aperture radar for oceanography --- Book p0234 A81-46104

Remote sounding of atmosphere and ocean for climate research /Appleton Lecture/ p0236 A81-47099

First results of the Intercosmos satellite IK-21 [IAF PAPER 81-214] p0274 A81-47409

An analysis of the data of synchronous measurements from the Meteor satellite and ships at the eastern coast of the Caspian Sea p0237 A81-48687

Satellites for oceanography - The promises and the realities p0237 A81-49126

Oceanography from satellites p0237 A81-49127

The promise of satellite altimetry --- for oceanography p0237 A81-49128

Climate, the oceans, and remote sensing p0237 A81-49132

Commercial applications of satellite oceanography p0237 A81-49133

Satellite oceanography - The instruments p0274 A81-49134

Compact and highly sensitive fluorescence lidar for oceanographic measurements p0237 A81-49378

Theoretical investigations concerning the measurement of the plankton concentration with the aid of satellites p0237 A81-49426

Meteosat experience in assisting commercial fishing p0239 A81-49807

Following oceanographic phenomena on the South Coast of Brazil with remote sensing from orbital distance [INPE-1975-RPE/280] p0240 N81-30498

OFFSHORE ENERGY SOURCES

Experimental use of real time SAR imagery in support of oil exploration in the Beaufort Sea p0227 A81-49767

OHIO

A practical method for the verification of computer-processed Landsat data p0261 A81-48943

OHIO RIVER (US)

NASA participation in the 1980 Persistent Elevated Pollution Episode/Northeast Regional Oxidant Study (PEPE/NROS) Project: Operational aspects [NASA-TM-83170] p0220 N81-32708

OIL EXPLORATION

The use of imagery of the earth to study the structure of degassing zones within oil and gas basins p0225 A81-42276

Gravimetric studies of the earth's crust in the oceans --- Russian book p0221 A81-43524

The use of satellite imagery for studying the structural features of the Caspian oil and gas region p0227 A81-48684

The interrelation of linear and isometric objects on satellite imagery and the oil and gas structures of the Buzuluk Basin p0227 A81-48685

Remote sensing in development --- for developing nations p0279 A81-48936

OIL FIELDS

Identification of subresolution high temperature sources using a thermal IR sensor p0273 A81-46401

OIL POLLUTION

Satellite detection of oil on the marine surface p0233 A81-43251

OIL SLICKS

Features of the radar detection of sea surface nonuniformities p0234 A81-43967

OKLAHOMA

Aircraft active microwave measurements for estimating soil moisture p0271 A81-43547

Active microwave measurements for estimating soil moisture in Oklahoma p0199 A81-43744

ONBOARD DATA PROCESSING

Earth applications orbit analysis for a shuttle-mounted Multispectral Mapper [AAS PAPER 81-182] p0271 A81-45836

Program and instrumentation of the satellite experiment Bulgaria-1300 II [IAF PAPER 81-91] p0273 A81-47345

Application of delta modulation in on-board and ground video data processing systems for the purposes of remote sensing [IAF PAPER 81-102] p0260 A81-47361

ONTARIO

Applicability of airborne SAR data to geological mapping p0227 A81-49769

SAR image response over a conifer regeneration site p0203 A81-49770

Application of synthetic aperture radar data to snow cover monitoring p0253 A81-49778

Digital enhancements for vegetation mapping in a subarctic environment p0262 A81-49793

OPTICAL DENSITY

Synergistic relationships among remote-sensing and geophysical media: Geological and hydrological applications --- detecting near-surface ground water in Minnesota p0255 N81-33553

OPTICAL MEASUREMENT

Investigation of the efficiency of the optical sounding of aerosol by the use of spectral photometers p0215 A81-45406

OPTICAL POLARIZATION

A model of plant canopy polarization response p0201 A81-46035

OPTICAL PROPERTIES

An analysis of haze effects on LANDSAT multispectral scanner data [E81-10162] p0263 N81-29497

OPTICAL RADAR

Compact and highly sensitive fluorescence lidar for oceanographic measurements p0237 A81-49378

OPTICAL SCANNERS

Particular features of the ocean glitter pattern observed from a sun-synchronous orbit p0234 A81-45436

OPTICAL THICKNESS

Satellite measurements of tropospheric aerosols [NASA-CR-3459] p0219 N81-31680

ORBIT CALCULATION

Earth applications orbit analysis for a shuttle-mounted Multispectral Mapper [AAS PAPER 81-182] p0271 A81-45836

ORBITAL ELEMENTS

Simulation of orbital image-sensor geometry p0260 A81-46192

The characteristics of combining devices with different survey bands aboard a satellite p0274 A81-48689

ORBITAL VELOCITY

Wave orbital velocity, fade and SAR response to azimuth waves p0265 N81-33345

OREGON

A photo interpretation approach to forest regrowth monitoring using side-looking airborne radar - Grant County, Oregon p0200 A81-45428

Airborne gamma-ray spectrometer and magnetometer survey: Canyon City quadrangle (Oregon), volume 2 [DE81-028682] p0229 N81-33584

Airborne gamma-ray spectrometer and magnetometer survey, Salem quadrangle (Oregon), volume 2 [DE81-028681] p0229 N81-33585

OROGRAPHY

Landsat derived snow cover as an input variable for snow melt runoff forecasting in South Central Colorado p0246 A81-43208

Multisensor analysis of hydrologic features with emphasis on the Seasat SAR p0251 A81-43544

ORTHOPHOTOGRAPHY

A rectification technique for digital orthophoto production p0257 A81-41067

Mapping wetlands using orthophotoquads and 35-mm aerial photographs p0251 A81-43543

Stereoorthophotos as aids in the mapping of high mountain regions p0221 A81-46678

OSTA-1 PAYLOAD

First Shuttle payload loading to begin p0273 A81-46461

OZONE

A differential inversion method for high resolution atmospheric remote sensing p0215 A81-45862

Role of multiple scattering in ozone profile retrieval from satellite measurements in the ultraviolet p0215 A81-45870

P

PACIFIC ISLANDS

Remote sensing of soil radionuclide fluxes in a tropical ecosystem --- Eniwetok and Bikini Atolls [UCRL-84501] p0219 N81-29517

PACIFIC NORTHWEST (US)

Technical aspects of forest inventory demonstrations using Landsat data - Projects in the Pacific Northwest States p0203 A81-49764

PACIFIC OCEAN

Satellite detection of oil on the marine surface p0233 A81-43251

Satellite-tracked drift buoy observations of the near-surface flow in the eastern mid-latitude North Pacific p0236 A81-47022

The occurrence of vertical tilt in tropical cyclones p0238 A81-49656

Eastern North Pacific tropical cyclones of 1980 p0238 A81-49657

Airborne remote sensing of sea surface chlorophyll and temperature along the outer British Columbia coast p0239 A81-49805

Drifting buoy data from the tropical Pacific Ocean during NORPAX equatorial test shuttle experiment [PB81-198939] p0240 N81-31807

PARALLEL PROCESSING (COMPUTERS)

Parallel processing implementations of a contextual classifier for multispectral remote sensing data p0272 A81-46028

Inventory estimation on the massively parallel processor --- from satellite based images p0259 A81-46052

PARAMETER IDENTIFICATION

Inversion of multiwavelength radiometer measurements by three-dimensional filtering p0271 A81-45873

PARTICLE SIZE DISTRIBUTION

Satellite measurements of atmospheric aerosols [AD-A103493] p0220 N81-33720

PATTERN RECOGNITION

Accuracy of transmission of spectral contrasts in multispectral aerial photography, with application to problems of object recognition p0257 A81-41479

Experience with image combination in multispectral aerial photography p0257 A81-41481

Practical application of the method of empty blocks for the computerized determination of the boundaries of agricultural objects p0197 A81-41489

A measure of reliability for classification of earth satellite data p0257 A81-42631

From landforms to avian habitat - A look at topology p0214 A81-43739

A comparison of automatic classification algorithms for land use map by remotely sensed data p0215 A81-44701

Progress in passive microwave remote sensing - Nonlinear retrieval techniques --- for meteorological parameters p0271 A81-45872

An assessment of Landsat data acquisition history on identification and area estimation of corn and soybeans p0200 A81-46032

Procedure M - A framework for stratified area estimation --- in multispectral scanner data processing p0201 A81-46036

Maximum likelihood estimation of label imperfection probabilities and its use in the identification of mislabeled patterns --- with application to Landsat MSS data processing p0259 A81-46040

Inventory estimation on the massively parallel processor --- from satellite based images p0259 A81-46052

Procedure 1 and forestland classification using Landsat data p0201 A81-46055

Integration and comparison of SAR and MSS data for potato crop area estimation p0203 A81-49766

Interpreter evaluations of airborne radar imagery for ecological and land/use cover classification in southern Manitoba p0218 A81-49773

Colour - The critical photointerpretation element in the identification of rangeland plant communities on colour and colour-infrared aerial photography p0203 A81-49786

Maximum likelihood clustering with dependent feature trees [E81-10186] p0263 N81-29502

Evaluation of large area crop estimation techniques using LANDSAT and ground-derived data --- Missouri [E81-10200] p0206 N81-29511

Interactive digital image processing for terrain data extraction [AD-A101321] p0264 N81-30499

Improved version of the split routine for CLASSY [E81-10210] p0264 N81-31600

Identifying igneous rocks in an arid environment on aerial photography by photo tone and photo texture [AD-A102808] p0228 N81-32587

Partially automated object extraction from aerial photographs and land maps p0266 N81-33528

The use of charge transfer devices for LANDSAT pattern classification [E81-10087] p0266 N81-33544

Evaluation of LANDSAT data analysis for forest survey --- northeastern aspen-birch survey unit in Minnesota - Carlton County [E81-10175] p0210 N81-33561

Maximum likelihood labeling [E81-10177] p0267 N81-33563

PATTERN REGISTRATION

Evaluation of multiband, multitemporal, and transformed LANDSAT MSS data for land cover area estimation --- North Central Missouri [E81-10161] p0219 N81-29496

A description of the reformatted spring small grains labeling procedure used in test 2, part 2 of the US/Canada wheat and barley exploratory experiment [E81-10206] p0207 N81-31597

An evaluation of MSS P-format data registration [E81-10171] p0267 N81-33557

As-built design specification of the automatic registration system for the cartographic technology laboratory [E81-10176] p0267 N81-33562

PEAT

Current resource mapping and environmental monitoring applications using Landsat MSS data in Scotland p0218 A81-49806

PENNSYLVANIA

Application of digital terrain data to quantify and reduce the topographic effect on Landsat data p0259 A81-45433

Space based topographic mapping experiment using Seasat synthetic aperture radar and LANDSAT 3 return beam vidicon imagery [NASA-CR-164675] p0223 N81-30496

PERFORMANCE TESTS

Performance evaluation of a spaceborne scatterometer p0269 A81-41920

PHENOLOGY

Remote sensing and mapping of pastures p0213 A81-42281

Rapeseed - Guidelines for operational monitoring p0203 A81-49784

Analysis of US spring wheat and spring barley periodic ground truth [E81-10203] p0208 N81-32576

Scatterometer measurements on crop and soil surfaces p0208 N81-33349

A project to evaluate moisture stress and phenological factors in corn and soybean areas of southwestern and south-central Minnesota p0209 N81-33554

Crop phenology and LANDSAT-based irrigated lands inventory in the high plains: Appendices [E81-10172] p0210 N81-33558

Crop phenology and LANDSAT-based irrigated lands inventory in the high plains [E81-10173] p0210 N81-33559

A crop moisture stress index for large areas and its application in the prediction of spring wheat phenology [E81-10202] p0210 N81-33573

PHILIPPINES

Tiwi geothermal project - The Philippines p0225 A81-41908

PHOTOGEOLOGY

Tiwi geothermal project - The Philippines p0225 A81-41908

The use of imagery of the earth to study the structure of degassing zones within oil and gas basins p0225 A81-42276

Concerning the hydrogeological significance of faults on platform regions, as revealed by space imagery p0225 A81-42277

Ring structures of Precambrian shields, based on the interpretation of space imagery p0225 A81-42278

Fitoexomorphogenic analysis of geological environment changes in the South Aral Sea, based on aerial and space imagery p0225 A81-42279

Space research on seismic regions p0225 A81-42280

Geological interpretation in an interactive mode in automated systems of digital image processing p0225 A81-42289

Hydrogeology of glacial deposits from aerial photographs p0252 A81-43548

The possibility of using an aerial thermal survey for studying the structure of the salt bed in the Gulf of Kara-Bogaz-Gol p0226 A81-44061

A radar image time series p0226 A81-45430

Ore-controlling space geological objects and their assessment techniques applied to mineral prediction [IAF PAPER 81-107] p0227 A81-47353

The informational estimation of the effectiveness of using satellite imagery in hydrogeological research p0227 A81-48683

The use of satellite imagery for studying the structural features of the Caspian oil and gas region p0227 A81-48684

The interrelation of linear and isometric objects on satellite imagery and the oil and gas structures of the Buzuluk Basin p0227 A81-48685

Complex processing of satellite images and the geological interpretation p0227 A81-48690

Interactive system for the regional prognosis of raw mineral resources, based on ground-based and satellite imagery data p0227 A81-48691

Lineaments - Problems and directions of studies by means of aerial and space tools and methods p0221 A81-48696

Landsat data as a basis for regional environmental assessment within the Columbia Plateau p0218 A81-49798

Geological and terrain analysis of the Annapolis County region of Nova Scotia - An application of digital Landsat, radar and colour infrared data p0227 A81-49802

Atmospheric correction to LANDSAT data for limonite discrimination p0228 N81-31594

Visual enhancement of images of natural resources: Applications in geology [E81-10181] p0228 N81-32575

Remote sensing for engineering site selection [AD-A102810] p0219 N81-32586

Identifying igneous rocks in an arid environment on aerial photography by photo tone and photo texture [AD-A102809] p0228 N81-32587

Comparison of laboratory reflectance spectra and LANDSAT multispectral images of Hawaiian lava flows [E81-10061] p0266 N81-33541

An investigation of vegetation and other Earth resource/feature parameters using LANDSAT and other remote sensing data. 1: LANDSAT. 2: Remote sensing of volcanic emissions [E81-10081] p0209 N81-33543

PHOTOGRAMMETRY

A rectification technique for digital orthophoto production p0257 A81-41057

Experience with the determination of optical image distortions of landscape elements on IR aerial photographs p0257 A81-41480

Experience with image combination in multispectral aerial photography p0257 A81-41481

Analysis of the geometry of a frame photograph p0221 A81-42554

Determination of the external-orientation elements of single photographs and stereopairs p0257 A81-42555

Topographic and cartographic applications of photogrammetry p0221 A81-42847

Multispectral kelp resource surveys p0232 A81-43244

Hardware aspects of digital mapping p0271 A81-43530

Correlation techniques and devices --- for photogrammetry p0258 A81-43531

Automation in photogrammetry p0258 A81-43532

Skylab in retrospect p0277 A81-43535

A capture-recapture approach for estimation of detection probabilities in aerial surveys p0258 A81-43546

Rainbow 80; Fall Technical Meeting, Niagara Falls, NY, October 7-10, 1980, ASP Technical Papers p0198 A81-43727

Manual versus digital Landsat analysis for modeling river flooding p0252 A81-43745

A radar image time series p0226 A81-45430

A comparison between two photographic methods for the determination of relative bidirectional reflectance p0259 A81-45431

A top-down approach to the use of simulation in computer system design --- of Edit Processor of Integrated Photogrammetric Instrument Network p0274 A81-48331

Image correlation algorithms p0261 A81-48473

The influence of the accuracy of determining the elements of the external orientation of a stereopair on the processing of aerial photographs on the basis of adjusting elements p0261 A81-48773

Application of new precision measuring systems for photogrammetric comparators [BMFT-FB-T-80-134] p0276 N81-32595

Photogrammetry in China p0222 N81-33526

Military geodesy and geospace science, unit one [AD-A104038] p0222 N81-33581

PHOTOGRAPHIC EQUIPMENT

The signal-to-noise ratio of a space photographic system p0269 A81-42284

PHOTOGRAPHIC PROCESSING

Accuracy of transmission of spectral contrasts in multispectral aerial photography, with application to problems of object recognition p0257 A81-41479

PHOTOGRAPHIC RECTIFIERS

A rectification technique for digital orthophoto production p0257 A81-41057

PHOTOGRAPHS

Determination of the external-orientation elements of single photographs and stereopairs p0257 A81-42555

Analysis of landfills with historic airphotos p0216 A81-46407

Interim catalog ground data summary, data acquisition year 1976 [E81-10132] p0209 N81-33546

PHOTOINTERPRETATION

Some results on the investigation of earth resources by aerial and polygon methods --- Russian book p0269 A81-41476

Pseudocolor representation of multispectral aerial images by means of a three-channel projector p0269 A81-41483

The use of the spectral and physical-geographic characteristics of natural objects for the interpretation of multispectral satellite images p0257 A81-41484

Determination of the types and state of crops from multispectral aerial photographs p0197 A81-41486

Evaluation of the possibility of using spectral-band and multispectral aerial photographs for the large-scale survey of natural pastures p0197 A81-41487

The possibilities of the automated classification of agricultural objects on the basis of their multispectral aerial-spaceborne images p0197 A81-41488

Practical application of the method of empty blocks for the computerized determination of the boundaries of agricultural objects p0197 A81-41489

Ring structures of Precambrian shields, based on the interpretation of space imagery p0225 A81-42278

Geological interpretation in an interactive mode in automated systems of digital image processing p0225 A81-42289

A measure of reliability for classification of earth satellite data p0257 A81-42631

Hydrogeologic interpretations of Landsat imagery in arid zones of South and West Africa p0248 A81-43229

Landsat classification of coastal wetlands in Texas p0248 A81-43234

A comparison of remote sensing techniques for Minnesota wetlands classification p0249 A81-43239

Landsat interpretation of prairie lakes and wetlands of eastern South Dakota p0249 A81-43240

Assessment and classifications of selected Illinois lakes through the application of space technology p0250 A81-43255

Mapping irrigated lands in Western Kansas from Landsat p0198 A81-43265

Comparison of sampling procedures and data analysis for a land-use and land-cover map p0213 A81-43533

Spatial correlation effects upon accuracy of supervised classification of land cover p0213 A81-43534

Rainforest species on large-scale color photos p0198 A81-43536

Extravisual damage detection - Defining the standard normal tree p0198 A81-43537

Vegetable crop management with remote sensing p0198 A81-43540

Wetland mapping from digitized aerial photography p0252 A81-43549

Urban area update procedures using Landsat data p0214 A81-43733

On the analysis of remote sensing data to predict selected vegetative variables p0258 A81-43736

Use of remote sensing in landscape stratification for environmental impact assessment p0214 A81-43748

A comparison of automatic classification algorithms for land use map by remotely sensed data p0215 A81-44701

A photo interpretation approach to forest regrowth monitoring using side-looking airborne radar - Grant County, Oregon p0200 A81-45428

Land use mapping of Hong Kong from Landsat images - An evaluation p0215 A81-45434

Procedure M - A framework for stratified area estimation --- in multispectral scanner data processing p0201 A81-46036

A case study of soil erosion detection by digital analysis of the remotely sensed multispectral Landsat scanner data of a semi-arid land in southern India p0201 A81-46050

Alternative 'scale up' estimators for aerial surveys where both detection and classification errors exist p0260 A81-46197

Microdensitometry to identify saline rangelands on 70-mm color-infrared aerial film p0202 A81-46406

Large-area histograms from Meteosat images p0260 A81-46917

The informational estimation of the effectiveness of using satellite imagery in hydrogeological research p0227 A81-48683

The interrelation of linear and isometric objects on satellite imagery and the oil and gas structures of the Buzuluk Basin p0227 A81-48685

Complex processing of satellite images and the geological interpretation p0227 A81-48690

Suburban soil loss and runoff simulation assisted by interpretation of large scale aerial photography p0253 A81-48941

ICAP - An Interactive Cluster Analysis Procedure for analyzing remotely sensed data p0261 A81-49346

Operational applications for analysis of agricultural crops and cultural practices p0203 A81-49756

Multistage remote sensing in exploratory ecodistrict land classification p0217 A81-49759

Application of temporal Landsat forest digital data for updating the Yukon RRAMS data base using Aries --- Renewable Resources And Management Statistics p0203 A81-49760

Colour - The critical photointerpretation element in the identification of rangeland plant communities on colour and colour-infrared aerial photography p0203 A81-49786

Photointerpretation of fire damage to trees in a ponderosa pine/bunchgrass community p0204 A81-49787

Interpretation techniques applied to mixed terrains p0218 A81-49788

Benefits of using airborne remote sensing for Thematic Mapping p0275 A81-49801

Role of aerial photographs in classification of Landsat data p0262 A81-49808

Space based topographic mapping experiment using Seasat synthetic aperture radar and LANDSAT 3 return beam vidicon imagery [NASA-CR-164675] p0223 N81-30496

Field Study for Remote Sensing: An instructor's manual [NASA-CP-2155] p0279 N81-32564

The workshop --- use and application of remotely sensed data p0280 N81-32566

Why surface-truth field study is needed in remote-sensing instruction p0280 N81-32567

LANDSAT C workshop field/laboratory exercises p0280 N81-32571

Photographic technology development project: Timber typing in the Tahoe Basin using high altitude panoramic photography [NASA-CR-161082] p0208 N81-32578

Identifying igneous rocks in an arid environment on aerial photography by photo tone and photo texture [AD-A102809] p0228 N81-32587

Partially automated object extraction from aerial photographs and land maps p0266 N81-33528

Comparison of laboratory reflectance spectra and LANDSAT multispectral images of Hawaiian lava flows [E81-10061] p0266 N81-33541

Development of alternative data analysis techniques for improving the accuracy and specificity of natural resource inventories made with remote sensing data p0266 N81-33551

PHOTOMAPPING

The use of satellite data in predicting spring flow in the basins of the upper Ob' and upper Enisei p0243 A81-41723

Remote sensing and mapping of pastures p0213 A81-42281

Analysis of the geometry of a frame photograph p0221 A81-42554

The use of spaceborne photography for topographic mapping p0221 A81-42556

Satellite hydrology. Proceedings of the Fifth Annual William T. Pecora Memorial Symposium on Remote Sensing, Sioux Falls, SD, June 10-15, 1979 p0243 A81-43176

Corps of Engineers utilization of satellites for hydrologic purposes p0244 A81-43180

Satellite snow mapping techniques with emphasis on the use of Landsat p0245 A81-43200

Landsat derived snow cover as an input variable for snow melt runoff forecasting in South Central Colorado p0246 A81-43208

Soil moisture applications of the heat capacity mapping mission p0197 A81-43224

Applications of Landsat imagery to a coastal inlet stability study p0250 A81-43249

Application of remote sensing for California irrigated lands assessment p0213 A81-43261

Hardware aspects of digital mapping p0271 A81-43530

Comparison of sampling procedures and data analysis for a land-use and land-cover map p0213 A81-43533

Spatial correlation effects upon accuracy of supervised classification of land cover p0213 A81-43534

Vegetable crop management with remote sensing p0198 A81-43540

Mapping wetlands using orthophotoquads and 35-mm aerial photographs p0251 A81-43543

Use of ocean color scanner data in water quality mapping p0251 A81-43545

Mapping the Great Salt Lake shoreline and associated waterfowl habitat from Landsat data p0252 A81-43742

Aerial thermal survey in the study of earth resources --- Russian book p0277 A81-43981

Water quality mapping from Landsat digital data p0252 A81-45429

Earth applications orbit analysis for a shuttle-mounted Multispectral Mapper [AAS PAPER 81-182] p0271 A81-45836

Application of multispectral reflectance studies of soils - Pre-Landsat p0200 A81-46031

Mapping alpine soils using color positive and color infrared photographs p0252 A81-46045

Geomorphic mapping from Landsat-3 Return Beam Vidicon /RBV/ imagery p0226 A81-46194

European industrial space projects [AAS PAPER 81-053] p0278 A81-46234

Stereoorthophotos as aids in the mapping of high mountain regions p0221 A81-46678

The space engineering use efficiency for forest study [IAF PAPER 81-108] p0202 A81-47354

Derivation of formulas for the correlation of coordinate points of different-scale photographs and quasi-photographs p0261 A81-48772

Oceanography from satellites p0237 A81-49127

Canadian Symposium on Remote Sensing, 6th, Halifax, Canada, May 21-23, 1980, Proceedings p0279 A81-49751

The integration of remote sensing in environmental decision making for the Maritimes p0217 A81-49752

Multistage remote sensing in exploratory ecodistrict land classification p0217 A81-49759

Present state of remote sensing development in Poland p0279 A81-49763

Principal components enhancements versus classifications of Landsat images for forestry applications p0203 A81-49782

Land use/cover mapping for Halifax County - Remote sensing alternatives p0218 A81-49783

Digital enhancements for vegetation mapping in a subarctic environment p0262 A81-49793

Resource inventory and terrain analysis in north western Manitoba from integrated remote sensing data p0218 A81-49803

Current resource mapping and environmental monitoring applications using Landsat MSS data in Scotland p0218 A81-49806

A simulation of Thematic Mapper performance in an agricultural application p0204 A81-49810

Generation and use of digital elevation data for large areas p0221 A81-49811

Military geodesy and geospace science, unit one [AD-A104038] p0222 N81-33581

PHOTORECONNAISSANCE

Aerial data acquisition systems using test-ground polygons p0269 A81-41477

PLAINS

Mapping irrigated cropland on the High Plains using Landsat p0198 A81-43266

PLANKTON

Remote sensing of oceanic phytoplankton - Present capabilities and future goals p0232 A81-42215

Remote sensing in biological oceanography p0237 A81-49130

Theoretical investigations concerning the measurement of the plankton concentration with the aid of satellites p0237 A81-49426

Airborne remote sensing of sea surface chlorophyll and temperature along the outer British Columbia coast p0239 A81-49805

Environmental assessment of the Alaskan continental shelf: Reports of principal investigators. Volume 1: Reactors - birds, plankton, littoral, benthos [PB81-196263] p0240 N81-30780

PLANT STRESS

The effect of sensor bandpass and spectral response in crop stress detection p0199 A81-43737

Large area application of a corn hazard model --- Soviet Union [E81-10164] p0205 N81-28497

Soil moisture inferences from thermal infrared measurements of vegetation temperatures [E81-10184] p0208 N81-29500

The environmental vegetation index: A tool potentially useful for arid land management --- Texas and Mexico, plant growth stress due to water deficits [E81-10191] p0206 N81-29505

A study of Minnesota land and water resources using remote sensing, Volume 14 [E81-10166] p0254 N81-33550

A project to evaluate moisture stress and phenological factors in corn and soybean areas of southwestern and south-central Minnesota p0209 N81-33554

A crop moisture stress index for large areas and its application in the prediction of spring wheat phenology [E81-10202] p0210 N81-33573

PLANTS (BOTANY)

A model of plant canopy polarization response p0201 A81-46035

Colour - The critical photointerpretation element in the identification of rangeland plant communities on colour and colour-infrared aerial photography p0203 A81-49786

PLASMA INTERACTIONS

New complex for ionosphere-magnetosphere study 'Intercosmos-Bulgaria-1300' [IAF PAPER 81-212] p0273 A81-47407

PLATEAUS

Interactive processing of Landsat image for morphopedological studies p0259 A81-46043

The informational estimation of the effectiveness of using satellite imagery in hydrogeological research p0227 A81-48683

PLAYAS

Optical and digital analyses of Landsat data depicting hydrogeological features of the Daryacheh-Ye-Namak area, Iran p0225 A81-43215

PLOWING

Experiment plan: Row and roughness effects on dependence of active microwave measurements of soil moisture [E81-10209] p0211 N81-33575

POINT SOURCES

Environmental measurements of power plant cooling tower and stack plumes [DOE/EV-02463/6] p0219 N81-30695

POLAND

Present state of remote sensing development in Poland p0279 A81-49763

POLAR METEOROLOGY

Possible applications of communication satellites for research tasks in polar regions [BMFT-FB-W-80-029] p0267 N81-33587

POLAR REGIONS

Satellite Image Atlas of the earth's glaciers p0246 A81-43202

POLARIZATION (WAVES)

Optimal polarization concept in radar imaging --- electromagnetic scattering p0265 N81-33350

POLLUTION MONITORING

Stratospheric sulfate from the Gareloi eruption, 1980 - Contribution to the 'ambient' aerosol by a poorly documented volcanic eruption p0213 A81-41404

Application of remote sensing to monitoring and studying dispersion in ocean dumping p0232 A81-42228

Remote sensing of coastal pollutants using multispectral data p0233 A81-43245

Satellite detection of oil on the marine surface p0233 A81-43251

Application of digital image processing techniques and information systems to water quality monitoring of Lake Tahoe p0251 A81-43258

Features of the radar detection of sea surface nonuniformities p0234 A81-43967

Airborne simultaneous spectroscopic detection of laser-induced water Raman backscatter and fluorescence from chlorophyll a and other naturally occurring pigments p0253 A81-47647

Comparative measurements of stratospheric CH4 and CO concentrations with spectrograph and correlation radiometers p0217 A81-49433

NASA participation in the 1980 Persistent Elevated Pollution Episode/Northeast Regional Oxidant Study (PEPE/NROS) Project: Operational aspects [NASA-TM-83170] p0220 N81-32708

Quantification of non-point source sedimentation through densitometric analysis of color infrared aerial photography [PB81-209157] p0255 N81-33599

POLLUTION TRANSPORT

Aerospace remote sensing of the coastal zone for water quality and biotic productivity applications p0233 A81-43246

Drift and dispersion studies of ocean-dumped waste using Landsat imagery and current drogues p0233 A81-43539

Environmental measurements of power plant cooling tower and stack plumes [DOE/EV-02463/6] p0219 N81-30695

NASA participation in the 1980 Persistent Elevated Pollution Episode/Northeast Regional Oxidant Study (PEPE/NROS) Project: Operational aspects [NASA-TM-83170] p0220 N81-32708

Some methods of multitemporal analysis of LANDSAT images resulting from a study on Venice Lagoon [E81-10205] p0267 N81-33574

POTATOES

Integration and comparison of SAR and MSS data for potato crop area estimation p0203 A81-49766

POWER SPECTRA

Geomagnetic field mapping from a satellite: Spatial power spectra of the geomagnetic field at various satellite altitudes relative to natural noise sources and instrument noise [PUBL-1810] p0275 N81-29480

PRECAMBRIAN PERIOD

Ring structures of Precambrian shields, based on the interpretation of space imagery p0225 A81-42278

PRESSURE ICE

Radar detection of sea-ice ridges and icebergs in frozen oceans at incidence angles from 0 deg to 90 deg p0238 A81-49775

PROBABILITY DISTRIBUTION FUNCTIONS

Histogram estimation for multiple-detector sensors p0262 A81-48812

PROBABILITY THEORY

A capture-recapture approach for estimation of detection probabilities in aerial surveys p0258 A81-43546

Q

QUEBEC

Principal components enhancements versus classifications of Landsat images for forestry applications p0203 A81-49782

Use of Landsat images in the monitoring and study of the LG 2 reservoir during the filling period p0254 A81-49797

R

RADAR CROSS SECTIONS

Look direction dependence of radar backscattering cross section for agricultural fields p0199 A81-43741

Altimeter rain detection [NASA-TM-73291] p0275 N81-29408

RADAR DETECTION

Radar detection of sea-ice ridges and icebergs in frozen oceans at incidence angles from 0 deg to 90 deg p0238 A81-49775

RADAR GEOLOGY

Use of imaging radar for geology and archeology p0226 A81-43730

Applicability of airborne SAR data to geological mapping p0227 A81-49769

RADAR IMAGERY

Imaging ocean waves by synthetic aperture radars with long integration times p0231 A81-42026

Wave direction measured by four different systems p0232 A81-42622

The use of radar imagery for surface water investigations p0247 A81-43211

A preliminary analysis of SAR mapping of the Manitoba flood, May 1979 p0248 A81-43220

Use of imaging radar for geology and archeology p0226 A81-43730

Training site statistics from Landsat and Seasat satellite imagery registered to a common map base p0258 A81-43734

Use of Seasat satellite radar imagery for the detection of standing water beneath forest vegetation p0199 A81-43743

Texture measurements from Seasat - SAR images for urban land use interpretation p0214 A81-43749

A photo interpretation approach to forest regrowth monitoring using side-looking airborne radar - Grant County, Oregon p0200 A81-45428

A radar image time series p0226 A81-45430

Crop classification with a Landsat/radar sensor combination p0200 A81-46033

Radar image preprocessing --- of SEASAT-A SAR data p0272 A81-46038

The methodology of CIAT's land resource study of tropical America p0216 A81-46046

Spaceborne synthetic aperture radar for oceanography --- Book p0234 A81-46104

SAR ocean imaging mechanisms p0234 A81-46107

Detection of the Gulf Stream p0235 A81-46115

A search for cold water rings p0235 A81-46116

Tracking of a warm water ring p0235 A81-46117

Use of elevation models for landform analysis by Seasat-SAR imagery [IAF PAPER 81-98] p0260 A81-47349

Radar-optical-topographic transformations for scene content analysis p0261 A81-48552

Canadian Symposium on Remote Sensing, 6th, Halifax, Canada, May 21-23, 1980, Proceedings p0279 A81-49751

The integration of remote sensing in environmental decision making for the Maritimes p0217 A81-49752

The airborne SAR project - Conclusions and applications p0275 A81-49765

Integration and comparison of SAR and MSS data for potato crop area estimation p0203 A81-49766

Experimental use of real time SAR imagery in support of oil exploration in the Beaufort Sea p0227 A81-49767

An investigation of the autocorrelation function of radar images p0262 A81-49768

Applicability of airborne SAR data to geological mapping p0227 A81-49769

SAR image response over a conifer regeneration site p0203 A81-49770

Airborne impulse radar sounding of sea ice p0238 A81-49771

The Lake Melville/Labrador offshore synthetic aperture radar study - Winter 1979 p0238 A81-49772

Interpreter evaluations of airborne radar imagery for ecological and land/use cover classification in southern Manitoba p0218 A81-49773

Single and multiple parameter microwave signatures of sea ice p0238 A81-49774

SAR processing of partially coherent and sinusoidally dynamic ocean waves p0239 A81-49776

Digital image analysis of SAR imagery for the detection of icebergs p0239 A81-49777

Application of synthetic aperture radar data to snow cover monitoring p0253 A81-49778

Optimizing imaging radar parameters for ice reconnaissance p0239 A81-49779

Cartographic accuracy of synthetic aperture radar imagery p0262 A81-49780

Land use/cover mapping for Halifax County - Remote sensing alternatives p0218 A81-49783

Acquisition and preprocessing of images collected by future European Space Agency satellites p0263 A81-49814

Space based topographic mapping experiment using Seasat synthetic aperture radar and LANDSAT 3 return beam vidicon imagery [NASA-CR-164675] p0223 N81-30486

Seasat satellite investigation of the structure of western Nebraska and its application to the evaluation of geothermal resources [LA-UR-81-1454] p0223 N81-30505

Coherent and incoherent radar scattering from rough surfaces and vegetated areas - conferences [ESA-SP-166] p0206 N81-33339

Introduction to the workshop --- on coherent and incoherent radar scattering from rough surfaces and vegetated areas p0276 N81-33340

Imaging radar systems --- ocean surface imaging p0240 N81-33342

Optimal polarization concept in radar imaging --- electromagnetic scattering p0265 N81-33350

RADAR MAPS

Multisensor analysis of hydrologic features with emphasis on the Seasat SAR p0251 A81-43544

Utilisation and benefits of SLAR in operational ice data acquisition p0253 A81-49761

RADAR MEASUREMENT

The study of mesoscale ocean winds p0235 A81-46110

Radar methods for studying the earth --- Russian book p0273 A81-46924

RADAR SCATTERING

Satellite scatterometer p0232 A81-42102

Potential application of satellite radar to monitor soil moisture p0270 A81-43223

Aircraft active microwave measurements for estimating soil moisture p0271 A81-43547

Features of the radar detection of sea surface nonuniformities p0234 A81-43967

Aerosol sounding by means of aircraft-borne optical radar p0217 A81-49431

Radar altimeter waveform modeled parameter recovery --- SEASAT-1 data [NASA-TM-73294] p0275 N81-30325

Coherent and incoherent radar scattering from rough surfaces and vegetated areas --- conferences [ESA-SP-166] p0206 N81-33339

Sea surface scattering p0241 N81-33344

Wave orbital velocity, fade and SAR response to azimuth waves p0265 N81-33345

Scattering theory with application to synthetic aperture radar p0265 N81-33348

Scatterometer measurements on crop and soil surfaces p0206 N81-33349

Optimal polarization concept in radar imaging --- electromagnetic scattering p0265 N81-33350

Scatterometer calibration and data correction p0265 N81-33351

RADIANCE

Determination of moisture from NOAA polar orbiting satellite sounding radiances p0243 A81-41158

The effect of angular distribution models on the estimation of the earth's albedo p0269 A81-41915

A new numerical treatment of the source function in the radiative transfer equation --- for vertical atmospheric temperature and humidity profile retrieval from satellite radiance measurements p0269 A81-41916

On the analysis of remote sensing data to predict selected vegetative variables p0258 A81-43736

Atmospheric correction of Nimbus-7 Coastal Zone Color Scanner imagery p0271 A81-45879

Generation and use of digital elevation data for large areas p0221 A81-49811

Histogram estimation for multiple-detector sensors p0262 A81-49812

A comparative study of the thematic mapper and LANDSAT spectral bands from field measurement data [E81-10165] p0209 N81-33549

RADIATION DOSAGE

Remote sensing of soil radionuclide fluxes in a tropical ecosystem --- Eniwetok and Bikini A tolls [UCRL-84501] p0219 N81-29517

RADIATION TRANSPORT

Theoretical investigations concerning the measurement of the plankton concentration with the aid of satellites p0237 A81-49426

RADIATIVE TRANSFER

A new numerical treatment of the source function in the radiative transfer equation --- for vertical atmospheric temperature and humidity profile retrieval from satellite radiance measurements p0269 A81-41916

Requirements of space-borne microwave radiometers for detecting soil moisture contents p0270 A81-43225

Study of the influence of the atmosphere on the performance of an imaging microwave radiometer [ESA-CR(P)-1421] p0275 N81-30342

A study of the effects of the atmosphere on thematic mapper observations [E81-10056] p0276 N81-33540

RADIO ALTIMETERS

A comparison of Seasat 1 altimeter measurements of wave height with measurements made by a pitch-roll buoy p0231 A81-42066

Land subsidence measured by satellite radar altimetry p0270 A81-43260

Orbit determination requirements for TOPEX --- NASA ocean surface TOPography mapping EXperiment [AAS PAPER 81-158] p0221 A81-45828

Radar altimeter for ocean remote sensing [IAF PAPER 81-94] p0236 A81-47348

Altimeter rain detection [NASA-TM-73291] p0275 N81-29408

Radar altimeter waveform modeled parameter recovery --- SEASAT-1 data [NASA-TM-73294] p0275 N81-30325

Ice sheet altimetry [NASA-CR-156877] p0240 N81-31605

Gulf of Mexico satellite radar altimetry [NASA-TM-73295] p0224 N81-33760

RADIOACTIVE ISOTOPES

Remote sensing of soil radionuclide fluxes in a tropical ecosystem --- Eniwetok and Bikini A tolls [UCRL-84501] p0219 N81-29517

RADIOMETERS

Radiometry with nighttime DMSP images in digital form --- satellite earth observations p0260 A81-46402

Histogram estimation for multiple-detector sensors p0262 A81-49812

RADIOMETRIC RESOLUTION

Experience with the determination of optical image distortions of landscape elements on IR aerial photographs p0257 A81-41480

An examination of spectral band ratioing to reduce the topographic effect on remotely sensed data p0221 A81-45427

Inversion of multiwavelength radiometer measurements by three-dimensional filtering p0271 A81-45873

Atmospheric correction of Nimbus-7 Coastal Zone Color Scanner imagery p0271 A81-45879

Does the use of two radiometers correct for irradiance changes during measurements p0272 A81-46196

Generation and use of digital elevation data for large areas p0221 A81-49811

Histogram estimation for multiple-detector sensors p0262 A81-49812

Atmospheric correction to LANDSAT data for limonite discrimination p0228 N81-31594

RAIN

Insights into errors of SMS-inferred GATE convective rainfall p0243 A81-42095

Satellite applications in river and flood forecasting p0243 A81-43178

A satellite derived technique for estimating rainfall from thunderstorms and hurricanes p0244 A81-43191

Utilizing GOES imagery to determine convective storm characteristics in data deficient regions p0245 A81-43192

Rain estimation over several areas of the globe using satellite imagery p0245 A81-43193

A statistical approach to rainfall estimation using satellite data p0245 A81-43198

Altimeter rain detection [NASA-TM-73291] p0275 N81-29408

RAIN FORESTS

Rainforest species on large-scale color photos p0198 A81-43536

RAIN GAGES

Utilizing GOES imagery to determine convective storm characteristics in data deficient regions p0245 A81-43192

RAMAN SPECTRA

Airborne simultaneous spectroscopic detection of laser-induced water Raman backscatter and fluorescence from chlorophyll a and other naturally occurring pigments p0253 A81-47647

Use of water Raman emission to correct airborne laser fluorosensor data for effects of water optical attenuation p0253 A81-47676

RANGELANDS

Use of Landsat digital data to assist in mapping soils on Arizona rangelands p0201 A81-46047

Microdensitometry to identify saline rangelands on 70-mm color-infrared aerial film p0202 A81-46406

Colour - The critical photointerpretation element in the identification of rangeland plant communities on colour and colour-infrared aerial photography p0203 A81-49786

Spectral measurement of rangeland p0218 A81-49790

Remote sensing and land use planning p0218 A81-49792

Role of aerial photographs in classification of Landsat data p0262 A81-49808

Spectral properties of Arizona soils and rangelands and their relationship to LANDSAT digital data p0207 N81-31595

Dryland pasture and crop conditions as seen by HCMM [E81-10080] p0209 N81-33542

RECLAMATION

Remote methods and desert conservation --- Russian book p0213 A81-43523

RECREATION

Research on assessment of the recreational value of forests using Landsat digital data p0203 A81-49785

REFERENCE SYSTEMS

Selection of reference zones for the automatic coordinate control of space images p0261 A81-48693

REFLECTANCE

A comparison between two photographic methods for the determination of relative bidirectional reflectance p0259 A81-45431

Interpretation of hydrographic features seen in the waters off Cape Cod [AD-A102343] p0240 N81-31803

Derivation of shallow ocean bottom reflectance values from color aerial photography [AD-A101105] p0241 N81-33763

REFRACTED WAVES

Refraction of coastal ocean waves p0235 A81-46113

REFRACTIVITY

Mineralogical, optical, and geochemical properties of John H. Kerr Reservoir sediment samples for AgRISTARS pollution research [E81-10155] p0229 N81-33548

REGIONAL PLANNING

Resource inventory and terrain analysis in north western Manitoba from integrated remote sensing data p0218 A81-49803

REGRESSION ANALYSIS

Regression techniques for oceanographic parameter retrieval using space-borne microwave radiometry p0239 A81-49967

RELIABILITY ANALYSIS

Concerning the reliability estimation of information obtained from several sources in earth survey tasks p0270 A81-42286

A measure of reliability for classification of earth satellite data p0257 A81-42631

RELIEF MAPS

Analysis of the geometry of a frame photograph p0221 A81-42554

From landforms to avian habitat - A look at topology p0214 A81-43739

Stereoorthophotos as aids in the mapping of high mountain regions p0221 A81-46678

REMOTE REGIONS

Monitoring Canada's water resources in remote regions by satellite telemetry p0244 A81-43188

REMOTE SENSING

Some results on the investigation of earth resources by aerial and polygon methods --- Russian book p0269 A81-41476

Concerning the reliability estimation of information obtained from several sources in earth survey tasks p0270 A81-42286

Passive microwave techniques for geophysical sensing of the earth from satellites p0270 A81-43071

Radar methods for studying the earth --- Russian book p0273 A81-46924

Program and instrumentation of the satellite experiment Bulgaria-1300 II [IAF PAPER 81-91] p0273 A81-47345

AgRISTARS (Agriculture And Resources Inventory Surveys Through Aerospace Remote Sensing) DC/LC (Domestic Crops and Land Rover) project summary crop area estimates for Kansas and Iowa, 1980 [PB81-196909] p0207 N81-30511

Remote sensing for engineering site selection [AD-A102810] p0219 N81-32586

Experimental investigation of the physical fundamentals for remote sensing of soil and vegetation moisture by active infrared reflectance spectroscopy using CO2 laser technique [BMFT-FB-W-80-037] p0211 N81-33588

REQUIREMENTS
Reports on Marine Science Affairs. Report 14: Satellite data requirements for marine meteorological services
[WMO-548] p0239 N81-28668
RESERVOIRS
Use of Landsat images in the monitoring and study of the LG 2 reservoir during the filling period p0254 A81-49797
Mineralogical, optical, and geochemical properties of John H. Kerr Reservoir sediment samples for AgRISTARS pollution research
[E81-10155] p0229 N81-33548
RESOURCES MANAGEMENT
Commercial operations in space - 1980-2000; Proceedings of the Eighteenth Goddard Memorial Symposium, Washington, DC, March 27, 28, 1980 p0277 A81-44635
What does space remote sensing provide p0278 A81-47826
Agricultural water demand prediction using remote sensing technology for Georgia resource management
[PB81-184137] p0207 N81-30508
A selected bibliography: Remote sensing applications in wildlife management
[PB81-215881] p0211 N81-33598
RETURN BEAM VIDICONS
Geomorphic mapping from Landsat-3 Return Beam Vidicon /RBV/ imagery p0226 A81-46194
RIVER BASINS
The use of satellite data in predicting spring flow in the basins of the upper Ob' and upper Enisei p0243 A81-41723
Improving stream flow estimates through the use of Landsat p0247 A81-43216
Manual versus digital Landsat analysis for delineating river flooding p0252 A81-46405
The interrelation of linear and isometric objects on satellite imagery and the oil and gas structures of the Buzuluk Basin p0227 A81-48685
RIVERS
Roles of satellites in hydrology p0245 A81-43199
An examination of fluvial morphological characteristics of western Amazon streams from Apollo-Soyuz photographs p0247 A81-43212
Assessing the Red River of the North 1978 flooding from NOAA satellite data p0248 A81-43219
A preliminary analysis of SAR mapping of the Manitoba flood, May 1979 p0248 A81-43220
Remote sensing of dinoflagellate blooms in a turbid estuary p0251 A81-43538
Manual versus digital Landsat analysis for modeling river flooding p0252 A81-43745
ROCKY MOUNTAINS (NORTH AMERICA)
Landsat derived snow cover as an input variable for snow melt runoff forecasting in South Central Colorado p0248 A81-43206
RUN TIME (COMPUTERS)
Parallel processing implementations of a contextual classifier for multispectral remote sensing data p0272 A81-46028

S

SALINITY
Microwave radiometer measurement of tidally induced salinity changes off the Georgia coast p0232 A81-42067
Microdensitometry to identify saline rangelands on 70-mm color-infrared aerial film p0202 A81-48406
SALT BEDS
Optical and digital analyses of Landsat data depicting hydrogeological features of the Daryacheh-Ye-Namak area, Iran p0225 A81-43215
The possibility of using an aerial thermal survey for studying the structure of the salt bed in the Gulf of Kara-Bogaz-Gol p0226 A81-44061
Infrared imagery for studying the Kara-Bogaz-Gol Bay p0236 A81-48681
SAN FRANCISCO BAY (CA)
Use of ocean color scanner data in water quality mapping p0251 A81-43545
Water quality mapping from Landsat digital data p0252 A81-45429
SAN JOAQUIN VALLEY (CA)
Land subsidence measured by satellite radar altimetry p0270 A81-43260
SANDS
Determination of beach sand parameters using remotely sensed aircraft reflectance data p0217 A81-49346
SASKATCHEWAN
Rapeseed - Guidelines for operational monitoring p0203 A81-49784
Spectral measurement of rangeland p0218 A81-49790
SATELLITE DESIGN
Conceptual design of an automated mapping satellite System (MAPSAT)
[PB81-185555] p0264 N81-29522
Coastal Oceans Monitoring Satellite System (COMSS) system evaluation study
[ESS/SS-1035] p0239 N81-30168
SATELLITE NAVIGATION SYSTEMS
Satellite aided coastal zone monitoring and vessel traffic system p0231 A81-41755
SATELLITE NETWORKS
Optimization of Doppler measurements in the satellite network of Eastern Europe p0221 A81-48678
Commercial applications of satellite oceanography p0237 A81-49133
The remote sensing satellite program of the European Space Agency p0279 A81-49762
SATELLITE OBSERVATION
A new numerical treatment of the source function in the radiative transfer equation --- for vertical atmospheric temperature and humidity profile retrieval from satellite radiance measurements p0269 A81-41916
Passive microwave techniques for geophysical sensing of the earth from satellites p0270 A81-43071
Remote sensing in hydrology - A challenge to scientists p0243 A81-43177
Physical and technical foundations for the development of subsatellite systems for the exploration of natural earth resources
[IAF PAPER 81-101] p0278 A81-47350
Reports on Marine Science Affairs. Report 14: Satellite data requirements for marine meteorological services
[WMO-548] p0239 N81-28668
SATELLITE ORBITS
Particular features of the ocean glitter pattern observed from a sun-synchronous orbit p0234 A81-45436
Orbit determination requirements for TOPEX --- NASA ocean surface TOPography mapping EXperiment
[AAS PAPER 81-158] p0221 A81-45828
SATELLITE SOUNDING
Determination of moisture from NOAA polar orbiting satellite sounding radiances p0243 A81-41158
Application of the truncated normal distribution technique to the derivation of sea surface temperatures p0234 A81-45881
Remote sounding of atmosphere and ocean for climate research /Appleton Lecture/ p0236 A81-47099
New complex for ionosphere-magnetosphere study 'Intercosmos-Bulgaria-1300'
[IAF PAPER 81-212] p0273 A81-47407
SATELLITE TELEVISION
Measurement of lengths, angles, and areas on the earth's spheroid p0221 A81-42846
Analysis of the November 23, 1980 earthquake as a design basis for satellite emergency communication
[IAF PAPER 81-269] p0216 A81-47433
SATELLITE-BORNE INSTRUMENTS
Performance evaluation of a spaceborne scatterometer p0269 A81-41920
Remote sensing of oceanic phytoplankton - Present capabilities and future goals p0232 A81-42215
Concerning the reliability estimation of information obtained from several sources in earth survey tasks p0270 A81-42286
Calibration validation for the GEOS 3 altimeter p0270 A81-42871
Satellite hydrology; Proceedings of the Fifth Annual William T. Pecora Memorial Symposium on Remote Sensing, Sioux Falls, SD, June 10-15, 1979 p0243 A81-43176
Corps of Engineers utilization of satellites for hydrologic purposes p0244 A81-43180
Satellite versus conventional methods in hydrology p0244 A81-43183
Advanced technology for satellite data collection systems p0270 A81-43190
Data collection and location by satellite - The Argos system
[IAF PAPER 81-80] p0273 A81-47338
The first ESA remote sensing satellite /ERS/ - The programme and the system
[IAF PAPER 81-90] p0236 A81-47344
Program and instrumentation of the satellite experiment Bulgaria-1300 II
[IAF PAPER 81-91] p0273 A81-47345
SPOT status of development
[IAF PAPER 81-92] p0278 A81-47346
An atmospheric study by 'Spectrum-15' onboard of the Salyut-6 orbital station
[IAF PAPER 81-120] p0216 A81-47359
New complex for ionosphere-magnetosphere study 'Intercosmos-Bulgaria-1300'
[IAF PAPER 81-212] p0273 A81-47407
First results of the Intercosmos satellite IK-21
[IAF PAPER 81-214] p0274 A81-47409
The SPOT satellite mission, applications aspects and data products p0278 A81-48549
Satellites for oceanography - The promises and the realities p0237 A81-49126
Coastal Oceans Monitoring Satellite System (COMSS) system evaluation study
[ESS/SS-1035] p0239 N81-30168
SATELLITE-BORNE PHOTOGRAPHY
Hurricane 'Flossie' /September 1978/ observed in the north Atlantic, by the Meteosat satellite p0213 A81-41061
Aerial data acquisition systems using test-ground polygons p0269 A81-41477
The possibilities of the automated classification of agricultural objects on the basis of their multispectral aerial-spaceborne images p0197 A81-41488
Practical application of the method of empty blocks for the computerized determination of the boundaries of agricultural objects p0197 A81-41489
The use of spaceborne photography for topographic mapping p0221 A81-42556
An introduction to satellite hydrology p0244 A81-43184
Remote sensing of coastal pollutants using multispectral data p0233 A81-43245
Aerospace remote sensing of the coastal zone for water quality and biotic productivity applications p0233 A81-43246
Mapping irrigated cropland on the High Plains using Landsat p0198 A81-43266
Skylab in retrospect p0277 A81-43635
Simulation of orbital image-sensor geometry p0260 A81-46192
Manual versus digital Landsat analysis for delineating river flooding p0252 A81-46405
Large-area histograms from Meteosat images p0260 A81-46917
Derivation of formulas for the correlation of coordinate points of different-scale photographs and quasi-photographs p0261 A81-48772
SATELLITE-BORNE RADAR
Detection of the Gulf Stream p0235 A81-46115
Radar methods for studying the earth --- Russian book p0273 A81-46924
SATELLITE-TO-SATELLITE TRACKING
Satellite To Satellite Doppler Tracking (SSDT) for mapping of the Earth's gravity field
[NASA-CR-164722] p0223 N81-31601
SCANNERS
The characteristics of combining devices with different survey bands aboard a satellite p0274 A81-48689
Geometric correction of scanner images of the earth's surface p0261 A81-48694
SCATTEROMETERS
Performance evaluation of a spaceborne scatterometer p0269 A81-41920
Coherent and incoherent radar scattering from rough surfaces and vegetated areas --- conferences
[ESA-SP-166] p0208 N81-33339
Scatterometer calibration and data correction p0265 N81-33351
SCENE ANALYSIS
Procedure 1 and forestland classification using Landsat data p0201 A81-46055
Radar-optical-topographic transformations for scene content analysis p0261 A81-48552
Evaluation of Thematic Mapper bands - A first step in feature selection p0206 A81-49815
LANDSAT C workshop field/laboratory exercises p0280 N81-32571
SCOTLAND
Current resource mapping and environmental monitoring applications using Landsat MSS data in Scotland p0218 A81-49806
SEA ICE
Evaluation of the effect of sea-ice roughness on the microwave emission of the ice p0231 A81-41490
Sea ice detection using enhanced infrared satellite data p0232 A81-42131
Operational use of satellite imagery in the Canadian ice program p0238 A81-49754
The use of satellite imagery as an aid to the Canadian Coast Guard ice operations p0238 A81-49758
Experimental use of real time SAR imagery in support of oil exploration in the Beaufort Sea p0227 A81-49767
Airborne impulse radar sounding of sea ice p0238 A81-49771
The Lake Melville/Labrador offshore synthetic aperture radar study - Winter 1979 p0238 A81-49772
Single and multiple parameter microwave signatures of sea ice p0238 A81-49774
Optimizing imaging radar parameters for ice reconnaissance p0239 A81-49779
Study of the influence of the atmosphere on the performance of an imaging microwave radiometer
[ESA-CR(P)-1421] p0275 N81-30342
A review of volume scatter theories for modeling applications p0265 N81-33347
Comparative analysis of sea ice features using Side-Looking Airborne Radar (SLAR) and LANDSAT imagery --- Beaufort Sea and Bering Sea
[E81-10044] p0241 N81-33539
SEA ROUGHNESS
Radar altimeter waveform modeled parameter recovery --- SEASAT-1 data
[NASA-TM-73294] p0275 N81-30325
SEA STATES
Imaging ocean waves by synthetic aperture radars with long integration times p0231 A81-42026
The promise of satellite altimetry --- for oceanography p0237 A81-49128
Gulf of Mexico satellite radar altimetry
[NASA-TM-73295] p0224 N81-33760
SEA TRUTH
A comparison of Seasat 1 altimeter measurements of wave height with measurements made by a pitch-roll buoy p0231 A81-42068
Wave direction measured by four different systems p0232 A81-42622
SEA WATER
An analysis of the data of synchronous measurements from the Meteor satellite and ships at the eastern coast of the Caspian Sea p0237 A81-48687

Compact and highly sensitive fluorescence lidar for oceanographic measurements p0237 A81-49378

SEAS

Fitoexomorphogenic analysis of geological environment changes in the South Aral Sea, based on aerial and space imagery p0225 A81-42279

SEASAT SATELLITES

Seasat data applications by commercial users p0231 A81-41974

SEAWEEDS

Multispectral kelp resource surveys p0232 A81-43244

SEDIMENT TRANSPORT

An examination of fluvial morphological characteristics of western Amazon streams from Apollo-Soyuz photographs p0247 A81-43212

Southern Chesapeake Bay circulation and suspended sediment transport analyzed using Landsat imagery p0252 A81-43747

SEDIMENTS

Bay of Fundy verification of a system for multidate Landsat measurement of suspended sediment p0250 A81-43254

Remote sensing of dinoflagellate blooms in a turbid estuary p0251 A81-43538

Mineralogical, optical, and geochemical properties of John H. Kerr Reservoir sediment samples for AgRISTARS pollution research [E81-10155] p0229 N81-33548

A study of Minnesota land and water resources using remote sensing, Volume 14 [E81-10166] p0254 N81-33550

Lakewide monitoring of suspended solids using satellite data --- Lake Superior water reclamation p0254 N81-33552

Quantification of non-point source sedimentation through densitometric analysis of color infrared aerial photography [PB81-209157] p0255 N81-33599

SEISMOLOGY

Space research on seismic regions p0225 A81-42280

Optimal polarization concept in radar imaging --- electromagnetic scattering p0265 N81-33350

SHALLOW WATER

Trophic state determination for shallow coastal lakes from Landsat imagery p0251 A81-43259

SHEAR FLOW

Method for estimation of ocean current velocity from satellite images p0231 A81-41350

SHIPS

Satellite aided coastal zone monitoring and vessel traffic system p0231 A81-41755

SHOALS

Interpretation of hydrographic features seen in the waters off Cape Cod [AD-A102343] p0240 N81-31803

SHORELINES

Mapping the Great Salt Lake shoreline and associated waterfowl habitat from Landsat data p0252 A81-43742

A remote sensing technique to monitor Cladophora in the Great Lakes [PB81-173841] p0254 N81-29520

SIBERIA

The use of satellite data in predicting spring flow in the basins of the upper Ob' and upper Enisei p0243 A81-41723

Soviet remote sensing of the earth's resources and interpretation of space data with reference to the Caspian Sea, Siberia and the Arctic Ocean [IAF PAPER 81-112] p0278 A81-47355

SIDE-LOOKING RADAR

Iceberg detectability problems using SAR and SLAR systems p0232 A81-43206

A photo interpretation approach to forest regrowth monitoring using side-looking airborne radar - Grant County, Oregon p0200 A81-45428

A radar image time series p0226 A81-45430

Utilisation and benefits of SLAR in operational ice data acquisition p0253 A81-49761

SIERRA NEVADA MOUNTAINS (CA)

Satellite snow mapping techniques with emphasis on the use of Landsat p0245 A81-43200

Application of snow covered area to runoff forecasting, in the Sierra Nevada, California p0245 A81-43201

Remote sensing aided procedure for conifer growth modeling in the northeastern Sierra Nevada p0199 A81-43740

SIGNAL DISTORTION

Experience with the determination of optical image distortions of landscape elements on IR aerial photographs p0257 A81-41480

SIGNAL PROCESSING

Some methods of multitemporal analysis of LANDSAT images resulting from a study on Venice Lagoon [E81-10205] p0267 N81-33574

SIGNAL TO NOISE RATIOS

The signal-to-noise ratio of a space photographic system p0269 A81-42284

SIGNATURE ANALYSIS

Comparison of Landsat-2 and field spectrometer reflectance signatures of south Texas rangeland plant communities p0201 A81-46034

Why surface-truth field study is needed in remote-sensing instruction p0280 N81-32567

SITE SELECTION

The use of CIR and airborne multispectral scanner techniques for wetland soils mapping of highway corridors p0215 A81-46044

Remote sensing for engineering site selection [AD-A102810] p0219 N81-32586

The development of a remote sensing applications program for Vermont [E81-10148] p0266 N81-33547

Cornell University Remote Sensing Program [E81-10174] p0255 N81-33560

SKYLAB PROGRAM

Skylab in retrospect p0277 A81-43535

SLOPES

Topographic slope correction for analysis of thermal infrared images [PB81-211781] p0224 N81-33589

SNOW COVER

The use of satellite data in predicting spring flow in the basins of the upper Ob' and upper Enisei p0243 A81-41723

Satellite applications in river and flood forecasting p0243 A81-43178

Satellite snow mapping techniques with emphasis on the use of Landsat p0245 A81-43200

Application of snow covered area to runoff forecasting, in the Sierra Nevada, California p0245 A81-43201

The satellite record of the winter of 1978-79 in North America p0246 A81-43203

Prediction of water yield using satellite imagery and a snowmelt simulation model p0246 A81-43205

Passive microwave sensing of snow characteristics over land p0246 A81-43207

Landsat derived snow cover as an input variable for snow melt runoff forecasting in South Central Colorado p0246 A81-43208

Monitoring snow with microwaves p0246 A81-43209

Operational use of satellite data for snow inventory and runoff forecast p0248 A81-43210

Flood applications of satellite imagery p0247 A81-43217

Correlation function studies for snow and ice p0260 A81-46378

Angular anisotropy of reflection from various types of underlying surface. I - Snow cover. II - Desert p0260 A81-47007

Passive microwave systems [IAF PAPER 81-88] p0273 A81-47342

Monitoring of snow covered area using satellite data [IAF PAPER 81-114] p0253 A81-47356

Landsat observations of snowcover depletion and flooding in the Chesapeake Bay area during the winter of 1979 p0253 A81-48942

Landsat - What is operational in water resources p0253 A81-49757

Application of synthetic aperture radar data to snow cover monitoring p0253 A81-49778

Computer analysis of Tiros-N/NOAA-6 satellite data for operational snow cover mapping p0262 A81-49795

Investigation of multispectral remote sensing of snow cover using a solar radiation model p0267 A81-49804

Current resource mapping and environmental monitoring applications using Landsat MSS data in Scotland p0218 A81-49806

Satellite monitoring of snow extent and condition in agricultural, transitional, and forested land cover areas [PB81-188625] p0254 N81-30509

A review of volume scatter theories for modeling applications p0265 N81-33347

SOCIAL FACTORS

Large scale human benefits of space industrialization p0277 A81-42513

SOIL EROSION

An application of Landsat and computer technology to potential water pollution from soil erosion p0250 A81-43253

Remote sensing of bank erosion along the Missouri River, South Dakota p0213 A81-43263

A case study of soil erosion detection by digital analysis of the remotely sensed multispectral Landsat scanner data of a semi-arid land in southern India p0201 A81-46050

Suburban soil loss and runoff simulation assisted by interpretation of large scale aerial photography p0253 A81-48941

SOIL MAPPING

Using Landsat MSS data with soils information to identify wetland habitats p0249 A81-43236

Application of multispectral reflectance studies of soils - Pre-Landsat p0200 A81-46031

Stratification of Landsat data by uniformity productivity of soils p0259 A81-46042

Interactive processing of Landsat image for morphopedological studies p0259 A81-46043

The use of CIR and airborne multispectral scanner techniques for wetland soils mapping of highway corridors p0215 A81-46044

Mapping alpine soils using color positive and color infrared photographs p0252 A81-46045

Use of Landsat digital data to assist in mapping soils on Arizona rangelands p0201 A81-46047

Development of a digital data base for reflectance-related soil information p0201 A81-46051

Suburban soil loss and runoff simulation assisted by interpretation of large scale aerial photography p0253 A81-48941

Operational applications for analysis of agricultural crops and cultural practices p0203 A81-49756

Evaluation of Thematic Mapper bands - A first step in feature selection p0205 A81-49815

Spectral properties of Arizona soils and rangelands and their relationship to LANDSAT digital data p0207 N81-31596

Landform-vegetation relationships in the northern Chihuahuan Desert [AD-A102896] p0208 N81-32588

SOIL MOISTURE

Satellite applications in river and flood forecasting p0243 A81-43178

NASA water resources/hydrology remote sensing program in the 1980's p0244 A81-43179

Agricultures's needs related to satellite hydrology p0197 A81-43181

Passive microwave sensing of snow characteristics over land p0246 A81-43207

Survey of in-situ and remote sensing methods for soil moisture determination p0197 A81-43221

Characteristics of microwave emission of significance to satellite remote sensing of soil water p0258 A81-43222

Potential application of satellite radar to monitor soil moisture p0270 A81-43223

Soil moisture applications of the heat capacity mapping mission p0197 A81-43224

Requirements of space-borne microwave radiometers for detecting soil moisture contents p0270 A81-43225

Ground water applications of the heat capacity mapping mission p0248 A81-43233

A multistage mapping approach for an irrigated croplands inventory p0198 A81-43262

Aircraft active microwave measurements for estimating soil moisture p0271 A81-43547

Look direction dependence of radar backscattering cross section for agricultural fields p0199 A81-43741

Active microwave measurements for estimating soil moisture in Oklahoma p0199 A81-43744

Preliminary survey of HCMM satellite thermal imagery as applied to hydrospherics p0252 A81-43746

Thermal inertia mapping of some areas of Quebec based on aerial and HCMM satellite data p0204 A81-49799

Evaluation of gravimetric ground truth soil moisture data collected for the agricultural soil moisture experiment, 1978 Colby, Kansas, aircraft mission [E81-10114] p0205 N81-29494

Soil moisture inferences from thermal infrared measurements of vegetation temperatures [E81-10184] p0206 N81-29500

The environmental vegetation index: A tool potentially useful for arid land management --- Texas and Mexico, plant growth stress due to water deficits [E81-10191] p0206 N81-29506

Descriptive and sensitivity analyses of WATBALI: A dynamic soil water model [E81-10193] p0206 N81-29507

Landform-vegetation relationships in the northern Chihuahuan Desert [AD-A102896] p0208 N81-32588

Scatterometer measurements on crop and soil surfaces p0208 N81-33349

Dryland pasture and crop conditions as seen by HCMM [E81-10080] p0209 N81-33542

Measurement of soil moisture trends with airborne scatterometers --- Texas [E81-10088] p0209 N81-33545

A study of Minnesota land and water resources using remote sensing, Volume 14 [E81-10166] p0254 N81-33550

A project to evaluate moisture stress and phenological factors in corn and soybean areas of southwestern and south-central Minnesota p0209 N81-33554

A crop moisture stress index for large areas and its application in the prediction of spring wheat phenology [E81-10202] p0210 N81-33573

Experiment plan: Row and roughness effects on dependence of active microwave measurements of soil moisture [E81-10208] p0211 N81-33575

Experimental investigation of the physical fundamentals for remote sensing of soil and vegetation moisture by active infrared reflectance spectroscopy using CO2 laser technique [BMFT-FB-W-80-037] p0211 N81-33588

SOIL SCIENCE

Machine processing of remotely sensed data and soil information systems and remote sensing and soil survey; Proceedings of the Sixth Annual Symposium, Purdue University, West Lafayette, IN, June 3-6, 1980 p0200 A81-46026

SOILS

Microdensitometry to identify saline rangelands on 70-mm color-infrared aerial film p0202 A81-46406

Remote sensing of soil radionuclide fluxes in a tropical ecosystem --- Eniwetok and Bikini Atolls [UCRL-84501] p0219 N81-29517

Synergistic relationships among remote-sensing and geophysical media: Geological and hydrological applications --- detecting near-surface ground water in Minnesota p0255 N81-33553

SOLAR FLUX DENSITY

Radiation studies in the atmosphere p0216 A81-47001

SOLAR RADIATION
Investigation of multispectral remote sensing of snow cover using a solar radiation model p0262 A81-49604
Effect of forest canopy closure on incoming solar radiance
[E81-10170] p0205 N81-28499
SOUTH AMERICA
The methodology of CIAT's land resource study of tropical America p0216 A81-46046
SOUTH DAKOTA
Soil moisture applications of the heat capacity mapping mission p0197 A81-43224
Landsat data for locating shallow glacial aquifers in eastern South Dakota p0226 A81-43228
Ground water applications of the heat capacity mapping mission p0248 A81-43233
Landsat interpretation of prairie lakes and wetlands of eastern South Dakota p0249 A81-43240
Remote sensing of bank erosion along the Missouri River, South Dakota p0213 A81-43263
SOUTHERN CALIFORNIA
Multispectral kelp resource surveys p0232 A81-43244
Satellite detection of oil on the marine surface p0233 A81-43251
Land subsidence measured by satellite radar altimetry p0270 A81-43260
SOVEREIGNTY
International monitoring from space /Problems of international law/ --- Russian book p02?9 A81-49468
SOYBEANS
Relating ground level reflected radiance measurements in the Landsat MSS bandpasses to satellite altitudes p0271 A81-43735
On the analysis of remote sensing data to predict selected vegetative variables p0258 A81-43736
An assessment of Landsat data acquisition history on identification and area estimation of corn and soybeans p0200 A81-46032
Users manual for the US baseline corn and soybean segment classification procedure
[E81-10190] p0206 N81-29504
AgRISTARS (Agriculture And Resources Inventory Surveys Through Aerospace Remote Sensing) DC/LC (Domestic Crops and Land Rover) project summary crop area estimates for Kansas and Iowa, 1980
[PB81-196909] p0207 N81-30611
Crop area estimates using ground-gathered and LANDSAT data. A multitemporal approach: Missouri, 1979
[PB81-186751] p0208 N81-31614
A project to evaluate moisture stress and phenological factors in corn and soybean areas of southwestern and south-central Minnesota p0209 N81-33554
SPACE INDUSTRIALIZATION
Large scale human benefits of space industrialization p0277 A81-42513
SPACE PLASMAS
New complex for ionosphere-magnetosphere study Intercosmos-Bulgaria-1300
[IAF PAPER 81-212] p0273 A81-47407
SPACE PLATFORMS
Passive microwave systems
[IAF PAPER 81-88] p0273 A81-47342
SPACE SHUTTLE ORBITERS
First Shuttle payload loading to begin p0273 A81-48461
SPACE SHUTTLE PAYLOADS
Earth applications orbit analysis for a shuttle-mounted Multispectral Mapper
[AAS PAPER 81-182] p0271 A81-45836
SPACE SHUTTLES
Commercial operations in space - 1980-2000; Proceedings of the Eighteenth Goddard Memorial Symposium, Washington, DC, March 27, 28, 1980 p0277 A81-44635
SPACEBORNE EXPERIMENTS
Main tasks and methods of operational planning of experiments concerning the observations of the earth from space p0277 A81-42288
SPACEBORNE PHOTOGRAPHY
Space research on seismic regions p0225 A81-42280
Remote sensing and mapping of pastures p0213 A81-42281
The signal-to-noise ratio of a space photographic system p0269 A81-42284
An examination of fluvial morphological characteristics of western Amazon streams from Apollo-Soyuz photographs p0247 A81-43212
Application of digital terrain data to quantify and reduce the topographic effect on Landsat data p0259 A81-45433
Land use mapping of Hong Kong from Landsat images - An evaluation p0215 A81-45434
SPACECRAFT COMMUNICATION
Analysis of the November 23, 1980 earthquake as a design basis for satellite emergency communication
[IAF PAPER 81-269] p0216 A81-47433
SPACELAB PAYLOADS
The remote sensing satellite program of the European Space Agency p0279 A81-49762
SPATIAL DISTRIBUTION
Practical application of the method of empty blocks for the computerized determination of the boundaries of agricultural objects p0197 A81-41489
Spatial evolution of ocean wave spectra p0235 A81-46112
Research on assessment of the recreational value of forests using Landsat digital data p0203 A81-49785
Development of advanced acreage estimation methods
[E81-10160] p0206 N81-29495
The multicategory case of the sequential Bayesian pixel selection and estimation procedure
[E81-10182] p0263 N81-29498
Estimation of proportions in mixed pixels through their region characterization
[E81-10199] p0264 N81-29510
SPATIAL RESOLUTION
A measure of reliability for classification of earth satellite data p0257 A81-42631
Geomagnetic field mapping from a satellite: Spatial power spectra of the geomagnetic field at various satellite altitudes relative to natural noise sources and instrument noise
[PUBL-1810] p0275 N81-29480
SPECKLE PATTERNS
Fourier modulus image construction
[AD-A101728] p0264 N81-30723
SPECTRAL BANDS
Multispectral texture analysis p0257 A81-41055
Training site statistics from Landsat and Seasat satellite imagery registered to a common map base p0258 A81-43734
Waveband evaluation of proposed thematic mapper in forest cover classification p0199 A81-43738
An examination of spectral band ratioing to reduce the topographic effect on remotely sensed data p0221 A81-45427
Procedures for change detection using Landsat digital data p0215 A81-45437
Application of multispectral reflectance studies of soils - Pre-Landsat p0200 A81-46031
Advanced synthetic aperture radar for remote sensing p0274 A81-48553
The characteristics of combining devices with different survey bands aboard a satellite p0274 A81-48689
Evaluation of Thematic Mapper bands - A first step in feature selection p0205 A81-49815
A comparative study of the thematic mapper and LANDSAT spectral bands from field measurement data
[E81-10165] p0209 N81-33549
SPECTRAL EMISSION
Concerning the possibility of improving the spectroradiometric accuracy of remote sensing of the earth by means of multispectral band scanners p0270 A81-42285
SPECTRAL RECONNAISSANCE
Methods development and applications evaluations of NURE aerial reconnaissance survey data for uranium resource evaluation: Beeville/Bay City and Crystal City quadrangles, Texas
[GJBX-69(81)] p0228 N81-30502
Airborne gamma-ray spectrometer and magnetometer survey: Canyon City quadrangle (Oregon), volume 2
[DE81-028682] p0229 N81-33584
Airborne gamma-ray spectrometer and magnetometer survey, Salem quadrangle (Oregon), volume 2
[DE81-028681] p0229 N81-33585
SPECTRAL REFLECTANCE
Relating ground level reflected radiance measurements in the Landsat MSS bandpasses to satellite altitudes p0271 A81-43735
The effect of sensor bandpass and spectral response in crop stress detection p0199 A81-43737
Features of the radar detection of sea surface nonuniformities p0234 A81-43967
Application of multispectral reflectance studies of soils - Pre-Landsat p0200 A81-46031
Comparison of Landsat-2 and field spectrometer reflectance signatures of south Texas rangeland plant communities p0201 A81-46034
Development of a digital data base for reflectance-related soil information p0201 A81-46051
Does the use of two radiometers correct for irradiance changes during measurements p0272 A81-46196
Correlation between integral and spectral albedos of clouds over water surfaces p0235 A81-47004
Angular anisotropy of reflection from various types of underlying surface. I - Snow cover. II - Desert p0260 A81-47007
Assessing winter wheat dry matter production via spectral reflectance measurements p0202 A81-49344
Determination of beach sand parameters using remotely sensed aircraft reflectance data p0217 A81-49346
Spectral measurement of rangeland p0218 A81-49790
The discrimination of cereal crops and legumes using reflectance data in the Landsat bandpasses p0204 A81-49794
Investigation of multispectral remote sensing of snow cover using a solar radiation model p0262 A81-49804
Spectral properties of Arizona soils and rangelands and their relationship to LANDSAT digital data p0207 N81-31595
Visual enhancement of images of natural resources: Applications in geology
[E81-10181] p0228 N81-32575
Comparison of laboratory reflectance spectra and LANDSAT multispectral images of Hawaiian lava flows
[E81-10061] p0266 N81-33541
Cornell University Remote Sensing Program
[E81-10174] p0255 N81-33560
SPECTRAL RESOLUTION
Computer analysis of Tiros-N/NOAA-6 satellite data for operational snow cover mapping p0262 A81-49795
A simulation of Thematic Mapper performance in an agricultural application p0204 A81-49810
SPECTRAL SENSITIVITY
Integration and comparison of SAR and MSS data for potato crop area estimation p0203 A81-49766
An analysis of haze effects on LANDSAT multispectral scanner data
[E81-10162] p0263 N81-29497
A comparative study of the thematic mapper and LANDSAT spectral bands from field measurement data
[E81-10165] p0209 N81-33549
SPECTRAL SIGNATURES
Multispectral kelp resource surveys p0232 A81-43244
Maximum likelihood estimation of label imperfection probabilities and its use in the identification of mislabeled patterns --- with application to Landsat MSS data processing p0259 A81-46040
A temporal/spectral analysis of small grain crops and confusion crops --- North Dakota
[E81-10167] p0205 N81-28498
A description of the reformatted spring small grains labeling procedure used in test 2, part 2 of the US/Canada wheat and barley exploratory experiment
[E81-10206] p0207 N81-31597
Classification of wheat: Badhwar profile similarity technique
[E81-10207] p0207 N81-31598
Synergistic relationships among remote-sensing and geophysical media: Geological and hydrological applications --- detecting near-surface ground water in Minnesota p0255 N81-33553
SPECTROPHOTOMETRY
Investigation of the efficiency of the optical sounding of aerosol by the use of spectral photometers p0215 A81-45406
SPECTRORADIOMETERS
A radiometric model of an earth radiation budget radiometer optical system with diffuse-specular surfaces p0269 A81-41919
Concerning the possibility of improving the spectroradiometric accuracy of remote sensing of the earth by means of multispectral band scanners p0270 A81-42285
A comparative study of the thematic mapper and LANDSAT spectral bands from field measurement data
[E81-10165] p0209 N81-33549
SPECTRUM ANALYSIS
Multispectral texture analysis p0257 A81-41055
Spectral properties of Arizona soils and rangelands and their relationship to LANDSAT digital data p0207 N81-31595
SPECULAR REFLECTION
A comparison between two photographic methods for the determination of relative bidirectional reflectance p0259 A81-45431
Particular features of the ocean glitter pattern observed from a sun-synchronous orbit p0234 A81-45436
A model of plant canopy polarization response p0201 A81-46035
SPHEROIDS
Measurement of lengths, angles, and areas on the earth's spheroid p0221 A81-42846
SPOT (FRENCH SATELLITE)
SPOT status of development
[IAF PAPER 81-92] p0278 A81-47346
Image quality for SPOT satellite - Specifications and budget
[IAF PAPER 81-104] p0261 A81-47352
The SPOT satellite mission, applications aspects and data products p0278 A81-48549
SPREAD REFLECTION
ISS-b experimental results on global distributions of ionospheric parameters and thunderstorm activity p0215 A81-44862
SPRINGS (WATER)
Applications of aerospace data for detection of submarine springs in Jamaica p0226 A81-43232
Satellite observations of a geothermal submarine spring off Florida west coast p0233 A81-43248
The detection of groundwater discharges /springs/ using aerial thermography p0254 A81-49800
STATISTICAL ANALYSIS
A capture-recapture approach for estimation of detection probabilities in aerial surveys p0258 A81-43546
Alternative 'scale up' estimators for aerial surveys where both detection and classification errors exist p0260 A81-46197
STATISTICAL CORRELATION
Correlation function studies for snow and ice p0260 A81-46378
STATISTICAL DISTRIBUTIONS
Context distribution estimation for contextual classification of multispectral image data p0259 A81-46041
STATISTICAL WEATHER FORECASTING
A statistical approach to rainfall estimation using satellite data p0245 A81-43198

STEREOPHOTOGRAPHY
Determination of the external-orientation elements of single photographs and stereopairs p0257 A81-42555
Stereoorthophotos as aids in the mapping of high mountain regions p0221 A81-46678
SPOT status of development [IAF PAPER 81-92] p0278 A81-47348
The SPOT satellite mission, applications aspects and data products p0278 A81-48549
Derivation of formulas for the correlation of coordinate points of different-scale photographs and quasi-photographs p0261 A81-48772
The influence of the accuracy of determining the elements of the external orientation of a stereopair on the processing of aerial photographs on the basis of adjusting elements p0261 A81-48773

STEREOSCOPY
Derivation of formulas for the correlation of coordinate points of different-scale photographs and quasi-photographs p0261 A81-48772

STORMS
Utilizing GOES imagery to determine convective storm characteristics in data deficient regions p0245 A81-43192

STRATIFICATION
Stratification of Landsat data by uniformity productivity of soils p0259 A81-46042
The multicategory case of the sequential Bayesian pixel selection and estimation procedure [E81-10182] p0263 N81-29498

STRATOSPHERE
Stratospheric sulfate from the Gareloi eruption, 1980 - Contribution to the 'ambient' aerosol by a poorly documented volcanic eruption p0213 A81-41404
Measurements of CF2Cl2, CFCl3, and N2O in the lower stratosphere between 2 deg S and 73 deg N latitude p0214 A81-44515
The distribution of the trace gases H2O, NO2, and HNO3 in the middle atmosphere on the basis of LIMS measurements --- Limb Infrared Monitor of Stratosphere p0217 A81-49407
Comparative measurements of stratospheric CH4 and CO concentrations with spectrograph and correlation radiometers p0217 A81-49433

STRIP MINING
Detection of changes in a coal surface mining area by ratioing multidate Landsat digital data p0228 A81-49809

STRUCTURAL BASINS
Observations on Lake Ontario basin hydrogeology from optical enhancements of Landsat imagery p0248 A81-43231
Dynamic ecosystem of the Aral Basin studied from satellite imagery p0217 A81-48682

STRUCTURAL PROPERTIES (GEOLOGY)
Correlation of geologic structure inferred from computer enhanced Landsat imagery with underground water supplies in Arizona p0225 A81-43227
Lineament mapping in northern Sweden from Landsat images using orthogonal image transforms p0226 A81-46039
Geomorphic mapping from Landsat-3 Return Beam Vidicon /RBV/ imagery p0226 A81-46194
Ore-controlling space geological objects and their assessment techniques applied to mineral prediction [IAF PAPER 81-107] p0227 A81-47353
The interrelation of linear and isometric objects on satellite imagery and the oil and gas structures of the Buzuluk Basin p0227 A81-48685
Complex processing of satellite images and the geological interpretation p0227 A81-48690
Lineaments - Problems and directions of studies by means of aerial and space tools and methods p0221 A81-48696
Geological and terrain analysis of the Annapolis County region of Nova Scotia - An application of digital Landsat, radar and colour infrared data p0227 A81-49802
Seasat satellite investigation of the structure of western Nebraska and its application to the evaluation of geothermal resources [LA-UR-81-1454] p0223 N81-30505

SUBARCTIC REGIONS
Digital enhancements for vegetation mapping in a subarctic environment p0262 A81-49793

SUBSIDENCE
Land subsidence measured by satellite radar altimetry p0270 A81-43260

SUBURBAN AREAS
Suburban soil loss and runoff simulation assisted by interpretation of large scale aerial photography p0253 A81-48941

SUDAN
Comparative experimental study on the use of original and compressed multispectral Landsat data of the Bayuda desert p0262 A81-49813

SUNLIGHT
A comparison of observed and analytically derived remote sensing penetration depths for turbid water [NASA-TM-83176] p0255 N81-33577

SURFACE LAYERS
Survey of in-situ and remote sensing methods for soil moisture determination p0197 A81-43221

SURFACE NAVIGATION
Satellite aided coastal zone monitoring and vessel traffic system p0231 A81-41755
Operational use of satellite imagery in the Canadian ice program p0238 A81-49754
Experimental use of real time SAR imagery in support of oil exploration in the Beaufort Sea p0227 A81-49767
Ocean services for the nation. National ocean goals and objectives for the 1980's [PB81-200602] p0240 N81-31808

SURFACE PROPERTIES
A review of volume scatter theories for modeling applications p0265 N81-33347

SURFACE ROUGHNESS
The use of radar imagery for surface water investigations p0247 A81-43211
Airborne microwave radiometer remote sensing of lake ice p0253 A81-48554
Scatterometer calibration and data correction p0265 N81-33351
Experiment plan: Row and roughness effects on dependence of active microwave measurements of soil moisture [E81-10209] p0211 N81-33575

SURFACE ROUGHNESS EFFECTS
Evaluation of the effect of sea-ice roughness on the microwave emission of the ice p0231 A81-41480
Introduction to the workshop --- on coherent and incoherent radar scattering from rough surfaces and vegetated areas p0276 N81-33340
Wave orbital velocity, fade and SAR response to azimuth waves p0265 N81-33345
Scatterometer calibration and data correction p0265 N81-33351

SURFACE TEMPERATURE
What has been learned from the scanning multi-channel microwave radiometers /SMMRs/ p0269 A81-41995
Satellite determination of the mesoscale variability of the sea surface temperature p0234 A81-44861
Application of the truncated normal distribution technique to the derivation of sea surface temperatures p0234 A81-45881
Application of GOES visible-infrared data to quantifying mesoscale ocean surface temperatures p0236 A81-47021
Infrared imagery for studying the Kara-Bogaz-Gol Bay p0236 A81-48681
Thermal inertia mapping of some areas of Quebec based on aerial and HCMM satellite data p0204 A81-49799
Airborne remote sensing of sea surface chlorophyll and temperature along the outer British Columbia coast p0239 A81-49805
Satellite identification of surface radiant temperature fields of subpixel resolution [PB81-184038] p0265 N81-31615
Topographic slope correction for analysis of thermal infrared images [PB81-211781] p0224 N81-33589

SURFACE WATER
The use of radar imagery for surface water investigations p0247 A81-43211

SURFACE WAVES
Gulf of Mexico satellite radar altimetry [NASA-TM-73285] p0224 N81-33760

SWEDEN
Lineament mapping in northern Sweden from Landsat images using orthogonal image transforms p0226 A81-46039

SYNOPTIC METEOROLOGY
Modeling the terrestrial hydrology for the global atmosphere - The future role of satellite data p0245 A81-43197

SYNTHETIC APERTURE RADAR
Future plans for NASA's Oceanic Processes Program p0231 A81-41997
Imaging ocean waves by synthetic aperture radars with long integration times p0231 A81-42026
Iceberg detectability problems using SAR and SLAR systems p0232 A81-43206
A preliminary analysis of SAR mapping of the Manitoba flood, May 1979 p0248 A81-43220
Multisensor analysis of hydrologic features with emphasis on the Seasat SAR p0251 A81-43544
Look direction dependence of radar backscattering cross section for agricultural fields p0199 A81-43741
Use of Seasat satellite radar imagery for the detection of standing water beneath forest vegetation p0199 A81-43743
Texture measurements from Seasat - SAR images for urban land use interpretation p0214 A81-43749
Radar image preprocessing --- of SEASAT-A SAR data p0272 A81-46038
Spaceborne synthetic aperture radar for oceanography --- Book p0234 A81-46104
The structure of short gravity waves on the ocean surface p0234 A81-46105
SAR ocean imaging mechanisms p0234 A81-46107
The wind speed dependency of ocean microwave backscatter p0234 A81-46109
The study of mesoscale ocean winds p0235 A81-46110
Spatial evolution of ocean wave spectra p0235 A81-46112
Refraction of coastal ocean waves p0235 A81-46113
Detection of the Gulf Stream p0235 A81-46115
A search for cold water rings p0235 A81-46116
Tracking of a warm water ring p0235 A81-46117
The European SAR-Project Convair 580 p0273 A81-48679
Use of elevation models for landform analysis by Seasat SAR imagery [IAF PAPER 81-98] p0260 A81-47349
Advanced synthetic aperture radar for remote sensing p0274 A81-48553
The airborne SAR project - Conclusions and applications p0275 A81-49765
Airborne impulse radar sounding of sea ice p0238 A81-49771
SAR processing of partially coherent and sinusoidally dynamic ocean waves p0239 A81-49776
Digital image analysis of SAR imagery for the detection of icebergs p0238 A81-49777
Application of synthetic aperture radar data to snow cover monitoring p0253 A81-49778
Optimizing imaging radar parameters for ice reconnaissance p0239 A81-49779
Cartographic accuracy of synthetic aperture radar imagery p0262 A81-49780
Seasat satellite investigation of the structure of western Nebraska and its application to the evaluation of geothermal resources [LA-UR-81-1454] p0223 N81-30505
Wave orbital velocity, fade and SAR response to azimuth waves p0265 N81-33345
Scattering theory with application to synthetic aperture radar p0265 N81-33348

T

TECHNOLOGICAL FORECASTING
Large scale human benefits of space industrialization p0277 A81-42513

TECHNOLOGY TRANSFER
Field Study for Remote Sensing: An instructor's manual [NASA-CP-2155] p0279 N81-32564
The workshop --- use and application of remotely sensed data p0280 N81-32566
Why surface-truth field study is needed in remote-sensing instruction p0280 N81-32567
LANDSAT C workshop field/laboratory exercises p0280 N81-32571

TECHNOLOGY UTILIZATION
Seasat data applications by commercial users p0231 A81-41974
Efficiency criteria of space systems for studying the earth's natural resources p0277 A81-42287
Ground water and satellites - An overview/introduction p0248 A81-43226
Crop reporting from space - Problems, promises, potential [AAS 80-062] p0200 A81-44637
European industrial space projects [AAS PAPER 81-053] p0278 A81-46234
Remote sensing in development --- for developing nations p0279 A81-48936
Space Benefits: The secondary application of aerospace technology in other sectors of the economy [NASA-CR-164733] p0279 N81-32086
An industrial perspective of the LANDSAT opportunity p0279 N81-32565

TECTONICS
Concerning the hydrogeological significance of faults on platform regions, as revealed by space imagery p0225 A81-42277
Space research on seismic regions p0225 A81-42280
Complex processing of satellite images and the geological interpretation p0227 A81-48690
NASA selects scientific investigations for Earth dynamics studies [NASA-NEWS-RELEASE-81-129] p0228 N81-29143

TELEMETRY
Remote sensing in hydrology - A challenge to scientists p0243 A81-43177
Adapting GOES DCS for use by Corps of Engineers --- for flood control p0244 A81-43186
Satellite telemetry of hydrologic data in California p0244 A81-43187
Monitoring Canada's water resources in remote regions by satellite telemetry p0244 A81-43188
U.S. geological survey application of satellite telemetry for the support of hydrologic data collection p0258 A81-43189
Advanced technology for satellite data collection systems p0270 A81-43190
Possible applications of communication satellites for research tasks in polar regions [BMFT-FB-W-80-029] p0267 N81-33587

TEMPERATE REGIONS
Satellite-tracked drift buoy observations of the near-surface flow in the eastern mid-latitude North Pacific p0236 A81-47022

TEMPERATURE DISTRIBUTION
Satellite identification of surface radiant temperature fields of subpixel resolution [PB81-184038] p0265 N81-31615

TEMPORAL RESOLUTION
Classification of wheat: Badhwar profile similarity technique [E81-10207] p0207 N81-31598

TERRAIN
Conceptual design of an automated mapping satellite System (MAPSAT)
[PB81-185555] p0264 N81-29522
An evaluation of detail in dynamic visual displays
[AD-A103378] p0222 N81-33578

TERRAIN ANALYSIS
The use of spaceborne photography for topographic mapping p0221 A81-42556
Landsat classification of coastal wetlands in Texas p0248 A81-43234
Land subsidence measured by satellite radar altimetry p0270 A81-43260
Use of imaging radar for geology and archeology p0226 A81-43730
From landforms to avian habitat - A look at topology p0214 A81-43739
Use of remote sensing in landscape stratification for environmental impact assessment p0214 A81-43748
Application of digital terrain data to quantify and reduce the topographic effect on Landsat data p0259 A81-45433
Change vector analysis - An approach for detecting forest changes with Landsat p0202 A81-46056
Correlation function studies for snow and ice p0260 A81-46378
Manual versus digital Landsat analysis for delineating river flooding p0252 A81-45405
Microdensitometry to identify saline rangelands on 70-mm color-infrared aerial film p0202 A81-46406
Analysis of landfills with historic airphotos p0216 A81-46407
First Shuttle payload loading to begin p0273 A81-46461
Stereoorthophotos as aids in the mapping of high mountain regions p0221 A81-46678
Use of elevation models for landform analysis by Seasat-SAR imagery
[IAF PAPER 81-98] p0260 A81-47349
Radar-optical-topographic transformations for scene content analysis p0261 A81-48552
Geological and terrain analysis of the Annapolis County region of Nova Scotia - An application of digital Landsat, radar and colour infrared data p0227 A81-49802
Resource inventory and terrain analysis in north western Manitoba from integrated remote sensing data p0218 A81-49803
Generation and use of digital elevation data for large areas p0221 A81-49811
The sensor image simulator
[AD-A101172] p0275 N81-29512
Interactive digital image processing for terrain data extraction
[AD-A101321] p0264 N81-30499
Knowledge-based image analysis
[AD-A101319] p0264 N81-30852
Terrain profiling from Seasat altimetry
[NASA-CR-156878] p0222 N81-31604
OVSUP: A program for computer-aided disentanglement of overlapping zones p0222 N81-33525

TERRESTRIAL RADIATION
Annual and interannual variations in outgoing longwave radiation over the tropics p0251 A81-43356
Methods of editing cloud and atmospheric layer affected pixels from satellite data --- in south Texas test area
[E81-10169] p0266 N81-33556

TEXAS
Simulation modeling of estuarine ecosystems p0243 A81-42229
A satellite derived technique for estimating rainfall from thunderstorms and hurricanes p0244 A81-43191
Hydrologic land use classification using Landsat p0247 A81-43213
Landsat classification of coastal wetlands in Texas p0248 A81-43234
Land subsidence measured by satellite radar altimetry p0270 A81-43260
Microdensitometry to identify saline rangelands on 70-mm color-infrared aerial film p0202 A81-46406
The environmental vegetation index: A tool potentially useful for arid land management --- Texas and Mexico, plant growth stress due to water deficits
[E81-10191] p0206 N81-29505
Methods development and applications evaluations of NURE aerial reconnaissance survey data for uranium resource evaluation: Beeville/Bay City and Crystal City quadrangles, Texas
[GJBX-69(81)] p0228 N81-30502
Landform-vegetation relationships in the northern Chihuahuan Desert
[AD-A102896] p0208 N81-32588
Measurement of soil moisture trends with airborne scatterometers --- Texas
[E81-10088] p0209 N81-33545
Methods of editing cloud and atmospheric layer affected pixels from satellite data --- in south Texas test area
[E81-10169] p0266 N81-33556

TEXTURES
Multispectral texture analysis p0257 A81-41055
Use of imaging radar for geology and archeology p0226 A81-43730
Texture measurements from Seasat - SAR images for urban land use interpretation p0214 A81-43749
Texture analysis and urban land use classification p0214 A81-44684
Application of multispectral reflectance studies of soils - Pre-Landsat p0200 A81-46031

THEMATIC MAPPING
The use of the spectral and physical-geographic characteristics of natural objects for the interpretation of multispectral satellite images p0257 A81-41484
Evaluation of the possibility of using spectral-band and multispectral aerial photographs for the large-scale survey of natural pastures p0197 A81-41487
NASA water resources/hydrology remote sensing program in the 1980's p0244 A81-43179
A comparison of remote sensing techniques for Minnesota wetlands classification p0249 A81-43239
Remote methods and desert conservation --- Russian book p0213 A81-43523
Wetland mapping from digitized aerial photography p0252 A81-43549
Rainbow 80; Fall Technical Meeting, Niagara Falls, NY, October 7-10, 1980, ASP Technical Papers p0198 A81-43727
Waveband evaluation of proposed thematic mapper in forest cover classification p0199 A81-43738
Texture analysis and urban land use classification p0214 A81-44684
A comparison of automatic classification algorithms for land use map by remotely sensed data p0215 A81-44701
European industrial space projects
[AAS PAPER 81-053] p0278 A81-46234
What does space remote sensing provide p0278 A81-47826
Research on assessment of the recreational value of forests using Landsat digital data p0203 A81-49785
Spectral measurement of rangeland p0218 A81-49790
Computer analysis of Tiros-N/NOAA-6 satellite data for operational snow cover mapping p0262 A81-49795
Benefits of using airborne remote sensing for Thematic Mapping p0275 A81-49801
A simulation of Thematic Mapper performance in an agricultural application p0204 A81-49810
Evaluation of Thematic Mapper bands - A first step in feature selection p0205 A81-49815
Photographic technology development project: Timber typing in the Tahoe Basin using high altitude panoramic photography
[NASA-CR-161082] p0208 N81-32578
A study of the effects of the atmosphere on thematic mapper observations
[E81-10056] p0276 N81-33540
Comparison of laboratory reflectance spectra and LANDSAT multispectral images of Hawaiian lava flows
[E81-10061] p0266 N81-33541
Measurement of soil moisture trends with airborne scatterometers --- Texas
[E81-10088] p0209 N81-33545
A comparative study of the thematic mapper and LANDSAT spectral bands from field measurement data
[E81-10165] p0209 N81-33549

THERMAL MAPPING
Potentials of mapping buried glacier ice with Landsat thermal imagery p0276 A81-43204
Survey of in-situ and remote sensing methods for soil moisture determination p0197 A81-43221
Soil moisture applications of the heat capacity mapping mission p0197 A81-43224
Ground water applications of the heat capacity mapping mission p0248 A81-43233
Combined satellite imagery for study of coastal circulation, Onslow Bay, North Carolina p0233 A81-43250
Thermal patterns of Lake Michigan and Lake Superior from satellite remote sensors and its uses p0250 A81-43256
Preliminary survey of HCMM satellite thermal imagery as applied to hydrospherics p0252 A81-43746
Aerial thermal survey in the study of earth resources --- Russian book p0277 A81-43881
The possibility of using an aerial thermal survey for studying the structure of the salt bed in the Gulf of Kara-Bogaz-Gol p0228 A81-44061
Infrared-temperature variability in a large agricultural field p0200 A81-45432
Identification of subresolution high temperature sources using a thermal IR sensor p0273 A81-46401
Remote sensing of thermal radiation from an aircraft - An analysis and evaluation of crop-freeze protection methods p0202 A81-46895
Infrared imagery for studying the Kara-Bogaz-Gol Bay p0236 A81-48881
Satellite observations of England and north-western Europe p0217 A81-49174
Thermal vegetation canopy model studies p0202 A81-49347
The application of thermography for locating potential frost pockets in forest cutovers p0204 A81-49789
Thermal inertia mapping of some areas of Quebec based on aerial and HCMM satellite data p0204 A81-49799
The detection of groundwater discharges /springs/ using aerial thermography p0254 A81-49800
Meteosat experience in assisting commercial fishing p0239 A81-49807
Soil moisture inferences from thermal infrared measurements of vegetation temperatures
[E81-10184] p0206 N81-29500
Following oceanographic phenomena on the South Coast of Brazil with remote sensing from orbital distance
[INPE-1975-RPE/280] p0240 N81-30488
Dryland pasture and crop conditions as seen by HCMM
[E81-10080] p0209 N81-33542
Methods of editing cloud and atmospheric layer affected pixels from satellite data --- in south Texas test area
[E81-10169] p0266 N81-33556
Topographic slope correction for analysis of thermal infrared images
[PB81-211781] p0224 N81-33589

THUNDERSTORMS
A satellite derived technique for estimating rainfall from thunderstorms and hurricanes p0244 A81-43191
ISS-b experimental results on global distributions of ionospheric parameters and thunderstorm activity p0215 A81-44882

TIDES
Method for estimation of ocean current velocity from satellite images p0231 A81-41350
Microwave radiometer measurement of tidally induced salinity changes off the Georgia coast p0232 A81-42067
Some methods of multitemporal analysis of LANDSAT images resulting from a study on Venice Lagoon
[E81-10205] p0267 N81-33574

TIMBER IDENTIFICATION
Rainforest species on large-scale color photos p0198 A81-43536
Thermal vegetation canopy model studies p0202 A81-49347
Forestry priorities and their implications for the Canadian Remote Sensing Program p0202 A81-49755
SAR image response over a conifer regeneration site p0203 A81-49770
Nationwide forestry applications program. Analysis of forest classification accuracy
[E81-10183] p0206 N81-29499
Photographic technology development project: Timber typing in the Tahoe Basin using high altitude panoramic photography
[NASA-CR-161082] p0208 N81-32578

TIMBER INVENTORY
A photo interpretation approach to forest regrowth monitoring using side-looking airborne radar - Grant County, Oregon p0200 A81-45428
Application of temporal Landsat forest digital data for updating the Yukon RRAMS data base using Aries --- Renewable Resources And Management Statistics p0203 A81-49760
Technical aspects of forest inventory demonstrations using Landsat data - Projects in the Pacific Northwest States p0203 A81-49764
Principal components enhancements versus classifications of Landsat images for forestry applications p0203 A81-49782
An investigation of vegetation and other Earth resource/feature parameters using LANDSAT and other remote sensing data. 1: LANDSAT. 2: Remote sensing of volcanic emissions
[E81-10081] p0209 N81-33543
Evaluation of LANDSAT data analysis for forest survey --- northeastern aspen-birch survey unit in Minnesota - Carlton County
[E81-10175] p0210 N81-33561

TIMBER VIGOR
Extravisual damage detection - Defining the standard normal tree p0198 A81-43537

TIROS N SERIES SATELLITES
Characteristics of TIROS, GOES, DMSP and LANDSAT systems
[E81-10192] p0263 N81-29506

TOPOGRAPHY
The use of spaceborne photography for topographic mapping p0221 A81-42556
Topographic and cartographic applications of photogrammetry p0221 A81-42847
An examination of spectral band ratioing to reduce the topographic effect on remotely sensed data p0221 A81-45427
Space based topographic mapping experiment using Seasat synthetic aperture radar and LANDSAT 3 return beam vidicon imagery
[NASA-CR-164675] p0223 N81-30496
Terrain profiling from Seasat altimetry
[NASA-CR-156878] p0222 N81-31604
Ice sheet altimetry
[NASA-CR-156877] p0240 N81-31605
Reports on cartography and geodesy, series 1: Original reports, Number 81
[ISSN-0469-4236] p0222 N81-33527
Topographic slope correction for analysis of thermal infrared images
[PB81-211781] p0224 N81-33589

TOPOLOGY
From landforms to avian habitat - A look at topology p0214 A81-43739

TRACE CONTAMINANTS
The distribution of the trace gases H2O, NO2, and HNO3 in the middle atmosphere on the basis of LIMS measurements --- Limb Infrared Monitor of Stratosphere p0217 A81-49407

TRANSFORMATIONS (MATHEMATICS)
Radar-optical-topographic transformations for scene content analysis p0261 A81-48552

TRANSMISSIVITY
A comparison of observed and analytically derived remote sensing penetration depths for turbid water [NASA-TM-83176] p0255 N81-33577
TRANSPIRATION
Descriptive and sensitivity analyses of WATBALI: A dynamic soil water model [E81-10193] p0206 N81-29507
TREES (PLANTS)
Mountain pine beetle damage surveys with high-altitude panoramic photography p0199 A81-43732
TRIANGULATION
Measurement of lengths, angles, and areas on the earth's spheroid p0221 A81-42846
Application of new precision measuring systems for photogrammetric comparators [BMFT-FB-T-80-134] p0276 N81-32595
TROPICAL METEOROLOGY
Hurricane 'Flossie' /September 1978/ observed in the north Atlantic, by the Meteosat satellite p0213 A81-41061
Rain estimation over several areas of the globe using satellite imagery p0245 A81-43193
Annual and interannual variations in outgoing longwave radiation over the tropics p0251 A81-43356
TROPICAL REGIONS
The methodology of CIAT's land resource study of tropical America p0216 A81-46046
Remote sensing of soil radionuclide fluxes in a tropical ecosystem --- Eniwetok and Bikini Atolls [UCRL-84501] p0219 N81-29517
Drifting buoy data from the tropical Pacific Ocean during NORPAX equatorial test shuttle experiment [PB81-198939] p0240 N81-31807
TROPICAL STORMS
The occurrence of vertical tilt in tropical cyclones p0238 A81-49656
Eastern North Pacific tropical cyclones of 1980 p0238 A81-49657
TROPOSPHERE
Satellite measurements of tropospheric aerosols [NASA-CR-3459] p0219 N81-31680
TROPOSPHERIC RADIATION
Determination of moisture from NOAA polar orbiting satellite sounding radiances p0243 A81-41158
TUNISIA
A comparison between two photographic methods for the determination of relative bidirectional reflectance p0259 A81-45431
TURBIDITY
A comparison of observed and analytically derived remote sensing penetration depths for turbid water [NASA-TM-83176] p0255 N81-33577

U

U.S.S.R.
Results of ground surveys, carried out in conjunction with satellite and aerial studies, of the state of winter wheat on the Kursk test polygon p0197 A81-41485
Determination of the types and state of crops from multispectral aerial photographs p0197 A81-41486
Evaluation of the possibility of using spectral-band and multispectral aerial photographs for the large-scale survey of natural pastures p0197 A81-41487
Concerning the hydrogeological significance of faults on platform regions, as revealed by space imagery p0225 A81-42277
Ring structures of Precambrian shields, based on the interpretation of space imagery p0225 A81-42278
Space research on seismic regions p0225 A81-42280
The space engineering use efficiency for forest study [IAF PAPER 81-108] p0202 A81-47354
Infrared imagery for studying the Kara-Bogaz-Gol Bay p0236 A81-48681
Dynamic ecosystem of the Aral Basin studied from satellite imagery p0217 A81-48682
The informational estimation of the effectiveness of using satellite imagery in hydrogeological research p0227 A81-48683
The interrelation of linear and isometric objects on satellite imagery and the oil and gas structures of the Buzuluk Basin p0227 A81-48685
Use of satellite pictures for agriculture p0205 N81-28120
Large area application of a corn hazard model --- Soviet Union [E81-10164] p0205 N81-28497
U.S.S.R. SPACE PROGRAM
Soviet remote sensing of the earth's resources and interpretation of space data with reference to the Caspian Sea, Siberia and the Arctic Ocean [IAF PAPER 81-112] p0278 A81-47355
Evaluation of the 1980 Cosmos program p0278 A81-47829
ULTRAVIOLET RADIATION
Role of multiple scattering in ozone profile retrieval from satellite measurements in the ultraviolet p0215 A81-45870
UPWELLING WATER
Following oceanographic phenomena on the South Coast of Brazil with remote sensing from orbital distance [INPE-1975-RPE/280] p0240 N81-30488
URANIUM
Methods development and applications evaluations of NURE aerial reconnaissance survey data for uranium resource evaluation. Beeville/Bay City and Crystal City quadrangles, Texas [GJBX-69(81)] p0228 N81-30502
Airborne gamma-ray spectrometer and magnetometer survey [DE81-027157] p0229 N81-32592
Airborne gamma-ray spectrometer and magnetometer survey. Canyon City quadrangle (Oregon), volume 2 [DE81-028682] p0229 N81-33584
Airborne gamma-ray spectrometer and magnetometer survey. Salem quadrangle (Oregon). volume 2 [DE81-028681] p0229 N81-33585
URBAN RESEARCH
Urban area update procedures using Landsat data p0214 A81-43733
Training site statistics from Landsat and Seasat satellite imagery registered to a common map base p0258 A81-43734
Texture measurements from Seasat - SAR images for urban land use interpretation p0214 A81-43749
Aerosol formation, transformation, and effects in Denver's emissions plume p0214 A81-44526
Texture analysis and urban land use classification p0214 A81-44684
Research on assessment of the recreational value of forests using Landsat digital data p0203 A81-49785
Remote sensing and land use planning p0218 A81-49792
USER MANUALS (COMPUTER PROGRAMS)
Conversion of SPU-Universal disk file to JSC-Universal tape storage. CONVRT user's guide [E81-10185] p0263 N81-29501
Users manual for the US baseline corn and soybean segment classification procedure [E81-10190] p0206 N81-29504
Computer program documentation user information for the RSO-tape print program (RSOPRNT) [E81-10198] p0264 N81-29509
As-built design specification of the automatic registration system for the cartographic technology laboratory [E81-10176] p0267 N81-33562
USER REQUIREMENTS
Seasat data applications by commercial users p0231 A81-41974
Oceanic Satellite Data Distribution System p0231 A81-41996
Efficiency criteria of space systems for studying the earth's natural resources p0277 A81-42287
Requirements on the data/information system --- of satellite systems for earth resources observation p0278 A81-48527
Commercial applications of satellite oceanography p0237 A81-49133
An industrial perspective of the LANDSAT opportunity p0279 N81-32565

V

VECTOR ANALYSIS
Change vector analysis - An approach for detecting forest changes with Landsat p0202 A81-46056
VEGETABLES
Vegetable crop management with remote sensing p0198 A81-43540
VEGETATION
Remote sensing and mapping of pastures p0213 A81-42281
Accuracy evaluation of Landsat digital classification of vegetation in the Great Dismal Swamp p0248 A81-43235
Landsat hydrobiological classification for an inland fresh water marsh within Everglades National Park p0249 A81-43238
Comparison of sampling procedures and data analysis for a land-use and land-cover map p0213 A81-43533
Mapping wetlands using orthophotoquads and 35-mm aerial photographs p0251 A81-43543
Use of Landsat digital data to assist in mapping soils on Arizona rangelands p0201 A81-46047
Interpreter evaluations of airborne radar imagery for ecological and land/use cover classification in southern Manitoba p0218 A81-49773
Applications of remote sensing to construction impact assessment at the Roberts Bank Port, British Columbia p0218 A81-49781
Principal components enhancements versus classifications of Landsat images for forestry applications p0203 A81-49782
Colour - The critical photointerpretation element in the identification of rangeland plant communities on colour and colour-infrared aerial photography p0203 A81-49786
Spectral measurement of rangeland p0218 A81-49790
Digital enhancements for vegetation mapping in a subarctic environment p0282 A81-49793
Use of Landsat images in the monitoring and study of the LG 2 reservoir during the filling period p0254 A81-49797
Resource inventory and terrain analysis in north western Manitoba from integrated remote sensing data p0218 A81-49803
Interactive digital image processing for terrain data extraction [AD-A101321] p0264 N81-30499
Agricultural water demand prediction using remote sensing technology for Georgia resource management [PB81-184137] p0207 N81-30506
Landform-vegetation relationships in the northern Chihuahuan Desert [AD-A102886] p0208 N81-32588
Introduction to the workshop --- on coherent and incoherent radar scattering from rough surfaces and vegetated areas p0276 N81-33340
A review of volume scatter theories for modeling applications p0265 N81-33347
Comparison of laboratory reflectance spectra and LANDSAT multispectral images of Hawaiian lava flows [E81-10061] p0266 N81-33541
A comparative study of the thematic mapper and LANDSAT spectral bands from field measurement data [E81-10165] p0209 N81-33549
VEGETATION GROWTH
A technique for improved assessment of flow resistance characteristics of natural wetlands using Landsat data p0249 A81-43241
Computer-implemented remote sensing techniques for measuring coastal productivity and nutrient transport systems p0250 A81-43243
Remote methods and desert conservation --- Russian book p0213 A81-43523
Remote sensing aided procedure for conifer growth modeling in the northeastern Sierra Nevada p0199 A81-43740
The environmental vegetation index: A tool potentially useful for arid land management --- Texas and Mexico, plant growth stress due to water deficits [E81-10191] p0206 N81-29506
Meteorological satellite data: A tool to describe the health of the world's agriculture [E81-10204] p0207 N81-31596
VERMONT
The development of a remote sensing applications program for Vermont [E81-10149] p0266 N81-33547
VIDEO DATA
Application of delta modulation in on board and ground video data processing systems for the purposes of remote sensing [IAF PAPER 81-102] p0260 A81-47351
VINEYARDS
Interpretation techniques applied to mixed terrains p0218 A81-49788
Cornell University Remote Sensing Program [E81-10174] p0255 N81-33560
VIRGINIA
Accuracy evaluation of Landsat digital classification of vegetation in the Great Dismal Swamp p0248 A81-43235
Spatial correlation effects upon accuracy of supervised classification of land cover p0213 A81-43534
Remote sensing of dinoflagellate blooms in a turbid estuary p0251 A81-43538
Mineralogical, optical, and geochemical properties of John H. Kerr Reservoir sediment samples for AgRISTARS pollution research [E81-10155] p0229 N81-33548
Evaluation of remote sensing data for input into Hydrological Simulation Program-FORTRAN (HSPF) --- modeling the Occoquan watershed in Virginia using LANDSAT imagery for parameter estimation [PB81-209561] p0255 N81-33593
VISIBILITY
NASA participation in the 1980 Persistent Elevated Pollution Episode/Northeast Regional Oxidant Study (PEPE/NROS) Project: Operational aspects [NASA-TM-83170] p0220 N81-32708
VISUAL AIDS
An evaluation of detail in dynamic visual displays [AD-A103378] p0222 N81-33578
VOLCANOES
Stratospheric sulfate from the Gareloi eruption, 1980 - Contribution to the 'ambient' aerosol by a poorly documented volcanic eruption p0213 A81-41404
An investigation of vegetation and other Earth resource/feature parameters using LANDSAT and other remote sensing data. 1: LANDSAT. 2: Remote sensing of volcanic emissions [E81-10081] p0209 N81-33543

W

WASHINGTON
An investigation of vegetation and other Earth resource/feature parameters using LANDSAT and other remote sensing data. 1: LANDSAT. 2: Remote sensing of volcanic emissions [E81-10081] p0209 N81-33543
WASTE DISPOSAL
Application of remote sensing to monitoring and studying dispersion in ocean dumping p0232 A81-42228
Analysis of landfills with historic airphotos p0216 A81-46407

WATER
A comparison of observed and analytically derived remote sensing penetration depths for turbid water
[NASA-TM-83176] p0255 N81-33577
WATER CIRCULATION
Combined satellite imagery for study of coastal circulation, Onslow Bay, North Carolina
p0233 A81-43250
Preliminary survey of HCMM satellite thermal imagery as applied to hydrospherics p0252 A81-43746
Southern Chesapeake Bay circulation and suspended sediment transport analyzed using Landsat imagery
p0252 A81-43747
WATER COLOR
Nimbus-7 Coastal-Zone Colour Scanner data processing for Earthnet Experience to date p0235 A81-46919
Coastal Oceans Monitoring Satellite System (COMSS) system evaluation study
[ESS/SS-1038] p0239 N81-30168
WATER CURRENTS
A note on indirect detection of seiches in Great Salt Lake, Utah, by NOAA and Landsat satellite imagery
p0247 A81-43218
WATER DEPTH
Derivation of shallow ocean bottom reflectance values from color aerial photography
[AD-A101106] p0241 N81-33763
WATER FLOW
A technique for improved assessment of flow resistance characteristics of natural wetlands using Landsat data
p0249 A81-43241
Descriptive and sensitivity analyses of WATBALI: A dynamic soil water model
[E81-10193] p0206 N81-29507
WATER MANAGEMENT
Landsat data for regulatory permit monitoring
p0247 A81-43214
WATER POLLUTION
Application of remote sensing to monitoring and studying dispersion in ocean dumping p0232 A81-42228
Simulation modeling of estuarine ecosystems
p0243 A81-42229
Remote sensing of coastal pollutants using multispectral data p0233 A81-43245
Satellite detection of oil on the marine surface
p0233 A81-43251
An application of Landsat and computer technology to potential water pollution from soil erosion
p0250 A81-43253
Features of the radar detection of sea surface nonuniformities p0234 A81-43967
Airborne simultaneous spectroscopic detection of laser-induced water Raman backscatter and fluorescence from chlorophyll a and other naturally occurring pigments
p0253 A81-47647
Mineralogical, optical, and geochemical properties of John H. Kerr Reservoir sediment samples for AgRISTARS pollution research
[E81-10155] p0229 N81-33548
Quantification of non-point source sedimentation through densitometric analysis of color infrared aerial photography
[PB81-209157] p0255 N81-33599
WATER QUALITY
Aerospace remote sensing of the coastal zone for water quality and biotic productivity applications
p0233 A81-43246
Using enhanced Landsat images for calibrating real time estuarine water quality models p0250 A81-43252
Bay of Fundy verification of a system for multidate Landsat measurement of suspended sediment
p0250 A81-43254
Assessment and classifications of selected Illinois lakes through the application of space technology
p0250 A81-43255
Lake Ontario dynamics and water quality observations using thematically enhanced Landsat data
p0251 A81-43257
Application of digital image processing techniques and information systems to water quality monitoring of Lake Tahoe p0251 A81-43258
Trophic state determination for shallow coastal lakes from Landsat imagery p0251 A81-43259
Use of ocean color scanner data in water quality mapping p0251 A81-43545
Water quality mapping from Landsat digital data
p0252 A81-45429
Use of water Raman emission to correct airborne laser fluorosensor data for effects of water optical attenuation
p0253 A81-47676
Landsat - What is operational in water resources
p0253 A81-49757
Airborne estimation of water quality parameters in Lake Ontario p0254 A81-49796
The development of a remote sensing applications program for Vermont
[E81-10149] p0266 N81-33547
A study of Minnesota land and water resources using remote sensing. Volume 14
[E81-10166] p0254 N81-33550
Lakewide monitoring of suspended solids using satellite data --- Lake Superior water reclamation
p0254 N81-33552
Cornell University Remote Sensing Program
[E81-10174] p0255 N81-33560
WATER RECLAMATION
Lakewide monitoring of suspended solids using satellite data --- Lake Superior water reclamation
p0254 N81-33552
WATER RESOURCES
Satellite hydrology; Proceedings of the Fifth Annual William T. Pecora Memorial Symposium on Remote Sensing, Sioux Falls, SD, June 10-15, 1979
p0243 A81-43176
Remote sensing in hydrology - A challenge to scientists p0243 A81-43177
Satellite applications in river and flood forecasting
p0243 A81-43178
NASA water resources/hydrology remote sensing program in the 1980's p0244 A81-43179
Satellite versus conventional methods in hydrology
p0244 A81-43183
An introduction to satellite hydrology
p0244 A81-43184
Satellite telemetry of hydrologic data in California
p0244 A81-43187
Monitoring Canada's water resources in remote regions by satellite telemetry p0244 A81-43188
Roles of satellites in hydrology p0245 A81-43199
The use of radar imagery for surface water investigations p0247 A81-43211
Improving stream flow estimates through the use of Landsat p0247 A81-43216
Ground water and satellites - An overview/introduction
p0248 A81-43226
Improvements in lake volume predictions using Landsat data p0249 A81-43237
Using Landsat imagery to study the Okavango Swamp, Botswana p0249 A81-43242
Application of remote sensing for California irrigated lands assessment p0213 A81-43261
WATER RUNOFF
Satellite snow mapping techniques with emphasis on the use of Landsat p0245 A81-43200
Application of snow covered area to runoff forecasting, in the Sierra Nevada, California p0245 A81-43201
Prediction of water yield using satellite imagery and a snowmelt simulation model p0246 A81-43205
Landsat derived snow cover as an input variable for snow melt runoff forecasting in South Central Colorado
p0246 A81-43208
Operational use of satellite data for snow inventory and runoff forecast p0246 A81-43210
Suburban soil loss and runoff simulation assisted by interpretation of large scale aerial photography
p0253 A81-48941
Landsat observations of snowcover depletion and flooding in the Chesapeake Bay area during the winter of 1979
p0253 A81-48942
WATER TEMPERATURE
Thermal patterns of Lake Michigan and Lake Superior from satellite remote sensors and its uses
p0250 A81-43256
Airborne remote sensing of sea surface chlorophyll and temperature along the outer British Columbia coast
p0239 A81-49805
WATER VAPOR
What has been learned from the scanning multi-channel microwave radiometers /SMMRs/ p0269 A81-41995
WATER WAVES
Imaging ocean waves by synthetic aperture radars with long integration times p0231 A81-42026
A comparison of Seasat 1 altimeter measurements of wave height with measurements made by a pitch-roll buoy p0231 A81-42066
Satellite detection of seiches in Great Salt Lake, Utah
p0243 A81-42126
Wave direction measured by four different systems
p0232 A81-42622
Particular features of the ocean glitter pattern observed from a sun-synchronous orbit p0234 A81-45436
SAR ocean imaging mechanisms p0234 A81-46107
Spatial evolution of ocean wave spectra
p0235 A81-46112
Refraction of coastal ocean waves p0235 A81-46113
SAR processing of partially coherent and sinusoidally dynamic ocean waves p0239 A81-49776
Sea surface scattering p0241 N81-33344
Wave orbital velocity, fade and SAR response to azimuth waves p0265 N81-33345
Gulf of Mexico satellite radar altimetry
[NASA-TM-73295] p0224 N81-33760
WATERFOWL
Mapping the Great Salt Lake shoreline and associated waterfowl habitat from Landsat data p0252 A81-43742
WATERSHEDS
A statistical approach to rainfall estimation using satellite data p0245 A81-43198
Application of snow covered area to runoff forecasting, in the Sierra Nevada, California p0245 A81-43201
Hydrologic land use classification using Landsat
p0247 A81-43213
An application of Landsat and computer technology to potential water pollution from soil erosion
p0250 A81-43253
Aircraft active microwave measurements for estimating soil moisture p0271 A81-43547
Active microwave measurements for estimating soil moisture in Oklahoma p0199 A81-43744
Landsat - What is operational in water resources
p0253 A81-49757
The detection of groundwater discharges /springs/ using aerial thermography p0254 A81-49800
Agricultural water demand prediction using remote sensing technology for Georgia resource management
[PB81-184137] p0207 N81-30506
Photographic technology development project: Timber typing in the Tahoe Basin using high altitude panoramic photography
[NASA-CR-161082] p0208 N81-32578
Dryland pasture and crop conditions as seen by HCMM
[E81-10080] p0209 N81-33542
Evaluation of remote sensing data for input into Hydrological Simulation Program-FORTRAN (HSPF) --- modeling the Occoquan watershed in Virginia using LANDSAT imagery for parameter estimation
[PB81-209561] p0255 N81-33593
Quantification of non-point source sedimentation through densitometric analysis of color infrared aerial photography
[PB81-209157] p0255 N81-33599
WAVE PROPAGATION
Method for estimation of ocean current velocity from satellite images p0231 A81-41350
WAVEFORMS
Radar altimeter waveform modeled parameter recovery --- SEASAT-1 data
[NASA-TM-73294] p0275 N81-30325
WEATHER FORECASTING
Meteorological applications of the ARGOS system
[IAF PAPER 81-121] p0273 A81-47360
Potential for detection of natural disasters via Meteosat
[IAF PAPER 81-263] p0216 A81-47430
Use of satellite pictures for agriculture
p0205 N81-28120
Ocean services for the nation. National ocean goals and objectives for the 1980's
[PB81-200602] p0240 N81-31808
WEATHER MODIFICATION
Basic problems of the physics and chemistry of contemporary changes of climate p0216 A81-47002
WETLANDS
Landsat classification of coastal wetlands in Texas
p0248 A81-43234
Using Landsat MSS data with soils information to identify wetland habitats p0249 A81-43236
Improvements in lake volume predictions using Landsat data p0249 A81-43237
A comparison of remote sensing techniques for Minnesota wetlands classification p0249 A81-43239
Landsat interpretation of prairie lakes and wetlands of eastern South Dakota p0249 A81-43240
A technique for improved assessment of flow resistance characteristics of natural wetlands using Landsat data
p0249 A81-43241
Mapping wetlands using orthophotoquads and 35-mm aerial photographs p0251 A81-43543
Wetland mapping from digitized aerial photography
p0252 A81-43549
Mapping the Great Salt Lake shoreline and associated waterfowl habitat from Landsat data p0252 A81-43742
The use of CIR and airborne multispectral scanner techniques for wetland soils mapping of highway corridors p0215 A81-46044
WHEAT
Results of ground surveys, carried out in conjunction with satellite and aerial studies, of the state of winter wheat on the Kursk test polygon p0197 A81-41485
Determination of the types and state of crops from multispectral aerial photographs p0197 A81-41486
Sampling Landsat classifications for crop area estimation p0202 A81-46404
Assessing winter wheat dry matter production via spectral reflectance measurements p0202 A81-49344
Soil moisture inferences from thermal infrared measurements of vegetation temperatures
[E81-10184] p0206 N81-29500
Evaluation of spring wheat and barley crop calender models for the 1979 crop year
[E81-10197] p0206 N81-29508
AgRISTARS (Agriculture And Resources Inventory Surveys Through Aerospace Remote Sensing) DC/LC (Domestic Crops and Land Rover) project summary crop area estimates for Kansas and Iowa, 1980
[PB81-196909] p0207 N81-30511
A description of the reformatted spring small grains labeling procedure used in test 2, part 2 of the US/Canada wheat and barley exploratory experiment
[E81-10206] p0207 N81-31597
Classification of wheat: Badhwar profile similarity technique
[E81-10207] p0207 N81-31598
Weather analysis and interpretation procedures developed for the US/Canada wheat and barley exploratory experiment
[E81-10208] p0207 N81-31599
Crop area estimates using ground-gathered and LANDSAT data. A multitemporal approach: Missouri, 1979
[PB81-186751] p0208 N81-31614
Analysis of US spring wheat and spring barley periodic ground truth
[E81-10203] p0208 N81-32576
Dryland pasture and crop conditions as seen by HCMM
[E81-10080] p0209 N81-33542

Australian transition year special studies
[E81-10179] p0210 N81-33565
A crop moisture stress index for large areas and its application in the prediction of spring wheat phenology
[E81-10202] p0210 N81-33573

WILDLIFE
A selected bibliography: Remote sensing applications in wildlife management
[PB81-215881] p0211 N81-33598

WIND MEASUREMENT
Performance evaluation of a spaceborne scatterometer
p0269 A81-41920
Satellite scatterometer p0232 A81-42102

WIND RIVER RANGE (WY)
Multisensor analysis of hydrologic features with emphasis on the Seasat SAR p0251 A81-43544

WIND VELOCITY
What has been learned from the scanning multi-channel microwave radiometers /SMMRs/ p0269 A81-41995
The wind speed dependency of ocean microwave backscatter p0234 A81-46109
The study of mesoscale ocean winds
p0235 A81-46110

WIND VELOCITY MEASUREMENT
The future for satellite-derived surface winds
p0237 A81-49129
Cornell University Remote Sensing Program
[E81-10174] p0255 N81-33560

WINTER
The satellite record of the winter of 1978-79 in North America p0246 A81-43203

WISCONSIN
Improving stream flow estimates through the use of Landsat p0247 A81-43216

WORLD METEOROLOGICAL ORGANIZATION
Meteorological applications of the ARGOS system
[IAF PAPER 81-121] p0273 A81-47360

WRANGELL MOUNTAINS (AK)
Potentials of mapping buried glacier ice with Landsat thermal imagery p0246 A81-43204

WYOMING
Multisensor analysis of hydrologic features with emphasis on the Seasat SAR p0251 A81-43544

Y

YIELD
Yield Model Development (YMD) implementation plan for fiscal years 1981 and 1982
[E81-10211] p0208 N81-32577

PERSONAL AUTHOR INDEX

Earth Resources/*A Continuing Bibliography (Issue 32)* JANUARY 1982

Typical Personal Author Index Listing

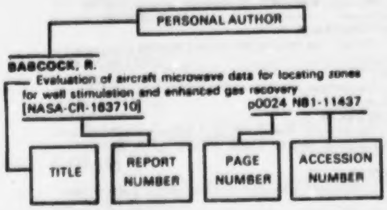
PERSONAL AUTHOR
BABCOCK, R.
Evaluation of aircraft microwave data for locating zones for well stimulation and enhanced gas recovery
[NASA-CR-163710]
p0024 N81-11437
TITLE
REPORT NUMBER
PAGE NUMBER
ACCESSION NUMBER

Listings in this index are arranged alphabetically by personal author. The title of the document provides the user with a brief description of the subject matter. The report number helps to indicate the type of document listed (e.g., NASA report, translation, NASA contractor report). The page and accession numbers are located beneath and to the right of the title, e.g., **p0024 N81-11437**. Under any one author's name the accession numbers are arranged in sequence with the AIAA accession numbers appearing first.

A

AASE, J. K
Assessing winter wheat dry matter production via spectral reflectance measurements p0202 A81-49344

ABBAS, M. M.
A differential inversion method for high resolution atmospheric remote sensing p0215 A81-45862

ADAMS, J. A. S.
Methods development and applications evaluations tof NURE aerial reconnaissance survey data for uranium resource evaluation: Beeville/Bay City and Crystal City quadrangles, Texas
[GJBX-69(81)] p0228 N81-30502

ADAMS, J. B.
Comparison of laboratory reflectance spectra and LANDSAT multispectral images of Hawaiian lava flows
[E81-10061] p0266 N81-33541

ADASKO, V.
New complex for ionosphere-magnetosphere study 'Intercosmos-Bulgaria-1300'
[IAF PAPER 81-212] p0273 A81-47407

AFOLDI, T. T.
Bay of Fundy verification of a system for multidate Landsat measurement of suspended sediment
p0250 A81-43254

AHERN, F. J.
Rapeseed - Guidelines for operational monitoring
p0203 A81-49784
Spectral measurement of rangeland
p0218 A81-49790
A simulation of Thematic Mapper performance in an agricultural application p0204 A81-49810
Evaluation of Thematic Mapper bands - A first step in feature selection p0205 A81-49815

AKHAVI, M. S.
Optical and digital analyses of Landsat data depicting hydrogeological features of the Daryacheh-Ye-Namak area, Iran p0225 A81-43215

ALANIZ, M. A.
Microdensitometry to identify saline rangelands on 70-mm color-infrared aerial film p0202 A81-46406

ALCARAZ, A.
Tiwi geothermal project - The Philippines
p0225 A81-41908

ALEXANDER, L.
An investigation of the autocorrelation function of radar images p0282 A81-49768

ALFANO, J. J.
Modeling the terrestrial hydrology for the global atmosphere - The future role of satellite data
p0245 A81-43197

ALFOLDI, T. T.
Canadian Symposium on Remote Sensing, 6th, Halifax, Canada, May 21-23, 1980, Proceedings
p0279 A81-49751

ALISHOUSE, J.
What has been learned from the scanning multi-channel microwave radiometers /SMMRs/ p0269 A81-41995

ALLORD, G. J.
Improving stream flow estimates through the use of Landsat p0247 A81-43216

ALPERS, W. R.
Imaging ocean waves by synthetic aperture radars with long integration times p0231 A81-42026

ALVO, M.
A measure of reliability for classification of earth satellite data p0257 A81-42631

AMANO, H.
Research on assessment of the recreational value of forests using Landsat digital data p0203 A81-49785

AMBROZIAK, R. A.
Yield Model Development (YMD) implementation plan for fiscal years 1981 and 1982
[E81-10211] p0208 N81-32577

AMIS, M. L.
Evaluation of large area crop estimation techniques using LANDSAT and ground-derived data
[E81-10200] p0206 N81-29511

AMOS, C. L.
Bay of Fundy verification of a system for multidate Landsat measurement of suspended sediment
p0250 A81-43254

AMURSKII, G. I.
The use of imagery of the earth to study the structure of degassing zones within oil and gas basins
p0225 AP1-42276

ANDERSEN, T.
Operational use of satellite data for snow inventory and runoff forecast p0246 A81-43210

ANDERSON, D. G.
Satellite versus conventional methods in hydrology
p0244 A81-43183
Roles of satellites in hydrology p0246 A81-43199

ANDERSON, I. C.
A top-down approach to the use of simulation in computer system design p0274 A81-48331

ANDERSSON, L. C.
Lineament mapping in northern Sweden from Landsat images using orthogonal image transforms
p0226 A81-48039

ANDREEV, G. G.
Machine method for the equalization of average phototone in an aerial photograph field
p0257 A81-41482
The possibilities of the automated classification of agricultural objects on the basis of their multispectral aerial-spaceborne images p0197 A81-41488
Practical application of the method of empty blocks for the computerized determination of the boundaries of agricultural objects p0197 A81-41489

ANTIKIDIS, J.-P.
Acquisition and preprocessing of images collected by future European Space Agency satellites
p0263 A81-49814

ANTIPOV, I. T.
Determination of the external-orientation elements of single photographs and stereopairs p0257 A81-42555

APOLLONI, A.
Use of elevation models for landform analysis by Seasat-SAR imagery
[IAF PAPER 81-98] p0260 A81-47349

AQUINO, R.
Tiwi geothermal project - The Philippines
p0225 A81-41908

AQUIPO, S.
Tiwi geothermal project - The Philippines
p0225 A81-41908

ARAUJO, E. O.
Visual enhancement of images of natural resources: Applications in geology
[E81-10181] p0228 N81-32575

ARGENTIERO, P. D.
Inventory estimation on the massively parallel processor p0259 A81-46052

ARMSTRONG, T. A.
Characteristics, of TIROS, GOES, DMSP and LANDSAT systems
[E81-10192] p0263 N81-29506

ARMSTRONG, T. E.
Australian transition year special studies
[E81-10179] p0210 N81-33565

ARSENAULT, L. D.
Single and multiple parameter microwave signatures of sea ice p0238 A81-49774
Radar detection of sea-ice ridges and icebergs in frozen oceans at incidence angles from 0 deg to 90 deg
p0238 A81-49775

ARYA, L. M.
Evaluation of gravimetric ground truth soil moisture data collected for the agricultural soil moisture experiment, 1978 Colby, Kansas, aircraft mission
[E81-10114] p0205 N81-29494
Experiment plan: Row and roughness effects on dependence of active microwave measurements of soil moisture
[E81-10209] p0211 N81-33575

ASHBURN, P.
Large area application of a corn hazard model
[E81-10164] p0205 N81-28497

ASTASHKIN, A. A.
Efficiency criteria of space systems for studying the earth's natural resources p0277 A81-42287
The characteristics of combining devices with different survey bands aboard a satellite p0274 A81-48889

AUGUSTINE, J. A.
Insights into errors of SMS inferred GATE convective rainfall p0243 A81-420'o5
Rain estimation over several areas of the globe using satellite imagery p0245 A81-43193

AUSTIN, W. W.
Classification of wheat: Badhwar profile similarity technique
[E81-10207] p0207 N81-31598

AVANESOV, G. A.
Selection of reference zones for the automatic coordinate control of space images p026-m A81-48693

AVDUEVSKII, V. S.
Efficiency criteria of space systems for studying the earth's natural resources p0277 A81-42287

B

BABCOCK, E. M.
Correlation of geologic structure inferred from computer enhanced Landsat imagery with underground water supplies in Arizona p0225 A81-43227

BACHAND, A.
Use of Landsat images in the monitoring and study of the I G 2 reservoir during the filling period
p0254 A81-49797

BADHWAR, G. D.
A comparative study of the thematic mapper and LANDSAT spectral bands from field measurement data
[E81-10165] p0209 N81-33549

BAGGETT, J.
A multistage mapping approach for an irrigated croplands inventory p0198 A81-43262

BAGOT, K. E.
Current resource mapping and environmental monitoring applications using Landsat MSS data in Scotland
p0218 A81-49806

BAKER, J. L.
Satellite aided coastal zone monitoring and vessel traffic system p0231 A81-41755

BAKER, V. R.
An examination of fluvial morphological characteristics of western Amazon streams from Apollo-Soyuz photographs p0247 A81-43212

BALEBANOV, V.
New complex for ionosphere-magnetosphere study 'Intercosmos-Bulgaria-1300'
[IAF PAPER 81-212] p0273 A81-47407

BALICK, L.
Thermal vegstation canopy model studies
p0202 A81-49347

BANNER, A.
The application of thermography for locating potential frost pockets in forest cutovers p0204 A81-49789

BARNES, J. C.
Satellite snow mapping techniques with emphasis on the use of Landsat p0245 A81-43200
Comparative analysis of sea ice features using Side-Looking Airborne Radar (SLAR) and LANDSAT imagery
[E81-10044] p0241 N81-33539

BASHKOVA, T. A.
Determination of the external-orientation elements of single photographs and stereopairs p0257 A81-42555

The influence of the accuracy of determining the elements of the external orientation of a stereopair on the processing of aerial photographs on the basis of adjusting elements
p0261 A81-48773

BATTEN, L. G.
Synergistic relationships among remote-sensing and geophysical media Geological and hydrological applications
p0255 N81-33553

BAUER, M. E.
An assessment of Landsat data acquisition history on identification and area estimation of corn and soybeans
p0200 A81-46032
Sampling Landsat classifications for crop area estimation
p0202 A81-46404

BAUMANN, W. T.
Inversion of multiwavelength radiometer measurements by three-dimensional filtering
p0271 A81-45873

BAUMGARDNER, M.
A case study of soil erosion detection by digital analysis of the remotely sensed multispectral Landsat scanner data of a semi-arid land in southern India
p0201 A81-46050

BAUMGARDNER, M. F.
Application of multispectral reflectance studies of soils - Pre-Landsat
p0200 A81-46031

BAUSCH, U.
Partially automated object extraction from aerial photographs and land maps
p0266 N81-33528

BEAL, R. C.
Spaceborne synthetic aperture radar for oceanography
p0234 A81-46104
Spatial evolution of ocean wave spectra
p0235 A81-46112

BEAUBIEN, J.
Principal components enhancements versus classifications of Landsat images for forestry applications
p0203 A81-49782

BEGNI, G.
Image quality for SPOT satellite - Specifications and budget
[IAF PAPER 81-104]
p0261 A81-47352

BELIAEV, M. IU.
Main tasks and methods of operational planning of experiments concerning the observations of the earth from space
p0277 A81-42288

BELIAEVA, N. V.
Results of ground surveys, carried out in conjunction with satellite and aerial studies, of the state of winter wheat on the Kursk test polygon
p0197 A81-41485
Evaluation of the possibility of using spectral-band and multispectral aerial photographs for the large-scale survey of natural pastures
p0197 A81-41487

BELIKOVA, T. P.
Geological interpretation in an interactive mode in automated systems of digital image processing
p0225 A81-42289

BELINSKII, A. N.
Experience with image combination in multispectral aerial photography
p0257 A81-41481
Pseudocolor representation of multispectral aerial images by means of a three-channel projector
p0269 A81-41483

BENDURA, R. J.
NASA participation in the 1980 Persistent Elevated Pollution Episode/Northeast Regional Oxidant Study (PEPE/NROS) Project Operational aspects
[NASA-TM-83170]
p0220 N81-32708

BENNY, A. H.
A technique for line extraction from LANDSAT multi-spectral scanner satellite data with some applications of the technique
[RAE-TR-81010]
p0265 N81-31613

BENSON, M. L.
Rainforest species on large-scale color photos
p0198 A81-43536

BENTLEY, C. R.
Investigation of Antarctic crust and upper mantle using Magsat and other geophysical data
[E81-10113]
p0222 N81-32574

BERG, C. P.
Satellite detection of seiches in Great Salt Lake, Utah
p0243 A81-42126
The satellite record of the winter of 1978-79 in North America
p0246 A81-43203
A note on indirect detection of seiches in Great Salt Lake, Utah, by NOAA and Landsat satellite imagery
p0247 A81-43218
Assessing the Red River of the North 1978 flooding from NOAA satellite data
p0248 A81-43219

BERGER, Z.
Suburban soil loss and runoff simulation assisted by interpretation of large scale aerial photography
p0253 A81-48941

BERNARDINI, G. C.
European industrial space projects
[AAS PAPER 81-053]
p0278 A81-46234

BERNIER, M.
Thermal inertia mapping of some areas of Quebec based on aerial and HCMM satellite data
p0204 A81-49799

BERNSTEIN, R.
Requirements on the data/information system
p0278 A81-48527

BERRETTA, G.
Analysis of the November 23, 1980 earthquake as a design basis for satellite emergency communication
[IAF PAPER 81-269]
p0216 A81-47433

BESSIS, J. L.
Data collection and location by satellite - The Argos system
[IAF PAPER 81-80]
p0273 A81-47338
Meteorological applications of the ARGOS system
[IAF PAPER 81-121]
p0273 A81-47360

BEST, R. G.
Landsat interpretation of prairie lakes and wetlands of eastern South Dakota
p0249 A81-43240

BHARTIA, P. K.
Role of multiple scattering in ozone profile retrieval from satellite measurements in the ultraviolet
p0215 A81-45870

BICE, K. L.
Mineralogical, optical, and geochemical properties of John H. Kerr Reservoir sediment samples for AgRISTARS pollution research
[E81-10155]
p0229 N81-33548

BIEHL, L. L.
Development of a digital data base for reflectance-related soil information
p0201 A81-46051

BINENKO, V. I.
Correlation between integral and spectral albedos of clouds over water surfaces
p0235 A81-47004

BIRNIE, R. W.
An investigation of vegetation and other Earth resource/feature parameters using LANDSAT and other remote sensing data 1 LANDSAT 2 Remote sensing of volcanic emissions
[E81-10081]
p0209 N81-33543

BISCHOFF, K.
First results of the Intercosmos satellite IK-21
[IAF PAPER 81-214]
p0274 A81-47409

BLACKWELL, R. J.
Application of digital image processing techniques and information systems to water quality monitoring of Lake Tahoe
p0251 A81-43258

BLANCHARD, B. J.
Dryland pasture and crop conditions as seen by HCMM
[E81-10080]
p0209 N81-33542

BLANTON, J. O.
Microwave radiometer measurement of tidally induced salinity changes off the Georgia coast
p0232 A81-42067

BLAZQUEZ, C. H.
Vegetable crop management with remote sensing
p0198 A81-43540

BLYSTONE, R. K.
On the analysis of remote sensing data to predict selected vegetative variables
p0258 A81-43736

BOCHEV, A.
New complex for ionosphere-magnetosphere study 'Intercosmos-Bulgaria-1300'
[IAF PAPER 81-212]
p0273 A81-47407

BOCK, P.
Modeling the terrestrial hydrology for the global atmosphere - The future role of satellite data
p0245 A81-43197

BOERNER, W. M.
Optimal polarization concept in radar imaging
p0265 N81-33350

BOGDANOV, A. A.
Concerning the possibility of improving the spectroradiometric accuracy of remote sensing of the earth by means of multispectral band scanners
p0270 A81-42285

BOISSONNAULT, J.
Mapping the Great Salt Lake shoreline and associated waterf[illegible] habitat from Landsat data
p0252 A81-43742

BOITR[illegible]T, C. A.
Measurements of CF2Cl2, CFCl3, and N2O in the lower stratosphere between 2 deg S and 73 deg N latitude
p0214 A81-44515

BOKSHTEIN, I. M.
Experience with image combination in multispectral aerial photography
p0257 A81-41481

BOLAND, D. H. P.
Assessment and classifications of selected Illinois lakes through the application of space technology
p0250 A81-43255

BOMMAS, G.
Possible applications of communication satellites for research tasks in polar regions
[BMFT-FB-W-80-029]
p0267 N81-33587

BONDAREVA, M. S.
The use of imagery of the earth to study the structure of degassing zones within oil and gas basins
p0225 A81-42276

BONN, F.
Thermal inertia mapping of some areas of Quebec based on aerial and HCMM satellite data
p0204 A81-49799

BORN, G. H.
Orbit determination requirements for TOPEX
[AAS PAPER 81-158]
p0221 A81-45828

BORSTAD, G. A.
Airborne remote sensing of sea surface chlorophyll and temperature along the outer British Columbia coast
p0239 A81-49805

BOSCHER, J.
Experimental investigation of the physical fundamentals for remote sensing of soil and vegetation moisture by active infrared reflectance spectroscopy using CO2 laser technique
[BMFT-FB-W-80-037]
p0211 N81-33588

BOWLEY, C. J.
Satellite snow mappin, techniques with emphasis on the use of Landsat
p0245 A81-43200
Comparative analysis of sea ice features using Side-Looking Airborne Radar (SLAR) and LANDSAT imagery
[E81-10044]
p0241 N81-33539

BRACALENTE, E. M.
Performance evaluation of a spaceborne scatterometer
p0269 A81-41920
The study of mesoscale ocean winds
p0235 A81-46110

BRADLEY, G. A.
Potential application of satellite radar to monitor soil moisture
p0270 A81-43223

BRETHERTON, F. P.
Climate, the oceans, and remote sensing
p0237 A81-49132

BRETON, D.
The remote sensing satellite program of the European Space Agency
p0279 A81-49762

BRISTOW, M.
Use of water Raman emission to correct airborne laser fluorosensor data for effects of water optical attenuation
p0253 A81-47676

BRITT, C. L., JR.
Performance evaluation of a spaceborne scatterometer
p0269 A81-41920

BROCHU, R.
Thermal inertia mapping of some areas of Quebec based on aerial and HCMM satellite data
p0204 A81-49799

BROOKS, R. L.
Land subsidence measured by satellite radar altimetry
p0270 A81-43260
Terrain profiling from Seasat altimetry
[NASA-CR-156878]
p0222 N81-31604
Ice sheet altimetry
[NASA-CR-156877]
p0240 N81-31605

BROWN, A. J.
Application of snow covered area to runoff forecasting, in the Sierra Nevada, California
p0245 A81-43201

BROWN, R. J.
Rapeseed - Guidelines for operational monitoring
p0203 A81-49784
Spectral measurement of rangeland
p0218 A81-49790
A simulation of Thematic Mapper performance in an agricultural application
p0204 A81-49810
Evaluation of Thematic Mapper bands - A first step in feature selection
p0205 A81-49815

BROWN, R. M.
Airborne remote sensing of sea surface chlorophyll and temperature along the outer British Columbia coast
p0239 A81-49805

BROWN, W. E., JR.
Advanced synthetic aperture radar for remote sensing
p0274 A81-48553

BROWNE, G. H.
Geomorphic mapping from Landsat-3 Return Beam Vidicon /RBV/ imagery
p0226 A81-46194

BRUCE, W. D.
Geological and terrain analysis of the Annapolis County region of Nova Scotia - An application of digital Landsat, radar and colour infrared data
p0227 A81-49802

BRYAN, M. L.
The use of radar imagery for surface water investigations
p0247 A81-43211

BUCKELEW, T. D.
Adapting GOES DCS for use by Corps of Engineers
p0244 A81-43186

BUNDY, D.
Use of water Raman emission to correct airborne laser fluorosensor data for effects of water optical attenuation
p0253 A81-47676

BURKE, H.-H. K.
Requirements of space-borne microwave radiometers for detecting soil moisture contents
p0270 A81-43225

BURKE, W. J.
Requirements of spac3-borne microwave radiometers for detecting soil moisture contents
p0270 A81-43225

BURLESHIN, M. I.
Concerning the hydrogeological significance of faults on platform regions, as revealed by space imagery
p0225 A81-42277
The informational estimation of the effectiveness of using satellite imagery in hydrogeological research
p0227 A81-48683

BURNS, E.
Mapping alpine soils using color positive and color infrared photographs
p0252 A81-46045

BURROFF, P. G.
Machine processing of remotely sensed data and soil information systems and remote sensing and soil survey, Proceedings of the Sixth Annual Symposium, Purdue University, West Lafayette, IN, June 3-6, 1980
p0200 A81-46026

BUTERA, M. K.
Computer-implemented remote sensing techniques for measuring coastal productivity and nutrient transport systems
p0250 A81-43243

BUTT, K. A.
Airborne impulse radar sounding of sea ice
p0238 A81-49771

C

CALABRESE, M. A.
NASA water resources/hydrology remote sensing program in the 1980's p0244 A81-43179

CALWELL, T. A.
Airborne estimation of water quality parameters in Lake Ontario p0254 A81-49796

CAMPBELL, J. B.
Spatial correlation effects upon accuracy of supervised classification of land cover p0213 A81-43534

CAMPBELL, W. J.
An application of Landsat and computer technology to potential water pollution from soil erosion p0250 A81-43253

CARNEGGIE, D. M.
A selected bibliography Remote sensing applications in wildlife management
[PB81-215881] p0211 N81-33598

CARNES, J. G.
Evaluation of spring wheat and barley crop calender models for the 1979 crop year
[E81-10197] p0206 N81-29508

CARRARA, A.
Use of elevation models for landform analysis by Seasat-SAR imagery
[IAF PAPER 81-98] p0260 A81-47349

CARTER, V.
Accuracy evaluation of Landsat digital classification of vegetation in the Great Dismal Swamp p0248 A81-43235

CASE, J. B.
Automation in photogrammetry p0258 A81-43532

CERMAK, R. J.
Hydrologic land use classification using Landsat p0247 A81-43213

CHAGARLAMUDI, P.
Stratification of Landsat data by uniformity productivity of soils p0259 A81-46042

CHANG, A.
Aircraft active microwave measurements for estimating soil moisture p0271 A81-43547
Active microwave measurements for estimating soil moisture in Oklahoma p0199 A81-43744

CHANG, A. T. C.
Passive microwave sensing of snow characteristics over land p0246 A81-43207
Freshwater ice thickness observations using passive microwave sensors p0254 A81-49968

CHAPKNOV, S.
New complex for ionosphere-magnetosphere study 'Intercosmos-Bulgaria-1300'
[IAF PAPER 81-212] p0273 A81-47407

CHAUME, D.
Interactive processing of Landsat image for morphopedological studies p0259 A81-46043

CHENEY, R. E.
A search for cold water rings p0235 A81-46116

CHERY, D. L.
Agricultural water demand prediction using remote sensing technology for Georgia resource management
[PB81-184137] p0207 N81-30508

CHITTINENI, C. B.
Maximum likelihood estimation of label imperfection probabilities and its use in the identification of mislabeled patterns p0259 A81-46040
Maximum likelihood clustering with dependent feature trees
[E81-10186] p0263 N81-29502
Estimation of proportions in mixed pixels through their region characterization
[E81-10199] p0264 N81-29510

CHOBAN, L. N.
Practical application of the method of empty blocks for the computerized determination of the boundaries of agricultural objects p0197 A81-41489

CHU, N. Y.
As-built design specification of the automatic registration system for the cartographic technology laboratory
[E81-10176] p0267 N81-33562

CHUMACHENKO, B. A.
Interactive system for the regional prognosis of raw mineral resources, based on ground-based and satellite imagery data p0227 A81-48691

CICONE, R. C.
Procedure M - A framework for stratified area estimation p0201 A81-46036

CIHLAR, J.
Interpreter evaluations of airborne radar imagery for ecological and land/use cover classification in southern Manitoba p0218 A81-49773

CITEAUX, J.
Meteosat experience in assisting commercial fishing p0239 A81-49807

CLARK, J.
Training site statistics from Landsat and Seasat satellite imagery registered to a common map base p0258 A81-43734

CLARK, R. A.
Satellite applications in river and flood forecasting p0243 A81-43178

CLARKE, R. P.
Assessment and classifications of selected Illinois lakes through the application of space technology p0250 A81-43255

CLEGG, B.
Remote sensing of soil radionuclide fluxes in a tropical ecosystem
[UCRL-84501] p0219 N81-29517

CLEMENT, S. C.
Mineralogical, optical, and geochemical properties of John H Kerr Reservoir sediment samples for AgRISTARS pollution research
[E81-10155] p0229 N81-33548

COCHRANE, G. R.
Geomorphic mapping from Landsat-3 Return Beam Vidicon /RBV/ imagery p0226 A81-46194

COCHRANE, T. T.
The methodology of CIAT's land resource study of tropical America p0216 A81-46046

COLEMAN, P. J., JR.
Geomagnetic field mapping from a satellite Spatial power spectra of the geomagnetic field at various satellite altitudes relative to natural noise sources and instrument noise
[PUBL-1810] p0275 N81-29480

COLLINS, A.
The use of satellite imagery as an aid to the Canadian Coast Guard ice operations p0238 A81-49758

COLOMBO, G.
Satellite To Satellite Doppler Tracking (SSDT) for mapping of the Earth's gravity field
[NASA-CR-164722] p0223 N81-31601

COLWELL, R.
Application of remote sensing for California irrigated lands assessment p0213 A81-43261
Users manual for the US baseline corn and soybean segment classification procedure
[E81-10190] p0206 N81-29504

CONGALTON, R. G.
Nationwide forestry applications program Analysis of forest classification accuracy
[E81-10183] p0206 N81-29499

CONNERS, R. W.
Texture analysis and urban land use classification p0214 A81-44684

COOK, A. F.
Remote sensing of thermal radiation from an aircraft - An analysis and evaluation of crop-freeze protection methods p0202 A81-46895

COOK, V. L.
Interim catalog ground data summary, data acquisition year 1978
[E81-10132] p0209 N81-33546

COONEY, G. C.
The discrimination of cereal crops and legumes using reflectance data in the Landsat bandpasses p0204 A81-49794

CORBELL, B. H.
Look direction dependence of radar backscattering cross section for agricultural fields p0199 A81-43741

CORNILLON, P.
Method for estimation of ocean current velocity from satellite images p0231 A81-41350

COTE, C. E.
Advanced technology for satellite data collection systems p0270 A81-43190

COURTOIS, M.
SPOT status of development
[IAF PAPER 81-92] p0278 A81-47346

COVAULT, C.
First Shuttle payload loading to begin p0273 A81-46461

COWELL, D. W.
The application of remote sensing techniques for an ecological land survey of the snow goose colony at Cape Henrietta Maria, Hudson Bay p0204 A81-49791

CRAGWALL, J. S., JR.
Remote sensing in hydrology A challenge to scientists p0243 A81-43177

CROFT, T. A.
Radiometry with nighttime DMSP images in digital form p0260 A81-46402

CURRAN, P. J.
A comparison between two photographic methods for the determination of relative bidirectional reflectance p0259 A81-45431

D

DACHEV, TS.
New complex for ionosphere-magnetosphere study 'Intercosmos-Bulgaria-1300'
[IAF PAPER 81-212] p0273 A81-47407

DAILY, M.
Use of imaging radar for geology and archeology p0226 A81-43730

DALY, P.
Analysis of the November 23, 1980 earthquake as a design basis for satellite emergency communication
[IAF PAPER 81-269] p0216 A81-47433

DAVIS, B. J.
Sampling Landsat classifications for crop area estimation p0202 A81-46404

DAVIS, J. B.
Urban area update procedures using Landsat data p0214 A81-43733

DAVIS, S.
Application of multispectral reflectance studies of soils - Pre-Landsat p0200 A81-46031

DAWE, B.
The use of satellite imagery as an aid to the Canadian Coast Guard ice operations p0238 A81-49758

DEALEMIDA, E. G.
Following oceanographic phenomena on the South Coast of Brazil with remote sensing from orbital distance
[INPE-1975-RPE/280] p0240 N81-30498

DEEPAK, A.
Remote sensing of atmospheres and oceans, Proceedings of the Interactive Workshop on Interpretation of Remotely Sensed Data, Williamsburg, VA, May 23-25, 1979 p0234 A81-45861

DEHN, M.
Multispectral texture analysis p0257 A81-41055

DEIMEL, L. E., JR.
A top-down approach to the use of simulation in computer system design p0274 A81-48331

DEJESUSPARADA, N.
Visual enhancement of images of natural resources Applications in geology
[E81-10181] p0228 N81-32575

DELEONIBUS, P. S.
Spaceborne synthetic aperture radar for oceanography p0234 A81-46104

DELNORE, V. E.
The study of mesoscale ocean winds p0235 A81-46110

DEMARCKE, J. S.
Look direction dependence of radar backscattering cross section for agricultural fields p0199 A81-43741
Use of Seasat satellite radar imagery for the detection of standing water beneath forest vegetation p0199 A81-43743

DENNIS, T. B.
The multicategory case of the sequential Bayesian pixel selection and estimation procedure
[E81-10182] p0263 N81-29498

DEPENA, R. G.
Environmental measurements of power plant cooling tower and stack plumes
[DOE/EV-02463/6] p0219 N81-30695

DERENYI, E. E.
Skylab in retrospect p0277 A81-43535
Cartographic accuracy of synthetic aperture radar imagery p0262 A81-49780

DESCHAMPS, P. Y.
Satellite determination of the mesoscale variability of the sea surface temperature p0234 A81-44861

DESLAURIERS, I.
The detection of groundwater discharges /springs/ using aerial thermography p0254 A81-49800

DESOUZA, R. C. M.
Visual enhancement of images of natural resources Applications in geology
[E81-10181] p0228 N81-32575

DEUELL, R. L.
Satellite monitoring of snow extent and condition in agricultural, transitional, and forested land cover areas
[PB81-188625] p0254 N81-30509

DEUTSCH, M.
Satellite hydrology, Proceedings of the Fifth Annual William T. Pecora Memorial Symposium on Remote Sensing, Sioux Falls, SD, June 10-15, 1979 p0243 A81-43176
Flood applications of satellite imagery p0247 A81-43217
Observations on Lake Ontario basin hydrogeology from optical enhancements of Landsat imagery p0248 A81-43231
Applications of aerospace data for detection of submarine springs in Jamaica p0226 A81-43232
Lake Ontario dynamics and water quality observations using thematically enhanced Landsat data p0251 A81-43257

DIADIUNOV, V. N.
An analysis of the data of synchronous measurements from the Meteor satellite and ships at the eastern coast of the Caspian Sea p0237 A81-48687

DIERCKS, J. W.
The occurrence of vertical tilt in tropical cyclones p0238 A81-49656

DILLMAN, R. D.
Mountain pine beetle damage surveys with high-altitude panoramic photography p0199 A81-43732

DINCER, T.
Using Landsat imagery to study the Okavango Swamp Botswana p0249 A81-43242

DIROSA, D. A.
Texture analysis and urban land use classification p0214 A81-44684

DIXON, R.
Resource inventory and terrain analysis in north western Manitoba from integrated remote sensing data p0218 A81-49803

DMITRIEVA, B. I.
The interrelation of linear and isometric objects on satellite imagery and the oil and gas structures of the Buzuluk Basin p0227 A81-48685

DOBROZRAKOV, A. D.
Aerial data acquisition systems using test ground polygons p0269 A81-41477

DOBSON, M. C.
Potential application of satellite radar to monitor soil moisture p0270 A81-43223

DORAISWAMY, P. C.
A crop moisture stress index for large areas and its application in the prediction of spring wheat phenology
[E81-10202] p0210 N81-33573

DOTTAVIO, C. L.
Effect of forest canopy closure on incoming solar radiance
[E81-10170] p0205 N81-28499

DOWNS, A. L.
Satellite monitoring of snow extent and condition in agricultural, transitional, and forested land cover areas
[PB81-188625] p0254 N81-30509

DOYLE, H. M.
Interim catalog ground data summary, data acquisition year 1978
[E81-10132] p0209 N81-33546

DOZIER, J.
Identification of subresolution high temperature sources using a thermal IR sensor p0273 A81-46401
Satellite identification of surface radiant temperature fields of subpixel resolution
[PB81-184038] p0265 N81-31615

DRIVER, J. M.
Earth applications orbit analysis for a shuttle-mounted Multispectral Mapper
[AAS PAPER 81-182] p0271 A81-45836

DUCKETT, C. C.
Drifting buoy data from the tropical Pacific Ocean during NORPAX equatorial test shuttle experiment
[PB81-198939] p0240 N81-31807

DUGGIN, M. J.
Relating ground level reflected radiance measurements in the Landsat MSS bandpasses to satellite altitudes p0271 A81-43735
On the analysis of remote sensing data to predict selected vegetative variables p0258 A81-43736
The effect of sensor bandpass and spectral response in crop stress detection p0199 A81-43737
The discrimination of cereal crops and legumes using reflectance data in the Landsat bandpasses p0204 A81-49794

DULEVICH, V. E.
Radar methods for studying the earth p0273 A81-46924

DYE, R. H.
Landsat technology transfer to the private and public sectors through community colleges and other locally available institutions p0277 A81-43750

DZHEMARDIAN, IU. A.
Accuracy of transmission of spectral contrasts in multispectral aerial photography, with application to problems of object recognition p0257 A81-41479

E

EASON, R.
AgRISTARS: Foreign commodity production forecasting. Program review presentation to level 1, Interagency Coordination Committee
[E81-10168] p0209 N81-33555

EAV, B. B.
Mountain pine beetle damage surveys with high-altitude panoramic photography p0199 A81-43732

EDWARDS, G. J.
Vegetable crop management with remote sensing p0198 A81-43540

EHLEN, J.
Identifying igneous rocks in an arid environment on aerial photography by photo tone and photo texture
[AD-A102809] p0228 N81-32587
Landform-vegetation relationships in the northern Chihuahuan Desert
[AD-A102896] p0208 N81-32588

ELLIOTT, R. A.
Vegetable crop management with remote sensing p0198 A81-43540

ELLIS, P. J.
Relating ground level reflected radiance measurements in the Landsat MSS bandpasses to satellite altitudes p0271 A81-43735

ENGMAN, E. T.
Agricultures's needs related to satellite hydrology p0197 A81-43181

EPSTEIN, E. E.
Millimeter-wave sensing of the environment: A bibliographic survey
[NASA-CR-156879] p0219 N81-32581

ERB, T. L.
Analysis of landfills with historic airphotos p0216 A81-46407

ERNST, C. L.
Using Landsat MSS data with soils information to identify wetland habitats p0249 A81-43236

ESAIAS, W. E.
Remote sensing of oceanic phytoplankton - Present capabilities and future goals p0232 A81-42215
Remote sensing in biological oceanography p0237 A81-49130

ESCOBAR, D. E.
Comparison of Landsat-2 and field spectrometer reflectance signatures of south Texas rangeland plant communities p0201 A81-46034

ESTES, J.
Application of remote sensing for California irrigated lands assessment p0213 A81-43261
A multistage mapping approach for an irrigated croplands inventory p0198 A81-43262

ESTES, J. E.
Multispectral kelp resource surveys p0232 A81-43244
Satellite detection of oil on the marine surface p0233 A81-43251

ESTES, R. H.
Early results from Magsat p0274 A81-48945

ETHRIDGE, L.
Correlation of geologic structure inferred from computer enhanced Landsat imagery with underground water supplies in Arizona p0225 A81-43227

ETLING, W.
Position measurements in Colombia by means of satellite observations p0222 N81-33522

EVANS, D. D.
Wave direction measured by four different systems p0232 A81-42622

EVANS, D. L.
Comparison of laboratory reflectance spectra and LANDSAT multispectral images of Hawaiian lava flows
[E81-10061] p0266 N81-33541

EVERITT, J. H.
Comparison of Landsat-2 and field spectrometer reflectance signatures of south Texas rangeland plant communities p0201 A81-46034
Microdensitometry to identify saline rangelands on 70-mm color-infrared aerial film p0202 A81-46406

EYTON, J. R.
Crop classification with a Landsat/radar sensor combination p0200 A81-46033

F

FAINTICH, M. B.
The sensor image simulator
[AD-A101172] p0275 N81-29512

FALCONER, A.
Observations on Lake Ontario basin hydrogeology from optical enhancement of Landsat imagery p0248 A81-43231
Lake Ontario dynamics and water quality observations using thematically enhanced Landsat data p0251 A81-43257

FARR, T. G.
Comparison of laboratory reflectance spectra and LANDSAT multispectral images of Hawaiian lava flows
[E81-10061] p0266 N81-33541

FASLER, F.
Texture measurements from Seasat - SAR images for urban land use interpretation p0214 A81-43749

FAVARD, J.-C.
Meteosat experience in assisting commercial fishing p0239 A81-49807

FEDOSH, M. S.
Southern Chesapeake Bay circulation and suspended sediment transport analyzed using Landsat imagery p0252 A81-43747

FEHRENBACH, L. K.
Derivation of shallow ocean bottom reflectance values from color aerial photography
[AD-A101105] p0241 N81-33763

FELDMAN, A.
Hydrologic land use classification using Landsat p0247 A81-43213

FERGG, F.
Comparative measurements of stratospheric CH4 and CO concentrations with spectrograph and correlation radiometers p0217 A81-49433

FERGUSON, H. L.
Flood applications of satellite imagery p0247 A81-43217

FERRIGNO, J. G.
Satellite Image Atlas of the earth's glaciers p0246 A81-43202

FFOLLIOTT, P. F.
Prediction of water yield using satellite imagery and a snowmelt simulation model p0246 A81-43205

FIENUP, J.
Fourier modulus image construction
[AD-A101728] p0284 N81-30723

FIGURA, P. C.
The sensor image simulator
[AD-A101172] p0275 N81-29512

FINLEY, R. J.
Landsat classification of coastal wetlands in Texas p0248 A81-43234

FINSTERWALDER, R.
Stereoorthophotos as aids in the mapping of high mountain regions p0221 A81-46678

FISCHER, H.
The distribution of the trace gases H2O, NO2, and HNO3 in the middle atmosphere on the basis of LIMS measurements p0217 A81-49407

FISCHER, H.-J.
First results of the Intercosmos satellite IK-21
[IAF PAPER 81-214] p0274 A81-47409

FITZPATRICK-LINS, K.
Comparison of sampling procedures and data analysis for a land-use and land-cover map p0213 A81-43533

FLEIG, A. J.
Role of multiple scattering in ozone profile retrieval from satellite measurements in the ultraviolet p0215 A81-45870

FLEMING, H. E.
A new numerical treatment of the source function in the radiative transfer equation p0269 A81-41916
Application of the truncated normal distribution technique to the derivation of sea surface temperatures p0234 A81-45881

FORD, J. P.
A radar image time series p0226 A81-45430

FORNARO, R. J.
A top-down approach to the use of simulation in computer system design p0274 A81-48331

FORREST, R. B.
Simulation of orbital image-sensor geometry p0260 A81-46192

FORSYTHE, R. G.
Gulf of Mexico satellite radar altimetry
[NASA-TM-73295] p0224 N81-33760

FOSTER, J.
Landsat observations of snowcover depletion and flooding in the Chesapeake Bay area during the winter of 1979 p0253 A81-48942

FOSTER, J. L.
Passive microwave sensing of snow characteristics over land p0246 A81-43207
Multisensor analysis of hydrologic features with emphasis on the Seasat SAR p0251 A81-43544
Satellite observations of England and north-western Europe p0217 A81-49174
Freshwater ice thickness observations using passive microwave sensors p0254 A81-49968

FOUQUET, J.-P.
The SPOT satellite mission, applications aspects and data products p0278 A81-48549

FRANZ, D. D.
Evaluation of remote sensing data for input into Hydrological Simulation Program-FORTRAN (HSPF)
[PB81-209561] p0255 N81-33593

FRASCA, J. W.
LANDSAT C workshop field/laboratory exercises p0280 N81-32571

FRITSCHEN, L.
Thermal vegetation canopy model studies p0202 A81-49347

FROMM, H.
Analysis of the November 23, 1980 earthquake as a design basis for satellite emergency communication
[IAF PAPER 81-269] p0216 A81-47433

FROST, R. E.
Remote sensing for engineering site selection
[AD-A102810] p0219 N81-32586

FROST, V. S.
Radar image preprocessing p0272 A81-46038

FROUIN, R.
Satellite determination of the mesoscale variability of the sea surface temperature p0234 A81-44861

FUCHS, H.
A radar image time series p0226 A81-45430

FUJIMURA, S.
A comparison of automatic classification algorithms for land use map by remotely sensed data p0215 A81-44701

FUNG, A. K.
A review of volume scatter theories for modeling applications p0265 N81-33.47

FURTEK, R.
Use of water Raman emission to correct airborne laser fluorosensor data for effects of water optical attenuation p0253 A81-47676

FUSCO, L.
Nimbus-7 Coastal-Zone Colour Scanner data processing for Earthnet Experience to date p0235 A81-46919

G

GAINANOV, A. G.
Gravimetric studies of the earth's crust in the oceans p0221 A81-43524

GAMBERG, J. B.
Airborne impulse radar sounding of sea ice p0238 A81-49771

GAMMON, P. T.
Accuracy evaluation of Landsat digital classification of vegetation in the Great Dismal Swamp p0248 A81-43235
Mapping wetlands using orthophotoquads and 35-mm aerial photographs p0251 A81-43543

GAPOSCHKIN, E. M.
Satellite To Satellite Doppler Tracking (SSDT) for mapping of the Earth's gravity field
[NASA-CR-164722] p0223 N81-31601

GAUCHER, D. W.
Derivation of shallow ocean bottom reflectance values from color aerial photography
[AD-A101105] p0241 N81-33763

GAUSMAN, H. W.
Comparison of Landsat-2 and field spectrometer reflectance signatures of south Texas rangeland plant communities p0201 A81-46034

GEHLHAAR, U.
Compact and highly sensitive fluorescence lidar for oceanographic measurements p0237 A81-49378

GENDLER, V. E.
Geological interpretation in an interactive mode in automated systems of digital image processing p0225 A81-42289

GEORGIEV, N.
Optimization of Doppler measurements in the satellite network of Eastern Europe p0221 A81-48678

GERBERMANN, A. H.
Microdensitometry to identify saline rangelands on 70-mm color-infrared aerial film p0202 A81-46406

GERGISHVILI, D.
Use of satellite pictures for agriculture p0205 N81-28120

GERGOV, TS.
Optimization of Doppler measurements in the satellite network of Eastern Europe p0221 A81-48678

GERSON, D. J.
Derivation of shallow ocean bottom reflectance values from color aerial photography
[AD-A101106] p0241 N81-33763

GERVIN, J. C.
Improvements in lake volume predictions using Landsat data p0249 A81-43237
A technique for improved assessment of flow resistance characteristics of natural wetlands using Landsat data p0249 A81-43241

GIBBS, P. M.
Computer program documentation user information for the RSO-tape print program (RSOPRNT)
[E81-10198] p0264 N81-29509

GILLE, J. C.
The distribution of the trace gases H2O, NO2, and HNO3 in the middle atmosphere on the basis of LIMS measurements p0217 A81-49407

GLASS, C. E.
Correlation of geologic structure inferred from computer enhanced Landsat imagery with underground water supplies in Arizona p0225 A81-43227

GLUCKSTEIN, S. A.
Airborne estimation of water quality parameters in Lake Ontario p0254 A81-49796

GLUKHOVSKII, M. Z.
Ring structures of Precambrian shields, based on the interpretation of space imagery p0225 A81-42278

GLUSHKOV, V. M.
Radar methods for studying the earth p0273 A81-46924

GNAUK, G.
Technical aspects of forest inventory demonstrations using Landsat data - Projects in the Pacific Northwest States p0203 A81-49764

GOEBEL, J. E.
Synergistic relationships among remote-sensing and geophysical media: Geological and hydrological applications p0255 N81-33553

GOEPFERT, W.
A rectification technique for digital orthophoto production p0257 A81-41057

GOETTELMAN, R. C.
Infrared-temperature variability in a large agricultural field p0200 A81-45432

GOGOSHEV, M.
New complex for ionosphere-magnetosphere study 'Intercosmos-Bulgaria-1300'
[IAF PAPER 81-212] p0273 A81-47407

GOLDBERG, M.
A measure of reliability for classification of earth satellite data p0257 A81-42631

GOLUB, V. B.
Evaluation of the possibility of using spectral-band and multispectral aerial photographs for the large-scale survey of natural pastures p0197 A81-41487

GONFREVILLE, P.
What does space remote sensing provide p0278 A81-47828

GOODENOUGH, D. G.
Integration and comparison of SAR and MSS data for potato crop area estimation p0203 A81-49766
Rapeseed - Guidelines for operational monitoring p0203 A81-49784
A simulation of Thematic Mapper performance in an agricultural application p0204 A81-49810

GOODIER, B. G.
Methods of editing cloud and atmospheric layer affected pixels from satellite data
[E81-10169] p0266 N81-33556

GOODISON, B. E.
Monitoring Canada's water resources in remote regions by satellite telemetry p0244 A81-43188
Application of synthetic aperture radar data to snow cover monitoring p0253 A81-49778

GOODY, R.
Satellites for oceanography - The promises and the realities p0237 A81-49126

GORBACHEV, V. V.
Experience with the determination of optical image distortions of landscape elements on IR aerial photographs p0257 A81-41480

GORDON, H. R.
Atmospheric correction of Nimbus-7 Coastal Zone Color Scanner imagery p0271 A81-45879

GORNYI, V. I.
The possibility of using an aerial thermal survey for studying the structure of the salt bed in the Gulf of Kara-Bogaz-Gol p0226 A81-44061
Infrared imagery for studying the Kara-Bogaz-Gol Bay p0236 A81-48681

GOULD, C. L.
Large scale human benefits of space industrialization p0277 A81-42513

GOWER, J. F. R.
Airborne remote sensing of sea surface chlorophyll and temperature along the outer British Columbia coast p0239 A81-49805

GRAHAM, D. S.
Using enhanced Landsat images for calibrating real time estuarine water quality models p0250 A81-43252

GRAHAM, M. H.
An evaluation of MSS P-format data registration
[E81-10171] p0267 N81-33557

GRANTHAM, W. L.
Performance evaluation of a spaceborne scatterometer p0269 A81-41920

GRAY, A. L.
Single and multiple parameter microwave signatures of sea ice p0238 A81-49774
Radar detection of sea-ice ridges and icebergs in frozen oceans at incidence angles from 0 deg to 90 deg p0238 A81-49775

GRAY, T. I., JR.
The environmental vegetation index: A tool potentially useful for arid land management
[E81-10191] p0206 N81-29505
Characteristics, of TIROS, GOES, DMSP and LANDSAT systems
[E81-10192] p0263 N81-29506
Meteorological satellite data: A tool to describe the health of the world's agriculture
[E81-10204] p0207 N81-31596

GRIFFITH, C. G.
Insights into errors of SMS-inferred GATE convective rainfall p0243 A81-42095
Rain estimation over several areas of the globe using satellite imagery p0245 A81-43193

GRIGGS, M.
Satellite measurements of tropospheric aerosols
[NASA-CR-3459] p0219 N81-31680
Satellite measurements of atmospheric aerosols
[AD-A103483] p0220 N81-33720

GROCH, W. D.
Partially automated object extraction from aerial photographs and land maps p0266 N81-33528

GROSSI, M.
Satellite To Satellite Doppler Tracking (SSDT) for mapping of the Earth's gravity field
[NASA-CR-164722] p0223 N81-31601

GUBIN, V. A.
Radar methods for studying the earth p0273 A81-46924

GUINDON, B.
Integration and comparison of SAR and MSS data for potato crop area estimation p0203 A81-49766

GUISSARD, A.
Study of the influence of the atmosphere on the performance of an imaging microwave radiometer
[ESA-CR(P)-1421] p0275 N81-30342

GUNN, K.
Crop phenology and LANDSAT-based irrigated lands inventory in the high plains
[E81-10173] p0210 N81-33559

GUNTHER, E. B.
Eastern North Pacific tropical cyclones of 1980 p0238 A81-49657

GUNTHER, K. P.
Compact and highly sensitive fluorescence lidar for oceanographic measurements p0237 A81-49378

GURAUS, E. A.
A comparison of observed and analytically derived remote sensing penetration depths for turbid water
[NASA-TM-83176] p0255 N81-33577

GURNEY, R. J.
Satellite observations of England and north-western Europe p0217 A81-49174

GURUSWAMY, V.
A case study of soil erosion detection by digital analysis of the remotely sensed multispectral Landsat scanner data of a semi-arid land in southern India p0201 A81-46050

GUSEMAN, L. F., JR.
Development of advanced acreage estimation methods
[E81-10160] p0205 N81-29485

GUYENNE, T. D.
Coherent and incoherent radar scattering from rough surfaces and vegetated areas
[ESA-SP-166] p0208 N81-33339

H

HADLEY, J., JR.
A practical method for the verification of computer-processed Landsat data p0261 A81-48943

HAFKER, W. R.
Manual versus digital Landsat analysis for modeling river flooding p0252 A81-43745
Manual versus digital Landsat analysis for delineating river flooding p0252 A81-46405

HAGEN, V. K.
Corps of Engineers utilization of satellites for hydrologic purposes p0244 A81-43180

HALL, D. K.
Passive microwave sensing of snow characteristics over land p0246 A81-43207
Multisensor analysis of hydrologic features with emphasis on the Seasat SAR p0251 A81-43544
Freshwater ice thickness observations using passive microwave sensors p0254 A81-49968

HALL, E. L.
Radar-optical-topographic transformations for scene content analysis p0261 A81-48552

HAMILTON, A. C.
The integration of remote sensing in environmental decision making for the Maritimes p0217 A81-49752

HAMILTON, G. D.
Reports on Marine Science Affairs. Report 14: Satellite data requirements for marine meteorological services
[WMO-548] p0239 N81-28668

HAMNAFORD, J. F.
Application of snow covered area to runoff forecasting in the Sierra Nevada, California p0245 A81-43201

HANKA, E.
Possible applications of communication satellites for research tasks in polar regions
[BMFT-FB-W-80-029] p0267 N81-33587

HANNAH, H. E.
Remote sensing of thermal radiation from an aircraft - An analysis and evaluation of crop-freeze protection methods p0202 A81-46896

HANSEN, D. V.
Drifting buoy data from the tropical Pacific Ocean during NORPAX equatorial test shuttle experiment
[PB81-198939] p0240 N81-31807

HANSEN, P. L.
Flood applications of satellite imagery p0247 A81-43217

HANSSEN, A. J.
Computer analysis of Tiros-N/NOAA-6 satellite data for operational snow cover mapping p0262 A81-49795

HARDY, N. E.
A photo interpretation approach to forest regrowth monitoring using side-looking airborne radar - Grant County, Oregon p0200 A81-45428

HARGER, R. O.
SAR ocean imaging mechanisms p0234 A81-46107

HARLAN, J. C.
Dryland pasture and crop conditions as seen by HCMM
[E81-10080] p0209 N81-33542

HARLOW, C. A.
Texture analysis and urban land use classification p0214 A81-44684

HARRILL, S. F.
Methods development and applications evaluations of NURE aerial reconnaissance survey data for uranium resource evaluation: Beeville/Bay City and Crystal City quadrangles, Texas
[GJBX-69(81)] p0228 N81-30502

HARRINGTON, L.
A capture-recapture approach for estimation of detection probabilities in aerial surveys p0258 A81-43546
Alternative 'scale up' estimators for aerial surveys where both detection and classification errors exist p0260 A81-46197

HARRINGTON, R. F.
Airborne microwave radiometer remote sensing of lake ice p0253 A81-48554

HARRISS, R. C.
Aerospace remote sensing of the coastal zone for water quality and biotic productivity applications p0233 A81-43246

HARTL, P.
The European SAR-Project Convair 580 p0273 A81-46679

HARWOOD, P.
Landsat classification of coastal wetlands in Texas p0248 A81-43234

HAUSKA, H.
The Lulea Image Processing System /LIPS/ - A versatile approach to earth resources data processing p0272 A81-46030
Lineament mapping in northern Sweden from Landsat images using orthogonal image transforms p0226 A81-46039

HAUSSMANN, J.
Possible applications of communication satellites for research tasks in polar regions
[BMFT-FB-W-80-029] p0267 N81-33587

HAWKINS, R. E.
Single and multiple parameter microwave signatures of sea ice p0238 A81-49774

HAWKINS, R. K.
Radar detection of sea-ice ridges and icebergs in frozen oceans at incidence angles from 0 deg to 90 deg p0238 A81-49775

HAY, C.
Users manual for the US baseline corn and soybean segment classification procedure
[E81-10190] p0206 N81-29504

HAYDEN, C. M.
Determination of moisture from NOAA polar orbiting satellite sounding radiances p0243 A81-41158

HAYES, R. M.
Detection of the Gulf Stream p0235 A81-46115

HEDDINGHAUS, T. R.
Annual and interannual variations in outgoing longwave radiation over the tropics p0251 A81-43356

HEIKEN, G.
Stratospheric sulfate from the Gareloi eruption, 1980 - Contribution to the 'ambient' aerosol by a poorly documented volcanic eruption p0213 A81-41404

HEILMAN, J. L.
Soil moisture applications of the heat capacity mapping mission p0197 A81-43224
Ground water applications of the heat capacity mapping mission p0248 A81-43233

HEIMBUCH, D. G.
Use of remote sensing in landscape stratification for environmental impact assessment p0214 A81-43748

HEINEN, J.
Nationwide forestry applications program. Analysis of forest classification accuracy
[E81-10183] p0206 N81-29499

HELD, D. N.
Radar image preprocessing p0272 A81-46038

HELLER, W. G.
Military geodesy and geospace science, unit one
[AD-A104038] p0222 N81-33581

HENDERSON, K. E.
A comparative study of the thematic mapper and LANDSAT spectral bands from field measurement data
[E81-10165] p0209 N81-33549

HENGEVELD, H. G.
Utilisation and benefits of SLAR in operational ice data acquisition p0253 A81-49761
Optimizing imaging radar parameters for ice reconnaissance p0239 A81-49779

HERMAN, L. D.
A statistical approach to rainfall estimation using satellite data p0245 A81-43198

HERSCHY, R. W.
Potential for detection of natural disasters via Meteosat
[IAF PAPER 81-263] p0216 A81-47430

HETTENYI, T.
First results of the Intercosmos satellite IK-21
[IAF PAPER 81-214] p0274 A81-47409

HEUTMAKER, J.
Synergistic relationships among remote-sensing and geophysical media. Geological and hydrological applications p0255 N81-33553

HEYDT, H. L.
Interactive digital image processing for terrain data extraction
[AD-A101321] p0264 N81-30499

HEYMANN, Y.
Interpretation techniques applied to mixed terrains p0218 A81-49788

HIGER, A. L.
Selected irrigation acreage estimates in northern Florida from Landsat data p0198 A81-43264

HILDRETH, W. W.
Descriptive and sensitivity analyses of WATBALI: A dynamic soil water model
[E81-10193] p0206 N81-29507

HILL, J. M.
Using enhanced Landsat images for calibrating real time estuarine water quality models p0250 A81-43252

HINKLE, R. E.
Mountain pine beetle damage surveys with high-altitude panoramic photography p0199 A81-43732

HIXSON, M. M.
An assessment of Landsat data acquisition history on identification and area estimation of corn and soybeans p0200 A81-46032
Sampling Landsat classifications for crop area estimation p0202 A81-46404

HODGES, T.
Analysis of US spring wheat and spring barley periodic ground truth
[E81-10203] p0208 N81-32576

HOFER, R.
Regression techniques for oceanographic parameter retrieval using space-borne microwave radiometry p0239 A81-49867

HOFFER, R. M.
Using Landsat MSS data with soils information to identify wetland habitats p0249 A81-43236
Waveband evaluation of proposed thematic mapper in forest cover classification p0199 A81-43738
Procedure 1 and forestland classification using Landsat data p0201 A81-46055
Evaluation of LANDSAT data analysis for forest survey
[E81-10175] p0210 N81-33561

HOFFMAN, H. W.
Thermal patterns of Lake Michigan and Lake Superior from satellite remote sensors and its uses p0250 A81-43258

HOGE, F. E.
Airborne simultaneous spectroscopic detection of laser-induced water Raman backscatter and fluorescence from chlorophyll a and other naturally occurring pigments p0253 A81-47647

HOGG, W. D.
Computer analysis of Tiros-N/NOAA-6 satellite data for operational snow cover mapping p0262 A81-49795

HOLBEN, B.
An examination of spectral band ratioing to reduce the topographic effect on remotely sensed data p0221 A81-45427

HOLBEN, B. N.
Application of digital terrain data to quantify and reduce the topographic effect on Landsat data p0259 A81-45433

HOLLADAY, G.
Remote sensing of soil radionuclide fluxes in a tropical ecosystem
[UCRL-84501] p0219 N81-29517

HOLLOWAY, J.
A multistage mapping approach for an irrigated croplands inventory p0198 A81-43262

HOLMAN, R. E., III
Trophic state determination for shallow coastal lakes from Landsat imagery p0251 A81-43259

HOLTZMAN, J. C.
Radar image preprocessing p0272 A81-46038

HOLZ, R. K.
An examination of fluvial morphological characteristics of western Amazon streams from Apollo-Soyuz photographs p0247 A81-43212

HONVAULT, C.
The first ESA remote sensing satellite /ERS/ - The programme and the system
[IAF PAPER 81-90] p0236 A81-47344

HORVATH, E. H.
Use of Landsat digital data to assist in mapping soils on Arizona rangelands p0201 A81-46047
Spectral properties of Arizona soils and rangelands and their relationship to LANDSAT digital data p0207 N81-31595

HORVATH, R.
Users manual for the US baseline corn and soybean segment classification procedure
[E81-10190] p0206 N81-29504

HOUGHTON, J. T.
Remote sounding of atmosphere and ocean for climate research /Appleton Lecture/ p0236 A81-47099

HOWARTH, P. J.
Procedures for change detection using Landsat digital data p0215 A81-45437
Digital enhancements for vegetation mapping in a subarctic environment p0262 A81-49793

HSIAO, S. V.
Wave direction measured by four different systems p0232 A81-42622

HUFFORD, G. L.
Sea ice detection using enhanced infrared satellite data p0232 A81-42131

HULL, G. A.
Field Study for Remote Sensing: An instructor's manual
[NASA-CP-2155] p0279 N81-32564

HUMPHRIES, L.
The use of satellite imagery as an aid to the Canadian Coast Guard ice operations p0238 A81-49758

HUNTLEY, J. E.
The occurrence of vertical tilt in tropical cyclones p0238 A81-49656

HUSSEY, W. J.
The National Oceanic Satellite System p0236 A81-48548

HUTCHISON, B.
Thermal vegetation canopy model studies p0202 A81-49347

HUTTON, S. M.
Using Landsat imagery to study the Okavango Swamp, Botswana p0249 A81-43242

HWANG, J. J.
Radar-optical-topographic transformations for scene content analysis p0261 A81-48552

I

IAKOVLEV, V. A.
Interactive system for the regional prognosis of raw mineral resources, based on ground-based and satellite imagery data p0227 A81-48691

IAKOVLEV, V. P.
Aerial data acquisition systems using test-ground polygons p0269 A81-41477

IAROSLAVSKII, L. P.
Geological interpretation in an interactive mode in automated systems of digital image processing p0225 A81-42289

INKSTER, D. R.
The airborne SAR project - Conclusions and applications p0275 A81-49765

INN, E. C. Y.
Measurements of CF2Cl2, CFCl3, and N2O in the lower stratosphere between 2 deg S and 73 deg N latitude p0214 A81-44515

IOSIFIAN, A.
New complex for ionosphere-magnetosphere study 'Intercosmos-Bulgaria-1300'
[IAF PAPER 81-212] p0273 A81-47407

IRONSIDE, G. R.
Multistage remote sensing in exploratory ecodistrict land classification p0217 A81-49759

ISMAILOV, T. K.
Physical and technical foundations for the development of subsatellite systems for the exploration of natural earth resources
[IAF PAPER 81-101] p0278 A81-47350

IUDIN, V. S.
Complex processing of satellite images and the geological interpretation p0227 A81-48690

IURKOV, IU. A.
Radar methods for studying the earth p0273 A81-46924

IVANOV, I.
New complex for ionosphere-magnetosphere study 'Intercosmos-Bulgaria-1300'
[IAF PAPER 81-212] p0273 A81-47407

IWAMOTO, I.
ISS-b experimental results on global distributions of ionospheric parameters and thunderstorm activity p0215 A81-44862

J

JACKSON, R. D.
Soil moisture inferences from thermal infrared measurements of vegetation temperatures
[E81-10184] p0206 N81-29500

JACKSON, T. J.
Survey of in-situ and remote sensing methods for soil moisture determination p0197 A81-43221
Aircraft active microwave measurements for estimating soil moisture p0271 A81-43547
Active microwave measurements for estimating soil moisture in Oklahoma p0199 A81-43744

JACOBOWITZ, H.
The effect of angular distribution models on the estimation of the earth's albedo p0269 A81-41915

JAIN, S. C.
Airborne estimation of water quality parameters in Lake Ontario p0254 A81-49796

JANO, A.
SAR image response over a conifer regeneration site p0203 A81-49770

JAWORKSI, E.
Landsat technology transfer to the private and public sectors through community colleges and other locally available institutions p0277 A81-43750

JENSEN, J. R.
Multispectral kelp resource surveys p0232 A81-43244
Suburban soil loss and runoff simulation assisted by interpretation of large scale aerial photography p0253 A81-48941
Agricultural water demand prediction using remote sensing technology for Georgia resource management
[PB81-184137] p0207 N81-30508

JOHNSON, A. H.
Photointerpretation of fire damage to trees in a ponderosa pine/bunchgrass community p0204 A81-49787

JOHNSON, G. R.
Role of aerial photographs in classification of Landsat data p0262 A81-49806

JOHNSON, M. P.
Methods of editing cloud and atmospheric layer affected pixels from satellite data
[E81-10169] p0266 N81-33556

JOHNSON, R. A.
Mapping irrigated cropland on the High Plains using Landsat p0198 A81-43266

JOHNSON, R. W.
Application of remote sensing to monitoring and studying dispersion in ocean dumping p0232 A81-42228
Simulation modeling of estuarine ecosystems p0243 A81-42229

JOHNSON, T. L.
Mapping irrigated cropland on the High Plains using Landsat p0198 A81-43266

JOHNSON, W. R.
A temporal/spectral analysis of small grain crops and confusion crops
[E81-10167] p0205 N81-28498
An analysis of haze effects on LANDSAT multispectral scanner data
[E81-10162] p0263 N81-29497

JOHNSTON, I. L.
Digital enhancements for vegetation mapping in a subarctic environment p0262 A81-49793

JOLLY, J. P.
Utilizing GOES imagery to determine convective storm characteristics in data deficient regions p0245 A81-43192

JONES, C.
Measurement of soil moisture trends with airborne scatterometers
[E81-10088] p0208 N81-33545

JONES, V. J.
Ocean services for the nation. National ocean goals and objectives for the 1980's
[PB81-200602] p0240 N81-31808

JONES, W. L.
The study of mesoscale ocean winds p0235 A81-46110

JONES, W. L., JR.
Performance evaluation of a spaceborne scatterometer p0269 A81-41920

JUSTICE, C.
An examination of spectral band ratioing to reduce the topographic effect on remotely sensed data p0221 A81-45427

JUSTICE, C. O.
Application of digital terrain data to quantify and reduce the topographic effect on Landsat data p0259 A81-45433

K

KALCIC, M. T.
Evaluation of multiband, multitemporal, and transformed LANDSAT MSS data for land cover area estimation
[E81-10161] p0219 N81-29496

KALMYKOV, A. I.
Features of the radar detection of sea surface nonuniformities p0234 A81-43967

KANAL, L. N.
Knowledge-based image analysis
[AD-A101319] p0264 N81-30852

KASISCHKE, E. S.
Refraction of coastal ocean waves p0235 A81-46113

KATZ, I.
Spaceborne synthetic aperture radar for oceanography p0234 A81-46104

KAUTH, R. J.
Procedure M - A framework for stratified area estimation p0201 A81-46036

KAVEESHWAR, V. G.
Role of multiple scattering in ozone profile retrieval from satellite measurements in the ultraviolet p0215 A81-45870

KAZMIERSKI, J.
Differential Doppler experiment /DIDEX/ for geodetic applications p0221 A81-47938

KEATING, T. J.
Quantification of non-point source sedimentation through densitometric analysis of color infrared aerial photography
[PB81-209157] p0255 N81-33599

KENDALL, B. M.
Microwave radiometer measurement of tidally induced salinity changes off the Georgia coast p0232 A81-42067

KENNEDY, M.
A capture-recapture approach for estimation of detection probabilities in aerial surveys p0258 A81-43546
Alternative 'scale up' estimators for aerial surveys where both detection and classification errors exist p0260 A81-46197

KERSCHGENS, M.
Theoretical investigations concerning the measurement of the plankton concentration with the aid of satellites p0237 A81-49426

KERUT, E.
Drifting buoy data from the tropical Pacific Ocean during NORPAX equatorial test shuttle experiment
[PB81-198939] p0240 N81-31807

KESTNER, W.
Partially automated object extraction from aerial photographs and land maps p0266 N81-33528

KHARIN, N. G.
Remote methods and desert conservation p0213 A81-43523

KHARITONOV, V. A.
Experience with the determination of optical image distortions of landscape elements on IR aerial photographs p0257 A81-41480

KHIZHNICHENKO, V. I.
Measurement of lengths, angles, and areas on the earth's spheroid p0221 A81-42846
Geometric correction of scanner images of the earth's surface p0261 A81-48694

KHORRAM, S.
Use of ocean color scanner data in water quality mapping p0251 A81-43545
Remote sensing aided procedure for conifer growth modeling in the northeastern Sierra Nevada p0199 A81-43740
Water quality mapping from Landsat digital data p0252 A81-45429

KHOVANSKII, B. N.
Space research on seismic regions p0225 A81-42280

KIEFER, R. W.
Wetland mapping from digitized aerial photography p0252 A81-43549

KIPP, E. R.
Crop phenology and LANDSAT-based irrigated lands inventory in the high plains
[E81-10173] p0210 N81-33559

KIRBY, M. E.
Iceberg detectability problems using SAR and SLAR systems p0232 A81-43206

KIRBY, W. E.
Digital image analysis of SAR imagery for the detection of icebergs p0239 A81-49777

KLAGES, W.
Possible applications of communication satellites for research tasks in polar regions
[BMFT-FB-W-80-029] p0267 N81-33587

KLEMAS, V.
Remote sensing of coastal pollutants using multispectral data p0233 A81-43245
Drift and dispersion studies of ocean-dumped waste using Landsat imagery and current drogues p0233 A81-43539

KLENK, K. F.
Role of multiple scattering in ozone profile retrieval from satellite measurements in the ultraviolet p0215 A81-45870

KLEWENO, D. D.
AgRISTARS (Agriculture And Resources Inventory Surveys Through Aerospace Remote Sensing) DC/LC (Domestic Crops and Land Rover) project summary crop area estimates for Kansas and Iowa, 1980
[PB81-198909] p0207 N81-30511

KOCH, D. W.
Inventory estimation on the massively parallel processor p0259 A81-46052

KOHOUT, F. A.
Applications of aerospace data for detection of submarine springs in Jamaica p0226 A81-43232
Satellite observations of a geothermal submarine spring off Florida west coast p0233 A81-43248

KOLENKIEWICZ, R.
Calibration validation for the GEOS 3 altimeter p0270 A81-42671

KOLIPINSKI, M. C.
Applications of aerospace data for detection of submarine springs in Jamaica p0226 A81-43232

KOLOSKOVA, V. N.
The informational estimation of the effectiveness of using satellite imagery in hydrogeological research p0227 A81-48683

KOMISSARENKO, S. V.
Accuracy of transmission of spectral contrasts in multispectral aerial photography, with application to problems of object recognition p0257 A81-41479

KONDRATEV, K. IA.
Radiation studies in the atmosphere p0216 A81-47001
Basic problems of the physics and chemistry of contemporary changes of climate p0216 A81-47002
Angular anisotropy of reflection from various types of underlying surface I - Snow cover II - Desert p0260 A81-47007

KONECNY, G.
Correlation techniques and devices p0258 A81-43531

KONG, J. A.
Correlation function studies for snow and ice p0260 A81-46378

KONIECZNY, J.
Present state of remote sensing development in Poland p0279 A81-49763

KOPTSEVA, N. N.
Machine method for the equalization of average phototone in an aerial photograph field p0257 A81-41482

KORANDA, J.
Remote sensing of soil radionuclide fluxes in a tropical ecosystem
[UCRL-84501] p0219 N81-29517

KORZOV, V. I.
Angular anisotropy of reflection from various types of underlying surface I - Snow cover II - Desert p0260 A81-47007

KOSIK, J. C.
Particular features of the ocean glitter pattern observed from a sun-synchronous orbit p0234 A81-45436

KOSTIN, B. S.
Investigation of the efficiency of the optical sounding of aerosol by the use of spectral photometers p0215 A81-45406

KOTAKI, M.
ISS-b experimental results on global distributions of ionospheric parameters and thunderstorm activity p0215 A81-44862

KOTLIAROV, I. I.
International monitoring from space /Problems of international law/ p0279 A81-48468

KOWALIK, W. S.
Atmospheric correction to LANDSAT data for limonite discrimination p0228 N81-31594

KRABILL, W. B.
Land subsidence measured by satellite radar altimetry p0270 A81-43260

KRIEGER, H.
Crop phenology and LANDSAT-based irrigated lands inventory in the high plains
[E81-10173] p0210 N81-33559

KRISHEN, K.
Advanced synthetic aperture radar for remote sensing p0274 A81-48553

KRISTOF, S. J.
Application of multispectral reflectance studies of soils Pre-Landsat p0200 A81-46031
A case study of soil erosion detection by digital analysis of the remotely sensed multispectral Landsat scanner data of a semi-arid land in southern India p0201 A81-46050

KRITIKOS, H.
An investigation of the autocorrelation function of radar images p0262 A81-49768

KRUCK, W.
Hydrogeologic interpretations of Landsat imagery in arid zones of South and West Africa p0248 A81-43229

KRUEGER, A. F.
Annual and interannual variations in outgoing longwave radiation over the tropics p0251 A81-43356

KRUUS, J.
Flood applications of satellite imagery p0247 A81-43217

KUDRIAVTSEV, V. S.
The space engineering use efficiency for forest study
[IAF PAPER 81-108] p0202 A81-47354

KUEHNLE, A.
Satellite scatterometer p0232 A81-42102

KUTIEV, I.
New complex for ionosphere-magnetosphere study 'Intercosmos-Bulgaria-1300'
[IAF PAPER 81-212] p0273 A81-47407

L

LAFRAMBOISE, P.
Use of Landsat images in the monitoring and study of the LG 2 reservoir during the filling period p0254 A81-49797

LAMBIRD, B. A.
Knowledge-based image analysis
[AD-A101319] p0264 N81-30852

LANGEL, R. A.
Magnetic space-based field measurements
[AAS PAPER 81-077] p0272 A81-46241
Early results from Magsat p0274 A81-48945

LANGHAM, E. J.
A review of Canada's present and future remote sensing activities relating to hydrology p0244 A81-43182
A preliminary analysis of SAR mapping of the Manitoba flood, May 1979 p0248 A81-43220
The Surveillance Satellite Program and the future of microwave remote sensing p0274 A81-49753
Application of synthetic aperture radar data to snow cover monitoring p0253 A81-49778
Interpretation techniques applied to mixed terrains p0218 A81-49788

LATKA, J.
Differential Doppler experiment /DIDEX/ for geodetic applications p0221 A81-47938

LATTY, R. S.
Waveband evaluation of proposed thematic mapper in forest cover classification p0199 A81-43738

LAURENT, D.
Evaluation of the 1980 Cosmos program p0278 A81-47829

LAVINE, D.
Knowledge-based image analysis
[AD-A101319] p0264 N81-30852

LAWRENCE, G. R.
The application of thermography for locating potential frost pockets in forest cutovers p0204 A81-49789
The detection of groundwater discharges /springs/ using aerial thermography p0254 A81-49800

LAWRENCE, M. B.
Atlantic hurricane season of 1980 p0238 A81-49649

LEAF, C. F.
Landsat derived snow cover as an input variable for snow melt runoff forecasting in South Central Colorado p0246 A81-43208

LEBERL, F.
A radar image time series p0226 A81-45430

LEE, P. S. T.
Remote sensing and land use planning p0218 A81-49792

LEE, Y. J.
Application of temporal Landsat forest digital data for updating the Yukon RRAMS data base using Aries p0203 A81-49760

LEHMAN, F.
Experimental investigation of the physical fundamentals for remote sensing of soil and vegetation moisture by active infrared reflectance spectroscopy using CO2 laser technique
[BMFT-FB-W-80-037] p0211 N81-33588

LENNERTZ, D.
The first ESA remote sensing satellite /ERS/ - The programme and the system
[IAF PAPER 81-90] p0236 A81-47344

LENNINGTON, R. K.
Evaluation of large area crop estimation techniques using LANDSAT and ground-derived data
[E81-10200] p0206 N81-29511

LEONHART, L. S.
Landsat data as a basis for regional environmental assessment within the Columbia Plateau p0218 A81-49798

LEROY, M. J.
Infrared-temperature variability in a large agricultural field p0200 A81-45432

LESCHACK, A. R.
Military geodesy and geospace science, unit one
[AD-A104038] p0222 N81-33581

LESHKEVICH, G. A.
Categorization of Northern Green Bay ice cover using LANDSAT 1 digital data A case study
[PB81-200438] p0265 N81-32602

LETOAN, T.
Scatterometer measurements on crop and soil surfaces p0208 N81-33349

LETTS, P. J.

Generation and use of digital elevation data for large areas p0221 A81-49811

LEVING, S. K.

Experimental use of real time SAR imagery in support of oil exploration in the Beaufort Sea p0227 A81-49767

LEVY, G.

Coherent and incoherent radar scattering from rough surfaces and vegetated areas [ESA-SP-166] p0208 N81-33339

LI, R. Y.

Crop classification with a Landsat/radar sensor combination p0200 A81-46033

LIANG, T.

Analysis of landfills with historic airphotos p0216 A81-46407

Cornell University Remote Sensing Program [E81-10174] p0255 N81-33560

LICHY, D. E.

Tracking of a warm water ring p0235 A81-46117

LIEU, S. M.

Evaluation of remote sensing data for input into Hydrological Simulation Program-FORTRAN (HSPF) [PB81-209561] p0255 N81-33593

LILLESAND, T. M.

Satellite monitoring of snow extent and condition in agricultural, transitional, and forested land cover areas [PB81-188625] p0254 N81-30509

Development of alternative data analysis techniques for improving the accuracy and specificity of natural resource inventories made with remote sensing data p0266 N81-33551

LIN, J. D.

Modeling the terrestrial hydrology for the global atmosphere - The future role of satellite data p0245 A81-43197

LINK, L. E.

Thermal vegetation canopy model studies p0202 A81-49347

LINSENBARTH, A.

Present state of remote sensing development in Poland p0279 A81-49763

LIPPENS, C.

Atmospheric nitric acid and chlorofluoromethane 11 from interferometric spectra obtained at the Observatoire du Pic du Midi [AERONOMICA-ACTA-A-227-1980] p0219 N81-30656

LIVINGSTONE, C. E.

Single and multiple parameter microwave signatures of sea ice p0238 A81-49774

Radar detection of sea-ice ridges and icebergs in frozen oceans at incidence angles from 0 deg to 90 deg p0238 A81-49775

LO, C. P.

Land use mapping of Hong Kong from Landsat images - An evaluation p0215 A81-45434

LOUGEAY, R.

Potentials of mapping buried glacier ice with Landsat thermal imagery p0246 A81-43204

LOWRY, J. D.

Quantification of non-point source sedimentation through densitometric analysis of color infrared aerial photography [PB81-209157] p0255 N81-33599

LOWRY, R. T.

Iceberg detectability problems using SAR and SLAR systems p0232 A81-43206

A preliminary analysis of SAR mapping of the Manitoba flood, May 1979 p0248 A81-43220

The airborne SAR project Conclusions and applications p0275 A81-49765

Experimental use of real time SAR imagery in support of oil exploration in the Beaufort Sea p0227 A81-49767

Optimizing imaging radar parameters for ice reconnaissance p0239 A81-49779

LUCAS, J. R.

Selected irrigation acreage estimates in northern Florida from Landsat data p0198 A81-43264

LUCAS, W. M.

Use of Landsat digital data to assist in mapping soils on Arizona rangelands p0201 A81-46047

LUEBBE, R. C.

An evaluation of MSS P-format data registration [E81-10171] p0267 N81-33557

LUEDECKE, C.

The distribution of the trace gases H2O, NO2, and HNO3 in the middle atmosphere on the basis of LIMS measurements p0217 A81-49407

LUTHER, J.

Compact and highly sensitive fluorescence lidar for oceanographic measurements p0237 A81-49378

LUTHER, M. R.

A radiometric model of an earth radiation budget radiometer optical system with diffuse-specular surfaces p0269 A81-41919

M

MACDONALD, H. C.

Look direction dependence of radar backscattering cross section for agricultural fields p0199 A81-43741

Use of Seasat satellite radar imagery for the detection of standing water beneath forest vegetation p0199 A81-43743

MACK, A. R.

Stratification of Landsat data by uniformity productivity of soils p0259 A81-46042

Operational applications for analysis of agricultural crops and cultural practices p0203 A81-49756

MADDREA, G. L., JR.

NASA participation in the 1980 Persistent Elevated Pollution Episode/Northeast Regional Oxidant Study (PEPE/NROS) Project Operational aspects [NASA-TM-83170] p0220 N81-32708

MADER, G. L.

Space based topographic mapping experiment using Seasat synthetic aperture radar and LANDSAT 3 return beam vidicon imagery [NASA-CR-164675] p0223 N81-30496

MAGNESS, E. R.

A description of the reformatted spring small grains labeling procedure used in test 2, part 2 of the US/Canada wheat and barley exploratory experiment [E81-10206] p0207 N81-31597

MAKAROV, V. I.

Lineaments - Problems and directions of studies by means of aerial and space tools and methods p0221 A81-48696

MAKAROVIC, B.

Image correlation algorithms p0261 A81-48473

MALILA, W. A.

Procedure M - A framework for stratified area estimation p0201 A81-46036

Change vector analysis - An approach for detecting forest changes with Landsat p0202 A81-46056

MANCINI, L. J.

Tracking of a warm water ring p0235 A81-46117

MARCHENKO, V. V.

Interactive system for the regional prognosis of raw mineral resources, based on ground-based and satellite imagery data p0227 A81-48691

MARRON, J. K.

Landsat derived snow cover as an input variable for snow melt runoff forecasting in South Central Colorado p0246 A81-43208

MARTIN, C. F.

Calibration validation for the GEOS 3 altimeter p0270 A81-42671

MARTIN, M. V.

Evaluation of large area crop estimation techniques using LANDSAT and ground-derived data [E81-10200] p0206 N81-29511

MARTINKO, E. A.

Crop phenology and LANDSAT-based irrigated lands inventory in the high plains [E81-10173] p0210 N81-33559

MARTSOLF, J. D.

Remote sensing of thermal radiation from an aircraft - An analysis and evaluation of crop-freeze protection methods p0202 A81-46895

MASCARENHAS, A. C.

Remote sensing in development p0279 A81-48936

MASCARENHAS, A. D. S., JR.

Method for estimation of ocean current velocity from satellite images p0231 A81-41350

MASCARENHAS, N. D. A.

Visual enhancement of images of natural resources: Applications in geology [E81-10181] p0228 N81-32575

MATEER, C. L.

Role of multiple scattering in ozone profile retrieval from satellite measurements in the ultraviolet p0215 A81-45870

MATIIASEVICH, L. M.

The signal-to-noise ratio of a space photographic system p0269 A81-42284

MATSON, M.

Satellite detection of seiches in Great Salt Lake, Utah p0243 A81-42126

A note on indirect detection of seiches in Great Salt Lake, Utah, by NOAA and Landsat satellite imagery p0247 A81-43218

Assessing the Red River of the North 1978 flooding from NOAA satellite data p0248 A81-43219

Preliminary survey of HCMM satellite thermal imagery as applied to hydrospherics p0252 A81-43746

Identification of subresolution high temperature sources using a thermal IR sensor p0273 A81-46401

MATSUMOTO, K.

Development of Marine Observation Satellite-1 [AAS PAPER 81-060] p0278 A81-46238

MATTIE, M. G.

Wave direction measured by four different systems p0232 A81-42622

Tracking of a warm water ring p0235 A81-46117

MATUURA, N.

ISS-b experimental results on global distributions of ionospheric parameters and thunderstorm activity p0215 A81-44862

MAUL, G. A.

Application of GOES visible-infrared data to quantifying mesoscale ocean surface temperatures p0236 A81-47021

MAXIM, L. D.

A capture-recapture approach for estimation of detection probabilities in aerial surveys p0258 A81-43546

Alternative 'scale up' estimators for aerial surveys where both detection and classification errors exist p0260 A81-46197

MAY, G. A.

Evaluation of multiband, multitemporal, and transformed LANDSAT MSS data for land cover area estimation [E81-10161] p0219 N81-29496

MAYHEW, M. A.

Early results from Magsat p0274 A81-48945

MCALLISTER, D. F.

A top-down approach to the use of simulation in computer system design p0274 A81-48331

MCCARTNEY, D. H.

Spectral measurement of rangeland p0218 A81-49790

MCCLAIN, E. P.

Environmental satellites p0277 A81-42231

MCCORMICK, J. A.

Rapeseed - Guidelines for operational monitoring p0203 A81-49784

MCCRARY, D. G.

The environmental vegetation index A tool potentially useful for arid land management [E81-10191] p0206 N81-29505

Characteristics, of TIROS, GOES, DMSP and LANDSAT systems [E81-10192] p0263 N81-29506

Meteorological satellite data A tool to describe the health of the world's agriculture [E81-10204] p0207 N81-31596

MCCULLOCH, B.

Landsat classification of coastal wetlands in Texas p0248 A81-43234

MCCULLOUGH, C. A.

Satellite telemetry of hydrologic data in California p0244 A81-43187

MCFARLAND, M. J.

Measurement of soil moisture trends with airborne scatterometers [E81-10088] p0209 N81-33545

MCGINNIS, D. F., JR.

Preliminary survey of HCMM satellite thermal imagery as applied to hydrospherics p0252 A81-43746

MCGUIRE, W. G.

Evaluation of large area crop estimation techniques using LANDSAT and ground-derived data [E81-10200] p0206 N81-29511

MCKIM, H. L.

Survey of in-situ and remote sensing methods for soil moisture determination p0197 A81-43221

MCLEAN, J. A.

Extravisual damage detection - Defining the standard normal tree p0198 A81-43537

MCLEOD, M. G.

Geomagnetic field mapping from a satellite Spatial power spectra of the geomagnetic field at various satellite altitudes relative to natural noise sources and instrument noise [PUBL-1810] p0275 N81-29480

MCLUCAS, J. L.

Commercial operations in space - 1980-2000; Proceedings of the Eighteenth Goddard Memorial Symposium, Washington, DC, March 27, 28, 1980 p0277 A81-44635

MCNALLEY, G.

Drifting buoy data from the tropical Pacific Ocean during NORPAX equatorial test shuttle experiment [PB81-198939] p0240 N81-31807

MCNALLY, G. J.

Satellite-tracked drift buoy observations of the near-surface flow in the eastern mid-latitude North Pacific p0236 A81-47022

MCPHERSON, C. A.

Radar-optical-topographic transformations for scene content analysis p0261 A81-48552

MEAD, R. A.

Mapping wetlands using orthophotoquads and 35-mm aerial photographs p0251 A81-43543

Nationwide forestry applications program Analysis of forest classification accuracy [E81-10183] p0206 N81-29499

MEISNER, D. E.

Satellite monitoring of snow extent and condition in agricultural, transitional, and forested land cover areas [PB81-188625] p0254 N81-30509

MEITIN, J. G.

Insights into errors of SMS-inferred GATE convective rainfall p0243 A81-42095

MEL, M.

Multispectral kelp resource surveys p0232 A81-43244

MELNIK, IU. A.

Radar methods for studying the earth p0273 A81-46924

MERCER, J. B.

Experimental use of real time SAR imagery in support of oil exploration in the Beaufort Sea p0227 A81-49767

MERGERSON, J. W.

Crop area estimation using ground-gathered and sampled LANDSAT data [PB81-192783] p0207 N81-30507

Crop area estimates using ground-gathered and LANDSAT data A multitemporal approach Missouri, 1979 [PB81-186751] p0208 N81-31614

METZIG, G.

Theoretical investigations concerning the measurement of the plankton concentration with the aid of satellites p0237 A81-49426

METZLER, M.
Users manual for the US baseline corn and soybean segment classification procedure
[E81-10190] p0206 N81-29504

MEYER, M. P.
A comparison of remote sensing techniques for Minnesota wetlands classification p0249 A81-43239

MIDDLETON, E. M.
Landsat - What is operational in water resources
p0253 A81-49757

MILLARD, J. P.
Infrared-temperature variability in a large agricultural field p0200 A81-45432

MILLER, C. E.
AgRISTARS (Agriculture And Resources Inventory Surveys Through Aerospace Remote Sensing) DC/LC (Domestic Crops and Land Rover) project summary crop area estimates for Kansas and Iowa. 1980
[PB81-196909] p0207 N81-30511

MILLER, W. A.
Role of aerial photographs in classification of Landsat data p0262 A81-49808

MILTON, E. J.
A comparison between two photographic methods for the determination of relative bidirectional reflectance
p0259 A81-45431
Does the use of two radiometers correct for irradiance changes during measurements p0272 A81-46196

MISHEV, D.
Program and instrumentation of the satellite experiment Bulgaria-1300 II
[IAF PAPER 81-91] p0273 A81-47345
Application of delta modulation in on-board and ground video data processing systems for the purposes of remote sensing
[IAF PAPER 81-102] p0260 A81-47351
An atmospheric study by 'Spectrum-15' onboard of the Salyut-6 orbital station
[IAF PAPER 81-120] p0216 A81-47359

MIYAZAKI, S.
ISS-b experimental results on global distributions of ionospheric parameters and thunderstorm activity
p0215 A81-44862

MOERL, P.
Aerosol sounding by means of aircraft-borne optical radar p0217 A81-49431

MOLLO-CHRISTENSEN, E.
Method for estimation of ocean current velocity from satellite images p0231 A81-41350

MONTGOMERY, D. R.
Seasat data applications by commercial users
p0231 A81-41974
Oceanic Satellite Data Distribution System
p0231 A81-41996
Commercial applications of satellite oceanography
p0237 A81-49133

MOORE, D. G.
Soil moisture applications of the heat capacity mapping mission p0197 A81-43224
Landsat data for locating shallow glacial aquifers in eastern South Dakota p0226 A81-43228
Ground water applications of the heat capacity mapping mission p0248 A81-43233
Landsat interpretation of prairie lakes and wetlands of eastern South Dakota p0249 A81-43240

MOORE, G. K.
An introduction to satellite hydrology
p0244 A81-43184

MOORE, R. K.
Sea surface scattering p0241 N81-33344
Scatterometer calibration and data correction
p0265 N81-33351

MORALEV, V. M.
Ring structures of Precambrian shields, based on the interpretation of space imagery p0225 A81-42278

MORGAN, J.
Potential for detection of natural disasters via Meteosat
[IAF PAPER 81-263] p0216 A81-47430

MOROZ, P. I.
The space engineering use efficiency for forest study
[IAF PAPER 81-108] p0202 A81-47354

MORRIS, W. D.
A comparison of observed and analytically derived remote sensing penetration depths for turbid water
[NASA-TM-83176] p0255 N81-33577

MORRISON, D. B.
Machine processing of remotely sensed data and soil information systems and remote sensing and soil survey; Proceedings of the Sixth Annual Symposium, Purdue University, West Lafayette, IN, June 3-6, 1980
p0200 A81-46026

MOZZHUKHIN, O. A.
A 'meteorological' method for calculating vertical refraction p0221 A81-48679

MROCZYNSKI, R. P.
Evaluation of LANDSAT data analysis for forest survey
[E81-10175] p0210 N81-33561

MROZ, E. J.
Stratospheric sulfate from the Gareloi eruption, 1980 - Contribution to the 'ambient' aerosol by a poorly documented volcanic eruption p0213 A81-41404

MUDRY, N.
A preliminary analysis of SAR mapping of the Manitoba flood, May 1979 p0248 A81-43220

MUELLER, J. L.
Atmospheric correction of Nimbus-7 Coastal Zone Color Scanner imagery p0271 A81-45879

MULLANE, T. F.
Operational use of satellite imagery in the Canadian ice program p0238 A81-49754

MULLER, C.
Atmospheric nitric acid and chlorofluoromethane 11 from interferometric spectra obtained at the Observatoire du Pic du Midi
[AERONOMICA-ACTA-A-227-1980] p0219 N81-30656

MUNDAY, J. C., JR.
Bay of Fundy verification of a system for multidate Landsat measurement of suspended sediment
p0250 A81-43254
Remote sensing of dinoflagellate blooms in a turbid estuary p0251 A81-43538
Southern Chesapeake Bay circulation and suspended sediment transport analyzed using Landsat imagery
p0252 A81-43747
Landsat - What is operational in water resources
p0253 A81-49757

MUNDAY, T. J.
A comparison between two photographic methods for the determination of relative bidirectional reflectance
p0259 A81-45431

MUNSON, R. C.
Satellite observations of a geothermal submarine spring off Florida west coast p0233 A81-43248

MURINO, P.
Use of elevation models for landform analysis by Seasat-SAR imagery
[IAF PAPER 81-98] p0260 A81-47349

MURTHA, P. A.
Extravisual damage detection - Defining the standard normal tree p0198 A81-43537
Photointerpretation of fire damage to trees in a ponderosa pine/bunchgrass community p0204 A81-49787

MUSGROVE, R. J.
Selected irrigation acreage estimates in northern Florida from Landsat data p0198 A81-43264

MUSSAKOWSKI, R.
Applicability of airborne SAR data to geological mapping p0227 A81-49769

MYERS, B. J.
Rainforest species on large-scale color photos
p0198 A81-43536

MYERS, L.
Observations on Lake Ontario basin hydrogeology from optical enhancements of Landsat imagery
p0248 A81-43231
Lake Ontario dynamics and water quality observations using thematically enhanced Landsat data
p0251 A81-43257

MYKOLENKO, O.
Users manual for the US baseline corn and soybean segment classification procedure
[E81-10190] p0206 N81-29504

N

NADBEREZHNYI, S. D.
Concerning the reliability estimation of information obtained from several sources in earth survey tasks
p0270 A81-42286

NALIMOV, V. N.
Concerning the possibility of improving the spectroradiometric accuracy of remote sensing of the earth by means of multispectral band scanners
p0270 A81-42285

NASH, T. L.
A practical method for the verification of computer-processed Landsat data p0261 A81-48943

NAZARE, C. V.
Evaluation of spring wheat and barley crop calender models for the 1979 crop year
[E81-10197] p0206 N81-29508

NELSON, M. L.
The GOES data collection system p0257 A81-43185

NELSON, R. F.
Procedure 1 and forestland classification using Landsat data p0201 A81-46055
Evaluation of LANDSAT data analysis for forest survey
[E81-10175] p0210 N81-33561

NEMIROVSKII, E. A.
Interactive system for the regional prognosis of raw mineral resources, based on ground-based and satellite imagery data p0227 A81-48691

NESTERENKO, O. P.
Concerning the reliability estimation of information obtained from several sources in earth survey tasks
p0270 A81-42286

NETO, G.
Visual enhancement of images of natural resources. Applications in geology
[E81-10181] p0228 N81-32575

NEWLAND, W.
Bulk processing techniques for very large areas - Landsat classification of California p0201 A81-46054

NEWTON, R. W.
Characteristics of microwave emission of significance to satellite remote sensing of soil water p0258 A81-43222

NGUYEN, D.
Thermal vegetation canopy model studies
p0202 A81-49347

NIELSEN, D.
Use of water Raman emission to correct airborne laser fluorosensor data for effects of water optical attenuation
p0253 A81-47676

NIKITIN, P. A.
Evaluation of the effect of sea-ice roughness on the microwave emission of the ice p0231 A81-41490

NIXON, P. R.
Methods of editing cloud and atmospheric layer affected pixels from satellite data
[E81-10169] p0266 N81-33558

NJOKU, E. G.
Regression techniques for oceanographic parameter retrieval using space-borne microwave radiometry
p0239 A81-49967

NOREN, D.
Technical aspects of forest inventory demonstrations using Landsat data - Projects in the Pacific Northwest States p0203 A81-49764

NORMAN, B.
Bulk processing techniques for very large areas - Landsat classification of California p0201 A81-46054

NUGENT, R. L.
As-built design specification of the automatic registration system for the cartographic technology laboratory
[E81-10176] p0267 N81-33562

O

OBRIEN, J. J.
The future for satellite-derived surface winds
p0237 A81-49129

OCHIAI, H.
Digital analysis of Landsat MSS data and application for coastal marine environment p0233 A81-43247
Monitoring of snow covered area using satellite data
[IAF PAPER 81-114] p0253 A81-47356

ODDO, J. E.
Methods development and applications evaluations of NURE aerial reconnaissance survey data for uranium resource evaluation: Beeville/Bay City and Crystal City quadrangles, Texas
[GJBX-69(81)] p0228 N81-30502

ODEGAARD, H.
Operational use of satellite data for snow inventory and runoff forecast p0246 A81-43210

ODENWELLER, J.
Users manual for the US baseline corn and soybean segment classification procedure
[E81-10190] p0206 N81-29504

ODERWALD, R. G.
Nationwide forestry applications program: Analysis of forest classification accuracy
[E81-10183] p0206 N81-29499

OHARA, D.
Measurements of CF2Cl2, CFCl3, and N2O in the lower stratosphere between 2 deg S and 73 deg N latitude
p0214 A81-44515

OHLEN, D. O.
Detection of changes in a coal surface mining area by ratioing multidate Landsat digital data
p0228 A81-49809
A selected bibliography: Remote sensing applications in wildlife management
[PB81-215881] p0211 N81-33598

OHLHORST, C. W.
Application of remote sensing to monitoring and studying dispersion in ocean dumping p0232 A81-42228

OKAMOTO, K.
Single and multiple parameter microwave signatures of sea ice p0238 A81-49774
Radar detection of sea-ice ridges and icebergs in frozen oceans at incidence angles from 0 deg to 90 deg
p0238 A81-49775

OLIVER, V. J.
A satellite derived technique for estimating rainfall from thunderstorms and hurricanes p0244 A81-43191

ONEILL, P. E.
Satellite detection of oil on the marine surface
p0233 A81-43251

ORLICEK, E.
First results of the Intercosmos satellite IK-21
[IAF PAPER 81-214] p0274 A81-47409

ORMSBY, J. P.
Satellite observations of England and north-western Europe p0217 A81-49174

OSTREM, G.
Operational use of satellite data for snow inventory and runoff forecast p0246 A81-43210

P

PAARLBERG, D.
Crop reporting from space - Problems, promises, potential
[AAS 80-062] p0200 A81-44637

PACI, G.
Particular features of the ocean glitter pattern observed from a sun-synchronous orbit p0234 A81-45436

PAINTER, J. E.

Advanced technology for satellite data collection systems p0270 A81-43190

PALA, S.

Applicability of airborne SAR data to geological mapping p0227 A81-49769

SAR image response over a conifer regeneration site p0203 A81-49770

PALMER, W. F.

A description of the reformatted spring small grains labeling procedure used in test 2, part 2 of the US/Canada wheat and barley exploratory experiment [E81-10206] p0207 N81-31597

PAPE, D.

Correlation techniques and devices p0258 A81-43531

PARASHAR, S. K.

The Lake Melville/Labrador offshore synthetic aperture radar study - Winter 1979 p0238 A81-49772

PARDINI, S.

Radar altimeter for ocean remote sensing [IAF PAPER 81-94] p0236 A81-47348

PARIS, J. F.

Experiment plan: Row and roughness effects on dependence of active microwave measurements of soil moisture [E81-10209] p0211 N81-33575

PARRA, C. G.

Gulf of Mexico satellite radar altimetry [NASA-TM-73295] p0224 N81-33760

PARSONS, C. L.

Gulf of Mexico satellite radar altimetry [NASA-TM-73295] p0224 N81-33760

PATZERT, W.

Drifting buoy data from the tropical Pacific Ocean during NORPAX equatorial test shuttle experiment [PB81-198939] p0240 N81-31807

PAUL, C. K.

Remote sensing in development p0279 A81-48936

PAULSON, R. W.

U.S. geological survey application of satellite telemetry for the support of hydrologic data collection p0258 A81-43189

PAYNE, R. W.

Australian transition year special studies [E81-10179] p0210 N81-33565

PEARCE, W. A.

A study of the effects of the atmosphere on thematic mapper observations [E81-10056] p0276 N81-33540

PEARSON, D.

Single and multiple parameter microwave signatures of sea ice p0238 A81-49774

Radar detection of sea-ice ridges and icebergs in frozen oceans at incidence angles from 0 deg to 90 deg p0238 A81-49775

PELISSIER, J. M.

Atlantic hurricane season of 1980 p0238 A81-49649

PENA, J. A.

Environmental measurements of power plant cooling tower and stack plumes [DOE/EV-02463/6] p0219 N81-30695

PEREBLEGIN, S. V.

Radar methods for studying the earth p0273 A81-46924

PESANT, C.

Monitoring Canada's water resources in remote regions by satellite telemetry p0244 A81-43188

PETERSON, C. J.

Interactive digital image processing for terrain data extraction [AD-A101321] p0264 N81-30499

PETERSON, D.

Bulk processing techniques for very large areas - Landsat classification of California p0201 A81-46054

PETERSON, D. L.

Technical aspects of forest inventory demonstrations using Landsat data - Projects in the Pacific Northwest States p0203 A81-49764

PETRIE, G.

Hardware aspects of digital mapping p0271 A81-43530

PETROV, P.

Application of delta modulation in on-board and ground video data processing systems for the purposes of remote sensing [IAF PAPER 81-102] p0260 A81-47351

PETTINGER, L. R.

A selected bibliography: Remote sensing applications in wildlife management [PB81-215881] p0211 N81-33598

PETTYJOHN, W. A.

Ground water and satellites - An overview/introduction p0246 A81-43226

PHILIPSON, W. R.

Manual versus digital Landsat analysis for modeling river flooding p0252 A81-43745

Manual versus digital Landsat analysis for delineating river flooding p0252 A81-46405

Analysis of landfills with historic airphotos p0216 A81-46407

Cornell University Remote Sensing Program [E81-10174] p0255 N81-33560

PHILLIPS, O. M.

The structure of short gravity waves on the ocean surface p0234 A81-46105

PHILPOT, W.

Remote sensing of coastal pollutants using multispectral data p0233 A81-43245

PHILPOT, W. D.

Drift and dispersion studies of ocean-dumped waste using Landsat imagery and current drogues p0233 A81-43539

PHINNEY, D. E.

Evaluation of gravimetric ground truth soil moisture data collected for the agricultural soil moisture experiment, 1978 Colby, Kansas, aircraft mission [E81-10114] p0205 N81-29494

PICARDI, G.

Radar altimeter for ocean remote sensing [IAF PAPER 81-94] p0236 A81-47348

PICHUGIN, A. P.

Features of the radar detection of sea surface nonuniformities p0234 A81-43967

PIECH, K. R.

Derivation of shallow ocean bottom reflectance values from color aerial photography [AD-A101105] p0241 N81-33763

PIERCE, T. W.

Multistage remote sensing in exploratory ecodistrict land classification p0217 A81-49759

PIETRAFESA, L. J.

Combined satellite imagery for study of coastal circulation, Onslow Bay, North Carolina p0233 A81-43250

POLAVARAPU, V. L.

Computer analysis of Tiros-N/NOAA-6 satellite data for operational snow cover mapping p0262 A81-49795

POLOVINKO, V. V.

Investigation of illumination in the image plane of the receiving optical system for the aerial or spaceborne photography of the world ocean p0232 A81-42553

POPESCU, J.

Soviet remote sensing of the earth's resources and interpretation of space data with reference to the Caspian Sea, Siberia and the Arctic Ocean [IAF PAPER 81-112] p0278 A81-47355

PORACSKY, J.

Mapping irrigated lands in Western Kansas from Landsat p0198 A81-43265

Crop phenology and LANDSAT-based irrigated lands inventory in the high plains [E81-10173] p0210 N81-33559

PORE, M. D.

The multicategory case of the sequential Bayesian pixel selection and estimation procedure [E81-10182] p0263 N81-29498

POST, D. F.

Use of Landsat digital data to assist in mapping soils on Arizona rangelands p0201 A81-46047

PRILL, J. C.

Mountain pine beetle damage surveys with high-altitude panoramic photography p0199 A81-43732

PRITCHARD, E. B.

Aerospace remote sensing of the coastal zone for water quality and biotic productivity applications p0233 A81-43246

PRITCHARD, J. A.

Preliminary survey of HCMM satellite thermal imagery as applied to hydrospherics p0252 A81-43746

PRONIN, V. G.

The use of satellite imagery for studying the structural features of the Caspian oil and gas region p0227 A81-48684

PROUT, N. A.

The airborne SAR project: Conclusions and applications p0275 A81-49765

Land use/cover mapping for Halifax County - Remote sensing alternatives p0218 A81-49783

PUESCHEL, R. F.

Aerosol formation, transformation, and effects in Denver's emissions plume p0214 A81-44526

Q

QUINN, E. W.

The sensor image simulator [AD-A101172] p0275 N81-29512

QUIRK, B. K.

Wetland mapping from digitized aerial photography p0252 A81-43549

R

RABUS, D.

Comparative measurements of stratospheric CH4 and CO concentrations with spectrograph and correlation radiometers p0217 A81-49433

RAHN, P. H.

Landsat data for locating shallow glacial aquifers in eastern South Dakota p0226 A81-43228

Remote sensing of bank erosion along the Missouri River, South Dakota p0213 A81-43263

RANEY, R. K.

The Surveillance Satellite Program and the future of microwave remote sensing p0274 A81-49753

The airborne SAR project: Conclusions and applications p0275 A81-49765

SAR processing of partially coherent and sinusoidally dynamic ocean waves p0239 A81-49776

Wave orbital velocity, fade and SAR response to azimuth waves p0265 N81-33345

RANGO, A.

Satellite hydrology; Proceedings of the Fifth Annual William T. Pecora Memorial Symposium on Remote Sensing, Sioux Falls, SD, June 10-15, 1979 p0243 A81-43176

Passive microwave sensing of snow characteristics over land p0246 A81-43207

Freshwater ice thickness observations using passive microwave sensors p0254 A81-49968

RANSON, K. J.

Thermal vegetation canopy model studies p0202 A81-49347

RASMUSSEN, W. O.

Prediction of water yield using satellite imagery and a snowmelt simulation model p0246 A81-43205

RASSBACH, M. E.

New output improvements for CLASSY [E81-10189] p0263 N81-29503

Improved version of the split routine for CLASSY [E81-10210] p0264 N81-31600

Maximum likelihood labeling [E81-10177] p0267 N81-33563

REA, D. K.

Determination of beach sand parameters using remotely sensed aircraft reflectance data p0217 A81-49346

REDFIELD, A. E.

The use of CIR and airborne multispectral scanner techniques for wetland soils mapping of highway corridors p0215 A81-46044

REDNER, R. A.

Maximum likelihood estimation for mixture models [E81-10178] p0210 N81-33564

REED, C. L.

Interpretation of hydrographic features seen in the waters off Cape Cod [AD-A102343] p0240 N81-31803

REGAN, R. D.

Reduction and analysis of satellite magnetometer data p0275 N81-29482

REID, I. A.

Monitoring Canada's water resources in remote regions by satellite telemetry p0244 A81-43188

REINHARDT, M. E.

Aerosol sounding by means of aircraft-borne optical radar p0217 A81-49431

RENGER, W.

Aerosol sounding by means of aircraft-borne optical radar p0217 A81-49431

REVZON, A. L.

Fitoexomorphogenic analysis of geological environment changes in the South Aral Sea, based on aerial and space imagery p0225 A81-42279

RHODE, W. G.

Role of aerial photographs in classification of Landsat data p0262 A81-49808

RICE, D.

Users manual for the US baseline corn and soybean segment classification procedure [E81-10190] p0206 N81-29504

RICHARDSON, A. J

Comparison of Landsat-2 and field spectrometer reflectance signatures of south Texas rangeland plant communities p0201 A81-46034

Methods of editing cloud and atmospheric layer affected pixels from satellite data [E81-10169] p0266 N81-33556

RIDINGS, T. F.

Airborne impulse radar sounding of sea ice p0238 A81-49771

RIES, J.

Orbit determination requirements for TOPEX [AAS PAPER 81-158] p0221 A81-45828

RINKER, J. N.

Remote sensing for engineering site selection [AD-A102810] p0219 N81-32586

RIVARD, A. I.

Interpretation techniques applied to mixed terrains p0218 A81-49788

ROBERT, P.

A project to evaluate moisture stress and phenological factors in corn and soybean areas of southwestern and south-central Minnesota p0209 N81-33554

ROBINSON, W.

Remote sensing of soil radionuclide fluxes in a tropical ecosystem [UCRL-84501] p0219 N81-29517

ROBSON, A.

Potential for detection of natural disasters via Meteosat [IAF PAPER 81-263] p0216 A81-47430

ROCHON, G.

Generation and use of digital elevation data for large areas p0221 A81-49811

ROESKA, K. O.

Large-area histograms from Meteosat5 images p0260 A81-46917

ROGERS, R. H.

Landsat technology transfer to the private and public sectors through community colleges and other locally available institutions p0277 A81-43750

ROHDE, W. G.
Accuracy evaluation of Landsat digital classification of vegetation in the Great Dismal Swamp p0248 A81-43235

RONCONI, R.
Radar altimeter for ocean remote sensing [IAF PAPER 81-94] p0236 A81-47348

ROSBOROUGH, G.
Orbit determination requirements for TOPEX [AAS PAPER 81-158] p0221 A81-45828

ROSE, P. W.
Landsat hydrobiological classification for an inland fresh water marsh within Everglades National Park p0249 A81-43238

ROSENDAHL, P. C.
Landsat hydrobiological classification for an inland fresh water marsh within Everglades National Park p0249 A81-43238

ROSENKRANZ, P. W.
Inversion of multiwavelength radiometer measurements by three-dimensional filtering p0271 A81-45873

ROSENTHAL, W. D.
Dryland pasture and crop conditions as seen by HCMM [E81-10080] p0209 N81-33542
Measurement of soil moisture trends with airborne scatterometers [E81-10088] p0209 N81-33545

ROSS, D. B.
The wind speed dependency of ocean microwave backscatter p0234 A81-46109

ROSS, R. E.
The application of remote sensing techniques for an ecological land survey of the snow goose colony at Cape Henrietta Maria, Hudson Bay p0204 A81-49791

ROSSIGNOLI, B.
Analysis of the November 23, 1980 earthquake as a design basis for satellite emergency communication [IAF PAPER 81-269] p0216 A81-47433

ROSSITER, J. R.
Airborne impulse radar sounding of sea ice p0238 A81-49771

ROTHERAM, S.
Scattering theory with application to synthetic aperture radar p0265 N81-33348

ROYAL, J. A.
Urban area update procedures using Landsat data p0214 A81-43733

ROYAL, W. R.
Satellite observations of a geothermal submarine spring off Florida west coast p0233 A81-43248

RUBEC, C. D. A.
Interpreter evaluations of airborne radar imagery for ecological and land/use cover classification in southern Manitoba p0218 A81-49773

RUFENACH, C. L.
Imaging ocean waves by synthetic aperture radars with long integration times p0231 A81-42026

RUSSELL, O.
Ground water exploration programs in Africa p0226 A81-43230

RUST, R. H.
A project to evaluate moisture stress and phenological factors in corn and soybean areas of southwestern and south-central Minnesota p0209 N81-33554

RYERSON, R. A.
Rapeseed - Guidelines for operational monitoring p0203 A81-49784
Benefits of using airborne remote sensing for Thematic Mapping p0275 A81-49801

RYLAND, W. E.
Conversion of SPU-Universal disk file to JSC-Universal tape storage. CONVRT user's guide [E81-10185] p0263 N81-29501

S

SADOV, A. V.
Concerning the hydrogeological significance of faults on platform regions, as revealed by space imagery p0225 A81-42277
Dynamic ecosystem of the Aral Basin studied from satellite imagery p0217 A81-48682

SAGAWA, E.
ISS-b experimental results on global distributions of ionospheric parameters and thunderstorm activity p0215 A81-44862

SAMPSEL, T. K.
Advanced synthetic aperture radar for remote sensing p0274 A81-48553

SATTERWHITE, M. B.
Landform-vegetation relationships in the northern Chihuahuan Desert [AD-A102896] p0208 N81-32588

SAUER, E. K.
Hydrogeology of glacial deposits from aerial photographs p0252 A81-43548

SAULSKII, V. K.
Efficiency criteria of space systems for studying the earth's natural resources p0277 A81-42287
The characteristics of combining devices with different survey bands aboard a satellite p0274 A81-48689

SAYN-WITTGENSTEIN, L.
Forestry priorities and their implications for the Canadian Remote Sensing Program p0202 A81-49755

SAZHIN, S. M.
An analysis of the data of synchronous measurements from the Meteor satellite and ships at the eastern coast of the Caspian Sea p0237 A81-48687

SCARPACE, F. L.
Improving stream flow estimates through the use of Landsat p0247 A81-43216
Wetland mapping from digitized aerial photography p0252 A81-43549

SCHAEFFER, D. J.
Assessment and classifications of selected Illinois lakes through the application of space technology p0250 A81-43255

SCHANDA, E.
Passive microwave systems [IAF PAPER 81-88] p0273 A81-47342

SCHITTENHELM, R.
OVSUP: A program for computer-aided disentanglement of overlapping zones p0222 N81-33525

SCHLUDE, F.
Imaging radar systems p0240 N81-33342

SCHMELOVSKY, K.-H.
First results of the Intercosmos satellite IK-21 [IAF PAPER 81-214] p0274 A81-47409

SCHMUGGE, T. J.
Survey of in-situ and remote sensing methods for soil moisture determination p0197 A81-43221
Aircraft active microwave measurements for estimating soil moisture p0271 A81-43547
Active microwave measurements for esSimating soil moisture in Oklahoma p0199 A81-43744

SCHNEIDER, E.
Millimeter-wave sensing of the environment: A bibliographic survey [NASA-CR-156879] p0219 N81-32581

SCHOLZ, D. K.
An assessment of Landsat data acquisition history on identification and area estimation of corn and soybeans p0200 A81-46032

SCHOWENGERDT, R.
Correlation of geologic structure inferred from computer enhanced Landsat imagery with underground water supplies in Arizona p0225 A81-43227

SCHROEDER, L. C.
Performance evaluation of a spaceborne scatterometer p0269 A81-41920

SCHUBERT, J.
Stratification of Landsat data by uniformity productivity of soils p0259 A81-46042

SCHUTZ, B. E.
Orbit determination requirements for TOPEX [AAS PAPER 81-158] p0221 A81-45828

SCHWEBEL, R.
Application of new precision measuring systems for photogrammetric comparators [BMFT-FB-T-80-134] p0276 N81-32595

SCOFIELD, R. A.
A satellite derived technique for estimating rainfall from thunderstorms and hurricanes p0244 A81-43191

SCOTT, L.
Meteorological satellite data: A tool to describe the health of the world's agriculture [E81-10204] p0207 N81-31596

SCQUIZZATO, N.
Automatic processing of computer compatible tapes with data from multispectral scanners installed in Landsat satellites p0272 A81-46029

SEDLACEK, W. A.
Stratospheric sulfate from the Gareloi eruption, 1980 - Contribution to the 'ambient' aerosol by a poorly documented volcanic eruption p0213 A81-41404

SEFTON, D. F.
Assessment and classifications of selected Illinois lakes through the application of space technology p0250 A81-43255

SERAFIMOV, K.
Program and instrumentation of the satellite experiment Bulgaria-1300 II [IAF PAPER 81-91] p0273 A81-47345
New complex for ionosphere-magnetosphere study 'Intercosmos-Bulgaria-1300' [IAF PAPER 81-212] p0273 A81-47407

SESTAK, M. L.
An analysis of haze effects on LANDSAT multispectral scanner data [E81-10162] p0263 N81-29497

SHAFER, B. A.
Landsat derived snow cover as an input variable for snow melt runoff forecasting in South Central Colorado p0246 A81-43208

SHANTON, J. A.
Applications of aerospace data for detection of submarine springs in Jamaica p0226 A81-43232

SHEFFIELD, C.
Commercial operations in space - 1980-2000; Proceedings of the Eighteenth Goddard Memorial Symposium, Washington, DC, March 27, 28, 1980 p0277 A81-44635

SHEN, S. S.
Evaluation of large area crop estimation techniques using LANDSAT and ground-derived data [E81-10200] p0206 N81-29511

SHIELDS, J. A.
Stratification of Landsat data by uniformity productivity of soils p0259 A81-46042

SHIH, S. F.
Improvements in lake volume predictions using Landsat data p0248 A81-43237
A technique for improved assessment of flow resistance characteristics of natural wetlands using Landsat data p0248 A81-43241

SHILIN, B. V.
Aerial thermal survey in the study of earth resources p0277 A81-43981

SHIUE, J. C.
Passive microwave sensing of snow characteristics over land p0246 A81-43207

SHOPE, W. G.
U.S. geological survey application of satellite telemetry for the support of hydrologic data collection p0258 A81-43189

SHUCHMAN, R. A.
Refraction of coastal ocean waves p0235 A81-46113
Determination of beach sand parameters using remotely sensed aircraft reflectance data p0217 A81-49346

SHULMIN, M. V.
Derivation of formulas for the correlation of coordinate points of different-scale photographs and quasi-photographs p0261 A81-48772

SIDDOWAY, F. H.
Assessing winter wheat dry matter production via spectral reflectance measurements p0202 A81-49344

SIEBER, A.
The European SAR-Project Convair 580 p0273 A81-46679
Introduction to the workshop p0276 N81-33340

SIEGEL, H. J.
Parallel processing implementations of a contextual classifier for multispectral remote sensing data p0272 A81-46028

SIMS, R. A.
The application of remote sensing techniques for an ecological land survey of the snow goose colony at Cape Henrietta Maria, Hudson Bay p0204 A81-49791

SINGHROY, V. H.
Geological and terrain analysis of the Annapolis County region of Nova Scotia - An application of digital Landsat, radar and colour infrared data p0227 A81-49802
Resource inventory and terrain analysis in north western Manitoba from integrated remote sensing data p0218 A81-49803

SKALEY, J. E.
From landforms to avian habitat - A look at topology p0214 A81-43739

SKROTSKII, V. G.
Accuracy of transmission of spectral contrasts in multispectral aerial photography, with application to problems of object recognition p0257 A81-41479

SLATER, P. N.
The effect of sensor bandpass and spectral response in crop stress detection p0199 A81-43737

SMART, M. A.
An evaluation of detail in dynamic visual displays [AD-A103378] p0222 N81-33578

SMITH, A. Y.
Application of digital image processing techniques and information systems to water quality monitoring of Lake Tahoe p0251 A81-43258

SMITH, B. W.
Parallel processing implementations of a contextual classifier for multispectral remote sensing data p0272 A81-46028

SMITH, H. G.
Remote sensing aided procedure for conifer growth modeling in the northeastern Sierra Nevada p0199 A81-43740

SMITH, J. A.
Thermal vegetation canopy model studies p0202 A81-49347

SMITH, R. S.
Quantification of non-point source sedimentation through densitometric analysis of color infrared aerial photography [PB81-209157] p0255 N81-33599

SMITH, W. L.
Determination of moisture from NOAA polar orbiting satellite sounding radiances p0243 A81-41158

SMOLIANINOV, IU. A.
Concerning the reliability estimation of information obtained from several sources in earth survey tasks p0270 A81-42286

SOKOLOV, IU. P.
Radar methods for studying the earth p0273 A81-46924

SOMMA, R.
Radar altimeter for ocean remote sensing [IAF PAPER 81-94] p0236 A81-47348

SOUTHWICK, D. L.
Synergistic relationships among remote-sensing and geophysical media: Geological and hydrological applications p0255 N81-33553

STAELIN, D. H.
Passive microwave techniques for geophysical sensing of the earth from satellites p0270 A81-43071
Progress in passive microwave remote sensing - Nonlinear retrieval techniques p0271 A81-45872

STAENZ, K.
Spectral measurement of rangeland p0218 A81-49790
Evaluation of Thematic Mapper bands - A first step in feature selection p0205 A81-49815

STANTURF, J. A.
Use of remote sensing in landscape stratification for environmental impact assessment p0214 A81-43748
Cornell University Remote Sensing Program
[E81-10174] p0255 N81-33560

STAVTSEV, A. L.
Ore-controlling space geological objects and their assessment techniques applied to mineral prediction
[IAF PAPER 81-107] p0227 A81-47353

STEPANENKO, V. D.
Radar methods for studying the earth
p0273 A81-46924

STEPHAN, J. G.
Landsat data as a basis for regional environmental assessment within the Columbia Plateau
p0218 A81-49798

STEVENS, G. R.
Geological and terrain analysis of the Annapolis County region of Nova Scotia - An application of digital Landsat, radar and colour infrared data p0227 A81-49802

STEWART, R. H.
Satellite oceanography - The instruments
p0274 A81-49134

STIES, M.
Partially automated object extraction from aerial photographs and land maps p0266 N81-33528

STILES, J. A.
Radar image preprocessing p0272 A81-46038

STILES, W. H.
Monitoring snow with microwaves p0246 A81-43209

STIX, J.
Seasat satellite investigation of the structure of western Nebraska and its application to the evaluation of geothermal resources
[LA-UR-81-1454] p0223 N81-30505

STOCKMAN, G. C.
Knowledge-based image analysis
[AD-A101319] p0264 N81-30852

STOIBER, R. E.
An investigation of vegetation and other Earth resource/feature parameters using LANDSAT and other remote sensing data 1: LANDSAT 2: Remote sensing of volcanic emissions
[E81-10081] p0209 N81-33543

STONER, E. R.
Development of a digital data base for reflectance-related soil information p0201 A81-46051
Evaluation of multiband, multitemporal, and transformed LANDSAT MSS data for land cover area estimation
[E81-10161] p0219 N81-29496

STOVE, G. C.
Current resource mapping and environmental monitoring applications using Landsat MSS data in Scotland
p0218 A81-49806

STRANG, R. M.
Photointerpretation of fire damage to trees in a ponderosa pine/bunchgrass community p0204 A81-49787

STRETTA, J.-M.
Meteosat experience in assisting commercial fishing
p0239 A81-49807

STROME, W. M.
Histogram estimation for multiple-detector sensors
p0262 A81-49812

STRONG, D. C.
The Lake Melville/Labrador offshore synthetic aperture radar study - Winter 1979 p0238 A81-49772

STRONG, J. P.
Inventory estimation on the massively parallel processor p0259 A81-46052

STUERZENHOFAECKER, P.
Possible applications of communication satellites for research tasks in polar regions
[BMFT-FB-W-80-029] p0267 N81-33587

SUKHOTKO, N. V.
Topographic and cartographic applications of photogrammetry p0221 A81-42847

SUTHERLAND, R. A.
Remote sensing of thermal radiation from an aircraft - An analysis and evaluation of crop-freeze protection methods p0202 A81-46895

SUZUKI, Y.
Digital analysis of Landsat MSS data and application for coastal marine environment p0233 A81-43247

SWAIN, P. H.
Parallel processing implementations of a contextual classifier for multispectral remote sensing data
p0272 A81-46028
Context distribution estimation for contextual classification of multispectral image data
p0259 A81-46041

SWIFT, C. T.
Airborne microwave radiometer remote sensing of lake ice p0253 A81-48554

SWIFT, R. N.
Airborne simultaneous spectroscopic detection of laser-induced water Raman backscatter and fluorescence from chlorophyll a and other naturally occurring pigments
p0253 A81-47647

SYCHEV, A. G.
Concerning the possibility of improving the spectroradiometric accuracy of remote sensing of the earth by means of multispectral band scanners
p0270 A81-42285

SYDOR, M.
Lakewide monitoring of suspended solids using satellite data p0254 N81-33552

SZABO, L.
Cartographic accuracy of synthetic aperture radar imagery p0262 A81-49780

T

TAKEDA, K.
Monitoring of snow covered area using satellite data
[IAF PAPER 81-114] p0253 A81-47356

TANAKA, K.
Following oceanographic phenomena on the South Coast of Brazil with remote sensing from orbital distance
[INPE-1975-RPE/280] p0240 N81-30498

TANG, C. C. H.
Earth applications orbit analysis for a shuttle-mounted Multispectral Mapper
[AAS PAPER 81-182] p0271 A81-45836

TANIS, F. J.
A remote sensing technique to monitor Cladophora in the Great Lakes
[PB81-173841] p0254 N81-29520

TAPLEY, B. D.
Orbit determination requirements for TOPEX
[AAS PAPER 81-158] p0221 A81-45828

TARAKANOV, V. G.
Analysis of the geometry of a frame photograph
p0221 A81-42554

TARNOPOLSKII, V. I.
Concerning the possibility of improving the spectroradiometric accuracy of remote sensing of the earth by means of multispectral band scanners
p0270 A81-42285

TAYLOR, S. L.
Role of multiple scattering in ozone profile retrieval from satellite measurements in the ultraviolet
p0215 A81-45870

TAYLOR, T. W.
Large area application of a corn hazard model
[E81-10164] p0205 N81-28497

TEILLET, P. M.
Integration and comparison of SAR and MSS data for potato crop area estimation p0203 A81-49766
Rapeseed - Guidelines for operational monitoring
p0203 A81-49784

TENG, W. L.
Analysis of landfills with historic airphotos
p0216 A81-46407

TER-MARKARIANTS, N. E.
Radiation studies in the atmosphere
p0216 A81-47001

TEREKHIN, G.
First results of the Intercosmos satellite IK-21
[IAF PAPER 81-214] p0274 A81-47409

THEIS, S. W.
Measurement of soil moisture trends with airborne scatterometers
[E81-10088] p0209 N81-33545

THELIN, G. P.
Mapping irrigated cropland on the High Plains using Landsat p0198 A81-43266

THIEN, N. P.
Interactive processing of Landsat image for morphopedological studies p0259 A81-46043

THOM, K. S.
The use of CIR and airborne multispectral scanner techniques for wetland soils mapping of highway corridors p0215 A81-46044

THOMAS, J.
Possible applications of communication satellites for research tasks in polar regions
[BMFT-FB-W-80-029] p0267 N81-33587

THOME, P. G.
NASA water resources/hydrology remote sensing program in the 1980's p0244 A81-43179

THOMPSON, D. R.
A crop moisture stress index for large areas and its application in the prediction of spring wheat phenology
[E81-10202] p0210 N81-33573

THOMSON, D. W.
Environmental measurements of power plant cooling tower and stack plumes
[DOE/EV-02463/6] p0219 N81-30696

THOMSON, K. P. B.
The airborne SAR project - Conclusions and applications p0275 A81-49765
Applications of remote sensing to construction impact assessment at the Roberts Bank Port, British Columbia
p0218 A81-49781
Rapeseed - Guidelines for operational monitoring
p0203 A81-49784
Spectral measurement of rangeland
p0218 A81-49790

THOMSON, K. P.-B.
A simulation of Thematic Mapper performance in an agricultural application p0204 A81-49810

THORNTON, H. F.
Airborne microwave radiometer remote sensing of lake ice p0253 A81-48554

TILTON, J. C.
Context distribution estimation for contextual classification of multispectral image data
p0259 A81-46041

TINNEY, L.
Application of remote sensing for California irrigated lands assessment p0213 A81-43261
A multistage mapping approach for an irrigated croplands inventory p0198 A81-43262

TISHCHENKO, A. P.
Some results on the investigation of earth resources by aerial and polygon methods p0269 A81-41476

TITS, D.
Analysis of the November 23, 1980 earthquake as a design basis for satellite emergency communication
[IAF PAPER 81-269] p0216 A81-47433

TOLL, D. L.
Urban area update procedures using Landsat data
p0214 A81-43733

TOLSTYKH, G. N.
Concerning the possibility of improving the spectroradiometric accuracy of remote sensing of the earth by means of multispectral band scanners
p0270 A81-42285

TOMLINS, G. F.
Applications of remote sensing to construction impact assessment at the Roberts Bank Port, British Columbia
p0218 A81-49781

TOYOTA, H.
A comparison of automatic classification algorithms for land use map by remotely sensed data
p0215 A81-44701

TRENCHARD, M. H.
Weather analysis and interpretation procedures developed for the US/Canada wheat and barley exploratory experiment
[E81-10208] p0207 N81-31599

TRIFONOV, IU.
Program and instrumentation of the satellite experiment Bulgaria-1300 II
[IAF PAPER 81-91] p0273 A81-47345

TRIVEDI, M. M.
Texture analysis and urban land use classification
p0214 A81-44684

TROFIMOV, D. M.
The interrelation of linear and isometric objects on satellite imagery and the oil and gas structures of the Buzuluk Basin p0227 A81-48685

TSVETAEVA, E. V.
Evaluation of the possibility of using spectral-band and multispectral aerial photographs for the large-scale survey of natural pastures p0197 A81-41487

TURNER, B. J.
ICAP - An Interactive Cluster Analysis Procedure for analyzing remotely sensed data p0261 A81-49345

TURNER, R. M.
Satellite observations of a geothermal submarine spring off Florida west coast p0233 A81-43248

TYSON, B. J.
Measurements of CF2Cl2, CFCl3, and N2O in the lower stratosphere between 2 deg S and 73 deg N latitude
p0214 A81-44515

U

ULABY, F. T.
Monitoring snow with microwaves p0246 A81-43209
Potential application of satellite radar to monitor soil moisture p0270 A81-43223
Crop classification with a Landsat/radar sensor combination p0200 A81-46033

ULBRICHT, K. A.
Comparative experimental study on the use of original and compressed multispectral Landsat data of the Bayuda desert p0262 A81-49813

USPENSKII, G. R.
Efficiency criteria of space systems for studying the earth's natural resources p0277 A81-42287
The characteristics of combining devices with different survey bands aboard a satellite p0274 A81-48689

USRY, J. W.
A comparison of observed and analytically derived remote sensing penetration depths for turbid water
[NASA-TM-83176] p0255 N81-33577

V

VALLESE, F.
Correlation function studies for snow and ice
p0260 A81-46378

VAN RYSWYK, A. L.
Colour - The critical photointerpretation element in the identification of rangeland plant communities on colour and colour-infrared aerial photography p0203 A81-49786

VAN VALIN, C. C.
Aerosol formation, transformation, and effects in Denver's emissions plume p0214 A81-44526

VANDERBILT, V. C.
A model of plant canopy polarization response
p0201 A81-46035

VANIUSHIN, G. P.
An analysis of the data of synchronous measurements from the Meteor satellite and ships at the eastern coast of the Caspian Sea p0237 A81-48687

VANKOUGHNETT, A. L.
The Surveillance Satellite Program and the future of microwave remote sensing p0274 A81-49753

VARDEMAN, S. B.
Context distribution estimation for contextual classification of multispectral image data p0259 A81-46041

VASIUKHINA, T. M.
Results of ground surveys, carried out in conjunction with satellite and aerial studies, of the state of winter wheat on the Kursk test polygon p0197 A81-41485
Determination of the types and state of crops from multispectral aerial photographs p0197 A81-41486

VASQUEZ-ESPINOSA, R. E.
Texture analysis and urban land use classification p0214 A81-44684

VAVAEV, V. A.
Selection of reference zones for the automatic coordinate control of space images p0261 A81-48693

VEDDER, J. F.
Measurements of CF2Cl2, CFCl3, and N2O in the lower stratosphere between 2 deg S and 73 deg N latitude p0214 A81-44515

VERBIN, V. E.
Selection of reference zones for the automatic coordinate control of space images p0261 A81-48693

VERESHCHAKA, T. V.
The use of spaceborne photography for topographic mapping p0221 A81-42556

VERETIAGIN, A. A.
Radar methods for studying the earth p0273 A81-46924

VETLOV, I.
Program and instrumentation of the satellite experiment Bulgaria-1300 II
[IAF PAPER 81-91] p0273 A81-47345

VINNICHENKO, N. K.
Some results on the investigation of earth resources by aerial and polygon methods p0269 A81-41476
Aerial data acquisition systems using test-ground polygons p0269 A81-41477
The use of the spectral and physical-geographic characteristics of natural objects for the interpretation of multispectral satellite images p0257 A81-41484
Determination of the types and state of crops from multispectral aerial photographs p0197 A81-41486

VINOGRADOV, B. V.
Remote sensing and mapping of pastures p0213 A81-42281

VLASOV, E. P.
Interactive system for the regional prognosis of raw mineral resources, based on ground-based and satellite imagery data p0227 A81-48691

VOLCHEGURSKII, L. F.
The use of satellite imagery for studying the structural features of the Caspian oil and gas region p0227 A81-48684

VOSTRIAKOVA, N. V.
The use of satellite data in predicting spring flow in the basins of the upper Ob' and upper Enisei p0243 A81-41723

W

WADDINGTON, J.
Spectral measurement of rangeland p0218 A81-49790

WAITE, W. P.
Look direction dependence of radar backscattering cross section for agricultural fields p0199 A81-43741
Use of Seasat satellite radar imagery for the detection of standing water beneath forest vegetation p0199 A81-43743

WAKE, W. H.
Field Study for Remote Sensing: An instructor's manual
[NASA-CP-2155] p0279 N81-32564
The workshop p0280 N81-32566
Why surface-truth field study is needed in remote-sensing instruction p0280 N81-32567

WALD, L.
Satellite determination of the mesoscale variability of the sea surface temperature p0234 A81-44861

WALL, S.
Application of remote sensing for California irrigated lands assessment p0213 A81-43261

WALLACE, D. E.
A report on the use of remote sensing techniques for the supervision of New England coastal salt marshes p0253 A81-48944

WALSH, E. J.
Altimeter rain detection
[NASA-TM-73291] p0275 N81-29408

WALTON, M.
Synergistic relationships among remote-sensing and geophysical media: Geological and hydrological applications p0255 N81-33553

WANG, Y.-H.
Applications of Landsat imagery to a coastal inlet stability study p0250 A81-43249

WANG, Z. Z.
Photogrammetry in China p0222 N81-33526

WARD, J. F.
Photographic technology development project: Timber typing in the Tahoe Basin using high altitude panoramic photography
[NASA-CR-161082] p0208 N81-32578

WARREN, G.
The use of satellite imagery as an aid to the Canadian Coast Guard ice operations p0238 A81-49758

WATERMAN, S. E.
Application of synthetic aperture radar data to snow cover monitoring p0253 A81-49778
Computer analysis of Tiros-N/NOAA-6 satellite data for operational snow cover mapping p0262 A81-49795
Investigation of multispectral remote sensing of snow cover using a solar radiation model p0262 A81-49804

WATSON, E. K.
Colour - The critical photointerpretation element in the identification of rangeland plant communities on colour and colour-infrared aerial photography p0203 A81-49786

WATSON, K.
Topographic slope correction for analysis of thermal infrared images
[PB81-211781] p0224 N81-33589

WEBB, D. J.
A comparison of Seasat 1 altimeter measurements of wave height with measurements made by a pitch-roll buoy p0231 A81-42066

WEBB, R. P.
Hydrologic land use classification using Landsat p0247 A81-43213

WEBSTER, K. B.
Selected irrigation acreage estimates in northern Florida from Landsat data p0198 A81-43264

WEDLER, E.
Applicability of airborne SAR data to geological mapping p0227 A81-49769
SAR image response over a conifer regeneration site p0203 A81-49770

WEISMILLER, R. A.
Application of multispectral reflectance studies of soils - Pre-Landsat p0200 A81-46031
Use of Landsat digital data to assist in mapping soils on Arizona rangelands p0201 A81-46047

WELBY, C. W.
Combined satellite imagery for study of coastal circulation, Onslow Bay, North Carolina p0233 A81-43250
Trophic state determination for shallow coastal lakes from Landsat imagery p0251 A81-43259

WELLMAN, D. L.
Aerosol formation, transformation, and effects in Denver's emissions plume p0214 A81-44526

WENTZ, F. J.
Performance evaluation of a spaceborne scatterometer p0269 A81-41920

WERTH, L. F.
A comparison of remote sensing techniques for Minnesota wetlands classification p0249 A81-43239

WESCOTT, T. F.
Interactive digital image processing for terrain data extraction
[AD-A101321] p0264 N81-30499

WHARTON, S. W.
Application of digital terrain data to quantify and reduce the topographic effect on Landsat data p0259 A81-45433
ICAP - An Interactive Cluster Analysis Procedure for analyzing remotely sensed data p0261 A81-49345

WHITE, D.
The detection of groundwater discharges /springs/ using aerial thermography p0254 A81-49800

WHITLOCK, C. H.
A comparison of observed and analytically derived remote sensing penetration depths for turbid water
[NASA-TM-83176] p0255 N81-33577

WHITMORE, R. A., JR.
The development of a remote sensing applications program for Vermont
[E81-10149] p0266 N81-33547

WHITNEY, L. F., JR.
A statistical approach to rainfall estimation using satellite data p0245 A81-43198

WICKWARE, G. H.
The application of remote sensing techniques for an ecological land survey of the snow goose colony at Cape Henrietta Maria, Hudson Bay p0204 A81-49791

WICKWARE, G. M.
Procedures for change detection using Landsat digital data p0215 A81-45437

WIEGAND, C. L.
Methods of editing cloud and atmospheric layer affected pixels from satellite data
[E81-10169] p0266 N81-33556

WIEGMANN, F.
First results of the Intercosmos satellite IK-21
[IAF PAPER 81-214] p0274 A81-47409

WIESNET, D. R.
Satellite hydrology: Proceedings of the Fifth Annual William T. Pecora Memorial Symposium on Remote Sensing, Sioux Falls, SD, June 10-15, 1979 p0243 A81-43176
The satellite record of the winter of 1978-79 in North America p0246 A81-43203
A note on indirect detection of seiches in Great Salt Lake, Utah, by NOAA and Landsat satellite imagery p0247 A81-43218
Assessing the Red River of the North 1978 flooding from NOAA satellite data p0248 A81-43219
Applications of aerospace data for detection of submarine springs in Jamaica p0228 A81-43232
Preliminary survey of HCMM satellite thermal imagery as applied to hydrospherics p0252 A81-43748

WIKEN, E. B.
Multistage remote sensing in exploratory ecodistrict land classification p0217 A81-49759

WILKINSON, T. L.
Single and multiple parameter microwave signatures of sea ice p0238 A81-49774
Radar detection of sea-ice ridges and icebergs in frozen oceans at incidence angles from 0 deg to 90 deg p0238 A81-49775

WILLIAMS, B. F.
An industrial perspective of the LANDSAT opportunity p0279 N81-32565

WILLIAMS, R. S., JR.
Satellite Image Atlas of the earth's glaciers p0246 A81-43202

WILLIAMS, T. H. L.
Mapping irrigated lands in Western Kansas from Landsat p0198 A81-43265

WILLIAMSON, A. N.
Landsat data for regulatory permit monitoring p0247 A81-43214

WILSON, C. L.
Landsat technology transfer to the private and public sectors through community colleges and other locally available institutions p0277 A81-43750

WILSON, M. J.
Satellite detection of oil on the marine surface p0233 A81-43251

WILSON, W. S.
Future plans for NASA's Oceanic Processes Program p0231 A81-41997
Oceanography from satellites p0237 A81-49127

WITHERSPOON, A. M.
Trophic state determination for shallow coastal lakes from Landsat imagery p0251 A81-43259

WITT, R. G.
Mapping the Great Salt Lake shoreline and associated waterfowl habitat from Landsat data p0252 A81-43742

WITTE, W. G.
A comparison of observed and analytically derived remote sensing penetration depths for turbid water
[NASA-TM-83176] p0255 N81-33577

WOODLEY, W. L.
Insights into errors of SMS-inferred GATE convective rainfall p0243 A81-42095
Rain estimation over several areas of the globe using satellite imagery p0245 A81-43193

WOOLF, H. M.
Determination of moisture from NOAA polar orbiting satellite sounding radiances p0243 A81-41158

WORSFOLD, R. D.
The Lake Melville/Labrador offshore synthetic aperture radar study - Winter 1979 p0238 A81-49772

WRIGLEY, R. C.
Atmospheric correction of Nimbus-7 Coastal Zone Color Scanner imagery p0271 A81-45879

WUNSCH, C.
The promise of satellite altimetry p0237 A81-49128

WYNN, S. L.
Wetland mapping from digitized aerial photography p0252 A81-43549

Y

YAMAMOTO, Y.
Geometric accuracy of Landsat images processed by NASDA p0263 A81-49818

Z

ZALL, L.
Ground water exploration programs in Africa p0226 A81-43230

ZANDONELLA, A.
Some methods of multitemporal analysis of LANDSAT images resulting from a study on Venice Lagoon
[E81-10206] p0267 N81-33574

ZANNI, S.
Hurricane 'Flossie' /September 1978/ observed in the north Atlantic, by the Meteosat satellite p0213 A81-41061

ZIELINSKI, J. B.
Differential Doppler experiment /DIDEX/ for geodetic applications p0221 A81-47938

ZIMMERMANN, G.
First results of the Intercosmos satellite IK-21
[IAF PAPER 81-214] p0274 A81-47409

ZSCHAU, J.
Potential for detection of natural disasters via Meteosat
[IAF PAPER 81-263] p0216 A81-47430

ZUBKOFF, P. L.
Remote sensing of dinoflagellate blooms in a turbid estuary p0251 A81-43538

ZUBKOVICH, S. G.
Radar methods for studying the earth
p0273 A81-46924
ZWICK, H. H.
Airborne estimation of water quality parameters in Lake Ontario
p0254 A81-49796

CORPORATE SOURCE INDEX

Typical Corporate Source Index Listing

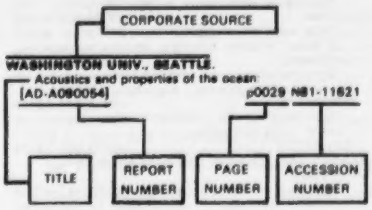

The title of the document is used to provide a brief description of the subject matter. The page number and the accession number are included in each entry to assist the user in locating the abstract in the abstract section. If applicable, a report number is also included as an aid in identifying the document.

A

AEROSPACE CORP., EL SEGUNDO, CALIF.
Millimeter-wave sensing of the environment: A bibliographic survey
[NASA-CR-156879] p0219 N81-32581

AIR FORCE INST. OF TECH., WRIGHT-PATTERSON AFB, OHIO.
An evaluation of detail in dynamic visual displays
[AD-A103378] p0222 N81-33578

ANALYTIC SCIENCES CORP., READING, MASS.
Military geodesy and geospace science, unit one
[AD-A104038] p0222 N81-33581

APPLIED PHYSICS LAB., JOHNS HOPKINS UNIV., LAUREL, MD.
Spatial evolution of ocean wave spectra
p0235 A81-46112

ARIZONA UNIV., TUCSON.
Spectral properties of Arizona soils and rangelands and their relationship to LANDSAT digital data
p0207 N81-31595

ARKANSAS UNIV., FAYETTEVILLE.
Look direction dependence of radar backscattering cross section for agricultural fields p0199 A81-43741

Use of Seasat satellite radar imagery for the detection of standing water beneath forest vegetation
p0199 A81-43743

ARMY COASTAL ENGINEERING RESEARCH CENTER, FORT BELVOIR, VA.
Wave direction measured by four different systems
p0232 A81-42622

ARMY COLD REGIONS RESEARCH AND ENGINEERING LAB., HANOVER, N. H.
Survey of in-situ and remote sensing methods for soil moisture determination p0197 A81-43221

ARMY ENGINEER TOPOGRAPHIC LABS., FORT BELVOIR, VA.
Remote sensing for engineering site selection
[AD-A102810] p0219 N81-32586

Identifying igneous rocks in an arid environment on aerial photography by photo tone and photo texture
[AD-A102809] p0228 N81-32587

Landform-vegetation relationships in the northern Chihuahuan Desert
[AD-A102896] p0206 N81-32588

ATMOSPHERIC ENVIRONMENT SERVICE, DOWNSVIEW (ONTARIO).
Role of multiple scattering in ozone profile retrieval from satellite measurements in the ultraviolet
p0215 A81-45870

Investigation of multispectral remote sensing of snow cover using a solar radiation model p0262 A81-49804

B

BATTELLE INST., FRANKFURT AM MAIN (WEST GERMANY).
Experimental investigation of the physical fundamentals for remote sensing of soil and vegetation moisture by active infrared reflectance spectroscopy using CO2 laser technique
[BMFT-FB-W-80-037] p0211 N81-33588

BEDFORD INST. OF OCEANOGRAPHY, DARTMOUTH (NOVA SCOTIA).
Bay of Fundy verification of a system for multidate Landsat measurement of suspended sediment
p0250 A81-43254

BENDIX FIELD ENGINEERING CORP., GRAND JUNCTION, COLO.
Methods development and applications evaluations of NURE aerial reconnaissance survey data for uranium resource evaluation: Beeville/Bay City and Crystal City quadrangles, Texas
[GJBX-69(81)] p0228 N81-30502

BOSTON COLL., CHESTNUT HILL, MASS.
Requirements of space-borne microwave radiometers for detecting soil moisture contents p0270 A81-43225

BRITISH AEROSPACE DYNAMICS GROUP, BRISTOL (ENGLAND).
Coastal Oceans Monitoring Satellite System (COMSS) system evaluation study
[ESS/SS-1035] p0239 N81-30168

BUSINESS AND TECHNOLOGICAL SYSTEMS, INC., SEABROOK, MD.
Early results from Magsat p0274 A81-48945

C

CALIFORNIA STATE COLL., BAKERSFIELD.
The workshop p0280 N81-32566
Why surface-truth field study is needed in remote-sensing instruction p0280 N81-32567

CALIFORNIA UNIV., BERKELEY.
Use of ocean color scanner data in water quality mapping p0251 A81-43545
Remote sensing aided procedure for conifer growth modeling in the northeastern Sierra Nevada
p0199 A81-43740
Water quality mapping from Landsat digital data
p0252 A81-45429
Users manual for the US baseline corn and soybean segment classification procedure
[E81-10190] p0206 N81-29504

CALIFORNIA UNIV., LIVERMORE. LAWRENCE LIVERMORE LAB.
Remote sensing of soil radionuclide fluxes in a tropical ecosystem
[UCRL-84501] p0219 N81-29517

CALIFORNIA UNIV., SANTA BARBARA.
Satellite detection of oil on the marine surface
p0233 A81-43251
Application of remote sensing for California irrigated lands assessment p0213 A81-43261

CALIFORNIA UNIV. AT BERKELEY.
Application of remote sensing for California irrigated lands assessment p0213 A81-43261

CALIFORNIA UNIV. AT LOS ANGELES.
Geomagnetic field mapping from a satellite: Spatial power spectra of the geomagnetic field at various satellite altitudes relative to natural noise sources and instrument noise
[PUBL-1810] p0275 N81-29480

CANADA CENTRE FOR REMOTE SENSING, OTTAWA (ONTARIO).
Bay of Fundy verification of a system for multidate Landsat measurement of suspended sediment
p0250 A81-43254
Wave orbital velocity, fade and SAR response to azimuth waves p0265 N81-33345

CENTRE NATIONAL DE LA RECHERCHE SCIENTIFIQUE, TOULOUSE (FRANCE).
Scatterometer measurements on crop and soil surfaces
p0208 N81-33349

COLLEGE OF WILLIAM AND MARY, WILLIAMSBURG, VA.
Mineralogical, optical, and geochemical properties of John H. Kerr Reservoir sediment samples for AgRISTARS pollution research
[E81-10155] p0229 N81-33548

COLORADO UNIV., BOULDER.
Mapping alpine soils using color positive and color infrared photographs p0252 A81-46046

COMMITTEE ON SCIENCE AND TECHNOLOGY (U. S. HOUSE).
NASA authorization, 1982, volume 4
[GPO-79-432-VOL-4] p0279 N81-31030

CONNECTICUT UNIV., STORRS.
Modeling the terrestrial hydrology for the global atmosphere - The future role of satellite data
p0245 A81-43197

CORNELL UNIV., ITHACA, N. Y.
Manual versus digital Landsat analysis for modeling river flooding p0252 A81-43745
Manual versus digital Landsat analysis for delineating river flooding p0252 A81-46405
Analysis of landfills with historic airphotos
p0216 A81-46407
Cornell University Remote Sensing Program
[E81-10174] p0255 N81-33560

D

DARTMOUTH COLL., HANOVER, N.H.
An investigation of vegetation and other Earth resource/feature parameters using LANDSAT and other remote sensing data. 1: LANDSAT. 2: Remote sensing of volcanic emissions
[E81-10081] p0209 N81-33543

DEFENSE MAPPING AGENCY AEROSPACE CENTER, ST. LOUIS, MO.
The sensor image simulator
[AD-A101172] p0275 N81-29512

DEFENSE MAPPING AGENCY HYDROGRAPHIC AND TOPOGRAPHIC CENTER, WASHINGTON, D.C.
Interpretation of hydrographic features seen in the waters off Cape Cod
[AD-A102343] p0240 N81-31803
Derivation of shallow ocean bottom reflectance values from color aerial photography
[AD-A101105] p0241 N81-33763

DELAWARE UNIV., NEWARK.
Drift and dispersion studies of ocean-dumped waste using Landsat imagery and current drogues p0233 A81-43539

DENVER RESEARCH INST., COLO.
Space Benefits: The secondary application of aerospace technology in other sectors of the economy
[NASA-CR-164733] p0279 N81-32086

DEPARTMENT OF AGRICULTURE, BELTSVILLE, MD.
Survey of in-situ and remote sensing methods for soil moisture determination p0197 A81-43221
Active microwave measurements for estimating soil moisture in Oklahoma p0199 A81-43744

DEPARTMENT OF AGRICULTURE, HOUSTON, TEX.
Large area application of a corn hazard model
[E81-10164] p0205 N81-28497
Yield Model Development (YMD) implementation plan for fiscal years 1981 and 1982
[E81-10211] p0208 N81-32577

DEPARTMENT OF AGRICULTURE, WASHINGTON, D.C.
Crop area estimation using ground-gathered and sampled LANDSAT data
[PB81-192783] p0207 N81-30507
AgRISTARS (Agriculture And Resources Inventory Surveys Through Aerospace Remote Sensing) DC/LC (Domestic Crops and Land Rover) project summary crop area estimates for Kansas and Iowa, 1980
[PB81-196909] p0207 N81-30511
Crop area estimates using ground-gathered and LANDSAT data. A multitemporal approach: Missouri, 1979
[PB81-186751] p0208 N81-31614
An evaluation of MSS P-format data registration
[E81-10171] p0267 N81-33557

DEPARTMENT OF AGRICULTURE, WESLACO, TEX.
Microdensitometry to identify saline rangelands on 70-mm color-infrared aerial film p0202 A81-46406

DEUTSCHE FORSCHUNGS- UND VERSUCHSANSTALT FUER LUFT- UND RAUMFAHRT, OBERPFAFFENHOFEN (WEST GERMANY).
Introduction to the workshop p0276 N81-33340
Imaging radar systems p0240 N81-33342

DORNIER-WERKE G.M.B.H., FRIEDRICHSHAFEN (WEST GERMANY).
Possible applications of communication satellites for research tasks in polar regions
[BMFT-FB-W-80-029] p0267 N81-33587

E

EG AND G WASHINGTON ANALYTICAL SERVICES CENTER, INC., POCOMOKE CITY, MD.
Airborne simultaneous spectroscopic detection of laser-induced water Raman backscatter and fluorescence from chlorophyll a and other naturally occurring pigments
p0253 A81-47647

EG & G WASHINGTON ANALYTICAL SERVICES CENTER, INC., RIVERDALE, MD.
Calibration validation for the GEOS 3 altimeter
p0270 A81-42671
A study of the effects of the atmosphere on thematic mapper observations
[E81-10056] p0276 N81-33540

ELOGIC, INC., HOUSTON, TEX.
New output improvements for CLASSY
[E81-10189] p0263 N81-29503
Improved version of the split routine for CLASSY
[E81-10210] p0264 N81-31600
Maximum likelihood labeling
[E81-10177] p0267 N81-33563

ENVIRONMENTAL RESEARCH AND TECHNOLOGY, INC., CONCORD, MASS.
Requirements of space-borne microwave radiometers for detecting soil moisture contents p0270 A81-43225
Comparative analysis of sea ice features using Side-Looking Airborne Radar (SLAR) and LANDSAT imagery
[E81-10044] p0241 N81-33539

ENVIRONMENTAL RESEARCH INST. OF MICHIGAN, ANN ARBOR.
Procedure M - A framework for stratified area estimation p0201 A81-46036
Refraction of coastal ocean waves p0235 A81-46113
Users manual for the US baseline corn and soybean segment classification procedure
[E81-10190] p0206 N81-29504
A remote sensing technique to monitor Cladophora in the Great Lakes
[PB81-173841] p0254 N81-29520
Fourier modulus image construction
[AD-A101728] p0264 N81-30723

EROS DATA CENTER, SIOUX FALLS, S. DAK.
An assessment of Landsat data acquisition history on identification and area estimation of corn and soybeans
p0200 A81-46032

EUROPEAN SPACE AGENCY, PARIS (FRANCE).
Coherent and incoherent radar scattering from rough surfaces and vegetated areas
[ESA-SP-166] p0208 N81-33339

F

FLORIDA UNIV., GAINESVILLE.
Remote sensing of thermal radiation from an aircraft - An analysis and evaluation of crop-freeze protection methods p0202 A81-46895

FLORIDA UNIV., LAKE ALFRED.
Vegetable crop management with remote sensing
p0198 A81-43540

G

GENERAL ELECTRIC CO., BELTSVILLE, MD.
Urban area update procedures using Landsat data
p0214 A81-43733

GENERAL ELECTRIC CO., LANHAM, MD.
Interactive digital image processing for terrain data extraction
[AD-A101321] p0264 N81-30499

GEOLOGICAL SURVEY, DENVER, COLO.
Topographic slope correction for analysis of thermal infrared images
[PB81-211781] p0224 N81-33589

GEORGIA INST. OF TECH., ATLANTA.
Agricultural water demand prediction using remote sensing technology for Georgia resource management
[PB81-184137] p0207 N81-30508

GEORGIA UNIV., ATHENS.
Agricultural water demand prediction using remote sensing technology for Georgia resource management
[PB81-184137] p0207 N81-30508

GEOSCIENCE RESEARCH CORP., SALISBURY, MD.
Terrain profiling from Seasat altimetry
[NASA-CR-156878] p0222 N81-31604
Ice sheet altimetry
[NASA-CR-156877] p0240 N81-31605

H

HIGH LIFE HELICOPTERS, INC., PUYALLUP, WASH.
Airborne gamma-ray spectrometer and magnetometer survey
[DE81-027157] p0229 N81-32592
Airborne gamma-ray spectrometer and magnetometer survey. Canyon City quadrangle (Oregon), volume 2
[DE81-028682] p0229 N81-33584
Airborne gamma-ray spectrometer and magnetometer survey. Salem quadrangle (Oregon), volume 2
[DE81-028681] p0229 N81-33585

HUGHES AIRCRAFT CO., EL SEGUNDO, CALIF.
Wave direction measured by four different systems
p0232 A81-42622

HYDROCOMP, INC., MOUNTAIN VIEW, CALIF.
Evaluation of remote sensing data for input into Hydrological Simulation Program-FORTRAN (HSPF)
[PB81-209561] p0255 N81-33593

I

ILLINOIS UNIV. AT CHICAGO CIRCLE, CHICAGO.
Optimal polarization concept in radar imaging
p0265 N81-33350

INSTITUT D'AERONOMIE SPATIALE DE BELGIQUE, BRUSSELS.
Atmospheric nitric acid and chlorofluoromethane 11 from interferometric spectra obtained at the Observatoire du Pic du Midi
[AERONOMICA-ACTA-A-227-1980] p0219 N81-30656

INSTITUT FUER ANGEWANDTE GEODAESIE, FRANKFURT AM MAIN (WEST GERMANY).
Position measurements in Colombia by means of satellite observations p0222 N81-33522
OVSUP: A program for computer-aided disentanglement of overlapping zones p0222 N81-33525
Photogrammetry in China p0222 N81-33526
Reports on cartography and geodesy, series 1: Original reports, Number 81
[ISSN-0469-4236] p0222 N81-33527
Partially automated object extraction from aerial photographs and land maps p0266 N81-33528

INSTITUTO DE PESQUISAS ESPACIAIS, SAO JOSE DOS CAMPOS (BRAZIL).
Following oceanographic phenomena on the South Coast of Brazil with remote sensing from orbital distance
[INPE-1975-RPE/280] p0240 N81-30498
Visual enhancement of images of natural resources: Applications in geology
[E81-10181] p0228 N81-32575

INTERNATIONAL BUSINESS MACHINES CORP., WHITE PLAINS, N.Y.
An industrial perspective of the LANDSAT opportunity
p0279 N81-32565

ITEK CORP., LEXINGTON, MASS.
Conceptual design of an automated mapping satellite System (MAPSAT)
[PB81-185555] p0264 N81-29522

J

JET PROPULSION LAB., CALIFORNIA INST. OF TECH., PASADENA.
Seasat data applications by commercial users
p0231 A81-41974
Wave direction measured by four different systems
p0232 A81-42622
The use of radar imagery for surface water investigations p0247 A81-43211
Application of digital image processing techniques and information systems to water quality monitoring of Lake Tahoe p0251 A81-43258
Use of imaging radar for geology and archeology
p0226 A81-43730
Training site statistics from Landsat and Seasat satellite imagery registered to a common map base
p0258 A81-43734
Texture measurements from Seasat - SAR images for urban land use interpretation p0214 A81-43749
A radar image time series p0226 A81-45430
Orbit determination requirements for TOPEX
[AAS PAPER 81-158] p0221 A81-45828
Earth applications orbit analysis for a shuttle-mounted Multispectral Mapper
[AAS PAPER 81-182] p0271 A81-45836
Radar image preprocessing p0272 A81-46038
Advanced synthetic aperture radar for remote sensing
p0274 A81-48553
Commercial applications of satellite oceanography
p0237 A81-49133
Satellite oceanography - The instruments
p0274 A81-49134
Regression techniques for oceanographic parameter retrieval using space-borne microwave radiometry
p0239 A81-49967
Space based topographic mapping experiment using Seasat synthetic aperture radar and LANDSAT 3 return beam vidicon imagery
[NASA-CR-164675] p0223 N81-30496

JOHNS HOPKINS UNIV., BALTIMORE, MD.
The structure of short gravity waves on the ocean surface p0234 A81-46105

JOINT PUBLICATIONS RESEARCH SERVICE, ARLINGTON, VA.
Use of satellite pictures for agriculture
p0205 N81-28120

K

KANSAS UNIV., LAWRENCE.
Mapping irrigated lands in Western Kansas from Landsat p0198 A81-43265
Radar image preprocessing p0272 A81-46038
A review of volume scatter theories for modeling applications p0265 N81-33347
Crop phenology and LANDSAT-based irrigated lands inventory in the high plains: Appendices
[E81-10172] p0210 N81-33558
Crop phenology and LANDSAT-based irrigated lands inventory in the high plains
[E81-10173] p0210 N81-33559

KANSAS UNIV. CENTER FOR RESEARCH, INC., LAWRENCE.
Monitoring snow with microwaves p0246 A81-43209
Potential application of satellite radar to monitor soil moisture p0270 A81-43223
Crop classification with a Landsat/radar sensor combination p0200 A81-46033
Sea surface scattering p0241 N81-33344
Scatterometer calibration and data correction
p0265 N81-33351

KENTRON INTERNATIONAL, INC., HAMPTON, VA.
The study of mesoscale ocean winds
p0235 A81-46110

L

L N K CORP., INC., SILVER SPRING, MD.
Knowledge-based image analysis
[AD-A101319] p0264 N81-30852

LOCKHEED ELECTRONICS CO., HOUSTON, TEX.
A comparison of remote sensing techniques for Minnesota wetlands classification p0249 A81-43239

LOCKHEED ENGINEERING AND MANAGEMENT SERVICES CO., INC., HOUSTON, TEX.
Maximum likelihood estimation of label imperfection probabilities and its use in the identification of mislabeled patterns p0259 A81-46040
A temporal/spectral analysis of small grain crops and confusion crops
[E81-10167] p0205 N81-28498
Evaluation of gravimetric ground truth soil moisture data collected for the agricultural soil moisture experiment, 1978 Colby, Kansas, aircraft mission
[E81-10114] p0205 N81-29494
An analysis of haze effects on LANDSAT multispectral scanner data
[E81-10162] p0263 N81-29497
The multicategory case of the sequential Bayesian pixel selection and estimation procedure
[E81-10182] p0263 N81-29498
Conversion of SPU-Universal disk file to JSC-Universal tape storage: CONVRT user's guide
[E81-10185] p0263 N81-29501
Maximum likelihood clustering with dependent feature trees
[E81-10186] p0263 N81-29502
Descriptive and sensitivity analyses of WATBALI: A dynamic soil water model
[E81-10193] p0206 N81-29507
Evaluation of spring wheat and barley crop calender models for the 1979 crop year
[E81-10197] p0206 N81-29508
Computer program documentation user information for the RSO-tape print program (RSOPRNT)
[E81-10198] p0264 N81-29509
Estimation of proportions in mixed pixels through their region characterization
[E81-10199] p0264 N81-29510
Evaluation of large area crop estimation techniques using LANDSAT and ground-derived data
[E81-10200] p0206 N81-29511
Meteorological satellite data: A tool to describe the health of the world's agriculture
[E81-10204] p0207 N81-31596
A description of the reformatted spring small grains labeling procedure used in test 2, part 2 of the US/Canada wheat and barley exploratory experiment
[E81-10206] p0207 N81-31597
Classification of wheat: Badhwar profile similarity technique
[E81-10207] p0207 N81-31598
Weather analysis and interpretation procedures developed for the US/Canada wheat and barley exploratory experiment
[E81-10208] p0207 N81-31599
Analysis of US spring wheat and spring barley periodic ground truth
[E81-10203] p0208 N81-32576

Photographic technology development project: Timber typing in the Tahoe Basin using high altitude panoramic photography
[NASA-CR-161082] p0208 N81-32578

Interim catalog ground data summary, data acquisition year 1978
[E81-10132] p0209 N81-33546

As-built design specification of the automatic registration system for the cartographic technology laboratory
[E81-10176] p0267 N81-33562

Maximum likelihood estimation for mixture models
[E81-10178] p0210 N81-33564

Australian transition year special studies
[E81-10179] p0210 N81-33565

A crop moisture stress index for large areas and its application in the prediction of spring wheat phenology
[E81-10202] p0210 N81-33573

Experiment plan: Row and roughness effects on dependence of active microwave measurements of soil moisture
[E81-10209] p0211 N81-33575

LOS ALAMOS SCIENTIFIC LAB., N. MEX.

Seasat satellite investigation of the structure of western Nebraska and its application to the evaluation of geothermal resources
[LA-UR-81-1454] p0223 N81-30505

M

MAINE UNIV., ORONO.

Quantification of non-point source sedimentation through densitometric analysis of color infrared aerial photography
[PB81-209157] p0255 N81-33599

MARCONI CO. LTD., CHELMSFORD (ENGLAND).

Scattering theory with application to synthetic aperture radar p0265 N81-33348

MASSACHUSETTS INST. OF TECH., CAMBRIDGE.

Passive microwave techniques for geophysical sensing of the earth from satellites p0270 A81-43071

Progress in passive microwave remote sensing - Nonlinear retrieval techniques p0271 A81-45872

Inversion of multiwavelength radiometer measurements by three-dimensional filtering p0271 A81-45873

Correlation function studies for snow and ice p0260 A81-46378

MIAMI UNIV., CORAL GABLES, FLA.

Atmospheric correction of Nimbus-7 Coastal Zone Color Scanner imagery p0271 A81-45879

MINNESOTA UNIV., DULUTH.

Lakewide monitoring of suspended solids using satellite data p0254 N81-33552

MINNESOTA UNIV., MINNEAPOLIS.

Satellite monitoring of snow extent and condition in agricultural, transitional, and forested land cover areas
[PB81-188625] p0254 N81-30509

A study of Minnesota land and water resources using remote sensing. Volume 14
[E81-10166] p0254 N81-33550

MINNESOTA UNIV., ST. PAUL.

A comparison of remote sensing techniques for Minnesota wetlands classification p0249 A81-43239

Development of alternative data analysis techniques for improving the accuracy and specificity of natural resource inventories made with remote sensing data p0266 N81-33551

Synergistic relationships among remote-sensing and geophysical media: Geological and hydrological applications p0255 N81-33553

A project to evaluate moisture stress and phenological factors in corn and soybean areas of southwestern and south-central Minnesota p0209 N81-33554

N

NATIONAL ADVISORY COMMITTEE ON OCEANS AND ATMOSPHERE, WASHINGTON, D.C.

Ocean services for the nation. National ocean goals and objectives for the 1980's
[PB81-200602] p0240 N81-31808

NATIONAL AERONAUTICS AND SPACE ADMINISTRATION, WASHINGTON, D. C.

Oceanic Satellite Data Distribution System p0231 A81-41996

Future plans for NASA's Oceanic Processes Program p0231 A81-41997

NASA water resources/hydrology remote sensing program in the 1980's p0244 A81-43179

Satellite detection of oil on the marine surface p0233 A81-43251

Oceanography from satellites p0237 A81-49127

NASA selects scientific investigations for Earth dynamics studies
[NASA-NEWS-RELEASE-81-129] p0228 N81-29143

NATIONAL AERONAUTICS AND SPACE ADMINISTRATION. AMES RESEARCH CENTER, MOFFETT FIELD, CALIF.

Measurements of CF2Cl2, CFCl3, and N2O in the lower stratosphere between 2 deg S and 73 deg N latitude p0214 A81-44515

Infrared-temperature variability in a large agricultural field p0200 A81-45432

Atmospheric correction of Nimbus-7 Coastal Zone Color Scanner imagery p0271 A81-45879

Bulk processing techniques for very large areas - Landsat classification of California p0201 A81-46054

Technical aspects of forest inventory demonstrations using Landsat data - Projects in the Pacific Northwest States p0203 A81-49764

Field Study for Remote Sensing: An instructor's manual
[NASA-CP-2155] p0279 N81-32564

NATIONAL AERONAUTICS AND SPACE ADMINISTRATION. EARTH RESOURCES LABS., BAY ST. LOUIS, MISS.

Computer-implemented remote sensing techniques for measuring coastal productivity and nutrient transport systems p0250 A81-43243

Development of a digital data base for reflectance-related soil information p0201 A81-46051

Evaluation of multiband, multitemporal, and transformed LANDSAT MSS data for land cover area estimation
[E81-10161] p0219 N81-29496

An evaluation of MSS P-format data registration
[E81-10171] p0267 N81-33557

NATIONAL AERONAUTICS AND SPACE ADMINISTRATION. GODDARD SPACE FLIGHT CENTER, GREENBELT, MD.

Calibration validation for the GEOS 3 altimeter p0270 A81-42671

Advanced technology for satellite data collection systems p0270 A81-43190

Passive microwave sensing of snow characteristics over land p0246 A81-43207

Survey of in-situ and remote sensing methods for soil moisture determination p0197 A81-43221

Improvements in lake volume predictions using Landsat data p0249 A81-43237

A technique for improved assessment of flow resistance characteristics of natural wetlands using Landsat data p0249 A81-43241

An application of Landsat and computer technology to potential water pollution from soil erosion p0250 A81-43253

Multisensor analysis of hydrologic features with emphasis on the Seasat SAR p0251 A81-43544

Aircraft active microwave measurements for estimating soil moisture p0271 A81-43547

Urban area update procedures using Landsat data p0214 A81-43733

Mapping the Great Salt Lake shoreline and associated waterfowl habitat from Landsat data p0252 A81-43742

Active microwave measurements for estimating soil moisture in Oklahoma p0199 A81-43744

An examination of spectral band ratioing to reduce the topographic effect on remotely sensed data p0221 A81-45427

Application of digital terrain data to quantify and reduce the topographic effect on Landsat data p0259 A81-45433

Role of multiple scattering in ozone profile retrieval from satellite measurements in the ultraviolet p0215 A81-45870

Atmospheric correction of Nimbus-7 Coastal Zone Color Scanner imagery p0271 A81-45879

Inventory estimation on the massively parallel processor p0259 A81-46052

Procedure 1 and forestland classification using Landsat data p0201 A81-46055

A search for cold water rings p0235 A81-46116

Magnetic space-based field measurements
[AAS PAPER 81-077] p0272 A81-46241

Landsat observations of snowcover depletion and flooding in the Chesapeake Bay area during the winter of 1979 p0253 A81-48942

Early results from Magsat p0274 A81-48945

ICAP - An Interactive Cluster Analysis Procedure for analyzing remotely sensed data p0261 A81-49345

Landsat - What is operational in water resources p0253 A81-49757

Freshwater ice thickness observations using passive microwave sensors p0254 A81-49968

Effect of forest canopy closure on incoming solar radiance
[E81-10170] p0205 N81-28499

NATIONAL AERONAUTICS AND SPACE ADMINISTRATION. LYNDON B. JOHNSON SPACE CENTER, HOUSTON, TEX.

Advanced synthetic aperture radar for remote sensing p0274 A81-48553

A comparative study of the thematic mapper and LANDSAT spectral bands from field measurement data
[E81-10165] p0209 N81-33549

AgRISTARS: Foreign commodity production forecasting Program review presentation to level 1, Interagency Coordination Committee
[E81-10168] p0209 N81-33555

A crop moisture stress index for large areas and its application in the prediction of spring wheat phenology
[E81-10202] p0210 N81-33573

Experiment plan: Row and roughness effects on dependence of active microwave measurements of soil moisture
[E81-10209] p0211 N81-33575

NATIONAL AERONAUTICS AND SPACE ADMINISTRATION. JOHN F. KENNEDY SPACE CENTER, COCOA BEACH, FLA.

Vegetable crop management with remote sensing p0198 A81-43540

NATIONAL AERONAUTICS AND SPACE ADMINISTRATION. LANGLEY RESEARCH CENTER, HAMPTON, VA.

A radiometric model of an earth radiation budget radiometer optical system with diffuse-specular surfaces p0269 A81-41919

Performance evaluation of a spaceborne scatterometer p0269 A81-41920

Microwave radiometer measurement of tidally induced salinity changes off the Georgia coast p0232 A81-42067

Remote sensing of oceanic phytoplankton - Present capabilities and future goals p0232 A81-42215

Application of remote sensing to monitoring and studying dispersion in ocean dumping p0232 A81-42228

Simulation modeling of estuarine ecosystems p0243 A81-42229

Aerospace remote sensing of the coastal zone for water quality and biotic productivity applications p0233 A81-43246

The study of mesoscale ocean winds p0235 A81-46110

Airborne microwave radiometer remote sensing of lake ice p0253 A81-48554

Remote sensing in biological oceanography p0237 A81-49130

NASA participation in the 1980 Persistent Elevated Pollution Episode/Northeast Regional Oxidant Study (PEPE/NROS) Project: Operational aspects
[NASA-TM-83170] p0220 N81-32708

A comparison of observed and analytically derived remote sensing penetration depths for turbid water
[NASA-TM-83176] p0255 N81-33577

NATIONAL AERONAUTICS AND SPACE ADMINISTRATION. WALLOPS FLIGHT CENTER, WALLOPS ISLAND, VA.

Land subsidence measured by satellite radar altimetry p0270 A81-43260

Airborne simultaneous spectroscopic detection of laser-induced water Raman backscatter and fluorescence from chlorophyll a and other naturally occurring pigments p0253 A81-47647

Altimeter rain detection
[NASA-TM-73291] p0275 N81-29408

Radar altimeter waveform modeled parameter recovery
[NASA-TM-73294] p0275 N81-30325

Gulf of Mexico satellite radar altimetry
[NASA-TM-73295] p0224 N81-33760

NATIONAL GOVERNORS ASSOCIATION/COUNCIL OF STATE PLANNING AGENCIES, WASHINGTON, D. C.

Landsat classification of coastal wetlands in Texas p0248 A81-43234

NATIONAL OCEANIC AND ATMOSPHERIC ADMINISTRATION, BOULDER, COLO.

Categorization of Northern Green Bay ice cover using LANDSAT 1 digital data: A case study
[PB81-200438] p0265 N81-32602

NATIONAL OCEANIC AND ATMOSPHERIC ADMINISTRATION, HOUSTON, TEX.

The environmental vegetation index: A tool potentially useful for arid land management
[E81-10191] p0206 N81-29505

Characteristics, of TIROS, GOES, DMSP and LANDSAT systems
[E81-10192] p0263 N81-29506

Meteorological satellite data: A tool to describe the health of the world's agriculture
[E81-10204] p0207 N81-31596

NATIONAL OCEANIC AND ATMOSPHERIC ADMINISTRATION, MIAMI, FLA.

Drifting buoy data from the tropical Pacific Ocean during NORPAX equatorial test shuttle experiment
[PB81-196939] p0240 N81-31807

NATIONAL OCEANIC AND ATMOSPHERIC ADMINISTRATION, ROCKVILLE, MD.

NOAA Climate Program plan
[PB81-193815] p0240 N81-30765

Environmental assessment of the Alaskan continental shelf: Reports of principal investigators. Volume 1: Reactors - birds, plankton, littoral, benthos
[PB81-196263] p0240 N81-30780

NATIONAL OCEANIC AND ATMOSPHERIC ADMINISTRATION, WASHINGTON, D. C.

Satellite identification of surface radiant temperature fields of subpixel resolution
[PB81-184038] p0265 N81-31615

NORTH CAROLINA STATE UNIV. AT RALEIGH.

Trophic state determination for shallow coastal lakes from Landsat imagery p0251 A81-43259

NORTH CAROLINA STATE UNIV., RALEIGH.

Water quality mapping from Landsat digital data p0252 A81-45429

The use of charge transfer devices for LANDSAT pattern classification
[E81-10087] p0266 N81-33544

P

PENNSYLVANIA STATE UNIV., UNIVERSITY PARK.
ICAP - An Interactive Cluster Analysis Procedure for analyzing remotely sensed data p0261 A81-49345
Environmental measurements of power plant cooling tower and stack plumes
[DOE/EV-02463/6] p0219 N81-30695

PHOENIX CORP., MCLEAN, VA.
Reduction and analysis of satellite magnetometer data p0275 N81-29482
Space based topographic mapping experiment using Seasat synthetic aperture radar and LANDSAT 3 return beam vidicon imagery
[NASA-CR-164675] p0223 N81-30496

PURDUE UNIV., LAFAYETTE, IND.
Using Landsat MSS data with soils information to identify wetland habitats p0249 A81-43236
Waveband evaluation of proposed thematic mapper in forest cover classification p0199 A81-43738
Parallel processing implementations of a contextual classifier for multispectral remote sensing data p0272 A81-46028
An assessment of Landsat data acquisition history on identification and area estimation of corn and soybeans p0200 A81-46032
A model of plant canopy polarization response p0201 A81-46035
Context distribution estimation for contextual classification of multispectral image data p0259 A81-46041
Development of a digital data base for reflectance-related soil information p0201 A81-46051
Procedure 1 and forestland classification using Landsat data p0201 A81-46055
Sampling Landsat classifications for crop area estimation p0202 A81-46404
Evaluation of LANDSAT data analysis for forest survey
[E81-10175] p0210 N81-33561

Q

QEB, INC., LAKEWOOD, COLO.
Airborne gamma-ray spectrometer and magnetometer survey. Canyon City quadrangle (Oregon), volume 2
[DE81-028682] p0229 N81-33584
Airborne gamma-ray spectrometer and magnetometer survey. Salem quadrangle (Oregon), volume 2
[DE81-028681] p0229 N81-33585

R

REMOTE SENSING SYSTEMS, SAUSALITO, CALIF.
Performance evaluation of a spaceborne scatterometer p0269 A81-41920

RICE UNIV., HOUSTON, TEX.
Methods development and applications evaluations of NURE aerial reconnaissance survey data for uranium resource evaluation: Beeville/Bay City and Crystal City quadrangles, Texas
[GJBX-69(81)] p0228 N81-30502

ROYAL AIRCRAFT ESTABLISHMENT, FARNBOROUGH (ENGLAND).
A technique for line extraction from LANDSAT multi-spectral scanner satellite data with some applications of the technique
[RAE-TR-81010] p0265 N81-31613

S

SCIENCE AND EDUCATION ADMINISTRATION, BELTSVILLE, MD.
Aircraft active microwave measurements for estimating soil moisture p0271 A81-43547

SCIENCE AND EDUCATION ADMINISTRATION, PHOENIX, ARIZ.
Soil moisture inferences from thermal infrared measurements of vegetation temperatures
[E81-10184] p0206 N81-29500

SCIENCE AND EDUCATION ADMINISTRATION, WESLACO, TEX.
Methods of editing cloud and atmospheric layer affected pixels from satellite data
[E81-10169] p0266 N81-33556

SCIENCE APPLICATIONS, INC., LA JOLLA, CALIF.
Satellite measurements of tropospheric aerosols
[NASA-CR-3459] p0219 N81-31680
Satellite measurements of atmospheric aerosols
[AD-A103493] p0220 N81-33720

SCRIPPS INSTITUTION OF OCEANOGRAPHY, LA JOLLA, CALIF.
Satellite oceanography - The instruments p0274 A81-49134

SKIDAWAY INST. OF OCEANOGRAPHY, SAVANNAH, GA.
Microwave radiometer measurement of tidally induced salinity changes off the Georgia coast p0232 A81-42067

SMITHSONIAN ASTROPHYSICAL OBSERVATORY, CAMBRIDGE, MASS.
Satellite To Satellite Doppler Tracking (SSDT) for mapping of the Earth's gravity field
[NASA-CR-164722] p0223 N81-31601

SONOMA STATE UNIV., CALIF.
LANDSAT C workshop field/laboratory exercises p0280 N81-32571

SOUTH CAROLINA UNIV., COLUMBIA.
Crop classification with a Landsat/radar sensor combination p0200 A81-46033

SOUTH DAKOTA STATE UNIV., BROOKINGS.
Soil moisture applications of the heat capacity mapping mission p0197 A81-43224
Ground water applications of the heat capacity mapping mission p0248 A81-43233

SRI INTERNATIONAL CORP., MENLO PARK, CALIF.
Radiometry with nighttime DMSP images in digital form p0260 A81-46402

STANFORD UNIV., CALIF.
Atmospheric correction to LANDSAT data for limonite discrimination p0228 N81-31594

SYSTEMS AND APPLIED SCIENCES CORP., RIVERDALE, MD.
Role of multiple scattering in ozone profile retrieval from satellite measurements in the ultraviolet p0215 A81-45870

SYSTEMS CONTROL, INC., WEST PALM BEACH, FLA.
Vegetable crop management with remote sensing p0198 A81-43540

T

TECHNICOLOR GRAPHIC SERVICES, INC., SIOUX FALLS, S. DAK.
A selected bibliography: Remote sensing applications in wildlife management
[PB81-215881] p0211 N81-33598

TECHNISCHE UNIV., GRAZ (AUSTRIA).
A radar image time series p0226 A81-45430

TELESPAZIO, S.P.A., ROME (ITALY).
Some methods of multitemporal analysis of LANDSAT images resulting from a study on Venice Lagoon
[E81-10205] p0267 N81-33574

TEXAS A&M UNIV., COLLEGE STATION.
Soil moisture applications of the heat capacity mapping mission p0197 A81-43224
Ground water applications of the heat capacity mapping mission p0248 A81-43233
Development of advanced acreage estimation methods
[E81-10160] p0205 N81-29495
Dryland pasture and crop conditions as seen by HCMM
[E81-10080] p0209 N81-33542
Measurement of soil moisture trends with airborne scatterometers
[E81-10088] p0209 N81-33545

TEXAS A&M UNIV., GALVESTON.
Applications of Landsat imagery to a coastal inlet stability study p0250 A81-43249

TEXAS UNIV., AUSTIN.
Landsat classification of coastal wetlands in Texas p0248 A81-43234
Orbit determination requirements for TOPEX
[AAS PAPER 81-158] p0221 A81-45828

TULSA UNIV., OKLA.
Maximum likelihood estimation for mixture models
[E81-10178] p0210 N81-33564

U

UNIVERSITE CATHOLIQUE DE LOUVAIN (BELGIUM).
Study of the influence of the atmosphere on the performance of an imaging microwave radiometer
[ESA-CR(P)-1421] p0275 N81-30342

UTAH UNIV., SALT LAKE CITY.
Mapping the Great Salt Lake shoreline and associated waterfowl habitat from Landsat data p0252 A81-43742

V

VERMONT UNIV., BURLINGTON.
The development of a remote sensing applications program for Vermont
[E81-10149] p0266 N81-33547

VIRGINIA INST. OF MARINE SCIENCE, GLOUCESTER POINT.
Bay of Fundy verification of a system for multidate Landsat measurement of suspended sediment p0250 A81-43254
Landsat - What is operational in water resources p0253 A81-49757

VIRGINIA POLYTECHNIC INST. AND STATE UNIV., BLACKSBURG.
Nationwide forestry applications program. Analysis of forest classification accuracy
[E81-10183] p0206 N81-29499

W

WASHINGTON UNIV., SEATTLE.
Comparison of laboratory reflectance spectra and LANDSAT multispectral images of Hawaiian lava flows
[E81-10061] p0266 N81-33541

WISCONSIN UNIV., MADISON.
Investigation of Antarctic crust and upper mantle using Magsat and other geophysical data
[E81-10113] p0222 N81-32574

WORLD METEOROLOGICAL ORGANIZATION, GENEVA (SWITZERLAND).
Reports on Marine Science Affairs. Report 14: Satellite data requirements for marine meteorological services
[WMO-548] p0239 N81-28668

Z

ZEISS (CARL), OBERKOCHEN (WEST GERMANY).
Application of new precision measuring systems for photogrammetric comparators
[BMFT-FB-T-80-134] p0276 N81-32595

CONTRACT NUMBER INDEX

Earth Resources/*A Continuing Bibliography (Issue 32)* JANUARY 1982

Typical Contract Number Index Listing

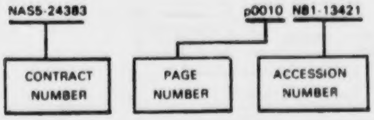

Listings in this index are arranged alphanumerically by contract number. Under each contract number, the accession numbers denoting documents that have been produced as a result of research done under that contract are arranged in ascending order with the AIAA accession numbers appearing first. The accession number denotes the number by which the citation is identified in the abstract section. Preceding the accession number is the page number on which the citation may be found.

AF PROJ 3204 p0222 N81-33581
AT(11-1)-2463 p0219 N81-30695
BLM-025-08 p0233 A81-43250
DAAG29-77-G-0075 p0272 A81-46038
DAAG29-79-C-0199 p0202 A81-49347
DAAG29-80-K-0018 p0265 N81-33347
DAAK70-77-C-0110 p0264 N81-30852
DAAK70-79-C-0153 p0264 N81-30499
DACW39-77-C-0073 p0202 A81-49347
DE-AC08-76NV-01183 p0228 N81-30502
DE-AC13-76GJ-01664 p0228 N81-30502
DE-AC13-79GJ-01692 p0229 N81-32592
p0229 N81-33584
p0229 N81-33585
DE-AS02-76EV-02463 p0219 N81-30695
DE-AS09-80EV-1033 p0232 A81-42067
DI PROJECT A-089-NY p0252 A81-43745
p0252 A81-46405
DI-B-066-ARIZ p0225 A81-43227
DI-14-08-0001-16439 p0211 N81-33598
DI-14-08-0001-18656 p0264 N81-29522
DOC/NA80AA-D-0019 p0254 N81-30509
DRXR-OPR-P-17227-EL p0265 N81-33350
DSS-1SB-79-00097 p0239 A81-49805
DSS-1SU-78-00347 p0238 A81-49771
E(11-1)-2463 p0219 N81-30695
EPA-R-803611 p0254 N81-29520
EPA-68-01-5801 p0255 N81-33593
ESA-3632/78-F-CG(SC) p0239 N81-30168
ESA-4428/80 p0236 A81-47348
ESTEC-4124/79-NL-DG(SC) p0275 N81-30342
EY-71-5-09-0802 p0233 A81-43250
F07401-78-C-0193 p0261 A81-48552
F19628-77-C-0152 p0222 N81-33581
F19628-80-C-0052 p0260 A81-46378
F30602-80-C-0002 p0264 N81-30723
JPL-954940 p0199 A81-43741
p0199 A81-43743
JPL-955998 p0223 N81-30496
NAG2-57 p0210 N81-33558
p0210 N81-33559
NAG5-10 p0270 A81-43071
NAG5-36 p0223 N81-31601
NAG5-141 p0260 A81-46378
NASA ORDER S-58376-G p0202 A81-46406
NASA ORDER S-75406-B p0266 N81-33556
NASA ORDER-S-40256-B p0224 N81-33589
NASW-3113 p0279 N81-32086
NAS1-16042 p0229 N81-33548
NAS3-21924 p0241 N81-33539
NAS5-2406 p0197 A81-43224
NAS5-20983 p0233 A81-43539
NAS5-20986 p0248 A81-43234
NAS5-22929 p0271 A81-45872
p0271 A81-45873
NAS5-22963 p0271 A81-45879
NAS5-23639 p0276 N81-33540
NAS5-23777 p0246 A81-43209
NAS5-24206 p0248 A81-43233
NAS5-24383 p0209 N81-33542
NAS5-25527 p0270 A81-43225
NAS5-25529 p0270 A81-43225
NAS5-25977 p0222 N81-32574
NAS6-2639 p0270 A81-43260
NAS6-2960 p0219 N81-32581
NAS6-3117 p0240 N81-31605
NAS7-100 p0231 A81-41974
p0232 A81-42622
p0247 A81-43211
p0258 A81-43734
p0214 A81-43749
p0226 A81-45430
p0271 A81-45836
p0272 A81-46038
p0237 A81-49133
p0239 A81-49967
NAS8-31984 p0251 A81-43259
NAS9-14052 p0270 A81-43223
NAS9-14251 p0199 A81-43741
NAS9-14565 p0206 N81-29504
NAS9-14689 p0205 N81-29495
NAS9-14970 p0202 A81-46404
NAS9-15421 p0200 A81-46033
NAS9-15466 p0272 A81-46028
p0200 A81-46032
p0201 A81-46035
p0259 A81-46041
p0201 A81-46051
NAS9-15476 p0201 A81-46036
p0206 N81-29504
NAS9-15683 p0263 N81-29502
NAS9-15800 p0259 A81-46040
p0205 N81-28498
p0205 N81-29494
p0263 N81-29497
p0263 N81-29498
p0263 N81-29501
p0206 N81-29507
p0206 N81-29508
p0264 N81-29509
p0264 N81-29510
p0207 N81-31596
p0207 N81-31597
p0207 N81-31598
p0207 N81-31599
p0208 N81-32576
p0209 N81-33546
p0267 N81-33562
p0210 N81-33564
p0210 N81-33565
p0210 N81-33573
NAS9-15889 p0199 A81-43738
NAS9-15981 p0263 N81-29503
p0264 N81-31600
p0267 N81-33563
NAS10-8920 p0202 A81-46895
NATO-SRG-10 p0231 A81-42026
NCC5-22 p0209 N81-33543
NGL-05-003-404 p0199 A81-43740
NGL-06-003-200 p0252 A81-46045
p0262 A81-49804
NGL-15-005-186 p0249 A81-43236
NGL-17-004-024 p0198 A81-43265
NGL-24-005-263 p0254 N81-33550
NGL-33-010-071 p0216 A81-46407
NGL-33-010-171 p0252 A81-43745
p0252 A81-46405
p0255 N81-33560
NGL-47-022-005 p0250 A81-43254
NGR-53-3182-0-29 p0208 N81-32578
NOAA-MO-A01-78-00-4330 p0235 A81-46112
NOAA-MO-A01-78-00-4339 p0235 A81-46113
NOAA-04-158-44046 p0250 A81-43252
NSERC-GA-5586 p0262 A81-49793
NSF ENG-79-09374 p0265 N81-33347
NSF MCS-78-04366 p0259 A81-46041
NSF OCE-16827 p0240 N81-31807
NSG-2208 p0213 A81-43261
NSG-5075 p0245 A81-43197
NSG-5134 p0209 N81-33545
NSG-5256 p0251 A81-43545
p0252 A81-45429
NSG-7453 p0266 N81-33547
N0014-74-C-0273 p0217 A81-49346
N0014-78-C-0458 p0217 A81-49346
N00014-75-C-0152 p0236 A81-47022
N00014-75-C-0291 p0231 A81-41350
N00014-77-C-0489 p0220 N81-33720
N00014-79-C-0413 p0231 A81-41350
N00014-79-G-0039 p0234 A81-45861
N00014-80-C-0073 p0265 N81-33350
N00014-80-C-0708 p0265 N81-33350
PROJ. AGRISTARS p0205 N81-28497
p0205 N81-28498
p0205 N81-28499
p0205 N81-29494
p0205 N81-29495
p0219 N81-29496
p0263 N81-29497
p0263 N81-29498
p0206 N81-29499
p0206 N81-29500
p0263 N81-29501
p0263 N81-29502
p0263 N81-29503
p0206 N81-29504
p0206 N81-29505
p0263 N81-29506
p0206 N81-29507
p0206 N81-29508
p0264 N81-29510
p0206 N81-29511
p0207 N81-31596
p0207 N81-31597
p0207 N81-31598
p0207 N81-31599
p0264 N81-31600
p0208 N81-32576
p0208 N81-32577
p0209 N81-33546
p0229 N81-33548
p0209 N81-33549
p0209 N81-33555
p0267 N81-33557
p0267 N81-33563
p0210 N81-33564
p0210 N81-33565
p0210 N81-33573
p0211 N81-33575
STU-76-6669 p0272 A81-46030
p0226 A81-46039
STU-77-6345 p0272 A81-46030
p0226 A81-46039
USBR-8-07-83-V0016 p0245 A81-43193
USDA-53-3187-8-25 p0199 A81-43732
USDA-53-3197 8-19 p0202 A81-46056
USGS-14-08-0001-3185 p0248 A81-43231
USGS-14-08-0001-12510 p0248 A81-43233
USGS-14-08-0001-13169 p0248 A81-43231
p0251 A81-43257
USGS-14-08-0001-13185 p0251 A81-43257
USGS-14-08-0001-13576 p0226 A81-43228
p0249 A81-43240
W-7405-ENG-36 p0223 N81-30505
W-7405-ENG-48 p0219 N81-29517
63-2455-2379 p0264 N81-29509
146-20-10-30 p0220 N81-32708
146-40-06 p0241 N81-33539
663-80-02-01 p0279 N81-32564
691-09-02-09 p0229 N81-33548

REPORT/ACCESSION NUMBER INDEX

Typical Report/Accession Number Index Listing

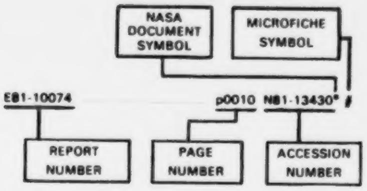

Listings in this index are arranged alphanumerically by report number. The page number indicates the page on which the citation is located. The accession number denotes the number by which the citation is identified. An asterisk (*) indicates that the item is a NASA report. A pound sign (#) indicates that the item is available on microfiche.

A-8336 p0279 N81-32564* #

AAS PAPER 81-053 p0278 A81-46234 #
AAS PAPER 81-060 p0278 A81-46238 #
AAS PAPER 81-077 p0272 A81-46241* #
AAS PAPER 81-158 p0221 A81-45828* #
AAS PAPER 81-182 p0271 A81-45836* #

AAS 80-062 p0200 A81-44637

AD-A101105 p0241 N81-33763 #
AD-A101172 p0275 N81-29512 #
AD-A101319 p0264 N81-30852 #
AD-A101321 p0264 N81-30499 #
AD-A101728 p0264 N81-30723 #
AD-A102343 p0240 N81-31803 #
AD-A102809 p0228 N81-32587 #
AD-A102810 p0219 N81-32586 #
AD-A102896 p0208 N81-32588 #
AD-A103378 p0222 N81-33578 #
AD-A103493 p0220 N81-33720 #
AD-A104038 p0222 N81-33581 #

AERONOMICA-ACTA-A-227-1980 p0219 N81-30656

AFGL-TR-81-0028 p0222 N81-33581 #

AFIT/GCS/EE/80-14 p0222 N81-33578 #

AGESS-810223 p0208 N81-31614 #
AGESS-810408 p0207 N81-30507 #
AGESS-810414 p0207 N81-30511 #

ATR-81(7805)-1 p0219 N81-32581* #

BF-R-64-028-01 p0211 N81-33588 #

BMFT-FB-T-80-134 p0276 N81-32595 #

BMFT-FB-W-80-029 p0267 N81-33587 #
BMFT-FB-W-80-037 p0211 N81-33588 #

BR78637 p0265 N81-31613 #

CONF-810557-1 p0223 N81-30505 #

DC-LI-04051 p0206 N81-29511* #

DC-Y1-04069 p0267 N81-33557* #
DC-Y1-04089 p0219 N81-29496* #

DE81-027157 p0229 N81-32592 #
DE81-028681 p0229 N81-33585 #
DE81-028682 p0229 N81-33584 #

DOE/EV-02463/6 p0219 N81-30695 #

EGG-004-77 p0276 N81-33540* #

EPA-600/3-80-075 p0254 N81-29520 #
EPA-600/3-81-037 p0255 N81-33593 #

ERC-07-80 p0207 N81-30508 #

ERIM-152400-1-X p0206 N81-29504* #

ESA-CR(P)-1421 p0275 N81-30342 #
ESA-CR(P)-1433 p0239 N81-30168 #

ESA-SP-166 p0208 N81-33339 #

ESS/SS-1035 p0239 N81-30168 #

ETL-R018 p0219 N81-32586 #
ETL-R019 p0228 N81-32587 #
ETL-R020 p0208 N81-32588 #

ETL-0241 p0264 N81-30499 #
ETL-0258 p0264 N81-30852 #

EW-LO-00706 p0263 N81-29501* #

EW-NI-04042 p0207 N81-31596* #
EW-NI-04076 p0206 N81-29505* #

EW-N1-04075 p0263 N81-29506* #

EW-UL-04074 p0205 N81-28497* #

EW-U1-04068 p0206 N81-29500* #

E81-10044 p0241 N81-33539* #
E81-10056 p0276 N81-33540* #
E81-10061 p0266 N81-33541* #
E81-10080 p0209 N81-33542* #
E81-10081 p0209 N81-33543* #
E81-10087 p0266 N81-33544* #
E81-10088 p0209 N81-33545* #
E81-10113 p0222 N81-32574* #
E81-10114 p0205 N81-29494* #
E81-10132 p0209 N81-33546* #
E81-10149 p0266 N81-33547* #
E81-10155 p0229 N81-33548* #
E81-10160 p0205 N81-29495* #
E81-10161 p0219 N81-29496* #
E81-10162 p0263 N81-29497* #
E81-10164 p0205 N81-28497* #
E81-10165 p0209 N81-33549* #
E81-10166 p0254 N81-33550* #
E81-10167 p0205 N81-28498* #
E81-10168 p0209 N81-33555* #
E81-10169 p0266 N81-33556* #
E81-10170 p0205 N81-28499* #
E81-10171 p0267 N81-33557* #
E81-10172 p0210 N81-33558* #
E81-10173 p0210 N81-33559* #
E81-10174 p0255 N81-33560* #
E81-10175 p0210 N81-33561* #
E81-10176 p0267 N81-33562* #
E81-10177 p0267 N81-33563* #
E81-10178 p0210 N81-33564* #
E81-10179 p0210 N81-33565* #
E81-10181 p0228 N81-32575* #
E81-10182 p0263 N81-29498* #
E81-10183 p0206 N81-28499* #
E81-10184 p0206 N81-29500* #
E81-10185 p0263 N81-29501* #
E81-10186 p0263 N81-29502* #
E81-10189 p0263 N81-29503* #
E81-10190 p0206 N81-29504* #
E81-10191 p0206 N81-29505* #
E81-10192 p0263 N81-29506* #
E81-10193 p0206 N81-29507* #
E81-10197 p0206 N81-29508* #
E81-10198 p0264 N81-29509* #
E81-10199 p0264 N81-29510* #
E81-10200 p0206 N81-29511* #
E81-10202 p0210 N81-33573* #
E81-10203 p0208 N81-32576* #
E81-10204 p0207 N81-31596* #
E81-10205 p0267 N81-33574* #
E81-10206 p0207 N81-31597* #
E81-10207 p0207 N81-31598* #
E81-10208 p0207 N81-31599* #
E81-10209 p0211 N81-33575* #
E81-10210 p0264 N81-31600* #
E81-10211 p0208 N81-32577* #

FC-E1-00712 p0206 N81-29504* #

FC-JO-04010 p0209 N81-33555* #

FC-LO-04000 p0207 N81-31597* #
FC-LO-04014 p0207 N81-31599* #

FC-L0-00464 p0210 N81-33565* #
FC-L1-04030 p0206 N81-29508* #

GJBX-69(81) p0228 N81-30502 #
GJBX-211(81) p0229 N81-32592 #
GJBX-240-81-VOL-2-(SALEM) p0229 N81-33585 #
GJBX-240-81-V2-(CANYON-CITY) p0229 N81-33584 #

GPO-79-432-VOL-4 p0279 N81-31030 #

IAF PAPER 81-80 p0273 A81-47338
IAF PAPER 81-88 p0273 A81-47342
IAF PAPER 81-90 p0236 A81-47344
IAF PAPER 81-91 p0273 A81-47345
IAF PAPER 81-92 p0278 A81-47346
IAF PAPER 81-94 p0236 A81-47348
IAF PAPER 81-98 p0260 A81-47349
IAF PAPER 81-101 p0278 A81-47350
IAF PAPER 81-102 p0260 A81-47351
IAF PAPER 81-104 p0261 A81-47352
IAF PAPER 81-107 p0227 A81-47353
IAF PAPER 81-108 p0202 A81-47354
IAF PAPER 81-112 p0278 A81-47355
IAF PAPER 81-114 p0253 A81-47356
IAF PAPER 81-120 p0216 A81-47359
IAF PAPER 81-121 p0273 A81-47360
IAF PAPER 81-212 p0273 A81-47407
IAF PAPER 81-214 p0274 A81-47409
IAF PAPER 81-263 p0216 A81-47430
IAF PAPER 81-289 p0216 A81-47433

INPE-1952-RPE/267 p0228 N81-32576* #
INPE-1975-RPE/280 p0240 N81-30498 #

ISBN-92-63-10548-0 p0239 N81-28668 #

ISSN-0170-1339 p0267 N81-33587 #
ISSN-0170-1339 p0211 N81-33588 #
ISSN-0340-7608 p0276 N81-32595 #
ISSN-0379-6566 p0208 N81-33339 #
ISSN-0469-4236 p0222 N81-33527 #

ITEK-81-8449A-2 p0264 N81-29522 #

JPL-9950582 p0223 N81-30496* #

JSC-16357 p0205 N81-29494* #
JSC-16368 p0210 N81-33565* #
JSC-16378 p0263 N81-29498* #
JSC-16821 p0263 N81-29501* #
JSC-16822 p0211 N81-33575* #
JSC-16826 p0207 N81-31598* #
JSC-16827 p0207 N81-31597* #
JSC-16832 p0210 N81-33564* #
JSC-16835 p0209 N81-33555* #
JSC-16837 p0208 N81-32576* #
JSC-16840 p0207 N81-31599* #
JSC-16846 p0206 N81-29507* #
JSC-16849 p0209 N81-33549* #
JSC-16850 p0206 N81-29508* #
JSC-16853 p0263 N81-29502* #
JSC-16857 p0208 N81-32577* #
JSC-17015 p0264 N81-29509* #
JSC-17017 p0267 N81-33562* #
JSC-17112 p0207 N81-31596* #
JSC-17116 p0206 N81-29511* #
JSC-17120 p0209 N81-33546* #
JSC-17121 p0210 N81-33573* #
JSC-17123 p0206 N81-29499* #
JSC-17124 p0264 N81-29510* #
JSC-17125 p0206 N81-29500* #
JSC-17127 p0263 N81-29497* #
JSC-17128 p0205 N81-28498* #
JSC-17130 p0205 N81-28497* #
JSC-17131 p0263 N81-29506* #
JSC-17132 p0206 N81-29505* #

L-14584 p0220 N81-32708* #

LA-UR-81-1454 p0223 N81-30505 #

LARS-TR-101880 p0210 N81-33561* #

LC-78-61696 p0279 N81-32564* #

LEMSCO-14600 p0205 N81-29494* #
LEMSCO-14807 p0263 N81-29498* #
LEMSCO-14808 p0210 N81-33565* #
LEMSCO-14880 p0210 N81-33564* #
LEMSCO-15181 p0211 N81-33575* #
LEMSCO-15305 p0207 N81-31598* #
LEMSCO-15404 p0207 N81-31597* #
LEMSCO-15608 p0263 N81-29501* #
LEMSCO-15612 p0207 N81-31599* #
LEMSCO-15676 p0205 N81-28498* #
LEMSCO-15683 p0263 N81-29502* #
LEMSCO-15691 p0208 N81-32578* #
LEMSCO-15698 p0208 N81-32576* #
LEMSCO-15763 p0206 N81-29511* #
LEMSCO-15903 p0264 N81-29509* #
LEMSCO-15904 p0267 N81-33562* #
LEMSCO-15936 p0206 N81-29508* #
LEMSCO-15971 p0263 N81-29497* #
LEMSCO-15978 p0207 N81-31596* #
LEMSCO-16021 p0264 N81-29510* #
LEMSCO-16216 p0210 N81-33573* #
LEMSCO-16325 p0209 N81-33546* #
LEMSCO-16572 p0206 N81-29507* #

MU-L1-04056 p0209 N81-33546* #

NACOA-18 p0240 N81-31808 #

NAS-811 p0263 N81-29503* #
NAS-811 p0267 N81-33563* #

NASA-CP-2155 p0279 N81-32564* #

NASA-CR-3459 p0219 N81-31680* #
NASA-CR-156877 p0240 N81-31605* #
NASA-CR-156878 p0222 N81-31604* #
NASA-CR-156879 p0219 N81-32581* #
NASA-CR-160938 p0263 N81-29501* #
NASA-CR-160939 p0263 N81-29502* #
NASA-CR-160948 p0267 N81-33563* #
NASA-CR-160949 p0206 N81-29499* #
NASA-CR-160951 p0208 N81-32577* #
NASA-CR-160953 p0207 N81-31596* #
NASA-CR-160954 p0206 N81-29500* #
NASA-CR-160961 p0267 N81-33562* #
NASA-CR-160965 p0263 N81-29498* #
NASA-CR-160966 p0205 N81-29494* #
NASA-CR-160967 p0210 N81-33564* #
NASA-CR-160968 p0210 N81-33565* #
NASA-CR-160969 p0207 N81-31597* #
NASA-CR-160970 p0207 N81-31598* #
NASA-CR-160971 p0207 N81-31599* #
NASA-CR-160973 p0264 N81-31600* #
NASA-CR-160974 p0263 N81-29503* #
NASA-CR-160975 p0206 N81-29504* #
NASA-CR-160977 p0206 N81-29508* #
NASA-CR-160978 p0206 N81-29505* #
NASA-CR-160979 p0263 N81-29506* #
NASA-CR-160980 p0206 N81-29507* #
NASA-CR-160983 p0205 N81-28498* #
NASA-CR-160984 p0263 N81-29497* #
NASA-CR-160985 p0205 N81-28497* #
NASA-CR-160998 p0206 N81-29511* #
NASA-CR-161000 p0264 N81-29509* #
NASA-CR-161001 p0264 N81-29510* #
NASA-CR-161004 p0205 N81-29495* #
NASA-CR-161005 p0208 N81-32576* #
NASA-CR-161035 p0209 N81-33546* #
NASA-CR-161082 p0208 N81-32578* #
NASA-CR-164107 p0222 N81-32574* #
NASA-CR-164565 p0210 N81-33558* #
NASA-CR-164566 p0210 N81-33559* #
NASA-CR-164567 p0255 N81-33560* #
NASA-CR-164675 p0223 N81-30496* #
NASA-CR-164693 p0228 N81-32575* #
NASA-CR-164722 p0223 N81-31601* #
NASA-CR-164733 p0279 N81-32086* #
NASA-CR-164748 p0266 N81-33541* #
NASA-CR-164749 p0209 N81-33542* #
NASA-CR-164750 p0209 N81-33543* #
NASA-CR-164751 p0266 N81-33544* #
NASA-CR-164752 p0209 N81-33545* #
NASA-CR-164754 p0210 N81-33561* #
NASA-CR-164768 p0254 N81-33550* #
NASA-CR-164769 p0266 N81-33556* #
NASA-CR-164770 p0267 N81-33574* #
NASA-CR-164871 p0266 N81-33547* #
NASA-CR-165335 p0241 N81-33539* #
NASA-CR-165762 p0229 N81-33548* #
NASA-CR-166660 p0276 N81-33540* #

NASA-NEWS-RELEASE-81-129 p0228 N81-29143*

NASA-TM-73291 p0275 N81-29408* #
NASA-TM-73294 p0275 N81-30325* #
NASA-TM-73295 p0224 N81-33760* #
NASA-TM-82113 p0205 N81-28499* #
NASA-TM-82289 p0219 N81-29496* #
NASA-TM-83170 p0220 N81-32708* #
NASA-TM-83176 p0255 N81-33577* #
NASA-TM-84030 p0209 N81-33555* #
NASA-TM-84032 p0209 N81-33549* #
NASA-TM-84033 p0267 N81-33557* #
NASA-TM-84035 p0210 N81-33573* #
NASA-TM-84048 p0211 N81-33575* #

NOAA-TM-ERL-AOML-45 p0240 N81-31807 #

NOAA-TM-ERL-GLERL-33 p0265 N81-32602 #

NOAA-TM-NESS-113 p0265 N81-31615 #

NOAA-81021104 p0254 N81-30509 #
NOAA-81021710 p0265 N81-31615 #
NOAA-81022305 p0240 N81-30765 #
NOAA-81031705 p0240 N81-31807 #
NOAA-81032301 p0265 N81-32602 #

NSTL/ERL-196 p0219 N81-29496* #
NSTL/ERL-197 p0267 N81-33557* #

OWRT-A-049-ME(2) p0255 N81-33599 #
OWRT-A-083-GA(1) p0207 N81-30508 #

P-3970-F p0241 N81-33539* #

PB81-173841 p0254 N81-29520 #
PB81-184038 p0265 N81-31615 #
PB81-184137 p0207 N81-30508 #
PB81-185555 p0264 N81-29522 #
PB81-186751 p0208 N81-31614 #
PB81-188625 p0254 N81-30509 #
PB81-192783 p0207 N81-30507 #
PB81-193815 p0240 N81-30765 #
PB81-196263 p0240 N81-30780 #
PB81-196909 p0207 N81-30511 #
PB81-198939 p0240 N81-31807 #
PB81-200438 p0265 N81-32602 #
PB81-200602 p0240 N81-31808 #
PB81-209157 p0255 N81-33599 #
PB81-209561 p0255 N81-33593 #
PB81-211781 p0224 N81-33589 #
PB81-215881 p0211 N81-33598 #

PR-3712-9 p0209 N81-33542* #

PUBL-1810 p0275 N81-29480* #

P81-10131 p0228 N81-29143*

QR-1 p0266 N81-33556* #
QR-2 p0266 N81-33556* #

QSTPR-4 p0222 N81-32574* #

RADC-TR-81-63 p0264 N81-30723 #

RAE-SPACE-592 p0265 N81-31613 #

RAE-TR-81010 p0265 N81-31613 #

REPT-14 p0239 N81-28668 #

RR-G1-04085 p0205 N81-28499* #

RR-U1-04086 p0206 N81-29499* #

RSC-3458-5 p0209 N81-33545* #

RSL-RR-80-6 p0254 N81-30509 #

SAI-131-80-578-LJ p0219 N81-31680* #
SAI-131-81-275-LJ p0220 N81-33720 #

SASR-3 p0209 N81-33543* #
SASR-18 p0255 N81-33560* #

SCIENTIFIC-5 p0222 N81-33581 #

SM-J0-00613 p0211 N81-33575* #

SM-L0-00441 p0205 N81-29494* #
SM-L0-04021 p0206 N81-29507* #

SR-IX-04046 p0264 N81-31600* #

SR-J0-04007 p0210 N81-33564* #
SR-J0-04029 p0209 N81-33549* #

SR-L0-00478 p0263 N81-29498* #
SR-L0-00499 p0207 N81-31598* #
SR-L0-04012 p0208 N81-32576* #

SR-L1-04031 p0263 N81-29502* #
SR-L1-04054 p0205 N81-28498* #
SR-L1-04064 p0210 N81-33573* #
SR-L1-04067 p0264 N81-29510* #
SR-L1-04071 p0263 N81-29497* #

SR-TI-04112 p0205 N81-29495* #

SR-XI-04053 p0263 N81-29503* #

SR-X1-04041 p0267 N81-33563* #

UCRL-84501 p0219 N81-29517 #

USGS-GD-81-002 p0224 N81-33589 #

USGS/NMD-81-001 p0264 N81-29522 #

WMO-548 p0239 N81-28668 #

W81-02428 p0207 N81-30508 #
W81-03252 p0255 N81-33599 #

YM-J1-C0618 p0208 N81-32577* #

1. Report No.
NASA SP-7041 (32)

2. Government Accession No.

3. Recipient's Catalog No.

4. Title and Subtitle
EARTH RESOURCES
A Continuing Bibliography (Issue 32)

5. Report Date
January 1982

6. Performing Organization Code

7. Author(s)

8. Performing Organization Report No.

9. Performing Organization Name and Address
National Aeronautics and Space Administration
Washington, D.C. 20546

10. Work Unit No.

11. Contract or Grant No.

12. Sponsoring Agency Name and Address

13. Type of Report and Period Covered

14. Sponsoring Agency Code

15. Supplementary Notes

16. Abstract

This bibliography list 580 reports, articles, and other documents introduced into the NASA scientific and technical information system between October 1 and December 31, 1981. Emphasis is placed on the use of remote sensing and geophysical instrumentation in spacecraft and aircraft to survey and inventory natural resources and urban areas. Subject matter is grouped according to agriculture and forestry, environmental changes and cultural resources, geodesy and cartography, geology and mineral resources, hydrology and water management, data processing and distribution systems, instrumentation and sensors, and economic analysis.

17. Key Words (Suggested by Author(s))
Bibliographies
Earth Resources
Remote Sensors

18. Distribution Statement
Unclassified - Unlimited

19. Security Classif. (of this report)
Unclassified

20. Security Classif. (of this page)
Unclassified

21. No. of Pages
146

22. Price*
$10.50 HC

*For sale by the National Technical Information Service, Springfield, Virginia 22161

NASA-Langley, 1982

PUBLIC COLLECTIONS OF NASA DOCUMENTS

DOMESTIC

NASA distributes its technical documents and bibliographic tools to eleven special libraries located in the organizations listed below. Each library is prepared to furnish the public such services as reference assistance, interlibrary loans, photocopy service, and assistance in obtaining copies of NASA documents for retention.

CALIFORNIA
University of California, Berkeley
COLORADO
University of Colorado, Boulder
DISTRICT OF COLUMBIA
Library of Congress
GEORGIA
Georgia Institute of Technology, Atlanta
ILLINOIS
The John Crerar Library, Chicago
MASSACHUSETTS
Massachusetts Institute of Technology, Cambridge
MISSOURI
Linda Hall Library, Kansas City
NEW YORK
Columbia University, New York
OKLAHOMA
University of Oklahoma, Bizzell Library
PENNSYLVANIA
Carnegie Library of Pittsburgh
WASHINGTON
University of Washington, Seattle

NASA publications (those indicated by an '*' following the accession number) are also received by the following public and free libraries:

CALIFORNIA
Los Angeles Public Library
San Diego Public Library
COLORADO
Denver Public Library
CONNECTICUT
Hartford Public Library
MARYLAND
Enoch Pratt Free Library, Baltimore
MASSACHUSETTS
Boston Public Library
MICHIGAN
Detroit Public Library
MINNESOTA
Minneapolis Public Library and Information Center
NEW JERSEY
Trenton Public Library
NEW YORK
Brooklyn Public Library
Buffalo and Erie County Public Library
Rochester Public Library
New York Public Library
OHIO
Akron Public Library
Cincinnati and Hamilton County Public Library
Cleveland Public Library
Dayton Public Library
Toledo and Lucas County Public Library
TEXAS
Dallas Public Library
Fort Worth Public Library
WASHINGTON
Seattle Public Library
WISCONSIN
Milwaukee Public Library

An extensive collection of NASA and NASA-sponsored documents and aerospace publications available to the public for reference purposes is maintained by the American Institute of Aeronautics and Astronautics, Technical Information Service, 555 West 57th Street, 12th Floor, New York, New York 10019.

EUROPEAN

An extensive collection of NASA and NASA-sponsored publications is maintained by the British Library Lending Division, Boston Spa, Wetherby, Yorkshire, England. By virtue of arrangements other than with NASA, the British Library Lending Division also has available many of the non-NASA publications cited in *STAR*. European requesters may purchase facsimile copy of microfiche of NASA and NASA-sponsored documents, those identified by both the symbols '#' and '*', from: ESA - Information Retrieval Service, European Space Agency, 8-10 rue Mario-Nikis, 75738 Paris CEDEX 15, France.

National Aeronautics and
Space Administration

Washington, D.C.
20546

Official Business
Penalty for Private Use, $300

THIRD-CLASS BULK RATE

Postage and Fees Paid
National Aeronautics and
Space Administration
NASA-451

U.S.MAIL

POSTMASTER: If Undeliverable (Section 158
Postal Manual) Do Not Return

7041 (33)

NASA

Earth Resources
A Continuing
Bibliography
with Indexes

NASA SP-7041(33)
April 1982

NEWARK PUBLIC LIBRARY

AUG 25 1982

U. S. GOVT. PUBS.
DEPOSITORY 376

National Aeronautics and
Space Administration

es Earth Resourc
s Earth Resources
arth Resources E
th Resources Ear
Resources Earth
esources Earth R
sources Earth Res

NAS 1.21:

NASA SP-7041(33)

Earth Resources
A Continuing Bibliography with Indexes

ACCESSION NUMBER RANGES

Accession numbers cited in this Supplement fall within the following ranges.

STAR (N-10000 Series)	N82-10001 - N82-16039
IAA (A-10000 Series)	A82-10001 - A82-18839

This bibliography was prepared by the NASA Scientific and Technical Information Facility operated for the National Aeronautics and Space Administration by PRC Government Information Systems.

NASA SP-7041(33)

EARTH RESOURCES

A CONTINUING BIBLIOGRAPHY WITH INDEXES

Issue 33

A selection of annotated references to unclassified reports and journal articles that were introduced into the NASA scientific and technical information system and announced between January 1 and March 31, 1982 in

- *Scientific and Technical Aerospace Reports (STAR)*
- *International Aerospace Abstracts (IAA).*

Scientific and Technical Information Branch 1982
National Aeronautics and Space Administration
Washington, DC

This supplement is available as NTISUB/038/093 from the National Technical Information Service (NTIS), Springfield, Virginia 22161 at the price of $10.50 domestic; $21.50 foreign for standing orders. Please note: Standing orders are subscriptions which do not terminate at the end of a year, as do regular subscriptions, but continue indefinitely unless specifically terminated by the subscriber.

INTRODUCTION

The technical literature described in this continuing bibliography may be helpful to researchers in numerous disciplines such as agriculture and forestry, geography and cartography, geology and mining, oceanography and fishing, environmental control, and many others. Until recently it was impossible for anyone to examine more than a minute fraction of the Earth's surface continuously. Now vast areas can be observed synoptically, and changes noted in both the Earth's lands and waters, by sensing instrumention on orbiting spacecraft or on aircraft.

This literature survey lists 436 reports, articles, and other documents announced between January 1 and March 31, 1982 in *Scientific and Technical Aerospace Reports (STAR)*, and *International Aerospace Abstracts (IAA)*.

The coverage includes documents related to the identification and evaluation by means of sensors in spacecraft and aircraft of vegetation, minerals, and other natural resources, and the techniques and potentialities of surveying and keeping up-to-date inventories of such riches. It encompasses studies of such natural phenomena as earthquakes, volcanoes, ocean currents, and magnetic fields; and such cultural phenomena as cities, transportation networks, and irrigation systems. Descriptions of the components and use of remote sensing and geophysical instrumentation, their subsystems, observational procedures, signature and analyses and interpretive techniques for gathering data are also included. All reports generated under NASA's Earth Resources Survey Program for the time period covered in this bibliography will also be included. The bibliography does not contain citations to documents dealing mainly with satellites or satellite equipment used in navigation or communication systems, nor with instrumentation not used aboard aerospace vehicles.

The selected items are grouped in nine categories. These are listed in the Table of Contents with notes regarding the scope of each category. These categories were especially chosen for this publication, and differ from those found in *STAR* and *IAA*.

Each entry consists of a standard bibliographic citation accompanied by an abstract. The citations and abstracts are reproduced exactly as they appeared originally in *STAR*, or *IAA*, including the original accession numbers from the respective announcement journals. This procedure, which saves time and money, accounts for the variation in citation appearance.

Under each of the nine categories, the entries are presented in one of two groups that appear in the following order:

IAA entries identified by accession number series A82-10,000 in ascending accession number order;

STAR entries identified by accession number series N82-10,000 in ascending accession number order.

After the abstract section, there are five indexes:

subject, personal author, corporate source, contract number and report/accession number.

AVAILABILITY OF CITED PUBLICATIONS

IAA ENTRIES (A82-10000 Series)

All publications abstracted in this Section are available from the Technical Information Service, American Institute of Aeronautics and Astronautics, Inc. (AIAA), as follows: Paper copies of accessions are available at $8.00 per document. Microfiche(1) of documents announced in *IAA* are available at the rate of $4.00 per microfiche on demand, and at the rate of $1.35 per microfiche for standing orders for all *IAA* microfiche.

Minimum air-mail postage to foreign countries is $2.50 and all foreign orders are shipped on payment of pro-forma invoices.

All inquiries and requests should be addressed to AIAA Technical Information Service. Please refer to the accession number when requesting publications.

STAR ENTRIES (N82-10000 Series)

One or more sources from which a document announced in *STAR* is available to the public is ordinarily given on the last line of the citation. The most commonly indicated sources and their acronyms or abbreviations are listed below. If the publication is available from a source other than those listed, the publisher and his address will be displayed on the availability line or in combination with the corporate source line.

Avail: NTIS. Sold by the National Technical Information Service. Prices for hard copy (HC) and microfiche (MF) are indicated by a price code preceded by the letters HC or MF in the *STAR* citation. Current values for the price codes are given in the tables on page vii.

Documents on microfiche are designated by a pound sign (#) following the accession number. The pound sign is used without regard to the source or quality of the microfiche.

Initially distributed microfiche under the NTIS SRIM (Selected Research in Microfiche) is available at greatly reduced unit prices. For this service and for information concerning subscription to NASA printed reports, consult the NTIS Subscription Section, Springfield, Va. 22161.

NOTE ON ORDERING DOCUMENTS: When ordering NASA publications (those followed by the * symbol), use the N accession number. NASA patent applications (only the specifications are offered) should be ordered by the US-Patent-Appl-SN number. Non-NASA publications (no asterisk) should be ordered by the AD, PB, or other *report* number shown on the last line of the citation, not by the N accession number. It is also advisable to cite the title and other bibliographic identification.

Avail: SOD (or GPO). Sold by the Superintendent of Documents, U.S. Government Printing Office, in hard copy. The current price and order number are given following the availability line. (NTIS will fill microfiche requests, at the standard $4.00 price, for those documents identified by a # symbol.)

Avail: NASA Public Document Rooms. Documents so indicated may be examined at or purchased from the National Aeronautics and Space Administration, Public Document Room (Room 126), 600 Independence Ave., S.W., Washington, D.C. 20546, or public document rooms located at each of the NASA research centers, the NASA Space Technology Laboratories, and the NASA Pasadena Office at the Jet Propulsion Laboratory.

---

(1) A microfiche is a transparent sheet of film, 105 by 148 mm in size containing as many as 60 to 98 pages of information reduced to micro images (not to exceed 26:1 reduction).

Avail: DOE Depository Libraries. Organizations in U.S. cities and abroad that maintain collections of Department of Energy reports, usually in microfiche form, are listed in *Energy Research Abstracts*. Services available from the DOE and its depositories are described in a booklet, *DOE Technical Information Center - Its Functions and Services* (TID-4660), which may be obtained without charge from the DOE Technical Information Center.

Avail: Univ. Microfilms. Documents so indicated are dissertations selected from *Dissertation Abstracts* and are sold by University Microfilms as xerographic copy (HC) and microfilm. All requests should cite the author and the Order Number as they appear in the citation.

Avail: USGS. Originals of many reports from the U.S. Geological Survey, which may contain color illustrations, or otherwise may not have the quality of illustrations preserved in the microfiche or facsimile reproduction, may be examined by the public at the libraries of the USGS field offices whose addresses are listed in this introduction. The libraries may be queried concerning the availability of specific documents and the possible utilization of local copying services, such as color reproduction.

Avail: HMSO. Publications of Her Majesty's Stationery Office are sold in the U.S. by Pendragon House, Inc. (PHI), Redwood City, California. The U.S. price (including a service and mailing charge) is given, or a conversion table may be obtained from PHI.

Avail: BLL (formerly NLL): British Library Lending Division, Boston Spa, Wetherby, Yorkshire, England. Photocopies available from this organization at the price shown. (If none is given, inquiry should be addressed to the BLL.)

Avail: Fachinformationszentrum, Karlsruhe. Sold by the Fachinformationszentrum Energie, Physik, Mathematik GMBH, Eggenstein Leopoldshafen, Federal Republic of Germany, at the price shown in deutschmarks (DM).

Avail: Issuing Activity, or Corporate Author, or no indication of availability. Inquiries as to the availability of these documents should be addressed to the organization shown in the citation as the corporate author of the document.

Avail: U.S. Patent and Trademark Office. Sold by Commissioner of Patents and Trademarks, U.S. Patent and Trademark Office, at the standard price of 50 cents each, postage free.

Other availabilities: If the publication is available from a source other than the above, the publisher and his address will be displayed entirely on the availability line or in combination with the corporate author line.

ADDRESSES OF ORGANIZATIONS

American Institute of Aeronautics and
Astronautics
Technical Information Service
555 West 57th Street, 12th Floor
New York, New York 10019

British Library Lending Division,
Boston Spa, Wetherby, Yorkshire,
England

Commissioner of Patents and
Trademarks
U.S. Patent and Trademark Office
Washington, D.C. 20231

Department of Energy
Technical Information Center
P.O. Box 62
Oak Ridge, Tennessee 37830

ESA-Information Retrieval Service
ESRIN
Via Galileo Galilei
00044 Frascati (Rome) Italy

Fachinformationszentrum Energie, Physik,
Mathematik GMBH
7514 Eggenstein Leopoldshafen
Federal Republic of Germany

Her Majesty's Stationery Office
P.O. Box 569, S.E. 1
London, England

NASA Scientific and Technical Information
Facility
P.O. Box 8757
B.W.I. Airport, Maryland 21240

National Aeronautics and Space
Administration
Scientific and Technical Information
Branch (NST-41)
Washington, D.C. 20546

National Technical Information Service
5285 Port Royal Road
Springfield, Virginia 22161

Pendragon House, Inc.
899 Broadway Avenue
Redwood City, California 94063

Superintendent of Documents
U.S. Government Printing Office
Washington, D.C. 20402

University Microfilms
A Xerox Company
300 North Zeeb Road
Ann Arbor, Michigan 48106

University Microfilms, Ltd.
Tylers Green
London, England

U.S. Geological Survey
1033 General Services Administration
Building
Washington, D.C. 20242

U.S. Geological Survey
601 E. Cedar Avenue
Flagstaff, Arizona 86002

U.S. Geological Survey
345 Middlefield Road
Menlo Park, California 94025

U.S. Geological Survey
Bldg. 25, Denver Federal Center
Denver, Colorado 80225

NTIS PRICE SCHEDULES

Schedule A

STANDARD PAPER COPY PRICE SCHEDULE

(Effective January 1, 1982)

Price Code	Page Range	North American Price	Foreign Price
A01	Microfiche	$ 4.00	$ 8.00
A02	001-025	6.00	12.00
A03	026-050	7.50	15.00
A04	051-075	9.00	18.00
A05	076-100	10.50	21.00
A06	101-125	12.00	24.00
A07	126-150	13.50	27.00
A08	151-175	15.00	30.00
A09	176-200	16.50	33.00
A10	201-225	18.00	36.00
A11	226-250	19.50	39.00
A12	251-275	21.00	42.00
A13	276-300	22.50	45.00
A14	301-325	24.00	48.00
A15	326-350	25.50	51.00
A16	351-375	27.00	54.00
A17	376-400	28.50	57.00
A18	401-425	30.00	60.00
A19	426-450	31.50	63.00
A20	451-475	33.00	66.00
A21	476-500	34.50	69.00
A22	501-525	36.00	72.00
A23	526-550	37.50	75.00
A24	551-575	39.00	78.00
A25	576-600	40.50	81.00
	601-up	-- 1/	-- 2/

A99 - Write for quote

1/ Add $1.50 for each additional 25 page increment or portion thereof for 601 pages up.

2/ Add $3.00 for each additional 25 page increment or portion thereof for 601 pages and more.

Schedule E

EXCEPTION PRICE SCHEDULE

Paper Copy & Microfiche

Price Code	North American Price	Foreign Price
E01	$ 6.50	$ 13.50
E02	7.50	15.50
E03	9.50	19.50
E04	11.50	23.50
E05	13.50	27.50
E06	15.50	31.50
E07	17.50	35.50
E08	19.50	39.50
E09	21.50	43.50
E10	23.50	47.50
E11	25.50	51.50
E12	28.50	57.50
E13	31.50	63.50
E14	34.50	69.50
E15	37.50	75.50
E16	40.50	81.50
E17	43.50	88.50
E18	46.50	93.50
E19	51.50	102.50
E20	61.50	123.50
E-99 - Write for quote		
N01	30.00	45.00

TABLE OF CONTENTS

Page

Category 01 Agriculture and Forestry 1

Includes crop forecasts, crop signature analysis, soil identification, disease detection, harvest estimates, range resources, timber inventory, forest fire detection, and wildlife migration patterns.

Category 02 Environmental Changes and Cultural Resources 7

Includes land use analysis, urban and metropolitan studies, environmental impact, air and water pollution, geographic information systems, and geographic analysis.

Category 03 Geodesy and Cartography 15

Includes mapping and topography.

Category 04 Geology and Mineral Resources 19

Includes mineral deposits, petroleum deposits, spectral properties of rocks, geological exploration, and lithology.

Category 05 Oceanography and Marine Resources 23

Includes sea-surface temperature, ocean bottom surveying imagery, drift rates, sea ice and icebergs, sea state, fish location

Category 06 Hydrology and Water Management 35

Includes snow cover and water runoff in rivers and glaciers, saline intrusion, drainage analysis, geomorphology of river basins, land uses, and estuarine studies.

Category 07 Data Processing and Distribution Systems 41

Includes film processing, computer technology, satellite and aircraft hardware, and imagery.

Category 08 Instrumentation and Sensors 49

Includes data acquisition and camera systems and remote sensors.

Category 09 General 55

Includes economic analysis.

Subject Index A-1
Personal Author Index B-1
Corporate Source Index C-1
Contract Number Index D-1
Report / Accession Number Index E-1

TYPICAL CITATION AND ABSTRACT FROM *STAR*

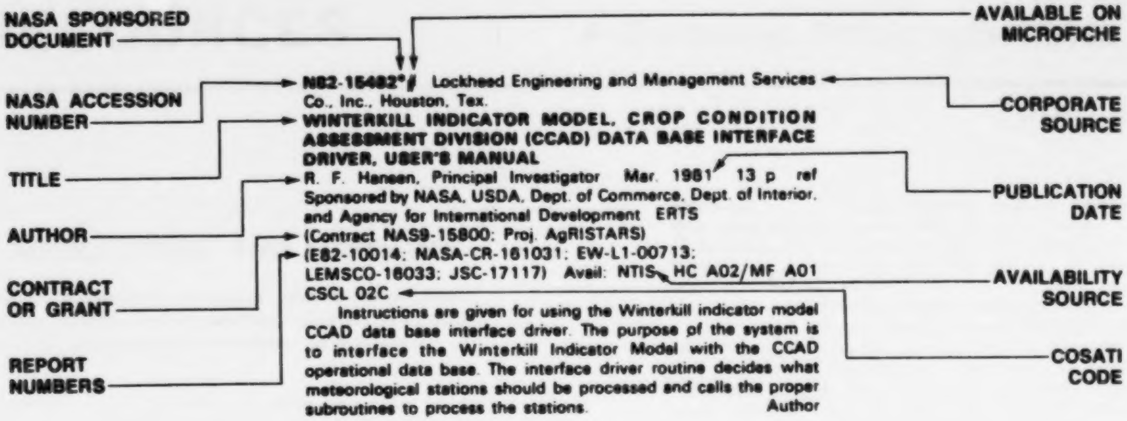
NASA SPONSORED DOCUMENT
AVAILABLE ON MICROFICHE
NASA ACCESSION NUMBER
CORPORATE SOURCE
TITLE
PUBLICATION DATE
AUTHOR
CONTRACT OR GRANT
AVAILABILITY SOURCE
REPORT NUMBERS
COSATI CODE

N82-15482*# Lockheed Engineering and Management Services Co., Inc., Houston, Tex.
WINTERKILL INDICATOR MODEL, CROP CONDITION ASSESSMENT DIVISION (CCAD) DATA BASE INTERFACE DRIVER, USER'S MANUAL
R. F. Hansen, Principal Investigator Mar. 1981 13 p ref
Sponsored by NASA, USDA, Dept. of Commerce, Dept. of Interior, and Agency for International Development ERTS
(Contract NAS9-15800; Proj. AgRISTARS)
(E82-10014; NASA-CR-161031; EW-L1-00713; LEMSCO-16033; JSC-17117) Avail: NTIS HC A02/MF A01
CSCL 02C

Instructions are given for using the Winterkill indicator model CCAD data base interface driver. The purpose of the system is to interface the Winterkill Indicator Model with the CCAD operational data base. The interface driver routine decides what meteorological stations should be processed and calls the proper subroutines to process the stations. Author

TYPICAL CITATION AND ABSTRACT FROM *IAA*

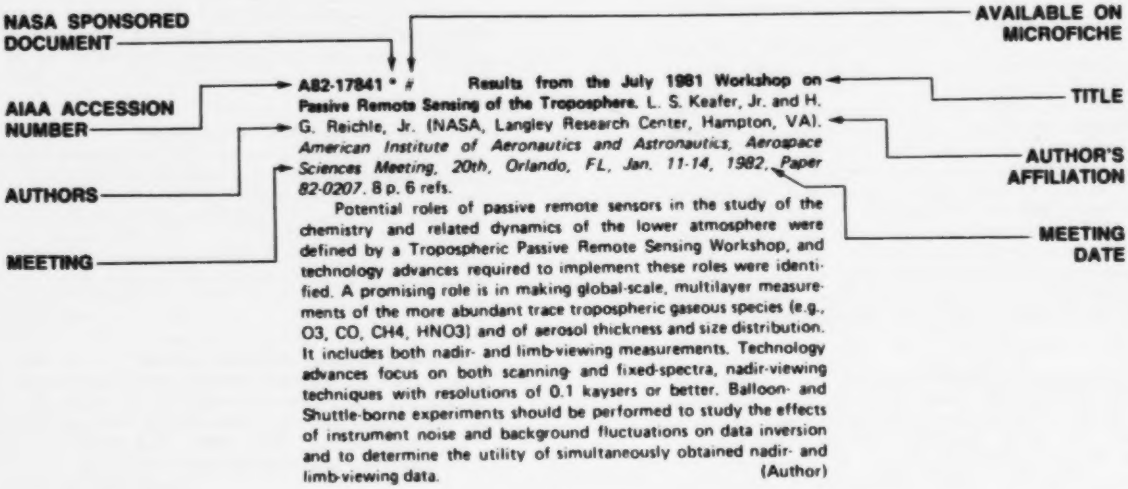
NASA SPONSORED DOCUMENT
AVAILABLE ON MICROFICHE
AIAA ACCESSION NUMBER
TITLE
AUTHORS
AUTHOR'S AFFILIATION
MEETING
MEETING DATE

A82-17841 * # **Results from the July 1981 Workshop on Passive Remote Sensing of the Troposphere.** L. S. Keafer, Jr. and H. G. Reichle, Jr. (NASA, Langley Research Center, Hampton, VA). *American Institute of Aeronautics and Astronautics, Aerospace Sciences Meeting, 20th, Orlando, FL, Jan. 11-14, 1982, Paper 82-0207*. 8 p. 6 refs.

Potential roles of passive remote sensors in the study of the chemistry and related dynamics of the lower atmosphere were defined by a Tropospheric Passive Remote Sensing Workshop, and technology advances required to implement these roles were identified. A promising role is in making global-scale, multilayer measurements of the more abundant trace tropospheric gaseous species (e.g., O3, CO, CH4, HNO3) and of aerosol thickness and size distribution. It includes both nadir- and limb-viewing measurements. Technology advances focus on both scanning- and fixed-spectra, nadir-viewing techniques with resolutions of 0.1 kaysers or better. Balloon- and Shuttle-borne experiments should be performed to study the effects of instrument noise and background fluctuations on data inversion and to determine the utility of simultaneously obtained nadir- and limb-viewing data. (Author)

EARTH RESOURCES

A Continuing Bibliography (Issue 33)

APRIL 1982

01
AGRICULTURE AND FORESTRY

Includes crop forecasts, crop signature analysis, soil identification, disease detection, harvest estimates, range resources, timber inventory, forest fire detection, and wildlife migration patterns.

A82-10039 **The effect of angular factors on popularly used indicators of vegetative vigor.** M. J. Duggin (New York, State University, Syracuse, NY). In: American Society of Photogrammetry, Annual Meeting, 46th, St. Louis, MO, March 9-14, 1980, ASP Technical Papers. Falls Church, VA, American Society of Photogrammetry, 1980, p.239-251. 19 refs.

Ground-based radiometric measurements of reflectance and radiometric data from airborne and spaceborne multispectral scanners and cameras have been used to experimentally determine biomass, vegetative cover, leaf area index, plant height, and disease severity for crops and (for some of these variables) for pastures. In studies so far reported, little or no attention has been given to the effect of sun-detector geometry on popular indices of these variables. It is shown using an experimental model that, for several different pasture targets, each angular variable (solar zenith angle, solar azimuth, and look angle) has an important effect on each of the indices. This implies that care is required in selecting angular regimes for the collection of data which can be interpreted unambiguously and for the meaningful comparison of data obtained on different occasions. B.J.

A82-10040 **Remote sensing techniques in the study of the agricultural potential of soils under the Cerrado vegetation /Brazil/.** G. J. Garcia and R. P. Harris (Universidade Estadual Paulista, Botucatu, São Paulo, Brazil). In: American Society of Photogrammetry, Annual Meeting, 46th, St. Louis, MO, March 9-14, 1980, ASP Technical Papers. Falls Church, VA, American Society of Photogrammetry, 1980, p. 252-260. 8 refs. Research supported by the Fundação de Amparo à Pesquisa do Estado de São Paulo.

A82-10041 **Mapping vegetation association boundaries with Landsat MSS data - An Oklahoma example.** J. A. Harrington, Jr. and C. W. Dunn, Jr. (Oklahoma, University, Norman, OK). In: American Society of Photogrammetry, Annual Meeting, 46th, St. Louis, MO, March 9-14, 1980, ASP Technical Papers. Falls Church, VA, American Society of Photogrammetry, 1980, p. 270-281. 15 refs.

The transition from oak forest to prairie grassland in central Oklahoma provides an excellent area to test the feasibility of using Landsat satellite remote sensing for vegetation mapping. An east-west oriented transect across the ecotone was identified as a study area for testing the mapping accuracy that is obtainable with both computer processing of the digital data and traditional aerial photographic interpretation of Landsat false color composites. Acreage statistics and locational measures of Landsat derived forest cover maps are compared with ground truth information obtained from interpretation of large scale panchromatic photography to suggest the relative accuracy of the analysis techniques. Potential applications of the use of Landsat satellite data for vegetation mapping are identified. (Author)

A82-10042 **Phytoecozonation of Sevier Lake region of Utah using digitized Landsat MSS data.** K. Lulla and P. Mausel (Indiana State University, Terre Haute, IN). In: American Society of Photogrammetry, Annual Meeting, 46th, St. Louis, MO, March 9-14, 1980, ASP Technical Papers. Falls Church, VA, American Society of Photogrammetry, 1980, p.282-292. 10 refs.

The practicality and value of Landsat MSS digital data using computer-assisted techniques were examined in a study of regional level phytoecozone identification in the Sevier Lake region of the Great Basin of Utah. Four band spectral responses from Landsat scene 73500200 (May 22, 1973) were converted into principal component (PC) and biomass ratios. Unsupervised results clearly indicate that Landsat MSS data in PC and biomass ratio form can be used to delineate major phytoecozone patterns at a map scale of 1:500,000 and also provide selected zonation information at 1:120,000 scale and larger. It was also found that combining PC, biomass ratio, and some original Landsat data gave the best results for delineating phytoecozone regions using nonparametric supervised classification techniques. B.J.

A82-10046 **Limitations in the spectral discrimination of the Landsat MSS.** M. J. Duggin (New York, State University, Syracuse, NY) and P. J. Ellis (Department of Scientific and Industrial Research, Physics and Engineering Laboratory, Lower Hutt, New Zealand). In: American Society of Photogrammetry, Annual Meeting, 46th, St. Louis, MO, March 9-14, 1980, ASP Technical Papers. Falls Church, VA, American Society of Photogrammetry, 1980, p.329-334. 7 refs.

The variation between the mean value in output for one bandpass for the Landsat 1, 2, and 3 multispectral scanners is nearly 10% for a target that shows variations in spectral response across the bandpass (e.g., vegetation) but is less than 1% for a target that does not (e.g., soil). This paper examines the above differences for real vegetation and soil targets to show that the differences in output between the channels for a given band of a given MSS are target-dependent; that is, striping on the MSS image is target-dependent. It is also shown that in the case of multitemporal studies involving the output of scanners on two or more satellites, the differences in mean output between like channels of scanners are target-dependent, being much larger for a target which shows variations in radiance across the scanner bandpass than for one which does not. B.J.

A82-10047 * **Remote sensing for vineyard management.** W. R. Philipson, T. L. Erb, D. Fernandez, and J. N. McLeester (Cornell University, Ithaca, NY). In: American Society of Photogrammetry, Annual Meeting, 46th, St. Louis, MO, March 9-14, 1980, ASP Technical Papers. Falls Church, VA, American Society of Photogrammetry, 1980, p.371-378. Grant No. NGL-33-010-171.

Cornell's Remote Sensing Program has been involved in a continuing investigation to assess the value of remote sensing for vineyard management. Program staff members have conducted a series of site and crop analysis studies. These include: (1) panchromatic aerial photography for planning artificial drainage in a new vineyard; (2) color infrared aerial photography for assessing crop vigor/health; and (3) color infrared aerial photography and aircraft multispectral scanner data for evaluating yield related factors. These studies and their findings are reviewed. (Author)

A82-10048 **Repetitive aerial photography for assessing marsh vegetation changes.** M. G. Weaver, G. H. Cross, and R. A. Mead

(Virginia Polytechnic Institute and State University, Blacksburg, VA). In: American Society of Photogrammetry, Annual Meeting, 46th, St. Louis, MO, March 9-14, 1980, ASP Technical Papers. Falls Church, VA, American Society of Photogrammetry, 1980, p. 395-408. 21 refs. Research supported by the Virginia Commission of Game and Inland Fisheries.

The dynamic conditions of two marshes on the Rappahannock River, Virginia, were investigated using sequential aerial photography. All the historical photography was 9 inch format, black and white panchromatic, and medium scale, purchased from various government agencies. Recent photos were large-scale 35 mm color infrared and natural color positive transparencies. Vegetative classes were delineated on the recent photographs to produce a large-scale 1:2,500 map useful in current resource planning and future monitoring. The black and white historical photos were interpreted using a generalized classification system. Comparisons of changes were made by reducing or enlarging the maps made from the historical and tabularly reducing the current vegetation classes to a common scale of 1:7,000. In addition, muskrat lodges were plotted on all photographs where resolution and quality permitted. Repetitive aerial photographs provided useful information on which to formulate hypotheses that would explain changes in marsh vegetation.

(Author)

A82-10862 **Stand density estimation on panoramic transparencies.** W. A. Befort, H. N. Anderson (Idaho, University, Moscow, ID), and B. L. Kessler (Idaho Department of Lands, Moscow, ID). *Photogrammetric Engineering and Remote Sensing,* vol. 47, Oct. 1981, p. 1477-1481. 9 refs.

Paired estimates of forest canopy density were made on optical bar panoramic CIR transparencies and on conventional black-and-white prints to see if different results would be obtained. Except in the portions of the photographs beyond about 36 deg of scan angle, estimates made on panoramic photos under 4x stereo magnification were not significantly different from estimates made on conventional photos with a 3x mirror stereoscope. (Author)

A82-10863 * **Spectral behavior of wheat yield variety trials.** J. L. Hatfield (California, University, Davis, CA). *Photogrammetric Engineering and Remote Sensing,* vol. 47, Oct. 1981, p. 1487-1491. 8 refs. Research supported by the U.S. Department of Agriculture; Grant No. NCA2-OR-180-607.

Little variation between varieties is seen at jointing, but the variability is found to increase during grain filling and decline again at maturity. No relationship is found between spectral response and yield, and when yields are segregated into various classes the spectral response is the same. Spring and winter nurseries are found to separate during the reproductive stage because of differences in dates of heading and maturity, but they exhibit similar spectral responses. The transformed normalized difference is at a minimum after the maximum grain weight occurs and the leaves begin to brown and fall off. These data of 100% ground cover demonstrate that it is not possible to predict grain yield from only spectral data. This, however, may not apply when reduced yields are caused by less-than-full ground cover.

C.R.

A82-10864 **Satellite sensing of irrigation patterns in semiarid areas - An Indian study.** S. Thiruvengadachari (National Remote Sensing Agency, Hyderabad, India). *Photogrammetric Engineering and Remote Sensing,* vol. 47, Oct. 1981, p. 1493-1499. 6 refs.

A82-12884 **Evaluation of digital photographic enhancement for Dutch elm disease detection.** T. M. Lillesand, D. E. Meisner, D. W. French, and W. L. Johnson (Minnesota, University, St. Paul, MN). *Photogrammetric Engineering and Remote Sensing,* vol. 47, Nov. 1981, p. 1581-1592. 11 refs. Research supported by the University of Minnesota.

A82-12886 * **Temporal spectral response of a corn canopy.** B. L. Markham, D. S. Kimes, C. J. Tucker (NASA, Goddard Space Flight Center, Earth Resources Branch, Greenbelt, MD), and J. E. McMurtrey, III (Science and Education Administration, Field Crops Laboratory, Beltsville, MD). *Photogrammetric Engineering and Remote Sensing,* vol. 47, Nov. 1981, p. 1599-1605. 14 refs.

Techniques developed for the prediction of winter wheat yields from remotely sensed data indicating crop status over the growing season are tested for their applicability to corn. Ground-based spectral measurements in the Landsat Thematic Mapper bands 3 (0.62-0.69 microns), 4 (0.76-0.90 microns) and 5 (1.55-1.75 microns) were performed at one-week intervals throughout the growing season for 24 plots of corn, and analyzed to derive spectral ratios and normalized spectral differences of the IR and shortwave IR bands with the red. The ratios of the near IR and shortwave IR bands are found to provide the highest and most consistent correlations with corn yield and dry matter accumulation, however the value of band 5 could not be tested due to the absence of water stress conditions. Integration of spectral ratios over several dates improved the correlations over those of any single date by achieving a seasonal, rather than instantaneous, estimate of crop status. Results point to the desirability of further tests under other growth conditions to determine whether satellite-derived data will be useful in providing corn yield information.

S.C.S.

A82-12887 **Identification of conifer species groupings from Landsat digital classifications.** K. E. Mayer and L. Fox, III (Humboldt State University, Arcata, CA). *Photogrammetric Engineering and Remote Sensing,* vol. 47, Nov. 1981, p. 1607-1614. 12 refs.

The development of computerized classification techniques for timber species groupings in Landsat digital data is discussed in light of the problems of spectrally inhomogeneous training fields, unique patterns not covered by limited numbers of training fields and spectral class labeling encountered in such situations. The combination of guided clustering with unsupervised classification is shown to have allowed inventorying of the timber resources of the McCloud Ranger District of the Shasta-Trinity National Forest in California. To complete the classification spectral classes were assigned to resource categories by the construction of spectral curves for each class from the mean digital values in spectral bands 4, 5, 6 and 7, in association with detailed photointerpretation. An overall classification accuracy for the identification of conifer species groupings, canopy density classes, and crown diameter categories of 0.83 was thus obtained.

S.C.S.

A82-15026 **The discrimination of winter wheat using a growth-state signature.** C. A. Hlavka, R. M. Haralick, S. M. Carlyle, and R. Yokoyama (Kansas, University, Lawrence, KS). *Remote Sensing of Environment,* vol. 9, June 1980, p. 277-294. 21 refs.

In this paper, a multitemporal classification procedure for crops in Landsat scenes is described. The method involves the creation of crop signatures which characterize multispectral observations as functions of phenological growth states. In this approach, crop spectral reflectance is modeled explicitly as a function of maturity rather than a function of date. This means that instead of stacking spectral vectors of one observation on another, as is usually done for multitemporal data, a correspondence of time to growth state is established for each possible crop category which minimizes the difference between the given multispectral multitemporal vector and the category mean vector indexed by growth state. The results of applying it to winter wheat show that the method is capable of discrimination with about the same degree of accuracy as more traditional multitemporal classifiers. It shows some potential to label degree of maturity of the crop without crop condition information in the training set.

V.L.

A82-15038 * **Temporal relationships between spectral response and agronomic variables of a corn canopy.** D. S. Kimes, B. L. Markham, C. J. Tucker (NASA, Goddard Space Flight Center, Earth Resources Branch, Greenbelt, MD), and J. E. McMurtrey, III (U.S. Science and Education Administration, Plant Genetics and Germplasm Institute, Beltsville, MD). *Remote Sensing of Environment,* vol. 11, Nov. 1981, p. 401-411. 15 refs.

Attention is given to an experiment in which spectral radiance data collected in three spectral regions are related to corn canopy variables. The study extends the work of Tucker et al. (1979) in that more detailed measurements of corn canopy variables were made using quantitative techniques. Wet and dry green leaf biomass is considered along with the green leaf area index, chlorotic leaf biomass, chlorotic leaf area, and leaf water content. In addition, spectral data were collected with a hand-held radiometer having Landsat-D Thematic Mapper (TM) bands TM3 (0.63-0.69 micrometers), TM4 (0.76-0.90 micrometers), and TM5 (1.55-1.75 micrometers). TM3, TM4, and TM5 seem to be well situated spectrally for making remotely sensed measurements related to chlorophyll concentration, leaf density, and leaf water content. G.R.

A82-15748 **A VHF homing system with VHF radiotelephony for area-representative strip-survey flights conducted, as part of combined forest inventories, with light aircraft carrying 70 mm and 35 mm cameras (Ein VHF-Homing-System mit VHF-Sprechfunk für flächenrepräsentative Streifenbefliegungen mit 70 mm und 35 mm Kameras von leichten Flugzeugen im Rahmen kombinierter Waldinventuren).** B. Rhody (Bundesforschungsanstalt für Forst- und Holzwirtschaft, Hamburg, West Germany). *Bildmessung und Luftbildwesen*, vol. 49, Nov. 1, 1981, p. 199-203. In German.

A82-15963 † **Study and mapping of agricultural land use, based on space images (Izuchenie i kartografirovanie sel'skokhoziaistvennogo ispol'zovaniia zemel' po kosmicheskim snimkam).** L. F. Ianvareva (Moskovskii Gosudarstvennyi Universitet, Moscow, USSR). *Issledovanie Zemli iz Kosmosa*, Sept.-Oct. 1981, p. 103-110. In Russian.

The possibilities of using multispectral images obtained at different times by the Fragment system to study the structure of agrarian lands and various forms of agriculture are assessed. A method is described for interpreting the agrarian areas, groups of agricultural cultures, and agrotechnical and land reclamation measures, which are based on a system of external features. The advantages of using space images as compared to ground-based methods are discussed, including the greater regional differentiation of space information. J.F.

A82-15964 † **Mapping of forest vegetation on the basis of space images (Kartografirovanie lesnoi rastitel'nosti po kosmicheskim snimkam).** T. V. Kotova, V. I. Kravtsova, and A. K. Makarevich (Moskovskii Gosudarstvennyi Universitet, Moscow, USSR). *Issledovanie Zemli iz Kosmosa*, Sept.-Oct. 1981, p. 111-116. In Russian.

Using the upper reaches of the Northern Dvina river as an example, the possibilities of studying and mapping forests by images obtained by the Fragment system were analyzed. The images were used to separate forest and non-forest areas, and to distinguish the forest areas as either coniferous, mixed, or deciduous. The outlines of forest and nonforest regions with areas greater than 0.5 sq km are established in detail, and the characteristics of the various species are discussed in general terms. J.F.

A82-16162 **Rural development in the humid tropics.** F. C. d'Audretsch and H. F. Gelens (International Institute for Aerial Survey and Earth Sciences, Enschede, Netherlands). *ITC Journal*, no. 3, 1981, p. 266-277.

The status of on-going rural development projects in Southeast Asia was the subject of a seven-week research tour of Thailand, Indonesia and the Philippines. The tour was jointly sponsored by the International Institute for Aerial Survey and Earth Sciences and the United Nations University. The study focused on the development of resources management in agro-forestry, forest conservation, reforestation and settlement in the humid tropics. Problems in the use of aerial photographs and coordination of resource management were identified. S.C.S.

A82-16622 † **Analysis of the information content of the polarimetric method of remote sensing (Analiz informativnosti poliarimetricheskogo metoda distantsionnogo zondirovaniia).** V. V. Egorov and B. S. Zhukov. In: Airborne and spaceborne multispectral photography of the earth. Moscow, Izdatel'stvo Nauka, 1981, p. 203-210. 8 refs. In Russian.

The comparative information content of polarization characteristics in remote sensing studies is analyzed. The optimal combination of spectral-polarization measurements is calculated for actual sets of soil-vegetation objects. Intensity and the degree of optical polarization were found to be the most informative polarization characteristics. B.J.

A82-17564 * **Aircraft radar response to soil moisture.** G. A. Bradley and F. T. Ulaby (University of Kansas Center for Research, Inc., Lawrence, KS). *Remote Sensing of Environment*, vol. 11, Dec. 1981, p. 419-438. 12 refs. Contracts No. NAS9-14052; Grant No. NAG5-30.

An analysis is presented of aircraft response to soil moisture in the upper surface layer of agricultural fields. Measurements (taken at 1.6 GHz and 4.75 GHz using HH and HV polarizations, and at 13.3 GHz using VV polarization from an experiment conducted in 1978 at Colby, Kansas) are used to derive the radar soil moisture sensitivities and correlations. It is shown that the aircraft response to soil moisture is optimum at C-band frequencies and incidence angles of 10-20 deg. confirming previous truck-radar results. Like-polarization radar response is unaffected by vegetation but is dependent on row-tillage patterns; cross-polarization response also is unaffected by vegetation but is approximately independent of tillage patterns. These results show that remote sensing radars can be used effectively for the detection and estimation of near-surface soil moisture in agricultural fields. (Author)

A82-17997 **Remote sensing of crop moisture status.** B. L. Blad, B. R. Gardner, D. G. Watts, and N. J. Rosenberg (Nebraska, University, Lincoln, NE). *Remote Sensing Quarterly*, vol. 3, Apr. 1981, p. 4-20. 11 refs. Research sponsored by the University of Nebraska.

Relations between crop temperatures and levels of water stress are determined to serve as a basis for the remote sensing of the extent and severity of water stress according to thermal imagery. Experiments were performed on stands of sorghum and corn grown near Mead and North Platte, Nebraska, respectively, under either full irrigation, a water gradient during the vegetative, pollination and grain-fill periods, or dryland conditions. Thermal imagery acquired at altitudes of 610 and 1220 m reveals the irrigated and nonirrigated sorghum plots to display the same temperatures in the morning, while the nonirrigated plot was a few degrees warmer in the afternoon and exhibited considerable temperature variability. Mid-afternoon temperature differences of up to 12.8 C are found in the corn plots accompanied by a great amount of interplot variability. Significant changes in crop temperature, particularly on nonirrigated lands, are observed under variably cloudy skies, making it difficult to quantify the degree of stress under these conditions from temperature data. The data reveal the optimum time of day for detecting maximum plant temperatures to be between 1300 and 1500 h. Crop temperatures measured by attached leaf thermocouples are found to be within 1.2 and 2.6 C of IR thermometer temperatures for the unstressed and stressed plants, respectively. Finally, differences in seasonal evapotranspiration are found to be correlated with seasonally accumulated temperature differences. A.L.W.

A82-17998 **The use of digitally processed Landsat imagery for vegetation mapping in Sulawesi, Indonesia.** R. M. Warwick-Smith (London, University, London, England). *Remote Sensing Quarterly*, vol. 3, Apr. 1981, p. 21-26. 13 refs. Research supported by the Royal Aircraft Establishment.

N82-10489# Intermountain Forest and Range Experiment Station, Ogden, Utah.

LARGE-SCALE COLOR AERIAL PHOTOGRAPHY AS A TOOL IN SAMPLING FOR MORTALITY RATES

David A. Hamilton, Jr. Jan. 1981 14 p refs Sponsored by USDA Forest Service
(PB81-214777; FSRP/INT-269) Avail: NTIS HC A02/MF A01 CSCL 02F

Mortality rates specify the proportion of trees with a given set of characteristics that are expected to die in a fixed time interval. Results indicate that 1 year mortality trees can be dated and species can be assigned to green trees and to 1 year mortality trees with acceptable accuracy on 70 mm color photography at scales of 1:1600 and 1:2400. GRA

N82-11910# Army Engineer Waterways Experiment Station, Vicksburg, Miss. Environmental Lab.

INCLUSION OF A SIMPLE VEGETATION LAYER IN TERRAIN TEMPERATURE MODELS FOR THERMAL INFRARED (IR) SIGNATURE PREDICTION Final Report, 1 Oct. 1979 - 1 Oct. 1980
Lee K. Balick, Randy K. Scoggins, and Lewis E. Link, Jr. Aug. 1981 44 p refs
(DA Proj. 4A7-62730-AT-42; DA Proj. 4A7-62719-AT-40)
(AD-A104469; WES/MP/EL-81-4) Avail: NTIS HC A03/MF A01 CSCL 17/5

Thermal infrared signatures of natural and cultural features are dynamic, varying with time and weather conditions. Prediction of thermal signatures for specific conditions requires first that the actual temperature of the features be determined; for vegetation canopies this involves the average temperatures of canopy components and for planar (nonvegetated) surfaces the temperature of the surface. Models have been developed to handle layered vegetation canopies and layered ground surfaces; however, efforts have only begun to formulate a comparable capability for intermediate conditions such as grass covered surfaces where both the terrain surface and vegetation influence the average surface temperature. This report presents a procedure, named VEGIE, that predicts the temperature of terrain surfaces which contain a simple layer of vegetation. VEGIE is designed as an interim procedure for immediate application in lieu of more sophisticated and theoretical treatments of this problem. Operational flexibility and simplicity are preserved by using VEGIE as a submodel to the Terrain Surface Temperature Model (TSTM) developed previously at the U.S. Army Engineer Waterways Experiment Station. The TSTM predicts the surface temperature of nonvegetated layer and planar features using material thermophysical properties and meteorological conditions. These models are applied to a deciduous and a coniferous canopy where the CSU model is valid but VEGIE is not. VEGIE is applied to the problem of estimating thermal signatures for terrain surfaces with less than total foliage cover, the consequences of changes in foliage cover, differing emissivities for the soil and vegetation, and reflected sky radiation. GRA

N82-12500*# California Univ., Berkeley.
VEGETATION PATTERNS
David M. Carneggie and Brain T. Fine (California Univ. at Davis) *In* NASA. Johnson Space Flight Center Skylab Explores the Earth 1977 p 243-262 refs

Avail: NTIS MF A01; SOD HC $16.50 CSCL 08F

In an effort to make meaningful observations of vegetation resources, the following sites and features were examined: (1) wheat in Argentina, Australia, and the U.S.; (2) rangelands in Australia, Africa, and the U.S.; (3) land use in Malaysia; (4) vegetation in New Zealand; (5) agriculture in California; (6) drought in northern Australia; (7) insect and disease damage in any of the sites; and (8) forest and range fires wherever found. The important factors that governed the ability of the crew to observe these features were angle of view from the spacecraft; atmospheric conditions; Sun angle; speed of the spacecraft; characteristics of natural and cultivated vegetation; and familiarity with the phenomena to be observed. User reaction to the imagery is discussed and photograph quality is evaluated. A.R.H.

N82-15480*# Environmental Research Inst. of Michigan, Ann Arbor. Infrared and Optics Div.
DEVELOPMENT AND EVALUATION OF AN AUTOMATIC LABELING TECHNIQUE FOR SPRING SMALL GRAINS Technical Report, 15 Nov. 1979 - 31 Dec. 1980
Eric P. Crist and William A. Malila, Principal Investigators Aug. 1981 67 p refs Sponsored by NASA, USDA, Dept. of Commerce, Dept. of Interior, and Agency for International Development ERTS
(Contract NAS9-15476; Proj. AgRISTARS)
(E82-10001; NASA-CR-161080; SR-EL-04065; ERIM-152400-3-T) Avail: NTIS HC A04/MF A01 CSCL 05A

A labeling technique is described which seeks to associate a sampling entity with a particular crop or crop group based on similarity of growing season and temporal-spectral patterns of development. Human analyst provide contextual information, after which labeling decisions are made automatically. Results of a test of the technique on a large, multi-year data set are reported. Grain labeling accuracies are similar to those achieved by human analysis techniques, while non-grain accuracies are lower. Recommendations for improvments and implications of the test results are discussed. Author

N82-15481*# South Dakota State Univ., Brookings. Remote Sensing Inst.
REMOTE SENSING APPLICATIONS TO RESOURCE PROBLEMS IN SOUTH DAKOTA Annual Progress Report, 1 Jul. 1980 - 30 Jun. 1981
Victor I. Myers, Principal Investigator 30 Jun. 1981 154 p refs Original contains color imagery. Original photography may be purchased from the EROS Data Center, Sioux Falls, S.D. 57198 ERTS
(Grant NGL-42-003-007)
(E82-10002; NASA-CR-164892; SDSU-RSI-81-11) Avail: NTIS HC A08/MF A01 CSCL 05A

The procedures used as well as the results obtained and conclusions derived are described for the following applications of remote sensing in South Dakota: (1) sage grouse management; (2) censusing Canada geese; (3) monitoring grasshopper infestation in rangeland; (4) detecting Dutch elm disease in an urban environment; (5) determining water usage from the Belle Fourche River; (6) resource management of the Lower James River; and (7) the National Model Implantation Program: Lake Herman watershed. A.R.H.

N82-15482*# California Univ., Berkeley. Space Sciences Lab.
APPLICATION OF REMOTE SENSING TO SELECTED PROBLEMS WITHIN THE STATE OF CALIFORNIA Annual Report
Robert N. Colwell, Principal Investigator, Andrew S. Benson, John E. Estes, and Claude Johnson 1 May 1981 258 p refs Original contains color imagery. Original photography may be purchased from the EROS Data Center, Sioux Falls, S.D. 57198. ERTS
(Grant NsG-7220)
(E82-10004; NASA-CR-164893; SSL-Ser-22-Issue-18) Avail: NTIS HC A12/MF A01 CSCL 05A

Specific case studies undertaken to demonstrate the usefulness of remote sensing technology to resource managers in California are highlighted. Applications discussed include the mapping and quantization of wildland fire fuels in Mendocino and Shasta Counties as well as in the Central Valley; the development of a digital spectral/terrain data set for Colusa County; the Forsythe Planning Experiment to maximize the usefulness of inputs from LANDSAT and geographic information systems to county planning in Mendocino County; the development of a digital data bank for Big Basin State Park in Santa Cruz County; the detection of salinity related cotton canopy reflectance differences in the Central Valley; and the surveying of avocado acreage and that of other fruits and nut crops in Southern California. Special studies include the interpretability of high altitude, large format photography of forested areas for coordinated resource planning using U-2 photographs of the NASA Bucks Lake Forestry test site in the Plumas National Forest in the Sierra Nevada Mountains. A.R.H.

N82-15485*# Instituto de Pesquisas Espaciais, Sao Jose dos Campos (Brazil).
WHEAT CULTIVATION: IDENTIFICATION AND ESTIMATION OF AREAS USING LANDSAT DATA [CULTURA DO TRIGO IDENTIFICACAO E AVALIACAO DE AREAS ATRAVES DE DADOS DO LANDSAT]
Nelson deJesusParada, Principal Investigator, Francisco Jose Mendonca, Dali Arthur Cottrell, Antonio Tebaldi Tardin, David Chung Liang Lee, Yosio Edemir Shimabukuro, Mauricio Alves Moreira, and Angela Maria deLimaeFernandoCelsoSoaresMaia May 1981 5 p refs In PORTUGUESE Sponsored by NASA ERTS
(E82-10007; NASA-CR-164905; INPE-2054-RPE/300) Avail: NTIS HC A02/MF A01 CSCL 02C

The feasibility of using automatically processed multispectral data obtained from LANDSAT to identify wheat and estimate the areas planted with this grain was investigated. Three 20 km by 40 km segments in a wheat growing region of Rio Grande do Sul were serially photographed using type 2443 Aerochrome film. Three maps corresponding to each segment were obtained from the analysis of the photographs which identified wheat, barley, fallow land, prepared soil, forests, and reforested land. Using basic information about the fields and maps made from the photographed areas, an automatic classification of wheat

was made using MSS data from two different periods: July to September and July to October 1979. Results show that orbital data is not only useful in characterizing the growth of wheat, but also provides information of the intensity and extent of adverse climate which affects cultivation. The temporal and spatial characteristics of LANDSAT data are also demonstrated.
Transl. by A.R.H.

N82-15490*# Instituto de Pesquisas Espaciais, Sao Jose dos Campos (Brazil).
REMOTE SENSING IN FORESTRY: APPLICATION TO THE AMAZON REGION
Nelson deJesusParada, Principal Investigator, Antonio T. Tardin, Armando dosSantos, Pedro Hernandez Filho, and Yosio E. Shimabukuro Apr. 1981 72 p refs Sponsored by NASA ERTS
(E82-10012; NASA-CR-164755; INPE-2035-RPE/292) Avail: NTIS HC A04/MF A01 CSCL 02F

The utilization of satellite remote sensing in forestry is reviewed with emphasis on studies performed for the Brazilian Amazon Region. Timber identification, deforestation, and pasture degradation after deforestation are discussed. A.R.H.

N82-15491*# Lockheed Engineering and Management Services Co., Inc., Houston, Tex.
FISCAL YEAR 1980-81 IMPLEMENTATION PLAN IN SUPPORT OF TECHNICAL DEVELOPMENT AND INTEGRATION OF SAMPLING AND AGGREGATION PROCEDURES
Mar. 1981 88 p refs Sponsored by NASA, USDA, Dept. of Commerce, Dept. of Interior, and Agency for International Development ERTS
(Contract NAS9-15800; Proj. AgRISTARS)
(E82-10013; NASA-CR-161030; FC-LO-00612; LEMSCO-15168; JSC-16819) Avail: NTIS HC A05/MF A01 CSCL 02C

The specific objectives of the FY 1980-81 tasks are: (1) further refinements to the weighted aggregation procedure; (2) improved approaches for estimating within-stratum variance; (3) more intensive investigation of alternative sampling strategies such as full-frame sampling strategy, and (4) further developments in regard to a simulated approach for assessing the performance of the overall designed sampling and aggregation system. Author

N82-15492*# Lockheed Engineering and Management Services Co., Inc., Houston, Tex.
WINTERKILL INDICATOR MODEL, CROP CONDITION ASSESSMENT DIVISION (CCAD) DATA BASE INTERFACE DRIVER, USER'S MANUAL
R. F. Hansen, Principal Investigator Mar. 1981 13 p ref Sponsored by NASA, USDA, Dept. of Commerce, Dept. of Interior, and Agency for International Development ERTS
(Contract NAS9-15800; Proj. AgRISTARS)
(E82-10014; NASA-CR-161031; EW-L1-00713; LEMSCO-16033; JSC-17117) Avail: NTIS HC A02/MF A01 CSCL 02C

Instructions are given for using the Winterkill indicator model CCAD data base interface driver. The purpose of the system is to interface the Winterkill Indicator Model with the CCAD operational data base. The interface driver routine decides what meteorological stations should be processed and calls the proper subroutines to process the stations. Author

N82-15494*# National Aeronautics and Space Administration. Lyndon B. Johnson Space Center, Houston, Tex.
US/CANADA WHEAT AND BARLEY CROP CALENDER EXPLORATORY EXPERIMENT IMPLEMENTATION PLAN
Sep. 1980 23 p refs Sponsored by NASA, USDA, Dept. of Commerce, Dept. of Interior, and Agency for International Development ERTS
(Proj. AgRISTARS)
(E82-10016; NASA-TM-84034; FC-JO-00611; JSC-16812) Avail: NTIS HC A02/MF A01 CSCL 02C

A plan is detailed for a supplemental experiment to evaluate several crop growth stage models and crop starter models. The objective of this experiment is to provide timely information to aid in understanding crop calendars and to provide data that will allow a selection between current crop calendar models.
Author

[illegible]

[illegible]

02

ENVIRONMENTAL CHANGES AND CULTURAL RESOURCES

Includes land use analysis, urban and metropolitan studies, environmental impact, air and water pollution, geographic information systems, and geographic analysis.

A82-10034 * **Introducing remote sensing to county-level agencies in Michigan through the Cooperative Extension Service.** W. R. Enslin and R. Hill-Rowley (Michigan State University, East Lansing, MI). In: American Society of Photogrammetry, Annual Meeting, 46th, St. Louis, MO, March 9-14, 1980, ASP Technical Papers. Falls Church, VA, American Society of Photogrammetry, 1980, p. 157-164. 11 refs. Research supported by the Michigan State University; Grant No. NGL-23-004-083.

State and regional planning agencies in Michigan are aware of remote sensing technology, however, many agencies at the county and township level have not been introduced to its potential. This paper describes an educational effort undertaken by the MSU Remote Sensing Project and the Michigan Cooperative Extension Service aimed at reaching local decision makers. Remote sensing materials and a questionnaire were used to elicit interest and aid in planning the program. A series of seven workshops were held throughout Michigan for governmental officials and the staff of public agencies from 38 counties. Emphasis was placed on the characteristics, availability and usefulness of remotely-sensed data through a series of successful applications conducted in the state. The workshops were highly successful and many local decision makers are not aware of a new tool to call upon in their responses to land use and natural resource concerns. (Author)

A82-10043 * **An improvement in land cover classification achieved by merging microwave data with Landsat multispectral scanner data.** S. T. Wu (NASA, National Space Technology Laboratories, Earth Resources Laboratory, Bay St. Louis, MS). In: American Society of Photogrammetry, Annual Meeting, 46th, St. Louis, MO, March 9-14, 1980, ASP Technical Papers. Falls Church, VA, American Society of Photogrammetry, 1980, p. 293-309. 5 refs.

The improvement in land cover classification achieved by merging microwave data with Landsat MSS data is examined. To produce a merged data set for analysis and comparison, a registration procedure by which a set of Seasat SAR digital data was merged with the MSS data is described. The Landsat MSS data and the merged Landsat/Seasat data sets were processed using conventional multichannel spectral pattern recognition techniques. An analysis of the classified data sets indicates that while Landsat data delineate different forest types (i.e., deciduous/coniferous) and allow some species separation, SAR data provide additional information related to plant canopy configuration and vegetation density as associated with varying water regimes, and therefore allow for further subdivision in the classification of forested wetlands of the coastal region of the southern United States. B.J.

A82-10044 * **Preliminary results of mapping urban land cover with Seasat SAR imagery.** F. M. Henderson (New York, State University, Albany, NY), S. W. Wharton, and D. L. Toll (NASA, Goddard Space Flight Center, Greenbelt, MD). In: American Society of Photogrammetry, Annual Meeting, 46th, St. Louis, MO, March 9-14, 1980, ASP Technical Papers. Falls Church, VA, American Society of Photogrammetry, 1980, p. 310-317.

The detectability of urban land cover types is explored using digitally processed Seasat SAR imagery of the Denver, Colorado area. Test sites within the metropolitan area were selected to include a cross section of Anderson, et. al. Level II land cover classes and cover types representative of the urban area growth stages. Using the Image 100 interactive processing system each test site was level sliced in an attempt to define specific reflectance boundaries for each cover type and to determine the spectral and spatial characteristics of homogeneous response regions. The rural-urban fringe boundary was readily definable, but a precise Level I and Level II land cover classification was not possible. High density housing could be separated from low density housing and from parks, but reflectance values were often look angle dependent. Confusion between some water and vegetation responses also posed problems. (Author)

A82-10616 **An investigation of a polar low with a spiral cloud structure.** E. Rasmussen (Copenhagen, University, Copenhagen, Denmark). *Journal of the Atmospheric Sciences*, vol. 38, Aug. 1981, p. 1785-1792. 9 refs.

A synoptic case study where a small-scale low, a so-called polar low, can be followed as a closed circulation on the surface maps around 2000 km from Iceland to the North Sea is presented. Satellite images show that the polar low develops a cloud pattern of convective clouds very much like that of a tropical cyclone. The 1000-500 mb thickness field shows that the polar low has a warm core during the time when it is best developed. It is concluded that the polar low discussed in this work probably is a phenomenon different from a comma cloud and also different from small-scale vortices associated with strong mid-tropospheric positive vorticity advection. (Author)

A82-10700 **Trace pollutant concentrations in a multiday smog episode in the California South Coast Air Basin by long path length Fourier transform infrared spectroscopy.** E. C. Tuazon, A. M. Winer, and J. N. Pitts, Jr. (California, University, Riverside, CA). *Environmental Science and Technology*, vol. 15, Oct. 1981, p. 1232-1237. 48 refs. U.S. Environmental Protection Agency Grant No. R-804546.

A82-11949 * **Automated analyzer for aircraft measurements of atmospheric methane and total hydrocarbons.** W. R. Cofer, III and G. C. Purgold (NASA, Langley Research Center, Hampton, VA). *Review of Scientific Instruments*, vol. 52, Oct. 1981, p. 1560-1564. 10 refs.

An automated methane/total hydrocarbon analyzer is presented, which can produce alternate methane/total hydrocarbon measurements every 7 seconds to provide the spatial resolution required for regional hydrocarbon measurements at aircraft speeds. The construction and sampling techniques developed for the aircraft mounted system are discussed. A technique to periodically measure atmosphere oxygen is incorporated into the analyzer to ensure accurate hydrocarbon measurements, and a data collection methodology is developed to minimize errors resulting from changes in flame ionization detector sensitivity at different altitudes. Aircraft data acquired at the 1979 Southeastern Virginia Urban Plume Study are also presented, which illustrate the application of the instrument to a troposphere pollution plume. D.L.G.

A82-12517 # **Spacelab-research of European regions with strong negative environmental influences, based on AVHRR-data of the satellites Tiros-N and NOAA.** H. Kaminski. In: International Scientific Conference on Space, 21st, Rome, Italy, March 25, 26, 1981, Proceedings. Rome, Rassegna Internazionale Elettronica Nucleare ed Aerospaziale, 1981, p. 197-206. 10 refs.

Remote sensing data from the Tiros-N-AVHRR satellites are considered as a base for further appraisals of air and water pollution in Europe by multispectral scanning from Spacelab. A short program is envisioned to verify the 10% anthropogenous induced clouding increase due to air traffic, as an aid to land use planning. Zones of meadows and woods between large towns are noted to be areas with no significant atmospheric heat build-up. Pollution from the Rhine and Po rivers has been sensed in the infrared and found to remain in coastal areas, mixing too slowly with sea water to disperse. A recommendation is offered to change the declination of Spacelab's orbit from 50 to 55 deg to allow more accurate sensing of pollutant problems in Belgium, the Netherlands, West Germany, and Italian industrialized regions. M.S.K.

A82-12591 **Areawide soil loss predictions using CIR airphotos.** K. M. Morgan (Texas Christian University, Fort Worth, TX) and R. Nalepa. In: Civil engineering applications of remote sensing; Proceedings of the Specialty Conference, Madison, WI, August 13, 14, 1980. New York, American Society of Civil

Engineers, 1980, p. 24-32. 10 refs. Research supported by the Texas Christian University Research Foundation.

It is pointed out that the Universal Soil Loss Equation (USLE) is a widely accepted tool for erosion prediction and conservation planning. In this study, manual interpretation of color infrared photography is used, along with the USLE and a computer-land information system, to identify critical areas of soil loss in Quil Miller Creek watershed in Johnson County, Texas. The low altitude color infrared photos used to record land use activities are at a scale of 1:48,000. C.R.

A82-12594 **Remote sensing that motivated community action.** R. H. Brownlee, J. P. Scherz (Wisconsin, University, Madison, WI), and J. M. Dennis (Chetek High School, Chetek, WI). In: Civil engineering applications of remote sensing; Proceedings of the Specialty Conference, Madison, WI, August 13, 14, 1980. New York, American Society of Civil Engineers, 1980, p. 60-77.

An account is given of the way in which the algal problem afflicting Prairie Lake, near Chetek, Wisconsin, was solved. Lake classification schemes developed at the University of Wisconsin with Multispectral Landsat Analysis indicated the source of pollution to be at the mouth of Rice Creek, which emptied into the lake. High-level and low-level aerial photos of the creek showed a cattle feedlot located near springs which fed into the creek. When residents of the area were shown the remote sensing data, they took steps to ensure that fewer cows used the spring. This solved the problem. C.R.

A82-12816 **Study of stack emissions by combination of lidar and correlation spectrometer.** P. Camagni, E. De Blust, C. Koechler, R. Michelon, A. Pedrini, M. De Groot, and S. Sandroni (Commission of the European Communities, Joint Research Centre, Ispra, Italy). *Nuovo Cimento C, Serie 1,* vol. 4C, May-June 1981, p. 359-371. 6 refs.

Examples are presented of the application of the combined techniques of lidar and correlation spectrometry to the monitoring of stack plume pollutants. Following a brief review of the principles of lidar observation of scattering particle spatial distribution and mask correlation spectrometer determination of gas integral-path thickness, attention is given to the results of combined measurements of particle and SO2 distributions above the three tallest stacks of the ENEL power plant at Turbigo, Italy. It is found that the plume aerosols behave differently from the gas component, which result demonstrates the potential of the combination technique in mass balance and mass flow evaluation. A.L.W.

A82-13268 * **Nitric oxide delta band emission in the earth's atmosphere - Comparison of a measurement and a theory.** D. W. Rusch (Colorado, University, Boulder, CO) and W. E. Sharp (Michigan, University, Ann Arbor, MI). *Journal of Geophysical Research,* vol. 86, Nov. 1, 1981, p. 10111-10114. 21 refs. Grants No. NsG-5372; No. NGR-23-005-360.

Attention is given to the altitude dependent emission rate in the delta-bands of nitric oxide as measured in the earth's atmosphere at night by a scanning ultraviolet spectrometer. It is noted that the reaction responsible is the two-body association of nitrogen and oxygen atoms. The measurements show a vertical intensity beneath the layer for the delta-band system of 19 R. The horizontal emission rate is found to increase from 70 R at 117 km to 140 R at 150 km. The data are analyzed with a one-dimensional, time-dependent, vertical-transport model of odd nitrogen photochemistry. The calculated and measured intensities agree so long as the quenching of N(2D) by atomic oxygen is near 5 x 10 to the -13 cu cm/sec. C.R.

A82-14320 **Radiative heating rates and some optical properties of the St. Louis aerosol, as inferred from aircraft measurements.** T. J. Method and T. N. Carlson (Pennsylvania State University, University Park, PA). *Atmospheric Environment,* vol. 16, no. 1, 1982, p. 53-66. 25 refs. U.S. Environmental Protection Agency Grants No. R-805500-01; No. R-806048-01-2.

Analyses of airborne measurements of solar and terrestrial radiation and aerosol profile measurements of the St. Louis boundary layer collected during two summers are summarized. Spectral pyranometers, radiometers, a pyrgeometer, an automatic particle counter, and an integrating nephelometer were used to collect data samples on 20 profile flights. Estimates of the vertical flux divergence and aerosol heating rates for solar, longwave, and total spectrum fluxes, in addition to total bulk estimates of aerosol parameters are provided. Results include a maximum aerosol heating in the visible exceeding three C/day near the bottom of the mixing layer, solar heating near one C/day near the ground, and zero heating near the top of the mixing layer. The total short and longwave radiative heating rates were slightly negative; with large particle aerosol concentration, the greatest extinction was near the surface. It is concluded that although St. Louis has a slightly greater aerosol loading than surrounding rural areas, the findings do not differ greatly from weakly absorbing natural soil particles commonly observed over nonurban and semiarid regions. M.S.K.

A82-15027 **Thermal inertia, thermal admittance, and the effect of layers.** G. F. Byrne and J. R. Davis (Commonwealth Scientific and Industrial Research Organization, Div. of Land Use Research, Canberra, Australia). *Remote Sensing of Environment,* vol. 9, June 1980, p. 295-300. 12 refs.

The effect of a diurnally varying flux on a solid surface is analysed in terms of thermal admittance, the reciprocal of complex thermal conductance. The presence of a surface layer of differing thermal characteristics from the bulk material, which can significantly affect the phase and amplitude of the temperature wave of the exposed surface, is discussed in terms of the admittance concept. It is suggested that the latter concept provides a better approach to the characterization of solid surfaces, particularly in the remote sensing context where varying water contents or organic materials are involved. (Author)

A82-15749 **Aerial-photography flights over Upper Franconia in 1980 - Operation and first application-related experience (Die Luftbildbefliegung Oberfranken 1980 - Ablauf und erste Anwendungserfahrungen).** B. Arnal (Höhere Landesplanungsbehörde, Bayreuth, West Germany). *Bildmessung und Luftbildwesen,* vol. 49, Nov. 1, 1981, p. 205-208. In German.

A82-15965 1 **Study of the anthropogenic influence on the environment, based on multispectral scanning images (Izuchenie antropogennogo vozdeistviia na prirodnuiu sredu po materialam mnogozonal'noi skanernoi s'emki).** V. I. Kravtsova and I. S. Nizkaia (Moskovskii Gosudarstvennyi Universitet, Moscow, USSR). *Issledovanie Zemli iz Kosmosa,* Sept.-Oct. 1981, p. 117-123. In Russian.

The possibilities of using images obtained by the Fragment multispectral scanning system to study the anthropogenic influence on the environment are analyzed. The analysis uses the taiga regions of the north European part of the USSR and the desert regions of Central Asia as examples. Maps are compiled of the anthropogenic influence on forest vegetation in the Kotlas region and on the desert landscapes of the central Ustiurt plateau. It is shown that the data obtained by the Fragment system are useful for establishing the occurrence, character, and degree of landscape changes; it can be used to compile thematic maps, to make recommendations on the use of resources, and to predict unfavorable effects of intense anthropogenic influences. J.F.

A82-15966 1 **Investigation and mapping of the erosion relief of the Kalachskaia upland on the basis of multispectral scanner images (Izuchenie i kartografirovanie erozionnogo rel'efa Kalachskoi vozvyshennosti po mnogozonal'nym skanernym snimkam).** N. I. Lapteva and N. N. Tal'skaia (Moskovskii Gosudarstvennyi Universitet, Moscow, USSR). *Issledovanie Zemli iz Kosmosa,* Sept.-Oct. 1981, p. 124-129. 5 refs. In Russian.

Geomorphological, lithological, and erosion maps were compiled for the Kalachskaia upland on the basis of the interpretation of multispectral scanner images obtained in different seasons with the Meteor-satellite Fragment system. The resolution and reliability of the images make it possible to convey the morphological structural plan of the region, the natural pattern, and the density of valleys and ravines. It is shown that the Fragment images can be effectively used to study the erosion relief of plains and to compile medium-scale geomorphological maps. B.J.

A82-15967 † Space photographs obtained with the Fragment system as a base for landscape mapping and physical-geographical classification of arid territories (Kosmicheskie snimki, poluchennye sistemoi 'Fragment' kak osnova landshaftnogo kartografirovaniia i fiziko-geograficheskogo raionirovaniia aridnykh territorii). L. I. Ivashutina and V. A. Nikolaev (Moskovskii Gosudarstvennyi Universitet, Moscow, USSR). *Issledovanie Zemli iz Kosmosa*, Sept.-Oct. 1981, p. 130-138. 9 refs. In Russian.

Space images obtained with the Meteor-satellite Fragment system have high landscape resolution and make it possible to investigate landscape structures of arid territories on several geosystem levels, from natural landscapes to physical-geographical regions. Detailed medium-scale landscape schemes of the southern Mugodzhar desert regions and of the northern Ustiurt were composed along with a consolidated scheme of physical-geographical division. Various interpretation criteria were used, the most important of which were optical density and image pattern. B.J.

A82-15968 Analysis of variance of thematic mapping experiment data. G. H. Rosenfield (U.S. Geological Survey, Reston, VA). *Photogrammetric Engineering and Remote Sensing*, vol. 47, Dec. 1981, p. 1685-1692. 23 refs.

The considered study has the objective to determine and document for the remote sensing researcher the minimum statistical methodology needed to perform and interpret an analysis of variance experiment. To illustrate the procedures, a set of data from the National Land Use and Land Cover Mapping Program of the U.S. Geological Survey was used. The set of proportions of correctly interpreted test data was subjected to three treatments of transformation as suggested by Snedecor and Cochran (1967). The transformed data were tested for the three assumptions of analysis of variance, taking into account normality, homogeneity of variance, and additivity. A weighted analysis of variance was performed, and multiple range tests were applied to those computed means deemed significant. From this research, a data analysis method and an operational computer program were developed to assist the analyst in considering the theoretical statistical concepts that are important for solving this type of problem. G.R.

A82-16325 Upper tropospheric cyclonic vortices in the tropical South Atlantic. V. E. Kousky and M. A. Gan (Conselho Nacional de Desenvolvimento Cientifico e Tecnológico, Instituto de Pesquisas Especiais, São Jose dos Campos, São Paulo, Brazil). *Tellus*, vol. 33, Dec. 1981, p. 538-551. 15 refs. Financiadora de Estudos e Projetos Contract No. B/28-79-002-00-00; Conselho Nacional de Pesquisas Contract No. 37/78.

An analysis of subtropical 200 mb cyclones is made for the South Atlantic. The cyclones are observed to occur primarily during the summer months and generally form near the axes of the mid-oceanic troughs. The relationship between cyclone formation and the presence of 200 mb anticyclones over the continental areas is discussed. Proposed mechanisms for cyclone formation are considered. The cyclones are characterized by a cold core and a direct thermal circulation - the cold air sinking and warm air on the periphery rising. The cloud pattern associated with the cyclones is found to depend on the direct thermal circulation, the vortex location and its direction of movement. The effects of South Atlantic 200 mb cyclonic vortices on Brazilian weather are discussed. (Author)

A82-16619 † Polarimetric surveys of oil slicks (Poliarizatsionnaia s'emka neftianykh zagriaznenii vodnoi poverkhnosti). B. S. Zhukov. In: Airborne and spaceborne multispectral photography of the earth. Moscow, Izdatel'stvo Nauka, 1981, p. 175-188. 16 refs. In Russian.

A theoretical study is presented of polarimetric remote-sensing surveys of oil slicks. The oil-water contrast is calculated as a function of the polarimetric analyzer, the spectral range, the thickness of the slick, and the transparence of the water. The influence of the atmosphere on the remote measurements of oil slicks is analyzed, and polarimetric measurement data on oil slicks are presented. B.J.

A82-16837 • A new method for inferring carbon monoxide concentrations from gas filter radiometer data. H. A. Wallio, H. G. Reichle, Jr. (NASA, Langley Research Center, Hampton, VA), J. C. Casas (Old Dominion University, Norfolk, VA), and B. B. Gormsen (Systems and Applied Sciences Corp., Hampton, VA). In: Conference on Atmospheric Radiation, 4th, Toronto, Canada, June 16-18, 1981, Preprints. Conference sponsored by the American Meteorological Society. Boston, MA, American Meteorological Society, 1981, p. 248-254. 14 refs.

A method for inferring carbon monoxide concentrations from gas filter radiometer data is presented. The technique can closely approximate the results of more costly line-by-line radiative transfer calculations over a wide range of altitudes, ground temperatures, and carbon monoxide concentrations. The technique can also be used over a larger range of conditions than those used for the regression analysis. Because the influence of the carbon monoxide mixing ratio requires only addition, multiplication and a minimum of logic, the method can be implemented on very small computers or microprocessors. D.L.G.

A82-17841 • # Results from the July 1981 Workshop on Passive Remote Sensing of the Troposphere. L. S. Keafer, Jr. and H. G. Reichle, Jr. (NASA, Langley Research Center, Hampton, VA). *American Institute of Aeronautics and Astronautics, Aerospace Sciences Meeting, 20th, Orlando, FL, Jan. 11-14, 1982, Paper 82-0207*. 8 p. 6 refs.

Potential roles of passive remote sensors in the study of the chemistry and related dynamics of the lower atmosphere were defined by a Tropospheric Passive Remote Sensing Workshop, and technology advances required to implement these roles were identified. A promising role is in making global-scale, multilayer measurements of the more abundant trace tropospheric gaseous species (e.g., O3, CO, CH4, HNO3) and of aerosol thickness and size distribution. It includes both nadir- and limb-viewing measurements. Technology advances focus on both scanning- and fixed-spectra, nadir-viewing techniques with resolutions of 0.1 kaysers or better. Balloon- and Shuttle-borne experiments should be performed to study the effects of instrument noise and background fluctuations on data inversion and to determine the utility of simultaneously obtained nadir- and limb-viewing data. (Author)

A82-18052 # The radiowave propagation environment - Science and technology objectives for the 80's. J. M. Goodman (U.S. Navy, E. O. Hulburt Center for Space Research, Washington, DC) and J. Aarons (USAF, Geophysics Laboratory, Bedford, MA). In: Symposium on the Effect of the Ionosphere on Radiowave Systems, Washington, DC, April 14-16, 1981, Preprints.
Washington, DC, U.S. Naval Research Laboratory, 1981. 10 p.

The ionosphere has a strong influence on the personality of radiowaves which propagate beneath, within, or through it; and this influence derives from the spatial and temporal nonuniformity in the refractivity of the magneto-ionic medium. Basic research objectives in environmental monitoring are examined, taking into account ionospheric research, magnetospheric research, interplanetary field and solar wind research, solar radiation and magnetic field research, and propagation studies. Operational systems which basic research will support are related to communications systems, navigation systems, and surveillance. Environmental effects/system deficiencies by frequency band are discussed, giving attention to the ELF frequency band (30-300 Hz), the VLF band (3-30 kHz), the MF/HF band (300 kHz - 30 MHz), and the UHF/SHF (300 MHz - 30 GHz). It is concluded that there is already a need to study the ionosphere and its coupling to the magnetosphere above and the troposphere below in order to more fully develop the insight required to specify the radiowave propagation effects introduced by the various media. G.R.

N82-11513*# Environmental Research and Technology, Inc., Concord, Mass.
AN EVALUATION OF THE SPATIAL RESOLUTION OF SOIL MOISTURE INFORMATION Final Report
Kenneth R. Hardy, Stephen H. Cohen, Linda Koshio Rogers, Hsiao-hua K. Burke, Robert C. Leupold, and Michael D. Smallwood
Mar. 1981 83 p refs
(Contract NAS5-25527)
(NASA-CR-166724; ERT-P-7505-F) Avail: NTIS
HC A05/MF A01 CSCL 08M

Rainfall-amount patterns in the central regions of the U.S.

were assessed. The spatial scales of surface features and their corresponding microwave responses in the mid western U.S. were investigated. The usefulness for U.S. government agencies of soil moisture information at scales of 10 km and 1 km. was ascertained. From an investigation of 494 storms, it was found that the rainfall resulting from the passage of most types of storms produces patterns which can be resolved on a 10 km scale. The land features causing the greatest problem in the sensing of soil moisture over large agricultural areas with a radiometer are bodies of water. Over the mid-western portions of the U.S., water occupies less than 2% of the total area, the consequently, the water bodies will not have a significant impact on the mapping of soil moisture. Over most of the areas, measurements at a 10-km resolution would adequately define the distribution of soil moisture. Crop yield models and hydrological models would give improved results if soil moisture information at scales of 10 km was available.
A.R.H.

N82-11514*# Jet Propulsion Lab., California Inst. of Tech., Pasadena.
RADAR MAPPING, ARCHAEOLOGY, AND ANCIENT LAND USE IN THE MAYA LOWLANDS
R. E. W. Adams (Cambridge Univ.), W. E. Brown, Jr., and T. Patrick Culbert (Arizona Univ.) 31 Mar. 1981 27 p refs
(Contract NAS7-100)
(NASA-CR-164931) Avail: NTIS HC A03/MF A01 CSCL 08B

Data from the use of synthetic aperture radar in aerial survey of the southern Maya lowlands suggest the presence of very large areas drained by ancient canals for the purpose of intensive cultivation. Preliminary ground checks in several very limited areas confirm the existence of canals and raised fields. Excavations and ground surveys by several scholars provide valuable comparative information. Taken together, the new data suggest that Late Classic period Maya civilization was firmly grounded in large-scale and intensive cultivation of swampy zones. A.R.H.

N82-11536# Hawaii Univ., Honolulu. Dept. of Planning and Economic Development.
A METHOD FOR USING AERIAL PHOTOS IN DELINEATING HISTORIC PATTERNS OF BEACH ACCRETION AND RETREAT
Dennis Hwang Dec. 1980 50 p refs
(Contract NA79AA-D-00085)
(PB81-223836; UNIHI-SG-CR-81-04; NOAA-81042706) Avail: NTIS HC A03/MF A01 CSCL 08C

A method is presented with a maximum estimated error of about 12 feet for measuring beach changes. This is believed to be an accurate estimate, as indicated by a comparison of field and photographic measurements and by the consistent distances obtained for nearby sections of the beach in the Kailua pilot study. The methods described in this report were applied for a pilot study of Kailua Beach.
GRA

N82-11635*# Mitre Corp., McLean, Va. Metrek Div.
SHUTTLE APPLICATIONS IN TROPOSPHERIC AIR QUALITY OBSERVATIONS Final Report
E. Friedman, J. Gupta, and J. Carmichael Aug. 1978 122 p refs Sponsored by NASA
(Contract F19628-78-C-001)
(NASA-CR-145374) Avail: NTIS HC A06/MF A01 CSCL 13B

The role which might be played by the space shuttle in obtaining data which describes the air quality of the north-eastern United States was investigated. The data requirements of users, a model for statistical interpretation of the observations, the influence of orbit parameters on the spatial and temporal sampling and an example of application of the the model were considered.
R.J.F.

N82-11639# Atmospheric Radiation Consultants, Action, Mass.
PROOF OF CONCEPT STUDY
A. S. Zachor, F. P. DelGreco, and M. Ahmadjian (AFGL) Hanscom AFB, Mass. AFGL 23 Mar. 1981 42 p refs Prepared for Utah State Univ., Logan
(Contract F19628-77-C-0203; AF Proj. 2310)
(AD-A104338; AFGL-TR-81-0134; SR-6) Avail: NTIS HC A03/MF A01 CSCL 17/5

Field test data were analyzed and computer simulations performed to validate the predictions of an earlier study, which calculated the minimum detectable quantities (MDQ's) of trace gases that can be detected remotely using high-resolution spectroscopy. The study demonstrates convincingly that reliable detection can be achieved near the MDQ level in a benign real-world environment.
Author (GRA)

N82-11649# Sandia Labs., Albuquerque, N. Mex.
ENVIRONMENTAL MONITORING REPORT, SANDIA NATIONAL LABS., ALBUQUERQUE, NEW MEXICO, 180
Gloria Chavez Millard, Theodore N. Simmons, Charles E. Gray, and Bill L. ONeal Apr. 1981 27 p refs
(Contract DE-AC04-76DP-00789)
(DE81-027839; SAND-81-0566) Avail: NTIS HC A03/MF A01

Radionuclides are potentially released from five technical areas from the laboratories research activities. The program searches for cesium-137, tritium, uranum, alpha emitters, and beta emitters in water, soil, air, and vegetation. No activity was found in public areas in excess of that found in local background in 1980. The Albuquerque population receives only 0.11 person-rem (estimated) from airborne radioactive releases. While national security research is the laboratories major responsibility, energy research is a major area of activity. Both these research areas cause radioactive releases.
T.M.

N82-11718 Washington Univ., Seattle.
ADAPTATION OF LAND USE TO SURFICIAL GEOLOGY IN METROPOLITAN WASHINGTON, D.C. Ph.D. Thesis
Robert Houston Alexander 1981 236 p
Avail: Univ. Microfilms Order No. 8121177

Implicit in the investigation is a process of communicating geologic information, and incorporating such information into land-use decisions. Land-use data were derived from high-altitude color infrared aerial photography, and the information on geologic suitability was obtained from a U.S. Geological Survey map of landforms and surface materials compiled to aid non-geologists in land use planning decisions. The new map was further interpreted and subdivided into those areas geologically suitable and unsuitable for residential and agricultural uses, respectively. The study found significant relationships among land uses and geologic map units, and significant differences in land-use and geologic suitability regimes in subregions based on distance from city center. More recently-developed areas near the urban core have higher proportional associations of residential and agricultural land use with appropriate surficial geologic characteristics than do the outlying areas on the metropolitan fringe. Dissert. Abstr.

N82-12499*# Texas Univ. at Austin.
CULTURAL FEATURES IMAGED AND OBSERVED FROM SKYLAB 4
Robert K. Holz *In* NASA. Johnson Space Flight Center Skylab Explores the Earth 1977 p 225-242 refs

Avail: NTIS MF A01; SOD HC $16.50 CSCL 08B

Data from Skylab 4 observations of metropolitan complexes are limited to city outline, major transportation arteries, suburban built-up areas, overall textural patterns of the city as compared to those of adjacent areas, and the color or albedo. Typical agricultural patterns, forest regions, and transportation networks on rural landscapes can be discerned, as well as the disturbances of soil during construction and mining which expose surface materials of a different albedo. Photographs of Denver, Colorado; San Antonio, Texas, Chicago, Illinois, and San Diego, California are analyzed.
A.R.H.

N82-12505*# Air Resources Lab., Las Vegas, Nev.
QUANTITATIVE ANALYSIS OF ATMOSPHERIC POLLUTION PHENOMENA
Darryl Randerson *In* NASA. Johnson Space Flight Center Skylab Explores the Earth 1977 p 381-406 refs

Avail: NTIS MF A01; SOD HC $16.50 CSCL 13B

Approximately 75 photographs of air pollution events were taken during the 84-day Skylab 4 mission. This imagery may be separated into two categories according to the sources of the pollution: natural pollution, which consists of dust generated by wind, naturally induced forest fires, and smoke generated by volcanic activity, and manmade pollution, which includes brush fires, smoke plumes from stacks or open burning, contrails, and

ship trails. Results of the analysis of some of the most interesting photographs are discussed in this section. Photographs of the following are analyzed: the Sakura-zime volcanic activity; dust clouds, the Los Angeles pollution pall; long smoke plums; an African brush fire, an Argentine forest fire, cirrus cloud plumes, and a snow streak.
A.R.H.

N82-12506*# National Aeronautics and Space Administration. Goddard Space Flight Center, Greenbelt, Md.
METEOROLOGICAL LAB APPLICATIONS OF SKYLAB HANDHELD-CAMERA PHOTOGRAPHS
W. C. Skillman and William E. Shenk *In* NASA. Johnson Space Flight Center Skylab Explores the Earth 1977 p 407-416

Avail: NTIS MF A01; SOD HC $16.50 CSCL 04B

The high resolution and image contrast of Skylab 4 photographs reveal details of the cloud structure associated with extratropical storms that normally cannot be seen in routinely available meteoriogical satellite images. A stereopair take over southern Arizona and northwestern Mexico east of the Gulf of California provides a good example of the cirrus clouds associated with a subtropical jet stream and demonstrates the height differences of multilayered clouds. The effects of cold air flowing over the warmer waters of the eastern Great Lakes, New York, southern New England, and the Atlantic Ocean are detailed as well as the cloud structure of an occluded cyclone. A.R.H.

N82-12507*# National Hurricane and Experimental Meteorology Lab., Coral Gables, Fla.
SOME ASPECTS OF TROPICAL STORM STRUCTURE REVEALED BY HANDHELD-CAMERA PHOTOGRAPHS FROM SPACE
Peter G. Black *In* NASA. Johnson Space Flight Center Skylab Explores the Earth 1977 p 417-462 refs

Avail: NTIS MF A01; SOD HC $16.50 CSCL 04B

The most important contribution to the fields of tropical storm research was the stereophotography of tropical storm Ellen during the Skylab 4 mission. Features of mature tropical storms revealed by Skylab 4 photographs are discussed and compared with data obtained by NOAA-2, Nimbus-5, and a DMSP satellite.
A.R.H.

N82-12508*# Chicago Univ., Ill.
MESOSCALE WAKE CLOUDS IN SKYLAB PHOTOGRAPHS
T. Theodore Fujita and Jaime J. Tecson *In* NASA. Johnson Space Flight Center Skylab Explores the Earth 1977 p 463-478 refs
Avail: NTIS MF A01; SOD HC $16.50 CSCL 04B

Examination of mesoscale cloud patterns within the wakes of obstacles seen in Skylab photographs reveals the existence of specific types of wake clouds. Cumulus streets occur when the lapse rate above the surface is adiabatic with a medium to slow flow rate. Karman vortex streets occur when the lapse rate above the surface is small, zero, or negative, with a slow to medium flow impinging against a relatively large obstacle. Wake waves occur when the lapse rate above the surface is small with a medium to fast flow rate impinging against a relatively small obstacle. When the flow rate exceeds a critical value, the transverse waves tend to disappear, leaving only the diverging waves. These phenomena are illustrated in Skylab photographs of the Aleutian Islands, the Kuril Islands, the Antipodes, South Pacific Islands, and the Bouvet Island in the South Atlantic.
A.R.H.

N82-12509*# National Aeronautics and Space Administration. Lyndon B. Johnson Space Center, Houston, Tex.
MESOSCALE CLOUD FEATURES OBSERVED FROM SKYLAB
David E. Pitts, J. T. Lee (National Severe Storms Lab.), J. Fein (Oklahoma Univ., Norman), Y. Sasaki (Oklahoma Univ., Norman), Kit Wagner, and R. Johnson (Lockheed Electronics Co., Houston, Tex.) *In its* Skylab Explores the Earth 1977 p 479-501 refs

Avail: NTIS MF A01; SOD HC $16.50 CSCL 04B

The Skylab 4 mission study of severe storm development was designed to photograph cloud-street patterns, to estimate the physical dimensions of cloud streets, and to describe their relationship to other cloud features and to land features. The moisture convergence of cloud streets and whether cloud-street curvature was an indicator of the source of angular momentum that results in the generation of rotating storms as precursors to tornadoes was analyzed from photographs taken over the Great Lakes and South America.
A.R.H.

N82-12511# Utah State Univ., Logan. Electro-Dynamics Lab.
LIMIT ON REMOTE FTIR DETECTION OF TRACE GASES
A. S. Zachor (Atmospheric Radiation Consultants, Inc.), B. Bartschi, and M. Ahmadjian (AFGL) Sep. 1981 7 p refs
(Contract F19628-77-C-0203; AF Proj. 7670)
(AD-A104842; AFGL-TR-81-0272) Avail: NTIS HC A02/MF A01 CSCL 20/6

We studied the capability of a Fourier spectrometer system to remotely detect trace gases in localized clouds, e.g., stationary source effluents. Detection is based on the degree to which the observed IR spectral radiance contrast between the cloud and adjacent background is correlated with a computed reference spectrum. It is shown that trace gases can be reliably detected when spectral features are well below the noise level. The minimum detectable quantities (MDQ's) for various trace gases at one atmosphere total pressure are given. The MDQ's determine the combinations of gas column thickness and gas-background temperature difference that correspond to 95 percent detection probability and one percent false detection probability when an FTS system with modest-size foreoptics views the target through a path equivalent to approximately one air mass. Author (GRA)

N82-12685* National Aeronautics and Space Administration. Pasadena Office, Calif.
MICROWAVE LIMB SOUNDER Patent
Jacob J. Gustincic, inventor (to NASA) (JPL, California Inst. of Tech., Pasadena) Issued 4 Aug. 1981 9 p Filed 24 Sep. 1979 Supersedes N79-34014 (17 - 24, p 3285) Sponsored by NASA
(NASA-Case-NPO-14544-1; US-Patent-4,282,525;
US-Patent-Appl-SN-078612; US-Patent-Class-343-100ME;
US-Patent-Class-343-100PE; US-Patent-Class-343-781P) Avail: US Patent and Trademark Office CSCL 04A

Trace gases in the upper atmosphere can be measured by comparing spectral noise content of limb soundings with the spectral noise content of cold space. An offset Cassegrain antenna system and tiltable input mirror alternately look out at the limb and up at cold space at an elevation angle of about 22. The mirror can also be tilted to look at a black body calibration target. Reflection from the mirror is directed into a radiometer whose head functions as a diplexer to combine the input radiation and a local oscillator (klystron) beam. The radiometer head is comprised of a Fabry-Perot resonator consisting of two Fabry-Perot cavities spaced a number of half wavelengths apart. Incoming radiation received on one side is reflected and rotated 90 deg in polarization by the resonator so that it will be reflected by an input grid into a mixer, while the klystron beam received on the other side is also reflected and rotated 90 deg, but not without passing some energy to be reflected by the input grid into the mixer.
Official Gazette of the U.S. Patent and Trademark Office

N82-12707# Automation Industries, Inc., Silver Spring, Md. Vitro Labs. Div.
ENVIRONMENTAL DATA FOR SITES IN THE NATIONAL SOLAR DATA NETWORK
Aug. 1981 176 p Prepared for Argonne National Lab.
(Contract DE-AC01-79CS-30027)
(DE82-000071; SOLAR/0010-81/08) Avail: NTIS HC A09/MF A01

Environmental information collected at the sites of the National Solar Data Network is tabulated for each solar site. The sites are grouped into 12 zones, each of which consists of several adjacent states. The insolation table presents the total, diffuse, direct, maximum, and extraterrestrial radiation for the site. It also shows the ratio of total to extraterrestrial radiation. The temperature table gives the average, daytime, nighttime, maximum, minimum, and inlet-water temperature for the site. All of the passive and some active solar sites are equipped with wind sensors which provide information on wind speed and direction. For some sites, a humidity tables provides relative humidity values for day and night. It also gives values for the maximum and minimum humidity for each day. A technical

discussion of the instruments and measurements used to obtain the data is included.
DOE

N82-12714 Meteorologisches Observatorium, Hohenpeissenberg (West Germany).
SPECIAL OBSERVATIONS BY THE HOHENPEISSENBERG METEOROLOGICAL OBSERVATORY. NUMBER 42: RESULTS OF AEROLOGICAL AND SURFACE OZONE MEASUREMENTS DURING THE FIRST SEMESTER OF 1980 [SONDERBEOBACHTUNGEN DES METEOROLOGISCHEN OBSERVATORIUMS HOHENPEISSENBERG. NR 42: ERGEBNISSE DER AEROLOGISCHEN UND BODENNAHEN OZONMESSUNGEN IM 1. HALBJAHR 1980]
1980 194 p refs In GERMAN and ENGLISH
(Sonderbeob-42; ISSN-0581-1287) Avail: Issuing Activity

Tabular and graphical ozonometry results are presented. Surface ozone measurement data cover day of measurement, daily mean of ozone near the ground (nbar), daily maximum of ozone near the ground (nbar), hour of maximum (GMT), duration of extreme values in excess of 100 nbar in tens of minutes, daily minimum (nbar), and monthly mean (without extreme values). Total ozone measurement data, determined by Dobson-spectrophotometer, include day of measurement, time of observation, type of measurement, i.e., direct Sun blue zenith, number of measurements for daily mean, and total ozone amount for AD and C wavelengths (daily mean values). The pairs of wavelengths used are: 305.5 nm, 325.4 nm; 311.45 nm, 332.4 nm; and 317.6 nm, 339.8 nm.
Author (ESA)

N82-13569# Meteorology Research, Inc., Santa Rosa, Calif.
AIRCRAFT DATA SUMMARIES OF THE SURE INTENSIVES, VOLUME 4 Final Report
W. S. Keifer, D. L. Blumenthal, J. B. Tommerdahl, J. A. Anderson, J. A. McDonald, R. B. Strong, and J. H. White Sep. 1981 190 p Sponsored by Electric Power Research Inst Prepared in cooperation with Research Triangle Inst., Research Triangle Park, N.C.
(EPRI Proj. RP-862)
(DE82-900311; EPRI-EA-1019-Vol-4) Avail: NTIS HC A09/MF A01

As part of the sulfate regional experient (SURE), six air quality sampling programs were conducted in the eastern United States using instrumented aircraft. The air quality and meteorological samples were taken near the Duncan Falls, Ohio sulfate regional experiment (SURE) Station and near the Research Triangle Park, North Carolina, SURE Station. Sampling data are presented for all measured parameters.
DOE

N82-13631# National Oceanic and Atmospheric Administration, Boulder, Colo.
GEOPHYSICAL MONITORING FOR CLIMATIC CHANGE, NUMBER 8: SUMMARY REPORT, 1979
Gary A. Herbert Dec. 1980 129 p refs
(PB81-233355; NOAA-81062615) Avail: NTIS HC A07/MF A01 CSCL 04B

Continuous measurement of CO2 and aerosol scattering at four wavelengths, using a nephelometer, began at the South Pole station. A filter collection system was installed at the Barrow station to make possible the determination of the mass of the carbonaceous aerosols. It is shown that graphic carbon makes up a significant part of the arctic haze, and because of its optical absorptivity, it may cause a significant contribution to the radiative energy budget. At the Mauna Loa Observatory a cooperative measurement program to obscure the chemical composition of aerosols was initiated.
GRA

N82-14572# Ecole Nationale Superieure des Mines, Sophia-Antipolis (France). Centre de Teledetection et d'Analyse des Milieux Naturels.
OIL SPILLS: LARGE SCALE MONITORING BY LANDSAT
M. Albuisson, J. M. Monget, and L. Wald *In* ESA Appl. of Remote Sensing Data on the Continental Shelf Jul. 1981 p 171-172 refs Sponsored by Joint Research Center of the European Communities

Avail: NTIS HC A13/MF A01; ESA, Paris FF 125

Oil pollution at sea using the LANDSAT multispectral scanner channel was detected. The variations of the reflection coefficient between rough sea and the oil spill was measured. The oil spill flattens the sea and reflects in only one direction while the capillary waves of rough sea scatter the light; a fraction of the incident light only reaches the satellite. An underestimate of pollution is expected during winter because of low solar elevation angles. This method is used to inventory pollution by hydrocarbons in the Mediterranean Sea. An estimation from 800 images shows the cumulative area covered by hydrocarbons, spread over the Mediterranean Sea each year, as 175,000 sq km.
Author (ESA)

N82-14573# Ministere de l'Environment et du Cadre de Vie, Neuilly (France). Direction de la Prevention des Pollutions.
THE OPERATIONAL OIL POLLUTION SURVEILLANCE SYSTEM BEING USED IN FRANCE: FORECASTED FUTURE DEVELOPMENTS IN CONSIDERATION OF THE NATO/CCMS REMOTE SENSING PILOT STUDY CONCLUSIONS
J. M. Massin *In* ESA Appl. of Remote Sensing Data on the Continental Shelf Jul. 1981 p 173-180 ref

Avail: NTIS HC A13/MF A01; ESA, Paris FF 125

The requirements of an ideal system for detecting, identifying, classifying, mapping, and tracking oil spills are defined. A core package consisting of a human observer, photographic cameras, side-looking airborne radar, infrared/ultraviolet line scanner, and passive television is proposed. The French airborne remote sensing system is shown to satisfy these requirements. Problems with a remote sensing system able to operate under all weather conditions, transmitting specific information in real time which permits the identification of hydrocarbons without having to check in situ, are discussed. Satellite possibilities are estimated.
Author (ESA)

N82-14588# Norwegian Air Survey Co., Oslo.
USE OF SIDE LOOKING AIRBORNE RADAR (SLAR) FOR OIL POLLUTION MONITORING IN NORWAY
Svein Erik Hoest *In* ESA Appl. of Remote Sensing Data on the Continental Shelf Jul. 1981 p 281-282 ref

Avail: NTIS HC A13/MF A01; ESA, Paris FF 125

Integration of the system with a data annotation unit and a navigation system is outlined. Position data, date, time, and mission parameters are annotated on film. Data are also displayed on a TV monitor while the radar image and data can be recorded on an onboard video cassette recorder. The installation of the system and its operation are covered and its potential use in oil spill monitoring (particularly at night and in low visibility) is explained. Other possible uses are summarized (search and rescue missions, geology, oceanography) together with possible future extensions of the sensor package and survey aircraft.
Author (ESA)

N82-14590# Atmospheric Sciences Lab., White Sands Missile Range, N. Mex.
SENSITIVITY ANALYSIS OF A MESOSCALE MOISTURE MODEL Final Report
James L. Cogan Mar. 1981 53 p refs
(DA Proj. 1L1-61102-B-53A)
(AD-A101528; ERADCOM/ASL-TR-0079) Avail: NTIS HC A04/MF A01 CSCL 04/1

Results from the model were computed for a variety of atmospheres and terrain types. A limited sensitivity analysis showed the effect of different model input parameters on meteorological variables for one vertical column through the atmosphere at a central horizontal grid point. A detailed analysis of selected cases for the entire domain of the model indicated the effect of input parameters on vertical velocity, precipitation amount, and precipitation rate. For one set of input parameters, analyses were performed of the variation of vertical velocity and precipitation every 2 hours for a 12-hour period. An example of a potential application to electro-optical algorithms is discussed and suggestions are made for future work.
T.M.

N82-14591# Aerospace Corp., El Segundo, Calif. Space Sciences Lab.
SATELLITE OBSERVATIONS OF THE MT. ST. HELENS' ERUPTION OF 18 MAY 1980
Carl J. Rice 21 Aug. 1981 32 p refs
(Contract F04701-80-C-0081)

(AD-A105784; TR-0081(6640)-3; SD-TR-81-70) Avail: NTIS HC A03/MF A01 CSCL 08/7

The explosive eruption of Mt. St. Helens on 18 May 1980 was monitored by infrared sensors aboard two U.S. Air Force satellites. Essentially continuous data are available following the initial sighting of the eruption cloud less than one minute after the earthquake which triggered the eruption. Dual monitoring permits triangulation so that both the horizontal and vertical development of the eruption can be determined with good temporal resolution. The sequence of events occurring early in the eruption can therefore be established. Author (GRA)

N82-15488*# Lockheed Engineering and Management Services Co., Inc., Houston, Tex.

INVESTIGATION OF THE APPLICATION OF REMOTE SENSING TECHNOLOGY TO ENVIRONMENTAL MONITORING

M. L. Rader, Principal Investigator Aug. 1980 76 p ERTS (Contract NAS9-15800)

(E82-10010; NASA-CR-161071; JSC-16759; LEMSCO-15175) Avail: NTIS HC A05/MF A01 CSCL 13B

Activities and results are reported of a project to investigate the application of remote sensing technology developed for the LACIE, AgRISTARS, Forestry and other NASA remote sensing projects for the environmental monitoring of strip mining, industrial pollution, and acid rain. Following a remote sensing workshop for EPA personnel, the EOD clustering algorithm CLASSY was selected for evaluation by EPA as a possible candidate technology. LANDSAT data acquired for a North Dakota test sight was clustered in order to compare CLASSY with other algorithms. A.R.H.

N82-15697# National Oceanic and Atmospheric Administration, Washington, D. C. Office of Federal Coordinator for Meteorological Services and Supporting Research.

NATIONAL HURRICANE OPERATIONS PLAN

May 1981 81 p

(PB81-247231; NOAA-FCM-P12-1981; NOAA-81071411) Avail: NTIS HC A05/MF A01 CSCL 04B

The hurricane warning service is an interdepartmental effort to provide the nation and designated international recipients with environmental data, forecasts, and assessments concerning tropical and subtropical weather systems. GRA

03

GEODESY AND CARTOGRAPHY

Includes mapping and topography.

A82-10028 **Digital image technology - MC&G impact.** M. Faintich (U.S. Defense Mapping Agency, Aerospace Center, St. Louis Air Force Station, MO). In: American Society of Photogrammetry, Annual Meeting, 46th, St. Louis, MO, March 9-14, 1980, ASP Technical Papers. Falls Church, VA, American Society of Photogrammetry, 1980, p. 32-43. 9 refs.

The Defense Mapping Agency Aerospace Center has developed a program to exploit digital image technology for the advancement of mapping, charting, and geodesy. Primary studies include image processing, analysis, and display techniques, and computer image generation. State-of-the-art digital image technology concepts have had a dramatic influence on the ability to analyze various digital data bases produced by the Defense Mapping Agency. In addition, emerging technologies in image processing and digital image analysis for automated feature extraction are demonstrating the potential for significant improvement in the utilization of imagery and significant reduction of production costs. Analyses of Landsat images and Viking Mars images are considered as examples. B.J.

A82-10029 **Factorial analysis of terrain feature positioning parameters used in combining radar and digital terrain model data.** R. Brock (New York, State University, Syracuse, NY) and D. I. Zulch (USAF, Rome Air Development Center, Griffiss AFB, NY). In: American Society of Photogrammetry, Annual Meeting, 46th, St. Louis, MO, March 9-14, 1980, ASP Technical Papers. Falls Church, VA, American Society of Photogrammetry, 1980, p. 44-51.

The significance of selected data collection parameters in the combination of radar data and digital terrain model data is evaluated in three phases: (1) the development of deterministic radar models from given digital terrain models and varying radar parameters; (2) the perturbation of the terrain feature coordinates which result from errors in radar position, radar orientation, range, and resolution; and (3) a factorial analysis of the terrain feature errors to establish the significance of the main fixed factors and their interactions; the main factors are azimuth from radar to terrain feature, range, resolution, terrain height, and coordinate. It is found that order of greatest to least importance of the factors is coordinate, range, resolution, terrain height, and azimuth. B.J.

A82-10056 **Application of satellite Doppler techniques to the national mapping program.** F. E. White, Jr. (U.S. Geological Survey, Topographic Div., Denver, CO). In: American Congress on Surveying and Mapping, Annual Meeting, 40th, St. Louis, MO, March 9-14, 1980, ACSM Technical Papers. Falls Church, VA, American Congress on Surveying and Mapping, 1981, p. 406-410.

Operational experience related to an employment of a Doppler system in Alaska during 1978 is discussed. There were certain problems in connection with equipment failure, poor weather conditions, and the destruction of one of the antennas by a grizzly bear. For a continuation of the operations, two MX 1502 Satellite Surveyor Systems were acquired in January 1979. Advantages of these systems over other systems currently in use are briefly examined. A description is presented of a research experiment which had been proposed in order to test and evaluate the acquired type of system at 29 deg, 40 deg, and 48 deg latitude. During the 1979 field season in Alaska, two teams established 45 Doppler stations and 65 electronic traverse stations from north of the Brooks Range area in the Arctic. Attention is given to a new instrument which would transcribe the cassette data of the Doppler Survey System to 9-track magnetic tape. G.R.

A82-10057 **Bureau of Land Management satellite Doppler positioning techniques.** W. E. Ball, Jr. (U.S. Bureau of Land Management, Denver, CO). In: American Congress on Surveying and Mapping, Annual Meeting, 40th, St. Louis, MO, March 9-14, 1980, ACSM Technical Papers. Falls Church, VA, American Congress on Surveying and Mapping, 1981, p. 411-421. 6 refs.

The U.S. Department of the Interior Bureau of Land Management has been using satellite Doppler positioning techniques to supplement existing survey control in Alaska since 1973. Multistation simultaneous positioning techniques are employed to obtain accurate relative positions among stations observed. Computed relative position coordinates are subsequently adjusted to conform to the known coordinates of the primary station, and to assure compatibility between all other satellite observation stations and existing local geodetic control stations. (Author)

A82-10645 * **GPS application to mapping, charting and geodesy.** W. J. Senus (U.S. Defense Mapping Agency, Advanced Technology Div., Washington, DC) and R. W. Hill (U.S. Navy, Naval Surface Weapons Center, Dahlgren, VA). *(Institute of Navigation, National Aerospace Meeting, Warminster, Pa., Apr. 8-10, 1981.) Navigation,* vol. 28, Summer 1981, p. 85-92. 6 refs. Research sponsored by the U.S. Defense Mapping Agency, U.S. Geological Survey, NASA, and NOAA.

GPSPAC, a receiver being developed for space applications by the Defense Mapping Agency and NASA, will use signals from GPS constellations to generate real-time values of host vehicle position and velocity. The GPSPAC has an L-band antenna and preamp capable of receiving the 1575 MHz and 1227 MHz spread spectrum signals; its stable oscillator at 5.115 MHz provides the basic frequency reference, resulting in a long term drift of less than one part in 10 to the -10th day. The GPSPAC performs many functions on board the spacecraft which were previously relegated to large-scale ground-based computer/receiver systems. A positional accuracy of better than 8 can be achieved for those periods when four or more NAVSTAR satellites are visible to the host satellite. The GPS geodetic receiver development, which will provide prototype receivers for utilization in terrestrial surveying operations, has the potential to significantly enhance the accuracy of point geodetic surveys over the current user hardware capability. J.F.

A82-10859 **Digitizing and automated output mapping errors.** L. G. S. Thompson (U.S. Military Academy, West Point, NY). *Photogrammetric Engineering and Remote Sensing,* vol. 47, Oct. 1981, p. 1455-1457.

Computer assisted cartography and mapping have become a reality. However, the errors concerned with these operations are still somewhat uncertain. Under the conditions found at the Army Survey Regiment, Bendigo, Australia, the errors associated with the digitizing of discrete points and the automated output of these points onto contact film were found to be 3.3 m and 1.9 m at ground scale (+ or - 0.082 mm and + or - 0.037 mm at table scale). The frequency of capturing digits and the expected errors when digitizing nondiscrete points (i.e., when the cursor is continuously in motion) are also discussed. (Author)

A82-12186 * **Magnetic field-aligned electron distributions in the dayside cusp.** L. J. Zanetti, T. A. Potemra (Johns Hopkins University, Laurel, MD), J. P. Doering, J. S. Lee (Johns Hopkins University, Baltimore, MD), and R. A. Hoffman (NASA, Goddard Space Flight Center, Greenbelt, MD). *Journal of Geophysical Research,* vol. 86, Oct. 1, 1981, p. 8957-8970. 35 refs. Contract No. NAS5-11415.

Observations of low-energy electron fluxes made over a 6 year period with the photoelectron spectrometer on the AE-C and AE-D satellite are used to investigate electron pitch angles in the low altitude cusp. A 16 point energy spectrum from 2 to 500 eV was obtained at every .25 s, and the location of the cusp was verified by the presence of protons detected by the low-energy electron instrument. Isotropic fluxes of precipitating electrons with Maxwellian energy spectra were observed in the low-altitude cusp, and the presence of low-energy electrons with pitch angles less than 15 deg was determined streaming into the cusp ionosphere. The energies of the streaming electrons sometimes appeared as a peak superimposed on the normal cusp Maxwellian background of isotropic electrons, and it is concluded that the energies and pitch angle distributions of the precipitating electrons may explain the enhancements of auroral emissions and discrete arcs. D.L.G.

A82-12215 **Distant magnetic field effects associated with Birkeland currents /made possible by the evaluation of TRIAD's**

attitude oscillations/. G. Gustafsson (Kiruna Geophysical Institute, Kiruna, Sweden), T. A. Potemra, S. Favin (Johns Hopkins University, Laurel, MD), and N. A. Saflekos (Boston College, Chestnut Hill, MA). *Journal of Geophysical Research,* vol. 86, Oct. 1, 1981, p. 9219-9223. 13 refs. NSF Navy-supported research.

Principal oscillations of the TRIAD satellite are studied in 150 passes and are identified as the librations of a gravity-stabilized satellite. The libration periods are T(O)/2 and T(O)/(3) exp 1/2, where T(O) is the orbit period of about 100 min. The amplitude and phase change over periods of a few days, sometimes vanishing altogether, and these attitude changes are numerically evaluated and removed. Data from three consecutive passes spanning over three hours show a magnetic profile which extends as far as 10 deg in latitude from a single region 1 Birkeland current sheet, confirming the permanent and global nature of large-scale Birkeland currents.

D.L.G.

A82-12912 † **Phototriangulation with map referencing of photographs in linear surveys (Fototriangulirovanie s priviazkoi snimkov k karte pri lineinykh izyskaniiakh).** A. I. Kaigorodov. *Geodeziia i Kartografiia,* Sept. 1981, p. 30, 31. In Russian.

A82-12914 † **A new method for computing distortion (O novom sposobe vychisleniia distorsii).** A. Sh. Shakhverdov and E. Z. Shliam. *Geodeziia i Kartografiia,* Sept. 1981, p. 34-36. In Russian.

An improved method is proposed for computing distortion arising in the calibration of aerial topographic cameras. The new method is especially suitable for implementation on a large computer, and was found to lead to a fivefold-to-sixfold improvement in the computation of distortion as compared with traditional methods.

B.J.

A82-12915 † **Aerial and space methods in cartography (Aerokosmicheskie metody v kartografii).** L. I. Zlobin and Iu. G. Kel'ner. *Geodeziia i Kartografiia,* Sept. 1981, p. 39-42. 9 refs. In Russian.

A82-15032 * **The surface albedo of the earth in the near ultraviolet /330-340 nm/.** J. E. Frederick (NASA, Goddard Space Flight Center, Laboratory for Planetary Atmospheres, Greenbelt, MD) and R. B. Abrams (Computer Sciences Corp., Silver Spring, MD). *Remote Sensing of Environment,* vol. 11, Nov. 1981, p. 337-347. 13 refs.

Satellite-borne measurements of solar radiation backscattered by the earth and atmosphere allow a determination of the surface albedo in the near ultraviolet. The data yielded albedos at tropical latitudes during a 15-month period in 1979-1980. The wavelengths studied are 331.2 and 339.8 nm. Sixty-nine percent of the measurements imply albedos less than 0.3. Higher values include a contribution due to reflection from clouds and are consistent with previous estimates of the fractional cloudover in the tropics. An albedo histogram based on a bin width of 0.1 shows results in the range 0.1-0.2 to be the most frequent, appearing in 29% of the cases, although values which span the entire range 0.0-1.0 are present. The derived albedos show no correlation with solar zenith angle. This result is consistent with the fact that, at the wavelengths considered, the diffuse integrated intensity is larger than the attenuated direct solar beam near the ground.

(Author)

A82-16161 **Some problem areas in the field of quality control for aerotriangulation.** M. Molenaar (International Institute for Aerial Survey and Earth Sciences, Enschede, Netherlands). *ITC Journal,* no. 3, 1981, p. 253-265. 20 refs.

Attention is given to problem areas in quality control for aerotriangulation. These include: (1) the possible occurrence of gross errors; (2) the presence of systematic deformations; (3) unified testing procedures; (4) the analysis of the stochastical model; (5) aerotriangular block accuracy as a function of ground control distribution; (6) variance component estimation; and (7) accuracy methods in practice.

S.C.S.

A82-16868 **Use of hydromagnetic waves to map geomagnetic field lines.** R. A. Greenwald, A. D. M. Walker (Johns Hopkins University, Laurel, MD), and M. Candidi (CNR, Laboratorio per il Plasma nello Spazio, Frascati, Italy). *Journal of Geophysical Research,* vol. 86, Dec. 1, 1981, p. 11251-11257. 12 refs. NSF Grant No. ATM-80-03300.

It is pointed out that if ionospheric and magnetospheric regions showing highly correlated temporal variations could be identified, it would be possible to determine the region in the ionosphere conjugate to a given location in the magnetosphere. A cross-correlation analysis is presented of Pc 5 magnetic field oscillations observed by GEOS 2 with drift velocity oscillations (electric field) observed with the STARE radars in the ionosphere. It is noted that GEOS 2 is in geostationary orbit with its conjugate point nominally located in the STARE field of view. Several comparisons are made over a 1-hour period in the early afternoon sector, and correlation coefficients reaching 0.84 over a limited area in the ionosphere are obtained. It is found that between the beginning and end of the hour, the measured footpoint is displaced by approximately 1 deg in latitude and approximately 2.5 deg in longitude.

C.R.

A82-18797 # **Space techniques to monitor movements in the earth's crust.** S. Hieber (ESA, Directorate of Application Programmes, Paris, France). *ESA Bulletin,* no. 28, Nov. 1981, p. 62-67.

Space techniques to monitor movements in the earth's crust such as very slow drift of tectonic plates or regional fault motions are discussed. Major research objectives in geodynamics are given. Space techniques include a number of satellite remote sensing missions, very-long-baseline interferometry and laser tracking methods, and satellite gradiometry. It is concluded that satellite imagery can be used in many more ways to enhance interdisciplinary research in geophysics and geology.

D.L.G.

N82-11696*# Smithsonian Astrophysical Observatory, Cambridge, Mass.
STUDY OF THE TIME EVOLUTION OF THE LITHOSPHERE Semiannual Progress Report, 1 Mar. - 31 Aug. 1981
Micheline C. Roufosse Nov 1981 7 p
(Grant NAG5-150)
(NASA-CR-164968; SAPR-1) Avail: NTIS HC A02/MF A01 CSCL 08G

A three dimensional geoid of all oceanic regions was obtained using a data set derived from the GEOS-3 radar altimeter. The editing and organization of the complete SEASAT geophysical data set are described. The geographical area located between 25 and 35 degrees south, and between 320 and 335 degrees east, around the Rio Grande Rise in the south Atlantic, was selected for continued study.

T.M.

N82-13606# National Geodetic Survey, Rockville, Md.
REPORT OF SURVEY FOR MCDONALD OBSERVATORY, HARVARD RADIO ASTRONOMY STATION, AND VICINITY
William E. Carter and James E. Pettey May 1981 91 p refs
(PB81-234338; NOAA-TM-NOS-NGS-32; NOAA-81062603)
Avail: NTIS HC A05/MF A01 CSCL 08E

A special purpose three dimensional geodetic survey was conducted near Ft. Davis, Texas. The observing program included astronomic positions and azimuths, zenith distances, electromagnetic distance measurements, leveling, gravity measurements, Doppler satellite positioning, and a variety of ancillary measurements. Information on the methods employed in the collection, reduction, and analysis of the survey data, tabulations of the observational data, and numerical and interpretive results is reported.

GRA

N82-14041*# National Aeronautics and Space Administration, Washington, D. C.
REPORTS OF PLANETARY GEOLOGY PROGRAM, 1981
Henry E. Holt, comp. Dec. 1981 580 p refs
(NASA-TM-84211) Avail: NTIS HC A25/MF A01 CSCL 03B

Abstracts of 205 reports from Principal investigators of NASA's Planetary Geology Program succinctly summarize work conducted and reflect the significant accomplishments. The entries are arranged under the following topics: (1) Saturnian satellites; (2) asteroids, comets and Galilean satellites; (3) cratering processes and landform development; (4) volcanic processes and landforms; (5) Aerolian processes and landforms; (6) fluvial, preglacial, and other processes of landform development; (7) Mars polar deposits, volatiles, and climate; (8) structure, tectonics, and stratigraphy; (9) remote sensing and regolith chemistry; (10) cartography and geologic mapping; and (11) special programs. A.R.H.

N82-15620# National Ocean Survey, Rockville, Md.
A HISTORY OF FLYING AND PHOTOGRAPHY: IN THE PHOTOGRAMMETRY DIVISION OF THE NATIONAL OCEAN SURVEY 1919 - 1979
John T. Smith, Jr. 1980 493 p refs
(PB81-246738; NOAA-81071405) Avail: NTIS HC A21/MF A01 CSCL 14E

A history of aerial photography and its impact on photogrammetric geodesy is presented. The work of pilots, navigators, and photographers as teams is narrated. Early mapping activities are reported. Development of the nine lens camera is described. Other topics include pilot training, testing of color and infrared photography, the B-17 photographic aircraft, beginning the Liberian survey, adaptation to new equipment, Saudi Arabia mapping, the Buffalo aircraft, and the RC-10 camera. GRA

N82-15812 Deutsches Geodaetisches Forschungsinstitut, Munich (West Germany).
DESCRIPTION AND COMPARISON OF ALGORITHMS FOR SOLVING LARGE SETS OF SPARSE MATRIX NORMAL EQUATIONS IN GEODESY AND PHOTOGRAMMETRY Ph.D. Thesis - Technischen Univ., Munich [DARSTELLUNG UND VERGLEICHE VON LOESUNGSSTRATEGIEN FUER GROSSE SCHWACH BESETZTE NORMALGLEICHUNGSSYSTEME IN DER GEODAESIE UND IN DER PHOTOGRAMMETRIE]
Franz Steidler Verlag der Bayerischen Akademie der Wissenschaften 1980 117 p refs In GERMAN
(Ser-C-261; ISSN-0065-5325; ISBN-3-7696-9313-2) Avail: Issuing Activity

Algorithms were investigated in relation to calculation time and data storage capability. For geodetic networks, direct techniques for sparse matrices are very well suited. For photogrammetric bundle-block adjustments with self calibration the conventional use of band algorithms is the best choice. For generating a digital terrain model following the finite element method, the band algorithm solves the normal equations in the fastest way. Author (ESA)

[illegible]

[illegible]

04

GEOLOGY AND MINERAL RESOURCES

Includes mineral deposits, petroleum deposits, spectral properties of rocks, geological exploration, and lithology.

A82-11039 * **A closer examination of the reduction of satellite magnetometer data for geological studies.** R. D. Regan (Barringer Resources, Golden, CO), D. W. Handschumacher (U.S. Navy, Naval Ocean Research and Development Activity, Bay St. Louis, MS), and M. Sugiura (NASA, Goddard Space Flight Center, Greenbelt, MD). *Journal of Geophysical Research*, vol. 86, Oct. 10, 1981, p. 9567-9573. 19 refs. Contracts No. N00014-79-C-0653; No. NAS5-25882.

Results of a detailed examination of magnetic field residuals obtained from POGO satellite magnetometer data are presented which illustrate some problems which may be encountered in the reduction and analysis of Magsat data. Comparisons of field residuals determined from OGO 2, 4 and 6 data for the region between 270 and 290 deg E reveals significant differences between the satellite data sets which are related to differences in the residual field level on individual satellites, external field contamination and effects from ring current correction in the data reduction process. When a new map is prepared from OGO 2 and 4 satellite data by compensating for these factors, dramatic differences with the original map are noted, including the disappearance of a major positive anomaly and the better definition of various magnetic highs and lows. The new map is also noted to be more consistent with conventional airborne and marine magnetic measurements. The results thus demonstrate the necessity for the inspection of satellite data and the adequate removal of the external field signal prior to geological analysis.
A.L.W.

A82-12366 * # **Coordinates of features on the Galilean satellites.** M. E. Davies and F. Y. Katayama (Rand Corp., Santa Monica, CA). *Journal of Geophysical Research*, vol. 86, Sept. 30, 1981, p. 8635-8657. 13 refs. Contracts No. JPL-953613; No. NASw-3321.

Control nets of the four Galilean satellites have been established photogrammetrically from pictures taken by the two Voyager spacecraft during their flybys of Jupiter in 1979. Coordinates of 504 points on Io, 112 points on Europa, 1547 points on Ganymede, and 439 points on Callisto are listed. Selected points are identified on U.S. Geological Survey maps of the satellites. Measurements of these points were made on 234 pictures of Io, 115 pictures of Europa, 282 pictures of Ganymede, and 200 pictures of Callisto. The systems of longitude were defined by craters on Europa, Ganymede, and Callisto. Preliminary solutions have been found for the directions of the axes of rotation of the Galilean satellites. New mean radii have been determined as 1815 + or - 5 km for Io, 1569 + or - 10 km for Europa, 2631 + or - 10 km for Ganymede, and 2400 + or - 10 km for Callisto.
(Author)

A82-12590 **Remote sensing study of sinkhole occurrence.** J. W. Casper, B. E. Ruth, M. Asce, and J. D. Degner (Florida, University, Gainesville, FL). In: Civil engineering applications of remote sensing; Proceedings of the Specialty Conference, Madison, WI, August 13, 14, 1980. New York, American Society of Civil Engineers, 1980, p. 1-14. 10 refs.

N82-10465 Utah Univ., Salt Lake City.
MORPHOSTRUCTURAL ANALYSES OF SPACE IMAGERY IN THE CENTRAL COLORADO PLATEAU Ph.D. Thesis
Abdelrahman Mohammad Shafik Maarouf 1981 130 p
Avail: Univ. Microfilms Order No. 8118146

Coincidences of increase or decrease in frequency of most of the lineament trends common to both Skylab and Landsat photos and images of the Colorado Plateau suggest that the peaks or troughs are not artificially introduced by sampling bias, and there are actual preferred orientations represented by peak or trough coincidences. Interpretation of lineaments from Skylab and Landsat data, along with study of magnetic and gravity maps, suggest strong correlation between lineaments and faults in the Precambrian basement. It is shown that the basement faults influenced the present surface drainage and structures through a sedimentary cover of more than 6 km. The faults were formed during the middle Precambrian, and were rejuvenated later in varying degrees and at various times. Dissert. Abstr.

N82-10476# Bendix Field Engineering Corp., Grand Junction, Colo.
STATISTICAL TECHNIQUES APPLIED TO AERIAL RADIOMETRIC SURVEYS (STAARS): SERIES INTRODUCTION AND THE PRINCIPAL-COMPONENTS-ANALYSIS METHOD
Fredric L. Pirkle Apr. 1981 62 p refs
(Contract DE-AC13-76GJ-01664)
(DE81-029177; GJBX-114(81)) Avail: NTIS HC A05/MF A01

A series of open-file reports established to provide the latest interpretation techniques to those using aerial radiometric data is announced. Geological applications of the technique are emphasized in case histories. A bibliography is provided which defines the detailed theory and statistics of the technique to assist researchers in ascertaining the statistical validity and merit of the technique. The use of multivariate statistical analysis in delineating regions favorable to uranium deposition in the Lubbock and Plainview quadrangles of Texas, and along the Texas Gulf coast is demonstrated in this issue. GRA

N82-10618 Idaho Univ., Moscow.
GEOLOGY AND LINEARS OF LIBYA Ph.D. Thesis
Milud Abdulkrim Mansur 1981 276 p
Avail: Univ. Microfilms Order No. 8119882

The geology of Libya is described in detail with some reference to economic resources. An analysis of LANDSAT space photographs revealed about 2,000 linears, unequally distributed in the different parts of the country, and characterized by considerable variations in their length, strike, and density. Some of them coincide with known structural features including fault scarps, topographic features, dikes, alignments of igneous bodies, and straight drainage systems. Dissert. Abstr.

N82-12491 Cornell Univ., Ithaca, N. Y.
REMOTE SENSING STUDIES OF SOME IRONSTONE GRAVELS AND PLINTHITE IN THAILAND Ph.D. Thesis
Pichit Jamnongpipatkul 1980 336 p
Avail: Univ. Microfilms Order No. 8177113

Ironstone gravels and plinthite in eastern Thailand were found to be associated with alluvial terraces as well as shale and basalt formation. Selected stereopairs of airphotos of known areas of ironstone gravels and plinthite were studied. The keys for airphoto interpretation were developed on the basis of the relation with types of landform, vegetation and appearance on the airphotos. Visual analysis of LANDSAT data provided information on the types of LANDSAT and vegetation which could lead to more detailed investigation of probable areas of ironstone gravels and plinthite. Digital analysis of LANDSAT data indicated that the difference of spectral reflectances from areas of ironstone gravels and those from the surrounding areas is considerable. Field study was conducted to verify the results of airphotos interpretation and LANDSAT data analysis and to obtain information in regard to genesis and morphology of soils with ironstone gravels and plinthite. Soil profile descriptions for typical soils with ironstone gravels and plinthite are included.
Dissert. Abstr.

N82-12492*# National Aeronautics and Space Administration. Lyndon B. Johnson Space Center, Houston, Tex.
SKYLAB EXPLORES THE EARTH
Washington 1977 512 p refs Original contains color illustrations
(NASA-SP-380; LC-77-829) Avail: NTIS MF A01; SOD HC $16.50 CSCL 08B

Data from visual observations are integrated with results of analyses of approxmately 600 of the nearly 2000 photographs taken of Earth during the 84-day Skylab 4 mission to provide additional information on (1) Earth features and processes; (2) operational procedures and constraints in observing and photographing the planet; and (3) the use of man in real-time analysis of oceanic and atmospheric phenomena.

N82-12493*# Geological Survey, Denver, Colo.
DESERT SAND SEAS
Edwin D. McKee, Carol S. Breed (Geological Survey, Flagstaff, Ariz.), and Steven G. Fryberger (Geological Survey, Flagstaff, Ariz.) *In* NASA. Johnson Space Flight Center Skylab Explores the Earth 1977 p 5-48 refs

Avail: NTIS MF A01; SOD HC $16.50 CSCL 08B

The usefulness of manned observations and handheld-camera photographs from space is confirmed by the immediate application of Skylab 4 data to the study of sand seas. The Skylab 4 crew provided information that: (1) confirms a tentative global classification of eolian sand deposits based on observed similarities in most of the major deserts of the world; (2) allows the preparation of maps that show the relationships of sand deposits to each other, to sand source areas, to natural sand distribution barriers, and to human land use; and (3) allows the regional patterns of large-scale dune morphology to be studied in relation to rainfall distribution and surface winds. Four sites in the Sahara and sub-Sahara of northern Africa, four in the Namib and Kalahari Deserts of southern Africa, two in the Empty Quarter of Saudi Arabia, five in the Takla Makan and Gobi Deserts of China, and three in the trans-Caspian deserts of the U.S.S.R. were selected as well as additional areas in northern Africa, India, Mexico, and Australia. A.R.H.

N82-12494*# Texas Univ. at Austin.
GLOBAL TECTONICS: SOME GEOLOGIC ANALYSES OF OBSERVATIONS AND PHOTOGRAPHS FROM SKYLAB
W. R. Muehlberger, P. R. Gucwa, A. W. Ritchie, and E. R. Swanson *In* NASA. Johnson Space Flight Center Skylab Explores the Earth 1977 p 49-88 refs

Avail: NTIS MF A01; SOD HC $16.50 CSCL 08G

Spreading zones, transform faults, and subduction zones were observed visually and by hand-held camera on Skylab 4. Geological studies of these observations are discussed for the Near and Middle East, the Atacama fault in Chile, the Alpine Fault zone in New Zealand, the Sierra Madre Occidental, in Mexico, and the Caribbean/Americas plate boundary in Guatemala and Southern Mexico. A.R.H.

N82-12495*# California Inst. of Tech., Pasadena.
GEOLOGICAL FEATURES OF SOUTHWESTERN NORTH AMERICA
L. T. Silter, T. H. Anderson, C. M. Conway, J. D. Murray, and R. E. Powell *In* NASA. Johnson Space Flight Center Skylab Explores the Earth 1977 p 89-136 refs

Avail: NTIS MF A01; SOD HC $16.50 CSCL 08G

Photographic and visual observation of geological target areas were integrated with other aspects of the ground investigations to: (1) identify and evaluate zones of major faulting in south eastern California, Baja California, and northwestern Sonora; (2) develop a new key to the regional stratigraphy of the prebatholithic rocks of northern Baja California; (3) discover the most southwesterly known occurrence of Precambrian crystalline rocks in North America; (4) discover a previously unmapped section of Mesozoic volcanic rocks in southeastern California; and (5) contribute important overview perspectives to many regional geologic problems. Skylab 4 data are discussed for the San Andreas fault system and architecture of Southern California; Nothern Baja, California; Sierra Mazatan and Sierra del Alamo in Sonora, Mexico; the northwest Sonora coast fault zones; and Arizona, including that portion of the Colorado Plateau in the vicinity of the Grand Canyon. A.R.H.

N82-12496*# Geological Survey, Denver, Colo.
SKYLAB 4 OBSERVATIONS OF VOLCANOES. PART A: VOLCANOES AND VOLCANIC LANDFORMS. PART B: SUMMIT ERUPTION OF FERNANDIAN CALDERA, GALAPAGOS ISLANDS, ECUADOR
Jules D. Friedman, Grant Heiken (Low Alamos Scientific Labs., New Mexico), Tom Simkin (Smithsonian Inst., Washington, D.C.), and Arthur F. Krueger (NOAA, Washington, D.C.) *In* NASA. Johnson Space Flight Center Skylab Explores the Earth 1977 p 137-173 refs
Avail: NTIS MF A01; SOD HC $16.50 CSCL 08K

Terrestrial volcanic features were observed and photographed from Skylab 4 under a variety of viewing conditions and Sun angles. Eruptions of Sakura-zima in southern Kyushu, Japan and the remote Fernandina volcano in the Galapagos Islands provided rare documentation of eruption clouds. Remote volcanic regions were also surveyed including the Tibesti volcanic massif and the Emi Koussi Caldera in Chad; the Altiplano volcanic field of Bolivia, Argentina, and Chile; the Kanchatcha Penninsula, U.S.S.R.; and the southeastern central plateau of Mexico. The landforms of volcanic provinces of Hawaii, southern Italy, the Aleutian Islands, Oregon, and Washington State were also investigated. Previously unobserved relationships between geomorphology and structure and previously unmapped tectonic ligaments were revealed as well as stratigraphic or relative age distinctions between partly overlapping basaltic flows. A.R.H.

N82-12497*# Energy, Mines and Resources Canada, Ottawa (Ontario).
THE MANICOUAGAN IMPACT STRUCTURE OBSERVED FROM SKYLAB
M. R. Dence *In* NASA. Johnson Space Flight Center Skylab Explores the Earth 1977 p 175-190 refs

(Contrib-544) Avail: NTIS MF A01; SOD HC $16.50 CSCL 08B

From comprehensive views of eastern Canada provided by Skylab oblique photographs, the main elements of the multi-ring Manicougan structure can be defined. By gravitational scaling, the structure is an analog for 200 km diameter structures on Mars and Mercury and 400 km to 500 km basins on the Moon. Because much larger structures on the other planets have rings spaced at intervals of 2 to the 1/2 power spacing, it is of interest to know if rings with intermediate spacing can be identified. A.R.H.

N82-12713# University Coll., Cardiff (Wales). Dept. of Applied Mathematics and Astronomy.
INFRARED SPECTROSCOPY OF MICROORGANISMS NEAR 3.4 MICRONS IN RELATION TO GEOLOGY AND ASTRONOMY
F. Hoyle, N. C. Wickramasinghe, S. Al-Mufti, and A. H. Olavesen Jun. 1981 11 p refs Submitted for publication
(Preprint-69) Avail: NTIS HC A02/MF A01

Cracking of microorganisms at high temperature and pressure were examined for the existence of microfossils in sedimentary rocks of the Isna series. Microorganism specimens were examined for degradation by infrared spectroscopy over the wavelength range from 2.5 microns to 15 microns. Stability up to 380 C after which there is degradation towards graphite is shown. It is concluded that the preservation of microfossils is feasible in rocks metamorphosized at temperatures of 400 C. Author (ESA)

N82-14600# Carson Helicopters, Inc., Perkasie, Pa.
NURE AERIAL GAMMA-RAY AND MAGNETIC RECONNAISSANCE SURVEY OF MAINE AND PORTIONS OF NEW YORK, VOLUME 2 Final Report
Jul. 1981 124 p refs
(Contract DE-AC13-76GJ-01664)
(DE82-000781; GJBX-327-81-Vol-2-SHERBROOKE) Avail: NTIS HC A06/MF A01

Contents includes: the flight line base map, anomaly maps (uranium, thorium, potassium, uranium/thorium, uranium/potassium, thorium/potassium), total count map, magnetic field map, uranium map, thorium map, potassium map, ratio maps for uranium/thorium, uranium/potassium, thorium/potassium, radiometric multiple-parameter stacked profiles, magnetic and ancillary stacked profile data, and histograms. DOE

N82-14601# Carson Helicopters, Inc., Perkasie, Pa.
NURE AERIAL GAMMA-RAY AND MAGNETIC RECONNAISSANCE SURVEY OF MAINE AND PORTIONS OF NEW YORK, VOLUME 2 Final Report
Jul. 1981 140 p refs
(Contract DE-AC13-76GJ-01664)
(DE82-000401; GJBX-327-81-Vol-2-OGDENSBURG) Avail: NTIS HC A07/MF A01

Content includes: the flight line base map anomaly maps (uranium, thorium, potassium, uranium/thorium, uranium/potassium, thorium/potassium), total count map, magnetic field map, uranium map, thorium map, potassium map, ratio maps for uranium/thorium, uranium/potassium, thorium/potassium, radiometric multiple-parameter stacked profiles, magnetic and ancillary stacked profile data, and historgrams. DOE

N82-14602# Carson Helicopters, Inc., Perkasie, Pa.
NURE AERIAL GAMMA-RAY AND MAGNETIC RECONNAISSANCE SURVEY OF MAINE AND PORTIONS OF NEW YORK, VOLUME 2 Final Report
Jun. 1981 168 p refs
(Contract DE-AC13-76GJ-01664)
(DE82-000780; GJBX-327-81-Vol-2-MILLINOCKET) Avail: NTIS HC A08/MF A01

Content contains: the flight line base map, anomaly maps (uranium, thorium, potassium, uranium/thorium, uranium/potassium, thorium/potassium), total count map, potassium map, ratio maps for uranium/thorium, uranium/potassium, thorium/potassium, rdiometric multiple-parameter stacked profiles, magnetic and ancillary stacked profile data, and histograms. DOE

N82-14603# Carson Helicopters, Inc., Perkasie, Pa.
NURE AERIAL GAMMA-RAY AND MAGNETIC RECONNAISSANCE SURVEY OF MAINE AND PORTIONS OF NEW YORK, VOLUME 2 Final Report
Jul. 1981 80 p refs
(Contract DE-AC13-76GJ-01664)
(DE82-000872; GJBX-327-81-Vol-2-LEWISTON) Avail: NTIS HC A05/MF A01

Content contains: the flight line base map, anomaly maps (uranium, thorium, potassium, uranium/thorium, uranium/potassium, thorium/potassium), total count map, magnetic field map, uranium map, thorium map, potassium map, ratio maps for U/T, U/K, T/K, radiometric multiple-parameter stacked profiles, magnetic and ancillary stacked profile data, and histograms. DOE

N82-14604# Carson Helicopters, Inc., Perkasie, Pa.
NURE AERIAL GAMMA-RAY AND MAGNETIC RECONNAISSANCE SURVEY OF MAINE AND PORTIONS OF NEW YORK, VOLUME 2 Final Report
Jun. 1981 306 p refs
(Contract DE-AC13-76GJ-01664)
(DE82-000772; GJBX-327-81-Vol-2-FREDERICTON) Avail: NTIS HC A14/MF A01

Content contains: the flight path maps, anomaly maps (uranium, thorium, potassium, uranium/thorium, uranium/potassium, thorium/potassium), radiometric multiple parameter stacked profiles, magnetic and ancillary stacked profile data, histograms, total count maps, magnetic field maps, uranium maps, thorium maps, potassium maps, ratio maps for U/T, U/K, and T/K. DOE

N82-14605# Carson Helicopters, Inc., Perkasie, Pa.
NURE AERIAL GAMMA-RAY AND MAGNETIC RECONNAISSANCE SURVEY OF MAINE AND PORTIONS OF NEW YORK, VOLUME 2 Final Report
Jun. 1981 242 p refs
(Contract DE-AC13-76GJ-01664)
(DE82-000785; GJBX-327-81-Vol-2-EDMUNDSTON) Avail: NTIS HC A11/MF A01

Content contains: the flight line base maps, nomaly maps (uranium, thorium, potassium, uranium/thorium, uranium/potassium, thorium/potassium), radiometric multiple parameter stacked profiles, magnetic and ancillary stacked profile data, histograms, total count maps, magnetic field maps, uranium maps, thorium maps, potassium maps, ratio maps for U/T, U/K, and T/K. DOE

N82-14606# Carson Helicopters, Inc., Perkasie, Pa.
NURE AERIAL GAMMA-RAY AND MAGNETIC RECONNAISSANCE SURVEY OF MAINE AND PORTIONS OF NEW YORK, VOLUME 2 Final Report
Jul. 1981 150 p refs
(Contract DE-AC13-76GT-01664)
(DE82-000869; GJBX-327-81-Vol-2-BINGHAMTON) Avail: NTIS HC A07/MF A01

Content contains: the flight line base map, anomaly maps (uranium, thorium, potassium, uranium/thorium, uranium/potassium, thorium/potassium), total count map, magnetic field map, uranium map, thorium map, potassium map, ratio maps for U/T, U/K, T/K, radiometric multiple parameter stacked profiles, magnetic and ancillary stacked profile data, and histograms. DOE

N82-14607# Carson Helicopters, Inc., Perkasie, Pa.
NURE AERIAL GAMMA-RAY AND MAGNETIC RECONNAISSANCE SURVEY OF MAINE AND PORTIONS OF NEW YORK, VOLUME 2 Final Report
Jul. 1981 260 p refs
(Contract DE-AC13-76GJ-01664)
(DE82-000794; GJBX-327-81-Vol-2-BANGOR) Avail: NTIS HC A12/MF A01

Content contains: the flight line base maps, anomaly maps (uranium, thorium, potassium, uranium/thorium, uranium/potassium, thorium/potassium), total count maps, magnetic field maps, uranium maps, thorium maps, potassium maps, ratio maps for U/T, U/K, T/K, radiometric multiple parameter stacked profiles, magnetic and ancillary stacked profile data, and histograms. DOE

N82-14608# Carson Helicopters, Inc., Perkasie, Pa.
NURE AERIAL GAMMA-RAY AND MAGNETIC RECONNAISSANCE SURVEY OF MAINE AND PORTIONS OF NEW YORK, VOLUME 2 Final Report
Jul. 1981 166 p refs
(Contract DE-AC13-76GJ-01664)
(DE82-000784; GJBX-327-81-Vol-2-UTICA) Avail: NTIS HC A08/MF A01

Content contains: the flight line base map, anomaly maps (uranium, thorium, potassium, uranium/thorium, uranium/potassium, thorium/potassium), radiometric multiple parameter stacked profiles, magnetic and ancillary stacked profile data, histograms, total count map, magnetic field map, uranium map, thorium map, potassium map, ratio maps for U/T, U/K, and T/K. DOE

N82-15487*# Massachusetts Univ., Amherst. Dept. of Geology.
THE MINERALOGY OF GLOBAL MAGNETIC ANOMALIES Progress Report, Jan. - Sep. 1981
Stephen E. Haggerty, Principal Investigator 19 Sep. 1981 27 p ERTS
(Contract NAS5-26414)
(E82-10009; NASA-CR-164907) Avail: NTIS HC A03/MF A01 CSCL 08G

Progress is reported in developing predictive abilities to evaluate the potential stabilities of magnetic minerals in the Earth crust and mantle by: (1) computing oxidation state profiling as a function of temperature and pressure; (2) compiling data on basalts to establish validity of the oxidation state profiles; (3) determining Fe-Ni alloys in association with magnetitie as a function of temperature and oxidation state; and (4) acquiring large chemical data banks on the mineral ilmenite which decomposes to mineral spinel in the presence of high sulfur or carbonate environments in the lower crust upper mantle. In addition to acquiring these data which are related to constraining Curie isotherm depths, an excellent correlation was found between MAGSAT anomaly data and the geology of West Africa. A.R.H.

N82-15489*# Geological Survey, Denver, Colo.
GEOLOGIC APPLICATIONS OF THERMAL-INERTIA MAPPING FROM SATELLITE Final Report
Terry W. Offield, Principal Investigator, Kenneth Watson, and Susanne Hummer-Miller Jul. 1981 109 p refs Original contains imagery. Original imagery may be purchased from NASA Goddard Space Flight Center, (Code 601), Greenbelt, Md. 20771. Domestic users send orders to 'Attn: National Space Science Data Center'; non-domestic users send orders to 'Attn: World Data Center A for Rockets and Satellites'. HCMM
(NASA Order S-40256-B)
(E82-10011; NASA-CR-164818) Avail: NTIS HC A06/MF A01 CSCL 08B

In the Powder River Basin, Wyo., narrow geologic units having thermal inertias which contrast with their surroundings can be discriminated in optimal images. A few subtle thermal inertia anomalies coincide with areas of helium leakage believed to be associated with deep oil and gas concentrations. The most important results involved delineation of tectonic framework elements some of which were not previously recognized. Thermal and thermal inertia images also permit mapping of geomorphic textural domains. A thermal lineament appears to reveal a basement discontinuity which involves the Homestake Mine in the Black Hill, a zone of Tertiary igneous activity and facies control in oil producing horizons. Applications of these data to the Cabeza Prieta, Ariz., area illustrate their potential for igneous rock type discrimination. Extension to Yellowstone National Park resulted in the detection of additional structural information but surface hydrothermal features could not be distinguished with any confidence. A thermal inertia mapping algorithm, a fast and accurate image registration technique, and an efficient topographic slope and elevation correction method were developed. Author

04 GEOLOGY AND MINERAL RESOURCES

N82-15505# Geological Survey, Denver, Colo.
PRELIMINARY ANALYSIS OF GRAVITY AND AEROMAGNETIC SURVEYS OF THE TIMBER MOUNTAIN AREA, SOUTHERN NEVADA
M. F. Kane, M. W. Webring, and B. K. Bhattacharyya 1981 143 p refs
(Contract DE-AI08-78ET-44802)
(DE81-029462; DOE/ET-44802/T2; USGS-Open-File-81-189)
Avail: NTIS HC A07/MF A01

Gravity and aeromagnetic surveys revealed details of subsurface structure and lithology. Information caused by volcanic events accommodated along straight line faults combining to give a curvilinear appearance to regional structure is suggested. The magnetic data suggest that rock units may have been altered, perhaps thermally, from their original state. The gravity data indicate that the south part of Timber Mountain is underlain by relatively dense and possibly intrusive rock, like that which crops out along its southeast side. The gravity data also suggest that the Silent Canyon caldera may extend considerably south of its presently indicated southern limit and may underlie much of the area of Timber Mountain. The most areas appear to be more rectangular or triangular than annular in shape. The southern part of Timber Mountain caldera is separated from the Yucca Mountain area to the south by a triangular horst. The structural relations of the rock units making up the horst are complex. Several linear terrain features in the southern part of the caldera area are closely alined with geophysical features, implying that the terrain features are fault controlled. DOE

N82-15925# Preussag A.G. Metall, Goslar (West Germany). Arbeitsgebiet Rohstoffe.
AN INVESTIGATION INTO THE APPLICABILITY OF THERMAL INFRARED SCANNING FOR EXPLORATION Final Report, Feb. 1981
Heribert Broicher Bonn Bundesministerium fuer Forschung und Technologie Jun. 1981 18 p refs In GERMAN; ENGLISH summary Sponsored by Bundesministerium fuer Forschung und Technologie
(BMFT-FB-T-81-087; ISSN-0340-7608) Avail: NTIS HC A02/MF A01; Fachinformationszentrum, Karlsruhe, West Germany DM 3,80

Pratt's theory of thermal inertia stripping lead to thermal inertia calculations for subsurface zones subjected to diurnal and annual temperature variations, as well as to temperatures at the zone limits. Thermal inertia mapping after separating these zones gains in importance for exploration since forebodies might cause detectable subsurface temperature anomalies. T.M.

05

OCEANOGRAPHY AND MARINE

Includes sea-surface temperature, ocean bottom surveying imagery, drift rates, sea ice and icebergs, sea state, fish location.

A82-10671 **Analysis of SEASAT wind observations over the Indian Ocean.** J. J. Fernandez-Partagas and M. A. Estoque (Miami, University, Miami, FL). *Tellus,* vol. 33, Oct. 1981, p. 463-475. Contract No. NOAA-NA-79SAC00737.

Surface winds as observed by the Seasat-A satellite over the Indian Ocean for the period July 15-17, 1978 are analyzed. The purposes of the analysis are: (1) to evaluate the accuracy of the Seasat wind measurements by comparing these measurements with ship observations and (2) to determine the improvement introduced to the description of the synoptic-scale wind field at the surface by adding Seasat data to ship and island wind observations. The results of the study indicate that: (1) on the synoptic scale, the accuracy of Seasat-derived winds is comparable to that of conventional surface observations and (2) a significant improvement in the surface wind analysis is achieved by incorporating Seasat wind information, especially in data sparse areas. (Author)

A82-11201 **The observation of tidal patterns, currents, and bathymetry with SLAR imagery of the sea.** G. P. De Loor (Centrale Organisatie voor Toegepast-Natuurwetenschappelijk Onderzoek, Physisch Laboratorium TNO, The Hague, Netherlands). *IEEE Journal of Oceanic Engineering,* vol. OE-6, Oct. 1981, p. 124-129. 9 refs.

Work done until 1978 on the visualization of currents, bathymetry, internal waves, etc., in SLAR imagery of the sea is reported. It did not receive much attention until the SEASAT SAR imagery showed these effects on a global scale. Although we know, qualitatively, how these images come about we are yet far from knowing how to extract more quantitative data from them on depth, current speed, etc. Much research effort is still needed here and for this work a simple real-aperture SLAR can be a very useful tool. (Author)

A82-11202 * **SAR imaging of ocean waves - Theory.** A. Jain (California Institute of Technology, Jet Propulsion Laboratory, Pasadena, CA). *IEEE Journal of Oceanic Engineering,* vol. OE-6, Oct. 1981, p. 130-139. 26 refs. Contract No. NAS7-100.

A SAR imaging integral for a rough surface is derived. Aspects of distributed target imaging and questions of ocean-wave imaging are considered. A description is presented of the results of analyses which are performed on aircraft and a spacecraft data in order to gain an understanding of the SAR imaging of ocean waves. The analyzed data illustrate the effect of radar resolution on the images of azimuthally traveling waves, the dependence of image distortion on the angle which the waves make with the radar flight path, and the dependence of the focusing parameter of the radar matched filter on the ocean wave period for azimuthally traveling waves. A dependence of ocean-wave modulation on significant wave height is also observed. The observed dependence of the modulations of azimuth waves on radar resolution is in contradiction to the hypothesis that these modulations are caused mainly by velocity bunching. G.R.

A82-11203 **Wave orbital velocity, fade, and SAR response to azimuth waves.** R. K. Raney (Canada Centre for Remote Sensing, Ottawa, Canada). *IEEE Journal of Oceanic Engineering,* vol. OE-6, Oct. 1981, p. 140-146. 18 refs.

Orbital motion of azimuth waves imposes differential Doppler shifts on wave imagery as seen by a SAR. This paper shows that these Doppler shifts are a function only of the wave and sensor geometry, and are not a function of SAR parameters. The azimuth wave reflectivity so modulated is equivalent to a redistributed scatterer density which can be used as an input with the SAR modulation transfer function for general distributed scenes to derive the azimuth wave image. The static scatterer density is calculated for a variety of sea states. Wave accelerations are not of first-order importance. Scatterer fade (decorrelation) is of central importance, as it impacts the SAR transfer function that is effective in wave imaging. (Author)

A82-12885 * **Synoptic thermal and oceanographic parameter distributions in the New York Bight Apex.** R. W. Johnson (NASA, Langley Research Center, Hampton, VA), G. S. Bahn (Kentron International, Inc., Hampton, VA), and J. P. Thomas (NOAA, Northeast Fisheries Center, Highlands, NJ). *Photogrammetric Engineering and Remote Sensing,* vol. 47, Nov. 1981, p. 1593-1598. 11 refs.

Concurrent surface water measurements made from a moving oceanographic research vessel were used to calibrate and interpret remotely sensed data collected over a plume in the New York Bight Apex on 23 June 1977. Multiple regression techniques were used to develop equations to map synoptic distributions of chlorophyll a and total suspended matter in the remotely sensed scene. Thermal (which did not have surface calibration values) and water quality parameter distributions indicated a cold mass of water in the Bight Apex with an overflowing nutrient-rich warm water plume that originated in the Sandy Hook Bay and flowed south near the New Jersey shoreline. Data analysis indicates that remotely sensed data may be particularly useful for studying physical and biological processes in the top several metres of surface water at plume boundaries. (Author)

A82-13214 **Oceanic wind and balanced pressure-height fields derived from satellite measurements.** R. M. Endlich, D. E. Wolf, C. T. Carlson, and J. W. Maresca, Jr. (SRI International, Menlo Park, CA). *Monthly Weather Review,* vol. 109, Sept. 1981, p. 2009-2016. 14 refs. Contract No. NOAA-NA-795AC0073.

The surface wind field over part of the northern Pacific on July 17 and October 3, 1978, was analyzed in light of (1) Seasat-A scatterometer system (SASS) measurements of wind speed and direction, and (2) GOES-2 satellite measurements of cloud motion directions. Agreement was found upon comparison of the surface pressure fields computed from the nondivergent, SASS-derived wind velocity fields using the balance equation with National Meteorological Center surface pressure fields. The linear correlation coefficient between the two fields was 0.91 for July 17 and 0.84 for October 3, indicating that the surface wind and pressure fields of the global oceans, excluding a narrow equatorial zone where the balance equation is invalid, can be determined with good accuracy by the exclusive use of satellite measurements. O.C.

A82-14586 # **Water vapour absorption in the 3.5-4.2 micron atmospheric window.** I. J. Barton (Oxford University, Oxford, England; Commonwealth Scientific and Industrial Research Organization, Div. of Atmospheric Physics, Aspendale, Victoria, Australia). *Royal Meteorological Society, Quarterly Journal,* vol. 107, Oct. 1981, p. 967-972. 16 refs. Research supported by the Natural Environment Research Council.

An analysis of the results of Nimbus 5 Chopper Radiometer data of sea surface water vapor temperature in the 3.5-4.2 micron interval are reported. The interval was chosen because the temperature dependence of the Planck radiance gives better temperature discrimination than at longer wavelengths and the water absorption is smaller, although e-type absorption was observed. Derivation of the absorption coefficients is described, along with measurement techniques used with the Nimbus-5 instruments. A transmittance model was developed to account for absorptances by atmospheric gases, resulting in a value of 4/g sq cm/atm for a self-broadened coefficient at 3.55 microns, implying the possibility of remotely sensing tropical sea surface temperatures to an accuracy of 1 K. M.S.K.

A82-14730 **Radar backscattering from ocean waves at low grazing angles.** H. C. Glaser and T. F. Havig (Boeing Aerospace Co., Seattle, WA). In: NAECON 1981; Proceedings of the National Aerospace and Electronics Conference, Dayton, OH, May 19-21, 1981. Volume 1. New York, Institute of Electrical and Electronics Engineers, Inc., 1981, p. 406-411. 6 refs.

Measurement of backscattering from sea clutter at grazing angles of zero to eight degrees is presented. During the qualification testing of the E-3A maritime radar (S-band, horizontally polarized, short pulse length), sea clutter data were recorded. Almost two billion range gate amplitudes were recorded over the period between

November 1979 and May 1980. Data judged outside the dynamic range of the system and that contaminated by land clutter were deleted. Conditions from flat calm to sea state five with forty knot winds have been recorded. Surface truth was reported by NOAA weather buoys every hour by satellite link. Wind speed was reported by the buoys and by the operator of the target vessel used in the testing. Absolute backscattering levels were determined by comparing the clutter returns with those from a dihedral reflector of measured cross section. Flight-to-flight variation in system gain is less than 2 dB, allowing reliable comparison between all of the data.

(Author)

A82-15030 **Comparison of polar and geostationary satellite infrared observations of sea surface temperatures in the Gulf of Maine.** R. Legeckis, E. Legg (NOAA, National Environmental Satellite Service, Washington, DC), and R. Limeburner (Woods Hole Oceanographic Institution, Woods Hole, MA). *Remote Sensing of Environment*, vol. 9, June 1980, p. 339-350. 10 refs. Grants No. NOAA-04-7-158-44104; No. NOAA-04-8-M01-149.

A82-15031 * **Remote sensing of benthic microalgal biomass with a tower-mounted multispectral scanner.** D. J. Jobson, S. J. Katzberg (NASA, Langley Research Center, Flight Electronics Div., Hampton, VA), and R. G. Zingmark (South Carolina, University, Columbia, SC). *Remote Sensing of Environment*, vol. 9, June 1980, p. 351-362. 18 refs. Grant No. NsG-1334.

A remote sensing instrument was mounted on a 50-ft tower overlooking North Inlet Estuary, South Carolina in order to conduct a remote sensing study of benthic microalgae. The instrument was programmed to take multispectral imagery data along a 90 deg horizontal frame in six spectral bands ranging from 400-1050 nm and had a ground resolution of about 3 cm. Imagery measurements were encoded in digital form on magnetic tape and were stored, decoded, and manipulated by computer. Correlation coefficients were calculated on imagery data and chlorophyll a concentrations derived from ground truth data. The most significant correlation occurred in the blue spectral band with numerical values ranging from -0.81 to -0.88 for three separate sampling periods. Mean values of chlorophyll a for a larger section of mudflat were estimated using regression equations. The scanner has provided encouraging results and promises to be a useful tool in sampling the biomass of intertidal benthic microalgae.

(Author)

A82-15076 **Ocean surface height-slope probability density function from SEASAT altimeter echo.** B. J. Lipa (SRI International, Menlo Park, CA) and D. E. Barrick (NOAA, Wave Propagation Laboratory, Boulder, CO). *Journal of Geophysical Research*, vol. 86, Nov. 20, 1981, p. 10921-10930. 25 refs. Grant No. NOAA-MO-A01-78-00-4319.

A82-15213 † **Determination of the length of sea waves by an airborne radar technique (Opredelenie dliny morskikh voln radiolokatsionnym metodom s letatel'nogo apparata).** A. A. Garnaker'ian, V. L. Karakush'ian, and V. D. Bukharin. *Radiotekhnika i Elektronika*, vol. 26, Nov. 1981, p. 2447-2450. 6 refs. In Russian.

A82-15318 * # **An analysis of short pulse and dual frequency radar techniques for measuring ocean wave spectra from satellites.** F. C. Jackson (NASA, Goddard Space Flight Center, Greenbelt, MD). *Radio Science*, vol. 16, Nov.-Dec. 1981, p. 1385-1400. 17 refs.

A four frequency moment characterization of backscatter from the near-vertical is applied to an analysis of the short pulse and dual frequency microwave techniques. The range reflectivity modulation spectrum closely approximates the directional wave slope spectrum, while harmonic distortion is small and is a minimum near 10 deg incidence. The short pulse measurement signal-to-noise ratio (SNR) is typically greater than the narrowband dual frequency SNR, with the difference being the ratio of the range beam extent to pulse length, minus the ratio of beam-limited to pulse-limited Doppler spreads. It is concluded that dual frequency measurements are basically impractical, although short pulse measurements are useful and can employ existing space-qualified microwave hardware.

D.L.G.

A82-15960 † **Investigation of survey conditions for the ocean surface in the 0.4-1.1 micron spectral range (Issledovanie uslovii s'emki poverkhnosti okeana v spektral'nom diapazone 0.4-1.1 mkm).** A. S. Selivanov, Iu. M. Gektin, A. S. Panfilov, and A. B. Fokin. *Issledovanie Zemli iz Kosmosa*, Sept.-Oct. 1981, p. 82-89. 18 refs. In Russian.

The optimal survey conditions were determined for frontal zones, meanders, eddies, and internal waves in the ocean, based on Meteor-satellite observations of the ocean surface in the visible and near-infrared spectral band. A theoretical model is presented, which takes into account these surface phenomena. It is shown that surveys should be performed in the sunny areas, where contrasts reach their maximum values; the maximum values of contrast were observed at solar zenith distances and at angles of sight of about 40 deg. The width of the spectral survey band does not have great significance in the study, since the observed phenomena do not have a marked spectral selectivity. Contrasts on the surfaces were found to disappear when the speed of the ocean surface wind exceeded 5-7 m/sec.

J.F.

A82-15962 † **Development of a coastal relief of the Gulf of Riga, based on results of an analysis of space images (Razvitie rel'efa poberezhii Rizhskogo zaliva po rezul'tatam analiza kosmicheskikh snimkov).** G. A. Saf'ianov and V. I. Kravtsova (Moskovskii Gosudarstvennyi Universitet, Moscow, USSR). *Issledovanie Zemli iz Kosmosa*, Sept.-Oct. 1981, p. 97-102. In Russian.

Based on an interpretation of relief forms of the coast of the Gulf of Riga, a geomorphological scheme of the coast was compiled, and an analysis of the dynamics of its development was performed. The direction of the alluvial drift in the past was established, and the main tendency of the dynamic processes of the coastal zone during the past thousand years were determined, namely, the separation of the single flow of deposits due to a change in the external conditions of their displacement.

J.F.

A82-16341 **U.S. Navy planning for satellite oceanographic data exploitation.** V. E. Noble (U.S. Navy, Naval Research Laboratory, Washington, DC) and R. Y. Felt (U.S. Navy, Naval Oceanography Div., Washington, DC). In: International space technical applications; Proceedings of the Nineteenth Goddard Memorial Symposium, Arlington, VA, March 26, 27, 1981.
San Diego, CA, Univelt, Inc., 1981, p. 117-130. (AAS 81-072)

The authors present an unofficial view of the basis for planning within the Navy Environmental Remote Sensing Program (NERSP). The NERSP includes all phases of research, development, and operational applications related to exploitation of oceanographic data from satellites. The existing 'end-to-end' system will be expanded to provide for: direct and central-site readout, assimilation of satellite data into analysis and prediction programs, dissemination and display of products, and generation of system-specific Tactical Decision Aids. NERSP priorities are driven by requirements, opportunities, and difficulty of R&D problems.

(Author)

A82-16620 † **Images of sea waves obtained in polarimetric surveys (Ob izobrazhenii volneniia pri poliarizatsionnoi s'emke).** V. V. Egorov and B. S. Zhukov. In: Airborne and spaceborne multispectral photography of the earth. Moscow, Izdatel'stvo Nauka, 1981, p. 188-196. 13 refs. In Russian.

An analysis is presented of the influence of the orientation of the analyzer on the structure and contrast of sea-wave images in polarimetric remote-sensing surveys. The imaging process is accompanied by a distinctive wave-filtering which depends on the survey conditions. Experimental results on such polarimetric surveys are presented.

B.J.

A82-17168 **Detection of monsoon inversion by TIROS-N satellite.** M. S. Narayanan and B. M. Rao (Space Applications Centre, Ahmedabad, India). *Nature*, vol. 294, Dec. 10, 1981, p. 546-548. 6 refs.

A link is established between the extent of inversion regions and the convective processes with the Indian monsoon at its different phases. TIROS N satellite data provided sea surface temperature (SST), a 15-layer atmospheric temperature profile from 1000 to 0.4 mbar, and three levels of water vapor content. A horizontal map of the SST and the 1000-850 mb layer-mean temperature with time and spatial averaging, confirmed by comparison with aircraft dropsonde data, revealed the inversion over the Arabian Sea. A 5 x 5 deg grid was devised to account for underlap of the maps, and showed a temperature increase west to east with the growth of a monsoon. A 10 min water vapor curve for tne 700-500 mbar level, drawn from the TIROS data, revealed higher values to the east, with the curve oscillating in weak, active, and revival periods of the monsoon. The middle level moisture changes were consistent with the shifts of low level inversions, and were linked to the monsoon circulation. D.H.K.

A82-17292 * # **Clear water radiances for atmospheric correction of coastal zone color scanner imagery.** H. R. Gordon (Miami, University, Coral Gables, FL) and D. K. Clark (NOAA, National Earth Satellite Service, Washington, DC). *Applied Optics,* vol. 20, Dec. 15, 1981, p. 4175-4180. 18 refs. Contract No. NAS5-22963; Grant No. NOAA-NA-79SA00741.

The possibility of computing the inherent sea surface radiance for regions of clear water from coastal zone color scanner (CZCS) imagery given only a knowledge of the local solar zenith angle is examined. The inherent sea surface radiance is related to the upwelling and downwelling irradiances just beneath the sea surface, and an expression is obtained for a normalized inherent sea surface radiance which is nearly independent of solar zenith angle for low phytoplankton pigment concentrations. An analysis of a data base consisting of vertical profiles of upwelled spectral radiance and pigment concentration, which was used in the development of the CZCS program, confirms the virtual constancy of the normalized inherent sea surface radiance at wavelengths of 520 and 550 nm for cases when the pigment concentration is less than 0.25 mg/cu m. A strategy is then developed for using the normalized inherent sea surface radiance in the atmospheric correction of CZCS imagery. A.L.W.

A82-17492 **The near-infrared radiation received by satellites from clouds.** G. J. Bell and M. C. Wong (Royal Observatory, Hong Kong). *Monthly Weather Review,* vol. 109, Oct. 1981, p. 2158-2163. 12 refs.

An analysis of certain Tiros N IR data of cloud tops and the sea at 3.7 microns which show that the sea is cooler than the clouds is presented. Noting that data taken at 10 microns showed the sea surface to be warmer than the clouds, the total radiation within the satellite's passband reaching the radiometer is defined by the net flux radiated by the element, the flux radiated by the atmospheric molecules and aerosols, and the solar flux reflected by the element. Calculations of the albedo of the clouds and sea show that under certain circumstances the reflected radiance from the sea will yield satellite IR scans which show that the sea is cooler than the clouds, because the sensor is receiving more radiation from the clouds. A steady decrease of albedo occurs with increasing wavelength and angle incidence. M.S.K.

A82-17494 **Annual and nonseasonal variability of monthly low-level wind fields over the Southeastern Tropical Pacific.** . B. Enfield (Oregon State University, Corvallis, OR). *Monthly Weather Review,* vol. 109, Oct. 1981, p. 2177-2190. 20 refs. NSF Grants No. ATM-78-20419; No. OCE-80-24116; Contract No. NOAA-NA-80RAC00003.

A82-17565 **The use of satellite infrared imagery for describing ocean processes in relation to spawning of the northern anchovy /Engraulis mordax/.** R. Lasker, R. M. Laurs (NOAA, Southwest Fisheries Center, La Jolla, CA), and J. Pelaez (California, University, San Diego, CA). *Remote Sensing of Environment,* vol. 11, Dec. 1981, p. 439-453. 10 refs.

Using satellite infrared thermal imagery in conjunction with extensive sampling for anchovy eggs and adults during March and April 1980, it is confirmed that large areas of the coastal ocean off California were avoided by anchovies during the peak of spawning due to entrainment into the California Current of water at a temperature of less than or equal to 14 C that upwelled north of Point Conception. Upwelling began coincident with the onset of winds from the north and proceeded in pulses separated by a few days. Plumes of upwelled water appeared to be advected southward in ladder-like rows by the California Current. A saline warm water pool more than 50 m deep 40 km off Ensenada, Baja California, Mexico also was avoided by anchovies. The appearance of an inshore 16 C refuge and an extensive 220-km warm-water 'wake' associated with Santa Catalina Island also were observed. Each of these oceanographic features was confirmed by ship observations. (Author)

A82-17567 **Variations in upper ocean heat storage determined from satellite data.** J. R. Miller (Rutgers University, New Brunswick, NJ). *Remote Sensing of Environment,* vol. 11, Dec. 1981, p. 473-482. 12 refs.

The development of new microwave sensors to measure oceanic surface parameters from satellites will provide information applicable to studies of variations in upper ocean heat storage. An algorithm was developed to use satellite-derived values of sea-surface temperature and surface wind speeds to predict changes in subsurface heat storage. The algorithm, which is based on a one-dimensional model of the upper ocean, is used to determine the effect of inherent limitations of satellite data, such as discontinuous coverage and errors in the derived fields. Errors in the temperature field become more important as the surface mixed-layer deepens, and accurate specification of the temperature field appears to be more important than accurate specification of the wind field. However, it is important to obtain information about high wind speed events when they occur. The technique, which also provides information on the total heat flux into the ocean between successive satellite passes, could be improved by obtaining information from more than one satellite and from multiple sensors. (Author)

A82-17915 # **The development of the Tiros Global Environmental Satellite System.** A. Schnapf. *American Institute of Aeronautics and Astronautics, Aerospace Sciences Meeting, 20th, Orlando, FL, Jan. 11-14, 1982, Paper 82-0383.* 11 p.

A table giving the orbital performance of the Tiros satellites is included. It is noted that the infrared data from the Tiros-N/NOAA satellites can be used to produce charts showing the sea-surface temperature over a larger area and with greater frequency than is possible from any other source. Satellite pictures display the extent and character of ice fields in the Arctic and Antarctic seas and on the Great Lakes with a frequency and geographic coverage never before attained. Tiros also collects and locates data from fixed or moving platforms and monitors electron and proton particles emanating from the sun. C.R.

A82-18074 # **Measurement of sea and ice backscatter reflectivity using an OTH radar system.** W. F. Ring and G. S. Sales (USAF, Rome Air Development Center, Bedford, MA). In: Symposium on the Effect of the Ionosphere on Radiowave Systems, Washington, DC, April 14-16, 1981, Preprints. Washington, DC, U.S. Naval Research Laboratory, 1981. (3B-2). 9 p. 8 refs.

Backscattered radio wave characteristics may permit the recognition of coastal regions or islands through differences in scattering by land and water. This technique is developed for the quantification of sea water, sea ice and Greenland ice cap surface reflectivities so that they may serve as references for the calibration of HF, Over-the-Horizon (OTH) radar sensitivity. Such references are necessary when no aircraft targets-of-opportunity are available to serve as calibration sources. Attention is drawn to the azimuthal or latitudinal variation in radar scattering cross section found. Previous measurements and models do not show the consistent increase in absorption from 65 to 72 deg geomagnetic latitude exhibited by the data presented. An ionospheric absorption or scattering loss mechanism is postulated as an explanation of this phenomenon. O.C.

A82-18716 * **Evaluation of the Seasat wind scatterometer.** W. L. Jones, E. M. Bracalente, L. C. Schroeder (NASA, Langley Research Center, Hampton, VA), D. H. Boggs, D. Shelton (California Institute of Technology, Jet Propulsion Laboratory, Pasadena, CA), R. A. Brown (Washington, University, Seattle, WA), and T. H. Guymer (Institute of Oceanographic Sciences, Wormley, Surrey, England). *Nature,* vol. 294, Dec. 24-31, 1981, p. 704-707. 16 refs.

Surface wind velocities have been derived from backscatter measurements of the ocean surface made by a satellite-borne, microwave sensor. Comparisons with high-quality surface-based measurements obtained during the Joint Air-Sea Interaction experiment are described. The accuracy of the scatterometer winds at this mid-latitude site, + or - 1.6 m/s in speed and + or - 18 deg in direction, for winds between 3 and 16 m/s is within the design specification. (Author)

A82-18724 * **Anomalous wind estimates from the Seasat scatterometer.** T. H. Guymer (Institute of Oceanographic Sciences, Wormley, Surrey, England), J. A. Businger (Washington, University, Seattle, WA), W. L. Jones (NASA, Langley Research Center, Hampton, VA), and R. H. Stewart (California Institute of Technology, Jet Propulsion Laboratory, Pasadena, CA). *Nature,* vol. 294, Dec. 24-31, 1981, p. 735-737. 10 refs.

The Seasat-A Satellite Scatterometer (SASS) measured the radar backscatter intensity from the sea surface using a four-beam microwave antenna. Estimates of wind speed and direction derived from these data agree well with surface measurements made during the Joint Air-Sea Interaction experiment, but there are occasions (3 out of 23 satellite passes) when the results are anomalous. One such occasion when the satellite measurements differed substantially from those at the surface of the sea has been studied, and it has been concluded that the interpretation of the SASS measurements may have been vitiated by a mid-level convective system deep enough to produce thunderstorms and lightning. (Author)

N82-10461# National Oceanic and Atmospheric Administration, Seattle, Wash
CTD/02 MEASUREMENTS DURING THE EQUATORIAL PACIFIC OCEAN CLIMATE STUDY (EPOCS) IN 1979
L. J. Mangum, N. N. Soreide, B. D. Davies, B. D. Spell, and S. P. Hayes Oct. 1980 641 p refs
(PB81-211203; NOAA-DR-ERL-PMEL-1; NOAA-81041501)
Avail: NTIS HC A99/MF A01 CSCL 08I

Neil Brown instrument System (NBIS) CTD/02 measurements recorded on five cruises are summarized. A description of the acquisition and processing systems and calibration techniques are presented. These data were collected along longitudes of 105 W and 110 W between 15 N and 5 S. Additional casts in the vicinity of 0 degrees, 153 W also presented. Station locations, meteorological conditions, and profiles of temperature, salinity, sigma T, and oxygen are shown for each cast. GRA

N82-10467 Danish Meteorological Inst., Copenhagen.
THE ICE-CONDITIONS IN THE GREENLAND WATERS, 1965. COASTAL MAPS
1980 66 p refs
(ISBN-87-7478-183-9) Avail: NTIS HC A04/MF A01

Maps indicating the size, distribution, and character of Greenland's coastal ice formations are presented. Data is derived from visual flight observations and supplemented by aerial radar reconnaissance and ship observations. Narrative evaluations of ice conditions for several coastal locations are presented. R.J.F.

N82-10473# Nova Univ., Dania, Fla.
SEASAT ALTIMETRY ADJUSTMENT MODEL INCLUDING TIDAL AND OTHER SEA SURFACE EFFECTS
Georges Blaha Hanscom AFB, Mass. AFGL Mar. 1981 113 p refs
(Contract F19628-78-C-0013; AF Proj. 2309)
(AD-A104188; SR-3; AFGL-TR-81-0152) Avail: NTIS HC A06/MF A01 CSCL 22/2

This study is a part of the on-going effort aimed at improved determinations of the Earth's gravity field through the adjustment of satellite altimeter data in the short-arc mode. Until recently the key role in such adjustments has been played by GEOS-3 altimeter data. However, Seasat altimetry is envisioned as providing a more accurate means for addressing this task. In view of the improved quality of altimeter data and of the corresponding more stringent requirements for the data reduction, several improvements in the existing altimetry model have been designed and are described herein. For example, the criteria have been established specifying the maximum and the mimimum allowable lengths of Seasat arcs. An important improvement in the economy has been achieved through a reduction in the number of spherical-harmonic potential coefficients entering the orbital integrator, without a noticeable compromise in the excellent quality of the Seasat observational system. GRA

N82-10486# Science Research Council, Slough (England).
STUDY ON SATELLITE RADAR ALTIMETRY IN CLIMATOLOGICAL AND OCEANOGRAPHIC RESEARCH, VOLUME 1 Final Report
Paris ESA Dec. 1980 450 p refs Prepared in cooperation with Natural Environment Research Council, Godalming, England 2 Vol.
(Contract ESA-4355/80/F-FC(SC))
(SP/153/06/01/FR(80)-Vol-1; ESA-CR(P)-1437-Vol-1) Avail: NTIS HC A19/MF A01

The contribution of satellite radar altimetry to climate, oceanographic and glaciological research is analyzed. The current position, the need for improved data and the relevance of existing altimeter data to climate, oceanographic and glaciological studies are discussed. Experience gained from previous missions is reviewed and the corrections which need to be made to the basic altimeter data are considered, along with the requirements for supporting measurements needed to aid in interpretation of this data. Sampling requirements in relation to particular aspects of oceanography and glaciology are treated. The role of circulation models in satellite altimetry, and those features of instrument design relating to scientific requirements, are examined. Supporting and complementary instruments are reviewed. The value of multi-satellite missions and possible future developments are discussed. Author (ESA)

N82-10487# Science Research Council, Slough (England).
STUDY ON SATELLITE RADAR ALTIMETRY IN CLIMATOLOGICAL AND OCEANOGRAPHIC RESEARCH, VOLUME 2 Final Report
Paris ESA Dec. 1980 47 p Prepared in cooperation with Natural Environment Research Council, Godalming, England 2 Vol.
(Contract ESA-4355/80/F-FC(SC))
(SP/153/06/01FR(80)-Vol-2; ESA-CR(P)-1437-Vol-2) Avail: NTIS HC A03/MF A01

The potential contribution of satellite radar altimetry to climatology, oceanography, and glaciology is discussed. The altimetry requirements for future programs are considered. Tradeoffs between spatial and temporal coverage, sampling rate and error budget, involved in defining an optimum mission are examined. Accuracy of + or - 10 cm, pulse lengths of 1.5 nsec and integration times of 3 sec are recommended. Orbital inclination should be between 60 and 65 deg. Author (ESA)

N82-10660 Texas Univ. at Arlington.
A GLOBAL ATLAS OF GEOS-3 SIGNIFICANT WAVEHEIGHT AND COMPARISON OF THE DATA WITH NATIONAL BUOY DATA Ph.D. Thesis
James Douglas McMillan 1981 147 p
Avail: Univ. Microfilms Order No. 8119337

The GEOS-3 significant waveheight estimation algorithm is derived by analyzing the return waveform characteristics of the altimeter. It is shown that the difference between the waveform expected from a flat surface and the actual waveform observed returning from a nonflat sea surface can be analyzed to determine the magnitude of the significant waveheight. This technique employs a curve fitting procedure utilizing least squares estimation. The rationale for a smoothing technique is presented and the convergence characteristics of the smoothed estimate are discussed. Then, a statistically representative sampling of GEOS-3 data is selected for comparison with buoy measurements and the accuracy of the GEOS-3 significant waveheight estimates is deduced, through statistical analysis, to be 50 cm. The GEOS-3 significant waveheight estimates gathered during the entire mission of the spacecraft are assembled in the form of a global atlas of contour maps. Both high and low sea state contour maps are presented, and the data are displayed both by seasons and for the entire duration of the GEOS-3 mission. The contour maps are then compared with contour maps compiled by the U.S. Navy and significant differences are found. Dissert. Abstr.

N82-10661*# National Aeronautics and Space Administration. Langley Research Center, Hampton, Va.
CHESAPEAKE BAY PLUME STUDY: SUPERFLUX 1980
Janet W. Campbell, ed. and James P. Thomas, ed. (National Marine Fisheries Service, Highland, N.J.) Oct. 1981 504 p refs Symp. held at Williamburg, Va., 21-23 Jan. 1981; sponsored in part by National Marine Fisheries Service, NOAA, and Dept. of Commerce
(NASA-CP-2188; L-14680;
NOAA/NEMP-111-81-ABCDFG-0042) Avail: NTIS HC A22/MF A01 CSCL 08C

The results of the Chesapeake Bay plume study are reported. The role of remote sensing in monitoring and assessing the effects of pollution of marine resources is delineated.

N82-10663*# National Marine Fisheries Service, Highlands, N.J. Div. of Environmental Assessment.

A MARINE ENVIRONMENTAL MONITORING AND ASSESSMENT PROGRAM

John B. Pearce *In* NASA. Langley Research Center Cheasapeake Bay Plume Study Oct. 1981 p 15-28 refs

Avail: NTIS HC A22/MF A01 CSCL 08C

The need for the use of modern, extremely sensitive techniques to aid in rapidly and synoptically assessing the relative health and production of coastal waters and estuaries is reported. Major emphasis is placed on establishing a solid foundation for the use of remote sensing in basic oceanographic studies and the management of human wastes. R.C.T.

N82-10664*# National Aeronautics and Space Administration. Langley Research Center, Hampton, Va.

SUPERFLUX I, II, AND III EXPERIMENT DESIGN: REMOTE SENSING ASPECTS

Janet W. Campbell, Wayne E. Esaias, and Warren D. Hypes *In its* Chesapeake Bay Plume Study Oct. 1981 p 29-42 refs

Avail: NTIS HC A22/MF A01 CSCL 08C

The Chesapeake Bay plume study called Superflux is described. The study was initiated to incorporate the disciplines of both resources management and remote sensing in accomplishing the following objectives: (1) process oriented research to understand the impact of estuarine outflows on continental shelf ecosystems; (2) monitoring and assessment to delineate the role of remote sensing in future monitoring and assessment programs; and (3) remote sensing research: to advance the state of the art in remote sensing systems as applied to sensing of the marine environment, thereby hastening the day when remote sensing can be used operationally for monitoring and assessment and for process oriented research. R.C.T.

N82-10665*# National Marine Fisheries Service, Highlands, N.J. Northeast Fisheries Center.

SUPERFLUX I, II, AND III EXPERIMENT DESIGNS: WATER SAMPLING AND ANALYSES

James P. Thomas *In* NASA. Langley Research Center Chesapeake Bay Plume Study Oct. 1981 p 43-60

Avail: NTIS HC A22/MF A01 CSCL 08C

Both airborne remote sensors and seagoing research vessels were used to study the effects of man's continual use of the Chesapeake Bay offshore environments. The major focus of the study was to: (1) advance the development and transfer of improved remote sensing systems and techniques for monitoring environmental quality and effects on living marine resources; (2) increase understanding of the influence of estuarine outwellings (plumes) on contiguous shelf ecosystems; and (3) provide a synoptic, integrated and timely data base for application to problems of marine resources and environmental quality. R.C.T.

N82-10668*# Research Triangle Inst., Research Triangle Park, N. C.

MONITORING THE CHESAPEAKE BAY USING SATELLITE DATA FOR SUPERFLUX III

Fred M. Vukovich and Bobby W. Crissman *In* NASA. Langley Research Center Chesapeake Bay Plume Study Oct. 1981 p 93-110

(Grant NA81FA-C-00002)

Avail: NTIS HC A22/MF A01 CSCL 08C

The TIROS-N and NOAA-6, and GOES visible infrared satellite data were used to identify and locate surface oceanographic thermal fronts for the purpose of issuing daily and premission advisory briefings in support of the Superflux 3 in situ and remote sensing experiment in the Chesapeake Bay region. Satellite data were collected for the period 1 - 22 October 1980. A summary of that data is presented. R.C.T.

N82-10670*# National Aeronautics and Space Administration. Langley Research Center, Hampton, Va.

REMOTE SENSING OF THE CHESAPEAKE BAY PLUME SALINITY VIA MICROWAVE RADIOMETRY

Bruche M. Kendall *In its* Chesapeake Bay Plume Study Oct. 1981 p 131-140 refs

Avail: NTIS HC A22/MF A01 CSCL 08C

The NASA-Langley-developed L-Band microwave radiometer was used to remotely measure sea surface salinity during the Chesapeake Bay plume studies. Obtained measurements of microwave brightness temperatures of the sea surface were combined with measurements of sea surface temperature obtained with an infrared radiometer and inverted to produce corresponding values of sea surface salinity. Results from the plume measurements, which indicate the southward extent of the plume along the Virginia-North Carolina coast, are presented and discussed. Additional measurements obtained for the Delaware Bay Mouth flight, and the James River-Shelf flight, are also discussed. R.C.T.

N82-10672*# National Aeronautics and Space Administration. Langley Research Center, Hampton, Va.

PRELIMINARY ANALYSIS OF OCEAN COLOR SCANNER DATA FROM SUPERFLUX III

Craig W. Ohlhorst *In its* Chesapeake Bay Plume Study Oct. 1981 p 159-174

Avail: NTIS HC A22/MF A01 CSCL 08C

The ocean color scanner collected data Superflux III Experiment. Single channel gray scale data products generated 5 minutes after the scanner data were collected showed details of the Chesapeake Plume structure, suggesting that this quick-look capability could have potential use to experimenters in real time. The Chesapeake Bay Plume extended offshore between 5 and 7 nautical miles on two occasions. The scanner data also show many other water features within the lower bay itself. R.C.T.

N82-10682*# National Aeronautics and Space Administration. Langley Research Center, Hampton, Va.

ANALYSIS OF TESTBED AIRBORNE MULTISPECTRAL SCANNER DATA FROM SUPERFLUX II

David E. Bowker, Charles A. Hardesty, Daniel J. Jobson, and Gilbert S. Bahn (Kentron International, Inc.) *In its* Chesapeake Bay Plume Study Oct. 1981 p 323-338

Avail: NTIS HC A22/MF A01 CSCL 08C

A test bed aircraft multispectral scanner (TBAMS) was flown during the James Shelf, Plume Scan, and Chesapeake Bay missions as part of the Superflux 2 experiment. Excellent correlations were obtained between water sample measurements of chlorophyll and sediment and TBAMS radiance data. The three-band algorithms used were insensitive to aircraft altitude and varying atmospheric conditions. This was particularly fortunate due to the hazy conditions during most of the experiments. A contour map of sediment, and also chlorophyll, was derived for the Chesapeake Bay plume along the southern Virginia-Carolina coastline. A sediment maximum occurs about 5 nautical miles off the Virginia Beach coast with a chlorophyll maximum slightly shoreward of this. During the James Shelf mission, a thermal anomaly (or front) was encountered about 50 miles from the coast. There was a minor variation in chlorophyll and sediment across the boundary. During the Chesapeake Bay mission, the Sun elevation increased from 50 degrees to over 70 degrees, interfering with the generation of data products. M.G.

N82-10684*# National Aeronautics and Space Administration. Wallops Flight Center, Wallops Island, Va.

APPLICATION OF THE NASA AIRBORNE OCEANOGRAPHIC LIDAR TO THE MAPPING OF CHLOROPHYLL AND OTHER ORGANIC PIGMENTS

F. E. Hoge and R. N. Swift (EG&G Washington Analytical Services Center, Inc.) *In* NASA. Langley Research Center Chesapeake Bay Plume Study Oct. 1981 p 349-374 refs

Avail: NTIS HC A22/MF A01 CSCL 08C

Laser fluorosensing techniques used for the airborne measurement of chlorophyll a and other naturally occurring waterborne pigments are reviewed. Previous experiments demonstrating the utility of the airborne oceanographic lidar (AOL) for assessment of various marine parameters are briefly discussed. The configuration of the AOL during the NOAA/NASA Superflux experiments is described. The participation of the AOL in these experiments is presented and the preliminary results are discussed. The importance of multispectral receiving capability in a laser fluorosensing system for providing reproducible measurements over wide areas having spatial variations in water column transmittance properties is addressed. This capability minimizes the number of truthing points required and is usable even in shallow estuarine areas where resuspension of bottom sediment is common. Finally, problems encountered on the Superflux missions and the resulting limitations on the AOL data sets are addressed and feasible solutions to these problems are provided. M.G.

N82-10694*# National Aeronautics and Space Administration. Langley Research Center, Hampton, Va.
ASSESSMENT OF SUPERFLUX RELATIVE TO REMOTE SENSING
Janet W. Campbell *In its* Chesapeake Bay Plume Study Oct. 1981 p 501-502
Avail: NTIS HC A22/MF A01 CSCL 08C

The state-of-the-art advancements in remote sensor technology due to the Superflux program are examined. Three major individual sensor technologies benefitted from the program: laser fluorosensors, optical-range scanners, and passive microwave sensors. Under Superflux, convincing evidence was obtained that the airborne oceanographic lidar fluorosensor can map chlorophyll, i.e., is linear, over a wide range from less than 0.5 to 5.0 mg/cu m. The lidar oceanographic probe dual-excitation concept for addressing phytoplankton color group composition was also demonstrated convincingly. Algorithm development, real time capabilities, and multisensor integration are also addressed. M.G.

N82-11511*# Ball Aerospace Systems Div., Boulder, Colo.
DEVELOPMENT OF THE COASTAL ZONE COLOR SCANNER FOR NIMBUS 7. VOLUME 1: MISSION OBJECTIVES AND INSTRUMENT DESCRIPTION Final Report
May 1979 76 p refs
(Contract NAS5-20900)
(NASA-CR-166720-Vol-1; F78-11-Rev-A) Avail: NTIS HC A05/MF A01 CSCL 14B

An Earth scanning six channel (detector) radiometer using a classical Cassegrain telescope and a Wadsworth type grating spectrometer was launched aboard Nimbus 7 in order to determine the abundance or density of chlorophyll at or near the sea surface in coastal waters. The instrument also measures the sediment or gelbstroffe (yellow stuff) in coastal waters, detects surface vegetation, and measures sea surface temperature. Block diagrams and schematics are presented, design features are discussed and each subsystem of the instrument is described. A mission overview is included. A.R.H.

N82-11515*# OAO Corp., Hampton, Va.
TECHNOLOGY TRANSFER OF NASA MICROWAVE REMOTE SENSING SYSTEM Final Report
N. D. Akey Oct. 1981 38 p refs
(Contract NAS1-16380)
(NASA-CR-165791) Avail: NTIS HC A03/MF A01 CSCL 14B

Viable techniques for effecting the transfer from NASA to a user agency of state-of-the-art airborne microwave remote sensing technology for oceanographic applications were studied. A detailed analysis of potential users, their needs and priorities; platform options; airborne microwave instrument candidates; ancillary instrumentation; and other, less obvious factors that must be considered were studied. Conclusions and recommendations for the development of an orderly and effective technology transfer of an airborne microwave system that could meet the specific needs of the selected user agencies are reported. R.J.F.

N82-11537# National Oceanic and Atmospheric Administration, Seattle, Wash. Pacific Marine Environmental Lab.
ICE CONDITIONS IN THE EASTERN BERING SEA FROM NOAA AND LANDSAT IMAGERY: WINTER CONDITIONS 1974, 1976, 1977, 1979
Lyn McNutt Feb. 1981 186 p refs Prepared in cooperation with Science Applications, Inc., Bellevue, Wash.
(PB81-220188; NOAA-TM-ERL-PMEL-24; CONTRIB-500; NOAA-81043005) Avail: NTIS HC A09/MF A01 CSCL 08L

The LANDSAT and NOAA satellite images from the University of Alaska LANDSAT library were used to make maps of ice conditions in the eastern Bering Sea. The analyses included daily charts of the ice, polynya locations, floe trajectories, and comparisons between data taken from the two sources. A zoom transfer scope (ZTS) was used to transfer the data from an image to a map base for later winter condition in 1974, 1976, 1977, and 1979. GRA

N82-11743# National Oceanic and Atmospheric Administration, Miami, Fla.
THE DETERMINATION OF NAVIGATIONAL AND METEOROLOGICAL VARIABLES MEASURED BY NOAA/RFC WP3D AIRCRAFT
Francis J. Merceret and Harlan W. Davis Apr. 1981 28 p refs
(PB81-225468; NOAA-TM-ERL-RFC-7; NOAA-81051503) Avail: NTIS HC A03/MF A01 CSCL 04B

For each variable, the sensor inputs and equations used are described and an estimate of the error in the result is provided. The report is divided into two sections: quantities displayed on-board in real-time and additional quantities computed and available to the user on request in the final data set. The aircraft and much of the instrumentation are described. T.M.

N82-12502# Office of Naval Research, Pasadena, Calif.
VISUAL OBSERVATIONS OF THE OCEAN
Robert E. Stevenson, L. David Carter (Geological Survey, Menlo Park, Calif.), Stephen P. VonderHaar (Univ. of Southern California, Los Angeles), and Richard O. Stone *In* NASA. Johnson Space Flight Center Skylab Explores the Earth 1977 p 287-338 refs
Avail: NTIS MF A01; SOD HC $16.50 CSCL 08J

The Skylab 4 mission allowed large scale, dynamic features such as ocean currents and associated eddies to be observed, described, and photographed repeatedly. Examples of regional and topical studies are included which discuss ocean currents, plankton, internal waves, coastal-sediment plumes, subtropical convergence, windborne sediment entering the ocean, and the interaction of ocean waves and currents. The importance of the observation of mesoscale phenomena is discussed as well as the amendement of charts of ocean currents. A.R.H.

N82-12503*# National Oceanic and Atmospheric Administration, Miami, Fla. Atlantic Oceanographic and Meteorological Labs.
AN ASSESSMENT OF THE POTENTIAL CONTRIBUTIONS TO OCEANOGRAPHY FROM SKYLAB VISUAL OBSERVATIONS AND HANDHELD-CAMERA PHOTOGRAPHS
George A. Maul and Michael McCaslin *In* NASA. Johnson Space Flight Center Skylab Explores the Earth 1977 p 339-352

Avail: NTIS MF A01; SOD HC $16.50 CSCL 08J

The possible roles that space observes may play in oceanographic experimentation are considered in a discussion of several ocean photographs and visual observations made during the Skylab 4 mission. While hand-held camera photography has a distinct role in reconnaissance, it cannot surpass the quantitativeness of a multispectral observation from a known altitude. Significantly, many of the most interesting scenes were taken by the S190B camera, which produced very high resolution photographs taken from a vertical position. From the standpoint of long term oceanographic observation, quantitative observations are needed with accurate geographical positioning. Concurrent ocean surface observations are also needed to correlate the data. A.R.H.

N82-12533# Danish Meteorological Inst., Copenhagen.
THE ICE CONDITIONS IN THE GREENLAND WATERS
1980 69 p
(ISBN-87-7478-183-9) Avail: NTIS HC A04/MF A01

Charts showing weekly ice conditions for 1965 are presented. Thickness of fast ice measured at coastal stations is given and the number of icebergs sighted is reported. Polar ice progress is followed. Information on the size, boundary, age, water features, and topography is provided. For ice of land origin, the relative frequencies of bergy bits and growlers are indicated. Author (ESA)

N82-12734*# EG and G Washington Analytical Services Center, Inc., Pocomoke City, Md.
BOUNDARY DETECTION CRITERIA FOR SATELLITE ALTIMETERS

C. F. Martin and R. L. Taylor Nov. 1981 61 p refs
(Contract NAS6-3075)
(NASA-CR-156880) Avail: NTIS HC A04/MF A01 CSCL 14B

A procedure for using satellite altimeter data to determine the time of crossing of a surface boundary, such as ocean land or ocean ice, with the primary objective to flag altimeter data that do not properly represent oceanographic measurements were studied. Water to land crossing and water to sea ice crossing were investigated. For ocean ice crossings, a large increase in AGC occurred. Waveform tests for increasing the probability of detecting an ocean land crossing were investigated. It is recommended that the boundary test be based on a fit of the full waveform to a limited parameter set at a rate of 5 to 10 second. E.A.K.

N82-13484# National Oceanic and Atmospheric Administration, Rockville, Md. Office of Marine Pollution Assessment.
DEEP OCEAN MINING ENVIRONMENTAL STUDY. ENVIRONMENTAL EFFECTS OF COMMERCIAL-SCALE MINING
Nov. 1980 319 p refs
(PB81-227753; NOAA-81052103) Avail: NTIS HC A14/MF A01 CSCL 08I

Papers on deep ocean mining environmental study are presented. The titles are: estimated discharge characteristics of a commercial nodule mining operation; dissolved components of the discharge; increased oxygen demand and microbial biomass; trace metal exchange between ferromanganese nodules and artificial seawater; dispersion of deep sea mining particulates and their effect on light in ocean surface layer; environmental investigation of the effect of deep sea mining on marine phytoplankton and primary productivity in the tropical eastern north Pacific ocean; potential effects on deep sea minerals mining on macrozooplankton in the north equatorial Pacific; dispersal and resedimentation of the benthic plume from deep sea mining operations; and limits in prediction and detecting benthic community response to manganese nodule mining. GRA

N82-13639# SACLANT ASW Research Center, La Spezia (Italy).
THE SACLANTCEN OCEANOGRAPHIC DATA BASE. VOLUME 1: DESIGN CRITERIA AND DATA STRUCTURE AND CONTENT
Richard F. J. Winterburn 15 Jun. 1981 30 p refs
(AD-A103277; SACLANTCEN-SM-150-Vol-1) Avail: NTIS HC A03/MF A01 CSCL 08/10

An oceanographic data base established at SACLANTCEN on a UNIVAC 1106 computer system is described. The design criteria used in setting up the data base, its structure and content, how data, were acquired either from outside institutions or from SACLANTCEN experiments are reformatted and entered are discussed. Data are accessed, interrogated, and display, including the plotting of charts with coastlines and of contoured data are described. Author

N82-13641# Naval Oceanographic Office, Bay St. Louis, Miss. Environmental Systems Div.
ICAPS OCEANOGRAPHIC DATA FOR THE INDIAN OCEAN Final Report
Dec. 1980 93 p refs
(AD-A103173; NOO-RP-32C) Avail: NTIS HC A05/MF A01 CSCL 08/10

The integrated command ASW prediction system (ICAPS) oceanographic data files for the Indian Ocean are presented. Graphic displays provide an illustration of the historical data stored within the ICAPS data base. Depth, temperature and salinity values are shown on a split-depth scale providing a depiction of the near surface strucutre and a less detailed picture of the slowly varying deeper structure. The corresponding oceanograhic data for the Atlantic Ocean and Mediterranean Sea and Pacific Ocean are presented in companion publications. Author

N82-13642# Massachusetts Inst. of Tech., Cambridge. Dept. of Meteorology.
SURFACE SIGNS OF INTERNAL OCEAN DYNAMICS
Erik Mollo-Christensen 1980 8 p refs
(Contract N00014-80-C-0273)
(AD-A101380) Avail: NTIS HC A02/MF A01 CSCL 08/3

There are various processes internal to the ocean that can interact with the surface. The resulting interaction causes changes in the surface wave structure that may well be recognizable by remote sensing systems. Vertical motion occurs when a wind driven surface Ekman layer is set up. Such 'pumping' can also take place in deeper Ekman layers especially over sloping bottom surfaces. Internal waves, topographic waves, and current shear can also cause changes in the surface wave field. A combination of ship, buoy, and remote sensors like those aboard LANDSAT and Seasat, coupled with the output of modeling analyses, can immeasurably improve our knowledge of ocean dynamics. Author

N82-14550*# National Aeronautics and Space Administration. Langley Research Center, Hampton, Va.
SPECTRAL ATMOSPHERIC OBSERVATIONS AT NANTUCKET ISLAND, MAY 7-14, 1981
T. A. Talay and L. R. Poole Nov. 1981 56 p refs
(NASA-TM-83196) Avail: NTIS HC A04/MF A01 CSCL 04A

An experiment was conducted by the National Langley Research Center to measure atmospheric optical conditions using a 10-channel solar spectral photometer system. This experiment was part of a larger series of multidisciplinary experiments performed in the area of Nantucket Shoals aimed at studying the dynamics of phytoplankton production processes. Analysis of the collected atmospheric data yield total and aerosol optical depths, transmittances, normalized sky radiance distributions, and total and sky irradiances. Results of this analysis may aid in atmospheric corrections of remote sensor data obtained by several sensors overflying the Nantucket Shoals area. Recommendations are presented concerning future experiments using the described solar photometer system and calibration and operational deficiencies uncovered during the experiment. A.R.H.

N82-14553# European Space Agency, Paris (France).
APPLICATION OF REMOTE SENSING DATA ON THE CONTINENTAL SHELF: PROCEEDINGS OF AN EARSeL-ESA SYMPOSIUM
N. Longdon, comp. and G. Levy, comp. Jul. 1981 298 p refs Symp. held in Voss, Norway, 19-20 May 1981 Prepared in cooperation with Royal Norwegian Council for Scientific and Industrial Research, Kjeller
(ESA-SP-167; ISSN-0379-6566) Avail: NTIS HC A13/MF A01; ESA, Paris FF 125

A symposium which studied the application of remote sensing techniques to oceanography, fishing, pollution monitoring, and coastal zone management is reported. National programs, operational requirements, and state of the art are reviewed. The use of satellites, including LANDSAT, Seasat and ERS is highlighted.

N82-14554# European Space Agency, Paris (France). Directorate of Application Programmes.
ERS-1: MISSION OBJECTIVES AND SYSTEM CONCEPT
G. Duchossois and D. Lannertz *In its* Appl. of Remote Sensing Data on the Continental Shelf Jul. 1981 p 5-16

Avail: NTIS HC A13/MF A01; ESA, Paris FF 125

The objectives of the first ESA remote sensing (ERS-1) satellite program are the development and promotion of commercial applications related to a better knowledge of ocean parameters; monitoring of sea ice and icebergs for industrial oceanic activities at high latitudes; and to increase understanding of coastal zones and global ocean processes which, together with the monitoring of the polar regions, can provide a major contribution to the World Climate Research Program. The ERS-1 system (space segment and ground segment) is described including the instruments which are part of the Earth applications payload, active microwave instrumentation, an ocean color monitor, and a radar altimeter. The procedures used in selecting the Earth sciences payload complement, the parameters which can be obtained from the applications payload, and a development plan for the ERS-1 system are outlined. Author (ESA)

N82-14556# Naval Oceanographic Office, Washington, D. C.
THE POTENTIAL AND REQUIREMENTS FOR SPACE OCEANOGRAPHY
Ross N. Williams *In* ESA Appl. of Rumote Sensing Data on the Continental Shelf Jul. 1981 p 23-27 refs

Avail: NTIS HC A13/MF A01; ESA, Paris FF 125

The use of satellite systems for communications, navigation, weather, oceanographic, and military purposes is reviewed. The trend is towards automated measurement, analysis, forecast and display of environmental effects. Both Marisat and Fleetsatcom, the shore based naval environmental data network and the commercial satellite data distribution system solve display and dissemination problems; and large dedicated computer capacity and atmospheric prediction models solve analysis and prediction software problems. Meteorological satellite programs together with more traditional atmospheric and oceanographic data imputs is used to demonstrate that globally sensed oceanographic data to initialize the models is not yet fully available, but could be determined with improved accuracy and resolution by employing an ocean satellite system, such as NOSS. Author (ESA)

N82-14557# Conoco Norway, Inc., Oslo.

OFFSHORE PETROLEUM INDUSTRY ENVIRONMENTAL DATA REQUIREMENTS: EMPHASIS ON REMOTE SENSING

Ronald L. Gratz *In* ESA Appl. of Remote Sensing Data on the Continental Shelf Jul. 1981 p 31-43 refs

Avail: NTIS HC A13/MF A01; ESA, Paris FF 125

Data quality and coverage requirements for the remote sensing of oceanographic and meteorological factors affecting the development of offshore hydrocarbon resources are considered, using a combination of fine-grid hindcasting and surface truth measurements. The establishment of data banks able to accumulate 20-30 years of climatological data for use in future designs is recommended. Special measurement programs are planned for data collection during storms. Remote sensing was used to measure several factors important to the petroleum industry, i.e., waves, winds, currents, and sea ice. Application to weather forecasting is shown. The use of surface truth data in the calibration and verification of measurements for remote sensing is suggested. Possible communications channels for the exchange of remote sensing data are assessed. Author (ESA)

N82-14558# Nice Univ. (France). Lab. d'Ocenagraphie Biologique.

REQUIREMENTS IN POLLUTION MONITORING AND COASTAL MANAGEMENT

J. Constans (Fondation Cousteau, Monaco) and G. Leger *In* ESA Appl. of Remote Sensing Data on the Continental Shelf Jul. 1981 p 45-46

Avail: NTIS HC A13/MF A01; ESA, Paris FF 125

Results of tests during a survey of Mediterranean coasts by the research vessel Calypso show general chemical pollution to be too low to justify the rapid decrease in fish, seaweed, and phanerogam populations. However, mechanical and/or physical attacks on the environment, such as land filling and associated constructions, or massive discharges of warm effluents have a devastating impact on coastal ecosystems. Development decision are based on individual/local perspectives. An approach, based on clear, overall, long-term strategies is called for before irreversible damage is done. Optimum use should be made of existing data aquisition techniques, such as ESA and Telespazio satellite imagery. Author (ESA)

N82-14559# Institute of Marine Research, Bergen (Norway).

FISHERIES INVESTIGATIONS AND MANAGEMENT BENEFITS FROM REMOTE SENSING

R. Ljoeen *In* ESA Appl. of Remote Sensing Data on the Continental Shelf Jul. 1981 p 47-54 refs

Avail: NTIS HC A13/MF A01; ESA, Paris FF 125

Physical and biological research in areas of particular interest to Norwegian fisheries is described and present problems connected with the management of cod, haddock and mackerel are indicated. Echo sounding techniques are used and salinity and water temperature at different depths are noted. The significance of ice edge dynamics, ocean fronts, and vertical stratification to biological conditions and fish distribution is surveyed. The application of remote sensing is primarily valued as a tool for providing real time physical data in order to optimize biological sampling programs and for indicating drift and variable distributions of eggs and young fish. The utility of IR and visible images from polar orbiting satellites for monitoring purposes is briefly considered. Author (ESA)

N82-14561# Jet Propulsion Lab., California Inst. of Tech., Pasadena.

THE SEASAT COMMERCIAL DEMONSTRATION PROGRAM

S. W. McCandless (User Systems Engineering, Annandale, Va.), B. P. Miller (Econ, Inc., Princeton, N.J.), and D. R. Montgomery *In* ESA Appl. of Remote Sensing Data on the Continental Shelf Jul 1981 p 59-72 refs

Avail: NTIS HC A13/MF A01; ESA, Paris FF 125

The background and development of the Seasat commercial demonstration program are reviewed and the Seasat spacecraft and its sensors (altimeter, wind field scatterometer, synthetic aperture radar, and scanning multichannel microwave radiometer) are described. The satellite data distribution system allows for selected sets of data, reformatted or tailored to specific needs and geographical regions, to be available to commercial users. Products include sea level and upper atmospheric pressure, sea surface temperature, marine winds, significant wave heights, primary wave direction and period, and spectral wave data. The results of a set of retrospective case studies performed for the commercial demonstration program are described. These are in areas of application such as marine weather and ocean condition forecasting, offshore resource exploration and development, commercial fishing, and marine transportation. Author (ESA)

N82-14562# Copenhagen Univ. (Denmark). Inst. of Physical Oceanography.

THE COLOR OF THE SEA AND ITS RELATION TO SURFACE CHLOROPHYLL AND DEPTH OF THE EUPHOTIC ZONE

N. K. Hoejerslev *In* ESA Appl. of Remote Sensing Data on the Continental Shelf Jul. 1981 p 73-76 refs

Avail: NTIS HC A13/MF A01; ESA, Paris FF 125

Algorithms based on signal ratios from the available channels in Nimbus 7, for the estimation of chlorophyll and phaeophytin are found to be inadequate. This is shown for coastal waters where the concentration of yellow substance (dissolved organic matter) which masks the chlorophyll signal can be variable by orders of more than 10. However, a single globally valid algorithm, based on two wavelengths in the blue and green parts of the spectrum, gives a good estimation of the depth of the euphotic zone as well as for intermediate quanta percentage levels. It is suggested that a relationship be sought involving the depth of the euphotic zone and plankton pigments, standing stock, and primary productivity. Author (ESA)

N82-14564# Oceanroutes, Inc., Palo Alto, Calif.

AN EVALUATION OF SEASAT-A DATA IN RELATION TO OPTIMUM TRACK SHIP WEATHER ROUTING AND SITE SPECIFIC FORECASTING FOR THE OFFSHORE OIL INDUSTRY

C. Daley, R. G. Johnson, and J. C. Thomson *In* ESA Appl. of Remote Sensing Data on the Continental Shelf Jul. 1981 p 93-102 refs

Avail: NTIS HC A13/MF A01; ESA, Paris FF 125

The usefulness of Seasat-A SASS and altimeter measurements is reviewed. Five oceanic areas were selected: the Gulf of Alaska, central and western north Atlantic, eastern north Pacific, southern Indian Ocean, and the North Sea. Both Seasat-aided and conventional analyses were used in offshore hindcast and optimum ship routing situations. Where conventional observations are relatively dense, Seasat wind and wave data have greater impact in determining the shape of major map features than in positioning the features. In data sparse areas, Seasat data permit greater definition of surface features as well as their precise location. The use of Seasat data in optimum ship routing is quantified by means of comparative studies in the Gulf of Alaska. Author (ESA)

N82-14565# University Coll., Galway (Ireland).

DETERMINATION OF SURFACE WIND SPEED FROM REMOTELY MEASURED WHITECAP COVERAGE, A FEASIBILITY ASSESSMENT

E. C. Monahan, I. G. Muircheartaigh, and M. P. Fitzgerald *In* ESA Appl. of Remote Sensing Data on the Continental Shelf Jul. 1981 p 103-109 refs

(Grant N00014-78-G-0052)
Avail: NTIS HC A13/MF A01; ESA, Paris FF 125

The relationship between wind speed and oceanic whitecap coverage was determined to facilitate the development of an algorithm for the remote determination of low elevation wind speed from the teledetected enhancement of sea surface microwave brightness temperature due to the presence of whitecaps. A basis is provided for estimating (and correcting for) the contribution to radiance, coming from whitecaps, in the various visible bands measured by satellite instruments. Combining results of the JASIN experiment with earlier observations, the effect of variations in air and sea surface temperature on this relationship is investigated. The wind speed at which whitecaps appear, and thus the lowest wind speed susceptible to teledetection via whiecap signature, is reassessed. Author (ESA)

N82-14566*# National Aeronautics and Space Administration. Langley Research Center, Hampton, Va.

THE NORWEGIAN REMOTE SENSING EXPERIMENT (NORSEX) IN A MARGINAL ICE ZONE

B. Farrelly (Bergen Univ.), J. Johannessen (Bergen Univ.), O. M. Johannessen (Bergen Univ.), E. Svendson (Bergen Univ.), K. Kloster (C. Michelson Inst.), I. Horjen (Norwegian Hydrodynamic Labs.), W. J. Campbell (Geological Survey, Tacoma, Wash.), J. Crawford, R. Harrington, L. Jones et al *In* ESA Appl. of Remote Sensing Data on the Continental Shelf Jul. 1981 p 113-118 refs Sponsored in cooperation with NASA Bergen Univ., and Royal Norwegian Council for Scientific and Industrial Research

(Grants N00014-80-G-0003; NATO-9-4-02-SRG.19)
Avail: NTIS HC A13/MF A01; ESA, Paris FF 125 CSCL 17I

Passive and active microwave measurements from surface based, airborne, and satellite instruments were obtained together with surface observations northwest of Svalbard. Emissivities of different ice patches in the ice edge region over the spectral range from 4.9 to 94 GHz are presented. The combination of a 6.6 GHz microwave radiometer with a 14.6 GHz scatterometer demonstrates the usefulness of an active/passive system in ice classification. A variety of mesoscale features under different meteorological conditions is revealed by a 1.36 GHz synthetic aperture radar. Ice edge location by Nimbus 7 scanning multifrequency microwave radiometer is shown accurate to 10 km when the 37 GHz horizontal polarized channel is used. Author (ESA)

N82-14567# Institute of Oceanographic Sciences, Wormley (England).

A PRELIMINARY EVALUATION OF SEASAT PERFORMANCE OVER THE AREA OF JASIN AND ITS RELEVANCE TO ERS-1

T. D. Allan and T. H. Guymer *In* ESA Appl. of Remote Sensing Data on the Continental Shelf Jul. 1981 p 119-127 refs

Avail: NTIS HC A13/MF A01; ESA, Paris FF 125

The microwave sensor data of Seasat was checked using Joint Air-Sea Interaction Experiment surface observations. The results of passes under light, and moderate to strong winds, show that sea surface conditions are revealed more accurately by Seasat than by weather charts based on ship reports. Wind observations are similar for satellite and surface observers. Author (ESA)

N82-14569# National Inst. of Oceanography, Goa (India).

STUDIES OF THE INDIAN CONTINENTAL SHELF: APPLICATION OF REMOTE SENSING DATA

L. V. GangadharaRao and V. R. Rao (Indian Space Research Organization, Bangalore) *In* ESA Appl. of Remote Sensing Data on the Continental Shelf Jul. 1981 p 131-141 refs

Avail: NTIS HC A13/MF A01; ESA, Paris FF 125

Early studies of coastal areas of India are reviewed and the state of the art of current studies is presented, including the identification of possible applications of remote sensing data in the context of ongoing programs and future study needs. Multidisciplinary studies with the Indian oceanographic research vessel RV Gaveshani are considered. Ocean engineering and coastal zone management (with application to offshore drilling and harbor development, fisheries, and pollution monitoring are discussed. Remote sensing data from satellites can contribute significantly to this program. Author (ESA)

N82-14570# Centre d'Etudes de Meteorologie Spatiale, Lannion (France). Antenne ORSTOM.

A SHORT REVIEW OF AN OCEANOGRAPHIC USE OF METEOSAT DATA BY THE ORSTOM REMOTE SENSING SERVICE

J. Citeau and F. Domain (Centre Oceanologique de Bretagne, France) *In* ESA Appl. of Remote Sensing Data on the Continental Shelf Jul. 1981 p 145-156 refs

Avail: NTIS HC A13/MF A01; ESA, Paris FF 125

Using the thermal infrared band, migration of schools of fish along coasts of Mauritania and Senegal was determined according to the latidudinal position of a thermal front and equatorial upwelling in the Gulf of Guinea was detected. For the latter study, an oceanographic program was instigated to furnish sea truth data. Despite a high degree of cloud cover, the Meteosat data shows good agreement on sea surface temperature. The beginning and development of the equatorial upwelling are adequately followed. The zonal extension of a large warm water band confirms that this upwelling is a phenomenon related to the equatorial process and that no advection from southern latitudes appears on the surface. Author (ESA)

N82-14571# Dundee Univ. (Scotland). Carnegie Lab. of Physics.

COASTAL ZONE RESEARCH USING REMOTE SENSING TECHNIQUES

A. P. Cracknell and S. M. Singh *In* ESA Appl. of Remote Sensing Data on the Continental Shelf Jul. 1981 p 157-168 refs

Avail: NTIS HC A13/MF A01; ESA, Paris FF 125

For the prelaunch exercise in connection with the EURASEP project, sea truth data was analyzed with data collected simultaneously from LANDSAT. Maps of chlorophyll and suspended sediment distributions over a substantial area of the North Sea off the Belgian and Dutch coastlines were generated. Analysis results of simultaneous airborne ocean color scanner data are compared. The NIMBUS 7 coastal zone color scanner (CZCS) in flight calibration data are compared with preflight calibration constants. Atmospheric corrections are applied. A satisfactory set of procedures for calibrating CZCS data, correlating that data with sea truth measurements, were established. Author (ESA)

N82-14574# Centre d'Etudes Techniques de l'Equipment, Aix-en-Provence (France).

OPERATIONAL USE OF REMOTE SENSING FOR COASTAL ZONE MANAGEMENT AND POSSIBLE CONTRIBUTION OF SPECIALIZED SATELLITES

C. Valerio *In* ESA Appl. of Remote Sensing Data on the Continental Shelf Jul. 1981 p 183-188

Avail: NTIS HC A13/MF A01; ESA, Paris FF 125

A multispectral remote sensing system, based on aerial photography, was developed in order to satisfy the requirements of coastal zone management. Data requirements (hydrodynamics, nature of the sea bottom, shore and land use) are interpreted in remote sensing terms. Technoeconomic results for study of the sewage treatment in Antibes on the Mediterranean coast are taken as a remote sensing example. Surface currents were investigated under different wind and climatic conditions. Vertical temperature and salinity profiles show vertical thermal stratification of the sea in that area. Author (ESA)

N82-14576# Swedish Meteorological and Hydrological Inst., Norkoeping.

MARINE ACTIVITIES IN SWEDEN FOR WHICH REMOTE SENSING DATA MAY BE OF INTEREST

Thomas Thompson *In* ESA Appl. of Remote Sensing Data on the Continental Shelf Jul. 1981 p 195-196

Avail: NTIS HC A13/MF A01; ESA, Paris FF 125

Coastal and offshore activities (physical oceanography, marine meteorology, fishing, marine transportation, environmental protection, and climatology) for which satellite data, particularly microwave measurements available on an operational basis is useful, were reviewed. These involve weather analyses and forecasting, ship routing, ice accretion measurement, sea ice surveillance, sea surface temperature measurement, wave analyses and forecasts, pollution surveillance, sea water level measurement, and surface currents monitoring. Present data has many deficiencies which can be remedied by remote sensing techniques, but a fully operational system is required. Author (ESA)

N82-14581# University Coll., Galway (Ireland).
THE FEASIBILITY OF USING REMOTELY SENSED COLOR AS AN INDEX OF IRISH COASTAL WATER PROPERTIES
E C Monahan, I G OMuircheartaigh, and M P Fitzgerald *In* ESA Appl of Remote Sensing Data on the Continental Shelf Jul 1981 p 233-237 refs

Avail NTIS HC A13/MF A01; ESA, Paris FF 125

Sea truth data collected at 250 oceanographic stations in coastal waters south and west of Ireland are used with statistical methodologies (including least squares fitting and the approach of Box and Cox) to obtain, where feasible, expressions for the relationships between water color and other surface water properties. Close correlation is found between surface salinity, Gelbstoff concentration and water color as expressed by Munsell hue. For the same waters, poor correlation is found between surface chlorophyll-a and water color. Such satellite instruments as the coastal zone color scanner are applicable to the delineation of coastal and offshore water boundaries near Ireland, but are not appropriate for estimating the standing crop of phytoplankton. Author (ESA)

N82-14582# Instituto de Investigaciones Pesqueras, Barcelona (Spain).
NECESSITY OF REMOTE SENSING FOR OCEAN STUDIES. PART 1: NORTHWEST AFRICAN MISSIONS, SAHARA-1 AND ATLOR-1
A. Ballester Nolla and C. Romeu Nedwed *In* ESA Appl. of Remote Sensing Data on the Continental Shelf Jul. 1981 p 239-241 refs
Avail. NTIS HC A13/MF A01; ESA, Paris FF 125

Results of two oceanographic missions studying the general conditions of the northwest African offshore upwelling are summarized. Strong correlation between temperature, nutrients (nitrate, phosphate, and silicate) and chlorophyll is found. The upwelling area, 60 to 100 miles offshore, does not correspond to normally accepted mechanisms. Preliminary results suggest a collision between intermediate subequatorial water masses and the southward surface Canary current. The hypothesis is supported by tests comparing sea truth data with remotely sensed temperature data (NOAA 2 VHRR). The employment of remotely sensed data as a formal method of study, and not simply as a complementary aid, is discussed. Author (ESA)

N82-14585# Deutsche Forschungs- und Versuchsanstalt fuer Luft- und Raumfahrt, Oberpfaffenhofen (West Germany). Inst. fuer Optoelektronik.
MARITIME APPLICATIONS OF IMAGE PROCESSING AT DFVLR, OBERPFAFFENHOFEN, WEST GERMANY
Klaus A. Ulbricht *In* ESA Appl. of Remote Sensing Data on the Continental Shelf Jul. 1981 p 255-261 refs

Avail: NTIS HC A13/MF A01; ESA, Paris FF 125

A digital interactive image analysis system is described and plans for a larger system are summarized. Examples of digital image processing of LANDSAT multispectral scanner images, showing contents otherwise easily missed, are given. Zones of different reflectivity, representing currents or drifts, are pointed out. The LANDSAT pictures of the Baltic Sea from four multispectral channels, processed to display the mass appearance of blue green algae, are included. Phytoplankton development in nearshore and inshore waters of the southwest Baltic, and its drift to deeper areas, are followed. Complexes of banks and channels revealed by LANDSAT in the Tay river and its delta in northeast Scotland are compared with current charts and maps of sediments. Author (ESA)

N82-14586# Atomic Energy Research Establishment, Harwell (England). Marine Technology Support Unit.
A LOOK AT NONSATELLITE REMOTE SENSING SYSTEMS FOR MARINE USE
R J Moulton *In* ESA Appl. of Remote Sensing Data of the Continental Shelf Jul. 1981 p 263-271 refs Sponsored by UK Dept. of Industry

Avail: NTIS HC A13/MF A01; ESA, Paris FF 125

Cost/benefit figures are given (but in some cases the costs are distorted by military investment). The main applications of remote sensing are fish location, pollution monitoring, shallow water bathymetry, and sea state measurement (with its implications for optimum ship routing). User needs for a system are classified by choice of function, operational choices, technical decisions, relevant sensors, and sensing techniques (H.F.; radar; u.v.; fluorimetry; pulsed laser bathymetry; low light television; cameras; passive multifrequency microwave imaging. The U.S. oil surveillance system as well as Swedish and French systems are described. Nonsatellite systems can be best used to verify satellite data. Author (ESA)

N82-14587# Indian Space Research Organization, Bangalore.
SCIENTIFIC STUDIES USING BHASKARA SATELLITE MICROWAVE RADIOMETER (SAMIR) DATA: A SHORT OVERVIEW
V, R. Rao IN ESA Appl. of Remote Sensing Data on the Continental Shelf Jul. 1981 p 273-278 refs

Avail: NTIS HC A13/MF A01; ESA, Paris FF 125

The three-channel microwave radiometric system SAMIR (two frequencies at 19 GHz and one at 22 Ghz) which is one of the two payloads on board the Bhaskara satellite, is described; along with the satellite itself and its complete payload. Data quality and methods of analysis are reviewed and the use of the data for investigation of sea states, water vapor and liquid water content in the atmosphere and over oceans adjoining India is examined. The derivation of these and further ocean related parameters (sea surface winds; rainfall rates) for monitoring sea state conditions in India was demonstrated. Author (ESA)

N82-14592# Kansas Univ. Center for Research, Inc., Lawrence. Remote Sensing Lab.
MEASUREMENTS OF RADAR BACKSCATTER FROM ARCTIC SEA ICE IN THE SUMMER
R. G. Onstott, S. Gogineni, C. V. Delker, and R. K. Moore Jul. 1981 16 p
(Contract N00014-76-C-1105)
(AD-A105586; CRINC/RSL-TR-331-20) Avail: NTIS HC A02/MF A01 CSCL 17/9

Measurements of radar backscatter from sea ice located near Svalbarb and Greenland were made during the summer of 1980 as part of Project YMER. These data were acquired using the University of Kansas helicopter-borne microwave active spectrometer (HELOSCAT II) which operated over a frequency range of 8 to 18 GHz and an angle of incidence range of 0 degrees to 50 degrees. The presence of meltponds, the transformation of the snowpack into an ice layer, and the warmer temperatures have contributed to radar signatures that may be significantly different than those observed during the winter and spring. A wide variety of ice conditions were investigated. These included multiyear, thick first-year, thin first-year, young, new, and pressure-ridged ice. The measurement program is described herein. Author (GRA)

N82-14593# Kansas Univ. Center for Research, Inc., Lawrence. Remote Sensing Lab.
MEASUREMENTS OF RADAR BACKSCATTER FROM ARCTIC SEA ICE IN THE SUMMER, APPENDICES A AND B
R. G. Onstott, S. Gogineni, R. K. Moore, and C. V. Delker Jul. 1981 96 p
(Contract N00014-76-C-1105)
(AD-A105736; CRINC/RSL-TR-331-22) Avail: NTIS HC A05/MF A01 CSCL 17/9

Computer output measurements of radar backscatter from arctic sea ice in the summer are presented, including raw radar backscatter data and sea ice salinity profiles N.W.

N82-14617# Physics Lab. RVO-TNO, The Hague (Netherlands). Research Group: Physics.
PROJECT NOORDWIJK. PART 1: MEASUREMENTS OF THE RADAR BACKSCATTER COEFFICIENT GAMMA (SIGMA DEG) IN 1977 AND 1978
G. P. deLoor Nov. 1979 42 p refs 2 Vol.
(PHL-1979-49-Pt-1; TDCK-73426) Avail: NTIS HC A03/MF A01

Radar backscatter measurements obtained from a sea platform are compared with airborne and spaceborne observations. A short range FM radar was mounted beside a television camera and directed into the prevailing winds. Upwind and crosswind data were collected, but downwind data are scarce, and more windspeed data are required. A systematic difference is observed between airborne and ground based data. The value of gamma is dependent on windspeed; dependency differs for the specular region (low incidence angles) and the diffuse (incidence angles > 45 deg). Author (ESA)

N82-14618# Physics Lab. RVO-TNO, The Hague (Netherlands). Research Group 4: Microwaves.

PROJECT NOORDWIJK. PART 2: RESULTS OF NORTH SEA CLUTTER MEASUREMENTS IN THE I-BAND PERFORMED FROM THE PLATFORM NOORDWIJK IN SEPTEMBER/OCTOBER 1977

H. Sittrop and H. Gravesteijn Aug. 1980 79 p refs 2 Vol. (PHL-1980-28-Pt-2; TDCK-74302) Avail: NTIS HC A05/MF A01

Radar backscatter off the sea at low incidence angles was measured. A low frequency spectral analysis method is used to show that an appreciable periodic content exists in the sea return. This component in the scintillation spectra is 0.14 Hz and is related to the sea wave period. Wind-wave interaction effects are observed for up, down and crosswind directions. The clutter patch size and the incidence angle are used as a parameter. An optimum spectral response exists for upwind observations at an incidence angle of 1 deg and pulselength 0.08 microsec. The radar cross section per unit area measured is compared with an experimental sea clutter model. For wind directions resulting in an adequate fetch over open sea, reasonable agreement is found. No significant conclusions can be drawn with respect to megaripple observations. Author (ESA)

N82-14789*# Illinois Univ., Urbana. Radio Research Lab.

REMOTE SENSING OF SEA STATE BY LASER ALTIMETERS

B. Tsai and C. S. Gardner Dec. 1981 51 p refs
(Grant NsG-5049)
(NASA-CR-165049; RRL-Publ-514) Avail: NTIS HC A04/MF A01 CSCL 08C

The reflection of short laser pulses from the ocean surface was analyzed based on the specular point theory of scattering. The expressions for the averaged received signal, shot noise and speckle induced noise were derived for a direct detection system. It is found that the reflected laser pulses have an average shape closely related to the probability density function associated with the surface profile. This result is applied to estimate the mean sea level and significant wave height from the receiver output of the laser altimeter. T.M.

N82-15498*# EG and G Washington Analytical Services Center, Inc., Pocomoke City, Md.

A GLOBAL ATLAS OF GEOS-3 SIGNIFICANT WAVEHEIGHT DATA AND COMPARISON OF THE DATA WITH NATIONAL BUOY DATA

J. D. McMillan Wallops Island, Va. NASA. Wallops Flight Center Nov. 1981 163 p refs
(Contract NAS6-2639)
(NASA-CR-156882) Avail: NTIS HC A08/MF A01 CSCL 08C

The accuracy of the GEOS-3 significant waveheight estimates compared with buoy measurements of significant waveheight were determined. A global atlas of the GEOS-3 significant waveheight estimates gathered is presented. The GEOS-3 significant waveheight estimation algorithm is derived by analyzing the return waveform characteristics of the altimeter. Convergence considerations are examined, the rationale for a smoothing technique is presented and the convergence characteristics of the smoothed estimate are discussed. The GEOS-3 data are selected for comparison with buoy measurements. The GEOS-3 significant waveheight estimates are assembled in the form of a global atlas of contour maps. Both high and low sea state contour maps are presented, and the data are displayed both by seasons and for the entire duration of the GEOS-3 mission. E.A.K.

N82-15684# Royal Netherlands Meteorological Inst., De Bilt. Oceanographic Research Div.

METEOROLOGICAL AND OCEANOGRAPHIC OBSERVATIONS ON BOARD NETHERLANDS LIGHTVESSELS AND THE LIGHTPLATFORM 'GOEREE' IN THE NORTH SEA Annual Report, 1976

1981 143 p In ENGLISH and DUTCH
(KNMI-141-28) Avail: NTIS HC A02/MF A01; KNMI, De Bilt, Netherlands FL 17.50

Three-hourly meteorological and wave observations as well as hourly current and salinity measurements were compiled. Tables show: (1) meteorological results; (2) oceanographic results; (3) general air circulation, air pressure, precipitation, and fog; (4) visibility and cloud amount; (5) air temperature; (6) sea surface temperature; (7) air-sea temperature differences; and (8) wind and wave frequencies. A.R.H.

READEX best copy available

06
HYDROLOGY AND WATER MANAGEMENT

Includes snow cover and water runoff in rivers and glaciers, saline intrusion, drainage analysis, geomorphology of river basins, land uses, and estuarine studies.

A82-10031 **Comparison of conventional and remotely sensed estimates of runoff curve numbers in southeastern Pennsylvania.** T. R. Bondelid, R. H. McCuen (Maryland, University, College Park, MD), and T. J. Jackson (Science and Education Administration, Plant Physiology Institute, Beltsville, MD). In: American Society of Photogrammetry, Annual Meeting, 46th, St. Louis, MO, March 9-14, 1980, ASP Technical Papers. Falls Church, VA, American Society of Photogrammetry, 1980, p. 81-96.

The present study compares estimates of runoff curve numbers obtained using three different methods of identifying land cover: conventional surveys, land cover maps developed by the U.S. Geological Survey, and Landsat data. Data were tested on three watersheds in southeastern Pennsylvania. Accuracy was evaluated for various levels of drainage basin size, land use, and inhomogeneity of land cover distribution. It is found that the estimates of the runoff curve number were not highly sensitive to the source of the land cover data for typical watershed sizes and characteristics in this study area. Thus, accurate estimates can be obtained using less expensive remote sensing techniques. B.J.

A82-10032 **Satellite rainfall estimation for hydrologic forecasting.** R. K. Farnsworth (NOAA, Hydrologic Research Laboratory, Silver Spring, MD) and R. P. Canterford. In: American Society of Photogrammetry, Annual Meeting, 46th, St. Louis, MO, March 9-14, 1980, ASP Technical Papers. Falls Church, VA, American Society of Photogrammetry, 1980, p. 97-105. 14 refs.

The paper presents a method for evaluating current rainfall estimation techniques in terms of the requirements for flood and stage forecasting of rivers. An evaluation scheme has been developed based on equivalent rain gage density (ERGD). This scheme involves assigning ERGDs to the satellite techniques for specified time and space scales down to the order of three hours and 1/4 deg x 1/4 deg latitude/longitude grids. The scheme makes it possible to make intercomparisons among satellite techniques and to measure their improvement, if any, over information from existing operational rain gage networks. B.J.

A82-10033 **Mapping of the 1978 Kentucky River Flood from NOAA-5 satellite thermal infrared data.** C. P. Berg, D. F. McGinnis, Jr., and D. G. Forsyth (NOAA, National Environmental Satellite Service, Washington, DC). In: American Society of Photogrammetry, Annual Meeting, 46th, St. Louis, MO, March 9-14, 1980, ASP Technical Papers. Falls Church, VA, American Society of Photogrammetry, 1980, p. 106-111.

The December 1978 Kentucky River Flood was analyzed using remotely sensed thermal infrared (IR) data from the Very High Resolution Radiometer (VHRR) onboard the NOAA-5 satellite. Computer-enhanced imagery and computer printouts permitted delineation of the flood boundaries; ground-based measurements indicate that this flood was a 200-year flood. Both manual photo-interpretive and automated computer analyses of the data indicate that NOAA-5 VHRR-IR data is a useful tool for flood delineation. (Author)

A82-10054 **Data sources for analyses of Great Lakes wetlands.** J. G. Lyon (Michigan, University, Ann Arbor, MI). In: American Society of Photogrammetry, Annual Meeting, 46th, St. Louis, MO, March 9-14, 1980, ASP Technical Papers. Falls Church, VA, American Society of Photogrammetry, 1980,p. 516-528. 14 refs. Grant No. NOAA-04-8-M01-134.

This paper presents a comparison of data sources for assessing quantity and variety of coastal zone wetlands. The information supplying capabilities of aerial photography, Landsat imagery and SEASAT radar data were evaluated. This was accomplished by mapping wetlands, and by a change-detection analysis of wetlands in relation to Great Lake water levels. The value of each source is examined in a framework of data gathering and analysis for purposes of coastal zone management. (Author)

A82-10208 **Analysis of bright bands from 3-D radar data.** C. G. Collier (Meteorological Office, Malvern, Worcs., England), S. Lovejoy, and G. L. Austin (McGill Radar Weather Observatory, Montreal, Canada). In: Conference on Radar Meteorology, 19th, Miami Beach, FL, April 15-18, 1980, Preprints. Boston, MA, American Meteorological Society, 1980, p. 44-47.

A practical scheme has been developed to automatically classify observed echo data into either stratiform rain, showers, or ground clutter using high resolution three-dimensional scanning radar. The technique involves the statistical determination of boundaries in n-dimensional space into m classes by the minimization of a general loss function, f. The reflectivity values are divided evenly into 30 classes, and a two-dimensional histogram of frequency-of-occurrence of the different 2-km, 3-km dBZ combinations is produced. The concentration of points is examined in relation to the line defined by reflectivity level at 3 km equals reflectivity level at 2 km. Points below the line indicate a positive vertical Z gradient, while points above indicate a negative one. Lines drawn to indicate the 50% contours represent the optimum boundaries for the technique when no more than two classes overlay at any one location with the two-dimensional 3 to 2 km reflectivity level plane. Errors in classification were found to be small (about 10%), and were usually a result of an error in only one category. J.F.

A82-10694 * # **A comparison of radiative transfer models for predicting the microwave emission from soils.** T. J. Schmugge (NASA, Goddard Space Flight Center, Hydrological Sciences Branch, Greenbelt, MD) and B. J. Choudhury (NASA, Goddard Space Flight Center, Hydrological Sciences Branch, Greenbelt; Computer Sciences Corp., Silver Spring, MD). *Radio Science,* vol. 16, Sept.-Oct. 1981, p. 927-938. 19 refs.

Noncoherent and coherent numerical models for predicting emission from soils are compared. Coherent models use the boundary conditions on the electric fields across the layer boundaries to calculate the radiation intensity, and noncoherent models consider radiation intensities directly. Interference may cause different results in the two approaches when coupling between soil layers in coherent models causes greater soil moisture sampling depths. Calculations performed at frequencies of 1.4 and 19.4 GHz show little difference between the models at 19.4 GHz, although differences are apparent at the lower frequency. A definition for an effective emissivity is also given for when a nonuniform temperature profile is present, and measurements made from a tower show good agreement with calculations from the coherent model. D.L.G.

A82-12553 **Effect of grain size and snowpack water equivalence on visible and near-infrared satellite observations of snow.** J. Dozier (California, University, Santa Barbara, CA), S. R. Schneider, and D. F. McGinnis, Jr. (NOAA, National Earth Satellite Service, Washington, DC). *Water Resources Research,* vol. 17, Aug. 1981, p. 1213-1221. 24 refs.

Satellite observations of snow in the near-infrared wavelengths can be used to roughly estimate snow grain size. When the grain size is large, it is possible to use measurements in the visible wavelengths to estimate snow water equivalence below some threshold value of around 100 mm. While sufficient data to fully evaluate these possibilities are not available, model calculations, selected satellite observations, and limited ground truth are in qualitative agreement. Complications arise because the effect of contamination by atmospheric aerosols is similar to that of finite depth, and because the near-infrared channel on the NOAA TIROS-N series satellites is not in the wavelength region where snow reflectance is most sensitive to grain size. (Author)

A82-12589 **Civil engineering applications of remote sensing; Proceedings of the Specialty Conference, University of Wisconsin, Madison, WI, August 13, 14, 1980.** Conference sponsored by ASCE, ASP, and University of Wisconsin. Edited by R. W. Kiefer (Wisconsin, University, Madison, WI). New York, American Society of Civil Engineers, 1980. 199 p. $19.50.

Topics discussed include land applications, water applications, thermography applications, and general applications of remote sensing. Papers are presented on Landsat imagery for hydrologic modeling, satellite imagery and shoreline erosion prediction, water temperature mappings by infrared scanner, and aerial photography in fire risk assessment. Attention is also given to a data base system for real-time hydrologic modeling, the application of Landsat to the inventory of dams, and the operational use of Landsat for lake quality assessment. C.R.

A82-12592 * Landsat imagery for hydrologic modeling. R. S. Taylor, R. P. Shubinski, and T. S. George (Camp, Dresser and McKee, Inc., Springfield, VA). In: Civil engineering applications of remote sensing; Proceedings of the Specialty Conference, Madison, WI, August 13, 14, 1980. New York, American Society of Civil Engineers, 1980, p. 44-52. NASA-supported research.

The cost and effectiveness of developing land cover information derived from Landsat imagery for hydrologic studies are compared with the cost and effectiveness of conventional sources. The analysis shows that the conventional and Landsat methods are nearly equally effective in providing adequate land cover data for hydrologic studies. The total cost effectiveness analysis demonstrates that the conventional method is cost effective for a study area of less than 26 sq km and that the Landsat method is to be preferred for areas of more than 26 sq km. C.R.

A82-12593 Application of Landsat to the inventory of DAMS. A. R. Blystra (FEderal Energy Regulatory Commission, Washington, DC) and R. R. Dumas (Chicago District, Corps of Engineers, Chicago, IL). In: Civil engineering applications of remote sensing; Proceedings of the Specialty Conference, Madison, WI, August 13, 14, 1980. New York, American Society of Civil Engineers, 1980, p. 54-59.

A82-12595 Satellite imagery and shoreline erosion prediction. C. W. Welby (North Carolina State University, Raleigh, NC). In: Civil engineering applications of remote sensing; Proceedings of the Specialty Conference, Madison, WI, August 13, 14, 1980. New York, American Society of Civil Engineers, 1980, p. 78-87. 11 refs.

A82-12596 * The operational use of Landsat for lake quality assessment. F. L. Scarpace (Wisconsin, University, Madison, WI) and L. T. Fisher (Maine, University, Orono, ME). In: Civil engineering applications of remote sensing; Proceedings of the Specialty Conference, Madison, WI, August 13, 14, 1980. New York, American Society of Civil Engineers, 1980, p. 88-100. 10 refs. Research supported by the Wisconsin Department of Natural Resources, U.S. Environmental Protection Agency, and NASA.

A cooperative program between the Wisconsin Department of Natural Resources and the University of Wisconsin for the assessment, with Landsat data, of the trophic status of all the significant inland lakes in Wisconsin is described. The analysis technique is a semiautomatic data acquisition and handling system which, in conjunction with an analytical categorization scheme, can be used for classifying inland lakes into one of seven categories of eutrophication and one of four problem types. C.R.

A82-12597 Field study for Landsat water quality verification. D. S. Graham and J. M. Hill (Louisiana State University, Baton Rouge, LA). In: Civil engineering applications of remote sensing; Proceedings of the Specialty Conference, Madison, WI, August 13, 14, 1980. New York, American Society of Civil Engineers, 1980, p. 101-117. 8 refs.

It is found that MSS data can be used to separate many water types in Apalachicola Bay, in Florida. Here, the images can be used to deduce circulation patterns. Circulation patterns for Landsat images are found to correspond clearly with both field data and numerical model results. The color intensity in the bay results from both dispersive mixing and a chemical reaction dependent on pH. C.R.

A82-12598 Water temperature mapping by infrared scanner. J. B. Evans (Texas Instruments, Inc., Dallas, TX). In: Civil engineering applications of remote sensing; Proceedings of the Specialty Conference, Madison, WI, August 13, 14, 1980. New York, American Society of Civil Engineers, 1980, p. 118-122.

The state-of-the-art method of mapping water temperature using an airborne calibrated infrared scanner combined with computer corrections is described. The radiation measurements are digitized and coded onto computer tape during airborne survey operations. It is noted that the computer corrects for atmospheric effects that also change with scan angle, physics of temperature to radiation, water surface cooling or heating, system parameters, and map linearities. Scale maps of temperature are printed or plotted in any form that is available to the computer. The accuracy thus obtained allows computer maps to be combined to cover a large area with one-half degree accuracy. C.R.

A82-15037 Use of visible and thermal satellite data to monitor an intermittently flooding marshland. G. F. Byrne, G. N. Goodrick (Commonwealth Scientific and Industrial Research Organization, Div. of Land Use Research, Canberra, Australia), and K. Dabrowska-Zielinska (Instytut Geodezji i Kartografii, Warsaw, Poland). *Remote Sensing of Environment*, vol. 11, Nov. 1981, p. 393-399. 5 refs.

Selected thermal and visible data from the Heat Capacity Mapping Mission satellite for the Macquarie Marshes of Eastern Central Australia are examined in the light of a substantial volume of data from other sources, including Landsat, with a view to evaluating meteorological satellite data as ecological monitors for this landform. The results indicate that at least four important components of marshland can be mapped using HCMM data. The ecological status of marshland is intimately connected to their water status and visible and thermal imagery appears to be an economical and effective method of monitoring such systems. (Author)

A82-15961 † Study of the dynamics of the Danube delta using space images (Izuchenie dinamiki del'ty Dunaia s ispol'zovaniem kosmicheskikh snimkov). O. N. Efremova and V. I. Kravtsova (Moskovskii Gosudarstvennyi Universitet, Moscow, USSR). *Issledovanie Zemli iz Kosmosa*, Sept.-Oct. 1981, p. 90-96. In Russian.

Multispectral scanning images of the Danube delta, obtained by the Fragment system in September 1980, were compared with analogous images obtained by the Landsat satellite in September 1972. A study of these images revealed the dynamics of the delta over an eight year period. A map was constructed, reflecting the seaward extension of the Kiliiskaia part of the delta; it revealed an increase in water supply in some parts of the inner delta, and a decrease in water supply in other parts; it also showed a significant growth in agricultural land, featuring the appearance of rice fields in drained marshes, as well as other crop fields on terraces. J.F.

A82-15969 * In situ spectral reflectance studies of tidal wetland grasses. D. S. Bartlett (NASA, Langley Research Center, Marine and Applications Technology Div., Hampton, VA) and V. Klemas (Delaware, University, Newark, DE). *Photogrammetric Engineering and Remote Sensing*, vol. 47, Dec. 1981, p. 1695-1703. 16 refs. Research supported by the University of Delaware; Contract No. NAS5-20983.

Field measurements of wetland spectral canopy reflectance in the Landsat-MSS wavebands were correlated with biotic factors. The highest single band correlations were observed between visible (MSS Band 4: 0.5 to 0.6 micron and Band 5: 0.6 to 0.7 micron) canopy reflectance and the percentage, by weight, of live (green) vegetation in the canopies of Spartina alterniflora (salt marsh cordgrass), Spartina patens (salt meadow grass), and Distichlis spicata (spike grass). Infrared canopy reflectance displayed significant but weaker dependence on canopy parameters such as live and total biomass and canopy height. The Band 7 (0.8 to 1.1 microns)/Band 5 (0.6 to 0.7 micron) reflectance ratio was found to be highly correlated with green biomass for S. alterniflora. Highest spectral seperability between the 'low marsh' S. alterniflora and the 'high marsh' Salt Hay (S. patens and D. spicata) communities in Delaware occurs during December. (Author)

A82-17892 # Role of remote sensing in the study of acid rain impact on aquatic systems. J. R. Schott (Rochester Institute of Technology, Rochester, NY) and M. A. Wilkinson (New York, State

University, Buffalo, NY). *American Institute of Aeronautics and Astronautics, Aerospace Sciences Meeting, 20th, Orlando, FL, Jan. 11-14, 1982, Paper 82-0336.* 10 p. 12 refs. Research supported by the New York State Energy Research and Development Authority.

Results are presented of a study of the capabilities of image analysis of remotely sensed data in the evaluation of the present state and past history of lakes subject to acidification by acid precipitation. Analysis of surface sampling data from nine Adirondack lakes reveals lake pH and alkalinity to be reflected in parameters related to optical properties, exhibiting a positive correlation with chlorophyll and total solids and a negative correlation with Secchi depth. Aerial photographic measurements of lake volume spectral reflectance, when compared with a simple laboratory model of the dependence of chlorophyll, lignin and humic acid contents of water on its optical properties, are also found to correlate with the differences between the in situ lake properties. Finally, analysis of Landsat band 4, 5 and 7 data obtained in September 1972 and 1979 for 18 lakes demonstrates the potential of the data for the isolation of lakes with low alkalinity, and for monitoring the rate of acidification over time providing data is properly calibrated for atmospheric, illumination and sensor response effects. Results thus demonstrate considerable potential for remote sensing in monitoring the impact of acidification on lakes, and point up the need for further studies of multi-temporal Landsat data and the techniques of aerial analysis. A.L.W.

A82-17999 **An application of Landsat derived data to a regional hydrologic model.** D. P. Killpack and R. M. McCoy (Utah, University, Salt Lake City, UT). *Remote Sensing Quarterly*, vol. 3, Apr. 1981, p. 27-33. 8 refs.

An empirical, regional hydrologic model for predicting stream flow is developed based on the use of planimetric terrain variables obtainable from satellite imagery without stereo coverage. Measurements of basin area, basin perimeter, network length and main channel length were obtained from topographic maps and from Landsat imagery for 12 undiverted gaged streams essentially free of reservoirs and lakes in the Wasatch Mountains, and compared with stream flow variables in order to derive a regression equation for estimating stream discharge. Use of the equation expressing runoff as a function of basin area to predict runoffs in eight additional basins results in a correlation coefficient between predicted and observed values of 0.92, thus demonstrating the validity of the approach. A.L.W.

A82-18000 **The potential for use of Landsat data in water resources planning for the Missouri River Basin.** T. W. Lowe (Missouri River Basin Commission, Omaha, NE). *Remote Sensing Quarterly*, vol. 3, Apr. 1981, p. 34-41. 10 refs.

A82-18166 **An inertially-aided aircraft track recovery system for coastal mapping.** D. B. Reid, W. S. Gesing, B. N. McWilliam (Philip A. Lapp, Ltd., Toronto, Canada), and J. R. Gibson (Canada Centre for Remote Sensing, Ottawa, Canada). In: PLANS '80 - Position Location and Navigation Symposium, Atlantic City, NJ, December 8-11, 1980, Record. New York, Institute of Electrical and Electronics Engineers, Inc., 1980, p. 422-429. 10 refs.

A description is given of a new airborne system developed for charting shallow coastal and inland waters. The main components of this system are an aerial survey camera, a profiling laser radar, an analytical stereo plotter, and a multisensor track recovery system (TRS). The TRS comprises a gimballed inertial navigation system and several auxiliary sensors which require redundant position and attitude information. The sensor data are combined postmission with the aid of a U-D factorized Kalman filter and modified Bryson-Frazier smoother to compute precise estimates of the orientation parameters of the survey camera at the times of film exposure. These parameters are used in order to position each overlapping pair of photographs on the analytical plotter to form a stereo image and a corresponding analytical stereomodel from which water depth measurements are made. Flight trial results demonstrate that the TRS is able to achieve radial position and attitude accuracies which exceed 1 meter and 2 arcmin (RMS), respectively, and that this level of performance is sufficient to enable water depth measurements to be made to an accuracy of better than 0.65 m (RMS). C.R.

N82-11530# National Oceanic and Atmospheric Administration, Boulder, Colo. Office of Weather Research and Modification.
A SYSTEMS APPROACH TO THE REAL-TIME RUNOFF ANALYSIS WITH A DETERMINISTIC RAINFALL-RUNOFF MODEL
Robert J. C. Burnash and R. Larry Ferral Apr. 1981 24 p refs
(PB81-224495; NOAA-TM-NWS-WR-162; NOAA-81050703)
Avail: NTIS HC A02/MF A01 CSCL 08H

The responsibility for providing the U.S. with warnings of river conditions was assigned to the National Weather Service in 1890. This requirement led to the development of a systems approach to hydrologic data collection, runoff computation, and forecast production. This system is focused on producing information on the future distribution of water in time and space which affects the safety, welfare, and economic well being of the nation and its inhabitats. A principal element of any hydrologic warning system is an effective rainfall-runoff model. GRA

N82-12498*# Environmental Research and Technology, Inc., Concord, Mass.
SNOW-MAPPING EXPERIMENT
James C. Barnes, Clinton J. Bowley, J. Thomas Parr, and Michael D. Smallwood *In* NASA. Johnson Space Flight Center Skylab Explores the Earth 1977 p 191-224 refs

Avail: NTIS MF A01; SOD HC $16.50 CSCL 08L

More than 300 hand-held camera photographs were taken of most part of the United States in which snow existed during the mission. The sites include the Sierra Nevada in California; the Salt-Verde Watershed in central Arizona; the Rocky Mountains in Colorado; the Great Salt Lake and Yellowstone Park in Utah and Wyoming; the Cascade Range in Washington and Oregon; the Black Hills in South Dakota; the Central Plains; and the Great Lakes. Snow in the European Alps; the Caucasus and Himalaya Mountains; the Pacific coastal areas of the U.S.S.R.; and New Zealand was also mapped. The experiment shows that: (1) a space observer can identify snow that photointerpreters cannot distinguish on a photograph of the same area, (2) can integrate, through partial cloud cover, to view the terrain, and (3) can select the optimum viewing angle and Sun angle and the appropriate film and filter combination to acquire the best data. A.R.H.

N82-12501*# American Univ., Washington, D. C. Drought Analysis Lab.
REPORT ON SKYLAB 4 AFRICAN DROUGHT AND ARID LAND EXPERIMENT
N. H. MacLeod, J. S. Schubert, and P. Anaejionu *In* NASA. Johnson Space Flight Center Skylab Explores the Earth 1977 p 263-286 refs
Avail: NTIS MF A01; SOD HC $16.50 CSCL 08B

Vegetation patterns, flooding, soil erosion, interdunal water accumulation, natural drainage systems, and drainage patterns in the Black Volta and White Volta River basins were observed and photographed in an effort to determine the causes of desertification in the Sahel. The Niger Island delta in Mali was selected to examine the distribution and changing patterns of vegetation and flooding of the major freshwater resources in that drought-prone area. Observations Nimbus-3, Apollo-9, and Skylab of dust and cloud movements, vegetation patterns, land surface features, the color and distribution of surface water, and color changes of lakes within the drought zone show that widespread destructice land practices contribute to the arid conditions. A.R.H.

N82-12504*# Geological Survey, Tacoma, Wash.
VISUAL OBSERVATIONS OF FLOATING ICE FROM SKYLAB
W. J. Campbell, R. O. Ramseier (Dept. of Environment, Ottawa, Ontario), W. F. Weeks (Cold Regions Research and Engineering Lab.), and J. A. Wayenberg *In* NASA. Johnson Space Flight Center Skylab Explores the Earth 1977 p 353-380 refs

Avail: NTIS MF A01; SOD HC $16.50 CSCL 08L

The lake and sea ice visual observation experiment performed during the Skylab 4 mission was very successful. In the initial experiment design, the Gulf of St. Lawrence and Lake Ontario were chosen as prime sites at which ground-truth measurements and aircraft remote-sensing data were to be obtained. In addition, the Skylab 4 astronauts obtained excellent photographs of sea ice in the Sea of Okhotsk and in the James

Bay portion of Hudson Bay and of icebergs in the Southern Ocean. Some of the sequential photographs contain very useful broad-scale information on the distribution of ice and ice types, the overall deformation patterns, and the amount of relative ice motion. A.R.H.

N82-12510*# Kansas Univ. Center for Research, Inc., Lawrence. Remote Sensing Lab.

PROGRESS IN RADAR SNOW RESEARCH

W. Stiles, F. T. Ulaby, A. K. Fung, and A. Aslam Feb. 1981 167 p refs
(Grant NsG-5335)
(NASA-CR-166709; RSL-TR-410-1) Avail: NTIS HC A08/MF A01 CSCL 08L

Multifrequency measurements of the radar backscatter from snow-covered terrain were made at several sites in Brookings, South Dakota, during the month of March of 1979. The data are used to examine the response of the scattering coefficient to the following parameters: (1) snow surface roughness, (2) snow liquid water content, and (3) snow water equivalent. The results indicate that the scattering coefficient is insensitive to snow surface roughness if the snow is drv. For wet snow, however, surface roughness can have a strong influence on the magnitude of the scattering coefficient. These observations confirm the results predicted by a theoretical model that describes the snow as a volume of Rayleig scatterers, bounded by a Gaussian random surface. In addition, empirical models were developed to relate the scattering coefficient to snow liquid water content and the dependence of the scattering coefficient on water equivalent was evaluated for both wet and dry snow conditions. Author

N82-14549*# National Aeronautics and Space Administration. Goddard Space Flight Center, Greenbelt, Md.

A SIMULATION STUDY OF THE RECESSION COEFFICIENT FOR ANTECEDENT PRECIPITATION INDEX

Bhaskar J. Choudhury and Bruce J. Blanchard Nov. 1981 25 p refs Submitted for publication
(NASA-TM-83860) Avail: NTIS HC A02/MF A01 CSCL 08M

The antecedent precipitation index (API) is a useful indicator of soil moisture conditions for watershed runoff calculations and recent attempts to correlate this index with spaceborne microwave observations have been fairly successful. It is shown that the prognostic equation for soil moisture used in some of the atmospheric general circulation models together with Thornthwaite-Mather parameterization of actual evapotranspiration leads to API equations. The recession coefficient for API is found to depend on climatic factors through potential evapotranspiration and on soil texture through the field capacity and the permanent wilting point. Climatologial data for Wisconsin together with a recently developed model for global isolation are used to simulate the annual trend of the recession coefficient. Good quantitative agreement is shown with the observed trend at Fennimore and Colby watersheds in Wisconsin. It is suggested that API could be a unifying vocabulary for watershed and atmospheric general circulation modelars. Author

N82-14575# Canada Centre for Remote Sensing, Ottawa (Ontario).

RECENT WORK IN PASSIVE OPTICAL IMAGING OF WATER

H. H. Zwick and S. C. Jain (Moniteq Ltd.) *In* ESA Appl. of Remote Sensing Data on the Continental Shelf Jul. 1981 p 189-194 refs
Avail: NTIS HC A13/MF A01; ESA, Paris FF 125

The estimation of water quality and bathymetry with passive optical multispectral data imagery are described. A water quality algorithm was developed from a coordinated set of airborne, multispectral scanner, in situ water, and ground based atmospheric measurements made during coastal zone color scanner NIMBUS 7 passes over Lake Ontario. Modeling of atmosphere, the air water interface, and macroscopic as well as microscopic water optical characteristics gives fresh water estimates of the independently varying chlorophyll-a and total suspended mineral concentrations. Remotely measured radiances are corrected for atmosphere, specular sky reflection, and water refractivity in effects. The required parameters are estimated using a computer optimization routine. Author (ESA)

N82-14579# Roskilde Univ. (Denmark). Institute of Geography, Socio-Economic Analysis and Computer Science.

MAPPING OF SURFACE CURRENTS IN GREENLAND FIORDS BY MEANS OF LANDSAT IMAGES

Sten Folving *In* ESA Appl. of Remote Sensing Data on the Continental Shelf Jul. 1981 p 211-219 refs

Avail: NTIS HC A13/MF A01; ESA, Paris FF 125

Data from LANDSAT were used to study the propagation of meltwater into Soendre Stroemfjord. Water masses are classified on the basis of intensity profiles. These data trace meltwater sediment plumes and the character of the fronts between meltwater and pure fiord water. The main currents are mapped. River discharge from the south side is always up fiord due to pronounced Coriolis influence. A permanent down fiord current is found on the north side, with very complex patterns of current arising when the direction of the fiord channel shifts significantly. Author (ESA)

N82-14580# Southampton Univ. (England).

THE USE OF LANDSAT MSS TO OBSERVE SEDIMENT DISTRIBUTION AND MOVEMENT IN THE SOLENT COASTAL AREA

I. S. Robinson and D. Srisaengthong *In* ESA Appl. of Remote Sensing Data on the Continental Shelf Jul. 1981 p 221-232 refs Sponsored by UK Dept. of Industry

Avail: NTIS HC A13/MF A01; ESA, Paris FF 125

The LANDSAT multispectral data from the Solent area was used to explore the potential value to marine scientists of archived data on estuaries and coastal regions. Ten images from the archives were digitally enhanced by color slicing, yielding useful qualitative information when interpreted as suspended sediment. Two further clear weather images were obtained. An approximate calibration algorithm based on six archives band-5 images and non coincident field observations show good agreement with a synoptic calibration of the last two images. The calibrated archived images show similar seasonal variations to those observed. The possibility, for certain estuaries, of obtaining quantitive information from archived data, using only recent field observations, is suggested. Author (ESA)

N82-14589# Virginia Univ., Charlottesville. Dept. of Environmental Sciences.

THE EFFECT OF SPATIAL VARIABILITY IN PRECIPITATION ON STREAMFLOW

Keith J. Beven and George M. Hornberger Sep. 1981 40 p refs Submitted for publication Prepared in cooperation with Illinois State Water Survey, Urbana
(Contract DAAG29-80-K-0053; Grant NSF ATM-78-08865)
(AD-A105955; TR-6; ARO-16816.3-GS) Avail: NTIS HC A03/MF A01 CSCL 04/2

In most approaches to modelling the rainfall/runoff process, a spatially lumped description of precipitation has been assumed adequate for modelling the important aspects of catchment response. However, theories of catchment hydrology as well as some recent modelling studies suggest that spatial variability in precipitation may be important in determining the characteristics of streamflow hydrographs. Data from two intensive rainfall recording experiments in Illinois have been used to examine the effects of rainfall pattern on stream hydrographs for summer convective storms. A threshold analysis was used to distinguish storms of markedly different pattern. A mixed deterministic/stochastic modelling procedure was used to determine the length of record required to differentiate the hydrograph characteristics resulting from storms of different patterns. It was found that differences in peak timing were highly significant but that differences in the distributions of peak flow and stormflow volumes were generally insignificant even given a long period of record. Author (GRA)

N82-14724# National Oceanic and Atmospheric Administration, Washington, D. C. Nationale Earth Satellite Service.

ANALYSIS OF RAINFALL FROM FLASH FLOOD PRODUCING THUNDERSTORMS, USING GOES DATA

Roderick A. Scofield *In* ESA Nowcasting: Mesoscale Observations and Short-Range Prediction Jun. 1981 p 51-58 refs

Avail: NTIS HC A19/MF A01; ESA, Paris FF 160 Member States, AU, CN and NO (+20% others)

The use of the Scofield-Oliver GOES technique for estimating convective precipitation from flash flood producing thunderstorms is discussed. The technique is applied using imagery displayed with a digital enhancement curve. Estimates of convective rainfall are done by comparing the changes in two consecutive pictures, both infrared and high resolution visible. The method is applied to two flash flood events. The estimates as compared to the observed rainfall are good. However, a warm top modification is needed for thunderstorms whose expected anvil temperatures are warmer than -62C. Author (ESA)

N82-15486*# Instituto de Pesquisas Espaciais, Sao Jose dos Campos (Brazil).
QUANTITATIVE ANALYSIS OF DRAINAGE OBTAINED FROM AERIAL PHOTOGRAPHS AND RBV/LANDSAT IMAGES [ANALISE QUANTITATIVA DA DRENAGEM OBTIDA ATRAVES DE FOTOGRAFIAS AEREAS E IMAGENS DO RBV/LANDSAT]
Nelson deJesusParada, Principal Investigator, Antonio Roberto Formaggio, Jose Carlos Neves Epiphanio, and Mario Valerio Filho
May 1981 29 p refs In PORTUGUESE; ENGLISH summary Presented at the 33rd Reuniao Anual de SBPC Sponsored by NASA ERTS
(E82-10008; NASA-CR-164906) Avail: NTIS HC A03/MF A01 CSCL 08H

Data obtained from aerial photographs (1:60,000) and LANDSAT return beam vidicon imagery (1:100,000) concerning drainage density, drainage texture, hydrography density, and the average length of channels were compared. Statistical analysis shows that significant differences exist in data from the two sources. The highly drained area lost more information than the less drained area. In addition, it was observed that the loss of information about the number of rivers was higher than that about the length of the channels. Author

N82-15673# California Univ., Santa Barbara. Computer Systems Lab.
USE OF ENVIRONMENTAL SATELLITE DATA FOR INPUT TO ENERGY BALANCE SNOWMELT MODELS Final Report
Jeff Dozier Dec. 1980 125 p refs
(Grant NOAA-04-8-MO)
(PB81-227795; TR-CSL-8001; NOAA-81050501) Avail: NTIS HC A06/MF A01 CSCL 04A

The development of solar and longwave radiation models for alpine snow covered terrain, techniques for atmospheric correction of satellite radiometric data and for snow albedo determination from satellite, a very fast solution to the terrain horizon problem, investigations of the use of NOAA satellite data for snow surface temperature, mapping, and work on canopy cover measurements from satellite for use in solar and longwave radiation models are described. GRA

07
DATA PROCESSING AND DISTRIBUTION SYSTEMS

Includes film processing, computer technology, satellite and aircraft hardware, and imagery.

A82-10027 **American Society of Photogrammetry, Annual Meeting, 46th, St. Louis, MO, March 9-14, 1980, ASP Technical Papers.** Falls Church, VA, American Society of Photogrammetry, 1980. 552 p. $10.

Consideration is given to such topics as digital classification accuracy, hydrometeorology, computational photogrammetry, digital image processing and rectification, the role of remote sensing in continuing education and professional development, digital displays, and the application of orthophotography in highway planning and construction. Also examined are the analysis of Landsat MSS data, remote sensor systems, close-range photogrammetry, the use of aerial photography in remote sensing, photogrammetric instruments, and automated cartography. B.J.

A82-10038 **Applications of digital displays in photointerpretation and digital mapping.** B. L. Schrock (U.S. Army, Computer Sciences Laboratory, Fort Belvoir, VA). In: American Society of Photogrammetry, Annual Meeting, 46th, St. Louis, MO, March 9-14, 1980, ASP Technical Papers. Falls Church, VA, American Society of Photogrammetry, 1980, p. 201-212.

The Digital Image Analysis Laboratory (DIAL) at USAETL is a large-scale interactive system designed for research and development activities in digital image processing. The system has been successfully applied to a variety of investigations in both digital mapping and photointerpretation as described in this presentation. Recently a Demonstration Image Processing System (DEMONS) has been added to the DIAL system to serve as a high-speed work station for processing very large digital images. Although DEMONS has been reasonably successful in manipulating large images, its limitations indicate that future such systems might be hybrid systems combining the best features of both hardcopy (film) and softcopy (cathode ray tube) exploitation systems. (Author)

A82-10860 **Two-dimensional resampling of line scan imagery by one-dimensional processing.** D. E. Friedmann (MacDonald, Dettwiller and Associates, Ltd., Richmond, British Columbia, Canada). *Photogrammetric Engineering and Remote Sensing,* vol. 47, Oct. 1981, p. 1459-1467. 33 refs. Research supported by the Department of Industry, Trade and Commerce.

Geometric correction of remote sensing data, such as Landsat MSS data, requires two-dimensional resampling. The resampling operation is typically carried out in two one-dimensional operations: along and across scan lines. The usual reasons given for validating the procedure are lower cost and higher speed. The theoretical assumptions under which one-dimensional processing is valid are presented in the light of current and future remote sensing sensors. It is shown that the assumptions are violated when a substantial amount of image rotation is incorporated into the precision processing. A method to perform image rotation with an additional step using one-dimensional processing is presented. The method makes precision correction and alignment of remote sensing data, to a map projection, both possible and accurate with one-dimensional processing. (Author)

A82-10861 **Estimation of atmospheric path-radiance by the covariance matrix method.** P. Switzer, W. S. Kowalik, and R. J. P. Lyon (Stanford University, Stanford, CA). *Photogrammetric Engineering and Remote Sensing,* vol. 47, Oct. 1981, p. 1469-1476. 16 refs.

A new method has been developed as an extension of Chavez's Regression Technique (Chavez, 1975) to provide estimates of the atmospheric path-radiance in the four Landsat MSS bands. The extension uses the correlation between all four bands of data simultaneously instead of in pairs. The Regression Method and this extension do not require auxiliary data, but operate solely upon the digital numbers recorded on the Landsat tapes. Furthermore, they do not require the presence of sites of low reflectance (basalt flows, clear lakes) or sites of low irradiance (shadows due to topography or clouds) in the Landsat data, or topographic slope data. Instead, we use Landsat data from areas of homogeneous reflectance in hilly terrain as test areas for estimation of the band-specific atmospheric path-radiances. The method has been applied to Landsat data from diverse terrain types and atmospheric conditions using three different Landsat images covering semi-arid western Nevada, temperate eastern Pennsylvania, and tropical central New Guinea. The method yields reasonable results from each area. (Author)

A82-12757 **A theory of wave scattering from an inhomogeneous layer with an irregular interface.** A. K. Fung and H. J. Eom (Kansas, University, Lawrence, KS). *IEEE Transactions on Antennas and Propagation,* vol. AP-29, Nov. 1981, p. 899-910. 10 refs. NSF Grant No. ENG-79-09374; Grant No. DAAG29-80-K-0018.

Bistatic wave scattering from a layer of Rayleigh scatterers with an irregular interface is studied by combining the doubling method in volume scattering with the Kirchhoff method in rough surface scattering. Theoretical results are presented illustrating the effect of the rough interface. It is found that for scattered and incident angles near the vertical, the rough interface brings about a substantial increase relative to the plane interface in both the like and cross-scattering coefficients over all azimuth angles. For large scattered and incident angles, however, the reverse is true, except for azimuth angles around the specular direction. C.R.

A82-12882 **Digital mapping using entities - A new concept.** S. E. Masry (New Brunswick, University, Fredericton, Canada). *Photogrammetric Engineering and Remote Sensing,* vol. 47, Nov. 1981, p. 1561-1565.

An approach to digital mapping using aerial or satellite photography is presented which is based on the use of linear features to establish the relationship between an image and a ground coordinate system in lieu of or in addition to individual control points. The concept is based on entity-to-entity correspondence, an entity being defined as a set of points describing part or the whole of a feature. It involves the transformation of the mathematical functions defining the observed entities in order that they become identical to the corresponding functions describing control entities obtained from a topographic data base or map. The concept has successfully been applied to carry out the absolute orientation of a stereomodel, and perform analytical space resection of an aerial photograph, with precision and convergence comparable to those derived from conventional control. S.C.S.

A82-12913 † **Aspects in the development of aerial-photography tasks (Voprosy razvitiia aerofotos'emochnykh rabot).** Iu. I. Poletaev. *Geodeziia i Kartografiia,* Sept. 1981, p. 32-34. In Russian.

Recent developments in aerial photography in the Soviet Union are briefly reviewed. Attention is given to calibration methods, ways to improve the quality of negatives, optimal exposure techniques, scaling, and automated processing. B.J.

A82-13121 **Interactive techniques for estimating precipitation from GOES imagery.** J. F. Moses, L. E. Spayd, Jr., R. S. Gird, and A. L. Siebers (NOAA, National Earth Satellite Service, Washington, DC). In: Joint Automatic Control Conference, Charlottesville, VA, June 17-19, 1981, Proceedings. Volume 2. New York, American Institute of Chemical Engineers, 1981. 9 p. (TP-6C). 6 refs.

Recent development of an interactive computer technique aids meteorologists in using geostationary satellite imagery to estimate precipitation. The interactive technique utilizes the interpretive abilities and experience of the meteorologist with the speed and accuracy of the computer to reduce the time and effort required by the previously developed manual method. An analysis of a precipitation event in Kansas on July 4-5, 1979, illustrates the technique. A comparison of satellite estimates to ground truth reports shows that the estimates indicate the areas of maximum observed precipitation accumulation. (Author)

07 DATA PROCESSING AND DISTRIBUTION SYSTEMS

A82-13633 † **Calculation of the decrease in the contrast of objects of a place due to light scattering in the atmosphere (O vychislenii padeniia kontrasta ob'ektov mestnosti iz-za rasseianiia sveta v atmosfere).** Iu. L. Biriukov and E. G. Markarian (Moskovskii Institut Inzhenerov Geodezii, Aerofotos'emki i Kartografii, Moscow, USSR). *Geodeziia i Aerofotos'emka,* no. 4, 1981, p. 80-86. 9 refs. In Russian.

With reference to aerial photography, an analytical method is presented for calculating the decrease in the image contrast of small-scale objects on the earth's surface due to light scattering in the atmosphere. An analysis is presented of the dependence of the contrast of the object and background, observed through the optical medium, on the optical thickness of the atmosphere, the solar zenith distance, the angles of sight, and the albedo of the object and background. Numerical results are presented. B.J.

A82-13634 † **Concerning the geometric accuracy of infrared scanner photographs (K voprosu o geometricheskoi tochnosti infrakrasnykh skanernykh snimkov).** O. I. Egorova (Moskovskii Institut Inzhenerov Geodezii, Aerofotos'emki i Kartografii, Moscow, USSR). *Geodeziia i Aerofotos'emka,* no. 4, 1981, p. 113-116. In Russian.

The sources of geometric errors of infrared scanner images are examined along with methods to eliminate these errors. Experimental results concerning the accuracy of infrared scanner photographs are presented. B.J.

A82-14860 **Reflectivity and emissivity of snow and ground at mm waves.** R. D. Hayes, N. C. Currie, and J. A. Scheer (Georgia Institute of Technology, Atlanta, GA). In: International Radar Conference, Arlington, VA, April 28-30, 1980, Record. New York, Institute of Electrical and Electronics Engineers, Inc., 1980, p. 67-72.

A summary is provided of the results of a test program conducted to determine the backscatter and emissivity characteristics of background clutter at millimeter wavelengths. The test was conducted during the late winter time frame to include snow and wet terrain as background types. It is pointed out that active and passive millimeter wave RF sensors are prime candidates for the role of air-to-surface anti-armor weapons applications because of certain advantages compared to microwave sensors and electro-optical sensors. However, the design, development, and evaluation of systems for such an application requires an extensive understanding of the millimeter wavelength reflectivity and emissivity characteristics of clutter and targets. It was found in the investigation that the radar reflectivity of the snow varies strongly with the diurnal freeze-melt cycle. Radar cross sections for short and tall grass are also considered. G.R.

A82-14870 * **A digital fast correlation approach to produce SEASAT SAR imagery.** C. Wu (California Institute of Technology, Jet Propulsion Laboratory, Pasadena, CA). In: International Radar Conference, Arlington, VA, April 28-30, 1980, Record. New York, Institute of Electrical and Electronics Engineers, Inc., 1980, p. 153-160. 9 refs. Contract No. NAS7-100.

This paper describes a digital processing algorithm and its associated system design for producing images from SEASAT Synthetic Aperture Radar (SAR) data. The proposed system uses the fast Fourier transform approach to perform the two-dimensional correlation process. The range migration problem, which is often a major obstacle to efficient processing, can be alleviated by approximating the locus of echoes from a point target by several linear segments. SAR data corresponding to each segment is correlated separately, and the results are coherently summed to produce full-resolution images. This processing approach exhibits high computation efficiency and simple processing control functions. It is particularly attractive for software implementation based on general purpose computer. Results of this implementation and examples of digitally correlated SEASAT SAR imagery are discussed. B.J.

A82-15003 # **Investigations concerning the image-controlled segmentation of objects in multispectral imagery data (Untersuchungen zur bildgesteuerten Separierung von Objekten in multispektralen Bilddaten).** R. Schärf. Karlsruhe, Universität, Fakultät für Elektrotechnik, Dr.-Ing. Dissertation, 1981. 157 p. 74 refs. In German.

The automatic segmentation of objects in an image represents an essential step in a procedure for the interpretation of images. The considered investigation is concerned with image-controlled processes, based on sequential operations, for the extraction of areal objects from real multispectral imagery. A survey is presented of various operational principles used for image segmentation, and a description is provided of the characteristics of multispectral imagery data. Problems of data compression are examined, and different segmentation procedures are compared. This comparison leads to the development of a two-stage procedure for the segmentation of objects on the basis of region growing. Important aspects of the new procedure are related to sequential iterative processing and the initial control of the processing steps by means of automatically extracted structural image elements. At a later stage, the characteristics and the position of the segmented objects provide additional control elements. G.R.

A82-15029 **Two-dimensional model variability in thermal inertia surveys.** D. A. Pratt (Newcastle, University, Newcastle, Australia). *Remote Sensing of Environment,* vol. 9, June 1980, p. 325-338. 20 refs. Research supported by the Australian Research Grants Committee.

Calibration of thermal inertia surveys requires the production of a numerical model where thermal inertia is expressed as a function of the diurnal ground surface temperature range and albedo. The model is calculated for a given set of local meteorological and surface conditions which must be assumed constant over the whole of the surveyed area. This paper reports the results of an investigation which estimates the magnitudes of thermal inertia errors as a function of the departure of the local conditions from those assumed. The parameters under investigation are wind speed, average air temperature, air-temperature fluctuations, surface roughness, slope and changes in the thermal inertia profile. (Author)

A82-15034 * **Texture transforms of remote sensing data.** J. R. Irons (NASA, Goddard Space Flight Center, Earth Resources Branch, Greenbelt, MD) and G. W. Petersen (Pennsylvania State University, University Park, PA). *Remote Sensing of Environment,* vol. 11, Nov. 1981, p. 359-370. 16 refs.

Tone and texture are fundamental interrelated visual concepts. The concepts are used for the digital analysis of remotely sensed image data. The reported investigation had the objective to develop software for the quantification of image texture and to apply the texture information to both image enhancement and thematic classification of remotely sensed data. The quantitative texture information was applied to the analysis of Landsat-2 Multispectral Scanner Subsystem (MSS) data. Attention is given to the characterization of image texture, textured transformations, the subtext program, and a description of methods and results. It is pointed out that the inability to use the texture transforms of the Landsat MSS data for the thematic mapping of the study area's land cover contrasts sharply with the reported results of the textural analysis of digitized aerial photography by Hsu (1978). G.R.

A82-15125 * **Optically processed Seasat radar mosaic of Florida.** M. L. Bryan (California Institute of Technology, Jet Propulsion Laboratory, Pasadena, CA). *Photogrammetric Engineering and Remote Sensing,* vol. 47, Sept. 1981, p. 1335-1337.

An uncontrolled mosaic of optically correlated Seasat radar imagery of Florida is presented to illustrate the data and the large area synoptic coverage made possible by combining multiple data sets. The images were taken from a total of 12 passes over 33 days from July 24, 1978 to August 27, 1978. The mosaic is controlled geometrically and with respect to image tone (representing radar backscatter). The SAR data was obtained at an L-band frequency (1.275 GHz, 23.5 cm) and in a horizontal transmit/receive mode, resulting in a 25 m resolution in 100 km swath widths. M.S.K.

A82-15764 **Compensation of systematic errors in bundle adjustment.** E. Kilpela, J. Heikkila, and K. Inkila (Helsinki University of Technology, Esbo, Finland). *Photogrammetria,* vol. 37, Nov. 1981, p. 1-13. 7 refs.

Results of the application of a bundle program to study the effects of weighted additional parameters on the accuracy and reliability of self-calibration are examined. Six additional parameter sets used with and without weighting, as well as a comparison of simultaneous and a posteriori self-calibration are studied. General features of the program are outlined, and the program is applied to photography of test areas at 1:4000 and 1:12,000 scales. Root mean square errors in planimetry and height are used as quantities for determining the effectiveness of compensation of systematic errors. Best results were obtained by employing weights corresponding to image point displacements of less than five micrometers, and weights equal to zero, especially in cases of minor side overlap. Simultaneous self-calibrations proved more efficient than a posteriori self-calibration. M.S.K.

A82-15765 **Compensation of systematic errors of image and model coordinates.** E. Kilpela (Helsinki University of Technology, Esbo, Finland). *Photogrammetria,* vol. 37, Nov. 1981, p. 15-44. 9 refs.

Compensation for systematic errors of image and model coordinates in different aerotriangulation methods is studied. Four test fields in Australia and Finland used for the photogrammetric adjustments were coordinated by a ground survey. Flight programs and measurements are outlined, and compensation procedures comprised reference adjustment, component calibration, test field calibration, and self calibration. Blockwise vs stripwise parameters, significance testing of additional parameters, weighting of additional parameters, correlations, and a priori data refinements, as well as side overlap, single vs double block, control point pattern, and the use of a reseau to correct film distortion were considered. Calibration improved the triangulation by 20%, self calibration produced results superior to test field calibration, and the introduction of strip invariant additional parameters was found to be ineffective. M.S.K.

A82-15970 **Cost effective computer processing of airborne scanner data for regional level mapping.** S. Thiruvengadachari (National Remote Sensing Agency, Hyderabad, India). *Photogrammetric Engineering and Remote Sensing,* vol. 47, Dec. 1981, p. 1705-1708.

The reported investigation concerning an optimization of the computer analysis of multispectral data was conducted in connection with an airborne scanner survey over an area of approximately 750 sq km in the northeastern part of India. The survey was conducted to obtain information with regard to flood inundation along a selected range of a major river system. Digital analysis was performed on the interactive Multispectral Data Analysis System, operated at the National Remote Sensing Agency facility at Hyderabad. An 11 channel scanner mounted on a DC-3 Dakota aircraft was used in the survey. Attention is given to the study background, analysis methodology, categorical analysis, and categorization accuracy. It was found that the computer analysis of 11-channel airborne scanner data can be made cost effective by the use of fewer channels, when regional selection of level information is to be obtained. G.R.

A82-15971 * **The Control Point Library Building System.** W. Niblack (IBM France, S.A., Paris, France). *Photogrammetric Engineering and Remote Sensing,* vol. 47, Dec. 1981, p. 1709-1715. 7 refs. Contracts No. NAS5-22999; No. NAS5-23790.

The Earth Resources Observation System (EROS) Data Center in Sioux Falls, South Dakota distributes precision corrected Landsat MSS and RBV data. These data are derived from master data tapes produced by the Master Data Processor (MDP), NASA's system for computing and applying corrections to the data. Included in the MDP is the Control Point Library Building System (CPLBS), an interactive, menu-driven system which permits a user to build and maintain libraries of control points. The control points are required to achieve the high geometric accuracy desired in the output MSS and RBV data. This paper describes the processing performed by CPLBS, the accuracy of the system, and the host computer and special image viewing equipment employed. (Author)

A82-15973 **Orientation and construction of models. III - Mathematical basis of the orientation problem of one-dimensional central perspective photographs.** A. Okamoto (Kyoto University, Kyoto, Japan). *Photogrammetric Engineering and Remote Sensing,* vol. 47, Dec. 1981, p. 1739-1752. 9 refs.

The reported analysis of the general orientation problem of one-dimensional central perspective photographs makes use of the mathematical basis employed in the orientation problem of two-dimensional (conventional) central perspective pictures. The general orientation problem of a stereoscopic pair of one-dimensional photographs is considered, taking into account also the special case in which the interior orientation parameters are known. Attention is given to the photogrammetric orientation problem of one-dimensional central-perspective photographs, and the orientation problem in the case of individual one-dimensional photographs. G.R.

A82-16160 **Spectral correlation filters and natural colour coding.** N. J. Mulder (International Institute for Aerial Survey and Earth Sciences, Enschede, Netherlands). *ITC Journal,* no. 3, 1981, p. 237-252.

A system utilizing spectral correlation filters and natural color coding has been developed for remote sensing. Studies of principal components (Mulder and Hempenius, 1974) have shown that there are only two or three independent factors in reflectance spectra of natural materials. Filters have thus been designed to store reflection spectra of water, dense green vegetation, and bare soil using a natural color coding scheme. Nearly all other natural reflection spectra can be described as a linear combination of these three spectra. The method has been tested for a simulation using Landsat data. S.C.S.

A82-16163 **Theoretical reliability of elementary photogrammetric procedures.** I. F. A. A. F. Amer (International Institute for Aerial Survey and Earth Sciences, Enschede, Netherlands). *ITC Journal,* no. 3, 1981, p. 278-307. 10 refs.

The reliability of elementary photogrammetric procedures for production photogrammetrists is presented. The derivation of the weight coefficient matrix of the residuals is obtained, noting its structure and the significance of its main and off-diagonal elements. For high homogeneous reliability, the main diagonal elements should be close to unity and equal. When all the main diagonal elements are equal the reference boundary value is achieved. The difference between detection and location of gross errors is illustrated. It is shown that a rejection matrix may be employed to evaluate the possibility of locating gross errors. S.C.S.

A82-16601 **Airborne and spaceborne multispectral photography of the earth (Mnogozonal'nye aerokosmicheskie s'emki zemli).** R. Z. Sagdeev. Moscow, Izdatel'stvo Nauka, 1981. 304 p. In Russian.

Multispectral scanning of earth resources is considered, with attention given to the Soyuz-22 Raduga experiment, optical scanning, remote spectroscopy, polarimetry methods, analog processing, and digital processing. Particular consideration is given to such topics as the parameter optimization of spaceborne photography systems, the instrumental interpretation of multispectral aerial and space photographs, a special-purpose optoelectronic system for the operational acquisition of multispectral image data, the energy calibration of multispectral scanner systems, and the maximum mean accuracy of classification of remote-sensing objects. B.J.

A82-16605 † **Evaluation of the information content of the channels of spaceborne multispectral photography of the Fergana region by the MKF-6 camera from Soyuz-22 (Otsenka i informativnosti kanalov mnogozonal'noi kosmicheskoi fotos'emki Ferganskogo uchastka kameroi MKF-6 s kosmicheskogo korablia 'Soiuz-22').** G. B. Gonin and V. P. Koroleva. In: Airborne and spaceborne multispectral photography of the earth. Moscow, Izdatel'stvo Nauka, 1981, p. 24-37. 10 refs. In Russian.

A82-16606 † **Geometric quality of MKF-6 photographs (Geometricheskoe kachestvo snimkov MKF-6).** Ia. L. Ziman, V. A. Krasikov, and V. I. Iurov. In: Airborne and spaceborne multispectral photography of the earth. Moscow, Izdatel'stvo Nauka, 1981, p. 37-43. In Russian.

The photogrammetric calibration and digital processing of multispectral photographs obtained with the MKF-6 camera in the Raduga experiment aboard Soyuz-22 are considered. It is shown that the MKF-6 photographs are topographic ones and can be used to solve many kinds of photogrammetric problem. B.J.

A82-16607 † **Methods of instrumental interpretation of multispectral aerial and space photographs (Metody izmeritel'nogo deshifrirovaniia mnogozonal'nykh aerokosmicheskikh snimkov).** I. A. Labutina and Iu. I. Fivenskii. In: Airborne and spaceborne multispectral photography of the earth. Moscow, Izdatel'stvo Nauka, 1981, p. 43-55. 7 refs. In Russian.

A82-16612 † **Spectrometric studies of the earth's surface (Spektrometricheskie issledovaniia zemnoi poverkhnosti).** G. A.

Avanesov and N. I. Snetkova. In: Airborne and spaceborne multispectral photography of the earth. Moscow, Izdatel'stvo Nauka, 1981, p. 100-117. 95 refs. In Russian.

A review of the literature on the remote spectroscopy of earth resources is presented. A classification of terrestrial features on the basis of spectral characteristics is considered. B.J.

A82-16614 † **The application of holographic gratings in spectrometers for the spatial-spectral analysis of the earth's surface from aerial and space platforms in the visible and near-infrared spectral regions (K voprosu o primenenii golograficheskikh reshetok v spektrometrakh dlia prostranstvenno-spektral'nogo analiza zemnoi poverkhnosti s aerokosmicheskikh platform v vidimom i blizhnem ik-diapazonakh spektra).** E. G. Lykasheva. In: Airborne and spaceborne multispectral photography of the earth. Moscow, Izdatel'stvo Nauka, 1981, p. 128-135. 6 refs. In Russian.

A82-16615 † **The maximum mean accuracy of classification of remote-sensing objects and the influence on this accuracy of data acquisition and processing methods (Dostizhimaia sredniaia tochnost' klassifikatsii ob'ektov distantsionnogo zondirovaniia i vliianie na nee metodov sbora i obrabotki dannykh).** B. M. Balter. In: Airborne and spaceborne multispectral photography of the earth. Moscow, Izdatel'stvo Nauka, 1981, p. 135-151. In Russian.

A review of the literature on the classification of remote-sensing objects is used to investigate the mean accuracy of classification. This accuracy was found to be 82% and (with a probability of 0.95) not lower than 55%. Current methods of automatic classification produce an increase of 8% compared with nonautomatic methods. The mean accuracy in the period 1972-1977 was found to increase by 1% every year. Such factors as type of sensor, platform, and data processing do not have an appreciable influence on the mean accuracy. B.J.

A82-16616 † **Characteristics of the photometry of small objects from aerial and space photographs (Osobennosti fotometrirovaniia malykh ob'ektov po aerokosmicheskim fotosnimkam).** Iu. I. Fivenskii and Iu. N. Kuznetsov. In: Airborne and spaceborne multispectral photography of the earth. Moscow, Izdatel'stvo Nauka, 1981, p. 152-164. 8 refs. In Russian.

The current status of the method of microphotometric determinations from remotely sensed images is described, and results of a laboratory experiment are presented. It is shown that the photometric properties are invariant to the geometry and distribution characteristics of small details on the photograph. Requirements on the photometric calibration of aerial and space photography systems are examined. B.J.

A82-16617 † **Estimation of the brightness field from results of multispectral photography of the earth from space (Otsenka iarkostnogo polia po rezul'tatam mnogozonal'nogo fotografirovaniia zemli iz kosmosa).** V. A. Kotsov. In: Airborne and spaceborne multispectral photography of the earth. Moscow, Izdatel'stvo Nauka, 1981, p. 165-169. In Russian.

A method for the statistical estimation of brightness and spectral contrasts for the territory of the USSR on the basis of data from the Soyuz-22 Raduga experiment is presented. The statistical characteristics of the contrasts are given. B.J.

A82-16618 † **The use of a priori information in the remote sensing of the earth from space (Ispol'zovanie apriornoi informatsii pri izuchenii zemli iz kosmosa).** V. A. Kottsov and I. B. Prokuronov. In: Airborne and spaceborne multispectral photography of the earth. Moscow, Izdatel'stvo Nauka, 1981, p. 170-174. 5 refs. In Russian.

The relationship between the concept of an object in remote sensing and the characteristics of a priori information is examined in the framework of pattern recognition theory. The improvement of remote sensing methods by using the representation of localized factors is considered. B.J.

A82-16621 † **The choice of the orientation of the analyzer in polarimetric surveys (O vybore orientatsii analizatora pri poliarizatsionnoi s'emke).** V. V. Egorov and B. S. Zhukov. In: Airborne and spaceborne multispectral photography of the. earth. Moscow, Izdatel'stvo Nauka, 1981, p. 197-202. In Russian.

An analysis is presented of the conditions of achieving maximum contrast in polarimetric remote-sensing surveys. It is found that for surveys of soil-vegetation objects the maximum contrast is generally attained when the analyzer is oriented parallel to the solar-vertical plane. Experimental results on such surveys are presented. B.J.

A82-16623 † **Analog methods for processing multispectral photographs (Ob analogovykh metodakh obrabotki mnogozonal'nykh fotosnimkov).** Iu. M. Chesnokov. In: Airborne and spaceborne multispectral photography of the earth. Moscow, Izdatel'stvo Nauka, 1981, p. 211-216. In Russian.

The possibilities of analog techniques for the processing of multispectral photographs are reviewed. Particular attention is given to the development of laser-based analog optoelectronic devices for the conversion of multispectral images into color images. B.J.

A82-16625 † **Structural analysis of aerial and space images (Strukturnyi analiz aerokosmicheskikh snimkov).** K. A. Kraush. In: Airborne and spaceborne multispectral photography of the earth. Moscow, Izdatel'stvo Nauka, 1981, p. 224-234. 10 refs. In Russian.

The theoretical principles of the structural analysis of remote sensing images are presented. A block diagram of an optoelectronic device for performing the structural analysis is given, and possible variants of the optical system are examined. The calculation of the intensity of the components of the spatial-frequency spectrum is considered, and the influence of noise is assessed. B.J.

A82-16626 † **Investigation of the spatial structure of space images of the earth's surface (Izuchenie prostranstvennoi struktury kosmicheskikh izobrazhenii zemnoi poverkhnosti).** V. V. Egorov and G. P. Arumov. In: Airborne and spaceborne multispectral photography of the earth. Moscow, Izdatel'stvo Nauka, 1981, p. 235-243. In Russian.

Aspects of the texture analysis of space photographs of the earth's surface are discussed. The analysis of the spatial structure was carried out by two methods: an analog technique for the formation of spatial-frequency spectra (Wiener spectra) and an analytic method for the component separation of mixtures of natural objects. Examples of analysis are presented. B.J.

A82-16627 † **Processing of multispectral image data on special-purpose computer systems (Obrabotka mnogozonal'noi videoinformatsii na spetsializirovannykh vychislitel'nykh kompleksakh).** V. A. Krasikov and V. A. Shamis. In: Airborne and spaceborne multispectral photography of the earth. Moscow, Izdatel'stvo Nauka, 1981, p. 244-248. In Russian.

The development of special-purpose operational systems for processing multispectral earth-resources data is considered. A Soviet system is described that assures effective access to the image. The library of application programs ensures effective thematic processing. B.J.

A82-16628 † **Programs for the statistical analysis of multispectral photographs (Programmy statisticheskogo analiza mnogozonal'nykh snimkov).** V. A. Krasikov, V. G. Sobchuk, V. A. Shamis, and M. V. Khatuntseva. In: Airborne and spaceborne multispectral photography of the earth. Moscow, Izdatel'stvo Nauka, 1981. p. 248-253. In Russian.

Minicomputer-implemented algorithms for the statistical analysis of multispectral photographs of earth resources are described. Particular attention is given to the computation and construction of brightness-distribution histograms, and to the computation of the vectors of mean and covariant matrices. B.J.

A82-16629 † **Linear combinations of multispectral images (Lineinye kombinatsii mnogozonal'nykh snimkov).** M. V. Khatuntseva. In: Airborne and spaceborne multispectral photography of the earth. Moscow, Izdatel'stvo Nauka, 1981, p. 253-261. In Russian.

The use of linear combinations of multispectral images in the thematic analysis and interpretation of multispectral photographs of the earth's surface is considered. Particular attention is given to the machine implementation of the method of principal components. B.J.

A82-16630 † **Coordinate referencing of MKF-6 photographs and their transformation to the cartographic projection (Koordinatnaia priviazka snimkov MKF-6 i preobrazovanie ikh v kartograficheskuiu proektsiiu).** Ia. L. Ziman, V. A. Krasikov, V. G. Sobchuk, and V. A. Shamis. In: Airborne and spaceborne multispectral photography of the earth. Moscow, Izdatel'stvo Nauka, 1981, p. 261-266. In Russian.

An analysis is presented of the use of affine transformations in the processing of multispectral photographs of earth resources and their transformation to the Kavraiskii cartographic projection. The optimization of access to the images is assured by a programmable virtual memory. B.J.

A82-18167 **Photo inertial positioning system development at the Canada Centre for Remote Sensing.** J. R. Gibson and J. E. Smyth (Canada Centre for Remote Sensing, Ottawa, Canada). In: PLANS '80 - Position Location and Navigation Symposium, Atlantic City, NJ, December 8-11, 1980, Record. New York, Institute of Electrical and Electronics Engineers, Inc., 1980, p. 436-438.

The system and projects described form part of the continuing development work on the Photo Inertial Positioning System at the Canada Centre for Remote Sensing. The system consists of an aerial camera having navigation systems and sensors hard-mounted to it. A general-purpose data acquisition system is used in time-correlating the data from these and other sensors. It is noted that during the past several years, the system development has been slanted toward the application of shallow water charting. The system is at present capable of providing postflight position accuracies of the order of 1 meter and attitude accuracies of 1 arcmin. C.R.

N82-10072*# General Electric Co., Lanham, Md. Space Div.
COMPUTATIONAL ASPECTS OF GEOMETRIC CORRECTION DATA GENERATION IN THE LANDSAT-D IMAGERY PROCESSING
I. Levine *In* NASA. Goddard Space Flight Center Sixth Ann. Flight Mech./Estimation Theory Symp. Oct. 1981 16 p ref

(Contract NAS5-25300)
Avail: NTIS HC A13/MF A01 CSCL 05B

A method is presented for systematic and geodetic correction data calculation. It is based on presentation of image distortions as a sum of nominal distortions and linear effects caused by variation of the spacecraft position and attitude variables from their nominals. The method may be used for both MSS and TM image data and it is incorporated into the processing by means of mostly offline calculations. Modeling shows that the maximal of the method are of the order of 5m at the worst point in a frame; the standard deviations of the average errors less than .8m. Author

N82-10466* National Aeronautics and Space Administration. Ames Research Center, Moffett Field, Calif.
MATE VAN: MOBILE ANALYSIS AND TRAINING EXTENSION
[1981] 7 p
(NASA-TM-84056) Avail: NASA Scientific and Technical Information Facility, P. O. Box 8757, B.W.I. Airport, Md. 21240 CSCL 05B

A modified 30-foot motor coach was equipped with modern data processing equipment in order to train personnel and demonstrate useful techniques and capabilities for analyzing and applying LANDSAT imagery in the western regional area. A block diagram of the interactive digital image manipulation system is presented and its processing features itemized. Specifications for the van and the equipment are listed. False color composites used to interpret and identify many LANDSAT technological applications are included. A.R.H.

N82-10469*# Martin Marietta Corp., Denver, Colo.
ONBOARD UTILIZATION OF GROUND CONTROL POINTS FOR IMAGE CORRECTION. VOLUME 1: EXECUTIVE SUMMARY Final Report
May 1981 30 p refs 4 Vol.
(Contract NAS5-26094)
(NASA-CR-166731; MCR-81-576-Vol-1) Avail: NTIS HC A03/MF A01 CSCL 05B

Operation of a navigation system, centered around image correction, was simulated and the system performance was analyzed. Onboard utilization of ground control points for image correction is summarized. Simulation results, and recommendations for future mission requirements are presented. E.A.K.

N82-10470*# Martin Marietta Corp., Denver, Colo.
ONBOARD UTILIZATION OF GROUND CONTROL POINTS FOR IMAGE CORRECTION. VOLUME 2: ANALYSIS AND SIMULATION RESULTS Final Report
May 1981 183 p refs 4 Vol.
(Contract NAS5-26094)
(NASA-CR-166732; MCR-81-576-Vol-2) Avail: NTIS HC A09/MF A01 CSCL 05B

An approach to remote sensing that meets future mission requirements was investigated. The deterministic acquisition of data and the rapid correction of data for radiometric effects and image distortions are the most critical limitations of remote sensing. The following topics are discussed: onboard image correction systems, GCP navigation system simulation, GCP analysis, and image correction analysis measurement. E.A.K.

N82-10471*# Martin Marietta Corp., Denver, Colo.
ONBOARD UTILIZATION OF GROUND CONTROL POINTS FOR IMAGE CORRECTION. VOLUME 3: GROUND CONTROL POINT SIMULATION SOFTWARE DESIGN Final Report
May 1981 409 p refs 4 Vol.
(Contract NAS5-26094)
(NASA-CR-166733; MCR-81-576-Vol-3) Avail: NTIS HC A18/MF A01 CSCL 05B

The software developed to simulate the ground control point navigation system is described. The Ground Control Point Simulation Program (GCPSIM) is designed as an analysis tool to predict the performance of the navigation system. The system consists of two star trackers, a global positioning system receiver, a gyro package, and a landmark tracker. E.A.K.

N82-10472*# Martin Marietta Corp., Denver, Colo.
ONBOARD UTILIZATION OF GROUND CONTROL POINTS FOR IMAGE CORRECTION. VOLUME 4: CORRELATION ANALYSIS SOFTWARE DESIGN Final Report
May 1981 86 p refs 4 Vol.
(Contract NAS5-26094)
(NASA-CR-166734; MCR-81-576-Vol-4) Avail: NTIS HC A05/MF A01 CSCL 05B

The software utilized for image correction accuracy measurement is described. The correlation analysis program is written to allow the user various tools to analyze different correlation algorithms. The algorithms were tested using LANDSAT imagery in two different spectral bands. Three classification algorithms are implemented. E.A.K.

N82-10485# Technical Research Centre of Finland, Espoo. Maankaeytoen Lab.
SMALL-SCALE TERRAIN MAPPING BASED ON NUMERICAL INTERPRETATION OF LANDSAT IMAGERY [LANDSAT-KUVIEN NUMEERISEEN TULKINTAAN PERUSTUVA PIENKAAVAINEN MAASTOKARTOITUS]
Esa Fransaila 1981 75 p refs In FINNISH; ENGLISH summary Original contains color illustrations
(VTT-40; ISBN-951-38-1180-8; ISSN-0355-3477) Avail: NTIS HC A04/MF A01

The usability of digital LANDSAT imagery for producing terrain data, the general map of Finland (1: 400,000) and other small-scale terrain maps was investigated. The image processing was based on numerical processing of: image correction to map projection; image interpretation; data generalization; and graphic output along with statistical summary data. In order to achieve an automated cartographic generalization, the scale caused details were effaced by applying alternative rules. Compared with the conventional generalization, the result is defective. Figure lines for cartographic presentation were produced. Author (ESA)

N82-11103*# Computer Sciences Corp., El Segundo, Calif.
MAGNETIC FIELD SATELLITE (MAGSAT) DATA PROCESSING SYSTEM SPECIFICATIONS
D. Berman, R. Gomez, and A. Miller Oct. 1980 136 p refs
(Contract NAS5-24391)
(NASA-CR-166737; CSC/TM-80/6214) Avail: NTIS HC A07/MF A01 CSCL 22B

The software specifications for the MAGSAT data processing system (MDPS) are presented. The MDPS is divided functionally into preprocessing of primary input data, data management, chronicle processing, and postprocessing. Data organization and validity, and checks of spacecraft and instrumentation are dicussed. Output products of the MDPS, including various plots and data tapes, are described. Formats for important tapes are presented. Dicussions and mathematical formulations for coordinate transformations and field model coefficients are included. S.L.

N82-11509 Washington Univ., Seattle.
IDENTIFICATION OF LITHOLOGIC UNITS USING MULTI-CHANNEL IMAGING SYSTEMS Ph.D. Thesis
Diane Louise Evans 1981 129 p
Avail: Univ. Microfilms Order No. 8121194

It is shown that is possible to compare laboratory reflectance spectra directly with multispectral images. The signal that would be produced if a particular laboratory sample were in a detector's field of view was calculated and converted into a digital number of DN value. Stacks of spatially registered multispectral images were then searched for materials that had spectral characteristics similar to the laboratory samples. When laboratory reflectance spectra of a suite of Hawaiian samples were compared to Viking Lander images of Mars, a weathered basaltic tephra from a Hawaiian cinder cone was found to have spectral characteristics that were similar in all bandpasses to surficial deposit at the Viking 1 site. When the reflectance spectra of the suite of samples were compared to Viking Orbiter images, the same Hawaiian tephra was found to correspons to a regional spectral unit in the low latitudes of Mars. It was also possible to compare laboratory reflectance spectra to Landsat images of the Earth. Comparison of laboratory reflectance spectra with multispectral images make it possible to derive compositional information from the images. Dissert. Abstr.

N82-13470*# Environmental Research and Technology, Inc., Concord, Mass.
ANALYSIS OF SOIL MOISTURE EXTRACTION ALGORITHM USING DATA FROM AIRCRAFT EXPERIMENTS Final Report
Hsiao-hua K. Burke and Jean-Hsien Ho Jun. 1981 37 p refs
(Contract NAS5-26361)
(NASA-CR-166719; P-A826) Avail: NTIS HC A03/MF A01 CSCL 08M

A soil moisture extraction algorithm is developed using a statistical parameter inversion method. Data sets from two aircraft experiments are utilized for the test. Multifrequency microwave radiometric data surface temperature, and soil moisture information are contained in the data sets. The surface and near surface (< or = 5 cm) soil moisture content can be extracted with accuracy of approximately 5% to 6% for bare fields and fields with grass cover by using L, C, and X band radiometer data. This technique is used for handling large amounts of remote sensing data from space. S.L.

N82-14548*# Applied Physics Lab., Johns Hopkins Univ., Laurel, Md.
RADAR CORRELATION WITH ICE DEPOLARIZATION MEASUREMENTS OF THE 28.56 GHz COMSTAR BEACON AND ASSOCIATED CROSS POLARIZATION STATISTICS
Julius Goldhirsh Aug. 1980 51 p refs
(NASA-CR-166717; JHU/APL-SIR-80U-026)
HC A04/MF A01 CSCL 08L

Two cases of radar correlation with significant ice depolarization events accompanied by low copolarization fades of the 28.56 CHz COMSTAR beacon signal are described. The copol and cross polarization levels of the 28.56 GHz beacon signal were sequentially monitored. A nearby high resolution S band radar pointing along the Earth satellite path monitored the simultaneous ice and rain reflectivity. For the first case, excellent correlation is noted between the cross polarization events and relatively large and extended ice reflectivities along a segment of the Earth satellite path at altitudes near and above the 0 C isotherm. In the second case, the radar and receiver data strongly suggest the cross polarization mechanism is due to a hailshaft which intersects the path at altitudes well below the 0 C isotherm. Extracted depolarization signals were statistically characterized for the 1979 data base in terms of a cumulative distribution as well as monthly and time of day statistics under the given condition that the copol fade is less than 2 dB. B.W.

N82-14568# Centre National d'Etudes Spatiales, Paris (France).
SPOT DATA SIMULATIONS: LITTORAL APPLICATIONS
N. Lannelongue *In* ESA Appl. of Remote Sensing Data on the Continental Shelf Jul. 1981 p 129-130

Avail: NTIS HC A13/MF A01; ESA, Paris FF 125

Remote sensing SPOT imagery was simulated. User plans for taking advantage of the data are elaborated and the adequacy of SPOT specifications is assessed. Since actual satellite data are not available, a set of aerial remote sensing images with a photographic camera and multispectral scanner was used. The Loire estuary is being studied. Data in the visible and near infrared, of high resolution and good accessibility, are being collected. Simulations show that images can be used immediately after launch. Author (ESA)

N82-14578# Consiglio Nazionale delle Ricerche, Venice (Italy).
MULTITEMPORAL CALIBRATION OF LANDSAT IMAGES: A METHOD FOR IMPROVING THE MARINE PHENOMENA RECOGNITION, WITH AS EXAMPLE THE VENICE LAGOON
L. Alberotanza and A. Zandonella (Telespazio S.p.a.) *In* ESA Appl. of Remote Sensing Data on the Continental Shelf Jul. 1981 p 205-209 refs

Avail: NTIS HC A13/MF A01; ESA, Paris FF 125

A method for LANDSAT data multitemporal calibration, developed during work on pollution diffusion in the Venice lagoon, was examined. The method consists of a projection, onto a like signal feature space, of images recorded in different time periods, with the aim of enhancing and analyzing the common features. An application in marine phenomena recognition (discrimination between water brightness image and haze image) is discussed together with the results. Author (ESA)

N82-14584# Norwegian Defence Research Establishment, Kjeller.
SEASAT SAR PROCESSING AT THE NORWEGIAN DEFENCE RESEARCH ESTABLISHMENT
E. A. Herland *In* ESA Appl. of Remote Sensing Data on the Continental Shelf Jul. 1981 p 247-253 refs

Avail: NTIS HC A13/MF A01; ESA, Paris FF 125

A digital processor which processes synthetic aperture radar (SAR) images from raw data gathered by a satellite platform is described. The basic principles of SAR are explained; the algorithms for the digital processor are given in terms of a block diagram, the different parts of which are considered separately. A routine for achieving automatic focusing in azimuth compression without satellite orbit information is discussed. Examples of imagery obtained by applying the algorithms to raw data from the Seasat-1 SAR system are shown. These indicate that it is possible to detect ships and that the system can be used for maritime surveillance purposes. Author (ESA)

N82-15484*# Energy Information Administration, Washington, D.C. Geomagnetic Service.
THE REDUCTION, VERIFICATION AND INTERPRETATION OF MAGSAT MAGNETIC DATA OVER CANADA Progress Report
R. L. Coles, Principal Investigator, E Dawson, G. V. Haines, G. Jansen vanBeek, J. K Walker, and L. R. Newitt Jul. 1981 3 p Sponsored by NASA ERTS
(E82-10006; NASA-CR-164904; PR-3) Avail: NTIS HC A02/MF A01 CSCL 05B

Magnetic anomalies of lithospheric origin are weak at Magsat altitudes (20 to 30 nT at most), and are easily masked by much larger effects caused by field-aligned and other currents at high latitudes. Most of Canada lies under the influence of ionospheric currents in the auroral zone and polar cap. A more refined selection of quiet Magsat data allowed a revised scalar magnetic anomaly map of the whole region north of about 40 deg N latitude. Very preliminary vector anomaly maps and absolute vector component maps were derived. The scalar magnitudes show great promise for mapping the total force and anomaly fields. The Z vector data also appear to be good. The horizontal X and Y vector data are seriously contaminated with external fields and maybe other effects. A.R.H.

N82-15602# Marconi Co. Ltd., Chelmsford (England). Communications Research Div.
SQUINTED SAR SYSTEM Final Report
In its Additional Studies of Earth Resources Syn. Aperture Radar Payload Oct. 1980 32 p refs

Avail: NTIS HC A06/MF A01

It is found that for conventional SAR systems pointing broadside to the satellite track it is impossible to obtain the required swarth width at several incidence angles with the same antenna design. It is suggested that the swath width might be increased by 'squinting' the beam forwards or backwards. A feasibility study of such a system is discussed. J.M.S.

N82-15603# Deutsche Forschungs- und Versuchsanstalt fuer Luft- und Raumfahrt, Oberpfaffenhofen (West Germany). Inst. fuer Hochfrequenztechnik.
VISUAL EVALUATION OF E-SLAR IMAGERY
Juergen Nithack Feb. 1981 52 p refs In GERMAN; ENGLISH summary Report will also be announced as translation (ESA-TT-734)
(DFVLR-FB-81-11) Avail: NTIS HC A04/MF A01; DFVLR, Cologne DM 13,10

Flights were conducted E-SLAR (side looking airborne radar) for remote sensing experiments with active microwave techniques (X-band). The analog recorded data were mainly evaluated by visual methods to judge the system and its usefulness to solve Earth scientific questions. J.M.S.

N82-15604# Naval Postgraduate School, Monterey, Calif. Dept. of Oceanography.
BIOLOGICAL PATCHINESS IN RELATION TO SATELLITE THERMAL IMAGERY AND ASSOCIATED CHEMICAL MESOSCALE FEATURES M.S. Thesis
Ronald Wayne Phoebus Jun. 1981 63 p refs
(AD-A105757) Avail: NTIS HC A04/MF A01 CSCL 08/1

The presence of biological patches, or communities, can have a direct effect on Naval operations, scientific research, and fisheries. It is shown that remote infrared satellite sensing may be used as a real-time tool to accurately locate thermally and biologically significant features. Several physical, chemical, and biological variables were sampled in the surface layer of mesoscale thermal features which were located using satellite imagery. The bio-chemical sampling produced replicate results from which the distribution of biomass could be inferred. Possible explanations are advanced for patch forming mechanisms and biomass distribution. Author (GRA)

N82-15698# National Oceanic and Atmospheric Administration, Washington, D. C.
ENVIRONMENTAL SATELLITE IMAGERY, MARCH 1981
May 1981 69 p refs
(PB81-248049; KMRD-5.4-8103) Avail: NTIS HC A04/MF A01 CSCL 04B

Current cloud data obtained by operational environmental satellites was documented. Daily global satellite imagery is recorded in condensed form as a guide to data stored in the NOAA archives and is designed to help users select data for research and climatological use. The polar hemispheric mosaics reproduced in this catalog are derived from the advanced very high resolution radiometer (AVHRR (GSC)) data, and prepared daily by high speed computers. Visible and infrared swaths obtained while the satellite is northbound are used in the 15L mosaics from TIROS-N and the infrared channel only in the 17L mosaics from NOAA-6, NOAA-7 will include both the infrared and visible mosaics from the 14L pass. Infrared data swaths obtained during southbound passage of TIROS-N are labeled 03L, NOAA-6 are labeled 07L and NOAA-7 will be labeled 02L. GRA

08

INSTRUMENTATION AND SENSORS

Includes data acquisition and camera systems and remote sensors.

A82-10045 **Data compression and reconstruction for mixed resolution multispectral sensors.** R. A. Schowengerdt (Arizona, University, Tucson, AZ). In: American Society of Photogrammetry, Annual Meeting, 46th, St. Louis, MO, March 9-14, 1980, ASP Technical Papers. Falls Church, VA, American Society of Photogrammetry, 1980, p. 318-328. 13 refs. Research supported by the U.S. Geological Survey.

A data compression technique that utilizes a mixture of spatial resolutions for a multispectral scanner is described. The complementary reconstruction procedure that extrapolates edge information from the high resolution band(s) to the low resolution bands is also discussed. Examples of Landsat MSS imagery that have been compressed and reconstructed to the original resolution are presented. Error rates are calculated for two types of scenes, one containing prominent topographic effects, the other of an agricultural area. Improvement in radiometric quality of up to 40% is achieved by application of the reconstruction procedure to the compressed data.

A82-10051 * **Absolute image registration for geosynchronous satellites.** R. Nankervis, D. Koch (NASA, Goddard Space Flight Center, Greenbelt, MD), H. Sielski (Computer Sciences Corp., Silver Spring, MD), and D. Hall (HRB Singer, Inc., State College, PA). In: American Society of Photogrammetry, Annual Meeting, 46th, St. Louis, MO, March 9-14, 1980, ASP Technical Papers. Falls Church, VA, American Society of Photogrammetry, 1980, p. 438-446. 6 refs.

A procedure for the absolute registration of earth images acquired by cameras on geosynchronous satellites is described. A conventional least squares process is used to estimate navigational parameters and camera pointing biases from observed minus computed landmark line and element numbers. These estimated parameters along with orbit and attitude dynamic models are used to register images, employing an automated grey-level correlation technique, inside the span represented by the landmark data. Experimental results obtained from processing the SMS-2 observation data base covering May 2, 1979 through May 20, 1979 show registration accuracies with a standard deviation of less than two pixels if the registration is within the landmark data span. It is also found that accurate registration can be expected for images obtained up to 48 hours outside of the landmark data span. B.J.

A82-10858 **Orientation and construction of models. I - The orientation problem in close-range photogrammetry.** A. Okamoto (Kyoto University, Kyoto, Japan). *Photogrammetric Engineering and Remote Sensing,* vol. 47, Oct. 1981, p. 1437-1454. 14 refs.

The orientation problem of a stereoscopic pair of photographs taken with nonmetric cameras is considered, first algebraically and then geometrically. Also, some orientation techniques are presented. The orientation theory given here is quite fundamental and is applicable to various photogrammetric problems such as the calibration problem of nonmetric cameras and the orientation problem of stereo-strip imagery. In particular, one promising calibration method can be developed to provide interior orientation parameters for each of a stereoscopic pair of photographs, respectively, by using only distances in the object space as control. (Author)

A82-11406 **A mathematical model of an over-sea airborne UHF radio link.** T. Slator. *Marconi Review,* vol. 44, 2nd Quarter, 1981, p. 101-118. 9 refs.

A mathematical model is described which enables the performance of an over-the-sea airborne UHF radio link to be estimated as a function of terminal height and separation distance taking account statistically of variations of signal level caused by such factors as irregular antenna radiation patterns and a rough sea surface. (Author)

A82-11533 * **Radiative transfer theory for passive microwave remote sensing of random media.** S. L. Chuang and J. A. Kong (MIT, Cambridge, MA). In: Research topics in electromagnetic wave theory. New York, Wiley-Interscience, 1981, p. 136-160. 14 refs. NSF Grant No. ENG-78-23145; Grant No. NAG5-16; Contract No. F19628-80-C-0052.

The radiative transfer theory is applied to a random medium for the case of passive remote sensing. A general numerical solution with Gaussian quadrature method is studied. For a medium with laminar structure or a medium with cylindrical structure, closed form solutions are obtained by solving the radiative transfer equations of a two-layer random medium. Numerical results for the general case and the two limiting cases are compared. V.L.

A82-12127 * # **Repeatability and measurement uncertainty of the United States meteorological rocketsonde.** F. J. Schmidlin (NASA, Wallops Flight Center, Wallops Island, VA). *(International Symposium on Middle Atmosphere Dynamics and Transport, University of Illinois, Urbana, IL, July 28-Aug. 1, 1980.) Journal of Geophysical Research,* vol. 86, Oct. 20, 1981, p. 9599-9603. 11 refs.

It is pointed out that rocketsondes provide the only in situ 'ground truth' data for altitudes above 30 km. The need for precise temperature information has, therefore, led to a study of rocketsonde instrument repeatability and measurement uncertainty. Results obtained from root-mean-square difference and linear regression techniques are consistent and strongly suggest that the Datasonde precision is better than 1 C up to an altitude of 53 or 54 km. This result excludes atmospheric variability, which may occur within 5 min, and effects owing to spatial differences, which are small for paired measurements. At altitudes of 55 km and higher it is possible that sensor and flight-related anomalies, differences in radiation corrections owing to differing solar angles because of varying launch times, or even seasonal variations may create conditions that affect the magnitude of the standard corrections. G.R.

A82-12600 * **Airborne laser acquisition of cross-section data.** J. G. Collins (U.S. Army, Engineer Waterways Experiment Station, Vicksburg, MS) and W. B. Krabill (NASA, Wallops Flight Center, Wallops Island, VA). In: Civil engineering applications of remote sensing; Proceedings of the Specialty Conference, Madison, WI, August 13, 14, 1980. New York, American Society of Civil Engineers, 1980, p. 175-181.

The feasibility of obtaining cross-section data from airborne remote sensing systems is investigated. Eleven test profiles in the Wolf River Basin, near Memphis, Tennessee, are selected. Each profile is characterized using conventional ground survey methods; under 'leaves-off' conditions, photogrammetric, airborne laser, and airborne radar data are obtained. Results indicate that valley profiles can be accurately characterized with an airborne laser system. C.R.

A82-13293 * **Intercalibration of Landsat 1-3 and NOAA 6 and 7 scanner data.** M. J. Duggin (New York, State University, Syracuse, NY). *Applied Optics,* vol. 20, Nov. 15, 1981, p. 3815, 3816. 14 refs. Contract No. JPL-916331.

A82-13547 **The influence of gravity waves on radiometric measurements - A case study.** M. T. Decker (NOAA, Wave Propagation Laboratory, Boulder, CO), F. Einaudi (Georgia Institute of Technology, Atlanta, GA), and J. J. Finnigan (Cooperative Institute for Research in Environmental Sciences, Boulder, CO; Commonwealth Scientific and Industrial Research Organization, Div. of Environmental Mechanics, Canberra, Australia). *Journal of Applied Meteorology,* vol. 20, Oct. 1981, p. 1231-1238. 26 refs.

During the 1978 PHOENIX experiment at the Boulder Atmospheric Observatory in Colorado, the presence of atmospheric gravity waves was detected by various independent remote sensing instruments. Fluctuations in the zenith atmospheric radiation were measured at 22.235 and 55.45 GHz in the water vapor and oxygen absorption bands and compared with corresponding fluctuations of surface pressure and the height of FM-CW radar echo returns. These fluctuations are explained, qualitatively and quantitatively, in terms of an internal gravity wave generated by wind shear above the boundary layer. The analysis shows that the oscillations at 22.235 GHz are essentially due to fluctuations of water vapor in the antenna beam while those at 55.45 GHz are due to temperature variations. (Author)

A82-13738 **Block adjustment with additional parameters.** F. Ackermann (Stuttgart, Universität, Stuttgart, West Germany).

Photogrammetria, vol. 36, Oct. 1981, p. 217-227. 25 refs.

The current status of the technique of systematic image error correction by block adjustment with additional parameters is reviewed. The technique, which has proven to be highly effective and widely applicable, is defined as based on the principle of aerial triangulation, with the parameters being additional unknowns, the magnitudes of which are estimated from observational data for a prefixed type of image deformation. Current research and development has centered on problems of the selection, reliability, determinability and statistical assessment of the additional parameters. Available results have shown that carefully applied additional parameters almost always give improved accuracy, depending on overlap, redundancy and control. The basic limitation of the method lies in the fact that additional parameters belong to the functional part of the mathematical adjustment model, and so are based on the erroneous assumption that image deformations are constant for a large group of photographs. S.C.S.

A82-14299 Characteristics of westward travelling surges during magnetospheric substorms. W. G. Tighe and G. Rostoker (Alberta, University, Edmonton, Canada). *Journal of Geophysics Zeitschrift für Geophysik,* vol. 50, no. 1, 1981, p. 51-67. 19 refs. Research supported by the Natural Sciences and Engineering Research Council of Canada.

Data from arrays of magnetometers along lines of constant magnetic latitude and longitude, supplemented with all-sky camera and riometer data, are used to study the temporal development and typical scale size of westward traveling surges which occur during magnetospheric substorms. It is found that the motion of the head of the surge can be quite irregular, and in extreme cases, the surge form may grow and decay in a confined longitudinal sector without any significant westward displacement. The positive D-component perturbation, the characteristic signature of a surge, is generally confined within a longitude range of 6-10 deg at about 70 deg N, and is believed to be generated by a filamentary southward ionospheric current flowing at the edge of the surge. A comprehensive model of the three-dimensional current system is presented by a detailed comparison of model and observed latitude and longitude profiles of the magnetic disturbance. It is found that the best agreement is obtained when the entire electrojet system flows from southeast to northwest relative to the lines of constant magnetic latitude. J.F.

A82-15039 * Availability of Seasat synthetic aperture radar imagery. B. Holt (California Institute of Technology, Jet Propulsion Laboratory, Pasadena, CA). *Remote Sensing of Environment,* vol. 11, Nov. 1981, p. 413-417. NASA-supported research.

One of the sensors of the Seasat satellite was a synthetic aperture radar (SAR), which was operated over both oceanic and land areas. The Seasat SAR was an active imaging microwave system which transmitted and received horizontally polarized radiation at L-band frequency (1.275 GHz, 23-cm wavelength). Extensive coverage was obtained over North America, Europe, the Eastern Pacific Ocean, the Western and Northern Atlantic Ocean, and the Beaufort Sea. Surface coverage was also acquired over limited portions of Central America, the Gulf of Mexico, and the Caribbean Sea. The majority of the data has been optically processed in a so-called survey mode. Each optically processed Seasat pass has a swath width of 100 km at a scale of 1:500,000. A subset of the SAR data has been digitally processed in a so-called high-resolution mode. Digital processing has been performed upon selected scenes with dimensions of 100 x 100 km. Digitally processed imagery has a nominal ground resolution of 25 m. G.R.

A82-15655 † Current aerial cameras (Sovremennye aerofotoapparaty). V. G. Afremov and V. B. Il'in. *Geodeziia i Kartografiia,* Oct. 1981, p. 40-42. 6 refs. In Russian.

The paper considers the development and operation of the TE and TES aerial cameras, having focal distances of 350, 100, 70, and 50 mm and FOV angles of 40, 103, 120, and 136.5 deg, respectively, for 18 x 18 cm frames. The basic technical characteristics and some applications of these cameras are presented. B.J.

A82-15920 Three bearing method for passive triangulation in systems with unknown deterministic biases. M. Mangel and C. F. Carter (California, University, Davis, CA). *IEEE Transactions on Aerospace and Electronic Systems,* vol. AES-17, Nov. 1981, p. 814-819. 5 refs. Contract No. N00014-81-K-0030.

The paper presents an operationally simple method for triangulation in systems with strong biases, which requires three bearing measurements and two turns of the aircraft. The triangulation problem is considered in the search for a stationary target, in which deterministic and random terms enter into the observed bearing. Numerical and flight testing are reported, and it is shown how the method can be modified to include random fluctuation and confidence contours about the point of triangulation. D.L.G.

A82-15951 † Satellites of the Meteor series, intended for earth studies from space (Sputniki serii 'Meteor', prednaznachennye dlia izucheniia zemli iz kosmosa). Iu. V. Trifonov. *Issledovanie Zemli iz Kosmosa,* Sept.-Oct. 1981, p. 8-20. 8 refs. In Russian.

The objectives and main results of the Soviet experimental program for the operational study of the earth from space by means of Meteor satellites are presented. Examples of the effective use of multispectral wide-angle television data of low and medium resolution in the fields of geology, hydrology, weather modification, hydrometeorology, forestry, and navigation are given. The specific features of the Meteor program for remote sensing are described. The ballistic design of the experimental remote sensing system is characterized, indicating a sun-synchronous orbit for the system. The advantage of using a low-thrust electrojet engine in the Meteor program is discussed. J.F.

A82-15952 † Technical equipment of an experiment for remote sensing of the earth from space (Kompleks tekhnicheskikh sredstv eksperimenta po distantsionnomu zondirovaniiu zemli iz kosmosa). Iu. V. Trifonov. *Issledovanie Zemli iz Kosmosa,* Sept.-Oct. 1981, p. 21-27. In Russian.

The equipment used in an experiment (1980-1981) to obtain multispectral television data of medium and high resolution using a second-generation Meteor satellite is described. The prospects of developing a continuously active space system for earth resources studies are characterized. The design features and structural characteristics of the spacecraft used in the experiment are noted. These features include the improved accuracy of three-axis attitude control and stabilization of the angular velocity; structural and weight improvements, and the increased possibilities for automatic control in transmitting and receiving data. J.F.

A82-15955 † Experimental telemetry system based on the Fragment multispectral scanning system (Eksperimental'nyi informatsionno-izmeritel'nyi kompleks na osnove mnogozonal'noi skaniruiushchei sistemy 'Fragment'). G. A. Avanesov (Akademiia Nauk SSSR, Institut Kosmicheskikh Issledovanii, Moscow, USSR). *Issledovanie Zemli iz Kosmosa,* Sept.-Oct. 1981, p. 40-44. 8 refs. In Russian.

The structure and functions of the main system of the experimental telemetry complex, based on the Fragment multispectral scanning system are considered. A preliminary analysis of the results of an experiment involving the operational acquisition and machine processing of multispectral data is given. The system is shown to be useful for the development of operational methods of earth-resources study. J.F.

A82-15958 † Metrological support of measurements of earth-surface brightness by the Fragment multispectral scanning system (Metrologicheskoe obespechenie izmerenii iarkosti zemnoi poverkhnosti mnogozonal'noi skaniruiushchei sistemoi 'Fragment'). G. A. Avanesov, Ia. L. Ziman, A. G. Sychev, and V. I. Tarnopol'skii (Akademiia Nauk SSSR, Institut Kosmicheskikh Issledovanii, Moscow, USSR). *Issledovanie Zemli iz Kosmosa,* Sept.-Oct. 1981, p. 65-77. 12 refs. In Russian.

A82-16164 The application of programmable pocket calculators for computations during survey flights. H. C. Zorn (International Institute for Aerial Survey and Earth Sciences, Enschede, Netherlands). *ITC Journal,* no. 3, 1981, p. 308-333.

Computation during survey flights can be effectively achieved using a programmable pocket calculator such as the Hewett-Packard C41 model. Using this calculator, formulas and programs have been developed for computing survey turns; wind star; heading and ground speed, given wind vector and required course; pressure altitude required to reach required true altitude; and true airspeed given indicated airspeed, air temperature, and pressure altitude. Other potential applications include the conversion of latitude and longitude to UTM zone and coordinates, and great circle and loxodrome computations. S.C.S.

A82-16447 * **Magnetic field observations on DE-A and -B.** W. H. Farthing, M. Sugiura, B. G. Ledley (NASA, Goddard Space Flight Center, Greenbelt, MD), and L. J. Cahill, Jr. (Minnesota, University, Minneapolis, MN). *Space Science Instrumentation,* vol. 5, Dec. 1981, p. 551-560. 14 refs.

Magnetic field observations are conducted on each of the DE-A and -B satellites by a triaxial fluxgate magnetometer. In the basic mode the instrumental resolution is + or - 1.5 nT; in addition, the DE-A magnetometer has two modes of higher resolution: + or - 0.25 nT and + or - 20 pT. The sampling rate is 16 vector samples per second in all modes. The experiment objectives include observations of field-aligned currents, magnetospheric equatorial currents, and ULF waves. These observations, taking full advantage of the specifically selected orbits of the two spacecraft and of the unique combination of instruments, are performed to achieve a better understanding of the electrodynamic coupling within the atmosphere-ionosphere-magnetosphere system and of wave-particle interactions which contribute to the coupling processes. (Author)

A82-16602 † **Main results of the Raduga experiment (Osnovnye itogi eksperimenta 'Raduga').** Ia. L. Ziman, Iu. M. Chesnokov, and V. V. Aksenov. In: Airborne and spaceborne multispectral photography of the earth. Moscow, Izdatel'stvo Nauka, 1981, p. 5-13. In Russian.

The Raduga experiment, involving the multispectral photography of earth resources from Soyuz-22, is described. Attention is given to the preflight testing and calibration of the multispectral cameras, the operational characteristics of the equipment, results of photointerpretation, and the success with which the goals of the experiment were carried out. It has been concluded that the MKF-6 and MSP-4 multispectral instrumentation is suitable for practical implementation in the remote sensing of earth resources. B.J.

A82-16613 † **Methodology and practice of spectroscopic measurements of landscape elements in the preparation and carrying out of down-looking experiments (Metodika i praktika spektrometricheskikh izmerenii elementov landshafta pri obespechenii i provedenii podsputnikovykh eksperimentov).** G. B. Gonin, A. A. Bartashevich, N. V. Kravchuk, N. N. Mozgov, and Iu. V. Ponomarenko. In: Airborne and spaceborne multispectral photography of the earth. Moscow, Izdatel'stvo Nauka, 1981, p. 118-128. 7 refs. In Russian.

Various aspects concerning the preparation and carrying out of down-looking experiments associated with multispectral scanning of landscape elements are considered. Particular consideration is given to the mathematical modeling of the earth-atmosphere system (with allowance for the scattering and turbulence properties of the atmosphere), and to calibration specifications in aerial spectroscopy experiments. B.J.

A82-17165 * **Global satellite measurements of water vapour, wind speed and wave height.** D. B. Chelton, K. J. Hussey, and M. E. Parke (California Institute of Technology, Jet Propulsion Laboratory, Pasadena, CA). *Nature,* vol. 294, Dec. 10, 1981, p. 529-532. 6 refs. NASA-supported research.

The results of global measurements of atmospheric water vapor by the Seasat Scanning Multichannel Microwave Radiometer and wave height and wind speed by the Seasat altimeter (ALT) are reported. The 13.5 GHz ALT has a 3.125 ns pulsewidth and 1022 Hz repetition rate, and measures surface height to a resolution exceeding 10 cm celative to a reference ellipsoid. Full ALT data comprise 135 km equatorial groundtracks, with about a 50 cm difference of sea wave height compared to buoy reference measurements, and wind-speed accuracy to within 0.25-1.58 m/sec up to 20 m/sec. Highest water vapor concentrations were observed in the tropics and the lowest at high latitudes. Wind speeds were highest for the north-east and south-east tradewinds in both the Atlantic and Pacific oceans. Average wave height is small in the summer North Hemisphere and the largest waves are in the winter Southern ocean, and lowest in western Atlantic and Pacific ocean areas where winds are lightest. D.H.K.

A82-17918 # **User needs and the future of operational meteorological satellites.** D. B. Miller and J. R. Silverman (NOAA, Advanced Systems Concepts Group, Washington, DC). *American Institute of Aeronautics and Astronautics, Aerospace Sciences Meeting, 20th, Orlando, FL, Jan. 11-14, 1982, Paper 82-0388.* 9 p.

Applications of the TIROS-N and GOES satellites are reviewed, and requirements for the next generation of meteorological satellites are discussed. TIROS N spacecraft were a joint effort of the U.S., U.K., and France, and carried instrumentation which provided information on oceanographic and hydrologic processes, agricultural products, meteorology, and digital imaging. The GOES satellites give continuous viewing of weather features and collect and relay meteorological data from remote platforms such as buoys, ships, stations, aircraft, and balloons. The next generation of GOES spacecraft are also intended for GEO, and instruments will provide imaging in the IR and visual with 1-2 and 0.5 km resolution, respectively, multispectral imaging, vertical temperature resolution in the troposphere to 1-5 km, and have solar X ray sensing capabilities, as well as for the atmospheric electron density. Further instrumentation additions and choice of orbits are examined, noting that a careful consideration of the capital return on investment will be required before any decision to fly new meteorological spacecraft. M.S.K.

N82-10071*# Scientific Analysts and Consultants, Inc., Rockville, Md.
DISTORTION-FREE MAPPING OF VISSR IMAGERY DATA FROM GEOSYNCHRONOUS SATELLITES
F. K. Chan *In* NASA. Goddard Space Flight Center Sixth Ann. Flight Mech./Estimation Theory Symp. Oct. 1981 35 p ref
(Contracts NOAA-01-8-MO1-1864; NOAA-NA79-KA-C-00026)
Avail: NTIS HC A13/MF A01 CSCL 22A

The formulation is rigorous and includes all misalignment angles of the VISSR, the sun sensor and the instantaneous spin axis with the satellite's body axis. It also includes the effects due to the motion of the satellite's suborbital point. All the mapping equations for distortion removal were reduced to simplest forms, and all the algorithms were optimized as much as possible. An approach was then formulated for implementing these algorithms for in-line operational use. It is concluded that in-line distortion removal is possible in real-time processing of infra-red but not visible VISSR imagery data. T.M.

N82-10073*# General Electric Co., Lanham, Md. Space Div.
THE MSS CONTROL POINT LOCATION ERROR FILTER FOR LANDSAT-D
I. Levine *In* NASA. Goddard Space Flight Center Sixth Ann. Flight Mech./Estimation Theory Symp. Oct. 1981 18 p refs

(Contract NAS5-25300)
Avail: NTIS HC A13/MF A01 CSCL 05B

The filter produces the maximum likelihood estimates for average values of the spacecraft position and attitude errors during a single scene. The quality of the filter performance is characterized by the maximal cross and along track residual errors for which probability distributions can be calculated analytically for a given pattern of control points. The filter with an automatic selection of the best set of estimates provides geodetic correction at 90% of pixels with residual errors less than 40 m for four or more control points and the mean squared measurement errors of the order of 20-25 m. The same accuracy can be preserved for eight or more control points and measurement errors of 30-35 m. T.M.

N82-10468*# National Aeronautics and Space Administration. Goddard Space Flight Center, Greenbelt, Md.
MAGSAT: VECTOR MAGNETOMETER ABSOLUTE SENSOR ALIGNMENT DETERMINATION
M. H. Acuna Sep. 1981 39 p refs
(NASA-TM-79648) Avail: NTIS HC A03/MF A01 CSCL 14B

A procedure is described for accurately determining the absolute alignment of the magnetic axes of a triaxial magnetometer sensor with respect to an external, fixed, reference coordinate system. The method does not require that the magnetic field vector orientation, as generated by a triaxial calibration coil system, be known to better than a few degrees from its true position, and minimizes the number of positions through which a sensor assembly must be rotated to obtain a solution. Computer simulations show that accuracies of better than 0.4 seconds of arc can be achieved under typical test conditions associated with existing magnetic test facilities. The basic approach is similar in nature to that presented by McPherron and Snare (1978) except that only three sensor positions are required and the system of equations to be solved is considerably simplified. Applications of the method to the case of the MAGSAT Vector Magnetometer are presented and the problems encountered discussed. A.R.H.

N82-10481# Research Inst. of National Defence, Linkoeping (Sweden). Huvudavdelning 3.
USE OF RADAR AND MICROWAVE RADIOMETRY FOR RECONNAISSANCE SATELLITES [ANVAENDNING AV RADAR OCH MIKROVAAGSRADIOMETRIE VID SPANINGSSATELLITER]
Hans Lok Oct. 1980 28 p refs In SWEDISH
(FOA-C-30204-E1) Avail: NTIS HC A03/MF A01

The advantages and disadvantages of side-looking radar and microwave radiometers for observations of Earth by satellite are discussed. Each system is examined with regards to field of view and instrument sensitivity. Microwave attenuation is also discussed. A.R.H.

N82-10484# Kiruna Geophysical Inst. (Sweden).
A SWEDISH PROPOSAL FOR AN EISCAT/GEOS-2 EXPERIMENT
Svante Westerlund, Georg Gustafsson, Aake Steen, John Murdin, Gudmund Wannberg, Rolf Bostroem (Uppasala Ionospheric Obs., Sweden), Aake Hedberg (Uppsala Ionospheric Obs., Sweden), Hermann Opgenoorth (Uppsala Ionospheric Obs., Sweden), Erling Nielsen (Max-Planck Inst. fuer Aeronomie, Katlenburg-Lindau, West Germany), Carl-Gunne Faelthammar (Royal Inst. of Technol., Stockholm) et al Mar. 1981 28 p refs
(KGI-175; ISSN-0347-6405) Avail: NTIS HC A03/MF A01

An experiment that uses GEOS to measure in the equatorial plane at the same time as EISCAT and other ground based instrumentation are monitoring the ionosphere is described. The generation, acceleration and loss of auroral particles are studied. Signatures of particle precipitation in the ionosphere and properties of the plasma and electric field in the equatorial plane are correlated. The position of the conjugate point of GEOS is determined during various conditions. Such data in conjunction with magnetic field models, make it feasible to identify and estimate the various effects that contribute to the field during disturbances, i.e. to improve geomagnetic field models. Author (ESA)

N82-10488# University Coll., Dublin (Ireland). Dept. of Physics.
STUDY ON CALIBRATION METHODS FOR EARTH OBSERVATION OPTICAL IMAGING INSTRUMENTS Final Report
E. O. Mongain Paris ESA Nov. 1980 230 p refs
(Contract ESA-4237/80/NL-PP(SC))
(UCD-207/1/80; ESA-CR(P)-1443) Avail: NTIS HC A11/MF A01

The properties and calibration of lamps diffusors, and detectors are considered. Measurements of solar irradiance from ground level are illustrated and the NASA solar spectral irradiance experiments are discussed with respect to the possibility of image striping as an inherent property of imaging arrays. Author (ESA)

N82-11512*# Research and Data Systems, Inc., Lanham, Md.
SMMR DATA SET DEVELOPMENT FOR GARP
John Kogut May 1981 60 p
(Contract NAS5-25781)
(NASA-CR-166721) Avail: NTIS HC A04/MF A01 CSCL 05B

The NIMBUS 7 Scanning Multichannel Microwave Radiometer (SMMR) data are analyzed. The impact of cross polarization and Faraday rotation on SMMR derived brightness temperatures is evaluated. The algorithms used to retrieve the geophysical parameters are tested, refined, and compared with values derived by other techniques. The technical approach taken is described and the results presented. S.L.

N82-12447*# EG & G Washington Analytical Services Center, Inc., Riverdale, Md.
IONOSPHERIC PROPAGATION CORRECTION MODELING FOR SATELLITE ALTIMETERS
George Nesterczuk Nov. 1981 14 p refs
(Contract NAS6-3075)
(NASA-CR-156881) Avail: NTIS HC A02/MF A01 CSCL 20D

The theoretical basis and avaliable accuracy verifications were reviewed and compared for ionospheric correction procedures based on a global ionospheric model driven by solar flux, and a technique in which measured electron content (using Faraday rotation measurements) for one path is mapped into corrections for a hemisphere. For these two techniques, RMS errors for correcting satellite altimeters data (at 14 GHz) are estimated to be 12 cm and 3 cm, respectively. On the basis of global accuracy and reliability after implementation, the solar flux model is recommended. Author

N82-13465* National Aeronautics and Space Administration. Goddard Space Flight Center, Greenbelt, Md.
SCANNER Patent
Robert F. Hummer (Santa Barbara Research Center) and Deane T. Upton, inventors (to NASA) (Santa Barbara Research Center) Issued 10 Nov. 1981 12 p Filed 19 May 1975 Supersedes N76-19408 (14 - 10, p 1252) Continuation of abandoned US Patent Appl. SN-583219, filed 30 Sep. 1966 Sponsored by NASA
(NASA-Case-GSC-12032-2; US-Patent-4,300,159; US-Patent-Appl-SN-578700; US-Patent-Appl-SN-583219; US-Patent-Class-358-109; US-Patent-Class-250-235; US-Patent-Class-250-236) Avail: US Patent and Trademark Office CSCL 20F

An aerial vehicle rotating in gyroscopic fashion about one of its axes has an optical system which scans an area below the vehicle in determined relation to vehicle rotation. A sensing device is provided to sense the physical condition of the area of scan and optical means are associated to direct the physical intelligence received from the scan area to the sensing means. Means are provided to incrementally move the optical means through a series of steps to effect sequential line scan of the area being viewed keyed to the rotational rate of the vehicle.
Official Gazette of the U.S. Patent and Trademark Office

N82-13469*# National Aeronautics and Space Administration. Goddard Space Flight Center, Greenbelt, Md.
INTERPOLATING FOR THE LOCATION OF REMOTE SENSOR DATA
Edward F. Puccinelli and Jack Kornfield (NSF) Jul. 1981 23 p refs
(NASA-TM-82169) Avail: NTIS HC A02/MF A01 CSCL 05B

An interpolation algorithm is presented as a practical alternative to common interpolation and approximation methods when applied to the problem of determining the location of remote sensor data. This algorithm is based upon knowledge of the geometry of the problem and is shown to be inherently more accurate than common interpolation schemes which may be applied to all types of data. A practical location problem is used to demonstrate its accuracy and computational cost.
Author

N82-14171# Officine Galileo S.p.A., Florence (Italy).
INFRARED RADIANCE MODEL VARIATION BY SENSOR FLIGHT MEASUREMENTS
R. BaldessiniFontana, D. Sciacovelli (ESTEC, Noordwijk, Netherlands), and L. Fraiture (ESOC, Darmstadt, West Germany) *In* ESA Spacecraft Flight Dyn. Aug. 1981 p 461-478 refs

Avail: NTIS HC A22/MF A01; ESA, Paris FF 160 Member States, AU, CN and NO (+20% others)

The NASA and BAC-ESR 4 IR radiance models of Earth, applied to attitude sensor calibration, are compared. The sensors are IR pencil beams on spinning satellites. Flight measurements of Geos 2 and OTS transfer orbits were compared to simulations from a model which describes the optics, detector and electronics of the beam, based on directly measured parameters and laboratory test data. The models performed equally well. It is shown that anomalies in preflight calibration can be detected. A small mismatch of the optical axis inclination of a Geos 2 IR telescope was observed. Author (ESA)

N82-14560# Centre National d'Etudes Spatiales, Toulouse (France).
STATE-OF-THE-ART IN USING A SPACEBORNE ALTIMETER AND SCATTEROMETER FOR THE DETERMINATION OF WIND, SEA STATE, AND MARINE AND ICE DYNAMICS
M. Lefebvre and J.-L. Hyacinthe (Centre National pour l'Exploitation des Oceans, Paris) *In* ESA Appl. of Remote Sensing Data on the Continental Shelf Jul. 1981 p 57-58

Avail: NTIS HC A13/MF A01; ESA, Paris FF 125

The accuracy of Seasat altimeter and scatterometer data is discussed. Sea state obtained through altimeter pulse shape and wind data obtained by altimeter pulse amplitude or, with direction by the scatterometer backscatter, are compared with model and map values. The altimeter performs well, but not the scatterometer. Altimeter data can be used to investigate marine and ice dynamics on a large scale, e.g., a sea. For seasonal and interannual fluctuation of oceanic circulation, a few cm accuracy on the relative satellite trajectory without geoid accuracy is needed. For the mean ocean circulation and the absolute determination of current, a 10 cm accurate geoid is needed. Author (ESA)

N82-14563# Canada Centre for Remote Sensing, Ottawa (Ontario).

A RECOMMENDED SENSOR PACKAGE FOR THE DETECTION AND TRACKING OF OIL SPILLS

H. H. Zwick, R. A. Neville, and R. A. ONeil *In* ESA Appl. of Remote Sensing Data on the Continental Shelf Jul. 1981 p 77-88 refs

Avail: NTIS HC A13/MF A01; ESA, Paris FF 125

Oil on open water under clear skies is a relatively easy target, oil under ice is very difficult. Results of remote sensing experiments acquiring data for system specification are discussed. Instruments assessed include active microwave sensors for the measurement of backscatter from oil slicks, scanners for oil thickness determination from the spectral character of reflected radiation and solar heating effects, and laser fluorosensors for oil-specific detection in oil and water and/or ice mixtures and for Raman scattering from the surface. The most effective system for the wide variety of conditions experienced in Canada consists of a laser fluorosensor, an ultraviolet/infrared line scanner, a side-looking airborne radar, low light level television and photographic cameras. These sensors are supported by real time data annotation, display, and analysis systems. Author (ESA)

N82-14577# Belfotop P.v.b.a., Wemmel (Belgium).

AIRBORNE REMOTE SENSING OF THE COASTAL ZONE

J. L. vanGenderen and G. DeMan *In* ESA Appl. of Remote Sensing Data on the Continental Shelf Jul. 1981 p 197-202

Avail: NTIS HC A13/MF A01; ESA, Paris FF 125

Using the European remote sensing aircraft platform, equipped with a digital multispectral scanner, two metric cameras, a realtime imaging system, and a digital navigation system, coastal zones were studied. The airborne platform and its operation are described. Practical problems associated with coastal airborne remote sensing are discussed (position fixing over water; day-night imaging; film processing; digital multispectral data processing) and examples from oil pollution monitoring, thermal discharge studies, coastal erosion, and surface wave direction analysis are given.
Author (ESA)

N82-14599# Carson Helicopters, Inc., Perkasie, Pa. Geoscience Div.

NURE AERIAL GAMMA-RAY AND MAGNETIC RECONNAISSANCE SURVEY OF MAINE AND PORTIONS OF NEW YORK. VOLUME 1: DATA ACQUISITION, REDUCTION AND INTERPRETATION Final Report

Aug. 1981 273 p refs

(Contract DE-AC13-76GJ-01664)

(DE82-000650; GJBX-327-81-Vol-1) Avail: NTIS HC A12/MF A01

A rotary wing high sensitivity radiometric and magnetic survey of the State of Maine and of Binghamton, Ogdensubrg and Utica in New York State was performed. The survey was flown with a Sikorsky S58T helicopter equipped with a high sensitivity calibrated gamma ray spectrometer. The radiometric data were processed to compensate for Compton scattering effects and altitude ariations. The data were normalized to 400 feet terrain clearance. The reduced data are presented in the form of stacked profiles, standard deviation anomaly plots, histogram plots and microfiche listings. DOE

N82-14616# Royal Aircraft Establishment, Farnborough (England). Remote Sensing Unit.

REMOTE SENSING INFORMATION BULLETIN; ISSUE NUMBER 6

Jul. 1981 33 p

Avail: NTIS HC A03/MF A01

The activities of the Center up to July 1981 are reported. Topics include: the United Kingdom report to the seventh Earthnet meeting, in June 1981; satellite status reports for LANDSAT 1, 2, 3, and D; microwave remote sensing, including Seasat synthetic aperture radar; Mapsat feasibility study; Eros field office; and symposia and conferences organized by the Center, including a summer school on remote sensing applications in marine science and technology. Author (ESA)

N82-14779# National Oceanic and Atmospheric Administration, Seattle, Wash. Pacific Marine Environmental Lab.

GEM: A SIMPLE METEOROLOGICAL BUOY WITH SATELLITE TELEMETRY

R. Michael Reynolds *In* ESA Nowcasting: Mesoscale Observations and Short-Range Prediction Jun. 1981 p 401-404 refs

Avail: NTIS HC A19/MF A01; ESA, Paris FF 160 Member States, AU, CN and NO (+20% others)

A small, easily deployable and inexpensive buoy was developed for mesoscale research. The synthesis of the detailed parameter fields necessary for mesometeorology necessitates the deployment of a network of buoys that are less expensive than most standard designs. Vector averaged winds, scaler winds, air temperature, water temperature, and gusts are measured. Compass readings provide surface current direction. The buoy transmits data via the GOES satellite which eliminates the need for internal tape recording. Computer processing of the data is described. Proper counterbalancing and vector averaging are shown to reduce the effects of buoy motion. Author (ESA)

N82-15110# Air Force Systems Command, Wright-Patterson AFB, Ohio.

METEOROLOGICAL SATELLITES

16 Oct. 1981 7 p refs Transl. into ENGLISH from Skrzydlata Polska (Poland) no. 27, 1979 21 p

(AD-A107427; FTD-ID(RS)T-1059-81) Avail: NTIS HC A02/MF A01 CSCL 22B

Meteor-2 (second generation meteorological satellite) and an experimental satellite on which instruments are being tested and modified for the requirements of hydrometeorology and a determination of natural resources are presently operational in the U.S.S.R. Television devices with a 1-10 km terrain image resolution operating in the visible and infrared region are used to determine the space system, velocity and direction of cloud movements and provide information about the snow and ice cover, cyclones, storms, vortices in the atmosphere, and velocity and direction of wind. Images with a 50-1000 m resolution make possible geological and hydrological surveys, an evaluation of the state of vegetation and crops, detection of forest fires, determination of pollution of the atmosphere and sea and determination of optimal fishing regions in the ocean. Measurement of the intensity of atmospheric radiation in narrow infrared regions and very high frequencies allows remote evaluation of the temperature and humidity distribution in the vertical cross section of the Earth's atmosphere. Author

N82-15483*# General Electric Co., Philadelphia, Pa. Space Div.

LANDSAT-2 AND LANDSAT-3 FLIGHT EVALUATION REPORT, 23 APRIL TO 23 JULY 1979

1 Aug. 1979 258 p ERTS

(Contract NAS5-21808)

(E82-10005; NASA-CR-163348; Doc-79SDS4242) Avail: NTIS HC A12/MF A01 CSCL 05B

The performance of satellite subsystems and the response of in-orbit payload systems are summarized. Graphs and tables show the values of the various parameters of these systems. A spacecraft orbit reference table is included. A.R.H.

N82-15493*# IBM Federal Systems Div., Houston, Texas.

ERSYS-SPP ACCESS METHOD SUBSYSTEM DESIGN SPECIFICATION

R. C. Weise, Principal Investigator Sep. 1980 74 p Sponsored by NASA, USDA, Dept. of Commerce, Dept. of Interior, and Agency for International Development ERTS

(Contract NAS9-14350; Proj. AgRISTARS)

(E82-10015; NASA-CR-161039; MU-11-00300; JSC-16918)

Avail: NTIS HC A04/MF A01 CSCL 02C

The STARAN special purpose processor (SPP) is a machine allowing the same operation to be performed on up to 512 different data elements simultaneously. In the ERSYS system, it is to be attached to a 4341 plug compatible machine (PCM) to do certain existing algorithms and, at a later date, to perform other to be specified algorithms. That part of the interface between the 4341 PCM and the SPP located in the 4341 PCM is known as the SPP access method (SPPAM). Access to the SPPAM will be obtained by use of the NQUEUE and DQUEUE commands. The subsystem design specification is to incorporate all applicable design considerations from the ERSYS system design specification and the Level B requirements documents relating to the SPPAM. It is intended as a basis for the preliminary design review and will expand into the subsystem detailed design specification. Author

N82-15495*# General Electric Co., Philadelphia, Pa. Space Div.
LANDSAT-2 AND LANDSAT-3 FLIGHT EVALUATION REPORT, 23 OCTOBER 1978 TO 23 JANUARY 1979
1 Feb. 1979 236 p ERTS
(Contract NAS5-21808)
(E82-10017; NASA-CR-166640; Doc-79SDS4201) Avail: NTIS HC A11/MF A01 CSCL 05B

Orbital parameters and adjustments are discussed and tabulated. The performance of the various subsystems and payloads on the two satellites is documented in tables. A.R.H.

N82-15500# Marconi Co. Ltd., Chelmsford (England). Communications Research Div.
ADDITIONAL STUDIES OF EARTH RESOURCES SYNTHETIC APERTURE RADAR PAYLOADS Final Report
A. P. Luscombe Paris ESA Oct. 1980 105 p refs
(Contract ESA-6225/80-F-CG(SC))
(MTR-80/90; ESA-CR(P)-1469) Avail: NTIS HC A06/MF A01

Results of design studies on the synthetic aperture radar payload are discussed. A new baseline system for an incidence angle of about 45 deg was specified, and its performance at smaller angles is assessed. A feasibility study of a squinted SAR system is described. For individual titles, see N82-15501 through N82-15502.

N82-15501# Marconi Co. Ltd., Chelmsford (England). Communications Research Div.
NEW BASELINE SYSTEM Final Report
In its Additional Studies of Earth Resources Syn. Aperture Radar Payload Oct. 1980 46 p refs

Avail: NTIS HC A06/MF A01

A baseline system with an incidence angle of around 45 deg was specified for the Earth resources SAR payload and its operation at smaller angles was investigated. The basic system design and method of analysis are described. The choices of pulse repetition frequency (PRF) for different incidence angles, the problem of ambiguities and their evaluation and the antenna beam patterns are covered along with the selection of major system parameters (beam pattern, PRF's and incidence angles). The detail and the baseline system suggested is analyzed in terms of the image quality specifications. Two more aspects of the SAR system, the transmitter power requirements and the variation in ground range resolution with incidence angle, are discussed. A listing of the basic results for four different incidence angles is given. J.M.S.

09
GENERAL

Includes economic analysis.

A82-12530 **Remote sensing contributions to the management of renewable resources.** C. Sheffield (Earth Satellite Corp., Washington, DC). In: The year of the Shuttle; Proceedings of the Eighteenth Space Congress, Cocoa Beach, FL, April 29-May 1, 1981. Cocoa Beach, FL, Canaveral Council of Technical Societies, 1981, p. 2-7 to 2-14. 9 refs.

Present and future contributions of space-derived remotely sensed data, obtained from observations of five major areas of renewable resources, are discussed. The data needs for the five resource areas - agriculture, forestry, rangeland management, coastal zones, and the ocean harvest - are described, and the principal satellites and sensors flown in space to cover these areas since 1972 are presented. Data sources and data needs are compared, and areas of data deficiency and limitation are identified. A profile of earth sensing satellites to fill these gaps in a 1985-1995 time frame is given. Cooperative international efforts to develop future earth resource satellites are suggested. J.F.

A82-12541 **The 1981 RCA space constellation.** A. Schnapf (RCA, Astro-Electronics Div., Princeton, NJ). In: The year of the Shuttle; Proceedings of the Eighteenth Space Congress, Cocoa Beach, FL, April 29-May 1, 1981. Cocoa Beach, FL, Canaveral Council of Technical Societies, 1981, p. 5-43 to 5-53.

The eight spacecraft scheduled for launch in 1981 are described. These are the RCA Satcom D and E commercial communication satellites, the U.S. Navy NOVA 1 and 2 navigation satellites, NASA's Dynamics Explorer A and B scientific satellites, the U.S. Department of Commerce NOAA-C operational meteorological satellite, and the Department of Defense DMSP Block 5D-2 operational meteorological satellite. It is noted that in addition a number of RCA color television camera systems will be carried on the Space Transportation System for aiding the astronauts in inspecting and deploying cargo from the cargo bay and for providing video transmissions of engineering and public relations activity in the Shuttle crew compartment. C.R.

A82-17307 # **ISRO satellite mission support facilities - Scope and future plans.** M. K. Sundararaman, V. S. Iyengar, and K. V. Venkatachary (Indian Space Research Organization, Sriharikota, India). In: Space tracking and data systems; Proceedings of the Symposium, Arlington, VA, June 16-18, 1981. New York, American Institute of Aeronautics and Astronautics, 1981, p. 51-63.

It is the objective of the Indian Space Research Organization (ISRO) to provide communication and education to widely dispersed rural communities in India, and to survey and manage the country's natural resources with the aid of satellite technology. India maintains also a modest scientific research program which employs satellite missions. A brief overview is provided of the Indian space program, giving attention to the network's current capabilities for satellite data acquisition, tracking activities, and data dissemination. A description is given of plans for the coming decade. G.R.

N82-10087*# **National Aeronautics and Space Administration. Goddard Space Flight Center, Greenbelt, Md.**
REPORT ON ACTIVE AND PLANNED SPACECRAFT AND EXPERIMENTS
Robert W. Vostreys, ed. and Harriet H. Maitson, ed. Aug. 1981 310 p refs
(NASA-TM-84025; NSSDC/WDC-A-R&S-81-10) Avail: NTIS HC A14/MF A01 CSCL 22A

Active and planned spacecraft activity and experiments between June 1, 1980 and May 31, 1981 known to the National Space Science Data Center are described. The information covers a wide range of disciplines: astronomy, Earth sciences, meteorology, planetary sciences, aeronomy, particles and fields, solar physics, life sciences, and material sciences. Each spacecraft and experiment is described and its current status presented. Descriptions of navigational and communications satellites and of spacecraft that contain only continuous radio beacons used for ionospheric studies are specifically excluded. J.D.H.

N82-10102*# National Aeronautics and Space Administration, Washington, D. C.
MISSION OPERATION REPORT: OSTA-1
26 Oct. 1981 28 p
(NASA-TM-84053; S-420-81-01) Avail: NTIS HC A03/MF A01 CSCL 22B

The Office of Space and Terrestrial Applications (OSTA 1) payload was designed to demonstrate shuttle's capability as a space research platform and the potential application of techniques for future remote sensing. Because thermal tests planned for STS-2 flight require that the payload bay to be pointed towards Earth, the experiments selected for OSTA 1 emphasize terrestrial sciences and are concerned with remote sensing for Earth resources, environmental quality, ocean conditions, meteorological phenomena, and life sciences. Characteristics of the STS-2 flight, the major events timeline, geopgraphical areas coverage, pallet experiments ground coverages, and experiment operating modes are described. The OSTA-1 pallet configuration, payload interface, and the instruments comprising each of the experiments are described and illustrated. Mission support stations, and the payload team are listed. Mission cost data are included. A.R.H.

N82-13010# Eurosat S.A., Geneva (Switzerland).
OVERALL ECONOMIC IMPACT OF AN OPERATIONAL METEOSAT SYSTEM Final Report
J. B. Lagarde, P. Brendle (BETA/ULP), C. Miller, and P. Cohendet (BETA/ULP) Paris ESA Jan. 1981 70 p refs
(Contract ESA-4421/80/F-FC(SC))
(ESA-CR(P)-1457) Avail: NTIS HC A04/MF A01

The METEOSAT concept through its development and well into its expected operational mode, up to 1990 was analyzed. Account was taken of the disturbance introduced by the METEOSAT 1 failure in November 1979, of the delay in the launch of METEOSAT 2, and of the uncertainties arising from the lack of decision, at the end of 1980, on the operational METEOSAT follow-on. Results show important positive economic effects both for the users community (direct benefits) and for the contracting industry concerned (induced benefits). Author (ESA)

N82-14555# European Space Agency, Paris (France).
THE NEED FOR INTEGRATED OFF-SHORE, REAL-TIME INFORMATION AND MANAGEMENT SYSTEMS
L. W. Morley *In its* Appl. of Remote Sensing Data on the Continental Shelf Jul. 1981 p 17-21 refs

Avail: NTIS HC A13/MF A01; ESA, Paris FF 125

Integrated planning, in which data from ships, aircraft, data buoys, and shore or satellite-borne radar are used for ocean surveillance is urged. The Atlantic coast of Canada is used as an example of the inefficiency of current management methods. Traffic control, search and rescue missions, pollution control, weather forecasting, and fisheries management are directed by separate government agencies, each with its own information system. A coordinated approach would reduce waste and allow full advantage to be taken of technological developments, e.g., satellites, unknown when the agencies were created. Author (ESA)

N82-14615# Erno Raumfahrttechnik G.m.b.H., Bremen (West Germany). Abteilung Satelliten und Sonden PRV-1.
STUDY OF A COMBINED SATELLITE SYSTEM FOR REMOTE SENSING AND EARTH-ORIENTED RESEARCH (LOCSS) Final Report, Jul. 1980
HansJuergen Guenther, Wolfgang Gericke, Hansjoerg Klotz, Rainer Krieger, Birgit Metzgar, Joachim Nauck, Klaus Plate, Rudolf Rohr, Gernot Schmidt, and Gerhard Schneider Bonn Bundesministerium fuer Forschung und Technologie Jan. 1981 222 p refs In GERMAN; ENGLISH summary Sponsored by Bundesministerium fuer Forschung und Technologie
(BMFT-FB-W-81-002; ISSN-0170-1339) Avail: NTIS HC A10/MF A01; Fachinformationszentrum, Karlsruhe, West Germany DM 38.60

The suitability of three European satellite platforms (ERDSAT, SPAS, SPOT) for a combined satellite system (remote sensing and Earth-oriented research) is discussed. The system consists of two Sun-synchronous orbiting satellites with a combined remote sensing and Earth-oriented research payload and of a pure climatography satellite on a drift orbit. All platforms can accommodate the basic payload, but SPAS offers some advantages and is the only platform able to accommodate the extended payload. The combined three-satellite system offers cost advantages over the four-satellite system only if the space shuttle is used as launcher. Hence, SPAS should be given preference over the other platforms for such a system. The subsystem design is presented and problem areas are discussed. Data acquisition and data processing of image and climatic data are the bottlenecks in existing systems. Author (ESA)

N82-15496*# Mississippi State Univ., Mississippi State. Remote Sensing Center.

A PROPOSAL FOR CONTINUATION OF SUPPORT FOR THE APPLICATION OF REMOTELY SENSED DATA TO STATE AND REGIONAL PROBLEMS. PART 1: TECHNICAL PROPOSAL

Jun. 1981 114 p ERTS
(Grant NGL-25-001-054)
(E82-10018; NASA-CR-164817) Avail: NTIS HC A06/MF A01 CSCL 05A

The objectives, procedures, accomplishments, plans, and ultimate uses of information from current projects at the Mississippi Remote Sensing Center are discussed for the following applications: (1) land use planning; (2) strip mine inventory and reclamation; (3) biological management for white tailed deer; (4) forest habitats in potential lignite areas; (5) change discrimination in gravel operations; (6) discrimination of freshwater wetlands for inventory and monitoring; and (7) remote sensing data analysis support systems. The initiation of a conceptual design for a LANDSAT based, state wide information system is proposed. A.R.H.

N82-15497# Committee on Science and Technology (U. S. House).

CIVIL LAND REMOTE SENSING SYSTEMS

Washington GPO 1981 370 p Joint hearings before the Subcomm. on Space Sci. and Appl. of the Comm. on Sci. and Technol. and the Subcomm. on Sci., Technol., and Space of the Comm. on Com., Sci., and Transportation, 97th Congr., 1st Sess., No. 40, 22-23 Jul. 1981
(GPO-35-265) Avail: Subcommittee on Space Science and Applications

Steps taken to facilitate NOAA assumption of responsibility for operating LANDSAT D and LANDSAT D prime are reviewed and institutional alternatives for transferring operational responsibility for the program to the private sector are examined. These include: (1) an existing private corporation; (2) a legislatively established for profit private corporation; (3) a government corporation; and (4) Federal agency ownership with private sector operation. The advantages and disadvantages of each of these options are considered as well as user participation. A.R.H.

N82-15499# Cologne Univ. (West Germany). Inst. fuer Geophysik und Meteorologie.

ANALYSIS OF SATELLITE OBSERVATIONS: THEORETICAL STUDIES ON THE SAMPLING PROBLEM [ANALYSE VON SATELLITENBEOBACHTUNGEN - THEORETISCHE UNTERSUCHUNGEN ZUM SAMPLING PROBLEM]

Hans Joachim Preuss 1981 68 p refs In GERMAN; ENGLISH summary
(Mitt-31; ISSN-0069-5882) Avail: NTIS HC A04/MF A01

In a general mission analysis, some orbital and measuring characteristics are simulated and their influence on the sampling investigated. The important role of a satellite with a moderate inclination (approximately 60 deg) is shown; with the drifting orbit homogeneous sampling of diurnal variations and of radiance distributions is possible in a global scale within about 15 days. More complex scan modes (off track, rotary or conical) may improve the angular sampling, especially in case of Sun synchronous satellites, but for studies in small temporal and spatial scales a system with at least three satellites is necessary. The general results are applied on the determination of the radiation balance. By means of models for the diurnal variations and anisotropic behavior, measurements are created and sampling errors demonstrated. Author

SUBJECT INDEX

EARTH RESOURCES / *A Continuing Bibliography (Issue 33)*

APRIL 1982

Typical Subject Index Listing

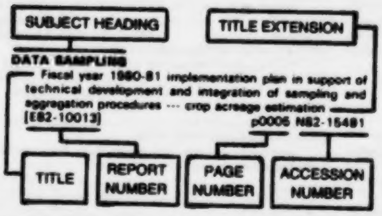
SUBJECT HEADING
TITLE EXTENSION
DATA SAMPLING
Fiscal year 1980-81 implementation plan in support of technical development and integration of sampling and aggregation procedures --- crop acreage estimation
[E82-10013]
p0005 N82-15481
TITLE
REPORT NUMBER
PAGE NUMBER
ACCESSION NUMBER

The subject heading is a key to the subject content of the document. The title is used to provide a description of the subject matter. When the title is insufficiently descriptive of the document content, the title extension is added, separated from the title by three hyphens. The (NASA or AIAA) accession number and the page number are included in each entry to assist the user in locating the abstract in the abstract section (of this supplement). If applicable, a report number is also included as an aid in identifying the document. Under any one subject heading, the accession numbers are arranged in sequence with the AIAA accession numbers appearing first.

A

ACID RAIN
Role of remote sensing in the study of acid rain impact on aquatic systems
[AIAA PAPER 82-0336] p0036 A82-17892
Investigation of the application of remote sensing technology to environmental monitoring
[E82-10010] p0013 N82-15488

ACIDITY
Role of remote sensing in the study of acid rain impact on aquatic systems
[AIAA PAPER 82-0336] p0036 A82-17892

AERIAL PHOTOGRAPHY
Aspects in the development of aerial-photography tasks p0041 A82-12913
Current aerial cameras p0050 A82-15655
Photo inertial positioning system development at the Canada Centre for Remote Sensing p0045 A82-18167

AERIAL RECONNAISSANCE
A history of flying and photography. In the Photogrammetry Division of the National Ocean Survey 1919 - 1979
[PB81-246738] p0017 N82-15520

AEROSOLS
Study of stack emissions by combination of lidar and correlation spectrometer p0006 A82-12816
Radiative heating rates and some optical properties of the St. Louis aerosol, as inferred from aircraft measurements p0008 A82-14320
Results from the July 1981 Workshop on Passive Remote Sensing of the Troposphere
[AIAA PAPER 82-0207] p0009 A82-17841

AEROSPACE TECHNOLOGY TRANSFER
Civil land remote sensing systems
[GPO-35-265] p0056 N82-15497

AFRICA
Skylab 4 observations of Volcanoes. Part A: Volcanoes and volcanic landforms. Part B: Summit eruption of Fernandian Caldera, Galapagos Islands, Ecuador p0020 N82-12496
Vegetation patterns p0004 N82-12500
Report on Skylab 4 African drought and arid land experiment p0037 N82-12501
Necessity of remote sensing for ocean studies. Part 1: Northwest African missions, Sahara-1 and Atlor-1 --- sea truth/remote sensing correlation of offshore upwelling p0032 N82-14582
The mineralogy of global magnetic anomalies
[E82-10009] p0021 N82-15487

AGRICULTURE
Remote sensing techniques in the study of the agricultural potential of soils under the Cerrado vegetation /Brazil/ p0001 A82-10040
Remote sensing contributions to the management of renewable resources p0055 A82-12530
Study and mapping of agricultural land use, based on space images p0003 A82-15963
Rural development in the humid tropics p0003 A82-16162
Cultural features imaged and observed from Skylab 4 p0010 N82-12499
Application of remote sensing to selected problems within the state of California
[E82-10004] p0004 N82-15482

AGROCLIMATOLOGY
Wheat cultivation: Identification and estimation of areas using LANDSAT data
[E82-10007] p0004 N82-15485

AGROMETEOROLOGY
Winterkill indicator model. Crop Condition Assessment Division (CCAD) data base interface driver, user's manual
[E82-10014] p0005 N82-15492

AIR LAND INTERACTIONS
Thermal inertia, thermal admittance, and the effect of layers p0008 A82-15027

AIR POLLUTION
Trace pollutant concentrations in a multiday smog episode in the California South Coast Air Basin by long path length Fourier transform infrared spectroscopy p0007 A82-10700
Spacelab-research of European regions with strong negative environmental influences, based on AVHRR-data of the satellites Tiros-N and NOAA p0007 A82-12517
Study of stack emissions by combination of lidar and correlation spectrometer p0006 A82-12816
Radiative heating rates and some optical properties of the St. Louis aerosol, as inferred from aircraft measurements p0008 A82-14320
Results from the July 1981 Workshop on Passive Remote Sensing of the Troposphere
[AIAA PAPER 82-0207] p0009 A82-17841
Proof of concept study
[AD-A104338] p0010 N82-11639
Quantitative analysis of atmospheric pollution phenomena p0010 N82-12505

AIR QUALITY
Shuttle applications in tropospheric air quality observations
[NASA-CR-145374] p0010 N82-11635
Aircraft data summaries of the SURE intensives, volume 4
[DE82-900311] p0012 N82-13569

AIR SAMPLING
Automated analyzer for aircraft measurements of atmospheric methane and total hydrocarbons p0007 A82-11949

AIR WATER INTERACTIONS
Analysis of SEASAT wind observations over the Indian Ocean p0023 A82-10671
Annual and nonseasonal variability of monthly low-level wind fields over the Southeastern Tropical Pacific p0025 A82-17494
Variations in upper ocean heat storage determined from satellite data p0025 A82-17567
Anomalous wind estimates from the Seasat scatterometer p0026 A82-18724
Meteorological lab applications of Skylab handheld-camera photographs p0011 N82-12506
Determination of surface wind speed from remotely measured whitecap coverage, a feasibility assessment p0030 N82-14565
The Norwegian remote sensing experiment (Norsex) in a marginal ice zone p0031 N82-14566
A preliminary evaluation of Seasat performance over the area of JASIN and its relevance to ERS-1 p0031 N82-14567
Project Noordwijk. Part 1: Measurements of the radar backscatter coefficient gamma (sigma deg) in 1977 and 1978 --- on a sea platform
[PHL-1979-49-PT-1] p0032 N82-14617
Project Noordwijk. Part 2: Results of North Sea clutter measurements in the I-band performed from the platform Noordwijk in September/October 1977
[PHL-1980-28-PT-2] p0033 N82-14618
Meteorological and oceanographic observations on board Netherlands lightvessels and the lightplatform 'Goeree' in the North Sea
[KNMI-141-28] p0033 N82-15684

AIR WATER INTERACTIONS GREAT LAKES (US)
Mesoscale cloud features observed from Skylab p0011 N82-12509

AIRSPEED
The application of programmable pocket calculators for computations during survey flights p0050 A82-16164

ALASKA
Application of satellite Doppler techniques to the national mapping program p0015 A82-10056
Bureau of Land Management satellite Doppler positioning techniques p0015 A82-10057
Geophysical monitoring for climatic change, number 8: Summary Report, 1979
[PB81-233355] p0012 N82-13631

ALBEDO
The near-infrared radiation received by satellites from clouds p0025 A82-17492
Use of environmental satellite data for input to energy balance snowmelt models
[PB81-227795] p0039 N82-15673

ALGAE
Remote sensing that motivated community action p0008 A82-12594
Remote sensing of benthic microalgal biomass with a tower-mounted multispectral scanner p0024 A82-15031

ALGORITHMS
Analysis of soil moisture extraction algorithm using data from aircraft experiments
[NASA-CR-166719] p0046 N82-13470

ALIGNMENT
MAGSAT: Vector magnetometer absolute sensor alignment determination
[NASA-TM-79648] p0051 N82-10468

ALTIMETERS
Seasat altimetry adjustment model including tidal and other sea surface effects
[AD-A104188] p0026 N82-10473
Ionospheric propagation correction modeling for satellite altimeters
[NASA-CR-156881] p0052 N82-12447

AMAZON REGION (SOUTH AMERICA)
Remote sensing in forestry: Application to the Amazon region
[E82-10012] p0005 N82-15490

ANGULAR RESOLUTION
The effect of angular factors on popularly used indicators of vegetative vigor p0001 A82-10039

ANNUAL VARIATIONS
Annual and nonseasonal variability of monthly low-level wind fields over the Southeastern Tropical Pacific p0025 A82-17494

ANTARCTIC REGIONS
Geophysical monitoring for climatic change, number 8: Summary Report, 1979
[PB81-233355] p0012 N82-13631

ANTENNA RADIATION PATTERNS
Additional studies of Earth resources synthetic aperture radar payloads
[MTR-80/90] p0054 N82-15500
New baseline system p0054 N82-15501
Squinted SAR system p0047 N82-15502

ARABIAN SEA
Detection of monsoon inversion by TIROS-N satellite p0024 A82-17168

ARCHAEOLOGY
Radar mapping, archaeology, and ancient land use in the Maya lowlands
[NASA-CR-164931] p0010 N82-11514

ARCTIC OCEAN
The ice-conditions in the Greenland waters, 1965. Coastal maps
[ISBN-87-7478-183-9] p0028 N82-10467
The ice conditions in the Greenland waters
[ISBN-87-7478-183-9] p0028 N82-12533
The Norwegian remote sensing experiment (Norsex) in a marginal ice zone p0031 N82-14566
Measurements of radar backscatter from Arctic Sea ice in the summer
[AD-A105586] p0032 N82-14592
Measurements of radar backscatter from Arctic Sea ice in the summer. Appendices A and B
[AD-A105736] p0032 N82-14593

ARGENTINA
Vegetation patterns p0004 N82-12500

ARID LANDS
Satellite sensing of irrigation patterns in semiarid areas An Indian study p0002 A82-10864
Space photographs obtained with the Fragment system as a base for landscape mapping and physical-geographical classification of arid territories p0009 A82-15967
Report on Skylab 4 African drought and arid land experiment p0037 N82-12501

ARIZONA
Geological features of southwestern North America p0020 N82-12495
Meteorological lab applications of Skylab handheld-camera photographs p0011 N82-12506

ASTRONOMICAL COORDINATES
Coordinates of features on the Galilean satellites p0019 A82-12366

ATLANTIC OCEAN
An investigation of a polar low with a spiral cloud structure p0007 A82-10616
Synoptic thermal and oceanographic parameter distributions in the New York Bight Apex p0023 A82-12885
Comparison of polar and geostationary satellite infrared observations of sea surface temperatures in the Gulf of Maine p0024 A82-15030
Upper tropospheric cyclonic vortices in the tropical South Atlantic p0009 A82-16325
Global satellite measurements of water vapour, wind speed and wave height p0051 A82-17165
Remote sensing of the Chesapeake Bay plume salinity via microwave radiometry p0027 N82-10670
Preliminary analysis of ocean color scanner data from Superflux III p0027 N82-10672
Analysis of testbed airborne multispectral scanner data from Superflux II --- Chesapeake Bay plume and James Shelf data p0027 N82-10682
An assessment of the potential contributions to oceanography from Skylab visual observations and handheld-camera photographs p0028 N82-12503
Meteorological lab applications of Skylab handheld-camera photographs p0011 N82-12506
The need for integrated off-shore, real-time information and management systems p0055 N82-14555
An evaluation of Seasat-A data in relation to optimum track ship weather routing and site specific forecasting for the offshore oil industry p0030 N82-14564
A short review of an oceanographic use of Meteosat data by the ORSTOM remote sensing service p0031 N82-14570
Necessity of remote sensing for ocean studies. Part 1: Northwest African missions, Sahara-1 and Atlor-1 --- sea truth/remote sensing correlation of offshore upwelling p0032 N82-14582

ATLANTIC OCEAN PACIFIC OCEAN
Availability of Seasat synthetic aperture radar imagery p0050 A82-15039

ATMOSPHERIC ATTENUATION
Water vapour absorption in the 3.5-4.2 micron atmospheric window p0023 A82-14586
The radiowave propagation environment - Science and technology objectives for the 80's p0009 A82-18052

ATMOSPHERIC CHEMISTRY
Trace pollutant concentrations in a multiday smog episode in the California South Coast Air Basin by long path length Fourier transform infrared spectroscopy p0007 A82-10700
Automated analyzer for aircraft measurements of atmospheric methane and total hydrocarbons p0007 A82-11949
Results from the July 1981 Workshop on Passive Remote Sensing of the Troposphere
[AIAA PAPER 82-0207] p0009 A82-17841

ATMOSPHERIC CIRCULATION
An investigation of a polar low with a spiral cloud structure p0007 A82-10616

ATMOSPHERIC MODELS
Ionospheric propagation correction modeling for satellite altimeters
[NASA-CR-156881] p0052 N82-12447

ATMOSPHERIC MOISTURE
Global satellite measurements of water vapour, wind speed and wave height p0051 A82-17165
Scientific studies using Bhaskara satellite microwave radiometer (SAMIR) data: A short overview --- calibration of the instrument and its use in the study of oceanographic parameters p0032 N82-14587
Sensitivity analysis of a mesoscale moisture model
[AD-A101528] p0012 N82-14590

ATMOSPHERIC OPTICS
Radiative heating rates and some optical properties of the St. Louis aerosol, as inferred from aircraft measurements p0008 A82-14320
Spectral atmospheric observations at Nantucket Island, May 7-14, 1981
[NASA-TM-83196] p0029 N82-14550

ATMOSPHERIC PRESSURE
Oceanic wind and balanced pressure-height fields derived from satellite measurements p0023 A82-13214

ATMOSPHERIC RADIATION
Estimation of atmospheric path-radiance by the covariance matrix method p0041 A82-10861
The influence of gravity waves on radiometric measurements - A case study p0049 A82-13547
Environmental Monitoring Report, Sandia National Labs., Albuquerque, New Mexico, 180
[DE81-027839] p0010 N82-11649

ATMOSPHERIC SCATTERING
Calculation of the decrease in the contrast of objects of a place due to light scattering in the atmosphere p0042 A82-13633

ATMOSPHERIC SOUNDING
Repeatability and measurement uncertainty of the United States meteorological rocketsonde p0049 A82-12127
Microwave limb sounder --- measuring trace gases in the upper atmosphere
[NASA-CASE-NPO-14544-1] p0011 N82-12685

ATMOSPHERIC TEMPERATURE
Repeatability and measurement uncertainty of the United States meteorological rocketsonde p0049 A82-12127
Thermal inertia, thermal admittance, and the effect of layers p0008 A82-15027

AURORAL ZONES
Characteristics of westward travelling surges during magnetospheric substorms p0050 A82-14299

AUSTRALIA
Use of visible and thermal satellite data to monitor an intermittently flooding marshland p0036 A82-15037
Compensation of systematic errors of image and model coordinates p0043 A82-15765
Vegetation patterns p0004 N82-12500

B

BACKSCATTERING
A theory of wave scattering from an inhomogeneous layer with an irregular interface p0041 A82-12757
Radar backscattering from ocean waves at low grazing angles p0023 A82-14730
The surface albedo of the earth in the near ultraviolet /330-340 nm/ p0016 A82-15032
Measurement of sea and ice backscatter reflectivity using an OTH radar system p0025 A82-18074
Evaluation of the Seasat wind scatterometer p0025 A82-18716
Anomalous wind estimates from the Seasat scatterometer p0026 A82-18724
Progress in radar snow research --- Brookings, South Dakota
[NASA-CR-166709] p0038 N82-12510
State-of-the-art in using a spaceborne altimeter and scatterometer for the determination of wind, sea state, and marine and ice dynamics --- Seasat instruments p0052 N82-14560
Measurements of radar backscatter from Arctic Sea ice in the summer, Appendices A and B
[AD-A105736] p0032 N82-14593
Project Noordwijk. Part 1: Measurements of the radar backscatter coefficient gamma (sigma deg) in 1977 and 1978 --- on a sea platform
[PHL-1979-49-PT-1] p0032 N82-14617

BALTIC SEA
Maritime applications of image processing at DFVLR, Oberpfaffenhofen, West Germany --- LANDSAT multispectral scanner images, digital interactive image analysis p0032 N82-14585

BARLEY
US/Canada wheat and barley crop calender exploratory experiment implementation plan
[E82-10016] p0005 N82-15494

BAYS (TOPOGRAPHIC FEATURES)
Field study for Landsat water quality verification p0036 A82-12597
Synoptic thermal and oceanographic parameter distributions in the New York Bight Apex p0023 A82-12885
Visual observations of floating ice from Skylab p0037 N82-12504

BEACHES
A method for using aerial photos in delineating historic patterns of beach accretion and retreat
[PB81-223836] p0010 N82-11536

BEARING (DIRECTION)
Three bearing method for passive triangulation in systems with unknown deterministic biases p0050 A82-15920

BERING SEA
Ice conditions in the eastern Bering Sea from NOAA and LANDSAT imagery: Winter conditions 1974, 1976, 1977, 1979
[PB81-220188] p0028 N82-11537

BIAS
Three bearing method for passive triangulation in systems with unknown deterministic biases p0050 A82-15920

BIBLIOGRAPHIES
Report on Active and Planned Spacecraft and experiments
[NASA-TM-84025] p0056 N82-10087

BIOMASS
Remote sensing of benthic microalgal biomass with a tower-mounted multispectral scanner p0024 A82-15031
Biological patchiness in relation to satellite thermal imagery and associated chemical mesoscale features
[AD-A105757] p0047 N82-15504

BIRDS
Remote sensing applications to resource problems in South Dakota
[E82-10002] p0004 N82-15481

BLIGHT
Evaluation of digital photographic enhancement for Dutch elm disease detection p0002 A82-12884

BLUE GREEN ALGAE
Maritime applications of image processing at DFVLR, Oberpfaffenhofen, West Germany --- LANDSAT multispectral scanner images, digital interactive image analysis p0032 N82-14585

BRAZIL
Remote sensing techniques in the study of the agricultural potential of soils under the Carrado vegetation /Brazil/ p0001 A82-10040
Wheat cultivation: Identification and estimation of areas using LANDSAT data
[E82-10007] p0004 N82-15485
Quantitative analysis of drainage obtained from aerial photographs and RBV/LANDSAT images
[E82-10008] p0039 N82-15486
Remote sensing in forestry: Application to the Amazon region
[E82-10012] p0006 N82-15490

BRIGHTNESS
Metrological support of measurements of earth-surface brightness by the Fragment multispectral scanning system p0050 A82-15958

BRIGHTNESS DISCRIMINATION
Multitemporal calibration of LANDSAT images: A method for improving the marine phenomena recognition, with as example the Venice lagoon --- brightness/green/yellow feature space, image enhancement p0046 N82-14578

BRIGHTNESS DISTRIBUTION
Estimation of the brightness field from results of multispectral photography of the earth from space p0044 A82-16617
Programs for the statistical analysis of multispectral photographs p0044 A82-16628

BRIGHTNESS TEMPERATURE
A comparison of radiative transfer models for predicting the microwave emission from soils p0035 A82-10694
Water vapour absorption in the 3.5-4.2 micron atmospheric window p0023 A82-14586
Remote sensing of the Chesapeake Bay plume salinity via microwave radiometry p0027 N82-10670
SMMR data set development for GARP --- impact of cross polarization and Faraday rotation on SMMR derived brightness temperatures
[NASA-CR-166721] p0052 N82-11512
Limit on remote FTIR detection of trace gases
[AD-A104842] p0011 N82-12511
Determination of surface wind speed from remotely measured whitecap coverage, a feasibility assessment p0030 N82-14565

BUOYS
GEM: A simple meteorological buoy with satellite telemetry p0053 N82-14779

C

CALCULATORS
The application of programmable pocket calculators for computations during survey flights p0050 A82-16164

CALDERAS
Skylab 4 observations of Volcanoes. Part A: Volcanoes and volcanic landforms. Part B: Summit eruption of Fernandian Caldera, Galapagos Islands, Ecuador p0020 N82-12496

CALIBRATING
Aspects in the development of aerial-photography tasks p0041 A82-12913
A new method for computing distortion p0016 A82-12914
Intercalibration of Landsat 1-3 and NOAA 6 and 7 scanner data p0049 A82-13293
Compensation of systematic errors of image and model coordinates p0043 A82-15765
Main results of the Raduga experiment p0051 A82-16602
Geometric quality of MKF-6 photographs p0043 A82-16606
Characteristics of the photometry of small objects from aerial and space photographs p0044 A82-16616
Measurement of sea and ice backscatter reflectivity using an OTH radar system p0025 A82-18074
Study on calibration methods for Earth observation optical imaging instruments
[UCD-207/1/80] p0052 N82-10488
Infrared radiance model variation by sensor flight measurements p0052 N82-14171
Coastal zone research using remote sensing techniques --- calibration of coastal zone color scanner p0031 N82-14571

CALIFORNIA
Spectral behavior of wheat yield variety trials p0002 A82-10863
Landsat imagery for hydrologic modeling p0036 A82-12592
Identification of conifer species groupings from Landsat digital classifications p0002 A82-12887
The use of satellite infrared imagery for describing ocean processes in relation to spawning of the northern anchovy /Engraulis mordax/ p0025 A82-17565
Geological features of southwestern North America p0020 N82-12495
Vegetation patterns p0004 N82-12500
Application of remote sensing to selected problems within the state of California
[E82-10004] p0004 N82-15482

CAMERAS
A new method for computing distortion p0016 A82-12914
Current aerial cameras p0050 A82-15655

A history of flying and photography: In the Photogrammetry Division of the National Ocean Survey 1919 - 1979
[PB81-246738] p0017 N82-15520

CANADA

The Manicouagan impact structure observed from Skylab
[CONTRIB-544] p0020 N82-12497

The need for integrated off-shore, real-time information and management systems p0055 N82-14555

The reduction, verification and interpretation of Magsat magnetic data over Canada
[E82-10006] p0046 N82-15484

US/Canada wheat and barley crop calender exploratory experiment implementation plan
[E82-10016] p0005 N82-15494

CANOPIES (VEGETATION)

An improvement in land cover classification achieved by merging microwave data with Landsat multispectral scanner data p0007 A82-10043

Stand density estimation on panoramic transparencies p0002 A82-10862

Spectral behavior of wheat yield variety trials p0002 A82-10863

Temporal spectral response of a corn canopy p0002 A82-12886

Temporal relationships between spectral response and agronomic variables of a corn canopy p0002 A82-15038

In situ spectral reflectance studies of tidal wetland grasses p0036 A82-15969

Inclusion of a simple vegetation layer in terrain temperature models for thermal infrared (IR) signature prediction
[AD-A104469] p0003 N82-11910

CARBON MONOXIDE

A new method for inferring carbon monoxide concentrations from gas filter radiometer data p0009 A82-16837

CENTRAL AMERICA

Availability of Seasat synthetic aperture radar imagery p0050 A82-15039

Radar mapping, archaeology, and ancient land use in the Maya lowlands
[NASA-CR-164931] p0010 N82-11514

CENTRAL PROCESSING UNITS

ERSYS-SPP access method subsystem design specification
[E82-10015] p0053 N82-15493

CHESAPEAKE BAY (US)

Chesapeake Bay Plume Study: Superflux 1980
[NASA-CP-2188] p0026 N82-10661

Superflux I, II, and III experiment design: Remote sensing aspects p0027 N82-10664

Superflux I, II, and III experiment designs: Water sampling and analyses --- Chespeake Bay, environmental monitoring and remote sensing p0027 N82-10665

Monitoring the Chesapeake Bay using satellite data for Superflux III p0027 N82-10668

Remote sensing of the Chesapeake Bay plume salinity via microwave radiometry p0027 N82-10670

Preliminary analysis of ocean color scanner data from Superflux III p0027 N82-10672

Analysis of testbed airborne multispectral scanner data from Superflux II --- Chesapeake Bay plume and James Shelf data p0027 N82-10682

Application of the NASA airborne oceanographic lidar to the mapping of chlorophyll and other organic pigments p0027 N82-10684

Assessment of Superflux relative to remote sensing --- airborne remote sensing of the Chesapeake Bay plume and shelf regions p0028 N82-10694

CHILE

Global Tectonics: Some Geologic analyses of observations and photographs from Skylab p0020 N82-12494

CHLOROPHYLLS

Synoptic thermal and oceanographic parameter distributions in the New York Bight Apex p0023 A82-12885

Remote sensing of benthic microalgal biomass with a tower-mounted multispectral scanner p0024 A82-15031

Temporal relationships between spectral response and agronomic variables of a corn canopy p0002 A82-15038

Role of remote sensing in the study of acid rain impact on aquatic systems
[AIAA PAPER 82-0336] p0036 A82-17892

Application of the NASA airborne oceanographic lidar to the mapping of chlorophyll and other organic pigments p0027 N82-10684

Assessment of Superflux relative to remote sensing --- airborne remote sensing of the Chesapeake Bay plume and shelf regions p0028 N82-10694

Development of the coastal zone color scanner for NIMBUS 7. Volume 1: Mission objectives and instrument description
[NASA-CR-166720-VOL-1] p0028 N82-11511

The color of the sea and its relation to surface chlorophyll and depth of the euphotic zone p0030 N82-14562

Coastal zone research using remote sensing techniques --- calibration of coastal zone color scanner p0031 N82-14571

Recent work in passive optical imaging of water --- space and aircraft derived data p0038 N82-14575

The feasibility of using remotely sensed color as an index of Irish coastal water properties --- statistical correlation of sea truth data p0032 N82-14581

Necessity of remote sensing for ocean studies. Part 1: Northwest African missions, Sahara-1 and Atlor-1 --- sea truth/remote sensing correlation of offshore upwelling p0032 N82-14582

CITIES

Cultural features imaged and observed from Skylab 4 p0010 N82-12499

CLASSIFICATIONS

Phytoecozonation of Sevier Lake region of Utah using digitized Landsat MSS data p0001 A82-10042

An improvement in land cover classification achieved by merging microwave data with Landsat multispectral scanner data p0007 A82-10043

Spectrometric studies of the earth's surface p0043 A82-16612

The maximum mean accuracy of classification of remote-sensing objects and the influence on this accuracy of data acquisition and processing methods p0044 A82-16615

Fiscal year 1980-81 implementation plan in support of technical development and integration of sampling and aggregation procedures --- crop acreage estimation
[E82-10013] p0005 N82-15491

CLIMATOLOGY

Upper tropospheric cyclonic vortices in the tropical South Atlantic p0009 A82-16325

CTD/02 measurements during the Equatorial Pacific Ocean Climate Study (EPOCS) in 1979
[PB81-211203] p0026 N82-10461

Study on satellite radar altimetry in climatological and oceanographic research, volume 1
[SP/153/06/01/FR(80)-VOL-1] p0026 N82-10486

Study on satellite radar altimetry in climatological and oceanographic research, volume 2
[SP/153/06/01FR(80)-VOL-2] p0026 N82-10487

Geophysical monitoring for climatic change, number 8: Summary Report, 1979
[PB81-233355] p0012 N82-13631

Environmental satellite imagery, March 1981
[PB81-248049] p0047 N82-15698

CLOUD COVER

The near-infrared radiation received by satellites from clouds p0025 A82-17492

CLOUD PHOTOGRAPHY

An investigation of a polar low with a spiral cloud structure p0007 A82-10616

Meteorological lab applications of Skylab handheld-camera photographs p0011 N82-12506

Some aspects of tropical storm structure revealed by handheld-camera photographs from space p0011 N82-12507

Mesoscale wake clouds in Skylab photographs p0011 N82-12508

Mesoscale cloud features observed from Skylab p0011 N82-12509

CLOUDS

Limit on remote FTIR detection of trace gases
[AD-A104842] p0011 N82-12511

COASTAL CURRENTS

Operational use of remote sensing for coastal zone management and possible contribution of specialized satellites --- aerial photography p0031 N82-14574

Mapping of surface currents in Greenland fiords by means of LANDSAT images --- multispectral photography p0038 N82-14579

Necessity of remote sensing for ocean studies. Part 1: Northwest African missions, Sahara-1 and Atlor-1 --- sea truth/remote sensing correlation of offshore upwelling p0032 N82-14582

COASTAL ECOLOGY

Data sources for analyses of Great Lakes wetlands p0035 A82-10054

A marine environmental monitoring and assessment program p0027 N82-10663

A method for using aerial photos in delineating historic patterns of beach accretion and retreat
[PB81-223836] p0010 N82-11536

Requirements in pollution monitoring and coastal management p0030 N82-14558

Studies of the Indian continental shelf: Application of remote sensing data p0031 N82-14569

Operational use of remote sensing for coastal zone management and possible contribution of specialized satellites --- aerial photography p0031 N82-14574

COASTAL WATER

Satellite imagery and shoreline erosion prediction p0036 A82-12595

Clear water radiances for atmospheric correction of coastal zone color scanner imagery p0025 A82-17292

The use of satellite infrared imagery for describing ocean processes in relation to spawning of the northern anchovy /Engraulis mordax/ p0025 A82-17565

An inertially-aided aircraft track recovery system for coastal mapping p0037 A82-18166

The ice-conditions in the Greenland waters, 1965. Coastal maps
[ISBN-87-7478-183-9] p0026 N82-10467

Analysis of testbed airborne multispectral scanner data from Superflux II --- Chesapeake Bay plume and James Shelf data p0027 N82-10682

The need for integrated off-shore, real-time information and management systems p0055 N82-14555

The color of the sea and its relation to surface chlorophyll and depth of the euphotic zone p0030 N82-14562

SPOT data simulations: Littoral applications p0046 N82-14568

A short review of an oceanographic use of Meteosat data by the ORSTOM remote sensing service p0031 N82-14570

Coastal zone research using remote sensing techniques --- calibration of coastal zone color scanner p0031 N82-14571

Marine activities in Sweden for which remote sensing data may be of interest --- oceanography, weather forecasting, and analysis p0031 N82-14576

Airborne remote sensing of the coastal zone p0053 N82-14577

The use of LANDSAT MSS to observe sediment distribution and movement in the Solent coastal area --- multispectral scannel (MSS) p0038 N82-14580

The feasibility of using remotely sensed color as an index of Irish coastal water properties --- statistical correlation of sea truth data p0032 N82-14581

Use of Side Looking Airborne Radar (SLAR) for oil pollution monitoring in Norway p0012 N82-14588

COASTAL ZONE COLOR SCANNER

Clear water radiances for atmospheric correction of coastal zone color scanner imagery p0025 A82-17292

Development of the coastal zone color scanner for NIMBUS 7. Volume 1: Mission objectives and instrument description
[NASA-CR-166720-VOL-1] p0028 N82-11511

Coastal zone research using remote sensing techniques --- calibration of coastal zone color scanner p0031 N82-14571

COASTS

Remote sensing contributions to the management of renewable resources p0055 A82-12530

Development of a coastal relief of the Gulf of Riga, based on results of an analysis of space images p0024 A82-15962

Application of remote sensing data on the continental shelf: Proceedings of an EARsL-ESA Symposium
[ESA-SP-167] p0029 N82-14553

COLOR CODING

Spectral correlation filters and natural colour coding p0043 A82-16160

COLOR INFRARED PHOTOGRAPHY

Areawide soil loss predictions using CIR airphotos p0007 A82-12591

COLOR TELEVISION

The 1981 RCA space constellation p0055 A82-12541

COLORADO

Preliminary results of mapping urban land cover with Seasat SAR imagery p0007 A82-10044

COLORADO PLATEAU (US)

Morphostructural analyses of space imagery in the central Colorado Plateau p0019 N82-10465

Geological features of southwestern North America p0020 N82-12495

COMPUTER GRAPHICS

Digital image technology - MC&G impact --- Mapping, Charting, & Geodesy p0015 A82-10028

Applications of digital displays in photointerpretation and digital mapping p0041 A82-10038

Digitizing and automated output mapping errors p0015 A82-10859

Interactive techniques for estimating precipitation from GOES imagery p0041 A82-13121

Small-scale terrain mapping based on numerical interpretation of LANDSAT imagery
[VTT-40] p0045 N82-10485

COMPUTER PROGRAMS

Compensation of systematic errors in bundle adjustment p0042 A82-15764

The application of programmable pocket calculators for computations during survey flights p0050 A82-16164

Programs for the statistical analysis of multispectral photographs p0044 A82-16628

Onboard utilization of ground control points for image correction. Volume 3: Ground control point simulation software design
[NASA-CR-166733] p0045 N82-10471

Onboard utilization of ground control points for image correction. Volume 4: Correlation analysis software design
[NASA-CR-166734] p0045 N82-10472

Magnetic Field Satellite (Magsat) data processing system specifications
[NASA-CR-166737] p0045 N82-11103

COMPUTER SYSTEMS DESIGN

ERSYS-SPP access method subsystem design specification
[E82-10015] p0053 N82-15493

COMPUTER TECHNIQUES

Mapping of the 1978 Kentucky River Flood from NOAA-5 satellite thermal infrared data p0035 A82-10033

Water temperature mapping by infrared scanner p0036 A82-12598

Identification of conifer species groupings from Landsat digital classifications p0002 A82-12887
A new method for computing distortion p0016 A82-12914
Cost effective computer processing of airborne scanner data for regional level mapping p0043 A82-15970
Analog methods for processing multispectral photographs p0044 A82-16623
Processing of multispectral image data on special-purpose computer systems p0044 A82-16627

COMPUTERIZED SIMULATION
SPOT data simulations: Littoral applications p0046 N82-14568

CONFERENCES
American Society of Photogrammetry, Annual Meeting, 46th, St Louis, MO, March 9-14, 1980, ASP Technical Papers p0041 A82-10027
Civil engineering applications of remote sensing; Proceedings of the Specialty Conference, University of Wisconsin, Madison, WI, August 13, 14, 1980 p0035 A82-12589
Chesapeake Bay Plume Study: Superflux 1980 [NASA-CP-2188] p0026 N82-10661
Application of remote sensing data on the continental shelf: Proceedings of an EARsL-ESA Symposium [ESA-SP-167] p0029 N82-14553

CONGRESSIONAL REPORTS
Civil land remote sensing systems [GPO-35-265] p0056 N82-15497

CONIFERS
Identification of conifer species groupings from Landsat digital classifications p0002 A82-12887

CONTINENTAL SHELVES
Analysis of testbed airborne multispectral scanner data from Superflux II --- Chesapeake Bay plume and James Shelf data p0027 N82-10682
Assessment of Superflux relative to remote sensing --- airborne remote sensing of the Chesapeake Bay plume and shelf regions p0028 N82-10694
Application of remote sensing data on the continental shelf: Proceedings of an EARsL-ESA Symposium [ESA-SP-167] p0029 N82-14553
Studies of the Indian continental shelf: Application of remote sensing data p0031 N82-14569

COORDINATE TRANSFORMATIONS
Coordinate referencing of MKF-6 photographs and their transformation to the cartographic projection p0045 A82-16630

COORDINATES
MAGSAT: Vector magnetometer absolute sensor alignment determination [NASA-TM-79648] p0051 N82-10468

CORN
Temporal spectral response of a corn canopy p0002 A82-12886
Temporal relationships between spectral response and agronomic variables of a corn canopy p0002 A82-15038
Remote sensing of crop moisture status p0003 A82-17997

COST EFFECTIVENESS
Landsat imagery for hydrologic modeling p0036 A82-12592

COVARIANCE
Estimation of atmospheric path-radiance by the covariance matrix method p0041 A82-10861

CROP CALENDARS
Development and evaluation of an automatic labeling technique for spring small grains [E82-10001] p0004 N82-15480
US/Canada wheat and barley crop calender exploratory experiment implementation plan [E82-10016] p0005 N82-15494

CROP GROWTH
Spectral behavior of wheat yield variety trials p0002 A82-10863
The discrimination of winter wheat using a growth-state signature p0002 A82-15026

CROP IDENTIFICATION
Limitations in the spectral discrimination of the Landsat MSS p0001 A82-10046
Temporal spectral response of a corn canopy p0002 A82-12886
Methods of instrumental interpretation of multispectral aerial and space photographs p0043 A82-16607

CROP INVENTORIES
Remote sensing for vineyard management p0001 A82-10047
Temporal relationships between spectral response and agronomic variables of a corn canopy p0002 A82-15038
Development and evaluation of an automatic labeling technique for spring small grains [E82-10001] p0004 N82-15480
Wheat cultivation: Identification and estimation of areas using LANDSAT data [E82-10007] p0004 N82-15485
Fiscal year 1980-81 implementation plan in support of technical development and integration of sampling and aggregation procedures --- crop acreage estimation [E82-10013] p0005 N82-15491

CROP VIGOR
The effect of angular factors on popularly used indicators of vegetative vigor p0001 A82-10039
Remote sensing for vineyard management p0001 A82-10047
Remote sensing of crop moisture status p0003 A82-17997
Winterkill indicator model. Crop Condition Assessment Division (CCAD) data base interface driver, user's manual [E82-10014] p0005 N82-15492

CROSS POLARIZATION
SMMR data set development for GARP --- impact of cross polarization and Faraday rotation on SMMR derived brightness temperatures [NASA-CR-166721] p0052 N82-11512
Radar correlation with ice depolarization measurements of the 28.56 GHz COMSTAR beacon and associated cross polarization statistics [NASA-CR-166717] p0046 N82-14548

CRUSTAL FRACTURES
Remote sensing study of sinkhole occurrence p0019 A82-12590
Morphostructural analyses of space imagery in the central Colorado Plateau p0019 N82-10465

CURRENT SHEETS
Distant magnetic field effects associated with Birkeland currents /made possible by the evaluation of TRIAD's attitude oscillations/ p0015 A82-12215

CYCLONES
An investigation of a polar low with a spiral cloud structure p0007 A82-10616
Upper tropospheric cyclonic vortices in the tropical South Atlantic p0009 A82-16325
Meteorological lab applications of Skylab handheld-camera photographs p0011 N82-12506

D

DAMS
Application of Landsat to the inventory of DAMS p0036 A82-12593

DATA ACQUISITION
LANDSAT-2 and LANDSAT-3 flight evaluation report, 23 April to 23 July 1979 [E82-10005] p0053 N82-15483
LANDSAT-2 and LANDSAT-3 flight evaluation report, 23 October 1978 to 23 January 1979 [E82-10017] p0054 N82-15495

DATA BASES
The SACLANTCEN oceanographic data base. Volume 1: Design criteria and data structure and content [AD-A103277] p0029 N82-13639

DATA COMPRESSION
Data compression and reconstruction for mixed resolution multispectral sensors p0049 A82-10045

DATA CORRELATION
Factorial analysis of terrain feature positioning parameters used in combining radar and digital terrain model data p0015 A82-10029
A digital fast correlation approach to produce SEASAT SAR imagery p0042 A82-14870
Interpolating for the location of remote sensor data [NASA-TM-82169] p0052 N82-13469

DATA PROCESSING
U.S. Navy planning for satellite oceanographic data exploitation [AAS 81-072] p0024 A82-16341
Magnetic Field Satellite (Magsat) data processing system specifications [NASA-CR-166737] p0045 N82-11103
Analysis of soil moisture extraction algorithm using data from aircraft experiments [NASA-CR-166719] p0046 N82-13470
Development and evaluation of an automatic labeling technique for spring small grains [E82-10001] p0004 N82-15480
ERSYS-SPP access method subsystem design specification [E82-10015] p0053 N82-15493

DATA PROCESSING EQUIPMENT
MATE VAN: Mobile analysis and training extension --- analyzing LANDSAT digital data [NASA-TM-84056] p0045 N82-10466

DATA REDUCTION
Bureau of Land Management satellite Doppler positioning techniques p0015 A82-10057
A closer examination of the reduction of satellite magnetometer data for geological studies p0019 A82-11039
A new method for inferring carbon monoxide concentrations from gas filter radiometer data p0009 A82-16837
MATE VAN: Mobile analysis and training extension --- analyzing LANDSAT digital data [NASA-TM-84056] p0045 N82-10466
Seasat altimetry adjustment model including tidal and other sea surface effects [AD-A104188] p0026 N82-10473
Statistical Techniques Applied to Aerial Radiometric Surveys (STAARS): Series introduction and the principal-components-analysis method --- National Uranium Resource Evaluation Program [DE81-029177] p0019 N82-10476
The reduction, verification and interpretation of Magsat magnetic data over Canada [E82-10006] p0046 N82-15484

DATA SAMPLING
Fiscal year 1980-81 implementation plan in support of technical development and integration of sampling and aggregation procedures --- crop acreage estimation [E82-10013] p0005 N82-15491
Analysis of satellite observations: Theoretical studies on the sampling problem [MITT-31] p0056 N82-15499

DATA SYSTEMS
The Control Point Library Building System --- for Landsat MSS and RBV geometric image correction p0043 A82-15971
U.S. Navy planning for satellite oceanographic data exploitation [AAS 81-072] p0024 A82-16341

DECIDUOUS TREES
Evaluation of digital photographic enhancement for Dutch elm disease detection p0002 A82-12884

DEER
A proposal for continuation of support for the application of remotely sensed data to state and regional problems. Part 1: Technical proposal [E82-10018] p0056 N82-15496

DEFORESTATION
Remote sensing in forestry: Application to the Amazon region [E82-10012] p0005 N82-15490

DELAWARE
In situ spectral reflectance studies of tidal wetland grasses p0036 A82-15969

DELAWARE BAY (US)
Remote sensing of the Chesapeake Bay plume salinity via microwave radiometry p0027 N82-10670

DELTAS
Study of the dynamics of the Danube delta using space images p0036 A82-15961

DEPOLARIZATION
Radar correlation with ice depolarization measurements of the 28.56 GHz COMSTAR beacon and associated cross polarization statistics [NASA-CR-166717] p0046 N82-14548

DESERTS
Study of the anthropogenic influence on the environment, based on multispectral scanning images p0008 A82-15965
Space photographs obtained with the Fragment system as a base for landscape mapping and physical-geographical classification of arid territories p0009 A82-15967
Desert sand seas p0020 N82-12493

DIGITAL DATA
Factorial analysis of terrain feature positioning parameters used in combining radar and digital terrain model data p0015 A82-10029
Phytoecozonation of Sevier Lake region of Utah using digitized Landsat MSS data p0001 A82-10042
Wheat cultivation: Identification and estimation of areas using LANDSAT data [E82-10007] p0004 N82-15485

DIGITAL TECHNIQUES
American Society of Photogrammetry, Annual Meeting, 46th, St. Louis, MO, March 9-14, 1980, ASP Technical Papers p0041 A82-10027
Digital image technology - MC&G impact --- Mapping, Charting, & Geodesy p0015 A82-10028
Applications of digital displays in photointerpretation and digital mapping p0041 A82-10038
Digitizing and automated output mapping errors p0015 A82-10859
Digital mapping using entities - A new concept p0041 A82-12882
Evaluation of digital photographic enhancement for Dutch elm disease detection p0002 A82-12884
A digital fast correlation approach to produce SEASAT SAR imagery p0042 A82-14870
The use of digitally processed Landsat imagery for vegetation mapping in Sulawesi, Indonesia p0003 A82-17998
Small-scale terrain mapping based on numerical interpretation of LANDSAT imagery [VTT-40] p0045 N82-10485
Some aspects of tropical storm structure revealed by handheld-camera photographs from space p0011 N82-12507
Seasat SAR processing at the Norwegian Defence Research Establishment --- design and operation of a digital process p0046 N82-14584
Maritime applications of image processing at DFVLR, Oberpfaffenhofen, West Germany --- LANDSAT multispectral scanner images, digital interactive image analysis p0032 N82-14585

DISTORTION
A new method for computing distortion p0016 A82-12914

DISTRICT OF COLUMBIA
Adaptation of land use to surficial geology in metropolitan Washington, D.C. p0010 N82-11718

DOMESTIC SATELLITE COMMUNICATIONS SYSTEMS
ISRO satellite mission support facilities - Scope and future plans p0055 A82-17307

DOPPLER EFFECT
Report of survey for McDonald Observatory, Harvard Radio Astronomy Station, and vicinity [PB81-234338] p0016 N82-13606

DOPPLER RADAR
Application of satellite Doppler techniques to the national mapping program p0015 A82-10056
Bureau of Land Management satellite Doppler positioning techniques p0015 A82-10057

DRAINAGE PATTERNS
Morphostructural analyses of space imagery in the central Colorado Plateau p0019 N82-10465
Report on Skylab 4 African drought and arid land experiment p0037 N82-12501
Quantitative analysis of drainage obtained from aerial photographs and RBV/LANDSAT images
[E82-10008] p0039 N82-15486

DROUGHT
Report on Skylab 4 African drought and arid land experiment p0037 N82-12501

DUNES
Desert sand seas p0020 N82-12493

DYNAMICS EXPLORER SATELLITES
Magnetic field observations on DE-A and -B --- Dynamics Explorer A and B satellites p0051 A82-16447

E

EARTH ALBEDO
The surface albedo of the earth in the near ultraviolet /330-340 nm/ p0016 A82-15032

EARTH ATMOSPHERE
Nitric oxide delta band emission in the earth's atmosphere Comparison of a measurement and a theory
p0008 A82-13268

EARTH CRUST
Space techniques to monitor movements in the earth's crust p0016 A82-18797
The mineralogy of global magnetic anomalies
[E82-10009] p0021 N82-15487

EARTH MOVEMENTS
Space techniques to monitor movements in the earth's crust p0016 A82-18797

EARTH OBSERVATIONS (FROM SPACE)
Skylab explores the Earth
[NASA-SP-380] p0019 N82-12492

EARTH RESOURCES INFORMATION SYSTEM
Civil land remote sensing systems
[GPO-35-265] p0056 N82-15497

EARTH SURFACE
Thermal inertia, thermal admittance, and the effect of layers p0008 A82-15027
The surface albedo of the earth in the near ultraviolet /330-340 nm/ p0016 A82-15032
Metrological support of measurements of earth surface brightness by the Fragment multispectral scanning system p0050 A82-15958

ECOLOGY
Use of visible and thermal satellite data to monitor an intermittently flooding marshland p0036 A82-15037
A proposal for continuation of support for the application of remotely sensed data to state and regional problems. Part 1: Technical proposal
[E82-10018] p0056 N82-15496

ECONOMIC IMPACT
Overall economic impact of an operational Meteosat system
[ESA-CR(P)-1457] p0055 N82-13010

ECOSYSTEMS
Phytoecozonation of Sevier Lake region of Utah using digitized Landsat MSS data p0001 A82-10042
Chesapeake Bay Plume Study: Superflux 1980
[NASA-CP-2188] p0026 N82-10661
Superflux I, II, and III experiment design: Remote sensing aspects p0027 N82-10664
Superflux I, II, and III experiment designs: Water sampling and analyses --- Chespeake Bay, environmental monitoring and remote sensing p0027 N82-10665
Deep Ocean Mining Environmental Study. Environmental effects of commercial-scale mining
[PB81-227753] p0029 N82-13484

ECUADOR
Skylab 4 observations of Volcanoes. Part A: Volcanoes and volcanic landforms. Part B: Summit eruption of Femandian Caldera, Galapagos Islands, Ecuador
p0020 N82-12496

EDUCATIONAL TELEVISION
ISRO satellite mission support facilities - Scope and future plans p0055 A82-17307

EISCAT RADAR SYSTEM (EUROPE)
A Swedish proposal for an EISCAT/GEOS-2 experiment --- geomagnetic field models
[KGI-175] p0052 N82-10484

EJECTA
Satellite observations of the Mt. St. Helens' eruption of 18 May 1980
[AD-A105784] p0012 N82-14591

ELECTROMAGNETIC FIELDS
Radiative transfer theory for passive microwave remote sensing of random media p0049 A82-11533

EMISSION SPECTRA
Nitric oxide delta band emission in the earth's atmosphere Comparison of a measurement and a theory
p0008 A82-13268

EMISSIVITY
Reflectivity and emissivity of snow and ground at mm waves p0042 A82-14860

ENGLAND
The use of LANDSAT MSS to observe sediment distribution and movement in the Solent coastal area --- multispectral scannel (MSS) p0038 N82-14580

ENVIRONMENT EFFECTS
Deep Ocean Mining Environmental Study. Environmental effects of commercial-scale mining
[PB81-227753] p0029 N82-13484

ENVIRONMENT MANAGEMENT
Requirements in pollution monitoring and coastal management p0030 N82-14558

ENVIRONMENTAL MONITORING
Civil engineering applications of remote sensing; Proceedings of the Specialty Conference, University of Wisconsin, Madison, WI, August 13, 14, 1980
p0035 A82-12589
Use of visible and thermal satellite data to monitor an intermittently flooding marshland p0036 A82-15037
Study of the anthropogenic influence on the environment, based on multispectral scanning images
p0008 A82-15965
ISRO satellite mission support facilities - Scope and future plans p0055 A82-17307
User needs and the future of operational meteorological satellites
[AIAA PAPER 82-0388] p0051 A82-17918
The radiowave propagation environment - Science and technology objectives for the 80's p0009 A82-18052
A marine environmental monitoring and assessment program p0027 N82-10663
Superflux I, II, and III experiment design: Remote sensing aspects p0027 N82-10664
Superflux I, II, and III experiment designs: Water sampling and analyses --- Chespeake Bay, environmental monitoring and remote sensing p0027 N82-10665
Monitoring the Chesapeake Bay using satellite data for Superflux III p0027 N82-10668
Shuttle applications in tropospheric air quality observations
[NASA-CR-145374] p0010 N82-11635
Environmental Monitoring Report, Sandia National Labs., Albuquerque, New Mexico, 180
[DE81-027839] p0010 N82-11649
Snow-mapping experiment p0037 N82-12498
Quantitative analysis of atmospheric pollution phenomena p0010 N82-12505
Limit on remote FTIR detection of trace gases
[AD-A104842] p0011 N82-12511
Environmental data for sites in the National Solar Data Network
[DE82-000071] p0011 N82-12707
Special observations by the Hohenpeissenberg Meteorological Observatory. Number 42: Results of aerological and surface ozone measurements during the first semester of 1980
[SONDERBEOB-42] p0012 N82-12714
Aircraft data summaries of the SURE intensives, volume 4
[DE82-900311] p0012 N82-13569
ERS-1: Mission objectives and system concept
p0029 N82-14554
The need for integrated off-shore, real-time information and management systems p0055 N82-14555
Offshore petroleum industry environmental data requirements: Emphasis on remote sensing
p0030 N82-14557
Fisheries investigations and management benefits from remote sensing --- fish tracking p0030 N82-14559
A look at nonsatellite remote sensing systems for marine use --- together with satellite systems, overall view of the technology p0032 N82-14586
Study of a combined satellite system for remote sensing and earth-oriented research (LOCSS) --- ESA satellite
[BMFT-FB-W-81-002] p0055 N82-14615
Meteorological satellites
[AD-A107427] p0053 N82-15110
Investigation of the application of remote sensing technology to environmental monitoring
[E82-10010] p0013 N82-15488
National Hurricane operations plan
[PB81-247231] p0013 N82-15697
Environmental satellite imagery, March 1981
[PB81-248049] p0047 N82-15698

EQUATORIAL REGIONS
CTD/02 measurements during the Equatorial Pacific Ocean Climate Study (EPOCS) in 1979
[PB81-211203] p0026 N82-10461

EROSION
Satellite imagery and shoreline erosion prediction
p0036 A82-12585
A method for using aerial photos in delineating historic patterns of beach accretion and retreat
[PB81-223836] p0010 N82-11536
Airborne remote sensing of the coastal zone
p0053 N82-14577

ERROR ANALYSIS
Factorial analysis of terrain feature positioning parameters used in combining radar and digital terrain model data
p0015 A82-10029
Digitizing and automated output mapping errors
p0015 A82-10859
Concerning the geometric accuracy of infrared scanner photographs p0042 A82-13634
Some problem areas in the field of quality control for aerotriangulation p0016 A82-16161

ERROR CORRECTING DEVICES
Block adjustment with additional parameters
p0049 A82-13738
The MSS control point location error filter for LANDSAT-D p0051 N82-10073

ERS-1 (ESA SATELLITE)
ERS-1: Mission objectives and system concept
p0029 N82-14554

ESA SATELLITES
Study of a combined satellite system for remote sensing and earth-oriented research (LOCSS) --- ESA satellite
[BMFT-FB-W-81-002] p0055 N82-14615

ESTUARIES
Field study for Landsat water quality verification
p0036 A82-12597
Remote sensing of benthic microalgal biomass with a tower-mounted multispectral scanner p0024 A82-15031
Chesapeake Bay Plume Study: Superflux 1980
[NASA-CP-2188] p0026 N82-10661
Superflux I, II, and III experiment design: Remote sensing aspects p0027 N82-10664
Remote sensing of the Chesapeake Bay plume salinity via microwave radiometry p0027 N82-10670
Preliminary analysis of ocean color scanner data from Superflux III p0027 N82-10672
SPOT data simulations: Littoral applications
p0046 N82-14568
The use of LANDSAT MSS to observe sediment distribution and movement in the Solent coastal area --- multispectral scannel (MSS) p0038 N82-14580

EUROPE
Spacelab-research of European regions with strong negative environmental influences, based on AVHRR-data of the satellites Tiros-N and NOAA p0007 A82-12517
Availability of Seasat synthetic aperture radar imagery
p0050 A82-15039

EUTROPHICATION
The operational use of Landsat for lake quality assessment p0036 A82-12596

EVAPOTRANSPIRATION
A simulation study of the recession coefficient for antecedent precipitation index --- soil moisture and water runoff estimation
[NASA-TM-83860] p0038 N82-14549

F

FARADAY EFFECT
SMMR data set development for GARP --- impact of cross polarization and Faraday rotation on SMMR derived brightness temperatures
[NASA-CR-166721] p0052 N82-11512

FARMLANDS
Satellite sensing of irrigation patterns in semiarid areas - An Indian study p0002 A82-10864
Study and mapping of agricultural land use, based on space images p0003 A82-15963
Aircraft radar response to soil moisture
p0003 A82-17564
Vegetation patterns p0004 N82-12500

FIELD OF VIEW
The choice of the orientation of the analyzer in polarimetric surveys p0044 A82-16621
Scanner --- photography from a spin stabilized synchronous satellite
[NASA-CASE-GSC-12032-2] p0052 N82-13465
Interpolating for the location of remote sensor data
[NASA-TM-82169] p0052 N82-13469

FINLAND
Compensation of systematic errors of image and model coordinates p0043 A82-15765
Small-scale terrain mapping based on numerical interpretation of LANDSAT imagery
[VTT-40] p0045 N82-10485

FIORDS
Mapping of surface currents in Greenland fiords by means of LANDSAT images --- multispectral photography
p0038 N82-14579

FIRES
Quantitative analysis of atmospheric pollution phenomena p0010 N82-12505

FISHERIES
The use of satellite infrared imagery for describing ocean processes in relation to spawning of the northern anchovy /Engraulis mordax/ p0025 A82-17565
Application of remote sensing data on the continental shelf: Proceedings of an EAReL-ESA Symposium
[ESA-SP-167] p0029 N82-14553
Fisheries investigations and management benefits from remote sensing --- fish tracking p0030 N82-14559
The Seasat commercial demonstration program
p0030 N82-14561
A short review of an oceanographic use of Meteosat data by the ORSTOM remote sensing service
p0031 N82-14570

FLIGHT TESTS
Three bearing method for passive triangulation in systems with unknown deterministic biases p0050 A82-15920

FLOOD PLAINS
Mapping of the 1978 Kentucky River Flood from NOAA-5 satellite thermal infrared data p0035 A82-10033

FLOOD PREDICTIONS
Satellite rainfall estimation for hydrologic forecasting
p0035 A82-10032

A systems approach to the real-time runoff analysis with a deterministic rainfall-runoff model
[PB81-224495] p0037 N82-11530
Analysis of rainfall from flash flood producing thunderstorms, using GOES data p0038 N82-14724

FLOODS
Use of visible and thermal satellite data to monitor an intermittently flooding marshland p0036 A82-15037
Cost effective computer processing of airborne scanner data for regional level mapping p0043 A82-15970

FLORIDA
Field study for Landsat water quality verification p0036 A82-12597
Optically processed Seasat radar mosaic of Florida p0042 A82-15125

FLUORESCENCE
Application of the NASA airborne oceanographic lidar to the mapping of chlorophyll and other organic pigments p0027 N82-10684
A recommended sensor package for the detection and tracking of oil spills p0053 N82-14563

FOREST FIRES
Quantitative analysis of atmospheric pollution phenomena p0010 N82-12505

FOREST MANAGEMENT
A VHF homing system with VHF radiotelephony for area-representative strip-survey flights conducted, as part of combined forest inventories, with light aircraft carrying 70 mm and 35 mm cameras p0003 A82-15748
Rural development in the humid tropics p0003 A82-16162
Large-scale color aerial photography as a tool in sampling for mortality rates
[PB81-214777] p0003 N82-10489

FORESTS
Mapping vegetation association boundaries with Landsat MSS data - An Oklahoma example p0001 A82-10041
Stand density estimation on panoramic transparencies p0002 A82-10862
Remote sensing contributions to the management of renewable resources p0055 A82-12530
Identification of conifer species groupings from Landsat digital classifications p0002 A82-12887
Mapping of forest vegetation on the basis of space images p0003 A82-15964
Study of the anthropogenic influence on the environment, based on multispectral scanning images p0008 A82-15965
The use of digitally processed Landsat imagery for vegetation mapping in Sulawesi, Indonesia p0003 A82-17998
Vegetation patterns p0004 N82-12500
Application of remote sensing to selected problems within the state of California
[E82-10004] p0004 N82-15482
Remote sensing in forestry. Application to the Amazon region
[E82-10012] p0005 N82-15490

FRAMING CAMERAS
Orientation and construction of models. I - The orientation problem in close-range photogrammetry p0049 A82-10858

FRANCE
The operational oil pollution surveillance system being used in France. Forecasted future developments in consideration of the NATO/CCMS remote sensing pilot study conclusions p0012 N82-14573

FRESH WATER
Recent work in passive optical imaging of water --- space and aircraft derived data p0038 N82-14575

FRONTS (METEOROLOGY)
An investigation of a polar low with a spiral cloud structure p0007 A82-10616

G

GALILEAN SATELLITES
Coordinates of features on the Galilean satellites p0019 A82-12366

GAS ANALYSIS
A new method for inferring carbon monoxide concentrations from gas filter radiometer data p0009 A82-16837
Proof of concept study
[AD-A104338] p0010 N82-11639

GEOCHRONOLOGY
Study of the time evolution of the lithosphere
[NASA-CR-164968] p0016 N82-11696

GEODESY
Digital image technology - MC&G impact --- Mapping, Charting, & Geodesy p0015 A82-10028
Space techniques to monitor movements in the earth's crust p0016 A82-18797
Study of the time evolution of the lithosphere
[NASA-CR-164968] p0016 N82-11696
Reports of Planetary Geology Program, 1981
[NASA-TM-84211] p0016 N82-14041
Description and comparison of algorithms for solving large sets of sparse matrix normal equations in geodesy and photogrammetry
[SER-C-261] p0017 N82-15812

GEODETIC SURVEYS
Application of satellite Doppler techniques to the national mapping program p0015 A82-10056
Bureau of Land Management satellite Doppler positioning techniques p0015 A82-10057
GPS application to mapping, charting and geodesy p0015 A82-10645
Phototriangulation with map referencing of photographs in linear surveys p0016 A82-12912
Some problem areas in the field of quality control for aerotriangulation p0016 A82-16161
Theoretical reliability of elementary photogrammetric procedures. I p0043 A82-16163
Report of survey for McDonald Observatory, Harvard Radio Astronomy Station, and vicinity
[PB81-234338] p0016 N82-13606
A history of flying and photography. In the Photogrammetry Division of the National Ocean Survey 1919 - 1979
[PB81-246738] p0017 N82-15520

GEOLOGICAL FAULTS
Morphostructural analyses of space imagery in the central Colorado Plateau p0019 N82-10465
Global Tectonics. Some Geologic analyses of observations and photographs from Skylab p0020 N82-12494

GEOLOGICAL SURVEYS
A closer examination of the reduction of satellite magnetometer data for geological studies p0019 A82-11039
Coordinates of features on the Galilean satellites p0019 A82-12366
Statistical Techniques Applied to Aerial Radiometric Surveys (STAARS). Series introduction and the principal-components-analysis method --- National Uranium Resource Evaluation Program
[DE81-029177] p0019 N82-10476
Skylab explores the Earth
[NASA-SP-380] p0019 N82-12492
Global Tectonics. Some Geologic analyses of observations and photographs from Skylab p0020 N82-12494
Geological features of southwestern North America p0020 N82-12495
Skylab 4 observations of Volcanoes. Part A: Volcanoes and volcanic landforms. Part B: Summit eruption of Fernandian Caldera, Galapagos Islands, Ecuador p0020 N82-12496
The Manicouagan impact structure observed from Skylab
[CONTRIB-544] p0020 N82-12497
Geologic applications of thermal-inertia mapping from satellite --- Powder River, Wyoming; Cubeza Prieta, Arizona, and Yellowstone National Park
[E82-10011] p0021 N82-15489
Preliminary analysis of gravity and aeromagnetic surveys of the Timber Mountain area, southern Nevada
[DE81-029462] p0022 N82-15506

GEOLOGY
Geology and linears of Libya p0019 N82-10618
Adaptation of land use to surficial geology in metropolitan Washington, D.C p0010 N82-11718

GEOMAGNETISM
A closer examination of the reduction of satellite magnetometer data for geological studies p0019 A82-11039
Magnetic field-aligned electron distributions in the dayside cusp p0015 A82-12186
Distant magnetic field effects associated with Birkeland currents /made possible by the evaluation of TRIAD's attitude oscillations/ p0015 A82-12215
Magnetic field observations on DE-A and -B --- Dynamics Explorer A and B satellites p0051 A82-16447
Use of hydromagnetic waves to map geomagnetic field lines p0016 A82-16868
A Swedish proposal for an EISCAT/GEOS-2 experiment --- geomagnetic field models
[KGI-175] p0052 N82-10484
Magnetic Field Satellite (Magsat) data processing system specifications
[NASA-CR-166737] p0045 N82-11103
The mineralogy of global magnetic anomalies
[E82-10009] p0021 N82-15487

GEOMETRIC RECTIFICATION (IMAGERY)
Factorial analysis of terrain feature positioning parameters used in combining radar and digital terrain model data p0015 A82-10029
Two-dimensional resampling of line scan imagery by one-dimensional processing p0041 A82-10860
Digital mapping using entities - A new concept p0041 A82-12882
A new method for computing distortion p0016 A82-12914
Concerning the geometric accuracy of infrared scanner photographs p0042 A82-13634
Block adjustment with additional parameters p0049 A82-13738
Compensation of systematic errors in bundle adjustment p0042 A82-15764
Compensation of systematic errors of image and model coordinates p0043 A82-15765
The Control Point Library Building System --- for Landsat MSS and RBV geometric image correction p0043 A82-15971
Computational aspects of geometric correction data generation in the LANDSAT-D imagery processing p0045 N82-10072

GEOMORPHOLOGY
Development of a coastal relief of the Gulf of Riga, based on results of an analysis of space images p0024 A82-15962
Investigation and mapping of the erosion relief of the Kalachskaia upland on the basis of multispectral scanner images p0008 A82-15966
Space photographs obtained with the Fragment system as a base for landscape mapping and physical-geographical classification of arid territories p0009 A82-15967
Morphostructural analyses of space imagery in the central Colorado Plateau p0019 N82-10465
Desert sand seas p0020 N82-12493

GEOPHYSICS
Analysis of satellite observations. Theoretical studies on the sampling problem
[MITT-31] p0056 N82-15499

GEOTHERMAL RESOURCES
Geologic applications of thermal-inertia mapping from satellite --- Powder River, Wyoming; Cubeza Prieta, Arizona, and Yellowstone National Park
[E82-10011] p0021 N82-15489

GLACIOLOGY
Study on satellite radar altimetry in climatological and oceanographic research, volume 1
[SP/153/06/01/FR(80)-VOL-1] p0026 N82-10486
Study on satellite radar altimetry in climatological and oceanographic research, volume 2
[SP/153/06/01FR(80)-VOL-2] p0026 N82-10487

GLOBAL AIR POLLUTION
A new method for inferring carbon monoxide concentrations from gas filter radiometer data p0009 A82-16837

GLOBAL ATMOSPHERIC RESEARCH PROGRAM
SMMR data set development for GARP --- impact of cross polarization and Faraday rotation on SMMR derived brightness temperatures
[NASA-CR-166721] p0052 N82-11512

GLOBAL POSITIONING SYSTEM
GPS application to mapping, charting and geodesy p0015 A82-10645
Onboard utilization of ground control points for image correction. Volume 1: Executive summary
[NASA-CR-166731] p0045 N82-10469
Onboard utilization of ground control points for image correction. Volume 2: Analysis and simulation results
[NASA-CR-166732] p0045 N82-10470
Onboard utilization of ground control points for image correction. Volume 3: Ground control point simulation software design
[NASA-CR-166733] p0045 N82-10471
Onboard utilization of ground control points for image correction. Volume 4: Correlation analysis software design
[NASA-CR-166734] p0045 N82-10472

GOES SATELLITES
User needs and the future of operational meteorological satellites
[AIAA PAPER 82-0388] p0051 A82-17918

GOVERNMENT/INDUSTRY RELATIONS
The Seasat commercial demonstration program p0030 N82-14561

GRAINS (FOOD)
Development and evaluation of an automatic labeling technique for spring small grains
[E82-10001] p0004 N82-15480

GRASSES
In situ spectral reflectance studies of tidal wetland grasses p0036 A82-15969

GRASSHOPPERS
Remote sensing applications to resource problems in South Dakota
[E82-10002] p0004 N82-15481

GRASSLANDS
The effect of angular factors on popularly used indicators of vegetative vigor p0001 A82-10039
Mapping vegetation association boundaries with Landsat MSS data - An Oklahoma example p0001 A82-10041

GRATINGS (SPECTRA)
The application of holographic gratings in spectrometers for the spatial-spectral analysis of the earth's surface from aerial and space platforms in the visible and near-infrared spectral regions p0044 A82-16614

GRAVELS
Remote sensing studies of some ironstone gravels and plinthite in Thailand p0019 N82-12491

GRAVIMETRY
Preliminary analysis of gravity and aeromagnetic surveys of the Timber Mountain area, southern Nevada
[DE81-029462] p0022 N82-15506

GRAVITY WAVES
The influence of gravity waves on radiometric measurements - A case study p0049 A82-13547

GRAZING INCIDENCE
Radar backscattering from ocean waves at low grazing angles p0023 A82-14730

GREAT BASIN (US)
Phytoecoronation of Sevier Lake region of Utah using digitized Landsat MSS data p0001 A82-10042

GREAT LAKES (NORTH AMERICA)
Data sources for analyses of Great Lakes wetlands p0035 A82-10054

GREAT PLAINS CORRIDOR (NORTH AMERICA)
US/Canada wheat and barley crop calender exploratory experiment implementation plan [E82-10016] p0005 N82-15494

GREENLAND
Measurement of sea and ice backscatter reflectivity using an OTH radar system p0025 A82-18074
The ice-conditions in the Greenland waters, 1965. Coastal maps [ISBN-87-7478-183-9] p0026 N82-10467
The ice conditions in the Greenland waters [ISBN-87-7478-183-9] p0028 N82-12533
Mapping of surface currents in Greenland fiords by means of LANDSAT images --- multispectral photography p0038 N82-14579

GROUND TRUTH
The mineralogy of global magnetic anomalies [E82-10009] p0021 N82-15487

GUATEMALA
Radar mapping, archaeology, and ancient land use in the Maya lowlands [NASA-CR-164931] p0010 N82-11514
Global Tectonics: Some Geologic analyses of observations and photographs from Skylab p0020 N82-12494

GULF OF ALASKA
An evaluation of Seasat-A data in relation to optimum track ship weather routing and site specific forecasting for the offshore oil industry p0030 N82-14564

GULFS
Comparison of polar and geostationary satellite infrared observations of sea surface temperatures in the Gulf of Maine p0024 A82-15030
Development of a coastal relief of the Gulf of Riga, based on results of an analysis of space images p0024 A82-15962
Visual observations of floating ice from Skylab p0037 N82-12504

H

HABITATS
Repetitive aerial photography for assessing marsh vegetation changes p0001 A82-10048
A proposal for continuation of support for the application of remotely sensed data to state and regional problems. Part 1: Technical proposal [E82-10018] p0056 N82-15496

HAWAII
A method for using aerial photos in delineating historic patterns of beach accretion and retreat [PB81-223836] p0010 N82-11536
Skylab 4 observations of Volcanoes. Part A: Volcanoes and volcanic landforms. Part B: Summit eruption of Fernandian Caldera, Galapagos Islands, Ecuador p0020 N82-12496

HAZE
Multitemporal calibration of LANDSAT images: A method for improving the marine phenomena recognition, with as example the Venice lagoon --- brightness/green/yellow feature space, image enhancement p0046 N82-14578

HEAT FLUX
Thermal inertia, thermal admittance, and the effect of layers p0008 A82-15027

HEAT STORAGE
Variations in upper ocean heat storage determined from satellite data p0025 A82-17567

HOLOGRAPHY
The application of holographic gratings in spectrometers for the spatial-spectral analysis of the earth's surface from aerial and space platforms in the visible and near-infrared spectral regions p0044 A82-16614

HOMING DEVICES
A VHF homing system with VHF radiotelephony for area-representative strip-survey flights conducted, as part of combined forest inventories, with light aircraft carrying 70 mm and 35 mm cameras p0003 A82-15748

HURRICANES
National Hurricane operations plan [PB81-247231] p0013 N82-15697

HYDROCARBONS
Automated analyzer for aircraft measurements of atmospheric methane and total hydrocarbons p0007 A82-11949

HYDROGRAPHY
Application of Landsat to the inventory of DAMS p0036 A82-12593
Study of the dynamics of the Danube delta using space images p0036 A82-15961
Quantitative analysis of drainage obtained from aerial photographs and RBV/LANDSAT images [E82-10008] p0039 N82-15486

HYDROLOGY
Satellite rainfall estimation for hydrologic forecasting p0035 A82-10032
Civil engineering applications of remote sensing; Proceedings of the Specialty Conference, University of Wisconsin, Madison, WI, August 13, 14, 1980 p0035 A82-12589
Landsat imagery for hydrologic modeling p0036 A82-12592
Field study for Landsat water quality verification p0036 A82-12597
Operational use of remote sensing for coastal zone management and possible contribution of specialized satellites --- aerial photography p0031 N82-14574
The effect of spatial variability in precipitation on streamflow [AD-A105955] p0038 N82-14589

HYDROLOGY MODELS
Civil engineering applications of remote sensing; Proceedings of the Specialty Conference, University of Wisconsin, Madison, WI, August 13, 14, 1980 p0035 A82-12589
An application of Landsat derived data to a regional hydrologic model p0037 A82-17999

HYDROMETEOROLOGY
A systems approach to the real-time runoff analysis with a deterministic rainfall-runoff model [PB81-224495] p0037 N82-11530
A simulation study of the recession coefficient for antecedent precipitation index --- soil moisture and water runoff estimation [NASA-TM-83860] p0038 N82-14549
Meteorological satellites [AD-A107427] p0053 N82-15110

I

ICE
Radar correlation with ice depolarization measurements of the 28.56 GHz COMSTAR beacon and associated cross polarization statistics [NASA-CR-166717] p0046 N82-14548

ICE MAPPING
The ice-conditions in the Greenland waters, 1965. Coastal maps [ISBN-87-7478-183-9] p0026 N82-10467
Ice conditions in the eastern Bering Sea from NOAA and LANDSAT imagery: Winter conditions 1974, 1976, 1977, 1979 [PB81-220188] p0028 N82-11537
The Norwegian remote sensing experiment (Norsex) in a marginal ice zone p0031 N82-14566

ICE REPORTING
Visual observations of floating ice from Skylab p0037 N82-12504
The ice conditions in the Greenland waters [ISBN-87-7478-183-9] p0028 N82-12533
Marine activities in Sweden for which remote sensing data may be of interest --- oceanography, weather forecasting, and analysis p0031 N82-14576

ILLINOIS
The effect of spatial variability in precipitation on streamflow [AD-A105955] p0038 N82-14589

IMAGE CONTRAST
Calculation of the decrease in the contrast of objects of a place due to light scattering in the atmosphere p0042 A82-13833
Estimation of the brightness field from results of multispectral photography of the earth from space p0044 A82-16617
Polarimetric surveys of oil slicks p0009 A82-16619
Images of sea waves obtained in polarimetric surveys p0024 A82-16620
The choice of the orientation of the analyzer in polarimetric surveys p0044 A82-16621

IMAGE ENHANCEMENT
Evaluation of digital photographic enhancement for Dutch elm disease detection p0002 A82-12884
Multitemporal calibration of LANDSAT images: A method for improving the marine phenomena recognition, with as example the Venice lagoon --- brightness/green/yellow feature space, image enhancement p0046 N82-14578

IMAGE FILTERS
Spectral correlation filters and natural colour coding p0043 A82-16160

IMAGE PROCESSING
American Society of Photogrammetry, Annual Meeting, 46th, St. Louis, MO, March 9-14, 1980, ASP Technical Papers p0041 A82-10027
Digital image technology - MC&G impact --- Mapping, Charting, & Geodesy p0015 A82-10028
Mapping of the 1978 Kentucky River Flood from NOAA-5 satellite thermal infrared data p0035 A82-10033
Applications of digital displays in photointerpretation and digital mapping p0041 A82-10038
An improvement in land cover classification achieved by merging microwave data with Landsat multispectral scanner data p0007 A82-10043
Preliminary results of mapping urban land cover with Seasat SAR imagery p0007 A82-10044
Absolute image registration for geosynchronous satellites p0049 A82-10051
Two-dimensional resampling of line scan imagery by one-dimensional processing p0041 A82-10860
Intercalibration of Landsat 1-3 and NOAA 6 and 7 scanner data p0049 A82-13293
Investigations concerning the image-controlled segmentation of objects in multispectral imagery data --- German thesis p0042 A82-15003
Texture transforms of remote sensing data p0042 A82-15034
Optically processed Seasat radar mosaic of Florida p0042 A82-15125
Analysis of variance of thematic mapping experiment data p0009 A82-15968
Cost effective computer processing of airborne scanner data for regional level mapping p0043 A82-15970
The Control Point Library Building System --- for Landsat MSS and RBV geometric image correction p0043 A82-15971
Airborne and spaceborne multispectral photography of the earth --- Russian book p0043 A82-16601
Geometric quality of MKF-6 photographs p0043 A82-16606
The maximum mean accuracy of classification of remote-sensing objects and the influence on this accuracy of data acquisition and processing methods p0044 A82-16615
Analog methods for processing multispectral photographs p0044 A82-16623
Structural analysis of aerial and space images p0044 A82-16625
Processing of multispectral image data on special-purpose computer systems p0044 A82-16627
Programs for the statistical analysis of multispectral photographs p0044 A82-16628
Coordinate referencing of MKF-6 photographs and their transformation to the cartographic projection p0045 A82-16630
The use of digitally processed Landsat imagery for vegetation mapping in Sulawesi, Indonesia p0003 A82-17998
Distortion-free mapping of VISSR imagery data from geosynchronous satellites p0051 N82-10071
Computational aspects of geometric correction data generation in the LANDSAT-D imagery processing p0045 N82-10072
MATE VAN: Mobile analysis and training extension --- analyzing LANDSAT digital data [NASA-TM-84056] p0045 N82-10466
Onboard utilization of ground control points for image correction. Volume 1: Executive summary [NASA-CR-166731] p0045 N82-10469
Onboard utilization of ground control points for image correction. Volume 2: Analysis and simulation results [NASA-CR-166732] p0045 N82-10470
Onboard utilization of ground control points for image correction. Volume 3: Ground control point simulation software design [NASA-CR-166733] p0045 N82-10471
Onboard utilization of ground control points for image correction. Volume 4: Correlation analysis software design [NASA-CR-166734] p0045 N82-10472
Small-scale terrain mapping based on numerical interpretation of LANDSAT imagery [VTT-40] p0045 N82-10485
Identification of lithologic units using multichannel imaging systems p0046 N82-11509
Airborne remote sensing of the coastal zone p0053 N82-14577
Seasat SAR processing at the Norwegian Defence Research Establishment --- design and operation of a digital process p0046 N82-14584
Maritime applications of image processing at DFVLR, Oberpfaffenhofen, West Germany --- LANDSAT multispectral scanner images, digital interactive image analysis p0032 N82-14585

IMAGE RECONSTRUCTION
Data compression and reconstruction for mixed resolution multispectral sensors p0049 A82-10045

IMAGE RESOLUTION
Data compression and reconstruction for mixed resolution multispectral sensors p0049 A82-10045
Aspects in the development of aerial-photography tasks p0041 A82-12913
A new method for computing distortion p0016 A82-12914
Characteristics of the photometry of small objects from aerial and space photographs p0044 A82-16616
Distortion-free mapping of VISSR imagery data from geosynchronous satellites p0051 N82-10071

IMAGE ROTATION
Two-dimensional resampling of line scan imagery by one-dimensional processing p0041 A82-10860

IMAGING TECHNIQUES
SAR imaging of ocean waves - Theory p0023 A82-11202
Study on calibration methods for Earth observation optical imaging instruments [UCD-207/1/80] p0052 N82-10488
A recommended sensor package for the detection and tracking of oil spills p0053 N82-14563

IN-FLIGHT MONITORING
Infrared radiance model variation by sensor flight measurements p0052 N82-14171

INCIDENCE
New baseline system p0054 N82-15501
Squinted SAR system p0047 N82-15502

INDIA
Satellite sensing of irrigation patterns in semiarid areas: An Indian study p0002 A82-10864
Cost effective computer processing of airborne scanner data for regional level mapping p0043 A82-15970
Detection of monsoon inversion by TIROS-N satellite p0024 A82-17168
Studies of the Indian continental shelf: Application of remote sensing data p0031 N82-14569

INDIAN OCEAN

Analysis of SEASAT wind observations over the Indian Ocean p0023 A82-10671

ICAPS oceanographic data for the Indian Ocean [AD-A103173] p0029 N82-13641

An evaluation of Seasat-A data in relation to optimum track ship weather routing and site specific forecasting for the offshore oil industry p0030 N82-14564

INDIAN SPACE PROGRAM

ISRO satellite mission support facilities - Scope and future plans p0055 A82-17307

INDIAN SPACECRAFT

Scientific studies using Bhaskara satellite microwave radiometer (SAMIR) data: A short overview --- calibration of the instrument and its use in the study of oceanographic parameters p0032 N82-14587

INDONESIA

Rural development in the humid tropics p0003 A82-16162

The use of digitally processed Landsat imagery for vegetation mapping in Sulawesi, Indonesia p0003 A82-17998

INERTIAL NAVIGATION

Photo inertial positioning system development at the Canada Centre for Remote Sensing p0045 A82-18167

INFESTATION

Vegetation patterns p0004 N82-12500

Remote sensing applications to resource problems in South Dakota [E82-10002] p0004 N82-15481

INFRARED ASTRONOMY

Infrared spectroscopy of microorganisms near 3.4 microns in relation to geology and astronomy [PREPRINT-69] p0020 N82-12713

INFRARED IMAGERY RADIOMETRIC RESOLUTION

Water temperature mapping by infrared scanner p0036 A82-12598

INFRARED PHOTOGRAPHY

Concerning the geometric accuracy of infrared scanner photographs p0042 A82-13634

INFRARED RADIATION

Biological patchiness in relation to satellite thermal imagery and associated chemical mesoscale features [AD-A105757] p0047 N82-15504

INFRARED REFLECTION

Mapping of the 1978 Kentucky River Flood from NOAA-5 satellite thermal infrared data p0035 A82-10033

Effect of grain size and snowpack water equivalence on visible and near-infrared satellite observations of snow p0035 A82-12553

INFRARED SPECTRA

Proof of concept study [AD-A104338] p0010 N82-11639

Inclusion of a simple vegetation layer in terrain temperature models for thermal infrared (IR) signature prediction [AD-A104469] p0003 N82-11910

Satellite observations of the Mt. St. Helens' eruption of 18 May 1980 [AD-A105784] p0012 N82-14591

INFRARED SPECTROSCOPY

Trace pollutant concentrations in a multiday smog episode in the California South Coast Air Basin by long path length Fourier transform infrared spectroscopy p0007 A82-10700

Infrared spectroscopy of microorganisms near 3.4 microns in relation to geology and astronomy [PREPRINT-69] p0020 N82-12713

INFRARED TRACKING

Satellite observations of the Mt. St. Helens' eruption of 18 May 1980 [AD-A105784] p0012 N82-14591

INLAND WATERS

The operational use of Landsat for lake quality assessment p0036 A82-12596

An inertially-aided aircraft track recovery system for coastal mapping p0037 A82-18166

INSOLATION

Environmental data for sites in the National Solar Data Network [DE82-000071] p0011 N82-12707

INSTRUMENT ERRORS

Ionospheric propagation correction modeling for satellite altimeters [NASA-CR-156881] p0052 N82-12447

INSTRUMENT ORIENTATION

Orientation and construction of models. III - Mathematical basis of the orientation problem of one-dimensional central perspective photographs p0043 A82-15973

Images of sea waves obtained in polarimetric surveys p0024 A82-16620

The choice of the orientation of the analyzer in polarimetric surveys p0044 A82-16621

An inertially-aided aircraft track recovery system for coastal mapping p0037 A82-18166

MAGSAT: Vector magnetometer absolute sensor alignment determination [NASA-TM-79648] p0051 N82-10468

Infrared radiance model variation by sensor flight measurements p0052 N82-14171

INTERNAL WAVES

Visual observations of the ocean p0028 N82-12502

An assessment of the potential contributions to oceanography from Skylab visual observations and handheld-camera photographs p0028 N82-12503

Surface signs of internal ocean dynamics [AD-A101380] p0029 N82-13642

INTERPOLATION

Interpolating for the location of remote sensor data [NASA-TM-82169] p0052 N82-13469

IONOSPHERE

A Swedish proposal for an EISCAT/GEOS-2 experiment --- geomagnetic field models [KGI-175] p0052 N82-10484

IONOSPHERIC CURRENTS

Characteristics of westward travelling surges during magnetospheric substorms p0050 A82-14299

IONOSPHERIC DRIFT

Use of hydromagnetic waves to map geomagnetic field lines p0016 A82-16868

IONOSPHERIC ELECTRON DENSITY

Magnetic field-aligned electron distributions in the dayside cusp p0015 A82-12186

IONOSPHERIC PROPAGATION

The radiowave propagation environment - Science and technology objectives for the 80's p0009 A82-18052

Ionospheric propagation correction modeling for satellite altimeters [NASA-CR-156881] p0052 N82-12447

IRELAND

The feasibility of using remotely sensed color as an index of Irish coastal water properties --- statistical correlation of sea truth data p0032 N82-14581

IRON COMPOUNDS

Remote sensing studies of some ironstone gravels and plinthite in Thailand p0019 N82-12491

IRRADIANCE

The color of the sea and its relation to surface chlorophyll and depth of the euphotic zone p0030 N82-14562

IRRIGATION

Satellite sensing of irrigation patterns in semiarid areas - An Indian study p0002 A82-10864

ISLANDS

Mesoscale wake clouds in Skylab photographs p0011 N82-12508

Boundary detection criteria for satellite altimeters [NASA-CR-156880] p0028 N82-12734

ITALY

Study of stack emissions by combination of lidar and correlation spectrometer p0008 A82-12816

Skylab 4 observations of Volcanoes. Part A: Volcanoes and volcanic landforms. Part B: Summit eruption of Femandian Caldera, Galapagos Islands, Ecuador p0020 N82-12496

J

JAPAN

Skylab 4 observations of Volcanoes. Part A: Volcanoes and volcanic landforms. Part B: Summit eruption of Femandian Caldera, Galapagos Islands, Ecuador p0020 N82-12496

JET STREAMS (METEOROLOGY)

Meteorological lab applications of Skylab handheld-camera photographs p0011 N82-12506

K

KANSAS

Interactive techniques for estimating precipitation from GOES imagery p0041 A82-13121

The discrimination of winter wheat using a growth-state signature p0002 A82-15026

Aircraft radar response to soil moisture p0003 A82-17564

KENTUCKY

Mapping of the 1978 Kentucky River Flood from NOAA-5 satellite thermal infrared data p0035 A82-10033

L

LAGOONS

Multitemporal calibration of LANDSAT images: A method for improving the marine phenomena recognition, with as example the Venice lagoon --- brightness/green/yellow feature space, image enhancement p0046 N82-14578

LAKE ICE

The development of the Tiros Global Environmental Satellite System [AIAA PAPER 82-0383] p0025 A82-17915

Visual observations of floating ice from Skylab p0037 N82-12504

LAKE ONTARIO

Visual observations of floating ice from Skylab p0037 N82-12504

Recent work in passive optical imaging of water --- space and aircraft derived data p0038 N82-14575

LAKES

Remote sensing that motivated community action p0008 A82-12594

The operational use of Landsat for lake quality assessment p0036 A82-12596

Role of remote sensing in the study of acid rain impact on aquatic systems [AIAA PAPER 82-0336] p0036 A82-17892

The Manicouagan impact structure observed from Skylab [CONTRIB-544] p0020 N82-12497

LAND ICE

Measurement of sea and ice backscatter reflectivity using an OTH radar system p0025 A82-18074

LAND MANAGEMENT

Remote sensing for vineyard management p0001 A82-10047

Bureau of Land Management satellite Doppler positioning techniques p0015 A82-10057

Civil engineering applications of remote sensing; Proceedings of the Specialty Conference, University of Wisconsin, Madison, WI, August 13, 14, 1980 p0035 A82-12589

Adaptation of land use to surficial geology in metropolitan Washington, D.C. p0010 N82-11718

LAND USE

Introducing remote sensing to county-level agencies in Michigan through the Cooperative Extension Service p0007 A82-10034

Remote sensing techniques in the study of the agricultural potential of soils under the Cerrado vegetation /Brazil/ p0001 A82-10040

Preliminary results of mapping urban land cover with Seasat SAR imagery p0007 A82-10044

Areawide soil loss predictions using CIR airphotos p0007 A82-12591

Study of the dynamics of the Danube delta using space images p0036 A82-15961

Study and mapping of agricultural land use, based on space images p0003 A82-15963

Study of the anthropogenic influence on the environment, based on multispectral scanning images p0008 A82-15965

Analysis of variance of thematic mapping experiment data p0009 A82-15968

An evaluation of the spatial resolution of soil moisture information [NASA-CR-166724] p0009 N82-11513

Radar mapping, archaeology, and ancient land use in the Maya lowlands [NASA-CR-164931] p0010 N82-11514

Adaptation of land use to surficial geology in metropolitan Washington, D.C. p0010 N82-11718

Cultural features imaged and observed from Skylab 4 p0010 N82-12499

Vegetation patterns p0004 N82-12500

Report on Skylab 4 African drought and arid land experiment p0037 N82-12501

A proposal for continuation of support for the application of remotely sensed data to state and regional problems. Part 1: Technical proposal [E82-10018] p0056 N82-15496

LANDSAT D

Computational aspects of geometric correction data generation in the LANDSAT-D imagery processing p0045 N82-10072

The MSS control point location error filter for LANDSAT-D p0051 N82-10073

LANDSAT 2

LANDSAT-2 and LANDSAT-3 flight evaluation report, 23 April to 23 July 1979 [E82-10005] p0053 N82-15483

LANDSAT-2 and LANDSAT-3 flight evaluation report, 23 October 1978 to 23 January 1979 [E82-10017] p0054 N82-15495

LANDSAT 3

LANDSAT-2 and LANDSAT-3 flight evaluation report, 23 April to 23 July 1979 [E82-10005] p0053 N82-15483

LANDSAT-2 and LANDSAT-3 flight evaluation report, 23 October 1978 to 23 January 1979 [E82-10017] p0054 N82-15495

LASER APPLICATIONS

Airborne laser acquisition of cross-section data p0049 A82-12600

Analog methods for processing multispectral photographs p0044 A82-16623

Space techniques to monitor movements in the earth's crust p0016 A82-18797

Remote sensing of sea state by laser altimeters [NASA-CR-165049] p0033 N82-14789

LIBERIA

A history of flying and photography: In the Photogrammetry Division of the National Ocean Survey 1919 - 1979 [PB81-246738] p0017 N82-15520

LIBRATION

Distant magnetic field effects associated with Birkeland currents /made possible by the evaluation of TRIAD's attitude oscillations/ p0015 A82-12215

LIBYA

Geology and linears of Libya p0019 N82-10818

LIGHT SCATTERING

Calculation of the decrease in the contrast of objects of a place due to light scattering in the atmosphere p0042 A82-13633

LIMNOLOGY

Data sources for analyses of Great Lakes wetlands p0035 A82-10054

Remote sensing that motivated community action p0008 A82-12594

The operational use of Landsat for lake quality assessment p0036 A82-12596

LINEAR FILTERS
The MSS control point location error filter for LANDSAT-D p0051 N82-10073
LITHOSPHERE
Study of the time evolution of the lithosphere [NASA-CR-164968] p0016 N82-11696
The reduction, verification and interpretation of Magsat magnetic data over Canada [E82-10006] p0046 N82-15484
LOWER CALIFORNIA (MEXICO)
The use of satellite infrared imagery for describing ocean processes in relation to spawning of the northern anchovy /Engraulis mordax/ p0025 A82-17565
Geological features of southwestern North America p0020 N82-12495

M

MAGNETIC ANOMALIES
A closer examination of the reduction of satellite magnetometer data for geological studies p0019 A82-11039
The reduction, verification and interpretation of Magsat magnetic data over Canada [E82-10006] p0046 N82-15484
The mineralogy of global magnetic anomalies [E82-10009] p0021 N82-15487
MAGNETIC EFFECTS
Distant magnetic field effects associated with Birkeland currents /made possible by the evaluation of TRIAD's attitude oscillations/ p0015 A82-12215
MAGNETIC FIELDS
Magnetic field-aligned electron distributions in the dayside cusp p0015 A82-12186
MAGSAT: Vector magnetometer absolute sensor alignment determination [NASA-TM-79648] p0051 N82-10468
MAGNETIC MEASUREMENT
Magnetic field observations on DE-A and -B --- Dynamics Explorer A and B satellites p0051 A82-16447
MAGNETIC STORMS
Characteristics of westward travelling surges during magnetospheric substorms p0050 A82-14299
MAGNETIC SURVEYS
Use of hydromagnetic waves to map geomagnetic field lines p0016 A82-16868
Space techniques to monitor movements in the earth's crust p0016 A82-18797
Magnetic Field Satellite (Magsat) data processing system specifications [NASA-CR-166737] p0045 N82-11103
NURE aerial gamma-ray and magnetic reconnaissance survey of Maine and portions of New York. Volume 1: Data acquisition, reduction and interpretation [DE82-000650] p0053 N82-14599
NURE aerial gamma-ray and magnetic reconnaissance survey of Maine and portions of New York, volume 2 [DE82-000781] p0020 N82-14600
NURE aerial gamma-ray and magnetic reconnaissance survey of Maine and portions of New York, volume 2 [DE82-000401] p0020 N82-14601
NURE aerial gamma-ray and magnetic reconnaissance survey of Maine and portions of New York, volume 2 [DE82-000780] p0021 N82-14602
NURE aerial gamma-ray and magnetic reconnaissance survey of Maine and portions of New York, volume 2 [DE82-000872] p0021 N82-14603
NURE aerial gamma-ray and magnetic reconnaissance survey of Maine and portions of New York, volume 2 [DE82-000772] p0021 N82-14604
NURE aerial gamma-ray and magnetic reconnaissance survey of Maine and portions of New York, volume 2 [DE82-000785] p0021 N82-14605
NURE aerial gamma-ray and magnetic reconnaissance survey of Maine and portions of New York, volume 2 [DE82-000869] p0021 N82-14606
NURE aerial gamma-ray and magnetic reconnaissance survey of Maine and portions of New York, volume 2 [DE82-000794] p0021 N82-14607
NURE aerial gamma-ray and magnetic reconnaissance survey of Maine and portions of New York, volume 2 [DE82-000784] p0021 N82-14608
Preliminary analysis of gravity and aeromagnetic surveys of the Timber Mountain area, southern Nevada [DE81-029462] p0022 N82-15506
MAGNETOHYDRODYNAMIC WAVES
Use of hydromagnetic waves to map geomagnetic field lines p0016 A82-16868
MAGNETOMETERS
Magnetic field observations on DE-A and -B --- Dynamics Explorer A and B satellites p0051 A82-16447
MAGSAT: Vector magnetometer absolute sensor alignment determination [NASA-TM-79648] p0051 N82-10468
MAGNETOSPHERE
Characteristics of westward travelling surges during magnetospheric substorms p0050 A82-14299
Use of hydromagnetic waves to map geomagnetic field lines p0016 A82-16868
MAGSAT SATELLITES
Magnetic Field Satellite (Magsat) data processing system specifications [NASA-CR-166737] p0045 N82-11103
MAINE
NURE aerial gamma-ray and magnetic reconnaissance survey of Maine and portions of New York. Volume 1: Data acquisition, reduction and interpretation [DE82-000650] p0053 N82-14599
NURE aerial gamma-ray and magnetic reconnaissance survey of Maine and portions of New York, volume 2 [DE82-000781] p0020 N82-14600
NURE aerial gamma-ray and magnetic reconnaissance survey of Maine and portions of New York, volume 2 [DE82-000401] p0020 N82-14601
NURE aerial gamma-ray and magnetic reconnaissance survey of Maine and portions of New York, volume 2 [DE82-000780] p0021 N82-146C2
NURE aerial gamma-ray and magnetic reconnaissance survey of Maine and portions of New York, volume 2 [DE82-000872] p0021 N82-14603
NURE aerial gamma-ray and magnetic reconnaissance survey of Maine and portions of New York, volume 2 [DE82-000772] p0021 N82-14604
NURE aerial gamma-ray and magnetic reconnaissance survey of Maine and portions of New York, volume 2 [DE82-000785] p0021 N82-14605
NURE aerial gamma-ray and magnetic reconnaissance survey of Maine and portions of New York, volume 2 [DE82-000869] p0021 N82-14606
NURE aerial gamma-ray and magnetic reconnaissance survey of Maine and portions of New York, volume 2 [DE82-000794] p0021 N82-14607
NURE aerial gamma-ray and magnetic reconnaissance survey of Maine and portions of New York, volume 2 [DE82-000784] p0021 N82-14608
MALAYA
Vegetation patterns p0004 N82-12500
MAN ENVIRONMENT INTERACTIONS
Spacelab-research of European regions with strong negative environmental influences, based on AVHRR-data of the satellites Tiros-N and NOAA p0007 A82-12517
Study of the anthropogenic influence on the environment, based on multispectral scanning images p0008 A82-15965
Cultural features imaged and observed from Skylab 4 p0010 N82-12499
MAPPING
Digital image technology - MC&G impact --- Mapping, Charting, & Geodesy p0015 A82-10028
Applications of digital displays in photointerpretation and digital mapping p0041 A82-10038
Application of satellite Doppler techniques to the national mapping program p0015 A82-10056
Bureau of Land Management satellite Doppler positioning techniques p0015 A82-10057
Cost effective computer processing of airborne scanner data for regional level mapping p0043 A82-15970
Small-scale terrain mapping based on numerical interpretation of LANDSAT imagery [VTT-40] p0045 N82-10485
Reports of Planetary Geology Program, 1981 [NASA-TM-84211] p0016 N82-14041
The reduction, verification and interpretation of Magsat magnetic data over Canada [E82-10006] p0046 N82-15484
MAPS
A global atlas of GEOS-3 significant waveheight and comparison of the data with national buoy data p0026 N82-10660
MARINE BIOLOGY
Fisheries investigations and management benefits from remote sensing --- fish tracking p0030 N82-14559
MARINE ENVIRONMENTS
A marine environmental monitoring and assessment program p0027 N82-10663
Monitoring the Chesapeake Bay using satellite data for Superflux III p0027 N82-10668
A look at nonsatellite remote sensing systems for marine use --- together with satellite systems, overall view of the technology p0032 N82-14586
MARINE METEOROLOGY
An investigation of a polar low with a spiral cloud structure p0007 A82-10616
Analysis of SEASAT wind observations over the Indian Ocean p0023 A82-10671
Oceanic wind and balanced pressure-height fields derived from satellite measurements p0023 A82-13214
Upper tropospheric cyclonic vortices in the tropical South Atlantic p0009 A82-16325
Detection of monsoon inversion by TIROS-N satellite p0024 A82-17168
CTD/02 measurements during the Equatorial Pacific Ocean Climate Study (EPOCS) in 1979 [PB81-211203] p0026 N82-10461
The potential and requirements for space oceanography --- National Oceanic Satellite system and U.S. Navy requirements p0029 N82-14556
Offshore petroleum industry environmental data requirements: Emphasis on remote sensing p0030 N82-14557
The Seasat commercial demonstration program p0030 N82-14561
Determination of surface wind speed from remotely measured whitecap coverage, a feasibility assessment p0030 N82-14565
Marine activities in Sweden for which remote sensing data may be of interest --- oceanography, weather forecasting, and analysis p0031 N82-14576
Scientific studies using Bhaskara satellite microwave radiometer (SAMIR) data: A short overview --- calibration of the instrument and its use in the study of oceanographic parameters p0032 N82-14587
GEM: A simple meteorological buoy with satellite telemetry p0053 N82-14779
Meteorological and oceanographic observations on board Netherlands lightvessels and the lightplatform 'Goeree' in the North Sea [KNMI-141-28] p0033 N82-15684
MARINE RESOURCES
Remote sensing contributions to the management of renewable resources p0055 A82-12530
Chesapeake Bay Plume Study: Superflux 1980 [NASA-CP-2188] p0026 N82-10661
Superflux I, II, and III experiment design: Remote sensing aspects p0027 N82-10664
Superflux I, II, and III experiment designs: Water sampling and analyses --- Chespeake Bay, environmental monitoring and remote sensing p0027 N82-10665
Application of the NASA airborne oceanographic lidar to the mapping of chlorophyll and other organic pigments p0027 N82-10684
Studies of the Indian continental shelf: Application of remote sensing data p0031 N82-14569
MARINE TRANSPORTATION
An evaluation of Seasat-A data in relation to optimum track ship weather routing and site specific forecasting for the offshore oil industry p0030 N82-14564
MARKING
Development and evaluation of an automatic labeling technique for spring small grains [E82-10001] p0004 N82-15480
MARSHLANDS
Repetitive aerial photography for assessing marsh vegetation changes p0001 A82-10048
Use of visible and thermal satellite data to monitor an intermittently flooding marshland p0036 A82-15037
MASSACHUSETTS
Spectral atmospheric observations at Nantucket Island, May 7-14, 1981 [NASA-TM-83196] p0029 N82-14550
MATHEMATICAL MODELS
A mathematical model of an over-sea airborne UHF radio link p0049 A82-11406
A Swedish proposal for an EISCAT/GEOS-2 experiment --- geomagnetic field models [KGI-175] p0052 N82-10484
Ionospheric propagation correction modeling for satellite altimeters [NASA-CR-156881] p0052 N82-12447
Sensitivity analysis of a mesoscale moisture model [AD-A101528] p0012 N82-14590
Winterkill indicator model, Crop Condition Assessment Division (CCAD) data base interface driver, user's manual [E82-10014] p0005 N82-15492
Use of environmental satellite data for input to energy balance snowmelt models [PB81-227795] p0039 N82-15673
MEDITERRANEAN SEA
Requirements in pollution monitoring and coastal management p0030 N82-14558
Oil spills: Large scale monitoring by LANDSAT p0012 N82-14572
Operational use of remote sensing for coastal zone management and possible contribution of specialized satellites --- aerial photography p0031 N82-14574
MESOMETEOROLOGY
GEM: A simple meteorological buoy with satellite telemetry p0053 N82-14779
MESOSCALE PHENOMENA
Visual observations of the ocean p0028 N82-12502
Mesoscale wake clouds in Skylab photographs p0011 N82-12508
Mesoscale cloud features observed from Skylab p0011 N82-12509
Sensitivity analysis of a mesoscale moisture model [AD-A101528] p0012 N82-14590
METEORITE CRATERS
The Manicouagan impact structure observed from Skylab [CONTRIB-544] p0020 N82-12497
METEOROLOGICAL PARAMETERS
Two-dimensional model variability in thermal inertia surveys p0042 A82-15029
The determination of navigational and meteorological variables measured by NOAA/RFC WP3D aircraft [PB81-225468] p0028 N82-11743
METEOROLOGICAL RADAR
Analysis of bright bands from 3-D radar data --- for snow/rain delineation p0035 A82-10208
METEOROLOGY
Meteorological lab applications of Skylab handheld-camera photographs p0011 N82-12506
Analysis of satellite observations: Theoretical studies on the sampling problem [MITT-31] p0056 N82-15499
METEOSAT SATELLITE
Overall economic impact of an operational Meteosat system [ESA-CR(P)-1457] p0055 N82-13010
METHANE
Automated analyzer for aircraft measurements of atmospheric methane and total hydrocarbons p0007 A82-11949

MEXICO

Radar mapping, archaeology, and ancient land use in the Maya lowlands
[NASA-CR-164931] p0010 N82-11514

Global Tectonics: Some Geologic analyses of observations and photographs from Skylab
p0020 N82-12494

Geological features of southwestern North America
p0020 N82-12495

MICHIGAN

Introducing remote sensing to county-level agencies in Michigan through the Cooperative Extension Service
p0007 A82-10034

Data sources for analyses of Great Lakes wetlands
p0035 A82-10064

MICROORGANISMS

Infrared spectroscopy of microorganisms near 3.4 microns in relation to geology and astronomy
[PREPRINT-69] p0020 N82-12713

MICROWAVE EMISSION

A comparison of radiative transfer models for predicting the microwave emission from soils p0035 A82-10694

SMMR data set development for GARP --- impact of cross polarization and Faraday rotation on SMMR derived brightness temperatures
[NASA-CR-166721] p0052 N82-11512

MICROWAVE IMAGERY

An improvement in land cover classification achieved by merging microwave data with Landsat multispectral scanner data p0007 A82-10043

A preliminary evaluation of Seasat performance over the area of JASIN and its relevance to ERS-1
p0031 N82-14567

Visual Evaluation of E-SLAR imagery
[DFVLR-FB-81-11] p0047 N82-15503

MICROWAVE RADIOMETERS

Use of radar and microwave radiometry for reconnaissance satellites
[FOA-C-30204-E1] p0052 N82-10481

Microwave limb sounder --- measuring trace gases in the upper atmosphere
[NASA-CASE-NPO-14544-1] p0011 N82-12685

Scientific studies using Bhaskara satellite microwave radiometer (SAMIR) data: A short overview --- calibration of the instrument and its use in the study of oceanographic parameters p0032 N82-14587

MICROWAVE SCATTERING

Radiative transfer theory for passive microwave remote sensing of random media p0049 A82-11533

Reflectivity and emissivity of snow and ground at mm waves p0042 A82-14860

Ocean surface height-slope probability density function from SEASAT altimeter echo p0024 A82-15076

An analysis of short pulse and dual frequency radar techniques for measuring ocean wave spectra from satellites p0024 A82-15318

State-of-the-art in using a spaceborne altimeter and scatterometer for the determination of wind, sea state, and marine and ice dynamics --- Seasat instruments
p0052 N82-14560

MICROWAVE SENSORS

Technology transfer of NASA microwave remote sensing system
[NASA-CR-165791] p0028 N82-11515

Remote Sensing Information Bulletin: Issue number 6
p0053 N82-14616

MILLIMETER WAVES

Reflectivity and emissivity of snow and ground at mm waves p0042 A82-14860

MINERAL DEPOSITS

Deep Ocean Mining Environmental Study. Environmental effects of commercial-scale mining
[PB81-227753] p0029 N82-13484

MINERAL EXPLORATION

Statistical Techniques Applied to Aerial Radiometric Surveys (STAARS): Series introduction and the principal-components-analysis method --- National Uranium Resource Evaluation Program
[DE81-029177] p0019 N82-10476

NURE aerial gamma-ray and magnetic reconnaissance survey of Maine and portions of New York. Volume 1: Data acquisition, reduction and interpretation
[DE82-000650] p0053 N82-14599

NURE aerial gamma-ray and magnetic reconnaissance survey of Maine and portions of New York, volume 2
[DE82-000781] p0020 N82-14600

NURE aerial gamma-ray and magnetic reconnaissance survey of Maine and portions of New York, volume 2
[DE82-000401] p0020 N82-14601

NURE aerial gamma-ray and magnetic reconnaissance survey of Maine and portions of New York, volume 2
[DE82-000780] p0021 N82-14602

NURE aerial gamma-ray and magnetic reconnaissance survey of Maine and portions of New York, volume 2
[DE82-000872] p0021 N82-14603

NURE aerial gamma-ray and magnetic reconnaissance survey of Maine and portions of New York, volume 2
[DE82-000772] p0021 N82-14604

NURE aerial gamma-ray and magnetic reconnaissance survey of Maine and portions of New York, volume 2
[DE82-000785] p0021 N82-14605

NURE aerial gamma-ray and magnetic reconnaissance survey of Maine and portions of New York, volume 2
[DE82-000869] p0021 N82-14606

NURE aerial gamma-ray and magnetic reconnaissance survey of Maine and portions of New York, volume 2
[DE82-000794] p0021 N82-14607

NURE aerial gamma-ray and magnetic reconnaissance survey of Maine and portions of New York, volume 2
[DE82-000784] p0021 N82-14608

Geologic applications of thermal-inertia mapping from satellite --- Powder River, Wyoming; Cubeza Prieta, Arizona, and Yellowstone National Park
[E82-10011] p0021 N82-15489

An investigation into the applicability of thermal infrared scanning for exploration
[BMFT-FB-T-81-087] p0022 N82-15925

MINERALOGY

The mineralogy of global magnetic anomalies
[E82-10009] p0021 N82-15487

MINES (EXCAVATION)

A proposal for continuation of support for the application of remotely sensed data to state and regional problems. Part 1: Technical proposal
[E82-10018] p0056 N82-15496

MINING

Deep Ocean Mining Environmental Study. Environmental effects of commercial-scale mining
[PB81-227753] p0029 N82-13484

MISSISSIPPI

A proposal for continuation of support for the application of remotely sensed data to state and regional problems. Part 1: Technical proposal
[E82-10018] p0056 N82-15496

MISSOURI

Radiative heating rates and some optical properties of the St. Louis aerosol, as inferred from aircraft measurements p0008 A82-14320

MISSOURI RIVER BASIN (US)

The potential for use of Landsat data in water resources planning for the Missouri River Basin p0037 A82-18000

MODULATION TRANSFER FUNCTION

Wave orbital velocity, fade, and SAR response to azimuth waves p0023 A82-11203

MOISTURE CONTENT

Effect of grain size and snowpack water equivalence on visible and near-infrared satellite observations of snow
p0035 A82-12553

Remote sensing of crop moisture status
p0003 A82-17997

Progress in radar snow research --- Brookings, South Dakota
[NASA-CR-166709] p0038 N82-12510

MOLECULAR SPECTROSCOPY

Nitric oxide delta band emission in the earth's atmosphere Comparison of a measurement and a theory
p0008 A82-13268

MONSOONS

Detection of monsoon inversion by TIROS-N satellite
p0024 A82-17168

MOUNTAINS

Snow-mapping experiment p0037 N82-12498

Preliminary analysis of gravity and aeromagnetic surveys of the Timber Mountain area, southern Nevada
[DE81-029462] p0022 N82-15506

Use of environmental satellite data for input to energy balance snowmelt models
[PB81-227795] p0039 N82-15673

MULTIPATH TRANSMISSION

A mathematical model of an over-sea airborne UHF radio link p0049 A82-11406

MULTISPECTRAL BAND CAMERAS

Main results of the Raduga experiment
p0051 A82-16602

MULTISPECTRAL BAND SCANNERS

Data compression and reconstruction for mixed resolution multispectral sensors p0049 A82-10045

Limitations in the spectral discrimination of the Landsat MSS p0001 A82-10046

Computational aspects of geometric correction data generation in the LANDSAT-D imagery processing
p0045 N82-10072

The MSS control point location error filter for LANDSAT-D p0051 N82-10073

MULTISPECTRAL PHOTOGRAPHY

Investigations concerning the image-controlled segmentation of objects in multispectral imagery data --- German thesis p0042 A82-15003

Experimental telemetry system based on the Fragment multispectral scanning system p0050 A82-15955

Study and mapping of agricultural land use, based on space images p0003 A82-15963

Airborne and spaceborne multispectral photography of the earth --- Russian book p0043 A82-16601

Main results of the Raduga experiment
p0051 A82-16602

Evaluation of the information content of the channels of spaceborne multispectral photography of the Fergana region by the MKF-6 camera from Soyuz-22
p0043 A82-16605

Geometric quality of MKF-6 photographs
p0043 A82-16606

Methods of instrumental interpretation of multispectral aerial and space photographs p0043 A82-16607

Characteristics of the photometry of small objects from aerial and space photographs p0044 A82-16616

Estimation of the brightness field from results of multispectral photography of the earth from space
p0044 A82-16617

Analog methods for processing multispectral photographs p0044 A82-16623

Processing of multispectral image data on special-purpose computer systems p0044 A82-16627

Programs for the statistical analysis of multispectral photographs p0044 A82-16628

Linear combinations of multispectral images
p0044 A82-16629

Coordinate referencing of MKF-6 photographs and their transformation to the cartographic projection
p0045 A82-16630

Identification of lithologic units using multichannel imaging systems p0046 N82-11509

Multitemporal calibration of LANDSAT images: A method for improving the marine phenomena recognition, with as example the Venice lagoon --- brightness/green/yellow feature space, image enhancement p0046 N82-14578

Mapping of surface currents in Greenland fiords by means of LANDSAT images --- multispectral photography
p0038 N82-14579

The use of LANDSAT MSS to observe sediment distribution and movement in the Solent coastal area --- multispectral scannel (MSS) p0038 N82-14580

Maritime applications of image processing at DFVLR, Oberpfaffenhofen, West Germany --- LANDSAT multispectral scanner images, digital interactive image analysis p0032 N82-14585

MULTIVARIATE STATISTICAL ANALYSIS

Statistical Techniques Applied to Aerial Radiometric Surveys (STAARS): Series introduction and the principal-components-analysis method --- National Uranium Resource Evaluation Program
[DE81-029177] p0019 N82-10476

Fiscal year 1980-81 implementation plan in support of technical development and integration of sampling and aggregation procedures --- crop acreage estimation
[E82-10013] p0005 N82-15491

N

NASA PROGRAMS

Reports of Planetary Geology Program, 1981
[NASA-TM-84211] p0016 N82-14041

NATIONAL OCEANIC SATELLITE SYSTEM

The potential and requirements for space oceanography --- National Oceanic Satellite system and U.S. Navy requirements p0029 N82-14556

NATIONAL SEVERE STORMS PROJECT

National Hurricane operations plan
[PB81-247231] p0013 N82-15697

NAVIGATION AIDS

The application of programmable pocket calculators for computations during survey flights p0050 A82-16164

NEAR INFRARED RADIATION

Effect of grain size and snowpack water equivalence on visible and near-infrared satellite observations of snow
p0035 A82-12553

The near-infrared radiation received by satellites from clouds p0025 A82-17492

NEARSHORE WATER

Synoptic thermal and oceanographic parameter distributions in the New York Bight Apex
p0023 A82-12885

NEBRASKA

Remote sensing of crop moisture status
p0003 A82-17997

The potential for use of Landsat data in water resources planning for the Missouri River Basin p0037 A82-18000

NEVADA

Estimation of atmospheric path-radiance by the covariance matrix method p0041 A82-10861

Preliminary analysis of gravity and aeromagnetic surveys of the Timber Mountain area, southern Nevada
[DE81-029462] p0022 N82-15506

NEW ENGLAND (US)

Meteorological lab applications of Skylab handheld-camera photographs p0011 N82-12506

NEW GUINEA (ISLAND)

Estimation of atmospheric path-radiance by the covariance matrix method p0041 A82-10861

NEW MEXICO

Environmental Monitoring Report, Sandia National Labs., Albuquerque, New Mexico, 180
[DE81-027839] p0010 N82-11649

Meteorological lab applications of Skylab handheld-camera photographs p0011 N82-12506

NEW YORK

Synoptic thermal and oceanographic parameter distributions in the New York Bight Apex
p0023 A82-12885

Role of remote sensing in the study of acid rain impact on aquatic systems
[AIAA PAPER 82-0336] p0036 A82-17892

Meteorological lab applications of Skylab handheld-camera photographs p0011 N82-12506

NURE aerial gamma-ray and magnetic reconnaissance survey of Maine and portions of New York. Volume 1: Data acquisition, reduction and interpretation
[DE82-000650] p0053 N82-14599

NURE aerial gamma-ray and magnetic reconnaissance survey of Maine and portions of New York, volume 2
[DE82-000781] p0020 N82-14600

NURE aerial gamma-ray and magnetic reconnaissance survey of Maine and portions of New York, volume 2
[DE82-000401] p0020 N82-14601
NURE aerial gamma-ray and magnetic reconnaissance survey of Maine and portions of New York, volume 2
[DE82-000780] p0021 N82-14602
NURE aerial gamma-ray and magnetic reconnaissance survey of Maine and portions of New York, volume 2
[DE82-000872] p0021 N82-14603
NURE aerial gamma-ray and magnetic reconnaissance survey of Maine and portions of New York, volume 2
[DE82-000772] p0021 N82-14604
NURE aerial gamma-ray and magnetic reconnaissance survey of Maine and portions of New York, volume 2
[DE82-000785] p0021 N82-14605
NURE aerial gamma-ray and magnetic reconnaissance survey of Maine and portions of New York, volume 2
[DE82-000869] p0021 N82-14606
NURE aerial gamma-ray and magnetic reconnaissance survey of Maine and portions of New York, volume 2
[DE82-000794] p0021 N82-14607
NURE aerial gamma-ray and magnetic reconnaissance survey of Maine and portions of New York, volume 2
[DE82-000784] p0021 N82-14608

NEW ZEALAND
Global Tectonics: Some Geologic analyses of observations and photographs from Skylab
p0020 N82-12494
Vegetation patterns p0004 N82-12500

NITRIC OXIDE
Nitric oxide delta band emission in the earth's atmosphere Comparison of a measurement and a theory
p0008 A82-13268

NORTH AMERICA
Availability of Seasat synthetic aperture radar imagery
p0050 A82-15039
Geological features of southwestern North America
p0020 N82-12495
Skylab 4 observations of Volcanoes. Part A: Volcanoes and volcanic landforms. Part B: Summit eruption of Femandian Caldera, Galapagos Islands, Ecuador
p0020 N82-12496

NORTH CAROLINA
Satellite imagery and shoreline erosion prediction
p0036 A82-12595
Aircraft data summaries of the SURE intensives, volume 4
[DE82-900311] p0012 N82-13569

NORTH SEA
An evaluation of Seasat-A data in relation to optimum track ship weather routing and site specific forecasting for the offshore oil industry p0030 N82-14564
Coastal zone research using remote sensing techniques --- calibration of coastal zone color scanner
p0031 N82-14571
Project Noordwijk. Part 1: Measurements of the radar backscatter coefficient gamma (sigma deg) in 1977 and 1978 --- on a sea platform
[PHL-1979-49-PT-1] p0032 N82-14617
Project Noordwijk. Part 2: Results of North Sea clutter measurements in the I-band performed from the platform Noordwijk in September/October 1977
[PHL-1980-28-PT-2] p0033 N82-14618
Meteorological and oceanographic observations on board Netherlands lightvessels and the lightplatform 'Goeree' in the North Sea
[KNMI-141-28] p0033 N82-15684

NORWAY
The Norwegian remote sensing experiment (Norsex) in a marginal ice zone p0031 N82-14566

O

OCEAN BOTTOM
Deep Ocean Mining Environmental Study. Environmental effects of commercial-scale mining
[PB81-227753] p0029 N82-13484
Operational use of remote sensing for coastal zone management and possible contribution of specialized satellites --- aerial photography p0031 N82-14574

OCEAN COLOR SCANNER
Preliminary analysis of ocean color scanner data from Superflux III p0027 N82-10672

OCEAN CURRENTS
The observation of tidal patterns, currents, and bathymetry with SLAR imagery of the sea
p0023 A82-11201
A short review of an oceanographic use of Meteosat data by the ORSTOM remote sensing service
p0031 N82-14570
Marine activities in Sweden for which remote sensing data may be of interest --- oceanography, weather forecasting, and analysis p0031 N82-14576

OCEAN DATA ACQUISITIONS SYSTEMS
U.S. Navy planning for satellite oceanographic data exploitation
[AAS 81-072] p0024 A82-16341
Technology transfer of NASA microwave remote sensing system
[NASA-CR-165791] p0028 N82-11515
The need for integrated off-shore, real-time information and management systems p0055 N82-14555
The potential and requirements for space oceanography --- National Oceanic Satellite system and U.S. Navy requirements p0029 N82-14556
Requirements in pollution monitoring and coastal management p0030 N82-14558
A look at nonsatellite remote sensing systems for marine use --- together with satellite systems, overall view of the technology p0032 N82-14586
GEM: A simple meteorological buoy with satellite telemetry p0053 N82-14779

OCEAN DYNAMICS
Surface signs of internal ocean dynamics
[AD-A101380] p0029 N82-13642
State-of-the-art in using a spaceborne altimeter and scatterometer for the determination of wind, sea state, and marine and ice dynamics --- Seasat instruments
p0052 N82-14560

OCEAN SURFACE
Analysis of SEASAT wind observations over the Indian Ocean p0023 A82-10671
Wave orbital velocity, fade, and SAR response to azimuth waves p0023 A82-11203
Water vapour absorption in the 3.5-4.2 micron atmospheric window p0023 A82-14586
Radar backscattering from ocean waves at low grazing angles p0023 A82-14730
Ocean surface height-slope probability density function from SEASAT altimeter echo p0024 A82-15076
Determination of the length of sea waves by an airborne radar technique p0024 A82-15213
An analysis of short pulse and dual frequency radar techniques for measuring ocean wave spectra from satellites p0024 A82-15318
Investigation of survey conditions for the ocean surface in the 0.4-1.1 micron spectral range p0024 A82-15960
Clear water radiances for atmospheric correction of coastal zone color scanner imagery p0025 A82-17292
The near-infrared radiation received by satellites from clouds p0025 A82-17492
Variations in upper ocean heat storage determined from satellite data p0025 A82-17567
Measurement of sea and ice backscatter reflectivity using an OTH radar system p0025 A82-18074
Seasat altimetry adjustment model including tidal and other sea surface effects
[AD-A104188] p0026 N82-10473
A global atlas of GEOS-3 significant waveheight and comparison of the data with national buoy data
p0026 N82-10660
Surface signs of internal ocean dynamics
[AD-A101380] p0029 N82-13642
Determination of surface wind speed from remotely measured whitecap coverage, a feasibility assessment
p0030 N82-14565
A preliminary evaluation of Seasat performance over the area of JASIN and its relevance to ERS-1
p0031 N82-14567
Oil spills: Large scale monitoring by LANDSAT
p0012 N82-14572
Airborne remote sensing of the coastal zone
p0053 N82-14577
Multitemporal calibration of LANDSAT images: A method for improving the marine phenomena recognition, with as example the Venice lagoon --- brightness/green/yellow feature space, image enhancement p0046 N82-14578
The feasibility of using remotely sensed color as an index of Irish coastal water properties --- statistical correlation of sea truth data p0032 N82-14581
Project Noordwijk. Part 1: Measurements of the radar backscatter coefficient gamma (sigma deg) in 1977 and 1978 --- on a sea platform
[PHL-1979-49-PT-1] p0032 N82-14617
Project Noordwijk. Part 2: Results of North Sea clutter measurements in the I-band performed from the platform Noordwijk in September/October 1977
[PHL-1980-28-PT-2] p0033 N82-14618
Remote sensing of sea state by laser altimeters
[NASA-CR-165049] p0033 N82-14789

OCEAN TEMPERATURE
Comparison of polar and geostationary satellite infrared observations of sea surface temperatures in the Gulf of Maine p0024 A82-15030
Detection of monsoon inversion by TIROS-N satellite
p0024 A82-17168
The use of satellite infrared imagery for describing ocean processes in relation to spawning of the northern anchovy /Engraulis mordax/ p0025 A82-17565
ICAPS oceanographic data for the Indian Ocean
[AD-A103173] p0029 N82-13641

OCEANOGRAPHIC PARAMETERS
Fisheries investigations and management benefits from remote sensing --- fish tracking p0030 N82-14559

OCEANOGRAPHY
SAR imaging of ocean waves - Theory
p0023 A82-11202
Synoptic thermal and oceanographic parameter distributions in the New York Bight Apex
p0023 A82-12885
Investigation of survey conditions for the ocean surface in the 0.4-1.1 micron spectral range p0024 A82-15960
Study on satellite radar altimetry in climatological and oceanographic research, volume 1
[SP/153/06/01/FR(80)-VOL-1] p0026 N82-10486
Study on satellite radar altimetry in climatological and oceanographic research, volume 2
[SP/153/06/01FR(80)-VOL-2] p0026 N82-10487
Application of the NASA airborne oceanographic lidar to the mapping of chlorophyll and other organic pigments
p0027 N82-10684
Assessment of Superflux relative to remote sensing --- airborne remote sensing of the Chesapeake Bay plume and shelf regions p0028 N82-10694
Visual observations of the ocean p0028 N82-12502
An assessment of the potential contributions to oceanography from Skylab visual observations and handheld-camera photographs p0028 N82-12503
Boundary detection criteria for satellite altimeters
[NASA-CR-156880] p0028 N82-12734
The SACLANTCEN oceanographic data base. Volume 1: Design criteria and data structure and content
[AD-A103277] p0029 N82-13639
ICAPS oceanographic data for the Indian Ocean
[AD-A103173] p0029 N82-13641
Application of remote sensing data on the continental shelf: Proceedings of an EAReL-ESA Symposium
[ESA-SP-167] p0029 N82-14553
ERS-1: Mission objectives and system concept
p0029 N82-14554
Offshore petroleum industry environmental data requirements: Emphasis on remote sensing
p0030 N82-14557
An evaluation of Seasat-A data in relation to optimum track ship weather routing and site specific forecasting for the offshore oil industry p0030 N82-14564
Studies of the Indian continental shelf: Application of remote sensing data p0031 N82-14569
Scientific studies using Bhaskara satellite microwave radiometer (SAMIR) data: A short overview --- calibration of the instrument and its use in the study of oceanographic parameters p0032 N82-14587
A global atlas of GEOS-3 significant waveheight data and comparison of the data with national buoy data
[NASA-CR-156882] p0033 N82-15498
Biological patchiness in relation to satellite thermal imagery and associated chemical mesoscale features
[AD-A105757] p0047 N82-15504
Meteorological and oceanographic observations on board Netherlands lightvessels and the lightplatform 'Goeree' in the North Sea
[KNMI-141-28] p0033 N82-15684

OFFSHORE ENERGY SOURCES
Offshore petroleum industry environmental data requirements: Emphasis on remote sensing
p0030 N82-14557
The Seasat commercial demonstration program
p0030 N82-14561

OHIO
Aircraft data summaries of the SURE intensives, volume 4
[DE82-900311] p0012 N82-13569

OIL EXPLORATION
Offshore petroleum industry environmental data requirements: Emphasis on remote sensing
p0030 N82-14557
Geologic applications of thermal-inertia mapping from satellite --- Powder River, Wyoming; Cubeza Prieta, Arizona, and Yellowstone National Park
[E82-10011] p0021 N82-15489

OIL POLLUTION
Oil spills: Large scale monitoring by LANDSAT
p0012 N82-14572
The operational oil pollution surveillance system being used in France: Forecasted future developments in consideration of the NATO/CCMS remote sensing pilot study conclusions p0012 N82-14573
Use of Side Looking Airborne Radar (SLAR) for oil pollution monitoring in Norway p0012 N82-14588

OIL SLICKS
Polarimetric surveys of oil slicks p0009 A82-16619
A recommended sensor package for the detection and tracking of oil spills p0053 N82-14563

OKLAHOMA
Mapping vegetation association boundaries with Landsat MSS data - An Oklahoma example p0001 A82-10041

ONBOARD DATA PROCESSING
Application of satellite Doppler techniques to the national mapping program p0015 A82-10056
GPS application to mapping, charting and geodesy
p0015 A82-10645
Onboard utilization of ground control points for image correction. Volume 2: Analysis and simulation results
[NASA-CR-166732] p0045 N82-10470
Onboard utilization of ground control points for image correction. Volume 3: Ground control point simulation software design
[NASA-CR-166733] p0045 N82-10471
Onboard utilization of ground control points for image correction. Volume 4: Correlation analysis software design
[NASA-CR-166734] p0045 N82-10472

OPERATIONAL PROBLEMS
LANDSAT-2 and LANDSAT-3 flight evaluation report, 23 April to 23 July 1979
[E82-10005] p0053 N82-15483
LANDSAT-2 and LANDSAT-3 flight evaluation report, 23 October 1978 to 23 January 1979
[E82-10017] p0054 N82-15495

OPTICAL CORRECTION PROCEDURE

A new method for computing distortion p0016 A82-12914

OPTICAL EQUIPMENT

Study on calibration methods for Earth observation optical imaging instruments [UCD-207/1/80] p0052 N82-10488

OPTICAL PATHS

Estimation of atmospheric path-radiance by the covariance matrix method p0041 A82-10861

OPTICAL POLARIZATION

Analysis of the information content of the polarimetric method of remote sensing p0003 A82-16822

OPTICAL RADAR

Application of the NASA airborne oceanographic lidar to the mapping of chlorophyll and other organic pigments p0027 N82-10684

OSTA-1 PAYLOAD

Mission operation report: OSTA-1 [NASA-TM-84053] p0055 N82-10102

OVER-THE-HORIZON RADAR

Measurement of sea and ice backscatter reflectivity using an OTH radar system p0025 A82-18074

OXYGEN

CTD/02 measurements during the Equatorial Pacific Ocean Climate Study (EPOCS) in 1979 [PB81-211203] p0026 N82-10461

OZONOMETRY

Trace pollutant concentrations in a multiday smog episode in the California South Coast Air Basin by long path length Fourier transform infrared spectroscopy p0007 A82-10700

Special observations by the Hohenpeissenberg Meteorological Observatory. Number 42: Results of aerological and surface ozone measurements during the first semester of 1980 [SONDERBEOB-42] p0012 N82-12714

P

PACIFIC OCEAN

Oceanic wind and balanced pressure-height fields derived from satellite measurements p0023 A82-13214

Global satellite measurements of water vapour, wind speed and wave height p0051 A82-17165

Annual and nonseasonal variability of monthly low-level wind fields over the Southeastern Tropical Pacific p0025 A82-17494

The use of satellite infrared imagery for describing ocean processes in relation to spawning of the northern anchovy /Engraulis mordax/ p0025 A82-17565

CTD/02 measurements during the Equatorial Pacific Ocean Climate Study (EPOCS) in 1979 [PB81-211203] p0026 N82-10461

An assessment of the potential contributions to oceanography from Skylab visual observations and handheld-camera photographs p0028 N82-12503

Deep Ocean Mining Environmental Study: Environmental effects of commercial-scale mining [PB81-227753] p0029 N82-13484

An evaluation of Seasat-A data in relation to optimum track ship weather routing and site specific forecasting for the offshore oil industry p0030 N82-14564

PARAMETER IDENTIFICATION

Absolute image registration for geosynchronous satellites p0049 A82-10051

PATENT POLICY

Microwave limb sounder --- measuring trace gases in the upper atmosphere [NASA-CASE-NPO-14544-1] p0011 N82-12685

PATTERN RECOGNITION

American Society of Photogrammetry, Annual Meeting, 46th, St. Louis, MO, March 9-14, 1980, ASP Technical Papers p0041 A82-10027

Digital image technology - MC&G impact --- Mapping, Charting, & Geodesy p0015 A82-10028

Investigations concerning the image-controlled segmentation of objects in multispectral imagery data --- German thesis p0042 A82-15003

The use of a priori information in the remote sensing of the earth from space p0044 A82-16618

Identification of lithologic units using multichannel imaging systems p0046 N82-11509

Vegetation patterns p0004 N82-12500

Development and evaluation of an automatic labeling technique for spring small grains [E82-10001] p0004 N82-15480

Wheat cultivation: Identification and estimation of areas using LANDSAT data [E82-10007] p0004 N82-15485

PATTERN REGISTRATION

An improvement in land cover classification achieved by merging microwave data with Landsat multispectral scanner data p0007 A82-10043

Absolute image registration for geosynchronous satellites p0049 A82-10051

PAYLOADS

LANDSAT-2 and LANDSAT-3 flight evaluation report, 23 April to 23 July 1979 [E82-10005] p0053 N82-15483

LANDSAT-2 and LANDSAT-3 flight evaluation report, 23 October 1978 to 23 January 1979 [E82-10017] p0054 N82-15495

PENNSYLVANIA

Comparison of conventional and remotely sensed estimates of runoff curve numbers in southeastern Pennsylvania p0035 A82-10031

Estimation of atmospheric path-radiance by the covariance matrix method p0041 A82-10861

PETROGRAPHY

The mineralogy of global magnetic anomalies [E82-10009] p0021 N82-15487

PHENOLOGY

The discrimination of winter wheat using a growth-state signature p0002 A82-15026

US/Canada wheat and barley crop calender exploratory experiment implementation plan [E82-10016] p0005 N82-15494

PHILIPPINES

Rural development in the humid tropics p0003 A82-16162

PHOTOGEOLOGY

Remote sensing study of sinkhole occurrence p0019 A82-12590

Development of a coastal relief of the Gulf of Riga, based on results of an analysis of space images p0024 A82-15962

Investigation and mapping of the erosion relief of the Kalachskaia upland on the basis of multispectral scanner images p0008 A82-15966

Space techniques to monitor movements in the earth's crust p0016 A82-18797

Geology and linears of Libya p0019 N82-10618

Remote sensing studies of some ironstone gravels and plinthite in Thailand p0019 N82-12491

Skylab explores the Earth [NASA-SP-380] p0019 N82-12492

Global Tectonics: Some Geologic analyses of observations and photographs from Skylab p0020 N82-12494

Geological features of southwestern North America p0020 N82-12495

Skylab 4 observations of Volcanoes. Part A: Volcanoes and volcanic landforms. Part B: Summit eruption of Fernandian Caldera, Galapagos Islands, Ecuador p0020 N82-12496

The Manicouagan impact structure observed from Skylab [CONTRIB-544] p0020 N82-12497

PHOTOGRAMMETRY

American Society of Photogrammetry, Annual Meeting, 46th, St. Louis, MO, March 9-14, 1980, ASP Technical Papers p0041 A82-10027

Orientation and construction of models. I - The orientation problem in close-range photogrammetry p0049 A82-10858

Digital mapping using entities - A new concept p0041 A82-12882

Phototriangulation with map referencing of photographs in linear surveys p0016 A82-12912

Aspects in the development of aerial-photography tasks p0041 A82-12913

Block adjustment with additional parameters p0049 A82-13738

Compensation of systematic errors in bundle adjustment p0042 A82-15764

Compensation of systematic errors of image and model coordinates p0043 A82-15765

Orientation and construction of models. III - Mathematical basis of the orientation problem of one-dimensional central perspective photographs p0043 A82-15973

Theoretical reliability of elementary photogrammetric procedures. I p0043 A82-16163

Geometric quality of MKF-6 photographs p0043 A82-16606

A history of flying and photography. In the Photogrammetry Division of the National Ocean Survey 1919 - 1979 [PB81-246738] p0017 N82-15520

Description and comparison of algorithms for solving large sets of sparse matrix normal equations in geodesy and photogrammetry [SER-C-281] p0017 N82-15812

PHOTOINTERPRETATION

Applications of digital displays in photointerpretation and digital mapping p0041 A82-10038

Remote sensing for vineyard management p0001 A82-10047

Repetitive aerial photography for assessing marsh vegetation changes p0001 A82-10048

Identification of conifer species groupings from Landsat digital classifications p0002 A82-12887

Interactive techniques for estimating precipitation from GOES imagery p0041 A82-13121

Investigations concerning the image-controlled segmentation of objects in multispectral imagery data --- German thesis p0042 A82-15003

The discrimination of winter wheat using a growth-state signature p0002 A82-15026

Space photographs obtained with the Fragment system as a base for landscape mapping and physical-geographical classification of arid territories p0009 A82-15967

Airborne and spaceborne multispectral photography of the earth --- Russian book p0043 A82-16601

Main results of the Raduga experiment p0051 A82-16602

Methods of instrumental interpretation of multispectral aerial and space photographs p0043 A82-16607

The maximum mean accuracy of classification of remote-sensing objects and the influence on this accuracy of data acquisition and processing methods p0044 A82-16615

Characteristics of the photometry of small objects from aerial and space photographs p0044 A82-16616

The use of a priori information in the remote sensing of the earth from space p0044 A82-16618

Analog methods for processing multispectral photographs p0044 A82-16623

Investigation of the spatial structure of space images of the earth's surface p0044 A82-16626

Processing of multispectral image data on special-purpose computer systems p0044 A82-16627

Linear combinations of multispectral images p0044 A82-16629

A method for using aerial photos in delineating historic patterns of beach accretion and retreat [PB81-223836] p0010 N82-11536

Skylab explores the Earth [NASA-SP-380] p0019 N82-12492

Visual observations of floating ice from Skylab p0037 N82-12504

Mesoscale wake clouds in Skylab photographs p0011 N82-12508

Mesoscale cloud features observed from Skylab p0011 N82-12509

Quantitative analysis of drainage obtained from aerial photographs and RBV/LANDSAT images [E82-10008] p0039 N82-15486

Visual Evaluation of E-SLAR imagery [DFVLR-FB-81-11] p0047 N82-15503

PHOTOMAPPING

Comparison of conventional and remotely sensed estimates of runoff curve numbers in southeastern Pennsylvania p0035 A82-10031

Data sources for analyses of Great Lakes wetlands p0035 A82-10054

GPS application to mapping, charting and geodesy p0015 A82-10645

Digitizing and automated output mapping errors p0015 A82-10859

Coordinates of features on the Galilean satellites p0019 A82-12366

Areawide soil loss predictions using CIR airphotos p0007 A82-12591

Satellite imagery and shoreline erosion prediction p0036 A82-12595

Digital mapping using entities - A new concept p0041 A82-12882

Phototriangulation with map referencing of photographs in linear surveys p0016 A82-12912

Aerial and space methods in cartography p0016 A82-12915

Investigations concerning the image-controlled segmentation of objects in multispectral imagery data --- German thesis p0042 A82-15003

A VHF homing system with VHF radiotelephony for area-representative strip-survey flights conducted, as part of combined forest inventories, with light aircraft carrying 70 mm and 35 mm cameras p0003 A82-15748

Aerial-photography flights over Upper Franconia in 1980 - Operation and first application-related experience p0008 A82-15749

Study and mapping of agricultural land use, based on space images p0003 A82-15963

Mapping of forest vegetation on the basis of space images p0003 A82-15964

Study of the anthropogenic influence on the environment, based on multispectral scanning images p0008 A82-15965

Space photographs obtained with the Fragment system as a base for landscape mapping and physical-geographical classification of arid territories p0009 A82-15967

Analysis of variance of thematic mapping experiment data p0009 A82-15968

Orientation and construction of models. III - Mathematical basis of the orientation problem of one-dimensional central perspective photographs p0043 A82-15973

Coordinate referencing of MKF-6 photographs and their transformation to the cartographic projection p0045 A82-16630

The development of the Tiros Global Environmental Satellite System [AIAA PAPER 82-0383] p0025 A82-17915

The use of digitally processed Landsat imagery for vegetation mapping in Sulawesi, Indonesia p0003 A82-17998

An inertially-aided aircraft track recovery system for coastal mapping p0037 A82-18166

Photo inertial positioning system development at the Canada Centre for Remote Sensing p0045 A82-18167

Large-scale color aerial photography as a tool in sampling for mortality rates [PB81-214777] p0003 N82-10489

Desert sand seas p0020 N82-12493

Snow-mapping experiment p0037 N82-12498

An assessment of the potential contributions to oceanography from Skylab visual observations and handheld-camera photographs p0028 N82-12503

Mapping of surface currents in Greenland fiords by means of LANDSAT images --- multispectral photography p0038 N82-14579

PHOTOMETRY
Characteristics of the photometry of small objects from aerial and space photographs p0044 A82-16616

PHOTORECONNAISSANCE
Current aerial cameras p0050 A82-15655
Quantitative analysis of atmospheric pollution phenomena p0010 N82-12505
Some aspects of tropical storm structure revealed by handheld-camera photographs from space p0011 N82-12507

PLAINS
Investigation and mapping of the erosion relief of the Kalachskaia upland on the basis of multispectral scanner images p0008 A82-15966

PLANETARY GEOLOGY
Reports of Planetary Geology Program, 1981 [NASA-TM-84211] p0016 N82-14041

PLANKTON
Development of the coastal zone color scanner for NIMBUS 7. Volume 1: Mission objectives and instrument description [NASA-CR-166720-VOL-1] p0028 N82-11511
Spectral atmospheric observations at Nantucket Island, May 7-14, 1981 [NASA-TM-83196] p0029 N82-14550
The color of the sea and its relation to surface chlorophyll and depth of the euphotic zone p0030 N82-14562
The feasibility of using remotely sensed color as an index of Irish coastal water properties --- statistical correlation of sea truth data p0032 N82-14581

PLANT STRESS
Remote sensing of crop moisture status p0003 A82-17997
Investigation of the application of remote sensing technology to environmental monitoring [E82-10010] p0013 N82-15488

PLANTS (BOTANY)
Phytoecozonation of Sevier Lake region of Utah using digitized Landsat MSS data p0001 A82-10042

POLAR CAPS
The ice conditions in the Greenland waters [ISBN-87-7478-183-9] p0028 N82-12533

POLAR METEOROLOGY
An investigation of a polar low with a spiral cloud structure p0007 A82-10616

POLAR REGIONS
ERS-1: Mission objectives and system concept p0029 N82-14554

POLARIMETRY
Polarimetric surveys of oil slicks p0009 A82-16619
Images of sea waves obtained in polarimetric surveys p0024 A82-16620
The choice of the orientation of the analyzer in polarimetric surveys p0044 A82-16621
Analysis of the information content of the polarimetric method of remote sensing p0003 A82-16622

POLARIZATION
Aircraft radar response to soil moisture p0003 A82-17564

POLLUTION MONITORING
Trace pollutant concentrations in a multiday smog episode in the California South Coast Air Basin by long path length Fourier transform infrared spectroscopy p0007 A82-10700
Automated analyzer for aircraft measurements of atmospheric methane and total hydrocarbons p0007 A82-11949
Spacelab-research of European regions with strong negative environmental influences, based on AVHRR-data of the satellites Tiros-N and NOAA p0007 A82-12517
Remote sensing that motivated community action p0008 A82-12594
Study of stack emissions by combination of lidar and correlation spectrometer p0008 A82-12816
Polarimetric surveys of oil slicks p0009 A82-16619
A new method for inferring carbon monoxide concentrations from gas filter radiometer data p0009 A82-16837
Role of remote sensing in the study of acid rain impact on aquatic systems [AIAA PAPER 82-0336] p0036 A82-17892
Shuttle applications in tropospheric air quality observations [NASA-CR-145374] p0010 N82-11635
Proof of concept study [AD-A104338] p0010 N82-11639
Quantitative analysis of atmospheric pollution phenomena p0010 N82-12505
Geophysical monitoring for climatic change, number 8: Summary Report, 1979 [PB81-233355] p0012 N82-13631
Application of remote sensing data on the continental shelf: Proceedings of an EAReL-ESA Symposium [ESA-SP-167] p0029 N82-14553
Requirements in pollution monitoring and coastal management p0030 N82-14558
A recommended sensor package for the detection and tracking of oil spills p0053 N82-14563
Studies of the Indian continental shelf: Application of remote sensing data p0031 N82-14569
Oil spills: Large scale monitoring by LANDSAT p0012 N82-14572
The operational oil pollution surveillance system being used in France: Forecasted future developments in consideration of the NATO/CCMS remote sensing pilot study conclusions p0012 N82-14573
Airborne remote sensing of the coastal zone p0053 N82-14577
Multitemporal calibration of LANDSAT images: A method for improving the marine phenomena recognition, with as example the Venice lagoon --- brightness/green/yellow feature space, image enhancement p0046 N82-14578
Use of Side Looking Airborne Radar (SLAR) for oil pollution monitoring in Norway p0012 N82-14588
Investigation of the application of remote sensing technology to environmental monitoring [E82-10010] p0013 N82-15488

POLLUTION TRANSPORT
Results from the July 1981 Workshop on Passive Remote Sensing of the Troposphere [AIAA PAPER 82-0207] p0009 A82-17841

POSITION (LOCATION)
Interpolating for the location of remote sensor data [NASA-TM-82169] p0052 N82-13469

POSITION ERRORS
Digitizing and automated output mapping errors p0015 A82-10859
Some problem areas in the field of quality control for aerotriangulation p0016 A82-16161
Theoretical reliability of elementary photogrammetric procedures. I p0043 A82-16163

POSITION INDICATORS
Photo inertial positioning system development at the Canada Centre for Remote Sensing p0045 A82-18167

PRECIPITATION (METEOROLOGY)
Interactive techniques for estimating precipitation from GOES imagery p0041 A82-13121
A simulation study of the recession coefficient for antecedent precipitation index --- soil moisture and water runoff estimation [NASA-TM-83860] p0038 N82-14549
The effect of spatial variability in precipitation on streamflow [AD-A105955] p0038 N82-14589

PREDICTION ANALYSIS TECHNIQUES
A comparison of radiative transfer models for predicting the microwave emission from soils p0035 A82-10694

PROJECT PLANNING
U.S. Navy planning for satellite oceanographic data exploitation [AAS 81-072] p0024 A82-16341

Q

QUALITY CONTROL
Some problem areas in the field of quality control for aerotriangulation p0016 A82-16161

QUEBEC
The Manicouagan impact structure observed from Skylab [CONTRIB-544] p0020 N82-12497

R

RADAR ATTENUATION
Radar correlation with ice depolarization measurements of the 28.56 GHz COMSTAR beacon and associated cross polarization statistics [NASA-CR-166717] p0046 N82-14548

RADAR BEACONS
Radar correlation with ice depolarization measurements of the 28.56 GHz COMSTAR beacon and associated cross polarization statistics [NASA-CR-166717] p0046 N82-14548

RADAR DATA
Analysis of bright bands from 3-D radar data --- for snow/rain delineation p0035 A82-10208

RADAR ECHOES
The influence of gravity waves on radiometric measurements - A case study p0049 A82-13547
Study on satellite radar altimetry in climatological and oceanographic research, volume 1 [SP/153/06/01/FR(80)-VOL-1] p0026 N82-10486
Study on satellite radar altimetry in climatological and oceanographic research, volume 2 [SP/153/06/01FR(80)-VOL-2] p0026 N82-10487

RADAR IMAGERY
Factorial analysis of terrain feature positioning parameters used in combining radar and digital terrain model data p0015 A82-10029
Remote sensing techniques in the study of the agricultural potential of soils under the Cerrado vegetation /Brazil/ p0001 A82-10040
Preliminary results of mapping urban land cover with Seasat SAR imagery p0007 A82-10044
The observation of tidal patterns, currents, and bathymetry with SLAR imagery of the sea p0023 A82-11201
SAR imaging of ocean waves - Theory p0023 A82-11202
Wave orbital velocity, fade, and SAR response to azimuth waves p0023 A82-11203
A digital fast correlation approach to produce SEASAT SAR imagery p0042 A82-14870
Availability of Seasat synthetic aperture radar imagery p0050 A82-15039
Optically processed Seasat radar mosaic of Florida p0042 A82-15125
A preliminary evaluation of Seasat performance over the area of JASIN and its relevance to ERS-1 p0031 N82-14567
Seasat SAR processing at the Norwegian Defence Research Establishment --- design and operation of a digital process p0046 N82-14584
Visual Evaluation of E-SLAR imagery [DFVLR-FB-81-11] p0047 N82-15503

RADAR MAPS
Radar mapping, archaeology, and ancient land use in the Maya lowlands [NASA-CR-164931] p0010 N82-11514

RADAR MEASUREMENT
Determination of the length of sea waves by an airborne radar technique p0024 A82-15213
An analysis of short pulse and dual frequency radar techniques for measuring ocean wave spectra from satellites p0024 A82-15318
Measurement of sea and ice backscatter reflectivity using an OTH radar system p0025 A82-18074

RADAR RESOLUTION
Additional studies of Earth resources synthetic aperture radar payloads [MTR-80/90] p0054 N82-15500
New baseline system p0054 N82-15501
Squinted SAR system p0047 N82-15502

RADAR SCATTERING
Radar backscattering from ocean waves at low grazing angles p0023 A82-14730
Aircraft radar response to soil moisture p0003 A82-17564
Measurement of sea and ice backscatter reflectivity using an OTH radar system p0025 A82-18074
Anomalous wind estimates from the Seasat scatterometer p0026 A82-18724
Progress in radar snow research --- Brookings, South Dakota [NASA-CR-166709] p0038 N82-12510
Project Noordwijk. Part 1: Measurements of the radar backscatter coefficient gamma (sigma deg) in 1977 and 1978 --- on a sea platform [PHL-1979-49-PT-1] p0032 N82-14617
Project Noordwijk. Part 2: Results of North Sea clutter measurements in the I-band performed from the platform Noordwijk in September/October 1977 [PHL-1980-28-PT-2] p0033 N82-14618

RADAR SIGNATURES
The determination of navigational and meteorological variables measured by NOAA/RFC WP3D aircraft [PB81-225468] p0028 N82-11743
Measurements of radar backscatter from Arctic Sea ice in the summer [AD-A105586] p0032 N82-14592
Measurements of radar backscatter from Arctic Sea ice in the summer. Appendices A and B [AD-A105736] p0032 N82-14593

RADAR TRACKING
The operational oil pollution surveillance system being used in France: Forecasted future developments in consideration of the NATO/CCMS remote sensing pilot study conclusions p0012 N82-14573

RADIANCE
Limitations in the spectral discrimination of the Landsat MSS p0001 A82-10046
Estimation of atmospheric path-radiance by the covariance matrix method p0041 A82-10861
Clear water radiances for atmospheric correction of coastal zone color scanner imagery p0025 A82-17292
The near-infrared radiation received by satellites from clouds p0025 A82-17492
Infrared radiance model variation by sensor flight measurements p0052 N82-14171

RADIATION ABSORPTION
Water vapour absorption in the 3.5-4.2 micron atmospheric window p0023 A82-14586

RADIATIVE HEAT TRANSFER
Radiative heating rates and some optical properties of the St. Louis aerosol, as inferred from aircraft measurements p0008 A82-14320

RADIATIVE TRANSFER
A comparison of radiative transfer models for predicting the microwave emission from soils p0035 A82-10694
Radiative transfer theory for passive microwave remote sensing of random media p0049 A82-11533
An evaluation of the spatial resolution of soil moisture information [NASA-CR-166724] p0009 N82-11513

RADIO ALTIMETERS
Ocean surface height-slope probability density function from SEASAT altimeter echo p0024 A82-15076
Seasat altimetry adjustment model including tidal and other sea surface effects [AD-A104188] p0026 N82-10473
Study on satellite radar altimetry in climatological and oceanographic research, volume 1 [SP/153/06/01/FR(80)-VOL-1] p0026 N82-10486
Study on satellite radar altimetry in climatological and oceanographic research, volume 2 [SP/153/06/01FR(80)-VOL-2] p0026 N82-10487

State-of-the-art in using a spaceborne altimeter and scatterometer for the determination of wind, sea state, and marine and ice dynamics --- Seasat instruments p0052 N82-14560

RADIO ATTENUATION
The radiowave propagation environment - Science and technology objectives for the 80's p0009 A82-18052

RADIO DIRECTION FINDERS
Three bearing method for passive triangulation in systems with unknown deterministic biases p0060 A82-15920

RADIO RELAY SYSTEMS
A mathematical model of an over-sea airborne UHF radio link p0049 A82-11406

RADIOACTIVE CONTAMINANTS
Environmental Monitoring Report, Sandia National Labs., Albuquerque, New Mexico, 180
[DE81-027838] p0010 N82-11649

RADIOMETRIC CORRECTION
Clear water radiances for atmospheric correction of coastal zone color scanner imagery p0025 A82-17292

RADIOMETRIC RESOLUTION
The effect of angular factors on popularly used indicators of vegetative vigor p0001 A82-10039
Data compression and reconstruction for mixed resolution multispectral sensors p0049 A82-10045
The influence of gravity waves on radiometric measurements - A case study p0049 A82-13547
Onboard utilization of ground control points for image correction. Volume 2: Analysis and simulation results
[NASA-CR-166732] p0045 N82-10470
Recent work in passive optical imaging of water --- space and aircraft derived data p0038 N82-14575
Use of environmental satellite data for input to energy balance snowmelt models
[PB81-227795] p0039 N82-15673

RADIOTELEPHONES
A VHF homing system with VHF radiotelephony for area-representative strip-survey flights conducted, as part of combined forest inventories, with light aircraft carrying 70 mm and 35 mm cameras p0003 A82-15748

RAIN
Satellite rainfall estimation for hydrologic forecasting p0035 A82-10032
Analysis of bright bands from 3-D radar data --- for snow/rain delineation p0035 A82-10208
An evaluation of the spatial resolution of soil moisture information
[NASA-CR-166724] p0009 N82-11513
A systems approach to the real-time runoff analysis with a deterministic rainfall-runoff model
[PB81-224495] p0037 N82-11530
Scientific studies using Bhaskara satellite microwave radiometer (SAMIR) data: A short overview --- calibration of the instrument and its use in the study of oceanographic parameters p0032 N82-14587
Analysis of rainfall from flash flood producing thunderstorms, using GOES data p0038 N82-14724

RANGELANDS
Remote sensing contributions to the management of renewable resources p0055 A82-12530
Vegetation patterns p0004 N82-12500

RAYLEIGH SCATTERING
A theory of wave scattering from an inhomogeneous layer with an irregular interface p0041 A82-12757

RECLAMATION
A proposal for continuation of support for the application of remotely sensed data to state and regional problems. Part 1: Technical proposal
[E82-10018] p0056 N82-15496

RECONNAISSANCE AIRCRAFT
The determination of navigational and meteorological variables measured by NOAA/RFC WP3D aircraft
[PB81-225408] p0028 N82-11743

REFLECTANCE
Effect of grain size and snowpack water equivalence on visible and near-infrared satellite observations of snow p0035 A82-12553
Oil spills: Large scale monitoring by LANDSAT p0012 N82-14572

REGIONAL PLANNING
Introducing remote sensing to county-level agencies in Michigan through the Cooperative Extension Service p0007 A82-10034
Aerial-photography flights over Upper Franconia in 1980 Operation and first application-related experience p0008 A82-15749
The potential for use of Landsat data in water resources planning for the Missouri River Basin p0037 A82-18000

RELIEF MAPS
Development of a coastal relief of the Gulf of Riga, based on results of an analysis of space images p0024 A82-15982

RESOURCES MANAGEMENT
Remote sensing for vineyard management p0001 A82-10047
Remote sensing contributions to the management of renewable resources p0055 A82-12530
Study of the anthropogenic influence on the environment, based on multispectral scanning images p0008 A82-15965
The potential for use of Landsat data in water resources planning for the Missouri River Basin p0037 A82-18000
Application of remote sensing data on the continental shelf: Proceedings of an EARseL-ESA Symposium
[ESA-SP-167] p0029 N82-14553
Fisheries investigations and management benefits from remote sensing --- fish tracking p0030 N82-14559
Application of remote sensing to selected problems within the state of California
[E82-10004] p0004 N82-15482

RIVER BASINS
Airborne laser acquisition of cross-section data p0049 A82-12600
Cost effective computer processing of airborne scanner data for regional level mapping p0043 A82-15970

RIVERS
Satellite rainfall estimation for hydrologic forecasting p0035 A82-10032
Study of the dynamics of the Danube delta using space images p0036 A82-15961
Visual observations of floating ice from Skylab p0037 N82-12504
Quantitative analysis of drainage obtained from aerial photographs and RBV/LANDSAT images
[E82-10006] p0039 N82-15486

ROADS
Cultural features imaged and observed from Skylab 4 p0010 N82-12499

ROCKET SOUNDING
Repeatability and measurement uncertainty of the United States meteorological rocketsonde p0049 A82-12127

ROCKY MOUNTAINS (NORTH AMERICA)
An application of Landsat derived data to a regional hydrologic model p0037 A82-17999

ROUTES
An evaluation of Seasat-A data in relation to optimum track ship weather routing and site specific forecasting for the offshore oil industry p0030 N82-14564

RURAL AREAS
Cultural features imaged and observed from Skylab 4 p0010 N82-12499

RURAL LAND USE
Rural development in the humid tropics p0003 A82-16162

S

S MATRIX THEORY
A theory of wave scattering from an inhomogeneous layer with an irregular interface p0041 A82-12757

SALINITY
Remote sensing of the Chesapeake Bay plume salinity via microwave radiometry p0027 N82-10670
Operational use of remote sensing for coastal zone management and possible contribution of specialized satellites --- aerial photography p0031 N82-14574
The feasibility of using remotely sensed color as an index of Irish coastal water properties --- statistical correlation of sea truth data p0032 N82-14581
Measurements of radar backscatter from Arctic Sea ice in the summer, Appendices A and B
[AD-A105736] p0032 N82-14593

SAN ANDREAS FAULT
Geological features of southwestern North America p0020 N82-12495

SANDS
Desert sand seas p0020 N82-12493

SATELLITE OBSERVATION
Magnetic field-aligned electron distributions in the dayside cusp p0015 A82-12186
The potential and requirements for space oceanography --- National Oceanic Satellite system and U.S. Navy requirements p0029 N82-14556
Analysis of satellite observations: Theoretical studies on the sampling problem
[MITT-31] p0056 N82-15499

SATELLITE ORBITS
Distant magnetic field effects associated with Birkeland currents /made possible by the evaluation of TRIAD's attitude oscillations/ p0015 A82-12215
LANDSAT-2 and LANDSAT-3 flight evaluation report, 23 April to 23 July 1979
[E82-10005] p0053 N82-15483
LANDSAT-2 and LANDSAT-3 flight evaluation report, 23 October 1978 to 23 January 1979
[E82-10017] p0054 N82-15495

SATELLITE SURFACES
Coordinates of features on the Galilean satellites p0019 A82-12366

SATELLITE TELEVISION
The 1981 RCA space constellation p0055 A82-12541
Satellites of the Meteor series, intended for earth studies from space p0050 A82-15951
Technical equipment of an experiment for remote sensing of the earth from space p0050 A82-15952

SATELLITE-BORNE INSTRUMENTS
Metrological support of measurements of earth-surface brightness by the Fragment multispectral scanning system p0050 A82-15958
Magnetic field observations on DE-A and -B --- Dynamics Explorer A and B satellites p0051 A82-16447

SATELLITE-BORNE PHOTOGRAPHY
Coordinates of features on the Galilean satellites p0019 A82-12366
Satellites of the Meteor series, intended for earth studies from space p0050 A82-15951
Technical equipment of an experiment for remote sensing of the earth from space p0050 A82-15952
Study of the anthropogenic influence on the environment, based on multispectral scanning images p0008 A82-15965
Processing of multispectral image data on special-purpose computer systems p0044 A82-16627
Computational aspects of geometric correction data generation in the LANDSAT-D imagery processing p0045 N82-10072
Scanner --- photography from a spin stabilized synchronous satellite
[NASA-CASE-GSC-12032-2] p0052 N82-13465

SATELLITE-BORNE RADAR
Study on satellite radar altimetry in climatological and oceanographic research, volume 2
[SP/153/06/01FR(80)-VOL-2] p0026 N82-10487

SAUDI ARABIA
A history of flying and photography: In the Photogrammetry Division of the National Ocean Survey 1919 - 1979
[PB81-246738] p0017 N82-15520

SCANNERS
Scanner --- photography from a spin stabilized synchronous satellite
[NASA-CASE-GSC-12032-2] p0052 N82-13465

SCANNING
Airborne and spaceborne multispectral photography of the earth --- Russian book p0043 A82-16601

SCATTERING CROSS SECTIONS
Airborne laser acquisition of cross-section data p0049 A82-12600

SCATTEROMETERS
Evaluation of the Seasat wind scatterometer p0025 A82-18716

SCENE ANALYSIS
Data compression and reconstruction for mixed resolution multispectral sensors p0049 A82-10045
MATE VAN: Mobile analysis and training extension --- analyzing LANDSAT digital data
[NASA-TM-84056] p0045 N82-10466
Application of remote sensing to selected problems within the state of California
[E82-10004] p0004 N82-15482

SEA ICE
The development of the Tiros Global Environmental Satellite System
[AIAA PAPER 82-0383] p0025 A82-17915
Measurement of sea and ice backscatter reflectivity using an OTH radar system p0025 A82-18074
The ice-conditions in the Greenland waters, 1965. Coastal maps
[ISBN-87-7478-183-9] p0026 N82-10467
Study on satellite radar altimetry in climatological and oceanographic research, volume 1
[SP/153/06/01/FR(80)-VOL-1] p0026 N82-10486
Ice conditions in the eastern Bering Sea from NOAA and LANDSAT imagery: Winter conditions 1974, 1976, 1977, 1979
[PB81-220188] p0028 N82-11537
Visual observations of floating ice from Skylab p0037 N82-12504
The ice conditions in the Greenland waters
[ISBN-87-7478-183-9] p0028 N82-12533
Boundary detection criteria for satellite altimeters
[NASA-CR-156880] p0028 N82-12734
ERS-1: Mission objectives and system concept p0029 N82-14554
The Norwegian remote sensing experiment (Norsex) in a marginal ice zone p0031 N82-14566
Marine activities in Sweden for which remote sensing data may be of interest --- oceanography, weather forecasting, and analysis p0031 N82-14576
Measurements of radar backscatter from Arctic Sea ice in the summer
[AD-A105586] p0032 N82-14592
Measurements of radar backscatter from Arctic Sea ice in the summer, Appendices A and B
[AD-A105736] p0032 N82-14593

SEA ROUGHNESS
SAR imaging of ocean waves - Theory p0023 A82-11202
A mathematical model of an over-sea airborne UHF radio link p0049 A82-11406
Ocean surface height-slope probability density function from SEASAT altimeter echo p0024 A82-15076
Images of sea waves obtained in polarimetric surveys p0024 A82-16620
Evaluation of the Seasat wind scatterometer p0025 A82-18716
Anomalous wind estimates from the Seasat scatterometer p0026 A82-18724
Visual observations of the ocean p0028 N82-12502
Determination of surface wind speed from remotely measured whitecap coverage, a feasibility assessment p0030 N82-14565
A preliminary evaluation of Seasat performance over the area of JASIN and its relevance to ERS-1 p0031 N82-14567
Oil spills: Large scale monitoring by LANDSAT p0012 N82-14572
Project Noordwijk. Part 1: Measurements of the radar backscatter coefficient gamma (sigma deg) in 1977 and 1978 --- on a sea platform
[PHL-1979-49-PT-1] p0032 N82-14617

Project Noordwijk. Part 2: Results of North Sea clutter measurements in the I-band performed from the platform Noordwijk in September/October 1977
[PHL-1980-28-PT-2] p0033 N82-14818
SEA STATES
Analysis of SEASAT wind observations over the Indian Ocean p0023 A82-10671
Radar backscattering from ocean waves at low grazing angles p0023 A82-14730
Investigation of survey conditions for the ocean surface in the 0.4-1.1 micron spectral range p0024 A82-15960
Global satellite measurements of water vapour, wind speed and wave height p0051 A82-17165
A global atlas of GEOS-3 significant waveheight and comparison of the data with national buoy data p0026 N82-10860
State-of-the-art in using a spaceborne altimeter and scatterometer for the determination of wind, sea state, and marine and ice dynamics --- Seasat instruments p0052 N82-14560
An evaluation of Seasat-A data in relation to optimum track ship weather routing and site specific forecasting for the offshore oil industry p0030 N82-14564
Scientific studies using Bhaskara satellite microwave radiometer (SAMIR) data: A short overview --- calibration of the instrument and its use in the study of oceanographic parameters p0032 N82-14587
Remote sensing of sea state by laser altimeters
[NASA-CR-165049] p0033 N82-14789
A global atlas of GEOS-3 significant waveheight data and comparison of the data with national buoy data
[NASA-CR-156882] p0033 N82-15498
SEA TRUTH
The Norwegian remote sensing experiment (Norsex) in a marginal ice zone p0031 N82-14566
Coastal zone research using remote sensing techniques --- calibration of coastal zone color scanner p0031 N82-14571
The feasibility of using remotely sensed color as an index of Irish coastal water properties --- statistical correlation of sea truth data p0032 N82-14581
Necessity of remote sensing for ocean studies. Part 1: Northwest African missions, Sahara-1 and Atlor-1 --- sea truth/remote sensing correlation of offshore upwelling p0032 N82-14582
A look at nonsatellite remote sensing systems for marine use --- together with satellite systems, overall view of the technology p0032 N82-14586
GEM: A simple meteorological buoy with satellite telemetry p0053 N82-14779
A global atlas of GEOS-3 significant waveheight data and comparison of the data with national buoy data
[NASA-CR-156882] p0033 N82-15498
SEA WATER
Variations in upper ocean heat storage determined from satellite data p0025 A82-17567
CTD/02 measurements during the Equatorial Pacific Ocean Climate Study (EPOCS) in 1979
[PB81-211203] p0026 N82-10461
Preliminary analysis of ocean color scanner data from Superflux III p0027 N82-10672
Development of the coastal zone color scanner for NIMBUS 7. Volume 1: Mission objectives and instrument description
[NASA-CR-166720-VOL-1] p0028 N82-11511
The color of the sea and its relation to surface chlorophyll and depth of the euphotic zone p0030 N82-14562
SEAMOUNTS
Visual observations of the ocean p0028 N82-12502
SEARCH RADAR
Three bearing method for passive triangulation in systems with unknown deterministic biases p0050 A82-15920
SEAS
Availability of Seasat synthetic aperture radar imagery p0050 A82-15039
Global Tectonics: Some Geologic analyses of observations and photographs from Skylab p0020 N82-12494
SEASAT SATELLITES
State-of-the-art in using a spaceborne altimeter and scatterometer for the determination of wind, sea state, and marine and ice dynamics --- Seasat instruments p0052 N82-14560
The Seasat commercial demonstration program p0030 N82-14561
SEDIMENT TRANSPORT
Mapping of surface currents in Greenland fiords by means of LANDSAT images --- multispectral photography p0038 N82-14579
The use of LANDSAT MSS to observe sediment distribution and movement in the Solent coastal area --- multispectral scannel (MSS) p0038 N82-14580
Maritime applications of image processing at DFVLR, Oberpfaffenhofen, West Germany --- LANDSAT multispectral scanner images, digital interactive image analysis p0032 N82-14585
SEDIMENTARY ROCKS
Remote sensing studies of some ironstone gravels and plinthite in Thailand p0019 N82-12491
SEDIMENTS
Recent work in passive optical imaging of water --- space and aircraft derived data p0038 N82-14575
The use of LANDSAT MSS to observe sediment distribution and movement in the Solent coastal area --- multispectral scannel (MSS) p0038 N82-14580
SENSITIVITY
Evaluation of the Seasat wind scatterometer p0025 A82-18716
Assessment of Superflux relative to remote sensing --- airborne remote sensing of the Chesapeake Bay plume and shelf regions p0028 N82-10694
SEWAGE
A marine environmental monitoring and assessment program p0027 N82-10663
Operational use of remote sensing for coastal zone management and possible contribution of specialized satellites --- aerial photography p0031 N82-14574
SHALLOW WATER
An inertially-aided aircraft track recovery system for coastal mapping p0037 A82-18166
Photo inertial positioning system development at the Canada Centre for Remote Sensing p0045 A82-18167
SHIP TERMINALS
A mathematical model of an over-sea airborne UHF radio link p0049 A82-11406
SHORELINES
Satellite imagery and shoreline erosion prediction p0036 A82-12595
SPOT data simulations: Littoral applications p0046 N82-14568
SIBERIA
Investigation of the spatial structure of space images of the earth's surface p0044 A82-16626
SIDE-LOOKING RADAR
The observation of tidal patterns, currents, and bathymetry with SLAR imagery of the sea p0023 A82-11201
Use of radar and microwave radiometry for reconnaissance satellites
[FOA-C-30204-E1] p0052 N82-10481
Use of Side Looking Airborne Radar (SLAR) for oil pollution monitoring in Norway p0012 N82-14588
SIGNAL PROCESSING
A digital fast correlation approach to produce SEASAT SAR imagery p0042 A82-14870
SINKHOLES
Remote sensing study of sinkhole occurrence p0019 A82-12590
SKY RADIATION
Spectral atmospheric observations at Nantucket Island, May 7-14, 1981
[NASA-TM-83196] p0029 N82-14550
SKYLAB 4
Skylab explores the Earth
[NASA-SP-380] p0019 N82-12492
SMOKE
Quantitative analysis of atmospheric pollution phenomena p0010 N82-12505
SNOW
Analysis of bright bands from 3-D radar data --- for snow/rain delineation p0035 A82-10208
SNOW COVER
Effect of grain size and snowpack water equivalence on visible and near-infrared satellite observations of snow p0035 A82-12553
Reflectivity and emissivity of snow and ground at mm waves p0042 A82-14860
Snow-mapping experiment p0037 N82-12498
Progress in radar snow research --- Brookings, South Dakota
[NASA-CR-166709] p0038 N82-12510
Use of environmental satellite data for input to energy balance snowmelt models
[PB81-227795] p0039 N82-15673
SOIL EROSION
Areawide soil loss predictions using CIR airphotos p0007 A82-12591
Investigation and mapping of the erosion relief of the Kalachskaia upland on the basis of multispectral scanner images p0008 A82-15966
Report on Skylab 4 African drought and arid land experiment p0037 N82-12501
SOIL MAPPING
Remote sensing techniques in the study of the agricultural potential of soils under the Cerrado vegetation /Brazil/ p0001 A82-10040
Limitations in the spectral discrimination of the Landsat MSS p0001 A82-10046
A comparison of radiative transfer models for predicting the microwave emission from soils p0035 A82-10694
Space photographs obtained with the Fragment system as a base for landscape mapping and physical-geographical classification of arid territories p0009 A82-15967
Aircraft radar response to soil moisture p0003 A82-17564
SOIL MOISTURE
Aircraft radar response to soil moisture p0003 A82-17564
Remote sensing of crop moisture status p0003 A82-17997
An evaluation of the spatial resolution of soil moisture information
[NASA-CR-166724] p0009 N82-11513
Analysis of soil moisture extraction algorithm using data from aircraft experiments
[NASA-CR-166719] p0046 N82-13470
A simulation study of the recession coefficient for antecedent precipitation index --- soil moisture and water runoff estimation
[NASA-TM-83860] p0038 N82-14549
Quantitative analysis of drainage obtained from aerial photographs and RBV/LANDSAT images
[E82-10008] p0039 N82-15486
SOILS
The choice of the orientation of the analyzer in polarimetric surveys p0044 A82-16621
Analysis of the information content of the polarimetric method of remote sensing p0003 A82-16622
Remote sensing studies of some ironstone gravels and plinthite in Thailand p0019 N82-12491
SOLAR FLUX DENSITY
Ionospheric propagation correction modeling for satellite altimeters
[NASA-CR-156881] p0052 N82-12447
SOLAR RADIATION
The surface albedo of the earth in the near ultraviolet /330-340 nm/ p0016 A82-15032
Use of environmental satellite data for input to energy balance snowmelt models
[PB81-227795] p0039 N82-15673
SORGHUM
Remote sensing of crop moisture status p0003 A82-17997
SOUNDING ROCKETS
Repeatability and measurement uncertainty of the United States meteorological rocketsonde p0049 A82-12127
SOUTH AMERICA
Upper tropospheric cyclonic vortices in the tropical South Atlantic p0009 A82-16325
Skylab 4 observations of Volcanoes. Part A: Volcanoes and volcanic landforms. Part B: Summit eruption of Fernandian Caldera, Galapagos Islands, Ecuador p0020 N82-12496
Mesoscale cloud features observed from Skylab p0011 N82-12509
SOUTH CAROLINA
Remote sensing of benthic microalgal biomass with a tower-mounted multispectral scanner p0024 A82-15031
SOUTH DAKOTA
Progress in radar snow research --- Brookings, South Dakota
[NASA-CR-166709] p0038 N82-12510
Remote sensing applications to resource problems in South Dakota
[E82-10002] p0004 N82-15481
SOUTHEAST ASIA
Rural development in the humid tropics p0003 A82-16162
SOUTHERN CALIFORNIA
Trace pollutant concentrations in a multiday smog episode in the California South Coast Air Basin by long path length Fourier transform infrared spectroscopy p0007 A82-10700
SOVIET SPACECRAFT
Satellites of the Meteor series, intended for earth studies from space p0050 A82-15951
Technical equipment of an experiment for remote sensing of the earth from space p0050 A82-15952
Meteorological satellites
[AD-A107427] p0053 N82-15110
SOYBEANS
Limitations in the spectral discrimination of the Landsat MSS p0001 A82-10046
SPACE MISSIONS
Report on Active and Planned Spacecraft and experiments
[NASA-TM-84025] p0055 N82-10087
SPACE SHUTTLE ORBITERS
Mission operation report: OSTA-1
[NASA-TM-84053] p0055 N82-10102
Shuttle applications in tropospheric air quality observations
[NASA-CR-145374] p0010 N82-11635
SPACE SHUTTLES
The 1981 RCA space constellation p0055 A82-12541
SPACEBORNE EXPERIMENTS
Report on Active and Planned Spacecraft and experiments
[NASA-TM-84025] p0055 N82-10087
Mission operation report: OSTA-1
[NASA-TM-84053] p0055 N82-10102
SPACECRAFT LAUNCHING
The 1981 RCA space constellation p0055 A82-12541
SPACECRAFT PERFORMANCE
LANDSAT-2 and LANDSAT-3 flight evaluation report, 23 April to 23 July 1979
[E82-10006] p0053 N82-15483
LANDSAT-2 and LANDSAT-3 flight evaluation report, 23 October 1978 to 23 January 1979
[E82-10017] p0054 N82-15495
SPACELAB
Spacelab-research of European regions with strong negative environmental influences, based on AVHRR-data of the satellites Tiros-N and NOAA p0007 A82-12517
SPATIAL DISTRIBUTION
The effect of spatial variability in precipitation on streamflow
[AD-A105955] p0038 N82-14589
SPATIAL RESOLUTION
Data compression and reconstruction for mixed resolution multispectral sensors p0049 A82-10045
Structural analysis of aerial and space images p0044 A82-16625
Investigation of the spatial structure of space images of the earth's surface p0044 A82-16626

An evaluation of the spatial resolution of soil moisture information
[NASA-CR-166724] p0009 N82-11513

SPECTRAL CORRELATION
In situ spectral reflectance studies of tidal wetland grasses p0036 A82-15969
Spectral correlation filters and natural colour coding p0043 A82-16160

SPECTRAL EMISSION
Nitric oxide delta band emission in the earth's atmosphere Comparison of a measurement and a theory p0008 A82-13268

SPECTRAL RECONNAISSANCE
Spectrometric studies of the earth's surface p0043 A82-16612
Methodology and practice of spectroscopic measurements of landscape elements in the preparation and carrying out of down-looking experiments p0051 A82-16613
The application of holographic gratings in spectrometers for the spatial-spectral analysis of the earth's surface from aerial and space platforms in the visible and near-infrared spectral regions p0044 A82-16614
Use of radar and microwave radiometry for reconnaissance satellites
[FOA-C-30204-E1] p0052 N82-10481
NURE aerial gamma-ray and magnetic reconnaissance survey of Maine and portions of New York. Volume 1: Data acquisition, reduction and interpretation
[DE82-000650] p0053 N82-14599
NURE aerial gamma-ray and magnetic reconnaissance survey of Maine and portions of New York, volume 2
[DE82-000781] p0020 N82-14600
NURE aerial gamma-ray and magnetic reconnaissance survey of Maine and portions of New York, volume 2
[DE82-000401] p0020 N82-14601
NURE aerial gamma-ray and magnetic reconnaissance survey of Maine and portions of New York, volume 2
[DE82-000780] p0021 N82-14602
NURE aerial gamma-ray and magnetic reconnaissance survey of Maine and portions of New York, volume 2
[DE82-000872] p0021 N82-14603
NURE aerial gamma-ray and magnetic reconnaissance survey of Maine and portions of New York, volume 2
[DE82-000772] p0021 N82-14604
NURE aerial gamma-ray and magnetic reconnaissance survey of Maine and portions of New York, volume 2
[DE82-000785] p0021 N82-14605
NURE aerial gamma-ray and magnetic reconnaissance survey of Maine and portions of New York, volume 2
[DE82-000869] p0021 N82-14606
NURE aerial gamma-ray and magnetic reconnaissance survey of Maine and portions of New York, volume 2
[DE82-000794] p0021 N82-14607
NURE aerial gamma-ray and magnetic reconnaissance survey of Maine and portions of New York, volume 2
[DE82-000784] p0021 N82-14608

SPECTRAL REFLECTANCE
The effect of angular factors on popularly used indicators of vegatative vigor p0001 A82-10039
Limitations in the spectral discrimination of the Landsat MSS p0001 A82-10046
Spectral behavior of wheat yield variety trials p0002 A82-10863
Intercalibration of Landsat 1-3 and NOAA 6 and 7 scanner data p0049 A82-13293
Reflectivity and emissivity of snow and ground at mm waves p0042 A82-14860
Temporal relationships between spectral response and agronomic variables of a corn canopy p0002 A82-15038
Metrological support of measurements of earth-surface brightness by the Fragment multispectral scanning system p0050 A82-15958
Investigation of survey conditions for the ocean surface in the 0.4-1.1 micron spectral range p0024 A82-15960
In situ spectral reflectance studies of tidal wetland grasses p0036 A82-15969
Measurement of sea and ice backscatter reflectivity using an OTH radar system p0025 A82-18074
Identification of lithologic units using multichannel imaging systems p0046 N82-11509

SPECTRAL RESOLUTION
Estimation of the brightness field from results of multispectral photography of the earth from space p0044 A82-16617

SPECTRAL SENSITIVITY
An improvement in land cover classification achieved by merging microwave data with Landsat multispectral scanner data p0007 A82-10043
Evaluation of the information content of the channels of spaceborne multispectral photography of the Fergana region by the MKF-6 camera from Soyuz-22 p0043 A82-16605
SPOT data simulations: Littoral applications p0046 N82-14568

SPECTRAL SIGNATURES
The discrimination of winter wheat using a growth-state signature p0002 A82-15026
Inclusion of a simple vegetation layer in terrain temperature models for thermal infrared (IR) signature prediction
[AD-A104469] p0003 N82-11910
A recommended sensor package for the detection and tracking of oil spills p0053 N82-14563

SPECTROMETERS
The application of holographic gratings in spectrometers for the spatial-spectral analysis of the earth's surface from aerial and space platforms in the visible and near-infrared spectral regions p0044 A82-16614

SPECTROPHOTOMETRY
Spectral atmospheric observations at Nantucket Island, May 7-14, 1981
[NASA-TM-83196] p0029 N82-14550

SPECTROSCOPY
Spectrometric studies of the earth's surface p0043 A82-16612
Methodology and practice of spectroscopic measurements of landscape elements in the preparation and carrying out of down-looking experiments p0051 A82-16613

SPOT (FRENCH SATELLITE)
SPOT data simulations: Littoral applications p0046 N82-14568

SPRINGS (WATER)
Remote sensing that motivated community action p0008 A82-12594

STACKS
Study of stack emissions by combination of lidar and correlation spectrometer p0008 A82-12816

STATISTICAL ANALYSIS
Factorial analysis of terrain feature positioning parameters used in combining radar and digital terrain model data p0015 A82-10029
Analysis of variance of thematic mapping experiment data p0009 A82-15968
Estimation of the brightness field from results of multispectral photography of the earth from space p0044 A82-16617
Programs for the statistical analysis of multispectral photographs p0044 A82-16628

STEREOPHOTOGRAPHY
Orientation and construction of models. I - The orientation problem in close-range photogrammetry p0049 A82-10858
Aerial-photography flights over Upper Franconia in 1980 Operation and first application-related experience p0008 A82-15749
Orientation and construction of models. III - Mathematical basis of the orientation problem of one-dimensional central perspective photographs p0043 A82-15973
An inertially-aided aircraft track recovery system for coastal mapping p0037 A82-18166

STORMS
An evaluation of the spatial resolution of soil moisture information
[NASA-CR-166724] p0009 N82-11513

STREAMS
An application of Landsat derived data to a regional hydrologic model p0037 A82-17999

STRIP MINING
Investigation of the application of remote sensing technology to environmental monitoring
[E82-10010] p0013 N82-15488

STRUCTURAL BASINS
An application of Landsat derived data to a regional hydrologic model p0037 A82-17999

STRUCTURAL PROPERTIES (GEOLOGY)
Morphostructural analyses of space imagery in the central Colorado Plateau p0019 N82-10465
Geology and linears of Libya p0019 N82-10618
The Manicouagan impact structure observed from Skylab
[CONTRIB-544] p0020 N82-12497
Reports of Planetary Geology Program, 1981
[NASA-TM-84211] p0016 N82-14041

SULFUR DIOXIDES
Study of stack emissions by combination of lidar and correlation spectrometer p0008 A82-12816
Aircraft data summaries of the SURE intensives, volume 4
[DE82-900311] p0012 N82-13569

SUPPORT SYSTEMS
ISRO satellite mission support facilities - Scope and future plans p0055 A82-17307

SURFACE LAYERS
Thermal inertia, thermal admittance, and the effect of layers p0008 A82-15027

SURFACE PROPERTIES
Metrological support of measurements of earth-surface brightness by the Fragment multispectral scanning system p0050 A82-15958
Investigation of survey conditions for the ocean surface in the 0.4-1.1 micron spectral range p0024 A82-15960

SURFACE ROUGHNESS
Airborne laser acquisition of cross-section data p0049 A82-12600
A theory of wave scattering from an inhomogeneous layer with an irregular interface p0041 A82-12757
A global atlas of GEOS-3 significant waveheight and comparison of the data with national buoy data p0026 N82-10660
Progress in radar snow research --- Brookings, South Dakota
[NASA-CR-166709] p0038 N82-12510

SURFACE TEMPERATURE
Two-dimensional model variability in thermal inertia surveys p0042 A82-15029
Comparison of polar and geostationary satellite infrared observations of sea surface temperatures in the Gulf of Maine p0024 A82-15030
Inclusion of a simple vegetation layer in terrain temperature models for thermal infrared (IR) signature prediction
[AD-A104469] p0003 N82-11910
Analysis of soil moisture extraction algorithm using data from aircraft experiments
[NASA-CR-166719] p0046 N82-13470
Necessity of remote sensing for ocean studies. Part 1: Northwest African missions, Sahara-1 and Atlor-1 --- sea truth/remote sensing correlation of offshore upwelling p0032 N82-14582
An investigation into the applicability of thermal infrared scanning for exploration
[BMFT-FB-T-81-087] p0022 N82-15925

SURFACE WATER
Application of Landsat to the inventory of DAMS p0036 A82-12593

SURGES
Characteristics of westward travelling surges during magnetospheric substorms p0050 A82-14299

SUSQUEHANNA RIVER BASIN (MD-NY-PA)
Texture transforms of remote sensing data p0042 A82-15034

SWEDEN
Marine activities in Sweden for which remote sensing data may be of interest --- oceanography, weather forecasting, and analysis p0031 N82-14576

SYNOPTIC METEOROLOGY
An investigation of a polar low with a spiral cloud structure p0007 A82-10816
Analysis of SEASAT wind observations over the Indian Ocean p0023 A82-10671

SYNTHETIC APERTURE RADAR
Preliminary results of mapping urban land cover with Seasat SAR imagery p0007 A82-10044
SAR imaging of ocean waves - Theory p0023 A82-11202
Wave orbital velocity, fade, and SAR response to azimuth waves p0023 A82-11203
A digital fast correlation approach to produce SEASAT SAR imagery p0042 A82-14870
Availability of Seasat synthetic aperture radar imagery p0050 A82-15039
Optically processed Seasat radar mosaic of Florida p0042 A82-15125
Seasat SAR processing at the Norwegian Defence Research Establishment --- design and operation of a digital process p0046 N82-14584
Remote Sensing Information Bulletin; Issue number 6 p0053 N82-14616
Additional studies of Earth resources synthetic aperture radar payloads
[MTR-80/90] p0054 N82-15500
New baseline system p0054 N82-15501
Squinted SAR system p0047 N82-15502

SYSTEMS SIMULATION
Onboard utilization of ground control points for image correction. Volume 1: Executive summary
[NASA-CR-166731] p0045 N82-10469

T

TECHNOLOGY TRANSFER
Introducing remote sensing to county-level agencies in Michigan through the Cooperative Extension Service p0007 A82-10034
MATE VAN: Mobile analysis and training extension --- analyzing LANDSAT digital data
[NASA-TM-84056] p0045 N82-10466
Technology transfer of NASA microwave remote sensing system
[NASA-CR-165791] p0028 N82-11515

TECTONIC PLATES
Global Tectonics: Some Geologic analyses of observations and photographs from Skylab p0020 N82-12494

TECTONICS
Space techniques to monitor movements in the earth's crust p0016 A82-18797

TELEMETRY
Technical equipment of an experiment for remote sensing of the earth from space p0050 A82-15952
Experimental telemetry system based on the Fragment multispectral scanning system p0050 A82-15955

TEMPERATURE INVERSIONS
Detection of monsoon inversion by TIROS-N satellite p0024 A82-17168

TENNESSEE
Airborne laser acquisition of cross-section data p0049 A82-12600

TERRAIN ANALYSIS
Factorial analysis of terrain feature positioning parameters used in combining radar and digital terrain model data p0015 A82-10029
Airborne laser acquisition of cross-section data p0049 A82-12600
Investigation and mapping of the erosion relief of the Kalachskaia upland on the basis of multispectral scanner images p0008 A82-15866

Space photographs obtained with the Fragment system as a base for landscape mapping and physical-geographical classification of arid territories p0009 A82-15967

Description and comparison of algorithms for solving large sets of sparse matrix normal equations in geodesy and photogrammetry
[SER-C-261] p0017 N82-15812

TERRESTRIAL RADIATION

Metrological support of measurements of earth-surface brightness by the Fragment multispectral scanning system p0050 A82-15958

Infrared radiance model variation by sensor flight measurements p0052 N82-14171

Analysis of satellite observations: Theoretical studies on the sampling problem
[MITT-31] p0056 N82-15499

TEXAS

Areawide soil loss predictions using CIR airphotos p0007 A82-12591

Statistical Techniques Applied to Aerial Radiometric Surveys (STAARS): Series introduction and the principal-components-analysis method --- National Uranium Resource Evaluation Program
[DE81-029177] p0019 N82-10476

Report of survey for McDonald Observatory, Harvard Radio Astronomy Station, and vicinity
[PB81-234338] p0016 N82-13606

TEXTURES

Texture transforms of remote sensing data p0042 A82-15034

Investigation of the spatial structure of space images of the earth's surface p0044 A82-16626

THAILAND

Rural development in the humid tropics p0003 A82-16162

Remote sensing studies of some ironstone gravels and plinthite in Thailand p0019 N82-12491

THEMATIC MAPPING

Mapping vegetation association boundaries with Landsat MSS data - An Oklahoma example p0001 A82-10041

An improvement in land cover classification achieved by merging microwave data with Landsat multispectral scanner data p0007 A82-10043

Preliminary results of mapping urban land cover with Seasat SAR imagery p0007 A82-10044

Repetitive aerial photography for assessing marsh vegetation changes p0001 A82-10048

Satellite sensing of irrigation patterns in semiarid areas An Indian study p0002 A82-10864

Temporal spectral response of a corn canopy p0002 A82-12886

Aerial and space methods in cartography p0016 A82-12915

Investigations concerning the image-controlled segmentation of objects in multispectral imagery data --- German thesis p0042 A82-15003

Analysis of variance of thematic mapping experiment data p0009 A82-15968

Processing of multispectral image data on special-purpose computer systems p0044 A82-16627

Linear combinations of multispectral images p0044 A82-16629

Application of the NASA airborne oceanographic lidar to the mapping of chlorophyll and other organic pigments p0027 N82-10684

The operational oil pollution surveillance system being used in France: Forecasted future developments in consideration of the NATO/CCMS remote sensing pilot study conclusions p0012 N82-14573

Remote sensing in forestry: Application to the Amazon region
[E82-10012] p0005 N82-15490

A global atlas of GEOS-3 significant waveheight data and comparison of the data with national buoy data
[NASA-CR-156882] p0033 N82-15498

THERMAL CONDUCTIVITY

Thermal inertia, thermal admittance, and the effect of layers p0008 A82-15027

THERMAL MAPPING

Mapping of the 1978 Kentucky River Flood from NOAA-5 satellite thermal infrared data p0035 A82-10033

Civil engineering applications of remote sensing; Proceedings of the Specialty Conference, University of Wisconsin, Madison, WI, August 13, 14, 1980 p0035 A82-12589

Water temperature mapping by infrared scanner p0036 A82-12598

Synoptic thermal and oceanographic parameter distributions in the New York Bight Apex p0023 A82-12885

Two-dimensional model variability in thermal inertia surveys p0042 A82-15029

Use of visible and thermal satellite data to monitor an intermittently flooding marshland p0036 A82-15037

The use of satellite infrared imagery for describing ocean processes in relation to spawning of the northern anchovy /Engraulis mordax/ p0025 A82-17565

Remote sensing of crop moisture status p0003 A82-17997

Inclusion of a simple vegetation layer in terrain temperature models for thermal infrared (IR) signature prediction
[AD-A104469] p0003 N82-11910

A recommended sensor package for the detection and tracking of oil spills p0053 N82-14563

A short review of an oceanographic use of Meteosat data by the ORSTOM remote sensing service p0031 N82-14570

Geologic applications of thermal-inertia mapping from satellite --- Powder River, Wyoming; Cubeza Prieta, Arizona, and Yellowstone National Park
[E82-10011] p0021 N82-15489

Biological patchiness in relation to satellite thermal imagery and associated chemical mesoscale features
[AD-A105757] p0047 N82-15504

An investigation into the applicability of thermal infrared scanning for exploration
[BMFT-FB-T-81-067] p0022 N82-15925

THERMAL POLLUTION

Airborne remote sensing of the coastal zone p0053 N82-14577

THERMAL RESISTANCE

Two-dimensional model variability in thermal inertia surveys p0042 A82-15029

THUNDERSTORMS

Analysis of rainfall from flash flood producing thunderstorms, using GOES data p0038 N82-14724

TIDAL FLATS

Remote sensing of benthic microalgal biomass with a tower-mounted multispectral scanner p0024 A82-15031

In situ spectral reflectance studies of tidal wetland grasses p0036 A82-15969

TIDAL WAVES

The observation of tidal patterns, currents, and bathymetry with SLAR imagery of the sea p0023 A82-11201

TIDES

Seasat altimetry adjustment model including tidal and other sea surface effects
[AD-A104188] p0026 N82-10473

TIMBER IDENTIFICATION

An improvement in land cover classification achieved by merging microwave data with Landsat multispectral scanner data p0007 A82-10043

Identification of conifer species groupings from Landsat digital classifications p0002 A82-12887

Remote sensing in forestry: Application to the Amazon region
[E82-10012] p0005 N82-15490

TIMBER INVENTORY

A VHF homing system with VHF radiotelephony for area-representative strip-survey flights conducted, as part of combined forest inventories, with light aircraft carrying 70 mm and 35 mm cameras p0003 A82-15748

Mapping of forest vegetation on the basis of space images p0003 A82-15964

TIMBER VIGOR

Evaluation of digital photographic enhancement for Dutch elm disease detection p0002 A82-12884

Large-scale color aerial photography as a tool in sampling for mortality rates
[PB81-214777] p0003 N82-10489

Remote sensing applications to resource problems in South Dakota
[E82-10002] p0004 N82-15481

TIROS N SERIES SATELLITES

User needs and the future of operational meteorological satellites
[AIAA PAPER 82-0388] p0051 A82-17918

TIROS SATELLITES

The development of the Tiros Global Environmental Satellite System
[AIAA PAPER 82-0383] p0025 A82-17915

TOPOGRAPHY

A new method for computing distortion p0016 A82-12914

Geometric quality of MKF-6 photographs p0043 A82-16606

Small-scale terrain mapping based on numerical interpretation of LANDSAT imagery
[VTT-40] p0045 N82-10485

TRACE CONTAMINANTS

Trace pollutant concentrations in a multiday smog episode in the California South Coast Air Basin by long path length Fourier transform infrared spectroscopy p0007 A82-10700

TRACE ELEMENTS

Proof of concept study
[AD-A104338] p0010 N82-11639

Limit on remote FTIR detection of trace gases
[AD-A104842] p0011 N82-12511

TRACKING NETWORKS

ISRO satellite mission support facilities - Scope and future plans p0055 A82-17307

TRAINING DEVICES

MATE VAN: Mobile analysis and training extension --- analyzing LANDSAT digital data
[NASA-TM-84056] p0045 N82-10466

TRANSFORMATIONS (MATHEMATICS)

Texture transforms of remote sensing data p0042 A82-15034

TRANSIT TIME DATA PROCESSING

Boundary detection criteria for satellite altimeters
[NASA-CR-156880] p0028 N82-12734

TREES (PLANTS)

Large-scale color aerial photography as a tool in sampling for mortality rates
[PB81-214777] p0003 N82-10489

TRIANGULATION

Phototriangulation with map referencing of photographs in linear surveys p0016 A82-12912

Block adjustment with additional parameters p0049 A82-13738

Compensation of systematic errors of image and model coordinates p0043 A82-15765

Three bearing method for passive triangulation in systems with unknown deterministic biases p0050 A82-15920

Some problem areas in the field of quality control for aerotriangulation p0016 A82-16161

TROPICAL METEOROLOGY

Upper tropospheric cyclonic vortices in the tropical South Atlantic p0009 A82-16325

Detection of monsoon inversion by TIROS-N satellite p0024 A82-17168

Annual and nonseasonal variability of monthly low-level wind fields over the Southeastern Tropical Pacific p0025 A82-17494

National Hurricane operations plan
[PB81-247231] p0013 N82-15697

TROPICAL REGIONS

Rural development in the humid tropics p0003 A82-16162

The use of digitally processed Landsat imagery for vegetation mapping in Sulawesi, Indonesia p0003 A82-17998

TROPICAL STORMS

Some aspects of tropical storm structure revealed by handheld-camera photographs from space p0011 N82-12507

TROPOSPHERE

Results from the July 1981 Workshop on Passive Remote Sensing of the Troposphere
[AIAA PAPER 82-0207] p0009 A82-17841

Shuttle applications in tropospheric air quality observations
[NASA-CR-145374] p0010 N82-11635

U

U.S.S.R.

Study of the anthropogenic influence on the environment, based on multispectral scanning images p0008 A82-15965

Space photographs obtained with the Fragment system as a base for landscape mapping and physical-geographical classification of arid territories p0009 A82-15967

Evaluation of the information content of the channels of spaceborne multispectral photography of the Fergana region by the MKF-6 camera from Soyuz-22 p0043 A82-16605

Spectrometric studies of the earth's surface p0043 A82-16612

Estimation of the brightness field from results of multispectral photography of the earth from space p0044 A82-16617

Linear combinations of multispectral images p0044 A82-16629

Skylab 4 observations of Volcanoes. Part A: Volcanoes and volcanic landforms. Part B: Summit eruption of Fernandian Caldera, Galapagos Islands, Ecuador p0020 N82-12496

U.S.S.R. SPACE PROGRAM

Satellites of the Meteor series, intended for earth studies from space p0050 A82-15951

Technical equipment of an experiment for remote sensing of the earth from space p0050 A82-15952

Experimental telemetry system based on the Fragment multispectral scanning system p0050 A82-15955

Metrological support of measurements of earth-surface brightness by the Fragment multispectral scanning system p0050 A82-15958

Investigation of survey conditions for the ocean surface in the 0.4-1.1 micron spectral range p0024 A82-15960

Study of the dynamics of the Danube delta using space images p0036 A82-15961

Development of a coastal relief of the Gulf of Riga, based on results of an analysis of space images p0024 A82-15962

Study and mapping of agricultural land use, based on space images p0003 A82-15963

Mapping of forest vegetation on the basis of space images p0003 A82-15964

Main results of the Raduga experiment p0051 A82-16602

U.S.S.R. THEMATIC MAPPING

Investigation and mapping of the erosion relief of the Kalachskaia upland on the basis of multispectral scanner images p0008 A82-15966

ULTRAHIGH FREQUENCIES

A mathematical model of an over-sea airborne UHF radio link p0049 A82-11406

UNDERWATER RESOURCES

Deep Ocean Mining Environmental Study. Environmental effects of commercial-scale mining
[PB81-227753] p0029 N82-13484

UNITED STATES OF AMERICA

Snow-mapping experiment p0037 N82-12498

UPPER ATMOSPHERE

Microwave limb sounder --- measuring trace gases in the upper atmosphere
[NASA-CASE-NPO-14544-1] p0011 N82-12685

UPWELLING WATER

The use of satellite infrared imagery for describing ocean processes in relation to spawning of the northern anchovy /Engraulis mordax/ p0025 A82-17565

A short review of an oceanographic use of Meteosat data by the ORSTOM remote sensing service p0031 N82-14570

Necessity of remote sensing for ocean studies. Part 1: Northwest African missions, Sahara-1 and Atlor-1 --- sea truth/remote sensing correlation of offshore upwelling p0032 N82-14582

URANIUM

Statistical Techniques Applied to Aerial Radiometric Surveys (STAARS): Series introduction and the principal-components-analysis method --- National Uranium Resource Evaluation Program [DE81-029177] p0019 N82-10476

NURE aerial gamma-ray and magnetic reconnaissance survey of Maine and portions of New York. Volume 1: Data acquisition, reduction and interpretation [DE82-000650] p0053 N82-14599

NURE aerial gamma-ray and magnetic reconnaissance survey of Maine and portions of New York, volume 2 [DE82-000781] p0020 N82-14600

NURE aerial gamma-ray and magnetic reconnaissance survey of Maine and portions of New York, volume 2 [DE82-000401] p0020 N82-14601

NURE aerial gamma-ray and magnetic reconnaissance survey of Maine and portions of New York, volume 2 [DE82-000780] p0021 N82-14602

NURE aerial gamma-ray and magnetic reconnaissance survey of Maine and portions of New York, volume 2 [DE82-000872] p0021 N82-14603

NURE aerial gamma-ray and magnetic reconnaissance survey of Maine and portions of New York, volume 2 [DE82-000772] p0021 N82-14604

NURE aerial gamma-ray and magnetic reconnaissance survey of Maine and portions of New York, volume 2 [DE82-000785] p0021 N82-14605

NURE aerial gamma-ray and magnetic reconnaissance survey of Maine and portions of New York, volume 2 [DE82-000869] p0021 N82-14606

NURE aerial gamma-ray and magnetic reconnaissance survey of Maine and portions of New York, volume 2 [DE82-000794] p0021 N82-14607

NURE aerial gamma-ray and magnetic reconnaissance survey of Maine and portions of New York, volume 2 [DE82-000784] p0021 N82-14608

URBAN RESEARCH

Preliminary results of mapping urban land cover with Seasat SAR imagery p0007 A82-10044

Radiative heating rates and some optical properties of the St. Louis aerosol, as inferred from aircraft measurements p0008 A82-14320

Adaptation of land use to surficial geology in metropolitan Washington, D.C. p0010 N82-11718

USER MANUALS (COMPUTER PROGRAMS)

Winterkill indicator model. Crop Condition Assessment Division (CCAD) data base interface driver, user's manual [E82-10014] p0005 N82-15492

USER REQUIREMENTS

Technology transfer of NASA microwave remote sensing system [NASA-CR-165791] p0028 N82-11515

UTAH

Phytoecozonation of Sevier Lake region of Utah using digitized Landsat MSS data p0001 A82-10042

V

VEGETATION

The effect of angular factors on popularly used indicators of vegetative vigor p0001 A82-10039

Remote sensing techniques in the study of the agricultural potential of soils under the Cerrado vegetation /Brazil/ p0001 A82-10040

Mapping vegetation association boundaries with Landsat MSS data - An Oklahoma example p0001 A82-10041

Mapping of forest vegetation on the basis of space images p0003 A82-15964

Methodology and practice of spectroscopic measurements of landscape elements in the preparation and carrying out of down-looking experiments p0051 A82-16613

The choice of the orientation of the analyzer in polarimetric surveys p0044 A82-16621

Analysis of the information content of the polarimetric method of remote sensing p0003 A82-16622

The use of digitally processed Landsat imagery for vegetation mapping in Sulawesi, Indonesia p0003 A82-17998

Inclusion of a simple vegetation layer in terrain temperature models for thermal infrared (IR) signature prediction [AD-A104469] p0003 N82-11910

Vegetation patterns p0004 N82-12500

Remote sensing in forestry. Application to the Amazon region [E82-10012] p0005 N82-15490

VEGETATION GROWTH

Repetitive aerial photography for assessing marsh vegetation changes p0001 A82-10048

VERY LONG BASE INTERFEROMETRY

Space techniques to monitor movements in the earth's crust p0016 A82-18797

VIDEO DATA

Investigations concerning the image-controlled segmentation of objects in multispectral imagery data --- German thesis p0042 A82-15003

VINEYARDS

Remote sensing for vineyard management p0001 A82-10047

VIRGINIA

Repetitive aerial photography for assessing marsh vegetation changes p0001 A82-10048

Analysis of testbed airborne multispectral scanner data from Superflux II --- Chesapeake Bay plume and James Shelf data p0027 N82-10682

VISIBLE INFRARED SPIN SCAN RADIOMETER

Distortion-free mapping of VISSR imagery data from geosynchronous satellites p0051 N82-10071

VISIBLE SPECTRUM

Effect of grain size and snowpack water equivalence on visible and near-infrared satellite observations of snow p0035 A82-12553

VISUAL OBSERVATION

Desert sand seas p0020 N82-12493

Global Tectonics: Some Geologic analyses of observations and photographs from Skylab p0020 N82-12494

Geological features of southwestern North America p0020 N82-12495

Skylab 4 observations of Volcanoes. Part A: Volcanoes and volcanic landforms. Part B: Summit eruption of Fernandian Caldera, Galapagos Islands, Ecuador p0020 N82-12496

Snow-mapping experiment p0037 N82-12498

Visual observations of the ocean p0028 N82-12502

An assessment of the potential contributions to oceanography from Skylab visual observations and handheld-camera photographs p0028 N82-12503

Visual observations of floating ice from Skylab p0037 N82-12504

VOLCANOES

Skylab 4 observations of Volcanoes. Part A: Volcanoes and volcanic landforms. Part B: Summit eruption of Fernandian Caldera, Galapagos Islands, Ecuador p0020 N82-12496

Quantitative analysis of atmospheric pollution phenomena p0010 N82-12505

Satellite observations of the Mt. St. Helens' eruption of 18 May 1980 [AD-A105784] p0012 N82-14591

W

WASHINGTON

Satellite observations of the Mt. St. Helens' eruption of 18 May 1980 [AD-A105784] p0012 N82-14591

WATER COLOR

Field study for Landsat water quality verification p0036 A82-12597

Preliminary analysis of ocean color scanner data from Superflux III p0027 N82-10672

Development of the coastal zone color scanner for NIMBUS 7. Volume 1: Mission objectives and instrument description [NASA-CR-166720-VOL-1] p0028 N82-11511

The color of the sea and its relation to surface chlorophyll and depth of the euphotic zone p0030 N82-14562

Coastal zone research using remote sensing techniques --- calibration of coastal zone color scanner pC031 N82-14571

The feasibility of using remotely sensed color as an index of Irish coastal water properties --- statistical correlation of sea truth data p0032 N82-14581

WATER CURRENTS

Maritime applications of image processing at DFVLR, Oberpfaffenhofen, West Germany --- LANDSAT multispectral scanner images, digital interactive image analysis p0032 N82-14585

WATER DEPTH

The observation of tidal patterns, currents, and bathymetry with SLAR imagery of the sea p0023 A82-11201

An inertially-aided aircraft track recovery system for coastal mapping p0037 A82-18166

Recent work in passive optical imaging of water --- space and aircraft derived data p0038 N82-14575

WATER FLOW

The effect of spatial variability in precipitation on streamflow [AD-A105955] p0038 N82-14589

WATER MANAGEMENT

Civil engineering applications of remote sensing; Proceedings of the Specialty Conference, University of Wisconsin, Madison, WI, August 13, 14, 1980 p0035 A82-12589

The potential for use of Landsat data in water resources planning for the Missouri River Basin p0037 A82-18000

Remote sensing applications to resource problems in South Dakota [E82-10002] p0004 N82-15481

WATER POLLUTION

Spacelab-research of European regions with strong negative environmental influences, based on AVHRR-data of the satellites Tiros-N and NOAA p0007 A82-12517

Remote sensing that motivated community action p0008 A82-12584

Polarimetric surveys of oil slicks p0009 A82-16619

Chesapeake Bay Plume Study: Superflux 1980 [NASA-CP-2188] p0026 N82-10661

Multitemporal calibration of LANDSAT images: A method for improving the marine phenomena recognition, with as example the Venice lagoon --- brightness/green/yellow feature space, image enhancement p0046 N82-14578

WATER QUALITY

The operational use of Landsat for lake quality assessment p0036 A82-12596

Field study for Landsat water quality verification p0036 A82-12597

Role of remote sensing in the study of acid rain impact on aquatic systems [AIAA PAPER 82-0336] p0036 A82-17892

Superflux I, II, and III experiment designs: Water sampling and analyses --- Chespeake Bay, environmental monitoring and remote sensing p0027 N82-10665

Application of the NASA airborne oceanographic lidar to the mapping of chlorophyll and other organic pigments p0027 N82-10684

Recent work in passive optical imaging of water --- space and aircraft derived data p0038 N82-14575

WATER RESOURCES

Landsat imagery for hydrologic modeling p0036 A82-12592

The potential for use of Landsat data in water resources planning for the Missouri River Basin p0037 A82-18000

WATER RUNOFF

Comparison of conventional and remotely sensed estimates of runoff curve numbers in southeastern Pennsylvania p0035 A82-10031

A systems approach to the real-time runoff analysis with a deterministic rainfall-runoff model [PB81-224495] p0037 N82-11530

A simulation study of the recession coefficient for antecedent precipitation index --- soil moisture and water runoff estimation [NASA-TM-83860] p0038 N82-14549

WATER TEMPERATURE

Water temperature mapping by infrared scanner p0036 A82-12598

Synoptic thermal and oceanographic parameter distributions in the New York Bight Apex p0023 A82-12885

Variations in upper ocean heat storage determined from satellite data p0025 A82-17567

The development of the Tiros Global Environmental Satellite System [AIAA PAPER 82-0383] p0025 A82-17915

ICAPS oceanographic data for the Indian Ocean [AD-A103173] p0029 N82-13641

Fisheries investigations and management benefits from remote sensing --- fish tracking p0030 N82-14559

A short review of an oceanographic use of Meteosat data by the ORSTOM remote sensing service p0031 N82-14570

Operational use of remote sensing for coastal zone management and possible contribution of specialized satellites --- aerial photography p0031 N82-14574

WATER VAPOR

Water vapour absorption in the 3.5-4.2 micron atmospheric window p0023 A82-14586

WATER WAVES

SAR imaging of ocean waves - Theory p0023 . 82-11202

Wave orbital velocity, fade, and SAR response to azimuth waves p0023 A82-11203

Radar backscattering from ocean waves at low grazing angles p0023 A82-14730

Ocean surface height-slope probability density function from SEASAT altimeter echo p0024 A82-15076

Determination of the length of sea waves by an airborne radar technique p0024 A82-15213

An analysis of short pulse and dual frequency radar techniques for measuring ocean wave spectra from satellites p0024 A82-15318

Images of sea waves obtained in polarimetric surveys p0024 A82-16620

Global satellite measurements of water vapour, wind speed and wave height p0051 A82-17165

A global atlas of GEOS-3 significant waveheight and comparison of the data with national buoy data p0026 N82-10660

Surface signs of internal ocean dynamics [AD-A101380] p0029 N82-13642

Determination of surface wind speed from remotely measured whitecap coverage, a feasibility assessment p0030 N82-14565

Airborne remote sensing of the coastal zone p0053 N82-14577

A global atlas of GEOS-3 significant waveheight data and comparison of the data with national buoy data [NASA-CR-156882] p0033 N82-15498

WATERSHEDS

Comparison of conventional and remotely sensed estimates of runoff curve numbers in southeastern Pennsylvania p0035 A82-10031

Areawide soil loss predictions using CIR airphotos
p0007 A82-12591

Landsat imagery for hydrologic modeling
p0036 A82-12592

An application of Landsat derived data to a regional hydrologic model
p0037 A82-17999

A simulation study of the recession coefficient for antecedent precipitation index --- soil moisture and water runoff estimation
[NASA-TM-83860] p0038 N82-14549

Remote sensing applications to resource problems in South Dakota
[E82-10002] p0004 N82-15481

WAVE REFLECTION
Wave orbital velocity, fade, and SAR response to azimuth waves
p0023 A82-11203

WAVE SCATTERING
A theory of wave scattering from an inhomogeneous layer with an irregular interface
p0041 A82-12757

WEATHER FORECASTING
A systems approach to the real-time runoff analysis with a deterministic rainfall-runoff model
[PB81-224495] p0037 N82-11530

Some aspects of tropical storm structure revealed by handheld-camera photographs from space
p0011 N82-12507

The Seasat commercial demonstration program
p0030 N82-14561

National Hurricane operations plan
[PB81-247231] p0013 N82-15697

WEST GERMANY
Aerial-photography flights over Upper Franconia in 1980 - Operation and first application-related experience
p0006 A82-15749

WETLANDS
An improvement in land cover classification achieved by merging microwave data with Landsat multispectral scanner data
p0007 A82-10043

Data sources for analyses of Great Lakes wetlands
p0035 A82-10054

In situ spectral reflectance studies of tidal wetland grasses
p0036 A82-15969

A proposal for continuation of support for the application of remotely sensed data to state and regional problems. Part 1: Technical proposal
[E82-10018] p0056 N82-15496

WHEAT
Spectral behavior of wheat yield variety trials
p0002 A82-10863

The discrimination of winter wheat using a growth-state signature
p0002 A82-15026

Vegetation patterns
p0004 N82-12500

Wheat cultivation: Identification and estimation of areas using LANDSAT data
[E82-10007] p0004 N82-15485

Winterkill indicator model. Crop Condition Assessment Division (CCAD) data base interface driver, user's manual
[E82-10014] p0005 N82-15492

US/Canada wheat and barley crop calender exploratory experiment implementation plan
[E82-10016] p0005 N82-15494

WILDERNESS
Application of remote sensing to selected problems within the state of California
[E82-10004] p0004 N82-15482

WIND DIRECTION
Evaluation of the Seasat wind scatterometer
p0025 A82-18716

Anomalous wind estimates from the Seasat scatterometer
p0026 A82-18724

WIND MEASUREMENT
Analysis of SEASAT wind observations over the Indian Ocean
p0023 A82-10671

WIND PROFILES
Annual and nonseasonal variability of monthly low-level wind fields over the Southeastern Tropical Pacific
p0025 A82-17494

WIND VELOCITY
Annual and nonseasonal variability of monthly low-level wind fields over the Southeastern Tropical Pacific
p0025 A82-17494

State-of-the-art in using a spaceborne altimeter and scatterometer for the determination of wind, sea state, and marine and ice dynamics --- Seasat instruments
p0052 N82-14560

WIND VELOCITY MEASUREMENT
Oceanic wind and balanced pressure-height fields derived from satellite measurements
p0023 A82-13214

Global satellite measurements of water vapour, wind speed and wave height
p0051 A82-17165

Evaluation of the Seasat wind scatterometer
p0025 A82-18716

Anomalous wind estimates from the Seasat scatterometer
p0026 A82-18724

Determination of surface wind speed from remotely measured whitecap coverage, a feasibility assessment
p0030 N82-14565

WINTER
Ice conditions in the eastern Bering Sea from NOAA and LANDSAT imagery: Winter conditions 1974, 1976, 1977, 1979
[PB81-220188] p0028 N82-11537

Winterkill indicator model. Crop Condition Assessment Division (CCAD) data base interface driver, user's manual
[E82-10014] p0005 N82-15492

WISCONSIN
Remote sensing that motivated community action
p0008 A82-12594

The operational use of Landsat for lake quality assessment
p0036 A82-12596

A simulation study of the recession coefficient for antecedent precipitation index --- soil moisture and water runoff estimation
[NASA-TM-83860] p0038 N82-14549

WYOMING
Geologic applications of thermal-inertia mapping from satellite --- Powder River, Wyoming; Cubeza Prieta, Arizona, and Yellowstone National Park
[E82-10011] p0021 N82-15489

Y

YELLOWSTONE NATIONAL PARK (ID-MT-WY)
Geologic applications of thermal-inertia mapping from satellite --- Powder River, Wyoming; Cubeza Prieta, Arizona, and Yellowstone National Park
[E82-10011] p0021 N82-15489

PERSONAL AUTHOR INDEX

EARTH RESOURCES / *A Continuing Bibliography (Issue 33)* **APRIL 1982**

Typical Personal Author Index Listing

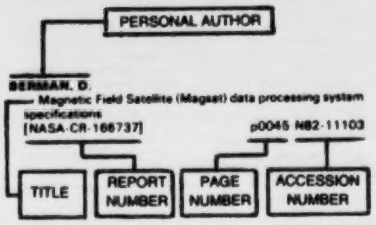

Listings in this index are arranged alphabetically by personal author. The title of the document provides the user with a brief description of the subject matter. The report number helps to indicate the type of document listed (e.g., NASA report, translation, NASA contractor report). The page and accession numbers are located beneath and to the right of the title, e.g., p0045 N82-11103. Under any one author's name the accession numbers are arranged in sequence with the AIAA accession numbers appearing first.

A

AARONS, J.
The radiowave propagation environment - Science and technology objectives for the 80's p0009 A82-18052

ABRAMS, R. B.
The surface albedo of the earth in the near ultraviolet /330-340 nm/ p0016 A82-15032

ACKERMANN, F.
Block adjustment with additional parameters p0049 A82-13738

ACUNA, M. H.
MAGSAT: Vector magnetometer absolute sensor alignment determination
[NASA-TM-79648] p0051 N82-10468

ADAMS, R. E. W.
Radar mapping, archaeology, and ancient land use in the Maya lowlands
[NASA-CR-164931] p0010 N82-11514

AFREMOV, V. G.
Current aerial cameras p0050 A82-15655

AHMADJIAN, M.
Proof of concept study
[AD-A104338] p0010 N82-11639
Limit on remote FTIR detection of trace gases
[AD-A104842] p0011 N82-12511

AKEY, N. D.
Technology transfer of NASA microwave remote sensing system
[NASA-CR-165791] p0028 N82-11515

AKSENOV, V. V.
Main results of the Raduga experiment p0051 A82-16602

AL-MUFTI, S.
Infrared spectroscopy of microorganisms near 3.4 microns in relation to geology and astronomy
[PREPRINT-69] p0020 N82-12713

ALBEROTANZA, L.
Multitemporal calibration of LANDSAT images: A method for improving the marine phenomena recognition, with as example the Venice lagoon p0046 N82-14578

ALBUISSON, M.
Oil spills: Large scale monitoring by LANDSAT p0012 N82-14572

ALEXANDER, R. H.
Adaptation of land use to surficial geology in metropolitan Washington, D.C. p0010 N82-11718

ALLAN, T. D.
A preliminary evaluation of Seasat performance over the area of JASIN and its relevance to ERS-1 p0031 N82-14567

AMER, F. A. A. F.
Theoretical reliability of elementary photogrammetric procedures. I p0043 A82-16163

ANAEJIONU, P.
Report on Skylab 4 African drought and arid land experiment p0037 N82-12501

ANDERSON, H. N.
Stand density estimation on panoramic transparencies p0002 A82-10862

ANDERSON, J. A.
Aircraft data summaries of the SURE intensives, volume 4
[DE82-900311] p0012 N82-13569

ANDERSON, T. H.
Geological features of southwestern North America p0020 N82-12495

ARNAL, B.
Aerial-photography flights over Upper Franconia in 1980 - Operation and first application-related experience p0008 A82-15749

ARUMOV, G. P.
Investigation of the spatial structure of space images of the earth's surface p0044 A82-16626

ASCE, M.
Remote sensing study of sinkhole occurrence p0019 A82-12590

ASLAM, A.
Progress in radar snow research
[NASA-CR-166709] p0038 N82-12510

AUSTIN, G. L.
Analysis of bright bands from 3-D radar data p0035 A82-10208

AVANESOV, G. A.
Experimental telemetry system based on the Fragment multispectral scanning system p0050 A82-15955
Metrological support of measurements of earth-surface brightness by the Fragment multispectral scanning system p0050 A82-15958
Spectrometric studies of the earth's surface p0043 A82-16612

B

BAHN, G. S.
Synoptic thermal and oceanographic parameter distributions in the New York Bight Apex p0023 A82-12885
Analysis of testbed airborne multispectral scanner data from Superflux II p0027 N82-10682

BALDASSINIFONTANA, R.
Infrared radiance model variation by sensor flight measurements p0052 N82-14171

BALICK, L. K.
Inclusion of a simple vegetation layer in terrain temperature models for thermal infrared (IR) signature prediction
[AD-A104469] p0003 N82-11910

BALL, W. E., JR.
Bureau of Land Management satellite Doppler positioning techniques p0015 A82-10057

BALTER, B. M.
The maximum mean accuracy of classification of remote sensing objects and the influence on this accuracy of data acquisition and processing methods p0044 A82-16615

BARNES, J. C.
Snow-mapping experiment p0037 N82-12498

BARRICK, D. E.
Ocean surface height-slope probability density function from SEASAT altimeter echo p0024 A82-15076

BARTASHEVICH, A. A.
Methodology and practice of spectroscopic measurements of landscape elements in the preparation and carrying out of down-looking experiments p0051 A82-16613

BARTLETT, D. S.
In situ spectral reflectance studies of tidal wetland grasses p0036 A82-15969

BARTON, I. J.
Water vapour absorption in the 3.5-4.2 micron atmospheric window p0023 A82-14586

BARTSCHI, B.
Limit on remote FTIR detection of trace gases
[AD-A104842] p0011 N82-12511

BEFORT, W. A.
Stand density estimation on panoramic transparencies p0002 A82-10862

BELL, G. J.
The near-infrared radiation received by satellites from clouds p0025 A82-17492

BENSON, A. S.
Application of remote sensing to selected problems within the state of California
[E82-10004] p0004 N82-15482

BERG, C. P.
Mapping of the 1978 Kentucky River Flood from NOAA-5 satellite thermal infrared data p0035 A82-10033

BERMAN, D.
Magnetic Field Satellite (Magsat) data processing system specifications
[NASA-CR-166737] p0045 N82-11103

BEVEN, K. J.
The effect of spatial variability in precipitation on streamflow
[AD-A105955] p0038 N82-14589

BHATTACHARYYA, B. K.
Preliminary analysis of gravity and aeromagnetic surveys of the Timber Mountain area, southern Nevada
[DE81-029462] p0022 N82-15506

BIRIUKOV, IU. L.
Calculation of the decrease in the contrast of objects of a place due to light scattering in the atmosphere p0042 A82-13633

BLACK, P. G.
Some aspects of tropical storm structure revealed by handheld-camera photographs from space p0011 N82-12507

BLAD, B. L.
Remote sensing of crop moisture status p0003 A82-17997

BLAHA, G.
Seasat altimetry adjustment model including tidal and other sea surface effects
[AD-A104188] p0026 N82-10473

BLANCHARD, B. J.
A simulation study of the recession coefficient for antecedent precipitation index
[NASA-TM-83860] p0038 N82-14549

BLUMENTHAL, D. L.
Aircraft data summaries of the SURE intensives, volume 4
[DE82-900311] p0012 N82-13569

BLYSTRA, A. R.
Application of Landsat to the inventory of DAMS p0036 A82-12593

BOGGS, D. H.
Evaluation of the Seasat wind scatterometer p0025 A82-18716

BONDELID, T. R.
Comparison of conventional and remotely sensed estimates of runoff curve numbers in southeastern Pennsylvania p0035 A82-10031

BOSTROEM, R.
A Swedish proposal for an EISCAT/GEOS-2 experiment
[KGI-176] p0052 N82-10484

BOWKER, D. E.
Analysis of testbed airborne multispectral scanner data from Superflux II p0027 N82-10682

BOWLEY, C. J.
Snow-mapping experiment p0037 N82-12498

BRACALENTE, E. M.
Evaluation of the Seasat wind scatterometer p0025 A82-18716

BRADLEY, G. A.
Aircraft radar response to soil moisture p0003 A82-17564

BREED, C. S.
Desert sand seas p0020 N82-12493

BRENDLE, P.
Overall economic impact of an operational Meteosat system
[ESA-CR(P)-1457] p0056 N82-13010

BROCK, R.
Factorial analysis of terrain feature positioning parameters used in combining radar and digital terrain model data p0015 A82-10029

BROICHER, H.
An investigation into the applicability of thermal infrared scanning for exploration
[BMFT-FB-T-81-087] p0022 N82-15925

BROWN, R. A.
Evaluation of the Seasat wind scatterometer p0025 A82-18716

BROWN, W. E., JR.
Radar mapping, archaeology, and ancient land use in the Maya lowlands
[NASA-CR-164931] p0010 N82-11514

BROWNLEE, R. H.
Remote sensing that motivated community action p0008 A82-12594

BRYAN, M. L.
Optically processed Seasat radar mosaic of Florida
p0042 A82-15125

BUKHARIN, V. D.
Determination of the length of sea waves by an airborne radar technique
p0024 A82-15213

BURKE, H. H. K.
An evaluation of the spatial resolution of soil moisture information
[NASA-CR-166724] p0009 N82-11513
Analysis of soil moisture extraction algorithm using data from aircraft experiments
[NASA-CR-166719] p0046 N82-13470

BURNASH, R. J. C.
A systems approach to the real-time runoff analysis with a deterministic rainfall-runoff model
[PB81-224495] p0037 N82-11530

BUSINGER, J. A.
Anomalous wind estimates from the Seasat scatterometer
p0026 A82-18724

BYRNE, G. F.
Thermal inertia, thermal admittance, and the effect of layers
p0008 A82-15027
Use of visible and thermal satellite data to monitor an intermittently flooding marshland
p0036 A82-15037

C

CAHILL, L. J., JR.
Magnetic field observations on DE-A and -B
p0051 A82-16447

CAMAGNI, P.
Study of stack emissions by combination of lidar and correlation spectrometer
p0008 A82-12816

CAMPBELL, J. W.
Chesapeake Bay Plume Study: Superflux 1980
[NASA-CP-2188] p0026 N82-10661
Superflux I, II, and III experiment design. Remote sensing aspects
p0027 N82-10664
Assessment of Superflux relative to remote sensing
p0028 N82-10694

CAMPBELL, W. J.
Visual observations of floating ice from Skylab
p0037 N82-12504
The Norwegian remote sensing experiment (Norsex) in a marginal ice zone
p0031 N82-14566

CANDIDI, M.
Use of hydromagnetic waves to map geomagnetic field lines
p0016 A82-16868

CANTERFORD, R. P.
Satellite rainfall estimation for hydrologic forecasting
p0035 A82-10032

CARLSON, C. T.
Oceanic wind and balanced pressure-height fields derived from satellite measurements
p0023 A82-13214

CARLSON, T. N.
Radiative heating rates and some optical properties of the St. Louis aerosol, as inferred from aircraft measurements
p0008 A82-14320

CARLYLE, S. M.
The discrimination of winter wheat using a growth-state signature
p0002 A82-15026

CARMICHAEL, J.
Shuttle applications in tropospheric air quality observations
[NASA-CR-145374] p0010 N82-11635

CARNEGGIE, D. M.
Vegetation patterns
p0004 N82-12500

CARTER, C. R.
Three bearing method for passive triangulation in systems with unknown deterministic biases
p0050 A82-15920

CARTER, L. D.
Visual observations of the ocean
p0028 N82-12502

CARTER, W. E.
Report of survey for McDonald Observatory, Harvard Radio Astronomy Station, and vicinity
[PB81-234338] p0016 N82-13606

CASAS, J. C.
A new method for inferring carbon monoxide concentrations from gas filter radiometer data
p0009 A82-16837

CASPER, J. W.
Remote sensing study of sinkhole occurrence
p0019 A82-12590

CHAN, F. K.
Distortion-free mapping of VISSR imagery data from geosynchronous satellites
p0051 N82-10071

CHELTON, D. B.
Global satellite measurements of water vapour, wind speed and wave height
p0051 A82-17165

CHESNOKOV, IU. M
Main results of the Raduga experiment
p0051 A82-16602
Analog methods for processing multispectral photographs
p0044 A82-16623

CHOUDHURY, B. J.
A comparison of radiative transfer models for predicting the microwave emission from soils
p0035 A82-10694
A simulation study of the recession coefficient for antecedent precipitation index
[NASA-TM-83860] p0038 N82-14549

CHUANG, S. L.
Radiative transfer theory for passive microwave remote sensing of random media
p0049 A82-11533

CITEAU, J.
A short review of an oceanographic use of Meteosat data by the ORSTOM remote sensing service
p0031 N82-14570

CLARK, D. K.
Clear water radiances for atmospheric correction of coastal zone color scanner imagery
p0025 A82-17292

COFER, W. R., III
Automated analyzer for aircraft measurements of atmospheric methane and total hydrocarbons
p0007 A82-11949

COGAN, J. L.
Sensitivity analysis of a mesoscale moisture model
[AD-A101528] p0012 N82-14590

COHEN, S. H.
An evaluation of the spatial resolution of soil moisture information
[NASA-CR-166724] p0009 N82-11513

COHENDET, P.
Overall economic impact of an operational Meteosat system
[ESA-CR(P)-1457] p0055 N82-13010

COLES, R. L.
The reduction, verification and interpretation of Magsat magnetic data over Canada
[E82-10006] p0046 N82-15484

COLLIER, C. G.
Analysis of bright bands from 3-D radar data
p0035 A82-10208

COLLINS, J. G.
Airborne laser acquisition of cross-section data
p0049 A82-12600

COLWELL, R. N.
Application of remote sensing to selected problems within the state of California
[E82-10004] p0004 N82-15482

CONSTANS, J.
Requirements in pollution monitoring and coastal management
p0030 N82-14558

CONWAY, C. M.
Geological features of southwestern North America
p0020 N82-12495

COTTRELL, D. A.
Wheat cultivation: Identification and estimation of areas using LANDSAT data
[E82-10007] p0004 N82-15485

CRACKNELL, A. P.
Coastal zone research using remote sensing techniques
p0031 N82-14571

CRAWFORD, J.
The Norwegian remote sensing experiment (Norsex) in a marginal ice zone
p0031 N82-14566

CRISSMAN, B. W.
Monitoring the Chesapeake Bay using satellite data for Superflux III
p0027 N82-10668

CRIST, E. P.
Development and evaluation of an automatic labeling technique for spring small grains
[E82-10001] p0004 N82-15480

CROSS, G. H.
Repetitive aerial photography for assessing marsh vegetation changes
p0001 A82-10048

CULBERT, T. P.
Radar mapping, archaeology, and ancient land use in the Maya lowlands
[NASA-CR-164931] p0010 N82-11514

CURRIE, N. C.
Reflectivity and emissivity of snow and ground at mm waves
p0042 A82-14860

D

DABROWSKA-ZIELINSKA, K.
Use of visible and thermal satellite data to monitor an intermittently flooding marshland
p0036 A82-15037

DALEY, C.
An evaluation of Seasat-A data in relation to optimum track ship weather routing and site specific forecasting for the offshore oil industry
p0030 N82-14564

DAUDRETSCH, F. C.
Rural development in the humid tropics
p0003 A82-16162

DAVIES, B. D.
CTD/02 measurements during the Equatorial Pacific Ocean Climate Study (EPOCS) in 1979
[PB81-211203] p0026 N82-10461

DAVIES, M. E.
Coordinates of features on the Galilean satellites
p0019 A82-12366

DAVIS, H. W.
The determination of navigational and meteorological variables measured by NOAA/RFC WP3D aircraft
[PB81-225468] p0028 N82-11743

DAVIS, J. R.
Thermal inertia, thermal admittance, and the effect of layers
p0008 A82-15027

DAWSON, E.
The reduction, verification and interpretation of Magsat magnetic data over Canada
[E82-10006] p0046 N82-15484

DE BLUST, E.
Study of stack emissions by combination of lidar and correlation spectrometer
p0008 A82-12816

DE GROOT, M.
Study of stack emissions by combination of lidar and correlation spectrometer
p0008 A82-12816

DE LOOR, G. P.
The observation of tidal patterns, currents, and bathymetry with SLAR imagery of the sea
p0023 A82-11201

DECKER, M. T.
The influence of gravity waves on radiometric measurements - A case study
p0049 A82-13547

DEGNER, J. D.
Remote sensing study of sinkhole occurrence
p0019 A82-12590

DEJESUSPARADA, N.
Wheat cultivation: Identification and estimation of areas using LANDSAT data
[E82-10007] p0004 N82-15485
Quantitative analysis of drainage obtained from aerial photographs and RBV/LANDSAT images
[E82-10008] p0039 N82-15486
Remote sensing in forestry: Application to the Amazon region
[E82-10012] p0005 N82-15490

DELGRECO, F. P.
Proof of concept study
[AD-A104338] p0010 N82-11639

DELIMAEFERNANDOCELSOSOARESMAIA, A. M.
Wheat cultivation: Identification and estimation of areas using LANDSAT data
[E82-10007] p0004 N82-15485

DELKER, C. V.
Measurements of radar backscatter from Arctic Sea ice in the summer
[AD-A105586] p0032 N82-14592
Measurements of radar backscatter from Arctic Sea ice in the summer. Appendices A and B
[AD-A105736] p0032 N82-14593

DELOOR, G. P.
Project Noordwijk. Part 1: Measurements of the radar backscatter coefficient gamma (sigma deg) in 1977 and 1978
[PHL-1979-49-PT-1] p0032 N82-14617

DEMAN, G.
Airborne remote sensing of the coastal zone
p0053 N82-14577

DENCE, M. R.
The Manicouagan impact structure observed from Skylab
[CONTRIB-544] p0020 N82-12497

DENNIS, J. M.
Remote sensing that motivated community action
p0006 A82-12594

DOERING, J. P.
Magnetic field-aligned electron distributions in the dayside cusp
p0015 A82-12186

DOMAIN, F.
A short review of an oceanographic use of Meteosat data by the ORSTOM remote sensing service
p0031 N82-14570

DOSSANTOS, A.
Remote sensing in forestry: Application to the Amazon region
[E82-10012] p0005 N82-15490

DOZIER, J.
Effect of grain size and snowpack water equivalence on visible and near-infrared satellite observations of snow
p0035 A82-12553
Use of environmental satellite data for input to energy balance snowmelt models
[PB81-227795] p0039 N82-15673

DUCHOSSOIS, G.
ERS-1: Mission objectives and system concept
p0029 N82-14554

DUGGIN, M. J.
The effect of angular factors on popularly used indicators of vegetative vigor
p0001 A82-10039
Limitations in the spectral discrimination of the Landsat MSS
p0001 A82-10046
Intercalibration of Landsat 1-3 and NOAA 6 and 7 scanner data
p0049 A82-13293

DUMAS, R. R.
Application of Landsat to the inventory of DAMS
p0036 A82-12593

DUNN, C. W., JR.
Mapping vegetation association boundaries with Landsat MSS data - An Oklahoma example
p0001 A82-10041

E

EFREMOVA, O. N.
Study of the dynamics of the Danube delta using space images
p0036 A82-15861

EGOROV, V. V.
Images of sea waves obtained in polarimetric surveys
p0024 A82-16620
The choice of the orientation of the analyzer in polarimetric surveys
p0044 A82-16621
Analysis of the information content of the polarimetric method of remote sensing
p0003 A82-16622
Investigation of the spatial structure of space images of the earth's surface
p0044 A82-16626

EGOROVA, O. I.
Concerning the geometric accuracy of infrared scanner photographs
p0042 A82-13634

EINAUDI, F.
The influence of gravity waves on radiometric measurements - A case study p0049 A82-13547

ELLIS, P. J.
Limitations in the spectral discrimination of the Landsat MSS p0001 A82-10046

ENDLICH, R. M.
Oceanic wind and balanced pressure-height fields derived from satellite measurements p0023 A82-13214

ENSLIN, W. R.
Introducing remote sensing to county-level agencies in Michigan through the Cooperative Extension Service p0007 A82-10034

EOM, H. J.
A theory of wave scattering from an inhomogeneous layer with an irregular interface p0041 A82-12757

EPIPHANIO, J. C. N.
Quantitative analysis of drainage obtained from aerial photographs and RBV/LANDSAT images
[E82-10008] p0039 N82-15486

ERB, T. L.
Remote sensing for vineyard management p0001 A82-10047

ESAIAS, W. E.
Superflux I, II, and III experiment design: Remote sensing aspects p0027 N82-10664

ESTES, J. E.
Application of remote sensing to selected problems within the state of California
[E82-10004] p0004 N82-15482

ESTOQUE, M. A.
Analysis of SEASAT wind observations over the Indian Ocean p0023 A82-10671

EVANS, D. L.
Identification of lithologic units using multichannel imaging systems p0046 N82-11509

EVANS, J. B.
Water temperature mapping by infrared scanner p0036 A82-12598

F

FAELTHAMMAR, C. G.
A Swedish proposal for an EISCAT/GEOS-2 experiment
[KGI-175] p0052 N82-10484

FAINTICH, M.
Digital image technology - MC&G impact p0015 A82-10028

FARNSWORTH, R. K.
Satellite rainfall estimation for hydrologic forecasting p0035 A82-10032

FARRELLY, B.
The Norwegian remote sensing experiment (Norsex) in a marginal ice zone p0031 N82-14566

FARTHING, W. H.
Magnetic field observations on DE-A and -B p0051 A82-16447

FAVIN, S.
Distant magnetic field effects associated with Birkeland currents /made possible by the evaluation of TRIAD's attitude oscillations/ p0015 A82-12215

FEIN, J.
Mesoscale cloud features observed from Skylab p0011 N82-12509

FELT, R. Y.
U.S. Navy planning for satellite oceanographic data exploitation
[AAS 81-072] p0024 A82-16341

FERNANDEZ-PARTAGAS, J. J.
Analysis of SEASAT wind observations over the Indian Ocean p0023 A82-10671

FERNANDEZ, D.
Remote sensing for vineyard management p0001 A82-10047

FERRAL, R. L.
A systems approach to the real-time runoff analysis with a deterministic rainfall-runoff model
[PB81-224496] p0037 N82-11530

FILHO, M. V.
Quantitative analysis of drainage obtained from aerial photographs and RBV/LANDSAT images
[E82-10008] p0039 N82-15486

FILHO, P. H.
Remote sensing in forestry: Application to the Amazon region
[E82-10012] p0005 N82-15490

FINE, B. T.
Vegetation patterns p0004 N82-12500

FINNIGAN, J. J.
The influence of gravity waves on radiometric measurements - A case study p0049 A82-13547

FISHER, L. T.
The operational use of Landsat for lake quality assessment p0036 A82-12596

FITZGERALD, M. P.
Determination of surface wind speed from remotely measured whitecap coverage, a feasibility assessment p0030 N82-14565
The feasibility of using remotely sensed color as an index of Irish coastal water properties p0032 N82-14581

FIVENSKII, IU. I.
Methods of instrumental interpretation of multispectral aerial and space photographs p0043 A82-16607
Characteristics of the photometry of small objects from aerial and space photographs p0044 A82-16616

FOKIN, A. B.
Investigation of survey conditions for the ocean surface in the 0.4-1.1 micron spectral range p0024 A82-15960

FOLVING, S.
Mapping of surface currents in Greenland fiords by means of LANDSAT images p0038 N82-14579

FORMAGGIO, A. R.
Quantitative analysis of drainage obtained from aerial photographs and RBV/LANDSAT images
[E82-10008] p0039 N82-15486

FORSYTH, D. G.
Mapping of the 1978 Kentucky River Flood from NOAA-5 satellite thermal infrared data p0035 A82-10033

FOX, L., III
Identification of conifer species groupings from Landsat digital classifications p0002 A82-12887

FRAITURE, L.
Infrared radiance model variation by sensor flight measurements p0052 N82-14171

FRANSSILA, E.
Small-scale terrain mapping based on numerical interpretation of LANDSAT imagery
[VTT-40] p0045 N82-10485

FREDERICK, J. E.
The surface albedo of the earth in the near ultraviolet /330-340 nm/ p0016 A82-15032

FRENCH, D. W.
Evaluation of digital photographic enhancement for Dutch elm disease detection p0002 A82-12884

FRIEDMAN, E.
Shuttle applications in tropospheric air quality observations
[NASA-CR-145374] p0010 N82-11635

FRIEDMAN, J. D.
Skylab 4 observations of Volcanoes. Part A: Volcanoes and volcanic landforms. Part B: Summit eruption of Fernandian Caldera, Galapagos Islands, Ecuador p0020 N82-12496

FRIEDMANN, D. E.
Two-dimensional resampling of line scan imagery by one-dimensional processing p0041 A82-10860

FRYBERGER, S. G.
Desert sand seas p0020 N82-12493

FUJITA, T. T.
Mesoscale wake clouds in Skylab photographs p0011 N82-12508

FUNG, A. K.
A theory of wave scattering from an inhomogeneous layer with an irregular interface p0041 A82-12757
Progress in radar snow research
[NASA-CR-166709] p0038 N82-12510

G

GAN, M. A.
Upper tropospheric cyclonic vortices in the tropical South Atlantic p0009 A82-16325

GANGADHARARAO, L. V.
Studies of the Indian continental shelf: Application of remote sensing data p0031 N82-14569

GARCIA, G. J.
Remote sensing techniques in the study of the agricultural potential of soils under the Cerrado vegetation /Brazil/ p0001 A82-10040

GARDNER, B. R.
Remote sensing of crop moisture status p0003 A82-17997

GARDNER, C. S.
Remote sensing of sea state by laser altimeters
[NASA-CR-165049] p0033 N82-14789

GARNAKERIAN, A. A.
Determination of the length of sea waves by an airborne radar technique p0024 A82-15213

GEKTIN, IU. M.
Investigation of survey conditions for the ocean surface in the 0.4-1.1 micron spectral range p0024 A82-15960

GELENS, H. F.
Rural development in the humid tropics p0003 A82-16162

GEORGE, T. S.
Landsat imagery for hydrologic modeling p0036 A82-12592

GERICKE, W.
Study of a combined satellite system for remote sensing and earth-oriented research (LOCSS)
[BMFT-FB-W-81-002] p0055 N82-14615

GESING, W. S.
An inertially-aided aircraft track recovery system for coastal mapping p0037 A82-18166

GIBSON, J. R.
An inertially-aided aircraft track recovery system for coastal mapping p0037 A82-18166
Photo inertial positioning system development at the Canada Centre for Remote Sensing p0045 A82-18167

GIRD, R. S.
Interactive techniques for estimating precipitation from GOES imagery p0041 A82-13121

GLASER, H. C.
Radar backscattering from ocean waves at low grazing angles p0023 A82-14730

GOGINENI, S.
Measurements of radar backscatter from Arctic Sea ice in the summer
[AD-A105586] p0032 N82-14592
Measurements of radar backscatter from Arctic Sea ice in the summer. Appendices A and B
[AD-A105736] p0032 N82-14593

GOLDHIRSH, J.
Radar correlation with ice depolarization measurements of the 28.56 GHz COMSTAR beacon and associated cross polarization statistics
[NASA-CR-166717] p0046 N82-14548

GOMEZ, R.
Magnetic Field Satellite (Magsat) data processing system specifications
[NASA-CR-166737] p0045 N82-11103

GONIN, G. B.
Evaluation of the information content of the channels of spaceborne multispectral photography of the Fergana region by the MKF-6 camera from Soyuz-22 p0043 A82-16605
Methodology and practice of spectroscopic measurements of landscape elements in the preparation and carrying out of down-looking experiments p0051 A82-16613

GOODMAN, J. M.
The radiowave propagation environment - Science and technology objectives for the 80's p0009 A82-18052

GOODRICK, G. N.
Use of visible and thermal satellite data to monitor an intermittently flooding marshland p0036 A82-15037

GORDON, H. R.
Clear water radiances for atmospheric correction of coastal zone color scanner imagery p0025 A82-17292

GORMSEN, B. B.
A new method for inferring carbon monoxide concentrations from gas filter radiometer data p0009 A82-16837

GRAHAM, D. S.
Field study for Landsat water quality verification p0036 A82-12597

GRATZ, R. L.
Offshore petroleum industry environmental data requirements: Emphasis on remote sensing p0030 N82-14557

GRAVESTEIJN, H.
Project Noordwijk. Part 2: Results of North Sea clutter measurements in the I-band performed from the platform Noordwijk in September/October 1977
[PHL-1980-28-PT-2] p0033 N82-14618

GRAY, C. E.
Environmental Monitoring Report, Sandia National Labs., Albuquerque, New Mexico, 180
[DE81-027839] p0010 N82-11649

GREENWALD, R. A.
Use of hydromagnetic waves to map geomagnetic field lines p0016 A82-16868

GUCWA, P. R.
Global Tectonics: Some Geologic analyses of observations and photographs from Skylab p0020 N82-12494

GUENTHER, H.
Study of a combined satellite system for remote sensing and earth-oriented research (LOCSS)
[BMFT-FB-W-81-002] p0055 N82-14615

GUPTA, J.
Shuttle applications in tropospheric air quality observations
[NASA-CR-145374] p0010 N82-11635

GUSTAFSSON, G.
Distant magnetic field effects associated with Birkeland currents /made possible by the evaluation of TRIAD's attitude oscillations/ p0015 A82-12215
A Swedish proposal for an EISCAT/GEOS-2 experiment
[KGI-175] p0052 N82-10484

GUSTINCIC, J. J.
Microwave limb sounder
[NASA-CASE-NPO-14544-1] p0011 N82-12685

GUYMER, T. H.
Evaluation of the Seasat wind scatterometer p0025 A82-18716
Anomalous wind estimates from the Seasat scatterometer p0026 A82-18724
A preliminary evaluation of Seasat performance over the area of JASIN and its relevance to ERS-1 p0031 N82-14567

H

HAGGERTY, S. E.
The mineralogy of global magnetic anomalies
[E82-10009] p0021 N82-15487

HAINES, G. V.
The reduction, verification and interpretation of Magsat magnetic data over Canada
[E82-10006] p0046 N82-15484

HALL, D.
Absolute image registration for geosynchronous satellites p0049 A82-10051

HAMILTON, D. A., JR.
Large-scale color aerial photography as a tool in sampling for mortality rates
[PB81-214777] p0003 N82-10489

HANDSCHUMACHER, D. W.
A closer examination of the reduction of satellite magnetometer data for geological studies p0019 A82-11039

HANSEN, R. F.
Winterkill indicator model, Crop Condition Assessment Division (CCAD) data base interface driver, user's manual [E82-10014] p0005 N82-15492

HARALICK, R. M.
The discrimination of winter wheat using a growth-state signature p0002 A82-15026

HARDESTY, C. A.
Analysis of testbed airborne multispectral scanner data from Superflux II p0027 N82-10682

HARDY, K. R.
An evaluation of the spatial resolution of soil moisture information [NASA-CR-166724] p0009 N82-11513

HARRINGTON, J. A., JR.
Mapping vegetation association boundaries with Landsat MSS data - An Oklahoma example p0001 A82-10041

HARRINGTON, R.
The Norwegian remote sensing experiment (Norsex) in a marginal ice zone p0031 N82-14566

HARRIS, R. P.
Remote sensing techniques in the study of the agricultural potential of soils under the Cerrado vegetation /Brazil/ p0001 A82-10040

HATFIELD, J. L.
Spectral behavior of wheat yield variety trials p0002 A82-10863

HAVIG, T. F.
Radar backscattering from ocean waves at low grazing angles p0023 A82-14730

HAYES, R. D.
Reflectivity and emissivity of snow and ground at mm waves p0042 A82-14860

HAYES, S. P.
CTD/02 measurements during the Equatorial Pacific Ocean Climate Study (EPOCS) in 1979 [PB81-211203] p0026 N82-10461

HEDBERG, A.
A Swedish proposal for an EISCAT/GEOS-2 experiment [KGI-175] p0052 N82-10484

HEIKEN, G.
Skylab 4 observations of Volcanoes. Part A: Volcanoes and volcanic landforms. Part B: Summit eruption of Fernandian Caldera, Galapagos Islands, Ecuador p0020 N82-12496

HEIKKILA, J.
Compensation of systematic errors in bundle adjustment p0042 A82-15764

HENDERSON, F. M.
Preliminary results of mapping urban land cover with Seasat SAR imagery p0007 A82-10044

HERBERT, G. A.
Geophysical monitoring for climatic change, number 8: Summary Report, 1979 [PB81-233355] p0012 N82-13631

HERLAND, E. A.
Seasat SAR processing at the Norwegian Defence Research Establishment p0046 N82-14584

HIEBER, S.
Space techniques to monitor movements in the earth's crust p0016 A82-18797

HILL-ROWLEY, R.
Introducing remote sensing to county-level agencies in Michigan through the Cooperative Extension Service p0007 A82-10034

HILL, J. M.
Field study for Landsat water quality verification p0036 A82-12597

HILL, R. W.
GPS application to mapping, charting and geodesy p0015 A82-10645

HLAVKA, C. A.
The discrimination of winter wheat using a growth-state signature p0002 A82-15026

HO, J. H.
Analysis of soil moisture extraction algorithm using data from aircraft experiments [NASA-CR-166719] p0046 N82-13470

HOEJERSLEV, N. K.
The color of the sea and its relation to surface chlorophyll and depth of the euphotic zone p0030 N82-14562

HOEST, S. E.
Use of Side Looking Airborne Radar (SLAR) for oil pollution monitoring in Norway p0012 N82-14588

HOFFMAN, R. A.
Magnetic field-aligned electron distributions in the dayside cusp p0015 A82-12186

HOGE, F. E.
Application of the NASA airborne oceanographic lidar to the mapping of chlorophyll and other organic pigments p0027 N82-10684

HOLT, B.
Availability of Seasat synthetic aperture radar imagery p0050 A82-15039

HOLT, H. E.
Reports of Planetary Geology Program, 1981 [NASA-TM-84211] p0016 N82-14041

HOLZ, R. K.
Cultural features imaged and observed from Skylab 4 p0010 N82-12489

HORJEN, I.
The Norwegian remote sensing experiment (Norsex) in a marginal ice zone p0031 N82-14566

HORNBERGER, G. M.
The effect of spatial variability in precipitation on streamflow [AD-A106955] p0038 N82-14589

HOYLE, F.
Infrared spectroscopy of microorganisms near 3.4 microns in relation to geology and astronomy [PREPRINT-69] p0020 N82-12713

HUMMER-MILLER, S.
Geologic applications of thermal-inertia mapping from satellite [E82-10011] p0021 N82-15489

HUMMER, R. F.
Scanner [NASA-CASE-GSC-12032-2] p0052 N82-13465

HUSSEY, K. J.
Global satellite measurements of water vapour, wind speed and wave height p0051 A82-17165

HWANG, D.
A method for using aerial photos in delineating historic patterns of beach accretion and retreat [PB81-223836] p0010 N82-11536

HYACINTHE, J. L.
State-of-the-art in using a spaceborne altimeter and scatterometer for the determination of wind, sea state, and marine and ice dynamics p0052 N82-14560

HYPES, W. D.
Superflux I, II, and III experiment design: Remote sensing aspects p0027 N82-10664

I

IANVAREVA, L. F.
Study and mapping of agricultural land use, based on space images p0003 A82-15963

ILIN, V. B.
Current aerial cameras p0050 A82-15655

INKILA, K.
Compensation of systematic errors in bundle adjustment p0042 A82-15764

IRONS, J. R.
Texture transforms of remote sensing data p0042 A82-15034

IUROV, V. I.
Geometric quality of MKF-6 photographs p0043 A82-16606

IVASHUTINA, L. I.
Space photographs obtained with the Fragment system as a base for landscape mapping and physical-geographical classification of arid territories p0009 A82-15967

IYENGAR, V. S.
ISRO satellite mission support facilities - Scope and future plans p0055 A82-17307

J

JACKSON, F. C.
An analysis of short pulse and dual frequency radar techniques for measuring ocean wave spectra from satellites p0024 A82-15318

JACKSON, T. J.
Comparison of conventional and remotely sensed estimates of runoff curve numbers in southeastern Pennsylvania p0035 A82-10031

JAIN, A.
SAR imaging of ocean waves - Theory p0023 A82-11202

JAIN, S. C.
Recent work in passive optical imaging of water p0038 N82-14575

JAMNONGPIPATKUL, P.
Remote sensing studies of some ironstone gravels and plinthite in Thailand p0019 N82-12491

JOBSON, D. J.
Remote sensing of benthic microalgal biomass with a tower-mounted multispectral scanner p0024 A82-15031
Analysis of testbed airborne multispectral scanner data from Superflux II p0027 N82-10682

JOHANNESSEN, J.
The Norwegian remote sensing experiment (Norsex) in a marginal ice zone p0031 N82-14566

JOHANNESSEN, O. M.
The Norwegian remote sensing experiment (Norsex) in a marginal ice zone p0031 N82-14566

JOHNSON, C.
Application of remote sensing to selected problems within the state of California [E82-10004] p0004 N82-15482

JOHNSON, R.
Mesoscale cloud features observed from Skylab p0011 N82-12509

JOHNSON, R. G.
An evaluation of Seasat-A data in relation to optimum track ship weather routing and site specific forecasting for the offshore oil industry p0030 N82-14564

JOHNSON, R. W.
Synoptic thermal and oceanographic parameter distributions in the New York Bight Apex p0023 A82-12885

JOHNSON, W. L.
Evaluation of digital photographic enhancement for Dutch elm disease detection p0002 A82-12884

JONES, L.
The Norwegian remote sensing experiment (Norsex) in a marginal ice zone p0031 N82-14566

JONES, W. L.
Evaluation of the Seasat wind scatterometer p0025 A82-18716
Anomalous wind estimates from the Seasat scatterometer p0026 A82-18724

K

KAIGORODOV, A. I.
Phototriangulation with map referencing of photographs in linear surveys p0016 A82-12912

KAMINSKI, H.
Spacelab-research of European regions with strong negative environmental influences, based on AVHRR-data of the satellites Tiros-N and NOAA p0007 A82-12517

KANE, M. F.
Preliminary analysis of gravity and aeromagnetic surveys of the Timber Mountain area, southern Nevada [DE81-029462] p0022 N82-15506

KARAKUSHIAN, V. L.
Determination of the length of sea waves by an airborne radar technique p0024 A82-15213

KATAYAMA, F. Y.
Coordinates of features on the Galilean satellites p0019 A82-12366

KATZBERG, S. J.
Remote sensing of benthic microalgal biomass with a tower-mounted multispectral scanner p0024 A82-15031

KEAFER, L. S., JR.
Results from the July 1981 Workshop on Passive Remote Sensing of the Troposphere [AIAA PAPER 82-0207] p0009 A82-17841

KEIFER, W. S.
Aircraft data summaries of the SURE intensives, volume 4 [DE82-900311] p0012 N82-13569

KELNER, IU. G.
Aerial and space methods in cartography p0016 A82-12915

KENDALL, B. M.
Remote sensing of the Chesapeake Bay plume salinity via microwave radiometry p0027 N82-10670

KESSLER, B. L.
Stand density estimation on panoramic transparencies p0002 A82-10862

KHATUNTSEVA, M. V.
Programs for the statistical analysis of multispectral photographs p0044 A82-16628
Linear combinations of multispectral images p0044 A82-16629

KIEFER, R. W.
Civil engineering applications of remote sensing; Proceedings of the Specialty Conference, University of Wisconsin, Madison, WI, August 13, 14, 1980 p0035 A82-12589

KILLPACK, D. P.
An application of Landsat derived data to a regional hydrologic model p0037 A82-17899

KILPELA, E.
Compensation of systematic errors in bundle adjustment p0042 A82-15764
Compensation of systematic errors of image and model coordinates p0043 A82-15765

KIMES, D. S.
Temporal spectral response of a corn canopy p0002 A82-12886
Temporal relationships between spectral response and agronomic variables of a corn canopy p0002 A82-15038

KLEMAS, V.
In situ spectral reflectance studies of tidal wetland grasses p0036 A82-15969

KLOSTER, K.
The Norwegian remote sensing experiment (Norsex) in a marginal ice zone p0031 N82-14566

KLOTZ, H.
Study of a combined satellite system for remote sensing and earth-oriented research (LOCSS) [BMFT-FB-W-81-002] p0055 N82-14615

KOCH, D.
Absolute image registration for geosynchronous satellites p0049 A82-10051

KOECHLER, C.
Study of stack emissions by combination of lidar and correlation spectrometer p0008 A82-12816

KOGUT, J.
SMMR data set development for GARP [NASA-CR-166721] p0052 N82-11512

KONG, J. A.
Radiative transfer theory for passive microwave remote sensing of random media p0049 A82-11533

KORNFIELD, J.
Interpolating for the location of remote sensor data [NASA-TM-82169] p0052 N82-13469

KOROLEVA, V. P.
Evaluation of the information content of the channels of spaceborne multispectral photography of the Fergana region by the MKF-6 camera from Soyuz-22 p0043 A82-16605

KOTOVA, T. V.
Mapping of forest vegetation on the basis of space images p0003 A82-15964

KOTSOV, V. A.
Estimation of the brightness field from results of multispectral photography of the earth from space p0044 A82-16617

KOTTSOV, V. A.
The use of a priori information in the remote sensing of the earth from space p0044 A82-16618

KOUSKY, V. E.
Upper tropospheric cyclonic vortices in the tropical South Atlantic p0009 A82-16325

KOWALIK, W. S.
Estimation of atmospheric path-radiance by the covariance matrix method p0041 A82-10861

KRABILL, W. B.
Airborne laser acquisition of cross-section data p0049 A82-12600

KRASIKOV, V. A.
Geometric quality of MKF-6 photographs p0043 A82-16606
Processing of multispectral image data on special-purpose computer systems p0044 A82-16627
Programs for the statistical analysis of multispectral photographs p0044 A82-16628
Coordinate referencing of MKF-6 photographs and their transformation to the cartographic projection p0045 A82-16630

KRAUSH, K. A.
Structural analysis of aerial and space images p0044 A82-16625

KRAVCHUK, N. V.
Methodology and practice of spectroscopic measurements of landscape elements in the preparation and carrying out of down-looking experiments p0051 A82-16613

KRAVTSOVA, V. I.
Study of the dynamics of the Danube delta using space images p0036 A82-15961
Development of a coastal relief of the Gulf of Riga, based on results of an analysis of space images p0024 A82-15962
Mapping of forest vegetation on the basis of space images p0003 A82-15964
Study of the anthropogenic influence on the environment, based on multispectral scanning images p0008 A82-15965

KRIEGER, R.
Study of a combined satellite system for remote sensing and earth-oriented research (LOCSS)
[BMFT-FB-W-81-002] p0055 N82-14615

KRUEGER, A. F.
Skylab 4 observations of Volcanoes. Part A: Volcanoes and volcanic landforms. Part B: Summit eruption of Fernandian Caldera, Galapagos Islands, Ecuador p0020 N82-12496

KUZNETSOV, IU. N.
Characteristics of the photometry of small objects from aerial and space photographs p0044 A82-16616

L

LABUTINA, I. A.
Methods of instrumental interpretation of multispectral aerial and space photographs p0043 A82-16607

LAGARDE, J. B.
Overall economic impact of an operational Meteosat system
[ESA-CR(P)-1457] p0055 N82-13010

LANNELONGUE, N.
SPOT data simulations: Littoral applications p0046 N82-14568

LAPTEVA, N. I.
Investigation and mapping of the erosion relief of the Kalachskaia upland on the basis of multispectral scanner images p0008 A82-15966

LASKER, R.
The use of satellite infrared imagery for describing ocean processes in relation to spawning of the northern anchovy /Engraulis mordax/ p0025 A82-17565

LAURS, R. M.
The use of satellite infrared imagery for describing ocean processes in relation to spawning of the northern anchovy /Engraulis mordax/ p0025 A82-17565

LEDLEY, B. G.
Magnetic field observations on DE-A and -B p0051 A82-16447

LEE, D. C. L.
Wheat cultivation: Identification and estimation of areas using LANDSAT data
[E82-10007] p0004 N82-15485

LEE, J. S.
Magnetic field-aligned electron distributions in the dayside cusp p0015 A82-12188

LEE, J. T.
Mesoscale cloud features observed from Skylab p0011 N82-12509

LEFEBVRE, M.
State-of-the-art in using a spaceborne altimeter and scatterometer for the determination of wind, sea state, and marine and ice dynamics p0052 N82-14560

LEGECKIS, R.
Comparison of polar and geostationary satellite infrared observations of sea surface temperatures in the Gulf of Maine p0024 A82-15030

LEGER, G.
Requirements in pollution monitoring and coastal management p0030 N82-14558

LEGG, E.
Comparison of polar and geostationary satellite infrared observations of sea surface temperatures in the Gulf of Maine p0024 A82-15030

LENNERTZ, D.
ERS-1: Mission objectives and system concept p0029 N82-14554

LEUPOLD, R. C.
An evaluation of the spatial resolution of soil moisture information
[NASA-CR-166724] p0009 N82-11513

LEVINE, I.
Computational aspects of geometric correction data generation in the LANDSAT-D imagery processing p0045 N82-10072
The MSS control point location error filter for LANDSAT-D p0051 N82-10073

LEVY, G.
Application of remote sensing data on the continental shelf: Proceedings of an EARcL-ESA Symposium
[ESA-SP-167] p0029 N82-14553

LILLESAND, T. M.
Evaluation of digital photographic enhancement for Dutch elm disease detection p0002 A82-12884

LIMEBURNER, R.
Comparison of polar and geostationary satellite infrared observations of sea surface temperatures in the Gulf of Maine p0024 A82-15030

LINK, L. E., JR.
Inclusion of a simple vegetation layer in terrain temperature models for thermal infrared (IR) signature prediction
[AD-A104469] p0003 N82-11910

LIPA, B. J.
Ocean surface height-slope probability density function from SEASAT altimeter echo p0024 A82-15076

LJOEEN, R.
Fisheries investigations and management benefits from remote sensing p0030 N82-14559

LOK, H.
Use of radar and microwave radiometry for reconnaissance satellites
[FOA-C-30204-E1] p0052 N82-10481

LONGDON, N.
Application of remote sensing data on the continental shelf: Proceedings of an EARcL-ESA Symposium
[ESA-SP-167] p0029 N82-14553

LOVEJOY, S.
Analysis of bright bands from 3-D radar data p0035 A82-10208

LOWE, T. W.
The potential for use of Landsat data in water resources planning for the Missouri River Basin p0037 A82-18000

LULLA, K.
Phytoecozonation of Sevier Lake region of Utah using digitized Landsat MSS data p0001 A82-10042

LUSCOMBE, A. P.
Additional studies of Earth resources synthetic aperture radar payloads
[MTR-80/90] p0054 N82-15500

LYKASHEVA, E. G.
The application of holographic gratings in spectrometers for the spatial-spectral analysis of the earth's surface from aerial and space platforms in the visible and near-infrared spectral regions p0044 A82-16614

LYON, J. G.
Data sources for analyses of Great Lakes wetlands p0035 A82-10054

LYON, R. J. P.
Estimation of atmospheric path-radiance by the covariance matrix method p0041 A82-10861

M

MAAROUF, A. M. S.
Morphostructural analyses of space imagery in the central Colorado Plateau p0019 N82-10465

MACLEOD, N. H.
Report on Skylab 4 African drought and arid land experiment p0037 N82-12501

MAITSON, H. H.
Report on Active and Planned Spacecraft and experiments
[NASA-TM-84025] p0055 N82-10087

MAKAREVICH, A. K.
Mapping of forest vegetation on the basis of space images p0003 A82-15964

MALILA, W. A.
Development and evaluation of an automatic labeling technique for spring small grains
[E82-10001] p0004 N82-15480

MANGEL, M.
Three bearing method for passive triangulation in systems with unknown deterministic biases p0050 A82-15920

MANGUM, L. J.
CTD/02 measurements during the Equatorial Pacific Ocean Climate Study (EPOCS) in 1979
[PB81-211203] p0026 N82-10461

MANSUR, M. A.
Geology and linears of Libya p0019 N82-10618

MARESCA, J. W., JR.
Oceanic wind and balanced pressure-height fields derived from satellite measurements p0023 A82-13214

MARKARIAN, E. G.
Calculation of the decrease in the contrast of objects of a place due to light scattering in the atmosphere p0042 A82-13633

MARKHAM, B. L.
Temporal spectral response of a corn canopy p0002 A82-12886
Temporal relationships between spectral response and agronomic variables of a corn canopy p0002 A82-15038

MARTIN, C. F.
Boundary detection criteria for satellite altimeters
[NASA-CR-156880] p0028 N82-12734

MASRY, S. E.
Digital mapping using entities - A new concept p0041 A82-12882

MASSIN, J. M.
The operational oil pollution surveillance system being used in France: Forecasted future developments in consideration of the NATO/CCMS remote sensing pilot study conclusions p0012 N82-14573

MAUL, G. A.
An assessment of the potential contributions to oceanography from Skylab visual observations and handheld-camera photographs p0028 N82-12503

MAUSEL, P.
Phytoecozonation of Sevier Lake region of Utah using digitized Landsat MSS data p0001 A82-10042

MAYER, K. E.
Identification of conifer species groupings from Landsat digital classifications p0002 A82-12887

MCCANDLESS, S. W.
The Seasat commercial demonstration program p0030 N82-14561

MCCASLIN, M.
An assessment of the potential contributions to oceanography from Skylab visual observations and handheld-camera photographs p0028 N82-12503

MCCOY, R. M.
An application of Landsat derived data to a regional hydrologic model p0037 A82-17999

MCCUEN, R. H.
Comparison of conventional and remotely sensed estimates of runoff curve numbers in southeastern Pennsylvania p0035 A82-10031

MCDONALD, J. A.
Aircraft data summaries of the SURE intensives, volume 4
[DE82-900311] p0012 N82-13569

MCGINNIS, D. F., JR.
Mapping of the 1978 Kentucky River Flood from NOAA-5 satellite thermal infrared data p0035 A82-10033
Effect of grain size and snowpack water equivalence on visible and near-infrared satellite observations of snow p0035 A82-12553

MCKEE, E. D.
Desert sand seas p0020 N82-12483

MCLEESTER, J. N.
Remote sensing for vineyard management p0001 A82-10047

MCMILLAN, J. D.
A global atlas of GEOS-3 significant waveheight and comparison of the data with national buoy data p0026 N82-10660
A global atlas of GEOS-3 significant waveheight data and comparison of the data with national buoy data
[NASA-CR-156882] p0033 N82-15499

MCMURTREY, J. E., III
Temporal spectral response of a corn canopy p0002 A82-12886
Temporal relationships between spectral response and agronomic variables of a corn canopy p0002 A82-15038

MCNUTT, L.
Ice conditions in the eastern Bering Sea from NOAA and LANDSAT imagery: Winter conditions 1974, 1976, 1977, 1979
[PB81-220188] p0028 N82-11537

MCWILLIAM, B. N.
An inertially-aided aircraft track recovery system for coastal mapping p0037 A82-18168

MEAD, R. A.
Repetitive aerial photography for assessing marsh vegetation changes p0001 A82-10048

MEISNER, D. E.
Evaluation of digital photographic enhancement for Dutch elm disease detection p0002 A82-12884

MENDONCA, F. J.
Wheat cultivation: Identification and estimation of areas using LANDSAT data
[E82-10007] p0004 N82-15485

MERCERET, F. J.
The determination of navigational and meteorological variables measured by NOAA/RFC WP3D aircraft
[PB81-225468] p0028 N82-11743

METHOD, T. J.
Radiative heating rates and some optical properties of the St. Louis aerosol, as inferred from aircraft measurements p0008 A82-14320

METZGAR, B.
Study of a combined satellite system for remote sensing and earth-oriented research (LOCSS)
[BMFT-FB-W-81-002] p0055 N82-14615

MICHELON, R.
Study of stack emissions by combination of lidar and correlation spectrometer p0008 A82-12816

MILLARD, G. C.
Environmental Monitoring Report, Sandia National Labs., Albuquerque, New Mexico, 180
[DE81-027839] p0010 N82-11649

MILLER, A.
Magnetic Field Satellite (Magsat) data processing system specifications
[NASA-CR-166737] p0045 N82-11103

MILLER, B. P.
The Seasat commercial demonstration program
p0030 N82-14561

MILLER, C.
Overall economic impact of an operational Meteosat system
[ESA-CR(P)-1457] p0055 N82-13010

MILLER, D. B.
User needs and the future of operational meteorological satellites
[AIAA PAPER 82-0388] p0051 A82-17918

MILLER, J. R.
Variations in upper ocean heat storage determined from satellite data p0025 A82-17567

MOLENAAR, M.
Some problem areas in the field of quality control for aerotriangulation p0016 A82-16161

MOLLO-CHRISTENSEN, E.
Surface signs of internal ocean dynamics
[AD-A101380] p0029 N82-13642

MONAHAN, E. C.
Determination of surface wind speed from remotely measured whitecap coverage, a feasibility assessment
p0030 N82-14565
The feasibility of using remotely sensed color as an index of Irish coastal water properties p0032 N82-14581

MONGAIN, E. O.
Study on calibration methods for Earth observation optical imaging instruments
[UCD-207/1/80] p0052 N82-10488

MONGET, J. M.
Oil spills: Large scale monitoring by LANDSAT
p0012 N82-14572

MONTGOMERY, D. R.
The Seasat commercial demonstration program
p0030 N82-14561

MOORE, R. K.
Measurements of radar backscatter from Arctic Sea ice in the summer
[AD-A105586] p0032 N82-14592
Measurements of radar backscatter from Arctic Sea ice in the summer, Appendices A and B
[AD-A105736] p0032 N82-14593

MOREIRA, M. A.
Wheat cultivation: Identification and estimation of areas using LANDSAT data
[E82-10007] p0004 N82-15485

MORGAN, K. M.
Areawide soil loss predictions using CIR airphotos
p0007 A82-12591

MORLEY, L. W.
The need for integrated off-shore, real-time information and management systems p0055 N82-14555

MOSES, J. F.
Interactive techniques for estimating precipitation from GOES imagery p0041 A82-13121

MOULTON, R. J.
A look at nonsatellite remote sensing systems for marine use p0032 N82-14586

MOZGOV, N. N.
Methodology and practice of spectroscopic measurements of landscape elements in the preparation and carrying out of down-looking experiments
p0051 A82-16613

MUEHLBERGER, W. R.
Global Tectonics: Some Geologic analyses of observations and photographs from Skylab
p0020 N82-12494

MUIRCHEARTAIGH, I. G.
Determination of surface wind speed from remotely measured whitecap coverage, a feasibility assessment
p0030 N82-14565

MULDER, N. J.
Spectral correlation filters and natural colour coding
p0043 A82-16160

MURDIN, J.
A Swedish proposal for an EISCAT/GEOS-2 experiment
[KGI-175] p0052 N82-10484

MURRAY, J. D.
Geological features of southwestern North America
p0020 N82-12495

MYERS, V. I.
Remote sensing applications to resource problems in South Dakota
[E82-10002] p0004 N82-15481

N

NALEPA, R.
Areawide soil loss predictions using CIR airphotos
p0007 A82-12591

NANKERVIS, R.
Absolute image registration for geosynchronous satellites p0049 A82-10061

NARAYANAN, M. S.
Detection of monsoon inversion by TIROS-N satellite
p0024 A82-17168

NAUCK, J.
Study of a combined satellite system for remote sensing and earth-oriented research (LOCSS)
[BMFT-FB-W-81-002] p0055 N82-14615

NEDWED, C. R.
Necessity of remote sensing for ocean studies. Part 1: Northwest African missions, Sahara-1 and Atlor-1
p0032 N82-14582

NESTERCZUK, G.
Ionospheric propagation correction modeling for satellite altimeters
[NASA-CR-156881] p0052 N82-12447

NEVILLE, R. A.
A recommended sensor package for the detection and tracking of oil spills p0053 N82-14583

NEWITT, L. R.
The reduction, verification and interpretation of Magsat magnetic data over Canada
[E82-10006] p0046 N82-15484

NIBLACK, W.
The Control Point Library Building System
p0043 A82-15971

NIELSEN, E.
A Swedish proposal for an EISCAT/GEOS-2 experiment
[KGI-175] p0052 N82-10484

NIKOLAEV, V. A.
Space photographs obtained with the Fragment system as a base for landscape mapping and physical-geographical classification of arid territories p0009 A82-15967

NITHACK, J.
Visual Evaluation of E-SLAR imagery
[DFVLR-FB-81-11] p0047 N82-15503

NIZKAIA, I. S.
Study of the anthropogenic influence on the environment, based on multispectral scanning images
p0008 A82-15965

NOBLE, V. E.
U.S. Navy planning for satellite oceanographic data exploitation
[AAS 81-072] p0024 A82-16341

NOLLA, A. B.
Necessity of remote sensing for ocean studies. Part 1: Northwest African missions, Sahara-1 and Atlor-1
p0032 N82-14582

O

OFFIELD, T. W.
Geologic applications of thermal-inertia mapping from satellite
[E82-10011] p0021 N82-15489

OHLHORST, C. W.
Preliminary analysis of ocean color scanner data from Superflux III p0027 N82-10672

OKAMOTO, A.
Orientation and construction of models. I - The orientation problem in close-range photogrammetry
p0049 A82-10858
Orientation and construction of models. III - Mathematical basis of the orientation problem of one-dimensional central perspective photographs p0043 A82-15973

OLAVESEN, A. H.
Infrared spectroscopy of microorganisms near 3.4 microns in relation to geology and astronomy
[PREPRINT-69] p0020 N82-12713

OMUIRCHEARTAIGH, I. G.
The feasibility of using remotely sensed color as an index of Irish coastal water properties p0032 N82-14581

ONEAL, B. L.
Environmental Monitoring Report, Sandia National Labs., Albuquerque, New Mexico, 180
[DE81-027839] p0010 N82-11649

ONEIL, R. A.
A recommended sensor package for the detection and tracking of oil spills p0053 N82-14583

ONSTOTT, R. G.
Measurements of radar backscatter from Arctic Sea ice in the summer
[AD-A105586] p0032 N82-14592
Measurements of radar backscatter from Arctic Sea ice in the summer, Appendices A and B
[AD-A105736] p0032 N82-14593

OPGENOORTH, H.
A Swedish proposal for an EISCAT/GEOS-2 experiment
[KGI-175] p0052 N82-10484

P

PANFILOV, A. S.
Investigation of survey conditions for the ocean surface in the 0.4-1.1 micron spectral range p0024 A82-15960

PARKE, M. E.
Global satellite measurements of water vapour, wind speed and wave height p0061 A82-17165

PARR, J. T.
Snow-mapping experiment p0037 N82-12498

PEARCE, J. B.
A marine environmental monitoring and assessment program p0027 N82-10663

PEDRINI, A.
Study of stack emissions by combination of lidar and correlation spectrometer p0008 A82-12816

PELAEZ, J.
The use of satellite infrared imagery for describing ocean processes in relation to spawning of the northern anchovy /Engraulis mordax/ p0025 A82-17565

PETERSEN, G. W.
Texture transforms of remote sensing data
p0042 A82-15034

PETTEY, J. E.
Report of survey for McDonald Observatory, Harvard Radio Astronomy Station, and vicinity
[PB81-234338] p0016 N82-13606

PHILIPSON, W. R.
Remote sensing for vineyard management
p0001 A82-10047

PHOEBUS, R. W.
Biological patchiness in relation to satellite thermal imagery and associated chemical mesoscale features
[AD-A105757] p0047 N82-15504

PIRKLE, F. L.
Statistical Techniques Applied to Aerial Radiometric Surveys (STAARS): Series introduction and the principal-components-analysis method
[DE81-029177] p0019 N82-10476

PITTS, D. E.
Mesoscale cloud features observed from Skylab
p0011 N82-12509

PITTS, J. N., JR.
Trace pollutant concentrations in a multiday smog episode in the California South Coast Air Basin by long path length Fourier transform infrared spectroscopy
p0007 A82-10700

PLATE, K.
Study of a combined satellite system for remote sensing and earth-oriented research (LOCSS)
[BMFT-FB-W-81-002] p0055 N82-14615

POLETAEV, IU. I.
Aspects in the development of aerial-photography tasks
p0041 A82-12913

PONOMARENKO, IU. V.
Methodology and practice of spectroscopic measurements of landscape elements in the preparation and carrying out of down-looking experiments
p0051 A82-16613

POOLE, L. R.
Spectral atmospheric observations at Nantucket Island, May 7-14, 1981
[NASA-TM-83196] p0029 N82-14550

POTEMRA, T. A.
Magnetic field-aligned electron distributions in the dayside cusp p0015 A82-12186
Distant magnetic field effects associated with Birkeland currents /made possible by the evaluation of TRIAD's attitude oscillations/ p0015 A82-12215

POWELL, R. E.
Geological features of southwestern North America
p0020 N82-12495

PRATT, D. A.
Two-dimensional model variability in thermal inertia surveys p0042 A82-15029

PREUSS, H. J.
Analysis of satellite observations: Theoretical studies on the sampling problem
[MITT-31] p0056 N82-15499

PROKURONOV, I. B.
The use of a priori information in the remote sensing of the earth from space p0044 A82-16818

PUCCINELLI, E. F.
Interpolating for the location of remote sensor data
[NASA-TM-82109] p0052 N82-13469

PURGOLD, G. C.
Automated analyzer for aircraft measurements of atmospheric methane and total hydrocarbons
p0007 A82-11949

R

RADER, M. L.
Investigation of the application of remote sensing technology to environmental monitoring
[E82-10010] p0013 N82-15488

RAMSEIER, R. O.
Visual observations of floating ice from Skylab
p0037 N82-12504

RANDERSON, D.
Quantitative analysis of atmospheric pollution phenomena p0010 N82-12505

RANEY, R. K.
Wave orbital velocity, fade, and SAR response to azimuth waves p0023 A82-11203

RAO, B. M.
Detection of monsoon inversion by TIROS-N satellite p0024 A82-17168

RAO, V. R.
Studies of the Indian continental shelf: Application of remote sensing data p0031 N82-14569
Scientific studies using Bhaskara satellite microwave radiometer (SAMIR) data: A short overview p0032 N82-14587

RASMUSSEN, E.
An investigation of a polar low with a spiral cloud structure p0007 A82-10616

REGAN, R. D.
A closer examination of the reduction of satellite magnetometer data for geological studies p0019 A82-11039

REICHLE, H. G., JR.
A new method for inferring carbon monoxide concentrations from gas filter radiometer data p0009 A82-16837
Results from the July 1981 Workshop on Passive Remote Sensing of the Troposphere
[AIAA PAPER 82-0207] p0009 A82-17841

REID, D. B.
An inertially-aided aircraft track recovery system for coastal mapping p0037 A82-18166

REYNOLDS, R. M.
GEM: A simple meteorological buoy with satellite telemetry p0053 N82-14779

RHODY, B.
A VHF homing system with VHF radiotelephony for area-representative strip-survey flights conducted, as part of combined forest inventories, with light aircraft carrying 70 mm and 35 mm cameras p0003 A82-15748

RICE, C. J.
Satellite observations of the Mt. St. Helens' eruption of 18 May 1980
[AD-A105784] p0012 N82-14591

RING, W. F.
Measurement of sea and ice backscatter reflectivity using an OTH radar system p0025 A82-18074

RITCHIE, A. W.
Global Tectonics: Some Geologic analyses of observations and photographs from Skylab p0020 N82-12494

ROBINSON, I. S.
The use of LANDSAT MSS to observe sediment distribution and movement in the Solent coastal area p0038 N82-14580

ROGERS, L. K.
An evaluation of the spatial resolution of soil moisture information
[NASA-CR-166724] p0009 N82-11513

ROHR, R.
Study of a combined satellite system for remote sensing and earth-oriented research (LOCSS)
[BMFT-FB-W-81-002] p0055 N82-14615

ROSENBERG, N. J.
Remote sensing of crop moisture status p0003 A82-17997

ROSENFIELD, G. H.
Analysis of variance of thematic mapping experiment data p0009 A82-15968

ROSTOKER, G.
Characteristics of westward travelling surges during magnetospheric substorms p0050 A82-14299

ROUFOSSE, M. C.
Study of the time evolution of the lithosphere
[NASA-CR-164968] p0016 N82-11696

RUSCH, D. W.
Nitric oxide delta band emission in the earth's atmosphere Comparison of a measurement and a theory p0008 A82-13268

RUTH, B. E.
Remote sensing study of sinkhole occurrence p0019 A82-12590

S

SAFIANOV, G. A.
Development of a coastal relief of the Gulf of Riga, based on results of an analysis of space images p0024 A82-15962

SAFLEKOS, N. A.
Distant magnetic field effects associated with Birkeland currents /made possible by the evaluation of TRIAD's attitude oscillations/ p0015 A82-12215

SAGDEEV, R. Z.
Airborne and spaceborne multispectral photography of the earth p0043 A82-16601

SALES, G. S.
Measurement of sea and ice backscatter reflectivity using an OTH radar system p0025 A82-18074

SANDRONI, S.
Study of stack emissions by combination of lidar and correlation spectrometer p0008 A82-12816

SASAKI, Y.
Mesoscale cloud features observed from Skylab p0011 N82-12509

SCARPACE, F. L.
The operational use of Landsat for lake quality assessment p0036 A82-12596

SCHAERF, R.
Investigations concerning the image-controlled segmentation of objects in multispectral imagery data p0042 A82-15003

SCHEER, J. A.
Reflectivity and emissivity of snow and ground at mm waves p0042 A82-14860

SCHERZ, J. P.
Remote sensing that motivated community action p0008 A82-12594

SCHMIDLIN, F. J.
Repeatability and measurement uncertainty of the United States meteorological rocketsonde p0049 A82-12127

SCHMIDT, G.
Study of a combined satellite system for remote sensing and earth-oriented research (LOCSS)
[BMFT-FB-W-81-002] p0055 N82-14615

SCHMUGGE, T. J.
A comparison of radiative transfer models for predicting the microwave emission from soils p0035 A82-10694

SCHNAPF, A.
The 1981 RCA space constellation p0055 A82-12541
The development of the Tiros Global Environmental Satellite System
[AIAA PAPER 82-0383] p0025 A82-17915

SCHNEIDER, G.
Study of a combined satellite system for remote sensing and earth-oriented research (LOCSS)
[BMFT-FB-W-81-002] p0055 N82-14615

SCHNEIDER, S. R.
Effect of grain size and snowpack water equivalence on visible and near-infrared satellite observations of snow p0035 A82-12553

SCHOTT, J. R.
Role of remote sensing in the study of acid rain impact on aquatic systems
[AIAA PAPER 82-0336] p0036 A82-17892

SCHOWENGERDT, R. A.
Data compression and reconstruction for mixed resolution multispectral sensors p0049 A82-10045

SCHROCK, B. L.
Applications of digital displays in photointerpretation and digital mapping p0041 A82-10038

SCHROEDER, L. C.
Evaluation of the Seasat wind scatterometer p0025 A82-18716

SCHUBERT, J. S.
Report on Skylab 4 African drought and arid land experiment p0037 N82-12501

SCIACOVELLI, D.
Infrared radiance model variation by sensor flight measurements p0052 N82-14171

SCOFIELD, R. A.
Analysis of rainfall from flash flood producing thunderstorms, using GOES data p0038 N82-14724

SCOGGINS, R. K.
Inclusion of a simple vegetation layer in terrain temperature models for thermal infrared (IR) signature prediction
[AD-A104469] p0003 N82-11910

SELIVANOV, A. S.
Investigation of survey conditions for the ocean surface in the 0.4-1.1 micron spectral range p0024 A82-15960

SENUS, W. J.
GPS application to mapping, charting and geodesy p0015 A82-10645

SHAKHVERDOV, A. SH.
A new method for computing distortion p0016 A82-12914

SHAMIS, V. A.
Processing of multispectral image data on special-purpose computer systems p0044 A82-16627
Programs for the statistical analysis of multispectral photographs p0044 A82-16628
Coordinate referencing of MKF-6 photographs and their transformation to the cartographic projection p0045 A82-16630

SHARP, W. E.
Nitric oxide delta band emission in the earth's atmosphere Comparison of a measurement and a theory p0008 A82-13268

SHEFFIELD, C.
Remote sensing contributions to the management of renewable resources p0055 A82-12530

SHELTON, D.
Evaluation of the Seasat wind scatterometer p0025 A82-18716

SHENK, W. E.
Meteorological lab applications of Skylab handheld-camera photographs p0011 N82-12506

SHIMABUKURO, Y. E.
Wheat cultivation: Identification and estimation of areas using LANDSAT data
[E82-10007] p0004 N82-15485
Remote sensing in forestry: Application to the Amazon region
[E82-10012] p0005 N82-15490

SHLIAM, E. Z.
A new method for computing distortion p0016 A82-12914

SHUBINSKI, R. P.
Landsat imagery for hydrologic modeling p0036 A82-12592

SIEBERS, A. L.
Interactive techniques for estimating precipitation from GOES imagery p0041 A82-13121

SIELSKI, H.
Absolute image registration for geosynchronous satellites p0049 A82-10051

SILTER, L. T.
Geological features of southwestern North America p0020 N82-12495

SILVERMAN, J. R.
User needs and the future of operational meteorological satellites
[AIAA PAPER 82-0388] p0051 A82-17918

SIMKIN, T.
Skylab 4 observations of Volcanoes. Part A: Volcanoes and volcanic landforms. Part B: Summit eruption of Femandian Caldera, Galapagos Islands, Ecuador p0020 N82-12496

SIMMONS, T. N.
Environmental Monitoring Report, Sandia National Labs., Albuquerque, New Mexico, 180
[DE81-027839] p0010 N82-11649

SINGH, S. M.
Coastal zone research using remote sensing techniques p0031 N82-14571

SITTROP, H.
Project Noordwijk. Part 2: Results of North Sea clutter measurements in the I-band performed from the platform Noordwijk in September/October 1977
[PHL-1980-28-PT-2] p0033 N82-14618

SKILLMAN, W. C.
Meteorological lab applications of Skylab handheld-camera photographs p0011 N82-12506

SLATOR, T.
A mathematical model of an over-sea airborne UHF radio link p0049 A82-11406

SMALLWOOD, M. D.
An evaluation of the spatial resolution of soil moisture information
[NASA-CR-166724] p0009 N82-11513
Snow-mapping experiment p0037 N82-12498

SMITH, J. T., JR.
A history of flying and photography: In the Photogrammetry Division of the National Ocean Survey 1919 - 1979
[PB81-246738] p0017 N82-15520

SMYTH, J. E.
Photo inertial positioning system development at the Canada Centre for Remote Sensing p0045 A82-18167

SNETKOVA, N. I.
Spectrometric studies of the earth's surface p0043 A82-16612

SOBCHUK, V. G.
Programs for the statistical analysis of multispectral photographs p0044 A82-16628
Coordinate referencing of MKF-6 photographs and their transformation to the cartographic projection p0045 A82-16630

SOREIDE, N. N.
CTD/O2 measurements during the Equatorial Pacific Ocean Climate Study (EPOCS) in 1979
[PB81-211203] p0026 N82-10481

SPAYD, L. E., JR.
Interactive techniques for estimating precipitation from GOES imagery p0041 A82-13121

SPELL, B. D.
CTD/O2 measurements during the Equatorial Pacific Ocean Climate Study (EPOCS) in 1979
[PB81-211203] p0026 N82-10481

SRISAENGTHONG, D.
The use of LANDSAT MSS to observe sediment distribution and movement in the Solent coastal area p0038 N82-14580

STEEN, A.
A Swedish proposal for an EISCAT/GEOS-2 experiment
[KGI-175] p0052 N82-10484

STEIDLER, F.
Description and comparison of algorithms for solving large sets of sparse matrix normal equations in geodesy and photogrammetry
[SER-C-261] p0017 N82-15812

STEVENSON, R. E.
Visual observations of the ocean p0028 N82-12502

STEWART, R. H.
Anomalous wind estimates from the Seasat scatterometer p0026 A82-18724

STILES, W.
Progress in radar snow research
[NASA-CR-166709] p0038 N82-12510

STONE, R. O.
Visual observations of the ocean p0028 N82-12502

STRONG, R. B.
Aircraft data summaries of the SURE intensives, volume 4
[DE82-900311] p0012 N82-13569

SUGIURA, M.
A closer examination of the reduction of satellite magnetometer data for geological studies p0019 A82-11039
Magnetic field observations on DE-A and -B p0051 A82-16447

SUNDARARAMAN, M. K.
ISRO satellite mission support facilities - Scope and future plans p0055 A82-17307

SVENDSON, E.
The Norwegian remote sensing experiment (Norsex) in a marginal ice zone p0031 N82-14566

SWANSON, E. R.
Global Tectonics: Some Geologic analyses of observations and photographs from Skylab
p0020 N82-12494

SWIFT, R. N.
Application of the NASA airborne oceanographic lidar to the mapping of chlorophyll and other organic pigments
p0027 N82-10684

SWITZER, P.
Estimation of atmospheric path-radiance by the covariance matrix method p0041 A82-10861

SYCHEV, A. G.
Metrological support of measurements of earth-surface brightness by the Fragment multispectral scanning system p0050 A82-15958

T

TALAY, T. A.
Spectral atmospheric observations at Nantucket Island, May 7-14, 1981
[NASA-TM-83196] p0029 N82-14550

TALSKAIA, N. N.
Investigation and mapping of the erosion relief of the Kalachskaia upland on the basis of multispectral scanner images p0008 A82-15966

TARDIN, A. T.
Wheat cultivation: Identification and estimation of areas using LANDSAT data
[E82-10007] p0004 N82-15485
Remote sensing in forestry: Application to the Amazon region
[E82-10012] p0005 N82-15490

TARNOPOLSKII, V. I.
Metrological support of measurements of earth-surface brightness by the Fragment multispectral scanning system p0050 A82-15958

TAYLOR, R. L.
Boundary detection criteria for satellite altimeters
[NASA-CR-156880] p0028 N82-12734

TAYLOR, R. S.
Landsat imagery for hydrologic modeling
p0036 A82-12592

TECSON, J. J.
Mesoscale wake clouds in Skylab photographs
p0011 N82-12506

THIRUVENGADACHARI, S.
Satellite sensing of irrigation patterns in semiarid areas: An Indian study p0002 A82-10864
Cost effective computer processing of airborne scanner data for regional level mapping p0043 A82-15970

THOMAS, J. P.
Synoptic thermal and oceanographic parameter distributions in the New York Bight Apex
p0023 A82-12885
Chesapeake Bay Plume Study: Superflux 1980
[NASA-CP-2188] p0026 N82-10661
Superflux I, II, and III experiment designs: Water sampling and analyses p0027 N82-10665

THOMPSON, L. G. S.
Digitizing and automated output mapping errors
p0015 A82-10859

THOMPSON, T.
Marine activities in Sweden for which remote sensing data may be of interest p0031 N82-14576

THOMSON, J. C.
An evaluation of Seasat-A data in relation to optimum track ship weather routing and site specific forecasting for the offshore oil industry p0030 N82-14564

TIGHE, W. G.
Characteristics of westward travelling surges during magnetospheric substorms p0050 A82-14299

TOLL, D. L.
Preliminary results of mapping urban land cover with Seasat SAR imagery p0007 A82-10044

TOMMERDAHL, J. B.
Aircraft data summaries of the SURE intensives, volume 4
[DE82-900311] p0012 N82-13569

TRIFONOV, IU. V.
Satellites of the Meteor series, intended for earth studies from space p0050 A82-15951
Technical equipment of an experiment for remote sensing of the earth from space p0050 A82-15952

TSAI, B.
Remote sensing of sea state by laser altimeters
[NASA-CR-165049] p0033 N82-14789

TUAZON, E. C.
Trace pollutant concentrations in a multiday smog episode in the California South Coast Air Basin by long path length Fourier transform infrared spectroscopy
p0007 A82-10700

TUCKER, C. J.
Temporal spectral response of a corn canopy
p0002 A82-12886
Temporal relationships between spectral response and agronomic variables of a corn canopy p0002 A82-15038

U

ULABY, F. T.
Aircraft radar response to soil moisture
p0003 A82-17564
Progress in radar snow research
[NASA-CR-166709] p0038 N82-12510

ULBRICHT, K. A.
Maritime applications of image processing at DFVLR, Oberpfaffenhofen, West Germany p0032 N82-14885

UPTON, D. T.
Scanner
[NASA-CASE-GSC-12032-2] p0052 N82-13465

V

VALERIO, C.
Operational use of remote sensing for coastal zone management and possible contribution of specialized satellites p0031 N82-14574

VANBEEK, G. J.
The reduction, verification and interpretation of Magsat magnetic data over Canada
[E82-10006] p0046 N82-15484

VANGENDEREN, J. L.
Airborne remote sensing of the coastal zone
p0053 N82-14577

VENKATACHARY, K. V.
ISRO satellite mission support facilities - Scope and future plans p0055 A82-17307

VONDERHAAR, S. P.
Visual observations of the ocean p0028 N82-12502

VOSTREYS, R. W.
Report on Active and Planned Spacecraft and experiments
[NASA-TM-84025] p0055 N82-10087

VUKOVICH, F. M.
Monitoring the Chesapeake Bay using satellite data for Superflux III p0027 N82-10668

W

WAGNER, K.
Mesoscale cloud features observed from Skylab
p0011 N82-12509

WALD, L.
Oil spills: Large scale monitoring by LANDSAT
p0012 N82-14572

WALKER, A. D. M.
Use of hydromagnetic waves to map geomagnetic field lines p0016 A82-16868

WALKER, J. K.
The reduction, verification and interpretation of Magsat magnetic data over Canada
[E82-10006] p0046 N82-15484

WALLIO, H. A.
A new method for inferring carbon monoxide concentrations from gas filter radiometer data
p0009 A82-16837

WANNBERG, G.
A Swedish proposal for an EISCAT/GEOS-2 experiment
[KGI-175] p0052 N82-10484

WARWICK-SMITH, R. M.
The use of digitally processed Landsat imagery for vegetation mapping in Sulawesi, Indonesia
p0003 A82-17998

WATSON, K.
Geologic applications of thermal-inertia mapping from satellite
[E82-10011] p0021 N82-15489

WATTS, D. G.
Remote sensing of crop moisture status
p0003 A82-17997

WAYENBERG, J. A.
Visual observations of floating ice from Skylab
p0037 N82-12504

WEAVER, M. G.
Repetitive aerial photography for assessing marsh vegetation changes p0001 A82-10048

WEBRING, M. W.
Preliminary analysis of gravity and aeromagnetic surveys of the Timber Mountain area, southern Nevada
[DE81-029462] p0022 N82-15506

WEEKS, W. F.
Visual observations of floating ice from Skylab
p0037 N82-12504

WEISE, R. C.
ERSYS-SPP access method subsystem design specification
[E82-10015] p0053 N82-15493

WELBY, C. W.
Satellite imagery and shoreline erosion prediction
p0036 A82-12595

WESTERLUND, S.
A Swedish proposal for an EISCAT/GEOS-2 experiment
[KGI-175] p0052 N82-10484

WHARTON, S. W.
Preliminary results of mapping urban land cover with Seasat SAR imagery p0007 A82-10044

WHITE, F. E., JR.
Application of satellite Doppler techniques to the national mapping program p0015 A82-10066

WHITE, J. H.
Aircraft data summaries of the SURE intensives, volume 4
[DE82-900311] p0012 N82-13569

WICKRAMASINGHE, N. C.
Infrared spectroscopy of microorganisms near 3.4 microns in relation to geology and astronomy
[PREPRINT-69] p0020 N82-12713

WILKINSON, M. A.
Role of remote sensing in the study of acid rain impact on aquatic systems
[AIAA PAPER 82-0336] p0036 A82-17892

WILLIAMS, R. N.
The potential and requirements for space oceanography
p0029 N82-14556

WINER, A. M.
Trace pollutant concentrations in a multiday smog episode in the California South Coast Air Basin by long path length Fourier transform infrared spectroscopy
p0007 A82-10700

WINTERBURN, R. F. J.
The SACLANTCEN oceanographic data base. Volume 1: Design criteria and data structure and content
[AD-A103277] p0029 N82-13639

WOLF, D. E.
Oceanic wind and balanced pressure-height fields derived from satellite measurements p0023 A82-13214

WONG, M. C.
The near-infrared radiation received by satellites from clouds p0025 A82-17492

WU, C.
A digital fast correlation approach to produce SEASAT SAR imagery p0042 A82-14870

WU, S. T.
An improvement in land cover classification achieved by merging microwave data with Landsat multispectral scanner data p0007 A82-10043

Y

YOKOYAMA, R.
The discrimination of winter wheat using a growth-state signature p0002 A82-15028

Z

ZACHOR, A. S.
Proof of concept study
[AD-A104338] p0010 N82-11639
Limit on remote FTIR detection of trace gases
[AD-A104842] p0011 N82-12511

ZANDONELLA, A.
Multitemporal calibration of LANDSAT images: A method for improving the marine phenomena recognition, with as example the Venice lagoon p0046 N82-14578

ZANETTI, L. J.
Magnetic field-aligned electron distributions in the dayside cusp p0015 A82-12186

ZHUKOV, B. S.
Polarimetric surveys of oil slicks p0009 A82-16619
Images of sea waves obtained in polarimetric surveys
p0024 A82-16620
The choice of the orientation of the analyzer in polarimetric surveys p0044 A82-16621
Analysis of the information content of the polarimetric method of remote sensing p0003 A82-16622

ZIMAN, IA. L.
Metrological support of measurements of earth-surface brightness by the Fragment multispectral scanning system p0050 A82-15958
Main results of the Raduga experiment
p0051 A82-16602
Geometric quality of MKF-6 photographs
p0043 A82-16606
Coordinate referencing of MKF-6 photographs and their transformation to the cartographic projection
p0045 A82-16630

ZINGMARK, R. G.
Remote sensing of benthic microalgal biomass with a tower-mounted multispectral scanner p0024 A82-15031

ZLOBIN, L. I.
Aerial and space methods in cartography
p0016 A82-12915

ZORN, H. C.
The application of programmable pocket calculators for computations during survey flights p0050 A82-16164

ZULCH, D. I.
Factorial analysis of terrain feature positioning parameters used in combining radar and digital terrain model data
p0015 A82-10029

ZWICK, H. H.
A recommended sensor package for the detection and tracking of oil spills p0053 N82-14563
Recent work in passive optical imaging of water
p0038 N82-14575

CORPORATE SOURCE INDEX

EARTH RESOURCES / *A Continuing Bibliography (Issue 33)* **APRIL 1982**

Typical Corporate Source Index Listing

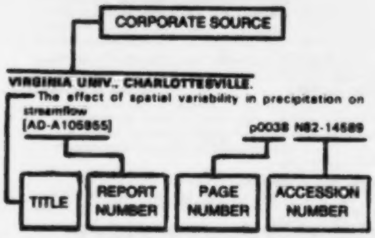
CORPORATE SOURCE
VIRGINIA UNIV., CHARLOTTESVILLE.
The effect of spatial variability in precipitation on streamflow
[AD-A105855]
p0038 N82-14589
TITLE
REPORT NUMBER
PAGE NUMBER
ACCESSION NUMBER

The title of the document is used to provide a brief description of the subject matter. The page number and the accession number are included in each entry to assist the user in locating the abstract in the abstract section. If applicable, a report number is also included as an aid in identifying the document.

A

AEROSPACE CORP., EL SEGUNDO, CALIF.
Satellite observations of the Mt. St. Helens' eruption of 18 May 1980
[AD-A105784] p0012 N82-14591

AIR FORCE SYSTEMS COMMAND, WRIGHT-PATTERSON AFB, OHIO.
Meteorological satellites
[AD-A107427] p0053 N82-15110

AIR RESOURCES LAB., LAS VEGAS, NEV.
Quantitative analysis of atmospheric pollution phenomena p0010 N82-12505

AMERICAN UNIV., WASHINGTON, D. C.
Report on Skylab 4 African drought and arid land experiment p0037 N82-12501

APPLIED PHYSICS LAB., JOHNS HOPKINS UNIV., LAUREL, MD.
Radar correlation with ice depolarization measurements of the 28.56 GHz COMSTAR beacon and associated cross polarization statistics
[NASA-CR-166717] p0046 N82-14548

ARGONNE NATIONAL LAB., ILL.
Environmental data for sites in the National Solar Data Network
[DE82-000071] p0011 N82-12707

ARMY ENGINEER WATERWAYS EXPERIMENT STATION, VICKSBURG, MISS.
Airborne laser acquisition of cross-section data
p0049 A82-12600
Inclusion of a simple vegetation layer in terrain temperature models for thermal infrared (IR) signature prediction
[AD-A104469] p0003 N82-11910

ATMOSPHERIC RADIATION CONSULTANTS, ACTON, MASS.
Proof of concept study
[AD-A104338] p0010 N82-11639

ATMOSPHERIC SCIENCES LAB., WHITE SANDS MISSILE RANGE, N. MEX.
Sensitivity analysis of a mesoscale moisture model
[AD-A101528] p0012 N82-14590

ATOMIC ENERGY RESEARCH ESTABLISHMENT, HARWELL (ENGLAND).
A look at nonsatellite remote sensing systems for marine use p0032 N82-14586

AUTOMATION INDUSTRIES, INC., SILVER SPRING, MD.
Environmental data for sites in the National Solar Data Network
[DE82-000071] p0011 N82-12707

B

BALL AEROSPACE SYSTEMS DIV., BOULDER, COLO.
Development of the coastal zone color scanner for NIMBUS 7. Volume 1: Mission objectives and instrument description
[NASA-CR-166720-VOL-1] p0028 N82-11611

BELFOTOP P.V.B.A., WEMMEL (BELGIUM).
Airborne remote sensing of the coastal zone
p0053 N82-14577

BENDIX FIELD ENGINEERING CORP., GRAND JUNCTION, COLO.
Statistical Techniques Applied to Aerial Radiometric Surveys (STAARS): Series introduction and the principal-components-analysis method
[DE81-029177] p0019 N82-10476

C

CALIFORNIA INST. OF TECH., PASADENA.
Geological features of southwestern North America
p0020 N82-12495

CALIFORNIA UNIV., BERKELEY.
Vegetation patterns p0004 N82-12500
Application of remote sensing to selected problems within the state of California
[E82-10004] p0004 N82-15482

CALIFORNIA UNIV., SANTA BARBARA.
Use of environmental satellite data for input to energy balance snowmelt models
[PB81-227795] p0039 N82-15673

CALIFORNIA UNIV. AT DAVIS.
Spectral behavior of wheat yield variety trials
p0002 A82-10863

CANADA CENTRE FOR REMOTE SENSING, OTTAWA (ONTARIO).
A recommended sensor package for the detection and tracking of oil spills p0053 N82-14563
Recent work in passive optical imaging of water
p0038 N82-14575

CARSON HELICOPTERS, INC., PERKASIE, PA.
NURE aerial gamma-ray and magnetic reconnaissance survey of Maine and portions of New York. Volume 1: Data acquisition, reduction and interpretation
[DE82-000850] p0053 N82-14599
NURE aerial gamma-ray and magnetic reconnaissance survey of Maine and portions of New York, volume 2
[DE82-000781] p0020 N82-14600
NURE aerial gamma-ray and magnetic reconnaissance survey of Maine and portions of New York, volume 2
[DE82-000401] p0020 N82-14601
NURE aerial gamma-ray and magnetic reconnaissance survey of Maine and portions of New York, volume 2
[DE82-000780] p0021 N82-14602
NURE aerial gamma-ray and magnetic reconnaissance survey of Maine and portions of New York, volume 2
[DE82-000872] p0021 N82-14603
NURE aerial gamma-ray and magnetic reconnaissance survey of Maine and portions of New York, volume 2
[DE82-000772] p0021 N82-14604
NURE aerial gamma-ray and magnetic reconnaissance survey of Maine and portions of New York, volume 2
[DE82-000785] p0021 N82-14605
NURE aerial gamma-ray and magnetic reconnaissance survey of Maine and portions of New York, volume 2
[DE82-000869] p0021 N82-14606
NURE aerial gamma-ray and magnetic reconnaissance survey of Maine and portions of New York, volume 2
[DE82-000794] p0021 N82-14607
NURE aerial gamma-ray and magnetic reconnaissance survey of Maine and portions of New York, volume 2
[DE82-000784] p0021 N82-14608

CENTRE D'ETUDES DE METEOROLOGIE SPATIALE, LANNION (FRANCE).
A short review of an oceanographic use of Meteosat data by the ORSTOM remote sensing service
p0031 N82-14570

CENTRE D'ETUDES TECHNIQUES DE L'EQUIPMENT, AIX-EN-PROVENCE (FRANCE).
Operational use of remote sensing for coastal zone management and possible contribution of specialized satellites p0031 N82-14574

CENTRE NATIONAL D'ETUDES SPATIALES, PARIS (FRANCE).
SPOT data simulations: Littoral applications
p0046 N82-14568

CENTRE NATIONAL D'ETUDES SPATIALES, TOULOUSE (FRANCE).
State-of-the-art in using a spaceborne altimeter and scatterometer for the determination of wind, sea state, and marine and ice dynamics p0052 N82-14560

CHICAGO UNIV., ILL.
Mesoscale wake clouds in Skylab photographs
p0011 N82-12508

COLOGNE UNIV. (WEST GERMANY).
Analysis of satellite observations: Theoretical studies on the sampling problem
[MITT-31] p0056 N82-15499

COLORADO UNIV., BOULDER.
Nitric oxide delta band emission in the earth's atmosphere - Comparison of a measurement and a theory
p0008 A82-13268

COMMITTEE ON SCIENCE AND TECHNOLOGY (U. S. HOUSE).
Civil land remote sensing systems
[GPO-35-265] p0056 N82-15497

COMPUTER SCIENCES CORP., EL SEGUNDO, CALIF.
Magnetic Field Satellite (Magsat) data processing system specifications
[NASA-CR-166737] p0045 N82-11103

COMPUTER SCIENCES CORP., SILVER SPRING, MD.
Absolute image registration for geosynchronous satellites p0049 A82-10061
A comparison of radiative transfer models for predicting the microwave emission from soils p0035 A82-10894
The surface albedo of the earth in the near ultraviolet /330-340 nm/ p0016 A82-15032

CONOCO NORWAY, INC., OSLO.
Offshore petroleum industry environmental data requirements: Emphasis on remote sensing
p0030 N82-14557

CONSIGLIO NAZIONALE DELLE RICERCHE, VENICE (ITALY).
Multitemporal calibration of LANDSAT images: A method for improving the marine phenomena recognition, with as example the Venice lagoon p0046 N82-14578

COPENHAGEN UNIV. (DENMARK).
The color of the sea and its relation to surface chlorophyll and depth of the euphotic zone p0030 N82-14562

CORNELL UNIV., ITHACA, N. Y.
Remote sensing for vineyard management
p0001 A82-10047
Remote sensing studies of some ironstone gravels and plinthite in Thailand p0019 N82-12491

D

DANISH METEOROLOGICAL INST., COPENHAGEN.
The ice-conditions in the Greenland waters, 1965. Coastal maps
[ISBN-87-7478-183-9] p0028 N82-10487
The ice conditions in the Greenland waters
[ISBN-87-7478-183-9] p0028 N82-12533

DEFENSE MAPPING AGENCY, WASHINGTON, D.C.
GPS application to mapping, charting and geodesy
p0015 A82-10645

DELAWARE UNIV., NEWARK.
In situ spectral reflectance studies of tidal wetland grasses p0036 A82-15969

DEUTSCHE FORSCHUNGS- UND VERSUCHSANSTALT FUER LUFT- UND RAUMFAHRT, OBERPFAFFENHOFEN (WEST GERMANY).
Maritime applications of image processing at DFVLR Oberpfaffenhofen, West Germany p0032 N82-14585
Visual Evaluation of E-SLAR imagery
[DFVLR-FB-81-11] p0047 N82-15503

DEUTSCHES GEODAETISCHES FORSCHUNGSINSTITUT, MUNICH (WEST GERMANY).
Description and comparison of algorithms for solving large sets of sparse matrix normal equations in geodesy and photogrammetry
[SER-C-261] p0017 N82-15812

DUNDEE UNIV. (SCOTLAND).
Coastal zone research using remote sensing techniques
p0031 N82-14571

E

ECOLE NATIONALE SUPERIEURE DES MINES, SOPHIA-ANTIPOLIS (FRANCE).
Oil spills: Large scale monitoring by LANDSAT
p0012 N82-14572

EG AND G WASHINGTON ANALYTICAL SERVICES CENTER, INC., POCOMOKE CITY, MD.
Boundary detection criteria for satellite altimeters
[NASA-CR-156880] p0028 N82-12734
A global atlas of GEOS-3 significant waveheight data and comparison of the data with national buoy data
[NASA-CR-156882] p0033 N82-15498
EG & G WASHINGTON ANALYTICAL SERVICES CENTER, INC., RIVERDALE, MD.
Ionospheric propagation correction modeling for satellite altimeters
[NASA-CR-156881] p0052 N82-12447
ENERGY INFORMATION ADMINISTRATION, WASHINGTON, D.C.
The reduction, verification and interpretation of Magsat magnetic data over Canada
[E82-10006] p0046 N82-15484
ENERGY, MINES AND RESOURCES CANADA, OTTAWA (ONTARIO).
The Manicouagan impact structure observed from Skylab
[CONTRIB-544] p0020 N82-12497
ENVIRONMENTAL RESEARCH AND TECHNOLOGY, INC., CONCORD, MASS.
An evaluation of the spatial resolution of soil moisture information
[NASA-CR-166724] p0009 N82-11513
Snow-mapping experiment p0037 N82-12498
Analysis of soil moisture extraction algorithm using data from aircraft experiments
[NASA-CR-166719] p0046 N82-13470
ENVIRONMENTAL RESEARCH INST. OF MICHIGAN, ANN ARBOR.
Development and evaluation of an automatic labeling technique for spring small grains
[E82-10001] p0004 N82-15480
ERNO RAUMFAHRTTECHNIK G.M.B.H., BREMEN (WEST GERMANY).
Study of a combined satellite system for remote sensing and earth-oriented research (LOCSS)
[BMFT-FB-W-81-002] p0055 N82-14615
EUROPEAN SPACE AGENCY, PARIS (FRANCE).
Application of remote sensing data on the continental shelf: Proceedings of an EARsL-ESA Symposium
[ESA-SP-167] p0029 N82-14553
ERS-1: Mission objectives and system concept
p0029 N82-14554
The need for integrated off-shore, real-time information and management systems p0055 N82-14555
EUROSAT S.A., GENEVA (SWITZERLAND).
Overall economic impact of an operational Meteosat system
[ESA-CR(P)-1457] p0055 N82-13010

G

GENERAL ELECTRIC CO., LANHAM, MD.
Computational aspects of geometric correction data generation in the LANDSAT-D imagery processing
p0045 N82-10072
The MSS control point location error filter for LANDSAT-D p0051 N82-10073
GENERAL ELECTRIC CO., PHILADELPHIA, PA.
LANDSAT-2 and LANDSAT-3 flight evaluation report, 23 April to 23 July 1979
[E82-10005] p0053 N82-15483
LANDSAT-2 and LANDSAT-3 flight evaluation report, 23 October 1978 to 23 January 1979
[E82-10017] p0054 N82-15495
GEOLOGICAL SURVEY, DENVER, COLO.
Desert sand seas p0020 N82-12493
Skylab 4 observations of Volcanoes. Part A: Volcanoes and volcanic landforms. Part B: Summit eruption of Fernandian Caldera, Galapagos Islands, Ecuador
p0020 N82-12496
Geologic applications of thermal-inertia mapping from satellite
[E82-10011] p0021 N82-15489
Preliminary analysis of gravity and aeromagnetic surveys of the Timber Mountain area, southern Nevada
[DE81-029462] p0022 N82-15506
GEOLOGICAL SURVEY, TACOMA, WASH.
Visual observations of floating ice from Skylab
p0037 N82-12504

H

HAWAII UNIV., HONOLULU.
A method for using aerial photos in delineating historic patterns of beach accretion and retreat
[PB81-223836] p0010 N82-11536
HRB-SINGER, INC., STATE COLLEGE, PA.
Absolute image registration for geosynchronous satellites p0049 A82-10051

I

IBM FEDERAL SYSTEMS DIV., HOUSTON, TEXAS.
ERSYS-SPP access method subsystem design specification
[E82-10015] p0053 N82-15493
IBM FRANCE S. A., PARIS.
The Control Point Library Building System
p0043 A82-15971
IDAHO UNIV., MOSCOW.
Geology and linears of Libya p0019 N82-10618
ILLINOIS STATE WATER SURVEY, URBANA.
The effect of spatial variability in precipitation on streamflow
[AD-A105955] p0036 N82-14589
ILLINOIS UNIV., URBANA.
Remote sensing of sea state by laser altimeters
[NASA-CR-165049] p0033 N82-14789
INDIAN SPACE RESEARCH ORGANIZATION, BANGALORE.
Scientific studies using Bhaskara satellite microwave radiometer (SAMIR) data: A short overview
p0032 N82-14587
INSTITUTE OF MARINE RESEARCH, BERGEN (NORWAY).
Fisheries investigations and management benefits from remote sensing p0030 N82-14558
INSTITUTE OF OCEANOGRAPHIC SCIENCES, WORMLEY (ENGLAND).
Evaluation of the Seasat wind scatterometer
p0025 A82-18716
Anomalous wind estimates from the Seasat scatterometer p0026 A82-18724
A preliminary evaluation of Seasat performance over the area of JASIN and its relevance to ERS-1
p0031 N82-14567
INSTITUTO DE INVESTIGACIONES PESQUERAS, BARCELONA (SPAIN).
Necessity of remote sensing for ocean studies. Part 1: Northwest African missions, Sahara-1 and Atlor-1
p0032 N82-14582
INSTITUTO DE PESQUISAS ESPACIAIS, SAO JOSE DOS CAMPOS (BRAZIL).
Wheat cultivation: Identification and estimation of areas using LANDSAT data
[E82-10007] p0004 N82-15485
Quantitative analysis of drainage obtained from aerial photographs and RBV/LANDSAT images
[E82-10008] p0039 N82-15486
Remote sensing in forestry: Application to the Amazon region
[E82-10012] p0005 N82-15490
INTERMOUNTAIN FOREST AND RANGE EXPERIMENT STATION, OGDEN, UTAH.
Large-scale color aerial photography as a tool in sampling for mortality rates
[PB81-214777] p0003 N82-10489

J

JET PROPULSION LAB., CALIFORNIA INST. OF TECH., PASADENA.
SAR imaging of ocean waves - Theory
p0023 A82-11202
A digital fast correlation approach to produce SEASAT SAR imagery p0042 A82-14870
Availability of Seasat synthetic aperture radar imagery
p0050 A82-15039
Optically processed Seasat radar mosaic of Florida
p0042 A82-15125
Global satellite measurements of water vapour, wind speed and wave height p0051 A82-17165
Evaluation of the Seasat wind scatterometer
p0025 A82-18716
Anomalous wind estimates from the Seasat scatterometer p0026 A82-18724
Radar mapping, archaeology, and ancient land use in the Maya lowlands
[NASA-CR-164931] p0010 N82-11514
Microwave limb sounder
[NASA-CASE-NPO-14544-1] p0011 N82-12685
The Seasat commercial demonstration program
p0030 N82-14561
JOHNS HOPKINS UNIV., BALTIMORE, MD.
Magnetic field-aligned electron distributions in the dayside cusp p0015 A82-12186
JOHNS HOPKINS UNIV., LAUREL, MD.
Magnetic field-aligned electron distributions in the dayside cusp p0015 A82-12186

K

KANSAS UNIV. CENTER FOR RESEARCH, INC., LAWRENCE.
Aircraft radar response to soil moisture
p0003 A82-17564
Progress in radar snow research
[NASA-CR-166708] p0038 N82-12510
Measurements of radar backscatter from Arctic Sea ice in the summer
[AD-A105586] p0032 N82-14592
Measurements of radar backscatter from Arctic Sea ice in the summer. Appendices A and B
[AD-A105736] p0032 N82-14593
KENTRON INTERNATIONAL, INC., HAMPTON, VA.
Synoptic thermal and oceanographic parameter distributions in the New York Bight Apex
p0023 A82-12885
KIRUNA GEOPHYSICAL INST. (SWEDEN).
A Swedish proposal for an EISCAT/GEOS-2 experiment
[KGI-175] p0052 N82-10484

L

LOCKHEED ENGINEERING AND MANAGEMENT SERVICES CO., INC., HOUSTON, TEX.
Investigation of the application of remote sensing technology to environmental monitoring
[E82-10010] p0013 N82-15488
Fiscal year 1980-81 implementation plan in support of technical development and integration of sampling and aggregation procedures
[E82-10013] p0005 N82-15491
Winterkill indicator model. Crop Condition Assessment Division (CCAD) data base interface driver, user's manual
[E82-10014] p0005 N82-15492

M

MAINE UNIV., ORONO.
The operational use of Landsat for lake quality assessment p0036 A82-12598
MARCONI CO. LTD., CHELMSFORD (ENGLAND).
Additional studies of Earth resources synthetic aperture radar payloads
[MTR-80/90] p0054 N82-15500
New baseline system p0054 N82-15501
Squinted SAR system p0047 N82-15502
MARTIN MARIETTA CORP., DENVER, COLO.
Onboard utilization of ground control points for image correction. Volume 1: Executive summary
[NASA-CR-166731] p0045 N82-10469
Onboard utilization of ground control points for image correction. Volume 2: Analysis and simulation results
[NASA-CR-166732] p0045 N82-10470
Onboard utilization of ground control points for image correction. Volume 3: Ground control point simulation software design
[NASA-CR-166733] p0045 N82-10471
Onboard utilization of ground control points for image correction. Volume 4: Correlation analysis software design
[NASA-CR-166734] p0045 N82-10472
MASSACHUSETTS INST. OF TECH., CAMBRIDGE.
Radiative transfer theory for passive microwave remote sensing of random media p0049 A82-11533
Surface signs of internal ocean dynamics
[AD-A101380] p0029 N82-13642
MASSACHUSETTS UNIV., AMHERST.
The mineralogy of global magnetic anomalies
[E82-10009] p0021 N82-15487
METEOROLOGISCHES OBSERVATORIUM, HOHENPEISSENBERG (WEST GERMANY).
Special observations by the Hohenpeissenberg Meteorological Observatory. Number 42: Results of aerological and surface ozone measurements during the first semester of 1980
[SONDERBEOB-42] p0012 N82-12714
METEOROLOGY RESEARCH, INC., SANTA ROSA, CALIF.
Aircraft data summaries of the SURE intensives, volume 4
[DE82-900311] p0012 N82-13569
MIAMI UNIV., CORAL GABLES, FLA.
Clear water radiances for atmospheric correction of coastal zone color scanner imagery p0025 A82-17292
MICHIGAN STATE UNIV., EAST LANSING.
Introducing remote sensing to county-level agencies in Michigan through the Cooperative Extension Service
p0007 A82-10034
MICHIGAN UNIV., ANN ARBOR.
Nitric oxide delta band emission in the earth's atmosphere Comparison of a measurement and a theory
p0008 A82-13268
MINISTERE DE L'ENVIRONMENT ET DU CADRE DE VIE, NEUILLY (FRANCE).
The operational oil pollution surveillance system being used in France: Forecasted future developments in consideration of the NATO/CCMS remote sensing pilot study conclusions p0012 N82-14573
MINNESOTA UNIV., MINNEAPOLIS.
Magnetic field observations on DE-A and -B
p0051 A82-16447
MISSISSIPPI STATE UNIV., MISSISSIPPI STATE.
A proposal for continuation of support for the application of remotely sensed data to state and regional problems. Part 1: Technical proposal
[E82-10018] p0056 N82-15496
MITRE CORP., MCLEAN, VA.
Shuttle applications in tropospheric air quality observations
[NASA-CR-145374] p0010 N82-11635

N

NATIONAL AERONAUTICS AND SPACE ADMINISTRATION, WASHINGTON, D. C.

Mission operation report: OSTA-1 [NASA-TM-84053] p0055 N82-10102

Reports of Planetary Geology Program, 1981 [NASA-TM-84211] p0016 N82-14041

NATIONAL AERONAUTICS AND SPACE ADMINISTRATION. AMES RESEARCH CENTER, MOFFETT FIELD, CALIF.

MATE VAN: Mobile analysis and training extension [NASA-TM-84056] p0045 N82-10466

NATIONAL AERONAUTICS AND SPACE ADMINISTRATION. GODDARD SPACE FLIGHT CENTER, GREENBELT, MD.

Preliminary results of mapping urban land cover with Seasat SAR imagery p0007 A82-10044

Absolute image registration for geosynchronous satellites p0049 A82-10051

A comparison of radiative transfer models for predicting the microwave emission from soils p0035 A82-10694

A closer examination of the reduction of satellite magnetometer data for geological studies p0019 A82-11039

Magnetic field-aligned electron distributions in the dayside cusp p0015 A82-12186

Temporal spectral response of a corn canopy p0002 A82-12886

The surface albedo of the earth in the near ultraviolet /330-340 nm/ p0016 A82-15032

Texture transforms of remote sensing data p0042 A82-15034

Temporal relationships between spectral response and agronomic variables of a corn canopy p0002 A82-15038

An analysis of short pulse and dual frequency radar techniques for measuring ocean wave spectra from satellites p0024 A82-15318

Magnetic field observations on DE-A and -B p0051 A82-16447

Report on Active and Planned Spacecraft and experiments [NASA-TM-84025] p0055 N82-10087

MAGSAT: Vector magnetometer absolute sensor alignment determination [NASA-TM-79648] p0051 N82-10468

Meteorological lab applications of Skylab handheld-camera photographs p0011 N82-12506

Scanner [NASA-CASE-GSC-12032-2] p0052 N82-13465

Interpolating for the location of remote sensor data [NASA-TM-82169] p0052 N82-13469

A simulation study of the recession coefficient for antecedent precipitation index [NASA-TM-83860] p0038 N82-14549

NATIONAL AERONAUTICS AND SPACE ADMINISTRATION. LYNDON B. JOHNSON SPACE CENTER, HOUSTON, TEX.

Skylab explores the Earth [NASA-SP-380] p0019 N82-12492

Mesoscale cloud features observed from Skylab p0011 N82-12509

US/Canada wheat and barley crop calender exploratory experiment implementation plan [E82-10016] p0005 N82-15494

NATIONAL AERONAUTICS AND SPACE ADMINISTRATION. LANGLEY RESEARCH CENTER, HAMPTON, VA.

Automated analyzer for aircraft measurements of atmospheric methane and total hydrocarbons p0007 A82-11949

Synoptic thermal and oceanographic parameter distributions in the New York Bight Apex p0023 A82-12885

Remote sensing of benthic microalgal biomass with a tower-mounted multispectral scanner p0024 A82-15031

In situ spectral reflectance studies of tidal wetland grasses p0036 A82-15989

A new method for inferring carbon monoxide concentrations from gas filter radiometer data p0009 A82-16837

Results from the July 1981 Workshop on Passive Remote Sensing of the Troposphere [AIAA PAPER 82-0207] p0009 A82-17841

Evaluation of the Seasat wind scatterometer p0025 A82-18716

Anomalous wind estimates from the Seasat scatterometer p0026 A82-18724

Chesapeake Bay Plume Study: Superflux 1980 [NASA-CP-2188] p0026 N82-10661

Superflux I, II, and III experiment design: Remote sensing aspects p0027 N82-10664

Remote sensing of the Chesapeake Bay plume salinity via microwave radiometry p0027 N82-10670

Preliminary analysis of ocean color scanner data from Superflux III p0027 N82-10672

Analysis of testbed airborne multispectral scanner data from Superflux II p0027 N82-10682

Assessment of Superflux relative to remote sensing p0028 N82-10694

Spectral atmospheric observations at Nantucket Island, May 7-14, 1981 [NASA-TM-83196] p0029 N82-14550

The Norwegian remote sensing experiment (Norsex) in a marginal ice zone p0031 N82-14566

NATIONAL AERONAUTICS AND SPACE ADMINISTRATION. NATIONAL SPACE TECHNOLOGY LABS., BAY SAINT LOUIS, MISS.

An improvement in land cover classification achieved by merging microwave data with Landsat multispectral scanner data p0007 A82-10043

NATIONAL AERONAUTICS AND SPACE ADMINISTRATION. PASADENA OFFICE, CALIF.

Microwave limb sounder [NASA-CASE-NPO-14544-1] p0011 N82-12685

NATIONAL AERONAUTICS AND SPACE ADMINISTRATION. WALLOPS FLIGHT CENTER, WALLOPS ISLAND, VA.

Repeatability and measurement uncertainty of the United States meteorological rocketsonde p0049 A82-12127

Airborne laser acquisition of cross-section data p0049 A82-12600

Application of the NASA airborne oceanographic lidar to the mapping of chlorophyll and other organic pigments p0027 N82-10684

NATIONAL GEODETIC SURVEY, ROCKVILLE, MD.

Report of survey for McDonald Observatory, Harvard Radio Astronomy Station, and vicinity [PB81-234338] p0016 N82-13606

NATIONAL HURRICANE AND EXPERIMENTAL METEOROLOGY LAB., CORAL GABLES, FLA.

Some aspects of tropical storm structure revealed by handheld-camera photographs from space p0011 N82-12507

NATIONAL INST. OF OCEANOGRAPHY, GOA (INDIA).

Studies of the Indian continental shelf: Application of remote sensing data p0031 N82-14569

NATIONAL MARINE FISHERIES SERVICE, HIGHLANDS, N. J.

A marine environmental monitoring and assessment program p0027 N82-10663

Superflux I, II, and III experiment designs: Water sampling and analyses p0027 N82-10665

NATIONAL OCEAN SURVEY, ROCKVILLE, MD.

A history of flying and photography: In the Photogrammetry Division of the National Ocean Survey 1919 - 1979 [PB81-246738] p0017 N82-15520

NATIONAL OCEANIC AND ATMOSPHERIC ADMINISTRATION, BOULDER, COLO.

A systems approach to the real-time runoff analysis with a deterministic rainfall-runoff model [PB81-224495] p0037 N82-11530

Geophysical monitoring for climatic change, number 8: Summary Report, 1979 [PB81-233355] p0012 N82-13631

NATIONAL OCEANIC AND ATMOSPHERIC ADMINISTRATION, HIGHLANDS, N. J.

Synoptic thermal and oceanographic parameter distributions in the New York Bight Apex p0023 A82-12885

NATIONAL OCEANIC AND ATMOSPHERIC ADMINISTRATION, MIAMI, FLA.

The determination of navigational and meteorological variables measured by NOAA/RFC WP3D aircraft [PB81-225468] p0028 N82-11743

An assessment of the potential contributions to oceanography from Skylab visual observations and handheld-camera photographs p0028 N82-12503

NATIONAL OCEANIC AND ATMOSPHERIC ADMINISTRATION, ROCKVILLE, MD.

Deep Ocean Mining Environmental Study. Environmental effects of commercial-scale mining [PB81-227753] p0029 N82-13464

NATIONAL OCEANIC AND ATMOSPHERIC ADMINISTRATION, SEATTLE, WASH.

CTD/02 measurements during the Equatorial Pacific Ocean Climate Study (EPOCS) in 1979 [PB81-211203] p0026 N82-10461

Ice conditions in the eastern Bering Sea from NOAA and LANDSAT imagery: Winter conditions 1974, 1976, 1977, 1979 [PB81-220188] p0028 N82-11537

GEM: A simple meteorological buoy with satellite telemetry p0053 N82-14779

NATIONAL OCEANIC AND ATMOSPHERIC ADMINISTRATION, WASHINGTON, D. C.

Analysis of rainfall from flash flood producing thunderstorms, using GOES data p0038 N82-14724

National Hurricane operations plan [PB81-247231] p0013 N82-15697

Environmental satellite imagery, March 1981 [PB81-248049] p0047 N82-15698

NATIONAL OCEANOGRAPHIC INSTRUMENTATION CENTER, WASHINGTON, D. C.

Clear water radiances for atmospheric correction of coastal zone color scanner imagery p0025 A82-17292

NATURAL ENVIRONMENT RESEARCH COUNCIL, GODALMING (ENGLAND).

Study on satellite radar altimetry in climatological and oceanographic research, volume 1 [SP/153/06/01/FR(80)-VOL-1] p0026 N82-10486

Study on satellite radar altimetry in climatological and oceanographic research, volume 2 [SP/153/06/01FR(80)-VOL-2] p0026 N82-10487

NAVAL OCEAN RESEARCH AND DEVELOPMENT ACTIVITY, BAY ST. LOUIS, MISS.

A closer examination of the reduction of satellite magnetometer data for geological studies p0019 A82-11039

NAVAL OCEANOGRAPHIC OFFICE, BAY ST. LOUIS, MISS.

ICAPS oceanographic data for the Indian Ocean [AD-A103173] p0029 N82-13641

NAVAL OCEANOGRAPHIC OFFICE, WASHINGTON, D. C.

The potential and requirements for space oceanography p0029 N82-14556

NAVAL POSTGRADUATE SCHOOL, MONTEREY, CALIF.

Biological patchiness in relation to satellite thermal imagery and associated chemical mesoscale features [AD-A105757] p0047 N82-15504

NAVAL SURFACE WEAPONS CENTER, DAHLGREN, VA.

GPS application to mapping, charting and geodesy p0015 A82-10645

NEW YORK STATE UNIV., SYRACUSE.

Intercalibration of Landsat 1-3 and NOAA 6 and 7 scanner data p0049 A82-13293

NICE UNIV. (FRANCE).

Requirements in pollution monitoring and coastal management p0030 N82-14558

NORWEGIAN AIR SURVEY CO., OSLO.

Use of Side Looking Airborne Radar (SLAR) for oil pollution monitoring in Norway p0012 N82-14588

NORWEGIAN DEFENCE RESEARCH ESTABLISHMENT, KJELLER.

Seasat SAR processing at the Norwegian Defence Research Establishment p0046 N82-14584

NOVA UNIV., DANIA, FLA.

Seasat altimetry adjustment model including tidal and other sea surface effects [AD-A104188] p0026 N82-10473

O

OAO CORP., HAMPTON, VA.

Technology transfer of NASA microwave remote sensing system [NASA-CR-165791] p0028 N82-11515

OCEANROUTES, INC., PALO ALTO, CALIF.

An evaluation of Seasat-A data in relation to optimum track ship weather routing and site specific forecasting for the offshore oil industry p0030 N82-14564

OFFICE OF NAVAL RESEARCH, PASADENA, CALIF.

Visual observations of the ocean p0028 N82-12502

OFFICINE GALILEO S.P.A., FLORENCE (ITALY).

Infrared radiance model variation by sensor flight measurements p0052 N82-14171

OLD DOMINION UNIV., NORFOLK, VA.

A new method for inferring carbon monoxide concentrations from gas filter radiometer data p0009 A82-16837

P

PENNSYLVANIA STATE UNIV., UNIVERSITY PARK.

Texture transforms of remote sensing data p0042 A82-15034

PHYSICS LAB. RVO-TNO, THE HAGUE (NETHERLANDS).

Project Noordwijk. Part 1: Measurements of the radar backscatter coefficient gamma (sigma deg) in 1977 and 1978 [PHL-1979-49-PT-1] p0032 N82-14617

Project Noordwijk. Part 2: Results of North Sea clutter measurements in the I-band performed from the platform Noordwijk in September/October 1977 [PHL-1980-28-PT-2] p0033 N82-14618

PREUSSAG A.G. METALL, GOSLAR (WEST GERMANY).

An investigation into the applicability of thermal infrared scanning for exploration [BMFT-FB-T-81-087] p0022 N82-15925

R

RAND CORP., SANTA MONICA, CALIF.

Coordinates of features on the Galilean satellites p0019 A82-12366

RESEARCH AND DATA SYSTEMS, INC., LANHAM, MD.

SMMR data set development for GARP [NASA-CR-166721] p0052 N82-11512

RESEARCH INST. OF NATIONAL DEFENCE, LINKOEPING (SWEDEN).

Use of radar and microwave radiometry for reconnaissance satellites [FOA-C-30204-E1] p0052 N82-10481

RESEARCH TRIANGLE INST., RESEARCH TRIANGLE PARK, N. C.

Monitoring the Chesapeake Bay using satellite data for Superflux III p0027 N82-10668

Aircraft data summaries of the SURE intensives, volume 4 [DE82-900311] p0012 N82-13569

ROSKILDE UNIV. (DENMARK).

Mapping of surface currents in Greenland fiords by means of LANDSAT images p0038 N82-14579

ROYAL AIRCRAFT ESTABLISHMENT, FARNBOROUGH (ENGLAND).
Remote Sensing Information Bulletin; Issue number 6
p0053 N82-14616

ROYAL NETHERLANDS METEOROLOGICAL INST., DE BILT.
Meteorological and oceanographic observations on board Netherlands lightvessels and the lightplatform 'Goeree' in the North Sea
[KNMI-141-28] p0033 N82-15684

ROYAL NORWEGIAN COUNCIL FOR SCIENTIFIC AND INDUSTRIAL RESEARCH, KJELLER.
Application of remote sensing data on the continental shelf: Proceedings of an EARSeL-ESA Symposium
[ESA-SP-167] p0029 N82-14553

S

SACLANT ASW RESEARCH CENTER, LA SPEZIA (ITALY).
The SACLANTCEN oceanographic data base. Volume 1: Design criteria and data structure and content
[AD-A103277] p0029 N82-13639

SANDIA LABS., ALBUQUERQUE, N. MEX.
Environmental Monitoring Report, Sandia National Labs., Albuquerque, New Mexico, 180
[DE81-027639] p0010 N82-11649

SANTA BARBARA RESEARCH CENTER, GOLETA, CALIF.
Scanner
[NASA-CASE-GSC-12032-2] p0062 N82-13465

SCIENCE AND EDUCATION ADMINISTRATION, BELTSVILLE, MD.
Temporal spectral response of a corn canopy
p0002 A82-12886

Temporal relationships between spectral response and agronomic variables of a corn canopy p0002 A82-15038

SCIENCE APPLICATIONS, INC., BELLEVUE, WASH.
Ice conditions in the eastern Bering Sea from NOAA and LANDSAT imagery: Winter conditions 1974, 1976, 1977, 1979
[PB81-220188] p0028 N82-11537

SCIENCE RESEARCH COUNCIL, SLOUGH (ENGLAND).
Study on satellite radar altimetry in climatological and oceanographic research, volume 1
[SP/153/06/01/FR(80)-VOL-1] p0026 N82-10486
Study on satellite radar altimetry in climatological and oceanographic research, volume 2
[SP/153/06/01FR(80)-VOL-2] p0026 N82-10487

SCIENTIFIC ANALYSTS AND CONSULTANTS, INC., ROCKVILLE, MD.
Distortion-free mapping of VISSR imagery data from geosynchronous satellites p0051 N82-10071

SMITHSONIAN ASTROPHYSICAL OBSERVATORY, CAMBRIDGE, MASS.
Study of the time evolution of the lithosphere
[NASA-CR-164968] p0016 N82-11696

SOUTH CAROLINA UNIV., COLUMBIA.
Remote sensing of benthic microalgal biomass with a tower-mounted multispectral scanner p0024 A82-15031

SOUTH DAKOTA STATE UNIV., BROOKINGS.
Remote sensing applications to resource problems in South Dakota
[E82-10002] p0004 N82-15481

SOUTHAMPTON UNIV. (ENGLAND).
The use of LANDSAT MSS to observe sediment distribution and movement in the Solent coastal area
p0038 N82-14580

STATE UNIV. OF NEW YORK, ALBANY.
Preliminary results of mapping urban land cover with Seasat SAR imagery p0007 A82-10044

SWEDISH METEOROLOGICAL AND HYDROLOGICAL INST., NORKOEPING.
Marine activities in Sweden for which remote sensing data may be of interest p0031 N82-14576

SYSTEMS AND APPLIED SCIENCES CORP., HAMPTON, VA.
A new method for inferring carbon monoxide concentrations from gas filter radiometer data
p0009 A82-16837

T

TECHNICAL RESEARCH CENTRE OF FINLAND, ESPOO.
Small-scale terrain mapping based on numerical interpretation of LANDSAT imagery
[VTT-40] p0045 N82-10485

TEXAS UNIV. AT ARLINGTON.
A global atlas of GEOS-3 significant waveheight and comparison of the data with national buoy data
p0026 N82-10660

TEXAS UNIV. AT AUSTIN.
Global Tectonics: Some Geologic analyses of observations and photographs from Skylab
p0020 N82-12494

Cultural features imaged and observed from Skylab 4
p0010 N82-12499

U

UNIVERSITY COLL., CARDIFF (WALES).
Infrared spectroscopy of microorganisms near 3.4 microns in relation to geology and astronomy
[PREPRINT-69] p0020 N82-12713

UNIVERSITY COLL., DUBLIN (IRELAND).
Study on calibration methods for Earth observation optical imaging instruments
[UCD-207/1/80] p0052 N82-10488

UNIVERSITY COLL., GALWAY (IRELAND).
Determination of surface wind speed from remotely measured whitecap coverage, a feasibility assessment
p0030 N82-14565

The feasibility of using remotely sensed color as an index of Irish coastal water properties p0032 N82-14581

UTAH STATE UNIV., LOGAN.
Proof of concept study
[AD-A104338] p0010 N82-11639
Limit on remote FTIR detection of trace gases
[AD-A104842] p0011 N82-12511

UTAH UNIV., SALT LAKE CITY.
Morphostructural analyses of space imagery in the central Colorado Plateau p0019 N82-10465

V

VIRGINIA UNIV., CHARLOTTESVILLE.
The effect of spatial variability in precipitation on streamflow
[AD-A105955] p0038 N82-14589

W

WASHINGTON UNIV., SEATTLE.
Evaluation of the Seasat wind scatterometer
p0025 A82-18716

Anomalous wind estimates from the Seasat scatterometer p0026 A82-18724
Identification of lithologic units using multichannel imaging systems p0046 N82-11509
Adaptation of land use to surficial geology in metropolitan Washington, D.C. p0010 N82-11718

WISCONSIN UNIV. - MADISON.
The operational use of Landsat for lake quality assessment p0036 A82-12596

CONTRACT NUMBER INDEX

Typical Contract Number Index Listing

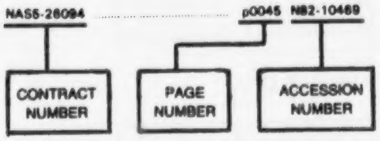

Listings in this index are arranged alphanumerically by contract number. Under each contract number, the accession numbers denoting documents that have been produced as a result of research done under that contract are arranged in ascending order with the AIAA accession numbers appearing first. The accession number denotes the number by which the citation is identified in the abstract section. Preceding the accession number is the page number on which the citation may be found.

AF PROJ. 2309 .... p0026 N82-10473
AF PROJ. 2310 .... p0010 N82-11639
AF PROJ. 7670 .... p0011 N82-12511
CNPQ-37/78 .... p0009 A82-16325
DA PROJ. 1L1-61102-B-53A p0012 N82-14590
DA PROJ. 4A7-62719-AT-40 .... p0003 N82-11910
DA PROJ. 4A7-62730-AT-42 .... p0003 N82-11910
DAAG29-80-K-0018 .... p0041 A82-12757
DAAG29-80-K-0053 .... p0038 N82-14589
DE-AC01-79CS-30027 .... p0011 N82-12707
DE-AC04-76DP-00789 .... p0010 N82-11649
DE-AC13-76GJ-01664 .... p0019 N82-10476
p0053 N82-14599
p0020 N82-14600
p0020 N82-14601
p0021 N82-14602
p0021 N82-14603
p0021 N82-14604
p0021 N82-14605
p0021 N82-14607
p0021 N82-14608
DE-AC13-76GT-01664 .... p0021 N82-14606
DE-AI08-78ET-44802 .... p0022 N82-15506
EPA-R-804546 .... p0007 A82-10700
EPA-R-805500-01 .... p0008 A82-14320
EPA-R-806048-01-2 .... p0008 A82-14320
EPRI PROJ. RP-862 .... p0012 N82-13569
ESA-4237/80/NL-PP(SC) p0052 N82-10488
ESA-4355/80/F-FC(SC) p0026 N82-10486
p0026 N82-10487
ESA-4421/80/F-FC(SC) p0055 N82-13010
ESA-6225/80-F-CG(SC) p0054 N82-15500
FINEP-B/28-79-002-00-00 .... p0009 A82-16325
F04701-80-C-0081 .... p0012 N82-14591
F19628-77-C-0203 .... p0010 N82-11639
p0011 N82-12511
F19628-78-C-001 .... p0010 N82-11635
F19628-78-C-0013 .... p0026 N82-10473
F19628-80-C-0052 .... p0049 A82-11533
JPL-916331 .... p0049 A82-13293
JPL-953613 .... p0019 A82-12366
NAG5-16 .... p0049 A82-11533
NAG5-30 .... p0003 A82-17564
NAG5-150 .... p0016 N82-11696
NASA ORDER S-40256-B p0021 N82-15489
NASW-3321 .... p0019 A82-12366
NAS1-16380 .... p0028 N82-11515
NAS5-11415 .... p0015 A82-12186
NAS5-20800 .... p0028 N82-11511
NAS5-20983 .... p0036 A82-15969
NAS5-21808 .... p0053 N82-15483
p0054 N82-15495
NAS5-22963 .... p0025 A82-17292
NAS5-22999 .... p0043 A82-15971
NAS5-23790 .... p0043 A82-15971
NAS5-24391 .... p0045 N82-11103
NAS5-25300 .... p0045 N82-10072
p0051 N82-10073
NAS5-25527 .... p0009 N82-11513
NAS5-25781 .... p0052 N82-11512
NAS5-25882 .... p0019 A82-11039
NAS5-26094 .... p0045 N82-10469
p0045 N82-10470
p0045 N82-10471
p0045 N82-10472
NAS5-26361 .... p0046 N82-13470
NAS5-26414 .... p0021 N82-15487
NAS6-2639 .... p0033 N82-15498
NAS6-3075 .... p0052 N82-12447
p0028 N82-12734
NAS7-100 .... p0023 A82-11202
p0042 A82-14870
p0010 N82-11514
NAS9-14052 .... p0003 A82-17564
NAS9-14350 .... p0053 N82-15493
NAS9-15476 .... p0004 N82-15480
NAS9-15800 .... p0013 N82-15488
p0005 N82-15491
p0005 N82-15492
NATO-9-4-02-SRG.19 .... p0031 N82-14566
NA79AA-D-00085 .... p0010 N82-11536
NA81FA-C-00002 .... p0027 N82-10868
NCA2-OR-180-607 .... p0002 A82-10863
NGL-23-004-083 .... p0007 A82-10034
NGL-25-001-054 .... p0056 N82-15496
NGL-33-010-171 .... p0001 A82-10047
NGL-42-003-007 .... p0004 N82-15481
NGR-23-005-360 .... p0008 A82-13268
NOAA-MO-A01-78-00-4319 .... p0024 A82-15076
NOAA-NA-79SAC00737 .... p0023 A82-10671
NOAA-NA-79SA00741 .... p0025 A82-17292
NOAA-NA-80RAC00003 .... p0025 A82-17494
NOAA-NA-79SAC0073 .... p0023 A82-13214
NOAA-NA79-KA-C-00026 .... p0051 N82-10071
NOAA-01-8-MO1-1864 .... p0051 N82-10071
NOAA-04-7-158-44104 .... p0024 A82-15030
NOAA-04-8-MO p0039 N82-15673
NOAA-04-8-M01-134 .... p0035 A82-10054
NOAA-04-8-M01-149 .... p0024 A82-15030
NSF ATM-78-08865 .... p0038 N82-14589
NSF ATM-78-20419 .... p0025 A82-17494
NSF ATM-80-03300 .... p0016 A82-16868
NSF ENG-78-23145 .... p0049 A82-11533
NSF ENG-79-09374 .... p0041 A82-12757
NSF OCE-80-24116 .... p0025 A82-17494
NSG-1334 .... p0024 A82-15031
NSG-5049 .... p0033 N82-14789
NSG-5335 .... p0038 N82-12510
NSG-5372 .... p0008 A82-13268
NSG-7220 .... p0004 N82-15482
N00014-76-C-1106 .... p0032 N82-14592
p0032 N82-14593
N00014-78-G-0052 .... p0030 N82-14565
N00014-79-C-0653 .... p0019 A82-11039
N00014-80-C-0273 .... p0029 N82-13642
N00014-80-G-0003 .... p0031 N82-14566
N00014-81-K-0030 .... p0050 A82-15920
PROJ. AGRISTARS p0004 N82-15480
p0005 N82-15491
p0005 N82-15492
p0053 N82-15493
p0005 N82-15494
146-40-15-07 .... p0029 N82-14550
146-40-15-50 .... p0026 N82-10661

REPORT/ACCESSION NUMBER INDEX

EARTH RESOURCES / *A Continuing Bibliography (Issue 33)* **APRIL 1982**

Typical Report/Accession Number Index Listing

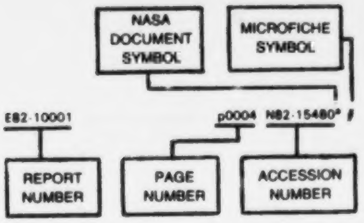

Listings in this index are arranged alphanumerically by report number. The page number indicates the page on which the citation is located. The accession number denotes the number by which the citation is identified. An asterisk (*) indicates that the item is a NASA report. A pound sign (#) indicates that the item is available on microfiche.

AAS 81-072 p0024 A82-16341

AD-A101380 p0029 N82-13642 #
AD-A101528 p0012 N82-14590 #
AD-A103173 p0029 N82-13641 #
AD-A103277 p0029 N82-13639 #
AD-A104188 p0026 N82-10473 #
AD-A104338 p0010 N82-11639 #
AD-A104469 p0003 N82-11910 #
AD-A104842 p0011 N82-12511 #
AD-A105586 p0032 N82-14592 #
AD-A105736 p0032 N82-14593 #
AD-A105757 p0047 N82-15504 #
AD-A105784 p0012 N82-14591 #
AD-A105955 p0038 N82-14589 #
AD-A107427 p0053 N82-15110 #

AFGL-TR-81-0134 p0010 N82-11639 #
AFGL-TR-81-0152 p0026 N82-10473 #
AFGL-TR-81-0272 p0011 N82-12511 #

AIAA PAPER 82-0207 p0009 A82-17841* #
AIAA PAPER 82-0336 p0036 A82-17892 #
AIAA PAPER 82-0383 p0025 A82-17915 #
AIAA PAPER 82-0388 p0051 A82-17918 #

ARO-16816.3-GS p0038 N82-14589 #

BMFT-FB-T-81-087 p0022 N82-15925 #

BMFT-FB-W-81-002 p0055 N82-14615 #

CONTRIB-500 p0028 N82-11537 #
CONTRIB-544 p0020 N82-12497* #

CRINC/RSL-TR-331-20 p0032 N82-14592 #
CRINC/RSL-TR-331-22 p0032 N82-14593 #

CSC/TM-80/6214 p0045 N82-11103* #

DE81-027839 p0010 N82-11649 #
DE81-029177 p0019 N82-10476 #
DE81-029462 p0022 N82-15506 #
DE82-000071 p0011 N82-12707 #
DE82-000401 p0020 N82-14601 #
DE82-000650 p0053 N82-14599 #
DE82-000772 p0021 N82-14604 #
DE82-000780 p0021 N82-14602 #
DE82-000781 p0020 N82-14600 #
DE82-000784 p0021 N82-14608 #
DE82-000785 p0021 N82-14605 #
DE82-000794 p0021 N82-14607 #
DE82-000869 p0021 N82-14606 #
DE82-000872 p0021 N82-14603 #
DE82-900311 p0012 N82-13569 #

DFVLR-FB-81-11 p0047 N82-15503 #

DOC-79SDS4201 p0054 N82-15495* #
DOC-79SDS4242 p0053 N82-15483* #

DOE/ET-44802/T2 p0022 N82-15506 #

EPRI-EA-1019-VOL-4 p0012 N82-13569 #

ERADCOM/ASL-TR-0079 p0012 N82-14590 #

ERIM-152400-3-T p0004 N82-15480* #

ERT-P-7505-F p0009 N82-11513* #

ESA-CR(P)-1437-VOL-1 p0026 N82-10486 #
ESA-CR(P)-1437-VOL-2 p0026 N82-10487 #
ESA-CR(P)-1443 p0052 N82-10488 #
ESA-CR(P)-1457 p0055 N82-13010 #
ESA-CR(P)-1469 p0054 N82-15500 #

ESA-SP-167 p0029 N82-14553 #

EW-L1-00713 p0005 N82-15492* #

E82-10001 p0004 N82-15480* #
E82-10002 p0004 N82-15481* #
E82-10004 p0004 N82-15482* #
E82-10005 p0053 N82-15483* #
E82-10006 p0046 N82-15484* #
E82-10007 p0004 N82-15485* #
E82-10008 p0039 N82-15486* #
E82-10009 p0021 N82-15487* #
E82-10010 p0013 N82-15488* #
E82-10011 p0021 N82-15489* #
E82-10012 p0005 N82-15490* #
E82-10013 p0005 N82-15491* #
E82-10014 p0005 N82-15492* #
E82-10015 p0053 N82-15493* #
E82-10016 p0005 N82-15494* #
E82-10017 p0054 N82-15495* #
E82-10018 p0056 N82-15496* #

FC-JO-00611 p0005 N82-15494* #

FC-LO-00612 p0005 N82-15491* #

FOA-C-30204-E1 p0052 N82-10481 #

FSRP/INT-269 p0003 N82-10489 #

FTD-ID(RS)T-1059-81 p0053 N82-15110 #

F78-11-REV-A p0028 N82-11511* #

GJBX-114(81) p0019 N82-10476 #
GJBX-327-81-VOL-1 p0053 N82-14599 #
GJBX-327-81-VOL-2-BANGOR p0021 N82-14607 #
GJBX-327-81-VOL-2-BINGHAMTON p0021 N82-14606 #
GJBX-327-81-VOL-2-EDMUNDSTON p0021 N82-14605 #
GJBX-327-81-VOL-2-FREDERICTON p0021 N82-14604 #
GJBX-327-81-VOL-2-LEWISTON p0021 N82-14603 #
GJBX-327-81-VOL-2-MILLINOCKET p0021 N82-14602 #
GJBX-327-81-VOL-2-OGDENSBURG p0020 N82-14601 #
GJBX-327-81-VOL-2-SHERBROOKE p0020 N82-14600 #
GJBX-327-81-VOL-2-UTICA p0021 N82-14608 #

GPO-35-265 p0056 N82-15497 #

INPE-2035-RPE/292 p0005 N82-15490* #
INPE-2054-RPE/300 p0004 N82-15485* #

ISBN-3-7696-9313-2 p0017 N82-15812
ISBN-87-7478-183-9 p0026 N82-10467
ISBN-87-7478-183-9 p0028 N82-12533 #
ISBN-951-38-1180-8 p0045 N82-10485 #

ISSN-0065-5325 p0017 N82-15812
ISSN-0069-5882 p0056 N82-15499 #
ISSN-0170-1339 p0055 N82-14615 #
ISSN-0340-7608 p0022 N82-15925 #
ISSN-0347-6405 p0052 N82-10484 #
ISSN-0355-3477 p0045 N82-10485 #
ISSN-0379-6566 p0029 N82-14553 #
ISSN-0581-1287 p0012 N82-12714

JHU/APL-SIR-80U-026 p0046 N82-14548* #

JSC-16759 p0013 N82-15488* #
JSC-16812 p0005 N82-15494* #
JSC-16819 p0005 N82-15491* #
JSC-16918 p0053 N82-15493* #
JSC-17117 p0005 N82-15492* #

KGI-175 p0052 N82-10484 #

KMRD-5.4-8103 p0047 N82-15698 #

KNMI-141-28 p0033 N82-15684 #

L-14680 p0026 N82-10661* #

LC-77-829 p0019 N82-12492* #

LEMSCO-15168 p0005 N82-15491* #
LEMSCO-15175 p0013 N82-15488* #
LEMSCO-16033 p0005 N82-15492* #

MCR-81-576-VOL-1 p0045 N82-10469* #
MCR-81-576-VOL-2 p0045 N82-10470* #
MCR-81-576-VOL-3 p0045 N82-10471* #
MCR-81-576-VOL-4 p0045 N82-10472* #

MITT-31 p0056 N82-15499 #

MTR-80/90 p0054 N82-15500 #

MU-11-00300 p0053 N82-15493* #

NASA-CASE-GSC-12032-2 p0052 N82-13465*

NASA-CASE-NPO-14544-1 p0011 N82-12685*

NASA-CP-2188 p0026 N82-10661* #

NASA-CR-145374 p0010 N82-11635* #
NASA-CR-156880 p0028 N82-12734* #
NASA-CR-156881 p0052 N82-12447* #
NASA-CR-156882 p0033 N82-15498* #
NASA-CR-161030 p0005 N82-15491* #
NASA-CR-161031 p0005 N82-15492* #
NASA-CR-161039 p0053 N82-15493* #
NASA-CR-161071 p0013 N82-15488* #
NASA-CR-161080 p0004 N82-15480* #
NASA-CR-163348 p0053 N82-15483* #
NASA-CR-164755 p0005 N82-15490* #
NASA-CR-164817 p0056 N82-15496* #
NASA-CR-164818 p0021 N82-15489* #
NASA-CR-164892 p0004 N82-15481* #
NASA-CR-164893 p0004 N82-15482* #
NASA-CR-164904 p0046 N82-15484* #
NASA-CR-164905 p0004 N82-15485* #
NASA-CR-164906 p0039 N82-15486* #
NASA-CR-164907 p0021 N82-15487* #
NASA-CR-164931 p0010 N82-11514* #
NASA-CR-164968 p0016 N82-11696* #
NASA-CR-165049 p0033 N82-14789* #
NASA-CR-165791 p0028 N82-11515* #
NASA-CR-166640 p0054 N82-15495* #
NASA-CR-166709 p0038 N82-12510* #
NASA-CR-166717 p0046 N82-14548* #
NASA-CR-166719 p0046 N82-13470* #
NASA-CR-166720-VOL-1 p0028 N82-11511* #
NASA-CR-166721 p0052 N82-11512* #
NASA-CR-166724 p0009 N82-11513* #
NASA-CR-166731 p0045 N82-10469* #
NASA-CR-166732 p0045 N82-10470* #
NASA-CR-166733 p0045 N82-10471* #
NASA-CR-166734 p0045 N82-10472* #
NASA-CR-166737 p0045 N82-11103* #

NASA-SP-380 p0019 N82-12492* #

NASA-TM-79648 p0051 N82-10468* #
NASA-TM-82169 p0052 N82-13469* #
NASA-TM-83196 p0029 N82-14550* #
NASA-TM-83860 p0038 N82-14549* #
NASA-TM-84025 p0055 N82-10087* #
NASA-TM-84034 p0005 N82-15494* #
NASA-TM-84053 p0055 N82-10102* #
NASA-TM-84056 p0045 N82-10466*
NASA-TM-84211 p0016 N82-14041* #

NOAA-DR-ERL-PMEL-1 p0026 N82-10461 #

NOAA-FCM-P12-1981 p0013 N82-15697 #

NOAA-TM-ERL-PMEL-24 p0028 N82-11537 #

NOAA-TM-ERL-RFC-7 p0028 N82-11743 #

NOAA-TM-NOS-NGS-32 p0016 N82-13606 #

NOAA-TM-NWS-WR-162 p0037 N82-11530 #

NOAA-81041501 p0026 N82-10461 #
NOAA-81042706 p0010 N82-11536 #
NOAA-81043008 p0028 N82-11537 #
NOAA-81050501 p0039 N82-15673 #
NOAA-81050703 p0037 N82-11530 #
NOAA-81051503 p0028 N82-11743 #
NOAA-81052103 p0029 N82-13484 #
NOAA-81062603 p0016 N82-13606 #
NOAA-81062615 p0012 N82-13631 #
NOAA-81071405 p0017 N82-15520 #
NOAA-81071411 p0013 N82-15697 #

NOAA/NEMP-111-81-ABCDFG-0042 p0026 N82-10661* #

NOO-RP-32C p0029 N82-13641 #

NSSDC/WDC-A-R&S-81-10 p0055 N82-10087* #

P-A826 p0046 N82-13470* #

PB81-211203 p0026 N82-10461 #
PB81-214777 p0003 N82-10489 #
PB81-220188 p0028 N82-11537 #
PB81-223836 p0010 N82-11536 #
PB81-224495 p0037 N82-11530 #
PB81-225468 p0028 N82-11743 #
PB81-227753 p0029 N82-13484 #
PB81-227795 p0039 N82-15673 #
PB81-233355 p0012 N82-13631 #
PB81-234338 p0016 N82-13606 #
PB81-246738 p0017 N82-15520 #
PB81-247231 p0013 N82-15697 #
PB81-248049 p0047 N82-15698 #

PHL-1979-49-PT-1 p0032 N82-14617 #
PHL-1980-28-PT-2 p0033 N82-14618 #

PR-3 p0046 N82-15484* #

PREPRINT-69 p0020 N82-12713 #

RRL-PUBL-514 p0033 N82-14789* #

RSL-TR-410-1 p0038 N82-12510* #

S-420-81-01 p0055 N82-10102* #

SACLANTCEN-SM-150-VOL-1 p0029 N82-13639 #

SAND-81-0566 p0010 N82-11649 #

SAPR-1 p0016 N82-11696* #

SD-TR-81-70 p0012 N82-14591 #

SDSU-RSI-81-11 p0004 N82-15481* #

SER-C-261 p0017 N82-15812

SOLAR/0010-81/08 p0011 N82-12707 #

SONDERBEOB-42 p0012 N82-12714

SP/153/06/01/FR(80)-VOL-1 p0026 N82-10486 #
SP/153/06/01FR(80)-VOL-2 p0026 N82-10487 #

SR-EL-04065 p0004 N82-15480* #

SR-3 p0026 N82-10473 #
SR-6 p0010 N82-11639 #

SSL-SER-22-ISSUE-18 p0004 N82-15482* #

TDCK-73426 p0032 N82-14617 #
TDCK-74302 p0033 N82-14618 #

TR-CSL-8001 p0039 N82-15673 #

TR-6 p0038 N82-14589 #
TR-0081(6640)-3 p0012 N82-14591 #

UCD-207/1/80 p0052 N82-10488 #

UNIHI-SG-CR-81-04 p0010 N82-11536 #

US-PATENT-APPL-SN-078612 p0011 N82-12685*
US-PATENT-APPL-SN-578700 p0052 N82-13465*
US-PATENT-APPL-SN-583219 p0052 N82-13465*

US-PATENT-CLASS-250-235 p0052 N82-13465*
US-PATENT-CLASS-250-236 p0052 N82-13465*
US-PATENT-CLASS-343-100ME p0011 N82-12685*
US-PATENT-CLASS-343-100PE p0011 N82-12685*
US-PATENT-CLASS-343-781P p0011 N82-12685*
US-PATENT-CLASS-356-109 p0052 N82-13465*

US-PATENT-4,282,525 p0011 N82-12685*
US-PATENT-4,300,159 p0052 N82-13465*

USGS-OPEN-FILE-81-189 p0022 N82-15506 #

VTT-40 p0045 N82-10485 #

WES/MP/EL-81-4 p0003 N82-11910 #

1. Report No.
NASA SP-7041 (33)

2. Government Accession No.

3. Recipient's Catalog No.

4. Title and Subtitle
EARTH RESOURCES
A Continuing Bibliography (Issue 33)

5. Report Date
April 1982

6. Performing Organization Code

7. Author(s)

8. Performing Organization Report No.

9. Performing Organization Name and Address

National Aeronautics and Space Administration
Washington, DC 20546

10. Work Unit No.

11. Contract or Grant No.

12. Sponsoring Agency Name and Address

13. Type of Report and Period Covered

14. Sponsoring Agency Code

15. Supplementary Notes

16. Abstract

This bibliography list 436 reports, articles, and other documents introduced into the NASA Scientific and Technical Information System between January 1 and March 31, 1982. Emphasis is placed on the use of remote sensing and geophysical instrumentation in spacecraft and aircraft to survey and inventory natural resources and urban areas. Subject matter is grouped according to agriculture and forestry, environmental changes and cultural resources, geodesy and cartography, geology and mineral resources, hydrology and water management, data processing and distribution systems, instrumentation and sensors, and economic analysis.

17. Key Words (Suggested by Author(s))
Bibliographies
Earth Resources
Remote Sensors

18. Distribution Statement
Unclassified - Unlimited

19. Security Classif. (of this report)
Unclassified

20. Security Classif. (of this page)
Unclassified

21. No. of Pages
104

22. Price*
$10.50 HC

*For sale by the National Technical Information Service, Springfield, Virginia 22161

NASA-Langley, 1982

PUBLIC COLLECTIONS OF NASA DOCUMENTS

DOMESTIC

NASA distributes its technical documents and bibliographic tools to eleven special libraries located in the organizations listed below. Each library is prepared to furnish the public such services as reference assistance, interlibrary loans, photocopy service, and assistance in obtaining copies of NASA documents for retention.

CALIFORNIA
University of California, Berkeley
COLORADO
University of Colorado, Boulder
DISTRICT OF COLUMBIA
Library of Congress
GEORGIA
Georgia Institute of Technology, Atlanta
ILLINOIS
The John Crerar Library, Chicago
MASSACHUSETTS
Massachusetts Institute of Technology, Cambridge
MISSOURI
Linda Hall Library, Kansas City
NEW YORK
Columbia University, New York
OKLAHOMA
University of Oklahoma, Bizzell Library
PENNSYLVANIA
Carnegie Library of Pittsburgh
WASHINGTON
University of Washington, Seattle

NASA publications (those indicated by an "*" following the accession number) are also received by the following public and free libraries:

CALIFORNIA
Los Angeles Public Library
San Diego Public Library
COLORADO
Denver Public Library
CONNECTICUT
Hartford Public Library
MARYLAND
Enoch Pratt Free Library, Baltimore
MASSACHUSETTS
Boston Public Library
MICHIGAN
Detroit Public Library
MINNESOTA
Minneapolis Public Library and Information Center
NEW JERSEY
Trenton Public Library
NEW YORK
Brooklyn Public Library
Buffalo and Erie County Public Library
Rochester Public Library
New York Public Library
OHIO
Akron Public Library
Cincinnati and Hamilton County Public Library
Cleveland Public Library
Dayton Public Library
Toledo and Lucas County Public Library
TEXAS
Dallas Public Library
Fort Worth Public Library
WASHINGTON
Seattle Public Library
WISCONSIN
Milwaukee Public Library

An extensive collection of NASA and NASA-sponsored documents and aerospace publications available to the public for reference purposes is maintained by the American Institute of Aeronautics and Astronautics, Technical Information Service, 555 West 57th Street, 12th Floor, New York, New York 10019.

EUROPEAN

An extensive collection of NASA and NASA-sponsored publications is maintained by the British Library Lending Division, Boston Spa, Wetherby, Yorkshire, England. By virtue of arrangements other than with NASA, the British Library Lending Division also has available many of the non-NASA publications cited in *STAR*. European requesters may purchase facsimile copy or microfiche of NASA and NASA-sponsored documents, those identified by both the symbols "#" and "*", from: ESA - Information Retrieval Service, European Space Agency, 8-10 rue Mario-Nikis, 75738 Paris CEDEX 15, France.

National Aeronautics and
Space Administration

Washington, D.C.
20546

Official Business
Penalty for Private Use, $300

THIRD-CLASS BULK RATE

Postage and Fees Paid
National Aeronautics and
Space Administration
NASA-451

U.S. MAIL

NASA

POSTMASTER: **If Undeliverable (Section 158**
Postal Manual) Do Not Return

7041(34)

NASA

Earth Resources
A Continuing
Bibliography
with Indexes

NASA SP-7041(34)
July 1982

NEWARK PUBLIC LIBRARY

NOV 8 1982

U. S. GOVT. PUBS.
DEPOSITORY 376

National Aeronautics and
Space Administration

es Earth Resourc
s Earth Resources
arth Resources E
th Resources Ear
Resources Earth
esources Earth
sources Earth Re

NAS 1.21:

ACCESSION NUMBER RANGES

Accession numbers cited in this Supplement fall within the following ranges.

STAR (N-10000 Series)	N82-16040 - N82-22140
IAA (A-10000 Series)	A82-18840 - A82-28538

This bibliography was prepared by the NASA Scientific and Technical Information Facility operated for the National Aeronautics and Space Administration by PRC Government Information Systems.

NASA SP-7041(34)

EARTH RESOURCES

A CONTINUING BIBLIOGRAPHY WITH INDEXES

Issue 34

A selection of annotated references to unclassified reports and journal articles that were introduced into the NASA scientific and technical information system and announced between April 1 and June 30, 1982 in

- *Scientific and Technical Aerospace Reports (STAR)*
- *International Aerospace Abstracts (IAA).*

NASA Scientific and Technical Information Branch 1982
National Aeronautics and Space Administration
Washington, DC

This supplement is available as NTISUB/038/093 from the National Technical Information Service (NTIS), Springfield, Virginia 22161 at the price of $10.50 domestic; $21.50 foreign for standing orders. Please note: Standing orders are subscriptions which do not terminate at the end of a year, as do regular subscriptions, but continue indefinitely unless specifically terminated by the subscriber.

INTRODUCTION

The technical literature described in this continuing bibliography may be helpful to researchers in numerous disciplines such as agriculture and forestry, geography and cartography, geology and mining, oceanography and fishing, environmental control, and many others. Until recently it was impossible for anyone to examine more than a minute fraction of the Earth's surface continuously. Now vast areas can be observed synoptically, and changes noted in both the Earth's lands and waters, by sensing instrumention on orbiting spacecraft or on aircraft.

This literature survey lists 567 reports, articles, and other documents announced between April 1 and June 30, 1982 in *Scientific and Technical Aerospace Reports (STAR)*, and *International Aerospace Abstracts (IAA).*

The coverage includes documents related to the identification and evaluation by means of sensors in spacecraft and aircraft of vegetation, minerals, and other natural resources, and the techniques and potentialities of surveying and keeping up-to-date inventories of such riches. It encompasses studies of such natural phenomena as earthquakes, volcanoes, ocean currents, and magnetic fields; and such cultural phenomena as cities, transportation networks, and irrigation systems. Descriptions of the components and use of remote sensing and geophysical instrumentation, their subsystems, observational procedures, signature and analyses and interpretive techniques for gathering data are also included. All reports generated under NASA's Earth Resources Survey Program for the time period covered in this bibliography will also be included. The bibliography does not contain citations to documents dealing mainly with satellites or satellite equipment used in navigation or communication systems, nor with instrumentation not used aboard aerospace vehicles.

The selected items are grouped in nine categories. These are listed in the Table of Contents with notes regarding the scope of each category. These categories were especially chosen for this publication, and differ from those found in *STAR* and *IAA*.

Each entry consists of a standard bibliographic citation accompanied by an abstract. The citations and abstracts are reproduced exactly as they appeared originally in *STAR*, or *IAA*, including the original accession numbers from the respective announcement journals. This procedure, which saves time and money, accounts for the variation in citation appearance.

Under each of the nine categories, the entries are presented in one of two groups that appear in the following order:

IAA entries identified by accession number series A82-10,000 in ascending accession number order;

STAR entries identified by accession number series N82-10,000 in ascending accession number order.

After the abstract section, there are five indexes:

subject, personal author, corporate source, contract number and report/accession number.

AVAILABILITY OF CITED PUBLICATIONS

IAA ENTRIES (A82-10000 Series)

All publications abstracted in this Section are available from the Technical Information Service. American Institute of Aeronautics and Astronautics, Inc. (AIAA), as follows: Paper copies of accessions are available at $8.00 per document. Microfiche(1) of documents announced in *IAA* are available at the rate of $4.00 per microfiche on demand, and at the rate of $1.35 per microfiche for standing orders for all *IAA* microfiche.

Minimum air-mail postage to foreign countries is $2.50 and all foreign orders are shipped on payment of pro-forma invoices.

All inquiries and requests should be addressed to AIAA Technical Information Service. Please refer to the accession number when requesting publications.

STAR ENTRIES (N82-10000 Series)

One or more sources from which a document announced in *STAR* is available to the public is ordinarily given on the last line of the citation. The most commonly indicated sources and their acronyms or abbreviations are listed below. If the publication is available from a source other than those listed, the publisher and his address will be displayed on the availability line or in combination with the corporate source line.

Avail: NTIS. Sold by the National Technical Information Service. Prices for hard copy (HC) and microfiche (MF) are indicated by a price code preceded by the letters HC or MF in the *STAR* citation. Current values for the price codes are given in the tables on page vii.

Documents on microfiche are designated by a pound sign (#) following the accession number. The pound sign is used without regard to the source or quality of the microfiche.

Initially distributed microfiche under the NTIS SRIM (Selected Research in Microfiche) is available at greatly reduced unit prices. For this service and for information concerning subscription to NASA printed reports, consult the NTIS Subscription Section, Springfield, Va. 22161.

NOTE ON ORDERING DOCUMENTS: When ordering NASA publications (those followed by the * symbol), use the N accession number. NASA patent applications (only the specifications are offered) should be ordered by the US-Patent-Appl-SN number. Non-NASA publications (no asterisk) should be ordered by the AD, PB, or other *report* number shown on the last line of the citation, not by the N accession number. It is also advisable to cite the title and other bibliographic identification.

Avail: SOD (or GPO). Sold by the Superintendent of Documents, U.S. Government Printing Office, in hard copy. The current price and order number are given following the availability line. (NTIS will fill microfiche requests, at the standard $4.00 price, for those documents identified by a # symbol.)

Avail: NASA Public Document Rooms. Documents so indicated may be examined at or purchased from the National Aeronautics and Space Administration, Public Document Room (Room 126), 600 Independence Ave., S.W., Washington, D.C. 20546, or public document rooms located at each of the NASA research centers, the NASA Space Technology Laboratories, and the NASA Pasadena Office at the Jet Propulsion Laboratory.

---

(1) A microfiche is a transparent sheet of film 105 by 148 mm in size containing as many as 60 to 98 pages of information reduced to micro images (not to exceed 26:1 reduction)

Avail: DOE Depository Libraries. Organizations in U.S. cities and abroad that maintain collections of Department of Energy reports, usually in microfiche form, are listed in *Energy Research Abstracts*. Services available from the DOE and its depositories are described in a booklet, *DOE Technical Information Center - Its Functions and Services* (TID-4660), which may be obtained without charge from the DOE Technical Information Center.

Avail: Univ. Microfilms. Documents so indicated are dissertations selected from *Dissertation Abstracts* and are sold by University Microfilms as xerographic copy (HC) and microfilm. All requests should cite the author and the Order Number as they appear in the citation.

Avail: USGS. Originals of many reports from the U.S. Geological Survey, which may contain color illustrations, or otherwise may not have the quality of illustrations preserved in the microfiche or facsimile reproduction, may be examined by the public at the libraries of the USGS field offices whose addresses are listed in this introduction. The libraries may be queried concerning the availability of specific documents and the possible utilization of local copying services, such as color reproduction.

Avail: HMSO. Publications of Her Majesty's Stationery Office are sold in the U.S. by Pendragon House, Inc. (PHI), Redwood City, California. The U.S. price (including a service and mailing charge) is given, or a conversion table may be obtained from PHI.

Avail: BLL (formerly NLL): British Library Lending Division, Boston Spa, Wetherby, Yorkshire, England. Photocopies available from this organization at the price shown. (If none is given, inquiry should be addressed to the BLL.)

Avail: Fachinformationszentrum, Karlsruhe. Sold by the Fachinformationszentrum Energie, Physik, Mathematik GMBH, Eggenstein Leopoldshafen, Federal Republic of Germany, at the price shown in deutschmarks (DM).

Avail: Issuing Activity, or Corporate Author, or no indication of availability. Inquiries as to the availability of these documents should be addressed to the organization shown in the citation as the corporate author of the document.

Avail: U.S. Patent and Trademark Office. Sold by Commissioner of Patents and Trademarks, U.S. Patent and Trademark Office, at the standard price of 50 cents each, postage free.

Other availabilities: If the publication is available from a source other than the above, the publisher and his address will be displayed entirely on the availability line or in combination with the corporate author line.

ADDRESSES OF ORGANIZATIONS

American Institute of Aeronautics and
Astronautics
Technical Information Service
555 West 57th Street, 12th Floor
New York, New York 10019

British Library Lending Division,
Boston Spa, Wetherby, Yorkshire,
England

Commissioner of Patents and
Trademarks
U.S. Patent and Trademark Office
Washington, D.C. 20231

Department of Energy
Technical Information Center
P.O. Box 62
Oak Ridge, Tennessee 37830

ESA-Information Retrieval Service
ESRIN
Via Galileo Galilei
00044 Frascati (Rome) Italy

Fachinformationszentrum Energie, Physik,
Mathematik GMBH
7514 Eggenstein Leopoldshafen
Federal Republic of Germany

Her Majesty's Stationery Office
P.O. Box 569, S.E. 1
London, England

NASA Scientific and Technical Information
Facility
P.O. Box 8757
B.W.I. Airport, Maryland 21240

National Aeronautics and Space
Administration
Scientific and Technical Information
Branch (NST-41)
Washington, D.C. 20546

National Technical Information Service
5285 Port Royal Road
Springfield, Virginia 22161

Pendragon House, Inc.
899 Broadway Avenue
Redwood City, California 94063

Superintendent of Documents
U.S. Government Printing Office
Washington, D.C. 20402

University Microfilms
A Xerox Company
300 North Zeeb Road
Ann Arbor, Michigan 48106

University Microfilms, Ltd.
Tylers Green
London, England

U.S. Geological Survey
1033 General Services Administration
Building
Washington, D.C. 20242

U.S. Geological Survey
601 E. Cedar Avenue
Flagstaff, Arizona 86002

U.S. Geological Survey
345 Middlefield Road
Menlo Park, California 94025

U.S. Geological Survey
Bldg. 25, Denver Federal Center
Denver, Colorado 80225

NTIS PRICE SCHEDULES

Schedule A

STANDARD PAPER COPY PRICE SCHEDULE

(Effective January 1, 1982)

Price Code	Page Range	North American Price	Foreign Price
A01	Microfiche	$ 4.00	$ 8.00
A02	001-025	6.00	12.00
A03	026-050	7.50	15.00
A04	051-075	9.00	18.00
A05	076-100	10.50	21.00
A06	101-125	12.00	24.00
A07	126-150	13.50	27.00
A08	151-175	15.00	30.00
A09	176-200	16.50	33.00
A10	201-225	18.00	36.00
A11	226-250	19.50	39.00
A12	251-275	21.00	42.00
A13	276-300	22.50	45.00
A14	301-325	24.00	48.00
A15	326-350	25.50	51.00
A16	351-375	27.00	54.00
A17	376-400	28.50	57.00
A18	401-425	30.00	60.00
A19	426-450	31.50	63.00
A20	451-475	33.00	66.00
A21	476-500	34.50	69.00
A22	501-525	36.00	72.00
A23	526-550	37.50	75.00
A24	551-575	39.00	78.00
A25	576-600	40.50	81.00
	601-up	-- 1/	-- 2/

A99 - Write for quote

1/ Add $1.50 for each additional 25 page increment or portion thereof for 601 pages up.

2/ Add $3.00 for each additional 25 page increment or portion thereof for 601 pages and more

Schedule E

EXCEPTION PRICE SCHEDULE

Paper Copy & Microfiche

Price Code	North American Price	Foreign Price
E01	$ 6.50	$ 13.50
E02	7.50	15.50
E03	9.50	19.50
E04	11.50	23.50
E05	13.50	27.50
E06	15.50	31.50
E07	17.50	35.50
E08	19.50	39.50
E09	21.50	43.50
E10	23.50	47.50
E11	25.50	51.50
E12	28.50	57.50
E13	31.50	63.50
E14	34.50	69.50
E15	37.50	75.50
E16	40.50	81.50
E17	43.50	88.50
E18	46.50	93.50
E19	51.50	102.50
E20	61.50	123.50

E-99 - Write for quote

N01	30.00'	45.00

TABLE OF CONTENTS

Page

Category 01 Agriculture and Forestry 57
Includes crop forecasts, crop signature analysis, soil identification, disease detection, harvest estimates, range resources, timber inventory, forest fire detection, and wildlife migration patterns.

Category 02 Environmental Changes and Cultural Resources 73
Includes land use analysis, urban and metropolitan studies, environmental impact, air and water pollution, geographic information systems, and geographic analysis.

Category 03 Geodesy and Cartography 81
Includes mapping and topography.

Category 04 Geology and Mineral Resources 89
Includes mineral deposits, petroleum deposits, spectral properties of rocks, geological exploration, and lithology.

Category 05 Oceanography and Marine Resources 93
Includes sea-surface temperature, ocean bottom surveying imagery, drift rates, sea ice and icebergs, sea state, fish location

Category 06 Hydrology and Water Management 101
Includes snow cover and water runoff in rivers and glaciers, saline intrusion, drainage analysis, geomorphology of river basins, land uses, and estuarine studies.

Category 07 Data Processing and Distribution Systems 111
Includes film processing, computer technology, satellite and aircraft hardware, and imagery.

Category 08 Instrumentation and Sensors 125
Includes data acquisition and camera systems and remote sensors.

Category 09 General 137
Includes economic analysis.

Subject Index A-1
Personal Author Index B-1
Corporate Source Index C-1
Contract Number Index D-1
Report / Accession Number Index E-1

TYPICAL CITATION AND ABSTRACT FROM *STAR*

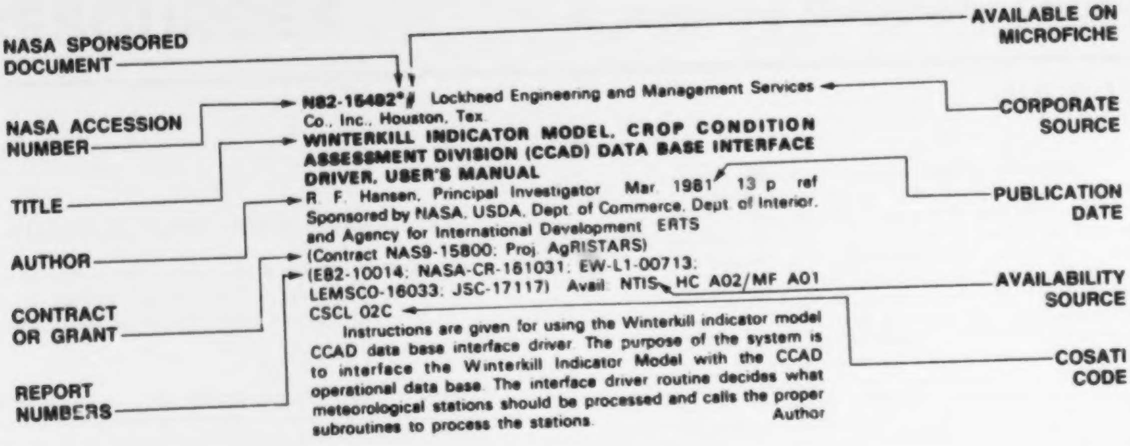
NASA SPONSORED DOCUMENT
NASA ACCESSION NUMBER
TITLE
AUTHOR
CONTRACT OR GRANT
REPORT NUMBERS
AVAILABLE ON MICROFICHE
CORPORATE SOURCE
PUBLICATION DATE
AVAILABILITY SOURCE
COSATI CODE

N82-16492*# Lockheed Engineering and Management Services Co., Inc., Houston, Tex.
WINTERKILL INDICATOR MODEL, CROP CONDITION ASSESSMENT DIVISION (CCAD) DATA BASE INTERFACE DRIVER, USER'S MANUAL
R. F. Hansen, Principal Investigator Mar. 1981 13 p ref
Sponsored by NASA, USDA, Dept. of Commerce, Dept. of Interior, and Agency for International Development ERTS
(Contract NAS9-15800; Proj. AgRISTARS)
(E82-10014; NASA-CR-161031; EW-L1-00713; LEMSCO-16033; JSC-17117) Avail: NTIS HC A02/MF A01 CSCL 02C

Instructions are given for using the Winterkill indicator model CCAD data base interface driver. The purpose of the system is to interface the Winterkill Indicator Model with the CCAD operational data base. The interface driver routine decides what meteorological stations should be processed and calls the proper subroutines to process the stations. Author

TYPICAL CITATION AND ABSTRACT FROM *IAA*

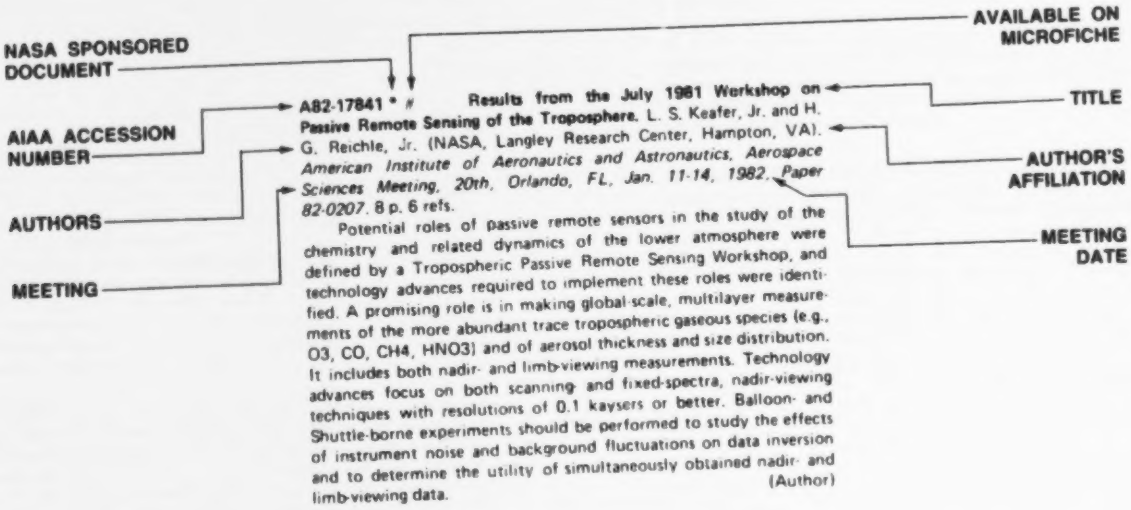
NASA SPONSORED DOCUMENT
AIAA ACCESSION NUMBER
AUTHORS
MEETING
AVAILABLE ON MICROFICHE
TITLE
AUTHOR'S AFFILIATION
MEETING DATE

A82-17841 * # **Results from the July 1981 Workshop on Passive Remote Sensing of the Troposphere.** L. S. Keafer, Jr. and H. G. Reichle, Jr. (NASA, Langley Research Center, Hampton, VA). *American Institute of Aeronautics and Astronautics, Aerospace Sciences Meeting, 20th, Orlando, FL, Jan. 11-14, 1982, Paper 82-0207.* 8 p. 6 refs.

Potential roles of passive remote sensors in the study of the chemistry and related dynamics of the lower atmosphere were defined by a Tropospheric Passive Remote Sensing Workshop, and technology advances required to implement these roles were identified. A promising role is in making global-scale, multilayer measurements of the more abundant trace tropospheric gaseous species (e.g., O3, CO, CH4, HNO3) and of aerosol thickness and size distribution. It includes both nadir- and limb-viewing measurements. Technology advances focus on both scanning- and fixed-spectra, nadir-viewing techniques with resolutions of 0.1 kaysers or better. Balloon- and Shuttle-borne experiments should be performed to study the effects of instrument noise and background fluctuations on data inversion and to determine the utility of simultaneously obtained nadir- and limb-viewing data. (Author)

TABLE OF CONTENTS

EARTH RESOURCES

A Continuing Bibliography (Issue 34)

JULY 1982

01
AGRICULTURE AND FORESTRY

Includes crop forecasts, crop signature analysis, soil identification, disease detection, harvest estimates, range resources, timber inventory, forest fire detection, and wildlife migration patterns.

A82-19529 # Soil moisture determination - Experiments with passive microwave radiometers. P. Meylan, C. Morzier, R. Caloz (Lausanne, Ecole Polytechnique Fédérale, Lausanne, Switzerland), E. Schanda, and Ch. Matzler (Bern, Universität, Berne, Switzerland). In: European Microwave Conference, 10th, Warsaw, Poland, September 8-12, 1980, Proceedings. Sevenoaks, Kent, England, Microwave Exhibitions and Publishers, Ltd., 1981, p. 256-260. 5 refs.

Long term observational programs have been followed in 1977 and 1978 for the determination of the relationship between emissivity and soil moisture on three test sites, representing three soil types. Five radiometers, whose frequencies are centered at 36, 21, 10.5, 4.9 and 1.8 GHz, were used. The interpretation of the measurements follows three ways: (1) analysis of the radiometer response versus scan angle; (2) factorial analysis of correspondences and clustering analysis; and (3) analysis of emissivity variation versus soil moisture content. In this last case a nonlinear function was fitted to the data and could be partially explained. An experiment was also conducted to determine the real penetration depth in a heavy soil. (Author)

A82-20349 † Experimental evaluation of methods of the automated interpretation of crops from a Fragment MSS image (Eksperimental'naia otsenka metodov avtomatizirovannogo deshifrirovaniia sel'skokhoziaistvennykh kul'tur po snimku s MSS 'Fragment'). I. A. Labutina and I. K. Lur'e (Moskovskii Gosudarstvennyi Universitet, Moscow, USSR). *Issledovanie Zemli iz Kosmosa,* Nov.-Dec. 1981, p. 89-92. In Russian.

Three methods of automated photointerpretation are examined and compared: the minimum distance method, the maximum likelihood method, and cluster analysis. The comparison involved crop identification from a Fragment MSS image of an area between the Don and Khoper rivers. Recommendations on the organization of automated image processing are given. B.J.

A82-20350 † Automation of the processing of aerial and space images for forest inventory (Avtomatizatsiia protsessa obrabotki aerokosmicheskikh snimkov v tseliakh inventarizatsii lesov). A. S. Alekseev, S. V. Vasil'ev, V. G. Mozalevskii, V. P. Piatkin, V. N. Sedykh, and V. S. Sidorova (Akademiia Nauk SSSR, Vychislitel'nyi Tsentr and Institut Lesa i Drevesiny, Novosibirsk, USSR). *Issledovanie Zemli iz Kosmosa,* Nov.-Dec. 1981, p. 93-100. 6 refs. In Russian.

Various aspects of the automated processing of remotely sensed images for purposes of forest inventory are considered. Particular attention is given to the use of textural features for image classification. B.J.

A82-20408 Manual and automatic crop identification with airborne radar imagery. B. Brisco and R. Protz (Guelph, University, Guelph, Ontario, Canada). *Photogrammetric Engineering and Remote Sensing,* vol. 48, Jan. 1982, p. 101-109. 16 refs. Department of Supply and Services Contract No. 08SU-01525-7-0198.

Woods, roughland and corn were identified with accuracies approaching or exceeding 90%, when image tone and texture were employed as the key discriminants, in manual and automatic crop discrimination by means of multi-date radar imagery. Hay-pasture and grain fields were, however, consistently confused, leading to identification accuracies of only about 50%. It is found that, while image enhancement prior to supervised classification was useful, increased class confusion resulted from the lack of textural information in the digital classification and its consequent overlapping of tonal distributions for the five investigated classes. For the more accurate identification of hay-pasture and grain fields, it is suggested that imagery be collected during the growing season. At that time, the two crop types exhibit the greatest difference in geometrical and dielectric properties. O.C.

A82-20422 * # Simple radiative transfer model for relationships between canopy biomass and reflectance. J. K. Park (Systems and Applied Sciences Corp., Riverdale, MD) and D. W. Deering (NASA, Goddard Space Flight Center, Earth Survey Applications Div., Greenbelt, MD). *Applied Optics,* vol. 21, Jan. 15, 1982, p. 303-309. 25 refs.

A modified Kubelka-Munk model has been utilized to derive useful equations for the analysis of apparent canopy reflectance. Based on the solution to the model simple working equations were formulated by employing reflectance characteristic parameters. The relationships derived show the asymptotic nature of reflectance data that is typically observed in remote sensing studies of plant biomass. They also establish the range of expected apparent canopy reflectance values for specific plant canopy types. The usefulness of the simplified equations was demonstrated by the exceptionally close fit of the theoretical curves to two separately acquired data sets for alfalfa and shortgrass prairie canopies. (Author)

A82-21026 The Dutch ROVE program. G. P. de Loor, P. Hoogeboom (Centrale Organisatie voor Toegepost-Natuurwetenschappelijk Onderzoek, Physisch Laboratorium TNO, The Hague, Netherlands), and E. P. W. Attema (Delft, Technische Hogeschool, Delft, Netherlands). *IEEE Transactions on Geoscience and Remote Sensing,* vol. GE-20, Jan. 1982, p. 3-11. 22 refs.

The Netherlands Radar Observation of Vegetation (ROVE) team efforts to employ radar as an all-weather, day and night remote sensing technique for observation and control of crops is described. Experiments involving X-band radar from TV towers, an X-band FM/CW system on rails, and an EMI X-band SLAR are reviewed and ground-based and airborne data collection and data are compared. Calibration angles for ground based observations of vegetation are under study, and a grazing angle of 75 deg has been found necessary for measuring soil moisture from the ground. Resolutions in white, black, and grey have been established for sugar beets, wheat, and potatoes, respectively, using airborne radar. Further programs are under way to define the effects on imaging of climate, season, irrigation, soil properties, soil treatment, sowing procedures, and fertilization. M.S.K.

A82-21028 Microwave radiometry of lands under natural and artificial moistening. A. M. Shutko (Akademiia Nauk SSSR, Institut Radiotekhniki i Elektroniki, Moscow, USSR). *IEEE Transactions on Geoscience and Remote Sensing,* vol. GE-20, Jan. 1982, p. 18-26. 13 refs.

The dielectric properties of soils and soil conditions are examined for the applications of microwave radiometry to agriculture, hydrogeology, and land reclamation. Fundamental relations are defined between radiation and soil-moisture content, and characteristics of the microwave emissivity of nonuniform moistened ground with either a flat or rough surface are analyzed. The effects of the uniformity or nonuniformity of the soil, of subsoil water, and of daily temperature variations are examined. Accuracy is found to be diminished by the presence of vegetation, and examples of applications of microwave sensing in agricultural fields, for irrigation quality control, for estimating subsoil water, to find areas with excessive drainage, and to determine the hydrologic regime of dry salt lakes are discussed. M.S.K.

A82-21029 **Microwave radiation peculiarities of vegetative covers.** A. M. Shutko and A. A. Chukhlantsev (Akademiia Nauk SSSR, Institut Radiotekhniki i Elektroniki, Moscow, USSR). *IEEE Transactions on Geoscience and Remote Sensing,* vol. GE-20, Jan. 1982, p. 27-29.

Theoretical and experimental results for determining the spectral peculiarities of soil-vegetation systems are reported. Vegetation covers were grouped into grain crops, grass and alfalfa, wide-leaf crops such as corn and beets, and bushes and woods. The type of vegetation showed the most influence in the cm band, and the wide-leaf crops were found to display a decrease in emissivity with an increase in wavelength. The total attenuation in vegetative covers was examined, and showed that attenuation is proportional to the water content in vegetation, with a proportionality coefficient which depends on the type of vegetation and its state of growth. A model was developed to take into account the scattering and absorption cross sections, and a formula is presented for the total attenuation in the chosen vegetation model. M.S.K.

A82-21030 **Mixture formulas applied in estimation of dielectric and radiative characteristics of soils and grounds at microwave frequencies.** A. M. Shutko and E. M. Reutov (Akademiia Nauk SSSR, Institut Radiotekhniki i Elektroniki, Moscow, USSR). *IEEE Transactions on Geoscience and Remote Sensing,* vol. GE-20, Jan. 1982, p. 29-32. 12 refs.

A82-21031 **Investigation of the vegetative covers on ploughed areas by SLAR.** A. G. Geller, E. N. Zotova, and M. I. Naumov (Akademiia Nauk SSSR, Institut Radiotekhniki i Elektroniki, Moscow, USSR). *IEEE Transactions on Geoscience and Remote Sensing,* vol. GE-20, Jan. 1982, p. 32-35. 7 refs.

Results of SLAR investigations of crop condition and the correlation of dependencies between the mean intensity of reflected signals and the biometrical parameters of the crops are reported. The experiments were made using K-band SLAR with HH polarization at a grazing angle of 12-24 deg, and corn, sugar beets, and winter wheat were examined in the middle of the growth cycle. Microphotometric techniques were used to process the radar data, and the phytomass and crop moisture content parameters were chosen to describe the crop state. The 80% confidence limits for the regression functions are provided, and differences in the scattered signal intensities from wide-leaf crops are accounted for by differences in surface roughness characteristics. The desired antenna pattern was achieved in sensing angles from 68-72 deg, and the use of dual frequency, dual polarization, and a calibrated radar to improve system efficiency is indicated. M.S.K.

A82-21032 **Volumetric effects in cross-polarized airborne radar data.** A. J. Blanchard, R. W. Newton, L. Tsang, and B. R. Jean (Texas A & M University, College Station, TX). *IEEE Transactions on Geoscience and Remote Sensing,* vol. GE-20, Jan. 1982, p. 36-41. 14 refs.

Experimental results and theoretical models for the sensitivity of radar backscatter return to soil moisture as a function of incident angle and the sensibility of the cross polarized radar return to surface roughness are presented. Additional attention is devoted to establishing the accuracy of cross-polarized radar backscatter measurements by the identification of specific criteria in terms of integrated antenna polarization isolation. NASA scatterometers were used in test runs at 1.6, 4.75, and 13.3 GHz to detect soil moisture. The Kirchhoff scattering theory and the Blanchard and Rouse surface/volume theory were used to test predictions for like-polarized backscatter as a function of moisture and incident angle. Volume dependent measurements were found to be possible independent of surface effects and incident angle. M.S.K.

A82-21033 * **Crop classification using airborne radar and Landsat data.** F. T. Ulaby, R. Y. Li, and K. S. Shanmugan (University of Kansas Center for Research, Inc., Lawrence, KS). *IEEE Transactions on Geoscience and Remote Sensing,* vol. GE-20, Jan. 1982, p. 42-51. 21 refs. Contract No. NAS9-15421.

NASA 13.3 GHz airborne radar data from a soil moisture measurement analysis is used to investigate the statistical nature of the radar backscattering coefficient for bare ground and three different crop types, and to evaluate the crop classification rates using Landsat data alone or combined with the airborne survey. The scatterometer was a fan-beam Doppler system, VV polarized, and is considered only for 50 deg angles of incidence. A total of 36 fields were covered a week apart by the aircraft and Landsat, and Rayleigh statistics were used in the frequency averaging to eliminate fluctuations due to random fluctuations. Within-field variances were calculated for the Landsat and the radar data and used to design optimum crop classification procedures. The Landsat Band 4 readings were 67% accurate, and an increase in accuracy of 10% was achieved by the addition of the radar data. M.S.K.

A82-21092 **Use of Landsat data for automatic classification and area estimation of sugar-cane plantation in Sao Paulo state, Brazil.** F. J. Mendonça (Instituto de Pesquisas Espaciais, São José dos Campos, São Paulo, Brazil). *International Journal of Remote Sensing,* vol. 2, Oct.-Dec. 1981, p. 361-368. 11 refs.

A sugar-cane inventory study of plantations in Sao Paulo state, Brazil is presented, in which sugar-cane was automatically classified and its area was estimated using an interactive image analysis system (Image-100) and Landsat digital data. Ten segments, 10 x 20 km, were aerially photographed from May 27-June 12, 1978; two Landsat passes were also made in April and July/August, 1978. Crop density, field size, and spatial distribution were all found to influence the spectral characteristics of the study crop. Classification of sugar-cane was found to be most difficult in the dry season (April) and easiest in July/August. The study area covered four Landsat paths: 235, 236, 237, and 238. The percentages of overall correct classification for the fourth paths ranged from 79.56 percent for path 238 to 95.59 percent for path 237. A difference of only 12.57 percent was encountered between sugar-cane estimates using Landsat data and those which used data from the Institute for Agricultural Economy. J.F.

A82-21093 **The estimation of the surface moisture of a vegetated soil using aerial infrared photography.** P. J. Curran (Reading, University, Reading, Berks., England). *International Journal of Remote Sensing,* vol. 2, Oct.-Dec. 1981, p. 369-378. 12 refs. Natural Environment Research Council Grant No. GR3/4076.

A remote sensing method for estimating the surface soil moisture of a soil with an incomplete vegetation cover is discussed. It has been shown that when the percentage cover of leaves and nongreen vegetation are known and constant, and the effect of shadow is minimal, the near infrared bidirectional reflectance from the vegetation canopy is negatively related to surface soil moisture. The near infrared bidirectional reflectance, surface soil moisture, and vegetation cover were measured at ten heathland sites on 18 different dates. It was found that the Y axis intercept of a regression between ground-based measurements of near infrared bidirectional reflectance (Y) and the percentage of green vegetation cover (X) was linearly related to surface soil moisture. This relationship between soil moisture and canopy reflectance was used to estimate the surface soil moisture of vegetated heathland in five flights of black and white infrared aerial photography. The resulting estimates had an accuracy of + or - 18.4% at the 95% confidence level. J.F.

A82-22142 **An airphoto key for major tropical crops.** W. R. Philipson and T. Liang (Cornell University, Ithaca, NY). *Photogrammetric Engineering and Remote Sensing,* vol. 48, Feb. 1982, p. 223-233. 15 refs.

A key is presented for identifying selected major crops of the tropics through stereoscopic analysis of medium-scale (1:10,000 to 1:30,000) panchromatic aerial photographs. The development of the key is based on representative photographs of crops as they occur throughout the tropics. The key recognizes certain field, management, and crop features which are frequently associated with crop occurrence. It is pointed out that positive crop identification normally requires ground verification. Attention has been given to crops of sugar cane, coffee, bananas, pineapple, rice, corn, tobacco, rubber, coconut, and cacao. G.R.

A82-22144 **Multispectral photographic remote sensing of green vegetation biomass and productivity.** P. J. Curran (Reading, University, Reading, Berks., England). *Photogrammetric Engineering and Remote Sensing,* vol. 48, Feb. 1982, p. 243-250. 13 refs. Natural Environment Research Council Grant No. GR/3/1481.

An investigation was conducted with the objective to demonstrate the importance of productivity to the relationship between green biomass and a bidirectional reflectance ratio. Using bidirectional reflectance data derived photographically from 22 sets of near vertical aerial photography and 56 sets of oblique ground photography, it was determined that the amount of bidirectional reflectance ratio variance accounted for by green biomass could be increased by around 6 percent with the addition of productivity. On a pasture site with low green biomass but high productivity, the bidirectional reflectance ratio was higher than for a high green biomass pasture site with lower productivity. G.R.

A82-24961 **Influence of illumination and viewing geometry and atmospheric composition on the 'tasseled cap' transformation of Landsat MSS data.** J. V. Dave (IBM Scientific Center, Palo Alto, CA). *Remote Sensing of Environment,* vol. 11, Mar. 1981, p. 37-55. 15 refs.

Various characteristics of a simulated tasseled cap (representing the spectral-temporal characteristics of wheat fields, as observed by the Landsat MSS sensors) are investigated as a function of the viewing and illumination geometry parameters, and atmospheric composition. Measured spectral reflectances of ten wheat fields in various growth stages and the satellite-level radiances, computed after taking into account all orders of scattering, are used in this investigation. It is shown that the procedure for normalizing the measured radiances by the cosine of the solar zenith angle is a less accurate approximation, and that the characteristics of the tasseled cap both in the greenness-brightness and yellowness-brightness hyperplanes are significantly affected by the geometric as well as the atmospheric parameters. (Author)

A82-24963 * **HCMM detection of high soil moisture areas.** J. L. Heilman (South Dakota State University, Brookings, SD; Texas A & M University, College Station, TX) and D. G. Moore (South Dakota State University, Brookings, SD). *Remote Sensing of Environment,* vol. 11, Mar. 1981, p. 73-76. Contract No. NAS5-24206.

It is noted that one objective of NASA's Heat Capacity Mapping Mission (HCMM) is to evaluate the feasibility of using HCMM data to assess soil moisture effects by observing temperatures near the maximum and minimum of the diurnal temperature cycle. The satellite, which carries a two-channel radiometer (0.5-1.1 and 10.5-12.5 microns) gathers data at 1:30 P.M. and 2:30 A.M. local time at midlatitudes, with a repeat cycle of 5 or 16 days depending on latitude. The spatial resolutions are 0.5 x 0.5 km at nadir for the visible channel and 0.6 x 0.6 km at nadir for the thermal infrared channel. An example is presented here of HCMM detection of a region of high soil moisture. C.R.

A82-25457 **Assessing mesquite-grass vegetation condition from Landsat.** K. C. McDaniel (New Mexico State University, Las Cruces, NM) and R. H. Haas (U.S. Geological Survey, EROS Data Center, Sioux Falls, SD). *Photogrammetric Engineering and Remote Sensing,* vol. 48, Mar. 1982, p. 441-450. 24 refs. Research supported by the E. Paul and Helen Buck Waggoner Foundation.

Regression analyses with Landsat MSS data and vegetation data collected on four dates from six study sites show the two vegetation index models, TVI 6 and GVI, to be highly correlated with such vegetation parameters associated with growing vegetation as green cover, green yield, and plant moisture content. This is seen as an indication of the possibility of vegetation condition quantitative measurement with Landsat MSS data. Because it is shown that land management practices do not seriously affect the relationship of Landsat MSS models with rangeland vegetation parameters obtained from a common vegetation-soil system, the stratifying of relatively uniform vegetation soil systems on Landsat imagery appears to be a useful first step in the vegetation survey use of Landsat MSS data. O.C.

A82-26577 † **The spectral reflectance of certain soils (Spektral'naia otrazhatel'naia sposobnost' nekotorykh pochv).** P. P. Fedchenko and K. Ia. Kondrat'ev. Leningrad, Gidrometeoizdat, 1981. 232 p. 121 refs. In Russian.

The principal factors affecting the reflectance properties of soils are investigated. Methods are proposed for aircraft and laboratory measurements of the spectral luminance factors of soils. Spectrometers currently in use for studying the reflectance properties of natural topographic features are described. It is shown that the theory of statistical pattern recognition makes possible soil mapping on the basis of reflection spectra. C.R.

A82-26842 * **Use of Landsat-derived temporal profiles for corn-soybean feature extraction and classification.** G. D. Badhwar (NASA, Johnson Space Center, Houston, TX), J. G. Carnes, and W. W. Austin (Lockheed Engineering and Management Services Co., Inc., Houston, TX). *Remote Sensing of Environment,* vol. 12, Mar. 1982, p. 57-79. 15 refs.

A physical model is presented, which has been derived from multitemporal-multispectral data acquired by Landsat satellites to describe the behavior and new features that are crop specific. A feasibility study over 40 sites was performed to classify the segment pixels into those of corn, soybeans, and others using the new features and a linear classifier. Results agree well with other existing methods, and it is shown the multitemporal-multispectral scanner data can be transformed into two parameters that are closely related to the target of interest and thus can be used in classification. The approach is less time intensive than other techniques and requires labeling of only pure pixels. D.L.G.

A82-27393 † **Evaluation of the state of crops from satellite data (Otsenka sostoianiia sel'skokhoziaistvennykh kul'tur po sputnikovym dannym).** G. I. Borisoglebskii and V. V. Kozoderov (Gosudarstvennyi Nauchno-Issledovatel'skii Tsentr Izucheniia Prirodnykh Resursov, USSR). *Meteorologiia i Gidrologiia,* Mar. 1982, p. 94-101. In Russian.

The paper examines the possibility of evaluating the dynamics of crop development from remote sensing images. Results are presented on the determination of the structure of agricultural lands and the state of winter crops in the Kherson territory of the USSR from medium-resolution satellite images. B.J.

A82-27397 **Remote sensing of the structure of taiga landscapes (Distantsionnaia indikatsiia struktury taezhnykh landshaftov).** Edited by V. V. Kuzmichev. Novosibirsk, Izdatel'stvo Nauka, 1981. 248 p. In Russian.

Papers are presented on the use of remote sensing to obtain information on the relationships between forests and other elements of the natural environment: soils, relief, the mineralogical composition of rocks, subsurface water, and animal habitats. Particular attention is given to such topics as the mapping of the post-fire stages of the formation of forests, the remote sensing of the dynamics of cedar forests in Siberia, the use of anthropogenic features in landscape studies (with Lake Baikal taken as an example), the use of remote sensing to study bird populations, and the relationship between taiga landscapes and geological structures. B.J.

A82-27586 * # **Stochastic models of cover class dynamics.** T. H. Barringer (Hunter College, New York, NY; Pennsylvania, University, Philadelphia, PA) and V. B. Robinson (Hunter College, New York, NY). In: International Symposium on Remote Sensing of Environment, 15th, Ann Arbor, MI, May 11-15, 1981, Proceedings. Volume 1. Ann Arbor, MI, Environmental Research Institute of Michigan, 1981, p. 125-144. 84 refs. Grant No. NsG-5325.

Investigations related to satellite remote sensing of vegetation have been concerned with questions of signature identification and extension, cover inventory accuracy, and change detection and monitoring. Attention is given to models of ecological succession, present directions in successional modeling and analysis, nondynamic spatial models, issues in the analysis of spatial data, and aspects of spatial modeling. Issues in time-series analysis are considered along with dynamic spatial models, and problems of model specification and identification. G.R.

A82-27588 # **Data base requirements in support of crop models.** A. B. Park (General Electric Co., Lanham, MD). In: International Symposium on Remote Sensing of Environment, 15th, Ann Arbor, MI, May 11-15, 1981, Proceedings. Volume 1. Ann Arbor, MI, Environmental Research Institute of Michigan, 1981, p. 165-174.

Problems regarding the data base design can be approached in at least two ways. For the design of a 'local' model, both the crop and its environment are confined to the research location, and there is no need to consider the spatial distribution complexity problem. However, in the case of the design of a 'global' model, it is necessary to account for the variability of both the crop and the environment in all possible geographic locations. During the development and test of the model, it is normally attempted to simplify this problem by using the 'homologue' approach. Requirements regarding the input of agronomic data are considered, taking into account the crop area, the cropping pattern, the crop calendar, crop varieties, yield, water culture, fertilizer, plant pests, soil, the meteorological station, and the terrain model. Meteorological input data requirements are also discussed. G.R.

A82-27601 # **Multiresource inventory methods pilot test.** R. T. Pelletier (U.S. Department of Agriculture, Forest Service, Washington, DC). In: International Symposium on Remote Sensing of Environment, 15th, Ann Arbor, MI, May 11-15, 1981, Proceedings. Volume 1. Ann Arbor, MI, Environmental Research Institute of Michigan, 1981, p. 339-355. 6 refs.

The test is being conducted by the Forest Service as an advanced demonstration of Landsat technology to supplement current methods of conducting recurrent inventories over large areas. It will test, validate, and, if deemed successful by the Forest Service, transfer new remote sensing capability to the inventory and planning process; this will offer new efficiencies benefiting resource managers and planners. The pilot test will be administered over a three-year period and will support major efforts in two geographical areas. C.R.

A82-27617 # **Dew and vapor pressure as complicating factors in the interpretation of spectral radiance from crops.** P. J. Pinter, Jr. and R. D. Jackson (U.S. Water Conservation Laboratory, Phoenix, AZ). In: International Symposium on Remote Sensing of Environment, 15th, Ann Arbor, MI, May 11-15, 1981, Proceedings. Volume 2. Ann Arbor, MI, Environmental Research Institute of Michigan, 1981, p. 547-554. 8 refs.

Ground-based radiometers, utilizing relatively wide-band spectral filters similar to those of present and anticipated satellites, are being used extensively to develop fundamental relationships between agricultural targets and their spectral characteristics. In the present investigation some of the unique operational characteristics of a hand-held 4-band radiometer are utilized to examine the effect of dew on the spectral characteristics of wheat and to study the influence of atmospheric vapor pressure on the spectral quality of radiance measured over soil and alfalfa canopy targets. It is found possible to detect and quantify the presence of dew on crops by monitoring the depression in a spectrally-based vegetation index. The timing of spectral data acquisition is a critical factor, because complications regarding the interpretation of data can arise in connection with the presence of dew on crop canopies. G.R.

A82-27621 # **A timely and accurate potato acreage estimate from Landsat - Results of a demonstration.** R. A. Ryerson, R. J. Brown (Canada Centre for Remote Sensing, Ottawa, Canada), J.-L. Tambay, L. A. Murphy (Statistics Canada, Ottawa, Canada), and B. McLaughlin (Statistics Canada, Truro, Nova Scotia, Canada). In: International Symposium on Remote Sensing of Environment, 15th, Ann Arbor, MI, May 11-15, 1981, Proceedings. Volume 2. Ann Arbor, MI, Environmental Research Institute of Michigan, 1981, p. 587-597. 10 refs.

The current statistical data collection system for obtaining crop area estimates is considered. The area for which an estimate was required is located in the upper St. John Valley in New Brunswick, Canada. The 1980 ground sample and data collection is considered along with the analysis of remotely sensed data, taking into account procedures to improve estimates and the generation of the 1980 estimate based on Landsat data. A highly accurate potato area estimate for the three major potato producing counties of New Brunswick was obtained. G.R.

A82-27622 # **Landsat feature enhancement - Or, can we separate vegetation from soil.** J. E. Colwell (Michigan, Environmental Research Institute, Ann Arbor, MI). In: International Symposium on Remote Sensing of Environment, 15th, Ann Arbor, MI, May 11-15, 1981, Proceedings. Volume 2. Ann Arbor, MI, Environmental Research Institute of Michigan, 1981, p. 599-621. 12 refs.

Two separate procedures are presented for enhancing certain features in Landsat data. One procedure is designed to be helpful in assessing soil features in situations where the soil is partially covered by variable amounts of green vegetation. This procedure results in the calculation of a parameter called 'Projected Soil Brightness'. The other procedure is designed to be an aid in interpreting separate soil and vegetation effects in areas with partial cover of nongreen vegetation. This procedure results in the calculation of parameters called 'Normalized Vegetation Shadow Measure' and 'Corrected Soil Brightness Measure'. G.R.

A82-27624 # **Scene analysis for wildland fire-fuel characteristics in a Mediterranean climate.** M. J. Cosentino, C. E. Woodcock, and J. Franklin (California, University, Santa Barbara, CA). In: International Symposium on Remote Sensing of Environment, 15th, Ann Arbor, MI, May 11-15, 1981, Proceedings. Volume 2. Ann Arbor, MI, Environmental Research Institute of Michigan, 1981, p. 635-646. 9 refs.

During the dry summer and fall seasons, wildfires are a threat to homes, lives, property, and natural resources in California. A computer program called FIREMOD, which will be used to predict fire spread rate and intensity, is currently being developed. A description is presented of the findings of a research project undertaken to evaluate the potential of using remotely sensed and collateral data in a geographic information system framework to provide maps of chaparral vegetation characteristics for input as a fuels database in the FIREMOD computer model. It is found that Landsat spectral data can be combined with a synthesized texture channel in an unsupervised classification procedure to provide a physiognomic vegetation classification which includes density distinctions. These vegetation classes are useful for fire spread simulation models because they contain meaningful distinctions related to fire behavior. G.R.

A82-27643 # **A vegetation response model applied to range inventory and monitoring using Landsat MSS data.** F. R. Honey and I. J. Tapley (Commonwealth Scientific and Industrial Research Organization, Div. of Land Resources Management, Perth, Australia). In: International Symposium on Remote Sensing of Environment, 15th, Ann Arbor, MI, May 11-15, 1981, Proceedings. Volume 2. Ann Arbor, MI, Environmental Research Institute of Michigan, 1981, p. 823-837. 7 refs.

A model describing the response of vegetation to rainfall from the standpoint of corresponding changes in reflectance, as measured by the Landsat MSS system, is presented. The main assumptions of the model are (1) that there is an exponential increase of fresh plant cells from such sources of new growth as seeds or buds, and (2) that the growth rates of the new cells is larger than their decay rate, so that some maximum is reached before the rate of production from the diminishing number of sources is less than the rate of decay. Because the shape of the response function curve will be independent of the means of measuring vegetation density and condition, curves from ground-collected biomass data should match those derived from Landsat vegetation indices. Results from data collected in Western Australia for three vegetation communities and plotted according to the model indicate that data must be collected intensively at the time of the peak. O.C.

A82-27644 # **Forest change detection.** J. E. Colwell (Michigan Environmental Research Institute, Ann Arbor, MI) and F. P. Weber (U.S. Forest Service, Houston, TX). In: International Symposium on Remote Sensing of Environment, 15th, Ann Arbor, MI, May 11-15, 1981, Proceedings. Volume 2. Ann Arbor, MI, Environmental Research Institute of Michigan, 1981, p. 839-852.

The U.S. Forest Service has a requirement to make periodic assessments of the renewable resources of the United States. This investigation was designed to examine the utility of Landsat data for assessing changes in renewable resources. Change was analyzed for a partially forested scene in Kershaw County, South Carolina based on Landsat data separated by two years in time. A variety of change detection procedures were investigated, including image analysis and two kinds of digital (automated) procedures. The most fundamental conclusion of this study is that the type of change detection procedure implemented can significantly affect the estimates of amount of change. (Author)

A82-27645 * # **Soybean canopy reflectance as a function of view and illumination geometry.** K. J. Ranson, V. C. Vanderbilt, L. L. Biehl, B. F. Robinson, and M. E. Bauer (Purdue University, West Lafayette, IN). In: International Symposium on Remote Sensing of Environment, 15th, Ann Arbor, MI, May 11-15, 1981, Proceedings. Volume 2. Ann Arbor, MI, Environmental Research Institute of Michigan, 1981, p. 853-865. 16 refs. Contract No. NAS9-15466.

Reflectances were calculated from measurements at four wavelength bands through eight view azimuth and seven view zenith directions, for various solar zenith and azimuth angles over portions of three days, in an experimental characterization of a soybean field by means of its reflectances and physical and agronomic attributes. Results indicate that the distribution of reflectance from a soybean field is a function of the solar illumination and viewing geometry, wavelength, and row direction, as well as the state of canopy development. Shadows between rows were found to affect visible wavelength band reflectance to a greater extent than near-IR reflectance. A model describing reflectance variation as a function of projected solar and viewing angles is proposed, which approximates the visible wavelength band reflectance variations of a canopy with a well-defined row structure. O.C.

A82-27646 # **The influence of illumination and viewing geometry on the reflectance factor of agricultural targets.** K. Staenz (Zürich, Universität, Zurich, Switzerland), F. J. Ahern, and R. J. Brown (Canada Centre for Remote Sensing, Ottawa, Canada). In: International Symposium on Remote Sensing of Environment, 15th, Ann Arbor, MI, May 11-15, 1981, Proceedings. Volume 2. Ann Arbor, MI, Environmental Research Institute of Michigan, 1981, p. 867-882. 25 refs.

The influence of illumination and viewing geometry on the reflectance factor of agricultural targets is investigated. Bare soil, small grains, and broadleaf crops are examined, and the reflectance factor of all three ground cover types shows significant variations with viewing angle. The reflectance factor increases when viewing away from the sun, and decreases when viewing toward the sun, although the effect is not usually symmetric about nadir. Curves showing the typical variation of reflectance factor in the thematic mapper bands as a function of viewing angle about their nadir are presented, and in general, the reflectance is a quasi-linear function of view angle for soil, but shows significant curvature for crops. D.L.G.

A82-27647 # **Digital analysis of spatial and spectral features from airborne MSS of a forested region.** P. M. Teillet, D. G. Goodenough, B. Guindon (Canada Centre for Remote Sensing, Ottawa, Canada), J.-F. Meunier, and K. Dickinson (INTERA Environmental Consultants, Ltd., Ottawa, Canada). In: International Symposium on Remote Sensing of Environment, 15th, Ann Arbor, MI, May 11-15, 1981, Proceedings. Volume 2. Ann Arbor, MI, Environmental Research Institute of Michigan, 1981, p. 883-903. 7 refs.

Forthcoming satellite imaging sensors will have increased spectral resolution and different spectral bandpasses compared to the current Landsat MSS. In order to assess improvements in information extraction anticipated from the use of these sensors, eleven-channel aircraft MSS data were acquired over a rugged forest site, located at Gun Lake near Bralorne, British Columbia. The aircraft MSS data set was rectified to the UTM projection while taking topography into account by means of a digital elevation map. Spatial features were generated using a variety of texture measures. Feature selection and classification were performed to investigate how well forest types can be distinguished and damaged stands can be detected using spatial and/or spectral features. B.J.

A82-27656 # **The potential of remote sensing to monitor soil erosion on cropland.** P. R. Stephens and J. Cihlar (Canada Centre for Remote Sensing, Applications Div., Ottawa, Canada). In: International Symposium on Remote Sensing of Environment, 15th, Ann Arbor, MI, May 11-15, 1981, Proceedings. Volume 2. Ann Arbor, MI, Environmental Research Institute of Michigan, 1981, p. 985-995. 18 refs.

Multitemporal satellite-borne multispectral scanner and thematic mapper digital data are assessed, following an erosion survey, by relating changes in farm crop rotation to changes in erosion rates according to the Universal Soil Loss Equation (USLE). Of the Landsat 2 and simulated Landsat-D and SPOT-1 data studied, SPOT-1 was evaluated to be the most accurate, with 94% classification accuracy for the case of spring imagery. SPOT-1 and Landsat-D summer imagery achieved the high relationship values of 0.97 and 0.95, respectively, between near-IR reflectance/red reflectance and the USLE C factor. While forest and cropland mapping accuracies were on the order of 90-97% for satellite digital data, pasture mapping accuracies were as low as 59-79%. Visual interpretation of medium-scale aerial photography should therefore be more accurate than satellite MSS data in the classification of spring pastures. O.C.

A82-27662 * # **Evaluation of large area crop estimation techniques.** M. L. Amis, R. K. Lennington, M. V. Martin, W. G. McGuire, and S. S. Shen (Lockheed Engineering and Management Services Co., Inc., Houston, TX). In: International Symposium on Remote Sensing of Environment, 15th, Ann Arbor, MI, May 11-15, 1981, Proceedings. Volume 2. Ann Arbor, MI, Environmental Research Institute of Michigan, 1981, p. 1047-1056. 9 refs. Contract No. NAS9-15800.

The performance of the USDAs EDITOR system is evaluated. The system processes Landsat imagery and estimates crop hectarage for large areas based on a regression estimator developed on a sample with known ground truth. It is found that use of multitemporal data over unitemporal significantly improves the hectarage estimates, and a 15% reduction in the r-squared of the regression occurs when independent and jackknifed test sets are used to evaluate the performance of the estimator. When an alternative clustering algorithm, CLASSY, is substituted for the current EDITOR method, estimator performance is improved with reduced need for analyst decisions. It is recommended that the CLASSY clustering algorithm and some form of jackknifing be implemented on EDITOR. D.L.G.

A82-27663 # **Potential utility of thematic mapper data in estimating crop areas.** R. Sigman and M. Craig (U.S. Department of Agriculture, Economics and Statistics Service, Washington, DC). In: International Symposium on Remote Sensing of Environment, 15th, Ann Arbor, MI, May 11-15, 1981, Proceedings. Volume 2. Ann Arbor, MI, Environmental Research Institute of Michigan, 1981, p. 1057-1064. 5 refs.

This paper predicts potential improvements offered by thematic mapper data over multispectral scanner data when utilized in regression estimation of crop areas. A study comparing Landsat data and simulated thematic mapper data is described. Quantitative measures of potential improvements in crop-area estimates of corn, soybeans, and dense woodlands are calculated, and the sensor characteristics causing these improvements are determined. (Author)

A82-27664 # **Automatic and semi-automatic classification of Landsat agricultural crops.** J. D. Tubbs (Arkansas, University, Fayetteville, AR). In: International Symposium on Remote Sensing of Environment, 15th, Ann Arbor, MI, May 11-15, 1981, Proceedings. Volume 2. Ann Arbor, MI, Environmental Research Institute of Michigan, 1981, p. 1065-1074. 10 refs.

One of the mathematical functions proposed by Crisp and Malila

(1980) for the modeling of crop spectral reflectance at different stages of physiological development is incorporated into an automatic classification procedure, or reference profile classifier, based upon the examination of unlabeled Landsat agricultural target development over an entire growing season and its matching with the closest reference profile. Although emphasis is put on incorporating a number of peculiar temporal profile aspects into a single decision rule, the concepts employed and difficulties encountered will arise in the development of any reference profile classification scheme. Attention is also given to the statistical problems affecting classification results, and a graphical procedure is adapted to the temporal-spectral classification problem in order to introduce an ancillary product useful in the definition of training inputs. O.C.

A82-27668 * # **Fanning - A classification algorithm for mixture landscapes applied to Landsat data of Maine forests.** S. G. Ungar (NASA, Goddard Institute for Space Studies, New York, NY) and E. Bryant (NASA, Goddard Institute for Space Studies, New York, NY; Dartmouth College, Hanover, NH). In: International Symposium on Remote Sensing of Environment, 15th, Ann Arbor, MI, May 11-15, 1981, Proceedings. Volume 3. Ann Arbor, MI, Environmental Research Institute of Michigan, 1981, p. 1113-1120. 6 refs.

It is pointed out that typical landscapes include a relatively small number of 'pure' land cover types which combine in various proportions to form a myriad of mixture types. Most Landsat classifications algorithms used today require a separate user specification for each category, including mixture categories. Attention is given to a simpler approach, which would require the user to specify only the 'pure' types. Mixture pixels would be classified on the basis of the proportion of the area covered by each pure type within the pixel. The 'fanning' algorithm quantifies varying proportions of two 'pure' land cover types in selected mixture pixels. This algorithm was applied to 200,000 ha of forest land in Maine, taking into account a comparison with standard inventory information. Results compared well with a discrete categories classification of the same area. G.R.

A82-27673 # **Monitoring forest land cover alteration in Thailand with the analysis of ancillary and digital Landsat data.** K. Nualchawee (Asian Institute of Technology, Bangkok, Thailand), L. D. Miller (Texas A & M University, College Station, TX), C. H. Tom (Science Applications, Inc., Golden, CO), and S. Wacharakitti (Kasetsart University, Bangkok, Thailand). In: International Symposium on Remote Sensing of Environment, 15th, Ann Arbor, MI, May 11-15, 1981, Proceedings. Volume 3. Ann Arbor, MI, Environmental Research Institute of Michigan, 1981, p. 1163-1172. 14 refs.

The present investigation was conducted to overlay ancillary map data onto a Landsat multispectral data base, create and test forest land cover change prediction models, determine forest land cover changes by means of image differencing procedures, and map forest land cover in a study site located in northern Thailand. The methods used in the investigation are discussed, taking into account aspects of map sampling and data plane compilation, a forest land cover projection, the determination of recent land cover dynamics, the Markov trend model of land cover, an initial spatial modeling test, and revised spatial models. G.R.

A82-27676 # **Crop area estimates using ground-gathered and Landsat data - A multitemporal approach.** J. W. Mergerson (U.S. Department of Agriculture, Statistical Research Div., Washington, DC). In: International Symposium on Remote Sensing of Environment, 15th, Ann Arbor, MI, May 11-15, 1981, Proceedings. Volume 3. Ann Arbor, MI, Environmental Research Institute of Michigan, 1981, p. 1211-1218. 5 refs.

The paper describes a comparative study in which a unitemporal approach for obtaining crop area estimates using ground-gathered and Landsat data was compared to a multitemporal approach. Four channel data were used for the unitemporal approach. Eight channel data consisting of four channels from each of two dates were used for the multitemporal approach. The multitemporal data set and the two corresponding unitemporal data sets were analyzed using various procedures. Results indicate that the use of multitemporal data can significantly improve the precision of crop area estimates for corn, soybeans and winter wheat, obtained using the unitemporal approach. (Author)

A82-27678 # **A technique for automatic labeling of Landsat agricultural scene elements by analysis of temporal-spectral patterns.** E. Crist and W. Malila (Michigan, Environmental Research Institute, Ann Arbor, MI). In: International Symposium on Remote Sensing of Environment, 15th, Ann Arbor, MI, May 11-15, 1981, Proceedings. Volume 3. Ann Arbor, MI, Environmental Research Institute of Michigan, 1981, p. 1227-1236. 11 refs.

A labeling technique is described which seeks to associate a sampling entity with a particular crop or crop group based on similarity of growing season and temporal-spectral patterns of development. Human analysts provide contextual information, after which labeling decisions are made automatically. Results of a test of the technique on a large, multi-year data set are reported. Grain labeling accuracies are similar to those achieved by human analysis techniques, while non-grain accuracies are lower. Recommendations for improvements and implications of the test results are discussed. (Author)

A82-27679 # **An invertible coniferous forest canopy reflectance model.** A. H. Strahler and L. Xiaowen (California, University, Santa Barbara, CA). In: International Symposium on Remote Sensing of Environment, 15th, Ann Arbor, MI, May 11-15, 1981, Proceedings. Volume 3. Ann Arbor, MI, Environmental Research Institute of Michigan, 1981, p. 1237-1244. 14 refs.

A mathematical model of the reflectance of a discontinuous forest canopy allows the direct calculation of the height and spacing of trees from remotely sensed reflectance values. The model is essentially geometric in character, treating trees as randomly positioned green cones on a contrasting background, and is driven by estimates of the proportion of each pixel in green canopy, shadow, and understory. The model is invertible, so that parameters of tree height and spacing can be directly inferred from spectral reflectance ratios. A simple version of the model assumes that tree heights are lognormally distributed and that tree spacing is distributed as a Poisson function. A more advanced version assumes an empirically calibrated height distribution and Neyman Type A spacing, and also corrects for the topographic orientation of the pixel. A preliminary test estimates height and density within about ten percent, as compared to values determined by photointerpretation. (Author)

A82-27680 # **An experiment in probabilistic relaxation for terrain cover classification of Kuwait from Landsat imagery.** R. Harris (Durham, University, Durham, England). In: International Symposium on Remote Sensing of Environment, 15th, Ann Arbor, MI, May 11-15, 1981, Proceedings. Volume 3. Ann Arbor, MI, Environmental Research Institute of Michigan, 1981, p. 1245-1252. 17 refs.

The stochastic probabilistic relaxation model developed by Rosenfeld et al. (1976) and others is described, and its relation to context classification discussed. Compatibility coefficients as correlation and as mutual information are given. An example of relaxation operations on a terrain cover classification of an area near Al Jahra, Kuwait is discussed, with poor results after the iterations to update the probabilities. (Author)

A82-27682 # **An autodigitizing procedure for ground-data labelling of Landsat pixels.** M. Ozga and R. Sigman (U.S. Department of Agriculture, Economics and Statistics Service, Washington, DC). In: International Symposium on Remote Sensing of Environment, 15th, Ann Arbor, MI, May 11-15, 1981, Proceedings. Volume 3. Ann Arbor, MI, Environmental Research Institute of Michigan, 1981, p. 1265-1273.

This paper describes an automatic digitizing procedure for use in ground-data labelling of Landsat pixels. The described procedure is based on video scanning of line tracings from aerial photographs containing identified ground-truth areas. The key feature of this procedure is that in the data processing of the scan data, no line-following algorithms are used. Instead the procedure directly maps scan pixel labels into Landsat pixel labels. An evaluation of the procedure on test cases, plus economic comparisons with alternative manual digitization methods, are presented. (Author)

A82-27687 # **Digital processing of tropical forest habitat in Bangladesh and the development of a low cost processing facility at the National Zoo, Smithsonian Institution.** K. M. Green (Smithsonian Institution; Howard University, Washington, DC). In: International Symposium on Remote Sensing of Environment, 15th, Ann Arbor, MI, May 11-15, 1981, Proceedings. Volume 3. Ann Arbor, MI, Environmental Research Institute of Michigan, 1981, p. 1315-1325. 12 refs.

A82-27691 # **Environmental studies by multispectral scanner under large-scale civil engineering construction.** S. Takeuchi (Remote Sensing Technology Center of Japan, Tokyo, Japan), A. Rikimaru (Pacific Aero Survey Co., Ltd., Tokyo, Japan), and T. Oshima (Hosei University, Tokyo, Japan). In: International Symposium on Remote Sensing of Environment, 15th, Ann Arbor, MI, May 11-15, 1981, Proceedings. Volume 3. Ann Arbor, MI, Environmental Research Institute of Michigan, 1981, p. 1363-1373.

A large-scale tunnel construction project has produced significant environmental effects related to changes in the distribution of underground water. An investigation was conducted with the objective to study these environmental effects. As forest trees occupy more than 70% of the total area covered with vegetation at the test site, the investigation has been mainly based on a consideration of the vitality of the forest trees. The investigation makes use of an airborne multispectral scanning (MSS) procedure. Attention has been given to the development of appropriate data analysis tools, a basic experiment on the spectral characteristics of trees, aspects of MSS data correction and calibration, and an evaluation of the year-to-year change of tree vitality. G.R.

A82-27697 # **Landsat MSS applied to rangeland management in Western Canada.** R. J. Brown, K. P. B. Thomson, F. J. Ahern, K. Staenz, J. Cihlar (Canada Centre for Remote Sensing, Ottawa, Canada), S. G. Klumph (Alberta Energy and Natural Resources, Calgary, Canada), and C. M. Pearce (Calgary, University, Calgary, Alberta, Canada). In: International Symposium on Remote Sensing of Environment, 15th, Ann Arbor, MI, May 11-15, 1981, Proceedings. Volume 3. Ann Arbor, MI, Environmental Research Institute of Michigan, 1981, p. 1435-1447. 23 refs. Research supported by the Alberta Environment.

Public lands in Alberta are administered by either the Alberta Forest Service or the Public Lands Division. Officers of these two administrative agencies regularly inspect the grazing lands to ensure that they are being properly managed. With the launch of Landsat-1 in 1972, came the expectation of developing techniques, which could be used to monitor, rapidly and inexpensively, the vast expanses of rangeland. In 1980, a project was initiated to determine the extent to which Landsat data could be used in an operational rangeland monitoring program. The project was divided into two segments, including a demonstration component and a research component. A description is presented of a part of the demonstration component, taking into account operational questions and a detailed analysis of Landsat imagery acquired for one of the test areas. G.R.

A82-27699 # **Development of a Canadian thermal infrared forest fire mapping operational program.** H. J. W. Shaw (Intertech Remote Sensing, Ltd., Calgary, Alberta, Canada). In: International Symposium on Remote Sensing of Environment, 15th, Ann Arbor, MI, May 11-15, 1981, Proceedings. Volume 3. Ann Arbor, MI, Environmental Research Institute of Michigan, 1981, p. 1465-1473. 11 refs.

Real-time reconnaissance information of active forest fires and the accurate location of holdover fires during mop-up operations have been identified as major requirements for successful forest fire management. Intertech Remote Sensing Limited has developed an operational thermal infrared forest fire mapping program to meet these requirements in a reliable and effective manner. This program has included the acquisition and processing of thermal data over active and smoulder fires, the interpretation, analysis and plotting to scale of all such data and the delivery of a final thermal-map product to the fire base or centre in near real-time. (Author)

A82-27700 # **Seasat imagery for detection of coastal Wetlands.** J. G. Lyon (Ohio State University, Columbus, OH) and J. F. McCarthy (Vermont, University, Burlington, VT). In: International Symposium on Remote Sensing of Environment, 15th, Ann Arbor, MI, May 11-15, 1981, Proceedings. Volume 3. Ann Arbor, MI, Environmental Research Institute of Michigan, 1981, p. 1475-1485. 11 refs. Grant No. NOAA-04-M01-134.

The research examined use of satellite radar imagery for locating wetlands in Michigan and Oregon. The information supplying capabilities of Seasat were evaluated through field work, review of literature and comparison with other sources of data. Application of radar imagery for management of wetlands is addressed. (Author)

A82-28131 † **Application of space remote sensing data in forestry (Primenenie kosmicheskoi informatsii v interesakh lesnogo khoziaistva).** P. I. Moroz. *(Vsesoiuznaia Konferentsiia po Problemam Issledovaniia Prirodnykh Resursov Zemli i Mirovogo Okeana, Aviatsionno-Kosmicheskimi Sredstvami, Moscow, USSR, Nov. 1980.) Geodeziia i Aerofotos'emka,* no. 1, 1982, p. 26-30. In Russian.

A82-28153 **Influence of solar illumination angle on soybean canopy reflectance.** J. C. Kollenkark, V. C. Vanderbilt, C. S. T. Daughtry, and M. E. Bauer (Purdue University, West Lafayette, IN). *Applied Optics,* vol. 21, Apr. 1, 1982, p. 1179-1184. 17 refs.

Remotely sensed spectral measurements taken over croplands are influenced not only by the cover type and condition, cultural practices, and environmental factors, but also by the solar illumination angle in relation to the scene. The reflectance of soybean canopies of differing row directions were measured at 15-min intervals during three clear days with a Landsat band radiometer to determine the interaction of the solar illumination angle and row azimuth angle on the measured reflectance factor of soybean canopies. Diurnal reflectance changes of as much as 140%, which were related to the fraction of shadow, were observed in the red wavelength region. As soil cover approached 100% the diurnal changes diminished. A function that describes the solar illumination angle with respect to the row azimuth explained most of the diurnal variation in the measured reflectance. Variation in near-infrared reflectance was much less and did not appear to be as strongly related to sun-row angle interactions as the visible region. (Author)

N82-16447*# Kansas Univ., Lawrence. Space Technology Center

THE APPLICATION OF REMOTE SENSING TO RESOURCE MANAGEMENT AND ENVIRONMENTAL QUALITY PROGRAMS IN KANSAS Annual Report, 1 Apr. 1980 - 31 Mar. 1981

B. G. Barr and E. A. Martinko, Principal Investigators Jul. 1981 164 p ERTS
(Grant NGL-17-004-024)
(E82-10029, NASA-CR-164756) Avail: NTIS HC A08/MF A01 CSCL 05A

Cooperative demonstration projects involved three principal areas of effort: agricultural and rural development; wildlife habitat and environmental quality; urban and regional planning. Several projects are reported including: an analysis of rangeland conditions in the Cimarron National Grasslands; an inventory of land use and land cover, particularly concerning forested lands, in two Indian reservations in northeast Kansas; an identification of homogeneous revenue regions in the state; an applied agricultural research and development project for Farmland Industries, Inc.; and an analysis of crop phenology and crop patterns in the high plains for identifying optimal dates of LANDSAT data for identifying irrigated lands. Several long-term projects include: weed pest surveys, irrigated lands data compilation from LANDSAT; and the development of an inventory of abandoned mined lands and potential hazard assessment in Kansas. T.M.

N82-16448*# Environmental Research Inst. of Michigan, Ann Arbor. Infrared and Optics Div.

DOCUMENTATION OF COMPUTER PROCEDURES FOR LABELING SPRING GRAINS AND DISCRIMINATING BETWEEN SPRING WHEAT AND BARLEY USING LANDSAT DATA

Robert Horvath, Principal Investigator, J. A. Finkler, and E. P. Crist Jul. 1981 81 p Sponsored by NASA, USDA, Dept. of Commerce, Dept. of the Interior, and Agency for International Development ERTS
(Contract NAS9-15476; Proj. AgRISTARS)
(E82-10030; NASA-CR-161081; SR-EI-04131;

ERIM-152400-5-T) Avail NTIS HC A05/MF A01 CSCL 02C

The computer software necessary to perform two research labeling procedures is described and documented The first labeling technique identifies spring small grain fields based on similarity of growing season and temporal spectral patterns of development in LANDSAT data The second technique further labels these fields as either wheat, barley or unknown spring grain, based on their spectral position in Tasseled Cap Greenness-Brightness space for a given day around the dough stage of wheat The subroutines which carry out the steps of the procedure are coded in PREFOR, a preprocessed FORTRAN The subroutines were designed to fit into the U.S Corn/Soybeam baseline procedure software developed for use in the AgRISTARS Program. Documentation of the subroutines are provided in an appendix.

Author

N82-16455# Colorado State Univ., Fort Collins Dept. of Forest and Wood Sciences.

THERMAL VEGETATION CANOPY MODEL STUDIES Final Report, 1 Oct. 1978 - 1 Feb. 1980

James A. Smith, K. Jon Ranson, Duong Nguyen, and Lewis E. Link (Army Engineer Waterways Experiment Station, Vicksburg, Miss.) Aug 1981 221 p refs
(Contract DACW39-77-C-0073; DA Proj 4A7-62730-AT-42)
(AD-A106422; WES/TR/EL-81-6) Avail NTIS HC A10/MF A01 CSCL 17/5

This is the final report in a series. Overall objectives of this project are concerned with developing comprehensive optical and thermal signature data bases, the development and evaluation of optical and thermal canopy radiation models, and the interpretation of these measurements Previous technical reports in this series have described optical and thermal measurements obtained over a coniferous site (Pinus contorta) in Leadville, Colorado This earlier data set served as a test bed for the development and initial evaluation of first, individual components, that is, needle and leaves, thermal models, and then a composite canopy terrain model

GRA

N82-17746# Instituto de Pesquisas Espaciais, Sao Jose dos Campos (Brazil).

THE SEVERITY OF THE BRAZILIAN FREEZE OF JULY 1981, AS MONITORED BY SATELLITE

Michael Allan Fortune Sep 1981 20 p refs
(INPE-2231-RPE/399) Avail: NTIS HC A02/MF A01

The location and intensity of freezing temperature during very cold nights ('geadas') in Brazil is discussed using satellite infrared television image data The data are needed to lay the groundwork for a short-term freeze forecast model, which is to be developed before winter 1982. A cold snap occurred on 20-22 July 1981, which destroyed a large part of the future coffee, sugar and other harvest is documented. The photographs of enhanced satellite images document the widespread occurrence of subfreezing temperature in the states of Parana, Sao Paulo, Mato Grosso do Sul, and Minas Gerais These sub-tropical areas are located north of the region which usually experiences frost, and thus damage to agriculture was particularly extensive. The synoptic factor responsible for the cold was a wandering cold-core cut-off low in the upper air, and not a strong cold front The data contained in the photographs, when combined with the meteorological observations also presented will be valuable in developing a prediction model for the occurrence of 'geadas'.

R.J.F.

N82-19607*# Lockheed Engineering and Management Services Co., Inc., Houston, Tex

WHEAT STRESS INDICATOR MODEL, CROP CONDITION ASSESSMENT DIVISION (CCAD) DATA BASE INTERFACE DRIVER, USER'S MANUAL

R F Hansen, Principal Investigator Feb 1981 15 p Sponsored by NASA, USDA, Dept of Commerce, Dept of the Interior, and Agency for International Development ERTS
(Contract NAS9-15800; Proj AgRISTARS)
(E82-10031; NASA-CR-161032; EW-L1-00711;
LEMSCO-16034; JSC-17114) Avail NTIS HC A02/MF A01 CSCL 02C

The use of the wheat stress indicator model CCAD data base interface driver is described The purpose of this system is to interface the wheat stress indicator model with the CCAD operational data base The interface driver routine decides what meteorological stations should be processed and calls the proper subroutines to process the stations

Author

N82-19608*# Lockheed Engineering and Management Services Co., Inc., Houston, Tex.

AGRISTARS: INTERIM CATALOG GROUND DATA SUMMARY, DATA ACQUISITION YEAR 1979

H. M. Doyle and V. L. Cook, Principal Investigators Feb. 1981 32 p Sponsored by NASA, USDA, Dept. of Commerce, Dept. of the Interior, and Agency for International Development ERTS
(Contract NAS9-15800; Proj. Agristars)
(E82-10032; NASA-CR 161033; MU-L1-04055;
LEMSCO-16207; JSC-17119) Avail: NTIS HC A03/MF A01 CSCL 02C

To honor numerous requests for information about data holdings, and to facilitate the requirements specifications process, a series of interim catalogs are being developed. The 1979 data acquisition year is covered in this volume with subsequent years to follow under different covers. This catalog lists by state those sample segment numbers for which aircraft data has been acquired and/or field inventory products produced.

A.R.H.

N82-19610*# Lockheed Engineering and Management Services Co., Inc., Houston, Tex.

RECOMMENDED DATA SETS, CORN SEGMENTS AND SPRING WHEAT SEGMENTS, FOR USE IN PROGRAM DEVELOPMENT

Willa W. Austin, Principal Investigator Apr. 1981 27 p Sponsored by NASA, USDA, Dept. of Commerce, Dept. of the Interior, and Agency for International Development ERTS
(Contract NAS9-15800; Proj. AgRISTARS)
(E82-10034; NASA-CR-161034; SR-L1-0409;
LEMSCO-15708; JSC-17137) Avail: NTIS HC A03/MF A01 CSCL 02C

The sets of Large Area Crop Inventory Experiment sites, crop year 1978, which are recommended for use in the development and evaluation of classification techniques based on LANDSAT spectral data are presented. For each site, the following exists: (1) accuracy assessment digitized ground truth; (2) a minimum of 5 percent of the scene ground truth identified as corn or spring wheat; and (3) at least four acquisitions of acceptable data quality during the growing season of the crop of interest The recommended data sets consist of 41 corn/soybean sites and 17 spring wheat sites

Author

N82-19614*# National Aeronautics and Space Administration Lyndon B. Johnson Space Center, Houston, Tex.

AGRISTARS: FOREIGN COMMODITY PRODUCTION FORECASTING. MINUTES OF THE ANNUAL FORMAL PROJECT MANAGER'S REVIEW, INCLUDING PRELIMINARY TECHNICAL REVIEW REPORTS OF FY80 EXPERIMENTS

24 Sep 1980 191 p Sponsored by NASA, USDA, Dept. of Commerce, Dept of the Interior, and Agency for International Development
(Proj. AgRISTARS)
(E82-10039; NASA-TM-84050; FC-J0-00502; JSC-16823) Avail NTIS HC A09/MF A01 CSCL 02C

The U.S./Canada wheat/barley exploratory experiment is discussed with emphasis on labeling, machine processing using P1A, and the crop calendar. Classification and the simulated aggregation test used in the U.S. corn/soybean exploratory experiment are also considered. Topics covered regarding the foreign commodity production forecasting project include: (1) the acquisition, handling, and processing of both U.S. and foreign agricultural data, as well as meteorological data. The accuracy assessment methodology, multicrop sampling and aggregation technology development, frame development, the yield project interface, and classification for area estimation are also examined.

A.R.H.

N82-19615*# Florida Univ., Gainesville. Inst. of Food and Agricultural Sciences.

USE OF THERMAL INERTIA DETERMINED BY HCMM TO PREDICT NOCTURNAL COLD PRONE AREAS IN FLORIDA Quarterly Report, 16 Mar. - 15 Jun. 1981

L. H. Allen, Jr., Principal Investigator, Ellen Chen, J. D. Martsolf, and P. H. Jones 15 Jun 1981 36 p refs Original contains color imagery. Original imagery may be purchased from NASA Goddard Space Flight Center, (Code 601), Greenbelt, Md 20771. Domestic users send orders to 'Attn: National Space Science Data Center', non-domestic users send orders to 'Attn: World

Data Center A for Rockets and Satellites'. HCMM
(Contract NAS5-26453)
(E82-10040; NASA-CR-164917; QR-1) Avail: NTIS HC A03/MF A01 CSCL 04B

The HCMM transparency scenes for the available winter of 1978-1979 were evaluated; scenes were identified on processed magnetic tapes; other remote sensing information was identified; and a soil heat flux model with variable-depth thermal profile was developed. The Image 100 system was used to compare HCMM and GOES transparent images of surface thermal patterns. Excellent correspondence of patterns was found, with HCMM giving the greater resolution. One image shows details of thermal patterns in Florida that are attributable to difference in near surface water contents. The wide range of surface temperatures attributable to surface thermal inertia that exist in the relatively flat Florida topography is demonstrated. A.R.H.

N82-19628*# Department of Agriculture, Houston, Tex.
AGRISTARS: SOIL MOISTURE/EARLY WARNING AND CROP CONDITION ASSESSMENT. INTERFACE CONTROL DOCUMENT
Nov. 1980 13 p Sponsored by NASA, USDA, Dept. of Commerce, Dept. of the Interior, and Agency for International Development ERTS
(Proj. AgRISTARS)
(E82-10053; NASA-CR-161028; MU-JO-0101; JSC-16842) Avail: NTIS HC A02/MF A01 CSCL 02C

The interactions and support functions required between the early warning/crop condition assessment (EW/CCA) project and soil moisture (SM) project are defined. The EW Project aims to develop, test and evaluate techniques and procedures for adapting remote sensing technology to provide early warning of events and the timely assessment of those factors which affect the quality and quantity of production of economically important crops. Those techniques to augment and reinforce the current assessment activities are to be developed to improve the definition of the relationship between the plant(s) and its environment. This assessment and evaluation will certainly include the need for soil moisture measurement and estimation. The SM Project aims to develop, test, and evaluate techniques and procedures to measure or predict soil moisture in the root zone using both contact and remote sensors. A.R.H.

N82-13629*# Department of Agriculture, Houston, Tex.
AGRISTARS: YIELD MODEL DEVELOPMENT/SOIL MOISTURE. INTERFACE CONTROL DOCUMENT
Nov. 1980 12 p refs Sponsored by NASA, USDA, Dept. of Commerce, Dept. of the Interior, and Agency for International Development ERTS
(Proj. AgRISTARS)
(E82-10054, NASA-CR-161029; MU-JO-0100; JSC-16841) Avail: NTIS HC A02/MF A01 CSCL 02C

The interactions and support functions required between the crop Yield Model Development (YMD) Project and Soil Moisture (SM) Project are defined. The requirements for YMD support of SM and vice-versa are outlined. Specific tasks in support of these interfaces are defined for development of support functions. J.D.H.

N82-19630*# Lockheed Engineering and Management Services Co., Inc., Houston, Tex.
AGRISTARS: EARLY WARNING AND CROP CONDITION ASSESSMENT. PATCH IMAGE PROCESSOR USER'S MANUAL
M. J. Nieves, Principal Investigator Sep. 1980 12 p Sponsored by NASA, USDA, Dept. of Commerce, Dept. of the Interior, and Agency for International Development ERTS
(Contract NAS9-15800; Proj. AgRISTARS)
(E82-10055; NASA-CR-161038; EW-LO-00707;
LEMSCO-15692; JSC-16833) Avail: NTIS HC A02/MF A01 CSCL 02C

The Patch Image Processor extracts patches in various size (32x32, 64x64, 128x128, and 256x256 pixels) from full-frame Landsat imagery data. With the patches that are extracted, a patch image mosaic is created in the image processing system, IMDACS, format. Author

N82-19631*# Lockheed Engineering and Management Services Co., Inc., Houston, Tex.
AGRISTARS: FOREIGN COMMODITY PRODUCTION FORECASTING. CORN/SOYBEAN DECISION LOGIC DEVELOPMENT AND TESTING
C. L. Dailey and K. M. Abotteen, Principal Investigators Oct. 1980 81 p refs Sponsored by NASA, USDA, Dept. of Commerce, Dept. of the Interior, and Agency for International Development
(Contract NAS9-15800; Proj. AgRISTARS)
(E82-10056; NASA-CR-161024; FC-LO-00480;
LEMSCO-14811; JSC-16380) Avail: NTIS HC A05/MF A01 CSCL 02C

The development and testing of an analysis procedure which was developed to improve the consistency and objectively of crop identification using LANDSAT data is described. The procedure was developed to identify corn and soybean crops in the U.S. corn belt region. The procedure consists of a series of decision points arranged in a tree-like structure, the branches of which lead an analyst to crop labels. The specific decision logic is designed to maximize the objectively of the identification process and to promote the possibility of future automation. Significant results are summarized. J.D.H.

N82-19632*# Lockheed Engineering and Management Services Co., Inc., Houston, Tex.
AGRICULTURAL SOIL MOISTURE EXPERIMENT, COLBY, KANSAS 1978: MEASURED AND PREDICTED HYDROLOGICAL PROPERTIES OF THE SOIL
L. M. Arya, Principal Investigator Oct. 1980 46 p refs Sponsored by NASA, USDA, Dept. of Commerce, Dept. of the Interior, and Agency for International Development ERTS
(Contract NAS9-15800; Proj. AgRISTARS)
(E82-10057; NASA-CR-161025; SM-LO-00463;
LEMSCO-14307; JSC-16366) Avail: NTIS HC A03/MF A01 CSCL 02C

Predictive procedures for developing soil hydrologic properties (i.e., relationships of soil water pressure and hydraulic conductivity to soil water content) are presented. Three models of the soil water pressure-water content relationship and one model of the hydraulic conductivity-water content relationship are discussed. Input requirements for the models are indicated, and computational procedures are outlined. Computed hydrologic properties for Keith silt loam, a soil typer near Colby, Kansas, on which the 1978 Agricultural Soil Moisture Experiment was conducted, are presented. A comparison of computed results with experimental data in the dry range shows that analytical models utilizing a few basic hydrophysical parameters can produce satisfactory data for large-scale applications. Author

N82-19633*# Department of Agriculture, Houston, Tex. Soil Conservation Service.
TAXONOMIC CLASSIFICATION OF WORLD MAP UNITS IN CROP PRODUCING AREAS OF ARGENTINA AND BRAZIL WITH REPRESENTATIVE US SOIL SERIES AND MAJOR LAND RESOURCE AREAS IN WHICH THEY OCCUR
Horace F. Huckle, Principal Investigator Oct. 1980 42 p refs Sponsored by NASA, USDA, Dept. of Commerce, Dept. of the Interior, and Agency for International Development ERTS
(Proj. AgRISTARS)
(E82-10058; NASA-CR-161021; SR-UO-00497; JSC-16824) Avail: NTIS HC A03/MF A01 CSCL 02C

The most probable current U.S. taxonomic classification of the soils estimated to dominate world soil map units (WSM)) in selected crop producing states of Argentina and Brazil are presented. Representative U.S. soil series the units are given. The map units occurring in each state are listed with areal extent and major U.S. land resource areas in which similar soils most probably occur. Soil series sampled in LARS Technical Report 111579 and major land resource areas in which they occur with corresponding similar WSM units at the taxonomic subgroup levels are given. Author

N82-19634*# Lockheed Engineering and Management Services Co., Inc., Houston, Tex.
PRELIMINARY EVALUATION OF SPECTRAL, NORMAL AND METEOROLOGICAL CROP STAGE ESTIMATION APPROACHES
R. B. Cate, J. A. Artley, P. C. Doraiswamy, T. Hodges, M. C. Kinsler, D. E. Phinney, and M. L. Sestak, Principal Investigators Oct. 1980 74 p refs Sponsored by NASA, USDA, Dept. of Commerce, Dept. of the Interior, and Agency for International Development ERTS
(Contract NAS9-15800; Proj. AgRISTARS)

(E82-10059: NASA-CR-161023: SR-LO-04002:
LEMSCO-14640: JSC-16830) Avail: NTIS HC A04/MF A01
CSCL 02C

Several of the projects in the AgRISTARS program require crop phenology information, including classification, acreage and yield estimation, and detection of episodal events. This study evaluates several crop calendar estimation techniques for their potential use in the program. The techniques, although generic in approach, were developed and tested on spring wheat data collected in 1978. There are three basic approaches to crop stage estimation: historical averages for an area (normal crop calendars), agrometeorological modeling of known crop-weather relationships agrometeorological (agromet) crop calendars, and interpretation of spectral signatures (spectral crop calendars). In all, 10 combinations of planting and biostage estimation models were evaluated. Dates of stage occurrence are estimated with biases between -4 and +4 days while root mean square errors range from 10 to 15 days. Results are inconclusive as to the superiority of any of the models and further evaluation of the models with the 1979 data set is recommended. Author

N82-19635*# Environmental Research Inst. of Michigan, Ann Arbor. Infrared and Optics Div.
NOTES FOR BRAZIL SAMPLING FRAME EVALUATION TRIP Technical Report, 1 - 19 Feb. 1981
Robert Horvath, Principal Investigator and David R. Hicks, comp. Aug. 1981 32 p ref Sponsored by NASA, USDA, Dept. of Commerce, Dept. of the Interior and Agency for International Development ERTS
(Contract NAS9-15476; Proj. AgRISTARS)
(E82-10060: NASA-CR-167420: SR-E1-04138:
ERIM-152400-7-T) Avail: NTIS HC A03/MF A01 CSCL 02C

Field notes describing a trip conducted in Brazil are presented. This trip was conducted for the purpose of evaluating a sample frame developed using LANDSAT full frame images by the USDA Economic and Statistics Service for the eventual purpose of cropland production estimation with LANDSAT by the Foreign Commodity Production Forecasting Project of the AgRISTARS program. Six areas were analyzed on the basis of land use, crop land in corn and soybean, field size and soil type. The analysis indicated generally successful use of LANDSAT images for purposes of remote large area land use stratification. Author

N82-19636*# Lockheed Engineering and Management Services Co., Inc., Houston, Tex.
SEGMENT-LEVEL EVALUATION OF THE SIMULATED AGGREGATION TEST: US CORN AND SOYBEAN EXPLORATORY EXPERIMENT
S. A. Davidson, Principal Investigator Oct. 1980 26 p refs Sponsored by NASA, USDA, Dept. of Commerce of the Interior, and Agency for International Development ERTS
(Contract NAS9-15800; Proj. AgRISTARS)
(E82-10061: NASA-CR-161022: FC-LO-00493:
LEMSCO-15116: JSC-16820) Avail: NTIS HC A03/MF A01
CSCL 02C

An evaluation of the corn and soybean proportion-estimation accuracy and dot labeling accuracy of the Simulated Aggregation Test, U.S. Corn and Soybean Exploratory Experiment, is presented. These results are in turn compared with the corn and soybean proportion-estimation accuracy and dot labeling accuracy of the Classification Procedures Verification Test. Author

N82-19639# Instituto de Pesquisas Espaciais, Sao Jose dos Campos (Brazil).
UTILIZATION OF AEROCHROME 2443 FILM FOR IDENTIFICATION AND ESTIMATING WHEAT GROWING AREAS
Francisco Jose Mendonca, Angela Maria DeLima, Antonio Teraldi Tardin, Armando P. Dossantos, Dall Arthur Cottrell, David C. L. Lee, Fernando C. S. Maia, Liane A. M. Lucht, Mauricio A. Moreira, and Rene Antonio Novaes Aug. 1981 10 p refs In PORTUGUESE; ENGLISH summary Submitted for publication
(INPE-2197-PRE/C06) Avail: NTIS HC A02/MF A01

To identify and estimate wheat area using remote sensing techniques, aerial photographs were taken using KODAK Aerochrome 2443, at Soledade, Cruz Alta, and Santa Angelo in the state of Rio Grande do Sul, the photographs were interpreted manually and maps indicating areas for wheat, barley, idle land, flowed land, pasture land, nature vegetation, reforestation and others were prepared for each segment. A.R.H.

N82-19640# Instituto de Pesquisas Espaciais, Sao Jose dos Campos (Brazil).
METHOD OF INTERPRETATION OF REMOTE SENSING DATA AND APPLICATIONS TO VEGETATION
Joao Roberto dosSantos, Pedro Hernandez Filho, and Yosio Edemir Shimabukuro Aug. 1981 54 p refs In PORTUGUESE; ENGLISH summary
(INPE-2215-MD/010) Avail: NTIS HC A03/MF A01

The material provided for remote sensing training course on vegetation is presented. Studies using remote sensing products for characterization and mapping, inventory or management problems in forestry were reviewed in the literature. The methodology of visual or automatic interpretation of those most commonly used LANDSAT data products in forestry studies is described. Case studies in natural or reforested vegetation, which were carried out in INPE, are included with the basic information. A.R.H.

N82-19715# Tennessee Valley Authority, Norris. Office of Natural Resources.
REMOTE SENSING OF SULFUR DIOXIDE EFFECTS ON VEGETATION. VOLUME 1: SUMMARY Final Report, 1976 - 1980
C. Daniel Sapp Washington EPA Jul. 1981 33 p 2 Vol.
(PB82-115122; TVA/ONR/ARP-81/5-Vol-1;
EPA-600/7-81-113) Avail: NTIS HC A03/MF A01 CSCL 06F

Three techniques for detecting and mapping sulfur dioxide (SO2) effects on the foliage of sensitive crops and trees near large, coal fired power plants were tested. These techniques used are spectroradiometry, photometric analysis of aerial photographs, and computer analysis of airborne multispectral scanner data. Airborne multispectral scanner data covering affected soybean fields were analyzed using three computer assisted procedures. GRA

N82-19716# Tennessee Valley Authority, Norris. Office of Natural Resources.
REMOTE SENSING OF SULFUR DIOXIDE EFFECTS ON VEGETATION. VOLUME 2: DATA Final Report, 1976 - 1980
C. Daniel Sapp Washington EPA Jul. 1981 284 p refs 2 Vol.
(PB82-115130; TVA/ONR/ARP-81/6-Vol-2;
EPA-600/7-81-114) Avail: NTIS HC A13/MF A01 CSCL 06F

Techniques for detecting and mapping sulfur dioxide (SO2) effects on foliage of sensitive crops and trees near large coal fired power plants were calculated. The techniques are: laboratory spectroradiometry field spectroradiometry; interpretation and analysis of aerial photographs; analysis of multispectral scanner data. GRA

N82-20590*# Purdue Univ., Lafayette, Ind. Lab. for Applications of Remote Sensing.
EVALUATION OF A SEGMENT-BASED LANDSAT FULL-FRAME APPROACH TO CORP AREA ESTIMATION
M. E. Bauer, Principal Investigator, M. M. Hixson, and S. M. Davis 23 Jun. 1981 22 p refs Sponsored by NASA, USDA, Dept. of Commerce, Dept. of the Interior, and Agency for International Development ERTS
(Contract NAS9-15466; Proj. AgRISTARS)
(E82-10067: NASA-CR-167400: NAS 1.26:167400:
FC-P1-04121: LARS-062381) Avail: NTIS HC A02/MF A01
CSCL 02C

As the registration of LANDSAT full frames enters the realm of current technology, sampling methods should be examined which utilize other than the segment data used for LACIE. The effect of separating the functions of sampling for training and sampling for area estimation. The frame selected for analysis was acquired over north central Iowa on August 9, 1978. A stratification of he full-frame was defined. Training data came from segments within the frame. Two classification and estimation procedures were compared: statistics developed on one segment were used to classify that segment, and pooled statistics from the segments were used to classify a systematic sample of pixels. Comparisons to USDA/ESCS estimates illustrate that the full-frame sampling approach can provide accurate and precise area estimates. A.R.H.

N82-20591*# Purdue Univ., Lafayette, Ind. Lab. for Applications of Remote Sensing.

EFFECTS OF NITROGEN NUTRITION ON THE GROWTH, YIELD AND REFLECTANCE CHARACTERISTICS OF CORN CANOPIES

M. E. Bauer, Principal Investigator, G. Walburg, and C. S. T. Daughtry May 1981 22 p refs Sponsored by NASA, USDA, Dept. of Commerce, Dept. of the Interior, and Agency for International Development ERTS
(Contract NAS9-15466; Proj. AgRISTARS)
(E82-10068; NASA-CR-165090; NAS 1.26:165090;
SR-P1-04044; LARS-030381) Avail: NTIS HC A02/MF A01
CSCL 02C

Spectral and agronomic measurements were collected from corn (Zea mays L.) canopies under four nitrogen treatment levels (0, 67, 134, and 202 kg/ha) on 11 dates during 1978 and 12 dates during 1979. Data were analyzed to determine the relationship between the spectral responses of canopies and their argonomic characteristics as well as the spectral separability of the four treatments. Red reflectance was increased, while the near infrared reflectance was decreased for canopies under nitrogen deprivation. Spectral differences between treatments were seen throughout each growing season. The near infrared/red reflectance ratio increased spectral treatment differences over those shown by single band reflectance measures. Of the spectral variables examined, the near infrared/red reflectance ratio most effectively separated the treatments. Differences in spectral response between treatments were attributed to varying soil cover, leaf area index, and leaf pigmentation values, all of which changed with N treatment. A.R.H.

N82-20594*# Instituto de Pesquisas Espaciais, Sao Jose dos Campos (Brazil).

SURVEY OF THE CANE-GROWING AREA OF THE STATE OF SAO PAULO USING LANDSAT DATA, SAFRA YEAR 1979/80, VOLUME 2 [LEVANTAMENTO JA AREA CANAVIEIRA DO ESTADO DE SAO PAULO, UTILIZANDO DADOS DO LANDSAT AND SAFRA 1979/80, VOLUME 2]

Nelson deJesusParada, Principal Investigator, Francisco Jose Mendonca, David Chung Liang Lee, Antonio Tebaldi Tardin, Yosio Edemir Shimabukuro, Sherry Chou Chen, Liane Antunes Maciel Lucht, Mauricio Alves Moreira, Angela Maria deLima, and Fernando Celso Soares Maia Mar. 1981 63 p In PORTUGUESE ERTS
(E82-10071; NASA-CR-165093; NAS 1.26:165093;
INPE-2021-RPE/288) Avail: NTIS HC A04/MF A01 CSCL
02C

Maps indicating areas of sugar cane cultivation in the state of Sao Paulo, Brazil are presented. J.D.H.

N82-20597*# Texas A&M Univ., College Station. Remote Sensing Center.

DRYLAND PASTURE AND CROP CONDITIONS AS SEEN BY HCMM Final Report, Jan. 1978 - Jan. 1981

J. C. Harlan, Principal Investigator, W. D. Rosenthal, and B. J. Blanchard Apr. 1981 8 p refs Sponsored by NASA HCMM
(E82-10074; NASA-CR-165096; NAS 1.26:165096) Avail:
NTIS HC A02/MF A01 CSCL 08F

The antecedent precipitation index (API) was related to surface temperatures as measured from the NASA C-130 and HCMM thermal data. Significant results from the aircraft flight in May 1978, include: (1) canopy temperature were measured accurately remotely; (2) pasture surface temperatures were related to pasture and wheat soil moisture conditions; (3) no relationship was developed with that data set between wheat yield and thermal infrared data due to a lack of moisture stress during the measurement period; and (4) lake surface temperatures were useful in normalizing the thermal IR data. Results from HCMM also suggested a relationship between thermal IR data and antecedent precipitation index. While HCMM was adequate in detecting relative soil moisture differences, the overpass timing was infrequent and prevented detailed analysis of the API/thermal relationship. A.R.H.

N82-20600*# Instituto de Pesquisas Espaciais, Sao Jose dos Campos (Brazil).

ELEVATION OF A CANE-GROWING AREA OF THE STATE OF SAO PAULO USING LANDSAT DATA [LEVANTAMENTO DA AREA CANAVIEIRA DO ESTADO DE SAO PAULO, UTLIZANDO DADOS DO LANDSAT ANO SAFRA: 1979/80]

Nelson deJesusParada, Principal Investigator, Francisco Jose Mendonca, David C. Liang Lee, Antonio Tebaldi Tardin, Yosio Edemir Shimabukuro, Sherry Chou Chen, Liane A. M. Lucht, Mauricio A. Moreira, Angela M. deLima, and Fernando C. S. Maia Aug. 1981 10 p refs In PORTUGUESE; ENGLISH summary Sponsored by NASA ERTS
(E82-10077; NASA-CR-168398; NAS 1.26:168399;
INPE-2199-RPE/007) Avail: NTIS HC A02/MF A01 CSCL
02C

Images at a scale of 1:250,000 were visually interpreted for identification and area estimates of sugar cane plantations in Sao Paulo. The basic criteria for crop identification were the spectral characteristics of channels 5 and 7 and their temporal variations observed from different LANDSAT passes. Using this technique, it was possible to map the sugar cane areas as well as the sugar cane already harvested. An area of 801,950 hectares was estimated within the study area. The confidence interval of correct classification ranged from 87.11% to 94.71%. T.M.

N82-20601*# Instituto de Pesquisas Espaciais, Sao Jose dos Campos (Brazil).

RELATION OF THE ACTIVITIES OF THE IPDF/INPE PROJECT (REFORESTATION SUBPROJECT) DURING THE YEAR 1979 [REALTORIO DAS ATIVIDADES DO PROJETO IBDF/INPE (SUBPROJETO REFLORESTAMENTO) DURANTE O ANO DE 179]

Nelson deJesusParada, Principal Investigator, Pedro Hernandez Filho, Yosio Edemir Shimabukuro, Jose Simeao deMedeiros, Carlito Chefer deSantana, and Eduardo Carlos Mignone Alves Aug. 1981 10 p In PORTUGUESE; ENGLISH summary Presented at the 11th Congr. Brasileiro de Engenharia Agricola, Brazil, 22-25 Jun. 1981 Sponsored by NASA ERTS
(E82-10078; NASA-CR-168399; NAS 1.26:168399;
INPE-2196-RPE/005) Avail: NTIS HC A02/MF A01 CSCL
02F

The state of Mato Grosso do Sul was selected as the study area to define the recognizable classes of Eucalyptus spp. and Pinus spp. by visual and automatic analyses. For visual analysis, a preliminary interpretation key and a legend of 6 groups were derived. Based on these six groups, three final classes were defined for analysis: (1) area prepared for reforestation; (2) area reforested with Eucalyptus spp.; and (3) area reforested with Pinus spp. For automatic interpretation the area along the highway from Ribas do Rio Pardo to Agua Clara was classified into the following classes: eucalytus, bare soil, plowed soil, pine and 'cerrado'. The results of visual analysis show that 67% of the reforested farms have relative differences in area estimate below 5%, 22%, between 5% and 10%, and 11% between 10% and 20%. The reforested eucalyptus area is 17 times greater than the area of reforested pine. Automatic classification of eucalyptus ranged from 73.03% to 92.30% in the training areas. Author

N82-20602*# Instituto de Pesquisas Espaciais, Sao Jose dos Campos (Brazil).

SYSTEM OF FORECASTING AGRICULTURAL CROPS USING SATELLITE OBSERVATIONS OF EARTH [SISTEMA DE PREVISAO DE SAFRAS AERICOLAS UTILIZANDO SATELITES DE OBSERVACAO DA TERRA]

Nelson deJesusParada, Principal Investigator, Rene Antonio Novaes, Derli M. Silva, Luiz Gylvan Meira Filho, Mucio R. Dias, Oscar P. Dias, Jr., and Fausto C. deAlmeida Jul. 1981 38 p In PORTUGUESE; ENGLISH summary Sponsored by NASA ERTS
(E82-10079; NASA-CR-168400; NAS 1.26:168400;
INPE-2163-RPE/381) Avail: NTIS HC A03/MF A01 CSCL
02C

A preliminary description of a crop forecasting system is presented. Ground and satellite observation are the main sources of data collection. T.M.

N82-20609*# Pennsylvania State Univ., University Park. Dept. of Agricultural Engineering.

[FREEZE PREDICTION MODEL] Final Report

C. Terry Morrow *In* Florida Univ. Appl. of Satellite Frost Forecast Technol. to Other Parts of the U.S., Phase 2 Nov. 1981 25 p refs (For primary document see N82-20607 11-43)
Avail: NTIS HC A12/MF A01 CSCL 02C

Measurements of wind speed, net irradiation, and of air, soil, and dew point temperatures in an orchard at the Rock

Springs Agricultural Research Center, as well as topographical and climatological data and a description of the major apple growing regions of Pennsylvania were supplied to the University of Florida for use in running the P-model, freeze prediction program. Results show that the P-model appears to have considerable applicability to conditions in Pennsylvania. Even though modifications may have to be made for use in the fruit growing regions, there are advantages for fruit growers with the model in its present form. A.R.H.

N82-20613*# Michigan State Univ., East Lansing. Dept. of Entomology.

APPLICABILITY OF SATELLITE FREEZE FORECASTING AND COLD CLIMATE MAPPING TO THE OTHER PARTS OF THE UNITED STATES Final Report

In Florida Univ. Appl. of Satellite Frost Forecast Technol. to Other Parts of the U.S., Phase 2 Nov. 1981 59 p refs Original contains color illustrations (For primary document see N82-20607 11-43)
Avail: NTIS HC A12/MF A01 CSCL 04B

Tasks performed to determine the value of using GOES satellite thermal imagery to enhance fruit crop production in Michigan are described. An overview is presented of the system developed for image processing and thermal image and surface environmental data bases prepared to assess the physical models developed in Florida. These data bases were used to identify correlations between satellite apparent temperatures patterns and Earth surface factors. Significant freeze events in 1981 and the physical models used to provide a perspective on how Florida models can be applied in the context of the Michigan environment are discussed. A.R.H.

N82-21635*# Lockheed Engineering and Management Services Co., Inc., Houston, Tex.

REGISTRATION VERIFICATION OF SEA/AR FIELDS

Willa W. Austin and Lyle Lautenschlager, Principal Investigators Jun. 1981 42 p Sponsored by NASA, USDA, Dept. of Commerce, Dept. of the Interior, and Agency for International Development ERTS
(Contract NAS9-15800; Proj. AgRISTARS)
(E82-10083; NASA-CR-161059; JSC-17251;
NAS 1.26:161059; EW-L1-04101; LEMSCO-16204) Avail: NTIS HC A03/MF A01 CSCL 02C

A method of field registration verification for 20 SEA/AR sites for the 1979 crop year is evaluated. Field delineations for the sites were entered into the data base, and their registration verified using single channel gray scale computer printout maps of LANDSAT data taken over the site. J.D.H.

N82-21636*# Lockheed Engineering and Management Services Co., Inc., Houston, Tex.

GROUND REGISTRATION OF DATA FROM AN AIRBORNE SCATTEROMETER

John C. Richter Jun. 1981 27 p Sponsored by NASA, USDA, Dept. of Commerce, Dept. of the Interior, and Agency for International Development ERTS
(Contract NAS9-15800; Proj. AgRISTARS)
(E82-10084; NASA-CR-161058; JSC-17296;
NAS 1.26:161058; SM-L1-04091; LEMSCO-16340) Avail: NTIS HC A03/MF A01 CSCL 02C

A portion of the data for the agricultural soil moisture experiment, conducted near Colby, Kansas, was collected from four scatterometers mounted on an aircraft. A method is outlined for locating the scatterometer footprints with respect to a ground-based coordinate system. The method requires the airplane's flight parameters along with aerial photography acquired simultaneously with the scatterometer data. Listings of the programs used in the registration process are included. A.R.H.

N82-21639*# Lockheed Engineering and Management Services Co., Inc., Houston, Tex.

AGRISTARS: FOREIGN COMMODITY PRODUCTION FORECASTING. PROJECT TEST REPORTS DOCUMENT, VOLUME 1

J. T. Waggoner and D. E. Phinney, Principal Investigators Jun. 1981 56 p Sponsored by NASA, USDA, Dept. of Commerce, Dept. of the Interior, and Agency for International Development ERTS
(Contract NAS9-15800; Proj. AgRISTARS)
(E82-10087; NASA-CR-161063; NAS 1.26:161063;
FC-L1-00718-Vol-1; JSC-17155-Vol-1; LEMSCO-16851-Vol-1)
Avail: NTIS HC A04/MF A01 CSCL 02C

Foreign Commodity Production Forecasting testing activities through June 1981 are documented. A log of test reports is presented. Standard documentation sets are included for each test. The documentation elements presented in each set are summarized. J.D.H.

N82-21640*# Lockheed Engineering and Management Services Co., Inc., Houston, Tex.

US CORN AND SOYBEANS EXPLORATORY EXPERIMENT

J. G. Carnes, Principal Investigator Jun. 1981 29 p Sponsored by NASA, USDA, Dept. of Commerce, Dept. of the Interior, and Agency for International Development ERTS
(Contract NAS9-15800; Proj. AgRISTARS)
(E82-10088; NASA-CR-161057; NAS 1.26:161057;
FC-L1-04073; JSC-17129; LEMSCO-16315) Avail: NTIS HC A03/MF A01 CSCL 02C

The results from the U.S. corn/soybeans exploratory experiment which was completed during FY 1980 are summarized. The experiment consisted of two parts: the classification procedures verification test and the simulated aggregation test. Evaluations of labeling, proportion estimation, and aggregation procedures are presented. J.D.H.

N82-21644*# Lockheed Engineering and Management Services Co., Inc., Houston, Tex.

AS-BUILT DESIGN SPECIFICATION FOR THE CLASFYG PROGRAM

C. L. Horton, Principal Investigator Jun. 1981 129 p Sponsored by NASA, USDA, Dept. of Commerce, Dept. of the Interior, and Agency for International Development ERTS
(Contract NAS9-15800; Proj. AgRISTARS)
(E82-10092; NASA-CR-161067; NAS 1.26:161067;
SR-L1-00304; JSC-17369; LEMSCO-16649) Avail: NTIS HC A07/MF A01 CSCL 02C

This program produces a file with a Universal-formatted header and data records in a nonstandard format. Trajectory coefficients are calculated from 5 to 8 acquisitions of radiance values in the training field corresponding to an agricultural product. These coefficients are then used to calculate a time of emergence and corresponding trajectory coefficients for each pixel in the test field. The time of emergence, two of the coefficients, and the sigma value for each pixel are written to the file. Author

N82-21645*# Lockheed Engineering and Management Services Co., Inc., Houston, Tex.

PROJECT COMMUNICATIONS/DOCUMENTATION STANDARDS MANUAL

J. T. Waggoner, Principal Investigators and D. E. Phinney Jun. 1981 32 p Sponsored by NASA, USDA, Dept. of Commerce, Dept. of the Interior, and Agency for International Development ERTS
(Contract NAS9-15800; Proj. AgRISTARS)
(E82-10093; NASA-CR-161055; NAS 1.26:161055;
FC-L1-00714; JSC-17141; LEMSCO-16850) Avail: NTIS HC A03/MF A01 CSCL 02C

The standards apply to the identification and description of remote sensing technical crop estimation analysis procedures. Standard working terminology for technical project and programmatic communications among and between FCPF project technologists and managers as well as with other AgRISTARS projects and program management is established. Basic reference material for FCPF project technologists is provided. The material presented can be used as introductory training material for new technical personnel. T.M.

N82-21647*# Purdue Univ., Lafayette, Ind. Lab. for Applications of Remote Sensing.

SOYBEAN CANOPY REFLECTANCE AS INFLUENCED BY CULTURAL PRACTICES

M. E. Bauer, Principal Investigator, J. C. Kollenkark, and C. S. T. Daughtry Mar. 1981 46 p refs Sponsored by NASA, USDA, Dept. of Commerce, Dept. of the Interior, and Agency for International Development ERTS
(Contract NAS9-15466; Proj. AgRISTARS)
(E82-10105; NASA-CR-167456; NAS 1.26:167456;
SR-P1-04038; LARS-021781) Avail: NTIS HC A03/MF A01 CSCL 02C

Experiments were conducted at West Lafayette, Indiana in 1978 and 1979 to study the reflectance factor of soybean canopies as affected by differences in row width, population, planting date, cultivar and soil type. Reflectance factor data were acquired throughout the growing season with a LANDSAT-band radiometer. Agronomic data included plant height, leaf area index, development stage, total fresh and dry biomass, percent soil cover, and grain yield. The results indicate that row width, planting date, and cultivar influence the percent soil cover, leaf area index, and biomass present, which are in turn related to the multispectral reflectance. Additionally, the reflectance data were quite sensitive to the onset of senescence. Soil color and moisture were found to be important factors influencing the reflectance in single LANDSAT bands, but the near infrared/red reflectance ratio and the greeness transformation were less sensitive than the single bands to the soil background present. Author

N82-21648*# Nebraska Univ., Lincoln. Dept. of Biology.
A GRADIENT MODEL OF VEGETATION AND CLIMATE UTILIZING NOAA SATELLITE IMAGERY. PHASE 1: TEXAS TRANSECT
David Greegor and Jim Norwine, Principal Investigators (Texas A & M Univ.) Aug. 1981 65 p refs Sponsored by NASA, USDA, Dept. of Commerce, Dept. of the Interior, and Agency for International Development ERTS
(Proj. AgRISTARS)
(E82-10107; NASA-CR-167454; NAS 1.26:167454; FC-J1-04176; JSC-17435) Avail: NTIS HC A04/MF A01 CSCL 02C

A climatological model/variable termed the sponge (a measure of moisture availability based on daily temperature maxima and minima, and precipitation) was tested for potential biogeograhic, ecological, and agro-climatological applications. Results, depicted in tabular and graphic form, suggest that, as generalized climatic index, sponge is particularly appropriate for large-area and global vegetation monitoring. The feasibility of utilizing NOAA/AVHRR data for vegetation classification was investigated and a vegetation gradient model that utilizes sponge and AVHRR data was initiated. Along an east-west Texas gradient, vegetation, sponge, and AVHRR pixel data (channels 1 and 2) were obtained for 12 locations. The normalized difference values for the AVHRR data when plotted against vegetation characteristics (biomass, net productivity, leaf area) and sponge values along the Texas gradient suggest that a multivariate gradient model incorporating AVHRR and sponge data may indeed be useful in global vegetation stratification and monitoring. A.R.H.

N82-21649*# Lockheed Engineering and Management Services Co., Inc., Houston, Tex.
SAN JUAN NATIONAL FOREST LAND MANAGEMENT PLANNING SUPPORT SYSTEM (LMPSS) REQUIREMENTS DEFINITION Final Report
Lee F. Werth, Principal Investigator Sep. 1981 41 p Sponsored by NASA, USDA, Dept. of Commerce, Dept. of the Interior, and Agency for International Development ERTS
(Contract NAS9-15800; Proj. AgRISTARS)
(E82-10108; NASA-CR-167448; NAS 1.26:167448; RR-L1-04146; JSC-17422; LEMSCO-17163) Avail: NTIS HC A03/MF A01 CSCL 02F

The role of remote sensing data as it relates to a three-component land management planning system (geographic information, data base management, and planning model) can be understood only when user requirements are known. Personnel at the San Juan National Forest in southwestern Colorado were interviewed to determine data needs for managing and monitoring timber, rangelands, wildlife, fisheries, soils, water, geology and recreation facilities. While all the information required for land management planning cannot be obtained using remote sensing techniques, valuable information can be provided for the geographic information system. A wide range of sensors such as small and large format cameras, synthetic aperture radar, and LANDSAT data should be utilized. Because of the detail and accuracy required, high altitude color infrared photography should serve as the baseline data base and be supplemented and updated with data from the other sensors. A.R.H.

N82-21650*# Lockheed Engineering and Management Services Co., Inc., Houston, Tex.
AN EVALUATION OF ISOCLS AND CLASSY CLUSTERING ALGORITHMS FOR FOREST CLASSIFICATION IN NORTHERN IDAHO
Lee F. Werth, Principal Investigator Sep. 1981 21 p refs Sponsored by NASA, USDA, Dept. of Commerce, Dept. of the Interior, and Agency for International Development ERTS
(Contract NAS9-15800; Proj. AgRISTARS)
(E82-10109; NASA-CR-167447; NAS 1.26:167447; RRI-L1-04143; JSC-17418; LEMSCO-17154) Avail: NTIS HC A02/MF A01 CSCL 02F

Both the iterative self-organizing clustering system (ISOCLS) and the CLASSY algorithms were applied to forest and nonforest classes for one 1:24,000 quadrangle map of northern Idaho and the classification and mapping accuracies were evaluated with 1:30,000 color infrared aerial photography. Confusion matrices for the two clustering algorithms were generated and studied to determine which is most applicable to forest and rangeland inventories in future projects. In an unsupervised mode, ISOCLS requires many trial-and-error runs to find the proper parameters to separate desired information classes. CLASSY tells more in a single run concerning the classes that can be separated, shows more promise for forest stratification than ISOCLS, and shows more promise for consistency. One major drawback to CLASSY is that important forest and range classes that are smaller than a minimum cluster size will be combined with other classes. The algorithm requires so much computer storage that only data sets as small as a quadrangle can be used at one time. A.R.H.

N82-21651*# Lockheed Engineering and Management Services Co., Inc., Houston, Tex.
TRANSITION YEAR LABELING ERROR CHARACTERIZATION STUDY Final Report
N. James Clinton, Principal Investigators Oct. 1980 81 p refs Sponsored by NASA, USDA, Dept. of Commerce, Dept. of the Interior, and Agency for International Development ERTS
(Contract NAS9-15800; Proj. AgRISTARS)
(E82-10111; NASA-CR-160887; NAS 1.26:160887; RC-L0-00479; LEMSCO-14056) Avail: NTIS HC A05/MF A01 CSCL 05B

Labeling errors made in the large area crop inventory experiment transition year estimates by Earth Observation Division image analysts are identified and quantified. The analysis was made from a subset of blind sites in six U.S. Great Plains states (Oklahoma, Kansas, Montana, Minnesota, North and South Dakota). The image interpretation basically was well done, resulting in a total omission error rate of 24 percent and a comission error rate of 4 percent. The largest amount of error was caused by factors beyond the control of the analysts who were following the interpretation procedures. The odd signatures, the largest error cause group, occurred mostly in areas of moisture abnormality. Multicrop labeling was tabulated showing the distribution of labeling for all crops. Author

N82-21652*# Lockheed Engineering and Management Services Co., Inc., Houston, Tex.
WHEAT STRESS INDICATOR MODEL, EARLY WARNING (EW) DATA BASE INTERFACE DRIVER, USER'S MANUAL
R. F. Hansen, Principal Investigator Nov. 1981 15 p Sponsored by NASA, USDA, Dept. of Commerce, Dept. of the Interior, and Agency for International Development ERTS
(Contract NAS9-15800; Proj. AgRISTARS)
(E82-10115; NASA-CR-167480; NAS 1.26:167480; EW-L1-00732; JSC-17793; LEMSCO-17179) Avail: HC A02/MF A01 CSCL 02C

Detailed instructions on the use of the wheat stress indicator model, early warning (EW) data base interface driver are given. The purpose of this system is to interface the wheat stress indicator model with the EW operational data base. The interface driver routine decides what meteorological stations data should be processed and calls the proper subroutines to process the stations data. M.G.

N82-21653*# Department of Agriculture, Washington, D.C.
AGRISTARS: AGRICULTURE AND RESOURCES INVENTORY SURVEYS THROUGH AEROSPACE REMOTE SENSING. ENUMERATOR'S MANUAL, 1981 GROUND DATA SURVEY
Jan. 1981 88 p Sponsored by NASA, USDA, Dept. of Commerce, Dept. of the Interior, and Agency for International Development ERTS
(Proj. AgRISTARS)
(E82-10116; NASA-CR-167434; NAS 1.26:167434; FC-J1-04108; JSC-16860) Avail: NTIS HC A05/MF A01 CSCL 05B

General information and administrative instructions are provided for individuals gathering ground truth data to support research and development techniques for estimating crop acreage and production by remote sensing by satellite. Procedures are given for personal safety with regards to organophosphorus insecticides, for conducting interviews for periodic observations, for coding the crops identified and their growth stages, and for selecting sites for placing rain gages. Forms are included for those citizens agreeing to monitor the gages and record the rainfall. Segment selection is also considered. A.R.H.

N82-21654*# Lockheed Engineering and Management Services Co., Inc., Houston, Tex.

DEVELOPMENT OF ROTATION SAMPLE DESIGNS FOR THE ESTIMATION OF CROP ACREAGES

T. G. Lycthuan-Lee, Principal Investigator Sep. 1981 126 p refs Sponsored by NASA, USDA, Dept. of Commerce, Dept. of the Interior, and Agency for International Development ERTS
(Contract NAS9-15800; Proj. AgRISTARS)
(E82-10117; NASA-CR-167438; NAS 1.26:167438;
FC-LI-04153; JSC-17427; LEMSCO-15409) Avail: NTIS HC A07/MF A01 CSCL 02C

The idea behind the use of rotation sample designs is that the variation of the crop acreage of a particular sample unit from year to year is usually less than the variation of crop acreage between units within a particular year. The estimation theory is based on an additive mixed analysis of variance model with years as fixed effects, (a sub t), and sample units as a variable factor. The rotation patterns are decided upon according to: (1) the number of sample units in the design each year; (2) the number of units retained in the following years; and (3) the number of years to complete the rotation pattern. Different analytic formulae for the variance of (a sub t) and the variance comparisons in using a complete survey of the rotation patterns. A.R.H.

N82-21655*# Lockheed Engineering and Management Services Co., Inc., Houston, Tex.

SAMPLE SELECTION IN FOREIGN SIMILARITY REGIONS FOR MULTICROP EXPERIMENTS

J. T. Malin, Principal Investigator Aug. 1981 44 p Sponsored by NASA, USDA, Dept. of Commerce, Dept. of the Interior, and Agency for International Development ERTS
(Contract NAS9-15800; Proj. AgRISTARS)
(E82-10118; NASA-CR-167439; NAS 1.26:167439;
FC-L1-04120; JSC-17401; LEMSCO-16663) Avail: NTIS HC A03/MF A01 CSCL 02C

The selection of sample segments in the U.S. foreign similarity regions for development of proportion estimation procedures and error modeling for Argentina, Australia, Brazil, and USSR in AgRISTARS is described. Each sample was chosen to be similar in crop mix to the corresponding indicator region sample. Data sets, methods of selection, and resulting samples are discussed. A.R.H.

N82-21657*# Lockheed Engineering and Management Services Co., Inc., Houston, Tex.

A LOOK AT THE COMMONLY USED LANDSAT VEGETATION INDICES

G. E. Miller, Principal Investigator Oct. 1981 37 p refs Sponsored by NASA, USDA, Dept. of Commerce, Dept. of the Interior, and Agency for International Development, ERTS
(Contract NAS9-15800; Proj. AgRISTARS)
(E82-10123; NASA-CR-167474; NAS 1.26:167474;
EW-L1-04134; JSC-17413; LEMSCO-16844) Avail: NTIS HC A03/MF A01 CSCL 02C

The origins, development, and logic of the indices are discussed. The relationships of the indices to ground-based measurements of vegetation are highlighted. An effort was made to preserve the order in which the various indices appeared in the literature in order to historically trace their underlying concepts. T.M.

N82-21658*# Environmental Research Inst. of Michigan, Ann Arbor.

THE 1981 ARGENTINA GROUND DATA COLLECTION

Robert Horvath, Robert N. Colwell, Principal Investigators, David Hicks, Buzz Sellman, Edwin Sheffner, Gene Thomas, and Byron Wood Oct. 1981 100 p refs Sponsored by NASA, USDA, Dept. of Commerce, Dept. of the Interior, and Agency for International Development. Prepared in cooperation with California Univ., Berkeley. Original contains imagery. Original photography may be purchased from the EROS Data Center, Sioux Falls, S.D. 57198 ERTS
(Contracts NAS9-15476; NAS9-14565; Proj. AgRISTARS)
(E82-10127; NASA-CR-167451; NAS 1.26:167451;
SR-E1-04174; ERIM-152400-12-T) Avail: NTIS HC A05/MF A01 CSCL 05B

Over 600 fields in the corn, soybean and wheat growing regions of the Argentine pampa were categorized by crop or cover type and ancillary data including crop calendars, historical crop production statistics and certain cropping practices were also gathered. A summary of the field work undertaken is included along with a country overview, a chronology of field trip planning and field work events, and the field work inventory of selected sample segments. LANDSAT images were annotated and used as the field work base and several hundred ground and aerial photographs were taken. These items along with segment descriptions are presented. Meetings were held with officials of the State Secretariat of Agriculture (SEAG) and the National Commission on Space Investigations (CNIE), and their support to the program are described. A.R.H.

N82-21661*# Lockheed Engineering and Management Services Co., Inc., Houston, Tex.

SONORA EXPLORATORY STUDY FOR THE DETECTION OF WHEAT-LEAF RUST

R. W. Payne, Principal Investigator Nov. 1980 43 p refs ERTS
(Contract NAS9-15800)
(E82-10133; NASA-CR-161051; JSC-16956;
NAS 1.26:161051; LEMSCO-15604) Avail: NTIS HC A03/MF A01 CSCL 02C

The applicability of LANDSAT remote sensing technology to the detection of a wheat-leaf-rust epidemic in Sonora, Mexico, during 1977 was investigated. LANDSAT data acquired during crop years 1975-76 and 1976-77 were clustered, classified, and analyzed in order to detect agricultural changes. Analysis of 1977 data indicates a significant proportion of the identified wheat is stressed (potentially rust-infected). Additional analyses show a significant increase in fallowing during the year, as well as a substantial decrease in reservoir levels in the Sonora agricultural region. Ground observations are required to substantiate these analyses. The possibility exists that heat-rust is not LANDSAT detectable and that the clusters identified as containing stressed signatures represent different varieties of wheat or perhaps nonwheat crops. A.R.H.

N82-21668*# Pennsylvania State Univ., University Park. Office for Remote Sensing of Earth Resources.

DELINEATION OF SOIL TEMPERATURE REGIMES FROM HCMM DATA Quarterly Report

Rick L. Day and Gary W. Petersen, Principal Investigators 31 Dec. 1981 3 p HCMM
(E82-10141; NASA-CR-168526; NAS 1.26:168526) Avail: NTIS HC A02/MF A01 CSCL 08M

Evaluation of LANDSAT and Heat Capacity Mapping Mission (HCMM) data as input into National Cooperative Soil Survey is discussed. Signature classification techniques were applied to 13 May 76 LANDSAT data. LANDSAT data was overlaid with HCMM data, revealing registration problems caused by a shortage of control points in LANDSAT data, and the WARP program developed to improve registration accuracy. Initial images for control point selection were produced using digital terrain elevation data. Statistical procedures for evaluating data classification and to describe spatial distribution of surface temperature and its correlation with soil surface conditions were investigated. J.D.

N82-21670*# Purdue Univ., Lafayette, Ind. Lab. for Applications of Remote Sensing.

SPECTRAL-AGRONOMIC RELATIONSHIPS OF CORN, SOYBEAN AND WHEAT CANOPIES

M. E. Bauer, Principal Investigator, C. S. T. Daughtry, and V. C. Vanderbilt Oct. 1981 19 p refs Presented at the Intern. Colloq. on Signatures of Remotely Sensed Objects, Avignon, France, 8-11 Sep. 1981 Sponsored by NASA, USDA, Dept. of Commerce, Dept. of the Interior, and Agency for International Development ERTS
(Contract NAS9-15466; Proj. AgRISTARS)

(E82-10143: NASA-CR-167510: NAS 1.26:167510.
SR-PI-04187: LARS-091281) Avail NTIS HC A02/MF A01
CSCL 20F

During the past six years several thousand reflectance spectra of corn, soybean, and wheat canopies were acquired and analyzed The relationships of biophysical variables, including leaf area index, percent soil cover, chlorophyll and water content, to the visible and infrared reflectance of canopies are described The effects on reflectance of cultural, environmental and stress factors such as planting data, seeding rate, row spacing, cultivar, soil type and nitrogen fertilization are also examined The conclusions are that several key agronomic variables including leaf area index, development stage and degree of stress are strongly related to spectral reflectance and that it should be possible to estimate these descriptions of crop condition from satellite acquired multispectral data A R H

N82-21671*# Purdue Univ., Lafayette, Ind Lab for Applications of Remote Sensing

SIMULATED RESPONSE OF A MULTISPECTRAL SCANNER OVER WHEAT AS A FUNCTION OF WAVELENGTH AND VIEW/ILLUMINATION DIRECTION

M E Bauer, Principal Investigator, V C Vanderbilt, B F Robinson, L L Biehl, and A S Vanderbilt Nov 1981 14 p refs
Sponsored by NASA, USDA, Dept of Commerce, Dept of the Interior, and Agency for International Development ERTS
(Contract NAS9-15466; Proj AgRISTARS)
(E82-10144; NASA-CR-167505; NAS 1.26:167505;
SR-P1-04202; LARS-071580) Avail NTIS HC A02/MF A01
CSCL 02C

The reflectance response with view angle of wheat, was analyzed The analyses, which assumes there are no atmospheric effects, and otherwise simulates the response of a multispectral scanner, is based upon spectra taken continuously in wavelength from 0.45 to 2.4 micrometers at more than 1200 view/illumination directions using an Exotech model 20C spectra radiometer Data were acquired six meters above four wheat canopies, each at a different growth stage The analysis shows that the canopy reflective response is a pronounced function of illumination angle, scanner view angle and wavelength The variation is greater at low solar elevations compared to high solar elevations A R H

N82-21672*# Purdue Univ., Lafayette, Ind Lab for Applications of Remote Sensing

VARIABILITY OF REFLECTANCE MEASUREMENTS WITH SENSOR ALTITUDE AND CANOPY TYPE

C S T Daughtry, V C Vanderbilt, and V J Pollara Nov 1981 24 p refs Sponsored by NASA, USDA, Dept of Commerce, Dept of the Interior, and Agency for International Development ERTS
(Contract NAS9-15466; Proj AgRISTARS)
(E82-10145; NASA-CR-167509; NAS 1.26:167509;
SR-P1-04191; LARS-111481) Avail NTIS HC A02/MF A01
CSCL 20F

Data were acquired on canopies of mature corn planted in 76 cm rows, mature soybeans planted in 96 cm rows with 71 percent soil cover, and mature soybeans planed in 76 cm rows with 100 percent soil cover A LANDSAT band radiometer with a 15 degree field of view was used at ten altitudes ranging from 0.2 m to 10 m above the canopy At each altitude, measurements were taken at 15 cm intervals also a 2.0 m transect perpendicular to the crop row direction Reflectance data were plotted as a function of altitude and horizontal position to verify that the variance of measurements at low altitudes was attributable to row effects which disappear at higher altitudes where the sensor integrate across several rows The coefficient of variation of reflectance decreased exponentially as the sensor was elevated Systematic sampling (at odd multiples of 0.5 times the row spacing interval) required fewer measurements than simple random sampling over row crop canopies A R H

N82-21673*# Purdue Univ., Lafayette, Ind Lab for Applications of Remote Sensing

DETERMINATION OF THE OPTIMAL LEVEL FOR COMBINING AREA AND YIELD ESTIMATES

Marvin E Bauer, Principal Investigator, M M Hixson, and C D Jobusch 12 Oct 1981 70 p Sponsored by NASA, USDA, Dept of Commerce, Dept of the Interior, and Agency for International Development ERTS
(Contract NAS9-15466; Proj AgRISTARS)
(E82-10146; NASA-CR-168531; NAS 1.26:168531;
FC-P1-04197; LARS-101281) Avail NTIS HC A04/MF A01
CSCL 02C

Several levels of obtaining both area and yield estimates of corn and soybeans in Iowa were considered county, refined strata, refined/split strata, crop reporting district, and state Using the CCEA model form and smoothed weather data, regression coefficients at each level were derived to compute yield and its variance Variances were also computed with stratum level The variance of the yield estimates was largest at the state and smallest at the county level for both crops The refined strata had somewhat larger variances than those associated with the refined/split strata and CRD For production estimates, the difference in standard deviations among levels was not large for corn, but for soybeans the standard deviation at the state level was more than 50% greater than for the other levels The refined strata had the smallest standard deviations The county level was not considered in evaluation of production estimates due to lack of county area variances A R H

N82-21676*# Lockheed Engineering and Management Services Co., Inc., Houston, Tex

AGRISTARS: SUPPORTING RESEARCH. CLASSIFICATION OF CORN: BADHWAR PROFILE SIMILARITY TECHNIQUE

Willa W Austin, Principal Investigator Aug 1981 46 p refs
Sponsored by NASA, USDA, Dept of Commerce, Dept of the Interior, and Agency for International Development ERTS
(Contract NAS9-15800; Proj AgRISTARS)
(E82-10150; NASA-CR-167409; JSC-17113;
NAS 1.26:167409; SR-L1-04049; LEMSCO-16035) Avail
NTIS HC A03/MF A01 CSCL 02C

The same software programs used to classify spring wheat are applied to the classification of corn in 26 segments in the corn belt Numerical results of the acreage estimation are given Potential problem areas defined in an earlier application are examined A R H

N82-21681*# Florida Univ., Gainesville Inst of Food and Agricultural Sciences

USE OF THERMAL INERTIA DETERMINED BY HCMM TO PREDICT NOCTURNAL COLD PRONE AREAS IN FLORIDA
Quarterly Report, 16 Jun. - 15 Sep. 1981

L H Allen, Jr., Principal Investigator, Ellen Chen, J D Martsolf, and P H Jones 15 Sep 1981 23 p ref Original contains imagery Original imagery may be purchased from NASA Goddard Space Flight Center, (code 601), Greenbelt, Md 20771 Domestic users send orders to 'Attn National Space Science Data Center', non-domestic users send orders to 'Attn World Data Center A for Rockets and Satellites' HCMM
(Contract NAS5-26453)
(E82-10157; NASA-CR-164927; NAS 1.26:164927; QR-2)
Avail NTIS HC A02/MF A01 CSCL 08F

Transparencies, prints, and computer compatible tapes of temperature differential and thermal inertia for the winter of 1978 to 1979 were obtained Thermal inertial differences in the South Florida depicted include drained organic soils of the Everglades agricultural area, undrained organic soils of the managed water conservation areas of the South Florida water management district, the urbanized area around Miami, Lake Okeechobee, and the mineral soil west of the Everglades agricultural area The range of wetlands and uplands conditions within the Suwanee River basin was also identified It is shown that the combination of wetlands uplands surface features of Florida yield a wide range of surface temperatures related to wetness of the surface features E A K

N82-21682*# Lockheed Engineering and Management Services Co., Inc., Houston, Tex

AGRISTARS: SUPPORTING RESEARCH. US CROP CALENDARS IN SUPPORT OF THE EARLY WARNING PROJECT

T Hodges, Principal Investigator Jul 1981 134 p refs
Sponsored by NASA, USDA, Dept of Commerce, Dept of the Interior, and Agency for International Development ERTS
(Contract NAS9-15800; Proj AgRISTARS)
(E82-10158; NASA-CR-167417; JSC-17402;
NAS 1.26:167417; SR-L1-04122; LEMSCO-14674) Avail
NTIS HC A07/MF A01 CSCL 05B

The crop calendars produced for the Large Area Crop Inventory

Experiment (LACIE) and crop calendar samples for Colorado, Iowa, Kansas, Minnesota, Montana, Nebraska, North Dakota, South Dakota, and Texas are presented. These calendars are based on weekly crop reporting district level observations of the percentage of various crops at several growth stages. A sample of the statistical treatments of the weekly data is provided. Four to five years of 50-percent dates for stages on a crop reporting district level for Arkansas, Iowa, Kentucky, Louisiana, Michigan, Mississippi, Ohio and Wisconsin are also given. M.G.

02

ENVIRONMENTAL CHANGES AND CULTURAL RESOURCES

Includes land use analysis, urban and metropolitan studies, environmental impact, air and water pollution, geographic information systems, and geographic analysis.

A82-19177 **Satellite observed cloud patterns associated with excessive precipitation outbreaks.** J. D. Clark, A. J. Lindner, R. Borneman, and R. E. Bell (NOAA, National Environmental Satellite Service, Camp Springs, MD). In: Conference on Weather Forecasting and Analysis, 8th, Denver, CO, June 10-13, 1980, Preprints. Boston, MA, American Meteorological Society, 1980, p. 463-473. 12 refs.

A description is provided of three convective system types in terms of cloud patterns, structure, and life cycle. If these systems move slowly, they are capable of producing excessive precipitation. Other convective occurrences also produce excessive precipitation, but are not as strongly associated with upper level cloud patterns which are easily identifiable in infrared satellite imagery. Each of the three convective types discussed has particular rain producing characteristics which are relevant to the forecasting of excessive precipitation. Synoptic type I systems tend to occur in the summer and early fall. Type II systems are most commonly observed in the spring and fall. Type III systems are generally observed over the eastern two thirds of the nation, but may be found in other areas as well. G.R.

A82-19179 **Modern methods for monitoring and controlling the timeliness, accuracy, and completeness of data for meteorological analysis.** A. R. Thomas (NOAA, National Meteorological Center, Washington, DC) and J. Kerlin (USAF, Offutt AFB, NE). In: Conference on Weather Forecasting and Analysis, 8th, Denver, CO, June 10-13, 1980, Preprints. Boston, MA, American Meteorological Society, 1980, p. 488-495. 6 refs.

The goals and applications of World Weather Watch (WWW) quality control procedures for meteorological data collection and recording are explored. The total systems concept possesses provisions for monitoring and quality control in telecommunication of data and data storage at meteorological centers. Radiosonde, rocketsonde, aircraft, and weather balloon observations are mentioned as part of the exponentially growing sources of mesoscale, synoptic, and asynoptic data where errors can occur in instruments, readings, corrections, signal processing, coding, and transmission. Checking procedures to maintain quality are outlined, and real-time and non-real-time data control are described, noting that the bulletins arrive from international sources. Future applications are indicated to concentrate on ecology, world food production, defense, energy use, and basic comfort and safety, in a climate of growing fiscal constraints. M.S.K.

A82-19826 † **Color characteristics of the earth's surface determined on the basis of spectroscopy results from Salyut 4 (Tsvetovye kharakteristiki pokrovov zemli po rezul'tatam spektrometrirovaniia s orbital'noi nauchnoi stantsii 'Saliut-4').** L. I. Kiselevskii, B. I. Beliaev, A. A. Kovalev, and V. E. Pliuta (Akademiia Nauk Belorusskoi SSR, Institut Fiziki, Minsk, Belorussian SSR). *Akademiia Nauk BSSR, Doklady,* vol. 26, no. 1, 1982, p. 21-24. 11 refs. In Russian.

Salyut-4 spectroscopy data were used to determine color characteristics for various types of underlying surfaces, including desert, vegetation, and water. The quantitative relationship of these color characteristics and Mancell's color-perception system is investigated, and the influence of the porthole on the colors of the underlying surfaces is analyzed. B.J.

A82-20226 **The use of the airborne lidar system 'ALEX F 1' for aerosol tracing in the lower troposphere.** P. Mörl, M. E. Reinhardt, W. Renger, and R. Schellhase (Deutsche Forschungs- und Versuchsanstalt für Luft- und Raumfahrt, Institut für Physik der Atmosphare, Oberpfaffenhofen, West Germany). *Beiträge zur Physik der Atmosphäre,* vol. 54, no. 4, 1981, p. 403-410. 9 refs. Research supported by the Bundesministerium fur Forschung und Technologie.

The characteristics and performance of the airborne lidar system ALEX F 1 are described, noting its potential applications on spacecraft. The laser is fixed to a downward looking telescope, which gathers backscattered light for detection by a silicon photodiode, which begins the IR and photomultiplier count. A sample rate of 100 MHz on one channel corresponds to a 1.5 m resolution, with the data recorded on magnetic tape. The strength of the lidar signal is related to a color scale, with different values of the backscatter coefficient yielding different color tones. Examples are provided for the mesoscale measurement of the aerosol in the [illegible] Valley, for the regional scale by imaging the Rhine Valley at a scale of 50 km, and a 5 km small scale aerosol from a point source. The use of multiwavelength laser systems for detecting invisible clouds which mask the results of remote sensing methods is indicated. M.S.K.

A82-20339 † **Landscape mapping and physical-geographical classification of the eastern part of the Chechen-Ingush, ASSR using space imagery (Landshaftnoe kartografirovanie i fizikogeograficheskoe raionirovanie vostochnoi chasti Checheno-Ingushskoi ASSR po kosmicheskim snimkam).** Iu. I. Kondratova and A. E. Fedina (Moskovskii Gosudarstvennyi Universitet, Moscow, USSR). *Issledovanie Zemli iz Kosmosa,* Nov.-Dec. 1981, p. 13-18. In Russian.

A82-20999 **Airborne in-situ measurement of particulate sulfur and sulfuric acid with flame photometry and thermal analysis.** W. G. Cobourn, J. Djukic-Husar, R. B. Husar, and S. Kohli (Washington University, St. Louis, MO). *(U.S. Environmental Protection Agency, Electric Power Research Institute, and U.S. National Park Service, Symposium on Plumes and Visibility: Measurements and Model Components, Grand Canyon, AZ, Nov. 10-14, 1980.)* *Atmospheric Environment,* vol. 15, no. 12, 1981, p. 2565-2571. 17 refs. U.S. Environmental Protection Agency Grant No. R-806606-02.

An airborne in-situ particulate sulfur monitor based on the FPD principle is developed and tested. The lower detection limit for particulate sulfur is [illegible] ppb (4 micrograms SO4 per cu m), with a time response to 90% of signal at 5 s. FPD zero drift caused by changes in pressure, humidity and other environmental factors is compensated for by including an automatic zeroing cycle so that the zero signal can be monitored with the sulfur signal. An accuracy of + or - 30% is attained, and an examination of field data indicates that plume profiles of particulate sulfur and sulfuric acid can be measured with good detail with vertical profiles of good quality. D.L.G.

A82-21217 **Ionospheric troughs in Antarctica.** J. R. Dudeney, M. J. Jarvis, R. I. Kressman, M. Pinnock, A. S. Rodger, and K. H. Wright (British Antarctic Survey, Cambridge, England). *Nature,* vol. 295, Jan. 28, 1982, p. 307, 308. 22 refs.

The first observations of the dynamics of both the mid-latitude and high-latitude troughs made by the Advanced Ionospheric Sounder (AIS) at Halley Station, Antarctica (76 deg S, 27 deg W; invariant lat. 61 deg) are reported. This experiment is part of a major international project to study the sub-auroral ionosphere and its associations with the magnetosphere. The analysis provides an accurate quantitative description of the latitudinal movements of these features and the first results delineating the orientation of the poleward edge of the mid-latitude trough. These results show that the AIS has a much greater potential for monitoring large scale ionospheric structures and for tracking their motions than more conventional radio wave experiments. (Author)

A82-21386 **Airborne lidar measurements of smoke plume distribution, vertical transmission, and particle size.** E. E. Uthe, B. M. Morley, and N. B. Nielsen (SRI International Atmospheric Science Center, Menlo Park, CA). *Applied Optics,* vol. 21, Feb. 1, 1982, p. 460-463. 12 refs. Research supported by SRI International.

Observations were made of a dense smoke plume downwind from a forest fire using the ALPHA-1 two-wavelength downward-looking airborne lidar system. Facsimile displays were derived which depict plume dimensions, boundary layer height, and underlying terrain elevations. Results show significantly greater plume attenuation at 0.53-micron wavelengths than at 1.06-micron wavelengths, which indicates about 0.1-micron mean particle diameters, or the presence of gaseous constituents that absorb the visible radiation. D.L.G.

A82-21432 Measurement of atmospheric emission using a balloon-borne cryogenic Fourier spectrometer. H. Sakai, T. C. Li (Massachusetts, University, Amherst, MA), J. Pritchard (Idealab, Inc., Franklin, MA), F. J. Murcray, F. H. Murcray, J. Williams (Denver, University, Denver, CO), and G. Vanasse (USAF, Geophysics Laboratory, Bedford, MA). In: International Conference on Fourier Transform Infrared Spectroscopy, Columbia, SC, June 8-12, 1981, Proceedings. Bellingham, WA, Society of Photo-Optical Instrumentation Engineers, 1981, p. 196-198. AF Project 2310, AF Task 2310G1.

In the lower atmosphere, the tropopause, and the stratosphere, the infrared emission radiance level directly relates to temperature and concentration of the molecules responsible for the emission. An experiment was conducted to obtain high precision data on altitude profiles of various atmospheric parameters by measuring the infrared emission spectrum of the atmosphere from a balloon-borne platform. The balloon flight took place on October 8, 1980. A spectrum was recovered from interferogram data taken at an altitude of approximately 5000 m. The maximum optical path difference was approximately 4 cm, producing a corresponding resolution of 0.12 per cm. The data indicate excellent sensitivity for detecting weak spectral lines. G.R.

A82-22143 A comparison between aerial photography and Landsat for computer land-cover mapping. B. K. Quirk and F. L. Scarpace (Wisconsin, University, Madison, WI). *Photogrammetric Engineering and Remote Sensing,* vol. 48, Feb. 1982, p. 235-240. 18 refs. NOAA-sponsored research.

In a number of applications, Landsat imagery resolution was found to be inadequate to meet mapping needs. An analysis of aerial photographs has, therefore, been considered to obtain required land-cover information. The considered investigation attempts to evaluate the potential of such an analysis on the basis of a comparison made between land-cover information provided from several sensors for an urbanizing area around Green Bay, Wisconsin. Land-cover information is important as an input to hydrologic models. Land-cover estimates from the computer analysis of Landsat and digitized aerial photography are compared to manual photointerpretations of black-and-white infrared and color infrared aerial photographs of the area within the watershed. It was found that computer analysis of a color infrared photograph provided more accurate land-cover estimates than Landsat when compared to a manual photointerpretation of an urban watershed. G.R.

A82-24958 A system for quantitative determination of species and vitalities of urban trees on color-infrared photographs. J. Fuhrer, K. H. Erismann, H. J. Keller, and A. Favre (Bern, Universitat, Berne, Switzerland). *Remote Sensing of Environment,* vol. 11, Mar. 1981, p. 1-8. 22 refs. Swiss National Science Foundation Grant No. 3,209,77.

Aerial color-infrared photographs of two Swiss cities (Bern and Lausanne) were taken to evaluate the potential use of automatic image analysis for the discrimination of urban tree species and their different vitalities. A TV-based hardware system under full software control measured five different functions at each of the 63 possible intensity levels at red (600 nm), green (550 nm), blue (470 nm), and white illumination. Eighty-three parameters per tree were derived from the corresponding intensity distributions describing tone and texture. Classification by supervised learning was carried out using stepwise discriminant analysis. The overall classification error for the discrimination of four deciduous tree species (horse chestnut, Norway maple, large-leaved lime, and London plane) was 4.9%. A higher error rate (6.2%) was found for the discrimination of five classes, namely healthy trees of the above mentioned four species and damaged horse chestnut trees. The practicability of the proposed system is discussed. (Author)

A82-24962 The Canadian north - Utility of remote sensing for environmental monitoring. B. Dey (Howard University, Washington, DC) and J. H. Richards (Saskatchewan, University, Saskatoon, Canada). *Remote Sensing of Environment,* vol. 11, Mar. 1981, p. 57-72. 31 refs.

Activities related to resource exploration have a great potential for causing environmental change and damage. In connection with a growing interest in northern mineral resources, environmental monitoring of the Canadian north has become important. Monitoring is undertaken so as to distinguish and record dynamic events such as weather, floods, forest fires, and ice break-up, as well as longer-term changes which may affect water quality, vegetation, and wildlife habitat. An investigation concerning the feasibility of remote sensing for environmental monitoring is conducted. It is found that the use of aircraft in remote sensing is becoming increasingly expensive, while the aircraft platform itself may be considered inadequate. In distinction, small-scale satellite imagery is relatively inexpensive, and the regularity and areal extent of satellite coverage is not in doubt. Inherent potentials will be more nearly realized with the aid of new techniques and satellites. G.R.

A82-25140 Building and road extraction from aerial photographs. M. Tavakoli (Shiraz University, Shiraz, Iran) and A. Rosenfeld (Maryland, University, College Park, MD). *IEEE Transactions on Systems, Man, and Cybernetics,* vol. SMC-12, Jan.-Feb. 1982, p. 84-91. 10 refs. Grant No. DAAG53-76-C-0138. DARPA Order 3206.

A method of extracting features such as buildings and roads from high-resolution aerial photographs is described. The approach involves several successive stages of grouping of edge segments. Straight line segments are fitted to sets of edge pixels; compatibilities between pairs of these segments, based on gray level and geometric information, are computed; and the segments are then grouped into building-like and road-like groupings based on these compatibilities. Examples of the results obtained using this approach are given, and some variations on the initial stages of the process are also investigated. (Author)

A82-25149 Mid-latitude summertime measurements of stratospheric NO2. J. B. Kerr, C. T. McElroy, and W. F. J. Evans (Department of the Environment, Atmospheric Environment Service, Downsview, Ontario, Canada). *Canadian Journal of Physics,* vol. 60, Feb. 1982, p. 196-200. 11 refs.

Measurements of the vertical distribution of stratospheric nitrogen dioxide made on Stratoprobe balloon flights in August from Yorkton, Saskatchewan are presented. The vertical profiles were calculated by the inversion of measurements of absorption at wavelengths of 437.7, 444.8 and 450.0 nm as a function of solar zenith angle during sunrise and sunset. Four pairs of observations were obtained which show variations in NO2 levels with 15% at all heights, demonstrating the reliability of the measurement and analysis methods. The average NO2 concentration at sunset is found to increase from about 0.3 ppbv at 10 km to 10 ppbv at 35 km, and at sunrise to increase from 0.2 to 5 ppbv. A.L.W.

A82-25452 * Analysis of two Seasat synthetic aperture radar images of an urban scene. M. L. Bryan (California Institute of Technology, Jet Propulsion Laboratory, Pasadena, CA). *Photogrammetric Engineering and Remote Sensing,* vol. 48, Mar. 1982, p. 393-398. 19 refs. Contract No. NAS7-100.

Because the Seasat satellite is not polar-orbiting, the look-directions of its SAR radar on the basic ascending and descending orbits were neither in the same direction, orthogonal to, nor opposite to, one another. This calls for a technique by means of which to identify those features within a given geographic region which were imaged from two directions by Seasat SAR and are sensitive to radar orientation. It is demonstrated that images from the two orbits with different look directions can be registered and subtracted from one another, with the resulting difference image highlighting those features that are direction-sensitive. Although this depends on a precise registration the subtraction technique is straightforward once such registration has been obtained. O.C.

A82-26329 An investigation of the ozone plume from a small city. C. W. Spicer, D. W. Joseph, and P. R. Sticksel (Battelle Columbus Laboratories, Columbus, OH). *Air Pollution Control*

Association, Journal, vol. 32, Mar. 1982, p. 278-281. 6 refs. U.S. Environmental Protection Agency Contract No. 68-02-2439.

The results of upwind and downwind flights around a large and small city (population less than 100,000) to determine if the small city contributed to downwind O3 pollution are reported. The flights were around St. Louis, MO and Springfield, IL on summer days. A small increase was noted downwind from Springfield, along with O3 precursors. Significant differences were observed on one occasion, and were found to correspond with atmospheric conditions conducive to photochemical formation of O3. M.S.K.

A82-26403 **A regional air quality model for the Kwinana industrial area of Western Australia.** F. H. Kamst and T. J. Lyons (Murdoch University, Murdoch, Australia). *Atmospheric Environment,* vol. 16, no. 3, 1982, p. 401-412. 30 refs.

The Kwinana industrial area lies 32 km south of the city of Perth, Western Australia. Since this area represents the major concentration of heavy industry near Perth, it is essential to have a clear understanding of its present and future impact on the regional air quality. A description is presented of the development of a regional air dispersion model wherein the initial development has been limited to the stable atmosphere. The model was used to predict SO2 concentrations in the Kwinana area during the night of August 1-2, 1978, between 2300 and 0445 h. The obtained results are presented in graphs. Attention is given to a sensitivity analysis, the determination of the input parameters to the model and a comparison of model results with photographs. G.R.

A82-26621 * # **The NASA participation in the 1980 EPA PEPE/NEROS field measurements program.** E. Remsberg and R. Bendura (NASA, Langley Research Center, Hampton, VA). *American Meteorological Society, Joint Conference on Applications of Air Pollution Meteorology, 3rd, San Antonio, TX, Jan. 11-15, 1982, Paper.* 4 p.

The Persistent Elevated Pollution Episode (PEPE)/Northeast Regional Oxidant Study (NEROS) Project consisted of a series of field measurements sponsored by the EPA during July and August, 1980. NASA participation in the Project had several purposes: (1) use remote sensing to help determine mixed layer height and ozone profiles regionally; and (2) provide opportunity for development, testing and evaluation of several NASA 'emerging' airborne remote sensing systems. NASA also provided information on the hazy pollution episodes throughout the summer of 1980 with satellite imagery. This paper describes findings on atmospheric aerosols, ozone profile and ozone column and discusses the instruments (airborne and ground-based sensors) and techniques used to obtain the relevant data. Associated archived data is also discussed. C.D.

A82-26700 **Diurnal variation of summer convection over West Africa and the Tropical Eastern Atlantic during 1974 and 1978.** R. J. Reed and K. D. Jaffe (Washington, University, Seattle, WA). *Monthly Weather Review,* vol. 109, Dec. 1981, p. 2527-2534. 12 refs. NOAA-supported research; NSF Grant No. ATM-81-03697.

The behavior of convection during the Greater Atlantic Tropical Experiment period is compared with data from the summer of 1978, the initial operation summer of Meteosat-1. IR imagery from Meteosat-1 taken at 4-hr intervals from July 1-Sept. 30 covered 3 deg squares. The GATE data was for 1974, and similarities between the two years included explosive convective processes over land in the afternoon over elevated terrain, a weak or absent diurnal cycle near Dakar, a noontime maximum in the south of the region offshore, a peak near midnight SE of Dakar, and weak diurnal variations in some ocean regions. The existence of a large diurnal cycle in an eastern Atlantic region downstream from a land area with a large diurnal variation indicated a possible connection between land and oceanic convection. M.S.K.

A82-26721 **Photogrammetry from aircraft side camera movies - Winter MONEX.** C. Warner (Virginia, University, Charlottesville, VA). *Journal of Applied Meteorology,* vol. 20, Dec. 1981, p. 1516-1526. 14 refs. NSF Grants No. ATM-79-00233; No. ATM-80-12214.

Side-looking cloud movie photogrammetry during the MONEX winter flights over the South China Sea in 1979 is described. The films were made along the line of flight parallel to the cloud movement at heights ascertained from meteorological stations. Theoretical underpinnings to the method of calculation of cloud height using the technique are provided. Examples are given for photogrammetry of fractus, humilis, mediocris, congestus, and cumulonimbus clouds, along with height and width measurements. A method is outlined for measuring the cloud density in a field by use of a cardboard cutout against a projection of the recorded images, and density measurements are noted to have a factor of 2 uncertainty. M.S.K.

A82-26844 **Humidity measurement by infrared thermometry.** S. B. Idso (U.S. Water Conservation Laboratory, Phoenix, AZ). *Remote Sensing of Environment,* vol. 12, Mar. 1982, p. 87-91. 12 refs.

A promising new approach to the remote sensing of plant water stress involves the evaluation of an index that is dependent upon air temperature and vapor pressure, in addition to the basic foliage temperature. The air temperature measurement is already being made by an appropriate sensor incorporated into some infrared thermometers; but the vapor pressure measurement has required a second instrument. This paper describes a technique for obtaining the vapor pressure measurement by viewing the cloudless sky directly overhead with the infrared thermometer itself, thus doing away with the need for a second instrument in the remote field assessment of plant water stress by infrared thermometry. (Author)

A82-26980 * **Low-latitude cloudiness and climate feedback - Comparative estimates from satellite data.** R. D. Cess (National Center for Atmospheric Research, Boulder, CO; New York, State University, Stony Brook, NY), B. P. Briegleb (National Center for Atmospheric Research, Boulder, CO), and M. S. Lian (New York, State University, Stony Brook, NY). *Journal of the Atmospheric Sciences,* vol. 39, Jan. 1982, p. 53-59. 19 refs. NSF Grant No. CME-79-09065; Contract No. NAS1-16444.

Three studies of the relative albedo to the IR components of cloud amount feedback are reviewed, and an approach to the seasonal variability in low-level cloud numbers is presented. Comparisons are made and uncertainties calculated for the predictions of cloud amounts from satellite data sets for outgoing IR flux. IR data is used directly for a linear regression analysis and seasonal and latitudinal variations are considered in terms of monthly-annual means for particular latitude zones. Investigations of NOAA-NESS satellite data revealed that cirrus clouds are transparent in the 10.5-12.5 microns range and cloud albedos decrease at wavelengths greater than 0.7 micron, which suggests a possibility of cloud-sky and clear-sky albedo comparisons at 0.5-0.7 micron. The inclusion of Rayleigh scattering and atmospheric water vapor absorption of sunlight is recommended to test the effects on observed contracts. M.S.K.

A82-27040 # **Detection of natural disasters via Meteosat.** A. Robson, J. Morgan (ESA, European Space Operations Centre, Darmstadt, West Germany), R. W. Herschy (Department of the Environment, Water Data Unit, Reading, England), and J. Zschau (Kiel, Neue Universität, Kiel, West Germany). *ESA Bulletin,* no. 29, Feb. 1982, p. 10-18.

The operations, characteristics, and data distribution capabilities of the Meteosat 1 and 2 spacecraft which, due to separate system malfunctions, perform the mission capabilities of one satellite, are described. The GEO-situated satellites generate images in the visible and with two channels in the IR, at 11 and 6 microns. Sightings are made of hurricanes, cyclones, extratropical depressions, droughts, and floods, with whole-earth images being produced every 30 min. Raw images are received at the European Space Operations Center in Darmstadt, processed, and then sent back through the satellite to a dozen digital and over 200 analog user stations. Data Collection Platforms on board the spacecraft broadcast collected images at scheduled time intervals, when interrogated, or during an alert status when immediate information is required. Further applications to detect storm surges and earthquake activity are outlined. M.S.K.

A82-27627 # **Analysis of a discrete-time linear model for geothermal flux reconnaissance from two or three aircraft infrared**

measurements. J. L. Farah (Universidad Nacional Autónoma de México, Mexico City, Mexico). In: International Symposium on Remote Sensing of Environment, 15th, Ann Arbor, MI, May 11-15, 1981, Proceedings. Volume 2. Ann Arbor, MI, Environmental Research Institute of Michigan, 1981, p. 663-670. 10 refs.

Attention is given to a model of the earth's surface temperature which is fully based on work reported by Jaeger (1953), extensions of this work, and applications to remote-sensing problems in geology. The present investigation has the objective to perform a mathematical analysis of linearizations of these models. The basic equations are considered along with a model for g, questions of model linearization, direct and inverse relationships, and practical numerical considerations. The use of the linear model in producing maps of thermal inertia and/or of geothermal flux as viewed in the investigation, appears to yield a powerful tool for applications, mainly because at least in the case of the three-flight problem, one can take full advantage of the Fast-Fourier-Transform algorithms and of only three one-dimensional tables. G.R.

A82-27650 # **Detection of volcanic ash fall area from Landsat MSS CCT data - Eruption of Mt. Ontake in 1979.** S. Kishi and S. Yazaki (National Research Center for Disaster Prevention, Sakura, Ibaraki, Japan). In: International Symposium on Remote Sensing of Environment, 15th, Ann Arbor, MI, May 11-15, 1981, Proceedings. Volume 2. Ann Arbor, MI, Environmental Research Institute of Michigan, 1981, p. 919-928. 7 refs.

Results are presented from a digital analysis study, conducted to detect the volcanic ash fall area from the October 1979 eruption of Mt. Ontake in Japan, using Landsat MSS imagery taken a few days before and after the event. The value difference of Bands 4 and 7 was found to be the most useful in detecting the ash fall area, which was covered by a layer more than 1 mm thick. O.C.

A82-27657 # **Detailed land use classification based on multitemporal Landsat-MSS-data.** J. Lichtenegger (Zürich, Universität, Zurich, Switzerland) and K. Seidel (Zürich, Eidgenössische Technische Hochschule, Zurich, Switzerland). In: International Symposium on Remote Sensing of Environment, 15th, Ann Arbor, MI, May 11-15, 1981, Proceedings. Volume 2.
Ann Arbor, MI, Environmental Research Institute of Michigan, 1981, p. 997-1005. 6 refs. Research supported by the Swiss National Science Foundation.

Use of the 'time dimension' is shown to improve the classification result in contrast to single frame analyses. Several Landsat multispectral scanner frames are registered by means of cross correlation and then superimposed on each other to form a multitemporal data set. These data are analyzed for detailed land use categories by a supervised classification algorithm. An example for the enhancement of the classification accuracy with a quantitative ground truth comparison is given. Finally data compression is performed by principal components analysis as a preprocessing procedure prior to conventional visual interpretation. A color representation of the main components demonstrates up to seven clearly distinguishable land use categories. (Author)

A82-27661 # **Thermal IR detection of submarine gas seepages in the western Istra off-shore area /Yugoslavia/.** M. Knapp and B. Koscec (Industroprojekt, Zagreb, Yugoslavia). In: International Symposium on Remote Sensing of Environment, 15th, Ann Arbor, MI, May 11-15, 1981, Proceedings. Volume 2.
Ann Arbor, MI, Environmental Research Institute of Michigan, 1981, p. 1039-1046.

A82-27665 * # **Land cover classification accuracy as a function of sensor spatial resolution.** B. L. Markham (NASA, Goddard Space Flight Center, Earth Survey Applications Div., Greenbelt, MD) and J. R. G. Townshend (NASA, Goddard Space Flight Center, Earth Survey Applications Div., Greenbelt, MD; Reading, University, Reading, Berks., England). In: International Symposium on Remote Sensing of Environment, 15th, Ann Arbor, MI, May 11-15, 1981, Proceedings. Volume 3.
Ann Arbor, MI, Environmental Research Institute of Michigan, 1981, p. 1075-1090. 12 refs.

The benefits obtained from sensor systems for monitoring earth resources will depend on the application and interpretation methods used. A frequently used analysis method is supervised per-pixel multispectral classification with a typical application being land cover classification. An investigation is conducted to evaluate the effect of spatial resolution on the ability to classify land cover types with per-pixel digital image classification techniques. Attention is also given to the documentation of changes in scene noise and the percentage of boundary pixels as a function of spatial resolution, in order to improve the understanding of the interrelationship between classification accuracy and spatial resolution. It is found that scene noise varies considerably between land cover categories. Changes in scene noise with coarsening resolution occur at different rates for different categories. G.R.

A82-27670 # **Phenomena modelling of remotely sensed data by image rationing.** J. Iisaka (IBM Japan, Ltd., Tokyo, Japan), N. Yoshimura, Y. Yasuda, and Y. Emori (Chiba University, Chiba, Japan). In: International Symposium on Remote Sensing of Environment, 15th, Ann Arbor, MI, May 11-15, 1981, Proceedings. Volume 3. Ann Arbor, MI, Environmental Research Institute of Michigan, 1981, p. 1127-1140.

Phenomena modelling represents a useful approach to extract objective information from remotely sensed data in cases in which the resolution size is larger than the object. The concept of phenomena modelling has been applied to soil mapping, taking into account an elimination of the vegetation factor by an image rationing procedure. The considered study is concerned with an attempt to utilize phenomena modelling for an interpretation of information regarding the metropolitan area of Tokyo. Attention is given to problems regarding the detection of roughness features in the metropolitan area, aspects of modelling for the estimation of building height, the conduction of an experiment, a two-feature model for building height estimation, and a three-feature model for the building height estimation. G.R.

A82-27690 # **Inventory of eroded areas in the state of Guanajuato Mexico, by automatic analysis of Landsat images.** A. Benitez, R. Sánchez, and R. Vital (Ministry of Agriculture and Hydraulic Resources, Mexico City, Mexico). In: International Symposium on Remote Sensing of Environment, 15th, Ann Arbor, MI, May 11-15, 1981, Proceedings. Volume 3.
Ann Arbor, MI, Environmental Research Institute of Michigan, 1981, p. 1353-1362. 6 refs.

A82-27696 # **Assessment of change in Bangladesh coastal regions.** M. A. H. Pramanik (Bangladesh Space Research and Remote Sensing Organization, Dacca, Bangladesh), F. C. Polcyn, and N. E. G. Roller (Michigan, Environmental Research Institute, Ann Arbor, MI). In: International Symposium on Remote Sensing of Environment, 15th, Ann Arbor, MI, May 11-15, 1981, Proceedings. Volume 3. Ann Arbor, MI, Environmental Research Institute of Michigan, 1981, p. 1425-1434. Research supported by the Food and Agriculture Organization.

A study was conducted with the objective to determine whether a net gain or loss of land occurred along the coastline of Bangladesh between 1972 and 1979. The information provided by the study is to furnish a basis for a prediction regarding the new land which will be formed in the future. It is hoped, that based on this quantitative assessment, it may be possible to define steps to accelerate the process of land formation and to stabilize any gains. Questions of methodology are examined, taking into account aspects of preprocessing, problems of categorization, questions of registration, change detection, and the output products. G.R.

A82-27701 # **Utilisation of remote sensing in resources identification and land use in India - An integrated approach.** R. K. Katti, M. G. Sardar, T. V. Pavate, and P. Venkatachalam (Indian Institute of Technology, Bombay, India). In: International Symposium on Remote Sensing of Environment, 15th, Ann Arbor, MI, May 11-15, 1981, Proceedings. Volume 3. Ann Arbor, MI, Environmental Research Institute of Michigan, 1981, p. 1487-1497.

In this paper, remotely sensed data from Landsat-I in the form of imagery, computer compatible tape (CCT) outputs, aerial photographs and topographic maps are used for forestry and terrain evaluation in geotechnical engineering appraisal. The study shows that it is possible to develop an integrated classification system encompassing forest resources evaluation and terrain evaluation for engineering uses in particular, and agriculture development and geological aspects in general. Thus the integrated approach helps in reducing repetitiveness of sampling on the one hand, and on the other facilitates the development of thematic maps in a more rational way. The approach concerns an understanding of the physical and chemical properties of deposits, and their relation to the surface features observed in remotely sensed data in the form of CCT digital output and imagery. Genetic and morphological factors are taken into account in the analysis. (Author)

A82-27704 # **Remote SO2 emission measurements with correlation spectrometers from volcanoes.** L. Daubner, J. Davies, M. Millan (Barringer Research, Ltd., Toronto, Canada), and R. Stoiber (Dartmouth College, Hanover, NH). In: International Symposium on Remote Sensing of Environment, 15th, Ann Arbor, MI, May 11-15, 1981, Proceedings. Volume 3. Ann Arbor, MI, Environmental Research Institute of Michigan, 1981, p. 1519-1526. 17 refs.

The way in which correlation spectrometers can be used in monitoring emissions of SO2 from volcanoes as an indicator of volcanic activity is described. It is shown that volcanic gas geochemistry can provide indications of increasing magmatic contributions to eruption. Mass flows of SO2 at Mount Etna are found to correlate well with a model of magma movement within the conduit system proposed by Wadge (1977). A table giving the specifications of a correlation spectrometer is included. C.R.

A82-28133 † **The atlas 'Geographical Results of Spaceborne Multispectral Experiments' (Atlas 'Geograficheskie rezul'taty mnogozonal'nykh kosmicheskikh eksperimentov').** Iu. F. Knizhnikov and V. I. Kravtsova. *(Vsesoiuznaia Konferentsiia po Problemam Issledovaniia Prirodnykh Resursov Zemli i Mirovogo Okeana, Aviatsionno-Kosmicheskimi Sredstvami, Moscow, USSR, Nov. 1980.) Geodeziia i Aerofotos'emka,* no. 1, 1982, p. 37-41. In Russian.

A82-28152 * **Model studies of laser absorption computed tomography for remote air pollution measurement.** D. C. Wolfe, Jr. and R. L. Byer (Stanford University, Stanford, CA). *Applied Optics,* vol. 21, Apr. 1, 1982, p. 1165-1178. 41 refs. Grant No. NsG-2289; Contract No. F4920-77-C-0092.

Model studies of the potential of laser absorption-computed tomography are presented which demonstrate the possibility of sensitive remote atmospheric pollutant measurements, over kilometer-sized areas, with two-dimensional resolution, at modest laser source powers. An analysis of this tomographic reconstruction process as a function of measurement SNR, laser power, range, and system geometry, shows that the system is able to yield two-dimensional maps of pollutant concentrations at ranges and resolutions superior to those attainable with existing, direct-detection laser radars. O.C.

A82-28295 * # **Precipitation measurements from space - Workshop summary 28 April-1 May 1981, Greenbelt, MD.** D. Atlas and O. W. Thiele (NASA, Goddard Space Flight Center, Laboratory for Atmospheric Sciences, Greenbelt, MD). *American Meteorological Society, Bulletin,* vol. 63, Jan. 1982, p. 59-63. 6 refs.

The goals and methods for global precipitation measurements from space are examined. Records currently exist only for visible and IR scans of cloud properties, and are applied from GEO for detecting diurnal variations in precipitation. Microwave radiometry is noted to be a suitable method for supplementing the visible and IR data for measuring stratiform oceanic precipitation, and when used at up to 3 microns can detect areas, if not amounts, of precipitation from GEO. Applications of radar altimeters are proposed in terms of modifications to the Seasat-type 2.2 cm radar, the use of surface target attentuation radar, of frequency agile rain radar, or of adaptive pointing radar. Soil moisture sensing is available with passive microwave radiometry in the 20-50 cm bands, or active sensing in the 5-8 cm bands. The utilization of GARP ground truth data is explored, along with statistical methods for treating the data samples. M.S.K.

N82-16443*# Instituto de Pesquisas Espaciais, Sao Jose dos Campos (Brazil).

REMOTE SENSING DATA APPLIED TO LAND-USE SURVEY AT THE PARAIBA VALLEY

Nelson deJesusParada, Principal Investigator, Magda Adelaide Lombardo, Evlyn Marcia Leao DeMoraesNovo, Madalena Niero, and Celina Foresti May 1981 10 p refs Presented at the 7th Intern. Symp. on Machine Process. of Remotely Sensed Data, West Lafayette, Ind., 23-26 Jun. 1981 Sponsored by NASA ERTS

(E82-10025; NASA-CR-164812; INPE-2081-RPE/315) Avail: NTIS HC A02/MF A01 CSCL 08B

The Paraiba Valley (state of Sao Paulo) was selected as the test site in a study to develop a methodology for land-use survey and to determine the land-use modification rates using data of LANDSAT system. Both visual and automatic interpretation methods were employed to analyze seven land-use classes. They are: urban area, industrial area, bare soil, cultivated area, pastureland, reforestation and natural vegetation. By means of visual interpretation little spectral differences among those classes were observed. The automatic classification of LANDSAT MSS data using maximum likelihood algorithm shows a 39% average error of omission and a 3.4% error of commission for the seven classes. The classification results were under the influences of the complexity of land-uses in the study area, the large spectral variations of analyzed classes and the low resolution of LANDSAT data. Author

N82-16613# National Oceanic and Atmospheric Administration, Silver Spring, Md. Air Resources Labs.

DEMONSTRATION OF A LONG-RANGE ATMOSPHERIC TRACER SYSTEM USING PERFLUOROCARBONS

Gilbert J. Ferber, Kosta Telegadas, Jerome L. Heffter, C. Ray Dickson, Russell N. Dietz, and Philip W. Krey Apr. 1981 84 p refs

(Contract DE-AI01-80EV-10081)

(PB82-106246; NOAA-TM-ERL-ARL-101; NOAA-81080301) Avail: NTIS HC A05/MF A01 CSCL 13B

Regional-scale tracer experiments are needed to validate atmospheric dispersion aspects of air pollution models. The capability of a new system, using perfluorocarbon tracers (PFTs), for long-range dispersion experiments at reasonable cost was demonstrated in two experiments. Two PFTs (C7F14 and C8F16) were released simultaneously with SF6 and two heavy methanes. The PFT system provides automatic sequential samplers and rapid, inexpensive analyses down to 2 parts per 10 to the + 15th power of air. PFT concentrations were measured 600 km away, up to three days after release. Performance of the PFT system was excellent and a consistent set of tracer data was obtained. GRA

N82-17562*# National Aeronautics and Space Administration. Goddard Space Flight Center, Greenbelt, Md.

CHARACTERIZING USER REQUIREMENTS FOR FUTURE LAND OBSERVING SATELLITES

J. L. Barker, P. J. Cressy, C. C. Schnetzler, and V. V. Salomonson Dec. 1981 56 p refs

(NASA-TM-83867) Avail: NTIS HC A04/MF A01 CSCL 05B

The objective procedure was developed for identifying probable sensor and mission characteristics for an operational satellite land observing system. Requirements were systematically compiled, quantified and scored by type of use, from surveys of federal, state, local and private communities. Incremental percent increases in expected value of data were estimated for critical system improvements. Comparisons with costs permitted selection of a probable sensor system, from a set of 11 options, with the following characteristics: 30 meter spatial resolution in 5 bands and 15 meters in 1 band, spectral bands nominally at Thematic Mapper (TM) bands 1 through 6 positions, and 2 day data turn around for receipt of imagery. Improvements are suggested for both the form of questions and the procedures for analysis of future surveys in order to provide a more quantitatively precise definition of sensor and mission requirements. A.R.H.

N82-18772*# National Aeronautics and Space Administration. Goddard Space Flight Center, Greenbelt, Md.

MULTIDIMENSIONAL ASPECTS: OZONE, TEMPERATURE AND TRANSPORT
In its The Stratosphere 1981 Jan 1982 99 p

Avail: NTIS HC A22/MF A01 CSCL 04A

The capability for obtaining four-dimensional data on stratospheric structure, dynamics, and zone is discussed. Progress in the development of multidimensional models of the stratosphere is reported. The discussion of multidimensional aspects of the stratosphere is divided into four major sections: observations, analysis and interpretation, modeling, and transport of trace species.

T.M.

N82-18808*# National Aeronautics and Space Administration. Goddard Space Flight Center, Greenbelt, Md.
CLIMATE OBSERVING SYSTEM STUDIES: AN ELEMENT OF THE NASA CLIMATE RESEARCH PROGRAM: WORKSHOP REPORT
Sep. 1980 154 p refs
(NASA-TM-84040) Avail: NTIS HC A08/MF A01 CSCL 04B

Plans for NASA's efforts in climatology were discussed. Targets for a comprehensive observing system for the early 1990's were considered. A program to provide useful data in the near and mid-term, and a program to provide for a feasibility assessment of instruments and methods for the development of a long-term system were discussed. Climate parameters that cannot be measured from space were identified. Long-term calibration, intercomparison, standards, and ground truth were discussed.

R.J.F.

N82-19256# Instituto de Pesquisas Espaciais, Sao Jose dos Campos (Brazil).
GENERAL CONFIGURATION AND INTERNAL DISPOSITION OF EQUIPMENT IN A SATELLITE FOR COLLECTING ENVIRONMENTAL DATA
Carlos deOliveira Lino and Aydano Barreto Carleial Oct. 1981 32 p refs In PORTUGUESE; ENGLISH summary Presented at 33d Ann. Meeting of SBPC, Salvador, 81-5 Jul. 1981
(INPE-2240-PRE/026) Avail: NTIS HC A03/MF A01

The general configuration of an experimental satellite for reception and retransmission to the Earth of environmental data is described. The data originates from small automatic Earth stations equipped with sensors and capable of operating in remote locations. The interrelationships among the equipment blocks constituting the satellite and between these and the outside medium, which were used in the search for an adequate disposition for the equipment blocks are presented. The proposed internal and external disposition for the blocks is presented in drawings. Some mechanical quantities (position of the center of mass, moments of inertia) resulting from the mass distribution inherent to the chosen configuration, are calculated.

S.L.

N82-19601* Michigan Energy and Resource Research Association, Detroit.
RESOURCEFUL DECISIONS: LANDSAT IN MICHIGAN
Todd Anuskiewicz, Principal Investigator and Roy Meador [1982] 29 p Sponsored by NASA Original contains color imagery. Original photography may be purchased from the EROS Data Center, Sioux Falls, S.D. 57198 ERTS
(E82-10037; NASA-CR-164771) Avail: SOD HC CSCL 05B

The capabilities of LANDSAT and the continuous advantages the satellite offers in remote sensing are reviewed. The processing and application of data from the satellite to the study of resource and environmental needs in Michigan highlighted include: land use; classification of trophic states in lakes and the monitoring of water quality; prospecting for oil, gas, minerals, and water; identifying wetlands, wildlife habitats, and recreation areas; forest management; routing power lines; transportation planning; and surveying the Great Lakes Basin. The work of the Environmental Research Institute of Michigan in solving modern sensor technological problems and in gathering ground truth is reported as well as activities available through the University of Michigan remote sensing program.

A.R.H.

N82-19609*# Mississippi State Univ., Mississippi State.
APPLICATION OF REMOTE SENSING TO STATE AND REGIONAL PROBLEMS Semiannual Progress Report, 1 Nov. 1980 - 30 Apr. 1981
W. Frank Miller, John S. Powers, Jon R. Clark, Jimmy L. Solomon, and Sidney G. Williams, Principal Investigators 30 Apr. 1981 106 p refs ERTS
(Grant NGL-25-001-054)
(E82-10033; NASA-CR-164746; SAPR-15) Avail: NTIS HC A06/MF A01 CSCL 05B

The methods and procedures used, accomplishments, current status, and future plans are discussed for each of the following applications of LANDSAT in Mississippi: (1) land use planning in Lowndes County; (2) strip mine inventory and reclamation; (3) white-tailed deer habitat evaluation; (4) remote sensing data analysis support systems; (5) discrimination of unique forest habitats in potential lignite areas; (6) changes in gravel operations; and (7) determining freshwater wetlands for inventory and monitoring. The documentation of all existing software and the integration of the image analysis and data base software into a single package are now considered very high priority items.

A.R.H.

N82-19641# Instituto de Pesquisas Espaciais, Sao Jose dos Campos (Brazil).
METHODOLOGY OF THE INTERPRETATION OF REMOTE SENSING DATA AND APPLICATIONS IN PEDOLOGY
Mario Valerio Filho, Jose Carlos Neves Epiphanio, and Antonio Roberto Formaggio Aug. 1981 55 p refs In PORTUGUESE; ENGLISH summary
(INPE-2211-MD/008) Avail: NTIS HC A03/MF A01

A global view of photointerpretation techniques in soil survey is presented. Photopedologic methods are described which served as a base for the systematic approach to orbital data interpretation for soil survey. Several pedology research projects in Brazil are described.

A.R.H.

N82-19740# Cologne Univ. (West Germany). Inst. fuer Geophysik und Meteorologie.
ATLAS OF THE GLOBAL DISTRIBUTION OF THE TOTAL OZONE CONCENTRATION ACCORDING TO SATELLITE MEASUREMENTS [ATLAS DER GLOBALVERTEILUNG DES GESAMTOZONBETRAGES NACH SATELLITENMESSUNGEN (APRIL 1970-MAY 1972)]
Anver Ghazi 1980 47 p refs In GERMAN
(Mitt-28; ISSN-0069-5882) Avail: NTIS HC A03/MF A01

An atlas of interdisciplinair research on the many different aspects of ozone research is presented. Maps were drawn from backscatter ultraviolet satellite observations. Data are compiled on global distribution of the total ozone layer.

E.A.K.

N82-20588*# Instituto de Pesquisas Espaciais, Sao Jose dos Campos (Brazil).
THE UTILIZATION OF ORBITAL IMAGES AS AN ADEQUATE FORM OF CONTROL OF PRESERVED AREAS [UTILIZACAO DE IMAGENS ORBITAIS, COMO FORMA ADEQUADA NO CONTROLE DE AREAS DE PRESERVACAO]
Nelson deJesusParada, Principal Investigator and Joao Roberto dosSantos May 1981 14 p refs In PORTUGUESE; ENGLISH summary Sponsored by NASA; submitted for publication ERTS
(E82-10065; NASA-CR-165087; NAS 1.26:165087; INPE-2064-RPE/306) Avail: NTIS HC A02/MF A01 CSCL 08B

The synoptic view and the repetitive acquisition of LANDSAT imagery provide precise information, in real-time, for monitoring preserved areas based on spectral, temporal and spatial properties. The purpose of this study was to monitor, with the use of multispectral imagery, the systematic annual burning, which causes the degradation of ecosystems in the National Park of Araguaia. LANDSAT imagery of channel 5 (0.6 a 0.7 microns) and 7 (0.8 a 1.1 microns), at the scale of 1:250,000, were used to identify and delimit vegetation units and burned area, based on photointerpretation parameter of tonality. The results show that the gallery forest can be discriminated from the seasonally flooded 'campo cerrado', and that 4.14% of the study area was burned. Conclusions point out that the LANDSAT images can be used for the implementation of environmental protection in national parks.

Author

N82-20592*# Instituto de Pesquisas Espaciais, Sao Jose dos Campos (Brazil).
AMAZONAS PROJECT: APPLICATION OF REMOTE SENSING TECHNIQUES FOR THE INTEGRATED SURVEY

OF NATURAL RESOURCES IN AMAZONAS [PROJETO AMAZONAS APLICACAO DAS TECNICAS DE SENSORIAMENTO REMOTO PARA LEVANTAMENTO INTEGRADO DOS RECURSOS NATURAIS DO AMAZONAS]
Nelson deJesusParada, Principal Investigator Mar. 1981 95 p refs In PORTUGUESE Sponsored by NASA ERTS
(E82-10069; NASA-CR-165091; NAS 1.26:165091;
INPE-2019-NTE/166) Avail: NTIS HC A05/MF A01 CSCL 08F

The use of LANDSAT multispectral scanner and return beam vidicon imagery for surveying the natural resources of the Brazilian Amazonas is described. Purposes of the Amazonas development project are summarized. The application of LANDSAT imagery to identification of vegetation coverage and soil use, identification of soil types, geomorphology, and geology and highway planning is discussed. An evaluation of the worth of LANDSAT imagery in mapping the region is presented. Maps generated by the project are included.
J.D.H.

N82-20593*# Canada Centre for Remote Sensing, Ottawa (Ontario).
HEAT CAPACITY MAPPING MISSION (HCMM): INTERPRETATION OF IMAGERY OVER CANADA Final Report
Josef Cihlar, Principal Investigator and R. G. Dixon Aug. 1981 72 p refs Sponsored by NASA Original contains imagery. Original imagery may be purchased from NASA Goddard Space Flight Center, (code 601), Greenbelt, Md. 20771. Domestic users send order to 'Attn: National Space Science Data Center'; non-domestic users send orders to 'Attn. World Data Center A for Rockets and Satellites'. HCMM 1
(E82-10070; NASA-CR-165092; NAS 1.26:165092) Avail: NTIS HC A04/MF A01 CSCL 05B

Visual analysis of HCMM images acquired over two sites in Canada and supporting aircraft and ground data obtained at a smaller subsite in Alberta show that nighttime surface temperature distribution is primarily related to the near-surface air temperature; the effects of topography, wind, and land cover were low or indirect through air temperature. Surface cover and large altitudinal differences were important parameters influencing daytime apparent temperature values. A quantitative analysis of the relationship between the antecedent precipitation index and the satellite thermal IR measurements did not yield statistically significant correlation coefficients, but the correlations had a definite temporal trend which could be related to the increasing uniformity of vegetation cover. The large pixel size (resulting in a mixture of cover types and soil/canopy temperatures measured by the satellite) and high cloud cover frequency found in images covering both Canadian sites and northern U.S. were considered the main deficiencies of the thermal satellite data.
A.R.H.

N82-20595*# Instituto de Pesquisas Espaciais, Sao Jose dos Campos (Brazil).
LAND USE IN THE PARAIBA VALLEY THROUGH REMOTELY SENSED DATA [USO DA TERRA NO VALE DO PARAIBA ATRAVES DE DADOS DE SENSORIAMENTO REMOTO - RELATORIO FINAL]
Nelson deJesusParada, Principal Investigator, Magda Adelaide Lombardo, Evlyn Marcia Leao deMoraes Novo, Madalena Niero, and Celina Foresti Dec. 1980 95 p refs In PORTUGUESE; ENGLISH summary Sponsored by NASA Original contains color imagery. Original photography may be purchased from the EROS Data Center, Sioux Falls, S.D. 57198. ERTS
(E82-10072; NASA-CR-165094; NAS 1.26:165094;
INPE-1972-RPE/278) Avail: NTIS HC A05/MF A01 CSCL 08B

A methodology for land use survey was developed and land use modification rates were determined using LANDSAT imagery of the Paraiba Valley (state of Sao Paulo). Both visual and automatic interpretation methods were employed to analyze seven land use classes: urban area, industrial area, bare soil, cultivated area, pastureland, reforestation and natural vegetation. By means of visual interpretation, little spectral differences are observed among those classes. The automatic classification of LANDSAT MSS data using maximum likelihood algorithm shows a 39% average error of omission and a 3.4% error of inclusion for the seven classes. The complexity of land uses in the study area, the large spectral variations of analyzed classes, and the low resolution of LANDSAT data influenced the classification results.
A.R.H.

N82-20615*# Florida Univ., Gainesville. Dept. of Fruit Crops.
A SATELLITE FROST FORECASTING SYSTEM FOR FLORIDA Final Report
J. David Martsolf *In its* Appl. of Satellite Frost Forecast Technol. to Other Parts of the U.S., Phase 2 Nov. 1981 42 p refs Presented at the Workshop on Appl. of Weather Data to Agr. and Forest Prod., Anaheim, Calif., 30-31 Mar. 1981; sponsored by American Meteorological Soc. and NSF
Avail: NTIS HC A12/MF A01 CSCL 04B

Since the first of two minicomputers that are the main components of the satellite frost forecast system was delivered in 1977, the system has evolved appreciably. A geostationary operational environmental satellite (GEOS) system provides the satellite data. The freeze of January 12-14, 1981, was documented with increasing interest in potential of such systems. Satellite data is now acquired digitally rather than by redigitizing the GOES-Tap transmissions. Data acquisition is now automated, i.e., the computers are programmed to operate the system with little, if any, operator intervention.
A.R.H.

N82-20776 Bundesgesundheitsamt, Berlin (West Germany). Inst. fuer Wasser-, Boden- und Lufthygiene.
OPTIMAL NETWORK DENSITY FOR ATMOSPHERIC RECORDING [OPTIMALE NETZDICHTE FUER ATMOSPHAERISCHE BEOBACHTUNGEN. GRUNDLEGENDE BETRACHTUNGEN IHRER EXISTENZ UND ERMITTLUNG]
Walter Fett *In* Deutscher Wetterdienst Soc. Meteorol. Palatina, 1780-1795 1980 p 167-168 ref In GERMAN; ENGLISH summary
Avail: Issuing Activity

Statistical parameters are derived in a theoretical-statistical manner for space-correlated events. The procedure is applied to the case of heavy precipitation in a long range dense recording network and to cases of air pollution measurements in an urban network.
J.M.S.

N82-20782 Deutsche Forschungs- und Versuchsanstalt fuer Luft- und Raumfahrt, Oberpfaffenhofen (West Germany). Inst. fuer Physik der Atmosphaere.
SOUNDING THE AEROSOL DISTRIBUTION OVER THE UPPER RHINE VALLEY IN THE VALLEY IN THE SPEYER AREA BY MEANS OF LIDAR [SONDIERUNG DER AEROSOLSCHICHTUNG UEBER DEM OBERRHEINGRABEN IN RAUM SPEYER MITTELS FLUGZEUG-LIDAR]
P. Moerl, M. E. Reinhardt, W. Renger, and R. Schellhase *In* Deutscher Wetterdienst Soc. Meteorol. Palatina, 1780-1795 1980 p 183-184 refs In GERMAN

Avail: Issuing Activity

The aerosol lidar system on meteorological research airplanes is outlined. The sonde method makes the following observations: (1) soil measurements (smog layers with temperature boundary effects), (2) control of harmful material emission by large industrial complexes; (3) determination of fresh air flow course as an aid in construction planning; (4) precision sounding of smoke plumes; (5) sounding upper layers of clouds; and (6) fine structure and dynamic methods of aerosol stratification.
Transl. by E.A.K.

N82-20802 Freie Univ., Berlin (West Germany). Inst. fuer Meteorologie.
DUST FROM THE SAHARA IN SATELLITE IMAGES [SAHARASTAUB IM SATELLITENBILD]
Ute Katergiannakis *In* Deutscher Wetterdienst Soc. Meteorol. Palatina, 1780-1795 1980 p 246-248 refs In GERMAN; ENGLISH summary

Avail: Issuing Activity

In satellite images of North Africa and the surrounding seas visibility is often obscured by sand and dust. This cloudiness appears in images of visible targets as a fine, light grey screen, which is probably a cirrostratus cloud. In infrared images sand and dust storms are seldom observed. Images of a dust wall in the inner Sahara desert, a sandstorm over the Mediterranean, and a dust cloud over the Atlantic ocean are shown.
E.A.K.

N82-21667*# Research Triangle Inst., Research Triangle Park, N.C.
A STUDY OF MODEL PARAMETERS ASSOCIATED WITH THE URBAN CLIMATE USING HCMM DATA Quarterly

Progress Report
Nov. 1981 5 p HCMM
(Contract NAS5-26442)
(E82-10140; NASA-CR-168525; NAS 1.26:168525) Avail: NTIS HC A02/MF A01 CSCL 13B

The use of infrared and visible data from the Heat Capacity Mapping Mission (HCMM) and in situ data to study the intensity of the urban heat island of Saint Louis is described. Analysis of HCMM data shows that an urban heat island exists day and night in all seasons when clear skies prevail. The lower albedo value of the urban region during the day suggests that the higher temperatures are due to more absorption of solar radiation. Preliminary analysis of in situ meteorological data was performed after merging with HCMM data, and surface roughness, the exchange coefficient, and the soil moisture were calculated. J.D.

N82-21683*# Research Triangle Inst., Research Triangle Park, N. C. Geosciences Dept.
A STUDY OF MODEL PARAMETERS ASSOCIATED WITH THE URBAN CLIMATE USING HCMM DATA Quarterly Progress Report
Jul. 1981 7 p HCMM
(Contract NAS5-26442)
(E82-10159; NASA-CR-168542; NAS 1.26:168542) Avail: NTIS HC A02/MF A01 CSCL 13B

Infrared and visible data from the Heat Capacity Mapping Mission (HCMM) satellite were used to study the intensity of the urban heat island, commonly defined as the temperature difference between the center of the city and the surrounding suburban and rural regions, as a function of changes in the season and changes in meteorological conditions in order to derive various parameters which may be used in numerical models for urban climate. The analysis was focused on the city of St. Louis; and in situ data from St. Louis was combined with HCMM data in order to derive the various parameters. The HCMM data were mapped onto a Mercator projection map of the city and ground temperatures were established using data corrected for the effects of atmospheric absorption. The corrected and uncorrected HCMM data were compared to determine the magnitude of the error induced by atmospheric effects. M.G.

N82-21684*# Research Triangle Inst., Research Triangle Park, N. C. Geosciences Dept.
A STUDY OF MODEL PARAMETERS ASSOCIATED WITH THE URBAN CLIMATE USING HCMM DATA Quarterly Progress Report
Apr. 1981 7 p HCMM
(Contract NAS5-26442)
(E82-10160; NASA-CR-168543; NAS 1.26:168543) Avail: NTIS HC A02/MF A01 CSCL 13B

Progress in the study of the intensity of the urban heat island is reported. The intensity of the heat island is commonly defined as the temperature difference between the center of the city and the surrounding suburban and rural regions. The intensity is considered as a function of changes in the season and changes in meteorological conditions in order to derive various parameters which may be used in numerical models for urban climate. Twelve case studies were selected and CCT's were ordered. In situ data was obtained from sixteen stations scattered about the city of St. Louis. Upper-air meteorological data were obtained and the water vapor and the temperature data were processed. Atmospheric transmissivities were computed for each of the case studies. T.M.

N82-21685*# Pennsylvania State Univ., University Park. Dept. of Meteorology.
APPLICATIONS OF HCMM SATELLITE DATA TO THE STUDY OF URBAN HEATING PATTERNS Final Report, Dec. 1977 - Dec. 1980
Toby N. Carlson, Principal Investigator 1 Dec. 1980 71 p refs Original contains imagery. Original imagery may be purchased from NASA Goddard Space Flight Center, (code 601), Greenbelt, Md. 20771. Domestic users send orders to 'Attn: National Space Science Data Center'; non-domestic users send orders to 'Attn: World Data Centr A for Rockets and Satellites'. HCMM
(Contract NAS5-24264)
(E82-10161; NASA-CR-168544; NAS 1.26:168544) Avail: NTIS HC A04/MF A01 CSCL 13B

A research summary is presented and is divided into two major areas, one developmental and the other basic science. In the first three sub-categories are discussed: image processing techniques, especially the method whereby surface temperature image are converted to images of surface energy budget, moisture availability and thermal inertia; model development; and model verification. Basic science includes the use of a method to further the understanding of the urban heat island and anthropogenic modification of the surface heating, evaporation over vegetated surfaces, and the effect of surface heat flux on plume spread. T.M.

READEX FICHE best copy available

03

GEODESY AND CARTOGRAPHY

Includes mapping and topography.

A82-20340 † **Reconstruction of a present-day landscape map of a central part of Italy using space images (Obnovlenie karty sovremennykh landshaftov tsentral'noi chasti Italii po kosmicheskim snimkam).** E. V. Glushko, E. P. Romanova, and K. N. Sukhanova (Moskovskii Gosudarstvennyi Universitet, Moscow, USSR). *Issledovanie Zemli iz Kosmosa,* Nov.-Dec. 1981, p. 19-26. 7 refs In Russian.

The possibility of reconstructing a landscape map on the basis of space images is demonstrated by the example of a landscape map of a portion of central Italy at a scale of 1:2,000,000. Multispectral scanner data were obtained on October 3, 1980 by the Meteor-satellite Fragment system in the 0.7-0.8 and 0.8-1.1 micron spectral bands for an area of 17,600 sq km. The images were used to produce a map scheme for interpreting the landscapes; this map is also compared with a natural-resources map of the same territory. B.J.

A82-20407 **Mapping in tropical forests - A new approach using the laser APR.** H. Arp, J. C. Griesbach (TRANARG CA, Caracas, Venezuela), and J. P. Burns. *Photogrammetric Engineering and Remote Sensing,* vol. 48, Jan. 1982, p. 91-100. 7 refs.

Novel techniques involving the Laser Airborne Profile Recorder (Laser APR) have been developed as a solution to the problem of topographic mapping in dense tropical forests. The narrow laser beam used is able not only to record profiles of the tree canopy, but penetrate through small openings to ground level. Tree heights are then determined by comparing recorded profiles. The system is applied to the mapping of the Rio Caura reservoir site in southern Venezuela, where topographic maps showing 5-10 m contours of the 800 sq km area were completed in five months by means of Laser APR flights at 1.5 km intervals. A special, three-channel Autotape, mounted on a helicopter, was used in photogrammetric control location by trilateration from ground stations to the hovering aircraft. Many Laser APR-derived elevations were identified on the existing, 1:50,000-scale photography used for the mapping. O.C.

A82-21036 **Application and experimental verification of an empirical backscattering cross section model for the earth's surface.** W. Keydel (Deutsche Forschungs- und Versuchsanstalt für Luft- und Raumfahrt, Institut für Hochfrequenztechnik, Oberpfaffenhofen, West Germany). *IEEE Transactions on Geoscience and Remote Sensing,* vol. GE-20, Jan. 1982, p. 67-71.

The spectral power density of ground clutter for a radar moving horizontally over the ground is calculated and the results are compared with measured values. An empirical model for the backscattering per unit area is employed to generate values for scattering cross sections from a sea surface. The predictions are found to agree well with 60% grazing angle measurements of the Baltic Sea. The analysis is concluded to hold for incoherent scattering, thereby extending the model's effectiveness into the statistical area. M.S.K.

A82-21037 **On randomly absorbing and scattering surface layers.** E. Schanda (Bern, Universität, Berne, Switzerland). *IEEE Transactions on Geoscience and Remote Sensing,* vol. GE-20, Jan. 1982, p. 72-76. 7 refs.

Radar wave scattering from a natural surface modelled as a heterogeneous layer of finite thickness consisting of randomly distributed concentrations and dilutions within a background dielectric is studied. The illumination of the modelled surface with a coherent plane wave yields a coherent and diffuse backscatter, and the dimensions of the fluctuations of the complex index of refraction is described by a delta correlation in the direction perpendicular to the mean surface and by a finitely extended correlation in the plane of the mean surface. A continuous distribution of random absorption and phase irregularities is formulated and consideration is given to albedo and emissivity. The replacement of the planar nature of the model with more realistic phase and absorption distributions, including the background medium and the natural parameters of the surface layer is indicated. M.S.K.

A82-21038 **A radar signature model for partially coherent scattering from irregular surfaces.** E. P. W. Attema, P. J. Van Kats, and L. Krul (Delft, Technische Hogeschool, Delft, Netherlands). *IEEE Transactions on Geoscience and Remote Sensing,* vol. GE-20, Jan. 1982, p. 76-84. 9 refs.

An electromagnetic scattering model for radar surface sensing is presented which accounts for spatial correlation beyond the contour of the illuminated area. Specifically, targets whose sizes of irregularities and radii of curvature are not larger than the radar wavelength and which have sizes which are not much smaller than the scanned area are considered. A two scale surface roughness is examined for small scale irregularities riding on gentle undulations. Particular attention is given to discrepancies between radar backscatter data from airborne scatterometry and from short-range scatterometry. The scattering model is compared with existing sea surface scatterometer data with favorable results. M.S.K.

A82-22147 **Landsat thermal imaging of alpine regions.** R. Lougeay (State University, New York, Geneseo, NY). *Photogrammetric Engineering and Remote Sensing,* vol. 48, Feb. 1982, p. 269-273. 15 refs.

Satellite-borne thermal data from Landsat are shown to be of utility in alpine regions. Even the highly degraded Landsat-3 thermal data are shown to contain information which aids in the interpretation of imagery depicting highly glacierized landscapes with extreme topographic texture. Comparison is given between Landsat-3 visible (MSS band 5,600-700 nm) and thermal infrared (MSS band 8, 10,400-12,600 nm) images. Thermal patterns displayed on the Landsat thermal image are compared with ground level observations of radiometric emittance. The thermal data are shown to provide a rendition of topographic texture lacking in other spectral bands of Landsat data. (Author)

A82-25234 † **Orbital methods of celestial geodesy (Orbital'nye metody kosmicheskoi geodezii).** M. S. Urmaev. Moscow, Izdatel'stvo Nedra, 1981. 256 p. 74 refs. In Russian.

The book presents the state-of-the-art in the mathematical treatment of measurements used in orbital methods of celestial geodesy for the determination of the coordinates of satellite observation points. Basic principles of the use of orbital methods are examined, with attention given to the linearization of the fundamental equations and the solution of the overdetermined system of equations by the least squares method. The theory of the two-body problem is considered as the theoretical basis of the method, and a model of perturbed motion of a satellite is analyzed. The theory and methods of the calculation of the matrixant, a matrix of derivatives of the changing orbital elements with respect to their initial values, are examined in detail, and the numerical integration of the differential equations of motion by the Runge-Kutta, Adams, sequential approximation, Shenks, Bulirsh and Stoer, and Everhart methods is considered. The problem of the coordinate-time coupling of the results of spaceborne photography of the earth and moon by orbital methods is also discussed, and the nature of the measurements of orbital methods is examined in relation to the problem of observability. A.L.W.

A82-26012 **A structural synthesis of Brazil, based on the study of major lineaments derived from remote sensing imagery interpretation.** O. P. G. Braun (Companhia de Pesquisa de Recursos Minerais, Rio de Janeiro, Brazil). *Photogrammetria,* vol. 37, Feb. 1982, p. 77-108. 11 refs. Translation. Research sponsored by the Companhia de Pesquisa de Recursos Minerais.

A structural synthesis of the Brazil topography is presented, based on SAR imagery from Landsat and SLAR data. Lineaments are divided into straight or curved alignments of discontinuous linear and congruent elements, and linear features extending several hundred kilometers. Manifestations of fracture zones are reviewed, including quartz bands, intercrossed faults, and volcanic rock dykes. The extended lineaments are noted to originate from fault zones with high angle planes, and main zones are distinguished in terms of post-Bambui activity and diastrophism-originated faults. Tectonic interpretations are given of the structural differences between the western and eastern parts of the country. Landsat topographic data was gathered on band 7 and phytophysiognomic properties on band 5. M.S.K.

A82-26048 **Area determination by means of the method of finite elements (Flächenbestimmung mit der Methode der Finiten Elemente).** G. Melykuti (Budapesti Muszaki Egyetem, Budapest, Hungary). *Bildmessung und Luftbildwesen,* vol. 50, Mar. 1, 1982, p. 49-58. In German. Research supported by the Alexander von Humboldt-Stiftung.

The method of finite elements provides very suitable approaches to take into consideration topographical characteristics and particularities in a mathematical description of the surface of the earth. The mathematical foundations of this method are discussed. The considered surface is a two-dimensional scalar field. The values of the scalar field and certain field characteristics are known at a finite number of points. Questions regarding the given relationships can be solved by differential geometry. The area can be determined with the aid of a differential equation and various boundary conditions. Approaches for solving the involved problems are discussed. An approximate solution can be obtained on the basis of the principle of the Ritz method by making use of a finite element procedure. This approach provides appropriate possibilities for taking into consideration the various boundary conditions. G.R.

A82-26266 * **Harmonic structure of Pc 3-4 pulsations.** K. Takahashi and R. L. McPherron (California, University, Los Angeles, CA). *Journal of Geophysical Research,* vol. 87, Mar. 1, 1982, p. 1504-1516. 49 refs. Grant No. NGL-05-007-004; Contract No. N00014-75-C-0396.

Power spectra of magnetic pulsations observed at synchronous orbit by the ATS 6 satellite often show several spectral peaks simultaneously. Such pulsations, called harmonic events because of the nearly constant separation between successive peaks, are continuously observed in the dayside in the Pc 3-4 frequency range (6.6-100 mHz). The harmonic events are seen clearly only in the east-west magnetic field component. The spectral peaks are regularly spaced with a typical minimum separation of 14 mHz in the morning gradually decreasing to 10 mHz in the afternoon. In the dynamic spectra of harmonic events, the fundamental mode is usually absent. In addition, the relative amplitudes of the higher harmonics depend on the magnetic latitude. These observed features can be explained by a standing Alfven wave consisting of many discrete harmonic frequencies. A statistical analysis of power spectra demonstrates that at least 10-30% of Pc 3 pulsations can be classified as harmonic events. For a selected event on August 7, 1975, the plasma mass density at the synchronous orbit is estimated to be 3-8 hydrogen mass/cu cm. (Author)

A82-26843 **Cliff and slope topography of part of the Grand Canyon, Arizona as characterized on a Seasat radar image.** G. L. Berlin, G. C. Schaber, R. C. Kozak, and P. Chavez, Jr. (U.S. Geological Survey, Flagstaff, AZ). *Remote Sensing of Environment,* vol. 12, Mar. 1982, p. 81-85.

A82-27507 † **Investigation of the earth on the basis of space photographic data (Issledovanie planety zemlia po materialam kosmicheskoi fotoinformatsii).** V. D. Bol'shakov. In: Scientific lectures on aviation and astronautics 1980. Moscow, Izdatel'stvo Nauka, 1981, p. 57-66. In Russian.

The remote sensing of the earth's surface using the Zond and Salyut spacecraft is discussed, with particular emphasis on the use of space data for small-scale mapping and the revision of existing maps. The significance of color and multispectral photography for the remote sensing of earth resources is considered, and results on the study of the earth's figure from its planetary photographs are presented. Attention is also given to the development of efficient and automated operational systems of complex and thematic interpretation. B.J.

A82-27584 # **Airborne laser systems use in terrain mapping.** L. E. Link and J. G. Collins (U.S. Army, Engineer Waterways Experiment Station, Vicksburg, MS). In: International Symposium on Remote Sensing of Environment, 15th, Ann Arbor, MI, May 11-15, 1981, Proceedings. Volume 1. Ann Arbor, MI, Environmental Research Institute of Michigan, 1981, p. 95-110. 21 refs.

Perhaps the most significant recent advancements in measurement technology have resulted from the invention of the laser. As early as the mid-1960's, lasers were being placed in aircraft to examine their applicability to terrain mapping. The emerging new mapping technique has the potential to dramatically improve the capability to map topographic features and to provide quantitative environmental quality data that was previously impractical to acquire over large areas. Airborne laser mapping systems have two major components. A laser altimeter accurately measures the distance from the aircraft to a reflecting surface. Simultaneously, the positioning system records the location and orientation of the aircraft. Attention is given to details of laser system operation, positioning system operation, the status of available airborne systems, and airborne laser systems applications. G.R.

A82-27611 # **Application of side-looking color infrared photography for structure detection in subtle topography.** J. Aghassy (Pittsburgh, University, Pittsburgh, PA) and Z. Berger (Exxon Production Research Co., Houston, TX). In: International Symposium on Remote Sensing of Environment, 15th, Ann Arbor, MI, May 11-15, 1981, Proceedings. Volume 1. Ann Arbor, MI, Environmental Research Institute of Michigan, 1981, p. 491-497. 7 refs.

Examples are cited from a pilot study evaluating surface-form relationships in subtle topographies. Sequential photography taken from 150 m, 300 m, and 500 m above ground level at varying distances from the rims surrounding certain geological structures illustrates that the optimal height coupled with the optimal distance can unveil important stream and slope elements that aid in identifying structures. In addition, a comparison between color photography and Side-Looking Color Infrared (SLCIR) shows that in regular color photography, the close elements of topography are clear whereas the more remote ones are masked by haze in spite of filtering devices. In color IR, the effect of haze on distant elements is much less pronounced, and the details of successive parallel ridges are more clearly visible. SLCIR photos provide valuable insight into the normal evolutionary erosional process of surface expression and drainage components generated above different geological structures, thereby aiding in the verification of anomalies observed in Landsat imagery. C.R.

A82-27615 # **Topographic mapping using Landsat data.** G. D. Lodwick (Calgary, University, Calgary, Alberta, Canada). In: International Symposium on Remote Sensing of Environment, 15th, Ann Arbor, MI, May 11-15, 1981, Proceedings. Volume 2. Ann Arbor, MI, Environmental Research Institute of Michigan, 1981, p. 527-534.

The reported work developed from a major research project recently completed, which resulted in the development of a comprehensive computer system to identify and monitor ecological changes in multitemporal Landsat data. The project involved investigation of a study area in the upper Hunter Valley of New South Wales, Australia. A sequence of seven images taken in 1976 was analyzed. The method of cartographic adjustment was to model the surface of each image using complete cubic polynomials, spatially resected onto 21 ground control points. Attention is given to the prediction of site slope and the refinement of slope prediction. For this research project, data interpretation is concerned with evaluating the principal components and their scores. This involves broad observation throughout the study area, as well as specific observation at 25 sample sites using scores from all seven Landsat images. G.R.

A82-27631 * # **Wide area, coarse resolution imaging with satellite-borne synthetic aperture radars in low-earth and geosynchronous orbits.** K. Tomiyasu (GE Valley Forge Space Center, Philadelphia, PA). In: International Symposium on Remote Sensing of Environment, 15th, Ann Arbor, MI, May 11-15, 1981, Proceedings. Volume 2. Ann Arbor, MI, Environmental Research Institute of Michigan, 1981, p.701-709. 9 refs. Contract No. NAS1-15657.

The LEOSAR (low-earth-orbit synthetic aperture radar) can map around the earth, while the GEOSAR (geosynchronous synthetic aperture radar) can map a large global area bounded in both longitudinal and latitudinal ranges. This paper presents the mapping capabilities and power requirements of both LEOSAR and GEOSAR. For a low-earth-orbit SAR, images of swath widths of the order of 700 km are possible with 100-m resolution and 300 watts of average transmitter power at 9375 MHz. From a SAR in a 50-deg inclined geosynchronous circular orbit, the contiguous United States can be imaged in about 6.4 hours with 100-m resolution, 345 watts of average transmitter power, and a data rate of 6 megabits/sec at 2450 MHz. B.J.

A82-27632 * # A shuttle scanning laser altimeter for topographic mapping. M. Kobrick and C. Elachi (California Institute of Technology, Jet Propulsion Laboratory, Pasadena, CA). In: International Symposium on Remote Sensing of Environment, 15th, Ann Arbor, MI, May 11-15, 1981, Proceedings. Volume 2. Ann Arbor, MI, Environmental Research Institute of Michigan, 1981, p. 711-714.

The shuttle scanning laser altimeter is an instrument, currently under development at JPL, capable of producing a three-dimensional elevation map of the topography along a wide swath beneath a spaceborne platform. Operating on the same principle as radar (broadcast of a short pulse of radiation and timing the reception of an echo) the very narrow beamwidths and high pulse rates of modern lasers would allow a significant breakthrough in the areal resolution capability of altimeters. Specifically, the copper vapor laser currently available and planned for use would provide 50 meter horizontal and 3 meter vertical resolution over a 10 kilometer continuous swath or, in a snapshot mode, a 50 kilometer square area. (Author)

A82-28134 † Analytic methods of geodetic referencing of nontopographic images (Analiticheskie metody geodezicheskoi priviazki netopograficheskikh izobrazhenii). V. I. Akovetskii, Iu. N. Korneev, and A. S. Sergeev. *(Vsesoiuznaia Konferentsiia po Problemam Issledovaniia Prirodnykh Resursov Zemli i Mirovogo Okeana, Aviatsionno-Kosmicheskimi Sredstvami, Moscow, USSR, Nov. 1980.) Geodeziia i Aerofotos'emka,* no. 1, 1982, p. 41-49. 6 refs. In Russian.

The paper examines the mathematical details of an analytic method for determining coordinates on the earth's surface from nontopographic images; the method can be used to solve a number of topographic and thematic problems. The method implemented on the Riad computer, has been experimentally verified and shown good results. The algorithm for solving a given problem consists of two independent elements: the solution of the direct photogrammetric intersection problem, and the solution of the inverse problem. B.J.

A82-28138 † Possibilities of using experience gained from the thematic mapping of the moon in studies of earth resources by remote sensing methods (O vozmozhnostiakh ispol'zovaniia opyta tematicheskogo kartografirovaniia luny pri issledovanii prirodnykh resursov zemli distantsionnymi metodami). N. N. Evsiukov, I. Iu. Levitskii, and I. G. Chervanev. *(Vsesoiuznaia Konferentsiia po Problemam Issledovaniia Prirodnykh Resursov Zemli i Mirovogo Okeana, Aviatsionno-Kosmicheskimi Sredstvami, Moscow, USSR, Nov. 1980.) Geodeziia i Aerofotos'emka,* no. 1, 1982, p. 66-72. 9 refs. In Russian.

Kharkov University has a facility that specializes in the mapping of the lunar surface on the basis of the photometric processing of photographic images; the facility incorporates automated processing of remote sensing images and mathematical techniques of cartographic analysis. This paper examines the possibility of applying techniques developed at this facility to the remote sensing and mapping of earth resources. Particular attention is given to the potential usefulness of a two-parameter map of the lunar surface. B.J.

A82-28139 † Potential use of space photographs obtained from the manned orbital station Salyut-5 in order to compile a set of small-scale thematic maps of mountain and piedmont regions of Central Asia (Vozmozhnosti ispol'zovaniia kosmicheskikh snimkov, poluchennykh s orbital'noi pilotiruemoi stantsii 'Saliut-5', dlia sostavleniia kompleksa [illegible]komasshtabnykh tematicheskikh kartskhem gornykh i predgo[illegible]ykh raionov Srednei Azii). G. G. Bakai and E. M. Nikolaeva. *(Vsesoiu[illegible] [illegible]nferentsiia po Problemam Issledovaniia Prirodnykh Resursov Zemli i Mirovogo Okeana, Aviatsionno-Kosmicheskimi Sredstvami, Moscow, USSR, Nov. 1980.) Geodeziia i Aerofotos'emka,* no. 1, 1982, p. 72-76. In Russian.

N82-17599 Colorado State Univ., Fort Collins.
REGIONAL PROPERTIES OF ANGULAR REFLECTANCE MODELS Ph.D. Thesis
John Michael Davis 1981 215 p
Avail: Univ. Microfilms Order No. 8126427

The inference of the reflected flux density from satellite radiance measurements requires a knowledge of the angular properties of the reflected radiance field. The angular dependence and the spatial variability of the radiance fields reflected from 30 regional atmospheric scenes were examined. The reflected radiance data set was collected from a high altitude aircraft during the Summer Monsoon Experiment using a unique multi-detector instrument which permitted an instantaneous sampling of the radiance fields from twelve angular veiwing coordinates. All of the scenes display sufficient anisotropy to conclude that neglecting the angular variation of the reflected radiances would lead to significant errors (10-100%) in the inferred flux density. Radiances over the relatively isotropic scenes converge to their regional mean values on a spatial scale which is small compared to that of the total region. Dissert. Abstr.

N82-17708*# Jet Propulsion Lab., California Inst. of Tech., Pasadena.
SESSION III OF THE VLBI/LASER INTERCOMPARISON TASK OF THE NASA CRUSTAL DYNAMICS PROJECT
Henry Fliegel 1 Nov. 1981 50 p refs
(Contract NAS7-100)
(NASA-CR-168427; JPL-Pub-81-96) Avail: NTIS HC A03/MF A01 CSCL 08E

Baseline vector measurements are reported for a line crossing most of the state of California from Quincy to Mt. Otay near the Mexican border. They were obtained to compare three space geodetic techniques: very long baseline interferometry, satellite laser ranging, and Doppler satellite tracking. A.R.H.

N82-17711# Instituto de Pesquisas Espaciais, Sao Jose dos Campos (Brazil).
PARTICLE PRECIPITATION AND ATMOSPHERIC X-AND GAMMA-RAYS IN THE SOUTH ATLANTIC MAGNETIC ANOMALY BY BALLOON EXPERIMENTS Progress Report, 1968 - 1981
Jose Marques daCosta Jun. 1981 10 p refs Presented at the 1st Aeronomy Workshop Brazil-Argentina, Foz do Iguacu, Brazil, 18-20 Jul. 1981 Sponsored in part by the Fundo Nacional de Desenvolvimento Cientifico e Technologico - FNDCT
(INPE-2119-RPE/343) Avail: NTIS HC A02/MF A01

Particle precipitation from the Van Allen belts into the atmosphere of the South Atlantic magnetic anomaly region, were observed with balloon-borne instrumentation. Balloons carrying onboard charged particle and X-and gamma ray detectors formed by plastic scintillators were used. Measurements of bremsstrahlung X-rays and low energy gamma rays as well as the charged particles themselves were made at the altitude of the stratospheric balloons, and simultaneous measurements of the geomagnetic variations were made by rapid run ground magnetometers. S.L.

N82-17714*# National Aeronautics and Space Administration. Goddard Space Flight Center, Greenbelt, Md.
SOME NEW METHODS IN GEOMAGNETIC FIELD MODELING APPLIED TO THE 1960 - 1980 EPOCH
R. A. Langel, R. H. Estes (Business and Technological Systems, Seabrook, Md.), and G. H. Mead Dec. 1981 42 p refs Submitted for publication
(NASA-TM-83868) Avail: NTIS HC A03/MF A01 CSCL 08N

The utilization of satellite and surface data together permitted the incorporation of a solution for the anomaly field at each observatory. The residuals of the observatory measurements to such models is commensurate with the actual measurment accuracy. Incorporation of the anomaly estimation enabled the inclusion of stable time derivatives of the spherical harmonic coefficients up to the third derivative. A spherical harmonic model is derived with degree and order 13 in its constant and first time derivative terms, six in its second derivative terms and four in its third derivative terms. E.A.K.

N82-17716*# National Aeronautics and Space Administration. Goddard Space Flight Center, Greenbelt, Md.

SATELLITE AND SURFACE GEOPHYSICAL EXPRESSION OF ANOMALOUS CRUSTAL STRUCTURE IN KENTUCKY AND TENNESSEE

M. A. Mayhew (BTS, Inc.), H. H. Thomas, and P. J. Wasilewski
Jul. 1981 29 p refs
(NASA-TM-82163) Avail: NTIS HC A03/MF A01 CSCL 08N

An equivalent layer magnetization model is discussed. Inversion of long wavelength satellite magnetic anomaly data indicates a very magnetic source region centered in south central Kentucky. Refraction profiles suggest that the source of the gravity anomaly is a large mass of rock occupying much of the crustal thickness. The outline of the source delineated by gravity contours is also discernible in aeromagnetic anomaly patterns. The mafic plutonic complex, and several lines of evidence are consistent with a rift association. The body is, however, clearly related to the inferred position of the Grenville Front. It is bounded on the north by the fault zones of the 38th Parallel Lineament. It is suggested that such magnetization levels are achieved with magnetic mineralogies produced by normal oxidation and metamorphic processes and enhanced by viscous build-up, especially in mafic rocks of alkaline character. E.A.K.

N82-18930# Defense Mapping Agency Aerospace Center, St. Louis, Mo.

MATRIX DATA ANALYSIS: COLOR/B AND W CODING IS NOT ALWAYS ENOUGH Interim Report, 1976 - 1981

Marshall B. Faintich 1981 6 p refs
(AD-A108406) Avail: NTIS HC A02/MF A01 CSCL 09/2

The Defense Mapping Agency produces digital data bases that describe the physical appearance of the surface of the Earth. These data bases include, but are not limited to, terrain elevation, culture including landscape characteristics, and vertical features. This data is collected from digitized source maps, from optically or digitally correlated stereopairs of photographic imagery, and from digital multi-spectral sensor data. A dramatic impact has been made in the ability to analyze these digital data bases by applying state-of-the-art digital image technology processing and display concepts. These include a variety of color and/or black and white displays of not only intensity/color coded matrix data, but also image processed data using specialized convolution filters, texture discrimination, and special color representation techniques. In addition, computer generated imagery from these data bases serve as a final analysis tool. Author (GRA)

N82-18931# Defense Mapping Agency Aerospace Center, St. Louis, Mo.

PROFILING SENSITIVITY TO IMAGE QUALITY Final Report

Dennis E. Moellman Oct. 1981 21 p refs
(AD-A108405) Avail: NTIS HC A02/MF A01 CSCL 09/2

This paper reports results from a study conducted by the Defense Mapping Agency (DMA) to determine the sensitivity of terrain profiling accuracy to input image quality. The study was accomplished by building a set of stereo test models over a test site; exercising those test models with current instruments; reducing the resultant profile data and comparing the results to existing ground control for the test site. The test models were produced from a single model by repeated steps of photographic enlargement, reduction and resolution degradation. The resultant 25 test models represented all combinations of five specific image scales and resolutions. The instruments were operated in both manual and automatic correlation modes. As a consequence the results portray the interdependence of profile accuracy with both scale and resolution as well as the effects of both manual and automatic profiling. The results also provide insight into the behavior of automatic correlation when approaching and exceeding the instrument's theoretical minimum resolution threshold. Author (GRA)

N82-19603 Deutsches Geodaetisches Forschungsinstitut, Munich (West Germany)

HELMUT WOLF: ON THE OCCASION OF HIS 70TH BIRTHDAY [HELMUT WOLF ZUM 70. GEBURTSTAG]

Verlag der Bayerischen Akademie der Wissenschaften 1980 45 p refs In GERMAN Presented at Bonn, 2 May 1980
(Ser-E-18; ISSN-0065-5341; ISBN-3-7696-9663-8) Copyright. Avail: Issuing Activity

The life and accomplishments of Helmut Wolf, and his contribution to theoretical geodesy are described. A collection of publications and lectures in the geodetic sciences is presented. Wolf's contribution to the development of geodestic surveys and to the mathematical and stochastic model of photogrammetry are outlined. Transl. by E.A.K.

N82-19604 Deutsches Geodaetisches Forschungsinstitut, Munich (West Germany).

DEVELOPMENTS IN GEODESY WITHIN THE SCOPE OF HELMUT WOLF'S WORK [DIE ENTWICKLUNG DER ERDMESSUNG IN SPIEGEL DES WERKES HELMUT WOLFS]

Helmut Moritz *In its* Helmut Wolf: On the Occasion of his 70th Birthday 1980 p 5-12 In GERMAN

Avail: Issuing Activity

Twenty years of progress in geodetic surveys, the use of artificial satellites and their practical applications are described. Gravimetric methods, astrogeodetic methods, statistical procedures in the physical geodesy, and geodetic problems in geodynamics are discussed. It is found that in the geometric reference system of deep geodynamic observations the axis of rotation of the Earth is a fundamental direction of reference which changes, whether it is in the universe or on terrestrial bodies. E.A.K.

N82-19605 Deutsches Geodaetisches Forschungsinstitut, Munich (West Germany).

MATHEMATICAL AND STOCHASTIC MODELS IN PHOTOGRAMMETRY RELATING TO HELMUT WOLF'S WORK [DAS MATHEMATISCHE UND STOCHASTISCHE MODELL DER PHOTOGRAMMETRIE MIT BEZUG AUF DAS WERK HELMUT WOLFS]

Hellmut Schmid *In its* Helmut Wolf: On the Occasion of his 70th Birthday 1980 p 13-27 In GERMAN

Avail: Issuing Activity

The development of a mathematical model which is applied to interpret the measured variables and random variables with their characteristic random noise is discussed. It is posited that for typical geometric problems, as well as for geodetic and photogrammetric tasks it is possible to analyze specific geometrically established solvent algorithms quantitatively and qualitatively. Such a computing method is often advantageous, especially because it can be applied to practical engineering. E.A.K.

N82-19616*# Business and Technological Systems, Inc., Seabrook, Md.

EQUIVALENT SOURCE MODELING OF THE MAIN FIELD USING MAGSAT DATA Quarterly Report, 1 Apr. - 30 Jun. 1981

11 Aug. 1981 4 p ERTS
(Contract NAS5-26047)
(E82-10041; NASA-CR-164918; QR-6) Avail: NTIS HC A02/MF A01 CSCL 08G

Magsat dipole solution models were obtained with both 32 deg and 21 deg resolution based on a data set extending over 4 months. Time dependence was modeled using first time derivatives for the dipole magnetization vector components. This doubles the n total number of parameters in the solution. The solutions displayed a very slow convergence in time derivatives although at each iteration the conversion of the dipole parameters to spherical harmonic coefficients showed close agreement with the MGST (12/80) spherical harmonic model to degree 13 in the constant terms and 8 in the secular variation terms. The program error in the option to simultaneously estimate observatory anomaly biases was found and corrected. A 32 deg resolution dipole model was generated using the selected magnetic observatory data from 1960-1977 used in the GSFC (9/80) spherical harmonic model. A.R.H.

N82-19618*# Brown Univ., Providence, R.I. Dept. of Geological Sciences.

ELECTROMAGNETIC DEEP-PROBING (100-1000 KMS) OF THE EARTH'S INTERIOR FROM ARTIFICIAL SATELLITES:

CONSTRAINTS ON THE REGIONAL EMPLACEMENT OF CRUSTAL RESOURCES Quarterly Progress Report, 30 Jun. - 30 Sep. 1981
John F. Hermance, Principal Investigator 30 Sep. 1981 9 p refs ERTS
(Contract NAS5-26138)
(E82-10043; NASA-CR-164920; QPR-5) Avail: NTIS HC A02/MF A01 CSCL 08G

An algorithm was developed to address the problem of electromagnetic coupling of ionospheric current systems to both a homogeneous Earth having finite conductivity, and to an Earth having gross lateral variations in its conductivity structure, e.g., the ocean-land interface. Typical results from the model simulation for ionospheric currents flowing parallel to a representative geologic discontinuity are shown. Although the total magnetic field component at the satellite altitude is an order of magnitude smaller than at the Earth's surface (because of cancellation effects from the source current), the anomalous behavior of the satellite observations as the vehicle passes over the geologic contact is relatively more important pronounced. The results discriminate among gross lithospheric structures because of difference in electrical conductivity. A.R.H.

N82-19619*# Brown Univ., Providence, R. I.
ELECTROMAGNETIC DEEP-PROBING (100-1000 KMS) OF THE EARTH'S INTERIOR FROM ARTIFICIAL SATELLITES: CONSTRAINTS ON THE REGIONAL EMPLACEMENT OF CRUSTAL RESOURCES Quarterly Progress Report, 31 Mar. 1980 - 30 Jun. 1981
John F. Hermance, Principal Investigator 30 Sep. 1981 5 p ERTS
(Contract NAS5-26138)
(E82-10044; NASA-CR-164921; QPR-4) Avail: NTIS HC A02/MF A01 CSCL 08G

Efforts continue in the development of a computer program for looking at the coupling of finite-dimensional source fields with a laterally heterogeneous Earth. An algorithm is also being developed for calculating a time-varying reference field using ground-based magnetic observatory data. It was discovered that ground-based standard magnetic observation is not as so available for the time of the MAGSAT mission as might be expected. Attempts are being made to determine the exact times and observatories from which data are available. A.R.H.

N82-19620*# Business and Technological Systems, Inc., Seabrook, Md.
MAGSAT SCIENCE INVESTIGATIONS Quarterly Report, 1 Jun. - 30 Aug. 1981
30 Aug. 1981 4 p ERTS
(Contract NAS5-26328)
(E82-10045; NASA-CR-164922; QR-4) Avail: NTIS HC A02/MF A01 CSCL 08G

The optimal source spacing for the computer delta-B data set was determined from the intermediate attitude tapes. A U.S. magnetization map based on this result is in preparation. Computed delta-B from the fine-attitude tapes is unexpectedly noisy; the reason for this is being sought. A.R.H.

N82-19625*# National Aeronautics and Space Administration. Goddard Space Flight Center, Greenbelt, Md.
STUDIES RELATED TO MAGSAT Progress Report, period ending Sep. 1981
David P. Stern, Principal Investigator 30 Sep. 1981 21 p ERTS
(E82-10050; NASA-TM-84129) Avail: NTIS HC A02/MF A01 CSCL 08G

The westward drift of the geomagnetic field was analyzed using models from Magsat which include secular variation. Two approaches were utilized. A straightforward covariance method gave large drift rates (0.25 degr./yr and up) and suggested that the drift was larger in the Southern Hemisphere than in the Northern, and was small near the poles. The drawback was a rather large noise level superimposed on a small signal. The other approach followed the method of A.D. Richmond and obtained drifts of the order of 0.1 deg/yr. The use of Magsat to study the Backus effect is explored. Particular attention is drawn to the comparison with resuls of general inverse analysis. A.R.H.

N82-19626*# Phoenix Corp., McLean, Va.
IMPROVED DEFINITION OF CRUSTAL ANOMALIES FOR MAGSAT DATA Quarterly Report
25 Mar. 1981 11 p ERTS
(Contract NAS5-25882)
(E82-10051; NASA-CR-164928; QR-6) Avail: NTIS HC A02/MF A01 CSCL 08G

A scheme was developed for separating the portions of the magnetic field measured by the Magsat 1 satellite that arise from internal and external sources. To test this method, a set of sample coefficients were used to compute the field values along a simulated satellite orbit. This data was then used to try to recover the original coefficients. Matrix inversion and recursive least squares methods were used to solve for the input coefficients. The accuracy of the two methods are compared. M.G.

N82-19648# Deutsches Geodaetisches Forschungsinstitut, Munich (West Germany).
THE DIAGNOSIS SETTLEMENT 1980 OF THE GERMAN MAIN TRIANGULATION NETWORK. PART 2: TRAJECTORIES [DIE DIAGNOSEAUSGLEICHUNG 1980 DES DEUTSCHEN HAUPTDREICKSNETZES. 2: STRECKEN]
Rudolf Schmidt Frankfurt am Main Verlag des Instituts fuer Angewandte Geodaesie 1981 501 p refs In GERMAN
(SER-B-253-Mitt-159-Pt-2; ISSN-0071-9196) Avail: NTIS HC A22/MF A01

Diagnostic balancing in triangulation networks was investigated. The purpose of defining the network for diagnostic balancing is to reduce the balance of the edge effect. The computer program is based on observations of the geographic coordinates system. The following tasks were performed: compilation of results from end to end measurements; execution of end to end measurements in the triangulation network; reduction of field length; and, calculation of end to end measurements. E.A.K.

N82-19731*# National Aeronautics and Space Administration. Goddard Space Flight Center, Greenbelt, Md.
INFORMATION THEORY LATERAL DENSITY DISTRIBUTION FOR EARTH INFERRED FROM GLOBAL GRAVITY FIELD
David Parry Rubincam Oct. 1981 64 p refs Submitted for publication
(NASA-TM-83825) Avail: NTIS HC A04/MF A01 CSCL 08N

Information Theory Inference, better known as the Maximum Entropy Method, was used to infer the lateral density distribution inside the Earth. The approach assumed that the Earth consists of indistinguishable Maxwell-Boltzmann particles populating infinitesimal volume elements, and followed the standard methods of statistical mechanics (maximizing the entropy function). The GEM 10B spherical harmonic gravity field coefficients, complete to degree and order 36, were used as constraints on the lateral density distribution. The spherically symmetric part of the density distribution was assumed to be known. The lateral density variation was assumed to be small compared to the spherically symmetric part. The resulting information theory density distribution for the cases of no crust removed, 30 km of compensated crust removed, and 30 km of uncompensated crust removed all gave broad density anomalies extending deep into the mantle, but with the density contrasts being the greatest towards the surface (typically + or 0.004 g cm 3 in the first two cases and + or - 0.04 g cm 3 in the third). None of the density distributions resemble classical organized convection cells. The information theory approach may have use in choosing Standard Earth Models, but, the inclusion of seismic data into the approach appears difficult. Author

N82-19732*# Woods Hole Oceanographic Institution, Mass.
GRAVITY AND GEOID ANOMALIES OF THE PHILIPPINE SEA: EVIDENCE ON THE DEPTH OF COMPENSATION FOR THE NEGATIVE RESIDUAL WATER DEPTH ANOMALY
Carl Bowin [1982] 27 p refs
(Grant NAG5-18)
(NASA-CR-168639; WHOI-4931) Avail: NTIS HC A03/MF A01 CSCL 08G

A negative free-air gravity anomaly which occurs in the central part of the Philippine Sea was examined to determine the distribution and nature of possible regional mass excesses or deficiencies. Geoid anomalies from GEOS-3 observation were positive. A negative residual geoid anomaly consistent with the area of negative free-air gravity anomalies were found. Theoretical gravity-topography and geoid-topography admittance functions indicated that high density mantle at about 60 km dept could account for the magnitudes of the gravity and residual geoid anomaly and the 1 km residual water depth anomaly in the Philippine Sea. The negative residual depth anomaly may be compensated for by excess density in the uppermost mantle, but the residual geoid and regional free-air gravity anomalies and a slow surface wave velocity structure might result from low-density warm upper mantle material lying beneath the zone of high-density uppermost mantle. From a horizontal disk approximation, the depth of the low-density warm mantle was estimated to be on the order of 200 km. M.D.K.

N82-20580# Bayerische Akademie der Wissenschaften, Munich (West Germany).

SOME CRITERIA FOR THE ACCURACY AND THE RELIABILITY OF NETWORKS

Hans Pelzer *In its* Contrib. from the Federal Rep. of Ger. to the 17th Gen. Assembly of Intern. Union of Geodesy and Geophys. 1980 p 55-67 refs

Avail: NTIS HC A06/MF A01

Design criteria for optimizing the quality of a geodetic network, taking both the functional and the stochastic model of the network into account, are derived. An effective global accuracy criterion is shown to be obtainable from the maximum eigenvalue of the cofactor matrix of the vector of points coordinates. The essential eigenvectors of the same matrix are identified as indicators for functions with maximum variance. A reliability criterion can be obtained by means of a reliability parameter constructed by gross error testing of each observation. To this end a nomogram is made available. Author (ESA)

N82-20581# Bayerische Akademie der Wissenschaften, Munich (West Germany).

EXPERIMENTS IN SATELLITE DOPPLER CONTROL POSITIONING AT SEA

Guenter Seeber, Delf Egge, and Hans Werner Schenke *In its* Contrib. from the Federal Rep. of Ger. to the 17th Gen. Assembly of Intern. Union of Geodesy and Geophys. 1980 p 69-80 refs Sponsored by Bundesministerium fuer Forschung- und Technologie and Deutsche Forschungsgeimschaft

Avail: NTIS HC A06/MF A01

Experiments on the application of the transit satellite system, which utilizes Doppler control positioning, for an extension of classical continental geodetic networks beyong the shore lines are described. The experiments were conducted in the North Sea area and deal with: (1) fixed point positioning on a platform; (2) positioning of a moored buoy; (3) positioning of a drifting buoy. The evaluation indicates that for fixed or stationary motion conditions no accuracy decrease occurs provided an accumulated solution is made. For nonstationary motion one has to resort to position fixes with single satellite passes so that no accumulated increase of precision can be obtained. Experiments to assess the inherent accuracy of the Doppler satellite method in a single pass solution are presently underway. Author (ESA)

N82-20583# Bayerische Akademie der Wissenschaften, Munich (West Germany).

RECENT RESULTS OF GEOID DETERMINATION BY COMBINATION TECHNIQUES IN THE NORTH SEA TEST AREA

Hans-Georg Wenzel *In its* Contrib. from the Federal Rep. of Ger. to the 17th Gen. Assembly of Intern. Union of Geodesy and Geophys. 1980 p 95-121 refs Sponsored by Deutsche Forschungsgeimschaft

Avail: NTIS HC A06/MF A01

Gravity anomalies, GEOS 3 satellite altimetry and astrogeodetic vertical deflections were used to determine gravimetric, altimetric and astrogeodetic geoids in the North Sea test area. The agreement between these independent geoids is below the 1 m level and no sea surface topography could be detected. Simple averaging techniques, and stokes and least square collocations are used to determine combined geoids with an accuracy believed to be below the 0.5 m level. Author (ESA)

N82-20585*# Wisconsin Univ., Madison.

INVESTIGATION OF ANTARCTIC CRUST AND UPPER MANTLE USING MAGSAT AND OTHER GEOPHYSICAL DATA Quarterly Progress Report

C. R. Bentley, Principal Investigator 9 Sep. 1981 2 p refs ERTS

(Contract NAS5-25977)

(E82-10062; NASA-CR-165084; NAS 1.26:165084; QPR-6) Avail: NTIS HC A02/MF A01 CSCL 08G

Progress in processing and analysis of Investigator B MAGSAT data is reported. Data processing tasks required prior to data analysis, including translation and reformatting of tapes and development of computer routines, were performed. A scalar anomaly map of Antarctica is near completion. Data analysis included a qualitative correlation of NASA's 4/81 scalar map of Antarctica with other geopotential data and correlation of POGO and continental scale gravity data with MAGSAT data. A magnetic high was found to exist over the Ross Embayment. J.D.H.

N82-20589*# Analytic Sciences Corp., Reading, Mass.

[MAGSAT ANOMALY PROFILES OF THE EASTERN INDIAN OCEAN] Quarterly Progress Report, 1 Apr. - 30 Jun. 1981

Richard V. Sailor, Principal Investigator and Andrew R. Lazarewicz 15 Aug. 1981 21 p refs ERTS

(Contract NAS5-26424)

(E82-10066; NASA-CR-165088; NAS 1.26:165088; PR-1325-2) Avail: NTIS HC A02/MF A01 CSCL 05B

Ground tracks from SEASAT were used in an effort to develop qualititative relationships between the gravity field and MAGSAT magnetic anomalies in the eastern Indian Ocean. Investigation of data quality led to analyses of the average value (over 80 vector data points, or approximately 36 km intervals) and of the standard deviation of this average, as a mean of identifying noisy portions of the data. It was discovered that the plots of the average value minus the individual (measured) point value are most useful for identifying noisy areas and data spikes. Spectrum analysis using edited (spikes removed) data show that the noise floor is less than 1 nT and the slope of the spectrum in the region of wavelengths between 1200 km and 250 km is approximately -3. Consequently the estimated resolution limit improved from approximately 360 km to approximately 250 km. A.R.H.

N82-20598*# Liverpool Univ. (England).

SPHERICAL HARMONIC REPRESENTATION OF THE MAIN GEOMAGNETIC FIELD FOR WORLD CHARTING AND INVESTIGATIONS OF SOME FUNDAMENTAL PROBLEMS OF PHYSICS AND GEOPHYSICS Progress Report

D. R. Barraclough, R. Hide, B. R. Leaton, F. J. Lowes, S. R. C. Malin, and R. L. Wilson, Principal Investigators 1 Oct. 1981 8 p refs Sponsored by NASA ERTS

(E82-10075; NASA-CR-165097; NAS 1.26:165097) Avail: NTIS HC A02/MF A01 CSCL 08G

Quiet-day data from MAGSAT were examined for effects which might test the validity of Maxwell's equations. Both external and toroidal fields which might represent a violation of the equations appear to exist, well within the associated errors. The external field might be associated with the ring current, and varies of a time-scale of one day or less. Its orientation is parallel to the geomagetic dipole. The toriodal field can be confused with an orientation in error (in yaw). It the toroidal field really exists, its can be related to either ionospheric currents, or to toroidal fields in the Earth's core in accordance with Einstein's unified field theory, or to both. Author

N82-21475# Canada Centre for Remote Sensing, Ottawa (Ontario).

RELIEF EFFECTS AND THE USE OF TERRAIN MODELS IN SAR IMAGE PROCESSING

B. Guindon, P. M. Teillet, D. G. Goodenough, K. Dickinson (INTERA Environmental Consultants, Calgary, Canada), and J. F. Meunier (INTERA Environmental Consultants, Calgary, Canada) *In* ESA SAR Image Quality Jun. 1981 p 89-92 refs

Avail: NTIS HC A05/MF A01; ESA, Paris FF 55 (US $12)

The use of digital terrain models in Canada to overcome the effects of topographic relief on geometric and radiometric fidelity of SAR imagery is discussed. Digital elevaton models (DEM) can reduce, to 15 m, errors incurred in overlaying multipass SAR imagery of mountainous terrain. Neglect of topography can result in errors of hundreds of meters. Shadow or layover problem areas can be identified using DEM's. Author (ESA)

N82-21659*# Paris VI Univ. (France).

PRELIMINARY MODELS OF THE CORE FIELD Progress Report

Jean-Louis LeMouel, Principal Investigator, Armand Galdeano, and Joel Ducruix 1 Aug. 1981 5 p Sponsored by NASA ERTS

(E82-10129; NASA-CR-168513; NAS 1.26:168513) Avail: NTIS HC A02/MF A01 CSCL 05B

Using the CHROFIN tapes containing MAGSAT data for the month of December, two spherical harmonic models were prepared. One of these models was specially designed to study the Bangui anomaly region. For this region an attempt was made to downward continue the data and to compare it with the existing ground level map. M.G.

N82-21674*# Wisconsin Univ., Madison.

INVESTIGATION OF ANTARCTIC CRUST AND UPPER MANTLE USING MAGSAT AND OTHER GEOPHYSICAL DATA Quarterly Status and Technical Progress Report

C. R. Bentley, Principal Investigator 30 Nov. 1981 6 p refs ERTS

(Contract NAS5-25977)

(E82-10147; NASA-CR-168532; NAS 1.26:168532; QTPR-7) Avail: NTIS HC A02/MF A01 CSCL 08G

The isolation of the crustal magnetic anomaly field is discussed. Slowly spatially varying ring current fields were modeled as a least squares fit to each MAGSAT pass over Antarctica. Selection criteria were applied to data from 3000 MAGSAT passes to remove field aligned currents, yielding 87 data sets used to construct a scalar magnetic anomaly map for regions south of 55 S latitude. Internal tests performed on MAGSAT data and omparisons with the POGO map indicated that the general anomaly features are of crustal origin. The sources of anomalies generated in continental and in oceanic regions are discussed. Correlations were found between crustal magnetic anomalies and known geologic features over West and East Antarctica and over the surrounding oceanic regions. J.D.

N82-21675*# Instituto de Pesquisas Espaciais, Sao Jose dos Campos (Brazil).

COMPARISON OF STORM-TIME CHANGES OF GEOMAGNETIC FIELD AT GROUND AND AT MAGSAT ALTITUDES Progress Report

Rajaram Purushottam Kane and Nalin Babulal Trivedi Dec. 1981 15 p refs Sponsored by NASA ERTS

(E82-10148; NASA-CR-168533; NAS 1.26:168533) Avail: NTIS HC A02/MF A01 CSCL 08G

Computations concerning variations of the geomagnetic field at MAGSAT altitudes were investigated. Using MAGSAT data for the X, Y, and Z components of the geomagnetic field, a computer conversion to yield the H component was performed. Two methods of determining delta H normalized to a constant geocentric distance R sub 0 = 6800 were investigated, and the utility of elta H at times of magnetic storms was considered. Delta H at a geographical latitude of 0 at dawn and dusk, the standard Dst, and K sub p histograms were plotted and compared. Magnetic anomalies are considered. Examination of data from the majority of the 400 passes of MAGSAT considered show a reasonable delta H versus latitude variation. Discrepancies in values are discussed. J.D.

N82-21679*# Brown Univ., Providence, R.I. Dept. of Geological Sciences.

ELECTROMAGNETIC DEEP-PROBING (100-1000 KMS) OF THE EARTH'S INTERIOR FROM ARTIFICIAL SATELLITES: CONSTRAINTS ON THE REGIONAL EMPLACEMENT OF CRUSTAL RESOURCES Quarterly Progress Report, 30 Sep. - 31 Dec. 1981

John F. Hermance, Principal Investigator 31 Dec. 1981 16 p refs ERTS

(Contract NAS5-26138)

(E82-10155; NASA-CR-168540; NAS 1.26:168540; QPR-6) Avail: NTIS HC A02/MF A01 CSCL 08G

Model simulations show that induction in a spherical Earth by distant magnetospheric sources can contribute magnetic field fluctuations at MAGSAT altitudes which are 30 to 40 percent of the external field amplitudes. When the characteristic dimensions (e.g. depth of penetration, etc) of a particular situations are small compared with the Earth's radius, the Earth can be approximated by a plane horizontal half space. In this case, electromagnetic energy is reflected with close to 100 percent efficiency from the Earth's surface. This implies that the total horizontal field is twice the source field when the source is above the satellite, but is reduced to values which are much smaller than the source field when the source is below the satellite. This latter effect tends to enhance the signature of gross electrical discontinuities in the lithosphere when observed at satellite altitudes. A.R.H.

N82-21686*# Colorado Univ., Boulder. Dept. of Astrogeophysics.

INVESTIGATION OF GEOMAGNETIC FIELD FORECASTING AND FLUID DYNAMICS OF THE CORE Quarterly Status Technical Progress Report, 1 Jul. - 30 Sep. 1981

Edward R. Benton, Principal Investigator 1 Oct. 1981 14 p ERTS

(Contract NAS5-25957)

(E82-10162; NASA-CR-168545; NAS 1.26:168545; QSTPR-7) Avail: NTIS HC A02/MF A01 CSCL 08G

The magnetic determination of the depth of the core-mantle boundary using MAGSAT data is discussed. Refinements to the approach of using the pole-strength of Earth to evaluate the radius of the Earth's core-mantle boundary are reported. The downward extrapolation through the electrically conducting mantle was reviewed. Estimates of an upper bound for the time required for Earth's liquid core to overturn completely are presented. High order analytic approximations to the unsigned magnetic flux crossing the Earth's surface are also presented. T.M.

N82-21689# Army Engineer Topographic Labs., Fort Belvoir, Va.

A DIGITAL TECHNIQUE FOR CONSTRUCTING VARIABLE-WIDTH LINES

Richard L. Rosenthal Mar. 1982 10 p

(AD-A110287; ETL-R031) Avail: NTIS HC A02/MF A01 CSCL 08/2

This paper describes a digital technique for constructing variable-width cartographic lines. Specifically, an algorithm is developed for generating symbolized lines using multiply-stoked centerline data. Algorithmic development considers three factors: cartographic principles, inherent problems with existing algorithms, and hardware constraints imposed by specific output devices including the Defense Mapping Agency's Laser Platemaker. Software developed from the algorithm uses simple trigonometric functions and may be implemented in applications using vector data with vector or raster plotters. Author (GRA)

N82-21690# Defense Mapping Agency Aerospace Center, St. Louis, Mo.

EXPERIENCES WITH DIGITAL TERRAIN ELEVATION DATA CONTOURING PROGRAMS Interim Report

Philip K. Alderman 26 Jan. 1982 12 p refs

(AD-A110280) Avail: NTIS HC A02/MF A01 CSCL 08/2

The DMA digital terrain elevation data base has been expanding steadily since its inception. With increasing coverage there has been a greater opportunity to apply this data, including the automatic derivation of contours from digital elevation data for aerospace charts. GRA

N82-21697# Royal Aircraft Establishment, Farnborough (England).

COMPUTER BASED TECHNIQUE FOR CONVERTING A CONTOUR MAP INTO AN EQUISPACED GRID OF POINTS

P. A. Roberts London HMSO Sep. 1980 68 p

(RAE-TR-80110; RAE-Space-586; BR77598) Avail: NTIS HC A04/MF A01

The purpose of the grid representation is to enable the map data to be handled more easily in a computer. Contours are assumed to represent some physical quantity and thus the variable represented by the contour height is a single valued function of the map coordinates. It is also assumed that the variable is smooth and continuous. The technique has applications in image processing where it may be necessary to compare (by ratioing) an image and a contour map. A grid representation is also an essential prerequisite for degrading the spatial resolution of a contour map by convolution, thus enabling contour maps having different resolutions to be compared at a common resolution. The interpolation algorithms and the reasons for their use are described in detail. Operations are described which may be required to be performed on a grid; those of expanding (or contracting) the number of data points in the grid, and the construction of cross sections. Listings of all programs, written in ANSI FORTRAN V are given. Author (ESA)

N82-21796*# Massachusetts Inst. of Tech., Cambridge. Dept. of Earth and Planetary Sciences.
APPLICATIONS TO EARTH PHYSICS: VERY-LONG-BASELINE INTERFEROMETRY AND DATA ANALYSIS Final Technical Report, 1 Apr. 1974 - 15 Mar. 1982
Charles C. Counselman, III and Irwin I. Shapiro Apr. 1982 197 p refs
(Contract NGR-22-009-839)
(NASA-CR-168743; NAS 1.26:168743) Avail: NTIS HC A09/MF A01 CSCL 08G

A range of very long baseline interferometry experiments applied to Earth physics are covered. N.W.

04
GEOLOGY AND MINERAL RESOURCES

Includes mineral deposits, petroleum deposits, spectral properties of rocks, geological exploration, and lithology.

A82-20338 † **Analysis of space imagery to compile a geomorphological map of the world (Analiz kosmicheskikh snimkov dlia sostavleniia geomorfologicheskoi karty mira).** N. V. Bashenina and N. N. Tal'skaia (Moskovskii Gosudarstvennyi Universitet, Moscow, USSR). *Issledovanie Zemli iz Kosmosa,* Nov.-Dec. 1981, p. 5-12. 10 refs. In Russian.

The paper presents and examines portions of a geomorphological map of the earth, with a scale of 1:15,000,000, compiled on the basis of space imagery and photomosaics. The use of space photographs has made it possible to delineate the general morphostructural plan of large areas of continents and the natural patterns of morphostructures. B.J.

A82-20341 † **The relationship between seismicity and lineaments of the Anatolian-Caucasian-Iranian segment of the Mediterranean fold belt (K voprosu o sootnoshenii seismichnosti s lineamentami Anatoliisko-Kavkazsko-Iranskogo segmenta Sredizemnomorskogo poiasa).** T. L. Korovina (Akademiia Nauk SSSR, Institut Kosmicheskikh Issledovanii, Moscow, USSR) and A. S. Karakhanian (Akademiia Nauk Armianskoi SSR, Institut Geologicheskikh Nauk, Yerevan, Armenian SSR). *Issledovanie Zemli iz Kosmosa,* Nov.-Dec. 1981, p. 27-34. 15 refs. In Russian.

A comparison of remotely sensed data from Meteor, Soyuz, and Salyut data with statistical data on seismic activity made it possible to determine the regional and superregional lineaments that control seismic activity in the Anatolian-Caucasian-Iranian segment of the Mediterranean fold belt. The junctions of the lineaments considered are the seismic foci of intense earthquake zones. The general relationship obtained here can be used as an additional criterion for the forecasting of earthquakes. B.J.

A82-20342 † **Structural analysis of the basement of the East European platform by remote sensing methods (Analiz struktur fundamenta Vostochno-Evropeiskoi platformy distantsionnymi metodami).** D. V. Lopatin (Akademiia Nauk SSSR, Institut Geologii i Geokhronologii Dokembriia, Leningrad, USSR). *Issledovanie Zemli iz Kosmosa,* Nov.-Dec. 1981, p. 35-40. 13 refs. In Russian.

It is shown that the interpretation of aerial and space imagery and geomorphological analysis can assist in the identification of Precambrian basement structures under sedimentary cover in Eastern Europe. The existence of early Archaen mobile zones dividing the platform into three large geoblocks was confirmed. In addition, early Proterozoic Rapakivi granitoid massifs were found to be volcano-plutonic structures of central type. B.J.

A82-25453 **Dip determinations in photogeology.** M. Ricci. *Photogrammetric Engineering and Remote Sensing,* vol. 48, Mar. 1982, p. 407-414. 21 refs.

A photogeological dip determination method which is free of conceptual error and, in addition, is both rapid and accurate, is presented. The method is based on (1) parallax difference measurements and (2) the use of a trigonometric formula which incorporates perspective correction, and is shown capable of determining dip angles independently of the position and orientation of the photographic inclined bed images for the entire range of angle values. Comparisons are presented of the present method's results with those of previously published methods. O.C.

A82-26013 **The Pampean Plain studied with Landsat images.** P. Pasotti and C. A. Canoba (Rosario, Universidad Nacional, Rosario, Argentina). *Photogrammetria,* vol. 37, Feb. 1982, p. 109-130. 31 refs.

Topographical charts, aerial photographs, and Landsat imagery from bands 5 and 7 were employed for a visual investigation of the tectonics in the Pampean Plain in the Sante Fe Province of Argentina. Satellite imagery was examined by magnifying glass inspection, and a mosaic of photographs was built to portray the low flooded zones. The last hydrographic network of the Pleistocene age was identified, and is formed of many parallel and straight depressions running SW-NE from the western mountains. A smooth sinusoidal flexure with a large radius of curvature generating one depressed and two uplifted subregions comprise the tectonic movements, and hydrographic studies are indicated to determine the characteristics of geofracture dividing the pampas. Additional color composites using different combinations of bands 4-7 were explored for information on lineaments, valleys, and the depressed zones. M.S.K.

A82-26014 **Remote sensing applied to basement tectonics of the calcareous High Atlas /Morocco/.** A. Bahmad (Service Régional de la Géologie, Midelt, Morocco), H. Chariai (Service Régional de la Géologie, Marrakech, Morocco), A. Djerrari, A. El Kochri (Paris VI, Université, Paris, France), E. A. Hilali (Direction de la Géologie, Rabat, Morocco), D. Ratz, A. L. G. Tamain (Paris XI, Université, Orsay, Essonne, France), and T. Saqalli (Société de Sel de Mohammedia, Mohammedia, Morocco). *Photogrammetria,* vol. 37, Feb. 1982, p. 131-150. 38 refs.

The use of Landsat generated imagery as the first step in geological research of the Moroccan High Atlas is reviewed. Initial examination of photographs results in the construction of structural and lineaments maps. Comparisons with existing geological maps yield further, structural and fractural charts. Little cloud cover was observed on the high summits, and the detection of anticlines, synclines, and continuous and discontinuous faults is discussed. A parallelism was found between the direction of the faults and the lengthening of the folded regions, indicating subvertical tectonic faults. The distribution of alkaline magmatism is outlined, having settled in the upper Jurassic to early Cretaceous periods, and dense wefts are taken as further evidence that the faults tend toward the vertical with greater depth. M.S.K.

A82-26015 **Relationship of hydrothermal phenomena within the Leinster Granite to crustal fractures delineated from Landsat imagery.** P. M. Brück (University College, Cork, Ireland) and P. J. O'Connor (Geological Survey of Ireland, Dublin, Ireland). *Photogrammetria,* vol. 37, Feb. 1982, p. 151-159. 16 refs.

Landsat imagery was combined with existing geologic maps of the Leinster Granite in SE Ireland to develop a model of hydrothermal processes in the area and detect the fracture zones. Observed linears were interpreted as fractures, and satellite imagery allowed the discernment of hydrothermal alteration zones, occurrences of spodume and red-feldspar pegmatites, and explosion breccias. Pb-Zn mineralization sites displayed a spatial association with a transverse fracture system, with galena and sphalerite the main ores in veins with thicknesses ranging from a few meters to a few cm. Hydrothermal processes which may have led to the formation of the Leinster Granite are detailed, along with a suggestion that fractures occuring late in the cooling granite's history formed channels for circulating ground waters. M.S.K.

A82-26016 **Geophysical and Landsat lineament mapping - An approach illustrated from west-central and south India.** M. N. Qureshy (Department of Science and Technology, New Delhi, India). *Photogrammetria,* vol. 37, Feb. 1982, p. 161-184. 35 refs.

Linear zones correlated with surface geology, geophysical data, and Landsat data for parts of India are reviewed, along with mappings of magnetic and gravitational anomalies correlated with the tectonic framework of the subcontinent. Reactivation tendencies were observed in a megalineament in west central India, and is taken as evidence of continued activity of global tectonic forces. Linears were detected to cluster around regions of a gravitational high, and the recurrence of particular mineral-bearing lineaments with successive phases of activity is suggested. The use of Landsat data in conjunction with photogeological studies at the surface is considered as useful for determining surface features which originate in processes in the mantle. M.S.K.

A82-26017 **One orogenic belt or two - A structural reinterpretation supported by Landsat data products of the Precam-**

brian metamorphics of Singhbhum, eastern India. A. N. Sarkar (Geological Survey of India, Map Div., Calcutta, India) and D. K. Chakraborti (Geological Survey of India, Agartala, India). *Photogrammetria,* vol. 37, Feb. 1982, p. 185-201. 27 refs.

A stratigraphic/tectonic analysis of the Singhbhum district in India, aided by imagery from Landsat I, is presented. Analyses of the rocks found in the area are reviewed, with particular attention to the potential existence of an Iron Ore and a Singhbhum Group of rocks of different geologic ages delineating northern metamorphic rocks and southern older rocks, with the southern rocks actually part of the same stratigraphic group as the northern rocks. An observed shear zone running E-W is concluded not to demarcate two different metamorphic belts, and deformation actually occurred during the orogenesis which ended in an ENE-WSW diagonal sinistral shearing in the western part of the district. M.S.K.

A82-26604 * **Ore deposits in Africa and their relation to the underlying mantle.** H.-S. Liu (NASA, Goddard Space Flight Center, Greenbelt, MD). *Modern Geology,* vol. 8, no. 1, 1981, p. 23-36. 70 refs.

African magmatism is largely related to the tensional stress regimes of the crust which are induced by the hotter upwelling mantle rocks. These mantle rocks may provide emanating forces and thermal energy for the upward movements of primary ore bodies with fluid inclusions in the tensional stress regimes of the crust. In this paper, the Goddard Earth Gravity Model is used to calculate a detailed subcrustal stress system exerted by mantle convection under Africa. The resulting system is found to be correlated with the African metallogenic provinces. Recognition of the full spectrum of ore deposits in Africa that may be associated with the hotter upwelling mantle rocks has provided an independent evidence to support the hypothesis of mantle-derived heat source for ore deposits. (Author)

A82-27466 † **Application of aerial and space photographic data in the study of subsurface water and tectonic structures (Primenenie materialov aerokosmicheskikh s'emok v issledovanii podzemnykh vod i tektonicheskikh struktur).** E. Radai. In: Aerospace methods for the study of water resources and their pollution. Leningrad, Gidrometeoizdat, 1981, p. 70-76. In Russian

The paper examines the use of aerial and space photography data to create a network for monitoring subsurface water in karst areas of the Danube region. The interpretation of space remote sensing images has made it possible to obtain new data on the geological structure of a basin in the area as well as to detect tectonic structures in two massifs. B.J.

A82-27600 * # **A data base of geologic field spectra.** A. B. Kahle, A. F. H. Goetz, H. N. Paley, R. E. Alley, and E. A. Abbott (California Institute of Technology, Jet Propulsion Laboratory, Pasadena, CA). In: International Symposium on Remote Sensing of Environment, 15th, Ann Arbor, MI, May 11-15, 1981, Proceedings. Volume 1. Ann Arbor, MI, Environmental Research Institute of Michigan, 1981, p. 329-337. NASA-supported research.

It is noted that field samples measured in the laboratory do not always present an accurate picture of the ground surface sensed by airborne or spaceborne instruments because of the heterogeneous nature of most surfaces and because samples are disturbed and surface characteristics changed by collection and handling. The development of new remote sensing instruments relies on the analysis of surface materials in their natural state. The existence of thousands of Portable Field Reflectance Spectrometer (PFRS) spectra has necessitated a single, all-inclusive data base that permits greatly simplified searching and sorting procedures and facilitates further statistical analyses. The data base developed at JPL for cataloging geologic field spectra is discussed. C.R.

A82-27612 # **Automatic linear recognition and analysis using computer program LIRA.** D. H. Coupland and R. K. Vincent (Geospectra Corp., Ann Arbor, MI). In: International Symposium on Remote Sensing of Environment, 15th, Ann Arbor, MI, May 11-15, 1981, Proceedings. Volume 1. Ann Arbor, MI, Environmental Research Institute of Michigan, 1981, p. 499-508.

Computer program LIRA will automatically recognize and map linear features in digital images. Input to the program is a magnetic tape containing the image to be analyzed; output is a list of linears found and a linear plot which overlays the original image. LIRA does not replace the human interpreter, but speeds his work and provides an objective criterion for interpreting linear features in tonal images. Linears recognized by LIRA map major faults, lithologic boundaries, drainage and erosional patterns, and other features of geologic interest. In Landsat frame La Ronge (northern Saskatchewan), linear recognition maps produced by LIRA show a detailed relationship to published geologic maps. Significant variations in linear density and azimuthal distribution are seen between major geologic regions. (Author)

A82-27635 # **Seasat satellite investigation of the structure of Western Nebraska and its application to the evaluation of geothermal resources.** J. Stix (Los Alamos National Laboratory, Los Alamos, NM). In: International Symposium on Remote Sensing of Environment, 15th, Ann Arbor, MI, May 11-15, 1981, Proceedings. Volume 2. Ann Arbor, MI, Environmental Research Institute of Michigan, 1981, p. 735-750. 43 refs.

Seasat synthetic aperture radar (SAR) satellite imagery was used to interpret the structural framework and, indirectly, the geothermal potential of an area in Western Nebraska. Lineaments were mapped from the imagery and then compared to known structure. It was found that Seasat does record surface manifestations of subtle basement structures, particularly faulting. Furthermore, four areas with geothermal potential were delineated using Seasat and other data. It is stressed that more subsurface geology and geophysical data are needed before a final evaluation of the geothermal potential can be made. Seasat imagery is a useful reconnaissance exploration tool in the interpretation of regional structure within areas of little topographic relief. (Author)

A82-27672 # **Integration of Landsat, geological and geophysical data for use in thematic mapping at regional scale.** C. M. Marino, G. Miglio, E. Zini (Milano, Università, Milan, Italy), and P. M. Rossi (CNR, Centro di Studio per la Stratigrafia e Petrografia delle Alpi Centrali, Milan, Italy). In: International Symposium on Remote Sensing of Environment, 15th, Ann Arbor, MI, May 11-15, 1981, Proceedings. Volume 3. Ann Arbor, MI, Environmental Research Institute of Michigan, 1981, p. 1153-1162. 12 refs.

This paper describes a study on the integration of Landsat, geological and geophysical data over a large test-site in the western portion of Northern Apennines Range. In this framework particular attention was devoted to the use of hydrographic network as a new parameter to be considered in the process of temporal classification of linear phenomena. Moreover reference is made to the regional contribution of geophysical data mainly to test the validity of some hypotheses arisen from the analysis of satellite images. (Author)

A82-27694 # **Non-parametric classification of abandoned coal mine features using multioriented and ratio transformed Landsat data.** P. W. Mausel, R. C. Howe, and K. Lulla (Indiana State University, Terre Haute, IN). In: International Symposium on Remote Sensing of Environment, 15th, Ann Arbor, MI, May 11-15, 1981, Proceedings. Volume 3. Ann Arbor, MI, Environmental Research Institute of Michigan, 1981, p. 1397-1409. 7 refs.

A82-27695 # **Airborne remote sensing in east Greenland.** J.-C. Favard (Centre National d'Etudes Spatiales, Toulouse, France), J. F. Scanvic (Bureau de Recherches Géologiques et Minières, Orléans, France), A. L. Friedman (Christian Rovsing A/S, Herlev, Denmark), and T. Thyrsted (Gronlands Geologiske Undersogelse, Copenhagen, Denmark). In: International Symposium on Remote Sensing of Environment, 15th, Ann Arbor, MI, May 11-15, 1981, Proceedings. Volume 3. Ann Arbor, MI, Environmental Research Institute of Michigan, 1981, p. 1411-1424.

A joint French-Danish investigation was conducted with the objective to study the feasibility of an employment of multispectra observation techniques in geological research projects. A region in east Greenland was selected as a test site in connection with a

number of advantages provided by the involved area. These advantages are related to a wind range of geological environments, a wide variety of mineralization types, and limitations with respect to vegetation and secondary cover. Three test areas were studied. Two multispectral scanners were employed in the investigation, including one instrument for the visible and near-infrared spectral region, and another instrument used as thermal scanner. Flight altitudes at 2,500 m and 5,000 m above ground were used. The obtained data are found to make a meaningful contribution to mining prospection, because they provide mapping precision or define original prospection aims.
G.R.

A82-27705 # Applications of aircraft and satellite data for the study of archaeology and environment - Mekong Delta, Vietnam. A. Lind (Vermont, University, Burlington, VT). In: International Symposium on Remote Sensing of Environment, 15th, Ann Arbor, MI, May 11-15, 1981, Proceedings. Volume 3.
Ann Arbor, MI, Environmental Research Institute of Michigan, 1981, p. 1529-1537.

An account is given of the way in which Landsat data have been used in conjunction with aerial photography to study and map the imprints of early hydraulic civilizations and the pattern of geomorphic changes of a dynamic delta environment. It is noted that many studies have demonstrated the applicability of remote sensing data to the investigation of fluvial and coastal environments. Data of this type are applied here to reconstructing geomorphic conditions in the Trans-Bassac, a plain bounded by the Bassac River and the Gulf of Thailand. Landsat is shown to provide a broader perspective of the canals previously discerned by aerial photography and to give clues to extensions of these canals.
C.R.

A82-28136 † Ring structures in the earth's crust, and their significance for geology and methods for their investigation (Kol'tsevye struktury zemnoi kory, ikh znachenie dlia geologii i metody izucheniia). A. E. Mikhailov. *(Vsesoiuznaia Konferentsiia po Problemam Issledovaniia Prirodnykh Resursov Zemli i Mirovogo Okeana, Aviatsionno-Kosmicheskimi Sredstvami, Moscow, USSR, Nov. 1980.) Geodeziia i Aerofotos'emka,* no. 1, 1982, p. 55-59. In Russian.

The use of satellite remote-sensing techniques to study ring structures is considered. The occurrence of ring structures on Soviet territory is discussed, and the volcano-plutonic mechanism for the formation of such structures is examined. Recommendations on the use of remote sensing techniques for the further study of these structures are given.
B.J.

N82-16442*# Instituto de Pesquisas Espaciais, Sao Jose dos Campos (Brazil).
REPORT ON A SHORT COURSE IN REMOTE SENSING AND THE GEOLOGICAL APPLICATIONS OF LANDSAT MSS IMAGERY AT INPE
Nelson deJesusParada, Principal Investigator and Kampta Persaud (Geological Survey Dept. (Guyana)) Oct. 1980 48 p refs Sponsored by NASA ERTS
(E82-10024; NASA-CR-164813; INPE-1923-RPE/249) Avail: NTIS HC A03/MF A01 CSCL 05B

Training in the theory of remote sensing in Brazil involves studying the principles of electromagnetic radiation and the instrumentation used to measure the radiation characteristics of a body. The overall LANDSAT system is considered with emphasis on the multispectral band scanner and Brazil's participation in the LANDSAT Program. Geologic information from MSS imagery is at a regional scale, and three basic types are available: rock and soil, geologic structures, and landforms. Discrimination between alluvium and sedimentary or crystalline bedrock, and between units in thick sedimentary sequences is best, primarily because of topographic expressions and vegetation differences. Discrimination between crystalline rock types is poor. Folds and fractures are the best displayed geologic features and are recognizable by topographic expressions, drainage patterns, and rock or vegetational tonal patterns. Landforms are easily discriminated by their familiar shapes and patterns. The IMAGE-100 computer has the ability to extract thematic information and to enhance the image.
A.R.H.

N82-16446*# Stanford Univ., Calif. Remote Sensing Lab.
INTEGRATION OF LANDSAT WITH GEOLOGY AND AIRBORNE GEOPHYSICS INTO AN OPERATIONAL MINERAL EXPLORATION SYSTEM Final Report, Jun. 1978 - Dec. 1980
R. J. P. Lyon and M. F. Crawford, Principal Investigators Mar. 1981 270 p refs Prepared for JPL, Pasadena, Calif. Original contains imagery. Original photography may be purchased from the EROS Data Center, Sioux Falls, S.D. 57198. ERTS
(Contract JPL-955047)
(E82-10028; NASA-CR-164433) Avail: NTIS HC A12/MF A01 CSCL 08G

Digital data, gamma-ray spectrometry and aeromagnetic data were digitally combined and analyzed for the Bearlodge area (northeastern Wyoming) where potential resources of thorium and rare earths occur. The combined LANDSAT-geophysical data set revealed several geologic structures that were not evident in a single data set for the study area. Both qualitative and quantitative methods of analysis were performed on the combined data sets. Qualitative analysis of the data was done on a computer controlled, interactive color TV display system by overlaying the various data sets in different colors. In the Bearlodge area, this analysis revealed a pair of northwest-southeast tranding lineaments in the LANDSAT image which appeared to truncate a zone of high radioactivity. An elliptical feature formed by drainages is found. An intense thorium-gamma ray anomaly which coincides with thorium-rare earth mineralization, occurs inside this elliptical feature.
T.M.

N82-19624*# Iowa Univ., Iowa City. Dept. of Geology.
USE OF MAGSAT ANOMALY DATA FOR CRUSTAL STRUCTURE AND MINERAL RESOURCES IN THE US MIDCONTINENT Quarterly Report, period ending 30 Sep. 1981
Robert S. Carmichael, Principal Investigator 28 Sep. 1981 10 p Original contains color illustrations ERTS
(Contract NAS5-26425)
(E82-10049; NASA-CR-164926; QR-3) Avail: NTIS HC A02/MF A01 CSCL 08G

Magnetic profiles on individual satellites tracks were examined to identify bad (nonterrestrially-based) data points r profiles. Anomaly profiles for the same satellite track, but at different passes were compared for parallel tracks and for tracks that cross. The selected and processed data were plotted and contoured to develop a preliminary magnetic anomaly map. The map is similar in general morphology to NASA's Magsat global scalar anomaly map, but has more detail which is related to crustal properties. Efforts have begun to interpret the satellite magnetic anomalies in terms of crustal character. The correlation of magnetics with crustal petrology may have a much larger tectonic implication. Th possibility of there being an ultramafic lower crust along one zone as a consequence of a continental collision/subduction which helped form the midcontinent craton in Precambrian times is being investigated.
A.R.H.

N82-19642# Instituto de Pesquisas Espaciais, Sao Jose dos Campos (Brazil).
METHODOLOGY OF THE INTERPRETATION OF REMOTE SENSING DATA AND APPLICATIONS IN GEOMORPHOLOGY
Tania Maria Sausen and Evlyn Marcia Leao deM. Novo Aug. 1981 42 p refs In PORTUGUESE; ENGLISH summary
(INPE-2209-MD/007) Avail: NTIS HC A03/MF A01

Remote sensing techniques not only permit the acquisition, in a short time, of a large volume of information about phenomena occurring at the Earth's surface, but also provide a constant flux of data showing variations in spatial distribution patterns, which is of value in predicting and controlling geomorphological events. The use of aerial panchromatic, color, and multispectral photography is discussed as well as the interpretation of radar and thermal infrared imagery. Methods for interpreting multispectral imagery from LANDSAT are examined.
A.R.H.

N82-20596*# Consiglio Nazionale delle Ricerche, Milan (Italy).
HEAT CAPACITY MAPPING MISSION (HCMM) PROGRAM: STUDY OF GEOLOGICAL STRUCTURE OF SICILY AND OTHER ITALIAN AREAS Final Report
Roberto Cassinis, Giovanni Lechi, Principal Investigators, Eugenio Zilioli, Alberto Marini, Pietro A. Brivio, and Nicola Tosi Aug. 1981 34 p refs Sponsored by NASA. Original contains imagery. Original imagery may be purchased from NASA Goddard Space Flight Center, (code 601), Greenbelt, Md. 20771. Domestic

users send orders to 'Attn: National Space Science Data Center'; non-domestic users send orders to 'Attn: World Data Center A for Rockets and Satellites'. HCMM
(E82-10073; NASA-CR-165095; NAS 1.26:165095) Avail: NTIS HC A03/MF A01 CSCL 05B

The usefulness of thermal inertia mapping in discriminating geolithological units was investigated using Sardinia and the Gulf of Orosei as test sites. Software designed for LANDSAT data were modified and improved for HCMM tapes. A first attempt was made to compare the geological cross section, the topography, the IR radiance, and the thermal inertia along selected profiles of the test site. Thermal inertia profiles appear smoothed in comparison with the thermal radiance. The lowest apparent thermal inertia (ATI) was found on granitic and basaltic outcrops where their image is of sufficient extent, while ATI is higher on carbonatic and dolomitic or moist deposits. Almost every fault is marked by a jump of ATI, the interval being sometimes of the order of one pixel. This seems to demonstrate the ability of ATI to detect contacts or tectonically disturbed zones with a good resolution. It seems more difficult to measure the differences in ATI between homogeneous materials having different lithology. Ground surveys conducted and a simulation model of diurnal temperatures of rocks having different thermal inertia are discussed. A.R.H.

N82-20599*# Instituto de Pesquisas Espaciais, Sao Jose dos Campos (Brazil)
STUDY PROJECT OF INTRUSIVE ROCKS: STATES OF ESPIRITO SANTO AND RIO DE JANEIRO, SOUTH AND EAST OF MINAS GERAIS AND SOUTHEAST OF THE STATE OF SAO PAULO [PROJETO ESTUDO DAS ROCHAS INTRUSIVAS: ESTADOS DO ESPIRITO SANTO E DU RIO DE JANEIRO, PARTES SUL E LESTE DE MINAS GERAIS E SUDESTE DO ESTADO DE SAO PAULO]
Nelson deJesusParada, Principal Investigator, Athos Ribeiro dosSantos, Celio Eustaquio dos Anjos, Marx Prestes Barbos, and Paulo Veneziani Jul. 1981 19 p refs In PORTUGUESE; ENGLISH summary Presented at the 3rd Simposio Regional de Geol., Curitiba, Brazil, 12-15 Nov. 1981 Sponsored by NASA ERTS
(E82-10076; NASA-CR-168397; NAS 1.26:168397; INPE-2190-RPE/002) Avail: NTIS HC A02/MF A01 CSCL 08B

The feasibility of mapping intrusive rocks in polycyclic and polymetamorphic areas using the logic method for photointerpretation of LANDSAT and radar imagery was investigated. The resolution, scale and spectral characteristics of the imagery were considered. Spectral characteristics of the intrusive rock units mapped using image 100 were investigated. It was determined that identification of acidic and basic intrusive bodies and determination of their relationships with principal structural directions using the logic method was feasible. Tectonic compartments were subdivided into units according to their predominant lithographic types, ignoring stratigraphy. The principal directions of various foliations, faults, megafolds, and fractural systems were defined. Delineation of the boundaries of intrusive bodies mapped using the spectral characteristics of Image 100 imagery ws determined to be more accurate than visual analysis. A 1:500,000 scale map of intrusions in the areas studied was generated. J.D.H.

N82-21662*# Stanford Univ., Calif. Dept of Geology.
HCMM: SOIL MOISTURE IN RELATION TO GEOLOGIC STRUCTURE AND LITHOLOGY, NORTHERN CALIFORNIA Final Report
Ernest I. Rich, Principal Investigator May 1981 26 p Original contains imagery. Original imagery may be purchased from NASA Goddard Space Flight Center, (code 601), Greenbelt, Md. 20771. Domestic users send orders to 'Attn: National Space Science Data Center'; non-domestic users send orders to 'Attn: World Data Center A for Rockets and Satellites'. HCMM
(Contract NAS5-24479)
(E82-10135; NASA-CR-168518; NAS 1.26:168518) Avail: NTIS HC A03/MF A01 CSCL 08G

Heat capacity mapping mission images of about 80,000 sq km in northern California were qualitatively evaluated for usefulness in regional geologic investigations of structure and lithology. The thermal characteristics recorded vary among the several geomorphic provinces and depend chiefly on the topographic expression and vegetation cover. Identification of rock types, or groups of rock types, was most successfully carried out within the semiarid parts of the region; however, extensive features, such as faults, folds and volcanic fields could be delineated. Comparisons of seasonally obtained HCMM images are of limited value except in semiarid regions. Author

N82-21664*# Geological Survey, Denver, Colo. Petrophysics and Remote Sensing.
APPLICATION OF HCMM DATA TO REGIONAL GEOLOGIC ANALYSIS FOR MINERAL AND ENERGY RESOURCE EVALUATION Progress Report, Jun. - Aug. 1981
Kenneth Watson, Principal Investigator and Susanne H-Miller Aug. 1981 4 p Sponsored by NASA HCMM
(E82-10137; NASA-CR-168522; NAS 1.26:168522) Avail: NTIS HC A02/MF A01 CSCL 08G

Experimentation with several potentially promising techniques led to the selection of a fairly simple scheme for registration of data from the HCMM using an affine transformation. A method based solely on remote sensing was developed to estimate those meteorological effects which are required for thermal inertia mapping. It assumes that the atmospheric fluxes are spatially invariant and that the solar, sky and sensible heat fluxes can be approximated by a simple mathematical form. Coefficients are determined from least squares method by fitting observational data to the thermal model.

N82-21677*# Iowa Univ., Iowa City. Dept. of Geology.
USE OF MAGSAT ANOMALY DATA FOR CRUSTAL STRUCTURE AND MINERAL RESOURCES IN THE US MIDCONTINENT Quarterly Report, period ending 30 Jun. 1981
Robert S. Carmichael, Principal Investigator 30 Jun. 1981 4 p ERTS
(Contract NAS5-26425)
(E82-10152; NASA-CR-168537; NAS 1.26:168537; QR-2) Avail: NTIS HC A02/MF A01 CSCL 08G

While the preliminary magnetic anomaly map for the centra midcontinent is only in the hand-drawn stage, it agrees in broad aspects with the preliminary global MAGSAT map provided by NASA. Because of data evaluation and finer scale averaging, there are more detailed features which hold promise for eventual geological/crustal interpretation. Some current analysis is directed at examining whether a map data feature such as an elongated anomaly or trend, which seems parallel to satellite data tracks, is likely of crustal origin or is an artifact of the data set. A.R.H.

05

OCEANOGRAPHY AND MARINE RESOURCES

Includes sea-surface temperature, ocean bottom surveying imagery, drift rates, sea ice and icebergs, sea state, fish location.

A82-19139 **Analyses of the Eastern Pacific without ship PAPA data.** J. Spagnol, M. Horita, and P. Haering (Department of the Environment, Pacific Weather Centre, Vancouver, Canada). In: Conference on Weather Forecasting and Analysis, 8th, Denver, CO, June 10-13, 1980, Preprints. Boston, MA, American Meteorological Society, 1980, p. 150-155.

Two cases (Oct. 21-22 and Oct. 25-26, 1979) were chosen to illustrate the effect of poor numerical analyses and the ability of improving them using the resources available at the Pacific Weather Centre. It was found that without adequate alternative data sources the loss of Ocean Station PAPA data can have a detrimental effect on the Canadian Meteorological Centre (CMC) objective analysis over the Eastern Pacific. In periods of intense weather activity, without the anchoring effect of this data the uncorrected errors in the analyses may propagate westward to the coast causing the rejection of valid coastal radiosonde observations. However, the Pacific Weather Centre regional analyses can complement the CMC national analyses and partly offset the expected data void created by the loss of Ocean Station PAPA data in 1981. G.R.

A82-19560 # **Microwave brightness temperature pattern over the Indian subcontinent and the surrounding oceans as observed by the satellite microwave radiometer /SAMIR/ onboard Bhaskara.** O. P. N. Calla, G. Raju, S. S. Rana, and S. Balasubramanian (Indian Space Research Organization, Space Applications Centre, Ahmedabad, India). In: European Microwave Conference, 10th, Warsaw, Poland, September 8-12, 1980, Proceedings. Sevenoaks, Kent, England, Microwave Exhibitions and Publishers, Ltd., 1981, p. 588-599.

A82-20344 † **The use of Meteor-satellite image data in oceanography (Opyt ispol'zovaniia videoinformatsii s ISZ 'Meteor' dlia issledovaniia iavlenii v okeane).** A. S. Kaz'min and V. E. Skliarov (Akademiia Nauk SSSR, Institut Okeanologii, Moscow, USSR). *Issledovanie Zemli iz Kosmosa,* Nov.-Dec. 1981, p. 48-57. 13 refs. In Russian.

A82-20445 * # **Influence of dissolved organic materials on turbid water optical properties and remote-sensing reflectance.** W. G. Witte, C. H. Whitlock, R. C. Harriss, J. W. Usry, L. R. Poole, W. M. Houghton, W. D. Morris, and E. A. Gurganus (NASA, Langley Research Center, Hampton, VA). *Journal of Geophysical Research,* vol. 87, Jan. 20, 1982, p. 441-446. 18 refs.

The effects of dissolved organic materials on turbid-water optical properties are assessed, by means of field measurements and laboratory simulations in which upwelled reflectance, attenuation, absorption, and backscatter spectral properties at wavelengths from 450 to 800 nm are examined in relation to water chemistry. The data show that dissolved organic materials decrease upwelled reflectance from turbid waters, and that the decrease in reflectance is a nonlinear function of concentration with the largest gradients at low carbon concentrations, depending on wavelength. Upwelled reflectance is found to be highly correlated with two backscatter-absorption parameters used in some optical models, which are nonlinear with dissolved organic material concentration change. O.C.

A82-20447 * # **Structure and variability of the Alboran Sea frontal system.** R. E. Cheney (NASA, Goddard Space Flight Center, Greenbelt, MD) and R. A. Doblar (U.S. Navy, Naval Ocean Research and Development Activity, Bay St. Louis, MS). *Journal of Geophysical Research,* vol. 87, Jan. 20, 1982, p. 585-594. 8 refs. Navy-sponsored research.

A distinct oceanic front coinciding with the jet of incoming North Atlantic water, and an associated anticyclonic gyre in the western half of the basin, were observed during a ship and aircraft survey of the physical characteristics of the Alboran Sea in the western Mediterranean in October 1977. The front was confined to the upper 200 m and was a continuous feature, extending from the Strait of Gibraltar 500 km eastward to the prime meridian. It is noted that in ten days between two surveys, the center of the gyre shifted 50 km westward. This variability of the anticyclonic gyre may correspond to changes of North Atlantic inflow strength, as inferred by local wind and the average atmospheric pressure over the western Mediterranean. O.C.

A82-21917 * **SASS measurements of the Ku-band radar signature of the ocean.** L. C. Schroeder, W. L. Grantham (NASA, Langley Research Center, Hampton, VA), J. L. Mitchell, and J. L. Sweet (Kentron Technical Center, Hampton, VA). *IEEE Journal of Oceanic Engineering,* vol. OE-7, Jan. 1982, p. 3-14. 13 refs.

SeaSat-A Satellite Scatterometer (SASS) measurements of normalized radar cross section (NRCS) have been merged with high quality surface-wind fields based on in situ, to create a large data base of NRCS-wind signature data. These data are compared to the existing NRCS-wind model used by the SASS to infer winds. False-color maps of SASS NRCS and ocean winds from multiple orbits show important synoptic trends. (Author)

A82-21921 **Some peculiarities of formulation and solution of inverse problems in microwave radiometry of the ocean surface and atmosphere.** A. M. Shutko and A. G. Grankov (Akademiia Nauk SSSR, Institut Radiotekhniki i Elektroniki, Moscow, USSR). *IEEE Journal of Oceanic Engineering,* vol. OE-7, Jan. 1982, p. 40-43. 10 refs.

The use of multifrequency radiometers to determine certain emission properties of the sea surface is considered, as is the dependence of the radiometer on wind speed, atmospheric water vapor content, and liquid water content in clouds. Attention is given to the sea state influence on the radiative characteristics of the ocean-atmosphere system and to calibrating the data of range measurement. Also considered is the problem of choosing those spectral bands which provide optimum accuracy for determining geophysical parameters with due regard to the spectral peculiarities of the functional relationships between the radiophysical and geophysical parameters and their uncertainties. Data are presented on an experiment for determining different hydrometeorological conditions and estimating the accuracy of applied retrieval procedures. C.R.

A82-24061 * **The Seasat low rate data processing system.** J. W. Brown, J. C. Klose, and M. L. MacMedan (California Institute of Technology, Jet Propulsion Laboratory, Pasadena, CA). In: Oceans '80; International Forum on Ocean Engineering in the '80s, Seattle, WA, September 8-10, 1980, Conference Record. New York, Institute of Electrical and Electronics Engineers, Inc., 1980, p. 518-526. 6 refs. Contract No. NAS7-100.

The development of the algorithms for data processing and distribution, the circuitry, and the performance of the Seasat low rate data processing system are reviewed. The system controls data from the radar altimeter, scatterometer, microwave radiometer, and the visible and IR radiometer for independent transmission of each instrument's readings. The downlink operates at 25 kb/sec, and a yearlong program of geophysical evaluation proceeded shortly after launch, allowing on-line engineering evaluation and alteration of the control algorithms in the system. Some data is preformatted for immediate distribution and storage in archival quality. A catalog and abstracts are provided to users allowing a RAM search from remote terminals for historical conditions. Procedures for verifying and altering the algorithms are detailed. M.S.K.

A82-24063 * **Comparison of conventionally measured sea surface temperature and wind speed with data retrieved from satellite-borne microwave radiometry.** R. Hofer and E. G. Njoku (California Institute of Technology, Jet Propulsion Laboratory, Pasadena, CA). In: Oceans '80; International Forum on Ocean Engineering in the '80s, Seattle, WA, September 8-10, 1980, Conference Record. New York, Institute of Electrical and Electronics Engineers, Inc., 1980, p. 531-534. Research supported by the National Academy of Sciences; Contract No. NAS7-100.

The Scanning Multichannel Microwave Radiometer aboard both the Seasat and Nimbus-7 satellites was designed to estimate sea surface temperature (SST) and wind speed (WS) over an extended range of atmospheric conditions. The retrieval technique is described briefly, and it is demonstrated in a case study that the instrument design goals (SST:1.5 C; WS:2 m/s) appear to be feasible. (Author)

A82-24822 **Workshop on the application of existing satellite data to the study of ocean surface energetics, 19-21 November 1980, University of Wisconsin-Madison.** C. Gautier (Wisconsin, University, Madison, WI) and D. McConnell (NOAA, National Climate Program Office, Rockville, MD). *American Meteorological Society, Bulletin,* vol. 62, Dec. 1981, p. 1679-1689.

A82-27091 * # **Topex orbit sustenance maneuver design.** J. A. Kechichian (California Institute of Technology, Jet Propulsion Laboratory, Pasadena, CA). *American Institute of Aeronautics and Astronautics, Aerospace Sciences Meeting, 20th, Orlando, FL, Jan. 11-14, 1982, Paper 82-0202.* 15 p. 6 refs. NASA-supported research.

A trade-off analysis between maneuver period, execution errors, and orbit determination uncertainties is carried out for the Ocean Topography Experiment spacecraft for a given nodal equatorial constraint. Semimajor axis and eccentricity are controlled with minimum impulse using the linear theory of optimal transfer between close coplanar near-circular orbits. Ellipses of equal minimum and average maneuver periods are presented in the (3 execution error, 3 orbit determination uncertainty) space for different nodal equatorial constraints enabling the determination of the appropriate combination of execution errors and orbit determination uncertainties that guarantees a mission required minimum maneuver period for a given nodal deadband. (Author)

A82-27596 * # **Optimal spatial filtering and transfer function for SAR ocean wave spectra.** A. D. Goldfinger, R. C. Beal, and D. G. Tilley (Johns Hopkins University, Laurel, MD). In: International Symposium on Remote Sensing of Environment, 15th, Ann Arbor, MI, May 11-15, 1981, Proceedings. Volume 1.
Ann Arbor, MI, Environmental Research Institute of Michigan, 1981, p. 291-297. 5 refs. NASA-supported research; Contract No. NOAA-MO-A01-78-00-4330.

The Seasat Synthetic Aperture Radar (SAR) has proved to be an instrument of great utility in the sensing of ocean conditions on a global scale. An analysis of oceanographic and atmospheric aspects of Seasat data has shown that the features observed in the imagery are linked to ocean phenomena such as storm sources and their resulting swell systems. However, there remains one central problem which has not been satisfactorily solved to date. This problem is related to the accurate measurement of wind-generated ocean wave spectra. Investigations addressing this problem are currently being conducted. The problem has two parts, including the accurate measurement of the image spectra and the inference of actual surface wave spectra from these measurements. A description is presented of the progress made towards solving the first part of the problem, taking into account a digital rather than optical computation of the image transforms. G.R.

A82-27602 # **Integrated sensor system for collection of wave data applied to coastal engineering design.** D. E. Lichy, T. L. Miloser, and D. W. Berg (U.S. Army, Coastal Engineering Research Center, Fort Belvoir, VA). In: International Symposium on Remote Sensing of Environment, 15th, Ann Arbor, MI, May 11-15, 1981, Proceedings. Volume 1. Ann Arbor, MI, Environmental Research Institute of Michigan, 1981, p. 357-365. 11 refs.

Ocean wave climate is a primary consideration in the design of coastal structures. Wave data are a major parameter for use in longshore current and transport mathematical models. During October and November 1980, more than 30 organizations took part in the 56-day Atlantic Remote Sensing Land Ocean Experiment (ARSLOE) near Duck, North Carolina. A total of 47 wave measuring devices, in situ to remote sensing, were tested. This paper discusses the various considerations involved in designing an integrated system for the collection of ocean wave data, along with the limitations and advantages of the systems tested during ARSLOE and other field experiments. B.J.

A82-27608 # **The first ESA remote sensing satellite system ERS-1.** G. Duchossois and C. Honvalut (ESA, Directorate of Application Programmes, Paris and Toulouse, France). In: International Symposium on Remote Sensing of Environment, 15th, Ann Arbor, MI, May 11-15, 1981, Proceedings. Volume 1. Ann Arbor, MI, Environmental Research Institute of Michigan, 1981, p. 461-477.

The mission objectives of the ESA remote sensing satellite system ERS-1 is to develop applications related to a better knowledge of ocean parameters and sea-state conditions and to increase scientific understanding of coastal zones and global ocean processes. In particular, offshore activities, ship routing, physical oceanography and glaciology, climate research, and marine biology will be benefited. The main payload will consist of a C-band active microwave instrumentation, and ocean color monitor, and a radar altimeter. Launched by Ariane 2 or 3, the system will use the Multimission Platform developed in the framework of the French national SPOT program. The requirements and constraints for the ERS-1 mission include coverage, instrument duty cycles, stations network, processing levels/products, and ground segment concept. The development program is described. ERS-1 will be both an experimental and an operational system. C.D.

A82-27619 # **Comparisons of laser profilometer sea ice roughness statistics with surface truthed data and SLAR imagery.** M. E. Kirby and J. T. Sutton (INTERA Environmental Consultants, Ltd., Ottawa, Canada). In: International Symposium on Remote Sensing of Environment, 15th, Ann Arbor, MI, May 11-15, 1981, Proceedings. Volume 2. Ann Arbor, MI, Environmental Research Institute of Michigan, 1981, p. 563-575. 6 refs.

In connection with programs related to the exploration and development of sources of petroleum in remote offshore regions of the high Arctic, the presence of sea ice has usually a significant effect on the activities involved in the implementation of such a program. In anticipation of year-round operations, models have been developed which calculate the predicted performance levels of ships and drill rigs under various design characteristics and ice conditions. These models are very dependent on historical ridge data sets. The method most widely used in the acquisition of ice ridge statistics involves the analysis of laser profilometer data. However, a detailed validation test of the laser profilometer method has not been conducted. The present investigation has the objective to compare airborne laser profilometer data of sea ice with measurements taken on the ice. A close positive correlation between radar brightness and ridge density could be observed. G.R.

A82-27620 # **A method for the retrieval of phytoplankton and suspended sediment concentrations from remote measurements of water colour.** S. Tassan (Commission of the European Communities, Joint Research Centre, Ispra, Italy). In: International Symposium on Remote Sensing of Environment, 15th, Ann Arbor, MI, May 11-15, 1981, Proceedings. Volume 2. Ann Arbor, MI, Environmental Research Institute of Michigan, 1981, p. 577-586. 19 refs.

A82-27640 # **High precision radiometric temperature measurements of the ocean surface.** K. Peacock, R. F. Gasparovic, and L. D. Tubbs (Johns Hopkins University, Laurel, MD). In: International Symposium on Remote Sensing of Environment, 15th, Ann Arbor, MI, May 11-15, 1981, Proceedings. Volume 2.
Ann Arbor, MI, Environmental Research Institute of Michigan, 1981, p. 793-802.

Characteristics of a unique imaging radiometer used to make measurements over areas of the North Atlantic at infrared wavelengths are described. Examples are presented of the surface temperature spatial variation, the radiometric temperature variation with viewing angle, atmospheric effects, influence of scattered clouds, and the wavenumber variance spectrum. The radiometric environment typically encountered is discussed. It is shown that the capabilities of the radiometer permit the obtaining of precise radiance data for estimating corrections necessary for extracting accurate sea surface temperatures. D.L.G.

A82-27674 # **A formation process of an oceanic vortex analyzed by multi-temporal remote sensing.** Y. Hatakeyama (Asia Air Survey Co., Ltd., Tokyo, Japan), S. Tanaka (Remote Sensing Technology Center of Japan, Tokyo, Japan), and T. Nishimura (Tokyo Science University, Noda, Japan). In: International Symposium on Remote Sensing of Environment, 15th, Ann Arbor, MI, May 11-15, 1981, Proceedings. Volume 3. Ann Arbor, MI, Environmental Research Institute of Michigan, 1981, p. 1173-1186. 6 refs.

Investigations of the flow characteristics in the coastal seas of Japan are required in connection with water-quality problems related to rapid urbanization or industrialization. The present study is concerned with an observation of the dynamic aspects of an interaction between the Kuroshio current and coastal water in October 1979, after Typhoon-20 had passed through Japan. The observational data were obtained with the aid of a multitemporal remote sensing method. A vortex at the mouth of Suruga Bay was detected on the basis of the fluid-mechanical interpretation of the data. Attention is given to the marine background of the site, an analysis of temporal static aspects of the vortex with the aid of Landsat data, the analysis of dynamic vortex processes, and approaches for observing a vortex with the aid of remote-sensing data. G.R.

A82-27684 # **Response of the marine community to satellite-derived oceanic information.** N. J. Hooper (Metrics, Inc., Atlanta, GA) and J. W. Sherman, III (NOAA, National Earth Satellite Service, Washington, DC). In: International Symposium on Remote Sensing of Environment, 15th, Ann Arbor, MI, May 11-15, 1981, Proceedings. Volume 3. Ann Arbor, MI, Environmental Research Institute of Michigan, 1981, p. 1285-1295. 8 refs.

The present investigation has the objective to merge the marine data requirements identified at the NOAA Workshop on Oceanic Remote Sensing with those reflected by the response of the marine community to the National Oceanic Satellite System (NOSS) Conference Worksheets. The result of such an effort provides a summary of the civil marine community's oceanic remote sensing data requirements as they are currently understood. Oceanic remote sensing had been defined as being restricted to the use of electromagnetic energy to observe or measure properties of the ocean while remotely located from that portion of the ocean being observed. G.R.

A82-28031 # **Estimation of sea surface temperature from remote sensing in the 3.7 micron window region.** T. Takashima and Y. Takayama (Meteorological Research Institute, Tsukuba, Ibaraki, Japan). *Meteorological Society of Japan, Journal,* vol. 59, Dec. 1981, p. 876-891. 16 refs.

Temperature measurement deviation in satellite remote sensing during day and night is considered. Atmospheric gases are taken as absorbent constituents and aerosols as scatterers in an atmosphere-ocean model. The solar input is chosen at 1.94 cal/min at the surface, and a standard atmosphere is assumed. Optical thickness calculations for the 3.7 micron band include the effects of water vapor lines and continua, the collision-induced N2 band near 4 microns, and mixed gases. The atmosphere is characterized by nine layers, each with 14 homogeneous sublayers. Optical thicknesses are calculated over the 9 layers, averaged and weighted by the NOAA-6 filter response. The refractive index is also calculated, and the surface is treated as a specular reflector. Except for sun glint, deviations in observed to measured temperatures were less in the day than at night. Greater than 50 deg differences were detected in the specular direction, and were correctable by simulation. The surface wind speeds are required in order to correct for sun glint. M.S.K.

A82-28135 † **Polarimetric method for the remote sensing of oil slicks on the sea surface (Poliarizatsionnyi metod distantsionnoi indikatsii plenok nefti na poverkhnosti moria).** A. A. Buznikov and G. A. Lakhtanov. *(Vsesoiuznaia Konferentsiia po Problemam Issledovaniia Prirodnykh Resursov Zemli i Mirovogo Okeana, Aviatsionno-Kosmicheskimi Sredstvami, Moscow, USSR, Nov. 1980.) Geodeziia i Aerofotos'emka,* no. 1, 1982, p. 50-54. 10 refs. In Russian.

The polarimetric method for the remote sensing of oil slicks on the sea surface is described, and some previous studies using this method are briefly reviewed. Particular attention is given to the use of lidar polarimeters, and results of single-channel polarimetric studies of pollution in the Caspian Sea are discussed. B.J.

A82-28145 † **The use of data from satellite-borne microwave scanning radiometers for the automated compilation of operational maps of ice cover for the Arctic Ocean (Ispol'zovanie dannykh sputnikovykh skaniruiushchikh SVCh radiometrov dlia avtomatizirovannogo sostavleniia operativnykh kart ledianogo pokrova Severnogo Ledovitogo Okeana).** V. V. Bogorodskii, N. D. Liubovnyi, and P. A. Nikitin. *(Vsesoiuznaia Konferentsiia po Problemam Issledovaniia Prirodnykh Resursov Zemli i Mirovogo Okeana, Aviatsionno-Kosmicheskimi Sredstvami, Moscow, USSR, Nov. 1980.) Geodeziia i Aerofotos'emka,* no. 1, 1982, p. 108-111. In Russian.

N82-16331# Mitre Corp., Bedford, Mass.

COHERENT SCATTER OF MICROWAVES FROM MODERATELY ROUGH SURFACES

M. M. Weiner and G. A. Robertshaw Aug. 1981 33 p refs
(Contract F19628-81-C-0001; AF Proj. 4290)
(AD-A106133; MTR-8299) Avail: NTIS HC A03/MF A01 CSCL 20/14

An improved model is reported for the effect of surface roughness on coherent scatter of microwaves from moderately rough terrain and sea surfaces. This model gives agreement with microwave and acoustical experimental data for surface height standard deviations as much as 400% larger than for a widely accepted model discussed by Beckmann and other investigators. The improved agreement with data is achieved by assuming a symmetrical exponential probability density of the surface height random variable. This model lends itself to an interesting physical interpretation of the stochastic process associated with the surface profile. Author (GRA)

N82-16683*# National Aeronautics and Space Administration. Wallops Flight Center, Wallops Island, Va.

NOSS ALTIMETER ALGORITHM SPECIFICATIONS

D. W. Hancock, R. G. Forsythe, and J. D. McMillan (Washington Analytical Services Center, Pocomoke City, Md.) Jan. 1982 112 p refs
(NASA-RP-1083) Avail: NTIS HC A06/MF A01 CSCL 08C

A description of all algorithms required for altimeter processing is given. Each description includes title, description, inputs/outputs, general algebraic sequences and data volume. All required input/output data files are described and the computer resources required for the entire altimeter processing system were estimated. The majority of the data processing requirements for any radar altimeter of the Seasat-1 type are scoped. Additions and deletions could be made for the specific altimeter products required by other projects. T.M.

N82-16697# SRI International Corp., Menlo Park, Calif.

AN EXPERIMENTAL PROGRAM TO PROVIDE REMOTE MEASUREMENT AND ANALYSIS OF OCEAN WAVES, SEA LEVEL WINDS AND BALANCED PRESSURE IN SUPPORT OF SEASAT-A Final Report

J. W. Maresca, Jr., R. M. Endlich, C. T. Carlson, and D. E. Wolf Feb. 1981 50 p refs
(Contract NA79SA-C-00738; SRI Proj. 8808)
(PB81-246035; NOAA-81071410) Avail: NTIS HC A03/MF A01 CSCL 08C

Wide Aperture Research Facility (WARF) HF skywave radar and Seasat-A measurements of rms wave height and wind direction were compared for 17 July and 3 October 1978. Estimates of rms wave height were made during the 2 October period from skywave radar data recorded directly below the satellite. Sea level balanced pressure fields were computed from the Seasat-A satellite scatterometer (SASS) derived wind field on both days and compared to the National Weather Service (NWS) surface pressure charts. GRA

N82-17561*# National Aeronautics and Space Administration. Goddard Space Flight Center, Greenbelt, Md.

AN OPTICAL MODEL FOR THE MICROWAVE PROPERTIES OF SEA ICE

P. Gloersen and J. K. Larabee Nov. 1981 28 p refs Submitted for publication
(NASA-TM-83865) Avail: NTIS HC A03/MF A01 CSCL 08L

The complex refractive index of sea ice is modeled and used to predict the microwave signatures of various sea ice types. Results are shown to correspond well with the observed values of the complex index inferred from dielectic constant and dielectric loss measurements performed in the field, and with observed microwave signatures of sea ice. The success of this modeling procedure vis a vis modeling of the dielectric properties of sea ice constituents used earlier by several others is explained. Multiple layer radiative transfer calculations are used to predict the microwave properties of first-year sea ice with and without snow, and multiyear sea ice. Author

N82-17563*# National Aeronautics and Space Administration. Goddard Space Flight Center, Greenbelt, Md.
SATELLITE-DERIVED ICE DATA SETS NO. 1: ANTARCTIC MONTHLY AVERAGE MICROWAVE BRIGHTNESS TEMPERATURES AND SEA-ICE CONCENTRATIONS, 1973 - 1976
H. J. Zwally Nov. 1981 35 p refs Submitted for publication
(NASA-TM-83812) Avail: NTIS HC A03/MF A01 CSCL 08L

A summary data set concerning 4 years of Antarctic sea-ice conditions was created and is available on magnetic tape. The data were derived from electrically scanning microwave radiometer brightness temperatures and were mapped into a polar stereographic grid enclosing the 50 deg S latitude circle. The grid size varies from about 32 by 32 sq km at the poles to about 28 by 28 sq km at 50 deg S. The microwave brightness temperatures of Antarctic sea ice are predominantly characteristic of first-year ice with an emissivity of 0.92 at 19 GHz frequency. Sea ice concentrations were calculated from the brightness temperature data for each grid element with an algorithm that uses an emissivity value of 0.92 and an ice physical temperature estimate from climatological surface air temperatures. Monthly, multiyear monthly, and yearly maps of brightness temperatures and sea ice concentrations were created for the 4 years, except for 7 months for which useable data were insufficient. Author

N82-17566# Research Inst. of National Defence, Stockholm (Sweden).
REMOTE SENSING TECHNIQUES SUITABLE FOR EXPLORATION AND NAVIGATION IN AND UNDER SEA ICE
Ragnar Thoren 1981 44 p refs Presented at Intern. Colloq. of the Intern. Soc. of Photogrammetry and Remote Sensing on Spectral Signatures of Objects in Remote Sensing, Avignon, France, 8-11 Sep., 1981
(FOA-Rept-Vol-15-No-2; FOA-B-60002-M7;
ISBN-91-7056-057-9) Avail: NTIS HC A03/MF A01; Research Inst. of National Defence, Stockholm Kr 9

The performance of advanced satellite navigation used aboard Swedish and Soviet icebreakers is reported. It is shown that the ships' position was obtained with very high precision in spite of frequent fog. Further development of remote sensing satellite systems for ocean monitoring, the development of LORAN C into an expanded and improved aid to navigation, and the importance of visual ice reconnaissance in combination with optical viewing systems in arctic waters are also addressed. Developments in underwater technology, including hydroacoustics, hydrooptics, laser depth sounding, underwater communication, and subsea exploratory drilling are included. J.M.S.

N82-17567# Office of Naval Research, Pasadena, Calif.
ARABIAN SEA PROJECT OF 1980: COMPOSITES OF INFRARED IMAGES
Ben J. Cagle and Robert Whritner Aug. 1981 67 p
(AD-A107910; ORNWEST-81-5) Avail: NTIS HC A04/MF A01 CSCL 08/1

A technique was developed for determining the mesoscale features of the Arabian Sea, and reported on in ONRWEST Report 81-3. A method for assembling composites of images in mosaic form is presented. Enhanced images are presented with surface interpretations for the spring and fall transition periods related to the Northeast and Southwest Monsoons, respectively. Author (GRA)

N82-17798*# Old Dominion Univ., Norfolk, Va. Dept. of Oceanography.
THE RELATIONSHIP AMONG SEA SURFACE ROUGHNESS VARIATIONS, OCEANOGRAPHIC ANALYSES, AND AIRBORNE REMOTE SENSING ANALYSES Final Report, 16 May - 31 Oct. 1981
George F. Oertel and Terry L. Wade Dec. 1981 252 p refs
(Grant NAG1-189)
(NASA-CR-168444; TR-81-2) Avail: NTIS HC A12/MF A01 CSCL 08C

The synthetic aperture radar (SAR) was studied to determine whether it could image large scale estuaries and oceanic features such as fronts and to explain the electromagnetic interaction between SAR and the individual surface front features. Fronts were observed to occur at the entrance to the Chesapeake Bay. The airborne measurements consisted of data collection by SAR onboard an F-4 aircraft and real aperture side looking radar (SLAR) in Mohawk aircraft. A total of 89 transects were flown. Surface roughness and color as well as temperature and salinity were evaluated. Cross-frontal surveys were made. Frontal shear and convergence flow were obtained. Surface active organic materials, it was indicated, are present at the air-sea interface. In all, 2000 analyses were conducted to characterize the spatial and temporal variabilities associated with water mass boundaries. N.W.

N82-17802# European Space Agency, Paris (France).
SEA STATE MEASUREMENT WITH A TWO FREQUENCY SCATTEROMETER (THEORY)
Michael Kleintz Dec. 1981 177 p refs Transl. into ENGLISH of "Seegangsbestimmung mit dem Zweifrequenz-Scatterometer (Theoretische Grundlagen)" Rept. DFVLR-FB-80-32 Oberpfaffenhofen, West Germany, May 1980 Original report in GERMAN previously announced as N81-22675
(ESA-TT-710; DFVLR-FB-80-32) Avail: NTIS HC A09/MF A01; DFVLR, Cologne DM 31,20

In the context of the Spacelab program, sea state measurements with a two frequency scatterometer are considered. A system analysis of two frequency scatterometry, especially signal analysis for stationary and airborne (aircraft; satellite) measurements, is presented, and an unambiguous method for wind direction determination is given. A statistical model of sea state, based on the frequency spectrum of the water wave height distribution, is used. The radar echo from the sea surface is characterized for a monochromatic ouptut signal. An autocorrelation function is developed, and application in consideration of the Doppler spectrum of the sea surface reflectance function is shown. Author (ESA)

N82-17803# National Oceanic and Atmospheric Administration, Rockville, Md. Ocean Technology and Engineering Services.
ERROR ANALYSIS OF PULSE LOCATION ESTIMATES FOR SIMULATED BATHYMETRIC LIDAR RETURNS
Gary C. Guenther and Robert W. L. Thomas Jul. 1981 59 p refs Prepared in cooperation with EG and G Washington Analytical Services Center, Inc., Rockville, Md.
(PB82-109448; NOAA-TR-OTES-1; NOAA-81081101) Avail: NTIS HC A04/MF A01 CSCL 08J

A Poisson count simulator is used to generate precision and offset results for the estimated temporal location of quantum limited laser pulses. Pulse sizes, shapes, and charge integration times are varied over appropriate ranges. A number of location estimators including variations on peak, centroid, and threshold detectors are examined. Comparisons with experimental results are presented. Hardware and software design parameters of an airborne lidar hydrography system are discussed. GRA

N82-17806# National Bureau of Standards, Boulder, Colo. Wave Propagation Lab.
RECOVERING OCEAN WAVEHEIGHT FROM HF RADAR SEA ECHOES DISTORTED BY IMPERFECT IONOSPHERIC REFLECTION
T. M. Georges, J. W. Maresca, C. T. Carlson, J. P. Riley, R. M. Jones, and D. E. Westover May 1981 156 p refs
(PB82-113283; NOAA-TM-ERL-WPL-73; NOAA-81081301) Avail: NTIS HC A08/MF A01 CSCL 08C

A real-time signal processing package to collect high-quality sea-echo Doppler spectra under many different ionospheric conditions found in nature was developed. Graphical displays and objective quality indices help the radar operator sort undistorted spectra from those distorted by imperfect ionospheric reflection, so that ocean wave height can be reliably estimated while the data are being collected. The package can be used either off-line on archival data or for on-line adaptive processing of radar data as part of an ocean-scanning strategy. Author (GRA)

N82-18860*# Jet Propulsion Lab., California Inst. of Tech., Pasadena.

SEASAT DATA UTILIZATION PROJECT Final Report

G. H. Born, D. N. Held, D. B. Lame, R. G. Lipes, D. R. Montgomery, P. J. Rygh, and J. F. Scott 30 Sep. 1981 62 p refs

(NASA-CR-168557; Rept-622-233) Avail: NTIS HC A04/MF A01 CSCL 05B

During the three months of orbital operations, the satellite returned data from the world's oceans. Dozens of tropical storms, hurricanes and typhoons were observed, and two planned major intensive surface truth experiments were conducted. The utility of the Seasat-A microwave sensors as oceanographic tools was determined. Sensor and geophysical evaluations are discussed, including surface observations, and evaluation summaries of an altimeter, a scatterometer, a scanning multichannel microwave radiometer, a synthetic aperture radar, and a visible and infrared radiometer. N.W.

N82-18844# Office of Technology Assessment, Washington, D. C.

TECHNOLOGY AND OCEANOGRAPHY: AN ASSESSMENT OF FEDERAL TECHNOLOGIES FOR OCEANOGRAPHIC RESEARCH AND MONITORING

Jun. 1981 27 p

(OTA-O-142) Avail: NTIS HC A03/MF A01

The status of technologies used to collect data about the ocean and to conduct experiments in the ocean is addressed. Problems and opportunities are analyzed and the Federal agencies and programs charged with conducting oceanic studies and providing the necessary management and hardware systems are examined. Selected national programs directed toward conserving and managing marine fishery resources, developing an oceanographic satellite system investigating the geology and possible resource potential of the continental margins beneath the deep ocean, and developing a climate prediction capability are analyzed. S.L.

N82-19435# Washington Univ., Seattle. Polar Science Center.

SEA ICE MOVEMENTS FROM SYNTHETIC APERTURE RADAR Final Report, 1 Apr. 1979 - 30 Jun. 1981

David A. Rothrock and Alan S. Thorndike 1 Dec. 1981 84 p refs

(Contract N00014-79-C-0418; NR Proj. 307-428)

(AD-A109002) Avail: NTIS HC A05/MF A01 CSCL 08/12

The spatial structure of the sea ice velocity field determines ridging, open water production and ice stress. The velocity has been measured roughly every 2 km along an 865 km track from SEASAT synthetic aperture radar. The movement shows individual pieces as large as 100 km. The spatial autocorrelation function of velocity has been estimated from these data and FGGE and AIDJEX buoy data, and has a length scale of roughly 1000 km. A model of the movement of a set of pieces shows the large uncertainty in opening and ridging estimated from velocities measured at only three points. Author (GRA)

N82-19704# Instituto de Pesquisas Espaciais, Sao Jose dos Campos (Brazil).

PRELIMINARY RESULTS OF A STUDY OF MAPPING THERMAL DISCHARGE IN THE OCEAN, USING REMOTE SENSING DATA

Merritt Raymond Stevenson, Carlos Alberto Steffen, and Hector Manual Inostroza Villagra Sep. 1981 23 p refs In PORTUGUESE; ENGLISH summary Presented at 33d Ann. Meeting of SBPC, Salvador, 8-15 Jul. 1981

(INPE-2229-PRE/021) Avail: NTIS HC A02/MF A01

The spatial and temporal variations of the sea surface temperature, utilizing data obtained from sea surface, aircraft and satellite platforms were studied. The objective of the study is the evaluation and mapping of small scale variations in the sea surface temperature, caused by the thermal discharge from a nuclear power plant at Angra dos Reis, Brazil. Evaluation of data from ANGRA 01, the first experiment made on December 19, 1980, showed the surface temperature to be quite isothermal. Temperature from the aircraft and satellite radiometers were about 0.6 C and 5.0 C cooler, respectively, than the temperatures measured from the boat. These thermal offsets are readily accounted for by differences in emissivities of the sea surface and the intervening water vapor in the lower atmosphere.Author

N82-19756 British Library Lending Div., Boston Spa (England).

CLASSIFICATION OF THE FIELDS OF ANOMALY IN MONTHLY WATER TEMPERATURE OF THE NORTH ATLANTIC DURING THE COLD HALF-YEAR

R. M. Vilfand 27 Jul. 1981 6 p refs Transl. into ENGLISH from Gidromet. Nauch.-Issled. Tsentr. SSSR (USSR), v. 231, 1980 p 123-126

(BLL-Trans-1509-(9022.552)) Avail: British Library Lending Div., Boston Spa, Engl.

The use of the thermal characteristics of ocean surface in making long-term forecasts is examined. Fields of anomaly in the mean monthly water temperature of the North Atlantic were classified and analyzed. R.J.F.

N82-19778# Instituto de Pesquisas Espaciais, Sao Jose dos Campos (Brazil).

CONVERGENCE ZONES IN THE SOUTH ATLANTIC AND THEIR INFLUENCE ON THE PRECIPITATION REGIME IN NORTHEASTERN BRAZIL M.S. Thesis [ZONAS DE CONVERGENCIA NO ATLANTICO SUL E SUAS INFLUENCIAS NO REGIME DE PRECIPITACAO NO NORDESTE DO BRASIL]

Lucimar Luciano deOliveira Jan. 1982 125 p refs In PORTUGUESE; ENGLISH summary

(INPE-2307-TDL/074) Avail: NTIS HC A06/MF A01

The relationship between the convergence zones in the South Atlantic and the rainfall variability on Northeast Brazil was studied. Radiosonde data from the Posto Oceanografico da Ilha da Trindade, wind charts from the National Meteorological Center, USA, precipitation data of selected coastal stations and satellite imagery were utilized. Monthly and half-yearly brightness charts were constructed from such satellite imagery between the parallels of 10 degrees N and 55 degrees S and the meridians of 010 degrees E and 080 degrees W, for a dry and a rainy year. The results reveal that dry years correspond to the permanence of the Spring pattern of interaction between the intertropical convergence zone and the South Atlantic convergence zones, the Bolivian high (in 200 mb) being more developed; in such dry years a stronger and more regular Walker circulation seems to be present. R.J.F.

N82-19781*# National Aeronautics and Space Administration. Goddard Space Flight Center, Greenbelt, Md.

ESTIMATING OCEAN-AIR HEAT FLUXES DURING COLD AIR OUTBREAKS BY SATELLITE

Shu-Hsien Chou and David Atlas Nov. 1981 52 p refs Submitted for publication Original contains color illustrations

(NASA-TM-83854) Avail: NTIS HC A04/MF A01 CSCL 04B

Nomograms of mean column heating due to surface sensible and latent heat fluxes were developed. Mean sensible heating of the cloud free region is related to the cloud free path (CFP, the distance from the shore to the first cloud formation) and the difference between land air and sea surface temperatures, theta sub 1 and theta sub 0, respectively. Mean latent heating is related to the CFP and the difference between land air and sea surface humidities q sub 1 and q sub 0 respectively. Results are also applicable to any path within the cloud free region. Corresponding heat fluxes may be obtained by multiplying the mean heating by the mean wind speed in the boundary layer. The sensible heating estimated by the present method is found to be in good agreement with that computed from the bulk transfer formula. The sensitivity of the solutions to the variations in the initial coastal soundings and large scale subsidence is also investigated. The results are not sensitive to divergence but are affected by the initial lapse rate of potential temperature; the greater the stability, the smaller the heating, other things being equal. Unless one knows the lapse rate at the shore, this requires another independent measurement. For this purpose the downwind slope of the square of the boundary layer height is used, the mean value of which is also directly proportional to the mean sensible heating. The height of the boundary layer should be measurable by future spaceborn lidar systems. B.W.

N82-19796# Florida State Univ., Tallahassee. Dept. of Meteorology.

COASTAL UPWELLING ECOSYSTEMS ANALYSIS. ATLAS OF THE JOINT I AIRCRAFT WINDS FOR THE 500 FOOT LEVEL Final Report

D. W. Stuart, A. I. Watson, and W. P. Duval Jun. 1981 73 p refs

(Grant NSF OCE-77-27735)
(PB82-114703; NSF/IDOE-81-44; FSU-MET-STU-81/2; NSF/IDOE/CUEA/TR-39) Avail: NTIS HC A04/MF A01 CSCL 04B

Maps of winds at 500 ft are presented for 17 individual flights and for 3 mean wind regimes using aircraft data gathered during daytime flights made in February-March 1974 as part of JOINT I. The total wind field is shown by maps of the streamlines and isotachs while the north-south component is shown by maps of isotachs and averaged offshore and alongshore profiles. GRA

N82-19801*# National Aeronautics and Space Administration, Washington, D. C.
NASA OCEANIC PROCESSES PROGRAM, FISCAL YEAR 1981 Annual Report
Mar 1982 132 p refs
(NASA-TM-84467) Avail: NTIS HC A07/MF A01 CSCL 08C

Summaries are included for Nimbus 7, Seasat, TIROS-N, Altimetry, Color Radiometry, in situ data collection systems, Synthetic Aperture Radar (SAR)/Open Ocean, SAR/Sea Ice, Scatterometry, National Oceanic Satellite System, Free Flying Imaging Radar Experiment, TIROS-N/Scatterometer and/or ocean color scanner, and Ocean Topography Experiment. Summaries of individual research projects sponsored by the Ocean Processes Program are given. Twelve investigations for which contracting services are provided by NOAA are included. N.W.

N82-19802# Electronics Research Lab., Adelaide (Australia).
AN AERIAL SURVEY OF WATER TURBIDITY AND LASER DEPTH SOUNDING PERFORMANCE ALONG THE QUEENSLAND COAST
D. M. Phillips and R. H. Abbot Apr. 1981 29 p refs
(AD-A109050; ERL-0192-TR) Avail: NTIS HC A03/MF A01 CSCL 08/10

The performance of the WRELADS laser airborne depth sounder has been assessed in North Queensland coastal waters from Townsville to Torres Strait. This was achieved by recording water turbidity and maximum sounding depth in the aircraft along the flight path. The parameter used in the aerial survey as a measure of water turbidity was related to beam attenuation coefficient measured from a boat in a joint aircraft and boat trial. Data relating the statistical distribution of turbidity to water depth were obtained and compared with the observed performance characteristic in order to indicate the proportion of Queensland coastal waters suitable for sounding with an airborne laser sounder. Author (GRA)

N82-19805# Ecole Nationale Superieure des Mines, Valbonne (France). Centre de Teledetection et d'Analyse des Milieux Naturels.
THE TOCIND EXPERIMENT Final Report [EXPERIENCE TOCIND]
L. Wald Paris ESA Jul. 1981 21 p refs In FRENCH
Sponsored in cooperation with CNES
(Contract ESA-4423/80/F-FC(SC))
(CTAMN/81/R/10; ESA-CR(P)-1479) Avail: NTIS HC A02/MF A01

The relation between surface isotherms and current is discussed. Predicting surface current from satellite thermographs is investigated. Ship measurements of Indian Ocean currents are compared with Meteosat images. Extensive cloud cover makes it impossible to compare results. Results from a horizontal heat advection model agree closely with measurements. Author (ESA)

N82-20823*# California Univ., La Jolla. Inst. of Marine Resources.
SHIP AND SATELLITE BIO-OPTICAL RESEARCH IN THE CALIFORNIA BIGHT
Raymond C. Smith and Karen S. Baker [1982] 23 p refs
(Grant NsG-1641)
(NASA-CR-168681; NAS 1.26:168681) Avail: NTIS HC A02/MF A01 CSCL 08A

Mesoscale biological patterns and processes in productive coastal waters were studied. The physical and biological processes leading to chlorophyll variability were investigated. The ecological and evolutionary significance of this variability, and its relation to the prediction of fish recruitment and marine mammal distributions was studied. Seasonal primary productivity (using chlorophyll as an indication of phytoplankton biomass) for the entire Southern California Bight region was assessed. Complementary and contemporaneous ship and satellite (Nimbus 7-CZCS) bio-optical data from the Southern California Bight and surrounding waters were obtained and analyzed. These data were also utilized for the development of multi-platform sampling strategies and the optimization of algorithms for the estimation of phytoplankton biomass and primary production from satellite imagery. R.J.F.

N82-20824# National Research Inst. for Oceanology, Stellenbosch (South Africa). Physical Oceanography Div.
INTERACTION BETWEEN THE AGULHAS CURRENT AND THE SUBTROPICAL CONVERGENCE
J. R. E. Lutjeharms Feb. 1981 42 p refs Presented at the 4th Natl. Oceanographic Symp., Cape Town, 10-13 Jul. 1979
(CSIR-RR-384) Avail: NTIS HC A03/MF A01

The Agulhas Current which loses its essential character as a western boundary current south of South Africa is discussed. This ocean area is known as an area of dramatic dynamical variability. To investigate this variability, and the mechanisms responsible, a number of satellite products covering a period of over two years were studied. A number of dynamical phenomena were observed and are described. These include the genesis and growth of sheer edge eddies on the landward border of the current, the nature and location of the Agulhas retroflection region, the formation of Agulhas rings in the south-east Atlantic Ocean, and the nature and variability of planetary waves in the subtropical convergence. The possible interaction between these features of the circulation is discussed in so far as the limited data allow this, and a conceptual image of the macroscale current dynamics in the area is presented. Author

N82-20827# Naval Research Lab., Washington, D. C. Aerospace Systems Div.
SURFACE WAVE STATISTICS AND SPECTRA DURING HIGH SEA STATE CONDITIONS IN THE NORTH ATLANTIC
C. R. McClain, D. T. Chen, and W. D. Hart 30 Dec. 1981 33 p refs
(RR0320841; WF59553000)
(AD-A109832; NRL-MR-4722) Avail: NTIS HC A03/MF A01 CSCL 08/3

Surface wave data collected using an airborne laser profilometer during high sea state conditions are analyzed to produce statistical cumulants up to the fifth order and power spectra. Theoretically, the third cumulant, skewness, is directly proportional to the wind-wave significant slope. This relationship is supported by wind-wave tank data, but little field data of this kind is available in the literature. Also, it has been suggested that if skewness can be derived from radar altimeter data, the significant slope would be computed and together with another altimeter product, the rms wave height, the wave spectra can be estimated using the Wallops Spectral Model (WSM). The results of this study indicate that the skewness relationship is valid for wind-wave dominated seas but as the swell contribution to rms wave height increases, the combined wave field skewness monotonically decreases below the predicted value. The WSM yields excellent reproductions of the wind-wave spectra even in multiple-peaked seas providing that the model inputs are properly determined for the wind-wave subfield. Finally the altimeter-WSM scheme should work reasonably well when the seas are wind-wave dominated provided that the altimeter can accurately measure skewness. More research on intermediate and swell dominated conditions is recommended. Author (GRA)

N82-21469# Deutsche Forschungs- und Versuchsanstalt fuer Luft- und Raumfahrt, Oberpfaffenhofen (West Germany).
TWO-DIMENSIONAL POWER SPECTRA OF SEASAT SAR IMAGERY
H. Seichter *In* ESA SAR Image Quality Jun. 1981 p 55-58

Avail: NTIS HC A05/MF A01; ESA, Paris FF 55 (US $12)

A least complication attempt was made to produce ocean wave power spectra of SEASAT SAR imagery. Two-dimensional power spectra of ocean SAR imagery with a pixel spacing of 12.5 m or multiples of it and side lengths of 1.6 km to 25.6 km were produced and converted to photo products. The most favorable sizes are dependent on wave properties. Author (ESA)

N82-21691# Naval Surface Weapons Center, Dahlgren, Va.
SOME ALTIMETRIC SIGNATURES FROM SEASAT OVER THE MID-PACIFIC SEAMOUNT RANGE Final Report
Bernd Zondek Oct. 1981 10 p ref
(AD-A110419; NSWC/TR-81-440) Avail: NTIS HC A02/MF A01 CSCL 08/10

Altimetric signatures from SEASAT tracks in the mid-Pacific seamount range reveal that some seamount signatures are not correlated with features in the reference bathymetry. GRA

06
HYDROLOGY AND WATER MANAGEMENT

Includes snow cover and water runoff in rivers and glaciers, saline intrusion, drainage analysis, geomorphology of river basins, land uses, and estuarine studies.

A82-19559 # **Microwave radiation from a natural snow field.** M. Tiuri and H. Schultz (Helsinki University of Technology, Esbo, Finland). In: European Microwave Conference, 10th, Warsaw, Poland, September 8-12, 1980, Proceedings.
Sevenoaks, Kent, England, Microwave Exhibitions and Publishers, Ltd., 1981, p. 574-578. 5 refs.

The brightness temperature of a natural snow field in Finland has been studied theoretically and experimentally at 5, 12 and 37 GHz for satellite remote sensing applications. A snow model consisting of ice spheres covered by a water shell has been used in theoretical calculations taking into account scattering and absorption. The brightness temperature of a natural snow field as a function of view angle has been measured from a tower in 1978 and 1979. The measured brightness temperature curves can be fitted with calculated ones by assuming reasonable values for the wetness and the particle size of snow. Experimental results also show that relatively small changes in the snow conditions cause large changes in the brightness temperature. (Author)

A82-19831 † **A photometric method for depth determination by aerial photography (O fotometricheskom sposobe opredeleniia glubin po aerofotosnimku).** E. S. Zubchenko and V. D. Kondiurin. *Geodeziia i Kartografiia*, Nov. 1981, p. 47-49. In Russian.

A modified photometric method for the determination of water depth based on an exponential approximation of the dependence of the brightness recorded by an aerial photograph on the depth is presented. The formulas employed calculate depth from measurements of the luminous flux having passed through the image, as well as the optical density of the image, so that it is not necessary to measure signals on portions of the photograph with optically infinite depths. Evaluation of the accuracy of the photometric method by comparison with results of sonic depth sounder measurements for a coastal region has shown it to be accurate to within 0.25 m rms for depths between 0.5 and 11.8 m, representing a significant improvement in accuracy. The method is thus recommended for use in bottom relief mapping in coastal shelf regions. A.L.W.

A82-20343 † **Investigation of the dynamics of the regional underground runoff of the Aral sea basin using space photography (Izuchenie dinamiki regional'nogo podzemnogo stoka basseina Aral'skogo moria s ispol'zovaniem s'emki iz kosmosa).** N. S. Semina (Vsesoiuznyi Nauchno-Issledovatel'skii Institut Gidrogeologii i Inzhenernoi Geologii, Moscow, USSR). *Issledovanie Zemli iz Kosmosa*, Nov.-Dec. 1981, p. 41-47. 6 refs. In Russian.

A82-21922 **Optical properties of snow.** S. G. Warren (Cooperative Institute for Research in Environmental Sciences, Boulder, CO). *Reviews of Geophysics and Space Physics*, vol. 20, Feb. 1982, p. 67-89. 99 refs. NSF Grant No. ATM-80-24641.

The reflection, absorption and transmission of light in the solar and infrared regions by snow are reviewed in light of the importance of optical properties in radiation budget and remote sensing studies. Measurements of snow albedo, bidirectional reflectance, flux extinction and intensity extinction are discussed, and the development of modeling of snow optical properties is outlined. Consideration is then given to the effects of snow grain size, liquid water content and impurities on snow albedo, and to spectrally integrated and spectral flux extinction in the transmission of light through snow. The dependence of snow and spectrally integrated planetary albedos on sun angle is examined, and effects of cloud cover are noted. A complete description of the bidirectional reflectance of snow is presented for use in satellite measurements, and the azimuthally averaged reflectance is supplied for flux calculations. Attention is also given to the thermal infrared emissivity and brightness temperature properties of snow and to the remote sensing of snow parameters based on solar infrared and microwave spectra. A.L.W.

A82-22145 **Use of GOES and TIROS/NOAA satellite data for snow-cover mapping.** T. M. Lillesand, D. E. Meisner, A. LaMois Downs, and R. L. Deuell (Minnesota, University, St. Paul, MN). *(American Society of Photogrammetry, Annual Convention, Washington, DC, Feb. 22-27, 1981.) Photogrammetric Engineering and Remote Sensing*, vol. 48, Feb. 1982, p. 251-259. 14 refs. Research supported by the University of Minnesota; Grant No. NOAA-NA-80AAD0019.

Using Minnesota as a test area, a study was conducted to evaluate the imaging characteristics of snow in open agricultural areas, under heavily forested conditions, and in zones of transition between the two cover types. Both GOES and NOAA/TIROS data were analyzed and both visual and digital data analysis techniques were employed. Satellite and ground-based snow survey data were compared for the winters of 1978-79 and 1979-80. Attention is given to aspects of data acquisition, visual image interpretation, and digital data analysis. It was found that visual interpretation of snow extent in nonforested regions would provide very useful input to the snow mapping techniques currently used in Minnesota. The satellite data provide an improved portrayal of the spatial distribution of snow when used in conjunction with ground data. GOES images were found to be more useful than TIROS/NOAA images. G.R.

A82-22873 **The use of satellite data in rainfall monitoring.** E. C. Barrett (Bristol, University, Bristol, England) and D. W. Martin (Madison, University, Madison, WI). London and New York, Academic Press, 1981. 350 p. 310 refs. $57.

Applications, limitations, and prospectives for future improvements in satellite data gathering for rainfall hydrometeorology are examined. Basic parameters of rainfall amenable to satellite observation are reviewed, along with existing satellites and systems for rainfall observations. Specific attention is given to observation methods such as preliminary studies, cloud-indexing, life-histories, bi-spectral and cloud model methods, rainfall detection from visible and IR images, and properties of microwave radiation in the atmosphere. Satellite rainfall monitoring applications are explored in terms of rainfall inventories on macro- and mesoscales, and for use in hydrology, for studying floods, droughts, and plagues, and for monitoring crop growth and production. Finally, future prospects are discussed for active microwave systems and integrated and international programs for rainfall monitoring. M.S.K.

A82-24959 **Change detection in the Peace-Athabasca Delta using digital Landsat data.** G. M. Wickware (Canada Centre for Inland Waters, Burlington, Ontario, Canada) and P. J. Howarth (McMaster University, Hamilton, Ontario, Canada). *Remote Sensing of Environment*, vol. 11, Mar. 1981, p. 9-25. 21 refs. Research supported by Parks Canada and Natural Sciences and Engineering Research Council of Canada.

The extensive Peace-Athabasca Delta has experienced major changes in water boundaries and vegetation types due to flooding. To determine the feasibility of Landsat digital data to monitor such changes, comparisons of parts of the delta under normal and flooded conditions have been made. The analysis involved supervised classification of the digital data on two dates followed by post-classification change detection. Comparison of the digital analysis results with aerial photography and existing maps showed good classification accuracy, although a considerable number of pixels remained unclassified. Change detection involved registration of the images on the Image 100 monitor followed by class comparison on a pixel-by-pixel basis. This demonstrated not only that changes had occurred, but also the nature of the changes. Evaluation of the original reflectance values for each class helped in the explanation of the known water and vegetational changes. Results of the study indicate that this type of wetland environment can be effectively mapped and changes readily determined using digital Landsat data. Care must be taken, however, in the analysis of statistical information generated on a pixel-by-pixel basis, particularly for linear features where there are frequent boundaries between classes. (Author)

06 HYDROLOGY AND WATER MANAGEMENT

A82-24960 * **Spectral reflectance of hydrophytes.** R. G. Best, M. E. Wehde, and R. L. Linder (South Dakota State University, Brookings, SD). *Remote Sensing of Environment,* vol. 11, Mar. 1981, p. 27-35. 9 refs. Research supported by the South Dakota State University, South Dakota Department of Game, Fish and Parks, and U.S. Fish and Wildlife Service; Grant No. NGL-42-003-007.

Identification of hydrophytes will improve the delineation and classification of wetlands on remotely sensed imagery. Spectral reflectance measurements of 10 species of hydrophytes were made with an Exotech radiometer during three phenological stages, flowering and early seed, senescent, and early emergent. Reflectance data were analyzed to determine significant (P not greater than 0.5) differences between species in each of four spectral regions during each phenological stage. Eight species had significantly (P not greater than 0.05) different reflectances during the flower and early seed stage. Among the ten species only one could not be spectrally isolated during at least 1 phenological stage. The results indicate that films sensitive to both visible and infrared spectra (e.g., Ektachrome infrared) should enable recognition of different species of hydrophytes. (Author)

A82-26838 **Geotechnical applications of Landsat image analysis of Bhakra Dam Reservoir, India.** R. P. Gupta and J. Bodechtel (Zentralstelle für Geo-Photogrammetrie und Fernerkundung, Munich, West Germany). *Remote Sensing of Environment,* vol. 12, Mar. 1982, p. 3-13. 16 refs.

Repetitive coverages of Landsat MSS images over Bhakra Dam Reservoir, India, are analyzed and processed on an optical-analog processing device for feature enhancement. The investigations are made with respect to the geological-structural set-up of the area, reservoir lake monitoring, and silting hazards in the reservoir, with emphasis on the importance of remote sensing in water resources management. A lineament-tectonic map of the area is prepared, and temporal variations in the lake reservoir are mapped from the images, the accuracy of which can be improved through digital processing. A method for volumetric estimation of stored water from the Landsat data is proposed. D.L.G.

A82-26839 * **Remote sensing of salinity in the San Francisco Bay Delta.** S. Khorram (California, University, Berkeley, CA; North Carolina State University, Raleigh, NC). *Remote Sensing of Environment,* vol. 12, Mar. 1982, p. 15-22. 32 refs. Research supported by the University of California; Grant No. NsG-5256.

Landsat multispectral scanner data and color and color infrared photographs acquired from a U-2 aircraft are combined with surface measurements for salinity mapping of the San Fransisco Bay Delta. A regression model is developed between the surface truth data and Landsat digital data for 29 sample sites, and is then extended over the entire study area. Results are in general agreement with reported salinity distribution values. It appears to be impossible to establish any quantitative judgement regarding the salinity values by visual interpretation of the imagery within the test site. D.L.G.

A82-27457 **Aerospace methods for the study of water resources and their pollution (Aerokosmicheskie metody pri issledovanii vodnykh resursov i ikh zagriazneniia).** Edited by V. V. Kupriianov and V. F. Usachev. Leningrad, Gidrometeoizdat (Gosudarstvennyi Gidrologicheskii Institut, Trudy, No. 285, 1981. 152 p. In Russian.

Papers are presented on such topics as the use of satellite remote sensing data to study meltage runoff in mountain basins, the investigation of the dynamics of snow cover, the use of satellite multispectral photography to study snow meltage fronts, and the evaluation of the pollution of snow cover in industrial regions on the basis of remote sensing data. Also considered are the determination of the albedo and brightness coefficients of snow cover, the use of remote sensing to study subsurface water and tectonic structures, the investigation of the thermal pollution of rivers on the basis of infrared aerial photography, remote sensing methods for monitoring water quality, and microwave sensing methods for the investigation of water resources and their pollution. B.J.

A82-27458 † **The possibilities of microwave remote sensing for the study of water resources and their pollution (Vozmozhnosti mikrovolnovoi distantsionnoi indikatsii dlia izucheniia vodnykh resursov i ikh zagriazneniia).** K. Ia. Kondrat'ev, Iu. I. Rabinovich, and E. M. Shul'gina. In: Aerospace methods for the study of water resources and their pollution. Leningrad, Gidrometeoizdat, 1981, p. 5-12. 7 refs. In Russian.

The application of microwave remote sensing to the following hydrological tasks is considered: (1) the mapping of water bodies and ice formations on these bodies; (2) the determination of soil moisture; (3) the evaluation of certain types of water-surface pollution; and (4) the sensing of precipitation zones. It is shown that the use of microwave sensing and active radar techniques in hydrological studies will provide important information on the state of the atmosphere and the underlying surfaces. B.J.

A82-27459 † **Remote-sensing functions in the interpretation of moisture from aerial and space images (Indikatsionnye funktsii pri deshifrirovanii uvlazhneniia po aerokosmicheskim izobrazheniiam).** B. V. Vinogradov. In: Aerospace methods for the study of water resources and their pollution. Leningrad, Gidrometeoizdat, 1981, p. 13-24. 17 refs. In Russian.

A remote-sensing function is a quantitative description of data transformations in the transition from the object under study to the remote image of the object. A remote-sensing function is determined by analytic functional relationships, modulation transfer functions, or statistical analysis. A complete remote-sensing function contains a number of data-transmission units: instrumental, atmospheric, botanical, soil-related, hydrological, and geological. Several different remote-sensing functions are examined, and approximating equations are obtained for geophysical, botanical, soil functions for soil moisture and ground water. B.J.

A82-27460 † **Remote-sensing determination of the characteristics of hydrological objects (Opredelenie kharakteristik gidrologicheskikh ob'ektov distantsionnym metodom).** G. Tovizi. In: Aerospace methods for the study of water resources and their pollution. Leningrad, Gidrometeoizdat, 1981, p. 25-28. In Russian.

Remote sensing studies of water resources in Hungary are described. Most favorable spectral regions have been established for shorelines (0.8-0.9 micron), bottoms (0.45-0.65 micron), geological and tectonic formations (0.6-1.1 micron), and snow and ice cover (0.5-0.7 micron). The use of aerial photography to study water turbidity, silt formation in reservoirs, water flow rate and temperature, and surface pollution of water is discussed. Spectral regions most suitable for the study of these characteristics are indicated. B.J.

A82-27461 † **Application of satellite data to analyze and predict meltage runoff in a mountain basin (Primenenie sputnikovoi informatsii dlia rascheta i prognoza talogo stoka v gornom basseine).** N. V. Vostriakova. In: Aerospace methods for the study of water resources and their pollution. Leningrad, Gidrometeoizdat, 1981, p. 29-37. 9 refs. In Russian.

The use of satellite remote sensing images to analyze and predict meltage runoff during spring and summer periods is examined using the basins of the Sayan-Altai river system as an example. The following relationships are examined: (1) the dependence of changes in basin snow cover on the sum of positive values of air temperature; (2) the relationship between the rate of rise of the snow line and the water content during the high-water period; (3) the dependence of runoff volume on the area of snow meltage and the heat influx to the remaining high-water period on the size of the snow-covered area of the basin. The need to use multispectral imagery to study mountain river runoff is emphasized. B.J.

A82-27462 † **Dynamics of snow cover in mountain regions of the Aral Sea basin, studied using satellite photographs (Dinamika snezhnogo pokrova v gornykh raionakh basseina Aral'skogo Moria po sputnikovym snimkam).** M. V. Sitnikova, B. K. Tsarev, and V. Iu. Chernov. In: Aerospace methods for the study of water resources and their pollution. Leningrad, Gidrometeoizdat, 1981, p. 38-44. 8 refs. In Russian.

A82-27463 † **The possibility of determining snow-meltage fronts using Meteor-satellite multispectral data /with Kazakhstan considered as an example/ (O vozmozhnosti opredeleniia fronta snegotaianiia po mnogozonal'noi informatsii s ISZ 'Meteor' /na primere Kazakhstana/).** E. I. Pankratova. In: Aerospace methods for

the study of water resources and their pollution.
Leningrad, Gidrometeoizdat, 1981, p. 47-55. 5 refs. In Russian.

A82-27464 † Evaluation of snow-cover pollution in industrial regions using satellite TV images (Otsenka zagriaznennosti snezhnogo pokrova promyshlennykh raionov po sputnikovym TV izobrazheniiam). V. N. Vasilenko, V. G. Prokacheva, and Sh. D. Fridman. In: Aerospace methods for the study of water resources and their pollution. Leningrad, Gidrometeoizdat, 1981, p. 56-63. In Russian.

A subsatellite experiment was conducted in the spring of 1978 to investigate the pollution of snow cover in the Vorkuta industrial center of the USSR; Meteor-satellite TV images were interpreted. In addition, ground-based measurements of albedo, snow height and density, and dust concentrations in the snow cover were carried out along with aerial visual and photographic observations over an area of about 2500 sq km. Preliminary relationships were obtained between albedo, dust density in the snow, and the brightness of the snow cover on satellite images. B.J.

A82-27465 † Albedo and brightness coefficients of snow cover (Ob al'bedo i koeffitsientakh iarkosti snezhnogo pokrova). V. F. Usachev, V. A. Mikhailov, and V. G. Prokacheva. In: Aerospace methods for the study of water resources and their pollution. Leningrad, Gidrometeoizdat, 1981, p. 64-69. In Russian.

Parallel measurements of integral albedo (0.3-2.4 microns) and spectral brightness coefficients (420, 525, 622, and 787 nm) of snow cover were carried out near the city of Monchegorsk during the period of snow meltage. The albedo was measured by the M-60 field albedometer, while the spectral brightness coefficients were measured photoelectrically using a four-channel spectrophotometer. The field measurements (64 series) showed that the relationship between the integral albedo and the spectral brightness coefficients is quasi-linear. The use of satellite TV imagery to determine the brightness of snow cover is considered. B.J.

A82-27467 † Survey and mapping of shallow water bodies and the distribution of the river runoff of solids on the basis of multispectral aerial and space photographs (Issledovanie i kartografirovanie melkovodnykh akvatorii i raspredeleniia tverdogo stoka rek po mnogozonal'nym aerokosmicheskim snimkam). Iu. F. Knizhnikov, V. I. Kravtsova, and I. A. Labutina. In: Aerospace methods for the study of water resources and their pollution. Leningrad, Gidrometeoizdat, 1981, p. 77-84. In Russian

Shallow areas of the northeastern Caspian were mapped using multispectral photographs from Soyuz-22. Geomorphological, bathymetric, relief, bottom-deposit, underwater-vegetation, and underwater-landscape maps were compiled. Attention is also given to general aspects of the use of multispectral photography to study the flow of suspensions carried by rivers into the coastal regions of seas and lakes. B.J.

A82-27468 † The use of space photographs for hydrogeological studies of the Baikal region and Mongolia (Ispol'zovanie kosmicheskikh snimkov dlia gidrogeologicheskikh issledovanii raionov Pribaikal'ia i Mongolii). Iu. L. Ob'edkov. In: Aerospace methods for the study of water resources and their pollution. Leningrad, Gidrometeoizdat, 1981, p. 85-96. 10 refs. In Russian.

The principles of the hydrogeological interpretation of space remote sensing images are discussed, with particular attention given to the determination of the relationship between various hydrogeological objects and landscape elements. A detailed analysis of space photographs makes it possible to determine the locations and boundaries of artesian basins, to characterize the water-conducting and collecting properties of water-containing rocks, and to evaluate subsurface water resources. The proposed method was used to study the hydrogeology of the Baikal region and the western part of central Mongolia. B.J.

A82-27469 † The effect of anthropogenic factors on the dynamics of lakes in the plains of Central Asia /studied on the basis of space photographs/ (Vliianie antropogennykh faktorov na dinamiku ravninnykh ozer Srednei Azii /po materialam kosmicheskikh s'emok/). A. M. Nikitin and Iu. N. Lesnik. In: Aerospace methods for the study of water resources and their pollution.
Leningrad, Gidrometeoizdat, 1981, p. 97-102. 5 refs. In Russian.

A82-27470 † Primary processing of and possibilities of using data from the meteorological satellite TIROS-N (Pervichnaia obrabotka i vazmozhnosti ispol'zovaniia dannykh meteorologicheskogo sputnika 'Tairos-N'). Sh. Kyevskii and V. Tollinger. In: Aerospace methods for the study of water resources and their pollution. Leningrad, Gidrometeoizdat, 1981, p. 103-107. In Russian.

Results of the primary processing of images of Czechoslovakia obtained with TIROS-N are presented. Geometric and radiative correction in three spectral intervals was used along with quantization and synthesis of images in conditional colors. The applicability of these data to hydrology is examined. B.J.

A82-27471 † Monitoring of the thermal pollution of natural channels of water using infrared aerial photography (Obsledovanie teplovogo zagriazneniia estestvennykh vodotokov s ispol'zovaniem infrakrasnoi aeros'emki). D. Domokosh. In: Aerospace methods for the study of water resources and their pollution.
Leningrad, Gidrometeoizdat, 1981, p. 108-113. In Russian.

It is proposed that infrared and aerial photography techniques be used to study river pollution resulting from power-plant emissions. As an illustration of the method, aerial photography in the visible (0.38-0.76 micron) and near IR (2.0-5.0 microns) was used to study the pollution of a section of the Danube in Hungary. A pollution distribution map of a 10-km section of the river was obtained (including the propagation of thermal waters only along the left bank). Stereophotogrammetry was used to determine the flow velocity. B.J.

A82-27472 † Investigation of silting and currents in Lake Balaton by use of hydraulic models and aerial and space photographs (Issledovanie zaileniia i techenii oz. Balaton s primeneniem gidravlicheskikh modelei i aerokosmicheskikh snimkov). L. Goda. In: Aerospace methods for the study of water resources and their pollution. Leningrad, Gidrometeoizdat, 1981, p. 114-119. In Russian.

A82-27473 † Interpretation of multispectral aerial photographs of Lake Müggelsee (Deshifrirovanie mnogozonal'nykh aerofotosnimkov oz. Miugel'zee). E. Iung. In: Aerospace methods for the study of water resources and their pollution.
Leningrad, Gidrometeoizdat, 1981, p. 120-122. In Russian.

A82-27474 † Spectrometric studies of the water composition of Lake Müggelsee (Spektrometricheskie issledovaniia sostava vod oz. Miugel'zee). D. Slavik. In: Aerospace methods for the study of water resources and their pollution.
Leningrad, Gidrometeoizdat, 198, p. 123-126. In Russian.

A hand-held spectrometer operating in the 335-1150 nm range was used to study the reflectance of water samples from Lake Müggelsee. The reflectance in this spectral range was studied as a function of the concentration of sediments in the water. The influence of suspensions of peat, green algae, and blue-green algae on the reflectance of the water is examined. B.J.

A82-27475 † Noncontact methods for the quality control of water resources (Nekontaktnye metody kontrolia kachestva vod). Iu. V. Zavolokin, L. A. Shliakhova, V. I. Rodzin, and V. A. Kriul'kov. In: Aerospace methods for the study of water resources and their pollution. Leningrad, Gidrometeoizdat, 1981, p. 127-134. 17 refs. In Russian.

Remote sensing methods for the operational quality control of water resources are described. Results of remote measurements of the physical and chemical properties of water bodies and water mineralization are presented. The recording, storage, and processing of the remote sensing data using television systems and analog/digital conversion techniques are considered. The development of a general model for the remote monitoring of water resources is discussed. B.J.

A82-27476 † Analog devices for the processing of aerial and space images for the study of water resources (Analogovye ustroistva

dlia obrabotki aerokosmicheskikh fotoizobrazhenii pri izuchenii vodnykh resursov). V. A. Mikhailov and V. F. Usachev. In: Aerospace methods for the study of water resources and their pollution. Leningrad, Gidrometeoizdat, 1981, p. 135-140. In Russian.

The paper examines the use of analog devices for the interpretation of remote sensing images, particularly, the delineation of contours of varying optical density and the determination of their areas. The application of such devices in the study of water resources is considered, and the incorporation of such devices in systems for the automated processing of remote sensing images is examined. B.J.

A82-27592 * # **Spatial reasoning in remotely sensed data.** J. Campbell, R. W. Ehrich, D. Elliott, R. M. Haralick, and S. Wang (Virginia Polytechnic Institute and State University, Blacksburg, VA). In: International Symposium on Remote Sensing of Environment, 15th, Ann Arbor, MI, May 11-15, 1981, Proceedings. Volume 1. Ann Arbor, MI, Environmental Research Institute of Michigan, 1981, p. 223-235. Contract No. NAS5-26276.

Photointerpreters employ a variety of implicit spatial models to provide interpretations from remotely sensed aerial or satellite imagery. In this paper one application is illustrated: how ridges and valleys can be automatically interpreted from Landsat imagery of a mountainous area, and how a relative elevation terrain model can be constructed from this interpretation. How to examine valleys for the possible presence of streams or rivers is shown, and how a spatial relational model can be set up to make a final interpretation of the river drainage network is explored. (Author)

A82-27610 # **Inland water quality assessment from Landsat data.** D. J. Carpenter (Australian National University, Canberra, Australia). In: International Symposium on Remote Sensing of Environment, 15th, Ann Arbor, MI, May 11-15, 1981, Proceedings. Volume 1. Ann Arbor, MI, Environmental Research Institute of Michigan, 1981, p. 483-490.

Landsat MSS data have been successfully applied to the collection of inland water quality data using multiple linear regressions. The data came from seven satellite acquisitions and simultaneous ground surveys of four lakes in the Southern Tablelands region of South East Australia. The linear models developed included the four band spectral radiances and the sun elevation as predictors and accounted for over 90% of the variance of the dependent variables. These were the water quality parameters turbidity and algal pigments. (Author)

A82-27613 # **Satellite sensing for extraction of groundwater resources information.** S. S. Kumar and S. Thiruvengadachari (National Remote Sensing Agency, Hyderabad, India). In: International Symposium on Remote Sensing of Environment, 15th, Ann Arbor, MI, May 11-15, 1981, Proceedings. Volume 1. Ann Arbor, MI, Environmental Research Institute of Michigan, 1981, p. 509-518.

Satellite derived data were used to generate regional level groundwater resources information in the chronically drought affected parts of central and southern India. Two different methodologies were adopted in the two different regions. In the first area, where geomorphology exercises a significant control over groundwater movement and occurrence, this relationship has been utilized to arrive at potential groundwater zones, whereas in Tamilnadu in south India basic resources information in regard to geology, geomorphology, hydrologic land use and soils were extracted and integrated to support a regional groundwater resources evaluation program. The two contrasting methodologies along with the case studies are described. Selection of suitable methodology in any area will depend upon the complexity of control over groundwater occurrence and movement, cost of survey and level of information required. (Author)

A82-27614 # **Snow cover monitoring using AVHRR data from TIROS and NOAA satellites.** G. Saint, P. Herbert (Centre National d'Etudes Spatiales, Toulouse, France), C. Leprieur (Grouppement pour le Développement de la Télédétection Aérospatiale, Toulouse, France), and M. Deneau (Electricité de France, Toulouse, France). In: International Symposium on Remote Sensing of Environment, 15th, Ann Arbor, MI, May 11-15, 1981, Proceedings. Volume 2. Ann Arbor, MI, Environmental Research Institute of Michigan, 1981, p. 519-526. 5 refs.

It is pointed out that the management of dams in hydroelectric projects could be substantially improved by monitoring the extent of the existing snow cover. In a study concerning the feasibility of such monitoring activities, it was found that the Advanced Very High Resolution Radiometer (AVHRR) carried by the TIROS-N series satellites would be the most suitable instrument for obtaining the required data. Attention is given to the characteristics of the AVHRR data, the principles of image segmentation, a description of the processing, the ground estimate, and a comparison of ground estimate and processing results. G.R.

A82-27634 # **Calcium carbonate precipitation in Pyramid Lake, Nevada, as monitored by satellite - 1978 and 1980.** C. P. Berg, S. R. Schneider (NOAA, National Earth Satellite Service, Washington, DC), and D. L. Galat (Colorado State University, Fort Collins, CO). In: International Symposium on Remote Sensing of Environment, 15th, Ann Arbor, MI, May 11-15, 1981, Proceedings. Volume 2. Ann Arbor, MI, Environmental Research Institute of Michigan, 1981, p. 721-731. 16 refs.

Satellite data from the summers of 1978 and 1980 on calcium carbonate precipitation in Pyramid Lake, Nevada, are presented. The whiting sequence, the growth, distribution pattern, and cessation of the phenomenon were documented by NASA's Landsat and NOAA's GOES. Results from water chemistry sampling verify the satellite imagery, and give evidence of a relationship between particulate calcium concentration and observed brightness. An optimum spectral interval of 0.5-0.6 microns is verified, and a significant reduction of light penetration into the lake, and therefore light available for photosynthesis, is found to be caused by the whitings. D.L.G.

A82-27637 # **Use of Landsat imagery to delineate glaciofluvial aquifers in southeast South Dakota.** E. F. Bugliosi (U.S. Geological Survey, Huron, SD). In: International Symposium on Remote Sensing of Environment, 15th, Ann Arbor, MI, May 11-15, 1981, Proceedings. Volume 2. Ann Arbor, MI, Environmental Research Institute of Michigan, 1981, p. 761-769. 7 refs.

An analysis of Landsat satellite imagery has been used in the delineation of buried glaciofluvial aquifers in southeastern South Dakota. A color and tonal pattern analysis was performed on a band 7 and a false color composite Landsat image obtained in April 1974 to detect linear and curvilinear patterns, and the patterns were compared with drainage and geomorphological overlays to locate any anomalies indicative of a buried glaciofluvial deposit. Test drilling at 50 locations within the Landsat area confirmed the presence or absence of aquifers predicted by the image analysis in 72% of the cases. Of the 17 holes drilled where Landsat predicted no deposits, 10 detected a glaciofluvial deposit, however five of these were either dry or located 30 m or more below the surface. Results demonstrate the feasibility of using Landsat images to delineate glaciofluvial aquifers at depths less than about 24 m below land surface. A.L.W.

A82-27639 # **Remote sensing of rainfall rates using airborne microwave rain-scatterometer/radiometer.** H. Inomata, K. Okamoto, T. Ojima, H. Masuko, S. Yoshikado, and N. Fugono (Ministry of Posts and Telecommunications, Radio Research Laboratories, Koganei, Tokyo, Japan). In: International Symposium on Remote Sensing of Environment, 15th, Ann Arbor, MI, May 11-15, 1981, Proceedings. Volume 2. Ann Arbor, MI, Environmental Research Institute of Michigan, 1981, p. 781-792.

Characteristics of an airborne microwave rain-scatterometer and radiometer operating at X-band and Ka-band are summarized. Data analysis techniques for deriving rainfall rates from the received powers of the scatterometer are briefly described. Some preliminary results of flight experiments performed in October 1980 for rain on the sea are discussed. Qualitative correlations between rainfall rates calculated from the X-band scatterometer data and antenna temperatures of the X-band radiometer data are clearly found. They also correlate fairly well with the attenuation of backscattered powers from sea surfaces. Typical displays of analyzed data in the flight experiment are shown. The ground-based experiment for strong rainfall from the rainfront stimulated by the typhoon in September 1980 are also discussed. An example of time sequential display of rainfall rates distribution are presented. Average wind speeds and falling speeds of raindrops can be easily estimated from the display. (Author)

A82-27692 # **Mapping of water quality using Landsat imagery.** L. T. Lindell (Statens Naturvardsverk, Uppsala, Sweden). In: International Symposium on Remote Sensing of Environment, 15th, Ann Arbor, MI, May 11-15, 1981, Proceedings. Volume 3. Ann Arbor, MI, Environmental Research Institute of Michigan, 1981, p. 1375-1385. 9 refs.

This paper discusses the possibilities of using Landsat imagery for purposes of mapping water quality. The methodology was first worked out on Lake Malaren, Sweden, where most of the practical procedures were tried and the variables to be mapped were chosen. The county of Orebro was selected as a test area for the country-wide mapping. This area contains more than 500 lakes larger than 10 ha ranging in trophic state from oligotrophic to eutrophic and, in elevation from mountain to lowland. Variables studied include turbidity, Secchi disc depth and lake surface area. The satellite data were geometrically corrected and color printed on a scale of 1:100 000 using an ink jet plotter. The experiences from this work will be used to develop a map of the water quality of Sweden. Mapping should be repeated frequently to record changes in water quality. Changes in water quality are displayed together with a separate field data base, which is used to determine possible causes for the changes. (Author)

A82-28137 † **The use of space photographs to compile water-amelioration maps (Ispol'zovanie kosmicheskikh snimkov pri sostavlenii meliorativno-vodokhoziaistvennykh kart).** T. V. Vereshchaka, B. V. Krasnopevtseva, and V. V. Usova. *(Vsesoiuznaia Konferentsiia po Problemam Issledovaniia Prirodnykh Resursov Zemli i Mirovogo Okeana, Aviatsionno-Kosmicheskimi Sredstvami, Moscow, USSR, Nov. 1980.) Geodeziia i Aerofotos'emka,* no. 1, 1982, p. 60-65. In Russian.

N82-16439*# Wisconsin Univ., Madison. Inst. for Environmental Studies.
MULTIDISCIPLINARY RESEARCH ON THE APPLICATION OF REMOTE SENSING TO WATER RESOURCES PROBLEMS Progress Report, Aug. 1979 - Jul. 1980
Ralph W. Kiefer, Principal Investigator Jul. 1980 45 p ERTS
(Grant NGL-50-002-127)
(E82-10021; NASA-CR-164815) Avail: NTIS HC A03/MF A01 CSCL 08H

Progress is reported in the following NASA-funded projects: (1) sediment plume study; (2) atmospheric correction to LANDSAT imagery; (3) demonstrating and evaluating opportunites for operational application of LANDSAT data in Wisconsin; and (4) the development of a facility to process imagery for the study of land cover, land use, water quality, electrophoresis gel analysis, prediction of storm and snow flow conditions, physical oceanography, and soils. Associated projects summarized are concerned with vegetation mapping in Sheboygan Marsh, surveying the Green Bay watershed to estimate the impact of land development on bay water quality; thermal scanning of ocean fronts; lake water quality, the Irondequoit River watershed, a model of thermal environment for land use planning, and changes in wetland vegetation near the Columbia Generating Station. Emphasis was focused on the selection of equipment for the efficient processing of images used for water-quality analysis and the development of supporting software for application by users. A.R.H.

N82-17601 Michigan Univ., Ann Arbor.
SPECTRAL REFLECTANCES OF FRESHWATER ICE AND SNOW FROM 340 THROUGH 1100 nm Ph.D. Thesis
Stanley Joseph Bolsenga 1981 159 p
Avail: Univ. Microfilms Order No. 8125073

Measured spectral reflectances of new and moderately metamorphosed snow were generally > 80% from 340 to 950 nm. From 950 to 100 nm a characteristic dip and rise of spectral reflectances occurred. One scan over a deteriorated snow patch showed much lower spectral reflectances than fresh snow, but the shape of the curve remained similar to fresher snow. Spectral reflectances for clear ice contrasted sharply with those for snow. In general, values were < 10% and the curves lacked distinctive shape. Higher spectral reflectances, due to lighter colored ice in the measurement area, were measured at some sites. Secondary ice types (refrozen slush, pancake, brash, slush curd) revealed spectral reflectance curves similar in form to each other, but which varied significantly in the range of spectral reflectances for each ice type. All measurements were acquired with a pair of scanning spectroradiometers adapted to obtain automatically simultaneous readings of incident and reflected radiation from 340 to 100 nm. Dissert. Abstr.

N82-17602 Colorado State Univ., Fort Collins.
WATERSHED MODEL STUDY USING LANDSAT DATA Ph.D. Thesis
Tien-Po Chang 1981 331 p
Avail: Univ. Microfilms Order No. 8126421

In connection with the use of remote sensing techniques, a digital terrain model that characterizes geometric features and other terrain conditions of a watershed is necessary for watershed modeling. As a result of constructing a watershed cell system on the digital terrain model, the mathematical formation on simulated physical processes can be simplified since the mathematical expressions only handle the small-sized, well-defined and relatively homogeneous components of the physical processes within a watershed cell. Four submodels that link the processing of the remote sensed data to the watershed analysis were developed. The submodels are LANDSAT image data processing model, digital terrain model, hydrologic simulation model, and landslide-hazard potential delineation model. The structure, function, and computer programs related to these models, along with the results of watershed simulation using the models, are presented and discussed. Dissert. Abstr.

N82-18469# Army Cold Regions Research and Engineering Lab., Hanover, N. H. Ice Engineering Research Branch.
ELECTROMAGNETIC SUBSURFACE MEASUREMENTS
Arnold M. Dean, Jr. Oct. 1981 24 p
(Proj. CWIS-31350)
(AD-A108192; CRREL-SR-81-23) Avail: NTIS HC A02/MF A01 CSCL 17/9

In 1974, personnel at the U.S. Army Cold Regions Research and Engineering Laboratory (CRREL) began using an impulse radar system to profile accumulations of ice forms. The system was modified for effective use as a profiling system in a ground or airborne configuration, in certain high-noise environments. The system can penetrate fresh water and media with a high water content. Frazil and brash ice accumulations with approximately 50% water were profiled to a depth of 25 to 35 ft. As a result of the CRREL modifications, the system has found extensive and varied applications as a low-level remote sensing tool. Applications include profiling ice accumulations (including ice jams), river beds, sheet ice, permafrost, subsurface ice masses, river bank revetments through air-entrained water, snow covers, sea ice, icebergs, and peat bogs. Limited laboratory work has also shown that the impulse radar system may be able to detect oil and gas under sea ice. Selected applications and data are presented. Since it was used mainly for research, the CRREL system needs further development to make it useful to operational units. Additional development of hardware and software is recommended. GRA

N82-18663*# National Aeronautics and Space Administration. Goddard Space Flight Center, Greenbelt, Md.
SPECTRAL ALBEDOS OF MIDLATITUDE SNOWPACKS
Bhaskar Choudhury Nov. 1981 41 p refs Submitted for publication
(NASA-TM-83858) Avail: NTIS HC A03/MF A01 CSCL 08L

Spectral albedos of impure-nonhomogeneous snowpacks, typical of midlatitudes, from 400 to 2200 nm were modeled through a numerical solution of the radiative transfer equation in the two-stream approximation. Discrete depth-dependent values of density, grain size and impurity concentration were used to characterize the snowpacks. The model is for diffuse incident radiation, and the numerical method is based on doubling and invariant imbedding. The effect of soot impurities on snowpack albedos is illustrated when a snowpack is several centimeters deep and soot reduces the albedos at visible wavelengths, however, when a snowpack is only a few centimeters deep, soot may increase the albedos at visible wavelengths. By adjusting soot content and snow grain size, good quantitative agreement with some observations at the Cascade Mountains (Washington) and at Point Barrow (Alaska) are obtained; however, the model grain sizes are found to be fifty to four hundred percent larger than the measured values. For satellite snowcover observations, a model for effective albedo of partially snow-covered areas was developed and compared with some NOAA-2 observations of the southeastern United States. T.M.

N82-18664*# National Aeronautics and Space Administration. Lewis Research Center, Cleveland, Ohio.
GROUND-TRUTH OBSERVATIONS OF ICE-COVERED NORTH SLOPE LAKES IMAGED BY RADAR
W. F. Weeks Oct. 1981 24 p refs Prepared in cooperation with CRREL, Hanover, N.H.
(NASA-TM-84127; AD-A108342; CRREL-81-19) Avail: NTIS HC A02/MF A01 CSCL 08/8

Field observations support the interpretation that differences in the strength of radar returns from the ice covers of lakes on the North Slope of Alaska can be used to determine where the lake is frozen completely to the bottom. An ice/frozen soil interface is indicated by a weak return and an ice/water interface by a strong return. The immediate value of this result is that SLAR (side-looking airborne radar) imagery can now be used to prepare maps of large areas of the North Slope showing where the lakes are shallower or deeper than 1.7m (the approximate draft of the lake ice at the time of the SLAR flights). The bathymetry of these shallow lakes is largely unknown and is not obvious from their sizes or outlines. Such information could be very useful, for example in finding suitable year-round water supplies. Author (GRA)

N82-18670# World Meteorological Organization, Geneva (Switzerland). Rapporteur on Sediment Transport.
MEASUREMENT OF RIVER SEDIMENTS
1981 69 p refs
(WMO-561; OHR-16; ISBN-92-63-10561-8) Avail: NTIS MF A01; print copy available at WMO, Geneva

Samples and remote sensing techniques for measuring sediment discharge in alluvial rivers are reviewed, noting that the simplest as well as sophisticated methods are not mutually exclusive. It is demonstrated that, in many cases, the optimum means for systematic sediment measurement is a combination of traditional and advanced methods and instruments. Areas where further improvement is needed, e.g., automation and telemetering as well as the international standardization of water pollution aspects of sediment monitoring, are indicated. Author (ESA)

N82-18671# World Meteorological Organization, Geneva (Switzerland).
FLASH FLOOD FORECASTING
A. J. Hall 1981 49 p refs
(WMO-577; OHR-18; ISBN-92-63-10577-4) Avail: NTIS MF A01; print copy available at WMO, Geneva SwFr 6

The problem of flash floods is reviewed and basic flash flood forecasting techniques, warning systems, and non-real time solutions to flash flooding are discussed. Data sources for flash flood forecasting are identified, including radar, satellites and quantitative precipitation forecasting. Flash flood forecasting can be based on meteorological, hydrological, meteorological-hydrological or dam break techniques. The design and establishment of flash flood warning systems, ranging from simple networks and procedures to sophisticated computerized automatic systems are described. The success of a flash flood warning system is measured by public response to warnings, the saving of life, and reduction of damage to property. Community involvement is evaluated, indicating the complex interactions among agencies, information dissemination subsystems and the public. Flood plain zoning, and basin management and the construction of engineering works are considered. The limitations and advantages of flood damage reduction measures are also analyzed. Author (ESA)

N82-19304# Instituto de Pesquisas Espaciais, Sao Jose dos Campos (Brazil).
DATA COLLECTION PLATFORMS: APPLICATIONS TO HYDROLOGY [PLATFORMAS DE COLETA DE DADOS: APLICACAO A HIDROLOGIA]
Jose Roberto deOliveira Oct. 1981 14 p refs In PORTUGUESE; ENGLISH summary Presented at 4th Brazilian Symp. on Hydrol. and Hydrol. Resources, 15-19 Nov. 1981
(INPE-2246-PRE/030) Avail: NTIS HC A02/MF A01

Data collection platforms which use artificial satellites as data relayers of meteorological data to receiving centers are discussed. The main systems available for data collection, and their advantages and limitations relative to hydrologic applications are discussed. R.J.F.

N82-19638*# Kansas Univ. Center for Research, Inc., Lawrence. Remote Sensing Lab.
DIELECTRIC PROPERTIES OF SNOW Interim Technical Report
W. H. Stiles and F. T. Ulaby Greenbelt, Md. NASA. Goddard Space Flight Center Dec. 1981 43 p refs
(Grant NAG5-163)
(NASA-CR-166764; RSL-TR-527-1) Avail: NTIS HC A03/MF A01 CSCL 08L

The dielectric properties of snow in the radio frequency range from 100 KHz to 35 GHz are reviewed. Applicable dielectric mixing formulas are discussed and compared to available experimental data. S.L.

N82-19646*# Kansas Univ. Center for Research, Inc., Lawrence. Remote Sensing Lab.
ACTIVE MICROWAVE INVESTIGATION OF SNOWPACKS: EXPERIMENTAL DOCUMENTATION, COLORADO 1979-1980
W. H. Stiles, Fawwaz T. Ulaby, A. Aslam, and M. Abdelrazik Jul. 1981 188 p refs
(Grant NsG-5335)
(NASA-CR-166727; RSL-TR-410-3) Avail: NTIS HC A09/MF A01 CSCL 08L

During the winter of 1979-1980, the University of Kansas Microwave Active Spectrometer systems measured the backscattering properties of snowpacks under varying conditions at four test sites in Colorado. In addition to the radar data over 1-35 GHz, ground-truth measurements of the atmospheric, snow, and soil characteristics were obtained for each radar data set. The test sites, data acquisition procedures, and data that were acquired in this experiment are presented and described. Author

N82-19790# Food and Agriculture Organization of the United Nations, Rome (Italy). Remote Sensing Centre.
PRECIPITATION ASSESSMENT FROM ENVIRONMENTAL SATELLITE DATA FOR NORTHWEST LIBYA INCLUDING THE GEFARA PLAN
A. vanDijk 1981 50 p refs
(RSC-4) Avail: NTIS HC A04/MF A01

The FAO precipitation assessment technique (satellite imagery combined with rain gage data) was applied to NW Libya to improve precipitation monitoring in this data sparse region. A 21 day period containing a few dry days, a heavy rainstorm, then a few more dry days was chosen. Rain gages reported 3 days of heavy rainfall, but failed to detect 2 further days with rain indicated by satellite data. The FAO rainfall maps appear more reliable than rain gage ones. The application of the technique to the whole of Libya, using Meteosat 2, and 10 reliable, well distributed rain gages, in combination with selected rain gages in South Italy, Tunisia and West Egypt is suggested. Author (ESA)

N82-20586*# Brigham Young Univ., Provo, Utah.
HCMM HYDROLOGICAL ANALYSIS IN UTAH
3 Sep. 1981 37 p refs Original contains imagery. Original imagery may be purchased from NASA Goddard Space Flight Center, (code 601), Greenbelt, Md. 20071. Domestic users send orders to 'Attn: National Space Science Data Center'; non-domestic users send orders to 'Attn: World Data Center A from Rockets and Satellites'. HCMM
(E82-10063; NASA-CR-165085; NAS 1.26:165085; QR-2) Avail: NTIS HC A03/MF A01 CSCL 08H

Progress in analysis of Heat Capacity Mapping Mission (HCMM) infrared and visible observations of the hydrology of Utah Lake is reported. Correlation between HCMM intensities converted to temperature and ground truth temperatures was investigated, and a conversion offset value determined. Ground truth surface temperatures minus HCMM temperatures were plotted against several hydrological parameters. Relationships among visible data, thermal data, and algae concentrations were considered, and summer concentrations of predominant algae species determined. Investigations on the effects of varying algae concentrations on evaporation rates are reported. Efforts to develop a model for evaporation estimation are reported. The relationship between air and water surface temperatures was studied and the temperature distribution in different segments of the lake investigated. Indications of the existence of thermal springs are reported. Correlation of HCMM surface temperature data and depth to groundwater were investigated. J.D.H.

N82-20587*# National Oceanic and Atmospheric Administration, Washington, D. C.
EVALUATION OF HCMM SATELLITE DATA FOR ESTUARINE TIDAL CIRCULATION PATTERNS AND THERMAL INERTIA SOIL MOISTURE MEASUREMENTS Final Report
Donald R. Wiesnet, David F. McGinnis, Jr., Principal Investigators, Michael Matson, and John A. Pritchard Jun. 1981 79 p refs Original contains color imagery. Original imagery may be purchased from NASA Goddard Space Flight Center, (code 601), Greenbelt, Md. 20071. Domestic users send orders to 'Attn: National Space Science Data Center'; non-domestic users send orders to 'Attn: World Data Center A for Rockets and Satellites'. HCMM
(NASA Order S-40229B)
(E82-10064; NASA-CR-165086; NAS 1.26:165086) Avail: NTIS HC A05/MF A01 CSCL 08C

Digital thermal maps of the Cooper River (SC) and the Potomac River estuaries were prepared from heat capacity mapping radiometer (HCMR) tapes. Tidal phases were correctly interpreted and verified. Synoptic surface circulation patterns were charted by location thermal fronts and water mass boundaries within the estuaries. Thermal anomalies were detected adjacent of a conventional power plant on the Potomac. Under optimum conditions, estuaries as small as the Cooper River can be monitored for generalized thermal/tidal circulation patterns by the HCMM-type IR sensors. The HCMM thermal inertia approach to estimating soil moisture at the Luverne (MN) test site was found to be unsatisfactory as a NESS operational satellite technique because of cloud cover interference. Thermal-IR data show similar structure of the Baltimore and Washington heat islands when compared to NOAA AVHHR thermal-IR data. Thermal anomalies from the warm water discharge water of a nuclear power plant were mapped in Lake Anna, Virginia. A.R.H.

N82-20606*# Instituto de Pesquisas Espaciais, Sao Jose dos Campos (Brazil).
DYNAMIC STUDY OF THE UPPER SAO FRANCISCO RIVER AND THE TRES MARIAS RESERVOIR USING MSS/LANDSAT IMAGES [ESTUDO DINAMICO DO ALTO RICO SAO FRANCISCO ERESERVATORIO DETRES MARIAS, ATRAVES DE IMAGENS MSS/LANDSAT]
Nelson deJesusParada, Principal Investigator and Tania Maria Sausen Jul. 1981 77 p refs In PORTUGUESE Presented at 33rd Reuniao Anual da SBPC, Salvador, Brazil, 8-15 Jun. 1981 Sponsored by NASA ERTS
(E82-10082; NASA-CR-168403; NAS 1.26:168403; INPE-2154-RPE/373) Avail: NTIS HC A05/MF A01 CSCL 08H

The use of LANDSAT multispectral ban scanner imagery to verify the relationship between the behavior of the Tres Marias reservoir and the dynamics of the Sao Francisco River supply basin is described. The dispersion of suspended sediments and their concentration in the surface layers of the water are considered. A five year survey of the region during both dry and rainy seasons was performed. The drainage network was analyzed based on the patterns of dessication, water rises and soil use in the supply basin. Surface layers of the reservoir were tabulated as a function of the levels of gray in the imagery. In situ observations of water depth and reflectance were performed. Ground truth and LANDSAT data were correlated to determine the factors affecting the dynamics of the supply basin. J.D.H.

N82-20617*# National Aeronautics and Space Administration. Goddard Space Flight Center, Greenbelt, Md.
APPLICATIONS SYSTEMS VERIFICATION AND TRANSFER PROJECT. VOLUME 1: OPERATIONAL APPLICATIONS OF SATELLITE SNOW COVER OBSERVATIONS: EXECUTIVE SUMMARY
Albert Rango Dec. 1981 81 p refs 8 Vol.
(NASA-TP-1822; NAS 1.60:1822; Rept-81F0060-Vol-1) Avail: NTIS HC A05/MF A01 CSCL 05B

Both LANDSAT and NOAA satellite data were used in improving snowmelt runoff forecasts. When the satellite snow cover data were tested in both empirical seasonal runoff estimation and short term modeling approaches, a definite potential for reducing forecast error was evident. A cost benefit analysis run in conjunction with the snow mapping indicated a $36.5 million annual benefit accruing from a one percent improvement in forecast accuracy using the snow cover data for the western United States. The annual cost of employing the system would be $505,000. The snow mapping has proven that satellite snow cover data can be used to reduce snowmelt runoff forecast error in a cost effective manner once all operational satellite data are available within 72 hours after acquisition. Executive summaries of the individual snow mapping projects are presented. J.M.S.

N82-20618*# Geological Survey, Phoenix, Ariz.
APPLICATIONS SYSTEMS VERIFICATION AND TRANSFER PROJECT. VOLUME 2: OPERATIONAL APPLICATIONS OF SATELLITE SNOW-COVER OBSERVATIONS AND DATA-COLLECTION SYSTEMS IN THE ARIZONA TEST SITE
Herbert H. Schumann Dec. 1981 62 p refs 8 Vol.
(NASA-TP-1823; NAS 1.60:1823; Rept-81F0061-Vol-2) Avail: NTIS HC A04/MF A01 CSCL 08L

Ground surveys and aerial observations were used to monitor rapidly changing moisture conditions in the Salt-Verde watershed. Repetitive satellite snow cover observations greatly reduce the necessity for routine aerial snow reconnaissance flights over the mountains. High resolution, multispectral imagery provided by LANDSAT satellite series enabled rapid and accurate mapping of snow-cover distributions for small- to medium-sized subwatersheds; however, the imagery provided only one observation every 9 days of about a third of the watershed. Low resolution imagery acquired by the ITOSa dn SMS/GOES meteorological satellite series provides the daily synoptic observation necessary to monitor the rapid changes in snow-covered area in the entire watershed. Short term runoff volumes can be predicted from daily sequential snow cover observations. J.M.S.

N82-20619*# California State Dept. of Water Resources, Sacramento.
APPLICATIONS SYSTEMS VERIFICATION AND TRANSFER PROJECT. VOLUME 3: OPERATIONAL APPLICATIONS OF SATELLITE SNOW COVER OBSERVATIONS IN CALIFORNIA
A. J Brown and J. F. Hannaford (Sierra Hydrotech, Placerville, Calif.) Dec. 1981 70 p refs 8 Vol.
(Contract NAS5-20831)
(NASA-TP-1824; NAS 1.60:1824; Rept-81F0062-Vol-3) Avail: NTIS HC A04/MF A01 CSCL 08L

Five southern Sierra snowmelt basins and two northern Sierra-Southern Cascade snowmelt basins were used to evaluate the effect on operational water supply forecasting from satellite imagery. Manual photointerpretation techniques were used to obtain SCA and equivalent snow line for the years 1973 to 1979 for the seven test basins using LANDSAT imagery and GOES imagery. The use of SCA was tested operationally in 1977-79. Results indicate the addition of SCA improve the water supply forecasts during the snowmelt phase for these basins where there may be an unusual distribution of snowpack throughout the basin, or where there is a limited amount of real time data available. A high correlation to runoff was obtained when SCA was combined with snow water content data obtained from reporting snow sensors. T.M.

N82-20620*# Soil Conservation Service, Denver, Colo.
APPLICATIONS SYSTEMS VERIFICATION AND TRANSFER PROJECT. VOLUME 4: OPERATIONAL APPLICATIONS OF SATELLITE SNOW COVER OBSERVATIONS. COLORADO FIELD TEST CENTER
Bernard A. Shafer, Charles F. Leaf, Jeris A. Danielson (Colorado State Engineers Office), and George F. Moravec (Colorado State Engineers Office) Dec. 1981 101 p refs 8 Vol.
(NASA-TP-1825; NAS 1.60:1825; Rept-81F0063-Vol-4) Avail: NTIS HC A06/MF A01 CSCL 08L

The study was conducted on six watersheds ranging in size from 277 km to 3460 km in the Rio Grande and Arkansas River basins of southwestern Colorado. Six years of satellite data in the period 1973-78 were analyzed and snowcover maps prepared for all available image dates. Seven snowmapping techniques were explored; the photointerpretative method was selected as the most accurate. Three schemes to forecast snowmelt runoff employing satellite snowcover observations were investigated. They included a conceptual hydrologic model, a statistical model, and a graphical method. A reduction of 10% in the current average forecast error is estimated when snowcover data in snowmelt runoff forecasting is shown to be extremely promising. Inability to obtain repetitive coverage due to the 18 day cycle of LANDSAT, the occurrence of cloud cover and slow image delivery are obstacles to the immediate implementation of satellite derived snowcover in operational streamflow forecasting programs. T.M.

N82-20621*# Bonneville Power Administration, Portland, Oreg.
APPLICATIONS SYSTEMS VERIFICATION AND TRANSFER PROJECT. VOLUME 5: OPERATIONAL APPLICATIONS OF SATELLITE SNOW-COVER OBSERVATIONS, NORTHWEST UNITED STATES
John P. Dillard Dec. 1981 84 p refs 8 Vol.
(Contract NASA Order S-53877)
(NASA-TP-1826; NAS 1.60:1826; Rept-81F0064-Vol-5) Avail: NTIS HC A05/MF A01 CSCL 08L

The study objective was to develop or modify methods in an operational framework that would allow incorporation of satellite derived snow cover observations for prediction of snowmelt derived runoff. Data were reviewed and verified for five basins in the Pacific Northwest. The data were analyzed for up to a 6-year period ending July 1978, and in all cases cover a low, average, and high snow cover/runoff year. Cloud cover is a major problem in these springtime runoff analyses and have hampered data collection for periods of up to 52 days. Tree cover and terrain are sufficiently dense and rugged to have caused problems. The interpretation of snowlines from satellite data was compared with conventional ground truth data and tested in operational streamflow forecasting models. When the satellite snow-covered area (SCA) data are incorporated in the SSARR (Streamflow Synthesis and Reservoir Regulation) model, there is a definite but minor improvement. T.M.

N82-20622*# National Environmental Satellite Service, Washington, D. C.
APPLICATIONS SYSTEMS VERIFICATION AND TRANSFER PROJECT. VOLUME 6: OPERATIONAL APPLICATIONS OF SATELLITE SNOW-COVER OBSERVATIONS NOAA/NESS SUPPORT STUDY Final Report, 1 Jan. 1975 - 31 Dec. 1978
Stanley R. Schneider Dec. 1981 68 p refs 8 Vol.
(NASA Order S-53772)
(NASA-TP-1827; NAS 1.60:1827; Rept-81F0065-Vol-6) Avail: NTIS HC A04/MF A01 CSCL 05B

Geostationary and polar orbiting satellite data from the National Oceanic and Atmospheric Administration were used to operationally provide field hydrologists with basin snowcover percentages for inclusion in runoff models. Data reduction is accomplished thru the use of optical rectification devices and electronic color density slicers. Over two thousand satellite-derived snow maps covering 30 different basins in the western United States were provided to users. Plans for improving snowmapping techniques on computer interactive systems and by all-digital analysis are presented. A description of the newest generation of NOAA polar orbiters, TIROS-N, and its potential for snowmapping is reviewed. Snowcover percentages for all basins determined between November 1974 and July 1978 are presented in tabular format. J.M.S.

N82-20623*# Ecosystems International, Inc., Gambrills, Md.
APPLICATIONS SYSTEMS VERIFICATION AND TRANSFER PROJECT. VOLUME 7: COST/BENEFIT ANALYSIS FOR THE ASVT ON OPERATIONAL APPLICATIONS OF SATELLITE SNOW-COVER OBSERVATIONS
P. Castruccio, H. Loats, D. Lloyd, and P. Newman Dec. 1981 245 p refs 8 Vol.
(Contract NAS5-23729)
(NASA-TP-1828; NAS 1.60:1818; Rept-81F0066-Vol-7) Avail: NTIS HC A11/MF A01 CSCL 08L

The results of the OASSO ASVT's were used to estimate the benefits accruing from the added information available from satellite snowcover area measurement. Estimates of the improvement in runoff prediction due to addition of SATSCAM were made by the Colorado ASVT personnel. The improvement estimate is 6-10%. Data were applied to subregions covering the Western States snow area amended by information from the ASVT and other watershed experts to exclude areas which are not impacted by snowmelt runoff. Benefit models were developed for irrigation and hydroenergy uses. The benefit/cost ratio is 72:1. Since only two major benefit contributors were used and since the forecast improvement estimate does not take into account future satellite capabilities these estimates are considered to be conservative. The large magnitude of the benefit/cost ratio supports the utility and applicability of SATSCAM. T.M.

N82-20624*# Environmental Research and Technology, Inc., Concord, Mass.
APPLICATIONS SYSTEMS VERIFICATION AND TRANSFER PROJECT. VOLUME 8: SATELLITE SNOW MAPPING AND RUNOFF PREDICTION HANDBOOK
Clinton J. Bowley, James C. Barnes, and Albert Rango (NASA. Goddard Space Flight Center) Dec. 1981 98 p refs 8 Vol.
(Contract NAS5-24410)
(NASA-TP-1829; NAS 1.60:1829; Rept-81F0067-Vol-8) Avail: NTIS HC A05/MF A01 CSCL 08L

The purpose of the handbook is to update the various snowcover interpretation techniques, document the snow mapping techniques used in the various ASVT study areas, and describe the ways snowcover data have been applied to runoff prediction. Through documentation in handbook form, the methodology developed in the Snow Mapping ASVT can be applied to other areas. T.M.

N82-20807*# Morgan State Univ., Baltimore, Md. Dept. of Mathematics and Computer Science.
ASSESSMENT OF THE QUALITY OF GATE AREA RAINFALL DATA FROM A NIMBUS-5 RADIOMETER Final Report
Nathaniel Knox 31 Mar. 1982 18 p refs
(Grant NAG5-14)
(NASA-CR-168512; NAS 1.26:168512) Avail: NTIS HC A02/MF A01 CSCL 04B

The quality of rainfall intensity estimates derived from passive microwave measurements by the Electrically Scanned Microwave Radiometer (ESMR-5) aboard the NIMBUS-5 satellite was evaluated. The microwave measurements used are those coincident with the GARP (Global Atmospheric Research Program) Atlantic Tropical Experiment (GATE). ESMR-5 derived rainfall intensity estimates are compared with hourly averaged GATE radar rainfall measurements. Using the radar measurements as ground truth it is determined that with the transfer curve derived herein the ratio (ESMR-5 derived rain rate)/radar measured rain rate has a mean of approximately 0.62. Author

N82-20822# Digital Programming Services, Inc., Waltham, Mass.
DEVELOPMENT AND APPLICATIONS OF TECHNIQUES TO PROCESS HYDROMETEOR DISTRIBUTION DATA Final Report, 1 May 1978 - 31 Jul. 1981
Lawrence E. Belksy, Fredric B. Kaplan, James P. Lally, D. Keith Roberts, and Terence OToole 31 Jul. 1981 636 p
(Contract F19628-78-C-0131; AF Proj. 627A)
(AD-A109929; AFGL-TR-81-0261) Avail: NTIS HC A99/MF A01 CSCL 04/2

This report summarizes the mathematical procedures used on a variety of standard and non-standard cloud physics data. It includes the complete descriptions and operating instructions for all programs developed under this contract. GRA

N82-21680*# Hydex Corp., Fairfax, Va.
STRATEGIES FOR USING REMOTELY SENSED DATA IN HYDROLOGIC MODELS Final Report
E. L. Peck, T. N. Keefer, and E. R. Johnson, Principal Investigators 31 Jul. 1981 85 p refs Sponsored by NASA, USDA, Dept. of Commerce, Dept. of the Interior, and Agency for International Development ERTS
(Contract NAS5-26446; Proj. AgRISTARS)
(E82-10156; NASA-CR-166729; NAS 1.26:166729) Avail: NTIS HC A05/MF A01 CSCL 05B

Present and planned remote sensing capabilities were evaluated. The usefulness of six remote sensing capabilities (soil moisture, land cover, impervious area, areal extent of snow cover, areal extent of frozen ground, and water equivalent of the snow cover) with seven hydrologic models (API, CREAMS, NWSRFS, STORM, STANFORD, SSARR, and NWSRFS Snowmelt) were reviewed. The results indicate remote sensing information has only limited value for use with the hydrologic models in their present form. With minor modifications to the models the usefulness would be enhanced. Specific recommendations are made for incorporating snow covered area measurements in the NWSRFS Snowmelt model. Recommendations are also made for incorporating soil moisture measurements in NWSRFS. Suggestions are made for incorporating snow covered area, soil moisture, and others in STORM and SSARR. General characteristics of a hydrologic model needed to make maximum use of remotely sensed data are discussed. Suggested goals for improvements in remote sensing for use in models are also established. Author

N82-21704# National Academy of Sciences - National Research Council, Washington, D. C.
REMOTE SENSING FOR WATER RESOURCES AND HYDROLOGY: AN ASSESSMENT OF THE CORPS OF ENGINEERS' PROGRAM Final Report
Nov. 1981 53 p refs
(Contract Dacw72-81-M-0342)
(PB82-137142) Avail: NTIS HC A04/MF A01 CSCL 13B

The U.S. Army Corps of Engineers' program of research and development and technology transfer on the application of remote sensing to problems of water resources and hydrology is reviewed. The Corps' current program consists of work units (coastal engineering, flood prediction and management, hydrology, environmental assessment, and development of techniques and equipment). Current research programs are reviewed and recommendations are made. Author (GRA)

N82-21774*# National Aeronautics and Space Administration. Langley Research Center, Hampton, Va.
LABORATORY UPWELLED RADIANCE AND REFLECTANCE SPECTRA OF KERR RESERVOIR SEDIMENT WATERS
William G. Witte, Charles H. Whitlock, W. Douglas Morris, and E. A. Gurganus Mar. 1982 22 p refs
(NASA-TP-1993; L-14992; NAS 1.60:1993) Avail: NTIS HC A02/MF A01 CSCL 13B

Reflectance, chromaticity, and several other physical and chemical properties were measured for various water mixtures of bottom sediments taken from two sites at Kerr Reservoir, Virginia. Mixture concentrations ranged from 5 to 1000 ppm by weight of total suspended solids (TSS) in filtered deionized tap water. The two sets of radiance and reflectance spectra obtained were similar in shape and magnitude for comparable values of TSS. Upwelled reflectance was observed to be a nonlinear function of TSS with the degree of curvature a function of wavelength. Sediment from the downstream site contained a greater amount of particulate organic carbon than from the upstream site. No strong conclusions can be made regarding the effects of this difference on the radiance and reflectance spectra. Near-infrared wavelengths appear useful for measuring highly turbid water with concentrations up to 1000 ppm or more. Chromaticity characteristics do not appear useful for monitoring sediment loads above 150 ppm. Author

07

DATA PROCESSING AND DISTRIBUTION SYSTEMS

Includes film processing, computer technology, satellite and aircraft hardware, and imagery.

A82-19833 † Optimal methods of computerized image conversion (Ob optimal'nykh sposobakh preobrazovaniia izobrazhenii na EVM). V. I. Krasnov, S. L. Krylov, and B. I. Savel'ev. *Geodeziia i Kartografiia,* Dec. 1981, p. 34-38. In Russian.

It is noted that digital methods of processing images are far more effective than analog methods. Because of the machine time required, however, these methods are less economical. A general model of image conversion using a computer and an input-output device for the images is considered. C.R.

A82-20347 † Diffusion model of cloud cover and its use in the analysis of satellite operations (Diffuzionnaia model' oblachnosti i ee ispol'zovanie pri analize raboty ISZ). V. K. Saul'skii. *Issledovanie Zemli iz Kosmosa,* Nov.-Dec. 1981, p. 73-78. In Russian.

A diffusion model is developed which can be used to analyze the effects of cloud cover on satellite observations of the earth surface. Cloud cover values are modeled as a continuous Markov process of diffusion type which is completely characterized by two parameters: the transport coefficient and the diffusion coefficient. The application of this model to operations involving the remote sensing of earth resources is considered. B.J.

A82-20401 The accuracy potential of the modern bundle block adjustment in aerial photogrammetry. A. Grün (München, Technische Universität, Munich, West Germany). *Photogrammetric Engineering and Remote Sensing,* vol. 48, Jan. 1982, p. 45-54. 24 refs.

The use of orthogonal bivariate polynomials as an additional parameter set, together with a gross error detection strategy, are shown to be necessary for self-calibrating bundle block adjustment photogrammetry accuracy. This is illustrated by the processing of data from four test field blocks, gathered by means of three different camera systems, proving empirically that 2.5-micron planimetry and 4.5-micron height accuracies can be achieved for photogrammetric coordinates. The use of dense control and 60/60% overlap, together with the additional parameter set, are demonstrated to be essential for the continuous achievement of such accuracy levels. These results are judged to carry analytical photogrammetry into such new fields of application as network densification and cadastral surveying. O.C.

A82-20402 Analytical triangulation of space photography. M. E. O. Ali (Gendron, Lefebvre, Inc., Laval, Quebec, Canada) and A. J. Brandenberger (Université Laval, Quebec, Canada). *Photogrammetric Engineering and Remote Sensing,* vol. 48, Jan. 1982, p. 55-65. 12 refs. Research sponsored by the Department of Energy, Mines and Resources and National Research Council of Canada.

A computer program implementing a mathematical model is used to assess the accuracy of analytical aerial triangulation using Skylab photography combined with high-altitude aircraft photography and Skylab orbital parameters. Two novel bundle adjustment methods are employed: (1) in which the coordinates of the ground control as well as the photo measurements are used as observations in the collinearity condition equations, and (2) in which the camera parameters, control point ground coordinates and the photo measurements are used as observations in the equations. The former method yielded root mean square errors of 53 m in planimetry and 148 m in height. Comparisons of tests to which both bundle adjustment methods were submitted show a significant improvement in planimetric accuracy with the latter method, although this may be due to inherent Skylab mission difficulties. O.C.

A82-20403 Calibration and model reconstruction in analytical close-range stereophotogrammetry. I - Mathematical fundamentals. W. Frobin and E. Hierholzer (Orthopädische Universitätsklinik, Münster, West Germany). *Photogrammetric Engineering and Remote Sensing,* vol. 48, Jan. 1982, p. 67-72. 10 refs. Research supported by the Deutsche Forschungsgemeinschaft.

A discussion is presented on the application of the photogrammetric bundle method to close-range problems, with respect to (1) stereophotography, (2) rasterstereography, or the use of a projected grid in stereophotogrammetry, (3) moiré topography, and (4) stereoradiography. After giving the mathematical principles of the method in a form appropriate for application to most close-range problems, a simplified procedure which employs alternating orientation and reconstruction steps is described. In addition, a discussion on the convergence of the solution of the bundle equations and an error analysis are given. O.C.

A82-20404 The location of three-dimensional linear objects by using multiple projections. S. Kondo, R. Ohba, and K. Murata (Hokkaido University, Sapporo, Japan). *Photogrammetric Engineering and Remote Sensing,* vol. 48, Jan. 1982, p. 73-79. 10 refs.

A novel method is proposed which determines the least-squares position of a point, a straight line or a curved line by means of plural projections. The method is characterized by the following features: (1) the influence of errors on measurements is minimized, since the result is obtained as the least-squares solution for all data points; (2) the relative positions of data points on the object are unnecessary for every projection; (3) the cost function value at the termination of iterative calculation indicates the variance of the distances between data lines and the least-squares position; (4) the number of calculations increases as more projections and data lines are acquired for higher accuracy; and (5) in the case of a complex object, it is often difficult to select the initial simplex within the domain of the peak containing the minimum cost function value. O.C.

A82-20409 The use of digital multi-date Landsat imagery in terrain classification. H. Schreier, L. M. Lavkulich (British Columbia, University, Vancouver, Canada), and L. C. Goodfellow (Canada Centre for Remote Sensing, Ottawa, Canada). *Photogrammetric Engineering and Remote Sensing,* vol. 48, Jan. 1982, p. 111-119. 21 refs. Research supported by the Defence Research Establishment.

A quantitative assessment was made of organic terrain in northern Canada, in order to predict off-road mobility conditions, by using multi-date satellite imagery which provides contrast between vegetation communities and surface materials. A principal component analysis was used to identify the two most important MSS bands for each image, and selected spectral data from two images were then combined and subjected to an unsupervised cluster analysis. The resulting, color-coded images were then related to ground conditions, and were found to be directly useful as thematic mobility maps for operational planning in such environments. O.C.

A82-20410 Techniques for combining Landsat and ancillary data for digital classification improvement. C. F. Hutchinson (Arizona, University, Tucson, AZ). *Photogrammetric Engineering and Remote Sensing,* vol. 48, Jan. 1982, p. 123-130. 17 refs. Research supported by the U.S. Geological Survey.

Such ancilliary data as digitized maps and terrain elevation data are combined with Landsat data in order to improve the digital classification in natural resource inventories. The combined data have been used in (1) preclassification scene stratification; (2) postclassification class sorting; and (3) classification modification through increases of the number of observation channels, the modification of prior probabilities, or the addition of a second stage to the classification. The two former uses of the data are found to be efficient, yet unsophisticated due to their reliance on deterministic decision rules. Of the later uses, stratification of the sample used for training by the ancilliary data is found to improve accuracy, as do the altering of prior probabilities and the incorporation of distribution models at the expense of additional sampling. O.C.

A82-20411 Sampling for thematic map accuracy testing. G. H. Rosenfield, K. Fitzpatrick-Lins, and H. S. Ling (U.S. Geological Survey, National Mapping Div., Reston, VA). *Photogrammetric Engineering and Remote Sensing,* vol. 48, Jan. 1982, p. 131-137. 13 refs.

The cumulative binomial distribution is used in thematic map accuracy testing to develop (1) the minimum sample size needed to validate the accuracy for each category with specified confidence, and (2) the critical level, which is used as the criterion for determining whether the identification from remotely sensed data of a thematic category meets a specified accuracy. The algorithm used in map accuracy testing employs a stratified, systematic, unaligned sampling technique based on the map as a whole, and an additional random sample of points for under-represented categories from all points in that category. Such a technique is implemented by a computer program prepared to select the sample from the Geographic Information Retrieval and Analysis System file. The estimated overall accuracy of the map, and the estimated accuracy for each category of the map, are considered, with associated confidence limits. O.C.

A82-20423 * **Contrast reduction by the atmosphere and retrieval of nonuniform surface reflectance.** Y. Mekler (Tel Aviv University, Tel Aviv, Israel) and Y. J. Kaufman (NASA, Goddard Space Flight Center, Laboratory for Atmospheric Sciences, Greenbelt, MD). *Applied Optics,* vol. 21, Jan. 15, 1982, p. 310-316. 21 refs.

A radiative transfer model is developed which gives the upward radiance at nadir for any 1-D Lambertian surface reflectance. This model is used to depict the atmospheric effect on the transmittance of contrast for any 1-D surface reflectance. Here by contrast we mean a general variation of the radiation field across the image. With the aid of this model an inversion algorithm is developed for retrieval of true surface reflectance from high resolution satellite data (e.g., Landsat). This inversion technique can be a useful tool for extraction of surface reflectance from satellite data in the case of a surface reflectance variable in one dimension only (e.g., seashore or near borders of big fields). A sensitivity study of the inversion procedure on the knowledge of atmospheric parameters and sensor calibration was performed. It is shown that this inversion technique is stable even in the presence of errors in the sensor calibration and the atmospheric parameters. The method was applied to Landsat data in two wavelengths. The results show reasonable dependence of the derived surface reflectance on the distance from the seashore. (Author)

A82-21039 * # **Comparison of sigma/deg/ obtained from the conventional definition with sigma/deg/ appearing in the radar equation for randomly rough surfaces.** D. M. LeVine (NASA, Goddard Space Flight Center, Greenbelt, MD). *IEEE Transactions on Geoscience and Remote Sensing,* vol. GE-20, Jan. 1982, p. 85-90. 18 refs.

Results from the radar cross section of rough surfaces calculated from a conventional definition and from a direct solution of the radar equation are compared. The purpose is to define conditions under which the conventional solution produces the same cross-section as the radar equation. A randomly rough conduction surface is considered for line sources and corrugated surfaces. Two problems are analyzed: first, a plane wave is assumed to be incident on the surface and the observed scattered fields are computed, and second, the scattered fields received by an antenna colocated with the emitting antenna are used to compute the available power. The fields are assumed to scatter incoherently and the stationary points are assumed to be homogeneously distributed over the surface. The cross sections are found to be equal if the observer is far from the surface compared to the radii of the surface at the specular points. M.S.K.

A82-21040 **Maximum likelihood estimation of label imperfection probabilities and its use in the identification of mislabeled patterns.** C. B. Chittineni (Conoco, Inc., Exploration Research Div., Ponca City, OK). *IEEE Transactions on Geoscience and Remote Sensing,* vol. GE-20, Jan. 1982, p. 99-111. 18 refs.

The estimation of recognition system performance and of the probabilities of label imperfections as maximum likelihood estimates from the classifier decisions of labeled and unlabeled patterns are considered. The classification of a set of labeled and unlabeled patterns are used to derive the maximum likelihood estimates of classification errors and a priori probabilities. Additionally, expressions for the asymptotic variances of probability of correct classification and proportions are presented. Imperfection in the labels are assumed, and simple models are developed for imperfections in the labels and classification errors. Dependencies between the imperfect, classifier, and true labels, and between the probabilities of label imperfections and the classification accuracies are accounted for. The techniques developed are applicable for processing remotely sensed multispectral data. M.S.K.

A82-21041 **Exterior algebraic processing for remotely sensed multispectral and multitemporal images.** M. Inamura, H. Toyota, and S. Fujimura (Tokyo, University, Tokyo, Japan). *IEEE Transactions on Geoscience and Remote Sensing,* vol. GE-20, Jan. 1982, p. 112-118. 5 refs. Research supported by the Japan Research Committee of Environmental Remote Sensing.

The application of Grassmann algebra to multispectral, multitemporal image processing is examined. The use of an exterior product, an inner product, and an inner product between two exterior products is introduced, and it is shown that a multispectral image and spectral images or a monochromatic image are representable by a vector image and a scalar image, respectively. The advantages of employing algebraic, as opposed to statistical, image processing are the simplicity of the algorithm because only the statistical mean values are used, and exterior image processing involves the algebraic relationship among spectral vectors or feature vectors. The method is noted to be the equivalent of a normalized correlation method. M.S.K.

A82-21089 **Information extraction from remotely sensed data - A user view.** J. Townshend (Reading University, Reading, Berks., England) and C. Justice (ESA, European Space Research Institute, Frascati, Italy). *(Remote Sensing Society, Conference on Image Processing - Enhancement or Degradation, University of London, London, England, Nov. 14, 1980.) International Journal of Remote Sensing,* vol. 2, Oct.-Dec. 1981, p. 313-329. 78 refs.

Digital image processing refers to a variety of transformations and manipulations for improving the ability to extract information from imagery. It is often difficult for the user to select the most suitable approach in computer-assisted information extraction. More objective assessments of the relative utility of the different supervised, unsupervised, and hybrid approaches, as well as the individual stages within each of them, is therefore required. The ultimate use of the information extracted from the data is also affected by its compatability with other geographical data planes. Four alternative strategies for incorporating remote sensing data into comprehensive automated geographic information systems are suggested, each of which differ according to flexibility and the quantity of data to be processed and stored. Finally, the success of image analysis and classification methods depends on the relationship between the capabilities of the sensing systems and the character of the phenomena being studied. J.F.

A82-21094 **The use of contextual information to improve land cover classification of digital remotely sensed data.** C. M. Gurney (Reading University, Reading, Berks., England). *International Journal of Remote Sensing,* vol. 2, Oct.-Dec. 1981, p. 379-388. 12 refs. Research supported by the Atomic Energy Research Establishment.

Errors frequently occur in land cover classifications which use remotely sensed data. Where the error is assumed to conform to particular spatial patterns, automated contextual correction methods may be applied. Various types of classification errors are described first, and possible contextual correction methods are suggested. Accuracy testing procedures applied both before and after correction are described. The error correction methods were applied to urban:nonurban classifications of four sets of Landsat data of the United Kingdom. The results of linear feature detection were added to the urban classification to reduce the confusion between roads and urban areas. The results were smoothed, and the objects below a given size were removed. Increases in accuracy were obtained which were statistically significant at the 95% confidence level. J.F.

A82-21398 **Digital photography techniques (Digitale Aufnahmetechnik).** O. Hofmann (Messerschmitt-Bölkow-Blohm GmbH, Munich, West Germany). *Bildmessung und Luftbildwesen,* vol. 50, Jan. 1, 1982, p. 16-32. 9 refs. In German.

Optoelectronic digital imagery technology has been developed for photographing the earth's surface from the air. The cameras operate according to a push-broom principle with high resolution, linear semiconductor photodetector arrays. Based on a successful 1978 flight, the Modular Optoelectric Multispectral Scanner (MOMS) was developed, which will be used on the SPAS platform of the 1983 Space Shuttle. Image data are recorded directly on high-density digital tapes, which are later transcribed on computer-compatible tapes for further processing. The image data are produced in graphic form in black-and-white or color by means of a raster plotter. Solutions are still being sought to handle the large data rates and storage requirements as well as to correct the geometric distortions of the scanning lines. J.F.

A82-22146 * **Registration of heat capacity mapping mission day and night images.** K. Watson, S. Hummer-Miller, and D. L. Sawatzky (U.S. Geological Survey, Denver, CO). *Photogrammetric Engineering and Remote Sensing,* vol. 48, Feb. 1982, p. 263-268. 14 refs. NASA Order S-40256-B.

Registration of thermal images is complicated by distinctive differences in the appearance of day and night features needed as control in the registration process. These changes are unlike those that occur between Landsat scenes and pose unique constraints. Experimentation with several potentially promising techniques has led to selection of a fairly simple scheme for registration of data from the experimental thermal satellite HCMM using an affine transformation. Two registration examples are provided. (Author)

A82-22891 # **Classification of ice radar imagery.** G. Y. Tang (National Taiwan University, Taipei, Republic of China). *Republic of China, National Science Council, Proceedings, Part A: Applied Sciences,* vol. 5, Oct. 1981, p. 287-296. National Science Council of Republic of China Grant No. 70-0404-E002-09; NSF Grant No. ECS-80-06884.

The development of algorithms for computerized radar ice-imagery processing is presented. Initial attempts have involved the establishment of statistical parameters for discerning different ice features from the radar images. Radar imagery is gathered by either side-looking airborne radar (SLAR) or by synthetic aperture side-looking airborne radar (SAR), with coordinates chosen as azimuth (flight path) and range direction, the direction of sensing. SLAR produces a two-dimensional image of the reflectivity distribution of the ground, while higher resolution has allowed SAR applications in satellites. Seasat-1 SAR images are cited as examples for grey level categorization of surface features, and analysis indicates that mean and variance of grey levels serve best for classification. M.S.K.

A82-25139 **Multispectral texture.** A. Rosenfeld (Maryland, University, College Park, MD), A. Y. Wu (Maryland, University, College Park, MD; American University, Washington, DC), and C.-Y. Wang. *IEEE Transactions on Systems, Man, and Cybernetics,* vol. SMC-12, Jan.-Feb. 1982, p. 79-84. 5 refs. Grant No. AF-AFOSR-77-3271.

Textures in single-band images are often characterized by statistics of the joint distributions of pairs of gray levels for pairs of pixels in given relative positions, or by statistics of absolute gray level differences for such pairs of pixels. Joint distributions of pairs of spectral vectors in multiband images are cumbersome, since for k bands they are 2k-dimensional, but absolute difference distributions are less so, e.g., for two bands they are only two-dimensional. The possibility is discussed of using statistics of absolute difference distributions for characterizing textures in multiband images, with emphasis on the two-band case. (Author)

A82-25454 **Increase in correlation accuracy of remote sensing imagery by digital filtering.** M. Ehlers (Hannover, Universität, Hanover, West Germany). *Photogrammetric Engineering and Remote Sensing,* vol. 48, Mar. 1982, p. 415-420. 8 refs.

For correlation of remote sensing photographs of Wetlands, a concept for rectification on a common reference image was developed at the University of Hanover. The results of two objective functions after previous filtering are compared to those obtained without filtering. It is shown that the accuracy and efficiency of the objective function at the correlation process is essentially increased by a low pass filter. (Author)

A82-25455 * **Modeling misregistration and related effects on multispectral classification.** F. C. Billingsley (California Institute of Technology, Jet Propulsion Laboratory, Pasadena, CA). *Photogrammetric Engineering and Remote Sensing,* vol. 48, Mar. 1982, p. 421-430. Contract No. NAS7-100.

Misregistration is but one of a group of parameters (noise, class separability, spatial transient response, field sizes) affecting the accuracy of multispectral classification. The entire group must be considered simultaneously. Any noise in the measurements (due to the scene, to the sensor, or to the analog/digital conversion) will cause a finite fraction of the measurements to fall outside of the classification limits, even within nominally uniform fields. For field boundaries, where the effects of misregistration are felt, additional pixels will be misclassified due to the mixture of materials in the pixels. Misregistration causes field borders in a given (set of) band(s) to be closer than expected to a given pixel, causing additional pixels to be misclassified. Simplified models of the various effects are used to gain conceptual understanding and to estimate the performance to be expected. (Author)

A82-25456 * **Using known map category marginal frequencies to improve estimates of thematic map accuracy.** D. H. Card (NASA, Ames Research Center, Moffett Field, CA). *Photogrammetric Engineering and Remote Sensing,* vol. 48, Mar. 1982, p. 431-439. 10 refs.

By means of two simple sampling plans suggested in the accuracy-assessment literature, it is shown how one can use knowledge of map-category relative sizes to improve estimates of various probabilities. The fact that maximum likelihood estimates of cell probabilities for the simple random sampling and map category-stratified sampling were identical has permitted a unified treatment of the contingency-table analysis. A rigorous analysis of the effect of sampling independently within map categories is made possible by results for the stratified case. It is noted that such matters as optimal sample size selection for the achievement of a desired level of precision in various estimators are irrelevant, since the estimators derived are valid irrespective of how sample sizes are chosen. O.C.

A82-26050 **A procedure for the interactive tracing of edges and lines by means of digital image processing (Ein Verfahren zur interaktiven Verfolgung von Kanten und Linien mit den Mitteln der Digitalen Bildverarbeitung).** B.-S. Schulz (Institut für angewandte Geodäsie, Frankfurt am Main, West Germany). *Bildmessung und Luftbildwesen,* vol. 50, Mar. 1, 1982, p. 69-79. 18 refs. In German.

The considered procedure is partly related to the realization that object boundaries in an aerial photograph can be determined only on the basis of density discontinuities. The method has been developed for the calculation and the tracing of edges. In the study of cartographic objects, a special case involves conditions in which object width and image element size are approximately equal. Such problems can also be solved with the aid of the reported method. The strategy of line tracing is considered, taking into account the utilization of a 3 x 3 matrix. A preprocessing step is employed to close small gaps automatically and to delete inadmissible line connections. With an arbitrary starting point on the line, the line is followed to the end or to a point where an interruption occurs. Aspects of method implementation are illustrated with the aid of specific examples. G.R.

A82-26726 † **Methods for the processing of synthetic-aperture radar signals when solving problems of the national economy /Review/ (Sposoby obrabotki signalov radiolokatorov s sinteziirovannoi aperturoi pri reshenii narodnokhoziaistvennykh zadach /Obzor/).** V. B. Shteinshleiger, A. N. Erkin, P. S. Lifanov, G. S. Misezhnikov, and A. V. Ianovich. *Radiotekhnika i Elektronika,* vol. 27, Feb. 1982, p. 193-213. 34 refs. In Russian.

The paper examines and compares various signal processing methods for synthetic-aperture radar systems used in the remote sensing of earth resources. Attention is given to optical processing, processing using CRTs with memory, and digital and hybrid processing. B.J.

A82-26840 **An automatic optimum kernel-size selection technique for edge enhancement.** P. Chavez, Jr. (U.S. Geological Survey, Flagstaff, AZ) and B. Bauer (U.S. Geological Survey, EROS Data Center, Sioux Falls, SD). *Remote Sensing of Environment,* vol. 12, Mar. 1982, p. 23-38. 5 refs. Research supported by the U.S.

07 DATA PROCESSING AND DISTRIBUTION SYSTEMS

Geological Survey.

An automatic optimum kernel-size selection technique for edge enhancement is presented, which is a correction for the modulation transfer function of an imaging system to a first order. The horizontal first difference is used to automatically select the optimum kernel size to enhance the edges contained in the image. The technique is easy to implement, works on a one-line-in/one-line-out basis, and the first difference and the subtractive rectangular filter are both efficient and simple. D.L.G.

A82-26841 **A relation between Landsat digital numbers, surface reflectance, and the cosine of the solar zenith angle.** W. S. Kowalik, S. E. Marsh (Stanford University, Stanford, CA; U.S. Geological Survey, Washington, DC), and R. J. P. Lyon (Stanford University, Stanford, CA). *Remote Sensing of Environment*, vol. 12, Mar. 1982, p. 39-55. 23 refs. Research supported by the U.S. Geological Survey.

A method for estimating the reflectance of ground sites from satellite radiance data is proposed and tested. The method uses the known ground reflectance from several sites and satellite data gathered over a wide range of solar zenith angles. The method was tested on each of 10 different Landsat images using 10 small sites in the Walker Lake, Nevada area. Plots of raw Landsat digital numbers (DNs) versus the cosine of the solar zenith angle (cos Z) for the test areas are linear, and the average correlation coefficients of the data for Landsat bands 4, 5, 6, and 7 are 0.94, 0.93, 0.94, and 0.94, respectively. Ground reflectance values for the 10 sites are proportional to the slope of the DN versus cos Z relation at each site. The slope of the DN versus cos Z relation for seven additional sites in Nevada and California were used to estimate the ground reflectances of those sites. The estimates for nearby sites are in error by an average of 1.2% and more distant sites are in error by 5.1%. The method can successfully estimate the reflectance of sites outside the original scene, but extrapolation of the reflectance estimation equations to other areas may violate assumptions of atmospheric homogeneity. (Author)

A82-27505 † **The effectiveness of instrumented visual studies of the earth from space (Ob effektivnosti vizual'no-instrumental'nykh issledovanii zemli iz kosmosa).** V. V. Kovalenok, A. D. Koval', and A. A. Tishchenko. In: Scientific lectures on aviation and astronautics 1980. Moscow, Izdatel'stvo Nauka, 1981, p. 39-49. In Russian.

Recommendations are presented on the equipment required for making visual observations of the earth's surface from orbital space stations. Attention is given to the effectiveness of human vision with regard to the interpretation, recognition, and study of various types of earth resources and terrestrial phenomena in a wide range of observation conditions. General criteria are developed for the quantitative assessment of the effectiveness of visual-observation systems. B.J.

A82-27587 # **Context dependent modeling.** P. R. Beaudet (Business and Technological Systems, Inc., Seabrook, MD). In: International Symposium on Remote Sensing of Environment, 15th, Ann Arbor, MI, May 11-15, 1981, Proceedings. Volume 1. Ann Arbor, MI, Environmental Research Institute of Michigan, 1981, p. 145-164. 23 refs.

In connection with remote-sensing operations, the need arises to incorporate a priori knowledge in the interpretation of the digital images in order to gain complete understanding of the data that is present. This need to incorporate a priori knowledge is found in every part of the processing algorithm. As a consequence, context-dependent modeling is much utilized today as a means of incorporating a priori knowledge in the interpretation process. In most of the context-dependent work, the information extraction process is partitioned into a set of parallel feature extraction routines embedded in a decision tree network. The notion of context-dependent modeling, as it applies to processing algorithms, is considered along with the role of a priori knowledge, and data interpretive tools. G.R.

A82-27590 # **Operational resampling for correcting images to a geocoded format.** D. E. Friedmann (MacDonald, Dettwiler and Associates, Ltd., Richmond, British Columbia, Canada). In: International Symposium on Remote Sensing of Environment, 15th, Ann Arbor, MI, May 11-15, 1981, Proceedings. Volume 1. Ann Arbor, MI, Environmental Research Institute of Michigan, 1981, p. 195-212. 24 refs. Research supported by the Department of Industry, Trade and Commerce. DITC Project 534-3203.

Accompanying the improved satellite imagery provided in connection with new remote-sensing developments is the increasing compilation of detailed, geographically oriented data bases from disparate sources. Image correction must evolve to cope with the new sources of data. Precision processed images with map accuracies are now available for a variety of remote sensing applications. In connection with a study of the new developments, it becomes apparent that geometric correction must be expanded to yield satellite independent images. These geocoded images are precision images that have been rotated through the spacecraft heading angle so that they are aligned with the output map projection. Attention is given to the theoretical arguments for validating one-dimensional precision processing of imagery data from present and future sensors. It is shown that a radiometrically and geometrically accurate geocoded image can be obtained by a series of three one-dimensional resampling passes. G.R.

A82-27607 # **Towards an operational SPOT system - A preliminary assessment.** G. Brachet and P. Gonfreville (Centre National d'Etudes Spatiales, Paris, France). In: International Symposium on Remote Sensing of Environment, 15th, Ann Arbor, MI, May 11-15, 1981, Proceedings. Volume 1. Ann Arbor, MI, Environmental Research Institute of Michigan, 1981, p. 445-460.

A description is presented of the SPOT system, whose operation is scheduled to begin in 1984 and which comprises both earth observation satellites and ground stations offering the greatest achievable adherence to user requirements. The vertical and oblique viewing capability of the system will minimize the time interval between consecutive observations of the same area. Stereoscopic image pairs will be obtained by oblique observations of a given area during different satellite passes, and the 10-m resolution offered will permit operations on a 1/50,000-scale and even 1/25,000-scale, in some cases. It is expected that renewable resources management will gradually replace the creation of image data banks for mining and oil companies, which will represent the system's principal activity during its first years of existence. O.C.

A82-27623 # **Enhancement of Landsat data for Hudson Bay lowlands vegetation.** I. L. Johnston and P. J. Howarth (McMaster University, Hamilton, Ontario, Canada). In: International Symposium on Remote Sensing of Environment, 15th, Ann Arbor, MI, May 11-15, 1981, Proceedings. Volume 2. Ann Arbor, MI, Environmental Research Institute of Michigan, 1981, p. 623-633. 18 refs. Research supported by McMaster University; Natural Sciences and Engineering Research Council of Canada Grant No. A-5586.

The two basic methods of Landsat digital analysis include classification and enhancement. In classification, spectral data are statistically sorted and displayed as different colors or symbols on a CRT monitor or line printer. There are sometimes difficulties related to the assignment of a unique description or to interpretation. In order to overcome these problems, image enhancement has been developed as a second and complementary method of digital analysis. Image enhancement maximizes the visual information presented on the CRT monitor so that subtle details in the image are clearly displayed. The present investigation is concerned with the assessment of the capabilities of three Landsat digital enhancements to differentiate major land cover types in a remote subarctic environment, giving attention to linear contrast stretch, band ratioing, and video filtering. G.R.

A82-27625 # **An evaluation of the utility of smaller Landsat resolution elements /Resolution of Landsat resolution/.** R. F. Hyde, N. J. Vesper, and I. A. Goldblatt (Butler University, Indianapolis, IN). In: International Symposium on Remote Sensing of Environment, 15th, Ann Arbor, MI, May 11-15, 1981, Proceedings. Volume 2. Ann Arbor, MI, Environmental Research Institute of Michigan, 1981, p. 647-652.

The considered project has the objective to make definitive statements on the spatial resolution level requirements or the optimum pixel size for several of the high volume Landsat data user disciplines. Several issues are examined in anticipation of future and proposed satellite derived smaller pixels (or ground resolution levels). This is accomplished by the construction of a detailed database which combines the two technical philosophies associated with Landsat data analysis and application, with Geographic Information System database development. Aspects of methodology are considered. In connection with a discussion of data base construction, attention is given to design, encoding, and computer generating. Questions of aggregation to various pixel sizes are considered along with the assignment of reflectance values, the classification of each new pixel resolution, and the interpretation of aggregate levels. G.R.

A82-27626 # **The use of digital terrain model in the rectification of satellite-borne imagery.** F. Wong, R. Orth, and D. E. Friedmann (MacDonald, Dettwiler and Associates, Ltd.; Richmond, British Columbia, Canada). In: International Symposium on Remote Sensing of Environment, 15th, Ann Arbor, MI, May 11-15, 1981, Proceedings. Volume 2. Ann Arbor, MI, Environmental Research Institute of Michigan, 1981, p. 653-662. 8 refs. Research supported by the Industrial Research Assistance Program.

The present investigation is concerned with the precision geometric rectification of satellite-borne imagery, including correction for relief displacement with the use of a digital terrain model. While relief displacement error is small in Multispectral Scanner System (Landsats -1, -2, and -3) imagery, it will become significant in imagery from future sensors due to increased resolution (Thematic Mapper on Landsat-D) and off-nadir pointing capabilities (linear arrays on SPOT). It is shown how the slow varying geometric distortion correction can be separated from the fast varying relief displacement correction. Experiments illustrate that subpixel geometric rectification accuracy can be achieved even in areas of severe high relief provided an accurate digital terrain model is used during the correction process. G.R.

A82-27629 # **An approach to path radiance correction in MSS images.** M. Onitsuka, K. Ohta (National Research Institute for Pollution and Resources, Yatabe, Ibaraki, Japan), N. Okami (Institute of Physical and Chemical Research, Wako, Saitama, Japan), and J. R. Miller (York University, Downsview, Ontario, Canada). In: International Symposium on Remote Sensing of Environment, 15th, Ann Arbor, MI, May 11-15, 1981, Proceedings. Volume 2. Ann Arbor, MI, Environmental Research Institute of Michigan, 1981, p. 681-689. 10 refs.

Problems related to providing accurate corrections for atmospheric scattering are a major obstacle to the use of remote sensing for determining changes in water quality with time. In the present investigation, published path radiance determinations are used to derive relationships which describe the systematic variation in the path radiance. Empirical equations are derived to relate the path radiance in Landsat bands 4, 5, and 6 to the path radiance in band 7. The algorithms are applied to a number of Landsat images acquired over Japanese coastal waters. G.R.

A82-27636 # **Strategies and uses of small distributed analysis centers as in the natural resource inventory of Venezuela.** R. J. P. Lyon, K. Lanz (Stanford University, Stanford, CA), and R. Lairet (Ministerio del Ambiente y de los Recursos Naturales Renovables, Caracas, Venezuela). In: International Symposium on Remote Sensing of Environment, 15th, Ann Arbor, MI, May 11-15, 1981, Proceedings. Volume 2. Ann Arbor, MI, Environmental Research Institute of Michigan, 1981, p. 751-759.

A82-27651 # **Field-by-field multitemporal analysis of aerial scanner data geometrically corrected by means of a sliding model.** R. Jeansoulin, J.-C. Darcos, and G. Rigal (CNRS, Langages et Systèmes Informatiques; Toulouse, Ecole Nationale Supérieure d'Electrotechnique, d'Electronique, d'Informatique et d'Hydraulique, Toulouse, France). In: International Symposium on Remote Sensing of Environment, 15th, Ann Arbor, MI, May 11-15, 1981, Proceedings. Volume 2. Ann Arbor, MI, Environmental Research Institute of Michigan, 1981, p. 929-938. 6 refs. Research supported by the Centre National d'Etudes Spatiales.

Field-by-field multitemporal analysis is the geometrical processing of multitemporal images of a given scene through automatic registration and overlapping, with emphasis on the processing of information lying within the same geographical entity in order to obtain the population distribution function for every date. Two techniques are proposed to this end: (1) the sliding model, in which a sequence of local, simple and independent models of the relative deformation is computed and adjacent local models are joined by sliding processing; and (2) the field-by-field correction method, which is based on the segmentation of intersecting areas into a reference image, and the assessment of the same area at different dates through computation of local relative deformation with the minimum number of nearest neighbors among the registered control points. O.C.

A82-27654 # **Effect of aerosols on optical remotely sensed data.** W. G. Egan (Grumman Aerospace Corp., Research Dept., Bethpage, NY) and G. E. Shaw (Alaska, University, Fairbanks, AK). In: International Symposium on Remote Sensing of Environment, 15th, Ann Arbor, MI, May 11-15, 1981, Proceedings. Volume 2. Ann Arbor, MI, Environmental Research Institute of Michigan, 1981, p. 959-973. 23 refs.

It has been found possible to validate and determine certain characteristics of atmospheric aerosols, as well as to typify their effects, in major experimental tests of two complementary aerosol modeling approaches: (1) the Dave (1972) radiative transfer program, applied to the Caribbean area of St. Thomas in 1972, and (2) the constrained linear inversion method, applied to the continental area of Ft. Collins, Colorado, in 1980. The aerosol optical thickness at 0.5-micron wavelength over Ft. Collins was about 0.07, and about 0.12 over St. Thomas. It is concluded that, by using ground-based observations, the Dave model provides detailed angular variation of sky radiance and solar flux to + or - 20% away from the solar aureole, while the constrained linear inversion model furnishes path-averaged optical depth to + or - 3%, and total downwelling diffuse radiation to + or - 1%, as well as aerosol size distribution. O.C.

A82-27655 # **HCMM night-time thermal IR imaging experiment in Michigan.** R. K. Vincent, J. B. Parrish, D. H. Coupland (Geospectra Corp., Ann Arbor, MI), and E. Jaworski (Eastern Michigan University, Ypsilanti, MI). In: International Symposium on Remote Sensing of Environment, 15th, Ann Arbor, MI, May 11-15, 1981, Proceedings. Volume 2. Ann Arbor, MI, Environmental Research Institute of Michigan, 1981, p. 975-980, 983, 984. 7 refs.

The Heat Capacity Mapping Mission satellite's 10.5-12.5-micron thermal IR channel obtained a color level-sliced image of Michigan during an August 21, 1978 overpass. Surface water, including most of the Great Lakes, was warmer than the land mass, and two area types in the southern peninsula of Michigan appear unusually cool: (1) forested valley areas with high soil infiltration rates, in the north-central region; and (2) small, flat, swampy areas in Sanilac County associated with peat bogs. Comparison with actual reported temperatures show an underestimation of temperature by the satellite of up to 8 C, perhaps due to atmospheric effects. O.C.

A82-27666 * # **ELAS - A geobased information system that is transferable to several computers.** S. L. Whitley, R. W. Pearson, B. R. Seyfarth, and M. H. Graham (NASA, National Space Technology Laboratories, Earth Resources Laboratory, Bay St. Louis, MS). In: International Symposium on Remote Sensing of Environment, 15th, Ann Arbor, MI, May 11-15, 1981, Proceedings. Volume 3. Ann Arbor, MI, Environmental Research Institute of Michigan, 1981, p. 1091-1098.

In the early years of remote sensing, emphasis was placed on the processing and analysis of data from a single multispectral sensor, such as the Landsat Multispectral Scanner System (MSS). However, in connection with attempts to use the data for resource management, it was realized that many deficiencies existed in single data sets. A need was established to geographically reference the MSS data and to register with it data from disparate sources. Technological transfer activities have required systems concepts that can be easily transferred to computers of different types in other organizations. ELAS (Earth Resources Laboratory Applications Software), a geographically based information system, was developed to meet the considered needs. ELAS accepts data from a variety of sources. It contains programs to geographically reference the data to the Universal Transverse Mercator grid. One of the primary functions of ELAS is to produce a surface cover map. G.R.

07 DATA PROCESSING AND DISTRIBUTION SYSTEMS

A82-27667 # Flexible processing of remote sensing data through integration of image processing and geobased information systems. W. A. Hallada (Computer Sciences Corp., Silver Spring, MD), F. C. Mertz, L. R. Tinney, M. J. Cosentino, and J. E. Estes (California, University, Santa Barbara, CA). In: International Symposium on Remote Sensing of Environment, 15th, Ann Arbor, MI, May 11-15, 1981, Proceedings. Volume 3. Ann Arbor, MI, Environmental Research Institute of Michigan, 1981, p. 1099-1111. 13 refs.

Integrating image processing and geobased information systems (GBIS) provides the analyst with many new options and opportunities for processing and using remotely sensed data. Even when remote sensing can provide a crucial input to an analysis, it is not uncommon for this input to be only one of many that must be considered. In a similar manner, many types of data (e.g. terrain and soils) can be very useful when deriving products from remotely sensed data. Research to date indicates that a systems concept employing geobased system and image processing technologies provides a flexible means of analyzing remotely sensed data for purposes of preprocessing, stratification, classification, and modeling. This paper presents examples of the use of an image based information system (IBIS) that allows the spatial integration of remotely sensed imagery with other types of geobased data. An automated cluster labeling procedure, an automated land management system, and an automated fire information management system are discussed within this paper. (Author)

A82-27671 # Interpretation of Heat Capacity Mapping Mission images over Canada. J. Cihlar (Canada Centre for Remote Sensing, Applications Div., Ottawa, Canada). In: International Symposium on Remote Sensing of Environment, 15th, Ann Arbor, MI, May 11-15, 1981, Proceedings. Volume 3. Ann Arbor, MI, Environmental Research Institute of Michigan, 1981, p. 1141-1152.

The influence of atmospheric and land surface variables on day and night Heat Capacity Mapping Mission (HCMM) thermal infrared data collected over two Canadian sites is analyzed for confirmation of the thermal inertia concept. Visual analysis of many images and digital nighttime apparent land temperature distribution was dominated by the near-surface air temperature and that the effects of typography, wind, and land cover were primarily indirect. In the daytime, surface cover was the most important variable, mainly because of the role of water in relation to cover type. The effect of soil moisture was very weak. Except for the land/water contrast, surface temperature differences were relatively small. Cloud cover was the dominant feature of daytime and nighttime thermal infrared images. (Author)

A82-27677 # Classification of Landsat MSS data for surface cover of small areas. Y. J. Chong, A. C. Yeo, and V. K. Vong (National University of Singapore, Singapore). In: International Symposium on Remote Sensing of Environment, 15th, Ann Arbor, MI, May 11-15, 1981, Proceedings. Volume 3. Ann Arbor, MI, Environmental Research Institute of Michigan, 1981, p. 1219-1225.

Multispectral scanner data acquired by Landsat 1, 2 and 3 have been studied for path 137 row 56 and path 137 row 57. Software has been developed to process the computer compatible tapes on a user terminal of a general purpose mini-computer utilizing only the standard input/output peripherals. Spectral classification of the data is done by identifying clusters in a four-dimensional vector space. An area of the sea in the vicinity of a tidal gauge station is chosen for study, both at high tide and at low tide. When the classified data is compared with a hydrographic map water depth boundaries are clearly discernible, even though the water in the area being influenced by river discharges is not particularly clear. (Author)

A82-27685 # An analysis of user requirements for operational land satellite data. G. W. Spann, N. J. Hooper (Metrics, Inc., Atlanta, GA), and D. J. Cotter (NOAA, National Earth Satellite Service, Washington, DC). In: International Symposium on Remote Sensing of Environment, 15th, Ann Arbor, MI, May 11-15, 1981, Proceedings. Volume 3. Ann Arbor, MI, Environmental Research Institute of Michigan, 1981, p. 1297-1303.

The National Oceanic and Atmospheric Administration/National Earth Satellite Service (NOAA/NESS), as the agency designated to implement and manage the U.S. operational land remote sensing satellite system, conducted a survey in March, 1980, to determine user needs for land satellite data in the context of an operational system. Analysis of the survey responses indicates that the operational requirements of most users can be met by data similar to that which can be provided by the MSS and/or TM instruments developed by NASA in the Landsat program. The analysis further indicates that users emphasize the timely, reliable delivery of data products as the essential element of an operational land satellite system. (Author)

A82-27686 * # Precision in the evaluation of Landsat autocorrelation - The terrain effect. R. G. Craig (Kent State University, Kent, OH). In: International Symposium on Remote Sensing of Environment, 15th, Ann Arbor, MI, May 11-15, 1981, Proceedings. Volume 3. Ann Arbor, MI, Environmental Research Institute of Michigan, 1981, p. 1305-1314. 14 refs. Contract No. NAS5-26111.

The autocorrelation present in Landsat data can be described by a two-parameter model. Presence of this autocorrelation seriously inflates estimates of the variance of a set of pixels. The degree of inflation is always serious but varies markedly according to the values of the parameters phi and Theta. Thus corrections of the effects of the model require precise estimates of these parameters. Two hypotheses are proposed to explain the variation of phi with location. Several lines of evidence are presented which support the idea that phi is induced directly by the autocorrelation structure of the terrain being sensed. It is suggested that use of this relation will allow economical estimates of phi for any scene of interest. (Author)

A82-27688 # Natural resources inventories by computer-satellite mapping techniques in Chaco State, Argentine Republic, South America. A. V. Gustin (State Institute of Ecology, Natural Resources and Technology, Resistencia, Chaco, Argentina) and L. L. Ledesma (National Institute of Agro-Technology, Roque Saénz Peña, Chaco, Argentina; Stanford University, San Francisco, CA). In: International Symposium on Remote Sensing of Environment, 15th, Ann Arbor, MI, May 11-15, 1981, Proceedings. Volume 3. Ann Arbor, MI, Environmental Research Institute of Michigan, 1981, p. 1327-1338. 9 refs. Research supported by the Quebracho Extract National Commission.

Information from satellites Landsat 1 and Landsat 2, launched by NASA in 1972 and 1975, were used to survey natural resources in Chaco State, Argentine. In order to get map representation by a digital system, computer processing was done defining spectral characteristics (Honey curves) which were used as survey patterns in the digital analysis. Results of this procedure are 1:100,000 and 1:25,000 dotprints maps and slides in false color, with band combination (4, 5, 6, 7). The multispectral analysis of Landsat C.C.T. data has shown to be useful for the characterization and correlation (based on field data, frames interpretation and aerial photo interpretation) for surveying and mapping natural resources in this State, because the site spectral values are well segregated by their own natural characteristics. (Author)

A82-27689 * # Ground level reflectance measurement techniques - An evaluation with emphasis on the importance of spectral calibration. M. J. Duggin (New York, State University, Syracuse, NY) and W. R. Philipson (Cornell University, Ithaca, NY). In: International Symposium on Remote Sensing of Environment, 15th, Ann Arbor, MI, May 11-15, 1981, Proceedings. Volume 3. Ann Arbor, MI, Environmental Research Institute of Michigan, 1981, p. 1339-1352. 36 refs. Research supported by the U.S. Department of Agriculture; Grant No. NGL-33-010-171.

The bandpasses, overflight conditions, and sensor geometry that will provide optimum target discrimination in remote-sensing studies can be determined only from spectral reflectance measurements made for various sun-target-sensor geometries, supplemented by model calculations which can be checked against field data. The accurate measurement of ground reflectance properties is critical to the design of future sensors and to the determination of imaging conditions. The current investigation has the objective to review typical methods of measuring spectral reflectance, to point out some of the problems inherent to reflectance measuring techniques, and to present a method of checking measurement accuracy. G.R.

A82-27693 # Application of machine processing of visible and thermal data to the study of the geothermal area of Cerro Prieto, Mexico. A. Jinich, J. L. Farah, M. Garza, C. Velarde, R. Méndez, J. Rosenblueth (Universidad Nacional Autónoma de México, Villa Obregón, Mexico), R. Alvarez, G. García, R. Hernández, and A. López (Comissión Federal de Electricidad, Mexico). In: International Symposium on Remote Sensing of Environment, 15th, Ann Arbor, MI, May 11-15, 1981, Proceedings. Volume 3.
Ann Arbor, MI, Environmental Research Institute of Michigan, 1981, p. 1387-1396. 13 refs. Research supported by the United Nations. UN Project MEX-120-8-004-05-X.

A82-27698 # Visual and digital analysis of H.C.M.M. data over eastern Canada. F. Bonn, M. Bernier, and R. Brochu (Sherbrooke, Université, Sherbrooke, Québec, Canada). In: International Symposium on Remote Sensing of Environment, 15th, Ann Arbor, MI, May 11-15, 1981, Proceedings. Volume 3.
Ann Arbor, MI, Environmental Research Institute of Michigan, 1981, p. 1449-1463. 21 refs. Natural Sciences and Engineering Council Grant No. A-6043.

It is pointed out that the Heat Capacity Mapping Mission (HCMM) has generated a great conceptual and research interest due to its theoretical ability to map subsurface features which were up to now invisible to sensors. A satellite equipped with a thermal channel providing a 12 hour coverage at adequate passing times might be of great value to investigators interested in physical aspects of rocks, soils, and water. The present analysis is concerned with two HCMM scenes, which were acquired on June 6th, 1978 over Montreal and Lake Ontario, and on September 19th, 1978 over the St. Lawrence Valley. A visual analysis of the images is considered, taking into account geology and geomorphology, topography and climate, landuse and human activities, and hydrology and water surfaces. Attention is given to day and night images, the temperature difference image, the thermal inertia image, the digital analysis of a subimage, and observed features unique to HCMM. G.R.

A82-27923 # The role of computer graphics in geographic research. F. T. Aldrich (Arizona State University, Tempe, AZ). In: Computer Graphics Symposium, Phoenix, AZ, April 24, 1982, Proceedings. New York, American Institute of Aeronautics and Astronautics, 1982, p. 38-41. 7 refs.

This paper discusses the way in which a geographer views computer graphics and the role this media plays in applied spatial research. A background perspective is presented which gives the scope of geographic research tasks and a discussion of manual cartographic displays, their characteristics and limitations. Advantages of digital production of conventional graphics is presented as well as a documenting of new capabilities available only by utilizing the media of computer graphics. These new capabilities involved the use of whole surface displays using perspective views, stereo perspective, and 'photogrammetric' surfaces. (Author)

A82-28141 † Correlation identification of stellar configurations for purposes of the coordinate referencing of aerial and space images (Korreliatsionnoe otozhdestvlenie zvezdnykh konfiguratsii dlia tselei koordinatnoi priviazki aerokosmicheskikh snimkov). V. K. Zlobin and V. N. Kobzev. *(Vsesoiuznaia Konferentsiia po Problemam Issledovaniia Prirodnykh Resursov Zemli i Mirovogo Okeana, Aviatsionno-Kosmicheskimi Sredstvami, Moscow, USSR, Nov. 1980.) Geodeziia i Aerofotos'emka,* no. 1, 1982, p. 83-88. 8 refs. In Russian.

Correlation algorithms are proposed for the identification of stellar configurations in the coordinate referencing of aerial and space remote-sensing images. In order to reduce the number of required computations, an image of the correlation-field fragment is constructed, and a search is carried out for the maximum of the cross correlation function of the real image and the reference image. B.J.

A82-28143 † Characteristics of the use of laser-mirror scanners for image processing in cartography and aerial photography (Osobennosti ispol'zovaniia lazernykh zerkal'nykh skanatorov dlia obrabotki izobrazhenii v kartografii i aerofotos'emke). I. M. Kol'tsov, V. P. Mikheev, and B. S. Rozov. *(Vsesoiuznaia Konferentsiia po Problemam Issledovaniia Prirodnykh Resursov Zemli i Mirovogo Okeana, Aviatsionno-Kosmicheskimi Sredstvami, Moscow, USSR, Nov. 1980.) Geodeziia i Aerofotos'emka,* no. 1, 1982, p. 94-99. In Russian.

A special-purpose laser-mirror scanner for the processing of aerial photographs is described. The system provides for synphase scanning of two photographs per line, whose length varies automatically from 0.5 to 10 mm. The size of the scanning spot varies from 30 to 300 mm, while the rms error of the position of the raster centers is about 3 microns. A schematic diagram of the scanning system is presented, and the basic characteristics of the scanner are given. B.J.

A82-28144 † Construction of digital models of statistically uniform characteristics on the basis of multispectral space imagery (Postroenie tsifrovykh modelei statisticheski odnorodnykh kharakteristik po spektrozonal'nym kosmicheskim materialam). N. P. Lavrova and G. Ia. Globa. *(Vsesoiuznaia Konferentsiia po Problemam Issledovaniia Prirodnykh Resursov Zemli i Mirovogo Okeana, Aviatsionno-Kosmicheskimi Sredstvami, Moscow, USSR, Nov. 1980.) Geodeziia i Aerofotos'emka,* no. 1, 1982, p. 99-108. In Russian.

The development of digital terrain models on the basis of multispectral remote-sensing data is considered. It is found that partial multispectral images can be subjected to statistical treatment using microphotometer data. Digital models are constructed for a portion of terrain having statistically uniform characteristics. B.J.

A82-28146 † Construction of a mathematical model for the recognition of identical images on a pair of photographs (O postroenii matematicheskoi modeli opoznavaniia identichnykh izobrazhenii na pare snimkov). I. G. Zhurkin. *(Vsesoiuznaia Konferentsiia po Problemam Issledovaniia Prirodnykh Resursov Zemli i Mirovogo Okeana, Aviatsionno-Kosmicheskimi Sredstvami, Moscow, USSR, Nov. 1980.) Geodeziia i Aerofotos'emka,* no. 1, 1982, p. 111-119. In Russian.

A82-28343 Earth-scanning satellites lead resource hunt. P. Kinnucan. *High Technology,* vol. 2, Mar.-Apr. 1982, p. 53-60.

Technology to be used for the acquisition of satellite imagery for earth resources applications is discussed. Advanced earth resource satellites to be launched in the 1980s by the United States, France and Japan will incorporate technical innovations increasing the value of satellite imagery for the mapping and monitoring of crops, mineral and petroleum deposits and other resources, including the Thematic Mapper to be carried on board the Landsat D satellites, data relay satellites to be used for image transmission to the ground, the pushbroom scanner to be used on the French SPOT satellites to provide high-resolution panchromatic and stereo images, and night and all-weather coverage offered by radar imaging from the Japanese ERS satellites. These technical innovations, however, raise sensitive issues concerning the need for specialized agricultural and geological satellites, the private operation of the Landsat satellites, the restriction of access to satellite data and national defense. A.L.W.

A82-28467 † Improving the quality of aerial photography /Concerning the 'Basic principles of aerial photography'/ (Povyshat' kachestvo aerofotos'emochnykh rabot /K Vypusku osnovnykh polozhenii po aerofotos'emke/). A. G. Vanin and Iu. I. Poletaev. *Geodeziia i Kartografiia,* Feb. 1982, p. 45-48. In Russian.

The paper reviews the contents of the normative document 'Basic principles of aerial photography', issued by the Krasovskii Institute of Geodesy, Cartography, and Aerial Photography. Particular consideration is given to techniques for improving the quality of aerial photography. B.J.

A82-28468 † Classification of systems for digital terrain simulation (K voprosu klassifikatsii sistem tsifrovogo modelirovaniia rel'efa mestnosti). A. S. Vasmut, A. V. Gusev, and Iu. A. Kravchenko. *Geodeziia i Kartografiia,* Feb. 1982, p. 53-57. 6 refs. In Russian.

A classification scheme for digital terrain models is examined. Particular attention is given to the three main classification characteristics: (1) data structures (the makeup and organization of terrain data interrelationships); (2) mathematical methods (i.e., recovery of relief at the required point); and (3) algorithms of data transformation. Interpolation methods for digital terrain models are considered. B.J.

N82-16437*# Wisconsin Univ. - Madison. Environmental Remote Sensing Center.

WETLAND MAPPING FROM DIGITIZED AERIAL PHOTOGRAPHY

F. L. Scarpace, B. K. Quirk, R. W. Kiefer, and S. L. Wynn, Principal Investigators [1982] 31 p refs Original contains color imagery. Original photography may be purchased from the EROS Data Center, Sioux Falls, S.D. 57198. ERTS
(E82-10019; NASA-CR-164816) Avail: NTIS HC A03/MF A01 CSCL 08B

Aerial photographic imagery of the Sheboygan Marsh in Wisconsin was scanned through three different narrow band interference filters centered at .45, .55, and .65 micrometers. The output data was transformed into log exposures and corrected for lens fall-off. The scanned area was approximately 253 hectares, with each pixel representing an area of 6.0 meters square on the ground. Training sets were extracted from the digital file of the imagery using the map generated from the photointerpretation and computer generated character displays from the digital file as first approximations. From these training sets, statistics were generated to be used with an elliptical classifier. The classifier generated a digital file from which color coded thematic representations of the classifications could be produced. A two stage table-look-up elliptical algorithm was used as the classification procedure. The wetland boundary was easily delineated, but there was difficulty in mapping the boundaries of vegetation within the wetland. A.R.H.

N82-16438*# Lockheed Engineering and Management Services Co., Inc., Houston, Tex.

PARTIALLY PROCESSED MULTISPECTRAL SCANNER LANDSAT HIGH-DENSITY TAPES REFORMATTING SYSTEM (HDT-AM/AMC) DESIGN SPECIFICATIONS

Omar J. Holguin, Principal Investigator Dec. 1980 37 p ERTS
(Contract NAS9-15800)
(E82-10020; NASA-CR-161046; JSC-17101; LEMSCO-15905) Avail: NTIS HC A03/MF A01 CSCL 05B

The data interface formats and communication conventions used by the system (HDTRS) are defined. They are used to retrieve partially processed MSS and return beam vidicon type data. T.M.

N82-16441*# Instituto de Pesquisas Espaciais, Sao Jose dos Campos (Brazil).

CNPQ/INPE: LANDSAT SYSTEM Progress Report, 1 Jun. 1980 - 30 Apr. 1981

Nelson deJesusParada, Principal Investigator and Marcio Nogueira Barbosa May 1981 26 p Sponsored by NASA Original contains color imagery. Original photography may be purchased from the EROS Data Center, Sioux Falls, S.D. 57198 ERTS
(E82-10023; NASA-CR-164814; INPE-2063-RPE/305) Avail: NTIS HC A03/MF A01 CSCL 05B

The current status of the Brazilian LANDSAT facilities is reported. The activities at the Cuiaba tracking and receiving station, and at the electronic processing and photo laboratories are presented. The image data bank is discussed. Operation statistics are given and include: scenes received and recorded, and scenes converted to images; images distributed to users and revenues; CCT's produced to users and revenues; images and CCT's distributed (summary); and LANDSAT data sales/distribution analysis for the year of 1980. The status of the LANDSAT-D project is also reported. T.M.

N82-16450# Instituto de Pesquisas Espaciais, Sao Jose dos Campos (Brazil).

SIMPLIFIED ALGORITHM FOR CALCULATING RADIATIVE TRANSFER IN SATELLITE IMAGES [ALGORITMO SIMPLIFICADO PARA CALCULO DE TRANSFERENCIA RADIATIVA EM IMAGENS DE SATELITE]

L. A. V. Dias, A. E. C. Pereira, and G. Camara Jul. 1981 17 p refs In PORTUGUESE; ENGLISH abstract Presented at the 33rd Reuniao Anual da SBPC, 8-15 Jul. 1981, Salvador, Brazil
(INPE-2169-RPE/385) Avail: NTIS HC A02/MF A01

Temporal variations of Earth's atmosphere may cause problems on remote sensing data analysis of satellites, such as LANDSAT, SKYLAB and NIMBUS-7. The apparent radiance of surface features which an orbiting spacecraft measures differs from the intrinsic surface radiance of the object, due to the presence of the intervening atmosphere of Earth. An algorithm for atmospheric correction is presented. J.D.H.

N82-16452*# Texas Univ. at Arlington. Applied Research Labs.

DIGITAL CORRELATION OF DDRS DATA Final Report, 1 Oct. 1980 - 30 Sep. 1981

Carroll R. Griffin and James M. Estes 24 Nov. 1981 42 p refs
(Contract NAS9-16208)
(NASA-CR-167494; ARL-TR-81-51) Avail: NTIS HC A03/MF A01 CSCL 05B

The reduction of digital SAR (synthetic aperture radar) data to radar images for use in remote sensing applications was investigated. The critical software operations are discussed in detail, and suggestions and recommendations are made for improving the algorithms currently being used. J.M.S.

N82-16677# National Weather Service, Fort Worth, Tex. Scientific Services Div.

WEATHER SATELLITE INTERPRETATION: INTRODUCTION TO WEATHER SATELLITE IMAGERY

David L. Carlson Jun. 1981 54 p refs
(PB82-107657; NOAA-TM-NWS-SR-103; NOAA-81081105) Avail: NTIS HC A04/MF A01 CSCL 04B

This manual was designed to be a basic self-study course for the new GOES (Geostationary Operational Environmental Satellite). They may also be referred to as SMS, Synchronous Meteorological Satellite. Five GOES satellites launched by the U.S. and two others launched by Europe and Japan provide global coverage plus backup capability. Content of the manual includes basic operation of the GOES system and detailed explanations of some of the most commonly used GOES photos. The test consists of two chapters, a criterion test at the end of each chapter, and a comprehensive photo interpretation examination. GRA

N82-17570# Inter-American Geodetic Survey, Fort Sam Houston, Tex.

PHOTOGRAMMETRY SOFTWARE. A PACKAGE FOR EVERYONE

James R. Hawk Oct. 1981 59 p
(AD-A108098) Avail: NTIS HC A04/MF A01 CSCL 08/2

An example photogrammetry software is presented for consideration. The system is being implemented throughout Latin America by IAGS. It includes both analytical and semi-analytical adjustments. It is a simplistic yet versatile system which has proven very successful. Author (GRA)

N82-18656 Old Dominion Univ., Norfolk, Va.

USAGE AND LIMITATIONS OF CHARACTERISTIC VECTOR ANALYSIS OF REMOTE SENSING MULTISPECTRAL DATA FOR THE IDENTIFICATION AND QUANTIFICATION OF WATER QUALITY PARAMETERS Ph.D. Thesis

Theodore A. Talay 1981 394 p
Avail: Univ. Microfilms Order No. 8128308

Characteristic vector analysis is investigated to determine how it resolves total radiance signals measured by a remote sensor into eigenvectors and associated scalar coefficients and their relationships to the identification and quantification of the in situ water constituents. Technique operation is checked against a progression of hypothetical test cases and a limited number of laboratory data sets. Under ideal conditions, characteristic vector analysis has the potential of identifying and quantifying individual constituents in water, even when in mixtures, with a minimum of surface truth data. Exact constituent identification, using characteristic vectors, and quantification, by scaling a scalar coefficients, is possible when the study constituents have a linear radiance concentration relationship, superimpose linearly in mixtures, and the measured radiance spectra are devoid of noise and atmospheric effects. As these conditions are relaxed, technique limitations and inexact solutions are encountered. Dissert. Abstr.

N82-18657 Royal Aircraft Establishment, Farnborough (England). Space Dept.

AUTOMATIC RELOCATION OF GROUND CONTROL POINTS IN LANDSAT IMAGERY

A. H. Benny 5 Jun. 1981 37 p refs
(RAE-TR-81071; RAE-Space-598; BR80598) Copyright. Avail: Issuing Activity

A computer program which relocates ground control points (GCP), used in the geometric transformation of satellite pictures is discussed. The GCP's are first located manually on the image and a map. A transformation matrix enables image locations to

be converted to map references. For subsequent images, the identity of a first GCP and an indication (not necessarily precise) of its position in the new image enable a spiral search to locate that GCP and then all the others. Accuracy of + or - 0.4 pixel is obtained for LANDSAT pictures. For similar seasons, proportion relocated approaches 100%. In worst cases (6 months difference between images, with snow in the second) 60% is achieved.
Author (ESA)

N82-19611*# National Aeronautics and Space Administration, Washington, D. C.
SATELLITE EARTH RESOURCES DATA, MODULE U-3
Jan. 1980 13 p Original contains color imagery. Original photography may be purchased from the EROS Data Center, Sioux Fals, S.D. 57198. ERTS
(E82-10035; NASA-TM-84130) Avail: NTIS
HC A02/MF A01 CSCL 05B

Satellite data image products potentially useful in solving Earth resource and environmental problems are described. Sources for satellite data and user information are given. Recommendations for suitability of use of data from each satellite are presented. Satellite sources of Earth resources data are summarized for satellites launched since 1965 and those projected for launch through the late 1980s. The sensors of interest on each satellite, the wavelength or frequency of operation, and the resolution are given. Color ranges are illustrated and compared. The form and utility of aircraft and LANDSAT images are compared. Data from the Gemini-Apollo photography, Skylab, meteorological satellites, the Heat Capacity Mapping Mission, the Coastal Zone Color Scanner, Seasat, LANDSAT, and projected future satellites are briefly described.
J.D.H.

N82-19612*# Consiglio Nazionale delle Ricerche, Venice (Italy). Lab. per lo Studio della Dinamica delle Grandi Masse.
LANDSAT IMAGERY OF THE VENETIAN LAGOON: A MULTITEMPORAL ANALYSIS
L. Alberotanza and A. Zandonella, Principal Investigators (Telespazio S.p.A., Rome) 1980 9 p refs Sponsored by NASA ERTS
(E82-10036; NASA-CR-164772) Avail: NTIS
HC A02/MF A01 CSCL 08H

The use of LANDSAT multispectral scanner images from 1975 to 1979 to determine pollution dispersion in the central basin of the lagoon under varying tidal conditions is described. Images taken during the late spring and representing both short and long range tidal dynamics were processed for partial haze removal and removal of residual striping. Selected spectral bands were correlated to different types of turbid water. The multitemporal data was calibrated, classified considering sea truth data, and evaluated. The classification differentiated tide diffusion, algae belts, and industrial, agricultural, and urban turbidity distributions. Pollution concentration is derived during the short time interval between inflow and outflow and from the distance between the two lagoon inlets and the industrial zones. Increasing pollution of the lagoon is indicated.
J.D.H.

N82-19613*# National Aeronautics and Space Administration. Goddard Space Flight Center, Greenbelt, Md.
A COMPARISON OF UNSUPERVISED CLASSIFICATION PROCEDURES ON LANDSAT MSS DATA FOR AN AREA OF COMPLEX SURFACE CONDITIONS IN BASILICATA, SOUTHERN ITALY
Chris Justice and John Townshend, Principal Investigators Mar. 1981 40 p refs Submitted for publication Original contains imagery. Original photography may be purchased from the EROS Data Center, Sioux, Falls, S.D. 57198. ERTS
(E82-10038; NASA-TM-82098) Avail: NTIS
HC A03/MF A01 CSCL 05B

Two unsupervised classification procedures were applied to ratioed and unratioed LANDSAT multispectral scanner data of an area of spatially complex vegetation and terrain. An objective accuracy assessment was undertaken on each classification and comparison was made of the classification accuracies. The two unsupervised procedures use the same clustering algorithm. By on procedure the entire area is clustered and by the other a representative sample of the area is clustered and the resulting statistics are extrapolated to the remaining area using a maximum likelihood classifier. Explanation is given of the major steps in the classification procedures including image preprocessing; classification; interpretation of cluster classes; and accuracy assessment. Of the four classifications undertaken, the monocluster block approach on the unratioed data gave the highest accuracy of 80% for five coarse cover classes. This accuracy was increased to 84% by applying a 3 x 3 contextual filter to the classified image. A detailed description and partial explanation is provided for the major misclassification. The classification of the unratioed data produced higher pecentage accuracies than for the ratioed data and the monocluster block approach gave higher accuracies than clustering the entire area. The moncluster block approach was additionally the most economical in terms of computing time.
Author

N82-19617*# Pennsylvania State Univ., University Park. Office for Remote Sensing of Earth Resources.
DELINEATION OF SOIL TEMPERATURE REGIMES FROM HCMM DATA Quarterly Report
Rick L. Day and Gary W. Petersen, Principal Investigators 30 Sep. 1981 3 p Sponsored by NASA HCMM
(E82-10042; NASA-CR-164919) Avail: NTIS
HC A02/MF A01 CSCL 08M

Supplementary data including photographs as well as topographic, geologic, and soil maps were obtained and evaluated for ground truth purposes and control point selection. A study area (approximately 450 by 450 pixels) was subset from LANDSAT scene No. 2477-17142. Geometric corrections and scaling were performed. Initial enhancement techniques were initiated to aid control point selection and soils interpretation. The SUBSET program was modified to read HCMM tapes and HCMM data were reformated so that they are compatible with the ORSER system. Initial NMAP products of geometrically corrected and scaled raw data tapes (unregistered) of the study were produced.
A.R.H.

N82-19621*# Agricultural Research Service, Weslaco, Tex.
METHODS OF EDITING CLOUD AND ATMOSPHERIC LAYER AFFECTED PIXELS FROM SATELLITE DATA Quarterly Progress Report, 5 Jun. - 5 Sep. 1981
Paul R. Nixon, Principal Investigator, Craig L. Wiegand, Arthur J. Richardson, Michael P. Johnson, and Benjamin G. Goodier Sep. 1981 10 p ERTS
(NASA Order S-75406-B)
(E82-10046; NASA-CR-164923; QPR-3) Avail: NTIS
HC A02/MF A01 CSCL 05B

The location and migration of cloud, land and water features were examined in spectral space (reflective VIS vs. emissive IR). Daytime HCMM data showed two distinct types of cloud affected pixels in the south Texas test area. High altitude cirrus and/or cirrostratus and 'subvisible cirrus' (SCi) reflected the same or only slightly more than land features. In the emissive band, the digital counts ranged from 1 to over 75 and overlapped land features. Pixels consisting of cumulus clouds, or of mixed cumulus and landscape, clustered in a different area of spectral space than the high altitude cloud pixels. Cumulus affected pixels were more reflective than land and water pixels. In August the high altitude clouds and SCi were more emissive than similar clouds were in July. Four-channel TIROS-N data were examined with the objective of developing a multispectral screening technique for removing SCi contaminated data.
Author

N82-19622*# Miami Univ., Fla. School of Marine and Atmospheric Science.
INVESTIGATIONS OF MEDIUM WAVELENGTH MAGNETIC ANOMALIES IN THE EASTERN PACIFIC USING MAGSAT DATA Interim Report, Apr. - Jun. 1981
Christopher G. A. Harrison, Principal Investigator Jun. 1981 3 p Sponsored by NASA ERTS
(E82-10047; NASA-CR-164924) Avail: NTIS
HC A02/MF A01 CSCL 08G

Processing continued on the data set covering the first three months of the mission. Orbits were selected over a specified range of longitude and latitude and those orbits falling within the geographical boundaries were stored on a disk and a listing made. To verify the quality of the data, plots were made showing altitude vs latitude, anomalous field vs latitude, and corrected anomalous field vs latitude. Results of the plotting showed that: (1) data from the first day of the mission are not usable because they are too noisy; (2) some orbits contain spikes, no doubt a processing error on the tape; (3) some orbits contain a 20 deg region in latitude, offset roughly 30 nT from the rest of the anomalous field profiles; and (4) the correlation between the adjacent orbits is poor. Even the new ring current coefficients provided with a later, corrected set of data tapes did not not yield the desired correlations. A.R.H.

N82-19623*# Pennsylvania State Univ., University Park. Dept. of Meteorology.
INTERACTIVE INITIALIZATION OF HEAT FLUX PARAMETERS FOR NUMERICAL MODELS USING SATELLITE TEMPERATURE MEASUREMENTS Quarterly Report, 1 Jun. - 31 Aug. 1981
Toby N. Carlson, Principal Investigator 31 Aug. 1981 5 p
Sponsored by NASA HCMM
(E82-10048; NASA-CR-164925; QR-2) Avail: NTIS HC A02/MF A01 CSCL 08M

Day/night Heat Capacity Mapping Mission image pairs over Kansas and Indiana were used to examine the spatial variation of moisture availability on the mesoscale. Of particular concern was whether patterns of moisture availability and thermal inertia, as well as surface heat fluxes, respond to significant spatial variations in the rainfall pattern. A temperature analysis for the Indiana case is presented. M.G.

N82-19644*# Business and Technological Systems, Inc., Seabrook, Md.
AN INFORMATION ADAPTIVE SYSTEM STUDY REPORT AND DEVELOPMENT PLAN
William S. Ataras, Kenneth Eng, John J. Morone, Paul R. Beaudet, and Roland Chin 9 May 1980 225 p
(Contract NAS5-25668)
(NASA-CR-166768; BTS-FR-80-117) Avail: NTIS HC A10/MF A01 CSCL 05B

The purpose of the information adaptive system (IAS) study was to determine how some selected Earth resource applications may be processed onboard a spacecraft and to provide a detailed preliminary IAS design for these applications. Detailed investigations of a number of applications were conducted with regard to IAS and three were selected for further analysis. Areas of future research and development include algorithmic specifications, system design specifications, and IAS recommended time lines. N.W.

N82-19645*# National Aeronautics and Space Administration. Goddard Space Flight Center, Greenbelt, Md.
THE EFFECT OF FINITE FIELD SIZE ON CLASSIFICATION AND ATMOSPHERIC CORRECTION
Yoram J. Kaufman and Robert S. Fraser Sep. 1981 53 p refs
(NASA-TM-83818) Avail: NTIS HC A04/MF A01 CSCL 20F

The atmospheric effect on the upward radiance of sunlight scattered from the Earth-atmosphere system is strongly influenced by the contrasts between fields and their sizes. For a given atmospheric turbidity, the atmospheric effect on classification of surface features is much stronger for nonuniform surfaces than for uniform surfaces. Therefore, the classification accuracy of agricultural fields and urban areas is dependent not only on the optical characteristics of the atmosphere, but also on the size of the surface do not account for the nonuniformity of the surface have only a slight effect on the classification accuracy in other cases the classification accuracy descreases. The radiances above finite fields were computed to simulate radiances measured by a satellite. A simulation case including 11 agricultural fields and four natural fields (water, soil, savanah, and forest) was used to test the effect of the size of the background reflectance and the optical thickness of the atmosphere on classification accuracy. It is concluded that new atmospheric correction methods, which take into account the finite size of the fields, have to be developed to improve significantly the classification accuracy. Author

N82-19649# British Aerospace Dynamics Group, Stevenage (England). Space and Communications Div.
STUDY OF EARTH RESOURCES SATELLITE (ERS) DATA REDUCTION UNIT
C. J. Collins, comp., F. A. C. Burke, comp., J. W. Pengelly, comp., P. Redstone, comp. (Logica Ltd.), C. Burrows, comp. (Logica Ltd.), and N. McEvoy, comp. (Logica Ltd.) Paris ESA Aug. 1981 188 p refs
(Contract ESA-4415/80/NL-PP(SC))
(BAe-TP-7905; ESA-CR(P)-1478) Avail: NTIS HC A09/MF A01

Techniques for reducing onboard, by a factor of 4, the data rate from imaging instruments on Earth resources satellites, especially from the ocean color monitor on ERS 1, were examined. Theoretical analysis and simulation with real images allow algorithms to be defined for implementation assessment. A tradeoff based on performance and engineering criteria shows that spatial resolution degrading unit (SRDU) and a fixed weight spectral transform followed by a Rice Machine (FWST + RM2) meet reduction criteria within the mass and power constraints. Costs (two model program) are comparable, the greater complexity of FWST + RM2 being largely offset by more advanced technology in SRDU. Before either option is adopted, further simulation and breadboarding are recommended. Author (ESA)

N82-19654# Engins Matra, Velizy (France). Lab. de Traitement des Images.
DATA RATE REDUCTION. IMPACT OF IMAGE DATA COMPRESSION ON END TO END DATA MANAGEMENT OF A MULTISPECTRAL PAYLOAD
G. E. Lowitz, J. M. Vivier, J. P. Camus, and B. H. Roy Paris ESA Jul. 1980 51 p refs
(Contract ESTEC-3749/78)
(Rept-44/130; ESA-CR(P)-1507) Avail: NTIS HC A04/MF A01

Satellite onboard data compression by clustering in the raw channels with a variable number of classes is discussed. The effect on the overall image chain is illustrated by land applications satellite system (LASS) data and LANDSAT ground stations processing and dissemination systems. Image quality, processing costs, software and hardware are considered. Onboard mechanization is efficient and the compression principles benefit user interpretation routines such as classification. Compressed data can be processed efficiently, yielding cost savings on the order of 100 to 1. A 512 X 512 pixel frame, including preprocessing, is treated in 5 min. The compressed imagery can be recognized, zones can be located and cloud cover can be assessed, making high quality quick looks possible. Author (ESA)

N82-19656# Saab-Scania, Linkoping (Sweden).
ON THE ACCURACY OF THERMAL INERTIA MAPPING BY INFRARED IMAGERY
Sune R. J. Axelsson 1981 20 p refs
(SAAB-REPR-AE-10) Avail: NTIS HC A02/MF A01

The influence of different interfering parameters on the estimation of the thermal inertia of the ground from the diurnal variations of the surface, temperature, using thermal infrared and albedo measuring imagery, was investigated. The strong influence of these parameters degrades the accuracy of the analysis and makes the interpretation complex. This influence was studied, starting from an improved analytic model of the surface temperature of a periodically heated ground surface. The errors in albedo and atmospheric heat exchange, and the limited accuracy of sensors and the model used in data processing, dominate the thermal inertia error. Further reductions of the accuracy are due to the translation of the thermal inertia map into user data like soil type, porosity and soil moisture. Upper bounds on the potential thermal inertia mapping accuracy are found by calculating the estimation error when the interfering parameters are known with specified accuracy. Author (ESA)

N82-19788# Wisconsin Univ. - Madison. Space Science and Engineering Center.
THE DEVELOPMENT AND TESTING OF METHODS TO INFER MIDLATITUDE PRECIPITATION INTENSITY FROM GEOSYNCHRONOUS SATELLITE INFRARED DATA
John V. Zapotocny, Donald R. Johnson, and Thomas M. Whittaker Hanscom AFB, Mass. AFGL 31 Jul. 1981 90 p refs
(Contract F19628-78-C-0137; AF Proj. 6670)
(AD-A106881; SCIENTIFIC-3; AFGL-TR-81-0252) Avail: NTIS HC A05/MF A01 CSCL 04/2

In an attempt to aid development of simple techniques applicable in middle latitudes, this study addresses the inference of precipitation intensity and its temporal change associated with imbedded convective activity at a location in areas of continuous stratiform precipitation from Geosynchronous Operational Environmental Satellite (GOES) IR digital data. Imbedded convective activity is easily identified in high resolution visible GOES imagery if high cloud layers are not present to obscure the convection. At low Sun angles with the shadowing effect of the convective towers, details of these convective areas are especially enhanced. However, with the need for these methods to be applicable during both daytime and nighttime hours, only the IR 11 micron channel data were used in this study which was based on several synoptic cases. In each of the cases examined, visible and IR imagery and loops were used to help pinpoint optimum areas for study. GRA

N82-19927# Instituto de Pesquisas Espaciais, Sao Jose dos Campos (Brazil).
SELECTION OF ATTRIBUTES APPLIED TO MULTISPECTRAL IMAGES [SELECAO DE ATRIBUTOS APLICADA A IMAGENS MULTISPECTRAIS]
Fernando A. Mitsuo Ii Jan. 1982 92 p refs In PORTUGUESE; ENGLISH summary
(INPE-2303-TDL/072) Avail: NTIS HC A05/MF A01

Classes of Gaussian distribution are defined, given a multispectral scene of 12 channels. The best channels for separating classes are identified using the J-M distance criterion. The quantitative analysis of these interclass separations is also discussed. M.G.

N82-20603*# Instituto de Pesquisas Espaciais, Sao Jose dos Campos (Brazil).
THE LANDSAT SYSTEM OPERATED IN BRAZIL BY CNPQ/INPE - RESULTS OBTAINED IN THE AREA OF MAPPING AND FUTURE PERSPECTIVES [O SISTEMA LANDSAT OPERADO NO BRASIL PELO CNPQ/INPE - RESULTADOS OBTIDOS NA AREA DE CARTOGRAFIA E PERSPECTIVAS FUTURAS]
Nelson deJesusParada, Principal Investigator and Marcio Nogueira Barbosa Jul. 1981 45 p refs In PORTUGUESE; ENGLISH summary Presented at the 10th Congr. Brasileiro de Cartografica, Brasil, 19-24 Jul. 1981 Sponsored by NASA ERTS
(E82-10080; NASA-CR-168401; NAS 1.26:168401; INPE-2191-RPE/003) Avail: NTIS HC A03/MF A01 CSCL 05B

The LANDSAT system, operated in the country by CNPg/INPE since 1973, systematically acquires, produces, and distributes both multispectral and panchromatic images obtained through remote sensing satellites to thousands of researchers and technicians involved in the natural resources survey. To cooperate in the solution of national problems, CNPq/INPE is developing efforts in the area of manipulation of those images with the objective of making them useful as planimetric bases for the simple revision of already published maps or for its utilization as basic material in regions not yet reliability mapped. The results obtained from performed tests are presented and the existing limitations are discussed. The new system purchased to handle data from the next series of LANDSAT as well as from MAPSAT and SPOT which will be in operation within the 80's decade, and are designed not only for natural resources survey but also for the solution of cartographic problems. Author

N82-20604*# Instituto de Pesquisas Espaciais, Sao Jose dos Campos (Brazil).
AN ALGORITHM FOR SPATIAL HEIRARCHY CLUSTERING [UM ALGORITMO PARA AGREGACAO HIERARQUICA ESPACIAL]
Nelson deJesusPar_da, Principal Investigator and Flavio Roberto Dias Velasco Jul. 1981 12 p refs In PORTUGUESE; ENGLISH summary ERTS
(E82-10081; NASA-CR-168402; NAS 1.26:168402; INPE-2170-RPE/386) Avail: NTIS HC A02/MF A01 CSCL 05B

A method for utilizing both spectral and spatial redundancy in compacting and preclassifying images is presented. In multispectral satellite images, a high correlation exists between neighboring image points which tend to occupy dense and restricted regions of the feature space. The image is divided into windows of the same size where the clustering is made. The classes obtained in several neighboring windows are clustered, and then again successively clustered until only one region corresponding to the whole image is obtained. By employing this algorithm only a few points are considered in each clustering, thus reducing computational effort. The method is illustrated as applied to LANDSAT images. J.D.H.

N82-20607*# Florida Univ., Gainesville. Climatology Lab.
APPLICATION OF SATELLITE FROST FORECAST TECHNOLOGY TO OTHER PARTS OF THE UNITED STATES, PHASE 2 Final Report
J. David Martsolf, Ellen Chen, C. Terry Morrow, Stuart H. Gage, and Jon F. Bartholic Nov. 1981 265 p refs Prepared in cooperation with Pennsylvania State Univ., University Park and Michigan State Univ., East Lansing Original contains color illustrations
(Contract NAS10-9876)
(NASA-CR-166827) Avail: NTIS HC A12/MF A01 CSCL 02C

Thermal infrared data taken from the GOES satellite over a period of several hours was color enhanced by computer according to temperature. The varying temperatures were then used to assist in frost forecasting. Input from Michigan and Pennsylvania to the cold climate mapping project is emphasized in the report of the second year's activities of a two-year effort.

N82-20608*# Florida Univ., Gainesville.
APPLICATION OF SATELLITE FROST FORECAST TECHNOLOGY TO OTHER PARTS OF THE UNITED STATES, PHASE 2, INTRODUCTION Final Report
In its Appl. of Satellite Frost Forecast Technol. to Other Parts of the U.S., Phase 2 Nov. 1981 31 p

Avail: NTIS HC A12/MF A01 CSCL 02C

The history and status of University of Michigan and University of Pennsylvania involvement in determining if P-model for frost prediction used in Florida is applicable to those geographic locations is reviewed. The possibility of using the S-model to develop a satellite frost forecast system that can recall the distribution of temperatures during previous freezes from a particular area and bring that cold climate climatology to bear on present forecasts is discussed as well as a proposed GOES satellite downlink system to sectionalize the data used in Florida. A.R.H.

N82-20612*# Pennsylvania State Univ., University Park.
THE OFFICE FOR REMOTE SENSING OF EARTH RESOURCES Final Report
In Florida Univ. Appl. of Satellite Frost Forecast Technol. to Other Parts of the U.S., Phase 2 Nov. 1981 6 p refs

Avail: NTIS HC A12/MF A01 CSCL 05B

The main effort of the University of Pennsylvania's office for remote sensing of Earth resources (ORSER) is the processing, analysis, and interpretation of multispectral data, most often supplied by NASA in the form of imagery and digital data. The facilities used for data reduction and image enhancement are described as well as the development of algorithms for producing a computer map showing various environmental and land use characteristics of data points in the analyzed scenes. The application of an (ORSER) capability for statewide monitoring of gypsy moth defoliation is discussed. A.R.H.

N82-20614*# Michigan State Univ., East Lansing.
MSU TEST OF P-MODEL Final Report
In Florida Univ. Appl. of Satellite Frost Forecast Technol. to Other Parts of the U.S., Phase 2 Nov. 1981 8 p refs

Avail: NTIS HC A12/MF A01 CSCL 05B

Results of running key station data (soil, air, and dew point temperatures, net irradiation, and wind direction and speed) from Michigan through the P-model are presented. The details of each of the 55 error calculations are shown in tables. A histogram is included showing errors in degrees Fahrenheit. A.R.H.

N82-20628# Army Engineer Topographic Labs., Fort Belvoir, Va.
COMPUTER-ASSISTED PHOTO INTERPRETATION RESEARCH AT USAETL
George E. Lukes 21 Apr. 1981 14 p refs
(AD-A109366; ETL-R028) Avail: NTIS HC A02/MF A01 CSCL 08/5

A program in computer-assisted photo interpretation research (CAPIR) has been initiated at the U.S. Army Engineer Topographic Laboratories. In a new laboratory, a photo interpreter (PI) analyzing high-resolution, aerial photography interfaces directly to a digital computer and geographic information system (GIS). A modified analytical plotter enables the PI to transmit encoded three dimensional spatial data from the stereomodel to the computer. Computer-generated graphics are displayed in the stereomodel for direct feedback of digital spatial data to the PI. Initial CAPIR capabilities include point positioning, mensuration, stereoscopic area search, GIS creation and playback, and elevation data extraction. New capabilities under development include stereographic superposition, a digital image workstation, and integration of panoramic Optical Bar Camera photography as a primary GIS data source. This project has been conceived as an evolutionary approach to the digital cartographic feature extraction problem. As a working feature extraction system, the CAPIR laboratory can serve as a testbed for new concepts emerging from image understanding and knowledge-based systems research. GRA

N82-21457*# Business and Technological Systems, Inc., Seabrook, Md.
CONTEXT SENSITIVE FORMULATIONS OF ANTENNA PATTERN CORRECTION AND SIDE LOBE COMPENSATION FOR NOSS/LAMMR REAL TIME PROCESSING Final Report
Roland T. Chin and Paul R. Beaudet 7 Oct. 1981 157 p
(Contract NAS5-26541)
(NASA-CR-166789; NAS 1.26:166789; BTS-FR-81-165) Avail: NTIS HC A08/MF A01 CSCL 20N

Large antenna multi-channel microwave radiometer (LAMMR) software specifications were written for LAMMR ground processing. There is a need to determine more computationally-efficient antenna temperature correction methods in compensating side lobe contributions especially near continents, islands and weather fronts. One of the major conclusions was that the antenna pattern corrections (APC) processes did not accomplish the implied goals of compensating for the antenna side lobe influences on brightness temperature. A-priori knowledge of land/water locations was shown to be needed and had to be incorporated in a context sensitive APC process if the artifacts caused by land presence is to be avoided. The high temperatures in land regions can severely bias the lower ocean response. R.J.F.

N82-21458# European Space Agency, Paris (France).
SAR IMAGE QUALITY
Jun. 1981 96 p refs Presented at EARTHNET/EARSel Workshop, Frascati, Italy, 11-12 Dec. 1980
(ESA-SP-172; ISSN-0379-6566) Avail: NTIS HC A05/MF A01; ESA, Paris FF 55 (US $12)

The processing and quality of synthetic aperture radar imagery is considered with particular attention on optimal multilook processing, simulation, beam tracking, speckle filtering, radiometric calibration, digital processing, ocean wave spectra, two-dimensional image spectrum, terrain models, etc.

N82-21474# Centre de Recherches en Physique de l'Environnement, Issy-les-Moulineaux (France).
DIRECT DETERMINATION OF THE TWO DIMENSIONAL IMAGE SPECTRUM FROM RAW SYNTHETIC APERTURE RADAR DATA
P. Martin *In* ESA SAR Image Quality Jun. 1981 p 81-87 refs Submitted for publication

Avail: NTIS HC A05/MF A01; ESA, Paris FF 55 (US $12)

An algorithm is described which computes the two-dimensional Fourier transform of a synthetic aperture radar image. This method is intended to replace the whole SAR processing and the two-dimensional Fourier transformation by a specialized processing scheme which, in terms of computational speed and complexity, will be of the order of a single two-dimensional autocorrelation. This processing approach is applied to the estimation of the wave directional spectrum from the raw data of the SAR sensor of SEASAT-1. Author (ESA)

N82-21499# Royal Signals and Radar Establishment, Malvern (England).
THE DESIGN AND IMPLEMENTATION OF AN OPERATIONAL, COMPUTER-BASED WEATHER RADAR SYSTEM
A. P. Ball, J. L. Clarke, M. J. Brien, A. H. Shaw, S. E. Trigg, and T. A. Vollier 1979 94 p refs Original contains color illustrations
(RSRE-MEMO-3151; BR71459) Avail: NTIS HC A05/MF A01

A system that provides quantitative rainfall data is described. It consists of an on-site PDP-11/40 computer used to process digitized radar data from a narrow beam, fully steerable radar aerial. The data are collected at several low elevation angles. The radar amplitude signals received are digitized and transferred to the computer by a special purpose radar signal averaging unit (RSAU). After processing, the signals are displayed as a color coded, Cartesian map of instantaneous rainfall rate and distribution on a modified color TV via a special data store. Similar data can be transmitted via the DATEL service to users remote from the radar and to a network center computer where a composited color TV picture of data is displayed. Hardware and software are described in detail. Author (ESA)

N82-21565# Royal Aircraft Establishment, Farnborough (England).
AN INTRODUCTION TO IMAGE PROCESSING AT ROYAL AIRCRAFT ESTABLISHMENT, FARNBOROUGH, ENGLAND
G. J. Davison London HMSO Sep. 1980 26 p refs
(RAE-TR-80107; RAE-SPACE-585; BR76808) Avail: NTIS HC A03/MF A01

Data collection and image processing for the generation of photographic products from SEASAT, LANDSAT, NIMBUS TIROS and METEOSAT 2 are described. The hardware facilities include a Linoscan 204 D composition device driven by a PRIME 200 computer, and a Plessey IDP 3000 interactive image display system. A disk based system enables the user to apply various processing algorithms to standard format data for display. Algorithms are described including: contrast enhancement by applying a mapping function to a set of pixel intensity values, a destriping algorithm which equates the means and variances of the radiance levels from each detector (LANDSAT), four principal components analysis, edge enhancement, and geometric transformations. Collaborative projects using remote sensing data by other government agencies are also mentioned. Author (ESA)

N82-21637*# Lockheed Engineering and Management Services Co., Inc., Houston, Tex.
AS-BUILT DESIGN SPECIFICATION FOR UNIV4VEC
Mary Ann Tompkins and Carol A. Sivillo, Principal Investigators Jun. 1981 32 p Sponsored by NASA, USDA, Dept. of Commerce, Dept. of the Interior, and Agency for International Development ERTS
(Contract NAS9-15800; Proj. AgRISTARS)
(E82-10085; NASA-CR-161060; JSC-17389;
NAS 1.26:161060; SR-L1-00301; LEMSCO-16676) Avail: NTIS HC A03/MF A01 CSCL 02C

The UNIV4VEC program which is part of the CLSFYG package is described. This program reads a CLASFYG vector parameter file and converts it to a four channel universal formatted file. A.R.H.

N82-21638*# Lockheed Engineering and Management Services Co., Inc., Houston, Tex.
AS-BUILT DOCUMENTATION OF PROGRAMS TO IMPLEMENT THE ROBERTSON AND DORAISWAMY/THOMPSON MODELS
D. J. Valenziano, Principal Investigator Jun. 1981 96 p Sponsored by NASA, USDA, Dept. of Commerce, Dept. of the Interior, and Agency for International Development ERTS
(Contract NAS9-15800; Proj. AgRISTARS)
(E82-10086; NASA-CR-161061; JSC-17400;
NAS 1.26:161061; SR-L1-00717; LEMSCO-16376) Avail: NTIS HC A05/MF A01 CSCL 02C

The software which implements two spring wheat phenology models is described. The main program routines for the Doraiswamy/Thompson crop phenology model and the basic Robertson crop phenology model are DTMAIN and BRMAIN. These routines read meteorological data files and coefficient files, accept the planting date information and other information from the user, and initiate processing. Daily processing for the basic Robertson program consists only of calculation of the basic Robertson increment of crop development. Additional processing in the Doraiswamy/Thompson program includes the calculation of a moisture stress index and correction of the basic increment of development. Output for both consists of listings of the daily results. T.M.

N82-21641*# Lockheed Engineering and Management Services Co., Inc., Houston, Tex.
AS-BUILT DESIGN SPECIFICATION FOR PARHIS
Mary Ann Tompkins, Principal Investigator Jun. 1981 122 p

Sponsored by NASA, USDA, Dept. of Commerce, Dept. of the Interior, and Agency for International Development ERTS
(Contract NAS9-15800; Proj. AgRISTARS)
(E82-10089; NASA-CR-161064; NAS 1.26:161064;
SR-L1-00305; JSC-17371; LEMSCO-16650) Avail: NTIS
HC A06/MF A01 CSCL 02C

The program is part of the CLASFYG package. It produces histograms of the greenness profile derived parameters alpha, beta, t sub o, and chi squared, which are computed by the CLASFYG program. Alpha is the approximate greenness rise time, beta is the approximate greennss decay time, t sub o is the spectral crop emergence date, and chi squared per degree of freedom is the goodness of fit of the actual data to the computed greenness profile. The program also produces statistical information concerning the parameters. T.M.

N82-21642*# Lockheed Engineering and Management Services Co., Inc., Houston, Tex.

AS-BUILT DESIGN SPECIFICATION FOR PARCLS

Mary Ann Tompkins, Principal Investigator Jun. 1981 113 p
Sponsored by NASA, USDA, Dept. of Commerce, Dept. of the Interior, and Agency for International Development ERTS
(Contract NAS9-15800; Proj. AgRISTARS)
(E82-10090; NASA-CR-161065; NAS 1.26:161065;
SR-L1-00302; JSC-17390; LEMSCO-16677) Avail: NTIS
HC A06/MF A01 CSCL 02C

The PARCLS program, part of the CLASFYG package, reads a parameter file created by the CLASFYG program and a pure pixel ground truth file in order to create to classification file of three separate crop categories in universal format. A.R.H.

N82-21643*# Lockheed Engineering and Management Services Co., Inc., Houston, Tex.

AS-BUILT DESIGN SPECIFICATION FOR MISMAP

P. M. Brown, D. E. Cheng, and M. A. Tompkins, Principal Investigators Jun. 1981 71 p Sponsored by NASA, USDA, Dept. of Commerce, Dept. of the Interior, and Agency for International Development ERTS
(Contract NAS9-15800; Proj. AgRISTARS)
(E82-10091; NASA-CR-161066; NAS 1.26:161066;
SR-L1-00307; JSC-17231; LEMSCO-16300) Avail: NTIS
HC A04/MF A01 CSCL 02C

The MISMAP program, which is part of the CLASFYT package, is described. The program is designed to compare classification values with ground truth values for a segment and produce a comparison map and summary table. A.R.H.

N82-21646*# Lockheed Engineering and Management Services Co., Inc., Houston, Tex.

AS-BUILT DESIGN SPECIFICATION FOR SEGMENT MAP (SGMAP) PROGRAM

Mary Ann Tompkins, Principal Investigator Jun. 1981 100 p
Sponsored by NASA, USDA, Dept. of Commerce, Dept. of the Interior, and Agency for International Development ERTS
(Contract NAS9-15800; Proj. AgRISTARS)
(E82-10094; NASA-CR-161056; NAS 1.26:161056;
SR-LI-00306; JSC-17037; LEMSCO-15937) Avail: NTIS
HC A05/MF A01 CSCL 02C

The segment map program (SGMAP), which is part of the CLASFYT package, is described in detail. This program is designed to output symbolic maps or numerical dumps from LANDSAT cluster/classification files or aircraft ground truth/processed ground truth files which are in 'universal' format. M.G.

N82-21656*# Research and Data Systems, Inc., Lanham, Md.

DEVELOPMENT OF A SURFACE ISOLATION ESTIMATION TECHNIQUE SUITABLE FOR APPLICATION OF POLAR ORBITING SATELLITE DATA

P. A. Davis and L. M. Penn, Principal Investigators Nov. 1981
77 p refs Sponsored by NASA, USDA, Dept. of Commerce, Dept. of the Interior, and Agency for International Development
Original contains imagery. Original photography may be purchased from the EROS Data Center, Sioux Falls, S.D. 57198. ERTS
(NASA Order C-00741; Proj. AgRISTARS)
(E82-10122; NASA-CR-167473; NAS 1.26:167473;
YM-N1-04198; JSC-17784) Avail: NTIS HC A05/MF A01
CSCL 04A

A technique is developed for the estimation of total daily insolation on the basis of data derivable from operational polar-orbiting satellites. Although surface insolation and meteorological observations are used in the development, the algorithm is constrained in application by the infrequent daytime polar-orbiter coverage.
Author

N82-21663*# North Carolina State Univ., Raleigh. Dept. of Marine, Earth and Atmospheric Sciences.

COMPATIBILITY STUDY OF THE MAGSAT DATA AND AEROMAGNETIC DATA Progress Report

I. J. Won, Principal Investigator Aug. 1981 15 p refs
(Contract NAS5-26157)
(E82-10136; NASA-CR-168521; NAS 1.26:168521) Avail:
NTIS HC A02/MF A01 CSCL 05B

The results of (1) an analysis of the fine attitude MAGSAT data covering the continental U.S., (2) analysis of the Project MAGNET U.S. aeromagnetic data in terms of its compatibility with the corresponding MAGSAT data, and finally, (3) analysis of MAGSAT data in the Pacific region and comparison with satellite gravity data are presented. All data reduction procedures are described and the resulting magnetic maps are given. The results indicate a general compatibility between the MAGSAT data and the MAGNET and gravity data. M.G.

N82-21665*# Paris VI Univ. (France).

CONTINUATION OF POTENTIAL FIELD DATA TO A COMMON ALTITUDE

Jean-Louis LeMouel, Principal Investigator and Joel Ducruix
1 Apr. 1981 3 p refs Sponsored by NASA ERTS
(E82-10138; NASA-CR-168523; NAS 1.26:168523) Avail:
NTIS HC A02/MF A01 CSCL 05B

It is noted that the distorsions introduced by the variation of distance between the sources and the measurement points can be important enough to create fake anomalies. The average amplitude of the anomalies at MAGSAT altitude is of the order of a few nT. Thus it is necessary to be careful in reducing MAGSAT data to a common elevation. The achievement of the corresponding anomaly map is of primary importance for the study of regional and long wave length anomalies. A method for the continuation of potential fields is described which consists in representing any harmonic function (in particular the anomaly is function of space coordinates) as a sum of elementary harmonic functions; the continuation being achieved by an inverse technique. Tests, made on a synthetic set of data, evaluate the method.
M.G.

N82-21666*# Paris VI Univ. (France).

SEPARATION OF INTERNAL AND EXTERNAL FIELDS: A NEW TECHNIQUE OF DATA SCREENING Progress Report

Jean-Louis LeMouel, Principal Investigator, Michel Menvielle, and Joel Ducruix 1 Dec. 1980 5 p ref Sponsored by NASA ERTS
(E82-10139; NASA-CR-168524; NAS 1.26:168524) Avail:
NTIS HC A02/MF A01 CSCL 05B

A method for eliminating transient variation from MAGSAT data is described. Instead of using the conventional Kp index, the Km index is used for the rejection of nonquiet data. To build the Km index, the surface of the Earth is divided in eight sectors. Each sector is defined by two or three magnetic observatories and its geographic limits. For each three hourly interval the MAGSAT tracks were drawn on a map showing the location of the station (the crosses), the limits of the sector, and the value of the mean K index inside each sector. No figure in a sector means that the activity level in this sector is lower than 5 nt; in a sector covered with number 1, the activity lies between 5 and 20 nt; 2 stands for any level greater than 20 nT. M.G.

N82-21678*# Agricultural Research Service, Weslaco, Tex.

METHODS OF EDITING CLOUD AND ATMOSPHERIC LAYER AFFECTED PIXELS FROM SATELLITE DATA Quarterly Progress Report, 5 Sep. - 5 Dec. 1981

Paul R. Nixon, Principal Investigator, Craig L. Wiegand, Arthur J. Richardson, and Michael P. Johnson Dec. 1981 6 p ref
HCMM
(NASA Order S-75406B)
(E82-10154; NASA-CR-168539; NAS 1.26:168539; PR-4)
Avail: NTIS HC A02/MF A01 CSCL 05B

Plotted transects made from south Texas daytime HCMM data show the effect of subvisible cirrus (SCI) clouds in the emissive (IR) band but the effect is unnoticable in the reflective (VIS) band. The depression of satellite indicated temperatures ws greatest in the center of SCi streamers and tapered off at the edges. Pixels of uncontaminated land and water features in the HCMM test area shared identical VIS and IR digital count combinations with other pixels representing similar features. A minimum of 0.015 percent repeats of identical VIS-IR combinations are characteristic of land and water features in a scene of 30 percent cloud cover. This increases to 0.021 percent of more when the scene is clear. Pixels having shared VIS-IR combinations less than these amounts are considered to be cloud contaminated in the cluster screening method. About twenty percent of SCi was machine indistinguishable from land features in two dimensional spectral space (VIS vs IR). T.M.

N82-21687*# National Aeronautics and Space Administration, Washington, D. C.
OBSERVATION OF THE EARTH BY RADAR
Charles Elachi (French Petroleum Inst.) Feb. 1982 33 p Transl. into ENGLISH from La Recherche (France), v. 12, no. 128, Dec. 1981 p 1366-1375 Transl. by Scientific Translation Service, Santa Barbara, Calif. Original doc. prep. by French Petroleum Inst.
(Contract NASw-3542)
(NASA-TM-76830; NAS 1.15:76830) Avail: NTIS HC A03/MF A01 CSCL 17I

Techniques and applications of radar observation from Earth satellites are discussed. Images processing and analysis of these images are discussed. Also discussed is radar imaging from aircraft. Uses of this data include ocean wave analysis, surface water evaluation, and topographic analysis. R.J.F.

N82-21698# Logica Ltd., London (England).
FUTURE EARTHNET DISSEMINATION SYSTEMS (FEDS) STUDY. EXECUTIVE SUMMARY Final Report
M. Macintyre, P. Norris, and P. Scragg Paris ESA Dec. 1980 47 p
(Contract ESA-4241/80/F-FC(SC))
(Rept-3318; ESA-CR(P)-1438) Avail: NTIS HC A03/MF A01

The preparation of Earthnet for the dissemination to users of data from the European remote sensing program is considered. Worldwide plans for remote sensing satellite systems, European and north African user demand, data acquisition subsystems, data processing subsystems, data archiving subsystems and data communications subsystems are covered. Subsystems configurations that would meet these performance requirement are studied. Results are integrated to define overall systems configurations that would meet the performance requirements. Alternate centralized acquires data at four Earth stations and stores it temporarily on magnetic tape. Data are forwarded by satellite and disseminated to users by satellite and terrestrial links. Raw data are stored in a permanent playback archive, on optical disks, at the central site. Author (ESA)

N82-21699# Logica Ltd., London (England).
INTERPRETATION OF REMOTELY SENSED IMAGE DATA AND IMPACT OF CLUSTER COMPRESSION
David J. Stanley Paris ESA Feb. 1981 154 p refs
(Contract ESA-3749/78/NL-HP)
(Rept-44.2866; ESA-CR(P)-1450) Avail: NTIS HC A08/MF A01

Image interpretation techniques are described and related to the needs of application areas. A survey of users and literature shows (1) little correlation between processing techniques and specific applications; (2) most users employ general purpose image analysis algorithms rather than developing special purpose techniques; (3) interpretation methodology frequently involves the use of several preprocessing, enhancement, and classification methods; (4) the majority of operational applications rely on manual photointerpretation, and (5) most digital image interpretation is done with general purpose software packages and/or special hard-wired image analysis systems. Operational users, (a minority), rely heavily on human photointerpretation, especially in geology, and at most use simple linear classifiers or enhancement techniques on interactive image processing systems. The impact of compression is limited because of academic and research user hostility, and decreasing cost of machine processing. Author (ESA)

N82-21700# European Space Agency, Paris (France).
ATLAS OF METEOSAT IMAGERY
C. A. Brimacombe (ESOC) May 1981 494 p refs In ENGLISH and FRENCH Original contains color illustrations
(ESA-SP-1030; ISSN-0379-6566) Avail: NTIS HC A21/MF A01; ESA, Paris FF 200 Member States, AU, CN, and NO (+20% others)

A selection of the images received from METEOSAT during its first two years of operation is presented. The METEOSAT system is described and characteristics of images as well as image processing are explained. Imagery is examined as to cloud classification, surface features, and mesoscale cloud formations. Synoptic scale cloud patterns, planetary scale cloud systems, and details of tropical cloud systems are also discussed. Miscellaneous aspects of satellite meteorology are included. Author (ESA)

08
INSTRUMENTATION AND SENSORS

Includes data acquisition and camera systems and remote sensors.

A82-21022 **Thermal viewing system for studying the earth's resources.** V. V. Perlov, D. N. Krasnikov, V. P. Sergeev, B. V. Ukhov, and G. I. Iasinskii. *(Optiko-Mekhanicheskaia Promyshlennost', vol. 48, Apr. 1981, p. 27-29.) Soviet Journal of Optical Technology*, vol. 48, Apr. 1981, p. 213-215. 5 refs. Translation.

The paper presents the Vulkan airborne thermal viewing system for remote studies of earth's resources, which operates simultaneously in two spectral bands of 3.8-5.2 microns. The construction and circuit features of the thermal viewer are examined, and further improvements for studying natural resources involving simultaneous radiometric measurements in several spectral channels are discussed.
D.L.G.

A82-21027 * **Sigma/deg/ signature of the Amazon rain forest obtained from the Seasat scatterometer.** I. J. Birrer, G. Berthold (University of Kansas Center for Research, Inc., Lawrence, KS), E. M. Bracalente (NASA, Langley Research Center, Hampton, VA), G. J. Dome (Bell Telephone Laboratories, Inc., Holmdel, NJ), and J. Sweet (Kentron Corp., Hampton, VA). *IEEE Transactions on Geoscience and Remote Sensing*, vol. GE-20, Jan. 1982, p. 11-17.

Scatterometer data from Seasat of the Amazon rain forest were examined to determine if the region is suitable to use as a reference for calibration of radars. The consistency of Skylab data viewing the Amazon region prompted the analyses, and the Seasat-A scatterometer system (SASS) gathered data of the same region at varying angles. The instrument employed a 100 W 14.6 GHz signal with the reflected power sampled 61 times during each 1.89 sec measurement period. Doppler filters were used in 15 parallel channels of reception, and represented areas 20 km by 50-70 km. Tests were made of regional and temporal stability of the Amazon area, with five measurement angles averaged at different incidence angles to find the mean deviation, which was found to be less than 0.5 dB. Diurnal effects were confined to early morning, and further tests are recommended to obtain results for an entire year, to develop screening methods for thick clouds and rain, and to determine the deviation more precisely.
M.S.K.

A82-21034 **Theoretical and experimental studies of microwave emission signatures of snow.** M. E. Tiuri (Helsinki University of Technology, Esbo, Finland). *IEEE Transactions on Geoscience and Remote Sensing*, vol. GE-20, Jan. 1982, p. 51-57. 11 refs.

Theoretical and experimental studies of the brightness temperature of snow are reported. A snow model was devised, with the dielectric constant for snow determined from the dielectric properties of ice and water. The equivalent scattering particle dielectric constant was calculated from the dielectric constant of snow, and the theory was expanded to consider different homogeneous layers. Radiometric readings at 4.8, 11.6, and 36.8 GHz were taken from a seven meter high tower in a snow field. The brightness temperature decreased rapidly with increasing frequencies, and the brightness temperature of snow covered land was found to be higher in cold weather than that of bare land.
M.S.K.

A82-21035 **Towards the definition of optimum sensor specifications for microwave remote sensing of snow.** C. Mätzler, E. Schanda (Bern, Universität, Berne, Switzerland), and W. Good (Eidgenössisches Institut für Schnee- und Lawinenforschung, Davos, Switzerland). *IEEE Transactions on Geoscience and Remote Sensing*, vol. GE-20, Jan. 1982, p. 57-66. 20 refs.

The inconsistencies in the relationships between microwave data and the water equivalent of the snowcover, and the disappearance of the contrast between snow and snow-free regions when the snow is wet were studied. A relationship between the water equivalent of a dry snow layer and the brightness temperature is discussed in terms of a complete set of snow radiometry data at 4.9, 10.4, 21, and 36 GHz. The combined effects of volume scattering on large crystals is shown to be a function of the water equivalent, which is determined from knowledge of the state of metamorphism. A strong decrease of the reflected wavelengths was found to be due to snow wetness, especially at higher frequencies. Multivariate data analysis was employed to analyze the data set to find the respective discriminant powers in splitting the ground-truth data-points of the changing snow cover.
M.S.K.

A82-21082 **Observation of the turbulent structure in the planetary boundary layer with a kytoon-mounted ultrasonic anemometer system.** Y. Ogawa (National Institute for Environmental Studies, Yatabe, Ibaraki, Japan) and T. Ohara (Hokkaido University, Sapporo, Japan). *Boundary-Layer Meteorology*, vol. 22, Jan. 1982, p. 123-131.

The development of a small, lightweight ultrasonic kytoon-mounted anemometer system for transmitting windspeed, momentum, and heat flux data to the ground in digital form by means of optical fibers is reported. The 70 cu m kytoon can lift 20-30 kg, and the weight of the instruments is 10 kg, with an optic fiber 1500 m long capable of carrying one megabyte/sec at 18 cycles/sec on 16 channels. Numerical filters are used to eliminate artificial velocities induced by swinging motion of the sensors, with calibration achieved in wind tunnel studies. Experimental data were gathered at heights of 50, 100, 200, 300, 400, 500, and 700 m, and the standard deviations for the u, v, and w components were found to stabilize at 400 m, and increase with decreasing height below that level. The kytoon-mounted system is suitable for operation in winds below 10 m/sec.
M.S.K.

A82-21090 **Image quality control in the Meteosat ground processing system.** M. Jones and N. C. Colombeski (ESA, European Space Research Operations Centre, Darmstadt, West Germany). *International Journal of Remote Sensing*, vol. 2, Oct.-Dec. 1981, p. 331-349. 11 refs.

The approach taken to image quality control in the European Space Agency's Meteosat project is discussed. User requirements, to both instrumental and physical accuracy, on the quality of the meteorological end-products and on the image quality are presented, and the effect of a deterioration in image quality on budget errors is discussed. Methods for evaluating image quality are described, and the implementation of these methods within the Meteosat Ground Computer System is reviewed. It is concluded, that the proper hardware and software must be provided to monitor the quality indicators and to allow for an adequate level of manning. This includes interactive displays permitting near real-time display of image data and key parameters, and facilities for a longer-term view of the evolution of the quality parameters. Image quality control should also be closely coupled with mission control. The radiometric and geometric quality from the F1-model of Meteosat is described as an example.
J.F.

A82-21091 **Effects of the atmosphere on the detection of surface changes from Landsat multispectral scanner data.** J. Otterman (U.S. Geological Survey, Reston, VA; Tel Aviv University, Tel Aviv, Israel) and C. J. Robinove (U.S. Geological Survey, Reston, VA). *International Journal of Remote Sensing*, vol. 2, Oct.-Dec. 1981, p. 351-360.

The atmospheric effects of radiometric data recorded in the Landsat multispectral scanner system bands are compiled for cases of representative and ideal atmospheric conditions. These effects are expressed as a difference between the actual spectral reflectivity measured close to the ground and the surface-atmosphere system reflectivity to zenith, derived from satellite data. The resulting formula includes two optical thickness parameters for backscattering and absorption as well as a function for the anisotropy of backscattering from the direct beam to the zenith. The expression is accurate only for an atmosphere of low optical thickness and large areas of uniform reflectivity. It is concluded that in the quantitative monitoring of surface changes from satellites, scattering effects will predominate in some cases (mapping coastal waters), while absorption effects will predominate in others (desert fringe regions). The measurements used for monitoring scattering effects are also shown to differ from those for monitoring absorption effects.
J.F.

A82-21399 **Analysis of the direction-dependent radiation behavior in multispectral scanning data (Untersuchung des richtungs-**

abhängigen Strahlungsverhaltens in multispektralen Abtastdaten). B. Pfeiffer (Karlsruhe, Universität, Karlsruhe, West Germany). *Bildmessung und Luftbildwesen,* vol. 50, Jan. 1, 1982, p. 35-47. 7 refs. In German.

The direction-dependent radiation behavior of several natural objects is analyzed, based on multispectral scanning data from a number of different flight altitudes. Results show a significant change in brightness with view angle and wavelength, and a comparison with atmospheric model calculations shows that the increase in directional behavior is caused more by the object itself than by the atmosphere. The position of the sun seemed to have a greater effect in changing the object-reflected signal than did height. The direction-dependence could not be corrected for all classes of objects and wavelengths due to variations in brightness as well as object-dependent color shifts. The application of a modified classification procedure by use of a direction dependent statistic greatly improved the results. J.F.

A82-21434 **Recent auroral measurements using a field-widened interferometer spectrometer.** A. J. Steed, D. J. Baker, B. Y. Bartschi (Utah State University of Agriculture and Applied Science, Logan, UT), and A. T. Stair, Jr. (USAF, Geophysics Laboratory, Bedford, MA). In: International Conference on Fourier Transform Infrared Spectroscopy, Columbia, SC, June 8-12, 1981, Proceedings. Bellingham, WA, Society of Photo-Optical Instrumentation Engineers, 1981, p. 202-205. 9 refs. USAF-sponsored research.

Questions regarding the evolution of field-widened interferometer (FWI) instruments are briefly considered. The first FWI instrument was designed for visible and near IR applications. In response to the need for a faster drive system for auroral work, a second generation instrument using a gas-lubricated bearing was developed in 1973. A description is presented of the field operating configuration of the second generation system, taking into account also recent auroral results. A third generation rocket-borne version of this instrument has been developed by Haycock et al. (1979). A presented graph shows one 40 second spectral scan of an auroral arc taken with the second generation FWI instrument in Andoya, Norway, on November 11, 1980. The instrument was pointed at the zenith, and a separate dual channel radiometer was co-aligned with the interferometer to provide long-term OH and O2 emission levels. G.R.

A82-22140 **Accuracy of the normal case of close-range photogrammetry.** Y. I. Abdel-Aziz (University of Petroleum and Minerals, Dhahran, Saudi Arabia). *Photogrammetric Engineering and Remote Sensing,* vol. 48, Feb. 1982, p. 207-213. 5 refs.

The photogrammetric technique is used for the three-dimensional recording of historical monuments. In connection with the recording operation, certain problems have to be solved concerning the establishment of the optimum location of the camera relative to the monument. So far, there have been no satisfactory formulas for the determination of the optimum positions of the two camera stations. The main objective of the considered investigation is related to the development of formulas which will make it possible to determine the object accuracy, for any camera setup, right in the field. The new formulas developed express the accuracy of the ground points as a function of the four parameters of external orientation. A description is provided of mathematical and experimental proofs regarding the correctness of the new formulas. G.R.

A82-22141 **Calibration and model reconstruction in analytical close-range stereophotogrammetry. II - Special evaluation procedures for rasterstereography and moiré topography.** W. Frobin and E. Hierholzer (Orthopädische Universitätsklinik, Münster, West Germany). *Photogrammetric Engineering and Remote Sensing,* vol. 48, Feb. 1982, p. 215-220. 8 refs. Research supported by the Deutsche Forschungsgemeinschaft.

It is pointed out that, in the case of rasterstereography and moiré topography, special provisions have to be made when standard photogrammetric procedures are employed. Rasterstereography is a modification of conventional stereophotography, in which one of the two cameras has been replaced by a projector with a regular (cross) raster diapositive. The raster lines are projected onto the surface to be measured and are photographed by the camera. The calibration of a rasterstereographic apparatus is discussed. In cross rasterstereography, there is an overdeterminancy regarding the reconstruction of the surface point. Either vertical or horizontal raster lines may be omitted. Special procedures employed in line rasterstereography are considered. Problems related to the use of moiré topography are also investigated, taking into account the projection method and the shadow method. G.R.

A82-22148 **Satellite photos can aid navigation on aerial photo missions.** R. J. Myhre (U.S. Forest Service, Fort Collins, CO). *Photogrammetric Engineering and Remote Sensing,* vol. 48, Feb. 1982, p. 275-279.

Accurate navigation is important to the success of aerial photo missions. The accuracy of the navigation on these missions depends on the amount of useful information available on the flight maps or photos. If satisfactory maps or aerial photos are not available, current satellite imagery (Landsat photos) can be enlarged for use as navigational aids. This technique has been tested and proven successful on operational aerial photography missions. Aspects of photo mission planning are considered, taking into account aerial photo coverage and satellite photo coverage. Attention is also given to questions regarding Landsat imagery and the two methods employed to enlarge the Landsat image to the desired scale. It is found to be important to select a satellite image which represents the time frame of the anticipated aerial photo mission. G.R.

A82-22397 † **Spaceborne photography for the study of earth resources (Kosmicheskaia fotos'emka dlia izucheniia prirodnykh resursov).** G. B. Bonin. Leningrad, Izdatel'stvo Nedra, 1980. 320 p. 564 refs. In Russian.

Various theoretical and practical aspects of spaceborne photography in the study of earth resources are reviewed, including problems of photogrammetric image processing. Particular consideration is given to the attitude control and stabilization of remote-sensing satellites; the effect of the atmosphere on the quality and photometric properties of the photographs; subsatellite experiments; and external-orientation elements of space imagery. Photogrammetric measurements on the basis of single images, the transformation of images, and elements of scanner photogrammetry are also discussed. B.J.

A82-22877 * **Microwave remote sensing: Active and passive. Volume 1 - Microwave remote sensing fundamentals and radiometry.** F. T. Ulaby, R. K. Moore, and A. K. Fung (Kansas, University, Lawrence, KS). Research supported by NASA, NSF, and DOD. Reading, MA, Addison-Wesley Publishing Co. (Remote Sensing, No. 2), 1981. 470 p. 267 refs. $46.50.

The three components of microwave remote sensing (sensor-scene interaction, sensor design, and measurement techniques), and the applications to geoscience are examined. The history of active and passive microwave sensing is reviewed, along with fundamental principles of electromagnetic wave propagation, antennas, and microwave interaction with atmospheric constituents. Radiometric concepts are reviewed, particularly for measurement problems for atmospheric and terrestrial sources of natural radiation. Particular attention is given to the emission by atmospheric gases, clouds, and rain as described by the radiative transfer function. Finally, the operation and performance characteristics of radiometer receivers are discussed, particularly for measurement precision, calibration techniques, and imaging considerations. M.S.K.

A82-23045 * **Superconducting tensor gravity gradiometer.** H. J. Paik (Maryland, University, College Park, MD). *(International Symposium on Inertial Technology for Surveying and Geodesy, 2nd, Banff, Alberta, Canada, June 1-5, 1981.) Bulletin Géodésique,* vol. 55, no. 4, 1981, p. 370-381. 12 refs. Contract No. NAS8-33822.

The employment of superconductivity and other material properties at cryogenic temperatures to fabricate sensitive, low-drift, gravity gradiometer is described. The device yields a reduction of noise of four orders of magnitude over room temperature gradiometers, and direct summation and subtraction of signals from accelerometers in varying orientations are possible with superconducting circuitry. Additional circuits permit determination of the linear and angular acceleration vectors independent of the measurement of the gravity gradient tensor. A dewar flask capable of maintaining helium in a liquid state for a year's duration is under development by NASA, and a superconducting tensor gravity gradiometer for the NASA Geodynamics Program is intended for a LEO polar trajectory to measure the harmonic expansion coefficients of the earth's gravity field up to order 300. M.S.K.

A82-24964 **Thermal infrared data from the Heat Capacity Mapping Mission.** *Remote Sensing of Environment,* vol. 11, Mar. 1981, p. 77-79.

The Heat Capacity Mapping Mission (HCMM) satellite, launched on April 26, 1978, was designed to experimentally evaluate the usefulness of remotely sensed surface temperature measurements for applications in geology, botany, ecology, hydrology and meteorology. The orbital characteristics of the satellite permit repetitive observations of midlatitude regions over the course of the diurnal heating cycle. This type of coverage is optimal for observing the temporal and spatial thermal contrasts within surface materials. HCMM thermal IR measurements can also be used to estimate the apparent thermal inertia of surface cover materials. A nighttime thermal IR image of Utah is examined. O.C.

A82-25460 **Satellite photograph interpretation.** C. Peebles. *Spaceflight,* vol. 24, Apr. 1982, p. 161-163. 10 refs.

The instrumentation and interpretation of satellite earth surface reconnaissance data are outlined. IR scanners, multispectral photo systems, and digitally returned optical sensor information are soon to be augmented by imaging radar and continuation of the use of the Big Bird satellites for high resolution photographic imaging. The photographs are sometimes scanned visually by using a 60% overlap to provide a stereo view and gain depth information on the observed scene. Human photointerpreters are mentioned as having an encyclopedic knowledge of particular areas of scanning, enabling immediate detection and educated guessing at the function of any change in a repeatedly monitored scene. Comparative covers is a process of historically referencing updated photos to determine increases or decreases in use of areas, or precise visual steps of weapons assembly. M.S.K.

A82-26000 # **Ideal phase in estimating the spatial gradient of magnetic daily variations recorded by magnetometer arrays.** F. E. M. Lilley and M. N. Sloane (Australian National University, Canberra, Australia). *Journal of Geomagnetism and Geoelectricity,* vol. 33, no. 9, 1981, p. 517-525. 14 refs.

A82-26049 **Evaluation of serial photogrammetric camera and aircraft scanner pictures from tidal lands - Digital correlation and classification of multitemporal imagery data (Auswertung von Reihenmesskammer- und Flugzeugabtasteraufnahmen aus Wattgebieten - Digitale Korrelation und Klassifizierung multitemporaler Bilddaten).** E. Dennert-Möller and M. Ehlers (Hannover, Universität, Hanover, West Germany). *Bildmessung und Luftbildwesen,* vol. 50, Mar. 1, 1982, p. 59-67. 14 refs. In German.

It has been found that large-scale aerial photographs are particularly suited for the study of the special conditions of the tidal lands at the German coast of the North Sea. Procedures of digital correlation make it possible to establish, for a comparison, relations between imagery obtained with various sensors at different scales and at different times. In the present investigation, photographs obtained with serial photogrammetric cameras, and aircraft scanner imagery are, after image correction, classified on an individual basis, and are compared with each other. A multitemporal picture is finally obtained and classified. The required digital processing operations are performed by making use of interactive image processing equipment and a Cyber 76-14 computer. G.R.

A82-26963 **Radiometric calibration of the Coastal Zone Color Scanner on Nimbus 7 - A proposed adjustment.** M. Viollier (Lille I, Université, Villeneuve d'Ascq, Nord, France). *Applied Optics,* vol. 21, Mar. 15, 1982, p. 1142-1145. 12 refs. Research supported by the Centre National d'Etudes Spatiales and Ministère de l'Environnement et du Cadre de Vie.

In conjunction with atmospheric effect computations, ground measurements of water reflectances for two very clear days are compared with Coastal Zone Color Scanner satellite data to point out scanner calibration errors. A new set of calibration constants is proposed which standardizes radiances relative to the extraterrestrial solar irradiance. It is emphasized that the suggested modification is theoretically valid only for the June and July, 1979 period of study alone, and for the corresponding electronic gain. It is expected that similar calibration error trends exist for the other gains and periods. O.C.

A82-27576 * **International Symposium on Remote Sensing of Environment, 15th, University of Michigan, Ann Arbor, MI, May 11-15, 1981, Proceedings. Volumes 1, 2 & 3.** Symposium sponsored by the Environmental Research Institute of Michigan, NOAA, NASA, et al. Ann Arbor, MI, Environmental Research Institute of Michigan, 1981. Vol. 1, 570 p.; vol. 2, 568 p.; vol. 3, 493 p. Price of three volumes, $88.

Developments related to advanced sensors and sensor systems are being examined, taking into account advanced aerospace remote sensing systems for global resource applications, spaceborne radar observation of the earth surface, a concept for an advanced earth resources satellite system, technologies for the multispectral mapping of earth resources, and the use of Landsat images and morphologic analogs in space exploration. Other topics discussed are related to modeling for terrain analysis, digital processing and analysis of remotely sensed data, microwave remote sensing, new discoveries from planetary remote sensing, and data base utilization. Advances in the area of luminescence are also considered along with future plans and prospects concerning the remote sensing of the earth from space. G.R.

A82-27577 * # **Advanced aerospace remote sensing systems for global resource applications.** J. V. Taranik (NASA, Office of Space and Terrestrial Applications, Washington, DC). In: International Symposium on Remote Sensing of Environment, 15th, Ann Arbor, MI, May 11-15, 1981, Proceedings. Volume 1. Ann Arbor, MI, Environmental Research Institute of Michigan, 1981, p. 3-20. 8 refs.

The Landsat program, which was concerned with testing the use of satellite data for global resource observations, has been an unqualified success, and users of Landsat data demand now that repetitive global multispectral data be provided on a routine basis for a wide variety of applications. A review is provided of the current status of NASA's land observation program, new developments in advanced aerospace remote sensing techniques, and issues related to the development and testing of new prototype systems by the U.S. The current Landsat program is considered along with developments in solid-state imaging technology, short wave infrared research using the Space Shuttle, the Shuttle Orbiter camera payload system large format camera, and advanced research in thermal remote sensing. Attention is also given to the potential of imaging radar for global resource observations, and research related to geopotential field mapping. G.R.

A82-27578 * # **Spaceborne radar observation of the earth surface.** C. Elachi (California Institute of Technology, Jet Propulsion Laboratory, Pasadena, CA). In: International Symposium on Remote Sensing of Environment, 15th, Ann Arbor, MI, May 11-15, 1981, Proceedings. Volume 1. Ann Arbor, MI, Environmental Research Institute of Michigan, 1981, p. 21-31. 9 refs. Contract No. NAS7-100.

Seasat SAR images are being analyzed to determine the potential of spaceborne radars for earth resources and ocean surface observation. Examples are presented for a variety of applications in structural mapping, lithological classification, soil moisture detection, polar ice motion monitoring and ocean features observation. These examples are briefly discussed with emphasis on the future research needed to further the capability of radar sensors, by themselves or in combination with other sensors. A brief discussion is then given on the spaceborne sensors which are required and planned to meet these needs. (Author)

A82-27579 # **A concept for an advanced earth resources satellite system.** G. T. Keene (Eastman Kodak Co., Rochester, NY). In: International Symposium on Remote Sensing of Environment, 15th, Ann Arbor, MI, May 11-15, 1981, Proceedings. Volume 1. Ann Arbor, MI, Environmental Research Institute of Michigan, 1981, p. 33-44. 5 refs.

Attention is given to a study concerned with the definition of a concept for an advanced sensor system to follow the Landsat D series. In this project NASA sought maximum operational reliability and minimum development risk by use of proven mechanisms and available technology, taking into account an employment of visible (VIS), shortwave infrared (SWIR), and thermal infrared (TIR) spectral bands. The TIR section was to be an optional modular unit, and all focal planes would utilize the inherent registration of solid state linear arrays with no moving parts while imaging, and passive thermal control. Attention is given to optics, detectors, thermal control, performance estimates, and recent modifications. G.R.

A82-27580 * # **Technologies for the multispectral mapping of earth resources.** J. B. Wellman (California Institute of Technology, Jet Propulsion Laboratory, Pasadena, CA). In: International Symposium on Remote Sensing of Environment, 15th, Ann Arbor, MI, May 11-15, 1981, Proceedings. Volume 1. Ann Arbor, MI, Environmental Research Institute of Michigan, 1981, p. 45-64. 16 refs. Contract No. NAS7-100.

The application of solid-state detector array imaging to the remote sensing of the earth as a follow-on to currently planned Landsat missions provides the opportunity to achieve significantly increased performance. First-order advantages to be anticipated are higher sensitivity resulting in greater radiometric accuracies and improved geometric fidelity. The Multispectral Mapper design concept is responsive to a broad range of user needs by incorporating in-flight selection of spectral bands, instantaneous fields of view, and swath width. This versatility is achieved by the use of an imaging spectrometer which permits both spatial and spectral sampling in the image plane using area array detectors. Other improvements over the current Landsat multispectral scanner and Thematic Mapper include higher spatial resolution and inherently precise registration of the spectral bands. The key technologies required in order to realize these improvements include short-wavelength infrared detectors, wide field of view, broad spectral coverage optics, focal plane cooling, and high-speed onboard signal processing. Significant development activities will be required if an advanced remote sensing capability is to be implemented. (Author)

A82-27581 # **Mapsat compared to other earth-sensing concepts.** A. P. Colvocoresses (U.S. Geological Survey, Reston, VA). In: International Symposium on Remote Sensing of Environment, 15th, Ann Arbor, MI, May 11-15, 1981, Proceedings. Volume 1. Ann Arbor, MI, Environmental Research Institute of Michigan, 1981, p. 65-72. 10 refs.

The acceptance and use of Landsat products clearly indicates that there is a need for a truly operational earth-sensing system. In December 1980 NASA issued a request for proposal of an MLA (multispectral linear array) Instrument Definition Study. The MLA study calls for two 'short-wave' infrared bands (1.55 to 1.75 micrometers and 2.08 to 2.35 micrometers). However, in connection with cost and complexity problems, it appears unlikely that these bands will be utilized on any operational system during the 1980's. The characteristics of available systems for imaging the earth are discussed. Attention is given to Mapsat which is the result of an effort to define an operational earth-sensing system. Mapsat is based on Landsat technology and will provide global coverage on a continuous basis. Aspects of mapping geometry are considered along with questions of resolution and data transmission, spectral bands, stereoscopic capability, and one-dimensional data processing. G.R.

A82-27583 * # **Information expectations from Landsat-D.** V. V. Salomonson, D. L. Williams, and J. L. Barker (NASA, Goddard Space Flight Center, Applications Directorate, Greenbelt, MD). In: International Symposium on Remote Sensing of Environment, 15th, Ann Arbor, MI, May 11-15, 1981, Proceedings. Volume 1. Ann Arbor, MI, Environmental Research Institute of Michigan, 1981, p. 81-93. 5 refs.

The first satellite of the Landsat-D Project is to be launched in the third quarter of 1982 with a second satellite to be prepared for launch 12 to 15 months later. Both spacecraft are to include the familiar Multispectral Scanner (MSS) and the advanced multispectral scanner called the Thematic Mapper (TM). The ground data processing system for the MSS data is to be ready to produce 200 scenes a day in 1982. The data processing systems for the TM are to be fully operational at the 50 to 100 scenes a day level in early 1985. The fabrication of the system components has proceeded well in recent months, and integration of the total system is under way. The procedures for processing the data and meeting specifications are nearly completed for the MSS and are outlined in detail for the TM. An outline of an investigation program stressing systems performance has been developed for the period 1982 to 1985. (Author)

A82-27589 # **Overview of digital processing of SAR data.** J. P. Guignard (ESA, Data Handling and Signal Processing Div., Noordwijk, Netherlands). In: International Symposium on Remote Sensing of Environment, 15th, Ann Arbor, MI, May 11-15, 1981, Proceedings. Volume 1. Ann Arbor, MI, Environmental Research Institute of Michigan, 1981, p. 179-194. 18 refs.

It is pointed out that before the launch of the Seasat-A spacecraft, the processing of synthetic aperture radar (SAR) data was mainly performed using optical correlators. Seasat offered the first opportunity to develop digital SAR processors. An overview is provided of the Seasat-A SAR digital processors, taking into account the MDA configuration, Communication Research Center processing, the RAE processor, the DFVLR-GSOC processor, the JPL processor, the Bendix SAR processor, the CCRS processors, the Mitsubishi Seasat processor, the Norway Defense Research Establishment processor, and the Nippon Electric Company processor. Attention is also given to algorithms, image quality experiments, and a number of new developments. G.R.

A82-27591 # **The logit classifier - A general maximum likelihood discriminant for remote sensing applications.** P. F. Maynard and A. H. Strahler (California, University, Santa Barbara, CA). In: International Symposium on Remote Sensing of Environment, 15th, Ann Arbor, MI, May 11-15, 1981, Proceedings. Volume 1. Ann Arbor, MI, Environmental Research Institute of Michigan, 1981, p. 213-222. 17 refs.

The most commonly used discriminant function in remote sensing applications is the Bayes maximum likelihood classifier (Bayes MLC). However, in an evaluation study it is found that Bayes MLC with parametric estimation of the probability density functions is not an optimal classifier for many remote sensing applications. It is pointed out that there are several statistically acceptable techniques for classifying nominal data such as the probit, logit, and arctan. However, the logit model has computational advantages since it is a closed (explicit) functional form with convenient curvature properties for numerical optimization. An investigation shows that the logit classifier is both theoretically and experimentally superior to the Bayes MLC with the simulated data and the Landsat Multispectral Scanner System (MSS) data employed in the study. G.R.

A82-27594 * # **Simulation and studies of spaceborne synthetic aperture radar image quality with reduced bit rate.** F. Li, D. Held, B. Huneycutt, and H. Zebker (California Institute of Technology, Jet Propulsion Laboratory, Pasadena, CA). In: International Symposium on Remote Sensing of Environment, 15th, Ann Arbor, MI, May 11-15, 1981, Proceedings. Volume 1. Ann Arbor, MI, Environmental Research Institute of Michigan, 1981, p. 259-270. 18 refs. Contract No. NAS7-100.

A computer simulation program that is used to study the effects of digitization in spaceborne synthetic aperture radar systems is described. An analytical study of the distortion noise introduced by the digitization process at various gain settings, sampling rates and bit error rates is presented and the results agree well with those obtained from the simulation program. The simulation program is also used to study the spatial frequency response of hard-limiting (quantizing to 1-bit) synthetic aperture radar systems. The implications of these results on synthetic aperture radar system design are discussed. (Author)

A82-27595 # **Features of a generalized digital Synthetic Aperture Radar processor.** J. R. Bennett, I. G. Cumming, P. R. McConnell, and L. Gutteridge (MacDonald, Dettwiler and Associates, Ltd., Richmond, British Columbia, Canada). In: International Symposium on Remote Sensing of Environment, 15th, Ann Arbor, MI, May 11-15, 1981, Proceedings. Volume 1. Ann Arbor, MI, Environmental Research Institute of Michigan, 1981, p. 271-290.

A summary of the planned or proposed international Synthetic

Aperture Radar (SAR) activity for the next decade is provided in a table. A large number of primarily Shuttle-based experimental missions carrying SARs are being considered. In terms of SAR processing requirements, this activity translates into a need for modest throughput, highly flexible processors. The required processors will have to be adaptable to SARs of different pulse coding schemes, frequency, antenna length (beam width), swath width, depression angle, altitude, squint angle, polarization, and data rates. Experimental flexibility will be required to process the data from a given SAR configuration in a variety of different ways, taking into account resolution, multilooks, and multisubapertures. A description is presented of a digital processor designed to service the needs of this projected SAR activity. G.R.

A82-27606 # **The Japanese MOS and Los program.** Y. Ishizawa (National Space Development Agency of Japan, Tokyo, Japan). In: International Symposium on Remote Sensing of Environment, 15th, Ann Arbor, MI, May 11-15, 1981, Proceedings. Volume 1. Ann Arbor, MI, Environmental Research Institute of Michigan, 1981, p. 433-443.

The status of the Japanese Earth Observation Satellite Program and sensor development program is reviewd, with emphasis on the Marine Observation Satellite-1 (MOS-1) to be launched in 1985. Mission objectives of the MOS-1 program are outlined, and the satellite and radiometers are described. Three sensors to be mounted on the satellite are presented, which are to observe visible, near visible, near infrared, infrared, and microwave regions. The MOS-1 is a three-axis stabilized satellite with a cubic body on which the three sensors and bus equipment are mounted. The overall height, including antennas, is about 300 cm, with a length and width of about 146 and 126 cm, respectively. D.L.G.

A82-27628 # **Implementation of the Space Oblique Mercator projection in a production environment.** J. Brooks, R. Kumar, and I. Levine (General Electric Co., Space Div., Lanham, MD). In: International Symposium on Remote Sensing of Environment, 15th, Ann Arbor, MI, May 11-15, 1981, Proceedings. Volume 2. Ann Arbor, MI, Environmental Research Institute of Michigan, 1981, p. 671-679. 5 refs.

The Space Oblique Mercator (SOM) projection, first considered by Colvocoresses (1974) is the first known map projection to provide continuous conformal mapping of satellite imagery true to scale along ground track, and accurate to within a few parts in a million. Although SOM was specifically designed for Landsat Imagery, it is also suitable for other near polar satellites. Snyder (1978) obtained a full mathematical derivation of the projection and developed a computer program for it (Snyder's Code). The present investigation has the objective to show that it is possible to incorporate the Snyder code output into Landsat-D Multispectral Scanner System (MSS) processing by means of mostly offline calculations. G.R.

A82-27633 # **Spectritek - A multispectral electron-optic pushbroom camera.** R. F. Lucy (Itek Corp., Optical Systems Div., Lexington, MA). In: International Symposium on Remote Sensing of Environment, 15th, Ann Arbor, MI, May 11-15, 1981, Proceedings. Volume 2. Ann Arbor, MI, Environmental Research Institute of Michigan, 1981, p. 715-720.

Spectritek is an electro-optic aircraft camera concept designed to provide multispectral imagery for earth resources exploration. The silicon CCD focal plane arrays provide registered imagery in three Landsat color bands. The camera sensitivity meets Landsat-MLA requirements. The data collected is recorded on magnetic tape. After ground processing and calibration the data is stored in a low-cost storage medium for use by earth resources investigators. The camera system provides the wide area coverage of a satellite sensor and the high resolution of an aircraft sensor. Spectritek complements a companion large format stereo film camera (Metritek). Another advantage of the aircraft approach is its ability to update data files rapidly and economically. (Author)

A82-27638 # **Locating prehistoric archaeological sites using Landsat.** I. Wells, J. Custer, and V. Klemas (Delaware, University, Newark, DE). In: International Symposium on Remote Sensing of Environment, 15th, Ann Arbor, MI, May 11-15, 1981, Proceedings. Volume 2. Ann Arbor, MI, Environmental Research Institute of Michigan, 1981, p. 771-780. 29 refs. Research supported by the Bureau of Archaeology and Historic Preservation of the State of Delaware.

It has been suggested that computer statistical techniques using Landsat digital imagery classifications can be applied over large areas and a large number of sites to locate areas that have a high probability of containing prehistoric sites. To test this hypothesis, an experiment has been performed on a selected area along the Appoquinimink River in New Castle County, Delaware. The results of the experiment suggest that Landsat data combined possibly with digital terrain data can provide the necessary consistent synoptic analysis of the landscape. B.J.

A82-27642 # **Passive bathymetric measurements in the Bruce Peninsula region of Ontario.** W. C. Weidmark, S. C. Jain (Moniteq, Ltd., Concord, Ontario, Canada), H. H. Zwick (Canada Centre for Remote Sensing, Ottawa, Canada), and J. R. Miller (York University, Downsview, Ontario, Canada). In: International Symposium on Remote Sensing of Environment, 15th, Ann Arbor, MI, May 11-15, 1981, Proceedings. Volume 2. Ann Arbor, MI, Environmental Research Institute of Michigan, 1981, p. 811-822. 12 refs. Research supported by the Canada Centre for Remote Sensing; Department of Supply and Services Contract No. OSQ-80-00097.

Airborne MSS measurements in the 400-1000 nm wavelength range were performed in the summer of 1980 over the Bruce Peninsula in order to evaluate techniques of computing water depth from MSS imagery. The spectral volume reflectance maps were processed using radiative transfer models to interpret the image in terms of water depth. Theoretical modelling shows that the modification of Hulbert's formulation of the two-flow model to include asymmetric attenuation of upwelling and downwelling radiation results in reflectance values which express accurately the exact Monte Carlo calculations. A value of asymmetry factor can be chosen for any scattering albedo and backscatter probability to ensure a good fit of the two-flow model results to the Monte Carlo calculations. B.J.

A82-27648 # **Utilization of spatial complexity in computer classified Landsat MSS data for multi-factoral thematic mapping.** J. W. Merchant (Kansas, University, Lawrence, KS). In: International Symposium on Remote Sensing of Environment, 15th, Ann Arbor, MI, May 11-15, 1981, Proceedings. Volume 2. Ann Arbor, MI, Environmental Research Institute of Michigan, 1981, p. 905-914. 32 refs.

Graphic displays of classified Landsat MSS data commonly exhibit substantial variations in the degree to which pixels of various cover types are fragmented, aggregated and interspersed within a scene. The nature of the spatial distribution of classified pixels, or 'spatial complexity', in a scene is discussed. The components of cover frequency, cover diversity and cover composition are defined and are employed to measure spatial complexity. Regions of similar spatial complexity are delimited in a Kansas test site and are found to be associated with independently defined multi-factoral landscape regions. Such multi-factoral regions are characterized by integrated complexes of physical and cultural phenomena. Potential applications of research results are considered. (Author)

A82-27649 # **Development and implementation of a low cost micro computer system for Landsat analysis and geographic data base application.** N. L. Faust, L. E. Jordon, III, and M. D. Furman (ERDAS, Inc., Atlanta, GA). In: International Symposium on Remote Sensing of Environment, 15th, Ann Arbor, MI, May 11-15, 1981, Proceedings. Volume 2. Ann Arbor, MI, Environmental Research Institute of Michigan, 1981, p. 915-917.

This paper addresses some of the issues involved in the design and operational use of a low-cost image processing system based on recent advances in micro-computer technology. Also discussed are the integration on the micro system of Landsat image processing and GIS capabilities, with an overview of existing software capabilities such as false color display, training field selection, geometric correction, and both supervised and unsupervised (cluster) classification. Considerations for the use of the system by 'non-computer types' provide the basis for a menu-selection approach using simple keywords. Future directions in the development of the micro system are also mentioned. (Author)

08 INSTRUMENTATION AND SENSORS

A82-27652 # **Instrumentation for remote reflectance and radiance measurements.** L. Daubner, J. Davies, R. Dick, and S. M. Till (Barringer Research, Ltd., Toronto, Canada). In: International Symposium on Remote Sensing of Environment, 15th, Ann Arbor, MI, May 11-15, 1981, Proceedings. Volume 2.
Ann Arbor, MI, Environmental Research Institute of Michigan, 1981, p. 939-948. 12 refs.

Reflectance spectroscopy has led to the development of a family of instruments capable of remote sensing applications. The various features in the reflectance spectra of soils, rocks, and other materials are dependent upon their constituent minerals. Attention is given to the Field Reflectance Spectrometer (REFSPEC), which is a self-contained dual beam scanning reflectance spectrometer. The optical train looks alternately at the target of choice and then at the solar radiation. REFSPEC comprises the optical head a battery pack, a standard reflectance target package, and a digital data logger. An analog output is also provided. Another instrument considered is the Hand Held Ratioing Radiometer (HHRR). This instrument measures the energy reflected by a target scene of interest. Applications for both instruments are related to general studies, agriculture, geobotany, geochemistry, geology, and oceanography. G.R.

A82-27653 # **Orbital performance of a 1.6 micrometer DMSP snow/cloud discrimination sensor.** A. W. Kimball (Westinghouse Electric Corp., Baltimore, MD). In: International Symposium on Remote Sensing of Environment, 15th, Ann Arbor, MI, May 11-15, 1981, Proceedings. Volume 2. Ann Arbor, MI, Environmental Research Institute of Michigan, 1981, p. 949-958. USAF-supported research.

A report on the orbital performance of a line array infrared (1.57 + or - 0.6 micron) sensor flown on DMSP satellite F4 in 1979 is given. Instrument characteristics are discussed briefly. Numerical data reduction and normalization methods are described. Samples of orbital data, normalized and compared to data in DMSP visible and thermal infrared channels, are presented. It is concluded that the instrument design performance was essentially as expected and that cloud/snow contrast ratios predicted to lie in the range of three to six were realized in analysis of daylight data over the Northern Hemisphere in December 1979. (Author)

A82-27659 # **University of Dundee satellite image data acquisition and archiving facility.** P. E. Baylis (Dundee, University, Dundee, Scotland). In: International Symposium on Remote Sensing of Environment, 15th, Ann Arbor, MI, May 11-15, 1981, Proceedings. Volume 2. Ann Arbor, MI, Environmental Research Institute of Michigan, 1981, p. 1017-1024. 10 refs.

The capabilities, operations and equipment of the facility for the reception and archiving of satellite image data maintained by the University of Dundee are presented. The Dundee station receives, records and stores data from the Very High Resolution Radiometer (VHRR) of the ITOS/NOAA satellites, the Advanced Very High Resolution Radiometer (AVHRR) of the Tiros-N/NOAA satellites, the Coastal Zone Color Scanner (CZCS) of the Nimbus 7 satellite, and the Visible and Infra-red Spin Scan Radiometer of the Meteosat satellite. Products available from the archive include hard copy and browse files of VHRR/AVHRR and CZCS images, and computer compatible tapes of AVHRR and CZCS scenes. Station equipment used to carry out the functions of the Dundee station consists of a spun aluminum antenna with computer-driven drive motors for satellite tracking purposes, connected with two front ends, telemetry receivers, a bit conditioner, frame synchronizer, and decommutator, and also includes a video processor and tape transports. A.L.W.

A82-27675 # **The use of wave contrast measurements in the evaluation of SAR/gravity models.** E. S. Kasischke and R. A. Shuchman (Michigan, Environmental Research Institute, Ann Arbor, MI). In: International Symposium on Remote Sensing of Environment, 15th, Ann Arbor, MI, May 11-15, 1981, Proceedings. Volume 3. Ann Arbor, MI, Environmental Research Institute of Michigan, 1981, p. 1187-1209. 36 refs. Contract No. N00014-76-C-1048.

A new method to measure the detectability of gravity waves imaged by a synthetic aperture radar (SAR) has been developed. This new method is called a peak-to-background ratio (PBR). The PBR was used in studying two different SAR data sets. X- and L-band aircraft SAR data collected over a Lake Michigan test site were used to study the effects of changing SAR processing parameters (telerotation adjustments and integration time) on wave visibility. A second data set was collected by the Seasat L-band SAR over the JASIN test array and was used to correlate PBRs to various wind and wave parameters. Results of this study indicate the peak-to-background ratio is an effective means to correlate SAR/oceanography theory with actual SAR data sets. (Author)

A82-27681 # **A low cost NOAA/TIROS AVHRR receiving station.** W. Carroll (Western Australia Institute of Technology, South Bentley, Australia), R. D. Cargill, and F. R. Honey (Commonwealth Scientific and Industrial Research Organization, Div. of Land Resources Management, Wembley, Australia). In: International Symposium on Remote Sensing of Environment, 15th, Ann Arbor, MI, May 11-15, 1981, Proceedings. Volume 3.
Ann Arbor, MI, Environmental Research Institute of Michigan, 1981, p. 1253-1264. 12 refs.

In August 1980, a project was initiated with the objective to build in Australia a facility for real-time reception, processing, and dissemination of data from the Advanced Very High Resolution Radiometer (AVHRR) on the NOAA satellites. Using existing equipment and developing some special purpose hardware and software, the facility cost approximately $5000, excluding labor costs. This facility will provide data for experiments on correlation of sea surface temperatures with fish catches around Australia, for cloud seeding experiments, and for regional geologic, soil moisture, and land system mapping. G.R.

A82-27683 # **Spatial resolution and geometric potential of planned earth satellite missions.** R. Welch (Georgia, University, Athens, GA). In: International Symposium on Remote Sensing of Environment, 15th, Ann Arbor, MI, May 11-15, 1981, Proceedings. Volume 3. Ann Arbor, MI, Environmental Research Institute of Michigan, 1981, p. 1275-1283. 14 refs.

Evidence to-date indicates that spatial resolutions of satellite sensor systems equivalent to 5 to 10 m IFOV will be required for the compilation of topographic maps at scales larger than 1:250,000, or for the preparation of land use maps depicting Level II and III classes of information. Film and line array cameras planned for use on satellite missions in the 1980's will provide image data meeting accepted accuracy standards for planimetric maps of 1:25,000 to 1:100,000 scale. Contour intervals of approximately 50 to 100 m appear feasible. Contour intervals of this magnitude are normally associated with topographic maps of 1:250,000 scale. (Author)

A82-27706 # **Geometric correction of airborne multispectral scanner images.** M. Kindelan (IBM Scientific Centre, Madrid, Spain), V. Moreno (Instituto Nacional de Técnica Aerospacial, Madrid, Spain), and A. Valverde (Escuela Técnica Superior de Ingenieros de Minas, Madrid, Spain). In: International Symposium on Remote Sensing of Environment, 15th, Ann Arbor, MI, May 11-15, 1981, Proceedings. Volume 3. Ann Arbor, MI, Environmental Research Institute of Michigan, 1981, p. 1539-1549. 17 refs.

The aim of this paper, is to compare different methods to correct the geometric distortions which are present in Multispectral Scanner Images, and to propose a method based on the orientation parameters which are recorded in flight in the same tape as the image data. This method has the advantage that it may be completed automatically, while their results are comparable or better than those of other methods. (Author)

A82-28127 † **Investigation of earth resources using rocket and space technology (Issledovanie zemnykh resursov pri pomoshchi raketno-kosmicheskoi tekhniki).** V. P. Mishin. *(Vsesoiuznaia Konferentsiia po Problemam Issledovaniia Prirodnykh Resursov Zemli i Mirovogo Okeana, Aviatsionno-Kosmicheskimi Sredstvami, Moscow, USSR, Nov. 1980.) Geodeziia i Aerofotos'emka*, no. 1, 1982, p. 9-11. In Russian.

Various applications of the remote sensing of earth resources are described, and the basic characteristics of the investigation of resources of land and sea from space are discussed. The features of a long-term remote sensing program are examined. B.J.

A82-28128 † **Structure of hardware and software at a regional center for the automated processing of aerial and space**

remote-sensing images (Struktura tekhnicheskikh i programmnykh sredstv regional'nogo tsentra avtomatizirovannoi obrabotki aerokosmicheskikh izobrazhenii). A. S. Alekseev, V. N. Dement'ev, B. K. Kozhevnikov, N. V. Kul'kov, V. P. Piatkin, R. M. Salavatov, and S. L. Shevelev. *(Vsesoiuznaia Konferentsiia po Problemam Issledovaniia Prirodnykh Resursov Zemli i Mirovogo Okeana, Aviatsionno-Kosmicheskimi Sredstvami, Moscow, USSR, Nov. 1980.) Geodeziia i Aerofotos'emka,* no. 1, 1982, p. 12-21. 8 refs. In Russian.

The paper describes a multiprocessor system for the processing of multispectral remote-sensing images, which features interactive thematic processing. Hardware and software structures for the system are described, and particular attention is given to the development of problem-oriented languages. B.J.

A82-28129 † The structure and basic parameters of a satellite system for the remote sensing of earth resources (O sostave i osnovnykh parametrakh kosmicheskoi sistemy issledovaniia prirodnykh resursov). A. S. Selivanov. *(Vsesoiuznaia Konferentsiia po Problemam Issledovaniia Prirodnykh Resursov Zemli i Mirovogo Okeana, Aviatsionno-Kosmicheskimi Sredstvami, Moscow, USSR, Nov. 1980.) Geodeziia i Aerofotos'emka,* no. 1, 1982, p. 22, 23. In Russian.

The characteristics of a remote sensing complex for the study of earth resources are briefly described. Particular attention is given to the characteristics and operation of a multispectral scanner of high and medium resolution. Also included in the complex are side-looking radar, a radar altimeter, and a microwave scanning radiometer. The organization of regional processing centers for the remote sensing data is considered. B.J.

A82-28130 † Experience with a variety of studies of earth resources in the Kalmyk ASSR using space imagery (Opyt kompleksnogo izucheniia prirodnykh resursov Kalmytskoi ASSR na osnove kosmicheskoi informatsii). I. N. El'vartynov and Iu. P. Kienko. *(Vsesoiuznaia Konferentsiia po Problemam Issledovaniia Prirodnykh Resursov Zemli i Mirovogo Okeana, Aviatsionno-Kosmicheskimi Sredstvami, Moscow, USSR, Nov. 1980.) Geodeziia i Aerofotos'emka,* no. 1, 1982, p. 23-26. In Russian.

Various applications of the remote sensing of earth resources in the Kalmyk ASSR are reviewed. These applications include structural mapping, gas and oil exploration, hydrogeology, soil studies, and the mapping of agricultural lands and pastures. B.J.

A82-28132 † The earth resources program for the long-term orbital station Salyut 6 (Programma IPRZ na dolgovremennoi orbital'noi stantsii 'Saliut-6'). V. V. Arkhipov, A. D. Koval', V. V. Kovalenok, A. A. Tishchenko, and L. A. Ronzhin. *(Vsesoiuznaia Konferentsiia po Problemam Issledovaniia Prirodnykh Resursov Zemli i Mirovogo Okeana, Aviatsionno-Kosmicheskimi Sredstvami, Moscow, USSR, Nov. 1980.) Geodeziia i Aerofotos'emka,* no. 1, 1982, p. 30-36. In Russian.

A general review is given of the basic features of the remote sensing of earth resources from Salyut 6. Particular attention is given to the development of the earth resources program, preparatory steps towards the implementation of the program, and the acquisition, processing, and application of the data. B.J.

A82-28140 † Complex of units for the storage and automated processing of research data (Kompleks sredstv dlia nakopleniia i avtomatizirovannoi obrabotki dannykh pri nauchnykh issledovaniiakh). N. I. Baklashov, G. M. Solodikhin, and L. V. Sergeev. *(Vsesoiuznaia Konferentsiia po Problemam Issledovaniia Prirodnykh Resursov Zemli i Mirovogo Okeana, Aviatsionno-Kosmicheskimi Sredstvami, Moscow, USSR, Nov. 1980.) Geodeziia i Aerofotos'emka,* no. 1, 1982, p. 76-82. 5 refs. In Russian.

The paper describes an onboard system for the acquisition, storage, and processing of remote sensing data. Various storage techniques are discussed, and block diagrams of the various elements of the system are presented. B.J.

A82-28142 † Machine implementation of algorithms for the mapping of soil moisture on the basis of microwave-radiometer measurements (Mashinnaia realizatsiia algoritmov kartirovaniia vlazhnosti pochvy po rezul'tatam SVCh-radiometricheskikh izmerenii). N. A. Armand, F. A. Mkrtchian, and A. M. Shutko. *(Vsesoiuznaia Konferentsiia po Problemam Issledovaniia Prirodnykh Resursov Zemli i Mirovogo Okeana, Aviatsionno-Kosmicheskimi Sredstvami, Moscow, USSR, Nov. 1980.) Geodeziia i Aerofotos'emka,* no. 1, 1982, p. 89-94. In Russian.

The paper describes a method for the compilation of soil moisture maps on the basis of microwave remote-sensing data. The technique involves the use of the BENSON graphic device, a general-purpose computer, and an analog-digital converter. The program for the implementation of the proposed algorithm is presented, and it is shown that the program makes it possible to obtain moisture maps of arbitrary gradation. B.J.

A82-28342 Instruments watch for impending earthquakes. B. C. Cole. *High Technology,* vol. 2, Mar.-Apr. 1982, p. 43-47, 50, 51.

The current state of the art of earthquake prediction techniques is discussed. Signs of an imminent earthquake detected upon the analysis of seismic records preceding the Sylmar quake in 1971 are described which have led to the development of more sophisticated instruments and procedures for monitoring seismic velocities and other precursors, including seismometers and seismographs, tiltmeters, linear-strain meters, creep meters, dilatometers, magnetometers, gravimeters, ohmmeters, well monitors, radon monitors and radio telescopes and satellites. Problems with the establishment of a useful earthquake theory on which to base a prediction model are considered, and plans for improving data collection and analysis, particularly from California and the western states, are outlined. The mixed record of previous earthquake predictions in the United States, the Soviet Union and China is noted, and indications of greater confidence in predictions over the next decade as the understanding of earthquake processes grows are pointed out. A.L.W.

A82-28466 † Complex examination of photorectifiers (Kompleksnoe issledovanie fototransformatorov). V. A. Moroz and L. I. Iablonskii. *Geodeziia i Kartografiia,* Feb. 1982, p. 42-44. In Russian.

A method for the complex investigation of photorectifiers is proposed which involves the simultaneous determination of instrumental accuracy and corrections to null points which characterize the operational accuracy of the basic elements of the instruments. This makes possible a more effective adjustment and improves the accuracy of transformation. B.J.

N82-16164*# National Aeronautics and Space Administration. Langley Research Center, Hampton, Va.
THE MICROWAVE RADIOMETER SPACECRAFT. A DESIGN STUDY: EXECUTIVE SUMMARY
Uriel M. Lovelace *In its* The Microwave Radiometer Spacecraft Dec. 1981 p 1-14 refs

Avail: NTIS HC A11/MF A01 CSCL 22B

A conceptual design was developed for a microwave radiometer spacecraft (MRS) using a large passive reflector, microwave radiometer, and advanced control concepts soil moisture mapping from microwave sensing for global crop forecasting. Mission requirements and tradeoffs were defined, and major subsystems (structural, electromagnetic surface, and attitude control) conceptually designed. An overview of the mission and a summary of the study results are presented. J.M.S.

N82-16165*# National Aeronautics and Space Administration. Langley Research Center, Hampton, Va.
MISSION DEFINITION FOR A LARGE-APERTURE MICROWAVE RADIOMETER SPACECRAFT
Lloyd S. Keafer, Jr. *In its* The Microwave Radiometer Spacecraft Dec. 1981 p 17-32 refs

Avail: NTIS HC A11/MF A01 CSCL 22B

An Earth-observation measurements mission is defined for a large-aperture microwave radiometer spacecraft. This mission is defined without regard to any particular spacecraft design concept. Space data application needs, the measurement selection rationale, and broad spacecraft design requirements and constraints are described. The effects of orbital parameters and image quality requirements on the spacecraft and mission performance are discussed. Over the land the primary measurand is soil moisture; over the coastal zones and the oceans important measurands are salinity, surface temperature, surface winds, oil spill dimensions and ice boundaries; and specific measurement requirements have been selected for each. Near-all-weather operation and good spatial resolution are assured by operating at low microwave frequencies using an extremely large aperture antenna in a low-Earth-orbit contiguous mapping mode. Author

N82-16440*# General Electric Co., Philadelphia, Pa. Space Div.
LANDSAT-2 AND LANDSAT-3 FLIGHT EVALUATION REPORT, 23 JANUARY TO 23 JULY 1980
1 Aug. 1980 241 p ERTS
(Contract NAS5-21808)
(E82-10022; NASA-CR-164392; Doc-80SDS4229) Avail: NTIS HC A11/MF A01 CSCL 05B

Flight performance analyses of LANDSAT 2 and LANDSAT 3 are presented. Spacecraft operations and orbital parameters are summarized for each spacecraft. Data are provided on the performance and operation of the following onboard subsystems: power; attitude control; command/clock; telemetry; orbit adjust; magnetic moment compensation assembly; unified S-band/premodulation processor; electrical interface; thermal; narrowband tape recorders; wideband tape recorders; return beam vidicon; multispace multispectral scanner; and data collection. Orbit reference tables for January 1980 through July 1981 are included. A.R.H.

N82-16444*# Instituto de Pesquisas Espaciais, Sao Jose dos Campos (Brazil).
BRAZILIAN REMOTE SENSING ACTIVITIES, CURRENT AND PROSPECTIVE NEEDS
Nelson deJesusParada, Principal Investigator Apr. 1981 55 p Presented at the United Nations Regional Seminar on Remote Sensing Appl. and Satellite Commun. for Education and Develop., Toulouse, 21-25 Apr. 1981 Sponsored by NASA ERTS
(E82-10026; NASA-CR-164811) Avail: NTIS HC A04/MF A01 CSCL 05A

Remote sensing activities began in Brazil in 1968 and are now concentrated in a satellite and a side-looking radar program. The radar program systematically surveys the natural resources of the whole national territory in a level of detail compatible with a 1:1,000,000 scale, focusing on geology, geomorphology, soil, agricultural aptitude, ecology, and potential land use. The satellite program receives, processes, and disseminates remotely sensed data (basically LANDSAT data) and develops methodologies for applying these data for surveying, monitoring and mapping. Special emphasis is given to national priorities, particularly food and energy. Major results obtained and difficulties encountered in the following applications are described: crop forecasting, reforestation, mineral exploration, fishing chart models, land use, sedimentation in reservoirs, and deforestation in the Amazon forest. A decision was made to upgrade existing LANDSAT reception and processing stations to receive and process MSS and thematic data from LANDSAT-D and from SPOT and to construct two satellites for launch in 1987-1990. A.R.H.

N82-16445*# South Dakota State Univ., Brookings. Remote Sensing Inst.
REMOTE SENSING APPLICATIONS TO RESOURCE PROBLEMS IN SOUTH DAKOTA Semiannual Progress Report, 1 Jul. 1980 - 1 Jan. 1981
Victor I. Myers, Principal Investigator, T. Bailey, R. G. Best, J. C. Eidenshink, D. Hause, H. Haivala, F. A. Schmer, M. Wehde, and K. Winks 1 Jan. 1981 102 p refs Original contains color imagery. Original photography may be purchased from the EROS Data Center, Sioux Falls, S.D. 57198. ERTS
(Grant NGL-42-003-007)
(E82-10027; NASA-CR-164810; SDSU-RSI-81-03) Avail: NTIS HC A06/MF A01 CSCL 05A

Data obtained from field studies, aerial color infrared photography, and LANDSAT imagery are being used for resources management in South Dakota. The procedures used and results obtained are described for the following applications: (1) detecting Dutch elm disease in the city of Watertown; (2) determining the distribution and abundance of grasshoppers in Corcon County; (3) inventorying sagebrush in Butte County to support sage grouse management; (4) computerized digitization of aerial thermography of the concentration of Canada geese on the Missouri River Reservoir; (5) surveying to determine the diversion of water along the Belle Fourche River from the Keyhole Reservoir in eastern Wyoming to the City of Belle Fourche in western South Dakota; (6) identifying and locating areas of the Lower James River where stream blockages, streambank erosion, and flooding occur; and (7) acquiring and analyzing data on the landcover in the Lake Herman watershed for the national pilot Model Implementation program. A.R.H.

N82-18466# Analysis and Technology, Inc., North Stonington, Conn.
EVALUATION OF TWO AN/APS-94 SIDE-LOOKING AIRBORNE RADAR SYSTEMS IN THE DETECTION OF SEARCH AND RESCUE TARGETS Interim Report, Jan. 1978 - Aug. 1981
S. R. Osmer, N. C. Edwards, Jr., G. L. Hover, and T. J. Mazour Aug. 1981 163 p refs
(Contract DTCG39-80-C-80052)
(AD-A108404; USCG-D-64-81) Avail: NTIS HC A08/MF A01 CSCL 17/9

Side-Looking Airborne Radar (SLAR) detection data were gathered in conjunction with four visual detection experiments designed to improve search planning guidance contained in the National Search and Rescue Manual. HC-130 aircraft, equipped with either the Airborne Oil Surveillance System (AOSS) or SLAR/radar image processor (SLAR/RIP) configuration of the AN/APS-94C or D SLAR, conducted controlled searches for life rafts, small boats, and 41- to 95-foot Coast Guard vessels in Block Island Sound or open ocean. Using a microwave tracking system and SLAR data, the positions of searchers and targets were accurately reconstructed to facilitate the verification of detections on SLAR films or video tape. These data were used to evaluate the effects of environmental and controllable parameters on SLAR detection of the various target types. Target size/composition search altitude, swell height, wind speed, and humidity/precipitation were found to have a significant influence of SLAR detection performance. Upper-bound lateral range curves and sweep widths for SLAR search are included. Real-time performance tests for AN/APS-94D SLAR and system performance tests for new SLARs (AN/APS-131) are recommended. GRA

N82-18481# Thomson-CSF, Meudon-la-Foret (France). Dept. Espace-Satellites.
STUDY OF SYNTHETIC APERTURE RADAR IN 2D - 2FS OPERATION OVER THE OCEAN Final Report
Paris ESA 5 Mar. 1981 25 p
(Contract ESA-4586/81/F-DD(SC))
(ESA-CR(P)-1475) Avail: NTIS HC A02/MF A01

Synthetic aperture radar operation (imaging mode) for the European Remote Sensing program is considered. The 2D - 2FS function consists in operating in a low power mode (100 W RF) for 1.5 sec every 15 sec in order to image patches on the sea surface of 5 km by 5 km every 100 km, with the 5 km squares in the center of the beam. The data stream needs to be buffered such that a continuous (300 kbit/sec) data stream is delivered. The impact of such a mode on hardware, especially in terms of mass and power consumption, was studied. Results show that the 2D - 2FS option requires minor changes. One additional dispersive line and one additional box, containing the added hardware for data handling, are necessary. This represents 7 kg more (with redundancy) for payload. The average power consumption in wave mode becomes 150 W. Author (ESA)

N82-18564# British Aerospace Dynamics Group, Bristol (England). Space and Communications Div.
IMAGING MICROWAVE RADIOMETER. PHASE A STUDY. VOLUME 1: EXECUTIVE SUMMARY Final Report
C. R. Francis Paris ESA Jul. 1980 50 p refs Prepared in cooperation with Dornier-Werke G.m.b.H., Friedrichshafen, West Germany, B and W Electronik and Tech. Univ. of Denmark Original contains color illustrations
(Contract ESA-4243/80/F-CG(SC))
(ESS/SS-1006; ESA-CR(P)-1468) Avail: NTIS HC A03/MF A01

An imaging microwave radiometer, a passive microwave instrument proposed for inclusion in the sensor payload of the Coastal Ocean Monitoring Satellite System (COMSS) spacecraft, was studied. The instrument detects microwave radiation at 5 frequencies in the range 6.8 to 36.5 GHz, each at vertical and horizontal polarization, and has an optional facility for measurements at 90 GHz. Results show that the instrument

meets the experiment requirements proposed by ESA and meets the accommodation constraints of the COMSS payload.
Author (ESA)

N82-18672# Research Inst. of National Defence, Linkoeping (Sweden). Huvudavdelning 3.
OBSERVATIONS WITH AN IMAGING 35 GHz RADIOMETER OF TERRAIN IN MALMSLATETT, JULY 1980
Gunnar Stenstroem and Ain Sume Oct. 1981 39 p refs
Original contains color illustrations
(FOA-C-30240-E1/E3) Avail: NTIS HC A03/MF A01

Microwave emission of militarily important terrain was studied, using Dicke radiometer measurements around an air traffic control tower. The radiometer has a 60 cm parabolic Cassegrain antenna, controlled through a desk top computer, which also manages the data sampling and recording. The radiometric images were color-coded and presented on-line on a TV monitor. A selected part of the scenery was monitored once every hour in order to examine time variations of the observed antenna temperature and their correlation with day-to-night and meteorological changes. The significance of reflected, cold sky radiation in smooth surfaces (metals, plastics, roads) is demonstrated, resulting in a contrast with the less reflective surroundings.
Author (ESA)

N82-18776*# National Aeronautics and Space Administration. Goddard Space Flight Center, Greenbelt, Md.
STRATOSPHERIC INSTRUMENTS AND ANALYSES
In its The Stratosphere 1981 Jan. 1982 26 p

Avail: NTIS HC A22/MF A01 CSCL 04A

The Instruments are divided into two groups, ground based instruments and satellite-borne instruments. The ground based instruments include a Dobson ozone spectrophotometer, a filter ozonometer, and ozonesondes. The satellite-borne instruments include: a backscatter ultraviolet spectrometer, a high resolution infrared radiation sounder, a infrared interferometer spectrometer, a limb radiance inversion radiometer, and multichannel filter radiometer. A list of investigations using stratospheric satellite data is presented.
T.M.

N82-18881# Instituto de Pesquisas Espaciais, Sao Jose dos Campos (Brazil).
A MICROCOMPUTER FOR CONTROL OF DATA COLLECTION PLATFORMS [UM MICROCOMPUTADOR PARA CONTROLE DE PLATAFORMAS DE COLETA DE BADOS]
Jose Bianchi Neto and E. W. Bergamini Jun. 1981 12 p refs In PORTUGUESE; ENGLISH summary Presented at the 2nd Natl. Meeting on Automation, Salvador, Bahia, Brazil, Jul. 1981
(INPE-2104-RPE/331) Avail: NTIS HC A02/MF A01

A microcomputer developed for application in an environmental data collection platform performs functions of data control, acquisition and processing of a self timed data collection platform compatible with the GOES (satellite) system. Block diagrams are presented and the data collection platform is described.
Author

N82-19520# Instituto de Pesquisas Espaciais, Sao Jose dos Campos (Brazil).
AUTOMATIC ANALYSIS OF MULTISPECTRAL IMAGES
Luciano Vieira Dutra, Ricado Cartaxo Modesto deSouza, Fernando Augusto Mitsuo, II, and Jose Carlos Moreira Aug. 1981 33 p refs In PORTUGUESE; ENGLISH summary
(INPE-2212-MD/009) Avail: NTIS HC A03/MF A01

Some ideas of automatic multispectral image analysis are introduced. Automatic multispectral image analysis plays a central role in numerically oriented remote sensing systems. It presupposes the utilization of electronic equipments, mainly computers and their peripherals, to help people to interpret the information contained in multispectral digital imagery. This necessity derives from the great amount of multispectral data gathered by remote sensors within satellites and airplanes. When the number of channels or spectral bands is increased, the interpretation becomes more complex and subjective. In some cases, for example, in harvest estimation in national or regional level, it is imperative to use computer systems to complete the work within the time required. Automatic analysis also aimes to eliminate subjective factors that appear in the human interpretation, so increasing the global precision.
R.J.F.

N82-19647*# Systematics General Corp., Sterling, Va.
GUIDELINES FOR SPACEBORNE MICROWAVE REMOTE SENSORS
Viqui Litman (Applied Media, Inc., Greenbelt, Md.) and John Nicholas Mar. 1982 87 p refs
(Contract NASw-3398)
(NASA-RP-1086) Avail: NTIS HC A05/MF A01 CSCL 14B

A handbook was developed to provide information and support to the spaceborne remote sensing and frequency management communities: to guide sensor developers in the choice of frequencies; to advise regulators on sensor technology needs and sharing potential; to present sharing analysis models and, through example, methods for determining sensor sharing feasibility; to introduce developers to the regulatory process; to create awareness of proper assignment procedures; to present sensor allocations; and to provide guidelines on the use and limitations of allocated bands. Controlling physical factors and user requirements and the regulatory environment are discussed. Sensor frequency allocation achievable performance and usefulness are reviewed. Procedures for national and international registration, the use of non-allocated bands and steps for obtaining new frequency allocations, and procedures for reporting interference are also discussed.
M.D.K.

N82-19650# Dornier-Werke G.m.b.H., Friedrichshafen (West Germany).
SATELLITE SCATTEROMETER FEASIBILITY STUDY. VOLUME 1: TECHNICAL RESULTS Final Report
R. Anders, G. Bommas, W. Gieraths, W. Gilg, P. Hans, M. Haimerl, H. Hoelzl, A. Kuehnle, H. Schuessler, P. Stuerzenhofaecker et al Paris ESA Apr. 1981 194 p refs 2 Vol.
(Contract ESA-4367/80/F-DD(SC))
(ESA-CR(P)-1492-Vol-1) Avail: NTIS HC A09/MF A01

A scatterometer for ERS 1 is described. A wind sensor determines vector fields within a 400 km sweep parallel to satellite motion. Individual vectors are extractable from 50 X 50 km cells. Wind speeds between 4 and 24 m/sec are measured with an angular accuracy of + or - 20 deg. A wave sensor handles spectra between 100 and 1000 m wavelength. Measurements are taken with a spacing of 100 km or less along the satellite track. Data are extractable from 5 x 5 km resolution cells. Wind speed and wind direction measurements are derived from Seasat data and of two-dimensional ocean wave spectra measurement are derived from the synthetic aperture radar mode.
Author (ESA)

N82-19651# Dornier-Werke G.m.b.H., Friedrichshafen (West Germany).
SATELLITE SCATTEROMETER FEASIBILITY STUDY. VOLUME 2: DATA EXTRACTION ALGORITHM AND ERROR SIMULATION FOR WIND SENSOR Final Report
P. Hans Paris ESA Apr. 1981 100 p ref 2 Vol.
(Contract ESA-4367/80/F-DD(SC))
(ESA-CR(P)-1492-Vol-2) Avail: NTIS HC A05/MF A01

The ERS 1 scatterometer operation was computer simulated to: (1) test the Moore's relationship between the backscattering coefficient sigma deg and wind speed/direction, (2) investigate the influence of statistical errors in the sigma deg measurement on the resultant wind parameters, and (3) investigate antenna configurations with respect to functional performance and hardwear realization. Erroneous a sub zero parameter values in the radar sea return model cause errors mainly in wind speed, while erroneous a sub 2 causes errors in wind direction, and a sub 1 has little effect. The dual beam/dual polarization concept is recommended.
Author (ESA)

N82-19652# Spar Aerospace Products Ltd., Toronto (Ontario).
STUDY OF A RADAR ALTIMETER FOR THE EUROPEAN REMOTE SENSING PROGRAM. VOLUME 1: EXECUTIVE SUMMARY
A. Thompson and S. J. Alexander Jun. 1981 90 p Prepared jointly with Dornier-Werke GmbH Friedrichshafen, West Germany
(Contract ESA-4427/80/F-DD(SC))
(Spar-R.1090-Issue-A; ESA-CR(P)-1502) Avail: NTIS HC A05/MF A01

Sea scattering, radar parameter selection, performance characteristics such as acquisition and tracking, and operation in rain and over land were studied in order to design a radar altimeter. Tradeoffs covering the antenna, microwave subsystem, signal processor, and altimeter controller were performed.

A configuration consisting of a full deramp radar pulse compression system operating at 13.7 GHz, with a maximum likelihood estimator tracker/processor is chosen. The design meets the specification in all respects, has better performance and less weight than the Seasat altimeter, yet is fully redundant. A costed development plan completely compatible with the ERS 1 schedule is outlined. Author (ESA)

N82-19653# Royal Netherlands Aircraft Factories Fokker, Schiphol-Oost.
DEVELOPMENT OF A BREADBOARD COOLER FOR INFRARED REMOTE SENSING PAYLOADS, PHASE 1 Final Report
E. G Overbosch and N. P. Enderberg Paris ESA 14 Mar. 1981 153 p
(Contract ESTEC-4484/80/NL-PP(SC))
(FOK-RV-R-81-064; ESA-CR(P)-1506) Avail: NTIS HC A08/MF A01

A multistage passive cryogenic cooler was designed for the ocean color monitor (OCM) for ERS 1. Mathematical models of thermal and mechanical behavior support the concept of a radiator located in a parabolic reflector. Technologically critical areas of the design are compared with corresponding components in the optical imaging instrument, i.e. the glass reinforced thermal insulation/suspension straps, the suspension system integrated in the cooler, the parabolic reflector, and the cold stage radiator. A set of critical components suitable for both coolers is feasible. A three stage breadboard cooler is described. The multilayer insulation (MLI) radiator cools the MLI support, the first stage cools the paraboloid. The second stage is the cold stage radiating its heat loads by the open faced honeycomb radiator to space. The suspension of the first stage consists of dummies representing the thermal behavior of the corresponding OCM straps. The outside mounting ring is sufficiently stiff to support the cooler, and is used for mounting the cooler in the test chamber. Author (ESA)

N82-20375# European Space Agency, Paris (France).
MRSE: A MICROWAVE REMOTE SENSING EXPERIMENT IN SPACELAB
Marian Werner *In its* On Radio Frequencies in Aerospace (ESA-TT-704) Dec. 1981 p 75-83 Transl into ENGLISH from "Beitraege zum Kolloq. 'Hochfrequenztech. in der Luft- u. Raumfahrt'", Rept. DFVLR-Mitt-80-10 DFVLR, Oberpfaffenhofen, West Germany, Jun. 1980

Avail: NTIS HC A06/MF A01; DFVLR, Cologne DM 21,80

The design and development of the microwave remote sensing experiment are discussed. The equipment allows for three operating modes: scatterometry, synthetic aperture radar, and microwave radiometry. Sea state measurement, radar imagery, and passive detection of terrestrial radiation are planned. Author (ESA)

N82-20491# Electronics Research Lab., Adelaide (Australia).
PROPOSED DIGITAL CARTRIDGE RECORDING SYSTEM FOR WRELADS
T. R. Adams and D. M. Phillips Aug. 1981 22 p
(AD-A109484; ERL-0210-TM) Avail: NTIS HC A02/MF A01 CSCL 09/2

The present data recording system in WRELADS II uses a hybrid tape recorder. Signal waveforms are recorded in analogue form while system parameters are recorded digitally. The hybrid recording system has several disadvantages that would be overcome by introducing a fully digital recording system. A proposal is described for developing a system to utilize two high-capacity digital cartridge recorders in conjunction with a microprocessor based cartridge controller. GRA

N82-20606*# National Aeronautics and Space Administration, Washington, D. C.
GRADIO: PROJECT PROPOSAL FOR SATELLITE GRADIOMETRY
G. Balmino, F. Barilier, A. Bernard, C. Bouzat, G. Riviera, and J. Runavot Dec. 1981 55 p refs Transl. into ENGLISH of "Gradio: Gradiometrie par Satellite Proposition de Projet" Rept. no. 244 PRT/AMP/AP (France), 8 Sep. 1981 p 1-51 Transl. by Kanner (Leo) Associates, Redwood City, Calif. Original doc. prep. by Centre National Etudes Spatiales
(Contract NASw-3541)
(NASA-TM-76796; NAS 1.15:76796) Avail: NTIS HC A04/MF A01 CSCL 08B

A gradiometric approach, rather than the more complicated satellite to satellite tracking, is proposed for studying anomalies in the gravitational fields of the Earth and, possibly, other telluric bodies. The first analyses of a gradiometer based on four of ONERA's CACTUS or SUPERCACTUS accelerometers are summarized. it is shown that the obstacles to achieving the required accuracy are not insuperable. The device will be carried in a 1000 kg lens shaped satellite in a heliosynchronous orbit 200 to 300 km in altitude. The first launching is planned for the end of 1987. Author

N82-20630# Naval Ocean Systems Center, San Diego, Calif.
SATELLITE-BORNE NON-DOD SENSORS FOR TERRESTRIAL OBSERVATIONS
H. M. Wight Aug. 1981 66 p refs
(AD-A109486; NOSC/TD-458) Avail: NTIS HC A04/MF A01 CSCL 22/2

This is a summary review that was made of satellite-borne 'non-DoD sensors' used for terrestrial observations. The term non-DoD sensors refers to 'civil' (as contrasted with 'military') remote sensing systems. The civil satellite-borne sensing systems were developed for the most part by NASA and are employed operationally by NOAA/NESS. Author (GRA)

N82-21669*# Purdue Univ., Lafayette, Ind. Lab. for Applications of Remote Sensing.
A MULTIBAND RADIOMETER AND DATA ACQUISITION SYSTEM FOR REMOTE SENSING FIELD RESEARCH
M. E. Bauer, Principal Investigator, B. F. Robinson, D. P. DeWitt, L. F. Silva, and V. C. Vanderbilt Nov. 1981 14 p refs Repr. from from Proc. of the Intern. Arch. of Photogrammetry (West Germany), v. 23(B8) p 783-793 Presented at the 14th Congr. of the Intern. Soc. for Photogrammetry, Hamburg, 13-25 Jul. 1980 Sponsored by NASA, USDA, Dept. of Commerce, Dept. of the Interior, and Agency for International Development ERTS
(Contract NAS9-15466; Proj. AgRISTARS)
(E82-10142; NASA-CR-167506; NAS 1.26:167506; SR-P1-04201; LARS-071480) Avail: NTIS HC A02/MF A01 CSCL 14B

Specifications are described for a recently developed prototype multispectral data acquisition system which consists of multiband radiometer with 8 bands between 0.4 and 12.5 micrometers and a data recording module to record data from the radometer and ancillary sources. The system is adaptable to helicopter, truck, or tripod platforms, as well as hand-held operation. The general characteristics are: (1) comparatively inexpensive to acquire, maintain and operate; (2) simple to operate and calibrate; (3) complete with data hardware and software; and (4) well documented for use by researchers. The instrument system is to be commercially available and can be utilized by many researchers to obtain large numbers of accurate, calibrated spectral measurements. It can be a key element in improving and advancing the capability for field research in remote sensing. A.R.H.

N82-21703# Tennessee Valley Authority, Chattanooga.
NATIONAL HIGH-ALTITUDE PHOTOGRAPHY (NHAP) OF THE TENNESSEE VALLEY REGION, VOLUME 1, NO. 1
31 Oct. 1981 19 p
(PB82-130899; TVA/ONR/NRO-82/3) Avail: NTIS HC A02/MF A01 CSCL 08B

The capabilities and activities of the photogrammetry and remote sensing section of the mapping services branch are described. The uses of aerial photography are briefly described. Plans for upgrading of services and equipment are discussed. GRA

N82-21808# Wyoming Univ., Laramie. Dept. of Physics and Astronomy.
OZONE MEASUREMENTS TO 48Km WITH CHEMILUMINESCENT OZONE DETECTORS Annual Progress Report
J. M. Rosen and D. J. Hofman Jan. 1982 9 p refs
(Contract N00014-76-C-0170)
(AD-A110342; AP-70) Avail: NTIS HC A02/MF A01 CSCL 07/1

An inflight ozone calibrator was tested both in a laboratory environmental chamber and on a balloon flight. The results demonstrate the need for an inflight calibrator and also indicate that there may be a serious and previously unobserved temperature sensitivity problem with one of the primary ozone detectors. Author (GRA)

N82-21626*# National Aeronautics and Space Administration. Goddard Space Flight Center, Greenbelt, Md.

CLOUD TOP SCANNING RADIOMETER (CTS): USER'S GUIDE

K. S. Brown Nov. 1981 30 p refs
(NASA-TM-83887; NAS 1.15:83887) Avail: NTIS HC A03/MF A01 CSCL 04B

The CTS maps the Earth's surface with a resolution of 0.1 km from an altitude of 18km with 60km side-to-side coverage of the field. It has three spectral channels. The 0.625 micrometer centered visual channel detects reflectance to within 1 percent. The 6.75 micrometer centered water vapor channel detects changes in temperature of less than one degree Kelvin at 175 K. The 11.5 micrometer centered infrared window channel detects changes of less one half degree Kelvin at 175 K. The data can be converted graphically into three display images of the scene. Values for scene temperature and albedo are calculated from calibration equations. The equations were derived from in-situ and laboratory measurements. Intercomparisons of the flight data temperatures with ground based and other remote sensor results established the certainty of the derived temperature values to within 3 K over a wide temperature range (180 to 320 K). The system performance, calibration, and operation is successful and the engineering information describing this system should prove useful to scientists and potential users of the data. T.M.

09
GENERAL

Includes economic analysis.

A82-20412 **Landsat classification accuracy assessment procedures.** R. A. Mead (Virginia Polytechnic Institute and State University, Blacksburg, VA) and J. Szajgin (Technicolor Graphic Services, Inc., Sioux Falls, SD). *Photogrammetric Engineering and Remote Sensing*, vol. 48, Jan. 1982, p. 139-141.

At the November 12-14, 1980 conference on Landsat classification accuracy assessment procedures, attention was given to sampling procedures, statistical analysis techniques, and examples of projects concerned with accuracy assessment as well as the associated costs, logistical problems, and value of accuracy data to the remote sensing and resource management fields. It was commented during the proceedings that national standards for reporting thematic map accuracy have not been established, so that potential users of Landsat classifications often do not know the relative accuracies achievable in the identification of land-cover types. Moreover, Landsat classification accuracy assessments are often made with inadequate reference data, such as maps, photointerpretations or visits to the field. These reference data should be distributed throughout the scene in such a way that all cover types and transition zones between them are adequately represented. O.C.

A82-21280 **The Landsat program - Moving ahead.** A. Chiaviello. *Satellite Communications*, vol. 6, Feb. 1982, p. 34-36.

The operations and accomplishments of Landsats 1-3 are reviewed, and attention is given to the capabilities and uses of Landsat D. Landsats 1-3 fly at a 510 mi altitude in polar orbits, taking photographs of 115 by 115 km areas of the earth surface for transmittance to cover 100 countries. False color composites are developed with color coding for vegetation, water, cities, and highways. Multispectral data on minerals and oil locations, population estimates, crop yield estimates, and for disaster warnings have been gathered, along with data for resources planning and environmental monitoring. The Landsat-D satellite will carry a Thematic Mapper besides the Multispectral Scanner in a 435 mi altitude orbit and transmit at X-band and S-band frequencies. The Thematic Mapper will have 30 m resolution and the whole package will generate 800 images/day. M.S.K.

A82-21875 **Remote sensing for natural resources: An international view of problems, promises and accomplishments.** Moscow, ID, University of Idaho, 1980. 527 p.

Aspects of remote sensing which were discussed included historical uses of remote sensing and reports on current applications in forestry, in international assistance programs, for spatial classification of multisource data types for lithologic mapping in Southwestern Idaho, and for rangeland sensing. Interactive roles between remote sensing and management information/mapping systems in resource inventories were discussed, along with Landsat contributions to national and regional resource inventories, techniques for obtaining multiresource information from remote sensing and ancillary data sources for resources in Costa Rica, and computer analysis of remote sensing data. Consideration was given to applications of remote sensing to pest control, in identifying wind energy sites, for crops identification, and for mapping world forests and nonrenewable resources. M.S.K.

A82-22149 **An intelligent earth sensing information system.** T. H. Fay (Southern Mississippi, University, Hattiesburg, MS), J. Nazemetz (Oklahoma State University, Stillwater, OK), D. M. Sandford (Rutgers University, New Brunswick, NJ), V. Taneja (Western Illinois University, Macomb, IL), and P. Walsh (Fairleigh Dickinson University, Teaneck, NJ). *Photogrammetric Engineering and Remote Sensing*, vol. 48, Feb. 1982, p. 281-286. 9 refs.

By the year 2000, problems related to the expected increase in the world population will require for their solution a highly effective widespread management of earth resources with the aid of remote earth sensing. The cost of operating an earth sensing system can be greatly reduced through the use of artificial intelligence techniques to achieve goal oriented data gathering, information extraction using a world model, and direct user interfacing. A technology feasibility study was conducted to investigate the use of advanced and intelligent automation in space. The concept of an ambitious earth resource monitoring system directed toward future needs was developed as a result of this study. A proposal is made for the extensive use of artificial intelligence techniques within an autonomous satellite system to acquire and interpret data required by future users at as low a cost as possible. G.R.

A82-24343 # **Remote sensing and international law.** C. Q. Christol (Southern California, University, Los Angeles, CA). In Annals of air and space law. Volume 5. Toronto, Carswell Co., Ltd.; Paris, Editions A. Pedone, 1980, p. 375-426. 90 refs.

Legal aspects of spaceborne remote sensing are reviewed, with consideration given to a definition of remote sensing, a functional approach to remote sensing, the emergence of contending positions on remote sensing, and the range of legal viewpoints in 1980. It is concluded that it has become increasingly evident during the COPUOS negotiations relating to the space-based remote sensing of the earth and its natural resources that substantial obstacles lie in the way of acceptance of fundamental principles concerning this matter. B.J.

A82-26123 **Some problems concerning the effective use of remote sensing (Zu einigen Problemen der effektiven Nutzung der Erdfernerkundung).** P. Bormann (Deutsche Akademie der Wissenschaften, Zentralinstitut für Physik der Erde, Potsdam, East Germany). *Gerlands Beiträge zur Geophysik*, vol. 91, no. 1, 1982, p. 13-24. 13 refs. In German.

The paper investigates a number of problems in remote sensing relating to data aquisition, information extraction, and the utilization of information, in an effort to increase its effectiveness. Emphasis is on the conception of suitable remote sensing systems; the importance of accessibility, continuity, and timelessness of data; and the acceptability and feasibility of a remote sensing system as related to the scientific-technical, economical, infrastructural and environmental conditions of a given country. The assessment of cost benefits of remote sensing is discussed, and information extraction and integration of results into traditional disciplines, information systems and decision making are considered. D.L.G.

A82-27169 **Imaging the earth. I - The troubled first decade of Landsat.** M. M. Waldrop. *Science*, vol. 215, Mar. 26, 1982, p. 1600-1603.

The coming launching of Landsat-D in July 1982 follows a decade of problems between NASA and users of Landsat data. The users wanted the continued use on Landsat-D of the multispectral scanner that had been aboard previous Landsats, since they had made heavy investments in computers, software and trained personnel to process the data obtained through that scanner. NASA, however, had planned to replace the scanner with a thematic mapper that advances the 80-meter resolution of the MSS to 30 meters and senses in not four spectral bands but seven. Users also wanted a far higher map production rate from NASA. Although it appeared that Landsat-D might go into orbit without the thematic mapper, the problems were finally resolved as NASA achieved high-volume map output and decided to put both the MSS and the mapper into orbit. C.D.

A82-27501 **Scientific lectures on aviation and astronautics 1980 (Nauchnye chteniia po aviatsii i kosmonavtike 1980 g.).** Edited by A. Iu. Ishlinskii. Moscow, Izdatel'stvo Nauka, 1981. 336 p. In Russian.

Papers from the 1979 and 1980 Gagarin Lectures on Aviation and Astronautics are presented. Attention is given to such topics as directional solidification in conditions of weightlessness, scientific-technical and organizational problems of cosmonaut training, the remote sensing of earth resources, the ballistic-navigational support for the Salyut 6-Soyuz-Progress complex, and the automation of the thermal-stress analysis of flight vehicles. Also considered are the development of spacecraft power supply systems, space biomedical studies, method for the design of flight-vehicle control systems, problems of space-flight mechanics, and the development of life support systems. B.J.

A82-27506 † **Present and future studies of natural resources and the environment from space (Kosmicheskoe prirodovedenie segodnia i zavtra).** Iu. P. Kienko. In: Scientific lectures on aviation and astronautics 1980. Moscow, Izdatel'stvo Nauka, 1981, p. 50-56. In Russian.

The advantages of space data on natural resources, as compared with conventional sources of such data, are described. Current trends in remote sensing technology are reviewed, and examples are presented illustrating the application of remote sensing data to solve various scientific and economic problems. B.J.

A82-27543 † **Development of cooperation between CMEA member countries in the development and utilization of space-based systems for the remote sensing of earth resources and the environment (Razvitie sotrudnichestva stran-chlenov SEV v oblasti sozdaniia i ispol'zovaniia kosmicheskikh sistem issledovaniia prirodnykh resursov i okruzhaiushchei sredy).** B. A. Chumachenko, V. V. Marchenko, Iu. A. Tiurin, and E. P. Vlasov. In: Problems of space studies. Moscow, Mezhdunarodnyi Tsentr Nauchnoi i Tekhnicheskoi Informatsii, 1981, p. 13-22. 10 refs. In Russian.

The development of remote sensing systems for geological services is examined with reference to cooperation between CMEA member countries. Attention is given to the organization of the sequential processing and complex integration of space and ground data in relation to the prediction of earth resources on the basis of a problem-oriented man-machine system. The Region system, dedicated to geological prediction, is considered as an example of such a system. B.J.

A82-27669 # **Earth sensing from space - Commercial and international aspects.** A. W. Frutkin (Burroughs Corp., Pacific Canada Div., Detroit, MI). In: International Symposium on Remote Sensing of Environment, 15th, Ann Arbor, MI, May 11-15, 1981, Proceedings. Volume 3. Ann Arbor, MI, Environmental Research Institute of Michigan, 1981, p. 1121-1126.

A critical evaluation is conducted of problems and promises related to earth sensing operations from space, taking into account developments occurring during the last two or three years. In a quick survey of the fundamental elements of the present situation, it is found that there were no changes with respect to the space segment during the last two years. Neither has there been any great increase in the use of the data during the same period. Attention is also given to the absence of substantial changes regarding the price of data, the transfer of responsibility for a future operational system to NOAA, national programs in France and Japan, and the absence of a real provision for continuity beyond Landsats D/D-prime. All hope and planning for the future seem to be a function of legislation to be proposed for a private sector follow-on to Landsats D/D-prime. After an investigation of the envisaged private-sector solution, it is concluded that the primary role should be played by government. G.R.

N82-17792# National Oceanic and Atmospheric Administration, Washington, D. C. National Earth Satellite Service
PUBLICATIONS AND REPORTS ON CONTRACTS AND GRANTS, 1980 Final Report
Nancy A. Everson May 1981 19 p refs
(PB82-103219; NOAA-TM-NESS-115; NOAA-81072202) Avail: NTIS HC A02/MF A01 CSCL 04B

This bibliography cites the titles and authors of 122 articles and reports published by or for the National Earth Satellite Service (NESS). The first section includes publications by NESS staff members and the second section includes final reports on contracts and grants sponsored by NESS GRA

N82-18669# Eurospace, Paris (France).
EXAMINATION OF THE OPERATIONAL PROSPECTS FOR REMOTE SENSING Final Report [EXAMEN DES PERSPECTIVES OPERATIONNELLES DE LA TELEDETECTION]
Eleonora Ambrosetti Paris ESA Dec. 1980 305 p refs In FRENCH
(Contract ESA-4080/79/F-FC(SC))
(ESA-CR(P)-1476) Avail: NTIS HC A14/MF A01

European remote sensing activities are reviewed while development and utilization trends are identified. Existing and planned satellite systems are described. Remote sensing applications are listed by country in the European Economic Community. Cartography, geology, agriculture, silviculture, and land and water resources management are mentioned among other user disciplines. Applications are summarized in three categories: terrestrial, maritime, and coastal. Although maritime and coastal uses of remote sensing data are less well developed than terrestrial applications, economic, social and political benefits which can be accrued by Europe are sure to provide a strong incentive to continuing development. Author (ESA)

N82-19627*# Public Technology, Inc., Washington, D. C.
REMOTE SENSING PROCUREMENT PACKAGE: A MANAGEMENT REPORT FOR STATE AND LOCAL GOVERNMENTS
Jun. 1981 21 p ERTS
(Contract NAS13-129)
(E82-10052; NASA-CR-168633) Avail: NTIS HC A02/MF A01 CSCL 05B

An overview of the remote sensing procurement process is presented for chief executives, senior administrators, and other local and state officials responsible for purchasing remote sensing products, services, or equipment. Guidelines are provided for planning, organizing, staffing, and implementing such a procurement project. Other sections of the four-volume package are described and their benefits examined. A.R.H.

N82-20626# Inter-American Geodetic Survey, Fort Sam Houston, Tex.
REMOTE SENSING IN LATIN AMERICA: TECHNOLOGY AND MARKETS FOR THE 1980'S
Lawrence J. Jungman Aug. 1981 16 p refs
(AD-A108784) Avail: NTIS HC A02/MF A01 CSCL 22/2

A review is made on the impact of satellite derived remote sensing data in Latin America. Data availability has generated a phenomenal growth in the user community in Latin America, and new sensor systems planned and proposed are viewed as a further impetus to an increased market in the Americas. The international institutionalization of remote sensing interests in the area is an indicator submitted as a viable force in the continued, future market and transfer of technology. The availability of required training and funding for special projects by these institutions is reviewed. Proposals are made for special training to prepare for increased digital and cartographic applications that will be required in the expanded users market of the 1980s. GRA

N82-21660*# Washington Univ., St. Louis, Mo. Center for Development Technology.
PROGRAM ON STIMULATING OPERATIONAL PRIVATE SECTOR USE OF EARTH OBSERVATION SATELLITE INFORMATION Final Report, 1 Nov. 1979 - 15 Jan. 1981
Lester F. Eastwood, Jr., Jerry Foshage, Guillermo Gomez, Becky Kirkpatrick, Barry Konig, and Robert Stein, Principal Investigators 15 Jan. 1981 216 p refs Original contains imagery. Original photography may be purchased from the EROS Data Center, Sioux Falls, S.D. 57198. ERTS
(Contract NASw-3331)
(E82-10131; NASA-CR-168515; NAS 1.26:168515) Avail: NTIS HC A10/MF A01 CSCL 05B

Ideas for new businesses specializing in using remote sensing and computerized spatial data systems were developd. Each such business serves as an 'information middleman', buying raw satellite or aircraft imagery, processing these data, combining them in a computer system with customer-specific information, and marketing the resulting information products. Examples of the businesses the project designed are: (1) an agricultural facility site evaluation firm; (2) a mass media grocery price and supply analyst and forecaster; (3) a management service for privately held woodlots; (4) a brokerage for insulation and roofing contractors, based on infrared imagery; (5) an expanded real estate information service. In addition, more than twenty-five other commercially attractive ideas in agribusiness, forestry, mining, real estate, urban planning and redevelopment, and consumer information were created. The commercial feasibility of the five business was assessed. This assessment included market surveys, revenue projections, cost analyses, and profitability studies. The results show that there are large and enthusiastic markets willing to pay for the services these businesses offer, and that the businesses could operate profitably. M.G.

SUBJECT INDEX

EARTH RESOURCES / *A Continuing Bibliography (Issue 34)* **JULY 1982**

Typical Subject Index Listing

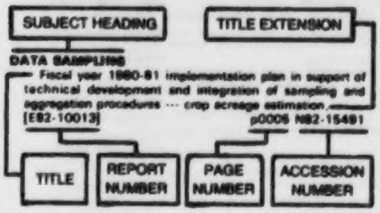
SUBJECT HEADING
TITLE EXTENSION
DATA SAMPLING
Fiscal year 1980-81 implementation plan in support of technical development and integration of sampling and aggregation procedures --- crop acreage estimation
[E82-10013]
p0005 N82-15491
TITLE
REPORT NUMBER
PAGE NUMBER
ACCESSION NUMBER

The subject heading is a key to the subject content of the document. The title is used to provide a description of the subject matter. When the title is insufficiently descriptive of the document content, the title extension is added, separated from the title by three hyphens. The (NASA or AIAA) accession number and the page number are included in each entry to assist the user in locating the abstract in the abstract section (of this supplement). If applicable, a report number is also included as an aid in identifying the document. Under any one subject heading, the accession numbers are arranged in sequence with the AIAA accession numbers appearing first.

A

ACCURACY

Modern methods for monitoring and controlling the timeliness, accuracy, and completeness of data for meteorological analysis p0073 A82-19179

Landsat classification accuracy assessment procedures p0137 A82-20412

Using known map category marginal frequencies to improve estimates of thematic map accuracy p0113 A82-25456

ADRIATIC SEA

Thermal IR detection of submarine gas seepages in the western Istra off-shore area /Yugoslavia/ p0076 A82-27661

LANDSAT imagery of the Venetian Lagoon: A multitemporal analysis
[E82-10036] p0119 N82-19612

AERIAL PHOTOGRAPHY

An airphoto key for major tropical crops p0058 A82-22142

Evaluation of aerial photogrammetric camera and aircraft scanner pictures from tidal lands - Digital correlation and classification of multitemporal imagery data p0127 A82-26049

AERIAL RECONNAISSANCE

Satellite photos can aid navigation on aerial photo missions p0126 A82-22148

Satellite Earth resources data, module U-3
[E82-10035] p0119 N82-19611

National High-Altitude Photography (NHAP) of the Tennessee Valley Region, volume 1, no. 1
[PB82-130899] p0134 N82-21703

AEROSOLS

The use of the airborne lidar system 'ALEX F 1' for aerosol tracing in the lower troposphere p0073 A82-20226

The NASA participation in the 1980 EPA PEPE/NEROS field measurements program p0075 A82-26621

Effect of aerosols on optical remotely sensed data p0115 A82-27654

Demonstration of a long-range atmospheric tracer system using perfluorocarbons
[PB82-106246] p0081 N82-16613

Sounding the aerosol distribution over the Upper Rhine Valley in the Valley in the Speyer area by means of lidar p0079 N82-20782

AFRICA

Ore deposits in Africa and their relation to the underlying mantle p0090 A82-26604

Diurnal variation of summer convection over West Africa and the Tropical Eastern Atlantic during 1974 and 1978 p0075 A82-26700

Preliminary models of the core field --- geomagnetic models
[E82-10129] p0087 N82-21659

AGRICULTURE

Utilisation of remote sensing in resources identification and land use in India - An integrated approach p0076 A82-27701

Examination of the operational prospects for remote sensing --- in Europe
[ESA-CR(P)-1476] p0138 N82-18669

Elevation of a cane-growing area of the state of Sao Paulo using LANDSAT data
[E82-10077] p0067 N82-20800

System of forecasting agricultural crops using satellite observations of Earth
[E82-10079] p0067 N82-20802

Soybean canopy reflectance as influenced by cultural practices --- West Lafayette, Indiana
[E82-10105] p0068 N82-21647

A look at the commonly used LANDSAT vegetation indices
[E82-10123] p0070 N82-21657

Sonora exploratory study for the detection of wheat-leaf rust
[E82-10133] p0070 N82-21661

Spectral-agronomic relationships of corn, soybean and wheat canopies
[E82-10143] p0070 N82-21670

AGROCLIMATOLOGY

A gradient model of vegetation and climate utilizing NOAA satellite imagery. Phase 1: Texas transect
[E82-10107] p0069 N82-21648

AGROMETEOROLOGY

Data base requirements in support of crop models p0060 A82-27588

Preliminary evaluation of spectral, normal and meteorological crop stage estimation approaches
[E82-10059] p0065 N82-19634

AIR POLLUTION

The use of the airborne lidar system 'ALEX F 1' for aerosol tracing in the lower troposphere p0073 A82-20226

Airborne in-situ measurement of particulate sulfur and sulfuric acid with flame photometry and thermal analysis p0073 A82-20999

An investigation of the ozone plume from a small city p0074 A82-26329

A regional air quality model for the Kwinana industrial area of Western Australia p0075 A82-26403

The NASA participation in the 1980 EPA PEPE/NEROS field measurements program p0075 A82-26621

Model studies of laser absorption computed tomography for remote air pollution measurement p0077 A82-28152

Demonstration of a long-range atmospheric tracer system using perfluorocarbons
[PB82-106246] p0081 N82-16613

Remote sensing of sulfur dioxide effects on vegetation. Volume 1: Summary
[PB82-115122] p0066 N82-19715

Remote sensing of sulfur dioxide effects on vegetation. Volume 2: Data
[PB82-115130] p0066 N82-19716

Sounding the aerosol distribution over the Upper Rhine Valley in the Valley in the Speyer area by means of lidar p0079 N82-20782

AIR QUALITY

A regional air quality model for the Kwinana industrial area of Western Australia p0075 A82-26403

AIR SAMPLING

An investigation of the ozone plume from a small city p0074 A82-26329

AIR WATER INTERACTIONS

Structure and variability of the Alboran Sea frontal system p0093 A82-20447

SASS measurements of the Ku-band radar signature of the ocean p0093 A82-21917

Some peculiarities of formulation and solution of inverse problems in microwave radiometry of the ocean surface and atmosphere p0093 A82-21921

Optimal spatial filtering and transfer function for SAR ocean wave spectra p0094 A82-27596

Estimation of sea surface temperature from remote sensing in the 3.7 micron window region p0095 A82-28031

Estimating ocean-air heat fluxes during cold air outbreaks by satellite
[NASA-TM-83854] p0097 N82-19781

AIRBORNE/SPACEBORNE COMPUTERS

The Seasat low rate data processing system p0093 A82-24061

Strategies and uses of small distributed analysis centers as in the natural resource inventory of Venezuela p0115 A82-27636

Utilization of spatial complexity in computer classified Landsat MSS data for multi-factoral thematic mapping p0129 A82-27648

Development and implementation of a low cost micro computer system for Landsat analysis and geographic data base application p0129 A82-27649

Structure of hardware and software at a regional center for the automated processing of aerial and space remote-sensing images p0130 A82-28128

Complex of units for the storage and automated processing of research data p0131 A82-28140

ALASKA

Landsat thermal imaging of alpine regions p0079 A82-22147

Ground-truth observations of ice-covered North Slope Lakes imaged by radar
[NASA-TM-84127] p0107 N82-18664

ALBEDO

Optical properties of snow p0101 A82-21922

Low-latitude cloudiness and climate feedback - Comparative estimates from satellite data p0075 A82-26980

Albedo and brightness coefficients of snow cover p0103 A82-27465

Spectral albedos of midlatitude snowpacks
[NASA-TM-83858] p0106 N82-18663

ALFALFA

Simple radiative transfer model for relationships between canopy biomass and reflectance p0057 A82-20422

Dew and vapor pressure as complicating factors in the interpretation of spectral radiance from crops p0060 A82-27617

ALGAE

Spectrometric studies of the water composition of Lake Mueggelsee p0104 A82-27474

Inland water quality assessment from Landsat data p0105 A82-27610

HCMM hydrological analysis in Utah --- Utah lake
[E82-10063] p0107 N82-20586

ALGEBRA

Exterior algebraic processing for remotely sensed multispectral and multitemporal images p0112 A82-21041

ALGORITHMS

Context dependent modeling --- for remote sensing data processing p0114 A82-27587

Automatic and semi-automatic classification of Landsat agricultural crops p0061 A82-27664

Fanning - A classification algorithm for mixture landscapes applied to Landsat data of Maine forests p0062 A82-27668

Simplified algorithm for calculating radiative transfer in satellite images
[INPE-2169-RPE/385] p0118 N82-16450

NOSS altimeter algorithm specifications
[NASA-RP-1083] p0095 N82-16683

An evaluation of ISOCLS and CLASSY clustering algorithms for forest classification in northern Idaho --- Elk River quadrange of the Clearwater National Forest
[E82-10109] p0069 N82-21650

ALLUVIUM

Measurement of river sediments
[WMO-561] p0107 N82-18670

ALPS MOUNTAINS (EUROPE)

Towards the definition of optimum sensor specifications for microwave remote sensing of snow p0125 A82-21035

AMAZON REGION (SOUTH AMERICA)

Sigma/deg/ signature of the Amazon rain forest obtained from the Seasat scatterometer p0125 A82-21027

Amazonas project: Application of remote sensing techniques for the integrated survey of natural resources in Amazonas --- Brazil
[E82-10069] p0078 N82-20592

ANALYSIS OF VARIANCE

Development of rotation sample designs for the estimation of crop acreages
[E82-10117] p0070 N82-21654

Determination of the optimal level for combining area and yield estimates
[E82-10146] p0071 N82-21673

ANGULAR DISTRIBUTION

Regional properties of angular reflectance models p0083 N82-17599

ANNUAL VARIATIONS

Low-latitude cloudiness and climate feedback - Comparative estimates from satellite data p0075 A82-26980

A study of model parameters associated with the urban climate using HCMM data --- analysis of St. Louis, Missouri infrared imagery [E82-10160] p0080 N82-21684

ANTARCTIC REGIONS

Ionospheric troughs in Antarctica p0073 A82-21217

Satellite-derived ice data sets no. 1. Antarctic monthly average microwave brightness temperatures and sea-ice concentrations, 1973 - 1976 [NASA-TM-83812] p0096 N82-17563

Investigation of Antarctic crust and upper mantle using MAGSAT and other geophysical data [E82-10062] p0086 N82-20585

Investigation of antarctic crust and upper mantle using MAGSAT and other geophysical data [E82-10147] p0087 N82-21674

ANTENNA DESIGN

The microwave radiometer spacecraft. A design study. Executive summary p0131 N82-16154

Mission definition for a large-aperture microwave radiometer spacecraft p0131 N82-16155

ANTENNA RADIATION PATTERNS

Context sensitive formulations of antenna pattern correction and side lobe compensation for NOSS/LAMMR real time processing [NASA-CR-166789] p0122 N82-21457

AQUIFERS

Use of Landsat imagery to delineate glaciofluvial aquifers in southeast South Dakota p0105 A82-27637

ARABIAN SEA

Arabian sea project of 1980. Composites of infrared images [AD-A107910] p0096 N82-17567

ARCHAEOLOGY

Locating prehistoric archaeological sites using Landsat p0129 A82-27638

Applications of aircraft and satellite data for the study of archaeology and environment - Mekong Delta, Vietnam p0091 A82-27705

ARCTIC OCEAN

The use of data from satellite-borne microwave scanning radiometers for the automated compilation of operational maps of ice cover for the Arctic Ocean p0095 A82-28145

ARGENTINA

The Pampean Plain studied with Landsat images p0089 A82-26013

Natural resources inventories by computer-satellite mapping techniques in Chaco State, Argentine Republic, South America p0116 A82-27688

Taxonomic classification of world map units in crop producing areas of Argentina and Brazil with representative US soil series and major land resource areas in which they occur [E82-10058] p0065 N82-19633

Sample selection in foreign similarity regions for multicrop experiments [E82-10118] p0070 N82-21655

The 1981 Argentina ground data collection [E82-10127] p0070 N82-21658

ARIZONA

Cliff and slope topography of part of the Grand Canyon, Arizona as characterized on a Seasat radar image p0082 A82-26843

Applications systems verification and transfer project. Volume 2: Operational applications of satellite snow-cover observations and data-collection systems in the Arizona test site [NASA-TP-1823] p0108 N82-20618

ARTIFICIAL INTELLIGENCE

An intelligent earth sensing information system p0137 A82-22149

ASHES

Detection of volcanic ash fall area from Landsat MSS CCT data Eruption of Mt. Ontake in 1979 p0076 A82-27650

ASIA

Potential use of space photographs obtained from the manned orbital station Salyut-5 in order to compile a set of small-scale thematic maps of mountain and piedmont regions of Central Asia p0083 A82-28139

ASTRONOMICAL COORDINATES

Correlation identification of stellar configurations for purposes of the coordinate referencing of aerial and space images p0117 A82-28141

ATLANTIC OCEAN

The use of Meteor-satellite image data in oceanography p0093 A82-20344

Structure and variability of the Alboran Sea frontal system p0093 A82-20447

Diurnal variation of summer convection over West Africa and the Tropical Eastern Atlantic during 1974 and 1978 p0075 A82-26700

High precision radiometric temperature measurements of the ocean surface p0094 A82-27640

Classification of the fields of anomaly in monthly water temperature of the North Atlantic during the cold half-year [BLL-TRANS-1509-(9022.552)] p0097 N82-19756

Convergence zones in the South Atlantic and their influence on the precipitation regime in Northeastern Brazil [INPE-2307-TDL/074] p0097 N82-19778

Interaction between the Agulhas current and the subtropical convergence [CSIR-RR-384] p0098 N82-20824

Surface wave statistics and spectra during high sea state conditions in the North Atlantic [AD-A109832] p0098 N82-20827

ATMOSPHERIC ATTENUATION

Dew and vapor pressure as complicating factors in the interpretation of spectral radiance from crops p0060 A82-27617

Simplified algorithm for calculating radiative transfer in satellite images [INPE-2169-RPE/385] p0118 N82-16450

Development of a surface isolation estimation technique suitable for application of polar orbiting satellite data [E82-10122] p0123 N82-21656

Methods of editing cloud and atmospheric layer affected pixels from satellite data [E82-10154] p0123 N82-21678

ATMOSPHERIC CHEMISTRY

Mid-latitude summertime measurements of stratospheric NO2 p0074 A82-25149

ATMOSPHERIC CIRCULATION

Multidimensional aspects. Ozone, temperature and transport p0081 N82-18772

ATMOSPHERIC COMPOSITION

A regional air quality model for the Kwinana industrial area of Western Australia p0075 A82-26403

Stratospheric instruments and analyses p0133 N82-18776

ATMOSPHERIC DIFFUSION

Diffusion model of cloud cover and its use in the analysis of satellite operations p0111 A82-20347

Demonstration of a long-range atmospheric tracer system using perfluorocarbons [PB82-106246] p0081 N82-16813

ATMOSPHERIC EFFECTS

Diffusion model of cloud cover and its use in the analysis of satellite operations p0111 A82-20347

Contrast reduction by the atmosphere and retrieval of nonuniform surface reflectance p0112 A82-20423

Effects of the atmosphere on the detection of surface changes from Landsat multispectral scanner data p0125 A82-21091

Spaceborne photography for the study of earth resources --- Russian book p0126 A82-22397

Influence of illumination and viewing geometry and atmospheric composition on the tasseled cap transformation of Landsat MSS data p0059 A82-24961

Effect of aerosols on optical remotely sensed data p0115 A82-27654

ATMOSPHERIC HEAT BUDGET

Low-latitude cloudiness and climate feedback - Comparative estimates from satellite data p0075 A82-26980

ATMOSPHERIC MODELS

Effect of aerosols on optical remotely sensed data p0115 A82-27654

Multidimensional aspects. Ozone, temperature and transport p0081 N82-18772

ATMOSPHERIC MOISTURE

Some peculiarities of formulation and solution of inverse problems in microwave radiometry of the ocean surface and atmosphere p0093 A82-21921

ATMOSPHERIC OPTICS

Effect of aerosols on optical remotely sensed data p0115 A82-27654

ATMOSPHERIC RADIATION

Measurement of atmospheric emission using a balloon-borne cryogenic Fourier spectrometer p0074 A82-21432

Particle precipitation and atmospheric X-and Gamma-rays in the South Atlantic magnetic anomaly by balloon experiments [INPE-2119-RPE/343] p0083 N82-17711

ATMOSPHERIC SCATTERING

Effects of the atmosphere on the detection of surface changes from Landsat multispectral scanner data p0125 A82-21091

Microwave remote sensing. Active and passive. Volume 1 - Microwave remote sensing fundamentals and radiometry --- Book p0126 A82-22877

An approach to path radiance correction in MSS images p0115 A82-27629

The effect of finite field size on classification and atmospheric correction [NASA-TM-83818] p0120 N82-19645

ATMOSPHERIC SOUNDING

Observation of the turbulent structure in the planetary boundary layer with a kytoon-mounted ultrasonic anemometer system p0125 A82-21082

Sounding the aerosol distribution over the Upper Rhine Valley in the Valley in the Speyer area by means of lidar p0079 N82-20782

ATMOSPHERIC TEMPERATURE

Multidimensional aspects. Ozone, temperature and transport p0081 N82-18772

MSU test of P-model p0121 N82-20614

AURORAL ZONES

Ionospheric troughs in Antarctica p0073 A82-21217

AURORAS

Recent auroral measurements using a field-widened interferometer spectrometer p0126 A82-21434

AUSTRALIA

A regional air quality model for the Kwinana industrial area of Western Australia p0075 A82-26403

Inland water quality assessment from Landsat data p0105 A82-27610

Topographic mapping using Landsat data p0082 A82-27615

A vegetation response model applied to range inventory and monitoring using Landsat MSS data p0060 A82-27643

A low cost NOAA/TIROS AVHRR receiving station --- Advanced Very High Resolution Radiometer p0130 A82-27681

An aerial survey of water turbidity and laser depth sounding performance along the Queensland Coast [AD-A109050] p0098 N82-19802

Sample selection in foreign similarity regions for multicrop experiments [E82-10118] p0070 N82-21655

AUTOCORRELATION

Precision in the evaluation of Landsat autocorrelation - The terrain effect p0116 A82-27686

B

BACKSCATTERING

Influence of dissolved organic materials on turbid water optical properties and remote-sensing reflectance p0093 A82-20445

Volumetric effects in cross-polarized airborne radar data p0058 A82-21032

Crop classification using airborne radar and Landsat data p0058 A82-21033

Application and experimental verification of an empirical backscattering cross section model for the earth's surface p0081 A82-21036

A radar signature model for partially coherent scattering from irregular surfaces p0079 A82-21038

Microwave remote sensing. Active and passive. Volume 1 - Microwave remote sensing fundamentals and radiometry --- Book p0126 A82-22877

Remote sensing of rainfall rates using airborne microwave rain-scatterometer/radiometer p0105 A82-27639

Active microwave investigation of snowpacks: Experimental documentation, Colorado 1979-1980 [NASA-CR-166727] p0107 N82-19646

Satellite scatterometer feasibility study. Volume 2: Data extraction algorithm and error simulation for wind sensor --- Earth Resources Satellite (ERS 1) [ESA-CR(P)-1492-VOL-2] p0133 N82-19651

Atlas of the global distribution of the total ozone concentration according to satellite measurements [MITT-28] p0078 N82-19740

BANGLADESH

Digital processing of tropical forest habitat in Bangladesh and the development of a low cost processing facility at the National Zoo, Smithsonian Institution p0063 A82-27687

Assessment of change in Bangladesh coastal regions p0076 A82-27696

BARLEY

Documentation of computer procedures for labeling spring grains and discriminating between spring wheat and barley using LANDSAT data [E82-10030] p0063 N82-16448

AgRISTARS: Foreign commodity production forecasting. Minutes of the annual formal project manager's review, including preliminary technical review reports of FY80 experiments --- wheat/barley and corn/soybean experiments [E82-10039] p0064 N82-19614

BAYS (TOPOGRAPHIC FEATURES)

Multidisciplinary research on the application of remote sensing to water resources problems --- Wisconsin [E82-10021] p0106 N82-16439

Ship and satellite bio-optical research in the California Bight [NASA-CR-168681] p0098 N82-20823

BIBLIOGRAPHIES

Publications and reports on contracts and grants, 1980 [PB82-103219] p0138 N82-17792

BIOGRAPHY

Helmut Wolf. On the occasion of his 70th birthday [SER-E-18] p0084 N82-19603

BIOMASS

Simple radiative transfer model for relationships between canopy biomass and reflectance p0057 A82-20422

Multispectral photographic remote sensing of green vegetation biomass and productivity p0059 A82-22144

BIRDS

Remote sensing applications to resource problems in South Dakota [E82-10027] p0132 N82-16445

BLIGHT

Sonora exploratory study for the detection of wheat-leaf rust [E82-10133] p0070 N82-21661

BOUNDARIES

Investigation of geomagnetic field forecasting and fluid dynamics of the core [E82-10162] p0087 N82-21686

BRAZIL

Use of Landsat data for automatic classification and area estimation of sugar-cane plantation in Sao Paulo state. Brazil p0058 A82-21092

A structural synthesis of Brazil, based on the study of major lineaments derived from remote sensing imagery interpretation p0079 A82-26012

CNPq/INPE LANDSAT system --- operations at the Cuiaba station and the electronic processing and photo laboratories
[E82-10023] p0118 N82-16441

Report on a short course in remote sensing and the geological applications of LANDSAT MSS imagery at INPE
[E82-10024] p0091 N82-16442

Remote sensing data applied to land-use survey at the Paraiba Valley --- Brazil
[E82-10025] p0081 N82-16443

Brazilian remote sensing activities current and prospective needs
[E82-10026] p0132 N82-16444

The severity of the Brazilian freeze of July 1981, as monitored by satellite
[INPE-2231-RPE/399] p0064 N82-17746

Taxonomic classification of world map units in crop producing areas of Argentina and Brazil with representative US soil series and major land resource areas in which they occur
[E82-10058] p0065 N82-19633

Notes for Brazil sampling frame evaluation trip
[E82-10060] p0066 N82-19635

Utilization of Aerochrome 2443 film for identification and estimating wheat growing areas --- Rio Grande do Sul, Brazil
[INPE-2197-PRE/006] p0066 N82-19639

Preliminary results of a study of mapping thermal discharge in the ocean, using remote sensing data
[INPE-2229-PRE/021] p0097 N82-19704

Convergence zones in the South Atlantic and their influence on the precipitation regime in Northeastern Brazil
[INPE-2307-TDL/074] p0097 N82-19778

The utilization of orbital images as an adequate form of control of preserved areas --- Araguaia National Park, Brazil
[E82-10065] p0078 N82-20588

Amazonas project Application of remote sensing techniques for the integrated survey of natural resources in Amazonas --- Brazil
[E82-10069] p0078 N82-20592

Survey of the cane-growing area of the state of Sao Paulo using LANDSAT data. Safra Year 1979/80, volume 2 --- maps, Brazil
[E82-10071] p0067 N82-20594

Land use in the Paraiba Valley through remotely sensed data --- Brazil
[E82-10072] p0079 N82-20595

Study project of intrusive rocks States of Espirito Santo and Rio de Janeiro, south and east of Minas Gerais and southeast of the state of Sao Paulo --- Brazil
[E82-10076] p0092 N82-20599

Elevation of a cane-growing area of the state of Sao Paulo using LANDSAT data
[E82-10077] p0067 N82-20600

Relation of the activities of the IPDF/INPE project (reforestation subproject) during the year 1979 --- Mato Grosso do Sul, Brazil
[E82-10078] p0067 N82-20601

The LANDSAT system operated in Brazil by CNPq/INPE - results obtained in the area of mapping and future perspectives
[E82-10080] p0121 N82-20603

Dynamic study of the upper Sao Francisco River and the Tres Marias reservoir using MSS/LANDSAT images --- Brazil
[E82-10082] p0108 N82-20605

Sample selection in foreign similarity regions for multicrop experiments
[E82-10118] p0070 N82-21655

BRIGHTNESS

Analysis of the direction-dependent radiation behavior in multispectral scanning data p0125 A82-21399

The spectral reflectance of certain soils --- Russian book p0059 A82-26577

Evaluation of snow-cover pollution in industrial regions using satellite TV images p0103 A82-27464

Landsat feature enhancement - Or, can we separate vegetation from soil p0060 A82-27622

A look at the commonly used LANDSAT vegetation indices
[E82-10123] p0070 N82-21657

BRIGHTNESS DISTRIBUTION

Albedo and brightness coefficients of snow cover p0103 A82-27465

BRIGHTNESS TEMPERATURE

Soil moisture determination - Experiments with passive microwave radiometers p0057 A82-19529

Microwave radiation from a natural snow field p0101 A82-19559

Microwave brightness temperature pattern over the Indian subcontinent and the surrounding oceans as observed by the satellite microwave radiometer /SAMIR/ onboard Bhaskara p0093 A82-19560

Theoretical and experimental studies of microwave emission signatures of snow p0125 A82-21034

Towards the definition of optimum sensor specifications for microwave remote sensing of snow p0125 A82-21035

Optical properties of snow p0101 A82-21922

An optical model for the microwave properties of sea ice
[NASA-TM-83865] p0095 N82-17561

Satellite-derived ice data sets no 1 Antarctic monthly average microwave brightness temperatures and sea-ice concentrations, 1973 - 1976
[NASA-TM-83812] p0096 N82-17563

Observations with an imaging 35 GHz radiometer of terrain in Malmslatett, July 1980
[FOA-C-30240-E1/E3] p0133 N82-18672

BUILDINGS

Building and road extraction from aerial photographs p0074 A82-25140

C

CALCIUM CARBONATES

Calcium carbonate precipitation in Pyramid Lake, Nevada, as monitored by satellite - 1978 and 1980 p0105 A82-27634

CALIBRATING

The accuracy potential of the modern bundle block adjustment in aerial photogrammetry p0111 A82-20401

Calibration and model reconstruction in analytical close-range stereophotogrammetry I - Mathematical fundamentals p0111 A82-20403

Calibration and model reconstruction in analytical close-range stereophotogrammetry II - Special evaluation procedures for rasterstereography and moire topography p0126 A82-22141

Radiometric calibration of the Coastal Zone Color Scanner on Nimbus 7 - A proposed adjustment p0127 A82-26963

Ground level reflectance measurement techniques - An evaluation with emphasis on the importance of spectral calibration p0116 A82-27689

Ozone measurements to 48Km with chemiluminescent ozone detectors
[AD-A110342] p0134 N82-21808

CALIFORNIA

Techniques for combining Landsat and ancillary data for digital classification improvement p0111 A82-20410

A relation between Landsat digital numbers, surface reflectance, and the cosine of the solar zenith angle p0114 A82-26841

Scene analysis for wildland fire-fuel characteristics in a Mediterranean climate p0060 A82-27624

Session III of the VLBI/Laser intercomparison task of the NASA crustal dynamics project
[NASA-CR-168427] p0083 N82-17708

Applications systems verification and transfer project. Volume 3 Operational applications of satellite snow cover observations in California
[NASA-TP-1824] p0108 N82-20619

HCMM Soil moisture in relation to geologic structure and lithology, northern California --- Northern Coast Range Sacramento Valley, and the Modoc Plateau
[E82-10135] p0092 N82-21662

CANADA

Analyses of the Eastern Pacific without ship PAPA data --- buoys, radar and satellite to replace weathership p0093 A82-19139

The use of digital multi-date Landsat imagery in terrain classification p0111 A82-20409

Change detection in the Peace-Athabasca Delta using digital Landsat data p0101 A82-24959

The Canadian north - Utility of remote sensing for environmental monitoring p0074 A82-24962

A timely and accurate potato acreage estimate from Landsat - Results of a demonstration p0060 A82-27621

Digital analysis of spatial and spectral features from airborne MSS of a forested region p0061 A82-27647

Interpretation of Heat Capacity Mapping Mission images over Canada p0116 A82-27671

Landsat MSS applied to rangeland management in Western Canada p0063 A82-27697

Visual and digital analysis of H C M M data over eastern Canada --- thermal imagery by Heat Capacity Mapping Mission p0117 A82-27698

Development of a Canadian thermal infrared forest fire mapping operational program p0063 A82-27699

Heat Capacity Mapping Mission (HCMM) Interpretation of imagery over Canada
[E82-10070] p0079 N82-20593

Relief effects and the use of terrain models in SAR image processing --- Anderson River test site, British Columbia p0086 N82-21475

CANALS

Applications of aircraft and satellite data for the study of archaeology and environment - Mekong Delta, Vietnam p0091 A82-27705

CANOPIES (VEGETATION)

Color characteristics of the earth's surface determined on the basis of spectroscopy results from Salyut 4 p0073 A82-19826

Mapping in tropical forests - A new approach using the laser APR --- Airborne Profile Recorder p0081 A82-20407

Simple radiative transfer model for relationships between canopy biomass and reflectance p0057 A82-20422

Microwave radiation peculiarities of vegetative covers p0058 A82-21029

Investigation of the vegetative covers on ploughed areas by SLAR p0058 A82-21031

The estimation of the surface moisture of a vegetated soil using aerial infrared photography p0058 A82-21093

Multispectral photographic remote sensing of green vegetation biomass and productivity p0059 A82-22144

Stochastic models of cover class dynamics --- remote sensing of vegetation p0059 A82-27586

Dew and vapor pressure as complicating factors in the interpretation of spectral radiance from crops p0060 A82-27617

Landsat feature enhancement - Or, can we separate vegetation from soil p0060 A82-27622

Enhancement of Landsat data for Hudson Bay lowlands vegetation p0114 A82-27623

Soybean canopy reflectance as a function of view and illumination geometry p0061 A82-27645

The influence of illumination and viewing geometry on the reflectance factor of agricultural targets p0061 A82-27646

An invertible coniferous forest canopy reflectance model p0062 A82-27679

Influence of solar illumination angle on soybean canopy reflectance p0063 A82-28153

The application of remote sensing to resource management and environmental quality programs in Kansas --- Cimarron National Grasslands, Prairie Potawatomi Reservation, and Kickapoo Reservation
[E82-10029] p0063 N82-16447

Thermal vegetation canopy model studies
[AD-A106422] p0064 N82-16455

Effects of nitrogen nutrition on the growth, yield and reflectance characteristics of corn canopies --- Purdue Agronomy Farm, Indiana
[E82-10068] p0067 N82-20591

Dryland pasture and crop conditions as seen by HCMM --- Washita River watershed
[E82-10074] p0067 N82-20597

Soybean canopy reflectance as influenced by cultural practices --- West Lafayette, Indiana
[E82-10106] p0068 N82-21647

A look at the commonly used LANDSAT vegetation indices
[E82-10123] p0070 N82-21657

Spectral-agronomic relationships of corn, soybean and wheat canopies
[E82-10143] p0070 N82-21670

Simulated response of a multispectral scanner over wheat as a function of wavelength and view/illumination direction
[E82-10144] p0071 N82-21671

Variability of reflectance measurements with sensor altitude and canopy type
[E82-10145] p0071 N82-21672

Applications of HCMM satellite data to the study of urban heating patterns
[E82-10161] p0080 N82-21685

CASCADE RANGE (CA-OR-WA)

Applications systems verification and transfer project. Volume 3 Operational applications of satellite snow cover observations in California
[NASA-TP-1824] p0108 N82-20619

CASPIAN SEA

Survey and mapping of shallow water bodies and the distribution of the river runoff of solids on the basis of multispectral aerial and space photographs p0103 A82-27467

Polarimetric method for the remote sensing of oil slicks on the sea surface p0095 A82-28135

CATALOGS (PUBLICATIONS)

AgRISTARS Interim catalog ground data summary, data acquisition year 1979
[E82-10032] p0064 N82-19608

CELESTIAL GEODESY

Orbital methods of celestial geodesy --- Russian book p0079 A82-25234

CELESTIAL REFERENCE SYSTEMS

Correlation identification of stellar configurations for purposes of the coordinate referencing of aerial and space images p0117 A82-28141

CENTRAL PROCESSING UNITS

Overview of digital processing of SAR data --- from Seasat-A p0128 A82-27589

Features of a generalized digital Synthetic Aperture Radar processor p0128 A82-27595

CHAPARRAL

Scene analysis for wildland fire-fuel characteristics in a Mediterranean climate p0060 A82-27624

CHEMILUMINESCENCE

Ozone measurements to 48Km with chemiluminescent ozone detectors
[AD-A110342] p0134 N82-21808

CHESAPEAKE BAY (US)

The relationship among sea surface roughness variations, oceanographic analyses, and airborne remote sensing analyses
[NASA-CR-168444] p0096 N82-17798

CHLOROPHYLLS

Ship and satellite bio-optical research in the California Bight
[NASA-CR-168681] p0098 N82-20823

As-built design specification for PARHIS
[E82-10089] p0122 N82-21641

CINEMATOGRAPHY

Photogrammetry from aircraft side camera movies - Winter MONEX p0075 A82-26721

CITIES

A system for quantitative determination of species and vitalities of urban trees on color-infrared photographs p0074 A82-24958

Analysis of two Seasat synthetic aperture radar images of an urban scene p0074 A82-25452

An investigation of the ozone plume from a small city p0074 A82-26329

Phenomena modelling of remotely sensed data by image rationing p0076 A82-27670

Visual and digital analysis of H C M M data over eastern Canada --- thermal imagery by Heat Capacity Mapping Mission p0117 A82-27698

The effect of finite field size on classification and atmospheric correction [NASA-TM-83818] p0120 N82-19645

A study of model parameters associated with the urban climate using HCMM data [E82-10159] p0080 N82-21683

A study of model parameters associated with the urban climate using HCMM data --- analysis of St. Louis, Missouri infrared imagery [E82-10160] p0080 N82-21684

Applications of HCMM satellite data to the study of urban heating patterns [E82-10161] p0080 N82-21685

CLASSIFICATIONS

Landscape mapping and physical-geographical classification of the eastern part of the Chechen-Ingush, ASSR using space imagery p0073 A82-20339

Automation of the processing of aerial and space images for forest inventory p0057 A82-20350

Techniques for combining Landsat and ancillary data for digital classification improvement p0111 A82-20410

Landsat classification accuracy assessment procedures p0137 A82-20412

Crop classification using airborne radar and Landsat data p0058 A82-21033

Maximum likelihood estimation of label imperfection probabilities and its use in the identification of mislabeled patterns p0112 A82-21040

Information extraction from remotely sensed data - A user view p0112 A82-21089

Use of Landsat data for automatic classification and area estimation of sugar-cane plantation in Sao Paulo state, Brazil p0058 A82-21092

The use of contextual information to improve land cover classification of digital remotely sensed data p0112 A82-21094

A system for quantitative determination of species and vitalities of urban trees on color-infrared photographs p0074 A82-24958

Change detection in the Peace-Athabasca Delta using digital Landsat data p0101 A82-24959

Spectral reflectance of hydrophytes p0102 A82-24960

Building and road extraction from aerial photographs p0074 A82-25140

Modeling misregistration and related effects on multispectral classification p0113 A82-25455

Using known map category marginal frequencies to improve estimates of thematic map accuracy p0113 A82-25456

Use of Landsat-derived temporal profiles for corn-soybean feature extraction and classification p0059 A82-26842

Development and implementation of a low cost micro computer system for Landsat analysis and geographic data base application p0129 A82-27649

Orbital performance of a 1.6 micrometer DMSP snow/cloud discrimination sensor p0130 A82-27653

Detailed land use classification based on multitemporal Landsat-MSS-data p0076 A82-27657

Automatic and semi-automatic classification of Landsat agricultural crops p0061 A82-27664

Fanning - A classification algorithm for mixture landscapes applied to Landsat data of Maine forests p0062 A82-27668

Classification of Landsat MSS data for surface cover of small areas p0116 A82-27677

An experiment in probabilistic relaxation for terrain cover classification of Kuwait from Landsat imagery p0062 A82-27680

Non-parametric classification of abandoned coal mine features using multioriented and ratio transformed Landsat data p0090 A82-27694

Remote sensing data applied to land-use survey at the Paraiba Valley --- Brazil [E82-10025] p0081 N82-16443

A comparison of unsupervised classification procedures on LANDSAT MSS data for an area of complex surface conditions in Basilicata, Southern Italy [E82-10038] p0119 N82-19613

Taxonomic classification of world map units in crop producing areas of Argentina and Brazil with representative US soil series and major land resource areas in which they occur [E82-10058] p0065 N82-19633

The effect of finite field size on classification and atmospheric correction [NASA-TM-83818] p0120 N82-19645

Selection of attributes applied to multispectral images [INPE-2303-TDL/072] p0121 N82-19827

Evaluation of a segment-based LANDSAT full-frame approach to corp area estimation [E82-10067] p0066 N82-20590

Land use in the Paraiba Valley through remotely sensed data --- Brazil [E82-10072] p0079 N82-20595

An algorithm for spatial heirarchy clustering [E82-10081] p0121 N82-20604

As-Built design specification for UNIV4VEC [E82-10085] p0122 N82-21637

US corn and soybeans exploratory experiment [E82-10088] p0068 N82-21640

As-built design specification for PARHIS [E82-10089] p0122 N82-21641

As-built design specification for PARCLS [E82-10090] p0123 N82-21642

As-built design specification for MISMAP [E82-10091] p0123 N82-21643

As-built design specification for the CLASFYG program [E82-10092] p0068 N82-21644

An evaluation of ISOCLS and CLASSY clustering algorithms for forest classification in northern Idaho --- Elk River quadrange of the Clearwater National Forest [E82-10109] p0069 N82-21650

Transition year labeling error characterization study --- Kansas, Minnesota, Montana, North Dakota, South Dakota, and Oklahoma [E82-10111] p0069 N82-21651

AgRISTARS: Supporting research. Classification of corn: Badhwar profile similarity technique --- us corn belt [E82-10150] p0071 N82-21676

CLIFFS

Cliff and slope topography of part of the Grand Canyon, Arizona as characterized on a Seasat radar image p0082 A82-26843

CLIMATE

Visual and digital analysis of H C M M data over eastern Canada --- thermal imagery by Heat Capacity Mapping Mission p0117 A82-27698

Application of satellite frost forecast technology to other parts of the United States, phase 2, introduction p0121 N82-20608

Freeze prediction model --- Pennsylvania p0067 N82-20609

Applicability of satellite freeze forecasting and cold climate mapping to the other parts of the United States --- Michigan p0068 N82-20613

MSU test of P-model p0121 N82-20614

A satellite frost forecasting system for Florida p0079 N82-20615

CLIMATOLOGY

Low-latitude cloudiness and climate feedback - Comparative estimates from satellite data p0075 A82-26980

Climate observing system studies: An element of the NASA Climate Research Program. Workshop report [NASA-TM-84040] p0078 N82-18808

Application of satellite frost forecast technology to other parts of the United States, phase 2 --- Pennsylvania, Michigan, and Florida [NASA-CR-166827] p0121 N82-20607

A study of model parameters associated with the urban climate using HCMM data [E82-10159] p0080 N82-21683

A study of model parameters associated with the urban climate using HCMM data --- analysis of St. Louis, Missouri infrared imagery [E82-10160] p0080 N82-21684

CLOUD COVER

Satellite observed cloud patterns associated with excessive precipitation outbreaks [PB80-215130] p0073 A82-19177

Diffusion model of cloud cover and its use in the analysis of satellite operations p0111 A82-20347

Low-latitude cloudiness and climate feedback - Comparative estimates from satellite data p0075 A82-26980

Interpretation of Heat Capacity Mapping Mission images over Canada p0116 A82-27671

Heat Capacity Mapping Mission (HCMM): Interpretation of imagery over Canada [E82-10070] p0079 N82-20593

Dust from the Sahara in satellite images p0079 N82-20802

Development of a surface isolation estimation technique suitable for application of polar orbiting satellite data [E82-10122] p0123 N82-21656

Methods of editing cloud and atmospheric layer affected pixels from satellite data [E82-10154] p0123 N82-21678

Atlas of METEOSAT imagery [ESA-SP-1030] p0124 N82-21700

CLOUD PHOTOGRAPHS

Atlas of METEOSAT imagery [ESA-SP-1030] p0124 N82-21700

CLOUD PHOTOGRAPHY

Photogrammetry from aircraft side camera movies - Winter MONEX p0075 A82-26721

CLOUD PHYSICS

Development and applications of techniques to process hydrometeor distribution data [AD-A109929] p0109 N82-20822

CLOUDS (METEOROLOGY)

Orbital performance of a 1.6 micrometer DMSP snow/cloud discrimination sensor p0130 A82-27653

Methods of editing cloud and atmospheric layer affected pixels from satellite data [E82-10046] p0119 N82-19621

COASTAL WATER

A photometric method for depth determination by aerial photography p0101 A82-19831

An approach to path radiance correction in MSS images p0115 A82-27629

A formation process of an oceanic vortex analyzed by multi-temporal remote sensing p0095 A82-27674

Imaging microwave radiometer. Phase A study. Volume 1: Executive summary --- instrument for the European Remote Sensing system payload [ESS/SS-1006] p0132 N82-18564

Coastal upwelling ecosystems analysis. Atlas of the JOINT I aircraft winds for the 500 foot level [PB82-114703] p0097 N82-19796

An aerial survey of water turbidity and laser depth sounding performance along the Queensland Coast [AD-A109050] p0098 N82-19802

Ship and satellite bio-optical research in the California Bight [NASA-CR-168681] p0098 N82-20823

COASTAL ZONE COLOR SCANNER

Radiometric calibration of the Coastal Zone Color Scanner on Nimbus 7 - A proposed adjustment p0127 A82-26863

COASTS

Integrated sensor system for collection of wave data applied to coastal engineering design p0094 A82-27602

Assessment of change in Bangladesh coastal regions p0076 A82-27696

Applications of aircraft and satellite data for the study of archaeology and environment - Mekong Delta, Vietnam p0091 A82-27705

Examination of the operational prospects for remote sensing --- in Europe [ESA-CR(P)-1476] p0138 N82-18569

Heat Capacity Mapping Mission (HCMM) program: Study of geological structure of Sicily and other Italian areas --- Sardinia and the Gulf of Orosei [E82-10073] p0091 N82-20596

COHERENT SCATTERING

A radar signature model for partially coherent scattering from irregular surfaces p0079 A82-21038

Coherent scatter of microwaves from moderateily rough surfaces [AD-A106133] p0095 N82-16331

COLD WEATHER

The severity of the Brazilian freeze of July 1981, as monitored by satellite [INPE-2231-RPE/399] p0064 N82-17746

Use of thermal inertia determined by HCMM to predict nocturnal cold prone areas in Florida [E82-10040] p0064 N82-19615

Application of satellite frost forecast technology to other parts of the United States, phase 2, introduction p0121 N82-20608

COLOR CODING

Development and implementation of a low coist micro computer system for Landsat analysis and geograpihc data base application p0129 A82-27649

Matrix data analysis: Color/B and W coding is not always enough [AD-A108406] p0084 N82-18930

COLOR INFRARED PHOTOGRAPHY

Application of side-looking color infrared photography for structure detection in subtle topography p0082 A82-27611

COLORADO

Effect of aerosols on optical remotely sensed data p0115 A82-27654

Active microwave investigation of snowpacks: Experimental documentation, Colorado 1979-1980) [NASA-CR-166727] p0107 N82-19646

Applications systems verification and transfer project. Volume 4: Operational applications of satellite snow cover observations: Colorado Field Test Center [NASA-TP-1825] p0108 N82-20620

Applications systems verification and transfer project. Volume 7: Cost/benefit analysis for the ASVT on operational applications of satellite snow-cover observations [NASA-TP-1828] p0109 N82-20623

Registration verification of SEA/AR fields --- Oregon, Texas, Montana, Nebraska, Washington, Colorado, Kansas, Oklahoma, and North Dakota [E82-10083] p0068 N82-21635

San Juan National Forest Land Management Planning Support System (LMPSS) requirements definition [E82-10108] p0069 N82-21649

COLORIMETRY

Color characteristics of the earth's surface determined on the basis of spectroscopy results from Salyut 4 p0073 A82-19826

COMMERCE

Program on stimulating operational private sector use of Earth observation satellite information [E82-10131] p0138 N82-21660

COMPUTER COMPATIBLE TAPES

Partially processed multispectral scanner LANDSAT high-density tapes reformatting system (HDT-AM/AMC) design specifications [E82-10020] p0118 N82-16438

COMPUTER GRAPHICS

A procedure for the interactive tracing of edges and lines by means of digital image processing p0113 A82-26050

Utilization of spatial complexity in computer classified Landsat MSS data for multi-factoral thematic mapping
p0129 A82-27648

The role of computer graphics in geographic research
p0117 A82-27923

Computer-assisted photo interpretation research at USAETL
[AD-A109366] p0121 N82-20628

The design and implementation of an operational, computer-based weather radar system --- rainfall maps
[RSRE-MEMO-3151] p0122 N82-21499

A digital technique for constructing variable-width lines
[AD-A110287] p0087 N82-21689

Experiences with digital terrain elevation data contouring programs
[AD-A110280] p0087 N82-21690

COMPUTER PROGRAMS

Automatic linear recognition and analysis using computer program LIRA --- satellite imagery for earth observations
p0090 A82-27612

Scene analysis for wildland fire-fuel characteristics in a Mediterranean climate p0060 A82-27624

Implementation of the Space Oblique Mercator projection in a production environment p0129 A82-27628

ELAS - A geobased information system that is transferable to several computers --- Earth resources Laboratory Applications Software p0115 A82-27666

Documentation of computer procedures for labeling spring grains and discriminating between spring wheat and barley using LANDSAT data
[E82-10030] p0063 N82-16448

Photogrammetry software A package for everyone
[AD-A108098] p0118 N82-17570

AgRISTARS Early warning and crop condition assessment. Patch image processor user's manual
[E82-10055] p0065 N82-19630

Development and applications of techniques to process hydrometeor distribution data
[AD-A109929] p0109 N82-20822

Ground registration of data from an airborne scatterometer
[E82-10084] p0068 N82-21636

As-Built documentation of programs to implement the Robertson and Doraiswamy/Thompson models
[E82-10086] p0122 N82-21638

As-built design specification for PARHIS
[E82-10089] p0172 N82-21641

As-built design specification for segment map (Sgmap) program
[E82-10094] p0123 N82-21646

Wheat stress indicator model. Early Warning (EW) data base interface driver, user's manual
[E82-10115] p0069 N82-21652

Experiences with digital terrain elevation data contouring programs
[AD-A110280] p0087 N82-21690

COMPUTER SYSTEMS PROGRAMS

As-Built design specification for UNIV4VEC
[E82-10085] p0122 N82-21637

As-built design specification for PARCLS
[E82-10090] p0123 N82-21642

As-built design specification for MISMAP
[E82-10091] p0123 N82-21643

As-built design specification for the CLASFYG program
[E82-10092] p0068 N82-21644

COMPUTER TECHNIQUES

Optimal methods of computerized image conversion
p0111 A82-19833

Analytical triangulation of space photography
p0111 A82-20402

Image quality control in the Meteosat ground processing system p0125 A82-21090

Use of Landsat data for automatic classification and area estimation of sugar-cane plantation in Sao Paulo state, Brazil p0058 A82-21092

Remote sensing for natural resources. An international view of problems, promises and accomplishments --- Book p0137 A82-21875

A comparison between aerial photography and Landsat for computer land-cover mapping p0074 A82-22143

Analog devices for the processing of aerial and space images for the study of water resources
p0104 A82-27476

Topographic mapping using Landsat data
p0082 A82-27615

Evaluation of large area crop estimation techniques
p0061 A82-27662

Classification of Landsat MSS data for surface cover of small areas p0116 A82-27677

Natural resources inventories by computer-satellite mapping techniques in Chaco State, Argentine Republic, South America p0116 A82-27688

Structure of hardware and software at a regional center for the automated processing of aerial and space remote-sensing images p0130 A82-28128

Analytic methods of geodetic referencing of nontopographic images p0083 A82-28134

Machine implementation of algorithms for the mapping of soil moisture on the basis of microwave-radiometer measurements p0131 A82-28142

Classification of systems for digital terrain simulation
p0117 A82-28468

Wetland mapping from digitized aerial photography --- Sheboygan Marsh, Wisconsin
[E82-10019] p0118 N82-16437

A satellite frost forecasting system for Florida
p0079 N82-20615

Context sensitive formulations of antenna pattern correction and side lobe compensation for NOSS/LAMMR real time processing
[NASA-CR-166789] p0122 N82-21457

Sonora exploratory study for the detection of wheat-leaf rust
[E82-10133] p0070 N82-21661

COMPUTERIZED SIMULATION

Accuracy of the normal case of close-range photogrammetry p0126 A82-22140

Simulation and studies of spaceborne synthetic aperture radar image quality with reduced bit rate
p0128 A82-27594

Satellite scatterometer feasibility study. Volume 2. Data extraction algorithm and error simulation for wind sensor --- Earth Resources Satellite (ERS 1)
[ESA-CR(P)-1492-VOL-2] p0133 N82-19651

CONFERENCES

International Symposium on Remote Sensing of Environment, 15th, University of Michigan, Ann Arbor, MI, May 11-15, 1981, Proceedings. Volumes 1, 2 & 3
p0127 A82-27576

Precipitation measurements from space - Workshop summary 28 April-1 May 1981, Greenbelt, MD
p0077 A82-28295

AgRISTARS. Foreign commodity production forecasting. Minutes of the annual formal project manager's review, including preliminary technical review reports of FY80 experiments --- wheat/barley and corn/soybean experiments
[E82-10039] p0064 N82-19614

SAR image quality --- conference, Frascati, Italy, 11-12 Dec. 1980, synthetic aperture radar (SAR)
[ESA-SP-172] p0122 N82-21458

CONFORMAL MAPPING

Implementation of the Space Oblique Mercator projection in a production environment p0129 A82-27628

CONGRESSIONAL REPORTS

Technology and oceanography. An assessment of Federal technologies for oceanographic research and monitoring
[OTA-O-142] p0097 N82-18844

CONIFERS

Remote sensing of the structure of taiga landscapes --- Russian book p0059 A82-27397

An invertible coniferous forest canopy reflectance model p0062 A82-27679

CONTEXT

The use of contextual information to improve land cover classification of digital remotely sensed data
p0112 A82-21094

Context dependent modeling --- for remote sensing data processing p0114 A82-27587

CONTOURS

Experiences with digital terrain elevation data contouring programs
[AD-A110280] p0087 N82-21690

Computer based technique for converting a contour map into an equispaced grid of points
[RAE-TR-80110] p0087 N82-21697

CONVECTION CURRENTS

The development and testing of methods to infer midlatitude precipitation intensity from geosynchronous satellite infrared data
[AD-A108881] p0120 N82-19788

COORDINATE TRANSFORMATIONS

Analytic methods of geodetic referencing of nontopographic images p0083 A82-28134

COORDINATES

Computer based technique for converting a contour map into an equispaced grid of points
[RAE-TR-80110] p0087 N82-21697

CORN

Manual and automatic crop identification with airborne radar imagery p0057 A82-20408

Use of Landsat-derived temporal profiles for corn-soybean feature extraction and classification p0059 A82-26842

Potential utility of thematic mapper data in estimating crop areas p0061 A82-27663

Crop area estimates using ground-gathered and Landsat data A multitemporal approach p0062 A82-27676

Recommended data sets, corn segments and spring wheat segments, for use in program development
[E82-10034] p0064 N82-19610

AgRISTARS. Foreign commodity production forecasting. Minutes of the annual formal project manager's review, including preliminary technical review reports of FY80 experiments --- wheat/barley and corn/soybean experiments
[E82-10039] p0064 N82-19614

AgRISTARS. Foreign commodity production forecasting. Corn/soybean decision logic development and testing
[E82-10056] p0065 N82-19631

Notes for Brazil sampling frame evaluation trip
[E82-10060] p0066 N82-19635

Segment-level evaluation of the simulated aggregation test. US corn and soybean exploratory experiment
[E82-10061] p0066 N82-19636

Evaluation of a segment-based LANDSAT full-frame approach to corp area estimation
[E82-10067] p0066 N82-20590

Effects of nitrogen nutrition on the growth, yield and reflectance characteristics of corn canopies --- Purdue Agronomy Farm, Indiana
[E82-10068] p0067 N82-20591

US corn and soybeans exploratory experiment
[E82-10088] p0068 N82-21640

The 1981 Argentina ground data collection
[E82-10127] p0070 N82-21658

Spectral-agronomic relationships of corn, soybean and wheat canopies
[E82-10143] p0070 N82-21670

Variability of reflectance measurements with sensor altitude and canopy type
[E82-10145] p0071 N82-21672

Determination of the optimal level for combining area and yield estimates
[E82-10146] p0071 N82-21673

AgRISTARS. Supporting research. Classification of corn Badhwar profile similarity technique --- us corn belt
[E82-10150] p0071 N82-21676

CORRELATION

Profiling sensitivity to image quality
[AD-A108405] p0084 N82-18931

CORRELATION COEFFICIENTS

Increase in correlation accuracy of remote sensing imagery by digital filtering p0113 A82-25454

CORRELATION DETECTION

Correlation identification of stellar configurations for purposes of the coordinate referencing of aerial and space images p0117 A82-28141

COST EFFECTIVENESS

Some problems concerning the effective use of remote sensing p0137 A82-26123

Applications systems verification and transfer project. Volume 7. Cost/benefit analysis for the ASVT on operational applications of satellite snow-cover observations
[NASA-TP-1828] p0109 N82-20623

CROP CALENDARS

Wheat stress indicator model. Crop Condition Assessment Division (CCAD) data base interface driver, user's manual
[E82-10031] p0064 N82-19607

AgRISTARS. Foreign commodity production forecasting. Minutes of the annual formal project manager's review, including preliminary technical review reports of FY80 experiments --- wheat/barley and corn/soybean experiments
[E82-10039] p0064 N82-19614

Preliminary evaluation of spectral, normal and meteorological crop stage estimation approaches
[E82-10059] p0065 N82-19634

Wheat stress indicator model. Early Warning (EW) data base interface driver, user's manual
[E82-10115] p0069 N82-21652

AgRISTARS. Supporting research. US crop calendars in support of the early warning project
[E82-10158] p0072 N82-21682

CROP GROWTH

Evaluation of the state of crops from satellite data
p0059 A82-27393

Automatic and semi-automatic classification of Landsat agricultural crops p0061 A82-27664

A technique for automatic labeling of Landsat agricultural scene elements by analysis of temporal-spectral patterns
p0062 A82-27678

Segment-level evaluation of the simulated aggregation test. US corn and soybean exploratory experiment
[E82-10061] p0066 N82-19636

System of forecasting agricultural crops using satellite observations of Earth
[E82-10079] p0067 N82-20602

Freeze prediction model --- Pennsylvania
p0067 N82-20609

As-Built documentation of programs to implement the Robertson and Doraiswamy/Thompson models
[E82-10086] p0122 N82-21638

AgRISTARS. Agriculture and Resources Inventory Surveys Through Aerospace Remote Sensing. Enumerator's manual, 1981 ground data survey
[E82-10116] p0069 N82-21653

CROP IDENTIFICATION

Experimental evaluation of methods of the automated interpretation of crops from a Fragment MSS image
p0057 A82-20349

Manual and automatic crop identification with airborne radar imagery p0057 A82-20408

Simple radiative transfer model for relationships between canopy biomass and reflectance p0057 A82-20422

The Dutch ROVE program --- Radar Observation of VEgetation p0057 A82-21026

Crop classification using airborne radar and Landsat data p0058 A82-21033

Remote sensing for natural resources. An international view of problems, promises and accomplishments --- Book p0137 A82 21875

An airphoto key for major tropical crops
p0058 A82-22142

Automatic and semi-automatic classification of Landsat agricultural crops p0061 A82 27664

A technique for automatic labeling of Landsat agricultural scene elements by analysis of temporal-spectral patterns
p0052 A82-27678

An autodigitizing procedure for ground-data labelling of Landsat pixels p0062 A82-27682

Documentation of computer procedures for labeling spring grains and discriminating between spring wheat and barley using LANDSAT data
[E82-10030] p0063 N82-16448

AgRISTARS: Foreign commodity production forecasting. Corn/soybean decision logic development and testing
[E82-10056] p0065 N82-19631

AgRISTARS: Foreign commodity production forecasting. Project test reports document, volume 1 --- using North Dakota, South Dakota, Montana, and Minnesota
[E82-10087] p0068 N82-21639

Transition year labeling error characterization study --- Kansas, Minnesota, Montana, North Dakota, South Dakota, and Oklahoma
[E82-10111] p0069 N82-21651

A look at the commonly used LANDSAT vegetation indices
[E82-10123] p0070 N82-21657

The 1981 Argentina ground data collection
[E82-10127] p0070 N82-21658

CROP INVENTORIES

Use of Landsat data for automatic classification and area estimation of sugar-cane plantation in Sao Paulo state, Brazil p0058 A82-21092

Use of Landsat-derived temporal profiles for corn-soybean feature extraction and classification p0059 A82-26842

Data base requirements in support of crop models p0060 A82-27588

A timely and accurate potato acreage estimate from Landsat - Results of a demonstration p0060 A82-27621

A vegetation response model applied to range inventory and monitoring using Landsat MSS data p0060 A82-27643

Evaluation of large area crop estimation techniques p0061 A82-27662

Potential utility of thematic mapper data in estimating crop areas p0061 A82-27663

Crop area estimates using ground-gathered and Landsat data A multitemporal approach p0062 A82-27676

Brazilian remote sensing activities, current and prospective needs
[E82-10026] p0132 N82-16444

AgRISTARS: Interim catalog ground data summary, data acquisition year 1979
[E82-10032] p0064 N82-19608

Recommended data sets, corn segments and spring wheat segments, for use in program development
[E82-10034] p0064 N82-19610

AgRISTARS: Foreign commodity production forecasting. Minutes of the annual formal project manager's review, including preliminary technical review reports of FY80 experiments --- wheat/barley and corn/soybean experiments
[E82-10039] p0064 N82-19614

Notes for Brazil sampling frame evaluation trip
[E82-10060] p0066 N82-19635

Segment-level evaluation of the simulated aggregation test: US corn and soybean exploratory experiment
[E82-10061] p0066 N82-19636

Utilization of Aerochrome 2443 film for identification and estimating wheat growing areas --- Rio Grande do Sul, Brazil
[INPE-2197-PRE/006] p0066 N82-19639

Evaluation of a segment-based LANDSAT full-frame approach to corp area estimation
[E82-10067] p0066 N82-20590

Survey of the cane-growing area of the state of Sao Paulo using LANDSAT data. Safra Year 1979/80, volume 2 --- maps, Brazil
[E82-10071] p0067 N82-20594

Elevation of a cane-growing area of the state of Sao Paulo using LANDSAT data
[E82-10077] p0067 N82-20600

Registration verification of SEA/AR fields --- Oregon, Texas, Montana, Nebraska, Washington, Colorado, Kansas, Oklahoma, and North Dakota
[E82-10083] p0068 N82-21635

As-Built documentation of programs to implement the Robertson and Doraiswamy/Thompson models
[E82-10086] p0122 N82-21638

AgRISTARS: Foreign commodity production forecasting. Project test reports document, volume 1 --- using North Dakota, South Dakota, Montana, and Minnesota
[E82-10087] p0068 N82-21639

US corn and soybeans exploratory experiment
[E82-10088] p0068 N82-21640

As-built design specification for PARCLS
[E82-10090] p0123 N82-21642

As-built design specification for the CLASFYG program
[E82-10092] p0068 N82-21644

Project communications/documentation standards manual
[E82-10093] p0068 N82-21645

AgRISTARS: Agriculture and Resources Inventory Surveys Through Aerospace Remote Sensing. Enumerator's manual, 1981 ground data survey
[E82-10116] p0069 N82-21653

Development of rotation sample designs for the estimation of crop acreages
[E82-10117] p0070 N82-21654

Sample selection in foreign similarity regions for multicrop experiments
[E82-10118] p0070 N82-21655

The 1981 Argentina ground data collection
[E82-10127] p0070 N82-21658

Determination of the optimal level for combining area and yield estimates
[E82-10146] p0071 N82-21673

AgRISTARS: Supporting research. Classification of corn: Badhwar profile similarity technique --- us corn belt
[E82-10150] p0071 N82-21676

CROP VIGOR

AgRISTARS: Soil moisture/early warning and crop condition assessment. Interface control document
[E82-10053] p0065 N82-19628

AgRISTARS: Early warning and crop condition assessment. Patch image processor user's manual
[E82-10055] p0065 N82-19630

As-built design specification for PARHIS
[E82-10089] p0122 N82-21641

CROSS POLARIZATION

Volumetric effects in cross-polarized airborne radar data p0058 A82-21032

CRUSTAL FRACTURES

Relationship of hydrothermal phenomena within the Leinster Granite to crustal fractures delineated from Landsat imagery p0089 A82-26015

CRYOGENIC COOLING

Development of a breadboard cooler for infrared remote sensing payloads, phase 1 --- Earth Resources Satellite ERS 1
[FOK-RV-R-81-064] p0134 N82-19653

CULTURAL RESOURCES

Accuracy of the normal case of close-range photogrammetry p0126 A82-22140

Locating prehistoric archaeological sites using Landsat p0129 A82-27638

CZECHOSLOVAKIA

Primary processing of and possibilities of using data from the meteorological satellite TIROS-N p0103 A82-27470

D

DATA ACQUISITION

Modern methods for monitoring and controlling the timeliness, accuracy, and completeness of data for meteorological analysis p0073 A82-19179

An intelligent earth sensing information system p0137 A82-22149

Some problems concerning the effective use of remote sensing p0137 A82-26123

University of Dundee satellite image data acquisition and archiving facility p0130 A82-27659

Data collection platforms: Applications to hydrology
[INPE-2246-PRE/030] p0107 N82-19304

Precipitation assessment from environmental satellite data for northwest Libya including the Gefara plan
[RSC-4] p0107 N82-19790

An introduction to image processing at Royal Aircraft Establishment, Farnborough, England --- U.S. and European satellite imagery
[RAE-TR-80107] p0122 N82-21565

AgRISTARS: Agriculture and Resources Inventory Surveys Through Aerospace Remote Sensing. Enumerator's manual, 1981 ground data survey
[E82-10116] p0069 N82-21653

A multiband radiometer and data acquisition system for remote sensing field research
[E82-10142] p0134 N82-21669

Some altimetric signatures from Seasat over the mid-Pacific Seamount Range
[AD-A110419] p0099 N82-21691

DATA BASES

Data base requirements in support of crop models p0060 A82-27588

A data base of geologic field spectra p0090 A82-27600

An evaluation of the utility of smaller Landsat resolution elements /Resolution of Landsat resolution/ p0114 A82-27625

Development and implementation of a low cost micro computer system for Landsat analysis and geographic data base application p0129 A82-27649

University of Dundee satellite image data acquisition and archiving facility p0130 A82-27659

DATA COLLECTION PLATFORMS

A microcomputer for control of data collection platforms --- GOES satellites
[INPE-2104-RPE/331] p0133 N82-18881

Data collection platforms: Applications to hydrology
[INPE-2246-PRE/030] p0107 N82-19304

DATA COMPRESSION

Study of Earth Resources Satellite (ERS) data reduction unit
[BAE-TP-7905] p0120 N82-19649

Data rate reduction: Impact of image data compression on end to end data management of a multispectral payload --- for satellite imagery
[REPT-44/130] p0120 N82-19654

An algorithm for spatial heirarchy clustering
[E82-10081] p0121 N82-20604

Interpretation of remotely sensed image data and impact of cluster compression --- impact of cluster compression, users
[REPT-44 2866] p0124 N82-21699

DATA CORRELATION

Evaluation of aerial photogrammetric camera and aircraft scanner pictures from tidal lands - Digital correlation and classification of multitemporal imagery data p0127 A82-26049

A relation between Landsat digital numbers, surface reflectance, and the cosine of the solar zenith angle p0114 A82-26841

Digital correlation of DDRS data
[NASA-CR-167494] p0118 N82-16452

LANDSAT imagery of the Venetian Lagoon: A multitemporal analysis
[E82-10036] p0119 N82-19612

Assessment of the quality of GATE area rainfall data from a Nimbus-5 radiometer
[NASA-CR-168512] p0109 N82-20807

Ground registration of data from an airborne scatterometer
[E82-10084] p0068 N82-21636

DATA MANAGEMENT

AgRISTARS: Interim catalog ground data summary, data acquisition year 1979
[E82-10032] p0064 N82-19608

DATA PROCESSING

The Seasat low rate data processing system p0093 A82-24061

Influence of illumination and viewing geometry and atmospheric composition on the 'tasseled cap' transformation of Landsat MSS data p0059 A82-24961

Mapsat compared to other earth-sensing concepts p0128 A82-27581

Information expectations from Landsat-D p0128 A82-27583

Context dependent modeling --- for remote sensing data processing p0114 A82-27587

Overview of digital processing of SAR data --- from Seasat-A p0128 A82-27589

Features of a generalized digital Synthetic Aperture Radar processor p0128 A82-27595

Strategies and uses of small distributed analysis centers as in the natural resource inventory of Venezuela p0115 A82-27636

Detection of volcanic ash fall area from Landsat MSS CCT data Eruption of Mt. Ontake in 1979 p0076 A82-27650

Orbital performance of a 1.6 micrometer DMSP snow/cloud discrimination sensor p0130 A82-27653

Detailed land use classification based on multitemporal Landsat-MSS-data p0076 A82-27657

University of Dundee satellite image data acquisition and archiving facility p0130 A82-27659

A low cost NOAA/TIROS AVHRR receiving station --- Advanced Very High Resolution Radiometer p0130 A82-27681

Precision in the evaluation of Landsat autocorrelation - The terrain effect p0116 A82-27686

Non-parametric classification of abandoned coal mine features using multioriented and ratio transformed Landsat data p0090 A82-27694

Structure of hardware and software at a regional center for the automated processing of aerial and space remote-sensing images p0130 A82-28128

The structure and basic parameters of a satellite system for the remote sensing of earth resources p0131 A82-28129

The earth resources program for the long-term orbital station Salyut 6 p0131 A82-28132

Partially processed multispectral scanner LANDSAT high-density tapes reformatting system (HDT-AM/AMC) design specifications
[E82-10020] p0118 N82-16438

NOSS altimeter algorithm specifications
[NASA-RP-1083] p0095 N82-16683

Study of synthetic aperture radar in 2D - 2FS operation over the ocean --- European Remote Sensing system
[ESA-CR(P)-1475] p0132 N82-18481

Usage and limitations of characteristic vector analysis of remote sensing multispectral data for the identification and quantification of water quality parameters p0118 N82-18656

Magsat science investigations
[E82-10045] p0085 N82-19620

Investigations of medium wavelength magnetic anomalies in the Eastern Pacific using Magsat data
[E82-10047] p0119 N82-19622

The LANDSAT system operated in Brazil by CNPq/INPE - results obtained in the area of mapping and future perspectives
[E82-10080] p0121 N82-20603

As-built design specification for segment map (Sgmap) program
[E82-10094] p0123 N82-21646

Methods of editing cloud and atmospheric layer affected pixels from satellite data
[E82-10154] p0123 N82-21678

DATA RECORDING

Proposed digital cartridge recording system for WRELADS --- laser airborne depth sounder
[AD-A109484] p0134 N82-20481

DATA REDUCTION

Use of GOES and TIROS/NOAA satellite data for snow-cover mapping p0101 A82-22145

Imaging the earth. I - The troubled first decade of Landsat p0137 A82-27169

Digital correlation of DDRS data
[NASA-CR-167494] p0118 N82-16452

Studies related to Magsat --- Backus effect and the westward drift
[E82-10050] p0085 N82-19625

Improved definition of crustal anomalies for Magsat data
[E82-10051] p0085 N82-19626

Study of Earth Resources Satellite (ERS) data reduction unit
[BAE-TP-7905] p0120 N82-19649

The Office for Remote Sensing of Earth Resources --- Pennsylvania p0121 N82-20612

Development and applications of techniques to process hydrometeor distribution data
[AD-A109929] p0109 N82-20822

An evaluation of ISOCLS and CLASSY clustering algorithms for forest classification in northern Idaho --- Elk River quadrange of the Clearwater National Forest
[E82-10109] p0069 N82-21650

Compatibility study of the MAGSAT data and aeromagnetic data
[E82-10136] p0123 N82-21663

Continuation of potential field data to a common altitude --- magsat data
[E82-10138] p0123 N82-21665

Separation of internal and external fields A new technique of data screening --- MAGSAT data
[E82-10139] p0123 N82-21666

DATA SAMPLING

Sampling for thematic map accuracy testing p0111 A82-20411

Landsat classification accuracy assessment procedures p0137 A82-20412

Development of rotation sample designs for the estimation of crop acreages
[E82-10117] p0070 N82-21654

Sample selection in foreign similarity regions for multicrop experiments
[E82-10118] p0070 N82-21655

DATA SMOOTHING

Determination of the optimal level for combining area and yield estimates
[E82-10146] p0071 N82-21673

DATA STORAGE

Complex of units for the storage and automated processing of research data p0131 A82-28140

DATA SYSTEMS

ELAS - A geobased information system that is transferable to several computers --- Earth resources Laboratory Applications Software p0115 A82-27666

Flexible processing of remote sensing data through integration of image processing and geobased information systems p0116 A82-27667

A microcomputer for control of data collection platforms --- GOES satellites
[INPE-2104-RPE/331] p0133 N82-18881

Wheat stress indicator model, Early Warning (EW) data base interface driver, user's manual
[E82-10115] p0069 N82-21652

Future Earthnet Dissemination Systems (FEDS) study Executive summary --- remote sensing data transmission
[REPT-3318] p0124 N82-21698

DATA TRANSMISSION

Future Earthnet Dissemination Systems (FEDS) study Executive summary --- remote sensing data transmission
[REPT-3318] p0124 N82-21698

DAYTIME

Registration of heat capacity mapping mission day and night images p0113 A82-22146

DECIDUOUS TREES

A system for quantitative determination of species and vitalities of urban trees on color-infrared photographs p0074 A82-24958

DEER

Application of remote sensing to state and regional problems --- mississippi
[E82-10033] p0078 N82-19809

DEFORESTATION

Amazonas project Application of remote sensing techniques for the integrated survey of natural resources in Amazonas --- Brazil
[E82-10069] p0078 N82-20592

DELAWARE

Locating prehistoric archaeological sites using Landsat p0129 A82-27638

DELAWARE BAY (US)

Evaluation of HCMM satellite data for estuarine tidal circulation patterns and thermal inertia soil moisture measurements --- Delaware Bay, Cooper River, and the Potomac River estuaries; Luverne, Minnesota, soil moisture, and water temperature of Lake Anna, Virginia
[E82-10064] p0108 N82-20587

DELTAS

Change detection in the Peace-Athabasca Delta using digital Landsat data p0101 A82-24959

Remote sensing of salinity in the San Francisco Bay Delta p0102 A82-26839

Assessment of change in Bangladesh coastal regions p0076 A82-27696

Applications of aircraft and satellite data for the study of archaeology and environment - Mekong Delta, Vietnam p0091 A82-27705

DENSITY DISTRIBUTION

Information theory lateral density distribution for Earth inferred from global gravity field
[NASA-TM-83825] p0085 N82-19731

DEPTH MEASUREMENT

A photometric method for depth determination by aerial photography p0101 A82-19831

Ground-truth observations of ice-covered North Slope Lakes imaged by radar
[NASA-TM-84127] p0107 N82-18664

An aerial survey of water turbidity and laser depth sounding performance along the Queensland Coast
[AD-A109060] p0098 N82-19802

Some altimetric signatures from Seasat over the mid-Pacific Seamount Range
[AD-A110419] p0099 N82-21891

DESERTS

Color characteristics of the earth's surface determined on the basis of spectroscopy results from Salyut 4 p0073 A82-19826

DIELECTRIC PROPERTIES

Mixture formulas applied in estimation of dielectric and radiative characteristics of soils and grounds at microwave frequencies p0058 A82-21030

Dielectric properties of snow
[NASA-CR-166764] p0107 N82-19638

DIGITAL DATA

The use of digital multi-date Landsat imagery in terrain classification p0111 A82-20409

The use of contextual information to improve land cover classification of digital remotely sensed data p0112 A82-21094

A relation between Landsat digital numbers, surface reflectance, and the cosine of the solar zenith angle p0114 A82-26841

Automatic linear recognition and analysis using computer program LIRA --- satellite imagery for earth observations p0090 A82-27612

Remote sensing in Latin America Technology and markets for the 1980's
[AD-A108784] p0138 N82-20626

Experiences with digital terrain elevation data contouring programs
[AD-A110280] p0087 N82-21690

DIGITAL FILTERS

Increase in correlation accuracy of remote sensing imagery by digital filtering p0113 A82-25454

DIGITAL RADAR SYSTEMS

Simulation and studies of spaceborne synthetic aperture radar image quality with reduced bit rate p0128 A82-27594

DIGITAL SIMULATION

Classification of systems for digital terrain simulation p0117 A82-28468

Watershed model study using LANDSAT data p0106 N82-17602

DIGITAL SYSTEMS

Proposed digital cartridge recording system for WRELADS --- laser airborne depth sounder
[AD-A109484] p0134 N82-20491

DIGITAL TECHNIQUES

Techniques for combining Landsat and ancillary data for digital classification improvement p0111 A82-20410

Information extraction from remotely sensed data - A user view p0112 A82-21089

Digital photography techniques p0112 A82-21398

Classification of ice radar imagery p0113 A82-22891

Change detection in the Peace-Athabasca Delta using digital Landsat data p0101 A82-24959

Evaluation of aerial photogrammetric camera and aircraft scanner pictures from tidal lands - Digital correlation and classification of multitemporal imagery data p0127 A82-26049

A procedure for the interactive tracing of edges and lines by means of digital image processing p0113 A82-26050

Methods for the processing of synthetic-aperture radar signals when solving problems of the national economy /Review/ p0113 A82-26726

An automatic optimum kernel-size selection technique for edge enhancement p0113 A82-26840

Features of a generalized digital Synthetic Aperture Radar processor p0128 A82-27595

Enhancement of Landsat data for Hudson Bay lowlands vegetation p0114 A82-27623

The use of digital terrain model in the rectification of satellite-borne imagery p0115 A82-27626

Forest change detection p0061 A82-27644

Digital analysis of spatial and spectral features from airborne MSS of a forested region p0061 A82-27647

Detection of volcanic ash fall area from Landsat MSS CCT data Eruption of Mt. Ontake in 1979 p0076 A82-27650

An autodigitizing procedure for ground-data labelling of Landsat pixels p0062 A82-27682

Digital processing of tropical forest habitat in Bangladesh and the development of a low cost processing facility at the National Zoo, Smithsonian Institution p0053 A82-27687

Visual and digital analysis of H C M M data over eastern Canada --- thermal imagery by Heat Capacity Mapping Mission p0117 A82-27698

The role of computer graphics in geographic research p0117 A82-27923

Construction of digital models of statistically uniform characteristics on the basis of multispectral space imagery p0117 A82-28144

Digital correlation of DDRS data
[NASA-CR-167494] p0118 N82-16452

Matrix data analysis Color/B and W coding is not always enough
[AD-A108406] p0084 N82-18930

The LANDSAT system operated in Brazil by CNPq/INPE - results obtained in the area of mapping and future perspectives
[E82-10080] p0121 N82-20603

Computer-assisted photo interpretation research at USAETL
[AD-A109366] p0121 N82-20628

Relief effects and the use of terrain models in SAR image processing --- Anderson River test site, British Columbia p0086 N82-21475

As-built design specification for segment map (Sgmap) program
[E82-10094] p0123 N82-21646

A digital technique for constructing variable-width lines
[AD-A110287] p0087 N82-21689

Computer based technique for converting a contour map into an equispaced grid of points
[RAE-TR-80110] p0087 N82-21697

DISASTERS

Detection of natural disasters via Meteosat p0075 A82-27040

DISCRIMINANT ANALYSIS (STATISTICS)

The logit classifier - A general maximum likelihood discriminant for remote sensing applications p0128 A82-27591

DISCRIMINATION

Methods of editing cloud and atmospheric layer affected pixels from satellite data
[E82-10154] p0123 N82-21678

DIURNAL VARIATIONS

HCMM detection of high soil moisture areas --- by diurnal temperature observation p0059 A82-24963

Ideal phase in estimating the spatial gradient of magnetic daily variations recorded by magnetometer arrays p0127 A82-26000

Diurnal variation of summer convection over West Africa and the Tropical Eastern Atlantic during 1974 and 1978 p0075 A82-26700

Interpretation of Heat Capacity Mapping Mission images over Canada p0116 A82-27671

Influence of solar illumination angle on soybean canopy reflectance p0063 A82-28153

Use of thermal inertia determined by HCMM to predict nocturnal cold prone areas in Florida
[E82-10040] p0064 N82-19615

On the accuracy of thermal inertia mapping by infrared imagery
[SAAB-REPR-AE-10] p0120 N82-19656

Comparison of storm-time changes of geomagnetic field at ground and at MAGSAT altitudes
[E82-10148] p0087 N82-21675

Use of thermal inertia determined by HCMM to predict nocturnal cold prone areas in Florida --- The Everglades agricultural area, Lake Okeechobee, and the Suwanee River basin
[E82-10157] p0071 N82-21681

DOPPLER EFFECT

Experiments in satellite Doppler control positioning at sea p0086 N82-20581

DOPPLER RADAR

Recovering ocean waveheight from HF radar sea echoes distorted by imperfect ionospheric reflection
[PB82-113283] p0096 N82-17806

DRAINAGE

Use of thermal inertia determined by HCMM to predict nocturnal cold prone areas in Florida --- The Everglades agricultural area, Lake Okeechobee, and the Suwanee River basin
[E82-10157] p0071 N82-21681

DRAINAGE PATTERNS

Application of side-looking color infrared photography for structure detection in subtle topography p0082 A82-27611

Watershed model study using LANDSAT data p0106 N82-17602

Methodology of the interpretation of remote sensing data and applications in pedology
[INPE-2211-MD/008] p0078 N82-19641

Dynamic study of the upper Sao Francisco River and the Tres Marias reservoir using MSS/LANDSAT images --- Brazil
[E82-10082] p0108 N82-20605

DROUGHT

Satellite sensing for extraction of groundwater resources information p0105 A82-27613

DUST STORMS

Dust from the Sahara in satellite images p0079 N82-20802

E

EARTH (PLANET)

Information theory lateral density distribution for Earth inferred from global gravity field
[NASA-TM-83825] p0085 N82-19731

EARTH ALBEDO
Regional properties of angular reflectance models
p0083 N82-17599

EARTH AXIS
Developments in geodesy within the scope of Helmut Wolf's work
p0084 N82-19604

EARTH CORE
Investigation of geomagnetic field forecasting and fluid dynamics of the core
[E82-10162]
p0087 N82-21686

EARTH CRUST
Ring structures in the earth's crust, and their significance for geology and methods for their investigation
p0081 A82-28136

Session III of the VLBI/Laser intercomparison task of the NASA crustal dynamics project
[NASA-CR-168427]
p0083 N82-17708

Satellite and surface geophysical expression of anomalous crustal structure in Kentucky and Tennessee
[NASA-TM-82163]
p0084 N82-17715

Electromagnetic deep-probing (100-1000 KMS) of the Earth's interior from artificial satellites Constraints on the regional emplacement of crustal resources
[E82-10043]
p0084 N82-19618

Electromagnetic deep-probing (100-1000 KMS) of the Earth's interior from artificial satellites Constraints on the regional emplacement of crustal resources
[E82-10044]
p0085 N82-19619

Use of Magsat anomaly data for crustal structure and mineral resources in the US midcontinent
[E82-10049]
p0091 N82-19624

Investigation of Antarctic crust and upper mantle using MAGSAT and other geophysical data
[E82-10062]
p0086 N82-20585

Investigation of antarctic crust and upper mantle using MAGSAT and other geophysical data
[E82-10147]
p0087 N82-21674

Use of MAGSAT anomaly data for crustal structure and mineral resources in the US midcontinent
[E82-10152]
p0092 N82-21677

EARTH MANTLE
Ore deposits in Africa and their relation to the underlying mantle
p0090 A82-26604

Electromagnetic deep-probing (100-1000 KMS) of the Earth's interior from artificial satellites Constraints on the regional emplacement of crustal resources
[E82-10044]
p0085 N82-19619

Gravity and geoid anomalies of the Philippine Sea Evidence on the depth of compensation for the negative residual water depth anomaly
[NASA-CR-168639]
p0085 N82-19732

Investigation of geomagnetic field forecasting and fluid dynamics of the core
[E82-10162]
p0087 N82-21686

EARTH OBSERVATIONS (FROM SPACE)
The effectiveness of instrumented visual studies of the earth from space
p0114 A82-27506

International Symposium on Remote Sensing of Environment, 15th, University of Michigan, Ann Arbor, MI, May 11-15, 1981, Proceedings Volumes 1, 2 & 3
p0127 A82-27576

Spaceborne radar observation of the earth surface
p0127 A82-27578

Characterizing user requirements for future land observing satellites
[NASA-TM-83867]
p0081 N82-17562

Satellite Earth resources data, module U-3
[E82-10035]
p0119 N82-19611

EARTH RESOURCES
Spaceborne radar observation of the earth surface
p0127 A82-27578

EARTH RESOURCES INFORMATION SYSTEM
Flexible processing of remote sensing data through integration of image processing and geobased information systems
p0116 A82-27667

EARTH SURFACE
Color characteristics of the earth's surface determined on the basis of spectroscopy results from Salyut 4
p0073 A82-19826

Analysis of space imagery to compile a geomorphological map of the world
p0089 A82-20338

Application and experimental verification of an empirical backscattering cross section model for the earth's surface
p0081 A82-21036

Effects of the atmosphere on the detection of surface changes from Landsat multispectral scanner data
p0125 A82-21091

Area determination by means of the method of finite elements
p0082 A82-26048

A relation between Landsat digital numbers, surface reflectance, and the cosine of the solar zenith angle
p0114 A82-26841

The effectiveness of instrumented visual studies of the earth from space
p0114 A82-27505

Interpretation of Heat Capacity Mapping Mission images over Canada
p0116 A82-27671

On the accuracy of thermal inertia mapping by infrared imagery
[SAAB-REPR-AE-10]
p0120 N82-19656

Cloud Top Scanning radiometer (CTS) User's guide
[NASA-TM-83887]
p0135 N82-21826

EARTHQUAKES
The relationship between seismicity and lineaments of the Anatolian-Caucasian-Iranian segment of the Mediterranean fold belt
p0089 A82-20341

Instruments watch for impending earthquakes
p0131 A82-28342

EAST GERMANY
Interpretation of multispectral aerial photographs of Lake Mueggelsee
p0104 A82-27473

Spectrometric studies of the water composition of Lake Mueggelsee
p0104 A82-27474

ECOLOGY
Topographic mapping using Landsat data
p0082 A82-27615

ECOSYSTEMS
Remote sensing of the structure of taiga landscapes --- Russian book
p0059 A82-27397

EDGES
A procedure for the interactive tracing of edges and lines by means of digital image processing
p0113 A82-26050

An automatic optimum kernel-size selection technique for edge enhancement
p0113 A82-26840

EDITING
Methods of editing cloud and atmospheric layer affected pixels from satellite data
[E82-10046]
p0119 N82-19621

Methods of editing cloud and atmospheric layer affected pixels from satellite data
[E82-10154]
p0123 N82-21678

EDUCATION
Report on a short course in remote sensing and the geological applications of LANDSAT MSS imagery at INPE
[E82-10024]
p0091 N82-16442

ELECTRIC POWER PLANTS
Remote sensing of sulfur dioxide effects on vegetation Volume 2 Data
[PB82-115130]
p0066 N82-19716

ELECTRO-OPTICAL PHOTOGRAPHY
Spectritek - A multispectral electron-optic pushbroom camera
p0129 A82-27633

ELECTRO-OPTICS
Digital photography techniques
p0112 A82-21398

ELECTROMAGNETIC ABSORPTION
On randomly absorbing and scattering surface layers
p0079 A82-21037

ELECTROMAGNETIC MEASUREMENT
Electromagnetic deep-probing (100-1000 KMS) of the Earth's interior from artificial satellites Constraints on the regional emplacement of crustal resources
[E82-10043]
p0084 N82-19618

Electromagnetic deep-probing (100-1000 KMS) of the Earth's interior from artificial satellites Constraints on the regional emplacement of crustal resources
[E82-10044]
p0085 N82-19619

ELECTROMAGNETISM
Electromagnetic deep-probing (100-1000 KMS) of the Earth's interior from artificial satellites Constraints on the regional emplacement of crustal resources
[E82-10155]
p0087 N82-21679

ELEVATION
Experiences with digital terrain elevation data contouring programs
[AD-A110280]
p0087 N82-21690

EMISSIVITY
Methods of editing cloud and atmospheric layer affected pixels from satellite data
[E82-10154]
p0123 N82-21678

END-TO-END DATA SYSTEMS
Data rate reduction Impact of image data compression on end to end data management of a multispectral payload --- for satellite imagery
[REPT-44/130]
p0120 N82-19654

ENERGY BUDGETS
Applications of HCMM satellite data to the study of urban heating patterns
[E82-10161]
p0080 N82-21685

ENVIRONMENT MODELS
Watershed model study using LANDSAT data
p0106 N82-17602

ENVIRONMENT POLLUTION
Evaluation of snow-cover pollution in industrial regions using satellite TV images
p0103 A82-27464

ENVIRONMENTAL MONITORING
Modern methods for monitoring and controlling the timeliness, accuracy, and completeness of data for meteorological analysis
p0073 A82-19179

The Canadian north - Utility of remote sensing for environmental monitoring
p0074 A82-24962

Detection of natural disasters via Meteosat
p0075 A82-27040

Present and future studies of natural resources and the environment from space
p0138 A82-27506

Development of cooperation between CMEA member countries in the development and utilization of space-based systems for the remote sensing of earth resources and the environment
p0138 A82-27543

Topographic mapping using Landsat data
p0082 A82-27615

Forest change detection
p0061 A82-27644

Monitoring forest land cover alteration in Thailand with the analysis of ancillary and digital Landsat data
p0062 A82-27673

Environmental studies by multispectral scanner under large-scale civil engineering construction
p0063 A82-27691

Remote SO2 emission measurements with correlation spectrometers from volcanoes
p0077 A82-27704

Polarimetric method for the remote sensing of oil slicks on the sea surface
p0095 A82-28135

Instruments watch for impending earthquakes
p0131 A82-28342

Multidisciplinary research on the application of remote sensing to water resources problems --- Wisconsin
[E82-10021]
p0106 N82-16439

Satellite-derived ice data sets no. 1: Antarctic monthly average microwave brightness temperatures and sea-ice concentrations, 1973 - 1976
[NASA-TM-83812]
p0096 N82-17563

Publications and reports on contracts and grants, 1980
[PB82-103219]
p0138 N82-17792

Imaging microwave radiometer Phase A study Volume 1 Executive summary --- instrument for the European Remote Sensing system payload
[ESS/SS-1006]
p0132 N82-18564

Measurement of river sediments
[WMO-561]
p0107 N82-18670

A microcomputer for control of data collection platforms --- GOES satellites
[INPE-2104-RPE/331]
p0133 N82-18881

General configuration and internal disposition of equipment in a satellite for collecting environmental data
[INPE-2240-PRE/026]
p0078 N82-19256

Resourceful decisions LANDAT in Michigan
[E82-10037]
p0078 N82-19601

The utilization of orbital images as an adequate form of control of preserved areas --- Araguaia National Park, Brazil
[E82-10065]
p0078 N82-20588

Applications systems verification and transfer project Volume 1 Operational applications of satellite snow cover observations Executive summary --- usefulness of satellite snow-cover data for water yield prediction
[NASA-TP-1822]
p0108 N82-20617

Applications systems verification and transfer project Volume 2 Operational applications of satellite snow-cover observations and data-collection systems in the Arizona test site
[NASA-TP-1823]
p0108 N82-20618

Optimal network density for atmospheric recording
p0079 N82-20776

Sounding the aerosol distribution over the Upper Rhine Valley in the Valley in the Speyer area by means of lidar
p0079 N82-20782

Remote sensing for water resources and hydrology An assessment of the Corps of Engineers' program
[PB82-137142]
p0110 N82-21704

ENVIRONMENTAL QUALITY
The application of remote sensing to resource management and environmental quality programs in Kansas --- Cimarron National Grasslands, Prairie Potawatomi Reservation, and Kickapoo Reservation
[E82-10029]
p0063 N82-16447

EROSION
Inventory of eroded areas in the state of Guanajuato Mexico, by automatic analysis of Landsat images
p0076 A82-27680

ERROR ANALYSIS
Modern methods for monitoring and controlling the timeliness, accuracy, and completeness of data for meteorological analysis
p0073 A82-19179

Maximum likelihood estimation of label imperfection probabilities and its use in the identification of mislabeled patterns
p0112 A82-21040

Modeling misregistration and related effects on multispectral classification
p0113 A82-25455

Error analysis of pulse location estimates for simulated bathymetric lidar returns
[PB82-109448]
p0096 N82-17803

Some criteria for the accuracy and the reliability of networks --- in geodesy
p0086 N82-20580

Transition year labeling error characterization study --- Kansas, Minnesota, Montana, North Dakota, South Dakota, and Oklahoma
[E82-10111]
p0069 N82-21651

ERROR CORRECTING DEVICES
The use of contextual information to improve land cover classification of digital remotely sensed data
p0112 A82-21094

ERS-1 (ESA SATELLITE)
The first ESA remote sensing satellite system ERS-1
p0094 A82-27608

Study of Earth Resources Satellite (ERS) data reduction unit
[BAE-TP-7905]
p0120 N82-19649

Satellite scatterometer feasibility study Volume 1 Technical results --- Earth Resources Satellite (ERS 1)
[ESA-CR(P)-1492-VOL-1]
p0133 N82-19650

Satellite scatterometer feasibility study Volume 2 Data extraction algorithm and error simulation for wind sensor --- Earth Resources Satellite (ERS 1)
[ESA-CR(P)-1492-VOL-2]
p0133 N82-19651

Study of a radar altimeter for the European remote sensing program Volume 1 Executive summary --- Earth Resources Satellite (ERS 1)
[SPAR-R-1090-ISSUE-A]
p0133 N82-19652

Development of a breadboard cooler for infrared remote sensing payloads, phase 1 --- Earth Resources Satellite ERS 1
[FOK-RV-R-81-064]
p0134 N82-19653

ESTIMATING

Preliminary evaluation of spectral, normal and meteorological crop stage estimation approaches
[E82-10059] p0065 N82-19634

Development of rotation sample designs for the estimation of crop acreages
[E82-10117] p0070 N82-21654

ESTUARIES

The relationship among sea surface roughness variations, oceanographic analyses, and airborne remote sensing analyses
[NASA-CR-168444] p0096 N82-17798

Evaluation of HCMM satellite data for estuarine tidal circulation patterns and thermal inertia soil moisture measurements --- Delaware Bay, Cooper River, and the Potomac River estuaries; Luverne, Minnesota, soil moisture, and water temperature of Lake Anna, Virginia
[E82-10064] p0108 N82-20587

EUROPE

Structural analysis of the basement of the East European platform by remote sensing methods p0089 A82-20342

Examination of the operational prospects for remote sensing --- in Europe
[ESA-CR(P)-1476] p0138 N82-18669

EVAPORATION RATE

HCMM hydrological analysis in Utah --- Utah lake
[E82-10063] p0107 N82-20586

EVAPOTRANSPIRATION

A gradient model of vegetation and climate utilizing NOAA satellite imagery. Phase 1: Texas transect
[E82-10107] p0069 N82-21648

Applications of HCMM satellite data to the study of urban heating patterns
[E82-10161] p0080 N82-21685

EVERGLADES (FL)

Use of thermal inertia determined by HCMM to predict nocturnal cold prone areas in Florida --- The Everglades agricultural area, Lake Okeechobee, and the Suwanee River basin
[E82-10157] p0071 N82-21681

F

FARM CROPS

Experimental evaluation of methods of the automated interpretation of crops from a Fragment MSS image
p0057 A82-20349

Manual and automatic crop identification with airborne radar imagery p0057 A82-20408

The Dutch ROVE program --- Radar Observation of VEgetation p0057 A82-21026

Investigation of the vegetative covers on ploughed areas by SLAR p0058 A82-21031

Crop classification using airborne radar and Landsat data p0058 A82-21033

Data base requirements in support of crop models
p0060 A82-27588

Dew and vapor pressure as complicating factors in the interpretation of spectral radiance from crops
p0060 A82-27617

Automatic and semi-automatic classification of Landsat agricultural crops p0061 A82-27664

AgRISTARS: Yield model development/soil moisture interface control document
[E82-10054] p0065 N82-19629

Remote sensing of sulfur dioxide effects on vegetation. Volume 1: Summary
[PB82-115122] p0066 N82-19715

Atlas of the global distribution of the total ozone concentration according to satellite measurements
[MITT-28] p0078 N82-19740

System of forecasting agricultural crops using satellite observations of Earth
[E82-10079] p0067 N82-20602

A look at the commonly used LANDSAT vegetation indices
[E82-10123] p0070 N82-21657

AgRISTARS: Supporting research. US crop calendars in support of the early warning project
[E82-10158] p0072 N82-21682

FARMLANDS

The influence of illumination and viewing geometry on the reflectance factor of agricultural targets
p0061 A82-27646

The potential of remote sensing to monitor soil erosion on cropland p0061 A82-27656

Experience with a variety of studies of earth resources in the Kalmyk ASSR using space imagery
p0131 A82-28130

The application of remote sensing to resource management and environmental quality programs in Kansas --- Cimarron National Grasslands, Prairie Potawatomi Reservation, and Kickapoo Reservation
[E82-10029] p0063 N82-16447

AgRISTARS: Foreign commodity production forecasting. Corn/soybean decision logic development and testing
[E82-10056] p0065 N82-19631

Taxonomic classification of world map units in crop producing areas of Argentina and Brazil with representative US soil series and major land resource areas in which they occur
[E82-10058] p0065 N82-19633

Notes for Brazil sampling frame evaluation trip
[E82-10060] p0066 N82-19635

The effect of finite field size on classification and atmospheric correction
[NASA-TM-83818] p0120 N82-19645

Elevation of a cane-growing area of the state of Sao Paulo using LANDSAT data
[E82-10077] p0067 N82-20600

FERTILIZERS

Effects of nitrogen nutrition on the growth, yield and reflectance characteristics of corn canopies --- Purdue Agronomy Farm, Indiana
[E82-10068] p0067 N82-20591

FIELD OF VIEW

A multiband radiometer and data acquisition system for remote sensing field research
[E82-10142] p0134 N82-21669

Variability of reflectance measurements with sensor altitude and canopy type
[E82-10145] p0071 N82-21672

FINITE ELEMENT METHOD

Area determination by means of the method of finite elements p0082 A82-26048

FINLAND

Microwave radiation from a natural snow field
p0101 A82-19559

Theoretical and experimental studies of microwave emission signatures of snow p0125 A82-21034

FIRE PREVENTION

Scene analysis for wildland fire-fuel characteristics in a Mediterranean climate p0060 A82-27624

FISHERIES

Brazilian remote sensing activities, current and prospective needs
[E82-10026] p0132 N82-16444

Technology and oceanography: An assessment of Federal technologies for oceanographic research and monitoring
[OTA-O-142] p0097 N82-18844

FLIGHT ALTITUDE

Analysis of the direction-dependent radiation behavior in multispectral scanning data p0125 A82-21399

FLOOD PLAINS

Change detection in the Peace-Athabasca Delta using digital Landsat data p0101 A82-24959

FLOOD PREDICTIONS

Satellite observed cloud patterns associated with excessive precipitation outbreaks
[PB80-215130] p0073 A82-19177

Dynamics of snow cover in mountain regions of the Aral Sea basin, studied using satellite photographs
p0102 A82-27462

Flash flood forecasting --- and damage control measures
[WMO-577] p0107 N82-18671

Remote sensing for water resources and hydrology: An assessment of the Corps of Engineers' program
[PB82-137142] p0110 N82-21704

FLORIDA

Use of thermal inertia determined by HCMM to predict nocturnal cold prone areas in Florida
[E82-10040] p0064 N82-19615

Application of satellite frost forecast technology to other parts of the United States, phase 2 --- Pennsylvania, Michigan, and Florida
[NASA-CR-166827] p0121 N82-20607

A satellite frost forecasting system for Florida
p0079 N82-20615

Use of thermal inertia determined by HCMM to predict nocturnal cold prone areas in Florida --- The Everglades agricultural area, Lake Okeechobee, and the Suwanee River basin
[E82-10157] p0071 N82-21681

FLUOROCARBONS

Demonstration of a long-range atmospheric tracer system using perfluorocarbons
[PB82-106246] p0081 N82-16613

FOLIAGE

Atlas of the global distribution of the total ozone concentration according to satellite measurements
[MITT-28] p0078 N82-19740

FOOTPRINTS

Ground registration of data from an airborne scatterometer
[E82-10084] p0068 N82-21636

FORECASTING

System of forecasting agricultural crops using satellite observations of Earth
[E82-10079] p0067 N82-20602

FOREST FIRE DETECTION

Flexible processing of remote sensing data through integration of image processing and geobased information systems p0116 A82-27667

Development of a Canadian thermal infrared forest fire mapping operational program p0063 A82-27699

FOREST FIRES

Airborne lidar measurements of smoke plume distribution, vertical transmission, and particle size p0073 A82-21386

Scene analysis for wildland fire-fuel characteristics in a Mediterranean climate p0060 A82-27624

The utilization of orbital images as an adequate form of control of preserved areas --- Araguaia National Park, Brazil
[E82-10065] p0078 N82-20588

FOREST MANAGEMENT

Automation of the processing of aerial and space images for forest inventory p0057 A82-20350

Multiresource inventory methods pilot test --- for forests p0060 A82-27601

Application of space remote sensing data in forestry
p0063 A82-28131

Examination of the operational prospects for remote sensing --- in Europe
[ESA-CR(P)-1476] p0138 N82-18669

Method of interpretation of remote sensing data and applications to vegetation
[INPE-2215-MD/010] p0066 N82-19640

Relation of the activities of the IPDF/INPE project (reforestation subproject) during the year 1979 --- Mato Grosso do Sul, Brazil
[E82-10078] p0067 N82-20601

FORESTS

Manual and automatic crop identification with airborne radar imagery p0057 A82-20408

Remote sensing of the structure of taiga landscapes --- Russian book p0059 A82-27397

Forest change detection p0061 A82-27644

Digital analysis of spatial and spectral features from airborne MSS of a forested region p0061 A82-27647

HCMM night-time thermal IR imaging experiment in Michigan --- Heat Capacity Mapping Mission
p0115 A82-27655

Potential utility of thematic mapper data in estimating crop areas p0061 A82-27663

Fanning - A classification algorithm for mixture landscapes applied to Landsat data of Maine forests
p0062 A82-27668

Monitoring forest land cover alteration in Thailand with the analysis of ancillary and digital Landsat data
p0062 A82-27673

An invertible coniferous forest canopy reflectance model p0062 A82-27679

Digital processing of tropical forest habitat in Bangladesh and the development of a low cost processing facility at the National Zoo, Smithsonian Institution
p0063 A82-27687

Environmental studies by multispectral scanner under large-scale civil engineering construction
p0063 A82-27691

Utilisation of remote sensing in resources identification and land use in India - An integrated approach
p0076 A82-27701

Application of space remote sensing data in forestry
p0063 A82-28131

Brazilian remote sensing activities, current and prospective needs
[E82-10026] p0132 N82-16444

The application of remote sensing to resource management and environmental quality programs in Kansas --- Cimarron National Grasslands, Prairie Potawatomi Reservation, and Kickapoo Reservation
[E82-10029] p0063 N82-16447

The effect of finite field size on classification and atmospheric correction
[NASA-TM-83818] p0120 N82-19645

San Juan National Forest Land Management Planning Support System (LMPSS) requirements definition
[E82-10108] p0069 N82-21649

An evaluation of ISOCLS and CLASSY clustering algorithms for forest classification in northern Idaho --- Elk River quadrange of the Clearwater National Forest
[E82-10109] p0069 N82-21650

FRENCH SPACE PROGRAMS

Earth sensing from space - Commercial and international aspects p0138 A82-27669

FREQUENCY ASSIGNMENT

Guidelines for spaceborne microwave remote sensors
[NASA-RP-1086] p0133 N82-19647

FRESH WATER

Spectral reflectances of freshwater ice and snow from 340 through 1100 nm p0106 N82-17601

FRONTS (METEOROLOGY)

Structure and variability of the Alboran Sea frontal system p0093 A82-20447

FROST

Application of satellite frost forecast technology to other parts of the United States, phase 2 --- Pennsylvania, Michigan, and Florida
[NASA-CR-166827] p0121 N82-20607

Application of satellite frost forecast technology to other parts of the United States, phase 2, introduction
p0121 N82-20608

Freeze prediction model --- Pennsylvania
p0067 N82-20609

Applicability of satellite freeze forecasting and cold climate mapping to the other parts of the United States --- Michigan p0068 N82-20613

MSU test of P-model p0121 N82-20614

A satellite frost forecasting system for Florida
p0079 N82-20615

Use of thermal inertia determined by HCMM to predict nocturnal cold prone areas in Florida --- The Everglades agricultural area, Lake Okeechobee, and the Suwanee River basin
[E82-10157] p0071 N82-21681

G

GARP ATLANTIC TROPICAL EXPERIMENT

Assessment of the quality of GATE area rainfall data from a Nimbus-5 radiometer [NASA-CR-168512] p0109 N82-20807

GAS DETECTORS

Ozone measurements to 48Km with chemiluminescent ozone detectors [AD-A110342] p0134 N82-21808

GAS POCKETS

Thermal IR detection of submarine gas seepages in the western Istra off-shore area /Yugoslavia/ p0076 A82-27661

GEOCHEMISTRY

Calcium carbonate precipitation in Pyramid Lake, Nevada, as monitored by satellite - 1978 and 1980 p0105 A82-27634

GEODESY

Session III of the VLBI/Laser intercomparison task of the NASA crustal dynamics project [NASA-CR-168427] p0083 N82-17708

Some criteria for the accuracy and the reliability of networks --- in geodesy p0086 N82-20580

Experiments in satellite Doppler control positioning at sea p0086 N82-20581

Recent results of geoid determination by combination techniques in the North Sea test area p0086 N82-20583

GEODETIC COORDINATES

Analytic methods of geodetic referencing of nontopographic images p0083 A82-28134

Mathematical and stochastic models in photogrammetry relating to Helmut Wolf's work p0084 N82-19605

The diagnosis settlement 1980 of the German main triangulation network. Part 2: Trajectories [SER-B-253-MITT-159-PT-2] p0085 N82-19648

Some criteria for the accuracy and the reliability of networks --- in geodesy p0086 N82-20580

Experiments in satellite Doppler control positioning at sea p0086 N82-20581

GEODETIC SURVEYS

Photogrammetry software: A package for everyone [AD-A108098] p0118 N82-17570

Helmut Wolf: On the occasion of his 70th birthday [SER-E-18] p0084 N82-19603

Developments in geodesy within the scope of Helmut Wolf's work p0084 N82-19604

Mathematical and stochastic models in photogrammetry relating to Helmut Wolf's work p0084 N82-19605

The diagnosis settlement 1980 of the German main triangulation network. Part 2: Trajectories [SER-B-253-MITT-159-PT-2] p0085 N82-19648

Applications to Earth physics: Very-long-baseline interferometry and data analysis [NASA-CR-168743] p0088 N82-21796

GEODYNAMICS

Developments in geodesy within the scope of Helmut Wolf's work p0084 N82-19604

GEOGRAPHY

The role of computer graphics in geographic research p0117 A82-27923

The atlas 'Geographical Results of Spaceborne Multispectral Experiments' p0077 A82-28133

GEOIDS

Gravity and geoid anomalies of the Philippine Sea: Evidence on the depth of compensation for the negative residual water depth anomaly [NASA-CR-168639] p0085 N82-19732

Recent results of geoid determination by combination techniques in the North Sea test area p0086 N82-20583

GEOLOGICAL FAULTS

Instruments watch for impending earthquakes p0131 A82-28342

GEOLOGICAL SURVEYS

Structural analysis of the basement of the East European platform by remote sensing methods p0089 A82-20342

Remote sensing for natural resources: An international view of problems, promises and accomplishments --- Book p0137 A82-21875

Dip determinations in photogeology p0089 A82-25453

Development of cooperation between CMEA member countries in the development and utilization of space-based systems for the remote sensing of earth resources and the environment p0138 A82-27543

Automatic linear recognition and analysis using computer program LIRA --- satellite imagery for earth observations p0090 A82-27612

Integration of Landsat, geological and geophysical data for use in thematic mapping at regional scale p0090 A82-27672

Airborne remote sensing in east Greenland p0090 A82-27695

Ring structures in the earth's crust, and their significance for geology and methods for their investigation p0091 A82-28136

Satellite and surface geophysical expression of anomalous crustal structure in Kentucky and Tennessee [NASA-TM-82163] p0084 N82-17715

Resourceful decisions: LANDAT in Michigan [E82-10037] p0078 N82-19601

Use of Magsat anomaly data for crustal structure and mineral resources in the US midcontinent [E82-10049] p0091 N82-19624

Amazonas project: Application of remote sensing techniques for the integrated survey of natural resources in Amazonas --- Brazil [E82-10069] p0078 N82-20592

Study project of intrusive rocks: States of Espirito Santo and Rio de Janeiro, south and east of Minas Gerais and southeast of the state of Sao Paulo --- Brazil [E82-10076] p0092 N82-20599

HCMM: Soil moisture in relation to geologic structure and lithology, northern California --- Northern Coast Range, Sacramento Valley, and the Modoc Plateau [E82-10135] p0092 N82-21662

Application of HCMM data to regional geologic analysis for mineral and energy resource evaluation [E82-10137] p0092 N82-21664

Use of MAGSAT anomaly data for crustal structure and mineral resources in the US midcontinent [E82-10152] p0092 N82-21677

GEOLOGY

Visual and digital analysis of H.C.M.M. data over eastern Canada --- thermal imagery by Heat Capacity Mapping Mission p0117 A82-27698

GEOMAGNETIC MICROPULSATIONS

Harmonic structure of Pc 3-4 pulsations p0082 A82-26266

GEOMAGNETISM

Ideal phase in estimating the spatial gradient of magnetic daily variations recorded by magnetometer arrays p0127 A82-26000

Harmonic structure of Pc 3-4 pulsations p0082 A82-26266

Particle precipitation and atmospheric X-and Gamma-rays in the South Atlantic magnetic anomaly by balloon experiments [INPE-2119-RPE/343] p0083 N82-17711

Some new methods in geomagnetic field modeling applied to the 1960 - 1980 epoch [NASA-TM-83868] p0083 N82-17714

Equivalent source modeling of the main field using Magsat data [E82-10041] p0084 N82-19616

Electromagnetic deep-probing (100-1000 KMS) of the Earth's interior from artificial satellites: Constraints on the regional emplacement of crustal resources [E82-10043] p0084 N82-19618

Electromagnetic deep-probing (100-1000 KMS) of the Earth's interior from artificial satellites: Constraints on the regional emplacement of crustal resources [E82-10044] p0085 N82-19619

Magsat science investigations [E82-10045] p0085 N82-19620

Investigations of medium wavelength magnetic anomalies in the Eastern Pacific using Magsat data [E82-10047] p0119 N82-19622

Studies related to Magsat --- Backus effect and the westward drift [E82-10050] p0085 N82-19625

Improved definition of crustal anomalies for Magsat data [E82-10051] p0085 N82-19626

Investigation of Antarctic crust and upper mantle using MAGSAT and other geophysical data [E82-10062] p0086 N82-20585

MAGSAT anomaly profiles of the eastern Indian Ocean [E82-10066] p0086 N82-20589

Spherical harmonic representation of the main geomagnetic field for world charting and investigations of some fundamental problems of physics and geophysics [E82-10075] p0086 N82-20598

Preliminary models of the core field --- geomagnetic models [E82-10129] p0087 N82-21659

Compatibility study of the MAGSAT data and aeromagnetic data [E82-10136] p0123 N82-21663

Continuation of potential field data to a common altitude --- magsat data [E82-10138] p0123 N82-21665

Separation of internal and external fields: A new technique of data screening --- MAGSAT data [E82-10139] p0123 N82-21666

Investigation of antarctic crust and upper mantle using MAGSAT and other geophysical data [E82-10147] p0087 N82-21674

Comparison of storm-time changes of geomagnetic field at ground and at MAGSAT altitudes [E82-10148] p0087 N82-21675

Use of MAGSAT anomaly data for crustal structure and mineral resources in the US midcontinent [E82-10152] p0092 N82-21677

Electromagnetic deep-probing (100-1000 KMS) of the Earth's interior from artificial satellites: Constraints on the regional emplacement of crustal resources [E82-10155] p0087 N82-21679

Investigation of geomagnetic field forecasting and fluid dynamics of the core [E82-10162] p0087 N82-21686

GEOMETRIC RECTIFICATION (IMAGERY)

Primary processing of and possibilities of using data from the meteorological satellite TIROS-N p0103 A82-27470

Operational resampling for correcting images to a geocoded format --- in remote sensing p0114 A82-27590

The use of digital terrain model in the rectification of satellite-borne imagery p0115 A82-27626

Development and implementation of a low cost micro computer system for Landsat analysis and geographic data base application p0129 A82-27649

Field-by-field multitemporal analysis of aerial scanner data geometrically corrected by means of a sliding model p0115 A82-27651

Geometric correction of airborne multispectral scanner images p0130 A82-27706

Automatic relocation of ground control points in LANDSAT imagery [RAE-TR-81071] p0118 N82-18657

Relief effects and the use of terrain models in SAR image processing --- Anderson River test site, British Columbia p0086 N82-21475

An introduction to image processing at Royal Aircraft Establishment, Farnborough, England --- U.S. and European satellite imagery [RAE-TR-80107] p0122 N82-21565

GEOMORPHOLOGY

Analysis of space imagery to compile a geomorphological map of the world p0089 A82-20338

Structural analysis of the basement of the East European platform by remote sensing methods p0089 A82-20342

A structural synthesis of Brazil, based on the study of major lineaments derived from remote sensing imagery interpretation p0079 A82-26012

Remote sensing applied to basement tectonics of the calcareous High Atlas /Morocco/ p0089 A82-26014

Area determination by means of the method of finite elements p0082 A82-26048

Satellite sensing for extraction of groundwater resources information p0105 A82-27613

Methodology of the interpretation of remote sensing data and applications in geomorphology [INPE-2209-MD/007] p0091 N82-19642

Heat Capacity Mapping Mission (HCMM) program: Study of geological structure of Sicily and other Italian areas --- Sardinia and the Gulf of Orosei [E82-10073] p0091 N82-20596

GEOPHYSICS

Investigation of geomagnetic field forecasting and fluid dynamics of the core [E82-10162] p0087 N82-21686

Applications to Earth physics: Very-long-baseline interferometry and data analysis [NASA-CR-168743] p0088 N82-21796

GEOTECHNICAL ENGINEERING

Geotechnical applications of Landsat image analysis of Bhakra Dam Reservoir, India p0102 A82-26838

GEOTEMPERATURE

Analysis of a discrete-time linear model for geothermal flux reconnaissance from two or three aircraft infrared measurements p0075 A82-27627

GEOTHERMAL RESOURCES

Seasat satellite investigation of the structure of Western Nebraska and its application to the evaluation of geothermal resources p0090 A82-27635

Application of machine processing of visible and thermal data to the study of the geothermal area of Cerro Prieto, Mexico p0117 A82-27693

GERMANY

The use of the airborne lidar system 'ALEX F 1' for aerosol tracing in the lower troposphere p0073 A82-20226

Evaluation of aerial photogrammetric camera and aircraft scanner pictures from tidal lands - Digital correlation and classification of multitemporal imagery data p0127 A82-26049

GLACIAL DRIFT

Use of Landsat imagery to delineate glaciofluvial aquifers in southeast South Dakota p0105 A82-27637

GOES SATELLITES

Weather satellite interpretation: Introduction to weather satellite imagery [PB82-107657] p0118 N82-16677

GOVERNMENT PROCUREMENT

Remote sensing procurement package: A management report for state and local governments [E82-10052] p0138 N82-19627

GOVERNMENT/INDUSTRY RELATIONS

Earth sensing from space - Commercial and international aspects p0138 A82-27669

GRAINS (FOOD)

Documentation of computer procedures for labeling spring grains and discriminating between spring wheat and barley using LANDSAT data [E82-10030] p0063 N82-16449

AgRISTARS: Foreign commodity production forecasting. Project test reports document, volume 1 --- using North Dakota, South Dakota, Montana, and Minnesota [E82-10087] p0068 N82-21639

GRAND CANYON (AZ)

Cliff and slope topography of part of the Grand Canyon, Arizona as characterized on a Seasat radar image p0082 A82-26843

GRASSES

Assessing mesquite-grass vegetation condition from Landsat p0059 A82-25457

GRASSHOPPERS

Remote sensing applications to resource problems in South Dakota [E82-10027] p0132 N82-16445

GRASSLANDS
Simple radiative transfer model for relationships between canopy biomass and reflectance p0057 A82-20422
Multispectral photographic remote sensing of green vegetation biomass and productivity p0059 A82-22144
The application of remote sensing to resource management and environmental quality programs in Kansas --- Cimarron National Grasslands, Prairie Potawatomi Reservation, and Kickapoo Reservation
[E82-10029] p0063 N82-16447
The effect of finite field size on classification and atmospheric correction
[NASA-TM-83818] p0120 N82-19645

GRAVIMETRY
Developments in geodesy within the scope of Helmut Wolf's work p0084 N82-19604

GRAVITATION
Ore deposits in Africa and their relation to the underlying mantle p0090 A82-26604

GRAVITATIONAL FIELDS
Information theory lateral density distribution for Earth inferred from global gravity field
[NASA-TM-83825] p0085 N82-19731

GRAVITY ANOMALIES
Geophysical and Landsat lineament mapping - An approach illustrated from west-central and south India p0089 A82-26016
Satellite and surface geophysical expression of anomalous crustal structure in Kentucky and Tennessee
[NASA-TM-82163] p0084 N82-17715
Gravity and geoid anomalies of the Philippine Sea. Evidence on the depth of compensation for the negative residual water depth anomaly
[NASA-CR-168639] p0085 N82-19732
Recent results of geoid determination by combination techniques in the North Sea test area p0086 N82-20583
Investigation of Antarctic crust and upper mantle using MAGSAT and other geophysical data
[E82-10062] p0086 N82-20585
Gradio: Project proposal for satellite gradiometry
[NASA-TM-76796] p0134 N82-20606

GRAVITY GRADIOMETERS
Superconducting tensor gravity gradiometer p0126 A82-23045
Gradio: Project proposal for satellite gradiometry
[NASA-TM-76796] p0134 N82-20606

GRAVITY WAVES
The use of wave contrast measurements in the evaluation of SAR/gravity models p0130 A82-27675

GREAT LAKES (NORTH AMERICA)
HCMM night-time thermal IR imaging experiment in Michigan --- Heat Capacity Mapping Mission p0115 A82-27655

GREAT PLAINS CORRIDOR (NORTH AMERICA)
Transition year labeling error characterization study --- Kansas, Minnesota, Montana, North Dakota, South Dakota, and Oklahoma
[E82-10111] p0069 N82-21651
AgRISTARS: Supporting research. US crop calendars in support of the early warning project
[E82-10158] p0072 N82-21682

GREEN WAVE EFFECT
As-built design specification for PARHIS
[E82-10089] p0122 N82-21641

GREENLAND
Airborne remote sensing in east Greenland p0090 A82-27695

GROUND STATIONS
University of Dundee satellite image data acquisition and archiving facility p0130 A82-27659
A low cost NOAA/TIROS AVHRR receiving station --- Advanced Very High Resolution Radiometer p0130 A82-27681
CNPq/INPE: LANDSAT system --- operations at the Cuiaba station and the electronic processing and photo laboratories
[E82-10023] p0118 N82-16441

GROUND TRUTH
Crop area estimates using ground-gathered and Landsat data A multitemporal approach p0062 A82-27676
An autodigitizing procedure for ground-data labelling of Landsat pixels p0062 A82-27682
AgRISTARS: Interim catalog ground data summary, data acquisition year 1979
[E82-10032] p0064 N82-19608
Recommended data sets, corn segments and spring wheat segments, for use in program development
[E82-10034] p0064 N82-19610
Agricultural soil moisture experiment, Colby, Kansas 1978: Measured and predicted hydrological properties of the soil
[E82-10057] p0065 N82-19632
Preliminary evaluation of spectral, normal and meteorological crop stage estimation approaches
[E82-10059] p0065 N82-19634
Notes for Brazil sampling frame evaluation trip
[E82-10060] p0066 N82-19635
As-built design specification for PARHIS
[E82-10089] p0122 N82-21641
As-built design specification for MISMAP
[E82-10091] p0123 N82-21643
AgRISTARS: Agriculture and Resources Inventory Surveys Through Aerospace Remote Sensing. Enumerator's manual, 1981 ground data survey
[E82-10116] p0069 N82-21653
The 1981 Argentina ground data collection
[E82-10127] p0070 N82-21658
A study of model parameters associated with the urban climate using HCMM data --- St. Louis, Missouri
[E82-10140] p0079 N82-21667
A multiband radiometer and data acquisition system for remote sensing field research
[E82-10142] p0134 N82-21669

GROUND WATER
Investigation of the dynamics of the regional underground runoff of the Aral sea basin using space photography p0101 A82-20343
Mixture formulas applied in estimation of dielectric and radiative characteristics of soils and grounds at microwave frequencies p0058 A82-21030
Remote-sensing functions in the interpretation of moisture from aerial and space images p0102 A82-27459
Application of aerial and space photographic data in the study of subsurface water and tectonic structures p0090 A82-27466
Satellite sensing for extraction of groundwater resources information p0105 A82-27613
Environmental studies by multispectral scanner under large-scale civil engineering construction p0063 A82-27691
HCMM hydrological analysis in Utah --- Utah lake
[E82-10063] p0107 N82-20586

H

HABITATS
Remote sensing of the structure of taiga landscapes --- Russian book p0059 A82-27397
Digital processing of tropical forest habitat in Bangladesh and the development of a low cost processing facility at the National Zoo, Smithsonian Institution p0063 A82-27687
The application of remote sensing to resource management and environmental quality programs in Kansas --- Cimarron National Grasslands, Prairie Potawatomi Reservation, and Kickapoo Reservation
[E82-10029] p0063 N82-16447
Application of remote sensing to state and regional problems --- mississippi
[E82-10033] p0078 N82-19609
San Juan National Forest Land Management Planning Support System (LMPSS) requirements definition
[E82-10106] p0069 N82-21649

HANDBOOKS
Applications systems verification and transfer project. Volume 8: Satellite snow mapping and runoff prediction handbook
[NASA-TP-1829] p0109 N82-20624

HEAT CAPACITY MAPPING MISSION
A study of model parameters associated with the urban climate using HCMM data
[E82-10159] p0080 N82-21683

HEAT FLUX
Analysis of a discrete-time linear model for geothermal flux reconnaissance from two or three aircraft infrared measurements p0075 A82-27627
Interactive initialization of heat flux parameters for numerical models using satellite temperature measurements
[E82-10048] p0120 N82-19623
Estimating ocean-air heat fluxes during cold air outbreaks by satellite
[NASA-TM-83854] p0097 N82-19781
Applications of HCMM satellite data to the study of urban heating patterns
[E82-10161] p0080 N82-21685

HEAT ISLANDS
A study of model parameters associated with the urban climate using HCMM data --- St. Louis, Missouri
[E82-10140] p0079 N82-21667
A study of model parameters associated with the urban climate using HCMM data
[E82-10159] p0080 N82-21683
A study of model parameters associated with the urban climate using HCMM data --- analysis of St. Louis, Missouri infrared imagery
[E82-10160] p0080 N82-21684
Applications of HCMM satellite data to the study of urban heating patterns
[E82-10161] p0080 N82-21685

HIGHWAYS
Amazonas project: Application of remote sensing techniques for the integrated survey of natural resources in Amazonas --- Brazil
[E82-10069] p0078 N82-20592

HUMIDITY MEASUREMENT
Humidity measurement by infrared thermometry p0075 A82-26844

HUNGARY
Remote-sensing determination of the characteristics of hydrological objects p0102 A82-27460
Monitoring of the thermal pollution of natural channels of water using infrared aerial photography p0104 A82-27471
Investigation of silting and currents in Lake Balaton by use of hydraulic models and aerial and space photographs p0104 A82-27472

HYDROGEOLOGY
Microwave radiometry of lands under natural and artificial moistening p0057 A82-21028
Mixture formulas applied in estimation of dielectric and radiative characteristics of soils and grounds at microwave frequencies p0058 A82-21030
Geotechnical applications of Landsat image analysis of Bhakra Dam Reservoir, India p0102 A82-26838
Remote-sensing determination of the characteristics of hydrological objects p0102 A82-27460
Application of aerial and space photographic data in the study of subsurface water and tectonic structures p0090 A82-27466
The use of space photographs for hydrogeological studies of the Baikal region and Mongolia p0103 A82-27468
Satellite sensing for extraction of groundwater resources information p0105 A82-27613
Use of Landsat imagery to delineate glaciofluvial aquifers in southeast South Dakota p0105 A82-27637
Experience with a variety of studies of earth resources in the Kalmyk ASSR using space imagery p0131 A82-28130

HYDROGRAPHY
The Pampean Plain studied with Landsat images p0089 A82-26013
Aerospace methods for the study of water resources and their pollution --- Russian book p0102 A82-27457
Interpretation of multispectral aerial photographs of Lake Mueggelsee p0104 A82-27473
Spectrometric studies of the water composition of Lake Mueggelsee p0104 A82-27474
Integration of Landsat, geological and geophysical data for use in thematic mapping at regional scale p0090 A82-27672
Classification of Landsat MSS data for surface cover of small areas p0116 A82-27677
Mapping of water quality using Landsat imagery p0106 A82-27692
The use of space photographs to compile water-amelioration maps p0106 A82-28137
Error analysis of pulse location estimates for simulated bathymetric lidar returns
[PB82-109448] p0096 N82-17803
Proposed digital cartridge recording system for WRELADS --- laser airborne depth sounder
[AD-A109484] p0134 N82-20491

HYDROLOGY
Investigation of the dynamics of the regional underground runoff of the Aral sea basin using space photography p0101 A82-20343
The possibilities of microwave remote sensing for the study of water resources and their pollution p0102 A82-27458
Remote-sensing determination of the characteristics of hydrological objects p0102 A82-27460
Application of satellite data to analyze and predict meltage runoff in a mountain basin p0102 A82-27461
Dynamics of snow cover in mountain regions of the Aral Sea basin, studied using satellite photographs p0102 A82-27462
Survey and mapping of shallow water bodies and the distribution of the river runoff of solids on the basis of multispectral aerial and space photographs p0103 A82-27467
Primary processing of and possibilities of using data from the meteorological satellite TIROS-N p0103 A82-27470
Noncontact methods for the quality control of water resources p0104 A82-27475
Analog devices for the processing of aerial and space images for the study of water resources p0104 A82-27476
Snow cover monitoring using AVHRR data from TIROS and NOAA satellites --- Advanced Very High Resolution Radiometer p0105 A82-27614
Visual and digital analysis of H.C.M.M. data over eastern Canada --- thermal imagery by Heat Capacity Mapping Mission p0117 A82-27698
Measurement of river sediments
[WMO-561] p0107 N82-18670
Data collection platforms: Applications to hydrology
[INPE-2246-PRE/030] p0107 N82-19304
Agricultural soil moisture experiment, Colby, Kansas 1978: Measured and predicted hydrological properties of the soil
[E82-10057] p0065 N82-19632
HCMM hydrological analysis in Utah --- Utah lake
[E82-10063] p0107 N82-20586
Dynamic study of the upper Sao Francisco River and the Tres Marias reservoir using MSS/LANDSAT images --- Brazil
[E82-10082] p0108 N82-20605
Applications systems verification and transfer project. Volume 4: Operational applications of satellite snow cover observations: Colorado Field Test Center
[NASA-TP-1825] p0108 N82-20620
Applications systems verification and transfer project. Volume 5: Operational applications of satellite snow-cover observations, northwest United States
[NASA-TP-1826] p0109 N82-20621
Applications systems verification and transfer project. Volume 6: Operational applications of satellite snow-cover observations NOAA/NESS support study
[NASA-TP-1827] p0109 N82-20622

Applications systems verification and transfer project. Volume 8 Satellite snow mapping and runoff prediction handbook
[NASA-TP-1829] p0109 N82-20624

Remote sensing for water resources and hydrology An assessment of the Corps of Engineers' program
[PB82-137142] p0110 N82-21704

HYDROLOGY MODELS

Investigation of silting and currents in Lake Balaton by use of hydraulic models and aerial and space photographs p0104 A82-27472

Watershed model study using LANDSAT data p0106 N82-17602

Strategies for using remotely sensed data in hydrologic models
[E82-10158] p0109 N82-21680

HYDROMETEOROLOGY

The use of satellite data in rainfall monitoring --- Book p0101 A82-22873

The possibility of determining snow-meltage fronts using Meteor-satellite multispectral data /with Kazakhstan considered as an example/ p0102 A82-27463

Publications and reports on contracts and grants, 1980
[PB82-103219] p0138 N82-17792

Flash flood forecasting --- and damage control measures
[WMO-577] p0107 N82-18671

Development and applications of techniques to process hydrometeor distribution data
[AD-A109929] p0109 N82-20822

I

ICE

Spectral reflectances of freshwater ice and snow from 340 through 1100 nm p0106 N82-17601

ICE MAPPING

Classification of ice radar imagery p0113 A82-22891

The possibilities of microwave remote sensing for the study of water resources and their pollution p0102 A82-27458

Remote-sensing determination of the characteristics of hydrological objects p0102 A82-27460

Land cover classification accuracy as a function of sensor spatial resolution p0076 A82-27665

The use of data from satellite-borne microwave scanning radiometers for the automated compilation of operational maps of ice cover for the Arctic Ocean p0095 A82-28145

Satellite-derived ice data sets no. 1 Antarctic monthly average microwave brightness temperatures and sea-ice concentrations, 1973 - 1976
[NASA-TM-83812] p0096 N82-17563

Electromagnetic subsurface measurements
[AD-A108192] p0106 N82-18469

Ground-truth observations of ice-covered North Slope Lakes imaged by radar
[NASA-TM-84127] p0107 N82-18664

Sea ice movements from synthetic aperture radar
[AD-A109002] p0097 N82-19435

ICE REPORTING

Comparisons of laser profilometer sea ice roughness statistics with surface truthed data and SLAR imagery p0094 A82-27619

IDAHO

Multiresource inventory methods pilot test --- for forests p0060 A82-27601

An evaluation of ISOCLS and CLASSY clustering algorithms for forest classification in northern Idaho --- Elk River quadrange of the Clearwater National Forest
[E82-10109] p0069 N82-21650

ILLINOIS

An investigation of the ozone plume from a small city p0074 A82-26329

ILLUMINATION

The influence of illumination and viewing geometry on the reflectance factor of agricultural targets p0061 A82-27646

IMAGE CONTRAST

Contrast reduction by the atmosphere and retrieval of nonuniform surface reflectance p0112 A82-20423

IMAGE CORRELATORS

Automatic relocation of ground control points in LANDSAT imagery
[RAE-TR-81071] p0118 N82-18657

IMAGE ENHANCEMENT

Geotechnical applications of Landsat image analysis of Bhakra Dam Reservoir, India p0102 A82-26838

An automatic optimum kernel-size selection technique for edge enhancement p0113 A82-26840

Landsat feature enhancement - Or, can we separate vegetation from soil p0060 A82-27622

Enhancement of Landsat data for Hudson Bay lowlands vegetation p0114 A82-27623

IMAGE FILTERS

Increase in correlation accuracy of remote sensing imagery by digital filtering p0113 A82-25454

IMAGE PROCESSING

Optimal methods of computerized image conversion p0111 A82-19833

Experimental evaluation of methods of the automated interpretation of crops from a Fragment MSS image p0057 A82-20349

Automation of the processing of aerial and space images for forest inventory p0057 A82-20350

The accuracy potential of the modern bundle block adjustment in aerial photogrammetry p0111 A82-20401

Exterior algebraic processing for remotely sensed multispectral and multitemporal images p0112 A82-21041

Information extraction from remotely sensed data - A user view p0112 A82-21089

The use of contextual information to improve land cover classification of digital remotely sensed data p0112 A82-21094

Registration of heat capacity mapping mission day and night images p0113 A82-22146

Spaceborne photography for the study of earth resources --- Russian book p0126 A82-22397

Classification of ice radar imagery p0113 A82-22891

Multispectral texture p0113 A82-25139

Building and road extraction from aerial photographs p0074 A82-25140

Increase in correlation accuracy of remote sensing imagery by digital filtering p0113 A82-25454

A procedure for the interactive tracing of edges and lines by means of digital image processing p0113 A82-26050

Primary processing of and possibilities of using data from the meteorological satellite TIROS-N p0103 A82-27470

Analog devices for the processing of aerial and space images for the study of water resources p0104 A82-27476

Operational resampling for correcting images to a geocoded format --- in remote sensing p0114 A82-27590

Topographic mapping using Landsat data p0082 A82-27615

Implementation of the Space Oblique Mercator projection in a production environment p0129 A82-27628

Development and implementation of a low cost micro computer system for Landsat analysis and geographic data base application p0129 A82-27649

Field-by-field multitemporal analysis of aerial scanner data geometrically corrected by means of a sliding model p0115 A82-27651

Evaluation of large area crop estimation techniques p0061 A82-27662

Flexible processing of remote sensing data through integration of image processing and geobased information systems p0116 A82-27667

Phenomena modelling of remotely sensed data by image rationing p0076 A82-27670

Classification of Landsat MSS data for surface cover of small areas p0116 A82-27677

Digital processing of tropical forest habitat in Bangladesh and the development of a low cost processing facility at the National Zoo, Smithsonian Institution p0063 A82-27687

Application of machine processing of visible and thermal data to the study of the geothermal area of Cerro Prieto, Mexico p0117 A82-27693

Visual and digital analysis of H.C.M.M. data over eastern Canada --- thermal imagery by Heat Capacity Mapping Mission p0117 A82-27698

Structure of hardware and software at a regional center for the automated processing of aerial and space remote-sensing images p0130 A82-28128

Possibilities of using experience gained from the thematic mapping of the moon in studies of earth resources by remote sensing methods p0083 A82-28138

Characteristics of the use of laser-mirror scanners for image processing in cartography and aerial photography p0117 A82-28143

Partially processed multispectral scanner LANDSAT high-density tapes reformatting system (HDT-AM/AMC) design specifications
[E82-10020] p0118 N82-16438

Multidisciplinary research on the application of remote sensing to water resources problems --- Wisconsin
[E82-10021] p0106 N82-16439

CNPq/INPE LANDSAT system --- operations at the Cuiaba station and the electronic processing and photo laboratories
[E82-10023] p0118 N82-16441

Simplified algorithm for calculating radiative transfer in satellite images
[INPE-2169-RPE/385] p0118 N82-16450

Evaluation of two AN/APS-94 side-looking airborne radar systems in the detection of search and rescue targets
[AD-A108404] p0132 N82-18466

Matrix data analysis Color/B and W coding is not always enough
[AD-A108406] p0084 N82-18930

Automatic analysis of multispectral images
[INPE-2212-MD/009] p0133 N82-19520

LANDSAT imagery of the Venetian Lagoon A multitemporal analysis
[E82-10036] p0119 N82-19612

A comparison of unsupervised classification procedures on LANDSAT MSS data for an area of complex surface conditions in Basilicata, Southern Italy
[E82-10038] p0119 N82-19613

Delineation of soil temperature regimes from HCMM data
[E82-10042] p0119 N82-19617

AgRISTARS Early warning and crop condition assessment Patch image processor user's manual
[E82-10055] p0065 N82-19630

Data rate reduction Impact of image data compression on end to end data management of a multispectral payload --- for satellite imagery
[REPT-44/130] p0120 N82-19654

Selection of attributes applied to multispectral images
[INPE-2303-TDL/072] p0121 N82-19927

Study project of intrusive rocks States of Espirito Santo and Rio de Janeiro, south and east of Minas Gerais and southeast of the state of Sao Paulo --- Brazil
[E82-10076] p0092 N82-20599

An algorithm for spatial heirarchy clustering
[E82-10081] p0121 N82-20604

Applicability of satellite freeze forecasting and cold climate mapping to the other parts of the United States --- Michigan p0068 N82-20613

Satellite-borne non-DOD sensors for terrestrial observations
[AD-A109486] p0134 N82-20630

Direct determination of the two dimensional image spectrum from raw synthetic aperture radar data p0122 N82-21474

Relief effects and the use of terrain models in SAR image processing --- Anderson River test site, British Columbia p0086 N82-21475

An introduction to image processing at Royal Aircraft Establishment, Farnborough, England --- U.S. and European satellite imagery
[RAE-TR-80107] p0122 N82-21565

Sonora exploratory study for the detection of wheat-leaf rust
[E82-10133] p0070 N82-21661

Observation of the Earth by radar
[NASA-TM-76830] p0124 N82-21687

Computer based technique for converting a contour map into an equispaced grid of points
[RAE-TR-80110] p0087 N82-21697

Interpretation of remotely sensed image data and impact of cluster compression --- impact of cluster compression, users
[REPT-44.2866] p0124 N82-21699

IMAGE RECONSTRUCTION

Reconstruction of a present-day landscape map of a central part of Italy using space images p0081 A82-20340

Calibration and model reconstruction in analytical close-range stereophotogrammetry I - Mathematical fundamentals p0111 A82-20403

Calibration and model reconstruction in analytical close-range stereophotogrammetry II - Special evaluation procedures for rasterstereography and moire topography p0126 A82-22141

IMAGE RESOLUTION

Image quality control in the Meteosat ground processing system p0125 A82-21090

The Landsat program - Moving ahead p0137 A82-21280

A comparison between aerial photography and Landsat for computer land-cover mapping p0074 A82-22143

An evaluation of the utility of smaller Landsat resolution elements /Resolution of Landsat resolution/ p0114 A82-27625

Improving the quality of aerial photography /Concerning the 'Basic principles of aerial photography'/ p0117 A82-28467

Profiling sensitivity to image quality
[AD-A108405] p0084 N82-18931

The LANDSAT system operated in Brazil by CNPq/INPE - results obtained in the area of mapping and future perspectives
[E82-10080] p0121 N82-20603

SAR image quality --- conference, Frascati, Italy, 11-12 Dec. 1980, synthetic aperture radar (SAR)
[ESA-SP-172] p0122 N82-21458

Two-dimensional power spectra of SEASAT SAR imagery --- ocean waves p0098 N82-21469

IMAGING TECHNIQUES

Digital photography techniques p0112 A82-21398

The use of satellite data in rainfall monitoring --- Book p0101 A82-22873

Detection of natural disasters via Meteosat p0075 A82-27040

The earth resources program for the long-term orbital station Salyut 6 p0131 A82-28132

Earth-scanning satellites lead resource hunt p0117 A82-28343

Observations with an imaging 35 GHz radiometer of terrain in Malmslatett, July 1980
[FOA-C-30240-E1/E3] p0133 N82-18672

INCIDENCE

Influence of solar illumination angle on soybean canopy reflectance p0063 A82-28153

INDEXES (RATIOS)

A look at the commonly used LANDSAT vegetation indices
[E82-10123] p0070 N82-21657

INDIA

Microwave brightness temperature pattern over the Indian subcontinent and the surrounding oceans as observed by the satellite microwave radiometer /SAMIR/ onboard Bhaskara p0093 A82-19560

Geophysical and Landsat lineament mapping - An approach illustrated from west-central and south India p0089 A82-26016

One orogenic belt or two - A structural reinterpretation supported by Landsat data products of the Precambrian metamorphics of Singhbhum, eastern India
p0089 A82-26017

Geotechnical applications of Landsat image analysis of Bhakra Dam Reservoir, India p0102 A82-26838

Satellite sensing for extraction of groundwater resources information p0106 A82-27613

Utilisation of remote sensing in resources identification and land use in India - An integrated approach
p0076 A82-27701

INDIAN OCEAN

Microwave brightness temperature pattern over the Indian subcontinent and the surrounding oceans as observed by the satellite microwave radiometer /SAMIR/ onboard Bhaskara p0093 A82-19560

The TOCIND experiment --- relation between surface isotherms and ocean currents
[CTAMN/81/R/10] p0098 N82-19805

MAGSAT anomaly profiles of the eastern Indian Ocean
[E82-10066] p0086 N82-20589

INDIANA

Non-parametric classification of abandoned coal mine features using multioriented and ratio transformed Landsat data p0090 A82-27694

Interactive initialization of heat flux parameters for numerical models using satellite temperature measurements
[E82-10048] p0120 N82-19623

Soybean canopy reflectance as influenced by cultural practices --- West Lafayette, Indiana
[E82-10105] p0068 N82-21647

INDUSTRIAL AREAS

A regional air quality model for the Kwinana industrial area of Western Australia p0075 A82-26403

INFESTATION

Remote sensing applications to resource problems in South Dakota
[E82-10027] p0132 N82-16445

The application of remote sensing to resource management and environmental quality programs in Kansas --- Cimarron National Grasslands, Prairie Potawatomi Reservation, and Kickapoo Reservation
[E82-10029] p0063 N82-16447

The Office for Remote Sensing of Earth Resources --- Pennsylvania p0121 N82-20612

INFORMATION ADAPTIVE SYSTEM

An information adaptive system study report and development plan
[NASA-CR-166768] p0120 N82-19644

INFORMATION DISSEMINATION

An analysis of user requirements for operational land satellite data p0116 A82-27685

CNPq/INPE LANDSAT system --- operations at the Cuiaba station and the electronic processing and photo laboratories
[E82-10023] p0118 N82-16441

AgRISTARS Soil moisture/early warning and crop condition assessment Interface control document
[E82-10053] p0065 N82-19628

Future Earthnet Dissemination Systems (FEDS) study Executive summary --- remote sensing data transmission
[REPT-3318] p0124 N82-21698

INFORMATION SYSTEMS

Information extraction from remotely sensed data - A user view p0112 A82-21089

Some problems concerning the effective use of remote sensing p0137 A82-26123

Program on stimulating operational private sector use of Earth observation satellite information
[E82-10131] p0138 N82-21660

INFRARED DETECTORS

Orbital performance of a 1.6 micrometer DMSP snow/cloud discrimination sensor p0130 A82-27653

INFRARED IMAGERY

Satellite observed cloud patterns associated with excessive precipitation outbreaks
[PB80-215130] p0073 N82-19177

Thermal viewing system for studying the earth's resources p0125 A82-21022

Thermal infrared data from the Heat Capacity Mapping Mission p0127 A82-24964

High precision radiometric temperature measurements of the ocean surface p0094 A82-27640

HCMM night-time thermal IR imaging experiment in Michigan --- Heat Capacity Mapping Mission
p0115 A82-27655

Thermal IR detection of submarine gas seepages in the western Istra off-shore area /Yugoslavia/
p0076 A82-27661

Arabian sea project of 1980 Composites of infrared images
[AD-A107910] p0096 N82-17567

On the accuracy of thermal inertia mapping by infrared imagery
[SAAB-REPR-AE-10] p0120 N82-19656

INFRARED PHOTOGRAPHY

The estimation of the surface moisture of a vegetated soil using aerial infrared photography p0058 A82-21093

A system for quantitative determination of species and vitalities of urban trees on color-infrared photographs
p0074 A82-24958

Remote sensing of sulfur dioxide effects on vegetation Volume 1 Summary
[PB82-115122] p0066 N82-19715

Remote sensing of sulfur dioxide effects on vegetation Volume 2: Data
[PB82-115130] p0066 N82-19716

INFRARED RADIATION

Low-latitude cloudiness and climate feedback - Comparative estimates from satellite data
p0075 A82-26980

INFRARED RADIOMETERS

Snow cover monitoring using AVHRR data from TIROS and NOAA satellites --- Advanced Very High Resolution Radiometer p0105 A82-27614

Analysis of a discrete-time linear model for geothermal flux reconnaissance from two or three aircraft infrared measurements p0075 A82-27627

Instrumentation for remote reflectance and radiance measurements p0130 A82-27652

INFRARED SCANNERS

Humidity measurement by infrared thermometry
p0075 A82-26844

INFRARED SPECTRA

Thermal vegetation canopy model studies
[AD-A106422] p0064 N82-16455

INFRARED SPECTROMETERS

Measurement of atmospheric emission using a balloon-borne cryogenic Fourier spectrometer
p0074 A82-21432

INFRARED SPECTROSCOPY

Recent auroral measurements using a field-widened interferometer spectrometer p0126 A82-21434

INLAND WATERS

Inland water quality assessment from Landsat data
p0105 A82-27610

INSOLATION

Development of a surface isolation estimation technique suitable for application of polar orbiting satellite data
[E82-10122] p0123 N82-21656

INSTRUMENT ERRORS

Radiometric calibration of the Coastal Zone Color Scanner on Nimbus 7 - A proposed adjustment
p0127 A82-26963

INTERFEROMETERS

Recent auroral measurements using a field-widened interferometer spectrometer p0126 A82-21434

INTERNATIONAL COOPERATION

Development of cooperation between CMEA member countries in the development and utilization of space-based systems for the remote sensing of earth resources and the environment p0138 A82-27543

INTERNATIONAL LAW

Remote sensing and international law
p0137 A82-24343

IONOSPHERIC CURRENTS

Electromagnetic deep-probing (100-1000 KMS) of the Earth's interior from artificial satellites Constraints on the regional emplacement of crustal resources
[E82-10043] p0084 N82-19618

IONOSPHERIC PROPAGATION

Recovering ocean waveheight from HF radar sea echoes distorted by imperfect ionospheric reflection
[PB82-113283] p0096 N82-17805

IONOSPHERIC SOUNDING

Ionospheric troughs in Antarctica p0073 A82-21217

IOWA

Evaluation of a segment-based LANDSAT full-frame approach to corp area estimation
[E82-10067] p0066 N82-20590

Determination of the optimal level for combining area and yield estimates
[E82-10146] p0071 N82-21673

IRAN

The relationship between seismicity and lineaments of the Anatolian-Caucasian-Iranian segment of the Mediterranean fold belt p0089 A82-20341

IRAQ

The relationship between seismicity and lineaments of the Anatolian-Caucasian-Iranian segment of the Mediterranean fold belt p0089 A82-20341

IRELAND

Relationship of hydrothermal phenomena within the Leinster Granite to crustal fractures delineated from Landsat imagery p0089 A82-26015

IRON ORES

One orogenic belt or two - A structural reinterpretation supported by Landsat data products of the Precambrian metamorphics of Singhbhum, eastern India
p0089 A82-26017

IRRIGATION

Microwave radiometry of lands under natural and artificial moistening p0057 A82-21028

The use of space photographs to compile water-amelioration maps p0106 A82-28137

ISOTHERMS

The TOCIND experiment --- relation between surface isotherms and ocean currents
[CTAMN/81/R/10] p0098 N82-19805

ITALY

The use of the airborne lidar system 'ALEX F 1' for aerosol tracing in the lower troposphere p0073 A82-20226

Reconstruction of a present-day landscape map of a central part of Italy using space images
p0081 A82-20340

Integration of Landsat, geological and geophysical data for use in thematic mapping at regional scale
p0090 A82-27672

LANDSAT imagery of the Venetian Lagoon A multitemporal analysis
[E82-10036] p0119 N82-19612

A comparison of unsupervised classification procedures on LANDSAT MSS data for an area of complex surface conditions in Basilicata, Southern Italy
[E82-10038] p0119 N82-19613

Heat Capacity Mapping Mission (HCMM) program: Study of geological structure of Sicily and other Italian areas --- Sardinia and the Gulf of Orosei
[E82-10073] p0091 N82-20596

J

JAPAN

An approach to path radiance correction in MSS images p0115 A82-27629

Detection of volcanic ash fall area from Landsat MSS CCT data Eruption of Mt. Ontake in 1979
p0076 A82-27650

Phenomena modelling of remotely sensed data by image rationing p0076 A82-27670

A formation process of an oceanic vortex analyzed by multi-temporal remote sensing p0095 A82-27674

JAPANESE SPACE PROGRAM

The Japanese MOS and Los program --- Marine Observation Satellite p0129 A82-27606

Earth sensing from space - Commercial and international aspects p0138 A82-27669

K

KANSAS

Crop classification using airborne radar and Landsat data p0058 A82-21033

Utilization of spatial complexity in computer classified Landsat MSS data for multi-factoral thematic mapping
p0129 A82-27648

The application of remote sensing to resource management and environmental quality programs in Kansas --- Cimarron National Grasslands, Prairie Potawatomi Reservation, and Kickapoo Reservation
[E82-10029] p0063 N82-16447

Interactive initialization of heat flux parameters for numerical models using satellite temperature measurements
[E82-10048] p0120 N82-19623

Agricultural soil moisture experiment, Colby, Kansas 1978 Measured and predicted hydrological properties of the soil
[E82-10057] p0065 N82-19632

Registration verification of SEA/AR fields --- Oregon, Texas, Montana, Nebraska, Washington, Colorado, Kansas, Oklahoma, and North Dakota
[E82-10083] p0068 N82-21635

Ground registration of data from an airborne scatterometer
[E82-10084] p0068 N82-21636

KARST

Application of aerial and space photographic data in the study of subsurface water and tectonic structures
p0090 A82-27466

KENTUCKY

Satellite and surface geophysical expression of anomalous crustal structure in Kentucky and Tennessee
[NASA-TM-8[illegible]163] p0084 N82-17715

KUWAIT

An experiment in probabilistic relaxation for terrain cover classification of Kuwait from Landsat imagery
p0062 A82-27680

L

LAGOONS

LANDSAT imagery of the Venetian Lagoon A multitemporal analysis
[E82-10036] p0119 N82-19612

LAKE ICE

Ground-truth observations of ice-covered North Slope Lakes imaged by radar
[NASA-TM-84127] p0107 N82-18664

LAKE MICHIGAN

The use of wave contrast measurements in the evaluation of SAR/gravity models p0130 A82-27675

LAKE ONTARIO

Visual and digital analysis of H.C.M.M. data over eastern Canada --- thermal imagery by Heat Capacity Mapping Mission p0117 A82-27698

LAKES

Geotechnical applications of Landsat image analysis of Bhakra Dam Reservoir, India p0102 A82-26838

Remote sensing of the structure of taiga landscapes --- Russian book p0059 A82-27397

The effect of anthropogenic factors on the dynamics of lakes in the plains of Central Asia /studied on the basis of space photographs/ p0103 A82-27469

Investigation of silting and currents in Lake Balaton by use of hydraulic models and aerial and space photographs p0104 A82-27472

Interpretation of multispectral aerial photographs of Lake Mueggelsee p0104 A82-27473

Spectrometric studies of the water composition of Lake Mueggelsee p0104 A82-27474

Inland water quality assessment from Landsat data p0105 A82-27610

Mapping of water quality using Landsat imagery p0106 A82-27692

Multidisciplinary research on the application of remote sensing to water resources problems --- Wisconsin [E82-10021] p0106 N82-16439

Ground-truth observations of ice-covered North Slope Lakes imaged by radar [NASA-TM-84127] p0107 N82-18664

Resourceful decisions LANDAT in Michigan [E82-10037] p0078 N82-19601

HCMM hydrological analysis in Utah --- Utah lake [E82-10063] p0107 N82-20586

LAND MANAGEMENT

Inventory of eroded areas in the state of Guanajuato Mexico, by automatic analysis of Landsat images p0076 A82-27690

Assessment of change in Bangladesh coastal regions p0076 A82-27696

Landsat MSS applied to rangeland management in Western Canada p0063 A82-27697

Seasat imagery for detection of coastal Wetlands p0063 A82-27700

Examination of the operational prospects for remote sensing --- in Europe [ESA-CR(P)-1476] p0138 N82-18669

San Juan National Forest Land Management Planning Support System (LMPSS) requirements definition [E82-10108] p0069 N82-21649

LAND USE

A comparison between aerial photography and Landsat for computer land cover mapping p0074 A82-22143

Detailed land use classification based on multitemporal Landsat-MSS-data p0076 A82-27657

Flexible processing of remote sensing data through integration of image processing and geobased information systems p0116 A82-27667

Visual and digital analysis of H C M M data over eastern Canada --- thermal imagery by Heat Capacity Mapping Mission p0117 A82-27698

Utilization of remote sensing in resources identification and land use in India - An integrated approach p0076 A82-27701

Remote sensing data applied to land-use survey at the Paraiba Valley --- Brazil [E82-10025] p0081 N82-16443

The application of remote sensing to resource management and environmental quality programs in Kansas --- Cimarron National Grasslands, Prairie Potawatomi Reservation, and Kickapoo Reservation [E82-10029] p0063 N82-16447

Resourceful decisions LANDAT in Michigan [E82-10037] p0078 N82-19601

Application of remote sensing to state and regional problems --- mississippi [E82-10033] p0078 N82-19609

Notes for Brazil sampling frame evaluation trip [E82-10060] p0066 N82-19635

Amazonas project Application of remote sensing techniques for the integrated survey of natural resources in Amazonas --- Brazil [E82-10069] p0078 N82-20592

Land use in the Paraiba Valley through remotely sensed data --- Brazil [E82-10072] p0079 N82-20595

AgRISTARS Agriculture and Resources Inventory Surveys Through Aerospace Remote Sensing Enumerator's manual, 1981 ground data survey [E82-10116] p0069 N82-21653

Strategies for using remotely sensed data in hydrologic models [E82-10156] p0109 N82-21680

LANDFORMS

Methods of editing cloud and atmospheric layer affected pixels from satellite data [E82-10154] p0123 N82-21678

LANDSAT D

Imaging the earth. I - The troubled first decade of Landsat p0137 A82-27169

Information expectations from Landsat-D p0128 A82-27583

Implementation of the Space Oblique Mercator projection in a production environment p0129 A82-27628

The potential of remote sensing to monitor soil erosion on cropland p0061 A82-27656

Earth sensing from space - Commercial and international aspects p0138 A82-27669

An analysis of user requirements for operational land satellite data p0116 A82-27685

LANDSAT D PRIME

Earth sensing from space - Commercial and international aspects p0138 A82-27669

An analysis of user requirements for operational land satellite data p0116 A82-27685

LANDSAT SATELLITES

Effects of the atmosphere on the detection of surface changes from Landsat multispectral scanner data p0125 A82-21091

The Landsat program - Moving ahead p0137 A82-21280

LANDSAT 2

LANDSAT-2 and LANDSAT-3 flight evaluation report, 23 January to 23 July 1980 [E82-10022] p0132 N82-16440

LANDSAT 3

LANDSAT-2 and LANDSAT-3 flight evaluation report, 23 January to 23 July 1980 [E82-10022] p0132 N82-16440

LARGE AREA CROP INVENTORY EXPERIMENT

Transition year labeling error characterization study --- Kansas, Minnesota, Montana, North Dakota, South Dakota, and Oklahoma [E82-10111] p0069 N82-21651

LARGE SPACE STRUCTURES

The microwave radiometer spacecraft. A design study. Executive summary p0131 N82-16154

LASER ALTIMETERS

Airborne laser systems use in terrain mapping p0082 A82-27584

A shuttle scanning laser altimeter for topographic mapping p0083 A82-27632

LASER APPLICATIONS

Mapping in tropical forests - A new approach using the laser APR --- Airborne Profile Recorder p0081 A82-20407

Comparisons of laser profilometer sea ice roughness statistics with surface truthed data and SLAR imagery p0094 A82-27619

Characteristics of the use of laser-mirror scanners for image processing in cartography and aerial photography p0117 A82-28143

Model studies of laser absorption computed tomography for remote air pollution measurement p0077 A82-28152

An aerial survey of water turbidity and laser depth sounding performance along the Queensland Coast [AD-A109050] p0098 N82-19802

LASER RANGE FINDERS

Session III of the VLBI/Laser intercomparison task of the NASA crustal dynamics project [NASA-CR-168427] p0083 N82-17708

LEAST SQUARES METHOD

The location of three-dimensional linear objects by using multiple projections p0111 A82-20404

LEAVES

Soybean canopy reflectance as influenced by cultural practices --- West Lafayette, Indiana [E82-10105] p0068 N82-21647

LIBYA

Precipitation assessment from environmental satellite data for northwest Libya including the Gefara plan [RSC-4] p0107 N82-19790

LIGHT SCATTERING

Simulated response of a multispectral scanner over wheat as a function of wavelength and view/illumination direction [E82-10144] p0071 N82-21671

LIGNITE

Application of remote sensing to state and regional problems --- mississippi [E82-10033] p0078 N82-19609

LIMNOLOGY

The effect of anthropogenic factors on the dynamics of lakes in the plains of Central Asia /studied on the basis of space photographs/ p0103 A82-27469

Calcium carbonate precipitation in Pyramid Lake, Nevada, as monitored by satellite - 1978 and 1980 p0105 A82-27634

LITHOLOGY

Heat Capacity Mapping Mission (HCMM) program Study of geological structure of Sicily and other Italian areas --- Sardinia and the Gulf of Orosei [E82-10073] p0091 N82-20596

HCMM Soil moisture in relation to geologic structure and lithology, northern California --- Northern Coast Range, Sacramento Valley, and the Modoc Plateau [E82-10135] p0092 N82-21662

Use of MAGSAT anomaly data for crustal structure and mineral resources in the US midcontinent [E82-10152] p0092 N82-21677

LITHOSPHERE

Electromagnetic deep-probing (100-1000 KMS) of the Earth's interior from artificial satellites Constraints on the regional emplacement of crustal resources [E82-10043] p0084 N82-19618

MAGSAT anomaly profiles of the eastern Indian Ocean [E82-10066] p0086 N82-20589

Electromagnetic deep-probing (100-1000 KMS) of the Earth's interior from artificial satellites Constraints on the regional emplacement of crustal resources [E82-10155] p0087 N82-21679

LONG RANGE WEATHER FORECASTING

Classification of the fields of anomaly in monthly water temperature of the North Atlantic during the cold half-year [BLL-TRANS-1509-(9022.552)] p0097 N82-19756

M

MAGNETIC ANOMALIES

Geophysical and Landsat lineament mapping - An approach illustrated from west-central and south India p0089 A82-26016

Harmonic structure of Pc 3-4 pulsations p0082 A82-26266

Particle precipitation and atmospheric X-and Gamma-rays in the South Atlantic magnetic anomaly by balloon experiments [INPE-2119-RPE/343] p0083 N82-17711

Some new methods in geomagnetic field modeling applied to the 1960 - 1980 epoch [NASA-TM-83868] p0083 N82-17714

Satellite and surface geophysical expression of anomalous crustal structure in Kentucky and Tennessee [NASA-TM-82163] p0084 N82-17715

Equivalent source modeling of the main field using Magsat data [E82-10041] p0084 N82-19616

Magsat science investigations [E82-10045] p0085 N82-19620

Investigations of medium wavelength magnetic anomalies in the Eastern Pacific using Magsat data [E82-10047] p0119 N82-19622

Use of Magsat anomaly data for crustal structure and mineral resources in the US midcontinent [E82-10049] p0091 N82-19624

Improved definition of crustal anomalies for Magsat data [E82-10051] p0085 N82-19626

MAGSAT anomaly profiles of the eastern Indian Ocean [E82-10066] p0086 N82-20589

Preliminary models of the core field --- geomagnetic models [E82-10129] p0087 N82-21659

Compatibility study of the MAGSAT data and aeromagnetic data [E82-10136] p0123 N82-21663

Continuation of potential field data to a common altitude --- magsat data [E82-10138] p0123 N82-21665

Investigation of antarctic crust and upper mantle using MAGSAT and other geophysical data [E82-10147] p0087 N82-21674

Use of MAGSAT anomaly data for crustal structure and mineral resources in the US midcontinent [E82-10152] p0092 N82-21677

MAGNETIC DIPOLES

Equivalent source modeling of the main field using Magsat data [E82-10041] p0084 N82-19616

MAGNETIC INDUCTION

Electromagnetic deep-probing (100-1000 KMS) of the Earth's interior from artificial satellites Constraints on the regional emplacement of crustal resources [E82-10044] p0085 N82-19619

MAGNETIC STORAGE

Partially processed multispectral scanner LANDSAT high-density tapes reformatting system (HDT-AM/AMC) design specifications [E82-10020] p0118 N82-16438

MAGNETIC STORMS

Comparison of storm-time changes of geomagnetic field at ground and at MAGSAT altitudes [E82-10148] p0087 N82-21675

MAGNETIC SURVEYS

Integration of LANDSAT with geology and airborne geophysics into an operational mineral exploration system --- the Bearlodge area of northeastern Wyoming [E82-10028] p0091 N82-16446

Improved definition of crustal anomalies for Magsat data [E82-10051] p0085 N82-19626

Investigation of Antarctic crust and upper mantle using MAGSAT and other geophysical data [E82-10062] p0086 N82-20585

Spherical harmonic representation of the main geomagnetic field for world charting and investigations of some fundamental problems of physics and geophysics [E82-10075] p0086 N82-20598

Preliminary models of the core field -- geomagnetic models [E82-10129] p0087 N82-21659

Compatibility study of the MAGSAT data and aeromagnetic data [E82-10136] p0123 N82-21663

Continuation of potential field data to a common altitude --- magsat data [E82-10138] p0123 N82-21665

Separation of internal and external fields A new technique of data screening --- MAGSAT data [E82-10139] p0123 N82-21666

Investigation of antarctic crust and upper mantle using MAGSAT and other geophysical data [E82-10147] p0087 N82-21674

Comparison of storm-time changes of geomagnetic field at ground and at MAGSAT altitudes [E82-10148] p0087 N82-21675

MAGNETIC VARIATIONS

Ideal phase in estimating the spatial gradient of magnetic daily variations recorded by magnetometer arrays p0127 A82-26000

Studies related to Magsat --- Backus effect and the westward drift [E82-10050] p0085 N82-19625

Electromagnetic deep-probing (100-1000 KMS) of the Earth's interior from artificial satellites Constraints on the regional emplacement of crustal resources [E82-10155] p0087 N82-21679

MAGNETIZATION

Satellite and surface geophysical expression of anomalous crustal structure in Kentucky and Tennessee
[NASA-TM-82163] p0084 N82-17715

MAINE

Fanning - A classification algorithm for mixture landscapes applied to Landsat data of Maine forests
p0082 A82-27668

MAN ENVIRONMENT INTERACTIONS

The effect of anthropogenic factors on the dynamics of lakes in the plains of Central Asia /studied on the basis of space photographs/ p0103 A82-27469

MAPPING

Reconstruction of a present-day landscape map of a central part of Italy using space images
p0081 A82-20340

Mapsat compared to other earth-sensing concepts
p0128 A82-27581

Airborne laser systems use in terrain mapping
p0082 A82-27584

Automatic linear recognition and analysis using computer program LIRA --- satellite imagery for earth observations
p0090 A82-27612

Topographic mapping using Landsat data
p0082 A82-27615

Wide area, coarse resolution imaging with satellite-borne synthetic aperture radars in low-earth and geosynchronous orbits p0082 A82-27631

The role of computer graphics in geographic research
p0117 A82-27923

Photogrammetry software A package for everyone
[AD-A108098] p0118 N82-17570

Matrix data analysis Color/B and W coding is not always enough
[AD-A108406] p0084 N82-18930

Profiling sensitivity to image quality
[AD-A108405] p0084 N82-18931

The LANDSAT system operated in Brazil by CNPq/INPE results obtained in the area of mapping and future perspectives
[E82-10080] p0121 N82-20603

Remote sensing in Latin America Technology and markets for the 1980's
[AD-A108784] p0138 N82-20626

As-built design specification for segment map (Sgmap) program
[E82-10094] p0123 N82-21646

Preliminary models of the core field - geomagnetic models
[E82-10129] p0087 N82-21659

A digital technique for constructing variable-width lines
[AD-A110287] p0087 N82-21689

Computer based technique for converting a contour map into an equispaced grid of points
[RAE-TP-80110] p0087 N82-21697

MAPS

Taxonomic classification of world map units in crop producing areas of Argentina and Brazil with representative US soil series and major land resource areas in which they occur
[E82-10058] p0065 N82-19633

MARINE ENVIRONMENTS

Recent results of geoid determination by combination techniques in the North Sea test area p0086 N82-20583

MARINE METEOROLOGY

Analyses of the Eastern Pacific without ship PAPA data --- buoys, radar and satellite to replace weathership
p0093 A82-19139

Structure and variability of the Alboran Sea frontal system p0093 A82-20447

Some peculiarities of formulation and solution of inverse problems in microwave radiometry of the ocean surface and atmosphere p0093 A82-21921

Diurnal variation of summer convection over West Africa and the Tropical Eastern Atlantic during 1974 and 1978
p0075 A82-26700

Photogrammetry from aircraft side camera movies - Winter MONEX p0075 A82-26721

Remote sensing of rainfall rates using airborne microwave rain-scatterometer/radiometer p0105 A82-27639

An experimental program to provide remote measurement and analysis of ocean waves, sea level winds and balanced pressure in support of Seasat-A
[PB81-246035] p0095 N82-16697

Classification of the fields of anomaly in monthly water temperature of the North Atlantic during the cold half-year
[BLL-TRANS-1509-(9022.552)] p0097 N82-19756

Convergence zones in the South Atlantic and their influence on the precipitation regime in Northeastern Brazil
[INPE-2307-TDL/074] p0097 N82-19778

Estimating ocean-air heat fluxes during cold air outbreaks by satellite
[NASA-TM-83854] p0097 N82-19781

MARINE RESOURCES

Brazilian remote sensing activities current and prospective needs
[E82-10026] p0132 N82-16444

Technology and oceanography An assessment of Federal technologies for oceanographic research and monitoring
[OTA-O-142] p0097 N82-18844

Ship and satellite bio-optical research in the California Bight
[NASA-CR-168681] p0098 N82-20823

MARITIME SATELLITES

The Japanese MOS and Los program --- Marine Observation Satellite p0129 A82-27606

MARKET RESEARCH

Program on stimulating operational private sector use of Earth observation satellite information
[E82-10131] p0138 N82-21660

MARKING

Documentation of computer procedures for labeling spring grains and discriminating between spring wheat and barley using LANDSAT data
[E82-10030] p0063 N82-16448

MARSHLANDS

HCMM night-time thermal IR imaging experiment in Michigan --- Heat Capacity Mapping Mission
p0115 A82-27655

MASSIFS

Application of aerial and space photographic data in the study of subsurface water and tectonic structures
p0090 A82-27466

MATHEMATICAL MODELS

Stochastic models of cover class dynamics --- remote sensing of vegetation p0059 A82-27586

Data base requirements in support of crop models
p0060 A82-27588

Analysis of a discrete-time linear model for geothermal flux reconnaissance from two or three aircraft infrared measurements p0075 A82-27627

The use of wave contrast measurements in the evaluation of SAR/gravity models p0130 A82-27675

An invertible coniferous forest canopy reflectance model p0062 A82-27679

Construction of a mathematical model for the recognition of identical images on a pair of photographs
p0117 A82-28146

An optical model for the microwave properties of sea ice
[NASA-TM-83865] p0095 N82-17561

Mathematical and stochastic models in photogrammetry relating to Helmut Wolf's work p0084 N82-19605

Wheat stress indicator model, Crop Condition Assessment Division (CCAD) data base interface driver, user's manual
[E82-10031] p0064 N82-19607

Equivalent source modeling of the main field using Magsat data
[E82-10041] p0084 N82-19616

Spherical harmonic representation of the main geomagnetic field for world charting and investigations of some fundamental problems of physics and geophysics
[E82-10075] p0086 N82-20598

Freeze prediction model --- Pennsylvania
p0067 N82-20609

MSU test of P-model p0121 N82-20614

A gradient model of vegetation and climate utilizing NOAA satellite imagery Phase 1 Texas transect
[E82-10107] p0069 N82-21648

MAXIMUM ENTROPY METHOD

Information theory lateral density distribution for Earth inferred from global gravity field
[NASA-TM-83825] p0085 N82-19731

MAXIMUM LIKELIHOOD ESTIMATES

Maximum likelihood estimation of label imperfection probabilities and its use in the identification of mislabeled patterns p0112 A82-21040

The logit classifier - A general maximum likelihood discriminant for remote sensing applications
p0128 A82-27591

MEDITERRANEAN SEA

The use of Meteor-satellite image data in oceanography p0093 A82-20344

Structure and variability of the Alboran Sea frontal system p0093 A82-20447

MELTING

The possibility of determining snow-meltage fronts using Meteor-satellite multispectral data /with Kazakhstan considered as an example/ p0102 A82-27463

MERCATOR PROJECTION

Implementation of the Space Oblique Mercator projection in a production environment p0129 A82-27628

MESOSCALE PHENOMENA

Arabian sea project of 1980 Composites of infrared images
[AD-A107910] p0096 N82-17567

METAL VAPOR LASERS

A shuttle scanning laser altimeter for topographic mapping p0083 A82-27632

METEOROLOGICAL CHARTS

The design and implementation of an operational, computer-based weather radar system --- rainfall maps
[RSRE-MEMO-3151] p0122 N82-21499

METEOROLOGICAL FLIGHT

Photogrammetry from aircraft side camera movies - Winter MONEX p0075 A82-26721

METEOROLOGICAL PARAMETERS

Modern methods for monitoring and controlling the timeliness, accuracy, and completeness of data for meteorological analysis p0073 A82-19179

A study of model parameters associated with the urban climate using HCMM data --- analysis of St Louis Missouri infrared imagery
[E82-10160] p0080 N82-21684

METEOROLOGICAL RADAR

The design and implementation of an operational, computer-based weather radar system --- rainfall maps
[RSRE-MEMO-3151] p0122 N82-21499

METEOROLOGICAL SATELLITES

Climate observing system studies An element of the NASA Climate Research Program Workshop report
[NASA-TM-84040] p0078 N82-18808

METEOROLOGICAL SERVICES

Analyses of the Eastern Pacific without ship PAPA data --- buoys, radar and satellite to replace weathership
p0093 A82-19139

Publications and reports on contracts and grants, 1980
[PB82-103219] p0138 N82-17792

METEOSAT SATELLITE

Detection of natural disasters via Meteosat
p0075 A82-27040

Atlas of METEOSAT imagery
[ESA-SP-1030] p0124 N82-21700

MEXICO

Inventory of eroded areas in the state of Guanajuato Mexico, by automatic analysis of Landsat images
p0076 A82-27690

Application of machine processing of visible and thermal data to the study of the geothermal area of Cerro Prieto, Mexico p0117 A82-27693

Sonora exploratory study for the detection of wheat leaf rust
[E82-10133] p0070 N82-21661

MICHIGAN

HCMM night-time thermal IR imaging experiment in Michigan --- Heat Capacity Mapping Mission
p0115 A82-27655

Seasat imagery for detection of coastal Wetlands
p0063 A82-27700

Resourceful decisions LANDAT in Michigan
[E82-10037] p0078 N82-19601

Application of satellite frost forecast technology to other parts of the United States, phase 2 --- Pennsylvania, Michigan, and Florida
[NASA-CR-166827] p0121 N82-20607

Application of satellite frost forecast technology to other parts of the United States, phase 2, introduction
p0121 N82-20608

Applicability of satellite freeze forecasting and cold climate mapping to the other parts of the United States --- Michigan p0068 N82-20613

MSU test of P-model p0121 N82-20614

MICROCOMPUTERS

Development and implementation of a low cost micro computer system for Landsat analysis and geographic data base application p0129 A82-27649

A microcomputer for control of data collection platforms --- GOES satellites
[INPE-2104-RPE/331] p0133 N82-18881

MICROWAVE EMISSION

Soil moisture determination - Experiments with passive microwave radiometers p0057 A82-19529

Microwave radiometry of lands under natural and artificial moistening p0057 A82-21028

Microwave radiation peculiarities of vegetative covers
p0058 A82-21029

Mixture formulas applied in estimation of dielectric and radiative characteristics of soils and grounds at microwave frequencies p0058 A82-21030

Theoretical and experimental studies of microwave emission signatures of snow p0125 A82-21034

Some peculiarities of formulation and solution of inverse problems in microwave radiometry of the ocean surface and atmosphere p0093 A82-21921

An optical model for the microwave properties of sea ice
[NASA-TM-83865] p0095 N82-17561

Satellite-derived ice data sets no 1 Antarctic monthly average microwave brightness temperatures and sea-ice concentrations, 1973 - 1976
[NASA-TM-83812] p0096 N82-17563

Observations with an imaging 35 GHz radiometer of terrain in Malmslatett, July 1980
[FOA-C-30240-E1/E3] p0133 N82-18672

MICROWAVE IMAGERY

Machine implementation of algorithms for the mapping of soil moisture on the basis of microwave-radiometer measurements p0131 A82-28142

MICROWAVE RADIOMETERS

Microwave brightness temperature pattern over the Indian subcontinent and the surrounding oceans as observed by the satellite microwave radiometer /SAMIR/ onboard Bhaskara p0093 A82-19560

Comparison of conventionally measured sea surface temperature and wind speed with data retrieved from satellite-borne microwave radiometry p0093 A82-24063

The structure and basic parameters of a satellite system for the remote sensing of earth resources
p0131 A82-28129

The microwave radiometer spacecraft A design study Executive summary p0131 N82-16154

Mission definition for a large-aperture microwave radiometer spacecraft p0131 N82-16155

Imaging microwave radiometer Phase A study Volume 1 Executive summary --- instrument for the European Remote Sensing system payload
[ESS/SS-1006] p0132 N82-18564

Assessment of the quality of GATE area rainfall data from a Nimbus-5 radiometer
[NASA-CR-168512] p0109 N82-20807

Context sensitive formulations of antenna pattern correction and side lobe compensation for NOSS/LAMMR real time processing
[NASA-CR-166789] p0122 N82-21457

MICROWAVE SCATTERING
Microwave radiation from a natural snow field p0101 A82-19559
The use of satellite data in rainfall monitoring --- Book p0101 A82-22873
Remote sensing of rainfall rates using airborne microwave rain-scatterometer/radiometer p0105 A82-27639
Coherent scatter of microwaves from moderately rough surfaces
[AD-A106133] p0095 N82-16331
Active microwave investigation of snowpacks. Experimental documentation. Colorado 1979-1980
[NASA-CR-166727] p0107 N82-19646
Ground registration of data from an airborne scatterometer
[E82-10084] p0068 N82-21636

MICROWAVE SENSORS
Towards the definition of optimum sensor specifications for microwave remote sensing of snow p0125 A82-21035
Microwave remote sensing. Active and passive. Volume 1 - Microwave remote sensing fundamentals and radiometry --- Book p0126 A82-22877
The possibilities of microwave remote sensing for the study of water resources and their pollution p0102 A82-27458
Guidelines for spaceborne microwave remote sensors
[NASA-RP-1086] p0133 N82-19647
MRSE: A Microwave Remote Sensing Experiment in Spacelab p0134 N82-20375

MIDLATITUDE ATMOSPHERE
Ionospheric troughs in Antarctica p0073 A82-21217
The development and testing of methods to infer midlatitude precipitation intensity from geosynchronous satellite infrared data
[AD-A108881] p0120 N82-19788

MINERAL DEPOSITS
Relationship of hydrothermal phenomena within the Leinster Granite to crustal fractures delineated from Landsat imagery p0089 A82-26015
One orogenic belt or two - A structural reinterpretation supported by Landsat data products of the Precambrian metamorphics of Singhbhum, eastern India p0089 A82-26017
Ore deposits in Africa and their relation to the underlying mantle p0090 A82-26604
Utilisation of remote sensing in resources identification and land use in India - An integrated approach p0076 A82-27701
Integration of LANDSAT with geology and airborne geophysics into an operational mineral exploration system --- the Bearlodge area of northeastern Wyoming
[E82-10028] p0091 N82-16446
Use of Magsat anomaly data for crustal structure and mineral resources in the US midcontinent
[E82-10049] p0091 N82-19624

MINERAL EXPLORATION
Towards an operational SPOT system - A preliminary assessment --- earth observation satellites for resources management p0114 A82-27607
Airborne remote sensing in east Greenland p0090 A82-27695
Earth-scanning satellites lead resource hunt p0117 A82-28343
Report on a short course in remote sensing and the geological applications of LANDSAT MSS imagery at INPE
[E82-10024] p0091 N82-16442
Brazilian remote sensing activities: current and prospective needs
[E82-10026] p0132 N82-16444
Integration of LANDSAT with geology and airborne geophysics into an operational mineral exploration system --- the Bearlodge area of northeastern Wyoming
[E82-10028] p0091 N82-16446
Technology and oceanography: An assessment of Federal technologies for oceanographic research and monitoring
[OTA-O-142] p0097 N82-18844
Application of HCMM data to regional geologic analysis for mineral and energy resource evaluation
[E82-10137] p0092 N82-21664

MINES (EXCAVATIONS)
Non-parametric classification of abandoned coal mine features using multioriented and ratio transformed Landsat data p0090 A82-27694

MINNESOTA
Use of GOES and TIROS/NOAA satellite data for snow cover mapping p0101 A82-22145

MISSION PLANNING
The Japanese MOS and Los program --- Marine Observation Satellite p0129 A82-27606
The first ESA remote sensing satellite system ERS-1 p0094 A82-27608
Mission definition for a large-aperture microwave radiometer spacecraft p0131 N82-16155

MISSISSIPPI
Application of remote sensing to state and regional problems --- mississippi
[E82-10033] p0078 N82-19609

MISSOURI
An investigation of the ozone plume from a small city p0074 A82-26329
A study of model parameters associated with the urban climate using HCMM data --- St. Louis, Missouri
[E82-10140] p0079 N82-21667
A study of model parameters associated with the urban climate using HCMM data
[E82-10159] p0080 N82-21683
A study of model parameters associated with the urban climate using HCMM data --- analysis of St. Louis, Missouri infrared imagery
[E82-10160] p0080 N82-21684

MODULATION TRANSFER FUNCTION
An automatic optimum kernel-size selection technique for edge enhancement p0113 A82-26840

MOIRE EFFECTS
Calibration and model reconstruction in analytical close-range stereophotogrammetry. II - Special evaluation procedures for rasterstereography and moire topography p0126 A82-22141

MOISTURE CONTENT
Microwave radiometry of lands under natural and artificial moistening p0057 A82-21028
Microwave radiation peculiarities of vegetative covers p0058 A82-21029
Investigation of the vegetative covers on ploughed areas by SLAR p0058 A82-21031
Towards the definition of optimum sensor specifications for microwave remote sensing of snow p0125 A82-21035
The estimation of the surface moisture of a vegetated soil using aerial infrared photography p0058 A82-21093
Remote-sensing functions in the interpretation of moisture from aerial and space images p0102 A82-27459
A gradient model of vegetation and climate utilizing NOAA satellite imagery. Phase 1: Texas transect
[E82-10107] p0069 N82-21648
Applications of HCMM satellite data to the study of urban heating patterns
[E82-10161] p0080 N82-21685

MONGOLIA
The use of space photographs for hydrogeological studies of the Baikal region and Mongolia p0103 A82-27468

MONOCHROMATORS
Stratospheric instruments and analyses p0133 N82-18776

MONSOONS
Photogrammetry from aircraft side camera movies - Winter MONEX p0075 A82-26721
Arabian sea project of 1980. Composites of infrared images
[AD-A107910] p0096 N82-17567

MONTANA
Registration verification of SEA/AR fields --- Oregon, Texas, Montana, Nebraska, Washington, Colorado, Kansas, Oklahoma, and North Dakota
[E82-10083] p0068 N82-21635

MOROCCO
Remote sensing applied to basement tectonics of the calcareous High Atlas /Morocco/ p0089 A82-26014

MOSAICS
Arabian sea project of 1980. Composites of infrared images
[AD-A107910] p0096 N82-17567

MOTHS
The Office for Remote Sensing of Earth Resources --- Pennsylvania p0121 N82-20612

MOUNTAINS
Landsat thermal imaging of alpine regions p0079 A82-22147
Remote sensing applied to basement tectonics of the calcareous High Atlas /Morocco/ p0089 A82-26014
Application of satellite data to analyze and predict meltage runoff in a mountain basin p0102 A82-27461
Integration of Landsat, geological and geophysical data for use in thematic mapping at regional scale p0090 A82-27672

MULTISPECTRAL BAND CAMERAS
Spectritek - A multispectral electron-optic pushbroom camera p0129 A82-27633

MULTISPECTRAL BAND SCANNERS
Effects of the atmosphere on the detection of surface changes from Landsat multispectral scanner data p0125 A82-21091
Digital photography techniques p0112 A82-21398
Analysis of the direction-dependent radiation behavior in multispectral scanning data p0125 A82-21399
Information expectations from Landsat-D p0128 A82-27563
Land cover classification accuracy as a function of sensor spatial resolution p0076 A82-27665
The structure and basic parameters of a satellite system for the remote sensing of earth resources p0131 A82-28129
Characterizing user requirements for future land observing satellites
[NASA-TM-83867] p0081 N82-17562

MULTISPECTRAL IMAGERY
Passive bathymetric measurements in the Bruce Peninsula region of Ontario p0129 A82-27642

MULTISPECTRAL LINEAR ARRAYS
A concept for an advanced earth resources satellite system p0127 A82-27579
Mapsat compared to other earth-sensing concepts p0128 A82-27581

MULTISPECTRAL PHOTOGRAPHY
Exterior algebraic processing for remotely sensed multispectral and multitemporal images p0112 A82-21041
Multispectral photographic remote sensing of green vegetation biomass and productivity p0059 A82-22144
Multispectral texture p0113 A82-25139
Imaging the earth. I - The troubled first decade of Landsat p0137 A82-27169
The possibility of determining snow-meltage fronts using Meteor-satellite multispectral data /with Kazakhstan considered as an example/ p0102 A82-27463
Survey and mapping of shallow water bodies and the distribution of the river runoff of solids on the basis of multispectral aerial and space photographs p0103 A82-27467
Technologies for the multispectral mapping of earth resources p0128 A82-27580
An approach to path radiance correction in MSS images p0115 A82-27629
Utilization of spatial complexity in computer classified Landsat MSS data for multi-factoral thematic mapping p01[illegible]9 A82-27648
Airborne remote sensing in east Greenland p0090 A82-27695
The atlas 'Geographical Results of Spaceborne Multispectral Experiments' p0077 A82-28133
Construction of digital models of statistically uniform characteristics on the basis of multispectral space imagery p0117 A82-28144
Automatic relocation of ground control points in LANDSAT imagery
[RAE-TR-81071] p0118 N82-18657
Automatic analysis of multispectral images
[INPE-2212-MD/009] p0133 N82-19520
Data rate reduction: Impact of image data compression on end to end data management of a multispectral payload --- for satellite imagery
[REPT-44/130] p0120 N82-19654
Selection of attributes applied to multispectral images
[INPE-2303-TDL/072] p0121 N82-19927
Atlas of METEOSAT imagery
[ESA-SP-1030] p0124 N82-21700

N

NASA PROGRAMS
Climate observing system studies: An element of the NASA Climate Research Program. Workshop report
[NASA-TM-84040] p0078 N82-18808
NASA Oceanic Processes Program, Fiscal Year 1981
[NASA-TM-84467] p0098 N82-19801

NATIONAL OCEANIC SATELLITE SYSTEM
NOSS altimeter algorithm specifications
[NASA-RP-1083] p0095 N82-16683

NATIONAL PARKS
The utilization of orbital images as an adequate form of control of preserved areas --- Araguaia National Park, Brazil
[E82-10065] p0078 N82-20588

NATURAL GAS
Thermal IR detection of submarine gas seepages in the western Istra off-shore area /Yugoslavia/ p0076 A82-27661

NATURAL GAS EXPLORATION
Experience with a variety of studies of earth resources in the Kalmyk ASSR using space imagery p0131 A82-28130

NAVIGATION AIDS
Satellite photos can aid navigation on aerial photo missions p0126 A82-22148

NEBRASKA
Seasat satellite investigation of the structure of Western Nebraska and its application to the evaluation of geothermal resources p0090 A82-27635
Registration verification of SEA/AR fields --- Oregon, Texas, Montana, Nebraska, Washington, Colorado, Kansas, Oklahoma, and North Dakota
[E82-10083] p0068 N82-21635

NEEDS (DATA SYSTEM)
An information adaptive system study report and development plan
[NASA-CR-166768] p0120 N82-19644

NETHERLANDS
The Dutch ROVE program --- Radar Observation of VEgetation p0057 A82-21026

NETWORK ANALYSIS
The diagnosis settlement 1980 of the German main triangulation network. Part 2: Trajectories
[SER-B-253-MITT-159-PT-2] p0085 N82-19648

NEVADA
A relation between Landsat digital numbers, surface reflectance, and the cosine of the solar zenith angle p0114 A82-26841
Calcium carbonate precipitation in Pyramid Lake, Nevada, as monitored by satellite - 1978 and 1980 p0105 A82-27634

NIGHT SKY
Registration of heat capacity mapping mission day and night images p0113 A82-22146

NITROGEN
Effects of nitrogen nutrition on the growth, yield and reflectance characteristics of corn canopies --- Purdue Agronomy Farm, Indiana
[E82-10068] p0067 N82-20681
NITROGEN DIOXIDE
Mid-latitude summertime measurements of stratospheric NO2 p0074 A82-25149
NORTH AMERICA
Use of Magsat anomaly data for crustal structure and mineral resources in the US midcontinent
[E82-10049] p0081 N82-19624
NORTH DAKOTA
Registration verification of SEA/AR fields --- Oregon, Texas, Montana, Nebraska, Washington, Colorado, Kansas, Oklahoma, and North Dakota
[E82-10083] p0068 N82-21635
NORTH SEA
Evaluation of aerial photogrammetric camera and aircraft scanner pictures from tidal lands - Digital correlation and classification of multitemporal imagery data
p0127 A82-26049
Experiments in satellite Doppler control positioning at sea p0086 N82-20581
Recent results of geoid determination by combination techniques in the North Sea test area p0086 N82-20583
NUCLEAR POWER PLANTS
Preliminary results of a study of mapping thermal discharge in the ocean, using remote sensing data
[INPE-2229-PRE/021] p0097 N82-19704

O

OCEAN BOTTOM
Gravity and geoid anomalies of the Philippine Sea: Evidence on the depth of compensation for the negative residual water depth anomaly
[NASA-CR-168639] p0085 N82-19732
Some altimetric signatures from Seasat over the mid-Pacific Seamount Range
[AD-A110419] p0099 N82-21691
OCEAN COLOR SCANNER
A method for the retrieval of phytoplankton and suspended sediment concentrations from remote measurements of water colour p0094 A82-27620
Study of Earth Resources Satellite (ERS) data reduction unit
[BAE-TP-7905] p0120 N82-19649
Development of a breadboard cooler for infrared remote sensing payloads, phase 1 --- Earth Resources Satellite ERS 1
[FOK-RV-R-81-064] p0134 N82-19653
OCEAN CURRENTS
A formation process of an oceanic vortex analyzed by multi-temporal remote sensing p0095 A82-27674
The TOCIND experiment --- relation between surface isotherms and ocean currents
[CTAMN/81/R/10] p0098 N82-19805
Interaction between the Agulhas current and the subtropical convergence
[CSIR-RR-384] p0098 N82-20824
OCEAN DATA ACQUISITIONS SYSTEMS
Integrated sensor system for collection of wave data applied to coastal engineering design p0094 A82-27602
The first ESA remote sensing satellite system ERS-1
p0094 A82-27608
Response of the marine community to satellite-derived oceanic information p0095 A82-27684
Examination of the operational prospects for remote sensing --- in Europe
[ESA-CR(P)-1476] p0138 N82-18669
Technology and oceanography: An assessment of Federal technologies for oceanographic research and monitoring
[OTA-O-142] p0097 N82-18844
NASA Oceanic Processes Program, Fiscal Year 1981
[NASA-TM-84467] p0098 N82-19801
An aerial survey of water turbidity and laser depth sounding performance along the Queensland Coast
[AD-A109050] p0098 N82-19802
Proposed digital cartridge recording system for WRELADS --- laser airborne depth sounder
[AD-A109484] p0134 N82-20491
OCEAN DYNAMICS
Workshop on the application of existing satellite data to the study of ocean surface energetics, 19-21 November 1980, University of Wisconsin-Madison
p0094 A82-24822
A formation process of an oceanic vortex analyzed by multi-temporal remote sensing p0095 A82-27674
NASA Oceanic Processes Program, Fiscal Year 1981
[NASA-TM-84467] p0098 N82-19801
Interaction between the Agulhas current and the subtropical convergence
[CSIR-RR-384] p0098 N82-20824
OCEAN SURFACE
Color characteristics of the earth's surface determined on the basis of spectroscopy results from Salyut 4
p0073 A82-19826
Some peculiarities of formulation and solution of inverse problems in microwave radiometry of the ocean surface and atmosphere p0093 A82-21921
Comparison of conventionally measured sea surface temperature and wind speed with data retrieved from satellite-borne microwave radiometry p0093 A82-24063
Workshop on the application of existing satellite data to the study of ocean surface energetics, 19-21 November 1980, University of Wisconsin-Madison
p0094 A82-24822
Optimal spatial filtering and transfer function for SAR ocean wave spectra p0094 A82-27596
High precision radiometric temperature measurements of the ocean surface p0094 A82-27640
Thermal IR detection of submarine gas seepages in the western Istra off-shore area /Yugoslavia/
p0076 A82-27661
Classification of Landsat MSS data for surface cover of small areas p0116 A82-27677
Estimation of sea surface temperature from remote sensing in the 3.7 micron window region
p0095 A82-28031
Polarimetric method for the remote sensing of oil slicks on the sea surface p0095 A82-28135
An experimental program to provide remote measurement and analysis of ocean waves, sea level winds and balanced pressure in support of Seasat-A
[PB81-246039] p0095 N82-16697
Recovering ocean waveheight from HF radar sea echoes distorted by imperfect ionospheric reflection
[PB82-113283] p0096 N82-17805
Study of synthetic aperture radar in 2D - 2FS operation over the ocean --- European Remote Sensing system
[ESA-CR(P)-1475] p0132 N82-18481
Preliminary results of a study of mapping thermal discharge in the ocean, using remote sensing data
[INPE-2229-PRE/021] p0097 N82-19704
Classification of the fields of anomaly in monthly water temperature of the North Atlantic during the cold half-year
[BLL-TRANS-1509-(9022.552)] p0097 N82-19756
Surface wave statistics and spectra during high sea state conditions in the North Atlantic
[AD-A109832] p0098 N82-20827
Two-dimensional power spectra of SEASAT SAR imagery --- ocean waves p0098 N82-21469
Direct determination of the two dimensional image spectrum from raw synthetic aperture radar data
p0122 N82-21474
OCEAN TEMPERATURE
Comparison of conventionally measured sea surface temperature and wind speed with data retrieved from satellite-borne microwave radiometry p0093 A82-24063
High precision radiometric temperature measurements of the ocean surface p0094 A82-27640
Estimation of sea surface temperature from remote sensing in the 3.7 micron window region
p0095 A82-28031
Preliminary results of a study of mapping thermal discharge in the ocean, using remote sensing data
[INPE-2229-PRE/021] p0097 N82-19704
Classification of the fields of anomaly in monthly water temperature of the North Atlantic during the cold half-year
[BLL-TRANS-1509-(9022.552)] p0097 N82-19756
Estimating ocean-air heat fluxes during cold air outbreaks by satellite
[NASA-TM-83854] p0097 N82-19781
OCEANOGRAPHIC PARAMETERS
Mission definition for a large-aperture microwave radiometer spacecraft p0131 N82-16155
The relationship among sea surface roughness variations, oceanographic analyses, and airborne remote sensing analyses
[NASA-CR-168444] p0096 N82-17798
OCEANOGRAPHY
The use of Meteor-satellite image data in oceanography p0093 A82-20344
SASS measurements of the Ku-band radar signature of the ocean p0093 A82-21917
Land cover classification accuracy as a function of sensor spatial resolution p0076 A82-27665
Response of the marine community to satellite-derived oceanic information p0095 A82-27684
Seasat data utilization project
[NASA-CR-168557] p0097 N82-18660
Technology and oceanography: An assessment of Federal technologies for oceanographic research and monitoring
[OTA-O-142] p0097 N82-18844
Satellite-borne non-DOD sensors for terrestrial observations
[AD-A109486] p0134 N82-20630
OFFSHORE ENERGY SOURCES
Thermal IR detection of submarine gas seepages in the western Istra off-shore area /Yugoslavia/
p0076 A82-27661
OIL EXPLORATION
Towards an operational SPOT system - A preliminary assessment --- earth observation satellites for resources management p0114 A82-27607
Comparisons of laser profilometer sea ice roughness statistics with surface truthed data and SLAR imagery
p0094 A82-27619
Experience with a variety of studies of earth resources in the Kalmyk ASSR using space imagery
p0131 A82-28130
OIL SLICKS
Polarimetric method for the remote sensing of oil slicks on the sea surface p0095 A82-28135
OKLAHOMA
Registration verification of SEA/AR fields --- Oregon, Texas, Montana, Nebraska, Washington, Colorado, Kansas, Oklahoma, and North Dakota
[E82-10083] p0068 N82-21635
ONBOARD DATA PROCESSING
An intelligent earth sensing information system
p0137 A82-22149
The Seasat low rate data processing system
p0093 A82-24061
Complex of units for the storage and automated processing of research data p0131 A82-28140
An information adaptive system study report and development plan
[NASA-CR-166768] p0120 N82-19644
Study of Earth Resources Satellite (ERS) data reduction unit
[BAE-TP-7905] p0120 N82-19649
Data rate reduction: Impact of image data compression on end to end data management of a multispectral payload --- for satellite imagery
[REPT-44/130] p0120 N82-19654
ONTARIO
Manual and automatic crop identification with airborne radar imagery p0057 A82-20408
Enhancement of Landsat data for Hudson Bay lowlands vegetation p0114 A82-27623
Passive bathymetric measurements in the Bruce Peninsula region of Ontario p0129 A82-27642
OPTICAL DATA PROCESSING
Methods for the processing of synthetic-aperture radar signals when solving problems of the national economy /Review/ p0113 A82-26726
OPTICAL DENSITY
Analog devices for the processing of aerial and space images for the study of water resources
p0104 A82-27476
OPTICAL EMISSION SPECTROSCOPY
Measurement of atmospheric emission using a balloon-borne cryogenic Fourier spectrometer
p0074 A82-21432
OPTICAL PROPERTIES
Influence of dissolved organic materials on turbid water optical properties and remote-sensing reflectance
p0093 A82-20445
Optical properties of snow p0101 A82-21922
An optical model for the microwave properties of sea ice
[NASA-TM-83865] p0095 N82-17561
OPTICAL RADAR
The use of the airborne lidar system 'ALEX F 1' for aerosol tracing in the lower troposphere p0073 A82-20226
Airborne lidar measurements of smoke plume distribution, vertical transmission, and particle size p0073 A82-21386
Error analysis of pulse location estimates for simulated bathymetric lidar returns
[PB82-109448] p0096 N82-17803
Sounding the aerosol distribution over the Upper Rhine Valley in the Valley in the Speyer area by means of lidar
p0079 N82-20782
OPTICAL SCANNERS
Characteristics of the use of laser-mirror scanners for image processing in cartography and aerial photography
p0117 A82-28143
OPTICAL THICKNESS
Development of a surface isolation estimation technique suitable for application of polar orbiting satellite data
[E82-10122] p0123 N82-21656
ORBIT CALCULATION
Orbital methods of celestial geodesy --- Russian book
p0079 A82-25234
ORBITAL ASSEMBLY
The microwave radiometer spacecraft: A design study. Executive summary p0131 N82-16154
ORBITAL MANEUVERS
Topex orbit sustenance maneuver design --- Ocean Topography Experiment spacecraft
[AIAA PAPER 82-0202] p0094 A82-27091
OREGON
Seasat imagery for detection of coastal Wetlands
p0063 A82-27700
Registration verification of SEA/AR fields --- Oregon, Texas, Montana, Nebraska, Washington, Colorado, Kansas, Oklahoma, and North Dakota
[E82-10083] p0068 N82-21635
OROGRAPHY
Spatial reasoning in remotely sensed data
p0105 A82-27592
Integration of Landsat, geological and geophysical data for use in thematic mapping at regional scale
p0090 A82-27672
OZONE
Multidimensional aspects: Ozone, temperature and transport p0081 N82-16772
Atlas of the global distribution of the total ozone concentration according to satellite measurements
[MITT-28] p0078 N82-19740
Ozone measurements to 48Km with chemiluminescent ozone detectors
[AD-A110342] p0134 N82-21808

OZONOMETRY

The NASA participation in the 1980 EPA PEPE/NEROS field measurements program p0075 A82-28621

Stratospheric instruments and analyses p0133 N82-18776

Atlas of the global distribution of the total ozone concentration according to satellite measurements [MITT-28] p0078 N82-19740

P

PACIFIC NORTHWEST (US)

Applications systems verification and transfer project. Volume 5: Operational applications of satellite snow-cover observations, northwest United States [NASA-TP-1826] p0109 N82-20621

PACIFIC OCEAN

Analyses of the Eastern Pacific without ship PAPA data --- buoys, radar and satellite to replace weathership p0093 A82-19139

The use of Meteor-satellite image data in oceanography p0093 A82-20344

A formation process of an oceanic vortex analyzed by multi-temporal remote sensing p0095 A82-27674

Investigations of medium wavelength magnetic anomalies in the Eastern Pacific using Magsat data [E82-10047] p0119 N82-19622

Gravity and geoid anomalies of the Philippine Sea: Evidence on the depth of compensation for the negative residual water depth anomaly [NASA-CR-168639] p0085 N82-19732

Ship and satellite bio-optical research in the California Bight [NASA-CR-168681] p0098 N82-20823

Compatibility study of the MAGSAT data and aeromagnetic data [E82-10136] p0123 N82-21663

Some altimetric signatures from Seasat over the mid-Pacific Seamount Range [AD-A110419] p0099 N82-21691

PAMPAS

The Pampean Plain studied with Landsat images p0089 A82-26013

PANORAMIC SCANNING

Field-by-field multitemporal analysis of aerial scanner data geometrically corrected by means of a sliding model p0115 A82-27651

PARTICLE SIZE DISTRIBUTION

Airborne lidar measurements of smoke plume distribution, vertical transmission, and particle size p0073 A82-21386

PARTICULATE SAMPLING

Airborne in-situ measurement of particulate sulfur and sulfuric acid with flame photometry and thermal analysis p0073 A82-20899

PATTERN RECOGNITION

Maximum likelihood estimation of label imperfection probabilities and its use in the identification of mislabeled patterns p0112 A82-21040

An airphoto key for major tropical crops p0058 A82-22142

Building and road extraction from aerial photographs p0074 A82-25140

The spectral reflectance of certain soils --- Russian book p0059 A82-26577

Use of Landsat-derived temporal profiles for corn-soybean feature extraction and classification p0059 A82-26842

Automatic linear recognition and analysis using computer program LIRA --- satellite imagery for earth observations p0090 A82-27612

Digital analysis of spatial and spectral features from airborne MSS of a forested region p0061 A82-27647

Construction of a mathematical model for the recognition of identical images on a pair of photographs p0117 A82-28146

Report on a short course in remote sensing and the geological applications of LANDSAT MSS imagery at INPE [E82-10024] p0091 N82-16442

Remote sensing data applied to land-use survey at the Paraiba Valley --- Brazil [E82-10025] p0081 N82-16443

Automatic analysis of multispectral images [INPE-2212-MD/009] p0133 N82-19520

Utilization of Aerochrome 2443 film for identification and estimating wheat growing areas --- Rio Grande do Sul, Brazil [INPE-2197-PRE/006] p0066 N82-19639

Methodology of the interpretation of remote sensing data and applications in pedology [INPE-2211-MD/008] p0078 N82-19641

Methodology of the interpretation of remote sensing data and applications in geomorphology [INPE-2208-MD/007] p0091 N82-19642

Land use in the Paraiba Valley through remotely sensed data --- Brazil [E82-10072] p0079 N82-20595

Relation of the activities of the IPDF/INPE project (reforestation subproject) during the year 1979 --- Mato Grosso do Sul, Brazil [E82-10078] p0067 N82-20601

Computer-assisted photo interpretation research at USAETL [AD-A109366] p0121 N82-20628

US corn and soybeans exploratory experiment [E82-10088] p0068 N82-21640

Interpretation of remotely sensed image data and impact of cluster compression --- impact of cluster compression; users [REPT-44 2866] p0124 N82-21899

PATTERN REGISTRATION

Registration of heat capacity mapping mission day and night images p0113 A82-22146

Automatic relocation of ground control points in LANDSAT imagery [RAE-TR-81071] p0116 N82-18657

Registration verification of SEA/AR fields --- Oregon, Texas, Montana, Nebraska, Washington, Colorado, Kansas, Oklahoma, and North Dakota [E82-10083] p0068 N82-21635

Application of HCMM data to regional geologic analysis for mineral and energy resource evaluation [E82-10137] p0092 N82-21664

Delineation of soil temperature regimes from HCMM data [E82-10141] p0070 N82-21668

PEAT

Spectrometric studies of the water composition of Lake Mueggelsee p0104 A82-27474

PENNSYLVANIA

Application of satellite frost forecast technology to other parts of the United States, phase 2 --- Pennsylvania, Michigan, and Florida [NASA-CR-166827] p0121 N82-20607

Application of satellite frost forecast technology to other parts of the United States, phase 2, introduction p0121 N82-20608

Freeze prediction model --- Pennsylvania p0067 N82-20609

The Office for Remote Sensing of Earth Resources --- Pennsylvania p0121 N82-20612

PERFORMANCE TESTS

An aerial survey of water turbidity and laser depth sounding performance along the Queensland Coast [AD-A109050] p0098 N82-19802

PERIODIC VARIATIONS

Development of a surface isolation estimation technique suitable for application of polar orbiting satellite data [E82-10122] p0123 N82-21656

PERMAFROST

Strategies for using remotely sensed data in hydrologic models [E82-10156] p0109 N82-21680

PERMITTIVITY

Mixture formules applied in estimation of dielectric and radiative characteristics of soils and grounds at microwave frequencies p0058 A82-21030

PETROLOGY

A data base of geologic field spectra p0090 A82-27600

PHENOLOGY

Evaluation of the state of crops from satellite data p0059 A82-27393

Automatic and semi-automatic classification of Landsat agricultural crops p0061 A82-27664

The application of remote sensing to resource management and environmental quality programs in Kansas --- Cimarron National Grasslands, Prairie Potawatomi Reservation, and Kickapoo Reservation [E82-10029] p0063 N82-16447

Preliminary evaluation of spectral, normal and meteorological crop stage estimation approaches [E82-10069] p0065 N82-19634

As-Built documentation of programs to implement the Robertson and Doraiswamy/Thompson models [E82-10086] p0122 N82-21638

PHOTOCHEMICAL OXIDANTS

An investigation of the ozone plume from a small city p0074 A82-26329

PHOTOCHEMICAL REACTIONS

Multidimensional aspects: Ozone, temperature and transport p0081 N82-18772

PHOTOGEOLOGY

The relationship between seismicity and lineaments of the Anatolian-Caucasian-Iranian segment of the Mediterranean fold belt p0089 A82-20341

Structural analysis of the basement of the East European platform by remote sensing methods p0089 A82-20342

Investigation of the dynamics of the regional underground runoff of the Aral sea basin using space photography p0101 A82-20343

Dip determinations in photogeology p0089 A82-25453

Geophysical and Landsat lineament mapping - An approach illustrated from west-central and south India p0089 A82-26016

Application of aerial and space photographic data in the study of subsurface water and tectonic structures p0090 A82-27466

A data base of geologic field spectra p0090 A82-27600

The atlas 'Geographical Results of Spaceborne Multispectral Experiments' p0077 A82-28133

Potential use of space photographs obtained from the manned orbital station Salyut-5 in order to compile a set of small-scale thematic maps of mountain and piedmont regions of Central Asia p0083 A82-28139

Report on a short course in remote sensing and the geological applications of LANDSAT MSS imagery at INPE [E82-10024] p0091 N82-16442

Integration of LANDSAT with geology and airborne geophysics into an operational mineral exploration system --- the Bearlodge area of northeastern Wyoming [E82-10028] p0091 N82-16446

Weather satellite interpretation: Introduction to weather satellite imagery [PB82-107657] p0118 N82-16677

Methodology of the interpretation of remote sensing data and applications in geomorphology [INPE-2208-MD/007] p0091 N82-19642

Study project of intrusive rocks: States of Espirito Santo and Rio de Janeiro, south and east of Minas Gerais and southeast of the state of Sao Paulo --- Brazil [E82-10076] p0092 N82-20599

San Juan National Forest Land Management Planning Support System (LMPSS) requirements definition [E82-10108] p0069 N82-21649

PHOTOGRAMMETRY

The accuracy potential of the modern bundle block adjustment in aerial photogrammetry p0111 A82-20401

Analytical triangulation of space photography p0111 A82-20402

Calibration and model reconstruction in analytical close-range stereophotogrammetry. I - Mathematical fundamentals p0111 A82-20403

The location of three-dimensional linear objects by using multiple projections p0111 A82-20404

Accuracy of the normal case of close-range photogrammetry p0126 A82-22140

Calibration and model reconstruction in analytical close-range stereophotogrammetry. II - Special evaluation procedures for rasterstereography and moire topography p0126 A82-22141

Spaceborne photography for the study of earth resources --- Russian book p0126 A82-22397

Area determination by means of the method of finite elements p0082 A82-26048

Evaluation of aerial photogrammetric camera and aircraft scanner pictures from tidal lands - Digital correlation and classification of multitemporal imagery data p0127 A82-26049

A procedure for the interactive tracing of edges and lines by means of digital image processing p0113 A82-26050

Photogrammetry from aircraft side camera movies - Winter MONEX p0075 A82-26721

Analytic methods of geodetic referencing of nontopographic images p0083 A82-28134

Complex examination of photorectifiers p0131 A82-28466

Improving the quality of aerial photography /Concerning the 'Basic principles of aerial photography'/ p0117 A82-28467

Photogrammetry software: A package for everyone [AD-A108098] p0118 N82-17570

Helmut Wolf: On the occasion of his 70th birthday [SER-E-18] p0084 N82-19603

Mathematical and stochastic models in photogrammetry relating to Helmut Wolf's work p0084 N82-19605

National High-Altitude Photography (NHAP) of the Tennessee Valley Region, volume 1, no. 1 [PB82-130899] p0134 N82-21703

PHOTOINTERPRETATION

Experimental evaluation of methods of the automated interpretation of crops from a Fragment MSS image p0057 A82-20349

Manual and automatic crop identification with airborne radar imagery p0057 A82-20408

The use of digital multi-date Landsat imagery in terrain classification p0111 A82-20409

Techniques for combining Landsat and ancillary data for digital classification improvement p0111 A82-20410

Landsat classification accuracy assessment procedures p0137 A82-20412

Crop classification using airborne radar and Landsat data p0068 A82-21033

Maximum likelihood estimation of label imperfection probabilities and its use in the identification of mislabeled patterns p0112 A82-21040

A comparison between aerial photography and Landsat for computer land-cover mapping p0074 A82-22143

A system for quantitative determination of species and vitalities of urban trees on color-infrared photographs p0074 A82-24958

Dip determinations in photogeology p0089 A82-25453

Modeling misregistration and related effects on multispectral classification p0113 A82-25455

Satellite photograph interpretation p0127 A82-25460

A procedure for the interactive tracing of edges and lines by means of digital image processing p0113 A82-26050

Evaluation of the state of crops from satellite data p0059 A82-27393

Remote-sensing functions in the interpretation of moisture from aerial and space images p0102 A82-27459

The use of space photographs for hydrogeological studies of the Baikal region and Mongolia p0103 A82-27468

Interpretation of multispectral aerial photographs of Lake Mueggelsee p0104 A82-27473

Analog devices for the processing of aerial and space images for the study of water resources p0104 A82-27476
Investigation of the earth on the basis of space photographic data p0082 A82-27507
Context dependent modeling --- for remote sensing data processing p0114 A82-27587
Spatial reasoning in remotely sensed data p0105 A82-27592
Application of side-looking color infrared photography for structure detection in subtle topography p0082 A82-27611
Land cover classification accuracy as a function of sensor spatial resolution p0076 A82-27665
An autodigitizing procedure for ground-data labelling of Landsat pixels p0062 A82-27682
Inventory of eroded areas in the state of Guanajuato Mexico, by automatic analysis of Landsat images p0076 A82-27690
The atlas 'Geographical Results of Spaceborne Multispectral Experiments' p0077 A82-28133
The use of space photographs to compile water-amelioration maps p0106 A82-28137
Characteristics of the use of laser-mirror scanners for image processing in cartography and aerial photography p0117 A82-28143
Construction of a mathematical model for the recognition of identical images on a pair of photographs p0117 A82-28146
Wetland mapping from digitized aerial photography --- Sheboygan Marsh, Wisconsin
[E82-10019] p0118 N82-16437
Weather satellite interpretation Introduction to weather satellite imagery
[PB82-107657] p0118 N82-16677
Arabian sea project of 1980 Composites of infrared images
[AD-A107910] p0086 N82-17567
Automatic analysis of multispectral images
[INPE-2212-MD/009] p0133 N82-19520
Utilization of Aerochrome 2443 film for identification and estimating wheat growing areas --- Rio Grande do Sul, Brazil
[INPE-2197-PRE/006] p0066 N82-19639
Method of interpretation of remote sensing data and applications to vegetation
[INPE-2215-MD/010] p0066 N82-19640
Methodology of the interpretation of remote sensing data and applications in pedology
[INPE-2211-MD/008] p0078 N82-19641
Methodology of the interpretation of remote sensing data and applications in geomorphology
[INPE-2209-MD/00., p0091 N82-19642
Land use in the Paraiba Valley through remotely sensed data --- Brazil
[E82-10072] p0079 N82-20595
Study project of intrusive rocks States of Espirito Santo and Rio de Janeiro, south and east of Minas Gerais and southeast of the state of Sao Paulo --- Brazil
[E82-10076] p0092 N82-20599
Relation of the activities of the IPDF/INPE project (reforestation subproject) during the year 1979 --- Mato Grosso do Sul, Brazil
[E82-10078] p0067 N82-20601
The Office for Remote Sensing of Earth Resources --- Pennsylvania p0121 N82-20612
Applications systems verification and transfer project. Volume 4: Operational applications of satellite snow cover observations Colorado Field Test Center
[NASA-TP-1825] p0108 N82-20620
Applications systems verification and transfer project. Volume 8 Satellite snow mapping and runoff prediction handbook
[NASA-TP-1829] p0109 N82-20624
Computer-assisted photo interpretation research at USAETL
[AD-A109366] p0121 N82-20628

PHOTOMAPPING
Analysis of space imagery to compile a geomorphological map of the world p0089 A82-20338
Analytical triangulation of space photography p0111 A82-20402
Mapping in tropical forests - A new approach using the laser APR --- Airborne Profile Recorder p0081 A82-20407
Sampling for thematic map accuracy testing p0111 A82-20411
Towards the definition of optimum sensor specifications for microwave remote sensing of snow p0125 A82-21035
Exterior algebraic processing for remotely sensed multispectral and multitemporal images p0112 A82-21041
Remote sensing for natural resources An international view of problems, promises and accomplishments --- Book p0137 A82-21875
A comparison between aerial photography and Landsat for computer land-cover mapping p0074 A82-22143
Use of GOES and TIROS/NOAA satellite data for snow-cover mapping p0101 A82-22145
A procedure for the interactive tracing of edges and lines by means of digital image processing p0113 A82-26050
The spectral reflectance of certain soils --- Russian book p0059 A82-26577
Remote sensing of the structure of taiga landscapes --- Russian book p0059 A82-27397
Survey and mapping of shallow water bodies and the distribution of the river runoff of solids on the basis of multispectral aerial and space photographs p0103 A82-27467
Primary processing of and possibilities of using data from the meteorological satellite TIROS-N p0103 A82-27470
Investigation of silting and currents in Lake Balaton by use of hydraulic models and aerial and space photographs p0104 A82-27472
Interpretation of multispectral aerial photographs of Lake Mueggelsee p0104 A82-27473
Investigation of the earth on the basis of space photographic data p0082 A82-27507
Technologies for the multispectral mapping of earth resources p0128 A82-27580
Spatial reasoning in remotely sensed data p0105 A82-27592
An evaluation of the utility of smaller Landsat resolution elements /Resolution of Landsat resolution/ p0114 A82-27625
Spatial resolution and geometric potential of planned earth satellite missions p0130 A82-27683
Natural resources inventories by computer-satellite mapping techniques in Chaco State, Argentine Republic, South America p0116 A82-27688
Assessment of change in Bangladesh coastal regions p0076 A82-27696
Potential use of space photographs obtained from the manned orbital station Salyut-5 in order to compile a set of small-scale thematic maps of mountain and piedmont regions of Central Asia p0083 A82-28139
Characteristics of the use of laser-mirror scanners for image processing in cartography and aerial photography p0117 A82-28143
Earth-scanning satellites lead resource hunt p0117 A82-28343
Applications systems verification and transfer project. Volume 1 Operational applications of satellite snow cover observations Executive summary --- Usefulness of satellite snow-cover data for water yield prediction
[NASA-TP-1822] p0108 N82-20617
Applications systems verification and transfer project. Volume 2 Operational applications of satellite snow-cover observations and data-collection systems in the Arizona test site
[NASA-TP-1823] p0108 N82-20618
Applications systems verification and transfer project. Volume 6 Operational applications of satellite snow-cover observations NOAA/NESS support study
[NASA-TP-1827] p0109 N82-20622
Computer-assisted photo interpretation research at USAETL
[AD-A109366] p0121 N82-20628
National High-Altitude Photography (NHAP) of the Tennessee Valley Region, volume 1, no. 1
[PB82-130899] p0134 N82-21703

PHOTOMAPS
Satellite photos can aid navigation on aerial photo missions p0126 A82-22148
AgRISTARS Interim catalog ground data summary data acquisition year 1979
[E82-10032] p0064 N82-19608

PHOTOMETRY
A photometric method for depth determination by aerial photography p0101 A82-19831
Investigation of earth resources using rocket and space technology p0130 A82-28127
Possibilities of using experience gained from the thematic mapping of the moon in studies of earth resources by remote sensing methods p0083 A82-28138

PHOTORECONNAISSANCE
Satellite photograph interpretation p0127 A82-25460

PIEDMONTS
Potential use of space photographs obtained from the manned orbital station Salyut-5 in order to compile a set of small-scale thematic maps of mountain and piedmont regions of Central Asia p0083 A82-28139

PLAINS
Precipitation assessment from environmental satellite data for northwest Libya including the Gefara plan
[RSC-4] p0107 N82-19790

PLANETARY BOUNDARY LAYER
Observation of the turbulent structure in the planetary boundary layer with a kytoon-mounted ultrasonic anemometer system p0125 A82-21082

PLANETARY MAPPING
A shuttle scanning laser altimeter for topographic mapping p0083 A82-27632

PLANETARY WAVES
Interaction between the Agulhas current and the subtropical convergence
[CSIR-RR-384] p0098 N82-20824

PLANKTON
A method for the retrieval of phytoplankton and suspended sediment concentrations from remote measurements of water colour p0084 A82-27620
Ship and satellite bio-optical research in the California Bight
[NASA-CR-168881] p0086 N82-20823

PLANT STRESS
Humidity measurement by infrared thermometry p0075 A82-26844
Wheat stress indicator model, Crop Condition Assessment Division (CCAD) data base interface driver, user's manual
[E82-10031] p0064 N82-19607
AgRISTARS Soil moisture/early warning and crop condition assessment Interface control document
[E82-10053] p0065 N82-19628
Remote sensing of sulfur dioxide effects on vegetation. Volume 1 Summary
[PB82-115122] p0066 N82-19715
Atlas of the global distribution of the total ozone concentration according to satellite measurements
[MITT-28] p0078 N82-19740
Dryland pasture and crop conditions as seen by HCMM --- Washita River watershed
[E82-10074] p0067 N82-20597
As-Built documentation of programs to implement the Robertson and Doraiswamy/Thompson models
[E82-10086] p0122 N82-21638
Soybean canopy reflectance as influenced by cultural practices --- West Lafayette, Indiana
[E82-10105] p0068 N82-21647
Wheat stress indicator model, Early Warning (EW) data base interface driver, user's manual
[E82-10115] p0069 N82-21652
A look at the commonly used LANDSAT vegetation indices
[E82-10123] p0070 N82-21657
Spectral-agronomic relationships of corn, soybean and wheat canopies
[E82-10143] p0070 N82-21670

PLANTS (BOTANY)
Spectral reflectance of hydrophytes p0102 A82-24960

PLOTTERS
A digital technique for constructing variable-width lines
[AD-A110287] p0087 N82-21689

PLUMES
Airborne in-situ measurement of particulate sulfur and sulfuric acid with flame photometry and thermal analysis p0073 A82-20999
Airborne lidar measurements of smoke plume distribution, vertical transmission, and particle size p0073 A82-21386
An investigation of the ozone plume from a small city p0074 A82-26329
Applications of HCMM satellite data to the study of urban heating patterns
[E82-10161] p0080 N82-21685

POLAR REGIONS
Ionospheric troughs in Antarctica p0073 A82-21217

POLARIMETRY
Polarimetric method for the remote sensing of oil slicks on the sea surface p0085 A82-28135

POLLUTION MONITORING
The use of the airborne lidar system 'ALEX F 1' for aerosol tracing in the lower troposphere p0073 A82-20226
Airborne in-situ measurement of particulate sulfur and sulfuric acid with flame photometry and thermal analysis p0073 A82-20999
Aerospace methods for the study of water resources and their pollution --- Russian book p0102 A82-27457
Evaluation of snow-cover pollution in industrial regions using satellite TV images p0103 A82-27464
Monitoring of the thermal pollution of natural channels of water using infrared aerial photography p0104 A82-27471
Noncontact methods for the quality control of water resources p0104 A82-27475
Model studies of laser absorption computed tomography for remote air pollution measurement p0077 A82-28152
Optimal network density for atmospheric recording p0079 N82-20776

POLLUTION TRANSPORT
An investigation of the ozone plume from a small city p0074 A82-26329
LANDSAT imagery of the Venetian Lagoon A multitemporal analysis
[E82-10036] p0119 N82-19612
Applications of HCMM satellite data to the study of urban heating patterns
[E82-10161] p0080 N82-21685

POSITION (LOCATION)
The location of three-dimensional linear objects by using multiple projections p0111 A82-20404
Accuracy of the normal case of close-range photogrammetry p0126 A82-22140

POSITION ERRORS
An evaluation of ISOCLS and CLASSY clustering algorithms for forest classification in northern Idaho --- Elk River quadrange of the Clearwater National Forest
[E82-10109] p0069 N82-21650

POSITION INDICATORS
Experiments in satellite Doppler control positioning at sea p0086 N82-20581

POTATOES
A timely and accurate potato acreage estimate from Landsat - Results of a demonstration p0060 A82-27621

POTENTIAL FIELDS
Continuation of potential field data to a common altitude --- magsat data
[E82-10138] p0123 N82-21665

POWER SPECTRA
Application and experimental verification of an empirical backscattering cross section model for the earth's surface p0081 A82-21036
Harmonic structure of Pc 3-4 pulsations p0082 A82-26266

Surface wave statistics and spectra during high sea state conditions in the North Atlantic
[AD-A109832] p0098 N82-20827
Two-dimensional power spectra of SEASAT SAR imagery --- ocean waves p0098 N82-21469

PRECIPITATION (METEOROLOGY)
Satellite observed cloud patterns associated with excessive precipitation outbreaks
[PB80-215130] p0073 A82-19177
Precipitation measurements from space - Workshop summary 28 April-1 May 1981, Greenbelt, MD p0077 A82-28295
Dryland pasture and crop conditions as seen by HCMM --- Washita River watershed
[E82-10074] p0067 N82-20597

PRECIPITATION PARTICLE MEASUREMENT
The development and testing of methods to infer midlatitude precipitation intensity from geosynchronous satellite infrared data
[AD-A108881] p0120 N82-19788

PREDICTION ANALYSIS TECHNIQUES
Agricultural soil moisture experiment, Colby, Kansas 1978: Measured and predicted hydrological properties of the soil
[E82-10057] p0065 N82-19632

PRESSURE DISTRIBUTION
An experimental program to provide remote measurement and analysis of ocean waves, sea level winds and balanced pressure in support of Seasat-A
[PB81-246035] p0095 N82-16697

PROCUREMENT MANAGEMENT
Remote sensing procurement package: A management report for state and local governments
[E82-10052] p0138 N82-19627

PROFILOMETERS
Comparisons of laser profilometer sea ice roughness statistics with surface truthed data and SLAR imagery p0094 A82-27619
Electromagnetic subsurface measurements
[AD-A108192] p0106 N82-18469

PROJECT MANAGEMENT
AgRISTARS: Soil moisture/early warning and crop condition assessment. Interface control document
[E82-10053] p0065 N82-19628
AgRISTARS: Yield model development/soil moisture. Interface control document
[E82-10054] p0065 N82-19629
Project communications/documentation standards manual
[E82-10093] p0068 N82-21645

PULSED LASERS
Error analysis of pulse location estimates for simulated bathymetric lidar returns
[PB82-109448] p0096 N82-17803

PUSHBROOM SENSOR MODES
Digital photography techniques p0112 A82-21398
Spectritek - A multispectral electron-optic pushbroom camera p0129 A82-27633

PYRAMID LAKE (NV)
Calcium carbonate precipitation in Pyramid Lake, Nevada, as monitored by satellite - 1978 and 1980 p0105 A82-27634

Q

QUALITY CONTROL
Image quality control in the Meteosat ground processing system p0125 A82-21090

R

RADAR CROSS SECTIONS
Comparison of sigma/deg/ obtained from the conventional definition with sigma/deg/ appearing in the radar equation for randomly rough surfaces p0112 A82-21039

RADAR DATA
NOSS altimeter algorithm specifications
[NASA-RP-1083] p0095 N82-16683
Study of synthetic aperture radar in 2D - 2FS operation over the ocean --- European Remote Sensing system
[ESA-CR(P)-1475] p0132 N82-18481
Active microwave investigation of snowpacks. Experimental documentation, Colorado 1979-1980
[NASA-CR-166727] p0107 N82-19646
The design and implementation of an operational, computer-based weather radar system --- rainfall maps
[RSRE-MEMO-3151] p0122 N82-21499

RADAR ECHOES
Recovering ocean waveheight from HF radar sea echoes distorted by imperfect ionospheric reflection
[PB82-113283] p0096 N82-17805

RADAR GEOLOGY
Cliff and slope topography of part of the Grand Canyon, Arizona as characterized on a Seasat radar image p0082 A82-26843
Comparisons of laser profilometer sea ice roughness statistics with surface truthed data and SLAR imagery p0094 A82-27619
Seasat satellite investigation of the structure of Western Nebraska and its application to the evaluation of geothermal resources p0090 A82-27635
Land cover classification accuracy as a function of sensor spatial resolution p0076 A82-27665

RADAR IMAGERY
Manual and automatic crop identification with airborne radar imagery p0057 A82-20408
Classification of ice radar imagery p0113 A82-22891
Analysis of two Seasat synthetic aperture radar images of an urban scene p0074 A82-25452
Spaceborne radar observation of the earth surface p0127 A82-27578
Overview of digital processing of SAR data --- from Seasat-A p0128 A82-27589
Simulation and studies of spaceborne synthetic aperture radar image quality with reduced bit rate p0128 A82-27594
Wide area, coarse resolution imaging with satellite-borne synthetic aperture radars in low-earth and geosynchronous orbits p0082 A82-27631
The use of wave contrast measurements in the evaluation of SAR/gravity models p0130 A82-27675
Seasat imagery for detection of coastal Wetlands p0063 A82-27700
Digital correlation of DDRS data
[NASA-CR-167494] p0118 N82-16452
SAR image quality --- conference, Frascati, Italy, 11-12 Dec. 1980, synthetic aperture radar (SAR)
[ESA-SP-172] p0122 N82-21458
Two-dimensional power spectra of SEASAT SAR imagery --- ocean waves p0098 N82-21469
Direct determination of the two dimensional image spectrum from raw synthetic aperture radar data p0122 N82-21474
Relief effects and the use of terrain models in SAR image processing --- Anderson River test site, British Columbia p0086 N82-21475
Observation of the Earth by radar
[NASA-TM-76830] p0124 N82-21687

RADAR MEASUREMENT
Airborne lidar measurements of smoke plume distribution, vertical transmission, and particle size p0073 A82-21386
Precipitation measurements from space - Workshop summary 28 April-1 May 1981, Greenbelt, MD p0077 A82-28295
Sea state measurement with a two frequency scatterometer (theory)
[ESA-TT-710] p0096 N82-17802
Electromagnetic subsurface measurements
[AD-A108192] p0106 N82-18469
Sea ice movements from synthetic aperture radar
[AD-A109002] p0097 N82-19435

RADAR SCATTERING
The Dutch ROVE program --- Radar Observation of VEgetation p0057 A82-21026
Sigma/deg/ signature of the Amazon rain forest obtained from the Seasat scatterometer p0125 A82-21027
Investigation of the vegetative covers on ploughed areas by SLAR p0058 A82-21031
Volumetric effects in cross-polarized airborne radar data p0058 A82-21032
Crop classification using airborne radar and Landsat data p0058 A82-21033
Application and experimental verification of an empirical backscattering cross section model for the earth's surface p0081 A82-21036
On randomly absorbing and scattering surface layers p0079 A82-21037
A radar signature model for partially coherent scattering from irregular surfaces p0079 A82-21038
Comparison of sigma/deg/ obtained from the conventional definition with sigma/deg/ appearing in the radar equation for randomly rough surfaces p0112 A82-21039

RADAR SIGNATURES
A radar signature model for partially coherent scattering from irregular surfaces p0079 A82-21038
SASS measurements of the Ku-band radar signature of the ocean p0093 A82-21917

RADIANCE
Measurement of atmospheric emission using a balloon-borne cryogenic Fourier spectrometer p0074 A82-21432
Dew and vapor pressure as complicating factors in the interpretation of spectral radiance from crops p0060 A82-27617
An approach to path radiance correction in MSS images p0115 A82-27629
High precision radiometric temperature measurements of the ocean surface p0094 A82-27640
Usage and limitations of characteristic vector analysis of remote sensing multispectral data for the identification and quantification of water quality parameters p0118 N82-18656
As-built design specification for the CLASFYG program
[E82-10082] p0068 N82-21644
Laboratory upwelled radiance and reflectance spectra of Kerr reservoir sediment waters
[NASA-TP-1993] p0110 N82-21774

RADIANT FLUX DENSITY
Regional properties of angular reflectance models p0083 N82-17599

RADIATION COUNTERS
Ozone measurements to 48Km with chemiluminescent ozone detectors
[AD-A110342] p0134 N82-21808

RADIATION MEASURING INSTRUMENTS
Analysis of the direction-dependent radiation behavior in multispectral scanning data p0125 A82-21399

RADIATIVE TRANSFER
Simple radiative transfer model for relationships between canopy biomass and reflectance p0057 A82-20422
Contrast reduction by the atmosphere and retrieval of nonuniform surface reflectance p0112 A82-20423
Mixture formulas applied in estimation of dielectric and radiative characteristics of soils and grounds at microwave frequencies p0058 A82-21030
Some peculiarities of formulation and solution of inverse problems in microwave radiometry of the ocean surface and atmosphere p0093 A82-21921
Optical properties of snow p0101 A82-21922
Microwave remote sensing: Active and passive. Volume 1 - Microwave remote sensing fundamentals and radiometry --- Book p0126 A82-22877
Passive bathymetric measurements in the Bruce Peninsula region of Ontario p0129 A82-27642
Simplified algorithm for calculating radiative transfer in satellite images
[INPE-2169-RPE/385] p0118 N82-16450
A study of model parameters associated with the urban climate using HCMM data --- St. Louis, Missouri
[E82-10140] p0079 N82-21667

RADIO ALTIMETERS
The structure and basic parameters of a satellite system for the remote sensing of earth resources p0131 A82-28129
NOSS altimeter algorithm specifications
[NASA-RP-1083] p0095 N82-16683
Study of a radar altimeter for the European remote sensing program. Volume 1: Executive summary --- Earth Resources Satellite (ERS 1)
[SPAR-R-1090-ISSUE-A] p0133 N82-19652

RADIO RECEPTION
A low cost NOAA/TIROS AVHRR receiving station --- Advanced Very High Resolution Radiometer p0130 A82-27681

RADIOMETERS
Microwave remote sensing: Active and passive. Volume 1 - Microwave remote sensing fundamentals and radiometry --- Book p0126 A82-22877
Stratospheric instruments and analyses p0133 N82-18776
A multiband radiometer and data acquisition system for remote sensing field research
[E82-10142] p0134 N82-21669
Cloud Top Scanning radiometer (CTS): User's guide
[NASA-TM-83887] p0135 N82-21826

RADIOMETRIC CORRECTION
Primary processing of and possibilities of using data from the meteorological satellite TIROS-N p0103 A82-27470
Context sensitive formulations of antenna pattern correction and side lobe compensation for NOSS/LAMMR real time processing
[NASA-CR-166789] p0122 N82 21457

RADIOMETRIC RESOLUTION
Image quality control in the Meteosat ground processing system p0125 A82-21090
Technologies for the multispectral mapping of earth resources p0128 A82-27580
Operational resampling for correcting images to a geocoded format --- in remote sensing p0114 A82-27590
Relief effects and the use of terrain models in SAR image processing --- Anderson River test site, British Columbia p0086 N82-21475

RAIN
The use of satellite data in rainfall monitoring --- Book p0101 A82-22873
Remote sensing of rainfall rates using airborne microwave rain-scatterometer/radiometer p0105 A82-27639
A vegetation response model applied to range inventory and monitoring using Landsat MSS data p0060 A82-27643
Convergence zones in the South Atlantic and their influence on the precipitation regime in Northeastern Brazil
[INPE-2307-TDL/074] p0097 N82-19778
Precipitation assessment from environmental satellite data for northwest Libya including the Gefara plan
[RSC-4] p0107 N82-19790
Assessment of the quality of GATE area rainfall data from a Nimbus-5 radiometer
[NASA-CR-168512] p0109 N82-20807

RAIN FORESTS
Mapping in tropical forests - A new approach using the laser APR --- Airborne Profile Recorder p0081 A82-20407
Sigma/deg/ signature of the Amazon rain forest obtained from the Seasat scatterometer p0125 A82-21027

RANDOM PROCESSES
On randomly absorbing and scattering surface layers p0079 A82-21037

RANDOM SAMPLING
Using known map category marginal frequencies to improve estimates of thematic map accuracy p0113 A82-25456
Development of rotation sample designs for the estimation of crop acreages
[E82-10117] p0070 N82-21654

RANGE LANDS
A vegetation response model applied to range inventory and monitoring using Landsat MSS data
p0050 A82-27643

RANGELANDS
Assessing mesquite-grass vegetation condition from Landsat p0059 A82-25457
Landsat MSS applied to rangeland management in Western Canada p0063 A82-27697
The application of remote sensing to resource management and environmental quality programs in Kansas --- Cimarron National Grasslands, Prairie Potawatomi Reservation, and Kickapoo Reservation
[E82-10029] p0063 N82-16447
San Juan National Forest Land Management Planning Support System (LMPSS) requirements definition
[E82-10108] p0069 N82-21649

RECLAMATION
Application of remote sensing to state and regional problems --- mississippi
[E82-10033] p0078 N82-19609

RECREATION
San Juan National Forest Land Management Planning Support System (LMPSS) requirements definition
[E82-10108] p0069 N82-21649

RECTIFIERS
Complex examination of photorectifiers
p0131 A82-28466

REFERENCE STARS
Correlation identification of stellar configurations for purposes of the coordinate referencing of aerial and space images p0117 A82-28141

REFLECTANCE
Simple radiative transfer model for relationships between canopy biomass and reflectance p0057 A82-20422
Contrast reduction by the atmosphere and retrieval of nonuniform surface reflectance p0112 A82-20423
Soybean canopy reflectance as a function of view and illumination geometry p0061 A82-27645
Regional properties of angular reflectance models
p0083 N82-17599
The effect of finite field size on classification and atmospheric correction
[NASA-TM-83818] p0120 N82-19645
A look at the commonly used LANDSAT vegetation indices
[E82-10123] p0070 N82-21657
A multiband radiometer and data acquisition system for remote sensing field research
[E82-10142] p0134 N82-21669
Methods of editing cloud and atmospheric layer affected pixels from satellite data
[E82-10154] p0123 N82-21678

REFRACTED WAVES
An optical model for the microwave properties of sea ice
[NASA-TM-83865] p0095 N82-17561

REGIONAL PLANNING
The application of remote sensing to resource management and environmental quality programs in Kansas --- Cimarron National Grasslands, Prairie Potawatomi Reservation, and Kickapoo Reservation
[E82-10029] p0063 N82-16447

REGRESSION ANALYSIS
Evaluation of large area crop estimation techniques
p0061 A82-27662
Potential utility of thematic mapper data in estimating crop areas p0061 A82-27663

RELAY SATELLITES
General configuration and internal disposition of equipment in a satellite for collecting environmental data
[INPE-2240-PRE/026] p0078 N82-19256

RELIEF MAPS
The use of digital terrain model in the rectification of satellite-borne imagery p0115 A82-27626
Experiences with digital terrain elevation data contouring programs
[AD-A110280] p0087 N82-21690
Computer based technique for converting a contour map into an equispaced grid of points
[RAE-TR-80110] p0087 N82-21697

REMOTE SENSING
Effects of the atmosphere on the detection of surface changes from Landsat multispectral scanner data
p0125 A82-21091
Remote sensing and international law
p0137 A82-24343
Land cover classification accuracy as a function of sensor spatial resolution p0076 A82-27665
Remote sensing of sulfur dioxide effects on vegetation. Volume 2: Data
[PB82-115130] p0066 N82-19716

REMOTE SENSORS
Advanced aerospace remote sensing systems for global resource applications p0127 A82-27577
Satellite Earth resources data, module U-3
[E82-10035] p0119 N82-19611
Cloud Top Scanning radiometer (CTS): User's guide
[NASA-TM-83887] p0135 N82-21826

RESCUE OPERATIONS
Evaluation of two AN/APS-94 side-looking airborne radar systems in the detection of search and rescue targets
[AD-A108404] p0132 N82-18466

RESERVOIRS
Geotechnical applications of Landsat image analysis of Bhakra Dam Reservoir, India p0102 A82-26838
Dynamic study of the upper Sao Francisco River and the Tres Marias reservoir using MSS/LANDSAT images --- Brazil
[E82-10082] p0108 N82-20605
Laboratory upwelled radiance and reflectance spectra of Kerr reservoir sediment waters
[NASA-TP-1993] p0110 N82-21774

RESOURCES MANAGEMENT
Remote sensing for natural resources: An international view of problems, promises and accomplishments --- Book p0137 A82-21875
Towards an operational SPOT system - A preliminary assessment --- earth observation satellites for resources management p0114 A82-27607
Strategies and uses of small distributed analysis centers as in the natural resource inventory of Venezuela
p0115 A82-27636
Remote sensing applications to resource problems in South Dakota
[E82-10027] p0132 N82-16445
Resourceful decisions: LANDAT in Michigan
[E82-10037] p0073 N82-19601

RETROREFLECTION
Interaction between the Agulhas current and the subtropical convergence
[CSIR-RR-384] p0098 N82-20824

RING CURRENTS
Investigations of medium wavelength magnetic anomalies in the Eastern Pacific using Magsat data
[E82-10047] p0119 N82-19622
Spherical harmonic representation of the main geomagnetic field for world charting and investigations of some fundamental problems of physics and geophysics
[E82-10075] p0086 N82-20598

RIVER BASINS
Application of satellite data to analyze and predict meltage runoff in a mountain basin p0102 A82-27461
Dynamics of snow cover in mountain regions of the Aral Sea basin, studied using satellite photographs
p0102 A82-27462
A comparison of unsupervised classification procedures on LANDSAT MSS data for an area of complex surface conditions in Basilicata, Southern Italy
[E82-10038] p0119 N82-19613
Dynamic study of the upper Sao Francisco River and the Tres Marias reservoir using MSS/LANDSAT images --- Brazil
[E82-10082] p0108 N82-20605
Applications systems verification and transfer project. Volume 4: Operational applications of satellite snow cover observations: Colorado Field Test Center
[NASA-TP-1825] p0108 N82-20620

RIVERS
Monitoring of the thermal pollution of natural channels of water using infrared aerial photography
p0104 A82-27471
Measurement of river sediments
[WMO-561] p0107 N82-18670
Evaluation of HCMM satellite data for estuarine tidal circulation patterns and thermal inertia soil moisture measurements --- Delaware Bay, Cooper River, and the Potomac River estuaries; Luverne, Minnesota soil moisture; and water temperature of Lake Anna, Virginia
[E82-10064] p0108 N82-20587

ROADS
Building and road extraction from aerial photographs
p0074 A82-25140

ROCK INTRUSIONS
Study project of intrusive rocks: States of Espirito Santo and Rio de Janeiro, south and east of Minas Gerais and southeast of the state of Sao Paulo --- Brazil
[E82-10076] p0092 N82-20599

ROCK MECHANICS
Ore deposits in Africa and their relation to the underlying mantle p0080 A82-26604

ROCKET-BORNE PHOTOGRAPHY
Investigation of earth resources using rocket and space technology p0130 A82-28127

ROCKS
One orogenic belt or two - A structural reinterpretation supported by Landsat data products of the Precambrian metamorphics of Singhbhum, eastern India
p0089 A82-26017
Heat Capacity Mapping Mission (HCMM) program: Study of geological structure of Sicily and other Italian areas --- Sardinia and the Gulf of Orosei
[E82-10073] p0091 N82-20596

RUST FUNGI
Sonora exploratory study for the detection of wheat-leaf rust
[E82-10133] p0070 N82-21661

S

SACRAMENTO VALLEY (CA)
HCMM: Soil moisture in relation to geologic structure and lithology, northern California --- Northern Coast Range, Sacramento Valley, and the Modoc Plateau
[E82-10135] p0092 N82-21662

SAFETY FACTORS
AgRISTARS: Agriculture and Resources Inventory Surveys Through Aerospace Remote Sensing. Enumerator's manual, 1981 ground data survey
[E82-10116] p0069 N82-21653

SAHARA DESERT (AFRICA)
Dust from the Sahara in satellite images
p0079 N82-20802

SALINITY
Remote sensing of salinity in the San Francisco Bay Delta p0102 A82-26839

SAMPLING
Evaluation of a segment-based LANDSAT full-frame approach to corp area estimation
[E82-10067] p0066 N82-20590

SAN FRANCISCO BAY (CA)
Remote sensing of salinity in the San Francisco Bay Delta p0102 A82-26839

SANDS
Dust from the Sahara in satellite images
p0079 N82-20802

SATELLITE ATTITUDE CONTROL
Spaceborne photography for the study of earth resources --- Russian book p0126 A82-22397

SATELLITE CONFIGURATIONS
The microwave radiometer spacecraft: A design study. Executive summary p0131 N82-16154
Mission definition for a large aperture microwave radiometer spacecraft p0131 N82-16155
General configuration and internal disposition of equipment in a satellite for collecting environmental data
[INPE-2240-PRE/026] p0078 N82-19256

SATELLITE NAVIGATION SYSTEMS
Remote sensing techniques suitable for exploration and navigation in and under sea ice
[FOA-REPT-VOL-15-NO-2] p0096 N82-17566

SATELLITE OBSERVATION
Detection of natural disasters via Meteosat
p0075 A82-27040
Satellite Earth resources data, module U-3
[E82-10035] p0119 N82-19611

SATELLITE ORBITS
Orbital methods of celestial geodesy --- Russian book
p0079 A82-25234

SATELLITE-BORNE INSTRUMENTS
The Landsat program - Moving ahead
p0137 A82-21280
Superconducting tensor gravity gradiometer
p0126 A82-23045
Comparison of conventionally measured sea surface temperature and wind speed with data retrieved from satellite-borne microwave radiometry p0093 A82-24063
International Symposium on Remote Sensing of Environment, 15th, University of Michigan, Ann Arbor, MI, May 11-15, 1981, Proceedings. Volumes 1, 2 & 3
p0127 A82-27576
Advanced aerospace remote sensing systems for global resource applications p0127 A82-27577
A concept for an advanced earth resources satellite system p0127 A82-27579
The Japanese MOS and Los program --- Marine Observation Satellite p0129 A82-27606
The first ESA remote sensing satellite system ERS-1
p0094 A82-27608
Orbital performance of a 1.6 micrometer DMSP snow/cloud discrimination sensor p0130 A82-27653
The structure and basic parameters of a satellite system for the remote sensing of earth resources
p0131 A82-28129
Seasat data utilization project
[NASA-CR-168557] p0097 N82-18660
General configuration and internal disposition of equipment in a satellite for collecting environmental data
[INPE-2240-PRE/026] p0078 N82-19256
Guidelines for spaceborne microwave remote sensors
[NASA-RP-1086] p0133 N82-19647
NASA Oceanic Processes Program, Fiscal Year 1981
[NASA-TM-84467] p0098 N82-19801
Satellite-borne non-DOD sensors for terrestrial observations
[AD-A109486] p0134 N82-20630

SATELLITE-BORNE PHOTOGRAPHY
Spaceborne photography for the study of earth resources --- Russian book p0126 A82-22397
The effect of anthropogenic factors on the dynamics of lakes in the plains of Central Asia /studied on the basis of space photographs/ p0103 A82-27469
Present and future studies of natural resources and the environment from space p0138 A82-27506
Investigation of the earth on the basis of space photographic data p0082 A82-27507
Calcium carbonate precipitation in Pyramid Lake, Nevada, as monitored by satellite - 1978 and 1980
p0105 A82-27634
University of Dundee satellite image data acquisition and archiving facility p0130 A82-27659
Satellite Earth resources data, module U-3
[E82-10035] p0119 N82-19611
Atlas of METEOSAT imagery
[ESA-SP-1030] p0124 N82-21700

SATELLITE-BORNE RADAR
Spaceborne radar observation of the earth surface
p0127 A82-27578

SCANNERS
A shuttle scanning laser altimeter for topographic mapping p0083 A82-27632
Cloud Top Scanning radiometer (CTS) User's guide [NASA-TM-83887] p0135 N82-21826
SCATTERING COEFFICIENTS
Sigma/deg/ signature of the Amazon rain forest obtained from the Seasat scatterometer p0125 A82-21027
SCATTERING CROSS SECTIONS
Application and experimental verification of an empirical backscattering cross section model for the earth's surface p0081 A82-21036
SCATTEROMETERS
SASS measurements of the Ku-band radar signature of the ocean p0083 A82-21917
Sea state measurement with a two frequency scatterometer (theory) [ESA-TT-710] p0096 N82-17802
Satellite scatterometer feasibility study. Volume 1. Technical results --- Earth Resources Satellite (ERS 1) [ESA-CR(P)-1492-VOL-1] p0133 N82-19650
Satellite scatterometer feasibility study. Volume 2. Data extraction algorithm and error simulation for wind sensor --- Earth Resources Satellite (ERS 1) [ESA-CR(P)-1492-VOL-2] p0133 N82-19651
MRSE: A Microwave Remote Sensing Experiment in Spacelab p0134 N82-20375
SCENE ANALYSIS
Building and road extraction from aerial photographs p0074 A82-25140
Scene analysis for wildland fire-fuel characteristics in a Mediterranean climate p0060 A82-27624
A technique for automatic labeling of Landsat agricultural scene elements by analysis of temporal-spectral patterns p0062 A82-27678
The Office for Remote Sensing of Earth Resources --- Pennsylvania p0121 N82-20612
SCIENTISTS
Helmut Wolf: On the occasion of his 70th birthday [SER-E-18] p0084 N82-19603
SCOTLAND
University of Dundee satellite image data acquisition and archiving facility p0130 A82-27659
SEA ICE
Comparisons of laser profilometer sea ice roughness statistics with surface truthed data and SLAR imagery p0094 A82-27619
The use of data from satellite-borne microwave scanning radiometers for the automated compilation of operational maps of ice cover for the Arctic Ocean p0095 A82-28145
An optical model for the microwave properties of sea ice [NASA-TM-83865] p0095 N82-17561
Satellite-derived ice data sets no. 1: Antarctic monthly average microwave brightness temperatures and sea-ice concentrations, 1973 - 1976 [NASA-TM-83812] p0096 N82-17563
Remote sensing techniques suitable for exploration and navigation in and under sea ice [FOA-REPT-VOL-15-NO-2] p0096 N82-17566
Sea ice movements from synthetic aperture radar [AD-A109002] p0097 N82-19435
SEA ROUGHNESS
Workshop on the application of existing satellite data to the study of ocean surface energetics. 19-21 November 1980. University of Wisconsin-Madison p0094 A82-24822
An experimental program to provide remote measurement and analysis of ocean waves, sea level winds and balanced pressure in support of Seasat-A [PB81-246035] p0095 N82-16697
The relationship among sea surface roughness variations, oceanographic analyses, and airborne remote sensing analyses [NASA-CR-168444] p0096 N82-17798
Recovering ocean waveheight from HF radar sea echoes distorted by imperfect ionospheric reflection [PB82-113283] p0096 N82-17805
Observation of the Earth by radar [NASA-TM-76830] p0124 N82-21687
SEA STATES
Some peculiarities of formulation and solution of inverse problems in microwave radiometry of the ocean surface and atmosphere p0093 A82-21921
Sea state measurement with a two frequency scatterometer (theory) [ESA-TT-710] p0096 N82-17802
Surface wave statistics and spectra during high sea state conditions in the North Atlantic [AD-A109837] p0098 N82-20827
SEA TRUTH
Comparisons of laser profilometer sea ice roughness statistics with surface truthed data and SLAR imagery p0094 A82-27619
SEA WATER
Influence of dissolved organic materials on turbid water optical properties and remote-sensing reflectance p0093 A82-20445
Structure and variability of the Alboran Sea frontal system p0093 A82-20447
Brazilian remote sensing activities, current and prospective needs [E82-10026] p0132 N82-16444
SEAMOUNTS
Some altimetric signatures from Seasat over the mid-Pacific Seamount Range [AD-A110419] p0099 N82-21691
SEARCH RADAR
Evaluation of two AN/APS-94 side-looking airborne radar systems in the detection of search and rescue targets [AD-A108404] p0132 N82-18466
SEASAT-A SATELLITE
Seasat data utilization project [NASA-CR-168557] p0097 N82-18860
SECULAR VARIATIONS
Studies related to Magsat --- Backus effect and the westward drift [E82-10050] p0085 N82-19625
SEDIMENT TRANSPORT
Investigation of silting and currents in Lake Balaton by use of hydraulic models and aerial and space photographs p0104 A82-27472
Measurement of river sediments [WMO-561] p0107 N82-18870
Dynamic study of the upper Sao Francisco River and the Tres Marias reservoir using MSS/LANDSAT images --- Brazil [E82-10082] p0108 N82-20605
SEDIMENTS
A method for the retrieval of phytoplankton and suspended sediment concentrations from remote measurements of water colour p0094 A82-27620
Laboratory upwelled radiance and reflectance spectra of Kerr reservoir sediment waters [NASA-TP-1993] p0110 N82-21774
SERVICES
National High-Altitude Photography (NHAP) of the Tennessee Valley Region, volume 1, no. 1 [PB82-130899] p0134 N82-21703
SHALLOW WATER
Survey and mapping of shallow water bodies and the distribution of the river runoff of solids on the basis of multispectral aerial and space photographs p0103 A82-27467
SIBERIA
Remote sensing of the structure of taiga landscapes --- Russian book p0059 A82-27397
Application of satellite data to analyze and predict meltage runoff in a mountain basin p0102 A82-27461
The use of space photographs for hydrogeological studies of the Baikal region and Mongolia p0103 A82-27468
SICILY
Remote SO2 emission measurements with correlation spectrometers from volcanoes p0077 A82-27704
Heat Capacity Mapping Mission (HCMM) program: Study of geological structure of Sicily and other Italian areas --- Sardinia and the Gulf of Orosei [E82-10073] p0091 N82-20596
SIDE-LOOKING RADAR
Investigation of the vegetative covers on ploughed areas by SLAR p0058 A82-21031
Classification of ice radar imagery p0113 A82-22891
Application of side-looking color infrared photography for structure detection in subtle topography p0082 A82-27611
The structure and basic parameters of a satellite system for the remote sensing of earth resources p0131 A82-28129
The relationship among sea surface roughness variations, oceanographic analyses, and airborne remote sensing analyses [NASA-CR-168444] p0096 N82-17798
Evaluation of two AN/APS-94 side-looking airborne radar systems in the detection of search and rescue targets [AD-A108404] p0132 N82-18466
SIDELOBE REDUCTION
Context sensitive formulations of antenna pattern correction and side lobe compensation for NOSS/LAMMR real time processing [NASA-CR-166789] p0122 N82-21457
SIERRA NEVADA MOUNTAINS (CA)
Applications systems verification and transfer project. Volume 3: Operational applications of satellite snow cover observations in California [NASA-TP-1824] p0108 N82-20619
SIGNAL ANALYSIS
Sea state measurement with a two frequency scatterometer (theory) [ESA-TT-710] p0096 N82-17802
SIGNAL PROCESSING
Methods for the processing of synthetic-aperture radar signals when solving problems of the national economy /Review/ p0113 A82-26726
Recovering ocean waveheight from HF radar sea echoes distorted by imperfect ionospheric reflection [PB82-113283] p0096 N82-17805
Study of a radar altimeter for the European remote sensing program. Volume 1: Executive summary --- Earth Resources Satellite (ERS 1) [SPAR-R-1090-ISSUE-A] p0133 N82-19652
SIGNAL TO NOISE RATIOS
Simulation and studies of spaceborne synthetic aperture radar image quality with reduced bit rate p0128 A82-27594
SIGNATURE ANALYSIS
AgRISTARS: Foreign commodity production forecasting. Corn/soybean decision logic development and testing [E82-10056] p0065 N82-19631
Dust from the Sahara in satellite images p0079 N82-20802
Delineation of soil temperature regimes from HCMM data [E82-10141] p0070 N82-21668
SLOPES
Cliff and slope topography of part of the Grand Canyon, Arizona as characterized on a Seasat radar image p0082 A82-26843
SMOKE
Airborne lidar measurements of smoke plume distribution, vertical transmission, and particle size p0073 A82-21386
SNOW
Optical properties of snow p0101 A82-21922
Orbital performance of a 1.6 micrometer DMSP snow/cloud discrimination sensor p0130 A82-27653
Spectral reflectances of freshwater ice and snow from 340 through 1100 nm p0106 N82-17601
Dielectric properties of snow [NASA-CR-166764] p0107 N82-19638
The development and testing of methods to infer midlatitude precipitation intensity from geosynchronous satellite infrared data [AD-A108881] p0120 N82-19788
SNOW COVER
Microwave radiation from a natural snow field p0101 A82-19559
Theoretical and experimental studies of microwave emission signatures of snow p0125 A82-21034
Towards the definition of optimum sensor specifications for microwave remote sensing of snow p0125 A82-21035
Use of GOES and TIROS/NOAA satellite data for snow-cover mapping p0101 A82-22146
Aerospace methods for the study of water resources and their pollution --- Russian book p0102 A82-27457
Remote-sensing determination of the characteristics of hydrological objects p0102 A82-27460
Application of satellite data to analyze and predict meltage runoff in a mountain basin p0102 A82-27461
Dynamics of snow cover in mountain regions of the Aral Sea basin, studied using satellite photographs p0102 A82-27462
The possibility of determining snow-meltage fronts using Meteor-satellite multispectral data /with Kazakhstan considered as an example/ p0102 A82-27463
Evaluation of snow-cover pollution in industrial regions using satellite TV images p0103 A82-27464
Albedo and brightness coefficients of snow cover p0103 A82-27465
Snow cover monitoring using AVHRR data from TIROS and NOAA satellites --- Advanced Very High Resolution Radiometer p0105 A82-27614
Spectral albedos of midlatitude snowpacks [NASA-TM-83858] p0106 N82-18663
Active microwave investigation of snowpacks. Experimental documentation, Colorado 1979-1980 [NASA-CR-166727] p0107 N82-19646
Applications systems verification and transfer project. Volume 1: Operational applications of satellite snow cover observations. Executive summary --- usefulness of satellite snow-cover data for water yield prediction [NASA-TP-1822] p0108 N82-20617
Applications systems verification and transfer project. Volume 2: Operational applications of satellite snow-cover observations and data-collection systems in the Arizona test site [NASA-TP-1823] p0108 N82-20618
Applications systems verification and transfer project. Volume 3: Operational applications of satellite snow cover observations in California [NASA-TP-1824] p0108 N82-20619
Applications systems verification and transfer project. Volume 4: Operational applications of satellite snow cover observations: Colorado Field Test Center [NASA-TP-1825] p0108 N82-20620
Applications systems verification and transfer project. Volume 5: Operational applications of satellite snow-cover observations, northwest United States [NASA-TP-1826] p0109 N82-20621
Applications systems verification and transfer project. Volume 6: Operational applications of satellite snow-cover observations NOAA/NESS support study [NASA-TP-1827] p0109 N82-20622
Applications systems verification and transfer project. Volume 7: Cost/benefit analysis for the ASVT on operational applications of satellite snow-cover observations [NASA-TP-1828] p0109 N82-20623
Applications systems verification and transfer project. Volume 8: Satellite snow mapping and runoff prediction handbook [NASA-TP-1829] p0109 N82-20624
Strategies for using remotely sensed data in hydrologic models [E82-10156] p0109 N82-21680
SOIL EROSION
The potential of remote sensing to monitor soil erosion on cropland p0061 A82-27656
SOIL MAPPING
A comparison between aerial photography and Landsat for computer land-cover mapping p0074 A82-22143
The spectral reflectance of certain soils --- Russian book p0059 A82-26577

Remote sensing of the structure of taiga landscapes --- Russian book p0059 A82-27397

Flexible processing of remote sensing data through integration of image processing and geobased information systems p0116 A82-27667

Inventory of eroded areas in the state of Guanajuato Mexico, by automatic analysis of Landsat images p0076 A82-27690

Machine implementation of algorithms for the mapping of soil moisture on the basis of microwave-radiometer measurements p0131 A82-28142

Delineation of soil temperature regimes from HCMM data [E82-10042] p0119 N82-19617

Taxonomic classification of world map units in crop producing areas of Argentina and Brazil with representative US soil series and major land resource areas in which they occur [E82-10058] p0065 N82-19633

Methodology of the interpretation of remote sensing data and applications in pedology [INPE-2211-MD/008] p0078 N82-19641

Amazonas project Application of remote sensing techniques for the integrated survey of natural resources in Amazonas --- Brazil [E82-10069] p0078 N82-20592

Delineation of soil temperature regimes from HCMM data [E82-10141] p0070 N82-21668

SOIL MOISTURE

Soil moisture determination - Experiments with passive microwave radiometers p0057 A82-19529

The Dutch ROVE program --- Radar Observation of VEgetation p0057 A82-21026

Microwave radiometry of lands under natural and artificial moistening p0057 A82-21028

Mixture formulas applied in estimation of dielectric and radiative characteristics of soils and grounds at microwave frequencies p0058 A82-21030

Volumetric effects in cross-polarized airborne radar data p0058 A82-21032

The estimation of the surface moisture of a vegetated soil using aerial infrared photography p0058 A82-21093

HCMM detection of high soil moisture areas --- by diurnal temperature observation p0059 A82-24963

The possibilities of microwave remote sensing for the study of water resources and their pollution p0102 A82-27458

Remote-sensing functions in the interpretation of moisture from aerial and space images p0102 A82-27459

Machine implementation of algorithms for the mapping of soil moisture on the basis of microwave-radiometer measurements p0131 A82-28142

Precipitation measurements from space - Workshop summary 28 April-1 May 1981, Greenbelt, MD p0077 A82-28295

Mission definition for a large-aperture microwave radiometer spacecraft p0131 N82-16155

The application of remote sensing to resource management and environmental quality programs in Kansas --- Cimarron National Grasslands, Prairie Potawatomi Reservation, and Kickapoo Reservation [E82-10029] p0063 N82-16447

Wheat stress indicator model, Crop Condition Assessment Division (CCAD) data base interface driver, user's manual [E82-10031] p0064 N82-19607

Use of thermal inertia determined by HCMM to predict nocturnal cold prone areas in Florida [E82-10040] p0064 N82-19615

Interactive initialization of heat flux parameters for numerical models using satellite temperature measurements [E82-10048] p0120 N82-19623

AgRISTARS Soil moisture/early warning and crop condition assessment Interface control document [E82-10053] p0065 N82-19628

AgRISTARS Yield model development/soil moisture. Interface control document [E82-10054] p0065 N82-19629

Agricultural soil moisture experiment, Colby, Kansas 1978 Measured and predicted hydrological properties of the soil [E82-10057] p0065 N82-19632

Evaluation of HCMM satellite data for estuarine tidal circulation patterns and thermal inertia soil moisture measurements --- Delaware Bay, Cooper River, and the Potomac River estuaries; Luverne, Minnesota, soil moisture, and water temperature of Lake Anna, Virginia [E82-10064] p0108 N82-20587

Heat Capacity Mapping Mission (HCMM) Interpretation of imagery over Canada [E82-10070] p0079 N82-20593

Dryland pasture and crop conditions as seen by HCMM --- Washita River watershed [E82-10074] p0067 N82-20597

Ground registration of data from an airborne scatterometer [E82-10084] p0068 N82-21636

As-Built documentation of programs to implement the Robertson and Doraiswamy/Thompson models [E82-10086] p0122 N82-21638

Soybean canopy reflectance as influenced by cultural practices --- West Lafayette, Indiana [E82-10105] p0068 N82-21647

Sonora exploratory study for the detection of wheat-leaf rust [E82-10133] p0070 N82-21661

HCMM Soil moisture in relation to geologic structure and lithology, northern California --- Northern Coast Range, Sacramento Valley, and the Modoc Plateau [E82-10135] p0092 N82-21662

A study of model parameters associated with the urban climate using HCMM data --- St. Louis, Missouri [E82-10140] p0079 N82-21667

Strategies for using remotely sensed data in hydrologic models [E82-10156] p0109 N82-21680

Use of thermal inertia determined by HCMM to predict nocturnal cold prone areas in Florida --- The Everglades agricultural area, Lake Okeechobee, and the Suwanee River basin [E82-10157] p0071 N82-21681

SOILS

Landsat feature enhancement - Or, can we separate vegetation from soil p0060 A82-27622

An experiment in probabilistic relaxation for terrain cover classification of Kuwait from Landsat imagery p0062 A82-27680

Taxonomic classification of world map units in crop producing areas of Argentina and Brazil with representative US soil series and major land resource areas in which they occur [E82-10058] p0065 N82-19633

Notes for Brazil sampling frame evaluation trip [E82-10060] p0066 N82-19635

The effect of finite field size on classification and atmospheric correction [NASA-TM-83818] p0120 N82-19645

On the accuracy of thermal inertia mapping by infrared imagery [SAAB-REPR-AE-10] p0120 N82-19656

Delineation of soil temperature regimes from HCMM data [E82-10141] p0070 N82-21668

SOLAR POSITION

A relation between Landsat digital numbers, surface reflectance, and the cosine of the solar zenith angle p0114 A82-26841

Simulated response of a multispectral scanner over wheat as a function of wavelength and view/illumination direction [E82-10144] p0071 N82-21671

SONIC ANEMOMETERS

Observation of the turbulent structure in the planetary boundary layer with a kytoon-mounted ultrasonic anemometer system p0125 A82-21082

SOUTH AMERICA

Remote sensing in Latin America Technology and markets for the 1980's [AD-A108784] p0138 N82-20626

SOUTH CAROLINA

Multiresource inventory methods pilot test --- for forests p0060 A82-27601

Forest change detection p0061 A82-27644

SOUTH DAKOTA

Use of Landsat imagery to delineate glaciofluvial aquifers in southeast South Dakota p0105 A82-27637

Remote sensing applications to resource problems in South Dakota [E82-10027] p0132 N82-16445

SOUTHEAST ASIA

Photogrammetry from aircraft side camera movies - Winter MONEX p0075 A82-26721

SOUTHERN CALIFORNIA

Analysis of two Seasat synthetic aperture radar images of an urban scene p0074 A82-25452

Scene analysis for wildland fire-fuel characteristics in a Mediterranean climate p0060 A82-27624

Ship and satellite bio-optical research in the California Bight [NASA-CR-168681] p0098 N82-20823

SOYBEANS

Use of Landsat-derived temporal profiles for corn-soybean feature extraction and classification p0059 A82-26842

Soybean canopy reflectance as a function of view and illumination geometry p0061 A82-27645

Potential utility of thematic mapper data in estimating crop areas p0061 A82-27663

Crop area estimates using ground-gathered and Landsat data A multitemporal approach p0062 A82-27676

Influence of solar illumination angle on soybean canopy reflectance p0063 A82-28153

AgRISTARS Foreign commodity production forecasting Minutes of the annual formal project manager's review, including preliminary technical review reports of FY80 experiments --- wheat/barley and corn/soybean experiments [E82-10039] p0064 N82-19614

AgRISTARS Foreign commodity production forecasting Corn/soybean decision logic development and testing [E82-10056] p0065 N82-19631

Notes for Brazil sampling frame evaluation trip [E82-10060] p0066 N82-19635

Segment-level evaluation of the simulated aggregation test US corn and soybean exploratory experiment [E82-10061] p0066 N82-19636

Evaluation of a segment-based LANDSAT full-frame approach to corp area estimation [E82-10067] p0066 N82-20590

US corn and soybeans exploratory experiment [E82-10088] p0068 N82-21640

Soybean canopy reflectance as influenced by cultural practices --- West Lafayette, Indiana [E82-10105] p0068 N82-21647

The 1981 Argentina ground data collection [E82-10127] p0070 N82-21656

Spectral-agronomic relationships of corn, soybean and wheat canopies [E82-10143] p0070 N82-21670

Variability of reflectance measurements with sensor altitude and canopy type [E82-10145] p0071 N82-21672

Determination of the optimal level for combining area and yield estimates [E82-10146] p0071 N82-21673

SPACE SHUTTLES

Advanced aerospace remote sensing systems for global resource applications p0127 A82-27577

SPACEBORNE PHOTOGRAPHY

Analytical triangulation of space photography p0111 A82-20402

Satellite Earth resources data, module U-3 [E82-10035] p0119 N82-19611

SPACECRAFT PERFORMANCE

LANDSAT-2 and LANDSAT-3 flight evaluation report, 23 January to 23 July 1980 [E82-10022] p0132 N82-16440

SPACELAB PAYLOADS

MRSE A Microwave Remote Sensing Experiment in Spacelab p0134 N82-20375

SPATIAL DISTRIBUTION

Use of GOES and TIROS/NOAA satellite data for snow-cover mapping p0101 A82-22145

Stochastic models of cover class dynamics --- remote sensing of vegetation p0059 A82-27586

Data base requirements in support of crop models p0060 A82-27588

Utilization of spatial complexity in computer classified Landsat MSS data for multi-factoral thematic mapping p0129 A82-27648

Sea ice movements from synthetic aperture radar [AD-A109002] p0097 N82-19435

Recommended data sets, corn segments and spring wheat segments, for use in program development [E82-10034] p0064 N82-19610

AgRISTARS Early warning and crop condition assessment Patch image processor user's manual [E82-10055] p0065 N82-19630

Methodology of the interpretation of remote sensing data and applications in geomorphology [INPE-2209-MD/007] p0081 N82-19642

An algorithm for spatial heirarchy clustering [E82-10081] p0121 N82-20604

Registration verification of SEA/AR fields --- Oregon, Texas, Montana, Nebraska, Washington, Colorado, Kansas, Oklahoma, and North Dakota [E82-10083] p0068 N82-21635

SPATIAL FILTERING

Optimal spatial filtering and transfer function for SAR ocean wave spectra p0094 A82-27596

SPATIAL RESOLUTION

Spatial reasoning in remotely sensed data p0105 A82-27592

An evaluation of the utility of smaller Landsat resolution elements /Resolution of Landsat resolution/ p0114 A82-27625

Digital analysis of spatial and spectral features from airborne MSS of a forested region p0061 A82-27647

Land cover classification accuracy as a function of sensor spatial resolution p0076 A82-27665

Spatial resolution and geometric potential of planned earth satellite missions p0130 A82-27683

Characterizing user requirements for future land observing satellites [NASA-TM-83867] p0081 N82-17562

SPECTRAL BANDS

Characterizing user requirements for future land observing satellites [NASA-TM-83867] p0081 N82-17562

A multiband radiometer and data acquisition system for remote sensing field research [E82-10142] p0134 N82-21669

SPECTRAL CORRELATION

Remote SO2 emission measurements with correlation spectrometers from volcanoes p0077 A82-27704

SPECTRAL EMISSION

Methods of editing cloud and atmospheric layer affected pixels from satellite data [E82-10046] p0119 N82-19621

SPECTRAL RECONNAISSANCE

Watershed model study using LANDSAT data p0106 N82-17602

SPECTRAL REFLECTANCE

The estimation of the surface moisture of a vegetated soil using aerial infrared photography p0058 A82-21093

Multispectral photographic remote sensing of green vegetation biomass and productivity p0059 A82-22144

Spectral reflectance of hydrophytes p0102 A82-24960

Influence of illumination and viewing geometry and atmospheric composition on the tasseled cap transformation of Landsat MSS data p0059 A82-24961

The spectral reflectance of certain soils --- Russian book p0059 A82-26577

A relation between Landsat digital numbers, surface reflectance, and the cosine of the solar zenith angle p0114 A82-26841

Radiometric calibration of the Coastal Zone Color Scanner on Nimbus 7 - A proposed adjustment p0127 A82-26963

Albedo and brightness coefficients of snow cover p0103 A82-27465

Interpretation of multispectral aerial photographs of Lake Mueggelsee p0104 A82-27473

Spectrometric studies of the water composition of Lake Mueggelsee p0104 A82-27474

A data base of geologic field spectra p0090 A82-27600

Dew and vapor pressure as complicating factors in the interpretation of spectral radiance from crops p0060 A82-27617

Landsat feature enhancement - Or, can we seperate vegetation from soil p0060 A82-27622

An approach to path radiance correction in MSS images p0115 A82-27629

Passive bathymetric measurements in the Bruce Peninsula region of Ontario p0129 A82-27642

A vegetation response model applied to range inventory and monitoring using Landsat MSS data p0060 A82-27643

The influence of illumination and viewing geometry on the reflectance factor of agricultural targets p0061 A82-27646

Instrumentation for remote reflectance and radiance measurements p0130 A82-27652

An invertible coniferous forest canopy reflectance model p0062 A82-27679

Ground level reflectance measurement techniques - An evaluation with emphasis on the importance of spectral calibration p0116 A82-27689

Influence of solar illumination angle on soybean canopy reflectance p0063 A82-28153

Spectral reflectances of freshwater ice and snow from 340 through 1100 nm p0106 N82-17601

Spectral albedos of midlatitude snowpacks
[NASA-TM-83858] p0106 N82-18663

Methods of editing cloud and atmospheric layer affected pixels from satellite data
[E82-10048] p0119 N82-19821

Effects of nitrogen nutrition on the growth, yield and reflectance characteristics of corn canopies --- Purdue Agronomy Farm, Indiana
[E82-10068] p0067 N82-20591

As-built design specification for PARHIS
[E82-10089] p0122 N82-21641

Soybean canopy reflectance as influenced by cultural practices --- West Lafayette, Indiana
[E82-10105] p0068 N82-21647

Spectral-agronomic relationships of corn, soybean and wheat canopies
[E82-10143] p0070 N82-21670

Simulated response of a multispectral scanner over wheat as a function of wavelength and view/illumination direction
[E82-10144] p0071 N82-21671

Variability of reflectance measurements with sensor altitude and canopy type
[E82-10145] p0071 N82-21672

Laboratory upwelled radiance and reflectance spectra of Kerr reservoir sediment waters
[NASA-TP-1993] p0110 N82-21774

SPECTRAL RESOLUTION

Digital analysis of spatial and spectral features from airborne MSS of a forested region p0061 A82-27647

SPECTRAL SENSITIVITY

Landsat thermal imaging of alpine regions p0079 A82-22147

Imaging the earth. I - The troubled first decade of Landsat p0137 A82-27169

Technologies for the multispectral mapping of earth resources p0128 A82-27580

SPECTRAL SIGNATURES

Environmental studies by multispectral scanner under large-scale civil engineering construction p0063 A82-27691

Remote sensing data applied to land-use survey at the Paraiba Valley --- Brazil
[E82-10075] p0081 N82-16443

Thermal vegetation canopy model studies
[AD-A106422] p0084 N82-16455

AgRISTARS. Soil moisture/early warning and crop condition assessment. Interface control document
[E82-10053] p0065 N82-19628

Data rate reduction. Impact of image data compression on end to end data management of a multispectral payload --- for satellite imagery
[REPT-44/130] p0120 N82-19654

AgRISTARS. Foreign commodity production forecasting. Project test reports document, volume 1 --- using North Dakota, South Dakota, Montana, and Minnesota
[E82-10087] p0068 N82-21639

Transition year labeling error characterization study --- Kansas, Minnesota, Montana, North Dakota, South Dakota and Oklahoma
[E82-10111] p0069 N82-21651

AgRISTARS. Supporting research. Classification of corn. Badhwar profile similarity technique --- us corn belt
[E82-10150] p0071 N82-21676

SPECTROMETERS

Instrumentation for remote reflectance and radiance measurements p0130 A82-27652

SPECTROPHOTOMETERS

Stratospheric instruments and analyses p0133 N82-18776

SPECTROSCOPY

Color characteristics of the earth's surface determined on the basis of spectroscopy results from Salyut 4 p0073 A82-19326

SPECTRUM ANALYSIS

MAGSAT anomaly profiles of the eastern Indian Ocean
[E82-10066] p0086 N82-20589

Direct determination of the two dimensional image spectrum from raw synthetic aperture radar data p0122 N82-21474

SPECULAR REFLECTION

Contrast reduction by the atmosphere and retrieval of nonuniform surface reflectance p0112 A82-20423

SPHERICAL HARMONICS

Some new methods in geomagnetic field modeling applied to the 1960 - 1980 epoch
[NASA-TM-83868] p0083 N82-17714

SPOT (FRENCH SATELLITE)

Towards an operational SPOT system - A preliminary assessment --- earth observation satellites for resources management p0114 A82-27607

The potential of remote sensing to monitor soil erosion on cropland p0061 A82-27656

STANDARDS

Project communications/documentation standards manual
[E82-10083] p0068 N82-21645

STATIONKEEPING

Topex orbit sustenance maneuver design --- Ocean Topography Experiment spacecraft
[AIAA PAPER 82-0202] p0094 A82-27091

STATISTICAL ANALYSIS

Multispectral texture p0113 A82-25139

Using known map category marginal frequencies to improve estimates of thematic map accuracy p0113 A82-25456

An experiment in probabilistic relaxation for terrain cover classification of Kuwait from Landsat imagery p0062 A82-27680

Surface wave statistics and spectra during high sea state conditions in the North Atlantic
[AD-A109832] p0098 N82-20827

STEPPES

Landscape mapping and physical-geographical classification of the eastern part of the Chechen-Ingush, ASSR using space imagery p0073 A82-20339

STEREOPHOTOGRAPHY

Calibration and model reconstruction in analytical close-range stereophotogrammetry. I - Mathematical fundamentals p0111 A82-20403

Calibration and model reconstruction in analytical close-range stereophotogrammetry. II - Special evaluation procedures for rasterstereography and moire topography p0126 A82-22141

STOCHASTIC PROCESSES

Stochastic models of cover class dynamics --- remote sensing of vegetation p0059 A82-27586

STRATIFICATION

Techniques for combining Landsat and ancillary data for digital classification improvement p0111 A82-20410

Notes for Brazil sampling frame evaluation trip
[E82-10060] p0066 N82-19635

Evaluation of a segment-based LANDSAT full-frame approach to corp area estimation
[E82-10067] p0066 N82-20590

Determination of the optimal level for combining area and yield estimates
[E82-10146] p0071 N82-21673

STRATIGRAPHY

One orogenic belt or two - A structural reinterpretation supported by Landsat data products of the Precambrian metamorphics of Singhbhum, eastern India p0089 A82-26017

Seasat satellite investigation of the structure of Western Nebraska and its application to the evaluation of geothermal resources p0090 A82-27635

STRATOSPHERE

Mid-latitude summertime measurements of stratospheric NO2 p0074 A82-25149

Multidimensional aspects. Ozone, temperature and transport p0081 N82-18772

Stratospheric instruments and analyses p0133 N82-18776

STRIP MINING

Application of remote sensing to state and regional problems --- mississippi
[E82-10033] p0078 N82-19609

STRUCTURAL PROPERTIES (GEOLOGY)

The relationship between seismicity and lineaments of the Anatolian-Caucasian-Iranian segment of the Mediterranean fold belt p0089 A82-20341

Dip determinations in photogeology p0089 A82-25453

A structural synthesis of Brazil, based on the study of major lineaments derived from remote sensing imagery interpretation p0079 A82-26012

Geophysical and Landsat lineament mapping - An approach illustrated from west-central and south India p0089 A82-26016

One orogenic belt or two - A structural reinterpretation supported by Landsat data products of the Precambrian metamorphics of Singhbhum, eastern India p0089 A82-26017

Application of aerial and space photographic data in the study of subsurface water and tectonic structures p0090 A82-27466

Application of side-looking color infrared photography for structure detection in subtle topography p0082 A82-27611

Seasat satellite investigation of the structure of Western Nebraska and its application to the evaluation of geothermal resources p0090 A82-27635

Ring structures in the earth's crust, and their significance for geology and methods for their investigation p0091 A82-28136

Report on a short course in remote sensing and the geological applications of LANDSAT MSS imagery at INPE
[E82-10024] p0091 N82-16442

Integration of LANDSAT with geology and airborne geophysics into an operational mineral exploration system --- the Bearlodge area of northeastern Wyoming
[E82-10028] p0091 N82-16446

HCMM. Soil moisture in relation to geologic structure and lithology, northern California --- Northern Coast Range, Sacramento Valley, and the Modoc Plateau
[E82-10135] p0092 N82-21662

Investigation of antarctic crust and upper mantle using MAGSAT and other geophysical data
[E82-10147] p0087 N82-21674

Use of MAGSAT anomaly data for crustal structure and mineral resources in the US midcontinent
[E82-10152] p0092 N82-21677

SUBARCTIC REGIONS

Enhancement of Landsat data for Hudson Bay lowlands vegetation p0114 A82-27623

SUBURBAN AREAS

A study of model parameters associated with the urban climate using HCMM data
[E82-10159] p0080 N82-21683

SUGAR CANE

Use of Landsat data for automatic classification and area estimation of sugar-cane plantation in Sao Paulo state, Brazil p0058 A82-21092

Survey of the cane-growing area of the state of Sao Paulo using LANDSAT data, Safra Year 1979/80, volume 2 --- maps, Brazil
[E82-10071] p0067 N82-20594

Elevation of a cane-growing area of the state of Sao Paulo using LANDSAT data
[E82-10077] p0067 N82-20600

SULFUR DIOXIDES

A regional air quality model for the Kwinana industrial area of Western Australia p0075 A82-26403

Remote SO2 emission measurements with correlation spectrometers from volcanoes p0077 A82-27704

Remote sensing of sulfur dioxide effects on vegetation. Volume 1: Summary
[PB82-115122] p0066 N82-19715

Remote sensing of sulfur dioxide effects on vegetation. Volume 2: Data
[PB82-115130] p0066 N82-19716

SULFURIC ACID

Airborne in-situ measurement of particulate sulfur and sulfuric acid with flame photometry and thermal analysis p0073 A82-20999

SUMMER

Diurnal variation of summer convection over West Africa and the Tropical Eastern Atlantic during 1974 and 1978 p0075 A82-26700

SUNLIGHT

Soybean canopy reflectance as a function of view and illumination geometry p0061 A82-27645

SUPERCONDUCTIVITY

Superconducting tensor gravity gradiometer p0126 A82-23045

SURFACE LAYERS

On randomly absorbing and scattering surface layers p0079 A82-21037

SURFACE NAVIGATION

Remote sensing techniques suitable for exploration and navigation in and under sea ice
[FOA-REPT-VOL-15-NO-2] p0096 N82-17566

Experiments in satellite Doppler control positioning at sea p0086 N82-20581

SURFACE ROUGHNESS

Volumetric effects in cross-polarized airborne radar data p0068 A82-21032

A radar signature model for partially coherent scattering from irregular surfaces p0079 A82-21038

Comparison of sigma/deg/ obtained from the conventional definition with sigma/deg/ appearing in the radar equation for randomly rough surfaces p0112 A82-21039

Comparisons of laser profilometer sea ice roughness statistics with surface truthed data and SLAR imagery p0094 A82-27619

Coherent scatter of microwaves from moderately rough surfaces
[AD-A106133] p0095 N82-16331

A study of model parameters associated with the urban climate using HCMM data --- St. Louis, Missouri
[E82-10140] p0079 N82-21667

SURFACE TEMPERATURE

Comparison of conventionally measured sea surface temperature and wind speed with data retrieved from satellite-borne microwave radiometry p0093 A82-24063

Thermal infrared data from the Heat Capacity Mapping Mission p0127 A82-24964

Analysis of a discrete-time linear model for geothermal flux reconnaissance from two or three aircraft infrared measurements p0075 A82-27627

High precision radiometric temperature measurements of the ocean surface p0094 A82-27640

Estimation of sea surface temperature from remote sensing in the 3 7 micron window region p0095 A82-28031

Use of thermal inertia determined by HCMM to predict nocturnal cold prone areas in Florida
[E82-10040] p0064 N82-19615

Delineation of soil temperature regimes from HCMM data
[E82-10042] p0119 N82-19617

Interactive initialization of heat flux parameters for numerical models using satellite temperature measurements
[E82-10048] p0120 N82-19623

On the accuracy of thermal inertia mapping by infrared imagery
[SAAB-REPR-AE-10] p0120 N82-19656

The TOCIND experiment --- relation between surface isotherms and ocean currents
[CTAMN/81/R/10] p0098 N82-19805

HCMM hydrological analysis in Utah --- Utah lake
[E82-10063] p0107 N82-20586

Heat Capacity Mapping Mission (HCMM) Interpretation of imagery over Canada
[E82-10070] p0079 N82-20593

Heat Capacity Mapping Mission (HCMM) program Study of geological structure of Sicily and other Italian areas --- Sardinia and the Gulf of Orosei
[E82-10073] p0091 N82-20596

Dryland pasture and crop conditions as seen by HCMM --- Washita River watershed
[E82-10074] p0067 N82-20597

Delineation of soil temperature regimes from HCMM data
[E82-10141] p0070 N82-21668

Use of thermal inertia determined by HCMM to predict nocturnal cold prone areas in Florida --- The Everglades agricultural area, Lake Okeechobee, and the Suwanee River basin
[E82-10157] p0071 N82-21681

A study of model parameters associated with the urban climate using HCMM data
[E82-10159] p0080 N82-21683

A study of model parameters associated with the urban climate using HCMM data --- analysis of St Louis, Missouri infrared imagery
[E82-10160] p0080 N82-21684

Applications of HCMM satellite data to the study of urban heating patterns
[E82-10161] p0080 N82-21685

SURFACE WATER

The possibilities of microwave remote sensing for the study of water resources and their pollution p0102 A82-27458

Interpretation of Heat Capacity Mapping Mission images over Canada p0116 A82-27671

Dynamic study of the upper Sao Francisco River and the Tres Marias reservoir using MSS/LANDSAT images --- Brazil
[E82-10082] p0108 N82-20605

Methods of editing cloud and atmospheric layer affected pixels from satellite data
[E82-10154] p0123 N82-21678

Strategies for using remotely sensed data in hydrologic models
[E82-10156] p0109 N82-21680

SURFACE WAVES

Surface wave statistics and spectra during high sea state conditions in the North Atlantic
[AD-A108832] p0098 N82-20827

SWEDEN

Mapping of water quality using Landsat imagery p0106 A82-27692

Observations with an imaging 35 GHz radiometer of terrain in Malmslatett, July 1980
[FOA-C-30240-E1/E3] p0133 N82-18672

SWITZERLAND

Soil moisture determination - Experiments with passive microwave radiometers p0057 A82-19529

A system for quantitative determination of species and vitalities of urban trees on color-infrared photographs p0074 A82-24958

SYNOPTIC METEOROLOGY

Satellite observed cloud patterns associated with excessive precipitation outbreaks
[PB80-215130] p0073 A82-19177

SYNTHETIC APERTURE RADAR

Classification of ice radar imagery p0113 A82-22891

Methods for the processing of synthetic-aperture radar signals when solving problems of the national economy /Review/ p0113 A82-26726

Spaceborne radar observation of the earth surface p0127 A82-27578

Overview of digital processing of SAR data --- from Seasat-A p0128 A82-27589

Simulation and studies of spaceborne synthetic aperture radar image quality with reduced bit rate p0128 A82-27594

Features of a generalized digital Synthetic Aperture Radar processor p0128 A82-27595

Optimal spatial filtering and transfer function for SAR ocean wave spectra p0094 A82-27596

Wide area, coarse resolution imaging with satellite-borne synthetic aperture radars in low-earth and geosynchronous orbits p0082 A82-27631

Seasat satellite investigation of the structure of Western Nebraska and its application to the evaluation of geothermal resources p0090 A82-27635

The use of wave contrast measurements in the evaluation of SAR/gravity models p0130 A82-27675

Digital correlation of DDRS data
[NASA-CR-167494] p0118 N82-16452

The relationship among sea surface roughness variations, oceanographic analyses, and airborne remote sensing analyses
[NASA-CR-168444] p0096 N82-17798

Study of synthetic aperture radar in 2D - 2FS operation over the ocean --- European Remote Sensing system
[ESA-CR(P)-1475] p0132 N82-18481

Sea ice movements from synthetic aperture radar
[AD-A109002] p0097 N82-19435

MRSE A Microwave Remote Sensing Experiment in Spacelab p0134 N82-20375

SAR image quality --- conference, Frascati, Italy, 11-12 Dec 1980, synthetic aperture radar (SAR)
[ESA-SP-172] p0122 N82-21458

Two-dimensional power spectra of SEASAT SAR imagery --- ocean waves p0098 N82-21469

Direct determination of the two dimensional image spectrum from raw synthetic aperture radar data p0122 N82-21474

Relief effects and the use of terrain models in SAR image processing --- Anderson River test site, British Columbia p0086 N82-21475

SYSTEMS ANALYSIS

CNPq/INPE LANDSAT system --- operations at the Cuiabe station and the electronic processing and photo laboratories
[E82-10023] p0118 N82-16441

SYSTEMS INTEGRATION

Flexible processing of remote sensing data through integration of image processing and geobased information systems p0116 A82-27667

T

TAXONOMY

Taxonomic classification of world map units in crop producing areas of Argentina and Brazil with representative US soil series and major land resource areas in which they occur
[E82-10058] p0065 N82-19633

TECHNOLOGY TRANSFER

Remote sensing in Latin America Technology and markets for the 1980's
[AD-A108784] p0138 N82-20626

TECHNOLOGY UTILIZATION

Some problems concerning the effective use of remote sensing p0137 A82-26123

Earth sensing from space - Commercial and international aspects p0138 A82-27669

Remote sensing procurement package A management report for state and local governments
[E82-10052] p0138 N82-19627

Program on stimulating operational private sector use of Earth observation satellite information
[E82-10131] p0138 N82-21660

TECTONICS

A structural synthesis of Brazil, based on the study of major lineaments derived from remote sensing imagery interpretation p0079 A82-26012

The Pampean Plain studied with Landsat images p0089 A82-26013

Remote sensing applied to basement tectonics of the calcareous High Atlas /Morocco/ p0089 A82-26014

Geophysical and Landsat lineament mapping - An approach illustrated from west-central and south India p0089 A82-26016

One orogenic belt or two - A structural reinterpretation supported by Landsat data products of the Precambrian metamorphics of Singhbhum, eastern India p0089 A82-26017

Application of aerial and space photographic data in the study of subsurface water and tectonic structures p0090 A82-27466

MAGSAT anomaly profiles of the eastern Indian Ocean
[E82-10066] p0086 N82-20589

TELLURIC CURRENTS

Electromagnetic deep-probing (100-1000 KMS) of the Earth's interior from artificial satellites Constraints on the regional emplacement of crustal resources
[E82-10155] p0087 N82-21679

TEMPERATE REGIONS

Spectral albedos of midlatitude snowpacks
[NASA-TM-83858] p0106 N82-18663

Interaction between the Agulhas current and the subtropical convergence
[CSIR-RR-384] p0098 N82-20824

TEMPORAL DISTRIBUTION

Use of Landsat-derived temporal profiles for corn-soybean feature extraction and classification p0059 A82-26842

Field-by-field multitemporal analysis of aerial scanner data geometrically corrected by means of a sliding model p0115 A82-27651

Crop area estimates using ground-gathered and Landsat data A multitemporal approach p0062 A82-27676

TENNESSEE

Satellite and surface geophysical expression of anomalous crustal structure in Kentucky and Tennessee
[NASA-TM-82163] p0084 N82-17715

TENNESSEE VALLEY (AL-KY-TN)

National High-Altitude Photography (NHAP) of the Tennessee Valley Region, volume 1, no 1
[PB82-130899] p0134 N82-21703

TERRAIN

Precision in the evaluation of Landsat autocorrelation - The terrain effect p0116 A82-27686

Observations with an imaging 35 GHz radiometer of terrain in Malmslatett, July 1980
[FOA-C-30240-E1/E3] p0133 N82-18672

Experiences with digital terrain elevation data contouring programs
[AD-A110280] p0087 N82-21690

TERRAIN ANALYSIS

The use of digital multi-date Landsat imagery in terrain classification p0111 A82-20409

Remote sensing of the structure of taiga landscapes --- Russian book p0059 A82-27397

Airborne laser systems use in terrain mapping p0082 A82-27584

Spatial reasoning in remotely sensed data p0105 A82-27592

The use of digital terrain model in the rectification of satellite-borne imagery p0115 A82-27626

Locating prehistoric archaeological sites using Landsat p0129 A82-27638

Non-parametric classification of abandoned coal mine features using multioriented and ratio transformed Landsat data p0090 A82-27694

Utilisation of remote sensing in resources identification and land use in India - An integrated approach p0076 A82-27701

Construction of digital models of statistically uniform characteristics on the basis of multispectral space imagery p0117 A82-28144

Classification of systems for digital terrain simulation p0117 A82-28468

Matrix data analysis Color/B and W coding is not always enough
[AD-A108406] p0084 N82-18930

Profiling sensitivity to image quality
[AD-A108405] p0084 N82-18931

A comparison of unsupervised classification procedures on LANDSAT MSS data for an area of complex surface conditions in Basilicata, Southern Italy
[E82-10038] p0119 N82-19613

Relief effects and the use of terrain models in SAR image processing --- Anderson River test site, British Columbia p0086 N82-21475

TERRESTRIAL RADIATION

Methods of editing cloud and atmospheric layer affected pixels from satellite data
[E82-10046] p0119 N82-19621

TEXAS

Assessing mesquite-grass vegetation condition from Landsat p0059 A82-25457

Methods of editing cloud and atmospheric layer affected pixels from satellite data
[E82-10046] p0119 N82-19621

Registration verification of SEA/AR fields --- Oregon, Texas, Montana, Nebraska, Washington, Colorado, Kansas, Oklahoma, and North Dakota
[E82-10083] p0068 N82-21635

A gradient model of vegetation and climate utilizing NOAA satellite imagery Phase 1 Texas transect
[E82-10107] p0069 N82-21648

TEXTURES

Automation of the processing of aerial and space images for forest inventory p0057 A82-20350

Multispectral texture p0113 A82-25139

THAILAND

Monitoring forest land cover alteration in Thailand with the analysis of ancillary and digital Landsat data p0062 A82-27673

THEMATIC MAPPING

Analysis of space imagery to compile a geomorphological map of the world p0089 A82-20338

Landscape mapping and physical-geographical classification of the eastern part of the Chechen-Ingush ASSR using space imagery p0073 A82-20339

The use of digital multi-date Landsat imagery in terrain classification p0111 A82-20409

Sampling for thematic map accuracy testing p0111 A82-20411

Landsat classification accuracy assessment procedures p0137 A82-20412

Use of Landsat data for automatic classification and area estimation of sugar-cane plantation in Sao Paulo state, Brazil p0058 A82-21092

The Landsat program - Moving ahead p0137 A82-21280

Remote sensing for natural resources: An international view of problems, promises and accomplishments --- Book p0137 A82-21875

Use of GOES and TIROS/NOAA satellite data for snow-cover mapping p0101 A82-22145

Using known map category marginal frequencies to improve estimates of thematic map accuracy p0113 A82-25456

Imaging the earth. I - The troubled first decade of Landsat p0137 A82-27169

Evaluation of the state of crops from satellite data p0059 A82-27393

Investigation of the earth on the basis of space photographic data p0082 A82-27507

International Symposium on Remote Sensing of Environment, 15th, University of Michigan, Ann Arbor, MI, May 11-15, 1981, Proceedings. Volumes 1, 2 & 3 p0127 A82-27576

Advanced aerospace remote sensing systems for global resource applications p0127 A82-27577

Information expectations from Landsat-D p0128 A82-27583

Utilization of spatial complexity in computer classified Landsat MSS data for multi-factoral thematic mapping p0129 A82-27648

The potential of remote sensing to monitor soil erosion on cropland p0061 A82-27656

Potential utility of thematic mapper data in estimating crop areas p0061 A82-27663

ELAS - A geobased information system that is transferable to several computers --- Earth resources Laboratory Applications Software p0115 A82-27666

Integration of Landsat, geological and geophysical data for use in thematic mapping at regional scale p0090 A82-27672

Classification of Landsat MSS data for surface cover of small areas p0116 A82-27677

An analysis of user requirements for operational land satellite data p0116 A82-27685

Natural resources inventories by computer-satellite mapping techniques in Chaco State, Argentine Republic, South America p0116 A82-27688

Mapping of water quality using Landsat imagery p0106 A82-27692

Utilisation of remote sensing in resources identification and land use in India - An integrated approach p0076 A82-27701

Experience with a variety of studies of earth resources in the Kalmyk ASSR using space imagery p0131 A82-28130

The use of space photographs to compile water-amelioration maps p0106 A82-28137

Possibilities of using experience gained from the thematic mapping of the moon in studies of earth resources by remote sensing methods p0083 A82-28138

Potential use of space photographs obtained from the manned orbital station Salyut-5 in order to compile a set of small-scale thematic maps of mountain and piedmont regions of Central Asia p0083 A82-28139

Earth-scanning satellites lead resource hunt p0117 A82-28343

Wetland mapping from digitized aerial photography --- Sheboygan Marsh, Wisconsin [E82-10019] p0118 N82-16437

A comparison of unsupervised classification procedures on LANDSAT MSS data for an area of complex surface conditions in Basilicata, Southern Italy [E82-10038] p0119 N82-19613

Utilization of Aerochrome 2443 film for identification and estimating wheat growing areas --- Rio Grande do Sul, Brazil [INPE-2197-PRE/006] p0066 N82-19639

Remote sensing of sulfur dioxide effects on vegetation. Volume 1: Summary [PB82-115122] p0066 N82-19715

Atlas of the global distribution of the total ozone concentration according to satellite measurements [MITT-28] p0078 N82-19740

The utilization of orbital images as an adequate form of control of preserved areas --- Araguaia National Park, Brazil [E82-10065] p0078 N82-20588

Amazonas project: Application of remote sensing techniques for the integrated survey of natural resources in Amazonas --- Brazil [E82-10069] p0078 N82-20592

Survey of the cane-growing area of the state of Sao Paulo using LANDSAT data. Safra Year 1979/80, volume 2 --- maps, Brazil [E82-10071] p0067 N82-20594

Elevation of a cane-growing area of the state of Sao Paulo using LANDSAT data [E82-10077] p0067 N82-20600

THERMAL MAPPING

Thermal viewing system for studying the earth's resources p0125 A82-21022

Registration of heat capacity mapping mission day and night images p0113 A82-22146

Landsat thermal imaging of alpine regions p0079 A82-22147

HCMM detection of high soil moisture areas --- by diurnal temperature observation p0059 A82-24963

Thermal infrared data from the Heat Capacity Mapping Mission p0127 A82-24964

Humidity measurement by infrared thermometry p0075 A82-26844

Advanced aerospace remote sensing systems for global resource applications p0127 A82-27577

Analysis of a discrete-time linear model for geothermal flux reconnaissance from two or three aircraft infrared measurements p0075 A82-27627

HCMM night-time thermal IR imaging experiment in Michigan --- Heat Capacity Mapping Mission p0115 A82-27655

Thermal IR detection of submarine gas seepages in the western Istra off-shore area /Yugoslavia/ p0076 A82-27661

Interpretation of Heat Capacity Mapping Mission images over Canada p0116 A82-27671

Application of machine processing of visible and thermal data to the study of the geothermal area of Cerro Prieto, Mexico p0117 A82-27693

Visual and digital analysis of H.C.M.M. data over eastern Canada --- thermal imagery by Heat Capacity Mapping Mission p0117 A82-27698

Development of a Canadian thermal infrared forest fire mapping operational program p0063 A82-27699

Thermal vegetation canopy model studies [AD-A106422] p0064 N82-16455

The severity of the Brazilian freeze of July 1981, as monitored by satellite [INPE-2231-RPE/399] p0064 N82-17746

Use of thermal inertia determined by HCMM to predict nocturnal cold prone areas in Florida [E82-10040] p0064 N82-19615

Delineation of soil temperature regimes from HCMM data [E82-10042] p0119 N82-19617

Interactive initialization of heat flux parameters for numerical models using satellite temperature measurements [E82-10048] p0120 N82-19623

Method of interpretation of remote sensing data and applications to vegetation [INPE-2215-MD/010] p0066 N82-19640

On the accuracy of thermal inertia mapping by infrared imagery [SAAB-REPR-AE-10] p0120 N82-19656

Preliminary results of a study of mapping thermal discharge in the ocean, using remote sensing data [INPE-2229-PRE/021] p0097 N82-19704

The TOCIND experiment --- relation between surface isotherms and ocean currents [CTAMN/81/R/10] p0098 N82-19805

HCMM hydrological analysis in Utah --- Utah lake [E82-10063] p0107 N82-20586

Evaluation of HCMM satellite data for estuarine tidal circulation patterns and thermal inertia soil moisture measurements --- Delaware Bay, Cooper River, and the Potomac River estuaries; Luverne, Minnesota, soil moisture, and water temperature of Lake Anna, Virginia [E82-10064] p0108 N82-20587

Heat Capacity Mapping Mission (HCMM): Interpretation of imagery over Canada [E82-10070] p0079 N82-20593

Heat Capacity Mapping Mission (HCMM) program: Study of geological structure of Sicily and other Italian areas --- Sardinia and the Gulf of Orosei [E82-10073] p0091 N82-20596

Dryland pasture and crop conditions as seen by HCMM --- Washita River watershed [E82-10074] p0067 N82-20597

Application of satellite frost forecast technology to other parts of the United States, phase 2 --- Pennsylvania, Michigan, and Florida [NASA-CR-168827] p0121 N82-20607

Application of satellite frost forecast technology to other parts of the United States, phase 2, introduction p0121 N82-20608

Applicability of satellite freeze forecasting and cold climate mapping to the other parts of the United States --- Michigan p0068 N82-20613

HCMM: Soil moisture in relation to geologic structure and lithology, northern California --- Northern Coast Range, Sacramento Valley, and the Modoc Plateau [E82-10135] p0092 N82-21662

Application of HCMM data to regional geologic analysis for mineral and energy resource evaluation [E82-10137] p0092 N82-21664

A study of model parameters associated with the urban climate using HCMM data --- St. Louis, Missouri [E82-10140] p0079 N82-21667

Delineation of soil temperature regimes from HCMM data [E82-10141] p0070 N82-21668

Use of thermal inertia determined by HCMM to predict nocturnal cold prone areas in Florida --- The Everglades agricultural area, Lake Okeechobee, and the Suwanee River basin [E82-10157] p0071 N82-21681

A study of model parameters associated with the urban climate using HCMM data [E82-10159] p0080 N82-21683

Applications of HCMM satellite data to the study of urban heating patterns [E82-10161] p0080 N82-21685

Cloud Top Scanning radiometer (CTS): User's guide [NASA-TM-83887] p0135 N82-21826

THERMAL POLLUTION

Monitoring of the thermal pollution of natural channels of water using infrared aerial photography p0104 A82-27471

Preliminary results of a study of mapping thermal discharge in the ocean, using remote sensing data [INPE-2229-PRE/021] p0097 N82-19704

TIDAL FLATS

Evaluation of aerial photogrammetric camera and aircraft scanner pictures from tidal lands - Digital correlation and classification of multitemporal imagery data p0127 A82-26049

TIDES

Evaluation of HCMM satellite data for estuarine tidal circulation patterns and thermal inertia soil moisture measurements --- Delaware Bay, Cooper River, and the Potomac River estuaries; Luverne, Minnesota, soil moisture, and water temperature of Lake Anna, Virginia [E82-10064] p0108 N82-20587

TIMBER IDENTIFICATION

A system for quantitative determination of species and vitalities of urban trees on color-infrared photographs p0074 A82-24958

Fanning - A classification algorithm for mixture landscapes applied to Landsat data of Maine forests p0062 A82-27668

Thermal vegetation canopy model studies [AD-A106422] p0064 N82-16455

TIMBER INVENTORY

Automation of the processing of aerial and space images for forest inventory p0057 A82-20350

A system for quantitative determination of species and vitalities of urban trees on color-infrared photographs p0074 A82-24958

Multiresource inventory methods pilot test --- for forests p0060 A82-27601

Potential utility of thematic mapper data in estimating crop areas p0061 A82-27663

Monitoring forest land cover alteration in Thailand with the analysis of ancillary and digital Landsat data p0062 A82-27673

An invertible coniferous forest canopy reflectance model p0062 A82-27679

Method of interpretation of remote sensing data and applications to vegetation [INPE-2215-MD/010] p0066 N82-19640

Relation of the activities of the IPDF/INPE project (reforestation subproject) during the year 1979 --- Mato Grosso do Sul, Brazil [E82-10078] p0067 N82-20601

San Juan National Forest Land Management Planning Support System (LMPSS) requirements definition [E82-10108] p0069 N82-21649

TIMBER VIGOR

A system for quantitative determination of species and vitalities of urban trees on color-infrared photographs p0074 A82-24958

Environmental studies by multispectral scanner under large-scale civil engineering construction p0063 A82-27691

Remote sensing applications to resource problems in South Dakota [E82-10027] p0132 N82-16445

TOMOGRAPHY

Model studies of laser absorption computed tomography for remote air pollution measurement p0077 A82-28152

TOPEX

Topex orbit sustenance maneuver design --- Ocean Topography Experiment spacecraft [AIAA PAPER 82-0202] p0094 A82-27091

TOPOGRAPHY

Calibration and model reconstruction in analytical close-range stereophotogrammetry. II - Special evaluation procedures for rasterstereography and moire topography p0126 A82-22141

Landsat thermal imaging of alpine regions p0079 A82-22147

A structural synthesis of Brazil, based on the study of major lineaments derived from remote sensing imagery interpretation p0079 A82-26012

Area determination by means of the method of finite elements p0082 A82-26048

Cliff and slope topography of part of the Grand Canyon, Arizona as characterized on a Seasat radar image p0082 A82-26843

Airborne laser systems use in terrain mapping p0082 A82-27584

Application of side-looking color infrared photography for structure detection in subtle topography p0082 A82-27611

Topographic mapping using Landsat data p0082 A82-27615

A shuttle scanning laser altimeter for topographic mapping p0083 A82-27632

Spatial resolution and geometric potential of planned earth satellite missions p0130 A82-27683

Coherent scatter of microwaves from moderately rough surfaces [AD-A106133] p0095 N82-16331

Matrix data analysis: Color/B and W coding is not always enough [AD-A108406] p0084 N82-18930

Profiling sensitivity to image quality [AD-A108405] p0084 N82-18931

Methodology of the interpretation of remote sensing data and applications in pedology
[INPE-2211-MD/008] p0078 N82-19641
Heat Capacity Mapping Mission (HCMM) Interpretation of imagery over Canada
[E82-10070] p0079 N82-20593
Observation of the Earth by radar
[NASA-TM-76830] p0124 N82-21687
Some altimetric signatures from Seasat over the mid-Pacific Seamount Range
[AD-A110419] p0099 N82-21691

TRANSFER FUNCTIONS
Optimal spatial filtering and transfer function for SAR ocean wave spectra p0094 A82-27596

TRANSPORT PROPERTIES
Multidimensional aspects Ozone, temperature and transport p0081 N82-18772

TREES (PLANTS)
Remote sensing of sulfur dioxide effects on vegetation Volume 1 Summary
[PB82-115122] p0066 N82-19715

TRIANGULATION
Analytical triangulation of space photography p0111 A82-20402
The diagnosis settlement 1980 of the German main triangulation network Part 2 Trajectories
[SER-B-253-MITT-159-PT-2] p0085 N82-19648

TROPICAL METEOROLOGY
Diurnal variation of summer convection over West Africa and the Tropical Eastern Atlantic during 1974 and 1978 p0075 A82-26700
Low-latitude cloudiness and climate feedback - Comparative estimates from satellite data p0075 A82-26980

TROPICAL REGIONS
Mapping in tropical forests - A new approach using the laser APR --- Airborne Profile Recorder p0081 A82-20407
An airphoto key for major tropical crops p0058 A82-22142
Digital processing of tropical forest habitat in Bangladesh and the development of a low cost processing facility at the National Zoo, Smithsonian Institution p0063 A82-27687
The utilization of orbital images as an adequate form of control of preserved areas --- Araguaia National Park, Brazil
[E82-10065] p0078 N82-20588
Interaction between the Agulhas current and the subtropical convergence
[CSIR-RR-384] p0098 N82-20824

TROPICAL STORMS
Seasat data utilization project
[NASA-CR-168557] p0097 N82-18660

TROPOSPHERE
The NASA participation in the 1980 EPA PEPE/NEROS field measurements program p0075 A82-26621

TURBIDITY
Inland water quality assessment from Landsat data p0105 A82-27610
Mapping of water quality using Landsat imagery p0106 A82-27692
LANDSAT imagery of the Venetian Lagoon A multitemporal analysis
[E82-10036] p0119 N82-19612
An aerial survey of water turbidity and laser depth sounding performance along the Queensland Coast
[AD-A109050] p0098 N82-19802

TURBULENT BOUNDARY LAYER
Observation of the turbulent structure in the planetary boundary layer with a kytoon-mounted ultrasonic anemometer system p0125 A82-21082

TURKEY
The relationship between seismicity and lineaments of the Anatolian-Caucasian-Iranian segment of the Mediterranean fold belt p0089 A82-20341

TWO FLUID MODELS
Passive bathymetric measurements in the Bruce Peninsula region of Ontario p0128 A82-27642

TYPHOONS
A formation process of an oceanic vortex analyzed by multi-temporal remote sensing p0095 A82-27674

U

U.S.S.R.
Landscape mapping and physical-geographical classification of the eastern part of the Chechen-Ingush ASSR using space imagery p0073 A82-20339
The relationship between seismicity and lineaments of the Anatolian-Caucasian-Iranian segment of the Mediterranean fold belt p0089 A82-20341
Investigation of the dynamics of the regional underground runoff of the Aral sea basin using space photography p0101 A82-20343
Experimental evaluation of methods of the automated interpretation of crops from a Fragment MSS image p0057 A82-20349
Evaluation of the state of crops from satellite data p0059 A82-27393
Dynamics of snow cover in mountain regions of the Aral Sea basin, studied using satellite photographs p0102 A82-27462
The possibility of determining snow-meltage fronts using Meteor-satellite multispectral data /with Kazakhstan considered as an example/ p0102 A82-27463
Evaluation of snow-cover pollution in industrial regions using satellite TV images p0103 A82-27464
Albedo and brightness coefficients of snow cover p0103 A82-27465
Experience with a variety of studies of earth resources in the Kalmyk ASSR using space imagery p0131 A82-28130
Ring structures in the earth's crust, and their significance for geology and methods for their investigation p0091 A82-28136
The use of space photographs to compile water-amelioration maps p0106 A82-28137
Sample selection in foreign similarity regions for multicrop experiments
[E82-10118] p0070 N82-21655

U.S.S.R. SPACE PROGRAM
Scientific lectures on aviation and astronautics 1980 --- Russian book p0137 A82-27501
Present and future studies of natural resources and the environment from space p0138 A82-27506
Investigation of the earth on the basis of space photographic data p0082 A82-27507
Development of cooperation between CMEA member countries in the development and utilization of space-based systems for the remote sensing of earth resources and the environment p0138 A82-27543
The earth resources program for the long-term orbital station Salyut 6 p0131 A82-28132

ULTRASONIC SCANNERS
Observation of the turbulent structure in the planetary boundary layer with a kytoon-mounted ultrasonic anemometer system p0125 A82-21082

ULTRAVIOLET SPECTROMETERS
Remote SO2 emission measurements with correlation spectrometers from volcanoes p0077 A82-27704
Atlas of the global distribution of the total ozone concentration according to satellite measurements
[MITT-28] p0078 N82-19740

UNDERWATER ACOUSTICS
Remote sensing techniques suitable for exploration and navigation in and under sea ice
[FOA-REPT-VOL-15-NO-2] p0096 N82-17566

UNDERWATER OPTICS
Remote sensing techniques suitable for exploration and navigation in and under sea ice
[FOA-REPT-VOL-15-NO-2] p0096 N82-17566

UNITED KINGDOM
The use of contextual information to improve land cover classification of digital remotely sensed data p0112 A82-21094

UNITED STATES OF AMERICA
AgRISTARS Interim catalog ground data summary, data acquisition year 1979
[E82-10032] p0064 N82-19608
Use of Magsat anomaly data for crustal structure and mineral resources in the US midcontinent
[E82-10049] p0091 N82-19624
Application of satellite frost forecast technology to other parts of the United States, phase 2 --- Pennsylvania, Michigan, and Florida
[NASA-CR-166827] p0121 N82-20807
AgRISTARS Foreign commodity production forecasting Project test reports document, volume 1 --- using North Dakota, South Dakota, Montana, and Minnesota
[E82-10087] p0068 N82-21639
US corn and soybeans exploratory experiment
[E82-10088] p0068 N82-21640
Compatibility study of the MAGSAT data and aeromagnetic data
[E82-10136] p0123 N82-21663
Use of MAGSAT anomaly data for crustal structure and mineral resources in the US midcontinent
[E82-10152] p0092 N82-21677

UPWELLING WATER
Influence of dissolved organic materials on turbid water optical properties and remote-sensing reflectance p0093 A82-20445
Coastal upwelling ecosystems analysis Atlas of the JOINT I aircraft winds for the 500 foot level
[PB82-114703] p0097 N82-19796
Laboratory upwelled radiance and reflectance spectra of Kerr reservoir sediment waters
[NASA-TP-1993] p0110 N82-21774

URBAN RESEARCH
An investigation of the ozone plume from a small city p0074 A82-26329
Resourceful decisions LANDAT in Michigan
[E82-10037] p0078 N82-19601
A study of model parameters associated with the urban climate using HCMM data --- St Louis, Missouri
[E82-10140] p0079 N82-21667
Applications of HCMM satellite data to the study of urban heating patterns
[E82-10161] p0080 N82-21685

US.S.R. SPACE PROGRAM
The effectiveness of instrumented visual studies of the earth from space p0114 A82-27505

USER MANUALS (COMPUTER PROGRAMS)
Wheat stress indicator model, Crop Condition Assessment Division (CCAD) data base interface driver, user's manual
[E82-10031] p0064 N82-19807
AgRISTARS Early warning and crop condition assessment Patch image processor user's manual
[E82-10055] p0065 N82-19630
As-Built design specification for UNIV4VEC
[E82-10085] p0122 N82-21637
As-built design specification for PARCLS
[E82-10090] p0123 N82-21642
As-built design specification for the CLASFYG program
[E82-10092] p0068 N82-21644
Wheat stress indicator model, Early Warning (EW) data base interface driver, user's manual
[E82-10115] p0069 N82-21652

USER REQUIREMENTS
Response of the marine community to satellite-derived oceanic information p0095 A82-27684
An analysis of user requirements for operational land satellite data p0116 A82-27685
Characterizing user requirements for future land observing satellites
[NASA-TM-83867] p0081 N82-17562
Remote sensing procurement package A management report for state and local governments
[E82-10052] p0138 N82-19627
Future Earthnet Dissemination Systems (FEDS) study Executive summary --- remote sensing data transmission
[REPT-3318] p0124 N82-21698
Interpretation of remotely sensed image data and impact of cluster compression --- impact of cluster compression users
[REPT-44 2866] p0124 N82-21699

UTAH
Thermal infrared data from the Heat Capacity Mapping Mission p0127 A82-24964
HCMM hydrological analysis in Utah --- Utah lake
[E82-10063] p0107 N82-20586

V

VALLEYS
Spatial reasoning in remotely sensed data p0105 A82-27592
Land use in the Paraiba Valley through remotely sensed data --- Brazil
[E82-10072] p0079 N82-20595

VAPOR PRESSURE
Humidity measurement by infrared thermometry p0075 A82-26844

VECTOR ANALYSIS
Usage and limitations of characteristic vector analysis of remote sensing multispectral data for the identification and quantification of water quality parameters p0118 N82-18656

VEGETATION
The use of digital multi-date Landsat imagery in terrain classification p0111 A82-20409
The Dutch ROVE program --- Radar Observation of VEgetation p0057 A82-21026
Microwave radiation peculiarities of vegetative covers p0058 A82-21029
Change detection in the Peace-Athabasca Delta using digital Landsat data p0101 A82-24959
Remote-sensing functions in the interpretation of moisture from aerial and space images p0102 A82-27459
Stochastic models of cover class dynamics --- remote sensing of vegetation p0059 A82-27586
An experiment in probabilistic relaxation for terrain cover classification of Kuwait from Landsat imagery p0062 A82-27680
Wetland mapping from digitized aerial photography --- Sheboygan Marsh, Wisconsin
[E82-10019] p0118 N82-16437
A comparison of unsupervised classification procedures on LANDSAT MSS data for an area of complex surface conditions in Basilicata, Southern Italy
[E82-10038] p0119 N82-19613
Method of interpretation of remote sensing data and applications to vegetation
[INPE-2215-MD/010] p0066 N82-19640
The utilization of orbital images as an adequate form of control of preserved areas --- Araguaia National Park, Brazil
[E82-10065] p0078 N82-20588
Amazonas project Application of remote sensing techniques for the integrated survey of natural resources in Amazonas --- Brazil
[E82-10069] p0078 N82-20592
A gradient model of vegetation and climate utilizing NOAA satellite imagery Phase 1 Texas transect
[E82-10107] p0069 N82-21648
A look at the commonly used LANDSAT vegetation indices
[E82-10123] p0070 N82-21657
HCMM Soil moisture in relation to geologic structure and lithology, northern California --- Northern Coast Range, Sacramento Valley, and the Modoc Plateau
[E82-10135] p0092 N82-21662

VEGETATION GROWTH
The use of contextual information to improve land cover classification of digital remotely sensed data p0112 A82-21094
Multispectral photographic remote sensing of green vegetation biomass and productivity p0059 A82-22144
Spectral reflectance of hydrophytes p0102 A82-24960

Assessing mesquite-grass vegetation condition from Landsat p0059 A82-25457
A vegetation response model applied to range inventory and monitoring using Landsat MSS data p0060 A82-27643
Effects of nitrogen nutrition on the growth, yield and reflectance characteristics of corn canopies --- Purdue Agronomy Farm, Indiana
[E82-10068] p0067 N82-20591

VENEZUELA
Mapping in tropical forests - A new approach using the laser APR --- Airborne Profile Recorder p0081 A82-20407
Strategies and uses of small distributed analysis centers as in the natural resource inventory of Venezuela p0115 A82-27636

VERTICAL DISTRIBUTION
Mid-latitude summertime measurements of stratospheric NO2 p0074 A82-25149

VERY LONG BASE INTERFEROMETRY
Session III of the VLBI/Laser intercomparison task of the NASA crustal dynamics project
[NASA-CR-168427] p0083 N82-17708
Applications to Earth physics. Very-long-baseline interferometry and data analysis
[NASA-CR-168743] p0088 N82-21796

VIETNAM
Applications of aircraft and satellite data for the study of archaeology and environment - Mekong Delta, Vietnam p0091 A82-27705

VIEW EFFECTS
Analysis of the direction-dependent radiation behavior in multispectral scanning data p0125 A82-21399
Influence of illumination and viewing geometry and atmospheric composition on the 'tasseled cap' transformation of Landsat MSS data p0059 A82-24961
Analysis of two Seasat synthetic aperture radar images of an urban scene p0074 A82-25452
Soybean canopy reflectance as a function of view and illumination geometry p0061 A82-27645
The influence of illumination and viewing geometry on the reflectance factor of agricultural targets p0061 A82-27646
Ground level reflectance measurement techniques - An evaluation with emphasis on the importance of spectral calibration p0116 A82-27689
Geometric correction of airborne multispectral scanner images p0130 A82-27706
Influence of solar illumination angle on soybean canopy reflectance p0063 A82-28153
Simulated response of a multispectral scanner over wheat as a function of wavelength and view/illumination direction
[E82-10144] p0071 N82-21671
Variability of reflectance measurements with sensor altitude and canopy type
[E82-10145] p0071 N82-21672

VIRGIN ISLANDS
Effect of aerosols on optical remotely sensed data p0115 A82-27654

VISUAL DISCRIMINATION
Remote sensing data applied to land-use survey at the Paraiba Valley --- Brazil
[E82-10025] p0081 N82-16443

VISUAL OBSERVATION
The effectiveness of instrumented visual studies of the earth from space p0114 A82-27505

VOLCANOES
Detection of volcanic ash fall area from Landsat MSS CCT data Eruption of Mt. Ontake in 1979 p0076 A82-27650

VOLCANOLOGY
Remote SO2 emission measurements with correlation spectrometers from volcanoes p0077 A82-27704

VORTICES
A formation process of an oceanic vortex analyzed by multi-temporal remote sensing p0095 A82-27674

W

WARNING SYSTEMS
Flash flood forecasting --- and damage control measures
[WMO-577] p0107 N82-18671

WASHINGTON
Registration verification of SEA/AR fields --- Oregon, Texas, Montana, Nebraska, Washington, Colorado, Kansas, Oklahoma and North Dakota
[E82-10083] p0068 N82-21635

WATER
The effect of finite field size on classification and atmospheric correction
[NASA-TM-83818] p0120 N82-19645

WATER CIRCULATION
Evaluation of HCMM satellite data for estuarine tidal circulation patterns and thermal inertia soil moisture measurements --- Delaware Bay, Cooper River, and the Potomac River estuaries; Luverne, Minnesota, soil moisture, and water temperature of Lake Anna, Virginia
[E82-10064] p0108 N82-20587

WATER COLOR
A method for the retrieval of phytoplankton and suspended sediment concentrations from remote measurements of water colour p0094 A82-27620
Measurement of river sediments
[WMO-561] p0107 N82-18670

WATER DEPTH
A photometric method for depth determination by aerial photography p0101 A82-19831
Passive bathymetric measurements in the Bruce Peninsula region of Ontario p0129 A82-27642
Classification of Landsat MSS data for surface cover of small areas p0116 A82-27677
Dynamic study of the upper Sao Francisco River and the Tres Marias reservoir using MSS/LANDSAT images --- Brazil
[E82-10082] p0108 N82-20605

WATER MANAGEMENT
Geotechnical applications of Landsat image analysis of Bhakra Dam Reservoir, India p0102 A82-26838
Snow cover monitoring using AVHRR data from TIROS and NOAA satellites --- Advanced Very High Resolution Radiometer p0105 A82-27614
The use of space photographs to compile water-amelioration maps p0106 A82-28137

WATER POLLUTION
Aerospace methods for the study of water resources and their pollution --- Russian book p0102 A82-27457
The possibilities of microwave remote sensing for the study of water resources and their pollution p0102 A82-27458
Remote-sensing determination of the characteristics of hydrological objects p0102 A82-27460
The effect of anthropogenic factors on the dynamics of lakes in the plains of Central Asia /studied on the basis of space photographs/ p0103 A82-27469
Monitoring of the thermal pollution of natural channels of water using infrared aerial photography p0104 A82-27471
Polarimetric method for the remote sensing of oil slicks on the sea surface p0095 A82-28135
LANDSAT imagery of the Venetian Lagoon. A multitemporal analysis
[E82-10036] p0119 N82-19612

WATER PRESSURE
Agricultural soil moisture experiment, Colby, Kansas 1978. Measured and predicted hydrological properties of the soil
[E82-10057] p0065 N82-19632

WATER QUALITY
Influence of dissolved organic materials on turbid water optical properties and remote-sensing reflectance p0093 A82-20445
Remote sensing of salinity in the San Francisco Bay Delta p0102 A82-26839
Investigation of silting and currents in Lake Balaton by use of hydraulic models and aerial and space photographs p0104 A82-27472
Interpretation of multispectral aerial photographs of Lake Mueggelsee p0104 A82-27473
Spectrometric studies of the water composition of Lake Mueggelsee p0104 A82-27474
Noncontact methods for the quality control of water resources p0104 A82-27475
Inland water quality assessment from Landsat data p0105 A82-27610
An approach to path radiance correction in MSS images p0115 A82-27629
Calcium carbonate precipitation in Pyramid Lake, Nevada, as monitored by satellite - 1978 and 1980 p0105 A82-27634
A formation process of an oceanic vortex analyzed by multi-temporal remote sensing p0095 A82-27674
Mapping of water quality using Landsat imagery p0106 A82-27692
Multidisciplinary research on the application of remote sensing to water resources problems --- Wisconsin
[E82-10021] p0106 N82-16439

WATER RESOURCES
Aerospace methods for the study of water resources and their pollution --- Russian book p0102 A82-27457
The use of space photographs for hydrogeological studies of the Baikal region and Mongolia p0103 A82-27468
The effect of anthropogenic factors on the dynamics of lakes in the plains of Central Asia /studied on the basis of space photographs/ p0103 A82-27469
Noncontact methods for the quality control of water resources p0104 A82-27475
Analog devices for the processing of aerial and space images for the study of water resources p0104 A82-27476
Satellite sensing for extraction of groundwater resources information p0105 A82-27613
Strategies for using remotely sensed data in hydrologic models
[E82-10156] p0109 N82-21680
Observation of the Earth by radar
[NASA-TM-76830] p0124 N82-21687
Remote sensing for water resources and hydrology. An assessment of the Corps of Engineers' program
[PB82-137142] p0110 N82-21704

WATER RUNOFF
Investigation of the dynamics of the regional underground runoff of the Aral sea basin using space photography p0101 A82-20343
Application of satellite data to analyze and predict meltage runoff in a mountain basin p0102 A82-27461
Dynamics of snow cover in mountain regions of the Aral Sea basin, studied using satellite photographs p0102 A82-27462
The possibility of determining snow-meltage fronts using Meteor-satellite multispectral data /with Kazakhstan considered as an example/ p0102 A82-27463
Applications systems verification and transfer project. Volume 1: Operational applications of satellite snow cover observations: Executive summary --- usefulness of satellite snow-cover data for water yield prediction
[NASA-TP-1822] p0108 N82-20617
Applications systems verification and transfer project. Volume 2: Operational applications of satellite snow-cover observations and data-collection systems in the Arizona test site
[NASA-TP-1823] p0108 N82-20618
Applications systems verification and transfer project. Volume 3: Operational applications of satellite snow cover observations in California
[NASA-TP-1824] p0108 N82-20619
Applications systems verification and transfer project. Volume 4: Operational applications of satellite snow cover observations: Colorado Field Test Center
[NASA-TP-1825] p0108 N82-20620
Applications systems verification and transfer project. Volume 5: Operational applications of satellite snow-cover observations, northwest United States
[NASA-TP-1826] p0109 N82-20621
Applications systems verification and transfer project. Volume 6: Operational applications of satellite snow-cover observations NOAA/NESS support study
[NASA-TP-1827] p0109 N82-20622
Applications systems verification and transfer project. Volume 7: Cost/benefit analysis for the ASVT on operational applications of satellite snow-cover observations
[NASA-TP-1828] p0109 N82-20623
Applications systems verification and transfer project. Volume 8: Satellite snow mapping and runoff prediction handbook
[NASA-TP-1829] p0109 N82-20624

WATER TEMPERATURE
HCMM hydrological analysis in Utah --- Utah lake
[E82-10063] p0107 N82-20586
Evaluation of HCMM satellite data for estuarine tidal circulation patterns and thermal inertia soil moisture measurements --- Delaware Bay, Cooper River, and the Potomac River estuaries; Luverne, Minnesota, soil moisture, and water temperature of Lake Anna, Virginia
[E82-10064] p0108 N82-20587

WATER VAPOR
A study of model parameters associated with the urban climate using HCMM data --- analysis of St. Louis, Missouri infrared imagery
[E82-10160] p0080 N82-21684

WATER WAVES
Optimal spatial filtering and transfer function for SAR ocean wave spectra p0094 A82-27596
Integrated sensor system for collection of wave data applied to coastal engineering design p0094 A82-27602
The use of wave contrast measurements in the evaluation of SAR/gravity models p0130 A82-27675
An experimental program to provide remote measurement and analysis of ocean waves, sea level winds and balanced pressure in support of Seasat-A
[PB81-246035] p0095 N82-16697
Sea state measurement with a two frequency scatterometer (theory)
[ESA-TT-710] p0096 N82-17802
Recovering ocean waveheight from HF radar sea echoes distorted by imperfect ionospheric reflection
[PB82-113283] p0096 N82-17805

WATERSHEDS
Investigation of the dynamics of the regional underground runoff of the Aral sea basin using space photography p0101 A82-20343
A comparison between aerial photography and Landsat for computer land-cover mapping p0074 A82-22143
Aerospace methods for the study of water resources and their pollution --- Russian book p0102 A82-27457
Application of satellite data to analyze and predict meltage runoff in a mountain basin p0102 A82-27461
Dynamics of snow cover in mountain regions of the Aral Sea basin, studied using satellite photographs p0102 A82-27462
Spatial reasoning in remotely sensed data p0105 A82-27592
Multidisciplinary research on the application of remote sensing to water resources problems --- Wisconsin
[E82-10021] p0106 N82-16439
Remote sensing applications to resource problems in South Dakota
[E82-10027] p0132 N82-16445
Watershed model study using LANDSAT data p0106 N82-17602
Dryland pasture and crop conditions as seen by HCMM --- Washita River watershed
[E82-10074] p0067 N82-20597
Dynamic study of the upper Sao Francisco River and the Tres Marias reservoir using MSS/LANDSAT images --- Brazil
[E82-10082] p0108 N82-20605

Applications systems verification and transfer project. Volume 2: Operational applications of satellite snow-cover observations and data-collection systems in the Arizona test site
[NASA-TP-1823] p0108 N82-20618

Applications systems verification and transfer project. Volume 3: Operational applications of satellite snow cover observations in California
[NASA-TP-1824] p0108 N82-20619

Applications systems verification and transfer project. Volume 4: Operational applications of satellite snow cover observations. Colorado Field Test Center
[NASA-TP-1825] p0108 N82-20620

Applications systems verification and transfer project. Volume 7: Cost/benefit analysis for the ASVT on operational applications of satellite snow-cover observations
[NASA-TP-1828] p0109 N82-20623

WEATHER

Preliminary evaluation of spectral, normal and meteorological crop stage estimation approaches
[E82-10059] p0065 N82-19634

WEATHER FORECASTING

Technology and oceanography: An assessment of Federal technologies for oceanographic research and monitoring
[OTA-O-142] p0097 N82-18844

Application of satellite frost forecast technology to other parts of the United States, phase 2 --- Pennsylvania, Michigan, and Florida
[NASA-CR-166827] p0121 N82-20607

Freeze prediction model --- Pennsylvania
p0067 N82-20609

Applicability of satellite freeze forecasting and cold climate mapping to the other parts of the United States --- Michigan p0068 N82-20613

MSU test of P-model p0121 N82-20614

A satellite frost forecasting system for Florida
p0079 N82-20615

The design and implementation of an operational, computer-based weather radar system --- rainfall maps
[RSRE-MEMO-3151] p0122 N82-21499

WEATHER STATIONS

Optimal network density for atmospheric recording
p0079 N82-20776

WEST GERMANY

Sounding the aerosol distribution over the Upper Rhine Valley in the Valley in the Speyer area by means of lidar
p0079 N82-20782

WEST VIRGINIA

Spatial reasoning in remotely sensed data
p0105 A82-27592

WETLANDS

Change detection in the Peace-Athabasca Delta using digital Landsat data p0101 A82-24959

Spectral reflectance of hydrophytes p0102 A82-24960

Increase in correlation accuracy of remote sensing imagery by digital filtering p0113 A82-25454

Seasat imagery for detection of coastal Wetlands
p0063 A82-27700

Wetland mapping from digitized aerial photography --- Sheboygan Marsh, Wisconsin
[E82-10019] p0118 N82-16437

Application of remote sensing to state and regional problems --- mississippi
[E82-10033] p0078 N82-19609

Use of thermal inertia determined by HCMM to predict nocturnal cold prone areas in Florida --- The Everglades agricultural area, Lake Okeechobee, and the Suwanee River basin
[E82-10157] p0071 N82-21681

WHEAT

Influence of illumination and viewing geometry and atmospheric composition on the tasseled cap transformation of Landsat MSS data p0059 A82-24961

Dew and vapor pressure as complicating factors in the interpretation of spectral radiance from crops
p0060 A82-27617

Crop area estimates using ground-gathered and Landsat data: A multitemporal approach p0062 A82-27676

Documentation of computer procedures for labeling spring grains and discriminating between spring wheat and barley using LANDSAT data
[E82-10030] p0063 N82-16448

Wheat stress indicator model, Crop Condition Assessment Division (CCAD) data base interface driver, user's manual
[E82-10031] p0064 N82-19607

Recommended data sets, corn segments and spring wheat segments, for use in program development
[E82-10034] p0064 N82-19610

AgRISTARS: Foreign commodity production forecasting. Minutes of the annual formal project manager's review, including preliminary technical review reports of FY80 experiments --- wheat/barley and corn/soybean experiments
[E82-10039] p0064 N82-19614

Preliminary evaluation of spectral, normal and meteorological crop stage estimation approaches
[E82-10059] p0065 N82-19634

Utilization of Aerochrome 2443 film for identification and estimating wheat growing areas --- Rio Grande do Sul, Brazil
[INPE-2197-PRE/006] p0066 N82-19639

Dryland pasture and crop conditions as seen by HCMM --- Washita River watershed
[E82-10074] p0067 N82-20597

Registration verification of SEA/AR fields --- Oregon, Texas, Montana, Nebraska, Washington, Colorado, Kansas, Oklahoma, and North Dakota
[E82-10083] p0068 N82-21635

As-Built documentation of programs to implement the Robertson and Doraiswamy/Thompson models
[E82-10086] p0122 N82-21638

Wheat stress indicator model, Early Warning (EW) data base interface driver, user's manual
[E82-10115] p0069 N82-21652

The 1981 Argentina ground data collection
[E82-10127] p0070 N82-21658

Sonora exploratory study for the detection of wheat-leaf rust
[E82-10133] p0070 N82-21661

Spectral-agronomic relationships of corn, soybean and wheat canopies
[E82-10143] p0070 N82-21670

Simulated response of a multispectral scanner over wheat as a function of wavelength and view/illumination direction
[E82-10144] p0071 N82-21671

WILDLIFE

Digital processing of tropical forest habitat in Bangladesh and the development of a low cost processing facility at the National Zoo, Smithsonian Institution
p0063 A82-27687

The application of remote sensing to resource management and environmental quality programs in Kansas --- Cimarron National Grasslands, Prairie Potawatomi Reservation, and Kickapoo Reservation
[E82-10029] p0063 N82-16447

WIND (METEOROLOGY)

An experimental program to provide remote measurement and analysis of ocean waves, sea level winds and balanced pressure in support of Seasat-A
[PB81-246035] p0095 N82-16697

Convergence zones in the South Atlantic and their influence on the precipitation regime in Northeastern Brazil
[INPE-2307-TDL/074] p0097 N82-19778

WIND DIRECTION

An experimental program to provide remote measurement and analysis of ocean waves, sea level winds and balanced pressure in support of Seasat-A
[PB81-246035] p0095 N82-16697

Sea state measurement with a two frequency scatterometer (theory)
[ESA-TT-710] p0096 N82-17802

Satellite scatterometer feasibility study. Volume 1: Technical results --- Earth Resources Satellite (ERS 1)
[ESA-CR(P)-1492-VOL-1] p0133 N82-19650

Satellite scatterometer feasibility study. Volume 2: Data extraction algorithm and error simulation for wind sensor --- Earth Resources Satellite (ERS 1)
[ESA-CR(P)-1492-VOL-2] p0133 N82-19651

WIND PROFILES

SASS measurements of the Ku-band radar signature of the ocean p0093 A82-21917

Coastal upwelling ecosystems analysis. Atlas of the JOINT I aircraft winds for the 500 foot level
[PB82-114703] p0097 N82-19796

WIND VELOCITY

Comparison of conventionally measured sea surface temperature and wind speed with data retrieved from satellite-borne microwave radiometry p0093 A82-24063

WIND VELOCITY MEASUREMENT

Observation of the turbulent structure in the planetary boundary layer with a kytoon-mounted ultrasonic anemometer system p0125 A82-21082

Satellite scatterometer feasibility study. Volume 1: Technical results --- Earth Resources Satellite (ERS 1)
[ESA-CR(P)-1492-VOL-1] p0133 N82-19650

Satellite scatterometer feasibility study. Volume 2: Data extraction algorithm and error simulation for wind sensor --- Earth Resources Satellite (ERS 1)
[ESA-CR(P)-1492-VOL-2] p0133 N82-19651

WINTER

Photogrammetry from aircraft side camera movies - Winter MONEX p0075 A82-26721

Classification of the fields of anomaly in monthly water temperature of the North Atlantic during the cold half-year
[BLL-TRANS-1509-(9022.552)] p0097 N82-19756

WISCONSIN

A comparison between aerial photography and Landsat for computer land-cover mapping p0074 A82-22143

Wetland mapping from digitized aerial photography --- Sheboygan Marsh, Wisconsin
[E82-10019] p0118 N82-16437

Multidisciplinary research on the application of remote sensing to water resources problems --- Wisconsin
[E82-10021] p0106 N82-16439

WORLD METEOROLOGICAL ORGANIZATION

Modern methods for monitoring and controlling the timeliness, accuracy, and completeness of data for meteorological analysis p0073 A82-19179

WRANGELL MOUNTAINS (AK)

Landsat thermal imaging of alpine regions
p0079 A82-22147

WYOMING

Integration of LANDSAT with geology and airborne geophysics into an operational mineral exploration system --- the Bearlodge area of northeastern Wyoming
[E82-10028] p0091 N82-16446

X

X RAY SPECTRA

Spectral reflectances of freshwater ice and snow from 340 through 1100 nm p0106 N82-17601

Y

YIELD

AgRISTARS: Yield model development/soil moisture interface control document
[E82-10054] p0065 N82-19629

YUGOSLAVIA

Thermal IR detection of submarine gas seepages in the western Istra off shore area /Yugoslavia/
p0076 A82-27661

Z

ZENITH

A relation between Landsat digital numbers, surface reflectance, and the cosine of the solar zenith angle
p0114 A82-26841

PERSONAL AUTHOR INDEX

Typical Personal Author Index Listing

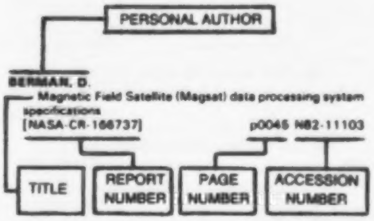
PERSONAL AUTHOR
BERMAN, D.
Magnetic Field Satellite (Magsat) data processing system specifications
[NASA-CR-166737] p0045 N82-11103
TITLE
REPORT NUMBER
PAGE NUMBER
ACCESSION NUMBER

Listings in this index are arranged alphabetically by personal author. The title of the document provides the user with a brief description of the subject matter. The report number helps to indicate the type of document listed (e.g., NASA report, translation, NASA contractor report). The page and accession numbers are located beneath and to the right of the title, e.g., p0045 N82-11103. Under any one author's name the accession numbers are arranged in sequence with the AIAA accession numbers appearing first.

A

ABBOT, R. H.
An aerial survey of water turbidity and laser depth sounding performance along the Queensland Coast
[AD-A109050] p0098 N82-19802

ABBOTT, E. A.
A data base of geologic field spectra
p0090 A82-27600

ABDEL-AZIZ, Y. I.
Accuracy of the normal case of close-range photogrammetry p0126 A82-22140

ABDELRAZIK, M.
Active microwave investigation of snowpacks Experimental documentation, Colorado 1979-1980
[NASA-CR-166727] p0107 N82-19646

ABOTTEEN, K. M.
AgRISTARS Foreign commodity production forecasting Corn/soybean decision logic development and testing
[E82-10056] p0065 N82-19631

ADAMS, T. R.
Proposed digital cartridge recording system for WRELADS
[AD-A109484] p0134 N82-20491

AGHASSY, J.
Application of side-looking color infrared photography for structure detection in subtle topography
p0082 A82-27611

AHERN, F. J.
The influence of illumination and viewing geometry on the reflectance factor of agricultural targets
p0061 A82-27646
Landsat MSS applied to rangeland management in Western Canada p0063 A82-27697

AKOVETSKII, V. I.
Analytic methods of geodetic referencing of nontopographic images p0083 A82-28134

ALBEROTANZA, L.
LANDSAT imagery of the Venetian Lagoon A multitemporal analysis
[E82-10036] p0119 N82-19612

ALDERMAN, P. K.
Experiences with digital terrain elevation data contouring programs
[AD-A110280] p0087 N82-21690

ALDRICH, F. T.
The role of computer graphics in geographic research
p0117 A82-27923

ALEKSEEV, A. S.
Automation of the processing of aerial and space images for forest inventory p0057 A82-20350
Structure of hardware and software at a regional center for the automated processing of aerial and space remote-sensing images p0130 A82-28128

ALEXANDER, S. J.
Study of a radar altimeter for the European remote sensing program Volume 1 Executive summary
[SPAR-R 1090-ISSUE-A] p0133 N82-19652

ALI, M. E. O.
Analytical triangulation of space photography
p0111 A82-20402

ALLEN, L. H., JR.
Use of thermal inertia determined by HCMM to predict nocturnal cold prone areas in Florida
[E82-10040] p0064 N82-19615
Use of thermal inertia determined by HCMM to predict nocturnal cold prone areas in Florida
[E82-10157] p0071 N82-21681

ALLEY, R. E.
A data base of geologic field spectra
p0090 A82-27600

ALVAREZ, R.
Application of machine processing of visible and thermal data to the study of the geothermal area of Cerro Prieto, Mexico p0117 A82-27693

ALVES, E. C. M.
Relation of the activities of the IPDF/INPE project (reforestation subproject) during the year 1979
[E82-10078] p0067 N82-20601

AMBROSETTI, E.
Examination of the operational prospects for remote sensing
[ESA-CR(P)-1476] p0138 N82-18669

AMIS, M. L.
Evaluation of large area crop estimation techniques
p0061 A82-27662

ANDERS, R.
Satellite scatterometer feasibility study Volume 1 Technical results
[ESA-CR(P)-1492-VOL-1] p0133 N82-19650

ANUSKIEWICZ, T.
Resourceful decisions LANDAT in Michigan
[E82-10037] p0078 N82-19601

ARKHIPOV, V. V.
The earth resources program for the long-term orbital station Salyut 6 p0131 A82-28132

ARMAND, N. A.
Machine implementation of algorithms for the mapping of soil moisture on the basis of microwave-radiometer measurements p0131 A82-28142

ARP, H.
Mapping in tropical forests - A new approach using the laser APR p0081 A82-20407

ARTLEY, J. A.
Preliminary evaluation of spectral normal and meteorological crop stage estimation approaches
[E82-10059] p0065 N82-19634

ARYA, L. M.
Agricultural soil moisture experiment, Colby, Kansas 1978 Measured and predicted hydrological properties of the soil
[E82-10057] p0065 N82-19632

ASLAM, A.
Active microwave investigation of snowpacks Experimental documentation, Colorado 1979-1980
[NASA-CR-166727] p0107 N82-19646

ATARAS, W. S.
An information adaptive system study report and development plan
[NASA-CR-166768] p0120 N82-19644

ATLAS, D.
Precipitation measurements from space - Workshop summary 28 April-1 May 1981, Greenbelt, MD
p0077 A82-28295
Estimating ocean-air heat fluxes during cold air outbreaks by satellite
[NASA-TM-83854] p0097 N82-19781

ATTEMA, E. P. W.
The Dutch ROVE program p0057 A82-21026
A radar signature model for partially coherent scattering from irregular surfaces p0079 A82-21038

AUSTIN, W. W.
Use of Landsat-derived temporal profiles for corn-soybean feature extraction and classification p0059 A82-26842
Recommended data sets, corn segments and spring wheat segments, for use in program development
[E82-10034] p0064 N82-19610
Registration verification of SEA/AR fields
[E82-10083] p0068 N82-21635
AgRISTARS Supporting research Classification of corn Badhwar profile similarity technique
[E82-10150] p0071 N82-21676

AXELSSON, S. R. J.
On the accuracy of thermal inertia mapping by infrared imagery
[SAAB-REPR-AE-10] p0120 N82-19656

B

BADHWAR, G. D.
Use of Landsat-derived temporal profiles for corn-soybean feature extraction and classification p0059 A82-26842

BAHMAD, A.
Remote sensing applied to basement tectonics of the calcareous High Atlas /Morocco/ p0089 A82-26014

BAILEY, T.
Remote sensing applications to resource problems in South Dakota
[E82-10027] p0132 N82-16445

BAKAI, G. G.
Potential use of space photographs obtained from the manned orbital station Salyut-5 in order to compile a set of small-scale thematic maps of mountain and piedmont regions of Central Asia p0083 A82-28139

BAKER, D. J.
Recent auroral measurements using a field-widened interferometer spectrometer p0126 A82-21434

BAKER, K. S.
Ship and satellite bio-optical research in the California Bight
[NASA-CR-168681] p0098 N82-20823

BAKLASHOV, N. I.
Complex of units for the storage and automated processing of research data p0131 A82-28140

BALASUBRAMANIAN, S.
Microwave brightness temperature pattern over the Indian subcontinent and the surrounding oceans as observed by the satellite microwave radiometer /SAMIR/ onboard Bhaskara p0093 A82-19560

BALL, A. P.
The design and implementation of an operational, computer-based weather radar system
[RSRE-MEMO-3151] p0122 N82-21499

BALMINO, G.
Gradio Project proposal for satellite gradiometry
[NASA-TM-76796] p0134 N82-20606

BARBOS, M. P.
Study project of intrusive rocks States of Espirito Santo and Rio de Janeiro, south and east of Minas Gerais and southeast of the state of Sao Paulo
[E82-10076] p0092 N82-20599

BARBOSA, M. N.
CNPq/INPE LANDSAT system
[E82-10023] p0118 N82-16441
The LANDSAT system operated in Brazil by CNPq/INPE - results obtained in the area of mapping and future perspectives
[E82-10080] p0121 N82-20603

BARLIER, F.
Gradio Project proposal for satellite gradiometry
[NASA-TM-76796] p0134 N82-20606

BARKER, J. L.
Information expectations from Landsat-D
p0128 A82-27583
Characterizing user requirements for future land observing satellites
[NASA-TM-83867] p0081 N82-17562

BARNES, J. C.
Applications systems verification and transfer project Volume 8 Satellite snow mapping and runoff prediction handbook
[NASA-TP-1829] p0109 N82-20624

BARR, B. G.
The application of remote sensing to resource management and environmental quality programs in Kansas
[E82-10029] p0063 N82-16447

BARRACLOUGH, D. R.
Spherical harmonic representation of the main geomagnetic field for world charting and investigations of some fundamental problems of physics and geophysics
[E82-10075] p0086 N82-20598

BARRETT, E. C.
The use of satellite data in rainfall monitoring
p0101 A82-22873

BARRINGER, T. H.
Stochastic models of cover class dynamics
p0059 A82-27586

BARTHOLIC, J. F.
Application of satellite frost forecast technology to other parts of the United States, phase 2
[NASA-CR-166827] p0121 N82-20807

BARTSCHI, B. Y.
Recent auroral measurements using a field-widened interferometer spectrometer p0126 A82-21434

BASHENINA, N. V.
Analysis of space imagery to compile a geomorphological map of the world p0089 A82-20338

BAUER, B.
An automatic optimum kernel-size selection technique for edge enhancement p0113 A82-26840

BAUER, M. E.
Soybean canopy reflectance as a function of view and illumination geometry p0061 A82-27645
Influence of solar illumination angle on soybean canopy reflectance p0063 A82-28153
Evaluation of a segment-based LANDSAT full-frame approach to corp area estimation
[E82-10067] p0066 N82-20590
Effects of nitrogen nutrition on the growth, yield and reflectance characteristics of corn canopies
[E82-10068] p0067 N82-20591
Soybean canopy reflectance as influenced by cultural practices
[E82-10106] p0068 N82-21647
A multiband radiometer and data acquisition system for remote sensing field research
[E82-10142] p0134 N82-21669
Spectral-agronomic relationships of corn, soybean and wheat canopies
[E82-10143] p0070 N82-21670
Simulated response of a multispectral scanner over wheat as a function of wavelength and view/illumination direction
[E82-10144] p0071 N82-21671
Determination of the optimal level for combining area and yield estimates
[E82-10146] p0071 N82-21673

BAYLIS, P. E.
University of Dundee satellite image data acquisition and archiving facility p0130 A82-27659

BEAL, R. C.
Optimal spatial filtering and transfer function for SAR ocean wave spectra p0094 A82-27596

BEAUDET, P. R.
Context dependent modeling p0114 A82-27587
An information adaptive system study report and development plan
[NASA-CR-166768] p0120 N82-19644
Context sensitive formulations of antenna pattern correction and side lobe compensation for NOSS/LAMMR real time processing
[NASA-CR-166789] p0122 N82-21457

BELIAEV, B. I.
Color characteristics of the earth's surface determined on the basis of spectroscopy results from Salyut 4
p0073 A82-19826

BELKSY, L. E.
Development and applications of techniques to process hydrometeor distribution data
[AD-A109929] p0109 N82-20822

BELL, R. E.
Satellite observed cloud patterns associated with excessive precipitation outbreaks
[PB80-215130] p0073 A82-19177

BENDURA, R.
The NASA participation in the 1980 EPA PEPE/NEROS field measurements program p0075 A82-26621

BENITEZ O., A.
Inventory of eroded areas in the state of Guanajuato Mexico, by automatic analysis of Landsat images
p0076 A82-27690

BENNETT, J. R.
Features of a generalized digital Synthetic Aperture Radar processor p0128 A82-27595

BENNY, A. H.
Automatic relocation of ground control points in LANDSAT imagery
[RAE-TR-81071] p0118 N82-18657

BENTLEY, C. R.
Investigation of Antarctic crust and upper mantle using MAGSAT and other geophysical data
[E82-10062] p0086 N82-20585
Investigation of antarctic crust and upper mantle using MAGSAT and other geophysical data
[E82-10147] p0087 N82-21674

BENTON, E. R.
Investigation of geomagnetic field forecasting and fluid dynamics of the core
[E82-10162] p0087 N82-21686

BERG, C. P.
Calcium carbonate precipitation in Pyramid Lake, Nevada, as monitored by satellite - 1978 and 1980
p0105 A82-27634

BERG, D. W.
Integrated sensor system for collection of wave data applied to coastal engineering design p0094 A82-27602

BERGAMINI, E. W.
A microcomputer for control of data collection platforms
[INPE-2104-RPE/331] p0133 N82-18881

BERGER, Z.
Application of side-looking color infrared photography for structure detection in subtle topography
p0082 A82-27611

BERLIN, G. L.
Cliff and slope topography of part of the Grand Canyon, Arizona as characterized on a Seasat radar image
p0082 A82-26843

BERNARD, A.
Gradio: Project proposal for satellite gradiometry
[NASA-TM-76796] p0134 N82-20606

BERNIER, M.
Visual and digital analysis of H.C.M.M. data over eastern Canada p0117 A82-27698

BERTHOLD, G.
Sigma/deg/ signature of the Amazon rain forest obtained from the Seasat scatterometer p0125 A82-21027

BEST, R. G.
Spectral reflectance of hydrophytes p0102 A82-24960
Remote sensing applications to resource problems in South Dakota
[E82-10027] p0132 N82-16445

BIEHL, L. L.
Soybean canopy reflectance as a function of view and illumination geometry p0061 A82-27645
Simulated response of a multispectral scanner over wheat as a function of wavelength and view/illumination direction
[E82-10144] p0071 N82-21671

BILLINGSLEY, F. C.
Modeling misregistration and related effects on multispectral classification p0113 A82-25455

BIRRER, I. J.
Sigma/deg/ signature of the Amazon rain forest obtained from the Seasat scatterometer p0125 A82-21027

BLANCHARD, A. J.
Volumetric effects in cross-polarized airborne radar data p0058 A82-21032

BLANCHARD, B. J.
Dryland pasture and crop conditions as seen by HCMM
[E82-10074] p0067 N82-20597

BODECHTEL, J.
Geotechnical applications of Landsat image analysis of Bhakra Dam Reservoir, India p0102 A82-26838

BOGORODSKII, V. V.
The use of data from satellite-borne microwave scanning radiometers for the automated compilation of operational maps of ice cover for the Arctic Ocean
p0095 A82-28145

BOLSENGA, S. J.
Spectral reflectances of freshwater ice and snow from 340 through 1100 nm p0106 N82-17601

BOLSHAKOV, V. D.
Investigation of the earth on the basis of space photographic data p0082 A82-27507

BOMMAS, G.
Satellite scatterometer feasibility study. Volume 1: Technical results
[ESA-CR(P)-1492-VOL-1] p0133 N82-19650

BONN, F.
Visual and digital analysis of H.C.M.M. data over eastern Canada p0117 A82-27698

BORISOGLEBSKII, G. I.
Evaluation of the state of crops from satellite data
p0059 A82-27393

BORMANN, P.
Some problems concerning the effective use of remote sensing p0137 A82-28123

BORN, G. H.
Seasat data utilization project
[NASA-CR-168557] p0097 N82-18660

BORNEMAN, R.
Satellite observed cloud patterns associated with excessive precipitation outbreaks
[PB80-215130] p0073 A82-19177

BOUZAT, C.
Gradio: Project proposal for satellite gradiometry
[NASA-TM-76796] p0134 N82-20606

BOWIN, C.
Gravity and geoid anomalies of the Philippine Sea: Evidence on the depth of compensation for the negative residual water depth anomaly
[NASA-CR-168639] p0085 N82-19732

BOWLEY, C. J.
Applications systems verification and transfer project. Volume 8: Satellite snow mapping and runoff prediction handbook
[NASA-TP-1829] p0109 N82-20624

BRACALENTE, E. M.
Sigma/deg/ signature of the Amazon rain forest obtained from the Seasat scatterometer p0125 A82-21027

BRACHET, G.
Towards an operational SPOT system - A preliminary assessment p0114 A82-27607

BRANDENBERGER, A. J.
Analytical triangulation of space photography
p0111 A82-20402

BRAUN, O. P. G.
A structural synthesis of Brazil, based on the study of major lineaments derived from remote sensing imagery interpretation p0079 A82-26012

BRIEGLEB, B. P.
Low-latitude cloudiness and climate feedback - Comparative estimates from satellite data
p0075 A82-26980

BRIEN, M. J.
The design and implementation of an operational, computer-based weather radar system
[RSRE-MEMO-3151] p0122 N82-21499

BRIMACOMBE, C. A.
Atlas of METEOSAT imagery
[ESA-SP-1030] p0124 N82-21700

BRISCO, B.
Manual and automatic crop identification with airborne radar imagery p0057 A82-20408

BRIVIO, P. A.
Heat Capacity Mapping Mission (HCMM) program. Study of geological structure of Sicily and other Italian areas
[E82-10073] p0091 N82-20596

BROCHU, R.
Visual and digital analysis of H.C.M.M. data over eastern Canada p0117 A82-27698

BROOKS, J.
Implementation of the Space Oblique Mercator projection in a production environment p0129 A82-27628

BROWN, A. J.
Applications systems verification and transfer project. Volume 3: Operational applications of satellite snow cover observations in California
[NASA-TP-1824] p0108 N82-20619

BROWN, J. W.
The Seasat low rate data processing system
p0083 A82-24061

BROWN, K. S.
Cloud Top Scanning radiometer (CTS): User's guide
[NASA-TM-83887] p0135 N82-21826

BROWN, P. M.
As-built design specification for MISMAP
[E82-10091] p0123 N82-21643

BROWN, R. J.
A timely and accurate potato acreage estimate from Landsat - Results of a demonstration p0060 A82-27621
The influence of illumination and viewing geometry on the reflectance factor of agricultural targets
p0061 A82-27646
Landsat MSS applied to rangeland management in Western Canada p0063 A82-27697

BRUECK, P. M.
Relationship of hydrothermal phenomena within the Leinster Granite to crustal fractures delineated from Landsat imagery p0089 A82-26015

BRYAN, M. L.
Analysis of two Seasat synthetic aperture radar images of an urban scene p0074 A82-25452

BRYANT, E.
Fanning - A classification algorithm for mixture landscapes applied to Landsat data of Maine forests
p0062 A82-27668

BUGLIOSI, E. F.
Use of Landsat imagery to delineate glaciofluvial aquifers in southeast South Dakota p0105 A82-27637

BURKE, F. A. C.
Study of Earth Resources Satellite (ERS) data reduction unit
[BAE-TP-7905] p0120 N82-19649

BURNS, J. P.
Mapping in tropical forests - A new approach using the laser APR p0081 A82-20407

BURROWS, C.
Study of Earth Resources Satellite (ERS) data reduction unit
[BAE-TP-7905] p0120 N82-19649

BUZNIKOV, A. A.
Polarimetric method for the remote sensing of oil slicks on the sea surface p0095 A82-28135

BYER, R. L.
Model studies of laser absorption computed tomography for remote air pollution measurement p0077 A82-28152

C

CAGLE, B. J.
Arabian sea project of 1980. Composites of infrared images
[AD-A107910] p0096 N82-17567

CALLA, O. P. N.
Microwave brightness temperature pattern over the Indian subcontinent and the surrounding oceans as observed by the satellite microwave radiometer /SAMIR/ onboard Bhaskara p0093 A82-19560

CALOZ, R.
Soil moisture determination - Experiments with passive microwave radiometers p0057 A82-19529

CAMARA, G.
Simplified algorithm for calculating radiative transfer in satellite images
[INPE-2169-RPE/385] p0118 N82-16450

CAMPBELL, J.
Spatial reasoning in remotely sensed data
p0106 A82-27592

CAMUS, J. P.
Data rate reduction: Impact of image data compression on end to end data management of a multispectral payload
[REPT-44/130] p0120 N82-19654

CANOBA, C. A.
The Pampean Plain studied with Landsat images
p0088 A82-28013

CARD, D. H.
Using known map category marginal frequencies to improve estimates of thematic map accuracy
p0113 A82-25456

CARGILL, R. D.
A low cost NOAA/TIROS AVHRR receiving station
p0130 A82-27681

CARLEIAL, A. B.
General configuration and internal disposition of equipment in a satellite for collecting environmental data
[INPE-2240-PRE/026] p0078 N82-19256

CARLSON, C. T.
An experimental program to provide remote measurement and analysis of ocean waves, sea level winds and balanced pressure in support of Seasat A
[PB81-246035] p0085 N82-16697
Recovering ocean waveheight from HF radar sea echoes distorted by imperfect ionospheric reflection
[PB82-113283] p0096 N82-17805

CARLSON, D. L.
Weather satellite interpretation Introduction to weather satellite imagery
[PB82-107657] p0118 N82-16677

CARLSON, T. N.
Interactive initialization of heat flux parameters for numerical models using satellite temperature measurements
[E82-10048] p0120 N82-19623
Applications of HCMM satellite data to the study of urban heating patterns
[E82-10161] p0080 N82-21685

CARMICHAEL, R. S.
Use of Magsat anomaly data for crustal structure and mineral resources in the US midcontinent
[E82-10049] p0091 N82-19624
Use of MAGSAT anomaly data for crustal structure and mineral resources in the US midcontinent
[E82-10152] p0092 N82-21677

CARNES, J. G.
Use of Landsat-derived temporal profiles for corn-soybean feature extraction and classification p0059 A82-26842
US corn and soybeans exploratory experiment
[E82-10088] p0068 N82-21640

CARPENTER, D. J.
Inland water quality assessment from Landsat data
p0105 A82-27610

CARROLL, W.
A low cost NOAA/TIROS AVHRR receiving station
p0130 A82-27681

CASSINIS, R.
Heat Capacity Mapping Mission (HCMM) program Study of geological structure of Sicily and other Italian areas
[E82-10073] p0091 N82-20596

CASTRUCCIO, P.
Applications systems verification and transfer project. Volume 7 Cost/benefit analysis for the ASVT on operational applications of satellite snow-cover observations
[NASA-TP-1828] p0109 N82-20623

CATE, R. B.
Preliminary evaluation of spectral, normal and meteorological crop stage estimation approaches
[E82-10059] p0065 N82-19634

CESS, R. D.
Low-latitude cloudiness and climate feedback - Comparative estimates from satellite data
p0075 A82-26980

CHAKRABORTI, D. K.
One orogenic belt or two - A structural reinterpretation supported by Landsat data products of the Precambrian metamorphics of Singhbhum, eastern India
p0089 A82-26017

CHANG, T. P.
Watershed model study using LANDSAT data
p0106 N82-17602

CHARIAI, H.
Remote sensing applied to basement tectonics of the calcareous High Atlas /Morocco/ p0089 A82-26014

CHAVEZ, P., JR.
An automatic optimum kernel-size selection technique for edge enhancement p0113 A82-26840
Cliff and slope topography of part of the Grand Canyon, Arizona as characterized on a Seasat radar image
p0082 A82-26843

CHEN, D. T.
Surface wave statistics and spectra during high sea state conditions in the North Atlantic
[AD-A109832] p0098 N82-20827

CHEN, E.
Use of thermal inertia determined by HCMM to predict nocturnal cold prone areas in Florida
[E82-10040] p0064 N82-19615
Application of satellite frost forecast technology to other parts of the United States, phase 2
[NASA-CR-166827] p0121 N82-20607
Use of thermal inertia determined by HCMM to predict nocturnal cold prone areas in Florida
[E82-10157] p0071 N82-21681

CHEN, S. C.
Survey of the cane-growing area of the state of Sao Paulo using LANDSAT data. Safra Year 1979/80, volume 2
[E82-10071] p0067 N82-20594
Elevation of a cane-growing area of the state of Sao Paulo using LANDSAT data
[E82-10077] p0067 N82-20800

CHENEY, R. E.
Structure and variability of the Alboran Sea frontal system p0093 A82-20447

CHENG, D. E.
As-built design specification for MISMAP
[E82-10091] p0123 N82-21643

CHERNOV, V. IU.
Dynamics of snow cover in mountain regions of the Aral Sea basin, studied using satellite photographs
p0102 A82 27462

CHERVANEV, I. G.
Possibilities of using experience gained from the thematic mapping of the moon in studies of earth resources by remote sensing methods p0083 A82-28138

CHIAVIELLO, A.
The Landsat program - Moving ahead
p0137 A82-21280

CHIN, R.
An information adaptive system study report and development plan
[NASA-CR-166768] p0120 N82-19644

CHIN, R. T.
Context sensitive formulations of antenna pattern correction and side lube compensation for NOSS/LAMMR real time processing
[NASA-CR-166789] p0122 N82-21457

CHITTINENI, C. B.
Maximum likelihood estimation of label imperfection probabilities and its use in the identification of mislabeled patterns p0112 A82-21040

CHONG, Y. J.
Classification of Landsat MSS data for surface cover of small areas p0116 A82-27677

CHOU, S. H.
Estimating ocean-air heat fluxes during cold air outbreaks by satellite
[NASA-TM-83854] p0097 N82 19781

CHOUDHURY, B.
Spectral albedos of midlatitude snowpacks
[NASA-TM-83858] p0106 N82-18663

CHRISTOL, C. Q.
Remote sensing and international law
p0137 A82-24343

CHUKHLANTSEV, A. A.
Microwave radiation peculiarities of vegetative covers
p0058 A82-21029

CHUMACHENKO, B. A.
Development of cooperation between CMEA member countries in the development and utilization of space-based systems for the remote sensing of earth resources and the environment p0138 A82-27543

CIHLAR, J.
The potential of remote sensing to monitor soil erosion on cropland p0061 A82-27656
Interpretation of Heat Capacity Mapping Mission images over Canada p0116 A82-27671
Landsat MSS applied to rangeland management in Western Canada p0063 A82-27697
Heat Capacity Mapping Mission (HCMM) Interpretation of imagery over Canada
[E82-10070] p0079 N82-20593

CLARK, J. D.
Satellite observed cloud patterns associated with excessive precipitation outbreaks
[PB80-215130] p0073 A82-19177

CLARK, J. R.
Application of remote sensing to state and regional problems
[E82-10033] p0078 N82-19609

CLARKE, J. L.
The design and implementation of an operational, computer-based weather radar system
[RSRE-MEMO-3151] p0122 N82-21499

CLINTON, N. J.
Transition year labeling error characterization study
[E82-10111] p0069 N82-21651

COBOURN, W. G.
Airborne in-situ measurement of particulate sulfur and sulfuric acid with flame photometry and thermal analysis
p0073 A82-20999

COLE, B. C.
Instruments watch for impending earthquakes
p0131 A82-28342

COLLINS, C. J.
Study of Earth Resources Satellite (ERS) data reduction unit
[BAE-TP-7905] p0120 N82-19649

COLLINS, J. G.
Airborne laser systems use in terrain mapping
p0082 A82-27584

COLOMBESKI, N. C.
Image quality control in the Meteosat ground processing system p0125 A82-21090

COLVOCORESSES, A. P.
Mapsat compared to other earth-sensing concepts
p0128 A82-27581

COLWELL, J. E.
Landsat feature enhancement - Or, can we separate vegetation from soil p0060 A82-27622
Forest change detection p0061 A82-27644

COLWELL, R. N.
The 1981 Argentina ground data collection
[E82-10127] p0070 N82-21658

COOK, V. L.
AgRISTARS Interim catalog ground data summary data acquisition year 1979
[E82-10032] p0064 N82-19608

COSENTINO, M. J.
Scene analysis for wildland fire-fuel characteristics in a Mediterranean climate p0060 A82-27624
Flexible processing of remote sensing data through integration of image processing and geobased information systems p0116 A82-27667

COTTER, D. J.
An analysis of user requirements for operational land satellite data p0116 A82-27685

COTTRELL, D. A.
Utilization of Aerochrome 2443 film for identification and estimating wheat growing areas
[INPE-2197-PRE/006] p0066 N82-19639

COUNSELMAN, C. C., III
Applications to Earth physics Very-long-baseline interferometry and data analysis
[NASA-CR-168743] p0088 N82-21796

COUPLAND, D. H.
Automatic linear recognition and analysis using computer program LIRA p0080 A82-27612
HCMM night-time thermal IR imaging experiment in Michigan p0115 A82-27655

CRAIG, M.
Potential utility of thematic mapper data in estimating crop areas p0061 A82-27663

CRAIG, R. G.
Precision in the evaluation of Landsat autocorrelation - The terrain effect p0116 A82-27686

CRAWFORD, M. F.
Integration of LANDSAT with geology and airborne geophysics into an operational mineral exploration system
[E82-10028] p0091 N82-16446

CRESSY, P. J.
Characterizing user requirements for future land observing satellites
[NASA-TM-83867] p0081 N82 17562

CRIST, E.
A technique for automatic labeling of Landsat agricultural scene elements by analysis of temporal-spectral patterns
p0062 A82-27678

CRIST, E. P.
Documentation of computer procedures for labeling spring grains and discriminating between spring wheat and barley using LANDSAT data
[E82-10030] p0063 N82-16448

CUMMING, I. G.
Features of a generalized digital Synthetic Aperture Radar processor p0128 A82-27595

CURRAN, P. J.
The estimation of the surface moisture of a vegetated soil using aerial infrared photography p0058 A82-21093
Multispectral photographic remote sensing of green vegetation biomass and productivity p0059 A82-22144

CUSTER, J.
Locating prehistoric archaeological sites using Landsat
p0129 A82-27638

D

DACOSTA, J. M.
Particle precipitation and atmospheric X-and Gamma-rays in the South Atlantic magnetic anomaly by balloon experiments
[INPE-2119-RPE/343] p0083 N82-17711

DAILEY, C. L.
AgRISTARS Foreign commodity production forecasting Corn/soybean decision logic development and testing
[E82-10056] p0065 N82-19631

DANIELSON, J. A.
Applications systems verification and transfer project. Volume 4 Operational applications of satellite snow cover observations Colorado Field Test Center
[NASA-TP-1825] p0108 N82-20620

DARCOS, J.-C.
Field-by-field multitemporal analysis of aerial scanner data geometrically corrected by means of a sliding model
p0115 A82-27651

DAUBNER, L.
Instrumentation for remote reflectance and radiance measurements p0130 A82-27652
Remote SO2 emission measurements with correlation spectrometers from volcanoes p0077 A82-27704

DAUGHTRY, C. S. T.
Influence of solar illumination angle on soybean canopy reflectance p0063 A82-28153
Effects of nitrogen nutrition on the growth, yield and reflectance characteristics of corn canopies
[E82-10068] p0067 N82-20591
Soybean canopy reflectance as influenced by cultural practices
[E82-10106] p0068 N82-21647
Spectral-agronomic relationships of corn, soybean and wheat canopies
[E82-10143] p0070 N82-21670
Variability of reflectance measurements with sensor altitude and canopy type
[E82-10145] p0071 N82-21672

DAVE, J. V.
Influence of illumination and viewing geometry and atmospheric composition on the tasseled cap transformation of Landsat MSS data p0059 A82-24961
DAVIDSON, S. A.
Segment-level evaluation of the simulated aggregation test. US corn and soybean exploratory experiment
[E82-10061] p0066 N82-19636
DAVIES, J.
Instrumentation for remote reflectance and radiance measurements p0130 A82-27652
Remote SO2 emission measurements with correlation spectrometers from volcanoes p0077 A82-27704
DAVIS, J. M.
Regional properties of angular reflectance models
p0083 N82-17599
DAVIS, P. A.
Development of a surface isolation estimation technique suitable for application of polar orbiting satellite data
[E82-10122] p0123 N82-21656
DAVIS, S. M.
Evaluation of a segment-based LANDSAT full-frame approach to corp area estimation
[E82-10067] p0066 N82-20590
DAVISON, G. J.
An introduction to image processing at Royal Aircraft Establishment, Farnborough, England
[RAE-TR-80107] p0122 N82-21565
DAY, R. L.
Delineation of soil temperature regimes from HCMM data
[E82-10042] p0119 N82-19617
Delineation of soil temperature regimes from HCMM data
[E82-10141] p0070 N82-21668
DE LOOR, G. P.
The Dutch ROVE program p0057 A82-21026
DEALMEIDA, F. C.
System of forecasting agricultural crops using satellite observations of Earth
[E82-10079] p0067 N82-20602
DEAN, A. M., JR.
Electromagnetic subsurface measurements
[AD-A108192] p0106 N82-18469
DEERING, D. W.
Simple radiative transfer model for relationships between canopy biomass and reflectance p0057 A82-20422
DEJESUSPARADA, N.
CNPq/INPE LANDSAT system
[E82-10023] p0118 N82-16441
Report on a short course in remote sensing and the geological applications of LANDSAT MSS imagery at INPE
[E82-10024] p0091 N82-16442
Remote sensing data applied to land-use survey at the Paraiba Valley
[E82-10025] p0081 N82-16443
Brazilian remote sensing activities, current and prospective needs
[E82-10026] p0132 N82-16444
The utilization of orbital images as an adequate form of control of preserved areas
[E82-10065] p0078 N82-20588
Amazonas project Application of remote sensing techniques for the integrated survey of natural resources in Amazonas
[E82-10069] p0078 N82-20592
Survey of the cane-growing area of the state of Sao Paulo using LANDSAT data, Safra Year 1979/80, volume 2
[E82-10071] p0067 N82-20594
Land use in the Paraiba Valley through remotely sensed data
[E82-10072] p0079 N82-20595
Study project of intrusive rocks States of Espirito Santo and Rio de Janeiro, south and east of Minas Gerais and southeast of the state of Sao Paulo
[E82-10076] p0092 N82-20599
Elevation of a cane-growing area of the state of Sao Paulo using LANDSAT data
[E82-10077] p0067 N82-20600
Relation of the activities of the IPDF/INPE project (reforestation subproject) during the year 1979
[E82-10078] p0067 N82-20601
System of forecasting agricultural crops using satellite observations of Earth
[E82-10079] p0067 N82-20602
The LANDSAT system operated in Brazil by CNPq/INPE - results obtained in the area of mapping and future perspectives
[E82-10080] p0121 N82-20603
An algorithm for spatial hoirarchy clustering
[E82-10081] p0121 N82-20604
Dynamic study of the upper Sao Francisco River and the Tres Marias reservoir using MSS/LANDSAT images
[E82-10082] p0108 N82-20605
DELIMA, A. M.
Utilization of Aerochrome 2443 film for identification and estimating wheat growing areas
[INPE-2197-PRE/006] p0066 N82-19639
Survey of the cane-growing area of the state of Sao Paulo using LANDSAT data, Safra Year 1979/80, volume 2
[E82-10071] p0067 N82-20594
Elevation of a cane-growing area of the state of Sao Paulo using LANDSAT data
[E82-10077] p0067 N82-20600
DEMEDEIROS, J. S.
Relation of the activities of the IPDF/INPE project (reforestation subproject) during the year 1979
[E82-10078] p0067 N82-20601
DEMENTEV, V. N.
Structure of hardware and software at a regional center for the automated processing of aerial and space remote-sensing images p0130 A82-28128
DEMORAESNOVO, E. M. L.
Remote sensing data applied to land-use survey at the Paraiba Valley
[E82-10025] p0081 N82-16443
DENEAU, M.
Snow cover monitoring using AVHRR data from TIROS and NOAA satellites p0105 A82-27614
DENNERT-MOELLER, E.
Evaluation of aerial photogrammetric camera and aircraft scanner pictures from tidal lands - Digital correlation and classification of multitemporal imagery data
p0127 A82-26049
DEOLIVEIRA, J. R.
Data collection platforms Applications to hydrology
[INPE-2246-PRE/030] p0107 N82-19304
DEOLIVEIRA, L. L.
Convergence zones in the South Atlantic and their influence on the precipitation regime in Northeastern Brazil
[INPE-2307-TDL/074] p0097 N82-19778
DESANTANA, C. C.
Relation of the activities of the IPDF/INPE project (reforestation subproject) during the year 1979
[E82-10078] p0067 N82-20601
DESOUZA, R. C. M.
Automatic analysis of multispectral images
[INPE-2212-MD/009] p0133 N82-19520
DEUELL, R. L.
Use of GOES and TIROS/NOAA satellite data for snow-cover mapping p0101 A82-22145
DEWITT, D. P.
A multiband radiometer and data acquisition system for remote sensing field research
[E82 10142] p0134 N82-21669
DEY, B.
The Canadian north - Utility of remote sensing for environmental monitoring p0074 A82-24962
DIAS, L. A. V.
Simplified algorithm for calculating radiative transfer in satellite images
[INPE-2169-RPE/385] p0118 N82-16450
DIAS, M. R.
System of forecasting agricultural crops using satellite observations of Earth
[E82-10079] p0067 N82-20602
DIAS, O. P., JR.
System of forecasting agricultural crops using satellite observations of Earth
[E82-10079] p0067 N82-20602
DICK, R.
Instrumentation for remote reflectance and radiance measurements p0130 A82-27652
DICKINSON, K.
Digital analysis of spatial and spectral features from airborne MSS of a forested region p0061 A82-27647
Relief effects and the use of terrain models in SAR image processing p0086 N82-21475
DICKSON, C. R.
Demonstration of a long-range atmospheric tracer system using perfluorocarbons
[PB82-106246] p0081 N82-16613
DIETZ, R. N.
Demonstration of a long-range atmospheric tracer system using perfluorocarbons
[PB82-106246] p0081 N82-16613
DILLARD, J. P.
Applications systems verification and transfer project Volume 5 Operational applications of satellite snow-cover observations, northwest United States
[NASA-TP-1826] p0109 N82-20621
DIXON, R. G.
Heat Capacity Mapping Mission (HCMM) Interpretation of imagery over Canada
[E82-10070] p0079 N82-20593
DJERRARI, A.
Remote sensing applied to basement tectonics of the calcareous High Atlas /Morocco/ p0089 A82-26014
DJUKIC-HUSAR, J.
Airborne in-situ measurement of particulate sulfur and sulfuric acid with flame photometry and thermal analysis
p0073 A82-20999
DOBLAR, R. A.
Structure and variability of the Alboran Sea frontal system p0093 A82-20447
DOME, G. J.
Sigma/deg/ signature of the Amazon rain forest obtained from the Seasat scatterometer p0125 A82-21027
DOMOKOSH, D.
Monitoring of the thermal pollution of natural channels of water using infrared aerial photography
p0104 A82-27471
DORAISWAMY, P. C.
Preliminary evaluation of spectral, normal and meteorological crop stage estimation approaches
[E82-10059] p0065 N82-19634
DOS ANJOS, C. E.
Study project of intrusive rocks States of Espirito Santo and Rio de Janeiro, south and east of Minas Gerais and southeast of the state of Sao Paulo
[E82-10076] p0092 N82-20599
DOSSANTOS, A. P.
Utilization of Aerochrome 2443 film for identification and estimating wheat growing areas
[INPE-2197-PRE/006] p0066 N82-19639
DOSSANTOS, A. R.
Study project of intrusive rocks States of Espirito Santo and Rio de Janeiro, south and east of Minas Gerais and southeast of the state of Sao Paulo
[E82 10076] p0092 N82-20599
DOSSANTOS, J. R.
Method of interpretation of remote sensing data and applications to vegetation
[INPE-2215-MD/010] p0066 N82-19640
The utilization of orbital images as an adequate form of control of preserved areas
[E82-10065] p0078 N82-20588
DOYLE, H. M.
AgRISTARS Interim catalog ground data summary, data acquisition year 1979
[E82-10032] p0064 N82-19608
DUCHOSSOIS, G.
The first ESA remote sensing satellite system ERS-1
p0094 A82-27608
DUCRUIX, J.
Preliminary models of the core field
[E82-10129] p0087 N82-21659
Continuation of potential field data to a common altitude
[E82-10138] p0123 N82-21665
Separation of internal and external fields A new technique of data screening
[E82-10139] p0123 N82-21666
DUDENEY, J. R.
Ionospheric troughs in Antarctica p0073 A82-21217
DUGGIN, M. J.
Ground level reflectance measurement techniques - An evaluation with emphasis on the importance of spectral calibration p0116 A82-27689
DUTRA, L. V.
Automatic analysis of multispectral images
[INPE-2212-MD/009] p0133 N82-19520
DUVAL, W. P.
Coastal upwelling ecosystems analysis Atlas of the JOINT I aircraft winds for the 500 foot level
[PB82-114703] p0097 N82-19796

E

EASTWOOD, L. F., JR.
Program on stimulating operational private sector use of Earth observation satellite information
[E82-10131] p0138 N82-21660
EDWARDS, N. C., JR.
Evaluation of two AN/APS-94 side-looking airborne radar systems in the detection of search and rescue targets
[AD-A108404] p0132 N82-18486
EGAN, W. G.
Effect of aerosols on optical remotely sensed data
p0115 A82-27654
EGGE, D.
Experiments in satellite Doppler control positioning at sea p0086 N82-20581
EHLERS, M.
Increase in correlation accuracy of remote sensing imagery by digital filtering p0113 A82-25454
Evaluation of aerial photogrammetric camera and aircraft scanner pictures from tidal lands - Digital correlation and classification of multitemporal imagery data
p0127 A82-26049
EHRICH, R. W.
Spatial reasoning in remotely sensed data
p0105 A82-27592
EIDENSHINK, J. C.
Remote sensing applications to resource problems in South Dakota
[E82-10027] p0132 N82-16445
EL KOCHRI, A.
Remote sensing applied to basement tectonics of the calcareous High Atlas /Morocco/ p0089 A82-26014
ELACHI, C.
Spaceborne radar observation of the earth surface
p0127 A82-27578
A shuttle scanning laser altimeter for topographic mapping p0083 A82-27632
Observation of the Earth by radar
[NASA-TM-76830] p0124 N82-21687
ELLIOTT, D.
Spatial reasoning in remotely sensed data
p0105 A82-27592
ELVARTYNOV, I. N.
Experience with a variety of studies of earth resources in the Kalmyk ASSR using space imagery
p0131 A82-28130

EMORI, Y.
Phenomena modelling of remotely sensed data by image rationing
p0076 A82-27670

ENDERBERG, N. P.
Development of a breadboard cooler for infrared remote sensing payloads, phase 1
[FOK-RV-R-81-064] p0134 N82-19653

ENDLICH, R. M.
An experimental program to provide remote measurement and analysis of ocean waves, sea level winds and balanced pressure in support of Seasat-A
[PB81-246035] p0095 N82-16697

ENG, K.
An information adaptive system study report and development plan
[NASA-CR-166768] p0120 N82-19644

EPIPHANIO, J. C. N.
Methodology of the interpretation of remote sensing data and applications in pedology
[INPE-2211-MD/008] p0078 N82-19641

ERISMANN, K. H.
A system for quantitative determination of species and vitalities of urban trees on color-infrared photographs
p0074 A82-24958

ERKIN, A. N.
Methods for the processing of synthetic-aperture radar signals when solving problems of the national economy /Review/
p0113 A82-26726

ESTES, J. E.
Flexible processing of remote sensing data through integration of image processing and geobased information systems
p0116 A82-27667

ESTES, J. M.
Digital correlation of DDRS data
[NASA-CR-167494] p0118 N82-16452

ESTES, R. H.
Some new methods in geomagnetic field modeling applied to the 1960 - 1980 epoch
[NASA-TM-83868] p0083 N82-17714

EVANS, W. F. J.
Mid-latitude summertime measurements of stratospheric NO2
p0074 A82-25149

EVERSON, N. A.
Publications and reports on contracts and grants, 1980
[PB82-103219] p0138 N82-17792

EVSIUKOV, N. N.
Possibilities of using experience gained from the thematic mapping of the moon in studies of earth resources by remote sensing methods
p0083 A82-28138

F

FAINTICH, M. B.
Matrix data analysis Color/B and W coding is not always enough
[AD-A108406] p0084 N82-18930

FARAH, J. L.
Analysis of a discrete-time linear model for geothermal flux reconnaissance from two or three aircraft infrared measurements
p0075 A82-27627
Application of machine processing of visible and thermal data to the study of the geothermal area of Cerro Prieto, Mexico
p0117 A82-27693

FAUST, N. L.
Development and implementation of a low cost micro computer system for Landsat analysis and geographic data base application
p0129 A82-27649

FAVARD, J.-C.
Airborne remote sensing in east Greenland
p0090 A82-27695

FAVRE, A.
A system for quantitative determination of species and vitalities of urban trees on color-infrared photographs
p0074 A82-24958

FAY, T. H.
An intelligent earth sensing information system
p0137 A82-22149

FEDCHENKO, P. P.
The spectral reflectance of certain soils
p0059 A82-26577

FEDINA, A. E.
Landscape mapping and physical-geographical classification of the eastern part of the Chechen-Ingush, ASSR using space imagery
p0073 A82-20339

FERBER, G. J.
Demonstration of a long-range atmospheric tracer system using perfluorocarbons
[PB82-106246] p0061 N82-16613

FETT, W.
Optimal network density for atmospheric recording
p0079 N82-20776

FILHO, L. G. M.
System of forecasting agricultural crops using satellite observations of Earth
[E82-10079] p0067 N82-20602

FILHO, M. V.
Methodology of the interpretation of remote sensing data and applications in pedology
[INPE-2211-MD/008] p0078 N82-19641

FILHO, P. H.
Method of interpretation of remote sensing data and applications to vegetation
[INPE-2215-MD/010] p0066 N82-19640
Relation of the activities of the IPDF/INPE project (reforestation subproject) during the year 1979
[E82-10078] p0067 N82-20601

FINKLER, J. A.
Documentation of computer procedures for labeling spring grains and discriminating between spring wheat and barley using LANDSAT data
[E82-10030] p0063 N82-16448

FITZPATRICK-LINS, K.
Sampling for thematic map accuracy testing
p0111 A82-20411

FLIEGEL, H.
Session III of the VLBI/Laser intercomparison task of the NASA crustal dynamics project
[NASA-CR-168427] p0063 N82-17708

FORESTI, C.
Remote sensing data applied to land use survey at the Paraiba Valley
[E82-10025] p0081 N82-16443
Land use in the Paraiba Valley through remotely sensed data
[E82-10072] p0079 N82-20595

FORMAGGIO, A. R.
Methodology of the interpretation of remote sensing data and applications in pedology
[INPE-2211-MD/008] p0078 N82-19641

FORSYTHE, R. G.
NOSS altimeter algorithm specifications
[NASA-RP-1083] p0095 N82-16683

FORTUNE, M. A.
The severity of the Brazilian freeze of July 1981, as monitored by satellite
[INPE-2231-RPE/399] p0064 N82-17746

FOSHAGE, J.
Program on stimulating operational private sector use of Earth observation satellite information
[E82-10131] p0138 N82-21660

FRANCIS, C. R.
Imaging microwave radiometer Phase A study Volume 1: Executive summary
[ESS/SS-1006] p0132 N82-18564

FRANKLIN, J.
Scene analysis for wildland fire-fuel characteristics in a Mediterranean climate
p0060 A82-27624

FRASER, R. S.
The effect of finite field size on classification and atmospheric correction
[NASA-TM-83818] p0120 N82-19645

FRIDMAN, SH. D.
Evaluation of snow-cover pollution in industrial regions using satellite TV images
p0103 A82-27464

FRIEDMAN, A. L.
Airborne remote sensing in east Greenland
p0090 A82-27695

FRIEDMANN, D. E.
Operational resampling for correcting images to a geocoded format
p0114 A82-27590
The use of digital terrain model in the rectification of satellite-borne imagery
p0115 A82-27626

FROBIN, W.
Calibration and model reconstruction in analytical close-range stereophotogrammetry I - Mathematical fundamentals
p0111 A82-20403
Calibration and model reconstruction in analytical close-range stereophotogrammetry II - Special evaluation procedures for rasterstereography and moire topography
p0126 A82-22141

FRUTKIN, A. W.
Earth sensing from space - Commercial and international aspects
p0138 A82-27669

FUGONO, N.
Remote sensing of rainfall rates using airborne microwave rain-scatterometer/radiometer
p0105 A82-27639

FUHRER, J.
A system for quantitative determination of species and vitalities of urban trees on color-infrared photographs
p0074 A82-24958

FUJIMURA, S.
Exterior algebraic processing for remotely sensed multispectral and multitemporal images
p0112 A82-21041

FUNG, A. K.
Microwave remote sensing. Active and passive Volume 1 - Microwave remote sensing fundamentals and radiometry
p0126 A82-22877

FURMAN, M. D.
Development and implementation of a low cost micro computer system for Landsat analysis and geographic data base application
p0129 A82-27649

G

GAGE, S. H.
Application of satellite frost forecast technology to other parts of the United States, phase 2
[NASA-CR-166827] p0121 N82-20607

GALAT, D. L.
Calcium carbonate precipitation in Pyramid Lake, Nevada, as monitored by satellite - 1978 and 1980
p0105 A82-27634

GALDEANO, A.
Preliminary models of the core field
[E82-10129] p0087 N82-21659

GARCIA, G.
Application of machine processing of visible and thermal data to the study of the geothermal area of Cerro Prieto, Mexico
p0117 A82-27693

GARZA, M.
Application of machine processing of visible and thermal data to the study of the geothermal area of Cerro Prieto, Mexico
p0117 A82-27693

GASPAROVIC, R. F.
High precision radiometric temperature measurements of the ocean surface
p0094 A82-27640

GAUTIER, C.
Workshop on the application of existing satellite data to the study of ocean surface energetics, 19-21 November 1980, University of Wisconsin-Madison
p0094 A82-24822

GELLER, A. G.
Investigation of the vegetative covers on ploughed areas by SLAR
p0058 A82-21031

GEORGES, T. M.
Recovering ocean waveheight from HF radar sea echoes distorted by imperfect ionospheric reflection
[PB82-113283] p0096 N82-17805

GHAZI, A.
Atlas of the global distribution of the total ozone concentration according to satellite measurements
[MITT-28] p0078 N82-19740

GIERATHS, W.
Satellite scatterometer feasibility study Volume 1 Technical results
[ESA-CR(P)-1492-VOL-1] p0133 N82-19650

GILG, W.
Satellite scatterometer feasibility study Volume 1 Technical results
[ESA-CR(P)-1492-VOL-1] p0133 N82-19650

GLOBA, G. IA.
Construction of digital models of statistically uniform characteristics on the basis of multispectral space imagery
p0117 A82-28144

GLOERSEN, P.
An optical model for the microwave properties of sea ice
[NASA-TM-83865] p0095 N82-17561

GLUSHKO, E. V.
Reconstruction of a present-day landscape map of a central part of Italy using space images
p0081 A82-20340

GODA, L.
Investigation of silting and currents in Lake Balaton by use of hydraulic models and aerial and space photographs
p0104 A82-27472

GOETZ, A. F. H.
A data base of geologic field spectra
p0090 A82-27600

GOLDBLATT, I. A.
An evaluation of the utility of smaller Landsat resolution elements /Resolution of Landsat resolution/
p0114 A82-27625

GOLDFINGER, A. D.
Optimal spatial filtering and transfer function for SAR ocean wave spectra
p0094 A82-27596

GOMEZ, G.
Program on stimulating operational private sector use of Earth observation satellite information
[E82-10131] p0138 N82-21660

GONFREVILLE, P.
Towards an operational SPOT system - A preliminary assessment
p0114 A82-27607

GONIN, G. B.
Spaceborne photography for the study of earth resources
p0126 A82-22397

GOOD, W.
Towards the definition of optimum sensor specifications for microwave remote sensing of snow
p0125 A82-21035

GOODENOUGH, D. G.
Digital analysis of spatial and spectral features from airborne MSS of a forested region p0061 A82-27647
Relief effects and the use of terrain models in SAR image processing
p0086 N82-21475

GOODFELLOW, L. C.
The use of digital multi-date Landsat imagery in terrain classification
p0111 A82-20409

GOODIER, B. G.
Methods of editing cloud and atmospheric layer affected pixels from satellite data
[E82-10046] p0119 N82-19621

GRAHAM, M. H.
ELAS - A geobased information system that is transferable to several computers p0115 A82-27666

GRANKOV, A. G.
Some peculiarities of formulation and solution of inverse problems in microwave radiometry of the ocean surface and atmosphere
p0093 A82-21921

GRANTHAM, W. L.
SASS measurements of the Ku band radar signature of the ocean
p0093 A82-21917

GREEGOR, D.
A gradient model of vegetation and climate utilizing NOAA satellite imagery Phase 1 Texas transect
[E82-10107] p0069 N82-21648

GREEN, K. M.
Digital processing of tropical forest habitat in Bangladesh and the development of a low cost processing facility at the National Zoo Smithsonian Institution
p0063 A82-27687

GRIESBACH, J. C.
Mapping in tropical forests - A new approach using the laser APR p0081 A82-20407

GRIFFIN, C. R.
Digital correlation of DDRS data
[NASA-CR-167494] p0118 N82-16452

GRUEN, A.
The accuracy potential of the modern bundle block adjustment in aerial photogrammetry p0111 A82-20401

GUENTHER, G. C.
Error analysis of pulse location estimates for simulated bathymetric lidar returns
[PB82-109448] p0096 N82-17803

GUIGNARD, J. P.
Overview of digital processing of SAR data
p0128 A82-27589

GUINDON, B.
Digital analysis of spatial and spectral features from airborne MSS of a forested region p0061 A82-27647
Relief effects and the use of terrain models in SAR image processing p0086 N82-21475

GUPTA, R. P.
Geotechnical applications of Landsat image analysis of Bhakra Dam Reservoir India p0102 A82-26838

GURGANUS, E. A.
Influence of dissolved organic materials on turbid water optical properties and remote-sensing reflectance
p0093 A82-20445
Laboratory upwelled radiance and reflectance spectra of Kerr reservoir sediment waters
[NASA-TP-1993] p0110 N82-21774

GURNEY, C. M.
The use of contextual information to improve land cover classification of digital remotely sensed data
p0112 A82-21094

GUSEV, A. V.
Classification of systems for digital terrain simulation
p0117 A82-28468

GUSTIN, A. V.
Natural resources inventories by computer-satellite mapping techniques in Chaco State. Argentine Republic. South America p0116 A82-27688

GUTTERIDGE, L.
Features of a generalized digital Synthetic Aperture Radar processor p0128 A82-27595

H

H-MILLER, S.
Application of HCMM data to regional geologic analysis for mineral and energy resource evaluation
[E82-10137] p0092 N82-21664

HAAS, R. H.
Assessing mesquite-grass vegetation condition from Landsat p0059 A82-25457

HAERING, P.
Analyses of the Eastern Pacific without ship PAPA data p0093 A82-19139

HAIMERL, M.
Satellite scatterometer feasibility study Volume 1 Technical results
[ESA-CR(P)-1492-VOL-1] p0133 N82-19650

HAIVALA, H.
Remote sensing applications to resource problems in South Dakota
[E82-10027] p0132 N82-16445

HALL, A. J.
Flash flood forecasting
[WMO-577] p0107 N82-18671

HALLADA, W. A.
Flexible processing of remote sensing data through integration of image processing and geobased information systems p0116 A82-27667

HANCOCK, D. W.
NOSS altimeter algorithm specifications
[NASA-RP-1064] p0095 N82-16683

HANNAFORD, J. F.
Applications systems verification and transfer project Volume 3 Operational applications of satellite snow cover observations in California
[NASA-TP-1824] p0108 N82-20619

HANS, P.
Satellite scatterometer feasibility study Volume 1 Technical results
[ESA-CR(P)-1492-VOL-1] p0133 N82-19650
Satellite scatterometer feasibility study Volume 2 Data extraction algorithm and error simulation for wind sensor
[ESA-CR(P)-1492-VOL-2] p0133 N82-19651

HANSEN, R. F.
Wheat stress indicator model. Crop Condition Assessment Division (CCAD) data base interface driver. user's manual
[E82-10031] p0064 N82-19607
Wheat stress indicator model. Early Warning (EW) data base interface driver. user's manual
[E82-10115] p0069 N82-21652

HARALICK, R. M.
Spatial reasoning in remotely sensed data
p0105 A82-27592

HARLAN, J. C.
Dryland pasture and crop conditions as seen by HCMM
[E82-10074] p0067 N82-20597

HARRIS, R.
An experiment in probabilistic relaxation for terrain cover classification of Kuwait from Landsat imagery
p0062 A82-27680

HARRISON, C. G. A.
Investigations of medium wavelength magnetic anomalies in the Eastern Pacific using Magsat data
[E82-10047] p0119 N82-19622

HARRISS, R. C.
Influence of dissolved organic materials on turbid water optical properties and remote-sensing reflectance
p0093 A82-20445

HART, W. D.
Surface wave statistics and spectra during high sea state conditions in the North Atlantic
[AD-A109832] p0098 N82-20827

HATAKEYAMA, Y.
A formation process of an oceanic vortex analyzed by multi-temporal remote sensing p0095 A82-27674

HAUSE, D.
Remote sensing applications to resource problems in South Dakota
[E82-10027] p0132 N82-16445

HAWK, J. R.
Photogrammetry software A package for everyone
[AD-A108098] p0118 N82-17570

HEFFTER, J. L.
Demonstration of a long-range atmospheric tracer system using perfluorocarbons
[PB82-106246] p0081 N82-16613

HEILMAN, J. L.
HCMM detection of high soil moisture areas
p0059 A82-24963

HELD, D.
Simulation and studies of spaceborne synthetic aperture radar image quality with reduced bit rate
p0128 A82-27594

HELD, D. N.
Seasat data utilization project
[NASA-CR-168557] p0097 N82-18660

HERBERT, P.
Snow cover monitoring using AVHRR data from TIROS and NOAA satellites p0105 A82-27614

HERMANCE, J. F.
Electromagnetic deep-probing (100-1000 KMS) of the Earth's interior from artificial satellites Constraints on the regional emplacement of crustal resources
[E82-10043] p0084 N82-19618
Electromagnetic deep-probing (100-1000 KMS) of the Earth's interior from artificial satellites Constraints on the regional emplacement of crustal resources
[E82-10044] p0085 N82-19619
Electromagnetic deep-probing (100-1000 KMS) of the Earth's interior from artificial satellites Constraints on the regional emplacement of crustal resources
[E82-10155] p0087 N82-21679

HERNANDEZ, R.
Application of machine processing of visible and thermal data to the study of the geothermal area of Cerro Prieto. Mexico p0117 A82-27693

HERSCHY, R. W.
Detection of natural disasters via Meteosat
p0075 A82-27040

HICKS, D.
The 1981 Argentina ground data collection
[E82-10127] p0070 N82-21658

HICKS, D. R.
Notes for Brazil sampling frame evaluation trip
[E82-10060] p0066 N82-19635

HIDE, R.
Spherical harmonic representation of the main geomagnetic field for world charting and investigations of some fundamental problems of physics and geophysics
[E82-10075] p0086 N82-20598

HIERHOLZER, E.
Calibration and model reconstruction in analytical close-range stereophotogrammetry I - Mathematical fundamentals p0111 A82-20403
Calibration and model reconstruction in analytical close-range stereophotogrammetry II - Special evaluation procedures for rasterstereography and moire topography
p0126 A82-22141

HILALI, E. A.
Remote sensing applied to basement tectonics of the calcareous High Atlas /Morocco/ p0089 A82-26014

HIXSON, M. M.
Evaluation of a segment-based LANDSAT full-frame approach to corp area estimation
[E82-10067] p0066 N82-20590
Determination of the optimal level for combining area and yield estimates
[E82-10146] p0071 N82-21673

HODGES, T.
Preliminary evaluation of spectral, normal and meteorological crop stage estimation approaches
[E82-10059] p0065 N82-19634
AgRISTARS Supporting research US crop calendars in support of the early warning project
[E82-10158] p0072 N82-21682

HOELZL, H.
Satellite scatterometer feasibility study Volume 1 Technical results
[ESA-CR(P)-1492-VOL-1] p0133 N82-19650

HOFER, R.
Comparison of conventionally measured sea surface temperature and wind speed with data retrieved from satellite-borne microwave radiometry p0093 A82-24063

HOFMAN, D. J.
Ozone measurements to 48Km with chemiluminescent ozone detectors
[AD-A110342] p0134 N82-21808

HOFMANN, O.
Digital photography techniques p0112 A82-21398

HOLGUIN, O. J.
Partially processed multispectral scanner LANDSAT high-density tapes reformatting system (HDT-AM/AMC) design specifications
[E82-10020] p0118 N82 16438

HONEY, F. R.
A vegetation response model applied to range inventory and monitoring using Landsat MSS data
p0060 A82-27643
A low cost NOAA/TIROS AVHRR receiving station
p0130 A82-27681

HONVALUT, C.
The first ESA remote sensing satellite system ERS-1
p0094 A82-27608

HOOGEBOOM, P.
The Dutch ROVE program p0057 A82-21026

HOOPER, N. J.
Response of the marine community to satellite-derived oceanic information p0095 A82-27684
An analysis of user requirements for operational land satellite data p0116 A82-27685

HORITA, M.
Analyses of the Eastern Pacific without ship PAPA data p0093 A82-19139

HORTON, C. L.
As-built design specification for the CLASFYG program
[E82-10092] p0068 N82-21644

HORVATH, R.
Documentation of computer procedures for labeling spring grains and discriminating between spring wheat and barley using LANDSAT data
[E82-10030] p0063 N82-16448
Notes for Brazil sampling frame evaluation trip
[E82-10060] p0066 N82-19635
The 1981 Argentina ground data collection
[E82-10127] p0070 N82-21658

HOUGHTON, W. M.
Influence of dissolved organic materials on turbid water optical properties and remote-sensing reflectance
p0093 A82-20445

HOVER, G. L.
Evaluation of two AN/APS-94 side-looking airborne radar systems in the detection of search and rescue targets
[AD-A108404] p0132 N82-18466

HOWARTH, P. J.
Change detection in the Peace-Athabasca Delta using digital Landsat data p0101 A82-24959
Enhancement of Landsat data for Hudson Bay lowlands vegetation p0114 A82-27623

HOWE, R. C.
Non-parametric classification of abandoned coal mine features using multioriented and ratio transformed Landsat data p0090 A82-27694

HUCKLE, H. F.
Taxonomic classification of world map units in crop producing areas of Argentina and Brazil with representative US soil series and major land resource areas in which they occur
[E82-10058] p0065 N82-19633

HUMMER-MILLER, S.
Registration of heat capacity mapping mission day and night images p0113 A82-22146

HUNEYCUTT, B.
Simulation and studies of spaceborne synthetic aperture radar image quality with reduced bit rate
p0128 A82-27594

HUSAR, R. B.
Airborne in-situ measurement of particulate sulfur and sulfuric acid with flame photometry and thermal analysis
p0073 A82-20999

HUTCHINSON, C. F.
Techniques for combining Landsat and ancillary data for digital classification improvement p0111 A82-20410

HYDE, R. F.
An evaluation of the utility of smaller Landsat resolution elements /Resolution of Landsat resolution/
p0114 A82-27625

I

IABLONSKII, L. I.
Complex examination of photorectifiers
p0131 A82-28466

IANOVICH, A. V.
Methods for the processing of synthetic-aperture radar signals when solving problems of the national economy /Review/ p0113 A82-26726

IASINSKII, G. I.
Thermal viewing system for studying the earth's resources p0125 A82-21022

IDSO, S. B.
Humidity measurement by infrared thermometry
p0075 A82-26844

II, F. A. M.
Selection of attributes applied to multispectral images
[INPE-2303 TDL/072] p0121 N82-19927

IISAKA, J.
Phenomena modelling of remotely sensed data by image rationing p0076 A82-27670

INAMURA, M.
Exterior algebraic processing for remotely sensed multispectral and multitemporal images
p0112 A82-21041

INOMATA, H.
Remote sensing of rainfall rates using airborne microwave rain-scatterometer/radiometer p0105 A82-27639

ISHIZAWA, Y.
The Japanese MOS and Los program
p0129 A82-27606

ISHLINSKII, A. IU.
Scientific lectures on aviation and astronautics 1980
p0137 A82-27501

IUNG, E.
Interpretation of multispectral aerial photographs of Lake Mueggelsee p0104 A82-27473

J

JACKSON, R. D.
Dew and vapor pressure as complicating factors in the interpretation of spectral radiance from crops
p0060 A82-27617

JAFFE, K. D.
Diurnal variation of summer convection over West Africa and the Tropical Eastern Atlantic during 1974 and 1978
p0075 A82-26700

JAIN, S. C.
Passive bathymetric measurements in the Bruce Peninsula region of Ontario p0129 A82-27642

JARVIS, M. J.
Ionospheric troughs in Antarctica p0073 A82-21217

JAWORSKI, E.
HCMM night-time thermal IR imaging experiment in Michigan p0115 A82-27655

JEAN, B. R.
Volumetric effects in cross-polarized airborne radar data p0058 A82-21032

JEANSOULIN, R.
Field-by-field multitemporal analysis of aerial scanner data geometrically corrected by means of a sliding model
p0115 A82-27651

JINICH, A.
Application of machine processing of visible and thermal data to the study of the geothermal area of Cerro Prieto, Mexico p0117 A82-27693

JOBUSCH, C. D.
Determination of the optimal level for combining area and yield estimates
[E82-10146] p0071 N82-21673

JOHNSON, D. R.
The development and testing of methods to infer midlatitude precipitation intensity from geosynchronous satellite infrared data
[AD-A108881] p0120 N82-19788

JOHNSON, E. R.
Strategies for using remotely sensed data in hydrologic models
[E82-10156] p0109 N82-21680

JOHNSON, M. P.
Methods of editing cloud and atmospheric layer affected pixels from satellite data
[E82-10046] p0119 N82-19621

Methods of editing cloud and atmospheric layer affected pixels from satellite data
[E82-10154] p0123 N82-21678

JOHNSTON, I. L.
Enhancement of Landsat data for Hudson Bay lowlands vegetation p0114 A82-27623

JONES, M.
Image quality control in the Meteosat ground processing system p0125 A82-21090

JONES, P. H.
Use of thermal inertia determined by HCMM to predict nocturnal cold prone areas in Florida
[E82-10040] p0064 N82-19615

Use of thermal inertia determined by HCMM to predict nocturnal cold prone areas in Florida
[E82-10157] p0071 N82-21681

JONES, R. M.
Recovering ocean waveheight from HF radar sea echoes distorted by imperfect ionospheric reflection
[PB82-113283] p0096 N82-17805

JORDON, L. E., III
Development and implementation of a low cost micro computer system for Landsat analysis and geographic data base application p0129 A82-27649

JOSEPH, D. W.
An investigation of the ozone plume from a small city
p0074 A82-26329

JUNGMAN, L. J.
Remote sensing in Latin America Technology and markets for the 1980's
[AD-A108784] p0138 N82-20626

JUSTICE, C.
Information extraction from remotely sensed data - A user view p0112 A82-21089

A comparison of unsupervised classification procedures on LANDSAT MSS data for an area of complex surface conditions in Basilicata, Southern Italy
[E82-10038] p0119 N82-19613

K

KAHLE, A. B.
A data base of geologic field spectra
p0090 A82-27600

KAMST, F. H.
A regional air quality model for the Kwinana industrial area of Western Australia p0075 A82-26403

KANE, R. P.
Comparison of storm-time changes of geomagnetic field at ground and at MAGSAT altitudes
[E82-10148] p0087 N82-21675

KAPLAN, F. B.
Development and applications of techniques to process hydrometeor distribution data
[AD-A109929] p0109 N82-20822

KARAKHANIAN, A. S.
The relationship between seismicity and lineaments of the Anatolian-Caucasian-Iranian segment of the Mediterranean fold belt p0089 A82-20341

KASISCHKE, E. S.
The use of wave contrast measurements in the evaluation of SAR/gravity models p0130 A82-27675

KATERGIANNAKIS, U.
Dust from the Sahara in satellite images
p0075 N82-20802

KATTI, R. K.
Utilisation of remote sensing in resources identification and land use in India - An integrated approach
p0076 A82-27701

KAUFMAN, Y. J.
Contrast reduction by the atmosphere and retrieval of nonuniform surface reflectance p0112 A82-20423

The effect of finite field size on classification and atmospheric correction
[NASA-TM-83818] p0120 N82-19645

KAZMIN, A. S.
The use of Meteor-satellite image data in oceanography p0093 A82-20344

KEAFER, L. S., JR.
Mission definition for a large-aperture microwave radiometer spacecraft p0131 N82-16155

KECHICHIAN, J. A.
Topex orbit sustenance maneuver design
[AIAA PAPER 82-0202] p0094 A82-27091

KEEFER, T. N.
Strategies for using remotely sensed data in hydrologic models
[E82-10156] p0109 N82-21680

KEENE, G. T.
A concept for an advanced earth resources satellite system p0127 A82-27579

KELLER, H. J.
A system for quantitative determination of species and vitalities of urban trees on color-infrared photographs
p0074 A82-24958

KERLIN, J.
Modern methods for monitoring and controlling the timeliness, accuracy, and completeness of data for meteorological analysis p0073 A82-19179

KERR, J. B.
Mid-latitude summertime measurements of stratospheric NO2 p0074 A82-25149

KEYDEL, W.
Application and experimental verification of an empirical backscattering cross section model for the earth's surface
p0081 A82-21036

KHORRAM, S.
Remote sensing of salinity in the San Francisco Bay Delta p0102 A82-26839

KIEFER, R. W.
Wetland mapping from digitized aerial photography
[E82-10019] p0118 N82-16437

Multidisciplinary research on the application of remote sensing to water resources problems
[E82-10021] p0106 N82-16439

KIENKO, IU. P.
Present and future studies of natural resources and the environment from space p0138 A82-27506

Experience with a variety of studies of earth resources in the Kalmyk ASSR using space imagery
p0131 A82-28130

KIMBALL, A. W.
Orbital performance of a 1.6 micrometer DMSP snow/cloud discrimination sensor p0130 A82-27653

KINDELAN, M.
Geometric correction of airborne multispectral scanner images p0130 A82-27706

KINNUCAN, P.
Earth-scanning satellites lead resource hunt
p0117 A82-28343

KINSLER, M. C.
Preliminary evaluation of spectral, normal and meteorological crop stage estimation approaches
[E82-10059] p0065 N82-19634

KIRBY, M. E.
Comparisons of laser profilometer sea ice roughness statistics with surface truthed data and SLAR imagery
p0094 A82-27619

KIRKPATRICK, B.
Program on stimulating operational private sector use of Earth observation satellite information
[E82-10131] p0138 N82-21660

KISELEVSKII, L. I.
Color characteristics of the earth's surface determined on the basis of spectroscopy results from Salyut 4
p0073 A82-19826

KISHI, S.
Detection of volcanic ash fall area from Landsat MSS CCT data Eruption of Mt Ontake in 1979
p0076 A82-27650

KLEINTZ, M.
Sea state measurement with a two frequency scatterometer (theory)
[ESA-TT-710] p0096 N82-17802

KLEMAS, V.
Locating prehistoric archaeological sites using Landsat
p0129 A82-27638

KLOSE, J. C.
The Seasat low rate data processing system
p0093 A82-24061

KLUMPH, S. G.
Landsat MSS applied to rangeland management in Western Canada p0063 A82-27697

KNAPP, M.
Thermal IR detection of submarine gas seepages in the western Istra off-shore area /Yugoslavia/
p0076 A82-27661

KNIZHNIKOV, IU. F.
Survey and mapping of shallow water bodies and the distribution of the river runoff of solids on the basis of multispectral aerial and space photographs
p0103 A82-27467

The atlas Geographical Results of Spaceborne Multispectral Experiments p0077 A82-28133

KNOX, N.
Assessment of the quality of GATE area rainfall data from a Nimbus-5 radiometer
[NASA-CR-168512] p0109 N82-20807

KOBRICK, M.
A shuttle scanning laser altimeter for topographic mapping p0083 A82-27632

KOBZEV, V. N.
Correlation identification of stellar configurations for purposes of the coordinate referencing of aerial and space images p0117 A82-28141

KOHLI, S.
Airborne in-situ measurement of particulate sulfur and sulfuric acid with flame photometry and thermal analysis
p0073 A82-20999

KOLLENKARK, J. C.
Influence of solar illumination angle on soybean canopy reflectance p0063 A82-28153

Soybean canopy reflectance as influenced by cultural practices
[E82-10105] p0068 N82-21647

KOLTSOV, I. M.
Characteristics of the use of laser-mirror scanners for image processing in cartography and aerial photography
p0117 A82-28143

KONDIURIN, V. D.
A photometric method for depth determination by aerial photography p0101 A82-19831

KONDO, S.
The location of three-dimensional linear objects by using multiple projections p0111 A82-20404

KONDRATEV, K. IA.
The spectral reflectance of certain soils
p0059 A82-26577

The possibilities of microwave remote sensing for the study of water resources and their pollution
p0102 A82-27458

KONDRATOVA, IU. I.
Landscape mapping and physical-geographical classification of the eastern part of the Chechen-Ingush ASSR using space imagery p0073 A82-20339

KONIG, B.
Program on stimulating operational private sector use of Earth observation satellite information
[E82-10131] p0138 N82-21660

KORNEEV, IU. N.
Analytic methods of geodetic referencing of nontopographic images p0083 A82-28134

KOROVINA, T. L.
The relationship between seismicity and lineaments of the Anatolian-Caucasian-Iranian segment of the Mediterranean fold belt p0089 A82-20341

KOSCEC, B.
Thermal IR detection of submarine gas seepages in the western Istra off-shore area /Yugoslavia/
p0076 A82-27661

KOVAL, A. D.
The effectiveness of instrumented visual studies of the earth from space p0114 A82-27505

The earth resources program for the long-term orbital station Salyut 6 p0131 A82-28132

KOVALENOK, V. V.
The effectiveness of instrumented visual studies of the earth from space p0114 A82-27505

The earth resources program for the long-term orbital station Salyut 6 p0131 A82-28132

KOVALEV, A. A.
Color characteristics of the earth's surface determined on the basis of spectroscopy results from Salyut 4 p0073 A82-19826

KOWALIK, W. S.
A relation between Landsat digital numbers, surface reflectance, and the cosine of the solar zenith angle p0114 A82-26841

KOZAK, R. C.
Cliff and slope topography of part of the Grand Canyon, Arizona as characterized on a Seasat radar image p0082 A82-26843

KOZHEVNIKOV, B. K.
Structure of hardware and software at a regional center for the automated processing of aerial and space remote-sensing images p0130 A82-28128

KOZODEROV, V. V.
Evaluation of the state of crops from satellite data p0059 A82-27393

KRASNIKOV, D. N.
Thermal viewing system for studying the earth's resources p0125 A82-21022

KRASNOPEVTSEVA, B. V.
The use of space photographs to compile water-amelioration maps p0106 A82-28137

KRASNOV, V. I.
Optimal methods of computerized image conversion p0111 A82-19833

KRAVCHENKO, IU. A.
Classification of systems for digital terrain simulation p0117 A82-28468

KRAVTSOVA, V. I.
Survey and mapping of shallow water bodies and the distribution of the river runoff of solids on the basis of multispectral aerial and space photographs p0103 A82-27467
The atlas 'Geographical Results of Spaceborne Multispectral Experiments p0077 A82-28133

KRESSMAN, R. I.
Ionospheric troughs in Antarctica p0073 A82-21217

KREY, P. W.
Demonstration of a long-range atmospheric tracer system using perfluorocarbons
[PB82-106246] p0081 N82-16613

KRIULKOV, V. A.
Noncontact methods for the quality control of water resources p0104 A82-27475

KRUL, L.
A radar signature model for partially coherent scattering from irregular surfaces p0079 A82-21038

KRYLOV, S. L.
Optimal methods of computerized image conversion p0111 A82-19833

KUEHNLE, A.
Satellite scatterometer feasibility study Volume 1 Technical results
[ESA-CR(P)-1492-VOL-1] p0133 N82-19650

KULKOV, N. V.
Structure of hardware and software at a regional center for the automated processing of aerial and space remote-sensing images p0130 A82-28128

KUMAR, R.
Implementation of the Space Oblique Mercator projection in a production environment p0129 A82-27628

KUMAR, S. S.
Satellite sensing for extraction of groundwater resources information p0105 A82-27613

KUPRIIANOV, V. V.
Aerospace methods for the study of water resources and their pollution p0102 A82-27457

KUZMICHEV, V. V.
Remote sensing of the structure of taiga landscapes p0059 A82-27397

KYEVSKII, SH.
Primary processing of and possibilities of using data from the meteorological satellite TIROS-N p0103 A82-27470

L

LABUTINA, I. A.
Experimental evaluation of methods of the automated interpretation of crops from a Fragment MSS image p0057 A82-20349
Survey and mapping of shallow water bodies and the distribution of the river runoff of solids on the basis of multispectral aerial and space photographs p0103 A82-27467

LAIRET, R.
Strategies and uses of small distributed analysis centers as in the natural resource inventory of Venezuela p0115 A82-27636

LAKHTANOV, G. A.
Polarimetric method for the remote sensing of oil slicks on the sea surface p0095 A82-28135

LALLY, J. P.
Development and applications of techniques to process hydrometeor distribution data
[AD-A109929] p0109 N82-20822

LAME, D. B.
Seasat data utilization project
[NASA CR-168557] p0097 N82-18660

LAMOIS DOWNS, A.
Use of GOES and TIROS/NOAA satellite data for snow-cover mapping p0101 A82-22145

LANGEL, R. A.
Some new methods in geomagnetic field modeling applied to the 1960 - 1980 epoch
[NASA-TM-83868] p0083 N82-17714

LANZ, K.
Strategies and uses of small distributed analysis centers as in the natural resource inventory of Venezuela p0115 A82-27636

LARABEE, J. K.
An optical model for the microwave properties of sea ice
[NASA-TM-83865] p0095 N82-17561

LAUTENSCHLAGER, L.
Registration verification of SEA/AR fields
[E82-10083] p0068 N82-21635

LAVKULICH, L. M.
The use of digital multi-date Landsat imagery in terrain classification p0111 A82-20409

LAVROVA, N. P.
Construction of digital models of statistically uniform characteristics on the basis of multispectral space imagery p0117 A82-28144

LAZAREWICZ, A. R.
MAGSAT anomaly profiles of the eastern Indian Ocean
[E82-10066] p0086 N82-20589

LEAF, C. F.
Applications systems verification and transfer project. Volume 4 Operational applications of satellite snow cover observations Colorado Field Test Center
[NASA-TP-1825] p0108 N82-20620

LEATON, B. R.
Spherical harmonic representation of the main geomagnetic field for world charting and investigations of some fundamental problems of physics and geophysics
[E82-10075] p0086 N82-20598

LECHI, G.
Heat Capacity Mapping Mission (HCMM) program Study of geological structure of Sicily and other Italian areas
[E82-10073] p0091 N82-20596

LEDESMA, L. L.
Natural resources inventories by computer-satellite mapping techniques in Chaco State, Argentine Republic, South America p0116 A82-27688

LEE, D. C. L.
Utilization of Aerochrome 2443 film for identification and estimating wheat growing areas
[INPE-2197-PRE/006] p0066 N82-19639
Survey of the cane-growing area of the state of Sao Paulo using LANDSAT data. Safra Year 1979/80, volume 2
[E82-10071] p0067 N82-20594
Elevation of a cane-growing area of the state of Sao Paulo using LANDSAT data
[E82-10077] p0067 N82-20600

LEMOUEL, J. L.
Preliminary models of the core field
[E82-10129] p0087 N82-21659
Continuation of potential field data to a common altitude
[E82-10138] p0123 N82-21665
Separation of internal and external fields A new technique of data screening
[E82-10139] p0123 N82-21666

LENNINGTON, R. K.
Evaluation of large area crop estimation techniques p0061 A82-27662

LEPRIEUR, C
Snow cover monitoring using AVHRR data from TIROS and NOAA satellites p0105 A82-27614

LESNIK, IU. N.
The effect of anthropogenic factors on the dynamics of lakes in the plains of Central Asia /studied on the basis of space photographs/ p0103 A82-27469

LEVINE, D. M.
Comparison of sigma/deg/ obtained from the conventional definition with sigma/deg/ appearing in the radar equation for randomly rough surfaces p0112 A82-21039

LEVINE, I.
Implementation of the Space Oblique Mercator projection in a production environment p0129 A82-27628

LEVITSKII, I. IU.
Possibilities of using experience gained from the thematic mapping of the moon in studies of earth resources by remote sensing methods p0083 A82-28138

LI, F.
Simulation and studies of spaceborne synthetic aperture radar image quality with reduced bit rate p0128 A82-27594

LI, R. Y.
Crop classification using airborne radar and Landsat data p0058 A82-21033

LI, T. C.
Measurement of atmospheric emission using a balloon-borne cryogenic Fourier spectrometer p0074 A82-21432

LIAN, M. S.
Low-latitude cloudiness and climate feedback - Comparative estimates from satellite data p0075 A82-26980

LIANG, T.
An airphoto key for major tropical crops p0058 A82-22142

LICHTENEGGER, J.
Detailed land use classification based on multitemporal Landsat-MSS-data p0076 A82-27657

LICHY, D. E.
Integrated sensor system for collection of wave data applied to coastal engineering design p0084 A82-27602

LIFANOV, P. S.
Methods for the processing of synthetic-aperture radar signals when solving problems of the national economy /Review/ p0113 A82-26726

LILLESAND, T. M.
Use of GOES and TIROS/NOAA satellite data for snow-cover mapping p0101 A82-22145

LILLEY, F. E. M.
Ideal phase in estimating the spatial gradient of magnetic daily variations recorded by magnetometer arrays p0127 A82-26000

LIND, A.
Applications of aircraft and satellite data for the study of archaeology and environment - Mekong Delta, Vietnam p0091 A82-27705

LINDELL, L. T.
Mapping of water quality using Landsat imagery p0106 A82-27692

LINDER, R. L.
Spectral reflectance of hydrophytes p0102 A82-24960

LINDNER, A. J.
Satellite observed cloud patterns associated with excessive precipitation outbreaks
[PB80-215130] p0073 A82-19177

LING, H. S.
Sampling for thematic map accuracy testing p0111 A82-20411

LINK, L. E.
Airborne laser systems use in terrain mapping p0082 A82-27584
Thermal vegetation canopy model studies
[AD-A106422] p0064 N82-16455

LINO, C. D.
General configuration and internal disposition of equipment in a satellite for collecting environmental data
[INPE-2240-PRE/020] p0078 N82-19256

LIPES, R. G.
Seasat data utilization project
[NASA-CR-168557] p0097 N82-18660

LITMAN, V.
Guidelines for spaceborne microwave remote sensors
[NASA-RP-1086] p0133 N82-19647

LIU, H.-S.
Ore deposits in Africa and their relation to the underlying mantle p0090 A82-26604

LIUBOVNYI, N. D.
The use of data from satellite-borne microwave scanning radiometers for the automated compilation of operational maps of ice cover for the Arctic Ocean p0095 A82-28145

LLOYD, D.
Applications systems verification and transfer project Volume 7 Cost/benefit analysis for the ASVT on operational applications of satellite snow-cover observations
[NASA-TP-1828] p0109 N82-20623

LOATS, H.
Applications systems verification and transfer project Volume 7. Cost/benefit analysis for the ASVT on operational applications of satellite snow-cover observations
[NASA-TP-1828] p0109 N82-20623

LODWICK, G. D.
Topographic mapping using Landsat data p0082 A82-27615

LOMBARDO, M. A.
Remote sensing data applied to land-use survey at the Paraiba Valley
[E82-10025] p0081 N82-16443
Land use in the Paraiba Valley through remotely sensed data
[E82-10072] p0079 N82-20595

LOPATIN, D. V.
Structural analysis of the basement of the East European platform by remote sensing methods p0089 A82-20342

LOPEZ, A.
Application of machine processing of visible and thermal data to the study of the geothermal area of Cerro Prieto, Mexico p0117 A82-27693

LOUGEAY, R.
Landsat thermal imaging of alpine regions p0079 A82-22147

LOVELACE, U. M.
The microwave radiometer spacecraft A design study Executive summary p0131 N82-16154

LOWES, F. J.
Spherical harmonic representation of the main geomagnetic field for world charting and investigations of some fundamental problems of physics and geophysics
[E82-10075] p0086 N82-20598

LOWITZ, G. E.
Data rate reduction Impact of image data compression on end to end data management of a multispectral payload
[REPT-44/130] p0120 N82-19654

LUCHT, L. A. M.
Utilization of Aerochrome 2443 film for identification and estimating wheat growing areas
[INPE-2197-PRE/006] p0066 N82-19639
Survey of the cane-growing area of the state of Sao Paulo using LANDSAT data. Safra Year 1979/80, volume 2
[E82-10071] p0067 N82-20594
Elevation of a cane-growing area of the state of Sao Paulo using LANDSAT data
[E82-10077] p0067 N82-20600

LUCY, R. F.
Spectritek - A multispectral electron-optic pushbroom camera p0129 A82-27633

LUKES, G. E.
Computer-assisted photo interpretation research at USAETL
[AD-A109366] p0121 N82-20628

LULLA, K.
Non-parametric classification of abandoned coal mine features using multioriented and ratio transformed Landsat data p0090 A82-27694

LURE, I. K.
Experimental evaluation of methods of the automated interpretation of crops from a Fragment MSS image p0057 A82-20349

LUTJENARMS, J. R. E.
Interaction between the Agulhas current and the subtropical convergence
[CSIR-RR-384] p0098 N82-20824

LYCTHUAN-LEE, T. G.
Development of rotation sample designs for the estimation of crop acreages
[E82-10117] p0070 N82-21654

LYON, J. G.
Seasat imagery for detection of coastal Wetlands p0063 A82-27700

LYON, R. J. P.
A relation between Landsat digital numbers, surface reflectance, and the cosine of the solar zenith angle p0114 A82-26841
Strategies and uses of small distributed analysis centers as in the natural resource inventory of Venezuela p0115 A82-27636
Integration of LANDSAT with geology and airborne geophysics into an operational mineral exploration system
[E82 10028] p0091 N82-16446

LYONS, T. J.
A regional air quality model for the Kwinana industrial area of Western Australia p0075 A82-26403

M

MACINTYRE, M.
Future Earthnet Dissemination Systems (FEDS) study Executive summary
[REPT-3318] p0124 N82-21698

MACMEDAN, M. L.
The Seasat low rate data processing system p0093 A82-24061

MAETZLER, C.
Towards the definition of optimum sensor specifications for microwave remote sensing of snow p0125 A82-21035

MAIA, F. C. S.
Utilization of Aerochrome 2443 film for identification and estimating wheat growing areas
[INPE-2197-PRE/006] p0066 N82-19639
Survey of the cane-growing area of the state of Sao Paulo using LANDSAT data. Safra Year 1979/80, volume 2
[E82-10071] p0067 N82-20594
Elevation of a cane-growing area of the state of Sao Paulo using LANDSAT data
[E82-10077] p0067 N82-20600

MALILA, W.
A technique for automatic labeling of Landsat agricultural scene elements by analysis of temporal-spectral patterns p0062 A82-27678

MALIN, J. T.
Sample selection in foreign similarity regions for multicrop experiments
[E82-10118] p0070 N82-21655

MALIN, S. R. C.
Spherical harmonic representation of the main geomagnetic field for world charting and investigations of some fundamental problems of physics and geophysics
[E82-10075] p0086 N82-20598

MARCHENKO, V. V.
Development of cooperation between CMEA member countries in the development and utilization of space-based systems for the remote sensing of earth resources and the environment p0138 A82-27543

MARESCA, J. W.
Recovering ocean waveheight from HF radar sea echoes distorted by imperfect ionospheric reflection
[PB82-113283] p0096 N82-17805

MARESCA, J. W., JR.
An experimental program to provide remote measurement and analysis of ocean waves, sea level winds and balanced pressure in support of Seasat-A
[PB81-246035] p0095 N82-16697

MARINI, A.
Heat Capacity Mapping Mission (HCMM) program Study of geological structure of Sicily and other Italian areas
[E82-10073] p0091 N82-20596

MARINO, C. M.
Integration of Landsat, geological and geophysical data for use in thematic mapping at regional scale p0090 A82-27672

MARKHAM, B. L.
Land cover classification accuracy as a function of sensor spatial resolution p0076 A82-27665

MARSH, S. E.
A relation between Landsat digital numbers, surface reflectance, and the cosine of the solar zenith angle p0114 A82-26841

MARTIN, D. W.
The use of satellite data in rainfall monitoring p0101 A82-22873

MARTIN, M. V.
Evaluation of large area crop estimation techniques p0061 A82-27662

MARTIN, P.
Direct determination of the two dimensional image spectrum from raw synthetic aperture radar data p0122 N82-21474

MARTINKO, E. A.
The application of remote sensing to resource management and environmental quality programs in Kansas
[E82-10029] p0063 N82-16447

MARTSOLF, J. D.
Use of thermal inertia determined by HCMM to predict nocturnal cold prone areas in Florida
[E82-10040] p0064 N82-19615
Application of satellite frost forecast technology to other parts of the United States, phase 2
[NASA-CR-166827] p0121 N82-20607
A satellite frost forecasting system for Florida p0079 N82-20615
Use of thermal inertia determined by HCMM to predict nocturnal cold prone areas in Florida
[E82-10157] p0071 N82-21681

MASUKO, H.
Remote sensing of rainfall rates using airborne microwave rain-scatterometer/radiometer p0105 A82-27639

MATSON, M.
Evaluation of HCMM satellite data for estuarine tidal circulation patterns and thermal inertia soil moisture measurements
[E82-10064] p0108 N82-20587

MATZLER, CH.
Soil moisture determination - Experiments with passive microwave radiometers p0057 A82-19529

MAUSEL, P. W.
Non-parametric classification of abandoned coal mine features using multioriented and ratio transformed Landsat data p0090 A82-27694

MAYHEW, M. A.
Satellite and surface geophysical expression of anomalous crustal structure in Kentucky and Tennessee
[NASA-TM-82163] p0084 N82-17715

MAYNARD, P. F.
The logit classifier - A general maximum likelihood discriminant for remote sensing applications p0128 A82-27591

MAZOUR, T. J.
Evaluation of two AN/APS-94 side-looking airborne radar systems in the detection of search and rescue targets
[AD-A108404] p0132 N82-18466

MCCARTHY, J. F.
Seasat imagery for detection of coastal Wetlands p0063 A82-27700

MCCLAIN, C. R.
Surface wave statistics and spectra during high sea state conditions in the North Atlantic
[AD-A109832] p0098 N82-20827

MCCONNELL, D.
Workshop on the application of existing satellite data to the study of ocean surface energetics, 19-21 November 1980, University of Wisconsin-Madison p0094 A82-24822

MCCONNELL, P. R.
Features of a generalized digital Synthetic Aperture Radar processor p0128 A82-27595

MCDANIEL, K. C.
Assessing mesquite-grass vegetation condition from Landsat p0059 A82-25457

MCELROY, C. T.
Mid-latitude summertime measurements of stratospheric NO2 p0074 A82-25149

MCEVOY, N.
Study of Earth Resources Satellite (ERS) data reduction unit
[BAE-TP-7905] p0120 N82-19649

MCGINNIS, D. F., JR.
Evaluation of HCMM satellite data for estuarine tidal circulation patterns and thermal inertia soil moisture measurements
[E82-10064] p0108 N82-20587

MCGUIRE, W. G.
Evaluation of large area crop estimation techniques p0061 A82-27662

MCLAUGHLIN, B.
A timely and accurate potato acreage estimate from Landsat - Results of a demonstration p0060 A82-27621

MCMILLAN, J. D.
NOSS altimeter algorithm specifications
[NASA-RP-1083] p0095 N82-16683

MCPHERRON, R. L.
Harmonic structure of Pc 3-4 pulsations p0082 A82-26266

MEAD, G. H.
Some new methods in geomagnetic field modeling applied to the 1960 - 1980 epoch
[NASA-TM-83868] p0083 N82-17714

MEAD, R. A.
Landsat classification accuracy assessment procedures p0137 A82-20412

MEADOR, R.
Resourceful decisions LANDAT in Michigan
[E82-10037] p0078 N82-19601

MEISNER, D. E.
Use of GOES and TIROS/NOAA satellite data for snow-cover mapping p0101 A82-22145

MEKLER, Y.
Contrast reduction by the atmosphere and retrieval of nonuniform surface reflectance p0112 A82-20423

MELYKUTI, G.
Area determination by means of the method of finite elements p0082 A82-26048

MENDEZ, R.
Application of machine processing of visible and thermal data to the study of the geothermal area of Cerro Prieto, Mexico p0117 A82-27693

MENDONCA, F. J.
Use of Landsat data for automatic classification and area estimation of sugar-cane plantation in Sao Paulo state, Brazil p0058 A82-21092
Utilization of Aerochrome 2443 film for identification and estimating wheat growing areas
[INPE-2197-PRE/006] p0066 N82-19639
Survey of the cane-growing area of the state of Sao Paulo using LANDSAT data. Safra Year 1979/80, volume 2
[E82-10071] p0067 N82-20594
Elevation of a cane-growing area of the state of Sao Paulo using LANDSAT data
[E82-10077] p0067 N82-20600

MENVIELLE, M.
Separation of internal and external fields A new technique of data screening
[E82-10139] p0123 N82-21666

MERCHANT, J. W.
Utilization of spatial complexity in computer classified Landsat MSS data for multi-factoral thematic mapping p0129 A82-27648

MERGERSON, J. W.
Crop area estimates using ground-gathered and Landsat data A multitemporal approach p0062 A82-27676

MERTZ, F. C.
Flexible processing of remote sensing data through integration of image processing and geobased information systems p0116 A82-27667

MEUNIER, J. F.
Relief effects and the use of terrain models in SAR image processing p0086 N82-21475

MEUNIER, J.-F.
Digital analysis of spatial and spectral features from airborne MSS of a forested region p0061 A82-27647

MEYLAN, P.
Soil moisture determination - Experiments with passive microwave radiometers p0057 A82-19529

MIGLIO, G.
Integration of Landsat, geological and geophysical data for use in thematic mapping at regional scale p0090 A82-27672

MIKHAILOV, A. E.
Ring structures in the earth s crust, and their significance for geology and methods for their investigation p0091 A82-28136

MIKHAILOV, V. A.
Albedo and brightness coefficients of snow cover p0103 A82-27465
Analog devices for the processing of aerial and space images for the study of water resources p0104 A82-27476

MIKHEEV, V. P.
Characteristics of the use of laser-mirror scanners for image processing in cartography and aerial photography p0117 A82-28143

MILLAN, M.
Remote SO2 emission measurements with correlation spectrometers from volcanoes p0077 A82-27704

MILLER, G. E.
A look at the commonly used LANDSAT vegetation indices
[E82-10123] p0070 N82-21657

MILLER, J. R.
An approach to path radiance correction in MSS images p0115 A82-27629
Passive bathymetric measurements in the Bruce Peninsula region of Ontario p0129 A82-27642

MILLER, L. D.
Monitoring forest land cover alteration in Thailand with the analysis of ancillary and digital Landsat data p0062 A82-27673

MILLER, W. F.
Application of remote sensing to state and regional problems
[E82-10033] p0078 N82-19609

MILOSER, T. L.

Integrated sensor system for collection of wave data applied to coastal engineering design p0094 A82-27602

MISEZHNIKOV, G. S.

Methods for the processing of synthetic-aperture radar signals when solving problems of the national economy /Review/ p0113 A82-26726

MISHIN, V. P.

Investigation of earth resources using rocket and space technology p0130 A82-28127

MITCHELL, J. L.

SASS measurements of the Ku-band radar signature of the ocean p0093 A82-21917

MITSUO, F. A., II

Automatic analysis of multispectral images
[INPE-2212-MD/009] p0133 N82-19520

MKRTCHIAN, F. A.

Machine implementation of algorithms for the mapping of soil moisture on the basis of microwave-radiometer measurements p0131 A82-28142

MOELLMAN, D. E.

Profiling sensitivity to image quality
[AD-A108405] p0084 N82-18931

MOERL, P.

The use of the airborne lidar system 'ALEX F 1' for aerosol tracing in the lower troposphere p0073 A82-20226

Sounding the aerosol distribution over the Upper Rhine Valley in the Valley in the Speyer area by means of lidar p0079 N82-20782

MONTGOMERY, D. R.

Seasat data utilization project
[NASA-CR-168557] p0097 N82-18660

MOORE, D. G.

HCMM detection of high soil moisture areas p0059 A82-24963

MOORE, R. K.

Microwave remote sensing: Active and passive. Volume 1 - Microwave remote sensing fundamentals and radiometry p0126 A82-22877

MORAVEC, G. F.

Applications systems verification and transfer project. Volume 4: Operational applications of satellite snow cover observations. Colorado Field Test Center
[NASA-TP-1825] p0108 N82-20620

MOREIRA, J. C.

Automatic analysis of multispectral images
[INPE-2212-MD/009] p0133 N82-19520

MOREIRA, M. A.

Utilization of Aerochrome 2443 film for identification and estimating wheat growing areas
[INPE-2197-PRE/006] p0066 N82-19639

Survey of the cane-growing area of the state of Sao Paulo using LANDSAT data. Safra Year 1979/80, volume 2
[E82-10071] p0067 N82-20594

Elevation of a cane-growing area of the state of Sao Paulo using LANDSAT data
[E82-10077] p0067 N82-20600

MORENO, V.

Geometric correction of airborne multispectral scanner images p0130 A82-27706

MORGAN, J.

Detection of natural disasters via Meteosat p0075 A82-27040

MORITZ, H.

Developments in geodesy within the scope of Helmut Wolf's work p0084 N82-19604

MORLEY, B. M.

Airborne lidar measurements of smoke plume distribution, vertical transmission, and particle size p0073 A82-21386

MORONE, J. J.

An information adaptive system study report and development plan
[NASA-CR-166768] p0120 N82-19644

MOROZ, P. I.

Application of space remote sensing data in forestry p0063 A82-28131

MOROZ, V. A.

Complex examination of photorectifiers p0131 A82-28466

MORRIS, W. D.

Influence of dissolved organic materials on turbid water optical properties and remote-sensing reflectance p0093 A82-20445

Laboratory upwelled radiance and reflectance spectra of Kerr reservoir sediment waters
[NASA-TP-1993] p0110 N82-21774

MORROW, C. T.

Application of satellite frost forecast technology to other parts of the United States, phase 2
[NASA-CR-166827] p0121 N82-20607

Freeze prediction model p0067 N82-20609

MORZIER, C.

Soil moisture determination - Experiments with passive microwave radiometers p0057 A82-19529

MOZALEVSKII, V. G.

Automation of the processing of aerial and space images for forest inventory p0057 A82-20350

MURATA, K.

The location of three-dimensional linear objects by using multiple projections p0111 A82-20404

MURCRAY, F. H.

Measurement of atmospheric emission using a balloon-borne cryogenic Fourier spectrometer p0074 A82-21432

MURCRAY, F. J.

Measurement of atmospheric emission using a balloon-borne cryogenic Fourier spectrometer p0074 A82-21432

MURPHY, L. A.

A timely and accurate potato acreage estimate from Landsat - Results of a demonstration p0060 A82-27621

MYERS, V. I.

Remote sensing applications to resource problems in South Dakota
[E82-10027] p0132 N82-16445

MYHRE, R. J.

Satellite photos can aid navigation on aerial photo missions p0126 A82-22148

N

NAUMOV, M. I.

Investigation of the vegetative covers on ploughed areas by SLAR p0058 A82-21031

NAZEMETZ, J.

An intelligent earth sensing information system p0137 A82-22149

NETO, J. B.

A microcomputer for control of data collection platforms
[INPE-2104-RPE/331] p0133 N82-18881

NEWMAN, P.

Applications systems verification and transfer project. Volume 7: Cost/benefit analysis for the ASVT on operational applications of satellite snow-cover observations
[NASA-TP-1828] p0109 N82-20623

NEWTON, R. W.

Volumetric effects in cross-polarized airborne radar data p0058 A82-21032

NGUYEN, D.

Thermal vegetation canopy model studies
[AD-A106422] p0064 N82-16455

NICHOLAS, J.

Guidelines for spaceborne microwave remote sensors
[NASA-RP-1086] p0133 N82-19647

NIELSEN, N. B.

Airborne lidar measurements of smoke plume distribution, vertical transmission, and particle size p0073 A82-21386

NIERO, M.

Remote sensing data applied to land-use survey at the Paraiba Valley
[E82-10025] p0081 N82-16443

Land use in the Paraiba Valley through remotely sensed data
[E82-10072] p0079 N82-20595

NIEVES, M. J.

AgRISTARS: Early warning and crop condition assessment. Patch image processor user's manual
[E82-10055] p0065 N82-19630

NIKITIN, A. M.

The effect of anthropogenic factors on the dynamics of lakes in the plains of Central Asia /studied on the basis of space photographs/ p0103 A82-27469

NIKITIN, P. A.

The use of data from satellite-borne microwave scanning radiometers for the automated compilation of operational maps of ice cover for the Arctic Ocean p0095 A82-28145

NIKOLAEVA, E. M.

Potential use of space photographs obtained from the manned orbital station Salyut-5 in order to compile a set of small-scale thematic maps of mountain and piedmont regions of Central Asia p0083 A82-28139

NISHIMURA, T.

A formation process of an oceanic vortex analyzed by multi-temporal remote sensing p0095 A82-27674

NIXON, P. R.

Methods of editing cloud and atmospheric layer affected pixels from satellite data
[E82-10046] p0119 N82-19621

Methods of editing cloud and atmospheric layer affected pixels from satellite data
[E82-10154] p0123 N82-21678

NJOKU, E. G.

Comparison of conventionally measured sea surface temperature and wind speed with data retrieved from satellite-borne microwave radiometry p0093 A82-24063

NORRIS, P.

Future Earthnet Dissemination Systems (FEDS) study. Executive summary
[REPT-3318] p0124 N82-21698

NORWINE, J.

A gradient model of vegetation and climate utilizing NOAA satellite imagery. Phase 1: Texas transect
[E82-10107] p0069 N82-21648

NOVAES, R. A.

Utilization of Aerochrome 2443 film for identification and estimating wheat growing areas
[INPE-2197-PRE/006] p0066 N82-19639

System of forecasting agricultural crops using satellite observations of Earth
[E82-10079] p0067 N82-20602

NOVO, E. M. L. D.

Methodology of the interpretation of remote sensing data and applications in geomorphology
[INPE-2209-MD/007] p0091 N82-19642

Land use in the Paraiba Valley through remotely sensed data
[E82-10072] p0079 N82-20595

NUALCHAWEE, K.

Monitoring forest land cover alteration in Thailand with the analysis of ancillary and digital Landsat data p0062 A82-27673

O

OBEDKOV, IU. L.

The use of space photographs for hydrogeological studies of the Baikal region and Mongolia p0103 A82-27468

OCONNOR, P. J.

Relationship of hydrothermal phenomena within the Leinster Granite to crustal fractures delineated from Landsat imagery p0089 A82-26015

OERTEL, G. F.

The relationship among sea surface roughness variations, oceanographic analyses, and airborne remote sensing analyses
[NASA-CR-168444] p0096 N82-17798

OGAWA, Y.

Observation of the turbulent structure in the planetary boundary layer with a kytoon-mounted ultrasonic anemometer system p0125 A82-21082

OHARA, T.

Observation of the turbulent structure in the planetary boundary layer with a kytoon-mounted ultrasonic anemometer system p0125 A82-21082

OHBA, R.

The location of three-dimensional linear objects by using multiple projections p0111 A82-20404

OHTA, K.

An approach to path radiance correction in MSS images p0115 A82-27629

OJIMA, T.

Remote sensing of rainfall rates using airborne microwave rain-scatterometer/radiometer p0105 A82-27639

OKAMI, N.

An approach to path radiance correction in MSS images p0115 A82-27629

OKAMOTO, K.

Remote sensing of rainfall rates using airborne microwave rain-scatterometer/radiometer p0105 A82-27639

ONITSUKA, M.

An approach to path radiance correction in MSS images p0115 A82-27629

ORTH, R.

The use of digital terrain model in the rectification of satellite-borne imagery p0115 A82-27626

OSHIMA, T.

Environmental studies by multispectral scanner under large-scale civil engineering construction p0063 A82-27691

OSMER, S. R.

Evaluation of two AN/APS-94 side-looking airborne radar systems in the detection of search and rescue targets
[AD-A108404] p0132 N82-18466

OTOOLE, T.

Development and applications of techniques to process hydrometeor distribution data
[AD-A109929] p0109 N82-20822

OTTERMAN, J.

Effects of the atmosphere on the detection of surface changes from Landsat multispectral scanner data p0125 A82-21091

OVERBOSCH, E. G.

Development of a breadboard cooler for infrared remote sensing payloads, phase 1
[FOK-RV-R-81-064] p0134 N82-19653

OZGA, M.

An autodigitizing procedure for ground-data labelling of Landsat pixels p0062 A82-27682

P

PAIK, H. J.

Superconducting tensor gravity gradiometer p0126 A82-23045

PALEY, H. N.

A data base of geologic field spectra p0090 A82-27600

PANKRATOVA, E. I.

The possibility of determining snow-meltage fronts using Meteor-satellite multispectral data /with Kazakhstan considered as an example/ p0102 A82-27463

PARK, A. B.

Data base requirements in support of crop models p0060 A82-27588

PARK, J. K.

Simple radiative transfer model for relationships between canopy biomass and reflectance p0057 A82-20422

PARRISH, J. B.

HCMM night-time thermal IR imaging experiment in Michigan p0115 A82-27655

PASOTTI, P.

The Pampean Plain studied with Landsat images p0089 A82-26013

READEX FICHE best copy available

PAVATE, T. V.
Utilisation of remote sensing in resources identification and land use in India - An integrated approach p0076 A82-27701

PAYNE, R. W.
Sonora exploratory study for the detection of wheat-leaf rust
[E82-10133] p0070 N82-21661

PEACOCK, K.
High precision radiometric temperature measurements of the ocean surface p0094 A82-27640

PEARCE, C. M.
Landsat MSS applied to rangeland management in Western Canada p0063 A82-27697

PEARSON, R. W.
ELAS - A geobased information system that is transferable to several computers p0115 A82-27666

PECK, E. L.
Strategies for using remotely sensed data in hydrologic models
[E82-10156] p0109 N82-21680

PEEBLES, C.
Satellite photograph interpretation p0127 A82-25460

PELLETIER, R. T.
Multiresource inventory methods pilot test p0060 A82-27601

PELZER, H.
Some criteria for the accuracy and the reliability of networks p0086 N82-20580

PENGELLY, J. W.
Study of Earth Resources Satellite (ERS) data reduction unit
[BAE-TP-7905] p0120 N82-19649

PENN, L. M.
Development of a surface isolation estimation technique suitable for application of polar orbiting satellite data
[E82-10122] p0123 N82-21656

PEREIRA, A. E. C.
Simplified algorithm for calculating radiative transfer in satellite images
[INPE-2169-RPE/385] p0118 N82-16450

PERLOV, V. V.
Thermal viewing system for studying the earth's resources p0125 A82-21022

PERSAUD, K.
Report on a short course in remote sensing and the geological applications of LANDSAT MSS imagery at INPE
[E82-10024] p0091 N82-16442

PETERSEN, G. W.
Delineation of soil temperature regimes from HCMM data
[E82-10042] p0119 N82-19617
Delineation of soil temperature regimes from HCMM data
[E82-10141] p0070 N82-21668

PFEIFFER, B.
Analysis of the direction-dependent radiation behavior in multispectral scanning data p0125 A82-21399

PHILIPSON, W. R.
An airphoto key for major tropical crops p0058 A82-22142
Ground level reflectance measurement techniques - An evaluation with emphasis on the importance of spectral calibration p0116 A82-27689

PHILLIPS, D. M.
An aerial survey of water turbidity and laser depth sounding performance along the Queensland Coast
[AD-A109050] p0098 N82-19802
Proposed digital cartridge recording system for WRELADS
[AD-A109484] p0134 N82-20491

PHINNEY, D. E.
Preliminary evaluation of spectral, normal and meteorological crop stage estimation approaches
[E82-10059] p0065 N82-19634
AgRISTARS: Foreign commodity production forecasting. Project test reports document, volume 1
[E82-10087] p0068 N82-21639
Project communications/documentation standards manual
[E82-10093] p0068 N82-21645

PIATKIN, V. P.
Automation of the processing of aerial and space images for forest inventory p0057 A82-20350
Structure of hardware and software at a regional center for the automated processing of aerial and space remote-sensing images p0130 A82-28128

PINNOCK, M.
Ionospheric troughs in Antarctica p0073 A82-21217

PINTER, P. J., JR.
Dew and vapor pressure as complicating factors in the interpretation of spectral radiance from crops p0060 A82-27617

PLIUTA, V. E.
Color characteristics of the earth's surface determined on the basis of spectroscopy results from Salyut 4 p0073 A82-19826

POLCYN, F. C.
Assessment of change in Bangladesh coastal regions p0076 A82-27696

POLETAEV, IU. I.
Improving the quality of aerial photography /Concerning the 'Basic principles of aerial photography'/ p0117 A82-28467

POLLARA, V. J.
Variability of reflectance measurements with sensor altitude and canopy type
[E82-10145] p0071 N82-21672

POOLE, L. R.
Influence of dissolved organic materials on turbid water optical properties and remote-sensing reflectance p0093 A82-20445

POWERS, J. S.
Application of remote sensing to state and regional problems
[E82-10033] p0078 N82-19609

PRAMANIK, M. A. H.
Assessment of change in Bangladesh coastal regions p0076 A82-27696

PRITCHARD, J.
Measurement of atmospheric emission using a balloon-borne cryogenic Fourier spectrometer p0074 A82-21432

PRITCHARD, J. A.
Evaluation of HCMM satellite data for estuarine tidal circulation patterns and thermal inertia soil moisture measurements
[E82-10064] p0108 N82-20587

PROKACHEVA, V. G.
Evaluation of snow-cover pollution in industrial regions using satellite TV images p0103 A82-27464
Albedo and brightness coefficients of snow cover p0103 A82-27465

PROTZ, R.
Manual and automatic crop identification with airborne radar imagery p0057 A82-20408

Q

QUIRK, B. K.
A comparison between aerial photography and Landsat for computer land-cover mapping p0074 A82-22143
Wetland mapping from digitized aerial photography
[E82-10019] p0118 N82-16437

QURESHY, M. N.
Geophysical and Landsat lineament mapping - An approach illustrated from west-central and south India p0089 A82-26016

R

RABINOVICH, IU. I.
The possibilities of microwave remote sensing for the study of water resources and their pollution p0102 A82-27458

RADAI, E.
Application of aerial and space photographic data in the study of subsurface water and tectonic structures p0090 A82-27466

RAJU, G.
Microwave brightness temperature pattern over the Indian subcontinent and the surrounding oceans as observed by the satellite microwave radiometer /SAMIR/ onboard Bhaskara p0093 A82-19560

RANA, S. S.
Microwave brightness temperature pattern over the Indian subcontinent and the surrounding oceans as observed by the satellite microwave radiometer /SAMIR/ onboard Bhaskara p0093 A82-19560

RANGO, A.
Applications systems verification and transfer project. Volume 1: Operational applications of satellite snow cover observations: Executive summary
[NASA-TP-1822] p0108 N82-20617
Applications systems verification and transfer project. Volume 8: Satellite snow mapping and runoff prediction handbook
[NASA-TP-1829] p0109 N82-20624

RANSON, K. J.
Soybean canopy reflectance as a function of view and illumination geometry p0061 A82-27645
Thermal vegetation canopy model studies
[AD-A106422] p0064 N82-16455

RATZ, D.
Remote sensing applied to basement tectonics of the calcareous High Atlas /Morocco/ p0089 A82-26014

REDSTONE, P.
Study of Earth Resources Satellite (ERS) data reduction unit
[BAE-TP-7905] p0120 N82-19649

REED, R. J.
Diurnal variation of summer convection over West Africa and the Tropical Eastern Atlantic during 1974 and 1978 p0075 A82-26700

REINHARDT, M. E.
The use of the airborne lidar system 'ALEX F 1' for aerosol tracing in the lower troposphere p0073 A82-20226
Sounding the aerosol distribution over the Upper Rhine Valley in the Valley in the Speyer area by means of lidar p0079 N82-20782

REMSBERG, E.
The NASA participation in the 1980 EPA PEPE/NEROS field measurements program p0075 A82-26621

RENGER, W.
The use of the airborne lidar system 'ALEX F 1' for aerosol tracing in the lower troposphere p0073 A82-20226
Sounding the aerosol distribution over the Upper Rhine Valley in the Valley in the Speyer area by means of lidar p0079 N82-20782

REUTOV, E. M.
Mixture formulas applied in estimation of dielectric and radiative characteristics of soils and grounds at microwave frequencies p0058 A82-21030

RICCI, M.
Dip determinations in photogeology p0089 A82-25453

RICH, E. I.
HCMM: Soil moisture in relation to geologic structure and lithology, northern California
[E82-10135] p0092 N82-21662

RICHARDS, J. H.
The Canadian north - Utility of remote sensing for environmental monitoring p0074 A82-24962

RICHARDSON, A. J.
Methods of editing cloud and atmospheric layer affected pixels from satellite data
[E82-10046] p0119 N82-19621
Methods of editing cloud and atmospheric layer affected pixels from satellite data
[E82-10154] p0123 N82-21678

RICHTER, J. C.
Ground registration of data from an airborne scatterometer
[E82-10084] p0068 N82-21636

RIGAL, G.
Field-by-field multitemporal analysis of aerial scanner data geometrically corrected by means of a sliding model p0115 A82-27651

RIKIMARU, A.
Environmental studies by multispectral scanner under large-scale civil engineering construction p0063 A82-27691

RILEY, J. P.
Recovering ocean waveheight from HF radar sea echoes distorted by imperfect ionospheric reflection
[PB82-113283] p0096 N82-17805

RIVIERA, G.
Gradio: Project proposal for satellite gradiometry
[NASA-TM-76796] p0134 N82-20606

ROBERTS, D. K.
Development and applications of techniques to process hydrometeor distribution data
[AD-A109929] p0109 N82-20822

ROBERTS, P. A.
Computer based technique for converting a contour map into an equispaced grid of points
[RAE-TR-80110] p0087 N82-21697

ROBERTSHAW, G. A.
Coherent scatter of microwaves from moderately rough surfaces
[AD-A106133] p0095 N82-16331

ROBINOVE, C. J.
Effects of the atmosphere on the detection of surface changes from Landsat multispectral scanner data p0125 A82-21091

ROBINSON, B. F.
Soybean canopy reflectance as a function of view and illumination geometry p0061 A82-27645
A multiband radiometer and data acquisition system for remote sensing field research
[E82-10142] p0134 N82-21669
Simulated response of a multispectral scanner over wheat as a function of wavelength and view/illumination direction
[E82-10144] p0071 N82-21671

ROBINSON, V. B.
Stochastic models of cover class dynamics p0059 A82-27586

ROBSON, A.
Detection of natural disasters via Meteosat p0075 A82-27040

RODGER, A. S.
Ionospheric troughs in Antarctica p0073 A82-21217

RODZIN, V. I.
Noncontact methods for the quality control of water resources p0104 A82-27475

ROLLER, N. E. G.
Assessment of change in Bangladesh coastal regions p0076 A82-27696

ROMANOVA, E. P.
Reconstruction of a present-day landscape map of a central part of Italy using space images p0081 A82-20340

RONZHIN, L. A.
The earth resources program for the long-term orbital station Salyut 6 p0131 A82-28132

ROSEN, J. M.
Ozone measurements to 48Km with chemiluminescent ozone detectors
[AD-A110342] p0134 N82-21808

ROSENBLUETH, J.
Application of machine processing of visible and thermal data to the study of the geothermal area of Cerro Prieto, Mexico p0117 A82-27693

ROSENFELD, A.
Multispectral texture p0113 A82-25139
Building and road extraction from aerial photographs p0074 A82-25140

ROSENFIELD, G. H.
Sampling for thematic map accuracy testing p0111 A82-20411

ROSENTHAL, R. L.
A digital technique for constructing variable-width lines
[AD-A110287] p0087 N82-21689

ROSENTHAL, W. D.
Dryland pasture and crop conditions as seen by HCMM
[E82-10074] p0067 N82-20597

ROSSI, P. M.
Integration of Landsat, geological and geophysical data for use in thematic mapping at regional scale
p0090 A82-27672

ROTHROCK, D. A.
Sea ice movements from synthetic aperture radar
[AD-A109002] p0097 N82-19435

ROY, B. H.
Data rate reduction Impact of image data compression on end to end data management of a multispectral payload
[REPT-44/130] p0120 N82-19854

ROZOV, B. S.
Characteristics of the use of laser-mirror scanners for image processing in cartography and aerial photography
p0117 A82-28143

RUBINCAM, D. P.
Information theory lateral density distribution for Earth inferred from global gravity field
[NASA-TM-83825] p0085 N82-19731

RUNAVOT, J.
Gradio Project proposal for satellite gradiometry
[NASA-TM-76796] p0134 N82-20606

RYERSON, R. A.
A timely and accurate potato acreage estimate from Landsat - Results of a demonstration p0080 A82-27621

RYGH, P. J.
Seasat data utilization project
[NASA-CR-168557] p0097 N82-18660

S

SAILOR, R. V.
MAGSAT anomaly profiles of the eastern Indian Ocean
[E82-10066] p0086 N82-20589

SAINT, G.
Snow cover monitoring using AVHRR data from TIROS and NOAA satellites p0105 A82-27614

SAKAI, H.
Measurement of atmospheric emission using a balloon-borne cryogenic Fourier spectrometer
p0074 A82-21432

SALAVATOV, R. M.
Structure of hardware and software at a regional center for the automated processing of aerial and space remote-sensing images p0130 A82-28128

SALOMONSON, V. V.
Information expectations from Landsat-D
p0128 A82-27583
Characterizing user requirements for future land observing satellites
[NASA-TM-83867] p0081 N82-17562

SANCHEZ S., R.
Inventory of eroded areas in the state of Guanajuato Mexico, by automatic analysis of Landsat images
p0076 A82-27690

SANDFORD, D. M.
An intelligent earth sensing information system
p0137 A82-22149

SAPP, C. D.
Remote sensing of sulfur dioxide effects on vegetation Volume 1 Summary
[PB82-115122] p0066 N82-19715
Remote sensing of sulfur dioxide effects on vegetation Volume 2 Data
[PB82-115130] p0066 N82-19716

SAQALLI, T.
Remote sensing applied to basement tectonics of the calcareous High Atlas /Morocco/ p0089 A82-26014

SARDAR, M. G.
Utilisation of remote sensing in resources identification and land use in India - An integrated approach
p0076 A82-27701

SARKAR, A. N.
One orogenic belt or two - A structural reinterpretation supported by Landsat data products of the Precambrian metamorphics of Singhbhum, eastern India
p0089 A82-26017

SAULSKII, V. K.
Diffusion model of cloud cover and its use in the analysis of satellite operations p0111 A82-20347

SAUSEN, T. M.
Methodology of the interpretation of remote sensing data and applications in geomorphology
[INPE-2209-MD/007] p0091 N82-19642
Dynamic study of the upper Sao Francisco River and the Tres Marias reservoir using MSS/LANDSAT images
[E82-10082] p0108 N82-20605

SAVELEV, B. I.
Optimal methods of computerized image conversion
p0111 A82-19833

SAWATZKY, D. L.
Registration of heat capacity mapping mission day and night images p0113 A82-22146

SCANVIC, J. F.
Airborne remote sensing in east Greenland
p0090 A82-27695

SCARPACE, F. L.
A comparison between aerial photography and Landsat for computer land-cover mapping p0074 A82-22143
Wetland mapping from digitized aerial photography
[E82-10019] p0118 N82-16437

SCHABER, G. C.
Cliff and slope topography of part of the Grand Canyon, Arizona as characterized on a Seasat radar image
p0082 A82-26843

SCHANDA, E.
Soil moisture determination - Experiments with passive microwave radiometers p0057 A82-19529
Towards the definition of optimum sensor specifications for microwave remote sensing of snow
p0125 A82-21035
On randomly absorbing and scattering surface layers
p0079 A82-21037

SCHELLHASE, R.
The use of the airborne lidar system 'ALEX F 1' for aerosol tracing in the lower troposphere p0073 A82-20226
Sounding the aerosol distribution over the Upper Rhine Valley in the Valley in the Speyer area by means of lidar
p0079 N82-20782

SCHENKE, H. W.
Experiments in satellite Doppler control positioning at sea p0086 N82-20581

SCHMER, F. A.
Remote sensing applications to resource problems in South Dakota
[E82-10027] p0132 N82-16445

SCHMID, H.
Mathematical and stochastic models in photogrammetry relating to Helmut Wolf's work p0084 N82-19605

SCHMIDT, R.
The diagnosis settlement 1980 of the German main triangulation network Part 2 Trajectories
[SER-B-253-MITT-159-PT-2] p0085 N82-19648

SCHNEIDER, S. R.
Calcium carbonate precipitation in Pyramid Lake, Nevada, as monitored by satellite - 1978 and 1980
p0105 A82-27634
Applications systems verification and transfer project Volume 6 Operational applications of satellite snow-cover observations NOAA/NESS support study
[NASA-TP-1827] p0109 N82-20622

SCHNETZLER, C. C.
Characterizing user requirements for future land observing satellites
[NASA-TM-83867] p0081 N82-17562

SCHREIER, H.
The use of digital multi-date Landsat imagery in terrain classification p0111 A82-20409

SCHROEDER, L. C.
SASS measurements of the Ku-band radar signature of the ocean p0093 A82-21917

SCHUESSLER, H.
Satellite scatterometer feasibility study Volume 1: Technical results
[ESA-CR(P)-1492-VOL-1] p0133 N82-19650

SCHULTZ, H.
Microwave radiation from a natural snow field
p0101 A82-19559

SCHULZ, B.-S.
A procedure for the interactive tracing of edges and lines by means of digital image processing p0113 A82-26050

SCHUMANN, H. H.
Applications systems verification and transfer project Volume 2 Operational applications of satellite snow-cover observations and data-collection systems in the Arizona test site
[NASA-TP-1823] p0108 N82-20618

SCOTT, J. F.
Seasat data utilization project
[NASA-CR-168557] p0097 N82-18660

SCRAGG, P.
Future Earthnet Dissemination Systems (FEDS) study Executive summary
[REPT-3318] p0124 N82-21698

SEDYKH, V. N.
Automation of the processing of aerial and space images for forest inventory p0057 A82-20350

SEEBER, G.
Experiments in satellite Doppler control positioning at sea p0086 N82-20581

SEICHTER, H.
Two-dimensional power spectra of SEASAT SAR imagery p0098 N82-21469

SEIDEL, K.
Detailed land use classification based on multitemporal Landsat-MSS-data p0076 A82-27657

SELIVANOV, A. S.
The structure and basic parameters of a satellite system for the remote sensing of earth resources
p0131 A82-28129

SELLMAN, B.
The 1981 Argentina ground data collection
[E82-10127] p0070 N82-21658

SEMINA, N. 3.
Investigation of the dynamics of the regional underground runoff of the Aral sea basin using space photography
p0101 A82-20343

SERGEEV, A. S.
Analytic methods of geodetic referencing of nontopographic images p0083 A82-28134

SERGEEV, L. V.
Complex of units for the storage and automated processing of research data p0131 A82-28140

SERGEEV, V. P.
Thermal viewing system for studying the earth's resources p0125 A82-21022

SESTAK, M. L.
Preliminary evaluation of spectral, normal and meteorological crop stage estimation approaches
[E82-10059] p0065 N82-19634

SEYFARTH, B. R.
ELAS - A geobased information system that is transferable to several computers p0115 A82-27666

SHAFER, B. A.
Applications systems verification and transfer project Volume 4 Operational applications of satellite snow cover observations Colorado Field Test Center
[NASA-TP-1825] p0108 N82-20620

SHANMUGAN, K. S.
Crop classification using airborne radar and Landsat data p0058 A82-21033

SHAPIRO, I. I.
Applications to Earth physics Very-long-baseline interferometry and data analysis
[NASA-CR-168743] p0088 N82-21796

SHAW, A. H.
The design and implementation of an operational, computer-based weather radar system
[RSRE-MEMO-3151] p0122 N82-21499

SHAW, G. E.
Effect of aerosols on optical remotely sensed data
p0115 A82-27654

SHAW, H. J. W.
Development of a Canadian thermal infrared forest fire mapping operational program p0063 A82-27699

SHEFFNER, E.
The 1981 Argentina ground data collection
[E82-10127] p0070 N82-21658

SHEN, S. S.
Evaluation of large area crop estimation techniques
p0061 A82-27662

SHERMAN, J. W., III
Response of the marine community to satellite-derived oceanic information p0095 A82-27684

SHEVELEV, S. L.
Structure of hardware and software at a regional center for the automated processing of aerial and space remote-sensing images p0130 A82-28128

SHIMABUKURO, Y. E.
Method of interpretation of remote sensing data and applications to vegetation
[INPE-2215-MD/010] p0066 N82-19640
Survey of the cane-growing area of the state of Sao Paulo using LANDSAT data, Safra Year 1979/80, volume 2
[E82-10071] p0067 N82-20594
Elevation of a cane-growing area of the state of Sao Paulo using LANDSAT data
[E82-10077] p0067 N82-20600
Relation of the activities of the IPDF/INPE project (reforestation subproject) during the year 1979
[E82-10078] p0067 N82-20601

SHLIAKHOVA, L. A.
Noncontact methods for the quality control of water resources p0104 A82-27475

SHTEINSHLEIGER, V. B.
Methods for the processing of synthetic-aperture radar signals when solving problems of the national economy /Review/ p0113 A82-26726

SHUCHMAN, R. A.
The use of wave contrast measurements in the evaluation of SAR/gravity models p0130 A82-27675

SHULGINA, E. M.
The possibilities of microwave remote sensing for the study of water resources and their pollution
p0102 A82-27458

SHUTKO, A. M.
Microwave radiometry of lands under natural and artificial moistening p0057 A82-21028
Microwave radiation peculiarities of vegetative covers
p0058 A82-21029
Mixture formulas applied in estimation of dielectric and radiative characteristics of soils and grounds at microwave frequencies p0058 A82-21030
Some peculiarities of formulation and solution of inverse problems in microwave radiometry of the ocean surface and atmosphere p0093 A82-21921
Machine implementation of algorithms for the mapping of soil moisture on the basis of microwave-radiometer measurements p0131 A82-28142

SIDOROVA, V. S.
Automation of the processing of aerial and space images for forest inventory p0057 A82-20350

SIGMAN, R.
Potential utility of thematic mapper data in estimating crop areas p0061 A82-27663
An autodigitizing procedure for ground-data labelling of Landsat pixels p0062 A82-27682

SILVA, D. M.
System of forecasting agricultural crops using satellite observations of Earth
[E82-10079] p0067 N82-20602

SILVA, L. F.
A multiband radiometer and data acquisition system for remote sensing field research
[E82-10142] p0134 N82-21669

SITNIKOVA, M. V.
Dynamics of snow cover in mountain regions of the Aral Sea basin, studied using satellite photographs
p0102 A82-27462

SIVILLO, C. A.
As-Built design specification for UNIV4VEC
[E82-10085] p0122 N82-21637

SKLIAROV, V. E.
The use of Meteor-satellite image data in oceanography p0093 A82-20344

SLAVIK, D.
Spectrometric studies of the water composition of Lake Mueggelsee p0104 A82-27474

SLOANE, M. N.
Ideal phase in estimating the spatial gradient of magnetic daily variations recorded by magnetometer arrays
p0127 A82-26000

SMITH, J. A.
Thermal vegetation canopy model studies
[AD-A106422] p0064 N82-16455

SMITH, R. C.
Ship and satellite bio-optical research in the California Bight
[NASA-CR-168681] p0098 N82-20823

SOLODIKHIN, G. M.
Complex of units for the storage and automated processing of research data p0131 A82-28140

SOLOMON, J. L.
Application of remote sensing to state and regional problems
[E82-10033] p0078 N82-19609

SPAGNOL, J.
Analyses of the Eastern Pacific without ship PAPA data p0093 A82-19139

SPANN, G. W.
An analysis of user requirements for operational land satellite data p0116 A82-27685

SPICER, C. W.
An investigation of the ozone plume from a small city
p0074 A82-26329

STAENZ, K.
The influence of illumination and viewing geometry on the reflectance factor of agricultural targets
p0061 A82-27646
Landsat MSS applied to rangeland management in Western Canada p0063 A82-27697

STAIR, A. T., JR.
Recent auroral measurements using a field-widened interferometer spectrometer p0126 A82-21434

STANLEY, D. J.
Interpretation of remotely sensed image data and impact of cluster compression
[REPT-44.2866] p0124 N82-21699

STEED, A. J.
Recent auroral measurements using a field-widened interferometer spectrometer p0126 A82-21434

STEFFEN, C. A.
Preliminary results of a study of mapping thermal discharge in the ocean, using remote sensing data
[INPE-2229-PRE/021] p0097 N82-19704

STEIN, R.
Program on stimulating operational private sector use of Earth observation satellite information
[E82-10131] p0138 N82-21660

STENSTROEM, G.
Observations with an imaging 35 GHz radiometer of terrain in Malmslatett, July 1980
[FOA-C-30240-E1/E3] p0133 N82-18672

STEPHENS, P. R.
The potential of remote sensing to monitor soil erosion on cropland p0061 A82-27656

STERN, D. P.
Studies related to Magsat
[E82-10050] p0085 N82-19625

STEVENSON, M. R.
Preliminary results of a study of mapping thermal discharge in the ocean, using remote sensing data
[INPE-2229-PRE/021] p0097 N82-19704

STICKSEL, P. R.
An investigation of the ozone plume from a small city
p0074 A82-26329

STILES, W. H.
Dielectric properties of snow
[NASA-CR-166764] p0107 N82-19638
Active microwave investigation of snowpacks. Experimental documentation, Colorado 1979-1980
[NASA-CR-166727] p0107 N82-19646

STIX, J.
Seasat satellite investigation of the structure of Western Nebraska and its application to the evaluation of geothermal resources p0090 A82-27635

STOIBER, R.
Remote SO2 emission measurements with correlation spectrometers from volcanoes p0077 A82-27704

STRAHLER, A. H.
The logit classifier - A general maximum likelihood discriminant for remote sensing applications
p0128 A82-27591
An invertible coniferous forest canopy reflectance model p0062 A82-27679

STUART, D. W.
Coastal upwelling ecosystems analysis. Atlas of the JOINT I aircraft winds for the 500 foot level
[PB82-114703] p0097 N82-19796

STUERZENHOFAECKER, P.
Satellite scatterometer feasibility study. Volume 1: Technical results
[ESA-CR(P)-1492-VOL-1] p0133 N82-19650

SUKHANOVA, K. N.
Reconstruction of a present-day landscape map of a central part of Italy using space images
p0081 A82-20340

SUME, A.
Observations with an imaging 35 GHz radiometer of terrain in Malmslatett, July 1980
[FOA-C-30240-E1/E3] p0133 N82-18672

SUTTON, J. T.
Comparisons of laser profilometer sea ice roughness statistics with surface truthed data and SLAR imagery
p0094 A82-27619

SWEET, J.
Sigma/deg/ signature of the Amazon rain forest obtained from the Seasat scatterometer p0125 A82-21027

SWEET, J. L.
SASS measurements of the Ku-band radar signature of the ocean p0093 A82-21917

SZAJGIN, J.
Landsat classification accuracy assessment procedures
p0137 A82-20412

T

TAKAHASHI, K.
Harmonic structure of Pc 3-4 pulsations
p0082 A82-26266

TAKASHIMA, T.
Estimation of sea surface temperature from remote sensing in the 3.7 micron window region
p0095 A82-28031

TAKAYAMA, Y.
Estimation of sea surface temperature from remote sensing in the 3.7 micron window region
p0095 A82-28031

TAKEUCHI, S.
Environmental studies by multispectral scanner under large-scale civil engineering construction
p0063 A82-27691

TALAY, T. A.
Usage and limitations of characteristic vector analysis of remote sensing multispectral data for the identification and quantification of water quality parameters
p0118 N82-18656

TALSKAIA, N. N.
Analysis of space imagery to compile a geomorphological map of the world p0089 A82-20338

TAMAIN, A. L. G.
Remote sensing applied to basement tectonics of the calcareous High Atlas /Morocco/ p0089 A82-26014

TAMBAY, J.-L.
A timely and accurate potato acreage estimate from Landsat - Results of a demonstration p0060 A82-27621

TANAKA, S.
A formation process of an oceanic vortex analyzed by multi-temporal remote sensing p0095 A82-27674

TANEJA, V.
An intelligent earth sensing information system
p0137 A82-22149

TANG, G. Y.
Classification of ice radar imagery p0113 A82-22891

TAPLEY, I. J.
A vegetation response model applied to range inventory and monitoring using Landsat MSS data
p0060 A82-27643

TARANIK, J. V.
Advanced aerospace remote sensing systems for global resource applications p0127 A82-27577

TARDIN, A. T.
Utilization of Aerochrome 2443 film for identification and estimating wheat growing areas
[INPE-2197-PRE/006] p0066 N82-19639
Survey of the cane-growing area of the state of Sao Paulo using LANDSAT data. Safra Year 1979/80, volume 2
[E82-10071] p0067 N82-20594
Elevation of a cane-growing area of the state of Sao Paulo using LANDSAT data
[E82-10077] p0067 N82-20600

TASSAN, S.
A method for the retrieval of phytoplankton and suspended sediment concentrations from remote measurements of water colour p0094 A82-27620

TAVAKOLI, M.
Building and road extraction from aerial photographs
p0074 A82-25140

TEILLET, P. M.
Digital analysis of spatial and spectral features from airborne MSS of a forested region p0061 A82-27647
Relief effects and the use of terrain models in SAR image processing p0086 N82-21475

TELEGADAS, K.
Demonstration of a long-range atmospheric tracer system using perfluorocarbons
[PB82-106246] p0081 N82-16613

THIELE, O. W.
Precipitation measurements from space - Workshop summary 28 April-1 May 1981, Greenbelt, MD
p0077 A82-26295

THIRUVENGADACHARI, S.
Satellite sensing for extraction of groundwater resources information p0105 A82-27613

THOMAS, A. R.
Modern methods for monitoring and controlling the timeliness, accuracy, and completeness of data for meteorological analysis p0073 A82-19179

THOMAS, G.
The 1981 Argentina ground data collection
[E82-10127] p0070 N82-21658

THOMAS, H. H.
Satellite and surface geophysical expression of anomalous crustal structure in Kentucky and Tennessee
[NASA-TM-82163] p0084 N82-17715

THOMAS, R. W. L.
Error analysis of pulse location estimates for simulated bathymetric lidar returns
[PB82-109448] p0096 N82-17803

THOMPSON, A.
Study of a radar altimeter for the European remote sensing program. Volume 1: Executive summary
[SPAR-R-1090-ISSUE-A] p0133 N82-19652

THOMSON, K. P. B.
Landsat MSS applied to rangeland management in Western Canada p0063 A82-27697

THOREN, R.
Remote sensing techniques suitable for exploration and navigation in and under sea ice
[FOA-REPT-VOL-15-NO-2] p0096 N82-17566

THORNDIKE, A. S.
Sea ice movements from synthetic aperture radar
[AD-A109002] p0097 N82-19435

THYRSTED, T.
Airborne remote sensing in east Greenland
p0090 A82-27695

TILL, S. M.
Instrumentation for remote reflectance and radiance measurements p0130 A82-27652

TILLEY, D. G.
Optimal spatial filtering and transfer function for SAR ocean wave spectra p0094 A82-27596

TINNEY, L. R.
Flexible processing of remote sensing data through integration of image processing and geobased information systems p0116 A82-27667

TISHCHENKO, A. A.
The effectiveness of instrumented visual studies of the earth from space p0114 A82-27505
The earth resources program for the long-term orbital station Salyut 6 p0131 A82-28132

TIURI, M.
Microwave radiation from a natural snow field
p0101 A82-19559

TIURI, M. E.
Theoretical and experimental studies of microwave emission signatures of snow p0125 A82-21034

TIURIN, IU. A.
Development of cooperation between CMEA member countries in the development and utilization of space-based systems for the remote sensing of earth resources and the environment p0138 A82-27543

TOLLINGER, V.
Primary processing of and possibilities of using data from the meteorological satellite TIROS-N p0103 A82-27470

TOM, C. H.
Monitoring forest land cover alteration in Thailand with the analysis of ancillary and digital Landsat data
p0062 A82-27673

TOMIYASU, K.
Wide area, coarse resolution imaging with satellite-borne synthetic aperture radars in low-earth and geosynchronous orbits p0082 A82-27631

TOMPKINS, M. A.
As-Built design specification for UNIV4VEC
[E82-10085] p0122 N82-21637
As-built design specification for PARHIS
[E82-10089] p0122 N82-21641
As-built design specification for PARCLS
[E82-10090] p0123 N82-21642
As-built design specification for MISMAP
[E82-10091] p0123 N82-21643
As-built design specification for segment map (Sgmap) program
[E82-10094] p0123 N82-21646

TOSI, N.
Heat Capacity Mapping Mission (HCMM) program. Study of geological structure of Sicily and other Italian areas
[E82-10073] p0091 N82-20596

TOVIZI, G.
Remote-sensing determination of the characteristics of hydrological objects p0102 A82-27460

TOWNSHEND, J.
Information extraction from remotely sensed data - A user view p0112 A82-21089
A comparison of unsupervised classification procedures on LANDSAT MSS data for an area of complex surface conditions in Basilicata, Southern Italy
[E82-10038] p0119 N82-19613

TOWNSHEND, J. R. G.
Land cover classification accuracy as a function of sensor spatial resolution p0076 A82-27665

TOYOTA, H.
Exterior algebraic processing for remotely sensed multispectral and multitemporal images
p0112 A82-21041

TRIGG, S. E.
The design and implementation of an operational, computer-based weather radar system
[RSRE-MEMO-3151] p0122 N82-21499

TRIVEDI, N. B.
Comparison of storm-time changes of geomagnetic field at ground and at MAGSAT altitudes
[E82-10148] p0087 N82-21675

TSANG, L.
Volumetric effects in cross-polarized airborne radar data p0058 A82-21032

TSAREV, B. K.
Dynamics of snow cover in mountain regions of the Aral Sea basin, studied using satellite photographs
p0102 A82-27462

TUBBS, J. D.
Automatic and semi-automatic classification of Landsat agricultural crops p0061 A82-27664

TUBBS, L. D.
High precision radiometric temperature measurements of the ocean surface p0094 A82-27640

U

UKHOV, B. V.
Thermal viewing system for studying the earth's resources p0125 A82-21022

ULABY, F. T.
Crop classification using airborne radar and Landsat data p0058 A82-21033
Microwave remote sensing. Active and passive. Volume 1 - Microwave remote sensing fundamentals and radiometry p0126 A82-22877
Dielectric properties of snow
[NASA-CR-166764] p0107 N82-19638
Active microwave investigation of snowpacks. Experimental documentation. Colorado 1979-1980
[NASA-CR-166727] p0107 N82-19646

UNGAR, S. G.
Fanning - A classification algorithm for mixture landscapes applied to Landsat data of Maine forests
p0062 A82-27668

URMAEV, M. S.
Orbital methods of celestial geodesy
p0079 A82-25234

USACHEV, V. F.
Aerospace methods for the study of water resources and their pollution p0102 A82-27457
Albedo and brightness coefficients of snow cover
p0103 A82-27465
Analog devices for the processing of aerial and space images for the study of water resources
p0104 A82-27476

USOVA, V. V.
The use of space photographs to compile water-amelioration maps p0106 A82-28137

USRY, J. W.
Influence of dissolved organic materials on turbid water optical properties and remote-sensing reflectance
p0093 A82-20445

UTHE, E. E.
Airborne lidar measurements of smoke plume distribution, vertical transmission, and particle size p0073 A82-21386

V

VALENZIANO, D. J.
As-Built documentation of programs to implement the Robertson and Doraiswamy/Thompson models
[E82-10086] p0122 N82-21638

VALVERDE, A.
Geometric correction of airborne multispectral scanner images p0130 A82-27706

VAN KATS, P. J.
A radar signature model for partially coherent scattering from irregular surfaces p0079 A82-21038

VANASSE, G.
Measurement of atmospheric emission using a balloon-borne cryogenic Fourier spectrometer
p0074 A82-21432

VANDERBILT, A. S.
Simulated response of a multispectral scanner over wheat as a function of wavelength and view/illumination direction
[E82-10144] p0071 N82-21671

VANDERBILT, V. C.
Soybean canopy reflectance as a function of view and illumination geometry p0061 A82-27645
Influence of solar illumination angle on soybean canopy reflectance p0063 A82-28153
A multiband radiometer and data acquisition system for remote sensing field research
[E82-10142] p0134 N82-21669
Spectral-agronomic relationships of corn, soybean and wheat canopies
[E82-10143] p0070 N82-21670
Simulated response of a multispectral scanner over wheat as a function of wavelength and view/illumination direction
[E82-10144] p0071 N82-21671
Variability of reflectance measurements with sensor altitude and canopy type
[E82-10145] p0071 N82-21672

VANDIJK, A.
Precipitation assessment from environmental satellite data for northwest Libya including the Gefara plan
[RSC-4] p0107 N82-19790

VANIN, A. G.
Improving the quality of aerial photography /Concerning the 'Basic principles of aerial photography'/
p0117 A82-28467

VASILENKO, V. N.
Evaluation of snow-cover pollution in industrial regions using satellite TV images p0103 A82-27464

VASILEV, S. V.
Automation of the processing of aerial and space images for forest inventory p0057 A82-20350

VASMUT, A. S.
Classification of systems for digital terrain simulation
p0117 A82-28468

VELARDE, C.
Application of machine processing of visible and thermal data to the study of the geothermal area of Cerro Prieto, Mexico p0117 A82-27693

VELASCO, F. R. D.
An algorithm for spatial heirarchy clustering
[E82-10081] p0121 N82-20604

VENEZIANI, P.
Study project of intrusive rocks: States of Espirito Santo and Rio de Janeiro, south and east of Minas Gerais and southeast of the state of Sao Paulo
[E82-10076] p0092 N82-20599

VENKATACHALAM, P.
Utilisation of remote sensing in resources identification and land use in India - An integrated approach
p0076 A82-27701

VERESHCHAKA, T. V.
The use of space photographs to compile water-amelioration maps p0106 A82-28137

VESPER, N. J.
An evaluation of the utility of smaller Landsat resolution elements /Resolution of Landsat resolution/
p0114 A82-27625

VILFAND, R. M.
Classification of the fields of anomaly in monthly water temperature of the North Atlantic during the cold half-year
[BLL-TRANS-1509-(9022.552)] p0097 N82-19756

VILLAGRA, H. M. I.
Preliminary results of a study of mapping thermal discharge in the ocean, using remote sensing data
[INPE-2229-PRE/021] p0097 N82-19704

VINCENT, R. K.
Automatic linear recognition and analysis using computer program LIRA p0090 A82-27612
HCMM night-time thermal IR imaging experiment in Michigan p0115 A82-27655

VINOGRADOV, B. V.
Remote-sensing functions in the interpretation of moisture from aerial and space images
p0102 A82-27459

VIOLLIER, M.
Radiometric calibration of the Coastal Zone Color Scanner on Nimbus 7 - A proposed adjustment
p0127 A82-26963

VITAL P., R.
Inventory of eroded areas in the state of Guanajuato Mexico, by automatic analysis of Landsat images
p0076 A82-27690

VIVIER, J. M.
Data rate reduction: Impact of image data compression on end to end data management of a multispectral payload
[REPT-44/130] p0120 N82-19654

VLASOV, E. P.
Development of cooperation between CMEA member countries in the development and utilization of space-based systems for the remote sensing of earth resources and the environment p0138 A82-2/543

VOLLER, T. A.
The design and implementation of an operational, computer-based weather radar system
[RSRE-MEMO-3151] p0122 N82-21499

VONG, V. K.
Classification of Landsat MSS data for surface cover of small areas p0116 A82-27677

VOSTRIAKOVA, N. V.
Application of satellite data to analyze and predict meltage runoff in a mountain basin p0102 A82-27461

W

WACHARAKITTI, S.
Monitoring forest land cover alteration in Thailand with the analysis of ancillary and digital Landsat data
p0062 A82-27673

WADE, T. L.
The relationship among sea surface roughness variations, oceanographic analyses, and airborne remote sensing analyses
[NASA-CR-168444] p0096 N82-17798

WAGGONER, J. T.
AgRISTARS: Foreign commodity production forecasting. Project test reports document, volume 1
[E82-10087] p0068 N82-21639
Project communications/documentation standards manual
[E82-10093] p0068 N82-21645

WALBURG, G.
Effects of nitrogen nutrition on the growth, yield and reflectance characteristics of corn canopies
[E82-10068] p0067 N82-20591

WALD, L.
The TOCIND experiment
[CTAMN/81/R/10] p0098 N82-19805

WALDROP, M. M.
Imaging the earth. I - The troubled first decade of Landsat p0137 A82-27169

WALSH, P.
An intelligent earth sensing information system
p0137 A82-22149

WANG, C.-Y.
Multispectral texture p0113 A82-25139

WANG, S.
Spatial reasoning in remotely sensed data
p0105 A82-27592

WARNER, C.
Photogrammetry from aircraft side camera movies - Winter MONEX p0075 A82-26721

WARREN, S. G.
Optical properties of snow p0101 A82-21922

WASILEWSKI, P. J.
Satellite and surface geophysical expression of anomalous crustal structure in Kentucky and Tennessee
[NASA-TM-82163] p0084 N82-17715

WATSON, A. I.
Coastal upwelling ecosystems analysis. Atlas of the JOINT I aircraft winds for the 500 foot level
[PB82-114703] p0097 N82-19796

WATSON, K.
Registration of heat capacity mapping mission day and night images p0113 A82-22146
Application of HCMM data to regional geologic analysis for mineral and energy resource evaluation
[E82-10137] p0092 N82-21664

WEBER, F. P.
Forest change detection p0061 A82-27644

WEEKS, W. F.
Ground-truth observations of ice-covered North Slope Lakes imaged by radar
[NASA-TM-84127] p0107 N82-18664

WEHDE, M.
Remote sensing applications to resource problems in South Dakota
[E82-10027] p0132 N82-16445

WEHDE, M. E.
Spectral reflectance of hydrophytes p0102 A82-24960

WEIDMARK, W. C.
Passive bathymetric measurements in the Bruce Peninsula region of Ontario p0129 A82-27642

WEINER, M. M.
Coherent scatter of microwaves from moderately rough surfaces
[AD-A106133] p0095 N82-16331

WELCH, R.
Spatial resolution and geometric potential of planned earth satellite missions p0130 A82-27683

WELLMAN, J. B.
Technologies for the multispectral mapping of earth resources p0128 A82-27580

WELLS, I.
Locating prehistoric archaeological sites using Landsat
p0129 A82-27638

WENZEL, H. G.
Recent results of geoid determination by combination techniques in the North Sea test area p0086 N82-20583

WERNER, M.
MRSE: A Microwave Remote Sensing Experiment in Spacelab p0134 N82-20375

WERTH, L. F.
San Juan National Forest Land Management Planning Support System (LMPSS) requirements definition
[E82-10108] p0069 N82-21649
An evaluation of ISOCLS and CLASSY clustering algorithms for forest classification in northern Idaho
[E82-10109] p0069 N82-21650

WESTOVER, D. E.
Recovering ocean waveheight from HF radar sea echoes distorted by imperfect ionospheric reflection
[PB82-113283] p0096 N82-17805

WHITLEY, S. L.
ELAS - A geobased information system that is transferable to several computers p0115 A82-27666

WHITLOCK, C. H.
Influence of dissolved organic materials on turbid water optical properties and remote-sensing reflectance
p0093 A82-20445
Laboratory upwelled radiance and reflectance spectra of Kerr reservoir sediment waters
[NASA-TP-1993] p0110 N82-21774

WHITTAKER, T. M.
The development and testing of methods to infer midlatitude precipitation intensity from geosynchronous satellite infrared data
[AD-A108881] p0120 N82-19788

WHRITNER, R.
Arabian sea project of 1980: Composites of infrared images
[AD-A107910] p0096 N82-17567

WICKWARE, G. M.
Change detection in the Peace-Athabasca Delta using digital Landsat data p0101 A82-24959

WIEGAND, C. L.
Methods of editing cloud and atmospheric layer affected pixels from satellite data
[E82-10046] p0119 N82-19621
Methods of editing cloud and atmospheric layer affected pixels from satellite data
[E82-10154] p0123 N82-21678

WIESNET, D. R.
Evaluation of HCMM satellite data for estuarine tidal circulation patterns and thermal inertia soil moisture measurements
[E82-10064] p0108 N82-20587

WIGHT, H. M.
Satellite-borne non-DOD sensors for terrestrial observations
[AD-A109486] p0134 N82-20630

WILLIAMS, D. L.
Information expectations from Landsat-D
p0128 A82-27583

WILLIAMS, J.
Measurement of atmospheric emission using a balloon-borne cryogenic Fourier spectrometer
p0074 A82-21432

WILLIAMS, S. G.
Application of remote sensing to state and regional problems
[E82-10033] p0078 N82-19609

WILSON, R. L.
Spherical harmonic representation of the main geomagnetic field for world charting and investigations of some fundamental problems of physics and geophysics
[E82-10075] p0086 N82-20598

WINKS, K.
Remote sensing applications to resource problems in South Dakota
[E82-10027] p0132 N82-16445

WITTE, W. G.
Influence of dissolved organic materials on turbid water optical properties and remote-sensing reflectance
p0093 A82-20445
Laboratory upwelled radiance and reflectance spectra of Kerr reservoir sediment waters
[NASA-TP-1993] p0110 N82-21774

WOLF, D. E.
An experimental program to provide remote measurement and analysis of ocean waves, sea level winds and balanced pressure in support of Seasat-A
[PB81-246035] p0095 N82-16697

WOLFE, D. C., JR.
Model studies of laser absorption computed tomography for remote air pollution measurement p0077 A82-28152

WON, I. J.
Compatibility study of the MAGSAT data and aeromagnetic data
[E82-10136] p0123 N82-21663

WONG, F.
The use of digital terrain model in the rectification of satellite-borne imagery p0115 A82-27626

WOOD, B.
The 1981 Argentina ground data collection
[E82-10127] p0070 N82-21658

WOODCOCK, C. E.
Scene analysis for wildland fire-fuel characteristics in a Mediterranean climate p0060 A82-27624

WRIGHT, K. H.
Ionospheric troughs in Antarctica p0073 A82-21217

WU, A. Y.
Multispectral texture p0113 A82-25139

WYNN, S. L.
Wetland mapping from digitized aerial photography
[E82-10019] p0118 N82-16437

X

XIAOWEN, L.
An invertible coniferous forest canopy reflectance model p0062 A82-27679

Y

YASUDA, Y.
Phenomena modelling of remotely sensed data by image rationing p0076 A82-27670

YAZAKI, S.
Detection of volcanic ash fall area from Landsat MSS CCT data Eruption of Mt. Ontake in 1979
p0076 A82-27650

YEO, A. C.
Classification of Landsat MSS data for surface cover of small areas p0116 A82-27677

YOSHIKADO, S.
Remote sensing of rainfall rates using airborne microwave rain-scatterometer/radiometer p0105 A82-27639

YOSHIMURA, N.
Phenomena modelling of remotely sensed data by image rationing p0076 A82-27670

Z

ZANDONELLA, A.
LANDSAT imagery of the Venetian Lagoon: A multitemporal analysis
[E82-10036] p0119 N82-19612

ZAPOTOCNY, J. V.
The development and testing of methods to infer midlatitude precipitation intensity from geosynchronous satellite infrared data
[AD-A108881] p0120 N82-19788

ZAVOLOKIN, IU. V.
Noncontact methods for the quality control of water resources p0104 A82-27475

ZEBKER, H.
Simulation and studies of spaceborne synthetic aperture radar image quality with reduced bit rate
p0128 A82-27594

ZHURKIN, I. G.
Construction of a mathematical model for the recognition of identical images on a pair of photographs
p0117 A82-28146

ZILIOLI, E.
Heat Capacity Mapping Mission (HCMM) program: Study of geological structure of Sicily and other Italian areas
[E82-10073] p0091 N82-20596

ZINI, E.
Integration of Landsat, geological and geophysical data for use in thematic mapping at regional scale
p0090 A82-27672

ZLOBIN, V. K.
Correlation identification of stellar configurations for purposes of the coordinate referencing of aerial and space images p0117 A82-28141

ZONDEK, B.
Some altimetric signatures from Seasat over the mid-Pacific Seamount Range
[AD-A110419] p0099 N82-21691

ZOTOVA, E. N.
Investigation of the vegetative covers on ploughed areas by SLAR p0058 A82-21031

ZSCHAU, J.
Detection of natural disasters via Meteosat
p0075 A82-27040

ZUBCHENKO, E. S.
A photometric method for depth determination by aerial photography p0101 A82-19831

ZWALLY, H. J.
Satellite-derived ice data sets no. 1: Antarctic monthly average microwave brightness temperatures and sea-ice concentrations, 1973 - 1976
[NASA-TM-83812] p0096 N82-17563

ZWICK, H. H.
Passive bathymetric measurements in the Bruce Peninsula region of Ontario p0129 A82-27642

CORPORATE SOURCE INDEX

Typical Corporate Source Index Listing

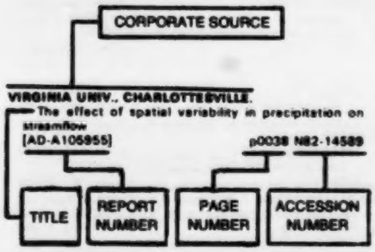
CORPORATE SOURCE
VIRGINIA UNIV., CHARLOTTESVILLE.
The effect of spatial variability in precipitation on streamflow
[AD-A105955]
p0038 N82-14589
TITLE
REPORT NUMBER
PAGE NUMBER
ACCESSION NUMBER

The title of the document is used to provide a brief description of the subject matter. The page number and the accession number are included in each entry to assist the user in locating the abstract in the abstract section. If applicable, a report number is also included as an aid in identifying the document.

A

AGRICULTURAL RESEARCH SERVICE, WESLACO, TEX.
Methods of editing cloud and atmospheric layer affected pixels from satellite data
[E82-10046] p0119 N82-19621
Methods of editing cloud and atmospheric layer affected pixels from satellite data
[E82-10154] p0123 N82-21678

ANALYSIS AND TECHNOLOGY, INC., NORTH STONINGTON, CONN.
Evaluation of two AN/APS-94 side-looking airborne radar systems in the detection of search and rescue targets
[AD-A108404] p0132 N82-18466

ANALYTIC SCIENCES CORP., READING, MASS.
MAGSAT anomaly profiles of the eastern Indian Ocean
[E82-10066] p0086 N82-20589

ARMY COLD REGIONS RESEARCH AND ENGINEERING LAB., HANOVER, N. H.
Electromagnetic subsurface measurements
[AD-A108192] p0106 N82-18469
Ground-truth observations of ice-covered North Slope Lakes imaged by radar
[NASA-TM-84127] p0107 N82-18664

ARMY ENGINEER TOPOGRAPHIC LABS., FORT BELVOIR, VA.
Computer-assisted photo interpretation research at USAETL
[AD-A109366] p0121 N82-20628
A digital technique for constructing variable-width lines
[AD-A110287] p0087 N82-21689

B

BAYERISCHE AKADEMIE DER WISSENSCHAFTEN, MUNICH (WEST GERMANY).
Some criteria for the accuracy and the reliability of networks p0086 N82-20580
Experiments in satellite Doppler control positioning at sea p0086 N82-20581
Recent results of geoid determination by combination techniques in the North Sea test area p0086 N82-20583

BELL TELEPHONE LABS., INC., HOLMDEL, N. J.
Sigma/deg/ signature of the Amazon rain forest obtained from the Seasat scatterometer p0125 A82-21027

BONNEVILLE POWER ADMINISTRATION, PORTLAND, OREG.
Applications systems verification and transfer project. Volume 5: Operational applications of satellite snow-cover observations, northwest United States
[NASA-TP-1826] p0109 N82-20621

BRIGHAM YOUNG UNIV., PROVO, UTAH.
HCMM hydrological analysis in Utah
[E82-10063] p0107 N82-20586

BRITISH AEROSPACE DYNAMICS GROUP, BRISTOL (ENGLAND).
Imaging microwave radiometer. Phase A study. Volume 1: Executive summary
[ESS/SS-1006] p0132 N82-18564

BRITISH AEROSPACE DYNAMICS GROUP, STEVENAGE (ENGLAND).
Study of Earth Resources Satellite (ERS) data reduction unit
[BAE-TP-7905] p0120 N82-19649

BRITISH LIBRARY LENDING DIV., BOSTON SPA (ENGLAND).
Classification of the fields of anomaly in monthly water temperature of the North Atlantic during the cold half-year
[BLL-TRANS-1509-(9022.552)] p0097 N82-19756

BROWN UNIV., PROVIDENCE, R. I.
Electromagnetic deep-probing (100-1000 KMS) of the Earth's interior from artificial satellites: Constraints on the regional emplacement of crustal resources
[E82-10043] p0084 N82-19618
Electromagnetic deep-probing (100-1000 KMS) of the Earth's interior from artificial satellites: Constraints on the regional emplacement of crustal resources
[E82-10044] p0085 N82-19619
Electromagnetic deep-probing (100-1000 KMS) of the Earth's interior from artificial satellites: Constraints on the regional emplacement of crustal resources
[E82-10155] p0087 N82-21879

BUNDESGESUNDHEITSAMT, BERLIN (WEST GERMANY).
Optimal network density for atmospheric recording
p0079 N82-20776

BUSINESS AND TECHNOLOGICAL SYSTEMS, INC., SEABROOK, MD.
Equivalent source modeling of the main field using Magsat data
[E82-10041] p0084 N82-19616
Magsat science investigations
[E82-10045] p0085 N82-19620
An information adaptive system study report and development plan
[NASA-CR-166768] p0120 N82-19644
Context sensitive formulations of antenna pattern correction and side lobe compensation for NOSS/LAMMR real time processing
[NASA-CR-166789] p0122 N82-21457

C

CALIFORNIA STATE DEPT. OF WATER RESOURCES, SACRAMENTO.
Applications systems verification and transfer project. Volume 3: Operational applications of satellite snow cover observations in California
[NASA-TP-1824] p0108 N82-20619

CALIFORNIA UNIV., BERKELEY.
Remote sensing of salinity in the San Francisco Bay Delta p0102 A82-26839
The 1981 Argentina ground data collection
[E82-10127] p0070 N82-21658

CALIFORNIA UNIV., LA JOLLA.
Ship and satellite bio-optical research in the California Bight
[NASA-CR-168681] p0098 N82-20823

CALIFORNIA UNIV., LOS ANGELES.
Harmonic structure of Pc 3-4 pulsations
p0082 A82-26266

CANADA CENTRE FOR REMOTE SENSING, OTTAWA (ONTARIO).
Heat Capacity Mapping Mission (HCMM): Interpretation of imagery over Canada
[E82-10070] p0079 N82-20593
Relief effects and the use of terrain models in SAR image processing p0086 N82-21475

CENTRE DE RECHERCHES EN PHYSIQUE DE L'ENVIRONNEMENT, ISSY-LES-MOULINEAUX (FRANCE).
Direct determination of the two dimensional image spectrum from raw synthetic aperture radar data
p0122 N82-21474

COLOGNE UNIV. (WEST GERMANY).
Atlas of the global distribution of the total ozone concentration according to satellite measurements
[MITT-28] p0078 N82-19740

COLORADO STATE UNIV., FORT COLLINS.
Thermal vegetation canopy model studies
[AD-A106422] p0064 N82-16455
Regional properties of angular reflectance models
p0083 N82-17599
Watershed model study using LANDSAT data
p0106 N82-17602

COLORADO UNIV., BOULDER.
Investigation of geomagnetic field forecasting and fluid dynamics of the core
[E82-10162] p0087 N82-21686

CONSIGLIO NAZIONALE DELLE RICERCHE, MILAN (ITALY).
Heat Capacity Mapping Mission (HCMM) program: Study of geological structure of Sicily and other Italian areas
[E82-10073] p0091 N82-20596

CONSIGLIO NAZIONALE DELLE RICERCHE, VENICE (ITALY).
LANDSAT imagery of the Venetian Lagoon: A multitemporal analysis
[E82-10036] p0119 N82-19612

CORNELL UNIV., ITHACA, N. Y.
Ground level reflectance measurement techniques - An evaluation with emphasis on the importance of spectral calibration p0116 A82-27689

D

DARTMOUTH COLL., HANOVER, N.H.
Fanning - A classification algorithm for mixture landscapes applied to Landsat data of Maine forests
p0052 A82-27668

DEFENSE MAPPING AGENCY AEROSPACE CENTER, ST. LOUIS, MO.
Matrix data analysis. Color/B and W coding is not always enough
[AD-A108406] p0084 N82-18930
Profiling sensitivity to image quality
[AD-A108405] p0084 N82-18931
Experiences with digital terrain elevation data contouring programs
[AD-A110280] p0087 N82-21690

DEPARTMENT OF AGRICULTURE, HOUSTON, TEX.
AgRISTARS: Soil moisture/early warning and crop condition assessment. Interface control document
[E82-10053] p0065 N82-19628
AgRISTARS: Yield model development/soil moisture. Interface control document
[E82-10054] p0065 N82-19629
Taxonomic classification of world map units in crop producing areas of Argentina and Brazil with representative US soil series and major land resource areas in which they occur
[E82-10058] p0065 N82-19633

DEPARTMENT OF AGRICULTURE, WASHINGTON, D.C.
AgRISTARS: Agriculture and Resources Inventory Surveys Through Aerospace Remote Sensing. Enumerator's manual, 1981 ground data survey
[E82-10116] p0069 N82-21653

DEUTSCHE FORSCHUNGS- UND VERSUCHSANSTALT FUER LUFT- UND RAUMFAHRT, OBERPFAFFENHOFEN (WEST GERMANY).
Sounding the aerosol distribution over the Upper Rhine Valley in the Valley in the Speyer area by means of lidar
p0079 N82-20782
Two-dimensional power spectra of SEASAT SAR imagery p0098 N82-21469

DEUTSCHES GEODAETISCHES FORSCHUNGSINSTITUT, MUNICH (WEST GERMANY).
Helmut Wolf: On the occasion of his 70th birthday
[SER-E-18] p0084 N82-19603
Developments in geodesy within the scope of Helmut Wolf's work p0084 N82-19604
Mathematical and stochastic models in photogrammetry relating to Helmut Wolf's work p0084 N82-19605
The diagnosis settlement 1980 of the German main triangulation network. Part 2: Trajectories
[SER-B-253-MITT-159-PT-2] p0085 N82-19648

DIGITAL PROGRAMMING SERVICES, INC., WALTHAM, MASS.
Development and applications of techniques to process hydrometeor distribution data
[AD-A109929] p0109 N82-20822

DORNIER-WERKE G.M.B.H., FRIEDRICHSHAFEN (WEST GERMANY).

Imaging microwave radiometer. Phase A study. Volume 1: Executive summary
[ESS/SS-1006] p0132 N82-18564

Satellite scatterometer feasibility study. Volume 1: Technical results
[ESA-CR(P)-1492-VOL-1] p0133 N82-19650

Satellite scatterometer feasibility study. Volume 2: Data extraction algorithm and error simulation for wind sensor
[ESA-CR(P)-1492-VOL-2] p0133 N82-19651

Study of a radar altimeter for the European remote sensing program. Volume 1: Executive summary
[SPAR-R 1090-ISSUE-A] p0133 N82-19652

E

ECOLE NATIONALE SUPERIEURE DES MINES, VALBONNE (FRANCE).

The TOCIND experiment
[CTAMN/81/R/10] p0098 N82-19805

ECOSYSTEMS INTERNATIONAL, INC., GAMBRILLS, MD.

Applications systems verification and transfer project. Volume 7: Cost/benefit analysis for the ASVT on operational applications of satellite snow-cover observations
[NASA-TP-1828] p0109 N82-20623

EG AND G WASHINGTON ANALYTICAL SERVICES CENTER, INC., ROCKVILLE, MD.

Error analysis of pulse location estimates for simulated bathymetric lidar returns
[PB82-109448] p0096 N82-17803

ELECTRONICS RESEARCH LAB., ADELAIDE (AUSTRALIA).

An aerial survey of water turbidity and laser depth sounding performance along the Queensland Coast
[AD-A109050] p0098 N82-19802

Proposed digital cartridge recording system for WRELADS
[AD-A109484] p0134 N82-20491

ENGINS MATRA, VELIZY (FRANCE).

Data rate reduction. Impact of image data compression on end to end data management of a multispectral payload
[REPT-44/130] p0120 N82-19654

ENVIRONMENTAL RESEARCH AND TECHNOLOGY, INC., CONCORD, MASS.

Applications systems verification and transfer project. Volume 8: Satellite snow mapping and runoff prediction handbook
[NASA-TP-1829] p0109 N82-20624

ENVIRONMENTAL RESEARCH INST. OF MICHIGAN, ANN ARBOR.

Documentation of computer procedures for labeling spring grains and discriminating between spring wheat and barley using LANDSAT data
[E82-10030] p0063 N82-16448

Notes for Brazil sampling frame evaluation trip
[E82-10060] p0066 N82-19635

The 1981 Argentina ground data collection
[E82-10127] p0070 N82-21658

EUROPEAN SPACE AGENCY, PARIS (FRANCE).

Sea state measurement with a two frequency scatterometer (theory)
[ESA-TT-710] p0096 N82-17802

MRSE: A Microwave Remote Sensing Experiment in Spacelab p0134 N82-20375

SAR image quality
[ESA-SP-172] p0122 N82-21458

Atlas of METEOSAT imagery
[ESA-SP-1030] p0124 N82-21700

EUROSPACE, PARIS (FRANCE).

Examination of the operational prospects for remote sensing
[ESA-CR(P)-1476] p0138 N82-18669

F

FLORIDA STATE UNIV., TALLAHASSEE.

Coastal upwelling ecosystems analysis. Atlas of the JOINT I aircraft winds for the 500 foot level
[PB82-114703] p0097 N82-19796

FLORIDA UNIV., GAINESVILLE.

Use of thermal inertia determined by HCMM to predict nocturnal cold prone areas in Florida
[E82-10040] p0064 N82-19615

Application of satellite frost forecast technology to other parts of the United States, phase 2
[NASA-CR-166827] p0121 N82-20607

Application of satellite frost forecast technology to other parts of the United States, phase 2, introduction
p0121 N82-20608

A satellite frost forecasting system for Florida
p0079 N82-20615

Use of thermal inertia determined by HCMM to predict nocturnal cold prone areas in Florida
[E82-10157] p0071 N82-21681

FOOD AND AGRICULTURE ORGANIZATION OF THE UNITED NATIONS, ROME (ITALY).

Precipitation assessment from environmental satellite data for northwest Libya including the Gefara plan
[RSC-4] p0107 N82-19790

FREIE UNIV., BERLIN (WEST GERMANY).

Dust from the Sahara in satellite images
p0079 N82-20802

G

GENERAL ELECTRIC CO., PHILADELPHIA, PA.

Wide area, coarse resolution imaging with satellite-borne synthetic aperture radars in low-earth and geosynchronous orbits p0082 A82-27631

LANDSAT-2 and LANDSAT-3 flight evaluation report, 23 January to 23 July 1980
[E82-10022] p0132 N82-16440

GEOLOGICAL SURVEY, DENVER, COLO.

Registration of heat capacity mapping mission day and night images p0113 A82-22146

Application of HCMM data to regional geologic analysis for mineral and energy resource evaluation
[E82-10137] p0092 N82-21664

GEOLOGICAL SURVEY, PHOENIX, ARIZ.

Applications systems verification and transfer project. Volume 2: Operational applications of satellite snow-cover observations and data-collection systems in the Arizona test site
[NASA-TP-1823] p0108 N82-20618

H

HUNTER COLL., NEW YORK.

Stochastic models of cover class dynamics
p0059 A82-27586

HYDEX CORP., FAIRFAX, VA.

Strategies for using remotely sensed data in hydrologic models
[E82-10156] p0109 N82-21680

I

INSTITUTO DE PESQUISAS ESPACIAIS, SAO JOSE DOS CAMPOS (BRAZIL).

CNPq/INPE: LANDSAT system
[E82-10023] p0118 N82-16441

Report on a short course in remote sensing and the geological applications of LANDSAT MSS imagery at INPE
[E82-10024] p0091 N82-16442

Remote sensing data applied to land-use survey at the Paraiba Valley
[E82-10025] p0081 N82-16443

Brazilian remote sensing activities, current and prospective needs
[E82-10026] p0132 N82-16444

Simplified algorithm for calculating radiative transfer in satellite images
[INPE-2169-RPE/385] p0118 N82-16450

Particle precipitation and atmospheric X-and Gamma-rays in the South Atlantic magnetic anomaly by balloon experiments
[INPE-2119-RPE/343] p0083 N82-17711

The severity of the Brazilian freeze of July 1981, as monitored by satellite
[INPE-2231-RPE/399] p0064 N82-17746

A microcomputer for control of data collection platforms
[INPE-2104-RPE/331] p0133 N82-18881

General configuration and internal disposition of equipment in a satellite for collecting environmental data
[INPE-2240-PRE/026] p0078 N82-19256

Data collection platforms: Applications to hydrology
[INPE-2246-PRE/030] p0107 N82-19304

Automatic analysis of multispectral images
[INPE-2212-MD/009] p0133 N82-19520

Utilization of Aerochrome 2443 film for identification and estimating wheat growing areas
[INPE-2197-PRE/006] p0066 N82-19639

Method of interpretation of remote sensing data and applications to vegetation
[INPE-2215-MD/010] p0066 N82-19640

Methodology of the interpretation of remote sensing data and applications in pedology
[INPE-2211-MD/008] p0078 N82-19641

Methodology of the interpretation of remote sensing data and applications in geomorphology
[INPE-2209-MD/007] p0091 N82-19642

Preliminary results of a study of mapping thermal discharge in the ocean, using remote sensing data
[INPE-2229-PRE/021] p0097 N82-19704

Convergence zones in the South Atlantic and their influence on the precipitation regime in Northeastern Brazil
[INPE-2307-TDL/074] p0097 N82-19778

Selection of attributes applied to multispectral images
[INPE-2303-TDL/072] p0121 N82-19927

The utilization of orbital images as an adequate form of control of preserved areas
[E82-10065] p0078 N82-20588

Amazonas project: Application of remote sensing techniques for the integrated survey of natural resources in Amazonas
[E82-10069] p0078 N82-20592

Survey of the cane-growing area of the state of Sao Paulo using LANDSAT data, Safra Year 1979/80, volume 2
[F82-10071] p0067 N82-20594

Land use in the Paraiba Valley through remotely sensed data
[E82-10072] p0079 N82-20595

Study project of intrusive rocks: States of Espirito Santo and Rio de Janeiro, south and east of Minas Gerais and southeast of the state of Sao Paulo
[E82-10076] p0092 N82-20599

Elevation of a cane-growing area of the state of Sao Paulo using LANDSAT data
[E82-10077] p0067 N82-20600

Relation of the activities of the IPDF/INPE project (reforestation subproject) during the year 1979
[E82-10078] p0067 N82-20601

System of forecasting agricultural crops using satellite observations of Earth
[E82-10079] p0067 N82-20602

The LANDSAT system operated in Brazil by CNPq/INPE - results obtained in the area of mapping and future perspectives
[E82-10080] p0121 N82-20603

An algorithm for spatial heirarchy clustering
[E82-10081] p0121 N82-20604

Dynamic study of the upper Sao Francisco River and the Tres Marias reservoir using MSS/LANDSAT images
[E82-10082] p0108 N82-20605

Comparison of storm-time changes of geomagnetic field at ground and at MAGSAT altitudes
[E82-10148] p0087 N82-21675

INTER-AMERICAN GEODETIC SURVEY, FORT SAM HOUSTON, TEX.

Photogrammetry software: A package for everyone
[AD-A108098] p0118 N82-17570

Remote sensing in Latin America: Technology and markets for the 1980's .
[AD-A108784] p0138 N82-20626

IOWA UNIV., IOWA CITY.

Use of Magsat anomaly data for crustal structure and mineral resources in the US midcontinent
[E82-10049] p0091 N82-19624

Use of MAGSAT anomaly data for crustal structure and mineral resources in the US midcontinent
[E82-10152] p0092 N82-21677

J

JET PROPULSION LAB., CALIFORNIA INST. OF TECH., PASADENA.

The Seasat low rate data processing system
p0093 A82-24061

Comparison of conventionally measured sea surface temperature and wind speed with data retrieved from satellite-borne microwave radiometry p0093 A82-24063

Analysis of two Seasat synthetic aperture radar images of an urban scene p0074 A82-25452

Modeling misregistration and related effects on multispectral classification p0113 A82-25455

Topex orbit sustenance maneuver design
[AIAA PAPER 82-0202] p0094 A82-27091

Spaceborne radar observation of the earth surface
p0127 A82-27578

Technologies for the multispectral mapping of earth resources p0128 A82-27580

Simulation and studies of spaceborne synthetic aperture radar image quality with reduced bit rate
p0128 A82-27594

A data base of geologic field spectra
p0090 A82-27600

A shuttle scanning laser altimeter for topographic mapping p0083 A82-27632

Integration of LANDSAT with geology and airborne geophysics into an operational mineral exploration system
[E82-10028] p0091 N82-16446

Session III of the VLBI/Laser intercomparison task of the NASA crustal dynamics project
[NASA-CR-168427] p0083 N82-17708

Seasat data utilization project
[NASA-CR-168557] p0097 N82-18660

JOHNS HOPKINS UNIV., LAUREL, MD.

Optimal spatial filtering and transfer function for SAR ocean wave spectra p0094 A82-27586

K

KANSAS UNIV., LAWRENCE.

Microwave remote sensing: Active and passive. Volume 1 - Microwave remote sensing fundamentals and radiometry p0126 A82-22877

The application of remote sensing to resource management and environmental quality programs in Kansas
[E82-10029] p0063 N82-16447

KANSAS UNIV. CENTER FOR RESEARCH, INC., LAWRENCE.

Sigma/deg/ signature of the Amazon rain forest obtained from the Seasat scatterometer p0125 A82-21027

Crop classification using airborne radar and Landsat data p0058 A82-21033

Dielectric properties of snow [NASA-CR-166764] p0107 N82-19638

Active microwave investigation of snowpacks: Experimental documentation, Colorado 1979-1980 [NASA-CR-168727] p0107 N82-19646

KENT STATE UNIV., OHIO.

Precision in the evaluation of Landsat autocorrelation - The terrain effect p0116 A82-27686

KENTRON INTERNATIONAL, INC., HAMPTON, VA.

SASS measurements of the Ku-band radar signature of the ocean p0093 A82-21917

L

LIVERPOOL UNIV. (ENGLAND).

Spherical harmonic representation of the main geomagnetic field for world charting and investigations of some fundamental problems of physics and geophysics [E82-10075] p0086 N82-20598

LOCKHEED ENGINEERING AND MANAGEMENT SERVICES CO., INC., HOUSTON, TEX.

Use of Landsat-derived temporal profiles for corn-soybean feature extraction and classification p0059 A82-26842

Evaluation of large area crop estimation techniques p0061 A82-27662

Partially processed multispectral scanner LANDSAT high-density tapes reformatting system (HDT-AM/AMC) design specifications [E82-10020] p0118 N82-16438

Wheat stress indicator model, Crop Condition Assessment Division (CCAD) data base interface driver, user's manual [E82-10031] p0064 N82-19607

AgRISTARS: Interim catalog ground data summary, data acquisition year 1979 [E82-10032] p0064 N82-19608

Recommended data sets, corn segments and spring wheat segments, for use in program development [E82-10034] p0064 N82-19610

AgRISTARS: Early warning and crop condition assessment. Patch image processor user's manual [E82-10055] p0065 N82-19630

AgRISTARS: Foreign commodity production forecasting. Corn/soybean decision logic development and testing [E82-10056] p0065 N82-19631

Agricultural soil moisture experiment, Colby, Kansas 1978: Measured and predicted hydrological properties of the soil [E82-10057] p0065 N82-19632

Preliminary evaluation of spectral, normal and meteorological crop stage estimation approaches [E82-10059] p0065 N82-19634

Segment-level evaluation of the simulated aggregation test: US corn and soybean exploratory experiment [E82-10061] p0066 N82-19636

Registration verification of SEA/AR fields [E82-10083] p0068 N82-21635

Ground registration of data from an airborne scatterometer [E82-10084] p0068 N82-21636

As-Built design specification for UNIV4VEC [E82-10085] p0122 N82-21637

As-Built documentation of programs to implement the Robertson and Doraiswamy/Thompson models [E82-10086] p0122 N82-21638

AgRISTARS: Foreign commodity production forecasting. Project test reports document, volume 1 [E82-10087] p0068 N82-21639

US corn and soybeans exploratory experiment [E82-10088] p0068 N82-21640

As-built design specification for PARHIS [E82-10089] p0122 N82-21641

As-built design specification for PARCLS [E82-10090] p0123 N82-21642

As-built design specification for MISMAP [E82-10091] p0123 N82-21643

As-built design specification for the CLASFYG program [E82-10092] p0068 N82-21644

Project communications/documentation standards manual [E82-10093] p0068 N82-21645

As-built design specification for segment map (Sgmap) program [E82-10094] p0123 N82-21646

San Juan National Forest Land Management Planning Support System (LMPSS) requirements definition [E82-10108] p0069 N82-21649

An evaluation of ISOCLS and CLASSY clustering algorithms for forest classification in northern Idaho [E82-10109] p0069 N82-21650

Transition year labeling error characterization study [E82-10111] p0069 N82-21651

Wheat stress indicator model, Early Warning (EW) data base interface driver, user's manual [E82-10115] p0069 N82-21652

Development of rotation sample designs for the estimation of crop acreages [E82-10117] p0070 N82-21654

Sample selection in foreign similarity regions for multicrop experiments [E82-10118] p0070 N82-21655

A look at the commonly used LANDSAT vegetation indices [E82-10123] p0070 N82-21657

Sonora exploratory study for the detection of wheat-leaf rust [E82-10133] p0070 N82-21661

AgRISTARS: Supporting research. Classification of corn: Badhwar profile similarity technique [E82-10150] p0071 N82-21676

AgRISTARS: Supporting research. US crop calendars in support of the early warning project [E82-10158] p0072 N82-21682

LOGICA LTD., LONDON (ENGLAND).

Future Earthnet Dissemination Systems (FEDS) study. Executive summary [REPT-3318] p0124 N82-21698

Interpretation of remotely sensed image data and impact of cluster compression [REPT-44.2866] p0124 N82-21699

M

MARYLAND UNIV., COLLEGE PARK.

Superconducting tensor gravity gradiometer p0126 A82-23045

MASSACHUSETTS INST. OF TECH., CAMBRIDGE.

Applications to Earth physics: Very-long-baseline interferometry and data analysis [NASA-CR-168743] p0088 N82-21796

MIAMI UNIV., FLA.

Investigations of medium wavelength magnetic anomalies in the Eastern Pacific using Magsat data [E82-10047] p0119 N82-19622

MICHIGAN ENERGY AND RESOURCE RESEARCH ASSOCIATION, DETROIT.

Resourceful decisions: LANDAT in Michigan [E82-10037] p0078 N82-19601

MICHIGAN STATE UNIV., EAST LANSING.

Application of satellite frost forecast technology to other parts of the United States, phase 2 [NASA-CR-166827] p0121 N82-20607

Applicability of satellite freeze forecasting and cold climate mapping to the other parts of the United States p0068 N82-20613

MSU test of P-model p0121 N82-20614

MICHIGAN UNIV., ANN ARBOR.

Spectral reflectances of freshwater ice and snow from 340 through 1100 nm p0106 N82-17601

MISSISSIPPI STATE UNIV., MISSISSIPPI STATE.

Application of remote sensing to state and regional problems [E82-10033] p0078 N82-19609

MITRE CORP., BEDFORD, MASS.

Coherent scatter of microwaves from moderately rough surfaces [AD-A106133] p0095 N82-16331

MORGAN STATE UNIV., BALTIMORE, MD.

Assessment of the quality of GATE area rainfall data from a Nimbus-5 radiometer [NASA-CR-168512] p0109 N82-20807

N

NATIONAL ACADEMY OF SCIENCES - NATIONAL RESEARCH COUNCIL, WASHINGTON, D. C.

Remote sensing for water resources and hydrology: An assessment of the Corps of Engineers' program [PB82-137142] p0110 N82-21704

NATIONAL AERONAUTICS AND SPACE ADMINISTRATION, WASHINGTON, D. C.

Advanced aerospace remote sensing systems for global resource applications p0127 A82-27577

Satellite Earth resources data, module U-3 [E82-10035] p0119 N82-19611

NASA Oceanic Processes Program, Fiscal Year 1981 [NASA-TM-84467] p0098 N82-19801

Gradio: Project proposal for satellite gradiometry [NASA-TM-76796] p0134 N82-20606

Observation of the Earth by radar [NASA-TM-76830] p0124 N82-21687

NATIONAL AERONAUTICS AND SPACE ADMINISTRATION. AMES RESEARCH CENTER, MOFFETT FIELD, CALIF.

Using known map category marginal frequencies to improve estimates of thematic map accuracy p0113 A82-25456

NATIONAL AERONAUTICS AND SPACE ADMINISTRATION. EARTH RESOURCES LABS., BAY ST. LOUIS, MISS.

ELAS - A geobased information system that is transferable to several computers p0115 A82-27666

NATIONAL AERONAUTICS AND SPACE ADMINISTRATION. GODDARD INST. FOR SPACE STUDIES, NEW YORK.

Fanning - A classification algorithm for mixture landscapes applied to Landsat data of Maine forests p0062 A82-27668

NATIONAL AERONAUTICS AND SPACE ADMINISTRATION. GODDARD SPACE FLIGHT CENTER, GREENBELT, MD.

Simple radiative transfer model for relationships between canopy biomass and reflectance p0067 A82-20422

Contrast reduction by the atmosphere and retrieval of nonuniform surface reflectance p0112 A82-20423

Structure and variability of the Alboran Sea frontal system p0093 A82-20447

Comparison of sigma/deg/ obtained from the conventional definition with sigma/deg/ appearing in the radar equation for randomly rough surfaces p0112 A82-21039

Ore deposits in Africa and their relation to the underlying mantle p0090 A82-26604

Information expectations from Landsat-D p0128 A82-27583

Land cover classification accuracy as a function of sensor spatial resolution p0076 A82-27665

Precipitation measurements from space - Workshop summary 28 April-1 May 1981, Greenbelt, MD p0077 A82-28295

An optical model for the microwave properties of sea ice [NASA-TM-83865] p0095 N82-17561

Characterizing user requirements for future land observing satellites [NASA-TM-83867] p0081 N82-17562

Satellite-derived ice data sets no. 1: Antarctic monthly average microwave brightness temperatures and sea-ice concentrations, 1973 - 1976 [NASA-TM-83812] p0096 N82-17563

Some new methods in geomagnetic field modeling applied to the 1960 - 1980 epoch [NASA-TM-83868] p0083 N82-17714

Satellite and surface geophysical expression of anomalous crustal structure in Kentucky and Tennessee [NASA-TM-82163] p0084 N82-17715

Spectral albedos of midlatitude snowpacks [NASA-TM-83858] p0106 N82-18663

Multidimensional aspects: Ozone, temperature and transport p0081 N82-18772

Stratospheric instruments and analyses p0133 N82-18776

Climate observing system studies: An element of the NASA Climate Research Program. Workshop report [NASA-TM-84040] p0078 N82-18808

A comparison of unsupervised classification procedures on LANDSAT MSS data for an area of complex surface conditions in Basilicata, Southern Italy [E82-10038] p0119 N82-19613

Studies related to Magsat [E82-10050] p0085 N82-19625

The effect of finite field size on classification and atmospheric correction [NASA-TM-83818] p0120 N82-19645

Information theory lateral density distribution for Earth inferred from global gravity field [NASA-TM-83825] p0085 N82-19731

Estimating ocean-air heat fluxes during cold air outbreaks by satellite [NASA-TM-83854] p0097 N82-19781

Applications systems verification and transfer project. Volume 1: Operational applications of satellite snow cover observations: Executive summary [NASA-TP-1822] p0108 N82-20617

Cloud Top Scanning radiometer (CTS): User's guide [NASA-TM-83887] p0135 N82-21826

NATIONAL AERONAUTICS AND SPACE ADMINISTRATION. LYNDON B. JOHNSON SPACE CENTER, HOUSTON, TEX.

Use of Landsat-derived temporal profiles for corn-soybean feature extraction and classification p0059 A82-26842

AgRISTARS: Foreign commodity production forecasting. Minutes of the annual formal project manager's review, including preliminary technical review reports of FY80 experiments [E82-10039] p0064 N82-19614

NATIONAL AERONAUTICS AND SPACE ADMINISTRATION. LANGLEY RESEARCH CENTER, HAMPTON, VA.

Influence of dissolved organic materials on turbid water optical properties and remote-sensing reflectance p0093 A82-20445

Sigma/deg/ signature of the Amazon rain forest obtained from the Seasat scatterometer p0125 A82-21027

SASS measurements of the Ku-band radar signature of the ocean p0093 A82-21917

The NASA participation in the 1980 EPA PEPE/NEROS field measurements program p0075 A82-26621

The microwave radiometer spacecraft: A design study. Executive summary p0131 N82-16154

Mission definition for a large-aperture microwave radiometer spacecraft p0131 N82-16155

Laboratory upwelled radiance and reflectance spectra of Kerr reservoir sediment waters [NASA-TP-1993] p0110 N82-21774

NATIONAL AERONAUTICS AND SPACE ADMINISTRATION. LEWIS RESEARCH CENTER, CLEVELAND, OHIO

Ground-truth observations of ice-covered North Slope Lakes imaged by radar [NASA-TM-84127] p0107 N82-18664

NATIONAL AERONAUTICS AND SPACE ADMINISTRATION. WALLOPS FLIGHT CENTER, WALLOPS ISLAND, VA.
NOSS altimeter algorithm specifications
[NASA-RP-1083] p0095 N82-16683

NATIONAL BUREAU OF STANDARDS, BOULDER, COLO.
Recovering ocean waveheight from HF radar sea echoes distorted by imperfect ionospheric reflection
[PB82-113283] p0096 N82-17805

NATIONAL CENTER FOR ATMOSPHERIC RESEARCH, BOULDER, COLO.
Low-latitude cloudiness and climate feedback - Comparative estimates from satellite data
p0075 A82-26980

NATIONAL ENVIRONMENTAL SATELLITE SERVICE, WASHINGTON, D. C.
Applications systems verification and transfer project. Volume 6: Operational applications of satellite snow-cover observations NOAA/NESS support study
[NASA-TP-1827] p0109 N82-20622

NATIONAL OCEANIC AND ATMOSPHERIC ADMINISTRATION, ROCKVILLE, MD.
Error analysis of pulse location estimates for simulated bathymetric lidar returns
[PB82-109448] p0096 N82-17803

NATIONAL OCEANIC AND ATMOSPHERIC ADMINISTRATION, SILVER SPRING, MD.
Demonstration of a long-range atmospheric tracer system using perfluorocarbons
[PB82-106246] p0081 N82-16613

NATIONAL OCEANIC AND ATMOSPHERIC ADMINISTRATION, WASHINGTON, D. C.
Publications and reports on contracts and grants, 1980
[PB82-103219] p0138 N82-17792
Evaluation of HCMM satellite data for estuarine tidal circulation patterns and thermal inertia soil moisture measurements
[E82-10064] p0108 N82-20587

NATIONAL RESEARCH INST. FOR OCEANOLOGY, STELLENBOSCH (SOUTH AFRICA).
Interaction between the Agulhas current and the subtropical convergence
[CSIR-RR-384] p0098 N82-20824

NATIONAL WEATHER SERVICE, FORT WORTH, TEX.
Weather satellite interpretation: Introduction to weather satellite imagery
[PB82-107657] p0118 N82-16677

NAVAL OCEAN RESEARCH AND DEVELOPMENT ACTIVITY, BAY ST. LOUIS, MISS.
Structure and variability of the Alboran Sea frontal system p0093 A82-20447

NAVAL OCEAN SYSTEMS CENTER, SAN DIEGO, CALIF.
Satellite-borne non-DOD sensors for terrestrial observations
[AD-A109486] p0134 N82-20630

NAVAL RESEARCH LAB., WASHINGTON, D. C.
Surface wave statistics and spectra during high sea state conditions in the North Atlantic
[AD-A109832] p0098 N82-20827

NAVAL SURFACE WEAPONS CENTER, DAHLGREN, VA.
Some altimetric signatures from Seasat over the mid-Pacific Seamount Range
[AD-A110419] p0099 N82-21691

NEBRASKA UNIV., LINCOLN.
A gradient model of vegetation and climate utilizing NOAA satellite imagery. Phase 1: Texas transect
[E82-10107] p0089 N82-21648

NORTH CAROLINA STATE UNIV., RALEIGH.
Remote sensing of salinity in the San Francisco Bay Delta p0102 A82-26839
Compatibility study of the MAGSAT data and aeromagnetic data
[E82-10136] p0123 N82-21663

O

OFFICE OF NAVAL RESEARCH, PASADENA, CALIF.
Arabian sea project of 1980: Composites of infrared images
[AD-A107910] p0096 N82-17567

OFFICE OF TECHNOLOGY ASSESSMENT, WASHINGTON, D. C.
Technology and oceanography: An assessment of Federal technologies for oceanographic research and monitoring
[OTA-O-142] p0097 N82-18844

OLD DOMINION UNIV., NORFOLK, VA.
The relationship among sea surface roughness variations, oceanographic analyses, and airborne remote sensing analyses
[NASA-CR-168444] p0096 N82-17798
Usage and limitations of characteristic vector analysis of remote sensing multispectral data for the identification and quantification of water quality parameters
p0118 N82-18656

P

PARIS VI UNIV. (FRANCE).
Preliminary models of the core field
[E82-10128] p0087 N82-21659
Continuation of potential field data to a common altitude
[E82-10138] p0123 N82-21665
Separation of internal and external fields: A new technique of data screening
[E82-10139] p0123 N82-21666

PENNSYLVANIA STATE UNIV., UNIVERSITY PARK.
Delineation of soil temperature regimes from HCMM data
[E82-10042] p0119 N82-19617
Interactive initialization of heat flux parameters for numerical models using satellite temperature measurements
[E82-10048] p0120 N82-19623
Application of satellite frost forecast technology to other parts of the United States, phase 2
[NASA-CR-166827] p0121 N82-20607
Freeze prediction model p0087 N82-20609
The Office for Remote Sensing of Earth Resources
p0121 N82-20612
Delineation of soil temperature regimes from HCMM data
[E82-10141] p0070 N82-21668
Applications of HCMM satellite data to the study of urban heating patterns
[E82-10161] p0080 N82-21685

PENNSYLVANIA UNIV., PHILADELPHIA.
Stochastic models of cover class dynamics
p0059 A82-27586

PHOENIX CORP., MCLEAN, VA.
Improved definition of crustal anomalies for Magsat data
[E82-10051] p0085 N82-19626

PUBLIC TECHNOLOGY, INC., WASHINGTON, D. C.
Remote sensing procurement package: A management report for state and local governments
[E82-10052] p0138 N82-19627

PURDUE UNIV., LAFAYETTE, IND.
Soybean canopy reflectance as a function of view and illumination geometry p0061 A82-27645
Evaluation of a segment-based LANDSAT full-frame approach to corp area estimation
[E82-10067] p0066 N82-20590
Effects of nitrogen nutrition on the growth, yield and reflectance characteristics of corn canopies
[E82-10068] p0067 N82-20591
Soybean canopy reflectance as influenced by cultural practices
[E82-10105] p0068 N82-21647
A multiband radiometer and data acquisition system for remote sensing field research
[E82-10142] p0134 N82-21669
Spectral-agronomic relationships of corn, soybean and wheat canopies
[E82-10143] p0070 N82-21670
Simulated response of a multispectral scanner over wheat as a function of wavelength and view/illumination direction
[E82-10144] p0071 N82-21671
Variability of reflectance measurements with sensor altitude and canopy type
[E82-10145] p0071 N82-21672
Determination of the optimal level for combining area and yield estimates
[E82-10146] p0071 N82-21673

R

READING UNIV. (ENGLAND).
Land cover classification accuracy as a function of sensor spatial resolution p0076 A82-27665

RESEARCH AND DATA SYSTEMS, INC., LANHAM, MD.
Development of a surface isolation estimation technique suitable for application of polar orbiting satellite data
[E82-10122] p0123 N82-21656

RESEARCH INST. OF NATIONAL DEFENCE, LINKOEPING (SWEDEN).
Observations with an imaging 35 GHz radiometer of terrain in Malmslatett, July 1980
[FOA-C-30240-E1/E3] p0133 N82-18672

RESEARCH INST. OF NATIONAL DEFENCE, STOCKHOLM (SWEDEN).
Remote sensing techniques suitable for exploration and navigation in and under sea ice
[FOA-REPT-VOL-15-NO-2] p0096 N82-17566

RESEARCH TRIANGLE INST., RESEARCH TRIANGLE PARK, N. C.
A study of model parameters associated with the urban climate using HCMM data
[E82-10140] p0079 N82-21667
A study of model parameters associated with the urban climate using HCMM data
[E82-10159] p0080 N82-21683
A study of model parameters associated with the urban climate using HCMM data
[E82-10160] p0080 N82-21684

ROYAL AIRCRAFT ESTABLISHMENT, FARNBOROUGH (ENGLAND).
Automatic relocation of ground control points in LANDSAT imagery
[RAE-TR-81071] p0118 N82-18657
An introduction to image processing at Royal Aircraft Establishment, Farnborough, England
[RAE-TR-80107] p0122 N82-21565
Computer based technique for converting a contour map into an equispaced grid of points
[RAE-TR-80110] p0087 N82-21697

ROYAL NETHERLANDS AIRCRAFT FACTORIES FOKKER, SCHIPHOL-OOST.
Development of a breadboard cooler for infrared remote sensing payloads, phase 1
[FOK-RV-R-81-064] p0134 N82-19653

ROYAL SIGNALS AND RADAR ESTABLISHMENT, MALVERN (ENGLAND).
The design and implementation of an operational, computer-based weather radar system
[RSRE-MEMO-3151] p0122 N82-21499

S

SAAB-SCANIA, LINKOPING (SWEDEN).
On the accuracy of thermal inertia mapping by infrared imagery
[SAAB-REPR-AE-10] p0120 N82-19656

SOIL CONSERVATION SERVICE, DENVER, COLO.
Applications systems verification and transfer project. Volume 4: Operational applications of satellite snow cover observations. Colorado Field Test Center
[NASA-TP-1825] p0108 N82-20620

SOUTH DAKOTA STATE UNIV., BROOKINGS.
Spectral reflectance of hydrophytes p0102 A82-24960
HCMM detection of high soil moisture areas
p0059 A82-24963
Remote sensing applications to resource problems in South Dakota
[E82-10027] p0132 N82-16445

SPAR AEROSPACE PRODUCTS LTD., TORONTO (ONTARIO).
Study of a radar altimeter for the European remote sensing program. Volume 1: Executive summary
[SPAR-R.1090-ISSUE-A] p0133 N82-19652

SRI INTERNATIONAL CORP., MENLO PARK, CALIF.
An experimental program to provide remote measurement and analysis of ocean waves, sea level winds and balanced pressure in support of Seasat-A
[PB81-246035] p0095 N82-16697

STANFORD UNIV., CALIF.
Model studies of laser absorption computed tomography for remote air pollution measurement p0077 A82-28152
Integration of LANDSAT with geology and airborne geophysics into an operational mineral exploration system
[E82-10028] p0091 N82-16446
HCMM: Soil moisture in relation to geologic structure and lithology, northern California
[E82-10135] p0092 N82-21662

STATE UNIV. OF NEW YORK, STONY BROOK.
Low-latitude cloudiness and climate feedback - Comparative estimates from satellite data
p0075 A82-26980

STATE UNIV. OF NEW YORK, SYRACUSE.
Ground level reflectance measurement techniques - An evaluation with emphasis on the importance of spectral calibration p0116 A82-27689

SYSTEMATICS GENERAL CORP., STERLING, VA.
Guidelines for spaceborne microwave remote sensors
[NASA-RP-1086] p0133 N82-19647

SYSTEMS AND APPLIED SCIENCES CORP., RIVERDALE, MD.
Simple radiative transfer model for relationships between canopy biomass and reflectance p0057 A82-20422

T

TEL-AVIV UNIV. (ISRAEL).
Contrast reduction by the atmosphere and retrieval of nonuniform surface reflectance p0112 A82-20423

TENNESSEE VALLEY AUTHORITY, CHATTANOOGA.
National High-Altitude Photography (NHAP) of the Tennessee Valley Region, volume 1, no. 1
[PB82-130899] p0134 N82-21703

TENNESSEE VALLEY AUTHORITY, NORRIS.
Remote sensing of sulfur dioxide effects on vegetation. Volume 1: Summary
[PB82-115122] p0066 N82-19715
Remote sensing of sulfur dioxide effects on vegetation. Volume 2: Data
[PB82-115130] p0066 N82-19716

TEXAS A&M UNIV., COLLEGE STATION.
HCMM detection of high soil moisture areas
p0059 A82-24963
Dryland pasture and crop conditions as seen by HCMM
[E82-10074] p0067 N82-20597

TEXAS UNIV. AT ARLINGTON.
Digital correlation of DDRS data
[NASA-CR-167494] p0118 N82-16452

THOMSON-CSF, MEUDON-LA-FORET (FRANCE).
Study of synthetic aperture radar in 2D - 2FS operation over the ocean
[ESA-CR(P)-1475] p0132 N82-18481

V

VIRGINIA POLYTECHNIC INST. AND STATE UNIV., BLACKSBURG.
Spatial reasoning in remotely sensed data
p0105 A82-27592

W

WASHINGTON UNIV., SEATTLE.
Sea ice movements from synthetic aperture radar
[AD-A109002] p0097 N82-19435
WASHINGTON UNIV., ST. LOUIS, MO.
Program on stimulating operational private sector use of Earth observation satellite information
[E82-10131] p0138 N82-21660
WISCONSIN UNIV. - MADISON.
Wetland mapping from digitized aerial photography
[E82-10019] p0118 N82-16437
The development and testing of methods to infer midlatitude precipitation intensity from geosynchronous satellite infrared data
[AD-A108881] p0120 N82-19788
WISCONSIN UNIV., MADISON.
Multidisciplinary research on the application of remote sensing to water resources problems
[E82-10021] p0106 N82-16439
Investigation of Antarctic crust and upper mantle using MAGSAT and other geophysical data
[E82-10062] p0088 N82-20585
Investigation of antarctic crust and upper mantle using MAGSAT and other geophysical data
[E82-10147] p0087 N82-21674
WOODS HOLE OCEANOGRAPHIC INSTITUTION, MASS.
Gravity and geoid anomalies of the Philippine Sea: Evidence on the depth of compensation for the negative residual water depth anomaly
[NASA-CR-168639] p0085 N82-19732
WORLD METEOROLOGICAL ORGANIZATION, GENEVA (SWITZERLAND).
Measurement of river sediments
[WMO-561] p0107 N82-18670
Flash flood forecasting
[WMO-577] p0107 N82-18671
WYOMING UNIV., LARAMIE.
Ozone measurements to 48Km with chemiluminescent ozone detectors
[AD-A110342] p0134 N82-21808

CONTRACT NUMBER INDEX

Typical Contract Number Index Listing

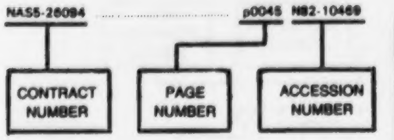

Listings in this index are arranged alphanumerically by contract number. Under each contract number, the accession numbers denoting documents that have been produced as a result of research done under that contract are arranged in ascending order with the AIAA accession numbers appearing first. The accession number denotes the number by which the citation is identified in the abstract section. Preceding the accession number is the page number on which the citation may be found.

AF PROJ. 627A p0109 N82-20822
AF PROJ. 4290 .... p0095 N82-16331
AF PROJ. 6670 .... p0120 N82-19788
AF PROJECT 2310 .... p0074 A82-21432
AF TASK 2310G1 .... p0074 A82-21432
AF-AFOSR-77-3271 .... p0113 A82-25139
DA PROJ. 4A7-62730-AT-42 .... p0064 N82-16455
DAAG53-76-C-0138 .... p0074 A82-25140
DACW39-77-C-0073 .... p0064 N82-16455
DACW72-81-M-0342 .... p0110 N82-21704
DARPA ORDER 3206 .... p0074 A82-25140
DE-AI01-80EV-10081 .... p0081 N82-16613
DITC PROJECT 534-3203 .... p0114 A82-27590
DSS-OSQ-80-00097 .... p0129 A82-27642
DSS-08SU-01525-7-0198 .... p0057 A82-20408
DTCG39-80-C-80052 .... p0132 N82-18466
EPA-R-806606-02 .... p0073 A82-20999
EPA-68-02-2439 .... p0074 A82-26329
ESA-3749/78/NL-HP p0124 N82-21699
ESA-4080/79/F-FC(SC) p0138 N82-18669
ESA-4241/80/F-FC(SC) p0124 N82-21698
ESA-4243/80/F-CG(SC) p0132 N82-18564
ESA-4367/80/F-DD(SC) p0133 N82-19650
p0133 N82-19651
ESA-4415/80/NL-PP(SC) p0120 N82-19649
ESA-4423/80/F-FC(SC) p0098 N82-19805
ESA-4427/80/F-DD(SC) p0133 N82-19652
ESA-4586/81/F-DD(SC) p0132 N82-18481
ESTEC-3749/78 .... p0120 N82-19654
ESTEC-4484/80/NL-PP(SC) p0134 N82-19653
F4920-77-C-0092 .... p0077 A82-28152
F19628-78-C-0131 .... p0109 N82-20822
F19628-78-C-0137 .... p0120 N82-19788
F19628-81-C-0001 .... p0095 N82-16331
JPL-955047 .... p0091 N82-16446
NAG1-189 .... p0096 N82-17798
NAG5-14 .... p0109 N82-20807
NAG5-18 .... p0085 N82-19732
NAG5-163 .... p0107 N82-19638
NASA ORDER C-00741 .... p0123 N82-21656
NASA ORDER S-40229B p0108 N82-20587
NASA ORDER S-40256-B p0113 A82-22146
NASA ORDER S-53772 .... p0109 N82-20622
NASA ORDER S-53877 .... p0109 N82-20621
NASA ORDER S-75406-B p0119 N82-19621
NASA ORDER S-75406B p0123 N82-21678
NASW-3331 .... p0138 N82-21660
NASW-3398 .... p0133 N82-19647
NASW-3541 .... p0134 N82-20606
NASW-3542 .... p0124 N82-21687
NAS1-15657 .... p0082 A82-27631
NAS1-16444 .... p0075 A82-26980
NAS5-20831 .... p0108 N82-20619
NAS5-21808 .... p0132 N82-16440
NAS5-23729 .... p0109 N82-20623
NAS5-24206 .... p0059 A82-24963
NAS5-24264 .... p0080 N82-21685
NAS5-24410 .... p0109 N82-20624
NAS5-24479 .... p0092 N82-21662
NAS5-25668 .... p0120 N82-19644
NAS5-25882 .... p0085 N82-19626
NAS5-25957 .... p0087 N82-21686
NAS5-25977 .... p0086 N82-20585
p0087 N82-21674
NAS5-26047 .... p0084 N82-19616
NAS5-26111 .... p0116 A82-27686
NAS5-26138 .... p0084 N82-19618
p0085 N82-19619
p0087 N82-21679
NAS5-26157 .... p0123 N82-21663
NAS5-26276 .... p0105 A82-27592
NAS5-26328 .... p0085 N82-19620
NAS5-26424 .... p0086 N82-20589
NAS5-26425 .... p0091 N82-19624
p0092 N82-21677
NAS5-26442 .... p0079 N82-21667
p0080 N82-21683
p0080 N82-21684
NAS5-26446 .... p0109 N82-21680
NAS5-26453 .... p0064 N82-19615
p0071 N82-21681
NAS5-26541 .... p0122 N82-21457
NAS7-100 .... p0093 A82-24061
p0093 A82-24063
p0074 A82-25452
p0113 A82-25455
p0127 A82-27578
p0128 A82-27580
p0128 A82-27594
p0083 N82-17708
NAS8-33822 .... p0126 A82-23045
NAS9-14565 .... p0070 N82-21658
NAS9-15421 .... p0058 A82-21033
NAS9-15486 .... p0061 A82-27645
p0066 N82-20590
p0067 N82-20591
p0068 N82-21647
p0134 N82-21669
p0070 N82-21670
p0071 N82-21671
p0071 N82-21672
p0071 N82-21673
NAS9-15476 .... p0063 N82-16448
p0066 N82-19635
p0070 N82-21658
NAS9-15800 .... p0081 A82-27662
p0118 N82-16438
p0064 N82-19607
p0064 N82-19608
p0064 N82-19610
p0065 N82-19630
p0065 N82-19631
p0065 N82-19632
p0065 N82-19634
p0066 N82-19636
p0068 N82-21635
p0068 N82-21636
p0122 N82-21637
p0122 N82-21638
p0068 N82-21639
p0068 N82-21640
p0122 N82-21641
p0123 N82-21642
p0123 N82-21643
p0068 N82-21644
p0068 N82-21645
p0123 N82-21646
p0069 N82-21649
p0069 N82-21650
p0069 N82-21651
p0069 N82-21652
p0070 N82-21654
p0070 N82-21655
p0070 N82-21657
p0070 N82-21661
p0071 N82-21676
p0072 N82-21682
NAS9-16208 .... p0118 N82-16452
NAS10-9876 .... p0121 N82-20607
NAS13-129 .... p0138 N82-19627
NA79SA-C-00738 .... p0095 N82-16697
NERC-GR/3/1481 .... p0059 A82-22144
NERC-GR/3/4076 .... p0058 A82-21093
NGL-05-007-004 .... p0082 A82-26266
NGL-17-004-024 .... p0063 N82-16447
NGL-25-001-054 .... p0078 N82-19609
NGL-33-010-171 .... p0116 A82-27689
NGL-42-003-007 .... p0102 A82-24960
p0132 N82-16445
NGL-50-002-127 .... p0106 N82-16439
NGR-22-009-839 .... p0088 N82-21796
NOAA-MO-A01-78-00-4330 .... p0094 A82-27596
NOAA-NA-80AAD0019 .... p0101 A82-22145
NOAA-04-M01-134 .... p0063 A82-27700
NR PROJ. 307-428 .... p0097 N82-19435
NSC-70-0404-E002-09 .... p0113 A82-22891
NSERC-A-5586 .... p0114 A82-27623
NSERC-A-6043 .... p0117 A82-27698
NSF ATM-79-00233 .... p0075 A82-26721
NSF ATM-80-12214 .... p0075 A82-26721
NSF ATM-80-24641 .... p0101 A82-21922
NSF ATM-81-03697 .... p0075 A82-26700
NSF CME-79-09065 .... p0075 A82-26980
NSF ECS-80-06884 .... p0113 A82-22891
NSF OCE-77-27735 .... p0097 N82-19796
NSG-1641 .... p0098 N82-20823
NSG-2289 .... p0077 A82-28152
NSG-5256 .... p0102 A82-26839
NSG-5325 .... p0059 A82-27586
NSG-5335 .... p0107 N82-19646
N00014-75-C-0396 .... p0082 A82-26266
N00014-76-C-0170 .... p0134 N82-21808
N00014-76-C-1048 .... p0130 A82-27675
N00014-79-C-0418 .... p0097 N82-19435
PROJ. AGRISTARS p0063 N82-16448
p0064 N82-19607
p0064 N82-19608
p0064 N82-19610
p0064 N82-19614
p0065 N82-19628
p0065 N82-19629
p0065 N82-19630
p0065 N82-19631
p0065 N82-19632
p0065 N82-19633
p0065 N82-19634
p0066 N82-19635
p0066 N82-19636
p0066 N82-20590
p0067 N82-20591
p0068 N82-21635
p0068 N82-21636
p0122 N82-21637
p0122 N82-21638
p0068 N82-21639
p0068 N82-21640
p0122 N82-21641
p0123 N82-21642
p0123 N82-21643
p0068 N82-21644
p0068 N82-21645
p0123 N82-21646
p0068 N82-21647
p0069 N82-21648
p0069 N82-21649
p0069 N82-21650
p0069 N82-21651
p0069 N82-21652
p0069 N82-21653
p0070 N82-21654
p0070 N82-21655
p0123 N82-21656
p0070 N82-21657
p0070 N82-21658
p0134 N82-21669
p0070 N82-21670
p0071 N82-21671
p0071 N82-21672
p0071 N82-21673
p0071 N82-21676
p0109 N82-21680
p0072 N82-21682
PROJ. CWIS-31350 .... p0106 N82-18469
RR0320841 .... p0098 N82-20827
SNSF-3,209,77 .... p0074 A82-24958
SRI PROJ. 8808 .... p0095 N82-16697
UN PROJECT MEX-120-8-004-05-X p0117 A82-27693
WF59553000 .... p0098 N82-20827
146-40-01-01 .... p0098 N82-19801
658-20-02 .... p0108 N82-20617
691-09-02-01 .... p0110 N82-21774
692-40-01 .... p0083 N82-17708

REPORT/ACCESSION NUMBER INDEX

EARTH RESOURCES / *A Continuing Bibliography (Issue 34)* **JULY 1982**

Typical Report/Accession Number Index Listing

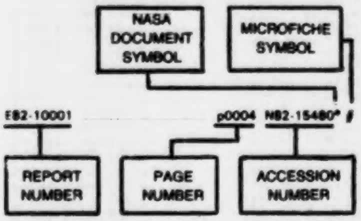

Listings in this index are arranged alphanumerically by report number. The page number indicates the page on which the citation is located. The accession number denotes the number by which the citation is identified. An asterisk (*) indicates that the item is a NASA report. A pound sign (#) indicates that the item is available on microfiche.

AD-A106133 p0095 N82-16331 #
AD-A106422 p0064 N82-16455 #
AD-A107910 p0096 N82-17567 #
AD-A108098 p0118 N82-17570 #
AD-A108192 p0106 N82-18469 #
AD-A108342 p0107 N82-18664* #
AD-A108404 p0132 N82-18466 #
AD-A108405 p0084 N82-18931 #
AD-A108406 p0084 N82-18930 #
AD-A108784 p0138 N82-20626 #
AD-A108881 p0120 N82-19788 #
AD-A109002 p0097 N82-19435 #
AD-A109050 p0098 N82-19802 #
AD-A109366 p0121 N82-20628 #
AD-A109484 p0134 N82-20491 #
AD-A109486 p0134 N82-20630 #
AD-A109832 p0098 N82-20827 #
AD-A109929 p0109 N82-20822 #
AD-A110280 p0087 N82-21690 #
AD-A110287 p0087 N82-21689 #
AD-A110342 p0134 N82-21808 #
AD-A110419 p0099 N82-21691 #

AFGL-TR-81-0252 p0120 N82-19788 #
AFGL-TR-81-0261 p0109 N82-20822 #

AIAA PAPER 82-0202 p0094 A82-27091* #

AP-70 p0134 N82-21808 #

ARL-TR-81-51 p0118 N82-16452* #

BAE-TP-7905 p0120 N82-19649 #

BLL-TRANS-1509-(9022.552) p0097 N82-19756

BR71459 p0122 N82-21499 #
BR76808 p0122 N82-21565 #
BR77598 p0087 N82-21697 #
BR80598 p0118 N82-18657

BTS-FR-80-117 p0120 N82-19644* #
BTS-FR-81-165 p0122 N82-21457* #

CRREL-SR-81-23 p0106 N82-18469 #

CRREL-81-19 p0107 N82-18664* #

CSIR-RR-384 p0098 N82-20824 #

CTAMN/81/R/10 p0098 N82-19805 #

DFVLR-FB-80-32 p0096 N82-17802 #

DOC-80SDS4229 p0132 N82-16440* #

EPA-600/7-81-113 p0066 N82-19715 #
EPA-600/7-81-114 p0066 N82-19716 #

ERIM-152400-5-T p0063 N82-16448* #
ERIM-152400-7-T p0066 N82-19635* #
ERIM-152400-12-T p0070 N82-21658* #

ERL-0192-TR p0098 N82-19802 #
ERL-0210-TM p0134 N82-20491 #

ESA-CR(P)-1438 p0124 N82-21698 #
ESA-CR(P)-1450 p0124 N82-21699 #
ESA-CR(P)-1468 p0132 N82-18564 #
ESA-CR(P)-1475 p0132 N82-18481 #
ESA-CR(P)-1476 p0138 N82-18669 #
ESA-CR(P)-1478 p0120 N82-19649 #
ESA-CR(P)-1479 p0098 N82-19805 #
ESA-CR(P)-1492-VOL-1 p0133 N82-19650 #
ESA-CR(P)-1492-VOL-2 p0133 N82-19651 #
ESA-CR(P)-1502 p0133 N82-19652 #
ESA-CR(P)-1506 p0134 N82-19653 #
ESA-CR(P)-1507 p0120 N82-19654 #

ESA-SP-172 p0122 N82-21458 #
ESA-SP-1030 p0124 N82-21700 #

ESA-TT-710 p0096 N82-17802 #

ESS/SS-1006 p0132 N82-18564 #

ETL-R028 p0121 N82-20628 #
ETL-R031 p0087 N82-21689 #

EW-LO-00707 p0065 N82-19630* #

EW-L1-00711 p0064 N82-19607* #
EW-L1-00732 p0069 N82-21652* #
EW-L1-04101 p0068 N82-21635* #
EW-L1-04134 p0070 N82-21657* #

E82-10019 p0118 N82-16437* #
E82-10020 p0118 N82-16438* #
E82-10021 p0106 N82-16439* #
E82-10022 p0132 N82-16440* #
E82-10023 p0118 N82-16441* #
E82-10024 p0091 N82-16442* #
E82-10025 p0081 N82-16443* #
E82-10026 p0132 N82-16444* #
E82-10027 p0132 N82-16445* #
E82-10028 p0091 N82-16446* #
E82-10029 p0063 N82-16447* #
E82-10030 p0063 N82-16448* #
E82-10031 p0064 N82-19607* #
E82-10032 p0064 N82-19608* #
E82-10033 p0078 N82-19609* #
E82-10034 p0064 N82-19610* #
E82-10035 p0119 N82-19611* #
E82-10036 p0119 N82-19612* #
E82-10037 p0078 N82-19601*
E82-10038 p0119 N82-19613* #
E82-10039 p0064 N82-19614* #
E82-10040 p0064 N82-19615* #
E82-10041 p0084 N82-19616* #
E82-10042 p0119 N82-19617* #
E82-10043 p0084 N82-19618* #
E82-10044 p0085 N82-19619* #
E82-10045 p0085 N82-19620* #
E82-10046 p0119 N82-19621* #
E82-10047 p0119 N82-19622* #
E82-10048 p0120 N82-19623* #
E82-10049 p0091 N82-19624* #
E82-10050 p0085 N82-19625* #
E82-10051 p0085 N82-19626* #
E82-10052 p0138 N82-19627* #
E82-10053 p0065 N82-19628* #
E82-10054 p0065 N82-19629* #
E82-10055 p0065 N82-19630* #
E82-10056 p0065 N82-19631* #
E82-10057 p0065 N82-19632* #
E82-10058 p0065 N82-19633* #
E82-10059 p0065 N82-19634* #
E82-10060 p0066 N82-19635* #
E82-10061 p0066 N82-19636* #
E82-10062 p0086 N82-20585* #
E82-10063 p0107 N82-20586* #
E82-10064 p0108 N82-20587* #
E82-10065 p0078 N82-20588* #
E82-10066 p0086 N82-20589* #
E82-10067 p0066 N82-20590* #
E82-10068 p0067 N82-20591* #
E82-10069 p0078 N82-20592* #
E82-10070 p0079 N82-20593* #
E82-10071 p0067 N82-20594* #
E82-10072 p0079 N82-20595* #
E82-10073 p0091 N82-20596* #
E82-10074 p0067 N82-20597* #
E82-10075 p0086 N82-20598* #
E82-10076 p0092 N82-20599* #
E82-10077 p0067 N82-20600* #
E82-10078 p0067 N82-20601* #
E82-10079 p0067 N82-20602* #
E82-10080 p0121 N82-20603* #
E82-10081 p0121 N82-20604* #
E82-10082 p0108 N82-20605* #
E82-10083 p0068 N82-21635* #
E82-10084 p0068 N82-21636* #
E82-10085 p0122 N82-21637* #
E82-10086 p0122 N82-21638* #
E82-10087 p0068 N82-21639* #
E82-10088 p0068 N82-21640* #
E82-10089 p0122 N82-21641* #
E82-10090 p0123 N82-21642* #
E82-10091 p0123 N82-21643* #
E82-10092 p0068 N82-21644* #
E82-10093 p0068 N82-21645* #
E82-10094 p0123 N82-21646* #
E82-10105 p0068 N82-21647* #
E82-10107 p0069 N82-21648* #
E82-10108 p0069 N82-21649* #
E82-10109 p0069 N82-21650* #
E82-10111 p0069 N82-21651* #
E82-10115 p0069 N82-21652* #
E82-10116 p0069 N82-21653* #
E82-10117 p0070 N82-21654* #
E82-10118 p0070 N82-21655* #
E82-10122 p0123 N82-21656* #
E82-10123 p0070 N82-21657* #
E82-10127 p0070 N82-21658* #
E82-10129 p0087 N82-21659* #
E82-10131 p0138 N82-21660* #
E82-10133 p0070 N82-21661* #
E82-10135 p0092 N82-21662* #
E82-10136 p0123 N82-21663* #
E82-10137 p0092 N82-21664* #
E82-10138 p0123 N82-21665* #
E82-10139 p0123 N82-21666* #
E82-10140 p0079 N82-21667* #
E82-10141 p0070 N82-21668* #
E82-10142 p0134 N82-21669* #
E82-10143 p0070 N82-21670* #
E82-10144 p0071 N82-21671* #
E82-10145 p0071 N82-21672* #
E82-10146 p0071 N82-21673* #
E82-10147 p0087 N82-21674* #
E82-10148 p0087 N82-21675* #
E82-10150 p0071 N82-21676* #
E82-10152 p0092 N82-21677* #
E82-10154 p0123 N82-21678* #
E82-10155 p0087 N82-21679* #
E82-10156 p0109 N82-21680* #
E82-10157 p0071 N82-21681* #
E82-10158 p0072 N82-21682* #
E82-10159 p0080 N82-21683* #
E82-10160 p0080 N82-21684* #
E82-10161 p0080 N82-21685* #
E82-10162 p0087 N82-21686* #

FC-J0-00502 p0064 N82-19614* #
FC-J1-04108 p0069 N82-21653* #
FC-J1-04176 p0069 N82-21646* #

FC-LI-04153 p0070 N82-21654* #

FC-LO-00480 p0065 N82-19631* #
FC-LO-00493 p0066 N82-19636* #

FC-L1-00714 p0068 N82-21645* #
FC-L1-00718-VOL-1 p0068 N82-21639* #
FC-L1-04073 p0068 N82-21640* #
FC-L1-04120-JSC-17401 p0070 N82-21655* #

FC-P1-04121 p0066 N82-20590* #
FC-P1-04197 p0071 N82-21673* #

FOA-B-60002-M7 p0096 N82-17566 #

FOA-C-30240-E1/E3 p0133 N82-18672 #

FOA-REPT-VOL-15-NO-2 p0096 N82-17566 #

FOK-RV-R-81-064 p0134 N82-19653 #

FSU-MET-STU-81/2 p0097 N82-19796 #

INPE-1923-RPE/249 p0091 N82-16442* #
INPE-1972-RPE/278 p0079 N82-20595* #
INPE-2019-NTE/166 p0078 N82-20592* #
INPE-2021-RPE/288 p0067 N82-20594* #
INPE-2063-RPE/305 p0118 N82-16441* #
INPE-2064-RPE/306 p0078 N82-20588* #
INPE-2081-RPE/315 p0081 N82-16443* #
INPE-2104-RPE/331 p0133 N82-18881 #
INPE-2119-RPE/343 p0083 N82-17711 #
INPE-2154-RPE/373 p0108 N82-20605* #
INPE-2163-RPE/381 p0067 N82-20602* #
INPE-2169-RPE/385 p0118 N82-16450 #
INPE-2170-RPE/386 p0121 N82-20604* #
INPE-2190-RPE/002 p0092 N82-20599* #
INPE-2191-RPE/003 p0121 N82-20603* #
INPE-2196-RPE/005 p0067 N82-20601* #
INPE-2197-PRE/006 p0066 N82-19639 #
INPE-2199-RPE/007 p0067 N82-20600* #
INPE-2209-MD/007 p0091 N82-19642 #
INPE-2211-MD/008 p0078 N82-19641 #
INPE-2212-MD/009 p0133 N82-19520 #
INPE-2215-MD/010 p0066 N82-19640 #
INPE-2229-PRE/021 p0097 N82-19704 #
INPE-2231-RPE/399 p0064 N82-17746 #
INPE-2240-PRE/026 p0078 N82-19256 #
INPE-2246-PRE/030 p0107 N82-19304 #
INPE-2303-TDL/072 p0121 N82-19927 #
INPE-2307-TDL/074 p0097 N82-19778 #

ISBN-3-7696-9663-8 p0084 N82-19603
ISBN-91-7056-057-9 p0096 N82-17566 #
ISBN-92-63-10561-8 p0107 N82-18670 #
ISBN-92-63-10577-4 p0107 N82-18671 #

ISSN-0065-5341 p0084 N82-19603
ISSN-0069-5882 p0078 N82-19740 #
ISSN-0071-9196 p0085 N82-19648 #
ISSN-0379-6566 p0122 N82-21458 #
ISSN-0379-6566 p0124 N82-21700 #

JPL-PUB-81-96 p0083 N82-17708* #

JSC-16366 p0065 N82-19632* #
JSC-16380 p0065 N82-19631* #
JSC-16820 p0066 N82-19636* #
JSC-16823 p0064 N82-19614* #
JSC-16824 p0065 N82-19633* #
JSC-16830 p0065 N82-19634* #
JSC-16833 p0065 N82-19630* #
JSC-16841 p0065 N82-19629* #
JSC-16842 p0065 N82-19628* #
JSC-16860 p0069 N82-21653* #
JSC-16956 p0070 N82-21661* #
JSC-17037 p0123 N82-21646* #
JSC-17101 p0118 N82-16438* #
JSC-17113 p0071 N82-21676* #
JSC-17114 p0064 N82-19607* #
JSC-17119 p0064 N82-19608* #
JSC-17129 p0068 N82-21640* #
JSC-17137 p0064 NP2-19610* #
JSC-17141 p0068 N82-21645* #
JSC-17155-VOL-1 p0068 N82-21639* #
JSC-17231 p0123 N82-21643* #
JSC-17251 p0068 N82-21635* #
JSC-17296 p0068 N82-21636* #
JSC-17369 p0068 N82-21644* #
JSC-17371 p0122 N82-21641* #
JSC-17389 p0122 N82-21637* #
JSC-17390 p0123 N82-21642* #
JSC-17400 p0122 N82-21638* #
JSC-17402 p0072 N82-21682* #
JSC-17413 p0070 N82-21657* #
JSC-17418 p0069 N82-21650* #
JSC-17422 p0069 N82-21649* #
JSC-17427 p0070 N82-21654* #
JSC-17435 p0069 N82-21648* #
JSC-17784 p0123 N82-21656* #
JSC-17793 p0069 N82-21652* #

L-14992 p0110 N82-21774* #

LARS-021781 p0068 N82-21647* #
LARS-030381 p0067 N82-20591* #
LARS-062381 p0066 N82-20590* #
LARS-071480 p0134 N82-21669* #
LARS-071580 p0071 N82-21671* #
LARS-091281 p0070 N82-21670* #
LARS-101281 p0071 N82-21673* #
LARS-111481 p0071 N82-21672* #

LEMSCO-14056 p0069 N82-21651* #
LEMSCO-14307 p0065 N82-19632* #
LEMSCO-14640 p0065 N82-19634* #
LEMSCO-14674 p0072 N82-21682* #
LEMSCO-14811 p0065 N82-19631* #
LEMSCO-15116 p0066 N82-19636* #
LEMSCO-15409 p0070 N82-21654* #
LEMSCO-15604 p0070 N82-21661* #
LEMSCO-15692 p0065 N82-19630* #
LEMSCO-15708 p0064 N82-19610* #
LEMSCO-15905 p0118 N82-16438* #
LEMSCO-15937 p0123 N82-21646* #
LEMSCO-16034 p0064 N82-19607* #
LEMSCO-16035 p0071 N82-21676* #
LEMSCO-16204 p0068 N82-21635* #
LEMSCO-16207 p0064 N82-19608* #
LEMSCO-16300 p0123 N82-21643* #
LEMSCO-16315 p0068 N82-21640* #
LEMSCO-16340 p0068 N82-21636* #
LEMSCO-16376 p0122 N82-21638* #
LEMSCO-16649 p0068 N82-21644* #
LEMSCO-16650 p0122 N82-21641* #
LEMSCO-16663 p0070 N82-21655* #
LEMSCO-16676 p0122 N82-21637* #
LEMSCO-16677 p0123 N82-21642* #
LEMSCO-16844 p0070 N82-21657* #
LEMSCO-16850 p0068 N82-21645* #
LEMSCO-16851-VOL-1 p0068 N82-21639* #
LEMSCO-17154 p0069 N82-21650* #
LEMSCO-17163 p0069 N82-21649* #
LEMSCO-17179 p0069 N82-21652* #

MITT-28 p0078 N82-19740 #

MTR-8299 p0095 N82-16331 #

MU-JO-0100 p0065 N82-19629* #
MU-JO-0101 p0065 N82-19628* #

MU-L1-04055 p0064 N82-19608* #

NAS 1.15:76796 p0134 N82-20606* #
NAS 1.15:76830 p0124 N82-21687* #
NAS 1.15:83887 p0135 N82-21826* #
NAS 1.26:160887 p0069 N82-21651* #
NAS 1.26:161051 p0070 N82-21661* #
NAS 1.26:161055 p0068 N82-21645* #
NAS 1.26:161056 p0123 N82-21646* #
NAS 1.26:161057 p0068 N82-21640* #
NAS 1.26:161058 p0068 N82-21636* #
NAS 1.26:161059 p0068 N82-21635* #
NAS 1.26:161060 p0122 N82-21637* #
NAS 1.26:161061 p0122 N82-21638* #
NAS 1.26:161063 p0068 N82-21639* #
NAS 1.26:161064 p0122 N82-21641* #
NAS 1.26:161065 p0123 N82-21642* #
NAS 1.26:161066 p0123 N82-21643* #
NAS 1.26:161067 p0068 N82-21644* #
NAS 1.26:164927 p0071 N82-21681* #
NAS 1.26:165084 p0086 N82-20585* #
NAS 1.26:165085 p0107 N82-20586* #
NAS 1.26:165086 p0108 N82-20587* #
NAS 1.26:165087 p0078 N82-20588* #
NAS 1.26:165088 p0086 N82-20589* #
NAS 1.26:165090 p0067 N82-20591* #
NAS 1.26:165091 p0078 N82-20592* #
NAS 1.26:165092 p0079 N82-20593* #
NAS 1.26:165093 p0067 N82-20594* #
NAS 1.26:165094 p0079 N82-20595* #
NAS 1.26:165095 p0091 N82-20596* #
NAS 1.26:165096 p0067 N82-20597* #
NAS 1.26:165097 p0086 N82-20598* #
NAS 1.26:166729 p0109 N82-21680* #
NAS 1.26:166789 p0122 N82-21457* #
NAS 1.26:167400 p0066 N82-20590* #
NAS 1.26:167409 p0071 N82-21676* #
NAS 1.26:167417 p0072 N82-21682* #
NAS 1.26:167434 p0069 N82-21653* #
NAS 1.26:167438 p0070 N82-21654* #
NAS 1.26:167439 p0070 N82-21655* #
NAS 1.26:167447 p0069 N82-21650* #
NAS 1.26:167448 p0069 N82-21649* #
NAS 1.26:167451 p0070 N82-21658* #
NAS 1.26:167454 p0069 N82-21648* #
NAS 1.26:167456 p0068 N82-21647* #
NAS 1.26:167473 p0123 N82-21656* #
NAS 1.26:167474 p0070 N82-21657* #
NAS 1.26:167480 p0069 N82-21652* #
NAS 1.26:167505 p0071 N82-21671* #
NAS 1.26:167506 p0134 N82-21669* #
NAS 1.26:167509 p0071 N82-21672* #
NAS 1.26:167510 p0070 N82-21670* #
NAS 1.26:168397 p0092 N82-20599* #
NAS 1.26:168399 p0067 N82-20600* #
NAS 1.26:168399 p0067 N82-20601* #
NAS 1.26:168400 p0067 N82-20602* #
NAS 1.26:168401 p0121 N82-20603* #
NAS 1.26:168402 p0121 N82-20604* #
NAS 1.26:168403 p0108 N82-20605* #
NAS 1.26:168512 p0109 N82-20807* #
NAS 1.26:168513 p0087 N82-21659* #
NAS 1.26:168515 p0138 N82-21660* #
NAS 1.26:168518 p0092 N82-21662* #
NAS 1.26:168521 p0123 N82-21663* #
NAS 1.26:168522 p0092 N82-21664* #
NAS 1.26:168523 p0123 N82-21665* #
NAS 1.26:168524 p0123 N82-21666* #
NAS 1.26:168525 p0079 N82-21667* #
NAS 1.26:168526 p0070 N82-21668* #
NAS 1.26:168531 p0071 N82-21673* #
NAS 1.26:168532 p0087 N82-21674* #
NAS 1.26:168533 p0087 N82-21675* #
NAS 1.26:168537 p0092 N82-21677* #
NAS 1.26:168539 p0123 N82-21678* #
NAS 1.26:168540 p0087 N82-21679* #
NAS 1.26:168542 p0080 N82-21683* #
NAS 1.26:168543 p0080 N82-21684* #
NAS 1.26:168544 p0080 N82-21685* #
NAS 1.26:168545 p0087 N82-21686* #
NAS 1,26:168681 p0098 N82-20823* #
NAS 1.26:168743 p0088 N82-21796* #
NAS 1.60:1818 p0109 N82-20623* #
NAS 1.60:1822 p0108 N82-20617* #
NAS 1.60:1823 p0108 N82-20618* #
NAS 1.60:1824 p0108 N82-20619* #
NAS 1.60:1825 p0108 N82-20620* #
NAS 1.60:1826 p0109 N82-20621* #
NAS 1.60:1827 p0109 N82-20622* #
NAS 1.60:1829 p0109 N82-20624* #
NAS 1.60:1993 p0110 N82-21774* #

NASA-CR-160887 p0069 N82-21651* #
NASA-CR-161021 p0065 N82-19633* #
NASA-CR-161022 p0066 N82-19636* #
NASA-CR-161023 p0065 N82-19634* #
NASA-CR-161024 p0065 N82-19631* #
NASA-CR-161025 p0065 N82-19632* #
NASA-CR-161028 p0065 N82-19628* #
NASA-CR-161029 p0065 N82-19629* #
NASA-CR-161032 p0064 N82-19607* #
NASA-CR-161033 p0064 N82-19608* #
NASA-CR-161034 p0064 N82-19610* #
NASA-CR-161038 p0065 N82-19630* #
NASA-CR-161046 p0118 N82-16438* #
NASA-CR-161051 p0070 N82-21661* #
NASA-CR-161055 p0068 N82-21645* #
NASA-CR-161056 p0123 N82-21646* #
NASA-CR-161057 p0068 N82-21640* #
NASA-CR-161058 p0068 N82-21636* #
NASA-CR-161059 p0068 N82-21635* #
NASA-CR-161060 p0122 N82-21637* #
NASA-CR-161061 p0122 N82-21638* #
NASA-CR-161063 p0068 N82-21639* #
NASA-CR-161064 p0122 N82-21641* #
NASA-CR-161065 p0123 N82-21642* #
NASA-CR-161066 p0123 N82-21643* #
NASA-CR-161067 p0068 N82-21644* #
NASA-CR-161081 p0063 N82-16448* #
NASA-CR-164392 p0132 N82-16440* #
NASA-CR-164433 p0091 N82-16446* #
NASA-CR-164746 p0078 N82-19609* #
NASA-CR-164756 p0063 N82-16447* #
NASA-CR-164771 p0078 N82-19601*
NASA-CR-164772 p0119 N82-19612* #
NASA-CR-164810 p0132 N82-16445* #
NASA-CR-164811 p0132 N82-16444* #
NASA-CR-164812 p0081 N82-16443* #
NASA-CR-164813 p0091 N82-16442* #
NASA-CR-164814 p0118 N82-16441* #
NASA-CR-164815 p0106 N82-16439* #
NASA-CR-164816 p0118 N82-16437* #
NASA-CR-164917 p0064 N82-19615* #
NASA-CR-164918 p0084 N82-19616* #
NASA-CR-164919 p0119 N82-19617* #
NASA-CR-164920 p0084 N82-19618* #
NASA-CR-164921 p0085 N82-19619* #
NASA-CR-164922 p0085 N82-19620* #
NASA-CR-164923 p0119 N82-19621* #
NASA-CR-164924 p0119 N82-19622* #
NASA-CR-164925 p0120 N82-19623* #
NASA-CR-164926 p0091 N82-19624* #
NASA-CR-164927 p0071 N82-21681* #
NASA-CR-164928 p0085 N82-19626* #
NASA-CR-165084 p0086 N82-20585* #
NASA-CR-165085 p0107 N82-20586* #
NASA-CR-165086 p0108 N82-20587* #
NASA-CR-165087 p0078 N82-20588* #
NASA-CR-165088 p0086 N82-20589* #
NASA-CR-165090 p0067 N82-20591* #
NASA-CR-165091 p0078 N82-20592* #
NASA-CR-165092 p0079 N82-20593* #
NASA-CR-165093 p0067 N82-20594* #
NASA-CR-165094 p0079 N82-20595* #
NASA-CR-165095 p0091 N82-20596* #
NASA-CR-165096 p0067 N82-20597* #
NASA-CR-165097 p0086 N82-20598* #
NASA-CR-166727 p0107 N82-19646* #
NASA-CR-166729 p0109 N82-21680* #
NASA-CR-166764 p0107 N82-19638* #
NASA-CR-166768 p0120 N82-19644* #
NASA-CR-166789 p0122 N82-21457* #
NASA-CR-166827 p0121 N82-20607* #
NASA-CR-167400 p0066 N82-20590* #
NASA-CR-167409 p0071 N82-21676* #
NASA-CR-167417 p0072 N82-21682* #
NASA-CR-167420 p0066 N82-19635* #
NASA-CR-167434 p0069 N82-21653* #
NASA-CR-167438 p0070 N82-21654* #
NASA-CR-167439 p0070 N82-21655* #
NASA-CR-167447 p0069 N82-21650* #
NASA-CR-167448 p0069 N82-21649* #
NASA-CR-167451 p0070 N82-21658* #
NASA-CR-167454 p0069 N82-21648* #
NASA-CR-167456 p0068 N82-21647* #
NASA-CR-167473 p0123 N82-21656* #
NASA-CR-167474 p0070 N82-21657* #
NASA-CR-167480 p0069 N82-21652* #
NASA-CR-167494 p0118 N82-16452* #
NASA-CR-167505 p0071 N82-21671* #
NASA-CR-167506 p0134 N82-21669* #
NASA-CR-167509 p0071 N82-21672* #

NASA-CR-167510 p0070 N82-21670* #
NASA-CR-168397 p0092 N82-20599* #
NASA-CR-168398 p0067 N82-20600* #
NASA-CR-168399 p0067 N82-20601* #
NASA-CR-168400 p0067 N82-20602* #
NASA-CR-168401 p0121 N82-20603* #
NASA-CR-168402 p0121 N82-20604* #
NASA-CR-168403 p0108 N82-20605* #
NASA-CR-168427 p0083 N82-17708* #
NASA-CR-168444 p0096 N82-17798* #
NASA-CR-168512 p0109 N82-20807* #
NASA-CR-168513 p0087 N82-21659* #
NASA-CR-168515 p0138 N82-21660* #
NASA-CR-168518 p0092 N82-21662* #
NASA-CR-168521 p0123 N82-21663* #
NASA-CR-168522 p0092 N82-21664* #
NASA-CR-168523 p0123 N82-21665* #
NASA-CR-168524 p0123 N82-21666* #
NASA-CR-168525 p0079 N82-21667* #
NASA-CR-168526 p0070 N82-21668* #
NASA-CR-168531 p0071 N82-21673* #
NASA-CR-168532 p0087 N82-21674* #
NASA-CR-168533 p0087 N82-21675* #
NASA-CR-168537 p0092 N82-21677* #
NASA-CR-168539 p0123 N82-21678* #
NASA-CR-168540 p0087 N82-21679* #
NASA-CR-168542 p0080 N82-21683* #
NASA-CR-168543 p0080 N82-21684* #
NASA-CR-168544 p0080 N82-21685* #
NASA-CR-168545 p0087 N82-21686* #
NASA-CR-168557 p0097 N82-18660* #
NASA-CR-168633 p0138 N82-19627* #
NASA-CR-168639 p0085 N82-19732* #
NASA-CR-168681 p0098 N82-20823* #
NASA-CR-168743 p0088 N82-21796* #

NASA-RP-1083 p0095 N82-16683* #
NASA-RP-1086 p0133 N82-19647* #

NASA-TM-76796 p0134 N82-20606* #
NASA-TM-76830 p0124 N82-21687* #
NASA-TM-82098 p0119 N82-19613* #
NASA-TM-82163 p0084 N82-17715* #
NASA-TM-83812 p0096 N82-17563* #
NASA-TM-83818 p0120 N82-19645* #
NASA-TM-83825 p0085 N82-19731* #
NASA-TM-83854 p0097 N82-19781* #
NASA-TM-83858 p0106 N82-18663* #
NASA-TM-83865 p0095 N82-17561* #
NASA-TM-83867 p0081 N82-17562* #
NASA-TM-83868 p0083 N82-17714* #
NASA-TM-83887 p0135 N82-21826* #
NASA-TM-84040 p0078 N82-18808* #
NASA-TM-84050 p0064 N82-19614* #
NASA-TM-84127 p0107 N82-18664* #
NASA-TM-84129 p0085 N82-19625* #
NASA-TM-84130 p0119 N82-19611* #
NASA-TM-84467 p0098 N82-19801* #

NASA-TP-1822 p0108 N82-20617* #
NASA-TP-1823 p0108 N82-20618* #
NASA-TP-1824 p0108 N82-20619* #
NASA-TP-1825 p0108 N82-20620* #
NASA-TP-1826 p0109 N82-20621* #
NASA-TP-1827 p0109 N82-20622* #
NASA-TP-1828 p0109 N82-20623* #
NASA-TP-1829 p0109 N82-20624* #
NASA-TP-1993 p0110 N82-21774* #

NOAA-TM-ERL-ARL-101 p0081 N82-16613 #

NOAA-TM-ERL-WPL-73 p0096 N82-17805 #

NOAA-TM-NESS-115 p0138 N82-17792 #

NOAA-TM-NWS-SR-103 p0118 N82-16677 #

NOAA-TR-OTES-1 p0096 N82-17803 #

NOAA-81071410 p0095 N82-16697 #
NOAA-81072202 p0138 N82-17792 #
NOAA-81080301 p0081 N82-16613 #
NOAA-81081101 p0096 N82-17803 #
NOAA-81081105 p0118 N82-16677 #
NOAA-81081901 p0096 N82-17805 #

NOSC/TD-458 p0134 N82-20630 #

NRL-MR-4722 p0098 N82-20827 #

NSF/IDOE-81-44 p0097 N82-19796 #

NSF/IDOE/CUEA/TR-39 p0097 N82-19796 #

NSWC/TR-81-440 p0099 N82-21691 #

OHR-16 p0107 N82-18670 #
OHR-18 p0107 N82-18671 #

ORNWEST-81-5 p0096 N82-17567 #

OTA-O-142 p0097 N82-18844 #

PB80-215130 p0073 A82-19177
PB81-246035 p0095 N82-16697 #

PB82-103219 p0138 N82-17792 #
PB82-106245 p0081 N82-16613 #
PB82-107657 p0118 N82-16677 #
PB82-109448 p0096 N82-17803 #
PB82-113283 p0096 N82-17805 #
PB82-114703 p0097 N82-19796 #
PB82-115122 p0066 N82-19715 #
PB82-115130 p0066 N82-19716 #
PB82-130899 p0134 N82-21703 #
PB82-137142 p0110 N82-21704 #

PR-4 p0123 N82-21678* #
PR-1325-2 p0086 N82-20589* #

QPR-3 p0119 N82-19621* #
QPR-4 p0085 N82-19619* #
QPR-5 p0084 N82-19618* #
QPR-6 p0086 N82-20585* #
QPR-6 p0087 N82-21679* #

QR-1 p0064 N82-19615* #
QR-2 p0120 N82-19623* #
QR-2 p0107 N82-20586* #
QR-2 p0092 N82-21677* #
QR-2 p0071 N82-21681* #
QR-3 p0091 N82-19624* #
QR-4 p0085 N82-19620* #
QR-6 p0084 N82-19616* #
QR-6 p0085 N82-19626* #

QSTPR-7 p0087 N82-21686* #

QTPR-7 p0087 N82-21674* #

RAE-SPACE-585 p0122 N82-21565 #
RAE-SPACE-586 p0087 N82-21697 #
RAE-SPACE-598 p0118 N82-18657

RAE-TR-80107 p0122 N82-21565 #
RAE-TR-80110 p0087 N82-21697 #
RAE-TR-81071 p0118 N82-18657

RC-LO-00479 p0069 N82-21651* #

REPT-44 2866 p0124 N82-21699 #
REPT-44/130 p0120 N82-19654 #
REPT-81F0060-VOL-1 p0108 N82-20617* #
REPT-81F0061-VOL-2 p0108 N82-20618* #
REPT-81F0062-VOL-3 p0108 N82-20619* #
REPT-81F0063-VOL-4 p0108 N82-20620* #
REPT-81F0064-VOL-5 p0109 N82-20621* #
REPT-81F0065-VOL-6 p0109 N82-20622* #
REPT-81F0066-VOL-7 p0109 N82-20623* #
REPT-81F0067-VOL-8 p0109 N82-20624* #
REPT-622-233 p0097 N82-18660* #
REPT-3318 p0124 N82-21698 #

RR-L1-04146 p0069 N82-21649* #

RRI-L1-04143 p0069 N82-21650* #

RSC-4 p0107 N82-19790 #

RSL-TR-410-3 p0107 N82-19646* #
RSL-TR-527-1 p0107 N82-19638* #

RSRE-MEMO-3151 p0122 N82-21499 #

SAAB-REPR-AE-10 p0120 N82-19656 #

SAPR-15 p0078 N82-19609* #

SCIENTIFIC-3 p0120 N82-19788 #

SDSU-RSI-81-03 p0132 N82-16445* #

SER-B-253-MITT-159-PT-2 p0085 N82-19648 #

SER-E-18 p0084 N82-19603

SM-LO-00463 p0065 N82-19632* #

SM-L1-04051 p0068 N82-21636* #

SPAR-R 1090-ISSUE-A p0133 N82-19652 #

SR-EL-04131 p0063 N82-16448* #

SR-E1-04138 p0066 N82-19635* #
SR-E1 04174 p0070 N82-21658* #

SR-LI-00306 p0123 N82-21646* #
SR-LI-04049 p0071 N82-21676* #

SR-LO-04002 p0065 N82-19634* #

SR-L1-0409 p0064 N82-19610* #
SR-L1-00301 p0122 N82-21637* #
SR-L1-00302 p0123 N82-21642* #
SR-L1-00304 p0068 N82-21644* #
SR-L1-00305 p0122 N82-21641* #
SR-L1-00307 p0123 N82-21643* #
SR-L1-00717 p0122 N82-21638* #
SR-L1-04122 p0072 N82-21682* #

SR-PI-04187 p0070 N82-21670* #

SR-P1-04038 p0068 N82-21647* #
SR-P1-04044 p0067 N82-20591* #
SR-P1-04191 p0071 N82-21672* #
SR-P1-04201 p0134 N82-21669* #
SR-P1-04202 p0071 N82-21671* #

SR-UO-00497 p0065 N82-19633* #

TR-81-2 p0096 N82-17798* #

TVA/ONR/ARP-81/5-VOL-1 p0066 N82-19715 #
TVA/ONR/ARP-81/6-VOL-2 p0066 N82-19716 #

TVA/ONR/NRO-82/3 p0134 N82-21703 #

USCG-D-64-81 p0132 N82-18466 #

WES/TR/EL-81-6 p0064 N82-16455 #

WHOI-4931 p0085 N82-19732* #

WMO-561 p0107 N82-18670 #
WMO-577 p0107 N82-18671 #

YM-N1-04198 p0123 N82-21656* #

1. Report No. NASA SP-7041 (34)	2. Government Accession No.	3. Recipient's Catalog No.
4. Title and Subtitle EARTH RESOURCES A Continuing Bibliography (Issue 34)		5. Report Date July 1982
		6. Performing Organization Code
7. Author(s)		8. Performing Organization Report No.
		10. Work Unit No.
9. Performing Organization Name and Address National Aeronautics and Space Administration Washington, DC 20546		11. Contract or Grant No.
		13. Type of Report and Period Covered
12. Sponsoring Agency Name and Address		14. Sponsoring Agency Code
15. Supplementary Notes		

16. Abstract

This bibliography list 567 reports, articles, and other documents introduced into the NASA Scientific and Technical Information System between April 1, and June 30, 1982. Emphasis is placed on the use of remote sensing and geophysical instrumentation in spacecraft and aircraft to survey and inventory natural resources and urban areas. Subject matter is grouped according to agriculture and forestry, environmental changes and cultural resources, geodesy and cartography, geology and mineral resources, hydrology and water management, data processing and distribution systems, instrumentation and sensors, and economic analysis.

17. Key Words (Suggested by Author(s)) Bibliographies Earth Resources Remote Sensors		18. Distribution Statement Unclassified - Unlimited	
19. Security Classif. (of this report) Unclassified	20. Security Classif. (of this page) Unclassified	21. No. of Pages 152	22. Price* $10.50 HC

*For sale by the National Technical Information Service, Springfield, Virginia 22161

NASA-Langley, 1982

PUBLIC COLLECTIONS OF NASA DOCUMENTS

DOMESTIC

NASA distributes its technical documents and bibliographic tools to eleven special libraries located in the organizations listed below. Each library is prepared to furnish the public such services as reference assistance, interlibrary loans, photocopy service, and assistance in obtaining copies of NASA documents for retention.

CALIFORNIA
University of California, Berkeley

COLORADO
University of Colorado, Boulder

DISTRICT OF COLUMBIA
Library of Congress

GEORGIA
Georgia Institute of Technology, Atlanta

ILLINOIS
The John Crerar Library, Chicago

MASSACHUSETTS
Massachusetts Institute of Technology, Cambridge

MISSOURI
Linda Hall Library, Kansas City

NEW YORK
Columbia University, New York

OKLAHOMA
University of Oklahoma, Bizzell Library

PENNSYLVANIA
Carnegie Library of Pittsburgh

WASHINGTON
University of Washington, Seattle

NASA publications (those indicated by an "*" following the accession number) are also received by the following public and free libraries:

CALIFORNIA
Los Angeles Public Library
San Diego Public Library

COLORADO
Denver Public Library

CONNECTICUT
Hartford Public Library

MARYLAND
Enoch Pratt Free Library, Baltimore

MASSACHUSETTS
Boston Public Library

MICHIGAN
Detroit Public Library

MINNESOTA
Minneapolis Public Library and Information Center

NEW JERSEY
Trenton Public Library

NEW YORK
Brooklyn Public Library
Buffalo and Erie County Public Library
Rochester Public Library
New York Public Library

OHIO
Akron Public Library
Cincinnati and Hamilton County Public Library
Cleveland Public Library
Dayton Public Library
Toledo and Lucas County Public Library

TEXAS
Dallas Public Library
Fort Worth Public Library

WASHINGTON
Seattle Public Library

WISCONSIN
Milwaukee Public Library

An extensive collection of NASA and NASA-sponsored documents and aerospace publications available to the public for reference purposes is maintained by the American Institute of Aeronautics and Astronautics, Technical Information Service, 555 West 57th Street, 12th Floor, New York, New York 10019.

EUROPEAN

An extensive collection of NASA and NASA-sponsored publications is maintained by the British Library Lending Division, Boston Spa, Wetherby, Yorkshire, England. By virtue of arrangements other than with NASA, the British Library Lending Division also has available many of the non-NASA publications cited in *STAR*. European requesters may purchase facsimile copy of microfiche of NASA and NASA-sponsored documents, those identified by both the symbols "#" and "*", from: ESA - Information Retrieval Service, European Space Agency, 8-10 rue Mario-Nikis, 75738 Paris CEDEX 15, France.

National Aeronautics and
Space Administration

Washington, D.C.
20546

Official Business
Penalty for Private Use, $300

THIRD-CLASS BULK RATE

Postage and Fees Paid
National Aeronautics and
Space Administration
NASA-451

U.S.MAIL

NASA

POSTMASTER: If Undeliverable (Section 158
Postal Manual) Do Not Return

7041(35)

NASA

Earth Resources
A Continuing
Bibliography
with Indexes

NASA SP-7041(35)
October 1982

NEWARK PUBLIC LIBRARY
FEB 3 1983
U. S. GOVT. PUBS.
DEPOSITORY 376

National Aeronautics and
Space Administration

es Earth Resource
s Earth Resources
Earth Resources E
th Resources Ear
Resources Earth
Resources Earth R
urces Earth Res

NAS1.21:

ACCESSION NUMBER RANGES

Accession numbers cited in this Supplement fall within the following ranges.

STAR (N-10000 Series)	N82-22141 - N82-28242
IAA (A-10000 Series)	A82-28539 - A82-38102

This bibliography was prepared by the NASA Scientific and Technical Information Facility operated for the National Aeronautics and Space Administration by PRC Government Information Systems.

NASA SP-7041(35)

EARTH RESOURCES

A CONTINUING BIBLIOGRAPHY WITH INDEXES

Issue 35

A selection of annotated references to unclassified reports and journal articles that were introduced into the NASA scientific and technical information system and announced between July 1 and September 30, 1982 in

- *Scientific and Technical Aerospace Reports (STAR)*
- *International Aerospace Abstracts (IAA).*

NASA Scientific and Technical Information Branch 1982
National Aeronautics and Space Administration
Washington, DC

This supplement is available as NTISUB/038/093 from the National Technical Information Service (NTIS), Springfield, Virginia 22161 at the price of $10.50 domestic; $21.50 foreign for standing orders. Please note: Standing orders are subscriptions which do not terminate at the end of a year, as do regular subscriptions, but continue indefinitely unless specifically terminated by the subscriber.

INTRODUCTION

The technical literature described in this continuing bibliography may be helpful to researchers in numerous disciplines such as agriculture and forestry, geography and cartography, geology and mining, oceanography and fishing, environmental control, and many others. Until recently it was impossible for anyone to examine more than a minute fraction of the Earth's surface continuously. Now vast areas can be observed synoptically, and changes noted in both the Earth's lands and waters, by sensing instrumention on orbiting spacecraft or on aircraft.

This literature survey lists 587 reports, articles, and other documents announced between July 1 and September 30, 1982 in *Scientific and Technical Aerospace Reports (STAR)*, and *International Aerospace Abstracts (IAA)*.

The coverage includes documents related to the identification and evaluation by means of sensors in spacecraft and aircraft of vegetation, minerals, and other natural resources, and the techniques and potentialities of surveying and keeping up-to-date inventories of such riches. It encompasses studies of such natural phenomena as earthquakes, volcanoes, ocean currents, and magnetic fields; and such cultural phenomena as cities, transportation networks, and irrigation systems. Descriptions of the components and use of remote sensing and geophysical instrumentation, their subsystems, observational procedures, signature and analyses and interpretive techniques for gathering data are also included. All reports generated under NASA's Earth Resources Survey Program for the time period covered in this bibliography will also be included. The bibliography does not contain citations to documents dealing mainly with satellites or satellite equipment used in navigation or communication systems, nor with instrumentation not used aboard aerospace vehicles.

The selected items are grouped in nine categories. These are listed in the Table of Contents with notes regarding the scope of each category. These categories were especially chosen for this publication, and differ from those found in *STAR* and *IAA*.

Each entry consists of a standard bibliographic citation accompanied by an abstract. The citations and abstracts are reproduced exactly as they appeared originally in *STAR*, or *IAA*, including the original accession numbers from the respective announcement journals. This procedure, which saves time and money, accounts for the variation in citation appearance.

Under each of the nine categories, the entries are presented in one of two groups that appear in the following order:

IAA entries identified by accession number series A82-10,000 in ascending accession number order;

STAR entries identified by accession number series N82-10,000 in ascending accession number order.

After the abstract section, there are six indexes:

subject, personal author, corporate source, contract number, report/accession number, and accession number.

AVAILABILITY OF CITED PUBLICATIONS

IAA ENTRIES (A82-10000 Series)

All publications abstracted in this Section are available from the Technical Information Service, American Institute of Aeronautics and Astronautics, Inc. (AIAA), as follows: Paper copies of accessions are available at $8.00 per document. Microfiche(1) of documents announced in *IAA* are available at the rate of $4.00 per microfiche on demand, and at the rate of $1.35 per microfiche for standing orders for all *IAA* microfiche.

Minimum air-mail postage to foreign countries is $2.50 and all foreign orders are shipped on payment of pro-forma invoices.

All inquiries and requests should be addressed to AIAA Technical Information Service. Please refer to the accession number when requesting publications.

STAR ENTRIES (N82-10000 Series)

One or more sources from which a document announced in *STAR* is available to the public is ordinarily given on the last line of the citation. The most commonly indicated sources and their acronyms or abbreviations are listed below. If the publication is available from a source other than those listed, the publisher and his address will be displayed on the availability line or in combination with the corporate source line.

Avail: NTIS. Sold by the National Technical Information Service. Prices for hard copy (HC) and microfiche (MF) are indicated by a price code preceded by the letters HC or MF in the *STAR* citation. Current values for the price codes are given in the tables on page vii.

Documents on microfiche are designated by a pound sign (#) following the accession number. The pound sign is used without regard to the source or quality of the microfiche.

Initially distributed microfiche under the NTIS SRIM (Selected Research in Microfiche) is available at greatly reduced unit prices. For this service and for information concerning subscription to NASA printed reports, consult the NTIS Subscription Section, Springfield, Va. 22161.

NOTE ON ORDERING DOCUMENTS: When ordering NASA publications (those followed by the * symbol), use the N accession number. NASA patent applications (only the specifications are offered) should be ordered by the US-Patent-Appl-SN number. Non-NASA publications (no asterisk) should be ordered by the AD, PB, or other *report* number shown on the last line of the citation, not by the N accession number. It is also advisable to cite the title and other bibliographic identification.

Avail: SOD (or GPO). Sold by the Superintendent of Documents, U.S. Government Printing Office, in hard copy. The current price and order number are given following the availability line. (NTIS will fill microfiche requests, at the standard $4.00 price, for those documents identified by a # symbol.)

Avail: NASA Public Document Rooms. Documents so indicated may be examined at or purchased from the National Aeronautics and Space Administration, Public Document Room (Room 126), 600 Independence Ave., S.W., Washington, D.C. 20546, or public document rooms located at each of the NASA research centers, the NASA Space Technology Laboratories, and the NASA Pasadena Office at the Jet Propulsion Laboratory.

---

(1) A microfiche is a transparent sheet of film, 105 by 148 mm in size containing as many as 60 to 98 pages of information reduced to micro images (not to exceed 26:1 reduction)

Avail: DOE Depository Libraries. Organizations in U.S. cities and abroad that maintain collections of Department of Energy reports, usually in microfiche form, are listed in *Energy Research Abstracts*. Services available from the DOE and its depositories are described in a booklet, *DOE Technical Information Center - Its Functions and Services* (TID-4660), which may be obtained without charge from the DOE Technical Information Center.

Avail: Univ. Microfilms. Documents so indicated are dissertations selected from *Dissertation Abstracts* and are sold by University Microfilms as xerographic copy (HC) and microfilm. All requests should cite the author and the Order Number as they appear in the citation.

Avail: USGS. Originals of many reports from the U.S. Geological Survey, which may contain color illustrations, or otherwise may not have the quality of illustrations preserved in the microfiche or facsimile reproduction, may be examined by the public at the libraries of the USGS field offices whose addresses are listed in this introduction. The libraries may be queried concerning the availability of specific documents and the possible utilization of local copying services, such as color reproduction.

Avail: HMSO. Publications of Her Majesty's Stationery Office are sold in the U.S. by Pendragon House, Inc. (PHI), Redwood City, California. The U.S. price (including a service and mailing charge) is given, or a conversion table may be obtained from PHI.

Avail: BLL (formerly NLL): British Library Lending Division, Boston Spa, Wetherby, Yorkshire, England. Photocopies available from this organization at the price shown. (If none is given, inquiry should be addressed to the BLL.)

Avail: Fachinformationszentrum, Karlsruhe. Sold by the Fachinformationszentrum Energie, Physik, Mathematik GMBH, Eggenstein Leopoldshafen, Federal Republic of Germany, at the price shown in deutschmarks (DM).

Avail: Issuing Activity, or Corporate Author, or no indication of availability. Inquiries as to the availability of these documents should be addressed to the organization shown in the citation as the corporate author of the document.

Avail: U.S. Patent and Trademark Office. Sold by Commissioner of Patents and Trademarks, U.S. Patent and Trademark Office, at the standard price of 50 cents each, postage free.

Other availabilities: If the publication is available from a source other than the above, the publisher and his address will be displayed entirely on the availability line or in combination with the corporate author line.

ADDRESSES OF ORGANIZATIONS

American Institute of Aeronautics and
Astronautics
Technical Information Service
555 West 57th Street, 12th Floor
New York, New York 10019

British Library Lending Division,
Boston Spa, Wetherby, Yorkshire,
England

Commissioner of Patents and
Trademarks
U.S. Patent and Trademark Office
Washington, D.C. 20231

Department of Energy
Technical Information Center
P.O. Box 62
Oak Ridge, Tennessee 37830

ESA-Information Retrieval Service
ESRIN
Via Galileo Galilei
00044 Frascati (Rome) Italy

Fachinformationszentrum Energie, Physik,
Mathematik GMBH
7514 Eggenstein Leopoldshafen
Federal Republic of Germany

Her Majesty's Stationery Office
P.O. Box 569, S.E. 1
London, England

NASA Scientific and Technical Information
Facility
P.O. Box 8757
B.W.I. Airport, Maryland 21240

National Aeronautics and Space
Administration
Scientific and Technical Information
Branch (NST-41)
Washington, D.C. 20546

National Technical Information Service
5285 Port Royal Road
Springfield, Virginia 22161

Pendragon House, Inc.
899 Broadway Avenue
Redwood City, California 94063

Superintendent of Documents
U.S. Government Printing Office
Washington, D.C. 20402

University Microfilms
A Xerox Company
300 North Zeeb Road
Ann Arbor, Michigan 48106

University Microfilms, Ltd.
Tylers Green
London, England

U.S. Geological Survey
1033 General Services Administration
Building
Washington, D.C. 20242

U.S. Geological Survey
601 E. Cedar Avenue
Flagstaff, Arizona 86002

U.S. Geological Survey
345 Middlefield Road
Menlo Park, California 94025

U.S. Geological Survey
Bldg. 25, Denver Federal Center
Denver, Colorado 80225

NTIS PRICE SCHEDULES

Schedule A

STANDARD PAPER COPY PRICE SCHEDULE

(Effective January 1, 1982)

Price Code	Page Range	North American Price	Foreign Price
A01	Microfiche	$ 4.00	$ 8.00
A02	001-025	6.00	12.00
A03	026-050	7.50	15.00
A04	051-075	9.00	18.00
A05	076-100	10.50	21.00
A06	101-125	12.00	24.00
A07	126-150	13.50	27.00
A08	151-175	15.00	30.00
A09	176-200	16.50	33.00
A10	201-225	18.00	36.00
A11	226-250	19.50	39.00
A12	251-275	21.00	42.00
A13	276-300	22.50	45.00
A14	301-325	24.00	48.00
A15	326-350	25.50	51.00
A16	351-375	27.00	54.00
A17	376-400	28.50	57.00
A18	401-425	30.00	60.00
A19	426-450	31.50	63.00
A20	451-475	33.00	66.00
A21	476-500	34.50	69.00
A22	501-525	36.00	72.00
A23	526-550	37.50	75.00
A24	551-575	39.00	78.00
A25	576-600	40.50	81.00
	601-up	-- 1/	-- 2/

A99 - Write for quote

1/ Add $1.50 for each additional 25 page increment or portion thereof for 601 pages up.

2/ Add $3.00 for each additional 25 page increment or portion thereof for 601 pages and more.

Schedule E

EXCEPTION PRICE SCHEDULE

Paper Copy & Microfiche

Price Code	North American Price	Foreign Price
E01	$ 6.50	$ 13.50
E02	7.50	15.50
E03	9.50	19.50
E04	11.50	23.50
E05	13.50	27.50
E06	15.50	31.50
E07	17.50	35.50
E08	19.50	39.50
E09	21.50	43.50
E10	23.50	47.50
E11	25.50	51.50
E12	28.50	57.50
E13	31.50	63.50
E14	34.50	69.50
E15	37.50	75.50
E16	40.50	81.50
E17	43.50	88.50
E18	46.50	93.50
E19	51.50	102.50
E20	61.50	123.50

E-99 - Write for quote

N01	30.00	45.00

TABLE OF CONTENTS

Page

Category 01 Agriculture and Forestry 1
Includes crop forecasts, crop signature analysis, soil identification, disease detection, harvest estimates, range resources, timber inventory, forest fire detection, and wildlife migration patterns.

Category 02 Environmental Changes and Cultural Resources 21
Includes land use analysis, urban and metropolitan studies, environmental impact, air and water pollution, geographic information systems, and geographic analysis.

Category 03 Geodesy and Cartography 31
Includes mapping and topography.

Category 04 Geology and Mineral Resources 40
Includes mineral deposits, petroleum deposits, spectral properties of rocks, geological exploration, and lithology.

Category 05 Oceanography and Marine Resources 49
Includes sea-surface temperature, ocean bottom surveying imagery, drift rates, sea ice and icebergs, sea state, fish location

Category 06 Hydrology and Water Management 59
Includes snow cover and water runoff in rivers and glaciers, saline intrusion, drainage analysis, geomorphology of river basins, land uses, and estuarine studies.

Category 07 Data Processing and Distribution Systems 63
Includes film processing, computer technology, satellite and aircraft hardware, and imagery.

Category 08 Instrumentation and Sensors 76
Includes data acquisition and camera systems and remote sensors.

Category 09 General 82
Includes economic analysis.

Subject Index A-1
Personal Author Index B-1
Corporate Source Index C-1
Contract Number Index D-1
Report / Accession Number Index E-1
Accession Number Index F-1

TYPICAL CITATION AND ABSTRACT FROM *STAR*

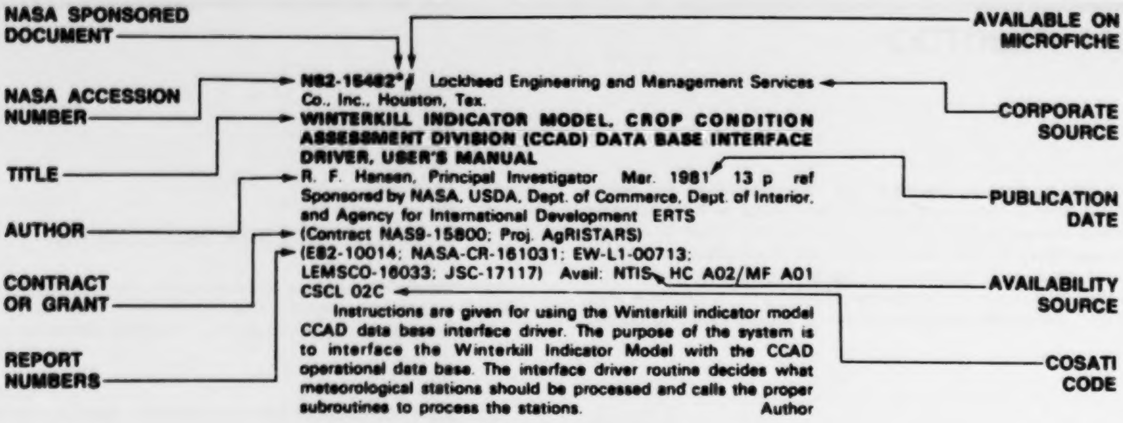
NASA SPONSORED DOCUMENT
AVAILABLE ON MICROFICHE
NASA ACCESSION NUMBER
CORPORATE SOURCE
TITLE
AUTHOR
PUBLICATION DATE
CONTRACT OR GRANT
AVAILABILITY SOURCE
REPORT NUMBERS
COSATI CODE

N82-16482*# Lockheed Engineering and Management Services Co., Inc., Houston, Tex.

WINTERKILL INDICATOR MODEL, CROP CONDITION ASSESSMENT DIVISION (CCAD) DATA BASE INTERFACE DRIVER, USER'S MANUAL

R. F. Hansen, Principal Investigator Mar. 1981 13 p ref
Sponsored by NASA, USDA, Dept. of Commerce, Dept. of Interior, and Agency for International Development ERTS
(Contract NAS9-15800; Proj. AgRISTARS)
(E82-10014; NASA-CR-161031; EW-L1-00713; LEMSCO-16033; JSC-17117) Avail: NTIS HC A02/MF A01 CSCL 02C

Instructions are given for using the Winterkill indicator model CCAD data base interface driver. The purpose of the system is to interface the Winterkill Indicator Model with the CCAD operational data base. The interface driver routine decides what meteorological stations should be processed and calls the proper subroutines to process the stations. Author

TYPICAL CITATION AND ABSTRACT FROM *IAA*

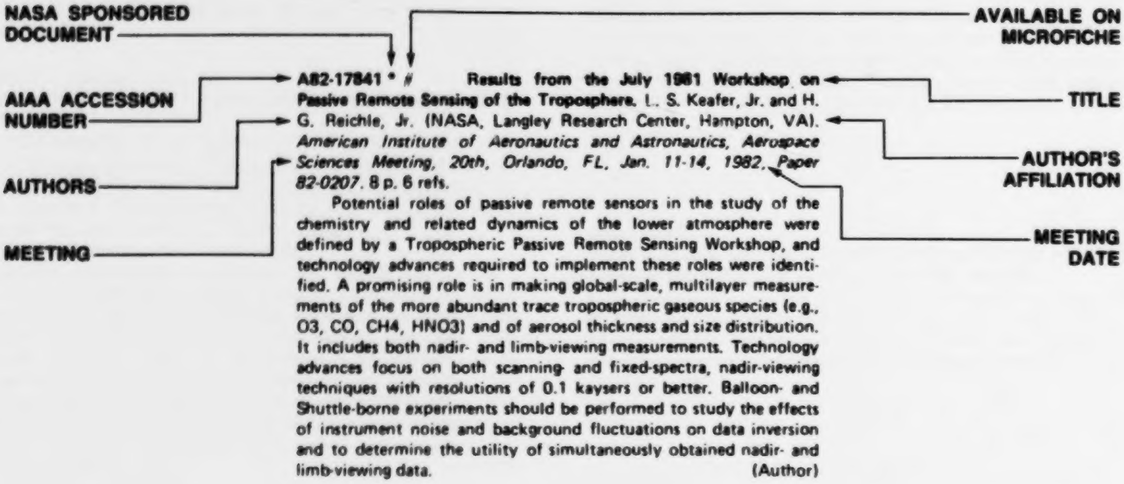
NASA SPONSORED DOCUMENT
AVAILABLE ON MICROFICHE
AIAA ACCESSION NUMBER
TITLE
AUTHORS
AUTHOR'S AFFILIATION
MEETING
MEETING DATE

A82-17841 * # **Results from the July 1981 Workshop on Passive Remote Sensing of the Troposphere.** L. S. Keafer, Jr. and H. G. Reichle, Jr. (NASA, Langley Research Center, Hampton, VA). *American Institute of Aeronautics and Astronautics, Aerospace Sciences Meeting, 20th, Orlando, FL, Jan. 11-14, 1982, Paper 82-0207*. 8 p. 6 refs.

Potential roles of passive remote sensors in the study of the chemistry and related dynamics of the lower atmosphere were defined by a Tropospheric Passive Remote Sensing Workshop, and technology advances required to implement these roles were identified. A promising role is in making global-scale, multilayer measurements of the more abundant trace tropospheric gaseous species (e.g., O3, CO, CH4, HNO3) and of aerosol thickness and size distribution. It includes both nadir- and limb-viewing measurements. Technology advances focus on both scanning- and fixed-spectra, nadir-viewing techniques with resolutions of 0.1 kaysers or better. Balloon- and Shuttle-borne experiments should be performed to study the effects of instrument noise and background fluctuations on data inversion and to determine the utility of simultaneously obtained nadir- and limb-viewing data. (Author)

EARTH RESOURCES

A Continuing Bibliography (Issue 35)

OCTOBER 1982

01

AGRICULTURE AND FORESTRY

Includes crop forecasts, crop signature analysis, soil identification, disease detection, harvest estimates, range resources, timber inventry, forest fire detection, and wildlife migration patterns.

A82-22539
A REPORT ON THE 'COSMIC RAY PROPAGATION PROBLEM'
P. S. FREIER (Minnesota, University, Minneapolis, MN) In: International Cosmic Ray Conference, 17th, Paris, France, July 13-25, 1981, Conference Papers. Volume 2. Gif-sur-Yvette, Essonne, France, Commissariat a l'Energie Atomique, 1981, p. 182-185. refs

Data on abundances of elements are now of such quality, that the major source of discrepancies in cosmic ray propagation results is believed to be due to a difference in the propagation programs being used by different groups. Nine groups were therefore asked to use a standardized source, E equals 2.3 GeV/n with no energy loss, and propagate it through a 5 g/sq cm exponential path length of hydrogen, using their values of the Silverberg and Tsao cross sections at 2.3 GeV/n (1973, 1977, 1979). Results indicate significant discrepancies arising from propagation, demonstrating the differences that can result when different physical conditions are assumed. J.F.

A82-22541* Chicago Univ., Ill.
THE QUESTION OF SHORT PATHLENGTHS IN INTERSTELLAR PROPAGATION
M. GARCIA-MUNOZ, T. G. GUZIK, J. A. SIMPSON, and J. P. WEFEL (Chicago, University, Chicago, IL) In: International Cosmic Ray Conference, 17th, Paris, France, July 13-25, 1981, Conference Papers. Volume 2. Gif-sur-Yvette, Essonne, France, Commissariat a l'Energie Atomique, 1981, p. 192-195. refs
(Contract NAS5-25731; NGL-14-001-006)

Interstellar propagation calculations for cosmic rays, He-4 - Ni-64, are compared with currently available abundance ratios for B/C and sub-Fe/Fe. The calculations show that an exponential pathlength distribution (leaky box model) cannot reproduce both secondary to primary ratios in the interval 0.5-1 GeV/n unless some values of the propagation parameters are modified. The calculated ratios are shown to be particularly sensitive to the adopted cross sections, the presence of the sub-Fe elements in the source regions, the shape of the source energy spectrum, and ionization energy loss. (Author)

A82-22542* National Aeronautics and Space Administration. Goddard Space Flight Center, Greenbelt, Md.
THE COSMIC RAY POSITRON SPECTRUM
R. J. PROTHEROE (NASA, Goddard Space Flight Center, Laboratory for High Energy Astrophysics, Greenbelt, MD) In: International Cosmic Ray Conference, 17th, Paris, France, July 13-25, 1981, Conference Papers. Volume 2. Gif-sur-Yvette, Essonne, France, Commissariat a l'Energie Atomique, 1981, p. 198-201. refs

A calculation is made of the flux of secondary positrons expected above 100 MeV for various disk-halo diffusion models, which are consistent with the observed grammage and Be-10 abundance. It is found that models which give a high surviving fraction of Be-10 (about 0.3) give a secondary positron spectrum which is consistent with the observations, while a model predicting a low Be-10 abundance (about 0.1 surviving) gives a poorer fit at high energies hinting at the presence of a primary positron component. Implications of these results are discussed. (Author)

A82-22543
THE ELECTRON AND POSITRON SPECTRA IN PRIMARY COSMIC RAYS
L. C. TAN and L. K. NG (University of Hong Kong, Hong Kong) In: International Cosmic Ray Conference, 17th, Paris, France, July 13-25, 1981, Conference Papers. Volume 2. Gif-sur-Yvette, Essonne, France, Commissariat a l'Energie Atomique, 1981, p. 202-205. refs

It is contended that variations in the results of various authors' positron calculations derive mainly from differences between the local interstellar electron spectrum and those derived from radio data. It is found that, among the spectra derived from radio data, that of Rockstroh and Webber (1978) is the most consistent with the description using the usual 'leaky box' model. In addition, it is shown that the electron injection spectrum with a single power law cannot satisfactorily explain the primary electron spectrum. Analysis also shows that the leaky box model is able to account for the mean behavior of interstellar positrons and electrons in a cosmic ray containment volume whose galactic scale height and width around the earth are, respectively, 0.5-1 kpc and 2-3 kpc. C.R.

A82-22544
COMPARISON OF THE MEASURED ANTIPROTON FLUX WITH THAT PREDICTED BY THE 'LEAKY BOX' MODEL
L. C. TAN and L. K. NG (University of Hong Kong, Hong Kong) In: International Cosmic Ray Conference, 17th, Paris, France, July 13-25, 1981, Conference Papers. Volume 2. Gif-sur-Yvette, Essonne, France, Commissariat a l'Energie Atomique, 1981, p. 210-213. refs

A82-22552
STEADY-STATE COSMIC RAY ELECTRON SPECTRUM UNDER DIFFUSION, CONVECTION, ADIABATIC DECELERATION AND SYNCHROTRON LOSSES
I. LERCHE (Chicago, University, Chicago, IL) and R. SCHLICKE6SER (Max-Planck-Institut fur Radioastronomie, Bonn, West Germany) In: International Cosmic Ray Conference, 17th, Paris, France, July 13-25, 1981, Conference Papers. Volume 2. Gif-sur-Yvette, Essonne, France, Commissariat a l'Energie Atomique, 1981, p. 244-247. Deutsche Forschungsgemeinschaft refs
(Contract DFG-SCHL-201/1)

A82-22557

MASS PER CHARGE RATIO IN HOT PLASMAS AND COSMIC RAY SOURCE COMPOSITION

C. J. CESARSKY, R. ROTHENFLUG, and M. CASSE (Commissariat a l'Energie Atomique, Centre d'Etudes Nucleaires de Saclay, Gif-sur-Yvette, Essonne, France) In: International Cosmic Ray Conference, 17th, Paris, France, July 13-25, 1981, Conference Papers. Volume 2. Gif-sur-Yvette, Essonne, France, Commissariat a l'Energie Atomique, 1981, p. 269-272. refs

Some models of shock acceleration of cosmic rays assume that particles are injected out of the thermal plasma behind the shock and are selected according to their effective charge (Eichler, 1979; Ellison et al., 1981). The pattern of compositions that could emerge from such a selection starting from plasmas in ionization equilibrium at various temperatures greater than or equal to 100,000 K and containing no grains is considered. It is found that, in the case of steady state ionization equilibrium and of time-dependent cooling of a hot plasma, which are possible descriptions of the hot ISM and of the halo gas, it is not possible to reproduce the observed cosmic ray composition with this simple scheme. (Author)

A82-22559

PHYSICAL STATE OF THE BIRTH PLACE OF COSMIC RAYS AND ITS IMPLICATION TO THE ACCELERATION PROCESSES

K. SAKURAI (Kanagawa University, Yokohama, Japan) In: International Cosmic Ray Conference, 17th, Paris, France, July 13-25, 1981, Conference Papers. Volume 2. Gif-sur-Yvette, Essonne, France, Commissariat a l'Energie Atomique, 1981, p. 277-280. refs

To explain the observed chemical composition of galactic cosmic rays at their sources, it is suggested that this composition is the result of an acceleration mechanism, possibly related to the charge states of particles ambient in the source regions. Since it is likely that most of the particles are partially ionized in these regions, the ambient temperature there will be less than 100,000 K before the start of acceleration. C.R.

A82-22560

ON VOLATILITY, FIRST IONIZATION POTENTIAL, AND S- AND R-PROCESSES

J. P. MEYER (Commissariat a l'Energie Atomique, Centre d'Etudes Nucleaires de Saclay, Gif-sur-Yvette, Essonne, France) In: International Cosmic Ray Conference, 17th, Paris, France, July 13-25, 1981, Conference Papers. Volume 2. Gif-sur-Yvette, Essonne, France, Commissariat a l'Energie Atomique, 1981, p. 281-284. refs

The possibility of a correlation between the first ionization potential and volatility (in that elements of low potential tend to be refractory and those of high potential volatile) is considered. It is noted that the apparent correlation between galactic cosmic ray source (GCRS) elemental abundances and the first ionization potential may in fact be based on volatility. Attention is given here to compositional clues which may determine whether volatility or the first ionization potential is the relevant parameter. The correlation between the first ionization potential and volatility is examined, and those elements which do not fit into the correlation are isolated. Attention is also given to possible ambiguities in interpreting the charge spectrum beyond Ni that derive from coincidences between regions of change in the first ionization (and volatility) and the s- and r-process peaks. C.R.

A82-22561

INTERSTELLAR GRAINS AS SEEDS FOR GALACTIC COSMIC RAYS

J.-P. BIBRING (CNRS, Centre de Spectrometrie Nucleaire et de Spectrometrie de Masse, Orsay, Essonne, France) and C. J. CESARSKY (Commissariat a l'Energie Atomique, Centre d'Etudes Nucleaires de Saclay, Gif-sur-Yvette, Essonne, France) In: International Cosmic Ray Conference, 17th, Paris, France, July 13-25, 1981, Conference Papers. Volume 2. Gif-sur-Yvette, Essonne, France, Commissariat a l'Energie Atomique, 1981, p. 289-291. refs

A82-22563

ORIGIN OF GALACTIC COSMIC RAYS FROM NE ISOTOPIC COMPOSITION

J. AUDOUZE (CNRS, Institut d'Astrophysique, Paris; CNRS, Centre de Spectrometrie Nucleaire et de Spectrometrie de Masse, Orsay, Essonne, France), M. CASSE, J. A. PAUL (Commissariat a l'Energie Atomique, Centre d'Etudes Nucleaires de Saclay, Gif-sur-Yvette, Essonne, France), J. P. CHIEZE (CNRS, Institut d'Astrophysique, Paris; Centre d'Etudes Nucleaires de Bruyere-le-Chatel, Montrouge, Hauts-de-Seine, France), and G. MALINIE (CNRS, Institut d'Astrophysique, Paris, France) In: International Cosmic Ray Conference, 17th, Paris, France, July 13-25, 1981, Conference Papers. Volume 2. Gif-sur-Yvette, Essonne, France, Commissariat a l'Energie Atomique, 1981, p. 296-298. refs

The possibility that a cosmic ray composition reflecting that of the interstellar medium may account for the observed enhancement of the cosmic ray Ne-22/Ne-20 abundance ratio with respect to the solar value is examined. Processes leading to the observed solar system abundances of Ne-22 are discussed, and it is suggested that explosive hydrogen burning might be a significant source, since secondary production of this isotope as a by-product of the CNO cycle in intermediate and massive stars is incapable of accounting for the present abundance. Calculations are presented which show that neither Ne-22 enrichment of the interstellar medium by low-mass stars after the birth of the sun nor a cosmic ray origin in the inner galaxy account for the observed cosmic ray enrichment. It is thus concluded that Ne-22 cannot have been significantly enriched in the interstellar medium during the last 4.6 billion years, and thus cosmic rays are accelerated in the vicinity of Ne-22 sources. A.L.W.

A82-22564

EVIDENCE FOR THE STOCHASTIC ACCELERATION OF COSMIC RAYS IN SUPERNOVA REMNANTS

T. W. HARQUIST (University College, London, England) and G. E. MORFILL (Max-Planck-Institut fuer Kernphysik, Heidelberg, West Germany) In: International Cosmic Ray Conference, 17th, Paris, France, July 13-25, 1981, Conference Papers. Volume 2. Gif-sur-Yvette, Essonne, France, Commissariat a l'Energie Atomique, 1981, p. 300-302. refs

Ionization rates in several locations in an expanding shell, probably formed by the passage of a shock driven by the expansion of an old supernova remnant in the Per OB2 association, have been derived from molecular observations. The production of 1-2 MeV cosmic rays by the second order Fermi mechanism in the ionized regions of the remnant would explain these and a number of other molecular observations. (Author)

A82-22565

THE GALACTIC ORIGIN OF COSMIC RAYS. I

S. A. COLGATE (Los Alamos National Laboratory, Los Alamos; New Mexico Institute of Mining and Technology, Socorro, NM) In: International Cosmic Ray Conference, 17th, Paris, France, July 13-25, 1981, Conference Papers. Volume 2. Gif-sur-Yvette, Essonne, France, Commissariat a l'Energie Atomique, 1981, p. 303-306. refs

(CONF-810711-1; LA-UR-81-965)

The theoretical basis for the supernova envelope shock origin of cosmic rays is reviewed. The theoretical explanation of the SN Type I light curve requires the ejection of a relativistic mass fraction. The criterion of the adiabatic deceleration by Alfven wave trapping neither applies in theory, when beta is greater than 1, or practice, as in the Starfish high-altitude nuclear explosion experiment. Arguments of delayed acceleration due to K-capture are not applicable to SN ejecta because a period of prompt recombination exists before subsequent stripping in propagation. (Author)

A82-22571

ORIGIN OF COSMIC RAYS IN GALACTIC CENTRE SOURCES

S. S. SAID, A. W. WOLFENDALE (Durham, University, Durham, England), M. GILER (Lodz, Uniwersytet, Lodz, Poland), and J. WDOWCZYK (Instytut Badan Jadrowych, Lodz, Poland) In: International Cosmic Ray Conference, 17th, Paris, France, July 13-25, 1981, Conference Papers. Volume 2. Gif-sur-Yvette, Essonne, France, Commissariat a l'Energie Atomique, 1981, p. 344-347. refs

A model is proposed which attributes the origin of cosmic rays to rare explosive events in galactic nuclei. In accordance with the model, the individual explosions are separated by times of the order of 100 million years, and the duration of each explosion is much shorter than the period of separation. Particles produced with a power-law spectrum would propagate by diffusion throughout the Galaxy, and in its simplest form, there would be simple three-dimensional diffusion with a diffusion coefficient independent of position. The proposed model could provide an explanation for the very low electron-to-proton ratio (about 3 percent at 1 GeV) of cosmic radiation at the earth. V.L.

A82-22572

ACCELERATION PROCESSES NEAR MASSIVE BLACK HOLES

M. KAFATOS (George Mason University, Fairfax, VA), R. SILBERBERG, and M. M. SHAPIRO (U.S. Navy, Naval Research Laboratory, Washington, DC) In: International Cosmic Ray Conference, 17th, Paris, France, July 13-25, 1981, Conference Papers. Volume 2. Gif-sur-Yvette, Essonne, France, Commissariat a l'Energie Atomique, 1981, p. 348-351. refs

Ultra-massive accreting black holes in the nuclei of active galaxies have been proposed as the central sources of energy emission, especially of the nonthermal kind. Accretion disks around massive black holes in the centers of active galactic nuclei are shown to be likely sites of particle acceleration. Electrons can be accelerated to relativistic energies by electromagnetic processes as well as purely gravitational processes (e.g., Penrose pair production). Protons are also accelerated to very high energies by processes such as (1) Fermi acceleration, (2) betatron acceleration, (3) shock wave acceleration, and (4) in beams via the electromagnetic dynamo process. The stochastic Fermi process acting over a period of only about a day in the ergosphere suffices for efficient acceleration of protons, even to high energies. (Author)

A82-22584* National Aeronautics and Space Administration. Goddard Space Flight Center, Greenbelt, Md.

INTERPLANETARY PARTICLE OBSERVATIONS ASSOCIATED WITH SOLAR FLARE GAMMA-RAY LINE EMISSION

T. T. VON ROSENVINGE, R. RAMATY, and V. REAMES (NASA, Goddard Space Flight Center, Laboratory for High Energy Astrophysics, Greenbelt, MD) In: International Cosmic Ray Conference, 17th, Paris, France, July 13-25, 1981, Conference Papers. Volume 3. Gif-sur-Yvette, Essonne, France, Commissariat a l'Energie Atomique, 1981, p. 28-31. refs

Observations of particle emissions during three solar flares which were observed to emit 2.22 MeV gamma rays as recorded by the Solar Maximum Mission are discussed. The 2.22 MeV line is produced by neutron capture by hydrogen, and additional attention is given to a 4.4 MeV emission line of June 7, 1980, with estimates made of the particle density 1 AU from the sun assuming a good magnetic connection between the earth and the sun. The measurements were made from the ISEE-3 and HELIOS-1 spacecraft. The connectedness of the earth and the sun in a magnetic field leads to conclusions that few particles actually escaped into interplanetary space. M.S.K.

A82-22587

COMPUTER SIMULATION OF THE TIME DEPENDENCE OF THE PHOTON ENERGY SPECTRA PRODUCED IN PROTON AND ELECTRON BREMSTRAHLUNG

S. R. KELNER, IU. D. KOTOV, A. S. ROSHAL, and V. N. RUSSKIKH (Moskovskii Inzherno-Fizicheskii Institut, Moscow, USSR) In: International Cosmic Ray Conference, 17th, Paris, France, July 13-25, 1981, Conference Papers. Volume 3. Gif-sur-Yvette, Essonne, France, Commissariat a l'Energie Atomique, 1981, p. 41-44. refs

An analytic model of the time dependence of the photon generation spectra resulting from proton and electron bremsstrahlung in matter is presented. The lifetimes of the protons and electrons with the same Lorentz factor are shown to differ by a factor of at least three, which implies that the time dependence of photon energy spectra resulting from pulse beam injection of accelerated particles into a generation region depends on the types of particles accelerated. Basic equations are formulated for the evolution of the proton distribution function in matter, with consideration given to path lengths which remain or pass from the matter. The proton energy spectrum is then defined and the generation function for the production of gamma rays in a target block is derived, taking into account the density of the target. Similar calculations for electrons showed that with time the energy spectra becames harder for electrons. M.S.K.

A82-22589

POSSIBLE EVIDENCE FOR ATTENUATION OF AN MHD SHOCK BY A MAGNETIC NEUTRAL SHEET IN THE SOLAR CORONA

D. J. MULLAN (Franklin Institute, Bartol Research Foundation, Newark, DE) In: International Cosmic Ray Conference, 17th, Paris, France, July 13-25, 1981, Conference Papers. Volume 3. Gif-sur-Yvette, Essonne, France, Commissariat a l'Energie Atomique, 1981, p. 51-54. refs

(Contract NSF ATM-78-20936-01)

The possibility that H-alpha filaments in the solar chromosphere are markers beneath regions where coronal shocks experience severe attenuation, and are thus the areas where particles can be ejected from the corona, is examined from data from flares of Aug. 4, 1972 and Nov. 9, 1979. Both flares produced gamma rays with 2.2 MeV energy, and data exists for the energetic protons received at earth stations. The efficiency of transport was high for the August event and two magnitudes lower for the November event. H-alpha filtergrams of the two flares show that in the second flare the shock propagation crossed two or three filaments lying in its path. The low efficiency of particle transport is taken to indicate a degraded shock in the region above the filaments, indicating that the particles needed a different route to escape. M.S.K.

A82-22591* Chicago Univ., Ill.

THE RELATION OF TYPE II RADIO BURSTS TO SOLAR ENERGETIC PARTICLES OBSERVED AT EARTH

P. EVENSON, P. MEYER (Chicago, University, Chicago, IL), and S. YANAGITA In: International Cosmic Ray Conference, 17th, Paris, France, July 13-25, 1981, Conference Papers. Volume 3. Gif-sur-Yvette, Essonne, France, Commissariat a l'Energie Atomique, 1981, p. 59-62. refs

(Contract NAS5-20674)

Observations of particle events associated with type II radio bursts as recorded on the ISEE-3 spacecraft are reported. Data on burst events following flares of Sept. 23,1978 and Aug. 18, 1979 yield time histories of the particle fluxes, which exceeded 25 MeV energy. The profiles of the Category-1 type II bursts display a continuous release of particles, which was concluded by no decrease in the fluxes until after the passage of the shock. The continuous nature of the recorded events suggests that the secondary acceleration process associated with the type II bursts is maintained as the flare shock propagates through interplanetary space, and may be the source of the energetic particles which propagate with the shock. M.S.K.

A82-22592* National Aeronautics and Space Administration. Goddard Space Flight Center, Greenbelt, Md.

A SURVEY OF SOLAR PROTONS AND ALPHA DIFFERENTIAL SPECTRA BETWEEN 1 AND GREATER THAN 400 MEV/NUCLEON

R. E. MCGUIRE, T. T. VON ROSENVINGE, and F. B. MACDONALD (NASA, Goddard Space Flight Center, Greenbelt; Maryland, University, College Park, MD) In: International Cosmic Ray Conference, 17th, Paris, France, July 13-25, 1981, Conference Papers. Volume 3. Gif-sur-Yvette, Essonne, France, Commissariat a l'Energie Atomique, 1981, p. 65-68. refs

Attempts to systematically measure and fit a large sample of flare spectra from IMP 7 and 8 satellite data to determine the spectral forms that characterize the data and the range of spectral slopes are reported. Proton spectra are constructed covering the range 0.9 to over 400 MeV, and alpha fluxes from 1.4-80 MeV/nucleon. The event spectra are composed of fluxes measured at different times at each energy, and fitting procedures were employed such as a power law in kinetic energy, an exponential in rigidity, an exponential in energy, and a Bessel function of momentum/nucleon. Best fits were obtained with the exponential in rigidity and the Bessel function, with the Bessel function having a better numerical accuracy for all 21 proton spectra considered. M.S.K.

A82-22593

ENERGETIC SOLAR PARTICLE SPECTRA ACCORDING TO VENERA-11, 12 AND PROGNOZ-5, 6

V. G. KURT, IU. I. LOGACHEV, V. G. STOLPOVSKII, and E. I. DAIBOG (Moskovskii Gosudarstvennyi Universitet, Moscow, USSR) In: International Cosmic Ray Conference, 17th, Paris, France, July 13-25, 1981, Conference Papers. Volume 3. Gif-sur-Yvette, Essonne, France, Commissariat a l'Energie Atomique, 1981, p. 69-72. refs

Proton and electron spectra of solar flares measured from 0.1-500 MeV and 0.03-3.0 MeV, respectively, on board the Venera 11, 12, and the Prognoz 5, 6, satellites are reported, along with analyses of the integral peak flux and density dependence in relation to the kinetic energy. All the spectra were fitted by either one or a set of two power functions, with the proton spectra having more complicated characteristics than the electron spectra. The number of high energy protons undergoing stochastic particle propagation was found to depend on the shock wave speed. Energy losses were calculated on the basis of deviation from a power law, of a deceleration down to the observation point, and from a numerical estimate of the rate of proton energy change in the adiabatic solar wind expansion. An event of Nov. 22, 1977 is notable for the absence of protons with energy less than 1 MeV. M.S.K.

A82-22594

EVOLUTION OF THE SOLAR PROTON SPECTRUM IN INTERPLANETARY SPACE

N. N. KONTOR (Moskovskii Gosudarstvennyi Universitet, Moscow, USSR) In: International Cosmic Ray Conference, 17th, Paris, France, July 13-25, 1981, Conference Papers. Volume 3. Gif-sur-Yvette, Essonne, France, Commissariat a l'Energie Atomique, 1981, p. 73-76. refs

Exponential forms suitable for describing two-three orders wide energy ranges of proton spectra emitted during solar flares are examined. The rigidity exponent form shows a good fit over a broad range except during the onset of a proton shower. A parabolic spectral shape is presented which becomes a power law at narrower energy ranges. Application of the parabolic formula to available flare data reveals that energetic protons arrive first at the detectors, followed by lower energy particles. M.S.K.

A82-22600

A DESCRIPTION OF RELATIVISTIC SOLAR PARTICLE PROPAGATION

H. DEBRUNNER, H. NEUENSCHWANDER, A. F. WAGNER (Bern, Universitaet, Berne, Switzerland), and J. A. LOCKWOOD (New Hampshire, University, Durham, NH) In: International Cosmic Ray Conference, 17th, Paris, France, July 13-25, 1981, Conference Papers. Volume 3. Gif-sur-Yvette, Essonne, France, Commissariat a l'Energie Atomique, 1981, p. 102-105. Research supported by the Swiss National Science Foundation and NSF.

The intensity-time profiles and anisotropies of the solar cosmic-ray ground level events (GLEs) on November 22, 1977 and May 7, 1978 were addressed by means of a Monte Carlo simulation of relativistic solar flare protons propagation in the interplanetary magnetic field. Pitch angle scattering mean free paths of 0.5 AU and more than 3 AU are deduced. The injection of the solar flare protons has an extended time structure, correlated with the X-ray burst profiles in the 1-8 A and 0.5-4.0 A bands, respectively, for the November 1977 and May 1978 GLEs. O.C.

A82-22601

NON-FLARE INJECTION OF PROTONS INTO INTERPLANETARY SPACE

V. DOMINGO, B. SANAHUJA, and K.-P. WENZEL (ESA, Space Science Dept., Noordwijk, Netherlands) In: International Cosmic Ray Conference, 17th, Paris, France, July 13-25, 1981, Conference Papers. Volume 3. Gif-sur-Yvette, Essonne, France, Commissariat a l'Energie Atomique, 1981, p. 109-112. refs

The superimposition of a second proton population associated with a solar wind regime, and bounded by a pair of shocks, is found to be superimposed upon the first in an investigation of 35-1600 KeV solar protons observed during an April, 1979 nonflare event by ISEE-3. The source of the particles and the solar wind regime appear to be closely associated with intense solar filament activity near the central meridian. The temporal evolution of velocity spectra and anisotropy distributions during this period are discussed. O.C.

A82-22602

LOW-ENERGY PARTICLES IN INTERPLANETARY MAGNETIC FIELD NEAR THE SECTORIAL BOUNDARY ON SEPTEMBER 26, 1977

M. A. ZELDOVICH and B. M. KUZHEVSKII (Moskovskii Gosudarstvennyi Universitet, Moscow, USSR) In: International Cosmic Ray Conference, 17th, Paris, France, July 13-25, 1981, Conference Papers. Volume 3. Gif-sur-Yvette, Essonne, France, Commissariat a l'Energie Atomique, 1981, p. 113-116. refs

Prognoz-6 data are used to examine effects of the sign reversal in the interplanetary magnetic field of September 26, 1977 on the 70-keV to 40 MeV proton fluxes, and the 10-30 keV and 40-500 keV electron fluxes. The sectorial boundary of interplanetary magnetic field traversed the earth at 2300 UT, and in that period the interplanetary space was filled with the solar cosmic ray particles generated in the flare of September 24, 1977, whose intensity decreased in time. Results indicate that the event of September 26, 1977 was the first observation where effects of the sectorial boundary were traced up to proton energies of 40-50 MeV. D.L.G.

A82-22610

COULOMBIAN ENERGY LOSSES AND THE NUCLEAR COMPOSITION OF THE SOLAR COSMIC RAYS

S. S. TRIVEDI and S. BISWAS (Tata Institute of Fundamental Research, Bombay, India) In: International Cosmic Ray Conference, 17th, Paris, France, July 13-25, 1981, Conference Papers. Volume 3. Gif-sur-Yvette, Essonne, France, Commissariat a l'Energie Atomique, 1981, p. 157-160. refs

Coulombian energy losses suffered by fast ions in a two component plasma are discussed quantitatively. Their dependence on the temperature and density of the ambient plasma is also investigated. It is shown that these losses coupled with the transient nature of the flare can give rise to selectivity effects. The ionic charge states are also discussed. (Author)

A82-22611* National Aeronautics and Space Administration. Goddard Space Flight Center, Greenbelt, Md.
HEAVY-ELEMENT ABUNDANCES IN HE/3/-RICH EVENTS
D. V. REAMES and T. T. VON ROSENVINGE (NASA, Goddard Space Flight Center, Laboratory for High Energy Astrophysics, Greenbelt, MD) In: International Cosmic Ray Conference, 17th, Paris, France, July 13-25, 1981, Conference Papers. Volume 3. Gif-sur-Yvette, Essonne, France, Commissariat a l'Energie Atomique, 1981, p. 162-165. refs

Abundances of the elements He through Fe observed on the ISEE-3 during He(3) rich events are reported. Ratios of He(3)-He(4) of not less than about 1, and Fe/O of greater than 1 are found, and rather large event-to-event variations in C, O, Ne, Mg, Si, and S are seen superposed upon the general trend of heavy element enhancement. It is concluded that the discontinuous variation of the neighboring elements in the He(3) rich events could result from differences in the electron temperature of the material prior to injection that give rise to differences in the dominant charge states and cyclotron frequencies of different elements. D.L.G.

A82-22612* Max-Planck-Institut fuer Physik und Astrophysik, Garching (West Germany).
A COMPARISON OF HELIUM AND HEAVY ION SPECTRA IN HE/3/ RICH SOLAR FLARES WITH A MODEL CALCULATION
E. MOBIUS, D. HOVESTADT, B. KLECKER, M. SCHOLER (Max-Planck-Institut fur Physik und Astrophysik, Garching, West Germany), and G. GLOECKLER (Maryland, University, College Park, MD) In: International Cosmic Ray Conference, 17th, Paris, France, July 13-25, 1981, Conference Papers. Volume 3. Gif-sur-Yvette, Essonne, France, Commissariat a l'Energie Atomique, 1981, p. 166-169. Bundesministerium fur Forschung und Technologie refs
(Contract BMFT-RV14-B8/74; NAS5-20062)

He isotopes, O and Fe in He(3) rich solar flares are studied during the 1977 to 1979 period with the MPI/UoMd particle experiment on ISEE-1 and ISEE-3. The study revealed that the He(3) spectrum is generally harder than that of He(4), and the O spectrum is harder than that of Fe. The spectra are compared with a stationary model based on stochastic Fermi acceleration in Alfven turbulence including a rigidity dependent particle loss. Model calculations fit the He(3) and He(4) spectra between 0.4 and 4.0 MeV/nucleon, with discrepancies at lower and higher energies, and the O and Fe spectra cannot be fitted simultaneously. D.L.G.

A82-22617
THE ENERGY SPECTRA OF COSMIC RAY VARIATIONS INFERRED FROM THE STRATOSPHERIC MEASUREMENTS IN 1972-1979
A. K. SVIRZHEVSKAIA, IU. I. STOZHKOV (Akademiia Nauk SSSR, Fizicheskii Institut, Moscow, USSR), and T. N. CHARAKHCHIAN (Moskovskii Gosudarstvennyi Universitet, Moscow, USSR) In: International Cosmic Ray Conference, 17th, Paris, France, July 13-25, 1981, Conference Papers. Volume 3. Gif-sur-Yvette, Essonne, France, Commissariat a l'Energie Atomique, 1981, p. 187-190.

A82-22618
PRIMARY SPECTRAL VARIATIONS OF COSMIC RAYS ABOVE 1 GV
P. H. STOKER (Potchefstroom University for Christian Higher Education, Potchefstroom, Republic of South Africa) In: International Cosmic Ray Conference, 17th, Paris, France, July 13-25, 1981, Conference Papers. Volume 3. Gif-sur-Yvette, Essonne, France, Commissariat a l'Energie Atomique, 1981, p. 193-196. refs

Observations on proton spectra of solar flare GLEs and data from a latitude survey are used to determine specific yield functions for the neutron moderated detector (4NMD) and the 3NM64 neutron monitor at Sanae, Antarctica. Monthly average count rates of the 4NMD and 3NM64 do not follow each other better than 1 percent on long term modulation. No definite physical explanation is singled out to account for the observed excessive variability, which is presumably related to a phase lag effect or hysteresis effect between changes in intensities of particles of different rigidities and the level of solar modulation. D.L.G.

A82-29435
REMOTE SENSING OF THE WEEDINESS OF CROP FIELDS [DISTANTSIONNOE OPREDELENIE ZASORENNOSTI SEL'SKOKHOZIAISTVENNYKH POLEI]
K. IA. KONDRATEV, A. I. BELIAVSKII, O. M. POKROVSKII, and P. P. FEDCHENKO (Glavnaia Geofizicheskaia Observatoriia, Leningrad, USSR) Akademiia Nauk SSSR, Doklady, vol. 263, Mar.-Apr. 1982, p. 251-253. In Russian.

A82-29526
COLOR AERIAL PHOTOGRAPHY IN THE PLANT SCIENCES AND RELATED FIELDS; PROCEEDINGS OF THE EIGHTH BIENNIAL WORKSHOP, LURAY, VA, APRIL 21-23, 1981
Workshop sponsored by the Society of American Foresters, American Society of Photogrammetry, U.S. Geological Survey, et al. Falls Church, VA, American Society of Photogrammetry, 1981. 174 p $20

Aerial photography methods, equipment, targets, and the effectiveness of remote sensing of vegetation are discussed. Analysis with color or IR equipment is examined, and color aerial photography of riparian vegetation in northeastern California, wildlife on an island, and the use of color IR photography for vegetative monitoring are described. Specific photography of loblolly pine plantations, Alaskan resources, forest land changes, rangeland cover proportions, Oregon vegetation, and fir trees infested by beetles are considered. Spectral scanning of SO2-affected winter wheat and soybeans is presented, along with IR color photography of damaged citrus crops, the application of a scanning microdensitometer in plant science studies, and the development of an IR exposure meter. M.S.K.

A82-29527
DEVELOPMENT AND APPLICATION OF PANORAMIC AERIAL PHOTOGRAPHY IN FOREST PEST MANAGEMENT
W. M. CIESLA (U.S. Forest Service, Davis, CA) In: Color aerial photography in the plant sciences and related fields; Proceedings of the Eighth Biennial Workshop, Luray, VA, April 21-23, 1981. Falls Church, VA, American Society of Photogrammetry, 1981, p. 19-28. refs

Characteristics of panoramic aerial photography and its use in forest pest management are reviewed. Applications to date include estimating losses caused by the mountain pine beetle and planning salvage operations of insect killed timber in California. Advantages of the optical bar panoramic aerial camera system include the ability to acquire high-resolution photography over large areas of land rapidly. Disadvantages include a relatively high acquisition cost, a limited acquisition capability, unconventional film size, and a changing photo scale. (Author)

A82-29528
RIPARIAN VEGETATION MAPPING IN NORTHEASTERN CALIFORNIA USING HIGH ALTITUDE COLOR INFRARED AERIAL PHOTOGRAPHY
K. G. BONNER (U.S. Forest Service, San Francisco, CA) In: Color aerial photography in the plant sciences and related fields; Proceedings of the Eighth Biennial Workshop, Luray, VA, April 21-23, 1981. Falls Church, VA, American Society of Photogrammetry, 1981, p. 29-37. Research supported by the California State Resources Agency. refs

A82-29529

INVENTORY OF WILDLIFE HABITAT FROM COLOR INFRARED AERIAL PHOTOGRAPHY FOR COBB ISLAND, VIRGINIA

J. T. HEINEN and R. A. MEAD (Virginia Polytechnic Institute and State University, Blacksburg, VA) In: Color aerial photography in the plant sciences and related fields; Proceedings of the Eighth Biennial Workshop, Luray, VA, April 21-23, 1981. Falls Church, VA, American Society of Photogrammetry, 1981, p. 39-44, 160. refs

A82-29530

CONSIDERATIONS IN USING COLOR INFRARED PHOTOGRAPHS FOR VEGETATIVE INTERPRETATION

P. M. SEEVERS (U.S. Geological Survey, EROS Data Center, Sioux Falls, SD) In: Color aerial photography in the plant sciences and related fields; Proceedings of the Eighth Biennial Workshop, Luray, VA, April 21-23, 1981. Falls Church, VA, American Society of Photogrammetry, 1981, p. 45-49. refs

The literature suggests that the infrared wavelengths are the most significant when color infrared film records the reflectance of vegetation. Some evidence, however, suggests that the relative sensitivity of the infrared sensitive emulsion layer of the film and the apparent intensity of near infrared reflectance from plants combine to saturate that layer when the film is used to photograph agricultural crops at low altitude. In addition, some physiological considerations of plant characteristics also suggest that the red- and green-sensitive emulsion layers would be affected before the infrared-sensitive layer. Observations indicate that tissue damage in most crops is relatively severe before it becomes detectable on color infrared film. It is also then visible to the human eye. This effect suggests that previsual detection of crop damage is not likely on color infrared film. Furthermore, the perceptability of color contrasts by the human eye tends to be a deterrent to visual detection of plant symptoms, both in the field and in the interpretations of color-infrared photographs. (Author)

A82-29531

COLOR AERIAL PHOTOGRAPHY DETECTS NUTRIENT STATUS OF LOBLOLLY PINE PLANTATIONS

A. LYONS and E. BUCKNER (Tennessee, University, Knoxville, TN) In: Color aerial photography in the plant sciences and related fields; Proceedings of the Eighth Biennial Workshop, Luray, VA, April 21-23, 1981. Falls Church, VA, American Society of Photogrammetry, 1981, p. 53-58. Research supported by the Champion International Corp. refs

A82-29532

MULTI-RESOURCE INVENTORY IN INTERIOR ALASKA

K. M. HEGG (U.S. Forest Service, Washington, DC), F. R. LARSON, D. R. MEAD, and K. C. WINTERBERGER (Pacific Northwest Forest and Range Experiment Station, Anchorage, AK) In: Color aerial photography in the plant sciences and related fields; Proceedings of the Eighth Biennial Workshop, Luray, VA, April 21-23, 1981. Falls Church, VA, American Society of Photogrammetry, 1981, p. 59-65. refs

Data reduction, conversion, and application of NASA small scale color IR photography for Alaskan renewable resource evaluation are described. The photographs are taken at a 1:120,000 scale, and special overlay ink and film allow suitable definitions of forest and woodland, although brush heights and tundra are undiscernable. The study is concentrated along the Susitna River basin, where rapid development is occurring along the road between Anchorage and Fairbanks. Interpretation involves classification of forest, woodland, nonforest, and nonvegetated groups, with forest and woodland further defined into closed or open crown areas, depending on exceeding 50% cover. It is recommended that relating ground sample selection based on photopoint interpretation to a digitized map be accomplished by completing the map digitization prior to field plot selection, and statistically tieing photointerpretation sampling schemes to detailed inplace digitized map sampling schemes. M.S.K.

A82-29533

APPLICATION OF 35MM COLOR AERIAL PHOTOGRAPHY TO FOREST LAND CHANGE DETECTION

N. L. MILLER and M. P. MEYER (Minnesota, University, St. Paul, MN) In: Color aerial photography in the plant sciences and related fields; Proceedings of the Eighth Biennial Workshop, Luray, VA, April 21-23, 1981. Falls Church, VA, American Society of Photogrammetry, 1981, p. 67-72. Research sponsored by the U.S. Forest Service.

Attention is called to the high cost ($280 per plot) of examining the sample plots that form the data base in forestry surveys. The use of 35-mm color aerial photography for detecting change in these plots is investigated. With the method envisaged here, only those sample plots found to be significantly changed (logging, fire, blowdown, insect damage, disease) would be examined; the rest would be updated by computer growth projection models. Trial runs with 35-mm color aerial photography in Minnesota and Michigan yielded good results at a cost estimated at $20 per plot. C.R.

A82-29534

ESTIMATING RANGELAND COVER PROPORTIONS WITH LARGE-SCALE COLOR-INFRARED AERIAL PHOTOGRAPHS

C. J. VAN ZEE (U.S. Geological Survey, EROS Data Center, Sioux Falls, SD) and K. G. BONNER (U.S. Forest Service, San Francisco, CA) In: Color aerial photography in the plant sciences and related fields; Proceedings of the Eighth Biennial Workshop, Luray, VA, April 21-23, 1981. Falls Church, VA, American Society of Photogrammetry, 1981, p. 73-82. refs

A82-29535

MAPPING RIPARIAN VEGETATION IN SOUTHEASTERN OREGON USING DIGITIZED LARGE SCALE COLOR INFRA-RED AERIAL PHOTOGRAPHY

D. S. LINDEN (Technicolor Graphic Services, Denver, CO) and D. M. CONCANNON (U.S. Bureau of Land Management, Denver, CO) In: Color aerial photography in the plant sciences and related fields; Proceedings of the Eighth Biennial Workshop, Luray, VA, April 21-23, 1981. Falls Church, VA, American Society of Photogrammetry, 1981, p. 83-89. refs

A82-29536

REMOTE SENSING OF DOUGLAS-FIR TREES NEWLY INFESTED BY BARK BEETLES

P. M. HALL, P. A. MURTHA, and J. A. MCLEAN (British Columbia, University, Vancouver, Canada) In: Color aerial photography in the plant sciences and related fields; Proceedings of the Eighth Biennial Workshop, Luray, VA, April 21-23, 1981. Falls Church, VA, American Society of Photogrammetry, 1981, p. 91-98, 157. refs

Two study plots containing Douglas-fir (Pseudotsuga menziesii /Mirb/ Franco) newly infested by Douglas-fir beetle (Dendroctonus pseudotsugae Hopk.) were photographed with large-scale (1:1000), color infrared film on July 29, 1979 - approximately three months after possible insect attack. Significant differences were found between the ratios of the optical density values of the images of healthy and attacked trees. It is concluded that trees which have been successfully attacked by beetles can be detected on color infrared air photos approximately three months after initial attack when the trees still support visually green, healthy-appearing foliage. (Author)

A82-29537#

SPECTRAL SCANNING OF EXPERIMENTAL PLOTS OF SO2-AFFECTED WINTER WHEAT AND SOYBEANS FOR MISSION PLANNING

C. D. SAPP (Tennessee Valley Authority, Chattanooga, TN) In: Color aerial photography in the plant sciences and related fields; Proceedings of the Eighth Biennial Workshop, Luray, VA, April 21-23, 1981. Falls Church, VA, American Society of Photogrammetry, 1981, p. 101-114. refs

A series of TVA experiments is described wherein plots of soybeans and winter wheat plants were grown to the critical seed-filling stage of development, exposed to controlled doses of SO2, observed systematically for foliar effects, then scanned row by row with a spectroradiometer. The spectral curves were statistically analyzed to determine the changes in spectral reflectance that occur after plants are stressed by SO2 emissions. For soybeans, the affected subplots had higher visible reflectance, lower IR reflectance, and a lower IR/red ratio. Variance analysis showed significant differences in IR and IR/red reflectance between chlorotic soybeans and unaffected ones; and in red reflectance, IR reflectance and IR/red ratio between necrotic and unaffected ones. Since the wheat subplots showed no chlorosis, analysis of reflectance data concentrates on necrosis, which showed a significant difference in red, IR, and IR/red reflectance between classes of differentially injured wheat. C.D.

A82-29538* National Aeronautics and Space Administration. John F. Kennedy Space Center, Cocoa Beach, Fla.

DETECTION AND DAMAGE ASSESSMENT OF CITRUS TREE LOSSES WITH AERIAL COLOR INFRARED PHOTOGRAPHY /ACIR/

C. H. BLAZQUEZ, F. W. HORN, JR. (NASA, Kennedy Space Center, Applications Projects Branch, Cocoa Beach, FL), and G. J. EDWARDS (Florida, University, Lake Alfred, FL) In: Color aerial photography in the plant sciences and related fields; Proceedings of the Eighth Biennial Workshop, Luray, VA, April 21-23, 1981. Falls Church, VA, American Society of Photogrammetry, 1981, p. 115-126. refs

Detection and disease damage assessment of citrus tree losses in a Florida citrus grove were made by establishing a registration (grove site location) coordinate system, developing a damage assessment system, and testing sequential aerial color infrared (ACIR) photography at the scale of 1 in. = 333 ft (2.5 cm = 100 m) during the winter, spring, and summer seasons of 1978 and spring of 1979. Spring photography was the easiest to photo interpret, showed the greatest differences between healthy and diseased trees, and had the least shadow and background interference for photo interpretation. Trees showing slight disease damage were detected in ACIR before they were found in ground surveys. (Author)

A82-29539* Minnesota Univ., St. Paul.

APPLICATION OF SCANNING MICRODENSITOMETER DATA IN SELECTED PLANT SCIENCE CASE STUDIES

T. M. LILLESAND and D. E. MEISNER (Minnesota, University, St. Paul, MN) In: Color aerial photography in the plant sciences and related fields; Proceedings of the Eighth Biennial Workshop, Luray, VA, April 21-23, 1981. Falls Church, VA, American Society of Photogrammetry, 1981, p. 127-136, 164, 165. Research supported by the Minnesota State Department of Agriculture and University of Minnesota refs
(Contract NGL-24-005-263)

This paper treats a representative sample of projects aimed at vegetation mapping and assessment via analysis of both digital photographic and Landsat data projects and illustrates the potential for using scanning microdensitometric data extracted from color infrared photographs in the following applications: freshwater wetlands mapping, tree type mapping, and yield vs. reflectance modeling in corn fertilization experiments. These case studies are presented to illustrate the general applicability of scanning microdensitometer data in the contexts of image classification and enhancement as well as quantitative modeling of ground parameters. (Author)

A82-29747

DESERT LOCUST HABITAT MONITORING WITH SATELLITE REMOTE SENSING A NEW TECHNOLOGY FOR AN OLD PROBLEM

J. U. HIELKEMA (United Nations, Food and Agriculture Organization, Rome, Italy) ITC Journal, no. 4, 1981, p. 387-417. refs

Precipitation and vegetation remote sensing techniques developed during Phase I of the UN Food and Agricultural Organization program to monitor rainfall and vegetation conditions known to presage desert locust plagues are described. Landsats 2 and 3 multispectral scanners were used, along with Tiros-N and Meteosat and Goes satellite data, to quantify the location, extent, duration, and intensity of rainfall events in the recession area, that region where locusts live as ordinary grasshoppers until conditions which lead to population explosions and subsequent swarming are present. Outbreak areas were sought, along with ecological conditions which induced the outbreaks. Landsat data handling procedures are reviewed, and it is noted that mosaic image construction has resulted in the construction of 10 maps for the north Africa locust recession area of Morocco, Algeria, Tunisia, and Libya. M.S.K.

A82-32701#

PANORAMIC AERIAL PHOTOGRAPHY IN FOREST PEST MANAGEMENT

W. M. CIESLA (U.S. Forest Service, Fort Collins, CO), R. A. ALLISON (U.S. Forest Service, Washington, DC), and F. P. WEBER (U.S. Forest Service, Houston, TX) Photogrammetric Engineering and Remote Sensing, vol. 48, May 1982, p. 719-723. refs

The combination of high image resolution and large-area coverage inherent in panoramic photography is shown to make possible 100% coverage of forest pest outbreak areas, as well as the extraction of both stratification and detailed crown counts from a single set of photos. Attention is given to the deployment of the KA-80A optical bar panoramic camera aboard the U-2 high-speed, high-altitude aircraft operated by NASA. Continuous coverage of forested areas allows photos acquired for vegetation damage assessment to be used by such other disciplines as land-use planning, watershed evaluation, road location, or timber-sale planning, suggesting the sharing of photo-acquisition costs. Unfortunately, no aircraft other than the U-2, with its 65,000-foot cruise altitude, is able to use this camera system efficiently. O.C.

A82-32703#

ESTIMATING BARK BEETLE-KILLED LODGEPOLE PINE WITH HIGH ALTITUDE PANORAMIC PHOTOGRAPHY

W. H. KLEIN (U.S. Forest Service, Davis, CA) Photogrammetric Engineering and Remote Sensing, vol. 48, May 1982, p. 733-737. refs

A82-32704#

ESTIMATING MOUNTAIN PINE BEETLE-KILLED PONDEROSA PINE OVER THE FRONT RANGE OF COLORADO WITH HIGH ALTITUDE PANORAMIC PHOTOGRAPHY

R. D. DILLMAN (Lockheed Engineering and Management Services Co., Inc., Houston, TX) and W. B. WHITE (U.S. Forest Service, Fort Collins, CO) Photogrammetric Engineering and Remote Sensing, vol. 48, May 1982, p. 741-747. U.S. Department of Agriculture refs
(Contract USDA-53-3187-8-25)

A82-32705#

OPTICAL BAR PANORAMIC PHOTOGRAPHY FOR PLANNING TIMBER SALVAGE IN DROUGHT-STRESSED FORESTS

J. CAYLOR, J. PIERCE, and W. SALAZAR (U.S. Forest Service, San Francisco, CA) Photogrammetric Engineering and Remote Sensing, vol. 48, May 1982, p. 749-753. refs

Panoramic aerial photographs were obtained over 40 million acres of forest land in northern California during the period July, 1978, through September, 1979. These were used as an aid in planning timber salvage sales to locate concentrations of bark beetle-caused tree mortality following a severe drought. Several innovative procedures devised to effectively use these unconventional format photographs under field conditions are described. The photos were used in 223 salvage sales, resulting in a harvest of 532.2 million board feet of bark beetle killed timber during the period July, 1978, through May 1979. (Author)

A82-32707
EVALUATION OF SPRUCE-FIR FORESTS USING SMALL-FORMAT PHOTOGRAPHS
J. MCCARTHY (Vermont, University, Burlington, VT), C. E. OLSON, JR., and J. A. WITTER (Michigan, University, Ann Arbor, MI) Photogrammetric Engineering and Remote Sensing, vol. 48, May 1982, p. 771-778. Research supported by the McIntire-Stennis Funds and University of Michigan; U.S. Department of Agriculture refs
(Contract USDA-23-178)

The effectiveness of large-scale, 1:4800 small-format color aerial photographs in the evaluation of tree conditions and identification of the balsam fir and white spruce hosts of the spruce budworm is assessed. Contingency tables allowed comparisons of tree condition and species identification from aerial and ground data. It is shown that photointerpretation of small-format photographs provided mean aerial estimates of tree conditions within one-half of a ranking class of the mean from ground truth data, with balsam fir and white spruce separable at a frequency of 80% and host specie mortality aerial estimates within 10% of the ground test data. O.C.

A82-32708* Cornell Univ., Ithaca, N. Y.
LANDSAT DETECTION OF HARDWOOD FOREST CLEARCUTS
W. R. HAFKER and W. R. PHILIPSON (Cornell University, Ithaca, NY) Photogrammetric Engineering and Remote Sensing, vol. 48, May 1982, p. 779, 780. refs
(Contract NGL-33-010-171)

In a study of hardwood forests in Pennsylvania, the detection of clearcuts by means of visual analysis of Landsat summer imagery was accomplished best using band 5 images; however, a higher percentage of clearcuts could be detected using bands 5 or 7 winter images acquired during periods of snow cover. (Author)

A82-32897* National Aeronautics and Space Administration. Goddard Space Flight Center, Greenbelt, Md.
REMOTE SENSING OF LEAF WATER CONTENT IN THE NEAR INFRARED
C. J. TUCKER (NASA, Goddard Space Flight Center, Earth Resources Branch, Greenbelt, MD) Remote Sensing of Environment, vol. 10, Aug. 1980, p. 23-32. refs
(Previously announced in STAR as N80-20768)

A82-32905* National Aeronautics and Space Administration. Goddard Space Flight Center, Greenbelt, Md.
EFFECTS OF VEGETATION CANOPY STRUCTURE ON REMOTELY SENSED CANOPY TEMPERATURES
D. S. KIMES (NASA, Goddard Space Flight Center, Earth Resources Branch, Greenbelt, MD) Remote Sensing of Environment, vol. 10, Nov. 1980, p. 165-174. refs
(Previously announced in STAR as N79-33530)

A82-32907
THE RESPONSE CHARACTERISTICS OF VEGETATION IN LANDSAT MSS DIGITAL DATA
K. R. MCCLOY (South Australian Institute of Technology, Ingle Farm, Australia) Remote Sensing of Environment, vol. 10, Nov. 1980, p. 185-190. refs

Empirical evidence is used to propose a model of the response due to a vegetative canopy. The model is a simplification, and hence approximation, of the complex relationship between physical conditions in the canopy and the resultant spectral reflectance. However, the model can be quantified to yield at least two, and possibly more, independent response parameters from the Landsat response data. These independent response parameters can be used to derive estimates of more than one independent physical characteristic of the canopy. Further, the model specifies its limitations, for a given data input; and indicates how further auxiliary data may be used to extract more information from the model. (Author)

A82-32909* National Aeronautics and Space Administration. Lyndon B. Johnson Space Center, Houston, Tex.
FIELD SIZE, LENGTH, AND WIDTH DISTRIBUTIONS BASED ON LACIE GROUND TRUTH DATA
D. E. PITTS and G. BADHWAR (NASA, Johnson Space Center, Houston, TX) Remote Sensing of Environment, vol. 10, Nov. 1980, p. 201-213. refs

The development of agricultural remote sensing systems requires knowledge of agricultural field size distributions so that the sensors, sampling frames, image interpretation schemes, registration systems, and classification systems can be properly designed. Malila et al. (1976) studied the field size distribution for wheat and all other crops in two Kansas LACIE (Large Area Crop Inventory Experiment) intensive test sites using ground observations of the crops and measurements of their field areas based on current year rectified aerial photomaps. The field area and size distributions reported in the present investigation are derived from a representative subset of a stratified random sample of LACIE sample segments. In contrast to previous work, the obtained results indicate that most field-size distributions are not log-normally distributed. The most common field size observed in this study was 10 acres for most crops studied. G.R.

A82-32913* National Aeronautics and Space Administration. Goddard Space Flight Center, Greenbelt, Md.
LANDSAT DIGITAL ANALYSIS OF THE INITIAL RECOVERY OF BURNED TUNDRA AT KOKOLIK RIVER, ALASKA
D. K. HALL, J. P. ORMSBY (NASA, Goddard Space Flight Center, Hydrological Sciences Branch, Greenbelt, MD), L. JOHNSON (U.S. Army, Cold Regions Research and Engineering Laboratory, Fairbanks, AK), and J. BROWN (U.S. Army, Cold Regions Research and Engineering Laboratory, Hanover, NH) Remote Sensing of Environment, vol. 10, Dec. 1980, p. 263-272. Research supported by the U.S. Geological Survey. refs
(Previously announced in STAR as N80-19588)

A82-32914* National Aeronautics and Space Administration. Goddard Space Flight Center, Greenbelt, Md.
VIEW ANGLE EFFECTS IN THE RADIOMETRIC MEASUREMENT OF PLANT CANOPY TEMPERATURES
D. S. KIMES (NASA, Goddard Space Flight Center, Earth Resources Branch, Greenbelt, MD), S. B. IDSO, P. J. PINTER, JR., R. J. REGINATO, and R. D. JACKSON (U.S. Water Conservation Laboratory, Phoenix, AZ) Remote Sensing of Environment, vol. 10, Dec. 1980, p. 273-284. refs

The thermal infrared sensor response from a wheat canopy was extremely non-Lambertian because of spatial variations in energy flow processes; the effective radiant temperature of the sensor varied as much as 13 C with changing view angle. This variation of sensor response was accurately quantified (root-mean-square of deviations between theoretical and measured responses reduced to 1.1 C) as a function of vegetation canopy geometry, vertical temperature distribution of canopy components, and sensor view angle. The results have important implications for optimizing sensor view angles for remote sensing missions. (Author)

A82-34179* New York State Univ., Syracuse.
EVALUATION OF NOAA-AVHRR DATA FOR CROP ASSESSMENT
M. J. DUGGIN, D. PIWINSKI (New York, State University, Syracuse, NY), V. WHITEHEAD, and G. RYLAND (Lockheed Engineering and Management Services Co., Inc., Houston, TX) Applied Optics, vol. 21, June 1, 1982, p. 1873-1875. refs
(Contract NAS9-16514)

A study has been carried out in order to determine the angular limits which should be imposed upon NOAA06 and -7 satellite advanced very high-resolution radiometer (AVHRR) data used in vegetation assessment. The study involved simulations of anticipated sensor output over a wheat crop and empirical investigation of sensor data over vegetated areas. The conclusion drawn from both approaches is that less than 10% variation in the simulated vegetative index may be anticipated across the swath of imagery used if only the central 512 pixels are utilized. V.L.

A82-34706

INTERPRETATION OF VEGETATIVE COVER IN WETLANDS USING FOUR-CHANNEL SAR IMAGERY

E. WEDLER (Ontario Centre for Remote Sensing, Toronto, Canada) and R. KESSLER (Freiburg, Universitaet, Freiburg im Breisgau, West Germany) In: American Society of Photogrammetry, Annual Meeting, 47th, Washington, DC, February 22-27, 1981, ASP Technical Papers. Falls Church, VA, American Society of Photogrammetry, 1981, p. 111-124. refs

As a part of a Canada-West Germany scientific exchange program, SAR imagery obtained over areas in Southern Ontario was investigated. A unique and varied image response was noted at certain wetland sites. A description is provided of the results of an extension of the early observations to other wetland sites, taking into account preliminary correlations between the SAR image response and the wetland cover type. It was found that the effects produced by wetland conditions in Southern Ontario on SAR X- and L-band backscatter make it possible to interpret vegetative cover and moisture conditions from SAR imagery. X-band SAR is sensitive to smaller-scale vegetative content in the wetlands, while L-band SAR is sensitive to larger-scale vegetative content in the wetlands. G.R.

A82-34710

PROBLEMS ASSOCIATED WITH REMOTELY DETECTING AND MONITORING SALINE SITES WITHIN IRRIGATED ALBERTA

D. B. HARKER (Alberta Agriculture, Irrigation Div., Lethbridge, Canada) In: American Society of Photogrammetry, Annual Meeting, 47th, Washington, DC, February 22-27, 1981, ASP Technical Papers. Falls Church, VA, American Society of Photogrammetry, 1981, p. 154-163. refs

Of the 400,000 ha of land irrigated in Alberta, from 10% to 30% has been estimated to be adversely affected by high water tables and soil salinity. To facilitate optimum rehabilitation planning, those lands which are affected or are likely to become affected under new irrigation must be identified and monitored. Over the last 25 years several attempts have been made to identify and monitor affected acreages using panchromatic air photos. Recently, 1:10,000 color and other photographic sensors and scales have been utilized and preliminary work with Landsat digital data has begun. In an evaluation of these activities, attention is given to mapping details, mapping efficiency, the affected area, visual pattern recognition problems, and ground truth requirements. Plans for future work are also discussed. G.R.

A82-34716

A COMPUTERIZED SPATIAL ANALYSIS SYSTEM FOR ASSESSING WILDLIFE HABITAT FROM VEGETATION MAPS

R. A. MEAD, T. L. SHARIK, S. P. PRISLEY, and J. T. HEINEN (Virginia Polytechnic Institute and State University, Blacksburg, VA) In: American Society of Photogrammetry, Annual Meeting, 47th, Washington, DC, February 22-27, 1981, ASP Technical Papers. Falls Church, VA, American Society of Photogrammetry, 1981, p. 212-220. refs

A82-34729* Florida Univ., Lake Alfred.

EFFECTS OF ALTITUDE, FOCAL LENGTH, AND FILTER COMBINATIONS ON COLOR INFRARED PHOTOGRAPHY OF CITRUS GROVES

C. H. BLAZQUEZ (Florida, University, Lake Alfred, FL), F. W. HORN, JR. (NASA, Kennedy Space Center, Cocoa Beach, FL), and E. RHODES (Florida, Dept. of Transportation, Tallahassee, FL) In: American Society of Photogrammetry, Annual Meeting, 47th, Washington, DC, February 22-27, 1981, ASP Technical Papers. Falls Church, VA, American Society of Photogrammetry, 1981, p. 351-366. refs

A82-34730* National Aeronautics and Space Administration. Goddard Space Flight Center, Greenbelt, Md.

DEFINING THE TEMPORAL WINDOW FOR MONITORING FOREST CANOPY DEFOLIATION USING LANDSAT

R. F. NELSON (NASA, Goddard Space Flight Center, Earth Resources Branch, Greenbelt, MD) In: American Society of Photogrammetry, Annual Meeting, 47th, Washington, DC, February 22-27, 1981, ASP Technical Papers. Falls Church, VA, American Society of Photogrammetry, 1981, p. 367-382. refs

An analysis of Landsat imagery of forested areas near Williamsport, Pennsylvania shows that the effects of defoliation by insects can be assessed over a two month period beginning in early June. Within this window heavily defoliated forest can be successfully delineated from moderately defoliated and healthy forest. Consequently, the effects of insect damage can be assessed at times other than peak defoliation, doubling the probability that useful satellite data can be acquired in the Williamsport area. (Author)

A82-34731

USE OF LANDSAT MULTISPECTRAL SCANNER DATA IN VEGETATION MAPPING OF A FORESTED AREA

S. KHORRAM and E. F. KATIBAH (California, University, Berkeley, CA) In: American Society of Photogrammetry, Annual Meeting, 47th, Washington, DC, February 22-27, 1981, ASP Technical Papers. Falls Church, VA, American Society of Photogrammetry, 1981, p. 383-392. refs

Landsat digital data combined with U-2 color infrared photography of the scale 1:120,000 are used for vegetation mapping of a forested area in northern California. The approach involves geometric correction of Landsat digital data, selection of ten training sites, unsupervised classification of training sites, and supervised classification of the entire study area. Best results for unsupervised classification are achieved when each training site is analyzed independently. USGS topographic maps of the scale 1:250,000 are useful in the location of control points, delineation of watershed boundary, and geometric correction of Landsat digital data. It is concluded that Landsat repetitive data are a useful means of mapping the area under investigation. D.L.G.

A82-34732

REMOTE SENSING - A POTENTIAL AID IN THE PREPARATION OF AN URBAN TREE INVENTORY

P. A. GOLDBERG In: American Society of Photogrammetry, Annual Meeting, 47th, Washington, DC, February 22-27, 1981, ASP Technical Papers. Falls Church, VA, American Society of Photogrammetry, 1981, p. 393-401. refs

Remote sensing is a reliable tool for the compilation of urban tree inventories. An assessment of the quantity and quality of the Omaha-Bellevue, Nebraska tree population was made the summer of 1979. After digitizing the data several analytical techniques were explored, among them factor analysis. Preliminary results indicated that the use of aerial surveys and computer analysis prove more cost effective and accurate than traditional forest field surveys. (Author)

A82-34733

MONITORING DEFORESTATION IN THE EASTERN PART OF THE STATE OF GUERRERO, MEXICO

D. RODRIGUEZ-BEJARANO (Guerrero, Universidad Autonoma, Chilpancingo, Mexico) In: American Society of Photogrammetry, Annual Meeting, 47th, Washington, DC, February 22-27, 1981, ASP Technical Papers. Falls Church, VA, American Society of Photogrammetry, 1981, p. 402-411. refs

A research project carried out by the University of Guerrero to investigate deforestation and other land use and land cover changes is described. Landsat imagery, aerial photographs, and cartographic maps are used in determining changes in forest vegetation between 1972 and 1979. The area covered by forest fell from 112,250 hectares to 76,250 hectares. During the period investigated, the population density rose from 35 persons/sq km to 46 persons/sq km. The forest cover comprises tropical and semitemperate forests. C.R.

A82-35139

STATUS AND PROSPECTS OF THE AUTOMATED PROCESSING OF REMOTE-SENSING DATA /USING FOREST SURVEYS AS AN EXAMPLE/ [SOSTOIANIE I PERSPEKTIVY AVTOMATIZATSII OBRABOTKI AEROKOSMICHESKOI INFORMATSII /NA PRIMERE MATERIALOV S'EMKI LESA/]

V. I. SUKHIKH and R. I. ELMAN In: Study of the hydrological cycle by aerospace methods. Moscow, Izdatel'stvo Radio i Sviaz', 1982, p. 80-85. In Russian.

Attention is given to the following techniques of the automated processing of remote-sensing data: the delineation of forest boundaries and homogeneous areas; the delineation of extended land areas and their schematic representation; and the determination of the reserves, completeness, diameter, and other characteristics of plantations. The automatic delineation of such land categories as forest-covered areas, fire-consumed areas, cleared spaces, and swamps is considered. It is shown that the most informative features for the determination of forest-evaluation indices are the combination of the image texture patterns of the delineated area with the landscape characteristics and generalized features of the external appearance of these images. B.J.

A82-37194

C-BAND RADAR FOR DETERMINING SURFACE SOIL MOISTURE

R. BERNARD, P. MARTIN, D. VIDAL-MADJAR (CNRS and CNET, Centre de Recherche en Physique de l'Environnement Terrestre et Planetaire, Issy-les-Moulineaux, Hauts-de-Seine, France), J. L. THONY, and M. VAUCLIN (Institut de Mecanique, Grenoble, France) Remote Sensing of Environment, vol. 12, July 1982, p. 189-200. Centre National d'Etudes Spatiales refs
(Contract CNES-214; CNES-272)

A C band radar calibration method is presented. The experiment has been conducted in an agricultural area near Paris on three different types of surface: wheat stubble, sugar beet, and corn. It has been found that the sensitivity of the radar backscattering coefficient to surface soil moisture agrees well with the results obtained by Ulaby et al. (1979) when soil moisture values are expressed as percentage of the field capacity. (Author)

A82-37503

REMOTE SENSING OF SALT MARSH VEGETATION IN THE FIRST FOUR PROPOSED THEMATIC MAPPER BANDS

J. T. C. BUDD (Portsmouth Polytechnic, Portsmouth, England) and E. J. MILTON (Southampton, University, Southampton, England) International Journal of Remote Sensing, vol. 3, Apr.-June 1982, p. 147-161. Research supported by Portsmouth Polytechnic and University of Reading. refs

The potential of the first four proposed TM bands for estimating above-ground biomass and discriminating species groups was evaluated in an area of intertidal salt marsh in Chichester Harbor, Southern England. Ground spectral data were collected using a portable multiband radiometer during August 1979. The correlation and variance-covariance matrices of the data are shown, as are the results of principal components analysis of the ground spectral data and of canonical variate analysis. Individual sites for four types of algae are graphed for principal components and canonical variates. For biomass estimation, the relationship between bidirectional reflectance and dry biomass is shown for the algae. C.D.

A82-37589

THE INFLUENCE OF SOIL CHARACTERISTICS ON REGIONAL CONVECTION DIFFERENCES ABOVE NORTHERN GERMANY [DIE AUSWIRKUNG VON BODENEIGENSCHAFTEN AUF DIE REGIONALEN KONVEKTIONSUNTERSCHIEDE UEBER NORDDEUTSCHLAND]

D. MUELLER and C. KOTTMEIER (Hannover, Technische Universitaet, Hanover, West Germany) Meteorologische Rundschau, vol. 35, June 1982, p. 84-91. In German. refs

The present investigation is concerned with the various factors which can affect the intensity of convection. Soil moisture and orography are found to have significant influence on the convection. Regional differences concerning soil and soil moisture are used as a basis to develop a map which can provide information regarding the local differences of the intensity of convection. The map shows good agreement with observations made by glider pilots above the North German Plain. However, in the mountainous area south of the northern lowlands, orography appears to have a greater effect than soil moisture. G.R.

N82-22623*# Purdue Univ., Lafayette, Ind. Lab. for Applications of Remote Sensing.

SPECTRAL PROPERTIES OF AGRICULTURAL CROPS AND SOILS MEASURED FROM SPACE, AERIAL, FIELD, AND LABORATORY SENSORS

M. E. BAUER, Principal Investigator, V. C. VANDERBILT, B. F. ROBINSON, and C. S. T. DAUGHTRY Nov. 1981 21 p refs
Repr. from Proc. of the Intern. Arch. of Photogrammetry, v. 23(B7) p 56-73 Presented at the 14th Congr. of the Intern. Soc. for photogrammetry, Hamburg, 13-15 Jul. 1980 Sponsored by NASA, USDA, Dept. of Commerce, Dept. of the Interior, and Agency for International Development ERTS
(Contract NAS9-15466; PROJ. AGRISTARS)
(E82-10189; NASA-CR-168617; SR-P1-04200; NAS 1.26:168617; LARS-07138) Avail: NTIS HC A02/MF A01 CSCL 20F

Investigations of the multispectral reflectance characteristics of crops and soils as measured from laboratory, field, aerial, and satellite sensor systems are reviewed. The relationships of important biological and physical characteristics to the spectral properties of crops and soils are addressed. J.D.

N82-22626*# Environmental Research Inst. of Michigan, Ann Arbor.

ANALYSIS OF SCANNER DATA FOR CROP INVENTORIES Progress Report, 15 Nov. 1980 - 14 Feb. 1981

R. HORVATH, Principal Investigator, R. C. CICONE, R. J. KAUTH, W. A. MALILA, W. PONT, B. THELEN, and A. SELLMAN Apr. 1981 141 p ERTS
(Contract NAS9-15476)
(E82-10192; NASA-CR-161047; NAS 1.26:161047; ERIM-152400-4-P) Avail: NTIS HC A07/MF A01 CSCL 02C

Accomplishments for a machine-oriented small grains labeler T&E, and for Argentina ground data collection are reported. Features of the small grains labeler include temporal-spectral profiles, which characterize continuous patterns of crop spectral development, and crop calendar shift estimation, which adjusts for planting date differences of fields within a crop type. Corn and soybean classification technology development for area estimation for foreign commodity production forecasting is reported. Presentations supporting quarterly project management reviews and a quarterly technical interchange meeting are also included. T.M.

N82-23116*# Evangel Coll., Springfield, Mo.

USE OF LANDSAT DATA TO DEFINE SOIL BOUNDARIES IN CARROLL COUNTY, MISSOURI

S. E. DAVIDSON *In* Houston Univ. The 1981 NASA ASEE Summer Fac. Fellowship Program, Vol. 1 12 p 20 Aug. 1981 refs
Avail: NTIS HC A14/MF A01 CSCL 08M

Bands 4, 5 and 7 false color composite photographs were prepared using data from LANDSAT scenes acquired during April 1977 and April 1981 on computer compatible tapes, and these color composites were compared with band 7 black and white photographs prepared for the entire county. Delineations of soil boundaries at the soil association level were achieved using LANDSAT spectral reflectance data and slope maps for a portion of Carroll County, Missouri. Forty two spectral reflectance classes from April 1977 LANDSAT data were overlaid on digitized slope maps of nine USGS 7.5 minute series topographic quadrangle slope maps to achieve boundary delineations of the soil associations. Author

N82-23133*# Mississippi State Univ., State College.

A COMPARISON OF STRATIFIED VERSUS REGRESSION ESTIMATORS Final Report

H. C. TAKACS *In* Houston Univ. The 1981 NASA ASEE Summer Fac. Fellowship Program, Vol. 2 17 p 20 Aug. 1981 refs

Avail: NTIS HC A17/MF A01 CSCL 05B

LANDSAT data acquired over an agricultural area along with ground enumeration of the same area are used to obtain crop acreage estimates which are better (as measured in terms of bias and variance) than can be obtained from either data source alone. Two basic approaches considered within the AgRISTARS program are a stratified crop acreage estimator and a regression estimator. A statement of the problem was mathematically formulated and some theorems were proved which relate to the variance of the two estimators. For a particular set of data, the regression and stratified estimators are compared in terms of certain easily computed parameters. S.L.

N82-23564*# National Aeronautics and Space Administration. Lyndon B. Johnson Space Center, Houston, Tex.

A METEOROLOGICALLY DRIVEN MAIZE STRESS INDICATOR MODEL

T. W. TAYLOR and F. W. RAVET, Principal Investigators Apr. 1981 20 p refs Sponsored by NASA, USDA, Dept. of Commerce, Dept. of the Interior, and Agency for International Development ERTS

(Contract PROJ. AGRISTARS)

(E82-10112; NASA-TM-84201; JSC-173991; NAS 1.15:84201; EW-UI-04119) Avail: NTIS HC A02/MF A01 CSCL 02C

A maize soil moisture and temperature stress model is described which was developed to serve as a meteorological data filter to alert commodity analysts to potential stress conditions in the major maize-producing areas of the world. The model also identifies optimum climatic conditions and planting/harvest problems associated with poor tractability. Author

N82-23565*# Lockheed Engineering and Management Services Co., Inc., Houston, Tex.

AGRISTARS: FOREIGN COMMODITY PRODUCTION FORECASTING. THE 1980 US/CANADA WHEAT AND BARLEY EXPLORATORY EXPERIMENT

R. W. PAYNE, Principal Investigator Jul. 1981 30 p refs Sponsored by NASA, USDA, Dept. of Commerce, Dept. of the Interior, and Agency for International Development ERTS

(Contract NAS9-15800; PROJ. AGRISTARS)

(E82-10126; NASA-CR-167404; JSC-17406; NAS 1.26:16740; LEMSCO-16921; FC-L1-04127) Avail: NTIS HC A03/MF A01 CSCL 02C

The crop identification procedures used performed were for spring small grains and are conducive to automation. The performance of the machine processing techniques shows a significant improvement over previously evaluated technology; however, the crop calendars require additional development and refinements prior to integration into automated area estimation technology. The integrated technology is capable of producing accurate and consistent spring small grains proportion estimates. Barley proportion estimation technology was not satisfactorily evaluated because LANDSAT sample segment data was not available for high density barley of primary importance in foreign regions and the low density segments examined were not judged to give indicative or unequvocal results. Generally, the spring small grains technology is ready for evaluation in a pilot experiment focusing on sensitivity analysis to a variety of agricultural and meteorological conditions representative of the global environment. Author

N82-23566*# Purdue Univ., Lafayette, Ind. Lab. for Applications of Remote Sensing.

DIURNAL CHANGES IN REFLECTANCE FACTOR DUE TO SUN-ROW DIRECTION INTERACTIONS

M. E. BAUER, Principal Investigator, V. C. VANDERBILT, J. C. KOLLENKARK, L. L. BIEHL, B. F. ROBINSON, and K. J. RANSON Sep. 1981 13 p refs Repr. from Intern. Colloq. on Spectral Signatures of Objects in Remote Sensing (France), 1980 Colloq. held in Avignon, France, 8-11 Sep. 1980 Sponsored by NASA, USDA, Dept. of Commerce, Dept. of the Interior, and Agency for International Development ERTS

(Contract NAS9-15466; PROJ. AGRISTARS)

(E82-10128; NASA-CR-167403; NAS 1.26:167403; LARS-090881; SR-P1-04140) Avail: NTIS HC A02/MF A01 CSCL 02C

Over a two year period, data were collected regarding the canopies of soybeans grown in rows in planter boxes placed on a turntable in an effort to investigate changes in the spectral reflectance factor related to row direction, Sun direction, soil background, and crop development stage. Results demonstrate that the direction of rows in a soybean canopy can affect the reflectance factor of the canopy by as much as 230%. The results for the red spectral region tend to support the validity of canopy reflectance models; results for the infrared region do not. A.R.H.

N82-23578*# Washington Univ., St. Louis, Mo. Dept. of Earth and Planetary Sciences.

STRUCTURE OF THE ST. FRANCOIS MOUNTAINS AND SURROUNDING LEAD BELT, S. E. MISSOURI: INFERENCES FROM THERMAL IR AND OTHER DATA SETS Quarterly Report, 1 Aug. - 31 Oct. 1981

R. E. ARVIDSON, Principal Investigator 15 Dec. 1981 5 p Original contains imagery. Original imagery may be purchased from NASA, Goddard Space Flight Center, (code 601), Greenbelt, Md. 20771. Domestic users send order to 'Attn.: National Space Science Data Center', nondomestic users send order to 'Attn.: World Data Center A for Rockets and Satellites . HCMM

(Contract NAS5-26533)

(E82-10205; NASA-CR-168632; NAS 1.26:168632) Avail: NTIS HC A02/MF A01 CSCL 08G

Day-IR, day-visible, and night-IR image data sets were analyzed. All three images were contrast enhanced, using a linear stretch. The night-IR image was destriped using a box-car filtering approach. Apparent thermal inertia images were generated from the data. The enhanced data and the apparent thermal inertia image were also registered and overlayed onto shaded relief images depicting topography and onto a colored version of the Missouri geologic map. The combination of the apparent thermal inertial image and the shaded relief map proved to have the greatest discriminability in terms of portraying linear features. The reason seems to be that the vegetation canopy on the Ozark Plateau is different topography, tend to emphasize subtle topographic effects. E.A.K.

N82-23579*# Lockheed Engineering and Management Services Co., Inc., Houston, Tex.

AGRISTARS: FOREIGN COMMODITY PRODUCTION FORECASTING. THE 1980 US CORN AND SOYBEANS EXPLORATORY EXPERIMENT Final Report

J. T. MALIN and J. G. CARNES, Principal Investigators Oct. 1981 183 p refs Sponsored by NASA, USDA, Dept. of Commerce, Dept. of the Interior and Agency for International Development ERTS

(Contract NAS9-15800; PROJ. AGRISTARS)

(E82-10206; NASA-CR-167485; JSC-17138; NAS 1.26:167485; LEMSCO-16573; FC-L1-04096) Avail: NTIS HC A09/MF A01 CSCL 02C

The U.S. corn and soybeans exploratory experiment is described which consisted of evaluations of two technology components of a production forecasting system: classification procedures (crop labeling and proportion estimation at the level of a sampling unit) and sampling and aggregation procedures. The results from the labeling evaluations indicate that the corn and soybeans labeling procedure works very well in the U.S. corn belt with full season (after tasseling) LANDSAT data. The procedure should be readily adaptable to corn and soybeans labeling required for subsequent exploratory experiments or pilot tests. The machine classification procedures evaluated in this experiment were not effective in improving the proportion estimates. The corn proportions produced by the machine procedures had a large bias when the bias correction was not performed. This bias was caused by the manner in which the machine procedures handled spectrally impure pixels. The simulation test indicated that the weighted aggregation procedure performed quite well. Although further work can be done to improve both the simulation tests and the aggregation procedure, the results of this test show that the procedure should serve as a useful baseline procedure in future exploratory experiments and pilot tests. M.G.

N82-23580*# Department of Agriculture, Houston, Tex.

EVALUATION OF THE DORAISWAMY-THOMPSON WINTER WHEAT CROP CALENDAR MODEL INCORPORATING A MODIFIED SPRING RESTART SEQUENCE

T. W. TAYLOR, F. W. RAVET, and D. SMIKA, Principal Investigators Nov. 1981 11 p refs Sponsored by NASA, USDA, Dept. of Commerce, Dept. of the Interior, and Agency for International Development ERTS
(Contract PROJ. AGRISTARS)
(E82-10207; NASA-CR-167486; JSC-17801; NAS 1.26:167486; EW-U1-04212) Avail: NTIS HC A02/MF A01 CSCL 02C

The Robertson phenology was used to provide growth stage information to a wheat stress indicator mode. A stress indicator model demands two acurate predictions from a crop calendar: date of spring growth initiation; and crop calendar stage at growth initiation. Several approaches for restarting the Robertson phenology model at spring growth initiation were studied. Although best results were obtained with a solar thermal unit method, an alternate approach which indicates soil temperature as the controlling parameter for spring growth initiation was selected and tested. The modified model (Doraiswamy-Thompson) is compared to LACIE-Robertson model predictions. E.A.K.

N82-23581*# Lockheed Engineering and Management Services Co., Inc., Houston, Tex.

AGRISTARS: SUPPORTING RESEARCH. SPRING SMALL GRAINS PLANTING DATE DISTRIBUTION MODEL

T. HODGES and J. A. ARTLEY, Principal Investigators Mar. 1981 33 p refs Sponsored by NASA, USDA, Dept. of Commerce, Dept. of the Interior, and Agency for International Development ERTS
(Contract NAS9-15800; PROJ. AGRISTARS)
(E82-10208; NASA-CR-167487; JSC-16858; NAS 1.26:167487; LEMSCO-16018; SR-L1-04032) Avail: NTIS HC A03/MF A01 CSCL 02C

A model was developed using 996 planting dates at 51 LANDSAT segments for spring wheat and spring barley in Minnesota, Montana, North Dakota, and South Dakota in 1979. Daily maximum and minimum temperatures and precipitation were obtained from the cooperative weather stations nearest to each segment. The model uses a growing degree day summation modified for daily temperature range to estimate the beginning of planting and uses a soil surface wetness variable to estimate how a fixed number of planting days are distributed after planting begins. For 1979, the model predicts first, median, and last planting dates with root mean square errors of 7.91, 6.61, and 7.09 days, respectively. The model also provides three or four dates to represent periods of planting activity within the planting season. Although the full model was not tested on an independent data set, it may be suitable in areas other than the U.S. Great Plains where spring small grains are planted as soon as soil and air temperatures become warm enough in the spring for plant growth. T.M.

N82-23582*# Lockheed Engineering and Management Services Co., Inc., Houston, Tex.

DESCRIPTION OF HISTORICAL CROP CALENDAR DATA BASES DEVELOPED TO SUPPORT FOREIGN COMMODITY PRODUCTION FORECASTING PROJECT EXPERIMENTS

W. L. WEST, III, Principal Investigator Oct. 1981 19 p refs Sponsored by NASA, USDA, Dept. of Commerce, Dept. of the Interior, and Agency for International Development ERTS
(Contract NAS9-15800; PROJ. AGRISTARS)
(E82-10209; NASA-CR-167488; JSC-17417; NAS 1.26:167488; LEMSCO-16929; FC-L1-04142) Avail: NTIS HC A02/MF A01 CSCL 02C

The content, format, and storage of data bases developed for the Foreign Commodity Production Forecasting project and used to produce normal crop calendars are described. In addition, the data bases may be used for agricultural meteorology, modeling of stage sequences and planting dates, and as indicators of possible drought and famine. M.G.

N82-23585*# Purdue Univ., Lafayette, Ind. Lab. for Applications of Remote Sensing.

SPECTRAL PROPERTIES OF AGRICULTURAL CROPS AND SOILS MEASURED FROM SPACE, AERIAL, FIELD, AND LABORATORY SENSORS

M. E. BAUER, Principal Investigator, V. C. VANDERBILT, B. F. ROBINSON, and C. S. T. DAUGHTRY Nov. 1982 21 p refs Repr. from Proc. of the Intern. Arch. of Photogrammetry (West Germany), v. 23(B7), 1980 p 56-73 Presented at the 14th Congr. of the Intern. Soc. for Photogrammetry, Hamburg, 13-15 Jul. 1980 Sponsored by NASA, USDA, Dept. of Commerce, Dept. of the Interior, and Agency for International Development ERTS
(Contract NAS9-15466; PROJ. AGRISTARS)
(E82-10212; NASA-CR-167507; SR-P1-04200; NAS 1.26:167507; LARS-071380) Avail: NTIS HC A02/MF A01 CSCL 02C

The state of knowledge of the multispectral reflectance characteristics of crops and soils as measured from laboratory, field, aerial, and satellite sensor systems is reviewed emphasizing current investigations. The relationships of important biological and physical characteristics to their spectral properties of crops and soils are addressed. Future research needs are defined. M.G.

N82-23588*# Purdue Univ., Lafayette, Ind. Lab. for Applications of Remote Sensing.

DETERMINATION OF THE OPTIMAL LEVEL FOR COMBINING AREA AND YIELD ESTIMATES

M. E. BAUER, Principal Investigator, M. M. HIXSON, and C. D. JOBUSCH 12 Oct. 1981 71 p refs Sponsored by NASA, USDA, Dept. of Commerce, Dept. of the Interior, and Agency for International Development ERTS
(Contract NAS9-15466; PROJ. AGRISTARS)
(E82-10215; NASA-CR-167511; FC-P1-04197; NAS 1.26:167511; LARS-101281) Avail: NTIS HC A04/MF A01 CSCL 02C

Several levels of obtaining both area and yield estimates are considered: county, refined strata, refined/split strata, crop reporting district, and state. Using the CCEA model form and smoothed weather data, regression coefficients at each level were derived to compute yield and its variance. The variance of the yield estimates was largest at the state and smallest at the county level for the two crops studied: corn and soybeans. The refined strata had somewhat larger variances than those associated with the refined/split strata and CRD. For production estimates, the difference in standard deviations among levels was not large for corn, but for soybeans the standard deviation at the state level was more than 50% greater than for the other levels. The refined strata had the smallest standard deviations. T.M.

N82-23589*# National Aeronautics and Space Administration. Lyndon B. Johnson Space Center, Houston, Tex.
AGRISTARS. PRELIMINARY TECHNICAL RESULTS REVIEW OF FY81 EXPERIMENTS, VOLUME 2: FISCAL YEAR 1981/1982 'CORN AND SOYBEANS PILOT' EXPERIMENT
29 Sep. 1981 170 p Sponsored by NASA, USDA, Dept. of Commerce, Dept. of the Interior, and Agency for International Development ERTS
(Contract PROJ. AGRISTARS)
(E82-10216; NASA-TM-84206; JSC-17433-VOL-2; NAS 1.15:84206; FC-J1-04175-VOL-2) Avail: NTIS HC A08/MF A01 CSCL 02C

The performance of the technology exhibited significant proportion estimation errors, specifically, high mean error in both corn and soybeans area estimation. The data systems, technical approaches, and data assessment of the pilot experiment were reviewed. Results of proportion estimations procedure performance evaluations, and sensitivity evaluations are presented. The role of the pilot experiment in foreign technology development is discussed.
T.M.

N82-23590*# Lockheed Engineering and Management Services Co., Inc., Houston, Tex.
APPLICATION OF THERMAL MODEL FOR PAN EVAPORATION TO THE HYDROLOGY OF A DEFINED MEDIUM, THE SPONGE
M. H. TRENCHARD and J. A. ARTLEY, Principal Investigators Nov. 1981 23 p refs Sponsored by NASA, USDA, Dept. of Commerce, Dept. of the Interior, and Agency for International Development ERTS
(Contract NAS9-15800; PROJ. AGRISTARS)
(E82-10217; NASA-CR-167479; JSC-17440; NAS 1.26:167479; LEMSCO-16935; FC-L1-04192) Avail: NTIS HC A02/MF A01 CSCL 02C

A technique is presented which estimates pan evaporation from the commonly observed values of daily maximum and minimum air temperatures. These two variables are transformed to saturation vapor pressure equivalents which are used in a simple linear regression model. The model provides reasonably accurate estimates of pan evaporation rates over a large geographic area. The derived evaporation algorithm is combined with precipitation to obtain a simple moisture variable. A hypothetical medium with a capacity of 8 inches of water is initialized at 4 inches. The medium behaves like a sponge: it absorbs all incident precipitation, with runoff or drainage occurring only after it is saturated. Water is lost from this simple system through evaporation just as from a Class A pan, but at a rate proportional to its degree of saturation. The contents of the sponge is a moisture index calculated from only the maximum and minium temperatures and precipitation.
T.M.

N82-23591*# National Aeronautics and Space Administration. Lyndon B. Johnson Space Center, Houston, Tex.
A METEOROLOGICALLY DRIVEN GRAIN SORGHUM STRESS INDICATOR MODEL
T. W. TAYLOR (Agricultural Research Service, Houston, Tex.) and F. W. RAVET, Principal Investigators Nov. 1981 18 p refs Sponsored by NASA, USDA, Dept. of Commerce, Dept. of the Interior, and Agency for International Development ERTS
(Contract PROJ. AGRISTARS)
(E82-10218; NASA-TM-84740; JSC-17797; NAS 1.15:84740; EW-U1-04208) Avail: NTIS HC A02/MF A01 CSCL 02C

A grain sorghum soil moisture and temperature stress model is described. It was developed to serve as a meteorological data filter to alert commodity analysts to potential stress conditions and crop phenology in selected grain sorghum production areas. The model also identifies optimum conditions on a daily basis and planting/harvest problems associated with poor tractability.
T.M.

N82-23592*# National Aeronautics and Space Administration. Lyndon B. Johnson Space Center, Houston, Tex.
AGRISTARS. PROJECT MANAGEMENT REPORT: PROGRAM REVIEW PRESENTATION TO LEVEL 1, INTERAGENCY COORDINATION COMMITTEE
3 Nov. 1981 105 p Sponsored by NASA, USDA, Dept. of Commerce, Dept. of the Interior, and Agency for International Development ERTS
(Contract PROJ. AGRISTARS)
(E82-10219; NASA-TM-84203; JSC-17792; NAS 1.15:84203; SR-J1-04195) Avail: NTIS HC A06/MF A01 CSCL 02C

The AgRISTARS supporting research projects in the areas of data systems, scene radiation, and pattern recognition are reviewed. The objectives, activities, and accomplishments of FY-80 and the objectives and status of FY-81 programs are described.
M.G.

N82-23593*# National Aeronautics and Space Administration. Ames Research Center, Moffett Field, Calif.
AIRBORNE OBSERVED SOLAR ELEVATION AND ROW DIRECTION EFFECTS ON THE NEAR-IR/RED RATIO OF COTTON
J. P. MILLARD, R. D. JACKSON (Science and Education Administration, Phoenix, Ariz.), R. C. GOETTELMAN (EAL Corp., Richmond, Calif.), and M. J. LEROY, Principal Investigators (DCA Corp., Palo Alto, Calif.) Aug. 1981 14 p refs Sponsored by NASA, USDA, Dept. of Commerce, Dept. of the Interior, and Agency for International Development ERTS
(Contract PROJ. AGRISTARS)
(E82-10220; NASA-TM-84204; JSC-17420; NAS 1.15:84204; EW-U1-04144) Avail: NTIS HC A02/MF A01 CSCL 02C

An airborne multispectral scanner was used to obtain data over two adjacent cotton fields having rows perpendicular to one another, at three times of day (different solar elevations), and on two dates (different plant size). The near IR/red ratios were displayed in image form, so that within-field variations and differences between fields could be easily assessed. The ratio varied with changing Sun elevation for north-south oriented rows, but no variation was detected for east-west oriented rows.
A.R.H.

N82-23594*# Lockheed Engineering and Management Services Co., Inc., Houston, Tex.
NORMAL CROP CALENDARS. VOLUME 3: THE CORN AND SOYBEAN STATES OF ILLINOIS, INDIANA, AND IOWA
W. L. WEST, III, Principal Investigator Oct. 1981 79 p refs Sponsored by NASA, USDA, Dept. of Commerce, Dept. of the Interior, and Agency for International Development
(Contract NAS9-15800; PROJ. AGRISTARS)
(E82-10221; NASA-CR-167446; JSC-17432; NAS 1.26:167446; LEMSCO-16944; FC-L1-04172) Avail: NTIS HC A05/MF A01 CSCL 02C

The state and crop reporting distric crop calendars for Iowa, Illinois, and Indiana are presented. Crop calendars for corn, soybeans, sorghum, oats, wheat, barley, clover, flax, sugar beets, and tobacco are included.
J.D.

N82-23595*# Lockheed Engineering and Management Services Co., Inc., Houston, Tex.
SELECTION OF THE AUSTRALIAN INDICATOR REGION
C. R. REED, Principal Investigator Sep. 1981 73 p refs Sponsored by NASA, USDA, Dept. of Commerce, Dept. of the Interior, and Agency for International Development ERTS
(Contract NAS9-15800; PROJ. AGRISTARS)
(E82-10222; NASA-CR-167406; JSC-17421; NAS 1.26:167406; LEMSCO-15682; FC-L1-04145) Avail: NTIS HC A04/MF A01 CSCL 02C

Each Australian state was examined for the availability of LANDSAT data, area, yield, and production characteristics, statistics, crop calendars, and other ancillary data. Agrophysical conditions that could influence labeling and classification accuracies were identified in connection with the highest producing states as determined from available Australian crop statistics.

Based primarily on these production statistics, Western Australia and New South Wales were selected as the wheat indicator region for Australia. The general characteristics of wheat in the indicator region, with potential problems anticipated for proportion estimation are considered. The varieties of wheat, the diseases and pests common to New South Wales, and the wheat growing regions of both states are examined. A.R.H.

N82-23597*# Lockheed Engineering and Management Services Co., Inc., Houston, Tex.

AGRISTARS: RENEWABLE RESOURCES INVENTORY. LAND INFORMATION SUPPORT SYSTEM IMPLEMENTATION PLAN AND SCHEDULE

S. S. YAO, Principal Investigator Sep. 1981 29 p Sponsored by NASA, USDA, Dept. of Commerce, Dept. of the Interior, and Agency for International Development ERTS
(Contract NAS9-15800; PROJ. AGRISTARS)
(E82-10224; NASA-CR-167441; JSC-17434; NAS 1.26:167441; LEMSCO-17276; RR-L1-00641) Avail: NTIS HC A03/MF A01 CSCL 05B

The planning and scheduling of the use of remote sensing and computer technology to support the land management planning effort at the national forests level are outlined. The task planning and system capability development were reviewed. A user evaluation is presented along with technological transfer methodology. A land management planning pilot test of the San Juan National Forest is discussed. T.M.

N82-23598*# Science and Education Administration, Weslaco, Tex.

AGRISTARS: EARLY WARNING AND CROP CONDITION ASSESSMENT. PLANT COVER, SOIL TEMPERATURE, FREEZE, WATER STRESS, AND EVAPOTRANSPIRATION CONDITIONS Final Report, 1 Dec. 1977 - Sep. 1 1980

C. L. WIEGAND, Principal Investigator, P. R. NIXON, H. W. GAUSMAN, L. N. NAMKEN, R. W. LEAMER, and A. J. RICHARDSON Aug. 1981 185 p refs Sponsored by NASA, USDA, Dept. of Commerce, Dept. of the Interior, and Agency for International Development ERTS
(Contract NASA ORDER S-40198B; PROJ. AGRISTARS)
(E82-10225; NASA-CR-167440; JSC-17143; NAS 1.26:167440; EW-U1-04103) Avail: NTIS HC A09/MF A01 CSCL 02C

Emissive (10.5 to 12.5 microns) and reflective (0.55 to 1.1 microns) data for ten day scenes and infrared data for six night scenes of southern Texas were analyzed for plant cover, soil temperature, freeze, water stress, and evapotranspiration. Heat capacity mapping mission radiometric temperatures were: within 2 C of dewpoint temperatures, significantly correlated with variables important in evapotranspiration, and related to freeze severity and planting depth soil temperatures. Author

N82-23600*# Purdue Univ., Lafayette, Ind. Lab. for Applications of Remote Sensing.

APPLICATION OF COMPUTER AXIAL TOMOGRAPHY (CAT) TO MEASURING CROP CANOPY GEOMETRY

M. E. BAUER, V. C. VANDERBILT, Principal Investigators, and R. W. KILGORE Jun. 1981 9 p refs Repr. from 1981 Intern. Geosci. and Remote Sensing Sym. (IGARSS'81), IEEE Catalog no. 81CH1656-8, 1981 p 1162-1167 Sym. held in Washington, D.C., 8-10 Jun. 1981 ERTS
(Contract NAS9-15466; PROJ. AGRISTARS)
(E82-10227; NASA-CR-167397; NAS 1.26:167397; LARS-TR-060881; SR-P1-04141) Avail: NTIS HC A02/MF A01 CSCL 02C

The feasibility of using the principles of computer axial topography (CAT) to quantify the structure of crop canopies was investigated because six variables are needed to describe the position-orientation with time of a small piece of canopy foliage. Several cross sections were cut through the foliage of healthy, green corn and soybean canopies in the dent and full pod development stages, respectively. A photograph of each cross section representing the intersection of a plane with the foliage was enlarged and the air-foliage boundaries delineated by the plane were digitized. A computer program was written and used to reconstruct the cross section of the canopy. The approach used in applying optical computer axial tomography to measuring crop canopy geometry shows promise of being able to provide needed geometric information for input data to canopy reflectance models. The difficulty of using the CAT scanner to measure large canopies of crops like corn is discussed and a solution is proposed involving the measurement of plants one at a time. A.R.H.

N82-23601*# Agricultural Research Services, Beltsville, Md.

AGRICULTURAL RESEARCH SERVICE RESEARCH HIGHLIGHTS IN REMOTE SENSING FOR CALENDAR YEAR 1980 Annual Report

J. C. RITCHIE, Principal Investigator Jul. 1981 27 p Sponsored by NASA, USDA, Dept. of Commerce, Dept. of the Interior, and Agency for International Development ERTS
(Contract PROJ. AGRISTARS)
(E82-10228; NASA-CR-167408; EW-R1-04147; NAS 1.26:167408) Avail: NTIS HC A03/MF A01 CSCL 02C

The AR research mission in remote sensing is to develop the basic understanding of the soil plant animal atmosphere continuum in agricultural ecosystems and to determine when remotely sensed data can be used to provide information about these agricultural ecosystems. A brief statement of the significant results of each project is given. A list of 1980 publication and location contacts is also given. T.M.

N82-23602*# Purdue Univ., Lafayette, Ind. Lab. for Applications of Remote Sensing.

LINEAR POLARIZATION OF LIGHT BY TWO WHEAT CANOPIES MEASURED AT MANY VIEW ANGLES

M. E. BAUER, Principal Investigator, V. C. VANDERBILT, L. L. BIEHL, B. F. ROBINSON, and A. S. VANDERBILT Sep. 1981 11 p refs Repr. from Intern. Colloq. on Spectral Signatures of Objects in Remote Sensing, 1980 Collog. held in Avignon, France, 8-11 Sep. 1980 Sponsored by NASA, USDA, Dept. of Commerce, Dept. of the Interior, and Agency for International Development ERTS
(Contract NAS9-15466; PROJ. AGRISTARS)
(E82-10229; NASA-CR-167419; NAS 1.26:167419; LARS-TR-090981; SR-P1-04139) Avail: NTIS HC A02/MF A01 CSCL 20F

The linear polarization and reflection of visible light by wheat as a function of sun-view diections, crop development stage, and wavelength were examined. Two-hundred spectra were taken continuously in wave-lengths from 0.45 to 0.72 Micron in 33 view directions using an Exotech model 20C spectroradiometer six meters above two wheat canopies in the boot and fully headed maturity stages. The analysis results show that the amount of linearly polarized light from the wheat canopies is greatest in the blue spectral region and decreases gradually with increasing wavelength. The results also show that the linearly polarized light from the canopies is generally greatest in the azimuth direction of the Sun and tends toward zero as the view direction tends toward the direction of the hot spot or anti-solar point. It is demonstrated that the single, angle of incidence of sunlight on the leaf, explains almost all of the variation of the amount of polarized light with Sun-view direction. M.G.

N82-23603*# Lockheed Engineering and Management Services Co., Inc., Houston, Tex.

EVALUATION OF THE PROCEDURE FOR SEPARATING BARLEY FROM OTHER SPRING SMALL GRAINS

E. R. MAGNESS, Principal Investigator Aug. 1980 77 p refs Sponsored by NASA, USDA, Dept. of Commerce, Dept. of the Interior, and Agency for International Development ERTS
(Contract NAS9-15800; PROJ. AGRISTARS)
(E82-10230; NASA-CR-160888; JSC-16752; NAS 1.26:160888; LEMSCO-14598; FC-LO-00472) Avail: NTIS HC A05/MF A01 CSCL 02C

The success of the Transition Year procedure to separate and label barley and the other small grains was assessed. It was decided that developers of the procedure would carry out the exercise in order to prevent compounding procedural problems with implementation problems. The evaluation proceeded by labeling the sping small grains first. The accuracy of this labeling was, on the average, somewhat better than that in the Transition Year operations. Other departures from the original procedure included a regionalization of the labeling process, the use of trend analysis, and the removal of time constraints from the actual processing. Segment selection, ground truth derivation, and data available for each segment in the analysis are discussed. Labeling accuracy is examined for North Dakota, South Dakota, Minnesota, and Montana as well as for the entire four-state area. Errors are characterized. A.R.H.

N82-23604*# National Aeronautics and Space Administration. Lyndon B. Johnson Space Center, Houston, Tex.

AGRISTARS. PROJECT MANAGEMENT REPORT: PROGRAM REVIEW PRESENTATION TO LEVEL 1, INTERAGENCY COORDINATION COMMITTEE Semiannual Report

Nov. 1981 232 p Sponsored by NASA, USDA, Dept. of Commerce, Dept. of the Interior, and Agency for International Development
(Contract PROJ. AGRISTARS)
(E82-10231; NASA-TM-84205; JSC-17438; NAS 1.15:84205; FC-J1-04181) Avail: NTIS HC A10/MF A01 CSCL 02C

Accomplishments relating to the development of crop calendars and production estimates for spring small grains, corn, and soybeans and the associated data acquisition and processing systems are reviewed. The areas of interest included the Great Plains Corridor and Argentina. M.G.

N82-23606*# Purdue Univ., Lafayette, Ind. Lab. for Applications of Remote Sensing.

A MODEL OF PLANT CANOPY POLARIZATION

V. C. VANDERBILT Jun. 1980 12 p refs Repr. from Machine Process. of Remotely Sensed Data, Jun. 1980 p 98-108 Sponsored by NASA, USDA, Dept. of Commerce, Dept. of the Interior, and Agency for International Development ERTS
(Contract NAS9-15466; PROJ. AGRISTARS)
(E82-10233; NASA-CR-167415; SR-P1-04170; NAS 1.26:167415; LARS-060580) Avail: NTIS HC A02/MF A01 CSCL 20F

A model for the amount of linearly polarized light reflected by the shiny leaves of grain crops is based on the morphological and phenological characteristics of the plant canopy and upon the Fresnel equations which describe the light reflection process at the smooth boundary separating two dielectrics. The theory used demonstrates that, potentially, measurements of the linearly polarized light from a crop canopy may be used as an additional feature to discriminate between crops such as wheat and barley, two crops which are so spectrally similar that they are misclassified with unacceptable frequency. Examination of the model suggests that, potentially, satellite polarization measurements may be used to monitor crop development stage, leaf water content, leaf area index, hail damage, and certain plant diseases. The information content of these measurements is needed to evaluate the proposed polarization sensor for the satellite-borne multispectral resource sampler. A.R.H.

N82-23607*# Lockheed Engineering and Management Services Co., Inc., Houston, Tex.

USE AND APPLICABILITY OF THE VEGETATION COMPONENT OF THE NATIONAL SITE CLASSIFICATION SYSTEM

C. A. CLARK, Principal Investigator Apr. 1981 43 p refs Sponsored by NASA, USDA, Dept. of Commerce, Dept. of the Interior, and Agency for International Development Original contains color imagery. Original photography may be purchased from the EROS Data Center, Sioux Falls, S.D. 57198 ERTS
(Contract NAS9-15800; PROJ. AGRISTARS)
(E82-10234; NASA-CR-167416; JSC-17122; NAS 1.26:167416; LEMSCO-15173; RR-LO-00466) Avail: NTIS HC A03/MF A01 CSCL 02C

Existing vegetation on a site in Sumter National Forest, South Carolina was classified using high altitude aerial optical bar color infrared photography in an effort to determine if the National Site Classification (NSC) system could be used in the heterogeneously forested southeastern United States where it had not previously been used. Results show that the revised UNESCO international classification and mapping of vegetation system, as incorporated into the NSCS, is general enough at the higher levels and specific enough at the lower levels to adequately accommodate densely forested, heterogeneous areas as well as the larger, more homogeneous regions of the Pacific Northwest. The major problem is of existing vegetation versus natural vegetation. A.R.H.

N82-23608*# Lockheed Engineering and Management Services Co., Inc., Houston, Tex.

DESCRIPTION OF THE FORTRAN IMPLEMENTATION OF THE SPRING SMALL GRAINS PLANTING DATE DISTRIBUTION MODEL

J. A. ARTLEY, Principal Investigator Aug. 1981 55 p refs Sponsored by NASA, USDA, Dept. of Commerce, Dept. of the Interior, and Agency for International Development ERTS
(Contract NAS9-15800; PROJ. AGRISTARS)
(E82-10235; NASA-CR-167411; JSC-17414; NAS 1.26:167411; LEMSCO-16854; SR-L1-00309) Avail: NTIS HC A04/MF A01 CSCL 02C

The Hodges-Artley spring small grains planting date distribution model was coded in FORTRAN. The PLDRVR program, which implements the model, is described and a copy of the code is provided. The purpose, calling procedure, local variables, and input/output devices for each subroutine are explained to supplement the user's guide. A.R.H.

N82-23609*# National Aeronautics and Space Administration. Lyndon B. Johnson Space Center, Houston, Tex.

AGRISTARS: AGRICULTURE AND RESOURCES INVENTORY SURVEYS THROUGH AEROSPACE REMOTE SENSING Annual Report

Jun. 1981 68 p Sponsored by NASA, USDA, Dept. of Commerce, Dept. of the Interior, and Agency for International Development ERTS
(Contract PROJ. AGRISTARS)
(E82-10236; NASA-TM-84202; JSC-17398; NAS 1.15:84202; AP-J0-04111) Avail: NTIS HC A04/MF A01 CSCL 02C

The major objectives and FY 1980 accomplishments are described of a long term program designed to determine the usefulness, cost, and extent to which aerospace remote sensing data can be integrated into existing or future USDA systems to improve the objectivity, reliability, timeliness, and adequacy of information. A general overview, the primary and participating agencies, and the technical highlights of each of the following projects are presented: early warning/crop condition assessment; foreign commodity production forecasting; yield model development; supporting research; soil moisture; domestic crops and land cover; renewable resources incentory; and conservation and pollution. A.R.H.

N82-23610*# Purdue Univ., Lafayette, Ind. Lab. for Applications of Remote Sensing.

CANOPY REFLECTANCE AS INFLUENCED BY SOLAR ILLUMINATION ANGLE

M. E. BAUER, Principal Investigator, J. C. KOLLENKARK, V. C. VANDERBILT, and C. S. T. DAUGHTRY Mar. 1981 24 p refs Sponsored by NASA, USDA, Dept. of Commerce, Dept. of the Interior, and Agency for International Development ERTS
(Contract NAS9-15466; PROJ. AGRISTARS)
(E82-10237; NASA-CR-167402; SR-P1-04039; NAS 1.26:167402; LRS-021681) Avail: NTIS HC A02/MF A01 CSCL 20F

The interaction of the solar illumination angle and row azimuth angle of the measured reflectance factor (RF) of soybean canopies was investigated. Diurnal changes of nearly 140% were observed in the red wavelength region when canopies covered 64% of the soil. The amount of shadow observed was a function of the plant geometry and row width. As soil cover approached 100%, the diurnal changes diminished. A function tht describes the solar illumination angle with respect to the row azimuth explained most of the diurnal variation in the measured RF. Variation in near infrared response was much less and did not appear to be as strongly related to Sun-row angle interactions. The near infrared/red ratio was highly sensitive to Sun angle-row direction interactions, whereas the greenness function, utilizing all four spectral bands, was not. J.D.

N82-23611*# National Aeronautics and Space Administration. Goddard Space Flight Center, Greenbelt, Md.

A MULTI-FREQUENCY RADIOMETRIC MEASUREMENT OF SOIL MOISTURE CONTENT OVER BARE AND VEGETATED FIELDS

J. R. WANG, T. J. SCHMUGGE, J. E. MCMURTREY, III (Dept. of Agriculture, Beltsville, Md.), W. I. GOULD, W. S. GLAZAR, and J. E. FUCHS, Principal Investigators Oct. 1981 16 p refs
Submitted for publication Sponsored by NASA, USDA, Dept. of Commerce, Dept. of the Interior, and Agency for International Development ERTS
(Contract PROJ. AGRISTARS)
(E82-10238; NASA-TM-83842; SM-GI-04178; NAS 1.15:83842)
Avail: NTIS HC A02/MF A01 CSCL 08M

A USDA Beltsville Agricultural Research Center site was used for an experiment in which soil moisture remote sensing over bare, grass, and alfalfa fields was conducted over a three-month period using 0.6 GHz, 1.4 GHz, and 10.6 GHz Dicke-type microwave radiometers mounted on mobile towers. Ground truth soil moisture content and ambient air and sil temperatures were obtained concurrently with the radiometric measurements. Biomass of the vegetation cover was sampled about once a week. Soil density for each of the three fields was measured several times during the course of the experiment. Results of the radiometric masurements confirm the frequency dependence of moisture sensing sensitivity reduction reported earlier. Observations over the bare, wet field show that the measured brightness temperature is lowest at 5.0 GHz and highest of 0.6 GHz frequency, a result contrary to expectation based on the estimated dielectric permittivity of soil water mixtures and current radiative transfer model in that frequency range. Author

N82-24519*# Environmental Research Inst. of Michigan, Ann Arbor.

ANALYSIS OF SCANNER DATA FOR CROP INVENTORIES Progress Report, 15 Feb. - 30 Jun. 1981

R. HORVATH, Principal Investigator, R. C. CICONE, R. J. KAUTH, and W. A. MALILA Aug. 1981 273 p refs Sponsored by NASA, USDA, Dept. of Commerce, Dept. of Interior and Agency for Intern. Develop. ERTS
(Contract NAS9-15476; PROJ. AGRISTARS)
(E82-10241; NASA-CR-167391; NAS 1.26:167391;
ERIM-152400-6-P) Avail: NTIS HC A12/MF A01 CSCL 02C

Progress and technical issues are reported in the development of corn/soybeans area estimation procedures for use on data from South America, with particular emphasis on Argentina. Aspects related to the supporting research section of the AgRISTARS Project discussed include: (1) multisegment corn/soybean estimation; (2) through the season separability of corn and soybeans within the U.S. corn belt; (3) TTS estimation; (4) insights derived from the baseline corn and soybean procedure; (5) small fields research; and (6) simulating the spectral appearance of wheat as a function of its growth and development. To assist the foreign commodity production forecasting, the performance of the baseline corn/soybean procedure was analyzed and the procedure modified. Fundamental limitations were found in the existing guidelines for discriminating these two crops. The temporal and spectral characteristics of corn and soybeans must be determined because other crops grow with them in Argentina. The state of software technology is assessed and the use of profile techniques for estimation is considered. A.R.H.

N82-24523*# National Aeronautics and Space Administration. Ames Research Center, Moffett Field, Calif.

MULTILEVEL MEASUREMENTS OF SURFACE TEMPERATURE OVER UNDULATING TERRAIN PLANTED TO BARLEY Final Report, 1 Nov. 1977 - 31 Oct. 1980

R. J. REGINATO, Principal Investigator (USDA, Phoenix, Ariz.), J. P. MILLARD, J. L. HATFIELD (California Univ., David), and R. D. JACKSON (USDA, Phoenix, Ariz.) Mar. 1981 74 p refs
Original contains color imagery. Original may be obtained from the EROS Data Center. Sioux Falls, S.D. 57198 ERTS
(Contract NASA ORDER S-40255-B)
(E82-10245; NASA-CR-168826; NAS 1.26:168826) Avail: NTIS HC A04/MF A01 CSCL 04B

A ground and aircraft program was conducted to extend ground based methods for measuring soil moisture and crop water stress to aircraft and satellite altitudes. A 260ha agricultural field in California was used over the 1977-78 growing season. For cloud free days ground based temperature measurements over bare soil were related to soil moisture content. Water stress resulted from too much water, not from lack of it, as was expected. A theoretical examination of the canopy air temperature difference as affected by vapor pressure deficit and net radiation was developed. This analysis shows why surface temperatures delineate crop water stress under conditions of low humidity, but not under high humidity conditions. Multilevel temperatures acquired from the ground, low and high altitude aircraft, and the Heat Capacity Mapping Mission (HCMM) spacecraft were compared for two day and one night overpasses. The U-2 and low altitude temperatures were within 0.5 C. The HCMM data were analyzed using both the pre- and post-launch calibrations, with the former being considerably closer in agreement with the aircraft data than the latter. M.G.

N82-24563*# National Aeronautics and Space Administration. National Space Technology Labs., Bay Saint Louis, Miss.

AN ANALYSIS OF LANDSAT MSS SCENE-TO-SCENE REGISTRATION ACCURACY

B. R. SEYFARTH and P. W. COOK, Principal Investigators (USDA) Dec. 1981 14 p Sponsored by NASA, USDA, Dept. of Commerce, Dept. of Interior, and Agency for International Development ERTS
(Contract PROJ. AGRISTARS)
(E82-10285; NASA-TM-84694; DC-Y1-04156; NSTL/ERL-198;
NAS 1.15:84694) Avail: NTIS HC A02/MF A01 CSCL 02C

Measurements were made for 12 registrations done by ERL for 8 registrations done by SRS. The results indicate that the ERL method is significantly more accurate in five of the eight comparison. The difference between the two methods are not significant in the other three cases. There are two possible reasons for the differences. First, the ERL model is a piecewise linear model and the EDITOR model is a cubic polynomial model. Second, the ERL program resamples using bilinear interpolation while the EDITOR software uses a nearest neighbor resampling. This study did not indicate how much of the difference is attributable to each factor. The average of all merged scene error values for ERL was 31.6 meters and the average for the eight common areas was 32.6 meters. The average of the eight merged scene error values for SRS was 40.1 meters. T.M.

N82-24564*# National Aeronautics and Space Administration. National Space Technology Labs., Bay Saint Louis, Miss.

AN ALGORITHM FOR AUTOMATING THE REGISTRATION OF USDA SEGMENT GROUND DATA TO LANDSAT MSS DATA

M. H. GRAHAM, Principal Investigator Dec. 1981 31 p refs
Sponsored by NASA, USDA, Dept. of Commerce, Dept. of Interior and Agency for International Development ERTS
(Contract PROJ. AGRISTARS)
(E82-10286; NASA-TM-84695; DC-YI-04211; NSTL/ERL-201;
NAS 1.15:84695) Avail: NTIS HC A03/MF A01 CSCL 02C

The algorithm is referred to as the Automatic Segment Matching Algorithm (ASMA). The ASMA uses control points or the annotation record of a P-format LANDSAT compter compatible tape as the initial registration to relate latitude and longitude to LANDSAT rows and columns. It searches a given area of LANDSAT data with a 2x2 sliding window and computes gradient values for bands 5 and 7 to match the segment boundaries. The gradient values are held in memory during the shifting (or matching) process. The reconstructed segment array, containing ones (1's) for boundaries and zeros elsewhere are computer compared to the LANDSAT array and the best match computed. Initial testing of the ASMA indicates that it has good potential for replacing the manual technique. T.M.

N82-24565*# National Aeronautics and Space Administration. National Space Technology Labs., Bay Saint Louis, Miss.

ANALYSIS OF THEMATIC MAPPER SIMULATOR DATA ACQUIRED DURING WINTER SEASON OVER PEARL RIVER, MISSISSIPPI, TEST SITE

J. E. ANDERSON and M. T. KALCIC, Principal Investigators Mar. 1982 45 p refs Sponsored by NASA, USDA, Dept. of Commerce Dept. of Interior and Agency for International Development Original contains color imagery. Original photography may be purchased from EROS Data Center, Sioux Falls, S.D. 57198 ERTS

(Contract PROJ. AGRISTARS)

(E82-10287; NASA-TM-84696, RR-Y1-04217; NSTL/ERL-202; NAS 1.15:84696) Avail: NTIS HC A03/MF A01 CSCL 05B

Digital processed aircraft-acquired thematic mapping simulator (TMS) data collected during the winter season over a forested site in southern Mississippi are presented to investigate the utility of TMS data for use in forest inventories and monitoring. Analyses indicated that TMS data are capable of delineating the mixed forest land cover type to an accuracy of 92.5 % correct. The accuracies associated with river bottom forest and pine forest were 95.5 and 91.5 % correct. The accuracies associated with river bottom forest and pine forest were 95.5 and 91.5 % correct, respectively. The figures reflect the performance for products produced using the best subset of channels for each forest cover type. It was found that the choice of channels (subsets) has a significant effect on the accuracy of classification produced, and that the same channels are not the most desirable for all three forest types studied. Both supervised and unsupervised spectral signature development techniques are evaluated; the unsupervised methods proved unacceptable for the three forest types considered. E.A.K.

N82-24574*# Pennsylvania State Univ., University Park. Office for Remote Sensing of Earth Resources.

DELINEATION OF SOIL TEMPERATURE REGIMES FROM HCMM DATA Quarterly Report

R. L. DAY and G. W. PETERSEN, Principal Investigators 31 Mar. 1982 3 p refs HCMM

(E82-10298; NASA-CR-168867; NAS 1.26:168867) Avail: NTIS HC A02/MF A01 CSCL 08M

The subsetting of HCMM data into ORSER format was completed for four dates using a modified SUBSET program. Large areas (approximately 2500 scan lines, 1680 elements) were selected to increase the occurrence of suitable control points for registration. Average daily temperatures (ADT) were calculated for each date. The MERGE program combined registered daytime temperature (DAY-IR) with nighttime temperature (NIGHT-IR) to form a separate two-channel data set. The SUBTRAN program averaged the DAY-IR and NIGHT-IR creating a third ADT channel. Registration equations for the four ADT data sets were generated. A one dimensional soil heat flow equation was modified to allow for mean annual soil temperature predictions using merged ADT data sets. A.R.H.

N82-24575*# Florida Univ., Gainesville.

USE OF THERMAL INERTIA DETERMINED BY HCMM TO PREDICT NOCTURNAL COLD PRONE AREAS IN FLORIDA Quarterly Report, 16 Sep. - 15 Dec. 1981

L. H. ALLEN, JR., Principal Investigator, E. CHEN, J. D. MARTSOLF, and P. H. JONES 15 Dec. 1981 15 p refs HCMM

(Contract NAS5-26453)

(E82-10299; NASA-CR-168868; NAS 1.26:168868) Avail: NTIS HC A02/MF A01 CSCL 04B

Surface temperatures derived from HCMM data were compared with to those obtained by GOES satellite and the apparent thermal inertia (ATI) calculated. For two dates, the HCMM temperatures appear to be about 5 C lower than the GOES temperatures. The ATI for excessively-drained to well-drained mineral soils was greater than for drained organic soils possibly because of long periods of low rainfall during late 1980 and early 1981. Organic soils cropped to sugar cane showed lower ATI after a severe killing freeze. With dead leaves, there was less transpiration and more solar radiation probably reached the dark soil surface. This would explain the larger diurnal temperature amplitude observed. A.R.H.

N82-24576*# Instituto Geografico Nacional, Madrid (Spain).

THERMAL MAPPING, GEOTHERMAL SOURCE LOCATION, NATURAL EFFLUENTS AND PLANT STRESS IN THE MEDITERRANEAN COAST OF SPAIN Final Report, Sep. 1978 - Aug. 1980

R. N. DELASCUEVAS, Principal Investigator and A. M. DEARAGON 31 Mar. 1981 218 p Sponsored by NASA Original contains color imagery. Original imagery may be purchased from NASA Goddard Space Flight Center, (code 601), Greenbelt, Md. 20070. Domestic users send orders to 'Attn: National Space Science Data Center'; non-domestic users send orders to 'Attn: World Data Center A for Rockets and Satellites'. HCMM

(E82-10300; NASA-CR-168869; NAS 1.26:168869) Avail: NTIS HC A10/MF A01 CSCL 08G

Data obtained by HCMM satellite over a complex area in eastern Spain were evaluated and found to be most useful in studying macrostructures in geology and in analyzing marine currents, layers, and areas (although other satellites provide more data). The upper scale to work with HCMM data appears to be 1:2.000.000. Techniques used in preprocessing, processing, and analyzing imagery are discussed as well as methods for pattern recognition. Surface temperatures obtained for soils, farmlands, forests, geological structures, and coastal waters are discussed. Suggestions are included for improvements needed to achieve better results in geographic areas similar to the study area. E.A.K.

N82-24585*# Pennsylvania State Univ., University Park. Dept. of Meteorology.

A METHOD FOR INFERRING AVAILABLE SURFACE MOISTURE USING REMOTE SURFACE TEMPERATURE MEASUREMENTS: AN ASSESSMENT

T. N. CARLSON, Principal Investigator Feb. 1982 33 p refs Sponsored by NASA ERTS

(E82-10311; NASA-CR-168886; NAS 1.26:168886) Avail: NTIS HC A03/MF A01 CSCL 08M

A method for inferring surface moisture availability, which combines a numerical boundary layer model with remote estimates of surface-temperature, is evaluated with regard to its ability to provide significant results. Some analyses of surface moisture availability based on GOES and on HCMM surface temperature measurements are presented for an urban area (St. Louis) and for a drought situation over Kansas. Patterns of moisture availability clearly indicate a relationship between land use, particularly vegetation cover, and derived moisture availability over urban areas and also suggest a relationship between antecedent rainfall and derived moisture availability over vegetated regions. Author

N82-24602*# South Dakota State Univ., Brookings. Remote Sensing Inst.

EVALUATION OF HCMM DATA FOR ASSESSING SOIL MOISTURE AND WATER TABLE DEPTH Final Report, Jun. 1977 - Mar. 1981

D. G. MOORE, J. L. HEILMAN, J. A. TUNHEIM, F. C. WESTIN, W. E. HEILMAN, G. A. BEUTLER, and S. D. NESS, Principal Investigators Aug. 1981 205 p refs Original contains imagery. Original imagery may be purchased from NASA Goddard Space Flight Center, (code 601), Greenbelt, Md. 20770 Domestic users send orders to 'Attn: National Space Science Data Center'; nondomestic users send orders to 'Attn: World Data Center A for Rockets and Satellites'. HCMM
(Contract NAS5-24206)
(E82-10329; NASA-CR-168944; NAS 1.26:168944; SDSU-RS1-81-04) Avail: NTIS HC A10/MF A01 CSCL 08M

Soil moisture in the 0-cm to 4-cm layer could be estimated with 1-mm soil temperatures throughout the growing season of a rainfed barley crop in eastern South Dakota. Empirical equations were developed to reduce the effect of canopy cover when radiometrically estimating the soil temperature. Corrective equations were applied to an aircraft simulation of HCMM data for a diversity of crop types and land cover conditions to estimate the soil moisture. The average difference between observed and measured soil moisture was 1.6% of field capacity. Shallow alluvial aquifers were located with HCMM predawn data. After correcting the data for vegetation differences, equations were developed for predicting water table depths within the aquifer. A finite difference code simulating soil moisture and soil temperature shows that soils with different moisture profiles differed in soil temperatures in a well defined functional manner. A significant surface thermal anomaly was found to be associated with shallow water tables. A.R.H.

N82-25605*# Texas A&M Univ., College Station. Remote Sensing Center.

ORBITING PASSIVE MICROWAVE SENSOR SIMULATION APPLIED TO SOIL MOISTURE ESTIMATION Final Report

R. W. NEWTON, Principal Investigator, B. V. CLARK, W. M. PITCHFORD, and J. F. PARIS (Houston Univ., Clear Lake City) Dec. 1979 219 p Original contains imagery. Original photography may be purchased from the EROS Data Center, Sioux Falls, S.D. 57198 ERTS
(Contract NSG-5266)
(E82-10343; NASA-CR-168960; NAS 1.26:168960; RSC-3753) Avail: NTIS HC A10/MF A01 CSCL 08M

A sensor/scene simulation program was developed and used to determine the effects of scene heterogeneity, resolution, frequency, look angle, and surface and temperature relations on the performance of a spaceborne passive microwave system designed to estimate soil water information. The ground scene is based on classified LANDSAT images which provide realistic ground classes, as well as geometries. It was determined that the average sensitivity of antenna temperature to soil moisture improves as the antenna footprint size increased. Also, the precision (or variability) of the sensitivity changes as a function of resolution. M.G.

N82-25606*# Purdue Univ., Lafayette, Ind. Lab. for Applications of Remote Sensing.

FOREST RESOURCE INFORMATION SYSTEM. PHASE 3: SYSTEM TRANSFER REPORT Final Report, 1 Apr. 1979 - 31 Dec. 1980

R. P. MROCZYNSKI, Principal Investigator 30 Jul. 1981 142 p refs Original contains imagery. Original photography may be purchased from the EROS Data Center, Sioux Falls, S.D. 57198 ERTS
(Contract NAS9-15325)
(E82-10344; NASA-CR-167544; NAS 1.26:167544; LARS-073081) Avail: NTIS HC A07/MF A01 CSCL 02F

Transfer of the forest reserve information system (FRIS) from the Laboratory for Applications of Remote Sensing to St. Regis Paper Company is described. Modifications required for the transfer of the LARYS image processing software are discussed. The reformatting, geometric correction, image registration, and documentation performed for preprocessing transfer are described. Data turnaround was improved and geometrically corrected and ground-registered CCT LANDSAT 3 data provided to the user. The technology transfer activities are summarized. An application test performed in order to assess a Florida land acquisition is described. A benefit/cost analysis of FRIS is presented. J.D.

N82-25607*# Utah Univ., Salt Lake City. Center for Remote Sensing and Cartography.

INVENTORY OF WETLANDS AND AGRICULTURAL LAND COVER IN THE UPPER SEVIER RIVER BASIN, UTAH

R. A. JAYNES, L. D. CLARK, JR., and K. F. LANDGRAF, Principal Investigator 31 Oct. 1981 40 p refs ERTS
(Contract NAGW-95)
(E82-10345; NASA-CR-168961) Avail: NTIS HC A03/MF A01 CSCL 08B

The use of color infrared aerial photography in the mapping of agricultural land use and wetlands in the Sevier River Basin of south central utah is described. The efficiency and cost effectiveness of utilizing LANDSAT multispectral scanner digital data to augment photographic interpretations are discussed. Transparent overlays for 27 quadrangles showing delineations of wetlands and agricultural land cover were produced. A table summarizing the acreage represented by each class on each quadrangle overlay is provided. J.D.

N82-25608*# National Aeronautics and Space Administration, Washington, D. C.

PLAN OF RESEARCH FOR INTEGRATED SOIL MOISTURE STUDIES. RECOMMENDATIONS OF THE SOIL MOISTURE WORKING GROUP

Oct. 1980 111 p refs
(NASA-TM-84731; NAS 1.15:84731) Avail: NTIS HC A06/MF A01 CSCL 08M

Soil moisture information is a potentially powerful tool for applications in agriculture, water resources, and climate. At present, it is difficult for users of this information to clearly define their needs in terms of accuracy, resolution and frequency because of the current sparsity of data. A plan is described for defining and conducting an integrated and coordinated research effort to develop and refine remote sensing techniques which will determine spatial and temporal variations of soil moisture and to utilize soil moisture information in support of agricultural, water resources, and climate applications. The soil moisture requirements of these three different application areas were reviewed in relation to each other so that one plan covering the three areas could be formulated. Four subgroups were established to write and compile the plan, namely models, ground-based studies, aircraft experiments, and spacecraft missions. A.R.H.

N82-26742*# Purdue Univ., Lafayette, Ind. Lab. for Applications of Remote Sensing.

SPECTRAL ESTIMATES OF SOLAR RADIATION INTERCEPTED BY CORN CANOPIES

M. E. BAUER, Principal Investigator, C. S. T. DAUGHTRY, and K. P. GALLO Mar. 1982 17 p refs Sponsored by NASA, USDA, Dept. of Commerce, Dept. of the Interior, and Agency for International Development ERTS
(Contract NAS9-15466; PROJ. AGRISTARS)
(E82-10003; NASA-CR-167643; SR-P2-04236; NAS 1.26:169032; LARS-030182) Avail: NTIS HC A02/MF A01 CSCL 20F

Reflectance factor data were acquired with a Landsat band radiometer throughout two growing seasons for corn (Zea mays L.) canopies differing in planting dates, populations, and soil types. Agronomic data collected included leaf area index (LAI), biomass, development stage, and final grain yields. The spectral variable, greenness, was associated with 78 percent of the variation in LAI over all treatments. Single observations of LAI or greenness have limited value in predicting corn yields. The proportions of solar radiation intercepted (SRI) by these canopies were estimated using either measured LAI or greenness. Both SRI estimates, when accumulated over the growing season, accounted for approximately

65 percent of the variation in yields. Models which simulated the daily effects of weather and intercepted solar radiation on growth had the highest correlations to grain yields. This concept of estimating intercepted solar radiation using spectral data represents a viable approach for merging spectral and meteorological data for crop yield models. Author

N82-26745*# Morgan State Coll., Baltimore, Md. Dept. of Biology.
RELATING THEMATIC MAPPER BANDS TM3, TM4, AND TM5 TO AGRONOMIC VARIABLES FOR CORN, COTTON, SUGARBEET, SOYBEAN, SORGHUM, SUNFLOWER AND TOBACCO Final Technical Report, 1 Apr. 1981 - 31 Mar. 1982
C. J. FAN, Principal Investigator 31 Mar. 1982 25 p refs ERTS
(Contract NAG5-12)
(E82-10347; NASA-CR-168856; NAS 1.26:168856) Avail: NTIS HC A02/MF A01 CSCL 02C

Red, photographic infrared, near infrared spectral data of corn, cotton, soybeans, sugar beets, sorghum, sunflowers and tobacco were collected throughout the entire growing season by using a three band handheld radiometer. Different radiance patterns were found among these crops based on their morphology, green biomass duration and leaf size. Results show near infrared radiance is a good indicator of water content in plant tissue under small scale experimental conditions. E.A.K.

N82-26747*# California Univ., Santa Barbara. Geography Remote Sensing Unit.
MULTISPECTRAL DETERMINATION OF SOIL MOISTURE-2 Annual Technical Report
J. E. ESTES, D. S. SIMONETT, Principal Investigators, E. J. HAJIC, B. M. HILTON, and R. D. LEES Apr. 1982 252 p refs
Prepared in cooperation with Texas A and M Univ., College Station ERTS
(Contract NCC5-5)
(E82-10349; NASA-CR-168967; NAS 1.26:168967) Avail: NTIS HC A12/MF A01 CSCL 08M

Soil moisture data obtained using scatterometers, modular multispectral scanners and passive microwave radiometers were revised and grouped into four field cover types for statistical anaysis. Guymon data are grouped as alfalfa, bare, milo with rows perpendicular to the field view, and milo viewed parallel to the field of view. Dalhart data are grouped as bare combo, stubble, disked stubble, and corn field. Summary graphs combine selected analyses to compare the effects of field cover. The analysis for each of the cover types is presented in tables and graphs. Other tables show elementary statistics, correlation matrices, and single variable regressions. Selected eigenvectors and factor analyses are included and the highest correlating sensor typs for each location are summarized. E.A.K.

N82-26749*# Kansas Univ. Center for Research, Inc., Lawrence. Remote Sensing Lab.
EVALUATION OF THE SOIL MOISTURE PREDICTION ACCURACY OF A SPACE RADAR USING SIMULATION TECHNIQUES Final Report
F. T. ULABY, Principal Investigator, M. C. DOBSON, J. A. STILES, R. K. MOORE, and J. C. HOLTZMAN May 1981 208 p refs
Original contains imagery. Original photography may be purchased from the EROS Data Center, Sioux Falls, S.D. 57198 ERTS
(Contract NAS5-25807)
(E82-10351; NASA-CR-166801; NAS 1.26:166801; RSL-TR-429-1)
Avail: NTIS HC A10/MF A01 CSCL 08M

Image simulation techniques were employed to generate synthetic aperture radar images of a 17.7 km x 19.3 km test site located east of Lawrence, Kansas. The simulations were performed for a space SAR at an orbital altitude of 600 km, with the following sensor parameters: frequency = 4.75 GHz, polarization = HH, and angle of incidence range = 7 deg to 22 deg from nadir. Three sets of images were produced corresponding to three different spatial resolutions; 20 m x 20 m with 12 looks, 100 m x 100 m with 23 looks, and 1 km x 1 km with 1000 looks. Each set consisted of images for four different soil moisture distributions across the test site. Results indicate that, for the agricultural portion of the test site, the soil moisture in about 90% of the pixels can be predicted with an accuracy of = + or - 20% of field capacity. Among the three spatial resolutions, the 1 km x 1 km resolution gave the best results for most cases, however, for very dry soil conditions, the 100 m x 100 m resolution was slightly superior. A.R.H.

N82-26751*# Environmental Research Inst. of Michigan, Ann Arbor. Infrared and Optics Div.
ASSOCIATION OF SPECTRAL DEVELOPMENT PATTERNS WITH DEVELOPMENT STAGES OF CORN Technical Report, 1 Nov. 1981 - 31 Jan. 1982
E. P. CRIST, Principal Investigator Feb. 1982 37 p refs
Sponsored by NASA, USDA, Dept. of Commerce, Dept. of the Interior, and Agency for International Development ERTS
(Contract NAS9-16538; PROJ. AGRISTARS)
(E82-10353; NASA-CR-167604; NAS 1.26:167604; IT-E2-04235; ERIM-160300-7-T) Avail: NTIS HC A03/MF A01 CSCL 02C

Association is made between the development stages of corn as defined by Hanway and the temporal-spectral development pattern of corn in a transformed data space derived from Landsat-MSS band reflectance values, using field-collected reflectance and associated data. Results indicate that the spectral vegetation index used (a reflectance equivalent of Tasseled Cap Greenness) reaches a maximum well before the stage at which corn is expected to achieve its peak leaf area index. Possible physiological and canopy geometry related causes for this and other results are presented. Author

N82-26752*# Utah Univ., Salt Lake City. Center for Remote Sensing and Cartography.
MAPPING OF WILDLIFE HABITAT IN FARMINGTON BAY, UTAH
R. A. JAYNES and R. D. WILLIE, Principal Investigators 1982 15 p refs ERTS
(Contract NAGW-95)
(E82-10354; NASA-CR-168975; NAS 1.26:168975; CRSC-82-1)
Avail: NTIS HC A02/MF A01 CSCL 08B

Mapping was accomplished through the interpretation of high-altitude color infrared photography. The feasibility of utilizing LANDSAT digital data to augment the analysis was explored; complex patterns of wildlife habitat and confusion of spectral classes resulted in the decision to make limited use of LANDSAT data in the analysis. The final product is a map which delineates wildlife habitat at a scale of 1:24,000. The map is registered to and printed on a screened U.S.G.S. quadrangle base map. Screened delineations of shoreline contours, mapped from a previous study, are also shown on the map. Intensive field checking of the map was accomplished for the Farmington Bay Waterfowl Management Area in August 1981; other areas on the map received only spot field checking. Author

N82-26753*# Utah Univ., Salt Lake City. Center for Remote Sensing and Cartography.
DETECTION OF VARIATIONS IN ASPEN FOREST HABITAT FROM LANDSAT DIGITAL DATA: BEAR RIVER RANGE, UTAH
J. A. MEROLA and R. A. JAYNES, Principal Investigators 17 Mar. 1982 34 p refs Sponsored in part by US Forest Service ERTS
(Contract NAGW-95; NSF SPI-80-03978)
(E82-10355; NASA-CR-168976; NAS 1.26:168976; CRSC-82-2)
Avail: NTIS HC A03/MF A01 CSCL 02F

The aspen forests of the Bear River Range were analyzed and mapped using data recorded on July 2, 1979 by the LANDSAT III satellite; study efforts yielded sixty-seven light signatures for the study area, of which three groups were identified as aspen and mapped at a scale of 1:24,000. Analysis and verification of the three groups were accomplished by random location of twenty-six field study plots within the LANDSAT-defined aspen areas. All study plots are included within the Cache portion of the

Wasatch-Cache National Forest. The following selected site characteristics were recorded for each study plot: a list of understory species present; average percent cover density for understory species; aspen canopy cover estimates and stem measurements; and general site topographic characteristics. The study plot data were then analyzed with respect to corresponding Landsat spectral signatures. Field studies show that all twenty-six study plots are associated with one of the three aspen groups. Further study efforts concentration on characterizing the differences between the site characteristics of plots falling into each of the three aspen groups. Author

N82-26754*# Utah Univ., Salt Lake City. Center for Remote Sensing and Cartography.

IRRIGATED ACREAGE IN THE BEAR RIVER BASIN AS OF THE 1975 GROWING SEASON

M. K. RIDD, R. A. JAYNES, K. F. LANDGRAF, and L. D. CLARK, JR., Principal Investigators 8 Apr. 1982 28 p refs Original contains color imagery. Original photography may be purchased from the EROS Data Center, Sioux Falls, S.D. 57198 ERTS
(Contract NAGW-95)
(E82-10356; NASA-CR-168977; NAS 1.26:168977; CRSC-82-3)
Avail: NTIS HC A03/MF A01 CSCL 02C

The irrigated cropland in the Bear River Basin as of the 1975 growing season was inventoried from satellite imagery. LANDSAT color infrared images (scale 1:125,000) were examined for early, mid, and late summer dates, and acreage was estimated by use of township/section overlays. The total basin acreage was estimated to be 573,435 acres, with individual state totals as follows: Idaho 234,370 acres; Utah 265,505 acres; and Wyoming 73,560 acres. As anticipated, wetland areas intermingled among cropland appears to have produced an over-estimation of irrigated acreage. According to a 2% random sample of test sites evaluated by personnel from the Soil Conservation Service such basin-wide over-estimation is 7.5%; individual counties deviate significantly from the basin-wide figure, depending on the relative amount of wetland areas intermingled with cropland. Author

N82-26755*# South Dakota State Univ., Brookings. Remote Sensing Inst.

IRRIGATION MANAGEMENT WITH REMOTE SENSING Final Technical Report, Apr. 1980 - Sep. 1981

C. HARLAN, J. HEILMAN, D. MOORE, and V. MYERS, Principal Investigators Feb. 1982 48 p refs
(Contract NAG5-37)
(E82-10357; NASA-CR-168978; NAS 1.26:168978; SDSU-RSI-82-02) Avail: NTIS HC A03/MF A01 CSCL 08H

Two visible/near IR hand held radiometers and a hand held thermoradiometer were used along with soil moisture and lysimetric measurements in a study of soil moisture distribution in afalfa fields on the Navajo Indian Irrigation Project near Farmington, New Mexico. Radiances from irrigated plots were measured and converted to reflectances. Surface soil water contents (o cm to 4 cm) were determined gravimetrically on samples collected at the same time as the spectral measurements. The relationship between the spectral measurements and the crop coefficient were evaluated to demonstrate potential for using spectral measurement to estimate crop coefficient. E.A.K.

N82-26759*# Texas A&M Univ., College Station. Remote Sensing Center.

MEASUREMENT OF SOIL MOISTURE TRENDS WITH AIRBORNE SCATTEROMETERS Final Report

C. L. JONES, M. J. MCFARLAND, W. D. ROSETHAL, and S. W. THEIS, Principal Investigators Feb. 1982 194 p refs ERTS
(Contract NSG-5134)
(E82-10361; NASA-CR-169010; NAS 1.26:169010; RSC-3458-131) Avail: NTIS HC A09/MF A01 CSCL 08M

In an effort to investigate aircraft multisensor responses to soil moisture and vegetation in agricultural fields, an intensive ground sampling program was conducted in Guymon, Oklahoma and Dalhart, Texas in conjunction with aircraft data collected for visible/infrared and passive and active microwave systems. Field selections, sampling techniques, data processing, and the aircraft schedule are discussed for both sites. Field notes are included along with final (normalized and corrected) data sets. A.R.H.

N82-26760*# Texas A&M Univ., College Station. Remote Sensing Center.

MULTIFREQUENCY REMOTE SENSING OF SOIL MOISTURE Final Report

S. W. THEIS, M. J. MCFARLAND, W. D. ROSENTHAL, and C. L. JONES, Principal Investigator Feb. 1982 145 p refs ERTS
(Contract NSG-5134)
(E82-10362; NASA-CR-169011; NAS 1.26:169011; RSC-3458-129) Avail: NTIS HC A07/MF A01 CSCL 08M

Multifrequency sensor data collected at Guymon, Oklahoma and Dalhart, Texas using NASA's C-130 aircraft were used to determine which of the all-weather microwave sensors demonstrated the highest correlation to surface soil moisture over optimal bare soil conditions, and to develop and test techniques which use visible/infrared sensors to compensate for the vegetation effect in this sensor's response to soil moisture. The L-band passive microwave radiometer was found to be the most suitable single sensor system to estimate soil moisture over bare fields. In comparison to other active and passive microwave sensors the L-band radiometer (1) was influenced least by ranges in surface roughness; (2) demonstrated the most sensitivity to soil moisture differences in terms of the range of return from the full range of soil moisture; and (3) was less sensitive to errors in measurement in relation to the range of sensor response. L-band emissivity related more strongly to soil moisture when moisture was expressed as percent of field capacity. The perpendicular vegetation index as determined from the visible/infrared sensors was useful as a measure of the vegetation effect on the L-band radiometer response to soil moisture. A.R.H.

N82-26761*# Texas A&M Univ., College Station. Remote Sensing Center.

DEVELOPMENT OF VISIBLE/INFRARED/MICROWAVE AGRICULTURE CLASSIFICATION AND BIOMASS ESTIMATION ALGORITHMS Final Report

W. D. ROSENTHAL, M. J. MCFARLAND, S. W. THEIS, and C. L. JONES, Principal Investigtors Feb. 1982 221 p refs ERTS
(Contract NSG-5134)
(E82-10363; NASA-CR-169012) Avail: NTIS HC A10/MF A01 CSCL 02C

Agricultural crop classification models using two or more spectral regions (visible through microwave) are considered in an effort to estimate biomass at Guymon, Oklahona Dalhart, Texas. Both grounds truth and aerial data were used. Results indicate that inclusin of C, L, and P band active microwave data, from look angles greater than 35 deg from nadir, with visible and infrared data improve crop discrimination and biomass estimates compared to results using only visible and infrared data. The microwave frequencies were sensitive to different biomass levels. The K and C band were sensitive to differences at low biomass levels, while P band was sensitive to differences at high biomass levels. Two indices, one using only active microwave data and the other using data from the middle and near infrared bands, were well correlated to total biomass. It is implied that inclusion of active microwave sensors with visible and infrared sensors on future satellites could aid in crop discrimination and biomass estimation. E.A.K.

N82-26762# California Univ., Santa Barbara.

THE USE OF SOIL TEXTURE AND FIELD CAPACITY TO NORMALIZE MICROWAVE SOIL MOISTURE MEASUREMENTS: SOME PROBLEMS M.S. Thesis

R. D. LEES May 1982 72 p refs Sponsored by Texas A & M Univ.
Avail: NTIS HC A04/MF A01

Soil moisture normalizing techniques attempt to explain variations in soil-water content between soils in terms of soil texture based on the percent sand, silt and clay in the soil. A critical analysis of these techniques was made to examine their effectiveness in comparing soils of varying texture and soil moisture content in relation to their microwave (radar) backscatter. While the particle size distribution is recognized as a significant factor in the soil-water relationship, its influence is regulated by a number of other factors. Results indicate that 'normalization' by use of field capacity - derived from the percentages of sand, silt and clay - actually reduced the sensitivity of backscattering coefficient to soil-water content. The water holding capacity of soils is variably influenced by properties such as soil structure, clay mineral type, organic matter content, aeration, soil layering, and hysteresis and related water addition and extraction processes. B.W.

02

ENVIRONMENTAL CHANGES AND CULTURAL RESOURCES

Includes land use analysis, urban and metroplitan studies, environmental impact, air and water pollution, geographic information systems, and geographic analysis.

A82-22545

DEPENDENCE OF EARTH SPECTRUM OF POSITRONS AND ANTIPROTONS ON PROPAGATION MODELS

S. A. STEPHENS (Tata Institute of Fundamental Research, Bombay, India) In: International Cosmic Ray Conference, 17th, Paris, France, July 13-25, 1981, Conference Papers. Volume 2. Gif-sur-Yvette, Essonne, France, Commissariat a l'Energie Atomique, 1981, p. 214-217. refs

A calculation of the equilibrium spectra of positrons and antiprotons for different models are presented. A total of five propagation models is considered, comprising a simple leak box, a modified leaky box, a nested leaky box, a simple closed galaxy, and a modified closed galaxy. The antiproton spectrum is noted to be dependent only on the propagation model and not on the solar modulation, which supports the use of an antiproton spectrometer in monitoring the degree of solar modulation. Kinetic energy fluxes are determined for the two components as predicted for each model, and observed antiproton fluxes are shown to rule out the modified and nested leaky box models. The modified closed galaxy model is found to accurately predict solar modulation from low energy data, and positron data at high energies is taken to quantify the mean gas density in a region of total confinement to be 0.05 atoms/cu cm. M.S.K.

A82-22562

ON THE STELLAR ORIGIN OF THE NE-22 EXCESS IN COSMIC RAYS

M. CASSE and J. A. PAUL (Commissariat a l'Energie Atomique, Centre d'Etudes Nucleaires de Saclay, Gif-sur-Yvette, Essonne, France) In: International Cosmic Ray Conference, 17th, Paris, France, July 13-25, 1981, Conference Papers. Volume 2. Gif-sur-Yvette, Essonne, France, Commissariat a l'Energie Atomique, 1981, p. 293-295. refs

A82-22566

COSMIC RAY ACCELERATION BY STELLAR WINDS. I - TOTAL DENSITY, PRESSURE AND ENERGY FLUX

G. M. WEBB, W. I. AXFORD (Max-Planck-Institut fuer Aeronomie, Katlenburg, West Germany), and M. A. FORMAN (New York, State University, Stony Brook, NY) In: International Cosmic Ray Conference, 17th, Paris, France, July 13-25, 1981, Conference Papers. Volume 2. Gif-sur-Yvette, Essonne, France, Commissariat a l'Energie Atomique, 1981, p. 309-312. refs

A82-22567

ON THE STELLAR ORIGIN OF LOW ENERGY COSMIC RAYS

S. BISWAS, N. DURGAPRASAD, and S. S. TRIVEDI (Tata Institute of Fundamental Research, Bombay, India) In: International Cosmic Ray Conference, 17th, Paris, France, July 13-25, 1981, Conference Papers. Volume 2. Gif-sur-Yvette, Essonne, France, Commissariat a l'Energie Atomique, 1981, p. 314-317. refs

The hypothesis is proposed that energetic ions of He, C, N, O, etc., in the low energy (1 to 50 MeV/amu) anomalous component of cosmic rays, originate from O-type stars which manifest very strong stellar winds with very high mass loss rates of about 3 x 10 to the -6th solar mass/yr. These have terminal velocities of 1200-4000 km/s which are typically several times their escape velocities. These velocities correspond to ion energies of 10 to 200 keV/amu. These ions of energy of about 100 keV/amu are in partly ionized states and are accelerated in the interstellar shock fronts to about 10 MeV/amu, thus accounting for the observed anomalous component of low-energy cosmic rays. (Author)

A82-22569

REMARKS ON COSMIC RAY ORIGIN

V. L. GINZBURG (Akademiia Nauk SSSR, Fizicheskii Institut, Moscow, USSR) and V. S. PTUSKIN (Akademiia Nauk SSSR, Institut Zemnogo Magnetizma Ionosfery i Rasprostraneniia Radiovoln, Troitsk, USSR) In: International Cosmic Ray Conference, 17th, Paris, France, July 13-25, 1981, Conference Papers. Volume 2. Gif-sur-Yvette, Essonne, France, Commissariat a l'Energie Atomique, 1981, p. 336-339. refs

Various problems related to current work on the origins of cosmic rays are considered. The acceleration of cosmic ray particles at the spherical front of an interstellar shock wave is analyzed, and a value of 10 to the 12th eV is obtained for the upper limit to accelerated particle energies. Transport in the Galaxy by means of large-scale turbulent motions is shown to produce a cosmic ray diffusion coefficient that is too low, while acceleration due to scattering by isotropic magnetohydrodynamic turbulence is also small. A possible method for the estimation of the contribution of local sources to cosmic ray concentrations observed near the earth is also presented, and possible explanations are suggested for the recent gamma ray observations of lowered cosmic ray electron concentrations at a distance less than 2 kpc from the galactic center. A.L.W.

A82-22570

PULSAR MODELS AND COSMIC-RAY ACCELERATION

F. C. MICHEL and A. J. DESSLER (Rice University, Houston, TX) In: International Cosmic Ray Conference, 17th, Paris, France, July 13-25, 1981, Conference Papers. Volume 2. Gif-sur-Yvette, Essonne, France, Commissariat a l'Energie Atomique, 1981, p. 340-343. refs

It is argued that radio pulsars and X-ray pulsars differ mainly in the fact that the the latter are surrounded by an inward moving accretion disk while the former are surrounded by an outward moving fossil collapse disk presumably left over from the formation event. Cosmic rays of more-or-less 'solar' composition can be accelerated to energies of 10 to the 20th eV shortly after the formation event. (Author)

A82-22583

SOLAR GAMMA-RAY EXPERIMENT ON ASTRO-A SATELLITE

K. OKUDAIRA, Y. HIRASIMA, M. YOSHIMORI (Rikkyo University, Tokyo, Japan), and I. KONDO (Tokyo, University, Tanashi, Japan) In: International Cosmic Ray Conference, 17th, Paris, France, July 13-25, 1981, Conference Papers. Volume 3. Gif-sur-Yvette, Essonne, France, Commissariat a l'Energie Atomique, 1981, p. 11-14. refs

The instrumentation and performance parameters of the Japanese Astro-A satellite for measuring solar gamma ray lines and continua associated with solar flares are described. A gamma ray spectrometer which is a phoswich scintillator covers the gamma ray range from 0.24-6.48 MeV with a resolution of 10 percent at 662 keV. Techniques to discern gamma ray from particle events are discussed, along with the 128 channel pulse height analyzer with three regions for the pulse height spectrum. Low bit rates are recorded during quiet modes, and high speed rates are enacted during a solar flare. The spacecraft was launched in Feb. 1981 and is in-flight calibrated by reference to the atmospheric positron annihilation line at 0.51 MeV.

M.S.K.

A82-22588

HIGH-ENERGY SOLAR PROTONS

N. N. VOLODICHEV and I. A. SAVENKO (Moskovskii Gosudarstvennyi Universitet, Moscow, USSR) In: International Cosmic Ray Conference, 17th, Paris, France, July 13-25, 1981, Conference Papers. Volume 3. Gif-sur-Yvette, Essonne, France, Commissariat a l'Energie Atomique, 1981, p. 45-48. refs

Evidence is presented for a second particle acceleration phase following the explosive phase of a solar flare. Cerenkov and scintillation counters were employed on the Prognoz satellite to detect the arrival of protons with energies greater than 100 MeV or 500 MeV, respectively. Delays of several minutes to several tens of minutes were observed for the arrival of protons from radiobursts in the cm range and X ray bursts during solar flare activity. A similar delay was recorded on the Proton-3 satellite during a burst event of Nov. 22, 1977, using the same measurement techniques. The existence of a second acceleration phase, when protons are accelerated to high energies and electrons up to relativistic energies, is noted to not contradict a model of the explosive phase of the flare as a process of disappearance and break of the current layer in the region of a highly dense plasma

M.S.K.

A82-22605* Maryland Univ., College Park.

TIME AND ENERGY DEPENDENCE OF HEAVY ION ABUNDANCES IN SOLAR FLARE ENERGETIC PARTICLE EVENTS

G. M. MASON, H. WEISS, G. GLOECKLER (Maryland, University, College Park, MD), and D. HOVESTADT (Max-Planck-Institut fuer Physik und Astrophysik, Garching, West Germany) In: International Cosmic Ray Conference, 17th, Paris, France, July 13-25, 1981, Conference Papers. Volume 3. Gif-sur-Yvette, Essonne, France, Commissariat a l'Energie Atomique, 1981, p. 124-127. refs (Contract NAS5-11063; NAS5-25735; NGR-21-002-316)

Data from a survey of solar flare events undertaken by the UMD/MPI ULET telescope on the IMP-8 satellite during the period 1973-1977 yields examples of time and energy dependence of the abundances and spectra of the He, C, O and Fe heavy ions. Time variations are found in the O/He, O/C and Fe/O ratios which appear to be inconsistent with models based entirely on rigidity-dependent propagation in the interplanetary medium. It is speculated that such other factors as the abundance differences at the flare site on the sun, or features of the acceleration and release mechanisms, may play an important role in the variations discussed.

O.C.

A82-22606* California Inst. of Tech., Pasadena.

HIGH RESOLUTION MEASUREMENTS OF SOLAR FLARE ISOTOPES

R. A. MEWALDT, J. D. SPALDING, E. C. STONE, and R. E. VOGT (California Institute of Technology, Pasadena, CA) In: International Cosmic Ray Conference, 17th, Paris, France, July 13-25, 1981, Conference Papers. Volume 3. Gif-sur-Yvette, Essonne, France, Commissariat a l'Energie Atomique, 1981, p. 131-134. refs (Contract NAS5-20721; NGR-05-002-160)

The individual isotopes of C, N and O are measured in the large solar particle event of August 1978. Limits are placed on mass dependent selection effects occurring in the solar flare by fitting a simple mass fractionation law to measurements of the C, N, O and Mg isotopes, to relate the SEP composition more directly to the composition of the sun. The individual isotopes are found to be consistent with solar system abundances, and the absence of any observable fractionation for C, O and Mg leads to the conclusion that solar neon is most likely neon-A with Ne-22/Ne-20 equals 0.12.

D.L.G.

A82-22616

11-YEAR MODULATION AND SPECTRUM OF COSMIC RAYS IN THE INTERSTELLAR SPACE

A. G. ZUSMANOVICH (Akademiia Nauk Kazakhskoi SSR, Sektor Ionosfery, Alma-Ata, Kazakh SSR) In: International Cosmic Ray Conference, 17th, Paris, France, July 13-25, 1981, Conference Papers. Volume 3. Gif-sur-Yvette, Essonne, France, Commissariat a l'Energie Atomique, 1981, p. 183-186. refs

The 11-year modulation in cosmic ray intensity is examined with a view towards the study of cosmic ray spectra in interstellar space. The steady-state, homogeneous solution of the cosmic ray modulation equation is used to determine a value of 0.4 plus or minus 0.1 for the modulation coefficient and a value between 15 and 20 GV for the rigidity of the unmodulated spectrum. Cosmic ray spectra outside the modulation region are then calculated from the modulation coefficient and differential energy spectra measured near earth at solar activity minimum, taking into account cosmic ray energy changes during passage through interplanetary space. Results are shown to be in agreement with measurements of galactic gamma ray intensities.

A.L.W.

A82-29327

DETECTION OF ENVIRONMENTAL DISTURBANCE USING COLOR AERIAL PHOTOGRAPHY AND THERMAL INFRARED IMAGERY

S. ARONOFF and G. A. ROSS (Calgary, University, Calgary, Alberta, Canada) Photogrammetric Engineering and Remote Sensing, vol. 48, Apr. 1982, p. 587-591. Research supported by the Alberta Oil Sands Environmental Research Program. refs

Characteristics of a program for satellite remote sensing for long-period environmental monitoring are examined, noting that establishing early mapping surveys of areas of concern aids in detection of stressful environmental conditions. The process is described with an example from IR and color photography of a 30,000 sq km area in the Athabasca Oil Sands, with the photography carried out from aircraft and satellite. The IR data was gathered between 8-14 microns and the photographs were taken at a 1:11,000 scale. Water-related disturbances detected included turbidity which indicated the possible presence of oil, and higher thermal emission near a tailings pond which also suggested an oil source. The presence of surface aquatic vegetation is an indicator of nutrient imbalance in a pond near a sewage pond. Finally, dead trees were observed near improperly installed culverts along new roads.

M.S.K.

A82-29332* South Carolina Univ., Columbia.

DETECTING RESIDENTIAL LAND-USE DEVELOPMENT AT THE URBAN FRINGE

J. R. JENSEN (South Carolina, University, Columbia, SC) and D. L. TOLL (NASA, Goddard Space Flight Center, Greenbelt, MD) Photogrammetric Engineering and Remote Sensing, vol. 48, Apr. 1982, p. 629-643. refs

Problems associated with the use of Landsat multispectral scanner (MSS) imagery for the detection of urban growth and land use patterns are discussed. The presence of vegetation, either original or added between scanning periods, has been found to dramatically effect the range of signatures in a given area. Different land use developmental stages have been successfully identified by means of 1:50,000 scale panchromatic aerial photography, a resolution only considered possible by spaceborne instrumentation with the advent of the Landsat D satellite. Textural information generated through the grey-tone spatial-dependency matrix for the Landsat band 5 data is compared for different years and a change detection algorithm is described. It is found that the addition of vegetation during development after the removal of natural vegetation resulted in error of omission in the single band data, which must therefore only be used in concert with other data sources.

M.S.K.

A82-30293

AIRCRAFT MONITORING OF SURFACE CARBON DIOXIDE EXCHANGE

R. L. DESJARDINS, E. J. BRACH (Agriculture Canada, Ottawa, Canada), P. ALVO, and P. H. SCHUEPP (McGill University, Sainte Anne de Bellevue, Quebec, Canada) Science, vol. 216, May 14, 1982, p. 733-735. Research supported by Agriculture Canada and National Research Council. refs

Aircraft-mounted sensors were used to measure the exchange of carbon dioxide above a cornfield, a forest, and a lake under midday conditions. Mean absorption values of 3400, 1200, and 100 milligrams of carbon dioxide per square meter per hour, respectively, are consistent with reported ground-based observations of carbon dioxide flux. Such information, gathered by aircraft, could be used to provide a quantitative evaluation of source and sink distributions of carbon dioxide in the biosphere, to establish a correlation between satellite data and near-surface measurements, and to monitor crop performance. (Author)

A82-30307

PROBLEMS OF THE INTERPRETATION OF AERIAL AND SATELLITE IMAGES OF INDUSTRIAL SMOKE [PROBLEMY INTERPRETACJI LOTNICZYCH I SATELITARNYCH ZDJEC DYMOW PRZEMYSLOWYCH]

T. Z. DWORAK (Instytut Meteorologii i Gospodarki Wodnej, Krakow, Poland) Przeglad Geofizyczny, vol. 25, no. 1, 1980, p. 33-38. In Polish. refs

Methods for the interpretation of aerial and satellite photographs of industrial smoke emissions are considered, with particular attention given to the difficulties of the qualitative interpretation of such images. Conditions that should be taken into account in an approximate solution of the radiative-transfer equations are examined. Recommendations on the practical solution of a specific satellite remote-sensing problem are presented. B.J.

A82-31295#

DETECTION OF VOLCANIC SMOKE AND ASH-FALL AREA AT VOLCANO ASO, FROM LANDSAT MSS DATA

Y. TANAKA (Meteorological Research Institute, Isukuba, Ibaraki, Japan), K. TSUCHIYA, and Y. YAMAURA (National Space Development Agency of Japan, Tokyo, Japan) Papers in Meteorology and Geophysics, vol. 32, Dec. 1981, p. 275-290. refs

Landsat imagery is employed to determine the extent of volcanic smoke and ashfall associated with the eruptions of the volcano ASO in 1979 and 1980, and a comparison is made with nearby meteorological data. Pictures from four bands 0.5-0.6, 0.6-0.7, 0.7-0.8, and 0.8-1.1 micron, are analyzed for information on volcanic smoke, polluted sea water, vegetation, clouds, and visibility over urban areas. The imagery comprises natural, false, and Ektachrome colors, taken from multispectral band scanners on Landsats 2 and 3. A qualitative analysis of volcanic smoke is developed, and a comparison of topographic data with the Landsat images showed that the Landsat pictures are useful and sufficiently accurate for detecting terrain changes due to the volcanic activity, including the forms of caldera. Assessment of the volcanic state, smoke, and ashfall were also possible using the Landsat imagery. M.S.K.

A82-31990* Lincoln Lab., Mass. Inst. of Tech., Lexington.

DETECTION OF REGIONAL AIR POLLUTION EPISODES UTILIZING SATELLITE DIGITAL DATA IN THE VISUAL RANGE

H.-H. K. BURKE (MIT, Lincoln Laboratory, Lexington, MA) IEEE Transactions on Geoscience and Remote Sensing, vol. GE-20, Apr. 1982, p. 154-158. refs
(Contract NAS1-15301)

Digital analyses of satellite visible data for selected high-sulfate cases over the northeastern U.S., on July 21 and 22, 1978, are compared with ground-based measurements. Quantitative information on total aerosol loading derived from the satellite digitized data using an atmospheric radiative transfer model is found to agree with the ground measurements, and it is shown that the extent and transport of the haze pattern may be monitored from the satellite data over the period of maximum intensity for the episode. Attention is drawn to the potential benefits of satellite monitoring of pollution episodes demonstrated by the model. O.C.

A82-32342* Liverpool Univ. (England).

SYSTEM ALBEDO AS SENSED BY SATELLITES - ITS DEFINITION AND VARIABILITY

N. A. HUGHES (Liverpool, University, Liverpool, England) and A. HENDERSON-SELLERS (NASA, Goddard Institute for Space Studies, New York, NY; Liverpool, University, Liverpool, England) International Journal of Remote Sensing, vol. 3, Jan.-Mar. 1982, p. 1-11. Natural Environment Research Council refs
(Contract NERC-GR3/3941)

System albedo, an important climatological and environmental parameter, is considered. Some of the problems and assumptions involved in evaluating albedo from satellite data are discussed. Clear-sky and cloud albedos over the United Kingdom and parts of northwest Europe are treated. Consideration is given to the spectral, temporal, and spatial variations and the effect of averaging. The implications of these results for those using and archiving albedo values and for future monitoring of system albedo are discussed. Normalization is of especial importance since this correction alters many albedo values. The pronounced difference in spectral albedo of the two visible channels reemphasizes the problem of attempting to calculate integrated albedo values from meteorological satellite data. The assumption of isotropic reflection is seen to be invalid, hindering the computation of accurate albedo values. C.R.

A82-32348* Alabama Univ., Huntsville.

REMOTE SENSING OF TORNADIC STORMS FROM GEOSYNCHRONOUS SATELLITE INFRARED DIGITAL DATA

R. J. HUNG (Alabama, University, Huntsville, AL) and R. E. SMITH (NASA, Marshall Space Flight Center, Huntsville, AL) International Journal of Remote Sensing, vol. 3, Jan.-Mar. 1982, p. 69-81. refs
(Contract NAS8-33726)

Two cases of GOES digital infrared data were analyzed during the three-hour period immediately prior to the tornado touchdown times. Clouds associated with tornadoes were compared to those without tornadoes using a combination of satellite infrared and rawinsonde data. On the basis of this limited data sample, it appears as if the altitude to which the overshooting cloud top penetrated above the tropopause is the factor which determines whether or not a tornado is formed. In these cases, the overshooting cloud top collapsed about 15 to 30 min before the tornado touchdown. (Author)

A82-32441* Jet Propulsion Lab., California Inst. of Tech., Pasadena.

RESOURCE INVENTORY TECHNIQUES USED IN THE CALIFORNIA DESERT CONSERVATION AREA

R. G. MCLEOD (California Institute of Technology, Jet Propulsion Laboratory Image Processing Laboratory, Pasadena, CA) and H. B. JOHNSON (U.S. Department of Agriculture, Grassland Soil and Water Research Laboratory, Temple, TX) In: Imaging spectroscopy; Proceedings of the Seminar, Los Angeles, CA, February 10, 11, 1981. Bellingham, WA, SPIE - The International Society for Optical Engineering, 1981, p. 2-16. refs
(Contract NAS7-100)

A variety of conventional and remotely sensed data for the 25 million acre California Desert Conservation Area (CDCA) have been integrated and analyzed to estimate range carrying capacity. Multispectral classification was performed on a digital mosaic of ten Landsat frames. Multispectral classes were correlated with low level aerial photography, quantified and aggregated by grazing allotment, land ownership, and slope. (Author)

A82-32711

SAMPLE DESIGN FOR ESTIMATING CHANGE IN LAND USE AND LAND COVER

G. H. ROSENFIELD (U.S. Geological Survey, Reston, VA) Photogrammetric Engineering and Remote Sensing, vol. 48, May 1982, p. 793-801. refs

The tasks of the field of applied statistics known as sample design are enumerated as: (1) sampling within a specified population; (2) consideration of sampling distribution; (3) determination of sample size; (4) determination of sample selection procedure; and (5) estimation of population means, totals, variances and confidence limits from the sample information. This methodology, which is used in the estimation of land use and land cover change, is sufficiently general to extend to the determination of change in any type of time-variant thematic mapping. An opportunity is presented for the determination of land use and land cover change in the state of Pennsylvania over a 20-year period. O.C.

A82-32899

IMPACTS OF REMOTE SENSING ON U.S. GEOGRAPHY

J. E. ESTES, D. S. SIMONETT (California, University, Santa Barbara, CA), and J. R. JENSEN (Georgia, University, Athens, GA) Remote Sensing of Environment, vol. 10, Aug. 1980, p. 43-80. refs

Attention is called to the fact that few senior academic geographers are doing research in remote sensing and that few economic geographers have even considered the possibilities opened up by this technique. This dearth of research is even more pronounced among regional geographers with interests in less-developed countries. Programs of study in remote sensing are considered vital because remote sensing can provide the geographer with significant improvements in the quantity, quality, and timeliness of data. C.R.

A82-32901

EFFECT OF ATMOSPHERIC CONDITIONS ON REMOTE SENSING OF VEGETATION PARAMETERS

J. V. DAVE (IBM Scientific Center, Palo Alto, CA) Remote Sensing of Environment, vol. 10, Sept. 1980, p. 87-99. refs

The effects of atmospheric and observational conditions on the remote sensing of vegetation parameters are studied in simulations of the ratios of radiances in the 0.76-0.90 micron and 0.52-0.60 micron bands (Landsat Thematic Mapper bands 4 and 2, respectively) as a function of leaf water content in blue grama grass. The simulations were performed based on spectral flux reflectance and canopy data for 35 plots with different leaf water levels and three different models of the cloud-free midlatitude summer atmosphere with no, moderate and high aerosol contents at solar zenith angles from 0 to 80 deg, heights from the top to the bottom of the atmosphere, nadir angles from 0 to 75 deg and azimuth angles from 0 to 180 deg. Selected results demonstrate that the slope and intercept of the straight line expressing the dependence of radiance ratio on leaf water content can be significantly affected by atmospheric conditions and viewing geometry. A.L.W.

A82-33652

SOUFRIERE VOLCANO, ST. VINCENT - OBSERVATIONS OF ITS 1979 ERUPTION FROM THE GROUND, AIRCRAFT, AND SATELLITES

R. S. FISKE (Smithsonian Institution, Washington, DC) and H. SIGURDSSON (Rhode Island, University, Kingston, RI) Science, vol. 216, June 4, 1982, p. 1105, 1106. refs

The 1979 eruption of Soufriere Volcano, St. Vincent, is described. The initial vulcanian explosive phase from April 13 to 26 was a series of discrete vertical explosions, blasting a new vent through the 1971-1972 lava island in the middle of the 1-km-wide crater lake. The second phase was characterized by the quiet extrusion of viscous basaltic andesite lava, resulting in the growth of a dome over the vent. The importance of the geologic, seismic and ground-deformation data gathered prior to the eruption is discussed. D.L.G.

A82-33654

GEOSTATIONARY SATELLITE OBSERVATIONS OF THE APRIL 1979 SOUFRIERE ERUPTIONS

A. F. KRUEGER (NOAA, National Weather Service, Washington, DC) Science, vol. 216, June 4, 1982, p. 1108, 1109. refs

Infrared images from the geostationary satellite SMS-1 were used to study the growth of the eight major eruptions of Soufriere, St. Vincent, during April, 1979. These eruptions differed considerably in growth and intensity, the most intense being that of April 17, which formed an ash cloud of 96,000 square kilometers in 4 hours. The weakest eruption formed a cloud of only 16,000 square kilometers. (Author)

A82-33655

METEOROLOGICAL ANALYSIS OF THE ERUPTION OF SOUFRIERE IN APRIL 1979

S. BARR (Los Alamos National Laboratory, Los Alamos, NM) and J. L. HEFFTER (NOAA, Air Resources Laboratory, Silver Spring, MD) Science, vol. 216, June 4, 1982, p. 1109-1111. refs

Meteorological upper-air data, in conjunction with satellite imagery, lidar light detection and ranging returns, and aircraft sampling, aid in the determination of plume altitude and transport. The estimated trajectories indicate that the ash was transported eastward across the Atlantic to Africa in 3 to 5 days and that there was modest meridional transport as far as 15 deg poleward during the first week of travel. (Author)

A82-33656

SKIRT CLOUDS ASSOCIATED WITH THE SOUFRIERE ERUPTION OF 17 APRIL 1979

S. BARR (Los Alamos National Laboratory, Los Alamos, NM) Science, vol. 216, June 4, 1982, p. 1111, 1112.

A fortuitous and dramatic photograph of the Soufriere eruption column of April 17, 1979 displays a series of highly structured skirt clouds. The gentle distortion of thin, quasi-horizontal layers of moist air has been documented in meteorological situations. It is proposed that at St. Vincent subhorizontal layers of moist air were intensely deformed by the rapidly rising eruption column and were carried to higher altitudes, where they condensed to form the skirt clouds. (Author)

A82-33657* National Aeronautics and Space Administration. Langley Research Center, Hampton, Va.

AIRBORNE LIDAR MEASUREMENTS OF THE SOUFRIERE ERUPTION OF 17 APRIL 1979

W. H. FULLER, JR., S. SOKOL (NASA, Langley Research Center, Hampton, VA), and W. H. HUNT (Wyle Laboratories, Hampton, VA) Science, vol. 216, June 4, 1982, p. 1113-1115. refs

At the time of the Soufriere, St. Vincent, volcanic eruption of April 17, 1979, a NASA P-3 aircraft with an uplooking lidar (light detection and ranging) system onboard was airborne 130 kilometers east of the island. Lidar measurements of the fresh volcanic ash were made approximately 2 hours after the eruption, 120 kilometers to the northeast and east. On the evening of April 18, the airborne lidar, on a southerly flight track, detected significant amounts of stratospheric material in layers at 16, 17, 18, and 19.5 kilometers. These data, and measurements to the north on April 19, indicate that the volcanic plume penetrated the stratosphere to an altitude of about 20 kilometers and moved south during the first 48 hours after the eruption. (Author)

A82-33659* National Aeronautics and Space Administration. Langley Research Center, Hampton, Va.

FINE PARTICLES IN THE SOUFRIERE ERUPTION PLUME

D. C. WOODS (NASA, Langley Research Center, Hampton, VA) and R. L. CHUAN (Brunswick Corp., Costa Mesa, CA) Science, vol. 216, June 4, 1982, p. 1118, 1119. refs

The size distributions of fine particles measured at tropospheric altitudes in the periphery of the eruption plume formed during the April 17, 1979 eruption of Soufriere Volcano and in the low-level effluents on May 15, 1979 were found to be bimodal, having peak concentrations at geometric mean diameters of 1.1 and 0.23 micrometers. Scanning electron microscopy and energy-dispersive

X-ray analysis of the samples revealed an abundance of aluminum and silicon and traces of sodium, magnesium, chlorine, potassium, calcium, and iron in the large-particle mode. The submicrometer-sized particles were covered with liquid containing sulfur, assumed to be in the form of liquid sulfuric acid. (Author)

A82-33865
EPA'S NEW BUBBLE AND BANKING POLICIES
M. R. DELAND (U.S. Environmental Protection Agency, Environmental Monitoring Systems Laboratory, Las Vegas, NV) Environmental Science and Technology, vol. 16, June 1982, p. 338A-346A. refs

The uses of multispectral scanning (MSS), laser technology, and aerial photography in remote sensing programs to monitor potential and existing environmental problems are examined. Airborne MSS applications involve the detection of visible and IR emissions from the earth's surface for electronic cleaning of the imagery and reproduction of the sensed scene. Spectroscopic coding of the images allows identification of pollutants, the health of vegetative cover, and the state of observable water quality. Airborne laser sensing of chlorophyll-a in water bodies has allowed association of dissolved organic nutrients, due mainly to sewage discharges, with increases in the population of the algae. Lidar measurements permit digitized air quality measurements from aircraft. The development of a differential absorption lidar (DIAL) system, using two lasers close in frequency output, is paving the way for specific species labeling. M.S.K.

A82-34218* National Aeronautics and Space Administration. Goddard Space Flight Center, Greenbelt, Md.
THE USE OF LANDSAT-3 THERMAL DATA TO HELP DIFFERENTIATE LAND COVERS
J. P. ORMSBY (NASA, Goddard Space Flight Center, Earth Survey Applications Div., Greenbelt, MD) Remote Sensing of Environment, vol. 12, May 1982, p. 97-105. refs

Landsat-3 Multispectral Scanner Subsystem (MSS) digital data of the Baltimore, Maryland area gathered on May 24, 1978, are examined to show the usefulness of thermal data in providing better discrimination between agricultural and residential areas, certain types of urban/industrial areas and water, cloud shadows and water, and bare-extractive areas and bright urban cover types. High altitude aircraft imagery taken on May 3, 1978, provides ground truth and training site verification. Two classifications are made for each training site: the initial one using bands 4, 5, and 7 and a second in which the thermal data are included with the visible and near infrared data. This permits a direct comparison of areas spectrally similar with and without the inclusion of the thermal data. Commission errors determined from selected subsets of the data show reductions of 95% for the urban/industrial versus water themes, 84% for the residential versus agriculture themes, 64.0% for the bare-extractive versus bright urban themes, and 24% for the cloud shadow versus water themes when the thermal data are included in the signature. C.R.

A82-34711
SITE SELECTION AND ENGINEERING ISSUES FOR A MAJOR INDUSTRIAL COMPLEX - APPLICATION OF IMAGE AND MAP INTERPRETATION
D. S. WAY (Harvard University, Cambridge, MA) In: American Society of Photogrammetry, Annual Meeting, 47th, Washington, DC, February 22-27, 1981, ASP Technical Papers. Falls Church, VA, American Society of Photogrammetry, 1981, p. 164-169.

A major port and industrial complex is being developed in Indonesia near Singapore. Little existing data is available facilitating application of remote sensing techniques for site evaluation and planning. Over eight hundred square kilometers of area was analyzed. Landsat images, aerial photographs, and topographic maps where interpreted for geology, geomorphology, soils, hydrology, and visual resources. Evaluations were made for both environmental and development/engineering issues culminating in a phased master plan. The data contributed by remote sensing represented a significant savings in site reconnaissance, design and construction. (Author)

A82-34739
A NEW APPROACH TO MULTIRESOURCE INVENTORIES USING REMOTE SENSING AND GEOGRAPHIC INFORMATION SYSTEMS TECHNOLOGIES
J. VAN ROESSEL, P. G. LANGLEY, C. SHEFFIELD, and M. C. PLACE (Earth Satellite Corp., Berkeley, CA) In: American Society of Photogrammetry, Annual Meeting, 47th, Washington, DC, February 22-27, 1981, ASP Technical Papers. Falls Church, VA, American Society of Photogrammetry, 1981, p. 499-510. refs

The design for a new multiresource inventory system is presented. Two geographic information systems are employed in concert to support a sampling system which can provide estimates for multiple resource parameters. One GIS (the upper level) is cell- and tape- oriented and incorporates various types of Landsat processing. The other (the lower level) is a disk-based polygon system that holds high resolution sample maps. The two systems are connected through a linear regression model. The results of a pilot test of a prototype system in South Carolina are presented. (Author)

A82-34743* Jet Propulsion Lab., California Inst. of Tech., Pasadena.
IMPROVED LAND USE CLASSIFICATION FROM LANDSAT AND SEASAT SATELLITE IMAGERY REGISTERED TO A COMMON MAP BASE
J. CLARK (California Institute of Technology, Jet Propulsion Laboratory, Pasadena, CA) In: American Society of Photogrammetry, Annual Meeting, 47th, Washington, DC, February 22-27, 1981, ASP Technical Papers. Falls Church, VA, American Society of Photogrammetry, 1981, p. 591-599. refs
(Contract NAS7-100)

In the case of Landsat Multispectral Scanner System (MSS) data, ambiguities in spectral signature can arise in urban areas. A study was initiated in the belief that Seasat digital SAR could help provide the spectral separability needed for a more accurate urban land use classification. A description is presented of the results of land use classifications performed on Landsat and preprocessed Seasat imagery that were registered to a common map base. The process of registering imagery and training site boundary coordinates to a common map has been reported by Clark (1980). It is found that preprocessed Seasat imagery provides signatures for urban land uses which are spectrally separable from Landsat signatures. This development appears to significantly improve land use classifications in an urban setting for class 12 (Commercial and Services), class 13 (Industrial), and class 14 (Transportation, Communications, and Utilities). G.R.

A82-34744* National Aeronautics and Space Administration. Goddard Inst. for Space Studies, New York.
LONGWAVE INFRARED OBSERVATION OF URBAN LANDSCAPES
S. N. GOWARD (NASA, Goddard Institute for Space Studies; Columbia University, New York, NY) In: American Society of Photogrammetry, Annual Meeting, 47th, Washington, DC, February 22-27, 1981, ASP Technical Papers. Falls Church, VA, American Society of Photogrammetry, 1981, p. 600-609. Research supported by the Indiana Academy of Science and Indiana State University. refs

An investigation is conducted regarding the feasibility to develop improved methods for the identification and analysis of urban landscapes on the basis of a utilization of longwave infrared observations. Attention is given to landscape thermal behavior, urban thermal properties, modeled thermal behavior of pavements and buildings, and observed urban landscape thermal emissions. The differential thermal behavior of buildings, pavements, and natural areas within urban landscapes is found to suggest that integrated multispectral solar radiant reflectance and terrestrial radiant emissions data will significantly increase potentials for analyzing urban landscapes. In particular, daytime satellite observations of the considered type should permit better identification of urban areas and an analysis of the density of buildings and pavements within urban areas. This capability should enhance the utility of satellite remote sensor data in urban applications. G.R.

A82-35534
OBSERVED MAGNETIC SUBSTORM SIGNATURES AT SYNCHRONOUS ALTITUDE
T. NAGAI Journal of Geophysical Research, vol. 87, June 1, 1982, p. 4405-4417. refs

Magnetic field data from the geostationary satellites GOES 2 and GOES 3 are examined to study the development of substorm activity in the near-earth nightside magnetosphere (around a radial distance of 6.6 earth radii). Substorm events are those in which a well-defined single onset is seen at low latitudes on the ground. The field configuration change from more taillike to more dipolelike starts initially in a longitudinally localized region in association with the ground onset, and it develops westward and eastward, even when the simultaneous onset of the low-latitude positive bay is recorded in a wide longitudinal region on the ground. It is also found that the variation caused by the field-aligned current starts at the ground onset and reaches a peak at the time of the field change. The present results are consistent with the view that a substorm is associated with a disruption and subsequent conversion of the cross-tail current to the field-aligned current connected with the polar ionosphere. It is indicated that the cross-tail current near synchronous orbit and its disruption are important in producing the field configuration change at synchronous orbit. (Author)

A82-35542* Maryland Univ., College Park.
GENERATION OF THE AURORAL KILOMETRIC RADIATION
C. S. WU, H. K. WONG (Maryland, University, College Park, MD), D. J. GORNEY (Aerospace Corp., Space Sciences Laboratory, El Segundo, CA), and L. C. LEE (Alaska, University, Fairbanks, AK) Journal of Geophysical Research, vol. 87, June 1, 1982, p. 4476-4487. refs
(Contract F04701-80-C-0081; NSF ATM-81-16045; NGL-21-002-005)

Data collected from the S3-3 spacecraft in the auroral kilometric radiation (AKR) source region are employed to form a stability theory from which numerical results are obtained and discussed. The distribution function was found to be isotropic outside the auroral atmospheric loss-cone region, which was partially filled with upcoming electrons. A parallel electric field was observed to be modifying the loss-cone distribution. A model distribution function is formulated, along with a magnetic field model expressed in terms of the electron cyclotron frequency. Models for the parallel electric field are also introduced, the first with the field distributed over a broad altitude range, while the second assumes a potential drop only above 4000 km. The presence of the field is found to enhance the growth rate of the AKR. At higher altitudes, the cutoff frequency of the X mode is affected by the rising energetic electrons. Finally, the folding distances of spatial amplification are calculated. M.S.K.

A82-35895
OBSERVATION OF THE DIURNAL VARIATION OF ATMOSPHERIC OZONE
J. L. LEAN (Adelaide, University, Adelaide, Australia) Journal of Geophysical Research, vol. 87, June 20, 1982, p. 4973-4980. Research supported by the World Meteorological Organization. refs

Ozone densities in the stratosphere and mesosphere have been derived from broad-band photometer measurements of Hartley band absorption of middle ultraviolet radiation. Seven rockets were launched during October-November 1979 from Wallops Island. Six rockets, each carrying one detector comprising two UV photometers, were launched at different times of the day. A seventh rocket, with three similar detectors each having three UV photometers, was launched at the time of a full moon and provided estimates of the nighttime ozone densities. Results from these rocket flights form a basis for investigating ozone diurnal variations. The number of flights provide greater statistical reliability for the ozone profiles than is generally afforded from in situ measurements with a single rocket. During the night, an enhancement in ozone densities occurred at altitudes above about 50 km. At 70 km, for example, the nighttime ozone was determined to be a factor of 6.4 greater than at sunset. In addition, these experiments suggest that near 40 km the magnitude of the ozone density at noon may be greater by 10-15% than the nighttime concentration. (Author)

A82-36053*# National Meteorological Center, Washington, D. C.
TOTAL OZONE VARIATIONS 1970-74 USING BACKSCATTERED ULTRAVIOLET /BUV/ AND GROUND-BASED OBSERVATIONS
A. J. MILLER, R. M. NAGATANI, T. G. ROGERS (NOAA, National Meteorological Center, Washington, DC), A. J. FLEIG, and D. F. HEATH (NASA, Goddard Space Flight Center, Greenbelt, MD) Journal of Applied Meteorology, vol. 21, May 1982, p. 621-630. NASA-supported research. refs

The most long-lived satellite set of ozone observations, to date, is that derived from the Backscatter Ultraviolet (BUV) ozone sensor on Nimbus 4 and extends from April 1970 through 1976. Unfortunately, this experiment suffered spacecraft power limitations which limited the spatial and temporal coverage and also appears to have suffered from long-term drifts which may be associated with changes in the instrument characteristics or the incident solar flux. Techniques have been developed to account for these problems, and this paper presents results of the BUV total ozone variations and compares them with those from ground-based observations, specifically the computations of Angell and Korshover (1978). After adjustments for the spatial gaps and comparison with concurrent Dobson ground-based observations, no significant trend was found in the BUV data over the years 1970-74. This finding is in contrast to a general decrease of about 2% during the same period appearing in the data of Angell and Korshover. The difference in these results is discussed in terms of the geographic sampling and the methods of hemispheric integration. (Author)

A82-36247#
AIRCRAFT MEASUREMENTS OF NO/X/ IN THE LOWER TROPOSPHERE ABOVE THE COAST OF JAPAN
Y. KONDO, M. TAKAGI, Y. MORITA, and A. IWATA Nagoya University, Research Institute of Atmospherics, Proceedings, vol. 29, Mar. 1982, p. 85-91. Research supported by the Nissan Science Foundation. refs

Concentrations of NO(x) in altitude regions of 0.5-3.0 km above the coastal area of Japan were measured. The measured mixing ratios range from 1 to 30 ppb depending on the altitude, location and time of the observations. From the measured mixing ratio, it can be said that relatively large amounts of NO(x) emitted at ground level are often transported at least as far as 3 km vertically and 200 km horizontally. (Author)

A82-36268
CHARACTERISTICS OF FIELD-ALIGNED E-REGION IRREGULARITIES OVER IIOKA /36 N/, JAPAN. I
T. TANAKA and S. V. VENKATESWARAN (California, University, Los Angeles, CA) Journal of Atmospheric and Terrestrial Physics, vol. 44, May 1982, p. 381-393, 395-397, 399-406. refs
(Contract NSF ATM-77-24843)

Measurements with a 25-MHz radar over Iioka, Japan, reveal that field-aligned E-region irregularities occur mainly at night in association with sporadic E (Es) layers at an altitude range of about 100-110 km and that they drift predominantly westward with speeds of the order of 60 m/s. It is shown that these observed characteristics of the irregularities are in reasonable agreement with quantitative predictions of the gradient drift instability theory. The predictions are based on appropriate models for neutral air densities and temperatures, ionic composition and ionospheric electric field, and available observations of electron density profiles of the E and Es layers. Observations of multifrequency (4-64 MHz) echoes with an oblique incidence ionosonde and of Doppler spectra with a fixed frequency (25 MHz) radar are then presented and discussed. It is shown that the ionosonde observations are capable of being explained in terms of the linear theory of cross-field or gradient-drift instability, which is presumed to generate the field-aligned irregularities. C.R.

A82-36292* National Aeronautics and Space Administration. Langley Research Center, Hampton, Va.

TROPOSPHERIC CO MEASUREMENT EXPERIMENT FROM THE SECOND SPACE SHUTTLE FLIGHT

H. G. REICHLE, JR. (NASA, Langley Research Center, Hampton, VA) American Meteorological Society, American Geophysical Union, and NASA, Symposium on the Composition of the Nonurban Troposphere, 2nd, Williamsburg, VA, May 25-28, 1982, Paper. 4 p. refs

The MAPS experiment was designed to remotely measure the mixing ratio of carbon monoxide in the middle and upper troposphere using a gas filter radiometer as the sensing instrument. The asymmetrical worldwide distribution of CO is discussed as background, and the experimental scientific and technical objectives are briefly stated. The gas filter radiometer is described in detail, and the second Shuttle mission is summarized. Auxiliary and correlative data were obtained in order to evaluate the performance of the measurement system, to assess the effect of stratospheric ozone on the radiometer signals, and to determine the effect of the underlying surface. The experiment acquired about 32 hours of data between 38 deg N and 38 deg S, signal-to-noise ratios were as predicted and the instrument achieved satisfactory stability in spite of large temperature variations. Data reduction is in progress. C.D.

A82-36293* National Aeronautics and Space Administration. Langley Research Center, Hampton, Va.

AMMONIA AND THE NOX BUDGET OF THE TROPOSPHERE

J. S. LEVINE, T. R. AUGUSTSSON, and J. M. HOELL (NASA, Langley Research Center, Hampton, VA) American Meteorological Society, American Geophysical Union, and NASA, Symposium on the Composition of the Nonurban Troposphere, 2nd, Williamsburg, VA, May 25-28, 1982, Paper. 3 p. refs

Liu et al. (1980) suggested that NOx transported from the stratosphere, as opposed to the anthropogenic source of NOx, may be the dominant source that controls the distribution of NOx in the global troposphere. These ideas require a reinvestigation, and, in particular, an assessment of the role of the oxidation of ammonia as a source of NOx. Attention is given to the results of an ammonia measurement program, in which the vertical distribution of ammonia in the troposphere and lower stratosphere could be studied with the aid of the Infrared Heterodyne Radiometer (IHR), a solar-viewing remote sensor. A one-dimensional photochemical model of the troposphere reported by Levine et al. (1980) was employed to study the chemical and physical processes that control the loss of ammonia in the troposphere. The results of the considered investigation suggest that the oxidation of ammonia may indeed be a significant source of NOx in the troposphere. G.R.

A82-36362*# National Aeronautics and Space Administration. Goddard Space Flight Center, Greenbelt, Md.

ATMOSPHERIC OZONE DETERMINATION BY SOLAR OCCULTATION USING THE UV SPECTROMETER ON THE SOLAR MAXIMUM MISSION

A. C. AIKIN, B. WOODGATE (NASA, Goddard Space Flight Center, Greenbelt, MD), and H. J. P. SMITH (Visidyne, Inc., Burlington, MA) Applied Optics, vol. 21, July 1, 1982, p. 2421-2424. refs

The UV spectrometer polarimeter instrument on the Solar Maximum Mission spacecraft has been used to measure ozone in the 53-75 km altitude interval by the technique of solar occultation. A 1 x 180 arcsec entrance aperture spectrometer with 0.04-A spectral resolution was employed. Resulting high-quality data are reduced by expressing measured UV attenuation as a Volterra integral equation. Solution of the equation is accomplished by expressing the integral in terms of a series representing the sum of ozone densities contained in concentric shells through tangent points separated by specified altitude increments. Sample ozone vs altitude profiles are presented for the equatorial region. These data show reproducibility to better than 10%. The density at 60 km is 7.3 + or - 0.15 x 10 to the 9th/cu cm for 2.5 deg latitude and longitudes between 81 and 105 deg west in September 1980. Density vs altitude profile exhibits changes in slope between 50 and 75 km. (Author)

A82-36405#

SENSITIVITY OF DOBSON TOTAL OZONE ESTIMATIONS TO WAVELENGTH BAND CALIBRATION UNCERTAINTIES

R. E. BASHER (New Zealand Meteorological Service, Wellington, New Zealand) In: Quadrennial International Ozone Symposium, Boulder, CO, August 4-9, 1980, Proceedings. Volume 1. Boulder, CO, International Association of Meteorology and Atmospheric Physics, 1981, p. 33-36. refs

It is pointed out that calibration uncertainties in the center wavelength, bandwidth, and shape of the Dobson instrument's bands propagate uncertainty into extraterrestrial constants, ozone absorption coefficients, standard lamp calibrations, and total ozone estimations. Detailed calculations of these uncertainties have been conducted for a wide range of conditions of calibration and operation. It is emphasized that all of the considered calculations refer to the defined 'well calibrated', 'well operated' instrument. It is found that the percent standard errors in total ozone are very dependent on airmass and ozone amount. The errors are greatest at low airmass and low ozone, especially for the D and CD band combinations. The AD combination generally has the least error of the double wavelength pairs, and for the directly intercompared instruments has a standard error of 1.1% or less. G.R.

A82-36406#

THE EFFECT OF THE SPECTRAL ATTENUATION OF UV RADIATION BY AEROSOL ON THE TOTAL OZONE MEASUREMENTS

A. DZIEWULSKA-LOSIOWA (Polska Akademia Nauk, Instytut Geofizyki, Warsaw, Poland) In: Quadrennial International Ozone Symposium, Boulder, CO, August 4-9, 1980, Proceedings. Volume 1. Boulder, CO, International Association of Meteorology and Atmospheric Physics, 1981, p. 38-45. U.S. Environmental Protection Agency refs

(Contract EPA-5-536-4)

The effect of aerosol in the atmosphere on ozone measurements is considered. Shah (1976) had concluded that changes in aerosol concentration and particle size distribution affect the measurement results only slightly. DeLuisi (1975), on the other hand, had found that substantial differences exist between values for ozone content obtained by taking into account scattering, and values calculated without regard to scattering effects. Instrumental errors are analyzed and the statistical relationship between measurements at different wavelengths are investigated. It is found that differences between the results of measurements related to different wavelength pairs are greater than instrumental errors. It is shown that these results are connected with the spectral extinction of the atmospheric aerosol. G.R.

A82-36414#

APPLICATION OF INFRARED TECHNIQUES TO THE STUDY OF ATMOSPHERIC OZONE [APPLICATION DES TECHNIQUES INFRAROUGES A L'ETUDE DE L'OZONE ATMOSPHERIQUE]

C. SECROUN, A. BARBE, P. MARCHE, and P. JOUVE (Reims, Universite, Reims, France) In: Quadrennial International Ozone Symposium, Boulder, CO, August 4-9, 1980, Proceedings. Volume 1. Boulder, CO, International Association of Meteorology and Atmospheric Physics, 1981, p. 108-113. In French. refs

The present investigation is concerned with the utilization of the infrared wavelength region for the study of the ozone in the atmosphere, taking into account three atmospheric windows including the wavelength ranges near 10, 5, and 3 micrometers. More than 3200 spectral lines could be assigned to different bands of the ozone spectrum. Laboratory studies formed one part of the investigation. Spectral frequencies, absorption line intensities, and linewidths were determined for ozone. Some of the obtained results were employed in connection with data provided by the radiometric probe LIMS on board the Nimbus-7 satellite. The second part of the investigation involved a study of the atmosphere. The same spectrometer as in the laboratory study was utilized, and the sun was employed as radiation source. The obtained results were compared with data provided by a Dobson spectrophotometer. Attention is also given to vertical concentration profiles. It is concluded that infrared absorption spectroscopy represents a suitable technique for studies of atmospheric ozone. G.R.

A82-36415*# Jet Propulsion Lab., California Inst. of Tech., Pasadena.

MICROWAVE MEASUREMENT OF STRATOSPHERIC AND MESOSPHERIC OZONE

J. W. WATERS (California Institute of Technology, Jet Propulsion Laboratory, Pasadena, CA) In: Quadrennial International Ozone Symposium, Boulder, CO, August 4-9, 1980, Proceedings. Volume 1. Boulder, CO, International Association of Meteorology and Atmospheric Physics, 1981, p. 114-121. refs

It is pointed out that ozone has a rich rotational spectrum with many lines at millimeter wavelengths. Measurement of these lines can provide a means of remotely sensing stratospheric and mesospheric ozone. Technology has recently advanced to the state where it is reasonable to consider monitoring upper atmospheric O3 on a global scale by microwave radiometers in earth orbit. An investigation indicates that approximately 1% accuracy and approximately 2 km vertical resolution O3 mixing ratio measurements are reasonable goals for limb-viewing microwave radiometers in earth orbit. Mesospheric ozone can also be measured by the considered techniques using stronger (but more temperature-sensitive) O3 lines. A balloon-borne microwave limb sounder has recently been constructed to test the practical limitations on the measurement concepts. Also under study is a microwave limb sounder for operation in earth orbit. G.R.

A82-36422#

TOTAL OZONE RETRIEVAL FROM SATELLITE METEOR 28 FOURIER SPECTROMETER MEASUREMENTS

U. FEISTER and D. SPAENKUCH (Meteorologisches Hauptobservatorium, Potsdam, East Germany) In: Quadrennial International Ozone Symposium, Boulder, CO, August 4-9, 1980, Proceedings. Volume 1. Boulder, CO, International Association of Meteorology and Atmospheric Physics, 1981, p. 168-175. refs

The efficiency and accuracy of four different algorithms for deriving total ozone from IR radiance measurements made with Fourier spectrometers are assessed. For a total of more than 1,100 spectrometer-interferometer spectra measured between July and September 1977, 40 corresponding Dobson ozone values are found with a maximum spatial distance between the subsatellite point and the Dobson station of 300 km and an average distance of 175 km; 35 values here are from midlatitudes of the Northern Hemisphere. The Dobson ozone values are used in determining a different number of coefficients for each method applying the least square method. With these coefficients, ozone values are calculated. The original number of spectral channels is then reduced to two intervals. It is found that a radiometer with one or two channels in the 9.6/micron band in the window and in the 15/micron band is sufficient for the total ozone determination. A highly significant positive correlation is found between spectrometer-interferometer ozone and calculated relative topographies of the lower stratosphere. This correlation holds even if the latitudinal dependence and autocorrelation of ozone values and relative topographies are eliminated. C.R.

A82-36428#

OPTICAL STOP AND FOCUSSING EFFECTS IN THE DOBSON INSTRUMENT

R. E. BASHER (New Zealand Meteorological Service, Wellington, New Zealand) In: Quadrennial International Ozone Symposium, Boulder, CO, August 4-9, 1980, Proceedings. Volume 1. Boulder, CO, International Association of Meteorology and Atmospheric Physics, 1981, p. 216-218.

The present investigation shows that the 'directional effect' observed in connection with the photoelectric spectrometer designed by Dobson (1931) is caused by defects in optical stopping and focusing. The considered effect consists of two parts, related to different field-of-view boundaries for the two wavelength bands being measured, and varying relative sensitivity across the field of view for the two bands. The stop problem is readily tested for and corrected, and it may affect only a limited number of instruments. The focussing problem, however, affects all but the earliest instruments, and its solution will require a careful consideration of the involved aspects. G.R.

A82-36431#

DOBSON SPECTROPHOTOMETER CALIBRATIONS, POSSIBLE ERRORS IN OZONE ABSORPTION COEFFICIENTS, AND ERRORS DUE TO INTERFERING POLLUTANT GASES

W. D. KOMHYR, R. D. GRASS (NOAA, Air Resources Laboratories, Boulder, CO), R. D. EVANS, and R. K. LEONARD (Cooperative Institute for Research in Environmental Sciences, Boulder, CO) In: Quadrennial International Ozone Symposium, Boulder, CO, August 4-9, 1980, Proceedings. Volume 1. Boulder, CO, International Association of Meteorology and Atmospheric Physics, 1981, p. 230-235. Research supported by the World Meteorological Organization; U.S. Department of Transportation refs
(Contract DOT-FA78WAI-850)

In connection with the employment of Dobson spectrophotometers as standard instruments for measurements of total ozone, it is imperative that the accuracy of the total ozone measurements be properly assessed. Research within the Geophysical Monitoring for Climatic Change program into the accuracy of ozone observations is currently focussed on possible variations of the Dobson instrument extraterrestrial constants. Attention is given to spectrophotometer calibrations, the systematic ozone measurement error, and interfering trace gas pollutants. It is pointed out that ozone produced photochemically in polluted air near ground level can also be considered an interferer since it renders unreliable background measurements of total ozone. G.R.

A82-36444#

OBSERVATIONS AND ANALYSES OF THE TOTAL AMOUNT OF ATMOSPHERIC OZONE IN THE BEIJING REGION AND IN THE REGION OF JOLMOLUNGMA MOUNTAIN IN TIBET

D. WEI (Chinese Academy of Sciences, Atmospheric Physics Institute, Beijing, People's Republic of China) and C. WEN (Sichuan, Institute of Geography, Sichuan, People's Republic of China) In: Quadrennial International Ozone Symposium, Boulder, CO, August 4-9, 1980, Proceedings. Volume 1. Boulder, CO, International Association of Meteorology and Atmospheric Physics, 1981, p. 340-346.

A82-36472#

OSO-8 LOWER MESOSPHERIC OZONE NUMBER DENSITY PROFILES

F. MILLIER (CNRS, Laboratoire de Physique Stellaire et Planetaire, Verrieres-le-Buisson, Essonne, France), B. A. EMERY, and R. G. ROBLE (National Center for Atmospheric Research, Boulder, CO) In: Quadrennial International Ozone Symposium, Boulder, CO, August 4-9, 1980, Proceedings. Volume 1. Boulder, CO, International Association of Meteorology and Atmospheric Physics, 1981, p. 572-579. refs

Solar occultation data gathered by the French ultraviolet spectrophotometer telescope on the NASA Orbiting Solar Observatory, scanning between about 50 deg N and 50 deg S between June 1975 and June 1976, are presented. The occultation profiles, observed near 2800 A, contain information on the ozone concentration at altitudes between about 52 and 75 km. Results obtained between June 5 and August 4, 1975 are discussed, longitudinal and latitudinal variations are demonstrated, and comparisons with published ozone density profiles are shown. C.D.

A82-36477#
COMPARISON OF OZONE IN POLLUTED AND CLEAN AIR MASSES OVER LAKE MICHIGAN
A. J. ALKEZWEENY, W. E. DAVIS, and R. C. EASTER (Battelle Pacific Northwest Laboratories, Richland, WA) In: Quadrennial International Ozone Symposium, Boulder, CO, August 4-9, 1980, Proceedings. Volume 1. Boulder, CO, International Association of Meteorology and Atmospheric Physics, 1981, p. 616-623. refs

A82-36534*# National Aeronautics and Space Administration. Goddard Space Flight Center, Greenbelt, Md.
THE SEASONAL VARIATIONS OF OZONE AND TEMPERATURE IN THE MIDDLE AND THE UPPER STRATOSPHERE
S. CHANDRA (NASA, Goddard Space Flight Center, Laboratory for Planetary Atmospheres, Greenbelt, MD) In: Quadrennial International Ozone Symposium, Boulder, CO, August 4-9, 1980, Proceedings. Volume 2. Boulder, CO, International Association of Meteorology and Atmospheric Physics, 1981, p. 1083-1090. refs

The seasonal variations in ozone and temperature inferred from the Nimbus-4 BUV (Backscatter Ultraviolet Spectrometer) and the SCR (Selective Chopper Radiometer) experiments are compared with predictions based on a simplified radiative photochemical model. It is shown that the observations, in agreement with the model calculations, show a systematic phase shift from a summer maximum at 10 mb to a winter maximum at 1 mb with equinoctial maxima at intermediate heights. In contrast, the temperature between these pressure levels shows no appreciable phase shift and the summer maximum prevails at all heights. The observed phase differences in ozone and temperature are shown to be a manifestation of the radiative feedback on the photochemistry of the upper stratosphere. (Author)

A82-36741
ON THE APPLICATION OF A MODEL OF BOUNDARY-LAYER FLOW OVER LOW HILLS TO REAL TERRAIN
J. L. WALMSLEY, J. R. SALMON, and P. A. TAYLOR (Department of the Environment, Atmospheric Environment Service, Downsview, Ontario, Canada) Boundary-Layer Meteorology, vol. 23, May 1982, p. 17-46. Research supported by the National Research Council of Canada. refs

Attempts to apply a computer model (Walmsley et al., 1980) to neutrally-stratified, boundary-layer flow over an isolated hill of moderate slope (Kettles Hill, Alberta) lead to velocity perturbation fields which probably overemphasize the impact of small-scale topographic features. Some numerical smoothing of the digitized terrain input field is found to be helpful in reducing this effect, although such a procedure is somewhat arbitrary. An extension of the original theory results in an improved representation of the effect of small-scale terrain components. These modifications are described and some results of an application of the extended model to Kettles Hill are presented (Author)

A82-37405* Aerospace Corp., El Segundo, Calif.
SOFT X-RAYS FROM THE SUNLIT EARTH'S ATMOSPHERE
D. L. MCKENZIE, H. R. RUGGE (Aerospace Corp., Space Sciences Laboratory, El Segundo, CA), and P. A. CHARLES (California, University, Berkeley, CA) Journal of Atmospheric and Terrestrial Physics, vol. 44, June 1982, p. 499-508. Research supported by the Aerospace Corp. refs
(Contract NAS8-33235; NASW-3338; CIT-44-727600; NAS5-23315 ; F04701-79-C-0080)

Observations of soft X-ray emission from the sunlit earth atmosphere are presented and compared with the predictions of an earth albedo X-ray theory. The exact theory accounts for the flux of Thomson scattered solar X rays and fluorescently excited K X rays that arise following the absorption of incident X rays as a function of observing geometry. Observations were made at widely separated geometries with the two low-energy detectors of the A-2 experiment on the HEAO-1 satellite. Fitting of the model to the observed spectra results in values for the solar coronal temperature and emission measure that are in good agreement with expected values for the nonflaring sun, indicating that X-ray observations of the sunlit atmosphere may be a useful monitor of solar activity for satellites unable to view the sun directly. The total measured fluorescent line flux is also in agreement with calculations, although the N/O line ratio is not. X-ray fluorescence measurements from the sunlit atmosphere will thus be useful in monitoring atmospheric composition only to the extent that the total line counting rates depend upon the composition. A.L.W.

A82-37502
SPATIAL RESOLUTION REQUIREMENTS FOR URBAN STUDIES
R. WELCH (Georgia, University, Athens, GA) International Journal of Remote Sensing, vol. 3, Apr.-June 1982, p. 139-146. refs

Remote sensor data with spatial resolutions corresponding to 0.5-10 m IFOV are required to define adequately the high frequency detail which characterizes the urban scene. Effective analyses of the small parcels, compact structures and narrow street patterns typical of Asian environments will necessitate data of much higher resolution than are required for Western countries. Consequently it is unlikely that satellite image data expected for the 1980s will replace aerial photographs as a primary source of information about urban areas. (Author)

N82-23043# Comptroller General of the United States, Washington, D.C.
STREAMLINING AND ENSURING MINERAL DEVELOPMENT MUST BEGIN AT LOCAL LAND MANAGEMENT LEVELS Report to the Chairman, Committee on Energy and Commerce, House of Representatives
4 Dec. 1981 24 p refs
(EMD-82-10; B-205344) Avail: SOD

A study of the use of Federal lands, particularily military lands, concluded that success in streamling and accelerating mineral development on Federal lands depends on the Bureau of Land Management state offices ultimately responsible for the implementation of Department of Interior minerals policies. It was found the eastern States Office of the Bureau of Land Management did not effectively deal with potential Federal mineral trespass in the East, and was unable to issue mineral leases and permits on a timely basis. Moreover, it was unable to effectively deal with new areas of mineral interest because of Department actions. Recommendations to improve the mineral trespass program help relieve lease and permit backlogs, maintain dedicated staff, and improve headquarters communications with State offices were made. R.J.F.

N82-23793# California Univ., Berkeley. Lawrence Berkeley Lab. Engineering and Technical Service Div.
ENVIRONMENTAL MONITORING REPORT OF THE LAWRENCE BERKELEY LABORATORY, 1980 Annual Report
G. E. SCHLEIMER, ed. Apr. 1981 33 p refs
(Contract W-7405-ENG-48)
(LBL-12604) Avail: NTIS HC A03/MF A01

The environmental monitoring program of the Lawrence Berkeley Laboratory is described. Data for 1980 are presented and general trends are discussed. Airborne and waterborne radionuclides are discussed. The radiation dose on the surrounding population is discussed. R.J.F.

N82-23891# National Oceanic and Atmospheric Administration, Washington, D. C. National Earth Satellite Service.
COMPARISON OF SATELLITE DERIVED RADIATION BUDGET MEASUREMENTS OVER MONEX DURING 1979 TO 1980
P. K. RAO IN WMO Intern. Conf. on Early Results of FGGE and Large-Scale Aspects of its Monsoon Expt. 7 p Apr. 1981
Avail: NTIS MF A01; HC WMO

Earth atmosphere radiation budgets derived from polar orbiting satellite radiometers are compared for May to August 1979 and 1980. The data are the differences in outgoing fluxes and albedos between 1980 and 1979. The low values in outgoing longwave radiation are associated with high and thick clouds which are relatively cold. High albedo values over this region are associated with clouds and snow over the mountains; moderately high values are observed over Saudi Arabia. Author (ESA)

N82-23963# Intermountain Forest and Range Experiment Station, Ogden, Utah. Aviation and Fire Management Staff.
REMOTE AUTOMATIC WEATHER STATION FOR RESOURCE AND FIRE MANAGEMENT AGENCIES
J. R. WARREN and D. L. VANCE Aug. 1981 15 p refs
(PB82-107335; FSGTR/INT-116) Avail: NTIS HC A02/MF A01
CSCL 04B

A weather station that operates automatically in remote areas, without power or communication lines was developed and is commercially available. Remote automatic weather stations (RAWS) transmit precipitation, windspeed, air temperature,temperature, humidity, and barometric pressure data via satellite. Data may be acquired by direct dialing or through a fire forecasting program. GRA

N82-24566*# Mississippi State Univ., Mississippi State. Remote Sensing Center.
APPLICATION OF REMOTE SENSING TO STATE AND REGIONAL PROBLEMS Semiannual Progress Report, 1 May - 31 Oct. 1981
W. F. MILLER, J. R. CLARK, J. L. SOLOMON, B. DUFFY, K. MINCHEW, and L. H. WRIGHT, Principal Investigator 1 Nov. 1981 89 p refs ERTS
(Contract NGL-25-001-054)
(E82-10288; NASA-CR-168857; NAS 1.26:168857; SAPR-16)
Avail: NTIS HC A05/MF A01 CSCL 06B

The objectives, accomplishments, and future plans of several LANDSAT applications projects in Mississippi are discussed. The applications include land use planning in Lowandes County, strip mine inventory and reclamation, white tailed deer habitat evaluation, data analysis support systems, discrimination of forest habitats in potential lignite areas, changes in gravel operations, and determination of freshwater wetlands for inventory and monitoring. In addition, a conceptual design for a LANDSAT based information system is discussed. M.G.

N82-24567*# Utah Univ., Salt Lake City. Center for Remote Sensing and Cartography.
IDENTIFYING ENVIRONMENTAL FEATURES FOR LAND MANAGEMENT DECISIONS Annual Report
27 Oct. 1981 55 p refs Original contains color imagery. Original photography may be purchased from the EROS Data Center, Sioux Falls, S. D. 57198 ERTS
(Contract NAGW-95)
(E82-10289; NASA-CR-168858) Avail: NTIS HC A04/MF A01
CSCL 05B

Advances in digital processing of LANDSAT imagery and in the interpretation of aerial photography are reported as well as the development of a geographic information system and the acquisition of cartographic equipment. Services to technical specialists and dignitaries are also described. The status of the following studies is discussed: Farmington Bay waterfowl; Sevier River wetland and agriculture; Davis County foothill development; Bear River Range aspen habitat; Wasatch-Cache riparian habitats; irrigated acreage in the Bear River Basin; the Parker Mountain rangeland inventory; and the development of techniques for inventorying aspen and aspen conifer stands. The cooperative project with NASA-Ames to verify LANDSAT digital maps of the forest and range resources on the LaSal Mountains is also considered. A.R.H.

N82-24598*# Instituto de Pesquisas Espaciais, Sao Jose dos Campos (Brazil).
COMPARISON OF STORM-TIME CHANGES OF GEOMAGNETIC FIELD AT GROUND AND AT MAGSAT ALTITUDES, PART 2
N. DEJESUSPARADA, Principal Investigator, R. P. KANE, and N. B. TRIVEDI Apr. 1982 42 p Sponsored by NASA ERTS
(E82-10325; NASA-CR-168904; NAS 1.26:168904;
INPE-2367-RA/161-PT-2) Avail: NTIS HC A03/MF A01 CSCL 08N

Geomagnetic field variations were studied by considering the parameter delta H which indicated H(observed) minus H(model), where H = (X squared + Y squared) (1/2) where X, Y, and Z are the components actually observed. Quiet time base values for 5 deg longitude belts were estimated. After subtracting these from the observed values, the residual delta H (dawn) and delta H (dusk) were studied for the two major storms. It was noticed that the dusk values attained larger (negative) values for a longer time, than the dawn value. Some changes in delta Y and delta Z were also noticed, indicating possibilities of either meridional currents and/or noncoincidence of the central plane of the ring current with the equatorial plane of the Earth. Other details are described. M.G.

N82-25661*# National Aeronautics and Space Administration. Langley Research Center, Hampton, Va.
IN SITU OZONE DATA FOR COMPARISON WITH LASER ABSORPTION REMOTE SENSOR: 1980 PEPE/NEROS PROGRAM
D. S. MCDOUGAL, R. B. LEE, III, and R. J. BENDURA May 1982 42 p refs
(NASA-TM-84471; NAS 1.15:84471) Avail: NTIS HC A03/MF A01 CSCL 13B

Several sets of in situ ozone (O3) measurements were made by a NASA aircraft in support of the laser absorption spectrometer (LAS) remote sensor. These measurements were designed to provide comparative O3 data for the LAS sensor. The LAS, which was flown on a second aircraft, remotely measured the vertical burden of O3 from the aircraft to the surface. In situ results of the air quality (O3 and B sub scat) and meteorological (temperature and dewpoint) parameters for three correlative missions are presented. The aircraft flight plans, in situ concentration profiles and vertical burdens, and measurement errors are summarized. B.W.

N82-26757*# Instituto de Pesquisas Espaciais, Sao Jose dos Campos (Brazil).
COMPARISON OF STORM-TIME CHANGES OF GEOMAGNETIC FIELD AT GROUND AND MAGSAT ALTITUDES
N. DEJESUSPARADA, Principal Investigator, R. P. KANE, and N. B. TRIVEDI Jan. 1982 17 p refs Sponsored by NASA and Fundo Nacional de Desenvolvimento Cientifico e Tecnologio ERTS
(E82-10359; NASA-CR-168980; NAS 1.26:168980;
INPE-2297-RPE/401) Avail: NTIS HC A02/MF A01 CSCL 04B

The MAGSAT data for the period Nov. 2-20, 1979 were studied. From the observed H, the HMD predicted by model was subtracted. The residue delta H = H-HMD shows storm-time variations similar to geomagnetic Dst, at least qualitatively. Delta H sub 0, i.e., equatorial values of delta H were studied separately for dusk and dawn and show some differences. T.M.

N82-27737# California Univ., Livermore. Lawrence Livermore Lab.
FEASIBILITY OF LASER-SEPARATION OF 36 S AND ITS USE AS AN ATMOSPHERIC TRACER
I. P. HERMAN 18 Aug. 1981 14 p refs
(Contract W-7405-ENG-48)
(DE82-000965; UCID-19167) Avail: NTIS HC A02/MF A01

The use of laser produced sulfur isotopes to analyze the acid rain situation is considered. The proposed use of isotopically labelled SO2, in particular of (56)SO2, as a tracer can help elucidate the chemical and transport facets in a unified experiment. Separation of a sufficient quantity of the rare (36)S isotope to perform several of these tracer studies appears to be practical and economical. T.M.

N82-27802# Tennessee Valley Authority, Chattanooga. Office of Natural Resources.
REMOTE SENSING OF SULFUR DIOXIDE EFFECTS ON VEGETATION. VOLUME 1: SUMMARY Final Report
C. D. SAPP Jul. 1981 31 p 2 Vol.
(Contract EPA-IAG-D8-E721)
(DE82-900580; TVA/ONR/ARP-81/5-VOL-1; EPA-660/7-81-113)
Avail: NTIS HC A03/MF A01

Three techniques for detecting and mapping sulfur dioxide (SO2) effects on the foliage of sensitive crops and trees near large, coal-fired power plants were tested and evaluated: spectroradiometry, photometric analysis of aerial photographs, and computer analysis of airborne multispectral scanner data. DOE

N82-27803# Tennessee Valley Authority, Chattanooga. Office of Natural Resources.
REMOTE SENSING OF SULFUR DIOXIDE EFFECTS ON VEGETATION. VOLUME 2: DATA Final Report
C. D. SAPP Jul. 1981 280 p refs 2 Vol.
(Contract EPA-IAG-D8-E721)
(DE82-900581; TVA/ONR/ARP-81/6-VOL-2; EPA-600/7-81-114)
Avail: NTIS HC A13/MF A01

Airborne multispectral scanner data covering affected soybean fields were analyzed using three computer-assisted procedures: unsupervised, supervised, and pseudosupervised. The last method provided the best results. LANDSAT imagery was also investigated, but the foliar effects of SO2 were too subtle to detect from orbit. DOE

03

GEODESY AND CARTOGRAPHY

Includes mapping and topography.

A82-22294* Pittsburg Univ., Pa.
A COLOR-RATIO MAP OF MERCURY
B. HAPKE, C. CHRISTMAN, B. RAVA (Pittsburgh, University, Pittsburgh, PA), and J. MOSHER (California Institute of Technology, Jet Propulsion Laboratory, Pasadena, CA) In: Lunar and Planetary Science Conference, 11th, Houston, TX, March 17-21, 1980, Proceedings. Volume 1. New York, Pergamon Press, 1980, p. 817-821. refs

Orange and UV frames are used to construct a color-ratio map of the portion of Mercury imaged by Mariner 10, with at least two independent color-ratio images being used for each region in order to prevent spurious, blemish-induced color. Color differences appear to be smaller than those of the moon, and many apparently fresh craters and their ray systems tend to be bluer than their surroundings. Regions of interesting color contrast are noted, and it is concluded that there is little evident correlation of color with either geology or topography. O.C.

A82-22595
PREFLARE INCREASES IN SOLAR COSMIC RAYS RELEVANT TO THE MODE OF ENERGY ACCUMULATION IN THE ACTIVE REGIONS ASSOCIATED WITH LARGE FLARES
G. M. BLOKH, O. P. GRIGORIAN, and B. M. KUZEVSKII (Moskovskii Gosudarstvennyi Universitet, Moscow, USSR) In: International Cosmic Ray Conference, 17th, Paris, France, July 13-25, 1981, Conference Papers. Volume 3. Gif-sur-Yvette, Essonne, France, Commissariat a l'Energie Atomique, 1981, p. 77-80. refs

Evidence of preflare increases in the electron and proton solar cosmic ray components is analyzed to develop a model of the processes involved. Data from the Prognoz-6 and Helios-1 and -2 satellites are cited as proof of a temporal form of particle arrival similar to a flare-produced event. The electron data indicates a set of individual events of acceleration up to 5 MeV and proton data shows the same process up to tens of MeV, implying a quasicontinuous generation of particles. The low-energy particle increase has been observed to occur several days in advance of a flare, with the particle acceleration happening in subregions of an imminent flare event. It is suggested that Coulomb interactions in the two-component plasma are responsible for the accelerations, which do not culminate in a flare until the ionization energy loss on the electrons and protons becomes insignificant compared to the acceleration rate. M.S.K.

A82-22596
COMPARISON OF SOLAR PROTON ACTIVITY IN 1967 AND 1969 WITH THAT IN 1978 AND 1979 AS MEASURED ONBOARD VENERA 4, 6, 11, 12 SPACE PROBES
S. I. ERMAKOV, N. N. KONTOR, G. P. LIUBIMOV, N. V. PERESLEGINA, and T. G. KHOTILOVSKAIA (Moskovskii Gosudarstvennyi Universitet, Moscow, USSR) In: International Cosmic Ray Conference, 17th, Paris, France, July 13-25, 1981, Conference Papers. Volume 3. Gif-sur-Yvette, Essonne, France, Commissariat a l'Energie Atomique, 1981, p. 81-84.

A comparison of the proton activity in 1967 and 1969 with that in 1978-1979 shows that proton activity in 1967 was much below the level of 1978-1979 owing to the high solar activity during the rise phase of the 21st cycle. It is also found that the activity in 1969 was much above the level of 1978-1979, although the smoothed sunspot number was approximately 110. This is seen as indicating that proton activity is weakly correlated with the smoothed sunspot number and is determined largely by the phase of the solar cycle. The greatest proton activity was observed in phases of maximum solar activity and solar activity decay. C.R.

A82-22598
SPACECRAFT DETERMINATION OF ENERGETIC PARTICLE PROPAGATION PARAMETERS - THE 1 JANUARY 1978 SOLAR EVENT
K. KECSKEMETY, T. I. GOMBOSI, A. J. SOMOGYI, A. SZENTGALI (Magyar Tudomanyos Akademia, Kozponti Fizikai Kutato Intezet, Budapest, Hungary), G. WIBBERENZ, G. GREEN, H. KUNOW, V. STEFFENS (Kiel, Neue Universitaet, Kiel, West Germany), V. G. KURT, and IU. I. LOGACHEV (Moskovskii Gosudarstvennyi Universitet, Moscow, USSR) In: International Cosmic Ray Conference, 17th, Paris, France, July 13-25, 1981, Conference Papers. Volume 3. Gif-sur-Yvette, Essonne, France, Commissariat a l'Energie Atomique, 1981, p. 89-92. refs

Intensity-time profiles in similar energy intervals measured by the longitudinally separated Helios 1/2 and Prognoz 6 spacecraft are used in studying coronal injection and interplanetary propagation. The scattering mean free path for the interplanetary propagation turns out to be in essence the same for the three locations. If the coronal propagation is described by a Reid-Axford type diffusion model, the diffusion coefficient is approximately constant below 200 MeV (about 0.1 AU); above this rigidity it exhibits a power law increase. C.R.

A82-22614
THE MODEL OF THE COSMIC RAY ENRICHMENT BY HELIUM-3
L. G. KOCHAROV (Leningradskii Politekhnicheskii Institut, Leningrad, USSR) In: International Cosmic Ray Conference, 17th, Paris, France, July 13-25, 1981, Conference Papers. Volume 3. Gif-sur-Yvette, Essonne, France, Commissariat a l'Energie Atomique, 1981, p. 175-178. refs

A model of He(3) enrichment is used to demonstrate that a stratified electron shock front propagating through the upper chromosphere may produce the He(3) enrichment in solar cosmic rays. The model also shows that bursts of hard X-rays, microwaves and UV radiation are produced. An analysis of available data shows that He(3) rich events are accompanied by hard X-rays, whose fluxes are in good agreement with theoretical estimations by Kocharov et al. (1980). D.L.G.

A82-29615*# National Aeronautics and Space Administration. Goddard Space Flight Center, Greenbelt, Md.
GRAVITY MODEL IMPROVEMENT FOR SEASAT
F. J. LERCH, J. G. MARSH (NASA, Goddard Space Flight Center, Geodynamics Branch, Greenbelt, MD), S. M. KLOSKO, and R. G. WILLIAMSON (EG&G Washington Analytical Services Center, Inc., Riverdale, MD) Journal of Geophysical Research, vol. 87, Apr. 30, 1982, p. 3281-3296. refs
(Previously announced in STAR as N80-20749)

A82-30306
WORK RELATED TO THE BLUE ROAD GEOTRAVERSE AT THE FINNISH GEODETIC INSTITUTE
J. MAKINEN (Geodeettinen Laitos, Helsinki, Finland) Earth Evolution Sciences, vol. 1, Mar. 1981, p. 71-76. refs

Finnish Geodetic Institute research work and research capabilities relevant to Blue Road Geotraverse studies are described. Institute activities cover precise levelling, high-precision gravimetry on land uplift gravity lines, earth tide observations, gravity mapping, geoid calculations, satellite geodesy, VLBI techniques, and geometric geodesy. O.C.

A82-30314
MAGNETIC ANOMALIES AS A REFERENCE FOR GROUND-SPEED AND MAP-MATCHING NAVIGATION
C. TYREN Journal of Navigation, vol. 35, May 1982, p. 242-254.

The use of the earth's magnetic field for ground referenced motion and position measurements is discussed. A magnetic terrain-navigation concept is set forth, and its sensor configuration, data processing and data storage unit, and navigation data interface unit are discussed. The navigational accuracy of the system is assessed; one particular advantage of terrain navigation systems is that ground-speed accuracy is independent of vehicle speed until speeds are reached at which the sensors and/or computer operations are too slow to track the vehicle path. The system is therefore excellent at low speeds and can advantageously be used for hovering operations. The results of field tests indicate that the feasibility of both ground-speed and map-matching methods is indeed promising. C.D.

A82-30778
MAGNETIC CHARTS OF CANADA DERIVED FROM MAGSAT DATA
L. R. NEWITT, E. DAWSON, R. L. COLES, and A. NANDI (Department of Energy, Mines, and Resources, Div. of Geomagnetism, Ottawa, Canada) Geophysical Research Letters, vol. 9, Apr. 1982, p. 246-249. refs

The feasibility of regional magnetic chart production by means of Magsat scalar and vector data is assessed through comparisons of Magsat north, east, vertical and total field charts with Canadian aeromagnetic data. After reducing all satellite and aeromagnetic data to sea-level, gridding at 1-deg intervals of longitude and latitude, and contouring the charts, it was determined that good agreement exists between the two data sets, with an overall rms difference of 150 nT. In all components, the greatest discrepancies between data sets occur in the northern U.S. and along the east coast of Canada. O.C.

A82-30784* National Aeronautics and Space Administration. Goddard Space Flight Center, Greenbelt, Md.
INITIAL SCALAR MAGNETIC ANOMALY MAP FROM MAGSAT
R. A. LANGEL (NASA, Goddard Space Flight Center, Greenbelt, MD), J. D. PHILLIPS (U.S. Geological Survey, Reston, VA), and R. J. HORNER (Computer Sciences Corp., Silver Spring, MD) Geophysical Research Letters, vol. 9, Apr. 1982, p. 269-272. refs

Magsat data acquired during the November 1979-June 1980 mission was used to derive a scalar magnetic anomaly map covering +50 to -50 deg geographic latitude, and the separation of anomaly fields from core and external fields was accomplished by techniques developed for POGO satellite data. Except in the Atlantic and Pacific at latitudes south of -15 deg, comparison of the Magsat map with its POGO data-derived counterpart shows basic anomaly patterns to be reproducible, and higher resolution due to Magsat's lower measurement altitude. Color-coded scalar anomaly maps are presented for both satellites. O.C.

A82-30785* National Aeronautics and Space Administration. Goddard Space Flight Center, Greenbelt, Md.
INITIAL VECTOR MAGNETIC ANOMALY MAP FROM MAGSAT
R. A. LANGEL, C. C. SCHNETZLER (NASA, Goddard Space Flight Center, Greenbelt, MD), J. D. PHILLIPS (U.S. Geological Survey, Reston, VA), and R. J. HORNER (Computer Sciences Corp., Silver Spring, MD) Geophysical Research Letters, vol. 9, Apr. 1982, p. 273-276. refs

Global magnetic component anomaly field maps have been derived from the Magsat vector magnetometer data obtained from November 1979 through May 1980. The amplitude of variations of the components over the maps are between 10 and 15 nT, well above the noise in the data. Averaged data, in 2-by-2 deg blocks, exhibit standard errors of the mean of about 1 nT over most of the X and Z maps, and about 2 nT over most of the Y maps. Errors rise to about twice these amounts near the auroral belts. Most of the anomalies in the component data are consistent with a crustal magnetization model which incorporates dipoles aligned only in the direction of the main field. However, there appear to be some regions which require dipoles aligned in some other direction i.e., remanent magnetization. (Author)

A82-30787* Wisconsin Univ., Madison.
MAGSAT MAGNETIC ANOMALIES OVER ANTARCTICA AND THE SURROUNDING OCEANS
M. H. RITZWOLLER and C. R. BENTLEY (Wisconsin, University, Madison, WI) Geophysical Research Letters, vol. 9, Apr. 1982, p. 285-288. refs
(Contract NAS5-25977)

A82-30788* Analytic Sciences Corp., Reading, Mass.
SPATIAL RESOLUTION AND REPEATABILITY OF MAGSAT CRUSTAL ANOMALY DATA OVER THE INDIAN OCEAN
R. V. SAILOR, A. R. LAZAREWICZ, and R. F. BRAMMER (Analytic Sciences Corp., Reading, MA) Geophysical Research Letters, vol. 9, Apr. 1982, p. 289-292. refs
(Contract NAS5-26424)

Preliminary results from analysis of individual Magsat tracks in the eastern Indian Ocean demonstrate the resolution capability and repeatability of these data. Spectrum analysis indicates that 250 km is the absolute lower limit for resolving crustal magnetic anomalies in Magsat along-track data. Spectral coherence analysis of closely-spaced tracks shows that magnetic anomaly features with wavelengths greater than 700 km are highly repeatable from track to track. (Author)

A82-30789* Purdue Univ., Lafayette, Ind.
VERIFICATION OF THE CRUSTAL COMPONENT IN SATELLITE MAGNETIC DATA
R. R. B. VON FRESE, W. J. HINZE, J. L. SEXTON, and L. W. BRAILE (Purdue University, West Lafayette, IN) Geophysical Research Letters, vol. 9, Apr. 1982, p. 293-295.
(Contract NAS5-25030)

A82-30790* North Carolina State Coll., Raleigh.
A PRELIMINARY COMPARISON OF THE MAGSAT DATA AND AEROMAGNETIC DATA IN THE CONTINENTAL U.S.
I. J. WON and K. H. SON (North Carolina State University, Raleigh, NC) Geophysical Research Letters, vol. 9, Apr. 1982, p. 296-298.
(Contract NAS5-26157)

A preliminary regional scale magnetic anomaly map derived from the Magsat data over the continental U.S. shows reasonably good correlations when compared with the corresponding aeromagnetic map. This conclusion is based upon the analysis of the fine attitude scalar Magsat data of about a two-month duration starting November 2, 1979 and the analysis of the Project Magnet U.S. aeromagnetic data in the same region. (Author)

A82-30795* Purdue Univ., Lafayette, Ind.

A SATELLITE MAGNETIC MODEL OF NORTHEASTERN SOUTH AMERICAN AULACOGENS

M. B. LONGACRE, W. J. HINZE, and R. R. B. VON FRESE (Purdue University, West Lafayette, IN) Geophysical Research Letters, vol. 9, Apr. 1982, p. 318-321. refs
(Contract NAS5-25030)

Magnetic modeling of the Amazon River and Takatu Aulacogens in northeastern South America illustrate the utility of satellite magnetic data in characterizing the properties and structure of the lithosphere. Specifically, reduction of preliminary Magsat scalar magnetic anomaly data to an equivalent condition of vertical polarization shows a general correlation between magnetic anomaly minima and the Amazon River and Takatu Aulacogens. Surface gravity data demonstrate a correlative positive anomaly. Spherical earth modeling of the magnetic data indicates a less magnetic crust associated with the aulacogens which is compatible with previous studies over the Mississippi River Aulacogen and Rio Grande Rift in North America. (Author)

A82-30796

PRELIMINARY INTERPRETATION OF MAGNETIC ANOMALIES OVER JAPAN AND ITS SURROUNDING AREA

M. YANAGISAWA, T. YUKUTAKE, N. FUKUSHIMA (Tokyo, University, Tokyo, Japan), and M. KONO (Tokyo Institute of Technology, Tokyo, Japan) Geophysical Research Letters, vol. 9, Apr. 1982, p. 322-324. refs

A82-30849

ALBEDO AND ANGULAR CHARACTERISTICS OF THE REFLECTANCE OF THE UNDERLYING SURFACE AND CLOUDS [AL'BEDO I UGLOVYE KHARAKTERISTIKI OTRAZHENIIA PODSTILAIUSHCHEI POVERKHNOSTI I OBLAKOV]

K. IA. KONDRATEV, V. I. BINENKO, L. N. DIACHENKO, V. I. KORZOV, and V. V. MUKHENBERG Leningrad, Gidrometeoizdat, 1981. 232 p. In Russian. refs

Information on the reflectance in the short-wave region of the spectrum of clouds and of the system comprising the earth's surface and atmosphere is discussed. Data are presented on the total albedo of the underlying surface and on the geographical distribution of albedo. Attention is given to the principles determining the spectral distribution of the albedo. Also considered are the laws governing the angular distribution of the reflectance of various types of natural formations. C.R.

A82-31994* Kansas Univ. Center for Research, Inc., Lawrence.

THE RECOGNITION OF EXTENDED TARGETS - SAR IMAGES FOR LEVEL AND HILLY TERRAIN

J. A. STILES, V. S. FROST, J. C. HOLTZMAN, and K. S. SHANMUGAM (University of Kansas Center for Research, Inc., Lawrence, KS) IEEE Transactions on Geoscience and Remote Sensing, vol. GE-20, Apr. 1982, p. 205-211. Research supported by the California Institute of Technology refs
(Contract NAS7-100)

Radar image simulation techniques are used to determine the character of SAR images of area-extensive targets, for the cases of flat underlying terrain and of moderate relief, with a view to the severity of elevation change effects on the detection and recognition of boundaries and shapes. The experiment, which demonstrated these effects on shapes and boundaries, was performed in order to establish Seasat-A SAR performance. Attention is given to the geometry/propagation effects in range perspective imaging that must be known for information extraction. O.C.

A82-32077* Ohio State Univ., Columbus.

REFERENCE COORDINATE SYSTEMS FOR EARTH DYNAMICS - A PREVIEW

I. I. MUELLER (Ohio State University, Columbus, OH) In: Reference coordinate systems for earth dynamics; Proceedings of the Fifty-sixth Colloquium, Warsaw, Poland, September 8-12, 1980. Dordrecht, D. Reidel Publishing Co., 1981, p. 1-22. Deutsche Forschungsgemeinschaft refs
(Contract DFG-4810/79; NSG-5265)
(Previously announced in STAR as N81-12525)

A82-32078* Joint Inst. for Lab. Astrophysics, Boulder, Colo.

ESTABLISHMENT OF TERRESTRIAL REFERENCE FRAMES BY NEW OBSERVATIONAL TECHNIQUES

P. L. BENDER (Joint Institute for Laboratory Astrophysics; National Bureau of Standards, Quantum Physics Div., Boulder, CO) In: Reference coordinate systems for earth dynamics; Proceedings of the Fifty-sixth Colloquium, Warsaw, Poland, September 8-12, 1980. Dordrecht, D. Reidel Publishing Co., 1981, p. 23-36. NBS-supported research refs
(Contract NASA ORDER S-65000-B)

It is anticipated that terrestrial reference systems for geodynamics studies which include adopted plate motion models will be introduced for the analysis of both LAGEOS satellite and very long baseline interferometry ranging data. One of the possible approaches involves adjustment of ground station coordinates in conjunction with solutions for Universal Time 1 (UT1) and polar motions as functions of time. Another method uses principal value decomposition to reduce the number of degrees of freedom being solved for by three. In a third alternative, the values of UT1 and polar motion derived from the available data by means of the initial set of coordinates are kept fixed, and an appropriate block of data is reanalyzed using the previously determined values of UT1 and polar motion so that a new set of station coordinates can be derived. O.C.

A82-32084

THE DEFINITION OF THE TERRESTRIAL COORDINATE FRAME BY LONG BASELINE INTERFEROMETRY

W. H. CANNON (York University, Toronto, Canada) and M. G. ROCHESTER (Newfoundland, Memorial University, St. John's, Canada) In: Reference coordinate systems for earth dynamics; Proceedings of the Fifty-sixth Colloquium, Warsaw, Poland, September 8-12, 1980. Dordrecht, D. Reidel Publishing Co., 1981, p. 111-118. refs

This paper examines the question of the definition of the celestial and terrestrial coordinate frames by the technique of long baseline interferometry. It demonstrates how the celestial coordinate frame may be usefully defined in terms of basis l-forms associated with the advancing phase fronts of the radiation fields from compact radio sources using only interferometer observables. The paper then proceeds to show how the terrestrial coordinate frame could be usefully defined, incorporating fully the effects of plate tectonics and secular motion of the observatories, by an application of the theory of continuum mechanics to interferometer observations. (Author)

A82-32090

ON REFERENCE COORDINATE SYSTEMS USED IN POLAR MOTION DETERMINATIONS

B. KOLACZEK (Polska Akademia Nauk, Centrum Badan Kosmicznych, Warsaw, Poland) and G. TELEKI (Astronomiska Opservatorija, Belgrade, Yugoslavia) In: Reference coordinate systems for earth dynamics; Proceedings of the Fifty-sixth Colloquium, Warsaw, Poland, September 8-12, 1980. Dordrecht, D. Reidel Publishing Co., 1981, p. 165-173. Research supported by the Smithsonian Institution. refs

A short review of the reference pole presently used in polar motion determinations by classical astrometric methods is followed by a discussion of the systematic differences between systems of polar coordinates and the influence of the mean latitude of stations on pole position. The importance of homogenous processing of astrometric data is stressed. (Author)

A82-32096

SOME CONSIDERATIONS IN THE USE OF VERY-LONG-BASELINE-INTERFEROMETRY TO ESTABLISH REFERENCE COORDINATE SYSTEMS FOR GEODYNAMICS

D. S. ROBERTSON (NOAA, National Geodetic Survey and National Ocean Survey, Rockville, MD) In: Reference coordinate systems for earth dynamics; Proceedings of the Fifty-sixth Colloquium, Warsaw, Poland, September 8-12, 1980. Dordrecht, D. Reidel Publishing Co., 1981, p. 205-216. refs

A82-32099

ORIGIN AND SCALE OF COORDINATE SYSTEMS IN SATELLITE GEODESY

J. B. ZIELINSKI (Polska Akademia Nauk, Centrum Badan Kosmicznych, Warsaw, Poland) In: Reference coordinate systems for earth dynamics; Proceedings of the Fifty-sixth Colloquium, Warsaw, Poland, September 8-12, 1980. Dordrecht, D. Reidel Publishing Co., 1981, p. 239-250. refs

The center of mass of the earth is commonly taken as origin for the coordinate systems used in satellite geodesy. In this paper the notion of the 'geocenter' is discussed from the point of view of mechanics and geophysics. It is shown that processes in and above the crust have practically no impact on the position of the geocenter. It is possible however that motions of the inner core may cause variations of the geocenter of the order of 1 m. Nevertheless the geocenter is the best point for the origin of a coordinate system. Mather's method of monitoring geocenter motion is discussed, and some other possibilities are mentioned. Concerning the scale problem, the role of the constant GM and time measurements in satellite net determinations are briefly discussed. (Author)

A82-32646* California Univ., Los Angeles.

GEOID HEIGHT-AGE RELATION FROM SEASAT ALTIMETER PROFILES ACROSS THE MENDOCINO FRACTURE ZONE

D. T. SANDWELL and G. SCHUBERT (California, University, Los Angeles, CA) Journal of Geophysical Research, vol. 87, May 10, 1982, p. 3949-3958. refs

(Contract NAG5-152)

Twenty-eight Seasat altimeter profiles crossing the Mendocino Fracture Zone are used together with seafloor ages determined from magnetic lineations to estimate the change in oceanic geoid height with age, between ages of 15 and 135 m.y. An unbiased estimate of the overall geoid offset along each profile is determined from a least-squares fit of the along-track derivative of the geoid to the geoid slope predicted from a simple two-layer gravitational edge effect model. Uncertainties based upon the statistical properties of each profile are also determined. A geoid slope-age relation is constructed by normalizing the geoid offsets and uncertainties by the age offsets. The results are in agreement with geoid slope-age relations determined from symmetrically spreading ridges (Sandwell and Schubert, 1980). However, the fracture zone estimates have smaller uncertainties and show less scatter. A comparison of these results with the geoid slope-age prediction of the boundary layer cooling model shows that the thermal structure begins to deviate from this model at an early age (20-40 m.y.). A plate cooling model with a thickness of 125 km is most compatible with the geoid slope-age estimates, although significant deviations occur; these may indicate that the lithospheric thermal structure is not entirely age dependent. (Author)

A82-33293

ESTABLISHING GEODETIC-GEODYNAMIC PARAMETERS USING LUNAR LASER RANGE MEASUREMENTS [DIE BESTIMMUNG GEODAETISCH-GEODYNAMISCHER PARAMETER MIT HILFE VON LASERDISTANZMESSUNGEN ZUM MOND]

L. BALLANI (Deutsche Akademie der Wissenschaften, Zentralinstitut fuer Physik der Erde, Potsdam, East Germany) Gerlands Beitraege zur Geophysik, vol. 91, no. 2, 1982, p. 121-140. In German. refs

The state of the art of lunar laser range measurements is reviewed. The transit time of the signals is simulated to determine if the effects of the final signal speed should be taken into account, and modeling of the signal time delay is treated in the frame of earth-moon dynamics. Results concerning coordinates and distances of laser stations in the United States, USSR and Austria, and essential UTO and UT1 analyses are presented. Conditions for establishing the geodetic-geodynamic parameters are determined, and preliminary estimations are made. (Author)

A82-33295

THE SIMULTANEOUS EMPLOYMENT OF GEODETIC MEASUREMENTS FOR BLOCK ADJUSTMENTS USING THE METHOD OF INDEPENDENT MODELS [EIN BEITRAG ZUR SIMULTANEN VERWENDUNG GEODAETISCHER MESSUNGEN BEI BLOCKAUSGLEICHUNGEN NACH DER METHODE DER UNABHAENGIGEN MODELLE]

R.-D. DUEPPE (Darmstadt, Technische Hochschule, Darmstadt, West Germany) Bildmessung und Luftbildwesen, vol. 50, May 1, 1982, p. 81-90. In German. refs

A method is proposed which involves the simultaneous adjustment of some types of geodetic measurements using independent models. Fields of application for the simultaneous adjustment are reviewed, and the photogrammetric consideration of geodetic measurements using the block adjustments with independent models is discussed. The method is presented with regard to a computer program development, and is demonstrated by several examples. D.L.G.

A82-34719

COMPARING LINEAMENTS INTERPRETED FROM LANDSAT IMAGERY AND TOPOGRAPHIC MAPS WITH REPORTED FAULTS IN SOUTHWEST MONTANA

R. C. HOWE and D. M. THOMPSON (Indiana State University, Terre Haute, IN) In: American Society of Photogrammetry, Annual Meeting, 47th, Washington, DC, February 22-27, 1981, ASP Technical Papers. Falls Church, VA, American Society of Photogrammetry, 1981, p. 237-246. refs

Poor resolution has usually prevented detection of features smaller than 60 by 80 meters on Landsat imagery. However, features previously not known to be related have been shown to be continuous or semicontinuous over large distances as a result of the synoptic view provided by satellites. In particular, numerous authors have noted the usefulness of Landsat imagery for lineament interpretations. The present investigation has the objective to compare the results of the lineament interpretation from Landsat imagery and topographic maps with reported faults in a portion of southwest Montana. The 1:1,000,000 color composite Landsat image was found to be clearly superior to 1:250,000 topographic maps for detecting lineaments. Almost twice as many lineaments were visible on the image as could be interpreted from the maps. However, the number of reported faults matching lineaments interpreted from each of these two data bases was similar. G.R.

A82-34918* National Aeronautics and Space Administration. Goddard Space Flight Center, Greenbelt, Md.

SATELLITE AND SURFACE GEOPHYSICAL EXPRESSION OF ANOMALOUS CRUSTAL STRUCTURE IN KENTUCKY AND TENNESSEE

M. A. MAYHEW (BTS, Inc., Seabrook, MD), H. H. THOMAS, and P. J. WASILEWSKI (NASA, Goddard Space Flight Center, Greenbelt, MD) Earth and Planetary Science Letters, vol. 58, no. 3, May 1982, p. 395-405. refs

(Previously announced in STAR as N82-17715)

A82-37175

THE PROCESSING OF SATELLITE NAVIGATION DATA FOR MARINE GEODESY [OBRABOTKA SPUTNIKOVOI NAVIGATSIONNOI INFORMATSII DLIA MORSKOI GEODEZII]

IU. G. FIRSOV and B. D. IAROVOI Geodeziia i Kartografiia, May 1982, p. 37-42. In Russian. refs

Various aspects of the use of satellite navigation systems to solve problems of marine geodesy, i.e., to determine ship coordinates, are examined. Particular consideration is given to the use of the integral Doppler method; the parametric equation and the solution of the problem in a spatial coordinate system; the determination of coordinates in a spatial polar system; allowance for different times of Doppler measurements in determining the coordinates of a mobile station; and tack equalization with allowance for feedback of satellite determinations. B.J.

A82-37962*# National Aeronautics and Space Administration. Goddard Space Flight Center, Greenbelt, Md.
INFORMATION THEORY LATERAL DENSITY DISTRIBUTION FOR EARTH INFERRED FROM GLOBAL GRAVITY FIELD
D. P. RUBINCAM (NASA, Goddard Space Flight Center, Geodynamics Branch, Greenbelt, MD) Journal of Geophysical Research, vol. 87, July 10, 1982, p. 5541-5552. NASA-supported research. refs
(Previously announced in STAR as N82-19731)

N82-22621*# Sao Paulo Univ. (Brazil).
STRUCTURE, COMPOSITION AND THERMAL STATE OF THE CRUST IN BRAZIL Progress Report, Feb. - May 1981
I. I. G. PACCA, Principal Investigator and W. SHUKOWSKY May 1981 41 p refs Sponsored by NASA ERTS
(E82-10187; NASA-CR-168615, NAS 1.26:168615) Avail: NTIS HC A03/MF A01 CSCL 08G

Efforts in support of a geomagnetic survey of the Brazilian area are described. Software to convert MAGSAT data tapes to the Burroughs/B-6700 binary format was developed and tested. A preliminary analysis of the first total intensity anomaly map was performed and methodologies for more intensive analysis were defined. The sources for correlative geological, aeromagnetic, and gravimetric data are described. M.G.

N82-22628*# Purdue Univ., Lafayette, Ind. Dept. of Geosciences.
STUDY OF GRAVITY AND MAGNETIC ANOMALIES USING MAGSAT DATA Quarterly Progress Report, Apr. - Jun. 1981
L. W. BRAILE, W. J. HINZE, and R. R. B. VONFRESE, Principal Investigators 1 Jul. 1981 9 p ERTS
(E82-10194; NASA-CR-168621; NAS 1.26:168621) Avail: NTIS HC A02/MF A01 CSCL 08B

The results of modeling satellite-elevation magnetic and gravity data using the constraints imposed by near surface data and seismic evidence shows that the magnetic minimum can be accounted for by either an intracrustal lithologic variation or by an upwarp of the Curie point isotherm. The long wavelength anomalies of the NOO's-vector magnetic survey of the conterminous U.S. were contoured and processed by various frequency filters to enhance particular characteristics. A preliminary inversion of the data was completed and the anomaly field calculated at 450 km from the equivalent magnet sources to compare with the POGO satellite data. Considerable progress was made in studing the satellite magnetic data of South America and adjacent marine areas. Preliminary versions of the 1 deg free-air gravity anomaly map (20 m gal contour interval) and the high cut (lambda approximately 8 deg) filtered anomaly maps are included. A.R.H.

N82-22832# National Academy of Sciences - National Research Council, Washington, D. C. Committee on Geodesy.
GEODETIC MONITORING OF TECTONIC INFORMATION. TOWARD A STRATEGY
1981 118 p refs
Avail: NTIS HC A06/MF A01 CSCL 08G

The time scale and time lapse over which crustal movements are traditionally monitored by geodesy and seismology was studied. Efforts are made to bridge this gap through increasing the frequency of geodetic measurements in the regions of particular interests, establishment of a global network of long and ultralong period seismometers, and development of geophysical and geodetic intrumentation that should be capable of measuring rates of crustal deformation over arbitrary time scales. The following measurements were undertaken: (1) on a global scale; (2) deformation near active plate boundaries; (3) deformation within plate interiors and other neotectonic motion; and (4) instrumentation for measuring tectonic deformation. E.A.K.

N82-22846*# National Academy of Sciences - National Research Council, Washington, D. C. Panel on Crustal Movement Measurements.
GEODETIC MONITORING OF TECTONIC DEFORMATION: TOWARD A STRATEGY Final Report
Nov. 1981 121 p refs Sponsored in part by Defense Mapping Agency, Washington; NASA, Washington; NOAA, Washington; and Geological Survey, Reston, Va.
(NASA-CR-168784; NAS 1.26:168784; PB82-137118) Avail: NTIS HC A06/MF A01 CSCL 08E

Issues of interest and importance to society and science are presented. The problems considered are of national concern; their solutions may contribute to a better understanding of tectonic deformation and earthquake hazards. The need for additional field data, the role of geodetic measurements, the importance of both ground and space techniques, and the need for advanced instrumentation development are discussed. GRA

N82-23563*# Consiglio Nazionale delle Ricerche, Naples (Italy). Osservatorio Vesuviano.
CRUSTAL STRUCTURES UNDER THE ACTIVE VOLCANIC AREAS OF CENTRAL AND EASTERN MEDITERRANEAN (M-44) Progress Report
P. GASPARINI, Principal Investigator, M. S. M. MANTOVANI, F. MONACO, D. PIERATTINI, and M. FEDI 10 Jan. 1981 4 p Sponsored by NASA ERTS
(E82-10096; NASA-CR-168845; NAS 1.26:168845) Avail: NTIS HC A02/MF A01 CSCL 08G

Programs are being adapted to the UNIVAC 1000 computer and others are being developed for immediate utilization in processing MAGSAT data. The magnetization intensity, susceptability, Koeningsberger ratio, NMR stbility against alternated fields and temperature, and the Curie temperature were determined for some rock formations with mineralogical compositions stable to the intermediate for lower continental crust and to upper manele conditions. Attempts to residuate crustal anomalies from one selected profile passing through western mediterranean using procedures commonly used at NASA yielded dubious results because of uncertainties in the adoption of coefficients in the expression accounting for the effect of equatorial ring currents and the empirical approach used for other corrections. Instead, filtering techniques are to be applied to each profile once invesigator B tapes relative to the whole planet are received. A.R.H.

N82-23571*# Colorado Univ., Boulder. Dept. of Astrogeophysics.
INVESTIGATION OF GEOMAGNETIC FIELD FORECASTING AND FLUID DYNAMICS OF THE CORE Quarterly Status Technical Progress Report, 1 Apr. - 30 Jun. 1981
E. R. BENTON, Principal Investigator 1 Jul. 1981 10 p ERTS
(Contract NAS5-25957)
(E82-10198; NASA-CR-168625; NAS 1.26:168625; QSTPR-6)
Avail: NTIS HC A02/MF A01 CSCL 08G

Progress in the use of MAGSAT data to confirm that the radius of the Earth's core-mantle boundary can be accurately determined magnatically is reported. The MAGSAT data was used in conjunction with a high quality manfield model for epoch 1965. The unsigned flux linking the core and mantle of the Earth is considered to be a legitimate invariant for a span of time. The value from MAGSAT of this constant is 16.056 GWb (gigawebers). J.D.

N82-23573*# Washington Univ., St. Louis, Mo. Dept. of Earth and Planetary Science.
STRUCTURE OF THE ST. FRANCOIS MOUNTAINS AND SURROUNDING LEAD BELT, S. E. MISSOURI: INFERENCES FROM THERMAL IR AND OTHER DATA SETS Quarterly Report, 13 May - 31 Jul. 1981
R. E. ARVIDSON, Principal Investigator 1 Nov. 1981 5 p HCMM
(Contract NAS5-26533)
(E82-10200; NASA-CR-168627; NAS 1.26:168627) Avail: NTIS HC A02/MF A01 CSCL 08G

Heat Capacity Mapping Mission (HCMM) in the form of an apparent thermal inertia image were merged with shaded relief maps and Bouguer gravity maps. The HCMM data show that the dominant structural grain in Missouri strikes in a northwesterly direction. The strike is the same as a major basement fault or flexure identified on the basis of gravity images. M.G.

N82-23577*# Analytic Sciences Corp., Reading, Mass.
BATHYMETRIC AND TECTONICS OF INDIAN OCEAN USING MAGSAT DATA Quarterly Progress Report, 1 Jul. - 30 Sep. 1981
R. V. SAILOR and A. R. LAZAREWICZ, Principal Investigators 15 Oct. 1981 22 p refs ERTS
(Contract NAS5-26424)
(E82-10204; NASA-CR-168631; NAS 1.26:168631) Avail: NTIS HC A02/MF A01 CSCL 05B

The quality of the MAGSAT data was assessed, especially the characterization of spikes. The spectral passbands of significance to geophysical analysis were analyzed, including computations of spectral coherence between nearby repeating satellite tracks. A spectrum modeling effort was begun which is designed to show the effect of spacecraft attitude on the observability of magnetic anomalies. The data obtained is to be used to compute crustal anomaly maps by modeling the equivalent dipoles in the project area. A.R.H.

N82-23587*# Geological Survey, Denver, Colo.
TOPOGRAPHIC SLOPE CORRECTION FOR ANALYSIS OF THERMAL INFRARED IMAGES
K. WATSON, Princpal Investigator 1982 14 p refs HCMM
(Contract NASA ORDER S-40256-B)
(E82-10214; NASA-CR-168774; NAS 1.26:168774) Avail: NTIS HC A02/MF A01 CSCL 08B

A simple topographic slope correction using a linearized thermal model and assuming slopes less than about 20 degrees is presented. The correction can be used to analyzed individual thermal images or composite products such as temperature difference or thermal inertia. Simple curves are provided for latitudes of 30 and 50 degrees. The form is easily adapted for analysis of HCMM images using the DMA digital terrain data. Author

N82-24520*# Purdue Univ., Lafayette, Ind. Dept. of Geosciences.
SPHERICAL-EARTH GRAVITY AND MAGNETIC ANOMALY MODELING BY GAUSS-LEGENDRE QUADRATURE INTEGRATION Quarterly Progress Report, Jul. - Sep. 1981
R. R. B. VONFRESE, W. J. HINZE, L. W. BRAILE, and A. J. LUCA, Principal Investigators (Chevron Geophysical Co., Calgary, Alberta) 1 Oct. 1981 11 p refs Repr. from J. Geophys. vol. 49, 1981 p 234-242 ERTS
(Contract NAS5-25030)
(E82-10242; NASA-CR-168823; NAS 1.26:168823) Avail: NTIS HC A03/MF A01 CSCL 05B

The anomalous potential of gravity and magnetic fields and their spatial derivatives on a spherical Earth for an arbitrary body represented by an equivalent point source distribution of gravity poles or magnetic dipoles were calculated. The distribution of equivalent point sources was determined directly from the coordinate limits of the source volume. Variable integration limits for an arbitrarily shaped body are derived from interpolation of points which approximate the body's surface envelope. The versatility of the method is enhanced by the ability to treat physical property variations within the source volume and to consider variable magnetic fields over the source and observation surface. A number of examples verify and illustrate the capabilities of the technique, including preliminary modeling of potential field signatures for Mississippi embayment crustal structure at satellite elevations. T.M.

N82-24522*# Tokyo Univ. (Japan). Geophysics Research Lab.
INVESTIGATION FROM JAPANESE MAGSAT TEAM. PART A. CRUSTAL STRUCTURE NEAR JAPAN AND IN ANTARCTIC STATION. PART B. ELECTRIC CURRENTS AND HYDROMAGNETIC WAVES IN THE IONOSPHERE AND THE MAGNETOSPHERE Progress Report, 15 Jul. - 15 Nov. 1981
N. FUKUSHIMA, Principal Investigator 15 Dec. 1981 13 p refs Sponsored by NASA ERTS
(E82-10244; NASA-CR-168825; NAS 1.26:168825; PR-4) Avail: NTIS HC A02/MF A01 CSCL 05B

Preliminary results of MAGSAT data analysis are described. Regional anomaly maps (deviations from the MGST model field) for X,Y,Z, and F in the area of 115 to 155 deg E and 20 to 60 deg N were obtained. A similar map for the geomagnetic total force anomaly in the vicinity of Japan showed that the observed anomaly can be explained by the difference in crustal magnetization between the Japan Sea and the Japan Island, which reflects a difference of 25 km in the thickness of the magnetized layer. The MAGSAT record of a sudden comencement of a magnetic storm above the South Atlantic Ocean showed a reverse impulse particularly in the D-component. Results relating to toroidal currents in the ionosphere, transverse and parallel perturbations over the polar regions, the relationship between field aligned currents and precipitating electrons, and the calculation of the subsatellite electric field are also discussed. M.G

N82-24573*# Business and Technological Systems, Inc., Seabrook, Md.
AN EQUIVALENT LAYER MAGNETIZATION MODEL FOR THE UNITED STATES DERIVED FROM MAGSAT DATA
M. A. MAYHEW and S. C. GALLIHER, Principal Investigators 1982 8 p refs ERTS
(Contract NAS5-26328)
(E82-10297; NASA-CR-168866; NAS 1.26:168866) Avail: NTIS HC A02/MF A01 CSCL 05B

Long wavelength anomalies in the total magnetic field measured field measured by MAGSAT over the United States and adjacent areas are inverted to an equivalent layer crustal magnetization distribution. The model is based on an equal area dipole grid at the Earth's surface. Model resolution having physical significance, is about 220 km for MAGSAT data in the elevation range 300-500 km. The magnetization contours correlate well with large-scale tectonic provinces. Author

N82-24577*# Analytic Sciences Corp., Reading, Mass.
ANALYZING THE BROKEN RIDGE AREA OF THE INDIAN OCEAN USING MAGNETIC AND GRAVITY ANOMALY MAPS AND GEOID UNDULATION AND BATHYMETRY DATA Quarterly Progress Report, 1 Jan. - 31 Mar. 1982
A. R. LAZAREWICZ and R. V. SAILOR, Principal Investigators 15 Apr. 1982 19 p refs ERTS
(Contract NAS5-26424)
(E82-10303; NASA-CR-168878; NAS 1.26:168878) Avail: NTIS HC A02/MF A01 CSCL 08G

A higher resolution anomaly map of the Broken Ridge area (2 degree dipole spacing) was produced and reduced to the pole using quiet time data for this area. The map was compared with equally scaled maps of gravity anomaly, geoid undulation, and bathymetry. The ESMAP results were compared with a NASA MAGSAT map derived by averaging data in two-degree bins. A survey simulation was developed to model the accuracy of MAGSAT anomaly maps as a function of satellite altitude, instrument noise level, external noise model, and crustal anomaly field model. A preliminary analysis of the geophysical structure of

Broken Ridge is presented and unresolved questions are listed.
A.R.H.

N82-24578*# Analytic Sciences Corp., Reading, Mass.
INVESTIGATING TECTONIC AND BATHYMETRIC FEATURES OF THE INDIAN OCEAN USING MAGSAT MAGNETIC ANOMALY DATA Quarterly Progress Report, 1 Sep. - 31 Dec. 1981
A. R. LAZAREWICZ and R. V. SAILOR, Principal Investigators 22 Jan. 1982 17 p refs ERTS
(Contract NAS5-26424)
(E82-10304; NASA-CR-168879; NAS 1.26:168879; PR-1325-4)
Avail: NTIS HC A02/MF A01 CSCL 08G

MAGSAT Investigator-B tapes were preprocessed by (1) removing all data points with obvious erroneous values and location errors; (2) removing smaller spikes (typically 15 nT or more), and deleting data tracks with fewer than 20 points; and (3) removing a linear trend from each track. The remaining data were recorded on tape for use by the equivalent source mapping (ESMAP) program which uses a least squares algorithm to fit the magnetization parameter of the grid of equivalent source dipoles in the crust to satellite data acquired at different times and locations. ESMAP was implemented on the TASC computing system and modified to read preprocessed MAGSAT tapes and interface with TASC plotting software. Some verification of the software was accomplished. Gridded 1-degree mean values of gravity anomaly and sea surface undulation computed from SEASAT radar altimeter were obtained and brought on line. A.R.H.

N82-24582*# Wisconsin Univ., Madison.
INVESTIGATION OF ANTARCTIC CRUST AND UPPER MANTLE USING MAGSAT AND OTHER GEOPHYSICAL DATA Quarterly Status Technical Progress Report
C. R. BENTLEY, Principal Investigator 14 Jan. 1982 1 p ERTS
(Contract NAS5-25977)
(E82-10308; NASA-CR-168883; NAS 1.26:168883; QSTPR-8)
Avail: NTIS HC A02/MF A01 CSCL 08G

Development of a spectral analysis technique to determine the depth to the Curie isotherm from MAGSAT data over Antarctica is reported. The analysis of the power spectra of a number of MAGSAT passes over Antarctica indicates on the average two power maxima for each flight pass, one with spatial wavelength of approximately 2000 km and the other with a wavelength of approximately 700 km. It was not determined whether these spectral peaks are geological or mathematical in origin. T.M.

N82-24583*# Wisconsin Univ., Madison.
INVESTIGATION OF ANTARCTIC CRUST AND UPPER MANTLE USING MAGSAT AND OTHER GEOPHYSICAL DATA Quarterly Status Technical Progress Report
C. R. BENTLEY, Principal Investigator 16 Apr. 1982 1 p ERTS
(Contract NAS5-25977)
(E82-10309; NASA-CR-168884; NAS 1.26:168884; QSTPR-9)
Avail: NTIS HC A02/MF A01 CSCL 08G

Plans to create an improved version of the MAGSAT magnetic anomaly map by more carefully scrutinizing the accepted data for field-aligned current effects are discussed. Data are continued to a 300 km surface for the compilation of a final map. Based on this set of data, vector anomaly maps over Antarctica are planned. A high-pass anomaly map with a cut-off wavelength of approximately 1500 km is also envisioned. It is suspected that longer-wavelength features have their origin outside the crust.
T.M.

N82-24584*# Colorado Univ., Boulder. Dept. of Astro-Geophysics.
INVESTIGATION OF GEOMAGNETIC FIELD FORECASTING AND FLUID DYNAMICS OF THE CORE Quarterly Progress Report, 1 Jan. - 31 Mar. 1982
E. R. BENTON, Principal Investigator 1 Apr. 1982 7 p refs ERTS
(Contract NAS5-25957)
(E82-10310; NASA-CR-168885; NAS 1.26:168885; QPR-9) Avail: NTIS HC A02/MF A01 CSCL 08G

It was established that the total absolute magnetic flux crossing the core- mantle boundary has been a constant of the core motion for the last 50 years. This provides a scalar constraint that could be added to the geometric modelling procedure. The GSFC 8 8/80 model is being evaluated. The absolute magnetic flux linking the CMB to that model was plotted as a function of time during the span covered by the data, and increasing truncation level. The inclusion of the standard error of each Gauss coefficient derived from the statistics of fit in the GSFC 9/80 model is useful. The magnitude and sense (upwelling or downe welling) of vertical fluid motion adjacent to the core-mantle boundary was calculated using the model. Standard errors were found to be sufficiently small at all but one or two of the 40 or more critical points of B sub r. They do not nearly overlap the value gamma u/gamma r = 0. It is concluded that the core is upwelling and downwelling at an observationally detectable level. A.R.H.

N82-24586*# Purdue Univ., Lafayette, Ind. Dept. of Geosciences.
MAGNETIC AND GRAVITY ANOMALIES IN THE AMERICAS Quarterly Progress Report, Oct. - Dec. 1981
L. W. BRAILE, W. J. HINZE, and R. R. B. VONFRESE, Principal Investigators 30 Dec. 1981 7 p Sponsored by NASA ERTS
(E82-10312; NASA-CR-168888; NAS 1.26:168888) Avail: NTIS HC A02/MF A01 CSCL 05B

The cleaning and magnetic tape storage of spherical Earth processing programs are reported. These programs include: NVERTSM which inverts total or vector magnetic anomaly data on a distribution of point dipoles in spherical coordinates; SMFLD which utilizes output from NVERTSM to compute total or vector magnetic anomaly fields for a distribution of point dipoles in spherical coordinates; NVERTG; and GFLD. Abstracts are presented for papers dealing with the mapping and modeling of magnetic and gravity anomalies, and with the verification of crustal components in satellite data. T.M.

N82-24587*# Phoenix Corp., McLean, Va.
IMPROVED DEFINITION OF CRUSTAL MAGNETIC ANOMALIES FOR MAGSAT DATA Final Report
R. D. BROWN, J. F. FRAWLEY, W. M. DAVIS, R. D. RAY, E. DIDWALL, and R. D. REGAN, Principal Investigators 15 Mar. 1982 23 p refs ERTS
(Contract NAS5-25882)
(E82-10314; NASA-CR-168889; NAS 1.26:168889) Avail: NTIS HC A02/MF A01 CSCL 08G

The routine correction of MAGSAT vector magnetometer data for external field effects such as the ring current and the daily variation by filtering long wavelength harmonics from the data is described. Separation of fields due to low altitude sources from those caused by high altitude sources is affected by means of dual harmonic expansions in the solution of Dirichlet's problem. This regression/harmonic filter procedure is applied on an orbit by orbit basis, and initial tests on MAGSAT data from orbit 1176 show reduction in external field residuals by 24.33 nT RMS in the horizontal component, and 10.95 nT RMS in the radial component. J.D.

N82-24589*# Technicolor Graphic Services, Inc., Sioux Falls, S. Dak.

AN INVESTIGATION OF MAGSAT AND COMPLEMENTARY DATA EMPHASIZING PRECAMBRIAN SHIELDS AND ADJACENT AREAS OF WEST AFRICA AND SOUTH AMERICA Quarterly Report, period ending 30 Sep. 1981

D. A. HASTINGS, Principal Investigator 30 Sep. 1981 34 p
Sponsored by NASA ERTS
(Contract DI-14-08-0001-16439)
(E82-10316; NASA-CR-168897; NAS 1.26:168897) Avail: NTIS HC A03/MF A01 CSCL 08B

Accomplishments with regard to the mapping and analysis of MAGSAT data for the investigation of correlations between the magnetic field characteristics of South American and African shields are reported. Significant results in the interpretation of the global total-field anomalies and the anomaly patterns of Africa and South America are discussed. The central position of the Brazilian shield tends to form a negative total-field anomaly, consistent with findings for shields in equatorial Africa. Sedimentary sequences in the Amazon basin and in the Rio de Janeiro-Sao Paolo areas exhibit positive anomalies, also consistent with equatorial Africa. Results for the Caribbean Sea and Guyana regions are also described.

M.G.

N82-24590*# Technicolor Graphic Services, Inc., Sioux Falls, S. Dak.

AN INVESTIGATION OF MAGSAT AND COMPLEMENTARY DATA EMPHASIZING PRECAMBRIAN SHIELDS AND ADJACENT AREAS OF WEST AFRICA AND SOUTH AMERICA Quarterly Report, 1 Oct. - 31 Dec. 1981

D. A. HASTINGS, Principal Investigator 31 Dec. 1981 13 p
Sponsored by NASA ERTS
(Contract DE-14-08-0001-16439)
(E82-10317; NASA-CR-168895; NAS 1.26:168895) Avail: NTIS HC A02/MF A01 CSCL 08G

Several possible causes for the east-west striping of the MAGSAT anomaly maps are listed and discussed including: (1) the inadequacy of the field model used for core-crustal separation of geomagnetic anomalies; (2) external field noise remaining in the available maps; (3) east-west trends of crustal uplift and depression; (4) east-west trends to convection patterns in the mantle; (5) bands of crustal materials of similar metamorphic grade; (6) variations in the depth of the Curie isotherm; and (7) the data processing techniques used to overcome the absence of tie lines and orbital path of MAGSAT.

M.G.

N82-24591*# Technicolor Graphic Services, Inc., Sioux Falls, S. Dak.

AN INVESTIGATION OF MAGSAT AND COMPLEMENTARY DATA EMPHASIZING PRECAMBRIAN SHIELDS AND ADJACENT AREAS OF WEST AFRICA AND SOUTH AMERICA Quarterly Report, 1 Jan. - 31 Mar. 1982

D. A. HASTINGS, Principal Investigator 31 Mar. 1982 14 p
Sponsored by NASA ERTS
(Contract DI-14-08-0001-21249)
(E82-10318; NASA-CR-168896; NAS 1.26:168896) Avail: NTIS HC A02/MF A01 CSCL 08B

The problems associated with the use of an interactive magnetic modeling program are reported and a publication summarizing the MAGSAT anomaly results for Africa and the possible tectonic associations of these anomalies is provided. An overview of the MAGSAT scalar anomaly map for Africa suggested a correlation of MAGSAT anomalies with major crustal blocks of uplift or depression and different degrees of regional metamorphism. The strongest MAGSAT anomalies in Africa are closely correlated spatially with major tectonic features. Results indicate that the Bangui anomaly may be caused by a central old Precambrian shield, flanked to the north and south by two relatively young sedimentary basins.

M.G.

N82-24592*# Texas Univ. at El Paso. Dept. of Geological Sciences.

THE CRUSTAL STRUCTURE AND TECTONICS OF SOUTH AMERICA Quarterly Report, 1 Jul. - 30 Sep. 1981

G. R. KELLER and E. G. LIDIAK, Principal Investigators 30 Sep. 1981 4 p refs ERTS
(Contract NAS5-26326)
(E82-10319; NASA-CR-168898; NAS 1.26:168898) Avail: NTIS HC A02/MF A01 CSCL 08G

A preliminary crustal structure map and a bibliography of crustal and upper mantle studies for South America are given. Work on the surface wave analysis and tectonic characterizations continues.

M.G.

N82-24593*# Texas Univ. at El Paso. Dept. of Geological Sciences.

GEOTECTONICS OF SOUTH AMERICA Quarterly Report, 1 Oct. 1981 - 31 Mar. 1982

G. R. KELLER and E. G. LIDIAK, Principal Investigators 31 Mar. 1982 36 p refs ERTS
(Contract NAS5-26326)
(E82-10320; NASA-CR-168899; NAS 1.26:168899) Avail: NTIS HC A03/MF A01 CSCL 08G

Preliminary satellite scalar magnetic anomaly data (MAGSAT) reduced to vertical polarization and long wavelength-pass filtered free air gravity anomaly data of South and Central America are compared to major tectonic features. In addition, a geotectonic overview of South America is presented.

M.G.

N82-24599*# Paris VI Univ. (France).

MAGSAT ANOMALY MAP AND CONTINENTAL DRIFT Progress Report

J. L. LEMOUEL, Principal Investigator, A. GALDEANO, and J. DUCRUIX 1 Dec. 1981 5 p refs Sponsored by NASA ERTS
(E82-10326; NASA-CR-168905; NAS 1.26:168905) Avail: NTIS HC A02/MF A01 CSCL 08G

Anomaly maps of high quality are needed to display unambiguously the so called long wave length anomalies. The anomalies were analyzed in terms of continental drift and the nature of their sources is discussed. The map presented confirms the thinness of the oceanic magnetized layer. Continental magnetic anomalies are characterized by elongated structures generally of east-west trend. Paleomagnetic reconstruction shows that the anomalies found in India, Australia, and Antarctic exhibit a fair consistency with the African anomalies. It is also shown that anomalies are locked under the continents and have a fixed geometry.

T.M.

N82-24603*# Miami Univ., Fla. School of Marine and Atmospheric Science.

INVESTIGATIONS OF MEDIUM WAVELENGTH MAGNETIC ANOMALIES IN THE EASTERN PACIFIC USING MAGSAT DATA Interim Report, Oct. - Dec. 1981

C. G. A. HARRISON, Principal Investigator Feb. 1982 3 p ERTS
(E82-10330; NASA-CR-168909; NAS 1.26:168909) Avail: NTIS HC A02/MF A01 CSCL 08G

Efforts concerning spherical harmonic modeling of the Earth's magnetic field and the use of such models in removing core produced magnetic fields from magnetic fields of crustal origin are discussed. Results indicate that the terms of a spherical harmonic expansion do not uniquely determine a given wavelength of signal as the terms in a Fourier series do. Addition of terms of higher degree and order to a spherical harmonic expansion tend to fine tune the amplitude of the terms of lower degree and order. As a result, removal of such a model from a regional data set will not remove long wavelengths completely.

M.G.

N82-25601*# Purdue Univ., Lafayette, Ind. Dept. of Geosciences.
AEROMAGNETIC AND SATELLITE MAGNETIC ANOMALLY MAPPING Quarterly Progress Report, Jan. - Mar. 1982
L. W. BRAILE, W. J. HINZE, and R. R. B. VONFRESE, Principal Investigators 31 Mar. 1982 8 p Sponsored by NASA ERTS
(E82-10339; NASA-CR-168958; NAS 1.26:168958) Avail: NTIS HC A02/MF A01 CSCL 05B

Efforts to process 2 deg-averaged MAGSAT data for a radially polarized map of Africa and western Europe and investigator B data tapes were initiated M.G.

N82-25604*# Colorado Univ., Boulder. Dept. of Astrogeophysics.
INVESTIGATION OF GEOMAGNETIC FIELD FORECASTING AND FLUID DYNAMICS OF THE CORE Quarterly Status Technical Progress Report, 1 Oct. - 31 Dec. 1981
E. R. BENTON, Principal Investigator 1 Jan. 1982 3 p ERTS
(Contract NAS5-25957)
(E82-10342; NASA-CR-168959; NAS 1.26:168959; QSTPR-8)
Avail: NTIS HC A02/MF A01 CSCL 08G

Accomplishments to date were summarized in three parts submitted for publication. Goddard models and MAGSAT data were used heavily in the investigation which address: (1) the sensitivity of selected geomagnetic properties to truncation level of spherical harmonic expansions; (2) the pole strength of the Earth from MAGSAT, and magnetic determination of the core radius; and (3) frozen flux upper limits to the MAGSAT geomagnetic coefficients and relative multipole indices for Earth. A.R.H.

N82-25748# Woods Hole Oceanographic Institution, Mass. Dept. of Geology and Geophysics.
COMPUTER-PROCESSED GEOPHYSICAL ATLAS OF DIGITAL DATA FOR THE EAST COAST MARGIN OF THE UNITED STATES FROM SURFACE AND SPACECRAFT DATA
C. BOWIN, J. MILLIGAN, and K. DUNKLE Dec. 1981 36 p refs Sponsored in part by Joint Oceanograph Inst., Inc.
(Contract N00014-82-C-0019)
(AD-A111388; WHOI-81-104) Avail: NTIS HC A03/MF A01 CSCL 08J

This atlas comprises maps for the East Coast margin of the United States of free-air gravity anomaly, geoid anomaly, regional geoid anomaly, residual geoid anomaly, magnetic crustal anomaly, and bathymetry. Data from surface measurements, GEOS-III and MAGSAT Satellites, GEM-9 spherical harmonic coefficients, and SYNBAPS bathymetry profiling systems were utilized. Estimated error maps for the geoid data are not included because for the marine areas, these data are uniformly of very low error. The data are presented in three sets of maps of northern, central, and southern portions of the margin. Author (GRA)

N82-26268# Defense Mapping Agency Hydrographic and Topographic Center, Washington, D.C.
A COMPARISON OF POLE POSITIONS DERIVED FROM GPS SATELLITE AND NAVY NAVIGATION SATELLITE OBSERVATIONS
W. H. WOODEN, II 6 Jan. 1982 18 p refs Presented at the 3rd Intern. Geodetic Symp. on Satellite Doppler Positioning
(AD-A110765) Avail: NTIS HC A02/MF A01 CSCL 17G

The observation of the motion of the Earth's spin axis with respect to the crust has been done continuously since the latter part of 1899 by the International Service. With the advent of new technologies, new determinations of polar motion have been possible. Doppler tracking of the Navy Navigation Satellites has provided estimates of the polar motion on a permanent basis since 1969. Currently, these estimates are done at the Defense Mapping Agency and are distributed to several agencies including the Bureau International de l'Heure (BIH), which has the responsibility of centralizing polar motion data. The NAVSTAR Global Positioning System (GPS) is a new navigation satellite system which will eventually replace the existing Navy Navigation Satellite System. As a byproduct of the orbit estimation process for the GPS satellites, values for the position of the pole are determined. In this paper the two different methods for computing the pole's position from satellite observations are described. The most recent results from each method are compared to each other and to the standard BIH values. Author (GRA)

N82-26746*# Washington Univ., St. Louis, Mo. Center for the Space Sciences.
STRUCTURE OF THE SAINT FRANCOIS MOUNTAINS AND SURROUNDING LEAD BELT, S.E. MISSOURI: INFERENCE FROM THERMAL IR AND OTHER DATA SETS Quarterly Report, 1 Nov. 1981 - 30 Apr. 1982
R. E. ARVIDSON, Principal Investigator 11 May 1982 65 p refs Original contains color imagery. Original imagery may be purchased from NASA Goddard Space Flight Center, (code 601), Greenbelt, Md. 20770. Domestic users send orders to Attn: National Space Science Data Center ; non-domestic users send orders to Attn: World Data Center A for Rockets and Satellites. . HCMM
(Contract NAS5-26533)
(E82-10350; NASA-CR-168969; NAS 1.26:168969) Avail: NTIS HC A04/MF A01 CSCL 08G

Progress in the preparation of manuscripts on the discovery of a Precambrian rift running NW-SE through Missouri as seen in free air and Bouguer gravity anomalies and in HCMM data, and on digital image processing of potential field and topographic data on the rift is reported. Copies of the papers are attached. Contrast-enhanced HCMM images that have been transformed to Mercator projections are presented. Shaded relief map overlays of thermal and apparent thermal inertia images used as part of a masers thesis examining correlations between HCMM data products, linears, and geologic units are presented. Progress in examination of the difference in information content of daytime infrared, night time infrared, albedo, and thermal inertia images and their application to he identification of linears not directly controlled by topography is repored. Thermal infrared and albedo data were coded as hue, saturation and brightness values to generate a color display, which is included. J.D.

N82-26915# California Univ., Livermore. Lawrence Livermore Lab.
SEISMIC AND GEODETIC STUDIES OF THE IMPERIAL VALLEY, CALIFORNIA Final Technical Report
D. D. JACKSON (UCLA) 1 May 1981 50 p refs
(Contract W-7405-ENG-48)
(DE82-001686; UCRL-15382) Avail: NTIS HC A03/MF A01

Patterns of gravitational and thermal anomalies, strike slip faulting, volcanism in the Imperial Valley were investigated. These patterns suggest that the continental crust may still be spreading. In recent years, the United States Geological Survey and Caltech have added new seismic stations into a dense network in the Imperial Valley to study in detail the relationship between geothermal areas and earthquakes, and to understand the tectonic processes taking place there. The following areas were examined: (1) crustal structure data on P wave arrival times of local earthquakes; (2) leveling data for evidence of tectonic subsidence or uplift; and (3) correlations between seismicity, seismic velocity, geodetic motion, geothermal activity, and local geology. DOE

N82-27882# National Oceanic and Atmospheric Administration, Boulder, Colo. Wave Propagation Lab.
FIELD MEASUREMENTS IN SUPPORT OF DISPERSION MODELING IN COMPLEX TERRAIN (1980) Annual Report
W. EBERHARD Jul. 1981 26 p refs
(PB82-148644; NOAA-81102005) Avail: NTIS HC A03/MF A01 CSCL 13B

The EPA is engaged in a concerted effort to develop models for prediction of air quality in complex terrain. Remote sensors and an instrumented aircraft from the Wave Propagation Laboratory and other elements of NOAA's Environmental Research Laboratory are participating with EPA in a series of field experiments that are necessary for development and validation of such models. A calibrated particulate mapping lidar with multiwavelength capability is the principal remote sensor. NOAA's accomplishments during the first year (February 1980 - January 1981) under the EPA-NOAA Interagency Agreement for Energy and Environment are participation by lidar and other sensors in EPA's Small Hill Impaction Study No. 1 studying plume impingement or elevated terrain; preliminary experiment by instrumented aircraft on power plant plumes near Farmington, New Mexico; lidar participation in DOE's 1980 ASCOT experiment investigating nocturnal drainage flows in mountainous terrain; and improvements to the lidar for plume mapping applications. GRA

N82-27900# Ohio State Univ., Columbus. Dept. of Geodetic Science and Surveying.
THE EARTH'S GRAVITY FIELD TO DEGREE AND ORDER 180 USING SEASAT ALTIMETER DATA, TERRESTRIAL GRAVITY DATA AND OTHER DATA
R. H. RAPP Hanscom AFB, Mass. AFGL Dec. 1981 58 p refs
(Contract F19628-79-C-0027; AF PROJ. 2309)
(AD-A113098; DGS-322; SCIENTIFIC-12; AFGL-TR-82-0019)
Avail: NTIS HCA04/MF A01 CSCL 08N

The spherical harmonic expansion of the Earth's gravitational field has been obtained to degree 180 by combining several sources of data. The first data set was an a priori set of potential coefficients to degree 36 based on number of recent solutions including a substantial of resonance terms. A second data set was a 1 x 1 deg anomaly field derived from the SEASAT data set, while the third data set was an updated 1 x 1 deg terrestrial field. The last two fields were combined into one set containing 56761 1 x 1 deg values. The remaining values were computed from the a priori potential coefficients. A rigorous combination solution was not carried out. Instead all anomalies were weighted in such a way that the normal equations were diagonal. The results of the adjustment were 64800 1 x 1 deg anomalies that were expanded into spherical harmonics using the optimum quadrature procedure developed by Colombo. Accuracy estimates for each coefficient were obtained considering noise propagation and sampling error caused by the finite block size in which the anomalies are given. The percentage error of the solution reaches 100% near degree 120. The coefficients and their accuracy to degree 50 are listed in an appendix. GRA

04

GEOLOGY AND MINERAL RESOURCES

Includes mineral deposits, petroleum deposits, spectral properties of rocks, geological exploration, and lithology.

A82-22574
EXTRAGALACTIC COSMIC RAYS, THEIR SOURCES AND SPECTRUM
R. SILBERBERG and M. M. SHAPIRO (U.S. Navy, Naval Research Laboratory, Washington, DC) In: International Cosmic Ray Conference, 17th, Paris, France, July 13-25, 1981, Conference Papers. Volume 2. Gif-sur-Yvette, Essonne, France, Commissariat a l'Energie Atomique, 1981, p. 356-359. refs

Studies of air showers, particularly by Watson et al. (1980), have shown that cosmic rays at energies above 10 to the 19th eV are likely to be extragalactic in origin. The energy density above 10 to the 19th eV is 3 x 10 to the -8th eV/cu cm, and the exponent of the integral energy spectrum is -1.4 plus or minus 0.1. For estimating the energy density of relativistic protons (E greater than GeV) in metagalactic space an energy input rate W sub p into protons similar to that for relativistic electrons (W sub e) in active galactic nuclei is assumed. For cosmic rays in the supercluster, W sub p is found to be 10 to the -4th (plus or minus 1) eV/cu cm. This estimate for W sub p is supported by the following internal consistency argument: this spectrum at 10 to the 9th eV, when extended with an exponent -1.4, smoothly joins the extragalactic spectrum at 10 to the 19th eV, having a similar spectral slope. (The exponent -1.4 also is that of galactic cosmic rays when corrected for rigidity-dependent leakage from the Galaxy.) (Author)

A82-22604
THE APPROXIMATE 1 GEV SOLAR COSMIC RAYS IN THE FORBUSH-EFFECT OF FEBRUARY 15, 1978
G. P. LIUBIMOV, V. I. TULUPOV, and E. A. CHUCHKOV (Moskovskii Gosudarstvennyi Universitet, Moscow, USSR) In: International Cosmic Ray Conference, 17th, Paris, France, July 13-25, 1981, Conference Papers. Volume 3. Gif-sur-Yvette, Essonne, France, Commissariat a l'Energie Atomique, 1981, p. 121-123. refs

Differences in the behavior of the galactic cosmic-ray intensity are studied using the data from the Alert and Deep River neutron monitors from February 14 to 17, 1978. The behavior of the intensity at Alert and Deep River is normalized to the initial stage of February 14, before the Forbush effect, and the additional differential flux reaches 15 percent. The observed anomalous differences are explained by an additional particle flux of about 1 GeV of solar origin in the Forbush effect. D.L.G.

A82-22607* Maryland Univ., College Park.
OBSERVATIONS OF THE IONIZATION STATES OF ENERGETIC PARTICLES ACCELERATED IN SOLAR FLARES
G. GLOECKLER, H. WEISS, F. M. IPAVICH (Maryland, University, College Park, MD), D. HOVESTADT, B. KLECKER, M. SCHOLER (Max-Planck-Institut fuer extraterrestrische Physik, Garching, West Germany), L. A. FISK (New Hampshire, University, Durham, NH), C. Y. FAN (Arizona, University, Tucson, AZ), and J. J. OGALLAGHER (Chicago, University, Chicago, IL) In: International Cosmic Ray Conference, 17th, Paris, France, July 13-25, 1981, Conference Papers. Volume 3. Gif-sur-Yvette, Essonne, France, Commissariat a l'Energie Atomique, 1981, p. 136-139. Bundesministerium fuer Forschung und Technologie refs
(Contract NAS5-20062; BMFT-RV14-B8/74;
BMFT-01-OI-017-ZA/WF/WRK-1754 ; NGR-21-002-224;
NGR-21-002-316)

The ionization states and spectra of 0.3 to 2.4 MeV/nuc He, C, O and Fe are measured in a survey of ten solar flare particle events. He(plus) is found to be present in all events, which indicates the common presence of energetic He(plus) in the source material from which solar particles are accelerated. The distribution functions of He(plus), He(plus plus) and heavier elements are represented by simple exponentials of the particle speed times its rigidity to a power n, where n is between 0 and 1, and equal e-folding values. Results are consistent with a model where ions are accelerated in the corona by multi-dimensional shocks out of a population taken from both hot and cold coronal regions. D.L.G.

A82-22609
A TENTATIVE ORDERING OF ALL AVAILABLE SOLAR ENERGETIC PARTICLES ABUNDANCE OBSERVATIONS. I - THE MASS UNBIASED BASELINE. II - DISCUSSION AND COMPARISON WITH CORONAL ABUNDANCES
J. P. MEYER (Commissariat a l'Energie Atomique, Centre d'Etudes Nucleaires de Saclay, Gif-sur-Yvette, Essonne, France) In: International Cosmic Ray Conference, 17th, Paris, France, July 13-25, 1981, Conference Papers. Volume 3. Gif-sur-Yvette, Essonne, France, Commissariat a l'Energie Atomique, 1981, p. 145-152. refs

A82-22613* Maryland Univ., College Park.
ON THE ANTICORRELATION BETWEEN THE HE/3//HE/4/ RATIO AND PROTON INTENSITY IN HE/3/ RICH FLARES
M. E. PESSES (Maryland, University, College Park, MD) In: International Cosmic Ray Conference, 17th, Paris, France, July 13-25, 1981, Conference Papers. Volume 3. Gif-sur-Yvette, Essonne, France, Commissariat a l'Energie Atomique, 1981, p. 171-174. refs
(Contract NAS5-20062)

A model is presented to explain the observed anticorrelation between the size of the He(3)/He(4) abundance ratio at not less than about 10 MeV/nuc and the peak intensity of about 10 MeV protons in the He(3) rich events. The anticorrelation is shown to be a natural consequence of producing abundance enhancement by a two step acceleration process, where He(3) is preaccelerated with respect to He(4) prior to the main ion acceleration phase, which has an effective injection cutoff varying from flare to flare. D.L.G.

A82-30304

REGIONAL GEOLOGICAL, TECTONIC AND GEOPHYSICAL FEATURES OF NORDLAND, NORWAY

R. H. GABRIELSEN, I. B. RAMBERG (Oslo, Universitetet, Oslo, Norway), M. B. E. MORK (Universitets Minelarogisk Geologiske Museum, Oslo, Norway), and B. TVEITEN (BP Petroleum Development of Norway, A/S, Stavanger, Norway) Earth Evolution Sciences, vol. 1, Mar. 1981, p. 14-26. Research supported by the Norges Almenvitenskapelige Forskningsrad, Committee for Geophysics and Geology and Norges Teknisk-Naturvitenskapelige Forskningsrad refs
(Contract NTNF PROJECT 18108075)

Foliation and lineament patterns from Landsat imagery, gravity and magnetic data mapping of Nordland, Norway shows a high degree of correlation with known tectonostratigraphic units and suggests other, previously unidentified tectonic units. Attention is given to regionally important lineament systems, one striking approximately ENE-WSW, and a younger one N-S. It is indicated by the large-scale residual gravity lows along the Norway-Sweden border, which are associated with basement domes, and by magnetic data and lineament patterns, that the eastern basement windows represent large-scale culminations. By contrast, the western domes represent smaller, perhaps granitic cores of recumbent fold nappes. A positive correlation is found between the seismotectonic coastal zones of Nordland and the area's Bouguer gravity anomally maximum gradient. O.C.

A82-30305

SATELLITE IMAGE INTERPRETATION OF THE EASTERN CALEDONIAN PART OF THE BLUE ROAD GEOTRAVERSE AND ITS GEOLOGICAL IMPLICATIONS /NORDLAND, VASTERBOTTEN, SCANDINAVIA/

R. GREILING (Mainz, Universitaet, Mainz, West Germany) Earth Evolution Sciences, vol. 1, Mar. 1981, p. 27-30. refs

An 80% coincidence of known geological features with the lineaments interpreted in the satellite image presented by Ehrenborg (1977) is found through the quantitative study of Landsat interpretations for the case of a Precambrian area in southeastern Sweden. Because of its probable connection with the quaternary glacial erosion, the distribution of joints and faults may be interpreted as (1) E-W-striking lineaments locally correlated with faults affecting Caledonian low-angle thrusts and folliations, (2) NW-SE lineaments locally correlated with leucocratic dikes, and (3) NNW-SSW lineaments generally parallel to the present coast which, by contrast to the region farther west, is of minor importance. O.C.

A82-30786* National Aeronautics and Space Administration. Goddard Space Flight Center, Greenbelt, Md.

MAGSAT SCALAR ANOMALY DISTRIBUTION - THE GLOBAL PERSPECTIVE

H. FREY (NASA, Goddard Space Flight Center, Geophysics Branch, Greenbelt, MD) Geophysical Research Letters, vol. 9, Apr. 1982, p. 277-280. refs

It is established that geographic coincidences exist between high-altitude Magsat scalar anomalies and major geologic and tectonic structures, with oceanic abyssal plains overlain by negative anomalies agreeing well in spatial extent and position and submarine platforms lying beneath positive scalar anomalies. In addition, geographic coincidence is found in the continents between many high-latitude positive anomalies and shields and cratons in North America, Eurasia and Australia. While these correlations are qualitative, they serve to identify regions for detailed study. The global distribution of anomalies provides a basis for comparative study which will be enhanced when reduced-to-pole versions of the Magsat data become available. O.C.

A82-32442* Jet Propulsion Lab., California Inst. of Tech., Pasadena.

SPECTROSCOPIC REMOTE SENSING FOR GEOLOGICAL APPLICATIONS

A. F. H. GOETZ (California Institute of Technology, Jet Propulsion Laboratory, Pasadena, CA) In: Imaging spectroscopy; Proceedings of the Seminar, Los Angeles, CA, February 10, 11, 1981. Bellingham, WA, SPIE - The International Society for Optical Engineering, 1981, p. 17-21. refs
(Contract NAS7-100)

Remote sensing is being used with increasing frequency in the development of geologic maps and in the exploration process. Spectral data from airborne and spaceborne multispectral scanners provide information on rock type and vegetation stress, important in geologic applications. Emphasis is now being placed on direct identification of materials rather than discrimination among geologic units. To do this, higher spectral resolution systems with wider spectral coverage than currently available are required. Imaging spectroscopy in the 0.4 - 14 microns region appears to be the answer. (Author)

A82-32898

POSSIBLE FAULT DETECTION IN COTTONBALL BASIN, CALIFORNIA AN APPLICATION OF RADAR REMOTE SENSING

G. L. BERLIN, G. G. SCHABER, and K. C. HORSTMAN (U.S. Geological Survey, Flagstaff, AZ) Remote Sensing of Environment, vol. 10, Aug. 1980, p. 33-42. refs

An analysis of a 3-cm wavelength radar image of Cottonball Basin in Death Valley National Monument has revealed the existence of two suspect fault traces in evaporite deposits that are less than 2000-yr old. The traces are well defined on the image because the radar system was able to differentiate surface roughness variations at the centimeter scale. The features are not recognizable on data sets recorded ,in the visible and near-infrared spectral bands. Results indicate the potential of radar images as a tool to help locate recent breaks along a fault when the disturbed zone is represented by a somewhat rougher surface than is found in immediately adjacent areas. (Author)

A82-33402

AEROGEOPHYSICAL METHODS OF FINDING URANIUM DEPOSITS [AEROGEOFIZICHESKIE METODY PROGNOZIROVANIIA MESTOROZHDENII URANA]

A. I. KRASNOV, E. B. VYSOKOOSTROVSKAIA, V. A. SMIRNOV, IU. B. NOVIKOV, E. I. ZUBOV, G. B. MUKAREVA, L. V. DIORDIENKO, and V. G. ZAITSEV Moscow, Atomizdat, 1980. 132 p. In Russian. refs

Geophysical prospecting for uranium with the aid of a large-scale, comprehensive gamma-spectrometric, aeromagnetic, and aeroelectric survey is considered. The development in the USSR and in other countries of aerogeophysical prospecting for uranium is surveyed. Features of geophysical fields that are characteristic of regions containing endogenous and exogenous deposits of uranium are analyzed. Direct and indirect radiogeochemical, magnetogeophysical, and electrogeophysical indicators of uranium-bearing structures are described. The methods described here rely on a comprehensive interpretation of aerogeophysical, geological, and other types of data. C.R.

A82-34721* National Aeronautics and Space Administration. Goddard Space Flight Center, Greenbelt, Md.
LANDSAT IN THE SEARCH FOR APPALACHIAN HYDROCARBONS
H. W. BLODGET (NASA, Goddard Space Flight Center, Eastern Regional Remote Sensing Applications Center, Greenbelt, MD) In: American Society of Photogrammetry, Annual Meeting, 47th, Washington, DC, February 22-27, 1981, ASP Technical Papers. Falls Church, VA, American Society of Photogrammetry, 1981, p. 259-262. refs

A study has been conducted to determine the applicability of enhanced Landsat imagery for oil and gas exploration in Appalachia. Attention was given to the feasibility to employ lineaments identified on Landsat imagery as a tool in petroleum exploration. Lineaments, as defined in this connection, are linear or sublinear traces seen on Landsat imagery. They frequently reflect subsurface geological structures. The investigation was conducted in two stages. The first was designed to identify the specific Landsat imagery enhancement best suited for displaying lineaments. The second stage consisted of plotting lineaments and conducting an analysis of the lineament trends with regard to both local geological structure and regional tectonics. A close relationship was observed between lineaments identified on Landsat imagery and known oil and gas reservoirs. This result suggests that lineaments can be related to the structural control of oil and gas reservoirs throughout Appalachia. G.R.

A82-36298* Lunar and Planetary Inst., Houston, Tex.
INFLUENCE OF CO2 ON MELTING OF MODEL GRANULITE FACIES ASSEMBLAGES - A MODEL FOR THE GENESIS OF CHARNOCKITES
R. F. WENDLANDT (Lunar and Planetary Institute, Houston, TX) American Mineralogist, vol. 66, 1981, 1164-1174. refs
(Contract NASW-3389)

A model is described for the melting of a simple granulite assemblage, in the presence of CO2-rich fluid phases, which can occur between 750 and 1000 C at crustal pressures and is therefore within the range estimated for such regional metamorphism as that of the Adirondacks. For melting which occurs at about 750 C in the presence of both H2O and CO2, pressures corresponding to the deep crust are required to generate a melt enriched in pyroxene and feldspar components, while melting the precense of pure CO2 at about 1000 C generates analogous melt compositions at lower pressures. These experimental reactions are in keeping with observations constraining charnockite occurrences: (1) pressure and temperature constraints; (2) mineralogical constraints; and (3) constraints on the compositions of volatiles associated with peak conditions of charnockite formation. O.C.

A82-37198
SIGNIFICANCE OF TECTONICS IN LINEAR FEATURE DETECTION AND INTERPRETATION ON SATELLITE IMAGES
F. CSILLAG (Eotvos Lorand Tudomanyegyetem, Budapest, Hungary) Remote Sensing of Environment, vol. 12, July 1982, p. 235-245. refs

There are two main concepts of linear feature evaluation based on satellite images. One puts emphasis on finding equivalence between the image and the field data, in the other, the basic aim is to correlate them after their more or less separate interpretation. A comparative study of the two methods has been carried out on a test field in Southwest Hungary using several kinds of geological and geophysical data as reference. Combining the statistical and deterministic approach a block-faulting mechanism can be recognized and described with ENE-WSW main axis. Correlation of satellite and reference data proved the tectonic difference of the northern and southern parts of the test field. This led to the conclusion that one can derive textural information on tectonics from a Landsat image concerning especially short lines. This implies that not only the present surface expression of faults and tectonics is detectable but the determination of the latest tectonically active surface is also possible. (Author)

N82-22624*# Bureau de Recherches Geologiques et Minieres, Minieres, Paris (France).
SPATIAL THERMAL RADIOMETRY CONTRIBUTION TO THE MASSIF ARMORICAIN AND THE MASSIF CENTRAL FRANCE LITHO-STRUCTURAL STUDY Final Report
J. Y. SCANVIC, Principal Investigator Nov. 1980 85 p refs
Sponsored by NASA Original contains imagery. Original imagery may be purchased from NASA Goddard Space Flight Center, (code 601), Greenbelt, Md. 20771. Domestic users send orders to 'Attn: National Space Science Data Center'; nondomestic users send orders to 'Attn: World Data Center A for Rockets and Satellites'. HCMM
(E82-10190; NASA-CR-168618; NAS 1.26:168618; REPT-80-SGN-848-GEO-REPT-3) Avail: NTIS HC A05/MF A01 CSCL 08G

Thermal zones delimited on HCMM images, by visual interpretation only, were correlated with geological units and carbonated rocks, granitic, and volcanic rocks were individualized rock signature is evolutive parameter and some distinctions were made by addition of day, night and seasonal thermal image interpretation. This analysis also demonstrated that forest cover does not mask the underlying rocks thermal signature. Thermal linears are associated with known tectonics but the observed thermal variations from day to night and from one to another represent a promising concept to be studied in function of neotectonics and hydrogeology. The thermal anomalies discovered represent a potential interest which is to be evaluated. Significant results were obtained in the Mont Dore area and additional geological targets were defined in the Paris Basin and the Montmarault granite. Author

N82-22636# Natural Environment Research Council, London (England).
OVERSEAS GEOLOGY AND MINERAL RESOURCES NUMBER 56: A GEOLOGICAL INTERPRETATION OF LANDSAT IMAGERY AND AIR PHOTOGRAPHY OF BOTSWANA
D. I. J. MALLICK, F. HABGOOD, and A. C. SKINNER 1981 41 p refs Original contains color maps Original contains color illustrations
(OGMR-56; ISBN-0-11-884138-6) Avail: NTIS HC A03/MF A01; HMSO 5

A 1:1 million geological map compiled from LANDSAT and air photography of Botswana and border areas is presented. The distribution of 22 geological units of Karoo and Precambrian age is shown together with the post-Karoo deposits, differentiated into 7 units, based on geomorphological criteria. The data help distinguish volcanics of the Kanye Group from those of the Ventersdorp Group, and the Transvaal Supergroup from those of the Waterberg Group at localities far from their better exposed outcrop areas in the southeast of the country. Eolian, lacustrine and alluvial components of Kalahari desert superficial deposits are differentiated. The fracture and lineament pattern is only partly evident from the photographs. Author (ESA)

N82-23569*# Texas Univ. at El Paso.
CHARACTERIZATION OF THE STRUCTURE AND TECTONIC OF SOUTH AMERICA Quarterly Report, 1 Mar. - 30 Jun. 1981
G. R. KELLER and E. G. LIDIAK, Principal Investigators 30 Jun. 1981 4 p ERTS
(Contract NAS5-26326)
(E82-10196; NASA-CR-168623; NAS 1.26:168623) Avail: NTIS HC A02/MF A01 CSCL 08G

Geologic studies of the South American plate were undertaken. The Guayana shield is reasonably well studied, and although data are sparce, the central Brazilian shield appears similar. Both the Amazon and Parnaiba basins seem to be related to an aulocogen structure. The collection of crustal structure information and the generation of measurement of surface wave dispersion in the shield areascontinues. Long period seismograms are digitized and analyzed. Exisiting crusted and upper mantle studies were indexed. Both MAGSAT scaler and vector magnetic anomaly data were used with regional gravity anomaly data to investigate the regional tectonic features of the South American plate. E.A.K.

N82-23621# Western Geophysical Co. of America, Houston, Tex. Aero Service Div.
AIRBORNE GAMMA-RAY SPECTROMETER AND MAGNETOMETER SURVEY. ROSEAU QUADRANGLE, MINNESOTA, VOLUME 1 Final Report
May 1981 98 p refs Prepared for Bendix Field Engineering Corp., Grand Junction, Colo. 2 Vol.
(Contract DE-AC13-76GJ-01664)
(DE82-001031; GJBX-329-81-VOL-1) Avail: NTIS HC A05/MF A01

An airborne high sensitivity gamma ray spectrometer and magnetometer survey was conducted over the Roseau map area in Minnesota. Radiometric multiple parameter, magnetic, and ancillary parameter stacked profiles are discussed. Hostograms, anomaly, and computer printer maps are also discussed. Stratigraphy is described. Geochemical, printer contour, and anomaly map analyses are provided. N.W.

N82-23623# Western Geophysical Co. of America, Houston, Tex. Aero Service Div.
AIRBORNE GAMMA-RAY SPECTROMETER AND MAGNETOMETER SURVEY. BARROW QUADRANGLE, ALASKA, VOLUME 1 Final Report
Mar. 1981 100 p refs 2 Vol.
(Contract DE-AC13-76GJ-01664)
(DE82-000334; GJBX-295-81-VOL-1) Avail: NTIS HC A05/MF A01

From July to August 1980, an airborne high sensitivity gamma ray spectrometer and magnetometer survey over eleven 30 by 10 and one 40 by 10 quadrangles of the Alaskan North Slope were conducted. The results obtained over the Barrow area are presented in four different forms: on magnetic tape; on microfiche; in graphic form as profiles and histograms; and in map form as anomaly maps, flight path maps, and computer printer maps. Complete data listings of both the reduced single record and the reduced averaged record data are given. DOE

N82-23624# Western Geophysical Co. of America, Houston, Tex. Aero Service Div.
AIRBORNE GAMMA-RAY SPECTROMETER AND MAGNETOMETER SURVEY. WAINWRIGHT QUADRANGLE, ALASKA, VOLUME 2 Final Report
Mar. 1981 125 p 2 Vol.
(Contract DE-AC13-76GJ-01664)
(DE82-000341; GJBX-296-81-VOL-2) Avail: NTIS HC A06/MF A01

The flight path map, multiparameter profiles, histograms, and anomaly maps for uranium, thorium, potassium, uranium/potassium, uranium/thorium, and thorium/potassium are given for the survey conducted in the Wainwright area, Alaska. DOE

N82-23625# Western Geophysical Co. of America, Houston, Tex. Aero Service Div.
AIRBORNE GAMMA-RAY SPECTROMETER AND MAGNETOMETER SURVEY, KENORA QUADRANGLE, MINNESOTA, VOLUME 1 Final Report
Mar. 1981 87 p refs
(Contract DE-AC13-76GJ-01664)
(DE82-001029; GJBX-328-81-VOL-1) Avail: NTIS HC A05/MF A01

During the months of June through October, 1980, Aero Service Division Western Geophysical Company of America conducted an airborne high sensitivity gamma-ray spectrometer and magnetometer survey over eleven (11) 20 x 10 NTMS quadrangles located in the states of Minnesota and Wisconsin and seven (7) 20 x 10 NTMS quadrangles in North and South Dakota. The results obtained over the Kenora map area of Minnesota are discussed. The final data are presented in four different forms: on magnetic tape; on microfiche; in graphic form as profiles and histograms: and in map form as anomaly maps, flight path maps, and computer printer maps. DOE

N82-23626# Western Geophysical Co. of America, Houston, Tex. Aero Service Div.
AIRBORNE GAMMA-RAY SPECTROMETER AND MAGNETOMETER SURVEY. MEADE RIVER QUADRANGLE, ALASKA, VOLUME 2 Final Report
Feb. 1981 173 p
(Contract DE-AC13-76GJ-01664)
(DE82-000340; GJBX-297-81-VOL-2) Avail: NTIS HC A08/MF A01

The flight path map, multiparameter profiles, histograms, and anomaly maps for uranium, thorium, potassium are given for the Beechey point area, Alaska. DOE

N82-23627# Western Geophysical Co. of America, Houston, Tex. Aero Service Div.
AIRBORNE GAMMA-RAY SPECTROMETER AND MAGNETOMETER SURVEY. TESHEKPUK QUADRANGLE, ALASKA, VOLUME 2 Final Report
Mar. 1981 88 p
(Contract DE-AC13-76GJ-01664)
(DE82-000310; GJBX-298-81-VOL-2) Avail: NTIS HC A05/MF A01

The flight path map, multiparameter profiles, histograms, and anomally maps for uranium, thorium, potassium uranium/potassium, uranium/thorium, and thorium/potassium are given. DOE

N82-23628# Western Geophysical Co. of America, Houston, Tex. Aero Service Div.
AIRBORNE GAMMA-RAY SPECTROMETER AND MAGNETOMETER SURVEY. HARRISON BAY QUADRANGLE, ALASKA, VOLUME 2 Final Report
Feb. 1981 120 p
(Contract DE-AC13-76GJ-016664)
(DE82-000315; GJBX-299-81-VOL-2) Avail: NTIS HC A06/MF A01

The flight path map, multiparameter profiles, histograms, and anomaly maps for uranium, thorium, potassium, uranium/potassium, uranium/thorium, and thorium/potassium are given. DOE

N82-23629# Western Geophysical Co. of America, Houston, Tex. Aero Service Div.
AIRBORNE GAMMA-RAY SPECTROMETER AND MAGNETOMETER SURVEY: BEECHEY PT., QUADRANGLE, ALASKA, VOLUME 2 Final Report
Feb. 1981 76 p
(Contract DE-AC13-76GJ-01664)
(DE82-000309; GJBX-300-81-VOL-2) Avail: NTIS HC A05/MF A01

Aerial survey data are presented including the flight path map, multiparameter profiles, histograms, and anomaly maps for uranium, thorium, potassium, uranium/potassium, uranium/thorium, and thorium/potassium. DOE

N82-23630# Western Geophysical Co. of America, Houston, Tex. Aero Service Div.
AIRBORNE GAMMA-RAY SPECTROMETER AND MAGNETOMETER SURVEY. POINT LAY QUADRANGLE, ALASKA, VOLUME 2 Final Report
Feb. 1981 101 p
(Contract DE-AC13-76GJ-01664)
(DE82-000308; GJBX-301-81-VOL-2) Avail: NTIS HC A06/MF A01

Data from magnetic and spectral surveys of the Point Lay area, Alaska are given including the flight path map, multiparameter profiles, histograms, and anomaly maps for uranium, thorium, and potassium. DOE

N82-23631# Western Geophysical Co. of America, Houston, Tex. Aero Service Div.
AIRBORNE GAMMA-RAY SPECTROMETER AND MAGNETOMETER SURVEY. UTUKIK RIVER QUADRANGLE, ALASKA, VOLUME 2 Final Report
Mar. 1981 208 p
(Contract DE-AC13-76GJ-01664)
(DE82-000316; GJBX-302-81-VOL-2) Avail: NTIS HC A10/MF A01

The flight path map, multiparameter profiles, histograms, and anomaly maps for uranium, thorium, potassium, uranium/potassium, uranium/thorium, and thorium/potassium are presented. DOE

N82-23632# Western Geophysical Co. of America, Houston, Tex. Aero Service Div.
AIRBORNE GAMMA-RAY SPECTROMETER AND MAGNETOMETER SURVEY. SAGAVANIRKTOK QUADRANGLE, ALASKA, VOLUME 2 Final Report
Mar. 1981 114 p
(Contract DE-AC13-76GJ-01664)
(DE82-000311; GJBX-306-81-VOL-2) Avail: NTIS HC A06/MF A01

Magnetic and gamma ray spectral data are given including the flight path map, multiparameter profiles, histograms, and anomaly maps for uranium, thorium, potassium, uranium/potassium, uranium/thorium, and thorium/potassium. DOE

N82-23633# Western Geophysical Co. of America, Houston, Tex. Aero Service Div.
AIRBORNE GAMMA-RAY SPECTROMETER AND MAGNETOMETER SURVEY: DULUTH QUADRANGLE, MINNESOTA, VOLUME 2 Final Report
Apr. 1981 56 p
(Contract DE-AC13-76GJ-01664)
(DE82-001027; GJBX-330-81-VOL-2) Avail: NTIS HC A04/MF A01

The flight path map, multiparameter profiles, histograms, and anomaly maps for uranium, thorium, potassium, uranium/potassium, uranium/thorium, and thorium/potassium are included. DOE

N82-23634# Western Geophysical Co. of America, Houston, Tex. Aero Service Div.
AIRBORNE GAMMA-RAY SPECTROMETER AND MAGNETOMETER SURVEY. ROSEAU QUADRANGLE, MINNESOTA, VOLUME 2 Final Report
Apr. 1981 50 p 2 Vol.
(Contract DE-AC13-76GJ-01664)
(DE82-001025; GJBX-329-81-VOL-2) Avail: NTIS HC A03/MF A01

Multiparameter profiles, histograms, and flight path and anomaly maps are provided for uranium, thorium and potassium deposits. N.W.

N82-23635# Western Geophysical Co. of America, Houston, Tex. Aero Service Div.
AIRBORNE GAMMA-RAY SPECTROMETER AND MAGNETOMETER SURVEY. DEVIL'S LAKE QUADRANGLE, NORTH DAKOTA, VOLUME 1 Final Report
May 1981 98 p refs 2 Vol.
(Contract DE-AC13-76GJ-01664)
(DE82-004161; GJBX-354-81-VOL-1) Avail: NTIS HC A05/MF A01

During the months of June through October, 1980, an airborne high sensitivity gamma ray spectrometer and magnetometer survey was conducted over eleven 20 X 10 NTMS quadrangles located in the states of Minnesota and Wisconsin and seven 20 x 10 NTMS quadrangles in North and South Dakota. The results obtained over the Devil's Lake map area of North Dakota are discussed. The final data are presented in four different forms: on magnetic tape; on microfiche; in graphic form as profiles and histograms; and in map form as anomaly maps, flight path maps, and computer printer maps. DOE

N82-23636# Western Geophysical Co. of America, Houston, Tex. Aero Service Div.
AIRBORNE GAMMA-RAY SPECTROMETER AND MAGNETOMETER SURVEY. DEVIL'S LAKE QUADRANGLE, NORTH DAKOTA, VOLUME 2 Final Report
Apr. 1981 98 p 2 Vol.
(Contract DE-AC13-76GJ-01664)
(DE82-004168; GJBX-354-81-VOL-2) Avail: NTIS HC A05/MF A01

Volume 2 on airborne gamma ray spectrometer and magnetometer surveys contains the flight path map, radiometric multiple parameter stacked profiles, magnetic and ancillary parameter stacked profiles, histograms, and anomaly maps for uranium, potassium, thorium, uranium/potassium, uranium/thorium, and thorium/potassium. DOE

N82-23637# Western Geophysical Co. of America, Houston, Tex. Aero Service Div.
AIRBORNE GAMMA-RAY SPECTROMETER AND MAGNETOMETER SURVEY. BEMIDJI QUADRANGLE, MINNESOTA, VOLUME 1 Final Report
May 1981 102 p refs 2 Vol.
(Contract DE-AC13-76GJ-01664)
(DE82-001032; GJBX-331-81-VOL-1) Avail: NTIS HC A06/MF A01

The results obtained over the Bemidji map area of Minnesota by airborne high sensitivity gamma ray spectrometer and magnetometer surveys are discussed. The final data are presented in four different forms: on magnetic tape; on microfiche; in graphic form as profiles and histograms; and in map form as anomaly maps, flight path maps, and computer printer maps. Complete data listings of both the reduced single record and the reduced averaged record data are also reported. DOE

N82-23638# Western Geophysical Co. of America, Houston, Tex. Aero Service Div.
AIRBORNE GAMMA-RAY SPECTROMETER AND MAGNETOMETER SURVEY. BEMIDJI QUADRANGLE, MINNESOTA, VOLUME 2 Final Report
Mar. 1981 50 p 2 Vol.
(Contract DE-AC13-76GJ-01664)
(DE82-001026; GJBX-331-81-VOL-2) Avail: NTIS HC A03/MF A01

Aerial surveys of the Bemidji quadrangle, Minnesota are reported. In volume 2 the flight path map, multiparameter profiles, histograms and anomaly maps fo uranium, thorium, potassium, uranium/potassium, uranium/thorium and thorium/potassium are presented. DOE

N82-23639# Western Geophysical Co. of America, Houston, Tex. Aero Service Div.
AIRBORNE GAMMA-RAY SPECTROMETER AND MAGNETOMETER SURVEY. HIBBING QUADRANGLE, MINNESOTA, VOLUME 1 Final Report
Apr. 1981 111 p refs 2 Vol.
(Contract DE-AC13-76GJ-01664)
(DE82-004159; GJBX-355-81-VOL-1) Avail: NTIS HC A06/MF A01

An airborne high sensitivity gamma-ray spectrometer and magnetometer survey over eleven 20 x 10 NTMS quadrangles located in the states of Minnesota and Wisconsin and seven 20 x 10 NTMS quadrangles in North and South Dakota was conducted. The results obtained over the Hibbing, Minnesota map area are presented in four different forms: on magnetic tape; on microfiche; in graphic form as profiles and histograms; and in map form as anomaly maps, flight path maps, and computer printer maps. DOE

N82-23640# Western Geophysical Co. of America, Houston, Tex. Aero Service Div.
AIRBORNE GAMMA-RAY SPECTROMETER AND MAGNETOMETER SURVEY. HIBBING QUADRANGLE, MINNESOTA, VOLUME 2 Final Report
Apr. 1981 138 p 2 Vol.
(Contract DE-AC13-76GJ-01664)
(DE82-004165; GJBX-355-81-VOL-2) Avail: NTIS HC A07/MF A01

The flight path map, radiometric multiple-parameter stacked profiles, magnetic and ancillary parameter stacked profiles, and histograms are presented. Anomaly maps for uranium, thorium, potassium, uranium/potassium, uranium/thorium, and thorium/potassium are included. DOE

N82-23641# Western Geophysical Co. of America, Houston, Tex. Aero Service Dept.
AIRBORNE GAMMA-RAY SPECTROMETER AND MAGNETOMETER SURVEY. ABERDEEN QUADRANGLE, SOUTH DAKOTA, VOLUME 1 Final Report
Apr. 1981 99 p refs 2 Vol.
(Contract DE-AC13-76GJ-01664)
(DE82-004152; GJBX-357-81-VOL-1) Avail: NTIS HC A05/MF A01

An airborne high sensitivity gamma-ray spectrometer and magnetometer survey over eleven 20 x 10 NTMS quadrangles located in the states of Minnesota and Wisconsin and seven 20 x 10 NTMS quadrangles in North and South Dakota were conducted. The results obtained over the Aberdeen, South Dakota map area are discussed. The final data are presented in four different forms: on magnetic tape; on microfiche; in graphic form as profiles and histograms; and in map form as anomaly maps, flight path maps, and computer printer maps. DOE

N82-23642# Western Geophysical Co. of America, Houston, Tex. Aero Service Div.
AIRBORNE GAMMA-RAY SPECTROMETER AND MAGNETOMETER SURVEY. ABERDEEN QUADRANGLE, SOUTH DAKOTA, VOLUME 2 Final Report
Apr. 1981 106 p 2 Vol.
(Contract DE-AC13-76GJ-01664)
(DE82-004164; GJBX-357-81-VOL-2) Avail: NTIS HC A06/MF A01

The flight path map, radiometric and multiple-parameter stacked profiles, magnetic and ancillary parameter stacked profiles, and histograms are presented. Anomaly maps for uranium, thorium, potassium, uranium/potassium, uranium/thorium, and thorium/potassium are included. DOE

N82-23643# Western Geophysical Co. of America, Houston, Tex. Aero Service Div.
AIRBORNE GAMMA-RAY SPECTROMETER AND MAGNETOMETER SURVEY. INTERNATIONAL FALLS QUADRANGLE, MINNESOTA, VOLUME 1 Final Report
Apr. 1981 107 p refs 2 Vol.
(Contract DE-AC13-76GJ-01664)
(DE82-004151; GJBX-356-81-VOL-1) Avail: NTIS HC A06/MF A01

Results obtained using an airborne high sensitivity gamma-ray spectrometer and magnetometer to survey the International Falls map area of Minnesota are presented on magnetic tape; on microfiche; in graphic form as profiles and histograms; and in map form as anomaly maps, flight path maps, and computer printer maps. DOE

N82-23644# Western Geophysical Co. of America, Houston, Tex. Aero Service Div.
AIRBORNE GAMMA-RAY SPECTROMETER AND MAGNETOMETER SURVEY. INTERNATIONAL FALLS QUADRANGLE, MINNESOTA, VOLUME 2 Final Report
Apr. 1981 104 p 2 Vol.
(Contract DE-AC13-76GJ-01664)
(DE82-004166; GJBX-356-81-VOL-2) Avail: NTIS HC A06/MF A01

The flight path map is presented as well as radiometric multiple-parameter stacked profiles, magnetic and ancillary parameter stacked profiles, histograms, and anomaly maps for uranium, potassium, thorium, uranium/potassium, thorium/potassium, and uranium/thorium. DOE

N82-24518*# Geological Survey, Denver, Colo.
APPLICATION OF HCMM DATA TO REGIONAL GEOLOGIC ANALYSIS FOR MINERAL AND ENERGY RESOURCE EVALUATION Progress Report, Sep. - Nov. 1981
K. WATSON, Principal Investigator and S. H. MILLER Nov. 1981 4 p Sponsored by NASA HCMM
(E82-10153; NASA-CR-168538; NAS 1.26:168538) Avail: NTIS HC A02/MF A01 CSCL 08G

A more accurate algorithm was developed to compute thermal inertia from temperature difference and albedo information. The error of this algorithm is about 1/3 of the measurement error in HCMM as opposed to the current algorithm which can have an error 5 times larger. A northeast trending lineament was discovered in southewestern Arizona on enhanced thermal inertia images. Author

N82-24521*# Geological Survey, Denver, Colo. Petrophysics and Remote Sensing Branch.
APPLICATION OF HCMM DATA TO REGIONAL GEOLOGIC ANALYSIS FOR MINERAL AND ENERGY RESOURCE EVALUATION Progress Report, Mar. - May 1981
K. WATSON, Principal Investigator and S. H. MILLER May 1981 4 p Sponsored by NASA HCMM
(E82-10243; NASA-CR-168824; NAS 1.26:168824) Avail: NTIS HC A02/MF A01 CSCL 08G

The effects of topographic elevation and slope on thermal images were examined using representative field obstructions of the solar and sky radiation and a simple linearized thermal model. The forms are easily adapted for analysis of HCMM images using the DMA digital terrain data. From a representative set of field observations, it was found that flux variations with elevation can cause changes in the mean diurnal temperature gradient from -4 deg to -14 deg per km evaluated at 2000 m. Changes in the temperature difference gradient of 1 to 2 C per km are also produced which is equivalent to an effective thermal inertia gradient of 100 W s to the 1/2 power/sq m K/1 per km. Exposed bedrock on topographic ridges will appear to have a lower thermal inertia due to the additional effect. E.A.K.

N82-24579*# Massachusetts Univ., Amherst. Dept. of Geology.
THE MINERALOGY OF GLOBAL MAGNETIC ANOMALIES Progress Report, Sep. 1981 - Jan. 1982
S. E. HAGGERTY, Principal Investigator 15 Feb. 1982 31 p refs ERTS
(Contract NAS5-26414)
(E82-10305; NASA-CR-168880; NAS 1.26:168880) Avail: NTIS HC A03/MF A01 CSCL 08G

Problems with the Curie balance, which severely hindered the acquisition of data, were rectified. Chemical analytical activities are proceeding satisfactorily. The magnetization characteristics of metamorphic suites were analyzed and susceptibility data for a wide range of metamorphic and igneous rocks. These rock magnetic signatures are discussed as well as the relationships between geology, gravity and MAGSAT anomalies of West Africa. A.R.H.

N82-24594*# Iowa Univ., Iowa City. Dept. of Geology.
USE OF MAGSAT ANOMALY DATA FOR CRUSTAL STRUCTURE AND MINERAL RESOURCES IN THE US MIDCONTINENT Quarterly Report, period ending 31 Mar. 1982
R. S. CARMICHAEL, Principal Investigatoret al. 24 Mar. 1982 2 p ERTS
(Contract NAS5-26425)
(E82-10321; NASA-CR-168900; NAS 1.26:168900; QR-5) Avail: NTIS HC A02/MF A01 CSCL 08G

Personnel matters related to the processing and interpretation of MAGSAT data are reported. Efforts are being initiated to determine the crustal geology, structure, and potential economic consequences to be deduced from the satellite magnetic anomalies in conjuction with correlative data. A.R.H.

N82-24596*# Iowa Univ., Iowa City. Dept. of Geology.
USE OF MAGSAT ANOMALY DATA FOR CRUSTAL STRUCTURE AND MINERAL RESOURCES IN THE US MIDCONTINENT Quarterly Report, period ending 31 Dec. 1981
R. S. CARMICHAEL, Principal Investigator 31 Dec. 1981 31 p refs ERTS
(Contract NAS5-26425)
(E82-10323; NASA-CR-168902; NAS 1.26:168902; QR-4) Avail: NTIS HC A03/MF A01 CSCL 08G

The analysis and preliminary interpretation of investigator-B MAGSAT data are addressed. The data processing included: (1) removal of spurious data points; (2) statistical smoothing along individual data tracks, to reduce the effect of geomagnetic transient disturbances; (3) comparison of data profiles spatially coincident in track location but acquired at different times; (4) reduction of data by weighted averaging to a grid with 1 deg xl deg latitude/longitude spacing, and with elevations interpolated and weighted to a common datum of 400 km; (5) wavelength filtering; and (6) reduction of the anomaly map to the magnetic pole. Agreement was found between a magnitude data anomaly map and a reduce-to-the-pole map supporting the general assumption that, on a large scale (long wavelength), it is induced crustal magnetization which is responsible for major anamalies. Anomalous features are identified and explanations are suggested with regard to crustal structure, petrologic characteristics, and Curie temperature isotherms. M.G.

N82-25603*# National Aeronautics and Space Administration. Goddard Space Flight Center, Greenbelt, Md.
THE INFLUENCE OF AUTOCORRELATION IN SIGNATURE EXTRACTION: AN EXAMPLE FROM A GEOBOTANICAL INVESTIGATION OF COTTER BASIN, MONTANA
M. L. LABOVITZ and E. J. MASUOKA, Principal Investigators Dec. 1981 28 p refs Submitted for publication ERTS
(E82-10341; NASA-TM-83871; NAS 1.15:83871) Avail: NTIS HC A03/MF A01 CSCL 05B

The presence of positive serial correlation (autocorrelation) in remotely sensed data results in an underestimate of the variance-covariance matrix when calculated using contiguous pixels. This underestimate produces an inflation in F statistics. For a set of Thematic Mapper Simulator data (TMS), used to test the ability to discriminate a known geobotanical anomaly from its background, the inflation in F statistics related to serial correlation is between 7 and 70 times. This means that significance tests of means of the spectral bands initially appear to suggest that the anomalous site is very different in spectral reflectance and emittance from its background sites. However, this difference often disappears and is always dramatically reduced when compared to frequency distributions of test statistics produced by the comparison of simulated training sets possessing equal means, but which are composed of autocorrelated observations. Author

N82-25620# High Life Helicopters, Inc., Puyallup, Wash.
AIRBORNE GAMMA-RAY SPECTROMETER AND MAGNETOMETER SURVEY, TORONTO QUADRANGLE NEW YORK, VOLUME 2A Final Report
1981 90 p refs Prepared in cooperation with QEB, Inc. 3 Vol.
(Contract DE-AC13-79GJ-01692)
(DE81-027158; GJBX-211-81-VOL-2A) Avail: NTIS HC A05/MF A01

No uranium anomalies meet the minimum statistical requirements as defined and no anomaly map is presented. Potassium (%K), equivalent Uranium (ppm eU), equivalent Thorium (ppm eTh), eU/eTh, eU/K, eTh/K, and magnetic pseudo-contour maps are presented. Stacked Profiles showing geologic strip maps along each flight-line, together with sensor data, and ancillary data are also presented. All maps and profiles were prepared on a scale of 1:250,000, but were reduced to 1:500,000 for presentation. DOE

N82-25621# High Life Helicopters, Inc., Puyallup, Wash.
AIRBORNE GAMMA-RAY SPECTROMETER AND MAGNETOMETER SURVEY, KINGSTON QUADRANGLE NEW YORK, VOLUME 2C Final Report
1981 64 p refs Prepared in cooperation with QEB, Inc. 3 Vol.
(Contract DE-AC13-79GJ-01692)
(DE81-027161; GJBX-211-81-VOL-2C) Avail: NTIS HC A04/MF A01

No uranium anomalies meet the minimum statistical requirements as defined. No Uranium Anomaly Map is given. Potassium (%K), equivalent Uranium (ppm eU), equivalent Thorium (ppm eTh), eU/eTh, eU/K, eTh/K, and magnetic pseudo-contour maps are presented. Stacked Profiles showing geologic strip maps along each flight-line, together with sensor data, and ancillary data are also presented. All maps and profiles were prepared on a scale of 1:250,000, but were reduced to 1:500,000 for presentation. DOE

N82-25622# High Life Helicopters, Inc., Puyallup, Wash.
AIRBORNE GAMMA-RAY SPECTROMETER AND MAGNETOMETER SURVEY, ROCHESTER QUADRANGLE NEW YORK, VOLUME 2D Final Report
1981 143 p refs Prepared in cooperation with QEB, Inc. 3 Vol.
(Contract DE-AC13-79GJ-01692)
(DE81-027156; GJBX-211-81-VOL-2D) Avail: NTIS HC A07/MF A01

One uranium anomaly met the minimum statistical requirements as defined. This anomaly is listed and is shown on the Uranium Anomaly Interpretation Map. Potassium (%K), equivalent Uranium (ppm eU), equivalent Thorium (ppm eTh), eU/eTh, eU/K, eTh/K, and magnetic pseudo-contour maps are also presented. Stacked Profiles showing geologic strip maps along each flight-line, together with sensor data, and ancillary data are presented. All maps and profiles were prepared on a scale of 1:250,000, but were reduced to 1:500,000 for presentation. Anomaly number 1 is over an area underlain by shale and dolomite of the upper Silurian Camillus and Syracuse formations (Scy). DOE

N82-25623# Western Geophysical Co. of America, Houston, Tex. Aero Service Div.
AIRBORNE GAMMA-RAY SPECTROMETER AND MAGNETOMETER SURVEY. BARROW QUADRANAGLE, ALASKA, VOLUME 2 Final Report
Mar. 1981 63 p refs 2 Vol.
(Contract DE-AC13-76GJ-01664)
(DE82-000342; GJBX-295-81-VOL-2) Avail: NTIS HC A04/MF A01

Volume II contains the flight path map, multiparamenter profiles, histograms, and anomaly maps for potassium, uranium, thorium, uranium/potassium, uranium/thorium, and thorium/potassium. GRA

N82-25625# Western Geophysical Co. of America, Houston, Tex. Aero Service Div.

AIRBORNE GAMMA-RAY SPECTROMETER AND MAGNETOMETER SURVEY. LOOKOUT RIDGE QUADRANGLE, ALASKA, VOLUME 2 Final Report

Feb. 1981 190 p refs 2 Vol.
(Contract DE-AC13-76GJ-01664)
(DE82-000313; GJBX-303-81-VOL-2) Avail: NTIS HC A09/MF A01

The flight path map, multiparameter profiles, histograms, and anomaly maps are included. Uranium, thorium, potassium, uranium/potassium, uranium/thorium, and thorium/potassium are investigated. DOE

N82-26750*# Brown Univ., Providence, R. I. Dept. of Geological Sciences.

AN INVESTIGATION INTO THE UTILIZATION OF HCMM THERMAL DATA FOR THE DISCRIMINATION OF VOLCANIC AND EOLIAN GEOLOGICAL UNITS Quarterly Progress Report, 1 Sep. 1981 - 28 Feb. 1982

J. W. HEAD, III, Principal Investigator 28 Feb. 1982 1 p HCMM
(Contract NAS5-26728)
(E82-10352; NASA-CR-168996; NAS 1.26:168996) Avail: NTIS HC A02/MF A01 CSCL 08G

The nature of the HCMM data set and the general geologic application of thermal inertia imaging using HCMM data were studied. The CCT's of five sites of interest were obtained and displayed. The upgrading of the image display system was investigated. Fragment/block size distributions in various terrain types wre characterized with emphasis on volcanic terrain. The SEASAT L-band radar images of volcanic landforms at Newberry Volcano, Oregon, were analyzed and compared to imagery from LANDSAT band 7. E.A.K.

N82-27804# Western Geophysical Co. of America, Houston, Tex. Aero Service Div.

AIRBORNE GAMMA-RAY SPECTROMETER AND MAGNETOMETER SURVEY: NORTH/SOUTH TIELINE, VOLUME 1 Final Report

May 1981 38 p refs 2 Vol.
(Contract DE-AC13-76GJ-01664)
(DE82-005542; GJBX-386-81-VOL-1) Avail: NTIS HC A03/MF A01

An airborne high sensitivity gamma ray spectrometer and magnetometer survey was conducted along the 990 longitude meridian from the Canadian border southward to the Mexican border. A total of 1555 line miles of geophysical data were acquired. The program acquires and compiles geologic and other information to assess the magnitude and distribution of uranium resources and to determine areas favorable for the occurrence of uranium in the United States. DOE

N82-27805# Western Geophysical Co. of America, Houston, Tex. Aero Service Div.

AIRBORNE GAMMA-RAY SPECTROMETER AND MAGNETOMETER SURVEY: NORTH/SOUTH TIELINE, VOLUME 2 Final Report

May 1981 108 p refs 2 Vol.
(Contract DE-AC13-76GJ-01664)
(DE82-005570; GJBX-386-81-VOL-2) Avail: NTIS HC A06/MF A01

Data from an airborne high sensitivity gamma-ray spectrometer and magnetometer survey along the 990 longitude meridian from the Canadian border southward to the Mexican border are presented. The purpose of this study is to acquire and compile geologic and other information with which to assess the magnitude and distribution of uranium resources and to determine areas favorable for the occurrence of uranium in the US. DOE

N82-27806# Western Geophysical Co. of America, Houston, Tex. Aero Service Div.

AIRBORNE GAMMA-RAY SPECTROMETER AND MAGNETOMETER SURVEY: SIOUX FALLS QUADRANGLE, SOUTH DAKOTA, VOLUME 1 Final Report

May 1981 99 p refs Sponsored in part by Bendix Field Engineering Corp. 2 Vol.
(Contract DE-AC13-76GJ-01664)
(DE82-005533; GJBX-389-81-VOL-1) Avail: NTIS HC A05/MF A01

Computer printer maps of the magnetic total intensity and the six radiometric parameters were prepared in addition to the radiometric anomaly maps for this area. The magnetic total intensity map displays a rather subdued response pattern of broad low amplitude anomalies over much of the area with an average magnetic intensity of approximately 58,900 gammas. The radiometric response over much of the area is relatively low. Equivalent concentrations of uranium, thorium and potassium only rarely exceed 3.2 ppM, 7.5 ppM and 1.4% respectively. A number of these zones of increased concentrations show corresponding anomalous responses on the uranium/potassium and/or uranium/thorium pseudo-contour maps. Based on this set of computer printer maps alone however, it is, at times, difficult to discern the contribution of coinciding local decreases in the potassium and thorium parameters to these ratio anomalies. Based on the criteria stated in the general section on interpretation, a total of seven uranium and seven thorium anomalies were outlined on the interpretation map. DOE

N82-27807# Western Geophysical Co. of America, Houston, Tex. Aero Service Div.

AIRBORNE GAMMA-RAY SPECTROMETER AND MAGNETOMETER SURVEY: SIOUX FALLS QUADRANGLE, SOUTH DAKOTA, VOLUME 2 Final Report

May 1981 132 p Sponsored in part by Bendix Field Engineering Corp. 2 Vol.
(Contract DE-AC13-76GJ-01664)
(DE82-005574; GJBX-389-81-VOL-2) Avail: NTIS HC A07/MF A01

The flight path, radiometric multiparameter stacked profiles, magnetic and ancillary parameter stacked profiles, histograms, and anomaly maps for the Sioux Falls Quadrangle in South Dakota are presented. These data are used to assess the magnitude and distribution of uranium resources and to determine areas favorable for the occurrence of uranium. DOE

N82-27808# Texas Univ., El Paso. Dept. of Geological Sciences.

EVALUATION AND COMBINED GEOPHYSICAL INTERPRETATIONS OF NURE AND RELATED GEOSCIENCE DATA IN THE VAN HORN, PECOS, MARFA, FORT STOCKTON, PRESIDIDO, AND EMORY PEAK QUADRANGLES, TEXAS, VOLUME 1 Final Report

G. R. KELLER, W. J. HINZE, C. L. V. AIKEN, P. C. GOODELL, R. F. ROY, and N. E. PINGITORE Sep. 1981 451 p refs 2 Vol.
(Contract DE-AC13-76GJ-01664)
(DE82-005554; GJBX-365-81) Avail: NTIS HC A20/MF A01

The six Trans-Pecos Texas quadrangles (Van Horn, Pecos, Marfa, Port Stockton, Presidio, and Emory Park) were surveyed. The aeromagnetic gravity and geochemical data, their processing, and their analysis are discussed. The geologic history and setting of the Trans-Pecos are discussed along with the uranium potential of the region. Uranium anomalies and occurrences are present in the study area, and information is presented on 33 drill holes into these targets. A folio of maps reduced to a scale of 1:500,000. Geologic maps for each of the six quadrangles are included and the geophysical maps have been prepared to be overlays for the geologic maps. Residual aeromagnetic anomaly, complete Bougner gravity anomaly, flight line index, gravity station index, and anomaly interpretative maps were prepared for each quadrangle. A large suite of digitally processed maps of gravity and aeromagnetic are included. DOE

N82-27809# Texas Univ., El Paso. Dept. of Geological Sciences.
EVALUATION AND COMBINED GEOPHYSICAL INTERPRETATIONS OF NURE AND RELATED GEOSCIENCE DATA IN THE VAN HORN, PECOS, MARFA, FORT STOCKTON, PRESIDIO, AND EMORY PEAK QUADRANGELS, TEXAS Final Report
G. R. KELLER, W. J. HINZE, C. L. V. AIKEN, R. C. GOODELL, R. F. ROY, and N. E. PINGITORE Sep. 1981 88 p 2 Vol.
(Contract DE-AC13-76GJ-01664)
(DE82-005560; GJBX-365-81-VOL-2) Avail: NTIS HC A05/MF A01

An atlas containing the geophysical data publicly available in the Van Horn, Pecos, Marfa, Fort Stockton, Presidio, and Emory Peak quadrangles and a major file of basic data which are the object of much industrial interest is presented. Narrative discussion of the maps and contour maps of the aeromagnetic and gravity data, as well as maps of flight path recovery and gravity station locations are included. Geologic maps, key radiometric data, and ground truth sample location and data are also displayed. A scale of 1:500,000 is employed so that the maps can be overlain for qualitative comparisons. The maps refer to the qualitative analysis, particularly the interpretative anomaly index maps. DOE

N82-27810# Carson Helicopters, Inc., Perkasie, Pa.
NURE AERIAL GAMMA-RAY AND MAGNETIC RECONNAISSANCE SURVEY OF PORTIONS OF NEW MEXICO, ARIZONA AND TEXAS. VOLUME 2: NEW MEXICO-CARLSBAD QUADRANGLE Final Report
Sep. 1981 184 p refs Prepared for Bendix Field Engineering Corp.
(Contract DE-AC13-76GJ-01664)
(DE82-005527; GJBX-412-81-VOL-2C) Avail: NTIS HC A09/MF A01

A rotary wing high sensitivity radiometric and magnetic survey was flown covering the Carlsbad Quadrangle of the State of New Mexico. The survey was flown with a Sikorsky S58T helicopter equipped with a high sensitivity gamma ray spectrometer and the dynamic test range at Lake Mead, Arizona. Instrumentation and data reduction methods are presented in Volume I of this report. The reduced data is presented in the form of stacked profiles, standard deviation anomaly plots, histogram plots and microfiche listings. The results of the geologic interpretation of the radiometric data together with the profiles, anomaly maps and histograms are presented in this Volume II final report. DOE

N82-27811# Bendix Field Engineering Corp., Grand Junction, Colo.
AIRBORNE GAMMA-RAY SPECTROMETER AND MAGNETOMETER SURVEY: SUSANVILLE QUADRANGLE, CALIFORNIA, VOLUME 1 Final Report
May 1981 115 p refs
(Contract DE-AC13-76GJ-01664)
(DE82-005538; GJBX-410-81-VOL-1) Avail: NTIS HC A06/MF A01

An airborne high sensitivity gamma ray spectrometer and magnetometer survey was conducted over ten areas over northern California and southwestern Oregon. These include the 20 x 10 NTMS quadrangles of Roseburg, Medford, Weed, Alturas, Redding, Susanville, Ukian, and Chico along with the 10 x 30 areas of the Coos bay quadrangle and the Crescent City/Eureka areas combined. Traverse lines were flown in an east-west direction at a line spacing of six (6) miles. The lines were flown north-south approximately eighteen (18) miles apart. A total of 16,880,5 line miles of geophysical data were acquired, compiled, and interpreted during the survey, of which 1642.8 line miles are in this quadrangle. Geologic and other information with which to assess the magnitude and distributing of uranium resources and to determine areas favorable for the occurrence of uranium in the United States were computed. Author

N82-27812# Bendix Field Engineering Corp., Grand Junction, Colo.
AIRBORNE GAMMA-RAY SPECTROMETER AND MAGNETOMETER SURVEY: ROSEBURG QUADRANGLE, OREGON, VOLUME 2 Final Report
Mar. 1981 134 p refs
(Contract DE-AC13-76GJ-01664)
(DE82-005568; GJBX-388-81-VOL-2) Avail: NTIS HC A07/MF A01

Data from an airborne high sensitivity gamma ray spectrometer and magnetometer survey of the Roseburg quadrangle, Oregon are presented. The magnitude and distribution of uranium resources and favorable areas for occurrence of uranium in the US are discussed. DOE

N82-27813# Western Geophysical Co. of America, Houston, Tex. Aero Service Div.
AIRBORNE GAMMA-RAY SPECTROMETER AND MAGNETOMETER SURVEY: UKIAH QUADRANGLE, CALIFORNIA, VOLUME 1 Final Report
May 1981 110 p refs Sponsored in part by Bendix Field Engineering Corp. 2 Vol.
(Contract DE-AC13-79GJ-01664)
(DE82-005541; GJBX-390-81-VOL-1) Avail: NTIS HC A06/MF A01

Transverse lines were flown in an east to west direction at a line spacing of six miles. Tie lines were flown north to south approximately eighteen miles apart. A total of 16,880.5 line miles of geophysical data were acquired, compiled and interpreted during the survey, of which 1517 line miles are in this quadrangle. Geologic and other information was compiled with which to assess the magnitude and distribution of uranium in the United States. DOE

N82-27814# Western Geophysical Co. of America, Houston, Tex. Aero Service Div.
AIRBORNE GAMMA-RAY SPECTROMETER AND MAGNETOMETER SURVEY: HURON QUADRANGLE, SOUTH DAKOTA Final Report
Apr 1981 98 p refs Prepared for Bendix Field Engineering Corp.
(Contract DE-AC13-76GJ-01664)
(DE82-005540; GJBX-405-81-VOL-1) Avail: NTIS HC A05/MF A01

Geologic and other information with which to assess the magnitude and distribution of uranium resources and to determine areas favorable for the occurrence of uranium in the United States were acquired. An airborne high sensitivity gamma ray spectrometer and magnetometer survey was conducted over eleven 20 x 10 NTMS quadrangles located in the states of Minnesota and Wisconsin and seven 20 x 10 NTMS quadrangles in North and South Dakota. The quadrangles located within the North and South Dakota survey area include Devil's Lake, New Rockford, Jamestown, Aberdeen, Huron, Mitchell, and Sioux Falls. The results obtained over the Huron map area are discussed. Traverse lines were flown in an east-west direction at a line spacing of six miles. The lines were flown north-south approximately 24 miles apart. DOE

N82-27815# Western Geophysical Co. of America, Houston, Tex. Aero Service Div.
AIRBORNE GAMMA-RAY SPECTROMETER AND MAGNETOMETER SURVEY: CHICO QUADRANGLE, CALIFORNIA Final Report
May 1981 127 p refs Prepared for Bendix Field Engineering Corp.
(Contract DE-AC13-76GJ-01664)
(DE82-005543; GJBX-407-81-VOL-1) Avail: NTIS HC A07/MF A01

The magnitude and distribution of uranium resources with which to assess the magnitude and distribution of uranium resources and to determine areas favorable for the occurrence of uranium in the United States was investigated. An airborne high sensitivity gamma ray spectrometer and magnetometer survey was conducted over 10 areas over northern California and southwestern Oregon. These include the 2° x 1° NTMS quadrangles of Roseburg, Medford, Weed, Alturas, Redding, Susanville, Ukian, and Chico along with the 1° x 2° areas of the Coos Bay quadrangle and the Crescent City/Eureka areas combined. The results obtained over the Chico, California, map area are discussed. DOE

05

OCEANOGRAPHY AND MARINE RESOURCES

Includes sea-surface temperature, ocean bottom surveying imagery, drift rates, sea ice and icebergs, sea state, fish location.

A82-22306* California Inst. of Tech., Pasadena.
LABORATORY STUDIES OF ACTINIDE METAL-SILICATE FRACTIONATION
J. H. JONES and D. S. BURNETT (California Institute of Technology, Pasadena, CA) In: Lunar and Planetary Science Conference, 11th, Houston, TX, March 17-21, 1980, Proceedings. Volume 2. New York, Pergamon Press, 1980, p. 995-1001. refs
(Contract NSG-7202)

Actinide and Sm partition coefficients between silicate melt and several metallic phases have been measured. Under reducing conditions Si, Th, U and Pu can be reduced to metals from silicate melts and alloyed with a platinum-gold alloy. U and Pu enter a molten Pt-Si alloy with roughly equal affinity but U strongly partitions into the solid Pt. Th behaves qualitatively the same as Pu but is much less readily reduced than U, and Sm appears to remain unreduced. Experiments with Fe metal have shown that the partition coefficients of the actinides between Fe and silicate liquid are extremely low, suggesting a very low actinide concentration in planetary cores. Experiments show that platinum metals can efficiently fractionate actinides and fractionate actinides from lanthanides and this process may be relevant to the condensation behavior of these elements from the solar nebula. Pt-metal grains in Allende Ca-Al-rich inclusions appear to be U-poor, although the sub-class of Zr-bearing Pt metals may have high U contents. (Author)

A82-22619
FEATURES OF COSMIC RAY VARIATIONS DUE TO VARIATIONS IN THE TOTAL MAGNETIC FIELD OF THE SUN
A. N. CHARAKHCHIAN (Akademiia Nauk SSSR, Fizicheskii Institut, Moscow, USSR) and T. N. CHARAKHCHIAN (Moskovskii Gosudarstvennyi Universitet, Moscow, USSR) In: International Cosmic Ray Conference, 17th, Paris, France, July 13-25, 1981, Conference Papers. Volume 3. Gif-sur-Yvette, Essonne, France, Commissariat a l'Energie Atomique, 1981, p. 202-205. refs

The characteristics of the large-scale variations in cosmic ray intensity associated with variations in the total solar magnetic field are discussed. Particular attention is given to cosmic ray effects connected with solar magnetic field inversion and the presence in the stratosphere of short-range particles during periods of increasing total solar magnetic field, and to zonal cosmic ray modulation in the primary energy range 5-20 GeV which is due largely to magnetic field variations at the periphery of the heliosphere. A.L.W.

A82-28907* National Aeronautics and Space Administration. Goddard Space Flight Center, Greenbelt, Md.
REMOTE SENSING OF PRECIPITABLE WATER OVER THE OCEANS FROM NIMBUS 7 MICROWAVE MEASUREMENTS
C. PRABHAKARA, A. T. C. CHANG (NASA, Goddard Space Flight Center, Laboratory for Atmospheric Sciences, Greenbelt, MD), and H. D. CHANG (NASA, Goddard Space Flight Center, Laboratory for Atmospheric Sciences, Greenbelt; Computer Sciences Corp., Silver Spring, MD) Journal of Applied Meteorology, vol. 21, Jan. 1982, p. 59-68. refs

(Previously announced in STAR as N81-24504)

A82-29601* Jet Propulsion Lab., California Inst. of Tech., Pasadena.
SEASAT MEASUREMENT SYSTEM EVALUATION - ACHIEVEMENTS AND LIMITATIONS
D. B. LAME and G. H. BORN (California Institute of Technology, Jet Propulsion Laboratory, Pasadena, CA) Journal of Geophysical Research, vol. 87, Apr. 30, 1982, p. 3175-3178. refs
(Contract NAS7-100)

The Seasat project, which demonstrated the feasibility of microwave oceanographic remote sensing, was sponsored by the National Aeronautics and Space Administration and managed by the Jet Propulsion Laboratory. The evaluation of the measurement system (elements of the satellite, the sensors, the data handling, and data processing subsystems) was a key activity of the Seasat project. This paper summarizes the primary achievements and highlights the generic limitations of the evaluation process. Other papers in this issue present details of the geophysical evaluation process carried out under the auspices of the Seasat project. (Author)

A82-29602* Texas Univ., Austin.
THE SEASAT ALTIMETER DATA AND ITS ACCURACY ASSESSMENT
B. D. TAPLEY (Texas, University, Austin, TX), G. H. BORN, and M. E. PARKE (California Institute of Technology, Jet Propulsion Laboratory, Pasadena, CA) Journal of Geophysical Research, vol. 87, Apr. 30, 1982, p. 3179-3188. NASA-supported research. refs

A description is given of the Seasat satellite radar altimeter, which was designed to measure (1) the altitude of the satellite above the ocean surface, (2) surface wave height, and (3) the ocean-surface backscatter coefficient from which wind speed may be inferred. The atmospheric and geophysical effects influencing radar altimeter measurement accuracies and the attendant correction models adopted for the altimeter geophysical data record are summarized, along with Seasat Altimeter/Precision Orbit Determination Experiment Team activities directed towards the validation and improvement of these models and investigations assessing the accuracy of both the altimeter measurements and the computed satellite altitude ephemeris. O.C.

A82-29603* National Aeronautics and Space Administration. Goddard Space Flight Center, Greenbelt, Md.
SEASAT ALTIMETER HEIGHT CALIBRATION
R. KOLENKIEWICZ (NASA, Goddard Space Flight Center, Geodynamics Branch, Greenbelt, MD) and C. F. MARTIN (EG&G Washington Analytical Services Center, Inc., Riverdale, MD) Journal of Geophysical Research, vol. 87, Apr. 30, 1982, p. 3189-3197. refs

(Previously announced in STAR as N81-19526)

A82-29604#
TIDAL AND GEODETIC OBSERVATIONS FOR THE SEASAT ALTIMETER CALIBRATION EXPERIMENT
J. M. DIAMANTE, B. C. DOUGLAS, D. L. PORTER, and R. P. MASTERSON, JR. (NOAA, National Ocean Survey, Rockville, MD) Journal of Geophysical Research, vol. 87, Apr. 30, 1982, p. 3199-3206. refs

As part of the Seasat calibration activities of September and October 1978, a tide gage was installed by the National Ocean Survey at an open coastal location on Bermuda to provide instantaneous sea surface height determinations during Seasat overflights of the island. Because the tide gage was geodetically tied to the laser tracking station on Bermuda, the satellite's position relative to the sea surface could be determined independently for comparison with altimeter measurements. A root sum square error of 4.0 cm in the laser's vertical position determination, relative to the sea surface, has been estimated apart from possible errors arising from the present lack of precise information on the elevation of the Bermuda geoid. O.C.

A82-29607* Jet Propulsion Lab., California Inst. of Tech., Pasadena.

AN EMPIRICAL DETERMINATION OF THE EFFECTS OF SEA STATE BIAS ON SEASAT ALTIMETRY

G. H. BORN, M. A. RICHARDS (California Institute of Technology, Jet Propulsion Laboratory, Pasadena, CA), and G. W. ROSBOROUGH (Texas, University, Austin, TX) Journal of Geophysical Research, vol. 87, Apr. 30, 1982, p. 3221-3226. NASA-supported research. refs

A linear empirical model has been developed for the correction of sea state bias effects, in Seasat altimetry data altitude measurements, that are due to (1) electromagnetic bias caused by the fact that ocean wave troughs reflect the altimeter signal more strongly than the crests, shifting the apparent mean sea level toward the wave troughs, and (2) an independent instrument-related bias resulting from the inability of height corrections applied in the ground processor to compensate for simplifying assumptions made for the processor aboard Seasat. After applying appropriate corrections to the altimetry data, an empirical model for the sea state bias is obtained by differencing significant wave height and height measurements from coincident ground tracks. Height differences are minimized by solving for the coefficient of a linear relationship between height differences and wave height differences that minimize the height differences. In more than 50% of the 36 cases examined, 7% of the value of significant wave height should be subtracted for sea state bias correction. O.C.

A82-29608*# National Aeronautics and Space Administration. Wallops Flight Center, Wallops Island, Va.

SEA-STATE-RELATED ALTITUDE ERRORS IN THE SEASAT RADAR ALTIMETER

G. S. HAYNE and D. W. HANCOCK, III (NASA, Wallops Flight Center, Wallops Island, VA) Journal of Geophysical Research, vol. 87, Apr. 30, 1982, p. 3227-3231. refs

A significant waveheight-dependent bias is identified in Seasat-measured surface heights which cannot be neglected when using Seasat data at accuracies within 10 cm. Ten-second averages of the data from 63 waveform sampling rates in the Seasat radar altimeter were least squares fitted with a six-parameter model, the time-origin parameter of which provides a measure of the position of the actual mean radar waveform relative to the sampling rate and therefore provides altitude measurement corrections. Attention is given to actual altimeter point target response function, waveform sampler noise baseline, waveform sampler gain calibration, attitude angle and sea surface skewness, as effects not accounted for in Seasat altimeter measurements and standard data processing. O.C.

A82-29609*# National Aeronautics and Space Administration. Goddard Space Flight Center, Greenbelt, Md.

SEASAT ALTIMETER TIMING BIAS ESTIMATION

J. G. MARSH (NASA, Goddard Space Flight Center, Geodynamics Branch, Greenbelt, MD) and R. G. WILLIAMSON (EG & G Washington Analytical Services Center, Inc., Riverdale, MD) Journal of Geophysical Research, vol. 87, Apr. 30, 1982, p. 3232-3238. refs

A technique developed for the solution of time lag bias based on the analysis of sea surface height discrepancies at ground track intersections, prompted by the presence of a time calibration bias in Seasat altimeter data that produced measurement errors in excess of 1 m, is shown to yield a separation of the dominant, once-per-revolution ephemeris error amounting to about 1.5 m rms from the timing error signature. The technique does not depend on precise geoid data, and in application to a global Seasat altimeter data set covering July 28-August 9, 1978, has yielded a time lag value of -81.0 + or - 2 msec. This corroborates the -79.4 msec revised value derived from a reexamination of internal instrument time delays. O.C.

A82-29610* Texas Univ., Austin.

EVALUATION OF THE SEASAT ALTIMETER TIME TAG BIAS

B. E. SCHUTZ, B. D. TAPLEY, and C. SHUM (Texas, University, Austin, TX) Journal of Geophysical Research, vol. 87, Apr. 30, 1982, p. 3239-3245. refs

(Contract NOAA-MO-A01-78-00-4325; JPL-954703)

Two methods were used in analyses of Seasat altimeter data, aimed at the corroboration of an inherent altimeter microprocessor delay compensation value of -79.4 msec, which benefited from a global data distribution in the oceanic areas: (1) the crossover method, using altimeter data differenced at points where the Seasat ground track intersected with itself, and (2) the direct use of the altimeter data. Because the former method is independent of errors in the geoid model, it is considered the more reliable. For all crossover method results, the adopted value of -79.4 msec is within the bounds of the standard deviation associated with the estimates, of which -78.1 + or - 2.0 msec is considered the best representative. O.C.

A82-29611*# National Aeronautics and Space Administration. Goddard Space Flight Center, Greenbelt, Md.

COMPARISON DATA FOR SEASAT ALTIMETRY IN THE WESTERN NORTH ATLANTIC

R. E. CHENEY (NASA, Goddard Space Flight Center, Geodynamics Branch, Greenbelt, MD) Journal of Geophysical Research, vol. 87, Apr. 30, 1982, p. 3247-3253. refs

(Previously announced in STAR as N81-19529)

A82-29612

WAVEHEIGHT AND WIND SPEED MEASUREMENTS FROM THE SEASAT RADAR ALTIMETER

L. S. FEDOR (NOAA, Wave Propagation Laboratory, Boulder, CO) and G. S. BROWN (Applied Science Associates, Inc., Apex, NC) Journal of Geophysical Research, vol. 87, Apr. 30, 1982, p. 3254-3260. refs

(Contract NOAA-NA-79SAC00723)

A similarity to the results of earlier comparisons with the GEOS-3 radar altimeter data is noted, in the mean difference of -0.25 m/sec and standard deviation of 1.56 m/sec found upon comparison of Seasat radar altimeter-derived winds with buoy-recorded winds in the 1-10 m/sec range. It has therefore been demonstrated by means of two different radars and data sets that radar altimetry can provide accurate estimates of ocean surface wind speeds. Although the altimeter cannot provide the large-swath coverage provided by the Seasat scatterometer, its ability to produce accurate, simultaneous estimates of wind speed and waveheight may be important to future oceanographic research O.C.

A82-29613* California Univ., La Jolla.

SEASAT ALTIMETER DETERMINATION OF OCEAN CURRENT VARIABILITY

R. L. BERNSTEIN, R. H. WHRITNER (California, University, La Jolla, CA), and G. H. BORN (California Institute of Technology, Jet Propulsion Laboratory, Pasadena, CA) Journal of Geophysical Research, vol. 87, Apr. 30, 1982, p. 3261-3268. refs

(Contract NAS7-100)

An experiment conducted in the Kuroshio Current, east of Japan, has confirmed the ability of radar altimeters of precision on the order of 10 cm, such as that of the Seasat satellite, to measure the small oceanic height variations associated with geostrophic ocean currents. Changes in surface dynamic height were inferred from data gathered by air-expendable barithermographs, which had been dropped to coincide with the Seasat subtrack, for the periods between the flights of September 25 and October 5 and 13, 1978. The changes registered generally agreed to within + or - 10 cm of the height changes observed in the altimeter data. O.C.

A82-29614*# National Aeronautics and Space Administration. Goddard Space Flight Center, Greenbelt, Md.
THE SEASAT ALTIMETER MEAN SEA SURFACE MODEL
J. G. MARSH (NASA, Goddard Space Flight Center, Geodynamics Branch, Greenbelt, MD) and T. V. MARTIN (EG & G Washington Analytical Services Center, Inc., Riverdale, MD) Journal of Geophysical Research, vol. 87, Apr. 30, 1982, p. 3269-3280. refs

Gridding techniques are used to combine an 18-day set of Seasat altimeter data and two precisely-computed Seasat ephemerides, in order to arrive at global contour maps of the mean sea surface topography. The altimeter data have an rms agreement of 111 cm with the SS3 mean sea surface computed by means of the PGS-S3 ephemerides, and of 70 cm with the SS4 mean surface derived from the PGS-S4 ephemerides. While comparisons with the GEM 10B 1 x 1 deg gravimetric geoid have yielded rms differences of 2.8 m, those with a global mean sea surface derived from GEOS 3 altimeter data show rms differences of 1.3 m and 1.1 m for the cases of the SS3 and SS4 surfaces, respectively. An SS4 mean sea surface topograph is featured among the study findings presented. Further improvements in the representation of mean sea surface topography are expected with the development of more accurate gravity models for orbit computation. O.C.

A82-29616*# General Electric Co., Philadelphia, Pa.
THE SEASAT-A SATELLITE SCATTEROMETER - THE GEOPHYSICAL EVALUATION OF REMOTELY SENSED WIND VECTORS OVER THE OCEAN
W. L. JONES (General Electric Co., Space Div., Philadelphia, PA), L. C. SCHROEDER, E. M. BRACALENTE (NASA, Langley Research Center, Hampton, VA), D. H. BOGGS (California Institute of Technology, Jet Propulsion Laboratory, Pasadena, CA), R. A. BROWN (Washington, University, Seattle, WA), G. J. DOME (University of Kansas Center for Research, Inc., Lawrence, KS), W. J. PIERSON (New York, City University, New York, NY), and F. J. WENTZ (Remote Sensing Systems, Inc., Sausalito, CA) Journal of Geophysical Research, vol. 87, Apr. 30, 1982, p. 3297-3317. refs

A description is given of the algorithm used to convert Seasat-A satellite microwave scatterometer measurements of ocean normalized radar cross section to the neutral stability vector wind at 19.5 m height, as well as to compare these winds with high-quality surface observations. The wind vector algorithm used an empirical normalized radar cross section model function to describe the ocean normalized radar cross section's dependence on the 19.5-m neutral stability wind vector. In addition, two model functions were evaluated by means of an independent set of in situ surface wind observations from the Joint Air Sea Interaction experiment (JASIN). Better results were produced by these comparisons than the stipulated Seasat wind speed and direction accuracy specifications of + or - 2 m/sec and + or - 20 deg, respectively, over the 0-16 m/sec range of winds observed during JASIN. O.C.

A82-29617*# National Aeronautics and Space Administration. Langley Research Center, Hampton, Va.
THE RELATIONSHIP BETWEEN WIND VECTOR AND NORMALIZED RADAR CROSS SECTION USED TO DERIVE SEASAT-A SATELLITE SCATTEROMETER WINDS
L. C. SCHROEDER, W. L. JONES (NASA, Langley Research Center, Hampton, VA), D. H. BOGGS, I. M. HALBERSTAM (California Institute of Technology, Jet Propulsion Laboratory, Pasadena, CA), G. DOME (University of Kansas Center for Research, Inc., Lawrence, KS), W. J. PIERSON (New York, City University, New York, NY), and F. J. WENTZ (Remote Sensing Systems, Inc., Sausalito, CA) Journal of Geophysical Research, vol. 87, Apr. 30, 1982, p. 3318-3336. refs

The Seasat-A Satellite Scatterometer (SASS) ocean normalized radar cross section (NRCS) dependence on the 19.5-m neutral stability wind vector may be specified as a function of radar incidence angle, the angle between wind direction and radar azimuth, and the neutral stability wind speed expressed in m/sec at a height of 19.5 m. An account is given of the development of models both expressing this relationship and providing the basis of inversion of NRCS to SASS winds, from initially aircraft scatterometer measurement-based forms to three Seasat field-validation experiments which furnish model NRCS versus surface windspeed data for comparison with SASS data. O.C.

A82-29618* Kansas Univ. Center for Research, Inc., Lawrence.
EVALUATION OF ATMOSPHERIC ATTENUATION FROM SMMR BRIGHTNESS TEMPERATURE FOR THE SEASAT SATELLITE SCATTEROMETER
R. K. MOORE, I. J. BIRRER (University of Kansas Center for Research, Inc., Lawrence, KS), E. M. BRACALENTE (NASA, Langley Research Center, Hampton, VA), G. J. DOME (Bell Telephone Laboratories, Inc., Holmdel, NJ), and F. J. WENTZ (Remote Sensing Systems, Inc., Sausalito, CA) Journal of Geophysical Research, vol. 87, Apr. 30, 1982, p. 3337-3354. refs

The effect of attenuation in precipitation regions of the sea, which must be considered in order to measure the radar backscatter from the ocean with sufficient accuracy to allow determination of the wind vector, can be ascertained from a knowledge of the brightness temperature observed by a microwave radiometer such as the Seasat multifrequency scanning radiometer. Two algorithms relating radiometric measurements and attenuation, and thereby correcting measured scattering coefficient values, were compared with wind vectors reported by surface observers and those determined by the Seasat scatterometer measurements with and without correction for atmospheric attenuation. Although the attenuation correction yields some improvements, it is constrained by both radiometer footprint differences and different scan patterns. O.C.

A82-29619* Washington Univ., Seattle.
SURFACE WIND ANALYSES FOR SEASAT
R. A. BROWN (Washington, University, Seattle, WA), V. J. CARDONE (Oceanweather, Inc., White Plains, NY), T. GUYMER (Institute of Oceanographic Sciences, Wormley, Surrey, England), J. HAWKINS (NOAA, National Hurricane and Experimental Meteorology Laboratory, Bay Saint Louis, MS), J. E. OVERLAND (NOAA, Pacific Marine Environment Laboratory, Seattle, WA), W. J. PIERSON (City College, New York, NY), S. PETEHERYCH (Department of the Environment, Atmospheric Environment Service, Downsview, Ontario, Canada), J. C. WILKERSON (NOAA, Camp Springs, MD), P. M. WOICESHYN (California Institute of Technology, Jet Propulsion Laboratory, Pasadena, CA), and M. WURTELE (California, University, Los Angeles, CA) Journal of Geophysical Research, vol. 87, Apr. 30, 1982, p. 3355-3364. refs

During the 99 days of Seasat operation, two large-scale experiments were conducted which established the satellite sensors' wind measuring capabilities: (1) the Gulf of Alaska Experiment (GOASEX), and (2) the Joint Air Sea Interaction Experiment (JASIN), which unlike GOASEX was independent of the Seasat program and undertook comprehensive air and sea investigations which furnished excellent comparison data for Seasat. Qualitative comparison windfields were also provided by several storms. The point measurements in GOASEX and JASIN were averaged in conjunction with Seasat scatterometer regions and, on the basis of comparisons between several anemometers on buoys and meteorological ships and the calculation of various averaging times, a 20-min average yields a scatterometer scale windfield accuracy of up to + or 1 m/sec and + or - 10 deg in well-behaved windfields. O.C.

A82-29621* Remote Sensing Systems, Sausalito, Calif.

INTERCOMPARISON OF WIND SPEEDS INFERRED BY THE SASS, ALTIMETER, AND SMMR

F. J. WENTZ (Remote Sensing Systems, Inc., Sausalito, CA), V. J. CARDONE (Oceanweather, Inc., White Plains, NY), and L. S. FEDOR (NOAA, Wave Propagation Laboratory, Boulder, CO) Journal of Geophysical Research, vol. 87, Apr. 30, 1982, p. 3378-3384. refs

(Contract NAS1-16032; NAS7-100)

The operational theory, control algorithms, and comparisons with surface-determined wind speeds for the scatterometer (SASS), altimeter (ALT), and passive microwave radiometer (SMMR) on board the Seasat satellite are presented. Radiative scattering combining specular reflections and Bragg resonance scattering are noted to occur at tilting waves and sea foam, two conditions highly correlated with wind speed. SASS scans swaths of 70, 200, and 700 km from nadir, the SMMR covers a 150 km strip. Normalized radar sections are derived from the SASS and ALT telemetry, and brightness temperature from the SMMR. ALT winds were found to be biased about 3 m/sec low, while intercomparison between the SMMR and SASS data showed a mean difference of 0.3 m/sec with a standard deviation from measured winds of 1.7 m/sec or less. The effects of land thermal emissions, rain, and sun glint are discussed, and good viewing conditions are concluded to result in 2 m/sec accuracy. M.S.K.

A82-29622* Jet Propulsion Lab., California Inst. of Tech., Pasadena.

DESCRIPTION OF SEASAT RADIOMETER STATUS AND RESULTS

R. G. LIPES (California Institute of Technology, Jet Propulsion Laboratory, Pasadena, CA) Journal of Geophysical Research, vol. 87, Apr. 30, 1982, p. 3385-3395. refs

(Contract NAS7-100)

Improved geophysical algorithms are shown to be able to determine sea surface temperature (SST) to an accuracy of 1 C (1 sigma) under favorable surface and atmospheric conditions over an SST range of 10-30 C. Under similar conditions, the radiometer wind retrievals track the scatterometer winds within a scatter of 2 m/s (1 sigma) over a wind speed range of 0-25 m/s. These conditions require that contamination from land, rain, sun glint, and radio frequency interference be avoided. What is more, water vapor determinations in the midlatitudes and in the tropical Pacific are found to agree with estimates of precipitable water from radiosondes to within 10%. C.R.

A82-29623* Stanford Univ., Calif.

THE OBSERVATION OF OCEAN SURFACE PHENOMENA USING IMAGERY FROM THE SEASAT SYNTHETIC APERTURE RADAR - AN ASSESSMENT

J. F. VESECKY (Stanford University, Stanford, CA) and R. H. STEWART (California Institute of Technology, Jet Propulsion Laboratory, Pasadena; California, University, La Jolla, CA) Journal of Geophysical Research, vol. 87, Apr. 30, 1982, p. 3397-3430. refs

(Contract N00014-75-C-0356; NOAA-MO-A01-78-00-4318)

The principles governing synthetic aperture radar (SAR) and its use on the Seasat spacecraft are reviewed. The way in which wind stress, surface currents, long gravity waves, and surface films modulate the scattering properties of resonant (approximately 30-cm-wavelength) waves is discussed, with particular emphasis placed on the mechanisms that could produce images of long gravity waves. Doppler effects by ocean motion are also described. Measurements of long (wavelength more than about 100 m) gravity waves made using Seasat SAR imagery are compared with surface measurements during several experiments. Combining these results, it is found that dominant wavelength and direction are measured by Seasat SAR within + or - 12% and + or - 15 deg, respectively. It is noted, however, that ocean waves are not always visible in SAR images, and detection criteria are discussed in terms of wave height, length, and direction. C.R.

A82-29624* National Oceanic and Atmospheric Administration, Seattle, Wash.

SEASAT WIND AND WAVE OBSERVATIONS OF NORTHEAST PACIFIC HURRICANE IVA, AUGUST 13, 1978

F. I. GONZALEZ (NOAA, Pacific Marine Environmental Laboratory, Seattle, WA), T. W. THOMPSON (Science Applications, Inc., Planetary Science Institute, Pasadena, CA), W. E. BROWN, JR. (California Institute of Technology, Jet Propulsion Laboratory, Pasadena, CA), and D. E. WEISSMAN (Hofstra University, Hempstead, NY) Journal of Geophysical Research, vol. 87, Apr. 30, 1982, p. 3431-3438. NOAA-supported research refs

(Contract NAS7-100)

The paper examines Seasat wind and wave observations collected in the eye of hurricane Iva on August 13, 1978 in the northeast Pacific. A maximum wind speed of 25-30 m/s is observed, along with a banana-shape high-wind-speed distribution. Two-dimensional Fourier transforms of selected SAR scenes show a dominant wavefield characterized by wavelengths of 166-211 m, with a fanlike distribution of propagation directions. A simple geometric model is proposed to explain the dominant wave field in terms of prior storm intensity and location, which is combined with the Ross parametric hurricane wave model and Seasat wind and wave data to estimate a value of 43 km for the effective radial distance from the storm center to the region of maximum winds. D.L.G.

A82-30666#

A STUDY OF THE EARTH'S RADIATION BUDGET USING A GENERAL CIRCULATION MODEL

J. M. SLINGO (Meteorological Office, Bracknell, Berks., England) Royal Meteorological Society, Quarterly Journal, vol. 108, Apr. 1982, p. 379-405. refs

A model clarifying the roles played by clouds and the surface in determining the seasonal variations in the radiation budget is described. The model employs an interactive radiation scheme with seasonally varying climatological sea surface temperatures, incoming solar radiation, and zonal mean climatological cloud amounts. Since its simulation of the various components of the earth's radiation compares favorably with results from satellites, its results are used in explaining certain aspects of the observed budgets. The model results are also used to estimate the earth's annual mean total energy budget and, in particular, the poleward flux of heat by the oceans. The oceanic heat flux implied by the model compares favorably with estimates based on observations, the main differences being at the equator and near the North Pole. C.R.

A82-30810

A SEARCH FOR SEAMOUNTS IN THE SOUTHERN COOK AND AUSTRAL REGION

K. LAMBECK and R. COLEMAN (Australian National University, Canberra, Australia) Geophysical Research Letters, vol. 9, Apr. 1982, p. 389-392. refs

A82-31294#

EMISSIVITY AND REFLECTANCE OF THE MODEL SEA SURFACE FOR THE USE OF AVHRR DATA OF NOAA SATELLITES

T. TAKASHIMA and Y. TAKAYAMA (Meteorological Research Institute, Tsukuba, Ibaraki, Japan) Papers in Meteorology and Geophysics, vol. 32, Dec. 1981, p. 267-274.

The emissivity and reflectance of the sea surface, modeled from AVHRR advanced radiometer sensing from the NOAA-6 satellites, are derived as a function of the incident and emergent directions of radiation. The sea surface is modeled numerically with slope components varying according to a gaussian distribution, including isotropy if independent of the wind direction, and anisotropy if dependent on the wind direction. The geometry of the slope with changing incident and reflecting angles is formulated in terms of spherical trigonometry. Treatment of the surface as a specular reflector is found to be acceptable except for visible light, where the reflection depends on the surface characteristics and a bivariate gaussian analysis is necessary. Additional influences due to oil slicks are considered, particularly for reflectance reduction. M.S.K.

A82-31995* National Aeronautics and Space Administration. Goddard Space Flight Center, Greenbelt, Md.

RETRIEVAL OF OCEAN SURFACE AND ATMOSPHERIC PARAMETERS FROM MULTICHANNEL MICROWAVE RADIOMETRIC MEASUREMENTS

A. T. C. CHANG (NASA, Goddard Space Flight Center, Earth Survey Application Div., Greenbelt, MD) and A. S. MILMAN (Systems and Applied Sciences Corp., Riverdale, MD) IEEE Transactions on Geoscience and Remote Sensing, vol. GE-20, Apr. 1982, p. 217-224. refs

Methods for the retrieval of ocean surface temperature, surface wind speed, rain rate, cloud height, and the amounts of water vapor and nonprecipitated liquid water over the ocean from Scanning Multichannel Microwave Radiometer (SMMR) data are presented. The sensitivity of retrieval algorithms for wind speed and sea surface temperature, in the absence of rain, to the undetected presence of rain, is discussed along with the accuracy of a more general method for the retrieval of rain rate in conjunction with other meteorological parameters. It is concluded that the inability to retrieve the average rain rate accurately at small rain angles is due to the inability of SMMR to distinguish between small raindrops and nonprecipitating droplets. O.C.

A82-32559#

LASER-INDUCED BIOLUMINESCENCE

G. D. HICKMAN (Applied Science Technology, Inc., Arlington, VA) and R. V. LYNCH, III (U.S. Navy, Naval Research Laboratory, Washington, DC) In: Los Alamos Conference on Optics '81, 2nd, Los Alamos, NM, April 7-10, 1981, Proceedings. Bellingham, WA, SPIE - The International Society for Optical Engineering, 1981, p 263-268. refs

(Contract N00014-80-C-0673)

A project has been initiated to determine the feasibility of developing a complete airborne remote sensing system for rapidly mapping high concentration patches of bioluminescent organisms in the world's oceans. Conceptually, this system would be composed of a laser illuminator to induce bioluminescence and a low light level image intensifier for detection of light. Initial laboratory measurements consisted of using a 2-J flash lamp pulsed optical dye laser to excite bioluminescence in the marine dinoflagellate Pyrocustis lunula at ambient temperature using Rhodamine 6G as the lasing dye (585 nm) and a laser pulse width of 1 microsec. After a latency period of 15-20 msec, the bioluminescence maximum occurred in the blue (480 nm is the wavelength maximum for most dinoflagellate bioluminescence) with the peaking occurring approximately 65 msec after the laser pulse. Planned experiments will investigate the effect of different excitation wavelengths and energies at various temperatures and salinities of the cultures. (Author)

A82-32651

A SHIP AND SATELLITE VIEW OF HYDROGRAPHIC FEATURES IN THE WESTERN GULF OF MEXICO

D. A. BROOKS (Texas A & M University, College Station, TX) and R. V. LEGECKIS (Texas A & M University, College Station, TX; NOAA National Earth Satellite Service, Washington, DC) Journal of Geophysical Research, vol. 87, May 20, 1982, p. 4195-4206. refs

(Contract NSF OCE-79-24606; NSF OCE-78-22481)

In April 1980, nearly synoptic hydrographic observations were obtained in the western Gulf of Mexico by satellite and ship. A meandering surface thermal front which turned northeastward from the Mexican coast near 23 deg N was prominent in the satellite infrared observations. The front separated a southern anticyclone and a northern cyclone, both of which had horizontal scales of several 100 km and were prominent in the subsurface hydrographic observations. The eastward geostrophic volume transport in the confluent leg of the two features was roughly equal to that of the Florida Current. A shallow layer of fresh, cool water from the Texas shelf region extended about 300 km seaward into the cyclone along the northern side of the front. Remnant Subtropical Underwater in the core of the April anticyclone indicates its origin in the eastern Gulf Loop Current. (Author)

A82-32881

ON THE SYNTHETIC APERTURE RADAR IMAGING OF OCEAN SURFACE WAVES

A. V. IVANOV (Akademiia Nauk SSSR, Institut Radiotekhniki i Elektroniki, Moscow, USSR) IEEE Journal of Oceanic Engineering, vol. OE-7, Apr. 1982, p. 96-103. refs

A process of synthetic aperture radar imaging of ocean surface waves is considered on the basis of the two-scale model of microwave scattering by a disturbed sea surface. Analytical expressions are obtained to relate characteristics of a large-scale wave image, averaged over an ensemble of realizations of the small-scale ripple, with the wave, radar, and viewing scheme as parameters. It is shown that the wave image would be defocused as an image of a target moving in the along-track direction with a speed equal to a half of the wave phase speed projection on the line of flight. The defocusing magnitude was measured experimentally for the ocean swells images, obtained with an airborne S-band radar, and the results are found to be in satisfactory agreement with the model prediction. (Author)

A82-32882* Jet Propulsion Lab., California Inst. of Tech., Pasadena.

OCEAN WAVE HEIGHT MEASUREMENT WITH SEASAT SAR USING SPECKLE DIVERSITY

A. JAIN, G. MEDLIN, and C. WU (California Institute of Technology, Jet Propulsion Laboratory, Pasadena, CA) IEEE Journal of Oceanic Engineering, vol. OE-7, Apr. 1982, p. 103-107. refs

(Contract NAS7-100)

Measurement of ocean wave heights with the synthetic aperture radar can be accomplished with high spatial resolution by determining the variation of speckle intensity with the frequency and angle of illumination. A comparison of data obtained by the SEASAT SAR with surface truth measurements obtained during the GOASEX and the JASIN experiments demonstrates this concept. (Author)

A82-32902

INFRARED SENSING OF SEA SURFACE TEMPERATURE FROM SPACE

M. SIDRAN (Bernard Baruch College, New York, NY) Remote Sensing of Environment, vol. 10, Sept. 1980, p. 101-114. refs

The retrieval of sea surface temperature information from the infrared signals received by remote sensing satellites is examined. Factors influencing the received signal are evaluated, including surface emissivity, spectral radiance, atmospheric transmittance, and sources of error in lengthy computer retrievals based on the integration of the radiative transfer equation related to imperfections in atmospheric transmittance models, uncertainties in the vertical profiles of atmospheric pressure, temperature and humidity profiles, temperature discontinuities at the air-sea interface, differences between surface and bulk water temperatures and the neglect of surface emissivity and reflectance are pointed out. The simple retrieval scheme of Prabhakara et al. (1974), which makes use of three spectral bands to achieve an rms error of + or - 1.1 K, is then reviewed, and a simplified version of this scheme based on only two bands is presented which reduces the rms error to + or - 1.0 K. A.L.W.

A82-32903

NEARSHORE CURRENT PATTERN OFF SOUTH TEXAS - AN INTERPRETATION FROM AERIAL PHOTOGRAPHS

R. E. HUNTER and G. W. HILL (U.S. Geological Survey, Menlo Park, CA) Remote Sensing of Environment, vol. 10, Sept. 1980, p. 115-134. refs

Turbidity patterns seen on aerial photographs of nearshore waters are analyzed to derive the current patterns in a 4-km wide zone along the south Texas coast. Series of color aerial photographs were taken vertically from an altitude of 3700 m on December 23, 1968, following the passage of a cold front accompanied by strong northwesterly to northeasterly winds. Examination of photographs taken from 6 to 80 min apart indicate the presence of southward currents nearly parallel to the shore, with velocities increasing from about 17 cm/sec off shore to about 40 cm/sec at the line of breaking waves. Rip-current plumes were observed to drift with the longshore current and be deformed by the horizontal shear. The turbidity by which these currents were traced originated in Aransas pass, a tidal inlet connecting several estuarine bays to the Gulf of Mexico, and a preceding ebb-tidal plume from the same inlet. A linear pattern of turbid and less turbid bands also suggests the development of Langmuir circulation with cell axes parallel to the shelf current. A.L.W.

A82-32917
MEASURING SEA SURFACE TEMPERATURE FROM SATELLITES - A GROUND TRUTH APPROACH
D. C. MCCONAGHY (NOAA, Southwest Fisheries Center, La Jolla, CA) Remote Sensing of Environment, vol. 10, Dec. 1980, p. 307-310.

Determining the correction for atmospheric attenuation is a major problem in processing thermal infrared digital data from very high resolution radiometers aboard NOAA Polar Orbiting Satellites. An empirical equation for estimating this correction is developed. The coefficients of the equation are determined by using regression techniques and comparing satellite observations to sea surface temperature measurements. Although there is not sufficient data to fully evaluate this procedure, initial satellite measurements are within 0.5 C of independent sea surface temperature measurements. (Author)

A82-33322*# National Aeronautics and Space Administration. Langley Research Center, Hampton, Va.
DEPRESSION OF BRIGHTNESS TEMPERATURE OF SEA SURFACES COVERED WITH MONOMOLECULAR OIL FILMS RELATIVE TO CLEAN WATER SURFACES AT 1.43 GHZ
H.-J. C. BLUME (NASA, Langley Research Center, Hampton, VA) Institute of Electrical and Electronics Engineers, International Geoscience and Remote Sensing Symposium, Munich, West Germany, June 1-4, 1982, Paper. 6 p. refs

A82-33438*# National Aeronautics and Space Administration. Langley Research Center, Hampton, Va.
CHARACTERISTICS OF 13.9 GHZ RADAR SCATTERING FROM OIL FILMS ON THE SEA SURFACE
J. W. JOHNSON and W. F. CROSWELL (NASA, Langley Research Center, Hampton, VA) Radio Science, vol. 17, May-June 1982, p. 611-617. refs

Aircraft microwave scatterometer measurements are presented, which were made in 1979 as part of a project to study the response of a number of active and passive microwave and optical remote sensors to an oil-covered sea surface conducted by NASA Langley Research Center. A 13.9-GHz Doppler scatterometer with a fan beam antenna and coherent detection was used to measure radar backscatter as a function of incidence angle. The radar scattering signature of the clear surface and signatures of the surface covered with various crude oil films are compared. Reductions in Ku band microwave backscatter up to 14 dB are observed for both treated and untreated LaRosa and Murban crude oil films deposited on the sea surface. Maximum Ku band sensitivity to the effects of the oil in terms of differential scatter is observed in the 25-35 deg incidence angle region. D.L.G.

A82-33717
SATELLITE OBSERVATIONS OF SEA SURFACE TEMPERATURE AROUND THE BRITISH ISLES
R. W. SAUNDERS, N. R. WARD, C. F. ENGLAND, and G. E. HUNT (University College, London, England) American Meteorological Society, Bulletin, vol. 63, Mar. 1982, p. 267-272. Research supported by the European Space Agency, Natural Environmental Research Council, and Science and Engineering Research Council. refs

TIROS-N Advanced Very High Resolution Radiometer (AVHRR) imagery has been used to study the temperature structure of the sea surface around the British Isles. The satellite imagery from both TIROS-N, METEOSAT and conventional synoptic data are combined to obtain a calibration for both 11-micron infrared channels, which gave sea surface temperatures accurate to + or - 1 K. The changes in the sea surface temperature around the British Isles for July 12, 1979 are shown well by the satellite data. In particular, a study is made of an anomalously warm patch in the North Sea that appeared at local noon over an area where the surface winds were weak, inhibiting surface mixing. (Author)

A82-34219
COASTAL ENVIRONMENT CHANGE ANALYSIS BY LANDSAT MSS DATA
J.-K. HONG (Tokyo University of Agriculture and Technology, Tokyo, Japan) and J. IISAKA (IBM Japan, Ltd., Tokyo, Japan) Remote Sensing of Environment, vol. 12, May 1982, p. 107-116. refs

A case study of coastal environmental change is conducted using computer-assisted analysis of Landsat scenes for three different years. The Kanto area in Japan is divided into three study areas on the basis of social and geographical factors. Land use changes along the bay from November 26, 1972, to November 11, 1980, are studied and the results are interpreted by referring to the ground truth data. The results show a continuous decrease in the area of shallow water along the bay and changes in land use in the coastal areas. The changes are recognized as being closely related to the bay area changes; they are found to correspond well to differences in social developments in the study areas. Landsat data are thus shown to provide sufficient information on the environmental changes taking place. C.R.

A82-36005
ESTIMATION OF THE TEMPERATURE OF THE UPPER BOUNDARY OF CLOUD COVER OVER THE WORLD OCEAN [OTSENKA TEMPERATURY VERKHNEI GRANITSY OBLACHNOSTI NAD MIROVYM OKEANOM]
O. AVASTE, O. KIARNER, and S. KEEVALLIK (Akademiia Nauk Estonskoi SSR, Institut Astrofiziki i Fiziki Atmosfery, Tartu, Estonian SSR) Meteorologiia i Gidrologiia, June 1982, p. 54-59. In Russian. refs

The temperature of the upper boundary of cloud cover over the world ocean is estimated on the basis of cloud-amount estimates made by Avaste et al. (1981), climatological means of ocean surface temperature, and mean monthly values of outgoing radiation fluxes. Mean monthly upper-cloud-boundary temperatures over the world ocean are estimated for the 30 deg N to 30 deg S latitude belt. Data from the Nimbus-3 and NOAA meteorological satellites were used in the estimation. B.J.

A82-36341
INTERANNUAL VARIATIONS OF OUTGOING IR ASSOCIATED WITH TROPICAL CIRCULATION CHANGES DURING 1974-1978
B. LIEBMANN and D. L. HARTMANN (Washington, University, Seattle, WA) Journal of the Atmospheric Sciences, vol. 39, May 1982, p. 1153-1162. refs
(Contract NSF 78-07369; NSF 81-06099)

Interannual variability of outgoing IR in the tropical Pacific Ocean is studied using measurements derived from the NOAA scanning radiometer. In addition to the usual mean maps, seasonal anomaly maps are constructed from June, July, August 1974-December 1977, and January, February 1978. Time series representing the equatorial eastern Pacific sea-surface temperature (SST) anomalies and monthly anomalies at various locations are also plotted. During this period a warming event occurs, in which SSTs in the eastern Pacific rapidly become anomalously warm. Dramatic changes in outgoing IR occur simultaneously with this SST increase. The region of convergence over Indonesia shifts eastward and connects to a well-developed intertropical convergence zone (ITCZ). The South Pacific convergence zone (SPCZ) is also connected to the Indonesian convergence zone, but develops more slowly and does not reach its maximum strength until more than a year after the SST increases occur. By this time the ITCZ has returned to its prewarming state. Eastward movement of the SPCZ is also apparent. (Author)

A82-37195

DETERMINATION OF WINTER TEMPERATURE PATTERNS, FRONTS, AND SURFACE CURRENTS IN THE YELLOW SEA AND EAST CHINA SEA FROM SATELLITE IMAGERY

Q. A. ZHENG and V. KLEMAS (Delaware, University, Newark, DE) Remote Sensing of Environment, vol. 12, July 1982, p. 201-218. refs

A82-37196

ESTIMATION OF THE PRECIPITABLE WATER FROM THE IR CHANNEL OF THE GEOSTATIONARY SATELLITE

T. AOKI (Meteorological Satellite Center, Kiyose, Tokyo, Japan) and T. INOUE (Meteorological Research Institute, Yatabe, Ibaraki, Japan) Remote Sensing of Environment, vol. 12, July 1982, p. 219-228. refs

It has been shown that over the tropical oceans the total precipitable water can be estimated from the infrared radiometer data (10.5-12.5 microns) of the Geostationary Meteorological Satellite. The satellite derived values are in good agreement with the radiosonde data, with a 0.53 g/sq cm rms difference. The weekly mean distribution of the precipitable water over the tropical ocean of western Pacific has been obtained in both summer and winter seasons. The pattern of this distribution is in reasonable agreement with other authors and climatological data. (Author)

A82-37390*# National Aeronautics and Space Administration. Wallops Flight Center, Wallops Island, Va.

PULSE-TO-PULSE CORRELATION IN SATELLITE RADAR ALTIMETERS

E. J. WALSH (NASA, Wallops Flight Center, Wallops Island, VA) Radio Science, vol. 17, July-Aug. 1982, p. 786-800. refs

Pulse-to-pulse correlation in satellite radar altimeters is examined to determine if range jitter in future altimeters could be reduced by increasing the pulse repetition frequency (PRF). Data from the Skylab radar altimeter is analyzed and compared with rules of thumb and the results of a Monte Carlo simulation. Altimeter range tracker configurations are reviewed and a simple curve is developed for the PRF below which decorrelation is assured. An adaptive PRF for future altimeters is recommended to conserve mission power while optimizing data collection during high-sea states. (Author)

A82-37505

A QUANTITATIVE MULTISPECTRAL ANALYSIS SYSTEM FOR AERIAL PHOTOGRAPHS APPLIED TO COASTAL PLANNING

C. VALERIO (Aix-en-Provence, Centre d'Etudes Techniques de l'Equipement, Les Milles, Bouches-du-Rhone, France) and A. LLEBARIA (CNRS, Laboratoire d'Astronomie Spatiale, Marseille, France) International Journal of Remote Sensing, vol. 3, Apr.-June 1982, p. 181-197. refs

A system that may be used to study the dispersion of effluents in the sea either by means of their color or by using a fluorescent tracer, rhodamine B, is described, and its use is illustrated with the study of the dispersion over one day of a release of rhodamine in seawater. The underlying principle is the adjustment of the data acquisition device to the optical properties of the phenomenon being studied, so that the signal-to-noise ratio is optimized. A very accurate digitizing microdensitometer is used, and the data processing system is adapted to allow for correction of radiometric, spatial, and temporal variations. A simple mathematical representation of the interaction of sunlight with the environments encountered before reaching the negative is employed. An experimental procedure that eliminates the need for sampling from boats is used to follow the evolution of the plume, giving maps showing quantity of rhodamine to an accuracy of about five percent. C.D.

N82-23614*# National Aeronautics and Space Administration. Langley Research Center, Hampton, Va.

ANALYSIS OF OCEAN COLOR SCANNER DATA FROM THE SUPERFLUX III EXPERIMENT

C. W. OHLHORST Mar. 1982 30 p refs
(NASA-TM-83290; NAS 1.15:83290) Avail: NTIS HC A03/MF A01 CSCL 08J

The scanner collected data on October 15, 20, and 22, 1980. Single-channel gray-scale data products generated 5 minutes after the scanner were collected and showed details of the Chesapeake plume structure, suggesting that this quick-look capability could have potential use for experiments in real time. The Chesapeake Bay plume extended offshore about 5 nautical miles on October 15, and 7 nautical miles on October 20. Using the October 15 1980, data, a correlation coefficient of r = 0.889 was obtained between chlorophyll 'A' and the ratio of band 7 (664-684 nanometers) to band 9 (746-766 nanometers). This ratio was then used to calculate the average surface chlorophyll 'A' concentration of the water flowing out of the Chesapeak Bay. A ratio from the Ocean Color Scanner bands was created to simulate the ratio that the Multichannel Ocean Color Sensor uses to calculate chlorophyll A concentrations. Using the October 15, 1980, data set, this ratio has a correlation coefficient of r = -0.739 with the log of the chlorophyll 'A' and the ratio of band 2 minus band 4 to band 2 plus band 4 of the Ocean Color Scanner. No correlation is found between the Ocean Color Scanner data and total suspended solid measurements made on October 15, 1980. T.M.

N82-23852# Wisconsin Univ., Madison.

THE IMPACT OF METEOROLOGICAL SATELLITES ON THE FIRST GARP GLOBAL EXPERIMENT (FGGE)

V. E. SUOMI *In* WMO Intern. Conf. on Early Results of FGGE and Large-Scale Aspects of its Monsoon Expt. 7 p Apr. 1981
Avail: NTIS MF A01; HC WMO

The impact of meteorological satellite observations is presented. Drifting buoys provide sea level atmospheric pressure and sea surface temperature for Tiros N temperature sounder retrievals. Geostationary satellites help to construct more accurate long range forecasting models. The Indian monsoon is observed. Author (ESA)

N82-23856# Commonwealth Scientific and Industrial Research Organization, Mordialoc (Australia). Div. of Atmospheric Physics.

MEAN SEA-LEVEL PRESSURE IN THE SOUTHERN HEMISPHERE DURING THE FGGE PERIOD

W. L. PHYSICK and G. B. TUCKER *In* WMO Intern. Conf. on Early Results of FGGE and Large-Scale Aspects of its Monsoon Expt. 5 p Apr. 1981 refs
Avail: NTIS MF A01; HC WMO

Drifting buoy recordings of mean sea level pressure (MSLP) are assessed as a means for investigating climate. Data from FGGE buoys were compared to long term MSLP's computed from daily numerical analyses and MSLP's from nine weather stations. Pressures observed in high latitude oceans during FGGE are lower than average for every month. The maximum difference is 12 mb. The MSLP is significantly different from normal. Mean zonal winds at 500 mb are significantly stronger by up to 50%. Buoys are useful data sources, but because the data is anomalous, they should not be used as reference points. Author (ESA)

N82-23879# Centre National de la Recherche Scientifique, Paris (France). Lab. de Meteorologie Dynamique.

REPRESENTATIVENESS OF CLOUD MOTION WINDS DEDUCED FROM GOES INDIAN OCEAN SATELLITE IMAGERY FOR THE DESCRIPTION OF THE INDIAN SUMMER MONSOON

M. DESBOIS *In* WMO Intern. Conf. on Early Results of FGGE and Large-Scale Aspects of its Monsoon Expt. 5 p Apr. 1981 refs
Avail: NTIS MF A01; HC WMO

A technique which extracts wind fields from cloud motions is described and data thus produced are compared with cloud winds extracted by standard methods, dropsondes and balloon winds of

the BALSAMINE experiment. A set of successive pictures is presented in loops. Each picture can be moved relative to the others. Pictures are aligned using landmarks and cloud motions are measured by moving the pictures so that the observed cloud appears motionless during the loop. The relative displacement of the pictures and the location of the cloud elements are recorded and the results are processed on a computer that plots them on a map. It takes 4 hr to obtain a field. Results compare well with other methods and indicate that low cloud tracers follow the wind like constant level balloons. Over the Indian Ocean low cloud winds are representative of the 900-850 mb layer. Cloud winds are advocated as a tool for investigating monsoons.
Author (ESA)

N82-23898# National Meteorological Center, Washington, D. C.
SHORT TERM INFLUENCE RADIUS OF MONSOONAL OVERTURNINGS
J. PAEGLE (Utah Univ.) *In* WMO Intern. Conf. on Early Results of FGGE and Large-Scale Aspects of its Monsoon Expt. 9 p Apr. 1981 refs
Avail: NTIS MF A01; HC WMO

The FGGE 3 b analyses and NOAA satellite data are used to delineate periods of intense convective activity over the central and western Pacific Ocean. For periods of stronger convection, the transient kinetic energy is relatively stronger over the deep tropics and into the subtropics than for times of less active tropical overturnings. Regions which are predominantly convective correspond to areas where the balance equation is nonelliptic. For these areas only steady states which are strongly divergent and with small or vanishing absolute vorticity are possible. Correlations of upper level outflows with wind components suggest substantial influence of the tropics upon the subtropics in time scales of 3 days. The need to include tropical processes in numerical weather prediction for tropical and subtropical numerical weather prediction is shown. Author (ESA)

N82-23900# Indian Inst. of Tropical Meteorology, Poona.
IMPACT OF ADDITIONAL SUMMER MONEX WIND DATA ON THE PREDICTION OF MONSOON DEPRESSIONS DURING JUNE - AUGUST 1979 WITH TWO VERSIONS OF PRIMITIVE EQUATION (PE) BAROTROPIC MODEL
D. R. SIKKA, S. SINHA, S. S. SINGH, P. L. KULKANNI, and A. A. KULKARNI *In* WMO Intern. Conf. on Early Results of FGGE and Large-Scale Aspects of its Monsoon Expt. 4 p Apr. 1981 refs Sponsored in part by Colorado State Univ.
Avail: NTIS MF A01; HC WMO

The reliability of barotropic prediction and the influence of MONEX data was investigated. Streamlines and isotachs data for 700 mb are analyzed using (1) regular weather station observations and (2) additional data from Monex platforms. Two versions of the P.E. barotropic model, which differ only in the dynamic initialization procedure, are used and it is found that they perform equally well. They perform best on those structures in which the easterly flow is of comparable strength to monsoon westerlies at 700 mb. The impact of additional data is not positive consistently because the easterlies around the depression are weaker than westerlies and the additional data are better defined the westerly maxima. Westward motion of monsoon depression is linked with the convergence ahead of the system and the preferential convection in the forward sector. It is concluded that the P.E. barotropic model is not the best one to study the impact of additional data. Author (ESA)

N82-23908# Miami Univ., Fla.
MONEX OCEANOGRAPHIC OBSERVATIONS ALONG THE EAST AFRICAN COAST
O. B. BROWN and F. SCHOTT *In* WMO Intern. Conf. on Early Results of FGGE and Large-Scale Aspects of its Monsoon Expt. 16 p Apr. 1981 refs
Avail: NTIS MF A01; HC WMO

Ship, buoy, and satellite current, temperature and air pressure data were used in order to study the Somali current. Wind field development, near surface circulation and upwelling were noted. Temperature, salinity, and potential density were recorded. The salinity profiles show several layers which deviate by more than 0.1 ppt from the mean. The density profile is smooth. So-called anomalous flow and expected flow often occur in the same year. Results suggest a mesoscale ocean-atmosphere interaction driven by the large horizontal difference in ocean surface temperature along the East African coast. Author (ESA)

N82-23909# Naval Physical and Oceanographic Lab., Cochin (India).
ON THE SPACE-TIME VARIABILITY OF OCEAN SURFACE MIXED LAYER CHARACTERISTICS OF CENTRAL AND EASTERN ARABIAN SEA DURING MONSOON-77
R. R. RAO, P. G. K. MURTY, M. G. JOSEPH, and K. V. S. RAMAN *In* WMO Intern. Conf. on Early Results of FGGE and Large-Scale Aspects of its Monsoon Expt. 8 p Apr. 1981 refs
Avail: NTIS MF A01; HC WMO

Surface mixed layer deepening and cooling of the Arabian Sea, which occurs in a nonhomogeneous manner during the monsoon season, is described. Ship polygons collected data on mixed layer (MLD) characteristics. Average MLD and vertical temperature gradient below MLD were recorded spatially and temporally. Deepening and cooling rates are higher over the central Arabian Sea than over the eastern Arabian Sea. In the central Arabian sea, deepening is greatest at the northern end. In the eastern Arabian Sea the layer deepening is higher at the southern location. The observed deepening shows good agreement with the computed layer depth, considering convective turnover caused by surface cooling. However, wind induced mixing contributes to the observed layer depth more in Phase-1U than Phase-2U. Vertical flow at the base of the mixed layer is upward, causing entrainment of colder waters from the upper thermocline and leading to mixed layer deepening and cooling. Author (ESA)

N82-23910# Wisconsin Univ., Madison.
ESTIMATES OF SEA SURFACE STRESS FOR SUMMER MONEX FROM CLOUD MOTIONS
B. B. HINTON and D. P. WYLIE *In* WMO Intern. Conf. on Early Results of FGGE and Large-Scale Aspects of its Monsoon Expt. 5 p Apr. 1981 refs
(Contract NSF ATM-79-13097)
Avail: NTIS MF A01; HC WMO

Numerical modeling of surface wind stress is described. Satellite winds, cloud motions and monthly ship data are analyzed. Cloud motion speed is plotted as a function of the speed measured by a collocated ship. A regression line extrapolates speed from cloud to ship level. Regression relations are exploited for direction changes, e.g. veering. Cloud and ship data are merged in order to produce daily stress maps. Results agree with observed published data. The method is accurate over a wide area, at a 2 deg or more resolution, for several days. Cross correlations indicate that gridded cloud motion measurements error characteristics are compatable with ship wind measurements. Author (ESA)

N82-23912# Australian Numerical Meteorology Research Center, Melbourne.
THE ONSET OF THE AUSTRALIAN NORTHWEST MONSOON DURING WINTER MONEX: BROADSCALE FLOW REVEALED BY AN OBJECTIVE ANALYSIS SCHEME
B. J. MCAVANEY, N. E. DAVIDSON, and J. L. MCBRIDE *In* WMO Intern. Conf. on Early Results of FGGE and Large-Scale Aspects of its Monsoon Expt. 5 p Apr. 1981
Avail: NTIS MF A01; HC WMO

The structure and time changes of the seasonal movement of the equatorial trough were studied using an univariate, three-dimensional optimum interpolation objective analysis scheme. Wind field and surface pressure are analyzed. Analyses are cycled so that the analysis from 12 hr previous is used as the first guess field. Ships, aircraft, land stations, ocean platforms, satellite and archive data are analyzed. The monsoon onset is a large scale event (10 deg latitude by 30 deg longitude). It is not preceeded by a similar change in the Northern Hemisphere. Forcing comes from changes in the Southern Hemisphere subtropical circulation. These changes are well simulated by numerical prediction models on the 3 to 4 day time scale. Author (ESA)

N82-23929# Brookhaven National Lab., Upton, N. Y. Atmospheric Sciences Div.

MARINE BOUNDARY LAYER WIND STRUCTURE OVER THE BAY OF BENGAL DURING MONEX-79

S. SETHURAMAN *In* WMO Intern. Conf. on Early Results of FGGE and Large-Scale Aspects of its Monsoon Expt. 7 p Apr. 1981 refs Sponsored by NSF
Avail: NTIS MF A01; HC WMO

The role of the atmospheric boundary layer in monsoon formation was investigated through a micrometeorological tower which observed turbulent fluxes of heat and momentum over the ocean, a weather station that continuously recorded mean parameters, and pilot balloon observations to a height of 1 km. Wind profiles and surface/layer fluxes of momentum and heat indicate a change in the direction of the heat flux (in a vertical plane). Surface heat flux is upward with small values for cases with large downward heat fluxes in the upper layers. This occurs when the monsoon trough is far northward causing a break in the monsoon. When the trough moves to its normal position, there is a strong convective boundary layer over the Bay of Bengal. Author (ESA)

N82-23939# Main Geophysical Observatory, Leningrad (USSR).

ESTIMATES OF THE STATISTICAL STRUCTURE OF THE ATMOSPHERIC PRESSURE FIELD IN SUMMER MONEX-79 AREA

I. A. DUYBKIN, E. A. SOSNINA, and N. A. SHKABURA *In* WMO Intern. Conf. on Early Results of FGGE and Large-Scale Aspects of its Monsoon Expt. 4 p Apr. 1981 refs
Avail: NTIS MF A01; HC WMO

Atmospheric pressure measurements (P) obtained from ships and three stationary polygons are presented. Diurnal course values, the temporal correlation structural functions, and their 95% confidence intervals were calculated using data with the diurnal course included and excluded. These show that in the northwest Indian Ocean the mean background of pressure oscillates within the limits 1011, 9 + or - 0, 7gPa and the scatter of singular measurements is within 1011, 9 + or - 2, 8gPa in the premonsoon period. During transition to monsoon circulation it is within 1008, 7 + or - 1, 2gPa and 1008, 7 + or - 3, 7gPa. During the monsoon onset it is 1007, 4 + or - 1, 2gPa and 1007, 4 + or - 3, 2gPa. The mean pressure field variability sigma p shows no significant differences for the polygons. It is within 1,4 sigma p 1, 7gPa. Author (ESA)

N82-23945# All-Union Scientific Research Inst. of Hydrometeorological Information, Moscow (USSR). World Data Centre.

ANALYSIS OF OCEAN AND ATMOSPHERE THERMODYNAMICAL CHARACTERISTICS DURING THE ONSET OF SOUTHWEST MONSOON OVER THE ARABIAN SEA

P. V. NUZHDIN *In* WMO Intern. Conf. on Early Results of FGGE and Large-Scale Aspects of its Monsoon Expt. 2 p Apr. 1981
Avail: NTIS MF A01; HC WMO

Ship surface and oceanographic data are used to analyze the onset of the Arabian Sea monsoon. Areas of marked heat storage, such as the central Arabian Sea are treated as centers of air sea coupling. A positive enthalpy anomaly is formed in this area from April to June, together with the Somali current, determines monsoon intensity. Enthalpy (H) and potential energy (Ep) were computed for the ocean layers 0 to 100 and 0 to 500 m as well as latent heat and sensible heat fluxes in the surface atmospheric layer over the ocean. The difference between the series of these characteristics for the premonsoon period and the period of the steady enthalpy decrease and heat and moisture flux increase is significant. Monsoon onset can be predicted from the moment when H and Ep stop oscillating drastically and H starts decreasing steadily. Author (ESA)

N82-24597*# Defence Science and Technology Organisation, Edgecliff (Australia).

HIGH RESOLUTION SATELLITE OBSERVATIONS OF MESOSCALE OCEANOGRAPHY IN THE TASMAN SEA, 1978 - 1979 Final Report, period ending 31 Mar. 1981

C. S. NILSSON, J. C. ANDREWS (Australian Inst. of Marine Science, Townsville), M. HORNIBROOK (CSIRO, North Ryde), A. R. LATHAM, G. C. SPEECHLEY, and P. SCULLY-POWER, Principal Investigators Feb. 1982 88 p refs Sponsored by NASA Original contains imagery. Original imagery may be purchased from NASA Goddard Space Flight Center, (code 601), Greenbelt, Md. 20770. Domestic users send orders to 'Attn: National Space Data Center'; non-domestic users send orders to 'Attn: World Data Center A for Rockets and Satellites'. HCMM
(E82-10324; NASA-CR-168903; NAS 1.26:168903; RANRL-1/82; AR-002-695) Avail: NTIS HC A05/MF A01 CSCL 08J

Of the Nearly 1000 standard infrared photographic images received, 273 images were on computer compatible tape. It proved necessary to digitally enhance the scene contrast to cover only a select few degrees K over the photographic grey scale appropriate to the scene-specific range of sea surface temperature (SST). Some 178 images were so enhanced. Comparison with sea truth show that SST, as seen by satellite, provides a good guide to the ocean currents and eddies off East Australia, both in summer and winter. This is in contrast, particularly in summer, to SST mapped by surface survey, which usually lacks the necessary spatial resolution. Author

N82-25609*# Jet Propulsion Lab., California Inst. of Tech., Pasadena.

SEA-ICE MISSION REQUIREMENTS FOR THE US FIREX AND CANADA RADARSAT PROGRAMS

F. D. CARSEY, R. O. RAMSEIER (Atmospheric Environment Service), and W. F. WEEKS (Army Cold Regions Research and Engineering Lab., Hanover, New Hampshire) Jan. 1982 83 p refs Presented at Bilateral Ice Study Team Workshop, Cornwall, Ontario, 11-13 Feb. 1981
(Contract NAS7-100)
(NASA-CR-168984; NAS 1.26:168984) Avail: NTIS HC A05/MF A01 CSCL 08F

A bilateral synthetic aperture radar (SAR) satellite program is defined. The studies include addressing the requirements supporting a SAR mission posed by a number of disciplines including science and operations in sea ice covered waters. Sea ice research problems such as ice information and total mission requirements, the mission components, the radar engineering parameters, and an approach to the transition of spacecraft SAR from a research to an operational tool were investigated. S.L.

N82-26525*# Remote Sensing Systems, Sausalito, Calif.

THE EFFECT OF SEA-SURFACE SUN GLITTER ON MICROWAVE RADIOMETER MEASUREMENTS

F. J. WENTZ 4 Nov. 1981 58 p refs
(Contract JPL-954958)
(NASA-CR-169083; JPL-9950-652; NAS 1.26:169083; RSS-TR-110481) Avail: NTIS HC A04/MF A01 CSCL 20N

A relatively simple model for the microwave brightness temperature of sea surface Sun glitter is presented. The model is an accurate closeform approximation for the fourfold Sun glitter integral. The model computations indicate that Sun glitter contamination of on orbit radiometer measurements is appreciable over a large swath area. For winds near 20 m/s, Sun glitter affects the retrieval of environmental parameters for Sun angles as large as 20 to 25 deg. The model predicted biases in retrieved wind speed and sea surface temperature due to neglecting Sun glitter are consistent with those experimentally observed in SEASAT SMMR retrievals. A least squares retrieval algorithm that uses a combined sea and Sun model function shows the potential of retrieving accurate environmental parameters in the presence of

Sun glitter so long as the Sun angles and wind speed are above 5 deg and 2 m/s, respectively. Author

N82-26758*# Instituto de Pesquisas Espaciais, Sao Jose dos Campos (Brazil).
A STUDY OF ATMOSPHERIC DIFFUSION FROM THE LANDSAT IMAGERY
N. DEJESUSPARADA, Principal Investigator, Y. VISWANADHAM, and J. A. TORSANI Dec. 1981 58 p refs Submitted for publication Sponsored by NASA Original contains color imagery. Original photography may be purchased from the EROS Data Center, Sioux Falls, S.D. 57198 ERTS
(E82-10360; NASA-CR-168981; NAS 1.26:168981; INPE-2284-PRE/060) Avail: NTIS HC A04/MF A01 CSCL 04A

LANDSAT multispectral scanner data of the smoke plumes which originated in eastern Cabo Frio, Brazil and crossed over into the Atlantic Ocean, are analyzed to illustrate how high resolution LANDSAT imagery can aid meteorologists in evaluating specific air pollution events. The eleven LANDSAT images selected are for different months and years. The results show that diffusion is governed primarily by water and air temperature differences. With colder water, low level air is very stable and the vertical diffusion is minimal; but water warmer than the air induces vigorous diffusion. The applicability of three empirical methods for determining the horizontal eddy diffusivity coefficient in the Gaussian plume formula was evaluated with the estimated standard deviation of the crosswind distribution of material in the plume from the LANDSAT imagery. The vertical diffusion coefficient in stable conditions is estimated using Weinstock's formulation. These results form a data base for use in the development and validation of meso scale atmospheric diffusion models. Author

N82-26764# Army Cold Regions Research and Engineering Lab., Hanover, N. H.
ICE DISTRIBUTION AND WINTER SURFACE CIRCULATION PATTERNS, KACHEMAK BAY, ALASKA
L. W. GATTO Dec. 1981 52 p refs
(AD-A110806; CRREL-81-22) Avail: NTIS HC A04/MF A01 CSCL 08C

Development of the hydropower potential of Bradley Lake, Alaska, would nearly double winter freshwater discharge from the Bradley River into upper Kachemak Bay, and the Corps of Engineers is concerned about possible subsequent increased ice formation and related ice-induced problems. The objectives of this investigation were to describe winter surface circulation in the bay and document ice distribution patterns for predicting where additional ice might be transported if it forms. Fifty-one LANDSAT MSS band 5 and 7 and RBV images with 70% cloud cover or less, taken between 1 November and 30 April each year, were analyzed for the eight winters from 1972 to 1980 with standard photointerpretation techniques. Results of this analysis showed that glacial sediment discharged into Kachemak Bay acts as a natural tracer in the water. Inner Kachemak Bay circulation in the winter is predominantly counterclockwise, with northeasterly nearshore currents along the south shore and southwesterly nearshore currents along the north shore. Most of the ice in the inner bay forms at its northeast end and is discharged by the Fox, Sheep and Bradley Rivers. Some ice becomes shorefast on the tidal flats at the head of the bay, while some moves southwestward along the north shore pushed by winds and currents. When this ice reaches Coal Bay, it accumulates between Homer Spit and the north shore. This buildup extended out to Coal Point at the tip of Homer Spit in February 1976 and 1979; ice was not observed in the nearshore zone along the south shore of the inner bay. GRA

N82-26766# Scripps Institution of Oceanography, La Jolla, Calif.
SATELLITE OBSERVATIONS IN FRONTS 80
M. L. VANWOERT Nov. 1981 44 p refs
(Contract N00014-80-C-0440)
(AD-A111080; SIO-REF-81-38) Avail: NTIS HC A03/MF A01 CSCL 08J

Early observations in the Central North Pacific indicate a general decrease in temperature and salinity as one moves northward from the equator. The change is not a smooth function of latitude, but rather, superimposed on a steady poleward decrease of temperature and salinity are regions of abrupt change called fronts (Seckel, 1968; Roden 1972). The general strength and location of the mid-ocean fronts are well-known. Near 45 deg. N latitude is the Pacific Subarctic Front. It separates the Pacific Subarctic water mass from the North Pacific Central water mass and is characterized by a change of 4 C per 30km and 0.6% per 30km across the front. In the vicinity of 32 deg. N is the Pacific Subtropical Front. It separates the North Pacific Central water mass from the Pacific Equatorial water mass and is characterized by a change of 2 deg. C per 30km and 0.25% per 30km across the front (Roden, 1975). A schematic map of the Central North Pacific Fronts is shown. Although the general location and strength of the mid-ocean fronts are well documented, little is known about variability associated with frontal strength and position. In December 1979 a large observational program (FRONTS 80) was undertaken to obtain basic scale information on a mid-ocean front. The North Pacific Subtropical Front, near 31 deg. N, 153 deg. W was chosen as the experiment site because of its logistical proximity to the U.S. mainland and Hawaii, and because extensive historical data exists for this region. GRA

N82-26944# Office of Technology Assessment, Washington, D.C.
TECHNOLOGY AND OCEANOGRAPHY: AN ASSESSMENT OF FEDERAL TECHNOLOGIES FOR OCEANOGRAPHIC RESEARCH AND MONITORING. VOLUME 2: WORKING PAPERS ON FISHERY RESEARCH TECHNOLOGY
Jun. 1981 245 p refs
Avail: NTIS HC A11/MF A01

The existing Federal research programs on ocean fisheries and other living oceanic resources are reviewed. The research technology and the programs provide the needed management information are evaluated and preparation for future demands on that technology and on the programs using it is discussed. The fishery research which is needed by international fishery agreements and by all regional fishery management councils is discussed. The stocks, measuring the abundance of each, and forecasting the effects on them of fishing and of environmental changes are described. E.A.K.

N82-26945# Naval Postgraduate School, Monterey, Calif. Dept. of Systems Technology.
RAPID OCEANOGRAPHIC DATA GATHERING: SOME PROBLEMS IN USING REMOTE SENSING TO DETERMINE THE HORIZONTAL AND VERTICAL THERMAL DISTRIBUTIONS IN THE NORTHEAST PACIFIC OCEAN M.S. Thesis
G. W. LUNDELL Sep. 1981 189 p refs
(AD-A111005; NPS68-81-006) Avail: NTIS HC A09/MF A01 CSCL 08J

NOAA-6 satellite AVHRR data and AXBT data were collected in the Northeast Pacific Ocean in late 1980 as part of the Naval Postgraduate School-sponsored Acoustic Storm Transfer and Response Experiment which was in turn part of the U.S.-Canadian Storm Transfer and Response Experiment (STREX). Some of the problems in transferring AXBT geographical positions to satellite images were solved by designing a computer program with accuracies of less than 2 pixels. Thermal comparisons were made between AXBT, NOAA-6, and GOSSTCOMP data with the result that NOAA-6 data was on the average of 2.9 C colder than AXBT data and 3.2 C colder than GOSSTCOMP data. Linear regression methods reduced to 0.3 C the difference between NOAA-6 and AXBT data. Use of this method over a period of 15 days produced a mean error of 0.5 C. Although NOAA-6 cannot sense directly the subsurface thermal structure, it is excellent for observing surface manifestations of horizontal thermal features. Further investigation into using satellite data as the basis of an empirical relationship between the surface temperature and the subsurface vertical thermal structure is warranted. Author (GRA)

N82-26948# Scripps Institution of Oceanography, La Jolla, Calif. Center for Coastal Studies.

FLUID-SEDIMENT INTERACTIONS ON BEACHES AND SHELVES Progress Report, 1980 - 1981

D. L. INMAN, C. D. WINANT, R. T. GUZA, and R. E. FLICK 11 Sep. 1981 91 p refs

(Contract N00014-75-C-0300)

(AD-A110838; SIO-REF-81-27) Avail: NTIS HC A05/MF A01 CSCL 08C

This research seeks to predict shelf and beach forms and their changes from knowledge of local bathymetry and the driving forces due to winds, waves and currents and their complicated interactions with nearshore sediments. The work falls into three distinct but interdependent areas of research: wave and current dynamics; fluid-sediment interactions; coastal zone remote sensing. The principal area of interest in wave and current dynamics continues to be wind generated, surface gravity waves and the currents and other fluid motions which derive their energy from surface waves. The fluid sediment interaction studies lead to an understanding of the shelf and beach sediment response including the fundamental rheology of granular fluids, the longshore and on-offshore transport of sand and the formation of features like cusps and bars. The coastal zone remote sensing tasks are largely exploratory in nature, with the general objective of determining the extent to which signatures from remote sensors can be used to define the broader spatial characteristics of driving forces, and the larger scale ocean surface patterns that are characteristic of nearshore dynamics. Author (GRA)

N82-26949# Florida State Univ., Tallahassee. Dept. of Meteorology.

METEOROLOGICAL AND AIRCRAFT DATA FOR CUE 2 1973

D. W. STUART and J. D. HAWKINS Jul. 1981 57 p refs

(Contract NSF OCE-77-27735)

(PB82-149246; CUEA-74; FSU-MET-STU-81/5; NSF/IDOE-81-88) Avail: NTIS HC A02/MF A01 CSCL 08J

Documentation of the various meteorological observations made in support of the CUE II experiment in coastal upwelling of Oregon during the summer 1975 is presented. Details of the instruments, observational techniques, and data recording systems, digitizing and reduction techniques are discussed. Selected parameters from land stations are presented as time plots. All sea surface temperature maps prepared via the aircraft are included. GRA

N82-27816# Technical Univ. of Denmark, Lyngby. Electromagnetics Inst.

MOVEMENT OF ICE MARKERS MEASURED BY SATELLITE RANGING

P. GUDMANDSEN, C. CARLE, and J. MAALOEE Paris ESA Jun. 1981 82 p refs

(Contract ESA-4634/81)

(R-240; ESA-CR(P)-1547) Avail: NTIS HC A05/MF A01

A method for determining the surface velocity of large ice sheets in Greenland and Antarctica involves measuring the change of distance between fixed markers and those on ice sheets, using ERS-1 for altimetry and radar ranging. An acceptable signal to noise ratio can be obtained with the ERS-1 high gain antenna and a marker, consisting of a square trihedral corner reflector, with side length = 1.5 m, radar cross section 55 dB. The high gain antenna limits the area investigated to an 18 km swath, assuming a 5 deg incidence angle. A Swerling type radar cross section of the corner reflector results in a 62% detection probability for 6-pulse integration. Displacement of markers can only be measured at crossing ground tracks when the satellite is operated in a rigid orbit mode, i.e., a 20 X 20 km area. Accuracy of 78 cm is possible. Author (ESA)

N82-27949# National Weather Service, Fort Worth, Tex. National Hurricane Center.

SOME EMPIRICAL RULES FOR FORECASTING FOG AND STATUS OVER NORTHERN FLORIDA, SOUTHERN GEORGIA AND ADJACENT COASTAL WATERS

E. L. RICKS Aug. 1981 15 p refs

(PB82-154006; NOAA-TM-NWS-SR-104; NOAA-81111608) Avail: NTIS HC A02/MF A01 CSCL 04B

Strong low-level winds, especially strong vertical wind shear, generate and maintain enough mixing below the subsidence inversion over southern Georgia and northern Florida to counteract, or inhibit, low stratus and fog formation. Weaker northeast and east winds flavor low stratus and fog formation over southern Georgia and northern Florida when the trajectory is from the Atlantic coast. GRA

06

HYDROLOGY AND WATER MANAGEMENT

Includes snow cover and water runoff in rivers and glaciers, saline intrusion, drainage analysis, geomorphology of river basins, land uses, and estuarine studies.

A82-13528#

EFFECTIVE ELECTROMAGNETIC SHIELDING IN MULTILAYER PRINTED CIRCUIT BOARDS

K. G. WILES and J. L. MOE (General Dynamics Corp., Fort Worth, TX) In: Digital Avionics Systems Conference, 4th, St. Louis, MO, November 17-19, 1981, Collection of Technical Papers. New York, American Institute of Aeronautics and Astronautics, 1981, p. 593-596.

(AIAA 81-2333)

Multilayer printed circuit boards have proven to be recurrent abettors of electromagnetic coupling problems created by the incessantly faster response times in integrated circuit technologies. Coupling within multilayer boards has not only inhibited meeting certain EMI requirements but has also precipitated 'self-inflicted' malfunctions commonly experienced during development of avionic systems. A recent avionic system, interfacing two asynchronous processors through a fourteen-layer motherboard, permitted coupling through ground plane connector apertures of sufficient amplitude and duration as to cause unintentional intercommunication and system malfunctions. The coupling mechanism and ground plane modifications which reduced this coupling by 40 dB and eliminated the incompatibility are discussed in this paper (Author)

A82-22615

THE MODULATION CHARACTERISTICS OF THE 19TH AND 20TH SOLAR ACTIVITY CYCLES

N. N. KONTOR, G. P. LIUBIMOV, N. V. PERESLEGINA, and T. I. STEPINA (Moskovskii Gosudarstvennyi Universitet, Moscow, USSR) In: International Cosmic Ray Conference, 17th, Paris, France, July 13-25, 1981, Conference Papers. Volume 3. Gif-sur-Yvette, Essonne, France, Commissariat a l'Energie Atomique, 1981, p. 179-182. refs

The intensity modulation of galactic cosmic rays at 1 AU from the sun is described in terms of the nonstationary model. The dependencies of the modulation coefficients are found, which characterize the galactic cosmic ray fluxes to and from the sun on the solar activity level, and consideration is given to the dependencies of the modulation parameters on time and cosmic ray energy. Significant variations are observed in the modulation factors, even for the smoothed data, and the transparency coefficient is proportional to the particle energy, while the transfer coefficient is inverse. D.L.G.

A82-29333

A SIMULATION STUDY OF SOIL MOISTURE ESTIMATION BY A SPACE SAR

F. T. ULABY, C. DOBSON, J. STILES, R. K. MOORE, and J. HOLTZMAN (University of Kansas Center for Research, Inc., Lawrence, KS) Photogrammetric Engineering and Remote Sensing, vol. 48, Apr. 1982, p. 645-660. refs

An evaluation of the accuracy of soil moisture estimates available from satellite radar remote sensing is made, along with an assessment of the effects of spatial resolution on the estimation accuracy. Synthetic aperture radar (SAR) images of a 17.7 x 19.3 km test site were generated by image simulation techniques for a space SAR orbiting at 600 km and operating at 4.75 GHz, an HH polarization, and an angle of incidence range between 7-22 deg from nadir. Data bases were constructed of U-2 color IR photographs, 20 m x 20 m pixel soil elements from the USDA totalling 800,000 pixels classified for target class, soil texture, and surface elevation. Three sets of images were generated for four varying soil moisture distributions across the site. Soil moisture in 90% of the 20 m x 20 m pixels were found to be predictable in terms of moisture capacity to within 20%. A 100 m x 100 m resolution was best for very dry soil conditions. M.S.K.

A82-32896* Texas Univ. at Austin.

INTERPRETATION OF SURFACE-WATER CIRCULATION, ARANSAS PASS, TEXAS, USING LANDSAT IMAGERY

R. J. FINLEY and R. W. BAUMGARDNER, JR. (Texas, University, Austin, TX) Remote Sensing of Environment, vol. 10, Aug. 1980, p.3-22. refs

(Contract NAS5-20986)

The development of plumes of turbid surface water in the vicinity of Aransas Pass, Texas has been analyzed using Landsat imagery. The shape and extent of plumes present in the Gulf of Mexico is dependent on the wind regime and astronomical tide prior to and at the time of satellite overpass. The best developed plumes are evident when brisk northerly winds resuspend bay-bottom muds and flow through Aransas Pass is increased by wind stress. Seaward diversion of nearshore waters by the inlet jetties was also observed. A knowledge of surface-water circulation through Aransas Pass under various wind conditions is potentially valuable for monitoring suspended and surface pollutants (Author)

A82-32910* National Aeronautics and Space Administration. Goddard Space Flight Center, Greenbelt, Md.

A COMPARATIVE STUDY OF MICROWAVE RADIOMETER OBSERVATIONS OVER SNOWFIELDS WITH RADIATIVE TRANSFER MODEL CALCULATIONS

A. T. C. CHANG and J. C. SHIUE (NASA, Goddard Space Flight Center, Laboratory for Atmospheric Sciences, Greenbelt, MD) Remote Sensing of Environment, vol. 10, Nov. 1980, p. 215-229. refs

(Previously announced in STAR as N79-30611)

A82-33329

THE GROWTH OF SNOW IN WINTER STORMS - AN AIRBORNE OBSERVATIONAL STUDY

K. K. LO and R. E. PASSARELLI, JR. (MIT, Cambridge, MA) Journal of the Atmospheric Sciences, vol. 39, Apr. 1982, p. 697-706. refs

(Contract F19628-80-C-0021)

In studies of precipitation growth, comparisons between theory and observation are difficult because of the problem in obtaining a complete four-dimensional (space and time) description of the kinematic, thermodynamic and microphysical properties of the atmosphere. A new flight plan has been devised which permits one to observe the height evolution of snow-size spectra in a reference frame where the effects of horizontal gradients and temporal changes are minimized. The flight plan, termed the advecting spiral descent (ASD), requires an aircraft to start aloft in a mesoscale precipitation area and then spiral downward in a constant bank angle, descending at approximately the mean fallspeed of snow. Qualitative comparisons between ASD observations and particle growth theory suggest that snow evolves through at least three stages characterized by deposition, aggregation and breakup. The breakup process serves to limit the number of large snow particles and interacts with aggregation to produce a limiting value of the slope of the snow-size spectrum. (Author)

A82-34734

AUTOMATED CLASSIFICATION OF RUNOFF COEFFICIENTS FROM LANDSAT MULTISPECTRAL DATA

F. ASKARI (Ohio State University, Columbus, OH) and N. L. FAUST (Georgia Institute of Technology, Atlanta, GA) In: American Society of Photogrammetry, Annual Meeting, 47th, Washington, DC, February 22-27, 1981, ASP Technical Papers. Falls Church, VA, American Society of Photogrammetry, 1981, p. 426-439. Research supported by the Ohio State University Research Foundation. refs

Multispectral data from Landsat are used with aircraft color infrared photography to derive the runoff coefficients for watersheds in Mill Creek, Ohio. Regression models are developed from the treatment of the runoff coefficient of each sample site as the dependent variable, and the mean radiance measurements in the four Landsat channels as the independent variables. A comparison of classification results illustrates the spatial and temporal variations of runoff potential for the surface. Single cover test fields and test watersheds are used to verify the model results, and the mean runoff coefficients derived for the test watersheds from the multispectral data analysis technique compare favorably with those obtained from ground truth. D.L.G.

A82-34735

DIGITAL AND VISUAL EVALUATION OF GOES AND TIROS/NOAA IMAGE DATA FOR COVER TYPE EFFECTS ON SNOWFIELD OBSERVATIONS

T. M. LILLESAND, D. E. MEISNER, A. L. DOWNS, and R. L. DEUELL (Minnesota, University, St. Paul, MN) In: American Society of Photogrammetry, Annual Meeting, 47th, Washington, DC, February 22-27, 1981, ASP Technical Papers. Falls Church, VA, American Society of Photogrammetry, 1981, p. 450-465. Research supported by the University of Minnesota refs

(Contract NOAA-NA-80AAD0019)

A82-34736* National Aeronautics and Space Administration. Goddard Space Flight Center, Greenbelt, Md.

USE OF AERIAL PHOTOGRAPHY IN DETERMINING LAND USE AND STREAMFLOW RELATIONSHIPS ON SMALL DEVELOPING WATERSHEDS

M. OWE (NASA, Goddard Space Flight Center, Hydrological Sciences Branch, Greenbelt, MD) In: American Society of Photogrammetry, Annual Meeting, 47th, Washington, DC, February 22-27, 1981, ASP Technical Papers. Falls Church, VA, American Society of Photogrammetry, 1981, p. 466-475. refs

Using aerial photographs dating back to 1937, the historical trends of five land use classes (crop, forest, open field, urban and suburban) are determined. The relationships between these and various flow regime parameters are investigated. Annual runoff is found to be 7.5 inches greater now than in the year 1932. It is also found that growing season runoff increased by 3.5 inches during the same period. This increase is approximately equivalent to 160 area inches of excess runoff during the 45-year period of observation. The increase in runoff is found to be positively correlated with the percent basin area in the urban, suburban and open field land use classes. A negative correlation is established with forest and crop land. Although poor correlations are found with high flow, low flow, flow interval and flow date data, it is thought that a more precise quantification of land use or a smaller basin area may possibly have yielded more positive results for streamflow timing data. C.R.

A82-34745

AERIAL PHOTOGRAPHY VS. LANDSAT FOR DIGITAL LAND-COVER MAPPING IN AN URBAN WATERSHED

B. K. QUIRK and F. L. SCARPACE (Wisconsin, University, Madison, WI) In: American Society of Photogrammetry, Annual Meeting, 47th, Washington, DC, February 22-27, 1981, ASP Technical Papers. Falls Church, VA, American Society of Photogrammetry, 1981, p. 610-617. refs

A comparison was made between digital analyses of color infrared film and Landsat to provide land-cover information in an urban watershed. The results were compared to a manual photo interpretation of a black and white infrared photograph. Both the color infrared and Landsat produced similar land-cover acreages and both were similar to the black and white interpretation. However, the color infrared was found to be a better representation. (Author)

A82-35126

STUDY OF THE HYDROLOGICAL CYCLE BY AEROSPACE METHODS [IZUCHENIE GIDROLOGICHESKOGO TSIKLA AEROKOSMICHESKIMI METODAMI]

K. IA. KONDRATEV, (ED.) and IU. V. KURILOVA Moscow, Izdatel'stvo Radio i Sviaz', 1982. 100 p. In Russian.

Topics discussed include principles and methods of the study of the hydrological cycle on the basis of remote-sensing methods, water-balance differentiation of natural complexes on the basis of satellite photographs, the use of remote sensing to study the hydrology of elementary watersheds, and methods for the analysis of the melting of firn complexes on the basis of satellite photographs. The mapping of snow lines in the central part of the European USSR, the forecasting of pluvial floods in Mongolia on the basis of remote-sensing data, the measurement of water-surface temperature by means of airborne infrared radiometers, the use of multispectral photography to study littoral zones, and the use of remote sensing to study the space-time variability of water quality are also considered. B.J.

A82-35127

PRINCIPLES AND METHODS OF THE STUDY OF THE HYDROLOGICAL CYCLE ON THE BASIS OF AEROSPACE DATA [PRINTSIPY I METODY IZLUCHENIIA GIDROLOGICHESKOGO TSIKLA PO AEROKOSMICHESKOI INFORMATSII]

IU. V. KURILOVA, A. M. GRIN, and P. A. KOLOSOV In: Study of the hydrological cycle by aerospace methods. Moscow, Izdatel'stvo Radio i Sviaz', 1982, p. 5-18. In Russian. refs

The paper examines the possibilities and advantages of using satellite data to study various aspects of the hydrological cycle. Methods for evaluating the separate components of the cycle are generalized. In addition, indirect methods for determining slowly and rapidly varying parameters of the cycle on the basis of global TV and IR data acquired by satellites are proposed. Attention is also given to the principles of dynamic regionalization according to types of processes and landscape features on the basis of multispectral data. B.J.

A82-35129

WATER-BALANCE DIFFERENTIATION OF NATURAL COMPLEXES ON THE BASIS OF SATELLITE PHOTOGRAPHS [VODNOBALANSOVAIA DIFFERENTSIATSIIA PRIRODNYKH KOMPLEKSOV NA OSNOVE ISPOL'ZOVANIIA KOSMICHESKIKH SNIMKOV]

A. V. LEBEDEV In: Study of the hydrological cycle by aerospace methods. Moscow, Izdatel'stvo Radio i Sviaz', 1982, p. 25-29. In Russian. refs

The paper examines methods for assessing the role of natural complexes, particularly forest complexes, in hydrology. These methods are then used to evaluate techniques of the differentiation and mapping of hydrological parameters on the basis of the structural elements of natural-territorial complexes. As an example, attention is given to the thermal and water-balance characteristics of the natural complexes of the middle and southern taiga of the Ob-Yenisei interfluve as determined from satellite photographs. B.J.

A82-35130

THE POSSIBILITY OF USING REMOTE-SENSING METHODS TO STUDY THE HYDROLOGY OF ELEMENTARY WATERSHEDS [VOZMOZHNOSTI PRIMENENIIA DISTANTSIONNYKH METODOV V OBLASTI GIDROLOGII ELEMENTARNYKH VODOSBOROV]

K. KASPRZHAK and F. SHABELA In: Study of the hydrological cycle by aerospace methods. Moscow, Izdatel'stvo Radio i Sviaz', 1982, p. 30-35. In Russian. refs

Theoretical and experimental determinations of the microwave radiation characteristics of wet soils are compared. A survey is then presented of methods for measuring the hydrological regimes of soils in the visible, infrared, and microwave ranges. Particular emphasis is placed on the use of active-radar techniques at wavelengths of 0.3-30 cm and even 100 cm, which make it possible to analyze the hydrological regimes of soils at great depths. B.J.

A82-35131

THE SEASONAL SNOW-LINE WITHIN THE FERGANA BASIN AND THE POSSIBILITY OF USING IT FOR HYDROLOGICAL FORECASTING [SEZONNAIA SNEGOVAIA GRANITSA V PREDELAKH FERGANSKOI KOTLOVINY I VOZMOZHNOSTI EE ISPOL'ZOVANIIA V GIDROPROGNOZAKH]

O. P. SHCHEGLOVA and V. IU. CHERNOV In: Study of the hydrological cycle by aerospace methods. Moscow, Izdatel'stvo Radio i Sviaz', 1982, p. 36-41. In Russian. refs

TV data acquired by meteorological satellites during 1969-1978 are used to study snow cover within the mountain region of the Fergana basin. The dynamics of the seasonal snow-line during spring thaw is investigated; and the positions of the seasonal snow-line for individual days in 1969 are given. The data are used to evaluate the possibility of making hydrological forecasts on the basis of relationships between the monthly average water discharge and the height of the snow line at the end of the preceding month. B.J.

A82-35132

THE USE OF SATELLITE PHOTOGRAPHS TO STUDY SNOW-COVER DYNAMICS AND TO DETERMINE THE AVERAGE WATER DISCHARGE OF THE AMUDARYA DURING A VEGETATION PERIOD [ISPOL'ZOVANIE SPUTNIKOVYKH SNIMKOV DLIA IZUCHENIIA DINAMIKI SNEZHNOGO POKROVA I OTSENKI SREDNEGO RASKHODA VODY AMUDAR'I ZA VEGETATSIONNYI PERIOD]

M. V. DZHORZHIO, M. V. SITNIKOVA, and B. K. TSAREV In: Study of the hydrological cycle by aerospace methods. Moscow, Izdatel'stvo Radio i Sviaz', 1982, p. 42-45. In Russian. refs

A82-35133

METHOD FOR THE ANALYSIS OF THE MELTING OF A FIRN COMPLEX ON THE BASIS OF AEROSPACE PHOTOGRAPHS [METODIKA RASCHETA TAIANIIA KOMPLEKSA SNEZHNIKOV PO AEROKOSMICHESKIM SNIMKAM]

N. I. OSOKIN In: Study of the hydrological cycle by aerospace methods. Moscow, Izdatel'stvo Radio i Sviaz', 1982, p. 46-49. In Russian. refs

The characteristics of firn melting are investigated on the basis of field studies performed in the polar Urals, Crimea, and Kamchatka, as well as on the basis of satellite data. It is shown that the intensity of melting is determined by the dimensions and shape of the firn basin. A dimensionless parameter for the shape of a firn basin is proposed which makes it possible to calculate the melting rate of individual firn basins as well as their complexes. Methods of automated processing of satellite photographs are examined, which may be used to determine this parameter in hydrometeorological calculation and forecasting. B.J.

A82-35134

EXPERIENCE WITH THE COMPILATION OF MAPS OF SNOW-COVER MELTING IN THE CENTRAL PART OF THE EUROPEAN USSR ON THE BASIS OF SATELLITE DATA [OPYT SOSTAVLENIIA KART SKHODA SNEZHNOGO POKROVA TSENTRAL'NOI CHASTI ETS PO DANNYM SPUTNIKOVOI INFORMATSII]

M. S. DELEUR, E. I. PANKRATOVA, and L. P. BABKINA In: Study of the hydrological cycle by aerospace methods. Moscow, Izdatel'stvo Radio i Sviaz', 1982, p. 50-54. In Russian.

The paper examines techniques for the compilation of snow-cover melting maps from satellite photographs as well as methods for the interpretation of snow-cover features for various territories. Attention is given to the possibility of determining the following features from satellite photographs: the position of snow lines and the velocity of their motion, and the extent of snow in river drainage systems. The accuracy with which snow lines can be depicted on maps is examined. B.J.

A82-35136

EVALUATION OF THE ACCURACY OF WATER-SURFACE TEMPERATURE MEASUREMENT BY MEANS OF AIRBORNE INFRARED RADIOMETERS [OTSENKA TOCHNOSTI IZMERENIIA TEMPERATURY POVERKHNOSTI VODY SAMOLETNYM RADIATSIONNYM TERMOMETROM]

A. M. NIKITIN and S. N. TEMNIKOV In: Study of the hydrological cycle by aerospace methods. Moscow, Izdatel'stvo Radio i Sviaz', 1982, p. 62-64. In Russian.

Two sets of experiments are described whose objective was to evaluate the accuracy of the MIR-3 small-scale infrared radiometer, installed on the Il-14 aircraft, for measuring the surface temperature of natural water bodies. The first set involved measurements of the surface temperature of Lake Issyk-Kul, carried out in July 1977. The second set involved five series of measurements of the surface temperature of the Aral Sea and five series of measurements of the surface temperature of Lake Issyk-Kul. The effect of atmospheric attenuation on the performance of the radiometers was evaluated. B.J.

A82-35138

THE USE OF REMOTE-SENSING DATA TO IDENTIFY THE SPACE-TIME VARIABILITY OF THE QUALITY OF NATURAL WATERS [ISPOL'ZOVANIE AEROKOSMICHESKOI INFORMATSII DLIA OBNARUZHENIIA PROSTRANSTVENNO-VREMENNOI IZMENCHIVOSTI KACHESTVA PRIRODNYKH VOD]

V. A. KRIULKOV, IU. V. ZAVOLOKIN, V. I. NOSACHEV, L. A. SHLIAKHOVA, and S. T. LAPCHENKOV In: Study of the hydrological cycle by aerospace methods. Moscow, Izdatel'stvo Radio i Sviaz', 1982, p. 75-79. In Russian.

Remote-sensing techniques for obtaining the quantitative characteristics of the space-time variability of water quality and reservoir pollution are assessed with particular attention given to the possibility of developing an operational system for the monitoring of water quality. Optimal spectral ranges of measurements, photointerpretation keys, and zones of relatively constant concentration values are determined on the basis of ground-based and airborne measurements. Algorithms for the processing of remote-sensing images obtained by different techniques are examined, and a hybrid system based on the synthesis of TV and digital data is proposed. B.J.

A82-35140

COMPARISON OF BRIGHTNESS INDICATRIXES OF SNOW COVER MEASURED FROM AN AIRCRAFT AND CALCULATED THEORETICALLY FOR DIFFERENT HEIGHTS OF THE ATMOSPHERE [SRAVNENIE INDIKATRIS IARKOSTI SNEZHNOGO POKROVA, IZMERENNYKH S SAMOLETA I RASSCHITANNYKH TEORETICHESKI DLIA OTDEL'NYKH VYSOT ATMOSFERY]

V. V. KOZODEROV In: Study of the hydrological cycle by aerospace methods. Moscow, Izdatel'stvo Radio i Sviaz', 1982, p. 86-88. In Russian. refs

A82-37174

THE USE OF SPACE PHOTOGRAPHS IN THE MAPPING OF GLACIERS AND WATER BODIES [ISPOL'ZOVANIE KOSMICHESKIKH SNIMKOV PRI KARTOGRAFIROVANII LEDNIKOV V VODNYKH OB'EKTOV]

M. A. ALIMUKHAMEDOV, IU. N. LESNIK, and A. M. TIMOSHENKO Geodeziia i Kartografiia, May 1982, p. 24-30. In Russian. refs

The use of black and white, multispectral, and color space photographs for the investigation of glaciers and water resources in the Middle Asiatic region has made possible the operational monitoring of their state and dynamics. Morphometric indices for the Fedchenko glacier, the Aidaro-Arnasaiskii water complex, and Lake Sarykamysh obtained from the interpretation of space photographs were found to be sufficiently accurate for various practical needs of the economy. B.J.

A82-37501

REMOTE SENSING IN SCOTLAND USING DATA RECEIVED FROM SATELLITES - A STUDY OF THE TAY ESTUARY REGION USING LANDSAT MULTISPECTRAL SCANNING IMAGERY

A. P. CRACKNELL, N. MACFARLANE, K. MCMILLAN, J. A. CHARLTON, J. MCMANUS (Dundee, University, Dundee, Scotland), and K. A. ULBRICHT (Deutsche Forschungsund Versuchsanstalt fuer Luft- und Raumfahrt, Oberpfaffenhofen, West Germany) International Journal of Remote Sensing, vol. 3, Apr.-June 1982, p. 113-137. Research supported by the Carnegie Trust and Science and Engineering Research Council. refs

Multispectral scanning data from Landsat are used to study the sandbanks and tidal flats in the Tay Estuary, and the specialized digital image-processing system used in the study is briefly described. Several examples of Landsat-2 images of the Tay Estuary and its environs are presented as false-color composites and monochrome pictures, and a qualitative interpretation and several quantitative ones are presented. The low-water mark for sandbanks in the upper and lower estuary is determined and the results are compared with existing charts and maps, showing that changes in the positions of sandbanks of the size found in the estuary can be monitored satisfactorily using satellite imagery. The position of an estuarine front is mapped and also observed in situ in the position indicated by this image. An attempt at quantitative bathymetry, using a high tide Landsat image, indicated that depths up to three or four meters can be determined from the satellite data, but the accuracy is rather poor. C.D.

N82-22625*# Environmental Research and Technology, Inc., Concord, Mass.

THE APPLICATION OF HEAT CAPACITY MAPPING MISSION (HCMM) THERMAL DATA TO SNOW HYDROLOGY Final Report, Sep. 1977 - Mar. 1981

J. C. BARNES, Principal Investigator, C. J. BOWLEY, M. D. SMALLWOOD, and J. H. WILLAND Mar. 1981 112 p refs Original contains imagery. Original imagery may be purchased from NASA Goddard Space Flight Center, (code 601), Greenbelt, Md. 20771. Domestic users send orders to 'Attn: National Space Science Data Center'; non-domestic users send orders to 'Attn: World Data Center A for Rockets and Satellites'. HCMM (Contract NAS5-24316)

(E82-10191; NASA-CR-168619; NAS 1.26:168619; ERT-P-2061-F) Avail: NTIS HC A06/MF A01 CSCL 08L

The application of HCMM thermal infrared data to snow hydrology and the prediction of snowmelt runoff was evaluated. Data for the Salt Verde watershed in central Arizona and the southern Sierra Nevada in California were analyzed and compared to LANDSAT and NOAA satellite data, U-2 thermal data, and other correlative data. It was determined that HCMM thermal imagery provides data as accurate for snow mapping as does visible imagery, and that in comparison with the reslution of other satellite imagery, it may be the most useful. Data from the HCMM thermal channel, with careful calibration, provides useful snow surface temperature data for hydrological purposes. An approach to an automated method of analysis is presented. J.D.

N82-22644# National Oceanic and Atmospheric Administration, Rockville, Md. Ocean Technology and Engineering Services Office.

BIAS CORRECTION PROCEDURES FOR AIRBORNE LASER HYDROGRAPHY

G. C. GUENTHER and R. W. L. THOMAS Aug. 1981 110 p refs Prepared in cooperation with EG and G Washington Analytical Services Center, Inc., Rockville, Md. sponsored in part by Naval Ocean Research and Development Activity, NSTL Station, Miss.

(PB82-130089; NOAA-TR-OTES-03; NOAA-8110502) Avail: NTIS HC A06/MF A01 CSCL 08J

Depending on the entry nadir angle of the beam and the optical properties of the water, one of two opposing effects, multiple scattering and geometric 'undercutting', will dominate and result in either a deep or shallow depth measurement bias, respectively. The magnitude of this bias can greatly exceed international hydrographic accuracy standards, and hence bias correctors must be calculated and applied to the raw depths in postflight data processing to attain the required accuracy for the overall system. The magnitudes of the bias correctors depend not only on the water and flight parameters, but also on the basic design of the receiver electronics. Several typical systems and procedures required to calculate a set of bias correctors for any given system are described and a cookbook approach for the necessary postflight data processing algorithms are included. GRA

N82-22854# National Oceanic and Atmospheric Administration, Rockville, Md. Earth Satellite Lab.

A STATISTICAL APPROACH TO RAINFALL ESTIMATION USING SATELLITE AND CONVENTIONAL DATA

L. F. WHITNEY, JR. Apr. 1982 55 p refs

(NOAA-TR-NESS-89) Avail: NTIS HC A04/MF A01

A statistical approach is employed in an attempt to estimate convective rainfall using both satellite and conventional data. A variety of variables derived from both satellite and conventional meteorological sources are presented. From among these variables, a screening regression method selects those which best explain area-averaged rainfall. Among the cases studied, the relationship of each variable to rainfall is weak to poor, particularly as cases are combined. Although multivariate selections improve the relationships, inconsistency of selection develops from one case to another and from one time to another, even in the same meteorological situation. Regression equations are found to estimate the amount inadequately, even when using dependent data. At best, rainfall is not likely to be measured quantitively by such an approach and, at worst, concern is raised about the validity of using the variables investigated to estimate rainfall. B.W.

N82-24569*# Instituto de Pesquisas Espaciais, Sao Jose dos Campos (Brazil).

DYNAMIC STUDY OF THE UPPER SAO FRANCISCO RIVER AND TRES MARIAS RESERVOIR USING MSS/LANDSAT IMAGES M.S. Thesis

N. DEJESUSPARADA, Principal Investigator and T. M. SAUSEN Oct. 1981 272 p refs In PORTUGUESE; ENGLISH summary ERTS

(E82-10291; NASA-CR-168860; NAS 1.26:168860; INPE-2249-TDL/066) Avail: NTIS HC A12/MF A01 CSCL 05B

The relationship between the dispersion and concentration of sediment in the superficial layers of the Tres Marias reservoir and the dynamics of the drainage basins of its tributaries was verified using LANDSAT MSS imagery. The drainage network, dissection patterns, and land use of each watershed were considered in an analysis of multispectral images, corresponding to bands 4,5, and 7, of dry and rainy seasons in 1973, 1975, 1977, and 1978. The superficial layer water layers of the reservoir were also divided according to the grey level pattern of each image. Two field trips were made to collect Secchi depths and in situ water reflectance. It is concluded that it is possible to determine the main factors that act in the dynamics of the drainage basins of a reservoir by simultaneous control of the physical variables and the antropic action of each basin. A.R.H.

N82-24601*# Brigham Young Univ., Provo, Utah. Dept. of Civil Engineering.

HCMM HYDROLOGICAL ANALYSIS IN UTAH Quarterly Progress Report

28 Feb. 1982 43 p Sponsored by NASA HCMM

(E82-10328; NASA-CR-168907; NAS 1.26:168907; QPR-3) Avail: NTIS HC A03/MF A01 CSCL 05B

Temperature calibration and groundwater depth location studies were finalized. Distinctions among algae species and among suspended materials (turbidity) using HCMM data were investigated. Field evaluations of algae's effect on evaporation pan readings were completed and related to the lake and HCMM data. Additional correlations among infrared and reflectivity data were made using the color graphics capabilities developed during this project. E.A.K.

07

DATA PROCESSING AND DISTRIBUTION SYSTEMS

Includes film processing, computer technology, satellite and aircraft hardware, and imagery.

A82-22538* New Hampshire Univ., Durham.

FRAGMENTATION OF FE NUCLEI ON CARBON, HYDROGEN AND CH2 TARGETS. I - INDIVIDUAL CHARGE CHANGING AND TOTAL CROSS SECTIONS. II - ISOTOPIC CROSS SECTIONS

D. A. BRAUTIGAM, J. H. CHAPELL, J. C. KISH, G. A. SIMPSON, and W. R. WEBBER (New Hampshire, University, Durham, NH) In: International Cosmic Ray Conference, 17th, Paris, France, July 13-25, 1981, Conference Papers. Volume 2. Gif-sur-Yvette, Essonne, France, Commissariat a l'Energie Atomique, 1981, p. 173-180. refs

(Contract NGR-30-002-052)

The fragmentation of Fe nuclei in carbon and CH2 targets at energies of 650, 800, and 950 MeV/nuc has been studied. Direct measurements of the interaction between Fe nuclei and the carbon and CH2 targets were carried out. The Fe to H charge changing cross sections derived for selected nuclei showed a clear energy dependence, consistent with the results of Westfall et al. (1979). Values for the total inelastic cross section Fe to H charge changing were obtained by two methods: the first method involved subtracting the total CH2 and C cross sections (values of 703 plus or minus 9 mb and 65 plus or minus 10 mb at 950 MeV/nuc and 650 MeV/nuc, respectively were obtained). The same cross sections were obtained by adding the individual charge changing cross sections. A cross section for Fe to fragment into lower mass Fe isotopes of 65 plus or minus 5 mb was also observed, giving total inelastic mass changing cross sections of 768 plus or minus 11 mb and 716 plus or minus 12 mb, respectively. In addition, the individual isotopic cross sections for Z equals 16-25 are reported. J.F.

A82-22540

ON THE CHARACTERISTICS OF THE VERY LOW ENERGY GALACTIC COSMIC RAYS IN THE INTERSTELLAR SPACE

M. B. KRAINEV (Akademiia Nauk SSSR, Fizicheskii Institut, Moscow, USSR) In: International Cosmic Ray Conference, 17th, Paris, France, July 13-25, 1981, Conference Papers. Volume 2. Gif-sur-Yvette, Essonne, France, Commissariat a l'Energie Atomique, 1981, p. 186-189. refs

The interstellar spectra of several cosmic ray nuclei and ions (H, He, C, O) are calculated in the energy range T less than 1 MeV/n, where the charge-exchange processes become significant. The ionization energy loss and the processes of electron loss and capture are taken into account. The cosmic ray intensity calculation is discussed in detail, and spectra results are presented and interpreted. J.F.

A82-22555* New Hampshire Univ., Durham.

THE CHARGE AND ISOTOPIC COMPOSITION OF Z EQUALS 7-16 COSMIC RAY NUCLEI AT THEIR SOURCE

W. R. WEBBER (New Hampshire, University, Durham, NH) In: International Cosmic Ray Conference, 17th, Paris, France, July 13-25, 1981, Conference Papers. Volume 2. Gif-sur-Yvette, Essonne, France, Commissariat a l'Energie Atomique, 1981, p. 261-264. refs

(Contract NGR-30-002-052)

Using the combined data from our 1976 and 1977 balloon flights, the charge and isotopic composition of Z equals 7-16 cosmic ray nuclei have been determined. A low abundance of both N and Ne in the cosmic ray source relative to solar cosmic rays is observed. However, the cosmic ray source ratio, Ne-22/Ne is 2.75 plus or minus 0.42 times the solar ratio. A possible enhancement of the Mg-26/Mg ratio, which is 1.29 plus or minus 0.14 times the solar ratio is also observed. (Author)

A82-22558

COSMIC RAY COMPOSITION FROM ACCELERATION OF THERMAL MATTER

J. PEREZ-PERAZA (Universidad Nacional Autonoma de Mexico, Villa Obregon, Mexico) In: International Cosmic Ray Conference, 17th, Paris, France, July 13-25, 1981, Conference Papers. Volume 2. Gif-sur-Yvette, Essonne, France, Commissariat a l'Energie Atomique, 1981, p. 273-276.

The source composition of cosmic rays is thought to be controlled by Coulombian interactions during the acceleration of thermal matter. A given element is representative of the source or depletion depending on whether the predominant ionic state at the temperature of the source is lower than a threshold imposed by Coulombian losses. Coupling this restriction to the theory of ionization equilibrium, the source abundances are calculated. The results corroborate sources of relatively low temperature. C.R.

A82-22568

ACCELERATION OF COSMIC RAYS IN ACCRETION SHOCKS

R. COWSIK (Tata Institute of Fundamental Research, Bombay, India) and M. A. LEE (New Hampshire, University, Durham, NH) In: International Cosmic Ray Conference, 17th, Paris, France, July 13-25, 1981, Conference Papers. Volume 2. Gif-sur-Yvette, Essonne, France, Commissariat a l'Energie Atomique, 1981, p. 318-321. refs

Spherically symmetric accretion around condensed astronomical objects like white dwarfs, neutron stars and black holes very often go through a quasi-stationary shock close to the object. The transport of radiation, energetic particles and neutrinos in such flows is studied, and it is found that these are accelerated to high energies very efficiently. The generated spectra are seen to have power-law behavior when the diffusion coefficient is independent of particle momentum. The possibility that the bulk of the galactic cosmic rays are accelerated by approximately 10,000 neutron stars which are surrounded by dense interstellar clouds is briefly discussed. (Author)

A82-22573

THE GALACTIC ORIGIN OF COSMIC RAYS. II

S. A. COLGATE (Los Alamos National Laboratory, Los Alamos; New Mexico Institute of Mining and Technology, Socorro, NM) In: International Cosmic Ray Conference, 17th, Paris, France, July 13-25, 1981, Conference Papers. Volume 2. Gif-sur-Yvette, Essonne, France, Commissariat a l'Energie Atomique, 1981, p. 352-355. refs

(CONF-810711-2; LA-UR-81-966)

The cosmic ray pressure limit to cosmic ray acceleration in the interstellar medium (ISM) is considered. It is found that the beta equals 1 Alfven speed streaming limit imposes a new and strong constraint on supernova-ISM shock models of cosmic-ray acceleration. A more detailed analysis is, therefore, required. Ultra-high energy cosmic rays are also discussed, giving attention to sources of cosmic rays inside and outside the Galaxy. In connection with complexities and constraints, one source for all energies within all galaxies is finally considered, taking into account a flattening of the source in slope and the characteristics of spectrum and flux produced by the shock ejection of the envelope of a type I supernova. G.R.

A82-22575

ASTROPHYSICAL SCENARIOS FOR CRITICALLY EVALUATING A ZERO-POINT FIELD ACCELERATION MECHANISM

A. RUEDA (Universidad de los Andes, Bogota, Colombia) In: International Cosmic Ray Conference, 17th, Paris, France, July 13-25, 1981, Conference Papers. Volume 2. Gif-sur-Yvette, Essonne, France, Commissariat a l'Energie Atomique, 1981, p. 361-364. refs

If the electromagnetic zero-point field of ordinary quantum theory is considered as a real field that may act on particles in the usual way that random fields act in classical electrodynamics, it is possible to show that electromagnetically interacting particles perform a random walk in velocity space to ever-increasing translational kinetic energies. As the zero-point field has a Lorentz invariant energy density spectrum, it can be shown that, in a very high vacuum an unconfined gas of infinitely many of those particle displays an energy spectrum of the form E to the (-eta) (eta is a parameter) when in equilibrium with the zero-point field. Scenarios are presented in order to critically discuss and evaluate the possible astrophysical relevance of the model as applied to the acceleration of particles in intergalactic space. (Author)

A82-22576

CALCULATION OF PRODUCTION RATES OF COSMOGENIC NUCLIDES BY MONTE CARLO METHOD

S. TOKAR and P. POVINEC (Komenskeho Univerzita, Bratislava, Czechoslovakia) In: International Cosmic Ray Conference, 17th, Paris, France, July 13-25, 1981, Conference Papers. Volume 2. Gif-sur-Yvette, Essonne, France, Commissariat a l'Energie Atomique, 1981, p. 374-377. refs

A method is presented for the calculation of production rates of cosmogenic nuclides based on Monte Carlo simulations of hadronic cascade processes in matter. Calculations are carried out for the case of a semi-infinite iron slab with a thickness of 2.5 m, and the hadronic cascade is assumed to consist only of nucleons and pions. The nuclide production is found to exhibit only a weak energy dependence, especially at higher energies. D.L.G.

A82-22577

MEASUREMENT OF COSMOGENIC NUCLIDES USING A MULTI-CRYSTAL GAMMA-RAY COINCIDENCE SPECTROMETER

J. C. BARTON (North London, Polytechnic, London, England) In: International Cosmic Ray Conference, 17th, Paris, France, July 13-25, 1981, Conference Papers. Volume 2. Gif-sur-Yvette, Essonne, France, Commissariat a l'Energie Atomique, 1981, p. 378-381.

The activities of Na-22 and Al-26 in a recently fallen meteorite, Mayo Belwa, have been measured using an improved gamma-ray spectrometer. This uses six sodium iodide detectors, arranged symmetrically, so that extended samples can be measured. By recording total rates, 2-fold and 3-fold coincidences simultaneously, it is possible to correct for source absorption and other instrumental effects. The absolute intensity of Al-26 was found to be comparable to that found in other meteorites, but that of Na-22 is anomalously high. (Author)

A82-22578

NUCLEOSYNTHESIS OF LIGHT AND BY-PASSED ISOTOPES IN THE SOLAR SYSTEM MATTER

A. K. LAVRUKHINA and R. I. KUZNETSOVA (Akademiia Nauk SSSR, Institut Geokhimii i Analiticheskoi Khimii, Moscow, USSR) In: International Cosmic Ray Conference, 17th, Paris, France, July 13-25, 1981, Conference Papers. Volume 2. Gif-sur-Yvette, Essonne, France, Commissariat a l'Energie Atomique, 1981, p. 382-385. refs

A model of nucleosynthesis of light and by-passed isotopes is proposed, which is based on the idea that a supernova event led simultaneously to nuclei explosion burning, to collective acceleration of particles up to relativistic energies by shock waves, and to spallation reactions. It is shown that solar system matter was formed in two main events of intensive nucleosynthesis. The first event led to the formation of about 99 percent of K-40, V-50, and the by-passed isotopes with A not less than 113. The second event led to the formation of observed abundances of isotopes and about 1 percent of other products of spallation reactions. Proton fluxes, the alpha/p value, the gamma value, irradiation duration, and the sequence of nucleosynthesis processes are obtained. D.L.G.

A82-22579

MAGNETIC MONOPOLE PAIR AND ITS OBSERVATION IN COSMIC RAYS

L. LUO (Nei Monggol University, Hohhot, People's Republic of China) and T. LU (Nanjing University, Nanjing, People's Republic of China) In: International Cosmic Ray Conference, 17th, Paris, France, July 13-25, 1981, Conference Papers. Volume 2. Gif-sur-Yvette, Essonne, France, Commissariat a l'Energie Atomique, 1981, p. 388-391.

The bound system of a magnetic monopole and an antimonopole is analyzed. It is pointed out that the angular momentum of the ground state may be 48 or 194. Some unexplained events in cosmic rays may be identified as the monopole pairs with high spin. (Author)

A82-22580

INTERNATIONAL COSMIC RAY CONFERENCE, 17TH, PARIS, FRANCE, JULY 13-25, 1981, CONFERENCE PAPERS. VOLUME 3 [CONFERENCE INTERNATIONALE SUR LE RAYONNEMENT COSMIQUE, 17TH, PARIS, FRANCE, JULY 13-25, 1981, CONFERENCE PAPERS. VOLUME 3]

Conference sponsored by CEA, IUPAP, CESR, et al. Gif-sur-Yvette, Essonne, France, Commissariat a l'Energie Atomique, 1981. 543 p. In French and English.

The sun and heliosphere are examined from satellite data of solar cosmic ray events recorded by satellite and theories of the interplanetary propagation of particles and particle acceleration within the heliosphere. Attention is given to X ray, radio, energetic electron, gamma ray, and nuclear reactions of energetic protons observations of solar activity. Ground-, balloon-, and satellite-based detection of particle events are discussed, along with data relevant to the propagation of particles, especially for He-3 enriched events. Modulation of galactic cosmic rays by the solar cycle is explored, and theories of the interplanetary propagation of particles and of the heliospheric medium are presented. Theoretical models of the acceleration of particles within the heliosphere are investigated, including the effect of planetary magnetospheres on the solar-accelerated particles. M.S.K.

A82-22581

MODEL FOR SOLAR HARD X-RAY BURSTS

M. YOSHIMORI (Rikkyo University, Tokyo, Japan) In: International Cosmic Ray Conference, 17th, Paris, France, July 13-25, 1981, Conference Papers. Volume 3. Gif-sur-Yvette, Essonne, France, Commissariat a l'Energie Atomique, 1981, p. 4-7.

Balloon-borne observations of the hard X ray burst event of Sept 19, 1979 are presented as a basis for a description of the temporal behavior of a number of electrons. One NaI(Tl) monitor and four NaI(Tl) counters provided measurements in the energy ranges 30-50, 50-80, 80-120, and 120-200 keV with a counting rate of 1 sec. The energy spectra of the hard X rays were correlated with solar flares and sunspots, and were fitted to power law forms evaluated at the sampling time. A trap-plus-precipitation model describes accelerated electrons as being magnetically trapped and precipitated onto a denser region, leading to hard X ray emission, yielding an electron/X ray ratio calculated to be 1,700,000, in accord with other observations. A thermal model approximated the energy spectrum of hard X-rays by the thermal radiation spectrum from hot plasma, with variations in temperature and emission. M.S.K.

A82-22582

THE DETERMINATION OF DIFFERENTIAL X-RAY SPECTRUM OF THE SOLAR FLARE USING IONOSPHERIC DATA

I. D. KOZIN (Akademiia Nauk Kazakhskoi SSR, Sektor Ionosfery, Alma-Ata, Kazakh SSR) In: International Cosmic Ray Conference, 17th, Paris, France, July 13-25, 1981, Conference Papers. Volume 3. Gif-sur-Yvette, Essonne, France, Commissariat a l'Energie Atomique, 1981, p. 8-10.

The ionization velocity of X rays from a solar flare entering the lower ionosphere is determined by first assuming that the X ray spectrum outside the atmosphere is described by a third degree polynomial. The absorption of monochromatic radiation is modeled as a function of atmospheric density, of the absorption cross-section, and of the path length. The ionosphere is divided into three levels, from which coefficients are calculated from data on ionization from the X ray flux. Substitution of the coefficients into the third degree polynomial equation yields the differential X ray spectrum. M.S.K.

A82-22585* Chicago Univ., Ill.

UNUSUAL PROPERTIES OF PARTICLE EVENTS ASSOCIATED WITH SOLAR FLARE GAMMA RAY EVENTS

P. EVENSON, P. MEYER, and S. YANAGITA (Chicago, University, Chicago, IL) In: International Cosmic Ray Conference, 17th, Paris, France, July 13-25, 1981, Conference Papers. Volume 3. Gif-sur-Yvette, Essonne, France, Commissariat a l'Energie Atomique, 1981, p. 32-35. refs

(Contract NAS5-20674)

An attempt to establish a link between gamma rays observed at the earth with solar flare areas highly enriched with electrons is presented. Two hour averages of the counting rates of 5-100 MeV electrons and 25-145 MeV protons performed on the ISEE-3 spacecraft were correlated with solar flares with a maximum intensity of 6-11 MeV electrons and 25-44 MeV protons recorded by other observers. The coverage was part of the Solar Maximum Mission, which attained a 50 percent coverage. Gamma ray associated events showed high ratios of electrons to protons, about 0.2, and electrons with energies greater than 80 MeV were observed, which are values high enough to produce the highest gamma rays observed, 40 MeV. The available data for electron, proton, and rare isotope fluxes and the time histories of the fluxes are noted to provide a data base for further information on solar flares and particle acceleration mechanisms. M.S.K.

A82-22586* Maryland Univ., College Park.

OBSERVATIONS OF INTERPLANETARY ENERGETIC CHARGED PARTICLES FROM GAMMA-RAY LINE SOLAR FLARES

M. E. PESSES, G. GLOECKLER (Maryland, University, College Park, MD), B. KLECKER, and D. HOVESTADT (Max-Planck-Institut fur extraterrestrische Physik, Garching, West Germany) In: International Cosmic Ray Conference, 17th, Paris, France, July 13-25, 1981, Conference Papers. Volume 3. Gif-sur-Yvette, Essonne, France, Commissariat a l'Energie Atomique, 1981, p. 36-39. Bundesministerium fur Forschung und Technologie refs

(Contract BMFT-RV14-B8/74;

BMFT-01-0I-017-ZA/WF/WRK-1754; NAS5-20062)

Results from ISEE-3 experiments on interplanetary energetic charged particles on June 7, June 21, and July 1, 1980 dealing with gamma ray producing solar flares are reported. The data were gathered by the Ultra Low Energy Wide Angle Telescope, which comprises a thin window, flow through proportional counter/solid-state detector composition telescope. Evidence of a specified time delay from an observed flare and the recording of 0.44-1.3 MeV electrons on ISEE-3 combined with quiescent periods of at least two hours before the observations and recording provides a link between the events. The data indicates interplanetary energetic particle enhancement, and a second, similar set of occurrences was also observed. Protons were accelerated up to 10-20 MeV. No enrichment of either He-3 or Fe was found. M.S.K.

A82-22590

AZIMUTHAL PROPAGATION OF FLARE PARTICLES IN THE HELIOSPHERE

J. PEREZ-PERAZA and J. MARTINELL (Universidad Nacional Autonoma de Mexico, Villa Obregon, Mexico) In: International Cosmic Ray Conference, 17th, Paris, France, July 13-25, 1981, Conference Papers. Volume 3. Gif-sur-Yvette, Essonne, France, Commissariat a l'Energie Atomique, 1981, p. 55-58. refs

Empirically determined properties of solar coronal particle transport are used to quantitatively describe coronal propagation. A velocity dependence of the transport is formulated based on the diffusive nature of the transport and the observation that a drift motion acts on the particles. Both characteristics are assumed to be applicable outside of the fast propagation region, where convective processes dominate. An evolution of particle density is defined, and time profiles of the distribution are calculated for the two regions just before propagation into outer space. A prediction of prompt particles is made, and is caused by contact between the expanding magnetic bottle and field lines of opposite polarity, which leads to a tearing mode instability and a transfer of energy excess to thermal particles. A calculation of the growth time of the instability shows that particles will be observed before the flare particles appear. M.S.K.

A82-22597

THE SOLAR PROTON FLUXES IN APRIL, 1979

S. I. ERMAKOV, N. N. KONTOR, T. I. MOROZOVA, T. I. STEPINA, and G. O. KHACHATURIAN (Moskovskii Gosudarstvennyi Universitet, Moscow, USSR) In: International Cosmic Ray Conference, 17th, Paris, France, July 13-25, 1981, Conference Papers. Volume 3. Gif-sur-Yvette, Essonne, France, Commissariat a l'Energie Atomique, 1981, p. 85-87.

Increases in the solar low-energy proton intensity near the earth detected in April 1979 by the Venera-11 space probe are discussed. During that period the probe was located at approximately 55 deg west of the sun-earth line. A comparison between the proton intensity profiles measured on Venera-11 and on earth shows that the proton propagation conditions during the period of high solar activity were essentially inhomogeneous in the azimuthal direction. C.R.

A82-28905

SURFACE TEMPERATURE DETERMINATION FROM AN AMALGAMATION OF GOES AND TIROS-N RADIANCE MEASUREMENTS

J. A. ZANDLO, W. P. MENZEL (Wisconsin, University, Madison, WI), W. L. SMITH, and C. M. HAYDEN (Wisconsin, University; NOAA, National Earth Satellite Service, Madison, WI) Journal of Applied Meteorology, vol. 21, Jan. 1982, p. 44-50.

A technique for exploiting the TIROS-N capability of measuring the earth skin surface temperature and the GOES ability to monitor surface changes with fine temporal and horizontal resolution is described. Atmospheric absorption due to water vapor is assumed to vary slowly in space and time relative to the same scales of the GOES observations, thus allowing a horizontally varying correction field derived from 6-hr TIROS-N data to be used to obtain quasi-continuous surface temperature features from the GOES data. Additionally, a field of temperature differences between the corrected TIROS-N window channel brightness temperatures and uncorrected GOES brightness temperatures are specified. The GOES temperatures are then correctable to within six hours. Two examples are provided of regional temperature assessments with comparison with surface-measured data and accuracy with the satellite data is within 1 K. M.S.K.

A82-29326* National Aeronautics and Space Administration. Earth Resources Labs., Bay St. Louis, Miss.

DEVELOPMENT OF THREE-DIMENSIONAL SPATIAL DISPLAYS USING A GEOGRAPHICALLY BASED INFORMATION SYSTEM

B. G. JUNKIN (NASA, National Space Technology Laboratories, Earth Resources Laboratory, Bay Saint Louis, MS) Photogrammetric Engineering and Remote Sensing, vol. 48, Apr. 1982, p. 577-586. refs

Procedures necessary for the development of a generalized three-dimensional perspective software capability in support of graphic, topographic, and color mapping of Landsat data are reviewed. The NASA Earth Resources Laboratory developed the procedures in order to facilitate the processing and analysis of disparate, geographically oriented base maps from aircraft and satellite sensors. Perspective displays are obtained through a translation of the space-viewed object to a vantage point coordinate system, followed by a rotation through two angles for alignment along the vantage line of sight, and finally a perspective transformation to yield two-dimensional displays with no hidden lines. Matrix equations for the transformations are reviewed, including scaling, and block diagrams are provided of the data and perspective software systems. The classification data plane may be mapped onto a topographic elevation data plane. M.S.K.

A82-29328

THE USE OF RESIDUAL IMAGES IN LANDSAT IMAGE ANALYSIS

D. L. B. JUPP and K. K. MAYO (Commonwealth Scientific and Industrial Research Organization, Div. of Land Use Research, Canberra, Australia) Photogrammetric Engineering and Remote Sensing, vol. 48, Apr. 1982, p. 595-604. refs

Methods of classification of Landsat data for interactive image display and analysis are reviewed, and the use of the residual image to improve the postclassification analysis is examined. The mean image is formed from an accumulation of the mean radiance values from four channels, while the residual image is generated in the form of pixels in terms of the difference between the class mean and the actual measured radiance. The residual image facilitates detection of departures from hierarchical classes and patterns. A reference model is developed to standardize residual images, and gains in texture analysis during visual analysis are noted with inclusion of the residual images. Examples are provided of land cover mapping an area in southeast Australia, and spectral class mapping on the northeast coast, where differences between inland and coastal vegetation are made visible using residual imagery. M.S.K.

A82-29409

DESCRIPTION OF GRAY LEVEL PICTURE USING A COLLECTION OF DENSITY CONTOUR LINES

T. AGUI, M. NAKAJIMA, and K. MATSUBARA (Tokyo Institute of Technology, Yokohama, Japan) Institute of Electronics and Communication Engineers of Japan, Transactions, Section E (English), vol. E 65, Jan. 1982, p. 36-43. refs

An extraction method of density contour lines of gray level pictures is described. Two kinds of quads composed of four image pixels and non-image pixels are defined for making the density contour lines simple closed paths. From the resultant density contour lines of simple closed paths, a tree graph is made for executing the recognition of a house included in a monochromatic aerial photo of an urban area. (Author)

A82-29762#

RELATING LANDSAT DIGITAL COUNT VALUES TO GROUND REFLECTANCE FOR OPTICALLY THIN ATMOSPHERIC CONDITIONS

A. J. RICHARDSON (U.S. Department of Agriculture, Agricultural Research Service, Weslaco, TX) Applied Optics, vol. 21, Apr. 15, 1982, p. 1457-1464. refs

The relation of Landsat digital count (DCc) values to ground-measured bidirectional reflectance (R), in data from seven previous investigations that are summarized and examined as a unified data set, is shown to be useful in the estimation of R by

READEX MICROPRINT best copy available

means of a simplified linear formulation for conditions approximating optically thin atmospheres. All digital count values and formulas were corrected to appear as though obtained at a sun zenith angle of 39 deg, with a Landsat-2 calibration for the January 22-July 15, 1975 period. The relations for R4-7 are: -5.9 + 0.476DCc4, -1.94 + 0.373DCc5, -1.40 + 0.412DCc6, and -0.49 + 1.220DCc7, respectively. O.C.

A82-32033

EXTRACTION OF LINE SHAPED OBJECTS FROM AERIAL IMAGES USING A SPECIAL OPERATOR TO ANALYZE THE PROFILES OF FUNCTIONS

W.-D. GROCH (Karlsruhe, Universitaet, Karlsruhe, West Germany) Computer Graphics and Image Processing, vol. 18, Apr. 1982, p. 347-358. Research supported by the Bundesministerium fuer Forschung und Technologie and U.S. Army. refs

Line-shaped objects are extracted sequentially by object-guided and object-specific methods with the facility for interactive support. The line following starts at locations which reliably are part of line-shaped objects. Two different object-guided methods may be initialized at these starting points. The methods follow the object by applying special operators to extract line segments. The operator is described that analyzes the function profiles, the detection of starting points, the two methods for line following and the combination of all methods in a system for the extraction of line-shaped objects from discrete gray level pictures. Results of a test are shown. C.D.

A82-32343* National Aeronautics and Space Administration. Goddard Space Flight Center, Greenbelt, Md.

PRELIMINARY EVIDENCE FOR THE INFLUENCE OF PHYSIOGRAPHY AND SCALE UPON THE AUTOCORRELATION FUNCTION OF REMOTELY SENSED DATA

M. L. LABOVITZ, D. L. TOLL (NASA, Goddard Space Flight Center, Greenbelt, MD), and R. E. KENNARD (Computer Sciences Corp., Silver Spring, MD) International Journal of Remote Sensing, vol. 3, Jan.-Mar. 1982, p. 13-30. refs

(Previously announced in STAR as N81-19530)

A82-32344

DEPENDENT FEATURE TREES FOR DENSITY APPROXIMATION. I - OPTIMAL CONSTRUCTION AND CLASSIFICATION RESULTS

C. B. CHITTINENI (Conoco, Inc., Ponca City, OK) International Journal of Remote Sensing, vol. 3, Jan.-Mar. 1982, p. 31-44. refs

This paper deals with the approximation of probability density functions with dependent feature trees. The optimal dependent feature trees are proposed to be constructed using criteria of mutual information and distance measures. Expressions are derived for the criteria when the distributions of the features are Gaussian. Expressions are developed for the covariances between the features connected by a path in a dependent feature tree. The case when the nodes in a dependent feature tree represent a set of features is also considered. Furthermore, experimental results from the classification of remotely sensed multispectral scanner imagery data are presented. (Author)

A82-32345* National Aeronautics and Space Administration. Goddard Space Flight Center, Greenbelt, Md.

EVALUATION OF TEMPORAL REGISTRATION OF LANDSAT SCENES

R. NELSON and G. GREBOWSKY (NASA, Goddard Space Flight Center, Greenbelt, MD) International Journal of Remote Sensing, vol. 3, Jan.-Mar. 1982, p. 45-50. refs

The registration of Landsat images is important for multitemporal classification and for detecting change. Landsat data are now rectified to a ground coordinate system during preprocessing, hence scenes obtained over the same area are registered. The machine responsible for preprocessing the Landsat multispectral scanner data is the master data processor (MDP). This paper describes the rectification approach taken by the MDP, reviews the accuracy standards of the resultant product, and provides an assessment of the accuracy of the scene to scene registration of two Landsat images. (Author)

A82-32346

THE USE OF CONTEXTUAL INFORMATION TO DETECT CUMULUS CLOUDS AND CLOUD SHADOWS IN LANDSAT DATA

C. M. GURNEY (Reading, University, Reading, England) International Journal of Remote Sensing, vol. 3, Jan.-Mar. 1982, p. 51-62. Research supported by the Atomic Energy Research Establishment. refs

The use of contextual information to identify areas of cloud and cloud shadow in digital Landsat data is described. The distance from cloud to shadow is calculated from sun elevation and azimuth, cloud base height and image geometry. Pixels with a gray level above a given threshold are considered to be potential cloud. A 3 x 3 pixel window centered at the calculated shadow position is searched. Pixels in this window with gray levels below a second threshold are classed as cloud shadow. If no shadow pixels are found the potential cloud is rejected. Modifications to allow for overlapping cloud and shadow are included. The detection procedure was found to work well for bands 5, 6, or 7 of Landsat data. (Author)

A82-32347

THE ESTIMATION OF WAVE HEIGHT FROM DIGITALLY PROCESSED SAR IMAGERY

M. H. B. THOMAS (Atomic Energy Research Establishment, Materials Physics Div., Harwell, Oxon, England) International Journal of Remote Sensing, vol. 3, Jan.-Mar. 1982, p. 63-68. Research supported by the Department of Industry. refs

A simple method has been developed for estimating wave height from synthetic aperture radar (SAR) imagery obtained by the Seasat satellite. The method is based on measuring the contrast of the image and the wavelength of the dominant wave. A calculation has been made for two orbits made by the satellite over the North Atlantic in 1978, using digitally processed data supplied by DFVLR in West Germany. Comparison with sea truth measurements shows agreement to within about 20 per cent. (Author)

A82-32507

DIGITALLY ENHANCED VISUAL DISPLAYS FACILITATE THE ANALYSIS OF LANDSAT IMAGERY

R. N. COLWELL (Earth Satellite Corp., Berkeley, CA) In: Display technology II; Proceedings of the Meeting, Los Angeles, CA, February 10, 11, 1981. Bellingham, WA, SPIE - The International Society for Optical Engineering, 1981, p. 118-126.

There have been efforts during most of the past decade to increase the interpretability of Landsat multispectral scanner (MSS) imagery through the performance of various kinds of image enhancement. Attention is given to research recently conducted for the U.S. Forest Service (USFS) with the objective to develop improved 'multiresource inventory methods' entailing the direct visual analysis of Landsat MSS imagery. The establishment of the resource categories to be identified is discussed along with approaches for producing the digitally enhanced visual displays, the preparation of the image analysis keys, the selection of personnel to evaluate the imagery, and the administration of the image interpretability tests. Preliminary results clearly showed that the studied procedure of enhanced visual display (color composite image in opaque print form) was significantly more interpretable than the conventional Landsat color composite imagery. G.R.

A82-32581* Lowell Observatory, Flagstaff, Ariz.
SUBTLETIES IN THE FLAT-FIELDING OF CHARGE-COUPLED DEVICE /CCD/ IMAGES
W. A. BAUM, B. THOMSEN, and T. J. KREIDL (Lowell Observatory, Flagstaff, AZ) In: Solid state imagers for astronomy; Proceedings of the Meeting, Cambridge, MA, June 10, 11, 1981. Bellingham, WA, SPIE - The International Society for Optical Engineering, 1981, p. 24-27.
(Contract NAS5-25451; NAS5-25488)

Astronomical photometry with CCDs will often involve relatively low signal levels (less than 1000 charge carriers per pixel), at which nonlinear effects sometimes become significant. These effects will probably play a role in the processing of Space Telescope data. The problem apparently arises because signal charges are not read out equally completely from all columns and all pixels. It is shown that, although a first-order correction can be made by subtracting a low-level flat field from all frames before conventional processing, higher accuracy can be achieved by modeling the response with a nonlinear function. B.J.

A82-32709
COMPUTATION WITH PHYSICAL VALUES FROM LANDSAT DIGITAL DATA
C. J. ROBINOVE (U.S. Geological Survey, Reston, VA) Photogrammetric Engineering and Remote Sensing, vol. 48, May 1982, p. 781-784.

Although the analysis of Landsat digital images by using the digital numbers for each pixel recorded on a computer-compatible magnetic tape may be adequate when only a single, internally-consistent image is used, incorrect results will be given by the procedure if more than one image is used for analysis, as in mosaics or temporal overlays. The digital numbers for each pixel should in such cases be converted to their dimensionless equivalents, such as (1) radiance, as measured at the satellite, in mW/sq cm per steradian (sr), or (2) reflectance, both of which vary depending on the calibration of satellite MSS, sun angle, atmospheric state, terrain slope and aspect, and surface cover. Equations are given for radiance and reflectance calculations for the cases of five radiometric conditions, neglecting atmospheric correction. O.C.

A82-32900
GEOGRAPHIC LOCATION OF INDIVIDUAL PIXELS
D. C. MCCONAGHY (NOAA, National Marine Fisheries Service, La Jolla, CA) Remote Sensing of Environment, vol. 10, Aug. 1980, p. 81-84. refs

A major problem in processing thermal infrared digital data from very high resolution radiometers aboard NOAA Polar Orbiting Satellites is the geographic placement of digital data fields. Geographic placement is especially difficult over oceanic areas because of the lack of landmarks. Using a series of geometric constructions, an analytical approach can be developed for geographic location of individual data pixels. The errors associated with this method are generally less than 0.1 deg latitude and longitude. (Author)

A82-32904* California Univ., Santa Barbara.
THE USE OF PRIOR PROBABILITIES IN MAXIMUM LIKELIHOOD CLASSIFICATION OF REMOTELY SENSED DATA
A. H. STRAHLER (California, University, Santa Barbara, CA) Remote Sensing of Environment, vol. 10, Sept. 1980, p. 135-163. refs
(Contract NAS9-15509; NAS7-100; NSG-2377)

Possibilities for the improvement of classification accuracies by the use of prior information about the expected distribution of classes in the maximum likelihood classification of remote sensing data are examined. The modification of the maximum likelihood decision rule to take into account one or several sets of probabilities for the occurrence of classes which probabilities are based on independent knowledge of the area surveyed is demonstrated. It is then shown that the use of prior probabilities is sufficiently versatile so as to allow the prior weighting of output classes based on their anticipated sizes as well as the merging of continuously varying measurements with discrete collateral information data sets and the construction of time-sequential classification systems in which an earlier classification modifies the outcome of a latter one. A.L.W.

A82-32906
MONITORING LAND-COVER CHANGE BY PRINCIPAL COMPONENT ANALYSIS OF MULTITEMPORAL LANDSAT DATA
G. F. BYRNE, P. F. CRAPPER, and K. K. MAYO (Commonwealth Scientific and Industrial Research Organization, Div. of Land Use Research, Canberra, Australia) Remote Sensing of Environment, vol. 10, Nov. 1980, p. 175-184. refs

Two four-channel Landsat scenes of the same area, which were recorded on different dates, were superimposed and treated as a single eight-dimensional (channel) data array. Principal component analysis (PCA) of this array resulted in the gross differences associated with overall radiation and atmospheric changes appearing in the major component images and statistically minor changes associated with local changes in land cover appearing in the minor component images. (Author)

A82-32911
TERRAIN ANALYSIS FROM LANDSAT USING A COLOR TV ENHANCEMENT SYSTEM
T. H. L. WILLIAMS (Kansas, University, Lawrence, KS) and J. M. GOODMAN (Oklahoma, University, Norman, OK) Remote Sensing of Environment, vol. 10, Nov. 1980, p. 231-237.

Visual interpretation of Landsat false-color composite imagery was employed to map terrain types on the Navajo Indian Reservation in northeastern Arizona and northwestern New Mexico. Three main difficulties were encountered in the visual analysis: (1) determination of the exact boundary positions; (2) repeatability of the boundary decisions over an area; and (3) discrimination among subtle tone differences associated with certain terrain type groupings. A simple image enhancement technique, based on a color television system was developed to make the visual analysis more accurate. A color TV camera was used to view the image and a color monitor used for the display. Image enhancement was achieved by use of the chroma, hue, contrast, and brightness controls on the monitor. The use of a zoom lens on the camera allowed rapid scale change and facilitated study of small areas of the image. By working directly from a color image, the technique obviated the need for separation positives with their attendant registration problems. (Author)

A82-32916
APPEARANCE OF IRREGULAR TREE CANOPIES IN NIGHTTIME HIGH-RESOLUTION THERMAL INFRARED IMAGERY
L. K. BALICK and S. K. WILSON (Los Alamos National Laboratory, Los Alamos, NM) Remote Sensing of Environment, vol. 10, Dec. 1980, p. 299-305. refs

A82-34225
SEPARATION OF DIFFUSE FROM SHARP-EDGED FEATURES IN DIGITAL IMAGERY
G. F. BYRNE, P. F. CRAPPER, B. G. WILLIAMS, and M. J. GOODSPEED (Commonwealth Scientific and Industrial Research Organization, Div. of Land Use Research, Canberra, Australia) Remote Sensing of Environment, vol. 12, May 1982, p. 181-186. refs

A new classification procedure that removes sharp-edge features from digital imagery and that more clearly reveals any patterns more diffuse in nature that may be present is proposed. The procedure relies on the hypothesis that the sharp edges separate areas of uniform but differing optical density. These differences are frequently sufficiently large to obscure other patterns that are more diffuse ('fuzzy') in nature. The technique is illustrated by application to a Landsat scene where a suspected mosaic arising from soil variability is overlain by agricultural fields. C.R.

A82-34469
EVALUATION OF THE EFFECTIVENESS OF SYSTEMATIC IMAGE DISTORTION COMPENSATION [OTSENKA EFFEKTIVNOSTI KOMPENSATSII SISTEMATICHESKIKH ISKAZHENII IZOBRAZHENIIA]
N. G. BARABANOVA, K. N. GERTSENOVA, and S. S. NEKHIN
Geodeziia i Kartografiia, Apr. 1982, p. 32-36. In Russian.

The improvements in image accuracy afforded by two methods for the compensation of systematic distortions in aerial photographs are studied. The techniques of field calibration, which involves the correction of image coordinates by interpolation from the coordinates of selected calibration points, and polynomial correction using additional reference points, in which the distortion field is approximated by second- and third-degree polynomials, were applied to aerial photographs subject to four different types of distortions. Examination of the errors in the determination of the coordinates of control points and the maximum errors of their mutual positioning indicates field calibration to be more effective for sign-changing point displacements, while polynomial approximation is more effective for regular displacements. A.L.W.

A82-34702
A PRACTICAL STUDY OF GROSS-ERROR DETECTION IN BUNDLE ADJUSTMENT
S. F. EL-HAKIM (National Research Council, Ottawa, Canada) In: American Society of Photogrammetry, Annual Meeting, 47th, Washington, DC, February 22-27, 1981, ASP Technical Papers. Falls Church, VA, American Society of Photogrammetry, 1981, p. 1-17. refs

A special bundle adjustment program has been developed with built-in automatic gross-error detector by the data snooping approach. The program computes, in an efficient way, the exact values of the redundancy numbers for each image point. Using actual data, many of the factors affecting the reliability of bundle adjustment and the ability of the technique to detect gross errors are studied. The effects of different block parameters, point type and location, and the use of additional constraints are presented. (Author)

A82-34717
AN INFORMATION-THEORIC SPATIAL TRANSFORM
J. S. POWERS (Mississippi State University, Mississippi State, MS) In: American Society of Photogrammetry, Annual Meeting, 47th, Washington, DC, February 22-27, 1981, ASP Technical Papers. Falls Church, VA, American Society of Photogrammetry, 1981, p. 221-225. refs

Significant improvements in the sensitivity of existing computer algorithms for digital remote-sensor image classification may be effected without involving any software modification of these systems. An information-theoric spatial transform may be applied to the raw multispectral data set, and synthetic channels thus created may be utilized in the classification process. The transform is analogous in operation to the transform which occurs in the retina of higher organisms; a processing stage which has been omitted in most existing classification schemes. The transform algorithm is described and preliminary results of the application of the algorithm to the study of forest ecosystems from Landsat MSS image data are discussed. (Author)

A82-34720* Jet Propulsion Lab., California Inst. of Tech., Pasadena.
BATHYMETRIC IMAGING
P. R. PALUZZI (California Institute of Technology, Jet Propulsion Laboratory, Pasadena, CA) and M. C. MALIN (Arizona State University, Tempe, AZ) In: American Society of Photogrammetry, Annual Meeting, 47th, Washington, DC, February 22-27, 1981, ASP Technical Papers. Falls Church, VA, American Society of Photogrammetry, 1981, p. 247-258. refs
(Contract NAS7-100)

Digital topography has, for some years, been formatted and processed into shaded relief images for specific studies involving land use and thermal properties. Application to bathymetry is a new and seemingly fruitful extension of these techniques. Digital terrain models of the earth - combining subaerial topography with an extensive collection of bathymetric soundings - have been processed to yield shaded relief images. These images provide new and exciting insights into submarine geomorphology and portray many aspects of plate tectonic physiography in a manner not previously possible. (Author)

A82-34722
A QUANTITATIVE METHOD TO TEST FOR SIMILARITY BETWEEN PHOTO INTERPRETERS
R. G. CONGALTON and R. A. MEAD (Virginia Polytechnic Institute and State University, Blacksburg, VA) In: American Society of Photogrammetry, Annual Meeting, 47th, Washington, DC, February 22-27, 1981, ASP Technical Papers. Falls Church, VA, American Society of Photogrammetry, 1981, p. 263-266.

Photo interpretation is the art and science of identifying objects and deducing their significance on aerial photos. The judgment involved is generally qualitative in nature, and, therefore, difficult to evaluate or compare with interpretations made by others. The present investigation is concerned with an approach which makes it possible to quantify photo interpretation results, taking into account a statistical method for comparing these results. The proposed procedure can be employed in tests regarding the degree of similarity between interpreters or the consistency of the same interpreter over time. The procedure is based on the employment of an error matrix and the conduction of a discrete multivariate analysis to test the degree of similarity between the error matrices. G.R.

A82-34723
TERRAIN CLASSIFICATION BY FOURIER ANALYSIS - ACCURACY AND ECONOMY
P. FREDERIKSEN and O. JACOBI (Danmarks Tekniske Hojskole, Lyngby, Denmark) In: American Society of Photogrammetry, Annual Meeting, 47th, Washington, DC, February 22-27, 1981, ASP Technical Papers. Falls Church, VA, American Society of Photogrammetry, 1981, p. 267-284. refs

The Fourier transformation is applied to terrain profiles for classification purposes. Areas with different geology are considered, and the power spectra are estimated. The spectrum is used to predict the accuracy of a digital terrain model and to calculate some economic consequences of the relation between type of terrain, accuracy of measurements, point density, and surveying expenses. (Author)

A82-34726
RAMS-1, A RESOURCE ANALYSIS AND MAPPING SYSTEM
R. J. MADILL (Systemhouse, Ltd., Ottawa, Canada) In: American Society of Photogrammetry, Annual Meeting, 47th, Washington, DC, February 22-27, 1981, ASP Technical Papers. Falls Church, VA, American Society of Photogrammetry, 1981, p. 306-310.

RAMS-1 is a Resource Analysis and Mapping System developed by Systemhouse. RAMS-1 will produce colour shaded thematic overlays as well as planimetric base maps. This paper describes the hardware configuration and software facilities of the SHL RAMS-1 system. (Author)

A82-34940
PRESENT STATUS OF ON-LINE ANALYTICAL TRIANGULATION
V. KRATKY (National Research Council, Ottawa, Canada) Photogrammetria, vol. 38, May 1982, p. 1-12. refs

Basic principles of solutions suitable for analytical aerial triangulation are outlined and analyzed in the context of existing on-line photogrammetric systems. Two basic categories of procedures are considered: those which primarily aim for a quality controlled data acquisition followed by an off-line adjustment, and those which make the adjustment a part of the on-line procedure proper. The discussion covers geometrical as well as numerical considerations and emphasizes practical and methodological aspects which may bring about a higher efficiency of work and a reduction of preparatory operations. (Author)

A82-35141

ALLOWANCE FOR THE EFFECT OF THE ATMOSPHERE IN THE PROCESSING OF SATELLITE REMOTE-SENSING IMAGES [UCHET VLIIANIIA ATMOSFERY PRI OBRABOTKE KOSMICHESKOI VIDEOINFORMATSII]

V. V. KOZODEROV and N. D. LIUBOVNYI In: Study of the hydrological cycle by aerospace methods. Moscow, Izdatel'stvo Radio i Sviaz', 1982, p. 90-94. In Russian. refs

A method for the radiative correction of multispectral imagery is proposed which relies on the physicomathematical modeling of the formation of the outgoing-radiation field on the basis of experimental data concerning the distribution of atmospheric aerosol and average statistical data on the distribution of the gaseous constituents of the atmosphere. As an example, attention is given to the radiative correction of Meteor-satellite data, realized by a special-purpose image-processing system. B.J.

A82-35650* National Aeronautics and Space Administration. Goddard Space Flight Center, Greenbelt, Md.

INFLUENCE OF SKY RADIANCE DISTRIBUTION ON THE RATIO TECHNIQUE FOR ESTIMATING BIDIRECTIONAL REFLECTANCE

J. A. KIRCHNER (NASA, Goddard Space Flight Center, Earth Resources Branch, Greenbelt, MD), S. YOUKHANA, and J. A. SMITH (Colorado State University, Fort Collins, CO) Photogrammetric Engineering and Remote Sensing, vol. 48, June 1982, p. 955-959. refs

(Contract DACW39-77-C-0073; DARG29-79-C-0199)

The technique of ratioing scene radiance to the radiance obtained from standard Lambertian reference panels in order to estimate bidirectional reflectance factors may depend on the angular distribution of the diffuse irradiance field as well as the direct solar irradiance. A simulation study was performed to estimate the magnitude of this effect for differing clear sky irradiance distributions for a variety of vegetated surfaces. For the seven surfaces and wavelengths analyzed, the error induced in the estimation of bidirectional reflectance factors using the standard ratio technique was less than 5 percent for zenith view and sun angles less than 55 degrees. (Author)

A82-35824* Business and Technological Systems, Inc., Seabrook, Md.

APPLICATION OF SATELLITE MAGNETIC ANOMALY DATA TO CURIE ISOTHERM MAPPING

M. A. MAYHEW (Business and Technological Systems, Inc., Seabrook, MD) Journal of Geophysical Research, vol. 87, June 10, 1982, p. 4846-4854. refs

(Contract NAS5-25720)

A82-36043#

THE METEOROLOGICAL PRODUCT - 'CLOUD-TOP HEIGHT'

R. A. BOWEN (ESA, European Space Operations Centre, Darmstadt, West Germany) ESA Bulletin, no. 30, May 1982, p. 16-20.

The rationale for choices made in the method of presenting Meteosat IR and visual imagery to commercial users for visual analyses are examined. IR, at 11 microns, and water vapor (WV), at 6 microns, channels are noted to produce pictures in 2500 x 2500 pixel grids, while the 0.4-11 micron visible channel yields 5000 x 2500 pixel images. It was found necessary to digitally compress every picture by four in both directions for direct transmission to users. A resolution of 20 km was then available at the subsatellite point. Eight grey levels showed clouds above 12,000 m height in 1500 m steps to the 300 m level. A correction for the semitransparency of clouds is numerically determined, particularly for overlying cirrus formations. User-activated corrections to images from remote terminals is described. A time lag of a little over two hours existed between Meteosat-1 acquisition and dissemination. M.S.K.

A82-36935

SATELLITE RADIATION MEASUREMENTS FOR THE RETRIEVAL OF THE VERTICAL TEMPERATURE PROFILES [PRZETWARZANIE SATELITARNYCH POMIAROW PROMIENIOWANIA NA PIONOWE PROFILE TEMPERATUR]

Z. BUNSCH-MAKAREWICZ, B. BRAUN, and R. GOSS-ZUREK Acta Geophysica Polonica, vol. 29, no. 3, 1981, p. 235-246. In Polish. refs

The physical basis underlying satellite IR determination of vertical temperature profiles in the atmosphere is detailed. The earth is treated as a black-body emitting radiation at temperatures dependent only on the concentration, temperature, and absorption coefficient of the absorbents present in the atmosphere. Consideration is given to regression analysis, the inverse matrix method, and direct retrieval techniques, noting that regression is preferred as the first choice in all cases and is the only method when transmission properties are not known. The level of agreement between derived profiles and measured values is shown to depend on the number of spectral frequency measurements. Good correlations are found, with the in situ data being slightly higher than the satellite figures. Examples are cited from TIROS N and NOAA spacecraft data. M.S.K.

A82-37048

DESIGN GUIDELINES FOR SATELLITE IMAGE DATA DISTRIBUTION SYSTEMS

D. L. HALL, K. H. MILLER, W. T. BISIGNANI, and J. W. VERA (Mitre Corp., McLean, VA) In: EASCON '81; Electronics and Aerospace Systems Conventions, Washington, DC, November 16-19, 1981, Record. New York, Institute of Electrical and Electronics Engineers, Inc., 1981, p. 328-337.

A modular, systems level design for satellite systems which produce images is presented. This is a three-stage, ten-step iterative design technique which applies to the data flow from the sensing instruments through the processing system to the image product users. Procedures for converting operational requirements into functional architectures are described. The resulting architectures are translated into a subsystem level design by using an array of building blocks. An important feature of this structured approach is the parametric characterization of the interfaces between building blocks. B.J.

A82-37200

LANDSAT D TO YIELD MORE PRECISE DATA

C. COVAULT Aviation Week and Space Technology, vol. 117, July 5, 1982, p. 40, 41, 46-48, 51.

The Landsat D spacecraft to be launched in mid 1982 will offer new multispectral and thermal imaging capabilities. The satellite is designed to improve the monitoring of renewable resources and to provide rock discrimination data for mineral and pertroleum geologists. The expanded features of the new satellite include a seven-band thematic mapper with spectral ranges from 0.45-0.52 microns to 2.08-2.35 microns and a multispectral scanner capable of higher resolution and spectral fidelity than used in previous Landsats. The development of the Landsat D has been complicated by project changes both in the Space Shuttle and the Tracking and Data Relay Satellite Program, which resulted in an increase in weight (now 4400 lb.), an additional hydrazine tank and narrow band tape recorders. Other details on the spacecraft include total array output power of 2200 W, operational altitude of 705 km and launching on a Delta 3920. N.B.

A82-37810*# National Aeronautics and Space Administration. Goddard Space Flight Center, Greenbelt, Md.
ADVANCED TECHNOLOGY FOR EARTH OBSERVATION - DATA PROCESSING
P. HEFFNER and E. CONNELL (NASA, Goddard Space Flight Center, Mission and Data Operations Directorate, Greenbelt, MD) American Astronautical Society and Deutsche Gesellschaft fuer Luft- und Raumfahrt, Goddard Memorial Symposium on Spacelab, Space Platforms and the Future, 20th, Greenbelt, MD, Mar. 17-19, 1982, AAS 18 p.
(AAS PAPER 82-130)

The Experimental Land Observing System (ELOS) is to demonstrate major advances in space-based land observation. Program success will depend upon successful demonstration of both space-segment performance and ground-system capabilities. Increases in data-rate, volume, and processing requirements present substantial challenges to the ground data processing system. ELOS is based on the utilization of the multispectral linear array (MLA) sensor, a solid-state, electronically scanned instrument. Current MLA instrument designs offer a number of capabilities beyond those provided in the Landsat imaging devices. These capabilities include greater resolution, inherent registration, onboard calibration, off-nadir pointing capability, and fore/aft pointing capability. The proposed MLA flight mission scenario will be one of continued growth and will include flights on the Space Transportation System. Attention is also given to ground-to-ground data transport, data capture, and the use of high speed computers. G.R.

N82-22622*# Herzberg Inst. of Astrophysics, Ottawa (Ontario).
STUDIES OF HIGH LATITUDE CURRENT SYSTEMS USING MAGSAT VECTOR DATA Progress Report, 16 Nov. 1980 - 31 Aug. 1981
J. R. BURROWS, Principal Investigator, T. J. HUGHES, D. D. WALLIS, and M. D. WILSON 31 Aug. 1981 19 p Sponsored by NASA ERTS
(E82-10188; NASA-CR-168616; NAS 1.26:168616; PR-3) Avail: NTIS HC A02/MF A01 CSCL 04A

The magnetic disturbance fields caused by global external current systems are considered with particular emphasis on improving the understanding of the physical processes which control high latitude current systems. Following processing the MAGSAT data were routinely plotted in the Universal Time (UT) format as well as in a polar plot format. The H'D'U' coordinate system, was adopted as the standard for representing the MAGSAT residual magnetic field vectors. A data file was generated and the TPOLAR computer code was developed to determine from the orbital elements, the time, latitude, and MLT of the extremum latitude of each transpolar segment of orbit. The precision of the vector data set from MAGSAT prompted an extended exploratory phase for data analysis procedures, modeling techniques and phenomenology. A.R.H.

N82-22627*# North Carolina State Univ., Raleigh. Dept. of Marine, Earth, and Atmospheric Sciences.
MAGSAT AND AEROMAGNETIC DATA IN THE NORTH AMERICAN CONTINENT Progress Report
8 Jun. 1981 2 p ERTS
(Contract NAS5-26157)
(E82-10193; NASA-CR-168620; NAS 1.26:168620) Avail: NTIS HC A02/MF A01 CSCL 05B

Problems were encountered in deriving a proper reference field to be subtracted from the aeromagnetic data obtained from Project MAGNET. Field models tried thus far do not seem to eliminate properly the main field. The MAGSAT data in the North American continent for the period November 1 to December 22, 1979 are being compiled and compared with MAGNET data. Efforts are being made to eliminate the orbital bias errors. A computer program was developed and successfully tested which computes a topographic profile of the Curie depth isotherm which fits best to the observed vector or scalar field magnetic data. A.R.H.

N82-22629*# Texas Univ. at Dallas, Richardson. Center for Space Sciences.
INVESTIGATION OF THE EFFECTS OF EXTERNAL CURRENT SYSTEMS ON THE MAGSAT DATA UTILIZING GRID CELL MODELING TECHNIQUES Quarterly Status Technical Progress Report, 1 Apr. - 30 Jun. 1981
D. M. KLUMPAR, Principal Investigator 8 Jul. 1981 12 p ERTS
(Contract NAS5-26309)
(E82-10195; NASA-CR-168622; NAS 1.26:168622; UTD-E0533-01; QSTRP-5) Avail: NTIS HC A02/MF A01 CSCL 05B

Refinements to the modeling procedure developed to compute the magnetic fields at satellite orbit due to current distributions in the ionosphere and magnetosphere are described. The modeling technique utilizes a linear current element representation of the large scale space current system. A model polar current system is presented and magnetic field perturbations resulting from this system are computed along two hypothetical satellite orbits. M.G.

N82-23567*# Business and Technological Systems, Inc., Seabrook, Md.
EQUIVALENT SOURCE MODELING OF THE MAIN FIELD USING MAGSAT DATA Quarterly Report, 1 Jan. - 31 Mar. 1981
31 Mar. 1981 4 p ERTS
(Contract NAS5-26047)
(E82-10151; NASA-CR-168536; NAS 1.26:168536; QR-5) Avail: NTIS HC A02/MF A01 CSCL 05B

Modeling and software development of the main field using MAGSAT data is discussed. The cause of the apparent bulge in the power spectrum of Dipole model no. 4 was investigated by simulation with POGO crustal anomaly field model. Results for cases with and without noise, and the spectra of selected resits are given. It is indicated that the beginning of the bump in the spectrum of Dipole no. 4 is due to crustal influence, while the departure of the spectrum from that of MGST (12/80-2) around expansion order 17 is due to the resolution limits of the Dipole density. E.A.K.

N82-23570*# Analytic Sciences Corp., Reading, Mass.
ANALYSES OF MAGSAT TRACKS CROSSING THE STUDY REGION IN THE INDIAN OCEAN Quarterly Progress Report, 2 Dec. 1980 - 31 Mar. 1981
R. V. SAILOR and A. R. LAZAREWICZ, Principal Investigators 7 May 1981 15 p ERTS
(Contract NAS5-26424)
(E82-10197; NASA-CR-168624; NAS 1.26:168624; PR-1325-1) Avail: NTIS HC A02/MF A01 CSCL 05B

Progress in software development and in preliminary analysis of MAGSAT tracks crossing the Indian Ocean is reported. Tracks crossing the Java Trench, Broken Ridge, the Southeast Indian Ridge, and the Ninetyeast Ridge show that magnetic anomalies correlate with some of these features. Preliminary study of anomaly profiles indicates that tracks of anomaly data (the observations minus a core field model) have a power spectrum decreasing as the inverse square of the spatial frequency. An apparent noise floor of about one to two gammas rms is reached at wavelengths of about 360 km, corresponding to approximately 10 samples of the decimated Investigator tape data at a sampling rate of approximately 4.9 sec/sample. J.D.

N82-23572*# Business and Technological Systems, Inc., Seabrook, Md.
MAGSAT SCIENCE INVESTIGATIONS Quarterly Report
1982 3 p ERTS
(Contract NAS5-26328)
(E82-10199; NASA-CR-168626) Avail: NTIS HC A02/MF A01 CSCL 05B

Progress in the development and modification of software to accommodate total field anomaly data and for spectral analysis of aeromagnetic profile data and computation of depth to magnetic bottom is reported. J.D.

N82-23574*# Applied Physics Lab., Johns Hopkins Univ., Laurel, Md.
INVESTIGATION OF MAGSAT AND TRIAD MAGNETOMETER DATA TO PROVIDE CORRECTIVE INFORMATION ON HIGH-LATITUDE EXTERNAL FIELDS Progress Report, 1 Jul. - 30 Sep. 1981
T. A. POTEMRA, Principal Investigator 4 Nov. 1981 10 p Sponsored by NASA Original contains color imagery. Original photography may be purchased from the EROS Data Center, Sioux Falls, S.D. 57198 ERTS
(E82-10201; NASA-CR-168628; NAS 1.26:168628) Avail: NTIS HC A02/MF A01 CSCL 04A

The compilation of a catalog of the MAGSAT-observed high altitude disturbances is discussed and an example of contents and format is given. The graphs allow the investigation of Birkeland current signatures which are superimposed upon the main geomagnetic field. An example of a display of the MAGSAT orbital tracks in a polar geomagnetic coordinate system with the locations, flow directions, and intensities of field aligned currents shown in color is also given. The display was generated using an interactive color graphics terminal. M.G.

N82-23575*# Indian Inst. of Geomagnetism, Bombay.
MAGSAT FOR GEOMAGNETIC STUDIES OVER INDIAN REGION Progress Report, 1 Jan. - 31 Oct. 1981
R. G. RASTOGI, B. N. BHARGAVA, B. P. SINGH, D. R. K. RAO, G. K. RANGARAJAN, R. RAJARAM, M. ROY, B. R. ARORA, and A. SETH, Principal Investigators 31 Oct. 1981 42 p refs Sponsored by NASA ERTS
(E82-10202; NASA-CR-168629; NAS 1.26:168629; PR-1) Avail: NTIS HC A03/MF A01 CSCL 08G

Progress in the preparation of software for converting data tapes produced on an IBM system to data readable on a DEC-10 system, in the creation of awareness of the utility of MAGSAT data among users in India, and in making computer programs supplied by NASA operational on the DEC-10 system is reported. Papers presented to Indian users, at the IAGA fourth scientific assembly, at a symposium on interdisciplinary approaches to geomagnetism, and a paper published in Science Today are included. J.D.

N82-23576*# Institute of Geological Sciences, Edinburgh (Scotland).
SPHERICAL HARMONIC REPRESENTATION OF THE MAIN GEOMAGNETIC FIELD FOR WORLD CHARTING AND INVESTIGATIONS OF SOME FUNDAMENTAL PROBLEMS OF PHYSICS AND GEOPHYSICS Progress Report
D. R. BARRACLOUGH, R. HIDE (Meteorological Office), B. R. LEATON, F. J. LOWES (Newcastle-Upon-Tyne Univ.), S. R. C. MALIN, and R. L. WILSON, Principal Investigators (Liverpool Univ.) 1 Jun. 1981 4 p Sponsored by NASA ERTS
(E82-10203; NASA-CR-168630; NAS 1.26:168630) Avail: NTIS HC A02/MF A01 CSCL 08G

The data processing of MAGSAT investigator B test tapes and data tapes, and tapes of selected data on 15 magnetically quiet days is reported. The 1980 World Chart spherical model was compared with the MAGSAT (3/80) and MAGSAT vector data were used in the models. An article on modelling the geomagnetic field using satellite data is included. T.M.

N82-23583*# Geological Survey, Denver, Colo.
REGISTRATION OF HEAT CAPACITY MAPPING MISSION DAY AND NIGHT IMAGES
K. WATSON, S. HUMMER-MILLER, and D. L. SAWATZKY, Principal Investigators 1982 17 p refs Submitted for publication Sponsored by NASA Original contains imagery. Original imagery may be purchased from NASA, Goddard Space Flight Center, (code 601), Greenbelt, Md. 20771. Domestic users send orders to 'Attn: National Space Science Data Center'; non-domestic users send orders to 'Attn: World Data Center A for Rockets and Satellites'. HCMM
(E82-10210; NASA-CR-168773) Avail: NTIS HC A02/MF A01 CSCL 05B

Neither iterative registration, using drainage intersection maps for control, nor cross correlation techniques were satisfactory in registering day and night HCMM imagery. A procedure was developed which registers the image pairs by selecting control points and mapping the night thermal image to the daytime thermal and reflectance images using an affine transformation on a 1300 by 1100 pixel image. The resulting image registration is accurate to better than two pixels (RMS) and does not exhibit the significant misregistration that was noted in the temperature-difference and thermal-inertia products supplied by NASA. The affine transformation was determined using simple matrix arithmetic, a step that can be performed rapidly on a minicomputer. A.R.H.

N82-23584*# Geological Survey, Denver, Colo.
GROUND SUPPORT DATA FROM JULY 10 TO JULY 29, 1978, FOR HCMM THERMAL SATELLITE DATA OF THE POWDER RIVER BASIN, WYOMING
S. HUMMER-MILLER, K. WATSON, and R. KIPFINGER, Principal Investigators 1980 48 p refs Sponsored by NASA HCMM
(E82-10211; NASA-CR-168772; NAS 1.26:168772; USGS-OFR-80-469) Avail: NTIS HC A03/MF A01 CSCL 08I

Radiometric and meteorological data acquired at three ground stations located approximately 150 km apart in the Powder River Basin, Wyoming, are summarized. The data were collected between July 10 and July 29, 1978, to support the HCMM thermal satellite data acquired during this time period. The parameters measured are direct solar radiance, total solar radiance, sky radiance, air temperature, relative humidity, wind speed, and wind direction. A tabulation of the measurement accuracies is presented. J.D.

N82-23586*# Purdue Univ., Lafayette, Ind. Lab. for Applications of Remote Sensing.
MULTISTAGE CLASSIFICATION OF MULTISPECTRAL EARTH OBSERVATIONAL DATA: THE DESIGN APPROACH
M. E. BAUER, Principal Investigators, M. J. MUASHER, and D. A. LANDGREBE Dec. 1981 181 p refs Sponsored by NASA, USDA, Dept. of Commerce, Dept. of the Interior, and Agency for International Development ERTS
(Contract NAS9-15466; PROJ. AGRISTARS)
(E82-10213; NASA-CR-167508; NAS 1.26:167508; LARS-101481; SR-P1-04194) Avail: NTIS HC A09/MF A01 CSCL 02C

An algorithm is proposed which predicts the optimal features at every node in a binary tree procedure. The algorithm estimates the probability of error by approximating the area under the likelihood ratio function for two classes and taking into account the number of training samples used in estimating each of these two classes. Some results on feature selection techniques, particularly in the presence of a very limited set of training samples, are presented. Results comparing probabilities of error predicted by the proposed algorithm as a function of dimensionality as compared to experimental observations are shown for aircraft and LANDSAT data. Results are obtained for both real and simulated data. Finally, two binary tree examples which use the algorithm are presented to illustrate the usefulness of the procedure. Author

N82-23596*# Lockheed Engineering and Management Services Co., Inc., Houston, Tex.
EVALUATION OF VICAR SOFTWARE CAPABILITY FOR LAND INFORMATION SUPPORT SYSTEM NEEDS
S. S. YAO, Principal Investigator Sep. 1981 19 p Sponsored by NASA, USDA, Dept. of Commerce, Dept. of the Interior, and Agency for International Development ERTS
(Contract NAS9-15800; PROJ. AGRISTARS)
(E82-10223; NASA-CR-167442; JSC-17431; NAS 1.26:167442; LEMSCO-17269; RR-L1-17269) Avail: NTIS HC A02/MF A01 CSCL 09B

A preliminary evaluation of the processing capability of the VICAR software for land information support system needs is presented. The geometric and radiometric properties of four sets of LANDSAT data taken over the Elk River, Idaho quadrangle were compared. Storage of data sets, the means of location, pixel resolution, and radiometric and geometric characteristics are described. Recommended modifications of VICAR programs are presented. J.D.

N82-23599*# Texas Univ. at Dallas. Center for Space Sciences.
INVESTIGATION OF THE EFFECTS OF EXTERNAL CURRENT SYSTEMS ON THE MAGSAT DATA UTILIZING GRID CELL MODELING TECHNIQUES Quarterly Status Technical Progress Report, 1 Oct. - 31 Dec. 1981
D. M. KLUMPAR, Principal Investigator 9 Jan. 1982 10 p ERTS
(Contract NAS5-26309)
(E82-10226; NASA-CR-168800; NAS 1.26:168800; QSTPR-5) Avail: NTIS HC A02/MF A01 CSCL 05B

Efforts in support of the development of a model of the magnetic fields due to ionospheric and magnetospheric electrical currents are discussed. Specifically, progress made in reading MAGSAT tapes and plotting the deviation of the measured magnetic field components with respect to a spherical harmonic model of the main geomagnetic field is reported. Initial tests of the modeling procedure developed to compute the ionosphere/magnetosphere-induced fields at satellite orbit are also described. The modeling technique utilizes a liner current element representation of the large scale current system. M.G.

N82-23605*# Texas Univ. at Dallas. Center for Space Sciences.
INVESTIGATION OF THE EFFECTS OF EXTERNAL CURRENT SYSTEMS ON THE MAGSAT DATA UTILIZING GRID CELL MODELING TECHNIQUES Quarterly Status Technical Progress Report, 1 Jul. - 30 Sep. 1981
D. M. KLUMPAR, Principal Investigator 12 Oct. 1981 9 p Original contains color imagery. Original photography may be purchased from the EROS Data Center, Sioux Falls, S.D. 57198. ERTS
(Contract NAS5-26309)
(E82-10232; NASA-CR-168801; NAS 1.26:168801; QSTPR-4) Avail: NTIS HC A02/MF A01 CSCL 08G

Progress is reported in reading MAGSAT tapes in modeling procedure developed to compute the magnetic fields at satellite orbit due to current distributions in the ionosphere. The modeling technique utilizes a linear current element representation of the large-scale space-current system. Author

N82-23612*# Tokyo Univ. (Japan).
INVESTIGATION FROM JAPANESE MAGSAT TEAM Progress Report, 15 Mar. 1980 - 15 Jul. 1981
N. FUKUSHIMA, Principal Investigator 20 Jul. 1981 10 p Sponsored by NASA ERTS
(E82-10239; NASA-CR-168755; NAS 1.26:168755; PR-3) Avail: NTIS HC A02/MF A01 CSCL 05B

The acquisition of tapes which contain vector and scalar data decimated at an interval of 0.5 sec, together with time and position data, is reported. Progress in the study of magnetic anomalies in the vicinity of Japan and in electric currents in the ionosphere and magnetosphere is also reported. MAGSAT data was used in obtaining a map of total force anomaly for the area of latitude 10-70 deg N and longitude 110-170 deg E. One of the outstanding features in the map of the magnetic anomaly is a negative magnetic anomaly in the Okhotsk Sea, which is of geophysical interest because of its possible connection with high heat flow values in that area. T.M.

N82-23613*# Miami Univ., Fla. School of Marine and Atmospheric Science.
INVESTIGATIONS OF MEDIUM WAVELENGTH MAGNETIC ANOMALIES IN THE EASTERN PACIFIC USING MAGSAT Interim Report, Jul. - Sep. 1981
C. G. A. HARRISON, Principal Investigator Nov. 1981 2 p Sponsored by NASA ERTS
(E82-10240; NASA-CR-168756; NAS 1.26:168756) Avail: NTIS HC A02/MF A01 CSCL 08G

Progress in study of the details of spherical harmonic representations of the Earth's magnetic field is reported. The first of the Investigator B quiet time tapes were received and determined to be error free. J.D.

N82-24517# Technische Hogeschool, Delft (Netherlands). Lab. of Engineering Mechanics.
NONLINEAR THEORY FOR ELASTIC BEAMS AND RODS AND ITS FINITE ELEMENT REPRESENTATION
J. F. BESSELING Oct. 1981 25 p refs
(WTHD-143) Avail: NTIS HC A02/MF A01

Expressions for large curvatures of elastic beams and rods are given in terms of displacement components and angular coordinates. The application of these expressions to bifurcation and stability problems, based on the principle of virtual work is discussed. This approach is compared with another finite element representation, and an error in this representation is corrected. The condition of zero extension of the axis in the case of the Euler column is shown to require division into a large number of finite elements in order to ensure an accurate result for the stability coefficient. The conditions of zero extension of the axis and zero curvature about one principal axis of the cross section in the case of the lateral buckling of the end loaded cantilever have similar consequences. Author (ESA)

N82-24570*# Survey of India, Dehra Dun. Geodetic and Research Branch.
REPORT OF MAGSAT PROJECT BY SURVEY OF INDIA Status Report
J. L. SAWHNEY 18 Aug. 1981 4 p refs Sponsored by NASA ERTS
(E82-10293; NASA-CR-168916; NAS 1.26:168916) Avail: NTIS HC A02/MF A01 CSCL 08G

Magsat data fo quiet days for the period 4.11.79, 17.11.79 to 24.11.79, which pertains to 44 passes, was screened to exclude the the period of exclude the period of maximum diurnal variation. The results of this screening process is a data set that has the effect, (or at least the major part of the effect), of the external field removed from it. Such a data set is the basis for further analysis which is in hand. The data set is now being reduced to horizontal plane. The mathematical techniques uses a finite harmonic series representation of the three dimensional data, combined with least squares approach for the solution of coefficients. A computer programme was developed to reduce satellite data to a common elevation. A.R.H.

N82-24572*# Indian Inst. of Geomagnetism, Bombay.
MAGSAT FOR GEOMAGNETIC STUDIES OVER INDIAN REGION Progress Report, 1 Nov. 1981 - 31 Mar. 1982
R. G. RASTOGI, B. P. SINGH, D. R. K. RAO, G. K. RANGARAJAN, R. RAJARAM, M. ROY, and B. R. ARORA, Principal Investigators 1 Apr. 1982 5 p ERTS
(E82-10296; NASA-CR-168865; NAS 1.26:168865; M-38; PR-2) Avail: NTIS HC A02/MF A01 CSCL 08G

The major activities of the period are summarized. Data tapes generated on an IBM system were read on DEC-10 system new tapes compatible with DEC-10 system were prepared for data sections of interest. Core and external current contributions were removed from selected passes over the Indian region and the residuals analyzed. Possible equatorial electrojet contributions to the MAGSAT data were studied. J.D.

N82-24580*# Texas Univ. at Dallas, Richardson. Center for Space Sciences.
INVESTIGATION OF THE EFFECTS OF EXTERNAL CURRENT SYSTEMS ON THE MAGSAT DATA UTILIZING GRID CELL MODELING TECHNIQUES Quarterly Status Technical Progress Report, 1 Jan. - 31 Mar. 1982
D. M. KLUMPAR, Principal Investigator 27 Apr. 1982 11 p ERTS
(Contract NAS5-26309)
(E82-10306; NASA-CR-168881; NAS 1.26:168881; STPR-6)
Avail: NTIS HC A02/MF A01 CSCL 05B

Progress made in reducing MAGSAT data and displaying magnetic field perturbations caused primarily by external currents is reported. A periodic and repeatable perturbation pattern is described that arises from external current effects but appears as unique signatures associated with upper middle latitudes on the Earth's surface. Initial testing of the modeling procedure that was developed to compute the magnetic fields at satellite orbit due to current distributions in the ionosphere and magnetosphere is also discussed. The modeling technique utilizes a linear current element representation of the large scale space current system. M.G.

N82-24581*# North Carolina State Univ., Raleigh. Dept. of Marine, Earth and Atmospheric Sciences.
MAGSAT SCALAR AND VECTOR ANOMALY DATA ANALYSIS Progress Report, period ending 31 Jan. 1982
1 Feb. 1982 1 p ERTS
(Contract NAS5-26157)
(E82-10307; NASA-CR-168882; NAS 1.26:168882) Avail: NTIS HC A02/MF A01 CSCL 08B

Efforts on the analysis of MAGSAT scalar anomaly data, the application of the scalar analysis results to three component vector data, and the comparison of MAGSAT data with corresponding MAGNET aeromagnetic and free air gravity anomaly data are briefly described. M.G.

N82-24588*# Zentralstelle fuer Geo-Photogrammetrie und Fernerkundung, Munich (West Germany).
MULTIDISCIPLINARY INVESTIGATIONS ON HCMM DATA OVER MIDDLE EUROPE AND MAROCCO Final Report, 1979 - 1981
R. HAYDN, Principal Investigator, G. DALKE, J. HENKEL, and H. KAUFMANN 10 Mar. 1982 86 p Sponsored by NASA, Deutsche Forschungsgemeinschaft and Bundesministerium fuer Forschung und Technologie Original contains color imagery. Original imagery may be purchased from NASA Goddard Space Flight Center, (code 601), Greenbelt, Md. 20070. Domestic users send orders to 'Attn: National Space Science Data Center'; nondomestic users send orders to 'Attn: World Data Center A for Rockets and Satellites'. HCMM
(E82-10315; NASA-CR-168910; NAS 1.26:168910) Avail: NTIS HC A05/MF A01 CSCL 05B

The development approaches in presenting HCMM data in combination with LANDSAT for improved interpretability is presented. The techniques are based on the IHS (intensity hue and saturation) concept which permits the calculation of LANDSAT/HCMM merges exhibiting the high spatial resolution of LANDSAT along with the HCMM thermal recordings coded into perceivable and interpretable colors. A further approach is based on the calculation of synthetic LANDSAT stereo images showing HCMM thermal recording as a quasitopography. The feasibility of these approaches are discussed on the tests The feasibility of these approaches are discussed on the basis of HCMM and LANDSAT images representing the test sites. On the basis of a scene covering an area of the Anti Atlas, the relationship between geological phenomena and their interpretability via LANDSAT/HCMM merged products. E.A.K.

N82-24595*# Tokyo Univ. (Japan). Geophysics Research Lab.
REPORT OF INVESTIGATION FROM JAPANESE MAGSAT TEAM Progress Report, 1 Dec. 1981 - 30 Mar. 1982
N. FUKUSHIMA, H. MAEDA, T. YUKUTAKE, M. TANAKA, S. OSHIMA, K. OGAWA, M. KAWAMURA, Y. MIYAZAKI, S. UYEDA, K. KOBAYASHI, Principal Investigatorset al. 5 Apr. 1982 13 p refs Submitted for publication ERTS
(E82-10322; NASA-CR-168901; NAS 1.26:168901; PR-5) Avail: NTIS HC A02/MF A01 CSCL 08G

Progress in the data processing and data acquisition of computer compatible MAGSAT tapes is reported. Investigations focused on the crustal structure near Japan and its Antarctic station, and electric currents and hydrodynamic waves in the ionosphere and the magnetosphere. The magnetization of the crust in the northwestern Pacific region is discussed. T.M.

N82-24600*# Paris VI Univ. (France).
MODELS AND MAPS OF THE MAIN FIELD Progress Report
J. L. LEMOUEL, Principal Investigator, C. GIRE, and J. DUCRUIX 1 Apr. 1982 13 p refs Sponsored by NASA ERTS
(E82-10327; NASA-CR-168906; NAS 1.26:168906) Avail: NTIS HC A02/MF A01 CSCL 08B

The difference between the models comes from the difference in the procedures of data selection and depends on the aim the model is intended for: regional studies necessitates locally higher density of data and for downward continuation the reduction of external variations must be as careful as possible. Refinements of preliminary models MAGP1 and MAGP2 are presented. Models MAGP1 and MAGP2 are found to have drawbacks coming from insufficient reduction of the external variations and from the inhomogeneity in the distribution of the measurement points. New analysis was performed to overcome these shortcomings. The quality of the new models is characterized by the average rms of the differences measurement model. T.M.

N82-25611# University of Southern California, Los Angeles. Image Processing Inst.
IMAGE UNDERSTANDING RESEARCH Final Technical Report, 1 Apr. - 30 Sep. 1981
R. NEVATIA and A. A. SAWCHUK 30 Sep. 1981 138 p refs
(Contract F33615-80-C-1080; DARPA ORDER 3119)
(AD-A110746; USCIPI-1050) Avail: NTIS HC A07/MF A01 CSCL 05H

This technical report summarizes the image understanding and VLSI system research activities performed by the University of Southern California and the Hughes Research Laboratories during 1 April 1981 through 30 September 1981 under contract number F-33615-80-C-1080 with the Defense Advanced Research Projects Agency, Information Processing Techniques Office. The purpose of this research program is to develop techniques and systems for understanding images, particularly for mapping applications. The research activity includes low level image analysis and feature extraction, statistical and structural texture analysis, symbolic image representations, and image to map correspondence using relational structures. Additional activity is concerned with VLSI architectures for implementation of image analysis and image understanding operations. GRA

N82-25612# Defense Mapping Agency Aerospace Center, St. Louis, Mo. Aerospace Cartography Dept.
MATRIX DATA ANALYSIS: COLOR/B AND W CODING IS NOT ALWAYS ENOUGH Interim Report, 1976 - 1981
M. B. FAINTICH, G. B. SIGLER, and J. D. SIMPSON 1981 31 p refs Presented at the Inter-Congr. Symp., Inter. Soc. of Phot. and Remote Sensing Comm. 3, Otaniemi, Finland, 7-11 Jun. 1982
(AD-A111401) Avail: NTIS HC A03/MF A01 CSCL 08B

The Defense Mapping Agency produces digital data bases that describe the physical appearance of the surface of the Earth. These data bases include, but are not limited to, terrain elevation, culture including landscape characteristics and vertical features. This data is collected from digitized source maps, from optically or digitally correlated stereo-pairs of photographic imagery, and from digital multi-spectral sensor data. A dramatic impact has been made in the ability to analyze these digital data bases by applying state-of-the-art digital image technology processing and display concepts. These include a variety of color and/or black and white displays of not only intensity/color coded matrix data, but also image processed data using specialized convolution filters, texture discrimination, and special color representation techniques. In addition, computer generated imagery from these data bases serves as a final analysis tool. GRA

N82-25613# Measurement Concept Corp., Rome, N. Y.
SOURCE ASSESSMENT SYSTEM Final Technical Report
R. H. SENN, M. L. TAYLOR, R. BURNS, and M. SMITH Griffiss AFB, N.Y. RADC Nov. 1981 153 p refs
(Contract F30602-80-C-0040; AF PROJ. 4303)
(AD-A111223; RADC-TR-81-303) Avail: NTIS HC A08/MF A01 CSCL 09B

This report contains an analysis of the Source Assessment Procedures at both Defense Mapping Agency (DMA) production facilities (Aerospace Center DMAAC in St. Louis MO and Hydrographic Topographic Center DMAHTC in Washington DC). Following the analysis, the report documents a design trade off of various approaches to a Source Assessment System. Finally, a Design Plan for the selected approach analog-digital video system, is presented. Author (GRA)

N82-25614# Army Engineer Topographic Labs., Fort Belvoir, Va.
COORDINATION OF STEREO IMAGE REGISTRATION AND PIXEL CLASSIFICATION Computer Sciences Lab.
M. A. CROMBIE 20 Mar. 1982 10 p refs Presented at the ACSM-ASP Ann. Conv., Denver, 1982
(AD-A111307; ETL-R034) Avail: NTIS HC A02/MF A01 CSCL 14E

An inadequate concept of how corresponding points relate to one another on dissimilar images has a greater effect than exposure geometry or data collection on registration problems in stereo photogrammetry. Conventional correlation, or one of its relatives, is the measure of similarity used in all automated stereo correlation systems. Correlation, a measure of the linear dependence between two sets of data, is an inadequate measure when there is less than, or more than, a moderate amount of image structure at and around points selected for image matching. The existence of structure should be recognized and utilized in an appropriate manner for image matching. Similarly, the absence of structure should be recognized, and the surrounding imagery should be used to complete matches where it is possible. The concurrent determination of what a pixel is, as well as where it is, can alleviate much of the registration problem. A variety of features including point-density data, texture, and edges, as well as existing cartographic knowledge, can be combined and organized through rules in order to more completely describe a point. The overall throughput of the compilation process will be improved in both time and accuracy if those functions which tend to support one another are concurrently, rather than sequentially, performed. If the compilation process takes place in image space, then the image matching operation as well as the other feature extraction operations, can be ordered by the data processing manager to best suit the function of the process. Author (GRA)

N82-26027# Instituto de Pesquisas Espaciais, Sao Jose dos Campos (Brazil).
SMS/GOES DATA COLLECTION PLATFORM SYSTEM [PLATFORMA DE COLETA DE DADOS SISTEMA SMS/GOES]
V. RODRIGUES *In its* Minutes of the 1st Seminar on Use of the Natl. System for Collection of Satellite Data p 21-30 Jul. 1981 In PORTUGUESE
Avail: NTIS HC A12/MF A01

The SMS/GOES synchronous meteorological satellite system, consisting of the satellite, ground stations, and data collection platforms, is described. The objectives of the system and the services it performs are listed. Applications of the data collection platforms are surveyed and the platforms described. The parameters of the data collected are listed. Transl. by J.D.

N82-26037# European Space Agency, Toulouse (France). METEOSAT Data Management Dept.
THE METEOSAT DATA COLLECTION SYSTEM AND ITS APPLICATION
A. ROBSON and H. HOVET *In* Instituto de Pesquisas Espaciais 1st Seminar on Use of the Natl. System for Collection of Satellite Data p 191-206 Jul. 1981
Avail: NTIS HC A12/MF A01

The METEOSAT data collection system and its applications are described. Use of the system for collection of meteorological data at remote land sites in Greenland, for meteorological and sea state monitoring at offshore sites in the North and Baltic Seas, for hydrological monitoring in Great Britain, and for meteorological data collection from aircraft is discussed. J.D.

N82-26756*# Survey of India, Dehra Dun.
ANALYSIS OF MAGSAT DATA OF THE INDIAN REGION Progress Report, 10 Jan. 1981 - 1 Feb. 1982
K. L. KHOSLA, Principal Investigators, M. G. ARUR, S. R. M. GUPTA, S. P. S. BAINS, S. J. LAL, J. G. NEGI (NGRI), P. K. AGARWAL (NGRI), B. N. P. AGARWAL (Indian School of Mines), and B. SAHAI (Space Application Centre, Ahmedabad, India) 31 Mar. 1982 3 p refs Sponsored by NASA ERTS
(E82-10358; NASA-CR-168979; NAS 1.26:168979; REPT-2; REPT-3) Avail: NTIS HC A02/MF A01 CSCL 05B

Progress in the development of software for reading MAGSAT data tapes and for the reduction of anomaly data, and in the preparation of data for magnetic anomaly maps is reported. J.D.

N82-26763*# Environmental Systems Research Inst., Redlands, Calif.
EXPLORATION INTO TECHNICAL PROCEDURES FOR VERTICAL INTEGRATION Final Contractor Report
R. J. MICHEL and K. D. MAW Sep. 1979 29 p refs
(Contract NASA ORDER A-65111-B)
(NASA-CR-166352; NAS 1.26:166352) Avail: NTIS HC A03/MF A01 CSCL 08G

Issues in the design and use of a digital geographic information system incorporating landuse, zoning, hazard, LANDSAT, and other data are discussed. An eleven layer database was generated. Issues in spatial resolution, registration, grid versus polygonal structures, and comparison of photointerpreted landuse to LANDSAT land cover are examined. Author

N82-26765# Earth Satellite Corp., Washington, D. C.
EXPERIMENTAL ASSESSMENT OF IMPROVED SPATIAL RESOLUTION LANDSAT DATA Final Report
C. SHEFFIELD, M. PLACE, D. GAROFALO, J. DYKSTRA, and L. HALL Ft. Belvoir, Va. ETL 30 Sep. 1981 82 p refs
(Contract DAAK70-80-C-0016)
(AD-A110538; E/S-1234; ETL-0268) Avail: NTIS HC A05/MF A01 CSCL 14E

This report describes the possible uses of higher resolution (25 meter) space-derived images for delineating and measuring surface features of interest in the Corps of Engineers' Civil Works Program. Following a discussion of imaging sensors and computer processing methods, test evaluations are described in which LANDSAT multispectral scanner data and SEASAT SAR data were interpreted for surface features. The comparative advantages of the two data sources are discussed, and the complementary nature of LANDSAT MSS and SEASAT SAR images is displayed in the image analyses. Image examples are included for both background discussion and test site evaluation. Author (GRA)

N82-26907# Massachusetts Univ., Amherst. Astronomy Research Facility.

STRATOSPHERIC EMISSION DATA ANALYSIS Final Report, 1 Jan. 1979 - 31 Jan. 1982

H. SAKAI Feb. 1982 32 p refs

(Contract F19628-79-C-0062; AF PROJ. 2310)

(AD-A112337; UMASS-ARF-82-321; AFGL-TR-82-0055) Avail: NTIS HC A03/MF A01 CSCL 04A

The work described in this report constitutes a data-processing and data analysis part of the AFGL SCRIBE (Stratospheric Cryogenic Interferometer Balloon Experiment) program. This work may be summarized into three major categories: (1) extraction of the interferogram data from the PCM telemetry data tape; (2) processing of the interferogram data for spectral retrieval; and (3) analysis of the obtained atmospheric emission data. GRA

08

INSTRUMENTATION AND SENSORS

Includes data acquisition and camera systems and remote sensors.

A82-22608

IS THE NEON COMPOSITION OF OUR SUN, PLANETARY OR SOLAR

M. N. RAO, C. M. NAUTIYAL, and T. R. VENKATESAN (Physical Research Laboratory, Ahmedabad, India) In: International Cosmic Ray Conference, 17th, Paris, France, July 13-25, 1981, Conference Papers. Volume 3. Gif-sur-Yvette, Essonne, France, Commissariat a l'Energie Atomique, 1981, p. 141-144. refs

The surficial solar wind from the feldspar grain-size separates of lunar soils is removed by selective chemical etching to determine whether the long term average solar flare Ne composition is planetary or solar. Mineral residues mostly containing solar flare implanted noble gas components are analyzed by step wise gas release mass spectrometric methods. Results do not show any major differences in the Ne ratios of solar flares and solar wind, and the long term average composition of low energy solar flares implanted Ne is similar to solar wind neon instead of planetary, although variations of Ne isotopic ratios in solar flares over short time scales is not ruled out. D.L.G.

A82-29541

AN INFRARED EXPOSURE METER

R. W. DANA (U.S. Forest Service, Fort Collins, CO) In: Color aerial photography in the plant sciences and related fields; Proceedings of the Eighth Biennial Workshop, Luray, VA, April 21-23, 1981. Falls Church, VA, American Society of Photogrammetry, 1981, p. 145-156. refs

It is noted that, since the commonly used color infrared aerial film has less latitude to variations in scene brightness than most normal color films, camera exposure adjustment is crucial in the infrared aerial photography of natural resources. A description is given of a spotmeter sensitive in the wavelength band of infrared films developed to aid the aerial photographer in adjusting camera settings for optimum exposure of a variety of scenes. Also discussed are airborne tests undertaken to evaluate the meter for agricultural, forest, and range cover. The problems encountered in using photographic photometry to evaluate luminance readings from a hand-held instrument fall into three groups: instrument pointing problems, film sensitometry, and camera calibration. The optimum exposure for quantitative density analysis is thought to be about three-fourths of a stop lower than for visual interpretation. The results of regression analysis suggest that the infrared meter marks an improvement over conventional spotmeters in predicting the infrared response of the film. C.R.

A82-29922

THERMOGRAPHY - A REMOTE SENSING METHOD WITH MANY PERSPECTIVES [THERMOGRAFIE - EINE PERSPEKTIVREICHE FERNERKUNDUNGSMETHODE]

A. GESCHKE (Gesellschaft fuer Internationalen Flugverkehr mbH, Berlin, East Germany) Technisch-oekonomische Information der zivilen Luftfahrt, vol. 17, no. 4, 1981, p. 169-171. In German.

Thermography, as considered in this report, is concerned with the utilization of the electromagnetic radiation of the far-infrared region for the formation of images. Possibilities for such a utilization improved greatly with the development of cooled semiconductor sensing devices during the last twenty years. Thermographs were designed as far-infrared image-forming devices which provide a thermal photograph by scanning a far-infrared image of an object or a scene. A description is provided of investigations in which such devices, carried on board of a helicopter or a fixed-wing aircraft, were used to obtain thermal images of an area on the ground. Thermography is found to be a valuable approach for the study of energetic aspects, geologic structures, groundwater budget questions, the vitality of forests and agricultural areas, and water pollution. G.R.

A82-31019

LARGE AMPLITUDE UNDULATIONS ON THE EQUATORWARD BOUNDARY OF THE DIFFUSE AURORA

A. T. Y. LUI, C.-I. MENG, and S. ISMAIL (Johns Hopkins University, Laurel, MD) Journal of Geophysical Research, vol. 87, Apr. 1, 1982, p. 2385-2400. refs

(Contract AF-AFOSR-79-0010; NSF ATM-79-23240; NSF ATM-79-25987)

A description is presented of the first observation of large scale undulations in the equatorward boundary of the diffuse aurora by pictures of global auroral displays in the afternoon-evening sector. These observations are made by a broad band scanning radiometer on the Defense Meteorological Satellite Program (DMSP) satellites. Attention is given to four periods during which the equatorward boundary of the diffuse aurora is undulated. Three of these are taken in the southern polar region and one in the northern polar region. The duration of the undulations is considered along with geomagnetic and interplanetary conditions. All undulations are found to occur during the period of a geomagnetic storm near the peak development of the storm-time ring current. All are accompanied by substorm patterns of discrete auroras. G.R.

A82-31020

EXTREMELY HIGH LATITUDE AURORAS

M. S. GUSSENHOVEN (Boston College, Chestnut Hill, MA) Journal of Geophysical Research, vol. 87, Apr. 1, 1982, p. 2401-2412. refs

(Contract F19628-81-K-0032; AF-AFOSR-79-0012)

It is pointed out that imaging devices on the polar orbiting ISIS and Defense Meteorological Satellite Program (DMSP) satellites have greatly increased the extent of polar cap and auroral zone coverage and have prompted several studies of polar cap arcs. A description is presented of a statistical study of the occurrence conditions for arcs recorded in DMSP images at extremely high latitudes, taking into account corrected geomagnetic latitudes equal to or greater than 80 deg. The 80 deg boundary is chosen to minimize the problems associated with defining a polar cap boundary. Attention is given to the data base and categorization of extremely high latitude auroras, the relationship to magnetic activity, and the relationship to solar wind conditions. It is found that one category of extremely high latitude auroras is distinctly different from the rest. This category includes the oval auroras which expand poleward in the midnight sector. G.R.

A82-31991

A SYSTEM DESIGN FOR A MULTISPECTRAL SENSOR USING TWO-DIMENSIONAL SOLID-STATE IMAGING ARRAYS

R. M. HODGSON (Canterbury, University, Christchurch, New Zealand), F. M. CADY (Montana State University, Bozeman, MT), and D. PAIRMAN (Department of Scientific and Industrial Research, Physics and Engineering Laboratories, Lower Hutt, New Zealand) IEEE Transactions on Geoscience and Remote Sensing, vol. GE-20, Apr. 1982, p. 177-179. Research supported by the University of Canterbury and University Grants Committee. refs

A system developed for remote sensing from light aircraft in the 400-1100 nm wavelength range possesses an architecture which permits the simultaneous capture of up to four images from solid-state, two-dimensional image sensors. In operation, the array sensor captures a series of relatively rapid, approximately 10 msec exposures at intervals as long as 10 sec. This mode of operation has the advantage of nearly the same degree of distortion due to aircraft roll in all image elements. The software generation of sensor drive signals is incorporated in the system. O.C.

A82-32440

IMAGING SPECTROSCOPY; PROCEEDINGS OF THE SEMINAR, LOS ANGELES, CA, FEBRUARY 10, 11, 1981

D. D. NORRIS, (ED.) (California Institute of Technology, Jet Propulsion Laboratory, Pasadena, CA) Seminar sponsored by SPIE - The International Society for Optical Engineering. Bellingham, WA, SPIE - The International Society for Optical Engineering (SPIE Proceedings. Volume 268), 1981. 204 p. MEMBERS, $34.; NONMEMBERS, $40

The seminar concentrated on the science applications of spectral imaging, multispectral imaging sensors, and spectral filtering. Papers are presented on spectroscopic remote sensing for geological applications, spectral mapping of Jupiter, system design of an interferometer imaging sounder and a common module imaging spectral radiometer. Other topics discussed include the performance and application of an intensified linear self-scanned array instrument, tunable optical filtering using an interferometer for selective modulation, design studies for a spectrally agile staring sensor system, and acousto-optic tunable filters for high-resolution spectral analysis. V.L.

A82-32443* Columbia Univ., New York.

HIGH SPECTRAL RESOLUTION AIRBORNE SPECTROMETRY

W. COLLINS, S. CHANG, J. T. KUO (Columbia University, New York, NY), M. DOUMA, S. MARSHALL (Massachusetts Manufacturing Corp., Cambridge, MA), and P. MURPHY (Sanders Associates, Inc., Nashua, NH) In: Imaging spectroscopy; Proceedings of the Seminar, Los Angeles, CA, February 10, 11, 1981. Bellingham, WA, SPIE - The International Society for Optical Engineering, 1981, p. 22-28
(Contract JPL-955832; NSF ENG-78-24432)

An airborne spectroradiometer system developed at Columbia University has been providing new spectral data for use in remote sensing for natural resources. The system has been improved by addition of a solid state silicon detector array, and has been extended into the infrared by addition of a 64 element lead sulfide detector array. The infrared data in the 2000 to 2500 nm region especially holds large potential for mineral and oil exploration. (Author)

A82-32447* Santa Barbara Research Center, Goleta, Calif.

THEMATIC MAPPER - AN OVERVIEW OF SPECTRAL BAND REGISTRATION

W. H. FREUDENSTEIN (Santa Barbara Research Center, Goleta, CA) In: Imaging spectroscopy; Proceedings of the Seminar, Los Angeles, CA, February 10,11, 1981. Bellingham, WA, SPIE - The International Society for Optical Engineering, 1981, p. 50-63.
(Contract NAS5-24200)

The Thematic Mapper (TM) is a high-resolution radiometer designed for earth resources classification and mapping. The TM employs multispectral scanning in a near polar orbit to sweep a 185-km swath. Data are obtained through a combination of spacecraft motion and the sweeping action of the scan mirror. These data are transmitted either directly to ground stations around the world or through a relay to the central data processing facility at White Sands, NM. Seven spectral passbands are employed, and applications include coastal water mapping, soil vegetation differentiation, biomass surveys, water body delineation, vegetation moisture measurement, plant heat stress management, and hydrothermal mapping. Attention is given to the scan mirror assembly, scan nonlinearities, the characterization and compensation of scan profiles, experimental performance, and a procedure for midscan correction. G.R.

A82-32448* Jet Propulsion Lab., California Inst. of Tech., Pasadena.

MULTISPECTRAL MAPPER - IMAGING SPECTROSCOPY AS APPLIED TO THE MAPPING OF EARTH RESOURCES

J. B. WELLMAN (California Institute of Technology, Jet Propulsion Laboratory, Observational Systems Div., Pasadena, CA) In: Imaging spectroscopy; Proceedings of the Seminar, Los Angeles, CA, February 10,11, 1981. Bellingham, WA, SPIE - The International Society for Optical Engineering, 1981, p. 64-73. refs
(Contract NAS7-100)

An instrument concept that uses solid-state array imaging has been developed for a future land observing system. The design concept is responsive to a variety of use needs and provides improved capabilities over the planned Landsat Thematic Mapper. A comparison of the differing approaches to the instrument design was made, resulting in the selection of a concept which uses a spectrograph coupled to a line-array imager to provide simultaneous spatial and spectral resolution. The design provides an inherent solution to the problem of achieving precise registration among the spectral bands. Data processing on the focal plane is used to select the spectral bands and their band widths. Onboard capabilities include radiometric correction, selection of instantaneous field-of-view and swath width, and data compression. (Author)

A82-32658* Massachusetts Inst. of Tech., Cambridge.

INVERSION OF DATA FROM DIFFRACTION-LIMITED MULTIWAVELENGTH REMOTE SENSORS. II - NONLINEAR DEPENDENCE OF OBSERVABLES ON THE GEOPHYSICAL PARAMETERS

P. W. ROSENKRANZ (MIT, Cambridge, MA) Radio Science, vol. 17, Jan.-Feb. 1982, p. 245-267. refs
(Contract NAS5-22929; NAG5-10)

Linear shift-invariant spatial filtering is applied to inversion of radiometric measurements of the earth in both polarizations at the following frequencies: 6.6, 10.7, 18, 21, and 37 GHz. For purposes of radiative transfer calculations at these frequencies, the state of the ocean-atmosphere system is described by a seven-parameter model. The parameters are near-surface wind speed, sea surface temperature, integrated water vapor mass, scale height of water vapor in an exponential distribution, integrated liquid water mass, height of the liquid water, and characteristic drop radius in a Best (1950) drop size distribution. Also described is a spatial filtering algorithm by means of which geophysical parameters are retrieved from measurements made over the ocean by the scanning multichannel microwave radiometer on the Nimbus 7 satellite. The parameters here are near-surface wind speed, sea surface temperature, rain rate, integrated atmospheric water vapor content, and integrated liquid water content (including rain). C.R.

A82-32702#

PHOTOGRAMMETRIC METHODS FOR MAPPING RESOURCE DATA FROM HIGH ALTITUDE PANORAMIC PHOTOGRAPHY

R. L. LISTON (U.S. Forest Service, Washington, DC) Photogrammetric Engineering and Remote Sensing, vol. 48, May 1982, p. 725-732. refs

Characteristics of the Itek KA-80A optical bar panoramic camera are discussed. Two computer based mapping systems designed to correct for variations in photo scale are described. Panoramic Grid (PANGRID) is a computer program that creates a panoramic

image overlay of an equal area grid assumed to lie on flat ground. The Photographic Mapping System (PMS) provides for the generation of both map registered grid overlays and mapping of digitized point, line, and polygon data. Both programs make use of single frame resection techniques and digital terrain data.
(Author)

A82-32766
SIMPLIFIED TECHNIQUES TO STUDY COMPONENTS OF SOLAR RADIATION UNDER HAZE AND CLOUDS
M. L. WESELY (Argonne National Laboratory, Argonne, IL) Journal of Applied Meteorology, vol. 21, Mar. 1982, p. 373-383. Research sponsored by the U.S. Department of Energy. refs

A82-32824#
AN OPTICAL OBJECTIVE LENS FOR EARTH OBSERVATIONS BY SATELLITES [UN OBJECTIF OPTIQUE POUR L'OBSERVATION DE LA TERRE A PARTIR DE SATELLITES]
E. MATHIEU (Wild Heerbrugg AG, Heerbrugg, Switzerland), E. SEIN (Centre National d'Etudes Spatiales, Centre Spatial de Toulouse, Toulouse, France), and J.-P. DURPAIRE (ESA, Toulouse, France) ESA Journal, vol. 6, no. 1, 1982, p. 71-81. In French. European Space Agency
(Contract ESA-4422/80)

The features and performance of objective lenses intended for transmission of optical images of the earth to deposition on the detectors of CCDs onboard the ESA land application satellite system/optical imaging instrument are described. Trials to determine satisfactory durability for space-based uses are reviewed. The lenses were required to have an angular field of 16 deg, a 105 mm aperture, cover the spectral bands 0.6, 0.69, 0.8, and 0.9 micron, the panchromatic band from 0.52-0.9 micron, have a focal distance to within 3 mm of 567 mm, cause less than 1 percent distortion in the image size, and less than 1.5 micron error in the spectral domain. Other requirements were for a 0.75 transmittance, polarization less than 1 percent, and a modulation transfer function close to theoretical limits, which was realized at less than 1 mm. The objective produced will have a resolution of around 15 m at the earth's surface from an orbit of 681 km and a total field of view of 167 km.
M.S.K.

A82-32912
QUANTITATIVE RELATIONSHIPS OF NEAR-SURFACE SPECTRA TO LANDSAT RADIOMETRIC DATA
S. E. MARSH and R. J. P. LYON (Stanford University, Stanford, CA) Remote Sensing of Environment, vol. 10, Dec. 1980, p. 241-261. Research supported by the U.S. Geological Survey. refs

It is shown that for typical homogeneous and moderately heterogeneous terrains, the number of samples required for estimating the mean reflectance of a pixel is small. No more than 9-20 samples are required to be within 2% reflectance at the 95% probability level. Coincident field measurements and satellite observations are used to test the equivalency and correlation of the reflectance data. It is noted that, before the Landsat data could be compared with the surface measurements, the satellite brightness values had to be converted to absolute radiometric units and corrected for atmospheric attenuation and scattering. A conversion method using a standard/target comparison, which indirectly compensates for atmospheric attenuation and scattering, produces a Landsat equivalent reflectance exhibiting a root-mean-square error of + or - 4% reflectance (compared with the surface measured value at 12 test sites).
C.R.

A82-32915* National Aeronautics and Space Administration. Goddard Space Flight Center, Greenbelt, Md.
SNOWPACK MONITORING IN NORTH AMERICA AND EURASIA USING PASSIVE MICROWAVE SATELLITE DATA
J. L. FOSTER, A. RANGO, D. K. HALL, A. T. C. CHANG, L. J. ALLISON, and B. C. DIESEN, III (NASA, Goddard Space Flight Center, Greenbelt, MD) Remote Sensing of Environment, vol. 10, Dec. 1980, p. 285-298. refs

Areas of the Canadian high plains, the Montana and North Dakota high plains, and the steppes of central Russia have been studied in an effort to determine the utility of spaceborne microwave radiometers for monitoring snow depths in different geographic areas. Significant regression relationships between snow depth and microwave brightness temperatures were developed for each of these homogeneous areas. In each of the study areas investigated in this paper, Nimbus-6 (0.81 cm) ESMR data produced higher correlations than Nimbus-5 (1.55 cm) ESMR data in relating microwave brightness temperature to snow depth. It is difficult to extrapolate relationships between microwave brightness temperature and snow depth from one area to another because different geographic areas are likely to have different snowpack conditions.
(Author)

A82-33296
INVESTIGATIONS OF POINT TRANSFER [UNTERSUCHUNGEN ZUR PUNKTUEBERTRAGUNG]
M. SIGLE (Stuttgart, Universitaet, Stuttgart, West Germany) Bildmessung und Luftbildwesen, vol. 50, May 1, 1982, p. 91-100. In German. refs

The effectiveness of various new instruments developed for point transfer in practical photogrammetry is discussed with emphasis on their accuracy and economy by controlled aerotriangulation. A comparison is made between signaled and artificially labeled connection points using controlled aerotriangulation selected according to the bundle method. Point transmission methods, picture coordinate measurements and block adjustments are discussed. Investigations are conducted using the equipment of the firms Zeiss and Kern, and no significant difference is found for the transcribers Zeiss PM1 and Kern PMG2 (CPM1).
D.L.G.

A82-33297
IMAGE QUALITY AND HEIGHT MEASUREMENT ACCURACY OF SERIAL SURVEY CAMERA IMAGERY FROM HIGH ALTITUDES [BEITRAEGE ZUR BILDQUALITAET UND HOEHENMESSGENAUIGKEIT VON REIHENMESSKAMMERAUFNAHMEN AUS GROESSEREN FLUGHOEHEN]
J. SIEVERS and K. SCHUERER (Institut fuer angewandte Geodaesie, Frankfurt am Main, West Germany) Bildmessung und Luftbildwesen, vol. 50, May 1, 1982, p. 101-118. In German. refs

The image quality for imagery obtained in photomissions flying from heights of 6 to 14 km is determined using four cameras of different focal lengths and the aerial film material Agfa Aviphot Pan 200. Resolving power is determined using a tri-bar test target, and a method is developed to estimate height accuracy with the aid of statistics. The influence of image quality on the model is taken into consideration, and a highlands area with differences in elevation up to 200 m is used as a terrestrial basis for comparison.
D.L.G.

A82-33442#
INFERENCE OF REFRACTIVITY PROFILES BY SATELLITE-TO-GROUND RF MEASUREMENTS
K. D. ANDERSON (U.S. Naval Ocean Systems Center, San Diego, CA) Radio Science, vol. 17, May-June 1982, p. 653-663. refs

A technique is described to infer an estimate of the tropospheric radio refractive index distribution from earth-based observations of a satellite-born beacon. This technique, known as the direct inference technique (DIT) predicts the refractivity profile by comparing the observed interference pattern, created as the satellite moves through low elevation angles, to patterns generated from a family of assumed refractivity profiles. It is shown that DID correctly predicts the ducting environment for 12 of 22 satellite-to-ground RF measurements made during July and August 1978. Although the inferred profile geometry can differ significantly from the refractivity profile measured by an upper air sounding, the technique is moderately successful in predicting whether the true profile contains a ground-based or elevated duct. However, the overall reliability of predicting the dominant features of the duct (e.g., refractive gradient through the trapping layer, top height of the duct) is not adequate for operational usage. (Author)

A82-34222* National Aeronautics and Space Administration. Goddard Space Flight Center, Greenbelt, Md.

IRRADIANCE MEASUREMENT ERRORS DUE TO THE ASSUMPTION OF A LAMBERTIAN REFERENCE PANEL

D. S. KIMES and J. A. KIRCHNER (NASA, Goddard Space Flight Center, Earth Resources Branch, Greenbelt, MD) Remote Sensing of Environment, vol. 12, May 1982, p. 141-149. refs

A technique is presented for determining the error in diurnal irradiance measurements that results from the non-Lambertian behavior of a reference panel under various irradiance conditions. Spectral biconical reflectance factors of a spray-painted barium sulfate panel, along with simulated sky radiance data for clear and hazy skies at six solar zenith angles, were used to calculate the estimated panel irradiances and true irradiances for a nadir-looking sensor in two wavelength bands. The inherent errors in total spectral irradiance (0.68 microns) for a clear sky were 0.60, 6.0, 13.0, and 27.0% for solar zenith angles of 0, 45, 60, and 75 deg, respectively. The technique can be used to characterize the error of a specific panel used in field measurements, and thus eliminate any ambiguity of the effects of the type, preparation, and aging of the paint. (Author)

A82-34470

TECHNICAL AND ECONOMICAL CHARACTERISTICS OF THE AFA-TES-10M AERIAL CAMERA [TEKHNIKO-EKONOMICHESKIE POKAZATELI AEROFOTOAPPARATA AFA-TES-10M]

A. G. VANIN Geodeziia i Kartografiia, Apr. 1982, p. 36-39. In Russian. refs

The technical characteristics and economics of the AFA-TES-10M aerial camera are compared with those of the AFA-TES-100M camera which it replaces. Although a focal length of 100 mm makes both suitable for large-scale cartography, the newer camera, which makes use of a Russar-71 objective, exhibits reduced objective distortion and increased resolution in comparison with the AFA-TES-100M. A shorter operating cycle and an extended exposure range also allow a wider applicability and greater effectiveness in large-scale cartography. Analysis of the costs involved in producing topographic maps of a rolling terrain at various scales by the AFA-TES-10M indicates an overall savings as a result of reductions in labor costs, the amount of field validation and cameral photogrammetric processes required and specific capital investment, as well as an increase in the productivity of survey work. Development costs of the new system would be recovered typically in two years. A.L.W.

A82-34471

ANALYTICAL PROCESSING OF PHOTOGRAPHS TAKEN BY PAIRED CAMERAS [ANALITICHESKAIA OBRABOTKA FOTOSNIMKOV, POLUCHENNYKH SPARENNYMI FOTOKAMERAMI]

G. P. KUDRIAVTSEV Geodeziia i Kartografiia, Apr. 1982, p. 39-41. In Russian.

The use of direct analytical methods for the processing of photographs taken simultaneously by pairs of cameras with parallel optical axes mounted on a moving airborne or ground vehicle is examined. A method is presented whereby the angular and linear components of the external orientation of a stereo model may be computed from the positions of three reference points visible on each of the photographs, and then used to derive the geodesic coordinates. A computer algorithm based on the method has been used to derive a topographic layout of the geometrical elements and transverse and longitudinal profiles of a road based on strip photography taken by a camera pair mounted on a moving automobile. A.L.W.

A82-34701

AMERICAN SOCIETY OF PHOTOGRAMMETRY, ANNUAL MEETING, 47TH, WASHINGTON, DC, FEBRUARY 22-27, 1981, ASP TECHNICAL PAPERS

Falls Church, VA, American Society of Photogrammetry, 1981. 662 p $12.50

Simple plotters for close-range photogrammetry are considered along with remote sensing of thermal subsurface terrain properties, the effect of mixtures of primary forest scence components on spectral variability, Landsat in the search for Appalachian hydrocarbons, and the exterior orientation of side looking sensors. Attention is given to image processing with microcomputers in remote sensing, sensitometry in Canadian aerial survey, aerial camera vibration, raster scanning and its application in automated cartography, improved land use classifications from Landsat and Seasat satellite imagery registered to a common map base, and a quantitative method to test for similarity between photo interpreters. Other topics explored are related to remote sensing of geomorphological factors affecting the visibility of archaeological materials, the use of Skylab S190-B photography for small scale mapping, an optical data link for an airborne scanning system, and new instrumentation for direct photogrammetric mapping. G.R.

A82-34708

IMAGE PROCESSING WITH MICROCOMPUTERS IN REMOTE SENSING

F. M. CADY (Montana State University, Bozeman, MT) and R. M. HODGSON (Canterbury, University, Christchurch, New Zealand) In: American Society of Photogrammetry, Annual Meeting, 47th, Washington, DC, February 22-27, 1981, ASP Technical Papers. Falls Church, VA, American Society of Photogrammetry, 1981, p. 140-149. refs

A description is given of a digital image processing system which has proved to be useful in a number of application areas. In connection with the employment of a relatively low resolution sensor, it was possible to use relatively inexpensive computing components, memory, and bulk storage devices. The speed of operation for a wide range of application programs was high enough to allow the system to be useful for interactive image processing. The experience gained with the aid of the considered system indicates that similar results can be obtained with higher resolution arrays by utilizing higher performance, new generation microprocessors. The discussed system is based on the use of an eight-bit microprocessor with an addressing space of 65,536 locations. G.R.

A82-34724

SENSITOMETRY IN CANADIAN AERIAL SURVEY

P. D. CARMAN (National Research Council, Ottawa, Canada) In: American Society of Photogrammetry, Annual Meeting, 47th, Washington, DC, February 22-27, 1981, ASP Technical Papers. Falls Church, VA, American Society of Photogrammetry, 1981, p. 285-295. refs

Since 1943, sensitometric control of the processing of aerial negatives has been used by the Royal Canadian Air Force (RCAF) in connection with the performance of its task to provide aerial photography for Canada. The sensitometers used by the RCAF suffered from a variety of problems which, however, could be overcome by making use of repair and recalibration facilities. The transfer of aerial photography assignments from the RCAF to a number of private companies in the 1950's made it appear desirable to employ sensitometers which could perform reliably without easy access to specialized repair facilities. Attention is given to a sensitometer which was designed to satisfy these requirements. The design features of the new instrument are discussed, taking into account the light source, the spectral quality of illumination, the shutter, and the electrical supply. Aspects of sensitometer calibration and verification are considered along with the uses of sensitometric control of aerial photography in Canada. G.R.

A82-34727

REMOTE SENSING OF THERMAL SUBSURFACE TERRAIN PROPERTIES

F. E. ALZOFON (Boeing Aerospace Co., Seattle, WA) In: American Society of Photogrammetry, Annual Meeting, 47th, Washington, DC, February 22-27, 1981, ASP Technical Papers. Falls Church, VA, American Society of Photogrammetry, 1981, p. 335-341. refs

It is noted that although the sensed radiation is generated and limited by heat flow through the material underlying the emitting surface, little attention appears to have been paid to the effect of variation in properties of the conducting materials on the information carried by the emitted radiation. As a consequence, variations in thermal radiation may be attributed solely to variation of the temperature and emissivity of the radiating surface. However, it is shown that variation in radiant emittance can equally well be dominated by variation in the thermal conductivity of the underlying material. Criteria are derived under which either thermal conductivity variations or emissivity variations dominate radiant emittance data. A definition is given of threshold temperature; below the threshold, emissivity variations dominate, above it thermal conductivity variations dominate. Expressions are presented for the threshold temperature for various kinds of surface cooling. C.R.

A82-34737

AN OPTICAL DATA LINK FOR AIRBORNE SCANNING SYSTEM

M. J. GREEN (Wisconsin, University, Madison, WI) In: American Society of Photogrammetry, Annual Meeting, 47th, Washington, DC, February 22-27, 1981, ASP Technical Papers. Falls Church, VA, American Society of Photogrammetry, 1981, p. 476-482.

In connection with a study of oceanic thermal fronts, the Navy is interested in a thermal scanning system which could be used with their P-3 patrol aircraft. A suitable scanning system would be the RS-18A scanning thermal IR radiometer. However, an obstacle regarding the envisaged use of the instrument is related to the necessity to employ the aircraft without an introduction of any modifications. The obstacle has been overcome by making use of an optical data link which replaces the hardwire connections between the scanner and the power supply. The optical link is housed in a ten inch diameter tube which is clamped in position directly behind the scanner head. G.R.

A82-34742

THE USE OF SKYLAB S-190B PHOTOGRAPHY FOR SMALL SCALE MAPPING

I. M. EL-HASSAN (Riyadh, University, Riyadh, Saudi Arabia) In: American Society of Photogrammetry, Annual Meeting, 47th, Washington, DC, February 22-27, 1981, ASP Technical Papers. Falls Church, VA, American Society of Photogrammetry, 1981, p. 536-543. refs

The use of the Skylab Earth Terrain Camera (S-190B) with 1:946,000 scale photography in small-scale mapping is investigated. The procedure used in making the measurements on the Skylab imagery is described. An analytical absolute orientation is performed, and the results show that the photography could be used for mapping at scales of 1:100,000 and smaller. The photography used in the test comprises a strip of three photographs exposed on the SO-242 high-resolution color film. Second generation film transparencies made from the original film are used in the actual test. C.R.

A82-34746

COMPARISONS OF LAND COVER CLASSIFICATIONS FROM SELECTED REMOTE SENSING SYSTEMS

J. B. CAMPBELL (Virginia Polytechnic Institute and State University, Blacksburg, VA) and F. M. HENDERSON (New York, State University, Albany, NY) In: American Society of Photogrammetry, Annual Meeting, 47th, Washington, DC, February 22-27, 1981, ASP Technical Papers. Falls Church, VA, American Society of Photogrammetry, 1981, p. 618-626. refs

The present investigation is concerned with differences in accuracy of land cover maps generated by manual interpretation of several forms of remote sensing imagery. An area near Harrisburg, PA was imaged by K-band SLAR, the Landsat-1 MSS, the Landsat-3 RBV, and two Seasat SAR passes. These images were manually interpreted to yield land cover parcels corresponding to the Level I categories considered by Anderson et al. (1976). The resulting interpretations were compared with the more detailed USGS land cover map of the same region to determine classification errors. It is pointed out, however, that the results of this comparison cannot be interpreted as definitive assessments of the merits of each sensor system. Continued research is necessary. According to the current study, airborne radar imagery produced the best overall accuracy. With respect to the four space-borne sensor systems the MSS and RBV images are preferable to the digitally processed Seasat SAR image with the optically processed Seasat SAR image being the least accurate system product. G.R.

A82-36018

THE USE OF MICROWAVE RADIOMETRY FOR THE DETERMINATION OF SNOW COVER HEIGHT [ISPOL'ZOVANIE SVCH RADIOMETRII DLIA OPREDELENIIA VYSOTY SNEZHNOGO POKROVA]

V. E. GERSHENZON, V. G. IRISOV, IU. B. KHAPIN, and V. S. ETKIN (Akademiia Nauk SSSR, Institut Kosmicheskikh Issledovanii, Moscow, USSR) Akademiia Nauk SSSR, Doklady, vol. 264, no. 3, 1982, p. 601-603. In Russian. refs

A method is proposed for determining the height of snow cover from remote measurements of the brightness temperatures in the wavelength range 1.5-0.34 cm. The method is validated by means of a model experiment and by comparing the results with direct measurements. The remote and direct measurements are found to correlate to within 5 cm. V.L.

A82-37809#

MICROWAVE SENSING FROM SPACE

H. SCHUESSLER (Dornier System GmbH, Friedrichshafen, West Germany) American Astronautical Society and Deutsche Gesellschaft fuer Luft- und Raumfahrt, Goddard Memorial Symposium on Spacelab, Space Platforms and the Future, 20th, Greenbelt, MD, Mar. 17-19, 1982, AAS 15 p. Research supported by the Bundesministerium fuer Forschung und Technologie. (AAS PAPER 82-127)

The design, functions, and performance of satellite microwave sensor systems for earth imaging are described. It is noted that microwave operations can be carried out in all weather and in day or night conditions, and that current satellite systems operate in the interval of 1-20 GHz. Applications for soil characterization, moisture, and wind vector measurements over the sea are described in terms of frequency selection, power, and antenna requirements. Sunsynchronous orbits offer the advantage of low power storage capabilities due to avoidance of eclipse conditions. Areas of development necessary to implement an SAR for GEO positioning are reviewed, and features of a microwave remote sensing experiment involving SAR operating at 9.6 GHz during the first Spacelab flight on the Shuttle are presented. Finally, details of the ERS-1 satellite, which will carry a radar altimeter, wind scatterometer, and SAR are outlined. M.S.K.

A82-37812*# National Aeronautics and Space Administration. Goddard Space Flight Center, Greenbelt, Md.

SOLID STATE INSTRUMENTATION CONCEPTS FOR EARTH RESOURCE OBSERVATION

H. L. RICHARD (NASA, Goddard Space Flight Center, Advanced Land Observing Systems Studies Office, Greenbelt, MD) American Astronautical Society and Deutsche Gesellschaft fuer Luft- und Raumfahrt, Goddard Memorial Symposium on Spacelab, Space Platforms and the Future, 20th, Greenbelt, MD, Mar. 17-19, 1982, AAS 18 p. refs

(AAS PAPER 82-132)

Late in 1980, specifications were prepared for detail design definition of a six band solid state multispectral instrument having three visible (VIS), one near infrared (NIR), and two short wave infrared (SWIR) bands. This instrument concept, known as the Multispectral Linear Array (MLA), also offered increased spatial resolution, on board gain and offset correction, and additional operational modes which would allow for cross track and stereoscopic viewing as well as a multialtitude operational capability. A description is presented of a summary of some of the salient features of four different MLA design concepts, as developed by four American companies. The designs ranged from the use of multiple refractive telescopes utilizing three groups of focal plane detectors electronic correlation processing for achieving spatial registration, and incorporating palladium silicide (PdSi) SWIR detectors, to a four-mirror all-reflective telecentric system utilizing a beam splitter for spatial registration. G.R.

N82-22643*# National Aeronautics and Space Administration. Goddard Space Flight Center, Greenbelt, Md.

USE OF NOAA/AVHRR VISIBLE AND NEAR-INFRARED DATA FOR LAND REMOTE SENSING

S. R. SCHNEIDER (NOAA)02(NOAA), D. F. MCGINNIS, JR., and J. A. GATLIN Sep. 1981 55 p refs Sponsored in part by NOAA Prepared in cooperation with Earth Satellite Corp.

(NASA-TM-84186; NAS 1.15:84186; PB82-129388; NOAA-TR-NESS-84; NOAA-81100501) Avail: NTIS HC A04/MF A01 CSCL 08L

The data were analyzed for their usefulness in monitoring lake ice, snowcover, water quality, crop condition and terrain classification on the H.P. 1000 computer interactive system. Terrain phenomena that were studied using LANDSAT MSS data could also be monitored with the NOAA-6 channels, but at a lesser resolution. T.M.

N82-22865*# National Aeronautics and Space Administration. Langley Research Center, Hampton, Va.

SEASAT: A SATELLITE SCATTEROMETER ILLUMINATION TIMES OF SELECTED IN SITU SITES

L. C. SCHROEDER, D. R. GOODRIDGE, J. C. BOBERLY, J. K. HUGHES, and J. L. SWEET Mar. 1982 120 p

(NASA-TM-83280; NAS 1.15:83280) Avail: NTIS HC A06/MF A01 CSCL 08J

A list of times that the SEASAT A Satellite Scatterometer (SASS) illuminated from directly above or directly abeam, selected surface sites where in situ winds were measured is provided. The list is ordered by the Greenwich Mean Time (GMT) of the midpoint of the illumination period (hit time) for a given surface site. The site identification, the orbit number and the direction from the subtrack in which the truth lies are provided. The accuracy of these times depends in part upon the ascending node times, which are estimated to be within +.1 sec, and on the illumination time relative to the ascending node, which is estimated to be within +6 seconds. The uncertainties in the times provided were judged to be sufficiently small to allow efficient and accurate extraction of SASS and in situ data at the selected surface sites. The list contains approximately six thousand hit times from 61 geographically dispersed sites. Author

N82-24264# Joint Publications Research Service, Arlington, Va.

PURPOSE, BACKGROUND OF 'INTERCOSMOS-21' MISSION

M. A. RIMSHA *In its* USSR Rept.: Space, No. 15 (JPRS-80424) p 94-98 29 Mar. 1982 Transl. into ENGLISH from Zemlya Vselennaya (USSR), no. 5, Sep. - Oct. 1981 p 39-41

Avail: NTIS HC A07/MF A01

Research performed with satellies of the 'Intercosmos' series is discussed. Scientists have investigated short wave emissions of the Sun and the Earth's ionosphere and magnetosphere, cosmic rays and meteorite flows. Various technical systems were tested in these satellites. A transmitter of the 'beacon' type operated successfully in the first 'Intercosmos' satellites, while a special telemetric system later functioned in space and was recommended for further use. The unified telemetric system transmitted information directly to ground stations without the use of spacecraft instruments. S.L.

N82-24489# Research Inst. of National Defence, Linkoeping (Sweden).

STUDY VISIT TO UNITED STATES LASER TECHNOLOGY CENTERS, 1981 [RAPPORT FRAAN USA-RESA INOM LASEROMRAADET, 1981]

O. STEINVALL Jan. 1982 29 p Partly in SWEDISH and ENGLISH

(FOA-C-30257-E1) Avail: NTIS HC A03/MF A01

Coherent infrared radar and coherent CO2 laser radar were studied. Information from visits to research laboratories and radar manufacturers is outlined, focusing on TEA lasers, heterodyne radiometers, laser absorption spectrometers, and transportable measurement radar. Airborne oceanographic lidar, laser cloud mappers, and oceanographic detection were examined. Infrared imaging systems, and hydrographic laser sounders were investigated. Author (ESA)

N82-25602*# General Software Corp., Landover, Md.

LANDSAT-D CONICAL SCANNER EVALUATION PLAN

S. BILANOW and L. C. CHEN, Principal Investigators Mar. 1982 102 p refs ERTS

(Contract NAS5-26205)

(E82-10340; NASA-CR-166790; NAS 1.26:166790; GSC-TR8203) Avail: NTIS HC A06/MF A01 CSCL 14B

The planned activities involved in the inflight sensor calibration and performance evaluation are discussed and the supporting software requirements are specified. The possible sensor error sources and their effects on sensor measurements are summarized. The methods by which the inflight sensor performance will be analyzed and the sensor modeling parameters will be calibrated are presented. In addition, a brief discussion on the data requirement for the study is provided. T.M.

N82-25610*# National Aeronautics and Space Administration. Langley Research Center, Hampton, Va.

RADIOMETER MISSION REQUIREMENTS FOR LARGE SPACE ANTENNA SYSTEMS

L. S. KEAFER, JR., P. SWANSON, and J. ECKERMAN May 1982 64 p refs

(NASA-TM-84478; NAS 1.15:84478) Avail: NTIS HC A04/MF A01 CSCL 20N

Requirements are defined for Earth observational microwave radiometry using large space antenna systems with apertures in the 50 to 200 meter range. General Earth observational needs, specific measurement requirements, orbital mission guidelines and constraints, and general radiometric requirements are defined. Specific measurements include soil moisture, water surface temperature, water roughness, ice boundaries, salinity, and water pollutants. Measurements with 10 to 1 km spatial resolution and 3 to 1 day temporal resolution are required. Author

N82-26642# Barringer Research Ltd., Rexdale (Ontario).
BREADBOARD GAS FILTER CORRELATION SPECTROMETER FOR ATMOSPHERIC MEASUREMENT OF HYDRAZINES AND NITROGEN DIOXIDE Final Report, Jan. 1977 - Apr. 1979
R. DICK Oct. 1981 31 p refs
(Contract F33615-77-C-0604; AF PROJ. 7930)
(AD-A110688; TR-79-281; SAM-TR-81-11) Avail: NTIS HC A03/MF A01 CSCL 14B

This report describes the efforts to build a breadboard Gas Filter Correlation Spectrometer (GFSC) for the atmospheric measurement of hydrazines and nitrogen dioxide. The instrument was configured for use as an ambient monitor, with the possibility of conversion to a remote sensor by addition of a telescope. The final detection limits for the gases were: N2H4 = .3 ppm, UDHM = .23 ppm, MMH = .22 ppm, and N02 = 9 ppm. GRA

N82-26741* National Aeronautics and Space Administration, Washington, D. C.
LANDSAT D TO TEST THEMATIC MAPPER, INAUGURATE OPERATIONAL SYSTEM
21 Jun. 1982 43 p
(NASA-NEWS-RELEASE-82-100; P82-10:03) Avail: NASA Scientific and Technical Information Facility, P. O. Box 8757, B.W.I. Airport, Md. 21240 CSCL 22A

NASA will launch the Landsat D spacecraft on July 9, 1982 aboard a new, up-rated Delta 3920 expendable launch vehicle. LANDSAT D will incorporate two highly sophisticated sensors; the flight proven multispectral scanner; and a new instrument expected to advance considerably the remote sensing capabilities of Earth resources satellites. The new sensor, the thematic mapper, provides data in seven spectral (light) bands with greatly improved spectral, spatial and radiometric resolution. L.F.M.

N82-26743*# Pennsylvania State Univ., University Park. Dept. of Meteorology.
INTERACTIVE INITIALIZATION OF HEAT FLUX PARAMETERS FOR NUMERICAL MODELS USING SATELLITE TEMPERATURE MEASUREMENTS Quarterly Report, 1 Nov. 1981 - 1 Jun. 1982
T. N. CARLSON, Principal Investigator 1 Jun. 1982 4 p HCMM
(Contract NAS5-26456)
(E82-10313; NASA-CR-168998; NAS 1.26:168998; QR-4) Avail: NTIS HC A02/MF A01 CSCL 05B

Progress made in HCMM research, including testing the interactive minicomputer system and preparation of a paper on the analysis of regional scale soil moisture patterns, is summarized. An exhibit on remote sensing including a videotape display of HCMM images, most of them of the State College area, was prepared. J.D.

N82-26744*# OAO Corp., Beltsville, Md.
LANDSAT-D THERMAL ANALYSIS AND DESIGN SUPPORT
1982 134 p ERTS
(Contract NAS5-25737)
(E82-10346; NASA-CR-166788; NAS 1.26:166788; OAO/TR-81/0033) Avail: NTIS HC A07/MF A01 CSCL 05B

Detailed thermal models of the LANDSAT-D Earth Sensor Assembly Module (ESAM), the Dummy Thematic Mapper (DTM), and a small thermal model of the LANDSAT-D spacecraft for a heater analysis were developed. These models were used to develop and verify the thermal design of the ESAM and DTM, to evaluate the aeroheating effects on ESAM during launch and to evaluate the thermal response of the LANDSAT-D assuming the hard-line heaters failed on with the spacecraft in the Space Transportation System (STS) orbiter bay. Results of model applications are summarized. T.M.

09

GENERAL

Includes economic analysis.

A82-22546
ANTIPROTONS FROM GALACTIC SOURCES OF COSMIC RAYS AND GAMMA RAYS
R. COWSIK (Franklin Institute, Bartol Research Foundation, Newark, DE; Tata Institute of Fundamental Research, Bombay, India) and T. K. GAISSER (Franklin Institute, Bartol Research Foundation, Newark, DE) In: International Cosmic Ray Conference, 17th, Paris, France, July 13-25, 1981, Conference Papers. Volume 2. Gif-sur-Yvette, Essonne, France, Commissariat a l'Energie Atomique, 1981, p. 218-221. Research supported by the U.S. Department of Energy. refs

Recent observations of discrete galactic sources of gamma rays are examined in terms of a modified version of the nested leaky box model of Cowsik and Wilson (1973, 1975). It is shown that the modified model can account for the observed high fluxes of antiprotons. The essential idea is that bright gamma-ray sources are surrounded by significantly more matter than most other sources of cosmic rays; they are thus strong sources of both secondary gamma rays and antiprotons, and at the same time efficient absorbers of heavy nuclei. V.L.

A82-22547* George Mason Univ., Fairfax, Va.
CONFINEMENT AND ACCELERATION OF COSMIC RAYS IN GALACTIC SUPERBUBBLES
M. KAFATOS (George Mason University, Fairfax, VA), F. BRUHWEILER, and S. SOFIA (NASA, Goddard Space Flight Center, Greenbelt, MD) In: International Cosmic Ray Conference, 17th, Paris, France, July 13-25, 1981, Conference Papers. Volume 2. Gif-sur-Yvette, Essonne, France, Commissariat a l'Energie Atomique, 1981, p. 222-225. refs

The role of the newly discovered galactic superbubbles on the confinement and acceleration of cosmic rays is examined. It is shown that these structures naturally account for the lifetime and the local origin of the cosmic rays, as well as for the location of galactic gamma-ray sources not associated with pulsars. (Author)

A82-22548
INTERACTIONS OF COSMIC RAYS WITH MOLECULAR CLOUDS
Y. FUKUI and S. HAYAKAWA (Nagoya University, Nagoya, Japan) In: International Cosmic Ray Conference, 17th, Paris, France, July 13-25, 1981, Conference Papers. Volume 2. Gif-sur-Yvette, Essonne, France, Commissariat a l'Energie Atomique, 1981, p. 226-228.

The optical thickness of HI, tau, obtained from the dip of 21 cm line for cold clouds is found to depend on the linear size d as tau varies as d to the 0.44 power. Cosmic rays responsible for the production of HI from H2 are appreciably absorbed in the inner part of the clouds. The tau-d relation indicates a nearly flat energy spectrum of cosmic rays at low energies. (Author)

A82-22549
DERIVATION OF THE DISTRIBUTION OF SYNCHROTRON EMISSIVITY IN THE GALAXY FROM THE 408 MHZ ALL-SKY SURVEY
S. PHILLIPPS, S. KEARSEY, J. L. OSBORNE (Durham, University, Durham, England), C. G. T. HASLAM, and H. STOFFEL (Max-Planck-Institut fuer Radioastronomie, Bonn, West Germany) In: International Cosmic Ray Conference, 17th, Paris, France, July 13-25, 1981, Conference Papers. Volume 2. Gif-sur-Yvette, Essonne, France, Commissariat a l'Energie Atomique, 1981, p. 229-232. refs

A82-22550

ANGULAR VARIATIONS OF NONTHERMAL RADIO EMISSION FROM THE GALAXY RELEVANT TO THE STRUCTURE OF INTERSTELLAR MAGNETIC FIELD

G. V. CHIBISOV (Akademiia Nauk SSSR, Fizicheskii Institut, Moscow, USSR) and V. S. PTUSKIN (Akademiia Nauk SSSR, Institut Zemnogo Magnetizma, Ionosfery i Rasprostraneniia Radiovoln, Troitsk, USSR) In: International Cosmic Ray Conference, 17th, Paris, France, July 13-25, 1981, Conference Papers. Volume 2. Gif-sur-Yvette, Essonne, France, Commissariat a l'Energie Atomique, 1981, p. 233-235.

The relation between the correlation function of the intensity of galactic radio-emission at different directions and the correlation function of interstellar magnetic field at different points is found. This relation is shown to be used for the determination of random and regular components of magnetic field. Measurements at different frequencies clarify the character of cosmic ray propagation in the Galaxy, and in particular, distinguish between the diffusive and convective transfer of cosmic rays. (Author)

A82-22551

CONVECTIVE OUTFLOW OF COSMIC RAYS FROM THE GALAXY AND BACKGROUND RADIO EMISSION

V. A. DOGIEL, V. M. KOVALENKO, and V. L. PRISHCHEP (Akademiia Nauk SSSR, Fizicheskii Institut, Moscow, USSR) In: International Cosmic Ray Conference, 17th, Paris, France, July 13-25, 1981, Conference Papers. Volume 2. Gif-sur-Yvette, Essonne, France, Commissariat a l'Energie Atomique, 1981, p. 236-239. refs

A82-22553

CONSEQUENCES OF AN INVERSE COMPTON EMISSION MODEL FOR EXTRAGALACTIC X-RAY SOURCES

P. BIERMANN and R. SCHLICKEISER (Max-Planck-Institut fuer Radioastronomie, Bonn, West Germany) In: International Cosmic Ray Conference, 17th, Paris, France, July 13-25, 1981, Conference Papers. Volume 2. Gif-sur-Yvette, Essonne, France, Commissariat a l'Energie Atomique, 1981, p. 252-255. refs

An X-ray survey of flat spectrum radio sources is carried out. All sources are detected, among them two highly compact BL Lac type objects which show aligned triple X-ray sources. Interpreting these features as very large jets radiating X rays by inverse Compton scattering of microwave background photons leads to strong constraints on the process of acceleration and the energetics of the sources. C.R.

A82-22554

CALCULATED ISOTOPIC SOURCE COMPOSITION AND TESTS FOR ORIGIN AND PROPAGATION OF COSMIC RAYS WITH MASS NUMBERS LESS THAN OR EQUAL TO 62

J. H. ADAMS, JR. and M. M. SHAPIRO (U.S. Navy, Naval Research Laboratory, Washington, DC) In: International Cosmic Ray Conference, 17th, Paris, France, July 13-25, 1981, Conference Papers. Volume 2. Gif-sur-Yvette, Essonne, France, Commissariat a l'Energie Atomique, 1981, p. 256-259. refs

Recent measurements of the nuclidic composition of cosmic-ray Ne and Mg are used to calculate their isotopic source compositions. In addition, the effects of these neutron-rich species on abundances of various secondary nuclides are presented. Implications of anomalies in the source composition for nucleosynthesis and/or evolution of the galactic composition are discussed. Finally, the arriving isotopic abundances Co-59, Co-57 and Ti-44, Ti-46 are calculated for time intervals much less than 50 years, much greater than 50 years, much less than 100,000 years, and much greater than 100,000 years between nucleosynthesis and acceleration to cosmic-ray energies. (Author)

A82-22556

COMPARATIVE ABUNDANCES IN SOLAR ENERGETIC PARTICLES AND IN GALACTIC COSMIC RAY SOURCES, AND THE NE-22 ANOMALY

J. P. MEYER (Commissariat a l'Energie Atomique, Centre d'Etudes Nucleaires de Saclay, Gif-sur-Yvette, Essonne, France) In: International Cosmic Ray Conference, 17th, Paris, France, July 13-25, 1981, Conference Papers. Volume 2. Gif-sur-Yvette, Essonne, France, Commissariat a l'Energie Atomique, 1981, p. 265-268. refs

A82-22599

ON THE PHYSICAL SENSE OF THE CONSTANT OF SOLAR COSMIC RAY CORONAL PROPAGATION

G. A. BAZILEVSKAIA (Akademiia Nauk SSSR, Fizicheskii Institut, Moscow, USSR) and E. V. VASHENIUK (Akademiia Nauk SSSR, Poliarnyi Geofizicheskii Institut, Apatity, USSR) In: International Cosmic Ray Conference, 17th, Paris, France, July 13-25, 1981, Conference Papers. Volume 3. Gif-sur-Yvette, Essonne, France, Commissariat a l'Energie Atomique, 1981, p. 93-96. refs

An analysis is made of the time dependence of solar cosmic ray intensity and anisotropy. Results show that the coronal time is the time of the escape of the bulk of the particles into the interplanetary space, and it is found that the generation of solar cosmic rays is almost simultaneous in the fast propagation region, which could be in the case of solar cosmic ray acceleration by the quasi-spheric shock wave. This result is in agreement with values found by Bazilevskaya and Vashenyuk (1979) for the transit time of the first particles in the corona for high energy solar cosmic rays. D.L.G.

A82-22603

THE INFLUENCE OF THE SECTOR STRUCTURE OF INTERPLANETARY MAGNETIC FIELD ON THE SOLAR COSMIC RAY CHARACTERISTICS

G. A. BAZILEVSKAIA (Akademiia Nauk SSSR, Fizicheskii Institut, Moscow, USSR) In: International Cosmic Ray Conference, 17th, Paris, France, July 13-25, 1981, Conference Papers. Volume 3. Gif-sur-Yvette, Essonne, France, Commissariat a l'Energie Atomique, 1981, p. 117-120. refs

A statistical study of solar cosmic-ray events from 1957 to 1968 is performed, taking into account only events with certain or probable association. The solar wind velocity is used to define the earth connection longitude on the sun and to map the longitude of sector boundaries. No sector boundary influence on registration probability of solar cosmic-rays is found, and the intensity time dependence seems to be controlled by coronal structures, which are situated lower in the solar atmosphere than where the sector boundaries are formed. D.L.G.

A82-30850

SPACE TO THE EARTH [KOSMOS - ZEMLE]

A. A. BOLSHOI, I. V. MESHCHERIAKOV, S. D. SILVESTROV, A. V. TSEPELEV, and V. A. MASHCHENKO Moscow, Izdatel'stvo Nauka, 1981. 152 p. In Russian. refs

Several applications of space technology are discussed. Attention is given to satellite communications systems, navigation satellites, space geodesy, meteorological satellites, and the remote sensing of earth resources. The principles underlying such applications and the design and operation of the appropriate systems are considered. B.J.

A82-31996

THE USE OF THE SPOT SATELLITE IN NATURAL RESOURCE EVALUATION [EL SATELITE SPOT EN LA EVALUACION DE LOS RECURSOS NATURALES]

P.-M. ADRIEN CIDA, vol. 5, no. 5, 1980, p. 31-36. In Spanish.

The practical application of the remote sensing satellite SPOT to natural resources assessment in Latin America are discussed. SPOT, which will be launched by the French government in 1984, will assume a nearly polar orbit at an altitude of 822 km and be able to scan a 60 km-wide area with 10-20 m sweeps of its multispectral scanner. Comparisons are made with the capabilities of the ARGOS satellite, which has been in operation since 1974. The data to be collected by SPOT will be pertinent to research in agricultural land use, agricultural meteorology, hydrology, forest management, and mineralogical resources. Attention is given to the coordination of such research and the dissemination of its data by French government agencies. O.C.

A82-33555

REMOTE SENSING OF THE EARTH'S RESOURCES - THE SOVIET EXPERIENCE

J. POPESCU British Interplanetary Society, Journal (Space Chronicle), vol. 35, June 1982, p. 273, 274.

The tools, techniques, and targets of Soviet remote sensing systems are explored. Satellite viewing results are rechecked by both aerial surveys and surface sampling for purposes of calibration and confirmation. A total of 1,260 Kosmos spacecraft were launched by 1979, and carried vidicons and microwave sensors for data acquisition. The Salyut space stations were also equipped with a multispectral scanner which featured 10 m resolution, could discern between wet and dry ground, and covered the range 0.46-0.89 microns. Additional instrumentation comprised a radio telescope, stereoscopic camera, and SAR. World grain crops are monitored to anticipate the world wheat market, regions of intense storm activity such as the Bermuda Triangle are studied, and weather conditions and evolution, particularly in Arctic shipping areas, are tracked. Telemetry stations are located in five countries outside the Soviet Union. Instances of successful cosmonaut remote sensing for mineral prospecting, glacier mapping, and sea ice tracking to protect ocean-going vessels are cited. M.S.K.

A82-34116#

EARTH OBSERVATIONS FROM SPACE - TRENDS AND PROSPECTS

G. BRACHET (Centre National d'Etudes Spatiales, Paris, France) In: International aerospace review; Proceedings of the First International Aerospace Symposium, Le Bourget, Seine-Saint-Denis, France, June 2, 3, 1981. New York, American Institute of Aeronautics and Astronautics, 1982, p. 215-223.

The instrumentation and missions of various earth observation satellites are outlined. Earth observation satellites are grouped into experimental types for testing instruments or observing techniques, operational meteorological satellites with on-line users, the Landsat series of satellites for performing whole-earth scanning using different EM wavelengths, and ocean and ice scanning satellites. The Tiros-N series of satellites included advanced very high resolution radiometers for sea-surface temperature measurements, a solar backscatter ultraviolet sensor for global ozone monitoring, and an advanced microwave sounding unit. The GOES-D spacecraft carries an improved imaging radiometer for atmospheric vertical sounding, while the European Meteosat features a water vapor channel at 6-7 microns for upper atmosphere water vapor content assays. Landsat data has been useful in areas such as agriculture, forestry, urban planning, mapping, cartography, water resources studies, and geology. M.S.K.

A82-34367#

ERS-1 EUROPEAN REMOTE SENSING SATELLITE

Dornier-Post (English Edition), no. 2, 1982, p. 24-29.

The mission objectives and the components developed for the ERS-1 remote sensing satellite are discussed. The spacecraft is intended for use in weather forecasting, sea state forecasting, off-shore activities support, ship routing, ice monitoring, ocean pollution monitoring, scientific investigations of complex ocean interactions, and microwave sensing of land surfaces and coastal zones. A supply module provides power for the instruments and earth pointing. The data will be transmitted and possibly stored on board. Launched by the Ariane into a 675 km sunsynchronous orbit, ERS-1 will carry a sidelooking radar with SAR for high resolution land and ocean imaging and wave spectra plotting, and a wind scatterometer for measurements from 4-24 m/sec over the oceans. A microwave radar serves for wave height, earth surface height, wind speed, and iced- or open-ocean determination. Launch is scheduled for 1987. M.S.K.

A82-36617*

SPACE SCIENCE FOR APPLICATIONS - THE HISTORY OF LANDSAT

P. E. MACH In: Space science comes of age: Perspectives in the history of the space sciences; Proceedings of the Symposium, Washington, DC, March 23, 24, 1981. Washington, DC, Smithsonian Institution Press, 1981, p. 135-148. NASA-supported research. refs

The history of the Landsat project is discussed in terms of three historical phases, each characterized by a dominant problem. From 1964 to 1967, the challenge was to develop interagency cooperation and to achieve consensus on basic plans for the satellite. Between 1968 and 1971, the cooperating agencies had to persuade the Bureau of the Budget to provide funding for the project. Since 1972, the challenge to NASA has been to encourage applications of the Landsat data and plan the shift from an experimental program to an operational one. The tension between experimental and operational goals has run through all these phases, and the conflicts between agencies is detailed, as well as the interaction between technological and political systems. C.D.

N82-22620*# Lockheed Engineering and Management Services Co., Inc., Houston, Tex.

TEN-ECOSYSTEM STUDY Final Report

A. V. MAZADE, Principal Investigator Aug. 1981 96 p refs
Sponsored in part by USDA Original contains color imagery. Original photography may be purchased from the EROS Data Center, Sioux Falls, S.D. 57198. ERTS
(Contract NAS9-15800; PROJ. AGRISTARS)
(E82-10186; NASA-CR-167457; NAS 1.26:167457;
LEMSCO-13491) Avail: NTIS HC A05/MF A01 CSCL 13B

Remote sensing methodology developed for the Nationwide Forestry Applications Program utilize computer data processing procedures for performing inventories from satellite imagery. The Ten-Ecosystem Study (TES) was developed to test the processing procedures in an intermediate-sized application study. The results of TES indicate that LANDSAT multispectral imagery and associated automatic data processing techniques can be used to distinguish softwood, hardwood, grassland, and water and make inventory of these classes with an accuracy of 70 percent or better. The technical problems encountered during the TES and the solutions and insights to these problems are discussed. The TES experience is useful in planning subsequent inventories utilizing remote sensing technology. T.M.

N82-22630# Committee on Science and Technology (U. S. House).

CIVIL LAND REMOTE SENSING SYSTEM

Washington GPO 1982 77 p Presented by the Subcom. on Space Sci. and Appl. of the Comm. on Sci. and Technol., 97th Congr., 1st Sess., Dec. 1981
(GPO-87-070) Avail: Subcommittee on Space Science and Applications

Current remote sensing research and development activities, current planning for an operational system, and international remote sensing activities are summarized. Significant issues considered include: the role of government vis-a-vis the private sector, the way in which it can best serve both the public and the private sector, its role in future research and development, and regulations and terms it must mandate for a civil land remote sensing system. Legislation needed for government/industry joint ventures is also examined. A.R.H.

N82-23258*# National Aeronautics and Space Administration, Washington, D. C.

OSTA-1 POST MISSION OPERATION REPORT

1982 17 p
(NASA-TM-84191; NAS 1.15:84191; S-420-81-01) Avail: NTIS HC A02/MF A01 CSCL 22A

The first science and applications payload for the space shuttle was carried on STS-2. The space shuttle's performance and systems were tested. The Shuttle's capability of providing a platform for scientific and applications research was demonstrated. The OSTA-1 payload was selected and developed to demonstrate this secondary objective. The experiments selected for the OSTA-1 payload were concerned with remote sensing of Earth resources, environmental quality, ocean conditions, meteorological phenomena and life sciences. These experiments demonstrated the Shuttle's capability for space research and the potential application of techniques for future remote sensing. S.L.

N82-23568*# Environmental Research Inst. of Michigan, Ann Arbor.
LANDSAT TECHNOLOGY TRANSFER TO THE PRIVATE AND PUBLIC SECTORS THROUGH COMMUNITY COLLEGES AND OTHER LOCALLY AVAILABLE INSTITUTIONS Final Report, 20 Dec. 1979 - 20 Dec. 1980
R. H. ROGERS, Principal Investigator Dec. 1980 59 p ERTS
(Contract NASW-3308)
(E82-10181; NASA-CR-168846; NAS 1.26:168846;
ERIM-147200-13-F) Avail: NTIS HC A04/MF A01 CSCL 05A

Major first year accomplishments are summarized and plans are provided for the next 12-month period for a program established by NASA with the Environmental Research Institute of Michigan to investigate methods of making LANDSAT technology readily available to a broader set of private sector firms through local community colleges. The program applies a network where the major participants are NASA, university or research institutes, community colleges, and obtain hands-on training in LANDSAT data analysis techniques, using a desk-top, interactive remote analysis station which communicates with a central computing facility via telephone line, and provides for generation of land cover maps and data products via remote command. A.R.H.

N82-24216# Centre National d'Etudes Spatiales, Toulouse (France).
HISTORY OF THE FRENCH SATELLITE SPACE PROGRAM [HISTORIQUE DU PROGRAMME SPATIALE SCIENTIFIQUE FRANCAIS]
J. C. HUSSON *In its* The Technol. of Spaceborne Sci. Expt. p 3-10 1981 In FRENCH
Avail: NTIS HC A99/MF A01

The amplitude of the French space program and the variety of research that supports it are discussed. Three objectives stand out: (1) develop space research and technology; (2) develop spacecraft and related technology; and (3) participate on a global scale in research into the terrestrial environment, space observation, and exploration of the solar system. Given this perspective, results concerning astronomy, planetology, geophysics, geodesy, meteorology, and biology are reviewed. Future projects in space manufacturing are also mentioned. Author (ESA)

N82-24263# Joint Publications Research Service, Arlington, Va.
COST-EFFECTIVENESS OF GEOGRAPHIC SURVEYING FROM SPACE
M. Y. LEMESHEV, Y. V. SUKHOTIN, and A. F. DEMIDOV *In its* USSR Rept.: Space, No. 15 (JPRS-80424) p 76-96 29 Mar. 1982 refs Transl. into ENGLISH from Ekon. Mat. Metody (USSR), v. 17, no. 5, Sep. - Oct. 1981 p 920-935
Avail: NTIS HC A07/MF A01

An economic evaluation of space based observation systems is presented. The cost effectiveness of these satellite systems is discussed. S.L.

N82-24568*# National Conference of State Legislatures, Denver, Colo. Remote Sensing Project.
A LEGISLATOR'S GUIDE TO LANDSAT
1982 33 p Sponsored by NASA. Original contains color imagery. Original photography may be purchased from the EROS Data Center, Sioux Falls, S.D. 57198 ERTS
(E82-10290; NASA-CR-168859; NAS 1.26:168859) Avail: NTIS HC A03/MF A01 CSCL 05B

The LANDSAT satellite is an effective tool in meeting the natural resources data requirements of state and federal legislation. The availability of data from the satellite is beginning to have an impact on state legislature activities. An overview of the history, operation, and data analysis techniques, is presented as well as a discussion of the advantages and limitations of this method of remote sensing. Applications are discussed in the areas of (1) land resource planning and management; (2) coastal zone management; (3) agriculture; (4) forestry; (5) routing and siting; (6) environmental monitoring; and (7) geological exploration. National and state sources from which information about LANDSAT technology is available are listed. A.R.H.

N82-26746*# Purdue Univ., Lafayette, Ind. Lab. of Applications of Remote Sensing.
KEY ISSUES IN THE ANALYSIS OF REMOTE SENSING DATA: A REPORT ON THE WORKSHOP
P. H. SWAIN, Principal Investigator Jun. 1981 41 p Workshop held in West Lafayette, Ind., 22-23 Jun. 1981 ERTS
(Contract NAS9-15466)
(E82-10348; NASA-CR-167570; NAS 1.26:167570;
LARS-TR-062481) Avail: NTIS HC A03/MF A01 CSCL 05B

The procedures of a workshop assessing the state of the art of machine analysis of remotely sensed data are summarized. Areas discussed were: data bases, image registration, image preprocessing operations, map oriented considerations, advanced digital systems, artificial intelligence methods, image classification, and improved classifier training. Recommendations of areas for further research are presented. J.D.

SUBJECT INDEX

EARTH RESOURCES / *A Continuing Bibliography (Issue 35)*

OCTOBER 1982

Typical Subject Index Listing

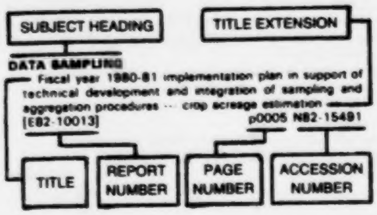
SUBJECT HEADING
TITLE EXTENSION
DATA SAMPLING
Fiscal year 1980-81 implementation plan in support of technical development and integration of sampling and aggregation procedures --- crop acreage estimation
[E82-10013]
p0005 N82-15491
TITLE
REPORT NUMBER
PAGE NUMBER
ACCESSION NUMBER

The subject heading is a key to the subject content of the document. The title is used to provide a description of the subject matter. When the title is insufficiently descriptive of the document content, the title extension is added, separated from the title by three hyphens. The (NASA or AIAA) accession number and the page number are included in each entry to assist the user in locating the abstract in the abstract section (of this supplement). If applicable, a report number is also included as an aid in identifying the document. Under any one subject heading, the accession numbers are arranged in sequence with the AIAA accession numbers appearing first.

A

ABSORPTION SPECTRA

Remote sensing of leaf water content in the near infrared p 8 A82-32897

In situ ozone data for comparison with laser absorption remote sensor: 1980 PEPE/NEROS program [NASA-TM-84471] p 30 N82-25661

ABSORPTION SPECTROSCOPY

Observation of the diurnal variation of atmospheric ozone p 26 A82-35895

ABSORPTIVITY

Sensitivity of Dobson total ozone estimations to wavelength band calibration uncertainties p 27 A82-36405

Dobson spectrophotometer calibrations, possible errors in ozone absorption coefficients, and errors due to interfering pollutant gases p 28 A82-36431

ABUNDANCE

The cosmic ray positron spectrum p 1 A82-22542

Calculated isotopic source composition and tests for origin and propagation of cosmic rays with mass numbers less than or equal to 62 p 83 A82-22554

Comparative abundances in solar energetic particles and in galactic cosmic ray sources, and the Ne-22 anomaly p 83 A82-22556

Mass per charge ratio in hot plasmas and cosmic ray source composition p 2 A82-22557

Cosmic ray composition from acceleration of thermal matter p 64 A82-22558

Interstellar grains as seeds for galactic cosmic rays p 2 A82-22561

On the stellar origin of the Ne-22 excess in cosmic rays p 21 A82-22562

Time and energy dependence of heavy ion abundances in solar flare energetic particle events p 22 A82-22605

High resolution measurements of solar flare isotopes p 22 A82-22606

Heavy-element abundances in He/3/-rich events p 5 A82-22611

A comparison of helium and heavy ion spectra in He/3/ rich solar flares with a model calculation p 5 A82-22612

On the anticorrelation between the He/3//He/4/ ratio and proton intensity in He/3/ rich flares p 40 A82-22613

ACCURACY

Investigations of point transfer p 78 A82-33296

Ten-Ecosystem Study --- Grand and Weld Counties, Colorado; Warren County, Pennsylvania; St. Louis County, Minnesota; Sandoval County, New Mexico; Kershaw County, South Carolina; Fort Yukon, Alaska; Grays Harbor County, Washington; and Washington County, Missouri [E82-10186] p 84 N82-22620

Analysis of scanner data for crop inventories [E82-10192] p 10 N82-22626

AgRISTARS. Preliminary technical results review of FY81 experiments, volume 2: Fiscal year 1981/1982 'corn and soybeans pilot' experiment [E82-10216] p 13 N82-23589

An analysis of LANDSAT MSS scene-to-scene registration accuracy [E82-10285] p 16 N82-24563

ACTINIDE SERIES

Laboratory studies of actinide metal-silicate fractionation p 49 A82-22306

AERIAL PHOTOGRAPHY

Detection of environmental disturbance using color aerial photography and thermal infrared imagery p 22 A82-29327

Description of gray level picture using a collection of density contour lines p 66 A82-29409

Color aerial photography in the plant sciences and related fields; Proceedings of the Eighth Biennial Workshop, Luray, VA, April 21-23, 1981 p 5 A82-29526

Development and application of panoramic aerial photography in forest pest management p 5 A82-29527

Riparian vegetation mapping in Northeastern California using high altitude color infrared aerial photography p 5 A82-29528

Inventory of wildlife habitat from color infrared aerial photography for Cobb Island, Virginia p 6 A82-29529

Considerations in using color infrared photographs for vegetative interpretation p 6 A82-29530

Color aerial photography detects nutrient status of loblolly pine plantations p 6 A82-29531

Application of 35mm color aerial photography to forest land change detection p 6 A82-29533

Estimating rangeland cover proportions with large-scale color-infrared aerial photographs p 6 A82-29534

Mapping riparian vegetation in Southeastern Oregon using digitized large scale color infra-red aerial photography p 6 A82-29535

Remote sensing of Douglas-fir trees newly infested by bark beetles p 6 A82-29536

Detection and damage assessment of citrus tree losses with aerial color infrared photography /ACIR/ p 7 A82-29538

An infrared exposure meter p 76 A82-29541

Thermography - A remote sensing method with many perspectives p 76 A82-29922

Problems of the interpretation of aerial and satellite images of industrial smoke p 23 A82-30307

Extraction of line shaped objects from aerial images using a special operator to analyze the profiles of functions p 67 A82-32033

Panoramic aerial photography in forest pest management p 7 A82-32701

Photogrammetric methods for mapping resource data from high altitude panoramic photography p 77 A82-32702

Estimating bark beetle-killed lodgepole pine with high altitude panoramic photography p 7 A82-32703

Estimating mountain pine beetle-killed ponderosa pine over the front range of Colorado with high altitude panoramic photography p 7 A82-32704

Optical bar panoramic photography for planning timber salvage in drought-stressed forests p 7 A82-32705

Evaluation of spruce-fir forests using small-format photographs p 8 A82-32707

Nearshore current pattern off south Texas - An interpretation from aerial photographs p 53 A82-32903

Image quality and height measurement accuracy of aerial survey camera imagery from high altitudes p 78 A82-33297

Skirt clouds associated with the Soufriere eruption of 17 April 1979 p 24 A82-33656

The use of Landsat-3 thermal data to help differentiate land covers p 25 A82-34218

Evaluation of the effectiveness of systematic image distortion compensation p 69 A82-34469

Technical and economical characteristics of the AFA-TES-10M aerial camera p 79 A82-34470

Analytical processing of photographs taken by paired cameras p 79 A82-34471

A quantitative method to test for similarity between photo interpreters p 69 A82-34722

Sensitometry in Canadian aerial survey p 79 A82-34724

Effects of altitude, focal length, and filter combinations on color infrared photography of citrus groves p 9 A82-34729

Remote sensing - A potential aid in the preparation of an urban tree inventory p 9 A82-34732

Use of aerial photography in determining land use and streamflow relationships on small developing watersheds p 60 A82-34736

Aerial photography vs. Landsat for digital land-cover mapping in an urban watershed p 61 A82-34745

Present status of on-line analytical triangulation p 69 A82-34940

A quantitative multispectral analysis system for aerial photographs applied to coastal planning p 55 A82-37505

AERIAL RECONNAISSANCE

Aerogeophysical methods of finding uranium deposits --- Russian book p 41 A82-33402

Airborne gamma-ray spectrometer and magnetometer survey. Roseau quadrangle, Minnesota, volume 1 [DE82-001031] p 43 N82-23621

Airborne gamma-ray spectrometer and magnetometer survey. Barrow quadrangle, Alaska, volume 1 [DE82-000334] p 43 N82-23623

Airborne gamma-ray spectrometer and magnetometer survey. Wainwright quadrangle, Alaska, volume 2 [DE82-000341] p 43 N82-23624

Airborne gamma-ray spectrometer and magnetometer survey. Devil's Lake quadrangle, North Dakota, volume 1 [DE82-004161] p 44 N82-23635

Airborne gamma-ray spectrometer and magnetometer survey. Devil's Lake quadrangle, North Dakota, volume 2 [DE82-004168] p 44 N82-23636

Airborne gamma-ray spectrometer and magnetometer survey. Bemidji quadrangle, Minnesota, volume 1 [DE82-001032] p 44 N82-23637

Airborne gamma-ray spectrometer and magnetometer survey. Bemidji quadrangle, Minnesota, volume 2 [DE82-001026] p 44 N82-23638

Airborne gamma-ray spectrometer and magnetometer survey. Barrow quadranagle, Alaska, volume 2 [DE82-000342] p 46 N82-25623

Airborne gamma-ray spectrometer and magnetometer survey: North/south tieline, volume 1 [DE82-005542] p 47 N82-27804

Airborne gamma-ray spectrometer and magnetometer survey: North/south tieline, volume 2 [DE82-005570] p 47 N82-27805

Evaluation and combined geophysical interpretations of NURE and related geoscience data in the Van Horn, Pecos, Marfa, Fort Stockton, Presidido, and Emory Peak quadrangles, Texas, volume 1 [DE82-005554] p 47 N82-27808

Airborne gamma-ray spectrometer and magnetometer survey: Huron Quadrangle, South Dakota [DE82-005540] p 48 N82-27814

Airborne gamma-ray spectrometer and magnetometer survey: Chico Quadrangle, California [DE82-005543] p 48 N82-27815

AEROSOLS

Effect of atmospheric conditions on remote sensing of vegetation parameters p 24 A82-32901

The effect of the spectral attenuation of UV radiation by aerosol on the total ozone measurements p 27 A82-36406

AFRICA

The mineralogy of global magnetic anomalies --- rock magnetic signatures and MAGSAT geological, and gravity correlations in West Africa [E82-10305] p 45 N82-24579

An investigation of MAGSAT and complementary data emphasizing precambrian shields and adjacent areas of West Africa and South America [E82-10316] p 38 N82-24589

An investigation of MAGSAT and complementary data emphasizing precambrian shields and adjacent areas of West Africa and South America [E82-10317] p 38 N82-24590

An investigation of MAGSAT and complementary data emphasizing precambrian shields and adjacent areas of West Africa and South America [E82-10318] p 38 N82-24591

Aeromagnetic and satellite magnetic anomaly mapping [E82-10339] p 39 N82-25601

AGRICULTURE

Remote sensing of leaf water content in the near infrared p 8 A82-32897

Analysis of scanner data for crop inventories [E82-10192] p 10 N82-22626

AgRISTARS: Supporting research. Spring small grains planting date distribution model [E82-10208] p 12 N82-23581

AgRISTARS. Preliminary technical results review of FY81 experiments, volume 2: Fiscal year 1981/1982 'corn and soybeans pilot' experiment [E82-10216] p 13 N82-23589

Application of thermal model for pan evaporation to the hydrology of a defined medium, the sponge [E82-10217] p 13 N82-23590

A meteorologically driven grain sorghum stress indicator model [E82-10218] p 13 N82-23591

Selection of the Australian indicator region [E82-10222] p 13 N82-23595

Agricultural Research Service research highlights in remote sensing for calendar year 1980 [E82-10228] p 14 N82-23601

AgRISTARS: Agriculture and resources inventory surveys through aerospace remote sensing [E82-10236] p 15 N82-23609

An analysis of LANDSAT MSS scene-to-scene registration accuracy [E82-10285] p 16 N82-24563

An algorithm for automating the registration of USDA segment ground data to LANDSAT MSS data [E82-10286] p 16 N82-24564

Plan of research for integrated soil moisture studies. Recommendations of the Soil Moisture Working Group [NASA-TM-84731] p 18 N82-25608

Association of spectral development patterns with development stages of corn [E82-10353] p 19 N82-26751

AGRISTARS PROJECT

AgRISTARS. Project management report: Program review presentation to level 1, interagency coordination committee [E82-10219] p 13 N82-23592

AgRISTARS: Agriculture and resources inventory surveys through aerospace remote sensing [E82-10236] p 15 N82-23609

AGROCLIMATOLOGY

A meteorologically driven maize stress indicator model [E82-10112] p 11 N82-23564

Selection of the Australian indicator region [E82-10222] p 13 N82-23595

AGROMETEOROLOGY

Spectral estimates of solar radiation intercepted by corn canopies [E82-10003] p 18 N82-26742

AIR LAND INTERACTIONS

On the application of a model of boundary-layer flow over low hills to real terrain p 29 A82-36741

AIR MASSES

Comparison of ozone in polluted and clean air masses over Lake Michigan p 29 A82-36477

AIR POLLUTION

Problems of the interpretation of aerial and satellite images of industrial smoke p 23 A82-30307

Detection of volcanic smoke and ash-fall area at volcano Aso, from Landsat MSS data p 23 A82-31295

Detection of regional air pollution episodes utilizing satellite digital data in the visual range p 23 A82-31990

Aircraft measurements of NO/x/ in the lower troposphere above the coast of Japan p 26 A82-36247

Tropospheric CO measurement experiment from the second Space Shuttle flight p 27 A82-36292

Dobson spectrophotometer calibrations, possible errors in ozone absorption coefficients, and errors due to interfering pollutant gases p 28 A82-36431

Comparison of ozone in polluted and clean air masses over Lake Michigan p 29 A82-36477

Breadboard gas filter correlation spectrometer for atmospheric measurement of hydrazines and nitrogen dioxide [AD-A110688] p 82 N82-26642

A study of atmospheric diffusion from the LANDSAT imagery --- pollution transport over the ocean [E82-10360] p 58 N82-26758

Feasibility of laser-separation of 36 S and its use as an atmospheric tracer [DE82-000965] p 30 N82-27737

Remote sensing of sulfur dioxide effects on vegetation. Volume 1: Summary [DE82-900580] p 31 N82-27802

Remote sensing of sulfur dioxide effects on vegetation. Volume 2: Data [DE82-900581] p 31 N82-27803

AIR QUALITY

In situ ozone data for comparison with laser absorption remote sensor: 1980 PEPE/NEROS program [NASA-TM-84471] p 30 N82-25661

Field measurements in support of dispersion modeling in complex terrain (1980) [PB82-148644] p 39 N82-27882

AIR SAMPLING

The growth of snow in winter storms - An airborne observational study p 60 A82-33329

AIR WATER INTERACTIONS

Remote sensing of precipitable water over the oceans from Nimbus 7 microwave measurements p 49 A82-28907

Surface wind analyses for Seasat p 51 A82-29619

Estimation of the temperature of the upper boundary of cloud cover over the world ocean p 54 A82-36005

Interannual variations of outgoing IR associated with tropical circulation changes during 1974-1978 p 54 A82-36341

Analysis of ocean and atmosphere thermodynamical characteristics during the onset of southwest monsoon over the Arabian Sea p 57 N82-23945

AIRBORNE EQUIPMENT

Aircraft monitoring of surface carbon dioxide exchange p 23 A82-30293

A system design for a multispectral sensor using two-dimensional solid-state imaging arrays p 77 A82-31991

High spectral resolution airborne spectrometry p 77 A82-32443

The growth of snow in winter storms - An airborne observational study p 60 A82-33329

EPA's new bubble and banking policies --- for environmental monitoring p 25 A82-33865

An optical data link for airborne scanning system p 80 A82-34737

Study of the hydrological cycle by aerospace methods --- Russian book p 61 A82-35126

Evaluation of the accuracy of water-surface temperature measurement by means of airborne infrared radiometers p 62 A82-35136

Comparison of brightness indicatrixes of snow cover measured from an aircraft and calculated theoretically for different heights of the atmosphere p 62 A82-35140

Airborne gamma-ray spectrometer and magnetometer survey, Kingston quadrangle New York, volume 2C [DE81-027161] p 46 N82-25621

Airborne gamma-ray spectrometer and magnetometer survey. Barrow quadranagle, Alaska, volume 2 [DE82-000342] p 46 N82-25623

AIRBORNE/SPACEBORNE COMPUTERS

Bathymetric imaging p 69 A82-34720

ALASKA

Landsat digital analysis of the initial recovery of burned tundra at Kokolik River, Alaska p 8 A82-32913

Airborne gamma-ray spectrometer and magnetometer survey. Barrow quadrangle, Alaska, volume 1 [DE82-000334] p 43 N82-23623

Airborne gamma-ray spectrometer and magnetometer survey. Wainwright quadrangle, Alaska, volume 2 [DE82-000341] p 43 N82-23624

Airborne gamma-ray spectrometer and magnetometer survey. Meade River quadrangle, Alaska, volume 2 [DE82-000340] p 43 N82-23626

Airborne gamma-ray spectrometer and magnetometer survey. Teshekpuk quadrangle, Alaska, volume 2 [DE82-000310] p 43 N82-23627

Airborne gamma-ray spectrometer and magnetometer survey. Harrison Bay quadrangle, Alaska, volume 2 [DE82-000315] p 43 N82-23628

Airborne gamma-ray spectrometer and magnetometer survey: Beechey Pt., quadrangle, Alaska, volume 2 [DE82-000309] p 43 N82-23629

Airborne gamma-ray spectrometer and magnetometer survey. Point Lay quadrangle, Alaska, volume 2 [DE82-000308] p 43 N82-23630

Airborne gamma-ray spectrometer and magnetometer survey. Utukik River quadrangle, Alaska, volume 2 [DE82-000316] p 44 N82-23631

Airborne gamma-ray spectrometer and magnetometer survey. Sagavanirktok quadrangle, Alaska, volume 2 [DE82-000311] p 44 N82-23632

Airborne gamma-ray spectrometer and magnetometer survey. Lookout Ridge quadrangle, Alaska, volume 2 [DE82-000313] p 47 N82-25625

Ice distribution and winter surface circulation patterns, Kachemak Bay, Alaska [AD-A110806] p 58 N82-26764

ALFALFA

Normal crop calendars. Volume 3: The corn and soybean states of Illinois, Indiana, and Iowa [E82-10221] p 13 N82-23594

A multi-frequency radiometric measurement of soil moisture content over bare and vegetated fields [E82-10238] p 16 N82-23611

ALGAE

HCMM hydrological analysis in Utah [E82-10328] p 63 N82-24601

ALGORITHMS

Multistage classification of multispectral Earth observational data: The design approach [E82-10213] p 72 N82-23586

ALTIMETERS

Intercomparison of wind speeds inferred by the SASS, altimeter, and SMMR p 52 A82-29621

Geoid height-age relation from Seasat altimeter profiles across the Mendocino Fracture Zone p 34 A82-32646

ALTITUDE

Effects of altitude, focal length, and filter combinations on color infrared photography of citrus groves p 9 A82-34729

Comparison of brightness indicatrixes of snow cover measured from an aircraft and calculated theoretically for different heights of the atmosphere p 62 A82-35140

AMMONIA

Ammonia and the NOx budget of the troposphere p 27 A82-36293

ANALYSIS OF VARIANCE

A comparison of stratified versus regression estimators p 11 N82-23133

ANGULAR CORRELATION

Angular variations of nonthermal radio emission from the Galaxy relevant to the structure of interstellar magnetic field p 83 A82-22550

ANGULAR DISTRIBUTION

Albedo and angular characteristics of the reflectance of the underlying surface and clouds --- Russian book p 33 A82-30849

Comparison of brightness indicatrixes of snow cover measured from an aircraft and calculated theoretically for different heights of the atmosphere p 62 A82-35140

ANGULAR MOMENTUM

Magnetic monopole pair and its observation in cosmic rays p 65 A82-22579

ANISOTROPY

On the physical sense of the constant of solar cosmic ray coronal propagation p 83 A82-22599

ANNUAL VARIATIONS

A study of the earth's radiation budget using a general circulation model p 52 A82-30666

The seasonal snow-line within the Fergana basin and the possibility of using it for hydrological forecasting p 61 A82-35131

Interannual variations of outgoing IR associated with tropical circulation changes during 1974-1978 p 54 A82-36341

Observations and analyses of the total amount of atmospheric ozone in the Beijing region and in the region of Jolmolungma Mountain in Tibet p 28 A82-36444

The seasonal variations of ozone and temperature in the middle and the upper stratosphere p 29 A82-36534

ANOMALIES

Airborne gamma-ray spectrometer and magnetometer survey, Toronto quadrangle New York, volume 2A [DE81-027158] p 46 N82-25620

Airborne gamma-ray spectrometer and magnetometer survey, Rochester quadrangle New York, volume 2D [DE81-027156] p 46 N82-25622

ANTARCTIC REGIONS

Magsat magnetic anomalies over Antarctica and the surrounding oceans p 32 A82-30787

Investigation of Antarctic crust and upper mantle using MAGSAT and other geophysical data [E82-10308] p 37 N82-24582

Investigation of Antarctic crust and upper mantle using MAGSAT and other geophysical data [E82-10309] p 37 N82-24583

ANTIPARTICLES

Magnetic monopole pair and its observation in cosmic rays p 65 A82-22579

ANTIPROTONS

Comparison of the measured antiproton flux with that predicted by the 'leaky box' model p 1 A82-22544

Dependence of earth spectrum of positrons and antiprotons on propagation models --- of cosmic radiation p 21 A82-22545

Antiprotons from galactic sources of cosmic rays and gamma rays p 82 A82-22546

ARABIAN SEA

On the space-time variability of ocean surface mixed layer characteristics of central and eastern Arabian sea during MONSOON-77 --- global atmospheric research program p 56 N82-23909

Analysis of ocean and atmosphere thermodynamical characteristics during the onset of southwest monsoon over the Arabian Sea p 57 N82-23945

ARCHITECTURE (COMPUTERS)

Design guidelines for satellite image data distribution systems p 70 A82-37048

ARCTIC OCEAN

Magsat magnetic anomalies over Antarctica and the surrounding oceans p 32 A82-30787

ARGENTINA

Analysis of scanner data for crop inventories [E82-10192] p 10 N82-22626

AgRISTARS. Project management report: Program review presentation to level 1, interagency coordination committee --- Brazil, Argentina, U.S. corn belt, Great Plains Corridor [E82-10231] p 15 N82-23604

Analysis of scanner data for crop inventories [E82-10241] p 16 N82-24519

ARIZONA

The application of Heat Capacity Mapping Mission (HCMM) thermal data to snow hydrology --- Salt Verde Watershed and the southern Sierra Nevada [E82-10191] p 62 N82-22625

Application of HCMM data to regional geologic analysis for mineral and energy resource evaluation [E82-10153] p 45 N82-24518

NURE aerial gamma-ray and magnetic reconnaissance survey of portions of New Mexico, Arizona and Texas. Volume 2: New Mexico-Carlsbad Quadrangle [DE82-005527] p 48 N82-27810

ARTIFICIAL INTELLIGENCE

Key Issues in the Analysis of Remote Sensing Data: A report on the workshop [E82-10348] p 85 N82-26746

ASTROMETRY

On reference coordinate systems used in polar motion determinations p 33 A82-32090

ASTRONOMICAL COORDINATES

The definition of the terrestrial coordinate frame by long baseline interferometry p 33 A82-32084

ASTRONOMICAL MAPS

A color-ratio map of Mercury p 31 A82-22294

ASTRONOMICAL MODELS

The cosmic ray positron spectrum p 1 A82-22542

Comparison of the measured antiproton flux with that predicted by the 'leaky box' model p 1 A82-22544

Dependence of earth spectrum of positrons and antiprotons on propagation models --- of cosmic radiation p 21 A82-22545

Consequences of an inverse Compton emission model for extragalactic X-ray sources p 83 A82-22553

Model for solar hard X-ray bursts p 65 A82-22581

ASTRONOMICAL PHOTOMETRY

Subtleties in the flat-fielding of charge-coupled device /CCD/ images p 68 A82-32581

ATLANTIC OCEAN

Comparison data for Seasat altimetry in the western North Atlantic p 50 A82-29611

A study of atmospheric diffusion from the LANDSAT imagery --- pollution transport over the ocean [E82-10360] p 58 N82-26758

ATMOSPHERIC ATTENUATION

Evaluation of atmospheric attenuation from SMMR brightness temperature for the Seasat satellite scatterometer p 51 A82-29618

Simplified techniques to study components of solar radiation under haze and clouds p 78 A82-32766

ATMOSPHERIC BOUNDARY LAYER

On the application of a model of boundary-layer flow over low hills to real terrain p 29 A82-36741

Marine boundary layer wind structure over the Bay of Bengal during Monex-79 --- Monsoon Experiment (MONEX) p 57 N82-23929

ATMOSPHERIC CHEMISTRY

Observation of the diurnal variation of atmospheric ozone p 26 A82-35895

The seasonal variations of ozone and temperature in the middle and the upper stratosphere p 29 A82-36534

ATMOSPHERIC CIRCULATION

Remote sensing of precipitable water over the oceans from Nimbus 7 microwave measurements p 49 A82-28907

A study of the earth's radiation budget using a general circulation model p 52 A82-30666

Interannual variations of outgoing IR associated with tropical circulation changes during 1974-1978 p 54 A82-36341

The impact of meteorological satellites on the First GARP Global Experiment (FGGE) --- First Global Atmospheric Research Program Global Experiment (FGGE) p 55 N82-23852

ATMOSPHERIC COMPOSITION

Total ozone variations 1970-74 using Backscattered Ultraviolet /BUV/ and ground-based observations p 26 A82-36053

Tropospheric CO measurement experiment from the second Space Shuttle flight p 27 A82-36292

Atmospheric ozone determination by solar occultation using the UV spectrometer on the Solar Maximum Mission p 27 A82-36362

Application of infrared techniques to the study of atmospheric ozone p 27 A82-36414

Total ozone retrieval from satellite Meteor 28 Fourier spectrometer measurements p 28 A82-36422

Observations and analyses of the total amount of atmospheric ozone in the Beijing region and in the region of Jolmolungma Mountain in Tibet p 28 A82-36444

In situ ozone data for comparison with laser absorption remote sensor: 1980 PEPE/NEROS program [NASA-TM-84471] p 30 N82-25661

ATMOSPHERIC DIFFUSION

A study of atmospheric diffusion from the LANDSAT imagery --- pollution transport over the ocean [E82-10360] p 58 N82-26758

ATMOSPHERIC EFFECTS

Effect of atmospheric conditions on remote sensing of vegetation parameters p 24 A82-32901

Allowance for the effect of the atmosphere in the processing of satellite remote-sensing images p 70 A82-35141

ATMOSPHERIC IONIZATION

The determination of differential X-ray spectrum of the solar flare using ionospheric data p 65 A82-22582

ATMOSPHERIC MODELS

A study of the earth's radiation budget using a general circulation model p 52 A82-30666

The growth of snow in winter storms - An airborne observational study p 60 A82-33329

ATMOSPHERIC MOISTURE

Remote sensing of precipitable water over the oceans from Nimbus 7 microwave measurements p 49 A82-28907

Description of Seasat radiometer status and results p 52 A82-29622

Estimation of the precipitable water from the IR channel of the geostationary satellite p 55 A82-37196

ATMOSPHERIC OPTICS

Relating Landsat digital count values to ground reflectance for optically thin atmospheric conditions p 66 A82-29762

ATMOSPHERIC PRESSURE

Mean sea-level pressure in the Southern Hemisphere during the FGGE period --- First Global Atmospheric Research Program Global Experiment (FGGE); buoys p 55 N82-23856

Estimates of the statistical structure of the atmospheric pressure field in summer Monex-79 area p 57 N82-23939

ATMOSPHERIC RADIATION

Soft X-rays from the sunlit earth's atmosphere p 29 A82-37405

ATMOSPHERIC SOUNDING

Total ozone variations 1970-74 using Backscattered Ultraviolet /BUV/ and ground-based observations p 26 A82-36053

Microwave measurement of stratospheric and mesospheric ozone p 28 A82-36415

ATMOSPHERIC TEMPERATURE

Estimation of the temperature of the upper boundary of cloud cover over the world ocean p 54 A82-36005

The seasonal variations of ozone and temperature in the middle and the upper stratosphere p 29 A82-36534

Satellite radiation measurements for the retrieval of the vertical temperature profiles p 70 A82-36935

A meteorologically driven maize stress indicator model [E82-10112] p 11 N82-23564

ATMOSPHERIC WINDOWS

Application of infrared techniques to the study of atmospheric ozone p 27 A82-36414

ATTITUDE CONTROL

LANDSAT-D conical scanner evaluation plan [E82-10340] p 81 N82-25602

AURORAL ARCS

Extremely high latitude auroras p 76 A82-31020

AURORAL IRRADIATION

Large amplitude undulations on the equatorward boundary of the diffuse aurora p 76 A82-31019

AURORAL ZONES

Generation of the auroral kilometric radiation p 26 A82-35542

AUSTRALIA

Selection of the Australian indicator region [E82-10222] p 13 N82-23595

The onset of the Australian Northwest monsoon during winter MONEX: Broadscale flow revealed by an objective analysis scheme p 56 N82-23912

AUTOCORRELATION

The influence of autocorrelation in signature extraction: An example from a geobotanical investigation of Cotter Basin, Montana [E82-10341] p 46 N82-25603

AUTOMATIC WEATHER STATIONS

Remote automatic weather station for resource and fire management agencies [PB82-107335] p 30 N82-23963

AUTOMATION

Extraction of line shaped objects from aerial images using a special operator to analyze the profiles of functions p 67 A82-32033

AVIONICS

Effective electromagnetic shielding in multilayer printed circuit boards [AIAA 81-2333] p 59 A82-13528

B

BALTIC SEA

The METEOSAT Data Collection System and its application p 75 N82-26037

BARLEY

AgRISTARS: Foreign commodity production forecasting. The 1980 US/Canada wheat and barley exploratory experiment [E82-10126] p 11 N82-23565

AgRISTARS: Supporting research. Spring small grains planting date distribution model [E82-10208] p 12 N82-23581

Evaluation of the procedure for separating barley from other spring small grains --- North Dakota, South Dakota, Minnesota and Montana [E82-10230] p 14 N82-23603

Description of the FORTRAN implementation of the spring small grains planting date distribution model [E82-10235] p 15 N82-23608

Multilevel measurements of surface temperature over undulating terrain planted to barley [E82-10245] p 16 N82-24523

Evaluation of HCMM data for assessing soil moisture and water table depth --- South Dakota [E82-10329] p 18 N82-24602

BAROTROPIC FLOW

Impact of additional summer MONEX wind data on the prediction of monsoon depressions during June - August 1979 with two versions of primitive equation (PE) barotropic model --- Monsoon Experiment (MONEX) p 56 N82-23900

BAROTROPISM

Estimates of sea surface stress for summer MONEX from cloud motions --- global atmospheric research program p 56 N82-23910

BARREN LAND

A multi-frequency radiometric measurement of soil moisture content over bare and vegetated fields [E82-10238] p 16 N82-23611

Multifrequency remote sensing of soil moisture --- Guymon, Oklahoma and Dalhart, Texas [E82-10362] p 20 N82-26760

BATHYMETERS

Bathymetric imaging p 69 A82-34720

BAY ICE

Ice distribution and winter surface circulation patterns, Kachemak Bay, Alaska [AD-A110606] p 58 N82-26764

BAYS (TOPOGRAPHIC FEATURES)

Marine boundary layer wind structure over the Bay of Bengal during Monex-79 --- Monsoon Experiment (MONEX) p 57 N82-23929

BEACHES
Fluid-sediment interactions on beaches and shelves
[AD-A110838] p 59 N82-26948
BEDROCK
Satellite image interpretation of the eastern Caledonian part of the Blue Road Geotraverse and its geological implications /Nordland, Vasterbotten, Scandinavia/
p 41 A82-30305
Characterization of the structure and tectonic of South America
[E82-10196] p 42 N82-23569
BEETLES
Remote sensing of Douglas-fir trees newly infested by bark beetles p 6 A82-29536
Estimating mountain pine beetle-killed ponderosa pine over the front range of Colorado with high altitude panoramic photography p 7 A82-32704
BERMUDA
Seasat altimeter height calibration --- related to sea surface heights near Bermuda p 49 A82-29603
BERYLLIUM 10
The cosmic ray positron spectrum p 1 A82-22542
BIBLIOGRAPHIES
The crustal structure and tectonics of South America
[E82-10319] p 38 N82-24592
BIOLUMINESCENCE
Laser-induced bioluminescence --- for remote sensing of marine organisms p 53 A82-32559
BIOMASS
Development of visible/infrared/microwave agriculture classification and biomass estimation algorithms --- Guyton, Oklahoma and Dalhart, Texas
[E82-10363] p 20 N82-26761
BLACK HOLES (ASTRONOMY)
Acceleration processes near massive black holes
p 3 A82-22572
BLIGHT
Detection and damage assessment of citrus tree losses with aerial color infrared photography /ACIR/
p 7 A82-29538
BOTSWANA
Overseas Geology And Mineral Resources number 56: A geological interpretation of LANDSAT imagery and air photography of Botswana
[OGMR-56] p 42 N82-22636
BOUNDARY LAYER FLOW
On the application of a model of boundary-layer flow over low hills to real terrain p 29 A82-36741
On the space-time variability of ocean surface mixed layer characteristics of central and eastern Arabian sea during MONSOON-77 --- global atmospheric research program p 56 N82-23909
BRAZIL
Structure, composition and thermal state of the crust in Brazil --- geomagnetic survey
[E82-10187] p 35 N82-22621
Dynamic study of the upper Sao Francisco river and Tres Marias reservoir using MSS/LANDSAT images --- BRazil
[E82-10291] p 63 N82-24569
A study of atmospheric diffusion from the LANDSAT imagery --- pollution transport over the ocean
[E82-10360] p 58 N82-26758
BREMSSTRAHLUNG
Computer simulation of the time dependence of the photon energy spectra produced in proton and electron bremstrahlung p 3 A82-22587
BRIGHTNESS DISTRIBUTION
Comparison of brightness indicatrixes of snow cover measured from an aircraft and calculated theoretically for different heights of the atmosphere p 62 A82-35140
BRIGHTNESS TEMPERATURE
Surface temperature determination from an amalgamation of GOES and TIROS-N radiance measurements p 66 A82-28905
Remote sensing of precipitable water over the oceans from Nimbus 7 microwave measurements
p 49 A82-28907
Evaluation of atmospheric attenuation from SMMR brighiness temperature foi the Seasat satellite scatterometer p 51 A82-29618
Snowpack monitoring in North America and Eurasia using passive microwave satellite data
p 78 A82-32915
Depression of brightness temperature of sea surfaces covered with monomolecular oil films relative to clean water surfaces at 1.43 GHz p 54 A82-33322
Analysis of scanner data for crop inventories
[E82-10192] p 10 N82-22626
A multi-frequency radiometric measurement of soil moisture content over bare and vegetated fields
[E82-10238] p 16 N82-23611
The effect of sea-surface Sun glitter on microwave radiometer measurements
[NASA-CR-169063] p 57 N82-26525
Relating thematic mapper bands TM3, TM4, and TM5 to agronomic variables for corn, cotton, sugarbeet, soybean, sorghum, sunflower and tobacco
[E82-10347] p 19 N82-26745
BUNDLES
A practical study of gross-error detection in bundle adjustment p 69 A82-34702
BUOYS
The impact of meteorological satellites on the First GARP Global Experiment (FGGE) --- First Global Atmospheric Research Program Global Experiment (FGGE) p 55 N82-23852

C

C BAND
C-band radar for determining surface soil moisture
p 10 A82-37194
CALIBRATING
Seasat altimeter height calibration --- related to sea surface heights near Bermuda p 49 A82-29603
Tidal and geodetic observations for the Seasat altimeter calibration experiment p 49 A82-29604
Sensitivity of Dobson total ozone estimations to wavelength band calibration uncertainties
p 27 A82-36405
Dobson spectrophotometer calibrations, possible errors in ozone absorption coefficients, and errors due to interfering pollutant gases p 28 A82-36431
C-band radar for determining surface soil moisture
p 10 A82-37194
CALIFORNIA
The application of Heat Capacity Mapping Mission (HCMM) thermal data to snow hydrology --- Salt Verde Watershed and the southern Sierra Nevada
[E82-10191] p 62 N82-22625
Multilevel measurements of surface temperature over undulating terrain planted to barley
[E82-10245] p 16 N82-24523
Airborne gamma-ray spectrometer and magnetometer survey: Ukiah quadrangle, California, volume 1 --- uranium exploration
[DE82-005541] p 48 N82-27813
Airborne gamma-ray spectrometer and magnetometer survey: Chico Quadrangle, California
[DE82-005543] p 48 N82-27815
CAMERAS
Image quality and height measurement accuracy of serial survey camera imagery from high altitudes
p 78 A82-33297
Analytical processing of photographs taken by paired cameras p 79 A82-34471
CANADA
Magnetic charts of Canada derived from Magsat data
p 32 A82-30778
AgRISTARS: Foreign commodity production forecasting. The 1980 US/Canada wheat and barley exploratory experiment
[E82-10126] p 11 N82-23565
CANOPIES (VEGETATION)
Effect of atmcspheric conditions on remote sensing of vegetation parameters p 24 A82-32901
The response characteristics of vegetation in Landsat MSS digital data p 8 A82-32907
View angle effects in the radiometric measurement of plant canopy temperatures p 8 A82-32914
Appearance of irregular tree canopies in nighttime high-resolution thermal infrared imagery
p 68 A82-32916
Spectral properties of agricultural crops and soils measured from space, aerial, field, and laboratory sensors
[E82-10189] p 10 N82-22623
Diurnal changes in reflectance factor due to Sun-row direction interactions
[E82-10128] p 11 N82-23566
Structure of the St. Francois Mountains and surrounding lead belt, S. E. Missouri: Inferences from thermal IR and other data sets --- Ozard Plateau and St. Francois Mountains
[E82-10205] p 11 N82-23578
Application of Computer Axial Tomography (CAT) to measuring crop canopy geometry --- corn and soybeans
[E82-10227] p 14 N82-23600
Linear polarization of light by two wheat canopies measured at many view angles
[E82-10229] p 14 N82-23602
A model of plant canopy polarization
[E82-10233] p 15 N82-23606
Canopy reflectance as influenced by solar illumination angle
[E82-10237] p 15 N82-23610
An analysis of LANDSAT MSS scene-to-scene registration accuracy
[E82-10285] p 16 N82-24563
An algorithm for automating the registration of USDA segment ground data to LANDSAT MSS data
[E82-10286] p 16 N82-24564
Evaluation of HCMM data for assessing soil moisture and water table depth --- South Dakota
[E82-10329] p 18 N82-24602
Spectral estimates of solar radiation intercepted by corn canopies
[E82-10003] p 18 N82-26742
Mapping of wildlife habitat in Farmington Bay, Utah
[E82-10354] p 19 N82-26752
Detection of variations in aspen forest habitat from LANDSAT digital data: Bear River Range, Utah
[E82-10355] p 19 N82-26753
CANTILEVER BEAMS
Nonlinear theory for elastic beams and rods and its finite element representation
[WTHD-143] p 73 N82-24517
CARBON DIOXIDE
Influence of CO2 on melting of model granulite facies assemblages - A model for the genesis of charnockites
p 42 A82-36298
CARBON DIOXIDE CONCENTRATION
Aircraft monitoring of surface carbon dioxide exchange p 23 A82-30293
CARBON MONOXIDE
Tropospheric CO measurement experiment from the second Space Shuttle flight p 27 A82-36292
CARBON STARS
On the stellar origin of the Ne-22 excess in cosmic rays p 21 A82-22562
CELESTIAL GEODESY
Space to the earth --- Russian book on space technology applications p 83 A82-30850
CELESTIAL REFERENCE SYSTEMS
Establishment of terrestrial reference frames by new observational techniques p 33 A82-32078
On reference coordinate systems used in polar motion determinations p 33 A82-32090
Some considerations in the use of very-long-baseline-interferometry to establish reference coordinate systems for geodynamics p 34 A82-32096
CENTRAL AMERICA
Geotectonics of South America --- regional magnetic and gravity anomalies of South America
[E82-10320] p 38 N82-24593
CHARGE COUPLED DEVICES
Subtleties in the flat-fielding of charge-coupled device /CCD/ images p 68 A82-32581
CHARGED PARTICLES
Mass per charge ratio in hot plasmas and cosmic ray source composition p 2 A82-22557
Observations of interplanetary energetic charged particles from gamma-ray line solar flares
p 65 A82-22586
CHECKOUT
Interactive initialization of heat flux parameters for numerical models using satellite temperature measurements
[E82-10313] p 82 N82-26743
CHEMICAL COMPOSITION
Calculated isotopic source composition and tests for origin and propagation of cosmic rays with mass numbers less than or equal to 62 p 83 A82-22554
The charge and isotopic composition of Z equals 7-16 cosmic ray nuclei at their source p 64 A82-22555
Physical state of the birth place of cosmic rays and its implication to the acceleration processes
p 2 A82-22559
High resolution measurements of solar flare isotopes
p 22 A82-22606
CHEMICAL EFFECTS
Spectral scanning of experimental plots of SO2-affected winter wheat and soybeans for mission planning
p 6 A82-29537
CHEMICAL FRACTIONATION
Laboratory studies of actinide metal-silicate fractionation p 49 A82-22306
CHESAPEAKE BAY (US)
Analysis of ocean color scanner data from the Superflux III Experiment
[NASA-TM-83290] p 55 N82-23614
CHLOROPHYLLS
Analysis of ocean color scanner data from the Superflux III Experiment
[NASA-TM-83290] p 55 N82-23614
CHROMOSPHERE
Possible evidence for attenuation of an MHD shock by a magnetic neutral sheet in the solar corona
p 3 A82-22589
The model of the cosmic ray enrichment by helium-3
p 31 A82-22614
CIRCUIT BOARDS
Effective electromagnetic shielding in multilayer printed circuit boards
[AIAA 81-2333] p 59 A82-13528

CITIES
Remote sensing - A potential aid in the preparation of an urban tree inventory p 9 A82-34732
Longwave infrared observation of urban landscapes p 25 A82-34744

CITRUS TREES
Detection and damage assessment of citrus tree losses with aerial color infrared photography /ACIR/ p 7 A82-29538
Effects of altitude, focal length, and filter combinations on color infrared photography of citrus groves p 9 A82-34729

CLASSIFICATIONS
The use of prior probabilities in maximum likelihood classification of remotely sensed data p 68 A82-32904
Ten-Ecosystem Study --- Grand and Weld Counties, Colorado; Warren County, Pennsylvania; St. Louis County, Minnesota; Sandoval County, New Mexico; Kershaw County, South Carolina; Fort Yukon, Alaska; Grays Harbor County, Washington; and Washington County, Missouri. [E82-10186] p 84 N82-22620
AgRISTARS: Foreign commodity production forecasting. The 1980 US corn and soybeans exploratory experiment [E82-10206] p 11 N82-23579
Multistage classification of multispectral Earth observational data: The design approach [E82-10213] p 72 N82-23586
Use and applicability of the vegetation component of the national site classification system --- Sumter National Forest, South Carolina [E82-10234] p 15 N82-23607
Analysis of scanner data for crop inventories [E82-10241] p 16 N82-24519
Analysis of thematic mapper simulator data acquired during winter season over Pearl River, Mississippi, test site [E82-10287] p 17 N82-24565
Key Issues in the Analysis of Remote Sensing Data: A report on the workshop [E82-10348] p 85 N82-26746
Development of visible/infrared/microwave agriculture classification and biomass estimation algorithms --- Guyton, Oklahoma and Dalhart, Texas [E82-10363] p 20 N82-26761

CLIMATE
The onset of the Australian Northwest monsoon during winter MONEX: Broadscale flow revealed by an objective analysis scheme p 56 N82-23912

CLIMATOLOGY
A study of the earth's radiation budget using a general circulation model p 52 A82-30666
System albedo as sensed by satellites - Its definition and variability p 23 A82-32342
Plan of research for integrated soil moisture studies. Recommendations of the Soil Moisture Working Group [NASA-TM-84731] p 18 N82-25608
Sea-Ice Mission Requirements for the US FIREX and Canada RADARSAT programs [NASA-CR-168984] p 57 N82-25609

CLOUD COVER
Simplified techniques to study components of solar radiation under haze and clouds p 78 A82-32766
Estimation of the temperature of the upper boundary of cloud cover over the world ocean p 54 A82-36005

CLOUD HEIGHT INDICATORS
The meteorological product - 'Cloud-top height' p 70 A82-36043

CLOUD PHOTOGRAPHY
Skirt clouds associated with the Soufriere eruption of 17 April 1979 p 24 A82-33656

CLOUD PHYSICS
Albedo and angular characteristics of the reflectance of the underlying surface and clouds --- Russian book p 33 A82-30849
Skirt clouds associated with the Soufriere eruption of 17 April 1979 p 24 A82-33656

CLOUDS (METEOROLOGY)
Representativeness of cloud motion winds deduced from GOES Indian Ocean satellite imagery for the description of the Indian summer monsoon --- superpressure balloons for the study of the Indian summer monsoon (BALSAMINE) p 55 N82-23879
Estimates of sea surface stress for summer MONEX from cloud motions --- global atmospheric research program p 56 N82-23910

COAL UTILIZATION
Remote sensing of sulfur dioxide effects on vegetation. Volume 1: Summary [DE82-900580] p 31 N82-27802
Remote sensing of sulfur dioxide effects on vegetation. Volume 2: Data [DE82-900581] p 31 N82-27803

COASTAL CURRENTS
Nearshore current pattern off south Texas - An interpretation from aerial photographs p 53 A82-32903
MONEX oceanographic observations along the East African coast --- global atmospheric research program p 56 N82-23908
Fluid-sediment interactions on beaches and shelves [AD-A110838] p 59 N82-26948

COASTAL WATER
Interpretation of surface-water circulation, Aransas Pass, Texas, using Landsat imagery p 60 A82-32896
A quantitative multispectral analysis system for aerial photographs applied to coastal planning p 55 A82-37505
Analysis of ocean color scanner data from the Superflux III Experiment [NASA-TM-83290] p 55 N82-23614
Thermal mapping, geothermal source location, natural effluents and plant stress in the Mediterranean coast of Spain [E82-10300] p 17 N82-24576
A study of atmospheric diffusion from the LANDSAT imagery --- pollution transport over the ocean [E82-10360] p 58 N82-26758
Meteorological and aircraft data for CUE 2 1973 [PB82-149246] p 59 N82-26949

COASTS
Coastal environment change analysis by Landsat MSS data p 54 A82-34219
Some empirical rules for forecasting fog and status over northern Florida, southern Georgia and adjacent coastal waters [PB82-154006] p 59 N82-27949

COHERENT RADAR
Study visit to United States laser technology centers, 1981 [FOA-C-30257-E1] p 81 N82-24439

COLD WEATHER
Use of thermal inertia determined by HCMM to predict nocturnal cold prone areas in Florida --- Everglades agricultural area and the west north central peninsula [E82-10299] p 17 N82-24575

COLOR CODING
Multidisciplinary investigations on HCMM data over middle Europe and Marocco --- southern Germany and Marrakesh, Morocco [E82-10315] p 74 N82-24588
Matrix data analysis: Color/B and W coding is not always enough [AD-A111401] p 74 N82-25612

COLOR INFRARED PHOTOGRAPHY
Riparian vegetation mapping in Northeastern California using high altitude color infrared aerial photography p 5 A82-29528
Inventory of wildlife habitat from color infrared aerial photography for Cobb Island, Virginia p 6 A82-29529
Considerations in using color infrared photographs for vegetative interpretation p 6 A82-29530
Multi-resource inventory in interior Alaska p 6 A82-29532
Estimating rangeland cover proportions with large-scale color-infrared aerial photographs p 6 A82-29534
Mapping riparian vegetation in Southeastern Oregon using digitized large scale color infra-red aerial photography p 6 A82-29535
Remote sensing of Douglas-fir trees newly infested by bark beetles p 6 A82-29536
Detection and damage assessment of citrus tree losses with aerial color infrared photography /ACIR/ p 7 A82-29538
An infrared exposure meter p 76 A82-29541
Estimating bark beetle-killed lodgepole pine with high altitude panoramic photography p 7 A82-32703
Effects of altitude, focal length, and filter combinations on color infrared photography of citrus groves p 9 A82-34729
Use of Landsat multispectral scanner data in vegetation mapping of a forested area p 9 A82-34731
Aerial photography vs. Landsat for digital land-cover mapping in an urban watershed p 61 A82-34745

COLOR PHOTOGRAPHY
A color-ratio map of Mercury p 31 A82-22294
Detection of environmental disturbance using color aerial photography and thermal infrared imagery p 22 A82-29327
Color aerial photography detects nutrient status of loblolly pine plantations p 6 A82-29531
Application of 35mm color aerial photography to forest land change detection p 6 A82-29533
Evaluation of spruce-fir forests using small-format photographs p 8 A82-32707
The use of Skylab S-190B photography for small scale mapping p 80 A82-34742
Multidisciplinary investigations on HCMM data over middle Europe and Marocco --- southern Germany and Marrakesh, Morocco [E82-10315] p 74 N82-24588
Mapping of wildlife habitat in Farmington Bay, Utah [E82-10354] p 19 N82-26752

COLOR TELEVISION
Terrain analysis from Landsat using a color TV enhancement system p 68 A82-32911

COLORADO
Application of thermal model for pan evaporation to the hydrology of a defined medium, the sponge [E82-10217] p 13 N82-23590
AgRISTARS: Renewable resources inventory. Land information support system implementation plan and schedule --- San Juan National Forest pilot test [E82-10224] p 14 N82-23597

COMMODITIES
A meteorologically driven grain sorghum stress indicator model [E82-10218] p 13 N82-23591

COMPARISON
An analysis of LANDSAT MSS scene-to-scene registration accuracy [E82-10285] p 16 N82-24563
An algorithm for automating the registration of USDA segment ground data to LANDSAT MSS data [E82-10286] p 16 N82-24564

COMPTON EFFECT
Consequences of an inverse Compton emission model for extragalactic X-ray sources p 83 A82-22553

COMPUTER COMPATIBLE TAPES
Computation with physical values from Landsat digital data p 68 A82-32709
Spherical harmonic representation of the main geomagnetic field for world charting and investigations of some fundamental problems of physics and geophysics [E82-10203] p 72 N82-23576
Investigation from Japanese MAGSAT team [E82-10239] p 73 N82-23612
An analysis of LANDSAT MSS scene-to-scene registration accuracy [E82-10285] p 16 N82-24563
An algorithm for automating the registration of USDA segment ground data to LANDSAT MSS data [E82-10286] p 16 N82-24564
Report of investigation from Japanese MAGSAT Team [E82-10322] p 74 N82-24595
Models and maps of the main field [E82-10327] p 74 N82-24600
Analysis of MAGSAT data of the Indian region [E82-10358] p 75 N82-26756
Comparison of storm-time changes of geomagnetic field at ground and MAGSAT altitudes [E82-10359] p 30 N82-26757

COMPUTER GRAPHICS
Development of three-dimensional spatial displays using a geographically based information system p 66 A82-29326
RAMS-1, a Resource Analysis and Mapping System p 69 A82-34726

COMPUTER PROGRAMS
The simultaneous employment of geodetic measurements for block adjustments using the method of independent models p 34 A82-33295
A practical study of gross-error detection in bundle adjustment p 69 A82-34702
Description of the FORTRAN implementation of the spring small grains planting date distribution model [E82-10235] p 15 N82-23608

COMPUTER SYSTEMS PROGRAMS
Development of three-dimensional spatial displays using a geographically based information system p 66 A82-29326

COMPUTER TECHNIQUES
A computerized spatial analysis system for assessing wildlife habitat from vegetation maps p 9 A82-34716
A quantitative method to test for similarity between photo interpreters p 69 A82-34722
Present status of on-line analytical triangulation p 69 A82-34940
Application of Computer Axial Tomography (CAT) to measuring crop canopy geometry --- corn and soybeans [E82-10227] p 14 N82-23600

COMPUTERIZED SIMULATION
Computer simulation of the time dependence of the photon energy spectra produced in proton and electron bremstrahlung p 3 A82-22587
A simulation study of soil moisture estimation by a space SAR p 60 A82-29333
Orbiting passive microwave sensor simulation applied to soil moisture estimation [E82-10343] p 18 N82-25605

CONFERENCES

International Cosmic Ray Conference, 17th, Paris, France, July 13-25, 1981, Conference Papers. Volume 3 p 65 A82-22580

Color aerial photography in the plant sciences and related fields; Proceedings of the Eighth Biennial Workshop, Luray, VA, April 21-23, 1981 p 5 A82-29526

Imaging spectroscopy; Proceedings of the Seminar, Los Angeles, CA, February 10, 11, 1981 p 77 A82-32440

American Society of Photogrammetry, Annual Meeting, 47th, Washington, DC, February 22-27, 1981, ASP Technical Papers p 79 A82-34701

CONGRESSIONAL REPORTS

Civil land remote sensing system [GPO-87-070] p 84 N82-22630

Streamlining and ensuring mineral development must begin at local land management levels [EMD-82-10] p 29 N82-23043

CONICAL SCANNING

LANDSAT-D conical scanner evaluation plan [E82-10340] p 81 N82-25602

CONIFERS

Remote sensing of Douglas-fir trees newly infested by bark beetles p 6 A82-29536

Estimating bark beetle-killed lodgepole pine with high altitude panoramic photography p 7 A82-32703

Estimating mountain pine beetle-killed ponderosa pine over the front range of Colorado with high altitude panoramic photography p 7 A82-32704

CONTINENTAL DRIFT

MAGSAT anomaly map and continental drift [E82-10326] p 38 N82-24599

CONTINENTS

MAGSAT anomaly map and continental drift [E82-10326] p 38 N82-24599

CONTOURS

Description of gray level picture using a collection of density contour lines p 66 A82-29409

CONVECTION

A statistical approach to rainfall estimation using satellite and conventional data [NOAA-TR-NESS-89] p 63 N82-22854

CONVECTION CURRENTS

The influence of soil characteristics on regional convection differences above Northern Germany p 10 A82-37589

CONVECTIVE FLOW

Convective outflow of cosmic rays from the Galaxy and background radio emission p 83 A82-22551

COORDINATES

Reference coordinate systems for earth dynamics - A preview p 33 A82-32077

CORN

A meteorologically driven maize stress indicator model [E82-10112] p 11 N82-23564

AgRISTARS: Foreign commodity production forecasting. The 1980 US corn and soybeans exploratory experiment [E82-10206] p 11 N82-23579

Determination of the optimal level for combining area and yield estimates [E82-10215] p 12 N82-23588

AgRISTARS. Preliminary technical results review of FY81 experiments, volume 2: Fiscal year 1981/1982 'corn and soybeans pilot' experiment [E82-10216] p 13 N82-23589

Application of Computer Axial Tomography (CAT) to measuring crop canopy geometry --- corn and soybeans [E82-10227] p 14 N82-23600

Analysis of scanner data for crop inventories [E82-10241] p 16 N82-24519

Spectral estimates of solar radiation intercepted by corn canopies [E82-10003] p 18 N82-26742

Association of spectral development patterns with development stages of corn [E82-10353] p 19 N82-26751

CORRELATION

On the anticorrelation between the He/3//He/4/ ratio and proton intensity in He/3/ rich flares p 40 A82-22613

COSMIC RAYS

Fragmentation of Fe nuclei on carbon, hydrogen and CH2 targets. I - Individual charge changing and total cross sections. II - Isotopic cross sections --- for interstellar cosmic ray propagation p 63 A82-22538

A report on the 'cosmic ray propagation problem' p 1 A82-22539

On the characteristics of the very low energy galactic cosmic rays in the interstellar space p 63 A82-22540

The question of short pathlengths in interstellar propagation p 1 A82-22541

Dependence of earth spectrum of positrons and antiprotons on propagation models --- of cosmic radiation p 21 A82-22545

Antiprotons from galactic sources of cosmic rays and gamma rays p 82 A82-22546

Confinement and acceleration of cosmic rays in galactic superbubbles p 82 A82-22547

Interactions of cosmic rays with molecular clouds p 82 A82-22548

Angular variations of nonthermal radio emission from the Galaxy relevant to the structure of interstellar magnetic field p 83 A82-22550

Convective outflow of cosmic rays from the Galaxy and background radio emission p 83 A82-22551

Steady-state cosmic ray electron spectrum under diffusion, convection, adiabatic deceleration and synchrotron losses p 1 A82-22552

Calculated isotopic source composition and tests for origin and propagation of cosmic rays with mass numbers less than or equal to 62 p 83 A82-22554

The charge and isotopic composition of Z equals 7-16 cosmic ray nuclei at their source p 64 A82-22555

Comparative abundances in solar energetic particles and in galactic cosmic ray sources, and the Ne-22 anomaly p 83 A82-22556

Mass per charge ratio in hot plasmas and cosmic ray source composition p 2 A82-22557

Cosmic ray composition from acceleration of thermal matter p 64 A82-22558

Physical state of the birth place of cosmic rays and its implication to the acceleration processes p 2 A82-22559

On volatility, first ionization potential, and s- and r-processes --- for Galactic cosmic ray sources p 2 A82-22560

Interstellar grains as seeds for galactic cosmic rays p 2 A82-22561

On the stellar origin of the Ne-22 excess in cosmic rays p 21 A82-22562

Origin of galactic cosmic rays from Ne isotopic composition p 2 A82-22563

Evidence for the stochastic acceleration of cosmic rays in supernova remnants p 2 A82-22564

Cosmic ray acceleration by stellar winds. I - Total density, pressure and energy flux p 21 A82-22566

On the stellar origin of low energy cosmic rays p 21 A82-22567

Acceleration of cosmic rays in accretion shocks p 64 A82-22568

Remarks on cosmic ray origin p 21 A82-22569

Pulsar models and cosmic-ray acceleration p 21 A82-22570

The galactic origin of cosmic rays. II [CONF-810711-2] p 64 A82-22573

Extragalactic cosmic rays, their sources and spectrum p 40 A82-22574

Calculation of production rates of cosmogenic nuclides by Monte Carlo method p 64 A82-22576

Measurement of cosmogenic nuclides using a multi-crystal gamma-ray coincidence spectrometer --- for Mayo Belwa meteorite study p 64 A82-22577

Magnetic monopole pair and its observation in cosmic rays p 65 A82-22579

International Cosmic Ray Conference, 17th, Paris, France, July 13-25, 1981, Conference Papers. Volume 3 p 65 A82-22580

The modulation characteristics of the 19th and 20th solar activity cycles p 59 A82-22615

11-year modulation and spectrum of cosmic rays in the interstellar space p 22 A82-22616

Features of cosmic ray variations due to variations in the total magnetic field of the sun p 49 A82-22619

COSMOCHEMISTRY

Laboratory studies of actinide metal-silicate fractionation p 49 A82-22306

The charge and isotopic composition of Z equals 7-16 cosmic ray nuclei at their source p 64 A82-22555

Nucleosynthesis of light and by-passed isotopes in the solar system matter p 64 A82-22578

COTTON

Airborne observed solar elevation and row direction effects on the near-IR/red ratio of cotton [E82-10220] p 13 N82-23593

COULOMB COLLISIONS

Cosmic ray composition from acceleration of thermal matter p 64 A82-22558

COULOMB POTENTIAL

Coulombian energy losses and the nuclear composition of the solar cosmic rays p 4 A82-22610

CROP CALENDARS

Analysis of scanner data for crop inventories [E82-10192] p 10 N82-22626

Evaluation of the Doraiswamy-Thompson winter wheat crop calendar model incorporating a modified spring restart sequence [E82-10207] p 12 N82-23580

AgRISTARS: Supporting research. Spring small grains planting date distribution model [E82-10208] p 12 N82-23581

Description of historical crop calendar data bases developed to support foreign commodity production forecasting project experiments [E82-10209] p 12 N82-23582

AgRISTARS. Preliminary technical results review of FY81 experiments, volume 2: Fiscal year 1981/1982 'corn and soybeans pilot' experiment [E82-10216] p 13 N82-23589

A meteorologically driven grain sorghum stress indicator model [E82-10218] p 13 N82-23591

AgRISTARS. Project management report: Program review presentation to level 1, interagency coordination committee [E82-10219] p 13 N82-23592

Selection of the Australian indicator region [E82-10222] p 13 N82-23595

AgRISTARS. Project management report: Program review presentation to level 1, interagency coordination committee --- Brazil, Argentina, U.S. corn belt, Great Plains Corridor [E82-10231] p 15 N82-23604

CROP GROWTH

Color aerial photography detects nutrient status of loblolly pine plantations p 6 A82-29531

Spectral scanning of experimental plots of SO2-affected winter wheat and soybeans for mission planning p 6 A82-29537

Evaluation of the Doraiswamy-Thompson winter wheat crop calendar model incorporating a modified spring restart sequence [E82-10207] p 12 N82-23580

AgRISTARS: Supporting research. Spring small grains planting date distribution model [E82-10208] p 12 N82-23581

Description of historical crop calendar data bases developed to support foreign commodity production forecasting project experiments [E82-10209] p 12 N82-23582

Application of thermal model for pan evaporation to the hydrology of a defined medium, the sponge [E82-10217] p 13 N82-23590

A meteorologically driven grain sorghum stress indicator model [E82-10218] p 13 N82-23591

AgRISTARS. Project management report: Program review presentation to level 1, interagency coordination committee [E82-10219] p 13 N82-23592

Relating thematic mapper bands TM3, TM4, and TM5 to agronomic variables for corn, cotton, sugarbeet, soybean, sorghum, sunflower and tobacco [E82-10347] p 19 N82-26745

Association of spectral development patterns with development stages of corn [E82-10353] p 19 N82-26751

CROP IDENTIFICATION

Field size, length, and width distributions based on LACIE ground truth data --- large area crop inventory experiment p 8 A82-32909

Evaluation of NOAA-AVHRR data for crop assessment --- Advanced Very High Resolution Radiometer p 8 A82-34179

Analysis of scanner data for crop inventories [E82-10192] p 10 N82-22626

AgRISTARS: Foreign commodity production forecasting. The 1980 US/Canada wheat and barley exploratory experiment [E82-10126] p 11 N82-23565

Agricultural Research Service research highlights in remote sensing for calendar year 1980 [E82-10228] p 14 N82-23601

Evaluation of the procedure for separating barley from other spring small grains --- North Dakota, South Dakota, Minnesota and Montana [E82-10230] p 14 N82-23603

AgRISTARS: Agriculture and resources inventory surveys through aerospace remote sensing [E82-10236] p 15 N82-23609

Canopy reflectance as influenced by solar illumination angle [E82-10237] p 15 N82-23610

An algorithm for automating the registration of USDA segment ground data to LANDSAT MSS data [E82-10286] p 16 N82-24564

Relating thematic mapper bands TM3, TM4, and TM5 to agronomic variables for corn, cotton, sugarbeet, soybean, sorghum, sunflower and tobacco [E82-10347] p 19 N82-26745

Development of visible/infrared/microwave agriculture classification and biomass estimation algorithms --- Guyton, Oklahoma and Dalhart, Texas [E82-10363] p 20 N82-26761

CROP INVENTORIES

Effects of altitude, focal length, and filter combinations on color infrared photography of citrus groves p 9 A82-34729

Analysis of scanner data for crop inventories [E82-10192] p 10 N82-22626

A comparison of stratified versus regression estimators p 11 N82-23133

Determination of the optimal level for combining area and yield estimates [E82-10215] p 12 N82-23588

AgRISTARS. Preliminary technical results review of FY81 experiments, volume 2: Fiscal year 1981/1982 'corn and soybeans pilot' experiment [E82-10216] p 13 N82-23589

Normal crop calendars. Volume 3: The corn and soybean states of Illinois, Indiana, and Iowa [E82-10221] p 13 N82-23594

Selection of the Australian indicator region [E82-10222] p 13 N82-23595

Analysis of scanner data for crop inventories [E82-10241] p 16 N82-24519

Inventory of wetlands and agricultural land cover in the upper Sevier River Basin, Utah [E82-10345] p 18 N82-25607

Spectral estimates of solar radiation intercepted by corn canopies [E82-10003] p 18 N82-26742

CROP VIGOR

Remote sensing of the weediness of crop fields p 5 A82-29435

Considerations in using color infrared photographs for vegetative interpretation p 6 A82-29530

Effects of vegetation canopy structure on remotely sensed canopy temperatures --- inferring plant water stress and yield p 8 A82-32905

Use of NOAA/AVHRR visible and near-infrared data for land remote sensing [NASA-TM-84186] p 81 N82-22643

AgRISTARS. Preliminary technical results review of FY81 experiments, volume 2: Fiscal year 1981/1982 'corn and soybeans pilot' experiment [E82-10216] p 13 N82-23589

A meteorologically driven grain sorghum stress indicator model [E82-10218] p 13 N82-23591

AgRISTARS: Early warning and crop condition assessment. Plant cover, soil temperature, freeze, water stress, and evapotranspiration conditions [E82-10225] p 14 N82-23598

Application of Computer Axial Tomography (CAT) to measuring crop canopy geometry --- corn and soybeans [E82-10227] p 14 N82-23600

Multispectral determination of soil moisture-2 --- Guymon, Oklahoma and Dalhart, Texas [E82-10349] p 19 N82-26747

CRUSTAL FRACTURES

Geoid height-age relation from Seasat altimeter profiles across the Mendocino Fracture Zone p 34 A82-32646

Geodetic monitoring of tectonic information. Toward a strategy p 35 N82-22832

Seismic and geodetic studies of the Imperial Valley, California [DE82-001686] p 39 N82-26915

CUMULONIMBUS CLOUDS

The onset of the Australian Northwest monsoon during winter MONEX: Broadscale flow revealed by an objective analysis scheme p 56 N82-23912

CUMULUS CLOUDS

The use of contextual information to detect cumulus clouds and cloud shadows in Landsat data p 67 A82-32346

The influence of soil characteristics on regional convection differences above Northern Germany p 10 A82-37589

CURIE TEMPERATURE

Application of satellite magnetic anomaly data to Curie isotherm mapping p 70 A82-35824

MAGSAT and aeromagnetic data in the North American continent [E82-10193] p 71 N82-22627

CYCLOGENESIS

Analysis of ocean and atmosphere thermodynamical characteristics during the onset of southwest monsoon over the Arabian Sea p 57 N82-23945

D

DAMAGE ASSESSMENT

Detection and damage assessment of citrus tree losses with aerial color infrared photography /ACIR/ p 7 A82-29538

DATA ACQUISITION

Application of satellite magnetic anomaly data to Curie isotherm mapping p 70 A82-35824

Source assessment system [AD-A111223] p 75 N82-25613

SMS/GOES data collection platform system p 75 N82-26027

DATA BASE MANAGEMENT SYSTEMS

Source assessment system [AD-A111223] p 75 N82-25613

DATA BASES

A tentative ordering of all available solar energetic particles abundance observations. I - The mass unbiased baseline. II - Discussion and comparison with coronal abundances p 40 A82-22609

Description of historical crop calendar data bases developed to support foreign commodity production forecasting project experiments [E82-10209] p 12 N82-23582

Matrix data analysis: Color/B and W coding is not always enough [AD-A111401] p 74 N82-25612

Key Issues in the Analysis of Remote Sensing Data: A report on the workshop [E82-10348] p 85 N82-26746

Exploration into technical procedures for vertical integration --- information systems [NASA-CR-166352] p 75 N82-26763

DATA COLLECTION PLATFORMS

The METEOSAT Data Collection System and its application p 75 N82-26037

DATA CONVERSION ROUTINES

MAGSAT for geomagnetic studies over Indian region [E82-10202] p 72 N82-23575

MAGSAT for geomagnetic studies over Indian region [E82-10296] p 73 N82-24572

DATA CORRELATION

Comparison data for Seasat altimetry in the western North Atlantic p 50 A82-29611

Preliminary evidence for the influence of physiography and scale upon the autocorrelation function of remotely sensed data p 67 A82-32343

Irrigation management with remote sensing --- Navajo Indian Irrigation Project [E82-10357] p 20 N82-26755

DATA LINKS

An optical data link for airborne scanning system p 80 A82-34737

DATA PROCESSING

The processing of satellite navigation data for marine geodesy p 34 A82-37175

Advanced technology for earth observation - Data processing [AAS PAPER 82-130] p 71 A82-37810

Ten-Ecosystem Study --- Grand and Weld Counties, Colorado; Warren County, Pennsylvania; St. Louis County, Minnesota; Sandoval County, New Mexico; Kershaw County, South Carolina; Fort Yukon, Alaska; Grays Harbor County, Washington; and Washington County, Missouri. [E82-10186] p 84 N82-22620

Use of NOAA/AVHRR visible and near-infrared data for land remote sensing [NASA-TM-84186] p 81 N82-22643

MAGSAT science investigations [E82-10199] p 71 N82-23572

Bathymetric and tectonics of Indian Ocean using MAGSAT data [E82-10204] p 36 N82-23577

AgRISTARS: Foreign commodity production forecasting. The 1980 US corn and soybeans exploratory experiment [E82-10206] p 11 N82-23579

Multistage classification of multispectral Earth observational data: The design approach [E82-10213] p 72 N82-23586

AgRISTARS. Project management report: Program review presentation to level 1, interagency coordination committee [E82-10219] p 13 N82-23592

An algorithm for automating the registration of USDA segment ground data to LANDSAT MSS data [E82-10286] p 16 N82-24564

Investigation of the effects of external current systems on the MAGSAT data utilizing grid cell modeling techniques [E82-10306] p 74 N82-24580

MAGSAT scalar and vector anomaly data analysis [E82-10307] p 74 N82-24581

An investigation of MAGSAT and complementary data emphasizing precambrian shields and adjacent areas of West Africa and South America [E82-10317] p 38 N82-24590

An investigation of MAGSAT and complementary data emphasizing precambrian shields and adjacent areas of West Africa and South America [E82-10318] p 38 N82-24591

Investigations of medium wavelength magnetic anomalies in the eastern Pacific using MAGSAT data [E82-10330] p 38 N82-24603

Aeromagnetic and satellite magnetic anomally mapping [E82-10339] p 39 N82-25601

Interactive initialization of heat flux parameters for numerical models using satellite temperature measurements [E82-10313] p 82 N82-26743

Measurement of soil moisture trends with airborne scatterometers --- Guymon, Oklahoma and Dalhart, Texas [E82-10361] p 20 N82-26759

DATA REDUCTION

The use of prior probabilities in maximum likelihood classification of remotely sensed data p 68 A82-32904

Studies of high latitude current systems using MAGSAT vector data [E82-10188] p 71 N82-22622

MAGSAT and aeromagnetic data in the North American continent [E82-10193] p 71 N82-22627

Investigation of the effects of external current systems on the MAGSAT data utilizing grid cell modeling techniques [E82-10195] p 71 N82-22629

LANDSAT technology transfer to the private and public sectors through community colleges and other locally available institutions [E82-10181] p 85 N82-23568

Investigation of MAGSAT and TRIAD magnetometer data to provide corrective information on high-latitude external fields [E82-10201] p 72 N82-23574

Investigation of the effects of external current systems on the MAGSAT data utilizing grid cell modeling techniques [E82-10226] p 73 N82-23599

Report of MAGSAT project by Survey of India [E82-10293] p 73 N82-24570

Analysis of MAGSAT data of the Indian region [E82-10358] p 75 N82-26756

DATA SAMPLING

Sample design for estimating change in land use and land cover p 24 A82-32711

Measurement of soil moisture trends with airborne scatterometers --- Guymon, Oklahoma and Dalhart, Texas [E82-10361] p 20 N82-26759

DATA SMOOTHING

Improved definition of crustal magnetic anomalies for MAGSAT data [E82-10314] p 37 N82-24587

DATA SYSTEMS

Design guidelines for satellite image data distribution systems p 70 A82-37048

AgRISTARS. Project management report: Program review presentation to level 1, interagency coordination committee --- Brazil, Argentina, U.S. corn belt, Great Plains Corridor [E82-10231] p 15 N82-23604

DATA TRANSMISSION

Purpose, background of 'Intercosmos-21' mission p 81 N82-24264

DEATH VALLEY (CA)

Possible fault detection in Cottonball Basin, California An application of radar remote sensing p 41 A82-32898

DEER

Application of remote sensing to state and regional problems [E82-10288] p 30 N82-24566

DEFOLIATION

Defining the temporal window for monitoring forest canopy defoliation using Landsat p 9 A82-34730

DEFORESTATION

Monitoring deforestation in the eastern part of the state of Guerrero, Mexico p 9 A82-34733

DEHYDRATION

Remote sensing of leaf water content in the near infrared p 8 A82-32897

DELINEATION

Status and prospects of the automated processing of remote-sensing data /using forest surveys as an example/ p 10 A82-35139

DENSITY (NUMBER/VOLUME)

OSO-8 lower mesospheric ozone number density profiles p 28 A82-36472

DENSITY DISTRIBUTION

Description of gray level picture using a collection of density contour lines p 66 A82-29409

Information theory lateral density distribution for earth inferred from global gravity field p 35 A82-37962

DEPOSITS
Evaluation and combined geophysical interpretations of NURE and related geoscience data in the Van Horn, Pecos, Marfa, Fort Stockton, Presidio, and Emory Peak quadrangels, Texas [DE82-005560] p 46 N82-27809

DESERTS
Desert locust habitat monitoring with satellite remote sensing A new technology for an old problem p 7 A82-29747
Resource inventory techniques used in the California Desert Conservation Area p 23 A82-32441

DIFFRACTION LIMITED CAMERAS
Inversion of data from diffraction-limited multiwavelength remote sensors. II - Nonlinear dependence of observables on the geophysical parameters p 77 A82-32658

DIFFUSE RADIATION
Large amplitude undulations on the equatorward boundary of the diffuse aurora p 76 A82-31019

DIGITAL DATA
Detection of regional air pollution episodes utilizing satellite digital data in the visual range p 23 A82-31990
Computation with physical values from Landsat digital data p 68 A82-32709
Use of NOAA/AVHRR visible and near-infrared data for land remote sensing [NASA-TM-84186] p 81 N82-22643
Computer-processed geophysical atlas of digital data for the East Coast margin of the United States from surface and spacecraft data [AD-A111388] p 39 N82-25748
Detection of variations in aspen forest habitat from LANDSAT digital data: Bear River Range, Utah [E82-10355] p 19 N82-26753

DIGITAL FILTERS
Matrix data analysis: Color/B and W coding is not always enough [AD-A111401] p 74 N82-25612

DIGITAL RADAR SYSTEMS
The estimation of wave height from digitally processed SAR imagery p 67 A82-32347

DIGITAL SYSTEMS
Separation of diffuse from sharp-edged features in digital imagery p 68 A82-34225

DIGITAL TECHNIQUES
Mapping riparian vegetation in Southeastern Oregon using digitized large scale color infra-red aerial photography p 6 A82-29535
Digitally enhanced visual displays facilitate the analysis of Landsat imagery p 67 A82-32507
The response characteristics of vegetation in Landsat MSS digital data p 8 A82-32907
Image processing with microcomputers in remote sensing p 79 A82-34708
Terrain classification by Fourier analysis - Accuracy and economy p 69 A82-34723
Aerial photography vs. Landsat for digital land-cover mapping in an urban watershed p 61 A82-34745
Matrix data analysis: Color/B and W coding is not always enough [AD-A111401] p 74 N82-25612
Key Issues in the Analysis of Remote Sensing Data: A report on the workshop [E82-10348] p 85 N82-26746

DISCONTINUITY
Satellite observations in FRONTS 80 [AD-A111080] p 58 N82-26766

DISPLAY DEVICES
Source assessment system [AD-A111223] p 75 N82-25613

DIURNAL VARIATIONS
Observation of the diurnal variation of atmospheric ozone p 26 A82-35895
Diurnal changes in reflectance factor due to Sun-row direction interactions [E82-10128] p 11 N82-23566
Registration of Heat Capacity Mapping Mission day and night images [E82-10210] p 72 N82-23583
Application of HCMM data to regional geologic analysis for mineral and energy resource evaluation [E82-10243] p 45 N82-24521
Delineation of soil temperature regimes from HCMM data [E82-10298] p 17 N82-24574
Magnetic and gravity anomalies in the Americas [E82-10312] p 37 N82-24586
Multidisciplinary investigations on HCMM data over middle Europe and Marocco --- southern Germany and Marrakesh, Morocco [E82-10315] p 74 N82-24588
HCMM hydrological analysis in Utah [E82-10328] p 63 N82-24601
Comparison of storm-time changes of geomagnetic field at ground and MAGSAT altitudes [E82-10359] p 30 N82-26757

DRAINAGE
The application of Heat Capacity Mapping Mission (HCMM) thermal data to snow hydrology --- Salt Verde Watershed and the southern Sierra Nevada [E82-10191] p 62 N82-22625

DRAINAGE PATTERNS
Dynamic study of the upper Sao Francisco river and Tres Marias reservoir using MSS/LANDSAT images --- BRazil [E82-10291] p 63 N82-24569

DROUGHT
Remote sensing of leaf water content in the near infrared p 8 A82-32897

DYNAMIC CHARACTERISTICS
Sea-Ice Mission Requirements for the US FIREX and Canada RADARSAT programs [NASA-CR-168984] p 57 N82-25609

DYNAMIC MODELS
Impact of additional summer MONEX wind data on the prediction of monsoon depressions during June - August 1979 with two versions of primitive equation (PE) barotropic model --- Monsoon Experiment (MONEX) p 56 N82-23900

E

E REGION
Characteristics of field-aligned E-region irregularities over lioka /36 N/, Japan. I p 26 A82-36268

EARTH (PLANET)
Reference coordinate systems for earth dynamics - A preview p 33 A82-32077
Some considerations in the use of very-long-baseline-interferometry to establish reference coordinate systems for geodynamics p 34 A82-32096
MAGSAT anomaly map and continental drift [E82-10326] p 38 N82-24599
Models and maps of the main field [E82-10327] p 74 N82-24600

EARTH ALBEDO
Albedo and angular characteristics of the reflectance of the underlying surface and clouds --- Russian book p 33 A82-30849
System albedo as sensed by satellites - Its definition and variability p 23 A82-32342
Comparison of satellite derived radiation budget measurements over MONEX during 1979 to 1980 --- Monsoon Experiment (MONEX) p 29 N82-23891

EARTH ATMOSPHERE
Soft X-rays from the sunlit earth's atmosphere p 29 A82-37405

EARTH CORE
Information theory lateral density distribution for earth inferred from global gravity field p 35 A82-37962
Investigation of geomagnetic field forecasting and fluid dynamics of the core --- determination of the bundary between the core and mantle of the Earth [E82-10198] p 35 N82-23571
Investigation of geomagnetic field forecasting and fluid dynamics of the core [E82-10310] p 37 N82-24584
Investigation of geomagnetic field forecasting and fluid dynamics of the core [E82-10342] p 39 N82-25604

EARTH CRUST
Initial vector magnetic anomaly map from Magsat p 32 A82-30785
Spatial resolution and repeatability of Magsat crustal anomaly data over the Indian Ocean p 32 A82-30788
Verification of the crustal component in satellite magnetic data p 32 A82-30789
Preliminary interpretation of magnetic anomalies over Japan and its surrounding area p 33 A82-30796
Influence of CO2 on melting of model granulite facies assemblages - A model for the genesis of charnockites p 42 A82-36298
Information theory lateral density distribution for earth inferred from global gravity field p 35 A82-37962
Structure, composition and thermal state of the crust in Brazil --- geomagnetic survey [E82-10187] p 35 N82-22621
Crustal structures under the active volcanic areas of central and eastern Mediterranean (M-44) [E82-10096] p 35 N82-23563
Equivalent source modeling of the main field using MAGSAT data [E82-10151] p 71 N82-23567
Spherical-Earth gravity and magnetic anomaly modeling by Gauss-Legendre quadrature integration [E82-10242] p 36 N82-24520
An equivalent layer magnetization model for the United States derived from MAGSAT data [E82-10297] p 36 N82-24573
Analyzing the Broken Ridge area of the Indian Ocean using magnetic and gravity anomaly maps and geoid undulation and bathymetry data [E82-10303] p 36 N82-24577
Investigating tectonic and bathymetric features of the Indian Ocean using MAGSAT magnetic anomaly data [E82-10304] p 37 N82-24578
Investigation of Antarctic crust and upper mantle using MAGSAT and other geophysical data [E82-10308] p 37 N82-24582
Investigation of Antarctic crust and upper mantle using MAGSAT and other geophysical data [E82-10309] p 37 N82-24583
Magnetic and gravity anomalies in the Americas [E82-10312] p 37 N82-24586
The crustal structure and tectonics of South America [E82-10319] p 38 N82-24592
Use of MAGSAT anomaly data for crustal structure and mineral resources in the US Midcontinent [E82-10321] p 46 N82-24594
Report of investigation from Japanese MAGSAT Team [E82-10322] p 74 N82-24595
Use of MAGSAT anomaly data for crustal structure and mineral resources in the US Midcontinent [E82-10323] p 46 N82-24596
MAGSAT anomaly map and continental drift [E82-10326] p 38 N82-24599
Investigations of medium wavelength magnetic anomalies in the eastern Pacific using MAGSAT data [E82-10330] p 38 N82-24603
Seismic and geodetic studies of the Imperial Valley, California [DE82-001686] p 39 N82-26915

EARTH MANTLE
Information theory lateral density distribution for earth inferred from global gravity field p 35 A82-37962
Investigation of geomagnetic field forecasting and fluid dynamics of the core --- determination of the bundary between the core and mantle of the Earth [E82-10198] p 35 N82-23571
Investigation of Antarctic crust and upper mantle using MAGSAT and other geophysical data [E82-10308] p 37 N82-24582
Investigation of Antarctic crust and upper mantle using MAGSAT and other geophysical data [E82-10309] p 37 N82-24583

EARTH MOVEMENTS
Geodetic monitoring of tectonic information. Toward a strategy p 35 N82-22832

EARTH OBSERVATIONS (FROM SPACE)
Space to the earth --- Russian book on space technology applications p 83 A82-30850
The use of the SPOT satellite in natural resource evaluation p 83 A82-31996
Spectroscopic remote sensing for geological applications p 41 A82-32442
Thematic mapper - An overview of spectral band registration p 77 A82-32447
An optical objective lens for earth observations by satellites p 78 A82-32824
Infrared sensing of sea surface temperature from space p 53 A82-32902
Inference of refractivity profiles by satellite-to-ground RF measurements p 78 A82-33442
Remote sensing of the earth's resources - The Soviet experience p 84 A82-33555
Earth observations from space - Trends and prospects p 84 A82-34116
ERS-1 European remote sensing satellite p 84 A82-34367
Microwave sensing from space [AAS PAPER 82-127] p 80 A82-37809
Advanced technology for earth observation - Data processing [AAS PAPER 82-130] p 71 A82-37810
Civil land remote sensing system [GPO-87-070] p 84 N82-22630
Radiometer mission requirements for large space antenna systems [NASA-TM-84478] p 81 N82-25610

EARTH PLANETARY STRUCTURE
The definition of the terrestrial coordinate frame by long baseline interferometry p 33 A82-32084
MAGSAT anomaly map and continental drift [E82-10326] p 38 N82-24599

EARTH RESOURCES
Multi-resource inventory in interior Alaska p 6 A82-29532
The use of the SPOT satellite in natural resource evaluation p 83 A82-31996
Thematic mapper - An overview of spectral band registration p 77 A82-32447

Multispectral mapper - Imaging spectroscopy as applied to the mapping of earth resources p 77 A82-32448
Photogrammetric methods for mapping resource data from high altitude panoramic photography p 77 A82-32702
Aerogeophysical methods of finding uranium deposits --- Russian book p 41 A82-33402
Remote sensing of the earth's resources - The Soviet experience p 84 A82-33555
RAMS-1, a Resource Analysis and Mapping System p 69 A82-34726
Landsat D to yield more precise data p 70 A82-37200
Solid state instrumentation concepts for earth resource observation [AAS PAPER 82-132] p 81 A82-37812
LANDSAT D to test thematic mapper, inaugurate operational system [NASA-NEWS-RELEASE-82-100] p 82 N82-26741

EARTH RESOURCES INFORMATION SYSTEM
A new approach to multiresource inventories using remote sensing and geographic information systems technologies p 25 A82-34739

EARTH RESOURCES PROGRAM
An infrared exposure meter p 76 A82-29541
Resource inventory techniques used in the California Desert Conservation Area p 23 A82-32441
High spectral resolution airborne spectrometry p 77 A82-32443
Irrigation management with remote sensing --- Navajo Indian Irrigation Project [E82-10357] p 20 N82-26755

EARTH RESOURCES SHUTTLE IMAGING RADAR
OSTA-1 Post Mission Operation Report [NASA-TM-84191] p 84 N82-23258

EARTH ROTATION
On reference coordinate systems used in polar motion determinations p 33 A82-32090

EARTH SATELLITES
Cost-effectiveness of geographic surveying from space p 85 N82-24263

EARTH SURFACE
Surface temperature determination from an amalgamation of GOES and TIROS-N radiance measurements p 66 A82-28905
Relating Landsat digital count values to ground reflectance for optically thin atmospheric conditions p 66 A82-29762
Albedo and angular characteristics of the reflectance of the underlying surface and clouds --- Russian book p 33 A82-30849
Simplified techniques to study components of solar radiation under haze and clouds p 78 A82-32766
Experimental assessment of improved spatial resolution LANDSAT data [AD-A110538] p 75 N82-26765

EARTH TIDES
Work related to the Blue Road Geotraverse at the Finnish Geodetic Institute p 32 A82-30306

EARTHQUAKES
Geodetic monitoring of tectonic deformation: Toward a strategy [NASA-CR-168784] p 35 N82-22846
Seismic and geodetic studies of the Imperial Valley, California [DE82-001686] p 39 N82-26915

ECOLOGY
Landsat digital analysis of the initial recovery of burned tundra at Kokolik River, Alaska p 8 A82-32913
Use and applicability of the vegetation component of the national site classification system --- Sumter National Forest, South Carolina [E82-10234] p 15 N82-23607

ECOSYSTEMS
Agricultural Research Service research highlights in remote sensing for calendar year 1980 [E82-10228] p 14 N82-23601

ELECTRIC CURRENT
Studies of high latitude current systems using MAGSAT vector data [E82-10188] p 71 N82-22622
Investigation from Japanese MAGSAT team [E82-10239] p 73 N82-23612
Investigation of Antarctic crust and upper mantle using MAGSAT and other geophysical data [E82-10309] p 37 N82-24583
Report of investigation from Japanese MAGSAT Team [E82-10322] p 74 N82-24595

ELECTRIC FIELDS
Generation of the auroral kilometric radiation p 26 A82-35542

ELECTROMAGNETIC FIELDS
Astrophysical scenarios for critically evaluating a zero-point field acceleration mechanism p 64 A82-22575

ELECTROMAGNETIC SHIELDING
Effective electromagnetic shielding in multilayer printed circuit boards [AIAA 81-2333] p 59 A82-13528

ELECTRON DIFFUSION
Convective outflow of cosmic rays from the Galaxy and background radio emission p 83 A82-22551

ELECTRON ENERGY
The electron and positron spectra in primary cosmic rays p 1 A82-22543
Generation of the auroral kilometric radiation p 26 A82-35542

ELECTRON FLUX DENSITY
The model of the cosmic ray enrichment by helium-3 p 31 A82-22614

ELECTROPHOTOMETERS
Optical stop and focussing effects in the Dobson instrument p 28 A82-36428

ELEMENTARY PARTICLE INTERACTIONS
Measurement of cosmogenic nuclides using a multi-crystal gamma-ray coincidence spectrometer --- for Mayo Belwa meteorite study p 64 A82-22577

EMISSION SPECTRA
The cosmic ray positron spectrum p 1 A82-22542
Consequences of an inverse Compton emission model for extragalactic X-ray sources p 83 A82-22553
Stratospheric emission data analysis [AD-A112337] p 76 N82-26907

EMISSIVITY
Derivation of the distribution of synchrotron emissivity in the Galaxy from the 408 MHz all-sky survey p 82 A82-22549
Emissivity and reflectance of the model sea surface for the use of AVHRR data of NOAA satellites p 52 A82-31294
Remote sensing of thermal subsurface terrain properties p 80 A82-34727

ENERGETIC PARTICLES
Comparative abundances in solar energetic particles and in galactic cosmic ray sources, and the Ne-22 anomaly p 83 A82-22556
Acceleration of cosmic rays in accretion shocks p 64 A82-22568
Observations of interplanetary energetic charged particles from gamma-ray line solar flares p 65 A82-22586
High-energy solar protons p 22 A82-22588
The relation of type II radio bursts to solar energetic particles observed at earth p 3 A82-22591
Energetic solar particle spectra according to Venera-11, 12 and Prognoz-5, 6 p 4 A82-22593
Evolution of the solar proton spectrum in interplanetary space p 4 A82-22594
Spacecraft determination of energetic particle propagation parameters - The 1 January 1978 solar event p 31 A82-22598
Time and energy dependence of heavy ion abundances in solar flare energetic particle events p 22 A82-22605
High resolution measurements of solar flare isotopes p 22 A82-22606
Observations of the ionization states of energetic particles accelerated in solar flares p 40 A82-22607
Is the neon composition of our sun, planetary or solar p 76 A82-22608
A tentative ordering of all available solar energetic particles abundance observations. I - The mass unbiased baseline. II - Discussion and comparison with coronal abundances p 40 A82-22609
On the anticorrelation between the He/3//He/4/ ratio and proton intensity in He/3/ rich flares p 40 A82-22613

ENERGY BUDGETS
Ammonia and the NOx budget of the troposphere p 27 A82-36293

ENERGY DISSIPATION
Steady-state cosmic ray electron spectrum under diffusion, convection, adiabatic deceleration and synchrotron losses p 1 A82-22552
Coulombian energy losses and the nuclear composition of the solar cosmic rays p 4 A82-22610

ENERGY SPECTRA
On the characteristics of the very low energy galactic cosmic rays in the interstellar space p 63 A82-22540
The electron and positron spectra in primary cosmic rays p 1 A82-22543
Dependence of earth spectrum of positrons and antiprotons on propagation models --- of cosmic radiation p 21 A82-22545
Extragalactic cosmic rays, their sources and spectrum p 40 A82-22574
Model for solar hard X-ray bursts p 65 A82-22581
Computer simulation of the time dependence of the photon energy spectra produced in proton and electron bremstrahlung p 3 A82-22587
A survey of solar protons and alpha differential spectra between 1 and greater than 400 MeV/nucleon p 4 A82-22592
Energetic solar particle spectra according to Venera-11, 12 and Prognoz-5, 6 p 4 A82-22593
Evolution of the solar proton spectrum in interplanetary space p 4 A82-22594
Preflare increases in solar cosmic rays relevant to the mode of energy accumulation in the active regions associated with large flares p 31 A82-22595
A comparison of helium and heavy ion spectra in He/3/ rich solar flares with a model calculation p 5 A82-22612
11-year modulation and spectrum of cosmic rays in the interstellar space p 22 A82-22616
The energy spectra of cosmic ray variations inferred from the stratospheric measurements in 1972-1979 p 5 A82-22617

ENTHALPY
Analysis of ocean and atmosphere thermodynamical characteristics during the onset of southwest monsoon over the Arabian Sea p 57 N82-23945

ENVIRONMENT EFFECTS
Landsat digital analysis of the initial recovery of burned tundra at Kokolik River, Alaska p 8 A82-32913

ENVIRONMENT POLLUTION
Environmental monitoring report of the Lawrence Berkeley Laboratory, 1980 [LBL-12604] p 29 N82-23793

ENVIRONMENTAL MONITORING
Detection of environmental disturbance using color aerial photography and thermal infrared imagery p 22 A82-29327
Desert locust habitat monitoring with satellite remote sensing A new technology for an old problem p 7 A82-29747
Aircraft monitoring of surface carbon dioxide exchange p 23 A82-30293
EPA's new bubble and banking policies --- for environmental monitoring p 25 A82-33865
Defining the temporal window for monitoring forest canopy defoliation using Landsat p 9 A82-34730
Monitoring deforestation in the eastern part of the state of Guerrero, Mexico p 9 A82-34733
Space science for applications - The history of Landsat p 84 A82-36617
Environmental monitoring report of the Lawrence Berkeley Laboratory, 1980 [LBL-12604] p 29 N82-23793
History of the French satellite space program p 85 N82-24216

ENVIRONMENTAL RESEARCH SATELLITES
ERS-1 European remote sensing satellite p 84 A82-34367

EQUATORIAL ELECTROJET
MAGSAT for geomagnetic studies over Indian region [E82-10296] p 73 N82-24572

EQUATORIAL REGIONS
Comparison of storm-time changes of geomagnetic field at ground and at MAGSAT altitudes, part 2 [E82-10325] p 30 N82-24598

ERROR ANALYSIS
Seasat altimeter timing bias estimation p 50 A82-29609
Evaluation of the Seasat altimeter time tag bias p 50 A82-29610
A practical study of gross-error detection in bundle adjustment p 69 A82-34702
A quantitative method to test for similarity between photo interpreters p 69 A82-34722
Dobson spectrophotometer calibrations, possible errors in ozone absorption coefficients, and errors due to interfering pollutant gases p 28 A82-36431

ERS-1 (ESA SATELLITE)
ERS-1 European remote sensing satellite p 84 A82-34367

ESTIMATES
Determination of the optimal level for combining area and yield estimates [E82-10215] p 12 N82-23588
AgRISTARS. Preliminary technical results review of FY81 experiments, volume 2: Fiscal year 1981/1982 'corn and soybeans pilot' experiment [E82-10216] p 13 N82-23589

ESTIMATING
Sample design for estimating change in land use and land cover p 24 A82-32711
A statistical approach to rainfall estimation using satellite and conventional data [NOAA-TR-NESS-89] p 63 N82-22854
A comparison of stratified versus regression estimators p 11 N82-23133

ESTUARIES
Remote sensing in Scotland using data received from satellites - A study of the Tay Estuary region using Landsat multispectral scanning imagery p 62 A82-37501

EUROPE
Crustal structures under the active volcanic areas of central and eastern Mediterranean (M-44)
[E82-10096] p 35 N82-23563
Aeromagnetic and satellite magnetic anomally mapping
[E82-10339] p 39 N82-25601

EUROPEAN SPACE AGENCY
ERS-1 European remote sensing satellite
p 84 A82-34367

EVALUATION
LANDSAT-D conical scanner evaluation plan
[E82-10340] p 81 N82-25602

EVAPORATION
A method for inferring available surface moisture using remote surface temperature measurements: An assessment --- Kansas and St. Louis, Missouri
[E82-10311] p 17 N82-24585

EVAPORATION RATE
Application of thermal model for pan evaporation to the hydrology of a defined medium, the sponge
[E82-10217] p 13 N82-23590

EVAPOTRANSPIRATION
Application of thermal model for pan evaporation to the hydrology of a defined medium, the sponge
[E82-10217] p 13 N82-23590
AgRISTARS: Early warning and crop condition assessment. Plant cover, soil temperature, freeze, water stress, and evapotranspiration conditions
[E82-10225] p 14 N82-23598

EXPERIMENTAL DESIGN
The impact of meteorological satellites on the First GARP Global Experiment (FGGE) --- First Global Atmospheric Research Program Global Experiment (FGGE) p 55 N82-23852

EXPLORATION
Airborne gamma-ray spectrometer and magnetometer survey. Devil's Lake quadrangle, North Dakota, volume 1
[DE82-004161] p 44 N82-23635

EXTRAGALACTIC RADIO SOURCES
Consequences of an inverse Compton emission model for extragalactic X-ray sources p 83 A82-22553

F

FAR INFRARED RADIATION
Thermography - A remote sensing method with many perspectives p 76 A82-29922

FARM CROPS
Remote sensing of the weediness of crop fields
p 5 A82-29435
Spectral properties of agricultural crops and soils measured from space, aerial, field, and laboratory sensors
[E82-10189] p 10 N82-22623
Analysis of scanner data for crop inventories
[E82-10192] p 10 N82-22626
Spectral properties of agricultural crops and soils measured from space, aerial, field, and laboratory sensors
[E82-10212] p 12 N82-23585
Application of thermal model for pan evaporation to the hydrology of a defined medium, the sponge
[E82-10217] p 13 N82-23590
AgRISTARS. Project management report: Program review presentation to level 1, interagency coordination committee
[E82-10219] p 13 N82-23592

FARMLANDS
Thermal mapping, geothermal source location, natural effluents and plant stress in the Mediterranean coast of Spain
[E82-10300] p 17 N82-24576
Irrigated acreage in the Bear River Basin as of the 1975 growing season --- Idaho, Utah, and Wyoming
[E82-10356] p 20 N82-26754
Measurement of soil moisture trends with airborne scatterometers --- Guymon, Oklahoma and Dalhart, Texas
[E82-10361] p 20 N82-26759

FELSITE
Influence of CO2 on melting of model granulite facies assemblages - A model for the genesis of charnockites
p 42 A82-36298

FERTILIZERS
Color aerial photography detects nutrient status of loblolly pine plantations p 6 A82-29531

FIELD THEORY (PHYSICS)
Astrophysical scenarios for critically evaluating a zero-point field acceleration mechanism
p 64 A82-22575

FINITE ELEMENT METHOD
Nonlinear theory for elastic beams and rods and its finite element representation
[WTHD-143] p 73 N82-24517

FIRE DAMAGE
Landsat digital analysis of the initial recovery of burned tundra at Kokolik River, Alaska p 8 A82-32913

FIRE PREVENTION
Remote automatic weather station for resource and fire management agencies
[PB82-107335] p 30 N82-23963

FISHERIES
Technology and oceanography: An assessment of Federal technologies for oceanographic research and monitoring. Volume 2: Working papers on fishery research technology p 56 N82-26944

FLAT PATTERNS
Subtleties in the flat-fielding of charge-coupled device /CCD/ images p 68 A82-32581

FLIGHT PATHS
Airborne gamma-ray spectrometer and magnetometer survey. Roseau quadrangle, Minnesota, volume 2
[DE82-001025] p 44 N82-23634

FLORIDA
Use of thermal inertia determined by HCMM to predict nocturnal cold prone areas in Florida --- Everglades agricultural area and the west north central peninsula
[E82-10299] p 17 N82-24575
Forest Resource Information System. Phase 3: System transfer report
[E82-10344] p 18 N82-25606

FLOW MEASUREMENT
Fluid-sediment interactions on beaches and shelves
[AD-A110838] p 59 N82-26948

FLUID DYNAMICS
Investigation of geomagnetic field forecasting and fluid dynamics of the core
[E82-10342] p 39 N82-25604

FLUID FLOW
Fluid-sediment interactions on beaches and shelves
[AD-A110838] p 59 N82-26948

FOCUSING
Optical stop and focussing effects in the Dobson instrument p 28 A82-36428

FOG
Some empirical rules for forecasting fog and status over northern Florida, southern Georgia and adjacent coastal waters
[PB82-154006] p 59 N82-27949

FOLIAGE
Remote sensing of leaf water content in the near infrared p 8 A82-32897
Application of Computer Axial Tomography (CAT) to measuring crop canopy geometry --- corn and soybeans
[E82-10227] p 14 N82-23600

FORBUSH DECREASES
The approximate 1 GeV solar cosmic rays in the Forbush-effect of February 15, 1978 p 40 A82-22604

FORECASTING
AgRISTARS: Foreign commodity production forecasting. The 1980 US corn and soybeans exploratory experiment
[E82-10206] p 11 N82-23579
Determination of the optimal level for combining area and yield estimates
[E82-10215] p 12 N82-23588
AgRISTARS. Preliminary technical results review of FY81 experiments, volume 2: Fiscal year 1981/1982 'corn and soybeans pilot' experiment
[E82-10216] p 13 N82-23589

FOREST MANAGEMENT
Development and application of panoramic aerial photography in forest pest management
p 5 A82-29527
Panoramic aerial photography in forest pest management p 7 A82-32701
Optical bar panoramic photography for planning timber salvage in drought-stressed forests p 7 A82-32705
Landsat detection of hardwood forest clearcuts
p 8 A82-32708
Defining the temporal window for monitoring forest canopy defoliation using Landsat p 9 A82-34730
AgRISTARS: Renewable resources inventory. Land information support system implementation plan and schedule --- San Juan National Forest pilot test
[E82-10224] p 14 N82-23597
Forest Resource Information System. Phase 3: System transfer report
[E82-10344] p 18 N82-25606

FORESTS
Application of 35mm color aerial photography to forest land change detection p 6 A82-29533
Evaluation of spruce-fir forests using small-format photographs p 8 A82-32707
Use of Landsat multispectral scanner data in vegetation mapping of a forested area p 9 A82-34731
Water-balance differentiation of natural complexes on the basis of satellite photographs p 61 A82-35129
Status and prospects of the automated processing of remote-sensing data /using forest surveys as an example/ p 10 A82-35139
Ten-Ecosystem Study --- Grand and Weld Counties, Colorado; Warren County, Pennsylvania; St. Louis County, Minnesota; Sandoval County, New Mexico; Kershaw County, South Carolina; Fort Yukon, Alaska; Grays Harbor County, Washington; and Washington County, Missouri.
[E82-10186] p 84 N82-22620
AgRISTARS: Renewable resources inventory. Land information support system implementation plan and schedule --- San Juan National Forest pilot test
[E82-10224] p 14 N82-23597
Use and applicability of the vegetation component of the national site classification system --- Sumter National Forest, South Carolina
[E82-10234] p 15 N82-23607
An analysis of LANDSAT MSS scene-to-scene registration accuracy
[E82-10285] p 16 N82-24563
Analysis of thematic mapper simulator data acquired during winter season over Pearl River, Mississippi, test site
[E82-10287] p 17 N82-24565
Identifying environmental features for land management decisions --- Utah
[E82-10289] p 30 N82-24567
Detection of variations in aspen forest habitat from LANDSAT digital data: Bear River Range, Utah
[E82-10355] p 19 N82-26753

FOURIER ANALYSIS
Terrain classification by Fourier analysis - Accuracy and economy p 69 A82-34723

FOURIER TRANSFORMATION
Terrain classification by Fourier analysis - Accuracy and economy p 69 A82-34723

FRAGMENTATION
Fragmentation of Fe nuclei on carbon, hydrogen and CH2 targets. I - Individual charge changing and total cross sections. II - Isotopic cross sections --- for interstellar cosmic ray propagation p 63 A82-22538

FRANCE
Spatial thermal radiometry contribution to the Massif Armoricain and the Massif Central France litho-structural study
[E82-10190] p 42 N82-22624

FREEZING
AgRISTARS: Early warning and crop condition assessment. Plant cover, soil temperature, freeze, water stress, and evapotranspiration conditions
[E82-10225] p 14 N82-23598

FRENCH SPACE PROGRAMS
History of the French satellite space program
p 85 N82-24216

FRESH WATER
Ice distribution and winter surface circulation patterns, Kachemak Bay, Alaska
[AD-A110806] p 58 N82-26764

G

GALACTIC NUCLEI
Origin of cosmic rays in galactic centre sources
p 3 A82-22571
Acceleration processes near massive black holes
p 3 A82-22572

GALACTIC RADIATION
On the characteristics of the very low energy galactic cosmic rays in the interstellar space p 63 A82-22540
Dependence of earth spectrum of positrons and antiprotons on propagation models --- of cosmic radiation p 21 A82-22545
Antiprotons from galactic sources of cosmic rays and gamma rays p 82 A82-22546
Confinement and acceleration of cosmic rays in galactic superbubbles p 82 A82-22547
Derivation of the distribution of synchrotron emissivity in the Galaxy from the 408 MHz all-sky survey
p 82 A82-22549
Angular variations of nonthermal radio emission from the Galaxy relevant to the structure of interstellar magnetic field p 83 A82-22550
Comparative abundances in solar energetic particles and in galactic cosmic ray sources, and the Ne-22 anomaly
p 83 A82-22556
Physical state of the birth place of cosmic rays and its implication to the acceleration processes
p 2 A82-22559
On volatility, first ionization potential, and s- and r-processes --- for Galactic cosmic ray sources
p 2 A82-22560
Interstellar grains as seeds for galactic cosmic rays
p 2 A82-22561

Origin of galactic cosmic rays from Ne isotopic composition p 2 A82-22563
The galactic origin of cosmic rays. I
[CONF-810711-1] p 2 A82-22565
Acceleration of cosmic rays in accretion shocks p 64 A82-22568
The galactic origin of cosmic rays. II
[CONF-810711-2] p 64 A82-22573
Extragalactic cosmic rays, their sources and spectrum p 40 A82-22574
International Cosmic Ray Conference, 17th, Paris, France, July 13-25, 1981, Conference Papers. Volume 3 p 65 A82-22580
The approximate 1 GeV solar cosmic rays in the Forbush-effect of February 15, 1978 p 40 A82-22604
The modulation characteristics of the 19th and 20th solar activity cycles p 59 A82-22615

GALACTIC RADIO WAVES
Convective outflow of cosmic rays from the Galaxy and background radio emission p 83 A82-22551

GAMMA RAY ASTRONOMY
Confinement and acceleration of cosmic rays in galactic superbubbles p 82 A82-22547
Origin of cosmic rays in galactic centre sources p 3 A82-22571
Measurement of cosmogenic nuclides using a multi-crystal gamma-ray coincidence spectrometer --- for Mayo Belwa meteorite study p 64 A82-22577
Solar gamma-ray experiment on Astro-A satellite p 21 A82-22583
Unusual properties of particle events associated with solar flare gamma ray events p 65 A82-22585

GAMMA RAY SPECTRA
Interplanetary particle observations associated with solar flare gamma-ray line emission p 3 A82-22584
Observations of interplanetary energetic charged particles from gamma-ray line solar flares p 65 A82-22586
Airborne gamma-ray spectrometer and magnetometer survey. International Falls quadrangle, Minnesota, volume 1
[DE82-004151] p 45 N82-23643
Airborne gamma-ray spectrometer and magnetometer survey. International Falls quadrangle, Minnesota, volume 2
[DE82-004166] p 45 N82-23644
Airborne gamma-ray spectrometer and magnetometer survey: Susanville quadrangle, California, volume 1
[DE82-005538] p 48 N82-27811
Airborne gamma-ray spectrometer and magnetometer survey: Roseburg quadrangle, Oregon, volume 2
[DE82-005568] p 48 N82-27812

GAMMA RAY SPECTROMETERS
Measurement of cosmogenic nuclides using a multi-crystal gamma-ray coincidence spectrometer --- for Mayo Belwa meteorite study p 64 A82-22577
Airborne gamma-ray spectrometer and magnetometer survey. Bemidji quadrangle, Minnesota, volume 1
[DE82-001032] p 44 N82-23637
Airborne gamma-ray spectrometer and magnetometer survey. Bemidji quadrangle, Minnesota, volume 2
[DE82-001026] p 44 N82-23638
Airborne gamma-ray spectrometer and magnetometer survey. Barrow quadranegle, Alaska, volume 2
[DE82-000342] p 46 N82-25623
Airborne gamma-ray spectrometer and magnetometer survey: North/south tieline, volume 1
[DE82-005542] p 47 N82-27804
NURE aerial gamma-ray and magnetic reconnaissance survey of portions of New Mexico, Arizona and Texas. Volume 2: New Mexico-Carlsbad Quadrangle
[DE82-005527] p 48 N82-27810
Airborne gamma-ray spectrometer and magnetometer survey: Huron Quadrangle, South Dakota
[DE82-005540] p 48 N82-27814
Airborne gamma-ray spectrometer and magnetometer survey: Chico Quadrangle, California
[DE82-005543] p 48 N82-27815

GAMMA RAYS
Antiprotons from galactic sources of cosmic rays and gamma rays p 82 A82-22546
Airborne gamma-ray spectrometer and magnetometer survey: North/south tieline, volume 2
[DE82-005570] p 47 N82-27805

GAS DETECTORS
Aircraft monitoring of surface carbon dioxide exchange p 23 A82-30293
Breadboard gas filter correlation spectrometer for atmospheric measurement of hydrazines and nitrogen dioxide
[AD-A110688] p 82 N82-26842

GAS EXCHANGE
Aircraft monitoring of surface carbon dioxide exchange p 23 A82-30293

GAS TRANSPORT
Comparison of ozone in polluted and clean air masses over Lake Michigan p 29 A82-36477

GEOBOTANY
The influence of autocorrelation in signature extraction: An example from a geobotanical investigation of Cotter Basin, Montana
[E82-10341] p 46 N82-25603

GEOCENTRIC COORDINATES
Establishment of terrestrial reference frames by new observational techniques p 33 A82-32078
Origin and scale of coordinate systems in satellite geodesy p 34 A82-32099

GEODESY
Seasat altimeter height calibration --- related to sea surface heights near Bermuda p 49 A82-29603
Gravity model improvement for Seasat p 32 A82-29615
Work related to the Blue Road Geotraverse at the Finnish Geodetic Institute p 32 A82-30306
Reference coordinate systems for earth dynamics - A preview p 33 A82-32077
Geodetic monitoring of tectonic deformation: Toward a strategy
[NASA-CR-168784] p 35 N82-22846

GEODETIC COORDINATES
Origin and scale of coordinate systems in satellite geodesy p 34 A82-32099
Investigations of point transfer p 78 A82-33296
The processing of satellite navigation data for marine geodesy p 34 A82-37175

GEODETIC SURVEYS
Tidal and geodetic observations for the Seasat altimeter calibration experiment p 49 A82-29604
Seasat altimeter timing bias estimation p 50 A82-29609
Establishing geodetic-geodynamic parameters using lunar laser range measurements p 34 A82-33293
The simultaneous employment of geodetic measurements for block adjustments using the method of independent models p 34 A82-33295
Geodetic monitoring of tectonic information. Toward a strategy p 35 N82-22832
Geodetic monitoring of tectonic deformation: Toward a strategy
[NASA-CR-168784] p 35 N82-22846
Seismic and geodetic studies of the Imperial Valley, California
[DE82-001686] p 39 N82-26915

GEODYNAMICS
Establishment of terrestrial reference frames by new observational techniques p 33 A82-32078
Some considerations in the use of very-long-baseline-interferometry to establish reference coordinate systems for geodynamics p 34 A82-32096
Establishing geodetic-geodynamic parameters using lunar laser range measurements p 34 A82-33293
Investigation of geomagnetic field forecasting and fluid dynamics of the core --- determination of the bundary between the core and mantle of the Earth
[E82-10196] p 35 N82-23571

GEOGRAPHY
Impacts of remote sensing on U.S. geography p 24 A82-32899
Exploration into technical procedures for vertical integration --- information systems
[NASA-CR-166352] p 75 N82-26763

GEOIDS
Geoid height-age relation from Seasat altimeter profiles across the Mendocino Fracture Zone p 34 A82-32646

GEOLOGICAL FAULTS
Satellite image interpretation of the eastern Caledonian part of the Blue Road Geotraverse and its geological implications /Nordland, Vasterbotten, Scandinavia/ p 41 A82-30305
Possible fault detection in Cottonball Basin, California An application of radar remote sensing p 41 A82-32898
Comparing lineaments interpreted from Landsat imagery and topographic maps with reported faults in southwest Montana p 34 A82-34719
Structure of the Saint Francois Mountains and surrounding lead belt, S.E. Missouri: Inference from thermal IR and other data sets
[E82-10350] p 39 N82-26748

GEOLOGICAL SURVEYS
Magsat scalar anomaly distribution - The global perspective p 41 A82-30786
Aerogeophysical methods of finding uranium deposits --- Russian book p 41 A82-33402
Satellite and surface geophysical expression of anomalous crustal structure in Kentucky and Tennessee p 34 A82-34918
Airborne gamma-ray spectrometer and magnetometer survey, Kenora quadrangle, Minnesota, volume 1
[DE82-001029] p 43 N82-23625
Airborne gamma-ray spectrometer and magnetometer survey. Roseau quadrangle, Minnesota, volume 2
[DE82-001025] p 44 N82-23634
Airborne gamma-ray spectrometer and magnetometer survey. Devil's Lake quadrangle, North Dakota, volume 1
[DE82-004161] p 44 N82-23635
Airborne gamma-ray spectrometer and magnetometer survey. Devil's Lake quadrangle, North Dakota, volume 2
[DE82-004168] p 44 N82-23636
Airborne gamma-ray spectrometer and magnetometer survey. Hibbing quadrangle, Minnesota, volume 1
[DE82-004159] p 44 N82-23639
Airborne gamma-ray spectrometer and magnetometer survey. Hibbing quadrangle, Minnesota, volume 2
[DE82-004165] p 45 N82-23640
Airborne gamma-ray spectrometer and magnetometer survey. Aberdeen quadrangle, South Dakota, volume 1
[DE82-004152] p 45 N82-23641
Airborne gamma-ray spectrometer and magnetometer survey. Aberdeen quadrangle, South Dakota, volume 2
[DE82-004164] p 45 N82-23642
Application of HCMM data to regional geologic analysis for mineral and energy resource evaluation
[E82-10243] p 45 N82-24521
Use of MAGSAT anomaly data for crustal structure and mineral resources in the US Midcontinent
[E82-10321] p 46 N82-24594
Use of MAGSAT anomaly data for crustal structure and mineral resources in the US Midcontinent
[E82-10323] p 46 N82-24596
Airborne gamma-ray spectrometer and magnetometer survey. Barrow quadranagle, Alaska, volume 2
[DE82-000342] p 46 N82-25623
An investigation into the utilization of HCMM thermal data for the discrimination of volcanic and Eolian geological units --- Newberry Volcano, Oregon
[E82-10352] p 47 N82-26750
Airborne gamma-ray spectrometer and magnetometer survey: North/south tieline, volume 1
[DE82-005542] p 47 N82-27804
Airborne gamma-ray spectrometer and magnetometer survey: Susanville quadrangle, California, volume 1
[DE82-005538] p 48 N82-27811

GEOLOGY
Geodetic monitoring of tectonic deformation: Toward a strategy
[NASA-CR-168784] p 35 N82-22846

GEOMAGNETIC HOLLOW
Satellite and surface geophysical expression of anomalous crustal structure in Kentucky and Tennessee p 34 A82-34918

GEOMAGNETISM
Regional geological, tectonic and geophysical features of Nordland, Norway p 41 A82-30304
Magnetic charts of Canada derived from Magsat data p 32 A82-30778
Initial scalar magnetic anomaly map from Magsat p 32 A82-30784
Initial vector magnetic anomaly map from Magsat p 32 A82-30785
Magsat scalar anomaly distribution - The global perspective p 41 A82-30786
Magsat magnetic anomalies over Antarctica and the surrounding oceans p 32 A82-30787
Spatial resolution and repeatability of Magsat crustal anomaly data over the Indian Ocean p 32 A82-30788
Verification of the crustal component in satellite magnetic data p 32 A82-30789
A preliminary comparison of the Magsat data and aeromagnetic data in the continental U.S. p 32 A82-30790
A satellite magnetic model of northeastern South American aulacogens p 33 A82-30795
Preliminary interpretation of magnetic anomalies over Japan and its surrounding area p 33 A82-30796
Observed magnetic substorm signatures at synchronous altitude p 26 A82-35534
Structure, composition and thermal state of the crust in Brazil --- geomagnetic survey
[E82-10187] p 35 N82-22621
Studies of high latitude current systems using MAGSAT vector data
[E82-10188] p 71 N82-22622
MAGSAT and aeromagnetic data in the North American continent
[E82-10193] p 71 N82-22627
Study of gravity and magnetic anomalies using MAGSAT data
[E82-10194] p 35 N82-22628
Equivalent source modeling of the main field using MAGSAT data
[E82-10151] p 71 N82-23567

Characterization of the structure and tectonic of South America
[E82-10196] p 42 N82-23569

Analyses of MAGSAT tracks crossing the study region in the Indian Ocean
[E82-10197] p 71 N82-23570

Investigation of geomagnetic field forecasting and fluid dynamics of the core --- determination of the bundary between the core and mantle of the Earth
[E82-10198] p 35 N82-23571

MAGSAT science investigations
[E82-10199] p 71 N82-23572

Investigation of MAGSAT and TRIAD magnetometer data to provide corrective information on high-latitude external fields
[E82-10201] p 72 N82-23574

MAGSAT for geomagnetic studies over Indian region
[E82-10202] p 72 N82-23575

Spherical harmonic representation of the main geomagnetic field for world charting and investigations of some fundamental problems of physics and geophysics
[E82-10203] p 72 N82-23576

Investigation of the effects of external current systems on the MAGSAT data utilizing grid cell modeling techniques
[E82-10226] p 73 N82-23599

Investigation of the effects of external current systems on the MAGSAT data utilizing grid cell modeling techniques
[E82-10232] p 73 N82-23605

Investigation from Japanese MAGSAT team
[E82-10239] p 73 N82-23612

Investigations of medium wavelength magnetic anomalies in the eastern Pacific using MAGSAT
[E82-10240] p 73 N82-23613

Airborne gamma-ray spectrometer and magnetometer survey. Devil's Lake quadrangle, North Dakota, volume 1
[DE82-004161] p 44 N82-23635

Airborne gamma-ray spectrometer and magnetometer survey. Devil's Lake quadrangle, North Dakota, volume 2
[DE82-004166] p 44 N82-23636

Airborne gamma-ray spectrometer and magnetometer survey. Bemidji quadrangle, Minnesota, volume 1
[DE82-001032] p 44 N82-23637

Spherical-Earth gravity and magnetic anomaly modeling by Gauss-Legendre quadrature integration
[E82-10242] p 36 N82-24520

Investigation from Japanese MAGSAT Team. Part A. Crustal structure near Japan and in Antarctic station. Part B. Electric currents and hydromagnetic waves in the ionosphere and the magnetosphere
[E82-10244] p 36 N82-24522

Report of MAGSAT project by Survey of India
[E82-10293] p 73 N82-24570

MAGSAT for geomagnetic studies over Indian region
[E82-10296] p 73 N82-24572

An equivalent layer magnetization model for the United States derived from MAGSAT data
[E82-10297] p 36 N82-24573

Investigation of the effects of external current systems on the MAGSAT data utilizing grid cell modeling techniques
[E82-10306] p 74 N82-24580

MAGSAT scalar and vector anomaly data analysis
[E82-10307] p 74 N82-24581

Investigation of geomagnetic field forecasting and fluid dynamics of the core
[E82-10310] p 37 N82-24584

Magnetic and gravity anomalies in the Americas
[E82-10312] p 37 N82-24586

Improved definition of crustal magnetic anomalies for MAGSAT data
[E82-10314] p 37 N82-24587

An investigation of MAGSAT and complementary data emphasizing precambrian shields and adjacent areas of West Africa and South America
[E82-10316] p 38 N82-24589

An investigation of MAGSAT and complementary data emphasizing precambrian shields and adjacent areas of West Africa and South America
[E82-10317] p 38 N82-24590

An investigation of MAGSAT and complementary data emphasizing precambrian shields and adjacent areas of West Africa and South America
[E82-10318] p 38 N82-24591

Report of investigation from Japanese MAGSAT Team
[E82-10322] p 74 N82-24595

Comparison of storm-time changes of geomagnetic field at ground and at MAGSAT altitudes, part 2
[E82-10325] p 30 N82-24598

MAGSAT anomaly map and continental drift
[E82-10326] p 38 N82-24599

Models and maps of the main field
[E82-10327] p 74 N82-24600

Investigations of medium wavelength magnetic anomalies in the eastern Pacific using MAGSAT data
[E82-10330] p 38 N82-24603

Aeromagnetic and satellite magnetic anomally mapping
[E82-10339] p 39 N82-25601

Investigation of geomagnetic field forecasting and fluid dynamics of the core
[E82-10342] p 39 N82-25604

A comparison of pole positions derived from GPS satellite and Navy navigation satellite observations
[AD-A110765] p 39 N82-26268

Comparison of storm-time changes of geomagnetic field at ground and MAGSAT altitudes
[E82-10359] p 30 N82-26757

The Earth's gravity field to degree and order 180 using SEASAT altimeter data, terrestrial gravity data and other data
[AD-A113098] p 40 N82-27900

GEOMETRIC RECTIFICATION (IMAGERY)

Evaluation of temporal registration of Landsat scenes
p 67 A82-32345

Evaluation of VICAR software capability for land information support system needs --- Elk River quadrangle, Idaho
[E82-10223] p 73 N82-23596

GEOMORPHOLOGY

Preliminary evidence for the influence of physiography and scale upon the autocorrelation function of remotely sensed data p 67 A82-32343

Soufriere Volcano, St. Vincent - Observations of its 1979 eruption from the ground, aircraft, and satellites
p 24 A82-33652

Overseas Geology And Mineral Resources number 56: A geological interpretation of LANDSAT imagery and air photography of Botswana
[OGMR-56] p 42 N82-22636

Analyses of MAGSAT tracks crossing the study region in the Indian Ocean
[E82-10197] p 71 N82-23570

Structure of the Saint Francois Mountains and surrounding lead belt, S.E. Missouri: Inference from thermal IR and other data sets
[E82-10350] p 39 N82-26748

GEOPHYSICAL FLUIDS

Investigation of geomagnetic field forecasting and fluid dynamics of the core
[E82-10342] p 39 N82-25604

GEOPHYSICAL SATELLITES

Satellite and surface geophysical expression of anomalous crustal structure in Kentucky and Tennessee
p 34 A82-34918

GEOPHYSICS

Origin and scale of coordinate systems in satellite geodesy p 34 A82-32099

Inversion of data from diffraction-limited multiwavelength remote sensors. II - Nonlinear dependence of observables on the geophysical parameters p 77 A82-32658

Spherical harmonic representation of the main geomagnetic field for world charting and investigations of some fundamental problems of physics and geophysics
[E82-10203] p 72 N82-23576

Computer-processed geophysical atlas of digital data for the East Coast margin of the United States from surface and spacecraft data
[AD-A111388] p 39 N82-25748

Airborne gamma-ray spectrometer and magnetometer survey: North/south tieline, volume 1
[DE82-005542] p 47 N82-27804

Evaluation and combined geophysical interpretations of NURE and related geoscience data in the Van Horn, Pecos, Marfa, Fort Stockton, Presidido, and Emory Peak quadrangles, Texas, volume 1
[DE82-005554] p 47 N82-27808

Evaluation and combined geophysical interpretations of NURE and related geoscience data in the Van Horn, Pecos, Marfa, Fort Stockton, Presidio, and Emory Peak quadrangels, Texas
[DE82-005560] p 48 N82-27809

NURE aerial gamma-ray and magnetic reconnaissance survey of portions of New Mexico, Arizona and Texas. Volume 2: New Mexico-Carlsbad Quadrangle
[DE82-005527] p 48 N82-27810

Airborne gamma-ray spectrometer and magnetometer survey: Susanville quadrangle, California, volume 1
[DE82-005538] p 48 N82-27811

Airborne gamma-ray spectrometer and magnetometer survey: Huron Quadrangle, South Dakota
[DE82-005540] p 48 N82-27814

Airborne gamma-ray spectrometer and magnetometer survey: Chico Quadrangle, California
[DE82-005543] p 48 N82-27815

GEOS 3 SATELLITE

A search for seamounts in the southern Cook and Austral region p 52 A82-30810

GLACIERS

The use of space photographs in the mapping of glaciers and water bodies p 62 A82-37174

GLINT

The effect of sea-surface Sun glitter on microwave radiometer measurements
[NASA-CR-169083] p 57 N82-26525

GLOBAL ATMOSPHERIC RESEARCH PROGRAM

The impact of meteorological satellites on the First GARP Global Experiment (FGGE) --- First Global Atmospheric Research Program Global Experiment (FGGE) p 55 N82-23852

Mean sea-level pressure in the Southern Hemisphere during the FGGE period --- First Global Atmospheric Research Program Global Experiment (FGGE); buoys
p 55 N82-23856

Comparison of satellite derived radiation budget measurements over MONEX during 1979 to 1980 --- Monsoon Experiment (MONEX) p 29 N82-23891

Short term influence radius of monsoonal overturnings --- First Global Atmospheric Research Program Global Experiment (FGGE) p 56 N82-23898

Impact of additional summer MONEX wind data on the prediction of monsoon depressions during June - August 1979 with two versions of primitive equation (PE) barotropic model --- Monsoon Experiment (MONEX)
p 56 N82-23900

GLOBAL POSITIONING SYSTEM

A comparison of pole positions derived from GPS satellite and Navy navigation satellite observations
[AD-A110765] p 39 N82-26268

GOES SATELLITES

Digital and visual evaluation of GOES and TIROS/NOAA image data for cover type effects on snowfield observations p 60 A82-34735

SMS/GOES data collection platform system
p 75 N82-26027

GOVERNMENT/INDUSTRY RELATIONS

Civil land remote sensing system
[GPO-87-070] p 84 N82-22630

LANDSAT technology transfer to the private and public sectors through community colleges and other locally available institutions
[E82-10181] p 85 N82-23568

GOVERNMENTS

A legislator's guide to LANDSAT
[E82-10290] p 85 N82-24568

GRAINS (FOOD)

Normal crop calendars. Volume 3: The corn and soybean states of Illinois, Indiana, and Iowa
[E82-10221] p 13 N82-23594

Evaluation of the procedure for separating barley from other spring small grains --- North Dakota, South Dakota, Minnesota and Montana
[E82-10230] p 14 N82-23603

AgRISTARS. Project management report: Program review presentation to level 1, interagency coordination committee --- Brazil, Argentina, U.S. corn belt, Great Plains Corridor
[E82-10231] p 15 N82-23604

Description of the FORTRAN implementation of the spring small grains planting date distribution model
[E82-10235] p 15 N82-23608

GRASSLANDS

Ten-Ecosystem Study --- Grand and Weld Counties, Colorado; Warren County, Pennsylvania; St. Louis County, Minnesota; Sandoval County, New Mexico; Kershaw County, South Carolina; Fort Yukon, Alaska; Grays Harbor County, Washington; and Washington County, Missouri.
[E82-10186] p 84 N82-22620

A multi-frequency radiometric measurement of soil moisture content over bare and vegetated fields
[E82-10238] p 16 N82-23611

GRAVIMETRY

Work related to the Blue Road Geotraverse at the Finnish Geodetic Institute p 32 A82-30306

GRAVITATIONAL FIELDS

Gravity model improvement for Seasat
p 32 A82-29615

The Earth's gravity field to degree and order 180 using SEASAT altimeter data, terrestrial gravity data and other data
[AD-A113098] p 40 N82-27900

GRAVITY ANOMALIES

Regional geological, tectonic and geophysical features of Nordland, Norway p 41 A82-30304

Work related to the Blue Road Geotraverse at the Finnish Geodetic Institute p 32 A82-30306

Study of gravity and magnetic anomalies using MAGSAT data
[E82-10194] p 35 N82-22628

Characterization of the structure and tectonic of South America
[E82-10196] p 42 N82-23569

Spherical-Earth gravity and magnetic anomaly modeling by Gauss-Legendre quadrature integration
[E82-10242] p 36 N82-24520
Analyzing the Broken Ridge area of the Indian Ocean using magnetic and gravity anomaly maps and geoid undulation and bathymetry data
[E82-10303] p 36 N82-24577
The mineralogy of global magnetic anomalies --- rock magnetic signatures and MAGSAT geological, and gravity correlations in West Africa
[E82-10305] p 45 N82-24579
Magnetic and gravity anomalies in the Americas
[E82-10312] p 37 N82-24586
Geotectonics of South America --- regional magnetic and gravity anomalies of South America
[E82-10320] p 38 N82-24593
Structure of the Saint Francois Mountains and surrounding lead belt, S.E. Missouri: Inference from thermal IR and other data sets
[E82-10350] p 39 N82-26748
The Earth's gravity field to degree and order 180 using SEASAT altimeter data, terrestrial gravity data and other data
[AD-A113098] p 40 N82-27900

GRAVITY GRADIOMETERS
Evaluation and combined geophysical interpretations of NURE and related geoscience data in the Van Horn, Pecos, Marfa, Fort Stockton, Presidio, and Emory Peak quadrangels, Texas
[DE82-005560] p 48 N82-27809

GRAVITY WAVES
The observation of ocean surface phenomena using imagery from the Seasat synthetic aperture radar - An assessment p 52 A82-29623

GREAT LAKES (NORTH AMERICA)
Airborne gamma-ray spectrometer and magnetometer survey. Bemidji quadrangle, Minnesota, volume 1
[DE82-001032] p 44 N82-23637
Airborne gamma-ray spectrometer and magnetometer survey. Hibbing quadrangle, Minnesota, volume 1
[DE82-004159] p 44 N82-23639
Airborne gamma-ray spectrometer and magnetometer survey. Hibbing quadrangle, Minnesota, volume 2
[DE82-004165] p 45 N82-23640

GREAT PLAINS CORRIDOR (NORTH AMERICA)
AgRISTARS: Foreign commodity production forecasting. The 1980 US/Canada wheat and barley exploratory experiment
[E82-10126] p 11 N82-23565
Evaluation of the procedure for separating barley from other spring small grains --- North Dakota, South Dakota, Minnesota and Montana
[E82-10230] p 14 N82-23603
AgRISTARS. Project management report: Program review presentation to level 1, interagency coordination committee --- Brazil, Argentina, U.S. corn belt, Great Plains Corridor
[E82-10231] p 15 N82-23604

GREAT SALT LAKE (UT)
Mapping of wildlife habitat in Farmington Bay, Utah
[E82-10354] p 19 N82-26752

GREEN WAVE EFFECT
Analysis of scanner data for crop inventories
[E82-10192] p 10 N82-22626

GREENLAND
The METEOSAT Data Collection System and its application p 75 N82-26037

GROUND SPEED
Magnetic anomalies as a reference for ground-speed and map-matching navigation p 32 A82-30314

GROUND TRUTH
Field size, length, and width distributions based on LACIE ground truth data --- large area crop inventory experiment p 8 A82-32909
Measuring sea surface temperature from satellites - A ground truth approach p 54 A82-32917
The use of Landsat-3 thermal data to help differentiate land covers p 25 A82-34218
Method for the analysis of the melting of a firn complex on the basis of aerospace photographs
p 61 A82-35133
Analysis of scanner data for crop inventories
[E82-10192] p 10 N82-22626
SEASAT: A satellite scatterometer illumination times of selected in situ sites
[NASA-TM-83280] p 81 N82-22865
AgRISTARS. Preliminary technical results review of FY81 experiments, volume 2: Fiscal year 1981/1982 'corn and soybeans pilot' experiment
[E82-10216] p 13 N82-23589
An algorithm for automating the registration of USDA segment ground data to LANDSAT MSS data
[E82-10286] p 16 N82-24564
The mineralogy of global magnetic anomalies --- rock magnetic signatures and MAGSAT geological, and gravity correlations in West Africa
[E82-10305] p 45 N82-24579
Irrigation management with remote sensing --- Navajo Indian Irrigation Project
[E82-10357] p 20 N82-26755
Comparison of storm-time changes of geomagnetic field at ground and MAGSAT altitudes
[E82-10359] p 30 N82-26757
Measurement of soil moisture trends with airborne scatterometers --- Guymon, Oklahoma and Dalhart, Texas
[E82-10361] p 20 N82-26759

GROUND WATER
Evaluation of HCMM data for assessing soil moisture and water table depth --- South Dakota
[E82-10329] p 18 N82-24602

GROUND WIND
Surface wind analyses for Seasat p 51 A82-29619

GULF OF MEXICO
A ship and satellite view of hydrographic features in the western Gulf of Mexico p 53 A82-32651

GULF STREAM
Comparison data for Seasat altimetry in the western North Atlantic p 50 A82-29611

H

HABITATS
Inventory of wildlife habitat from color infrared aerial photography for Cobb Island, Virginia p 6 A82-29529
Desert locust habitat monitoring with satellite remote sensing A new technology for an old problem
p 7 A82-29747
A computerized spatial analysis system for assessing wildlife habitat from vegetation maps p 9 A82-34716
Application of remote sensing to state and regional problems
[E82-10288] p 30 N82-24566
Identifying environmental features for land management decisions --- Utah
[E82-10289] p 30 N82-24567
Mapping of wildlife habitat in Farmington Bay, Utah
[E82-10354] p 19 N82-26752
Detection of variations in aspen forest habitat from LANDSAT digital data: Bear River Range, Utah
[E82-10355] p 19 N82-26753

HARMONIC ANALYSIS
Gravity model improvement for Seasat
p 32 A82-29615

HAZE
Simplified techniques to study components of solar radiation under haze and clouds p 78 A82-32766

HEAT FLUX
Interactive initialization of heat flux parameters for numerical models using satellite temperature measurements
[E82-10313] p 82 N82-26743

HEAT ISLANDS
A method for inferring available surface moisture using remote surface temperature measurements: An assessment --- Kansas and St Louis, Missouri
[E82-10311] p 17 N82-24585

HEAT TRANSMISSION
Remote sensing of thermal subsurface terrain properties p 80 A82-34727

HEAVY IONS
Time and energy dependence of heavy ion abundances in solar flare energetic particle events
p 22 A82-22605
A comparison of helium and heavy ion spectra in He/3/ rich solar flares with a model calculation
p 5 A82-22612

HEAVY NUCLEI
Fragmentation of Fe nuclei on carbon, hydrogen and CH2 targets. I - Individual charge changing and total cross sections. II - Isotopic cross sections --- for interstellar cosmic ray propagation p 63 A82-22538
A report on the 'cosmic ray propagation problem'
p 1 A82-22539
Heavy-element abundances in He/3/-rich events
p 5 A82-22611

HELIOSPHERE
Azimuthal propagation of flare particles in the heliosphere p 66 A82-22590

HELIUM ISOTOPES
Heavy-element abundances in He/3/-rich events
p 5 A82-22611
A comparison of helium and heavy ion spectra in He/3/ rich solar flares with a model calculation
p 5 A82-22612
On the anticorrelation between the He/3//He/4/ ratio and proton intensity in He/3/ rich flares
p 40 A82-22613
The model of the cosmic ray enrichment by helium-3
p 31 A82-22614

HIGH ALTITUDE
Estimating mountain pine beetle-killed ponderosa pine over the front range of Colorado with high altitude panoramic photography p 7 A82-32704

HIGH ALTITUDE TESTS
Image quality and height measurement accuracy of serial survey camera imagery from high altitudes
p 78 A82-33297

HIGH ENERGY ELECTRONS
Origin of cosmic rays in galactic centre sources
p 3 A82-22571
A survey of solar protons and alpha differential spectra between 1 and greater than 400 MeV/nucleon
p 4 A82-22592

HIGH RESOLUTION
High spectral resolution airborne spectrometry
p 77 A82-32443
Evaluation of NOAA-AVHRR data for crop assessment --- Advanced Very High Resolution Radiometer
p 8 A82-34179

HIGH TEMPERATURE PLASMAS
Mass per charge ratio in hot plasmas and cosmic ray source composition p 2 A82-22557

HISTOGRAMS
Airborne gamma-ray spectrometer and magnetometer survey. Roseau quadrangle, Minnesota, volume 1
[DE82-001031] p 43 N82-23621
Airborne gamma-ray spectrometer and magnetometer survey. Roseau quadrangle, Minnesota, volume 2
[DE82-001025] p 44 N82-23634
Airborne gamma-ray spectrometer and magnetometer survey. Bemidji quadrangle, Minnesota, volume 2
[DE82-001026] p 44 N82-23638

HISTORIES
Space science for applications - The history of Landsat p 84 A82-36617

HURRICANES
Seasat wind and wave observations of northeast Pacific hurricane Iva, August 13, 1978 p 52 A82-29624

HYDRAZINES
Breadboard gas filter correlation spectrometer for atmospheric measurement of hydrazines and nitrogen dioxide
[AD-A110688] p 82 N82-26642

HYDROCARBONS
Landsat in the search for Appalachian hydrocarbons
p 42 A82-34721

HYDRODYNAMICS
The use of satellite photographs to study snow-cover dynamics and to determine the average water discharge of the Amudarya during a vegetation period
p 61 A82-35132

HYDROGEN ATOMS
Interactions of cosmic rays with molecular clouds
p 82 A82-22548

HYDROGEOLOGY
Spatial thermal radiometry contribution to the Massif Armoricain and the Massif Central France litho-structural study
[E82-10190] p 42 N82-22624

HYDROGRAPHY
A ship and satellite view of hydrographic features in the western Gulf of Mexico p 53 A82-32651
Bias correction procedures for airborne laser hydrography
[PB82-130089] p 63 N82-22644

HYDROLOGY
Automated classification of runoff coefficients from Landsat multispectral data p 60 A82-34734
Study of the hydrological cycle by aerospace methods --- Russian book p 61 A82-35126
Principles and methods of the study of the hydrological cycle on the basis of aerospace data p 61 A82-35127
Water-balance differentiation of natural complexes on the basis of satellite photographs p 61 A82-35129
The possibility of using remote-sensing methods to study the hydrology of elementary watersheds
p 61 A82-35130
The use of space photographs in the mapping of glaciers and water bodies p 62 A82-37174
The application of Heat Capacity Mapping Mission (HCMM) thermal data to snow hydrology --- Salt Verde Watershed and the southern Sierra Nevada
[E82-10191] p 62 N82-22625
Application of thermal model for pan evaporation to the hydrology of a defined medium, the sponge
[E82-10217] p 13 N82-23590
AgRISTARS: Agriculture and resources inventory surveys through aerospace remote sensing
[E82-10236] p 15 N82-23609
HCMM hydrological analysis in Utah
[E82-10328] p 63 N82-24601

Plan of research for integrated soil moisture studies. Recommendations of the Soil Moisture Working Group [NASA-TM-84731] p 18 N82-25608

The METEOSAT Data Collection System and its application p 75 N82-26037

Ice distribution and winter surface circulation patterns, Kachemak Bay, Alaska [AD-A110806] p 58 N82-26764

HYGROSCOPICITY

Application of thermal model for pan evaporation to the hydrology of a defined medium, the sponge [E82-10217] p 13 N82-23590

I

ICE FORMATION

Sea-Ice Mission Requirements for the US FIREX and Canada RADARSAT programs [NASA-CR-168984] p 57 N82-25609

Ice distribution and winter surface circulation patterns, Kachemak Bay, Alaska [AD-A110806] p 58 N82-26764

ICE MAPPING

The use of space photographs in the mapping of glaciers and water bodies p 62 A82-37174

Movement of ice markers measured by satellite ranging [R-240] p 59 N82-27816

ICE REPORTING

Sea-Ice Mission Requirements for the US FIREX and Canada RADARSAT programs [NASA-CR-168984] p 57 N82-25609

IDAHO

Evaluation of VICAR software capability for land-information support system needs --- Elk River quadrangle, Idaho [E82-10223] p 73 N82-23596

Irrigated acreage in the Bear River Basin as of the 1975 growing season --- Idaho, Utah, and Wyoming [E82-10356] p 20 N82-26754

ILLINOIS

Normal crop calendars. Volume 3: The corn and soybean states of Illinois, Indiana, and Iowa [E82-10221] p 13 N82-23594

IMAGE CORRELATORS

Analytical processing of photographs taken by paired cameras p 79 A82-34471

IMAGE ENHANCEMENT

Digitally enhanced visual displays facilitate the analysis of Landsat imagery p 67 A82-32507

Terrain analysis from Landsat using a color TV enhancement system p 68 A82-32911

Separation of diffuse from sharp-edged features in digital imagery p 68 A82-34225

Evaluation of the effectiveness of systematic image distortion compensation p 69 A82-34469

Allowance for the effect of the atmosphere in the processing of satellite remote-sensing images p 70 A82-35141

Structure of the St. Francois Mountains and surrounding lead belt, S. E. Missouri: Inferences from thermal IR and other data sets --- Ozard Plateau and St. Francois Mountains [E82-10205] p 11 N82-23578

IMAGE MOTION COMPENSATION

Evaluation of the effectiveness of systematic image distortion compensation p 69 A82-34469

IMAGE PROCESSING

Development of three-dimensional spatial displays using a geographically based information system p 66 A82-29326

The use of residual images in Landsat image analysis p 66 A82-29328

Description of gray level picture using a collection of density contour lines p 66 A82-29409

Evaluation of temporal registration of Landsat scenes p 67 A82-32345

The estimation of wave height from digitally processed SAR imagery p 67 A82-32347

Inversion of data from diffraction-limited multiwavelength remote sensors. II - Nonlinear dependence of observables on the geophysical parameters p 77 A82-32658

Evaluation of NOAA-AVHRR data for crop assessment --- Advanced Very High Resolution Radiometer p 8 A82-34179

Coastal environment change analysis by Landsat MSS data p 54 A82-34219

Separation of diffuse from sharp-edged features in digital imagery p 68 A82-34225

A practical study of gross-error detection in bundle adjustment p 69 A82-34702

Image processing with microcomputers in remote sensing p 79 A82-34708

An information-theoric spatial transform p 69 A82-34717

Improved land use classification from Landsat and Seasat satellite imagery registered to a common map base p 25 A82-34743

Status and prospects of the automated processing of remote-sensing data /using forest surveys as an example/ p 10 A82-35139

Allowance for the effect of the atmosphere in the processing of satellite remote-sensing images p 70 A82-35141

Design guidelines for satellite image data distribution systems p 70 A82-37048

Ten-Ecosystem Study --- Grand and Weld Counties, Colorado; Warren County, Pennsylvania; St. Louis County, Minnesota; Sandoval County, New Mexico; Kershaw County, South Carolina; Fort Yukon, Alaska; Grays Harbor County, Washington; and Washington County, Missouri. [E82-10186] p 84 N82-22620

Registration of Heat Capacity Mapping Mission day and night images [E82-10210] p 72 N82-23583

Evaluation of VICAR software capability for land information support system needs --- Elk River quadrangle, Idaho [E82-10223] p 73 N82-23596

Application of HCMM data to regional geologic analysis for mineral and energy resource evaluation [E82-10243] p 45 N82-24521

Delineation of soil temperature regimes from HCMM data [E82-10298] p 17 N82-24574

Thermal mapping, geothermal source location, natural effluents and plant stress in the Mediterranean coast of Spain [E82-10300] p 17 N82-24576

Multidisciplinary investigations on HCMM data over middle Europe and Marocco --- southern Germany and Marrakesh, Morocco [E82-10315] p 74 N82-24588

Forest Resource Information System. Phase 3: System transfer report [E82-10344] p 18 N82-25606

Image understanding research [AD-A110746] p 74 N82-25611

Matrix data analysis: Color/B and W coding is not always enough [AD-A111401] p 74 N82-25612

Coordination of stereo image registration and pixel classification [AD-A111307] p 75 N82-25614

Key Issues in the Analysis of Remote Sensing Data: A report on the workshop [E82-10348] p 85 N82-26746

IMAGE RESOLUTION

Appearance of irregular tree canopies in nighttime high-resolution thermal infrared imagery p 68 A82-32916

Image quality and height measurement accuracy of serial survey camera imagery from high altitudes p 78 A82-33297

Spatial resolution requirements for urban studies p 29 A82-37502

Evaluation of the soil moisture prediction accuracy of a space radar using simulation techniques --- Kansas [E82-10351] p 19 N82-26749

IMAGING TECHNIQUES

Imaging spectroscopy; Proceedings of the Seminar, Los Angeles, CA, February 10, 11, 1981 p 77 A82-32440

Subtleties in the flat-fielding of charge-coupled device /CCD/ images p 68 A82-32581

Evaluation of the effectiveness of systematic image distortion compensation p 69 A82-34469

Bathymetric imaging p 69 A82-34720

Comparisons of land cover classifications from selected remote sensing systems p 80 A82-34746

Coordination of stereo image registration and pixel classification [AD-A111307] p 75 N82-25614

INDIA

MAGSAT for geomagnetic studies over Indian region [E82-10202] p 72 N82-23575

On the space-time variability of ocean surface mixed layer characteristics of central and eastern Arabian sea during MONSOON-77 --- global atmospheric research program p 56 N82-23909

Report of MAGSAT project by Survey of India [E82-10293] p 73 N82-24570

MAGSAT for geomagnetic studies over Indian region [E82-10296] p 73 N82-24572

Analysis of MAGSAT data of the Indian region [E82-10358] p 75 N82-26756

INDIAN OCEAN

Spatial resolution and repeatability of Magsat crustal anomaly data over the Indian Ocean p 32 A82-30788

Analyses of MAGSAT tracks crossing the study region in the Indian Ocean [E82-10197] p 71 N82-23570

Bathymetric and tectonics of Indian Ocean using MAGSAT data [E82-10204] p 36 N82-23577

Analyzing the Broken Ridge area of the Indian Ocean using magnetic and gravity anomaly maps and geoid undulation and bathymetry data [E82-10303] p 36 N82-24577

Investigating tectonic and bathymetric features of the Indian Ocean using MAGSAT magnetic anomaly data [E82-10304] p 37 N82-24578

INDIANA

Normal crop calendars. Volume 3: The corn and soybean states of Illinois, Indiana, and Iowa [E82-10221] p 13 N82-23594

INDUSTRIAL AREAS

Site selection and engineering issues for a major industrial complex - Application of image and map interpretation p 25 A82-34711

INDUSTRIAL WASTES

Problems of the interpretation of aerial and satellite images of industrial smoke p 23 A82-30307

INERTIAL COORDINATES

Reference coordinate systems for earth dynamics - A preview p 33 A82-32077

INFESTATION

Development and application of panoramic aerial photography in forest pest management p 5 A82-29527

Remote sensing of Douglas-fir trees newly infested by bark beetles p 6 A82-29536

Estimating bark beetle-killed lodgepole pine with high altitude panoramic photography p 7 A82-32703

Estimating mountain pine beetle-killed ponderosa pine over the front range of Colorado with high altitude panoramic photography p 7 A82-32704

Defining the temporal window for monitoring forest canopy defoliation using Landsat p 9 A82-34730

INFORMATION DISSEMINATION

Design guidelines for satellite image data distribution systems p 70 A82-37048

LANDSAT technology transfer to the private and public sectors through community colleges and other locally available institutions [E82-10181] p 85 N82-23568

INFORMATION SYSTEMS

Cost-effectiveness of geographic surveying from space p 85 N82-24263

Forest Resource Information System. Phase 3: System transfer report [E82-10344] p 18 N82-25606

Exploration into technical procedures for vertical integration --- information systems [NASA-CR-166352] p 75 N82-26763

INFORMATION THEORY

An information-theoric spatial transform p 69 A82-34717

Information theory lateral density distribution for earth inferred from global gravity field p 35 A82-37962

INFRARED DETECTORS

An infrared exposure meter p 76 A82-29541

INFRARED IMAGERY

Detection of environmental disturbance using color aerial photography and thermal infrared imagery p 22 A82-29327

Remote sensing of leaf water content in the near infrared p 8 A82-32897

View angle effects in the radiometric measurement of plant canopy temperatures p 8 A82-32914

Appearance of irregular tree canopies in nighttime high-resolution thermal infrared imagery p 68 A82-32916

Satellite radiation measurements for the retrieval of the vertical temperature profiles p 70 A82-36935

Determination of winter temperature patterns, fronts, and surface currents in the Yellow Sea and East China Sea from satellite imagery p 55 A82-37195

Estimation of the precipitable water from the IR channel of the geostationary satellite p 55 A82-37196

A statistical approach to rainfall estimation using satellite and conventional data [NOAA-TR-NESS-89] p 63 N82-22854

Registration of Heat Capacity Mapping Mission day and night images [E82-10210] p 72 N82-23583

Use of thermal inertia determined by HCMM to predict nocturnal cold prone areas in Florida --- Everglades agricultural area and the west north central peninsula [E82-10299] p 17 N82-24575

INFRARED INSTRUMENTS

Infrared sensing of sea surface temperature from space p 53 A82-32902

INFRARED PHOTOGRAPHY

Color aerial photography in the plant sciences and related fields; Proceedings of the Eighth Biennial Workshop, Luray, VA, April 21-23, 1981 p 5 A82-29526

Thermography - A remote sensing method with many perspectives p 76 A82-29922
Geostationary satellite observations of the April 1979 Soufriere eruptions p 24 A82-33654
Mapping of wildlife habitat in Farmington Bay, Utah [E82-10354] p 19 N82-26752

INFRARED RADAR
Study visit to United States laser technology centers, 1981 [FOA-C-30257-E1] p 81 N82-24489

INFRARED RADIATION
Interannual variations of outgoing IR associated with tropical circulation changes during 1974-1978 p 54 A82-36341
Structure of the Saint Francois Mountains and surrounding lead belt, S.E. Missouri: Inference from thermal IR and other data sets [E82-10350] p 39 N82-26748

INFRARED RADIOMETERS
High spectral resolution airborne spectrometry p 77 A82-32443
Evaluation of the accuracy of water-surface temperature measurement by means of airborne infrared radiometers p 62 A82-35136
OSTA-1 Post Mission Operation Report [NASA-TM-84191] p 84 N82-23258

INFRARED SCANNERS
Remote sensing of tornadic storms from geosynchronous satellite infrared digital data p 23 A82-32348
Longwave infrared observation of urban landscapes p 25 A82-34744
LANDSAT-D conical scanner evaluation plan [E82-10340] p 81 N82-25602

INFRARED SPECTRA
Airborne observed solar elevation and row direction effects on the near-IR/red ratio of cotton [E82-10220] p 13 N82-23593
Development of visible/infrared/microwave agriculture classification and biomass estimation algorithms --- Guyton, Oklahoma and Dalhart, Texas [E82-10363] p 20 N82-26761

INFRARED SPECTROMETERS
Total ozone retrieval from satellite Meteor 28 Fourier spectrometer measurements p 28 A82-36422

INFRARED SPECTROSCOPY
Application of infrared techniques to the study of atmospheric ozone p 27 A82-36414

INSOLATION
Ground support data from July 10 to July 29, 1978, for HCMM thermal satellite data of the Powder River Basin, Wyoming [E82-10211] p 72 N82-23584

INSTRUMENT ERRORS
Sea-state-related altitude errors in the Seasat radar altimeter p 50 A82-29608
Evaluation of the Seasat altimeter time tag bias p 50 A82-29610
Magnetic anomalies as a reference for ground-speed and map-matching navigation p 32 A82-30314
Irradiance measurement errors due to the assumption of a Lambertian reference panel p 79 A82-34222
The effect of the spectral attenuation of UV radiation by aerosol on the total ozone measurements p 27 A82-36406
Optical stop and focussing effects in the Dobson instrument p 28 A82-36428

INSTRUMENT PACKAGES
LANDSAT-D thermal analysis and design support [E82-10346] p 82 N82-26744

INSTRUMENTS
Investigations of point transfer p 78 A82-33296

INTEGRATED CIRCUITS
Image understanding research [AD-A110746] p 74 N82-25611

INTERCOSMOS SATELLITES
Purpose, background of 'Intercosmos-21' mission p 81 N82-24264

INTERGALACTIC MEDIA
Extragalactic cosmic rays, their sources and spectrum p 40 A82-22574
Astrophysical scenarios for critically evaluating a zero-point field acceleration mechanism p 64 A82-22575

INTERPLANETARY MAGNETIC FIELDS
A description of relativistic solar particle propagation p 4 A82-22600
Low-energy particles in interplanetary magnetic field near the sectorial boundary on September 26, 1977 p 4 A82-22602
The influence of the sector structure of interplanetary magnetic field on the solar cosmic ray characteristics p 83 A82-22603

INTERPLANETARY MEDIUM
Time and energy dependence of heavy ion abundances in solar flare energetic particle events p 22 A82-22605

INTERPLANETARY SPACE
Interplanetary particle observations associated with solar flare gamma-ray line emission p 3 A82-22584
Observations of interplanetary energetic charged particles from gamma-ray line solar flares p 65 A82-22586
Evolution of the solar proton spectrum in interplanetary space p 4 A82-22594
Spacecraft determination of energetic particle propagation parameters - The 1 January 1978 solar event p 31 A82-22598
On the physical sense of the constant of solar cosmic ray coronal propagation p 83 A82-22599
Non-flare injection of protons into interplanetary space p 4 A82-22601

INTERSTELLAR MAGNETIC FIELDS
Angular variations of nonthermal radio emission from the Galaxy relevant to the structure of interstellar magnetic field p 83 A82-22550

INTERSTELLAR MATTER
Confinement and acceleration of cosmic rays in galactic superbubbles p 82 A82-22547
Steady-state cosmic ray electron spectrum under diffusion, convection, adiabatic deceleration and synchrotron losses p 1 A82-22552
Interstellar grains as seeds for galactic cosmic rays p 2 A82-22561
On the stellar origin of low energy cosmic rays p 21 A82-22567

INTERSTELLAR RADIATION
The question of short pathlengths in interstellar propagation p 1 A82-22541
The electron and positron spectra in primary cosmic rays p 1 A82-22543

INTERSTELLAR SPACE
On the characteristics of the very low energy galactic cosmic rays in the interstellar space p 63 A82-22540
Remarks on cosmic ray origin p 21 A82-22569
11-year modulation and spectrum of cosmic rays in the interstellar space p 22 A82-22616

INVENTORIES
Multi-resource inventory in interior Alaska p 6 A82-29532
A new approach to multiresource inventories using remote sensing and geographic information systems technologies p 25 A82-34739

INVERSE SCATTERING
Consequences of an inverse Compton emission model for extragalactic X-ray sources p 83 A82-22553

ION EMISSION
Coulombian energy losses and the nuclear composition of the solar cosmic rays p 4 A82-22610

ION IMPLANTATION
Is the neon composition of our sun, planetary or solar p 76 A82-22608

ION MOTION
On the stellar origin of low energy cosmic rays p 21 A82-22567

ION PRODUCTION RATES
Evidence for the stochastic acceleration of cosmic rays in supernova remnants p 2 A82-22564

IONIZATION CROSS SECTIONS
Observations of the ionization states of energetic particles accelerated in solar flares p 40 A82-22607

IONIZATION POTENTIALS
On volatility, first ionization potential, and s- and r-processes --- for Galactic cosmic ray sources p 2 A82-22560
A tentative ordering of all available solar energetic particles abundance observations. I - The mass unbiased baseline. II - Discussion and comparison with coronal abundances p 40 A82-22609

IONOSPHERE
Investigation from Japanese MAGSAT team [E82-10239] p 73 N82-23612
Report of investigation from Japanese MAGSAT Team [E82-10322] p 74 N82-24595

IONOSPHERIC CURRENTS
Investigation of the effects of external current systems on the MAGSAT data utilizing grid cell modeling techniques [E82-10195] p 71 N82-22629
Investigation of the effects of external current systems on the MAGSAT data utilizing grid cell modeling techniques [E82-10226] p 73 N82-23599
Investigation of the effects of external current systems on the MAGSAT data utilizing grid cell modeling techniques [E82-10232] p 73 N82-23605
Investigation from Japanese MAGSAT team [E82-10239] p 73 N82-23612
Investigation from Japanese MAGSAT Team. Part A. Crustal structure near Japan and in Antarctic station. Part B. Electric currents and hydromagnetic waves in the ionosphere and the magnetosphere [E82-10244] p 36 N82-24522
Investigation of the effects of external current systems on the MAGSAT data utilizing grid cell modeling techniques [E82-10306] p 74 N82-24580
Report of investigation from Japanese MAGSAT Team [E82-10322] p 74 N82-24595

IONOSPHERIC DRIFT
Characteristics of field-aligned E-region irregularities over Iioka /36 N/, Japan. I p 26 A82-36268

IONOSPHERIC ELECTRON DENSITY
Generation of the auroral kilometric radiation p 26 A82-35542

IONOSPHERIC SOUNDING
The determination of differential X-ray spectrum of the solar flare using ionospheric data p 65 A82-22582

IOWA
Determination of the optimal level for combining area and yield estimates [E82-10215] p 12 N82-23588
Normal crop calendars. Volume 3: The corn and soybean states of Illinois, Indiana, and Iowa [E82-10221] p 13 N82-23594

IRON
Fragmentation of Fe nuclei on carbon, hydrogen and CH2 targets. I - Individual charge changing and total cross sections. II - Isotopic cross sections --- for interstellar cosmic ray propagation p 63 A82-22538

IRRADIANCE
Irradiance measurement errors due to the assumption of a Lambertian reference panel p 79 A82-34222

IRRIGATION
Problems associated with remotely detecting and monitoring saline sites within irrigated Alberta p 9 A82-34710
Irrigated acreage in the Bear River Basin as of the 1975 growing season --- Idaho, Utah, and Wyoming [E82-10356] p 20 N82-26754

ISOTHERMS
Application of satellite magnetic anomaly data to Curie isotherm mapping p 70 A82-35824

ISOTOPE EFFECT
Airborne gamma-ray spectrometer and magnetometer survey: Huron Quadrangle, South Dakota [DE82-005540] p 48 N82-27814

ISOTOPES
Nucleosynthesis of light and by-passed isotopes in the solar system matter p 64 A82-22578
High resolution measurements of solar flare isotopes p 22 A82-22606

ISOTOPIC ENRICHMENT
The charge and isotopic composition of Z equals 7-16 cosmic ray nuclei at their source p 64 A82-22555
The model of the cosmic ray enrichment by helium-3 p 31 A82-22614

ISOTOPIC LABELING
Feasibility of laser-separation of 36 S and its use as an atmospheric tracer [DE82-000965] p 30 N82-27737

ITALY
Crustal structures under the active volcanic areas of central and eastern Mediterranean (M-44) [E82-10096] p 35 N82-23563

J

JAPAN
Investigation from Japanese MAGSAT team [E82-10239] p 73 N82-23612
Investigation from Japanese MAGSAT Team. Part A. Crustal structure near Japan and in Antarctic station. Part B. Electric currents and hydromagnetic waves in the ionosphere and the magnetosphere [E82-10244] p 36 N82-24522
Report of investigation from Japanese MAGSAT Team [E82-10322] p 74 N82-24595

K

KALIHARI BASIN (AFRICA)
Overseas Geology And Mineral Resources number 56: A geological interpretation of LANDSAT imagery and air photography of Botswana [OGMR-56] p 42 N82-22636

KANSAS
Application of thermal model for pan evaporation to the hydrology of a defined medium, the sponge [E82-10217] p 13 N82-23590

Evaluation of the soil moisture prediction accuracy of a space radar using simulation techniques --- Kansas
[E82-10351] p 19 N82-26749

KENTUCKY
Satellite and surface geophysical expression of anomalous crustal structure in Kentucky and Tennessee
p 34 A82-34918

KILOMETRIC WAVES
Generation of the auroral kilometric radiation
p 26 A82-35542

KINETIC EQUATIONS
Estimates of sea surface stress for summer MONEX from cloud motions --- global atmospheric research program p 56 N82-23910

L

LAKE ICE
Use of NOAA/AVHRR visible and near-infrared data for land remote sensing
[NASA-TM-84166] p 81 N82-22643

LAKE MICHIGAN
Comparison of ozone in polluted and clean air masses over Lake Michigan p 29 A82-36477

LAMBERT SURFACE
Irradiance measurement errors due to the assumption of a Lambertian reference panel p 79 A82-34222

LAND MANAGEMENT
Resource inventory techniques used in the California Desert Conservation Area p 23 A82-32441
Problems associated with remotely detecting and monitoring saline sites within irrigated Alberta
p 9 A82-34710
AgRISTARS: Renewable resources inventory. Land information support system implementation plan and schedule --- San Juan National Forest pilot test
[E82-10224] p 14 N82-23597
Identifying environmental features for land management decisions --- Utah
[E82-10289] p 30 N82-24567

LAND USE
Detecting residential land-use development at the urban fringe p 22 A82-29332
Preliminary evidence for the influence of physiography and scale upon the autocorrelation function of remotely sensed data p 67 A82-32343
Sample design for estimating change in land use and land cover p 24 A82-32711
Site selection and engineering issues for a major industrial complex - Application of image and map interpretation p 25 A82-34711
Use of aerial photography in determining land use and streamflow relationships on small developing watersheds
p 60 A82-34736
Improved land use classification from Landsat and Seasat satellite imagery registered to a common map base p 25 A82-34743
Aerial photography vs. Landsat for digital land-cover mapping in an urban watershed p 61 A82-34745
Comparisons of land cover classifications from selected remote sensing systems p 80 A82-34746
Spatial resolution requirements for urban studies
p 29 A82-37502
Streamlining and ensuring mineral development must begin at local land management levels
[EMD-82-10] p 29 N82-23043
AgRISTARS. Preliminary technical results review of FY81 experiments, volume 2: Fiscal year 1981/1982 'corn and soybeans pilot' experiment
[E82-10216] p 13 N82-23589
AgRISTARS: Renewable resources inventory. Land information support system implementation plan and schedule --- San Juan National Forest pilot test
[E82-10224] p 14 N82-23597
An analysis of LANDSAT MSS scene-to-scene registration accuracy
[E82-10285] p 16 N82-24563
Application of remote sensing to state and regional problems
[E82-10288] p 30 N82-24566
A method for inferring available surface moisture using remote surface temperature measurements: An assessment --- Kansas and St. Louis, Missouri
[E82-10311] p 17 N82-24585
Forest Resource Information System. Phase 3: System transfer report
[E82-10344] p 18 N82-25606
Inventory of wetlands and agricultural land cover in the upper Sevier River Basin, Utah
[E82-10345] p 18 N82-25607
Exploration into technical procedures for vertical integration --- information systems
[NASA-CR-166352] p 75 N82-26763

LANDSAT D
Landsat D to yield more precise data
p 70 A82-37200
LANDSAT-D conical scanner evaluation plan
[E82-10340] p 81 N82-25602
LANDSAT D to test thematic mapper, inaugurate operational system
[NASA-NEWS-RELEASE-82-100] p 82 N82-26741
LANDSAT-D thermal analysis and design support
[E82-10346] p 82 N82-26744

LANDSAT SATELLITES
Development of three-dimensional spatial displays using a geographically based information system
p 66 A82-29326
The use of residual images in Landsat image analysis
p 66 A82-29328
Desert locust habitat monitoring with satellite remote sensing A new technology for an old problem
p 7 A82-29747
Relating Landsat digital count values to ground reflectance for optically thin atmospheric conditions
p 66 A82-29762
Regional geological, tectonic and geophysical features of Nordland, Norway p 41 A82-30304
Satellite image interpretation of the eastern Caledonian part of the Blue Road Geotraverse and its geological implications /Nordland, Vasterbotten, Scandinavia/
p 41 A82-30305
Detection of volcanic smoke and ash-fall area at volcano Aso, from Landsat MSS data p 23 A82-31295
Evaluation of temporal registration of Landsat scenes
p 67 A82-32345
Resource inventory techniques used in the California Desert Conservation Area p 23 A82-32441
Digitally enhanced visual displays facilitate the analysis of Landsat imagery p 67 A82-32507
Computation with physical values from Landsat digital data p 68 A82-32709
Monitoring land-cover change by principal component analysis of multitemporal Landsat data
p 68 A82-32906
The response characteristics of vegetation in Landsat MSS digital data p 8 A82-32907
Quantitative relationships of near-surface spectra to Landsat radiometric data p 78 A82-32912
Coastal environment change analysis by Landsat MSS data p 54 A82-34219
An information-theoric spatial transform
p 69 A82-34717
Defining the temporal window for monitoring forest canopy defoliation using Landsat p 9 A82-34730
Use of Landsat multispectral scanner data in vegetation mapping of a forested area p 9 A82-34731
Automated classification of runoff coefficients from Landsat multispectral data p 60 A82-34734
A new approach to multiresource inventories using remote sensing and geographic information systems technologies p 25 A82-34739
Improved land use classification from Landsat and Seasat satellite imagery registered to a common map base p 25 A82-34743
Aerial photography vs. Landsat for digital land-cover mapping in an urban watershed p 61 A82-34745
Space science for applications - The history of Landsat p 84 A82-36617
Remote sensing in Scotland using data received from satellites - A study of the Tay Estuary region using Landsat multispectral scanning imagery p 62 A82-37501
Remote sensing of salt marsh vegetation in the first four proposed Thematic Mapper bands
p 10 A82-37503
Use of LANDSAT data to define soil boundaries in Carroll County, Missouri p 10 N82-23116
A legislator's guide to LANDSAT
[E82-10290] p 85 N82-24568
Exploration into technical procedures for vertical integration --- information systems
[NASA-CR-166352] p 75 N82-26763
Experimental assessment of improved spatial resolution LANDSAT data
[AD-A110538] p 75 N82-26765

LANDSAT 3
The use of Landsat-3 thermal data to help differentiate land covers p 25 A82-34218

LARGE AREA CROP INVENTORY EXPERIMENT
Field size, length, and width distributions based on LACIE ground truth data --- large area crop inventory experiment p 8 A82-32909

LARGE SPACE TELESCOPE
Radiometer mission requirements for large space antenna systems
[NASA-TM-84478] p 81 N82-25610

LASER APPLICATIONS
Laser-induced bioluminescence --- for remote sensing of marine organisms p 53 A82-32559
Bias correction procedures for airborne laser hydrography
[PB82-130089] p 83 N82-22644
Study visit to United States laser technology centers, 1981
[FOA-C-30257-E1] p 81 N82-24489
Feasibility of laser-separation of 36 S and its use as an atmospheric tracer
[DE82-000965] p 30 N82-27737

LASER RANGE FINDERS
Establishing geodetic-geodynamic parameters using lunar laser range measurements p 34 A82-33293

LASER SPECTROMETERS
In situ ozone data for comparison with laser absorption remote sensor: 1980 PEPE/NEROS program
[NASA-TM-84471] p 30 N82-25661

LEASING
Streamlining and ensuring mineral development must begin at local land management levels
[EMD-82-10] p 29 N82-23043

LEAVES
Remote sensing of leaf water content in the near infrared p 8 A82-32897
Spectral properties of agricultural crops and soils measured from space, aerial, field, and laboratory sensors
[E82-10189] p 10 N82-22623

LENSES
An optical objective lens for earth observations by satellites p 78 A82-32824

LESSER ANTILLES
Soufriere Volcano, St. Vincent - Observations of its 1979 eruption from the ground, aircraft, and satellites
p 24 A82-33652

LIGNITE
Application of remote sensing to state and regional problems
[E82-10288] p 30 N82-24566

LINEAR POLARIZATION
Linear polarization of light by two wheat canopies measured at many view angles
[E82-10229] p 14 N82-23602

LITHOLOGY
Spatial thermal radiometry contribution to the Massif Armoricain and the Massif Central France litho-structural study
[E82-10190] p 42 N82-22624
Crustal structures under the active volcanic areas of central and eastern Mediterranean (M-44)
[E82-10096] p 35 N82-23563

LITHOSPHERE
A satellite magnetic model of northeastern South American aulacogens p 33 A82-30795

LOCUSTS
Desert locust habitat monitoring with satellite remote sensing A new technology for an old problem
p 7 A82-29747

LONG RANGE WEATHER FORECASTING
On the space-time variability of ocean surface mixed layer characteristics of central and eastern Arabian sea during MONSOON-77 --- global atmospheric research program p 56 N82-23909

LUNAR RANGEFINDING
Establishing geodetic-geodynamic parameters using lunar laser range measurements p 34 A82-33293

LUNAR SOIL
Is the neon composition of our sun, planetary or solar
p 76 A82-22608

M

MAGNESIUM ISOTOPES
Calculated isotopic source composition and tests for origin and propagation of cosmic rays with mass numbers less than or equal to 62 p 83 A82-22554

MAGNETIC ANOMALIES
Magnetic anomalies as a reference for ground-speed and map-matching navigation p 32 A82-30314
Initial scalar magnetic anomaly map from Magsat
p 32 A82-30784
Initial vector magnetic anomaly map from Magsat
p 32 A82-30785
Magsat scalar anomaly distribution - The global perspective p 41 A82-30786
Magsat magnetic anomalies over Antarctica and the surrounding oceans p 32 A82-30787
Spatial resolution and repeatability of Magsat crustal anomaly data over the Indian Ocean p 32 A82-30788
Verification of the crustal component in satellite magnetic data p 32 A82-30789
A preliminary comparison of the Magsat data and aeromagnetic data in the continental U.S.
p 32 A82-30790
A satellite magnetic model of northeastern South American aulacogens p 33 A82-30795

Preliminary interpretation of magnetic anomalies over Japan and its surrounding area p 33 A82-30796
Satellite and surface geophysical expression of anomalous crustal structure in Kentucky and Tennessee p 34 A82-34918
Application of satellite magnetic anomaly data to Curie isotherm mapping p 70 A82-35824
Structure, composition and thermal state of the crust in Brazil --- geomagnetic survey
[E82-10187] p 35 N82-22621
Study of gravity and magnetic anomalies using MAGSAT data
[E82-10194] p 35 N82-22628
Crustal structures under the active volcanic areas of central and eastern Mediterranean (M-44)
[E82-10096] p 35 N82-23563
Characterization of the structure and tectonic of South America
[E82-10196] p 42 N82-23569
Analyses of MAGSAT tracks crossing the study region in the Indian Ocean
[E82-10197] p 71 N82-23570
MAGSAT science investigations
[E82-10199] p 71 N82-23572
MAGSAT for geomagnetic studies over Indian region
[E82-10202] p 72 N82-23575
Bathymetric and tectonics of Indian Ocean using MAGSAT data
[E82-10204] p 36 N82-23577
Investigation from Japanese MAGSAT team
[E82-10239] p 73 N82-23612
Investigations of medium wavelength magnetic anomalies in the eastern Pacific using MAGSAT
[E82-10240] p 73 N82-23613
Airborne gamma-ray spectrometer and magnetometer survey. Roseau quadrangle, Minnesota, volume 1
[DE82-001031] p 43 N82-23621
Airborne gamma-ray spectrometer and magnetometer survey. Hibbing quadrangle, Minnesota, volume 1
[DE82-004159] p 44 N82-23639
Airborne gamma-ray spectrometer and magnetometer survey. Hibbing quadrangle, Minnesota, volume 2
[DE82-004165] p 45 N82-23640
Airborne gamma-ray spectrometer and magnetometer survey. Aberdeen quadrangle, South Dakota, volume 1
[DE82-004152] p 45 N82-23641
Airborne gamma-ray spectrometer and magnetometer survey. Aberdeen quadrangle, South Dakota, volume 2
[DE82-004164] p 45 N82-23642
Spherical-Earth gravity and magnetic anomaly modeling by Gauss-Legendre quadrature integration
[E82-10242] p 36 N82-24520
Investigation from Japanese MAGSAT Team. Part A. Crustal structure near Japan and in Antarctic station. Part B. Electric currents and hydromagnetic waves in the ionosphere and the magnetosphere
[E82-10244] p 36 N82-24522
Report of MAGSAT project by Survey of India
[E82-10293] p 73 N82-24570
MAGSAT for geomagnetic studies over Indian region
[E82-10296] p 73 N82-24572
An equivalent layer magnetization model for the United States derived from MAGSAT data
[E82-10297] p 36 N82-24573
Analyzing the Broken Ridge area of the Indian Ocean using magnetic and gravity anomaly maps and geoid undulation and bathymetry data
[E82-10303] p 36 N82-24577
Investigating tectonic and bathymetric features of the Indian Ocean using MAGSAT magnetic anomaly data
[E82-10304] p 37 N82-24578
The mineralogy of global magnetic anomalies --- rock magnetic signatures and MAGSAT geological, and gravity correlations in West Africa
[E82-10305] p 45 N82-24579
MAGSAT scalar and vector anomaly data analysis
[E82-10307] p 74 N82-24581
Investigation of Antarctic crust and upper mantle using MAGSAT and other geophysical data
[E82-10308] p 37 N82-24582
Investigation of Antarctic crust and upper mantle using MAGSAT and other geophysical data
[E82-10309] p 37 N82-24583
Magnetic and gravity anomalies in the Americas
[E82-10312] p 37 N82-24586
Improved definition of crustal magnetic anomalies for MAGSAT data
[E82-10314] p 37 N82-24587
An investigation of MAGSAT and complementary data emphasizing precambrian shields and adjacent areas of West Africa and South America
[E82-10316] p 38 N82-24589
An investigation of MAGSAT and complementary data emphasizing precambrian shields and adjacent areas of West Africa and South America
[E82-10317] p 38 N82-24590
An investigation of MAGSAT and complementary data emphasizing precambrian shields and adjacent areas of West Africa and South America
[E82-10318] p 38 N82-24591
Geotectonics of South America --- regional magnetic and gravity anomalies of South America
[E82-10320] p 38 N82-24593
Use of MAGSAT anomaly data for crustal structure and mineral resources in the US Midcontinent
[E82-10321] p 46 N82-24594
Report of investigation from Japanese MAGSAT Team
[E82-10322] p 74 N82-24595
Use of MAGSAT anomaly data for crustal structure and mineral resources in the US Midcontinent
[E82-10323] p 46 N82-24596
Comparison of storm-time changes of geomagnetic field at ground and at MAGSAT altitudes, part 2
[E82-10325] p 30 N82-24598
MAGSAT anomaly map and continental drift
[E82-10326] p 38 N82-24599
Models and maps of the main field
[E82-10327] p 74 N82-24600
Investigations of medium wavelength magnetic anomalies in the eastern Pacific using MAGSAT data
[E82-10330] p 38 N82-24603
Aeromagnetic and satellite magnetic anomally mapping
[E82-10339] p 39 N82-25601
Airborne gamma-ray spectrometer and magnetometer survey, Kingston quadrangle New York, volume 2C
[DE81-027161] p 46 N82-25621
Analysis of MAGSAT data of the Indian region
[E82-10358] p 75 N82-26756

MAGNETIC DISTURBANCES
Studies of high latitude current systems using MAGSAT vector data
[E82-10188] p 71 N82-22622

MAGNETIC EFFECTS
Features of cosmic ray variations due to variations in the total magnetic field of the sun p 49 A82-22619

MAGNETIC FIELDS
Investigation of the effects of external current systems on the MAGSAT data utilizing grid cell modeling techniques
[E82-10306] p 74 N82-24580

MAGNETIC FLUX
Investigation of geomagnetic field forecasting and fluid dynamics of the core --- determination of the bundary between the core and mantle of the Earth
[E82-10198] p 35 N82-23571
Investigation of geomagnetic field forecasting and fluid dynamics of the core
[E82-10310] p 37 N82-24584

MAGNETIC MEASUREMENT
Airborne gamma-ray spectrometer and magnetometer survey: Susanville quadrangle, California, volume 1
[DE82-005538] p 48 N82-27811
Airborne gamma-ray spectrometer and magnetometer survey: Roseburg quadrangle, Oregon, volume 2
[DE82-005568] p 48 N82-27812

MAGNETIC MONOPOLES
Magnetic monopole pair and its observation in cosmic rays p 65 A82-22579

MAGNETIC POLES
A comparison of pole positions derived from GPS satellite and Navy navigation satellite observations
[AD-A110765] p 39 N82-26268

MAGNETIC SIGNATURES
Observed magnetic substorm signatures at synchronous altitude p 26 A82-35534
Investigation of MAGSAT and TRIAD magnetometer data to provide corrective information on high-latitude external fields
[E82-10201] p 72 N82-23574

MAGNETIC STORMS
Comparison of storm-time changes of geomagnetic field at ground and MAGSAT altitudes
[E82-10359] p 30 N82-26757

MAGNETIC SURVEYS
Magnetic charts of Canada derived from Magsat data p 32 A82-30778
Verification of the crustal component in satellite magnetic data p 32 A82-30789
Structure, composition and thermal state of the crust in Brazil --- geomagnetic survey
[E82-10187] p 35 N82-22621
MAGSAT and aeromagnetic data in the North American continent
[E82-10193] p 71 N82-22627
Investigation of the effects of external current systems on the MAGSAT data utilizing grid cell modeling techniques
[E82-10195] p 71 N82-22629
Equivalent source modeling of the main field using MAGSAT data
[E82-10151] p 71 N82-23567
MAGSAT for geomagnetic studies over Indian region
[E82-10202] p 72 N82-23575
Spherical harmonic representation of the main geomagnetic field for world charting and investigations of some fundamental problems of physics and geophysics
[E82-10203] p 72 N82-23576
Investigation of the effects of external current systems on the MAGSAT data utilizing grid cell modeling techniques
[E82-10226] p 73 N82-23599
Investigation of the effects of external current systems on the MAGSAT data utilizing grid cell modeling techniques
[E82-10232] p 73 N82-23605
Investigation from Japanese MAGSAT team
[E82-10239] p 73 N82-23612
Airborne gamma-ray spectrometer and magnetometer survey. Roseau quadrangle, Minnesota, volume 1
[DE82-001031] p 43 N82-23621
Airborne gamma-ray spectrometer and magnetometer survey. Barrow quadrangle, Alaska, volume 1
[DE82-000334] p 43 N82-23623
Airborne gamma-ray spectrometer and magnetometer survey. Wainwright quadrangle, Alaska, volume 2
[DE82-000341] p 43 N82-23624
Airborne gamma-ray spectrometer and magnetometer survey. Meade River quadrangle, Alaska, volume 2
[DE82-000340] p 43 N82-23626
Airborne gamma-ray spectrometer and magnetometer survey. Teshekpuk quadrangle, Alaska, volume 2
[DE82-000310] p 43 N82-23627
Airborne gamma-ray spectrometer and magnetometer survey. Harrison Bay quadrangle, Alaska, volume 2
[DE82-000315] p 43 N82-23628
Airborne gamma-ray spectrometer and magnetometer survey: Beechey Pt., quadrangle, Alaska, volume 2
[DE82-000309] p 43 N82-23629
Airborne gamma-ray spectrometer and magnetometer survey. Point Lay quadrangle, Alaska, volume 2
[DE82-000308] p 43 N82-23630
Airborne gamma-ray spectrometer and magnetometer survey. Utukik River quadrangle, Alaska, volume 2
[DE82-000316] p 44 N82-23631
Airborne gamma-ray spectrometer and magnetometer survey. Sagavanirktok quadrangle, Alaska, volume 2
[DE82-000311] p 44 N82-23632
Airborne gamma-ray spectrometer and magnetometer survey: Duluth quadrangle, Minnesota, volume 2
[DE82-001027] p 44 N82-23633
Airborne gamma-ray spectrometer and magnetometer survey. Devil's Lake quadrangle, North Dakota, volume 1
[DE82-004161] p 44 N82-23635
Airborne gamma-ray spectrometer and magnetometer survey. Devil's Lake quadrangle, North Dakota, volume 2
[DE82-004168] p 44 N82-23636
Airborne gamma-ray spectrometer and magnetometer survey. Bemidji quadrangle, Minnesota, volume 1
[DE82-001032] p 44 N82-23637
Airborne gamma-ray spectrometer and magnetometer survey. International Falls quadrangle, Minnesota, volume 1
[DE82-004151] p 45 N82-23643
Airborne gamma-ray spectrometer and magnetometer survey. International Falls quadrangle, Minnesota, volume 2
[DE82-004166] p 45 N82-23644
Investigation from Japanese MAGSAT Team. Part A. Crustal structure near Japan and in Antarctic station. Part B. Electric currents and hydromagnetic waves in the ionosphere and the magnetosphere
[E82-10244] p 36 N82-24522
MAGSAT for geomagnetic studies over Indian region
[E82-10296] p 73 N82-24572
Investigation of geomagnetic field forecasting and fluid dynamics of the core
[E82-10310] p 37 N82-24584
Use of MAGSAT anomaly data for crustal structure and mineral resources in the US Midcontinent
[E82-10323] p 46 N82-24596
Investigation of geomagnetic field forecasting and fluid dynamics of the core
[E82-10342] p 39 N82-25604
Airborne gamma-ray spectrometer and magnetometer survey, Toronto quadrangle New York, volume 2A
[DE81-027158] p 46 N82-25620
Airborne gamma-ray spectrometer and magnetometer survey, Kingston quadrangle New York, volume 2C
[DE81-027161] p 46 N82-25621
Airborne gamma-ray spectrometer and magnetometer survey, Rochester quadrangle New York, volume 2D
[DE81-027156] p 46 N82-25622
Airborne gamma-ray spectrometer and magnetometer survey. Lookout Ridge quadrangle, Alaska, volume 2
[DE82-000313] p 47 N82-25625

Airborne gamma-ray spectrometer and magnetometer survey: North/south tieline, volume 1 [DE82-005542] p 47 N82-27804

Airborne gamma-ray spectrometer and magnetometer survey: North/south tieline, volume 2 [DE82-005570] p 47 N82-27805

Evaluation and combined geophysical interpretations of NURE and related geoscience data in the Van Horn, Pecos, Marfa, Fort Stockton, Presidido, and Emory Peak quadrangles, Texas, volume 1 [DE82-005554] p 47 N82-27808

Evaluation and combined geophysical interpretations of NURE and related geoscience data in the Van Horn, Pecos, Marfa, Fort Stockton, Presidio, and Emory Peak quadrangels, Texas [DE82-005560] p 48 N82-27809

NURE aerial gamma-ray and magnetic reconnaissance survey of portions of New Mexico, Arizona and Texas. Volume 2: New Mexico-Carlsbad Quadrangle [DE82-005527] p 48 N82-27810

Airborne gamma-ray spectrometer and magnetometer survey: Ukiah quadrangle, California, volume 1 --- uranium exploration [DE82-005541] p 48 N82-27813

Airborne gamma-ray spectrometer and magnetometer survey: Huron Quadrangle, South Dakota [DE82-005540] p 48 N82-27814

Airborne gamma-ray spectrometer and magnetometer survey: Chico Quadrangle, California [DE82-005543] p 48 N82-27815

MAGNETIC VARIATIONS

Comparison of storm-time changes of geomagnetic field at ground and at MAGSAT altitudes, part 2 [E82-10325] p 30 N82-24598

Comparison of storm-time changes of geomagnetic field at ground and MAGSAT altitudes [E82-10359] p 30 N82-26757

MAGNETIZATION

Satellite and surface geophysical expression of anomalous crustal structure in Kentucky and Tennessee p 34 A82-34918

MAGNETOHYDRODYNAMIC WAVES

The galactic origin of cosmic rays. I [CONF-810711-1] p 2 A82-22565

Possible evidence for attenuation of an MHD shock by a magnetic neutral sheet in the solar corona p 3 A82-22589

MAGNETOMETERS

Airborne gamma-ray spectrometer and magnetometer survey. Barrow quadranagle, Alaska, volume 2 [DE82-000342] p 46 N82-25623

MAGNETOSPHERE

Investigation of the effects of external current systems on the MAGSAT data utilizing grid cell modeling techniques [E82-10232] p 73 N82-23605

Investigation from Japanese MAGSAT team [E82-10239] p 73 N82-23612

Investigation from Japanese MAGSAT Team. Part A. Crustal structure near Japan and in Antarctic station. Part B. Electric currents and hydromagnetic waves in the ionosphere and the magnetosphere [E82-10244] p 36 N82-24522

Investigation of the effects of external current systems on the MAGSAT data utilizing grid cell modeling techniques [E82-10306] p 74 N82-24580

Report of investigation from Japanese MAGSAT Team [E82-10322] p 74 N82-24595

MAGSAT SATELLITES

Initial scalar magnetic anomaly map from Magsat p 32 A82-30784

Initial vector magnetic anomaly map from Magsat p 32 A82-30785

Magsat scalar anomaly distribution - The global perspective p 41 A82-30786

Magsat magnetic anomalies over Antarctica and the surrounding oceans p 32 A82-30787

Spatial resolution and repeatability of Magsat crustal anomaly data over the Indian Ocean p 32 A82-30788

Verification of the crustal component in satellite magnetic data p 32 A82-30789

A preliminary comparison of the Magsat data and aeromagnetic data in the continental U.S. p 32 A82-30790

A satellite magnetic model of northeastern South American aulacogens p 33 A82-30795

Preliminary interpretation of magnetic anomalies over Japan and its surrounding area p 33 A82-30796

MANAGEMENT INFORMATION SYSTEMS

AgRISTARS: Renewable resources inventory. Land information support system implementation plan and schedule --- San Juan National Forest pilot test [E82-10224] p 14 N82-23597

MANNED SPACECRAFT

Remote sensing of the earth's resources - The Soviet experience p 84 A82-33555

MAP MATCHING GUIDANCE

Magnetic anomalies as a reference for ground-speed and map-matching navigation p 32 A82-30314

MAPPING

Work related to the Blue Road Geotraverse at the Finnish Geodetic Institute p 32 A82-30306

American Society of Photogrammetry, Annual Meeting, 47th, Washington, DC, February 22-27, 1981, ASP Technical Papers p 79 A82-34701

Comparisons of land cover classifications from selected remote sensing systems p 80 A82-34746

Study of gravity and magnetic anomalies using MAGSAT data [E82-10194] p 35 N82-22628

Airborne gamma-ray spectrometer and magnetometer survey. Roseau quadrangle, Minnesota, volume 1 [DE82-001031] p 43 N82-23621

Airborne gamma-ray spectrometer and magnetometer survey. Roseau quadrangle, Minnesota, volume 2 [DE82-001025] p 44 N82-23634

Airborne gamma-ray spectrometer and magnetometer survey. Bemidji quadrangle, Minnesota, volume 2 [DE82-001026] p 44 N82-23638

Airborne gamma-ray spectrometer and magnetometer survey. Hibbing quadrangle, Minnesota, volume 1 [DE82-004159] p 44 N82-23639

Airborne gamma-ray spectrometer and magnetometer survey. Hibbing quadrangle, Minnesota, volume 2 [DE82-004165] p 45 N82-23640

Airborne gamma-ray spectrometer and magnetometer survey. Aberdeen quadrangle, South Dakota, volume 1 [DE82-004152] p 45 N82-23641

Airborne gamma-ray spectrometer and magnetometer survey. Aberdeen quadrangle, South Dakota, volume 2 [DE82-004164] p 45 N82-23642

Report of MAGSAT project by Survey of India [E82-10293] p 73 N82-24570

Magnetic and gravity anomalies in the Americas [E82-10312] p 37 N82-24586

Image understanding research [AD-A110746] p 74 N82-25611

Matrix data analysis: Color/B and W coding is not always enough [AD-A111401] p 74 N82-25612

Source assessment system [AD-A111223] p 75 N82-25613

Airborne gamma-ray spectrometer and magnetometer survey: Chico Quadrangle, California [DE82-005543] p 48 N82-27815

MAPS

The crustal structure and tectonics of South America [E82-10319] p 38 N82-24592

Report of investigation from Japanese MAGSAT Team [E82-10322] p 74 N82-24595

MAGSAT anomaly map and continental drift [E82-10326] p 38 N82-24599

Models and maps of the main field [E82-10327] p 74 N82-24600

Computer-processed geophysical atlas of digital data for the East Coast margin of the United States from surface and spacecraft data [AD-A111388] p 39 N82-25748

Evaluation and combined geophysical interpretations of NURE and related geoscience data in the Van Horn, Pecos, Marfa, Fort Stockton, Presidio, and Emory Peak quadrangels, Texas [DE82-005560] p 48 N82-27809

MARINE BIOLOGY

Laser-induced bioluminescence --- for remote sensing of marine organisms p 53 A82-32559

Technology and oceanography: An assessment of Federal technologies for oceanographic research and monitoring. Volume 2: Working papers on fishery research technology p 58 N82-26944

MARINE ENVIRONMENTS

A study of atmospheric diffusion from the LANDSAT imagery --- pollution transport over the ocean [E82-10360] p 58 N82-26758

MARINE METEOROLOGY

Retrieval of ocean surface and atmospheric parameters from multichannel microwave radiometric measurements p 53 A82-31995

Estimation of the temperature of the upper boundary of cloud cover over the world ocean p 54 A82-36005

Estimation of the precipitable water from the IR channel of the geostationary satellite p 55 A82-37196

Marine boundary layer wind structure over the Bay of Bengal during Monex-79 --- Monsoon Experiment (MONEX) p 57 N82-23929

MARINE RESOURCES

Technology and oceanography: An assessment of Federal technologies for oceanographic research and monitoring. Volume 2: Working papers on fishery research technology p 58 N82-26944

MARINE TECHNOLOGY

The processing of satellite navigation data for marine geodesy p 34 A82-37175

Technology and oceanography: An assessment of Federal technologies for oceanographic research and monitoring. Volume 2: Working papers on fishery research technology p 58 N82-26944

MARINER 10 SPACE PROBE

A color-ratio map of Mercury p 31 A82-22294

MARSHLANDS

Remote sensing of salt marsh vegetation in the first four proposed Thematic Mapper bands p 10 A82-37503

MASS RATIOS

Mass per charge ratio in hot plasmas and cosmic ray source composition p 2 A82-22557

MASSIFS

Spatial thermal radiometry contribution to the Massif Armoricain and the Massif Central France litho-structural study [E82-10190] p 42 N82-22624

MATCHING

An algorithm for automating the registration of USDA segment ground data to LANDSAT MSS data [E82-10286] p 16 N82-24564

MATHEMATICAL MODELS

A comparison of helium and heavy ion spectra in He/3/ rich solar flares with a model calculation p 5 A82-22612

Gravity model improvement for Seasat p 32 A82-29615

A comparative study of microwave radiometer observations over snowfields with radiative transfer model calculations --- for water runoff estimation p 60 A82-32910

Application of satellite magnetic anomaly data to Curie isotherm mapping p 70 A82-35824

A meteorologically driven maize stress indicator model [E82-10112] p 11 N82-23564

Topographic slope correction for analysis of thermal infrared images [E82-10214] p 36 N82-23587

Report of MAGSAT project by Survey of India [E82-10293] p 73 N82-24570

An equivalent layer magnetization model for the United States derived from MAGSAT data [E82-10297] p 36 N82-24573

MATRICES (MATHEMATICS)

Matrix data analysis: Color/B and W coding is not always enough [AD-A111401] p 74 N82-25612

MAXIMUM ENTROPY METHOD

Information theory lateral density distribution for earth inferred from global gravity field p 35 A82-37962

MAXIMUM LIKELIHOOD ESTIMATES

The use of prior probabilities in maximum likelihood classification of remotely sensed data p 68 A82-32904

MEAN FREE PATH

Spacecraft determination of energetic particle propagation parameters - The 1 January 1978 solar event p 31 A82-22598

MEASUREMENT

Movement of ice markers measured by satellite ranging [R-240] p 59 N82-27816

MEDITERRANEAN SEA

Crustal structures under the active volcanic areas of central and eastern Mediterranean (M-44) [E82-10096] p 35 N82-23563

Thermal mapping, geothermal source location, natural effluents and plant stress in the Mediterranean coast of Spain [E82-10300] p 17 N82-24576

MELTING

The use of satellite photographs to study snow-cover dynamics and to determine the average water discharge of the Amudarya during a vegetation period p 61 A82-35132

Method for the analysis of the melting of a firn complex on the basis of aerospace photographs p 61 A82-35133

Experience with the compilation of maps of snow-cover melting in the central part of the European USSR on the basis of satellite data p 62 A82-35134

MELTS (CRYSTAL GROWTH)

Influence of CO2 on melting of model granulite facies assemblages - A model for the genesis of charnockites p 42 A82-36298

MERCURY (PLANET)

A color-ratio map of Mercury p 31 A82-22294

MESON-MESON INTERACTIONS
Magnetic monopole pair and its observation in cosmic rays p 65 A82-22579
MESOSCALE PHENOMENA
High resolution satellite observations of mesoscale oceanography in the Tasman Sea, 1978 - 1979
[E82-10324] p 57 N82-24597
MESOSPHERE
Observation of the diurnal variation of atmospheric ozone p 26 A82-35895
Microwave measurement of stratospheric and mesospheric ozone p 28 A82-36415
OSO-8 lower mesospheric ozone number density profiles p 28 A82-36472
METEORITIC COMPOSITION
Measurement of cosmogenic nuclides using a multi-crystal gamma-ray coincidence spectrometer --- for Mayo Belwa meteorite study p 64 A82-22577
METEOROLOGICAL CHARTS
Meteorological and aircraft data for CUE 2 1973
[PB82-149246] p 59 N82-26949
METEOROLOGICAL PARAMETERS
Retrieval of ocean surface and atmospheric parameters from multichannel microwave radiometric measurements p 53 A82-31995
Meteorological analysis of the eruption of Soufriere in April 1979 p 24 A82-33655
The meteorological product - 'Cloud-top height' p 70 A82-36043
Ground support data from July 10 to July 29, 1978, for HCMM thermal satellite data of the Powder River Basin, Wyoming
[E82-10211] p 72 N82-23584
A meteorologically driven grain sorghum stress indicator model
[E82-10218] p 13 N82-23591
METEOROLOGICAL SATELLITES
System albedo as sensed by satellites - Its definition and variability p 23 A82-32342
The seasonal snow-line within the Fergana basin and the possibility of using it for hydrological forecasting p 61 A82-35131
Estimation of the temperature of the upper boundary of cloud cover over the world ocean p 54 A82-36005
METEOROLOGY
The METEOSAT Data Collection System and its application p 75 N82-26037
METEOSAT SATELLITE
The meteorological product - 'Cloud-top height' p 70 A82-36043
MEXICO
Monitoring deforestation in the eastern part of the state of Guerrero, Mexico p 9 A82-34733
MICROCOMPUTERS
Image processing with microcomputers in remote sensing p 79 A82-34708
MICRODENSITOMETERS
Application of scanning microdensitometer data in selected plant science case studies p 7 A82-29539
MICROWAVE EMISSION
A multi-frequency radiometric measurement of soil moisture content over bare and vegetated fields
[E82-10238] p 16 N82-23611
MICROWAVE EQUIPMENT
Intercomparison of wind speeds inferred by the SASS, altimeter, and SMMR p 52 A82-29621
MICROWAVE IMAGERY
Remote sensing of precipitable water over the oceans from Nimbus 7 microwave measurements p 49 A82-28907
MICROWAVE RADIOMETERS
Evaluation of atmospheric attenuation from SMMR brightness temperature for the Seasat satellite scatterometer p 51 A82-29618
Intercomparison of wind speeds inferred by the SASS, altimeter, and SMMR p 52 A82-29621
Description of Seasat radiometer status and results p 52 A82-29622
Retrieval of ocean surface and atmospheric parameters from multichannel microwave radiometric measurements p 53 A82-31995
Inversion of data from diffraction-limited multiwavelength remote sensors. II - Nonlinear dependence of observables on the geophysical parameters p 77 A82-32658
A comparative study of microwave radiometer observations over snowfields with radiative transfer model calculations --- for water runoff estimation p 60 A82-32910
Snowpack monitoring in North America and Eurasia using passive microwave satellite data p 78 A82-32915
The use of microwave radiometry for the determination of snow cover height p 80 A82-36018
Microwave measurement of stratospheric and mesospheric ozone p 28 A82-36415
Orbiting passive microwave sensor simulation applied to soil moisture estimation
[E82-10343] p 18 N82-25605
Radiometer mission requirements for large space antenna systems
[NASA-TM-84478] p 81 N82-25610
MICROWAVE SCATTERING
Intercomparison of wind speeds inferred by the SASS, altimeter, and SMMR p 52 A82-29621
On the synthetic aperture radar imaging of ocean surface waves p 53 A82-32881
Characteristics of 13.9 GHz radar scattering from oil films on the sea surface p 54 A82-33438
MICROWAVE SENSORS
Seasat measurement system evaluation - Achievements and limitations p 49 A82-29601
Microwave sensing from space
[AAS PAPER 82-127] p 80 A82-37809
Orbiting passive microwave sensor simulation applied to soil moisture estimation
[E82-10343] p 18 N82-25605
Multifrequency remote sensing of soil moisture --- Guymon, Oklahoma and Dalhart, Texas
[E82-10362] p 20 N82-26760
The use of soil texture and field capacity to normalize microwave soil moisture measurements: Some problems p 20 N82-26762
MICROWAVE SPECTRA
Development of visible/infrared/microwave agriculture classification and biomass estimation algorithms --- Guyton, Oklahoma and Dalhart, Texas
[E82-10363] p 20 N82-26761
MICROWAVES
The possibility of using remote-sensing methods to study the hydrology of elementary watersheds p 61 A82-35130
The effect of sea-surface Sun glitter on microwave radiometer measurements
[NASA-CR-169083] p 57 N82-26525
MIDLATITUDE ATMOSPHERE
Characteristics of field-aligned E-region irregularities over Iioka /36 N/, Japan. I p 26 A82-36268
MILKY WAY GALAXY
Derivation of the distribution of synchrotron emissivity in the Galaxy from the 408 MHz all-sky survey p 82 A82-22549
Angular variations of nonthermal radio emission from the Galaxy relevant to the structure of interstellar magnetic field p 83 A82-22550
Convective outflow of cosmic rays from the Galaxy and background radio emission p 83 A82-22551
MINERAL DEPOSITS
Overseas Geology And Mineral Resources number 56: A geological interpretation of LANDSAT imagery and air photography of Botswana
[OGMR-56] p 42 N82-22636
Streamlining and ensuring mineral development must begin at local land management levels
[EMD-82-10] p 29 N82-23043
Airborne gamma-ray spectrometer and magnetometer survey. Roseau quadrangle, Minnesota, volume 1
[DE82-001031] p 43 N82-23621
Airborne gamma-ray spectrometer and magnetometer survey. Barrow quadrangle, Alaska, volume 1
[DE82-000334] p 43 N82-23623
Airborne gamma-ray spectrometer and magnetometer survey. Wainwright quadrangle, Alaska, volume 2
[DE82-000341] p 43 N82-23624
Airborne gamma-ray spectrometer and magnetometer survey, Kenora quadrangle, Minnesota, volume 1
[DE82-001029] p 43 N82-23625
Airborne gamma-ray spectrometer and magnetometer survey. Roseau quadrangle, Minnesota, volume 2
[DE82-001025] p 44 N82-23634
Airborne gamma-ray spectrometer and magnetometer survey. Hibbing quadrangle, Minnesota, volume 1
[DE82-004159] p 44 N82-23639
Airborne gamma-ray spectrometer and magnetometer survey. Hibbing quadrangle, Minnesota, volume 2
[DE82-004165] p 45 N82-23640
Airborne gamma-ray spectrometer and magnetometer survey. Aberdeen quadrangle, South Dakota, volume 1
[DE82-004152] p 45 N82-23641
Airborne gamma-ray spectrometer and magnetometer survey. Aberdeen quadrangle, South Dakota, volume 2
[DE82-004164] p 45 N82-23642
Use of MAGSAT anomaly data for crustal structure and mineral resources in the US Midcontinent
[E82-10321] p 46 N82-24594
Airborne gamma-ray spectrometer and magnetometer survey, Toronto quadrangle New York, volume 2A
[DE81-027158] p 46 N82-25620
Airborne gamma-ray spectrometer and magnetometer survey, Rochester quadrangle New York, volume 2D
[DE81-027156] p 46 N82-25622
Evaluation and combined geophysical interpretations of NURE and related geoscience data in the Van Horn, Pecos, Marfa, Fort Stockton, Presidido, and Emory Peak quadrangles, Texas, volume 1
[DE82-005554] p 47 N82-27808
NURE aerial gamma-ray and magnetic reconnaissance survey of portions of New Mexico, Arizona and Texas. Volume 2: New Mexico-Carlsbad Quadrangle
[DE82-005527] p 48 N82-27810
MINERAL EXPLORATION
Aerogeophysical methods of finding uranium deposits --- Russian book p 41 A82-33402
Landsat in the search for Appalachian hydrocarbons p 42 A82-34721
Airborne gamma-ray spectrometer and magnetometer survey. Barrow quadrangle, Alaska, volume 1
[DE82-000334] p 43 N82-23623
Airborne gamma-ray spectrometer and magnetometer survey. Wainwright quadrangle, Alaska, volume 2
[DE82-000341] p 43 N82-23624
Airborne gamma-ray spectrometer and magnetometer survey. Meade River quadrangle, Alaska, volume 2
[DE82-000340] p 43 N82-23626
Airborne gamma-ray spectrometer and magnetometer survey. Teshekpuk quadrangle, Alaska, volume 2
[DE82-000310] p 43 N82-23627
Airborne gamma-ray spectrometer and magnetometer survey. Harrison Bay quadrangle, Alaska, volume 2
[DE82-000315] p 43 N82-23628
Airborne gamma-ray spectrometer and magnetometer survey: Beechey Pt., quadrangle, Alaska, volume 2
[DE82-000309] p 43 N82-23629
Airborne gamma-ray spectrometer and magnetometer survey. Point Lay quadrangle, Alaska, volume 2
[DE82-000308] p 43 N82-23630
Airborne gamma-ray spectrometer and magnetometer survey. Utukik River quadrangle, Alaska, volume 2
[DE82-000316] p 44 N82-23631
Airborne gamma-ray spectrometer and magnetometer survey. Sagavanirktok quadrangle, Alaska, volume 2
[DE82-000311] p 44 N82-23632
Airborne gamma-ray spectrometer and magnetometer survey: Duluth quadrangle, Minnesota, volume 2
[DE82-001027] p 44 N82-23633
Airborne gamma-ray spectrometer and magnetometer survey. International Falls quadrangle, Minnesota, volume 1
[DE82-004151] p 45 N82-23643
Airborne gamma-ray spectrometer and magnetometer survey. International Falls quadrangle, Minnesota, volume 2
[DE82-004166] p 45 N82-23644
Application of HCMM data to regional geologic analysis for mineral and energy resource evaluation
[E82-10153] p 45 N82-24518
Application of HCMM data to regional geologic analysis for mineral and energy resource evaluation
[E82-10243] p 45 N82-24521
Use of MAGSAT anomaly data for crustal structure and mineral resources in the US Midcontinent
[E82-10323] p 46 N82-24596
Airborne gamma-ray spectrometer and magnetometer survey, Kingston quadrangle New York, volume 2C
[DE81-027161] p 46 N82-25621
Airborne gamma-ray spectrometer and magnetometer survey. Barrow quadranagle, Alaska, volume 2
[DE82-000342] p 46 N82-25623
Airborne gamma-ray spectrometer and magnetometer survey. Lookout Ridge quadrangle, Alaska, volume 2
[DE82-000313] p 47 N82-25625
Airborne gamma-ray spectrometer and magnetometer survey: North/south tieline, volume 2
[DE82-005570] p 47 N82-27805
Airborne gamma-ray spectrometer and magnetometer survey: Sioux Falls quadrangle, South Dakota, volume 1
[DE82-005533] p 47 N82-27806
Airborne gamma-ray spectrometer and magnetometer survey: Sioux Falls quadrangle, South Dakota, volume 2
[DE82-005574] p 47 N82-27807
Airborne gamma-ray spectrometer and magnetometer survey: Ukiah quadrangle, California, volume 1 --- uranium exploration
[DE82-005541] p 48 N82-27813
MINERALOGY
Influence of CO2 on melting of model granulite facies assemblages - A model for the genesis of charnockites p 42 A82-36298
The mineralogy of global magnetic anomalies --- rock magnetic signatures and MAGSAT geological, and gravity correlations in West Africa
[E82-10305] p 45 N82-24579
MINICOMPUTERS
Interactive initialization of heat flux parameters for numerical models using satellite temperature measurements
[E82-10313] p 82 N82-26743

MINNESOTA

AgRISTARS: Supporting research. Spring small grains planting date distribution model
[E82-10208] p 12 N82-23581

Airborne gamma-ray spectrometer and magnetometer survey: Duluth quadrangle, Minnesota, volume 2
[DE82-001027] p 44 N82-23633

Airborne gamma-ray spectrometer and magnetometer survey. Bemidji quadrangle, Minnesota, volume 1
[DE82-001032] p 44 N82-23637

Airborne gamma-ray spectrometer and magnetometer survey. Bemidji quadrangle, Minnesota, volume 2
[DE82-001026] p 44 N82-23638

Airborne gamma-ray spectrometer and magnetometer survey. Hibbing quadrangle, Minnesota, volume 1
[DE82-004159] p 44 N82-23639

Airborne gamma-ray spectrometer and magnetometer survey. Hibbing quadrangle, Minnesota, volume 2
[DE82-004165] p 45 N82-23640

Airborne gamma-ray spectrometer and magnetometer survey. International Falls quadrangle, Minnesota, volume 1
[DE82-004151] p 45 N82-23643

Airborne gamma-ray spectrometer and magnetometer survey. International Falls quadrangle, Minnesota, volume 2
[DE82-004166] p 45 N82-23644

MISSISSIPPI

Analysis of thematic mapper simulator data acquired during winter season over Pearl River, Mississippi, test site
[E82-10287] p 17 N82-24565

Application of remote sensing to state and regional problems
[E82-10288] p 30 N82-24566

MISSOURI

Structure of the St. Francois Mountains and surrounding lead belt, S. E. Missouri: Inferences from thermal IR and other data sets
[E82-10200] p 36 N82-23573

Structure of the St. Francois Mountains and surrounding lead belt, S. E. Missouri: Inferences from thermal IR and other data sets --- Ozard Plateau and St. Francois Mountains
[E82-10205] p 11 N82-23578

Structure of the Saint Francois Mountains and surrounding lead belt, S.E. Missouri: Inference from thermal IR and other data sets
[E82-10350] p 39 N82-26748

MODELS

Investigation of the effects of external current systems on the MAGSAT data utilizing grid cell modeling techniques
[E82-10226] p 73 N82-23599

MODULATION TRANSFER FUNCTION

11-year modulation and spectrum of cosmic rays in the interstellar space p 22 A82-22616

MOISTURE CONTENT

Remote sensing of leaf water content in the near infrared p 8 A82-32897

Effect of atmospheric conditions on remote sensing of vegetation parameters p 24 A82-32901

Application of thermal model for pan evaporation to the hydrology of a defined medium, the sponge
[E82-10217] p 13 N82-23590

Relating thematic mapper bands TM3, TM4, and TM5 to agronomic variables for corn, cotton, sugarbeet, soybean, sorghum, sunflower and tobacco
[E82-10347] p 19 N82-26745

MOLECULAR CLOUDS

Interactions of cosmic rays with molecular clouds
p 82 A82-22548

MONOMOLECULAR FILMS

Depression of brightness temperature of sea surfaces covered with monomolecular oil films relative to clean water surfaces at 1.43 GHz p 54 A82-33322

MONSOONS

The impact of meteorological satellites on the First GARP Global Experiment (FGGE) --- First Global Atmospheric Research Program Global Experiment (FGGE) p 55 N82-23852

Representativeness of cloud motion winds deduced from GOES Indian Ocean satellite imagery for the description of the indian summer monsoon --- superpressure balloons for the study of the Indian summer monsoon (BALSAMINE) p 55 N82-23879

Comparison of satellite derived radiation budget measurements over MONEX during 1979 to 1980 --- Monsoon Experiment (MONEX) p 29 N82-23891

Short term influence radius of monsoonal overturnings --- First Global Atmospheric Research Program Global Experiment (FGGE) p 56 N82-23898

Impact of additional summer MONEX wind data on the prediction of monsoon depressions during June - August 1979 with two versions of primitive equation (PE) barotropic model --- Monsoon Experiment (MONEX)
p 56 N82-23900

MONEX oceanographic observations along the East African coast --- global atmospheric research program
p 56 N82-23908

Estimates of sea surface stress for summer MONEX from cloud motions --- global atmospheric research program p 56 N82-23910

The onset of the Australian Northwest monsoon during winter MONEX: Broadscale flow revealed by an objective analysis scheme p 56 N82-23912

Marine boundary layer wind structure over the Bay of Bengal during Monex-79 --- Monsoon Experiment (MONEX) p 57 N82-23929

Estimates of the statistical structure of the atmospheric pressure field in summer Monex-79 area
p 57 N82-23939

Analysis of ocean and atmosphere thermodynamical characteristics during the onset of southwest monsoon over the Arabian Sea p 57 N82-23945

MONTANA

AgRISTARS: Supporting research. Spring small grains planting date distribution model
[E82-10208] p 12 N82-23581

The influence of autocorrelation in signature extraction: An example from a geobotanical investigation of Cotter Basin, Montana
[E82-10341] p 46 N82-25603

MONTE CARLO METHOD

Calculation of production rates of cosmogenic nuclides by Monte Carlo method p 64 A82-22576

A description of relativistic solar particle propagation
p 4 A82-22600

MOROCCO

Multidisciplinary investigations on HCMM data over middle Europe and Marocco --- southern Germany and Marrakesh, Morocco
[E82-10315] p 74 N82-24588

MOUNTAINS

Method for the analysis of the melting of a firn complex on the basis of aerospace photographs
p 61 A82-35133

Structure of the St. Francois Mountains and surrounding lead belt, S. E. Missouri: Inferences from thermal IR and other data sets
[E82-10200] p 36 N82-23573

Structure of the Saint Francois Mountains and surrounding lead belt, S.E. Missouri: Inference from thermal IR and other data sets
[E82-10350] p 39 N82-26748

MULTISPECTRAL BAND SCANNERS

Detecting residential land-use development at the urban fringe p 22 A82-29332

Detection of volcanic smoke and ash-fall area at volcano Aso, from Landsat MSS data p 23 A82-31295

A system design for a multispectral sensor using two-dimensional solid-state imaging arrays
p 77 A82-31991

Spectroscopic remote sensing for geological applications p 41 A82-32442

Thematic mapper - An overview of spectral band registration p 77 A82-32447

Multispectral mapper - Imaging spectroscopy as applied to the mapping of earth resources p 77 A82-32448

The use of prior probabilities in maximum likelihood classification of remotely sensed data
p 68 A82-32904

Quantitative relationships of near-surface spectra to Landsat radiometric data p 78 A82-32912

EPA's new bubble and banking policies --- for environmental monitoring p 25 A82-33865

The use of Landsat-3 thermal data to help differentiate land covers p 25 A82-34218

Coastal environment change analysis by Landsat MSS data p 54 A82-34219

Use of Landsat multispectral scanner data in vegetation mapping of a forested area p 9 A82-34731

Comparisons of land cover classifications from selected remote sensing systems p 80 A82-34746

Remote sensing in Scotland using data received from satellites - A study of the Tay Estuary region using Landsat multispectral scanning imagery p 62 A82-37501

Remote sensing of salt marsh vegetation in the first four proposed Thematic Mapper bands
p 10 A82-37503

Solid state instrumentation concepts for earth resource observation
[AAS PAPER 82-132] p 81 A82-37812

OSTA-1 Post Mission Operation Report
[NASA-TM-84191] p 84 N82-23258

LANDSAT D to test thematic mapper, inaugurate operational system
[NASA-NEWS-RELEASE-82-100] p 82 N82-26741

MULTISPECTRAL LINEAR ARRAYS

Advanced technology for earth observation - Data processing
[AAS PAPER 82-130] p 71 A82-37810

MULTISPECTRAL PHOTOGRAPHY

Imaging spectroscopy; Proceedings of the Seminar, Los Angeles, CA, February 10, 11, 1981 p 77 A82-32440

Resource inventory techniques used in the California Desert Conservation Area p 23 A82-32441

Landsat detection of hardwood forest clearcuts
p 8 A82-32708

An information-theoric spatial transform
p 69 A82-34717

Allowance for the effect of the atmosphere in the processing of satellite remote-sensing images
p 70 A82-35141

Landsat D to yield more precise data
p 70 A82-37200

A quantitative multispectral analysis system for aerial photographs applied to coastal planning
p 55 A82-37505

Ten-Ecosystem Study --- Grand and Weld Counties, Colorado; Warren County, Pennsylvania; St. Louis County, Minnesota; Sandoval County, New Mexico; Kershaw County, South Carolina; Fort Yukon, Alaska; Grays Harbor County, Washington; and Washington County, Missouri.
[E82-10186] p 84 N82-22620

An analysis of LANDSAT MSS scene-to-scene registration accuracy
[E82-10285] p 16 N82-24563

N

NAUTICAL CHARTS

A search for seamounts in the southern Cook and Austral region p 52 A82-30810

NAVIGATION

Spherical harmonic representation of the main geomagnetic field for world charting and investigations of some fundamental problems of physics and geophysics
[E82-10203] p 72 N82-23576

NAVIGATION INSTRUMENTS

Magnetic anomalies as a reference for ground-speed and map-matching navigation p 32 A82-30314

NAVIGATION SATELLITES

The processing of satellite navigation data for marine geodesy p 34 A82-37175

NEARSHORE WATER

Nearshore current pattern off south Texas - An interpretation from aerial photographs
p 53 A82-32903

NEON ISOTOPES

Calculated isotopic source composition and tests for origin and propagation of cosmic rays with mass numbers less than or equal to 62 p 83 A82-22554

Comparative abundances in solar energetic particles and in galactic cosmic ray sources, and the Ne-22 anomaly
p 83 A82-22556

On the stellar origin of the Ne-22 excess in cosmic rays p 21 A82-22562

Origin of galactic cosmic rays from Ne isotopic composition p 2 A82-22563

Is the neon composition of our sun, planetary or solar
p 76 A82-22608

NEUTRAL SHEETS

Possible evidence for attenuation of an MHD shock by a magnetic neutral sheet in the solar corona
p 3 A82-22589

NEUTRON FLUX DENSITY

The approximate 1 GeV solar cosmic rays in the Forbush-effect of February 15, 1978 p 40 A82-22604

Primary spectral variations of cosmic rays above 1 GV
p 5 A82-22618

NEUTRON SPECTRA

Primary spectral variations of cosmic rays above 1 GV
p 5 A82-22618

NEUTRON SPECTROMETERS

Primary spectral variations of cosmic rays above 1 GV
p 5 A82-22618

NEUTRON STARS

Acceleration of cosmic rays in accretion shocks
p 64 A82-22568

Pulsar models and cosmic-ray acceleration
p 21 A82-22570

NEW MEXICO

NURE aerial gamma-ray and magnetic reconnaissance survey of portions of New Mexico, Arizona and Texas. Volume 2: New Mexico-Carlsbad Quadrangle
[DE82-005527] p 48 N82-27810

NIMBUS SATELLITES

Snowpack monitoring in North America and Eurasia using passive microwave satellite data
p 78 A82-32915

NIMBUS 4 SATELLITE
- Total ozone variations 1970-74 using Backscattered Ultraviolet /BUV/ and ground-based observations p 26 A82-36053

NITROGEN
- Soft X-rays from the sunlit earth's atmosphere p 29 A82-37405

NITROGEN DIOXIDE
- Breadboard gas filter correlation spectrometer for atmospheric measurement of hydrazines and nitrogen dioxide [AD-A110688] p 82 N82-25642

NITROGEN OXIDES
- Aircraft measurements of NO/x/ in the lower troposphere above the coast of Japan p 26 A82-36247
- Ammonia and the NOx budget of the troposphere p 27 A82-36293

NOAA SATELLITES
- Geographic location of individual pixels --- for thermal infrared digital data processing p 68 A82-32900
- Measuring sea surface temperature from satellites - A ground truth approach p 54 A82-32917
- Short term influence radius of monsoonal overturnings --- First Global Atmospheric Research Program Global Experiment (FGGE) p 56 N82-23898

NOAA 6 SATELLITE
- Evaluation of NOAA-AVHRR data for crop assessment --- Advanced Very High Resolution Radiometer p 8 A82-34179

NONLINEAR SYSTEMS
- Nonlinear theory for elastic beams and rods and its finite element representation [WTHD-143] p 73 N82-24517

NORTH AMERICA
- Study of gravity and magnetic anomalies using MAGSAT data [E82-10194] p 35 N82-22628
- Use of MAGSAT anomaly data for crustal structure and mineral resources in the US Midcontinent [E82-10321] p 46 N82-24594

NORTH DAKOTA
- AgRISTARS: Supporting research. Spring small grains planting date distribution model [E82-10208] p 12 N82-23581
- Application of thermal model for pan evaporation to the hydrology of a defined medium, the sponge [E82-10217] p 13 N82-23590
- Airborne gamma-ray spectrometer and magnetometer survey. Devil's Lake quadrangle, North Dakota, volume 1 [DE82-004161] p 44 N82-23635
- Airborne gamma-ray spectrometer and magnetometer survey. Devil's Lake quadrangle, North Dakota, volume 2 [DE82-004168] p 44 N82-23636

NORTH SEA
- The METEOSAT Data Collection System and its application p 75 N82-26037

NUCLEAR FUSION
- Nucleosynthesis of light and by-passed isotopes in the solar system matter p 64 A82-22578

NUCLIDES
- Calculated isotopic source composition and tests for origin and propagation of cosmic rays with mass numbers less than or equal to 62 p 83 A82-22554
- Calculation of production rates of cosmogenic nuclides by Monte Carlo method p 64 A82-22576
- Measurement of cosmogenic nuclides using a multi-crystal gamma-ray coincidence spectrometer --- for Mayo Belwa meteorite study p 64 A82-22577

NUMERICAL ANALYSIS
- Generation of the auroral kilometric radiation p 26 A82-35542

NUTRIENTS
- Color aerial photography detects nutrient status of loblolly pine plantations p 6 A82-29531

O

O STARS
- On the stellar origin of low energy cosmic rays p 21 A82-22567

OCCULTATION
- OSO-8 lower mesospheric ozone number density profiles p 28 A82-36472

OCEAN BOTTOM
- Geoid height-age relation from Seasat altimeter profiles across the Mendocino Fracture Zone p 34 A82-32646

OCEAN COLOR SCANNER
- Analysis of ocean color scanner data from the Superflux III Experiment [NASA-TM-83290] p 55 N82-23614

OCEAN CURRENTS
- Seasat altimeter determination of ocean current variability p 50 A82-29613
- A ship and satellite view of hydrographic features in the western Gulf of Mexico p 53 A82-32651
- Determination of winter temperature patterns, fronts, and surface currents in the Yellow Sea and East China Sea from satellite imagery p 55 A82-37195
- Ice distribution and winter surface circulation patterns, Kachemak Bay, Alaska [AD-A110806] p 58 N82-26764

OCEAN DATA ACQUISITIONS SYSTEMS
- Technology and oceanography: An assessment of Federal technologies for oceanographic research and monitoring. Volume 2: Working papers on fishery research technology p 58 N82-26944

OCEAN DYNAMICS
- Estimates of sea surface stress for summer MONEX from cloud motions --- global atmospheric research program p 56 N82-23910
- Satellite observations in FRONTS 80 [AD-A111080] p 58 N82-26766

OCEAN MODELS
- An empirical determination of the effects of sea state bias on Seasat altimetry p 50 A82-29607
- The Seasat altimeter mean sea surface model p 51 A82-29614

OCEAN SURFACE
- Remote sensing of precipitable water over the oceans from Nimbus 7 microwave measurements p 49 A82-28907
- The Seasat altimeter data and its accuracy assessment p 49 A82-29602
- Seasat altimeter height calibration --- related to sea surface heights near Bermuda p 49 A82-29603
- Tidal and geodetic observations for the Seasat altimeter calibration experiment p 49 A82-29604
- An empirical determination of the effects of sea state bias on Seasat altimetry p 50 A82-29607
- Sea-state-related altitude errors in the Seasat radar altimeter p 50 A82-29608
- Seasat altimeter timing bias estimation p 50 A82-29609
- The Seasat altimeter mean sea surface model p 51 A82-29614
- The Seasat-A satellite scatterometer - The geophysical evaluation of remotely sensed wind vectors over the ocean p 51 A82-29616
- The relationship between wind vector and normalized radar cross section used to derive Seasat-A Satellite Scatterometer winds p 51 A82-29617
- Surface wind analyses for Seasat p 51 A82-29619
- The observation of ocean surface phenomena using imagery from the Seasat synthetic aperture radar - An assessment p 52 A82-29623
- Seasat wind and wave observations of northeast Pacific hurricane Iva, August 13, 1978 p 52 A82-29624
- Emissivity and reflectance of the model sea surface for the use of AVHRR data of NOAA satellites p 52 A82-31294
- On the synthetic aperture radar imaging of ocean surface waves p 53 A82-32881
- Ocean wave height measurement with SEASAT SAR using speckle diversity p 53 A82-32882
- Infrared sensing of sea surface temperature from space p 53 A82-32902
- Measuring sea surface temperature from satellites - A ground truth approach p 54 A82-32917
- Depression of brightness temperature of sea surfaces covered with monomolecular oil films relative to clean water surfaces at 1.43 GHz p 54 A82-33322
- Characteristics of 13.9 GHz radar scattering from oil films on the sea surface p 54 A82-33438
- Satellite observations of sea surface temperature around the British Isles p 54 A82-33717
- Pulse-to-pulse correlation in satellite radar altimeters --- for ocean wave height measurement p 55 A82-37390
- Mean sea-level pressure in the Southern Hemisphere during the FGGE period --- First Global Atmospheric Research Program Global Experiment (FGGE); buoys p 55 N82-23856
- On the space-time variability of ocean surface mixed layer characteristics of central and eastern Arabian sea during MONSOON-77 --- global atmospheric research program p 56 N82-23909
- Estimates of sea surface stress for summer MONEX from cloud motions --- global atmospheric research program p 56 N82-23910
- Analysis of ocean and atmosphere thermodynamical characteristics during the onset of southwest monsoon over the Arabian Sea p 57 N82-23945
- The effect of sea-surface Sun glitter on microwave radiometer measurements [NASA-CR-169083] p 57 N82-26525
- Ice distribution and winter surface circulation patterns, Kachemak Bay, Alaska [AD-A110806] p 58 N82-26764
- Satellite observations in FRONTS 80 [AD-A111080] p 58 N82-26766

OCEAN TEMPERATURE
- Seasat altimeter determination of ocean current variability p 50 A82-29613
- Description of Seasat radiometer status and results p 52 A82-29622
- Infrared sensing of sea surface temperature from space p 53 A82-32902
- Measuring sea surface temperature from satellites - A ground truth approach p 54 A82-32917
- Satellite observations of sea surface temperature around the British Isles p 54 A82-33717
- Interannual variations of outgoing IR associated with tropical circulation changes during 1974-1978 p 54 A82-36341
- On the space-time variability of ocean surface mixed layer characteristics of central and eastern Arabian sea during MONSOON-77 --- global atmospheric research program p 56 N82-23909
- Rapid oceanographic data gathering: Some problems in using remote sensing to determine the horizontal and vertical thermal distributions in the Northeast Pacific Ocean [AD-A111005] p 58 N82-26945

OCEANOGRAPHIC PARAMETERS
- Waveheight and wind speed measurements from the Seasat radar altimeter p 50 A82-29612
- Retrieval of ocean surface and atmospheric parameters from multichannel microwave radiometric measurements p 53 A82-31995
- MONEX oceanographic observations along the East African coast --- global atmospheric research program p 56 N82-23908

OCEANOGRAPHY
- Seasat measurement system evaluation - Achievements and limitations p 49 A82-29601
- Magsat magnetic anomalies over Antarctica and the surrounding oceans p 32 A82-30787
- A search for seamounts in the southern Cook and Austral region p 52 A82-30810
- The processing of satellite navigation data for marine geodesy p 34 A82-37175
- High resolution satellite observations of mesoscale oceanography in the Tasman Sea, 1978 - 1979 [E82-10324] p 57 N82-24597
- Ice distribution and winter surface circulation patterns, Kachemak Bay, Alaska [AD-A110806] p 58 N82-26764
- Meteorological and aircraft data for CUE 2 1973 [PB82-149246] p 59 N82-26949

OIL SLICKS
- Emissivity and reflectance of the model sea surface for the use of AVHRR data of NOAA satellites p 52 A82-31294
- Depression of brightness temperature of sea surfaces covered with monomolecular oil films relative to clean water surfaces at 1.43 GHz p 54 A82-33322
- Characteristics of 13.9 GHz radar scattering from oil films on the sea surface p 54 A82-33438

OKLAHOMA
- Application of thermal model for pan evaporation to the hydrology of a defined medium, the sponge [E82-10217] p 13 N82-23590

ON-LINE SYSTEMS
- Present status of on-line analytical triangulation p 69 A82-34940

OPTICAL FILTERS
- Effects of altitude, focal length, and filter combinations on color infrared photography of citrus groves p 9 A82-34729

OPTICAL PROPERTIES
- Bias correction procedures for airborne laser hydrography [PB82-130089] p 63 N82-22644

OPTICAL RADAR
- Airborne lidar measurements of the Soufriere eruption of 17 April 1979 p 24 A82-33657

OPTICAL SCANNERS
- An optical data link for airborne scanning system p 80 A82-34737

OPTICAL THICKNESS
- Interactions of cosmic rays with molecular clouds p 82 A82-22548
- Relating Landsat digital count values to ground reflectance for optically thin atmospheric conditions p 66 A82-29762

OPTIMIZATION
- Determination of the optimal level for combining area and yield estimates [E82-10215] p 12 N82-23588

OREGON

An investigation into the utilization of HCMM thermal data for the discrimination of volcanic and Eolian geological units --- Newberry Volcano, Oregon
[E82-10352] p 47 N82-26750

Meteorological and aircraft data for CUE 2 1973
[PB82-149246] p 59 N82-26949

Airborne gamma-ray spectrometer and magnetometer survey: Chico Quadrangle, California
[DE82-005543] p 48 N82-27815

OROGRAPHY

On the application of a model of boundary-layer flow over low hills to real terrain p 29 A82-36741

The influence of soil characteristics on regional convection differences above Northern Germany p 10 A82-37569

OSCILLATIONS

Fluid-sediment interactions on beaches and shelves
[AD-A110838] p 59 N82-26948

OSO-8

OSO-8 lower mesospheric ozone number density profiles p 28 A82-36472

OSTA-1 PAYLOAD

OSTA-1 Post Mission Operation Report
[NASA-TM-84191] p 84 N82-23258

OXYGEN SPECTRA

Soft X-rays from the sunlit earth's atmosphere p 29 A82-37405

OZONE

Total ozone variations 1970-74 using Backscattered Ultraviolet /BUV/ and ground-based observations p 26 A82-36053

Atmospheric ozone determination by solar occultation using the UV spectrometer on the Solar Maximum Mission p 27 A82-36362

Application of infrared techniques to the study of atmospheric ozone p 27 A82-36414

Observations and analyses of the total amount of atmospheric ozone in the Beijing region and in the region of Jolmolungma Mountain in Tibet p 28 A82-36444

Comparison of ozone in polluted and clean air masses over Lake Michigan p 29 A82-36477

The seasonal variations of ozone and temperature in the middle and the upper stratosphere p 29 A82-36534

In situ ozone data for comparison with laser absorption remote sensor: 1980 PEPE/NEROS program
[NASA-TM-84471] p 30 N82-25661

OZONOMETRY

Observation of the diurnal variation of atmospheric ozone p 26 A82-35895

Sensitivity of Dobson total ozone estimations to wavelength band calibration uncertainties p 27 A82-36405

The effect of the spectral attenuation of UV radiation by aerosol on the total ozone measurements p 27 A82-36406

Microwave measurement of stratospheric and mesospheric ozone p 28 A82-36415

Total ozone retrieval from satellite Meteor 28 Fourier spectrometer measurements p 28 A82-36422

Dobson spectrophotometer calibrations, possible errors in ozone absorption coefficients, and errors due to interfering pollutant gases p 28 A82-36431

OSO-8 lower mesospheric ozone number density profiles p 28 A82-36472

P

PACIFIC OCEAN

A search for seamounts in the southern Cook and Austral region p 52 A82-30810

Investigations of medium wavelength magnetic anomalies in the eastern Pacific using MAGSAT
[E82-10240] p 73 N82-23613

Short term influence radius of monsoonal overturnings --- First Global Atmospheric Research Program Global Experiment (FGGE) p 56 N82-23898

High resolution satellite observations of mesoscale oceanography in the Tasman Sea, 1978 - 1979
[E82 10324] p 57 N82-24597

Investigations of medium wavelength magnetic anomalies in the eastern Pacific using MAGSAT data
[E82-10330] p 38 N82-24603

Satellite observations in FRONTS 80
[AD-A111080] p 58 N82-26766

Rapid oceanographic data gathering: Some problems in using remote sensing to determine the horizontal and vertical thermal distributions in the Northeast Pacific Ocean
[AD-A111005] p 58 N82-26945

PAIN

Thermal mapping, geothermal source location, natural effluents and plant stress in the Mediterranean coast of Spain
[E82-10300] p 17 N82-24576

PALEOMAGNETISM

MAGSAT anomaly map and continental drift
[E82-10326] p 38 N82-24599

PANORAMIC CAMERAS

Development and application of panoramic aerial photography in forest pest management p 5 A82-29527

Photogrammetric methods for mapping resource data from high altitude panoramic photography p 77 A82-32702

Estimating mountain pine beetle-killed ponderosa pine over the front range of Colorado with high altitude panoramic photography p 7 A82-32704

Optical bar panoramic photography for planning timber salvage in drought-stressed forests p 7 A82-32705

Technical and economical characteristics of the AFA-TES-10M aerial camera p 79 A82-34470

PANORAMIC SCANNING

Panoramic aerial photography in forest pest management p 7 A82-32701

PARTICLE ACCELERATION

Confinement and acceleration of cosmic rays in galactic superbubbles p 82 A82-22547

Cosmic ray composition from acceleration of thermal matter p 64 A82-22558

Physical state of the birth place of cosmic rays and its implication to the acceleration processes p 2 A82-22559

Evidence for the stochastic acceleration of cosmic rays in supernova remnants p 2 A82-22564

The galactic origin of cosmic rays. I
[CONF-810711-1] p 2 A82-22565

Cosmic ray acceleration by stellar winds. I - Total density, pressure and energy flux p 21 A82-22566

Acceleration of cosmic rays in accretion shocks p 64 A82-22568

Remarks on cosmic ray origin p 21 A82-22569

Pulsar models and cosmic-ray acceleration p 21 A82-22570

Acceleration processes near massive black holes p 3 A82-22572

The galactic origin of cosmic rays. II
[CONF-810711-2] p 64 A82-22573

Astrophysical scenarios for critically evaluating a zero-point field acceleration mechanism p 64 A82-22575

Interplanetary particle observations associated with solar flare gamma-ray line emission p 3 A82-22584

Computer simulation of the time dependence of the photon energy spectra produced in proton and electron bremstrahlung p 3 A82-22587

High-energy solar protons p 22 A82-22588

A survey of solar protons and alpha differential spectra between 1 and greater than 400 MeV/nucleon p 4 A82-22592

Preflare increases in solar cosmic rays relevant to the mode of energy accumulation in the active regions associated with large flares p 31 A82-22595

On the physical sense of the constant of solar cosmic ray coronal propagation p 83 A82-22599

Time and energy dependence of heavy ion abundances in solar flare energetic particle events p 22 A82-22605

Observations of the ionization states of energetic particles accelerated in solar flares p 40 A82-22607

Coulombian energy losses and the nuclear composition of the solar cosmic rays p 4 A82-22610

PARTICLE DIFFUSION

The cosmic ray positron spectrum p 1 A82-22542

PARTICLE EMISSION

Interplanetary particle observations associated with solar flare gamma-ray line emission p 3 A82-22584

Unusual properties of particle events associated with solar flare gamma ray events p 65 A82-22585

PARTICLE ENERGY

On the characteristics of the very low energy galactic cosmic rays in the interstellar space p 63 A82-22540

Cosmic ray acceleration by stellar winds. I - Total density, pressure and energy flux p 21 A82-22566

On the stellar origin of low energy cosmic rays p 21 A82-22567

11-year modulation and spectrum of cosmic rays in the interstellar space p 22 A82-22616

PARTICLE FLUX DENSITY

Comparison of the measured antiproton flux with that predicted by the 'leaky box' model p 1 A82-22544

Cosmic ray acceleration by stellar winds. I - Total density, pressure and energy flux p 21 A82-22566

Energetic solar particle spectra according to Venera-11, 12 and Prognoz-5, 6 p 4 A82-22593

The modulation characteristics of the 19th and 20th solar activity cycles p 59 A82-22615

Features of cosmic ray variations due to variations in the total magnetic field of the sun p 49 A82-22619

PARTICLE INTERACTIONS

Interactions of cosmic rays with molecular clouds p 82 A82-22548

Cosmic ray composition from acceleration of thermal matter p 64 A82-22558

Calculation of production rates of cosmogenic nuclides by Monte Carlo method p 64 A82-22576

PARTICLE MOTION

A report on the 'cosmic ray propagation problem' p 1 A82-22539

Azimuthal propagation of flare particles in the heliosphere p 66 A82-22590

Spacecraft determination of energetic particle propagation parameters - The 1 January 1978 solar event p 31 A82-22598

PARTICLE PRODUCTION

Extragalactic cosmic rays, their sources and spectrum p 40 A82-22574

Calculation of production rates of cosmogenic nuclides by Monte Carlo method p 64 A82-22576

PARTICLE SIZE DISTRIBUTION

Fine particles in the Soufriere eruption plume p 24 A82-33659

The effect of the spectral attenuation of UV radiation by aerosol on the total ozone measurements p 27 A82-36406

PARTICLE SPIN

Magnetic monopole pair and its observation in cosmic rays p 65 A82-22579

PARTICLE TRAJECTORIES

The question of short pathlengths in interstellar propagation p 1 A82-22541

PARTICULATE SAMPLING

Fine particles in the Soufriere eruption plume p 24 A82-33659

PATTERN RECOGNITION

Description of gray level picture using a collection of density contour lines p 66 A82-29409

Separation of diffuse from sharp-edged features in digital imagery p 68 A82-34225

Multistage classification of multispectral Earth observational data: The design approach
[E82-10213] p 72 N82-23586

AgRISTARS. Project management report: Program review presentation to level 1, interagency coordination committee
[E82-10219] p 13 N82-23592

Analysis of scanner data for crop inventories
[E82-10241] p 16 N82-24519

Analysis of thematic mapper simulator data acquired during winter season over Pearl River, Mississippi, test site
[E82-10287] p 17 N82-24565

Thermal mapping, geothermal source location, natural effluents and plant stress in the Mediterranean coast of Spain
[E82-10300] p 17 N82-24576

Image understanding research
[AD-A110746] p 74 N82-25611

Association of spectral development patterns with development stages of corn
[E82-10353] p 19 N82-26751

PATTERN REGISTRATION

Registration of Heat Capacity Mapping Mission day and night images
[E82-10210] p 72 N82-23583

An analysis of LANDSAT MSS scene-to-scene registration accuracy
[E82-10285] p 16 N82-24563

An algorithm for automating the registration of USDA segment ground data to LANDSAT MSS data
[E82-10286] p 16 N82-24564

Forest Resource Information System. Phase 3: System transfer report
[E82-10344] p 18 N82-25606

Key Issues in the Analysis of Remote Sensing Data: A report on the workshop
[E82-10348] p 85 N82-26746

PENNSYLVANIA

Interactive initialization of heat flux parameters for numerical models using satellite temperature measurements
[E82-10313] p 82 N82-26743

PERFORMANCE PREDICTION

Investigations of point transfer p 78 A82-33296

PERFORMANCE TESTS

The simultaneous employment of geodetic measurements for block adjustments using the method of independent models p 34 A82-33295

PERIODIC VARIATIONS

Features of cosmic ray variations due to variations in the total magnetic field of the sun p 49 A82-22619

Principles and methods of the study of the hydrological cycle on the basis of aerospace data p 61 A82-35127

PERTURBATION

Investigation of the effects of external current systems on the MAGSAT data utilizing grid cell modeling techniques
[E82-10226] p 73 N82-23599

PETROLOGY

Influence of CO2 on melting of model granulite facies assemblages - A model for the genesis of charnockites
p 42 A82-36298

PHENOLOGY

A meteorologically driven maize stress indicator model
[E82-10112] p 11 N82-23564

AgRISTARS: Foreign commodity production forecasting. The 1980 US/Canada wheat and barley exploratory experiment
[E82-10126] p 11 N82-23565

Evaluation of the Doraiswamy-Thompson winter wheat crop calendar model incorporating a modified spring restart sequence
[E82-10207] p 12 N82-23580

AgRISTARS: Supporting research. Spring small grains planting date distribution model
[E82-10208] p 12 N82-23581

A meteorologically driven grain sorghum stress indicator model
[E82-10218] p 13 N82-23591

PHOTOGEOLOGY

Spectroscopic remote sensing for geological applications p 41 A82-32442

Possible fault detection in Cottonball Basin, California An application of radar remote sensing
p 41 A82-32898

Aerogeophysical methods of finding uranium deposits --- Russian book p 41 A82-33402

Comparing lineaments interpreted from Landsat imagery and topographic maps with reported faults in southwest Montana p 34 A82-34719

Landsat in the search for Appalachian hydrocarbons
p 42 A82-34721

Significance of tectonics in linear feature detection and interpretation on satellite images p 42 A82-37198

Overseas Geology And Mineral Resources number 56: A geological interpretation of LANDSAT imagery and air photography of Botswana
[OGMR-56] p 42 N82 22636

Multidisciplinary investigations on HCMM data over middle Europe and Marocco --- southern Germany and Marrakesh, Morocco
[E82-10315] p 74 N82-24588

An investigation into the utilization of HCMM thermal data for the discrimination of volcanic and Eolian geological units --- Newberry Volcano, Oregon
[E82-10352] p 47 N82-26750

PHOTOGONIOMETERS

Irradiance measurement errors due to the assumption of a Lambertian reference panel p 79 A82-34222

PHOTOGRAMMETRY

Photogrammetric methods for mapping resource data from high altitude panoramic photography
p 77 A82-32702

Geographic location of individual pixels --- for thermal infrared digital data processing p 68 A82-32900

The simultaneous employment of geodetic measurements for block adjustments using the method of independent models p 34 A82-33295

Investigations of point transfer p 78 A82-33296

American Society of Photogrammetry, Annual Meeting, 47th, Washington, DC, February 22-27, 1981, ASP Technical Papers p 79 A82-34701

A practical study of gross-error detection in bundle adjustment p 69 A82-34702

Present status of on-line analytical triangulation
p 69 A82-34940

Coordination of stereo image registration and pixel classification
[AD-A111307] p 75 N82-25614

PHOTOGRAPHIC FILM

Considerations in using color infrared photographs for vegetative interpretation p 6 A82-29530

An infrared exposure meter p 76 A82-29541

Image quality and height measurement accuracy of serial survey camera imagery from high altitudes
p 78 A82-33297

Sensitometry in Canadian aerial survey
p 79 A82-34724

PHOTOGRAPHIC PROCESSING

Analytical processing of photographs taken by paired cameras p 79 A82-34471

PHOTOGRAPHY

Detection and damage assessment of citrus tree losses with aerial color infrared photography /ACIR/
p 7 A82-29538

PHOTOINTERPRETATION

Detecting residential land-use development at the urban fringe p 22 A82-29332

Development and application of panoramic aerial photography in forest pest management
p 5 A82-29527

Considerations in using color infrared photographs for vegetative interpretation p 6 A82-29530

Multi-resource inventory in interior Alaska
p 6 A82-29532

Estimating rangeland cover proportions with large-scale color-infrared aerial photographs p 6 A82-29534

Detection and damage assessment of citrus tree losses with aerial color infrared photography /ACIR/
p 7 A82-29538

Application of scanning microdensitometer data in selected plant science case studies p 7 A82-29539

Satellite image interpretation of the eastern Caledonian part of the Blue Road Geotraverse and its geological implications /Nordland, Vasterbotten, Scandinavia/
p 41 A82-30305

Problems of the interpretation of aerial and satellite images of industrial smoke p 23 A82-30307

Extraction of line shaped objects from aerial images using a special operator to analyze the profiles of functions p 67 A82-32033

Dependent feature trees for density approximation. I - Optimal construction and classification results
p 67 A82-32344

The use of contextual information to detect cumulus clouds and cloud shadows in Landsat data
p 67 A82-32346

Evaluation of spruce-fir forests using small-format photographs p 8 A82-32707

Sample design for estimating change in land use and land cover p 24 A82-32711

Interpretation of surface-water circulation, Aransas Pass, Texas, using Landsat imagery p 60 A82-32896

Monitoring land-cover change by principal component analysis of multitemporal Landsat data
p 68 A82-32906

Terrain analysis from Landsat using a color TV enhancement system p 68 A82-32911

Coastal environment change analysis by Landsat MSS data p 54 A82-34219

Site selection and engineering issues for a major industrial complex - Application of image and map interpretation p 25 A82-34711

A computerized spatial analysis system for assessing wildlife habitat from vegetation maps p 9 A82-34716

Comparing lineaments interpreted from Landsat imagery and topographic maps with reported faults in southwest Montana p 34 A82-34719

A quantitative method to test for similarity between photo interpreters p 69 A82-34722

Digital and visual evaluation of GOES and TIROS/NOAA image data for cover type effects on snowfield observations p 60 A82-34735

Status and prospects of the automated processing of remote-sensing data /using forest surveys as an example/ p 10 A82-35139

Significance of tectonics in linear feature detection and interpretation on satellite images p 42 A82-37198

LANDSAT technology transfer to the private and public sectors through community colleges and other locally available institutions
[E82-10181] p 85 N82-23568

Multidisciplinary investigations on HCMM data over middle Europe and Marocco --- southern Germany and Marrakesh, Morocco
[E82-10315] p 74 N82-24588

Mapping of wildlife habitat in Farmington Bay, Utah
[E82-10354] p 19 N82-26752

Irrigated acreage in the Bear River Basin as of the 1975 growing season --- Idaho, Utah, and Wyoming
[E82-10356] p 20 N82-26754

Exploration into technical procedures for vertical integration --- information systems
[NASA-CR-166352] p 75 N82-26763

PHOTOMAPPING

Riparian vegetation mapping in Northeastern California using high altitude color infrared aerial photography
p 5 A82-29528

Multi-resource inventory in interior Alaska
p 6 A82-29532

Mapping riparian vegetation in Southeastern Oregon using digitized large scale color infra-red aerial photography p 6 A82-29535

Application of scanning microdensitometer data in selected plant science case studies p 7 A82-29539

Regional geological, tectonic and geophysical features of Nordland, Norway p 41 A82-30304

Dependent feature trees for density approximation. I - Optimal construction and classification results
p 67 A82-32344

Spectroscopic remote sensing for geological applications p 41 A82-32442

Multispectral mapper - Imaging spectroscopy as applied to the mapping of earth resources p 77 A82-32448

Digitally enhanced visual displays facilitate the analysis of Landsat imagery p 67 A82-32507

Landsat detection of hardwood forest clearcuts
p 8 A82-32706

Computation with physical values from Landsat digital data p 68 A82-32709

Impacts of remote sensing on U.S. geography
p 24 A82-32899

Geographic location of individual pixels --- for thermal infrared digital data processing p 68 A82-32900

Technical and economical characteristics of the AFA-TES-10M aerial camera p 79 A82-34470

A computerized spatial analysis system for assessing wildlife habitat from vegetation maps p 9 A82-34716

Use of Landsat multispectral scanner data in vegetation mapping of a forested area p 9 A82-34731

The use of Skylab S-190B photography for small scale mapping p 80 A82-34742

Aerial photography vs. Landsat for digital land-cover mapping in an urban watershed p 61 A82-34745

The use of space photographs in the mapping of glaciers and water bodies p 62 A82-37174

Relating thematic mapper bands TM3, TM4, and TM5 to agronomic variables for corn, cotton, sugarbeet, soybean, sorghum, sunflower and tobacco
[E82-10347] p 19 N82-26745

Mapping of wildlife habitat in Farmington Bay, Utah
[E82-10354] p 19 N82-26752

PHOTOMAPS

Experience with the compilation of maps of snow-cover melting in the central part of the European USSR on the basis of satellite data p 62 A82-35134

PHOTON BEAMS

Computer simulation of the time dependence of the photon energy spectra produced in proton and electron bremstrahlung p 3 A82-22587

PHOTOOXIDATION

Ammonia and the NOx budget of the troposphere
p 27 A82-36293

PHOTOSYNTHESIS

Spectral estimates of solar radiation intercepted by corn canopies
[E82-10003] p 18 N82-26742

PLANET EPHEMERIDES

The Seasat altimeter data and its accuracy assessment p 49 A82-29602

The Seasat altimeter mean sea surface model
p 51 A82-29614

PLANETARY MAGNETIC FIELDS

MAGSAT anomaly map and continental drift
[E82-10326] p 38 N82-24599

Models and maps of the main field
[E82-10327] p 74 N82-24600

PLANETARY MAPPING

A color-ratio map of Mercury p 31 A82-22294

Initial vector magnetic anomaly map from Magsat
p 32 A82-30785

PLANKTON

HCMM hydrological analysis in Utah
[E82-10328] p 63 N82-24601

PLANT STRESS

A meteorologically driven maize stress indicator model
[E82-10112] p 11 N82-23564

Evaluation of the Doraiswamy-Thompson winter wheat crop calendar model incorporating a modified spring restart sequence
[E82-10207] p 12 N82-23580

A meteorologically driven grain sorghum stress indicator model
[E82-10218] p 13 N82-23591

AgRISTARS: Early warning and crop condition assessment. Plant cover, soil temperature, freeze, water stress, and evapotranspiration conditions
[E82-10225] p 14 N82-23598

Multilevel measurements of surface temperature over undulating terrain planted to barley
[E82-10245] p 16 N82-24523

Thermal mapping, geothermal source location, natural effluents and plant stress in the Mediterranean coast of Spain
[E82-10300] p 17 N82-24576

Multispectral determination of soil moisture-2 --- Guymon, Oklahoma and Dalhart, Texas
[E82-10349] p 19 N82-26747

PLANTING

Diurnal changes in reflectance factor due to Sun-row direction interactions
[E82-10128] p 11 N82-23566

AgRISTARS: Supporting research. Spring small grains planting date distribution model
[E82-10208] p 12 N82-23581

A meteorologically driven grain sorghum stress indicator model [E82-10218] p 13 N82-23591
Airborne observed solar elevation and row direction effects on the near-IR/red ratio of cotton [E82-10220] p 13 N82-23593
Description of the FORTRAN implementation of the spring small grains planting date distribution model [E82-10235] p 15 N82-23608

PLANTS (BOTANY)
Color aerial photography in the plant sciences and related fields; Proceedings of the Eighth Biennial Workshop, Luray, VA, April 21-23, 1981 p 5 A82-29526
Remote sensing of leaf water content in the near infrared p 8 A82-32897
Landsat digital analysis of the initial recovery of burned tundra at Kokolik River, Alaska p 8 A82-32913
The influence of autocorrelation in signature extraction: An example from a geobotanical investigation of Cotter Basin, Montana [E82-10341] p 46 N82-25603

PLASMA COMPOSITION
A tentative ordering of all available solar energetic particles abundance observations. I - The mass unbiased baseline. II - Discussion and comparison with coronal abundances p 40 A82-22609

PLATES (TECTONICS)
Regional geological, tectonic and geophysical features of Nordland, Norway p 41 A82-30304
A satellite magnetic model of northeastern South American aulacogens p 33 A82-30795
An investigation of MAGSAT and complementary data emphasizing precambrian shields and adjacent areas of West Africa and South America [E82-10316] p 38 N82-24589
An investigation of MAGSAT and complementary data emphasizing precambrian shields and adjacent areas of West Africa and South America [E82-10317] p 38 N82-24590
An investigation of MAGSAT and complementary data emphasizing precambrian shields and adjacent areas of West Africa and South America [E82-10318] p 38 N82-24591
Geotectonics of South America --- regional magnetic and gravity anomalies of South America [E82-10320] p 38 N82-24593

PLUMES
Meteorological analysis of the eruption of Soufriere in April 1979 p 24 A82-33655
Airborne lidar measurements of the Soufriere eruption of 17 April 1979 p 24 A82-33657
Fine particles in the Soufriere eruption plume p 24 A82-33659
In situ ozone data for comparison with laser absorption remote sensor: 1980 PEPE/NEROS program [NASA-TM-84471] p 30 N82-25661

POGO
Verification of the crustal component in satellite magnetic data p 32 A82-30789

POLAR CAPS
Extremely high latitude auroras p 76 A82-31020

POLAR ORBITS
Comparison of satellite derived radiation budget measurements over MONEX during 1979 to 1980 --- Monsoon Experiment (MONEX) p 29 N82-23891

POLAR REGIONS
Studies of high latitude current systems using MAGSAT vector data [E82-10188] p 71 N82-22622
Investigation from Japanese MAGSAT Team. Part A. Crustal structure near Japan and in Antarctic station. Part B. Electric currents and hydromagnetic waves in the ionosphere and the magnetosphere [E82-10244] p 36 N82-24522

POLAR SUBSTORMS
Observed magnetic substorm signatures at synchronous altitude p 26 A82-35534

POLAR WANDERING (GEOLOGY)
On reference coordinate systems used in polar motion determinations p 33 A82-32090
A comparison of pole positions derived from GPS satellite and Navy navigation satellite observations [AD-A110765] p 39 N82-26268

POLARIZED LIGHT
A model of plant canopy polarization [E82-10233] p 15 N82-23606

POLLUTION MONITORING
Problems of the interpretation of aerial and satellite images of industrial smoke p 23 A82-30307
Detection of regional air pollution episodes utilizing satellite digital data in the visual range p 23 A82-31990
Depression of brightness temperature of sea surfaces covered with monomolecular oil films relative to clean water surfaces at 1.43 GHz p 54 A82-33322
EPA's new bubble and banking policies --- for environmental monitoring p 25 A82-33865
The use of remote-sensing data to identify the space-time variability of the quality of natural waters p 62 A82-35138
Aircraft measurements of NO/x/ in the lower troposphere above the coast of Japan p 26 A82-36247
Tropospheric CO measurement experiment from the second Space Shuttle flight p 27 A82-36292
A quantitative multispectral analysis system for aerial photographs applied to coastal planning p 55 A82-37505
Feasibility of laser-separation of 36 S and its use as an atmospheric tracer [DE82-000965] p 30 N82-27737

POLLUTION TRANSPORT
Aircraft measurements of NO/x/ in the lower troposphere above the coast of Japan p 26 A82-36247
A study of atmospheric diffusion from the LANDSAT imagery --- pollution transport over the ocean [E82-10360] p 58 N82-26758
Feasibility of laser-separation of 36 S and its use as an atmospheric tracer [DE82-000965] p 30 N82-27737
Field measurements in support of dispersion modeling in complex terrain (1980) [PB82-148644] p 39 N82-27882

POSITION (LOCATION)
A comparison of pole positions derived from GPS satellite and Navy navigation satellite observations [AD-A110765] p 39 N82-26268

POSITRONS
The cosmic ray positron spectrum p 1 A82-22542
The electron and positron spectra in primary cosmic rays p 1 A82-22543
Dependence of earth spectrum of positrons and antiprotons on propagation models --- of cosmic radiation p 21 A82-22545

POSTMISSION ANALYSIS (SPACECRAFT)
OSTA-1 Post Mission Operation Report [NASA-TM-84191] p 84 N82-23258

POTASSIUM
Airborne gamma-ray spectrometer and magnetometer survey. Roseau quadrangle, Minnesota, volume 2 [DE82-001025] p 44 N82-23634
Airborne gamma-ray spectrometer and magnetometer survey. Bemidji quadrangle, Minnesota, volume 2 [DE82-001026] p 44 N82-23638
Airborne gamma-ray spectrometer and magnetometer survey, Kingston quadrangle New York, volume 2C [DE81-027161] p 46 N82-25621
Airborne gamma-ray spectrometer and magnetometer survey, Rochester quadrangle New York, volume 2D [DE81-027156] p 46 N82-25622
Airborne gamma-ray spectrometer and magnetometer survey. Lookout Ridge quadrangle, Alaska, volume 2 [DE82-000313] p 47 N82-25625
Airborne gamma-ray spectrometer and magnetometer survey: Sioux Falls quadrangle, South Dakota, volume 1 [DE82-005533] p 47 N82-27806

POTENTIAL FIELDS
Spherical-Earth gravity and magnetic anomaly modeling by Gauss-Legendre quadrature integration [E82-10242] p 36 N82-24520

POWER SPECTRA
Terrain classification by Fourier analysis - Accuracy and economy p 69 A82-34723
Investigation of Antarctic crust and upper mantle using MAGSAT and other geophysical data [E82-10308] p 37 N82-24582

PRECIPITATION (METEOROLOGY)
Remote sensing of precipitable water over the oceans from Nimbus 7 microwave measurements p 49 A82-28907

PRIMARY COSMIC RAYS
The electron and positron spectra in primary cosmic rays p 1 A82-22543
Comparison of the measured antiproton flux with that predicted by the 'leaky box' model p 1 A82-22544
The galactic origin of cosmic rays. I [CONF-810711-1] p 2 A82-22565
Origin of cosmic rays in galactic centre sources p 3 A82-22571
The energy spectra of cosmic ray variations inferred from the stratospheric measurements in 1972-1979 p 5 A82-22617
Primary spectral variations of cosmic rays above 1 GV p 5 A82-22618

PRIMITIVE EQUATIONS
Impact of additional summer MONEX wind data on the prediction of monsoon depressions during June - August 1979 with two versions of primitive equation (PE) barotropic model --- Monsoon Experiment (MONEX) p 56 N82-23900

PRINTED CIRCUITS
Effective electromagnetic shielding in multilayer printed circuit boards [AIAA 81-2333] p 59 A82-13528

PROBABILITY DENSITY FUNCTIONS
Dependent feature trees for density approximation. I - Optimal construction and classification results p 67 A82-32344

PROBABILITY THEORY
The use of prior probabilities in maximum likelihood classification of remotely sensed data p 68 A82-32904

PROJECT PLANNING
Plan of research for integrated soil moisture studies. Recommendations of the Soil Moisture Working Group [NASA-TM-84731] p 18 N82-25608

PROPAGATION MODES
A report on the 'cosmic ray propagation problem' p 1 A82-22539

PROTON ENERGY
Origin of cosmic rays in galactic centre sources p 3 A82-22571
High-energy solar protons p 22 A82-22588

PROTON FLUX DENSITY
Evolution of the solar proton spectrum in interplanetary space p 4 A82-22594
Comparison of solar proton activity in 1967 and 1969 with that in 1978 and 1979 as measured onboard Venera 4, 6, 11, 12 space probes p 31 A82-22596
The solar proton fluxes in April, 1979 p 66 A82-22597
A description of relativistic solar particle propagation p 4 A82-22600
Non-flare injection of protons into interplanetary space p 4 A82-22601
On the anticorrelation between the He/3//He/4/ ratio and proton intensity in He/3/ rich flares p 40 A82-22613
The energy spectra of cosmic ray variations inferred from the stratospheric measurements in 1972-1979 p 5 A82-22617

PULSARS
Pulsar models and cosmic-ray acceleration p 21 A82-22570

PULSE RADAR
Pulse-to-pulse correlation in satellite radar altimeters --- for ocean wave height measurement p 55 A82-37390

Q

QUANTITATIVE ANALYSIS
Quantitative relationships of near-surface spectra to Landsat radiometric data p 78 A82-32912

QUANTUM THEORY
Astrophysical scenarios for critically evaluating a zero-point field acceleration mechanism p 64 A82-22575

QUARTZ
Influence of CO2 on melting of model granulite facies assemblages - A model for the genesis of charnockites p 42 A82-36298

R

RADAR
Movement of ice markers measured by satellite ranging [R-240] p 59 N82-27816

RADAR CROSS SECTIONS
The relationship between wind vector and normalized radar cross section used to derive Seasat-A Satellite Scatterometer winds p 51 A82-29617

RADAR DETECTION
Possible fault detection in Cottonball Basin, California An application of radar remote sensing p 41 A82-32896

RADAR ECHOES
Characteristics of field-aligned E region irregularities over Iioka /36 N/, Japan. I p 26 A82-36268

RADAR EQUIPMENT
Pulse-to-pulse correlation in satellite radar altimeters --- for ocean wave height measurement p 55 A82-37390

RADAR GEOLOGY
An investigation into the utilization of HCMM thermal data for the discrimination of volcanic and Eolian geological units --- Newberry Volcano, Oregon [E82-10352] p 47 N82-26750

RADAR IMAGERY
A simulation study of soil moisture estimation by a space SAR p 60 A82-29333
The observation of ocean surface phenomena using imagery from the Seasat synthetic aperture radar - An assessment p 52 A82-29623

The estimation of wave height from digitally processed SAR imagery p 67 A82-32347
On the synthetic aperture radar imaging of ocean surface waves p 53 A82-32881
Ocean wave height measurement with SEASAT SAR using speckle diversity p 53 A82-32882
Possible fault detection in Cottonball Basin, California An application of radar remote sensing p 41 A82-32898
Interpretation of vegetative cover in wetlands using four-channel SAR imagery p 9 A82-34706
C-band radar for determining surface soil moisture p 10 A82-37194
Evaluation of the soil moisture prediction accuracy of a space radar using simulation techniques --- Kansas [E82-10351] p 19 N82-26749
RADAR MEASUREMENT
Airborne lidar measurements of the Soufriere eruption of 17 April 1979 p 24 A82-33657
The use of soil texture and field capacity to normalize microwave soil moisture measurements: Some problems p 20 N82-26762
RADAR SCATTERING
Characteristics of 13.9 GHz radar scattering from oil films on the sea surface p 54 A82-33438
The use of soil texture and field capacity to normalize microwave soil moisture measurements: Some problems p 20 N82-26762
RADAR TARGETS
The recognition of extended targets - SAR images for level and hilly terrain p 33 A82-31994
RADIANCE
Surface temperature determination from an amalgamation of GOES and TIROS-N radiance measurements p 66 A82-28905
Effect of atmospheric conditions on remote sensing of vegetation parameters p 24 A82-32901
Influence of sky radiance distribution on the ratio technique for estimating bidirectional reflectance p 70 A82-35650
Ground support data from July 10 to July 29, 1978, for HCMM thermal satellite data of the Powder River Basin, Wyoming [E82-10211] p 72 N82-23584
RADIANT FLUX DENSITY
The charge and isotopic composition of Z equals 7-16 cosmic ray nuclei at their source p 64 A82-22555
Comparison of brightness indicatrixes of snow cover measured from an aircraft and calculated theoretically for different heights of the atmosphere p 62 A82-35140
RADIATION COUNTERS
Relating Landsat digital count values to ground reflectance for optically thin atmospheric conditions p 66 A82-29762
RADIATION DISTRIBUTION
Derivation of the distribution of synchrotron emissivity in the Galaxy from the 408 MHz all-sky survey p 82 A82-22549
Influence of sky radiance distribution on the ratio technique for estimating bidirectional reflectance p 70 A82-35650
RADIATION HAZARDS
Environmental monitoring report of the Lawrence Berkeley Laboratory, 1980 [LBL-12604] p 29 N82-23793
RADIATION MEASUREMENT
Comparison of satellite derived radiation budget measurements over MONEX during 1979 to 1980 --- Monsoon Experiment (MONEX) p 29 N82-23891
RADIATION PRESSURE
Cosmic ray acceleration by stellar winds. I - Total density, pressure and energy flux p 21 A82-22566
RADIATION SOURCES
The charge and isotopic composition of Z equals 7-16 cosmic ray nuclei at their source p 64 A82-22555
Mass per charge ratio in hot plasmas and cosmic ray source composition p 2 A82-22557
The galactic origin of cosmic rays. II [CONF-810711-2] p 64 A82-22573
RADIATION SPECTRA
Airborne gamma-ray spectrometer and magnetometer survey. Roseau quadrangle, Minnesota, volume 1 [DE82-001031] p 43 N82-23621
Airborne gamma-ray spectrometer and magnetometer survey. Hibbing quadrangle, Minnesota, volume 1 [DE82-004159] p 44 N82-23639
Airborne gamma-ray spectrometer and magnetometer survey. Hibbing quadrangle, Minnesota, volume 2 [DE82-004165] p 45 N82-23640
Airborne gamma-ray spectrometer and magnetometer survey. Aberdeen quadrangle, South Dakota, volume 1 [DE82-004152] p 45 N82-23641
Airborne gamma-ray spectrometer and magnetometer survey. Aberdeen quadrangle, South Dakota, volume 2 [DE82-004164] p 45 N82-23642
RADIATIVE TRANSFER
A comparative study of microwave radiometer observations over snowfields with radiative transfer model calculations --- for water runoff estimation p 60 A82-32910
Spatial thermal radiometry contribution to the Massif Armoricain and the Massif Central France litho-structural study [E82-10190] p 42 N82-22624
Application of HCMM data to regional geologic analysis for mineral and energy resource evaluation [E82-10243] p 45 N82-24521
Multispectral determination of soil moisture-2 --- Guymon, Oklahoma and Dalhart, Texas [E82-10349] p 19 N82-26747
RADIO ALTIMETERS
The Seasat altimeter data and its accuracy assessment p 49 A82-29602
Seasat altimeter height calibration --- related to sea surface heights near Bermuda p 49 A82-29603
Tidal and geodetic observations for the Seasat altimeter calibration experiment p 49 A82-29604
An empirical determination of the effects of sea state bias on Seasat altimetry p 50 A82-29607
Sea-state-related altitude errors in the Seasat radar altimeter p 50 A82-29608
Seasat altimeter timing bias estimation p 50 A82-29609
Evaluation of the Seasat altimeter time tag bias p 50 A82-29610
Comparison data for Seasat altimetry in the western North Atlantic p 50 A82-29611
Waveheight and wind speed measurements from the Seasat radar altimeter p 50 A82-29612
Seasat altimeter determination of ocean current variability p 50 A82-29613
The Seasat altimeter mean sea surface model p 51 A82-29614
Pulse-to-pulse correlation in satellite radar altimeters --- for ocean wave height measurement p 55 A82-37390
RADIO AURORAS
Large amplitude undulations on the equatorward boundary of the diffuse aurora p 76 A82-31019
RADIO EMISSION
Angular variations of nonthermal radio emission from the Galaxy relevant to the structure of interstellar magnetic field p 83 A82-22550
RADIO FREQUENCY INTERFERENCE
Inference of refractivity profiles by satellite-to-ground RF measurements p 78 A82-33442
RADIO PROBING
Influence of sky radiance distribution on the ratio technique for estimating bidirectional reflectance p 70 A82-35650
RADIO SOURCES (ASTRONOMY)
The definition of the terrestrial coordinate frame by long baseline interferometry p 33 A82-32084
Some considerations in the use of very-long-baseline-interferometry to establish reference coordinate systems for geodynamics p 34 A82-32096
RADIO WAVE REFRACTION
Inference of refractivity profiles by satellite-to-ground RF measurements p 78 A82-33442
RADIOMETERS
Evaluation of NOAA-AVHRR data for crop assessment --- Advanced Very High Resolution Radiometer p 8 A82-34179
Airborne gamma-ray spectrometer and magnetometer survey. Devil's Lake quadrangle, North Dakota, volume 2 [DE82-004168] p 44 N82-23636
Airborne gamma-ray spectrometer and magnetometer survey, Toronto quadrangle New York, volume 2A [DE81-027158] p 46 N82-25620
Airborne gamma-ray spectrometer and magnetometer survey, Rochester quadrangle New York, volume 2D [DE81-027156] p 46 N82-25622
Irrigation management with remote sensing --- Navajo Indian Irrigation Project [E82-10357] p 20 N82-26755
Satellite observations in FRONTS 80 [AD-A111080] p 58 N82-26766
Airborne gamma-ray spectrometer and magnetometer survey: North/south tieline, volume 1 [DE82-005542] p 47 N82-27804
RADIOMETRIC CORRECTION
Quantitative relationships of near-surface spectra to Landsat radiometric data p 78 A82-32912
View angle effects in the radiometric measurement of plant canopy temperatures p 8 A82-32914
Measuring sea surface temperature from satellites - A ground truth approach p 54 A82-32917
RADIOMETRIC RESOLUTION
Evaluation of VICAR software capability for land information support system needs --- Elk River quadrangle, Idaho [E82-10223] p 73 N82-23596
RAIN
A statistical approach to rainfall estimation using satellite and conventional data [NOAA-TR-NESS-89] p 63 N82-22854
RANGELANDS
Estimating rangeland cover proportions with large-scale color-infrared aerial photographs p 6 A82-29534
An analysis of LANDSAT MSS scene-to-scene registration accuracy [E82-10285] p 16 N82-24563
REFLECTANCE
Application of Computer Axial Tomography (CAT) to measuring crop canopy geometry --- corn and soybeans [E82-10227] p 14 N82-23600
Canopy reflectance as influenced by solar illumination angle [E82-10237] p 15 N82-23610
Irrigated acreage in the Bear River Basin as of the 1975 growing season --- Idaho, Utah, and Wyoming [E82-10356] p 20 N82-26754
REFLECTED WAVES
System albedo as sensed by satellites - Its definition and variability p 23 A82-32342
REFRACTIVITY
Inference of refractivity profiles by satellite-to-ground RF measurements p 78 A82-33442
REGIONAL PLANNING
A legislator's guide to LANDSAT [E82-10290] p 85 N82-24568
REGRESSION ANALYSIS
A comparison of stratified versus regression estimators p 11 N82-23133
RELATIVISTIC ELECTRON BEAMS
Steady-state cosmic ray electron spectrum under diffusion, convection, adiabatic deceleration and synchrotron losses p 1 A82-22552
RELATIVISTIC PARTICLES
A description of relativistic solar particle propagation p 4 A82-22600
RELIABILITY ENGINEERING
A practical study of gross-error detection in bundle adjustment p 69 A82-34702
RELIEF MAPS
Bathymetric imaging p 69 A82-34720
REMOTE SENSING
Detection of environmental disturbance using color aerial photography and thermal infrared imagery p 22 A82-29327
A simulation study of soil moisture estimation by a space SAR p 60 A82-29333
Remote sensing of the weediness of crop fields p 5 A82-29435
Color aerial photography in the plant sciences and related fields; Proceedings, of the Eighth Biennial Workshop, Luray, VA, April 21-23, 1981 p 5 A82-29526
Development and application of panoramic aerial photography in forest pest management p 5 A82-29527
Riparian vegetation mapping in Northeastern California using high altitude color infrared aerial photography p 5 A82-29528
Inventory of wildlife habitat from color infrared aerial photography for Cobb Island, Virginia p 6 A82-29529
Color aerial photography detects nutrient status of loblolly pine plantations p 6 A82-29531
Application of 35mm color aerial photography to forest land change detection p 6 A82-29533
Remote sensing of Douglas-fir trees newly infested by bark beetles p 6 A82-29536
Spectral scanning of experimental plots of SO2-affected winter wheat and soybeans for mission planning p 6 A82-29537
Application of scanning microdensitometer data in selected plant science case studies p 7 A82-29539
The Seasat-A satellite scatterometer - The geophysical evaluation of remotely sensed wind vectors over the ocean p 51 A82-29616
Desert locust habitat monitoring with satellite remote sensing A new technology for an old problem p 7 A82-29747
Thermography - A remote sensing method with many perspectives p 76 A82-29922
Space to the earth --- Russian book on space technology applications p 83 A82-30850
The use of the SPOT satellite in natural resource evaluation p 83 A82-31996
Extraction of line shaped objects from aerial images using a special operator to analyze the profiles of functions p 67 A82-32033

Remote sensing of tornadic storms from geosynchronous satellite infrared digital data
p 23 A82-32348

Imaging spectroscopy; Proceedings of the Seminar, Los Angeles, CA, February 10, 11, 1981 p 77 A82-32440

Spectroscopic remote sensing for geological applications p 41 A82-32442

High spectral resolution airborne spectrometry
p 77 A82-32443

Laser-induced bioluminescence --- for remote sensing of marine organisms p 53 A82-32559

Impacts of remote sensing on U.S. geography
p 24 A82-32899

Effect of atmospheric conditions on remote sensing of vegetation parameters p 24 A82-32901

Infrared sensing of sea surface temperature from space p 53 A82-32902

Nearshore current pattern off south Texas - An interpretation from aerial photographs
p 53 A82-32903

The use of prior probabilities in maximum likelihood classification of remotely sensed data
p 68 A82 32904

Quantitative relationships of near-surface spectra to Landsat radiometric data p 78 A82-32912

Snowpack monitoring in North America and Eurasia using passive microwave satellite data
p 78 A82-32915

Appearance of irregular tree canopies in nighttime high-resolution thermal infrared imagery
p 68 A82-32916

Remote sensing of the earth's resources - The Soviet experience p 84 A82-33555

Irradiance measurement errors due to the assumption of a Lambertian reference panel p 79 A82-34222

ERS-1 European remote sensing satellite
p 84 A82-34367

American Society of Photogrammetry, Annual Meeting, 47th, Washington, DC, February 22-27, 1981, ASP Technical Papers p 79 A82-34701

Image processing with microcomputers in remote sensing p 79 A82-34708

Site selection and engineering issues for a major industrial complex - Application of image and map interpretation p 25 A82-34711

RAMS-1, a Resource Analysis and Mapping System
p 69 A82 34726

Remote sensing of thermal subsurface terrain properties p 80 A82-34727

Remote sensing - A potential aid in the preparation of an urban tree inventory p 9 A82-34732

Monitoring deforestation in the eastern part of the state of Guerrero, Mexico p 9 A82-34733

Digital and visual evaluation of GOES and TIROS/NOAA image data for cover type effects on snowfield observations p 60 A82-34735

A new approach to multiresource inventories using remote sensing and geographic information systems technologies p 25 A82-34739

Comparisons of land cover classifications from selected remote sensing systems p 80 A82-34746

Study of the hydrological cycle by aerospace methods --- Russian book p 61 A82-35126

Principles and methods of the study of the hydrological cycle on the basis of aerospace data p 61 A82-35127

The possibility of using remote-sensing methods to study the hydrology of elementary watersheds
p 61 A82-35130

The seasonal snow-line within the Fergana basin and the possibility of using it for hydrological forecasting
p 61 A82-35131

The use of remote-sensing data to identify the space-time variability of the quality of natural waters
p 62 A82-35138

Status and prospects of the automated processing of remote-sensing data /using forest surveys as an example/ p 10 A82-35139

Allowance for the effect of the atmosphere in the processing of satellite remote-sensing images
p 70 A82-35141

The use of microwave radiometry for the determination of snow cover height p 80 A82-36018

Microwave measurement of stratospheric and mesospheric ozone p 28 A82-36415

Space science for applications - The history of Landsat p 84 A82-36617

Satellite radiation measurements for the retrieval of the vertical temperature profiles p 70 A82-36935

Landsat D to yield more precise data
p 70 A82-37200

Spatial resolution requirements for urban studies
p 29 A82-37502

Remote sensing of salt marsh vegetation in the first four proposed Thematic Mapper bands
p 10 A82-37503

Advanced technology for earth observation - Data processing
[AAS PAPER 82-130] p 71 A82-37810

Solid state instrumentation concepts for earth resource observation
[AAS PAPER 82-132] p 81 A82-37812

Civil land remote sensing system
[GPO-87-070] p 84 N82-22630

Use of NOAA/AVHRR visible and near-infrared data for land remote sensing
[NASA-TM-84186] p 81 N82-22643

AgRISTARS: Renewable resources inventory. Land information support system implementation plan and schedule --- San Juan National Forest pilot test
[E82-10224] p 14 N82-23597

Agricultural Research Service research highlights in remote sensing for calendar year 1980
[E82-10228] p 14 N82-23601

Cost-effectiveness of geographic surveying from space p 85 N82-24263

Plan of research for integrated soil moisture studies. Recommendations of the Soil Moisture Working Group
[NASA-TM-84731] p 18 N82-25608

Experimental assessment of improved spatial resolution LANDSAT data
[AD-A110538] p 75 N82-26765

Rapid oceanographic data gathering: Some problems in using remote sensing to determine the horizontal and vertical thermal distributions in the Northeast Pacific Ocean
[AD-A111005] p 58 N82-26945

Remote sensing of sulfur dioxide effects on vegetation. Volume 1: Summary
[DE82-900580] p 31 N82-27802

Remote sensing of sulfur dioxide effects on vegetation. Volume 2: Data
[DE82-900581] p 31 N82-27803

REMOTE SENSORS

Magnetic anomalies as a reference for ground-speed and map-matching navigation p 32 A82-30314

A system design for a multispectral sensor using two-dimensional solid-state imaging arrays
p 77 A82-31991

Inversion of data from diffraction-limited multiwavelength remote sensors. II - Nonlinear dependence of observables on the geophysical parameters p 77 A82-32658

An optical objective lens for earth observations by satellites p 78 A82-32824

View angle effects in the radiometric measurement of plant canopy temperatures p 8 A82-32914

Characteristics of 13.9 GHz radar scattering from oil films on the sea surface p 54 A82-33438

EPA's new bubble and banking policies --- for environmental monitoring p 25 A82-33865

An information-theoric spatial transform
p 69 A82-34717

Bathymetric imaging p 69 A82-34720

Longwave infrared observation of urban landscapes
p 25 A82-34744

Evaluation of the accuracy of water-surface temperature measurement by means of airborne infrared radiometers
p 62 A82-35136

Microwave sensing from space
[AAS PAPER 82-127] p 80 A82-37809

Orbiting passive microwave sensor simulation applied to soil moisture estimation
[E82-10343] p 18 N82-25605

In situ ozone data for comparison with laser absorption remote sensor: 1980 PEPE/NEROS program
[NASA-TM-84471] p 30 N82-25661

RESEARCH

Agricultural Research Service research highlights in remote sensing for calendar year 1980
[E82-10228] p 14 N82-23601

RESEARCH FACILITIES

Environmental monitoring report of the Lawrence Berkeley Laboratory, 1980
[LBL-12604] p 29 N82-23793

RESEARCH MANAGEMENT

Plan of research for integrated soil moisture studies. Recommendations of the Soil Moisture Working Group
[NASA-TM-84731] p 18 N82-25608

RESERVOIRS

Dynamic study of the upper Sao Francisco river and Tres Marias reservoir using MSS/LANDSAT images --- BRazil
[E82-10291] p 63 N82-24569

RESIDENTIAL AREAS

Detecting residential land-use development at the urban fringe p 22 A82-29332

RESOURCES MANAGEMENT

Multi-resource inventory in interior Alaska
p 6 A82-29532

Streamlining and ensuring mineral development must begin at local land management levels
[EMD-82-10] p 29 N82-23043

Agricultural Research Service research highlights in remote sensing for calendar year 1980
[E82-10228] p 14 N82-23601

AgRISTARS: Agriculture and resources inventory surveys through aerospace remote sensing
[E82-10236] p 15 N82-23609

Remote automatic weather station for resource and fire management agencies
[PB82-107335] p 30 N82-23963

A legislator's guide to LANDSAT
[E82-10290] p 85 N82-24568

RESPONSE BIAS

Bias correction procedures for airborne laser hydrography
[PB82-130089] p 63 N82-22644

RETURN BEAM VIDICONS

Comparisons of land cover classifications from selected remote sensing systems p 80 A82-34746

RHEOLOGY

Fluid-sediment interactions on beaches and shelves
[AD-A110838] p 59 N82-26948

RING CURRENTS

Improved definition of crustal magnetic anomalies for MAGSAT data
[E82-10314] p 37 N82-24587

RIVER BASINS

The seasonal snow-line within the Fergana basin and the possibility of using it for hydrological forecasting
p 61 A82-35131

The use of satellite photographs to study snow-cover dynamics and to determine the average water discharge of the Amudarya during a vegetation period
p 61 A82-35132

Analysis of thematic mapper simulator data acquired during winter season over Pearl River, Mississippi, test site
[E82-10287] p 17 N82-24565

Irrigated acreage in the Bear River Basin as of the 1975 growing season --- Idaho, Utah, and Wyoming
[E82-10356] p 20 N82-26754

RIVERS

The use of satellite photographs to study snow-cover dynamics and to determine the average water discharge of the Amudarya during a vegetation period
p 61 A82-35132

Airborne gamma-ray spectrometer and magnetometer survey. Utukik River quadrangle, Alaska, volume 2
[DE82-000316] p 44 N82-23631

Dynamic study of the upper Sao Francisco river and Tres Marias reservoir using MSS/LANDSAT images --- BRazil
[E82-10291] p 63 N82-24569

ROCKS

The mineralogy of global magnetic anomalies --- rock magnetic signatures and MAGSAT geological, and gravity correlations in West Africa
[E82-10305] p 45 N82-24579

RODS

Nonlinear theory for elastic beams and rods and its finite element representation
[WTHD-143] p 73 N82-24517

RURAL LAND USE

Monitoring deforestation in the eastern part of the state of Guerrero, Mexico p 9 A82-34733

Analysis of scanner data for crop inventories
[E82-10192] p 10 N82-22626

Determination of the optimal level for combining area and yield estimates
[E82-10215] p 12 N82-23588

S

SALINITY

Problems associated with remotely detecting and monitoring saline sites within irrigated Alberta
p 9 A82-34710

SANDS

Remote sensing in Scotland using data received from satellites - A study of the Tay Estuary region using Landsat multispectral scanning imagery p 62 A82-37501

Fluid-sediment interactions on beaches and shelves
[AD-A110838] p 59 N82-26948

SATELLITE ANTENNAS

Movement of ice markers measured by satellite ranging
[R-240] p 59 N82-27816

SATELLITE DESIGN

LANDSAT-D thermal analysis and design support
[E82-10346] p 82 N82-26744

SATELLITE GROUND SUPPORT

Advanced technology for earth observation - Data processing
[AAS PAPER 82-130] p 71 A82-37810

SATELLITE GROUND TRACKS
Evaluation of the Seasat altimeter time tag bias p 50 A82-29610
SATELLITE OBSERVATION
Solar gamma-ray experiment on Astro-A satellite p 21 A82-22583
The relation of type II radio bursts to solar energetic particles observed at earth p 3 A82-22591
A survey of solar protons and alpha differential spectra between 1 and greater than 400 MeV/nucleon p 4 A82-22592
Energetic solar particle spectra according to Venera-11, 12 and Prognoz-5, 6 p 4 A82-22593
Spacecraft determination of energetic particle propagation parameters - The 1 January 1978 solar event p 31 A82-22598
Low-energy particles in interplanetary magnetic field near the sectorial boundary on September 26, 1977 p 4 A82-22602
Surface temperature determination from an amalgamation of GOES and TIROS-N radiance measurements p 66 A82-28905
The observation of ocean surface phenomena using imagery from the Seasat synthetic aperture radar - An assessment p 52 A82-29623
A study of the earth's radiation budget using a general circulation model p 52 A82-30666
Magsat scalar anomaly distribution - The global perspective p 41 A82-30786
A satellite magnetic model of northeastern South American aulacogens p 33 A82-30795
Extremely high latitude auroras p 76 A82-31020
Emissivity and reflectance of the model sea surface for the use of AVHRR data of NOAA satellites p 52 A82-31294
Origin and scale of coordinate systems in satellite geodesy p 34 A82-32099
System albedo as sensed by satellites - Its definition and variability p 23 A82-32342
Geoid height-age relation from Seasat altimeter profiles across the Mendocino Fracture Zone p 34 A82-32646
An optical objective lens for earth observations by satellites p 78 A82-32824
Geostationary satellite observations of the April 1979 Soufriere eruptions p 24 A82-33654
Earth observations from space - Trends and prospects p 84 A82-34116
Observed magnetic substorm signatures at synchronous altitude p 26 A82-35534
Estimation of the precipitable water from the IR channel of the geostationary satellite p 55 A82-37196
Soft X-rays from the sunlit earth's atmosphere p 29 A82-37405
Microwave sensing from space
[AAS PAPER 82-127] p 80 A82-37809
A statistical approach to rainfall estimation using satellite and conventional data
[NOAA-TR-NESS-89] p 63 N82-22854
Comparison of satellite derived radiation budget measurements over MONEX during 1979 to 1980 --- Monsoon Experiment (MONEX) p 29 N82-23891
History of the French satellite space program p 85 N82-24216
A comparison of pole positions derived from GPS satellite and Navy navigation satellite observations
[AD-A110765] p 39 N82-26268
SATELLITE SOUNDING
Magnetic charts of Canada derived from Magsat data p 32 A82-30778
Initial scalar magnetic anomaly map from Magsat p 32 A82-30784
Remote sensing of tornadic storms from geosynchronous satellite infrared digital data p 23 A82-32348
Satellite observations of sea surface temperature around the British Isles p 54 A82-33717
Total ozone retrieval from satellite Meteor 28 Fourier spectrometer measurements p 28 A82-36422
Satellite radiation measurements for the retrieval of the vertical temperature profiles p 70 A82-36935
SATELLITE TELEVISION
The seasonal snow-line within the Fergana basin and the possibility of using it for hydrological forecasting p 61 A82-35131
SATELLITE TEMPERATURE
LANDSAT-D thermal analysis and design support
[E82-10346] p 82 N82-26744
SATELLITE TRACKING
Spatial resolution and repeatability of Magsat crustal anomaly data over the Indian Ocean p 32 A82-30788
Representativeness of cloud motion winds deduced from GOES Indian Ocean satellite imagery for the description of the Indian summer monsoon --- superpressure balloons for the study of the Indian summer monsoon (BALSAMINE) p 55 N82-23879
SATELLITE TRANSMISSION
Purpose, background of 'Intercosmos-21' mission p 81 N82-24264
SATELLITE-BORNE INSTRUMENTS
Seasat measurement system evaluation - Achievements and limitations p 49 A82-29601
The Seasat altimeter data and its accuracy assessment p 49 A82-29602
Tidal and geodetic observations for the Seasat altimeter calibration experiment p 49 A82-29604
Waveheight and wind speed measurements from the Seasat radar altimeter p 50 A82-29612
Seasat altimeter determination of ocean current variability p 50 A82-29613
The Seasat altimeter mean sea surface model p 51 A82-29614
The Seasat-A satellite scatterometer - The geophysical evaluation of remotely sensed wind vectors over the ocean p 51 A82-29616
The relationship between wind vector and normalized radar cross section used to derive Seasat-A Satellite Scatterometer winds p 51 A82-29617
Evaluation of atmospheric attenuation from SMMR brightness temperature for the Seasat satellite scatterometer p 51 A82-29618
Intercomparison of wind speeds inferred by the SASS, altimeter, and SMMR p 52 A82-29621
Description of Seasat radiometer status and results p 52 A82-29622
Seasat wind and wave observations of northeast Pacific hurricane Iva, August 13, 1978 p 52 A82-29624
Space to the earth --- Russian book on space technology applications p 83 A82-30850
Inference of refractivity profiles by satellite-to-ground RF measurements p 78 A82-33442
Evaluation of NOAA-AVHRR data for crop assessment --- Advanced Very High Resolution Radiometer p 8 A82-34179
Allowance for the effect of the atmosphere in the processing of satellite remote-sensing images p 70 A82-35141
Application of satellite magnetic anomaly data to Curie isotherm mapping p 70 A82-35824
Pulse-to-pulse correlation in satellite radar altimeters --- for ocean wave height measurement p 55 A82-37390
Advanced technology for earth observation - Data processing
[AAS PAPER 82-130] p 71 A82-37810
LANDSAT-D conical scanner evaluation plan
[E82-10340] p 81 N82-25602
Orbiting passive microwave sensor simulation applied to soil moisture estimation
[E82-10343] p 18 N82-25605
SATELLITE-BORNE PHOTOGRAPHY
The use of residual images in Landsat image analysis p 66 A82-29328
Satellite image interpretation of the eastern Caledonian part of the Blue Road Geotraverse and its geological implications /Nordland, Vasterbotten, Scandinavia/ p 41 A82-30305
Problems of the interpretation of aerial and satellite images of industrial smoke p 23 A82-30307
Large amplitude undulations on the equatorward boundary of the diffuse aurora p 76 A82-31019
Detection of volcanic smoke and ash-fall area at volcano Aso, from Landsat MSS data p 23 A82-31295
Detection of regional air pollution episodes utilizing satellite digital data in the visual range p 23 A82-31990
Dependent feature trees for density approximation. I - Optimal construction and classification results p 67 A82-32344
Evaluation of temporal registration of Landsat scenes p 67 A82-32345
The use of contextual information to detect cumulus clouds and cloud shadows in Landsat data p 67 A82-32346
Resource inventory techniques used in the California Desert Conservation Area p 23 A82-32441
Digitally enhanced visual displays facilitate the analysis of Landsat imagery p 67 A82-32507
A ship and satellite view of hydrographic features in the western Gulf of Mexico p 53 A82-32651
Landsat detection of hardwood forest clearcuts p 8 A82-32708
Computation with physical values from Landsat digital data p 68 A82-32709
Geographic location of individual pixels --- for thermal infrared digital data processing p 68 A82-32900
Monitoring land-cover change by principal component analysis of multitemporal Landsat data p 68 A82-32906
The response characteristics of vegetation in Landsat MSS digital data p 8 A82-32907
Field size, length, and width distributions based on LACIE ground truth data --- large area crop inventory experiment p 8 A82-32909
Terrain analysis from Landsat using a color TV enhancement system p 68 A82-32911
Problems associated with remotely detecting and monitoring saline sites within irrigated Alberta p 9 A82-34710
Comparing lineaments interpreted from Landsat imagery and topographic maps with reported faults in southwest Montana p 34 A82-34719
Landsat in the search for Appalachian hydrocarbons p 42 A82-34721
Digital and visual evaluation of GOES and TIROS/NOAA image data for cover type effects on snowfield observations p 60 A82-34735
A new approach to multiresource inventories using remote sensing and geographic information systems technologies p 25 A82-34739
The use of Skylab S-190B photography for small scale mapping p 80 A82-34742
Study of the hydrological cycle by aerospace methods --- Russian book p 61 A82-35126
Principles and methods of the study of the hydrological cycle on the basis of aerospace data p 61 A82-35127
Water-balance differentiation of natural complexes on the basis of satellite photographs p 61 A82-35129
The use of satellite photographs to study snow-cover dynamics and to determine the average water discharge of the Amudarya during a vegetation period p 61 A82-35132
Method for the analysis of the melting of a firn complex on the basis of aerospace photographs p 61 A82-35133
Experience with the compilation of maps of snow-cover melting in the central part of the European USSR on the basis of satellite data p 62 A82-35134
Status and prospects of the automated processing of remote-sensing data /using forest surveys as an example/ p 10 A82-35139
The meteorological product - 'Cloud-top height' p 70 A82-36043
Space science for applications - The history of Landsat p 84 A82-36617
Design guidelines for satellite image data distribution systems p 70 A82-37048
The use of space photographs in the mapping of glaciers and water bodies p 62 A82-37174
Determination of winter temperature patterns, fronts, and surface currents in the Yellow Sea and East China Sea from satellite imagery p 55 A82-37195
Significance of tectonics in linear feature detection and interpretation on satellite images p 42 A82-37198
Landsat D to yield more precise data p 70 A82-37200
SCALE (RATIO)
Origin and scale of coordinate systems in satellite geodesy p 34 A82-32099
SCANNING
Application of scanning microdensitometer data in selected plant science case studies p 7 A82-29539
SCATTEROMETERS
The Seasat-A satellite scatterometer - The geophysical evaluation of remotely sensed wind vectors over the ocean p 51 A82-29616
The relationship between wind vector and normalized radar cross section used to derive Seasat-A Satellite Scatterometer winds p 51 A82-29617
Evaluation of atmospheric attenuation from SMMR brightness temperature for the Seasat satellite scatterometer p 51 A82-29618
Surface wind analyses for Seasat p 51 A82-29619
Intercomparison of wind speeds inferred by the SASS, altimeter, and SMMR p 52 A82-29621
SEASAT: A satellite scatterometer illumination times of selected in situ sites
[NASA-TM-83280] p 81 N82-22865
Measurement of soil moisture trends with airborne scatterometers --- Guymon, Oklahoma and Dalhart, Texas
[E82-10361] p 20 N82-26759
SCENE ANALYSIS
Landsat digital analysis of the initial recovery of burned tundra at Kokolik River, Alaska p 8 A82-32913
Coastal environment change analysis by Landsat MSS data p 54 A82-34219
Separation of diffuse from sharp-edged features in digital imagery p 68 A82-34225
An analysis of LANDSAT MSS scene-to-scene registration accuracy
[E82-10285] p 16 N82-24563
Image understanding research
[AD-A110746] p 74 N82-25611

SCHEDULES
AgRISTARS: Renewable resources inventory. Land information support system implementation plan and schedule --- San Juan National Forest pilot test [E82-10224] p 14 N82-23597
SEA ICE
Sea-Ice Mission Requirements for the US FIREX and Canada RADARSAT programs [NASA-CR-168984] p 57 N82-25609
SEA STATES
Seasat altimeter height calibration --- related to sea surface heights near Bermuda p 49 A82-29603
An empirical determination of the effects of sea state bias on Seasat altimetry p 50 A82-29607
Sea-state-related altitude errors in the Seasat radar altimeter p 50 A82-29608
The METEOSAT Data Collection System and its application p 75 N82-26037
SEA TRUTH
A ship and satellite view of hydrographic features in the western Gulf of Mexico p 53 A82-32651
SEA WATER
Technology and oceanography: An assessment of Federal technologies for oceanographic research and monitoring. Volume 2: Working papers on fishery research technology p 58 N82-26944
SEAMOUNTS
A search for seamounts in the southern Cook and Austral region p 52 A82-30810
SEAS
High resolution satellite observations of mesoscale oceanography in the Tasman Sea, 1978 - 1979 [E82-10324] p 57 N82-24597
SEASAT SATELLITES
Seasat measurement system evaluation - Achievements and limitations p 49 A82-29601
The Seasat altimeter data and its accuracy assessment p 49 A82-29602
Tidal and geodetic observations for the Seasat altimeter calibration experiment p 49 A82-29604
An empirical determination of the effects of sea state bias on Seasat altimetry p 50 A82-29607
Sea-state-related altitude errors in the Seasat radar altimeter p 50 A82-29608
Seasat altimeter timing bias estimation p 50 A82-29609
Evaluation of the Seasat altimeter time tag bias p 50 A82-29610
Waveheight and wind speed measurements from the Seasat radar altimeter p 50 A82-29612
Seasat altimeter determination of ocean current variability p 50 A82-29613
The Seasat altimeter mean sea surface model p 51 A82-29614
Gravity model improvement for Seasat p 32 A82-29615
Evaluation of atmospheric attenuation from SMMR brightness temperature for the Seasat satellite scatterometer p 51 A82-29618
Intercomparison of wind speeds inferred by the SASS, altimeter, and SMMR p 52 A82-29621
Description of Seasat radiometer status and results p 52 A82-29622
The observation of ocean surface phenomena using imagery from the Seasat synthetic aperture radar - An assessment p 52 A82-29623
Seasat wind and wave observations of northeast Pacific hurricane Iva, August 13, 1978 p 52 A82-29624
A search for seamounts in the southern Cook and Austral region p 52 A82-30810
The estimation of wave height from digitally processed SAR imagery p 67 A82-32347
Ocean wave height measurement with SEASAT SAR using speckle diversity p 53 A82-32882
Improved land use classification from Landsat and Seasat satellite imagery registered to a common map base p 25 A82-34743
SEASAT-A SATELLITE
Seasat altimeter height calibration --- related to sea surface heights near Bermuda p 49 A82-29603
The Seasat-A satellite scatterometer - The geophysical evaluation of remotely sensed wind vectors over the ocean p 51 A82-29616
The relationship between wind vector and normalized radar cross section used to derive Seasat-A Satellite Scatterometer winds p 51 A82-29617
Surface wind analyses for Seasat p 51 A82-29619
SEASAT: A satellite scatterometer illumination times of selected in situ sites [NASA-TM-83280] p 81 N82-22865
SECONDARY COSMIC RAYS
The cosmic ray positron spectrum p 1 A82-22542
SECULAR VARIATIONS
Investigation of geomagnetic field forecasting and fluid dynamics of the core [E82-10310] p 37 N82-24584
SEDIMENT TRANSPORT
Dynamic study of the upper Sao Francisco river and Tres Marias reservoir using MSS/LANDSAT images --- BRazil [E82-10291] p 63 N82-24569
SEDIMENTS
Fluid-sediment interactions on beaches and shelves [AD-A110838] p 59 N82-26948
SEISMOLOGY
Geodetic monitoring of tectonic information. Toward a strategy p 35 N82-22832
Seismic and geodetic studies of the Imperial Valley, California [DE82-001686] p 39 N82-26915
SENSITIVITY
Orbiting passive microwave sensor simulation applied to soil moisture estimation [E82-10343] p 18 N82-25605
SENSITOMETRY
Sensitometry in Canadian aerial survey p 79 A82-34724
SHADOWS
The use of contextual information to detect cumulus clouds and cloud shadows in Landsat data p 67 A82-32346
SHOCK FRONTS
The model of the cosmic ray enrichment by helium-3 p 31 A82-22614
SHOCK WAVE PROPAGATION
Possible evidence for attenuation of an MHD shock by a magnetic neutral sheet in the solar corona p 3 A82-22589
On the physical sense of the constant of solar cosmic ray coronal propagation p 83 A82-22599
SHOCK WAVES
Mass per charge ratio in hot plasmas and cosmic ray source composition p 2 A82-22557
Observations of the ionization states of energetic particles accelerated in solar flares p 40 A82-22607
SHORELINES
Airborne gamma-ray spectrometer and magnetometer survey. Meade River quadrangle, Alaska, volume 2 [DE82-000340] p 43 N82-23626
Airborne gamma-ray spectrometer and magnetometer survey. Harrison Bay quadrangle, Alaska, volume 2 [DE82-000315] p 43 N82-23628
Airborne gamma-ray spectrometer and magnetometer survey: Beechey Pt., quadrangle, Alaska, volume 2 [DE82-000309] p 43 N82-23629
Airborne gamma-ray spectrometer and magnetometer survey. Point Lay quadrangle, Alaska, volume 2 [DE82-000308] p 43 N82-23630
Airborne gamma-ray spectrometer and magnetometer survey. Utukik River quadrangle, Alaska, volume 2 [DE82-000316] p 44 N82-23631
Identifying environmental features for land management decisions --- Utah [E82-10289] p 30 N82-24567
Fluid-sediment interactions on beaches and shelves [AD-A110838] p 59 N82-26948
SIERRA NEVADA MOUNTAINS (CA)
The application of Heat Capacity Mapping Mission (HCMM) thermal data to snow hydrology --- Salt Verde Watershed and the southern Sierra Nevada [E82-10191] p 62 N82-22625
SIGNAL PROCESSING
Ocean wave height measurement with SEASAT SAR using speckle diversity p 53 A82-32882
SIGNAL TRANSMISSION
Establishing geodetic-geodynamic parameters using lunar laser range measurements p 34 A82-33293
SIGNATURE ANALYSIS
Irrigation management with remote sensing --- Navajo Indian Irrigation Project [E82-10357] p 20 N82-26755
SILICATES
Laboratory studies of actinide metal-silicate fractionation p 49 A82-22306
SILICON RADIATION DETECTORS
Simplified techniques to study components of solar radiation under haze and clouds p 78 A82-32766
SITE SELECTION
Site selection and engineering issues for a major industrial complex - Application of image and map interpretation p 25 A82-34711
SEASAT: A satellite scatterometer illumination times of selected in situ sites [NASA-TM-83280] p 81 N82-22865
SKY RADIATION
Influence of sky radiance distribution on the ratio technique for estimating bidirectional reflectance p 70 A82-35650
SKYLAB PROGRAM
The use of Skylab S-190B photography for small scale mapping p 80 A82-34742
SLOPES
Structure of the St. Francois Mountains and surrounding lead belt, S. E. Missouri: Inferences from thermal IR and other data sets --- Ozard Plateau and St. Francois Mountains [E82-10205] p 11 N82-23578
Topographic slope correction for analysis of thermal infrared images [E82-10214] p 36 N82-23587
Application of HCMM data to regional geologic analysis for mineral and energy resource evaluation [E82-10243] p 45 N82-24521
SMOKE
Problems of the interpretation of aerial and satellite images of industrial smoke p 23 A82-30307
Detection of volcanic smoke and ash-fall area at volcano Aso, from Landsat MSS data p 23 A82-31295
SMS 1
Geostationary satellite observations of the April 1979 Soufriere eruptions p 24 A82-33654
SNOW
The growth of snow in winter storms - An airborne observational study p 60 A82-33329
SNOW COVER
A comparative study of microwave radiometer observations over snowfields with radiative transfer model calculations --- for water runoff estimation p 60 A82-32910
Snowpack monitoring in North America and Eurasia using passive microwave satellite data p 78 A82-32915
Digital and visual evaluation of GOES and TIROS/NOAA image data for cover type effects on snowfield observations p 60 A82-34735
The seasonal snow-line within the Fergana basin and the possibility of using it for hydrological forecasting p 61 A82-35131
The use of satellite photographs to study snow-cover dynamics and to determine the average water discharge of the Amudarya during a vegetation period p 61 A82-35132
Method for the analysis of the melting of a firn complex on the basis of aerospace photographs p 61 A82-35133
Experience with the compilation of maps of snow-cover melting in the central part of the European USSR on the basis of satellite data p 62 A82-35134
Comparison of brightness indicatrixes of snow cover measured from an aircraft and calculated theoretically for different heights of the atmosphere p 62 A82-35140
The use of microwave radiometry for the determination of snow cover height p 80 A82-36018
The application of Heat Capacity Mapping Mission (HCMM) thermal data to snow hydrology --- Salt Verde Watershed and the southern Sierra Nevada [E82-10191] p 62 N82-22625
Use of NOAA/AVHRR visible and near-infrared data for land remote sensing [NASA-TM-84186] p 81 N82-22643
SOIL MAPPING
Problems associated with remotely detecting and monitoring saline sites within irrigated Alberta p 9 A82-34710
The influence of soil characteristics on regional convection differences above Northern Germany p 10 A82-37589
Overseas Geology And Mineral Resources number 56: A geological interpretation of LANDSAT imagery and air photography of Botswana [OGMR-56] p 42 N82-22636
Use of LANDSAT data to define soil boundaries in Carroll County, Missouri p 10 N82-23116
AgRISTARS: Agriculture and resources inventory surveys through aerospace remote sensing [E82-10236] p 15 N82-23609
SOIL MOISTURE
A simulation study of soil moisture estimation by a space SAR p 60 A82-29333
Remote sensing of leaf water content in the near infrared p 8 A82-32897
Landsat digital analysis of the initial recovery of burned tundra at Kokolik River, Alaska p 8 A82-32913
The possibility of using remote-sensing methods to study the hydrology of elementary watersheds p 61 A82-35130
C-band radar for determining surface soil moisture p 10 A82-37194
The influence of soil characteristics on regional convection differences above Northern Germany p 10 A82-37589
A meteorologically driven maize stress indicator model [E82-10112] p 11 N82-23564
Spectral properties of agricultural crops and soils measured from space, aerial, field, and laboratory sensors [E82-10212] p 12 N82-23585

Application of thermal model for pan evaporation to the hydrology of a defined medium, the sponge
[E82-10217] p 13 N82-23590

A meteorologically driven grain sorghum stress indicator model
[E82-10218] p 13 N82-23591

AgRISTARS: Early warning and crop condition assessment. Plant cover, soil temperature, freeze, water stress, and evapotranspiration conditions
[E82-10225] p 14 N82-23598

A multi-frequency radiometric measurement of soil moisture content over bare and vegetated fields
[E82-10238] p 16 N82-23611

Multilevel measurements of surface temperature over undulating terrain planted to barley
[E82-10245] p 16 N82-24523

Thermal mapping, geothermal source location, natural effluents and plant stress in the Mediterranean coast of Spain
[E82-10300] p 17 N82-24576

A method for inferring available surface moisture using remote surface temperature measurements: An assessment --- Kansas and St. Louis, Missouri
[E82-10311] p 17 N82-24585

Evaluation of HCMM data for assessing soil moisture and water table depth --- South Dakota
[E82-10329] p 18 N82-24602

Orbiting passive microwave sensor simulation applied to soil moisture estimation
[E82-10343] p 18 N82-25605

Plan of research for integrated soil moisture studies. Recommendations of the Soil Moisture Working Group
[NASA-TM-84731] p 18 N82-25608

Interactive initialization of heat flux parameters for numerical models using satellite temperature measurements
[E82-10313] p 82 N82-26743

Multispectral determination of soil moisture-2 --- Guymon, Oklahoma and Dalhart, Texas
[E82-10349] p 19 N82-26747

Evaluation of the soil moisture prediction accuracy of a space radar using simulation techniques --- Kansas
[E82-10351] p 19 N82-26749

Detection of variations in aspen forest habitat from LANDSAT digital data: Bear River Range, Utah
[E82-10355] p 19 N82-26753

Measurement of soil moisture trends with airborne scatterometers --- Guymon, Oklahoma and Dalhart, Texas
[E82-10361] p 20 N82-26759

Multifrequency remote sensing of soil moisture --- Guymon, Oklahoma and Dalhart, Texas
[E82-10362] p 20 N82-26760

The use of soil texture and field capacity to normalize microwave soil moisture measurements: Some problems p 20 N82-26762

SOIL SCIENCE

Use of LANDSAT data to define soil boundaries in Carroll County, Missouri p 10 N82-23116

SOILS

Spectral properties of agricultural crops and soils measured from space, aerial, field, and laboratory sensors
[E82-10189] p 10 N82-22623

Spectral properties of agricultural crops and soils measured from space, aerial, field, and laboratory sensors
[E82-10212] p 12 N82-23585

Delineation of soil temperature regimes from HCMM data
[E82-10298] p 17 N82-24574

Use of thermal inertia determined by HCMM to predict nocturnal cold prone areas in Florida --- Everglades agricultural area and the west north central peninsula
[E82-10299] p 17 N82-24575

The use of soil texture and field capacity to normalize microwave soil moisture measurements: Some problems p 20 N82-26762

SOLAR ACTIVITY

Comparison of solar proton activity in 1967 and 1969 with that in 1978 and 1979 as measured onboard Venera 4, 6, 11, 12 space probes p 31 A82-22596

The solar proton fluxes in April, 1979
p 66 A82-22597

Non-flare injection of protons into interplanetary space
p 4 A82-22601

SOLAR ACTIVITY EFFECTS

International Cosmic Ray Conference, 17th, Paris, France, July 13-25, 1981, Conference Papers. Volume 3
p 65 A82-22580

Model for solar hard X-ray bursts p 65 A82-22581

Solar gamma-ray experiment on Astro-A satellite
p 21 A82-22583

High-energy solar protons p 22 A82-22588

Preflare increases in solar cosmic rays relevant to the mode of energy accumulation in the active regions associated with large flares p 31 A82-22595

The modulation characteristics of the 19th and 20th solar activity cycles p 59 A82-22615

SOLAR ATMOSPHERE

Azimuthal propagation of flare particles in the heliosphere p 66 A82-22590

The influence of the sector structure of interplanetary magnetic field on the solar cosmic ray characteristics
p 83 A82-22603

SOLAR CORONA

Possible evidence for attenuation of an MHD shock by a magnetic neutral sheet in the solar corona
p 3 A82-22589

Azimuthal propagation of flare particles in the heliosphere p 66 A82-22590

On the physical sense of the constant of solar cosmic ray coronal propagation p 83 A82-22599

Observations of the ionization states of energetic particles accelerated in solar flares p 40 A82-22607

A tentative ordering of all available solar energetic particles abundance observations. I - The mass unbiased baseline. II - Discussion and comparison with coronal abundances p 40 A82-22609

SOLAR CORPUSCULAR RADIATION

Azimuthal propagation of flare particles in the heliosphere p 66 A82-22590

The relation of type II radio bursts to solar energetic particles observed at earth p 3 A82-22591

Energetic solar particle spectra according to Venera-11, 12 and Prognoz-5, 6 p 4 A82-22593

A tentative ordering of all available solar energetic particles abundance observations. I - The mass unbiased baseline. II - Discussion and comparison with coronal abundances p 40 A82-22609

Heavy-element abundances in He/3/-rich events
p 5 A82-22611

SOLAR COSMIC RAYS

Comparative abundances in solar energetic particles and in galactic cosmic ray sources, and the Ne-22 anomaly
p 83 A82-22556

International Cosmic Ray Conference, 17th, Paris, France, July 13-25, 1981, Conference Papers. Volume 3
p 65 A82-22580

Preflare increases in solar cosmic rays relevant to the mode of energy accumulation in the active regions associated with large flares p 31 A82-22595

On the physical sense of the constant of solar cosmic ray coronal propagation p 83 A82-22599

A description of relativistic solar particle propagation
p 4 A82-22600

Low-energy particles in interplanetary magnetic field near the sectorial boundary on September 26, 1977
p 4 A82-22602

The influence of the sector structure of interplanetary magnetic field on the solar cosmic ray characteristics
p 83 A82-22603

The approximate 1 GeV solar cosmic rays in the Forbush-effect of February 15, 1978 p 40 A82-22604

Coulombian energy losses and the nuclear composition of the solar cosmic rays p 4 A82-22610

The model of the cosmic ray enrichment by helium-3
p 31 A82-22614

Primary spectral variations of cosmic rays above 1 GV
p 5 A82-22618

SOLAR CYCLES

The modulation characteristics of the 19th and 20th solar activity cycles p 59 A82-22615

SOLAR ELECTRONS

Unusual properties of particle events associated with solar flare gamma ray events p 65 A82-22585

Low-energy particles in interplanetary magnetic field near the sectorial boundary on September 26, 1977
p 4 A82-22602

SOLAR FLARES

International Cosmic Ray Conference, 17th, Paris, France, July 13-25, 1981, Conference Papers. Volume 3
p 65 A82-22580

Model for solar hard X-ray bursts p 65 A82-22581

The determination of differential X-ray spectrum of the solar flare using ionospheric data p 65 A82-22582

Solar gamma-ray experiment on Astro-A satellite
p 21 A82-22583

Interplanetary particle observations associated with solar flare gamma-ray line emission p 3 A82-22584

Unusual properties of particle events associated with solar flare gamma ray events p 65 A82-22585

Observations of interplanetary energetic charged particles from gamma-ray line solar flares
p 65 A82-22586

High-energy solar protons p 22 A82-22588

Azimuthal propagation of flare particles in the heliosphere p 66 A82-22590

The relation of type II radio bursts to solar energetic particles observed at earth p 3 A82-22591

A survey of solar protons and alpha differential spectra between 1 and greater than 400 MeV/nucleon
p 4 A82-22592

Energetic solar particle spectra according to Venera-11, 12 and Prognoz-5, 6 p 4 A82-22593

Evolution of the solar proton spectrum in interplanetary space p 4 A82-22594

Preflare increases in solar cosmic rays relevant to the mode of energy accumulation in the active regions associated with large flares p 31 A82-22595

Spacecraft determination of energetic particle propagation parameters - The 1 January 1978 solar event p 31 A82-22598

The influence of the sector structure of interplanetary magnetic field on the solar cosmic ray characteristics
p 83 A82-22603

Time and energy dependence of heavy ion abundances in solar flare energetic particle events
p 22 A82-22605

High resolution measurements of solar flare isotopes
p 22 A82-22606

Observations of the ionization states of energetic particles accelerated in solar flares p 40 A82-22607

Is the neon composition of our sun, planetary or solar
p 76 A82-22608

A comparison of helium and heavy ion spectra in He/3/ rich solar flares with a model calculation
p 5 A82-22612

On the anticorrelation between the He/3//He/4/ ratio and proton intensity in He/3/ rich flares
p 40 A82-22613

Primary spectral variations of cosmic rays above 1 GV
p 5 A82-22618

SOLAR FLUX DENSITY

The solar proton fluxes in April, 1979
p 66 A82-22597

SOLAR MAGNETIC FIELD

Features of cosmic ray variations due to variations in the total magnetic field of the sun p 49 A82-22619

SOLAR MAXIMUM MISSION

Interplanetary particle observations associated with solar flare gamma-ray line emission p 3 A82-22584

Unusual properties of particle events associated with solar flare gamma ray events p 65 A82-22585

Atmospheric ozone determination by solar occultation using the UV spectrometer on the Solar Maximum Mission p 27 A82-36362

SOLAR ORBITS

Some considerations in the use of very-long-baseline-interferometry to establish reference coordinate systems for geodynamics p 34 A82-32096

SOLAR POSITION

Diurnal changes in reflectance factor due to Sun-row direction interactions
[E82-10128] p 11 N82-23566

Airborne observed solar elevation and row direction effects on the near-IR/red ratio of cotton
[E82-10220] p 13 N82-23593

Canopy reflectance as influenced by solar illumination angle
[E82-10237] p 15 N82-23610

The effect of sea-surface Sun glitter on microwave radiometer measurements
[NASA-CR-169083] p 57 N82-26525

SOLAR PROMINENCES

Non-flare injection of protons into interplanetary space
p 4 A82-22601

SOLAR PROTONS

Unusual properties of particle events associated with solar flare gamma ray events p 65 A82-22585

High-energy solar protons p 22 A82-22588

A survey of solar protons and alpha differential spectra between 1 and greater than 400 MeV/nucleon
p 4 A82-22592

Evolution of the solar proton spectrum in interplanetary space p 4 A82-22594

Comparison of solar proton activity in 1967 and 1969 with that in 1978 and 1979 as measured onboard Venera 4, 6, 11, 12 space probes p 31 A82-22596

The solar proton fluxes in April, 1979
p 66 A82-22597

Non-flare injection of protons into interplanetary space
p 4 A82-22601

Low-energy particles in interplanetary magnetic field near the sectorial boundary on September 26, 1977
p 4 A82-22602

SOLAR RADIATION

Simplified techniques to study components of solar radiation under haze and clouds p 78 A82-32766

Spectral estimates of solar radiation intercepted by corn canopies
[E82-10003] p 18 N82-26742

SOLAR SYSTEM

Nucleosynthesis of light and by-passed isotopes in the solar system matter p 64 A82-22578

SOLAR WIND
High resolution measurements of solar flare isotopes p 22 A82-22606
Is the neon composition of our sun, planetary or solar p 76 A82-22608
11-year modulation and spectrum of cosmic rays in the interstellar space p 22 A82-22616
SOLAR WIND VELOCITY
Non-flare injection of protons into interplanetary space p 4 A82-22601
The influence of the sector structure of interplanetary magnetic field on the solar cosmic ray characteristics p 83 A82-22603
SOLAR X-RAYS
Model for solar hard X-ray bursts p 65 A82-22581
The determination of differential X-ray spectrum of the solar flare using ionospheric data p 65 A82-22582
Solar gamma-ray experiment on Astro-A satellite p 21 A82-22583
Interplanetary particle observations associated with solar flare gamma-ray line emission p 3 A82-22584
Observations of interplanetary energetic charged particles from gamma-ray line solar flares p 65 A82-22586
Soft X-rays from the sunlit earth's atmosphere p 29 A82-37405
SOLID STATE DEVICES
A system design for a multispectral sensor using two-dimensional solid-state imaging arrays p 77 A82-31991
Solid state instrumentation concepts for earth resource observation
[AAS PAPER 82-132] p 81 A82-37812
SOMALIA
MONEX oceanographic observations along the East African coast --- global atmospheric research program p 56 N82-23908
SORGHUM
A meteorologically driven grain sorghum stress indicator model
[E82-10218] p 13 N82-23591
Normal crop calendars. Volume 3: The corn and soybean states of Illinois, Indiana, and Iowa
[E82-10221] p 13 N82-23594
SOUTH AMERICA
Study of gravity and magnetic anomalies using MAGSAT data
[E82-10194] p 35 N82-22628
Characterization of the structure and tectonic of South America
[E82-10196] p 42 N82-23569
Magnetic and gravity anomalies in the Americas
[E82-10312] p 37 N82-24586
An investigation of MAGSAT and complementary data emphasizing precambrian shields and adjacent areas of West Africa and South America
[E82-10316] p 38 N82-24589
An investigation of MAGSAT and complementary data emphasizing precambrian shields and adjacent areas of West Africa and South America
[E82-10317] p 38 N82-24590
The crustal structure and tectonics of South America
[E82-10319] p 38 N82-24592
Geotectonics of South America --- regional magnetic and gravity anomalies of South America
[E82-10320] p 38 N82-24593
SOUTH CAROLINA
Use and applicability of the vegetation component of the national site classification system --- Sumter National Forest, South Carolina
[E82-10234] p 15 N82-23607
SOUTH DAKOTA
AgRISTARS: Supporting research. Spring small grains planting date distribution model
[E82-10208] p 12 N82-23581
Airborne gamma-ray spectrometer and magnetometer survey. Aberdeen quadrangle, South Dakota, volume 1
[DE82-004152] p 45 N82-23641
Airborne gamma-ray spectrometer and magnetometer survey. Aberdeen quadrangle, South Dakota, volume 2
[DE82-004164] p 45 N82-23642
Evaluation of HCMM data for assessing soil moisture and water table depth --- South Dakota
[E82-10329] p 18 N82-24602
Airborne gamma-ray spectrometer and magnetometer survey: Sioux Falls quadrangle, South Dakota, volume 1
[DE82-005533] p 47 N82-27806
Airborne gamma-ray spectrometer and magnetometer survey: Sioux Falls quadrangle, South Dakota, volume 2
[DE82-005574] p 47 N82-27807
Airborne gamma-ray spectrometer and magnetometer survey: Huron Quadrangle, South Dakota
[DE82-005540] p 48 N82-27814
SOUTHERN HEMISPHERE
Mean sea-level pressure in the Southern Hemisphere during the FGGE period --- First Global Atmospheric Research Program Global Experiment (FGGE); buoys p 55 N82-23856
SOYBEANS
Spectral scanning of experimental plots of SO2-affected winter wheat and soybeans for mission planning p 6 A82-29537
Effects of vegetation canopy structure on remotely sensed canopy temperatures --- inferring plant water stress and yield p 8 A82-32905
Diurnal changes in reflectance factor due to Sun-row direction interactions
[E82-10128] p 11 N82-23566
AgRISTARS: Foreign commodity production forecasting. The 1980 US corn and soybeans exploratory experiment
[E82-10206] p 11 N82-23579
Determination of the optimal level for combining area and yield estimates
[E82-10215] p 12 N82-23588
AgRISTARS. Preliminary technical results review of FY81 experiments, volume 2: Fiscal year 1981/1982 'corn and soybeans pilot' experiment
[E82-10216] p 13 N82-23589
Normal crop calendars. Volume 3: The corn and soybean states of Illinois, Indiana, and Iowa
[E82-10221] p 13 N82-2359[illegible]
Application of Computer Axial Tomography (CAT) to measuring crop canopy geometry --- corn and soybeans
[E82-10227] p 14 N82-23600
AgRISTARS. Project management report: Program review presentation to level 1, interagency coordination committee --- Brazil, Argentina, U.S. corn belt, Great Plains Corridor
[E82-10231] p 15 N82-23604
Canopy reflectance as influenced by solar illumination angle
[E82-10237] p 15 N82-23610
Analysis of scanner data for crop inventories
[E82-10241] p 16 N82-24519
SPACE EXPLORATION
History of the French satellite space program p 85 N82-24216
SPACE MISSIONS
ERS-1 European remote sensing satellite p 84 A82-34367
SPACE NAVIGATION
Space to the earth --- Russian book on space technology applications p 83 A82-30850
SPACE PLATFORMS
SMS/GOES data collection platform system p 75 N82-26027
SPACE TRANSPORTATION SYSTEM 2 FLIGHT
Tropospheric CO measurement experiment from the second Space Shuttle flight p 27 A82-36292
OSTA-1 Post Mission Operation Report
[NASA-TM-84191] p 84 N82-23258
SPACE-TIME FUNCTIONS
On the space-time variability of ocean surface mixed layer characteristics of central and eastern Arabian sea during MONSOON-77 --- global atmospheric research program p 56 N82-23909
SPACEBORNE PHOTOGRAPHY
Imaging spectroscopy; Proceedings of the Seminar, Los Angeles, CA, February 10, 11, 1981 p 77 A82-32440
SPACEBORNE TELESCOPES
An optical objective lens for earth observations by satellites p 78 A82-32824
SPACECRAFT COMMUNICATION
Space to the earth --- Russian book on space technology applications p 83 A82-30850
SPACECRAFT INSTRUMENTS
Purpose, background of 'Intercosmos 21' mission p 81 N82-24264
SPACECRAFT LAUNCHING
LANDSAT D to test thematic mapper, inaugurate operational system
[NASA-NEWS-RELEASE-82-100] p 82 N82-26741
SPACECRAFT MODULES
LANDSAT-D thermal analysis and design support
[E82-10346] p 82 N82-26744
SPACETENNAS
Radiometer mission requirements for large space antenna systems
[NASA-TM-84478] p 81 N82-25610
SPATIAL DISTRIBUTION
The use of remote-sensing data to identify the space-time variability of the quality of natural waters p 62 A82-35138
SPATIAL FILTERING
Inversion of data from diffraction-limited multiwavelength remote sensors. II - Nonlinear dependence of observables on the geophysical parameters p 77 A82-32658
SPATIAL RESOLUTION
Spatial resolution requirements for urban studies p 29 A82-37502
SPECKLE PATTERNS
Ocean wave height measurement with SEASAT SAR using speckle diversity p 53 A82-32882
SPECTRAL BANDS
Measurement of soil moisture trends with airborne scatterometers --- Guymon, Oklahoma and Dalhart, Texas
[E82-10361] p 20 N82-26759
Development of visible/infrared/microwave agriculture classification and biomass estimation algorithms --- Guyton, Oklahoma and Dalhart, Texas
[E82-10363] p 20 N82-26761
SPECTRAL RECONNAISSANCE
Agricultural Research Service research highlights in remote sensing for calender year 1980
[E82-10228] p 14 N82-23601
Airborne gamma-ray spectrometer and magnetometer survey. Barrow quadrangle, Alaska, volume 1
[DE82-000334] p 43 N82-23623
Airborne gamma-ray spectrometer and magnetometer survey. Meade River quadrangle, Alaska, volume 2
[DE82-000340] p 43 N82-23626
Airborne gamma-ray spectrometer and magnetometer survey. Teshekpuk quadrangle, Alaska, volume 2
[DE82-000310] p 43 N82-23627
Airborne gamma-ray spectrometer and magnetometer survey. Harrison Bay quadrangle, Alaska, volume 2
[DE82-000315] p 43 N82-23628
Airborne gamma-ray spectrometer and magnetometer survey: Beechey Pt., quadrangle, Alaska, volume 2
[DE82-000309] p 43 N82-23629
Airborne gamma-ray spectrometer and magnetometer survey. Point Lay quadrangle, Alaska, volume 2
[DE82-000308] p 43 N82-23630
Airborne gamma-ray spectrometer and magnetometer survey. Utukik River quadrangle, Alaska, volume 2
[DE82-000316] p 44 N82-23631
Airborne gamma-ray spectrometer and magnetometer survey. Sagavanirktok quadrangle, Alaska, volume 2
[DE82-000311] p 44 N82-23632
Airborne gamma-ray spectrometer and magnetometer survey: Duluth quadrangle, Minnesota, volume 2
[DE82-001027] p 44 N82-23633
Airborne gamma-ray spectrometer and magnetometer survey: Ukiah quadrangle, California, volume 1 --- uranium exploration
[DE82-005541] p 48 N82-27813
SPECTRAL REFLECTANCE
Remote sensing of the weediness of crop fields p 5 A82-29435
Spectral scanning of experimental plots of SO2-affected winter wheat and soybeans for mission planning p 6 A82-29537
Relating Landsat digital count values to ground reflectance for optically thin atmospheric conditions p 66 A82-29762
Albedo and angular characteristics of the reflectance of the underlying surface and clouds --- Russian book p 33 A82-30849
Emissivity and reflectance of the model sea surface for the use of AVHRR data of NOAA satellites p 52 A82-31294
System albedo as sensed by satellites - Its definition and variability p 23 A82-32342
Remote sensing of leaf water content in the near infrared p 8 A82-32897
Quantitative relationships of near-surface spectra to Landsat radiometric data p 78 A82-32912
Influence of sky radiance distribution on the ratio technique for estimating bidirectional reflectance p 70 A82-35650
Spectral properties of agricultural crops and soils measured from space, aerial, field, and laboratory sensors
[E82-10189] p 10 N82-22623
Analysis of scanner data for crop inventories
[E82-10192] p 10 N82-22626
Diurnal changes in reflectance factor due to Sun-row direction interactions
[E82-10128] p 11 N82-23566
Spectral properties of agricultural crops and soils measured from space, aerial, field, and laboratory sensors
[E82-10212] p 12 N82-23585
Airborne observed solar elevation and row direction effects on the near-IR/red ratio of cotton
[E82-10220] p 13 N82-23593
Relating thematic mapper bands TM3, TM4, and TM5 to agronomic variables for corn, cotton, sugarbeet, soybean, sorghum, sunflower and tobacco
[E82-10347] p 19 N82-26745

Association of spectral development patterns with development stages of corn
[E82-10353] p 19 N82-26751

Detection of variations in aspen forest habitat from LANDSAT digital data: Bear River Range, Utah
[E82-10355] p 19 N82-26753

SPECTRAL SENSITIVITY

Sensitivity of Dobson total ozone estimations to wavelength band calibration uncertainties
p 27 A82-36405

Optical stop and focussing effects in the Dobson instrument p 28 A82-36428

Analysis of thematic mapper simulator data acquired during winter season over Pearl River, Mississippi, test site
[E82-10287] p 17 N82-24565

Multifrequency remote sensing of soil moisture --- Guymon, Oklahoma and Dalhart, Texas
[E82-10362] p 20 N82-26760

Development of visible/infrared/microwave agriculture classification and biomass estimation algorithms --- Guyton, Oklahoma and Dalhart, Texas
[E82-10363] p 20 N82-26761

SPECTRAL SIGNATURES

Landsat digital analysis of the initial recovery of burned tundra at Kokolik River, Alaska p 8 A82-32913

Improved land use classification from Landsat and Seasat satellite imagery registered to a common map base p 25 A82-34743

Spectral properties of agricultural crops and soils measured from space, aerial, field, and laboratory sensors
[E82-10189] p 10 N82-22623

Spectral properties of agricultural crops and soils measured from space, aerial, field, and laboratory sensors
[E82-10212] p 12 N82-23585

Airborne observed solar elevation and row direction effects on the near-IR/red ratio of cotton
[E82-10220] p 13 N82-23593

Linear polarization of light by two wheat canopies measured at many view angles
[E82-10229] p 14 N82-23602

Canopy reflectance as influenced by solar illumination angle
[E82-10237] p 15 N82-23610

Analysis of scanner data for crop inventories
[E82-10241] p 16 N82-24519

Analysis of thematic mapper simulator data acquired during winter season over Pearl River, Mississippi, test site
[E82-10287] p 17 N82-24565

The influence of autocorrelation in signature extraction: An example from a geobotanical investigation of Cotter Basin, Montana
[E82-10341] p 46 N82-25603

Spectral estimates of solar radiation intercepted by corn canopies
[E82-10003] p 18 N82-26742

Multispectral determination of soil moisture-2 --- Guymon, Oklahoma and Dalhart, Texas
[E82-10349] p 19 N82-26747

Detection of variations in aspen forest habitat from LANDSAT digital data: Bear River Range, Utah
[E82-10355] p 19 N82-26753

SPECTROMETERS

Breadboard gas filter correlation spectrometer for atmospheric measurement of hydrazines and nitrogen dioxide
[AD-A110688] p 82 N82-26642

Airborne gamma-ray spectrometer and magnetometer survey: North/south tieline, volume 2
[DE82-005570] p 47 N82-27805

SPECTROPHOTOMETERS

Optical stop and focussing effects in the Dobson instrument p 28 A82-36428

Observations and analyses of the total amount of atmospheric ozone in the Beijing region and in the region of Jolmolungma Mountain in Tibet p 28 A82-36444

SPECTRORADIOMETERS

Emissivity and reflectance of the model sea surface for the use of AVHRR data of NOAA satellites
p 52 A82-31294

High spectral resolution airborne spectrometry
p 77 A82-32443

Thematic mapper - An overview of spectral band registration p 77 A82-32447

SPECTROSCOPIC ANALYSIS

Imaging spectroscopy; Proceedings of the Seminar, Los Angeles, CA, February 10, 11, 1981 p 77 A82-32440

Multispectral mapper - Imaging spectroscopy as applied to the mapping of earth resources p 77 A82-32446

SPECTRUM ANALYSIS

Spectroscopic remote sensing for geological applications p 41 A82-32442

Total ozone retrieval from satellite Meteor 28 Fourier spectrometer measurements p 28 A82-36422

Observations and analyses of the total amount of atmospheric ozone in the Beijing region and in the region of Jolmolungma Mountain in Tibet p 28 A82-36444

MAGSAT science investigations
[E82-10199] p 71 N82-23572

Investigation of Antarctic crust and upper mantle using MAGSAT and other geophysical data
[E82-10308] p 37 N82-24582

Irrigation management with remote sensing --- Navajo Indian Irrigation Project
[E82-10357] p 20 N82-26755

SPECULAR REFLECTION

A model of plant canopy polarization
[E82-10233] p 15 N82-23606

SPHERICAL HARMONICS

Spherical harmonic representation of the main geomagnetic field for world charting and investigations of some fundamental problems of physics and geophysics
[E82-10203] p 72 N82-23576

Improved definition of crustal magnetic anomalies for MAGSAT data
[E82-10314] p 37 N82-24587

SPIRAL GALAXIES

Derivation of the distribution of synchrotron emissivity in the Galaxy from the 408 MHz all-sky survey
p 82 A82-22549

SPONGES (MATERIALS)

Application of thermal model for pan evaporation to the hydrology of a defined medium, the sponge
[E82-10217] p 13 N82-23590

SPOT (FRENCH SATELLITE)

The use of the SPOT satellite in natural resource evaluation p 83 A82-31996

STATISTICAL ANALYSIS

Monitoring land-cover change by principal component analysis of multitemporal Landsat data
p 68 A82-32906

Image quality and height measurement accuracy of serial survey camera imagery from high altitudes
p 78 A82-33297

The effect of the spectral attenuation of UV radiation by aerosol on the total ozone measurements
p 27 A82-36406

A statistical approach to rainfall estimation using satellite and conventional data
[NOAA-TR-NESS-89] p 63 N82-22854

Estimates of the statistical structure of the atmospheric pressure field in summer Monex-79 area
p 57 N82-23939

STEADY STATE

Steady-state cosmic ray electron spectrum under diffusion, convection, adiabatic deceleration and synchrotron losses p 1 A82-22552

STELLAR EVOLUTION

Nucleosynthesis of light and by-passed isotupes in the solar system matter p 64 A82-22578

STELLAR MAGNETIC FIELDS

Acceleration processes near massive black holes
p 3 A82-22572

STELLAR MASS ACCRETION

Acceleration of cosmic rays in accretion shocks
p 64 A82-22568

STELLAR MODELS

Pulsar models and cosmic-ray acceleration
p 21 A82-22570

STELLAR OCCULTATION

Atmospheric ozone determination by solar occultation using the UV spectrometer on the Solar Maximum Mission p 27 A82-36362

STELLAR RADIATION

On the stellar origin of the Ne-22 excess in cosmic rays p 21 A82-22562

On the stellar origin of low energy cosmic rays
p 21 A82-22567

STELLAR WINDS

Cosmic ray acceleration by stellar winds. I - Total density, pressure and energy flux p 21 A82-22566

STEREOPHOTOGRAPHY

Application of 35mm color aerial photography to forest land change detection p 6 A82-29533

Analytical processing of photographs taken by paired cameras p 79 A82-34471

STEREOSCOPY

Coordination of stereo image registration and pixel classification
[AD-A111307] p 75 N82-25614

STOCHASTIC PROCESSES

Evidence for the stochastic acceleration of cosmic rays in supernova remnants p 2 A82-22564

Preliminary evidence for the influence of physiography and scale upon the autocorrelation function of remotely sensed data p 67 A82-32343

STORMS (METEOROLOGY)

The growth of snow in winter storms - An airborne observational study p 60 A82-33329

Comparison of storm-time changes of geomagnetic field at ground and at MAGSAT altitudes, part 2
[E82-10325] p 30 N82-24598

STRATIFICATION

A comparison of stratified versus regression estimators p 11 N82-23133

STRATIFIED FLOW

On the application of a model of boundary-layer flow over low hills to real terrain p 29 A82-36741

STRATOSPHERE

Airborne lidar measurements of the Soufriere eruption of 17 April 1979 p 24 A82-33657

Observation of the diurnal variation of atmospheric ozone p 26 A82-35895

Microwave measurement of stratospheric and mesospheric ozone p 28 A82-36415

The seasonal variations of ozone and temperature in the middle and the upper stratosphere
p 29 A82-36534

STRATOSPHERE RADIATION

The energy spectra of cosmic ray variations inferred from the stratospheric measurements in 1972-1979
p 5 A82-22617

Stratospheric emission data analysis
[AD-A112337] p 76 N82-26907

STREAMS

Use of aerial photography in determining land use and streamflow relationships on small developing watersheds
p 60 A82-34736

STRESS (BIOLOGY)

Remote sensing of leaf water content in the near infrared p 8 A82-32897

Effects of vegetation canopy structure on remotely sensed canopy temperatures --- inferring plant water stress and yield p 8 A82-32905

STRESS MEASUREMENT

Estimates of sea surface stress for summer MONEX from cloud motions --- global atmospheric research program p 56 N82-23910

STRIP MINING

Application of remote sensing to state and regional problems
[E82-10288] p 30 N82-24566

STRUCTURAL BASINS

The influence of autocorrelation in signature extraction: An example from a geobotanical investigation of Cotter Basin, Montana
[E82-10341] p 46 N82-25603

STRUCTURAL PROPERTIES (GEOLOGY)

Regional geological, tectonic and geophysical features of Nordland, Norway p 41 A82-30304

Satellite image interpretation of the eastern Caledonian part of the Blue Road Geotraverse and its geological implications /Nordland, Vasterbotten, Scandinavia/
p 41 A82-30305

Comparing lineaments interpreted from Landsat imagery and topographic maps with reported faults in southwest Montana p 34 A82-34719

Terrain classification by Fourier analysis - Accuracy and economy p 69 A82-34723

Significance of tectonics in linear feature detection and interpretation on satellite images p 42 A82-37198

Spatial thermal radiometry contribution to the Massif Armoricain and the Massif Central France litho-structural study
[E82-10190] p 42 N82-22624

Geodetic monitoring of tectonic information. Toward a strategy p 35 N82-22832

Structure of the St. Francois Mountains and surrounding lead belt, S. E. Missouri: Inferences from thermal IR and other data sets
[E82-10200] p 36 N82-23573

Application of HCMM data to regional geologic analysis for mineral and energy resource evaluation
[E82-10153] p 45 N82-24518

Thermal mapping, geothermal source location, natural effluents and plant stress in the Mediterranean coast of Spain
[E82-10300] p 17 N82-24576

Analyzing the Broken Ridge area of the Indian Ocean using magnetic and gravity anomaly maps and geoid undulation and bathymetry data
[E82-10303] p 36 N82-24577

Investigating tectonic and bathymetric features of the Indian Ocean using MAGSAT magnetic anomaly data
[E82-10304] p 37 N82-24578

Magnetic and gravity anomalies in the Americas
[E82-10312] p 37 N82-24586

STRUCTURAL STABILITY

Nonlinear theory for elastic beams and rods and its finite element representation
[WTHD-143] p 73 N82-24517

SUGAR BEETS

Normal crop calendars. Volume 3: The corn and soybean states of Illinois, Indiana, and Iowa [E82-10221] p 13 N82-23594

SUGAR CANE

Use of thermal inertia determined by HCMM to predict nocturnal cold prone areas in Florida --- Everglades agricultural area and the west north central peninsula [E82-10299] p 17 N82-24575

SULFUR DIOXIDES

Spectral scanning of experimental plots of SO2-affected winter wheat and soybeans for mission planning p 6 A82-29537

Remote sensing of sulfur dioxide effects on vegetation. Volume 1: Summary [DE82-900580] p 31 N82-27802

Remote sensing of sulfur dioxide effects on vegetation. Volume 2: Data [DE82-900581] p 31 N82-27803

SUMMER

Impact of additional summer MONEX wind data on the prediction of monsoon depressions during June - August 1979 with two versions of primitive equation (PE) barotropic model --- Monsoon Experiment (MONEX) p 56 N82-23900

Estimates of sea surface stress for summer MONEX from cloud motions --- global atmospheric research program p 56 N82-23910

SUPERNOVA REMNANTS

Evidence for the stochastic acceleration of cosmic rays in supernova remnants p 2 A82-22564

SUPERNOVAE

The galactic origin of cosmic rays. I [CONF-810711-1] p 2 A82-22565

Nucleosynthesis of light and by-passed isotopes in the solar system matter p 64 A82-22578

SURFACE PROPERTIES

Experimental assessment of improved spatial resolution LANDSAT data [AD-A110538] p 75 N82-26765

SURFACE ROUGHNESS

Multispectral determination of soil moisture-2 --- Guymon, Oklahoma and Dalhart, Texas [E82-10349] p 19 N82-26747

Evaluation of the soil moisture prediction accuracy of a space radar using simulation techniques --- Kansas [E82-10351] p 19 N82-26749

Multifrequency remote sensing of soil moisture --- Guymon, Oklahoma and Dalhart, Texas [E82-10362] p 20 N82-26760

SURFACE TEMPERATURE

Surface temperature determination from an amalgamation of GOES and TIROS-N radiance measurements p 66 A82-28905

Infrared sensing of sea surface temperature from space p 53 A82-32902

Effects of vegetation canopy structure on remotely sensed canopy temperatures --- inferring plant water stress and yield p 8 A82-32905

Measuring sea surface temperature from satellites - A ground truth approach p 54 A82-32917

Satellite observations of sea surface temperature around the British Isles p 54 A82-33717

Evaluation of the accuracy of water-surface temperature measurement by means of airborne infrared radiometers p 62 A82-35136

Determination of winter temperature patterns, fronts, and surface currents in the Yellow Sea and East China Sea from satellite imagery p 55 A82-37195

The application of Heat Capacity Mapping Mission (HCMM) thermal data to snow hydrology --- Salt Verde Watershed and the southern Sierra Nevada [E82-10191] p 62 N82-22625

Evaluation of the Doraiswamy-Thompson winter wheat crop calendar model incorporating a modified spring restart sequence [E82-10207] p 12 N82-23580

AgRISTARS: Early warning and crop condition assessment. Plant cover, soil temperature, freeze, water stress, and evapotranspiration conditions [E82-10225] p 14 N82-23598

Delineation of soil temperature regimes from HCMM data [E82-10298] p 17 N82-24574

Use of thermal inertia determined by HCMM to predict nocturnal cold prone areas in Florida --- Everglades agricultural area and the west north central peninsula [E82-10299] p 17 N82-24575

Thermal mapping, geothermal source location, natural effluents and plant stress in the Mediterranean coast of Spain [E82-10300] p 17 N82-24576

A method for inferring available surface moisture using remote surface temperature measurements: An assessment --- Kansas and St. Louis, Missouri [E82-10311] p 17 N82-24585

High resolution satellite observations of mesoscale oceanography in the Tasman Sea, 1978 - 1979 [E82-10324] p 57 N82-24597

SURFACE WATER

Interpretation of surface-water circulation, Aransas Pass, Texas, using Landsat imagery p 60 A82-32896

SYNCHRONOUS METEOROLOGICAL SATELLITE

SMS/GOES data collection platform system p 75 N82-26027

SYNCHRONOUS SATELLITES

Observed magnetic substorm signatures at synchronous altitude p 26 A82-35534

SYNCHROTRON RADIATION

Derivation of the distribution of synchrotron emissivity in the Galaxy from the 408 MHz all-sky survey p 82 A82-22549

Steady-state cosmic ray electron spectrum under diffusion, convection, adiabatic deceleration and synchrotron losses p 1 A82-22552

SYNTHETIC APERTURE RADAR

A simulation study of soil moisture estimation by a space SAR p 60 A82-29333

The observation of ocean surface phenomena using imagery from the Seasat synthetic aperture radar - An assessment p 52 A82-29623

The recognition of extended targets - SAR images for level and hilly terrain p 33 A82-31994

The estimation of wave height from digitally processed SAR imagery p 67 A82-32347

On the synthetic aperture radar imaging of ocean surface waves p 53 A82-32881

Ocean wave height measurement with SEASAT SAR using speckle diversity p 53 A82-32882

Interpretation of vegetative cover in wetlands using four-channel SAR imagery p 9 A82-34706

Comparisons of land cover classifications from selected remote sensing systems p 80 A82-34746

Microwave sensing from space [AAS PAPER 82-127] p 80 A82-37809

Evaluation of the soil moisture prediction accuracy of a space radar using simulation techniques --- Kansas [E82-10351] p 19 N82-26749

SYSTEMS

Meteorological and aircraft data for CUE 2 1973 [PB82-149246] p 59 N82-26949

SYSTEMS ENGINEERING

A system design for a multispectral sensor using two-dimensional solid-state imaging arrays p 77 A82-31991

Design guidelines for satellite image data distribution systems p 70 A82-37048

T

TARGET RECOGNITION

The recognition of extended targets - SAR images for level and hilly terrain p 33 A82-31994

TECHNOLOGY ASSESSMENT

Seasat measurement system evaluation - Achievements and limitations p 49 A82-29601

Impacts of remote sensing on U.S. geography p 24 A82-32899

TECHNOLOGY TRANSFER

Civil land remote sensing system [GPO-87-070] p 84 N82-22630

LANDSAT technology transfer to the private and public sectors through community colleges and other locally available institutions [E82-10181] p 85 N82-23568

Forest Resource Information System. Phase 3: System transfer report [E82-10344] p 18 N82-25606

TECTONICS

Significance of tectonics in linear feature detection and interpretation on satellite images p 42 A82-37198

Geodetic monitoring of tectonic information. Toward a strategy p 35 N82-22832

Geodetic monitoring of tectonic deformation: Toward a strategy [NASA-CR-168784] p 35 N82-22846

Characterization of the structure and tectonic of South America [E82-10196] p 42 N82-23569

Bathymetric and tectonics of Indian Ocean using MAGSAT data [E82-10204] p 36 N82-23577

An equivalent layer magnetization model for the United States derived from MAGSAT data [E82-10297] p 36 N82-24573

Analyzing the Broken Ridge area of the Indian Ocean using magnetic and gravity anomaly maps and geoid undulation and bathymetry data [E82-10303] p 36 N82-24577

Investigating tectonic and bathymetric features of the Indian Ocean using MAGSAT magnetic anomaly data [E82-10304] p 37 N82-24578

The crustal structure and tectonics of South America [E82-10319] p 38 N82-24592

Geotectonics of South America --- regional magnetic and gravity anomalies of South America [E82-10320] p 38 N82-24593

Seismic and geodetic studies of the Imperial Valley, California [DE82-001686] p 39 N82-26915

TELEMETRY

Purpose, background of 'Intercosmos-21' mission p 81 N82-24264

TEMPERATURE DISTRIBUTION

Surface temperature determination from an amalgamation of GOES and TIROS-N radiance measurements p 66 A82-28905

Effects of vegetation canopy structure on remotely sensed canopy temperatures --- inferring plant water stress and yield p 8 A82-32905

Rapid oceanographic data gathering: Some problems in using remote sensing to determine the horizontal and vertical thermal distributions in the Northeast Pacific Ocean [AD-A111005] p 58 N82-26945

TEMPERATURE EFFECTS

A meteorologically driven grain sorghum stress indicator model [E82-10218] p 13 N82-23591

LANDSAT-D thermal analysis and design support [E82-10346] p 82 N82-26744

TEMPERATURE MEASUREMENT

View angle effects in the radiometric measurement of plant canopy temperatures p 8 A82-32914

Appearance of irregular tree canopies in nighttime high-resolution thermal infrared imagery p 68 A82-32916

Measuring sea surface temperature from satellites - A ground truth approach p 54 A82-32917

Evaluation of the accuracy of water-surface temperature measurement by means of airborne infrared radiometers p 62 A82-35136

Interactive initialization of heat flux parameters for numerical models using satellite temperature measurements [E82-10313] p 82 N82-26743

TEMPERATURE PROFILES

Satellite radiation measurements for the retrieval of the vertical temperature profiles p 70 A82-36935

TEMPORAL DISTRIBUTION

The use of remote-sensing data to identify the space-time variability of the quality of natural waters p 62 A82-35138

TERRADYNAMICS

Origin and scale of coordinate systems in satellite geodesy p 34 A82-32099

TERRAIN ANALYSIS

The recognition of extended targets - SAR images for level and hilly terrain p 33 A82-31994

Terrain analysis from Landsat using a color TV enhancement system p 68 A82-32911

Bathymetric imaging p 69 A82-34720

Terrain classification by Fourier analysis - Accuracy and economy p 69 A82-34723

Remote sensing of thermal subsurface terrain properties p 80 A82-34727

Use of NOAA/AVHRR visible and near-infrared data for land remote sensing [NASA-TM-84186] p 81 N82-22643

Topographic slope correction for analysis of thermal infrared images [E82-10214] p 36 N82-23587

Field measurements in support of dispersion modeling in complex terrain (1980) [PB82-148644] p 39 N82-27882

TERRESTRIAL RADIATION

A study of the earth's radiation budget using a general circulation model p 52 A82-30666

TEXAS

AgRISTARS: Early warning and crop condition assessment. Plant cover, soil temperature, freeze, water stress, and evapotranspiration conditions [E82-10225] p 14 N82-23598

Evaluation and combined geophysical interpretations of NURE and related geoscience data in the Van Horn, Pecos, Marfa, Fort Stockton, Presidido, and Emory Peak quadrangles, Texas, volume 1 [DE82-005554] p 47 N82-27808

Evaluation and combined geophysical interpretations of NURE and related geoscience data in the Van Horn, Pecos, Marfa, Fort Stockton, Presidio, and Emory Peak quadrangels, Texas [DE82-005560] p 48 N82-27809

TEXTURES
The use of soil texture and field capacity to normalize microwave soil moisture measurements: Some problems p 20 N82-26762

THEMATIC MAPPING
Preliminary evidence for the influence of physiography and scale upon the autocorrelation function of remotely sensed data p 67 A82-32343
Thematic mapper - An overview of spectral band registration p 77 A82-32447
Multispectral mapper - Imaging spectroscopy as applied to the mapping of earth resources p 77 A82-32448
RAMS-1, a Resource Analysis and Mapping System p 69 A82-34726
Improved land use classification from Landsat and Seasat satellite imagery registered to a common map base p 25 A82-34743
Water-balance differentiation of natural complexes on the basis of satellite photographs p 61 A82-35129
Remote sensing of salt marsh vegetation in the first four proposed Thematic Mapper bands p 10 A82-37503
Overseas Geology And Mineral Resources number 56: A geological interpretation of LANDSAT imagery and air photography of Botswana
[OGMR-56] p 42 N82-22636
Analysis of thematic mapper simulator data acquired during winter season over Pearl River, Mississippi, test site
[E82-10287] p 17 N82-24565
Identifying environmental features for land management decisions --- Utah
[E82-10289] p 30 N82-24567
A legislator's guide to LANDSAT
[E82-10290] p 85 N82-24568
The influence of autocorrelation in signature extraction: An example from a geobotanical investigation of Cotter Basin, Montana
[E82-10341] p 46 N82-25603
LANDSAT D to test thematic mapper, inaugurate operational system
[NASA-NEWS-RELEASE-82-100] p 82 N82-26741
Relating thematic mapper bands TM3, TM4, and TM5 to agronomic variables for corn, cotton, sugarbeet, soybean, sorghum, sunflower and tobacco
[E82-10347] p 19 N82-26745
Detection of variations in aspen forest habitat from LANDSAT digital data: Bear River Range, Utah
[E82-10355] p 19 N82-26753
Evaluation and combined geophysical interpretations of NURE and related geoscience data in the Van Horn, Pecos, Marfa, Fort Stockton, Presidio, and Emory Peak quadrangels, Texas
[DE82-005560] p 48 N82-27809

THERMAL CONDUCTIVITY
Remote sensing of thermal subsurface terrain properties p 80 A82-34727

THERMAL MAPPING
Thermography - A remote sensing method with many perspectives p 76 A82-29922
Geographic location of individual pixels --- for thermal infrared digital data processing p 68 A82-32900
View angle effects in the radiometric measurement of plant canopy temperatures p 8 A82-32914
Appearance of irregular tree canopies in nighttime high-resolution thermal infrared imagery p 68 A82-32916
The use of Landsat-3 thermal data to help differentiate land covers p 25 A82-34218
An optical data link for airborne scanning system p 80 A82-34737
Longwave infrared observation of urban landscapes p 25 A82-34744
Application of satellite magnetic anomaly data to Curie isotherm mapping p 70 A82-35824
Landsat D to yield more precise data p 70 A82-37200
Spatial thermal radiometry contribution to the Massif Armoricain and the Massif Central France litho-structural study
[E82-10190] p 42 N82-22624
The application of Heat Capacity Mapping Mission (HCMM) thermal data to snow hydrology --- Salt Verde Watershed and the southern Sierra Nevada
[E82-10191] p 62 N82-22625
Structure of the St. Francois Mountains and surrounding lead belt, S. E. Missouri: Inferences from thermal IR and other data sets
[E82-10200] p 36 N82-23573
Structure of the St. Francois Mountains and surrounding lead belt, S. E. Missouri: Inferences from thermal IR and other data sets --- Ozard Plateau and St. Francois Mountains
[E82-10205] p 11 N82-23578
Registration of Heat Capacity Mapping Mission day and night images
[E82-10210] p 72 N82-23583
Topographic slope correction for analysis of thermal infrared images
[E82-10214] p 36 N82-23587
Application of HCMM data to regional geologic analysis for mineral and energy resource evaluation
[E82-10153] p 45 N82-24518
Application of HCMM data to regional geologic analysis for mineral and energy resource evaluation
[E82-10243] p 45 N82-24521
Multilevel measurements of surface temperature over undulating terrain planted to barley
[E82-10245] p 16 N82-24523
Delineation of soil temperature regimes from HCMM data
[E82-10298] p 17 N82-24574
Use of thermal inertia determined by HCMM to predict nocturnal cold prone areas in Florida --- Everglades agricultural area and the west north central peninsula
[E82-10299] p 17 N82-24575
Thermal mapping, geothermal source location, natural effluents and plant stress in the Mediterranean coast of Spain
[E82-10300] p 17 N82-24576
A method for inferring available surface moisture using remote surface temperature measurements: An assessment --- Kansas and St. Louis, Missouri
[E82-10311] p 17 N82-24585
Multidisciplinary investigations on HCMM data over middle Europe and Marocco --- southern Germany and Marrakesh, Morocco
[E82-10315] p 74 N82-24588
High resolution satellite observations of mesoscale oceanography in the Tasman Sea, 1978 - 1979
[E82-10324] p 57 N82-24597
HCMM hydrological analysis in Utah
[E82-10328] p 63 N82-24601
Evaluation of HCMM data for assessing soil moisture and water table depth --- South Dakota
[E82-10329] p 18 N82-24602
Structure of the Saint Francois Mountains and surrounding lead belt, S.E. Missouri: Inference from thermal IR and other data sets
[E82-10350] p 39 N82-26748
An investigation into the utilization of HCMM thermal data for the discrimination of volcanic and Eolian geological units --- Newberry Volcano, Oregon
[E82-10352] p 47 N82-26750
Evaluation and combined geophysical interpretations of NURE and related geoscience data in the Van Horn, Pecos, Marfa, Fort Stockton, Presidido, and Emory Peak quadrangles, Texas, volume 1
[DE82-005554] p 47 N82-27808

THERMAL RADIATION
Cosmic ray composition from acceleration of thermal matter p 64 A82-22558
Effects of vegetation canopy structure on remotely sensed canopy temperatures --- inferring plant water stress and yield p 8 A82-32905
Remote sensing of thermal subsurface terrain properties p 80 A82-34727

THORIUM
Airborne gamma-ray spectrometer and magnetometer survey. Roseau quadrangle, Minnesota, volume 2
[DE82-001025] p 44 N82-23634
Airborne gamma-ray spectrometer and magnetometer survey. Bemidji quadrangle, Minnesota, volume 2
[DE82-001026] p 44 N82-23638
Airborne gamma-ray spectrometer and magnetometer survey. Lookout Ridge quadrangle, Alaska, volume 2
[DE82-000313] p 47 N82-25625
Airborne gamma-ray spectrometer and magnetometer survey: Sioux Falls quadrangle, South Dakota, volume 1
[DE82-005533] p 47 N82-27806

TIDAL FLATS
Remote sensing in Scotland using data received from satellites - A study of the Tay Estuary region using Landsat multispectral scanning imagery p 62 A82-37501

TIDES
Tidal and geodetic observations for the Seasat altimeter calibration experiment p 49 A82-29604

TIMBER INVENTORY
Optical bar panoramic photography for planning timber salvage in drought-stressed forests p 7 A82-32705
Landsat detection of hardwood forest clearcuts p 8 A82-32708
Remote sensing - A potential aid in the preparation of an urban tree inventory p 9 A82-34732
Ten-Ecosystem Study --- Grand and Weld Counties, Colorado; Warren County, Pennsylvania; St. Louis County, Minnesota; Sandoval County, New Mexico; Kershaw County, South Carolina; Fort Yukon, Alaska; Grays Harbor County, Washington; and Washington County, Missouri.
[E82-10186] p 84 N82-22620
AgRISTARS: Renewable resources inventory. Land information support system implementation plan and schedule --- San Juan National Forest pilot test
[E82-10224] p 14 N82-23597
Analysis of thematic mapper simulator data acquired during winter season over Pearl River, Mississippi, test site
[E82-10287] p 17 N82-24565

TIMBER VIGOR
Remote sensing of Douglas-fir trees newly infested by bark beetles p 6 A82-29536
Panoramic aerial photography in forest pest management p 7 A82-32701
Estimating bark beetle-killed lodgepole pine with high altitude panoramic photography p 7 A82-32703
Evaluation of spruce-fir forests using small-format photographs p 8 A82-32707

TIME DEPENDENCE
Computer simulation of the time dependence of the photon energy spectra produced in proton and electron bremstrahlung p 3 A82-22587

TIME LAG
Seasat altimeter timing bias estimation p 50 A82-29609
Evaluation of the Seasat altimeter time tag bias p 50 A82-29610
Geodetic monitoring of tectonic information. Toward a strategy p 35 N82-22832

TIROS N SERIES SATELLITES
Digital and visual evaluation of GOES and TIROS/NOAA image data for cover type effects on snowfield observations p 60 A82-34735

TOBACCO
Normal crop calendars. Volume 3: The corn and soybean states of Illinois, Indiana, and Iowa
[E82-10221] p 13 N82-23594

TOMOGRAPHY
Application of Computer Axial Tomography (CAT) to measuring crop canopy geometry --- corn and soybeans
[E82-10227] p 14 N82-23600

TOPOGRAPHY
Comparison data for Seasat altimetry in the western North Atlantic p 50 A82-29611
The simultaneous employment of geodetic measurements for block adjustments using the method of independent models p 34 A82-33295
Structure of the St. Francois Mountains and surrounding lead belt, S. E. Missouri: Inferences from thermal IR and other data sets --- Ozard Plateau and St. Francois Mountains
[E82-10205] p 11 N82-23578
Topographic slope correction for analysis of thermal infrared images
[E82-10214] p 36 N82-23587

TORNADOES
Remote sensing of tornadic storms from geosynchronous satellite infrared digital data p 23 A82-32348

TRACE CONTAMINANTS
Dobson spectrophotometer calibrations, possible errors in ozone absorption coefficients, and errors due to interfering pollutant gases p 28 A82-36431

TRANSFORMATIONS (MATHEMATICS)
An information-theoric spatial transform p 69 A82-34717

TRANSMITTANCE
Spectral properties of agricultural crops and soils measured from space, aerial, field, and laboratory sensors
[E82-10189] p 10 N82-22623

TRAVELING IONOSPHERIC DISTURBANCES
Characteristics of field-aligned E-region irregularities over Iioka /36 N/, Japan. I p 26 A82-36268

TREES (MATHEMATICS)
Dependent feature trees for density approximation I - Optimal construction and classification results p 67 A82-32344

TREES (PLANTS)
Remote sensing - A potential aid in the preparation of an urban tree inventory p 9 A82-34732
Ten-Ecosystem Study --- Grand and Weld Counties, Colorado; Warren County, Pennsylvania; St. Louis County, Minnesota; Sandoval County, New Mexico; Kershaw County, South Carolina; Fort Yukon, Alaska; Grays Harbor County, Washington; and Washington County, Missouri.
[E82-10186] p 84 N82-22620

TRIANGULATION
Present status of on-line analytical triangulation p 69 A82-34940

TROPICAL METEOROLOGY
Interannual variations of outgoing IR associated with tropical circulation changes during 1974-1978 p 54 A82-36341

TROPICAL REGIONS

The impact of meteorological satellites on the First GARP Global Experiment (FGGE) --- First Global Atmospheric Research Program Global Experiment (FGGE) p 55 N82-23852

TROPOSPHERE

Fine particles in the Soufriere eruption plume p 24 A82-33659

Aircraft measurements of NO/x/ in the lower troposphere above the coast of Japan p 26 A82-36247

Tropospheric CO measurement experiment from the second Space Shuttle flight p 27 A82-36292

Ammonia and the NOx budget of the troposphere p 27 A82-36293

TROPOSPHERIC SCATTERING

Inference of refractivity profiles by satellite-to-ground RF measurements p 78 A82-33442

TUNDRA

Landsat digital analysis of the initial recovery of burned tundra at Kokolik River, Alaska p 8 A82-32913

TURBIDITY

Interpretation of surface-water circulation, Aransas Pass, Texas, using Landsat imagery p 60 A82-32896

Nearshore current pattern off south Texas - An interpretation from aerial photographs p 53 A82-32903

TYPE 2 BURSTS

The relation of type II radio bursts to solar energetic particles observed at earth p 3 A82-22591

U

U.S.S.R. SPACE PROGRAM

Remote sensing of the earth's resources - The Soviet experience p 84 A82-33555

ULTRAVIOLET ABSORPTION

The effect of the spectral attenuation of UV radiation by aerosol on the total ozone measurements p 27 A82-36406

ULTRAVIOLET SPECTROMETERS

Atmospheric ozone determination by solar occultation using the UV spectrometer on the Solar Maximum Mission p 27 A82-36362

ULTRAVIOLET SPECTROPHOTOMETERS

Sensitivity of Dobson total ozone estimations to wavelength band calibration uncertainties p 27 A82-36405

Dobson spectrophotometer calibrations, possible errors in ozone absorption coefficients, and errors due to interfering pollutant gases p 28 A82-36431

OSO-8 lower mesospheric ozone number density profiles p 28 A82-36472

UNDERWATER OPTICS

Bias correction procedures for airborne laser hydrography [PB82-130089] p 63 N82-22644

UNITED KINGDOM

Satellite observations of sea surface temperature around the British Isles p 54 A82-33717

The METEOSAT Data Collection System and its application p 75 N82-26037

UNITED STATES OF AMERICA

MAGSAT and aeromagnetic data in the North American continent [E82-10193] p 71 N82-22627

AgRISTARS: Foreign commodity production forecasting. The 1980 US/Canada wheat and barley exploratory experiment [E82-10126] p 11 N82-23565

An equivalent layer magnetization model for the United States derived from MAGSAT data [E82-10297] p 36 N82-24573

Magnetic and gravity anomalies in the Americas [E82-10312] p 37 N82-24586

Use of MAGSAT anomaly data for crustal structure and mineral resources in the US Midcontinent [E82-10321] p 46 N82-24594

Use of MAGSAT anomaly data for crustal structure and mineral resources in the US Midcontinent [E82-10323] p 46 N82-24596

UNIVERSITY PROGRAM

LANDSAT technology transfer to the private and public sectors through community colleges and other locally available institutions [E82-10181] p 85 N82-23568

UPWELLING WATER

Meteorological and aircraft data for CUE 2 1973 [PB82-149246] p 59 N82-26949

URANIUM

Airborne gamma-ray spectrometer and magnetometer survey. Barrow quadrangle, Alaska, volume 1 [DE82-000334] p 43 N82-23623

Airborne gamma-ray spectrometer and magnetometer survey. Wainwright quadrangle, Alaska, volume 2 [DE82-000341] p 43 N82-23624

Airborne gamma-ray spectrometer and magnetometer survey, Kenora quadrangle, Minnesota, volume 1 [DE82-001029] p 43 N82-23625

Airborne gamma-ray spectrometer and magnetometer survey. Meade River quadrangle, Alaska, volume 2 [DE82-000340] p 43 N82-23626

Airborne gamma-ray spectrometer and magnetometer survey. Teshekpuk quadrangle, Alaska, volume 2 [DE82-000310] p 43 N82-23627

Airborne gamma-ray spectrometer and magnetometer survey. Harrison Bay quadrangle, Alaska, volume 2 [DE82-000315] p 43 N82-23628

Airborne gamma-ray spectrometer and magnetometer survey: Beechey Pt., quadrangle, Alaska, volume 2 [DE82-000309] p 43 N82-23629

Airborne gamma-ray spectrometer and magnetometer survey. Point Lay quadrangle, Alaska, volume 2 [DE82-000308] p 43 N82-23630

Airborne gamma-ray spectrometer and magnetometer survey. Utukik River quadrangle, Alaska, volume 2 [DE82-000316] p 44 N82-23631

Airborne gamma-ray spectrometer and magnetometer survey. Sagavanirktok quadrangle, Alaska, volume 2 [DE82-000311] p 44 N82-23632

Airborne gamma-ray spectrometer and magnetometer survey: Duluth quadrangle, Minnesota, volume 2 [DE82-001027] p 44 N82-23633

Airborne gamma-ray spectrometer and magnetometer survey. Roseau quadrangle, Minnesota, volume 2 [DE82-001025] p 44 N82-23634

Airborne gamma-ray spectrometer and magnetometer survey. Devil's Lake quadrangle, North Dakota, volume 1 [DE82-004161] p 44 N82-23635

Airborne gamma-ray spectrometer and magnetometer survey. Devil's Lake quadrangle, North Dakota, volume 2 [DE82-004168] p 44 N82-23636

Airborne gamma-ray spectrometer and magnetometer survey. Bemidji quadrangle, Minnesota, volume 1 [DE82-001032] p 44 N82-23637

Airborne gamma-ray spectrometer and magnetometer survey. Bemidji quadrangle, Minnesota, volume 2 [DE82-001026] p 44 N82-23638

Airborne gamma-ray spectrometer and magnetometer survey. Hibbing quadrangle, Minnesota, volume 1 [DE82-004159] p 44 N82-23639

Airborne gamma-ray spectrometer and magnetometer survey. Hibbing quadrangle, Minnesota, volume 2 [DE82-004165] p 45 N82-23640

Airborne gamma-ray spectrometer and magnetometer survey. Aberdeen quadrangle, South Dakota, volume 1 [DE82-004152] p 45 N82-23641

Airborne gamma-ray spectrometer and magnetometer survey. Aberdeen quadrangle, South Dakota, volume 2 [DE82-004164] p 45 N82-23642

Airborne gamma-ray spectrometer and magnetometer survey. International Falls quadrangle, Minnesota, volume 1 [DE82-004151] p 45 N82-23643

Airborne gamma-ray spectrometer and magnetometer survey. International Falls quadrangle, Minnesota, volume 2 [DE82-004166] p 45 N82-23644

Airborne gamma-ray spectrometer and magnetometer survey, Toronto quadrangle New York, volume 2A [DE81-027158] p 46 N82-25620

Airborne gamma-ray spectrometer and magnetometer survey, Kingston quadrangle New York, volume 2C [DE81-027161] p 46 N82-25621

Airborne gamma-ray spectrometer and magnetometer survey, Rochester quadrangle New York, volume 2D [DE81-027156] p 46 N82-25622

Airborne gamma-ray spectrometer and magnetometer survey. Barrow quadranagle, Alaska, volume 2 [DE82-000342] p 46 N82-25623

Airborne gamma-ray spectrometer and magnetometer survey. Lookout Ridge quadrangle, Alaska, volume 2 [DE82-000313] p 47 N82-25625

Airborne gamma-ray spectrometer and magnetometer survey: North/south tieline, volume 2 [DE82-005570] p 47 N82-27805

Airborne gamma-ray spectrometer and magnetometer survey: Sioux Falls quadrangle, South Dakota, volume 1 [DE82-005533] p 47 N82-27806

Airborne gamma-ray spectrometer and magnetometer survey: Sioux Falls quadrangle, South Dakota, volume 2 [DE82-005574] p 47 N82-27807

Airborne gamma-ray spectrometer and magnetometer survey: Susanville quadrangle, California, volume 1 [DE82-005538] p 48 N82-27811

Airborne gamma-ray spectrometer and magnetometer survey: Roseburg quadrangle, Oregon, volume 2 [DE82-005568] p 48 N82-27812

Airborne gamma-ray spectrometer and magnetometer survey: Ukiah quadrangle, California, volume 1 --- uranium exploration [DE82-005541] p 48 N82-27813

URBAN RESEARCH

Spatial resolution requirements for urban studies p 29 A82-37502

A legislator's guide to LANDSAT [E82-10290] p 85 N82-24568

USER MANUALS (COMPUTER PROGRAMS)

Description of the FORTRAN implementation of the spring small grains planting date distribution model [E82-10235] p 15 N82-23608

UTAH

Identifying environmental features for land management decisions --- Utah [E82-10289] p 30 N82-24567

HCMM hydrological analysis in Utah [E82-10328] p 63 N82-24601

Inventory of wetlands and agricultural land cover in the upper Sevier River Basin, Utah [E82-10345] p 18 N82-25607

Mapping of wildlife habitat in Farmington Bay, Utah [E82-10354] p 19 N82-26752

Detection of variations in aspen forest habitat from LANDSAT digital data: Bear River Range, Utah [E82-10355] p 19 N82-26753

Irrigated acreage in the Bear River Basin as of the 1975 growing season --- Idaho, Utah, and Wyoming [E82-10356] p 20 N82-26754

V

VARIABILITY

Determination of the optimal level for combining area and yield estimates [E82-10215] p 12 N82-23588

On the space-time variability of ocean surface mixed layer characteristics of central and eastern Arabian sea during MONSOON-77 --- global atmospheric research program p 56 N82-23909

VEGETATION

Color aerial photography in the plant sciences and related fields; Proceedings of the Eighth Biennial Workshop, Luray, VA, April 21-23, 1981 p 5 A82-29526

Estimating rangeland cover proportions with large-scale color-infrared aerial photographs p 6 A82-29534

Mapping riparian vegetation in Southeastern Oregon using digitized large scale color infra-red aerial photography p 6 A82-29535

Application of scanning microdensitometer data in selected plant science case studies p 7 A82-29539

Effects of vegetation canopy structure on remotely sensed canopy temperatures --- inferring plant water stress and yield p 8 A82-32905

Interpretation of vegetative cover in wetlands using four-channel SAR imagery p 9 A82-34706

Use of Landsat multispectral scanner data in vegetation mapping of a forested area p 9 A82-34731

Remote sensing of salt marsh vegetation in the first four proposed Thematic Mapper bands p 10 A82-37503

Use and applicability of the vegetation component of the national site classification system --- Sumter National Forest, South Carolina [E82-10234] p 15 N82-23607

AgRISTARS: Agriculture and resources inventory surveys through aerospace remote sensing [E82-10236] p 15 N82-23609

A method for inferring available surface moisture using remote surface temperature measurements: An assessment --- Kansas and St. Louis, Missouri [E82-10311] p 17 N82-24585

Measurement of soil moisture trends with airborne scatterometers --- Guymon, Oklahoma and Dalhart, Texas [E82-10361] p 20 N82-26759

Multifrequency remote sensing of soil moisture --- Guymon, Oklahoma and Dalhart, Texas [E82-10362] p 20 N82-26760

Remote sensing of sulfur dioxide effects on vegetation. Volume 1: Summary [DE82-900580] p 31 N82-27802

Remote sensing of sulfur dioxide effects on vegetation. Volume 2: Data [DE82-900581] p 31 N82-27803

VEGETATION GROWTH

Riparian vegetation mapping in Northeastern California using high altitude color infrared aerial photography p 5 A82-29528

Landsat digital analysis of the initial recovery of burned tundra at Kokolik River, Alaska p 8 A82-32913

Multispectral determination of soil moisture-2 --- Guymon, Oklahoma and Dalhart, Texas [E82-10349] p 19 N82-26747

Development of visible/infrared/microwave agriculture classification and biomass estimation algorithms --- Guyton, Oklahoma and Dalhart, Texas [E82-10363] p 20 N82-26761

VENERA SATELLITES

Comparison of solar proton activity in 1967 and 1969 with that in 1978 and 1979 as measured onboard Venera 4, 6, 11, 12 space probes p 31 A82-22596

VENERA 11 SATELLITE

The solar proton fluxes in April, 1979 p 66 A82-22597

VERTICAL DISTRIBUTION

Aircraft measurements of NO/x/ in the lower troposphere above the coast of Japan p 26 A82-36247

Ammonia and the NOx budget of the troposphere p 27 A82-36293

VERY LONG BASE INTERFEROMETRY

Work related to the Blue Road Geotraverse at the Finnish Geodetic Institute p 32 A82-30306

The definition of the terrestrial coordinate frame by long baseline interferometry p 33 A82-32084

Some considerations in the use of very-long-baseline-interferometry to establish reference coordinate systems for geodynamics p 34 A82-32096

VIEW EFFECTS

Effect of atmospheric conditions on remote sensing of vegetation parameters p 24 A82-32901

View angle effects in the radiometric measurement of plant canopy temperatures p 8 A82-32914

VISUAL AIDS

Interactive initialization of heat flux parameters for numerical models using satellite temperature measurements [E82-10313] p 82 N82-26743

VISUAL OBSERVATION

Detection of regional air pollution episodes utilizing satellite digital data in the visual range p 23 A82-31990

VOLATILITY

On volatility, first ionization potential, and s- and r-processes --- for Galactic cosmic ray sources p 2 A82-22560

VOLCANOES

Soufriere Volcano, St. Vincent - Observations of its 1979 eruption from the ground, aircraft, and satellites p 24 A82-33652

Crustal structures under the active volcanic areas of central and eastern Mediterranean (M-44) [E82-10096] p 35 N82-23563

An investigation into the utilization of HCMM thermal data for the discrimination of volcanic and Eolian geological units --- Newberry Volcano, Oregon [E82-10352] p 47 N82-26750

VOLCANOLOGY

Detection of volcanic smoke and ash-fall area at volcano Aso, from Landsat MSS data p 23 A82-31295

Geostationary satellite observations of the April 1979 Soufriere eruptions p 24 A82-33654

Meteorological analysis of the eruption of Soufriere in April 1979 p 24 A82-33655

Skirt clouds associated with the Soufriere eruption of 17 April 1979 p 24 A82-33656

Airborne lidar measurements of the Soufriere eruption of 17 April 1979 p 24 A82-33657

Fine particles in the Soufriere eruption plume p 24 A82-33659

Overseas Geology And Mineral Resources number 56: A geological interpretation of LANDSAT imagery and air photography of Botswana [OGMR-56] p 42 N82-22636

Seismic and geodetic studies of the Imperial Valley, California [DE82-001686] p 39 N82-26915

W

WATER BALANCE

Water-balance differentiation of natural complexes on the basis of satellite photographs p 61 A82-35129

The possibility of using remote-sensing methods to study the hydrology of elementary watersheds p 61 A82-35130

WATER CIRCULATION

Interpretation of surface-water circulation, Aransas Pass, Texas, using Landsat imagery p 60 A82-32896

Sea-Ice Mission Requirements for the US FIREX and Canada RADARSAT programs [NASA-CR-168984] p 57 N82-25609

WATER COLOR

Analysis of ocean color scanner data from the Superflux III Experiment [NASA-TM-83290] p 55 N82-23614

WATER DEPTH

Bias correction procedures for airborne laser hydrography [PB82-130089] p 63 N82-22644

Bathymetric and tectonics of Indian Ocean using MAGSAT data [E82-10204] p 36 N82-23577

Analyzing the Broken Ridge area of the Indian Ocean using magnetic and gravity anomaly maps and geoid undulation and bathymetry data [E82-10303] p 36 N82-24577

Investigating tectonic and bathymetric features of the Indian Ocean using MAGSAT magnetic anomaly data [E82-10304] p 37 N82-24578

WATER FLOW

The use of satellite photographs to study snow-cover dynamics and to determine the average water discharge of the Amudarya during a vegetation period p 61 A82-35132

WATER POLLUTION

Characteristics of 13.9 GHz radar scattering from oil films on the sea surface p 54 A82-33438

A quantitative multispectral analysis system for aerial photographs applied to coastal planning p 55 A82-37505

WATER QUALITY

The use of remote-sensing data to identify the space-time variability of the quality of natural waters p 62 A82-35138

Use of NOAA/AVHRR visible and near-infrared data for land remote sensing [NASA-TM-84186] p 81 N82-22643

HCMM hydrological analysis in Utah [E82-10328] p 63 N82-24601

WATER RESOURCES

A comparative study of microwave radiometer observations over snowfields with radiative transfer model calculations --- for water runoff estimation p 60 A82-32910

Use of aerial photography in determining land use and streamflow relationships on small developing watersheds p 60 A82-34736

The possibility of using remote-sensing methods to study the hydrology of elementary watersheds p 61 A82-35130

The seasonal snow-line within the Fergana basin and the possibility of using it for hydrological forecasting p 61 A82-35131

The use of remote-sensing data to identify the space-time variability of the quality of natural waters p 62 A82-35138

Ten-Ecosystem Study --- Grand and Weld Counties, Colorado; Warren County, Pennsylvania; St. Louis County, Minnesota; Sandoval County, New Mexico; Kershaw County, South Carolina; Fort Yukon, Alaska; Grays Harbor County, Washington; and Washington County, Missouri. [E82-10186] p 84 N82-22620

WATER RUNOFF

A comparative study of microwave radiometer observations over snowfields with radiative transfer model calculations --- for water runoff estimation p 60 A82-32910

Automated classification of runoff coefficients from Landsat multispectral data p 60 A82-34734

The application of Heat Capacity Mapping Mission (HCMM) thermal data to snow hydrology --- Salt Verde Watershed and the southern Sierra Nevada [E82-10191] p 62 N82-22625

WATER TABLES

Evaluation of HCMM data for assessing soil moisture and water table depth --- South Dakota [E82-10329] p 18 N82-24602

WATER TEMPERATURE

Evaluation of the accuracy of water-surface temperature measurement by means of airborne infrared radiometers p 62 A82-35136

WATER VAPOR

Estimation of the precipitable water from the IR channel of the geostationary satellite p 55 A82-37196

WATER WAVES

The Seasat altimeter data and its accuracy assessment p 49 A82-29602

An empirical determination of the effects of sea state bias on Seasat altimetry p 50 A82-29607

Sea-state-related altitude errors in the Seasat radar altimeter p 50 A82-29608

Waveheight and wind speed measurements from the Seasat radar altimeter p 50 A82-29612

Seasat wind and wave observations of northeast Pacific hurricane Iva, August 13, 1978 p 52 A82-29624

The estimation of wave height from digitally processed SAR imagery p 67 A82-32347

On the synthetic aperture radar imaging of ocean surface waves p 53 A82-32881

Ocean wave height measurement with SEASAT SAR using speckle diversity p 53 A82-32882

Pulse-to-pulse correlation in satellite radar altimeters --- for ocean wave height measurement p 55 A82-37390

WATERSHEDS

Automated classification of runoff coefficients from Landsat multispectral data p 60 A82-34734

Use of aerial photography in determining land use and streamflow relationships on small developing watersheds p 60 A82-34736

Dynamic study of the upper Sao Francisco river and Tres Marias reservoir using MSS/LANDSAT images --- BRazil [E82-10291] p 63 N82-24569

WAVE ATTENUATION

Possible evidence for attenuation of an MHD shock by a magnetic neutral sheet in the solar corona p 3 A82-22589

WAVE FRONTS

Satellite observations in FRONTS 80 [AD-A111080] p 58 N82-26766

WAVEFORMS

Sea-state-related altitude errors in the Seasat radar altimeter p 50 A82-29608

WEATHER FORECASTING

Impact of additional summer MONEX wind data on the prediction of monsoon depressions during June - August 1979 with two versions of primitive equation (PE) barotropic model --- Monsoon Experiment (MONEX) p 56 N82-23900

Some empirical rules for forecasting fog and status over northern Florida, southern Georgia and adjacent coastal waters [PB82-154006] p 59 N82-27949

WEST GERMANY

Multidisciplinary investigations on HCMM data over middle Europe and Marocco --- southern Germany and Marrakesh, Morocco [E82-10315] p 74 N82-24588

WEST INDIES

An investigation of MAGSAT and complementary data emphasizing precambrian shields and adjacent areas of West Africa and South America [E82-10316] p 38 N82-24589

WETLANDS

Interpretation of vegetative cover in wetlands using four-channel SAR imagery p 9 A82-34706

Application of remote sensing to state and regional problems [E82-10288] p 30 N82-24566

Identifying environmental features for land management decisions --- Utah [E82-10289] p 30 N82-24567

Inventory of wetlands and agricultural land cover in the upper Sevier River Basin, Utah [E82-10345] p 18 N82-25607

Irrigated acreage in the Bear River Basin as of the 1975 growing season --- Idaho, Utah, and Wyoming [E82-10356] p 20 N82-26754

WHEAT

Spectral scanning of experimental plots of SO2-affected winter wheat and soybeans for mission planning p 6 A82-29537

AgRISTARS: Foreign commodity production forecasting. The 1980 US/Canada wheat and barley exploratory experiment [E82-10126] p 11 N82-23565

Evaluation of the Doraiswamy-Thompson winter wheat crop calendar model incorporating a modified spring restart sequence [E82-10207] p 12 N82-23580

AgRISTARS: Supporting research. Spring small grains planting date distribution model [E82-10208] p 12 N82-23581

Selection of the Australian indicator region [E82-10222] p 13 N82-23595

Linear polarization of light by two wheat canopies measured at many view angles [E82-10229] p 14 N82-23602

A model of plant canopy polarization [E82-10233] p 15 N82-23606

Description of the FORTRAN implementation of the spring small grains planting date distribution model [E82-10235] p 15 N82-23608

WILDLIFE

Inventory of wildlife habitat from color infrared aerial photography for Cobb Island, Virginia p 6 A82-29529

A computerized spatial analysis system for assessing wildlife habitat from vegetation maps p 9 A82-34716

Mapping of wildlife habitat in Farmington Bay, Utah [E82-10354] p 19 N82-26752

WIND DIRECTION

Some empirical rules for forecasting fog and status over northern Florida, southern Georgia and adjacent coastal waters
[PB82-154006] p 59 N82-27949

WIND MEASUREMENT

The Seasat-A satellite scatterometer - The geophysical evaluation of remotely sensed wind vectors over the ocean p 51 A82-29616

The relationship between wind vector and normalized radar cross section used to derive Seasat-A Satellite Scatterometer winds p 51 A82-29617

Surface wind analyses for Seasat p 51 A82-29619

Seasat wind and wave observations of northeast Pacific hurricane Iva, August 13, 1978 p 52 A82-29624

SEASAT: A satellite scatterometer illumination times of selected in situ sites
[NASA-TM-83280] p 81 N82-22865

WIND VARIATIONS

Representativeness of cloud motion winds deduced from GOES Indian Ocean satellite imagery for the description of the Indian summer monsoon --- superpressure balloons for the study of the Indian summer monsoon (BALSAMINE) p 55 N82-23879

Estimates of sea surface stress for summer MONEX from cloud motions --- global atmospheric research program p 56 N82-23910

WIND VELOCITY

On the application of a model of boundary-layer flow over low hills to real terrain p 29 A82-36741

The effect of sea-surface Sun glitter on microwave radiometer measurements
[NASA-CR-169083] p 57 N82-26525

WIND VELOCITY MEASUREMENT

The Seasat altimeter data and its accuracy assessment p 49 A82-29602

Waveheight and wind speed measurements from the Seasat radar altimeter p 50 A82-29612

Intercomparison of wind speeds inferred by the SASS, altimeter, and SMMR p 52 A82-29621

Description of Seasat radiometer status and results p 52 A82-29622

WINDOWS (INTERVALS)

Defining the temporal window for monitoring forest canopy defoliation using Landsat p 9 A82-34730

WINTER

The growth of snow in winter storms - An airborne observational study p 60 A82-33329

Determination of winter temperature patterns, fronts, and surface currents in the Yellow Sea and East China Sea from satellite imagery p 55 A82-37195

The onset of the Australian Northwest monsoon during winter MONEX: Broadscale flow revealed by an objective analysis scheme p 56 N82-23912

Analysis of thematic mapper simulator data acquired during winter season over Pearl River, Mississippi, test site
[E82-10287] p 17 N82-24565

Ice distribution and winter surface circulation patterns, Kachemak Bay, Alaska
[AD-A110806] p 58 N82-26764

WOLF-RAYET STARS

On the stellar origin of the Ne-22 excess in cosmic rays p 21 A82-22562

WYOMING

Ground support data from July 10 to July 29, 1978, for HCMM thermal satellite data of the Powder River Basin, Wyoming
[E82-10211] p 72 N82-23584

Irrigated acreage in the Bear River Basin as of the 1975 growing season --- Idaho, Utah, and Wyoming
[E82-10356] p 20 N82-26754

X

X RAY SOURCES

Consequences of an inverse Compton emission model for extragalactic X-ray sources p 83 A82-22553

X RAY SPECTRA

The determination of differential X-ray spectrum of the solar flare using ionospheric data p 65 A82-22582

Y

YIELD

AgRISTARS: Supporting research Spring small grains planting date distribution model
[E82-10208] p 12 N82-23581

Determination of the optimal level for combining area and yield estimates
[E82-10215] p 12 N82-23588

AgRISTARS. Preliminary technical results review of FY81 experiments, volume 2: Fiscal year 1981/1982 'corn and soybeans pilot' experiment
[E82-10216] p 13 N82-23589

Association of spectral development patterns with development stages of corn
[E82-10353] p 19 N82-26751

Z

ZERO POINT ENERGY

Astrophysical scenarios for critically evaluating a zero-point field acceleration mechanism
p 64 A82-22575

PERSONAL AUTHOR INDEX

Typical Personal Author Index Listing

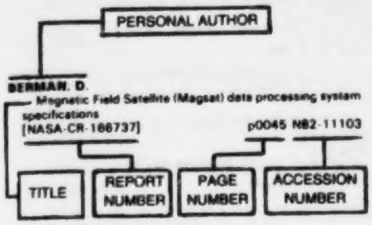

Listings in this index are arranged alphabetically by personal author. The title of the document provides the user with a brief description of the subject matter. The report number helps to indicate the type of document listed (e.g., NASA report, translation, NASA contractor report). The page and accession numbers are located beneath and to the right of the title, e.g., p0045 N82-11103. Under any one author's name the accession numbers are arranged in sequence with the AIAA accession numbers appearing first

A

ADAMS, J. H., JR.
Calculated isotopic source composition and tests for origin and propagation of cosmic rays with mass numbers less than or equal to 62 p 83 A82-22554

ADRIEN, P.-M.
The use of the SPOT satellite in natural resource evaluation p 83 A82-31996

AGARWAL, B. N. P.
Analysis of MAGSAT data of the Indian region
[E82-10358] p 75 N82-26756

AGARWAL, P. K.
Analysis of MAGSAT data of the Indian region
[E82-10358] p 75 N82-26756

AGUI, T.
Description of gray level picture using a collection of density contour lines p 66 A82 29409

AIKEN, C. L. V.
Evaluation and combined geophysical interpretations of NURE and related geoscience data in the Van Horn, Pecos, Marfa, Fort Stockton, Presidido, and Emory Peak quadrangles, Texas, volume 1
[DE82-005554] p 47 N82-27808
Evaluation and combined geophysical interpretations of NURE and related geoscience data in the Van Horn, Pecos, Marfa, Fort Stockton, Presidio, and Emory Peak quadrangels, Texas
[DE82-005560] p 48 N82-27809

AIKIN, A. C.
Atmospheric ozone determination by solar occultation using the UV spectrometer on the Solar Maximum Mission p 27 A82-36362

ALIMUKHAMEDOV, M. A.
The use of space photographs in the mapping of glaciers and water bodies p 62 A82-37174

ALKEZWEENY, A. J.
Comparison of ozone in polluted and clean air masses over Lake Michigan p 29 A82-36477

ALLEN, L. H., JR.
Use of thermal inertia determined by HCMM to predict nocturnal cold prone areas in Florida
[E82-10299] p 17 N82-24575

ALLISON, L. J.
Snowpack monitoring in North America and Eurasia using passive microwave satellite data
p 78 A82-32915

ALLISON, R. A.
Panoramic aerial photography in forest pest management p 7 A82-32701

ALVO, P.
Aircraft monitoring of surface carbon dioxide exchange p 23 A82-30293

ALZOFON, F. E.
Remote sensing of thermal subsurface terrain properties p 80 A82-34727

ANDERSON, J. E.
Analysis of thematic mapper simulator data acquired during winter season over Pearl River, Mississippi, test site
[E82-10287] p 17 N82-24565

ANDERSON, K. D.
Inference of refractivity profiles by satellite-to-ground RF measurements p 78 A82-33442

ANDREWS, J. C.
High resolution satellite observations of mesoscale oceanography in the Tasman Sea, 1978 - 1979
[E82-10324] p 57 N82-24597

AOKI, T.
Estimation of the precipitable water from the IR channel of the geostationary satellite p 55 A82-37196

ARONOFF, S.
Detection of environmental disturbance using color aerial photography and thermal infrared imagery
p 22 A82-29327

ARORA, B. R.
MAGSAT for geomagnetic studies over Indian region
[E82-10202] p 72 N82-23575
MAGSAT for geomagnetic studies over Indian region
[E82-10296] p 73 N82-24572

ARTLEY, J. A.
AgRISTARS: Supporting research. Spring small grains planting date distribution model
[E82-10208] p 12 N82-23581
Application of thermal model for pan evaporation to the hydrology of a defined medium, the sponge
[E82-10217] p 13 N82-23590
Description of the FORTRAN implementation of the spring small grains planting date distribution model
[E82-10235] p 15 N82-23608

ARUR, M. G.
Analysis of MAGSAT data of the Indian region
[E82-10358] p 75 N82-26756

ARVIDSON, R. E.
Structure of the St. Francois Mountains and surrounding lead belt, S. E. Missouri: Inferences from thermal IR and other data sets
[E82-10200] p 36 N82-23573
Structure of the St. Francois Mountains and surrounding lead belt, S. E. Missouri: Inferences from thermal IR and other data sets
[E82-10205] p 11 N82-23578
Structure of the Saint Francois Mountains and surrounding lead belt, S.E. Missouri: Inference from thermal IR and other data sets
[E82-10350] p 39 N82-26748

ASKARI, F.
Automated classification of runoff coefficients from Landsat multispectral data p 60 A82-34734

AUDOUZE, J.
Origin of galactic cosmic rays from Ne isotopic composition p 2 A82-22563

AUGUSTSSON, T. R.
Ammonia and the NOx budget of the troposphere
p 27 A82-36293

AVASTE, O.
Estimation of the temperature of the upper boundary of cloud cover over the world ocean p 54 A82-36005

AXFORD, W. I.
Cosmic ray acceleration by stellar winds. I - Total density, pressure and energy flux p 21 A82-22566

B

BABKINA, L. P.
Experience with the compilation of maps of snow-cover melting in the central part of the European USSR on the basis of satellite data p 62 A82-35134

BADHWAR, G.
Field size, length, and width distributions based on LACIE ground truth data p 8 A82-32909

BAINS, S. P. S.
Analysis of MAGSAT data of the Indian region
[E82-10358] p 75 N82-26756

BALICK, L. K.
Appearance of irregular tree canopies in nighttime high-resolution thermal infrared imagery
p 68 A82-32916

BALLANI, L.
Establishing geodetic-geodynamic parameters using lunar laser range measurements p 34 A82-33293

BARABANOVA, N. G.
Evaluation of the effectiveness of systematic image distortion compensation p 69 A82-34469

BARBE, A.
Application of infrared techniques to the study of atmospheric ozone p 27 A82-36414

BARNES, J. C.
The application of Heat Capacity Mapping Mission (HCMM) thermal data to snow hydrology
[E82-10191] p 62 N82-22625

BARR, S.
Meteorological analysis of the eruption of Soufriere in April 1979 p 24 A82-33655
Skirt clouds associated with the Soufriere eruption of 17 April 1979 p 24 A82-33656

BARRACLOUGH, D. R.
Spherical harmonic representation of the main geomagnetic field for world charting and investigations of some fundamental problems of physics and geophysics
[E82-10203] p 72 N82-23576

BARTON, J. C.
Measurement of cosmogenic nuclides using a multi-crystal gamma-ray coincidence spectrometer
p 64 A82-22577

BASHER, R. E.
Sensitivity of Dobson total ozone estimations to wavelength band calibration uncertainties
p 27 A82-36405
Optical stop and focussing effects in the Dobson instrument p 28 A82-36428

BAUER, M. E.
Spectral properties of agricultural crops and soils measured from space, aerial, field, and laboratory sensors
[E82-10189] p 10 N82-22623
Diurnal changes in reflectance factor due to Sun-row direction interactions
[E82-10128] p 11 N82-23566
Spectral properties of agricultural crops and soils measured from space, aerial, field, and laboratory sensors
[E82-10212] p 12 N82-23585
Multistage classification of multispectral Earth observational data: The design approach
[E82-10213] p 72 N82-23586
Determination of the optimal level for combining area and yield estimates
[E82-10215] p 12 N82-23588
Application of Computer Axial Tomography (CAT) to measuring crop canopy geometry
[E82-10227] p 14 N82-23600
Linear polarization of light by two wheat canopies measured at many view angles
[E82-10229] p 14 N82-23602
Canopy reflectance as influenced by solar illumination angle
[E82-10237] p 15 N82-23610
Spectral estimates of solar radiation intercepted by corn canopies
[E82-10003] p 18 N82-26742

BAUM, W. A.
Subtleties in the flat-fielding of charge-coupled device /CCD/ images p 68 A82-32581

BAUMGARDNER, R. W., JR.
Interpretation of surface-water circulation, Aransas Pass, Texas, using Landsat imagery p 60 A82-32896
BAZILEVSKAIA, G. A.
On the physical sense of the constant of solar cosmic ray coronal propagation p 83 A82-22599
The influence of the sector structure of interplanetary magnetic field on the solar cosmic ray characteristics p 83 A82-22603
BELIAVSKII, A. I.
Remote sensing of the weediness of crop fields p 5 A82-29435
BENDER, P. L.
Establishment of terrestrial reference frames by new observational techniques p 33 A82-32078
BENDURA, R. J.
In situ ozone data for comparison with laser absorption remote sensor: 1980 PEPE/NEROS program [NASA-TM-84471] p 30 N82-25661
BENTLEY, C. R.
Magsat magnetic anomalies over Antarctica and the surrounding oceans p 32 A82-30787
Investigation of Antarctic crust and upper mantle using MAGSAT and other geophysical data [E82-10308] p 37 N82-24582
Investigation of Antarctic crust and upper mantle using MAGSAT and other geophysical data [E82-10309] p 37 N82-24583
BENTON, E. R.
Investigation of geomagnetic field forecasting and fluid dynamics of the core [E82-10198] p 35 N82-23571
Investigation of geomagnetic field forecasting and fluid dynamics of the core [E82-10310] p 37 N82-24584
Investigation of geomagnetic field forecasting and fluid dynamics of the core [E82-10342] p 39 N82-25604
BERLIN, G. L.
Possible fault detection in Cottonball Basin, California An application of radar remote sensing p 41 A82-32898
BERNARD, R.
C-band radar for determining surface soil moisture p 10 A82-37194
BERNSTEIN, R. L.
Seasat altimeter determination of ocean current variability p 50 A82-29613
BESSELING, J. F.
Nonlinear theory for elastic beams and rods and its finite element representation [WTHD-143] p 73 N82-24517
BEUTLER, G. A.
Evaluation of HCMM data for assessing soil moisture and water table depth [E82-10329] p 18 N82-24602
BHARGAVA, B. N.
MAGSAT for geomagnetic studies over Indian region [E82-10202] p 72 N82-23575
BIBRING, J.-P.
Interstellar grains as seeds for galactic cosmic rays p 2 A82-22561
BIEHL, L. L.
Diurnal changes in reflectance factor due to Sun-row direction interactions [E82-10128] p 11 N82-23566
Linear polarization of light by two wheat canopies measured at many view angles [E82-10229] p 14 N82-23602
BIERMANN, P.
Consequences of an inverse Compton emission model for extragalactic X-ray sources p 83 A82-22553
BILANOW, S.
LANDSAT-D conical scanner evaluation plan [E82-10340] p 81 N82-25602
BINENKO, V. I.
Albedo and angular characteristics of the reflectance of the underlying surface and clouds p 33 A82-30849
BIRRER, I. J.
Evaluation of atmospheric attenuation from SMMR brightness temperature for the Seasat satellite scatterometer p 51 A82-29618
BISIGNANI, W. T.
Design guidelines for satellite image data distribution systems p 70 A82-37048
BISWAS, S.
On the stellar origin of low energy cosmic rays p 21 A82-22567
Coulombian energy losses and the nuclear composition of the solar cosmic rays p 4 A82-22610
BLAZQUEZ, C. H.
Detection and damage assessment of citrus tree losses with aerial color infrared photography /ACIR/ p 7 A82-29538
Effects of altitude, focal length, and filter combinations on color infrared photography of citrus groves p 9 A82-34729
BLODGET, H. W.
Landsat in the search for Appalachian hydrocarbons p 42 A82-34721
BLOKH, G. M.
Preflare increases in solar cosmic rays relevant to the mode of energy accumulation in the active regions associated with large flares p 31 A82-22505
BLUME, H.-J. C.
Depression of brightness temperature of sea surfaces covered with monomolecular oil films relative to clean water surfaces at 1.43 GHz p 54 A82-33322
BOBERLY, J. C.
SEASAT: A satellite scatterometer illumination times of selected in situ sites [NASA-TM-83280] p 81 N82-22865
BOGGS, D. H.
The Seasat-A satellite scatterometer - The geophysical evaluation of remotely sensed wind vectors over the ocean p 51 A82-29616
The relationship between wind vector and normalized radar cross section used to derive Seasat-A Satellite Scatterometer winds p 51 A82-29617
BOLSHOI, A. A.
Space to the earth p 83 A82-30850
BONNER, K. G.
Riparian vegetation mapping in Northeastern California using high altitude color infrared aerial photography p 5 A82-29526
Estimating rangeland cover proportions with large-scale color-infrared aerial photographs p 6 A82-29534
BORN, G. H.
Seasat measurement system evaluation - Achievements and limitations p 49 A82-29601
The Seasat altimeter data and its accuracy assessment p 49 A82-29602
An empirical determination of the effects of sea state bias on Seasat altimetry p 50 A82-29607
Seasat altimeter determination of ocean current variability p 50 A82-29613
BOWEN, R. A.
The meteorological product - 'Cloud-top height' p 70 A82-36043
BOWIN, C.
Computer-processed geophysical atlas of digital data for the East Coast margin of the United States from surface and spacecraft data [AD-A111388] p 39 N82-25748
BOWLEY, C. J.
The application of Heat Capacity Mapping Mission (HCMM) thermal data to snow hydrology [E82-10191] p 62 N82-22625
BRACALENTE, E. M.
The Seasat-A satellite scatterometer - The geophysical evaluation of remotely sensed wind vectors over the ocean p 51 A82-29616
Evaluation of atmospheric attenuation from SMMR brightness temperature for the Seasat satellite scatterometer p 51 A82-29618
BRACH, E. J.
Aircraft monitoring of surface carbon dioxide exchange p 23 A82-30293
BRACHET, G.
Earth observations from space - Trends and prospects p 84 A82-34116
BRAILE, L. W.
Verification of the crustal component in satellite magnetic data p 32 A82-30789
Study of gravity and magnetic anomalies using MAGSAT data [E82-10194] p 35 N82-22628
Spherical-Earth gravity and magnetic anomaly modeling by Gauss-Legendre quadrature integration [E82-10242] p 36 N82-24520
Magnetic and gravity anomalies in the Americas [E82-10312] p 37 N82-24586
Aeromagnetic and satellite magnetic anomally mapping [E82-10339] p 39 N82-25601
BRAMMER, R. F.
Spatial resolution and repeatability of Magsat crustal anomaly data over the Indian Ocean p 32 A82-30788
BRAUN, B.
Satellite radiation measurements for the retrieval of the vertical temperature profiles p 70 A82-36935
BRAUTIGAM, D. A.
Fragmentation of Fe nuclei on carbon, hydrogen and CH2 targets. I - Individual charge changing and total cross sections. II - Isotopic cross sections p 63 A82-22538
BROOKS, D. A.
A ship and satellite view of hydrographic features in the western Gulf of Mexico p 53 A82-32651
BROWN, G. S.
Waveheight and wind speed measurements from the Seasat radar altimeter p 50 A82-29612
BROWN, J.
Landsat digital analysis of the initial recovery of burned tundra at Kokolik River, Alaska p 8 A82-32913
BROWN, O. B.
MONEX oceanographic observations along the East African coast p 56 N82-23908
BROWN, R. A.
The Seasat-A satellite scatterometer - The geophysical evaluation of remotely sensed wind vectors over the ocean p 51 A82-29616
Surface wind analyses for Seasat p 51 A82-29619
BROWN, R. D.
Improved definition of crustal magnetic anomalies for MAGSAT data [E82-10314] p 37 N82-24587
BROWN, W. E., JR.
Seasat wind and wave observations of northeast Pacific hurricane Iva, August 13, 1978 p 52 A82-29624
BRUHWEILER, F.
Confinement and acceleration of cosmic rays in galactic superbubbles p 82 A82-22547
BUCKNER, E.
Color aerial photography detects nutrient status of loblolly pine plantations p 6 A82-29531
BUDD, J. T. C.
Remote sensing of salt marsh vegetation in the first four proposed Thematic Mapper bands p 10 A82-37503
BUNSCH-MAKAREWICZ, Z.
Satellite radiation measurements for the retrieval of the vertical temperature profiles p 70 A82-36935
BURKE, H.-H. K.
Detection of regional air pollution episodes utilizing satellite digital data in the visual range p 23 A82-31990
BURNETT, D. S.
Laboratory studies of actinide metal-silicate fractionation p 49 A82-22306
BURNS, R.
Source assessment system [AD-A111223] p 75 N82-25613
BURROWS, J. R.
Studies of high latitude current systems using MAGSAT vector data [E82-10188] p 71 N82-22622
BYRNE, G. F.
Monitoring land-cover change by principal component analysis of multitemporal Landsat data p 68 A82-32906
Separation of diffuse from sharp-edged features in digital imagery p 68 A82-34225

C

CADY, F. M.
A system design for a multispectral sensor using two-dimensional solid-state imaging arrays p 77 A82-31991
Image processing with microcomputers in remote sensing p 79 A82-34708
CAMPBELL, J. B.
Comparisons of land cover classifications from selected remote sensing systems p 80 A82-34746
CANNON, W. H.
The definition of the terrestrial coordinate frame by long baseline interferometry p 33 A82-32084
CARDONE, V. J.
Surface wind analyses for Seasat p 51 A82-29619
Intercomparison of wind speeds inferred by the SASS, altimeter, and SMMR p 52 A82-29621
CARLE, C.
Movement of ice markers measured by satellite ranging [R-240] p 59 N82-27816
CARLSON, T. N.
A method for inferring available surface moisture using remote surface temperature measurements: An assessment [E82-10311] p 17 N82-24585
Interactive initialization of heat flux parameters for numerical models using satellite temperature measurements [E82-10313] p 82 N82-26743
CARMAN, P. D.
Sensitometry in Canadian aerial survey p 79 A82-34724
CARMICHAEL, R. S.
Use of MAGSAT anomaly data for crustal structure and mineral resources in the US Midcontinent [E82-10321] p 46 N82-24594

Use of MAGSAT anomaly data for crustal structure and mineral resources in the US Midcontinent
[E82-10323] p 46 N82-24596

CARNES, J. G.
AgRISTARS: Foreign commodity production forecasting. The 1980 US corn and soybeans exploratory experiment
[E82-10206] p 11 N82-23579

CARSEY, F. D.
Sea-Ice Mission Requirements for the US FIREX and Canada RADARSAT programs
[NASA-CR-166984] p 57 N82-25609

CASSE, M.
Mass per charge ratio in hot plasmas and cosmic ray source composition p 2 A82-22557
On the stellar origin of the Ne-22 excess in cosmic rays p 21 A82-22562
Origin of galactic cosmic rays from Ne isotopic composition p 2 A82-22563

CAYLOR, J.
Optical bar panoramic photography for planning timber salvage in drought-stressed forests p 7 A82-32705

CESARSKY, C. J.
Mass per charge ratio in hot plasmas and cosmic ray source composition p 2 A82-22557
Interstellar grains as seeds for galactic cosmic rays p 2 A82-22561

CHANDRA, S.
The seasonal variations of ozone and temperature in the middle and the upper stratosphere p 29 A82-36534

CHANG, A. T. C.
Remote sensing of precipitable water over the oceans from Nimbus 7 microwave measurements p 49 A82-28907
Retrieval of ocean surface and atmospheric parameters from multichannel microwave radiometric measurements p 53 A82-31995
A comparative study of microwave radiometer observations over snowfields with radiative transfer model calculations p 60 A82-32910
Snowpack monitoring in North America and Eurasia using passive microwave satellite data p 78 A82-32915

CHANG, H. D.
Remote sensing of precipitable water over the oceans from Nimbus 7 microwave measurements p 49 A82-28907

CHANG, S.
High spectral resolution airborne spectrometry p 77 A82-32443

CHAPELL, J. H.
Fragmentation of Fe nuclei on carbon, hydrogen and CH2 targets. I - Individual charge changing and total cross sections. II - Isotopic cross sections p 63 A82-22538

CHARAKHCHIAN, A. N.
Features of cosmic ray variations due to variations in the total magnetic field of the sun p 49 A82-22619

CHARAKHCHIAN, T. N.
The energy spectra of cosmic ray variations inferred from the stratospheric measurements in 1972-1979 p 5 A82-22617
Features of cosmic ray variations due to variations in the total magnetic field of the sun p 49 A82-22619

CHARLES, P. A.
Soft X-rays from the sunlit earth's atmosphere p 29 A82-37405

CHARLTON, J. A.
Remote sensing in Scotland using data received from satellites - A study of the Tay Estuary region using Landsat multispectral scanning imagery p 62 A82-37501

CHEN, E.
Use of thermal inertia determined by HCMM to predict nocturnal cold prone areas in Florida
[E82-10299] p 17 N82-24575

CHEN, L. C.
LANDSAT-D conical scanner evaluation plan
[E82-10340] p 81 N82-25602

CHENEY, R. E.
Comparison data for Seasat altimetry in the western North Atlantic p 50 A82-29611

CHERNOV, V. IU.
The seasonal snow-line within the Fergana basin and the possibility of using it for hydrological forecasting p 61 A82-35131

CHIBISOV, G. V.
Angular variations of nonthermal radio emission from the Galaxy relevant to the structure of interstellar magnetic field p 83 A82-22550

CHIEZE, J. P.
Origin of galactic cosmic rays from Ne isotopic composition p 2 A82-22563

CHITTINENI, C. B.
Dependent feature trees for density approximation. I - Optimal construction and classification results p 67 A82-32344

CHRISTMAN, C.
A color-ratio map of Mercury p 31 A82-22294

CHUAN, R. L.
Fine particles in the Soufriere eruption plume p 24 A82-33659

CHUCHKOV, E. A.
The approximate 1 GeV solar cosmic rays in the Forbush-effect of February 15, 1978 p 40 A82-22604

CICONE, R. C.
Analysis of scanner data for crop inventories
[E82-10192] p 10 N82-22626
Analysis of scanner data for crop inventories
[E82-10241] p 16 N82-24519

CIESLA, W. M.
Development and application of panoramic aerial photography in forest pest management p 5 A82-29527
Panoramic aerial photography in forest pest management p 7 A82-32701

CLARK, B. V.
Orbiting passive microwave sensor simulation applied to soil moisture estimation
[E82-10343] p 18 N82-25605

CLARK, C. A.
Use and applicability of the vegetation component of the national site classification system
[E82-10234] p 15 N82-23607

CLARK, J.
Improved land use classification from Landsat and Seasat satellite imagery registered to a common map base p 25 A82-34743

CLARK, J. R.
Application of remote sensing to state and regional problems
[E82-10288] p 30 N82-24566

CLARK, L. D., JR.
Inventory of wetlands and agricultural land cover in the upper Sevier River Basin, Utah
[E82-10345] p 18 N82-25607
Irrigated acreage in the Bear River Basin as of the 1975 growing season
[E82-10356] p 20 N82-26754

COLEMAN, R.
A search for seamounts in the southern Cook and Austral region p 52 A82-30810

COLES, R. L.
Magnetic charts of Canada derived from Magsat data p 32 A82-30778

COLGATE, S. A.
The galactic origin of cosmic rays. I
[CONF-810711-1] p 2 A82-22565
The galactic origin of cosmic rays. II
[CONF-810711-2] p 64 A82-22573

COLLINS, W.
High spectral resolution airborne spectrometry p 7/ A82-32443

COLWELL, R. N.
Digitally enhanced visual displays facilitate the analysis of Landsat imagery p 67 A82-32507

CONCANNON, D. M.
Mapping riparian vegetation in Southeastern Oregon using digitized large scale color infra-red aerial photography p 6 A82-29535

CONGALTON, R. G.
A quantitative method to test for similarity between photo interpreters p 69 A82-34722

CONNELL, E.
Advanced technology for earth observation - Data processing
[AAS PAPER 82-130] p 71 A82-37810

COOK, P. W.
An analysis of LANDSAT MSS scene-to-scene registration accuracy
[E82-10285] p 16 N82-24563

COVAULT, C.
Landsat D to yield more precise data p 70 A82-37200

COWSIK, R.
Antiprotons from galactic sources of cosmic rays and gamma rays p 82 A82-22546
Acceleration of cosmic rays in accretion shocks p 64 A82-22568

CRACKNELL, A. P.
Remote sensing in Scotland using data received from satellites - A study of the Tay Estuary region using Landsat multispectral scanning imagery p 62 A82-37501

CRAPPER, P. F.
Monitoring land-cover change by principal component analysis of multitemporal Landsat data p 68 A82-32906
Separation of diffuse from sharp-edged features in digital imagery p 68 A82-34225

CRIST, E. P.
Association of spectral development patterns with development stages of corn
[E82-10353] p 19 N82-26751

CROMBIE, M. A.
Coordination of stereo image registration and pixel classification
[AD-A111307] p 75 N82-25614

CROSWELL, W. F.
Characteristics of 13.9 GHz radar scattering from oil films on the sea surface p 54 A82-33438

CSILLAG, F.
Significance of tectonics in linear feature detection and interpretation on satellite images p 42 A82-37198

D

DAIBOG, E. I.
Energetic solar particle spectra according to Venera-11, 12 and Prognoz-5, 6 p 4 A82-22593

DALKE, G.
Multidisciplinary investigations on HCMM data over middle Europe and Marocco
[E82-10315] p 74 N82-24568

DANA, R. W.
An infrared exposure meter p 76 A82-29541

DAUGHTRY, C. S. T.
Spectral properties of agricultural crops and soils measured from space, aerial, field, and laboratory sensors
[E82-10189] p 10 N82-22623
Spectral properties of agricultural crops and soils measured from space, aerial, field, and laboratory sensors
[E82-10212] p 12 N82-23585
Canopy reflectance as influenced by solar illumination angle
[E82-10237] p 15 N82-23610
Spectral estimates of solar radiation intercepted by corn canopies
[E82-10003] p 18 N82-26742

DAVE, J. V.
Effect of atmospheric conditions on remote sensing of vegetation parameters p 24 A82-32901

DAVIDSON, N. E.
The onset of the Australian Northwest monsoon during winter MONEX: Broadscale flow revealed by an objective analysis scheme p 56 N82-23912

DAVIDSON, S. E.
Use of LANDSAT data to define soil boundaries in Carroll County, Missouri p 10 N82-23116

DAVIS, W. E.
Comparison of ozone in polluted and clean air masses over Lake Michigan p 29 A82-36477

DAVIS, W. M.
Improved definition of crustal magnetic anomalies for MAGSAT data
[E82-10314] p 37 N82-24587

DAWSON, E.
Magnetic charts of Canada derived from Magsat data p 32 A82-30778

DAY, R. L.
Delineation of soil temperature regimes from HCMM data
[E82-10298] p 17 N82-24574

DEARAGON, A. M.
Thermal mapping, geothermal source location, natural effluents and plant stress in the Mediterranean coast of Spain
[E82-10300] p 17 N82-24576

DEBRUNNER, H.
A description of relativistic solar particle propagation p 4 A82-22600

DEJESUSPARADA, N.
Dynamic study of the upper Sao Francisco river and Tres Marias reservoir using MSS/LANDSAT images
[E82-10291] p 63 N82-24569
Comparison of storm-time changes of geomagnetic field at ground and at MAGSAT altitudes, part 2
[E82-10325] p 30 N82-24598
Comparison of storm-time changes of geomagnetic field at ground and MAGSAT altitudes
[E82-10359] p 30 N82-26757
A study of atmospheric diffusion from the LANDSAT imagery
[E82-10360] p 58 N82-26758

DELAND, M. R.
EPA's new bubble and banking policies p 25 A82-33865

DELASCUEVAS, R. N.
Thermal mapping, geothermal source location, natural effluents and plant stress in the Mediterranean coast of Spain
[E82-10300] p 17 N82-24576

DELEUR, M. S.
Experience with the compilation of maps of snow-cover melting in the central part of the European USSR on the basis of satellite data p 62 A82-35134

DEMIDOV, A. F.
Cost-effectiveness of geographic surveying from space p 85 N82-24263

DESBOIS, M.
Representativeness of cloud motion winds deduced from GOES Indian Ocean satellite imagery for the description of the Indian summer monsoon p 55 N82-23879

DESJARDINS, R. L.
Aircraft monitoring of surface carbon dioxide exchange p 23 A82-30293

DESSLER, A. J.
Pulsar models and cosmic-ray acceleration p 21 A82-22570

DEUELL, R. L.
Digital and visual evaluation of GOES and TIROS/NOAA image data for cover type effects on snowfield observations p 60 A82-34735

DIACHENKO, L. N.
Albedo and angular characteristics of the reflectance of the underlying surface and clouds p 33 A82-30849

DIAMANTE, J. M.
Tidal and geodetic observations for the Seasat altimeter calibration experiment p 49 A82-29604

DICK, R.
Breadboard gas filter correlation spectrometer for atmospheric measurement of hydrazines and nitrogen dioxide
[AD-A110688] p 82 N82-26642

DIDWALL, E.
Improved definition of crustal magnetic anomalies for MAGSAT data
[E82-10314] p 37 N82-24587

DIESEN, B. C., III
Snowpack monitoring in North America and Eurasia using passive microwave satellite data p 78 A82-32915

DILLMAN, R. D.
Estimating mountain pine beetle-killed ponderosa pine over the front range of Colorado with high altitude panoramic photography p 7 A82-32704

DIORDIENKO, L. V.
Aerogeophysical methods of finding uranium deposits p 41 A82-33402

DOBSON, C.
A simulation study of soil moisture estimation by a space SAR p 60 A82-29333

DOBSON, M. C.
Evaluation of the soil moisture prediction accuracy of a space radar using simulation techniques
[E82-10351] p 19 N82-26749

DOGIEL, V. A.
Convective outflow of cosmic rays from the Galaxy and background radio emission p 83 A82-22551

DOME, G.
The relationship between wind vector and normalized radar cross section used to derive Seasat-A Satellite Scatterometer winds p 51 A82-29617

DOME, G. J.
The Seasat-A satellite scatterometer - The geophysical evaluation of remotely sensed wind vectors over the ocean p 51 A82-29616
Evaluation of atmospheric attenuation from SMMR brightness temperature for the Seasat satellite scatterometer p 51 A82-29618

DOMINGO, V.
Non-flare injection of protons into interplanetary space p 4 A82-22601

DOUGLAS, B. C.
Tidal and geodetic observations for the Seasat altimeter calibration experiment p 49 A82-29604

DOUMA, M.
High spectral resolution airborne spectrometry p 77 A82-32443

DOWNS, A. L.
Digital and visual evaluation of GOES and TIROS/NOAA image data for cover type effects on snowfield observations p 60 A82-34735

DUCRUIX, J.
MAGSAT anomaly map and continental drift
[E82-10326] p 38 N82-24599
Models and maps of the main field
[E82-10327] p 74 N82-24600

DUEPPE, R.-D.
The simultaneous employment of geodetic measurements for block adjustments using the method of independent models p 34 A82-33295

DUFFY, B.
Application of remote sensing to state and regional problems
[E82-10288] p 30 N82-24566

DUGGIN, M. J.
Evaluation of NOAA-AVHRR data for crop assessment p 8 A82-34179

DUNKLE, K.
Computer-processed geophysical atlas of digital data for the East Coast margin of the United States from surface and spacecraft data
[AD-A111388] p 39 N82-25748

DURGAPRASAD, N.
On the stellar origin of low energy cosmic rays p 21 A82-22567

DURPAIRE, J.-P.
An optical objective lens for earth observations by satellites p 78 A82-32824

DUYBKIN, I. A.
Estimates of the statistical structure of the atmospheric pressure field in summer Monex-79 area p 57 N82-23939

DWORAK, T. Z.
Problems of the interpretation of aerial and satellite images of industrial smoke p 23 A82-30307

DYKSTRA, J.
Experimental assessment of improved spatial resolution LANDSAT data
[AD-A110538] p 75 N82-26765

DZHORZHIO, M. V.
The use of satellite photographs to study snow-cover dynamics and to determine the average water discharge of the Amudarya during a vegetation period p 61 A82-35132

DZIEWULSKA-LOSIOWA, A.
The effect of the spectral attenuation of UV radiation by aerosol on the total ozone measurements p 27 A82-36406

E

EASTER, R. C.
Comparison of ozone in polluted and clean air masses over Lake Michigan p 29 A82-36477

EBERHARD, W.
Field measurements in support of dispersion modeling in complex terrain (1980)
[PB82-148644] p 39 N82-27882

ECKERMAN, J.
Radiometer mission requirements for large space antenna systems
[NASA-TM-84478] p 81 N82-25610

EDWARDS, G. J.
Detection and damage assessment of citrus tree losses with aerial color infrared photography /ACIR/ p 7 A82-29538

EL-HAKIM, S. F.
A practical study of gross-error detection in bundle adjustment p 69 A82-34702

EL-HASSAN, I. M.
The use of Skylab S-190B photography for small scale mapping p 80 A82-34742

ELMAN, R. I.
Status and prospects of the automated processing of remote-sensing data /using forest surveys as an example/ p 10 A82-35139

EMERY, B. A.
OSO-8 lower mesospheric ozone number density profiles p 28 A82-36472

ENGLAND, C. F.
Satellite observations of sea surface temperature around the British Isles p 54 A82-33717

ERMAKOV, S. I.
Comparison of solar proton activity in 1967 and 1969 with that in 1978 and 1979 as measured onboard Venera 4, 6, 11, 12 space probes p 31 A82-22596
The solar proton fluxes in April, 1979 p 66 A82-22597

ESTES, J. E.
Impacts of remote sensing on U.S. geography p 24 A82-32699
Multispectral determination of soil moisture-2
[E82-10349] p 19 N82-26747

ETKIN, V. S.
The use of microwave radiometry for the determination of snow cover height p 80 A82-36018

EVANS, R. D.
Dobson spectrophotometer calibrations, possible errors in ozone absorption coefficients, and errors due to interfering pollutant gases p 28 A82-36431

EVENSON, P.
Unusual properties of particle events associated with solar flare gamma ray events p 65 A82-22585
The relation of type II radio bursts to solar energetic particles observed at earth p 3 A82-22591

F

FAINTICH, M. B.
Matrix data analysis: Color/B and W coding is not always enough
[AD-A111401] p 74 N82-25612

FAN, C. J.
Relating thematic mapper bands TM3, TM4, and TM5 to agronomic variables for corn, cotton, sugarbeet, soybean, sorghum, sunflower and tobacco
[E82-10347] p 19 N82-26745

FAN, C. Y.
Observations of the ionization states of energetic particles accelerated in solar flares p 40 A82-22607

FAUST, N. L.
Automated classification of runoff coefficients from Landsat multispectral data p 60 A82-34734

FEDCHENKO, P. P.
Remote sensing of the weediness of crop fields p 5 A82-29435

FEDI, M.
Crustal structures under the active volcanic areas of central and eastern Mediterranean (M-44)
[E82-10096] p 35 N82-23563

FEDOR, L. S.
Waveheight and wind speed measurements from the Seasat radar altimeter p 50 A82-29612
Intercomparison of wind speeds inferred by the SASS, altimeter, and SMMR p 52 A82-29621

FEISTER, U.
Total ozone retrieval from satellite Meteor 28 Fourier spectrometer measurements p 28 A82-36422

FINLEY, R. J.
Interpretation of surface-water circulation, Aransas Pass, Texas, using Landsat imagery p 60 A82-32896

FIRSOV, IU. G.
The processing of satellite navigation data for marine geodesy p 34 A82-37175

FISK, L. A.
Observations of the ionization states of energetic particles accelerated in solar flares p 40 A82-22607

FISKE, R. S.
Soufriere Volcano, St. Vincent - Observations of its 1979 eruption from the ground, aircraft, and satellites p 24 A82-33652

FLEIG, A. J.
Total ozone variations 1970-74 using Backscattered Ultraviolet /BUV/ and ground-based observations p 26 A82-36053

FLICK, R. E.
Fluid-sediment interactions on beaches and shelves
[AD-A110838] p 59 N82-26948

FORMAN, M. A.
Cosmic ray acceleration by stellar winds. I - Total density, pressure and energy flux p 21 A82-22566

FOSTER, J. L.
Snowpack monitoring in North America and Eurasia using passive microwave satellite data p 78 A82-32915

FRAWLEY, J. F.
Improved definition of crustal magnetic anomalies for MAGSAT data
[E82-10314] p 37 N82-24587

FREDERIKSEN, P.
Terrain classification by Fourier analysis - Accuracy and economy p 69 A82-34723

FREIER, P. S.
A report on the 'cosmic ray propagation problem' p 1 A82-22539

FREUDENSTEIN, W. H.
Thematic mapper - An overview of spectral band registration p 77 A82-32447

FREY, H.
Magsat scalar anomaly distribution - The global perspective p 41 A82-30786

FROST, V. S.
The recognition of extended targets - SAR images for level and hilly terrain p 33 A82-31994

FUCHS, J. E.
A multi-frequency radiometric measurement of soil moisture content over bare and vegetated fields
[E82-10236] p 16 N82-23611

FUKUI, Y.
Interactions of cosmic rays with molecular clouds p 82 A82-22548

FUKUSHIMA, N.
Preliminary interpretation of magnetic anomalies over Japan and its surrounding area p 33 A82-30796
Investigation from Japanese MAGSAT team
[E82-10239] p 73 N82-23612
Investigation from Japanese MAGSAT Team. Part A. Crustal structure near Japan and in Antarctic station. Part B. Electric currents and hydromagnetic waves in the ionosphere and the magnetosphere
[E82-10244] p 36 N82-24522

Report of investigation from Japanese MAGSAT Team
[E82-10322] p 74 N82-24595

FULLER, W. H., JR.
Airborne lidar measurements of the Soufriere eruption of 17 April 1979 p 24 A82-33657

G

GABRIELSEN, R. H.
Regional geological, tectonic and geophysical features of Nordland, Norway p 41 A82-30304

GAISSER, T. K.
Antiprotons from galactic sources of cosmic rays and gamma rays p 82 A82-22546

GALDEANO, A.
MAGSAT anomaly map and continental drift
[E82-10326] p 38 N82-24599

GALLIHER, S. C.
An equivalent layer magnetization model for the United States derived from MAGSAT data
[E82-10297] p 36 N82-24573

GALLO, K. P.
Spectral estimates of solar radiation intercepted by corn canopies
[E82-10003] p 18 N82-26742

GARCIA-MUNOZ, M.
The question of short pathlengths in interstellar propagation p 1 A82-22541

GAROFALO, D.
Experimental assessment of improved spatial resolution LANDSAT data
[AD-A110538] p 75 N82-26765

GASPARINI, P.
Crustal structures under the active volcanic areas of central and eastern Mediterranean (M-44)
[E82-10096] p 35 N82-23563

GATLIN, J. A.
Use of NOAA/AVHRR visible and near-infrared data for land remote sensing
[NASA-TM-84186] p 81 N82-22643

GATTO, L. W.
Ice distribution and winter surface circulation patterns, Kachemak Bay, Alaska
[AD-A110606] p 58 N82-26764

GAUSMAN, H. W.
AgRISTARS: Early warning and crop condition assessment. Plant cover, soil temperature, freeze, water stress, and evapotranspiration conditions
[E82-10225] p 14 N82-23598

GERSHENZON, V. E.
The use of microwave radiometry for the determination of snow cover height p 80 A82-36018

GERTSENOVA, K. N.
Evaluation of the effectiveness of systematic image distortion compensation p 69 A82-34469

GESCHKE, A.
Thermography - A remote sensing method with many perspectives p 76 A82-29922

GILER, M.
Origin of cosmic rays in galactic centre sources
p 3 A82-22571

GINZBURG, V. L.
Remarks on cosmic ray origin p 21 A82-22569

GIRE, C.
Models and maps of the main field
[E82-10327] p 74 N82-24600

GLAZAR, W. S.
A multi-frequency radiometric measurement of soil moisture content over bare and vegetated fields
[E82-10238] p 16 N82-23611

GLOECKLER, G.
Observations of interplanetary energetic charged particles from gamma-ray line solar flares
p 65 A82-22586

Time and energy dependence of heavy ion abundances in solar flare energetic particle events
p 22 A82-22605

Observations of the ionization states of energetic particles accelerated in solar flares p 40 A82-22607

A comparison of helium and heavy ion spectra in He/3/ rich solar flares with a model calculation
p 5 A82-22612

GOETTELMAN, R. C.
Airborne observed solar elevation and row direction effects on the near-IR/red ratio of cotton
[E82-10220] p 13 N82-23593

GOETZ, A. F. H.
Spectroscopic remote sensing for geological applications p 41 A82-32442

GOLDBERG, P. A.
Remote sensing - A potential aid in the preparation of an urban tree inventory p 9 A82-34732

GOMBOSI, T. I.
Spacecraft determination of energetic particle propagation parameters - The 1 January 1978 solar event p 31 A82-22598

GONZALEZ, F. I.
Seasat wind and wave observations of northeast Pacific hurricane Iva, August 13, 1978 p 52 A82-29624

GOODELL, P. C.
Evaluation and combined geophysical interpretations of NURE and related geoscience data in the Van Horn, Pecos, Marfa, Fort Stockton, Presidido, and Emory Peak quadrangles, Texas, volume 1
[DE82-005554] p 47 N82-27808

GOODELL, R. C.
Evaluation and combined geophysical interpretations of NURE and related geoscience data in the Van Horn, Pecos, Marfa, Fort Stockton, Presidio, and Emory Peak quadrangels, Texas
[DE82-005560] p 48 N82-27809

GOODMAN, J. M.
Terrain analysis from Landsat using a color TV enhancement system p 68 A82-32911

GOODRIDGE, D. R.
SEASAT: A satellite scatterometer illumination times of selected in situ sites
[NASA-TM-83280] p 81 N82-22865

GOODSPEED, M. J.
Separation of diffuse from sharp-edged features in digital imagery p 68 A82-34225

GORNEY, D. J.
Generation of the auroral kilometric radiation
p 26 A82-35542

GOSS-ZUREK, R.
Satellite radiation measurements for the retrieval of the vertical temperature profiles p 70 A82-36935

GOULD, W. I.
A multi-frequency radiometric measurement of soil moisture content over bare and vegetated fields
[E82-10238] p 16 N82-23611

GOWARD, S. N.
Longwave infrared observation of urban landscapes
p 25 A82-34744

GRAHAM, M. H.
An algorithm for automating the registration of USDA segment ground data to LANDSAT MSS data
[E82-10266] p 16 N82-24564

GRASS, R. D.
Dobson spectrophotometer calibrations, possible errors in ozone absorption coefficients, and errors due to interfering pollutant gases p 28 A82-36431

GREBOWSKY, G.
Evaluation of temporal registration of Landsat scenes
p 67 A82-32345

GREEN, G.
Spacecraft determination of energetic particle propagation parameters - The 1 January 1978 solar event p 31 A82-22598

GREEN, M. J.
An optical data link for airborne scanning system
p 80 A82-34737

GREILING, R.
Satellite image interpretation of the eastern Caledonian part of the Blue Road Geotraverse and its geological implications /Nordland, Vasterbotten, Scandinavia/
p 41 A82-30305

GRIGORIAN, O. P.
Preflare increases in solar cosmic rays relevant to the mode of energy accumulation in the active regions associated with large flares p 31 A82-22595

GRIN, A. M.
Principles and methods of the study of the hydrological cycle on the basis of aerospace data p 61 A82-35127

GROCH, W.-D.
Extraction of line shaped objects from aerial images using a special operator to analyze the profiles of functions p 67 A82-32033

GUDMANDSEN, P.
Movement of ice markers measured by satellite ranging
[R-240] p 59 N82-27816

GUENTHER, G. C.
Bias correction procedures for airborne laser hydrography
[PB82-130089] p 63 N82-22644

GUPTA, S. R. M.
Analysis of MAGSAT data of the Indian region
[E82-10358] p 75 N82-26756

GURNEY, C. M.
The use of contextual information to detect cumulus clouds and cloud shadows in Landsat data
p 67 A82-32346

GUSSENHOVEN, M. S.
Extremely high latitude auroras p 76 A82-31020

GUYMER, T.
Surface wind analyses for Seasat p 51 A82-29619

GUZA, R. T.
Fluid-sediment interactions on beaches and shelves
[AD-A110838] p 59 N82-26948

GUZIK, T. G.
The question of short pathlengths in interstellar propagation p 1 A82-22541

H

HABGOOD, F.
Overseas Geology And Mineral Resources number 56: A geological interpretation of LANDSAT imagery and air photography of Botswana
[OGMR-56] p 42 N82-22636

HAFKER, W. R.
Landsat detection of hardwood forest clearcuts
p 8 A82-32708

HAGGERTY, S. E.
The mineralogy of global magnetic anomalies
[E82-10305] p 45 N82-24579

HAJIC, E. J.
Multispectral determination of soil moisture-2
[E82-10349] p 19 N82-26747

HALBERSTAM, I. M.
The relationship between wind vector and normalized radar cross section used to derive Seasat-A Satellite Scatterometer winds p 51 A82-29617

HALL, D. K.
Landsat digital analysis of the initial recovery of burned tundra at Kokolik River, Alaska p 8 A82-32913

Snowpack monitoring in North America and Eurasia using passive microwave satellite data
p 78 A82-32915

HALL, D. L.
Design guidelines for satellite image data distribution systems p 70 A82-37048

HALL, L.
Experimental assessment of improved spatial resolution LANDSAT data
[AD-A110538] p 75 N82-26765

HALL, P. M.
Remote sensing of Douglas-fir trees newly infested by bark beetles p 6 A82-29536

HANCOCK, D. W., III
Sea-state-related altitude errors in the Seasat radar altimeter p 50 A82-29606

HAPKE, B.
A color-ratio map of Mercury p 31 A82-22294

HARKER, D. B.
Problems associated with remotely detecting and monitoring saline sites within irrigated Alberta
p 9 A82-34710

HARLAN, C.
Irrigation management with remote sensing
[E82-10357] p 20 N82-26755

HARQUIST, T. W.
Evidence for the stochastic acceleration of cosmic rays in supernova remnants p 2 A82-22564

HARRISON, C. G. A.
Investigations of medium wavelength magnetic anomalies in the eastern Pacific using MAGSAT
[E82-10240] p 73 N82-23613

Investigations of medium wavelength magnetic anomalies in the eastern Pacific using MAGSAT data
[E82-10330] p 38 N82-24603

HARTMANN, D. L.
Interannual variations of outgoing IR associated with tropical circulation changes during 1974-1978
p 54 A82-36341

HASLAM, C. G. T.
Derivation of the distribution of synchrotron emissivity in the Galaxy from the 408 MHz all-sky survey
p 82 A82-22549

HASTINGS, D. A.
An investigation of MAGSAT and complementary data emphasizing precambrian shields and adjacent areas of West Africa and South America
[E82-10316] p 38 N82-24589

An investigation of MAGSAT and complementary data emphasizing precambrian shields and adjacent areas of West Africa and South America
[E82-10317] p 38 N82-24590

An investigation of MAGSAT and complementary data emphasizing precambrian shields and adjacent areas of West Africa and South America
[E82-10318] p 38 N82-24591

HATFIELD, J. L.
Multilevel measurements of surface temperature over undulating terrain planted to barley
[E82-10245] p 16 N82-24523

HAWKINS, J.
Surface wind analyses for Seasat p 51 A82-29619

HAWKINS, J. D.
Meteorological and aircraft data for CUE 2 1973
[PB82-149246] p 59 N82-26949

HAYAKAWA, S.
Interactions of cosmic rays with molecular clouds
p 82 A82-22548

HAYDEN, C. M.
Surface temperature determination from an amalgamation of GOES and TIROS-N radiance measurements p 66 A82-28905

HAYDN, R.
Multidisciplinary investigations on HCMM data over middle Europe and Marocco
[E82-10315] p 74 N82-24588

HAYNE, G. S.
Sea-state-related altitude errors in the Seasat radar altimeter p 50 A82-29606

HEAD, J. W., III
An investigation into the utilization of HCMM thermal data for the discrimination of volcanic and Eolian geological units
[E82-10352] p 47 N82-26750

HEATH, D. F.
Total ozone variations 1970-74 using Backscattered Ultraviolet /BUV/ and ground-based observations
p 26 A82-36053

HEFFNER, P.
Advanced technology for earth observation - Data processing
[AAS PAPER 82-130] p 71 A82-37810

HEFFTER, J. L.
Meteorological analysis of the eruption of Soufriere in April 1979 p 24 A82-33655

HEGG, K. M.
Multi-resource inventory in interior Alaska
p 6 A82-29532

HEILMAN, J.
Irrigation management with remote sensing
[E82-10357] p 20 N82-26755

HEILMAN, J. L.
Evaluation of HCMM data for assessing soil moisture and water table depth
[E82-10329] p 18 N82-24602

HEILMAN, W. E.
Evaluation of HCMM data for assessing soil moisture and water table depth
[E82-10329] p 18 N82-24602

HEINEN, J. T.
Inventory of wildlife habitat from color infrared aerial photography for Cobb Island, Virginia p 6 A82-29529
A computerized spatial analysis system for assessing wildlife habitat from vegetation maps p 9 A82-34716

HENDERSON-SELLERS, A.
System albedo as sensed by satellites - Its definition and variability p 23 A82-32342

HENDERSON, F. M.
Comparisons of land cover classifications from selected remote sensing systems p 60 A82-34746

HENKEL, J.
Multidisciplinary investigations on HCMM data over middle Europe and Marocco
[E82-10315] p 74 N82-24588

HERMAN, I. P.
Feasibility of laser-separation of 36 S and its use as an atmospheric tracer
[DE82-000965] p 30 N82-27737

HICKMAN, G. D.
Laser-induced bioluminescence p 53 A82-32559

HIDE, R.
Spherical harmonic representation of the main geomagnetic field for world charting and investigations of some fundamental problems of physics and geophysics
[E82-10203] p 72 N82-23576

HIELKEMA, J. U.
Desert locust habitat monitoring with satellite remote sensing A new technology for an old problem
p 7 A82-29747

HILL, G. W.
Nearshore current pattern off south Texas - An interpretation from aerial photographs
p 53 A82-32903

HILTON, B. M.
Multispectral determination of soil moisture-2
[E82-10349] p 19 N82-26747

HINTON, B. B.
Estimates of sea surface stress for summer MONEX from cloud motions p 56 N82-23910

HINZE, W. J.
Verification of the crustal component in satellite magnetic data p 32 A82-30789
A satellite magnetic model of northeastern South American aulacogens p 33 A82-30795
Study of gravity and magnetic anomalies using MAGSAT data
[E82-10194] p 35 N82-22628
Spherical-Earth gravity and magnetic anomaly modeling by Gauss-Legendre quadrature integration
[E82-10242] p 36 N82-24520
Magnetic and gravity anomalies in the Americas
[E82-10312] p 37 N82-24586
Aeromagnetic and satellite magnetic anomally mapping
[E82-10339] p 39 N82-25601
Evaluation and combined geophysical interpretations of NURE and related geoscience data in the Van Horn, Pecos, Marfa, Fort Stockton, Presidido, and Emory Peak quadrangles, Texas, volume 1
[DE82-005554] p 47 N82-27808
Evaluation and combined geophysical interpretations of NURE and related geoscience data in the Van Horn, Pecos, Marfa, Fort Stockton, Presidio, and Emory Peak quadrangles, Texas
[DE82-005560] p 48 N82-27809

HIRASIMA, Y.
Solar gamma-ray experiment on Astro-A satellite
p 21 A82-22583

HIXSON, M. M.
Determination of the optimal level for combining area and yield estimates
[E82-10215] p 12 N82-23588

HODGES, T.
AgRISTARS: Supporting research. Spring small grains planting date distribution model
[E82-10208] p 12 N82-23581

HODGSON, R. M.
A system design for a multispectral sensor using two-dimensional solid-state imaging arrays
p 77 A82-31991
Image processing with microcomputers in remote sensing p 79 A82-34708

HOELL, J. M.
Ammonia and the NOx budget of the troposphere
p 27 A82-36293

HOLTZMAN, J.
A simulation study of soil moisture estimation by a space SAR p 60 A82-29333

HOLTZMAN, J. C.
The recognition of extended targets - SAR images for level and hilly terrain p 33 A82-31994
Evaluation of the soil moisture prediction accuracy of a space radar using simulation techniques
[E82-10351] p 19 N82-26749

HONG, J.-K.
Coastal environment change analysis by Landsat MSS data p 54 A82-34219

HORN, F. W., JR.
Detection and damage assessment of citrus tree losses with aerial color infrared photography /ACIR/
p 7 A82-29538
Effects of altitude, focal length, and filter combinations on color infrared photography of citrus groves
p 9 A82-34729

HORNER, R. J.
Initial scalar magnetic anomaly map from Magsat
p 32 A82-30784
Initial vector magnetic anomaly map from Magsat
p 32 A82-30785

HORNIBROOK, M.
High resolution satellite observations of mesoscale oceanography in the Tasman Sea, 1978 - 1979
[E82-10324] p 57 N82-24597

HORSTMAN, K. C.
Possible fault detection in Cottonball Basin, California An application of radar remote sensing
p 41 A82-32898

HORVATH, R.
Analysis of scanner data for crop inventories
[E82-10192] p 10 N82-22626
Analysis of scanner data for crup inventories
[E82-10241] p 16 N82-24519

HOVESTADT, D.
Observations of interplanetary energetic charged particles from gamma-ray line solar flares
p 65 A82-22586
Time and energy dependence of heavy ion abundances in solar flare energetic particle events
p 22 A82-22605
Observations of the ionization states of energetic particles accelerated in solar flares p 40 A82-22607
A comparison of helium and heavy ion spectra in He/3/ rich solar flares with a model calculation
p 5 A82-22612

HOVET, H.
The METEOSAT Data Collection System and its application p 75 N82-26037

HOWE, R. C.
Comparing lineaments interpreted from Landsat imagery and topographic maps with reported faults in southwest Montana p 34 A82-34719

HUGHES, J. K.
SEASAT: A satellite scatterometer illumination times of selected in situ sites
[NASA-TM-83280] p 81 N82-22865

HUGHES, N. A.
System albedo as sensed by satellites - Its definition and variability p 23 A82-32342

HUGHES, T. J.
Studies of high latitude current systems using MAGSAT vector data
[E82-10188] p 71 N82-22622

HUMMER-MILLER, S.
Registration of Heat Capacity Mapping Mission day and night images
[E82-10210] p 72 N82-23583
Ground support data from July 10 to July 29, 1978, for HCMM thermal satellite data of the Powder River Basin, Wyoming
[E82-10211] p 72 N82-23584

HUNG, R. J.
Remote sensing of tornadic storms from geosynchronous satellite infrared digital data
p 23 A82-32348

HUNT, G. E.
Satellite observations of sea surface temperature around the British Isles p 54 A82-33717

HUNT, W. H.
Airborne lidar measurements of the Soufriere eruption of 17 April 1979 p 24 A82-33657

HUNTER, R. E.
Nearshore current pattern off south Texas - An interpretation from aerial photographs
p 53 A82-32903

HUSSON, J. C.
History of the French satellite space program
p 85 N82-24216

I

IAROVOI, B. D.
The processing of satellite navigation data for marine geodesy p 34 A82-37175

IDSO, S. B.
View angle effects in the radiometric measurement of plant canopy temperatures p 8 A82-32914

IISAKA, J.
Coastal environment change analysis by Landsat MSS data p 54 A82-34219

INMAN, D. L.
Fluid-sediment interactions on beaches and shelves
[AD-A110838] p 59 N82-26948

INOUE, T.
Estimation of the precipitable water from the IR channel of the geostationary satellite p 55 A82-37196

IPAVICH, F. M.
Observations of the ionization states of energetic particles accelerated in solar flares p 40 A82-22607

IRISOV, V. G.
The use of microwave radiometry for the determination of snow cover height p 80 A82-36018

ISMAIL, S.
Large amplitude undulations on the equatorward boundary of the diffuse aurora p 76 A82-31019

IVANOV, A. V.
On the synthetic aperture radar imaging of ocean surface waves p 53 A82-32881

IWATA, A.
Aircraft measurements of NO/x/ in the lower troposphere above the coast of Japan
p 26 A82-36247

J

JACKSON, D. D.
Seismic and geodetic studies of the Imperial Valley, California
[DE82-001686] p 39 N82-26915

JACKSON, R. D.
View angle effects in the radiometric measurement of plant canopy temperatures p 8 A82-32914
Airborne observed solar elevation and row direction effects on the near-IR/red ratio of cotton
[E82-10220] p 13 N82-23593
Multilevel measurements of surface temperature over undulating terrain planted to barley
[E82-10245] p 16 N82-24523

JACOBI, O.
Terrain classification by Fourier analysis - Accuracy and economy p 69 A82-34723

JAIN, A.
Ocean wave height measurement with SEASAT SAR using speckle diversity p 53 A82-32882

JAYNES, R. A.
Inventory of wetlands and agricultural land cover in the upper Sevier River Basin, Utah
[E82-10345] p 18 N82-25607
Mapping of wildlife habitat in Farmington Bay, Utah
[E82-10354] p 19 N82-26752

Detection of variations in aspen forest habitat from LANDSAT digital data: Bear River Range, Utah
[E82-10355] p 19 N82-26753

Irrigated acreage in the Bear River Basin as of the 1975 growing season
[E82-10356] p 20 N82-26754

JENSEN, J. R.

Detecting residential land-use development at the urban fringe p 22 A82-29332

Impacts of remote sensing on U.S. geography
p 24 A82-32899

JOBUSCH, C. D.

Determination of the optimal level for combining area and yield estimates
[E82-10215] p 12 N82-23588

JOHNSON, H. B.

Resource inventory techniques used in the California Desert Conservation Area p 23 A82-32441

JOHNSON, J. W.

Characteristics of 13.9 GHz radar scattering from oil films on the sea surface p 54 A82-33438

JOHNSON, L.

Landsat digital analysis of the initial recovery of burned tundra at Kokolik River, Alaska p 8 A82-32913

JONES, C. L.

Measurement of soil moisture trends with airborne scatterometers
[E82-10361] p 20 N82-26759

Multifrequency remote sensing of soil moisture
[E82-10362] p 20 N82-26760

Development of visible/infrared/microwave agriculture classification and biomass estimation algorithms
[E82-10363] p 20 N82-26761

JONES, J. H.

Laboratory studies of actinide metal-silicate fractionation p 49 A82-22306

JONES, P. H.

Use of thermal inertia determined by HCMM to predict nocturnal cold prone areas in Florida
[E82-10299] p 17 N82-24575

JONES, W. L.

The Seasat-A satellite scatterometer - The geophysical evaluation of remotely sensed wind vectors over the ocean p 51 A82-29616

The relationship between wind vector and normalized radar cross section used to derive Seasat-A Satellite Scatterometer winds p 51 A82-29617

JOSEPH, M. G.

On the space-time variability of ocean surface mixed layer characteristics of central and eastern Arabian sea during MONSOON-77 p 56 N82-23909

JOUVE, P.

Application of infrared techniques to the study of atmospheric ozone p 27 A82-36414

JUNKIN, B. G.

Development of three-dimensional spatial displays using a geographically based information system
p 66 A82-29326

JUPP, D. L. B.

The use of residual images in Landsat image analysis
p 66 A82-29328

K

KAFATOS, M.

Confinement and acceleration of cosmic rays in galactic superbubbles p 82 A82-22547

Acceleration processes near massive black holes
p 3 A82-22572

KALCIC, M. T.

Analysis of thematic mapper simulator data acquired during winter season over Pearl River, Mississippi, test site
[E82-10287] p 17 N82-24565

KANE, R. P.

Comparison of storm-time changes of geomagnetic field at ground and at MAGSAT altitudes, part 2
[E82-10325] p 30 N82-24598

Comparison of storm-time changes of geomagnetic field at ground and MAGSAT altitudes
[E82-10359] p 30 N82-26757

KASPRZHAK, K.

The possibility of using remote-sensing methods to study the hydrology of elementary watersheds
p 61 A82-35130

KATIBAH, E. F.

Use of Landsat multispectral scanner data in vegetation mapping of a forested area p 9 A82-34731

KAUFMANN, H.

Multidisciplinary investigations on HCMM data over middle Europe and Marocco
[E82-10315] p 74 N82-24588

KAUTH, R. J.

Analysis of scanner data for crop inventories
[E82-10192] p 10 N82-22626

Analysis of scanner data for crop inventories
[E82-10241] p 16 N82-24519

KAWAMURA, M.

Report of investigation from Japanese MAGSAT Team
[E82-10322] p 74 N82-24595

KEAFER, L. S., JR.

Radiometer mission requirements for large space antenna systems
[NASA-TM-84478] p 81 N82-25610

KEARSEY, S.

Derivation of the distribution of synchrotron emissivity in the Galaxy from the 408 MHz all-sky survey
p 82 A82-22549

KECSKEMETY, K.

Spacecraft determination of energetic particle propagation parameters - The 1 January 1978 solar event p 31 A82-22598

KEEVALLIK, S.

Estimation of the temperature of the upper boundary of cloud cover over the world ocean p 54 A82-36005

KELLER, G. R.

Characterization of the structure and tectonic of South America
[E82-10196] p 42 N82-23569

The crustal structure and tectonics of South America
[E82-10319] p 38 N82-24592

Geotectonics of South America
[E82-10320] p 38 N82-24593

Evaluation and combined geophysical interpretations of NURE and related geoscience data in the Van Horn, Pecos, Marfa, Fort Stockton, Presidido, and Emory Peak quadrangles, Texas, volume 1
[DE82-005554] p 47 N82-27808

Evaluation and combined geophysical interpretations of NURE and related geoscience data in the Van Horn, Pecos, Marfa, Fort Stockton, Presidio, and Emory Peak quadrangels, Texas
[DE82-005560] p 48 N82-27809

KELNER, S. R.

Computer simulation of the time dependence of the photon energy spectra produced in proton and electron bremstrahlung p 3 A82-22587

KENNARD, R. E.

Preliminary evidence for the influence of physiography and scale upon the autocorrelation function of remotely sensed data p 67 A82-32343

KESSLER, R.

Interpretation of vegetative cover in wetlands using four-channel SAR imagery p 9 A82-34706

KHACHATURIAN, G. O.

The solar proton fluxes in April, 1979
p 66 A82-22597

KHAPIN, IU. B.

The use of microwave radiometry for the determination of snow cover height p 80 A82-36018

KHORRAM, S.

Use of Landsat multispectral scanner data in vegetation mapping of a forested area p 9 A82-34731

KHOSLA, K. L.

Analysis of MAGSAT data of the Indian region
[E82-10358] p 75 N82-26756

KHOTILOVSKAIA, T. G.

Comparison of solar proton activity in 1967 and 1969 with that in 1978 and 1979 as measured onboard Venera 4, 6, 11, 12 space probes p 31 A82-22596

KIARNER, O.

Estimation of the temperature of the upper boundary of cloud cover over the world ocean p 54 A82-36005

KILGORE, R. W.

Application of Computer Axial Tomography (CAT) to measuring crop canopy geometry
[E82-10227] p 14 N82-23600

KIMES, D. S.

Effects of vegetation canopy structure on remotely sensed canopy temperatures p 8 A82-32905

View angle effects in the radiometric measurement of plant canopy temperatures p 8 A82-32914

Irradiance measurement errors due to the assumption of a Lambertian reference panel p 79 A82-34222

KIPFINGER, R.

Ground support data from July 10 to July 29, 1978, for HCMM thermal satellite data of the Powder River Basin, Wyoming
[E82-10211] p 72 N82-23584

KIRCHNER, J. A.

Irradiance measurement errors due to the assumption of a Lambertian reference panel p 79 A82-34222

Influence of sky radiance distribution on the ratio technique for estimating bidirectional reflectance
p 70 A82-35650

KISH, J. C.

Fragmentation of Fe nuclei on carbon, hydrogen and CH2 targets. I - Individual charge changing and total cross sections. II - Isotopic cross sections p 63 A82-22538

KLECKER, B.

Observations of interplanetary energetic charged particles from gamma-ray line solar flares
p 65 A82-22586

Observations of the ionization states of energetic particles accelerated in solar flares p 40 A82-22607

A comparison of helium and heavy ion spectra in He/3/ rich solar flares with a model calculation
p 5 A82-22612

KLEIN, W. H.

Estimating bark beetle-killed lodgepole pine with high altitude panoramic photography p 7 A82-32703

KLEMAS, V.

Determination of winter temperature patterns, fronts, and surface currents in the Yellow Sea and East China Sea from satellite imagery p 55 A82-37195

KLOSKO, S. M.

Gravity model improvement for Seasat
p 32 A82-29615

KLUMPAR, D. M.

Investigation of the effects of external current systems on the MAGSAT data utilizing grid cell modeling techniques
[E82-10195] p 71 N82-22629

Investigation of the effects of external current systems on the MAGSAT data utilizing grid cell modeling techniques
[E82-10226] p 73 N82-23599

Investigation of the effects of external current systems on the MAGSAT data utilizing grid cell modeling techniques
[E82-10232] p 73 N82-23605

Investigation of the effects of external current systems on the MAGSAT data utilizing grid cell modeling techniques
[E82-10306] p 74 N82-24580

KOBAYASHI, K.

Report of investigation from Japanese MAGSAT Team
[E82-10322] p 74 N82-24595

KOCHAROV, L. G.

The model of the cosmic ray enrichment by helium-3
p 31 A82-22614

KOLACZEK, B.

On reference coordinate systems used in polar motion determinations p 33 A82-32090

KOLENKIEWICZ, R.

Seasat altimeter height calibration p 49 A82-29603

KOLLENKARK, J. C.

Diurnal changes in reflectance factor due to Sun-row direction interactions
[E82-10128] p 11 N82-23566

Canopy reflectance as influenced by solar illumination angle
[E82-10237] p 15 N82-23610

KOLOSOV, P. A.

Principles and methods of the study of the hydrological cycle on the basis of aerospace data p 61 A82-35127

KOMHYR, W. D.

Dobson spectrophotometer calibrations, possible errors in ozone absorption coefficients, and errors due to interfering pollutant gases p 28 A82-36431

KONDO, I.

Solar gamma-ray experiment on Astro-A satellite
p 21 A82-22583

KONDO, Y.

Aircraft measurements of NO/x/ in the lower troposphere above the coast of Japan
p 26 A82-36247

KONDRATEV, K. IA.

Remote sensing of the weediness of crop fields
p 5 A82-29435

Albedo and angular characteristics of the reflectance of the underlying surface and clouds p 33 A82-30849

Study of the hydrological cycle by aerospace methods
p 61 A82-35126

KONO, M.

Preliminary interpretation of magnetic anomalies over Japan and its surrounding area p 33 A82-30796

KONTOR, N. N.

Evolution of the solar proton spectrum in interplanetary space p 4 A82-22594

Comparison of solar proton activity in 1967 and 1969 with that in 1978 and 1979 as measured onboard Venera 4, 6, 11, 12 space probes p 31 A82-22596

The solar proton fluxes in April, 1979
p 66 A82-22597

The modulation characteristics of the 19th and 20th solar activity cycles p 59 A82-22615

KORZOV, V. I.

Albedo and angular characteristics of the reflectance of the underlying surface and clouds p 33 A82-30849

KOTOV, IU. D.

Computer simulation of the time dependence of the photon energy spectra produced in proton and electron bremstrahlung p 3 A82-22587

KOTTMEIER, C.
The influence of soil characteristics on regional convection differences above Northern Germany
p 10 A82-37589
KOVALENKO, V. M.
Convective outflow of cosmic rays from the Galaxy and background radio emission p 83 A82-22551
KOZIN, I. D.
The determination of differential X-ray spectrum of the solar flare using ionospheric data p 65 A82-22582
KOZODEROV, V. V.
Comparison of brightness indicatrixes of snow cover measured from an aircraft and calculated theoretically for different heights of the atmosphere p 62 A82-35140
Allowance for the effect of the atmosphere in the processing of satellite remote-sensing images
p 70 A82-35141
KRAINEV, M. B.
On the characteristics of the very low energy galactic cosmic rays in the interstellar space p 63 A82-22540
KRASNOV, A. I.
Aerogeophysical methods of finding uranium deposits
p 41 A82-33402
KRATKY, V.
Present status of on-line analytical triangulation
p 69 A82-34940
KREIDL, T. J.
Subtleties in the flat-fielding of charge-coupled device /CCD/ images p 68 A82-32581
KRIULKOV, V. A.
The use of remote-sensing data to identify the space-time variability of the quality of natural waters
p 62 A82-35138
KRUEGER, A. F.
Geostationary satellite observations of the April 1979 Soufriere eruptions p 24 A82-33654
KUDRIAVTSEV, G. P.
Analytical processing of photographs taken by paired cameras p 79 A82-34471
KULKANNI, P. L.
Impact of additional summer MONEX wind data on the prediction of monsoon depressions during June - August 1979 with two versions of primitive equation (PE) barotropic model p 56 N82-23900
KULKARNI, A. A.
Impact of additional summer MONEX wind data on the prediction of monsoon depressions during June - August 1979 with two versions of primitive equation (PE) barotropic model p 56 N82-23900
KUNOW, H.
Spacecraft determination of energetic particle propagation parameters - The 1 January 1978 solar event p 31 A82-22598
KUO, J. T.
High spectral resolution airborne spectrometry
p 77 A82-32443
KURILOVA, IU. V.
Study of the hydrological cycle by aerospace methods
p 61 A82-35126
Principles and methods of the study of the hydrological cycle on the basis of aerospace data p 61 A82-35127
KURT, V. G.
Energetic solar particle spectra according to Venera-11, 12 and Prognoz-5, 6 p 4 A82-22593
Spacecraft determination of energetic particle propagation parameters - The 1 January 1978 solar event p 31 A82-22598
KUZEVSKII, B. M.
Preflare increases in solar cosmic rays relevant to the mode of energy accumulation in the active regions associated with large flares p 31 A82-22595
KUZHEVSKII, B. M.
Low-energy particles in interplanetary magnetic field near the sectional boundary on September 26, 1977
p 4 A82-22602
KUZNETSOVA, R. I.
Nucleosynthesis of light and by-passed isotopes in the solar system matter p 64 A82-22578

L

LABOVITZ, M. L.
Preliminary evidence for the influence of physiography and scale upon the autocorrelation function of remotely sensed data p 67 A82-32343
The influence of autocorrelation in signature extraction: An example from a geobotanical investigation of Cotter Basin, Montana
[E82-10341] p 46 N82-25603
LAL, S. J.
Analysis of MAGSAT data of the Indian region
[E82-10358] p 75 N82-26756
LAMBECK, K.
A search for seamounts in the southern Cook and Austral region p 52 A82-30810
LAME, D. B.
Seasat measurement system evaluation - Achievements and limitations p 49 A82-29601
LANDGRAF, K. F.
Inventory of wetlands and agricultural land cover in the upper Sevier River Basin, Utah
[E82-10345] p 18 N82-25607
Irrigated acreage in the Bear River Basin as of the 1975 growing season
[E82-10356] p 20 N82-26754
LANDGREBE, D. A.
Multistage classification of multispectral Earth observational data: The design approach
[E82-10213] p 72 N82-23586
LANGEL, R. A.
Initial scalar magnetic anomaly map from Magsat
p 32 A82-30784
Initial vector magnetic anomaly map from Magsat
p 32 A82-30785
LANGLEY, P. G.
A new approach to multiresource inventories using remote sensing and geographic information systems technologies p 25 A82-34739
LAPCHENKOV, S. T.
The use of remote-sensing data to identify the space-time variability of the quality of natural waters
p 62 A82-35138
LARSON, F. R.
Multi-resource inventory in interior Alaska
p 6 A82-29532
LATHAM, A. R.
High resolution satellite observations of mesoscale oceanography in the Tasman Sea, 1978 - 1979
[E82-10324] p 57 N82-24597
LAVRUKHINA, A. K.
Nucleosynthesis of light and by-passed isotopes in the solar system matter p 64 A82-22578
LAZAREWICZ, A. R.
Spatial resolution and repeatability of Magsat crustal anomaly data over the Indian Ocean p 32 A82-30788
Analyses of MAGSAT tracks crossing the study region in the Indian Ocean
[E82-10197] p 71 N82-23570
Bathymetric and tectonics of Indian Ocean using MAGSAT data
[E82-10204] p 36 N82-23577
Analyzing the Broken Ridge area of the Indian Ocean using magnetic and gravity anomaly maps and geoid undulation and bathymetry data
[E82-10303] p 36 N82-24577
Investigating tectonic and bathymetric features of the Indian Ocean using MAGSAT magnetic anomaly data
[E82-10304] p 37 N82-24578
LEAMER, R. W.
AgRISTARS: Early warning and crop condition assessment. Plant cover, soil temperature, freeze, water stress, and evapotranspiration conditions
[E82-10225] p 14 N82-23598
LEAN, J. L.
Observation of the diurnal variation of atmospheric ozone p 26 A82-35895
LEATON, B. R.
Spherical harmonic representation of the main geomagnetic field for world charting and investigations of some fundamental problems of physics and geophysics
[E82-10203] p 72 N82-23576
LEBEDEV, A. V.
Water-balance differentiation of natural complexes on the basis of satellite photographs p 61 A82-35129
LEE, L. C.
Generation of the auroral kilometric radiation
p 26 A82-35542
LEE, M. A.
Acceleration of cosmic rays in accretion shocks
p 64 A82-22568
LEE, R. B., III
In situ ozone data for comparison with laser absorption remote sensor: 1980 PEPE/NEROS program
[NASA-TM-84471] p 30 N82-25661
LEES, R. D.
Multispectral determination of soil moisture-2
[E82-10349] p 19 N82-26747
The use of soil texture and field capacity to normalize microwave soil moisture measurements: Some problems p 20 N82-26762
LEGECKIS, R. V.
A ship and satellite view of hydrographic features in the western Gulf of Mexico p 53 A82-32651
LEMESHEV, M. Y.
Cost-effectiveness of geographic surveying from space p 85 N82-24263
LEMOUEL, J. L.
MAGSAT anomaly map and continental drift
[E82-10326] p 38 N82-24599
Models and maps of the main field
[E82-10327] p 74 N82-24600
LEONARD, R. K.
Dobson spectrophotometer calibrations, possible errors in ozone absorption coefficients, and errors due to interfering pollutant gases p 28 A82-36431
LERCH, F. J.
Gravity model improvement for Seasat
p 32 A82-29615
LERCHE, I.
Steady-state cosmic ray electron spectrum under diffusion, convection, adiabatic deceleration and synchrotron losses p 1 A82-22552
LEROY, M. J.
Airborne observed solar elevation and row direction effects on the near-IR/red ratio of cotton
[E82-10220] p 13 N82-23593
LESNIK, IU. N.
The use of space photographs in the mapping of glaciers and water bodies p 62 A82-37174
LEVINE, J. S.
Ammonia and the NOx budget of the troposphere
p 27 A82-36293
LIDIAK, E. G.
Characterization of the structure and tectonic of South America
[E82-10196] p 42 N82-23569
The crustal structure and tectonics of South America
[E82-10319] p 38 N82-24592
Geotectonics of South America
[E82-10320] p 38 N82-24593
LIEBMANN, B.
Interannual variations of outgoing IR associated with tropical circulation changes during 1974-1978
p 54 A82-36341
LILLESAND, T. M.
Application of scanning microdensitometer data in selected plant science case studies p 7 A82-29539
Digital and visual evaluation of GOES and TIROS/NOAA image data for cover type effects on snowfield observations p 60 A82-34735
LINDEN, D. S.
Mapping riparian vegetation in Southeastern Oregon using digitized large scale color infra-red aerial photography p 6 A82-29535
LIPES, R. G.
Description of Seasat radiometer status and results
p 52 A82-29622
LISTON, R. L.
Photogrammetric methods for mapping resource data from high altitude panoramic photography
p 77 A82-32702
LIUBIMOV, G. P.
Comparison of solar proton activity in 1967 and 1969 with that in 1978 and 1979 as measured onboard Venera 4, 6, 11, 12 space probes p 31 A82-22596
The approximate 1 GeV solar cosmic rays in the Forbush-effect of February 15, 1978 p 40 A82-22604
The modulation characteristics of the 19th and 20th solar activity cycles p 59 A82-22615
LIUBOVNYI, N. D.
Allowance for the effect of the atmosphere in the processing of satellite remote-sensing images
p 70 A82-35141
LLEBARIA, A.
A quantitative multispectral analysis system for aerial photographs applied to coastal planning
p 55 A82-37505
LO, K. K.
The growth of snow in winter storms - An airborne observational study p 60 A82-33329
LOCKWOOD, J. A.
A description of relativistic solar particle propagation
p 4 A82-22600
LOGACHEV, IU. I.
Energetic solar particle spectra according to Venera-11, 12 and Prognoz-5, 6 p 4 A82-22593
Spacecraft determination of energetic particle propagation parameters - The 1 January 1978 solar event p 31 A82-22598
LONGACRE, M. B.
A satellite magnetic model of northeastern South American aulacogens p 33 A82-30795
LOWES, F. J.
Spherical harmonic representation of the main geomagnetic field for world charting and investigations of some fundamental problems of physics and geophysics
[E82-10203] p 72 N82-23576
LU, T.
Magnetic monopole pair and its observation in cosmic rays p 65 A82-22579
LUCA, A. J.
Spherical-Earth gravity and magnetic anomaly modeling by Gauss-Legendre quadrature integration
[E82-10242] p 36 N82-24520
LUI, A. T. Y.
Large amplitude undulations on the equatorward boundary of the diffuse aurora p 76 A82-31019

LUNDELL, G. W.
Rapid oceanographic data gathering: Some problems in using remote sensing to determine the horizontal and vertical thermal distributions in the Northeast Pacific Ocean
[AD-A111005] p 58 N82-26945

LUO, L.
Magnetic monopole pair and its observation in cosmic rays p 65 A82-22579

LYNCH, R. V., III
Laser-induced bioluminescence p 53 A82-32559

LYON, R. J. P.
Quantitative relationships of near-surface spectra to Landsat radiometric data p 78 A82-32912

LYONS, A.
Color aerial photography detects nutrient status of loblolly pine plantations p 6 A82-29531

M

MAALOEE, J.
Movement of ice markers measured by satellite ranging
[R-240] p 59 N82-27816

MACDONALD, F. B.
A survey of solar protons and alpha differential spectra between 1 and greater than 400 MeV/nucleon
p 4 A82-22592

MACFARLANE, N.
Remote sensing in Scotland using data received from satellites - A study of the Tay Estuary region using Landsat multispectral scanning imagery p 62 A82-37501

MACH, P. E.
Space science for applications - The history of Landsat p 84 A82-36617

MADILL, R. J.
RAMS-1, a Resource Analysis and Mapping System
p 69 A82-34726

MAEDA, H.
Report of investigation from Japanese MAGSAT Team
[E82-10322] p 74 N82-24595

MAGNESS, E. R.
Evaluation of the procedure for separating barley from other spring small grains
[E82-10230] p 14 N82-23603

MAKINEN, J.
Work related to the Blue Road Geotraverse at the Finnish Geodetic Institute p 32 A82-30306

MALILA, W. A.
Analysis of scanner data for crop inventories
[E82-10192] p 10 N82-22626
Analysis of scanner data for crop inventories
[E82-10241] p 16 N82-24519

MALIN, J. T.
AgRISTARS: Foreign commodity production forecasting. The 1980 US corn and soybeans exploratory experiment
[E82-10206] p 11 N82-23579

MALIN, M. C.
Bathymetric imaging p 69 A82-34720

MALIN, S. R. C.
Spherical harmonic representation of the main geomagnetic field for world charting and investigations of some fundamental problems of physics and geophysics
[E82-10203] p 72 N82-23576

MALINIE, G.
Origin of galactic cosmic rays from Ne isotopic composition p 2 A82-22563

MALLICK, D. I. J.
Overseas Geology And Mineral Resources number 56: A geological interpretation of LANDSAT imagery and air photography of Botswana
[OGMR-56] p 42 N82-22636

MANTOVANI, M. S. M.
Crustal structures under the active volcanic areas of central and eastern Mediterranean (M-44)
[E82-10096] p 35 N82-23563

MARCHE, P.
Application of infrared techniques to the study of atmospheric ozone p 27 A82-36414

MARSH, J. G.
Seasat altimeter timing bias estimation
p 50 A82-29609
The Seasat altimeter mean sea surface model
p 51 A82-29614
Gravity model improvement for Seasat
p 32 A82-29615

MARSH, S. E.
Quantitative relationships of near-surface spectra to Landsat radiometric data p 78 A82-32912

MARSHALL, S.
High spectral resolution airborne spectrometry
p 77 A82-32443

MARTIN, C. F.
Seasat altimeter height calibration p 49 A82-29603

MARTIN, P.
C-band radar for determining surface soil moisture
p 10 A82-37194

MARTIN, T. V.
The Seasat altimeter mean sea surface model
p 51 A82-29614

MARTINELL, J.
Azimuthal propagation of flare particles in the heliosphere p 66 A82-22590

MARTSOLF, J. D.
Use of thermal inertia determined by HCMM to predict nocturnal cold prone areas in Florida
[E82-10299] p 17 N82-24575

MASHCHENKO, V. A.
Space to the earth p 83 A82-30850

MASON, G. M.
Time and energy dependence of heavy ion abundances in solar flare energetic particle events
p 22 A82-22605

MASTERSON, R. P., JR.
Tidal and geodetic observations for the Seasat altimeter calibration experiment p 49 A82-29604

MASUOKA, E. J.
The influence of autocorrelation in signature extraction: An example from a geobotanical investigation of Cotter Basin, Montana
[E82-10341] p 46 N82-25603

MATHIEU, E.
An optical objective lens for earth observations by satellites p 78 A82-32824

MATSUBARA, K.
Description of gray level picture using a collection of density contour lines p 66 A82-29409

MAW, K. D.
Exploration into technical procedures for vertical integration
[NASA-CR-166352] p 75 N82-26763

MAYHEW, M. A.
Satellite and surface geophysical expression of anomalous crustal structure in Kentucky and Tennessee
p 34 A82-34918
Application of satellite magnetic anomaly data to Curie isotherm mapping p 70 A82-30824
An equivalent layer magnetization model for the United States derived from MAGSAT data
[E82-10287] p 36 N82-24573

MAYO, K. K.
The use of residual images in Landsat image analysis
p 66 A82-29328
Monitoring land-cover change by principal component analysis of multitemporal Landsat data
p 68 A82-32906

MAZADE, A. V.
Ten-Ecosystem Study
[E82-10186] p 84 N82-22620

MCAVANEY, B. J.
The onset of the Australian Northwest monsoon during winter MONEX: Broadscale flow revealed by an objective analysis scheme p 56 N82-23912

MCBRIDE, J. L.
The onset of the Australian Northwest monsoon during winter MONEX: Broadscale flow revealed by an objective analysis scheme p 56 N82-23912

MCCARTHY, J.
Evaluation of spruce-fir forests using small-format photographs p 8 A82-32707

MCCLOY, K. R.
The response characteristics of vegetation in Landsat MSS digital data p 8 A82-32907

MCCONAGHY, D. C.
Geographic location of individual pixels
p 68 A82-32900
Measuring sea surface temperature from satellites - A ground truth approach p 54 A82-32917

MCDOUGAL, D. S.
In situ ozone data for comparison with laser absorption remote sensor: 1980 PEPE/NEROS program
[NASA-TM-84471] p 30 N82-25661

MCFARLAND, M. J.
Measurement of soil moisture trends with airborne scatterometers
[E82-10361] p 20 N82-26759
Multifrequency remote sensing of soil moisture
[E82-10362] p 20 N82-26760
Development of visible/infrared/microwave agriculture classification and biomass estimation algorithms
[E82-10363] p 20 N82-26761

MCGINNIS, D. F., JR.
Use of NOAA/AVHRR visible and near-infrared data for land remote sensing
[NASA-TM-84186] p 81 N82-22643

MCGUIRE, R. E.
A survey of solar protons and alpha differential spectra between 1 and greater than 400 MeV/nucleon
p 4 A82-22592

MCKENZIE, D. L.
Soft X-rays from the sunlit earth's atmosphere
p 29 A82-37405

MCLEAN, J. A.
Remote sensing of Douglas-fir trees newly infested by bark beetles p 6 A82-29536

MCLEOD, R. G.
Resource inventory techniques used in the California Desert Conservation Area p 23 A82-32441

MCMANUS, J.
Remote sensing in Scotland using data received from satellites - A study of the Tay Estuary region using Landsat multispectral scanning imagery p 62 A82-37501

MCMILLAN, K.
Remote sensing in Scotland using data received from satellites - A study of the Tay Estuary region using Landsat multispectral scanning imagery p 62 A82-37501

MCMURTREY, J. E., III
A multi-frequency radiometric measurement of soil moisture content over bare and vegetated fields
[E82-10238] p 16 N82-23611

MEAD, D. R.
Multi-resource inventory in interior Alaska
p 6 A82-29532

MEAD, R. A.
Inventory of wildlife habitat from color infrared aerial photography for Cobb Island, Virginia p 6 A82-29529
A computerized spatial analysis system for assessing wildlife habitat from vegetation maps p 9 A82-34716
A quantitative method to test for similarity between photo interpreters p 69 A82-34722

MEDLIN, G.
Ocean wave height measurement with SEASAT SAR using speckle diversity p 53 A82-32682

MEISNER, D. E.
Application of scanning microdensitometer data in selected plant science case studies p 7 A82-29539
Digital and visual evaluation of GOES and TIROS/NOAA image data for cover type effects on snowfield observations p 60 A82-34735

MENG, C.-I.
Large amplitude undulations on the equatorward boundary of the diffuse aurora p 76 A82-31019

MENZEL, W. P.
Surface temperature determination from an amalgamation of GOES and TIROS-N radiance measurements p 66 A82-28905

MEROLA, J. A.
Detection of variations in aspen forest habitat from LANDSAT digital data: Bear River Range, Utah
[E82-10355] p 19 N82-26753

MESHCHERIAKOV, I. V.
Space to the earth p 83 A82-30850

MEWALDT, R. A.
High resolution measurements of solar flare isotopes
p 22 A82-22606

MEYER, J. P.
Comparative abundances in solar energetic particles and in galactic cosmic ray sources, and the Ne-22 anomaly
p 63 A82-22556
On volatility, first ionization potential, and s- and r-processes p 2 A82-22560
A tentative ordering of all available solar energetic particles abundance observations. I - The mass unbiased baseline. II - Discussion and comparison with coronal abundances p 40 A82-22609

MEYER, M. P.
Application of 35mm color aerial photography to forest land change detection p 6 A82-29533

MEYER, P.
Unusual properties of particle events associated with solar flare gamma ray events p 65 A82-22585
The relation of type II radio bursts to solar energetic particles observed at earth p 3 A82-22591

MICHEL, F. C.
Pulsar models and cosmic-ray acceleration
p 21 A82-22570

MICHEL, R. J.
Exploration into technical procedures for vertical integration
[NASA-CR-166352] p 75 N82-26763

MILLARD, J. P.
Airborne observed solar elevation and row direction effects on the near-IR/red ratio of cotton
[E82-10220] p 13 N82-23593
Multilevel measurements of surface temperature over undulating terrain planted to barley
[E82-10245] p 16 N82-24523

MILLER, A. J.
Total ozone variations 1970-74 using Backscattered Ultraviolet /BUV/ and ground-based observations
p 26 A82-36053

MILLER, K. H.
Design guidelines for satellite image data distribution systems p 70 A82-37048

MILLER, N. L.
Application of 35mm color aerial photography to forest land change detection p 6 A82-29533

MILLER, S. H.
Application of HCMM data to regional geologic analysis for mineral and energy resource evaluation
[E82-10153] p 45 N82-24518
Application of HCMM data to regional geologic analysis for mineral and energy resource evaluation
[E82-10243] p 45 N82-24521

MILLER, W. F.
Application of remote sensing to state and regional problems
[E82-10288] p 30 N82-24566

MILLIER, F.
OSO-8 lower mesospheric ozone number density profiles p 28 A82-36472

MILLIGAN, J.
Computer-processed geophysical atlas of digital data for the East Coast margin of the United States from surface and spacecraft data
[AD-A111388] p 39 N82-25748

MILMAN, A. S.
Retrieval of ocean surface and atmospheric parameters from multichannel microwave radiometric measurements p 53 A82-31995

MILTON, E. J.
Remote sensing of salt marsh vegetation in the first four proposed Thematic Mapper bands p 10 A82-37503

MINCHEW, K.
Application of remote sensing to state and regional problems
[E82-10288] p 30 N82-24566

MIYAZAKI, Y.
Report of investigation from Japanese MAGSAT Team
[E82-10322] p 74 N82-24595

MOBIUS, E.
A comparison of helium and heavy ion spectra in He/3/ rich solar flares with a model calculation p 5 A82-22612

MOE, J. L.
Effective electromagnetic shielding in multilayer printed circuit boards
[AIAA 81-2333] p 59 A82-13526

MONACO, F.
Crustal structures under the active volcanic areas of central and eastern Mediterranean (M-44)
[E82-10096] p 35 N82-23563

MOORE, D.
Irrigation management with remote sensing
[E82-10357] p 20 N82-26755

MOORE, D. G.
Evaluation of HCMM data for assessing soil moisture and water table depth
[E82-10329] p 18 N82-24602

MOORE, R. K.
A simulation study of soil moisture estimation by a space SAR p 60 A82-29333
Evaluation of atmospheric attenuation from SMMR brightness temperature for the Seasat satellite scatterometer p 51 A82-29618
Evaluation of the soil moisture prediction accuracy of a space radar using simulation techniques
[E82-10351] p 19 N82-26749

MORFILL, G. E.
Evidence for the stochastic acceleration of cosmic rays in supernova remnants p 2 A82-22564

MORITA, Y.
Aircraft measurements of NO/x/ in the lower troposphere above the coast of Japan p 26 A82-36247

MORK, M. B. E.
Regional geological, tectonic and geophysical features of Nordland, Norway p 41 A82-30304

MOROZOVA, T. I.
The solar proton fluxes in April, 1979 p 66 A82-22597

MOSHER, J.
A color-ratio map of Mercury p 31 A82-22294

MROCZYNSKI, R. P.
Forest Resource Information System. Phase 3: System transfer report
[E82-10344] p 18 N82-25606

MUASHER, M. J.
Multistage classification of multispectral Earth observational data: The design approach
[E82-10213] p 72 N82-23586

MUELLER, D.
The influence of soil characteristics on regional convection differences above Northern Germany p 10 A82-37589

MUELLER, I. I.
Reference coordinate systems for earth dynamics - A preview p 33 A82-32077

MUKAREVA, G. B.
Aerogeophysical methods of finding uranium deposits p 41 A82-33402

MUKHENBERG, V. V.
Albedo and angular characteristics of the reflectance of the underlying surface and clouds p 33 A82-30849

MULLAN, D. J.
Possible evidence for attenuation of an MHD shock by a magnetic neutral sheet in the solar corona p 3 A82-22589

MURPHY, P.
High spectral resolution airborne spectrometry p 77 A82-32443

MURTHA, P. A.
Remote sensing of Douglas-fir trees newly infested by bark beetles p 6 A82-29536

MURTY, P. G. K.
On the space-time variability of ocean surface mixed layer characteristics of central and eastern Arabian sea during MONSOON-77 p 56 N82-23909

MYERS, V.
Irrigation management with remote sensing
[E82-10357] p 20 N82-26755

N

NAGAI, T.
Observed magnetic substorm signatures at synchronous altitude p 26 A82-35534

NAGATANI, R. M.
Total ozone variations 1970-74 using Backscattered Ultraviolet /BUV/ and ground-based observations p 26 A82-36053

NAKAJIMA, M.
Description of gray level picture using a collection of density contour lines p 66 A82-29409

NAMKEN, L. N.
AgRISTARS: Early warning and crop condition assessment. Plant cover, soil temperature, freeze, water stress, and evapotranspiration conditions
[E82-10225] p 14 N82-23598

NANDI, A.
Magnetic charts of Canada derived from Magsat data p 32 A82-30778

NAUTIYAL, C. M.
Is the neon composition of our sun, planetary or solar p 76 A82-22608

NEGI, J. G.
Analysis of MAGSAT data of the Indian region
[E82-10358] p 75 N82-26756

NEKHIN, S. S.
Evaluation of the effectiveness of systematic image distortion compensation p 69 A82-34469

NELSON, R.
Evaluation of temporal registration of Landsat scenes p 67 A82-32345

NELSON, R. F.
Defining the temporal window for monitoring forest canopy defoliation using Landsat p 9 A82-34730

NESS, S. D.
Evaluation of HCMM data for assessing soil moisture and water table depth
[E82-10329] p 18 N82-24602

NEUENSCHWANDER, H.
A description of relativistic solar particle propagation p 4 A82-22600

NEVATIA, R.
Image understanding research
[AD-A110746] p 74 N82-25611

NEWITT, L. R.
Magnetic charts of Canada derived from Magsat data p 32 A82-30778

NEWTON, R. W.
Orbiting passive microwave sensor simulation applied to soil moisture estimation
[E82-10343] p 18 N82-25605

NG, L. K.
The electron and positron spectra in primary cosmic rays p 1 A82-22543
Comparison of the measured antiproton flux with that predicted by the 'leaky box' model p 1 A82-22544

NIKITIN, A. M.
Evaluation of the accuracy of water-surface temperature measurement by means of airborne infrared radiometers p 62 A82-35136

NILSSON, C. S.
High resolution satellite observations of mesoscale oceanography in the Tasman Sea, 1978 - 1979
[E82-10324] p 57 N82-24597

NIXON, P. R.
AgRISTARS: Early warning and crop condition assessment. Plant cover, soil temperature, freeze, water stress, and evapotranspiration conditions
[E82-10225] p 14 N82-23598

NORRIS, D. D.
Imaging spectroscopy; Proceedings of the Seminar, Los Angeles, CA, February 10, 11, 1981 p 77 A82-32440

NOSACHEV, V. I.
The use of remote-sensing data to identify the space-time variability of the quality of natural waters p 62 A82-35138

NOVIKOV, IU. B.
Aerogeophysical methods of finding uranium deposits p 41 A82-33402

NUZHDIN, P. V.
Analysis of ocean and atmosphere thermodynamical characteristics during the onset of southwest monsoon over the Arabian Sea p 57 N82-23945

O

OGALLAGHER, J. J.
Observations of the ionization states of energetic particles accelerated in solar flares p 40 A82-22607

OGAWA, K.
Report of investigation from Japanese MAGSAT Team
[E82-10322] p 74 N82-24595

OHLHORST, C. W.
Analysis of ocean color scanner data from the Superflux III Experiment
[NASA-TM-83290] p 55 N82-23614

OKUDAIRA, K.
Solar gamma-ray experiment on Astro-A satellite p 21 A82-22583

OLSON, C. E., JR.
Evaluation of spruce-fir forests using small-format photographs p 8 A82-32707

ORMSBY, J. P.
Landsat digital analysis of the initial recovery of burned tundra at Kokolik River, Alaska p 8 A82-32913
The use of Landsat-3 thermal data to help differentiate land covers p 25 A82-34218

OSBORNE, J. L.
Derivation of the distribution of synchrotron emissivity in the Galaxy from the 408 MHz all-sky survey p 82 A82-22549

OSHIMA, S.
Report of investigation from Japanese MAGSAT Team
[E82-10322] p 74 N82-24595

OSOKIN, N. I.
Method for the analysis of the melting of a firn complex on the basis of aerospace photographs p 61 A82-35133

OVERLAND, J. E.
Surface wind analyses for Seasat p 51 A82-29619

OWE, M.
Use of aerial photography in determining land use and streamflow relationships on small developing watersheds p 60 A82-34736

P

PACCA, I. I. G.
Structure, composition and thermal state of the crust in Brazil
[E82-10187] p 35 N82-22621

PAEGLE, J.
Short term influence radius of monsoonal overturnings p 56 N82-23898

PAIRMAN, D.
A system design for a multispectral sensor using two-dimensional solid-state imaging arrays p 77 A82-31991

PALUZZI, P. R.
Bathymetric imaging p 69 A82-34720

PANKRATOVA, E. I.
Experience with the compilation of maps of snow-cover melting in the central part of the European USSR on the basis of satellite data p 62 A82-35134

PARIS, J. F.
Orbiting passive microwave sensor simulation applied to soil moisture estimation
[E82-10343] p 18 N82-25605

PARKE, M. E.
The Seasat altimeter data and its accuracy assessment p 49 A82-29602

PASSARELLI, R. E., JR.
The growth of snow in winter storms - An airborne observational study p 60 A82-33329

PAUL, J. A.
On the stellar origin of the Ne-22 excess in cosmic rays p 21 A82-22562
Origin of galactic cosmic rays from Ne isotopic composition p 2 A82-22563

PAYNE, R. W.
AgRISTARS: Foreign commodity production forecasting. The 1980 US/Canada wheat and barley exploratory experiment [E82-10126] p 11 N82-23565

PERESLEGINA, N. V.
Comparison of solar proton activity in 1967 and 1969 with that in 1978 and 1979 as measured onboard Venera 4, 6, 11, 12 space probes p 31 A82-22596
The modulation characteristics of the 19th and 20th solar activity cycles p 59 A82-22615

PEREZ-PERAZA, J.
Cosmic ray composition from acceleration of thermal matter p 64 A82-22558
Azimuthal propagation of flare particles in the heliosphere p 66 A82-22590

PESSES, M. E.
Observations of interplanetary energetic charged particles from gamma-ray line solar flares p 65 A82-22586
On the anticorrelation between the He/3//He/4/ ratio and proton intensity in He/3/ rich flares p 40 A82-22613

PETEHERYCH, S.
Surface wind analyses for Seasat p 51 A82-29619

PETERSEN, G. W.
Delineation of soil temperature regimes from HCMM data [E82-10298] p 17 N82-24574

PHILIPSON, W. R.
Landsat detection of hardwood forest clearcuts p 8 A82-32708

PHILLIPPS, S.
Derivation of the distribution of synchrotron emissivity in the Galaxy from the 408 MHz all-sky survey p 82 A82-22549

PHILLIPS, J. D.
Initial scalar magnetic anomaly map from Magsat p 32 A82-30784
Initial vector magnetic anomaly map from Magsat p 32 A82-30785

PHYSICK, W. L.
Mean sea-level pressure in the Southern Hemisphere during the FGGE period p 55 N82-23856

PIERATTINI, D.
Crustal structures under the active volcanic areas of central and eastern Mediterranean (M-44) [E82-10096] p 35 N82-23563

PIERCE, J.
Optical bar panoramic photography for planning timber salvage in drought-stressed forests p 7 A82-32705

PIERSON, W. J.
The Seasat-A satellite scatterometer - The geophysical evaluation of remotely sensed wind vectors over the ocean p 51 A82-29616
The relationship between wind vector and normalized radar cross section used to derive Seasat-A Satellite Scatterometer winds p 51 A82-29617
Surface wind analyses for Seasat p 51 A82-29619

PINGITORE, N. E.
Evaluation and combined geophysical interpretations of NURE and related geoscience data in the Van Horn, Pecos, Marfa, Fort Stockton, Presidio, and Emory Peak quadrangles, Texas, volume 1 [DE82-005554] p 47 N82-27808
Evaluation and combined geophysical interpretations of NURE and related geoscience data in the Van Horn, Pecos, Marfa, Fort Stockton, Presidio, and Emory Peak quadrangels, Texas [DE82-005560] p 48 N82-27809

PINTER, P. J., JR.
View angle effects in the radiometric measurement of plant canopy temperatures p 8 A82-32914

PITCHFORD, W. M.
Orbiting passive microwave sensor simulation applied to soil moisture estimation [E82-10343] p 18 N82-25605

PITTS, D. E.
Field size, length, and width distributions based on LACIE ground truth data p 8 A82-32909

PIWINSKI, D.
Evaluation of NOAA-AVHRR data for crop assessment p 8 A82-34179

PLACE, M.
Experimental assessment of improved spatial resolution LANDSAT data [AD-A110538] p 75 N82-26765

PLACE, M. C.
A new approach to multiresource inventories using remote sensing and geographic information systems technologies p 25 A82-34739

POKROVSKII, O. M.
Remote sensing of the weediness of crop fields p 5 A82-29435

PONT, W.
Analysis of scanner data for crop inventories [E82-10192] p 10 N82-22626

POPESCU, J.
Remote sensing of the earth's resources - The Soviet experience p 84 A82-33555

PORTER, D. L.
Tidal and geodetic observations for the Seasat altimeter calibration experiment p 49 A82-29604

POTEMRA, T. A.
Investigation of MAGSAT and TRIAD magnetometer data to provide corrective information on high-latitude external fields [E82-10201] p 72 N82-23574

POVINEC, P.
Calculation of production rates of cosmogenic nuclides by Monte Carlo method p 64 A82-22576

POWERS, J. S.
An information-theoric spatial transform p 69 A82-34717

PRABHAKARA, C.
Remote sensing of precipitable water over the oceans from Nimbus 7 microwave measurements p 49 A82-28907

PRISHCHEP, V. L.
Convective outflow of cosmic rays from the Galaxy and background radio emission p 83 A82-22551

PRISLEY, S. P.
A computerized spatial analysis system for assessing wildlife habitat from vegetation maps p 9 A82-34716

PROTHEROE, R. J.
The cosmic ray positron spectrum p 1 A82-22542

PTUSKIN, V. S.
Angular variations of nonthermal radio emission from the Galaxy relevant to the structure of interstellar magnetic field p 83 A82-22550
Remarks on cosmic ray origin p 21 A82-22569

Q

QUIRK, B. K.
Aerial photography vs. Landsat for digital land-cover mapping in an urban watershed p 61 A82-34745

R

RAJARAM, R.
MAGSAT for geomagnetic studies over Indian region [E82-10202] p 72 N82-23575
MAGSAT for geomagnetic studies over Indian region [E82-10296] p 73 N82-24572

RAMAN, K. V. S.
On the space-time variability of ocean surface mixed layer characteristics of central and eastern Arabian sea during MONSOON-77 p 56 N82-23909

RAMATY, R.
Interplanetary particle observations associated with solar flare gamma-ray line emission p 3 A82-22584

RAMBERG, I. B.
Regional geological, tectonic and geophysical features of Nordland, Norway p 41 A82-30304

RAMSEIER, R. O.
Sea-Ice Mission Requirements for the US FIREX and Canada RADARSAT programs [NASA-CR-168984] p 57 N82-25609

RANGARAJAN, G. K.
MAGSAT for geomagnetic studies over Indian region [E82-10202] p 72 N82-23575
MAGSAT for geomagnetic studies over Indian region [E82-10296] p 73 N82-24572

RANGO, A.
Snowpack monitoring in North America and Eurasia using passive microwave satellite data p 78 A82-32915

RANSON, K. J.
Diurnal changes in reflectance factor due to Sun-row direction interactions [E82-10128] p 11 N82-23566

RAO, D. R. K.
MAGSAT for geomagnetic studies over Indian region [E82-10202] p 72 N82-23575
MAGSAT for geomagnetic studies over Indian region [E82-10296] p 73 N82-24572

RAO, M. N.
Is the neon composition of our sun, planetary or solar p 76 A82-22608

RAO, P. K.
Comparison of satellite derived radiation budget measurements over MONEX during 1979 to 1980 p 29 N82-23891

RAO, R. R.
On the space-time variability of ocean surface mixed layer characteristics of central and eastern Arabian sea during MONSOON-77 p 56 N82-23909

RAPP, R. H.
The Earth's gravity field to degree and order 180 using SEASAT altimeter data, terrestrial gravity data and other data [AD-A113098] p 40 N82-27900

RASTOGI, R. G.
MAGSAT for geomagnetic studies over Indian region [E82-10202] p 72 N82-23575
MAGSAT for geomagnetic studies over Indian region [E82-10296] p 73 N82-24572

RAVA, B.
A color-ratio map of Mercury p 31 A82-22294

RAVET, F. W.
A meteorologically driven maize stress indicator model [E82-10112] p 11 N82-23564
Evaluation of the Doraiswamy-Thompson winter wheat crop calendar model incorporating a modified spring restart sequence [E82-10207] p 12 N82-23580
A meteorologically driven grain sorghum stress indicator model [E82-10218] p 13 N82-23591

RAY, R. D.
Improved definition of crustal magnetic anomalies for MAGSAT data [E82-10314] p 37 N82-24587

REAMES, D. V.
Heavy-element abundances in He/3/-rich events p 5 A82-22611

REAMES, V.
Interplanetary particle observations associated with solar flare gamma-ray line emission p 3 A82-22584

REED, C. R.
Selection of the Australian indicator region [E82-10222] p 13 N82-23595

REGAN, R. D.
Improved definition of crustal magnetic anomalies for MAGSAT data [E82-10314] p 37 N82-24587

REGINATO, R. J.
View angle effects in the radiometric measurement of plant canopy temperatures p 8 A82-32914
Multilevel measurements of surface temperature over undulating terrain planted to barley [E82-10245] p 16 N82-24523

REICHLE, H. G., JR.
Tropospheric CO measurement experiment from the second Space Shuttle flight p 27 A82-36292

RHODES, E.
Effects of altitude, focal length, and filter combinations on color infrared photography of citrus groves p 9 A82-34729

RICHARD, H. L.
Solid state instrumentation concepts for earth resource observation [AAS PAPER 82-132] p 81 A82-37812

RICHARDS, M. A.
An empirical determination of the effects of sea state bias on Seasat altimetry p 50 A82-29607

RICHARDSON, A. J.
Relating Landsat digital count values to ground reflectance for optically thin atmospheric conditions p 66 A82-29762
AgRISTARS: Early warning and crop condition assessment. Plant cover, soil temperature, freeze, water stress, and evapotranspiration conditions [E82-10225] p 14 N82-23598

RICKS, E. L.
Some empirical rules for forecasting fog and status over northern Florida, southern Georgia and adjacent coastal waters [PB82-154006] p 59 N82-27949

RIDD, M. K.
Irrigated acreage in the Bear River Basin as of the 1975 growing season [E82-10356] p 20 N82-26754

RIMSHA, M. A.
Purpose, background of 'Intercosmos-21' mission p 81 N82-24264

RITCHIE, J. C.
Agricultural Research Service research highlights in remote sensing for calendar year 1980 [E82-10228] p 14 N82-23601

RITZWOLLER, M. H.
Magsat magnetic anomalies over Antarctica and the surrounding oceans p 32 A82-30787

ROBERTSON, D. S.
Some considerations in the use of very-long-baseline-interferometry to establish reference coordinate systems for geodynamics p 34 A82-32096

ROBINOVE, C. J.
Computation with physical values from Landsat digital data p 68 A82-32709

ROBINSON, B. F.
Spectral properties of agricultural crops and soils measured from space, aerial, field, and laboratory sensors
[E82-10189] p 10 N82-22623
Diurnal changes in reflectance factor due to Sun-row direction interactions
[E82-10128] p 11 N82-23566
Spectral properties of agricultural crops and soils measured from space, aerial, field, and laboratory sensors
[E82-10212] p 12 N82-23585
Linear polarization of light by two wheat canopies measured at many view angles
[E82-10229] p 14 N82-23602

ROBLE, R. G.
OSO-8 lower mesospheric ozone number density profiles p 28 A82-36472

ROBSON, A.
The METEOSAT Data Collection System and its application p 75 N82-26037

ROCHESTER, M. G.
The definition of the terrestrial coordinate frame by long baseline interferometry p 33 A82-32084

RODRIGUES, V.
SMS/GOES data collection platform system p 75 N82-26027

RODRIGUEZ-BEJARANO, D.
Monitoring deforestation in the eastern part of the state of Guerrero, Mexico p 9 A82-34733

ROGERS, R. H.
LANDSAT technology transfer to the private and public sectors through community colleges and other locally available institutions
[E82-10181] p 85 N82-23568

ROGERS, T. G.
Total ozone variations 1970-74 using Backscattered Ultraviolet /BUV/ and ground-based observations p 26 A82-36053

ROSBOROUGH, G. W.
An empirical determination of the effects of sea state bias on Seasat altimetry p 50 A82-29607

ROSENFIELD, G. H.
Sample design for estimating change in land use and land cover p 24 A82-32711

ROSENKRANZ, P. W.
Inversion of data from diffraction-limited multiwavelength remote sensors. II - Nonlinear dependence of observables on the geophysical parameters p 77 A82-32658

ROSENTHAL, W. D.
Multifrequency remote sensing of soil moisture
[E82-10362] p 20 N82-26760
Development of visible/infrared/microwave agriculture classification and biomass estimation algorithms
[E82-10363] p 20 N82-26761

ROSETHAL, W. D.
Measurement of soil moisture trends with airborne scatterometers
[E82-10361] p 20 N82-26759

ROSHAL, A. S.
Computer simulation of the time dependence of the photon energy spectra produced in proton and electron bremstrahlung p 3 A82-22587

ROSS, G. A.
Detection of environmental disturbance using color aerial photography and thermal infrared imagery p 22 A82-29327

ROTHENFLUG, R.
Mass per charge ratio in hot plasmas and cosmic ray source composition p 2 A82-22557

ROY, M.
MAGSAT for geomagnetic studies over Indian region
[E82-10202] p 72 N82-23575
MAGSAT for geomagnetic studies over Indian region
[E82-10296] p 73 N82-24572

ROY, R. F.
Evaluation and combined geophysical interpretations of NURE and related geoscience data in the Van Horn, Pecos, Marfa, Fort Stockton, Presidido, and Emory Peak quadrangles, Texas volume 1
[DE82-005554] p 47 N82-27808
Evaluation and combined geophysical interpretations of NURE and related geoscience data in the Van Horn, Pecos, Marfa, Fort Stockton, Presidio, and Emory Peak quadrangels, Texas
[DE82-005560] p 48 N82-27809

RUBINCAM, D. P.
Information theory lateral density distribution for earth inferred from global gravity field p 35 A82-37962

RUEDA, A.
Astrophysical scenarios for critically evaluating a zero-point field acceleration mechanism p 64 A82-22575

RUGGE, H. R.
Soft X-rays from the sunlit earth's atmosphere p 29 A82-37405

RUSSKIKH, V. N.
Computer simulation of the time dependence of the photon energy spectra produced in proton and electron bremstrahlung p 3 A82-22587

RYLAND, G.
Evaluation of NOAA-AVHRR data for crop assessment p 8 A82-34179

S

SAHAI, B.
Analysis of MAGSAT data of the Indian region
[E82-10358] p 75 N82-26756

SAID, S. S.
Origin of cosmic rays in galactic centre sources p 3 A82-22571

SAILOR, R. V.
Spatial resolution and repeatability of Magsat crustal anomaly data over the Indian Ocean p 32 A82-30788
Analyses of MAGSAT tracks crossing the study region in the Indian Ocean
[E82-10197] p 71 N82-23570
Bathymetric and tectonics of Indian Ocean using MAGSAT data
[E82-10204] p 36 N82-23577
Analyzing the Broken Ridge area of the Indian Ocean using magnetic and gravity anomaly maps and geoid undulation and bathymetry data
[E82-10303] p 36 N82-24577
Investigating tectonic and bathymetric features of the Indian Ocean using MAGSAT magnetic anomaly data
[E82-10304] p 37 N82-24578

SAKAI, H.
Stratospheric emission data analysis
[AD-A112337] p 76 N82-26907

SAKURAI, K.
Physical state of the birth place of cosmic rays and its implication to the acceleration processes p 2 A82-22559

SALAZAR, W.
Optical bar panoramic photography for planning timber salvage in drought-stressed forests p 7 A82-32705

SALMON, J. R.
On the application of a model of boundary-layer flow over low hills to real terrain p 29 A82-36741

SANAHUJA, B.
Non-flare injection of protons into interplanetary space p 4 A82-22601

SANDWELL, D. T.
Geoid height-age relation from Seasat altimeter profiles across the Mendocino Fracture Zone p 34 A82-32646

SAPP, C. D.
Spectral scanning of experimental plots of SO2-affected winter wheat and soybeans for mission planning p 6 A82-29537
Remote sensing of sulfur dioxide effects on vegetation. Volume 1: Summary
[DE82-900580] p 31 N82-27802
Remote sensing of sulfur dioxide effects on vegetation. Volume 2: Data
[DE82-900581] p 31 N82-27803

SAUNDERS, R. W.
Satellite observations of sea surface temperature around the British Isles p 54 A82-33717

SAUSEN, T. M.
Dynamic study of the upper Sao Francisco river and Tres Marias reservoir using MSS/LANDSAT images
[E82-10291] p 63 N82-24569

SAVENKO, I. A.
High-energy solar protons p 22 A82-22588

SAWATZKY, D. L.
Registration of Heat Capacity Mapping Mission day and night images
[E82-10210] p 72 N82-23583

SAWCHUK, A. A.
Image understanding research
[AD-A110746] p 74 N82-25611

SAWHNEY, J. L.
Report of MAGSAT project by Survey of India
[E82-10293] p 73 N82-24570

SCANVIC, J. Y.
Spatial thermal radiometry contribution to the Massif Armoricain and the Massif Central France litho-structural study
[E82-10190] p 42 N82-22624

SCARPACE, F. L.
Aerial photography vs. Landsat for digital land-cover mapping in an urban watershed p 61 A82-34745

SCHABER, G. G.
Possible fault detection in Cottonball Basin, California An application of radar remote sensing p 41 A82-32898

SCHLEIMER, G. E.
Environmental monitoring report of the Lawrence Berkeley Laboratory, 1980
[LBL-12604] p 29 N82-23793

SCHLICKEISER, R.
Consequences of an inverse Compton emission model for extragalactic X-ray sources p 83 A82-22553

SCHLICKE6SER, R.
Steady-state cosmic ray electron spectrum under diffusion, convection, adiabatic deceleration and synchrotron losses p 1 A82-22552

SCHMUGGE, T. J.
A multi-frequency radiometric measurement of soil moisture content over bare and vegetated fields
[E82-10238] p 16 N82-23611

SCHNEIDER, S. R.
Use of NOAA/AVHRR visible and near-infrared data for land remote sensing
[NASA-TM-84186] p 81 N82-22643

SCHNETZLER, C. C.
Initial vector magnetic anomaly map from Magsat p 32 A82-30785

SCHOLER, M.
Observations of the ionization states of energetic particles accelerated in solar flares p 40 A82-22607
A comparison of helium and heavy ion spectra in He/3/ rich solar flares with a model calculation p 5 A82-22612

SCHOTT, F.
MONEX oceanographic observations along the East African coast p 56 N82-23908

SCHROEDER, L. C.
The Seasat-A satellite scatterometer - The geophysical evaluation of remotely sensed wind vectors over the ocean p 51 A82-29616
The relationship between wind vector and normalized radar cross section used to derive Seasat-A Satellite Scatterometer winds p 51 A82-29617
SEASAT: A satellite scatterometer illumination times of selected in situ sites
[NASA-TM-83280] p 81 N82-22865

SCHUBERT, G.
Geoid height-age relation from Seasat altimeter profiles across the Mendocino Fracture Zone p 34 A82-32646

SCHUEPP, P. H.
Aircraft monitoring of surface carbon dioxide exchange p 23 A82-30293

SCHUERER, K.
Image quality and height measurement accuracy of serial survey camera imagery from high altitudes p 78 A82-33297

SCHUESSLER, H.
Microwave sensing from space
[AAS PAPER 82-127] p 80 A82-37809

SCHUTZ, B. E.
Evaluation of the Seasat altimeter time tag bias p 50 A82-29610

SCULLY-POWER, P.
High resolution satellite observations of mesoscale oceanography in the Tasman Sea, 1978 - 1979
[E82-10324] p 57 N82-24597

SECROUN, C.
Application of infrared techniques to the study of atmospheric ozone p 27 A82-36414

SEEVERS, P. M.
Considerations in using color infrared photographs for vegetative interpretation p 6 A82-29530

SEIN, E.
An optical objective lens for earth observations by satellites p 76 A82-32824

SELLMAN, A.
Analysis of scanner data for crop inventories
[E82-10192] p 10 N82-22626

SENN, R. H.
Source assessment system
[AD-A111223] p 75 N82-25613

SETH, A.
MAGSAT for geomagnetic studies over Indian region
[E82-10202] p 72 N82-23575

SETHURAMAN, S.
Marine boundary layer wind structure over the Bay of Bengal during Monex-79 p 57 N82-23929

SEXTON, J. L.
Verification of the crustal component in satellite magnetic data p 32 A82-30789

SEYFARTH, B. R.
An analysis of LANDSAT MSS scene-to-scene registration accuracy
[E82-10285] p 16 N82-24563

SHABELA, F.
The possibility of using remote-sensing methods to study the hydrology of elementary watersheds p 61 A82-35130

SHANMUGAM, K. S.
The recognition of extended targets - SAR images for level and hilly terrain p 33 A82-31994

SHAPIRO, M. M.
Calculated isotopic source composition and tests for origin and propagation of cosmic rays with mass numbers less than or equal to 62 p 83 A82-22554
Acceleration processes near massive black holes p 3 A82-22572
Extragalactic cosmic rays, their sources and spectrum p 40 A82-22574

SHARIK, T. L.
A computerized spatial analysis system for assessing wildlife habitat from vegetation maps p 9 A82-34716

SHCHEGLOVA, O. P.
The seasonal snow-line within the Fergana basin and the possibility of using it for hydrological forecasting p 61 A82-35131

SHEFFIELD, C.
A new approach to multiresource inventories using remote sensing and geographic information systems technologies p 25 A82-34739
Experimental assessment of improved spatial resolution LANDSAT data
[AD-A110538] p 75 N82-26765

SHIUE, J. C.
A comparative study of microwave radiometer observations over snowfields with radiative transfer model calculations p 60 A82-32910

SHKABURA, N. A.
Estimates of the statistical structure of the atmospheric pressure field in summer Monex-79 area p 57 N82-23939

SHLIAKHOVA, L. A.
The use of remote-sensing data to identify the space-time variability of the quality of natural waters p 62 A82-35138

SHUKOWSKY, W.
Structure, composition and thermal state of the crust in Brazil
[E82-10187] p 35 N82-22621

SHUM, C.
Evaluation of the Seasat altimeter time tag bias p 50 A82-29610

SIDRAN, M.
Infrared sensing of sea surface temperature from space p 53 A82-32902

SIEVERS, J.
Image quality and height measurement accuracy of serial survey camera imagery from high altitudes p 78 A82-33297

SIGLE, M.
Investigations of point transfer p 78 A82-33296

SIGLER, G. B.
Matrix data analysis: Color/B and W coding is not always enough
[AD-A111401] p 74 N82-25612

SIGURDSSON, H.
Soufriere Volcano, St. Vincent - Observations of its 1979 eruption from the ground, aircraft, and satellites p 24 A82-33652

SIKKA, D. R.
Impact of additional summer MONEX wind data on the prediction of monsoon depressions during June - August 1979 with two versions of primitive equation (PE) barotropic model p 56 N82-23900

SILBERBERG, R.
Acceleration processes near massive black holes p 3 A82-22572
Extragalactic cosmic rays, their sources and spectrum p 40 A82-22574

SILVESTROV, S. D.
Space to the earth p 83 A82-30850

SIMONETT, D. S.
Impacts of remote sensing on U.S. geography p 24 A82-32899
Multispectral determination of soil moisture-2
[E82-10349] p 19 N82-26747

SIMPSON, G. A.
Fragmentation of Fe nuclei on carbon, hydrogen and CH2 targets. I - Individual charge changing and total cross sections. II - Isotopic cross sections p 63 A82-22538

SIMPSON, J. A.
The question of short pathlengths in interstellar propagation p 1 A82-22541

SIMPSON, J. D.
Matrix data analysis: Color/B and W coding is not always enough
[AD-A111401] p 74 N82-25612

SINGH, B. P.
MAGSAT for geomagnetic studies over Indian region
[E82-10202] p 72 N82-23575
MAGSAT for geomagnetic studies over Indian region
[E82-10296] p 73 N82-24572

SINGH, S. S.
Impact of additional summer MONEX wind data on the prediction of monsoon depressions during June - August 1979 with two versions of primitive equation (PE) barotropic model p 56 N82-23900

SINHA, S.
Impact of additional summer MONEX wind data on the prediction of monsoon depressions during June - August 1979 with two versions of primitive equation (PE) barotropic model p 56 N82-23900

SITNIKOVA, M. V.
The use of satellite photographs to study snow-cover dynamics and to determine the average water discharge of the Amudarya during a vegetation period p 61 A82-35132

SKINNER, A. C.
Overseas Geology And Mineral Resources number 56: A geological interpretation of LANDSAT imagery and air photography of Botswana
[OGMR-56] p 42 N82-22636

SLINGO, J. M.
A study of the earth's radiation budget using a general circulation model p 52 A82-30666

SMALLWOOD, M. D.
The application of Heat Capacity Mapping Mission (HCMM) thermal data to snow hydrology
[E82-10191] p 62 N82-22625

SMIKA, D.
Evaluation of the Doraiswamy-Thompson winter wheat crop calendar model incorporating a modified spring restart sequence
[E82-10207] p 12 N82-23580

SMIRNOV, V. A.
Aerogeophysical methods of finding uranium deposits p 41 A82-33402

SMITH, H. J. P.
Atmospheric ozone determination by solar occultation using the UV spectrometer on the Solar Maximum Mission p 27 A82-36362

SMITH, J. A.
Influence of sky radiance distribution on the ratio technique for estimating bidirectional reflectance p 70 A82-35650

SMITH, M.
Source assessment system
[AD-A111223] p 75 N82-25613

SMITH, R. E.
Remote sensing of tornadic storms from geosynchronous satellite infrared digital data p 23 A82-32348

SMITH, W. L.
Surface temperature determination from an amalgamation of GOES and TIROS-N radiance measurements p 66 A82-28905

SOFIA, S.
Confinement and acceleration of cosmic rays in galactic superbubbles p 82 A82-22547

SOKOL, S.
Airborne lidar measurements of the Soufriere eruption of 17 April 1979 p 24 A82-33657

SOLOMON, J. L.
Application of remote sensing to state and regional problems
[E82-10288] p 30 N82-24566

SOMOGYI, A. J.
Spacecraft determination of energetic particle propagation parameters - The 1 January 1978 solar event p 31 A82-22598

SON, K. H.
A preliminary comparison of the Magsat data and aeromagnetic data in the continental U.S. p 32 A82-30790

SOSNINA, E. A.
Estimates of the statistical structure of the atmospheric pressure field in summer Monex-79 area p 57 N82-23939

SPAENKUCH, D.
Total ozone retrieval from satellite Meteor 28 Fourier spectrometer measurements p 28 A82-36422

SPALDING, J. D.
High resolution measurements of solar flare isotopes p 22 A82-22606

SPEECHLEY, G. C.
High resolution satellite observations of mesoscale oceanography in the Tasman Sea, 1978 - 1979
[E82-10324] p 57 N82-24597

STEFFENS, V.
Spacecraft determination of energetic particle propagation parameters - The 1 January 1978 solar event p 31 A82-22598

STEINVALL, O.
Study visit to United States laser technology centers, 1981
[FOA-C-30257-E1] p 81 N82-24489

STEPHENS, S. A.
Dependence of earth spectrum of positrons and antiprotons on propagation models p 21 A82-22545

STEPINA, T. I.
The solar proton fluxes in April, 1979 p 66 A82-22597
The modulation characteristics of the 19th and 20th solar activity cycles p 59 A82-22615

STEWART, R. H.
The observation of ocean surface phenomena using imagery from the Seasat synthetic aperture radar - An assessment p 52 A82-29623

STILES, J.
A simulation study of soil moisture estimation by a space SAR p 60 A82-29333

STILES, J. A.
The recognition of extended targets - SAR images for level and hilly terrain p 33 A82-31994
Evaluation of the soil moisture prediction accuracy of a space radar using simulation techniques
[E82-10351] p 19 N82-26749

STOFFEL, H.
Derivation of the distribution of synchrotron emissivity in the Galaxy from the 408 MHz all-sky survey p 82 A82-22549

STOKER, P. H.
Primary spectral variations of cosmic rays above 1 GV p 5 A82-22618

STOLPOVSKII, V. G.
Energetic solar particle spectra according to Venera 11, 12 and Prognoz-5, 6 p 4 A82-22593

STONE, E. C.
High resolution measurements of solar flare isotopes p 22 A82-22606

STOZHKOV, IU. I.
The energy spectra of cosmic ray variations inferred from the stratospheric measurements in 1972-1979 p 5 A82-22617

STRAHLER, A. H.
The use of prior probabilities in maximum likelihood classification of remotely sensed data p 68 A82-32904

STUART, D. W.
Meteorological and aircraft data for CUE 2 1973
[PB82-149246] p 59 N82-26949

SUKHIKH, V. I.
Status and prospects of the automated processing of remote-sensing data /using forest surveys as an example/ p 10 A82-35139

SUKHOTIN, Y. V.
Cost-effectiveness of geographic surveying from space p 85 N82-24263

SUOMI, V. E.
The impact of meteorological satellites on the First GARP Global Experiment (FGGE) p 55 N82-23852

SVIRZHEVSKAIA, A. K.
The energy spectra of cosmic ray variations inferred from the stratospheric measurements in 1972-1979 p 5 A82-22617

SWAIN, P. H.
Key Issues in the Analysis of Remote Sensing Data: A report on the workshop
[E82-10348] p 85 N82-26746

SWANSON, P.
Radiometer mission requirements for large space antenna systems
[NASA-TM-84478] p 81 N82-25610

SWEET, J. L.
SEASAT: A satellite scatterometer illumination times of selected in situ sites
[NASA-TM-83280] p 81 N82-22865

SZENTGALI, A.
Spacecraft determination of energetic particle propagation parameters - The 1 January 1978 solar event p 31 A82-22598

T

TAKACS, H. C.
A comparison of stratified versus regression estimators p 11 N82-23133

TAKAGI, M.
Aircraft measurements of NO/x/ in the lower troposphere above the coast of Japan p 26 A82-36247

TAKASHIMA, T.
Emissivity and reflectance of the model sea surface for the use of AVHRR data of NOAA satellites p 52 A82-31294

TAKAYAMA, Y.
Emissivity and reflectance of the model sea surface for the use of AVHRR data of NOAA satellites p 52 A82-31294

TAN, L. C.
The electron and positron spectra in primary cosmic rays p 1 A82-22543
Comparison of the measured antiproton flux with that predicted by the 'leaky box' model p 1 A82-22544

TANAKA, M.
Report of investigation from Japanese MAGSAT Team
[E82-10322] p 74 N82-24595

TANAKA, T.
Characteristics of field-aligned E-region irregularities over Iioka /36 N/, Japan. I p 26 A82-36268
TANAKA, Y.
Detection of volcanic smoke and ash-fall area at volcano Aso, from Landsat MSS data p 23 A82-31295
TAPLEY, B. D.
The Seasat altimeter data and its accuracy assessment p 49 A82-29602
Evaluation of the Seasat altimeter time tag bias p 50 A82-29610
TAYLOR, M. L.
Source assessment system
[AD-A111223] p 75 N82-25613
TAYLOR, P. A.
On the application of a model of boundary-layer flow over low hills to real terrain p 29 A82-36741
TAYLOR, T. W.
A meteorologically driven maize stress indicator model
[E82-10112] p 11 N82-23564
Evaluation of the Doraiswamy-Thompson winter wheat crop calendar model incorporating a modified spring restart sequence
[E82-10207] p 12 N82-23580
A meteorologically driven grain sorghum stress indicator model
[E82-10218] p 13 N82-23591
TELEKI, G.
On reference coordinate systems used in polar motion determinations p 33 A82-32090
TEMNIKOV, S. N.
Evaluation of the accuracy of water-surface temperature measurement by means of airborne infrared radiometers p 62 A82-35136
THEIS, S. W.
Measurement of soil moisture trends with airborne scatterometers
[E82-10361] p 20 N82-26759
Multifrequency remote sensing of soil moisture
[E82-10362] p 20 N82-26760
Development of visible/infrared/microwave agriculture classification and biomass estimation algorithms
[E82-10363] p 20 N82-26761
THELEN, B.
Analysis of scanner data for crop inventories
[E82-10192] p 10 N82-22626
THOMAS, H. H.
Satellite and surface geophysical expression of anomalous crustal structure in Kentucky and Tennessee p 34 A82-34918
THOMAS, M. H. B.
The estimation of wave height from digitally processed SAR imagery p 67 A82-32347
THOMAS, R. W. L.
Bias correction procedures for airborne laser hydrography
[PB82-130089] p 63 N82-22644
THOMPSON, D. M.
Comparing lineaments interpreted from Landsat imagery and topographic maps with reported faults in southwest Montana p 34 A82-34719
THOMPSON, T. W.
Seasat wind and wave observations of northeast Pacific hurricane Iva, August 13, 1978 p 52 A82-29624
THOMSEN, B.
Subtleties in the flat-fielding of charge-coupled device /CCD/ images p 68 A82-32581
THONY, J. L.
C-band radar for determining surface soil moisture p 10 A82-37194
TIMOSHENKO, A. M.
The use of space photographs in the mapping of glaciers and water bodies p 62 A82-37174
TOKAR, S.
Calculation of production rates of cosmogenic nuclides by Monte Carlo method p 64 A82-22576
TOLL, D. L.
Detecting residential land-use development at the urban fringe p 22 A82-29332
Preliminary evidence for the influence of physiography and scale upon the autocorrelation function of remotely sensed data p 67 A82-32343
TORSANI, J. A.
A study of atmospheric diffusion from the LANDSAT imagery
[E82-10360] p 58 N82-26758
TRENCHARD, M. H.
Application of thermal model for pan evaporation to the hydrology of a defined medium, the sponge
[E82-10217] p 13 N82-23590
TRIVEDI, N. B.
Comparison of storm-time changes of geomagnetic field at ground and at MAGSAT altitudes, part 2
[E82-10325] p 30 N82-24598
Comparison of storm-time changes of geomagnetic field at ground and MAGSAT altitudes
[E82-10359] p 30 N82-26757
TRIVEDI, S. S.
On the stellar origin of low energy cosmic rays p 21 A82-22567
Coulombian energy losses and the nuclear composition of the solar cosmic rays p 4 A82-22610
TSAREV, B. K.
The use of satellite photographs to study snow-cover dynamics and to determine the average water discharge of the Amudarya during a vegetation period p 61 A82-35132
TSEPELEV, A. V.
Space to the earth p 83 A82-30850
TSUCHIYA, K.
Detection of volcanic smoke and ash-fall area at volcano Aso, from Landsat MSS data p 23 A82-31295
TUCKER, C. J.
Remote sensing of leaf water content in the near infrared p 8 A82-32897
TUCKER, G. B.
Mean sea-level pressure in the Southern Hemisphere during the FGGE period p 55 N82-23856
TULUPOV, V. I.
The approximate 1 GeV solar cosmic rays in the Forbush-effect of February 15, 1978 p 40 A82-22604
TUNHEIM, J. A.
Evaluation of HCMM data for assessing soil moisture and water table depth
[E82-10329] p 18 N82-24602
TVEITEN, B.
Regional geological, tectonic and geophysical features of Nordland, Norway p 41 A82-30304
TYREN, C.
Magnetic anomalies as a reference for ground-speed and map-matching navigation p 32 A82-30314

U

ULABY, F. T.
A simulation study of soil moisture estimation by a space SAR p 60 A82-29333
Evaluation of the soil moisture prediction accuracy of a space radar using simulation techniques
[E82-10351] p 19 N82-26749
ULBRICHT, K. A.
Remote sensing in Scotland using data received from satellites - A study of the Tay Estuary region using Landsat multispectral scanning imagery p 62 A82-37501
UYEDA, S.
Report of investigation from Japanese MAGSAT Team
[E82-10322] p 74 N82-24595

V

VALERIO, C.
A quantitative multispectral analysis system for aerial photographs applied to coastal planning p 55 A82-37505
VAN ROESSEL, J.
A new approach to multiresource inventories using remote sensing and geographic information systems technologies p 25 A82-34739
VAN ZEE, C. J.
Estimating rangeland cover proportions with large-scale color-infrared aerial photographs p 6 A82-29534
VANCE, D. L.
Remote automatic weather station for resource and fire management agencies
[PB82-107335] p 30 N82-23963
VANDERBILT, A. S.
Linear polarization of light by two wheat canopies measured at many view angles
[E82-10229] p 14 N82-23602
VANDERBILT, V. C.
Spectral properties of agricultural crops and soils measured from space, aerial, field, and laboratory sensors
[E82-10189] p 10 N82-22623
Diurnal changes in reflectance factor due to Sun-row direction interactions
[E82-10126] p 11 N82-23566
Spectral properties of agricultural crops and soils measured from space, aerial, field, and laboratory sensors
[E82-10212] p 12 N82-23585
Application of Computer Axial Tomography (CAT) to measuring crop canopy geometry
[E82-10227] p 14 N82-23600
Linear polarization of light by two wheat canopies measured at many view angles
[E82-10229] p 14 N82-23602
A model of plant canopy polarization
[E82-10233] p 15 N82-23606
Canopy reflectance as influenced by solar illumination angle
[E82-10237] p 15 N82-23610
VANIN, A. G.
Technical and economical characteristics of the AFA-TES-10M aerial camera p 79 A82-34470
VANWOERT, M. L.
Satellite observations in FRONTS 80
[AD-A111080] p 58 N82-26766
VASHENIUK, E. V.
On the physical sense of the constant of solar cosmic ray coronal propagation p 83 A82-22599
VAUCLIN, M.
C-band radar for determining surface soil moisture p 10 A82-37194
VENKATESAN, T. R.
Is the neon composition of our sun, planetary or solar p 76 A82-22608
VENKATESWARAN, S. V.
Characteristics of field-aligned E-region irregularities over Iioka /36 N/, Japan. I p 26 A82-36268
VERA, J. W.
Design guidelines for satellite image data distribution systems p 70 A82-37048
VESECKY, J. F.
The observation of ocean surface phenomena using imagery from the Seasat synthetic aperture radar - An assessment p 52 A82-29623
VIDAL-MADJAR, D.
C-band radar for determining surface soil moisture p 10 A82-37194
VISWANADHAM, Y.
A study of atmospheric diffusion from the LANDSAT imagery
[E82-10360] p 58 N82-26758
VOGT, R. E.
High resolution measurements of solar flare isotopes p 22 A82-22606
VOLODICHEV, N. N.
High-energy solar protons p 22 A82-22588
VON FRESE, R. R. B.
Verification of the crustal component in satellite magnetic data p 32 A82-30789
A satellite magnetic model of northeastern South American aulacogens p 33 A82-30795
VON ROSENVINGE, T. T.
Interplanetary particle observations associated with solar flare gamma-ray line emission p 3 A82-22584
A survey of solar protons and alpha differential spectra between 1 and greater than 400 MeV/nucleon p 4 A82-22592
Heavy-element abundances in He/3/-rich events p 5 A82-22611
VONFRESE, R. R. B.
Study of gravity and magnetic anomalies using MAGSAT data
[E82-10194] p 35 N82-22628
Spherical-Earth gravity and magnetic anomaly modeling by Gauss-Legendre quadrature integration
[E82-10242] p 36 N82-24520
Magnetic and gravity anomalies in the Americas
[E82-10312] p 37 N82-24586
Aeromagnetic and satellite magnetic anomally mapping
[E82-10339] p 39 N82-25601
VYSOKOOSTROVSKAIA, E. B.
Aerogeophysical methods of finding uranium deposits p 41 A82-33402

W

WAGNER, A. F.
A description of relativistic solar particle propagation p 4 A82-22600
WALLIS, D. D.
Studies of high latitude current systems using MAGSAT vector data
[E82-10188] p 71 N82-22622
WALMSLEY, J. L.
On the application of a model of boundary-layer flow over low hills to real terrain p 29 A82-36741
WALSH, E. J.
Pulse-to-pulse correlation in satellite radar altimeters p 55 A82-37390
WANG, J. R.
A multi-frequency radiometric measurement of soil moisture content over bare and vegetated fields
[E82-10236] p 16 N82-23611
WARD, N. R.
Satellite observations of sea surface temperature around the British Isles p 54 A82-33717

WARREN, J. R.
Remote automatic weather station for resource and fire management agencies
[PB82-107335] p 30 N82-23963

WASILEWSKI, P. J.
Satellite and surface geophysical expression of anomalous crustal structure in Kentucky and Tennessee p 34 A82-34918

WATERS, J. W.
Microwave measurement of stratospheric and mesospheric ozone p 28 A82-36415

WATSON, K.
Registration of Heat Capacity Mapping Mission day and night images
[E82-10210] p 72 N82-23583
Ground support data from July 10 to July 29, 1978, for HCMM thermal satellite data of the Powder River Basin, Wyoming
[E82-10211] p 72 N82-23584
Topographic slope correction for analysis of thermal infrared images
[E82-10214] p 36 N82-23587
Application of HCMM data to regional geologic analysis for mineral and energy resource evaluation
[E82-10153] p 45 N82-24518
Application of HCMM data to regional geologic analysis for mineral and energy resource evaluation
[E82-10243] p 45 N82-24521

WAY, D. S.
Site selection and engineering issues for a major industrial complex - Application of image and map interpretation p 25 A82-34711

WDOWCZYK, J.
Origin of cosmic rays in galactic centre sources p 3 A82-22571

WEBB, G. M.
Cosmic ray acceleration by stellar winds. I - Total density, pressure and energy flux p 21 A82-22566

WEBBER, W. R.
Fragmentation of Fe nuclei on carbon, hydrogen and CH2 targets. I - Individual charge changing and total cross sections. II - Isotopic cross sections p 63 A82-22538
The charge and isotopic composition of Z equals 7-16 cosmic ray nuclei at their source p 64 A82-22555

WEBER, F. P.
Panoramic aerial photography in forest pest management p 7 A82-32701

WEDLER, E.
Interpretation of vegetative cover in wetlands using four-channel SAR imagery p 9 A82-34706

WEEKS, W. F.
Sea-Ice Mission Requirements for the US FIREX and Canada RADARSAT programs
[NASA-CR-168984] p 57 N82-25609

WEFEL, J. P.
The question of short pathlengths in interstellar propagation p 1 A82-22541

WEI, D.
Observations and analyses of the total amount of atmospheric ozone in the Beijing region and in the region of Jolmolungma Mountain in Tibet p 28 A82-36444

WEISS, H.
Time and energy dependence of heavy ion abundances in solar flare energetic particle events p 22 A82-22605
Observations of the ionization states of energetic particles accelerated in solar flares p 40 A82-22607

WEISSMAN, D. E.
Seasat wind and wave observations of northeast Pacific hurricane Iva, August 13, 1978 p 52 A82-29624

WELCH, R.
Spatial resolution requirements for urban studies p 29 A82-37502

WELLMAN, J. B.
Multispectral mapper - Imaging spectroscopy as applied to the mapping of earth resources p 77 A82-32448

WEN, C.
Observations and analyses of the total amount of atmospheric ozone in the Beijing region and in the region of Jolmolungma Mountain in Tibet p 28 A82-36444

WENDLANDT, R. F.
Influence of CO2 on melting of model granulite facies assemblages - A model for the genesis of charnockites p 42 A82-36298

WENTZ, F. J.
The Seasat-A satellite scatterometer - The geophysical evaluation of remotely sensed wind vectors over the ocean p 51 A82-29616
The relationship between wind vector and normalized radar cross section used to derive Seasat-A Satellite Scatterometer winds p 51 A82-29617
Evaluation of atmospheric attenuation from SMMR brightness temperature for the Seasat satellite scatterometer p 51 A82-29618
Intercomparison of wind speeds inferred by the SASS, altimeter, and SMMR p 52 A82-29621
The effect of sea-surface Sun glitter on microwave radiometer measurements
[NASA-CR-169083] p 57 N82-26525

WENZEL, K.-P.
Non-flare injection of protons into interplanetary space p 4 A82-22601

WESELY, M. L.
Simplified techniques to study components of solar radiation under haze and clouds p 78 A82-32766

WEST, W. L., III
Description of historical crop calendar data bases developed to support foreign commodity production forecasting project experiments
[E82-10209] p 12 N82-23582
Normal crop calendars. Volume 3: The corn and soybean states of Illinois, Indiana, and Iowa
[E82-10221] p 13 N82-23594

WESTIN, F. C.
Evaluation of HCMM data for assessing soil moisture and water table depth
[E82-10329] p 18 N82-24602

WHITE, W. B.
Estimating mountain pine beetle-killed ponderosa pine over the front range of Colorado with high altitude panoramic photography p 7 A82-32704

WHITEHEAD, V.
Evaluation of NOAA-AVHRR data for crop assessment p 8 A82-34179

WHITNEY, L. F., JR.
A statistical approach to rainfall estimation using satellite and conventional data
[NOAA-TR-NESS-89] p 63 N82-22854

WHRITNER, R. H.
Seasat altimeter determination of ocean current variability p 50 A82-29613

WIBBERENZ, G.
Spacecraft determination of energetic particle propagation parameters - The 1 January 1978 solar event p 31 A82-22598

WIEGAND, C. L.
AgRISTARS: Early warning and crop condition assessment. Plant cover, soil temperature, freeze, water stress, and evapotranspiration conditions
[E82-10225] p 14 N82-23598

WILES, K. G.
Effective electromagnetic shielding in multilayer printed circuit boards
[AIAA 81-2333] p 59 A82-13528

WILKERSON, J. C.
Surface wind analyses for Seasat p 51 A82-29619

WILLAND, J. H.
The application of Heat Capacity Mapping Mission (HCMM) thermal data to snow hydrology
[E82-10191] p 62 N82-22625

WILLIAMS, B. G.
Separation of diffuse from sharp-edged features in digital imagery p 68 A82-34225

WILLIAMS, T. H. L.
Terrain analysis from Landsat using a color TV enhancement system p 68 A82-32911

WILLIAMSON, R. G.
Seasat altimeter timing bias estimation p 50 A82-29609
Gravity model improvement for Seasat p 32 A82-29615

WILLIE, R. D.
Mapping of wildlife habitat in Farmington Bay, Utah
[E82-10354] p 19 N82-26752

WILSON, M. D.
Studies of high latitude current systems using MAGSAT vector data
[E82-10188] p 71 N82-22622

WILSON, R. L.
Spherical harmonic representation of the main geomagnetic field for world charting and investigations of some fundamental problems of physics and geophysics
[E82-10203] p 72 N82-23576

WILSON, S. K.
Appearance of irregular tree canopies in nighttime high-resolution thermal infrared imagery p 68 A82-32916

WINANT, C. D.
Fluid-sediment interactions on beaches and shelves
[AD-A110838] p 59 N82-26948

WINTERBERGER, K. C.
Multi-resource inventory in interior Alaska p 6 A82-29532

WITTER, J. A.
Evaluation of spruce-fir forests using small-format photographs p 8 A82-32707

WOICESHYN, P. M.
Surface wind analyses for Seasat p 51 A82-29619

WOLFENDALE, A. W.
Origin of cosmic rays in galactic centre sources p 3 A82-22571

WON, I. J.
A preliminary comparison of the Magsat data and aeromagnetic data in the continental U.S. p 32 A82-30790

WONG, H. K.
Generation of the auroral kilometric radiation p 26 A82-35542

WOODEN, W. H., II
A comparison of pole positions derived from GPS satellite and Navy navigation satellite observations
[AD-A110765] p 39 N82-26268

WOODGATE, B.
Atmospheric ozone determination by solar occultation using the UV spectrometer on the Solar Maximum Mission p 27 A82-36362

WOODS, D. C.
Fine particles in the Soufriere eruption plume p 24 A82-33659

WRIGHT, L. H.
Application of remote sensing to state and regional problems
[E82-10288] p 30 N82-24566

WU, C.
Ocean wave height measurement with SEASAT SAR using speckle diversity p 53 A82-32882

WU, C. S.
Generation of the auroral kilometric radiation p 26 A82-35542

WURTELE, M.
Surface wind analyses for Seasat p 51 A82-29619

WYLIE, D. P.
Estimates of sea surface stress for summer MONEX from cloud motions p 56 N82-23910

Y

YAMAURA, Y.
Detection of volcanic smoke and ash-fall area at volcano Aso, from Landsat MSS data p 23 A82-31295

YANAGISAWA, M.
Preliminary interpretation of magnetic anomalies over Japan and its surrounding area p 33 A82-30796

YANAGITA, S.
Unusual properties of particle events associated with solar flare gamma ray events p 65 A82-22585
The relation of type II radio bursts to solar energetic particles observed at earth p 3 A82-22591

YAO, S. S.
Evaluation of VICAR software capability for land information support system needs
[E82-10223] p 73 N82-23596
AgRISTARS: Renewable resources inventory. Land information support system implementation plan and schedule
[E82-10224] p 14 N82-23597

YOSHIMORI, M.
Model for solar hard X-ray bursts p 65 A82-22581
Solar gamma-ray experiment on Astro-A satellite p 21 A82-22583

YOUKHANA, S.
Influence of sky radiance distribution on the ratio technique for estimating bidirectional reflectance p 70 A82-35650

YUKUTAKE, T.
Preliminary interpretation of magnetic anomalies over Japan and its surrounding area p 33 A82-30796
Report of investigation from Japanese MAGSAT Team
[E82-10322] p 74 N82-24595

Z

ZAITSEV, V. G.
Aerogeophysical methods of finding uranium deposits p 41 A82-33402

ZANDLO, J. A.
Surface temperature determination from an amalgamation of GOES and TIROS-N radiance measurements p 66 A82-28905

ZAVOLOKIN, IU. V.
The use of remote-sensing data to identify the space-time variability of the quality of natural waters p 62 A82-35138

ZELDOVICH, M. A.
Low-energy particles in interplanetary magnetic field near the sectorial boundary on September 26, 1977 p 4 A82-22602

ZHENG, Q. A.
Determination of winter temperature patterns, fronts, and surface currents in the Yellow Sea and East China Sea from satellite imagery p 55 A82-37195

ZIELINSKI, J. B.
Origin and scale of coordinate systems in satellite geodesy p 34 A82-32099

ZUBOV, E. I.
Aerogeophysical methods of finding uranium deposits
p 41 A82-33402

ZUSMANOVICH, A. G.
11-year modulation and spectrum of cosmic rays in the interstellar space
p 22 A82-22616

CORPORATE SOURCE INDEX

Typical Corporate Source Index Listing

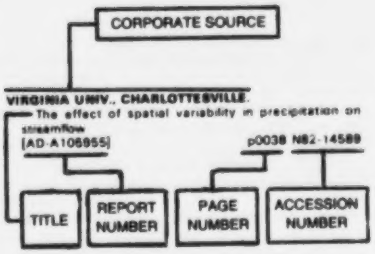
CORPORATE SOURCE
VIRGINIA UNIV., CHARLOTTESVILLE.
The effect of spatial variability in precipitation on streamflow
[AD-A106955]
p0038 N82-14589
TITLE
REPORT NUMBER
PAGE NUMBER
ACCESSION NUMBER

The title of the document is used to provide a brief description of the subject matter. The page number and the accession number are included in each entry to assist the user in locating the abstract in the abstract section. If applicable, a report number is also included as an aid in identifying the document.

A

Aerospace Corp., El Segundo, Calif.
Generation of the auroral kilometric radiation p 26 A82-35542
Soft X-rays from the sunlit earth's atmosphere p 29 A82-37405

Agricultural Research Services, Beltsville, Md.
Agricultural Research Service research highlights in remote sensing for calendar year 1980 [E82-10228] p 14 N82-23601

Alabama Univ., Huntsville.
Remote sensing of tornadic storms from geosynchronous satellite infrared digital data p 23 A82-32348

Alaska Univ., Fairbanks.
Generation of the auroral kilometric radiation p 26 A82-35542

All-Union Scientific Research Inst. of Hydrometeorological Information. Moscow (USSR).
Analysis of ocean and atmosphere thermodynamical characteristics during the onset of southwest monsoon over the Arabian Sea p 57 N82-23945

Analytic Sciences Corp., Reading, Mass.
Spatial resolution and repeatability of Magsat crustal anomaly data over the Indian Ocean p 32 A82-30788
Analyses of MAGSAT tracks crossing the study region in the Indian Ocean [E82-10197] p 71 N82-23570
Bathymetric and tectonics of Indian Ocean using MAGSAT data [E82-10204] p 36 N82-23577
Analyzing the Broken Ridge area of the Indian Ocean using magnetic and gravity anomaly maps and geoid undulation and bathymetry data [E82-10303] p 36 N82-24577
Investigating tectonic and bathymetric features of the Indian Ocean using MAGSAT magnetic anomaly data [E82-10304] p 37 N82-24578

Applied Physics Lab., Johns Hopkins Univ., Laurel, Md.
Investigation of MAGSAT and TRIAD magnetometer data to provide corrective information on high-latitude external fields [E82-10201] p 72 N82-23574

Arizona State Univ., Tempe.
Bathymetric imaging p 69 A82-34720

Arizona Univ., Tucson.
Observations of the ionization states of energetic particles accelerated in solar flares p 40 A82-22607

Army Cold Regions Research and Engineering Lab., Hanover, N. H.
Landsat digital analysis of the initial recovery of burned tundra at Kokolik River, Alaska p 8 A82-32913
Ice distribution and winter surface circulation patterns, Kachemak Bay, Alaska [AD-A110806] p 58 N82-26764

Army Engineer Topographic Labs., Fort Belvoir, Va.
Coordination of stereo image registration and pixel classification [AD-A111307] p 75 N82-25614

Atmospheric Environment Service, Downsview (Ontario).
Surface wind analyses for Seasat p 51 A82-29619

Australian cal Meteorology Research Center, Melbourne.
The onset of the Australian Northwest monsoon during winter MONEX: Broadscale flow revealed by an objective analysis scheme p 56 N82-23912

B

Barringer Research Ltd., Rexdale (Ontario).
Breadboard gas filter correlation spectrometer for atmospheric measurement of hydrazines and nitrogen dioxide [AD-A110688] p 82 N82-26642

Bell Telephone Labs., Inc., Holmdel, N. J.
Evaluation of atmospheric attenuation from SMMR brightness temperature for the Seasat satellite scatterometer p 51 A82-29618

Bendix Field Engineering Corp., Grand Junction, Colo.
Airborne gamma-ray spectrometer and magnetometer survey. Roseau quadrangle, Minnesota, volume 1 [DE82-001031] p 43 N82-23621
NURE aerial gamma-ray and magnetic reconnaissance survey of portions of New Mexico, Arizona and Texas. Volume 2: New Mexico-Carlsbad Quadrangle [DE82-005527] p 48 N82-27810
Airborne gamma-ray spectrometer and magnetometer survey: Susanville quadrangle, California, volume 1 [DE82-005538] p 48 N82-27811
Airborne gamma-ray spectrometer and magnetometer survey: Roseburg quadrangle, Oregon, volume 2 [DE82-005568] p 48 N82-27812
Airborne gamma-ray spectrometer and magnetometer survey: Huron Quadrangle, South Dakota [DE82-005540] p 48 N82-27814
Airborne gamma-ray spectrometer and magnetometer survey: Chico Quadrangle, California [DE82-005543] p 48 N82-27815

Brigham Young Univ., Provo, Utah.
HCMM hydrological analysis in Utah [E82-10328] p 63 N82-24601

Brookhaven National Lab., Upton, N. Y.
Marine boundary layer wind structure over the Bay of Bengal during Monex-79 p 57 N82-23929

Brown Univ., Providence, R. I.
An investigation into the utilization of HCMM thermal data for the discrimination of volcanic and Eolian geological units [E82-10352] p 47 N82-26750

Brunswick Corp., Costa Mesa, Calif.
Fine particles in the Soufriere eruption plume p 24 A82-33659

Bureau de Recherches Geologiques et Minieres, Minieres, Paris (France).
Spatial thermal radiometry contribution to the Massif Armoricain and the Massif Central France litho-structural study [E82-10190] p 42 N82-22624

Business and Technological Systems, Inc., Seabrook, Md.
Application of satellite magnetic anomaly data to Curie isotherm mapping p 70 A82-35824
Equivalent source modeling of the main field using MAGSAT data [E82-10151] p 71 N82-23567
MAGSAT science investigations [E82-10199] p 71 N82-23572
An equivalent layer magnetization model for the United States derived from MAGSAT data [E82-10297] p 36 N82-24573

C

California Inst. of Tech., Pasadena.
Laboratory studies of actinide metal-silicate fractionation p 49 A82-22306
High resolution measurements of solar flare isotopes p 22 A82-22606

California Univ., Berkeley. Lawrence Berkeley Lab.
Environmental monitoring report of the Lawrence Berkeley Laboratory, 1980 [LBL-12604] p 29 N82-23793

California Univ., La Jolla.
Seasat altimeter determination of ocean current variability p 50 A82-29613
The observation of ocean surface phenomena using imagery from the Seasat synthetic aperture radar - An assessment p 52 A82-29623

California Univ., Livermore. Lawrence Livermore Lab.
Seismic and geodetic studies of the Imperial Valley, California [DE82-001686] p 39 N82-26915
Feasibility of laser-separation of 36 S and its use as an atmospheric tracer [DE82-000965] p 30 N82-27737

California Univ., Los Angeles.
Surface wind analyses for Seasat p 51 A82-29619
Geoid height-age relation from Seasat altimeter profiles across the Mendocino Fracture Zone p 34 A82-32646

California Univ., Santa Barbara.
The use of prior probabilities in maximum likelihood classification of remotely sensed data p 68 A82-32904
Multispectral determination of soil moisture-2 [E82-10349] p 19 N82-26747
The use of soil texture and field capacity to normalize microwave soil moisture measurements: Some problems p 20 N82-26762

Carson Helicopters, Inc., Perkasie, Pa.
NURE aerial gamma-ray and magnetic reconnaissance survey of portions of New Mexico, Arizona and Texas. Volume 2: New Mexico-Carlsbad Quadrangle [DE82-005527] p 48 N82-27810

Centre National d'Etudes Spatiales, Toulouse (France).
History of the French satellite space program p 85 N82-24216

Centre National de la Recherche Scientifique, Paris (France).
Representativeness of cloud motion winds deduced from GOES Indian Ocean satellite imagery for the description of the Indian summer monsoon p 55 N82-23879

Chicago Univ., Ill.
The question of short pathlengths in interstellar propagation p 1 A82-22541
Unusual properties of particle events associated with solar flare gamma ray events p 65 A82-22585
The relation of type II radio bursts to solar energetic particles observed at earth p 3 A82-22591
Observations of the ionization states of energetic particles accelerated in solar flares p 40 A82-22607

City Coll. of the City Univ. of New York.
Surface wind analyses for Seasat p 51 A82-29619

City Univ. of New York, N. Y.
The Seasat-A satellite scatterometer - The geophysical evaluation of remotely sensed wind vectors over the ocean p 51 A82-29616
The relationship between wind vector and normalized radar cross section used to derive Seasat-A Satellite Scatterometer winds p 51 A82-29617

Colorado State Univ., Fort Collins.
Influence of sky radiance distribution on the ratio technique for estimating bidirectional reflectance p 70 A82-35650

Colorado Univ., Boulder.
Investigation of geomagnetic field forecasting and fluid dynamics of the core
[E82-10198] p 35 N82-23571
Investigation of geomagnetic field forecasting and fluid dynamics of the core
[E82-10310] p 37 N82-24584
Investigation of geomagnetic field forecasting and fluid dynamics of the core
[E82-10342] p 39 N82-25604

Columbia Univ., New York.
High spectral resolution airborne spectrometry
p 77 A82-32443
Longwave infrared observation of urban landscapes
p 25 A82-34744

Committee on Science and Technology (U. S. House).
Civil land remote sensing system
[GPO-87-070] p 84 N82-22630

Commonwealth Scientific and Industrial Research Organization, Mordialoc (Australia).
Mean sea-level pressure in the Southern Hemisphere during the FGGE period p 55 N82-23856

Comptroller General of the United States, Washington, D.C.
Streamlining and ensuring mineral development must begin at local land management levels
[EMD-82-10] p 29 N82-23043

Computer Sciences Corp., Silver Spring, Md.
Remote sensing of precipitable water over the oceans from Nimbus 7 microwave measurements
p 49 A82-28907
Initial scalar magnetic anomaly map from Magsat
p 32 A82-30784
Initial vector magnetic anomaly map from Magsat
p 32 A82-30785
Preliminary evidence for the influence of physiography and scale upon the autocorrelation function of remotely sensed data p 67 A82-32343

Consiglio Nazionale delle Ricerche, Naples (Italy).
Crustal structures under the active volcanic areas of central and eastern Mediterranean (M-44)
[E82-10096] p 35 N82-23563

Cornell Univ., Ithaca, N. Y.
Landsat detection of hardwood forest clearcuts
p 8 A82-32708

D

Defence Science and Technology Organisation, Edgecliff (Australia).
High resolution satellite observations of mesoscale oceanography in the Tasman Sea, 1978 - 1979
[E82-10324] p 57 N82-24597

Defense Mapping Agency Aerospace Center, St. Louis, Mo.
Matrix data analysis: Color/B and W coding is not always enough
[AD-A111401] p 74 N82-25612

Defense Mapping Agency Hydrographic and Topographic Center, Washington, D.C.
A comparison of pole positions derived from GPS satellite and Navy navigation satellite observations
[AD-A110765] p 39 N82-26268

Department of Agriculture, Houston, Tex.
Evaluation of the Doraiswamy-Thompson winter wheat crop calendar model incorporating a modified spring restart sequence
[E82-10207] p 12 N82-23580

E

Earth Satellite Corp., Washington, D. C.
Use of NOAA/AVHRR visible and near-infrared data for land remote sensing
[NASA-TM-84186] p 81 N82-22643
Experimental assessment of improved spatial resolution LANDSAT data
[AD-A110538] p 75 N82-26765

Environmental Research and Technology, Inc., Concord, Mass.
The application of Heat Capacity Mapping Mission (HCMM) thermal data to snow hydrology
[E82-10191] p 62 N82-22625

Environmental Research Inst. of Michigan, Ann Arbor.
Analysis of scanner data for crop inventories
[E82-10192] p 10 N82-22626
LANDSAT technology transfer to the private and public sectors through community colleges and other locally available institutions
[E82-10181] p 85 N82-23568
Analysis of scanner data for crop inventories
[E82-10241] p 16 N82-24519
Association of spectral development patterns with development stages of corn
[E82-10353] p 19 N82-26751

Environmental Systems Research Inst., Redlands, Calif.
Exploration into technical procedures for vertical integration
[NASA-CR-166352] p 75 N82-26763

European Space Agency, Toulouse (France).
The METEOSAT Data Collection System and its application p 75 N82-26037

Evangel Coll., Springfield, Mo.
Use of LANDSAT data to define soil boundaries in Carroll County, Missouri p 10 N82-23[illegible]6

EG & G Washington Analytical Services Center, Inc., Riverdale, Md.
Seasat altimeter height calibration p 49 A82-29603
Seasat altimeter timing bias estimation
p 50 A82-29609
The Seasat altimeter mean sea surface model
p 51 A82-29614
Gravity model improvement for Seasat
p 32 A82-29615

EG and G Washington Analytical Services Center, Inc., Rockville, Md.
Bias correction procedures for airborne laser hydrography
[PB82-130089] p 63 N82-22644

F

Florida Dept. of Transportation, Tallahassee.
Effects of altitude, focal length, and filter combinations on color infrared photography of citrus groves
p 9 A82-34729

Florida State Univ., Tallahassee.
Meteorological and aircraft data for CUE 2 1973
[PB82-149246] p 59 N82-26949

Florida Univ., Gainesville.
Use of thermal inertia determined by HCMM to predict nocturnal cold prone areas in Florida
[E82-10299] p 17 N82-24575

Florida Univ., Lake Alfred.
Detection and damage assessment of citrus tree losses with aerial color infrared photography /ACIR/
p 7 A82-29538
Effects of altitude, focal length, and filter combinations on color infrared photography of citrus groves
p 9 A82-34729

G

General Electric Co., Philadelphia, Pa.
The Seasat-A satellite scatterometer - The geophysical evaluation of remotely sensed wind vectors over the ocean p 51 A82-29616

General Software Corp., Landover, Md.
LANDSAT-D conical scanner evaluation plan
[E82-10340] p 81 N82-25602

Geological Survey, Denver, Colo.
Registration of Heat Capacity Mapping Mission day and night images
[E82-10210] p 72 N82-23583
Ground support data from July 10 to July 29, 1978, for HCMM thermal satellite data of the Powder River Basin, Wyoming
[E82-10211] p 72 N82-23584
Topographic slope correction for analysis of thermal infrared images
[E82-10214] p 36 N82-23587
Application of HCMM data to regional geologic analysis for mineral and energy resource evaluation
[E82-10153] p 45 N82-24518
Application of HCMM data to regional geologic analysis for mineral and energy resource evaluation
[E82-10243] p 45 N82-24521

Geological Survey, Reston, Va.
Initial scalar magnetic anomaly map from Magsat
p 32 A82-30784
Initial vector magnetic anomaly map from Magsat
p 32 A82-30785

George Mason Univ., Fairfax, Va.
Confinement and acceleration of cosmic rays in galactic superbubbles p 82 A82-22547

H

Herzberg Inst. of Astrophysics, Ottawa (Ontario).
Studies of high latitude current systems using MAGSAT vector data
[E82-10188] p 71 N82-22622

High Life Helicopters, Inc., Puyallup, Wash.
Airborne gamma-ray spectrometer and magnetometer survey, Toronto quadrangle New York, volume 2A
[DE81-027158] p 46 N82-25620
Airborne gamma-ray spectrometer and magnetometer survey, Kingston quadrangle New York, volume 2C
[DE81-027161] p 46 N82-25621
Airborne gamma-ray spectrometer and magnetometer survey, Rochester quadrangle New York, volume 2D
[DE81-027156] p 46 N82-25622

Hofstra Univ., Hempstead, N. Y.
Seasat wind and wave observations of northeast Pacific hurricane Iva, August 13, 1978 p 52 A82-29624

I

Indian Inst. of Geomagnetism, Bombay.
MAGSAT for geomagnetic studies over Indian region
[E82-10202] p 72 N82-23575
MAGSAT for geomagnetic studies over Indian region
[E82-10296] p 73 N82-24572

Indian Inst. of Tropical Meteorology, Poona.
Impact of additional summer MONEX wind data on the prediction of monsoon depressions during June - August 1979 with two versions of primitive equation (PE) barotropic model p 56 N82-23[illegible]0

Institute of Geological Sciences, Edinburgh (Scotland).
Spherical harmonic representation of the main geomagnetic field for world charting and investigations of some fundamental problems of physics and geophysics
[E82-10203] p 72 N82-23576

Institute of Oceanographic Sciences, Wormley (England).
Surface wind analyses for Seasat p 51 A82-29619

Instituto de Pesquisas Espaciais, Sao Jose dos Campos (Brazil).
Dynamic study of the upper Sao Francisco river and Tres Marias reservoir using MSS/LANDSAT images
[E82-10291] p 63 N82-24569
Comparison of storm-time changes of geomagnetic field at ground and at MAGSAT altitudes, part 2
[E82-10325] p 30 N82-24598
SMS/GOES data collection platform system
p 75 N82-26027
Comparison of storm-time changes of geomagnetic field at ground and MAGSAT altitudes
[E82-10359] p 30 N82-26757
A study of atmospheric diffusion from the LANDSAT imagery
[E82-10360] p 58 N82-26758

Instituto Geografico Nacional, Madrid (Spain).
Thermal mapping, geothermal source location, natural effluents and plant stress in the Mediterranean coast of Spain
[E82-10300] p 17 N82-24576

Intermountain Forest and Range Experiment Station, Ogden, Utah.
Remote automatic weather station for resource and fire management agencies
[PB82-107335] p 30 N82-23963

Iowa Univ., Iowa City.
Use of MAGSAT anomaly data for crustal structure and mineral resources in the US Midcontinent
[E82-10321] p 46 N82-24594
Use of MAGSAT anomaly data for crustal structure and mineral resources in the US Midcontinent
[E82-10323] p 46 N82-24596

J

Jet Propulsion Lab., California Inst. of Tech., Pasadena.
A color-ratio map of Mercury p 31 A82-22294
Seasat measurement system evaluation - Achievements and limitations p 49 A82-29601
The Seasat altimeter data and its accuracy assessment p 49 A82-29602
An empirical determination of the effects of sea state bias on Seasat altimetry p 50 A82-29607
Seasat altimeter determination of ocean current variability p 50 A82-29613
The Seasat-A satellite scatterometer - The geophysical evaluation of remotely sensed wind vectors over the ocean p 51 A82-29616
The relationship between wind vector and normalized radar cross section used to derive Seasat-A Satellite Scatterometer winds p 51 A82-29617
Surface wind analyses for Seasat p 51 A82-29619
Description of Seasat radiometer status and results
p 52 A82-29622
The observation of ocean surface phenomena using imagery from the Seasat synthetic aperture radar - An assessment p 52 A82-29623

Seasat wind and wave observations of northeast Pacific hurricane Iva, August 13, 1978 p 52 A82-29624
Resource inventory techniques used in the California Desert Conservation Area p 23 A82-32441
Spectroscopic remote sensing for geological applications p 41 A82-32442
Multispectral mapper - Imaging spectroscopy as applied to the mapping of earth resources p 77 A82-32448
Ocean wave height measurement with SEASAT SAR using speckle diversity p 53 A82-32882
Bathymetric imaging p 69 A82-34720
Improved land use classification from Landsat and Seasat satellite imagery registered to a common map base p 25 A82-34743
Microwave measurement of stratospheric and mesospheric ozone p 28 A82-36415
Sea-Ice Mission Requirements for the US FIREX and Canada RADARSAT programs
[NASA-CR-168984] p 57 N82-25609

Joint Inst. for Lab. Astrophysics, Boulder, Colo.
Establishment of terrestrial reference frames by new observational techniques p 33 A82-32078

Joint Publications Research Service, Arlington, Va.
Cost-effectiveness of geographic surveying from space p 85 N82-24263
Purpose, background of 'Intercosmos-21' mission p 81 N82-24264

K

Kansas Univ. Center for Research, Inc., Lawrence.
The Seasat-A satellite scatterometer - The geophysical evaluation of remotely sensed wind vectors over the ocean p 51 A82-29616
The relationship between wind vector and normalized radar cross section used to derive Seasat-A Satellite Scatterometer winds p 51 A82-29617
Evaluation of atmospheric attenuation from SMMR brightness temperature for the Seasat satellite scatterometer p 51 A82-29618
The recognition of extended targets - SAR images for level and hilly terrain p 33 A82-31994
Evaluation of the soil moisture prediction accuracy of a space radar using simulation techniques
[E82-10351] p 19 N82-26749

L

Lincoln Lab., Mass. Inst. of Tech., Lexington.
Detection of regional air pollution episodes utilizing satellite digital data in the visual range p 23 A82-31990

Liverpool Univ. (England).
System albedo as sensed by satellites - Its definition and variability p 23 A82-32342

Lockheed Engineering and Management Services Co., Inc., Houston, Tex.
Evaluation of NOAA-AVHRR data for crop assessment p 8 A82-34179
Ten-Ecosystem Study
[E82-10186] p 84 N82-22620
AgRISTARS: Foreign commodity production forecasting. The 1980 US/Canada wheat and barley exploratory experiment
[E82-10126] p 11 N82-23565
AgRISTARS: Foreign commodity production forecasting. The 1980 US corn and soybeans exploratory experiment
[E82-10206] p 11 N82-23579
AgRISTARS: Supporting research. Spring small grains planting date distribution model
[E82-10208] p 12 N82-23581
Description of historical crop calendar data bases developed to support foreign commodity production forecasting project experiments
[E82-10209] p 12 N82-23582
Application of thermal model for pan evaporation to the hydrology of a defined medium, the sponge
[E82-10217] p 13 N82-23590
Normal crop calendars. Volume 3: The corn and soybean states of Illinois, Indiana, and Iowa
[E82-10221] p 13 N82-23594
Selection of the Australian indicator region
[E82-10222] p 13 N82-23595
Evaluation of VICAR software capability for land information support system needs
[E82-10223] p 73 N82-23596
AgRISTARS: Renewable resources inventory. Land information support system implementation plan and schedule
[E82-10224] p 14 N82-23597
Evaluation of the procedure for separating barley from other spring small grains
[E82-10230] p 14 N82-23603
Use and applicability of the vegetation component of the national site classification system
[E82-10234] p 15 N82-23607
Description of the FORTRAN implementation of the spring small grains planting date distribution model
[E82-10235] p 15 N82-23608

Lowell Observatory, Flagstaff, Ariz.
Subtleties in the flat-fielding of charge-coupled device /CCD/ images p 68 A82-32581

Lunar and Planetary Inst., Houston, Tex.
Influence of CO2 on melting of model granulite facies assemblages - A model for the genesis of charnockites p 42 A82-36298

M

Main Geophysical Observatory, Leningrad (USSR).
Estimates of the statistical structure of the atmospheric pressure field in summer Monex-79 area p 57 N82-23939

Maryland Univ., College Park.
Observations of interplanetary energetic charged particles from gamma-ray line solar flares p 65 A82-22586
A survey of solar protons and alpha differential spectra between 1 and greater than 400 MeV/nucleon p 4 A82-22592
Time and energy dependence of heavy ion abundances in solar flare energetic particle events p 22 A82-22605
Observations of the ionization states of energetic particles accelerated in solar flares p 40 A82-22607
A comparison of helium and heavy ion spectra in He/3/ rich solar flares with a model calculation p 5 A82-22612
On the anticorrelation between the He/3//He/4/ ratio and proton intensity in He/3/ rich flares p 40 A82-22613
Generation of the auroral kilometric radiation p 26 A82-35542

Massachusetts Inst. of Tech., Cambridge.
Inversion of data from diffraction-limited multiwavelength remote sensors. II - Nonlinear dependence of observables on the geophysical parameters p 77 A82-32658

Massachusetts Univ., Amherst.
The mineralogy of global magnetic anomalies
[E82-10305] p 45 N82-24579
Stratospheric emission data analysis
[AD-A112337] p 76 N82-26907

Max-Planck-Institut fuer Extraterrestrische Physik, Garching (West Germany).
Observations of interplanetary energetic charged particles from gamma-ray line solar flares p 65 A82-22586
Observations of the ionization states of energetic particles accelerated in solar flares p 40 A82-22607

Max-Planck-Institut fuer Physik und Astrophysik, Garching (West Germany).
Time and energy dependence of heavy ion abundances in solar flare energetic particle events p 22 A82-22605
A comparison of helium and heavy ion spectra in He/3/ rich solar flares with a model calculation p 5 A82-22612

Measurement Concept Corp., Rome, N. Y.
Source assessment system
[AD-A111223] p 75 N82-25613

Miami Univ., Fla.
Investigations of medium wavelength magnetic anomalies in the eastern Pacific using MAGSAT
[E82-10240] p 73 N82-23613
MONEX oceanographic observations along the East African coast p 56 N82-23908
Investigations of medium wavelength magnetic anomalies in the eastern Pacific using MAGSAT data
[E82-10330] p 38 N82-24603

Minnesota Univ., St. Paul.
Application of scanning microdensitometer data in selected plant science case studies p 7 A82-29539

Mississippi State Univ., Mississippi State.
Application of remote sensing to state and regional problems
[E82-10288] p 30 N82-24566

Mississippi State Univ., State College.
A comparison of stratified versus regression estimators p 11 N82-23133

Morgan State Coll., Baltimore, Md.
Relating thematic mapper bands TM3, TM4, and TM5 to agronomic variables for corn, cotton, sugarbeet, soybean, sorghum, sunflower and tobacco
[E82-10347] p 19 N82-26745

N

National Academy of Sciences - National Research Council, Washington, D. C.
Geodetic monitoring of tectonic information. Toward a strategy p 35 N82-22832
Geodetic monitoring of tectonic deformation: Toward a strategy
[NASA-CR-168784] p 35 N82-22846

National Aeronautics and Space Administration. Ames Research Center, Moffett Field, Calif.
Airborne observed solar elevation and row direction effects on the near-IR/red ratio of cotton
[E82-10220] p 13 N82-23593
Multilevel measurements of surface temperature over undulating terrain planted to barley
[E82-10245] p 16 N82-24523

National Aeronautics and Space Administration. Earth Resources Labs., Bay St. Louis, Miss.
Development of three-dimensional spatial displays using a geographically based information system p 66 A82-29326

National Aeronautics and Space Administration. Goddard Inst. for Space Studies, New York.
System albedo as sensed by satellites - Its definition and variability p 23 A82-32342
Longwave infrared observation of urban landscapes p 25 A82-34744

National Aeronautics and Space Administration. Goddard Space Flight Center, Greenbelt, Md.
The cosmic ray positron spectrum p 1 A82-22542
Confinement and acceleration of cosmic rays in galactic superbubbles p 82 A82-22547
Interplanetary particle observations associated with solar flare gamma-ray line emission p 3 A82-22584
A survey of solar protons and alpha differential spectra between 1 and greater than 400 MeV/nucleon p 4 A82-22592
Heavy-element abundances in He/3/-rich events p 5 A82-22611
Remote sensing of precipitable water over the oceans from Nimbus 7 microwave measurements p 49 A82-28907
Detecting residential land-use development at the urban fringe p 22 A82-29332
Seasat altimeter height calibration p 49 A82-29603
Seasat altimeter timing bias estimation p 50 A82-29609
Comparison data for Seasat altimetry in the western North Atlantic p 50 A82-29611
The Seasat altimeter mean sea surface model p 51 A82-29614
Gravity model improvement for Seasat p 32 A82-29615
Initial scalar magnetic anomaly map from Magsat p 32 A82-30784
Initial vector magnetic anomaly map from Magsat p 32 A82-30785
Magsat scalar anomaly distribution - The global perspective p 41 A82-30786
Retrieval of ocean surface and atmospheric parameters from multichannel microwave radiometric measurements p 53 A82-31995
Preliminary evidence for the influence of physiography and scale upon the autocorrelation function of remotely sensed data p 67 A82-32343
Evaluation of temporal registration of Landsat scenes p 67 A82-32345
Remote sensing of leaf water content in the near infrared p 8 A82-32897
Effects of vegetation canopy structure on remotely sensed canopy temperatures p 8 A82-32905
A comparative study of microwave radiometer observations over snowfields with radiative transfer model calculations p 60 A82-32910
Landsat digital analysis of the initial recovery of burned tundra at Kokolik River, Alaska p 8 A82-32913
View angle effects in the radiometric measurement of plant canopy temperatures p 8 A82-32914
Snowpack monitoring in North America and Eurasia using passive microwave satellite data p 78 A82-32915
The use of Landsat-3 thermal data to help differentiate land covers p 25 A82-34218
Irradiance measurement errors due to the assumption of a Lambertian reference panel p 79 A82-34222
Landsat in the search for Appalachian hydrocarbons p 42 A82-34721
Defining the temporal window for monitoring forest canopy defoliation using Landsat p 9 A82-34730
Use of aerial photography in determining land use and streamflow relationships on small developing watersheds p 60 A82-34736
Satellite and surface geophysical expression of anomalous crustal structure in Kentucky and Tennessee p 34 A82-34918

Influence of sky radiance distribution on the ratio technique for estimating bidirectional reflectance
p 70 A82-35650

Total ozone variations 1970-74 using Backscattered Ultraviolet /BUV/ and ground-based observations
p 26 A82-36053

Atmospheric ozone determination by solar occultation using the UV spectrometer on the Solar Maximum Mission p 27 A82-36362

The seasonal variations of ozone and temperature in the middle and the upper stratosphere
p 29 A82-36534

Advanced technology for earth observation - Data processing
[AAS PAPER 82-130] p 71 A82-37810

Solid state instrumentation concepts for earth resource observation
[AAS PAPER 82-132] p 81 A82-37812

Information theory lateral density distribution for earth inferred from global gravity field p 35 A82-37962

Use of NOAA/AVHRR visible and near-infrared data for land remote sensing
[NASA-TM-84186] p 81 N82-22643

A multi-frequency radiometric measurement of soil moisture content over bare and vegetated fields
[E82-10238] p 16 N82-23611

The influence of autocorrelation in signature extraction: An example from a geobotanical investigation of Cotter Basin, Montana
[E82-10341] p 46 N82-25603

National Aeronautics and Space Administration. John F. Kennedy Space Center, Cocoa Beach, Fla.

Detection and damage assessment of citrus tree losses with aerial color infrared photography /ACIR/
p 7 A82-29538

Effects of altitude, focal length, and filter combinations on color infrared photography of citrus groves
p 9 A82-34729

National Aeronautics and Space Administration. Langley Research Center, Hampton, Va.

The Seasat-A satellite scatterometer - The geophysical evaluation of remotely sensed wind vectors over the ocean p 51 A82-29616

The relationship between wind vector and normalized radar cross section used to derive Seasat-A Satellite Scatterometer winds p 51 A82-29617

Evaluation of atmospheric attenuation from SMMR brightness temperature for the Seasat satellite scatterometer p 51 A82-29618

Depression of brightness temperature of sea surfaces covered with monomolecular oil films relative to clean water surfaces at 1.43 GHz p 54 A82-33322

Characteristics of 13.9 GHz radar scattering from oil films on the sea surface p 54 A82-33438

Airborne lidar measurements of the Soufriere eruption of 17 April 1979 p 24 A82-33657

Fine particles in the Soufriere eruption plume
p 24 A82-33659

Tropospheric CO measurement experiment from the second Space Shuttle flight p 27 A82-36292

Ammonia and the NOx budget of the troposphere
p 27 A82-36293

SEASAT: A satellite scatterometer illumination times of selected in situ sites
[NASA-TM-83280] p 81 N82-22865

Analysis of ocean color scanner data from the Superflux III Experiment
[NASA-TM-83290] p 55 N82-23614

Radiometer mission requirements for large space antenna systems
[NASA-TM-84478] p 81 N82-25610

In situ ozone data for comparison with laser absorption remote sensor: 1980 PEPE/NEROS program
[NASA-TM-84471] p 30 N82-25661

National Aeronautics and Space Administration. Lyndon B. Johnson Space Center, Houston, Tex.

Field size, length, and width distributions based on LACIE ground truth data p 8 A82-32909

A meteorologically driven maize stress indicator model
[E82-10112] p 11 N82-23564

AgRISTARS: Preliminary technical results review of FY81 experiments, volume 2: Fiscal year 1981/1982 'corn and soybeans pilot' experiment
[E82-10216] p 13 N82-23589

A meteorologically driven grain sorghum stress indicator model
[E82-10218] p 13 N82-23591

AgRISTARS: Project management report: Program review presentation to level 1, interagency coordination committee
[E82-10219] p 13 N82-23592

AgRISTARS: Project management report: Program review presentation to level 1, interagency coordination committee
[E82-10231] p 15 N82-23604

AgRISTARS: Agriculture and resources inventory surveys through aerospace remote sensing
[E82-10236] p 15 N82-23609

National Aeronautics and Space Administration. Marshall Space Flight Center, Huntsville, Ala.

Remote sensing of tornadic storms from geosynchronous satellite infrared digital data
p 23 A82-32348

National Aeronautics and Space Administration. National Space Technology Labs., Bay Saint Louis, Miss.

An analysis of LANDSAT MSS scene-to-scene registration accuracy
[E82-10285] p 16 N82-24563

An algorithm for automating the registration of USDA segment ground data to LANDSAT MSS data
[E82-10286] p 16 N82-24564

Analysis of thematic mapper simulator data acquired during winter season over Pearl River, Mississippi, test site
[E82-10287] p 17 N82-24565

National Aeronautics and Space Administration. Wallops Flight Center, Wallops Island, Va.

Sea-state-related altitude errors in the Seasat radar altimeter p 50 A82-29608

Pulse-to-pulse correlation in satellite radar altimeters
p 55 A82-37390

National Aeronautics and Space Administration, Washington, D. C.

OSTA-1 Post Mission Operation Report
[NASA-TM-84191] p 84 N82-23258

Plan of research for integrated soil moisture studies. Recommendations of the Soil Moisture Working Group
[NASA-TM-84731] p 18 N82-25608

LANDSAT D to test thematic mapper, inaugurate operational system
[NASA-NEWS-RELEASE-82-100] p 82 N82-26741

National Bureau of Standards, Boulder, Colo.

Establishment of terrestrial reference frames by new observational techniques p 33 A82-32078

National Conference of State Legislatures, Denver, Colo.

A legislator's guide to LANDSAT
[E82-10290] p 65 N82-24568

National Meteorological Center, Washington, D. C.

Total ozone variations 1970-74 using Backscattered Ultraviolet /BUV/ and ground-based observations
p 26 A82-36053

Short term influence radius of monsoonal overturnings
p 56 N82-23898

National Oceanic and Atmospheric Administration, Bay St. Louis, Miss.

Surface wind analyses for Seasat p 51 A82-29619

National Oceanic and Atmospheric Administration, Boulder, Colo.

Intercomparison of wind speeds inferred by the SASS, altimeter, and SMMR p 52 A82-29621

Field measurements in support of dispersion modeling in complex terrain (1980)
[PB82-148644] p 39 N82-27882

National Oceanic and Atmospheric Administration, Rockville, Md.

Bias correction procedures for airborne laser hydrography
[PB82-130089] p 63 N82-22644

A statistical approach to rainfall estimation using satellite and conventional data
[NOAA-TR-NESS-89] p 63 N82-22854

National Oceanic and Atmospheric Administration, Seattle, Wash.

Surface wind analyses for Seasat p 51 A82-29619

Seasat wind and wave observations of northeast Pacific hurricane Iva, August 13, 1978 p 52 A82-29624

National Oceanic and Atmospheric Administration, Washington, D. C.

Comparison of satellite derived radiation budget measurements over MONEX during 1979 to 1980
p 29 N82-23891

National Weather Service, Fort Worth, Tex.

Some empirical rules for forecasting fog and status over northern Florida, southern Georgia and adjacent coastal waters
[PB82-154006] p 59 N82-27949

Natural Environment Research Council, London (England).

Overseas Geology And Mineral Resources number 56. A geological interpretation of LANDSAT imagery and air photography of Botswana
[OGMR-56] p 42 N82-22636

Naval Physical and Oceanographic Lab., Cochin (India).

On the space-time variability of ocean surface mixed layer characteristics of central and eastern Arabian sea during MONSOON-77 p 56 N82-23909

Naval Postgraduate School, Monterey, Calif.

Rapid oceanographic data gathering: Some problems in using remote sensing to determine the horizontal and vertical thermal distributions in the Northeast Pacific Ocean
[AD-A111005] p 58 N82-26945

New Hampshire Univ., Durham.

Fragmentation of Fe nuclei on carbon, hydrogen and CH2 targets. I - Individual charge changing and total cross sections. II - Isotopic cross sections p 63 A82-22538

The charge and isotopic composition of Z equals 7-16 cosmic ray nuclei at their source p 64 A82-22555

Observations of the ionization states of energetic particles accelerated in solar flares p 40 A82-22607

New York State Univ., Syracuse.

Evaluation of NOAA-AVHRR data for crop assessment p 8 A82-34179

North Carolina State Coll., Raleigh.

A preliminary comparison of the Magsat data and aeromagnetic data in the continental U.S.
p 32 A82-30790

North Carolina State Univ., Raleigh.

MAGSAT and aeromagnetic data in the North American continent
[E82-10193] p 71 N82-22627

MAGSAT scalar and vector anomaly data analysis
[E82-10307] p 74 N82-24581

O

Ocean Weather, Inc., White Plains, N.Y.

Surface wind analyses for Seasat p 51 A82-29619

Intercomparison of wind speeds inferred by the SASS, altimeter, and SMMR p 52 A82-29621

Office of Technology Assessment, Washington, D. C.

Technology and oceanography: An assessment of Federal technologies for oceanographic research and monitoring. Volume 2: Working papers on fishery research technology p 58 N82-26944

Ohio State Univ., Columbus.

Reference coordinate systems for earth dynamics - A preview p 33 A82-32077

The Earth's gravity field to degree and order 180 using SEASAT altimeter data, terrestrial gravity data and other data
[AD-A113098] p 40 N82-27900

OAO Corp., Beltsville, Md.

LANDSAT-D thermal analysis and design support
[E82-10346] p 82 N82-26744

P

Paris VI Univ. (France).

MAGSAT anomaly map and continental drift
[E82-10326] p 38 N82-24599

Models and maps of the main field
[E82-10327] p 74 N82-24600

Pennsylvania State Univ., University Park.

Delineation of soil temperature regimes from HCMM data
[E82-10298] p 17 N82-24574

A method for inferring available surface moisture using remote surface temperature measurements: An assessment
[E82-10311] p 17 N82-24585

Interactive initialization of heat flux parameters for numerical models using satellite temperature measurements
[E82-10313] p 82 N82-26743

Phoenix Corp., McLean, Va.

Improved definition of crustal magnetic anomalies for MAGSAT data
[E82-10314] p 37 N82-24587

Pittsburg Univ., Pa.

A color-ratio map of Mercury p 31 A82-22294

Planetary Science Inst., Pasadena, Calif.

Seasat wind and wave observations of northeast Pacific hurricane Iva, August 13, 1978 p 52 A82-29624

Purdue Univ., Lafayette, Ind.

Verification of the crustal component in satellite magnetic data p 32 A82-30789

A satellite magnetic model of northeastern South American aulacogens p 33 A82-30795

Spectral properties of agricultural crops and soils measured from space, aerial, field, and laboratory sensors
[E82-10189] p 10 N82-22623

Study of gravity and magnetic anomalies using MAGSAT data
[E82-10194] p 35 N82-22628

Diurnal changes in reflectance factor due to Sun-row direction interactions
[E82-10128] p 11 N82-23566

Spectral properties of agricultural crops and soils measured from space, aerial, field, and laboratory sensors
[E82-10212] p 12 N82-23585

Multistage classification of multispectral Earth observational data: The design approach
[E82-10213] p 72 N82-23586

Determination of the optimal level for combining area and yield estimates
[E82-10215] p 12 N82-23588

Application of Computer Axial Tomography (CAT) to measuring crop canopy geometry
[E82-10227] p 14 N82-23600

Linear polarization of light by two wheat canopies measured at many view angles
[E82-10229] p 14 N82-23602

A model of plant canopy polarization
[E82-10233] p 15 N82-23606

Canopy reflectance as influenced by solar illumination angle
[E82-10237] p 15 N82-23610

Spherical-Earth gravity and magnetic anomaly modeling by Gauss-Legendre quadrature integration
[E82-10242] p 36 N82-24520

Magnetic and gravity anomalies in the Americas
[E82-10312] p 37 N82-24586

Aeromagnetic and satellite magnetic anomaly mapping
[E82-10339] p 39 N82-25601

Forest Resource Information System. Phase 3: System transfer report
[E82-10344] p 18 N82-25606

Spectral estimates of solar radiation intercepted by corn canopies
[E82-10003] p 18 N82-26742

Key Issues in the Analysis of Remote Sensing Data: A report on the workshop
[E82-10348] p 85 N82-26746

Q

QEB, Inc., Lakewood, Colo.

Airborne gamma-ray spectrometer and magnetometer survey, Toronto quadrangle New York, volume 2A
[DE81-027158] p 46 N82-25620

Airborne gamma-ray spectrometer and magnetometer survey, Kingston quadrangle New York, volume 2C
[DE81-027161] p 46 N82-25621

Airborne gamma-ray spectrometer and magnetometer survey, Rochester quadrangle New York, volume 2D
[DE81-027156] p 46 N82-25622

R

Remote Sensing Systems, Sausalito, Calif.

The Seasat-A satellite scatterometer - The geophysical evaluation of remotely sensed wind vectors over the ocean p 51 A82-29616

The relationship between wind vector and normalized radar cross section used to derive Seasat-A Satellite Scatterometer winds p 51 A82-29617

Evaluation of atmospheric attenuation from SMMR brightness temperature for the Seasat satellite scatterometer p 51 A82-29618

Intercomparison of wind speeds inferred by the SASS, altimeter, and SMMR p 52 A82-29621

The effect of sea-surface Sun glitter on microwave radiometer measurements
[NASA-CR-169083] p 57 N82-26525

Research Inst. of National Defence, Linkoeping (Sweden).

Study visit to United States laser technology centers, 1981
[FOA-C-30257-E1] p 81 N82-24489

S

Sanders Associates, Inc., Nashua, N. H.

High spectral resolution airborne spectrometry
p 77 A82-32443

Santa Barbara Research Center, Goleta, Calif.

Thematic mapper - An overview of spectral band registration p 77 A82-32447

Sao Paulo Univ. (Brazil).

Structure, composition and thermal state of the crust in Brazil
[E82-10187] p 35 N82-22621

Science and Education Administration, Weslaco, Tex.

AgRISTARS: Early warning and crop condition assessment. Plant cover, soil temperature, freeze, water stress, and evapotranspiration conditions
[E82-10225] p 14 N82-23598

Scripps Institution of Oceanography, La Jolla, Calif.

Satellite observations in FRONTS 80
[AD-A111080] p 58 N82-26766

Fluid-sediment interactions on beaches and shelves
[AD-A110838] p 59 N82-26948

South Carolina Univ., Columbia.

Detecting residential land-use development at the urban fringe p 22 A82-29332

South Dakota State Univ., Brookings.

Evaluation of HCMM data for assessing soil moisture and water table depth
[E82-10329] p 18 N82-24602

Irrigation management with remote sensing
[E82-10357] p 20 N82-26755

Stanford Univ., Calif.

The observation of ocean surface phenomena using imagery from the Seasat synthetic aperture radar - An assessment p 52 A82-29623

Survey of India, Dehra Dun.

Report of MAGSAT project by Survey of India
[E82-10293] p 73 N82-24570

Analysis of MAGSAT data of the Indian region
[E82-10358] p 75 N82-26756

Systems and Applied Sciences Corp., Riverdale, Md.

Retrieval of ocean surface and atmospheric parameters from multichannel microwave radiometric measurements
p 53 A82-31995

T

Technical Univ. of Denmark, Lyngby.

Movement of ice markers measured by satellite ranging
[R-240] p 59 N82-27816

Technicolor Graphic Services, Inc., Sioux Falls, S. Dak.

An investigation of MAGSAT and complementary data emphasizing precambrian shields and adjacent areas of West Africa and South America
[E82-10316] p 38 N82-24589

An investigation of MAGSAT and complementary data emphasizing precambrian shields and adjacent areas of West Africa and South America
[E82-10317] p 38 N82-24590

An investigation of MAGSAT and complementary data emphasizing precambrian shields and adjacent areas of West Africa and South America
[E82-10318] p 38 N82-24591

Technische Hogeschool, Delft (Netherlands).

Nonlinear theory for elastic beams and rods and its finite element representation
[WTHD-143] p 73 N82-24517

Tennessee Valley Authority, Chattanooga.

Remote sensing of sulfur dioxide effects on vegetation. Volume 1: Summary
[DE82-900580] p 31 N82-27802

Remote sensing of sulfur dioxide effects on vegetation. Volume 2: Data
[DE82-900581] p 31 N82-27803

Texas A&M Univ., College Station.

Orbiting passive microwave sensor simulation applied to soil moisture estimation
[E82-10343] p 18 N82-25605

Multispectral determination of soil moisture-2
[E82-10349] p 19 N82-26747

Measurement of soil moisture trends with airborne scatterometers
[E82-10361] p 20 N82-26759

Multifrequency remote sensing of soil moisture
[E82-10362] p 20 N82-26760

Development of visible/infrared/microwave agriculture classification and biomass estimation algorithms
[E82-10363] p 20 N82-26761

Texas Univ. at Austin.

Interpretation of surface-water circulation, Aransas Pass, Texas, using Landsat imagery p 60 A82-32896

Texas Univ. at Dallas.

Investigation of the effects of external current systems on the MAGSAT data utilizing grid cell modeling techniques
[E82-10226] p 73 N82-23599

Investigation of the effects of external current systems on the MAGSAT data utilizing grid cell modeling techniques
[E82-10232] p 73 N82-23605

Texas Univ. at Dallas, Richardson.

Investigation of the effects of external current systems on the MAGSAT data utilizing grid cell modeling techniques
[E82-10195] p 71 N82-22629

Investigation of the effects of external current systems on the MAGSAT data utilizing grid cell modeling techniques
[E82-10306] p 74 N82-24580

Texas Univ. at El Paso.

Characterization of the structure and tectonic of South America
[E82-10196] p 42 N82-23569

The crustal structure and tectonics of South America
[E82-10319] p 38 N82-24592

Geotectonics of South America
[E82-10320] p 38 N82-24593

Texas Univ., Austin.

The Seasat altimeter data and its accuracy assessment p 49 A82-29602

An empirical determination of the effects of sea state bias on Seasat altimetry p 50 A82-29607

Evaluation of the Seasat altimeter time tag bias
p 50 A82-29610

Texas Univ., El Paso.

Evaluation and combined geophysical interpretations of NURE and related geoscience data in the Van Horn, Pecos, Marfa, Fort Stockton, Presidido, and Emory Peak quadrangles, Texas, volume 1
[DE82-005554] p 47 N82-27808

Evaluation and combined geophysical interpretations of NURE and related geoscience data in the Van Horn, Pecos, Marfa, Fort Stockton, Presidio, and Emory Peak quadrangels, Texas
[DE82-005560] p 48 N82-27809

Tokyo Univ. (Japan).

Investigation from Japanese MAGSAT team
[E82-10239] p 73 N82-23612

Investigation from Japanese MAGSAT Team. Part A. Crustal structure near Japan and in Antarctic station. Part B. Electric currents and hydromagnetic waves in the ionosphere and the magnetosphere
[E82-10244] p 36 N82-24522

Report of investigation from Japanese MAGSAT Team
[E82-10322] p 74 N82-24595

U

University of Southern California, Los Angeles.

Image understanding research
[AD-A110746] p 74 N82-25611

Utah Univ., Salt Lake City.

Identifying environmental features for land management decisions
[E82-10289] p 30 N82-24567

Inventory of wetlands and agricultural land cover in the upper Sevier River Basin, Utah
[E82-10345] p 18 N82-25607

Mapping of wildlife habitat in Farmington Bay, Utah
[E82-10354] p 19 N82-26752

Detection of variations in aspen forest habitat from LANDSAT digital data: Bear River Range, Utah
[E82-10355] p 19 N82-26753

Irrigated acreage in the Bear River Basin as of the 1975 growing season
[E82-10356] p 20 N82-26754

V

Visidyne, Inc., Woburn, Mass.

Atmospheric ozone determination by solar occultation using the UV spectrometer on the Solar Maximum Mission p 27 A82-36362

W

Washington Univ., Seattle.

The Seasat-A satellite scatterometer - The geophysical evaluation of remotely sensed wind vectors over the ocean p 51 A82-29616

Surface wind analyses for Seasat p 51 A82-29619

Washington Univ., St. Louis, Mo.

Structure of the St. Francois Mountains and surrounding lead belt, S. E. Missouri: Inferences from thermal IR and other data sets
[E82-10200] p 36 N82-23573

Structure of the St. Francois Mountains and surrounding lead belt, S. E. Missouri: Inferences from thermal IR and other data sets
[E82-10205] p 11 N82-23578

Structure of the Saint Francois Mountains and surrounding lead belt, S.E. Missouri: Inference from thermal IR and other data sets
[E82-10350] p 39 N82-26748

Western Geophysical Co. of America, Houston, Tex.

Airborne gamma-ray spectrometer and magnetometer survey. Roseau quadrangle, Minnesota, volume 1
[DE82-001031] p 43 N82-23621

Airborne gamma-ray spectrometer and magnetometer survey. Barrow quadrangle, Alaska, volume 1
[DE82-000334] p 43 N82-23623

Airborne gamma-ray spectrometer and magnetometer survey. Wainwright quadrangle, Alaska, volume 2
[DE82-000341] p 43 N82-23624

Airborne gamma-ray spectrometer and magnetometer survey, Kenora quadrangle, Minnesota, volume 1
[DE82-001029] p 43 N82-23625

Airborne gamma-ray spectrometer and magnetometer survey. Meade River quadrangle, Alaska, volume 2
[DE82-000340] p 43 N82-23626

Airborne gamma-ray spectrometer and magnetometer survey. Teshekpuk quadrangle, Alaska, volume 2
[DE82-000310] p 43 N82-23627

Airborne gamma-ray spectrometer and magnetometer survey. Harrison Bay quadrangle, Alaska, volume 2
[DE82-000315] p 43 N82-23628

Airborne gamma-ray spectrometer and magnetometer survey: Beechey Pt., quadrangle, Alaska, volume 2
[DE82-000309] p 43 N82-23629

Airborne gamma-ray spectrometer and magnetometer survey. Point Lay quadrangle, Alaska, volume 2
[DE82-000308] p 43 N82-23630

Airborne gamma-ray spectrometer and magnetometer survey. Utukok River quadrangle, Alaska, volume 2
[DE82-000316] p 44 N82-23631

Airborne gamma-ray spectrometer and magnetometer survey. Segavanirktok quadrangle, Alaska, volume 2
[DE82-000311] p 44 N82-23632

Airborne gamma-ray spectrometer and magnetometer survey: Duluth quadrangle, Minnesota, volume 2
[DE82-001027] p 44 N82-23633

Airborne gamma-ray spectrometer and magnetometer survey. Roseau quadrangle, Minnesota, volume 2
[DE82-001025] p 44 N82-23634

Airborne gamma-ray spectrometer and magnetometer survey. Devil's Lake quadrangle, North Dakota, volume 1
[DE82-004161] p 44 N82-23635

Airborne gamma-ray spectrometer and magnetometer survey. Devil's Lake quadrangle, North Dakota, volume 2
[DE82-004168] p 44 N82-23636

Airborne gamma-ray spectrometer and magnetometer survey. Bemidji quadrangle, Minnesota, volume 1
[DE82-001032] p 44 N82-23637

Airborne gamma-ray spectrometer and magnetometer survey. Bemidji quadrangle, Minnesota, volume 2
[DE82-001026] p 44 N82-23638

Airborne gamma-ray spectrometer and magnetometer survey. Hibbing quadrangle, Minnesota, volume 1
[DE82-004159] p 44 N82-23639

Airborne gamma-ray spectrometer and magnetometer survey. Hibbing quadrangle, Minnesota, volume 2
[DE82-004165] p 45 N82-23640

Airborne gamma-ray spectrometer and magnetometer survey. Aberdeen quadrangle, South Dakota, volume 1
[DE82-004152] p 45 N82-23641

Airborne gamma-ray spectrometer and magnetometer survey. Aberdeen quadrangle, South Dakota, volume 2
[DE82-004164] p 45 N82-23642

Airborne gamma-ray spectrometer and magnetometer survey. International Falls quadrangle, Minnesota, volume 1
[DE82-004151] p 45 N82-23643

Airborne gamma-ray spectrometer and magnetometer survey. International Falls quadrangle, Minnesota, volume 2
[DE82-004166] p 45 N82-23644

Airborne gamma-ray spectrometer and magnetometer survey. Barrow quadranagle, Alaska, volume 2
[DE82-000342] p 46 N82-25623

Airborne gamma-ray spectrometer and magnetometer survey. Lookout Ridge quadrangle, Alaska, volume 2
[DE82-000313] p 47 N82-25625

Airborne gamma-ray spectrometer and magnetometer survey: North/south tieline, volume 1
[DE82-005542] p 47 N82-27804

Airborne gamma-ray spectrometer and magnetometer survey: North/south tieline, volume 2
[DE82-005570] p 47 N82-27805

Airborne gamma-ray spectrometer and magnetometer survey: Sioux Falls quadrangle, South Dakota, volume 1
[DE82-005533] p 47 N82-27806

Airborne gamma-ray spectrometer and magnetometer survey: Sioux Falls quadrangle, South Dakota, volume 2
[DE82-005574] p 47 N82-27807

Airborne gamma-ray spectrometer and magnetometer survey: Ukiah quadrangle, California, volume 1
[DE82-005541] p 48 N82-27813

Airborne gamma-ray spectrometer and magnetometer survey: Huron Quadrangle, South Dakota
[DE82-005540] p 48 N82-27814

Airborne gamma-ray spectrometer and magnetometer survey: Chico Quadrangle, California
[DE82-005543] p 48 N82-27815

Wisconsin Univ., Madison.

Magsat magnetic anomalies over Antarctica and the surrounding oceans p 32 A82-30787

The impact of meteorological satellites on the First GARP Global Experiment (FGGE) p 55 N82-23852

Estimates of sea surface stress for summer MONEX from cloud motions p 56 N82-23910

Investigation of Antarctic crust and upper mantle using MAGSAT and other geophysical data
[E82-10308] p 37 N82-24582

Investigation of Antarctic crust and upper mantle using MAGSAT and other geophysical data
[E82-10309] p 37 N82-24583

Woods Hole Oceanographic Institution, Mass.

Computer-processed geophysical atlas of digital data for the East Coast margin of the United States from surface and spacecraft data
[AD-A111388] p 39 N82-25746

Wyle Labs., Inc., Hampton, Va.

Airborne lidar measurements of the Soufriere eruption of 17 April 1979 p 24 A82-33657

Z

Zentralstelle fuer Geo-Photogrammetrie und Fernerkundung, Munich (West Germany).

Multidisciplinary investigations on HCMM data over middle Europe and Marocco
[E82-10315] p 74 N82-24588

CONTRACT NUMBER INDEX

Typical Contract Number Index Listing

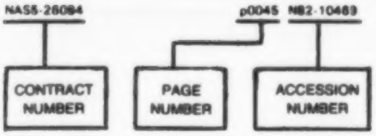

Listings in this index are arranged alphanumerically by contract number. Under each contract number, the accession numbers denoting documents that have been produced as a result of research done under that contract are arranged in ascending order with the AIAA accession numbers appearing first. The accession number denotes the number by which the citation is identified in the abstract section. Preceding the accession number is the page number on which the citation may be found.

AF PROJ. 2309 p 40 N82-27900
AF PROJ. 2310 p 76 N82-26907
AF PROJ. 4303 p 75 N82-25613
AF PROJ. 7930 p 82 N82-26642
AF-AFOSR-79-0010 p /6 A82-31019
AF-AFOSR-79-0012 p 76 A82-31020
BMFT-RV14-B8/74 p 65 A82-22586
p 40 A82-22607
p 5 A82-22612
BMFT-01-OI-017-ZA/WF/WRK-1754 p 40 A82-22607
BMFT-01-0I-017-ZA/WF/WRK-1754 p 65 A82-22586
CIT-44-727600 p 29 A82-37405
CNES-214 p 10 A82-37194
CNES-272 p 10 A82-37194
DAAK70-80-C-0016 p 75 N82-26765
DACW39-77-C-0073 p 70 A82-35650
DARG29-79-C-0199 p 70 A82-35650
DARPA ORDER 3119 p 74 N82-25611
DE-AC13-76GJ-01664 p 43 N82-23621
p 43 N82-23623
p 43 N82-23624
p 43 N82-23625
p 43 N82-23626
p 43 N82-23627
p 43 N82-23629
p 43 N82-23630
p 44 N82-23631
p 44 N82-23632
p 44 N82-23633
p 44 N82-23634
p 44 N82-23635
p 44 N82-23636
p 44 N82-23637
p 44 N82-23638
p 44 N82-23639
p 45 N82-23640
p 45 N82-23641
p 45 N82-23642
p 45 N82-23643
p 45 N82-23644
p 46 N82-25623
p 47 N82-25625
p 47 N82-27804
p 47 N82-27805
p 47 N82-27806
p 47 N82-27807
p 47 N82-27808
p 48 N82-27809
p 48 N82-27810
p 48 N82-27811
p 48 N82-27812
p 48 N82-27814
p 48 N82-27815
DE-AC13-76GJ-016664 p 43 N82-23628
DE-AC13-79CJ-01692 p 46 N82-25621
DE-AC13-79GJ-01664 p 48 N82-27813
DE-AC13-79GJ-01692 p 46 N82-25620
p 46 N82-25622
DE-14-08-0001-16439 p 38 N82-24590
DFG-SCHL-201/1 p 1 A82-22552
DFG-4810/79 p 33 A82-32077
DI-14-08-0001-16439 p 38 N82-24589
DI-14-08-0001-21249 p 38 N82-24591
DOT-FA78WAI-850 p 28 A82-36431
EPA-IAG-D8-E721 p 31 N82-27802
p 31 N82-27803
EPA-5-536-4 p 27 A82-36406
ESA-4422/80 p 78 A82-32824
ESA-4634/81 p 59 N82-27816
F04701-79-C-0080 p 29 A82-37405
F04701-80-C-0081 p 26 A82-35542
F19628-79-C-0027 p 40 N82-27900
F19628-79-C-0062 p 76 N82-26907
F19628-80-C-0021 p 60 A82-33329
F19628-81-K-0032 p 76 A82-31020
F30602-80-C-0040 p 75 N82-25613
F33615-77-C-0604 p 82 N82-26642
F33615-80-C-1080 p 74 N82-25611
JPL-954703 p 50 A82-29610
JPL-954958 p 57 N82-26525
JPL-955832 p 77 A82-32443
NAGW-95 p 30 N82-24567
p 18 N82-25607
p 19 N82-26752
p 19 N82-26753
p 20 N82-26754
NAG5-10 p 77 A82-32658
NAG5-12 p 19 N82-26745
NAG5-152 p 34 A82-32646
NAG5-37 p 20 N82-26755
NASA ORDER A-65111-B p 75 N82-26763
NASA ORDER S-40198B p 14 N82-23598
NASA ORDER S-40255-B p 16 N82-24523
NASA ORDER S-40256-B p 36 N82-23587
NASA ORDER S-65000-B p 33 A82-32078
NASW-3308 p 65 N82-23568
NASW-3338 p 29 A82-37405
NASW-3389 p 42 A82-36298
NAS1-15301 p 23 A82-31990
NAS1-16032 p 52 A82-29621
NAS5-11063 p 22 A82-22605
NAS5-20062 p 65 A82-22586
p 40 A82-22607
p 5 A82-22612
p 40 A82-22613
NAS5-20674 p 65 A82-22585
p 3 A82-22591
NAS5-20721 p 22 A82-22606
NAS5-20966 p 60 A82-32896
NAS5-22929 p 77 A82-32658
NAS5-23315 p 29 A82-37405
NAS5-24200 p 77 A82-32447
NAS5-24206 p 18 N82-24602
NAS5-24316 p 62 N82-22625
NAS5-25030 p 32 A82-30789
p 33 A82-30795
p 36 N82-24520
NAS5-25451 p 68 A82-32581
NAS5-25488 p 68 A82-32581
NAS5-25720 p 70 A82-35824
NAS5-25731 p 1 A82-22541
NAS5-25735 p 22 A82-22605
NAS5-25737 p 82 N82-26744
NAS5-25807 p 19 N82-26749
NAS5-25882 p 37 N82-24587
NAS5-25957 p 35 N82-23571
p 37 N82-24584
p 39 N82-25604
NAS5-25977 p 32 A82-30787
p 37 N82-24582
p 37 N82-24583
NAS5-26047 p 71 N82-23567
NAS5-26157 p 32 A82-30790
p 71 N82-22627
p 74 N82-24581
NAS5-26205 p 81 N82-25602
NAS5-26309 p 71 N82-22629
p 73 N82-23599
p 73 N82-23605
p 74 N82-24580
NAS5-26326 p 42 N82-23569
p 38 N82-24592
p 38 N82-24593
NAS5-26328 p 71 N82-23572
p 36 N82-24573
NAS5-26414 p 45 N82-24579
NAS5-26424 p 32 A82-30788
p 71 N82-23570
p 36 N82-23577
p 36 N82-24577
p 37 N82-24578
NAS5-26425 p 46 N82-24594
p 46 N82-24596
NAS5-26453 p 17 N82-24575
NAS5-26456 p 82 N82-26743
NAS5-26533 p 36 N82-23573
p 11 N82-23578
p 39 N82-26748
NAS5-26728 p 47 N82-26750
NAS7-100 p 49 A82-29601
p 50 A82-29613
p 52 A82-29621
p 52 A82-29622
p 52 A82-29624
p 33 A82-31994
p 23 A82-32441
p 41 A82-32442
p 77 A82-32448
p 53 A82-32882
p 68 A82-32904
p 69 A82-34720
p 25 A82-34743
p 57 N82-25609
NAS8-33235 p 29 A82-37405
NAS8-33726 p 23 A82-32348
NAS9-15325 p 18 N82-25606
NAS9-15466 p 10 N82-22623
p 11 N82-23566
p 12 N82-23585
p 72 N82-23586
p 12 N82-23588
p 14 N82-23600
p 14 N82-23602
p 15 N82-23606
p 15 N82-23610
p 18 N82-26742
p 85 N82-26746
NAS9-15476 p 10 N82-22626
p 16 N82-24519
NAS9-15509 p 68 A82-32904
NAS9-15800 p 84 N82-22620
p 11 N82-23565
p 11 N82-23579
p 12 N82-23581
p 12 N82-23582
p 13 N82-23590
p 13 N82-23594
p 13 N82-23595
p 73 N82-23596
p 14 N82-23597
p 14 N82-23603
p 15 N82-23607
p 15 N82-23608
NAS9-16514 p 8 A82-34179
NAS9-16538 p 19 N82-26751
NCC5-5 p 19 N82-26747
NERC-GR3/3941 p 23 A82-32342
NGL-14-001-006 p 1 A82-22541
NGL-21-002-005 p 26 A82-35542
NGL-24-005-263 p 7 A82-29539
NGL-25-001-054 p 30 N82-24566
NGL-33-010-171 p 8 A82-32708
NGR-05-002-160 p 22 A82-22606
NGR-21-002-224 p 40 A82-22607
NGR-21-002-316 p 22 A82-22605
p 40 A82-22607
NGR-30-002-052 p 63 A82-22538

p 64 A82-22555
NOAA-MO-A01-78-00-4318 .... p 52 A82-29623
NOAA-MO-A01-78-00-4325 .... p 50 A82-29610
NOAA-NA-79SAC00723 .... p 50 A82-29612
NOAA-NA-80AAD0019 .... p 60 A82-34735
NSF ATM-77-24843 .... p 26 A82-36268
NSF ATM-78-20936-01 .... p 3 A82-22589
NSF ATM-79-13097 .... p 56 N82-23910
NSF ATM-79-23240 .... p 76 A82-31019
NSF ATM-79-25987 .... p 76 A82-31019
NSF ATM-81-16045 .... p 26 A82-35542
NSF ENG-78-24432 .... p 77 A82-32443
NSF OCE-77-27735 .... p 59 N82-26949
NSF OCE-78-22481 .... p 53 A82-32651
NSF OCE-79-24606 .... p 53 A82-32651
NSF SPI-80-03978 .... p 19 N82-26753
NSF 78-07369 .... p 54 A82-36341
NSF 81-06099 .... p 54 A82-36341
NSG-2377 .... p 68 A82-32904
NSG-5134 .... p 20 N82-26759
p 20 N82-26760
p 20 N82-26761
NSG-5265 .... p 33 A82-32077
NSG-5266 .... p 18 N82-25605
NSG-7202 .... p 49 A82-22306
NTNF PROJECT 18108075 .... p 41 A82-30304
N00014-75-C-0300 .... p 59 N82-26948
N00014-75-C-0356 .... p 52 A82-29623
N00014-80-C-0440 .... p 56 N82-26766
N00014-80-C-0673 .... p 53 A82-32559
N00014-82-C-0019 .... p 39 N82-25748
PROJ. AGRISTARS .... p 84 N82-22620
p 10 N82-22623
p 11 N82-23564
p 11 N82-23565
p 11 N82-23566
p 11 N82-23579
p 12 N82-23580
p 12 N82-23581
p 12 N82-23582
p 12 N82-23585
p 72 N82-23586
p 12 N82-23588
p 13 N82-23589
p 13 N82-23590
p 13 N82-23591
p 13 N82-23592
p 13 N82-23593
p 13 N82-23594
p 13 N82-23595
p 73 N82-23596
p 14 N82-23597
p 14 N82-23598
p 14 N82-23600
p 14 N82-23601
p 14 N82-23602
p 14 N82-23603
p 15 N82-23604
p 15 N82-23606
p 15 N82-23607
p 15 N82-23608
p 15 N82-23609
p 15 N82-23610
p 16 N82-23611
p 16 N82-24519
p 16 N82-24563
p 16 N82-24564
p 17 N82-24565
p 18 N82-26742
p 19 N82-26751
USDA-23-178 .... p 8 A82-32707
USDA-53-3187-8-25 .... p 7 A82-32704
W-7405-ENG-48 .... p 29 N82-23793
p 39 N82-26915
p 30 N82-27737
146-20-10-29 .... p 30 N82-25661
146-40-01-04 .... p 57 N82-25609
146-40-05-05 .... p 81 N82-22865
146-40-15-07 .... p 55 N82-23614
506-62-43-01 .... p 81 N82-25610

REPORT/ACCESSION NUMBER INDEX

Typical Report/Accession Number Index Listing

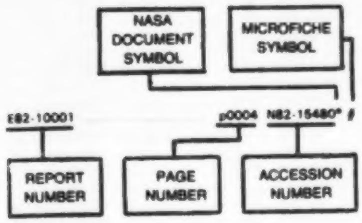

Listings in this index are arranged alphanumerically by report number. The page number indicates the page on which the citation is located. The accession number denotes the number by which the citation is identified. An asterisk (*) indicates that the item is a NASA report. A pound sign (#) indicates that the item is available on microfiche.

AAS PAPER 82-127 p 80 A82-37609 #
AAS PAPER 82-130 p 71 A82-37810* #
AAS PAPER 82-132 p 81 A82-37812* #

AD-A110538 p 75 N82-26765 #
AD-A110688 p 82 N82-26642 #
AD-A110746 p 74 N82-25611 #
AD-A110765 p 39 N82-26268 #
AD-A110806 p 58 N82-26764 #
AD-A110838 p 59 N82-26948 #
AD-A111005 p 58 N82-26945 #
AD-A111080 p 58 N82-26766 #
AD-A111223 p 75 N82-25613 #
AD-A111307 p 75 N82-25614 #
AD-A111388 p 39 N82-25748 #
AD-A111401 p 74 N82-25612 #
AD-A112337 p 76 N82-26907 #
AD-A113098 p 40 N82-27900 #

AFGL-TR-82-0019 p 40 N82-27900 #
AFGL-TR-82-0055 p 76 N82-26907 #

AIAA 81-2333 p 59 A82-13528 #

AP-J0-04111 p 15 N82-23609* #

AR-002-695 p 57 N82-24597* #

B-205344 p 29 N82-23043 #

CONF-810711-1 p 2 A82-22565 #
CONF-810711-2 p 64 A82-22573 #

CRREL-81-22 p 58 N82-26764 #

CRSC-82-1 p 19 N82-26752* #
CRSC-82-2 p 19 N82-26753* #
CRSC-82-3 p 20 N82-26754* #

CUEA-74 p 59 N82-26949 #

DC-YI-04211 p 16 N82-24564* #

DC-Y1-04156 p 16 N82-24563* #

DE81-027156 p 46 N82-25622 #
DE81-027158 p 46 N82-25620 #
DE81-027161 p 46 N82-25621 #
DE82-000308 p 43 N82-23630 #
DE82-000309 p 43 N82-23629 #
DE82-000310 p 43 N82-23627 #
DE82-000311 p 44 N82-23632 #
DE82-000313 p 47 N82-25625 #
DE82-000315 p 43 N82-23628 #
DE82-000316 p 44 N82-23631 #
DE82-000334 p 43 N82-23623 #
DE82-000340 p 43 N82-23626 #
DE82-000341 p 43 N82-23624 #
DE82-000342 p 46 N82-25623 #
DE82-000965 p 30 N82-27737 #
DE82-001025 p 44 N82-23634 #
DE82-001026 p 44 N82-23638 #
DE82-001027 p 44 N82-23633 #
DE82-001029 p 43 N82-23625 #
DE82-001031 p 43 N82-23621 #
DE82-001032 p 44 N82-23637 #
DE82-001686 p 39 N82-26915 #
DE82-004151 p 45 N82-23643 #
DE82-004152 p 45 N82-23641 #
DE82-004159 p 44 N82-23639 #
DE82-004161 p 44 N82-23635 #
DE82-004164 p 45 N82-23642 #
DE82-004165 p 45 N82-23640 #
DE82-004166 p 45 N82-23644 #
DE82-004168 p 44 N82-23636 #
DE82-005527 p 48 N82-27810 #
DE82-005533 p 47 N82-27806 #
DE82-005538 p 48 N82-27811 #
DE82-005540 p 48 N82-27814 #
DE82-005541 p 48 N82-27813 #
DE82-005542 p 47 N82-27804 #
DE82-005543 p 48 N82-27815 #
DE82-005554 p 47 N82-27808 #
DE82-005560 p 48 N82-27809 #
DE82-005568 p 48 N82-27812 #
DE82-005570 p 47 N82-27805 #
DE82-005574 p 47 N82-27807 #
DE82-900580 p 31 N82-27802 #
DE82-900581 p 31 N82-27803 #

DGS-322 p 40 N82-27900 #

E/S-1234 p 75 N82-26765 #

EMD-82-10 p 29 N82-23043 #

EPA-600/7-81-114 p 31 N82-27803 #
EPA-660/7-81-113 p 31 N82-27802 #

ERIM-147200-13-F p 85 N82-23568* #
ERIM-152400-4-P p 10 N82-22626* #
ERIM-152400-6-P p 16 N82-24519* #
ERIM-160300-7-T p 19 N82-26751* #

ERT-P-2061-F p 62 N82-22625* #

ESA-CR(P)-1547 p 59 N82-27816 #

ETL-R034 p 75 N82-25614 #

ETL-0268 p 75 N82-26765 #

EW-R1-04147 p 14 N82-23601* #

EW-UI-04119 p 11 N82-23564* #

EW-U1-04103 p 14 N82-23598* #
EW-U1-04144 p 13 N82-23593* #
EW-U1-04208 p 13 N82-23591* #
EW-U1-04212 p 12 N82-23580* #

E82-10003 p 18 N82-26742* #
E82-10096 p 35 N82-23563* #
E82-10112 p 11 N82-23564* #
E82-10126 p 11 N82-23565* #
E82-10128 p 11 N82-23566* #
E82-10151 p 71 N82-23567* #
E82-10153 p 45 N82-24518* #
E82-10181 p 85 N82-23568* #
E82-10186 p 84 N82-22620* #
E82-10187 p 35 N82-22621* #
E82-10188 p 71 N82-22622* #
E82-10189 p 10 N82-22623* #
E82-10190 p 42 N82-22624* #
E82-10191 p 62 N82-22625* #
E82-10192 p 10 N82-22626* #
E82-10193 p 71 N82-22627* #
E82-10194 p 35 N82-22628* #
E82-10195 p 71 N82-22629* #
E82-10196 p 42 N82-23569* #
E82-10197 p 71 N82-23570* #
E82-10198 p 35 N82-23571* #
E82-10199 p 71 N82-23572* #
E82-10200 p 36 N82-23573* #
E82-10201 p 72 N82-23574* #
E82-10202 p 72 N82-23575* #
E82-10203 p 72 N82-23576* #
E82-10204 p 36 N82-23577* #
E82-10205 p 11 N82-23578* #
E82-10206 p 11 N82-23579* #
E82-10207 p 12 N82-23580* #
E82-10208 p 12 N82-23581* #
E82-10209 p 12 N82-23582* #
E82-10210 p 72 N82-23583* #
E82-10211 p 72 N82-23584* #
E82-10212 p 12 N82-23585* #
E82-10213 p 72 N82-23586* #
E82-10214 p 36 N82-23587* #
E82-10215 p 12 N82-23588* #
E82-10216 p 13 N82-23589* #
E82-10217 p 13 N82-23590* #
E82-10218 p 13 N82-23591* #
E82-10219 p 13 N82-23592* #
E82-10220 p 13 N82-23593* #
E82-10221 p 13 N82-23594* #
E82-10222 p 13 N82-23595* #
E82-10223 p 73 N82-23596* #
E82-10224 p 14 N82-23597* #
E82-10225 p 14 N82-23598* #
E82-10226 p 73 N82-23599* #
E82-10227 p 14 N82-23600* #
E82-10228 p 14 N82-23601* #
E82-10229 p 14 N82-23602* #
E82-10230 p 14 N82-23603* #
E82-10231 p 15 N82-23604* #
E82-10232 p 73 N82-23605* #
E82-10233 p 15 N82-23606* #
E82-10234 p 15 N82-23607* #
E82-10235 p 15 N82-23608* #
E82-10236 p 15 N82-23609* #
E82-10237 p 15 N82-23610* #
E82-10238 p 16 N82-23611* #
E82-10239 p 73 N82-23612* #
E82-10240 p 73 N82-23613* #
E82-10241 p 16 N82-24519* #
E82-10242 p 36 N82-24520* #
E82-10243 p 45 N82-24521* #
E82-10244 p 36 N82-24522* #
E82-10245 p 16 N82-24523* #
E82-10285 p 16 N82-24563* #
E82-10286 p 16 N82-24564* #
E82-10287 p 17 N82-24565* #
E82-10288 p 30 N82-24566* #
E82-10289 p 30 N82-24567* #
E82-10290 p 85 N82-24568* #
E82-10291 p 63 N82-24569* #
E82-10293 p 73 N82-24570* #
E82-10296 p 73 N82-24572* #
E82-10297 p 36 N82-24573* #
E82-10298 p 17 N82-24574* #
E82-10299 p 17 N82-24575* #
E82-10300 p 17 N82-24576* #
E82-10303 p 36 N82-24577* #
E82-10304 p 37 N82-24578* #
E82-10305 p 45 N82-24579* #
E82-10306 p 74 N82-24580* #
E82-10307 p 74 N82-24581* #
E82-10308 p 37 N82-24582* #
E82-10309 p 37 N82-24583* #
E82-10310 p 37 N82-24584* #
E82-10311 p 17 N82-24585* #
E82-10312 p 37 N82-24586* #
E82-10313 p 82 N82-26743* #
E82-10314 p 37 N82-24587* #
E82-10315 p 74 N82-24588* #
E82-10316 p 38 N82-24589* #
E82-10317 p 38 N82-24590* #
E82-10318 p 38 N82-24591* #
E82-10319 p 38 N82-24592* #
E82-10320 p 38 N82-24593* #
E82-10321 p 46 N82-24594* #

E82-10322 p 74 N82-24595* #
E82-10323 p 46 N82-24596* #
E82-10324 p 57 N82-24597* #
E82-10325 p 30 N82-24598* #
E82-10326 p 38 N82-24599* #
E82-10327 p 74 N82-24600* #
E82-10328 p 63 N82-24601* #
E82-10329 p 18 N82-24602* #
E82-10330 p 38 N82-24603* #
E82-10339 p 39 N82-25601* #
E82-10340 p 81 N82-25602* #
E82-10341 p 46 N82-25603* #
E82-10342 p 39 N82-25604* #
E82-10343 p 18 N82-25605* #
E82-10344 p 18 N82-25606* #
E82-10345 p 18 N82-25607* #
E82-10346 p 82 N82-26744* #
E82-10347 p 19 N82-26745* #
E82-10348 p 85 N82-26746* #
E82-10349 p 19 N82-26747* #
E82-10350 p 39 N82-26748* #
E82-10351 p 19 N82-26749* #
E82-10352 p 47 N82-26750* #
E82-10353 p 19 N82-26751* #
E82-10354 p 19 N82-26752* #
E82-10355 p 19 N82-26753* #
E82-10356 p 20 N82-26754* #
E82-10357 p 20 N82-26755* #
E82-10358 p 75 N82-26756* #
E82-10359 p 30 N82-26757* #
E82-10360 p 58 N82-26758* #
E82-10361 p 20 N82-26759* #
E82-10362 p 20 N82-26760* #
E82-10363 p 20 N82-26761* #

FC-J1-04175-VOL-2 p 13 N82-23589* #
FC-J1-04181 p 15 N82-23604* #

FC-LO-00472 p 14 N82-23603* #

FC-L1-04096 p 11 N82-23579* #
FC-L1-04127 p 11 N82-23565* #
FC-L1-04142 p 12 N82-23582* #
FC-L1-04145 p 13 N82-23595* #
FC-L1-04172 p 13 N82-23594* #
FC-L1-04192 p 13 N82-23590* #

FC-P1-04197 p 12 N82-23588* #

FOA-C-30257-E1 p 81 N82-24489 #

FSGTR/INT-116 p 30 N82-23963 #

FSU-MET-STU-81/5 p 59 N82-26949 #

GJBX-211-81-VOL-2A p 46 N82-25620 #
GJBX-211-81-VOL-2C p 46 N82-25621 #
GJBX-211-81-VOL-2D p 46 N82-25622 #
GJBX-295-81-VOL-1 p 43 N82-23623 #
GJBX-295-81-VOL-2 p 46 N82-25623 #
GJBX-296-81-VOL-2 p 43 N82-23624 #
GJBX-297-81-VOL-2 p 43 N82-23626 #
GJBX-298-81-VOL-2 p 43 N82-23627 #
GJBX-299-81-VOL-2 p 43 N82-23628 #
GJBX-300-81-VOL-2 p 43 N82-23629 #
GJBX-301-81-VOL-2 p 43 N82-23630 #
GJBX-302-81-VOL-2 p 44 N82-23631 #
GJBX-303-81-VOL-2 p 47 N82-25625 #
GJBX-306-81-VOL-2 p 44 N82-23632 #
GJBX-328-81-VOL-1 p 43 N82-23625 #
GJBX-329-81-VOL-1 p 43 N82-23621 #
GJBX-329-81-VOL-2 p 44 N82-23634 #
GJBX-330-81-VOL-2 p 44 N82-23633 #
GJBX-331-81-VOL-1 p 44 N82-23637 #
GJBX-331-81-VOL-2 p 44 N82-23638 #
GJBX-354-81-VOL-1 p 44 N82-23635 #
GJBX-354-81-VOL-2 p 44 N82-23636 #
GJBX-355-81-VOL-1 p 44 N82-23639 #
GJBX-355-81-VOL-2 p 45 N82-23640 #
GJBX-356-81-VOL-1 p 45 N82-23643 #
GJBX-356-81-VOL-2 p 45 N82-23644 #
GJBX-357-81-VOL-1 p 45 N82-23641 #
GJBX-357-81-VOL-2 p 45 N82-23642 #
GJBX-365-81 p 47 N82-27808 #
GJBX-365-81-VOL-2 p 48 N82-27809 #
GJBX-386-81-VOL-1 p 47 N82-27804 #
GJBX-386-81-VOL-2 p 47 N82-27805 #
GJBX-388-81-VOL-2 p 48 N82-27812 #
GJBX-389-81-VOL-1 p 47 N82-27806 #
GJBX-389-81-VOL-2 p 47 N82-27807 #
GJBX-390-81-VOL-1 p 48 N82-27813 #
GJBX-405-81-VOL-1 p 48 N82-27814 #
GJBX-407-81-VOL-1 p 48 N82-27815 #
GJBX-410-81-VOL-1 p 48 N82-27811 #
GJBX-412-81-VOL-2C p 48 N82-27810 #

GPO-87-070 p 84 N82-22630 #

GSC-TR8203 p 81 N82-25602* #

INPE-2249-TDL/066 p 63 N82-24569* #
INPE-2284-PRE/060 p 58 N82-26758* #
INPE-2297-RPE/401 p 30 N82-26757* #
INPE-2367-RA/161-PT-2 p 30 N82-24598* #

ISBN-0-11-884138-6 p 42 N82-22636 #

IT-E2-04235 p 19 N82-26751* #

JPL-9950-652 p 57 N82-26525* #

JSC-16752 p 14 N82-23603* #
JSC-16858 p 12 N82-23581* #
JSC-17122 p 15 N82-23607* #
JSC-17138 p 11 N82-23579* #
JSC-17143 p 14 N82-23598* #
JSC-17398 p 15 N82-23609* #
JSC-173991 p 11 N82-23564* #
JSC-17406 p 11 N82-23565* #
JSC-17414 p 15 N82-23608* #
JSC-17417 p 12 N82-23582* #
JSC-17420 p 13 N82-23593* #
JSC-17421 p 13 N82-23595* #
JSC-17431 p 73 N82-23596* #
JSC-17432 p 13 N82-23594* #
JSC-17433-VOL-2 p 13 N82-23589* #
JSC-17434 p 14 N82-23597* #
JSC-17438 p 15 N82-23604* #
JSC-17440 p 13 N82-23590* #
JSC-17792 p 13 N82-23592* #
JSC-17797 p 13 N82-23591* #
JSC-17801 p 12 N82-23580* #

LA-UR-81-965 p 2 A82-22565 #
LA-UR-81-966 p 64 A82-22573 #

LARS-TR-060881 p 14 N82-23600* #
LARS-TR-062481 p 85 N82-26746* #
LARS-TR-030981 p 14 N82-23602* #

LARS-030182 p 18 N82-26742* #
LARS-060580 p 15 N82-23606* #
LARS-07138 p 10 N82-22623* #
LARS-071380 p 12 N82-23585* #
LARS-073081 p 18 N82-25606* #
LARS-090881 p 11 N82-23566* #
LARS-101281 p 12 N82-23588* #
LARS-101481 p 72 N82-23586* #

LBL-12604 p 29 N82-23793 #

LEMSCO-13491 p 84 N82-22620* #
LEMSCO-14598 p 14 N82-23603* #
LEMSCO-15173 p 15 N82-23607* #
LEMSCO-15682 p 13 N82-23595* #
LEMSCO-16018 p 12 N82-23581* #
LEMSCO-16573 p 11 N82-23579* #
LEMSCO-16854 p 15 N82-23608* #
LEMSCO-16921 p 11 N82-23565* #
LEMSCO-16929 p 12 N82-23582* #
LEMSCO-16935 p 13 N82-23590* #
LEMSCO-16944 p 13 N82-23594* #
LEMSCO-17269 p 73 N82-23596* #
LEMSCO-17276 p 14 N82-23597* #

LRS-021681 p 15 N82-23610* #

M-38 p 73 N82-24572* #

NAS 1.15:83280 p 81 N82-22865* #
NAS 1.15:83290 p 55 N82-23614* #
NAS 1.15:83842 p 16 N82-23611* #
NAS 1.15:83871 p 46 N82-25603* #
NAS 1.15:84186 p 81 N82-22643* #
NAS 1.15:84191 p 84 N82-23258* #
NAS 1.15:84201 p 11 N82-23564* #
NAS 1.15:84202 p 15 N82-23609* #
NAS 1.15:84203 p 13 N82-23592* #
NAS 1.15:84204 p 13 N82-23593* #
NAS 1.15:84205 p 15 N82-23604* #
NAS 1.15:84206 p 13 N82-23589* #
NAS 1.15:84471 p 30 N82-25661* #
NAS 1.15:84478 p 81 N82-25610* #
NAS 1.15:84694 p 16 N82-24563* #
NAS 1.15:84695 p 16 N82-24564* #
NAS 1.15:84696 p 17 N82-24565* #
NAS 1.15:84731 p 18 N82-25608* #
NAS 1.15:84740 p 13 N82-23591* #
NAS 1.26:16740 p 11 N82-23565* #
NAS 1.26:160888 p 14 N82-23603* #
NAS 1.26:161047 p 10 N82-22626* #
NAS 1.26:166352 p 75 N82-26763* #
NAS 1.26:166788 p 82 N82-26744* #
NAS 1.26:166790 p 81 N82-25602* #
NAS 1.26:166801 p 19 N82-26749* #
NAS 1.26:167391 p 16 N82-24519* #
NAS 1.26:167397 p 14 N82-23600* #
NAS 1.26:167402 p 15 N82-23610* #
NAS 1.26:167403 p 11 N82-23566* #
NAS 1.26:167406 p 13 N82-23595* #
NAS 1.26:167408 p 14 N82-23601* #
NAS 1.26:167411 p 15 N82-23608* #
NAS 1.26:167415 p 15 N82-23606* #
NAS 1.26:167416 p 15 N82-23607* #
NAS 1.26:167419 p 14 N82-23602* #
NAS 1.26:167440 p 14 N82-23598* #
NAS 1.26:167441 p 14 N82-23597* #
NAS 1.26:167442 p 73 N82-23596* #
NAS 1.26:167446 p 13 N82-23594* #
NAS 1.26:167457 p 84 N82-22620* #
NAS 1.26:167479 p 13 N82-23590* #
NAS 1.26:167485 p 11 N82-23579* #
NAS 1.26:167486 p 12 N82-23580* #
NAS 1.26:167487 p 12 N82-23581* #
NAS 1.26:167488 p 12 N82-23582* #
NAS 1.26:167507 p 12 N82-23585* #
NAS 1.26:167508 p 72 N82-23586* #
NAS 1.26:167511 p 12 N82-23588* #
NAS 1.26:167544 p 18 N82-25606* #
NAS 1.26:167570 p 85 N82-26746* #
NAS 1.26:167604 p 19 N82-26751* #
NAS 1.26:168536 p 71 N82-23567* #
NAS 1.26:168538 p 45 N82-24518* #
NAS 1.26:168615 p 35 N82-22621* #
NAS 1.26:168616 p 71 N82-22622* #
NAS 1.26:168617 p 10 N82-22623* #
NAS 1.26:168618 p 42 N82-22624* #
NAS 1.26:168619 p 62 N82-22625* #
NAS 1.26:168620 p 71 N82-22627* #
NAS 1.26:168621 p 35 N82-22628* #
NAS 1.26:168622 p 71 N82-22629* #
NAS 1.26:168623 p 42 N82-23569* #
NAS 1.26:168624 p 71 N82-23570* #
NAS 1.26:168625 p 35 N82-23571* #
NAS 1.26:168627 p 36 N82-23573* #
NAS 1.26:168628 p 72 N82-23574* #
NAS 1.26:168629 p 72 N82-23575* #
NAS 1.26:168630 p 72 N82-23576* #
NAS 1.26:168631 p 36 N82-23577* #
NAS 1.26:168632 p 11 N82-23578* #
NAS 1.26:168755 p 73 N82-23612* #
NAS 1.26:168756 p 73 N82-23613* #
NAS 1.26:168772 p 72 N82-23584* #
NAS 1.26:168774 p 36 N82-23587* #
NAS 1.26:168784 p 35 N82-22846* #
NAS 1.26:168800 p 73 N82-23599* #
NAS 1.26:168801 p 73 N82-23605* #
NAS 1.26:168823 p 36 N82-24520* #
NAS 1.26:168824 p 45 N82-24521* #
NAS 1.26:168825 p 36 N82-24522* #
NAS 1.26:168826 p 16 N82-24523* #
NAS 1.26:168845 p 35 N82-23563* #
NAS 1.26:168846 p 85 N82-23568* #
NAS 1.26:168856 p 19 N82-26745* #
NAS 1.26:168857 p 30 N82-24566* #
NAS 1.26:168859 p 85 N82-24568* #
NAS 1.26:168860 p 63 N82-24569* #
NAS 1.26:168865 p 73 N82-24572* #
NAS 1.26:168866 p 36 N82-24573* #
NAS 1.26:168867 p 17 N82-24574* #
NAS 1.26:168868 p 17 N82-24575* #
NAS 1.26:168869 p 17 N82-24576* #
NAS 1.26:168878 p 36 N82-24577* #
NAS 1.26:168879 p 37 N82-24578* #
NAS 1.26:168880 p 45 N82-24579* #
NAS 1.26:168881 p 74 N82-24580* #
NAS 1.26:168882 p 74 N82-24581* #
NAS 1.26:168883 p 37 N82-24582* #
NAS 1.26:168884 p 37 N82-24583* #
NAS 1.26:168885 p 37 N82-24584* #
NAS 1.26:168886 p 17 N82-24585* #
NAS 1.26:168888 p 37 N82-24586* #
NAS 1.26:168889 p 37 N82-24587* #
NAS 1.26:168895 p 38 N82-24590* #
NAS 1.26:168896 p 38 N82-24591* #
NAS 1.26:168897 p 38 N82-24589* #
NAS 1.26:165898 p 38 N82-24592* #
NAS 1.26:168899 p 38 N82-24593* #
NAS 1.26:168900 p 46 N82-24594* #
NAS 1.26:168901 p 74 N82-24595* #
NAS 1.26:168902 p 46 N82-24596* #
NAS 1.26:168903 p 57 N82-24597* #
NAS 1.26:168904 p 30 N82-24598* #
NAS 1.26:168905 p 38 N82-24599* #
NAS 1.26:168906 p 74 N82-24600* #
NAS 1.26:168907 p 63 N82-24601* #
NAS 1.26:168909 p 38 N82-24603* #
NAS 1.26:168910 p 74 N82-24588* #

NAS 1.26:168916 ..... p 73 N82-24570* #
NAS 1.26:168944 ..... p 18 N82-24602* #
NAS 1.26:168958 ..... p 39 N82-25601* #
NAS 1.26:168959 ..... p 39 N82-25604* #
NAS 1.26:168960 ..... p 18 N82-25605* #
NAS 1.26:168967 ..... p 19 N82-26747* #
NAS 1.26:168969 ..... p 39 N82-26748* #
NAS 1.26:168975 ..... p 19 N82-26752* #
NAS 1.26:168976 ..... p 19 N82-26753* #
NAS 1.26:168977 ..... p 20 N82-26754* #
NAS 1.26:168978 ..... p 20 N82-26755* #
NAS 1.26:168979 ..... p 75 N82-26756* #
NAS 1.26:168980 ..... p 30 N82-26757* #
NAS 1.26:168981 ..... p 58 N82-26758* #
NAS 1.26:168984 ..... p 57 N82-25609* #
NAS 1.26:168996 ..... p 47 N82-26750* #
NAS 1.26:168998 ..... p 82 N82-26743* #
NAS 1.26:169010 ..... p 20 N82-26759* #
NAS 1.26:169011 ..... p 20 N82-26760* #
NAS 1.26:169032 ..... p 18 N82-26742* #
NAS 1.26:169083 ..... p 57 N82-26525* #

NASA-CR-160888 ..... p 14 N82-23603* #
NASA-CR-161047 ..... p 10 N82-22626* #
NASA-CR-166352 ..... p 75 N82-26763* #
NASA-CR-166786 ..... p 82 N82-26744* #
NASA-CR-166790 ..... p 81 N82-25602* #
NASA-CR-166801 ..... p 19 N82-26749* #
NASA-CR-167391 ..... p 16 N82-24519* #
NASA-CR-167397 ..... p 14 N82-23600* #
NASA-CR-167402 ..... p 15 N82-23610* #
NASA-CR-167403 ..... p 11 N82-23566* #
NASA-CR-167404 ..... p 11 N82-23565* #
NASA-CR-167406 ..... p 13 N82-23595* #
NASA-CR-167408 ..... p 14 N82-23601* #
NASA-CR-167411 ..... p 15 N82-23608* #
NASA-CR-167415 ..... p 15 N82-23606* #
NASA-CR-167416 ..... p 15 N82-23607* #
NASA-CR-167419 ..... p 14 N82-23602* #
NASA-CR-167440 ..... p 14 N82-23598* #
NASA-CR-167441 ..... p 14 N82-23597* #
NASA-CR-167442 ..... p 73 N82-23596* #
NASA-CR-167446 ..... p 13 N82-23594* #
NASA-CR-167457 ..... p 84 N82-22620* #
NASA-CR-167479 ..... p 13 N82-23590* #
NASA-CR-167485 ..... p 11 N82-23579* #
NASA-CR-167486 ..... p 12 N82-23580* #
NASA-CR-167487 ..... p 12 N82-23581* #
NASA-CR-167488 ..... p 12 N82-23582* #
NASA-CR-167507 ..... p 12 N82-23585* #
NASA-CR-167508 ..... p 72 N82-23586* #
NASA-CR-167511 ..... p 12 N82-23588* #
NASA-CR-167544 ..... p 18 N82-25606* #
NASA-CR-167570 ..... p 85 N82-26746* #
NASA-CR-167604 ..... p 19 N82-26751* #
NASA-CR-167643 ..... p 18 N82-26742* #
NASA-CR-168536 ..... p 71 N82-23567* #
NASA-CR-168538 ..... p 45 N82-24518* #
NASA-CR-168615 ..... p 35 N82-22621* #
NASA-CR-168616 ..... p 71 N82-22622* #
NASA-CR-168617 ..... p 10 N82-22623* #
NASA-CR-168618 ..... p 42 N82-22624* #
NASA-CR-168619 ..... p 62 N82-22625* #
NASA-CR-168620 ..... p 71 N82-22627* #
NASA-CR-168621 ..... p 35 N82-22628* #
NASA-CR-168622 ..... p 71 N82-22629* #
NASA-CR-168623 ..... p 42 N82-23569* #
NASA-CR-168624 ..... p 71 N82-23570* #
NASA-CR-168625 ..... p 35 N82-23571* #
NASA-CR-168626 ..... p 71 N82-23572* #
NASA-CR-168627 ..... p 36 N82-23573* #
NASA-CR-168628 ..... p 72 N82-23574* #
NASA-CR-168629 ..... p 72 N82-23575* #
NASA-CR-168630 ..... p 72 N82-23576* #
NASA-CR-168631 ..... p 36 N82-23577* #
NASA-CR-168632 ..... p 11 N82-23578* #
NASA-CR-168755 ..... p 73 N82-23612* #
NASA-CR-168756 ..... p 73 N82-23613* #
NASA-CR-168772 ..... p 72 N82-23584* #
NASA-CR-168773 ..... p 72 N82-23583* #
NASA-CR-168774 ..... p 36 N82-23587* #
NASA-CR-168784 ..... p 35 N82-22846* #
NASA-CR-168800 ..... p 73 N82-23599* #
NASA-CR-168801 ..... p 73 N82-23605* #
NASA-CR-168823 ..... p 36 N82-24520* #
NASA-CR-168824 ..... p 45 N82-24521* #
NASA-CR-168825 ..... p 36 N82-24522* #
NASA-CR-168826 ..... p 16 N82-24523* #
NASA-CR-168845 ..... p 35 N82-23563* #
NASA-CR-168846 ..... p 85 N82-23568* #
NASA-CR-168856 ..... p 19 N82-26745* #
NASA-CR-168857 ..... p 30 N82-24566* #
NASA-CR-168858 ..... p 30 N82-24567* #
NASA-CR-168859 ..... p 85 N82-24568* #
NASA-CR-168860 ..... p 63 N82-24569* #
NASA-CR-168865 ..... p 73 N82-24572* #
NASA-CR-168866 ..... p 36 N82-24573* #
NASA-CR-168867 ..... p 17 N82-24574* #
NASA-CR-168868 ..... p 17 N82-24575* #
NASA-CR-168869 ..... p 17 N82-24576* #
NASA-CR-168878 ..... p 36 N82-24577* #
NASA-CR-168879 ..... p 37 N82-24578* #
NASA-CR-168880 ..... p 45 N82-24579* #
NASA-CR-168881 ..... p 74 N82-24580* #
NASA-CR-168882 ..... p 74 N82-24581* #
NASA-CR-168883 ..... p 37 N82-24582* #
NASA-CR-168884 ..... p 37 N82-24583* #
NASA-CR-168885 ..... p 37 N82-24584* #
NASA-CR-168886 ..... p 17 N82-24585* #
NASA-CR-168888 ..... p 37 N82-24586* #
NASA-CR-168889 ..... p 37 N82-24587* #
NASA-CR-168895 ..... p 38 N82-24590* #
NASA-CR-168896 ..... p 38 N82-24591* #
NASA-CR-168897 ..... p 38 N82-24589* #
NASA-CR-168898 ..... p 38 N82-24592* #
NASA-CR-168899 ..... p 38 N82-24593* #
NASA-CR-168900 ..... p 46 N82-24594* #
NASA-CR-168901 ..... p 74 N82-24595* #
NASA-CR-168902 ..... p 46 N82-24596* #
NASA-CR-168903 ..... p 57 N82-24597* #
NASA-CR-168904 ..... p 30 N82-24598* #
NASA-CR-168905 ..... p 38 N82-24599* #
NASA-CR-168906 ..... p 74 N82-24600* #
NASA-CR-168907 ..... p 63 N82-24601* #
NASA-CR-168909 ..... p 38 N82-24603* #
NASA-CR-168910 ..... p 74 N82-24588* #
NASA-CR-168916 ..... p 73 N82-24570* #
NASA-CR-168944 ..... p 18 N82-24602* #
NASA-CR-168958 ..... p 39 N82-25601* #
NASA-CR-168959 ..... p 39 N82-25604* #
NASA-CR-168960 ..... p 18 N82-25605* #
NASA-CR-168961 ..... p 18 N82-25607* #
NASA-CR-168967 ..... p 19 N82-26747* #
NASA-CR-168969 ..... p 39 N82-26748* #
NASA-CR-168975 ..... p 19 N82-26752* #
NASA-CR-168976 ..... p 19 N82-26753* #
NASA-CR-168977 ..... p 20 N82-26754* #
NASA-CR-168978 ..... p 20 N82-26755* #
NASA-CR-168979 ..... p 75 N82-26756* #
NASA-CR-168980 ..... p 30 N82-26757* #
NASA-CR-168981 ..... p 58 N82-26758* #
NASA-CR-168984 ..... p 57 N82-25609* #
NASA-CR-168996 ..... p 47 N82-26750* #
NASA-CR-168998 ..... p 82 N82-26743* #
NASA-CR-169010 ..... p 20 N82-26759* #
NASA-CR-169011 ..... p 20 N82-26760* #
NASA-CR-169012 ..... p 20 N82-26761* #
NASA-CR-169083 ..... p 57 N82-26525* #

NASA-NEWS-RELEASE-82-100 ... p 82 N82-26741* #

NASA-TM-83280 ..... p 81 N82-22865* #
NASA-TM-83290 ..... p 55 N82-23614* #
NASA-TM-83842 ..... p 16 N82-23611* #
NASA-TM-83871 ..... p 46 N82-25603* #
NASA-TM-84186 ..... p 81 N82-22643* #
NASA-TM-84191 ..... p 84 N82-23258* #
NASA-TM-84201 ..... p 11 N82-23564* #
NASA-TM-84202 ..... p 15 N82-23609* #
NASA-TM-84203 ..... p 13 N82-23592* #
NASA-TM-84204 ..... p 13 N82-23593* #
NASA-TM-84205 ..... p 15 N82-23604* #
NASA-TM-84206 ..... p 13 N82-23589* #
NASA-TM-84471 ..... p 30 N82-25661* #
NASA-TM-84478 ..... p 81 N82-25610* #
NASA-TM-84694 ..... p 16 N82-24563* #
NASA-TM-84695 ..... p 16 N82-24564* #
NASA-TM-84696 ..... p 17 N82-24565* #
NASA-TM-84731 ..... p 18 N82-25608* #
NASA-TM-84740 ..... p 13 N82-23591* #

NOAA-TM-NWS-SR-104 ..... p 59 N82-27949 #

NOAA-TR-NESS-84 ..... p 81 N82-22643* #
NOAA-TR-NESS-89 ..... p 63 N82-22854 #

NOAA-TR-OTES-03 ..... p 63 N82-22644 #

NOAA-81100501 ..... p 81 N82-22643* #
NOAA-81102005 ..... p 39 N82-27882 #
NOAA-8110502 ..... p 63 N82-22644 #
NOAA-81111608 ..... p 59 N82-27949 #

NPS68-81-006 ..... p 58 N82-26945 #

NSF/IDOE-81-88 ..... p 59 N82-26949 #

NSTL/ERL-198 ..... p 16 N82-24563* #
NSTL/ERL-201 ..... p 16 N82-24564* #
NSTL/ERL-202 ..... p 17 N82-24565* #

OAO/TR-81/0033 ..... p 82 N82-26744* #

OGMR-56 ..... p 42 N82-22636 #

PB82-107335 ..... p 30 N82-23963 #
PB82-129388 ..... p 81 N82-22643* #
PB82-130089 ..... p 63 N82-22644 #
PB82-137118 ..... p 35 N82-22846* #
PB82-148644 ..... p 39 N82-27882 #
PB82-149246 ..... p 59 N82-26949 #
PB82-154006 ..... p 59 N82-27949 #

PR-1 ..... p 72 N82-23575* #
PR-1325-1 ..... p 71 N82-23570* #
PR-1325-4 ..... p 37 N82-24578* #
PR-2 ..... p 73 N82-24572* #
PR-3 ..... p 71 N82-22622* #
PR-3 ..... p 73 N82-23612* #
PR-4 ..... p 36 N82-24522* #
PR-5 ..... p 74 N82-24595* #

P82-10:03 ..... p 82 N82-26741* #

QPR-3 ..... p 63 N82-24601* #
QPR-9 ..... p 37 N82-24584* #

QR-4 ..... p 46 N82-24596* #
QR-4 ..... p 82 N82-26743* #
QR-5 ..... p 71 N82-23567* #
QR-5 ..... p 46 N82-24594* #

QSTPR-4 ..... p 73 N82-23605* #
QSTPR-5 ..... p 73 N82-23599* #
QSTPR-6 ..... p 35 N82-23571* #
QSTPR-8 ..... p 37 N82-24582* #
QSTPR-8 ..... p 39 N82-25604* #
QSTPR-9 ..... p 37 N82-24583* #

QSTRP-5 ..... p 71 N82-22629* #

R-240 ..... p 59 N82-27816 #

RADC-TR-81-303 ..... p 75 N82-25613 #

RANRL-1/82 ..... p 57 N82-24597* #

REPT-2 ..... p 75 N82-26756* #
REPT-3 ..... p 75 N82-26756* #
REPT-80-SGN-848-GEO-REPT-3 . p 42 N82-22624* #

RR-LO-00466 ..... p 15 N82-23607* #

RR-L1-00641 ..... p 14 N82-23597* #
RR-L1-17269 ..... p 73 N82-23596* #

RR-Y1-04217 ..... p 17 N82-24565* #

RSC-3458-129 ..... p 20 N82-26760* #
RSC-3458-131 ..... p 20 N82-26759* #
RSC-3753 ..... p 18 N82-25605* #

RSL-TR-429-1 ..... p 19 N82-26749* #

RSS-TR-110481 ..... p 57 N82-26525* #

S-420-81-01 ..... p 84 N82-23258* #

SAM-TR-81-11 ..... p 82 N82-26642 #

SAPR-16 ..... p 30 N82-24566* #

SCIENTIFIC-12 ..... p 40 N82-27900 #

SDSU-RSI-82-02 ..... p 20 N82-26755* #

SDSU-RS1-81-04 ..... p 18 N82-24602* #

SIO-REF-81-27 ..... p 59 N82-26948 #
SIO-REF-81-38 ..... p 58 N82-26766 #

SM-GI-04178 ..... p 16 N82-23611* #

SR-J1-04195 ..... p 13 N82-23592* #

SR-L1-00309 ..... p 15 N82-23608* #
SR-L1-04032 ..... p 12 N82-23581* #

SR-P1-04039 ..... p 15 N82-23610* #
SR-P1-04139 ..... p 14 N82-23602* #
SR-P1-04140 ..... p 11 N82-23566* #
SR-P1-04141 ..... p 14 N82-23600* #
SR-P1-04170 ..... p 15 N82-23606* #
SR-P1-04194 ..... p 72 N82-23586* #
SR-P1-04200 ..... p 10 N82-22623* #
SR-P1-04200 ..... p 12 N82-23585* #
SR-P2-04236 ..... p 18 N82-26742* #

STPR-6 ..... p 74 N82-24580* #

TR-79-281 .... p 82 N82-26642 #

TVA/ONR/ARP-81/5-VOL-1 .... p 31 N82-27802 #
TVA/ONR/ARP-81/6-VOL-2 .... p 31 N82-27803 #

UCID-19167 .... p 30 N82-27737 #

UCRL-15382 .... p 39 N82-26915 #

UMASS-ARF-82-321 .... p 76 N82-26907 #

USCIPI-1050 .... p 74 N82-2561* #

USGS-OFR-80-469 .... p 72 N82-23584* #

UTD-E0533-01 .... p 71 N82-22629* #

WHOI-81-104 .... p 39 N82-25748 #

WTHD-143 .... p 73 N82-24517 #

ACCESSION NUMBER INDEX

EARTH RESOURCES / *A Continuing Bibliography (Issue 35)* OCTOBER 1982

Typical Accession Number Index Listing

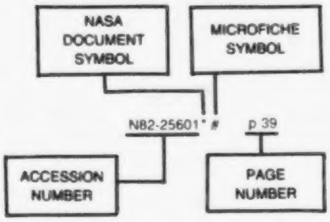

Listings in this index are arranged alphanumerically by accession number. The page number listed to the right indicates the page on which the citation is located. An asterisk (*) indicates that the item is a NASA report. A pound sign (#) indicates that the item is available on microfiche.

A82-13528 # p 58
A82-22294* # p 31
A82-22306* # p 49
A82-22538* # p 63
A82-22539 # p 1
A82-22540 # p 63
A82-22541* # p 1
A82-22542* # p 1
A82-22543 # p 1
A82-22544 # p 1
A82-22545 # p 21
A82-22546 # p 82
A82-22547* # p 82
A82-22548 # p 82
A82-22549 # p 82
A82-22550 # p 83
A82-22551 # p 83
A82-22552 # p 1
A82-22553 # p 83
A82-22554 # p 83
A82-22555* # p 64
A82-22556 # p 83
A82-22557 # p 2
A82-22558 # p 64
A82-22559 # p 2
A82-22560 # p 2
A82-22561 # p 2
A82-22562 # p 21
A82-22563 # p 2
A82-22564 # p 2
A82-22565 # p 2
A82-22566 # p 21
A82-22567 # p 21
A82-22568 # p 64
A82-22569 # p 21
A82-22570 # p 21
A82-22571 # p 3
A82-22572 # p 3
A82-22573 # p 64
A82-22574 # p 40
A82-22575 # p 64
A82-22576 # p 64
A82-22577 # p 64
A82-22578 # p 64
A82-22579 # p 65
A82-22580 p 65
A82-22581 # p 65
A82-22582 # p 65
A82-22583 # p 21
A82-22584* # p 3
A82-22585* # p 65
A82-22586* # p 65
A82-22587 # p 3
A82-22588 # p 22
A82-22589 # p 3
A82-22590 # p 66
A82-22591* # p 3
A82-22592* # p 4
A82-22593 # p 4
A82-22594 # p 4
A82-22595 # p 31
A82-22596 # p 31
A82-22597 # p 66
A82-22598 # p 31
A82-22599 # p 83
A82-22600 # p 4
A82-22601 # p 4
A82-22602 # p 4
A82-22603 # p 83
A82-22604 # p 40
A82-22605* # p 22
A82-22606* # p 22
A82-22607* # p 40
A82-22608 # p 76
A82-22609 # p 40
A82-22610 # p 4
A82-22611* # p 5
A82-22612* # p 5
A82-22613* # p 40
A82-22614 # p 31
A82-22615 # p 59
A82-22616 # p 22
A82-22617 # p 5
A82-22618 # p 5
A82-22619 # p 49
A82-28905 # p 66
A82-28907* # p 49
A82-29326* # p 66
A82-29327 # p 22
A82-29328 # p 66
A82-29332* # p 22
A82-29333 # p 60
A82-29409 # p 66
A82-29435 # p 5
A82-29526 p 5
A82-29527 # p 5
A82-29528 # p 5
A82-29529 # p 6
A82-29530 # p 6
A82-29531 # p 6
A82-29532 # p 6
A82-29533 # p 6
A82-29534 # p 6
A82-29535 # p 6
A82-29536 # p 6
A82-29537 # p 6
A82-29538* # p 7
A82-29539* # p 7
A82-29541 # p 76
A82-29601* # p 49
A82-29602* # p 49
A82-29603* # p 49
A82-29604 # p 49
A82-29607* # p 50
A82-29608* # p 50
A82-29609* # p 50
A82-29610* # p 50
A82-29611* # p 50
A82-29612 # p 50
A82-29613* # p 50
A82-29614* # p 51
A82-29615* # p 32
A82-29616* # p 51
A82-29617* # p 51
A82-29618* # p 51
A82-29619* # p 51
A82-29621* # p 52
A82-29622* # p 52
A82-29623* # p 52
A82-29624* # p 52
A82-29747 # p 7
A82-29762 # p 66
A82-29922 # p 76
A82-30293 # p 23
A82-30304 # p 41
A82-30305 # p 41
A82-30306 # p 32
A82-30307 # p 23
A82-30314 # p 32
A82-30666 # p 52
A82-30778 # p 32
A82-30784* # p 32
A82-30785* # p 32
A82-30786* # p 41
A82-30787* # p 32
A82-30788* # p 32
A82-30789* # p 32
A82-30790* # p 32
A82-30795* # p 33
A82-30796 # p 33
A82-30810 # p 52
A82-30849 # p 33
A82-30850 # p 83
A82-31019 # p 76
A82-31020 # p 76
A82-31294 # p 52
A82-31295 # p 23
A82-31990* # p 23
A82-31991 # p 77
A82-31994* # p 33
A82-31995* # p 53
A82-31996 # p 83
A82-32033 # p 67
A82-32077* # p 33
A82-32078* # p 33
A82-32084 # p 33
A82-32090 # p 33
A82-32096 # p 34
A82-32099 # p 34
A82-32342* # p 23
A82-32343* # p 67
A82-32344 # p 67
A82-32345* # p 67
A82-32346 # p 67
A82-32347 # p 67
A82-32348* # p 23
A82-32440 p 77
A82-32441* # p 23
A82-32442* # p 41
A82-32443* # p 77
A82-32447* # p 77
A82-32448* # p 77
A82-32507 # p 67
A82-32559 # p 53
A82-32581* # p 68
A82-32646* # p 34
A82-32651 # p 53
A82-32658* # p 77
A82-32701 # p 7
A82-32702 # p 77
A82-32703 # p 7
A82-32704 # p 7
A82-32705 # p 7
A82-32707 # p 8
A82-32708* # p 8
A82-32709 # p 68
A82-32711 # p 24
A82-32766 # p 78
A82-32824 # p 78
A82-32881 # p 53
A82-32882* # p 53
A82-32896* # p 60
A82-32897* # p 8
A82-32898 # p 41
A82-32899 # p 24
A82-32900 # p 68
A82-32901 # p 24
A82-32902 # p 53
A82-32903 # p 53
A82-32904* # p 68
A82-32905* # p 8
A82-32906 # p 68
A82-32907 # p 8
A82-32909* # p 8
A82-32910* # p 60
A82-32911 # p 68
A82-32912 # p 78
A82-32913* # p 8
A82-32914* # p 8
A82-32915* # p 78
A82-32916 # p 68
A82-32917 # p 54
A82-33293 # p 34
A82-33295 # p 34
A82-33296 # p 78
A82-33297 # p 78
A82-33322* # p 54
A82-33329 # p 60
A82-33402 # p 41
A82-33438* # p 54
A82-33442 # p 78
A82-33555 # p 84
A82-33652 # p 24
A82-33654 # p 24
A82-33655 # p 24
A82-33656 # p 24
A82-33657* # p 24
A82-33659* # p 24
A82-33717 # p 54
A82-33865 # p 25
A82-34116 # p 84
A82-34179* # p 8
A82-34218* # p 25
A82-34219 # p 54
A82-34222* # p 79
A82-34225 # p 68
A82-34367 # p 84
A82-34469 # p 69
A82-34470 # p 79
A82-34471 # p 79
A82-34701 p 79
A82-34702 # p 69
A82-34706 # p 9
A82-34708 # p 79
A82-34710 # p 9
A82-34711 # p 25
A82-34716 # p 9
A82-34717 # p 69
A82-34719 # p 34
A82-34720* # p 69
A82-34721* # p 42
A82-34722 # p 69
A82-34723 # p 69
A82-34724 # p 79
A82-34726 # p 69
A82-34727 # p 80
A82-34729* # p 9
A82-34730* # p 9
A82-34731 # p 9
A82-34732 # p 9
A82-34733 # p 9
A82-34734 # p 60
A82-34735 # p 60
A82-34736* # p 60
A82-34737 # p 80
A82-34739 # p 25
A82-34742 # p 80
A82-34743* # p 25
A82-34744* # p 25
A82-34745 # p 61
A82-34746 # p 80
A82-34918* # p 34
A82-34940 # p 69
A82-35126 p 61
A82-35127 # p 61
A82-35129 # p 61
A82-35130 # p 61
A82-35131 # p 61
A82-35132 # p 61
A82-35133 # p 61
A82-35134 # p 62
A82-35136 # p 62
A82-35138 # p 62
A82-35139 # p 10
A82-35140 # p 62
A82-35141 # p 70
A82-35534 # p 26
A82-35542* # p 26
A82-35650* # p 70
A82-35824* # p 70
A82-35895 # p 26
A82-36005 # p 54
A82-36018 # p 80
A82-36043 # p 70
A82-36053* # p 26
A82-36247 # p 26
A82-36266 # p 26
A82-36292* # p 27
A82-36293* # p 27
A82-36298* # p 42
A82-36341 # p 54
A82-36362* # p 27
A82-36405 # p 27
A82-36406 # p 27
A82-36414 # p 27
A82-36415* # p 28
A82-36422 # p 28
A82-36428 # p 28
A82-36431 # p 28
A82-36444 # p 28
A82-36472 # p 28
A82-36477 # p 29
A82-36534* # p 29
A82-36617* # p 84
A82-36741 # p 29
A82-36935 # p 70
A82-37048 # p 70
A82-37174 # p 62
A82-37175 # p 34
A82-37194 # p 10
A82-37195 # p 55
A82-37196 # p 55
A82-37198 # p 42
A82-37200 # p 70
A82-37390* # p 55
A82-37405* # p 29
A82-37501 # p 62
A82-37502 # p 29
A82-37503 # p 10
A82-37505 # p 55
A82-37589 # p 10
A82-37809 # p 80
A82-37810* # p 71
A82-37812* # p 81
A82-37962* # p 35

N82-22620* # p 84
N82-22621* # p 35
N82-22622* # p 71
N82-22623* # p 10
N82-22624* # p 42
N82-22625* # p 62
N82-22626* # p 10
N82-22627* # p 71
N82-22628* # p 35
N82-22629* # p 71
N82-22630 # p 84
N82-22636 # p 42
N82-22643* # p 81

N82-22644 # p 63
N82-22832 # p 35
N82-22846* # p 35
N82-22854 # p 63
N82-22865* # p 81
N82-23043 # p 29
N82-23116* # p 10
N82-23133* # p 11
N82-23258* # p 84
N82-23563* # p 35
N82-23564* # p 11
N82-23565* # p 11
N82-23566* # p 11
N82-23567* # p 71
N82-23568* # p 85
N82-23569* # p 42
N82-23570* # p 71
N82-23571* # p 35
N82-23572* # p 71
N82-23573* # p 36
N82-23574* # p 72
N82-23575* # p 72
N82-23576* # p 72
N82-23577* # p 36
N82-23578* # p 11
N82-23579* # p 11
N82-23580* # p 12
N82-23581* # p 12
N82-23582* # p 12
N82-23583* # p 72
N82-23584* # p 72
N82-23585* # p 12
N82-23586* # p 72
N82-23587* # p 36
N82-23588* # p 12
N82-23589* # p 13
N82-23590* # p 13
N82-23591* # p 13
N82-23592* # p 13
N82-23593* # p 13
N82-23594* # p 13
N82-23595* # p 13
N82-23596* # p 73
N82-23597* # p 14
N82-23598* # p 14
N82-23599* # p 73
N82-23600* # p 14
N82-23601* # p 14
N82-23602* # p 14
N82-23603* # p 14
N82-23604* # p 15
N82-23605* # p 73
N82-23606* # p 15
N82-23607* # p 15
N82-23608* # p 15
N82-23609* # p 15
N82-23610* # p 15
N82-23611* # p 16
N82-23612* # p 73
N82-23613* # p 73
N82-23614* # p 55
N82-23621 # p 43
N82-23623 # p 43
N82-23624 # p 43
N82-23625 # p 43
N82-23626 # p 43
N82-23627 # p 43
N82-23628 # p 43
N82-23629 # p 43
N82-23630 # p 43
N82-23631 # p 44
N82-23632 # p 44
N82-23633 # p 44
N82-23634 # p 44
N82-23635 # p 44
N82-23636 # p 44
N82-23637 # p 44
N82-23638 # p 44
N82-23639 # p 44
N82-23640 # p 45
N82-23641 # p 45
N82-23642 # p 45
N82-23643 # p 45
N82-23644 # p 45
N82-23793 # p 29
N82-23852 p 55
N82-23856 p 55
N82-23879 p 55
N82-23891 p 29
N82-23898 p 56
N82-23900 p 56
N82-23908 p 56
N82-23909 p 56
N82-23910 p 56
N82-23912 p 56
N82-23929 p 57
N82-23939 p 57
N82-23945 # p 57
N82-23963 # p 30
N82-24216 # p 85
N82-24263 # p 85
N82-24264 # p 81
N82-24489 # p 81
N82-24517 # p 73
N82-24518* # p 45
N82-24519* # p 16
N82-24520* # p 36
N82-24521* # p 45
N82-24522* # p 36
N82-24523* # p 16
N82-24563* # p 16
N82-24564* # p 16
N82-24565* # p 17
N82-24566* # p 30
N82-24567* # p 30
N82-24568* # p 85
N82-24569* # p 63
N82-24570* # p 73
N82-24572* # p 73
N82-24573* # p 36
N82-24574* # p 17
N82-24575* # p 17
N82-24576* # p 17
N82-24577* # p 36
N82-24578* # p 37
N82-24579* # p 45
N82-24580* # p 74
N82-24581* # p 74
N82-24582* # p 37
N82-24583* # p 37
N82-24584* # p 37
N82-24585* # p 17
N82-24586* # p 37
N82-24587* # p 37
N82-24588* # p 74
N82-24589* # p 38
N82-24590* # p 38
N82-24591* # p 38
N82-24592* # p 38
N82-24593* # p 38
N82-24594* # p 46
N82-24595* # p 74
N82-24596* # p 46
N82-24597* # p 57
N82-24598* # p 30
N82-24599* # p 38
N82-24600* # p 74
N82-24601* # p 63
N82-24602* # p 18
N82-24603* # p 38
N82-25601* # p 39
N82-25602* # p 81
N82-25603* # p 46
N82-25604* # p 39
N82-25605* # p 18
N82-25606* # p 18
N82-25607* # p 18
N82-25608* # p 18
N82-25609* # p 57
N82-25610* # p 81
N82-25611 # p 74
N82-25612 # p 74
N82-25613 # p 75
N82-25614 # p 75
N82-25620 # p 46
N82-25621 # p 46
N82-25622 # p 46
N82-25623 # p 46
N82-25625 # p 47
N82-25661* # p 30
N82-25748 # p 39
N82-26027 # p 75
N82-26037 # p 75
N82-26268 # p 39
N82-26525* # p 57
N82-26642 # p 82
N82-26741* # p 82
N82-26742* # p 18
N82-26743* # p 82
N82-26744* # p 82
N82-26745* # p 19
N82-26746* # p 85
N82-26747* # p 19
N82-26748* # p 39
N82-26749* # p 19
N82-26750* # p 47
N82-26751* # p 19
N82-26752* # p 19
N82-26753* # p 19
N82-26754* # p 20
N82-26755* # p 20
N82-26756* # p 75
N82-26757* # p 30
N82-26758* # p 58
N82-26759* # p 20
N82-26760* # p 20
N82-26761* # p 20
N82-26762 # p 20
N82-26763* # p 75
N82-26764 # p 58
N82-26765 # p 75
N82-26766 # p 58
N82-26907 # p 76
N82-26915 # p 39
N82-26944 # p 58
N82-26945 # p 58
N82-26948 # p 59
N82-26949 # p 59
N82-27737 # p 30
N82-27802 # p 31
N82-27803 # p 31
N82-27804 # p 47
N82-27805 # p 47
N82-27806 # p 47
N82-27807 # p 47
N82-27808 # p 47
N82-27809 # p 48
N82-27810 # p 48
N82-27811 # p 48
N82-27812 # p 48
N82-27813 # p 48
N82-27814 # p 48
N82-27815 # p 48
N82-27816 # p 59
N82-27882 # p 39
N82-27900 # p 40
N82-27949 # p 59

1. Report No. NASA SP-7041(35)	2. Government Accession No.	3. Recipient's Catalog No.
4. Title and Subtitle EARTH RESOURCES A Continuing Bibliography (Issue 35)		5. Report Date October 1982
		6. Performing Organization Code
7. Author(s)		8. Performing Organization Report No.
9. Performing Organization Name and Address National Aeronautics and Space Administration Washington, D.C. 20546		10. Work Unit No.
		11. Contract or Grant No.
12. Sponsoring Agency Name and Address		13. Type of Report and Period Covered
		14. Sponsoring Agency Code
15. Supplementary Notes		

16. Abstract

This bibliography list 587 reports, articles, and other documents introduced into the NASA Scientific and Technical Information System between July 1, and September 30, 1982. Emphasis is placed on the use of remote sensing and geophysical instrumentation in spacecraft and aircraft to survey and inventory natural resources and urban areas. Subject matter is grouped according to agriculture and forestry, environmental changes and cultural resources, geodesy and cartography, geology and mineral resources, hydrology and water management, data processing and distribution systems, instrumentation and sensors, and economic analysis.

17. Key Words (Suggested by Author(s)) Bibliographies Earth Resources Remote Sensors	18. Distribution Statement Unclassified - Unlimited		
19. Security Classif. (of this report) Unclassified	20. Security Classif. (of this page) Unclassified	21. No. of Pages 164	22. Price* $10.50 HC

*For sale by the National Technical Information Service, Springfield, Virginia 22161

NASA-Langley, 1982

PUBLIC COLLECTIONS OF NASA DOCUMENTS

DOMESTIC

NASA distributes its technical documents and bibliographic tools to eleven special libraries located in the organizations listed below. Each library is prepared to furnish the public such services as reference assistance, interlibrary loans, photocopy service, and assistance in obtaining copies of NASA documents for retention.

CALIFORNIA
University of California, Berkeley
COLORADO
University of Colorado, Boulder
DISTRICT OF COLUMBIA
Library of Congress
GEORGIA
Georgia Institute of Technology, Atlanta
ILLINOIS
The John Crerar Library, Chicago
MASSACHUSETTS
Massachusetts Institute of Technology, Cambridge
MISSOURI
Linda Hall Library, Kansas City
NEW YORK
Columbia University, New York
OKLAHOMA
University of Oklahoma, Bizzell Library
PENNSYLVANIA
Carnegie Library of Pittsburgh
WASHINGTON
University of Washington, Seattle

NASA publications (those indicated by an '*' following the accession number) are also received by the following public and free libraries

CALIFORNIA
Los Angeles Public Library
San Diego Public Library
COLORADO
Denver Public Library
CONNECTICUT
Hartford Public Library
MARYLAND
Enoch Pratt Free Library, Baltimore
MASSACHUSETTS
Boston Public Library
MICHIGAN
Detroit Public Library
MINNESOTA
Minneapolis Public Library and Information Center
NEW JERSEY
Trenton Public Library
NEW YORK
Brooklyn Public Library
Buffalo and Erie County Public Library
Rochester Public Library
New York Public Library
OHIO
Akron Public Library
Cincinnati and Hamilton County Public Library
Cleveland Public Library
Dayton Public Library
Toledo and Lucas County Public Library
TEXAS
Dallas Public Library
Fort Worth Public Library
WASHINGTON
Seattle Public Library
WISCONSIN
Milwaukee Public Library

An extensive collection of NASA and NASA-sponsored documents and aerospace publications available to the public for reference purposes is maintained by the American Institute of Aeronautics and Astronautics, Technical Information Service, 555 West 57th Street, 12th Floor, New York, New York 10019

EUROPEAN

An extensive collection of NASA and NASA-sponsored publications is maintained by the British Library Lending Division, Boston Spa, Wetherby, Yorkshire, England. By virtue of arrangements other than with NASA, the British Library Lending Division also has available many of the non-NASA publications cited in *STAR*. European requesters may purchase facsimile copy of microfiche of NASA and NASA-sponsored documents, those identified by both the symbols # and * from: ESA - Information Retrieval Service, European Space Agency, 8-10 rue Mario-Nikis, 75738 Paris CEDEX 15, France.

National Aeronautics and
Space Administration

Washington, D.C.
20546

Official Business
Penalty for Private Use, $300

SPECIAL FOURTH CLASS MAIL
BOOK

Postage and Fees Paid
National Aeronautics and
Space Administration
NASA-451

U.S. MAIL

NASA

POSTMASTER: If Undeliverable (Section 158
Postal Manual) Do Not Return